Munich Personal RePEc Archive

# Handbook of Sustainable Finance

Roncalli, Thierry

University of Paris-Saclay

1 January 2024

Online at https://mpra.ub.uni-muenchen.de/123868/
MPRA Paper No. 123868, posted 14 Mar 2025 08:01 UTC

# Handbook of Sustainable Finance

**Thierry Roncalli**

Université Paris-Saclay

Copyright © 2022–2024 by Thierry Roncalli

This book is published under a CC BY license (Creative Commons Attribution 4.0 International License)

https://creativecommons.org/licenses/by/4.0

This version: March 7, 2025.

# Contents

**Contents** vii

**Preface** ix

**List of Symbols and Notations** xi

**Abbreviations** xix

**1 Introduction** 1
- 1.1 Definition . . . 1
- 1.2 Short history of responsible and ethical investing . . . 2
- 1.3 The ESG ecosystem . . . 6
  - 1.3.1 Sustainable investment forum . . . 7
  - 1.3.2 Initiatives . . . 7
  - 1.3.3 Regulators . . . 13
  - 1.3.4 Reporting frameworks . . . 18
  - 1.3.5 Rating agencies and data providers . . . 25
- 1.4 Regulatory framework . . . 28
  - 1.4.1 EU taxonomy regulation . . . 33
  - 1.4.2 Climate benchmarks . . . 36
  - 1.4.3 Sustainable finance disclosure regulation . . . 36
  - 1.4.4 MiFID II and sustainable preferences . . . 38
  - 1.4.5 Corporate sustainability reporting directive . . . 39
- 1.5 The market of ESG investing . . . 42
  - 1.5.1 ESG strategies . . . 42
  - 1.5.2 The market share of ESG investing . . . 45
- 1.6 Conclusion . . . 48

**I ESG Risk** 51

**2 ESG Scoring** 53
- 2.1 Data and variables . . . 54
  - 2.1.1 Sovereign ESG data . . . 54
  - 2.1.2 Corporate ESG data . . . 65
- 2.2 Scoring system . . . 75
  - 2.2.1 ESG and scoring theory . . . 76
  - 2.2.2 Tree-based scoring methods . . . 77

2.2.3 Other statistical methods . . . 93
2.2.4 Performance evaluation criteria . . . 93
2.3 Rating system . . . 112
2.3.1 Definition . . . 112
2.3.2 ESG rating process . . . 113
2.3.3 Rating migration matrix . . . 117
2.3.4 Comparison with credit ratings . . . 131
2.4 Exercises . . . 132
2.4.1 Score normalization when the features are independent . . . 132
2.4.2 Probability distribution of an ESG score . . . 134

**3 Impact of ESG Investing on Asset Prices and Portfolio Returns 137**
3.1 Theoretical models . . . 138
3.1.1 An introduction to modern portfolio theory . . . 138
3.1.2 ESG risk premium . . . 151
3.1.3 ESG efficient frontier . . . 169
3.2 Empirical results . . . 178
3.2.1 Equity markets . . . 178
3.2.2 Fixed-income markets . . . 199
3.3 Cost of capital . . . 209
3.3.1 Cost of equity . . . 209
3.3.2 Cost of debt . . . 213
3.3.3 The case of sovereign issuers . . . 217
3.4 Exercises . . . 227
3.4.1 Equity portfolio optimization with ESG scores . . . 227

**4 Sustainable Financial Products 229**
4.1 ESG mutual funds . . . 229
4.1.1 Regulation . . . 230
4.1.2 Sustainable labels . . . 246
4.1.3 The market of ESG funds . . . 257
4.2 Green and social bonds . . . 266
4.2.1 Green bonds . . . 267
4.2.2 Social bonds . . . 281
4.2.3 Other sustainability-related instruments . . . 285
4.3 Sustainable alternative assets . . . 287
4.3.1 ESG private equity and debt funds . . . 292
4.3.2 Sustainable infrastructure . . . 294
4.3.3 Sustainable real estate . . . 296

**5 Impact Investing 297**
5.1 Definition . . . 299
5.1.1 Impact investing frameworks . . . 300
5.1.2 Historical perspectives . . . 307
5.1.3 Investing FOR impact vs. investing WITH impact . . . 315
5.1.4 Impact measurement . . . 320
5.2 Sustainable Development Goals . . . 325
5.2.1 Where we stand with the SDGs . . . 326

5.2.2 SDGs and impact investing . . . 333
5.2.3 SDG funds . . . 335
5.3 The market of impact investing . . . 342
5.3.1 Market size . . . 342
5.3.2 Market products . . . 348
5.4 An example with the biodiversity risk . . . 365
5.4.1 Definition . . . 366
5.4.2 Ecosystem functions and services . . . 394
5.4.3 Biodiversity threats and risks . . . 428
5.4.4 Biodiversity measurement . . . 539
5.4.5 Biodiversity governance and regulation . . . 549
5.4.6 Investment approaches . . . 559
5.5 Exercises . . . 564
5.5.1 Calculating the prevalence of undernourishment . . . 564
5.5.2 Calculating the species-area relationship using the theory of island biogeography 566
5.5.3 Species abundance models . . . 568
5.5.4 Valuation of risks to life and health . . . 569

**6 Engagement & Voting Policy 573**
6.1 Active ownership . . . 574
6.1.1 Definition . . . 574
6.1.2 The various forms of active ownership . . . 575
6.1.3 Individual versus collective engagement . . . 586
6.1.4 The role of institutional investors . . . 588
6.1.5 Performance of active ownership . . . 592
6.2 ESG voting . . . 593
6.2.1 Voting process . . . 593
6.2.2 Proxy voting . . . 593
6.2.3 Defining a voting policy . . . 595
6.2.4 Statistics about ESG voting . . . 597

**7 Extra-financial Accounting 609**
7.1 Historical perspectives . . . 609
7.2 Single vs. double materiality . . . 609
7.3 Environmental accounting . . . 609
7.3.1 National environmental accounts . . . 609
7.3.2 Corporate environmental accounts . . . 609
7.4 Sustainability accounting . . . 609
7.4.1 Social issues . . . 609
7.4.2 Governance factors . . . 609

**II Climate Risk 611**

**8 The Physics and Economics of Climate Change 613**
8.1 Awareness of climate change impacts . . . 614
8.1.1 Scientific evidence of global warming . . . 614
8.1.2 From the Holocene to the Anthropocene? . . . 624

8.1.3 The physics of climate change . . . 659
8.2 The ecosystem of climate change . . . 710
8.2.1 Scientists . . . 710
8.2.2 Conferences of the Parties . . . 723
8.2.3 Regulation policies . . . 739
8.3 Integrated assessment models . . . 750
8.3.1 The DICE model . . . 750
8.3.2 Other models . . . 774
8.3.3 Scenarios . . . 781
8.4 Environmentally-extended input-output model . . . 807
8.4.1 Input-output analysis . . . 807
8.4.2 Application to environmental problems . . . 819
8.4.3 Estimation of first-tier and indirect emissions . . . 823
8.4.4 Imported and exported carbon emissions . . . 836
8.4.5 Taxation, pass-through and price dynamics . . . 846
8.5 Exercises . . . 867

**9 Climate Risk Measures 869**
9.1 Carbon emissions . . . 870
9.1.1 Global warming potential . . . 870
9.1.2 Consolidation accounting at the company level . . . 876
9.1.3 Scope 1, 2 and 3 emissions . . . 878
9.1.4 Carbon emissions of investment portfolios . . . 894
9.1.5 Statistics . . . 896
9.1.6 Negative emissions, avoided emissions, and carbon offsetting . . . 899
9.2 Carbon intensity . . . 907
9.2.1 Physical intensity ratios . . . 907
9.2.2 Monetary intensity ratios . . . 908
9.2.3 Statistics . . . 911
9.3 Dynamic risk measures . . . 914
9.3.1 Carbon budget . . . 914
9.3.2 Carbon trend . . . 920
9.3.3 Participation, ambition and credibility for an alignment strategy . . . 929
9.3.4 Illustration . . . 934
9.4 Greenness measures . . . 938
9.4.1 Green taxonomy . . . 938
9.4.2 Green revenue share . . . 939
9.4.3 Green capex . . . 942
9.4.4 Other metrics . . . 942
9.5 Exercises . . . 942

**10 Transition Risk Modeling 943**
10.1 A primer on the economic analysis of negative externalities . . . 944
10.1.1 Optimal taxation . . . 944
10.1.2 Economic theory of quotas . . . 944
10.1.3 Game theory . . . 944
10.1.4 Uncertainty . . . 944
10.1.5 Irreversibility . . . 944

10.1.6 Cost-benefit analysis versus option theory . . . 944
10.2 Carbon tax and pricing . . . 944
10.2.1 Mathematics of carbon tax . . . 944
10.2.2 Abatement cost . . . 944
10.2.3 Cap-and-trade . . . 944
10.3 Stranded assets . . . 944
10.4 Decarbonization pathway . . . 945
10.4.1 Global analysis . . . 945
10.4.2 Sector analysis . . . 945
10.5 Transition risk measures . . . 945
10.5.1 Temperature rating modeling . . . 945
10.6 Exercises . . . 945

**11 Climate Portfolio Construction** **947**
11.1 Portfolio optimization in practice . . . 948
11.1.1 Equity portfolios . . . 948
11.1.2 Bond portfolios . . . 954
11.1.3 Advanced optimization problems . . . 961
11.2 Portfolio decarbonization . . . 967
11.2.1 Global reduction of the carbon footprint . . . 967
11.2.2 Sector-specific constraints . . . 973
11.2.3 Empirical results . . . 979
11.3 Net-zero investing . . . 991
11.3.1 Integrated approach . . . 991
11.3.2 Core-satellite approach . . . 1017
11.4 Exercise . . . 1029
11.4.1 Equity and bond portfolio optimization with green preferences . . . 1029
11.4.2 Monotonicity property of the order-statistic and naive approaches . . . 1032

**12 Physical Risk Modeling** **1033**
12.1 General circulation model . . . 1034
12.1.1 Carbon cycle . . . 1034
12.1.2 Greenhouse gas chemistry . . . 1034
12.1.3 Horizontal and vertical heat transport . . . 1034
12.1.4 Oceans . . . 1034
12.1.5 Carbon sinks . . . 1034
12.2 Statistical modeling of climate hazards . . . 1034
12.2.1 Chronic risk . . . 1034
12.2.2 Acute risk . . . 1034
12.3 Geolocation . . . 1035
12.3.1 Climate hazard location . . . 1035
12.3.2 Asset location . . . 1035
12.4 Applications . . . 1036
12.4.1 Cyclones and hurricanes . . . 1036
12.4.2 Drought . . . 1036
12.4.3 Floods . . . 1036
12.4.4 Extreme heat . . . 1036
12.4.5 Water stress . . . 1036

12.4.6 Wildfire . . . 1036
12.5 Exercises . . . 1036

**13 Climate Stress Testing and Risk Management 1037**
13.1 Transmission channels . . . 1038
13.1.1 Direct and indirect transmission . . . 1038
13.1.2 Credit transmission channel . . . 1038
13.1.3 Market transmission channel . . . 1038
13.1.4 Systemic risk . . . 1038
13.2 Climate risk hedging . . . 1039
13.3 Climate value-at-risk . . . 1039
13.4 Climate stress testing . . . 1039
13.5 Exercises . . . 1039

**Conclusion 1041**

**A Technical Appendix 1045**
A.1 Mathematical tools . . . 1045
A.1.1 Linear algebra . . . 1045
A.1.2 Optimization . . . 1047
A.1.3 Quadratic form . . . 1054
A.1.4 Nonnegative matrix . . . 1056
A.2 Statistical and probability analysis . . . 1057
A.2.1 Probability distributions . . . 1057
A.2.2 Copula functions . . . 1066
A.2.3 Estimation methods . . . 1077
A.3 Stochastic analysis . . . 1086
A.3.1 Stochastic optimal control . . . 1086
A.3.2 Jump-diffusion processes . . . 1086
A.4 Spatial data . . . 1086
A.4.1 Spherical coordinates . . . 1086
A.4.2 Geographic coordinate systems . . . 1086
A.4.3 Network common data form . . . 1086

**B Solutions to the Tutorial Exercises 1087**
B.1 Exercises related to ESG risk . . . 1087
B.1.1 Score normalization when the features are independent (Exercise 2.4.1) . . . 1087
B.1.2 Probability distribution of ESG scores (Exercise 2.4.4) . . . 1087
B.1.3 Equity Portfolio optimization with ESG scores (Exercise 3.4.1) . . . 1097
B.1.4 Calculating the prevalence of undernourishment (Exercise 5.5.1) . . . 1107
B.1.5 Calculating the species-area relationship using the theory of island biogeography (Exercise 5.5.2) . . . 1114
B.1.6 Species abundance models (Exercise 5.5.3) . . . 1124
B.1.7 Valuation of risks to life and health (Exercise 5.5.4) . . . 1129
B.2 Exercises related to climate risk . . . 1135
B.2.1 Equity and bond portfolio optimization with green preferences (Exercise 11.4.1) 1136

**Bibliography 1149**

**Subject Index** **1213**

**Author Index** **1225**

# Preface

## Teaching sustainable finance

I started teaching finance at the University of Bordeaux in 1995. My first course was called *Stochastic Finance* and was dedicated to option pricing and stochastic calculus. At that time I was also working as a consultant for a bank to develop numerical methods for some exotic payoffs. I realized that this academic course could benefit from this professional position. Indeed, I learnt that the main problem of traders is not the calculation of the option price, but the definition of the hedging strategy. Combining academic theory with professional practice has been a constant theme of my teaching career. In the 2000s, my risk management courses made extensive use of the risk management knowledge acquired at the Groupe de Recherche Opérationnelle (GRO) at Crédit Lyonnais and Crédit Agricole between 1999 and 2005. In the 2010s, my courses in asset management were largely based on the professional experience developed at SGAM AI and Lyxor Asset Management between 2005 and 2016. This sustainable finance course follows the same path. It is largely based on the ESG and climate investing research I have conducted at Amundi Asset Management since 2018.

Although this course has many features in common with the previous ones, sustainable finance is not as mature as option pricing, risk management and asset management. In particular, regulation is in its infancy and not yet stabilized, academic models are still in their infancy, data are noisy, biased and of poor quality, and even concepts are not well defined. In this context, all actors (investors, issuers, financial institutions, regulators, etc.) are adopting a *learning-by-doing* approach. This has important implications for the development of a training course. Each year, the course needs to be updated by incorporating new advances in modeling, adjusting definitions, changing the structure of the lecture notes, removing obsolete sections and adding new paragraphs. Since its inception, the course has been a continuous work in progress.

The issue of sustainable economic growth is a major change in the way economics and finance are taught. However, most academic models do not take climate change into account because they were developed in the 19th and 20th centuries. Taking climate change into account requires a complete overhaul of economic theory and many related concepts: economic growth, negative externality, moral hazard, labor productivity, economic rationality, consumption maximization, social welfare, Pareto optimality, invisible hand, market efficiency, utility function, homo economicus, capital allocation, risk theory, golden rule, overlapping generations model, steady state, non-cooperative games, etc. As teachers, it is difficult to adapt to this new world because we lack distance and cannot benefit from well-established textbooks. However, we cannot wait because time is running out. Therefore, we have a heavy responsibility to educate students about these important issues without adequate tools and a normative framework. This explains why there are thousands of ways to teach sustainable finance. It is not a science. Then be careful about the content, because it necessarily reflects our personal beliefs and experiences. And so I claim the right to be biased.

## About these lecture notes

In January 2019, I started to introduce some elements of ESG and climate investing in my course *Advanced Asset Management*. At that time, it was only about portfolio optimization with ESG scores and carbon footprints. Over the years, the part dedicated to sustainable finance has increased and now makes up 25% of the course. In 2021, we had some discussions at the University of Paris-Saclay about the future development of the Masters in Finance. We decided to create a full and comprehensive course in sustainability finance, going beyond portfolio allocation. For the 2021/2022 academic year, I then put together a set of 770 slides for the first course at Paris-Saclay University. During the year, Peter Tankov also offered to share his course *Green Finance* at ENSAE Paris. Today, sustainable finance is taught in four master's programs: *Master in Risk and Asset Management* (Paris-Saclay University), *Master in Quantitative Finance* (Paris-Saclay University), *Master in Banking & Finance* (Paris-Saclay University), *Master in Statistics, Finance and Actuarial Science* (ENSAE Paris and Paris Cité University). These three courses differ in the number of hours and the scientific approach (qualitative/quantitative and economics/mathematics). Unfortunately, creating three different lecture notes was not effective because there was a lot of overlap between them. Therefore, I decided to write a single set of lecture notes and use them for each course. This explains why some parts of this handbook are very descriptive, but other parts are technical and require a mathematical background in probability, statistics, machine learning, linear algebra, optimization and stochastic analysis.

The publication of my previous lecture notes on risk management (Roncalli, 2020a, Handbook of Financial Risk Management) was a great disappointment. In fact, the publisher has set a high price that is prohibitive for my students. Therefore, I have decided to publish this manual for free. Whatever happens, the electronic version of this manual is and will remain free for my students and everyone else. It is available at the following web site:

http://www.thierry-roncalli.com/SustainableFinanceBook.html

## Acknowledgments

I would like to thank the various people who helped me organize these academic courses, in alphabetical order: Michel Guillard, Eleni Iliopulos, Claire Loupias, Fabrice Pansard, Peter Tankov and Fabien Tripier. I would also like to thank all the Masters students who participated in my Sustainable Finance courses.

I would also like to thank all my co-authors at Amundi Asset Management, in particular Inès Barahhou, Mohamed Ben Slimane, Leila Bennani, Amina Cherief, Baptiste Desnos, Angelo Drei, Théo Le Guenedal, Frédéric Lepetit, Edmond Lezmi, Dorianne Lucius, François Lombard, Noureddine Oulid Azouz, Théo Roncalli, Raphaël Semet, Lauren Stagnol, Takaya Sekine and Jiali Xu. I have been learning about the practice of sustainable finance since I joined Amundi's quantitative research team. The writing of these lecture notes is therefore heavily influenced by the materials and models developed at Amundi.

I would also like to thank Mohamed Ben Slimane, Amina Cherief, Frédéric Lepetit, Wassim Le Lann, Théo Roncalli and Jiali Xu for helping with the data, reading and commenting on some parts of this book, or testing the exercises.

Paris, October 2023 Thierry Roncalli

# List of Symbols and Notations

## Symbol Description

| | |
|---|---|
| $\times$ | Arithmetic multiplication |
| $\cdot$ | Scalar, vector and matrix multiplication |
| $*$ | Convolution |
| $\circ$ | Hadamard product $(x \circ y)_i = x_i y_i$ |
| $\otimes$ | Kronecker product $A \otimes B$ |
| $\lvert\mathcal{E}\rvert$ | Cardinality of the set $\mathcal{E}$ |
| $\prec$ | Preference ordering |
| $\langle x, x' \rangle$ | Inner product of $x$ and $x'$ |
| | |
| $\mathbf{0}$ (or $\mathbf{0}_n$) | Vector of zeros |
| $\mathbf{1}$ (or $\mathbf{1}_n$) | Vector of ones |
| $\mathbb{1}\{\mathcal{A}\}$ | The indicator function is equal to 1 if $\mathcal{A}$ is true, 0 otherwise |
| $\mathbb{1}_{\mathcal{A}}\{x\}$ | The characteristic function is equal to 1 if $x \in \mathcal{A}$, 0 otherwise |
| | |
| $a$ | Subarea $a \subseteq A$ |
| $A$ | Area $A$ |
| $(A_{i,j})$ | Matrix $A$ with entry $A_{i,j}$ in row $i$ and column $j$ |
| $A^{-1}$ | Inverse of the matrix $A$ |
| $A^{\top}$ | Transpose of the matrix $A$ |
| $A^{+}$ | Moore-Penrose pseudo-inverse of the matrix $A$ |
| $\boldsymbol{\mathcal{AE}}$ | Avoided emissions |
| $\mathrm{AS}(w \mid b)$ | Asset-based active share |
| $\mathrm{AS}_{\boldsymbol{\mathcal{S}}ector}(w \mid b)$ | Sector-based active share |
| $\alpha_p$ | Planetary albedo (default value = 0.29) |
| | |
| $b$ | Vector of weights $(b_1, \ldots, b_n)$ for the benchmark $b$ |
| $\mathfrak{b}$ | $\mathfrak{b}$-score (or Beta score) |
| $B_\lambda(\lambda, \mathcal{T})$ | Planck radiation law |
| $\mathcal{B}(p)$ | Bernoulli distribution with parameter $p$ |
| $\mathcal{B}(n, p)$ | Binomial distribution with parameters $n$ and $p$ |
| $\mathcal{B}ates(n)$ | Bates distribution with parameter $n$ |
| $\mathcal{B}(\alpha, \beta)$ | Beta distribution with parameters $\alpha$ and $\beta$ |
| $\beta_i$ | Beta of asset $i$ with respect to portfolio $w$ |
| $\beta_i(w)$ | Another notation for the symbol $\beta_i$ |
| $\beta(w \mid b)$ | Beta of portfolio $w$ when the benchmark is $b$ |
| | |
| $c$ | Specific heat capacity |
| $\mathrm{cov}(X)$ | Covariance of the random vector $X$ |
| $\mathcal{C}_i$ | Carry of bond $i$ |
| $\mathbb{C}$ (or $\rho$) | Correlation matrix |

| | |
|---|---|
| $\mathbb{C}_n(\rho)$ | Constant correlation matrix of size $n$ with uniform correlation $\rho$ |
| $[C]$ | Concentration |
| $\boldsymbol{\mathcal{CB}}(t_1, t_2)$ | Carbon budget between $t_1$ and $t_2$ |
| $\mathcal{CC}$ | Concentration rate |
| $\boldsymbol{\mathcal{CE}}$ | Carbon emissions |
| $\boldsymbol{\mathcal{CI}}$ | Carbon intensity |
| $\boldsymbol{\mathcal{CI}}^{\star}$ | Maximum carbon intensity value or threshold |
| $\boldsymbol{\mathcal{CM}}$ | Carbon momentum |
| $\boldsymbol{\mathcal{CM}}^{\mathcal{L}ong}$ | Long-term carbon momentum |
| $\boldsymbol{\mathcal{CM}}^{Short}$ | Short-term carbon momentum |
| CPI | Consumer price index |
| | |
| $d$ | Distance |
| $\det(A)$ | Determinant of the matrix $A$ |
| $\operatorname{diag}(a)$ | Diagonal matrix with elements $(a_1, \ldots, a_n)$ |
| $D$ | Covariance matrix of idiosyncratic risks |
| $\mathcal{D}^{\eta}(p)$ | Hill number (or diversity index of order $\eta$) |
| $\mathcal{D}(x)$ | Discriminant curve |
| $\mathcal{D}(a)$ | Diagonal matrix $\mathcal{D}(a) = \operatorname{diag}(a)$ with elements $(a_1, \ldots, a_n)$ |
| $\mathrm{DTS}_i$ | Duration-times-spread factor of bond $i$ |
| $\mathrm{DTS}(w)$ | Duration-times-spread factor of portfolio $w$ |
| $\delta(t)$ | Net diversification rate |
| $\delta\mathrm{D}$ | Deuterium isotope ratio ($^2\mathrm{H}/^1\mathrm{H}$) |
| $\delta^{13}\mathrm{C}$ | Carbon isotope ratio ($^{13}\mathrm{C}/^{12}\mathrm{C}$) |
| $\delta^{18}\mathrm{O}$ | Oxygen isotope ratio ($^{18}\mathrm{O}/^{16}\mathrm{O}$) |
| | |
| $\mathbf{e}_i$ | The value of the vector is 1 for the row $i$ and 0 elsewhere |
| $E_a$ | Expected number of species endemic to the subarea $a \subseteq A$ |
| $\exp(A)$ | Exponential of the matrix $A$ |
| $\mathbb{E}[X]$ | Mathematical expectation of the random variable $X$ |
| $\mathcal{E}$ | Set of edges in a graph |
| $\mathcal{E}(\lambda)$ | Exponential probability distribution with parameter $\lambda$ |
| $\boldsymbol{\mathcal{E}}$ | Energy flux (or radiation flux) |
| $\mathrm{EAR}(a)$ | Endemics-area relationship in subarea $a \subseteq A$ |
| $\boldsymbol{\mathcal{EF}}$ | Emission factor |
| $\varepsilon$ | Emissivity |
| | |
| $f(x)$ | Probability density function |
| $F$ | Climate forcing |
| $F_{\mathrm{solar}}$ | Incoming solar radiation (default value = $242.82\,\mathrm{W/m^2}$) |
| $\mathbf{F}(x)$ | Cumulative distribution function |
| $\mathbf{F}^{-1}(\alpha)$ | Quantile function |
| $\mathcal{F}$ | Vector of risk factors $(\mathcal{F}_1, \ldots, \mathcal{F}_m)$ |
| $\mathcal{F}_j$ | Risk factor $j$ |
| $\mathcal{F}_t$ | Filtration |
| | |
| $\boldsymbol{g}$ | Greenium |
| $\boldsymbol{\mathcal{G}}$ | Greenness measure |
| $\mathcal{G}(p)$ | Geometric distribution with parameter $p$ |
| $\mathcal{G} = (\mathcal{V}, \mathcal{E})$ | Graph with vertices $\mathcal{V}$ and edges $\mathcal{E}$ |
| $\boldsymbol{\mathcal{GI}}$ | Green intensity |
| $\mathcal{G}ini$ | Gini coefficient |
| $\boldsymbol{\mathcal{GRS}}$ | Green revenue share |
| $\gamma$ | Risk-tolerance coefficient |

| | |
|---|---|
| $\bar{\gamma}$ | Risk-aversion coefficient |
| $\gamma_1$ | Skewness |
| $\gamma_2$ | Excess kurtosis |
| $\mathcal{H}(p)$ | Herfindahl index |
| $i$ | Asset (or component) $i$ |
| $I_n$ | Identity matrix of dimension $n$ |
| $\mathcal{I}(p)$ | Shannon entropy of the distribution $p$ |
| $\mathcal{I}(X)$ | Shannon entropy of the random variable $X$ |
| $\mathcal{I}(X,Y)$ | Shannon entropy of the random vector $(X,Y)$ |
| $\mathcal{I}(X \cap Y)$ | Mutual information of the random vector $(X,Y)$ |
| $\mathcal{I}^{\star}(p)$ | Shannon diversity index |
| $\mathcal{IG}(\mu,\lambda)$ | Inverse Gaussian distribution with parameters $\mu$ and $\lambda$ |
| $\mathrm{IR}(w \mid b)$ | Information ratio of portfolio $w$ with respect to the benchmark $b$ |
| $\mathbb{K}$ | State space $(1,\ldots,K)$ |
| $\boldsymbol{\kappa}_j^{\mathrm{up}}$ | Upstreamness index of sector $j$ |
| $\boldsymbol{\kappa}_j^{\mathrm{down}}$ | Downstreamness index of sector $j$ |
| $\mathrm{LE}(t;\varrho)$ | Discounted lifetime expectancy |
| $\ln(A)$ | Logarithm of the matrix $A$ |
| $\boldsymbol{\ell}(\theta)$ | Log-likelihood function with $\theta$ the vector of parameters to estimate |
| $\boldsymbol{\ell}_t$ | Log-likelihood function for the observation $t$ |
| $\mathcal{L}(x;\lambda)$ | Lagrange function, whose Lagrange multiplier is $\lambda$ |
| $\boldsymbol{\mathcal{L}}$ | Leontief inverse matrix |
| $\tilde{\boldsymbol{\mathcal{L}}}$ | Dual inverse matrix (or upstream multiplier matrix) |
| $\breve{\boldsymbol{\mathcal{L}}}$ | Downstream multiplier matrix |
| $\lambda(t)$ | Origination (or speciation) rate |
| $\lambda(p)$ | Simpson index |
| $\mathit{m}$ | $\mathit{m}$-score (or min-max score) |
| $\mathcal{M}ap$ | Map function |
| $\mathrm{MD}_i$ | Modified duration of bond $i$ |
| $\mathrm{MD}(w)$ | Modified duration of portfolio $w$ |
| $\mu$ | Vector of expected returns $(\mu_1,\ldots,\mu_n)$ |
| $\mu_i$ | Expected return of asset $i$ |
| $\mu_m$ | Expected return of the market portfolio |
| $\hat{\mu}$ | Empirical mean |
| $\mu(w)$ | Expected return of portfolio $w$ |
| $\mu(X)$ | Mean of the random vector $X$ |
| $\mu_m(X)$ | $m$-th centered moment of the random vector $X$ |
| $\mu'_m(X)$ | $m$-th moment of the random vector $X$ |
| $\mu(t)$ | Extinction rate |
| $n_i$ | Abundance (number of individuals) of species $i$ (rank abundance distribution) |
| $n_S$ | Number of scenarios or simulations |
| $\mathcal{N}(\mu,\sigma^2)$ | Normal distribution with mean $\mu$ and standard deviation $\sigma$ |
| $\mathcal{N}(\mu,\Sigma)$ | Multivariate normal distribution with mean $\mu$ and covariance matrix $\Sigma$ |
| $\mathcal{NRD}(\mu_x,\sigma_x^2,\mu_y,\sigma_y^2)$ | Ratio distribution of $Z = X/Y$ where $X \sim \mathcal{N}(\mu_x,\sigma_x^2)$ and $Y \sim \mathcal{N}(\mu_y,\sigma_y^2)$ |
| $\Omega$ | Covariance matrix of risk factors |
| $p(k)$ | Probability mass function of an integer-valued random variable |
| $P$ | Markov transition matrix |

| | |
|---|---|
| $P(t)$ | Transition matrix at time $t$ |
| $P(\Sigma)$ | Cholesky decomposition of $\Sigma$ |
| $\mathcal{P}(\lambda)$ | Poisson distribution with parameter $\lambda$ |
| $\mathcal{P}(x)$ | Performance curve |
| PPI | Producer price index |
| $\pi$ | Vector of risk premia |
| $\pi^\star$ | Stationary distribution |
| $\pi_{\text{cpi}}$ | Inflation rate (consumer price index) |
| $\pi_m$ | Market risk premium |
| $\pi_n^-$ | 1-diversity distribution |
| $\pi_n^+$ | $n$-diversity distribution |
| $\pi_{\text{ppi}}$ | Inflation rate (producer price index) |
| $\phi(x)$ | Probability density function of the standardized normal distribution |
| $\phi_2(x_1, x_2; \rho)$ | Probability density function of the bivariate normal distribution with correlation $\rho$ |
| $\phi_n(x; \Sigma)$ | Probability density function of the multivariate normal distribution with covariance matrix $\Sigma$ |
| $\Phi(x)$ | Cumulative density function of the standardized normal distribution |
| $\Phi^{-1}(\alpha)$ | Inverse of the cdf of the standardized normal distribution |
| $\Phi_2(x_1, x_2; \rho)$ | Cumulative density function of the bivariate normal distribution with correlation $\rho$ |
| $\Phi_n(x; \Sigma)$ | Cumulative density function of the multivariate normal distribution with covariance matrix $\Sigma$ |
| | |
| $q$ | $q$-score (or quantile score) |
| $\text{QALE}(t; \varrho)$ | Value of per statistical life year |
| $\mathcal{QF}(x; Q, R, c)$ | Quality-adjusted life expectancy |
| | |
| $r$ | Radius |
| $r$ | Return of the risk-free asset |
| $R$ | Vector of asset returns $(R_1, \ldots, R_n)$ |
| $R_i$ | Return of asset $i$ |
| $R_{i,t}$ | Return of asset $i$ at time $t$ |
| $R_{m,t}$ | Return of the market portfolio at time $t$ |
| $R(w)$ | Return of portfolio $w$ |
| $\mathcal{R}(t)$ | Rating of the entity at time $t$ |
| $\mathcal{R}(w)$ | Risk measure of portfolio $w$ |
| $\boldsymbol{\mathcal{R}}$ | Reduction rate of carbon emissions |
| $\boldsymbol{\mathcal{R}}(w \mid b)$ | Carbon footprint reduction rate of portfolio $w$ wrt benchmark $b$ |
| $\mathfrak{R}^2$ | Coefficient of determination |
| $\mathcal{RN}(\mu, \sigma^2)$ | Reciprocal normal distribution of $Y = 1/X$ where $X \sim \mathcal{N}(\mu, \sigma^2)$ |
| $\varrho$ | Discount rate |
| $\rho$ (or $\mathbb{C}$) | Correlation matrix of asset returns |
| $\rho_{i,j}$ | Correlation between asset returns $i$ and $j$ |
| $\rho(x, y)$ | Correlation between portfolios $x$ and $y$ |
| | |
| $s$ | Credit spread |
| $s(j)$ | Number of species with exactly $j$ individuals (species abundance distribution) |
| $\boldsymbol{s}_j$ | Mapping vector of sector $j$ |
| $\boldsymbol{\mathcal{S}}ector_j$ | Sector $j$ |
| $S$ | Number of species |
| $\boldsymbol{\mathcal{S}}$ | ESG score |
| $\boldsymbol{\mathcal{S}}^\star$ | Minimum ESG score or threshold |
| $S_0$ | Total solar irradiance or solar constant (default value = $1\,368\,\text{W/m}^2$) |
| $\mathcal{S}(x)$ | Selection curve |
| $\mathcal{S}(t)$ | Survival function |

| | |
|---|---|
| $S_a$ | Expected number of species in subarea $a \subseteq A$ — $S_a = \mathbb{E}\left[\tilde{S}_a\right]$ |
| $\tilde{S}_a$ | Random number of species in subarea $a \subseteq A$ |
| $\text{SAR}(a)$ | Species-area relationship in subarea $a \subseteq A$ |
| $\boldsymbol{\mathcal{SC}}_1$ | Scope 1 |
| $\boldsymbol{\mathcal{SC}}_2$ | Scope 2 |
| $\boldsymbol{\mathcal{SC}}_3^{\text{up}}$ | Upstream scope 3 |
| $\boldsymbol{\mathcal{SC}}_3^{\text{down}}$ | Downstream scope 3 |
| $\boldsymbol{\mathcal{SC}}_3$ | Scope 3 ($= \boldsymbol{\mathcal{SC}}_3^{\text{up}} + \boldsymbol{\mathcal{SC}}_3^{\text{down}}$) |
| $\boldsymbol{\mathcal{SC}}_{1-2}$ | Scope 1 and 2 |
| $\boldsymbol{\mathcal{SC}}_{1-3}^{\text{up}}$ | Scope 1, 2 and upstream 3 ($= \boldsymbol{\mathcal{SC}}_1 + \boldsymbol{\mathcal{SC}}_2 + \boldsymbol{\mathcal{SC}}_3^{\text{up}}$) |
| $\boldsymbol{\mathcal{SC}}_{1-3}$ | Scope 1, 2 and 3 |
| $\text{SR}(w \mid r)$ | Sharpe ratio of portfolio $w$ when the risk-free rate is equal to $r$ |
| $\sigma$ | Stefan-Boltzmann constant (default value $= 5.67 \times 10^{-8}\,\text{W/m}^2\,\text{K}^{-4}$) |
| $\sigma_i$ | Volatility of asset $i$ |
| $\sigma_m$ | Volatility of the market portfolio |
| $\tilde{\sigma}_i$ | Idiosyncratic volatility of asset $i$ |
| $\hat{\sigma}$ | Empirical volatility |
| $\sigma(w)$ | Volatility of portfolio $w$ |
| $\sigma(w \mid b)$ | Tracking error volatility of portfolio $w$ wrt benchmark $b$ |
| $\sigma_{\text{AS}}(w \mid b)$ | Active share active risk of portfolio $w$ wrt benchmark $b$ |
| $\sigma_{\text{MD}}(w \mid b)$ | Duration active risk of portfolio $w$ wrt benchmark $b$ |
| $\sigma_{\text{DTS}}(w \mid b)$ | DTS active risk of portfolio $w$ wrt benchmark $b$ |
| $\sigma(X)$ | Standard deviation of the random variable $X$ |
| $\Sigma$ | Covariance matrix |
| $\hat{\Sigma}$ | Empirical covariance matrix |
| | |
| $t_\nu$ | Student's $t$ distribution with $\nu$ degrees of freedom |
| $t_n(\Sigma, \nu)$ | Multivariate $t$ distribution with $\nu$ degrees of freedom and covariance matrix $\Sigma$ |
| $\text{trace}(A)$ | Trace of the matrix $A$ |
| $\mathbf{T}(x; \nu)$ | Cumulative density function of the Student's $t$ distribution with $\nu$ degrees of freedom |
| $\mathbf{T}^{-1}(\alpha; \nu)$ | Inverse of the cdf of the Student's $t$ distribution with $\nu$ degrees of freedom |
| $\mathbf{T}_n(x; \Sigma, \nu)$ | Cumulative density function of the $t$ distribution with parameters $\Sigma$ and $\nu$ |
| $\mathbf{T}_2(x_1, x_2; \rho, \nu)$ | Cumulative density function of the bivariate $t$ distribution with parameters $\rho$ and $\nu$ |
| $\mathcal{T}(u)$ | Matrix $\mathcal{T}(u) = uu^\top$ of dimension $n \times n$ where $a$ is a $n \times 1$ vector |
| $\mathcal{T} = (\mathcal{V}, \mathcal{E})$ | Tree with vertices $\mathcal{V}$ and edges $\mathcal{E}$ |
| $\mathcal{T}$ | Temperature |
| $\mathcal{T}_a$ | Air/atmospheric temperature |
| $\mathcal{T}_e$ | Effective temperature (default value $= degK255.81$ or $-17.34°\text{C}$) |
| $\mathcal{T}_s$ | Earth's surface temperature |
| $\boldsymbol{\mathcal{TS}}$ | Temperature score |
| $\tau$ | Relaxation time (or half-life) |
| $\boldsymbol{\tau}$ | Hitting time |
| $\theta$ | Vector of parameters |
| $\hat{\theta}$ | Estimator of $\theta$ |
| | |
| $\mathcal{U}_{[a,b]}$ | Uniform distribution between $a$ and $b$ |
| $\boldsymbol{\mathcal{U}}(W)$ | Utility function of the wealth $W$ |
| | |
| $\text{var}(X)$ | Variance of the random variable $X$ |
| $\mathcal{V}$ | Set of vertices in a graph |
| $\text{VSL}(t)$ | Value of a statistical life |
| $\text{VSLY}(t)$ | Value of per statistical life year |

| | |
|---|---|
| $w$ | Vector of weights $(w_1, \ldots, w_n)$ for portfolio $w$ |
| $w^\star$ | Mean-variance optimized portfolio |
| $w^*$ | Tangency portfolio |
| $w_i$ | Weight of asset $i$ in portfolio $w$ |
| $w_{\text{gmv}}$ | Global minimum variance portfolio |
| $w_m$ | Market portfolio |
| $W$ | Wealth |
| $x^+$ | Maximum value between $x$ and 0 |
| $X$ | Random variable |
| $X_{i:n}$ | $i^{\text{th}}$ order statistic of a sample of size $n$ |
| $y$ | Yield to maturity |
| $z$ | Altitude |
| $z$ | Exponent of the species-area relationship $S = cA^z$ |
| $z$ | $z$-score (or Gaussian score) |

## Other scientific conventions

| | |
|---|---|
| YYYY-MM-DD | We use the international standard date notation where YYYY is the year in the usual Gregorian calendar, MM is the month of the year between 01 (January) and 12 (December), and DD is the day of the month between 01 and 31. |
| AD | Anno Domini |
| BP | Before present (1950) |
| Kyr/kyr/ka | 1 000 years |
| Myr/myr/Ma | 1 000 000 years |
| Gyr/byr/Ga | 1 000 000 000 years |
| USD (or \$) | US dollar |
| EUR (or €) | Euro |
| KUSD | One thousand dollars |
| \$1 mn/bn/tn | One million/billion/trillion dollars |
| % | Percent or 0.01 |
| ‰ | Per mil or 0.1% |
| bp | Basis point or 0.01% |
| E/MSY | Number of extinctions per million species per year |
| Mbp | Million base pairs |
| $2n$ | Diploid number of chromosomes |
| pg | C-value of DNA (picogram) |
| ha | Hectare (square with 100-meter sides = 10 000 $\text{m}^2$) |
| Mha | Million hectares |
| \$/ha/yr | Value of ecosystem services in international dollars per hectare per year (alternative notation: \$ $\text{ha}^{-1}$ $\text{yr}^{-1}$) |
| \$ bn/yr, \$ tn/yr | Value of ecosystem services in billions/trillions of dollars per year |
| ppm | Part per million |
| ppmv | Part per million by volume |
| ppb | Part per billion |
| ppbv | Part per billion by volume |

| | |
|---|---|
| AS | Arsenic |
| B(a)P | Benzo[a]pyrene |
| Cd | Cadmium |
| $CH_4$ | Methane |
| CO | Carbon monoxide |
| $CO_2$ | Carbon dioxide |
| $CO_2e$ | Carbon dioxide equivalent |
| Cr | Chromium |
| $H_2O$ | Water vapor |
| Hg | Mercury |
| $N_2O$ | Nitrous oxide |
| $NH_3$ | Ammonia |
| Ni | Nickel |
| $NO_2$ | Nitrogen dioxide |
| $NO_x$ | Nitrogen oxides |
| $O_3$ | Ozone |
| Pb | Lead |
| $PM_{2.5}$ | Particulate matter |
| $PM_{10}$ | Particulate matter |
| $SO_2$ | Sulfur dioxide |
| | |
| $gCO_2e$ | One gram of $CO_2e$ |
| $kgCO_2e$ | One kilogram of $CO_2e$ (= 1 000 $gCO_2e$) |
| $tCO_2e$ | One tonne of $CO_2e$ (= 1 000 $kgCO_2e$) |
| $ktCO_2e$ | One kilotonne of $CO_2e$ (= 1 000 $tCO_2e$) |
| $MtCO_2e$ | One megatonne of $CO_2e$ (= $10^6$ $tCO_2e$) |
| $GtCO_2e$ | One gigatonne of $CO_2e$ (= $10^9$ $tCO_2e$) |
| $gCO_2e$/$ | One gram of $CO_2e$ per one dollar |
| $tCO_2e$/$ mn | One tonne of $CO_2e$ per one million of dollar |
| | |
| Ton | Imperial unit of weight equivalent to 1 016.047 kilograms |
| Tonne | Metric unit of weight equivalent to 1 000 kilograms (also known as a metric ton) |
| | |
| Cal (or kcal) | Calorie, kilocalorie or 1 000 calories |
| Hz | Frequency (Hertz or $s^{-1}$) |
| J | Energy (Joule or $m^2\,kg\,s^{-2}$ or $N\,m$) |
| K | Temperature (Kelvin) |
| kg | Mass (kilogram) |
| m | Length (meter) |
| $m^2$ | Area (square meter) |
| $m\,s^{-2}$ | Acceleration (meter per square second) |
| N | Force (Newton or $m\,kg\,s^{-2}$) |
| Pa | Pressure (Pascal or $m^{-1}\,kg\,s^{-2}$ or $N\,m^{-2}$) |
| s | Time (second) |
| W | Power (Watt or $m^2\,kg\,s^{-3}$ or $J\,s^{-1}$) |
| $W\,m^{-2}$ | Irradiance (Watt per square meter or $kg\,s^{-3}$) |

# Abbreviations

**ACPR** Autorité de contrôle prudentiel et de résolution
**ADB** Asian development bank
**AGM** Annual general meeting
**AI** Artificial intelligence
**AIF** Alternative investment fund
**AMOC** Atlantic meridional overturning circulation
**APS** Announced pledges scenario
**AQI** Air quality index
**AUM** Assets under management

**B-Corp** Benefit corporation
**BAU** Business as usual
**BCBS** Basel committee on banking supervision
**BECCS** Bio-energy carbon capture and storage
**BII** Biodiversity intactness index
**BIS** Bank for international settlements
**BMI** Body mass index
**BMR** EU benchmark regulation
**BoE** Bank of England

**CAPM** Capital asset pricing model
**CAT** Cap-and-trade
**CBAM** Carbon border adjustment mechanism
**CBD** Convention on biological diversity
**CBI** Climate bonds initiative
**CBIRC** China banking and insurance regulatory commission
**CCF** Corporate carbon footprint
**CCUS** Carbon capture, use, and storage
**CDP** Carbon disclosure project
**CDR** Carbon dioxide removal
**CDSB** Climate disclosure standards board
**CE** Carbon emissions
**CEO** Chief executive officer
**Ceres** Coalition for environmentally responsible economies
**CFP** Corporate financial performance
**CI** Carbon intensity
**CICES** Common International Classification of Ecosystem Services
**CITES** Convention on international trade in endangered species of wild fauna and flora
**CMA** Conference of the parties serving as the meeting of the parties to the Paris Agreement
**CMP** Conference of the parties serving as the meeting of the parties to the Kyoto Protocol
**COP** Conference of the parties
**CPI** Consumer price index
**CRA** Credit rating agency
**CRF** Concentration-response function
**CSDDD** Corporate sustainability due diligence directive
**CSP** Corporate social performance
**CSR** Corporate social responsibility
**CSRD** Corporate sustainability reporting directive
**CTB** Climate transition benchmark

**DAC** Direct air capture
**DACCS** Direct air carbon capture with carbon storage
**DALY** Disability-adjusted life years
**DDQ** Due diligence questionnaire
**DEC** Dietary energy consumption
**DFI** Development finance institution
**DIB** Development impact bond
**DICE** Dynamic integrated climate-economy model
**DNSH** Do no significant harm
**DTS** Duration-times-spread factor

**EAR** Endemics-area relationship

**EBA** European banking authority
**EC** European Commission
**ECB** European central bank
**ECS** Equilibrium climate sensitivity
**EDCI** ESG data convergence initiative
**EDGAR** Emission database for global atmospheric research
**EEA** European economic area
**EEA** European environment agency
**EEIO** Environmentally-extended input-output model
**EET** European ESG template
**EFAMA** European fund and asset management association
**EFDB** Emission factor database
**EFRAG** European financial reporting advisory group
**EIB** European investment bank
**EIOPA** European insurance and occupational pensions authority
**ENCORE** Exploring natural capital opportunities, risks and exposure
**ENSO** El Niño Southern Oscillation
**EPA** Environmental protection agency
**EPICA** European project for ice coring in Antarctica
**ERA** Extra-financial rating agency
**ERF** Effective radiative forcing
**ESA** European supervisory authority
**ESFS** European system of financial supervision
**ESG** Environmental, social and governance
**ESM** European stability mechanism
**ESMA** European securities and markets authority
**ESRS** European sustainability reporting standards
**ETC** Energy transitions commission
**ETS** Emissions trading scheme
**EUGBR** EU green bonds regulation
**Eurosif** European sustainable investment forum
**EUTR** European Union taxonomy regulation for sustainable activities

**FA** Financial advisor
**FAO** Food and agriculture organization
**FCA** Financial conduct authority
**FDI** Foreign direct investment
**FDIC** Federal deposit insurance corporation
**FIO** Federal insurance office
**FMP** Financial market participant
**FRB** Board of governors of the federal reserve system
**FSB** Financial stability board
**FSOC** Financial stability oversight council
**FUND** Climate framework for uncertainty, negotiation, and distribution

**GB** Green bond
**GBF** Kunming-Montreal global biodiversity framework
**GBP** Green bond principles
**GC** Global Compact
**GCM** General circulation model
**GEVA** Greenhouse gas emissions per unit of value added
**GFANZ** Glasgow financial alliance for net zero
**GHG** Greenhouse gaz
**GICS** Global industry classification standard
**GIIN** Global impact investing network
**GISP** Greenland ice sheet project
**GLP** Green loans principles
**GMO** Genetically modified organism
**GMV** Global minimum variance portfolio
**GQE** Green quantitative easing
**GRI** Global reporting initiative
**GRIP** Greenland ice core project
**GRS** Green revenue share
**GSAT** Global mean surface air temperature
**GSIA** Global sustainable investment alliance
**GSIR** Global sustainable investment review
**GSS** Green, social and sustainability bonds
**GTAP** Global trade analysis project
**GTB** Green-to-brown ratio
**GTP** global temperature potential
**GTS** Geologic time scale
**GWP** Global warming potential

**HCIS** High climate impact sector
**HKMA** Hong Kong monetary authority
**HLEG** High-level expert group on sustainable finance

**IAIS** International association of insurance supervisors
**IAM** Integrated assessment model
**IAS** Invasive alien species
**IASB** International accounting standards board

**IBAT** Integrated Biodiversity Assessment Tool
**ICMA** International capital market association
**IDD** Insurance distribution directive
**IEA** International energy agency
**IFC** International finance corporation
**IFRS** International financial reporting standards
**IIASA** International institute for applied systems analysis
**IIRC** International integrated reporting council
**ILO** International labour organization
**IMF** International monetary fund
**IOPS** International organisation of pensions supervisors
**IOSCO** International organization of securities commissions
**IOT** Input-output table
**IPBES** Intergovernmental science-policy platform on biodiversity and ecosystem services
**IPCC** Intergovernmental panel on climate change
**IPSL** Institut Pierre-Simon Laplace
**ISSB** International sustainabilityÂăstandards board
**ITR** Implied temperature rating
**IUCN** International union for conservation of nature

**JSIF** Japan sustainable investment forum

**KF** Kalman filter
**KPI** Key performance indicator

**LCA** Life cycle assessment
**LP** Linear programming
**LPI** Living planet index
**LSEG** London Stock Exchange Group
**LULUCF** Land use, land-use change, and forestry

**MAC** Marginal abatement cost
**MACC** Marginal abatement cost curve
**MAS** Monetary authority of Singapore
**MD** Modified duration
**MDB** Multilateral development bank
**MDER** Minimum dietary energy requirement
**MFI** Microfinance institution
**MiFID** Markets in financial instruments directive
**MRIO** Multi-regional input-output model
**MSA** Mean species abundance
**MSY** Maximum sustainable yield
**MVO** Mean-variance optimized portfolio

**NACE** Nomenclature statistique des activités économiques dans la Communauté Européenne
**NCA** National competent authority
**NCAR** National center for atmospheric research
**NCAVES** Natural capital accounting and valuation of ecosystem services
**NDC** Nationally determined contribution
**NET** Negative emissions technology
**NFRD** Non-financial reporting directive
**NGFS** Network of central banks and supervisors for greening the financial system
**NGO** Non-governmental organization
**NGRIP** North Greenland ice core project
**NICE** Nested inequalities climate-economy model
**NIR** National inventory report
**NLP** Natural langage processing
**NOAA** National oceanic and atmospheric administration
**NRSRO** Nationally recognized statistical rating organization
**NZAM** Net zero asset managers initiative
**NZAOA** Net zero asset owner alliance
**NZBA** Net zero banking alliance
**NZE** Net zero emissions scenario
**NZFSPA** Net zero financial service providers alliance
**NZIA** Net zero insurance alliance
**NZICI** Net zero investment consultants initiative

**OCC** Office of the comptroller of the currency
**OCIO** Outsourced chief investment officer
**OCR** Office of credit ratings
**OECD** Organisation for economic cooperation and development
**OLR** Outgoing longwave radiation
**OLS** Ordinary least squares
**OPS** One planet summit
**OPSWF** One planet sovereign wealth fund
**ORSE** Observatoire de la responsabilité sociétale des entreprises

**PAB** Paris aligned benchmark
**PAGE** Policy analysis of the greenhouse gas effect
**PAI** Principal adverse impact
**PAII** Paris aligned investment initiative
**PBOC** People's Bank of China
**PBR** Payment-by-results
**PCAF** Partnership for carbon accounting financials
**PCF** Product carbon footprint
**PDB** Pee Dee Belemnite
**PDF** Potentially disappeared fraction
**PF** Pension fund
**PIK** Potsdam institute for climate impact research
**PM** Particulate matter
**POP** Persistent organic pollutant
**PPI** Producer price index
**PRI** Principles for responsible investment

**QALE** Quality-adjusted life expectancy
**QALY** Quality-adjusted life year
**QP** Quadratic programming

**RCP** Representative concentration pathway
**RIAA** Responsible investment association Australasia
**RICE** Regional integrated climate-economy model
**RLI** Red list index
**RLS** Recursive least squares
**RTS** Regulatory technical standard

**SAC** Species accumulation curve
**SAD** Species abundance distribution
**SAR** Species-area relationship
**SASB** Sustainability accounting standards board
**SB** Social bond
**SBE** Sustainable blue economy
**SBP** Social bond principles
**SBTi** Science-based targets initiative
**SCC** Social cost of carbon
**SDA** Sectoral decarbonisation approach
**SDG** Sustainable development goal
**SDR** Sustainability disclosure requirement
**SDTF** Sudan divestment task force
**SEC** Securities and exchange commission
**SEEA** System of environmental-economic accounting
**SF** Sustainable finance
**SFDR** Sustainable finance disclosure reporting
**SIB** Social impact bond
**SIF** Sustainable investment forum
**SLB** Sustainability-linked bond
**SMOW** Standard mean ocean water
**SOC** Social outcomes contract
**SPO** Second party opinion
**SREP** Supervisory review and evaluation process
**SRI** Socially responsible investing
**SRP** Supervisory review process
**SSP** Shared socioeconomic pathway
**STAR** Species Threat Abatement and Restoration metric
**STEPS** Stated policies scenario
**SWF** Sovereign wealth fund

**TAB** Taxonomy-aligning benchmark
**TCFD** Task force on climate-related financial disclosures
**TEEB** The economics of ecosystems and biodiversity
**TEG** Technical expert group on sustainable finance
**TFP** Total factor productivity
**TIB** Theory of island biogeography
**TNFD** Task force on nature-related financial disclosures
**TSI** Total solar irradiance

**UCITS** Undertakings for collective investment in transferable securities
**UK SIF** UK sustainable investment and finance association
**UN** United Nations
**UN PRI** UN principles for responsible investment
**UNDP** United Nations development programme
**UNECE** United Nations Economic Commission for Europe
**UNEP** United Nations environment program
**UNEP FI** United Nations environment program finance initiative
**UNFCCC** UN framework convention on climate change

**UNICEF** United Nations children's fund
**US SIF** Forum for sustainable & responsible investment

**VBDO** Vereniging van beleggers voor duurzame ontwikkeling
**VCM** Voluntary carbon market
**VOLY** Value of life year
**VSL** Value of statistical life
**VSLY** Value per statistical life year

**WACC** Weighted average cost of capital
**WACI** Weighted average carbon intensity
**WAIS** West Antarctic ice sheet project
**WBCSD** World business council for sustainable development
**WCW** Who cares wins
**WDPA** World Database on Protected Areas
**WEF** World economic forum
**WHO** World health organization
**WIOD** World input-output database
**WMO** World meteorological organization
**WRI** World resources institute
**WTP** willingness-to-pay

**YLD** Years lived with disability
**YLL** Years of life lost

# Chapter 1

# Introduction

In this chapter, we first define the concept of sustainable finance (SF) and discuss its historical origins, particularly the motivations of responsible investors. We also present the responsible investing ecosystem and the related regulatory framework. Finally, we provide some figures on the sustainable finance market.

## 1.1 Definition

The European Commission (EC) defines the concept of sustainable finance as follows[1]:

> "*Sustainable finance refers to the process of taking* ***environmental, social and governance (ESG) considerations*** *into account when making investment decisions in the financial sector, leading to more long-term investments in sustainable economic activities and projects.* ***Environmental considerations*** *might include climate change mitigation and adaptation, as well as the environment more broadly, for instance the preservation of biodiversity, pollution prevention and the circular economy.* ***Social considerations*** *could refer to issues of inequality, inclusiveness, labour relations, investment in human capital and communities, as well as human rights issues. The* ***governance*** *of public and private institutions — including management structures, employee relations and executive remuneration — plays a fundamental role in ensuring the inclusion of social and environmental considerations in the decision-making process.*"

In this definition, the EC also introduces the concept of ESG (Environmental, Social and Governance), which is very popular among asset owners and managers. For example, unlike business-as-usual (BAU) or traditional investing, the goal of ESG investing is to incorporate extra-financial analysis into asset selection. Nevertheless, the boundary between SF and ESG is not very clear. This is also the case with other commonly used terms such as responsible investment (RI), sustainable investing (SI) and, socially responsible investing (SRI). Here are a few definitions we found in financial textbooks:

- **Responsible investment** is an approach to investing that explicitly recognizes the relevance to the investor of environmental, social and governance factors, as well as the long-term health of the market as a whole.
- **Sustainable investing** is an investment approach that considers environmental, social and governance factors in portfolio selection.

[1] See the webpage https://finance.ec.europa.eu/sustainable-finance/overview-sustainable-finance_en.

- **Socially responsible investing** is an investment strategy that is considered socially responsible, because it invests in companies that have ethical practices.
- **ESG** refers to the factors that measure the sustainability of an investment.

In fact, it is really difficult to make the difference between all these concepts, because they all encompass the same underlying idea. Therefore, we can consider them as the same topic (Figure 1.1). We can complete this list with other terms such as green finance, climate finance, blue finance, etc. In general, the term green finance is reserved for the environmental pillar, while blue finance is an emerging area of climate finance and concerns the ocean economy (IFC, 2022).

Figure 1.1: Many words, one concept

## 1.2 Short history of responsible and ethical investing

From a historical point of view, we observe three phases. In the 1990s and 2000s, the word "*sustainable finance*" is not really used. The term "*responsible investment*" is preferred because of ethical considerations of some end investors and asset owners. In the 2010s, "*ESG investing*" takes the lead as it gains momentum in the asset management industry. In addition, ESG rating agencies have adopted the breakdown of extra-financial information into environmental, social and governance pillars. Finally, the concept of ESG is spreading to all financial actors and sectors (*e.g.*, companies, banks, regulators, policy makers and central banks). In this context, it affects not only the investment side, but also regulation, society and public policy. Therefore, it is better to use the term "*sustainable finance*", which is more generic than responsible or ESG investing.

The previous evolution (responsible investment → ESG → sustainable finance) can be explained by the history of ethical investing. Religious motivations explain the earliest examples of responsible (or faith-based) investing. In 1758, the Quaker Philadelphia yearly meeting prohibited its members from participating in the slave trade (buying or selling humans). They were followed by religious groups (*e.g.*, Muslims, or Methodists), which urged people and members to avoid investing in companies related to weapons, tobacco, alcohol, or gambling. According to Beabout and Schmiesing (2003), the first SRI mutual fund (Pioneer Fund) was created in 1928 by Philip Carret for evangelical

Protestants. The years 1930–1960 saw the emergence of several investment doctrines. In particular, a series of corporate scandals led to an increased focus on governance issues. During the Vietnam War, shareholders organized resolutions against the production of napalm[2] and Agent Orange[3]. So we see the development of engagement policies alongside exclusion policies. In 1971, two members of the United Methodist Church (Luther Tyson and Jack Corbett) and the portfolio manager Tony Brown launched the Pax World Fund, which can also claim to be the first sustainable mutual fund in the United States. In fact, the fund's strategy mixed both financial and social criteria. This is a step forward because the fund considers selection screening, not just exclusion screening. Moskowitz (1972) published a first list of socially responsible stocks, including Chase Manhattan, Johnson Products, Levi Strauss, New York Times, Whirlpool and Xerox. These stocks are challenged by Vance (1975), who found that they largely underperformed the Dow Jones from 1972 to 1975. The concept of "*sin stocks*" was born, and the relationship between responsible investing and profitability led to many academic publications on these topics. This first period of sustainable finance can be summarized as follows:

> "*Do no harm. That is the central concept of traditional faith-based investing and, to some degree, the central concept of socially responsible investing: Avoiding products or industries that conflict with a set of moral values.*" (Townsend, 2020, page 2).

The question of moral values is also the main factor explaining the development of corporate social responsibility (CSR). This theory begins with the publication of "*Social Responsibilities of the Businessman*" by Bowen (1953). In this book, the author analyzes the responsibilities that corporations have to society. Considered the "*father of corporate social responsibility*" (Carroll, 1999), Howard Bowen argued that "*CSR can help business reach the goals of social justice and economic prosperity by creating welfare for a broad range of social groups, beyond the corporations and their shareholders.*" Viewed as an alternative to socialism and pure capitalism, CSR has been rejected by neoclassical economists. One of its most famous opponents is Milton Friedman:

> "*There is one and only one social responsibility of business — to use its resources and engage in activities designed to increase its profits so long as it stays within the rules of the game, which is to say, engages in open and free competition without deception or fraud.*" (Friedman, 1962).

In particular, his article published in the New York Times (Friedman, 1970) has had a major impact on the shareholder vs. stakeholder debate. Stakeholder theory suggests that the true success of a company lies in satisfying all of its stakeholders, not just shareholders (Freeman, 2004). The stakeholder ecosystem includes customers, suppliers, employees, local communities, government agencies, financiers, and others. In this theory, each business entity creates and sometimes destroys value for each stakeholder group. Again, much academic research has been published on this topic, particularly on how to define corporate social performance (CSP), and its relationship to corporate financial performance (CFP). However, even though the debate is still raging, stakeholder theory has profoundly changed the vision of business. Indeed, there's now a broad consensus that the purpose of business objective should be more than just profit maximization. One example is the Global Compact (GC) initiative launched by the UN Secretary-General Kofi Annan in July 2000. It is a voluntary initiative based on CEO commitments to implement a set of human rights, labor,

[2] In 1968, the Medical Committee for Human Rights bought shares in Dow Chemical to stop the sale of napalm.

[3] Agent Orange is a mixture of two herbicides. It was used by the US military to defoliate forests and terrorize the people of South Vietnam (Townsend, 2020, page 3).

environmental, and anti-corruption principles[4]. The UN Global Compact is widely used by responsible investors to define lists of excluded issuers, to engage with companies, and to develop impact investing products. The 10 principles are:

- Human rights
  1. Businesses should support and respect the protection of internationally proclaimed human rights;
  2. Ensure that they are not complicit in human rights abuses;
- Labor
  3. Businesses should uphold the freedom of association and the effective recognition of the right to collective bargaining;
  4. The elimination of all forms of forced and compulsory labor;
  5. The effective abolition of child labor;
  6. The elimination of discrimination in respect of employment and occupation;
- Environment
  7. Businesses should support a precautionary approach to environmental challenges;
  8. Take initiatives to promote greater environmental responsibility;
  9. Promote the development and diffusion of environmentally friendly technologies;
- Anti-corruption
  10. Businesses should work against corruption in all its forms, including extortion and bribery.

From 2004 to 2008, the UN Global Compact, the International Finance Corporation (IFC) and the Swiss government sponsored a series of annual conferences for investment professionals, asset managers, and financial institutions to develop guidelines and recommendations on how to better integrate environmental, social and corporate governance issues. The term ESG was first coined in the 2004 conference report "*Who Cares Wins — Connecting Financial Markets to a Changing World*" (WCW, 2004) and popularized by the next four reports[5].

Socially responsible investing applies not only to companies, but also to sovereigns and countries. For instance, in 1986, the US Congress passed the "*Comprehensive Anti-Apartheid Act*", which banned new investments in South Africa. Similarly, the Sudan Divestment Task Force (SDTF) was formed in 2005 to coordinate and provide resources for the Sudan divestment campaign in response to the genocide occurring in the Darfur region. The US "*Sudan Accountability and Divestment Act*" came into force in December 2007. It authorizes a state or local government to divest assets in companies that engages in business operations in Sudan that include power production activities, mineral extraction activities, oil-related activities, or the production of military equipment.

[4]The Global Compact initiative has its roots in the code of conduct for companies developed in 1977 by Leon Sullivan, a clergyman and civil rights leader. The original Sullivan Principles consisted of seven requirements to be met by a company operating in South Africa. They were a response to apartheid and an alternative to total divestment, which was perceived as a costly strategy (Grossman and Sharpe, 1986; Rudd, 1979).

[5]The titles of the four conference reports are "*Investing for Long-Term Value — Integrating Environmental, Social and Governance Value Drivers in Asset Management and Financial Research*" (2005), "*Communicating ESG Value Drivers at the Company-Investor Interface*" (2006), "*New Frontiers in Emerging Markets Investment*" (2007) and "*Future Proof? Embedding Environmental, Social and Governance Issues in Investment Markets*" (2008).

According to Townsend (2020), the current concept of sustainable finance mixes "*the traditional North American model for socially responsible investing, and ESG, which first took hold in Europe.*" It is true that the Who Cares Wins (WCW) conferences have had a more European focus, with participants coming primarily from European asset owners and managers, especially the 2005 conference (WCW, 2005). While SRI is more an exclusion and qualitative process at its inception in North America, ESG is a best-in-class and quantitative process when implemented in the early 2000s. The growth of ESG data and ESG rating agencies[6] largely explains this shift. One reason is "*the strong intellectual and legal debate on the relationship between fiduciary duty and issues of sustainability*" (Townsend, 2020, page 6). In 2005, UNEP invited the law firm Freshfields Bruckhaus Deringer to prepare a report on the legal use of ESG integration by pension funds (PFs), insurance companies and asset managers. The objective of the report was to answer the following question:

> "*Is the integration of environmental, social and governance issues into investment policy (including asset allocation, portfolio construction and stock-picking or bond-picking) voluntarily permitted, legally required or hampered by law and regulation; primarily as regards public and private pension funds, secondarily as regards insurance company reserves and mutual funds?*" (Freshfields Bruckhaus Deringer, 2005, page 6).

The 154-page report analyzed the legal frameworks for institutions in Australia, Canada, France, Germany, Italy, Japan, Spain, the United Kingdom and the United States. While the analysis is highly technical and results vary by jurisdiction, the report concludes that integrating ESG issues is consistent with fiduciary duty when ESG factors impact investment value and long-term risks. In this context, we are seeing a growing shift among European institutional investors who consider that their fiduciary duty requires them to integrate ESG into their investment analysis. As institutional investors are sophisticated investors and base their decisions on in-depth quantitative analysis, this has meant transforming the original qualitative approach based on discretionary exclusions to a more systematic model based on extra-financial quantitative data.

A second reason that explains the shift from a qualitative SRI to a quantitative ESG is the factor of climate change. In response to global warming, the Intergovernmental Panel on Climate Change (IPCC) was established in 1988 by the World Meteorological Organization (WMO) and the United Nations Environment Programme (UNEP). The IPCC produces periodic assessment reports on the state of knowledge about climate change. The first assessment report (AR1) was published in March 1990, while the synthesis of the latest assessment report (AR6) was completed in March 2023. These reports are used extensively at the United Nations conferences on climate change. In June 1992, the Earth Summit held in Rio de Janeiro produced two important legal agreements: the Convention on Biological Diversity (CBD) and the UN Framework Convention on Climate Change (UNFCCC). The objective of this international treaty is to reduce global environmental impacts. The implementation of the UNFCCC to combat global warming is an ongoing process. For instance, the Kyoto Protocol negotiated in 1997 and the Paris Agreement adopted in 2015 are certainly the two most famous international treaties on climate change. On the investor side, the Coalition for environmentally responsible economies (Ceres) was founded in 1989 with the goal of changing corporate environmental practices. In the wake of the Exxon Valdez oil spill, Ceres developed the Valdez Principles[7]. In 2000, it also launched the Global Reporting Initiative (GRI) to standardize corporate disclosure on ESG issues.

[6] This topic will be discussed in more detail in the next chapter.

[7] The 10 principles are (1) protection of the biosphere, (2) sustainable use of natural resources, (3) reduction and disposal of wastes, (4) energy conservation, (5) risk reduction, (6) safe products and services, (7) environmental restoration, (8) informing the public, (9) management commitment, and (10) audits and reporting.

The last twenty years have strengthened the place of ESG in finance, not only on the investment side, but also on the financing side[8]. Regulators are now involved, accounting standards have been developed, climate change is recognized as a key risk factor, controversies can damage a company's reputation, social pressure affects corporate governance, and so on. In the next chapters, we will extensively document the evolution of sustainable finance over the last period. The motivations for implementing socially responsible investment are now many and varied. In Figure 1.2, we show some of them. They can be divided into two groups. The first (economic sustainability, moral values and social pressure) is related to the "*do no harm principle*", and can be applied to many situations or decisions. The second group, which includes financial performance, fiduciary duty, and risk management, is related to investment principles. The underlying idea is that ESG risks need to be managed and cannot be ignored in portfolio construction.

Figure 1.2: The raison d'être of sustainable finance

## 1.3 The ESG ecosystem

As we have just seen, the ESG landscape involves many financial actors. First, investors are at the center of the ecosystem. We generally distinguish between asset owners and managers. Asset owners correspond to end investors and include pension funds (PFs), institutional investors, sovereign wealth funds (SWFs), insurance companies, endowments and foundations, family offices, retail investors, etc. The asset management industry, on the other hand, manages funds for end-investors. In this category we have mutual funds, hedge funds, private equity funds, infrastructure funds, third-party distributors, etc. We could also mention ESG index providers, as they are essential for passive management. Asset managers then act as financial intermediaries between the financial markets (*e.g.*, equity and bond markets) and the savings of households, companies and organizations. While asset owners and managers form the investment side, banks and issuers form the financing side. Sustainable finance therefore also involves the issuance of debt and the structuring of ESG products such as green bonds.

[8] However, we observe an ESG backlash in the US starting in 2021, with high political polarization and a setback or slowdown in the momentum of ESG regulation in the United States.

### 1.3.1 Sustainable investment forum

The sustainable investment forums (SIFs) are membership-based sustainable and responsible investment organizations. They work to promote the wider adoption of sustainable and responsible investment practices and, more generally, the mainstreaming of sustainability issues into financial markets and the investment chain. They are organized on a country or regional basis. For example, the European Sustainable Investment Forum (Eurosif) was established in 2001 and brings together Forum per la Finanza Sostenibile (Italy), Forum Nachhaltige Geldanlagen (Germany), Forum pour l'Investissement Responsable (France), Foro de Inversión Sostenible (Spain), Sustainable Finance Ireland, Swiss Sustainable Finance (Switzerland) and UK Sustainable Investment and Finance Association. Other SIFs include the Responsible Investment Association Australasia[9] (RIAA), the Responsible Investment Association Canada (RIA Canada), The Forum for Sustainable & Responsible Investment (US SIF), the Dutch Association of Investors for Sustainable Development[10] (VBDO) and the the Japan Sustainable Investment Forum (JSIF). All of these organizations are members of the Global Sustainable Investment Alliance (GSIA).

These forums were created at different times, reflecting the evolution of sustainable finance. US SIF was founded in 1984 and is the oldest SIF. It is followed by RIA Canada in 1990, UK SIF in 1991 and VBDO in 1995. Most of the European forums were established in 2001 (*e.g.*, Germany, France, Italy). The main activities of these sustainable investment forums are public policy, education, training, research and promotion of sustainable investment best practices. Founded in 2010, the GSIA is charged with aggregating responsible investment market data from its members in order to analyze the global sustainable investment market and the evolution of ESG trends. In particular, it publishes a Global Sustainable Investment Review or GSIR every two years (GSIA, 2013, 2015, 2017, 2019, 2021, 2023). We will make extensive use of these reports in Section 1.5 on page 42 when we analyze the market for ESG investing.

Figure 1.3: 2018, 2020 & 2022 GSIA reports

### 1.3.2 Initiatives

In this section, we highlight the most relevant initiatives (PRI, Climate action 100+, and net-zero alliances). We also list other initiatives that are part of the ESG ecosystem. Some of these are discussed in more detail in the following chapters.

[9] It covers both Australia and New Zealand.
[10] The Dutch name is Vereniging van Beleggers voor Duurzame Ontwikkeling.

### Principles for responsible investment

In early 2005, UN Secretary-General Kofi Annan invited a group of the world's largest institutional investors to participate in a process to develop the Principles for Responsible Investment[11] (PRI). A group of 20 investors from institutions in 12 countries was supported by a group of 70 experts from the investment industry, intergovernmental organizations and civil society. The PRI were launched at the New York Stock Exchange in April 2006.

Box 1.1: PRI signatories' commitment

"As institutional investors, we have a duty to act in the best long-term interests of our beneficiaries. In this fiduciary role, we believe that environmental, social, and corporate governance (ESG) issues can affect the performance of investment portfolios (to varying degrees across companies, sectors, regions, asset classes and through time).
We also recognise that applying these Principles may better align investors with broader objectives of society. Therefore, where consistent with our fiduciary responsibilities, we commit to the following:

- Principle 1: We will incorporate ESG issues into investment analysis and decision-making processes.
- Principle 2: We will be active owners and incorporate ESG issues into our ownership policies and practices.
- Principle 3: We will seek appropriate disclosure on ESG issues by the entities in which we invest.
- Principle 4: We will promote acceptance and implementation of the Principles within the investment industry.
- Principle 5: We will work together to enhance our effectiveness in implementing the Principles.
- Principle 6: We will each report on our activities and progress towards implementing the Principles.

The Principles for Responsible Investment were developed by an international group of institutional investors reflecting the increasing relevance of environmental, social and corporate governance issues to investment practices. The process was convened by the United Nations Secretary-General.
In signing the Principles, we as investors publicly commit to adopt and implement them, where consistent with our fiduciary responsibilities. We also commit to evaluate the effectiveness and improve the content of the Principles over time. We believe this will improve our ability to meet commitments to beneficiaries as well as better align our investment activities with the broader interests of society.
We encourage other investors to adopt the Principles."

Source: https://www.unpri.org.

[11] UN PRI and PRI are two interchangeable terms. For example, the website URL is https://www.unpri.org. However, PRI is the official term.

Signatories' commitment is reported in Box 1.1. The principles are voluntary and aspirational, and offer a range of possible actions to integrate ESG issues into investment practice. For example, here are some possible actions for Principle 1:

- Address ESG issues in investment policy statements;
- Support the development of ESG-related tools, metrics, and analysis;
- Promote ESG training for investment professionals;

Becoming a signatory requires the payment of an annual fee[12], but there are no other formal requirements for signing the membership agreement. However, signatories are required to report annually on their responsible investment activities. Members' responses, which make up the transparency report, are public and available to anyone[13]. Starting in 2019, members will also be required to complete a climate transparency report, which includes specific indicators on the management of risks and opportunities related to climate change. These indicators are modeled on the disclosure framework of the Task Force on Climate-related Disclosures (TCFD). Based on the transparency report, PRI produces an assessment report for each member, which consists of a series of scores on several dimensions (from 0 to 100) and a rating system (from one to five stars). The assessment report is confidential, unless the member chooses to make it public. It is also used by PRI to verify that signatories meet minimum requirements. If not, PRI engages with the member (one-on-one meetings, action plans, etc.). Delisting is a last resort if a signatory has not met the requirements after the two-year period. From 2018 to 2020, 165 signatories were identified as not meeting the minimum requirements. PRI has delisted 5 signatories, and 23 other members of the 165 identified have voluntarily delisted.

Table 1.1: Number of PRI signatories by region and year

| Region | 2015 | 2016 | 2017 | 2018 | 2019 | 2020 | 2021 | 2022 | 2023 |
|---|---|---|---|---|---|---|---|---|---|
| Africa | 2 | 3 | 6 | 3 | 11 | 11 | 23 | 19 | 12 |
| Asia | 9 | 21 | 25 | 31 | 49 | 57 | 122 | 107 | 79 |
| Australasia | 6 | 8 | 18 | 11 | 21 | 23 | 45 | 28 | 19 |
| Europe | 67 | 94 | 129 | 188 | 293 | 433 | 532 | 374 | 221 |
| Latin America | 1 | 1 | 8 | 12 | 26 | 59 | 66 | 49 | 20 |
| Middle East | 2 | 0 | 1 | 1 | 2 | 8 | 10 | 8 | 9 |
| North America | 38 | 41 | 66 | 85 | 137 | 187 | 260 | 191 | 105 |
| Total | 125 | 168 | 253 | 331 | 539 | 778 | 1 058 | 776 | 465 |

Source: PRI (2024), https://www.unpri.org/signatories/signatory-resources/signatory-directory & Author's calculations.

Figure 1.4 shows the growth of the PRI. At inception, most of the 63 founding signatories were asset owners[14] with a few asset managers[15] and data providers[16]. They were mainly located in

[12]The fee for 2022/23 ranges from £478 to £14 222 depending on the size and category (asset owner, investment manager and service provider) of the signatory.

[13]Reports from 2014 to 2020 are available on the website https://www.unpri.org/signatories/reporting-and-assessment/public-signatory-reports, while more recent reports can be downloaded from the data portal (or PRI's central depository for signatories' reporting data): https://ctp.unpri.org/dataportalv2.

[14]The most important were AP2, BT Pension Scheme, CDC, CDPQ, CalPERS, CPPIB, ERAFP, FRR, NYCERS, NZSF, NGPF, PGGM, TIAA-CREF, UNJSPF and USS.

[15]The best known asset managers were ABN AMRO Asset Management, Aviva Investors, BNP PAM, Candriam, CAAM (now Amundi), Daiwa AM, Henderson Global Investors and Threadneedle AM.

[16]*e.g.*, Ethix, Trucost and Vigeo.

Figure 1.4: PRI signatory growth 2006–2021

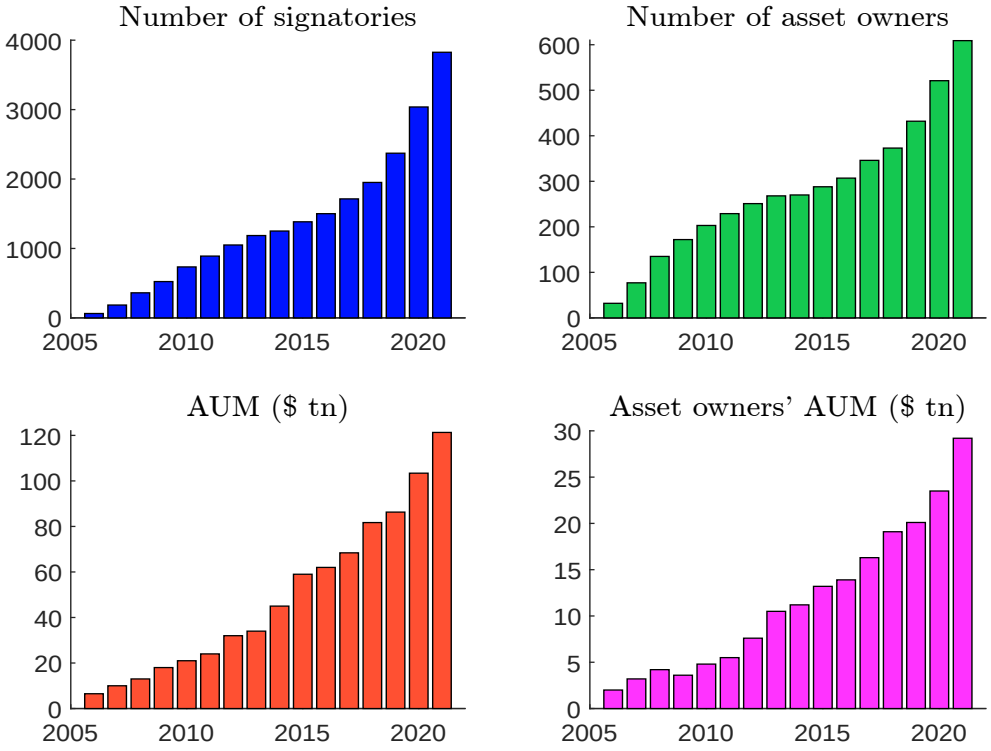


Source: https://www.unpri.org.

the US, Canada, UK, France[17], the Netherlands and the Nordics. As of September 2022, the PRI has 5 020 signatories representing approximately $121 trillion in assets under management (AUM). Investment managers are the most represented category (76%) followed by asset owners (14%) and service providers (10%). We observe a rapid evolution since 2015 and even an acceleration in 2020 and 2021, followed by a slowdown in 2022 and 2023, as the number of potential candidates remains limited. In total, the PRI has 5 372 of signatories on 31 December 2023, of which 740 are asset owners. Table 1.1 shows the current picture of where the signatories are located. More than half of them are located in Europe, with North America (Canada and the United States) being the second largest region. In terms of signatories by country, the United States is the largest, followed by the United Kingdom and France.

### Climate action 100+

Climate Action 100+ is a collaborative investor initiative to ensure that the world's largest corporate greenhouse gas emitters take necessary action on climate change. It was formed in the wake of the 2015 Paris Agreement, and is launched in December 2017. It is supported by 700 investors, responsible for over $68 trillion in assets under management. Climate Action 100+ focuses on engagement and coordinates the efforts of investor signatories. In a nutshell, engagement corresponds to the active dialogue between the investor and the company by discussing sustainability risks and communicating the investor's expectations for corporate behavior. The main objectives are to improve the climate performance of the company, reduce GHG emissions across the value chain and

[17] There are 8 founding signatories: BNP PAM, CDC, CAAM (now Amundi), ERAFP, FRR, Groupama AM, Macif Gestion and Vigeo.

ensure transparent disclosure. The engagement process can be described as follows:

- Engagement with focus company executives and board members is led by one or more Lead Investors, working with a number of Collaborating Investors and supported by technical experts.
- When signing up for the initiative, investors are asked to nominate which focus companies they would like to work with and whether they would like to be a lead or co-investor.
- Engagement takes a variety of forms, including meeting with companies, making a statement at a company AGM, supporting shareholder resolutions on climate change, and voting to remove directors who fail to address climate change risks.

As of 1 January 2024, Climate Action 100+ engagement focuses on 168 companies that account for up to 80% of global corporate industrial greenhouse gas emissions. The geographic breakdown is as follows: 1.8% in Africa, 20.4% in Asia, 9.0% in Australasia, 33.5% in Europe, 32.3% in North America, and 3.0% in South America. The sector distribution is shown in Table 1.2, where we indicate the number of companies and the market capitalization[18]. For example, the 5 focus companies for the airlines sector are Air France, American Airlines, Delta Air Lines, Qantas Airways, United Airlines, the 12 focus companies for the automobile sector are BMW, Ford, General Motors, Honda, Mercedez-Benz, Nissan, Renault, SAIC, Stellantis, Suzuki, Toyota, Volkswagen, etc.

Table 1.2: Sector breakdown of Climate Action 100+ engagement

| Sector | Frequency | | Market capitalisation | |
|---|---|---|---|---|
| | Number | in % | in $ bn | in % |
| Airlines | 5 | 3.0% | 57.7 | 0.6% |
| Automobiles | 12 | 7.1% | 737 | 7.1% |
| Cement | 11 | 6.5% | 181 | 1.8% |
| Chemicals | 8 | 4.8% | 287 | 2.8% |
| Coal mining | 3 | 1.8% | 68.5 | 0.7% |
| Consumer goods & services | 12 | 7.1% | 1 900 | 18.4% |
| Diversified mining | 11 | 6.5% | 484 | 4.7% |
| Electric utilities | 31 | 18.5% | 1 000 | 9.7% |
| Oil & gas | 40 | 23.8% | 3 700 | 35.8% |
| Oil & gas distribution | 2 | 1.2% | 160 | 1.5% |
| Other industrials | 15 | 8.9% | 1 100 | 10.6% |
| Other transportation | 7 | 4.2% | 501 | 4.8% |
| Paper | 2 | 1.2% | 33.6 | 0.3% |
| Shipping | 1 | 0.6% | 39 | 0.4% |
| Steel | 8 | 4.8% | 85 | 0.8% |
| Total | 168 | 100.0% | 10 334 | 100.0% |

Source: https://www.climateaction100.org/whos-involved/companies.

With the advent of the net-zero emissions goal, most of the actions coordinated by Climate Action 100+ focus on net-zero corporate policies. According to the 2023 Progress Update report, this year's engagement wins include National Grid, Volkswagen, Engie, CEZ, AES, Petroleo Brasil S.A., American Electric, Incitec Pivot and Toray Industries.

[18]Market capitalization is computed as of 15 December 2020.

### Net-zero alliances

Net-zero emissions refers to a state in which greenhouse gas emissions to the atmosphere are balanced by removals from the land and ocean (carbon sink). This is a condition for stopping global warming. According to IPCC (2018), the global temperature increase must be limited to 1.5°C above pre-industrial levels to mitigate the worst impacts of climate change and preserve a livable planet. In general, we assume that net zero emissions must be achieved by 2050 (IEA, 2021), otherwise several tipping points with irreversible consequences could be triggered.

The concept of "*Net-Zero Alliance*" starts with the launch of the Net Zero Asset Owner Alliance (NZAOA) in September 2019 under the umbrella of UNEP FI. As of January 2024, the Alliance counts 88 members representing $9.5 tn in AUM (UNEP, 2022). These members must adhere to a common protocol for target setting and reporting based on four components:

1. Engagement targets
   - Engage with 20 companies, focusing on those with the highest owned emissions or those responsible for a combined 65% of owned emissions in the portfolio;
2. Sub-portfolio emission targets
   - 22 to 32% $CO_2e$ reduction by 2025 (per IPCC 1.5°C SR scenarios);
   - 40 to 60% $CO_2e$ reduction by 2030 (per IPCC 1.5°C SR scenarios);
   - Cover portfolio Scope 1 + 2 emissions, track Scope 3 emissions, and use absolute or intensity-based reduction KPIs;
3. Sector targets
   - Use absolute or intensity-based reductions on all material sectors;
   - Scope 3 to be included wherever possible;
   - Sector specific intensity KPIs recommended;
4. Financing transition targets
   - Reporting progress on a climate-positive trend for all Alliance members internally to the Alliance;
   - Build solutions or enhance climate solution reporting.

For example, the targets[19] defined by Munich Re are the following: (1) concentrate on and engage with large contributors of financed emissions within the listed equity and corporate bond portfolios; (2) reduce absolute emissions from the listed equity, corporate bond and real estate portfolios by 25-29% (Scope $1+2$ emissions of investee companies) by 2025; (3) reduce emissions from listed equities and corporate bonds for thermal coal ($-35\%$) and oil & gas ($-25\%$); (4) double the renewable portfolio (equity and debt) from €1.6 bn to €3 bn.

In June 2020, the UNFCCC launches the "*Race to Zero*" campaign, which has significantly accelerated net-zero commitments. For example, the Glasgow Financial Alliance for Net Zero (GFANZ)

[19] The reader can consult the web page https://www.unepfi.org/net-zero-alliance/resources/member-targets to retrieve the 2025 member targets.

is created in April 2021 by Mark Carney[20] and the COP26 presidency to coordinate efforts across all sectors of the financial system to accelerate the transition to a net-zero global economy[21]. GFANZ is an umbrella organisation covering seven net-zero initiatives: NZAOA, the Net Zero Asset Managers initiative (NZAM), the Paris Aligned Investment Initiative (PAII), the Net Zero Banking Alliance (NZBA), the Net Zero Insurance Alliance (NZIA), Net Zero Financial Service Providers Alliance (NZFSPA) and the Net Zero Investment Consultants Initiative (NZICI).

#### Other initiatives

There is a growing list of initiatives related to ESG issues. Here are are some examples related to the three pillars:

- Environmental
  Asia Investor Group On Climate Change (AIGCC), Finance for Biodiversity Pledge, Finance for Tomorrow, Institutional Investors Group on Climate Change (IIGCC), Montreal Carbon Pledge, One Planet Sovereign Wealth Fund (OPSWF), Portfolio Decarbonization Coalition, etc.

- Social
  Platform Living Wage Financials (PLWF), PRI Human Rights Engagement, Tobacco-Free Finance Pledge, Workforce Disclosure Initiative (WDI), etc.

- Governance
  Australian Shareholders' Association (ASA), European Corporate Governance Institute (ECGI), International Corporate Governance Network (ICGN), Say on Climate, etc.

### 1.3.3 Regulators

While regulators and supervisors have long been absent from the ESG ecosystem, they are now at the forefront of the ESG debate. This is largely due to the phenomenal growth of ESG and climate investing, as well as changing motivations. When responsible investing was driven by moral values, ESG investing affected a small market of investors. Today, ESG has become a marketing argument and the risk of ESG-washing and greenwashing has become very high. We need to differentiate between two types of risk: (1) explicit & deliberate greenwashing; (2) unintentional greenwashing. Deliberate greenwashing is a mis-selling risk that is closely scrutinized by regulators. One example is the DWS scandal[22]. Unintentional greenwashing is a risk of misinterpretation that needs to be addressed by regulators[23]. One example is the definition of a net-zero investment policy. In this context, clients need to be protected from both types of greenwashing risk. Another reason for

[20] Mark Carney was the governor of the Bank of Canada from 2008 to 2013, the governor of the Bank of England from 2013 to 2020 and the chairman of the Financial Stability Board (FSB) from 2011 to 2018. Since 2020, he has been a United Nations special envoy for climate action and finance.

[21] We report here the press release of November 3, 2021 during the COP 26 summit: "*Today, through the Glasgow Financial Alliance for Net Zero (GFANZ), over $130 trillion of private capital is committed to transforming the economy for net zero. These commitments, from over 450 firms across 45 countries, can deliver the estimated $100 trillion of finance needed for net zero over the next three decades.*"

[22] Read about litigation issues in ESG investing in the Financial Times: `https://www.ft.com/content/1094d5da-70bf-40b5-98f4-725d50620a5a`.

[23] Here we make the difference between regulation and supervision from a risk management point of view (Roncalli, 2020a, page 12). The regulator is responsible for setting rules and policy guidelines. The supervisor assesses the safety and soundness of financial institutions and verifies that regulatory rules are being applied. For example, in Europe, the regulator of the banking sector is EBA while the supervisor is ECB.

the recent interest of regulators is the political will to mitigate global warming. Indeed, financial regulation is undoubtedly one of the most important instruments for achieving this goal. It is therefore no coincidence that the financial sector is expected to play a key role in the decarbonization of the corporate sector.

Table 1.3: The supervision institutions in finance

| | Banks | Insurers | Markets | All sectors |
|---|---|---|---|---|
| Global | BCBS | IAIS | IOSCO | FSB |
| EU | EBA/ECB | EIOPA | ESMA | ESFS |
| US | FDIC/FRB | FIO | SEC | FSOC |

The regulators responsible for sustainable risk are the same as those responsible for traditional risk (*e.g.*, market risk, credit risk, or liquidity risk). In Table 1.3 we have provided a list of financial regulators. At the global level, four international authorities have primary responsibility for financial regulation: the Basel Committee on Banking Supervision (BCBS), the International Association of Insurance Supervisors (IAIS), the International Organization of Securities Commissions (IOSCO), and the Financial Stability Board (FSB). The FSB, which is responsible for regulating systemic risk, identified climate risk at a very early stage. The speech "*Breaking the tragedy of the horizon*" by Mark Carney, Chairman of the FSB, in London on September 29, 2015, marked a turning point in the recognition of climate change as a major risk to financial stability (Carney, 2015). According to Mark Carney, financial stability can be affected through three channels: physical risk (the impact of extreme climatic events occurring today on insurance liabilities and financial assets), liability risk (the impact that could occur tomorrow as parties harmed by climate change seek compensation from those they hold responsible) and transition risk (the financial risk that could result from the process of adapting to a lower-carbon economy). Following the G20 Antalya Summit, the FSB proposed then to "*establish an industry-led disclosure task force, to design and deliver voluntary standards for effective disclosures that meet the needs of investors and creditors*" (FSB, 2015). The Task Force on Climate-related Financial Disclosures (TCFD) was established in December 2015 under the chairmanship of Michael Bloomberg. In June 2017, the TCFD released its final recommendations for climate-related financial disclosures. The first status report on disclosure practices was published in September 2018. Disclosure is the first pillar of the FSB roadmap, which covers three other areas: (1) data, (2) vulnerability analysis, and (3) regulatory and supervisory practices and tools (Figure 1.5).

The disclosure recommendations for climate-related reporting have been widely adopted, notably through the ISSB's sustainability disclosure standards. The FSB supports these standards to achieve global consistency in reporting. In addition, the FSB has asked the ISSB to take over the monitoring of corporate climate-related disclosures from the TCFD starting in 2024, as outlined in the TCFD's 2023 annual status report. On the data pillar, the FSB has tasked the Network for Greening the Financial System (NGFS) to work on this issue, and the NGFS published its final report on identifying and filling data gaps in July 2022. To develop vulnerability analysis, the FSB is promoting the adoption of scenario analysis based on the climate scenarios provided by the NGFS. Finally, under the regulatory and supervisory pillar, the FSB continues to work with the BCBS, IAIS and IOSCO to strengthen the regulation of climate risks for banks, insurance companies and asset managers, with a particular focus on the integrity of capital markets and the mitigation of greenwashing. In 2023, the FSB updated its roadmap to encompass risks related to nature or biodiversity, while various international organizations such as NGFS, OECD, and the World Bank are actively engaged in crafting analyses and policy frameworks concerning these environmental risks.

Figure 1.5: Stylised overview of the FSB roadmap for addressing climate-related financial risks (July 2021)

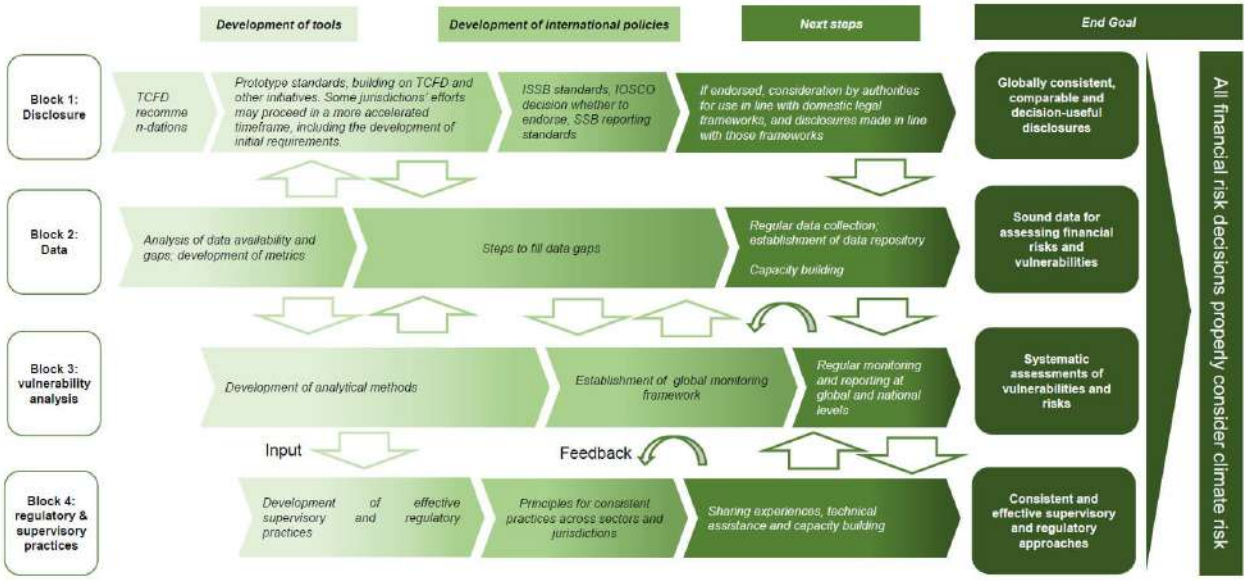


Source: Financial Stability Board (2021), www.fsb.org/work-of-the-fsb/financial-innovation-and-structural-change/climate-related-risks.

The Basel Committee on Banking Supervision (BCBS) provides a forum for regular cooperation on banking supervisory matters. Its main objective is to improve the quality of banking supervision worldwide. Its first publication on climate-related financial risks dates back to April 2020. In June 2022, the BCBS released its first guidelines on this topic (BCBS, 2022). These guidelines include 12 principles for effective risk management of climate risks and 6 principles for the supervisory review process (SRP). We report here on the first principle, which states that climate risk must be managed like financial risks (*e.g.*, market risk or credit risk):

> "*Banks should develop and implement a sound process for understanding and assessing the potential impacts of climate-related risk drivers on their businesses and on the environments in which they operate. Banks should consider material climate-related financial risks that could materialise over various time horizons and incorporate these risks into their overall business strategies and risk management frameworks.*" (BCBS, 2022).

Knowing that the BCBS is capable of developing new regulatory frameworks quickly, we can expect the publication of new standards including climate risk in the coming years. For example, the Basel Committee issued a public consultation paper on a Pillar 3 disclosure framework for climate-related financial risks in November 2023 (BCBS, 2023). This consultation is aligned with the TCFD, and the proposed Pillar 3 regime includes disclosure of qualitative information (governance, strategy, risk management, transition risk, physical risk, and concentration risk) and quantitative information (exposures and financed emissions by sector, exposures subject to physical risks, real estate exposures in the mortgage portfolio by energy efficiency level, emission intensity per physical output and by sector, facilitated emissions related to capital markets and financial advisory activities by sector). As for the other two global supervision institutions, IOSCO has produced a report on ESG rating agencies and data providers (IOSCO, 2021) and analyzed the supervisory practices to address

greenwashing (IOSCO, 2023), while the IAIS focuses more on climate risk and its supervision in the insurance sector (IAIS, 2021). In March 2023, the IAIS launched its first consultation to propose changes to the Insurance Core Principles (ICPs) on governance, risk management and internal controls. In November 2023, the IAIS published two draft application papers on climate risk in the insurance sector, one on market conduct in relation to greenwashing and natural catastrophes, and another on scenario analysis for assessing insurance risks. It is interesting to note that asset management supervisors are more focused on ESG data and greenwashing, while insurance supervisors are more concerned with physical risk.

We are also seeing rapid changes in the regulatory framework at the regional or national level. For example, a new SEC rule requiring all registrants to disclose information on climate risks was proposed in March 2022, but the SEC has since delayed releasing a final version[24]. The reason for this is mainly political, due to the anti-ESG movement we are seeing in a number of US states. At the same time, however, California Governor Gavin Newsom signed a climate disclosure bill in October 2023 that will require private and public companies doing business in California to disclose their Scope 1, 2 and 3 emissions from 2026. In Europe, the sustainable finance roadmap 2022–2024 identifies three priorities for ESMA[25]: (1) tackling greenwashing and promoting transparency, (2) building NCAs' and ESMA's capacities and, (3) monitoring, assessing and analysing ESG markets and risks. Banking supervisors have already conducted several climate stress tests (ACPR, 2021; Bank of England, 2022; ECB, 2022). Central banks have also been very active. Thus, the Network of Central Banks and Supervisors for Greening the Financial System (NGFS) was launched at the Paris One Planet Summit (OPS) in December 2017. Its 8 founding members are Banco de Mexico, Bank of England (BoE), Banque de France, Dutch Central Bank, Deutsche Bundesbank, Swedish FSA, Hong Kong Monetary Authority (HKMA), Monetary Authority of Singapore (MAS) and The People's Bank of China (PBOC). As of 27 December 2023, the NGFS consists of 134 members and 21 observers[26]. In addition to its methodological publications, the NGFS is known for its database of climate scenarios[27].

Sustainable finance is not only regulated by financial regulators. Figures 1.6 and 1.7 shows charts from the MSCI website, listing ESG regulations by type of regulator or by type of regulated party. We find that the number of regulations is greater for issuers than for investors. In addition, bodies other than financial regulators are involved in the ESG regulatory landscape, notably governments. For instance, the French law "*Climat et Résilience*" (Climate and Resilience) of 22 August 2021 implements part of the 146 proposals of the Citizen's Climate Convention adopted by the French government to reduce greenhouse gas emissions by 40% by 2030 in a spirit of social justice. In Europe, most ESG regulations are defined by the European Commission (EC) and the European Parliament. This is for example the case of the EU Non-Financial Reporting Directive (NFRD, 2014), the EU Taxonomy Regulation for sustainable activities (EUTR, 2020) and the EU Sustainable Finance Disclosure Regulation (SFDR, 2021). All of these policy initiatives are part of the "*European Green Deal*", whose aim is making the European Union climate neutral by 2050. New legislations on the circular economy, building renovation, biodiversity, agriculture and innovation are underway. In order to define these guidelines, the EC is supported by technical working groups such as the High-Level Expert Group on sustainable finance (HLEG) or the Technical Expert Group on sustainable finance (TEG). For example, the EC has mandated the European Financial Reporting Advisory Group (EFRAG) to carry out work for the development of the new EU Corporate Sustainability Reporting Directive (CSRD) in 2020, which will amend the current NFRD.

[24] Visit https://www.sec.gov/news/press-release/2022-46.
[25] Visit https://www.esma.europa.eu/policy-activities/sustainable-finance.
[26] Including BIS, BCBS, ESM, FSB, IAIS, IMF, IOPS, IOSCO and OECD.
[27] They can be found at https://www.ngfs.net/ngfs-scenarios-portal.

Figure 1.6: Who will regulate ESG? — The regulators viewpoint (MSCI, 2022)

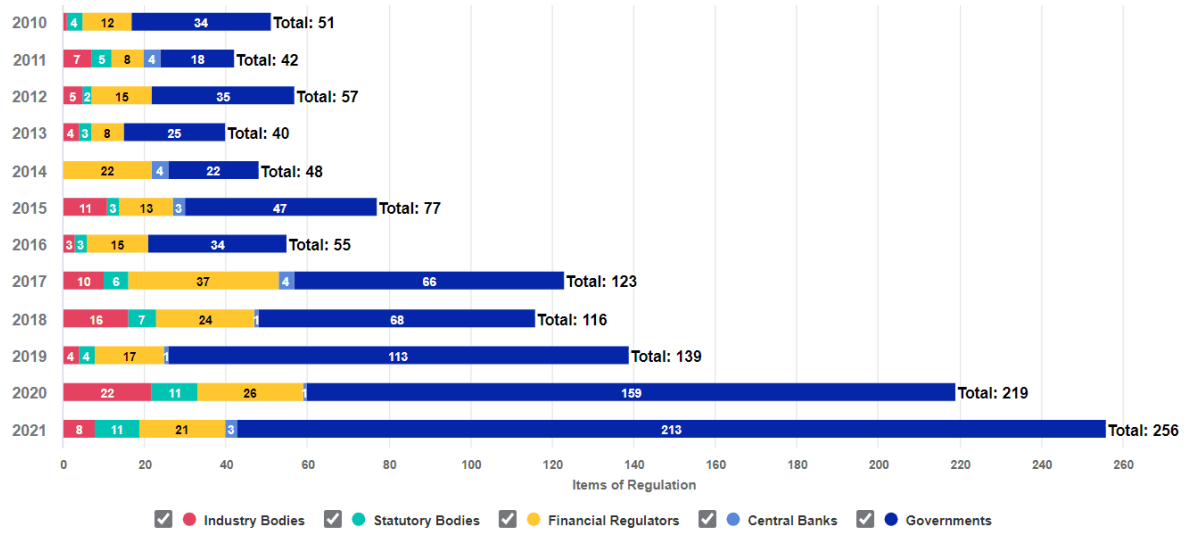


Source: https://www.msci.com/who-will-regulate-esg.

Figure 1.7: Who will regulate ESG? — The regulated viewpoint (MSCI, 2022)

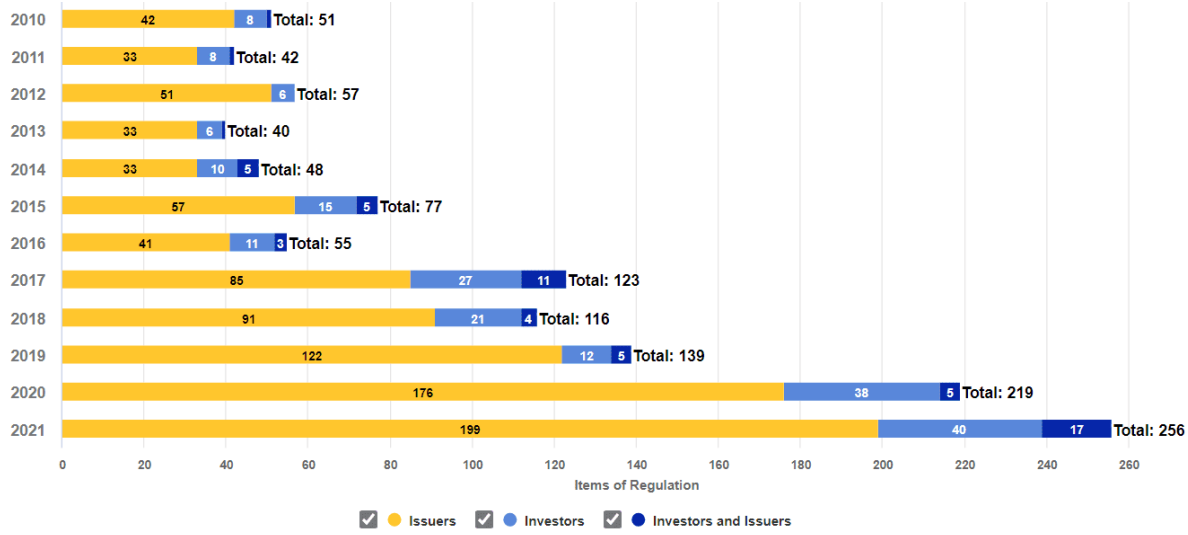


Source: https://www.msci.com/who-will-regulate-esg.

### 1.3.4 Reporting frameworks

As we have seen, reporting is a key element in understanding the ESG and climate policies of issuers and investors. Over the past 20 years, we have seen a proliferation of new reporting frameworks. Table 1.4 lists the most prominent. For each report, we indicate the date the initiative was created and the date the standards were implemented. The first two reporting frameworks were the Global Reporting Initiative (GRI) and the GHG Protocol. The most recent is the International Sustainability Standards Board (ISSB). In the following, we distinguish between sustainability reporting and climate-specific reporting.

Table 1.4: List of the main reporting frameworks

| Perimeter | Acronym | Name | Dates |
|---|---|---|---|
| General | GC | UN Global Compact Initiative | 2000/2000 |
| | GRI | Global Reporting Initiative | 1997/2000 |
| | IIRC | International Integrated Reporting Council | 2010/2013 |
| | ISSB | International SustainabilityÂăStandards Board | 2021/2024 |
| | SASB | Sustainability Accounting Standards Board | 2011/2016 |
| | SDGs | UN Sustainable Development Goals | 2015/2016 |
| Climate | CDP | Carbon Disclosure Project | 2000/2000 |
| | CDSB | Climate Disclosure Standards Board | 2007/2015 |
| | GHG Protocol | Greenhouse Gas Protocol | 1998/2001 |
| | PCAF | Partnership for Carbon Accounting Financials | 2019/2020 |
| | SBTi | Science Based Targets initiative | 2015/2015 |
| | TCFD | Task Force on Climate-Related Financial Disclosures | 2015/2017 |

#### Sustainability reporting

**International Sustainability Standards Board** After a decade of framework proliferation, the sustainability reporting landscape has changed significantly in the past three years. In June 2021, SASB and IIRC permanently merged into one organization to form the Value Reporting Foundation (VRF). On 3 November 2021, the IFRS Foundation Trustees announced the creation of the International Sustainability Standards Board (ISSB), chaired by Emmanuel Faber[28], with the goal of providing a comprehensive global baseline of sustainability disclosure standards. On 31 January 2022, the Climate Disclosure Standards Board (CDSB) was consolidated into the IFRS Foundation to support the work of ISSB. On 1 August 2022, the IFRS Foundation completes a new consolidation with VRF. On 10 July 2023, a new stage in the convergence of sustainability reporting has been reached with the Financial Stability Board's announcement that it will transfer the responsibility for monitoring progress on firms' disclosures from the TCFD to the ISSB in 2024. Although the previous frameworks will continue to exist and be used by companies, it is clear that the ISSB reporting framework is now the benchmark for sustainability reporting standards and will be used more and more in the future.

The ISSB standards are part of the larger body of IFRS standards and are referred to as IFRS-S (S for sustainability) to distinguish them from the accounting standards issued by the International Accounting Standards Board (IASB). In March 2022, ISSB published the drafts of its first proposed standards, which are definitively adopted in June 2023 with implementation in 2024:

[28] Emmanual Faber was CEO and Chair of the Board at multi-national food products company Danone.

- IFRS S1 general requirements for disclosure of sustainability-related financial information (ISSB, 2022a);
- IFRS S2 climate-related disclosures (ISSB, 2022b).

IFRS S1 requires companies to identify sustainability-related risks and opportunities until the SASB standards are replaced by the IFRS Sustainability Disclosure Standards. IFRS S2 builds on the TCFD recommendations and can be seen as a new version of the TCFD reporting. On October 2022, the ISSB decided to include Scope 3 GHG emissions in the climate reporting according to the fifteen Scope 3 categories described in the GHG Protocol. Although the ISSB standards have definitely taken the lead in sustainability reporting, one of the biggest concerns is the adoption of the single materiality approach rather than the double materiality approach[29], which is at odds with European standards such as the CSRD.

Figure 1.8: The SDGs icons

Source: https://sdgs.un.org/goals#icons.

**Sustainable Development Goals** The SDGs are a set of 17 interrelated global goals that serve as a "*blueprint to achieve a better and more sustainable future for all.*" They were adopted by the United Nations in 2015 and are to be achieved by 2030. The 17 SDGs are listed in Table 1.5. Each goal is defined by specific targets, and the progress toward each target is measured by indicators. In total, there are 69 goals and 231 unique indicators. The Goal.Target.Indicator numbering system is used to structure the SDGs tree map. For instance, the first target of the first goal is: 1.1 — By 2030,

[29]Single materiality refers to how climate and other ESG risks and opportunities affect a company's financial performance and position. In contrast, double materiality considers how the company also impacts the climate and the environment.

Table 1.5: The 17 SDGs

| # | Name | Description | E | S | G |
|---|---|---|---|---|---|
| 1 | No poverty | End poverty in all its forms everywhere | | ✓ | |
| 2 | Zero hunger | End hunger, achieve food security and improved nutrition and promote sustainable agriculture | | ✓ | |
| 3 | Good health and well-being | Ensure healthy lives and promote well-being for all at all ages | | ✓ | |
| 4 | Quality education | Ensure inclusive and equitable quality education and promote lifelong learning opportunities for all | | ✓ | |
| 5 | Gender equality | Achieve gender equality and empower all women and girls | | ✓ | ✓ |
| 6 | Clean water and sanitation | Ensure availability and sustainable management of water and sanitation for all | ✓ | ✓ | |
| 7 | Affordable and clean energy | Ensure access to affordable, reliable, sustainable and modern energy for all | ✓ | | |
| 8 | Decent work and economic growth | Promote sustained, inclusive and sustainable economic growth, full and productive employment and decent work for all | | ✓ | ✓ |
| 9 | Industry, innovation and infrastructure | Build resilient infrastructure, promote inclusive and sustainable industrialization and foster innovation | ✓ | ✓ | ✓ |
| 10 | Reduced inequality | Reduce inequality within and among countries | | ✓ | |
| 11 | Sustainable cities and communities | Make cities and human settlements inclusive, safe, resilient and sustainable | ✓ | | ✓ |
| 12 | Responsible consumption and production | Ensure sustainable consumption and production patterns | ✓ | ✓ | ✓ |
| 13 | Climate action | Take urgent action to combat climate change and its impacts | ✓ | | ✓ |
| 14 | Life below water | Conserve and sustainably use the oceans, seas and marine resources for sustainable development | ✓ | | |
| 15 | Life on land | Protect, restore and promote sustainable use of terrestrial ecosystems, sustainably manage forests, combat desertification, and halt and reverse land degradation and halt biodiversity loss | ✓ | | |
| 16 | Peace, justice, and strong institutions | Promote peaceful and inclusive societies for sustainable development, provide access to justice for all and build effective, accountable and inclusive institutions at all levels | | ✓ | ✓ |
| 17 | Partnerships for the goals | Strengthen the means of implementation and revitalize the Global Partnership for Sustainable Development | | | ✓ |

Source: https://sdgs.un.org/goals.

eradicate extreme poverty for all people everywhere, currently measured as people living on less than \$1.25 a day. This target is measured by only one indicator: 1.1.1 — Proportion of the population living below the international poverty line by sex, age, employment status and geographic location. The fifth target of the first goal is: 1.5 — By 2030, build the resilience of the poor and those in vulnerable situations and reduce their exposure and vulnerability to climate-related extreme events and other economic, social and environmental shocks and disasters. This target is measured by three indicators: 1.5.1 — Number of deaths, missing persons and directly affected persons attributed to disasters per 100 000 population, 1.5.2 — Direct economic loss attributed to disasters in relation to global gross domestic product and 1.5.3 — Number of countries that adopt and implement national disaster risk reduction strategies in line with the Sendai Framework for Disaster Risk Reduction 2015–2030. Initially, the SDGs are built to assess the progress of each country on the different pillars. We can then analyze the evolution of each indicator per country and per year. Synthetic scores are also available at the country or goal level. A compilation of these scores[30] can be found in Sachs *et al.* (2024).

The SDGs have been quickly adopted by financial institutions as a framework for impact investing. In Table 1.5, we map the 17 SDGs and the 3 ESG pillars. Therefore, we can assign the SDGs targets to each ESG dimension. An example applied to artificial intelligence companies is provided by Sætra (2022). The SDGs have also been used to assess the ESG objectives of sustainable financial products. For example, ICMA has published a mapping[31] to the SDGs for green and social bonds (ICMA, 2022), where the targets are linked to GBP and SBP categories.

### Climate reporting

**GHG Protocol** The GHG Protocol was created in 1998 by WRI and WBCSD with the goal of "*establishing comprehensive global standardized frameworks to measure and manage greenhouse gas emissions from private and public sector operations, value chains and mitigation actions.*" First published in 2001, the standard defines the accounting and reporting of six greenhouse gases covered by the Kyoto Protocol, including carbon dioxide (CO2) and methane (CH4).

The GHG Protocol corporate standard classifies a company's greenhouse gas emissions into three scopes (GHG Protocol, 2004):

- Scope 1 refers to direct GHG emissions from sources owned and controlled by the issuer.
- Scope 2 represents the indirect GHG emissions from the consumption of purchased electricity, heat, or steam.
- Scope 3 are other indirect emissions (not included in Scope 2) from the entire value chain.

Scope 2 emissions can be computed using two methods[32] (GHG Protocol, 2015):

1. the energy mix of the countries (location-based);
2. the energy mix of the utilities supplying the electricity (market-based).

[30] They are also available at the web page `https://dashboards.sdgindex.org`.

[31] The link to the Excel mapping file is `https://www.icmagroup.org/assets/documents/Sustainable-finance/2022-updates/Mapping-to-SDGs_June-2022-280622.xlsx`.

[32] The exact definitions are the following: "a *location-based method reflects the average emissions intensity of grids on which energy consumption occurs (using mostly grid-average emission factor data)*", while "a *market-based method reflects emissions from electricity that companies have purposefully chosen (or their lack of choice).*"

Scope 3 is based on 15 sub-categories (GHG Protocol, 2011, 2013), which are divided into two main categories[33]:

- Upstream Scope 3 emissions are defined as indirect carbon emissions related to the upstream value chain. More specifically, Upstream Scope 3 is based on 8 sub-categories: (1) purchased goods and services, (2) capital goods, (3) fuel and energy related activities, (4) upstream transportation and distribution, (5) waste generated in operations, (6) business travel, (7) employee commuting and (8) upstream leased assets.

- Downstream Scope 3 emissions are defined as indirect carbon emissions associated with the downstream value chain. They correspond to these 7 sub-categories: (9) downstream transportation and distribution, (10) processing of sold products, (11) use of sold products, (12) end-of-life treatment of sold products, (13) downstream leased assets, (14) franchises and (15) investments.

Scope 1 emissions are also called direct emissions, while indirect emissions include both Scope 2 and 3 GHG emissions. Unlike Scope 1 and 2, Scope 3 is an optional reporting category.

**Carbon Disclosure Project** The CDP (formerly the Carbon Disclosure Project) is a UK-based not-for-profit charity[34] co-founded by Paul Dickinson and Tessa Tennant in 2000. CDP manages a global disclosure system for investors, companies, cities, states and regions to manage their environmental impacts. Each year, CDP sends a questionnaire to organizations and collects information on three environmental dimensions:

1. Climate change (based on the GHG Protocol[35]).

2. Forest management;

3. Water security.

In addition, CDP introduces a pilot questionnaire for biodiversity in 2022 and plastics in 2023. The CDP database[36] is extensively used to measure the carbon footprint of companies, cities and governments. In 2022, more than 18 700 companies and 1 100 cities, states and regions have completed the questionnaire. This represents half of the global market capitalization. In 2023, the number of disclosures increases by 24% and there are now more than 18 700 companies disclosing through CDP. There is also strong demand for biodiversity reporting, with 2 800 companies disclosing on all biodiversity issues in 2022.

**Remark 1** *Because CDP is the most comprehensive reporting database for carbon emissions*[37]*, CDP data is used extensively by commercial data providers (e.g., Trucost and MSCI) to provide carbon footprint estimates.*

[33] The upstream value chain includes all activities related to the suppliers whereas the downstream value chain refers to post-manufacturing activities.

[34] The global budget of CDP is approximately $30 mn. CDP's funding comes primarily from philanthropic grants (32%), service-based memberships (30%), and government grants (12%).

[35] The differences between the GHG Protocol and CDP reporting templates are as follows The GHG Protocol reporting is more focused on numbers, while the CDP reporting includes more open-ended questions and comments. In addition, the CDP report is slightly more comprehensive as it also covers forest management and water security.

[36] It is available at https://www.cdp.net/en/data.

[37] The fact that the CDP report is an Excel file may explain why it has been more successful than the GHG Protocol report, which is a Word file. However, they are very similar in terms of carbon disclosure.

**TCFD** The Task Force on Climate Related Financial Disclosures (TCFD) was established by the FSB in 2015 to develop a set of voluntary and consistent disclosure recommendations that companies can used to inform investors, lenders and insurance underwriters about their climate-related financial risks. The TCFD consists of 31 members from the G20, representing both preparers and users of financial disclosures and is chaired by Michael Bloomberg. The TCFD framework is published in June 2017 and the 11 recommendations are organized around 4 core elements: (1) governance, (2) strategy, (3) risk management, and (4) metrics and targets (Table 1.6). The first core element describes the organization's governance of climate-related risks and opportunities, while the second core element lists the actual and potential impacts of climate-related risks and opportunities on the organization's business, strategy, and financial planning. The processes used by the organization to identify, assess, and manage climate-related risks are specified in the risk management tag. Finally, the last core element defines the metrics and targets used to measure and manage relevant climate-related risks and opportunities. The implementation of the reporting framework is extensively described in TCFD (2021a,b), and many examples can be found in CDSB (2021c) and TCFD (2022).

Table 1.6: The 11 recommended disclosures (TCFD, 2017)

| Recommendation | # | Recommended Disclosure |
|---|---|---|
| Governance | 1 | Board oversight |
| | 2 | Management's role |
| Strategy | 3 | Risks and opportunities |
| | 4 | Impact on organization |
| | 5 | Resilience of strategy |
| Risk management | 6 | Risk ID and assessment processes |
| | 7 | Risk management processes |
| | 8 | Integration into overall risk management |
| Metrics and targets | 9 | Climate-related metrics |
| | 10 | Scope 1, 2, 3 GHG emissions |
| | 11 | Climate-related targets |

Source: https://www.fsb-tcfd.org.

Unlike other climate frameworks (*e.g.*, GHG Protocol and CDP), the TCFD framework is a risk reporting, and not just a carbon emission reporting. For instance, below are some examples of recommended metrics (TCFD, 2022, pages 16-17):

- GHG emissions (absolute scope 1, scope 2, and scope 3 GHG emissions; financed emissions by asset class; weighted average carbon intensity);
- Transition risks (volume of real estate collaterals highly exposed to transition risk; concentration of credit exposure to carbon-related assets; percent of revenue from coal mining);
- Physical risks (number and value of mortgage loans in 100-year flood zones; revenue associated with water withdrawn and consumed in regions of high or extremely high baseline water stress; proportion of property, infrastructure, or other alternative asset portfolios in an area subject to flooding, heat stress, or water stress; proportion of real assets exposed to 1:100 or 1:200 climate-related hazards);
- Climate-related opportunities (net premiums written related to energy efficiency and low-

carbon technology; revenues from products or services that support the transition to a low-carbon economy; proportion of green buildings);

- Capital deployment (percentage of annual revenue invested in R&D of low-carbon products/services; investment in climate adaptation measures);
- Internal carbon prices (internal carbon price, shadow carbon price);
- Remuneration (portion of employee's annual discretionary bonus linked to investments in climate-related products; weighting of climate goals on long-term incentive; scorecards for executive directors).

Similarly, targets are more general and not limited to reducing carbon emissions. For example, they may relate to the amount of executive compensation influenced by climate considerations by 2025, the internal price of carbon by 2030, the amount invested in green buildings by 2035, and so on.

Figure 1.9: Examples of TCFD reports

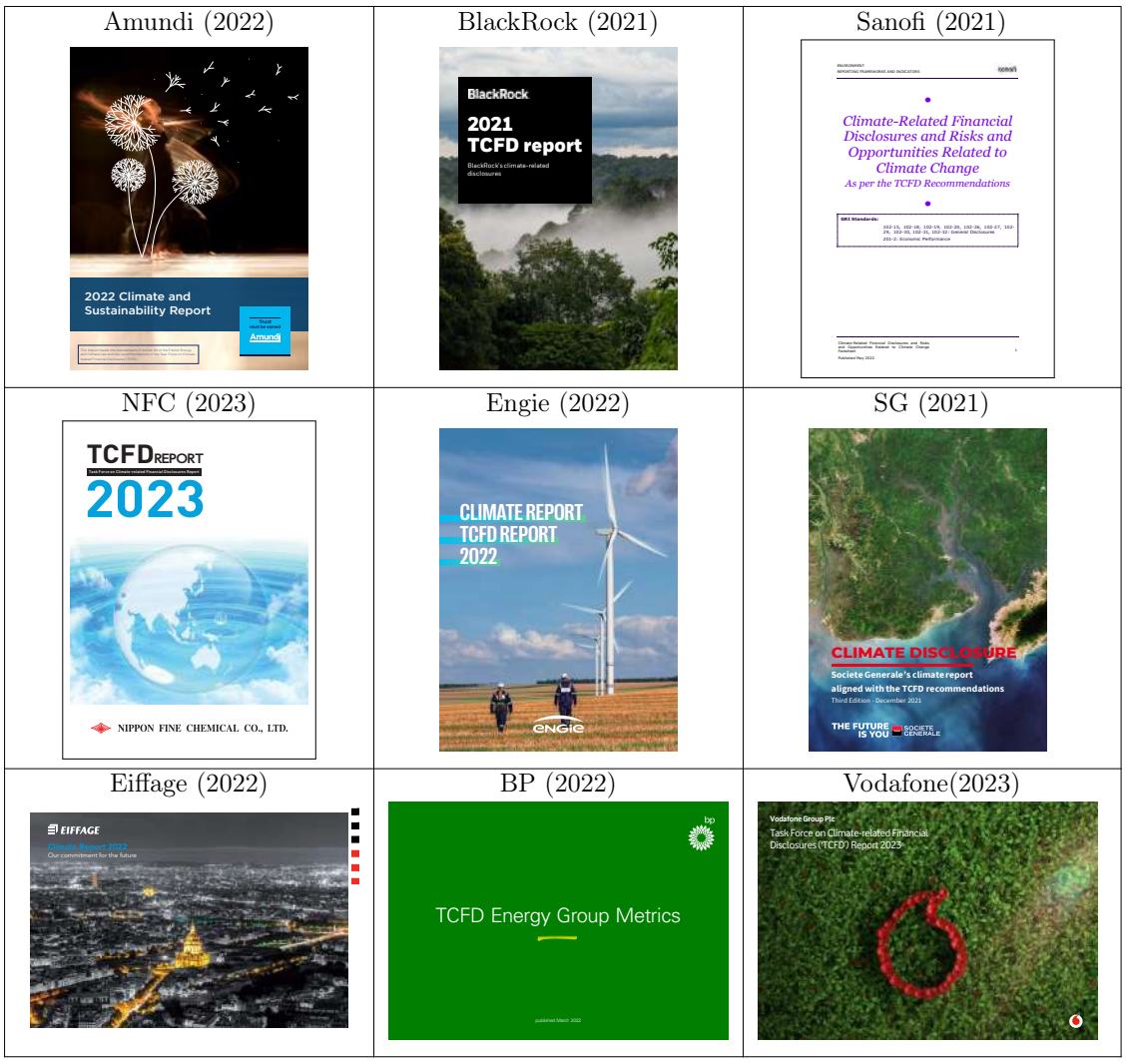


Source: Corporate websites.

**Remark 2** *Examples of TCFD reporting are given in Figure 1.9. We can generally find TCFD and climate reports by using the* Google *search bar with the keywords* `year + "TCFD report" + corporate name` *or* `year + "climate report" + corporate name`*. As we can see, the formats of TCFD reports are diverse. They can correspond to a PowerPoint file or a written document, the number of pages ranges from 3 to 100, etc.*

The TCFD framework is endorsed by many international bodies and regulators: European Commission, IFRS, IOSCO, Singapore Exchange Regulation, Central Bank of Brazil, Australian Prudential Regulatory Authority, Canadian Securities Administrators, etc. In this context, it has become the most popular reporting framework from a regulatory perspective. However, much progress remains to be made as this reporting is voluntary and not mandatory. For fiscal year 2021 reporting, "80% *of companies disclosed in line with at least one of the 11 recommended disclosures; however, only* 4% *disclosed in line with all 11 recommended disclosures and only around* 40% *disclosed in line with at least five* " (TCFD, 2022, page 5). The average level of disclosure is 60% for European companies, 36% for Asia Pacific companies and 29% for North American companies. Nearly 50% of asset managers and 75% of asset owners reported information consistent with at least five of the 11 recommended disclosures. The most popular recommended disclosures were (#3) risks and opportunities (61%), (#4) impact on organization (47%), and (#9) climate-related metrics (47%), while the less popular items were (#5) resilience of strategy (16%), (#2) management's role (22%) and (#1) board oversight (29%). On average, we see an increase of 20% between fiscal years for companies that report on climate risks. For example, for fiscal year 2022 reporting, 58% of companies disclosed in line with at least five of the eleven recommended disclosures (TCFD, 2023). However, the number of companies disclosing in line with all eleven recommendations remains at 4%. With the transfer of responsibility for monitoring progress from the TCFD to the ISSB, we can expect this situation to evolve rapidly.

### 1.3.5 Rating agencies and data providers

To implement ESG strategies, we need extra-financial data. In the 1980s and 1990s, several research firms were established to provide research on responsible investing. These small firms tend to specialize in a particular dimension and region. Some focus on the environmental pillar, but most specialize in the social pillar. In addition to research and advisory activities, they begin to collect a lot of extra-financial data and build sustainability scores. After an initial period of expansion and innovation, they structure themselves as global rating agencies following the model of credit rating agencies (CRA). We then observe a concentration of the industry and a period of consolidation in the 2010s.

#### The early stage of extra-financial rating agencies

In 2001, the French observatory centre for the corporate social responsibility[38] ORSE published a guide of companies specialized in ESG analysis (ORSE, 2001). This guide has been updated several times until 2012. For instance, in the 2005 edition, ORSE listed 34 sustainability research organizations of which 25 are located in Europe, 5 in North America and 4 in the rest of the world (Australia, Japon, South Korea). This number did not change much during the 2000s. In fact, most of the extra-financial rating agencies were created in the 1990s. Here is a list[39] of some well-known

[38] The French name is Observatoire de la Responsabilité Sociétale des Entreprises.
[39] This list is based on the works of Eccles and Stroehle (2018) and the company profiles provided by ORSE (2007).

entities[40]: Ethical Investment Research Services Ltd. (Eiris[41], 1983, UK), Institutional Shareholder Services (ISS[42], 1985, UK), Kinder, Lydenberg, Domini & Co. (KLD[43], 1988, US), Jantzi Research (Jantzi Research[44], 1992, Canada), Global Engagement Services (GES[45], 1992, Sweden), Innovest Strategic Value Advisors (Innovest[46], 1995, US), Sustainable Asset Management Ltd. (SAM[47], 1995, Switzerland), RepRisk (RepRisk[48], 1998, Switzerland), Oekom Research AG (Oekom[49], 1999, Germany), Ethix SRI Advisors (Ethix[50], 1999, Sweden), Trucost Plc (Trucost[51], 2000, UK), Inrate (Inrate[52], 2001, Switzerland), Vigeo (Vigeo[53], 2002, France), Dutch Sustainability Research (DSR[54], 2002, Netherlands), EthiFinance (EthiFinance[55], 2004, France).

### The consolidation of the industry

As shown by Eccles and Stroehle (2018) and Demartini (2020), we are seeing a period of consolidation in the 2010s. Here are some examples:

- Vigeo and Eiris merged in October 2015 to form Vigeo-Eiris (V.E), which will be acquired by Moody's in April 2019.
- In September 2015 and March 2018, ISS acquired Ethix SRI Advisors and Oekom to form ISS ESG solutions (ISS-ethix, ISS-climate and ISS-oekom). In November 2020, ISS is majority owned by Deutsche Börse Group.
- In February and November 2009, RiskMetrics acquired Innovest and KLD. RiskMetrics is bought by MSCI in 2010, froming MSCI ESG Research LLC.
- In September 2009, DSR and Jantzi Research merged to form Sustainalytics. In the 2010s, Sustainalytics acquired Responsible Research (Singapore), ESG Analytics (Switzerland), Solaron

[40] The date of creation and the country are shown in the parentheses.

[41] EIRIS was founded in 1983 by charities and churches as the UK's first independent research service for ethical investors.

[42] Institutional Shareholder Services was originally founded in 1985 by Robert Monks, an ESG advocate. It began offering proxy voting services in 1992.

[43] KLD was founded in 1989 by Amy Domini, Peter Kinder and Steve Lydenberg to provide institutional investors with social research on US companies. In May 1990, the firm launched the Domini 400 Social Index (DSI).

[44] Founded in 1992 by Michael Jantzi, Jantzi Research became a pioneer in the field of ESG research in Canada. In January 2000, it launched the Jantzi Social Index (JSI) consisting of 50 Canadian stocks.

[45] Caring Capitalism was founded in 1992 and renamed Global Engagement Services in 2003.

[46] Innovest was founded by Matthew Kierman and Hewson Batlzell as "*a green analogy to Moody's*" (Eccles *et al.*, 2020). In its early years, it focused on environmental screening. Later, it created the IVA ratings using the credit-like rating scale (AAA, AA, A, BBB, BB, B, and CCC).

[47] SAM was founded in 1995. In 1999, SAM and Dow Jones launched the Dow Jones Sustainability Indexes. In 2001, SAM launched the first global sustainable water fund (SAM Sustainable Water Fund). In 2006, SAM was acquired by Robeco and renamed RobecoSAM in 2013.

[48] RepRisk was established in 1998. The RepRisk database was launched later, starting in January 2007.

[49] The environmental publishing house ökom was founded in 1989. In 1993, ökom GmbH was created to provide environmental research. Oekom research AG became independent in 1999, focusing on corporate responsibility ratings.

[50] Established in 1999, Ethix developed norm-based screening in 2000 and expanded to emerging markets in 2005.

[51] Trucost was established in 2000 to help organizations, investors and governments understand and quantify the environmental impacts of business activities. Trucost's database was launched later, starting with the 2005 fiscal year.

[52] Inrate was officially created in 2001, but its roots go back to 1990 with the creation of Centre Info.

[53] Founded in 1997, Arese was the first SRI rating agency in France. In June 2002, it became Vigeo under the leadership of Nicole Notat, former General Secretary of the labor union CFDT. In June 2005, Vigeo merged with the Belgian agency Ethibel.

[54] DSR was the research team of Triodos Bank, a Dutch niche player in sustainable finance founded in 1980. In 2008 it changed its name to Sustainalytics.

[55] EthiFinance was founded in 2004. It merged with Spread Research in 2017.

(India) and GES (Sweden). In April 2020, Sustainalytics becomes a wholly owned subsidiary of Morningstar.

- S&P Global acquired Trucost in October 2016 and the ESG ratings business of RobecoSAM in November 2019.

Today, the industry of extra-financial analysis and ESG ratings is dominated by ISS-Oekom, MSCI, Refinitiv[56], Reprisk, S&P Global, Sustainalytics and Moody's.

**Remark 3** *In Chapter 2 we will see that these ESG rating agencies are specialized and do not offer the same solutions. For instance, on controversy risk, the main players are MSCI, Reprisk and Sustainalytics. For climate risk, CDP, MSCI and Trucost are the leading agencies, while Verisk Maplecroft is the specialized agency for sovereign ESG risk.*

**Remark 4** *Even if we observe a consolidation, this does not mean that we observe a convergence of ESG methodologies (Chatterji et al., 2016; Berg et al., 2022). This point will be discussed in the next chapter.*

### The current business of extra-financial data

As noted by Demartini (2020), the industry consists mainly of large Anglo-Saxon companies (US and UK) and small European start-ups. More precisely, it can be divided into three main categories:

1. Market data providers
   This category includes financial information providers (Bloomberg, Morningstar), index sponsors (Bloomberg, FTSE Russell, MSCI, Solactive) and stock exchanges (LSEG, Deutsche Börse Group).

2. Financial rating agencies
   Moody's, S&P Global and Fitch are now involved in the ESG landscape.

3. Specialized ESG firms
   In this category, we generally find a few pioneering companies such as Inrate, ISS ESG, RepRisk and Sustainalytics.

4. Technology start-ups
   Most of the new entrants use artificial intelligence (AI), big data, natural language processing (NLP), sentiment analysis and quantitative approaches. Some examples include Arabesque, Covalence, OWL ESG, and Truvalue Labs.

This explains the discrepancy in the number of ESG analysts between the companies. About 20% of extra-financial rating agencies have more than 200 ESG analysts[57], while 30% have less than 20 analysts (Demartini, 2020, page 11). Another difference is the wide range of activities: provision of raw data, provision of processed data (indicators, scores and ratings), ESG index creation, ESG screening, portfolio analysis, normative analysis, ESG controversy tracking, engagement monitoring, proxy advisory services, consulting, etc. (Demartini, 2020). These activities explain that the business model of extra-financial rating is based on the investor-pays principle, in contrast to credit rating

[56] Refinitiv is the former financial and risk unit of Thomson Reuters (including Eikon and Datastream). It is now part of the London Stock Exchange Group (LSEG), which has also acquired FTSE Russell (and Beyond Ratings).

[57] For instance, Sustainalytics has more than 800 ESG analysts (source: https://www.sustainalytics.com/about-us).

agencies, whose historical model was mainly driven by the issuer-pays principle. This means that investors pay a fee to access data, but issuers don't pay to be rated.

The issue of certification and supervision is on everyone's lips. For instance, credit rating agencies registered in the EU are supervised by ESMA[58] (Regulation 462/2013/EU and Directive 2013/14/EU). In the US, the Office of Credit Ratings (OCR) assists the Security and Exchange Commission (SEC) in overseeing those registered as nationally recognized statistical rating organizations[59] (NRSRO). As the market for ESG ratings is expected to grow, the supervision of this industry and the protection of investors are becoming an unavoidable topic. For instance, on April 2022, the EC launched a targeted consultation on the functioning of the ESG rating market in the European Union and on the consideration of ESG factors in credit ratings (EC, 2022a). The summary report, based on 204 responses[60] is published in August 2022. Its main conclusions are:

> "*The large majority of respondents (over 84%) consider that the market is not functioning well today. On the quality of ESG ratings, two thirds of respondents consider the quality to be fine to very good, with about one third considering it poor. A large majority of respondents (83%) consider that the lack of transparency on the methodologies used by the providers is a problem in the ESG ratings market. The vast majority of respondents (91%) also consider that there are significant biases with the methodology used by providers [...] Almost all respondents (94%) consider that intervention is necessary, of which the large majority (80%+) support a legislative intervention with the remainder supporting the development of non-regulatory intervention in the form of guidelines, code of conduct. Respondents largely indicated (90%+) that the main element to be addressed by the intervention should be improving transparency on the methodology used by ESG rating provider [...] The vast majority of respondents (82%) consider that ESG rating providers should be subject to some form of authorisation/registration regime in order to offer their services in the EU.*" (EC, 2022b, pages 3-4).

These results confirm previous analyses that found that the most common shortcomings are: (1) a lack of coverage, (2) data quality and, (3) a lack of transparency around the methodologies used by ESG rating providers (Boffo and Patalano, 2020). We can then expect that regulators will certainly provide regulatory safeguards for the use of ESG ratings in the near future.

## 1.4 Regulatory framework

The number of ESG regulations has increased dramatically in recent years. In Figure 1.10, we report on the global evolution and the breakdown by region. According to PRI (2022b), there are 868 policies and guidelines worldwide that encourage or require investors to consider ESG factors. Most have been developed since 2000, and we are seeing an acceleration that coincides with the Paris Agreement for climate change. The breakdown by region is shown in Figure 1.11. We observe that ESG regulations have gained the most momentum in Europe, but they are increasing in the other regions as well. By analyzing the PRI's regulation database, we obtain the following results[61]:

[58] The list of certified credit rating agencies is available at https://www.esma.europa.eu/supervision/credit-rating-agencies/risk.

[59] The list of certified NRSROs is available at https://www.sec.gov/ocr/ocr-current-nrsros.html.

[60] Including 21 ESG rating providers, 48 rating users (investors), 49 rated companies and 18 rating users (company).

[61] For each item, we indicate the frequency in %. Because each policy can apply to multiple items, the frequencies may not add up to 100%. For example, a policy may apply to both asset owners, issuers and asset managers.

Figure 1.10: Total number of ESG regulations

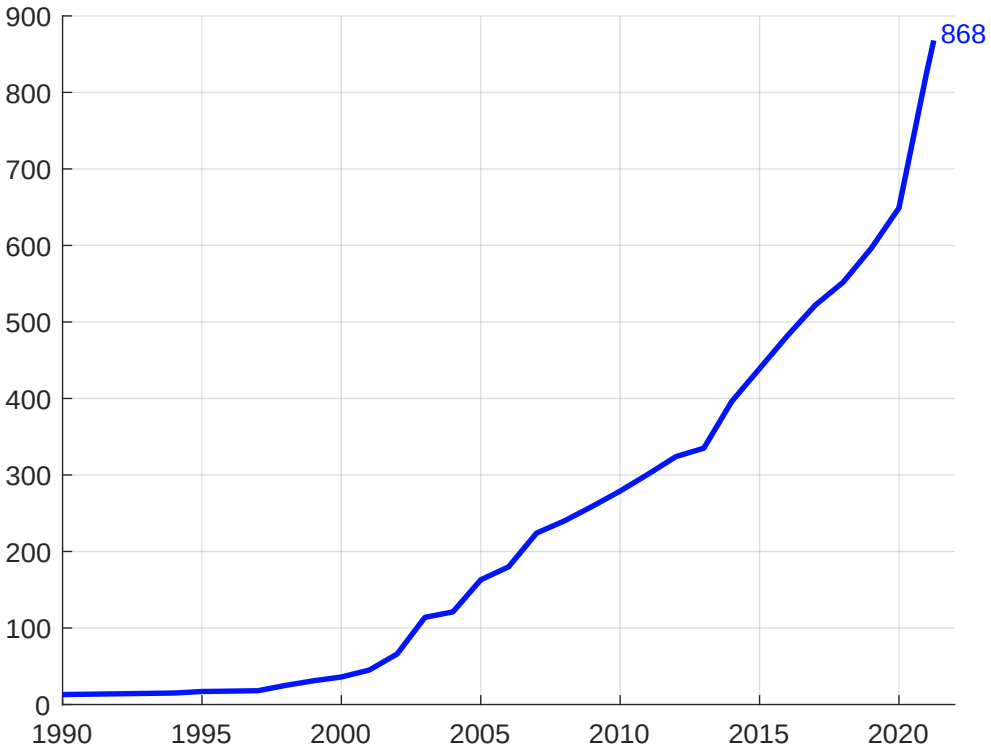


Source: PRI (2022b), https://www.unpri.org/policy/regulation-database.

Figure 1.11: Number of ESG regulations per region

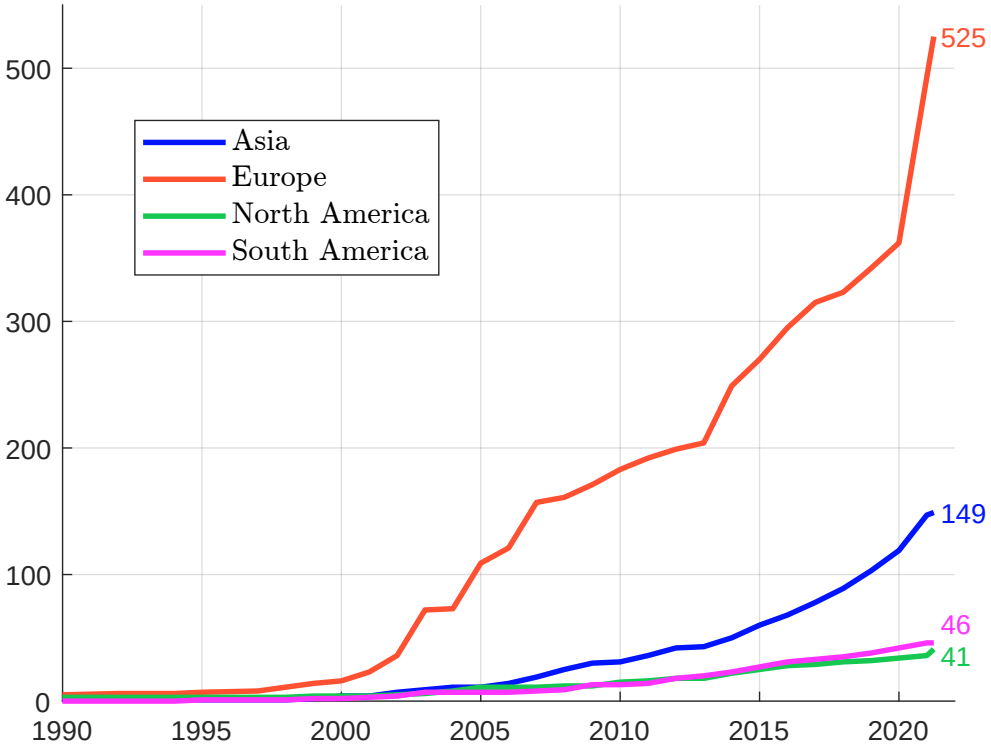


Source: PRI (2022b), https://www.unpri.org/policy/regulation-database.

- Policies are primarily issued by governments and regulators (78.8%). 19% are issued by industry associations, including stock exchanges. Finally, less than 3% are issued by international organizations (OECD, UN, ILO, etc.).
- Most of these policies are mandatory. Nevertheless, the number of voluntary-based approaches is significant[62], as they represent 33.2% of the sample.
- Four types of policy dominate: corporate ESG disclosure (61.5%), investor ESG disclosure (24.2%), investor ESG integration (20.3%) and national sustainable finance strategy (10.8%). The other types are sector-specific policies (5.6%), financial products[63] (4.5%), stewardship codes (2.6%) and taxonomy (1.6%).
- The application of these policies mainly concerns corporations (72.4%), asset owners (60.9%), investment managers (40%) and insurance companies (28.2%). The other categories are financial services providers (16.2%) and credit rating agencies (6.5%).
- If we focus on countries, we get the following ranking: China (49 policies), Germany (31), European Union (29), Italy (28), Spain (26), France (24), USA (23), Netherlands (22), Japan (22) and UK (20).

Most of policies are national. They may also be specific-sector. For instance, if we focus on regulations aiming to promote the improvement of the energy performance of buildings, and their reduction of GHG emissions and energy consumption, we find many legislative policies, such as the energy performance of buildings directive (EPBD) in Europe, the French high environmental quality (HQE) certification, the German building energy act (Gebäudeenergiegesetz or GEG), the German sustainable building certification (Deutsche Gesellschaft für Nachhaltiges Bauen or DGNB), the Italian energy-efficient construction and renovation certification (CasaClima), the Spanish climate change and energy transition law, etc. In this context, it is not realistic to have an overview of the regulations in the world[64]. This is why we will focus on the European Union[65].

The European regulatory framework is articulated around a series of policy initiatives by the European Commission:

- The action plan on sustainable finance (May 2018);
- The European Green Deal (December 2019);
- The Fit for 55 package (July 2021);
- The REPowerEU plan or energy security package (May 2022).

In December 2016, the EC established a high-level expert group on sustainable finance (HLEG), composed of 20 senior experts. HLEG (2018) published its final report on 31 January 2018 with

[62] Especially when they are issued by industry bodies.

[63] This category includes green bonds, social bonds, green labels, etc.

[64] Section 8.2.3 on page 739 provides a more comprehensive overview of climate-related regulations in the European Union and the rest of the world.

[65] We will not talk about the situation in the US, because it is not stable, especially with the recent emergence of the anti-ESG movement. The issue seems to be highly controversial. On May 25, 2022, the US Securities and Exchange Commission (SEC) proposed new rules and reporting forms to improve the regulatory framework for disclosure of funds' and advisers' consideration of ESG factors. However, these rules are still under discussion. At the same time, we are seeing political moves in the US against ESG investing (*e.g.*, Texas, Florida). Therefore, these backlashes place the US in an uncertain ESG environment.

several recommendations and proposals: (1) a classification system (or taxonomy) to provide market clarity on what is sustainable, (2) clarification of investors' obligations to achieve a more sustainable financial system, (3) improved disclosure by financial institutions and companies on how sustainability is taken into account in their decision-making, (4) an EU-wide label for green investment funds, (5) inclusion of sustainability in the mandates of European Supervisory Authorities (ESAs), and (6) a European standard for green bonds. All of these recommendations have been endorsed by the EC and form the basis of the action plan on sustainable finance adopted by the EC in March 2018 and by the European Parliament in May 2018. In July 2018, a technical expert group on sustainable finance (TEG) was established to assist the EC in developing an EU green taxonomy (1), guidelines to improve corporate disclosure of climate-related information (3), an EU green bond standard (6) and methodologies for EU climate benchmarks. In December 2019, the EC proposed a set of climate change policies including biodiversity, circular economy, construction, energy, food, forests and transport. The overall goal of this European Green Deal is for the European Union to become the world's first climate neutral continent by 2050. To finance this climate change strategy, the EC adopted in July 2021 the Renewed Sustainable Finance Strategy, a package of measures to help improve the flow of money to finance the transition to a sustainable economy. The goal is to mobilize at least €1 tn of financing over the decade. At the same time, a new cycle of legislative packages are proposed under the European Green Deal framework. In particular, the EC adopted the Fit for 55 package, a set of policies to achieve the target of reducing GHG emissions by 55% by 2030 compared to 1990 levels[66]. The plan is based on four pillars:

1. A more pronounced industrial transformation, with a wider application of the EU Emissions Trading System[67] (ETS) to new sectors, along with a tightening of the ETS itself;
2. A faster transition to clean mobility and aviation;
3. A significant growth in renewable energy[68] and energy efficiency;
4. The restoration of natural ecosystems and forestry to absorb carbon from natural sinks.

On 18 May 2022, the EC published the REPowerEU plan, which includes a series of measures to phase out Russian fossil fuels by 2027 and boost EU renewable energy production and energy efficiency measures. The REPowerEU plan is presented as "*the response of the EC to the hardships and global energy market disruption caused by Russia's invasion of Ukraine.*" The goal is clearly to reduce the gas dependence of the European Union. It is also an extension of the Fit for 55 package with four objectives: saving energy, diversifying supplies, accelerating the deployment of renewable energy, and reducing fossil fuel consumption in industry and transport.

**Remark 5** *The European Green Deal, the Fit for 55 package and the REPowerEU plan form the global climate strategy of the European Union. At first glance, one might think that they are almost exclusively about climate investing and not about ESG investing. Nevertheless, the EU climate strategy supports a just transition mechanism. According to ILO, "a just transition means greening the economy in a way that is as fair and inclusive as possible to everyone concerned, creating decent work opportunities and leaving no one behind." This means that the* S *and* G *pillars of ESG factors cannot be ignored. For instance, to ensure a socially fair transition, the EC proposed the creation of a social climate fund of €86 bn. The aim of this fund is to protect the poorest citizens who are most affected by energy and mobility costs.*

[66] With existing measures, EU carbon emissions are expected to fall only 36% below 1990 levels.
[67] Emissions trading systems are presented in Chapter 10 on page 944.
[68] The target for the share of renewable energy is set at 42.5% in 2030.

Figure 1.12: Sustainable finance action plan timeline

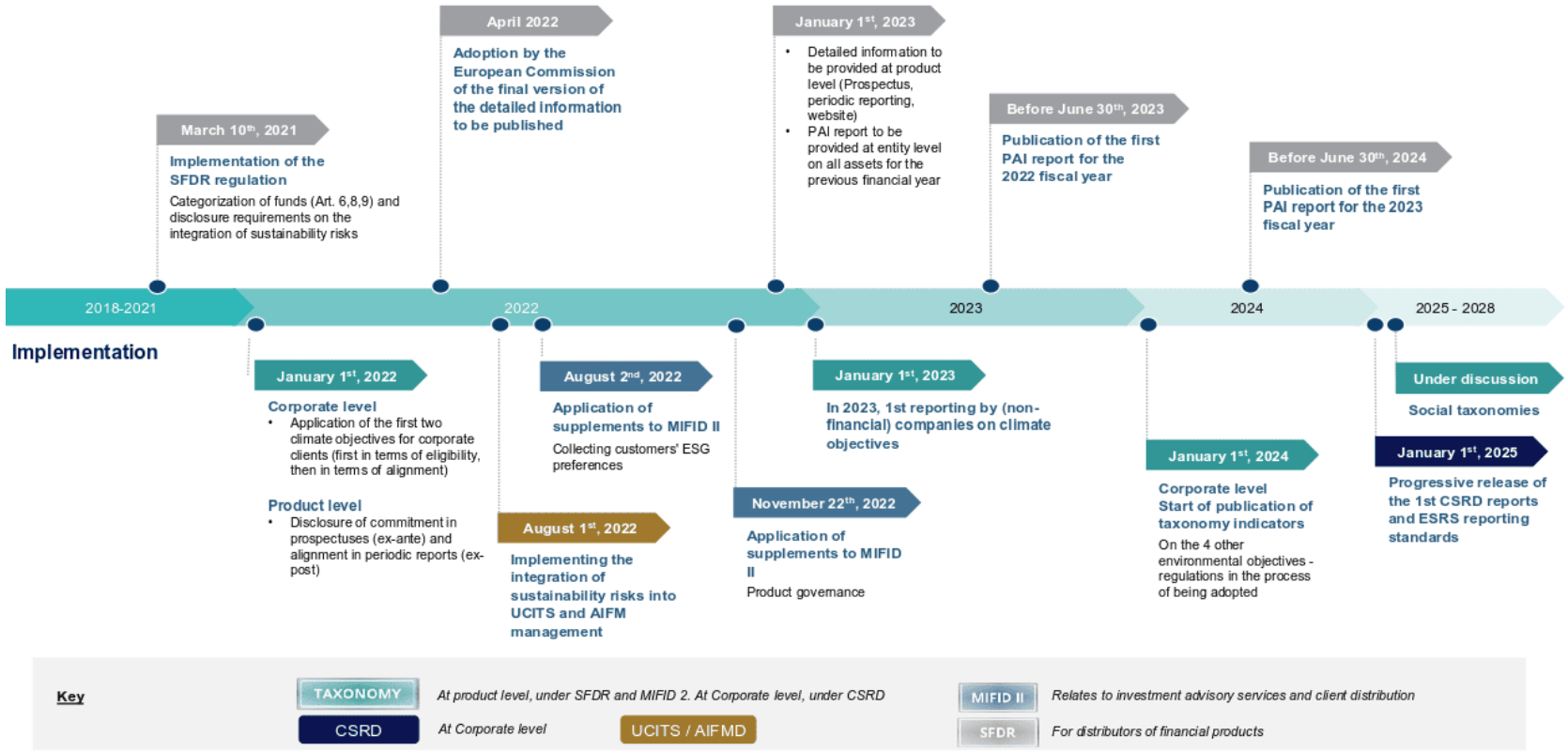


Source: Amundi Asset Management & Jaulin *et al.* (2022, page 10).

The implementation timeline shown in Figure 1.12 illustrates that the European ESG regulation is a continuous work in progress, which means that most of the frameworks discussed below are not yet finalized or may change.

### 1.4.1 EU taxonomy regulation

The purpose of a green financial taxonomy is to define what is green, and its objective is to inform investors about the greenness of their investments. This allows them to evaluate whether or not the green intensity of their portfolios meets their expectations. According to the European Commission[69], the EU taxonomy for sustainable activities is "*a classification system, establishing a list of environmentally sustainable economic activities. [...] The EU taxonomy would provide companies, investors and policymakers with appropriate definitions for which economic activities can be considered environmentally sustainable. In this way, it should create security for investors, protect private investors from greenwashing, help companies to become more climate-friendly, mitigate market fragmentation and help shift investments where they are most needed.*" In this context, the EU taxonomy is a common basis for other ESG regulations (BMR, SFDR, MiFID II, IDD, CSRD), acting as a "*common language*" around sustainable economic activities.

Developed by the Technical Expert Group on sustainable finance (TEG, 2020), the EU green taxonomy defines economic activities that make a significant contribution to at least one of the following six environmental objectives:

1. Climate change mitigation
2. Climate change adaptation
3. Sustainable use and protection of water and marine resources
4. Transition to a circular economy
5. Pollution prevention and control
6. Protection and restoration of biodiversity and ecosystem

To be considered sustainable, a business activity must also meet two other criteria. Namely, the activity must not cause significant harm to other environmental objectives (DNSH constraint) and it must comply with minimum social safeguards[70] (MS constraint). Figure 1.13 summarizes the different steps. However, according to the European Commission, the EU taxonomy is not a mandatory list for investors to invest in, and investors are free to choose what to invest in, but it is expected that over time the taxonomy will encourage a transition towards sustainability in order to meet the EU's climate and environmental goals.

In Table 1.7, we have listed the activities that are eligible for six environmental objectives. For example, the activity "*Human health and social work activities*" is eligible for the adaptation objective, but not for the five other objectives. For each activity, we have also indicated the number of sub-activities concerned. For instance, the activity "*Financial and insurance activities*" has only two eligible sub-activities: #10.1 Non-life insurance: underwriting of climate-related perils and #10.2 Reinsurance. For each sub-activity, the taxonomy also indicates the corresponding NACE

[69] See the EU website: https://ec.europa.eu/info/business-economy-euro/banking-and-finance/sustainable-finance_en.

[70] For example, the UN guiding principles on business and human rights.

Figure 1.13: EU taxonomy for sustainable activities

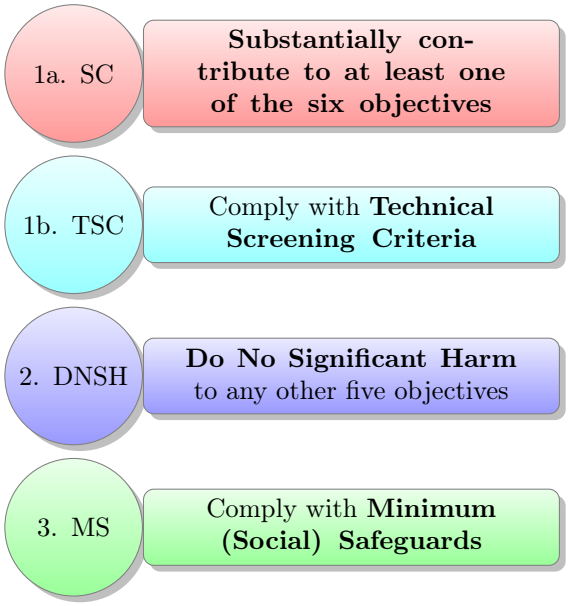


Table 1.7: Activities eligible for the six environmental objectives

| Activity name | # of activity numbers | | | | | |
|---|---|---|---|---|---|---|
| | (1) | (2) | (3) | (4) | (5) | (6) |
| Accommodation activities | | | | | | 1 |
| Arts, entertainment and recreation | | 3 | | | | |
| Construction and real estate | 7 | 7 | | 5 | | |
| Disaster risk management | | 2 | 1 | | | |
| Education | | 1 | | | | |
| Energy | 31 | 31 | | | | |
| Environmental protection and restoration activities | 1 | 1 | | | | 1 |
| Financial and insurance activities | | 2 | | | | |
| Forestry | 4 | 4 | | | | |
| Human health and social work activities | | 1 | | | | |
| Information and communication | 2 | 4 | 1 | 1 | | |
| Manufacturing | 21 | 17 | 1 | 2 | 2 | |
| Professional, scientific and technical activities | 3 | 3 | | | | |
| Services | | | | 6 | | |
| Transport | 20 | 20 | | | | |
| Water supply, sewerage, waste management and remediation | 12 | 13 | 3 | 7 | 4 | |
| Total | 101 | 106 | 6 | 21 | 6 | 2 |

Source: EU Taxonomy Compass, https://ec.europa.eu/sustainable-finance-taxonomy.

sectors[71], and the different criteria (technical screening and DNSH) for eligibility certification[72]. Looking at Table 1.7, there is an asymmetry between the first two objectives and the last four objectives. In fact, climate change mitigation and adaptation concerns more than 100 sub-activities, while there are only 2 sub-activities for the biodiversity objective, 6 for water management and pollution prevention, and 21 for the circular economy. The calculation of green intensities using the EU taxonomy is then biased towards climate change activities.

The EU's green taxonomy is of interest to a wide range of stakeholders because it defines the activities that need to be developed to achieve a low-carbon economy by 2050, with the goal of being net zero:

- All companies covered by NFRD and CSRD fall within the scope of the taxonomy. In fact, the green measurement tools and sustainability criteria developed for these two directives are aligned with the EU green taxonomy. These alignment indicators can then be found in companies' extra-financial reports.

- All financial products covered by SFDR must use the EU taxonomy to calculate the green metrics, some of the principal adverse impacts and the percentage of alignment with the European taxonomy. This information must be included in the prospectus and periodic reports of the funds and financial products.

- More generally, the EU taxonomy is widely used to define sustainable financial products. For example, the European green bond standard relies on the detailed criteria of the EU taxonomy to define green economic activities. While the EU climate-related benchmarks (CTB and PAB) do not specifically mention the taxonomy, most asset managers add green criteria that are aligned with the EU taxonomy. This is also the case for net-zero investment portfolios.

- For 2024, we expect the creation of two taxonomy-related benchmarks. On 13 December 2023, the EU Platform on Sustainable Finance published for consultation a draft report including proposals for EU taxonomy-aligning benchmarks (TAB). The two types proposed are a taxonomy-aligned benchmark (TAB) and a taxonomy-aligned benchmark excluding specific fossil fuel-related activities (TABex). The minimum standards for both TAB and TABex include at least a 7% average annual reduction in $CO_2e$ intensity by 2050 and at least a 5% annual increase in taxonomy-aligned CapEx, with a minimum exposure to CapEx securities at least equal to the equity market benchmark exposure, and an additional minimum set of exclusions for TABEx related to coal, oil and gas activities. The consultation is open until 13 March 2024.

**Remark 6** *The EU Taxonomy Regulation cannot be reduced to a green taxonomy. Indeed, the environmental taxonomy is the most advanced area, but the objective is to cover other topics. In February 2022, the EU Platform on Sustainable Finance published a final report on social taxonomy, but there is no sign of progress on the creation of a social taxonomy since the publication of this report. Similarly, there has been discussion of an expanded taxonomy in March 2022 to introduce additional levels of performance, in particular amber for intermediate performance and red for significantly harmful (SH) performance. This could form the basis of a future brown taxonomy.*

[71] NACE is the industry standard classification system used in the European Union. It is the abbreviation of the French term "*Nomenclature statistique des Activités économiques dans la Communauté Européenne*" (in English, statistical classification of economic activities in the European Community).

[72] All this information can be found in the EU Taxonomy Compass Excel file, which corresponds to Annex 1 and Annex 2 of the Delegated Act on the climate objectives (Delegated Regulation 2021/2139 of 4 June 2021) and the Complementary Climate Delegated Act (Delegated Regulation 2022/1214 of 9 March 2022).

### 1.4.2 Climate benchmarks

In September 2019, the EU Technical Expert Group on sustainable finance (TEG) proposed the creation of two climate benchmark labels[73]: climate transition benchmark (CTB) and Paris aligned benchmark (PAB). These labels are structured according to the following common principles:

1. A year-on-year self-decarbonization of 7% on average per year, based on Scope 1, 2 and 3 emissions;
2. A minimum reduction $\mathcal{R}^-$ in carbon intensity compared to the investable universe;
3. A minimum exposure to sectors highly exposed to climate change.

For the CTB label, the minimum reduction $\mathcal{R}^-$ is set at 30%, while for the PAB label it is set at 50%. Other restrictions are also imposed such as issuer exclusions (controversial weapons and violators of societal norms), a minimum green revenue share ratio (or green-to-brown ratio[74]), or some activity exclusions. These climate labels are now part of the EU Benchmarks Regulation (BMR), which also specifies ESG disclosure requirements for all benchmarks[75]. In particular, an index sponsor must disclose whether its benchmarks pursue ESG objectives and provide an explanation of the methodology used by those benchmarks to incorporate ESG factors. As mentioned above, we expect the creation of taxonomy-aligned benchmarks in 2024 to complete the European Union's climate change benchmarking framework. These various benchmarks are used in both passive and active management. In passive management, index sponsors create investable indexes that are replicated by asset managers. In active management, these climate indexes serve as benchmarks to measure the performance of climate-related and net-zero investment portfolios and to help identify responsible investment products.

### 1.4.3 Sustainable finance disclosure regulation

The SFDR is a European disclosure regulation[76] that applies at the entity level and product level. The aim is to encourage capital flows towards more sustainable investments and to prevent greenwashing. The SFDR covers websites of financial market participants (Article 4), remuneration policies in relation to the integration of sustainability risks (Article 5), the disclosure of principal adverse impacts (Article 7), the promotion of ESG on websites (Article 10), and periodic and annual reports (Article 11). The level of disclosure depends on the ESG degree of the product and the following product/fund classification:

- Article 6 (or non-ESG products)
  It covers standard financial products that cannot be Article 8 or Article 9.
- Article 8 (or ESG products)
  It corresponds to financial products which "*promote, among other characteristics, environmental or social characteristics, or a combination of those characteristics, provided that the companies in which the investments are made follow good governance practices.*"

[73] According to the TEG (2019a), "*a climate benchmark is defined as an investment benchmark that incorporates — next to financial investment objectives — specific objectives related to greenhouse gas (GHG) emission reductions and the transition to a low-carbon economy through the selection and weighting of underlying benchmark constituents.*"

[74] The implementation of GRS or GTB ratios is delayed, because it requires a comprehensive definition of green/brown taxonomies.

[75] With the exception of interest rate and currency benchmarks.

[76] Regulation (EU) 2019/2088 of the European Parliament and of the Council of 27 November 2019 on sustainability-related disclosures in the financial services sector.

- Article 9 (or sustainable products)
  In addition to the points covered by Article 8, these financial products have a sustainable investment objective.

For Article 8 and Article 9 products, the SFDR implies disclosure of qualitative and quantitative ESG information (ex-ante requirements for KIID, prospectus and websites, and ex-post requirements for annual reports and MiFID client reports). In particular, pre-contractual documents must indicate ex-ante minimum and planned percentage of sustainable investment (SI) according to following breakdown:

- SI with environmental objective
  - in economic activities that are taxonomy-aligned;
  - in economic activities that are not taxonomy-aligned.
- SI with social objective

They must also indicate how the portfolio manager considers principal adverse impacts (PAI). Among the 64 PAI indicators, some are mandatory and others are voluntary. Table 1.8 shows the 18 mandatory PAI indicators, which depend on the type of investment (exposure on corporations, investment in sovereign and supranational securities, real estate assets). In addition to these mandatory indicators, the SFDR RTS[77] also defines 22 and 24 optional PAI indicators for the E and S pillars[78], respectively.

The first level (SFDR Level I) came into force on 10 March 2021. It requires financial market participants (FMPs) to disclose general SFDR information at the entity level and SFDR classification at the product level. As SFDR Level I does not directly address all technical details, it was complemented[80] by SFDR Level II or SFDR Regulatory Technical Standards (RTS) and further amendments[81] on 20 February 2023. On 1st January 2023, SFDR Level 2 came into effect, requiring the publication of PAI indicators for Article 8 and Article 9 products. PAI reporting at the entity level for the fiscal years 2022 and 2023 must be published before June 2023 and June 2024, respectively.

Since August 2022, financial advisors (FAs) have to assess the sustainability preferences of their clients (MiFID II & IDD). For this purpose, FinDatEx has developed the European ESG Template (EET) to facilitate the exchange of ESG-related data between market participants. The EET is an Excel file containing qualitative information (*e.g.*, fund's name, isin, currency, SFDR classification) and quantitative data, in particular PAI indicators and taxonomy figures. The EET can be used as an SFDR/taxonomy template. The latest version is available at `https://findatex.eu`.

[77] In European Union, a Regulatory Technical Standard RTS is a delegated act, technical, prepared by a European Supervisory Authority (ESA). It should further develop, specify and determine the conditions for consistent harmonisation of the rules included in the basic legislative act. For instance, the SFDR RTS has been developed by ESMA, EBA, EIOPA and the ESAs' Joint Committee.

[78] The comprehensive list of PAI indicators and their associated metrics is given in Chapter 4 on page 233.

[79] Final Report on draft Regulatory Technical Standards with regard to the content, methodologies and presentation of disclosures pursuant to Article 2a(3), Article 4(6) and (7), Article 8(3), Article 9(5), Article 10(2) and Article 11(4) of Regulation (EU) 2019/2088

[80] Corrigendum to Commission Delegated Regulation (EU) 2022/1288 of 6 April 2022 supplementing Regulation (EU) 2019/2088 of the European Parliament and of the Council with regard to regulatory technical standards.

[81] Commission Delegated Regulation (EU) 2023/363 of 31 October 2022 amending and correcting the regulatory technical standards laid down in Delegated Regulation (EU) 2022/1288.

Table 1.8: The 18 mandatory PAI indicators

| | |
|---|---|
| Corporates | |
| Climate and other environment-related indicators | |
| 1 | GHG emissions |
| 2 | Carbon footprint |
| 3 | GHG intensity of investee companies |
| 4 | Exposure to companies active in the fossil fuel sector |
| 5 | Share of non renewable energy consumption and production |
| 6 | Energy consumption intensity per high impact climate sector |
| 7 | Activities negatively affecting biodiversity sensitive areas |
| 8 | Emissions to water |
| 9 | Hazardous waste ratio |
| Social and employee, respect for human rights, anti-corruption and anti-bribery matters | |
| 10 | Violations of UN Global Compact principles and OECD Guidelines for Multinational Enterprises |
| 11 | Lack of processes and compliance mechanisms to monitor compliance with UN Global Compact principles and OECD Guidelines for MNEs |
| 12 | Unadjusted gender pay gap |
| 13 | Board gender diversity |
| 14 | Exposure to controversial weapons (anti personnel mines, cluster munitions, chemical weapons and biological weapons) |
| Sovereigns and supranationals | |
| Climate and other environment-related indicators | |
| 15 | GHG intensity |
| Social and employee, respect for human rights, anti-corruption and anti-bribery matters | |
| 16 | Investee countries subject to social violations |
| Real estate assets | |
| Climate and other environment-related indicators | |
| 17 | Exposure to fossil fuels through real estate assets |
| 18 | Exposure to energy-inefficient real estate assets |

Source: SFDR RTS[79] (2 February 2021).

### 1.4.4 MiFID II and sustainable preferences

MiFID is the Markets in Financial Instruments Directive (2004/39/EC). It has applied to investment advice and portfolio management throughout the European Union since November 2007. Its aim is to standardize practices across the EU for investment services and activities and to ensure a high degree of harmonised protection for investors in financial instruments. MiFID II is a revised version of the original MiFID and came into force in 2018. It covers organizational requirements for investment firms, regulatory reporting to prevent market abuse, over-the-counter trading, cost transparency, etc.

In terms of investor protection, financial advisors must make a suitability and appropriateness assessment when providing individual portfolio management or advice on financial instruments. This means that FAs must obtain information from the client before providing investment advice or individual portfolio management. The MiFID II Suitability Test includes questions about the investor's knowledge and experience, financial situation, and investment objectives. In September

2022, ESMA has published its guidelines on the integration of ESG risks and factors into MiFID II (ESMA, 2022). There are two main implications:

1. Integration of sustainability preferences to define the suitable product;
2. Integration of ESG criteria in the product governance.

The first point ensures that the product is in line with investors' values when providing financial advice and portfolio management services. This requires a new version of the suitability and appropriateness assessment (profiling questionnaire, suitability test, adequacy report). The second point concerns the product offering of FMPs. Indeed, manufacturers and distributors must specify their target markets and the sustainability goals with which the product is compatible.

"*Sustainability preferences*" is the key concept when selling an ESG product[82]. If the client has sustainability preferences (yes/no), they must select one or a combination of the following criteria:

1. Minimum percentage in environmentally sustainable investments aligned to the EU taxonomy;
2. Minimum percentage invested in sustainable investments as defined in the SFDR (Articles 8 and 9);
3. Quantitative/qualitative elements of principal adverse impacts defined by the client.

Once the selection has been made, the financial advisor can sell a product to the client after ensuring that the product meets the client's sustainability preferences.

**Remark 7** *The integration of sustainability preferences is not limited to financial investment products and MiFID II. It also applies to insurance-based investment products and the Insurance Distribution Directive (IDD).*

### 1.4.5 Corporate sustainability reporting directive

The Corporate Sustainability Reporting Directive (CSRD) requires companies to disclose sustainability information in their financial reports. It has replaced the NFRD on 5 January 2023. The CSRD applies to all listed companies in the EU and all large European companies that meet at least two of the following criteria: (1) 250 employees, (2) €50 mn turnover and, (3) €25 mn total assets. This represents approximately 50 000 companies and 75% of the total turnover of companies in the EU, while the NFRD covered about 11 700 large companies. According to EFRAG (2022), the sustainable reporting standards shall address the following topics:

- **E**nvironmental factors: (1) climate change mitigation; (2) climate change adaptation; (3) water and marine resources; (4) resource use and circular economy; (5) pollution; (6) biodiversity and ecosystems.
- **S**ocial factors: (1) equal treatment and opportunities for all; (2) working conditions; (3) respect for the human rights, fundamental freedoms and democratic principles.
- **G**overnance factors: (1) role and composition of administrative, management and supervisory bodies; (2) features of the undertaking's internal control and risk management systems, in relation to the sustainability reporting; (3) business ethics and corporate culture, including anti-corruption and anti-bribery; (4) political engagements of the undertaking, including its lobbying activities; (5) management and quality of relationships with business partners.

[82] Client's sustainability preferences are required since August 2022.

For the environmental factors, we recognize the 6 goals of the green taxonomy. It is no coincidence that the CSRD must be consistent with the SFDR and the European taxonomy. In fact, it must help financial institutions calculate ESG and climate metrics in a more robust and effective way. In addition to current KPIs, the CSRD also requires the company measure and assess its targets. This type of forward-looking information is helpful to investors, for example, in defining their net-zero investment policies. However, the CSRD has another ambition by considering double materiality. It is a first step in the development of a comprehensive extra-financial/climate accounting statement[83]. Materiality is an accounting principle that states that information about an entity is material if it is reasonably likely to influence an investor's decision. Therefore, it must be recorded or reported in the financial statements. It is now widely accepted that climate-related impacts on a company can be material and therefore require disclosure. This approach is known as financial or single materiality. The concept of double materiality is an extension of single materiality by considering the company's negative externalities. In this case, we need to consider two materiality perspectives:

- How do sustainability factors affect the financial value of the company?
- How does the company impact the environment, society, and people?

The first corresponds to financial (or outside-in) materiality, while the second defines impact (or inside-out) materiality. For example, the SASB framework is based on the financial materiality. In contrast, the GRI framework has adopted an inside-out materiality by reporting on the impact of companies on people and the planet. In the case of the CSRD, EFRAG has chosen to consider the double materiality assessment.

On 31 July 2023, the European Commission published a first set of 12 European Sustainability Reporting Standards (ESRS) developed by EFRAG (2022) (Figure 1.14). The two cross-cutting standards are ESRS 1, which covers general requirements, and ESRS 2 which adresses general disclosures:

- ESRS 1 describes the architecture of ESRS standards, explains drafting conventions and fundamental concepts, and sets out general requirements for the preparation and presentation of sustainability-related information: qualitative characteristics of information, double materiality, due diligence, value chain, etc.
- ESRS 2 sets out disclosure requirements for the information that the company should provide at a general level on all material sustainability issues in the reporting areas of governance, strategy, impact, risk and opportunity management, and metrics and targets.

In addition to the two cross-cutting standards, there are 10 topical ESRS that cover a sustainability topic and are organized into topics and sub-topics:

- ESRS E1 climate change: climate change adaptation, climate change mitigation, energy.
- ESRS E2 pollution: pollution of air, pollution of water, pollution of soil, pollution of living organisms and food resources, substances of concern, substances of very high concern, microplastics.
- ESRS E3 water and marine resources: water (water consumption, water withdrawals, water discharges), marine resources (water discharges in the oceans, extraction and use of marine resources).

[83] The CSRD standards are defined by EFRAG (European Financial Reporting Advisory Group), which represents the European accounting profession and the European voice in financial reporting. In particular, it participates in the standard setting process of the IASB and develops European views on international accounting standards (IFRS).

Figure 1.14: ESRS standards

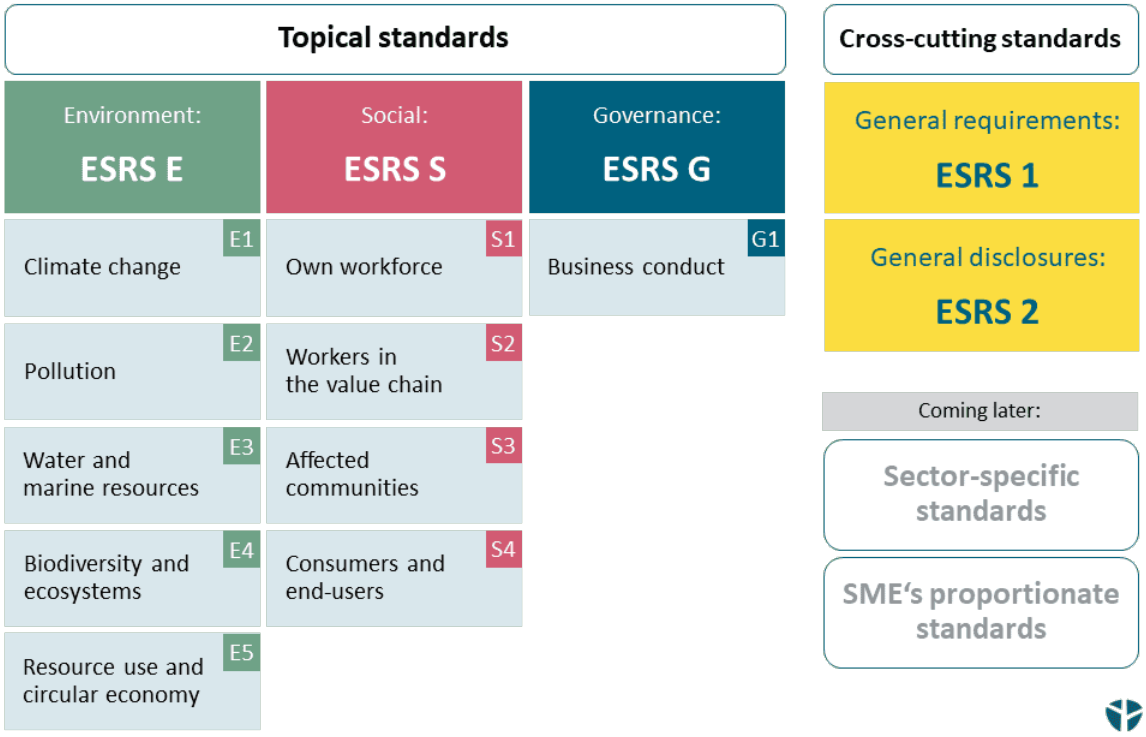


Source: https://denkstatt.eu/esrs-standards-explained.

- ESRS E4 biodiversity and ecosystems: direct impact drivers of biodiversity loss (land-use change, fresh water-use change and sea-use change, direct exploitation, invasive alien species), impacts on the state of species, impacts on the extent and condition of ecosystems, impacts and dependencies on ecosystem services.

- ESRS E5 circular economy: resources inflows, including resource use, resource outflows related to products and services, waste.

- ESRS S1 own workforce: working conditions (secure employment, working time, adequate wages, social dialogue, freedom of association, collective bargaining, work-life balance, health and safety), equal treatment and opportunities for all (gender equality and equal pay for work of equal value, training and skills development, employment and inclusion of persons with disabilities, measures against violence and harassment in the workplace, diversity), other work-related rights (child labour, forced labour, adequate housing, privacy).

- ESRS S2 workers in the value chain: working conditions, equal treatment and opportunities for all, other work-related rights.

- ESRS S3 affected communities: communities' economic, social and cultural rights (adequate housing, adequate food, water and sanitation, land-related impacts, security-related impacts), communities' civil and political rights (freedom of expression, freedom of assembly, impacts on human rights defenders), rights of indigenous peoples (free, prior and informed consent, self-determination, cultural rights).

- ESRS S4 consumers and end-users: information-related impacts for consumers and/or end-users (privacy, freedom of expression, access to quality information), personal safety of consumers and/or end-users (health and safety, security of a person, protection of children), social inclusion of consumers and/or end-users (non-discrimination, access to products and services, responsible marketing practices).
- ESRS G1 business conduct: corporate culture, protection of whistle-blowers, animal welfare, political engagement and lobbying activities, management of relationships with suppliers including payment practices, corruption and bribery (prevention and detection including training, incidents).

These first 12 ESRS cover all companies subject to the CSRD. Sector-specific and SME-specific ESRS are expected to follow. Obviously, reporting on all of these dimensions requires the calculation of hundreds of metrics and data points, is time-consuming, and can be relatively costly. For this reason, the European Commission has introduced a phased approach to reporting requirements. The ESRS will apply first to companies that were previously subject to the NFRD. They will publish the first CSRD report in 2025 for data collected in the 2024 financial year. Other large companies that were not subject to the NFRD will publish in 2026 for data collected in the 2025 financial year. Finally, listed SMEs will publish in 2027.

According to the European Commission[84], they have worked to "*ensure a very high level of alignment between ESRS and the standards of the International Sustainability Standards Board (ISSB) and the Global Reporting Initiative (GRI). From the beginning of the development of draft ESRS by EFRAG, the GRI served as an important reference point, and many of the reporting requirements in ESRS were inspired by the GRI standards. The ESRS and the first two standards of the ISSB (IFRS S1 and S2) have been developed in parallel. Intensive and constructive discussions between the Commission, EFRAG and the ISSB have ensured a very high degree of alignment where the two sets of standards overlap.*" However, we remind that there is a big difference between the ESRS and ISSB standards since the former is based on double materiality while the latter has adopted single materiality.

## 1.5 The market of ESG investing

In this section, we provide a global overview of the ESG market from an investment perspective. First, we define the various ESG strategies and provide some examples. We then discuss some figures on the ESG market and its growth.

### 1.5.1 ESG strategies

In Figure 1.15 we define the different types of ESG strategies. This list is based on several reports (Eurosif, 2018; GSIA, 2021; PRI, 2020). Depending on the region and the organization, these categories may have different names. For example, in the case of the seventh category, the term "*community investing*" is widely used in North America (RIA Canada, US SIF), while we prefer the term "*microfinance*" in Europe.

Most of these categories are based on the concept of screening, which refers to investment filters. Negative screening is an approach that excludes certain investments or groups of assets from the investable universe, such as companies, sectors or countries that do not meet specific ESG criteria. When applied to companies, it is also referred to as a worst-in-class exclusion strategy. In this

[84] See the website https://ec.europa.eu/commission/presscorner/detail/en/qanda_23_4043.

Figure 1.15: The 7 categories of ESG strategies

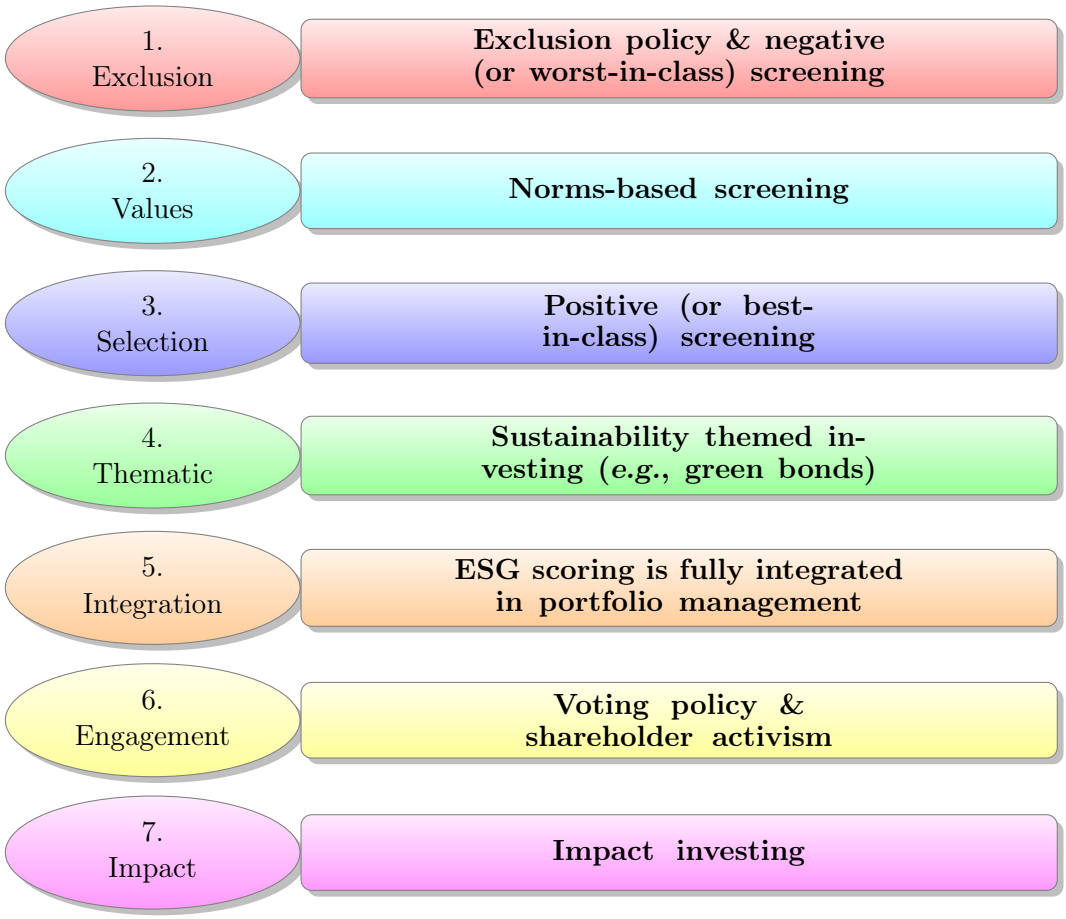


Source: Eurosif (2021), https://www.eurosif.org/responsible-investment-strategies.

Table 1.9: Comparison of Eurosif, GSIA and PRI classifications

| # | Eurosif | GSIA | PRI |
|---|---|---|---|
| 1 | Exclusions | Negative/exclusionary screening | Negative screening |
| 2 | Norms-based screening | Norms-based screening | Norms-based screening |
| 3 | Best-in-class | Best-in-class/positive screening | Positive screening |
| 4 | Sustainability themed | Sustainability themed/thematic investing | Thematic |
| 5 | ESG integration | ESG integration | Integration of ESG issues |
| 6 | Engagement & voting | Corporate engagement & shareholder action | Engagement/proxy voting |
| 7 | Impact investing | Impact/community investing | Sustainability impact |

case, the investor can systematically exclude issuers with the worst rating (*e.g.*, companies rated CCC). This category also covers sector or sub-industry exclusions (*e.g.*, coal & consumable fuels, fossil fuel production, conventional weapons, civilian firearms). This approach may also include certain activities, because they are inconsistent with the investor's values (*e.g.*, pornography, tobacco, alcohol, gambling, genetically modified organisms). In most cases, the investor defines an exclusion list of individual issuers.

Norm-based screening consists of excluding companies that have been called into question for violating international standards and norms on social or environmental issues, such as those issued by the OECD, ILO, UN Global Compact and UNICEF. The first category is closed to this second category, but the latter is based on international values, while the former is based on individual values. For example, a company that meets all the minimum standards of business practice based on international norms may be excluded in the negative screening approach because it has a very poor ESG rating or belongs to a sector that the investor does not want to finance. Considering the first two categories, the top exclusion criteria in Europe are (1) controversial weapons (Ottawa and Oslo treaties), (2), tobacco, (3) all weapons, (4) gambling, (5) pornography, (6) nuclear energy, (7) alcohol, (8) genetically modified organisms and (9) animal testing (Eurosif, 2018).

The third category invests in issuers, sectors or projects selected for positive ESG performance relative to industry peers. For this reason, the selection category is also referred to as positive screening. For example, the best-in-class ESG strategy selects issuers with the best ESG ratings (*e.g.*, AAA, AA and A), while the ESG momentum strategy selects issuers that have improved their ESG rating.

The goal of sustainability thematic investing is to invest in companies whose activities are related to sustainability, such as clean energy, green technology, sustainable agriculture, sustainable infrastructure, natural resources, biodiversity. ESG thematic investing considers all ESG issues, not just the environmental pillar. For example, it involves investing in social issues (*e.g.*, health, food security, diversity) and governance issues (*e.g.*, gender equality, inclusive boards). Generally, these thematic investments are implemented through mutual funds.

ESG integration is the systematic and explicit incorporation of ESG factors by investment managers into financial analysis and asset allocation. This strategy can be seen as an extension of exclusion and best-in-class strategies. For example, the stock or bond picking score may be a mix of the fundamental score and the ESG score. Some asset managers also require funds to have an ESG score greater than the ESG score of their benchmarks.

The sixth category uses shareholder power and active ownership to influence corporate behavior, including through direct corporate engagement, (*i.e.*, communication with company management and/or boards of directors), filing or co-filing shareholder proposals, and proxy voting that is guided by ESG guidelines. Examples of engagement activities include voting policy, public divestment, engagement with target companies on a specific subject (*e.g.*, pay ratio, living wage), proposing shareholder resolutions, public litigation, etc.

Impact investing is the term used to describe investments made with the intention of generating a positive, measurable social and environmental impact in addition to a financial return. Unlike thematic investing, which focuses on corporate stocks and bonds, impact investing considers assets and securities that finance specific projects. For example, impact investing includes microfinance, community investing, social entrepreneurship funds, funds with a social impact objective, and green and social bonds. Since the goal is to achieve positive social and environmental impacts, it is necessary to measure and report on these extra-financial impacts. Extra-financial reporting is then the key element of impact investing, as it must clearly define and measure the ESG objectives. (*e.g.*, GHG emissions avoided per €1 mn invested per year, percentage of water consumption savings).

**Remark 8** *We notice that these seven categories can be divided into two groups of strategies. The first takes into account the ESG scores when building an investment portfolio (exclusion, selection, thematic and integration). The primary objective of these strategies remains the financial performance of the portfolio. The second group places a high priority on ethical behavior (norm-based screening, engagement and impact investing) and can be related to signaling theory. In this approach, investors send a negative signal to the market and to companies when they apply norm-based screening or engage with a company*[85]*. Conversely, investors send a positive signal when they implement impact investing.*

### 1.5.2 The market share of ESG investing

In this section, we present a global view of ESG investment market growth[86] based on the Global Sustainable Investment Reviews (GSIA, 2017, 2019, 2021). For each report, Figures 1.16, 1.17 and 1.18 show the AUM of responsible investments, the corresponding market share, the global growth and the breakdown by country. According to GSIA (2021), sustainable investments represented \$35.3 tn of assets under management at the beginning of 2020, *i.e* a market share of 36%. They continue to grow in most regions[87], with Canada experiencing the largest increase (48% growth), followed by the United States (42% growth). On a regional analysis, the market share of sustainable investments is 62% in Canada, 42% in Europe, 38% in Australasia, 33% in the United States, and 24% in Japan.

Table 1.10: ESG asset growth by region

| Region | Asset under management (in \$ bn) | | | | Asset growth (in %) | | | |
|---|---|---|---|---|---|---|---|---|
| | 2016 | 2018 | 2020 | 2022 | 2016 | 2018 | 2020 | 2022 |
| Europe | 12 040 | 14 075 | 12 017 | 14 054 | 12% | 11% | −13% | 31% |
| Canada | 1 086 | 1 699 | 2 423 | 2 358 | 49% | 42% | 48% | −5% |
| Australasia | 516 | 734 | 906 | 1 220 | 248% | 46% | 25% | 30% |
| Japan | 474 | 2 180 | 2 874 | 4 289 | 6 692% | 307% | 34% | 59% |
| Sub-total | 14 116 | 18 688 | 18 220 | 21 921 | 21% | 32% | −3% | 20% |
| United Sates | 8 723 | 11 995 | 17 081 | 8 400 | 33% | 38% | 42% | −51% |
| Total | 22 839 | 30 683 | 35 301 | 30 321 | 25% | 34% | 15% | −14% |

Source: GSIA (2015, 2017, 2019, 2021, 2023) & Author's calculations.

The 2022 GSIR paints a different picture of the ESG investment market (Table 1.10). We see strong growth in Europe (+31% between 2020 and 2022), Australasia (+30%) and Japan (+59%). Over the same period, there is a decline in North America, particularly in the United States. As there is a change in the assets collected by the US SIF in the United States, it is difficult to know whether the decline is due to the change in methodology or whether it is a setback in the US due to the ESG backlash[88].

[85] Because the investor is not satisfied with the company's environmental, social or governance policies.

[86] The figures concerning specific segments (mutual funds, ETFs, green financing, etc.) are given in Chapters 2 and 10.

[87] The case of Europe (13% decline in the growth of sustainable investment assets between 2018 and 2020) is due to a change in the measurement methodology from which European data are collected and to European regulations, in particular the SFDR. We must therefore be cautious before drawing conclusions. In fact, these data do not take into account how ESG factors are truly implemented.

[88] GSIA (2023, page 8) gives the following reasons: "*The US SIF modified their methodology for the latest edition of the US SIF Trends report, which is used as the basis for the Global Sustainable Investment Review. The revised*

Figure 1.16: Sustainable investment assets at the start of 2016

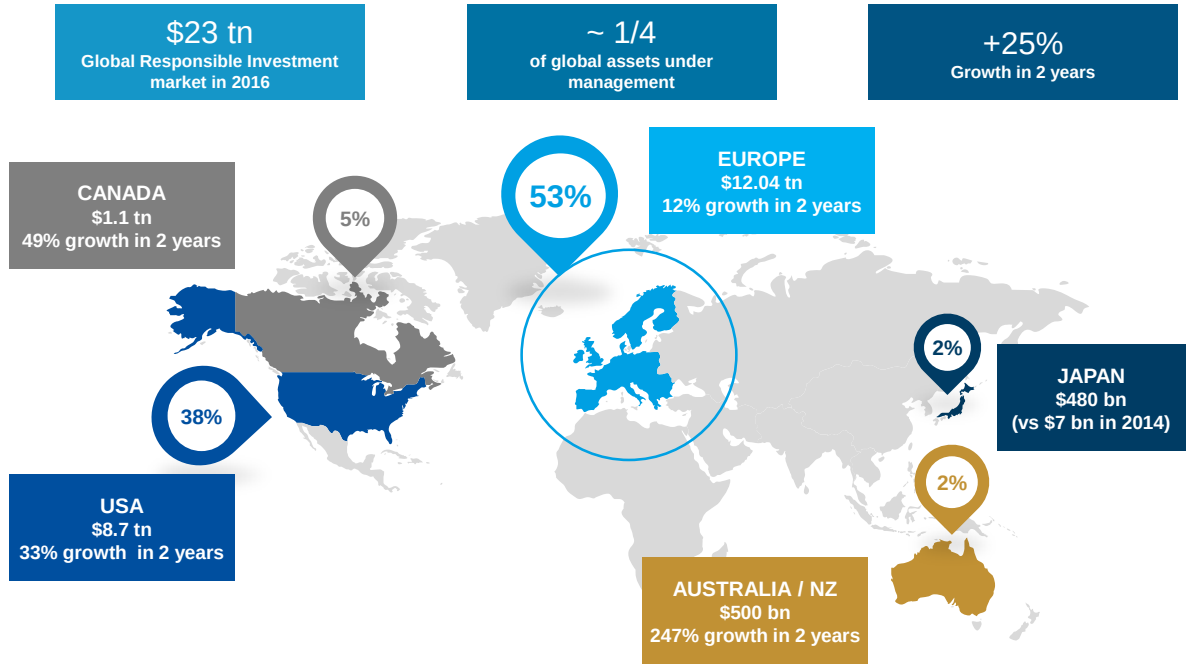


Source: GSIA (2017).

Figure 1.17: Sustainable investment assets at the start of 2018

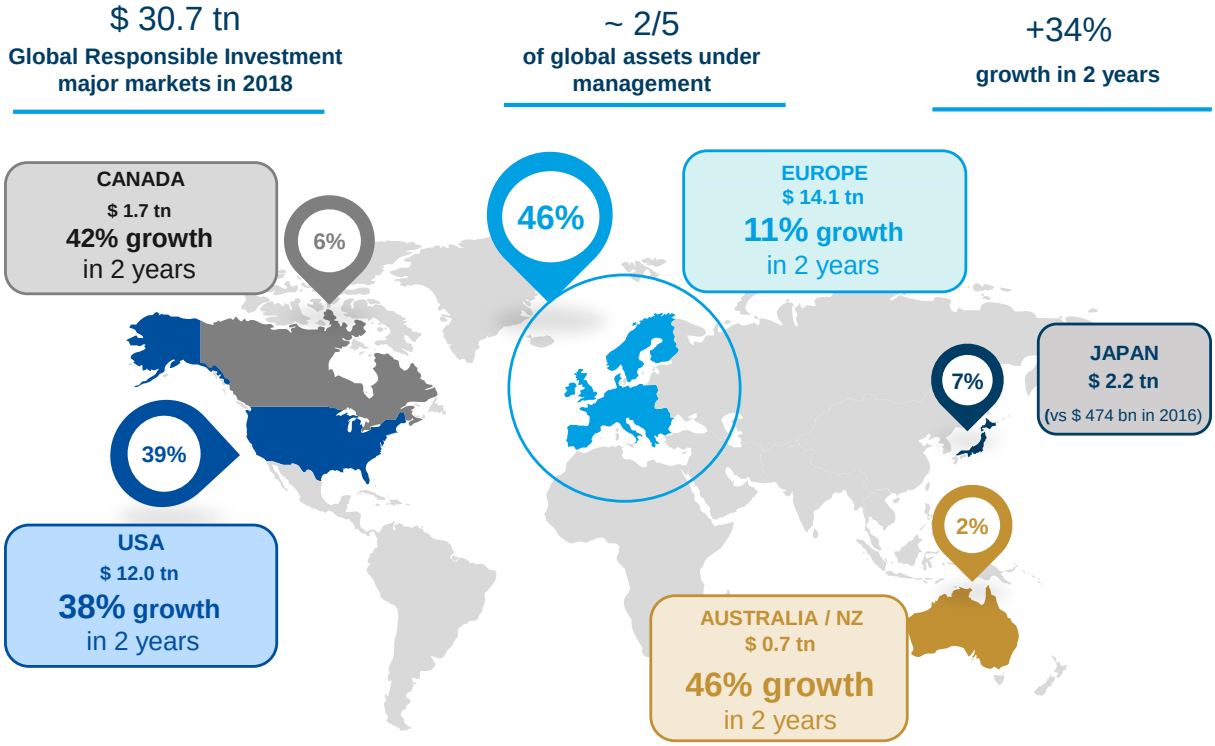


Source: GSIA (2019).

Figure 1.18: Sustainable investment assets at the start of 2020

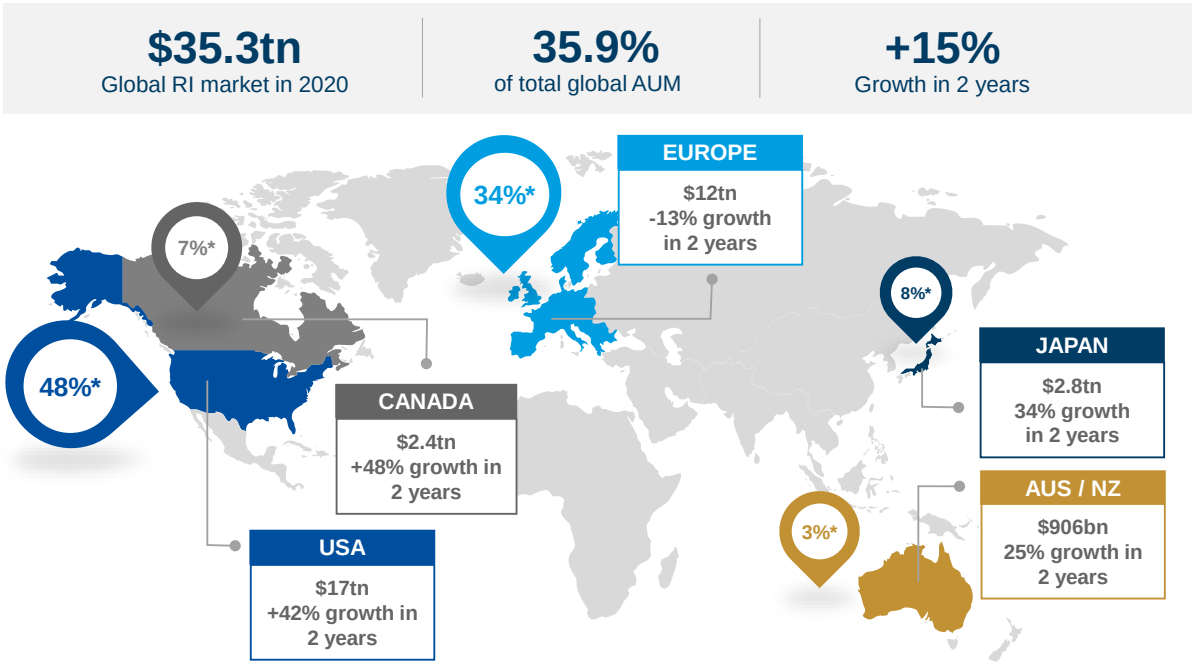


Source: GSIA (2021).

Figure 1.19: Asset values of ESG strategies between 2014 and 2022

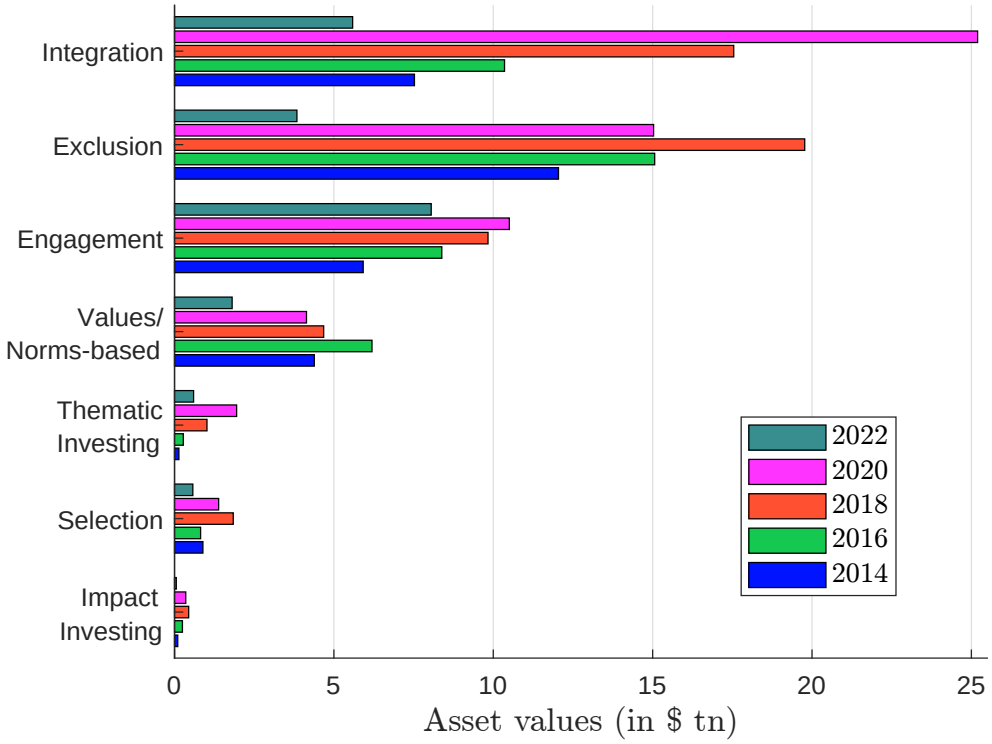


Source: GSIA (2015, 2017, 2019, 2021, 2023) & Author's calculations.

Figure 1.19 shows changes in asset values by ESG category. For many years, negative screening and exclusion dominated the other strategies. In 2020, ESG integration has become the most implemented approach. We also notice that some categories are less represented: thematic investing, best-in-class/selection and impact investing. However, we observe that thematic investing is the category with the highest growth in assets. Again, the 2022 figures are not comparable to the 2020 figures due to the change in methodology[89]. However, we note that engagement takes the lead, followed by integration and exclusion (Table 1.11).

Table 1.11: ESG asset growth by strategy

| # | ESG strategy | Asset growth | | | AUM (in $ bn) | |
|---|---|---|---|---|---|---|
| | | 2014–2016 | 2016–2018 | 2018–2020 | 2020 | 2022 |
| 1 | Exclusion | 11.7% | 14.6% | −24.0% | 15 030 | 3 840 |
| 2 | Values/Norms-based | 19.0% | −13.1% | −11.5% | 4 140 | 1 807 |
| 3 | Selection | 7.6% | 50.1% | −24.9% | 1 384 | 574 |
| 4 | Thematic Investing | 55.1% | 92.0% | 91.4% | 1 948 | 598 |
| 5 | Integration | 17.4% | 30.2% | 43.6% | 25 195 | 5 588 |
| 6 | Engagement | 18.9% | 8.3% | 6.8% | 10 504 | 8 053 |
| 7 | Impact Investing | 56.8% | 33.7% | −20.8% | 352 | 55 |
| | Total | | | | 58 553 | 20 515 |

Source: GSIA (2015, 2017, 2019, 2021, 2023) & Author's calculations.

If we focus on asset ownership, the ESG market is driven primarily by institutional investors. They currently account for 75% of the market, with the remaining 25% being retail assets. However, we are seeing a fundamental shift as the split in 2012 was 89% vs. 11% (GSIA, 2021, page 13). This is particularly true in Europe, where retail investors are increasingly interested in understanding the impact of their investments on the world, as demonstrated by both market developments and academic research (GSIA, 2023, page 22). It seems that this trend is also present in Japan, but not in the UK and the US. We also note that institutional and retail investors have different beliefs about ESG. For example, Giglio *et al.* (2023a) found that retail investors generally expect ESG investments to underperform the market, while institutional investors in Europe believe that ESG can improve the risk management of their portfolios.

## 1.6 Conclusion

This little-boring introduction provides a global overview of the sustainable finance landscape. As a student, you need to understand who does what, the outlines of the various regulations, and some figures about sustainable finance. However, a course in sustainable finance cannot be summarized by

*methodology does not include the AUM of investors who stated that they practice firmwide ESG integration but did not provide information on any specific ESG criteria they used (such as biodiversity, human rights or tobacco) in their investment decision-making. Additionally, several asset managers in the 2022 Trends Information Request reported far lower sustainable investing AUM than they had in 2020 (in some cases, in the magnitude of billions and trillions of dollars). The modified methodology and change in money manager reporting led to a significant drop in total reported ESG AUM, as well as ESG AUM for specific criteria.*"

[89] "*In previous years, respondents have been able to select multiple sustainable investing strategies. This has meant that the value across the categories has often exceeded the total ESG AUM (150-200%). In this year's report respondents from the US and Canada selected the predominant category and were required to validate selection with provision of AUM incorporating this strategy. As a result of this change the value across the categories does not meet the total ESG AUM, representing around 66%.*" (GSIA, 2023, page 8).

a set of acronyms (Figure 1.20). We also need to understand the data we are manipulating. Because the data are very noisy and not exhaustive, probability and quantitative modeling is important for two main reasons. The first is to estimate the limits of what professionals do. The second reason is to measure the relationships between the various factors from an ex-ante point of view and to make some convictions, because data and numbers can lie to us.

Figure 1.20: The ESG world of acronyms

# Part I

# ESG Risk

# Chapter 2

# ESG Scoring

To develop ESG analysis, we need extra-financial data provided by companies, reporting frameworks, academic institutions, research centers, international bodies, etc. In general, this heterogeneous data is collected by ESG data providers. These data are available for two levels of use. First, they are widely used by ESG analysts to assess the sustainability risks of companies and countries. Second, they provide the raw material for ESG scoring systems. Like credit scoring models, such systems are of paramount importance for risk assessment and decision making. In the case of credit scoring, the decision is whether or not to grant credit. Therefore, credit scoring models are at the center of the lending process. In the case of ESG scoring, the issue is a bit different. Of course, we can use ESG scores to decide whether or not to invest in a company, but exclusion is not the only strategy, as we saw in the previous chapter. For example, ESG scores are fully embedded in the strategy of ESG integration. In this approach, they play the role of screening rules for portfolio selection. ESG scoring is therefore more than a traditional scoring model. Nevertheless, the analogy between ESG scoring and credit scoring remains essential and poses several challenges in terms of performance evaluation, score consistency and backtesting. This is particularly true as ESG risk ratings are generated from these scoring systems. From this perspective, the concept of ESG model validation takes on a new dimension. We recall that any internal risk model must comply with an independent model validation process that is highly binding and formal from a regulatory standpoint (FRB, 2011; EBA, 2014). Moreover, the validation process is not limited to credit, market, operational and liquidity risks. For example, it also applies to compliance risks: statistical models developed for anti-money laundering detection, transaction monitoring, anomaly detection scenarios, list filtering, etc. The systematic validation approach of any model (risk-based, behavioral, rules-based and AI-based) has recently been reinforced in the US with the interagency guidance on model risk management (FRB, 2021). As ESG scoring models become more widely used by financial institutions, we can easily predict that they will be regulated in the near future, just like the other risk models. Therefore, in this chapter, we adopt the basic idea that a scoring system needs to be validated from an ex-post viewpoint. To do so, we make extensive use of the mathematical and statistical tools available to us in the fields of scoring theory and Markov-based rating methods (Roncalli, 2020a, Section 3.3.3 and Chapter 15). This chapter is then organized as follows. Section 1 presents the ESG data and the sources of extra-financial information. The construction of ESG scores and the performance evaluation of ESG scoring models are discussed in Section 2. Finally, we examine ESG rating systems and assess the consistency of ESG migration matrices.

## 2.1 Data and variables

In this section, we list the most important variables or indicators that are used in an ESG scoring system. For that, we distinguish between sovereign and corporate data since the sources are not the same and their access is more or less easy. As the adage says that "*we can only measure what we can define*", we must first specify the meaning of the three ESG factors, because the objective of an ESG score is to measure the risk and opportunities of an entity with respect to environmental, social and governance dimensions. If we consider the definition on page 1, we notice that each factor is defined by encompassing several issues:

- **E** climate change mitigation, climate change adaptation, preservation of biodiversity, pollution prevention, circular economy;
- **S** inequality, inclusiveness, labor relations, investment in human capital and communities, human rights;
- **G** management structure, employee relations, executive remuneration.

Of course, this list is non-exhaustive and must be adapted to show the difference between sovereign and corporate entities. Let us consider an example. According to the Universal Declaration of Human Rights[1], States have obligations and duties under international law to respect, protect and fulfill human rights:

> "*The obligation to respect means that States must refrain from interfering with or curtailing the enjoyment of human rights. The obligation to protect requires States to protect individuals and groups against human rights abuses. The obligation to fulfill means that States must take positive action to facilitate the enjoyment of basic human rights.* "

For a sovereign, the issue of human rights concerns both social (*e.g.*, access to health and education, labor rights) and governance (*e.g.*, safeguarding of civil and political rights) pillars, while it is more related to the social pillar (*e.g.*, ethical supply chain, employment conditions) of a company. Therefore, it is certainly easier to define the three dimensions with examples.

### 2.1.1 Sovereign ESG data

#### The World Bank framework

The World Bank database dedicated to sovereign ESG indicators is certainly the easiest way to understand the most common topics relevant to ESG analysis. The database is available at the following webpage: https://datatopics.worldbank.org/esg. It contains 67 ESG indicators grouped into 17 themes. In Table 2.1, we have reported these categories and the corresponding number of indicators. For example, the **E** pillar is made up of 5 categories, such as emissions and pollution that contains 5 indicators. In total, we have 5 **E**, 6 **S** and 6 **G** themes. We observe that global warming and its consequences are the main drivers of the environmental pillar. If we analyse the 27 indicators (Table 2.2), two categories are related to the measurement of climate change (emissions & pollution, environment/climate risk & resilience), one category is related to the mitigation risks of climate change (natural capital endowment & management, energy use & security), and the last category concerns the impact of climate change on food security. If we focus on the **S** pillar, the sources of social risks are related to inclusiveness and inequality (education & skills, poverty & inequality, health & nutrition, access to services), in particular the literacy rate, the school enrollment,

[1] See https://www.ohchr.org/en/ohchr_homepage.

Table 2.1: The World Bank database of sovereign ESG indicators

**Environmental (27)**

- Emissions & pollution (5)
- Natural capital endowment & management (6)
- Energy use & security (7)
- Environment/climate risk & resilience (6)
- Food security (3)

**Social (22)**

- Education & skills (3)
- Employment (3)
- Demography (3)
- Poverty & inequality (4)
- Health & nutrition (5)
- Access to services (4)

**Governance (18)**

- Human rights (2)
- Government effectiveness (2)
- Stability & rule of law (4)
- Economic environment (3)
- Gender (4)
- Innovation (3)

Table 2.2: Indicators of the environmental pillar (World Bank database)

- **Emissions & pollution** (1) CO2 emissions (metric tons per capita); (2) GHG net emissions/removals by LULUCF (Mt of CO2 equivalent); (3) Methane emissions (metric tons of CO2 equivalent per capita); (4) Nitrous oxide emissions (metric tons of CO2 equivalent per capita); (5) PM2.5 air pollution, mean annual exposure (micrograms per cubic meter);
- **Natural capital endowment & management**: (1) Adjusted savings: natural resources depletion (% of GNI); (2) Adjusted savings: net forest depletion (% of GNI); (3) Annual freshwater withdrawals, total (% of internal resources); (4) Forest area (% of land area); (5) Mammal species, threatened; (6) Terrestrial and marine protected areas (% of total territorial area);
- **Energy use & security**: (1) Electricity production from coal sources (% of total); (2) Energy imports, net (% of energy use); (3) Energy intensity level of primary energy (MJ/$2011 PPP GDP); (4) Energy use (kg of oil equivalent per capita); (5) Fossil fuel energy consumption (% of total); (6) Renewable electricity output (% of total electricity output); (7) Renewable energy consumption (% of total final energy consumption);
- **Environment/climate risk & resilience**: (1) Cooling degree days (projected change in number of degree Celsius); (2) Droughts, floods, extreme temperatures (% of population, average 1990–2009); (3) Heat Index 35 (projected change in days); (4) Maximum 5-day rainfall, 25-year return level (projected change in mm); (5) Mean drought index (projected change, unitless); (6) Population density (people per sq. km of land area)
- **Food security**: (1) Agricultural land (% of land area); (2) Agriculture, forestry, and fishing, value added (% of GDP); (3) Food production index (2004–2006 = 100);

Source: https://datatopics.worldbank.org/esg/framework.html.

Table 2.3: Indicators of the social pillar (World Bank database)

- **Education & skills**: (1) Government expenditure on education, total (% of government expenditure); (2) Literacy rate, adult total (% of people ages 15 and above); (3) School enrollment, primary (% gross);
- **Employment**: (1) Children in employment, total (% of children ages 7-14); (2) Labor force participation rate, total (% of total population ages 15-64) (modeled ILO estimate); (3) Unemployment, total (% of total labor force) (modeled ILO estimate);
- **Demography**: (1) Fertility rate, total (births per woman); (2) Life expectancy at birth, total (years); (3) Population ages 65 and above (% of total population);
- **Poverty & inequality**: (1) Annualized average growth rate in per capita real survey mean consumption or income, total population (%); (2) Gini index (World Bank estimate); (3) Income share held by lowest 20%; (4) Poverty headcount ratio at national poverty lines (% of population);
- **Health & nutrition**: (1) Cause of death, by communicable diseases and maternal, prenatal and nutrition conditions (% of total); (2) Hospital beds (per 1,000 people); (3) Mortality rate, under-5 (per 1,000 live births); (4) Prevalence of overweight (% of adults); (5) Prevalence of undernourishment (% of population);
- **Access to services**: (1) Access to clean fuels and technologies for cooking (% of population); (2) Access to electricity (% of population); (3) People using safely managed drinking water services (% of population); (4) People using safely managed sanitation services (% of population);

Table 2.4: Indicators of the governance pillar (World Bank database)

- **Human rights**: (1) Strength of legal rights index (0 = weak to 12 = strong); (2) Voice and accountability (estimate);
- **Government effectiveness**: (1) Government effectiveness (estimate); (2) Regulatory quality (estimate);
- **Stability & rule of law**: (1) Control of corruption (estimate); (2) Net migration; (3) Political stability and absence of violence/terrorism (estimate); (4) Rule of law (estimate)
- **Economic environment**: (1) Ease of doing business index (1 = most business-friendly regulations); (2) GDP growth (annual %); (3) Individuals using the internet (% of population);
- **Gender**: (1) Proportion of seats held by women in national parliaments (%); (2) Ratio of female to male labor force participation rate (%) (modeled ILO estimate); (3) School enrollment, primary and secondary (gross), gender parity index (GPI); (4) Unmet need for contraception (% of married women ages 15-49);
- **Innovation**: (1) Patent applications, residents; (2) Research and development expenditure (% of GDP); (3) Scientific and technical journal articles;

Source: https://datatopics.worldbank.org/esg/framework.html.

the Gini index[2], the income share held by the lowest 20%, etc. We also notice that the integration of some indicators from the categories employment and demography is disturbing. Indeed, we may wonder how the fertility rate is related to the social pillar. For instance, does a high fertility rate increase or decrease social risk? The G pillar includes two classical governance categories (government effectiveness, stability & rule of law), two economic categories (economic development, innovation) and two social-based categories (human rights, gender). In this last case, the frontier between social and governance is blurred. For instance, we can classify the four indicators of the gender category in the social pillar as a non-discrimination category.

**Remark 9** *The definition of each indicator can be found on the website* https://datatopics.worldbank.org/esg/framework.html. *Most of these variables are intuitive and easy to understand. Some of them are more technical and less comprehensible, especially some technical variables of the governance pillar. Therefore, we report in footnotes the definition provided by the World Bank for the following indicators: strength of legal rights index*[3]*; voice and accountability*[4]*, government effectiveness*[5]*; regulatory quality*[6]*; rule of law*[7]*.*

Certainly, one of the difficulties when building an ESG score is the data gathering, which requires the use of many internal and external sources. In the case of the World Bank framework, the data comes from[8]:

- National accounts statistics collected by Eurostat, OECD (https://www.oecd-ilibrary.org/statistics), United Nations Statistics Division (UNSD, https://unstats.un.org) and the World Bank;
- Internal departments and specialized databases of the World Bank: World Bank Open Data (https://data.worldbank.org), Business Enabling Environment (BEE), Climate Change Knowledge Portal (CCKP, https://climateknowledgeportal.worldbank.org), Global Database of Shared Prosperity (GDSP), Global Electrification Database (GEP), and Poverty and Inequality Platform (PIP, https://pip.worldbank.org);
- International organizations: Emission Database for Global Atmospheric Research (EDGAR, https://edgar.jrc.ec.europa.eu), Food and Agriculture Organization (FAO, https://www.fao.org/faostat), International Energy Agency (IEA, https://www.iea.org/data-and-statistics), International Labour Organization (ILO, https://ilostat.ilo.org), International Renewable Energy Agency (IRENA, https://www.irena.org/Data), UNESCO Institute for Statistics (UIS, http://uis.unesco.org), United Nations Population Division

[2] The Gini index is a measure of income inequality among individuals. It is based on the comparison of cumulative proportions of the population against cumulative proportions of income they receive, and it ranges between 0 in the case of perfect equality and 1 in the case of perfect inequality. Its computation is derived from the Lorenz curve.

[3] "*Strength of legal rights index measures the degree to which collateral and bankruptcy laws protect the rights of borrowers and lenders and thus facilitate lending.*"

[4] "*Voice and accountability captures perceptions of the extent to which a country's citizens are able to participate in selecting their government, as well as freedom of expression, freedom of association, and a free media.*"

[5] "*Government effectiveness captures perceptions of the quality of public services, the quality of the civil service and the degree of its independence from political pressures, the quality of policy formulation and implementation, and the credibility of the government's commitment to such policies.*"

[6] "*Regulatory quality captures perceptions of the ability of the government to formulate and implement sound policies and regulations that permit and promote private sector development.*"

[7] "*Rule of law captures perceptions of the extent to which agents have confidence in and abide by the rules of society, and in particular the quality of contract enforcement, property rights, the police, and the courts, as well as the likelihood of crime and violence.*"

[8] The list is not exhaustive.

(DESA, https://population.un.org), World Health Organization (WHO, https://www.who.int/data), World Intellectual Property Organization (WIPO, https://www.wipo.int/ipstats);

- National agencies and non-governmental organizations: Climate Watch (https://www.climatewatchdata.org), Netherlands Environmental Assessment Agency (PBL, https://www.pbl.nl), World Database on Protected Areas (WDPA, https://www.protectedplanet.net/en/thematic-areas/wdpa);

- Academic resources: Kaufmann *et al.* (2010), Cohen *et al.* (2017), and the international disasters database (EM-DAT) of the Centre for Research on the Epidemiology of Disasters (CRED, Université Catholique de Louvain).

Some of these databases are more relevant than others. If we would like to focus on a small number, our preferences are CCKP, EDGAR and Climate Watch for the E pillar, FAO, ILO and WHO for the S pillar, and the Worldwide Governance Indicators (WGI, https://info.worldbank.org/governance/wgi produced by Daniel Kaufmann and Aart Kraay for the G pillar.

Table 2.5: Sovereign ESG taxonomy

| Environmental | Social | Governance |
|---|---|---|
| • Biodiversity & land use | • Civil unrest | • Business & economic environment |
| • $CO_2$e emissions | • Demography | • Corruption & money laundering |
| • Compliance with environnemental standards | • Education | • Governance effectiveness |
| • Energy security & renewables | • Gender | • Infrastructure and mobility |
| • Emissions reduction targeting | • Health | • International relations |
| • Food security | • Income inequality & poverty | • Justice |
| • Fossil fuel dependency | • Labour rights & working conditions | • National security |
| • Green economy | • Living standards | • Political stability & institutional strength |
| • Physical risk exposure | • Migration | • Personal freedom & civil liberties |
| • Pollution & waste management | • Human rights & local communities | • Rights of shareholders |
| • Temperature | • Non-discrimination | • Rule of law |
| • Transition risk | • Social cohesion | |
| • Water management | • Water and electricity access | |

Source: Author's research based on the works of Bouyé and Menville (2021), Gratcheva *et al.* (2020) and Semet *et al.* (2021).

### Other frameworks

Most ESG rating agencies provide sovereign ESG data. The most known are FTSE (Beyond Ratings), Moody's (Vigeo-Eiris), MSCI, Sustainalytics and RepRisk. One of the most comprehensive databases is certainly Verisk Mapplecroft (https://www.maplecroft.com), which is a global company covering country risk. If we make the union of the different categories, we obtain a taxonomy that looks like the one in Table 2.5. There are many categories, much greater than for the World Bank framework or the PRI taxonomy[9]. If we consider the indicators, the number of variables is large, much greater than 400. Nevertheless, as explained by Bouyé and Menville (2021) and Semet *et al.* (2021), they are highly correlated. If we perform a principal component analysis, there are few independent dimensions (less than 10). In fact, many of these indicators are correlated to the GDP. For instance, Gratcheva *et al.* (2020) found that the average correlation between sovereign ESG scores and national income is equal to 81% for aggregate ESG, 51% for E pillar, 85% for S pillar, and 70% for G pillar. If we consider correlations for ESG providers, the lowest correlations are obtained for the E pillar of ISS (7%), MSCI (10%) and V.E (23%), and the G pillar of RepRisk (37%) and V.E (39%), but they are generally high. Therefore, although all these providers use very different indicators, we notice a relative convergence between them[10].

Table 2.6: Correlation of ESG scores with country's national income (GNI per capita)

| Factor | ESG | E | S | G |
|---|---|---|---|---|
| ISS | 68% | 7% | 86% | 77% |
| FTSE (Beyond Ratings) | 91% | 74% | 88% | 84% |
| MSCI | 84% | 10% | 90% | 77% |
| RepRisk | 78% | 79% | 75% | 37% |
| RobecoSAM | 89% | 82% | 85% | 85% |
| Sustainalytics | 95% | 83% | 94% | 93% |
| V.E | 60% | 23% | 79% | 39% |
| Total | 81% | 51% | 85% | 70% |

Source: Gratcheva *et al.* (2020, Table 3.1, page 32).

### The mushrooming growth of data

We observe among ESG data providers a mushrooming of indicators and data sources. This concerns the first well-established variables. For a very long time, income inequality was mainly measured by the Gini coefficient or the Lorenz curve, even if there were many other academic measures. It seems that data providers have recently rediscovered and embraced the academic literature. Thus, income inequality may also be measured by the Palma ratio, the S80/S20 (or 20:20) ratio, the Atkinson index, the percentile ratios (P90/P10, P90/P50, P50/P10), the Pietra index, the coefficient of variation or the Theil index. Nevertheless, the mushrooming growth of data mainly concerns non-economic variables. We provide some examples in Figures 2.1–2.4 with palm oil production and

[9] PRI (2019a) identifies 4 environmental factors (natural resources, physical risks, energy transition risk, energy security), 4 social factors (demographic change, education and human capital, living standards and income inequality, social cohesion) and 4 governance factors (institutional strength, political stability, government effectiveness, regulatory effectiveness).

[10] Gratcheva *et al.* (2020, Table 2.3, page 27) found that the average cross-correlation between these providers is equal to 85% for the ESG score, 42% for the environmental score, 85% for the social score and 71% for the governance score. These results are confirmed by the study of Bouyé and Menville (2021, Table 4, page 14).

Figure 2.1: Palm oil production (2019)

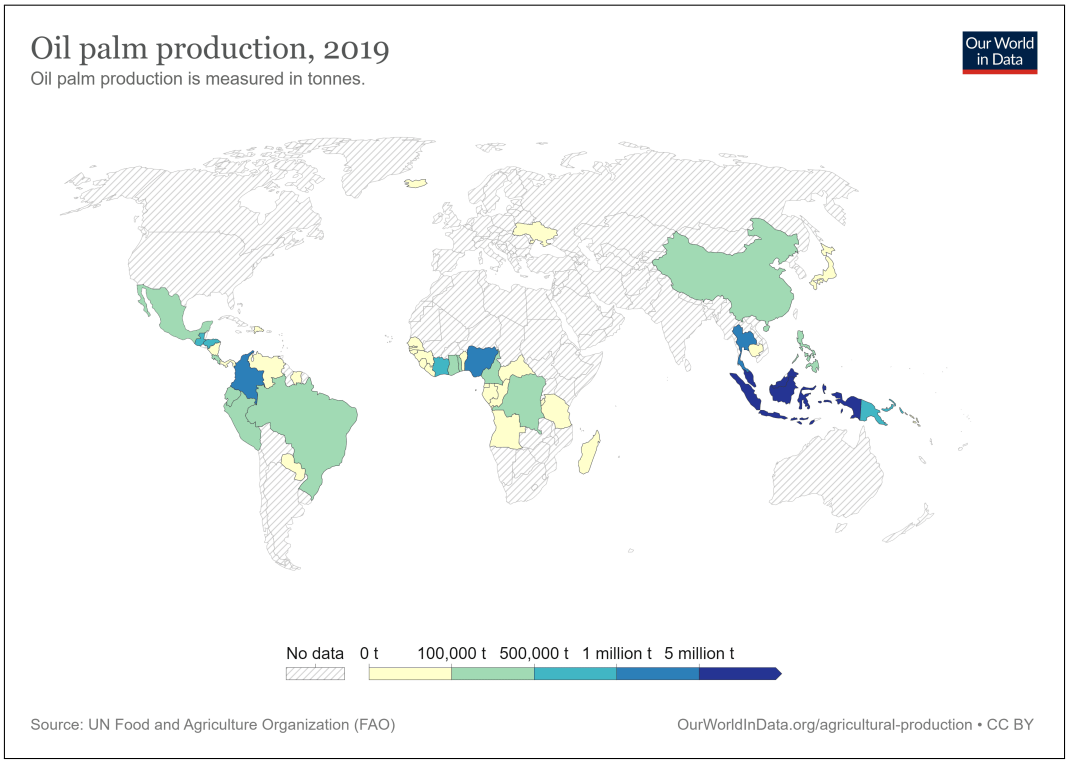


Source: Our World in Data, https://ourworldindata.org/palm-oil.

Figure 2.2: Palm oil imports (2019)

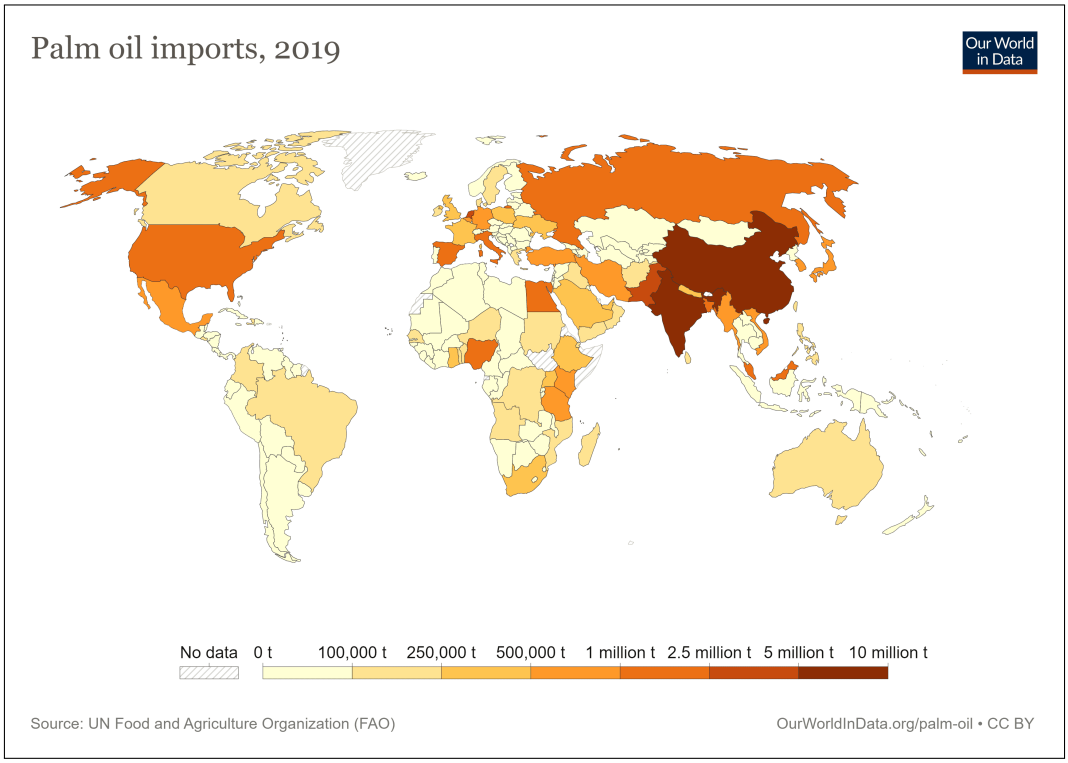


Source: Our World in Data, https://ourworldindata.org/palm-oil.

Figure 2.3: Share of global annual deforestation (2015)

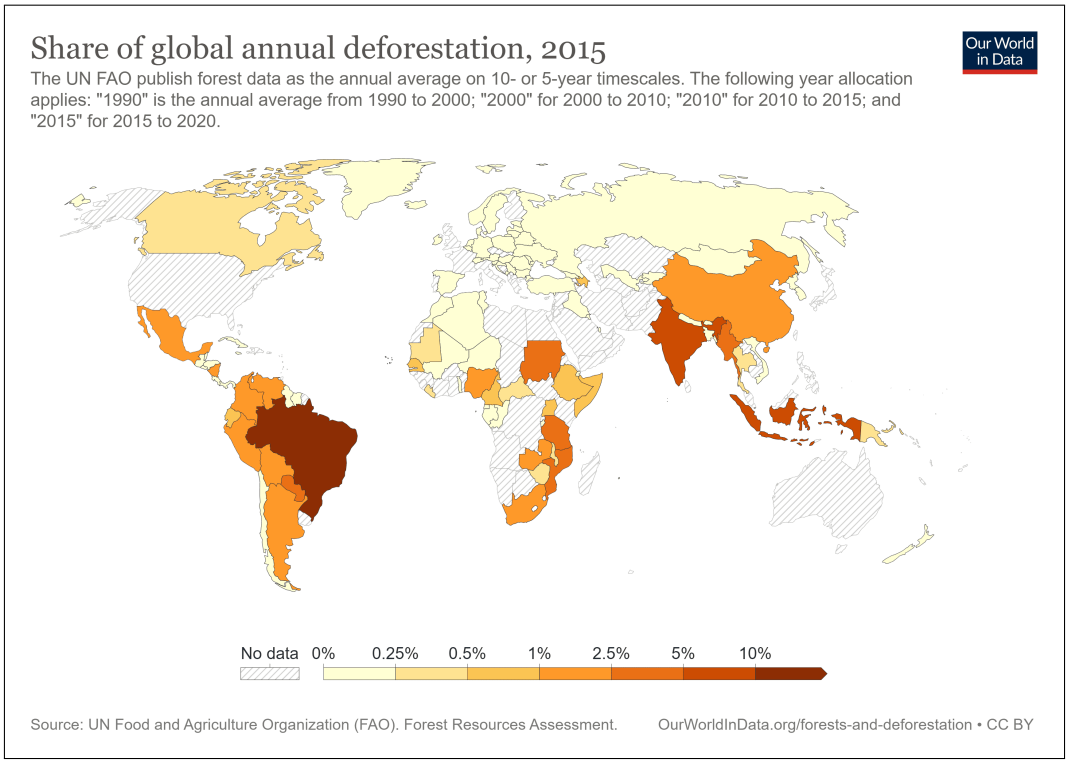


Source: Our World in Data, https://ourworldindata.org/deforestation.

Figure 2.4: Threatened mammal species (2018)

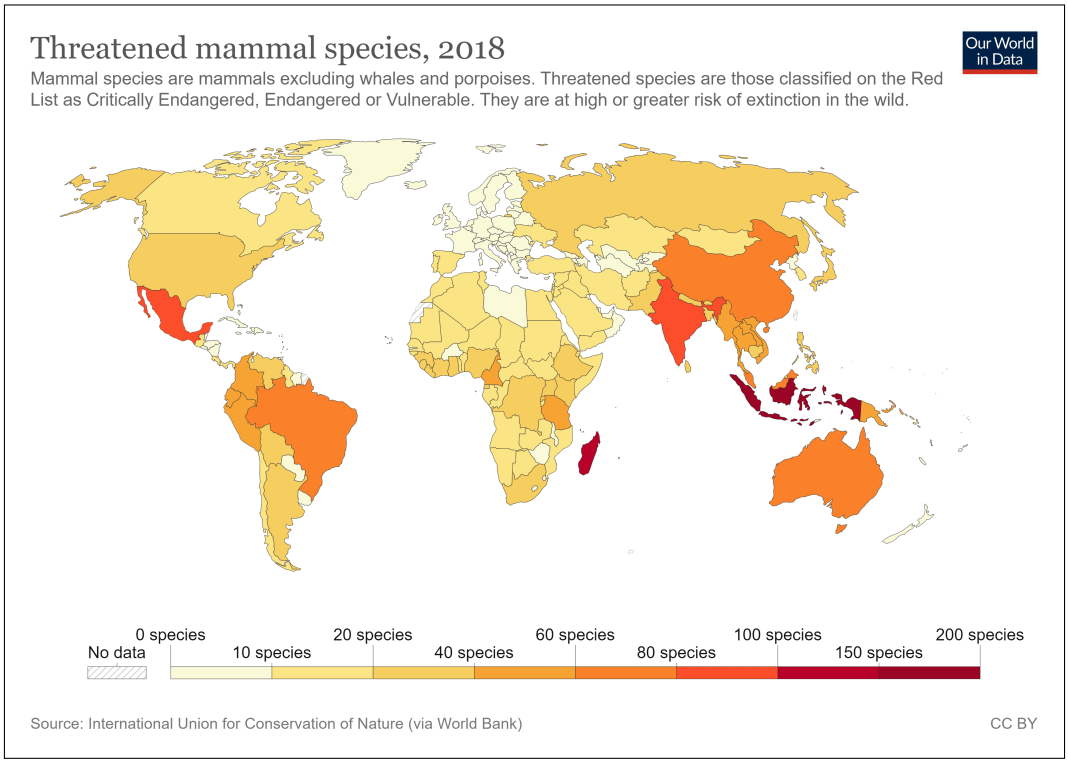


Source: Our World in Data, https://ourworldindata.org/biodiversity.

consumption, deforestation and threatened mammal species. In particular, we notice the increasing use of geo-location data, real-time data, or satellite data, for example, the data provided by the World Resources Institute (WRI) and its different data platforms (https://www.wri.org/data/data-platforms). The most interesting are Ocean Watch (data on ocean economies and management), Aqueduct (cutting-edge data to identify and evaluate water risks), Global Forest Watch (data on forest economies and management) and LandMark (global data of indigenous and community lands). For instance, we can collect data on coastal eutrophication risk, mangrove extent change, coral reef locations, seagrass, salt marshes, soil erosion, chlorophyll-a concentration, etc.

Figure 2.5: Global living planet index

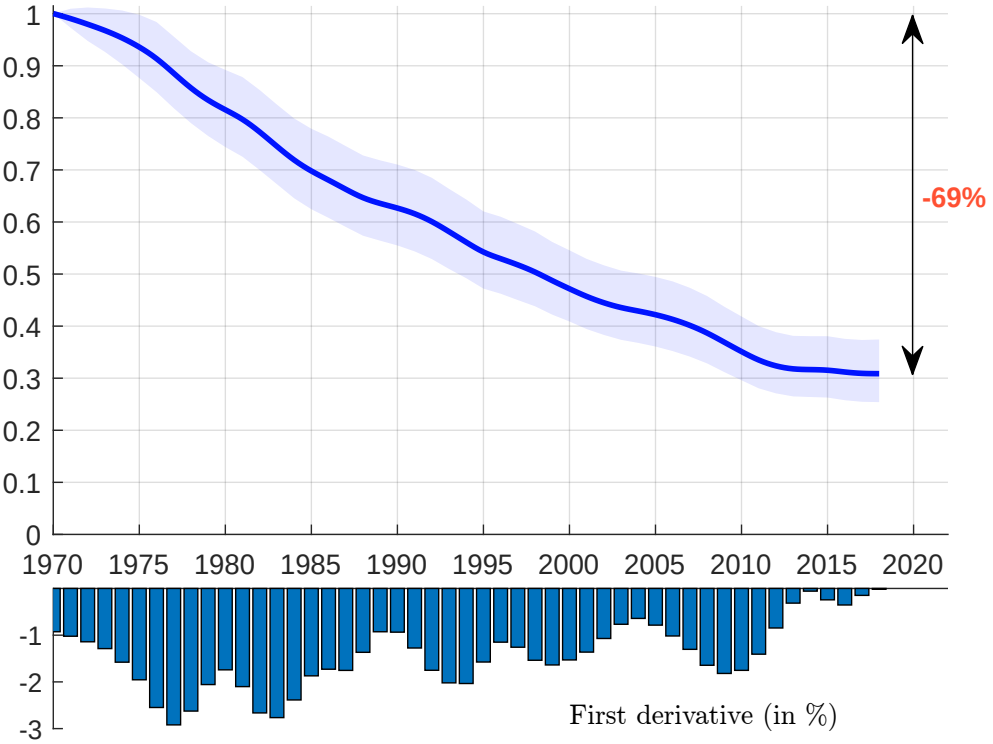


Source: https://livingplanetindex.org/latest_results & Author's calculations.

One of the hot topics is currently the biodiversity. A quick search on the web produces dozen of internet pages[11]. Financial institutions have also launched another initiative: Finance For Biodiversity Pledge (https://www.financeforbiodiversity.org). The UN Biodiversity Conference (COP 15), which is organized by the CBD in Montreal, Canada from 7 to 19 December 2022, has certainly given a special impulse, and may explain this new interest. However, biodiversity loss[12] is a very old topic and has been scientifically documented since the 1990s (Cardinale *et al.*, 2012). According to Almond *et al.* (2022), biodiversity, as measured by the Living Planet Index[13], has decreased by 69%

[11] For example, "*Why biodiversity is moving to top of mind for investors*" (Lazard Asset Management, February 2022), "*Investors grapple with complexities of biodiversity*" (Financial Times, September 2022), "*Asset Management, a lever for preserving biodiversity*" (BNP Paribas, September 2022), "*Biodiversity quickly rises up the ESG investing agenda*" (Financial Times, September 2022), "*Biodiversity: why investors should care*" (Pictet AM, October 2022), "*More asset owners and managers sign biodiversity pledge*" (Pensions&Investments, October 2022), etc.

[12] Biodiversity loss describes the decline in the number, genetic variability, and variety of species, and the biological communities in a given area.

[13] The LPI is computed using a subset of 31 821 populations of 5 230 species and a statistical model (Westveer *et al.*, 2022, page 28-31).

on average since 1970, but with a lot of heterogeneity across regions[14]. Even if the biodiversity loss has decreased these last years (Figure 2.5), this will inevitably result in negative consequences on global wealth in the long run. The seminal work of Costanza *et al.* (1997) estimated that the annual economic value of natural capital is on average two times the annual economic value of global GNP, explaining that "*ecosystem services provide a significant portion of the total contribution to human welfare on this planet.*"

Box 2.1: Ecological diversity indexes

Let $p = (p_1, \ldots, p_{n_S})$ be the proportion vector of species where $p_i$ is the relative abundance[a] of the $i^{\text{th}}$ specie. The Hill diversity coefficient of order $\eta \geq 0$ is defined as:

$$\mathcal{D}^{\eta}(p) = \left( \sum_{i=1}^{n_S} p_i^{\eta} \right)^{1/(1-\eta)}$$

We can show that $1 \leq \mathcal{D}^{\eta}(p) \leq n_s$ and the bounds are reached for the 1- and $n$-diversity distributions[b] $\pi_n^-$ and $\pi_n^+$. The Hill number measures the "*effective number of species*", meaning that the system holds a diversity equivalent to $\mathcal{D}^{\eta}(p)$ equally distributed species. The parameter $\eta$ defines the sensitivity of the true diversity to rare versus. abundant species by modifying the weight given to specie abundances. When $\eta = 0$, $\mathcal{D}^{\eta}(p)$ is equal the current number $n_S$ of species or the richness of species. When $\eta \to 1$, we obtain the Shannon diversity index $\mathcal{I}^{\star}(p)$, which is equal to the exponential of the Shannon entropy $\mathcal{I}(p)$:

$$\mathcal{D}^1(p) = \mathcal{I}^{\star}(p) = \exp\left(\mathcal{I}(p)\right) = \exp\left( -\sum_{i=1}^{n_S} p_i \ln p_i \right)$$

When $\eta = 2$, we obtain:

$$\mathcal{D}^2(p) = \left( \sum_{i=1}^{n_S} p_i^2 \right)^{-1}$$

We recognize the inverse of the Herfindahl index $\mathcal{H}(p) = \sum_{i=1}^{n_S} p_i^2$ (also called the Simpson index $\lambda(p)$ in ecology). Finally, when $\eta \to \infty$, the Hill index converges to the proportional abundance of the most abundant specie:

$$\mathcal{D}^{\infty}(p) = \max_i p_i$$

$\mathcal{D}^{\infty}(p)$ is then equal to the infinite norm of $p$.

[a] It is equal to number of individuals in the $i^{\text{th}}$ specie relative to the total number of individuals in the population.

[b] See their definition on page 1058.

The sudden interest of financial institutions in biodiversity may be explained by climate change, but also by a greater awareness of its critical functions (food security, health, etc.). Moreover, the seventh mandatory PAI indicator requires reporting the share of investments that negatively affect biodiversity sensitive areas[15], and the sixth objective of the EUTR is dedicated to the "*protec-*

[14] This figure is respectively equal to −18% in Europe and Central Asia, −20% in North America, −55% in Asia and the Pacific, −66% in Africa, and −94% in Latin America.

[15] See Table 1.8 on page 38.

Figure 2.6: Aggregate national RLI

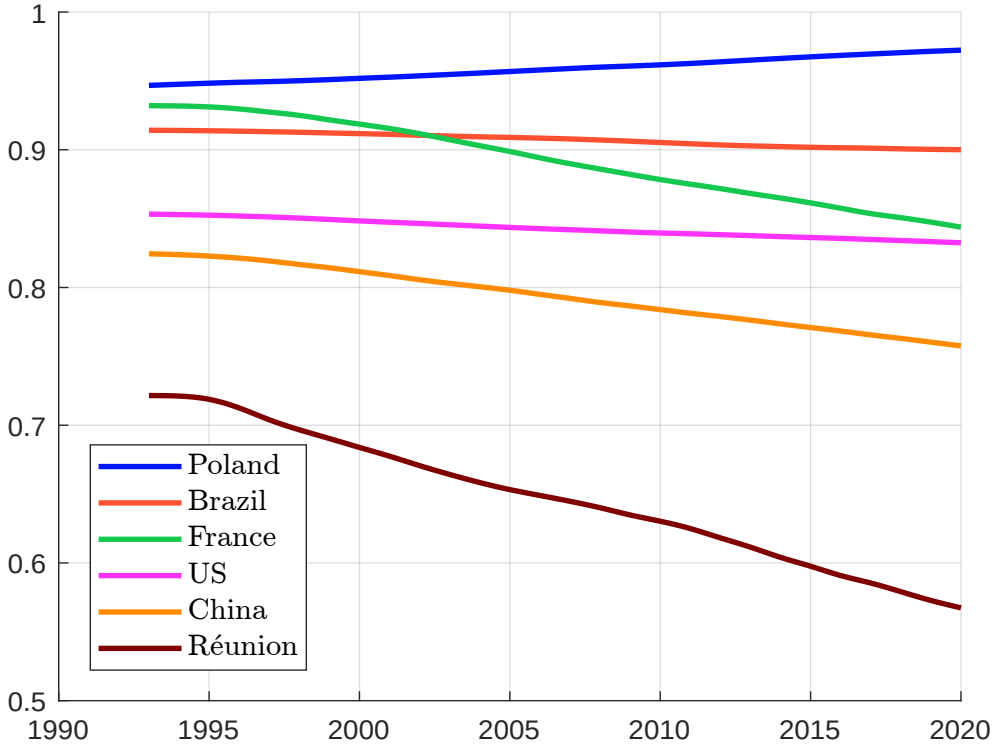


Source: https://www.iucnredlist.org/search & IUCN (2022).

*tion and restoration of biodiversity and ecosystem.*" All this obviously creates a high demand for biodiversity data and new opportunities for data providers, but as mentioned by Bowker (2000), biodiversity implies data diversity. Again, we are dealing with a huge amount of data[16]. For example, Icerberg Data Lab[17] (corporate biodiversity footprint or CBF), Carbon 4 (global biodiversity score[18] or GBS), CDC Biodiversité (global biodiversity score for financial institutions[19] or GBSFI), ISS ESG[20] (mean species abundance or MSA, potentially disappeared fraction of species or PDF) and Verisk Maplecroft (biodiversity and protected areas index score[21] or BPAI) have already developed biodiversity scores. For countries, most biodiversity data are open source[22] (Stephenson and Stengel, 2020):

- the Red List Index (RLI, https://www.iucnredlist.org)
  The RLI is an index of extinction risk for species of plants and animals. It is computed[23] by the IUCN and is available for five taxonomic groups: birds, mammals, amphibians, cycads and warm-water reef-forming corals. It can be disaggregated in various ways: subset of species (pollinator species, forest-specialist species, invasive alien species, etc.), country, region, etc.

[16] And also with a lot of diversity measures (Bandeira *et al.*, 2013; Ohlmann *et al.*, 2019).
[17] https://icebergdatalab.com.
[18] https://www.carbon4finance.com/product/biodiversity-impacts.
[19] https://www.cdc-biodiversite.fr/le-global-biodiversity-score.
[20] https://www.issgovernance.com/esg/biodiversity-impact-assessment-tool.
[21] https://www.maplecroft.com/insights/analysis/mining-operations-face-growing-biodiversity-risks.
[22] See the *Guide on Biodiversity Measurement Approaches* produced by the Finance for Biodiversity Pledge for a comparison of commercial and open source databases (https://www.financeforbiodiversity.org/publications/guide-on-biodiversity-measurement-approaches).
[23] The methodology is described in Butchart *et al.* (2007).

For instance, we report in Figure 2.6 the aggregate RLI for Brazil, China, France, Poland, La Réunion and US.

- World Database on Protected Areas (WDPA, https://www.protectedplanet.net)
- Integrated Biodiversity Assessment Tool (IBAT, https://www.ibat-alliance.org), including the Species Threat Abatement and Restoration metric (STAR)
- Exploring Natural Capital Opportunities, Risks and Exposure (ENCORE, https://encore.naturalcapital.finance)
- Etc.

**Remark 10** *Biodiversity risk is a key element for impact investing. We refer to Chapter 5 for an extensive study of this risk (Section 5.4 on page 365).*

### 2.1.2 Corporate ESG data

Compared to sovereign ESG data, the collection, understanding and use of corporate ESG data is much more complicated and requires a lot of time and resources. In the first case, we have about 200 countries in the world, many international organizations that produce country data for decades, and vast academic research on this topic. For instance, the economic literature on income inequality starts in the early twentieth century with the seminal publications of Lorenz (1905) and Gini (1921). Since that time, the number of research studies on income inequality has grown exponentially[24]. In the case of corporate ESG data, data production has just become very recently, and the data dimension is not comparable. According to the World Federation of Exchanges (WFE), there are nearly 58 200 listed companies in the world at the end of Q1 2022. Moreover, data collection is not easier because it has concerned private data for a very long time. It is only recently that extra-financial reporting frameworks for corporate issuers exist, and most of them are voluntary. Finally, the last issue when using corporate ESG data is that most of indicators does not have a universal definition. In a nutshell, there are 3 main challenges and barriers to corporate ESG data:

1. Data coverage (how to collect data for all the listed companies?);
2. Data sourcing (where to find the data?);
3. Data quality (what is the accuracy of the collected data?)

#### Main indicators

As we have previously seen, we must distinguish several levels of data. Indeed, raw data are generally transformed into ESG metrics, and these metrics are used to define an ESG score. The main difficulty is collecting the raw data. In the case of corporates, this process is time-consuming and manual. The main sources of raw data are:

1. Corporate publications (self-reporting)
   (a) Annual reports
   (b) Corporate sustainability reports

[24] According to Google scholar, there are more than 5 700 published papers on this topic from 1950 to 1980, and already about 270 before 1950.

Figure 2.7: From raw data to ESG pillars

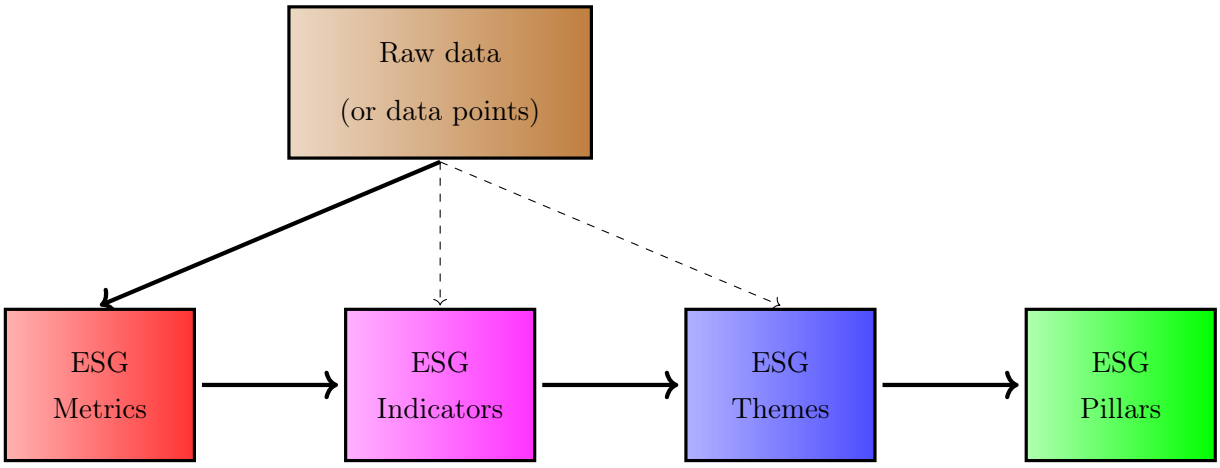


2. Financial and regulatory filings (standardized reporting)
   (a) Mandatory reports (SFDR, CSRD, EUTR, etc.)
   (b) Non-mandatory frameworks (PRI, TCFD, CDP, etc.)

For instance, the CDP database is the basic raw material used by all ESG rating agencies for measuring the carbon footprint of issuers. It can be viewed as the entry point and gives a first picture. Then, rating agencies will complete these data by gathering information from annual reports and other sources such as:

3 News and other media

4 NGO reports and websites

5 Company assessment and due diligence questionnaire (DDQ)

For example, S&P Global uses a 230-pages company questionnaire[25] called *Corporate Sustainability Assessment*. At the end of the collection data process, we may have missing data, noisy data or heterogeneous data. Therefore, the data are completed or adjusted by considering internal statistical models, *e.g.*, industry-based clustering methods. This can be considered as a sixth source of data:

6 Internal models

Once these raw data are collected and cleaned, they can be used to calculate ESG metrics (second level of ESG variables). They are then grouped to define ESG indicators (third level of ESG variables), which are combined to form the basic ESG themes (fourth level of ESG variables). In the sequel, an ESG criterion is a generic term to name ESG variables: it may be an ESG metric, an ESG indicator or an ESG theme. Finally, ESG Pillars are generally based on a few number of ESG themes. This slicing method of ESG variables is illustrated in Figure 2.7. ESG rating agencies do not publicly disclose the raw data they use. Generally, they stop on the theme stage, sometimes on the indicator stage. To better understand the slotting method, we report an example of ESG criteria in Table 2.7. In this example, the E S and G pillars are made up of 9 environmental themes, 7 social themes and 8 governance themes. Here, we do not have access to the ESG indicators. We

[25] It can be downloaded at https://portal.csa.spglobal.com/survey/documents/CSA_Companion.pdf.

notice that some criteria are global and concerns all the issuers (*e.g.*, carbon emissions), but other are specific to a given industry (*e.g.*, green cars for the automobile sector, green financing for the banking sector). The choice of the themes/indicators will be done by the ESG rating agency, and the distinction between the two levels is not always obvious. For instance, if the board diversity is measured by the male-female ratio[26], the ESG theme is measured by a single ESG indicator. In this case, it is difficult to make a distinction between the two levels. Another issue concerns the classification of ESG themes. Let us consider the supply chain for example. It is a social issue if we would like to measure whether or not the suppliers of the company respect human rights and labor standards, but it can be an environmental issue if we would like to measure the impact of the suppliers on climate change and pollution. In Table 2.7, we also observe that the choice of ESG themes may be subjective. For example, we can merge the two categories *Pollution* and *Waste disposal* into one category *Pollution & waste disposal*, we can name *Corporate ethics* instead of *Corporate behaviour*, we can split *Biodiversity* into two categories (fauna & wildlife conservation; flora & land management), etc.

Table 2.7: An example of ESG criteria

| **E**nvironmental | **S**ocial | **G**overnance |
|---|---|---|
| • Biodiversity | • Access to medicine | • Audit and control |
| • Carbon emissions | • Community involvement & human rights | • Board diversity |
| • Green cars$^\star$ | • Customer concern & responsibility | • Board independence |
| • Green financing$^\star$ | • Diversity | • Corporate behaviour |
| • Energy use | • Employment conditions & labor standards | • CSR strategy |
| • Pollution | • Gender equality | • Executive compensation |
| • Renewable energy | • Supply chain | • Management compensation |
| • Waste disposal | | • Shareholder' rights |
| • Water use | | |

In what follows, we give some insight into the themes and indicators used by rating agencies. This public information about the ESG criteria has been collected from their website, and varies considerably between providers.

- Bloomberg rates 11 800 public companies. They use more than 120 ESG indicators and 2 000+ data points.
- ISS ESG rates about 10 000 issuers. They use more than 800 indicators and apply approximately 100 indicators per company[27].

[26] It is the ratio of men to women or the proportion of women in the company board.

[27] E.g, climate change strategy, eco-efficiency, energy management, environmental impact of product portfolio, environmental management, water risk and impact for the E pillar; equal opportunities, freedom of association, health and safety, human rights, product responsibility, social impact of product portfolio, supply chain management, taxes for the S pillar; business ethics, compliance, independence of the board, voting rights, shareholder participation, remuneration for the G pillar.

Table 2.8: MSCI ESG key issue hierarchy

| Pillar | # | Theme | # | Indicator |
|---|---|---|---|---|
| Environment | 1 | Climate Change | 1 | Carbon Emissions |
| | | | 2 | Product Carbon Footprint |
| | | | 3 | Financing Environmental Impact |
| | | | 4 | Climate Change Vulnerability |
| | 2 | Natural Capital | 5 | Water Stress |
| | | | 6 | Biodiversity & Land Use |
| | | | 7 | Raw Material Sourcing |
| | 3 | Pollution & Waste | 8 | Toxic Emissions & Waste |
| | | | 9 | Packaging Material & Waste |
| | | | 10 | Electronic Waste |
| | 4 | Environmental Opportunities | 11 | Opportunities in Clean Tech |
| | | | 12 | Opportunities in Green Building |
| | | | 13 | Opportunities in Renewable Energy |
| Social | 5 | Human Capital | 14 | Labor Management |
| | | | 15 | Health & Safety |
| | | | 16 | Human Capital Development |
| | | | 17 | Supply Chain Labor Standards |
| | 6 | Product Liability | 18 | Product Safety & Quality |
| | | | 19 | Chemical Safety |
| | | | 20 | Consumer Financial Protection |
| | | | 21 | Privacy & Data Security |
| | | | 22 | Responsible Investment |
| | | | 23 | Health & Demographic Risk |
| | 7 | Stakeholder Opposition | 24 | Controversial Sourcing |
| | | | 25 | Community Relations |
| | 8 | Social Opportunities | 26 | Access to Communications |
| | | | 27 | Access to Finance |
| | | | 28 | Access to Health Care |
| | | | 29 | Opportunities in Nutrition & Health |
| Governance | 9 | Corporate Governance | 30 | Ownership & Control |
| | | | 31 | Board |
| | | | 32 | Pay |
| | | | 33 | Accounting |
| | 10 | Corporate Behavior | 34 | Business Ethics |
| | | | 35 | Tax Transparency |

Source: MSCI (2022, Exhibit 2, page 4).

Table 2.9: Refinitiv materiality matrix

| Pillar | # | Theme | Metrics | # | Indicator |
|---|---|---|---|---|---|
| Environment | 1 | Emissions | 28 | 1 | Emissions |
| | | | | 2 | Waste |
| | | | | 3 | Biodiversity |
| | | | | 4 | Environmental Management Systems |
| | 2 | Innovation | 20 | 5 | Product Innovation |
| | | | | 6 | Green Revenues, Green R&D and Green CapEx |
| | 3 | Resource Use | 20 | 7 | Water |
| | | | | 8 | Energy |
| | | | | 9 | Sustainable Packaging |
| | | | | 10 | Environmental Supply Chain |
| Social | 4 | Community | 14 | 11 | Community |
| | 5 | Human Rights | 8 | 12 | Human Rights |
| | 6 | Product Responsibility | 10 | 13 | Responsible Marketing |
| | | | | 14 | Product Quality |
| | | | | 15 | Data privacy |
| | 7 | Workforce | 30 | 16 | Diversity & Inclusion |
| | | | | 17 | Career Development & Training |
| | | | | 18 | Working Conditions |
| | | | | 19 | Health & Safety |
| Governance | 8 | CSR Strategy | 9 | 20 | CSR Strategy |
| | | | | 21 | ESG Reporting & Transparency |
| | 9 | Management | 35 | 22 | Structure (independence, diversity, committees) |
| | | | | 23 | Compensation |
| | 10 | Shareholders | 12 | 24 | Shareholder Rights |
| | | | | 25 | Takeover Defenses |

Source: Refinitiv (2022, page 10).

- FTSE Russell rates about 7 200 securities. They use more than 300 indicators and 14 themes: biodiversity, climate change, pollution and resources, supply chain and water security for the E pillar; customer responsibility, health and safety, human rights and community, labor standards and supply chain for the S pillar; anti-corruption, corporate governance, risk management and tax transparency for the G pillar. Each theme contains 10 to 35 indicators, and an average of 125 indicators are applied per company.

- Moody's V.E rates more than 5 000 companies. They consider six pillars (corporate governance, business behavior, environment, human rights, human resources, community involvement) and 38 ESG indicators[28].

[28]Moody's has also developed a methodology for assessing ESG risks in credit analysis based on 15 themes: carbon transition, physical climate risks, water management, waste & pollution, natural capital for the E pillar; customer relations, human capital, demographic & societal trends, health & safety, responsible production for the S pillar; financial strategy & risk management, management credibility & track record, organizational structure, compliance & reporting, board structure & procedures for the G pillars.

- MSCI (2022) rates 10 000 companies (14 000 issuers including subsidiaries) and 680 000 securities globally. Using 1000+ data points, they consider two families of metrics: 80 exposure metrics (how exposed is the company to each material issue?) and 250+ management metrics (how is the company managing each material issue?). These metrics are then combined into 35 key issues selected annually for each industry. These key metrics are reported in Table 2.8 and are combined to build 10 main themes.
- Refinitiv (2022) rates 12 000 public and private companies. They consider 10 themes: resource use, emissions and innovation for the E pillar; workforce, human rights, community and product responsibility for the S pillar; management, shareholders and responsibility (CSR) strategy for the G pillar. These themes are built using 186 metrics and 630+ data points. Table 2.9 shows the materiality matrix of themes, indicators and the number of metrics per theme.
- S&P Dow Jones Indices uses between 16 to 27 criteria scores, a questionnaire-based analysis process with 80-120 industry-specific questions and 1 000 data points.
- Sustainalytics rates more than 16 300 companies. They consider 20 material ESG issues, based on 350+ indicators.

**Remark 11** *Contrary to sovereign issuers, raw data for corporate issuers are more difficult to find, because they are not in open source data or they can only be manually collected (e.g., annual reporting). The ESG Data Cartography*[29]*, which has been developed by the Louis Bachelier Institute, proposes a comprehensive list of ESG data with 140+ data sources. The user can filter the databases by accessibility (free, open source, partially free and proprietary).*

**Exercise 1** *Berg et al. (2022) consider a common taxonomy based on 64 indicators to compare the different ESG rating providers: access to basic services; access to healthcare; animal welfare; anti-competitive practices; audit; biodiversity; board; board diversity; business ethics; chairperson-CEO separation; child labor; climate risk management; clinical trials; collective bargaining; community & society; corporate governance; corruption; customer relationship; diversity; ESG incentives; electromagnetic fields; employee development; employee turnover; energy; environmental fines; environmental management system; environmental policy; environmental reporting; financial inclusion; forests; GHG emissions; GHG policies; GMOs; Global Compact membership; green buildings; green products; HIV programs; hazardous waste; health & safety; human rights; indigenous rights; labor practices; lobbying; non-GHG air emissions; ozone-depleting gases; packaging; philanthropy; privacy & IT; product safety; public health; remuneration; reporting quality; resource efficiency; responsible marketing; shareholders; site closure; supply chain; sustainable finance; systemic risk; taxes; toxic spills; unions; waste; water. For each pillar, give the list of indicators that fall in the category. We consider a very basic ESG classification matrix with 12 themes:*

| E | S | G |
|---|---|---|
| *Global warming* | *Health* | *Board* |
| *Green opportunities* | *Human rights* | *Corporate ethics* |
| *Natural resource* | *Workforce* | *CSR strategy* |
| *Transition risk* | *Social responsibility* | *Shareholder* |

*For each indicator, associate the right ESG theme*[30]*.*

[29] The website is https://www.institutlouisbachelier.org/en/esg-data-cartography.
[30] There may be no or several valid answers.

### The race for alternative data

Alternative data corresponds to data that is not available through traditional channels (corporate publications, sustainable reporting, etc.). It includes non-structured data such as images or textual contents. The case of ESG ratings mainly concerns three types of data:

- Internet traffic, browsing activity, web scraping, product reviews, social media and sentiment data;
- Satellite imagery, geotracking data, sensor data[31];
- Supply-chain data.

Brière *et al.* (2022) discuss several uses of alternative data sets. The most famous application is the tracking and measurement of ESG controversies. A controversy risk occurs when allegations concerning a company could lead to reputational risk[32] and financial losses. Everybody knows the famous quotes of Warren Buffet about building and destroying a reputation:

> "*It takes 20 years to build a reputation and five minutes to ruin it. If you think about that, you'll do things differently. [...] We can afford to lose money — even a lot of money. But we can't afford to lose reputation — even a shred of reputation. [...] Should you find yourself in a chronically leaking boat, energy devoted to changing vessels is likely to be more productive than energy devoted to patching leaks. [...] Lose money for the firm, and I will be understanding. Lose a shred of reputation for the firm, and I will be ruthless.*"

The allegations can be reported by media, NGOs, social networks and stakeholders. Data providers generally use text mining and natural language processing (NLP) to analyze an enormous amount of information, detect controversial events and measure the severity of the reputational risk. For example, Refinitiv (2022) completes the traditional ESG score with a controversy score for the 10 ESG themes presented in Table 2.9 on page 69. This score is updated on a weekly basis. The ESG controversies score is calculated based on 23 ESG controversy topics:

- Community: (1) anti-competition controversy, (2) business ethics controversies, (3) intellectual property controversies, (4) critical countries controversies, (5) public health controversies, (6) tax fraud controversies;
- Human rights: (7) child labour controversies, (8) human rights controversies;
- Management: (9) management compensation controversies count;
- Product responsibility: (10) consumer controversies, (11) customer health and safety controversies; (12) privacy controversies; (13) product access controversies; (14) responsible marketing controversies; (15) responsible R&D controversies;
- Resource use: (16) environmental controversies;
- Shareholders: (17) accounting controversies count, (18) insider dealings controversies, (19) shareholder rights controversies;

[31] *E.g.*, temperature, humidity, pressure, chemical levels.

[32] Some famous examples are the *Mexico oil spill* (BP, 2010), *dieselgate* affair (Volkswagen, 2015), the gender pay gap (BBC, 2017), the Cambridge Analytica scandal (Facebook, 2018), the opioid epidemic (Purdue Pharma, 2019), the Ehpad scandal (Orpea, 2021), the Pegasus software (NSO, 2021), the greenwashing (DWS, 2022), etc.

- Workforce: (20) diversity and opportunity controversies; (21) employee health and safety controversies; (22) wages or working conditions controversies; (23) strikes.

One of the most famous controversy data providers is the Swiss company RepRisk (https://www.reprisk.com), which was created in Zurich in 1998. They are specialized in ESG data science and machine learning. In November 2021, they published their comprehensive methodology (RepRisk, 2022) and Jupyter Notebooks. To identify and classify ESG risks consistent with how key international standards and norms define ESG, they consider a 3-step process:

1. Daily, they collect 500 000+ documents from 100 000+ sources[33] in 23 languages;

2. These documents are scraped from online sources and fed to machine learning (ML) applications, which predict relevant and unique ESG risk incidents. Results are sent to the ML reducer, in particular, irrelevant results are discarded and predictions fed to the multilingual queue;

3. Then, documents are sorted in priority order. A team of 150+ human analysts confirm and correct ML predictions, assess severity, reach, and novelty, and write risk incident summaries; Final results are incorporated into RepRisk databases[34].

**Exercise 2** *RepRisk (2022) uses 73 controversial topics: abusive/illegal fishing; access to products and services; agricultural commodity speculation; airborne pollutants; alcohol; animal transportation; arctic drilling; asbestos; automatic and semi-automatic weapons; biological weapons; chemical weapons; cluster munitions; coal-fired power plants; conflict minerals; coral reefs; cyberattack; deep sea drilling; depleted uranium munitions; diamonds; drones; economic impact; endangered species; energy management; epidemics/pandemics; forest burning; frocking; fur and exotic animal skins; gambling; gender inequality; genetically modified organisms (GMOs); genocide/ethnic cleansing; greenhouse gas (GHG) emissions; health impact; high conservation value forests; human trafficking; hydropower (dams); illegal logging; indigenous people; involuntary resettlement; land ecosystems; land grabbing; land mines; lobbying; marijuana/cannabis; marine/coastal ecosystems; migrant labor; monocultures; mountaintop removal mining; negligence; nuclear power; nuclear weapons; offshore drilling; oil sands; opioids; palm oil; plastics; pornography; predatory lending; privacy violations; protected areas; racism/racial inequality; rare earths; salaries and benefits; sand mining and dredging; seabed mining; security services; ship breaking and scrapping; soy; tax havens; tobacco; wastewater management; water management; water scarcity. For each topic, associate the right ESG pillar.*

Besides controversy risk, text mining and NLP techniques became recently an essential ML tool for different ESG applications. For example, they are more and more used for assessing company disclosures and verifying their credibility. Friederich *et al.* (2021) use the language model BERT[35] to automatically identify disclosures of climate-related risks from corporates' annual reports. In a similar way, Bingler *et al.* (2022) analyse climate risk disclosures along the TCFD categories and conclude that "*the firms' TCFD support is mostly cheap talk and that firms cherry-pick to report primarily non-material climate risk information.*" Always using the same machine learning model

[33] These include government agencies, news sites, newsletters, NGOs, print media, regulators, research firms, social media blogs, think tanks and twitter messages.

[34] As of July 2022, the RepRisk dataset includes more than 205 000 companies that are associated with risk incidents. Of these 205 000 companies, approximately 7% are listed companies and 93% are non-listed companies (RepRisk, 2022, page 5).

[35] Bidirectional Encoder Representations from Transformers (BERT) is a transformer-based machine learning technique for NLP pre-training developed by Google.

BERT, Kölbel *et al.* (2022) consider the impact of climate risk disclosures on the CDS market and find that disclosing transition risks increases CDS spreads, which is not the case for physical risks.

Figure 2.8: Geolocation of world power plants by energy source

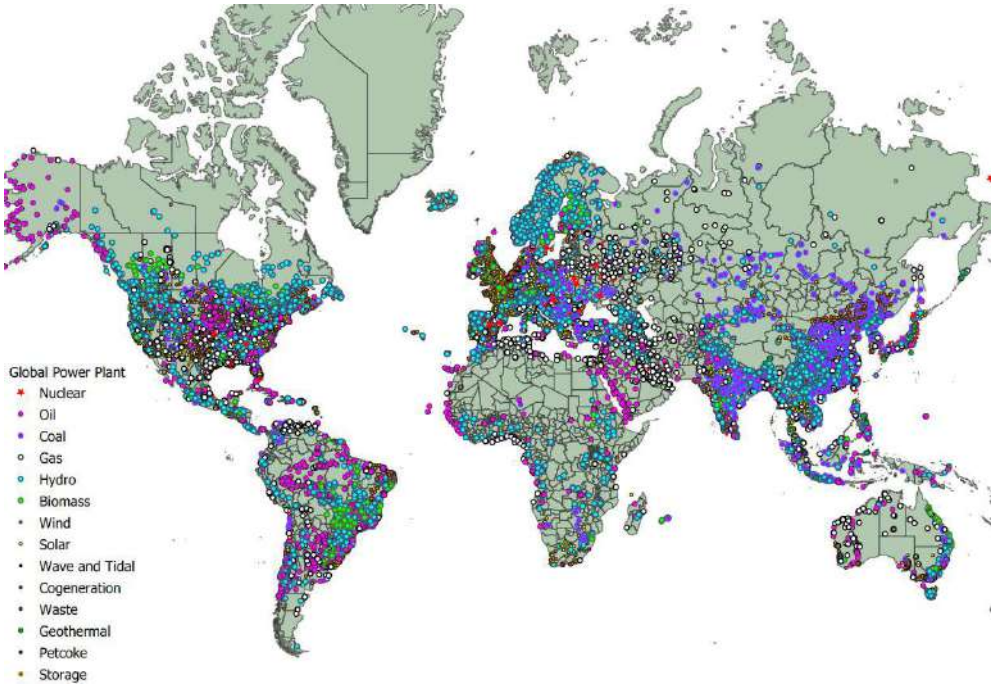


Source: Global Power Database version 1.3 (June 2021).

Another application of alternative data is the estimation of physical risk exposures. They correspond to the potential financial losses that companies can suffer, and includes droughts, floods, storms, etc. This risk is more difficult to quantify, and its evaluation requires multidisciplinary methodologies: climate modeling, physical asset geolocation, financial loss estimation, etc. In this case, asset tracking is really the crux of physical risk modeling. An example of spatial data is provided in Figure 2.8. This type of geolocalized data is extensively used by Le Guenedal *et al.* (2021, 2022) when developing a fully integrated methodology to measure cyclone-related physical risk. Until now, most of the models have been developed for countries and regions (Burke *et al.*, 2021)(Burke *et al.*, 2021). When dealing with corporate ESG, data providers generally use input-output matrices in order to compute the risk exposure or contribution of each firm. It is for example the case for biodiversity risk. Nevertheless, we have recently observed some initiatives to provide geospatial data and asset tracking directly at the company level. Even if these solutions are not yet mature, they are very promising[36].

**Remark 12** *Apart from controversies and physical risk, we also notice a third application of alternative data, which consists in building more reactive or real-time ESG scores. Ben Dor et al. (2022) propose to monitor planned sustainability-related corporate activities based on firms' actions, rather than relying solely on their announcements. For that, they use job postings and NLP to identify ESG-related openings and ESG-related activities of firms. This technique can be used to understand the dynamics of sustainability within a firm.*

[36]You can visit the website of the French technology company Kayrros (`https://www.kayrros.com`), which received the Financial TimesâĂŹ Tech Champions award for its innovation in the IT & Software sector. Kayrros uses satellite observation and AI to analyse trends in emissions and deforestation.

Figure 2.9: ESG rating disagreement

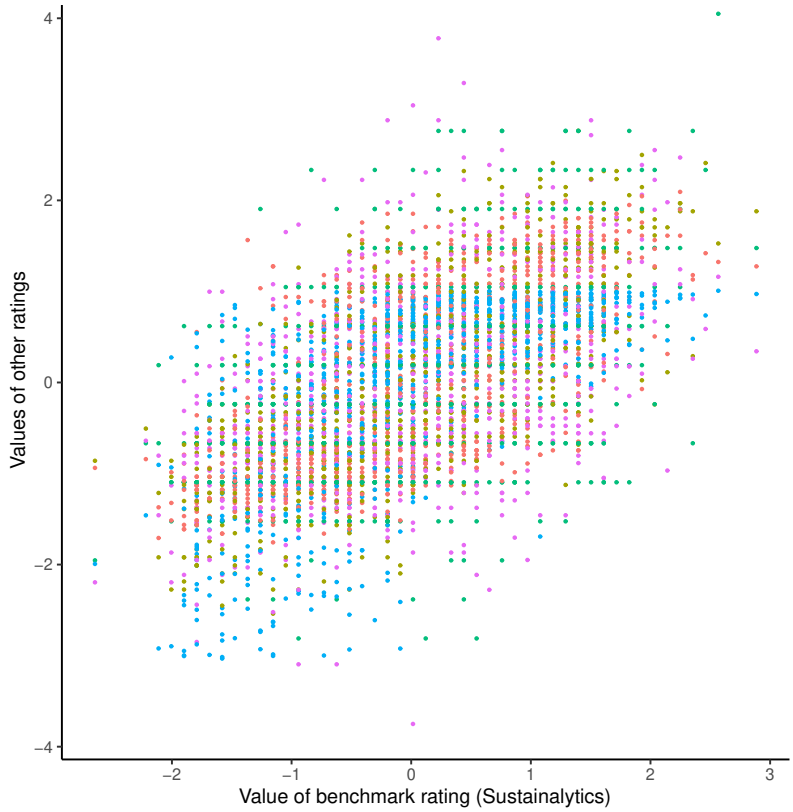


Source: Berg *et al.* (2022).

"*This graph illustrates the ESG rating divergence. The horizontal axis indicates the value of the Sustainalytics rating as a benchmark for each firm ($n = 924$). Rating values by the other five raters are plotted on the vertical axis in different colors*. For each rater, the distribution of values has been normalized to zero mean and unit variance. The Sustainalytics rating has discrete values that show up visually as vertical lines where several companies have the same rating value.*"

### The divergence of corporate ESG ratings

Corporate ESG data are very different than sovereign ESG data in terms of standardization. Therefore, we must expect more discrepancies in ESG ratings. In Figure 2.9, we have reported one of the most famous illustrations[37] about this rating disagreement extracted from the pioneering research of Berg *et al.* (2022). These authors investigate the divergence of ESG ratings from six prominent rating agencies: KLD, Moody's ESG, MSCI, Refinitiv, S&P Global and Sustainalytics. Using the ESG metrics of these data providers, they reconstruct synthetic ratings based on a common taxonomy of 64 indicators[38]. They identify three sources of divergence:

1. "**Measurement** *divergence refers to situation where rating agencies measure the same indicator using different ESG metrics;*

2. **Scope** *divergence refers to situation where ratings are based on different set of ESG indicators*;

[37] We have the following mapping: *S&P Global, Moody's ESG, KLD, Refinitiv, MSCI.
[38] See Exercise 1 on page 70 for the list of ESG indicators

3. **Weight** *divergence emerges when rating agencies take different views on the relative importance of ESG indicators.*"

They find that measurement contributes to 56% of the divergence, scope 38% and weight 6%.

Since this publication, the standardization issue of data and methodologies has been an ongoing discussion among practitioners and academics. For instance, Billio *et al.* (2021) analyze ESG ratings and indexes agreement and find that "*it is extremely difficult to measure the ability of a fund manager if financial performances are strongly conditioned by the chosen ESG benchmark*" and "*disagreement in the scores provided by the rating agencies disperses the effect of preferences of ESG investors on asset prices.*" In Table 2.10, we report their rank correlation matrix. On average, they obtain a mean correlation of 58% for corporate ESG ratings vs. 85% for sovereign ESG scores (Gratcheva *et al.*, 2020).

Table 2.10: Rank correlation among ESG ratings

| | MSCI | Refinitiv | S&P Global | |
|---|---|---|---|---|
| MSCI | 100% | | | |
| Refinitiv | 43% | 100% | | |
| S&P Global | 45% | 69% | 100% | |
| Sustainalytics | 53% | 64% | 69% | 100% |

Source: Billio *et al.* (2021, Table 3, page 1432) .

## 2.2 Scoring system

A scoring model is a mathematical model that forms the basis for risk stratification. For example, credit scoring refers to statistical models used to measure the creditworthiness of a company or individual (Roncalli, 2020a). In particular, the Altman $Z$ score is probably the most famous score for predicting the bankruptcy of commercial companies (Altman, 1968). However, scoring models can be found in many areas. For example, anti-money laundering (AML) scoring is a rating model used to assess the risk profile of customers (Chen *et al.*, 2018). The goal of trauma and field triage scoring systems is to predict the severity of injury or estimate the prognosis of trauma patients (Senkowski and McKenney, 1999). The Apgar score assesses the physical condition of newborns shortly after birth (Finster *et al.*, 2005). In the case of medicine, we find many scoring systems: ACR score (rheumatoid arthritis symptoms), Alvarado score (appendicitis), Framingham and QRISK scores (cardiovascular risk), Geneva score (pulmonary embolism), etc.

At first glance, we might think that ESG scoring is an extension of credit scoring using extra-financial data instead of financial data. And there are many similarities between the two concepts: ESG ratings vs. credit ratings, ESG materiality vs. credit materiality, ESG risk vs. credit risk, etc. However, from a mathematical point of view, they are two different concepts. In fact, ESG scoring is an unsupervised approach to risk materiality, while credit scoring is a supervised approach to risk materiality[39]. In the case of credit, we want to measure the one-year probability of default.

[39] Unsupervised learning is a branch of statistical learning in which the test data does not contain a response variable. It is in contrast to supervised learning, where the goal is to predict the value of the response variable $Y$ given a set of explanatory variables $X$. In unsupervised learning, we only know the $X$ values, because the $Y$ values do not exist or are not observed. Supervised and unsupervised learning methods are also called "*learning with/without a teacher*" (Hastie *et al.*, 2009). This metaphor means that in supervised learning we have access to the correct answer provided by the supervisor (or teacher). In unsupervised learning, we have no feedback on the correct answer. For example,

Therefore, credit scoring models are calibrated with a historical database of borrower default events. The response variable is then a binary variable that is 1 if the borrower has defaulted and 0 otherwise. In the case of ESG, we want to measure the sustainability of issuers, but we face an endogenous puzzle because the ESG score is already the sustainability measure. The big problem with ESG scoring systems is how to define the response variable. In most cases, the scoring model is not calibrated and is a simple rule-based method. For this reason, we generally consider ESG scoring to be an unsupervised statistical approach. This has several drawbacks in terms of performance evaluation, score consistency and backtesting. Nevertheless, we will see that we can define some proxies for the response variable and use traditional statistical tools to assess the quality of ESG scores.

### 2.2.1 ESG and scoring theory

The goal of scoring models is to produce a numeric score $\boldsymbol{\mathcal{S}}$. This score can take values between a lower bound $\boldsymbol{\mathcal{S}}^-$ and an upper bound $\boldsymbol{\mathcal{S}}^+$. We generally assume that a high value of $\boldsymbol{\mathcal{S}}$ is a good risk, while a low value of $\boldsymbol{\mathcal{S}}$ is a bad risk. Scoring systems are then used for two main types of decisions: selection and exclusion. A selection process consists of selecting the good risks so that $\boldsymbol{\mathcal{S}} \geq s_1$, while an exclusion process consists of excluding the bad risks so that $\boldsymbol{\mathcal{S}} \leq s_2$. The choice of the thresholds $s_1$ and $s_2$ is important and depends on the process. For example, suppose the score is between 0 and 1 000. We can formulate the following rule:

$$\begin{cases} \boldsymbol{\mathcal{S}} \geq 500 \Rightarrow \text{good risk} \Rightarrow \text{selection} \\ \boldsymbol{\mathcal{S}} \leq 500 \Rightarrow \text{bad risk} \Rightarrow \text{exclusion} \end{cases}$$

Obviously, separating the population into two groups (bad and good risks) is a difficult task. Another approach is to use stricter decision rules:

$$\begin{cases} \boldsymbol{\mathcal{S}} \geq 600 \Rightarrow \text{good risk} \Rightarrow \text{selection} \\ \boldsymbol{\mathcal{S}} \leq 300 \Rightarrow \text{bad risk} \Rightarrow \text{exclusion} \end{cases}$$

Here we see that there is an asymmetry in the definition of good and bad risks. The choice of the threshold is as important as the construction of the score. However, we have an endogenous problem because the threshold depends on the model itself. In the case of ESG, scores can be designed to define an exclusion process or a selection process, but in most cases they are used to perform both or they are used to define an integration process. This implies that the previous binary choice is replaced by the preference ordering:

$$\boldsymbol{\mathcal{S}}_1 \succ \boldsymbol{\mathcal{S}}_2 \Leftrightarrow \text{issuer } \#1 \text{ is a better ESG risk than issuer } \#2$$

This approach to scoring is different from the traditional approach. We face a problem here because ESG scores are generally the result of an unsupervised statistical method. Therefore, the development of ESG scoring has been done outside the framework of scoring theory. In fact, unsupervised statistical methods are generally used for clustering and classification. They are then adapted to a multimodal statistical problem, such as a binary statistical model (bad risk versus good risk). ESG scoring is more of an expert system than a true scoring model. In what follows, we try to provide a theoretical framework for ESG scoring, but we must be careful. This theoretical framework is limited for all the reasons mentioned above.

**Remark 13** *The fact that ESG scoring is designed as an unsupervised statistical process makes it difficult to assess the quality of ESG rating systems, particularly with respect to materiality.*

linear regression is a typical supervised learning model, while principal component analysis is an unsupervised learning approach.

### 2.2.2 Tree-based scoring methods

#### Tree structure

To understand a tree-based scoring model, we first consider the one-level tree structure. Let $X_1, \ldots, X_m$ be $m$ features. These metrics are linearly combined to obtain a score:

$$\mathcal{S} = \sum_{j=1}^{m} \omega_j X_j$$

where $\omega_j$ is the weight of the $j^{\text{th}}$ metric. Generally, the weights are normalized such that $\sum_{j=1}^{m} \omega_j = 1$. This is the most simple scoring model. For instance, the original bankruptcy score of Altman (1968) was equal to:

$$Z = 1.2 \cdot X_1 + 1.4 \cdot X_2 + 3.3 \cdot X_3 + 0.6 \cdot X_4 + 1.0 \cdot X_5$$

where the variables $X_j$ represent the following financial ratios:

| $X_j$ | Ratio |
|---|---|
| $X_1$ | Working capital / Total assets |
| $X_2$ | Retained earnings / Total assets |
| $X_3$ | Earnings before interest and tax / Total assets |
| $X_4$ | Market value of equity / Total liabilities |
| $X_5$ | Sales / Total assets |

If we note $Z_i$ the score of the firm $i$, we can calculate the normalized score $Z_i^\star = (Z_i - m_z)/\sigma_z$ where $m_z$ and $\sigma_z$ are the mean and standard deviation of the observed scores. $Z_i^\star$ can then be compared to the quantile of the Gaussian distribution or the empirical distribution. A low value of $Z_i^\star$ (for instance $Z_i^\star < -2.5$) indicates that the firm has a high probability of default, while companies with high scores above (for instance $Z_i^\star > 3$) are not likely to go bankrupt.

We can extend the previous approach to a two-level tree structure. We first begin to compute intermediary scores:

$$\mathcal{S}_k^{(1)} = \sum_{j=1}^{m} \omega_{j,k}^{(1)} X_j$$

Then we obtain a set of $m_{(1)}$ intermediary scores ($k = 1, \ldots, m_{(1)}$), which are combined to obtain the final score:

$$\mathcal{S} := \mathcal{S}_1^{(0)} = \sum_{k=1}^{m_{(1)}} \omega_k^{(0)} \mathcal{S}_k^{(1)}$$

The exponents (0) and (1) indicate the level of the tree. An example of two-level tree structure is given in Figure 2.10. For the first level, we have:

$$\begin{cases} \mathcal{S}_1^{(1)} = 0.5 \cdot X_1 + 0.25 \cdot X_2 + 0.25 \cdot X_3 \\ \mathcal{S}_2^{(1)} = 0.5 \cdot X_4 + 0.5 \cdot X_5 \\ \mathcal{S}_3^{(1)} = X_6 \end{cases}$$

The final score is the average of the three intermediary scores:

$$\mathcal{S} = \frac{\mathcal{S}_1^{(1)} + \mathcal{S}_2^{(1)} + \mathcal{S}_3^{(1)}}{3}$$

Figure 2.10: A two-level tree

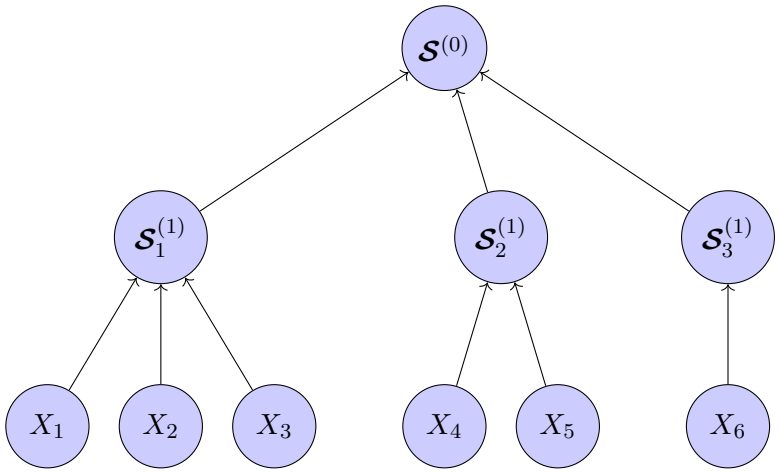


- Level 1: $\omega_{1,1}^{(1)} = 50\%$; $\omega_{2,1}^{(1)} = 25\%$; $\omega_{3,1}^{(1)} = 25\%$; $\omega_{4,2}^{(1)} = 50\%$; $\omega_{5,2}^{(1)} = 50\%$; $\omega_{6,3}^{(1)} = 100\%$;
- Level 0: $\omega_1^{(0)} = \omega_2^{(0)} = \omega_3^{(0)} = 33.33\%$;

Figure 2.11: A two-level overlapping graph

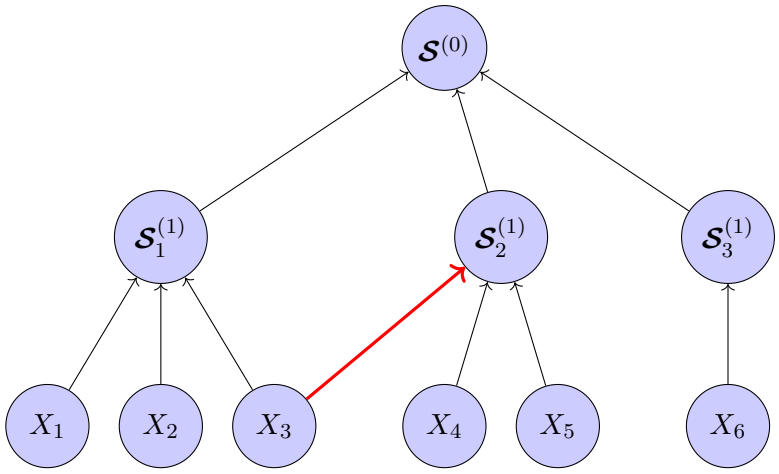


- Level 1: $\omega_{1,1}^{(1)} = 50\%$; $\omega_{2,1}^{(1)} = 25\%$; $\omega_{3,1}^{(1)} = 25\%$; $\omega_{3,2}^{(1)} = 25\%$; $\omega_{4,2}^{(1)} = 25\%$; $\omega_{5,2}^{(1)} = 50\%$; $\omega_{6,3}^{(1)} = 100\%$;
- Level 0: $\omega_1^{(0)} = \omega_2^{(0)} = \omega_3^{(0)} = 33.33\%$;

This tree is a non-overlapping graph because each child node is related to a single parent node, otherwise it is an overlapping graph (but it is not a tree). For example, if we assume that the score $\mathcal{S}_2^{(1)}$ also depends on the metric $X_3$, we obtain the overlapping graph structure given in Figure 2.11. In this case, the first level becomes:

$$\begin{cases} \mathcal{S}_1^{(1)} = 0.5 \cdot X_1 + 0.25 \cdot X_2 + 0.25 \cdot X_3 \\ \mathcal{S}_2^{(1)} = 0.25 \cdot X_3 + 0.25 \cdot X_4 + 0.5 \cdot X_5 \\ \mathcal{S}_3^{(1)} = X_6 \end{cases}$$

Box 2.2: Tree and graph theory

A scoring tree is a special case of a tree data structure, which is defined as a collection of nodes that are organized in a hierarchical structure (see Figure 2.A). A tree is also a connected graph without any circuits[a]. Therefore, the terminology of trees derives from the graph theory. A node (or a vertex) is the basic unit that may contain data and links to other nodes. A connection between two nodes is called an edge. In a tree, edges are directed and are also called arcs or arrows. For instance, our example has 13 nodes $\mathcal{V} = (A, \ldots, M)$ and 12 edges $\mathcal{E} = (\{K, H\}, \{L, J\}, \ldots, \{C, A\}, \{D, A\})$. Mathematically, the tree $\mathcal{T}$ is defined by the set $\mathcal{V}$ of nodes (or vertices) and the set $\mathcal{E}$ of edges: $\mathcal{T} = (\mathcal{V}, \mathcal{E})$. In a tree, the first node is called the root node $(A)$. Any node within a tree can be viewed as a root of its own subtree. By definition, The subtree $\mathcal{T}_{(v)}$ with $v$ as its root is also a tree consisting of $v$ and its descendants. $\mathcal{T}_{(v)}$ is defined by $\left(\mathcal{V}_{(v)}, \mathcal{E}_{(v)}\right)$, where $\mathcal{V}_{(v)}$ and $\mathcal{E}_{(v)}$ are the sets of vertices and edges of the subgraph. Each edge (or directed path) has a child and a parent (or an internal node). For example, $C$ is the parent node of $(H, I)$ and $H$ is a child node of $C$. Our example tree has then 6 parent nodes $\mathcal{P} = (A, B, C, D, H, J)$ and 12 children[b]. $B$ has three children $(E, F, G)$ and $B$ is a child of $A$. Child nodes with the same parent are sibling nodes, while a leaf node (or external node) is a node without child nodes. In the example tree, $(B, C, D)$, $(E, F, G)$, $(H, I)$ are siblings. The leaf nodes are $(E, F, G, I, K, L, M)$. The degree of a node is its number of children. It is equal to 3 for $(A, B)$, 2 for $(C, J)$ and 1 for $(H, D)$ and 0 for the leaves. The degree of a tree is equal to the maximum degree of nodes. Our example tree has a degree 3. The level of a node refers to the distance between the node and the root. We deduce that the root node is at level 0. Children of the root are at level 1 $(B, C, D)$. Level 2 corresponds to the nodes $(E, F, G, H, I, J)$ and we have 3 nodes at level 3 $(K, L, M)$. The depth of a tree is the level of the deepest node. It is equal to 3 in our example tree.

Figure 2.A: Tree data structure

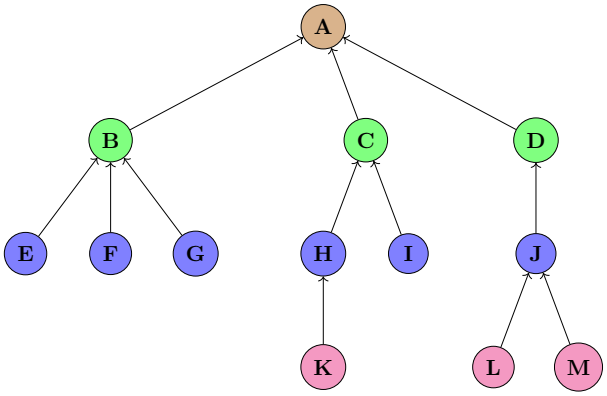


[a] We have the following properties:

- There is one and only one path between every pair of nodes in a tree;
- A tree with $n$ nodes has exactly $n - 1$ edges;
- A graph is a tree if and only if it is minimally connected;
- Any connected graph with $n$ nodes and $n - 1$ edges is a tree.

[b] In a tree, the number of children is exactly equal to the number of edges.

The two-level tree structure can be extended to multi-level tree structures. Let $L$ be the number of levels. At level $\ell$, the value of the $k^{\text{th}}$ node is given by:

$$\boldsymbol{\mathcal{S}}_k^{(\ell)} = \sum_{j=1}^{m_{(\ell+1)}} \omega_{j,k}^{(\ell)} \boldsymbol{\mathcal{S}}_j^{(\ell+1)} \tag{2.1}$$

where $m_{(\ell+1)}$ is the number of scores at level $\ell+1$, $\boldsymbol{\mathcal{S}}_j^{(\ell+1)}$ is the $j^{\text{th}}$ score at level $\ell+1$ and $\omega_{j,k}^{(\ell)}$ is the weight of the $j^{\text{th}}$ score at level $\ell+1$ for the $k^{\text{th}}$ score at level $\ell$. By construction, the scores at level $L$ are exactly equal to the features: $\boldsymbol{\mathcal{S}}_j^{(L)} = X_j$. We verify that the final score $\boldsymbol{\mathcal{S}}$ corresponds to the root score $\boldsymbol{\mathcal{S}}_1^{(0)}$. It can be computed by Algorithm 1. If we would like to target a specific level $\ell^\star$, we replace the **for** statement $t = 1 : L$ by $t = 1 : L + 1 - \ell^\star$.

**Algorithm 1** Recursive tree-based algorithm for computing the final score

Compute the final score $\boldsymbol{\mathcal{S}}_1^{(1)}$
**Input:** $L$ the number of levels, $(X_1, \ldots, X_m)$ the vector of the metrics and $\left\{\omega_{j,k}^{(\ell)}\right\}$ the weight tensor
**Initialize** $m_{(L)} = m$
**for** $j = 1 : m_{(L)}$ **do**
  $\boldsymbol{\mathcal{S}}_j^{(L)} \leftarrow X_j$
**end for**
**for** $t = 1 : L$ **do**
  {Change the value of $L$ by $L - \ell^\star$ if you target the level $\ell^\star$}
  $\ell \leftarrow L - t$
  **for** $k = 1 : m_{(\ell)}$ **do**
    $\boldsymbol{\mathcal{S}}_k^{(\ell)} \leftarrow 0$
    **for** $j = 1 : m_{(\ell+1)}$ **do**
      $\boldsymbol{\mathcal{S}}_k^{(\ell)} \leftarrow \boldsymbol{\mathcal{S}}_k^{(\ell)} + \omega_{j,k}^{(\ell)} \boldsymbol{\mathcal{S}}_j^{(\ell+1)}$
    **end for**
  **end for**
**end for**
$\boldsymbol{\mathcal{S}} \leftarrow \boldsymbol{\mathcal{S}}_1^{(0)}$
**return** $\boldsymbol{\mathcal{S}}$

The multi-level tree structure is very popular for computing ESG scores. For instance, the final ESG score corresponds to level 0. It is the weighted average of the E, S and G scores, which form the first level. Each pillar depends on a number of ESG themes, which constitutes the second level. As we have seen previously, an ESG theme is made up of several indicators. These last ones are located at the third level of the scoring tree. The computation of indicators requires some ESG metrics. Therefore, an ESG scoring model has at least four levels. For example, we have reported in Figure 2.12 an example of a tree from the MSCI scoring model. *Carbon emissions management and exposure* are two metrics (level 4). They are combined to form the indicator *carbon emissions* (level 3). MSCI uses this indicator and four others to define the *climate change* theme (level 2). It is one of the four themes of the environmental pillar (level 1).

Figure 2.12: An example of ESG scoring tree (MSCI methodology)

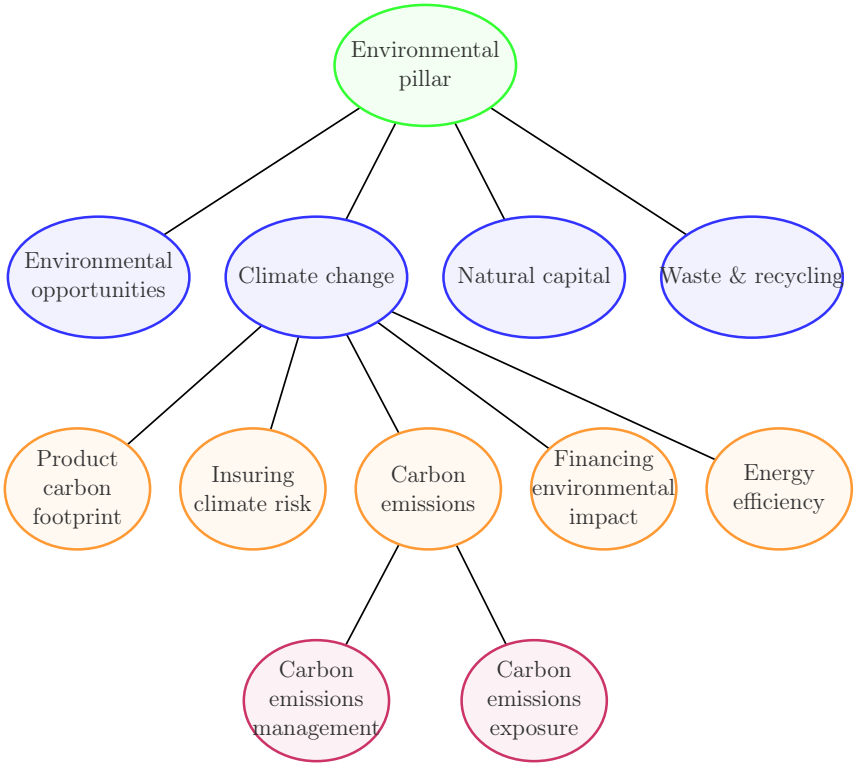


Source: MSCI (2020).

### Score normalization

**Why we need to normalize** Let $\omega_{(\ell)}$ be the $m_{(\ell+1)} \times m_{(\ell)}$ matrix, whose elements are $\omega_{j,k}^{(\ell)}$ for $j = 1, \ldots, m_{(\ell+1)}$ and $k = 1, \ldots, m_{(\ell)}$. We note $\boldsymbol{\mathcal{S}}^{(\ell)} = \left(\boldsymbol{\mathcal{S}}_1^{(\ell)}, \ldots, \boldsymbol{\mathcal{S}}_{m_{(\ell)}}^{(\ell)}\right)$ the vector of scores at the tree level $\ell$. We have:

$$\boldsymbol{\mathcal{S}}^{(\ell)} = \omega_{(\ell)}^\top \boldsymbol{\mathcal{S}}^{(\ell+1)}$$

At level 1, we obtain $\boldsymbol{\mathcal{S}}_1^{(1)} = \omega_{(1)}^\top \boldsymbol{\mathcal{S}}^{(2)}$. Since we have $\boldsymbol{\mathcal{S}}^{(2)} = \omega_{(2)}^\top \boldsymbol{\mathcal{S}}^{(3)}$, we deduce that $\boldsymbol{\mathcal{S}}_1^{(1)} = \omega_{(1)}^\top \omega_{(2)}^\top \boldsymbol{\mathcal{S}}^{(3)}$. By iterating the previous equation and noting that $\boldsymbol{\mathcal{S}}^{(L)} = X$, the final score is equal to:

$$\boldsymbol{\mathcal{S}} = \omega^\top X \tag{2.2}$$

where:

$$\omega = \omega_{(L-1)} \cdots \omega_{(1)} \omega_{(0)}$$

If we are interested in an intermediary score, we proceed in a similar way and we have:

$$\begin{aligned} \boldsymbol{\mathcal{S}}_k^{(\ell)} &= \mathbf{e}_k^\top \boldsymbol{\mathcal{S}}^{(\ell)} \\ &= \omega^\top X \end{aligned}$$

where:

$$\omega = \omega_{(L-1)} \cdots \omega_{(\ell-1)} \omega_{(\ell)}$$

We conclude that all the scores are a weighted average of initial metrics.

Let us consider the scoring tree given in Figure 2.11. We have:

$$\omega_{(1)} = \begin{bmatrix} 0.5 & 0 & 0 \\ 0.25 & 0 & 0 \\ 0.25 & 0.25 & 0 \\ 0 & 0.25 & 0 \\ 0 & 0.5 & 0 \\ 0 & 0 & 1 \end{bmatrix}$$

and:

$$\omega_{(0)} = \frac{1}{3} \begin{bmatrix} 1 \\ 1 \\ 1 \end{bmatrix}$$

We deduce that:

$$\omega = \omega_{(1)}\omega_{(0)} = \frac{1}{12} \begin{bmatrix} 2 \\ 1 \\ 2 \\ 1 \\ 2 \\ 4 \end{bmatrix}$$

The expression of the final score is:

$$\boldsymbol{\mathcal{S}} = \frac{2X_1 + X_2 + 2X_3 + X_4 + 2X_5 + 4X_3}{12}$$

Let us assume that $X$ follows a multivariate probability distribution $\mathbf{F}$. We deduce that $\boldsymbol{\mathcal{S}}$ follows the univariate probability distribution $\mathbf{G}$ defined by:

$$\begin{aligned} \mathbf{G}(s) &= \Pr\{\boldsymbol{\mathcal{S}} \leq s\} \\ &= \Pr\left\{\omega^\top X \leq s\right\} \\ &= \int \cdots \int \mathbb{1}\left\{\omega^\top x \leq s\right\} \mathrm{d}\mathbf{F}(x) \\ &= \int \cdots \int \mathbb{1}\left\{\sum_{j=1}^{m} \omega_j x_j \leq s\right\} \mathrm{d}\mathbf{F}(x_1, \ldots, x_m) \\ &= \int \cdots \int \mathbb{1}\left\{\sum_{j=1}^{m} \omega_j x_j \leq s\right\} \mathrm{d}\mathbf{C}(\mathbf{F}_1(x_1), \ldots, \mathbf{F}_m(x_m)) \end{aligned}$$

Therefore, the distribution $\mathbf{G}$ depends on the copula function $\mathbf{C}$ and the marginals $(\mathbf{F}_1, \ldots, \mathbf{F}_m)$ of $\mathbf{F}$.

We first investigate the independent case. It follows that:

$$\mathbf{G}(s) = \int \cdots \int \mathbb{1}\left\{\sum_{j=1}^{m} \omega_j x_j \leq s\right\} \prod_{j=1}^{m} \mathrm{d}\mathbf{F}_j(x_j)$$

We deduce that $\mathbf{G}$ is a convolution probability distribution. In some cases, it corresponds to a well-known probability distribution. For example, if $X_j \sim \mathcal{N}\left(\mu_j, \sigma_j^2\right)$, we have $\omega_j X_j \sim \mathcal{N}\left(\omega_j\mu_j, \omega_j^2\sigma_j^2\right)$. We deduce that:

$$\boldsymbol{\mathcal{S}} \sim \mathcal{N}\left(\sum_{j=1}^{m}\omega_j\mu_j, \sum_{j=1}^{m}\omega_j^2\sigma_j^2\right) \equiv \mathcal{N}\left(\omega^\top\mu, \omega^\top\Sigma\omega\right)$$

where $\mu = (\mu_1, \ldots, \mu_m)$ and $\Sigma = \operatorname{diag}\left(\sigma_1^2, \ldots, \sigma_m^2\right)$. In Figure 2.13, we have reported the density function of the intermediary and final scores for the tree 2.10 when $X_j \sim \mathcal{N}(0,1)$. The four scores $\boldsymbol{\mathcal{S}}_1^{(1)}$, $\boldsymbol{\mathcal{S}}_2^{(1)}$, $\boldsymbol{\mathcal{S}}_3^{(1)}$ and $\boldsymbol{\mathcal{S}}$ are Gaussian, centered at 0 with different standard deviations[40]. We face here an issue because we cannot compare the different scores and it is impossible to have a homogeneous rule to assess whether a score is good or not.

Figure 2.13: Probability distribution of the scores (Tree 2.10)

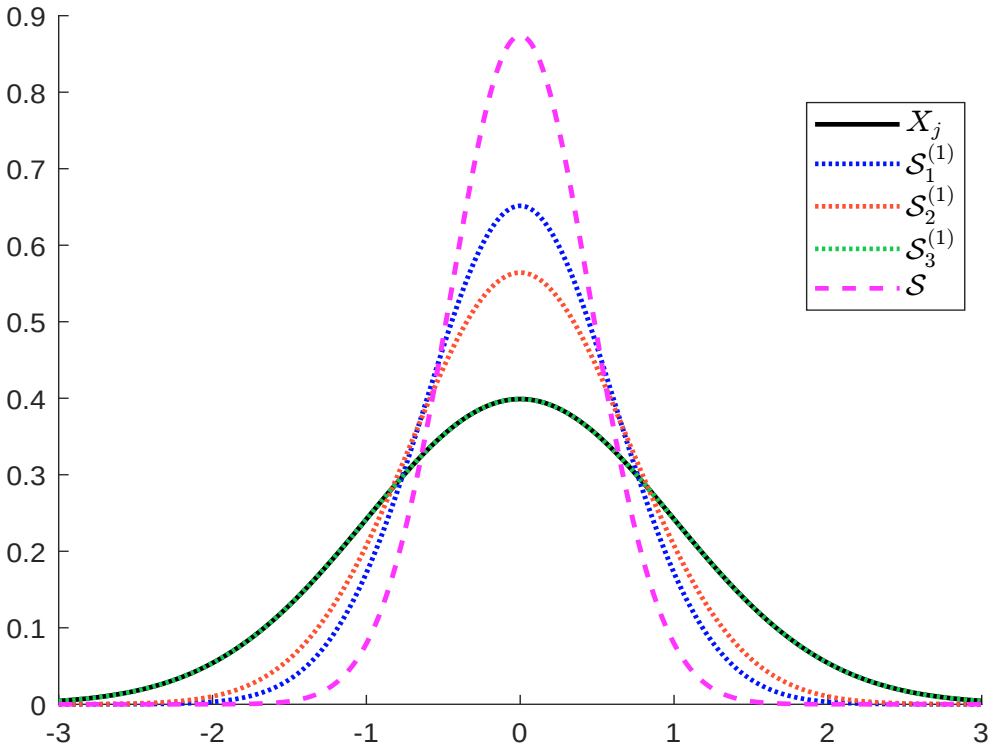


**Example 3** *We assume that* $X_1 \sim \mathcal{U}_{[0,1]}$ *and* $X_2 \sim \mathcal{U}_{[0,1]}$ *are two independent random variables. We consider the score* $\boldsymbol{\mathcal{S}}$ *defined as:*

$$\boldsymbol{\mathcal{S}} = \frac{X_1 + X_2}{2}$$

We have $\boldsymbol{\mathcal{S}} \in [0,1]$. In Figure 2.14, we consider a geometric interpretation of the probability mass function $\Pr\{\boldsymbol{\mathcal{S}} \leq s\} = \Pr\{X_1 + X_2 \leq 2s\}$. We distinguish two cases. The first case (a) corresponds to $s \leq 0.5$. The probability mass corresponds then to the right triangle with vertices $(0,0)$, $(0,2s)$ and $(2s,0)$. It is equal to one-half the square, whose length is $2s$. The second case (b) corresponds to $0.5 \leq s \leq 1$. Here the probability mass is equal to the area of the polygon shape, whose vertices

[40] They are equal to 0.6124 for $\boldsymbol{\mathcal{S}}_1^{(1)}$, 0.7071 for $\boldsymbol{\mathcal{S}}_2^{(1)}$, 1 for $\boldsymbol{\mathcal{S}}_3^{(1)}$ and 0.4564 for $\boldsymbol{\mathcal{S}}$.

Figure 2.14: Geometric interpretation of the probability mass function (Example 3)

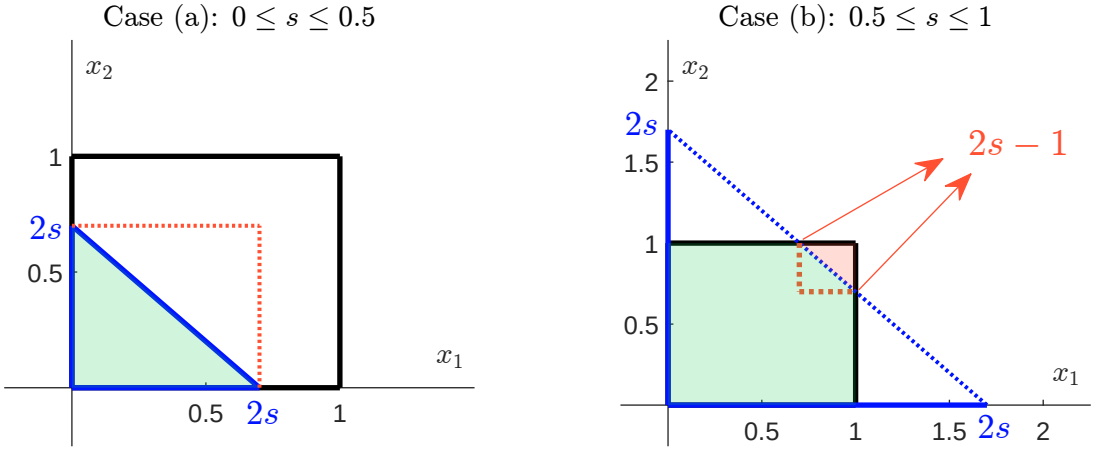


are $(0,0)$, $(1,0)$, $(1,2s-1)$, $(2s-1,1)$ and $(0,1)$. This is equivalent to computing the area of the unit square minus the right triangle with vertices $(1,2s-1)$, $(1,1)$ and $(2s-1,1)$. We notice that the area of the right triangle is equal to one-half the square, whose length is $2-2s$. We deduce that:

$$\Pr\{\boldsymbol{\mathcal{S}} \leq s\} = \begin{cases} \frac{1}{2}(2s)^2 & \text{if} \quad 0 \leq s \leq \frac{1}{2} \\ 1 - \frac{1}{2}(2-2s)^2 & \text{if} \quad \frac{1}{2} \leq s \leq 1 \end{cases}$$

Finally, we obtain:

$$\mathbf{G}(s) = \begin{cases} 2s^2 & \text{if} \quad 0 \leq s \leq \frac{1}{2} \\ -1 + 4s - 2s^2 & \text{if} \quad \frac{1}{2} \leq s \leq 1 \end{cases}$$

The density function is then:

$$g(s) = \begin{cases} 4s & \text{if} \quad 0 \leq s \leq \frac{1}{2} \\ 4 - 4s & \text{if} \quad \frac{1}{2} \leq s \leq 1 \end{cases}$$

The previous results can be extended to the case $m > 2$. We can show that the score follows the Bates distribution[41]:

$$\boldsymbol{\mathcal{S}} = \frac{X_1 + X_2 + \cdots + X_m}{m} \sim \mathfrak{Bates}(m)$$

In Figures 2.15 and 2.16, we report the density and distribution functions of the score for several values of $m$. We verify that the shape of the score depends on the number $m$ of features. In particular, we observe that the score tends to the Dirac distribution $\delta(x - 1/2)$.

Let us now investigate the dependent case. If we assume that $X \sim \mathcal{N}(\mu, \Sigma)$, the score $\boldsymbol{\mathcal{S}} = \omega^\top X$ is normally distributed: $\boldsymbol{\mathcal{S}} \sim \mathcal{N}(\omega^\top \mu, \omega^\top \Sigma \omega)$. We consider that $\mu_j = 0$, $\sigma_j = 1$ and $\rho_{j,k} = \rho$ for $j \neq k$. Since the covariance matrix is the constant correlation matrix $\mathbb{C}_m(\rho)$, we deduce that

[41] See Exercise 2.4.1 on page 132.

Figure 2.15: Probability density function of $\boldsymbol{\mathcal{S}}$ (uniform distribution)

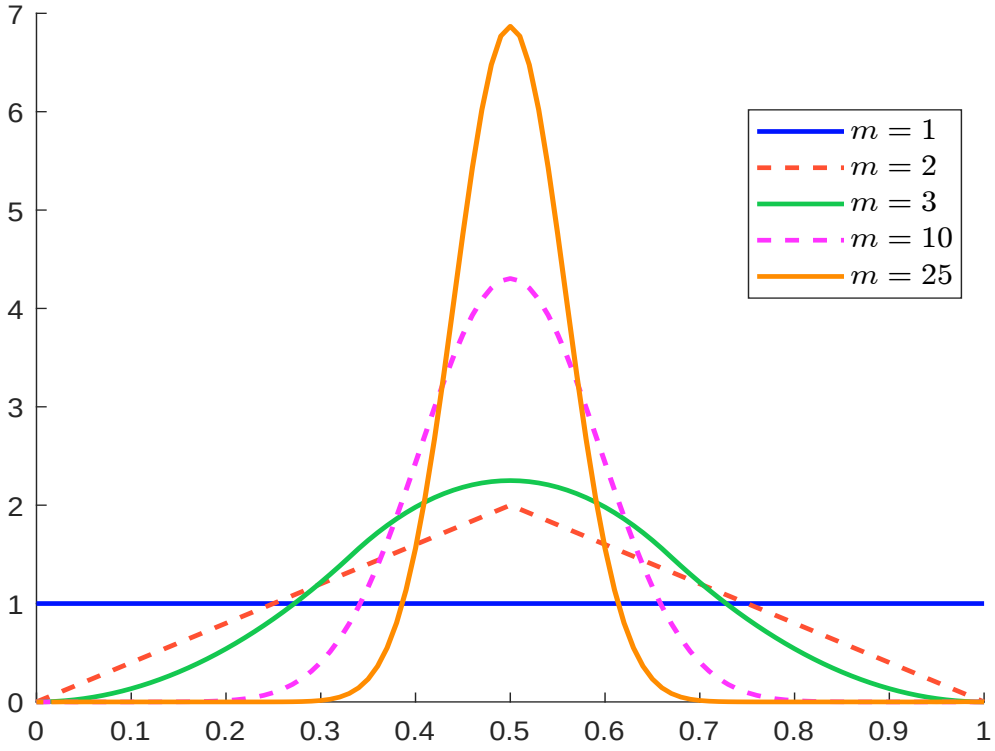


Figure 2.16: Cumulative distribution function of $\boldsymbol{\mathcal{S}}$ (uniform distribution)

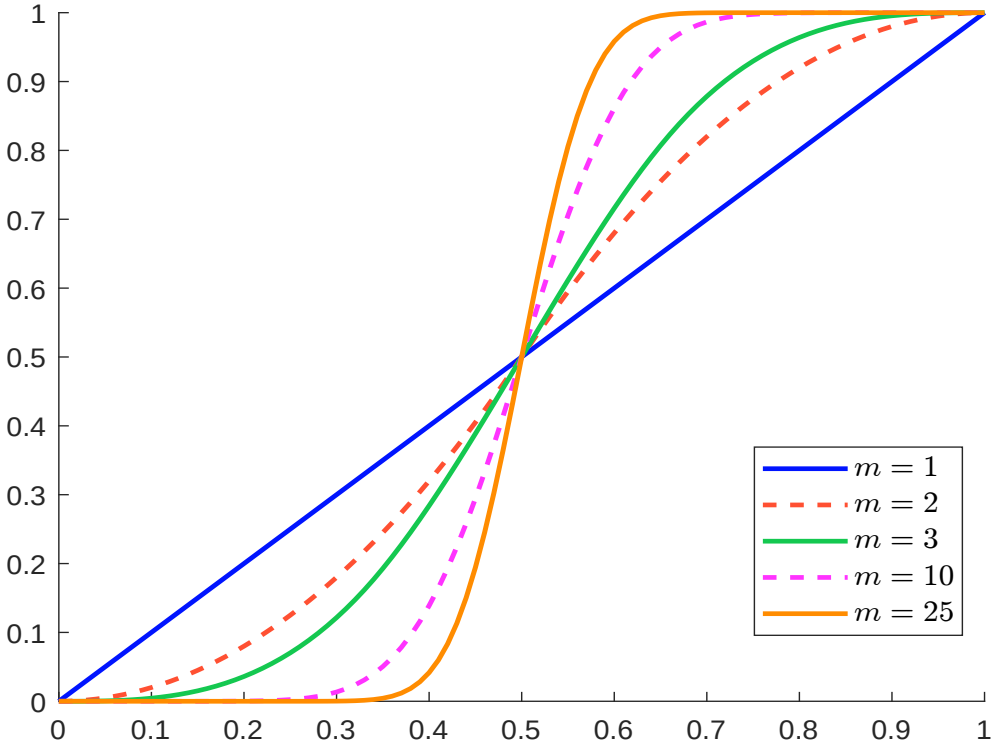

$\mathbb{E}[\boldsymbol{\mathcal{S}}] = 0$ and[42]:

$$\begin{aligned}
\text{var}(\boldsymbol{\mathcal{S}}) &= \omega^\top \mathbb{C}_m(\rho)\,\omega \\
&= \sum_{j=1}^m \sum_{k=1}^m \omega_j\omega_k\rho_{j,k} + \left(\sum_{j=1}^m \omega_j^2\rho - \sum_{j=1}^m \omega_j^2\rho\right) \\
&= \rho\sum_{j=1}^m \sum_{k=1}^m \omega_j\omega_k + (1-\rho)\sum_{j=1}^m \omega_j^2 \\
&= \rho\mathcal{S}^2(w) + (1-\rho)\,\mathcal{H}(\omega)
\end{aligned}$$

where $\mathcal{S}(w) = \sum_{j=1}^m \omega_j$ is the sum index and $\mathcal{H}(\omega) = \sum_{j=1}^m \omega_j^2$ is the Herfindahl index. Generally, the weights are normalized and we obtain $\boldsymbol{\mathcal{S}} \sim \mathcal{N}\left(0, \sigma_{\boldsymbol{\mathcal{S}}}^2\right)$ where:

$$\sigma_{\boldsymbol{\mathcal{S}}} = \sqrt{\rho + (1-\rho)\,\mathcal{H}(\omega)}$$

Since $0 \leq \mathcal{H}(\omega) \leq 1$, $\sigma_{\boldsymbol{\mathcal{S}}} \in \left[\sqrt{\rho}, 1\right]$. When the weights are equal ($\omega_j = 1/m$), the previous formula reduces to[43]:

$$\sigma_{\boldsymbol{\mathcal{S}}} = \sqrt{\rho + \frac{(1-\rho)}{m}}$$

Let us build the confidence interval of the score at the confidence level $\alpha$. We have $\Pr\{\boldsymbol{\mathcal{S}} \in [\boldsymbol{\mathcal{S}}^-(m,\alpha), \boldsymbol{\mathcal{S}}^+(m,\alpha)]\} = \alpha$. Since the expectation of the score is equal to zero, we consider an interval centered at 0. We deduce that:

$$\boldsymbol{\mathcal{S}}^+(m,\alpha) = \Phi^{-1}\left(\frac{1+\alpha}{2}\right)\sqrt{\rho + \frac{(1-\rho)}{m}}$$

and $\boldsymbol{\mathcal{S}}^-(m,\alpha) = -\boldsymbol{\mathcal{S}}^+(m,\alpha)$.

In Figure 2.17, we illustrate the shrinkage issue of the score when $\alpha$ is set to 99.75%. At this confidence level, a standard normal random variable lies between $-3$ and $+3$. This is the range that we have in mind when we build a $z$-score. We observe that the shrinkage begins when the score is made up of three features and a correlation lower than 80%. The shrinkage issue increases with the number of features. Let us consider for example an ESG score that depends on 20 ESG metrics, that have an average correlation of 20%. While the range of the features is between $-3$ and $+3$, the aggregate ESG score lies between $-1.5$ and $+1.5$, meaning that the support of the score has been divided by a factor of two!

**How to normalize?** The previous analysis implies that we must normalize the raw data and the scores at the different levels such that they follow the same probability distribution $\mathbf{F}_{\boldsymbol{\mathcal{S}}}$. Equation (2.1) is no longer valid and we deduce that the node values of the multi-level tree structure are equal to:

$$\boldsymbol{\mathcal{S}}_k^{(\ell)} = \varphi\left(\sum_{j=1}^{m_{(\ell+1)}} \omega_{j,k}^{(\ell)}\boldsymbol{\mathcal{S}}_j^{(\ell+1)}\right) \tag{2.3}$$

where $\varphi(s)$ is the normalization function. We also have $\boldsymbol{\mathcal{S}}_j^{(L)} = \varphi(X_j)$.

Let $X$ be a variable to normalize and $\{x_1, \ldots, x_n\}$ a sample of $n$ observations. In practice, there are three main approaches:

[42] We note $\mathcal{S}(w) = \sum_{j=1}^m \omega_j$. We deduce that $\left(\sum_{j=1}^m \omega_j\right)^2 = \sum_{j=1}^m \sum_{k=1}^m \omega_j\omega_k = \mathcal{S}^2(w)$.

[43] We have $\mathcal{H}(\omega) = \sum_{j=1}^m (1/m)^2 = 1/m$.

Figure 2.17: Upper and lower bounds of the aggregate score when $\alpha = 99.75\%$

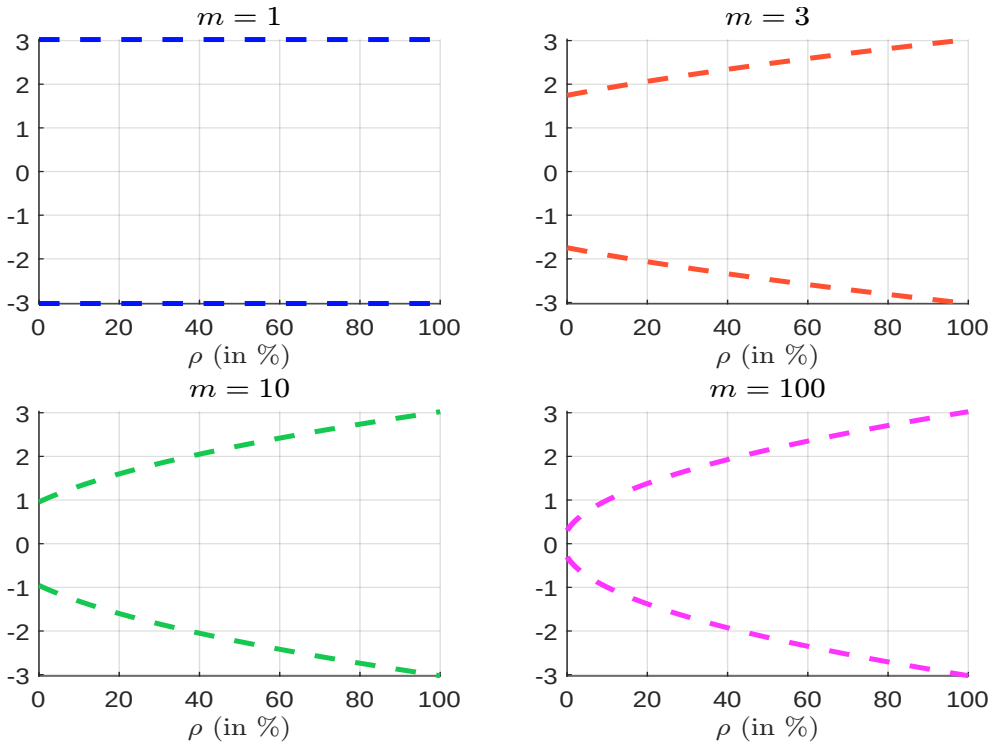


1. The first one is the $m$-score (or min-max) normalization:

$$m_i = \frac{x_i - x^-}{x^+ - x^-}$$

where $x^- = \min x_i$ and $x^+ = \max x_i$. This is the most naive approach to obtain a 0/1 normalization.

2. The second approach is the $q$-score (or quantile) normalization:

$$q_i = \mathbf{H}(x_i)$$

where $\mathbf{H}$ is the distribution function of $X$. When the distribution of $X$ is unknown, we replace $\mathbf{H}$ by the empirical distribution $\hat{\mathbf{H}}$: $q_i = \hat{\mathbf{H}}(x_i)$. In both cases, we obtain a 0/1 normalization.

3. The third method is the famous $z$-score normalization:

$$z_i = \frac{x_i - \mu}{\sigma}$$

where $\mu$ and $\sigma$ are the mathematical expectation and standard deviation of $X$. Again, when the distribution of $X$ is unknown, we use the empirical mean and standard deviation of the sample:

$$z_i = \frac{x_i - \hat{\mu}}{\hat{\sigma}}$$

By construction, we have $z_i \in (-\infty, \infty)$. Nevertheless, we have seen that $\Pr\{-3 \leq N(0,1) \leq 3\} \approx 99.75\%$. Generally, we consider that the $z$-score method produces a $-3/+3$ normalization.

Among the three approaches, only the second approach satisfies the consistency property. Indeed, if $X \sim \mathbf{H}$ and is continuous, we know that $Y = \mathbf{H}(X)$ is a uniform random variable[44]. $Y = \mathbf{H}(X)$ defines the *probability integral transform*, which plays an important role in statistics and probability. The min-max approach is consistent only if $X \sim \mathcal{U}_{[x^-,x^+]}$, whereas the $z$-score normalization is consistent if the original data are normally distributed.

Box 2.3: Computing the empirical distribution $\hat{\mathbf{H}}$

Let $\{x_1, x_2, \ldots, x_n\}$ be the sample. We have:

$$q_i = \hat{\mathbf{H}}(x_i) = \Pr\{X \leq x_i\} = \frac{\#\{x_j \leq x_i\}}{n_q}$$

We can use two normalization factors: $n_q = n$ or $n_q = n + 1$. For example, if $n = 4$, we have $q_i \in \{0.25, 0.5, 0.75, 1\}$ if $n_q = n$, and $q_i \in \{0.2, 0.4, 0.6, 0.8\}$ if $n_q = n + 1$. The second solution is better because $q_i \in ]0, 1[$. Therefore, we can transform $q_i$ into a random variable $Y$ with probability distribution $\mathbf{G}$ by considering the inverse probability integral transform:

$$Y = \mathbf{G}^{-1}(q_i) \sim \mathbf{G}$$

For example, we can transform a $q$-score into a $z$-score by considering the Gaussian quantile function:

$$z = \Phi^{-1}(q)$$

With the second solution, we are sure that $z \notin (-\infty, \infty)$.

To obtain an $a/b$ normalization, we consider the following property:

$$\mathcal{U}_{[a,b]} = a + (b - a)\,\mathcal{U}_{[0,1]}$$

Therefore, we apply the following transform to obtain the new score:

$$q' = a + (b - a)\,q$$

The $q$-score is distributed according to the uniform distribution. It has the advantage to be normalized between 0 and 1. However, it has the disadvantage to be a flat score, meaning that the extreme scores have the same probability to occur as the mean score. The $z$-score is distributed according to the Gaussian distribution. It has a bell-curve shape, meaning that the extreme scores have a lower probability to occur than the mean score. Therefore, it is interesting to combine the two properties to obtain a discriminant score between 0 and 1. This is done by considering the $b$-score using a Beta distribution $\mathcal{B}(\alpha, \beta)$. In this case, we have:

$$b_i = \mathfrak{B}^{-1}(\mathbf{H}(x_i); \alpha, \beta)$$

[44] We have $Y \in [0, 1]$ and:

$$\begin{aligned} \Pr\{Y \leq y\} &= \Pr\{\mathbf{H}(X) \leq y\} \\ &= \Pr\left\{X \leq \mathbf{H}^{-1}(y)\right\} \\ &= \mathbf{H}\left(\mathbf{H}^{-1}(y)\right) \\ &= y \end{aligned}$$

We deduce that $Y \sim \mathcal{U}_{[0,1]}$.

When $\alpha = \beta$, This creates a symmetric score around 0.5. To obtain a left-skewed score (when having more best-in-class issuers than worst-in-class issuers), we use $\alpha > \beta$. The case $\alpha < \beta$ produces a right-skewed score (when having more worst-in-class issuers than best-in-class issuers). The standard values for parameters are $\alpha = \beta = 2$.

**Example 4** *The data are normally distributed with mean $\mu = 5$ and standard deviation $\sigma = 2$. To map these data into a $0/1$ score, we consider the following transform:*

$$s := \varphi(x) = \mathfrak{B}^{-1}\left(\Phi\left(\frac{x-5}{2}\right); \alpha, \beta\right)$$

*In Figure 2.18, we report the transform function $\varphi(x)$ and the final distribution for three sets of parameters $(\alpha, \beta)$.*

Figure 2.18: Transforming data into $\mathcal{b}$-score using the Beta distribution

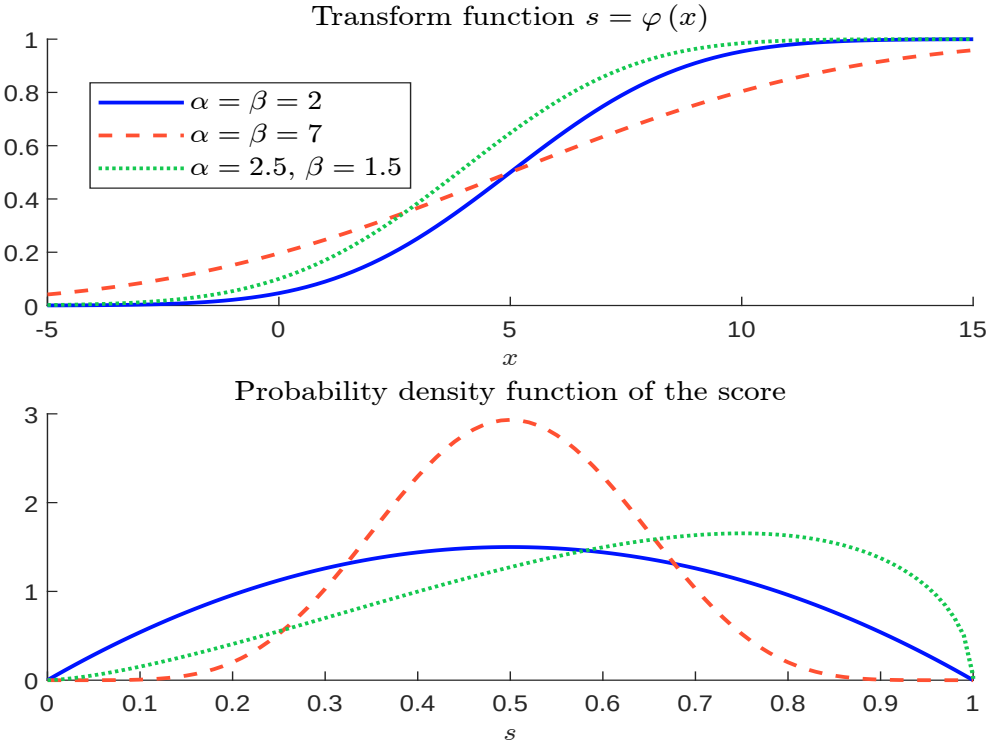


**Remark 14** *ESG data providers do not publish their statistical methodology for computing ESG scores*[45]*. It is then difficult to know which normalization approach is used. Nevertheless, they give the scale of the scores. Bloomberg, S&P Global and Sustainalytics use a range from 0 to 100, Refinitiv from 1 to 100, MSCI from 0 to 10, ISS ESG from 1 to 10, etc. Some asset managers use a scale between $-3$ and $+3$.*

[45] Only S&P Dow Jones Indices (2022, page 8) indicates that "*the normalization is performed by a sigmoid-function on a standard z-score*":

$$\mathcal{S} = \frac{2}{1+e^{-z}} - 1 \in [-1, 1]$$

**Example 5** *We consider the raw data of* 9 *companies in Table 2.11. These companies belong to the same industry. The first variable measures the carbon intensity of scope* $1+2$ *in 2020, while the second variable is the variation of carbon emissions between 2015 and* 2020*. We would like to create the score* $\boldsymbol{\mathcal{S}} \equiv 70\% \cdot X_1 + 30\% \cdot X_2$.

Table 2.11: Raw data of 9 companies (carbon emissions and carbon momentum)

| Firm | Carbon intensity (in $tCO_2e$/\$ mn) | Carbon momentum (in %) |
|---|---|---|
| 1 | 94.0 | −3.0 |
| 2 | 38.6 | −5.5 |
| 3 | 30.6 | 5.6 |
| 4 | 74.4 | −1.3 |
| 5 | 97.1 | −16.8 |
| 6 | 57.1 | −3.5 |
| 7 | 132.4 | 8.5 |
| 8 | 92.5 | −9.1 |
| 9 | 64.9 | −4.6 |

To create the synthetic score, we must analyze the data. An ESG investor prefers to be exposed to low-carbon companies than to high-carbon companies. Similarly, he favors firms that have reduced their carbon emissions in the past. If we consider the raw variables as the two features, a high value of the score will indicate a worst-in-class company while a low value of the score will indicate a best-in-class company. If we prefer that high scores correspond to best-in-class scores, we need to take the opposite of these data. We consider the first choice. In Table 2.12, we report the computation of the score by using a $q$-score 0/100 normalization. For instance, company #7 has the highest carbon emission and then the highest score $q_1 = 90$. It is followed by company #5 which has a score of 80. We verify that the mean of $q_1$ is equal to $(0+100)/2$ and its standard deviation is approximately[46] equal to $\sqrt{(100-0)^2/12}$. For the carbon momentum, the best issuer is company #5 with a trend of −16.8%, and its $q$-score is equal to 10. We compute then the score $s = 0.7 \cdot q_1 + 0.3 \cdot q_2$. This indicates that the ESG investor is more sensitive to carbon intensity than carbon intensity. Said differently, he would like to build a score primarily based on the carbon intensity, but he would like to penalize companies that increase their carbon emissions. For the first firm, we obtain $s = 0.7 \times 70 + 0.3 \times 60 = 67$. We notice that the standard deviation of the variable $s$ is equal to 20.60, which is lower than 27.39. Again, we have to normalize the variable $s$ and we obtain the final score. We also report the rank $\mathfrak{R}$ and we obtain the following ordering:

$$\#2 \succ \#3 \succ \#6 \succ \#9 \succ \#8 \succ \#4 \succ \#5 \succ \#1 \succ \#7$$

We deduce that the best-in-class and worst-in-class issuers are respectively companies #2 and #7. If we consider the $z$-score normalization, the results are given in Table 2.13. For example, $z_1$ and $z_2$ are equal to $(92.5 - 75.73)/31.95 = 0.525$ and $(-9.10 + 3.30)/7.46 = -0.778$ for company #8. We deduce that $s = 0.7 \times 0.525 + 0.3 \times (-0.778) = 0.134$. Again we observe that the variable $s$ is not normalized since its standard deviation is not equal to 1. We deduce that $\boldsymbol{\mathcal{S}} = (0.134 - 0.000)/0.759 = 0.177$. Finally, we obtain the following ordering:

$$\#2 \succ \#3 \succ \#6 \succ \#9 \succ \#5 \succ \#4 \succ \#8 \succ \#1 \succ \#7$$

We conclude that the two approaches produce two different rankings.

Table 2.12: Computation of the score $\boldsymbol{\mathcal{S}} \equiv 70\% \cdot X_1 + 30\% \cdot X_2$ ($q$-score 0/100 normalization)

| # | $X_1$ | $q_1$ | $X_2$ | $q_2$ | $s$ | $\boldsymbol{\mathcal{S}}$ | $\mathfrak{R}$ |
|---|---|---|---|---|---|---|---|
| 1 | 94.00 | 70.00 | −3.00 | 60.00 | 67.00 | 80.00 | 8 |
| 2 | 38.60 | 20.00 | −5.50 | 30.00 | 23.00 | 10.00 | 1 |
| 3 | 30.60 | 10.00 | 5.60 | 80.00 | 31.00 | 20.00 | 2 |
| 4 | 74.40 | 50.00 | −1.30 | 70.00 | 56.00 | 60.00 | 6 |
| 5 | 97.10 | 80.00 | −16.80 | 10.00 | 59.00 | 70.00 | 7 |
| 6 | 57.10 | 30.00 | −3.50 | 50.00 | 36.00 | 30.00 | 3 |
| 7 | 132.40 | 90.00 | 8.50 | 90.00 | 90.00 | 90.00 | 9 |
| 8 | 92.50 | 60.00 | −9.10 | 20.00 | 48.00 | 50.00 | 5 |
| 9 | 64.90 | 40.00 | −4.60 | 40.00 | 40.00 | 40.00 | 4 |
| Mean | 75.73 | 50.00 | −3.30 | 50.00 | 50.00 | 50.00 | |
| Std-dev. | 31.95 | 27.39 | 7.46 | 27.39 | 20.60 | 27.39 | |

Table 2.13: Computation of the score $\boldsymbol{\mathcal{S}} \equiv 70\% \cdot X_1 + 30\% \cdot X_2$ ($z$-score normalization)

| # | $X_1$ | $z_1$ | $X_2$ | $z_2$ | $s$ | $\boldsymbol{\mathcal{S}}$ | $\mathfrak{R}$ |
|---|---|---|---|---|---|---|---|
| 1 | 94.00 | 0.572 | −3.00 | 0.040 | 0.412 | 0.543 | 8 |
| 2 | 38.60 | −1.162 | −5.50 | −0.295 | −0.902 | −1.188 | 1 |
| 3 | 30.60 | −1.413 | 5.60 | 1.193 | −0.631 | −0.831 | 2 |
| 4 | 74.40 | −0.042 | −1.30 | 0.268 | 0.051 | 0.067 | 6 |
| 5 | 97.10 | 0.669 | −16.80 | −1.810 | −0.075 | −0.099 | 5 |
| 6 | 57.10 | −0.583 | −3.50 | −0.027 | −0.416 | −0.548 | 3 |
| 7 | 132.40 | 1.774 | 8.50 | 1.582 | 1.716 | 2.261 | 9 |
| 8 | 92.50 | 0.525 | −9.10 | −0.778 | 0.134 | 0.177 | 7 |
| 9 | 64.90 | −0.339 | −4.60 | −0.174 | −0.290 | −0.382 | 4 |
| Mean | 75.73 | 0.000 | −3.30 | 0.000 | 0.000 | 0.000 | |
| Std-dev. | 31.95 | 1.000 | 7.46 | 1.000 | 0.759 | 1.000 | |

Table 2.14: Comparison of the different scoring methods

| # | $q$ | | $z$ | | $qz$ | | $zq$ | | $bz$ | | $bz^\star$ | |
|---|---|---|---|---|---|---|---|---|---|---|---|---|
| | $\boldsymbol{\mathcal{S}}$ | $\mathfrak{R}$ | $\boldsymbol{\mathcal{S}}$ | $\mathfrak{R}$ | $\boldsymbol{\mathcal{S}}$ | $\mathfrak{R}$ | $\boldsymbol{\mathcal{S}}$ | $\mathfrak{R}$ | $\boldsymbol{\mathcal{S}}$ | $\mathfrak{R}$ | $\boldsymbol{\mathcal{S}}$ | $\mathfrak{R}$ |
| 1 | 80.00 | 8 | 0.54 | 8 | 76.27 | 8 | 0.84 | 8 | 0.66 | 8 | 0.81 | 8 |
| 2 | 10.00 | 1 | −1.19 | 1 | 9.19 | 1 | −1.28 | 1 | 0.20 | 1 | 0.30 | 1 |
| 3 | 20.00 | 2 | −0.83 | 2 | 21.37 | 2 | −0.84 | 2 | 0.29 | 2 | 0.38 | 2 |
| 4 | 60.00 | 6 | 0.07 | 6 | 54.13 | 5 | 0.25 | 6 | 0.52 | 6 | 0.70 | 6 |
| 5 | 70.00 | 7 | −0.10 | 5 | 56.65 | 6 | 0.52 | 7 | 0.51 | 5 | 0.64 | 5 |
| 6 | 30.00 | 3 | −0.55 | 3 | 24.42 | 3 | −0.52 | 3 | 0.34 | 3 | 0.50 | 3 |
| 7 | 90.00 | 9 | 2.26 | 9 | 98.04 | 9 | 1.28 | 9 | 0.93 | 9 | 0.96 | 9 |
| 8 | 50.00 | 5 | 0.18 | 7 | 60.39 | 7 | 0.00 | 5 | 0.56 | 7 | 0.72 | 7 |
| 9 | 40.00 | 4 | −0.38 | 4 | 30.96 | 4 | −0.25 | 4 | 0.39 | 4 | 0.56 | 4 |
| Mean | 50.00 | | 0.00 | | 47.94 | | 0.00 | | 0.49 | | 0.62 | |
| Std-dev. | 27.39 | | 1.00 | | 28.79 | | 0.82 | | 0.22 | | 0.21 | |

In Table 2.14, we compare the scores and the ranks obtained for different scoring schemes. Besides the $q$- and $z$-scores, we consider the following transforms:

- The $qz$-score is defined as:
$$qz = c \cdot \Phi(z) \in [0, c]$$
where $c = 100$ is the scaling factor.
- The $zq$-score is defined as:
$$zq = \Phi^{-1}\left(\frac{q}{c}\right) \in [-3, 3]$$
- The $\mathfrak{b}z$-score is defined as:
$$\mathfrak{b}z = \mathfrak{B}^{-1}(\Phi(z); \alpha, \beta) \in [0, 1]$$
where $\alpha = \beta = 2$.
- The $\mathfrak{b}z^\star$-score is a modification of the $\mathfrak{b}z$-score by using $\alpha = 2.5$ and $\beta = 1.5$.

We verify that the $\mathfrak{b}z^\star$-score is left-skewed and the mean is above $1/2$.

**Remark 15** *Most ESG scoring systems are sector neutral, meaning that the normalization is done at the sector (or industry) level, not at the issuer universe level. ESG scores are then* ***relative*** *scores (with respect to the sector/industry), not* ***absolute*** *scores. This is the concept of best-in-class/worst-in-class issuers. A best-in-class company is then not a best-in-universe issuer. Let us consider the example where the score of corporate $A$ is $\boldsymbol{\mathcal{S}}_A = +2$ and the score of corporate $B$ is $\boldsymbol{\mathcal{S}}_B = +1$. We have:*

- *If $A$ and $B$ belong to the same sector, we have $A \succ B$;*
- *If $A$ and $B$ belong to two different sectors, we may have $A \succ B$ or $B \succ A$.*

*The preference ordering $\succ$ is then partial and not total.*

**An example with the CEO pay ratio** The CEO pay ratio is calculated by dividing the CEO's compensation by the pay of the median employee. It is one of the key metrics for the G pillar. It has been imposed by the Dodd-Frank Act, which requires that publicly traded companies disclose:

1. the median total annual compensation of all employees other than the CEO;
2. the ratio of the CEO's annual total compensation to that of the median employee;
3. the wage ratio of the CEO to the median employee.

According to the American Federation of Labor and Congress of Industrial Organizations (AFL-CIO, https://aflcio.org), the average S&P 500 company's CEO-to-worker pay ratio was 324-to-1 in 2021. In Table 2.15, we have reported some data collected by this organization ($P$ is the median worker pay (in \$) and $R$ is the CEO pay ratio).

Computing the scores for the pay ratio is a real challenge, because the probability distribution of the pay ratio has both a high skew and a big kurtosis. To illustrate these issues, Figure 2.19 shows the histogram of the CEO pay ratios for all US public companies[47] for the fiscal year 2021. If we

[46] Since we have only 9 observations, we observe a small difference between the true and the sample values.

[47] We use the database *Fiscal 2021 CEO Pay Ratios* by Mark Siciliano, which can be downloaded at the University of Alabama: https://ir.ua.edu/handle/123456789/8639.

Table 2.15: Examples of CEO pay ratio (June 2021)

| Company name | $P$ | $R$ | Company name | $P$ | $R$ |
|---|---|---|---|---|---|
| Abercrombie & Fitch | 1 954 | 4,293 | Netflix | 202 931 | 190 |
| McDonald's | 9 291 | 1,939 | BlackRock | 133 644 | 182 |
| Coca-Cola | 11 285 | 1,657 | Pfizer | 98 972 | 181 |
| Gap | 6 177 | 1,558 | Goldman Sachs | 138 854 | 178 |
| Alphabet | 258 708 | 1,085 | MSCI | 55 857 | 165 |
| Walmart | 22 484 | 983 | Verisk Analytics | 77 055 | 117 |
| Estee Lauder | 30 733 | 697 | Facebook | 247 883 | 94 |
| Ralph Lauren | 21 358 | 570 | Invesco | 125 282 | 92 |
| NIKE | 25 386 | 550 | Boeing | 158 869 | 90 |
| Citigroup | 52 988 | 482 | Citrix Systems | 181 769 | 80 |
| PepsiCo | 45 896 | 368 | Harley-Davidson | 187 157 | 59 |
| Microsoft | 172 512 | 249 | Amazon.com | 28 848 | 58 |
| Apple | 57 596 | 201 | Berkshire Hathaway | 65 740 | 6 |

Source: https://aflcio.org (June 2021)

compute the $z$-score directly from the pay ratio, we obtain the blue histogram in Figure 2.20. This $z$-score has a mean around 0 and a standard deviation of 1, but we have $z \in (-0.338, 38.669)$. If we do the same exercise with the logarithm of the CEO pay ratio, we obtain the red histogram. In this case, we have $z \in (-3.561, 4.545)$. This is better, but it is not perfect. This example demonstrates that we must conduct a deep analysis of each data before applying a blind scoring approach. Most ESG data are skewed with fat tails, some of them are binary, others take discrete values, etc. In this context, data analysis is essential to choose the right normalization and scoring transform.

**Exercise 6** *The database of the CEO pay ratios for all US public companies contains several sector/industry variables. Compute the z-score of the CEO pay ratio and its logarithm at the sector level. Identify the most problematic sectors. Same question if we consider the industry level.*

### 2.2.3 Other statistical methods

Since ESG scoring is an unsupervised statistical method, the use of alternative statistical methods is limited. Indeed, we can use $K$-means clustering, hierarchical clustering, and principal component analysis to perform dimension reduction of the variables or to create synthetic features. However, it is difficult to go further with these methods. The use of classical parametric supervised methods, such as discriminant analysis and binary choice models, is not well suited except when the goal is to identify bad ESG risks. They are not used in practice. In fact, the only alternative statistical method that adds some value is the lasso method, which is described in Appendix A.2.3 on page 1079. The underlying idea is to perform the penalized linear regression $\boldsymbol{\mathcal{S}} = \beta^\top X + U$ subject to the $\mathcal{L}_1$-norm constraint $\|\beta\|_1 \leq \tau$ and identify the most important variables of the ESG scoring system. The lasso regression is then used as an ex-post statistical method to estimate the contribution of each variable. In practice, we find that a complex ESG scoring system based on more than 100 variables can be replicated with fewer variables.

### 2.2.4 Performance evaluation criteria

This section is dedicated to the performance assessment of a score. Backtesting an ESG score is relatively close to backtesting a credit score. Even if the tree-based scoring model is an unsuper-

Figure 2.19: Histogram of the CEO pay ratio

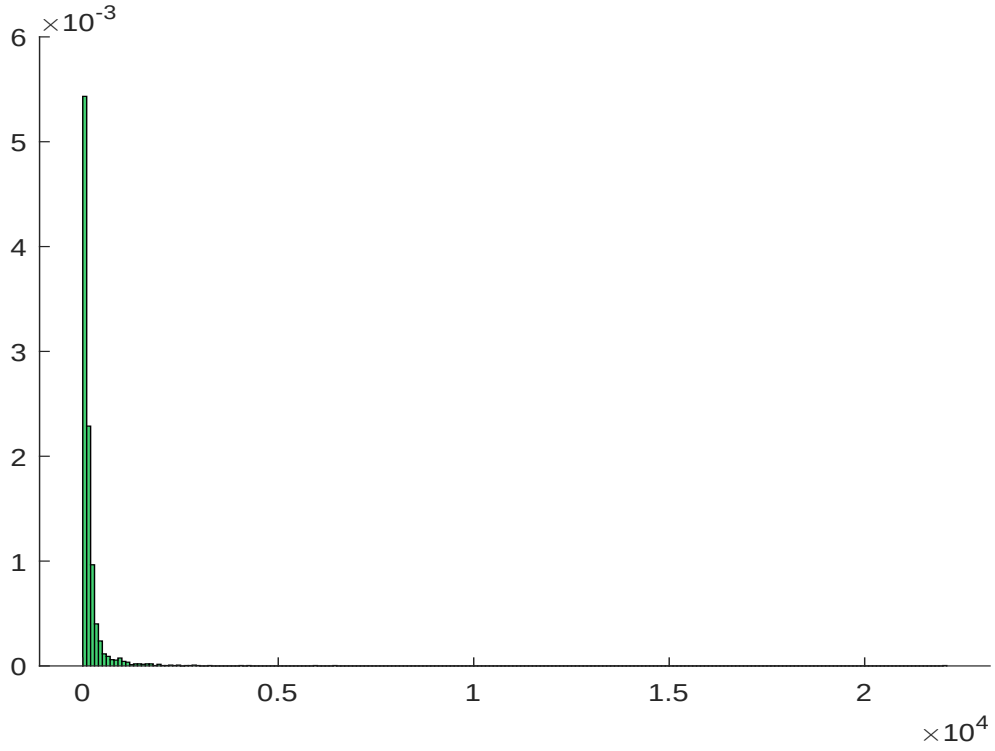


Figure 2.20: Histogram of $z$-score applied to the CEO pay ratio

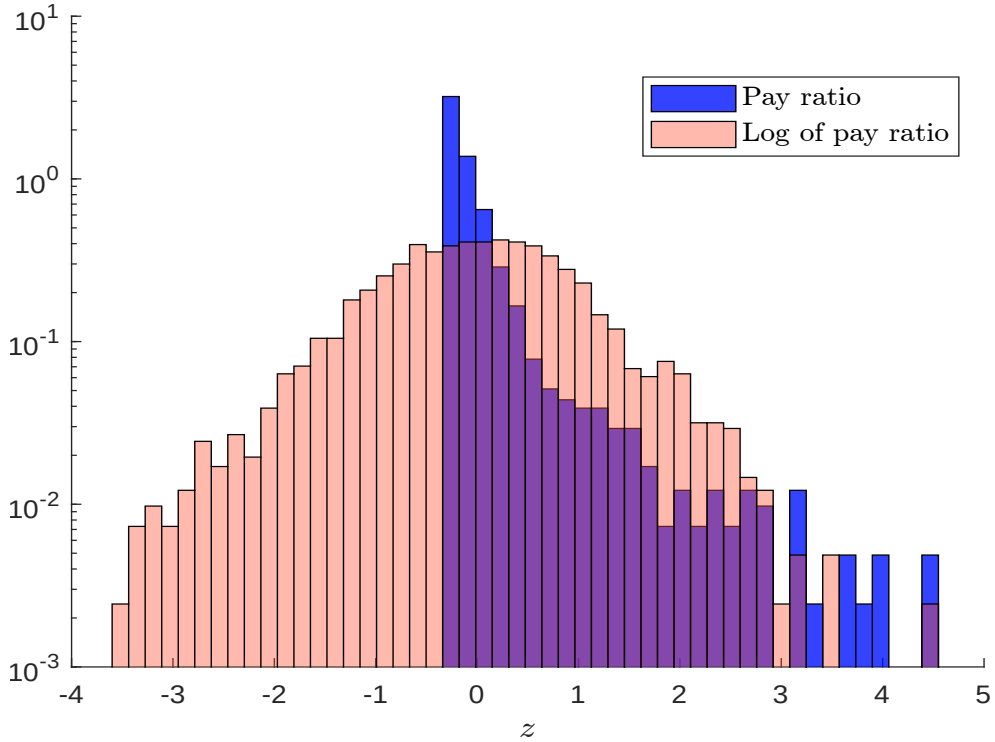

vised learning approach, we have seen that it is possible to build supervised models by using a control variable. The response function can be exogenous such as the controversy index $\mathcal{C}(t)$ or the controversy indicator $I(t) = \mathbb{1}\{\mathcal{C}(t) > 0\}$. It can also be endogenous by considering control variables based on the score $\boldsymbol{\mathcal{S}}(t+\delta)$ in the future. Examples are the best-in-class risk indicator $\mathcal{G}(t,\delta) = \mathbb{1}\{\boldsymbol{\mathcal{S}}(t+\delta) \geq s^\star\}$ or the worst-in-class risk indicator $\mathcal{B}(t,\delta) = \mathbb{1}\{\boldsymbol{\mathcal{S}}(t+\delta) \leq s^\star\}$. They are noted $\mathcal{G}$ and $\mathcal{B}$ by analogy with the risk theory that distinguishes good and bad risk. For instance, credit scoring models are mainly based on bad risk detection. This is also the same thing in the case of responsible investing. Nevertheless, we might also want to have a statistical model, whose main objective is to select the good issuers. In the case of the ESG momentum strategy, the response variable depends on the improvement of the ESG score. It can be defined as[48] $\mathcal{M}(t,\delta) = \mathbb{1}\{\boldsymbol{\mathcal{S}}(t+\delta) - \boldsymbol{\mathcal{S}}(t) \geq \Delta_s^\star\}$.

**Remark 16** *In this section, the score $\boldsymbol{\mathcal{S}}$ is not necessarily the final ESG score. It corresponds to any score or screening rule derived from the ESG scoring model. For instance, it may corresponds to a selection score, an exclusion score, etc.*

We notice that most control variables are binary. Therefore, we can use the classical tool of credit scoring and follow Roncalli (2020a, Chapter 15) to assess the performance of scoring models. In the first paragraph, we use information theory to know if the scoring system is informative or not. The second paragraph presents the graphical tools to measure the classification accuracy of the score. We then define the different statistical measures to estimate the score performance. Finally, we consider the assessment tools when there is no response function.

### Shannon entropy

**Definition and properties** The entropy is a measure of unpredictability or uncertainty of a random variable. Let $(X,Y)$ be a random vector where $p_{i,j} = \Pr\{X = x_i, Y = y_j\}$, $p_i = \Pr\{X = x_i\}$ and $p_j = \Pr\{Y = y_j\}$. The Shannon entropy of the discrete random variable $X$ is given by[49]:

$$\mathcal{I}(X) = -\sum_{i=1}^{n} p_i \ln p_i$$

We have the property $0 \leq \mathcal{I}(X) \leq \ln n$. The entropy is equal to zero if there is a state $i$ such that $p_i = 1$ and is equal to $\ln n$ in the case of the uniform distribution ($p_i = 1/n$). The Shannon entropy is a measure of the average information of the system. The lower the Shannon entropy, the more informative the system. For a random vector $(X,Y)$, we have:

$$\mathcal{I}(X,Y) = -\sum_{i=1}^{n}\sum_{j=1}^{n} p_{i,j} \ln p_{i,j}$$

We deduce that the conditional information of $Y$ given $X$ is equal to:

$$\begin{aligned}
\mathcal{I}(Y \mid X) &= \mathbb{E}[\mathcal{I}(Y \mid X = x)] \\
&= -\sum_{i=1}^{n}\sum_{j=1}^{n} p_{i,j} \ln \frac{p_{i,j}}{p_i} \\
&= \mathcal{I}(X,Y) - \mathcal{I}(X)
\end{aligned}$$

We have the following properties:

[48] Alternative measures are $\mathcal{M}(t,\delta) = \mathbb{1}\{\boldsymbol{\mathcal{S}}(t+\delta) - \boldsymbol{\mathcal{S}}(t) > \Delta_s^\star | \boldsymbol{\mathcal{S}}(t) \geq s^\star\}$ when we prefer to select companies among the best-in-class issuers and $\mathcal{M}(t,\delta) = \mathbb{1}\{\boldsymbol{\mathcal{S}}(t+\delta) - \boldsymbol{\mathcal{S}}(t) > \Delta_s^\star | \boldsymbol{\mathcal{S}}(t) \leq s^\star\}$ when we want to detect worst-in-class issuers that will improve their ESG score.

[49] We use the convention $p_i \ln p_i = 0$ when $p_i$ is equal to zero.

- if $X$ and $Y$ are independent, we have $\mathcal{I}(Y \mid X) = \mathcal{I}(Y)$ and $\mathcal{I}(X,Y) = \mathcal{I}(Y) + \mathcal{I}(X)$;
- if $X$ and $Y$ are perfectly dependent, we have $\mathcal{I}(Y \mid X) = 0$ and $\mathcal{I}(X,Y) = \mathcal{I}(X)$.

The amount of information obtained about one random variable, through the other random variable is measured by the mutual information:

$$\begin{aligned}\mathcal{I}(X \cap Y) &= \mathcal{I}(Y) + \mathcal{I}(X) - \mathcal{I}(X,Y) \\ &= \sum_{i=1}^{n}\sum_{j=1}^{n} p_{i,j} \ln \frac{p_{i,j}}{p_i p_j}\end{aligned}$$

Figure 2.21: Examples of Shannon entropy calculation

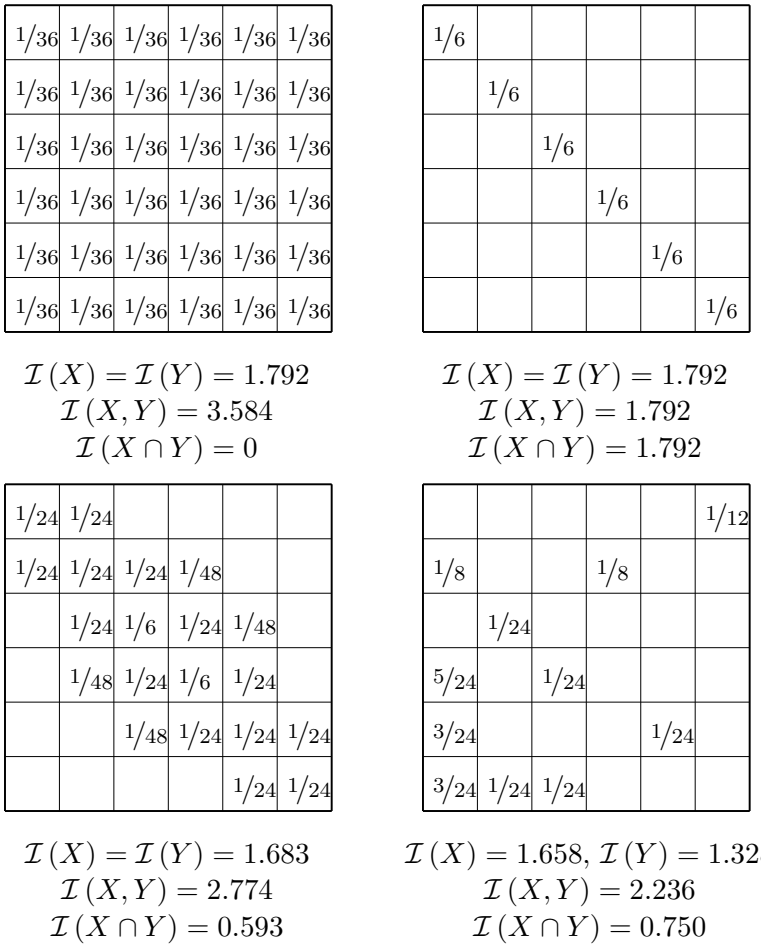


Figure 2.21 shows some examples of Shannon entropy calculation. For each example, we indicate the probabilities $p_{i,j}$ and the values taken by $\mathcal{I}(X)$, $\mathcal{I}(Y)$, $\mathcal{I}(X,Y)$ and $\mathcal{I}(X \cap Y)$. The top/left panel corresponds to a diffuse system. The value of $\mathcal{I}(X,Y)$ is maximum, meaning that the system is extremely disordered. The top/right panel represents a highly ordered system in the bivariate case and a diffuse system in the univariate case. We have $\mathcal{I}(X \mid Y) = \mathcal{I}(Y \mid X) = 0$, implying that the knowledge of $X$ is sufficient to find the state of $Y$. Generally, the system is not perfectly ordered or perfectly disordered. For instance, in the case of the system described in the bottom/left panel, the knowledge of $X$ informs us about the state of $Y$. Indeed, if $X$ is in the third state, then we

know that $Y$ cannot be in the first or sixth state. Another example is provided in the bottom/right panel.

**Remark 17** *If we apply the Shannon entropy to the transition matrix of a Markov chain, we set* $X = \mathcal{R}(s)$ *and* $Y = \mathcal{R}(t)$ *where* $\mathcal{R}(t)$ *is the state variable at the date* $t$*. We obtain:*

$$\mathcal{I}(\mathcal{R}(t) \mid \mathcal{R}(s)) = -\sum_{i=1}^{K} \pi_i^\star \sum_{j=1}^{K} p_{i,j}^{(t-s)} \ln p_{i,j}^{(t-s)}$$

*where* $p_{i,j} = \Pr\{\mathcal{R}(t+1) = j \mid \mathcal{R}(t) = i\}$, $\mathbb{K} = \{1, 2, \ldots, K\}$ *is the state space of the Markov chain and* $\pi^\star$ *is the associated stationary distribution.*

**Application to scoring** Let $\boldsymbol{\mathcal{S}}$ and $Y$ be the score and the control variable. For instance, $Y$ is a binary random variable that may indicate a bad ESG risk ($Y = 0$) or a good ESG risk ($Y = 1$). $Y$ may also correspond to classes defined by some quantiles. With Shannon entropy, we can measure the information of the system $(\boldsymbol{\mathcal{S}}, Y)$. We can also compare two scores $\boldsymbol{\mathcal{S}}_1$ and $\boldsymbol{\mathcal{S}}_2$ by using the statistical measures $\mathcal{I}(\boldsymbol{\mathcal{S}}_1 \cap Y)$ and $\mathcal{I}(\boldsymbol{\mathcal{S}}_2 \cap Y)$. Let $\boldsymbol{\mathcal{S}}_3$ be the aggregated score obtained from the two individual scores $\boldsymbol{\mathcal{S}}_1$ and $\boldsymbol{\mathcal{S}}_2$. We can calculate the information contribution of each score with respect to the global score. Therefore, we can verify that a score really adds an information.

We consider the following decision rule:

$$\begin{cases} \boldsymbol{\mathcal{S}} \leq 0 \Rightarrow \boldsymbol{\mathcal{S}}^\star = 0 \\ \boldsymbol{\mathcal{S}} > 0 \Rightarrow \boldsymbol{\mathcal{S}}^\star = 1 \end{cases}$$

We note $n_{i,j}$ the number of observations such that $\boldsymbol{\mathcal{S}}^\star = i$ and $Y = j$. We obtain the following system $(\boldsymbol{\mathcal{S}}^\star, Y)$:

| | $Y = 0$ | $Y = 1$ |
|---|---|---|
| $\boldsymbol{\mathcal{S}}^\star = 0$ | $n_{0,0}$ | $n_{0,1}$ |
| $\boldsymbol{\mathcal{S}}^\star = 1$ | $n_{1,0}$ | $n_{1,1}$ |

where $n = n_{0,0} + n_{0,1} + n_{1,0} + n_{1,1}$ is the total number of observations. The hit rate is the ratio of good bets:

$$H = \frac{n_{0,0} + n_{1,1}}{n}$$

This statistic can be viewed as an information measure of the system $(\boldsymbol{\mathcal{S}}, Y)$. When there are more states, we can consider the Shannon entropy. In Figure 2.22, we report the contingency table of two scores $\boldsymbol{\mathcal{S}}_1$ and $\boldsymbol{\mathcal{S}}_2$ for 100 observations[50]. We have $\mathcal{I}(\boldsymbol{\mathcal{S}}_1 \cap Y) = 0.763$ and $\mathcal{I}(\boldsymbol{\mathcal{S}}_2 \cap Y) = 0.636$. We deduce that $\boldsymbol{\mathcal{S}}_1$ is more informative than $\boldsymbol{\mathcal{S}}_2$.

### Graphical methods

We assume that the control variable $Y$ can takes two values: $Y = 0$ corresponds to a bad risk (or bad signal) while $Y = 1$ corresponds to a good risk (or good signal). Gouriéroux (1992) introduced three graphical tools for assessing the quality of a score: the performance curve, the selection curve and the discrimination curve[51]. In the following, we assume that the probability $\Pr\{Y = 1 \mid \boldsymbol{\mathcal{S}} \geq s\}$ is increasing with respect to the level[52] $s \in [0, 1]$, which corresponds to the rate of acceptance. We deduce that the decision rule is the following:

[50] Each score is divided into 6 intervals $(s_1, \ldots, s_6)$ while the dependent variable is divided into 5 intervals $(y_1, \ldots, y_5)$.

[51] See also Gouriéroux and Jasiak (2007).

[52] We assume that the score is based on the 0/1 normalization, but this assumption is not important since we can always map a general score into a 0/1 score.

Figure 2.22: Scorecards $\boldsymbol{\mathcal{S}}_1$ and $\boldsymbol{\mathcal{S}}_2$ (100 observations)

| | $y_1$ | $y_2$ | $y_3$ | $y_4$ | $y_5$ |
|---|---|---|---|---|---|
| $s_1$ | 10 | 9 | | | |
| $s_2$ | 7 | 9 | | | |
| $s_3$ | 3 | | 7 | 2 | |
| $s_4$ | | 2 | 10 | 4 | 5 |
| $s_5$ | | | | 10 | 2 |
| $s_6$ | | | 3 | 4 | 13 |

$\mathcal{I}(\boldsymbol{\mathcal{S}}_1) = 1.767$
$\mathcal{I}(Y) = 1.609$
$\mathcal{I}(\boldsymbol{\mathcal{S}}_1, Y) = 2.614$
$\mathcal{I}(\boldsymbol{\mathcal{S}}_1 \cap Y) = 0.763$

| | $y_1$ | $y_2$ | $y_3$ | $y_4$ | $y_5$ |
|---|---|---|---|---|---|
| $s_1$ | 7 | 10 | | | |
| $s_2$ | 10 | 8 | | | |
| $s_3$ | | | 5 | 4 | 3 |
| $s_4$ | 3 | | 10 | 6 | 4 |
| $s_5$ | 2 | | | 5 | 8 |
| $s_6$ | | | 5 | 5 | 5 |

$\mathcal{I}(\boldsymbol{\mathcal{S}}_2) = 1.771$
$\mathcal{I}(Y) = 1.609$
$\mathcal{I}(\boldsymbol{\mathcal{S}}_2, Y) = 2.745$
$\mathcal{I}(\boldsymbol{\mathcal{S}}_2 \cap Y) = 0.636$

- if the score of the observation is above the threshold $s$, the observation is selected;
- if the score of the observation is below the threshold $s$, the observation is not selected.

If $s$ is equal to one, we select no observation. If $s$ is equal to zero, we select all the observations. In a scoring system, the threshold $s$ is given. Below, we assume that $s$ is varying and we analyze the relevance of the score with respect to this parameter.

**Performance curve, selection curve and discriminant curve** The performance curve is the parametric function $y = \mathcal{P}(x)$ defined by:

$$\begin{cases} x(s) = \Pr\{\boldsymbol{\mathcal{S}} \geq s\} \\ y(s) = \dfrac{\Pr\{Y = 0 \mid \boldsymbol{\mathcal{S}} \geq s\}}{\Pr\{Y = 0\}} \end{cases}$$

where $x(s)$ corresponds to the proportion of selected observations and $y(s)$ corresponds to the ratio between the proportion of selected bad risks and the proportion of bad risks in the population. The score is efficient if the ratio is below one. If $y(s) > 1$, the score selects more bad risks than those we can find in the population[53]. If $y(s) = 1$, the score is random and the performance is equal to zero. In this case, the selected population is representative of the total population.

The selection curve is the parametric curve $y = \mathcal{S}(x)$ defined by:

$$\begin{cases} x(s) = \Pr\{\boldsymbol{\mathcal{S}} \geq s\} \\ y(s) = \Pr\{\boldsymbol{\mathcal{S}} \geq s \mid Y = 0\} \end{cases}$$

where $y(s)$ corresponds to the ratio of observations that are wrongly selected. By construction, we would like that the curve $y = \mathcal{S}(x)$ is located below the bisecting line $y = x$ in order to verify that $\Pr\{\boldsymbol{\mathcal{S}} \geq s \mid Y = 0\} < \Pr\{\boldsymbol{\mathcal{S}} \geq s\}$.

[53] In this case, we have $\Pr\{Y = 0 \mid \boldsymbol{\mathcal{S}} \geq s\} > \Pr\{Y = 0\}$.

**Remark 18** *The performance and selection curves are related as follows*[54]*:*

$$\mathcal{S}(x) = x\mathcal{P}(x)$$

The discriminant curve is the parametric curve $y = \mathcal{D}(x)$ defined by:

$$\mathcal{D}(x) = g_1\left(g_0^{-1}(x)\right)$$

where:

$$g_y(s) = \Pr\{\boldsymbol{\mathcal{S}} \geq s \mid Y = y\}$$

It represents the proportion of good risks in the selected population with respect to the proportion of bad risks in the selected population. The score is said to be discriminant if the curve $y = \mathcal{D}(x)$ is located above the bisecting line $y = x$.

**Some properties** We first notice that the previous parametric curves do not depend on the probability distribution of the score $\boldsymbol{\mathcal{S}}$, but only on the ranking of the observations. They are then invariant if we apply an increasing function to the score. Gouriéroux (1992) also established the following properties:

1. the performance curve (respectively, the selection curve) is located below the line $y = 1$ (respectively, the bisecting line $y = x$) if and only if $\operatorname{cov}(f(Y), g(\boldsymbol{\mathcal{S}})) \geq 0$ for any increasing functions $f$ and $g$;
2. the performance curve is increasing if and only if:

   $$\operatorname{cov}(f(Y), g(\boldsymbol{\mathcal{S}}) \mid \boldsymbol{\mathcal{S}} \geq s) \geq 0$$

   for any increasing functions $f$ and $g$, and any threshold level $s$;
3. the selection curve is convex if and only if $\mathbb{E}[f(Y) \mid \boldsymbol{\mathcal{S}} = s]$ is increasing with respect to the threshold level $s$ for any increasing function $f$.

**Remark 19** *The first property is the least restrictive. It allows us to verify that the score $\boldsymbol{\mathcal{S}}$ is better than a random score. We can show that* (3) ⇒ (2) ⇒ (1)*. The last property is then the most restrictive.*

A score is perfect or optimal if there is a threshold level $s^\star$ such that $\Pr\{Y = 1 \mid \boldsymbol{\mathcal{S}} \geq s^\star\} = 1$ and $\Pr\{Y = 0 \mid \boldsymbol{\mathcal{S}} < s^\star\} = 1$. It separates the population between good and bad risks. Graphically, the selection curve of a perfect score is equal to:

$$y = \mathbb{1}\{x > \Pr\{Y = 1\}\} \cdot \left(1 + \frac{x - 1}{\Pr\{Y = 0\}}\right)$$

[54] We have:

$$\begin{aligned}
\Pr\{\boldsymbol{\mathcal{S}} \geq s \mid Y = 0\} &= \frac{\Pr\{\boldsymbol{\mathcal{S}} \geq s, Y = 0\}}{\Pr\{Y = 0\}} \\
&= \Pr\{\boldsymbol{\mathcal{S}} \geq s\} \cdot \frac{\Pr\{\boldsymbol{\mathcal{S}} \geq s, Y = 0\}}{\Pr\{\boldsymbol{\mathcal{S}} \geq s\}\Pr\{Y = 0\}} \\
&= \Pr\{\boldsymbol{\mathcal{S}} \geq s\} \cdot \frac{\Pr\{Y = 0 \mid \boldsymbol{\mathcal{S}} \geq s\}}{\Pr\{Y = 0\}}
\end{aligned}$$

Using the relationship $\mathcal{S}(x) = x\mathcal{P}(x)$, we deduce that the performance curve of a perfect score is given by:

$$y = \mathbb{1}\{x > \Pr\{Y = 1\}\} \cdot \left(\frac{x - \Pr\{Y = 1\}}{x \cdot \Pr\{Y = 0\}}\right)$$

For the discriminant curve, a perfect score satisfies $\mathcal{D}(x) = 1$. When the score is random, we have $\mathcal{S}(x) = \mathcal{D}(x) = x$ and $\mathcal{P}(x) = 1$. In Figure 2.23, we have reported the performance, selection and discriminant curves of a given score $S$. We also show the curves obtained with an optimal (or perfect) score and a random score. A score must be located in the area between the curve computed with a random score and the curve computed with a perfect score, except if the score ranks the observations in a worst way than a random score.

Gouriéroux (1992) also established two properties for comparing two scores $\boldsymbol{\mathcal{S}}_1$ and $\boldsymbol{\mathcal{S}}_2$:

- the score $\boldsymbol{\mathcal{S}}_1$ is more performing on the population $P_1$ than the score $S_2$ on the population $P_2$ if and only if the performance (or selection) curve of $(\boldsymbol{\mathcal{S}}_1, P_1)$ is below the performance (or selection) curve of $(\boldsymbol{\mathcal{S}}_2, P_2)$;
- the score $\boldsymbol{\mathcal{S}}_1$ is more discriminatory on the population $P_1$ than the score $\boldsymbol{\mathcal{S}}_2$ on the population $P_2$ if and only if the discriminant curve of $(\boldsymbol{\mathcal{S}}_1, P_1)$ is above the discriminant curve of $(\boldsymbol{\mathcal{S}}_2, P_2)$.

Figure 2.24 illustrates the case where the score $\boldsymbol{\mathcal{S}}_1$ is better than the score $\boldsymbol{\mathcal{S}}_2$. However, the order is only partial. Most of the time, the two scores cannot be globally compared. An example is provided in Figure 2.25. The second score is not very good to distinguish good and bad risks when it takes small values, but it is close to a perfect score when it takes high values.

Figure 2.23: Performance, selection and discriminant curves

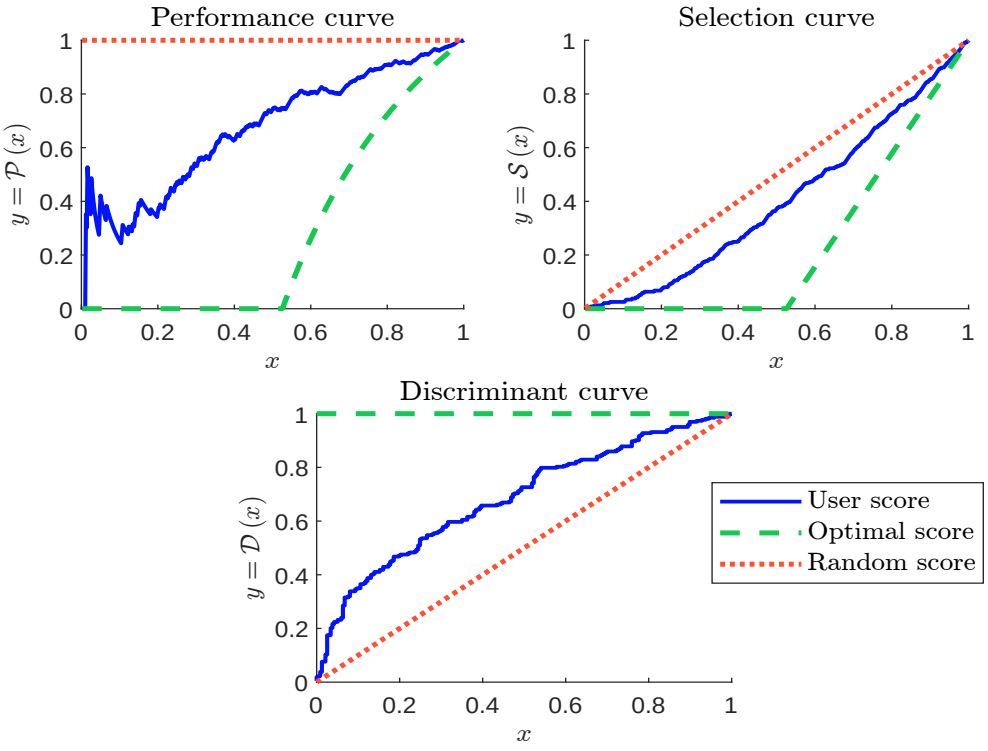

Figure 2.24: The score $S_1$ is better than the score $S_2$

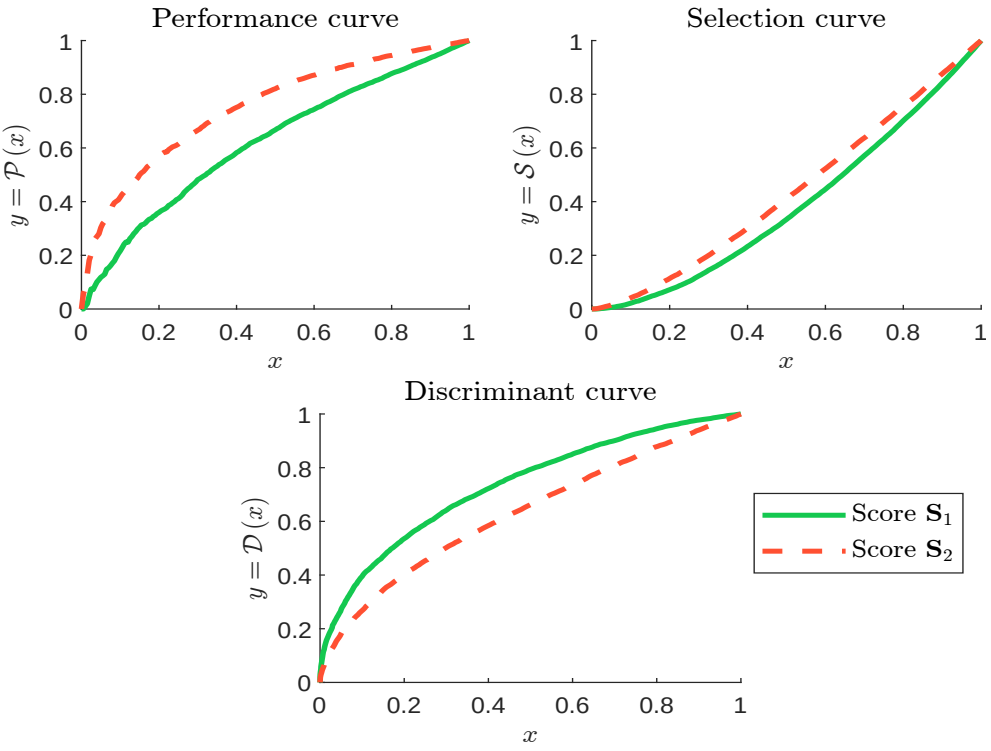


Figure 2.25: Illustration of the partial ordering between two scores

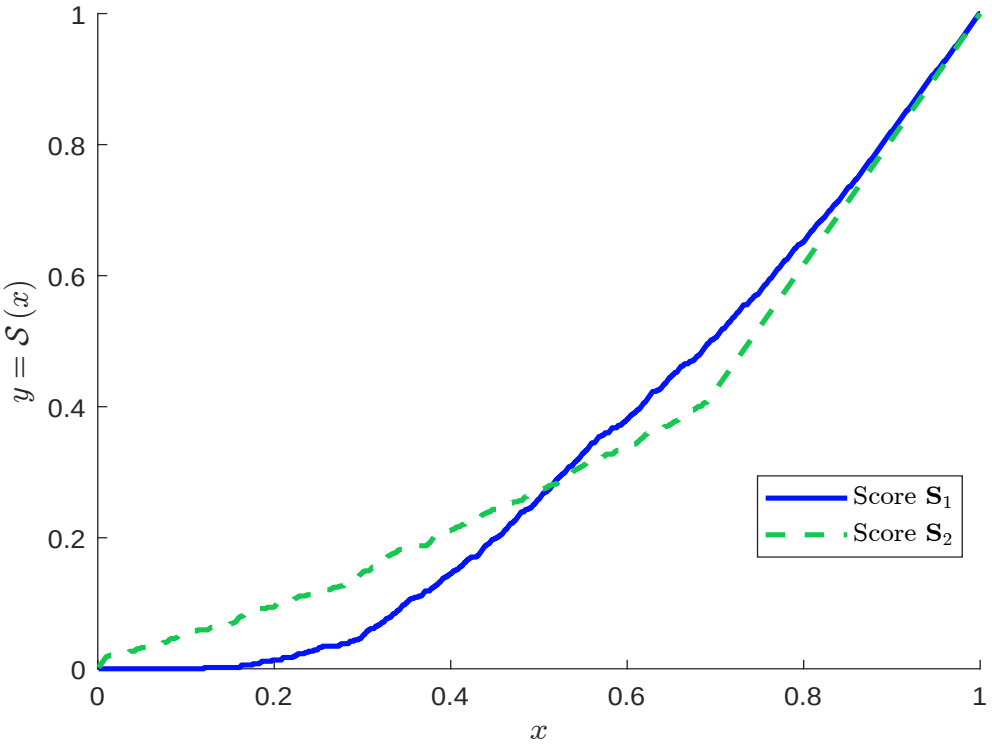

### Statistical methods

Since the quantitative tools for comparing two scores are numerous, we focus on two non-parametric measures: the Kolmogorov-Smirnov test and the Gini coefficient.

**Kolmogorov-Smirnov test** We consider the cumulative distribution functions:

$$\mathbf{F}_0(s) = \Pr\{\boldsymbol{\mathcal{S}} \leq s \mid Y = 0\}$$

and:

$$\mathbf{F}_1(s) = \Pr\{\boldsymbol{\mathcal{S}} \leq s \mid Y = 1\}$$

The score $\boldsymbol{\mathcal{S}}$ is relevant if we have the stochastic dominance order $\mathbf{F}_0 \succ \mathbf{F}_1$. In this case, the score quality is measured by the Kolmogorov-Smirnov statistic:

$$\text{KS} = \max_s |\mathbf{F}_0(s) - \mathbf{F}_1(s)|$$

It takes the value 1 if the score is perfect. The KS statistic may be used to verify that the score is not random. We then test the assumption $\mathcal{H}_0 : \text{KS} = 0$ by using the tabulated critical values[55]. In Figure 2.26, we give an example with 5 000 observations. The KS statistic is equal to 36%, which implies that $\mathcal{H}_0$ is rejected at the confidence level 1%.

### Gini coefficient

**The Lorenz curve** The Gini coefficient is the statistic, which is the most used for measuring the performance of a score. It is related to the concept of Lorenz curve, which is a graphical representation of the concentration. Let $X$ and $Y$ be two random variables. The Lorenz curve $y = \mathcal{L}(x)$ is the parametric curve defined by:

$$\begin{cases} x = \Pr\{X \leq x\} \\ y = \Pr\{Y \leq y \mid X \leq x\} \end{cases}$$

In economics, $x$ represents the proportion of individuals that are ranked by income while $y$ represents the proportion of income. In this case, the Lorenz curve is a graphical representation of the distribution of income and is used for illustrating inequality of the wealth distribution between individuals. For example, we observe that 70% of individuals have only 34% of total income in Figure 2.27.

**Definition of the Gini coefficient** The Lorenz curve has two limit cases. If the wealth is perfectly concentrated, one individual holds 100% of the total wealth. If the wealth is perfectly allocated between all the individuals, the corresponding Lorenz curve is the bisecting line. We define the Gini coefficient by:

$$\mathcal{G}ini(\mathcal{L}) = \frac{A}{A+B}$$

[55] The critical values at the 5% confidence level are equal to:

| $n$ | 10 | 50 | 100 | 500 | 5000 |
|---|---|---|---|---|---|
| CV | 40.9% | 18.8% | 13.4% | 6.0% | 1.9% |

More generally, the null hypothesis is rejected at the confidence level $\alpha$ if we have:

$$\text{KS} > \sqrt{\frac{1}{2n} \ln\left(\frac{2}{\alpha}\right)}$$

Figure 2.26: Comparison of the distributions $\mathbf{F}_0(s)$ and $\mathbf{F}_1(s)$

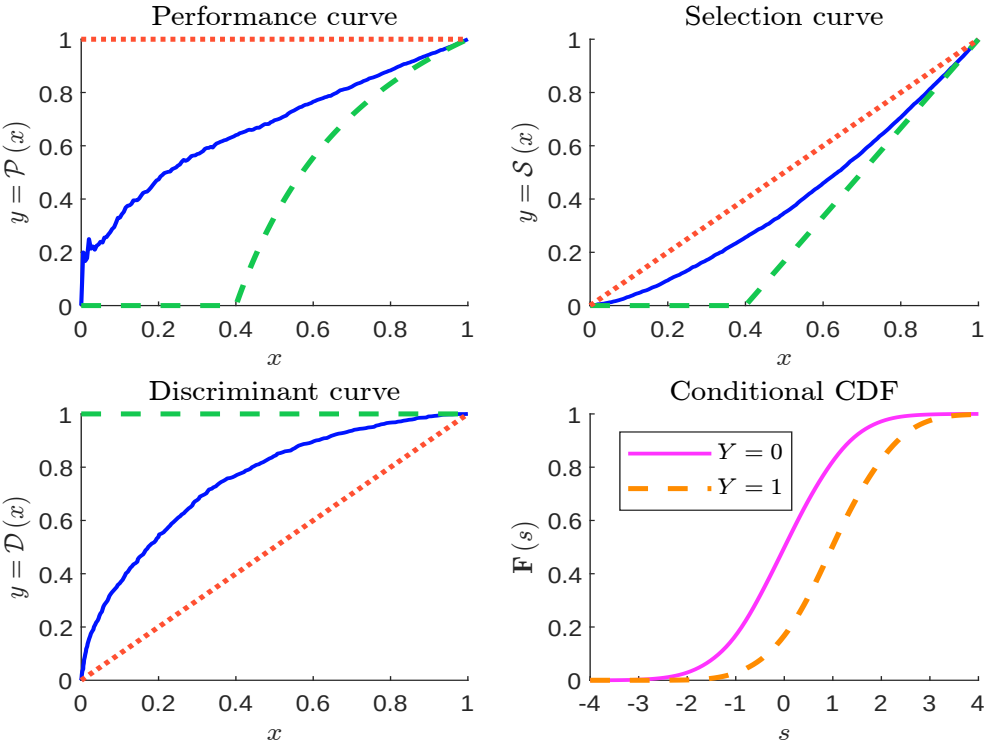


Figure 2.27: An example of Lorenz curve

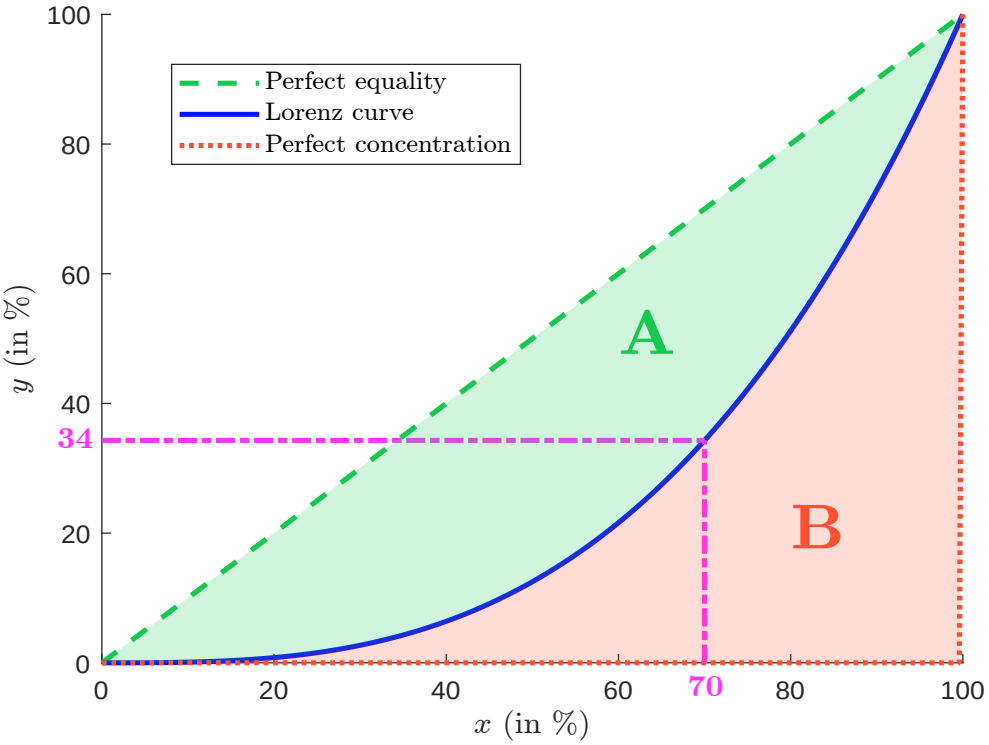

where $A$ is the area between the Lorenz curve and the curve of perfect equality, and $B$ is the area between the curve of perfect concentration and the Lorenz curve. By construction, we have $0 \leq \mathcal{G}ini(\mathcal{L}) \leq 1$. The Gini coefficient is equal to zero in the case of perfect equality and one in the case of perfect concentration. We have:

$$\mathcal{G}ini(\mathcal{L}) = 1 - 2\int_0^1 \mathcal{L}(x)\,\mathrm{d}x$$

**Application to scoring** We can interpret the selection curve as a Lorenz curve. We recall that $\mathbf{F}(s) = \Pr\{\boldsymbol{\mathcal{S}} \leq s\}$, $\mathbf{F}_0(s) = \Pr\{\boldsymbol{\mathcal{S}} \leq s \mid Y = 0\}$ and $\mathbf{F}_1(s) = \Pr\{\boldsymbol{\mathcal{S}} \leq s \mid Y = 1\}$. The selection curve is defined by the following parametric coordinates:

$$\begin{cases} x(s) = 1 - \mathbf{F}(s) \\ y(s) = 1 - \mathbf{F}_0(s) \end{cases}$$

The selection curve measures the capacity of the score for not selecting bad risks. We could also build the Lorenz curve that measures the capacity of the score for selecting good risks:

$$\begin{cases} x(s) = \Pr\{\boldsymbol{\mathcal{S}} \geq s\} = 1 - \mathbf{F}(s) \\ y(s) = \Pr\{\boldsymbol{\mathcal{S}} \geq s \mid Y = 1\} = 1 - \mathbf{F}_1(s) \end{cases}$$

It is called the precision curve. Another popular graphical tool is the receiver operating characteristic (or ROC) curve (Powers, 2011), which is defined by:

$$\begin{cases} x(s) = \Pr\{\boldsymbol{\mathcal{S}} \geq s \mid Y = 0\} = 1 - \mathbf{F}_0(s) \\ y(s) = \Pr\{\boldsymbol{\mathcal{S}} \geq s \mid Y = 1\} = 1 - \mathbf{F}_1(s) \end{cases}$$

An example for a given score $\boldsymbol{\mathcal{S}}$ is provided in Figure 2.28. For all the three curves, we can calculate the Gini coefficient. Since the precision and ROC curves are located above the bisecting line, the Gini coefficient associated to the Lorenz curve $\mathcal{L}$ becomes[56]:

$$\mathcal{G}ini(\mathcal{L}) = 2\int_0^1 \mathcal{L}(x)\,\mathrm{d}x - 1$$

The Gini coefficient of the score $\boldsymbol{\mathcal{S}}$ is then computed as follows:

$$\mathcal{G}ini^\star(\boldsymbol{\mathcal{S}}) = \frac{\mathcal{G}ini(\mathcal{L})}{\mathcal{G}ini(\mathcal{L}^\star)}$$

where $\mathcal{L}^\star$ is the Lorenz curve associated to the perfect score.

**Remark 20** *The Gini coefficient is not necessarily the same for the three curves. However, if the population is homogeneous, we generally obtain very similar figures*[57].

[56] An alternative to the Gini coefficient is the AUC measure, which corresponds to the area under the ROC curve. However, they give the same information since they are related by the equation:

$$\mathcal{G}ini(\text{ROC}) = 2 \times \text{AUC}(\text{ROC}) - 1$$

[57] For instance, we obtain the following results with the score $\boldsymbol{\mathcal{S}}$ that has been used in Figure 2.28:

| Curve | $\mathcal{G}ini(\mathcal{L})$ | $\mathcal{G}ini(\mathcal{L}^\star)$ | $\mathcal{G}ini^\star(S)$ |
|---|---|---|---|
| Selection | 20.41% | 40.02% | 51.01% |
| Precision | 30.62% | 59.98% | 51.05% |
| ROC | 51.03% | 100.00% | 51.03% |

Figure 2.28: Selection, precision and ROC curves

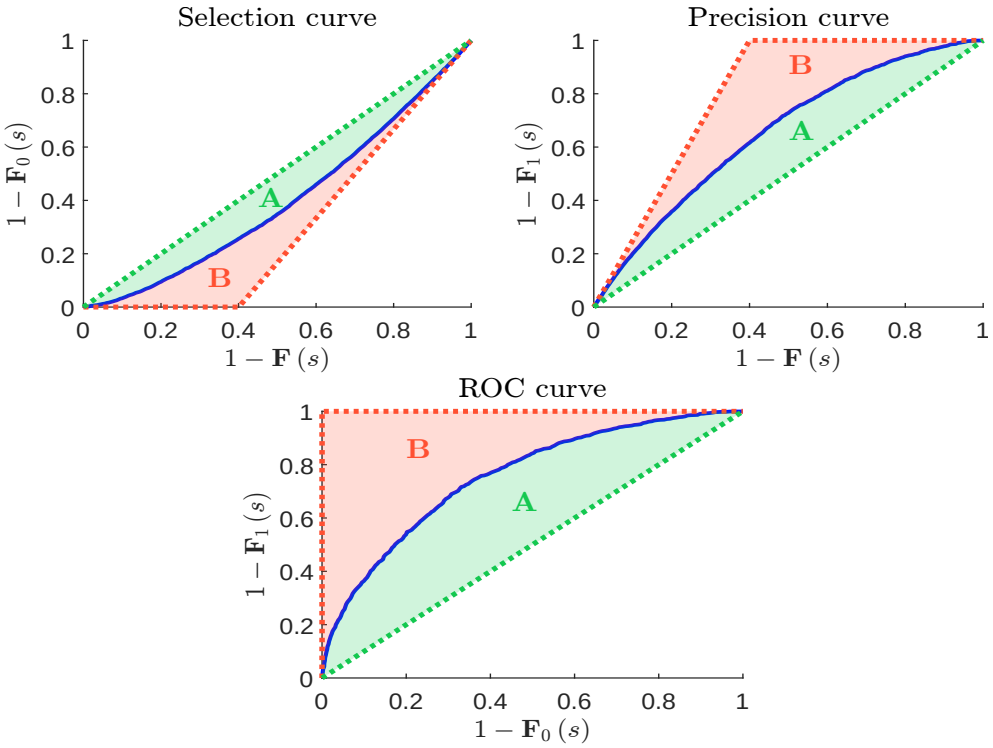


**Choice of the optimal cut-off** The choice of the optimal cut-off $s^\star$ depends on the objective function. For instance, we can calibrate $s^\star$ in order to achieve a minimum universe size of ESG assets. We can also fix a given selection rate. From a statistical point of view, we must distinguish the construction of the scoring model and the decision rule. In statistical learning, we generally consider three datasets: the training set, the validation set and the test set. The training set is used for calibrating the model and its parameters whereas the validation set helps to avoid overfitting. But the decision rule is based on the test set.

**Confusion matrix** A confusion matrix is a special case of contingency matrix. Each row of the matrix represents the frequency in a predicted class while each column represents the frequency in an actual class. Using the test set, it takes the following form:

| | $Y = 0$ | $Y = 1$ |
|---|---|---|
| $\boldsymbol{\mathcal{S}} < s$ | $n_{0,0}$ | $n_{0,1}$ |
| $\boldsymbol{\mathcal{S}} \geq s$ | $n_{1,0}$ | $n_{1,1}$ |
| | $n_0 = n_{0,0} + n_{1,0}$ | $n_1 = n_{0,1} + n_{1,1}$ |

where $n_{i,j}$ represents the number of observations of the cell $(i, j)$. The interpretation of the confusion matrix is given in Table 2.16. The cells $(\boldsymbol{\mathcal{S}} < s, Y = 0)$ and $(\boldsymbol{\mathcal{S}} \geq s, Y = 1)$ correspond to observations that are well-classified: true negative (TN) and true positive (TP). The cells $(\boldsymbol{\mathcal{S}} \geq s, Y = 0)$ and $(\boldsymbol{\mathcal{S}} < s, Y = 1)$ correspond to two types of errors:

1. A false positive (FP) can induce a future loss, because the risk can materialize: this is a type I error;

2. A false negative (FN) potentially corresponds to a an opportunity cost: this is a type II error.

Table 2.16: Interpretation of the confusion matrix

| | $Y = 0$ | $Y = 1$ |
|---|---|---|
| $\mathcal{S} < s$ | It is rejected and it is a bad risk (true negative) | It is rejected, but it is a good risk (false negative) |
| $\mathcal{S} \geq s$ | It is accepted, but it is a bad risk (false positive) | It is accepted and it is a good risk (true positive) |
| | (negative) | (positive) |

**Classification ratios** Binary classification defines many metrics for measuring the performance of the classifier[58] (Fawcett, 2006):

$$\begin{aligned}
&\text{True Positive Rate} && \text{TPR} = \frac{\text{TP}}{\text{TP} + \text{FN}} \\
&\text{False Negative Rate} && \text{FNR} = \frac{\text{FN}}{\text{FN} + \text{TP}} = 1 - \text{TPR} \\
&\text{True Negative Rate} && \text{TNR} = \frac{\text{TN}}{\text{TN} + \text{FP}} \\
&\text{False Positive Rate} && \text{FPR} = \frac{\text{FP}}{\text{FP} + \text{TN}} = 1 - \text{TNR}
\end{aligned}$$

The true positive rate (TPR) is also known as the sensitivity or the recall. It measures the proportion of real good risks that are correctly predicted good risk. Fawcett (2006) also defines the precision or the positive predictive value (PPV):

$$\text{PPV} = \frac{\text{TP}}{\text{TP} + \text{FP}}$$

It measures the proportion of predicted good risks that are correctly real good risk. Besides these metrics, statisticians also use three generic metrics:

1. The accuracy considers the classification of both negatives and positives:

$$\text{ACC} = \frac{\text{TP} + \text{TN}}{\text{P} + \text{N}} = \frac{\text{TP} + \text{TN}}{\text{TP} + \text{FN} + \text{TN} + \text{FP}}$$

2. The $F_1$ score is the harmonic mean of precision and sensitivity:

$$\begin{aligned}
F_1 &= \frac{2}{1/\text{precision} + 1/\text{sensitivity}} \\
&= \frac{2 \cdot \text{PPV} \cdot \text{TPR}}{\text{PPV} + \text{TPR}}
\end{aligned}$$

[58] We rewrite the confusion matrix as follows:

| | $Y = 0$ | $Y = 1$ |
|---|---|---|
| $\mathcal{S} < s$ | TN | FN |
| $\mathcal{S} \geq s$ | FP | TP |
| | $\text{N} = \text{TN} + \text{FP}$ | $\text{P} = \text{FN} + \text{TP}$ |

3. The $\phi$ coefficient or the Matthews correlation coefficient (MCC) is a measure of association between $\boldsymbol{\mathcal{S}}$ and $Y$:

$$\phi = \text{MCC} = \frac{\text{TP} \cdot \text{TN} - \text{FP} \cdot \text{FN}}{\sqrt{(\text{TP} + \text{FP}) \cdot (\text{TP} + \text{FN}) \cdot (\text{TN} + \text{FP}) \cdot (\text{TN} + \text{FN})}}$$

$\boldsymbol{\mathcal{S}}$ and $Y$ are positively associated if most of the observations fall along the diagonal cells.

Table 2.17: Confusion matrix of three scoring systems and three cut-off values $s$

| Score | $s = 100$ | | $s = 200$ | | $s = 500$ | |
|---|---|---|---|---|---|---|
| $\boldsymbol{\mathcal{S}}_1$ | 386 | 616 | 698 | 1 304 | 1 330 | 3 672 |
| | 1 614 | 7 384 | 1 302 | 6 696 | 670 | 4 328 |
| $\boldsymbol{\mathcal{S}}_2$ | 372 | 632 | 700 | 1 304 | 1 386 | 3 616 |
| | 1 628 | 7 368 | 1 300 | 6 696 | 614 | 4 384 |
| $\boldsymbol{\mathcal{S}}_3$ | 382 | 616 | 656 | 1 344 | 1 378 | 3 624 |
| | 1 618 | 7 384 | 1 344 | 6 656 | 622 | 4 376 |
| Perfect | 1 000 | 0 | 2 000 | 0 | 2 000 | 3 000 |
| | 1 000 | 8 000 | 0 | 8 000 | 0 | 5 000 |

**Example 7** *We consider three scoring systems that have been calibrated on a training set. These systems produce a score between* 0 *and* 1 000*. A low value predicts a bad risk while a high value predicts a good risk. In order to calibrate the cut-off, we consider a test set, which is composed of* 10 000 *new observations. In Table 2.17, we report the confusion matrix of each scoring system for different cut-off values (*100*,* 200 *and* 500*).*

Table 2.18: Binary classification ratios (in %) of the three scoring systems

| Score | $s$ | TPR | FNR | TNR | FPR | PPV | ACC | $F_1$ |
|---|---|---|---|---|---|---|---|---|
| | 100 | 92.3 | 7.7 | 19.3 | 80.7 | 82.1 | 77.7 | 86.9 |
| $\boldsymbol{\mathcal{S}}_1$ | 200 | 83.7 | 16.3 | 34.9 | 65.1 | 83.7 | 73.9 | 83.7 |
| | 500 | 54.1 | 45.9 | 66.5 | 33.5 | 86.6 | 56.6 | 66.6 |
| | 100 | 92.1 | 7.9 | 18.6 | 81.4 | 81.9 | 77.4 | 86.7 |
| $\boldsymbol{\mathcal{S}}_2$ | 200 | 83.7 | 16.3 | 35.0 | 65.0 | 83.7 | 74.0 | 83.7 |
| | 500 | 54.8 | 45.2 | 69.3 | 30.7 | 87.7 | 57.7 | 67.5 |
| | 100 | 92.3 | 7.7 | 19.1 | 80.9 | 82.0 | 77.7 | 86.9 |
| $\boldsymbol{\mathcal{S}}_3$ | 200 | 83.2 | 16.8 | 32.8 | 67.2 | 83.2 | 73.1 | 83.2 |
| | 500 | 54.7 | 45.3 | 68.9 | 31.1 | 87.6 | 57.5 | 67.3 |
| | 100 | 100.0 | 0.0 | 50.0 | 50.0 | 88.9 | 90.0 | 94.1 |
| Perfect | 200 | 100.0 | 0.0 | 100.0 | 0.0 | 100.0 | 100.0 | 100.0 |
| | 500 | 62.5 | 37.5 | 100.0 | 0.0 | 100.0 | 70.0 | 76.9 |
| Best | 100 | $\boldsymbol{\mathcal{S}}_1/\boldsymbol{\mathcal{S}}_3$ | $\boldsymbol{\mathcal{S}}_1/\boldsymbol{\mathcal{S}}_3$ | $\boldsymbol{\mathcal{S}}_1$ | $\boldsymbol{\mathcal{S}}_1$ | $\boldsymbol{\mathcal{S}}_1$ | $\boldsymbol{\mathcal{S}}_1$ | $\boldsymbol{\mathcal{S}}_1$ |
| scoring | 200 | $\boldsymbol{\mathcal{S}}_1/\boldsymbol{\mathcal{S}}_2$ | $\boldsymbol{\mathcal{S}}_1/\boldsymbol{\mathcal{S}}_2$ | $\boldsymbol{\mathcal{S}}_2$ | $\boldsymbol{\mathcal{S}}_2$ | $\boldsymbol{\mathcal{S}}_2$ | $\boldsymbol{\mathcal{S}}_2$ | $\boldsymbol{\mathcal{S}}_2$ |
| system | 500 | $\boldsymbol{\mathcal{S}}_2$ | $\boldsymbol{\mathcal{S}}_2$ | $\boldsymbol{\mathcal{S}}_2$ | $\boldsymbol{\mathcal{S}}_2$ | $\boldsymbol{\mathcal{S}}_2$ | $\boldsymbol{\mathcal{S}}_2$ | $\boldsymbol{\mathcal{S}}_2$ |

Using confusion matrices given in Table 2.17, we calculate the different classification ratios and report them in Table 2.18. In addition to the three scoring systems, we have also considered a

perfect score in order to show what the best value is for each classification ratio, and we indicate the best scoring system. We notice that it depends on the ratio and on the value of the cut-off. For instance, if we want to maximize the true positive ratio or minimize the false negative ratio, $\boldsymbol{\mathcal{S}}_1$ is the best scoring system for low value of $s$ while $\boldsymbol{\mathcal{S}}_2$ is better when $s$ is equal to 500. For the other ratios, $\boldsymbol{\mathcal{S}}_1$ seems to be the best scoring system when $s = 100$, otherwise $\boldsymbol{\mathcal{S}}_2$ dominates $\boldsymbol{\mathcal{S}}_1$ and $\boldsymbol{\mathcal{S}}_3$ when $s = 200$ or $s = 500$.

**Remark 21** *We recall that* $\mathbf{F}_0(s) = \Pr\{\boldsymbol{\mathcal{S}} \leq s \mid Y = 0\}$ *and* $\mathbf{F}_1(s) = \Pr\{\boldsymbol{\mathcal{S}} \leq s \mid Y = 1\}$. *We deduce that* $\text{TNR} = \mathbf{F}_0(s)$, $\text{FNR} = \mathbf{F}_1(s)$, $\text{FPR} = 1 - \mathbf{F}_0(s)$ *and* $\text{TPR} = 1 - \mathbf{F}_1(s)$. *Therefore, the ROC curve is the parametric curve, where the x-coordinates are the false positive rates and the y-coordinates are the true positive rates. Generally, we note* $\alpha$ *and* $\beta$ *the type I and II errors. We may also interpret the ROC curve as the relationship of* $1 - \beta(s)$ *with respect to* $\alpha(s)$.

**Backtesting of unsupervised scoring systems**

To understand how to implement a backtesting procedure, we take the example of credit scoring models. Let $\boldsymbol{\mathcal{S}}_i(t)$ be the credit score of individual/company $i$ at time $t$. The response variable is the default indicator variable $Y_i(t)$:

$$Y_i(t) = \mathbb{1}\{\tau_i \geq t + \delta\} = \mathbb{1}\{D_i(t + \delta) = 0\}$$

where $\tau_i$ and $D_i$ are the default time and the default indicator function, and $\delta$ is the time horizon (*e.g.*, one year). In this problem, $\boldsymbol{\mathcal{S}}_i(t)$ is used to predict the default time $\tau_i$ and the decision process is:

$$\begin{cases} \boldsymbol{\mathcal{S}}_i(t) \leq s^\star \Rightarrow i \text{ is a bad risk} \Rightarrow Y_i(t) = 0 \\ \boldsymbol{\mathcal{S}}_i(t) > s^\star \Rightarrow i \text{ is not a bad risk} \Rightarrow Y_i(t) = 1 \end{cases}$$

The calibration problem for the credit scoring model is therefore:

$$\Pr\{Y_i(t) = 0\} = f(\boldsymbol{\mathcal{S}}_i(t))$$

where $f$ is an increasing function. We obtain a binary choice model that can be calibrated using discriminant analysis, clustering methods or logit/probit regression. The backtesting procedure consists of verifying that $\hat{Y}_i(t) = \mathbb{1}\{\boldsymbol{\mathcal{S}}_i(t) > s^\star\}$ is a good estimator of $Y_i(t)$. Building a backtesting procedure for ESG scores then requires defining an ad hoc response variable.

**Static analysis** Let $\boldsymbol{\mathcal{S}}_i(t)$ be the ESG score of company $i$ at time $t$. The endogenous response variable can be defined as follows:

| Scoring system | Risk class | $Y_i(t)$ |
|---|---|---|
| Best-in-class oriented | Good risk | $\mathbb{1}\{\boldsymbol{\mathcal{S}}_i(t + \delta) \geq s^\star\}$ |
| Worst-in-class oriented | Bad risk | $\mathbb{1}\{\boldsymbol{\mathcal{S}}_i(t + \delta) \leq s^\star\}$ |

where $s^\star$ is the best-in-class/worst-in-class threshold to determine. $Y_i(t)$ is endogenous because it depends on the future value of the score. Here, the backtesting procedure can be seen as a stability test of the ESG scoring system. An alternative is to use an exogenous response variable based on controversies. For example, to predict bad risks, we can use the binary response $Y_i(t) = \mathbb{1}\{\mathcal{C}_i(t + \delta) \geq 0\}$ where $\mathcal{C}_i(t)$ is the controversy index.

**Dynamic analysis** The static analysis can be extended to the dynamic case. Instead of using the ESG score, we consider the past momentum $\mathcal{M}_i(t, h) = \boldsymbol{\mathcal{S}}_i(t) - \boldsymbol{\mathcal{S}}_i(t - h)$ where $h$ is typically the year, while the response variable is based on the future momentum $\boldsymbol{\mathcal{S}}_i(t + \delta) - \boldsymbol{\mathcal{S}}_i(t)$.

**Illustration using an ESG scoring system** We consider the scoring system of an ESG rating agency. We normalize the published scores in order to obtain $z$-scores and apply the backtesting procedure to these latter numbers. We consider four risk classes:

| Risk class | Definition | $Y_i(t)$ |
|---|---|---|
| Worst-in-class | $\boldsymbol{\mathcal{S}}_i(t) \leq \hat{\mathbf{F}}^{-1}(20\%)$ | $\mathbb{1}\{\boldsymbol{\mathcal{S}}_i(t+\delta) \leq s^\star\}$ |
| Bad risk | $\boldsymbol{\mathcal{S}}_i(t) \leq \bar{\boldsymbol{\mathcal{S}}}$ | $\mathbb{1}\{\boldsymbol{\mathcal{S}}_i(t+\delta) \leq s^\star\}$ |
| Good risk | $\boldsymbol{\mathcal{S}}_i(t) \geq \bar{\boldsymbol{\mathcal{S}}}$ | $\mathbb{1}\{\boldsymbol{\mathcal{S}}_i(t+\delta) \geq s^\star\}$ |
| Best-in-class | $\boldsymbol{\mathcal{S}}_i(t) \geq \hat{\mathbf{F}}^{-1}(80\%)$ | $\mathbb{1}\{\boldsymbol{\mathcal{S}}_i(t+\delta) \geq s^\star\}$ |

where $\hat{\mathbf{F}}$ is the empirical distribution of the score and $\bar{\boldsymbol{\mathcal{S}}}$ is the average of scores. For each risk class, we compute the classification ratios ACC, $F_1$, and $\phi$ and the Shannon entropy $\mathcal{I}(\boldsymbol{\mathcal{S}} \cap Y)$ with respect to the cut-off value $s$. The results, expressed in %, are shown in Figures 2.29 to 2.32 when we consider the MSCI World and MSCI EM universes.

Table 2.19: Optimal cut-off $s^\star$ (MSCI World)

| Risk class | $\delta = 3$ months | | | | $\delta = 12$ months | | | |
|---|---|---|---|---|---|---|---|---|
| | ACC | $F_1$ | $\phi$ | $\mathcal{I}(\boldsymbol{\mathcal{S}} \cap Y)$ | ACC | $F_1$ | $\phi$ | $\mathcal{I}(\boldsymbol{\mathcal{S}} \cap Y)$ |
| Worst-in-class | −0.91 | −0.61 | −0.68 | −0.58 | −0.96 | −0.58 | −0.67 | −0.54 |
| Bad risk | −0.01 | 0.18 | 0.02 | 0.02 | 0.01 | 0.24 | 0.04 | 0.05 |
| Good risk | −0.02 | −0.18 | 0.01 | 0.02 | −0.01 | −0.20 | 0.03 | 0.04 |
| Best-in-class | 1.05 | 0.79 | 0.85 | 0.77 | 1.08 | 0.76 | 0.83 | 0.72 |

Table 2.20: Optimal cut-off $s^\star$ (MSCI EM)

| Risk class | $\delta = 3$ months | | | | $\delta = 12$ months | | | |
|---|---|---|---|---|---|---|---|---|
| | ACC | $F_1$ | $\phi$ | $\mathcal{I}(\boldsymbol{\mathcal{S}} \cap Y)$ | ACC | $F_1$ | $\phi$ | $\mathcal{I}(\boldsymbol{\mathcal{S}} \cap Y)$ |
| Worst-in-class | −1.87 | −1.19 | −1.29 | −1.15 | −2.00 | −1.17 | −1.30 | −1.12 |
| Bad risk | 0.13 | 0.23 | −0.03 | −0.10 | 0.16 | 0.28 | −0.05 | −0.14 |
| Good risk | 0.13 | −0.15 | −0.03 | −0.14 | 0.16 | −0.22 | −0.05 | −0.24 |
| Best-in-class | 0.48 | 0.14 | 0.22 | 0.11 | 0.56 | 0.13 | 0.24 | 0.11 |

We can then estimate the optimal cut-off $s^\star$, which is the value $s$ that maximizes the backtesting metric. Results are given in Tables 2.19 and 2.20. Theoretically, the optimal cut-off is $s^\star = \Phi^{-1}(20\%) = -0.8416$ for the worst-in-class category, $s^\star = \mathbb{E}[\mathcal{N}(0,1)] = 0$ for the bad-risk and good-risk categories and $s^\star = \Phi^{-1}(80\%) = 0.8416$ for the best-in-class category, because the backtesting procedure concerns $z$-scores. For the MSCI World universe, the estimated cut-offs are not that far from the theoretical cut-offs. Moreover, we do not observe a large difference between the three-month and the twelve-month horizons. For the MSCI World universe, we face two problems. First, the backtesting of the worst-in-class category implies an optimal cut-off that is well below the theoretical cut-off, meaning that the worst-in-class universe is not adequately defined. Second, the scoring system is not really able to discriminate between bad risk and worst-in-class categories because the optimal cut-off for the latter category is close to zero.

**Remark 22** *The previous example illustrates that the robustness of an ESG scoring system can vary depending on the investment universe.*

Figure 2.29: Backtesting of ESG scores (worst-in-class & bad risk, MSCI World)

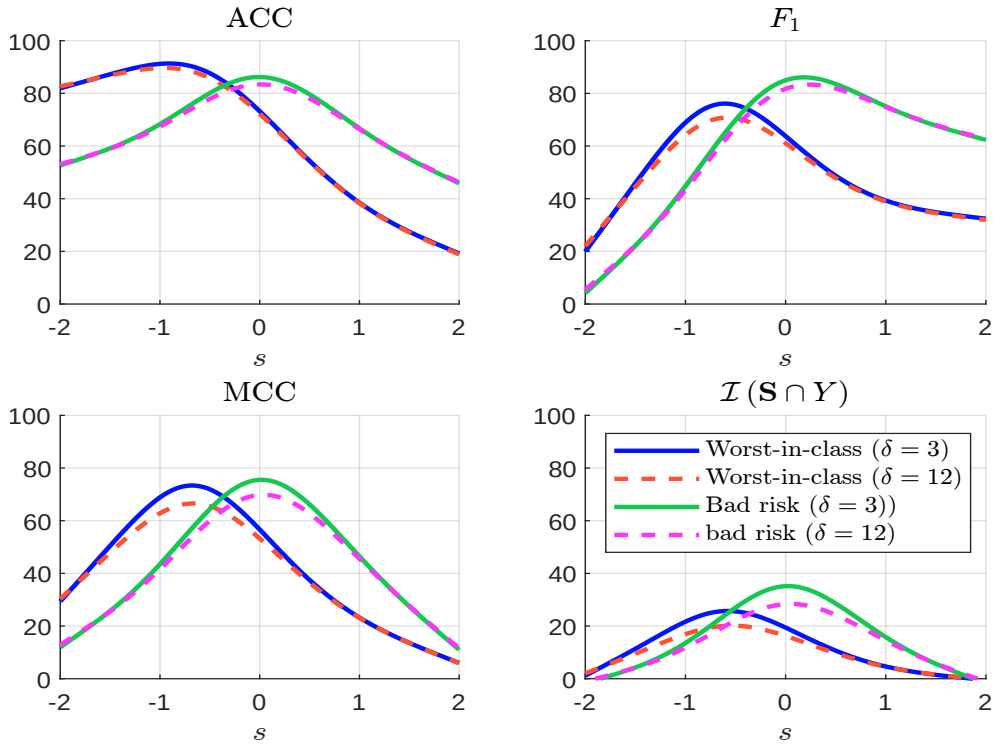


Figure 2.30: Backtesting of ESG scores (best-in-class & good risk, MSCI World)

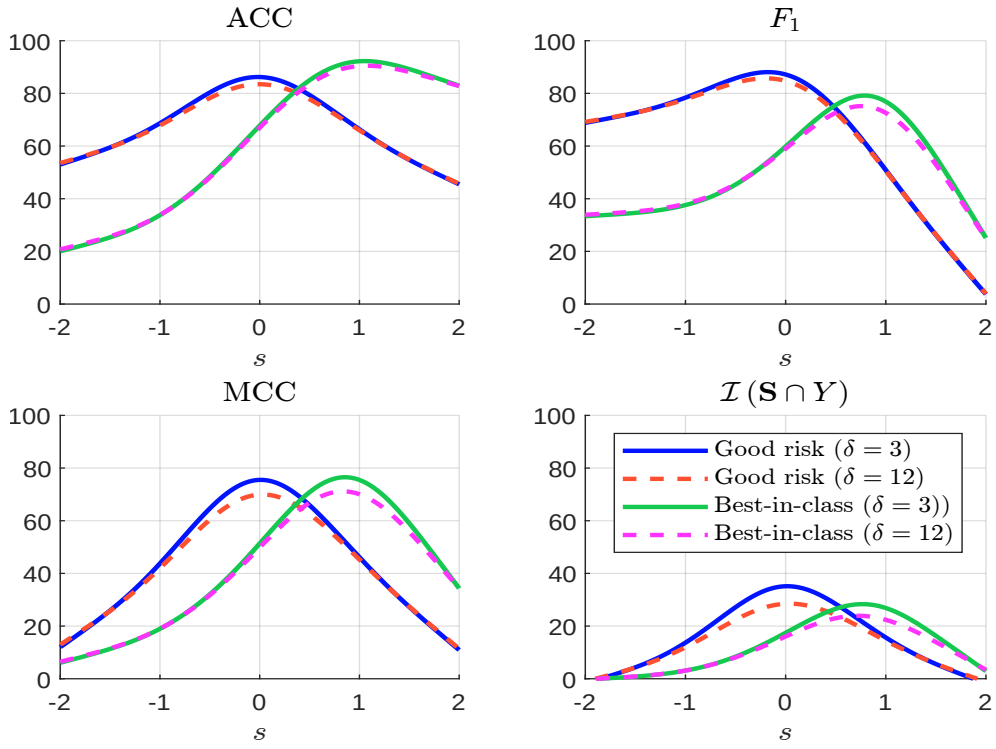

Figure 2.31: Backtesting of ESG scores (worst-in-class & bad risk, MSCI EM)

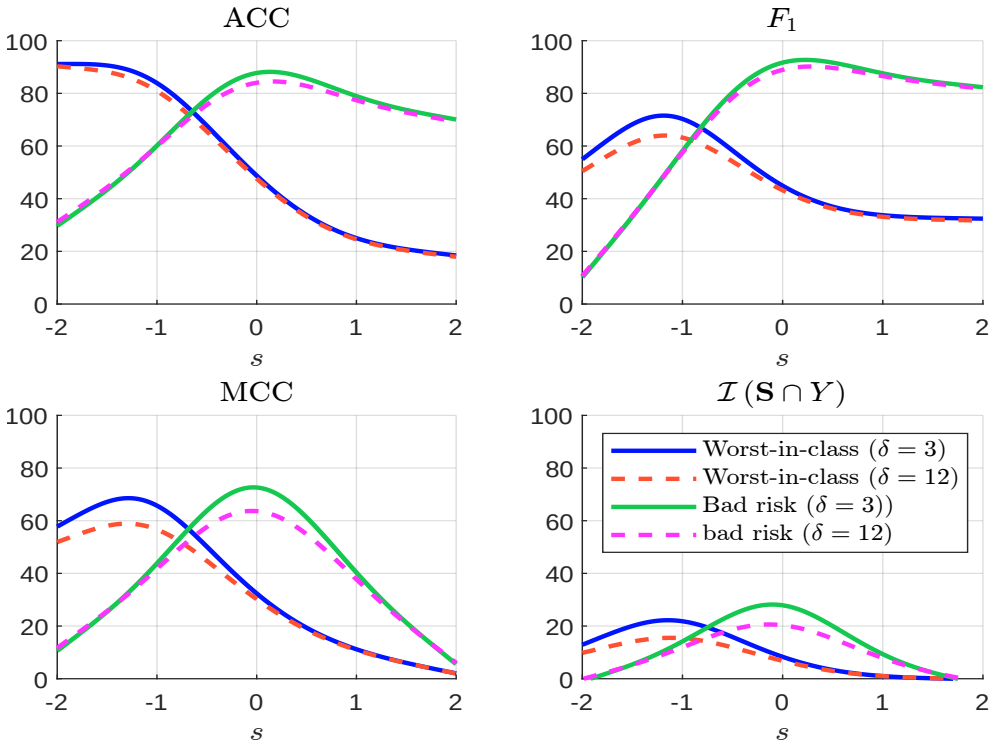


Figure 2.32: Backtesting of ESG scores (best-in-class & good risk, MSCI EM)

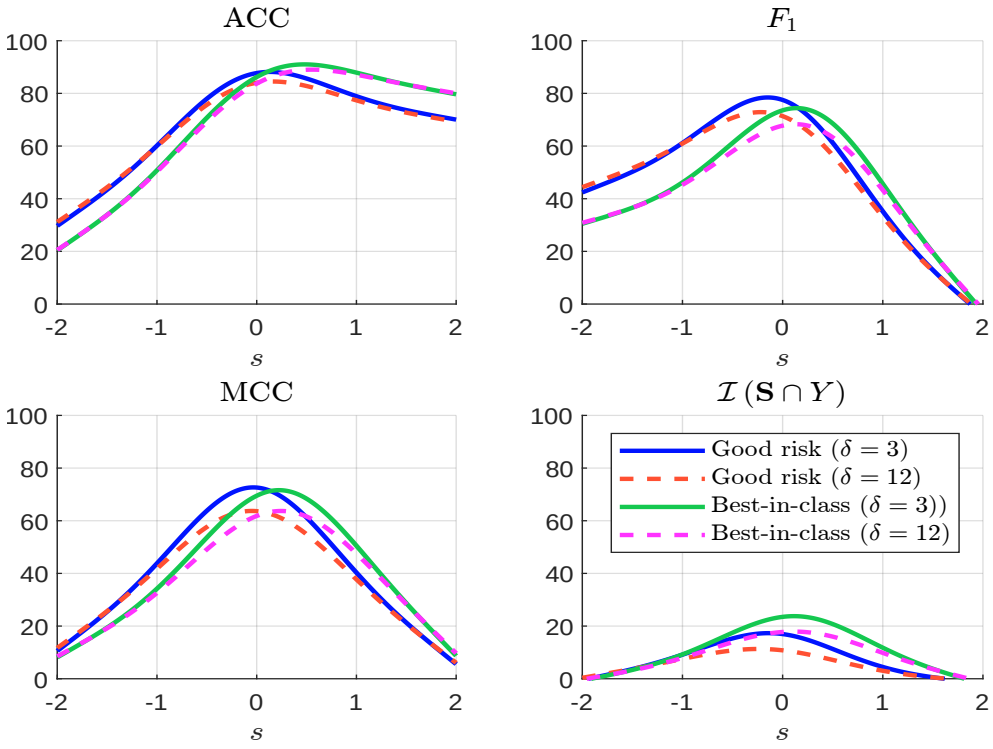

## 2.3 Rating system

As we have seen, a scoring model provides an automatic and statistical score. It is a pure quantitative approach. There may be the intervention of an analyst, but it is limited to data quality checks or forcing of input data[59]. A rating (or a notation) is different from a score, because it implies a quality scale. Since it implies a value judgement, a rating is generally produced by an analyst. For example, this is the case of credit ratings, which are made by an analyst who takes into account several quantitative scores, qualitative data, private and meeting information. Nevertheless, the balance between quantitative and qualitative judgements depends on the type of issuers. For retail borrowers, the rating is mainly explained by the scoring model. For blue chip and mega-cap companies, the rating highly depends on the qualitative assessment of the credit risk. If we consider ESG risk, the rating process shares similar patterns. The ESG score is generally the key component of the ESG rating. It is validated by an extra-financial analyst and it may be *forced* based on his qualitative information and experience. This explains why extra-financial analysis is organized with respect to sectors. An ESG analyst, who is specialized in a given sector, can then have a better view of all the ratings produced for this sector. This is particularly true for the strategic sectors: automobiles, coal, ciment, oil & gas, fertilizers & agricultural chemicals, utilities, etc. Nevertheless, there is a strong difference between credit and ESG rating processes from an investor viewpoint. Indeed, the number of rated companies for ESG analysis bears no comparison with the number of rated companies for credit analysis, because only few corporates have access to bond markets. On the contrary, a comprehensive ESG rating system must encompass all the securities and assets, notably all listed corporates and some private companies. In this context, the impact and the implication of the extra-financial analyst decrease with the firm size. This is why there is a strong small size bias in ESG rating systems.

### 2.3.1 Definition

ESG rating systems are based on the terminology of credit ratings (Box 2.4). For example, MSCI (2022) uses a 7-grade rating scale based on the grades AAA, AA, A, BBB, BB, B and CCC (Table 2.21). The number of grades, the rating symbols (letter, numeric) and the ordering of the system (low/worst rating to high/best rating vs. high/best to low/worst rating) differs from one provider to another provider[60]:

- Amundi: A (high), B,... to G (low) — 7-grade scale
- FTSE Russell: 0 (low), 1,... to 5 (high) — 6-grade scale
- ISS ESG: 1 (high), 2,... to 10 (low) — 10-grade scale
- MSCI: AAA (high), AA,... to CCC (low) — 7-grade scale
- Refinitiv: A+ (high), A, A-, B+,... to D- (low) — 12-grade scale
- RepRisk: AAA (high), AA,... to D (low) — 8-grade scale
- Sustainanalytics: 1 (low), 2,... to 5 (high) — 5-grade scale

We notice the high heterogeneity of rating scales. Nevertheless, we observe that they are less granular than those used by credit rating agencies. On average, an ESG rating system is made up of 7 grades vs. 20 grades for a credit rating system.

[59] In some cases, the analyst may also validate the score.

[60] In this list, we have included the asset manager Amundi, because ESG ratings are not only built by ESG rating agencies. Some investors (asset owners and managers) have defined their own internal ESG ratings.

Box 2.4: Terminology of credit ratings

A rating system is a symbolic or numeric classification according to grade, which indicates a degree or step in a scale. For example, the credit rating systems of S&P, Moody's and Fitch is reported in Table 2.B. They are all based on a rating scale of 20 grades[a]. The symbolic rank AA+ (or BBB) is then a grade or a rating in the S&P classification. A notch means the difference between a particular rating and the next lower. For example, in the case of Moody's, the difference between Baa1 and Baa2 constitutes one Notch, whereas the difference between Aaa and Aa2 corresponds to two notches. When a credit rating agency revises the credit risk of a company, it may upgrade its rating by one notch (+1 notch), two notches (+2 notches), etc. or it may downgrade its rating by one notch (−1 notch), two notches (−2 notches), etc.

Table 2.B: Credit rating system of S&P, Moody's and Fitch

| | Prime Maximum Safety | High Grade High Quality | | | Upper Medium Grade | | | Lower Medium Grade | | |
|---|---|---|---|---|---|---|---|---|---|---|
| S&P/Fitch | AAA | AA+ | AA | AA− | A+ | A | A− | BBB+ | BBB | BBB− |
| Moody's | Aaa | Aa1 | Aa2 | Aa3 | A1 | A2 | A3 | Baa1 | Baa2 | Baa3 |

| | Non Investment Grade Speculative | | | Highly Speculative | | | Substantial Risk | In Poor Standing | | Extremely Speculative |
|---|---|---|---|---|---|---|---|---|---|---|
| S&P/Fitch | BB+ | BB | BB− | B+ | B | B− | CCC+ | CCC | CCC− | CC |
| Moody's | Ba1 | Ba2 | Ba3 | B1 | B2 | B3 | Caa1 | Caa2 | Caa3 | Ca |

[a]Or 21 grades if we include the issuer default. Nevertheless, D is not considered as a rating.

Table 2.21: ESG rating system of Moody's

| Leader | | Average | | | Laggard | |
|---|---|---|---|---|---|---|
| AAA | AA | A | BBB | BB | B | CCC |

Source: MSCI (2022, Exhibit 8, page 12).

**Remark 23** *In the sequel, we use the 7-grade scale based on the ratings* AAA, AA, A, BBB, BB, B *and* CCC. *We think that it is easier to manipulate and understand from a pedagogical point of view. A company rated* AAA *is a good company (or a good ESG risk) and a company rated* CCC *is a bad company (or a bad ESG risk).*

### 2.3.2 ESG rating process

The construction of ESG ratings follows the same process than credit ratings (Figure 2.33). We need to define the map function that converts an ESG score into an ESG rating. In the case of credit risk, the estimate of the one-year probability of default is converted into credit ratings[61]. In the case of ESG risk, the ESG score is converted into an ESG rating such that the best scores correspond to the best ratings and the worst scores correspond to the worst ratings.

[61]For instance, a CCC-rated company has a one-year probability of default of 25%; a B-rated company has a 5% probability to default in the next year; for a BB-rated company, the one-year probability of default is equal to 1%; etc.

Figure 2.33: From ESG score to ESG rating

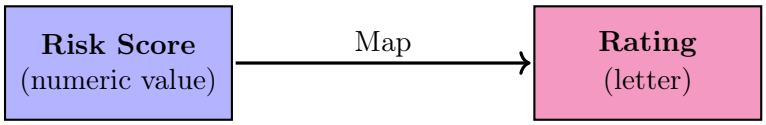


The first step consists in specifying the map function:

$$\begin{array}{rccc} \mathcal{M}ap: & \Omega_{\boldsymbol{\mathcal{S}}} & \longrightarrow & \Omega_{\mathcal{R}} \\ & \boldsymbol{\mathcal{S}} & \longmapsto & \mathcal{R} = \mathcal{M}ap\left(\boldsymbol{\mathcal{S}}\right) \end{array}$$

where $\Omega_{\boldsymbol{\mathcal{S}}}$ is the support of ESG scores, $\Omega_{\mathcal{R}}$ is the ordered state space of ESG ratings and $\mathcal{R}$ is the ESG rating. By construction, $\mathcal{M}ap$ is a monotone function in order to preserve the preference ordering. In the case where $\mathcal{M}ap$ is increasing, we verify that:

$$\boldsymbol{\mathcal{S}}_2 > \boldsymbol{\mathcal{S}}_1 \Leftrightarrow \mathcal{M}ap\left(\boldsymbol{\mathcal{S}}_2\right) \succ \mathcal{M}ap\left(\boldsymbol{\mathcal{S}}_1\right)$$

The second step is the validation (and the possible *forcing*) of the rating by the analyst.

Let us see some examples. MSCI (2022, page 12) explains that they use they use a uniform map function where $\Omega_{\boldsymbol{\mathcal{S}}} = [0, 10]$ and $\Omega_{\mathcal{R}} = \{\mathsf{CCC}, \mathsf{B}, \mathsf{BB}, \mathsf{BBB}, \mathsf{A}, \mathsf{AA}, \mathsf{AAA}\}$. The score is then divided into 7 equally-sized intervals and we have:

$$\mathcal{M}ap\left(s\right) = \begin{cases} \mathsf{CCC} & \text{if } \boldsymbol{\mathcal{S}} \in [0, 10/7] & (0 - 1.429) \\ \mathsf{B} & \text{if } \boldsymbol{\mathcal{S}} \in [10/7, 20/7] & (1.429 - 2.857) \\ \mathsf{BB} & \text{if } \boldsymbol{\mathcal{S}} \in [20/7, 30/7] & (2.857 - 4.286) \\ \mathsf{BBB} & \text{if } \boldsymbol{\mathcal{S}} \in [30/7, 40/7] & (4.286 - 5.714) \\ \mathsf{A} & \text{if } \boldsymbol{\mathcal{S}} \in [40/7, 50/7] & (5.714 - 7.143) \\ \mathsf{AA} & \text{if } \boldsymbol{\mathcal{S}} \in [50/7, 60/7] & (7.143 - 8.571) \\ \mathsf{AAA} & \text{if } \boldsymbol{\mathcal{S}} \in [60/7, 10] & (8.571 - 10) \end{cases}$$

For instance, if the ESG score of the company is equal to 5, we assign the grade BBB, a score of 8 corresponds to the grade AA, etc. Refinitiv (2022, page 7) also considers a uniform map function, implying that $\Omega_{\boldsymbol{\mathcal{S}}}$ is divided by 12 equally-sized intervals:

> "*[...] 'D' score* (D-, D and D+) *indicates poor relative ESG performance and insufficient degree of transparency in reporting material ESG data publicly. 'C' score* (C-, C and C+) *indicates satisfactory relative ESG performance and moderate degree of transparency in reporting material ESG data publicly. 'B' score* (B-, B and B+) *indicates good relative ESG performance and above average degree of transparency in reporting material ESG data publicly. 'A' score* (A-, A and A+) *indicates excellent relative ESG performance and high degree of transparency in reporting material ESG data publicly.*"

We assume that the map function is an increasing piecewise function, $\boldsymbol{\mathcal{S}} \sim \mathbf{F}$ and $\boldsymbol{\mathcal{S}} \in (s^-, s^+)$. We note $s_1^\star, \ldots, s_{K-1}^\star$ the knots of the piecewise function, $K$ the number of ratings and $\Omega_{\mathcal{R}} = \{R_1, \ldots, R_K\}$ the set of grades. We set $s_0^\star = s^-$ and $s_K^\star = s^+$. We deduce that:

$$\begin{aligned} p_k &= \Pr\left\{\mathcal{R} = R_k\right\} \\ &= \Pr\left\{s_{k-1}^\star \leq \boldsymbol{\mathcal{S}} < s_k^\star\right\} \\ &= \mathbf{F}\left(s_k^\star\right) - \mathbf{F}\left(s_{k-1}^\star\right) \end{aligned}$$

Using this equation, we can then compute the frequency distribution of the ratings. The set of frequencies $\{p_1, \ldots, p_K\}$ is denoted by $\mathbb{P}$. If we don't know the distribution $\mathbf{F}$, we consider the empirical distribution $\hat{\mathbf{F}}$ and the estimated frequency is equal to $\hat{p}_k = \hat{\mathbf{F}}(s_k^\star) - \hat{\mathbf{F}}(s_{k-1}^\star)$. If we would like to build a rating system with pre-defined frequencies $(p_1, \ldots, p_K)$, we have to solve the following equation:

$$\mathbf{F}(s_k^\star) - \mathbf{F}(s_{k-1}^\star) = p_k$$

We deduce that:

$$\begin{aligned}
\mathbf{F}(s_k^\star) &= p_k + \mathbf{F}(s_{k-1}^\star) \\
&= p_k + p_{k-1} + \mathbf{F}(s_{k-2}^\star) \\
&= \left(\sum_{j=1}^{k} p_j\right) + \mathbf{F}(s_0^\star)
\end{aligned}$$

Since $\mathbf{F}(s_0^\star) = 0$, we conclude that:

$$s_k^\star = \mathbf{F}^{-1}\left(\sum_{j=1}^{k} p_j\right)$$

**Remark 24** *The discrete probability space of the rating system is denoted by* $(\Omega_{\mathcal{R}}, \Omega_{\mathcal{R}}, \mathbb{P})$ *and we have:*

$$\mathcal{E} := \Omega_{\mathcal{R}} \times \mathbb{P} = \{(R_1, p_1), \ldots, (R_K, p_K)\}$$

Let us consider a uniform score $\boldsymbol{\mathcal{S}} \sim \mathcal{U}_{[a,b]}$. We have $\mathbf{F}(s) = (s-a)/(b-a)$. The rating system consists in $K$ equally-sized intervals. The knots of the map function are then equal to:

$$s_k^\star = a + \frac{(b-a)}{K} k$$

It follows that:

$$\begin{aligned}
p_k &= \mathbf{F}\left(a + \frac{(b-a)}{K} k\right) - \mathbf{F}\left(a + \frac{(b-a)}{K}(k-1)\right) \\
&= \frac{a + \dfrac{(b-a)}{K} k - a}{b-a} - \frac{a + \dfrac{(b-a)}{K}(k-1) - a}{b-a} \\
&= \frac{1}{K}
\end{aligned}$$

We obtain a trivial result: the rating frequencies are all equal. In the case where we impose pre-defined frequencies $(p_1, \ldots, p_K)$, the knots of the map function are equal to[62]:

$$s_k^\star = a + (b-a)\left(\sum_{j=1}^{k} p_j\right)$$

If we consider a 0/100 uniform score, we deduce that $s_k^\star = 100 \cdot \sum_{j=1}^{k} p_j$. For example, if $\Omega_{\mathcal{R}} \times \mathbb{P} = \{(\mathsf{CCC}, 5\%), (\mathsf{B}, 10\%), (\mathsf{BB}, 20\%), (\mathsf{BBB}, 30\%), (\mathsf{A}, 20\%), (\mathsf{AA}, 10\%), (\mathsf{AAA}, 5\%)\}$, we obtain the trivial piecewise function where[63] $s_{\mathsf{CCC}}^\star = 5$, $s_{\mathsf{B}}^\star = 15$, $s_{\mathsf{BB}}^\star = 35$, $s_{\mathsf{BBB}}^\star = 65$, $s_{\mathsf{A}}^\star = 85$ and $s_{\mathsf{AA}}^\star = 95$.

Figure 2.34: Map function of a $z$-score (equal-space ratings)

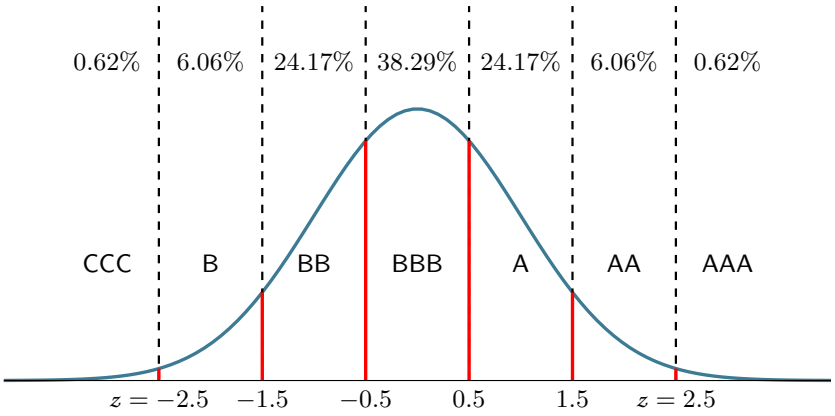


For a $z$-score system, we assume that $\boldsymbol{\mathcal{S}} \sim \mathcal{N}(0,1)$ and we obtain:

$$p_k = \Phi\left(s_k^\star\right) - \Phi\left(s_{k-1}^\star\right)$$

If we consider the 7-grade rating system with the classical knots $(-2.5, -1.5, -0.5, 0.5, 1.5, 2.5)$, we obtain the map function given in Figure 2.34 where[64]:

$$p_k = \Phi(-3.5 + k) - \Phi(-4.5 + k)$$

The rating system with equal frequencies is obtained by using the following knots:

$$s_k^\star = \Phi^{-1}\left(\frac{k}{K}\right) \qquad \text{for } k = 1, \ldots, K$$

In the case $K = 7$, the map function is given in Figure 2.35.

Figure 2.35: Map function of a $z$-score (equal-frequency ratings)

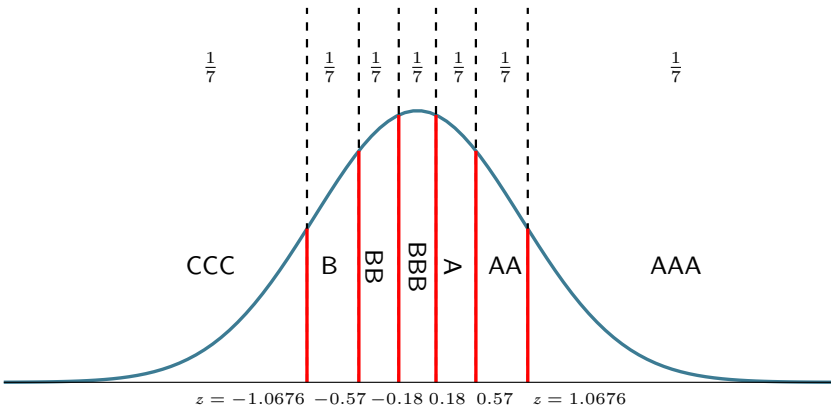


**Remark 25** *We recall that the role of the ESG analyst is to verify the consistency of the rated companies. This is why we generally observe forced ratings (or scores).*

[62] We have $\mathbf{F}(s) = u \Leftrightarrow (s-a)/(b-a) = u$. We deduce that $s = \mathbf{F}^{-1}(u) = a + (b-a)\,u$.

[63] By construction, the knot $s_{\mathsf{AAA}}^\star = 100$ is not necessarily to be defined because we always have $s_{\mathsf{AAA}}^\star = s^+$.

[64] We obtain the following results: $p_{\mathsf{CCC}} = \Phi(-2.5) = 0.62\%$, $p_{\mathsf{B}} = \Phi(-1.5) - \Phi(-2.5) = 6.06\%$, $p_{\mathsf{BB}} = \Phi(-0.5) - \Phi(-1.5) = 24.17\%$, $p_{\mathsf{BBB}} = \Phi(0.5) - \Phi(-0.5) = 38.29\%$, $p_{\mathsf{A}} = \Phi(1.5) - \Phi(0.5) = 24.17\%$, $p_{\mathsf{AA}} = \Phi(2.5) - \Phi(1.5) = 6.06\%$ and $p_{\mathsf{AAA}} = 1 - \Phi(2.5) = 0.62\%$.

Box 2.5: Asymmetric rating system

In a symmetric rating system, the probability of the $k^{\text{th}}$ rating class is equal to the probability of the $(K-k+1)^{\text{th}}$ rating class[a], *e.g.*, $p_{\mathsf{CCC}} = p_{\mathsf{AAA}}$, $p_{\mathsf{B}} = p_{\mathsf{A}}$ and $p_{\mathsf{BB}} = p_{\mathsf{A}}$. To obtain an asymmetric rating system, the first approach is to define the frequencies $p_k$ such that $\exists k : p_k \neq p_{K-k+1}$. We note $P_{worst} = \sum_{k=1}^{\lfloor K/2 \rfloor} p_k$ and $P_{best} = \sum_{\lceil K/2+1 \rceil}^{K} p_k$ the probability to be below and average the median rating. The rating process is said to be a *losing-oriented* system if $P_{worst} \geq P_{best}$, otherwise it is a *winning-oriented* system. This means that companies with bad ESG risk are more prevalent than companies with good ESG risk. For instance, $\Omega_{\mathcal{R}} \times \mathbb{P} = \{(\mathsf{CCC}, 5\%), (\mathsf{B}, 10\%), (\mathsf{BB}, 25\%), (\mathsf{BBB}, 40\%), (\mathsf{A}, 15\%), (\mathsf{AA}, 4\%), (\mathsf{AAA}, 1\%)\}$ is a *losing-oriented* system. The choice of an asymmetric rating system may be motivated by the underlying ESG strategy. For instance, implementing an exclusion ESG policy is not equivalent to considering a selection ESG policy. The investor may then want to adapt his rating system to take into account the objective of the strategy. The second approach to obtain an asymmetric rating system is to consider a $\mathcal{b}$-score normalization with $\alpha \neq \beta$. Some examples are provided in Table 2.C.

Table 2.C: Frequency distribution of ESG ratings (in %)

| Parameters | | Rating | | | | | | |
|---|---|---|---|---|---|---|---|---|
| $\alpha$ | $\beta$ | CCC | B | BB | BBB | A | AA | AAA |
| 1 | 1 | 14.3 | 14.3 | 14.3 | 14.3 | 14.3 | 14.3 | 14.3 |
| 2 | 2 | 5.5 | 14.3 | 19.5 | 21.3 | 19.5 | 14.3 | 5.5 |
| 3 | 3 | 2.3 | 12.1 | 22.3 | 26.4 | 22.3 | 12.1 | 2.3 |
| 0.25 | 0.25 | 33.9 | 7.5 | 5.9 | 5.5 | 5.9 | 7.5 | 33.9 |
| 2.5 | 1.5 | 1.5 | 6.4 | 12.4 | 18.1 | 22.3 | 23.2 | 16.0 |
| 1.5 | 2.5 | 16.0 | 23.2 | 22.3 | 18.1 | 12.4 | 6.4 | 1.5 |
| 0.75 | 1 | 23.2 | 15.8 | 13.9 | 12.8 | 12.0 | 11.4 | 10.9 |

[a] We reiterate that we only consider rating systems that satisfy a comprehensive preference ordering: $\forall k : \mathcal{R}_k \succ \mathcal{R}_{k-1}$.

### 2.3.3 Rating migration matrix

One important issue concerns the consistency of the rating system. In particular, we may wonder whether it is relevant to use an equal-frequency, an equal-space or an asymmetric rating scheme. In the case of credit rating systems, we generally observe that medium risk classes have a higher frequency than extreme (low/high) risk classes. For instance, there are more BBB-rated companies than CCC-rated companies, the less frequent class is by far the AAA rating (less than 1%), etc. In the case of ESG rating systems, there is no consensus. Therefore, to assess the consistency and robustness of the rating system, we need to use probabilistic tools based on transition probability matrices (Norris, 1997).

#### Discrete-time modeling

**Markov chain model** We consider a time-homogeneous Markov chain $\mathcal{R}$, whose transition matrix is $P = (p_{i,j})$. We note $\Omega_{\mathcal{R}} = \{R_1, \ldots, R_K\}$ the state space of the chain and $\mathbb{K} = \{1, \ldots, K\}$ the corresponding index set. $p_{i,j}$ is the probability that the entity migrates from rating $R_i$ to rating $R_j$.

The matrix $P$ satisfies the following properties:

- $\forall i, j \in \mathbb{K}$, $p_{i,j} \geq 0$;
- $\forall i \in \mathbb{K}$, $\sum_{j=1}^{K} p_{i,j} = 1$.

Let $\mathcal{R}(t)$ be the value of the state at time $t$. We define $p(s, i; t, j)$ as the probability that the entity reaches the state $R_j$ at time $t$ given that it has reached the state $R_i$ at time $s$. We have:

$$p(s, i; t, j) = \Pr\{\mathcal{R}(t) = R_j \mid \mathcal{R}(s) = R_i\} = p_{i,j}^{(t-s)}$$

This probability only depends on the duration between $s$ and $t$ because of the Markov property. Therefore, we can restrict the analysis by calculating the $n$-step transition probability:

$$p_{i,j}^{(n)} = \Pr\{\mathcal{R}(t+n) = R_j \mid \mathcal{R}(t) = R_i\}$$

and the associated $n$-step transition matrix $P^{(n)} = \left(p_{i,j}^{(n)}\right)$. For $n = 2$, we obtain:

$$\begin{aligned}
p_{i,j}^{(2)} &= \Pr\{\mathcal{R}(t+2) = R_j \mid \mathcal{R}(t) = R_i\} \\
&= \sum_{k=1}^{K} \Pr\{\mathcal{R}(t+2) = R_j, \mathcal{R}(t+1) = R_k \mid \mathcal{R}(t) = R_i\} \\
&= \sum_{k=1}^{K} \Pr\{\mathcal{R}(t+2) = R_j \mid \mathcal{R}(t+1) = R_k\} \cdot \Pr\{\mathcal{R}(t+1) = R_k \mid \mathcal{R}(t) = R_i\} \\
&= \sum_{k=1}^{K} p_{i,k} \cdot p_{k,j}
\end{aligned}$$

In a similar way, we obtain:

$$p_{i,j}^{(n+m)} = \sum_{k=1}^{K} p_{i,k}^{(n)} \cdot p_{k,j}^{(m)} \qquad \forall n, m > 0 \tag{2.4}$$

This equation is called the forward Chapman-Kolmogorov equation. In matrix form, we have:

$$P^{(n+m)} = P^{(n)} \cdot P^{(m)}$$

with the convention $P^{(0)} = I$. In particular, we have:

$$\begin{aligned}
P^{(n)} &= P^{(n-1)} \cdot P^{(1)} \\
&= P^{(n-2)} \cdot P^{(1)} \cdot P^{(1)} \\
&= \prod_{t=1}^{n} P^{(1)} \\
&= P^{n}
\end{aligned}$$

We deduce that:

$$p(t, i; t+n, j) = p_{i,j}^{(n)} = \mathbf{e}_i^\top P^n \mathbf{e}_j \tag{2.5}$$

When we apply this framework to ESG risk, $\mathcal{R}(t)$ denotes the rating (or the risk class) of the company at time $t$ and $p_{i,j}$ is the one-period transition probability from rating $R_i$ to rating $R_j$.

Table 2.22: ESG migration matrix #1 (one-year transition probability in %)

| | AAA | AA | A | BBB | BB | B | CCC |
|---|---|---|---|---|---|---|---|
| AAA | 92.76 | 5.66 | 0.90 | 0.45 | 0.23 | 0.00 | 0.00 |
| AA | 4.15 | 82.73 | 11.86 | 0.89 | 0.30 | 0.07 | 0.00 |
| A | 0.18 | 15.47 | 72.98 | 10.46 | 0.82 | 0.09 | 0.00 |
| BBB | 0.07 | 1.32 | 19.60 | 69.49 | 9.03 | 0.42 | 0.07 |
| BB | 0.04 | 0.19 | 1.55 | 19.36 | 70.88 | 7.75 | 0.23 |
| B | 0.00 | 0.05 | 0.24 | 1.43 | 21.54 | 74.36 | 2.38 |
| CCC | 0.00 | 0.00 | 0.22 | 0.44 | 2.21 | 13.24 | 83.89 |

In Table 2.22, we report an example of transition probability matrix. We read the figures as follows[65]: a company rated AAA has a one-year probability of 92.76% to remain AAA; its probability to become AA is 5.66%; a company rated CCC has a probability of 16.11% to improve its rating, etc. In Tables 2.23 and 2.24, we have reported the two-year and five-year transition matrices. We detail below the calculation of $p^{(2)}_{\mathsf{AAA},\mathsf{AAA}}$:

$$\begin{aligned} p^{(2)}_{\mathsf{AAA},\mathsf{AAA}} &= p_{\mathsf{AAA},\mathsf{AAA}} \times p_{\mathsf{AAA},\mathsf{AAA}} + p_{\mathsf{AAA},\mathsf{AA}} \times p_{\mathsf{AA},\mathsf{AAA}} + p_{\mathsf{AAA},\mathsf{A}} \times p_{\mathsf{A},\mathsf{AAA}} + p_{\mathsf{AAA},\mathsf{BBB}} \times p_{\mathsf{BBB},\mathsf{AAA}} + \\ &\quad p_{\mathsf{AAA},\mathsf{BB}} \times p_{\mathsf{BB},\mathsf{AAA}} + p_{\mathsf{AAA},\mathsf{B}} \times p_{\mathsf{B},\mathsf{AAA}} + p_{\mathsf{AAA},\mathsf{CCC}} \times p_{\mathsf{CCC},\mathsf{AAA}} \\ &= 0.9276^2 + 0.0566 \times 0.0415 + 0.0090 \times 0.0018 + 0.0045 \times 0.0007 + 0.0023 \times 0.0004 \\ &= 86.28\% \end{aligned}$$

Table 2.23: Two-year transition probability in % (migration matrix #1)

| | AAA | AA | A | BBB | BB | B | CCC |
|---|---|---|---|---|---|---|---|
| AAA | 86.28 | 10.08 | 2.25 | 0.92 | 0.44 | 0.02 | 0.00 |
| AA | 7.30 | 70.52 | 18.68 | 2.67 | 0.66 | 0.15 | 0.00 |
| A | 0.95 | 24.24 | 57.16 | 15.20 | 2.19 | 0.25 | 0.01 |
| BBB | 0.21 | 5.06 | 28.22 | 52.11 | 12.93 | 1.33 | 0.14 |
| BB | 0.09 | 0.79 | 6.07 | 27.45 | 53.68 | 11.37 | 0.55 |
| B | 0.01 | 0.18 | 0.98 | 6.26 | 31.47 | 57.28 | 3.82 |
| CCC | 0.00 | 0.05 | 0.50 | 1.32 | 6.31 | 21.13 | 70.70 |

Table 2.24: Five-year transition probability in % (migration matrix #1)

| | AAA | AA | A | BBB | BB | B | CCC |
|---|---|---|---|---|---|---|---|
| AAA | 70.45 | 18.69 | 6.97 | 2.61 | 1.08 | 0.18 | 0.01 |
| AA | 13.13 | 50.21 | 26.03 | 7.90 | 2.22 | 0.48 | 0.03 |
| A | 4.35 | 33.20 | 37.78 | 17.99 | 5.52 | 1.08 | 0.09 |
| BBB | 1.50 | 16.49 | 32.49 | 30.90 | 14.61 | 3.63 | 0.38 |
| BB | 0.50 | 5.98 | 17.83 | 30.10 | 31.35 | 12.85 | 1.39 |
| B | 0.15 | 1.90 | 7.40 | 18.95 | 35.11 | 31.26 | 5.23 |
| CCC | 0.05 | 0.64 | 2.55 | 6.93 | 17.96 | 38.54 | 43.33 |

[65]The rows represent the initial rating whereas the columns indicate the final rating.

Box 2.6: Stationary distribution of a Markov chain

We note $\pi_k^{(n)}$ the probability of the state $R_k$ at time $n$:

$$\pi_k^{(n)} = \Pr\left\{\mathcal{R}(n) = R_k\right\}$$

and $\pi^{(n)} = \left(\pi_1^{(n)}, \ldots, \pi_K^{(n)}\right)$ the probability distribution. By construction, we have:

$$\pi^{(n+1)} = P^\top \pi^{(n)}$$

The Markov chain $\mathcal{R}$ admits a stationary distribution $\pi^\star$ if[a]:

$$\pi^\star = P^\top \pi^\star$$

In this case, $\pi_k^\star$ is the limiting probability of state $R_k$:

$$\lim_{n\to\infty} p_{i,k}^{(n)} = \pi_k^\star \qquad \forall i$$

We can interpret $\pi_k^\star$ as the average duration spent by the chain $\mathcal{R}$ in the state $R_k$. Let $\mathcal{T}_k$ be the return period[b] of state $R_k$:

$$\mathcal{T}_k = \inf\left\{n : \mathcal{R}(n) = R_k \mid \mathcal{R}(0) = R_k\right\}$$

The average return period is then equal to:

$$\boldsymbol{\tau}_k := \mathbb{E}\left[\mathcal{T}_k\right] = \frac{1}{\pi_k^\star}$$

[a] Not all Markov chains behave in this way, meaning that $\pi^\star$ does not necessarily exist.
[b] $\mathcal{T}_k$ is a stopping time. It is also called the *first-passage time*.

We compute the stationary distribution[66] and we obtain:

$$\pi^\star = (17.78\%, 29.59\%, 25.12\%, 15.20\%, 8.35\%, 3.29\%, 0.67\%)$$

The average return periods are then equal to 5.6, 3.4, 4.0, 6.6, 12.0, 30.4 and 149.0 years. The interpretation of these results is the following. In the long term, the probability to observe a AAA-rated company is equal to 17.78%, while the probability to observe a CCC-rated company is equal to 0.67%. The probability $\pi_k^\star$ is then the long-term equivalent of the current (or sample) frequency $p_k$. Similarly, the expected time to reach the worst-in-class state is equal to 149 years. These results show that the rating system #1 is clearly a winning-oriented system, where more than 70% of corporates are expected to have a rating above BBB.

[66] There are three numerical approaches to compute $\pi^\star$. The first one is to approximate $P^{(\infty)}$ by $P^{(n)}$ with $n$ sufficient large ($n > 100$) and take any rows of the matrix $P^{(\infty)}$. The second method is to compute the eigendecomposition $V\Lambda V^{-1}$ of $P^\top$ and return the left eigenvector whose eigenvalue is exactly equal to 1. This second approach uses the fact that $\pi^\star = P^\top \pi^\star$ defines an eigenvalue problem $\left(P^\top - \lambda I_K\right)\pi^\star = \mathbf{0}$ with $\lambda = 1$. Finally, the third method directly solves the equation $\left(P^\top - I_K\right)\pi^\star = \mathbf{0}$ by computing an orthonormal basis for the null space of $P^\top - I_K$. For the last two methods, we normalize the solution such that $\mathbf{1}^\top \pi^\star = 1$.

Table 2.25: ESG migration matrix #2 (one-month transition probability in %)

| | AAA | AA | A | BBB | BB | B | CCC |
|---|---|---|---|---|---|---|---|
| AAA | 93.50 | 5.00 | 0.50 | 0.50 | 0.50 | 0.00 | 0.00 |
| AA | 2.00 | 93.00 | 4.00 | 0.50 | 0.50 | 0.00 | 0.00 |
| A | 0.00 | 3.00 | 93.00 | 3.90 | 0.10 | 0.00 | 0.00 |
| BBB | 0.00 | 0.10 | 2.80 | 94.00 | 3.00 | 0.10 | 0.00 |
| BB | 0.00 | 0.00 | 0.10 | 3.50 | 94.50 | 1.80 | 0.10 |
| B | 0.00 | 0.00 | 0.00 | 0.10 | 3.70 | 96.00 | 0.20 |
| CCC | 0.00 | 0.00 | 0.00 | 0.40 | 0.50 | 0.60 | 98.50 |

In Table 2.25, we now consider the ESG migration matrix #2, which has been computed on a monthly basis. If we would like to compare the two rating systems, we can compute the one-year probability transition matrix (Table 2.26). We observe that the two transition matrices are very different. Indeed, the second rating system is more reactive than the first rating system. If we compute the stationary distribution of the second rating system, we obtain:

$$\pi^\star = (3.11\%, 10.10\%, 17.46\%, 27.76\%, 25.50\%, 12.68\%, 3.39\%)$$

implying that the average return periods are equal to 32.2, 9.9, 5.7, 3.6, 3.9, 7.9 and 29.5 years. These results show that the rating system #2 is a balanced system.

Table 2.26: One-year probability transition in % (migration matrix #2)

| | AAA | AA | A | BBB | BB | B | CCC |
|---|---|---|---|---|---|---|---|
| AAA | 48.06 | 29.71 | 10.34 | 6.42 | 4.95 | 0.49 | 0.03 |
| AA | 11.65 | 49.25 | 24.10 | 9.60 | 4.87 | 0.49 | 0.03 |
| A | 2.02 | 17.51 | 49.67 | 24.72 | 5.52 | 0.54 | 0.03 |
| BBB | 0.27 | 3.53 | 17.46 | 55.50 | 20.21 | 2.88 | 0.16 |
| BB | 0.03 | 0.60 | 4.21 | 23.43 | 57.45 | 13.27 | 1.01 |
| B | 0.00 | 0.08 | 0.74 | 5.94 | 27.10 | 64.18 | 1.96 |
| CCC | 0.00 | 0.07 | 0.57 | 4.22 | 5.77 | 5.85 | 83.51 |

Table 2.27: One-month probability transition in % (migration matrix #1)

| | AAA | AA | A | BBB | BB | B | CCC |
|---|---|---|---|---|---|---|---|
| AAA | 99.36 | 0.53 | 0.05 | 0.04 | 0.02 | 0.00 | 0.00 |
| AA | 0.39 | 98.31 | 1.26 | 0.01 | 0.03 | 0.01 | 0.00 |
| A | −0.02 | 1.65 | 97.14 | 1.21 | 0.02 | 0.01 | 0.00 |
| BBB | 0.01 | −0.07 | 2.28 | 96.72 | 1.06 | −0.01 | 0.01 |
| BB | 0.00 | 0.02 | −0.12 | 2.29 | 96.92 | 0.88 | 0.01 |
| B | 0.00 | 0.00 | 0.04 | −0.15 | 2.45 | 97.42 | 0.25 |
| CCC | 0.00 | 0.00 | 0.02 | 0.04 | 0.05 | 1.37 | 98.53 |

**Remark 26** *Another approach to analyze the two rating systems is to compute the monthly transition matrix associated to the migration matrix #1. In this case, we have to find the matrix $M$ such*

*that* $M^{(12)} = P$*. The solution*[67] *is given by* $M = P^{1/12}$ *and reported in Table 2.27. We can compare it with the matrix in Table 2.25. Because* $M$ *has some negative probabilities, it is not a transition matrix, which indicates that the rating system #1 does not satisfy the Markov property*[68]*.*

Box 2.7: Mean hitting time

Let $\mathcal{A} \subset \mathbb{K}$ be a given subset. The first hitting time of $\mathcal{A}$ is given by:

$$\mathcal{T}(\mathcal{A}) = \inf\{n : \mathcal{R}(n) \in \mathcal{A}\}$$

$\mathcal{T}(\mathcal{A})$ measures how long it takes to reach the target states $j \in \mathcal{A}$. We can show that it is a stopping time. The mean first hitting (or passage) time to target $\mathcal{A}$ from state $k$ is defined as:

$$\boldsymbol{\tau}_k(\mathcal{A}) = \mathbb{E}[\mathcal{T}(\mathcal{A}) \mid \mathcal{R}(0) = R_k]$$

Let $\boldsymbol{\tau}(\mathcal{A}) = (\boldsymbol{\tau}_1(\mathcal{A}), \ldots, \boldsymbol{\tau}_K(\mathcal{A}))$ be the vector of mean first hitting times. Norris (1997) showed that:

$$\boldsymbol{\tau}_k(\mathcal{A}) = 1 + \sum_{j=1}^{K} p_{k,j}\boldsymbol{\tau}_j(\mathcal{A})$$

By construction, we have $\boldsymbol{\tau}_k(\mathcal{A}) = 0$ if $k \in \mathcal{A}$. In fact, $\boldsymbol{\tau}_k(\mathcal{A})$ is the minimal non negative solution to the previous system. It follows that $\|\boldsymbol{\tau}(\mathcal{A})\| = \sum_{k=1}^{K} |\boldsymbol{\tau}_k(\mathcal{A})| = \sum_{k=1}^{K} \boldsymbol{\tau}_k(\mathcal{A})$ because $\boldsymbol{\tau}_k(\mathcal{A}) \geq 0$. We deduce that:

$$\begin{aligned} \boldsymbol{\tau}(\mathcal{A}) &= \arg\min \sum_{k=1}^{K} x_k \\ &\text{s.t.} \begin{cases} x_k = 0 & \text{if } k \in \mathcal{A} \\ x_k = 1 + \sum_{j=1}^{K} p_{k,j} x_j & \text{if } k \notin \mathcal{A} \\ x_k \geq 0 \end{cases} \end{aligned}$$

We obtain a linear programming problem with $K + 1$ equally constraints and $K$ lower bounds:

$$\begin{aligned} \boldsymbol{\tau}(\mathcal{A}) &= \arg\min \sum_{k=1}^{K} x_k \\ &\text{s.t.} \begin{cases} x_k = 0 & \text{if } k \in \mathcal{A} \\ \sum_{j \notin \mathcal{A}} p_{k,j} x_j = -1 & \\ \sum_{j \notin \mathcal{A} \cup \{k\}} p_{k,j} x_j + (p_{k,k} - 1) x_k = -1 & \text{if } k \notin \mathcal{A} \\ x_k \geq 0 \end{cases} \end{aligned}$$

[67] Since $f(x) = x^\alpha$ with $\alpha > 1$ is a transcendental function, we use the Schur decomposition $P = QTQ^*$ to compute numerically the matrix $M$. Using Appendix A.1.1, we deduce that $M = QT^{1/12}Q^*$.

[68] The Markov property of ESG ratings is discussed later on page 127.

Let $\mathcal{B} = \{\mathsf{AAA}, \mathsf{AA}, \mathsf{A}\}$ and $\mathcal{W} = \{\mathsf{BB}, \mathsf{B}, \mathsf{CCC}\}$ be the best-in-class and worst-in-class sets. We obtain the following mean hitting times (in years) for the two rating systems:

| Rating | $\mathcal{W}$-target | | | | $\mathcal{B}$-target | | | |
|---|---|---|---|---|---|---|---|---|
| system | AAA | AA | A | BBB | BBB | BB | B | CCC |
| #1 | 79.21 | 70.04 | 62.34 | 46.54 | 7.50 | 13.28 | 17.58 | 22.68 |
| #2 | 10.24 | 9.92 | 9.13 | 6.68 | 8.68 | 11.99 | 14.26 | 17.54 |

**Estimation of the transition matrix** Using Bayes theorem, we have:

$$\begin{aligned} p_{i,j} &= \Pr\{\mathcal{R}(t+1) = R_j \mid \mathcal{R}(t) = R_i\} \\ &= \frac{\Pr\{\mathcal{R}(t+1) = R_j, \mathcal{R}(t) = R_i\}}{\Pr\{\mathcal{R}(t) = R_i\}} \end{aligned}$$

We reiterate that[69] $\mathcal{R}(t) = R_k \Leftrightarrow \boldsymbol{\mathcal{S}}(t) \in \left[s_{k-1}^\star, s_k^\star\right]$. We have seen that:

$$\Pr\{\mathcal{R}(t) = R_k\} = \mathbf{F}(s_k^\star) - \mathbf{F}\left(s_{k-1}^\star\right) = p_k$$

where $\mathbf{F}(s)$ is the probability distribution of the score $\boldsymbol{\mathcal{S}}(t)$. We assume that[70]:

$$\Pr\left\{\boldsymbol{\mathcal{S}}(t) \leq s, \boldsymbol{\mathcal{S}}(t+1) \leq s'\right\} = \mathbf{C}\left(\mathbf{F}(s), \mathbf{F}\left(s'\right)\right)$$

where $\mathbf{C}$ is the copula function of the random vector $(\boldsymbol{\mathcal{S}}(t), \boldsymbol{\mathcal{S}}(t+1))$. We deduce that:

$$\begin{aligned} \Pr\{\mathcal{R}(t+1) = R_j, \mathcal{R}(t) = R_i\} &= \Pr\left\{s_{i-1}^\star \leq \boldsymbol{\mathcal{S}}(t) \leq s_i^\star, s_{j-1}^\star \leq \boldsymbol{\mathcal{S}}(t+1) \leq s_j^\star\right\} \\ &= \mathbf{C}\left(\mathbf{F}(s_i^\star), \mathbf{F}\left(s_j^\star\right)\right) - \mathbf{C}\left(\mathbf{F}\left(s_{i-1}^\star\right), \mathbf{F}\left(s_j^\star\right)\right) - \\ &\quad \mathbf{C}\left(\mathbf{F}(s_i^\star), \mathbf{F}\left(s_{j-1}^\star\right)\right) + \mathbf{C}\left(\mathbf{F}\left(s_{i-1}^\star\right), \mathbf{F}\left(s_{j-1}^\star\right)\right) \end{aligned}$$

Finally, we obtain:

$$p_{i,j} = \frac{\mathbf{C}\left(\mathbf{F}(s_i^\star), \mathbf{F}\left(s_j^\star\right)\right) - \mathbf{C}\left(\mathbf{F}\left(s_{i-1}^\star\right), \mathbf{F}\left(s_j^\star\right)\right) - \mathbf{C}\left(\mathbf{F}(s_i^\star), \mathbf{F}\left(s_{j-1}^\star\right)\right) + \mathbf{C}\left(\mathbf{F}\left(s_{i-1}^\star\right), \mathbf{F}\left(s_{j-1}^\star\right)\right)}{\mathbf{F}(s_i^\star) - \mathbf{F}\left(s_{i-1}^\star\right)}$$

This is the theoretical expression of the probability transition $p_{i,j}$. In practice, we do not know the probability functions $\mathbf{F}$ and $\mathbf{C}$. Therefore, we can estimate them and the estimated value of $p_{i,j}$ is equal to:

$$\hat{p}_{i,j} = \frac{\hat{\mathbf{C}}\left(\hat{\mathbf{F}}(s_i^\star), \hat{\mathbf{F}}\left(s_j^\star\right)\right) - \hat{\mathbf{C}}\left(\hat{\mathbf{F}}\left(s_{i-1}^\star\right), \hat{\mathbf{F}}\left(s_j^\star\right)\right) - \hat{\mathbf{C}}\left(\hat{\mathbf{F}}(s_i^\star), \hat{\mathbf{F}}\left(s_{j-1}^\star\right)\right) + \hat{\mathbf{C}}\left(\hat{\mathbf{F}}\left(s_{i-1}^\star\right), \hat{\mathbf{F}}\left(s_{j-1}^\star\right)\right)}{\hat{\mathbf{F}}(s_i^\star) - \hat{\mathbf{F}}\left(s_{i-1}^\star\right)}$$

This parametric estimation approach is interesting when we specify the parametric functions $\mathbf{F}(s;\theta_1)$ and $\mathbf{C}(s, s';\theta_2)$, and we estimate the parameters $\theta_1$ and $\theta_2$.

Generally, we have no idea about the probability functions $\mathbf{F}$ and $\mathbf{C}$. We can then adopt a non-parametric estimation approach. The first idea is to replace $\mathbf{F}$ and $\mathbf{C}$ by the empirical distribution of $\boldsymbol{\mathcal{S}}(t)$ and the empirical copula of $(\boldsymbol{\mathcal{S}}(t), \boldsymbol{\mathcal{S}}(t+1))$. In practice, we can simplify this approach by estimating directly the empirical probability. Thanks to the Bayes theorem, we have:

$$\hat{p}_{i,j}(t) = \frac{\#\{\mathcal{R}(t+1) = R_j, \mathcal{R}(t) = R_i\}}{\#\{\mathcal{R}(t) = R_i\}}$$

[69] In this analysis, we have the following correspondance: $R_1 = \mathsf{CCC}, R_2 = \mathsf{B}, \ldots, R_K = \mathsf{AAA}$.

[70] There is no reason that the probability distribution of $\boldsymbol{\mathcal{S}}(t+1)$ is different than this of $\boldsymbol{\mathcal{S}}(t)$.

We consider a cohort of issuers for a given period $[t, t+1]$. Let $n_{i,\cdot}(t)$ be the number of issuers rated $R_i$ at the beginning of the period $t$. Let $n_{i,j}(t)$ be the number of issuers rated $R_i$ at the beginning of the period $t$ and $R_j$ at the end of the period $t$. We deduce that $\hat{p}_{i,j}$ is the ration between the two quantities:

$$\hat{p}_{i,j}(t) = \frac{n_{i,j}(t)}{n_{i,\cdot}(t)}$$

When the period is the year YYYY, the cohort starts on 1 January YYYY and ends on 31 December YYYY. If we have several annual cohorts, we can average the empirical probabilities:

$$\hat{p}_{i,j} = \frac{1}{T}\sum_{t=1}^{T}\hat{p}_{i,j}(t) = \frac{1}{T}\sum_{t=1}^{T}\frac{n_{i,j}(t)}{n_{i,\cdot}(t)}$$

Another approach is to use the pooling method:

$$\hat{p}_{i,j} = \frac{\sum_{t=1}^{T} n_{i,j}(t)}{\sum_{t=1}^{T} n_{i,\cdot}(t)}$$

The two approaches give different results. In the first case, each annual cohort has the same weight. In the second case, the approach puts more weight on the year which is more representative[71].

Table 2.28: Number of observations $n_{i,j}$ (migration matrix #1)

| $n_{i,j}$ | AAA | AA | A | BBB | BB | B | CCC | $n_{i,\cdot}(t)$ | $\hat{p}_{i,\cdot}(t)$ |
|---|---|---|---|---|---|---|---|---|---|
| AAA | 2 050 | 125 | 20 | 10 | 5 | 0 | 0 | 2 210 | 3.683% |
| AA | 280 | 5 580 | 800 | 60 | 20 | 5 | 0 | 6 745 | 11.242% |
| A | 20 | 1 700 | 8 020 | 1 150 | 90 | 10 | 0 | 10 990 | 18.317% |
| BBB | 10 | 190 | 2 820 | 10 000 | 1 300 | 60 | 10 | 14 390 | 23.983% |
| BB | 5 | 25 | 200 | 2 500 | 9 150 | 1 000 | 30 | 12 910 | 21.517% |
| B | 0 | 5 | 25 | 150 | 2 260 | 7 800 | 250 | 10 490 | 17.483% |
| CCC | 0 | 0 | 5 | 10 | 50 | 300 | 1 900 | 2 265 | 3.775% |
| $n_{\cdot,j}(t)$ | 2 365 | 7 625 | 11 890 | 13 850 | 12 875 | 9 175 | 2 190 | 60 000 | |
| $\hat{p}_{\cdot,j}(t)$ | 3.942% | 12.708% | 19.817% | 23.133% | 21.458% | 15.292% | 3.650% | | 100.00% |

In Table 2.28, we report all the information[72] for estimating the migration matrix #1. We have used the pooling method with 60 000 observations. For 2 050 observations, the initial rating on 1 January YYYY is AAA and the final rating on 31 December YYYY is AAA. We observe 125 cases where a AAA-rated issuer has been downgraded by one notch. If we compute the sum, we obtain 2 210 AAA-rated observations at the beginning of the year and 2 365 AAA-rated observations at the end of the year. We can then compute the transition probabilities: $\hat{p}_{\mathsf{AAA},\mathsf{AAA}} = \dfrac{2\,050}{2\,210} = 92.76\%$, $\hat{p}_{\mathsf{AAA},\mathsf{AA}} = \dfrac{125}{2\,210} = 5.66\%$, ...., $\hat{p}_{\mathsf{CCC},\mathsf{CCC}} = \dfrac{1\,900}{2\,265} = 83.89\%$.

Previously, we have seen that the stationary distribution of the migration matrix #1 is equal to:

$$\pi^\star = (17.78\%, 29.59\%, 25.12\%, 15.20\%, 8.35\%, 3.29\%, 0.67\%)$$

[71] From a theoretical viewpoint, this second method is biased. However, it is extensively used in particular when the number of observations is low for each period.

[72] We have $n(t) = \sum_{i=1}^{K} n_{i,\cdot}(t)$, $\hat{p}_{i,\cdot}(t) = n_{i,\cdot}(t)/n(t)$, $n'(t) = \sum_{j=1}^{K} n_{j,\cdot}(t)$, $\hat{p}_{j,\cdot}(t) = n_{j,\cdot}(t)/n'(t)$.

In Table 2.28, we observe that the initial empirical distribution of ratings is:

$$\hat{\pi}^{(0)} = (3.683\%, 11.242\%, 18.317\%, 23.983\%, 21.517\%, 17.483\%, 3.775\%)$$

We conclude that the long-term dynamics of the Markov chain has dramatically change the initial probability distribution. In Table 2.28, we also observe that the final distribution of ratings after one year is:

$$\hat{\pi}^{(1)} = (3.942\%, 12.708\%, 19.817\%, 23.133\%, 21.458\%, 15.290\%, 3.650\%)$$

We reiterate that the Kolmogorov equation applied to the distribution[73] $\pi^{(n)}$ is given by $\pi^{(n+1)} = P^\top \pi^{(n)}$. In particular, we verify that $\hat{\pi}^{(1)} = \hat{P}^\top \hat{\pi}^{(0)}$ where $\hat{P} = (\hat{p}_{i,j})$. In Figure 2.36, we have reported the dynamics of $\pi^{(n)}$ with $\pi^{(0)} = \hat{\pi}^{(0)}$. We conclude that the distribution of the score $\boldsymbol{\mathcal{S}}(t)$ is not stationary.

Figure 2.36: Dynamics of the probability distribution $\pi^{(n)}$ (migration matrix #1)

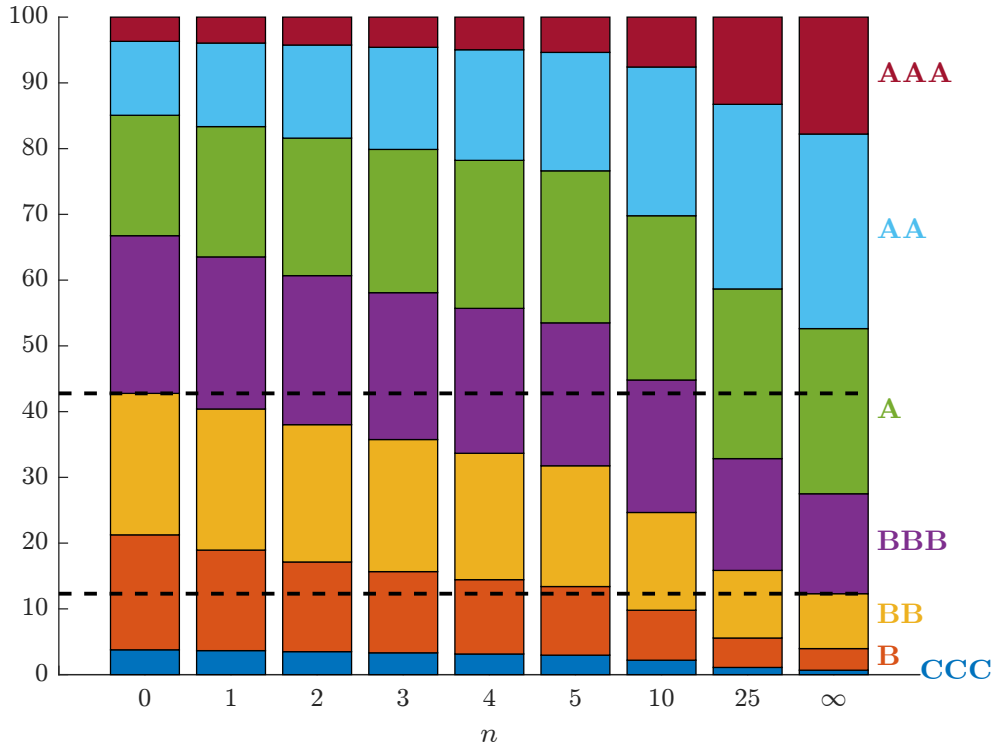


### Continuous-time modeling

**Markov generator** We now consider the case $t \in \mathbb{R}_+$. We note $P(s;t)$ the transition matrix defined as follows:

$$P_{i,j}(s;t) = p(s,i;t,j) = \Pr\{\mathcal{R}(t) = R_j \mid \mathcal{R}(s) = R_i\}$$

Assuming that the Markov chain is time-homogenous, we have $P(t) = P(0;t)$. Jarrow *et al.* (1997) introduce the generator matrix $\Lambda = (\lambda_{i,j})$ where $\lambda_{i,j} \geq 0$ for all $i \neq j$ and $\lambda_{i,i} = -\sum_{j \neq i}^{K} \lambda_{i,j}$. In this case, the transition matrix satisfies the following relationship:

$$P(t) = \exp(t\Lambda) \tag{2.6}$$

[73] We have $\pi_k^{(n)} = \Pr\{\mathcal{R}(n) = R_k\}$.

where $\exp(A)$ is the matrix exponential of $A$. Let us give a probabilistic interpretation of $\Lambda$. If we assume that the probability of jumping from rating $R_i$ to rating $R_j$ in a short time period $\Delta t$ is proportional to $\Delta t$, we have $p(t, i; t + \Delta t, j) = \lambda_{i,j} \Delta t$. The matrix form of this equation is $P(t; t + \Delta t) = \Lambda \, \Delta t$. We deduce that:

$$P(t + \Delta t) = P(t) \, P(t; t + \Delta t) = P(t) \, \Lambda \, \Delta t$$

and:

$$\mathrm{d}P(t) = P(t) \, \Lambda \, \mathrm{d}t$$

Because we have $\exp(\mathbf{0}) = I$, we obtain the solution $P(t) = \exp(t\Lambda)$. We then interpret $\lambda_{i,j}$ as the instantaneous transition rate of jumping from rating $R_i$ to rating $R_j$.

**Remark 27** *In Appendix A.1.1, we present the matrix exponential function and its mathematical properties. In particular, we have* $e^{A+B} = e^A e^B$ *and* $e^{A(s+t)} = e^{As} e^{At}$ *where* $A$ *and* $B$ *are two square matrices such that* $AB = BA$ *and* $s$ *and* $t$ *are two real numbers.*

**Example 8** *We consider a rating system with three states:* A *(good rating),* B *(average rating) and* C *(bad rating). The Markov generator is equal to:*

$$\Lambda = \begin{pmatrix} -0.30 & 0.20 & 0.10 \\ 0.15 & -0.40 & 0.25 \\ 0.10 & 0.15 & -0.25 \end{pmatrix}$$

The one-year transition probability matrix is equal to:

$$P(1) = e^{\Lambda} = \begin{pmatrix} 75.63\% & 14.84\% & 9.53\% \\ 11.63\% & 69.50\% & 18.87\% \\ 8.52\% & 11.73\% & 79.75\% \end{pmatrix}$$

For the two-year maturity, we get:

$$P(2) = e^{2\Lambda} = \begin{pmatrix} 59.74\% & 22.65\% & 17.61\% \\ 18.49\% & 52.24\% & 29.27\% \\ 14.60\% & 18.76\% & 66.63\% \end{pmatrix}$$

We verify that $P(2) = P(1) \cdot P(1)$. This derives from the property of the matrix exponential:

$$P(t) = e^{t\Lambda} = \left(e^{\Lambda}\right)^t = P(1)^t$$

The continuous-time framework allows to calculate transition matrices for non-integer maturities, which do not correspond to full years. For instance, the one-month transition probability matrix of the previous example is equal to:

$$P\left(\frac{1}{12}\right) = e^{\frac{1}{12}\Lambda} = \begin{pmatrix} 97.54\% & 1.62\% & 0.83 \\ 1.22\% & 96.74\% & 2.03 \\ 0.82\% & 1.22\% & 97.95 \end{pmatrix}$$

Box 2.8: Estimation of the Markov generator

One of the issues with the continuous-time framework is to estimate the Markov generator $\Lambda$. One solution consists in using the empirical transition matrix $\hat{P}(t)$, which have been calculated for a given time horizon $t$. In this case, the estimate $\hat{\Lambda}$ must satisfy the relationship $\hat{P}(t) = \exp\left(t\hat{\Lambda}\right)$. We deduce that:

$$\hat{\Lambda} = \frac{1}{t}\ln\left(\hat{P}(t)\right)$$

where $\ln A$ is the matrix logarithm of $A$. However, the matrix $\hat{\Lambda}$ cannot verify the Markov conditions $\hat{\lambda}_{i,j} \geq 0$ for all $i \neq j$ and $\sum_{j=1}^{K} \lambda_{i,j} = 0$. Therefore, Israel *et al.* (2001) propose two estimators to obtain a valid generator:

1. the first approach consists in adding the negative values back into the diagonal values:
$$\begin{cases} \bar{\lambda}_{i,j} = \max\left(\hat{\lambda}_{i,j}, 0\right) & i \neq j \\ \bar{\lambda}_{i,i} = \hat{\lambda}_{i,i} + \sum_{j \neq i} \min\left(\hat{\lambda}_{i,j}, 0\right) \end{cases}$$
2. in the second method, we carry forward the negative values on the matrix entries which have the correct sign:
$$\begin{cases} G_i = \left|\hat{\lambda}_{i,i}\right| + \sum_{j \neq i} \max\left(\hat{\lambda}_{i,j}, 0\right) \\ B_i = \sum_{j \neq i} \max\left(-\hat{\lambda}_{i,j}, 0\right) \\ \tilde{\lambda}_{i,j} = \begin{cases} 0 & \text{if } i \neq j \text{ and } \hat{\lambda}_{i,j} < 0 \\ \hat{\lambda}_{i,j} - B_i \left|\hat{\lambda}_{i,j}\right| / G_i & \text{if } G_i > 0 \\ \hat{\lambda}_{i,j} & \text{if } G_i = 0 \end{cases} \end{cases}$$

**Markov property** The Markov property refers to the lack of memory of stochastic processes. This implies that the probability distribution of future states of the process conditional on both past and present values depends only upon the present state. Therefore, given the present, the future does not depend on the past. In order to better understand the implications of this property, we consider the following example with three companies:

| $t-2$ | | $t-1$ | | $t$ | | $t+1$ |
|---|---|---|---|---|---|---|
| AAA | $\longrightarrow$ | BBB | $\longrightarrow$ | BBB | $\longrightarrow$ | ? |
| BBB | $\longrightarrow$ | BBB | $\longrightarrow$ | BBB | $\longrightarrow$ | ? |
| BB | $\longrightarrow$ | BB | $\longrightarrow$ | BBB | $\longrightarrow$ | ? |

Today, the three companies are rated BBB. We would like to predict the ESG rating of those companies at time $t+1$. If the ESG ratings are Markovian, these entities are equivalent and have the same conditional probabilities to become AAA, AA, etc. Otherwise, this means that the conditional probabilities depend on the past trajectory. In this case, we have:

$$\Pr\left\{\mathcal{R}_{c_1}(t+1) = R_j \mid \mathcal{R}_{c_1}(t) = R_i\right\} \neq \Pr\left\{\mathcal{R}_{c_2}(t+1) = R_j \mid \mathcal{R}_{c_2}(t) = R_i\right\}$$

for two different companies $c_1$ and $c_2$. In our example, the firms have different past trajectories. They don't have the same transition matrix if the rating process has not the Markov property.

To verify the Markov property, we compute the matrix $\Lambda' = \ln(P)$ and measure whether $\Lambda'$ is a Markov generator or not. Using the rating migration matrix #1, we obtain the results given in Table 2.29. We notice that $\ln P$ is not a Makov generator since 11 off-diagonal elements are not positive. Using the first method of Israel *et al.* (2001) described in Box 2.8, we transform this matrix into a Markov generator[74] $\bar{\Lambda}$ (Table 2.30). We recompute the one-year transition matrix $\bar{P}(1) = \exp\left(\bar{\Lambda}\right)$ and observe some small differences with the original transition matrix (see Table 2.31 vs. Table 2.22).

Table 2.29: Non-Markov generator $\Lambda' = \ln(P)$ of the migration matrix #1 (in %)

| | AAA | AA | A | BBB | BB | B | CCC |
|---|---|---|---|---|---|---|---|
| AAA | −7.663 | 6.427 | 0.542 | 0.466 | 0.245 | −0.016 | −0.000 |
| AA | 4.770 | −20.604 | 15.451 | −0.001 | 0.318 | 0.066 | −0.001 |
| A | −0.267 | 20.259 | −35.172 | 14.953 | 0.152 | 0.083 | −0.008 |
| BBB | 0.102 | −1.051 | 28.263 | −40.366 | 13.100 | −0.128 | 0.080 |
| BB | 0.032 | 0.307 | −1.762 | 28.351 | −37.889 | 10.832 | 0.129 |
| B | −0.005 | −0.008 | 0.503 | −2.240 | 30.227 | −31.482 | 3.006 |
| CCC | 0.000 | −0.024 | 0.194 | 0.469 | 0.365 | 16.806 | −17.810 |

Table 2.30: Markov generator of the migration matrix #1 (in %)

| | AAA | AA | A | BBB | BB | B | CCC |
|---|---|---|---|---|---|---|---|
| AAA | −7.679 | 6.427 | 0.542 | 0.466 | 0.245 | 0.000 | 0.000 |
| AA | 4.770 | −20.606 | 15.451 | 0.000 | 0.318 | 0.066 | 0.000 |
| A | 0.000 | 20.259 | −35.447 | 14.953 | 0.152 | 0.083 | 0.000 |
| BBB | 0.102 | 0.000 | 28.263 | −41.545 | 13.100 | 0.000 | 0.080 |
| BB | 0.032 | 0.307 | 0.000 | 38.351 | −39.651 | 10.832 | 0.129 |
| B | 0.000 | 0.000 | 0.503 | 0.000 | 30.227 | −33.735 | 3.006 |
| CCC | 0.000 | 0.000 | 0.194 | 0.469 | 0.365 | 16.806 | −17.834 |

Table 2.31: ESG migration Markov matrix #1 (one-year transition probability in %)

| | AAA | AA | A | BBB | BB | B | CCC |
|---|---|---|---|---|---|---|---|
| AAA | 92.75 | 5.66 | 0.90 | 0.45 | 0.23 | 0.01 | 0.00 |
| AA | 4.17 | 82.73 | 11.85 | 0.89 | 0.30 | 0.07 | 0.00 |
| A | 0.40 | 15.51 | 72.79 | 10.39 | 0.81 | 0.10 | 0.01 |
| BBB | 0.12 | 2.11 | 19.60 | 68.69 | 8.91 | 0.50 | 0.07 |
| BB | 0.04 | 0.43 | 2.79 | 19.25 | 69.65 | 7.61 | 0.23 |
| B | 0.01 | 0.09 | 0.65 | 2.98 | 21.21 | 72.71 | 2.35 |
| CCC | 0.00 | 0.02 | 0.25 | 0.58 | 2.19 | 13.09 | 83.87 |

[74] The matrix $\bar{\Lambda}$ is the best Markov generator that minimize the $\mathcal{L}_1$-norm distance to $P$.

**Dynamic analysis** We have now all the tools to conduct a dynamic analysis of the ESG rating system. There is tremendous potential. For instance, we compute the probability to reach the states $\mathcal{A}$ with the following formula:

$$\pi_k(t, \mathcal{A}) = \Pr\{\mathcal{R}(t) \in \mathcal{A} \mid \mathcal{R}(0) = k\} = \sum_{j \in \mathcal{A}} \mathbf{e}_k^\top e^{t\Lambda} \mathbf{e}_j^\top$$

Some examples are given in Figure 2.37. We can also use the continuous-time framework to investigate the probability density function of conditional events, the probability over a given interval, the $m$-order derivative of time functions, etc. We use the properties $\partial_t \exp(\Lambda t) = \Lambda \exp(\Lambda t)$, $\partial_t^m \exp(\Lambda t) = \Lambda^m \exp(\Lambda t)$ and[75] $\int_0^t e^{\Lambda s}\,\mathrm{d}s = \left(e^{\Lambda t} - I_K\right)\Lambda^{-1}$. For example, we have:

$$\pi_k^{(m)}(t, \mathcal{A}) := \frac{\partial\, \pi_k(t, \mathcal{A})}{\partial\, t^m} = \sum_{j \in \mathcal{A}} \mathbf{e}_k^\top \Lambda^m e^{t\Lambda} \mathbf{e}_j^\top$$

$\pi_k^{(1)}(t, \mathcal{A})$ may be interpreted as a "*time density function*". In Figure 2.37, we report $\pi_k(t, \mathsf{AAA})$, $\pi_k^{(1)}(t, \mathsf{AAA})$, $\pi_k(t, \mathsf{CCC})$ and $\pi_k^{(1)}(t, \mathsf{CCC})$. We observe the strange behavior of the CCC rating towards the AAA rating.

Figure 2.37: Probability $\pi_k(t, \mathcal{A})$ to reach $\mathcal{A}$ at time t (migration matrix #1)

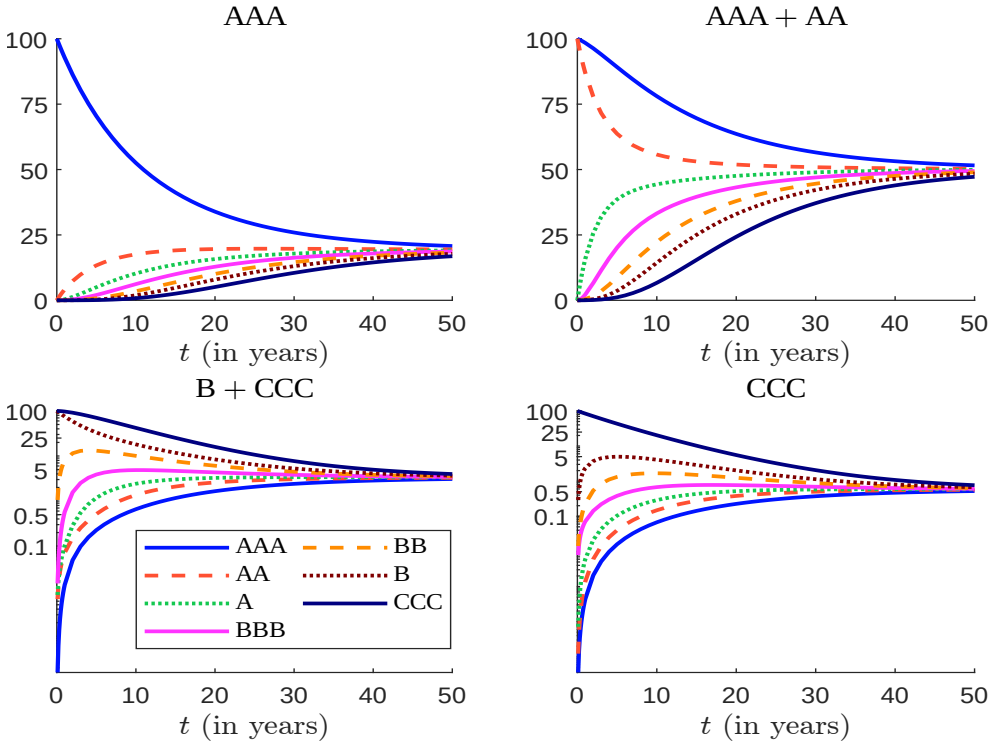


**Remark 28** *The previous analysis can be used to check consistency of ratings. In particular, the fact that ratings satisfy ordering preferences implies that we must generally observe a monotone behavior of quantities that are a non-decreasing and concave function of ratings.*

[75] For more general integrals of type $\int_0^t e^{\Lambda s} Q f(s)\,\mathrm{d}s$, we use the numerical algorithms developed by Van Loan (1978).

Figure 2.38: Time functions $\pi_k(t, \mathsf{AAA})$, $\pi_k^{(1)}(t, \mathsf{AAA})$, $\pi_k(t, \mathsf{CCC})$ and $\pi_k^{(1)}(t, \mathsf{CCC})$ (migration matrix #1)

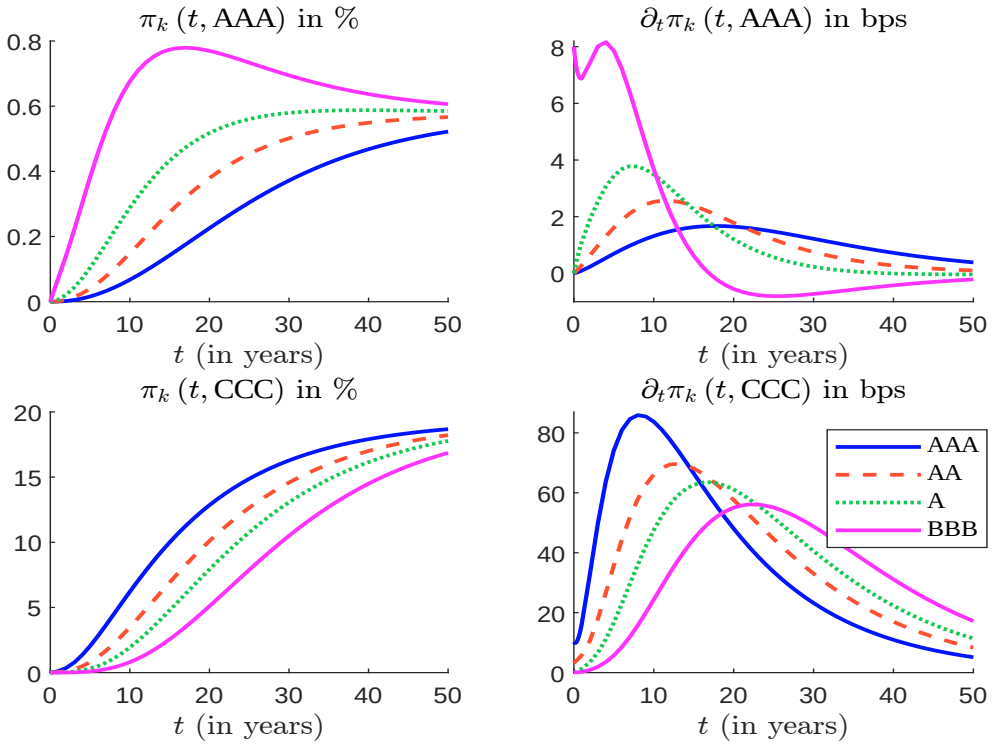


Box 2.9: Computing statistical moments with continuous-time Markov chains

The distribution $\pi(t)$ follows the Kolmogorov equation:

$$\frac{\mathrm{d}\pi(t)}{\mathrm{d}t} = \Lambda\pi(t)$$

It follows that $\pi(t) = e^{\Lambda t}\pi(0)$. Let $Y(t) = \phi(\mathcal{R}(t))$ be a random variable that depends on the ratings. We have:

$$\mu(t) = \sum_{k=1}^{K} \phi(R_k)\,\pi_k(t)$$

and:

$$\sigma^2(t) = \sum_{k=1}^{K} (\phi(R_k) - \mu(t))^2\,\pi_k(t)$$

### 2.3.4 Comparison with credit ratings

The modeling of credit ratings is similar than this of ESG ratings, but there is one important difference. The states include the default state. This means that $R_K$ is the absorbing state, implying that any entity which has reached this state remains in this state. In this case, $p_{i,K}$ is the one-period default probability of rating $R_i$ and we have $p_{K,K} = 1$. An example of credit migration matrix is given in Table 2.32. It is the S&P one-year transition probability matrix for corporate bonds estimated by Kavvathas (2001) for the period 1960–1998. More recent credit migration matrices[76] are given in Table 2.33.

Table 2.32: Example of credit migration matrix (one-year probability transition in %)

| | AAA | AA | A | BBB | BB | B | CCC | D |
|---|---|---|---|---|---|---|---|---|
| AAA | 92.82 | 6.50 | 0.56 | 0.06 | 0.06 | 0.00 | 0.00 | 0.00 |
| AA | 0.63 | 91.87 | 6.64 | 0.65 | 0.06 | 0.11 | 0.04 | 0.00 |
| A | 0.08 | 2.26 | 91.66 | 5.11 | 0.61 | 0.23 | 0.01 | 0.04 |
| BBB | 0.05 | 0.27 | 5.84 | 87.74 | 4.74 | 0.98 | 0.16 | 0.22 |
| BB | 0.04 | 0.11 | 0.64 | 7.85 | 81.14 | 8.27 | 0.89 | 1.06 |
| B | 0.00 | 0.11 | 0.30 | 0.42 | 6.75 | 83.07 | 3.86 | 5.49 |
| CCC | 0.19 | 0.00 | 0.38 | 0.75 | 2.44 | 12.03 | 60.71 | 23.50 |
| D | 0.00 | 0.00 | 0.00 | 0.00 | 0.00 | 0.00 | 0.00 | 100.00 |

Source: Kavvathas (2001).

Table 2.33: Credit migration matrix in % (Moody's, 1983–2021)

| | Aaa | Aa | A | Baa | Ba | B | Caa | W | D |
|---|---|---|---|---|---|---|---|---|---|
| Sovereign issuers | | | | | | | | | |
| Aaa | 96.99 | 2.87 | 0.03 | 0.08 | 0.00 | 0.00 | 0.00 | 0.03 | 0.00 |
| Aa | 2.73 | 93.52 | 2.56 | 0.62 | 0.09 | 0.00 | 0.00 | 0.47 | 0.00 |
| A | 0.00 | 3.60 | 92.17 | 3.19 | 0.98 | 0.06 | 0.00 | 0.00 | 0.00 |
| Baa | 0.00 | 0.00 | 5.43 | 89.17 | 4.98 | 0.39 | 0.03 | 0.00 | 0.00 |
| Ba | 0.00 | 0.00 | 0.00 | 6.91 | 85.72 | 6.53 | 0.29 | 0.10 | 0.44 |
| B | 0.00 | 0.00 | 0.00 | 0.00 | 4.31 | 88.49 | 4.50 | 0.26 | 2.43 |
| Caa | 0.00 | 0.00 | 0.00 | 0.00 | 0.06 | 13.60 | 73.24 | 0.75 | 12.35 |
| Corporates issuers | | | | | | | | | |
| Aaa | 87.16 | 8.05 | 0.45 | 0.08 | 0.03 | 0.00 | 0.00 | 4.23 | 0.00 |
| Aa | 0.70 | 85.02 | 8.57 | 0.42 | 0.06 | 0.04 | 0.02 | 5.17 | 0.02 |
| A | 0.05 | 2.44 | 86.84 | 5.15 | 0.45 | 0.10 | 0.04 | 4.88 | 0.05 |
| Baa | 0.02 | 0.12 | 3.73 | 86.43 | 3.42 | 0.65 | 0.16 | 5.31 | 0.15 |
| Ba | 0.00 | 0.03 | 0.38 | 6.02 | 75.95 | 7.19 | 0.86 | 8.78 | 0.77 |
| B | 0.01 | 0.03 | 0.12 | 0.42 | 4.73 | 73.61 | 7.34 | 10.79 | 2.95 |
| Caa | 0.00 | 0.01 | 0.02 | 0.07 | 0.26 | 5.58 | 70.41 | 14.82 | 8.83 |

Source: Moody's (2020).

[76] W means that the issuer has required to stop the rating (withdrawn).

Since there are few research on ESG ratings, credit migration matrices can be used as a benchmark to compare the two rating systems. For that, we consider the trace statistics:

$$\lambda(t) = \frac{\text{trace}\left(e^{t\Lambda}\right)}{K}$$

It is the average of the diagonal transition probabilities. It measures the average probability to remain in its state[77]. Results are reported in Figure 2.39. Even if the two ESG rating systems used here are fictitious examples, we generally conclude that ESG rating systems are less stable than credit rating systems, and the time horizon of ESG ratings for prediction is shorter.

Figure 2.39: Trace statistics of credit and ESG migration matrices

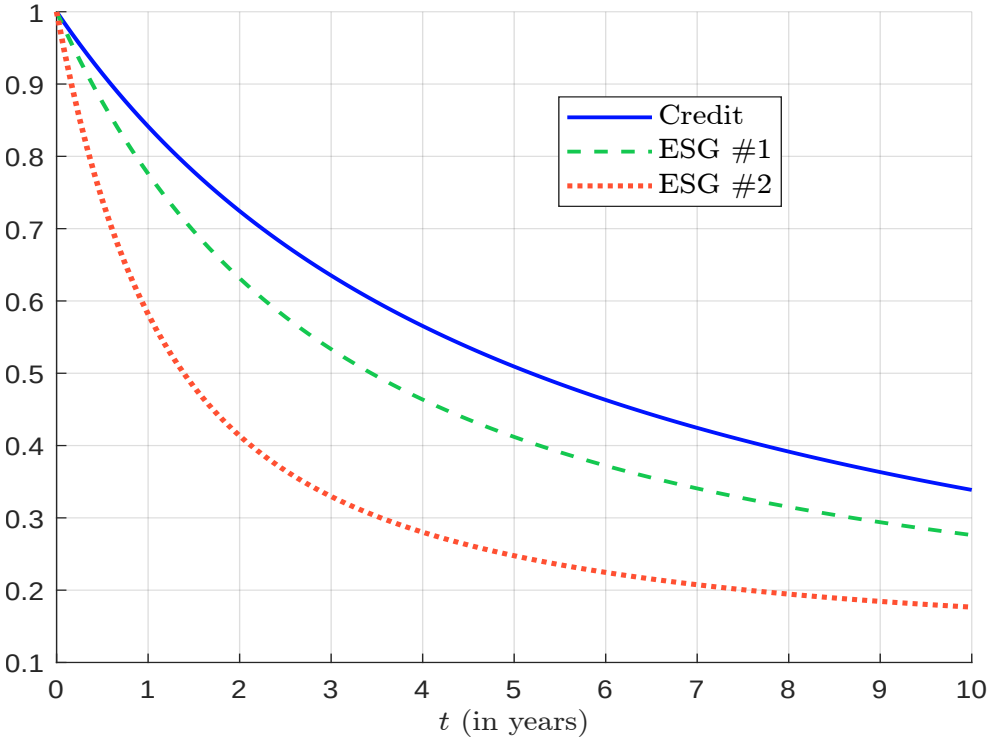


## 2.4 Exercises

### 2.4.1 Score normalization when the features are independent

We study the behavior of the score defined as:

$$\mathcal{S} = \frac{X_1 + X_2 + \cdots + X_m}{m}$$

where $X_1, \ldots, X_m$ is a sequence of *iid* uniform random variables, whose distribution is $\mathbf{F}$.

1. We consider the case $m = 2$ and $X_j \sim \mathcal{U}_{[0,1]}$. The score is a weighted average of $X_1$ and $X_2$:

$$\mathcal{S} = \omega X_1 + (1 - \omega) X_2$$

where $\omega \in [0, 1]$.

[77] For a credit migration matrix, we consider all the states except the absorbing state. In this case, we have $\lim_{t\to\infty} \lambda(t) = 0$.

(a) Let $s \in [0,1]$. Find the points of intersection between the curve $x_2 = (s - \omega X_1) / (1 - \omega)$ and the unit square. Discuss the different cases.

(b) For each case, compute the area $\mathcal{A}(s)$ defined as:

$$\mathcal{A}(s) = \iint_{\Omega(s)} \mathrm{d}x_1 \, \mathrm{d}x_2$$

where $\Omega(s) = \left\{(x_1, x_2) \in [0,1]^2 : \omega x_1 + (1-\omega) x_2 \leq s\right\}$. Deduce the cumulative distribution function $\mathbf{G}$ of the score.

(c) Compute the density function $g$.

(d) Find $\mathbf{G}$ and $g$ when $X_j \sim \mathcal{U}_{[a,b]}$ where $b > a$.

2. We consider the case $m = 3$ and $X_j \sim \mathcal{U}_{[0,1]}$. The volume $\mathcal{V}(s)$ is equal to:

$$\mathcal{V}(s) = \iiint_{\Omega(s)} \mathrm{d}x_1 \, \mathrm{d}x_2 \, \mathrm{d}x_3$$

where $\Omega(s) = \left\{(x_1, x_2, x_3) \in [0,1]^3 : x_1 + x_2 + x_3 \leq s\right\}$.

(a) Compute the volume $\mathcal{V}(s)$ when $0 \leq s \leq 1$.

(b) Compute the volume difference $\mathcal{V}(s) - \mathcal{V}(1)$ when $1 \leq s \leq 2$.

(c) Compute the volume difference $\mathcal{V}(s) - \mathcal{V}(2)$ when $1 \leq s \leq 2$.

(d) Deduce the cumulative distribution function $\mathbf{G}$ of the score.

(e) Compute the density function $g$.

3. We consider that $X_j \sim \mathcal{U}_{[0,1]}$ and $m \geq 1$. We note $\mathbf{G}_m(s)$ the probability $\Pr\{\boldsymbol{\mathcal{S}} \leq s\}$.

(a) Give the expression of $\mathbf{G}_m(s)$ and the associate density function $g_m(s)$.

(b) We assume that $X_j \sim \mathcal{U}_{[a,b]}$ where $b > a$. Deduce the expressions of the density and distribution functions of the score $\boldsymbol{\mathcal{S}}$.

4. We assume that $X_j \sim \mathcal{G}(\alpha_j, \beta)$ where $\alpha_j > 0$ and $\beta > 0$.

(a) Compute the cumulative distribution function $\mathbf{G}$ of the score.

(b) Deduce the density function $g$.

(c) Compute the mean and the variance of $\boldsymbol{\mathcal{S}}$.

(d) We assume that $\alpha_j = 2$ and $\beta = 2$.

i. Draw the functions $\mathbb{E}[\boldsymbol{\mathcal{S}}]$ and $\mathrm{var}(\boldsymbol{\mathcal{S}})$ with respect to the number $m$ of features.

ii. Find the value $m^+(p, \varepsilon)$ such that:

$$m^+(p, \varepsilon) = \{\inf m : \Pr\{2 - \varepsilon \leq \boldsymbol{\mathcal{S}} \leq 2 - \varepsilon\} \leq p\}$$

for the pairs $(p, \varepsilon) = (99\%, 5\%)$.

iii. Draw the function $m^+(p, \varepsilon)$ with respect to $p$ when $\varepsilon = 1\%$.

iv. Draw the function $m^+(p, \varepsilon)$ with respect to $\varepsilon$ when $p = 99.99\%$.

### 2.4.2 Probability distribution of an ESG score

1. We consider an investment universe of 8 issuers with the following ESG scores:

| Issuer | #1 | #2 | #3 | #4 | #5 | #6 | #7 | #8 |
|---|---|---|---|---|---|---|---|---|
| E | −2.80 | −1.80 | −1.75 | 0.60 | 0.75 | 1.30 | 1.90 | 2.70 |
| S | −1.70 | −1.90 | 0.75 | −1.60 | 1.85 | 1.05 | 0.90 | 0.70 |
| G | 0.30 | −0.70 | −2.75 | 2.60 | 0.45 | 2.35 | 2.20 | 1.70 |

   (a) Calculate the ESG score of the issuers if we assume the following weighting scheme: 40% for E, 40% for S and 20% for G.

   (b) Calculate the ESG score of the equally-weighted portfolio $x_{\text{ew}}$.

2. We assume that the ESG scores are *iid* and follow a standard Gaussian distribution:

$$\boldsymbol{\mathcal{S}}_i \sim \mathcal{N}(0,1)$$

   (a) We note $x_{\text{ew}}^{(n)}$ the equally-weighted portfolio composed of $n$ issuers. Calculate the distribution of the ESG score $\boldsymbol{\mathcal{S}}\left(x_{\text{ew}}^{(n)}\right)$ of the portfolio $x_{\text{ew}}^{(n)}$.

   (b) What is the ESG score of a well-diversified portfolio?

   (c) We note $T \sim \mathbf{F}_\alpha$ where $\mathbf{F}_\alpha(t) = t^\alpha$, $t \in [0,1]$ and $\alpha \geq 0$. Draw the graph of the probability density function $f_\alpha(t)$ when $\alpha$ is respectively equal to 0.5, 1.5, 2.5 and 70. What do you notice?

   (d) We assume that the weights of the portfolio[78] $x = (x_1, \ldots, x_n)$ follow a power-law distribution $\mathbf{F}_\alpha$:

$$x_i \sim cT_i$$

   where $T_i \sim \mathbf{F}_\alpha$ are *iid* random variables and $c$ is a normalization constant. Explain how to simulate the portfolio weights $x = (x_1, \ldots, x_n)$. Represent one simulation of the portfolio $x$ for the previous values of $\alpha$. Comment on these results. Deduce the relationship between the Herfindahl index $\mathcal{H}_\alpha(x)$ of the portfolio weights $x$ and the parameter $\alpha$.

   (e) We assume that the weight $x_i$ and the ESG score $\boldsymbol{\mathcal{S}}_i$ of the issuer $i$ are independent. How to simulate the portfolio's score $\boldsymbol{\mathcal{S}}(x)$? Using 50 000 replications, estimate the probability distribution function of $\boldsymbol{\mathcal{S}}(x)$ by the Monte Carlo method. Comment on these results.

   (f) We now assume that the weight $x_i$ and the ESG score $\boldsymbol{\mathcal{S}}_i$ of the issuer $i$ are positively correlated. More precisely, the dependence function between $x_i$ and $\boldsymbol{\mathcal{S}}_i$ is the Normal copula function with parameter $\rho$. Show that this is also the copula function between $T_i$ and $\boldsymbol{\mathcal{S}}_i$. Deduce an algorithm to simulate $\boldsymbol{\mathcal{S}}(x)$.

   (g) Using 50 000 replications, estimate the probability distribution function of $\boldsymbol{\mathcal{S}}(x)$ by the Monte Carlo method when the correlation parameter $\rho$ is set to 50%. Comment on these results.

   (h) Estimate the relationship between the correlation parameter $\rho$ and the expected ESG score $\mathbb{E}[\boldsymbol{\mathcal{S}}(x)]$ of the portfolio $x$. Comment on these results.

   (i) How are the previous results related to the size bias of ESG scoring?

[78] We use $n = 50$ in the rest of the exercise.

3. Let $\boldsymbol{\mathcal{S}}$ be the ESG score of the issuer. We assume that the ESG score follows a standard Gaussian distribution:

$$\boldsymbol{\mathcal{S}} \sim \mathcal{N}(0,1)$$

The ESG score $\boldsymbol{\mathcal{S}}$ is also converted into an ESG rating $\mathcal{R}$, which can take the values[79] **A**, **B**, **C** and **D**.

   (a) We assume that the breakpoints of the rating system are $-1.5$, 0 and $+1.5$. Compute the frequencies of the ratings.

   (b) We would like to build a rating system such that each category has the same frequency. Find the mapping function.

   (c) We would like to build a rating system such that the frequency of the median ratings **B** and **C** is 40% and the frequency of the extreme ratings **A** and **D** is 10%. Find the mapping function.

4. Let $\boldsymbol{\mathcal{S}}(t)$ be the ESG score of the issuer at time $t$. The ESG scoring system is evaluated every month. The index time $t$ corresponds to the current month, whereas the previous month is $t-1$. We assume that:

   i. The ESG score at time $t-1$ follows a standard Gaussian distribution:

$$\boldsymbol{\mathcal{S}}(t-1) \sim \mathcal{N}(0,1)$$

   ii. The variation of the ESG score is Gaussian between two months:

$$\Delta\boldsymbol{\mathcal{S}}(t) = \boldsymbol{\mathcal{S}}(t) - \boldsymbol{\mathcal{S}}(t-1) \sim \mathcal{N}\left(0, \sigma^2\right)$$

   iii. The ESG score $\boldsymbol{\mathcal{S}}(t-1)$ and the variation $\Delta\boldsymbol{\mathcal{S}}(t)$ are independent.

   The ESG score $\boldsymbol{\mathcal{S}}(t)$ is converted into an ESG rating $\mathcal{R}(t)$, which can take following grades:

$$\mathcal{R}_1 \prec \mathcal{R}_2 \prec \cdots \prec \mathcal{R}_k \prec \cdots \prec \mathcal{R}_{K-1} \prec \mathcal{R}_K$$

   We assume that the breakpoints of the rating system are $(s_1, s_2, \ldots, s_{K-1})$. We also note $s_0 = -\infty$ and $s_K = +\infty$.

   (a) Compute the bivariate probability distribution of the random vector $(\boldsymbol{\mathcal{S}}(t-1), \Delta\boldsymbol{\mathcal{S}}(t))$.

   (b) Compute the bivariate distribution of the random vector $(\boldsymbol{\mathcal{S}}(t-1), \boldsymbol{\mathcal{S}}(t))$.

   (c) Compute the probability $p_k = \Pr\{\mathcal{R}(t-1) = \mathcal{R}_k\}$.

   (d) Compute the joint probability $\Pr\{\mathcal{R}(t) = \mathcal{R}_k, \mathcal{R}(t-1) = \mathcal{R}_j\}$.

   (e) Compute the transition probability $p_{j,k} = \Pr\{\mathcal{R}(t) = \mathcal{R}_k \mid \mathcal{R}(t-1) = \mathcal{R}_j\}$.

   (f) Compute the monthly turnover $\mathcal{T}(\mathcal{R}_k)$ of the ESG rating $\mathcal{R}_k$.

   (g) Compute the monthly turnover $\mathcal{T}(\mathcal{R}_1, \ldots, \mathcal{R}_K)$ of the ESG rating system.

   (h) For each rating system given in Questions 3.a, 3.b and 3.c, compute the corresponding migration matrix and the monthly turnover of the rating system if we assume that $\sigma$ is equal to 10%. What is the best ESG rating system if we would like to control the turnover of ESG ratings?

[79] **A** is the best rating and **D** is the worst rating.

(i) Draw the relationship between the parameter $\sigma$ and the turnover $\mathcal{T}(\mathcal{R}_1, \ldots, \mathcal{R}_K)$ for the three ESG rating systems.

(j) We consider a uniform ESG rating system where:

$$\Pr\{\mathcal{R}(t-1) = \mathcal{R}_k\} = \frac{1}{K}$$

Draw the relationship between the number of notches $K$ and the turnover $\mathcal{T}(\mathcal{R}_1, \ldots, \mathcal{R}_K)$ when the parameter $\sigma$ takes the values 5%, 10% and 25%.

(k) Why is an ESG rating system different than a credit rating system? What do you conclude from the previous analysis? What is the issue of ESG exclusion policy and negative screening?

# Chapter 3

# Impact of ESG Investing on Asset Prices and Portfolio Returns

The question of ESG performance is on everyone's lips. This question is linked to several other questions, which can be summarized as follows: What is the impact of ESG on corporate financial performance? What is the impact of ESG investing on risk premia? How does ESG screening affect portfolio returns? Is there a difference between ESG investing and climate investing? In fact, we can multiply the questions because the term *ESG performance* covers different topics, and we need to be more precise when we talk about it. First, we need to distinguish between operational performance, social performance, accounting performance, market performance, etc. For example, it is not the same thing to measure performance based on financial statements (balance sheet and income statement) or share price evolution. Second, we can measure performance from an investor's or issuer's perspective. The third ambiguity concerns the nature of the financial assets. Are they stocks or bonds? Because we know that fixed-income and equity markets react differently. Another important source of discrepancy is the choice of financial instruments. We can compare the performance of securities, mutual funds, asset owners or backtests. For example, simulated performance must be different from live performance. The fifth issue is the investment universe and sample. We can imagine that the impact of ESG is different from one region to another, from one sector to another, one period to another, etc. Finally, if we focus on the financial performance of ESG strategies, the last question is the implementation of the portfolio strategy. Are we talking about an exclusion, selection, integration or momentum strategy? Are we talking about active or passive management? Moreover, since ESG scores vary widely from one rating agency to another, we are not sure that we are capturing the performance of the ESG market, but perhaps some idiosyncratic patterns. There are therefore many factors to consider, and it is no coincidence that there are many academic studies with different conclusions. It is impossible to cite all of them, even the most famous. They are described in meta-analyses, *e.g.*, Orlitzky *et al.* (2003), Margolis *et al.* (2009), Friede *et al.* (2015), Atz *et al.* (2022) and Coqueret (2022). Rather than delve into all these empirical studies, we take a different approach. In fact, fifteen or twenty years ago, ESG investing did not exist or was so marginal. Moreover, ESG data is certainly not robust or relevant before 2010. Therefore, it is better to focus on theoretical research when analyzing the performance of ESG investing. This first section is mainly based on the work of Pástor *et al.* (2021) and Pedersen *et al.* (2021). It will help us understand when, where and why ESG investing may underperform or outperform business-as-usual investing. The second section is devoted to empirical studies, but we make a selection to illustrate the theoretical results and concepts defined in the first section. Finally, the third section examines the impact of ESG on the cost of capital.

## 3.1 Theoretical models

Before discussing the impact of ESG on the theory of risk premia and security selection, we summarize the main results of modern portfolio theory as presented in Roncalli (2013).

### 3.1.1 An introduction to modern portfolio theory

The concept of the market portfolio has a long history, dating back to the seminal work of Markowitz (1952). He showed that an efficient portfolio is the portfolio that maximizes the expected return for a given level of risk. Markowitz concluded that there is not just one optimal portfolio, but a set of optimal portfolios called the efficient frontier. By studying the liquidity preference, Tobin (1958) showed that the efficient frontier becomes a straight line in the presence of a risk-free asset. In this case, optimal portfolios correspond to a combination of the risk-free asset and a particular efficient portfolio named the tangency portfolio. Sharpe (1964) summarized the results of Markowitz and Tobin as follows: "*the process of investment choice can be broken down into two phases: first, the choice of a unique optimum combination of risky assets*[1]*; and second, a separate choice concerning the allocation of funds between such a combination and a single riskless asset.*" This two-step process is today known as the *mutual fund separation theorem*. In this seminal research paper, Sharpe developed the CAPM theory and emphasized the relationship between the risk premium of the asset (the difference between the expected return and the risk-free rate) and its beta (the systematic risk with respect to the tangency portfolio). Assuming that the market is at equilibrium, he showed that asset prices are such that the tangency portfolio is the market portfolio, which is composed of all risky assets in proportion to their market capitalization.

#### The efficient frontier

**The optimization problem** Seventy years ago, Markowitz introduced the concept of the efficient frontier. Consider a universe of $n$ assets. Let $w = (w_1, \ldots, w_n)$ be the vector of weights in the portfolio. We assume that the portfolio is fully invested, so $\sum_{i=1}^n w_i = \mathbf{1}_n^\top w = 1$. We denote $R = (R_1, \ldots, R_n)$ the vector of asset returns where $R_i$ is the return of asset $i$. The portfolio return is then $R(w) = \sum_{i=1}^n w_i R_i = w^\top R$. Let $\mu = \mathbb{E}[R]$ and $\Sigma = \mathbb{E}\left[(R-\mu)(R-\mu)^\top\right]$ be the vector of expected returns and the covariance matrix of asset returns. The expected return $\mu(w) := \mathbb{E}[R(w)]$ of the portfolio is equal to:

$$\mu(w) = \mathbb{E}\left[w^\top R\right] = w^\top \mathbb{E}[R] = w^\top \mu$$

while its variance $\sigma^2(w) := \operatorname{var}(R(w))$ is given by:

$$\begin{aligned}
\sigma^2(w) &= \mathbb{E}\left[(R(w) - \mu(w))(R(w) - \mu(w))^\top\right] \\
&= \mathbb{E}\left[w^\top (R-\mu)(R-\mu)^\top w\right] \\
&= w^\top \Sigma w
\end{aligned}$$

We can then formulate the investor's financial problem as follows:

1. Maximize the expected return of the portfolio under a volatility constraint ($\sigma$-problem):

$$\max \mu(w) \quad \text{s.t.} \quad \sigma(w) \leq \sigma^\star \tag{3.1}$$

[1] It is precisely the tangency portfolio.

2. Or minimize the volatility of the portfolio under a return constraint ($\mu$-problem):

$$\min \sigma(w) \quad \text{s.t.} \quad \mu(w) \geq \mu^\star \tag{3.2}$$

By considering all the portfolios belonging to the simplex set defined by $\left\{w \in [0,1]^n : \mathbf{1}_n^\top w = 1\right\}$, we can compute the expected return and volatility bounds of the portfolios: $\mu^- \leq \mu(w) \leq \mu^+$ and $\sigma^- \leq \sigma(w) \leq \sigma^+$. There is also a solution to the first problem if $\sigma^\star \geq \sigma^-$. The second problem has a solution if $\mu^\star \leq \mu^+$. When these two conditions are verified, the inequality constraints become $\sigma(w) = \min(\sigma^\star, \sigma^+)$ and $\mu(w) = \max(\mu^-, \mu^\star)$.

The key idea of Markowitz (1956) was to transform the original nonlinear optimization problem (3.1) into a quadratic optimization problem which is easier to solve numerically. To do this, he introduced the mean-variance (or quadratic) utility function:

$$\boldsymbol{\mathcal{U}}(w) := \mathbb{E}[R(w)] - \frac{\bar{\gamma}}{2}\operatorname{var}(R(w)) = w^\top \mu - \frac{\bar{\gamma}}{2} w^\top \Sigma w$$

where $\bar{\gamma}$ is the absolute risk-aversion parameter. We get the following problem:

$$\begin{aligned} w^\star(\bar{\gamma}) &= \arg\max \left\{\boldsymbol{\mathcal{U}}(w) = w^\top \mu - \frac{\bar{\gamma}}{2} w^\top \Sigma w\right\} \\ &\text{s.t.} \quad \mathbf{1}_n^\top w = 1 \end{aligned} \tag{3.3}$$

If $\bar{\gamma} = 0$, the optimized portfolio is the one that maximizes the expected return and we have $\mu(w^\star(0)) = \mu^+$. If $\bar{\gamma} = \infty$, the risk-aversion parameter is maximum, we obtain the global minimum variance (GMV) portfolio:

$$\begin{aligned} w^\star(\infty) &= \arg\min \frac{1}{2} w^\top \Sigma w \\ &\text{s.t.} \quad \mathbf{1}_n^\top w = 1 \end{aligned}$$

and we have $\sigma(w^\star(\infty)) = \sigma^-$. In practice, we formulate the optimization problem (3.3) as follows:

$$\begin{aligned} w^\star(\gamma) &= \arg\min \frac{1}{2} w^\top \Sigma w - \gamma w^\top \mu \\ &\text{s.t.} \quad \mathbf{1}_n^\top w = 1 \end{aligned} \tag{3.4}$$

where $\gamma = \bar{\gamma}^{-1}$ is the inverse of the risk-aversion parameter and is called the risk-tolerance coefficient. The reason is that this new formulation is a standard quadratic programming (QP) problem[2]. From a numerical point of view, it is therefore better to use Problem (3.4). In this case, the minimum variance portfolio corresponds to $\gamma = 0$. The set of solutions $\{w^\star(\gamma), \gamma \geq 0\}$ corresponds to mean-variance optimized (MVO) portfolios.

**Example 9** *Consider an investment universe with five assets. Their expected returns are equal to* 5%, 7%, 6%, 10% *and* 8% *while their volatilities are equal to* 18%, 20%, 22%, 25% *and* 30%. *The correlation matrix of the asset returns is given by the following matrix:*

$$\mathbb{C} = \begin{pmatrix} 100\% & & & & \\ 70\% & 100\% & & & \\ 20\% & 30\% & 100\% & & \\ -30\% & 20\% & 10\% & 100\% & \\ 0\% & 0\% & 0\% & 0\% & 100\% \end{pmatrix}$$

Figure 3.1: Efficient frontier (Example 9)

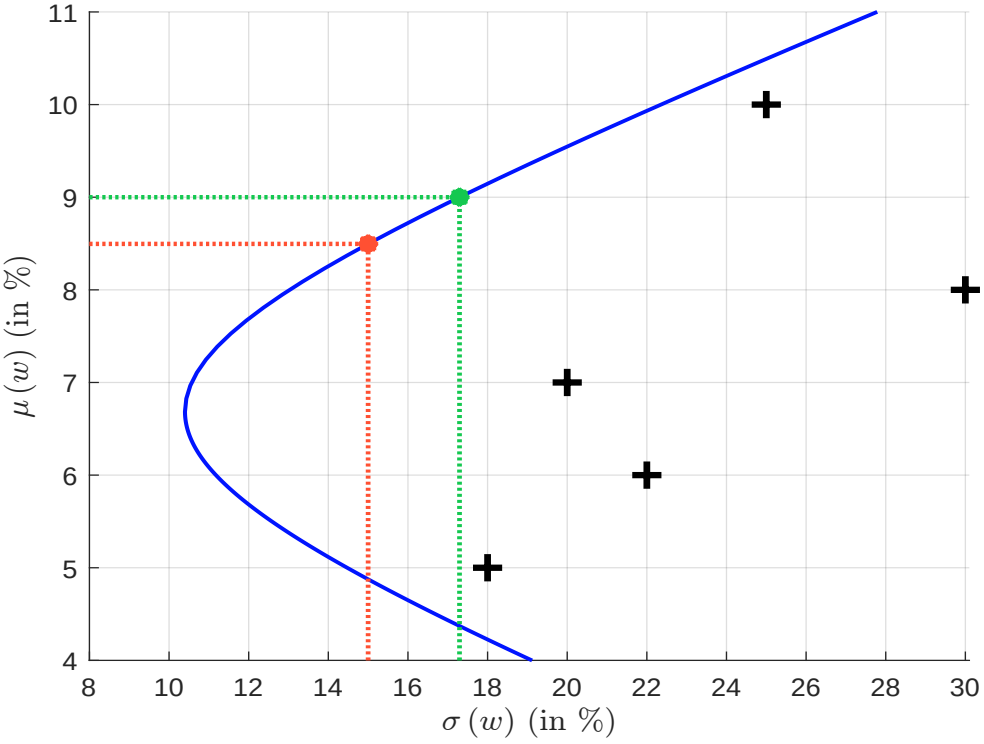


In Figure 3.1, we report the efficient frontier $\{\sigma(w^\star(\gamma)), \mu(w^\star(\gamma))\}$ by considering several values[3] of $\gamma \in [-0.5, 1]$. We see that the optimized portfolios significantly improve the risk/return profile with respect to the five assets represented by the cross symbol. Some special solutions are given in Table 3.1. The portfolio weights, its return and its volatility are expressed in %. For instance, the GMV portfolio is obtained with $\gamma = 0$. The solution is $(66.35\%, -28.52\%, 15.31\%, 34.85\%, 12.02\%)$ and it is not possible to find a portfolio whose volatility is less than 10.40%.

Table 3.1: Solution of the Markowitz optimization problem (in %)

| $\gamma$ | 0.00 | 0.10 | 0.20 | 0.50 | 1.00 | 5.00 |
|---|---|---|---|---|---|---|
| $w_1^\star(\gamma)$ | 66.35 | 58.25 | 50.14 | 25.84 | −14.67 | −338.72 |
| $w_2^\star(\gamma)$ | −28.52 | −22.67 | −16.82 | 0.74 | 30.00 | 264.12 |
| $w_3^\star(\gamma)$ | 15.31 | 13.30 | 11.30 | 5.28 | −4.74 | −84.93 |
| $w_4^\star(\gamma)$ | 34.85 | 37.65 | 40.44 | 48.82 | 62.78 | 174.50 |
| $w_5^\star(\gamma)$ | 12.02 | 13.48 | 14.94 | 19.32 | 26.62 | 85.03 |
| $\mu(w^\star(\gamma))$ | 6.69 | 6.97 | 7.25 | 8.09 | 9.49 | 20.71 |
| $\sigma(w^\star(\gamma))$ | 10.40 | 10.53 | 10.93 | 13.35 | 19.71 | 84.38 |

Solving the $\mu$-problem or the $\sigma$-problem is equivalent to finding the optimal value of $\gamma$ such that $\mu(w^\star(\gamma)) = \mu^\star$ or $\sigma(w^\star(\gamma)) = \sigma^\star$. We know that the functions $\mu(w^\star(\gamma))$ and $\sigma(w^\star(\gamma))$ are increasing in $\gamma$ and bounded. The optimal value of $\gamma$ can then be easily computed using the bisection

[2]See Appendix A.1.2 on page 1052.

[3]If $\gamma < 0$, $w^\star(\gamma)$ is not a MVO portfolio because it has a lower expected return than the GMV portfolio with higher volatility. In fact, Problem (3.4) defines the convex hull $\{\mu(w), \sigma(w)\}$ of all possible portfolios $\{w : \mathbf{1}_n^\top w = 1\}$.

algorithm described on page 1047. This is the approach used in practice, because it benefits from the numerical efficiency of quadratic programming solvers[4]. For instance, if we want a portfolio with $\sigma^\star = 15\%$, we know that $\gamma \in [0.5, 1]$. The optimal solution $w^\star$ is $(14.06\%, 9.25\%, 2.37\%, 52.88\%, 21.44\%)$. The bisection algorithm returns $\gamma = 0.6455$. In this case, we get $\mu(w^\star(\gamma)) = 8.50\%$. Now consider a $\mu$-problem with $\mu^\star = 9\%$. We find $\gamma = 0.8252$, $w^\star = (-0.50\%, 19.77\%, -1.23\%, 57.90\%, 24.07)$ and $\sigma(w^\star(\gamma)) = 17.30\%$.

**Adding some constraints** The Lagrange function of the optimization problem (3.4) is equal to:

$$\mathcal{L}(w; \lambda_0) = \frac{1}{2} w^\top \Sigma w - \gamma w^\top \mu + \lambda_0 \left( \mathbf{1}_n^\top w - 1 \right)$$

where $\lambda_0$ is the Lagrange coefficient associated with the constraint $\mathbf{1}_n^\top w = 1$. The solution $w^\star$ verifies the following first-order conditions:

$$\begin{cases} \partial_w \mathcal{L}(w; \lambda_0) = \Sigma w - \gamma \mu + \lambda_0 \mathbf{1}_n = \mathbf{0}_n \\ \partial_{\lambda_0} \mathcal{L}(w; \lambda_0) = \mathbf{1}_n^\top w - 1 = 0 \end{cases}$$

We obtain $w = \Sigma^{-1}(\gamma\mu - \lambda_0 \mathbf{1}_n)$. Since $\mathbf{1}_n^\top w - 1 = 0$, we have $\gamma \mathbf{1}_n^\top \Sigma^{-1} \mu - \lambda_0 \mathbf{1}_n^\top \Sigma^{-1} \mathbf{1}_n = 1$. It follows that:

$$\lambda_0 = \frac{\gamma \mathbf{1}_n^\top \Sigma^{-1} \mu - 1}{\mathbf{1}_n^\top \Sigma^{-1} \mathbf{1}_n}$$

The solution is then:

$$\begin{aligned} w^\star(\gamma) &= \frac{\Sigma^{-1}\mathbf{1}_n}{\mathbf{1}_n^\top \Sigma^{-1} \mathbf{1}_n} + \gamma \frac{\left(\mathbf{1}_n^\top \Sigma^{-1} \mathbf{1}_n\right) \Sigma^{-1} \mu - \left(\mathbf{1}_n^\top \Sigma^{-1} \mu\right) \Sigma^{-1} \mathbf{1}_n}{\mathbf{1}_n^\top \Sigma^{-1} \mathbf{1}_n} \\ &= w_{\text{gmv}} + \gamma w_{\text{lsp}} \end{aligned}$$

where $w_{\text{gmv}} = \left(\Sigma^{-1}\mathbf{1}_n\right) / \left(\mathbf{1}_n^\top \Sigma^{-1} \mathbf{1}_n\right)$ is the global minimum variance portfolio and $w_{\text{lsp}}$ is a long/short cash-neutral portfolio[5] such that $\mathbf{1}_n^\top w_{\text{lsp}} = 0$. We deduce that a QP solver is not needed to find the solution of the optimization problem (3.4). For example, analytic calculus gives $w_{\text{gmv}} = (66.35\%, -28.52\%, 15.31\%, 34.85\%, 12.02\%)$ and $w_{\text{lsp}} = (-81.01\%, 58.53\%, -20.05\%, 27.93\%, 14.60\%)$. Using the numerical results in Table 3.1, we verify that the equation $w^\star(\gamma) = w_{\text{gmv}} + \gamma w_{\text{lsp}}$ is satisfied. However, these solutions are not realistic because they correspond to leveraged long/short portfolios, but most investors cannot have short positions. In addition, short selling can only be implemented for a few assets that are very liquid and highly tradable. Otherwise, the cost of short selling is enormous. Therefore, in practice, portfolio optimization takes other constraints into account:

$$\begin{aligned} w^\star(\gamma) &= \arg\min \frac{1}{2} w^\top \Sigma w - \gamma w^\top \mu \\ &\text{s.t.} \begin{cases} \mathbf{1}_n^\top w = 1 \\ w \in \Omega \end{cases} \end{aligned} \tag{3.5}$$

where $w \in \Omega$ is the set of restrictions. The most common constraints are certainly the no short-selling restriction and the asset bounds. In the first case, $w_i \geq 0$ and $\Omega = [0, 1]^n$. The second constraint imposes $w_i \leq w^+$ to ensure that the portfolio is not concentrated in a small number of assets.

[4] From a numerical point of view, it is generally better to solve several QP problems than one nonlinear optimization problem.

[5] We have $\mathbf{1}_n^\top w^\star(\gamma) = 1 \Leftrightarrow \mathbf{1}_n^\top w_{\text{gmv}} + \gamma \mathbf{1}_n^\top w_{\text{lsp}} = 1 \Leftrightarrow \mathbf{1}_n^\top w_{\text{lsp}} = 0$ because $\mathbf{1}_n^\top w_{\text{gmv}} = 1$.

Let us introduce some constraints in Example 9. In Figure 3.2, we have plotted two constrained efficient frontiers, the first by imposing no short selling and the second by imposing that the weights are between 0% and 33%. We verify that investment constraints can significantly reduce opportunity arbitrage.

Figure 3.2: Impact of constraints on the efficient frontier (Example 9)

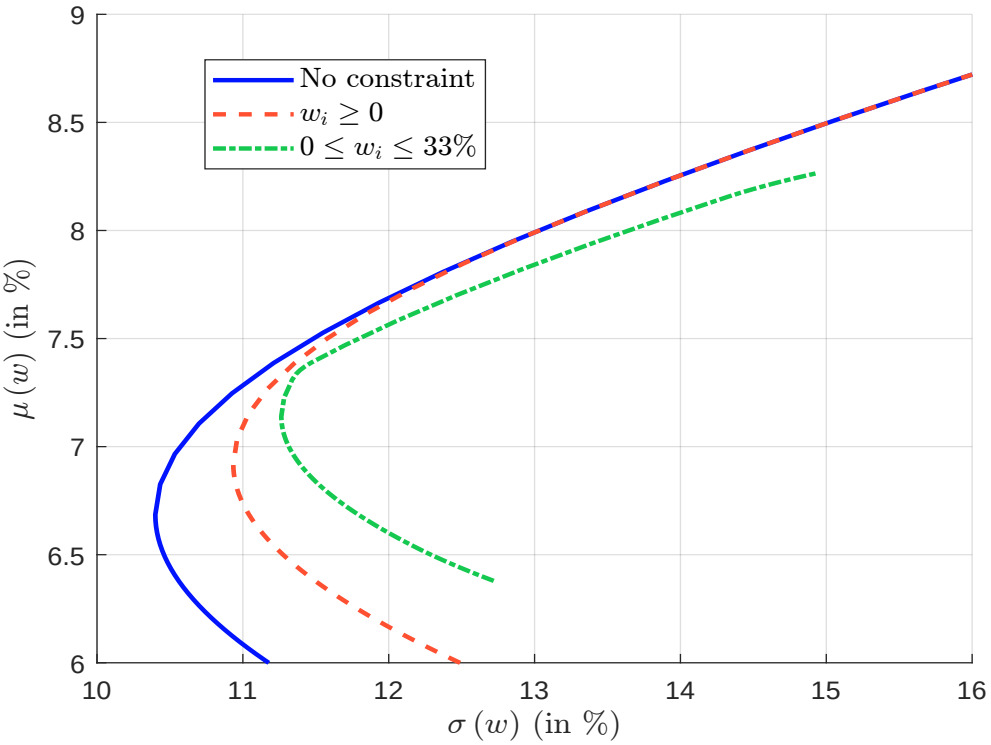


### The tangency portfolio

**Two-fund separation theorem** We recall that in Markowitz's view, there is a set of optimized portfolios. However, Tobin (1958) showed that one optimized portfolio dominates all others if there is a risk-free asset. Consider a combination of the risk-free asset and a portfolio $w$. We denote the return on the risk-free asset by $r$. We have[6]:

$$R(\tilde{w}) = (1-\alpha)\, r + \alpha R(w)$$

where $\tilde{w} = (\alpha w, 1-\alpha)$ is a vector of dimension $(n+1)$ and $\alpha \geq 0$ is the fraction of wealth invested in the risky portfolio. It follows that:

$$\mu(\tilde{w}) = (1-\alpha)\, r + \alpha\mu(w) = r + \alpha(\mu(w) - r)$$

and:

$$\sigma^2(\tilde{w}) = \alpha^2\sigma^2(w)$$

We deduce that:

$$\mu(\tilde{w}) = r + \frac{(\mu(w) - r)}{\sigma(w)}\sigma(\tilde{w}) \tag{3.6}$$

[6]We have $n+1$ assets in the universe, where the first $n$ assets correspond to the previous risky assets and the last asset is the risk-free asset.

It is the equation of a linear function between the expected return and the volatility of the combined portfolio $\tilde{w}$. In Figure 3.3, we plot the previous (unconstrained) efficient frontier. The dashed line corresponds to the combination between the risk-free asset ($r$ equals 3%) and the optimized portfolio $w^\star$. Nevertheless this combination is suboptimal because it is dominated by other combinations. We notice that one straight line dominates all other straight lines and the efficient frontier. This line is tangent to the efficient frontier and is called the capital market line. It implies that an optimized risky portfolio dominates all other risky portfolios, namely the tangency (or tangent) portfolio. We denote it by $w^*$.

Figure 3.3: Capital market line (Example 9)

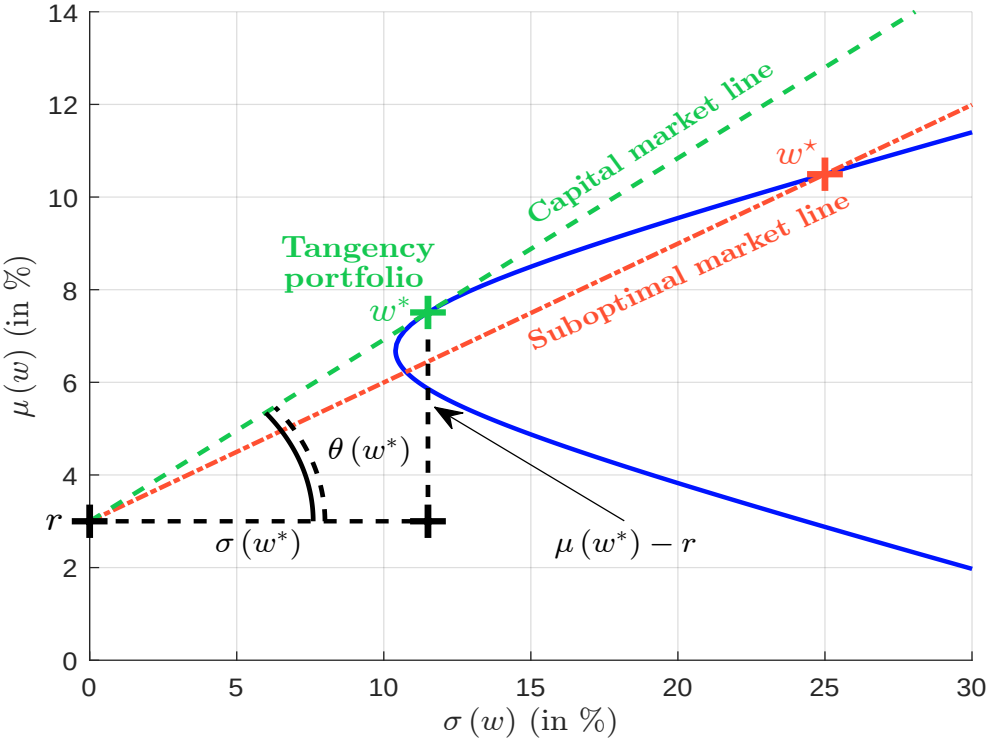


Let $\mathrm{SR}(w \mid r)$ be the Sharpe ratio of portfolio $w$:

$$\mathrm{SR}(w \mid r) = \frac{\mu(w) - r}{\sigma(w)}$$

Notice that we can write Equation (3.6) as follows:

$$\frac{\mu(\tilde{w}) - r}{\sigma(\tilde{w})} = \frac{\mu(w) - r}{\sigma(w)} \Leftrightarrow \mathrm{SR}(\tilde{w} \mid r) = \mathrm{SR}(w \mid r)$$

We deduce that the tangency portfolio is the one that maximizes the angle $\theta(w)$ or equivalently $\tan\theta(w)$ which is equal to the Sharpe ratio. The tangency portfolio is also the risky portfolio corresponding to the maximum Sharpe ratio. We also note that any portfolio belonging to the capital market line has the same Sharpe ratio. If we look at our example with $r = 3\%$, the composition of the tangency portfolio $w^*$ is $(42.57\%, -11.35\%, 9.43\%, 43.05\%, 16.30\%)$ and we have $\mu(w^*) = 7.51\%$, $\sigma(w^*) = 11.50\%$, $\mathrm{SR}(w^* \mid r) = 0.39$ and $\theta(w^*) = 21.40$ degrees.

**Augmented optimization problem** If the risk-free asset belongs to the investment universe, the optimization problem becomes:

$$\begin{aligned} \tilde{w}^\star(\gamma) &= \arg\min \frac{1}{2}\tilde{w}^\top \tilde{\Sigma}\tilde{w} - \gamma \tilde{w}^\top \tilde{\mu} \\ &\text{s.t.} \begin{cases} \mathbf{1}_n^\top \tilde{w} = 1 \\ \tilde{w} \in \Omega \end{cases} \end{aligned} \tag{3.7}$$

where $\tilde{w} = (w, w_r)$ is the augmented allocation vector of dimension $n+1$. It follows that:

$$\tilde{\Sigma} = \begin{pmatrix} \Sigma & \mathbf{0}_n \\ \mathbf{0}_n^\top & 0 \end{pmatrix} \quad \text{and} \quad \tilde{\mu} = \begin{pmatrix} \mu \\ r \end{pmatrix}$$

In the case where $\Omega = \mathbb{R}^{n+1}$, Roncalli (2013, pages 13-14) showed that the optimal solution is equal to:

$$\tilde{w}^\star(\gamma) = \underbrace{\alpha \begin{pmatrix} w^* \\ 0 \end{pmatrix}}_{\text{risky assets}} + \underbrace{(1-\alpha) \begin{pmatrix} \mathbf{0}_n \\ 1 \end{pmatrix}}_{\text{risk-free asset}}$$

where $w^*$ is the tangency portfolio:

$$w^* = \frac{\Sigma^{-1}(\mu - r\mathbf{1}_n)}{\mathbf{1}_n^\top \Sigma^{-1}(\mu - r\mathbf{1}_n)}$$

and the proportion of risky assets is equal to $\alpha = \gamma \mathbf{1}_n^\top \Sigma^{-1}(\mu - r\mathbf{1}_n)$. It follows that the risk-tolerance coefficient associated with the tangency portfolio is given by:

$$\gamma(w^*) = \frac{1}{\mathbf{1}_n^\top \Sigma^{-1}(\mu - r\mathbf{1}_n)}$$

When $\alpha \neq 1$, the weights $\tilde{w}^\star(\gamma)$ of the optimal portfolio are proportional to the weights $w^*$ of the tangency portfolio, while the wealth invested in the risk-free asset is the complement $(1-\alpha)$ to obtain a total exposure of 100%. We then retrieve the *two-fund separation theorem*.

### Market equilibrium and CAPM

**Risk premium and beta** Based on the results of Markowitz and Tobin, Sharpe (1964) developed the capital asset pricing model (CAPM). Let $w^*$ be the tangency portfolio. On the efficient frontier, we have seen that every portfolio $w$ satisfies the capital market line:

$$\mu(w) = r + \frac{\sigma(w)}{\sigma(w^*)}(\mu(w^*) - r)$$

We consider a portfolio $x$ with a fraction $\omega$ invested in the asset $i$ and a fraction $(1-\omega)$ invested in the tangency portfolio $w^*$. We have[7] $\mu(x) = \omega\mu_i + (1-\omega)\mu(w^*)$ and $\sigma^2(x) = \omega^2\sigma_i^2 + (1-\omega)^2\sigma^2(w^*) + 2\omega(1-\omega)\rho(\mathbf{e}_i, w^*)\sigma_i\sigma(w^*)$. It follows that:

$$\frac{\partial \mu(x)}{\partial \sigma(x)} = \frac{\mu_i - \mu(w^*)}{\left(\omega\sigma_i^2 + (\omega-1)\sigma^2(w^*) + (1-2\omega)\rho(\mathbf{e}_i, w^*)\sigma_i\sigma(w^*)\right)\sigma^{-1}(x)}$$

[7] $\mathbf{e}_i$ is the unit vector with 1 in the $i^{\text{th}}$ position and 0 elsewhere. It then corresponds to the portfolio fully invested in asset $i$.

When $\omega = 0$, the portfolio $x$ is the tangency portfolio $w^*$ and the previous derivative is equal to the Sharpe ratio $\mathrm{SR}(w^* \mid r)$:

$$\lim_{\omega \to 0} \frac{\partial \mu(x)}{\partial \sigma(x)} = \tan \theta(w^*) = \frac{\mu(w^*) - r}{\sigma(w^*)}$$

We deduce that:

$$\frac{(\mu_i - \mu(w^*))\,\sigma(w^*)}{\rho(\mathbf{e}_i, w^*)\,\sigma_i \sigma(w^*) - \sigma^2(w^*)} = \frac{\mu(w^*) - r}{\sigma(w^*)}$$

which is equivalent to:

$$\pi_i := \mu_i - r = \beta_i(\mu(w^*) - r) \tag{3.8}$$

where $\pi_i$ is the risk premium of the asset $i$ and:

$$\beta_i = \frac{\rho(\mathbf{e}_i, w^*)\,\sigma_i}{\sigma(w^*)} = \frac{\mathrm{cov}(R_i, R(w^*))}{\mathrm{var}(R(w^*))} \tag{3.9}$$

The coefficient $\beta_i$ is the ratio of the covariance between the return of asset $i$ and the return of the tangency portfolio to the variance of the tangency portfolio return. Equation (3.8) tells us that the risk premium of asset $i$ is equal to its beta times the excess return of the tangency portfolio. It is easy to show that this relationship holds for any portfolio $w$ and not just for the assets that make up the tangency portfolio.

Box 3.1: Computation of the beta coefficient

Let $R_{i,t}$ and $R_t(w)$ be the returns of asset $i$ and portfolio $w$ at time $t$. We consider the linear regression:

$$R_{i,t} = \alpha_i + \beta_i R_t(w) + \varepsilon_{i,t}$$

where $\varepsilon_{i,t}$ is a white noise process. The OLS coefficient $\hat{\beta}_i$ is an estimate of the beta $\beta_i$ of the asset $i$. We can generalize this approach to estimate the beta of a portfolio $x$ with respect to another portfolio $w$. We have:

$$R_t(x) = \alpha + \beta R_t(w) + \varepsilon_t$$

Another way to calculate beta is to use the following relationship:

$$\beta(x \mid w) = \frac{\sigma(x, w)}{\sigma^2(w)} = \frac{x^\top \Sigma w}{w^\top \Sigma w}$$

We deduce that the expression for the beta of asset $i$ is also:

$$\beta_i = \beta(\mathbf{e}_i \mid w) = \frac{\mathbf{e}_i^\top \Sigma w}{w^\top \Sigma w} = \frac{(\Sigma w)_i}{w^\top \Sigma w}$$

It follows that the beta of a portfolio is the weighted average of the betas of the assets that make up the portfolio:

$$\beta(x \mid w) = \frac{x^\top \Sigma w}{w^\top \Sigma w} = x^\top \frac{\Sigma w}{w^\top \Sigma w} = \sum_{i=1}^{n} x_i \beta_i$$

The relationship (3.8) is very important and highlights the role of the beta coefficient. However, this result is not the only main finding of Sharpe (1964). In his article, Sharpe also showed that

when the market is at equilibrium, the prices of assets are such that the tangency portfolio $w^*$ is the market portfolio $w_m$ (or the market-cap portfolio). With this result, the characterization of the tangency portfolio does not depend on assumptions about expected returns, volatilities, and correlations.

In the case of Example 9, we have seen that the composition of the tangency portfolio is $w^* = (42.57\%, -11.35\%, 9.43\%, 43.05\%, 16.30\%)$. Since its expected return is $\mu(w^*) = 7.51\%$ and $r = 3\%$, we deduce that the market risk premium is 4.51%. In Table 3.2, we report the beta of each asset and two portfolios: the equally weighted (EW) portfolio $w_{\text{ew}}$ and the GMV portfolio $w_{\text{gmv}}$. We compute the associated expected return $\mu(w) = w^\top \mu$ and the risk premium explained by the tangency portfolio $\pi(w \mid w^*) = \beta(w \mid w^*)(\mu(w^*) - r)$. We check the relationship $\pi(w \mid w^*) = \mu(w) - r$. For instance, the beta of the first asset is 0.444 and we have $0.444 \times 4.51\% = 2\%$, which is also the difference between 5% and 3%. For the EW portfolio, the risk premium is equal to $0.932 \times 4.51\% = 4.20\%$. We also check that it is equal to the difference between the expected return of 7.20% and the risk-free rate of 3%.

Table 3.2: Computation of beta and risk premium (Example 9)

| Portfolio | $\mu(w)$ | $\mu(w) - r$ | $\beta(w \mid w^*)$ | $\pi(w \mid w^*)$ |
|---|---|---|---|---|
| $\mathbf{e}_1$ | 5.00% | 2.00% | 0.444 | 2.00% |
| $\mathbf{e}_2$ | 7.00% | 4.00% | 0.887 | 4.00% |
| $\mathbf{e}_3$ | 6.00% | 3.00% | 0.665 | 3.00% |
| $\mathbf{e}_4$ | 10.00% | 7.00% | 1.553 | 7.00% |
| $\mathbf{e}_5$ | 8.00% | 5.00% | 1.109 | 5.00% |
| $w_{\text{ew}}$ | 7.20% | 4.20% | 0.932 | 4.20% |
| $w_{\text{gmv}}$ | 6.69% | 3.69% | 0.817 | 3.69% |

**Risk premium and alpha return** Jensen (1968) analyzed the performance of active management by using the following regression model:

$$R_{j,t} - r = \alpha_j + \beta_j (R_t(w_m) - r) + \varepsilon_{j,t}$$

where $R_{j,t}$ is the return of the mutual fund $j$ at time $t$, $R_t(w_m)$ is the return of the market portfolio and $\varepsilon_{j,t}$ is an idiosyncratic risk. If the mutual fund outperforms the market portfolio, the assumption $\alpha_j > 0$ is not rejected. However, Jensen rejected this assumption for most mutual funds and concluded that active management does not generate alpha. More generally, alpha is defined as the difference between the risk premium $\pi(w)$ of portfolio $w$ and the beta[8] $\beta(w)$ of the portfolio times the market risk premium $\pi_m$:

$$\begin{aligned} \alpha &= (\mu(w) - r) - \beta(w \mid w_m)(\mu(w_m) - r) \\ &= \pi(w) - \beta(w)\pi_m \end{aligned}$$

If we now impose a no short-selling constraint by using a lower bound $x_i \geq 0$, the tangency portfolio becomes $w^\star = (33.62\%, 0\%, 8.79\%, 40.65\%, 16.95\%)$ in our previous example. We check that the portfolio has no short exposure to the second asset. Since we have $\mu(w^*) = 7.63\%$ and $r = 3\%$, we deduce that the market risk premium is 4.63%. It is higher than in the unconstrained case. We report the beta and the risk premium in Table 3.3. We notice that the equality $\mu(w) - r = \beta(w)(\mu_m - r)$ is

[8] The notation $\beta(w)$ means that the beta is calculated with respect to the market portfolio.

Box 3.2: Computing the implied risk premia of investors

Consider the optimization problem[a]:

$$\begin{aligned} w^\star &= \arg\min \frac{1}{2} w^\top \Sigma w - \gamma w^\top (\mu - r\mathbf{1}_n) \\ &\text{s.t.} \begin{cases} \mathbf{1}_n^\top w = 1 \\ w \in \Omega \end{cases} \end{aligned}$$

If we omit the constraints, the solution is $w^\star = \gamma\Sigma^{-1}(\mu - r\mathbf{1}_n)$. In the Markowitz model, the unknown variable is the vector $w$ of weights. We now assume that the investor has a current asset allocation $w_0$. By construction, $w_0$ is the optimal portfolio for this investor, otherwise he will change his investment policy. We deduce that[b]:

$$w_0 = \gamma\Sigma^{-1}(\mu - r\mathbf{1}_n) \Leftrightarrow \tilde{\pi} = \mu - r\mathbf{1}_n = \frac{1}{\gamma}\Sigma w_0 \tag{3.10}$$

We can interpret $\tilde{\pi}$ as the vector of risk premia consistent with the portfolio $w_0$ (Black and Litterman, 1991, 1992). $\tilde{\pi}$ is then the risk premium priced by the portfolio manager. Calculating $\tilde{\pi}$ requires specifying the investor's risk tolerance. Let us assume that the investor targets a Sharpe ratio $\mathrm{SR}(w_0 \mid r)$ for his portfolio. We deduce that:

$$\mathrm{SR}(w_0 \mid r) = \frac{\mu(w_0) - r}{\sigma(w_0)} = \frac{w_0^\top(\mu - r\mathbf{1}_n)}{\sqrt{w_0^\top \Sigma w_0}} = \frac{1}{\gamma}\sqrt{w_0^\top \Sigma w_0}$$

Finally, we obtain:

$$\tilde{\pi} = \mathrm{SR}(w_0 \mid r) \cdot \frac{\Sigma w_0}{\sqrt{w_0^\top \Sigma w_0}}$$

Let us consider Example 9. We assume that the current allocation $w_0$ is equal to $(35\%, 25\%, 15\%, 15\%, 10\%)$. The volatility of the portfolio is then equal to $\sigma(x_0) = 12.52\%$. The objective of the portfolio manager is to target a Sharpe ratio of 0.25. The implied risk tolerance is $\gamma = 0.50$ and the implied risk premia are $\tilde{\pi} = (3.36\%, 4.45\%, 2.83\%, 1.59\%, 1.80\%)$.

[a] We notice that the excess expected return is equal to $w^\top(\mu - r\mathbf{1}_n) = w^\top\mu - r$. Adding the risk-free rate has no effect on the mean-variance utility function.

[b] From this equation we also deduce the following relationship: $\tilde{\pi}(w_0) = \gamma^{-1}\sigma^2(w_0)$.

not always satisfied. This is especially true for the second asset, which has a negative alpha of 49 bps. We know that the true risk premium of this asset is 4%. Nevertheless, investors are constrained and cannot short this asset. Theoretically, the optimal demand for this asset must be negative. Because of the lower bound $x_i \geq 0$, the market demand is higher than the expected demand derived from the CAPM. Therefore, there is a upward pressure on the price of this asset due to the lack of arbitrage. The risk premium perceived by the market is then higher, creating a negative alpha because the price is overvalued. Since the equally-weighted portfolio is long this asset, it also has a negative alpha. This is not the case for the GMV portfolio, which is short this asset (its weight is −28.52% — see Table 3.1 on page 140).

Table 3.3: Computation of alpha return (Example 9)

| Portfolio | $\mu(w)$ | $\mu(w) - r$ | $\beta(w \mid w^*)$ | $\pi(w \mid w^*)$ | $\alpha(w \mid w^*)$ |
|---|---|---|---|---|---|
| $\mathbf{e}_1$ | 5.00% | 2.00% | 0.432 | 2.00% | 0.00% |
| $\mathbf{e}_2$ | 7.00% | 4.00% | 0.970 | 4.49% | −0.49% |
| $\mathbf{e}_3$ | 6.00% | 3.00% | 0.648 | 3.00% | 0.00% |
| $\mathbf{e}_4$ | 10.00% | 7.00% | 1.512 | 7.00% | 0.00% |
| $\mathbf{e}_5$ | 8.00% | 5.00% | 1.080 | 5.00% | 0.00% |
| $w_{\text{ew}}$ | 7.20% | 4.20% | 0.929 | 4.30% | −0.10% |
| $w_{\text{gmv}}$ | 6.69% | 3.69% | 0.766 | 3.55% | 0.14% |

The previous analysis can be applied to a more general framework. There are two main explanations for alpha generation. The first concerns the assumptions of the CAPM. In particular, this model assumes that investors are not constrained in terms of leverage, short selling, transaction costs, etc. In practice, investors are highly constrained, especially large institutional investors. Since they cannot leverage their portfolios, they will not use the tangency portfolio. They will prefer a portfolio with a lower Sharpe ratio but a higher expected return. This explains why the demand for high beta assets is greater than the demand predicted by the CAPM. Therefore, we observe a positive alpha return for low beta assets and a negative alpha return for high beta assets (Black, 1972; Frazzini and Pedersen, 2014). The second explanation is the existence of other risk factors that are not priced by the CAPM (Ross, 1976). The development of factor investing and alternative risk premia in the aftermath of the 2008 global financial crisis is related to this issue. If investors use systematic strategies with the same approach and these strategies are very popular, they can affect asset prices (Roncalli, 2017). In both cases, alpha generation is rooted in the imbalance between supply and demand and the dynamics of investment flows.

### Portfolio optimization in the presence of a benchmark

**Utility function revisited** The Markowitz approach to portfolio optimization assumes that the investor has a mean-variance utility function without reference to a given investment policy. We now extend the optimization problem when a strategic asset allocation imposes a benchmark represented by a portfolio $b$. The tracking error between the active portfolio $w$ and its benchmark $b$ is the difference between the return of the portfolio and the return of the benchmark:

$$\epsilon = R(w) - R(b) = \sum_{i=1}^{n} w_i R_i - \sum_{i=1}^{n} b_i R_i = w^\top R - b^\top R = (w-b)^\top R$$

The tracking error $\epsilon$ is a stochastic random variable. The expected excess return is equal to:

$$\mu(w \mid b) := \mathbb{E}[\epsilon] = (w-b)^\top \mu$$

whereas the volatility of the tracking error is defined as:

$$\sigma(w \mid b) := \sigma(\epsilon) = \sqrt{(w-b)^\top \Sigma (w-b)}$$

The investor's objective is then to maximize the expected tracking error, subject to a constraint on the tracking error volatility:

$$\begin{aligned} w^\star &= \arg\max \mu(w \mid b) \\ &\text{s.t.} \begin{cases} \mathbf{1}_n^\top x = 1 \\ \sigma(w \mid b) \leq \sigma^\star \end{cases} \end{aligned} \tag{3.11}$$

Like the Markowitz problem, we transform this $\sigma$-problem into a $\gamma$-problem:

$$w^\star(\gamma) = \arg\min f(w \mid b)$$

where:

$$\begin{aligned} f(w \mid b) &= \frac{1}{2}\sigma^2(w \mid b) - \gamma\mu(w \mid b) \\ &= \frac{1}{2}(w-b)^\top \Sigma (w-b) - \gamma(w-b)^\top \mu \\ &= \frac{1}{2}w^\top \Sigma w - w^\top(\gamma\mu + \Sigma b) + \underbrace{\frac{1}{2}b^\top \Sigma b + \gamma b^\top \mu}_{\text{constant}} \end{aligned}$$

Again, we recognize a quadratic programming problem. The efficient frontier is then the parametric curve $(\sigma(w^\star(\gamma) \mid b), \mu(w^\star(\gamma) \mid b))$ with $\gamma \geq 0$.

**Remark 29** *Using Equation (3.10), we find that* $w^\top(\gamma\mu + \Sigma b) = 2\gamma w^\top\left(\frac{\pi + \tilde{\pi}}{2}\right) - \gamma$ *where* $\tilde{\pi}$ *is the implied risk premia associated with the benchmark* $b$*. We obtain a Markowitz problem where the vector of expected returns is replaced by an average of the true and implied risk premia.*

**Example 10** *Consider an investment universe with four assets. Their expected returns are* 5%*,* 6.5%*,* 8% *and* 6.5% *while their volatilities are* 15%*,* 20%*,* 25% *and* 30%*. The correlation matrix of the asset returns is given by the following matrix:*

$$\mathbb{C} = \begin{pmatrix} 100\% & & & \\ 10\% & 100\% & & \\ 40\% & 70\% & 100\% & \\ 50\% & 40\% & 80\% & 100\% \end{pmatrix}$$

We consider Example 10 with the benchmark $b = (60\%, 40\%, 20\%, -20\%)$. In Figure 3.4, we have represented the corresponding efficient frontier. We verify that it is a straight line if there is no constraint (Roll, 1992). If we impose that $w_i \geq -10\%$, the efficient frontier is shifted to the right. For the third case, we assume that the weights are between a lower bound and an upper bound: $w_i^- \leq w_i \leq w_i^+$ with $w_i^+ = 50\%$. For the first three assets, the lower bound $w_i^-$ is set to 0, while for the fourth asset it is $-20\%$.

**Information ratio** To compare the performance of different portfolios, a better measure than the Sharpe ratio is the information ratio which is defined as follows:

$$\mathrm{IR}(w \mid b) = \frac{\mu(w \mid b)}{\sigma(w \mid b)} = \frac{(w-b)^\top \mu}{\sqrt{(w-b)^\top \Sigma (w-b)}}$$

If we consider a combination of the benchmark $b$ and the active portfolio $w$, the composition of the portfolio is:

$$x = (1-\alpha)b + \alpha w$$

where $\alpha \geq 0$ is the proportion of wealth invested in the portfolio $w$. It follows that:

$$\mu(x \mid b) = (x-b)^\top \mu = \alpha\mu(w \mid b)$$

Figure 3.4: Efficient frontier with a benchmark (Example 10)

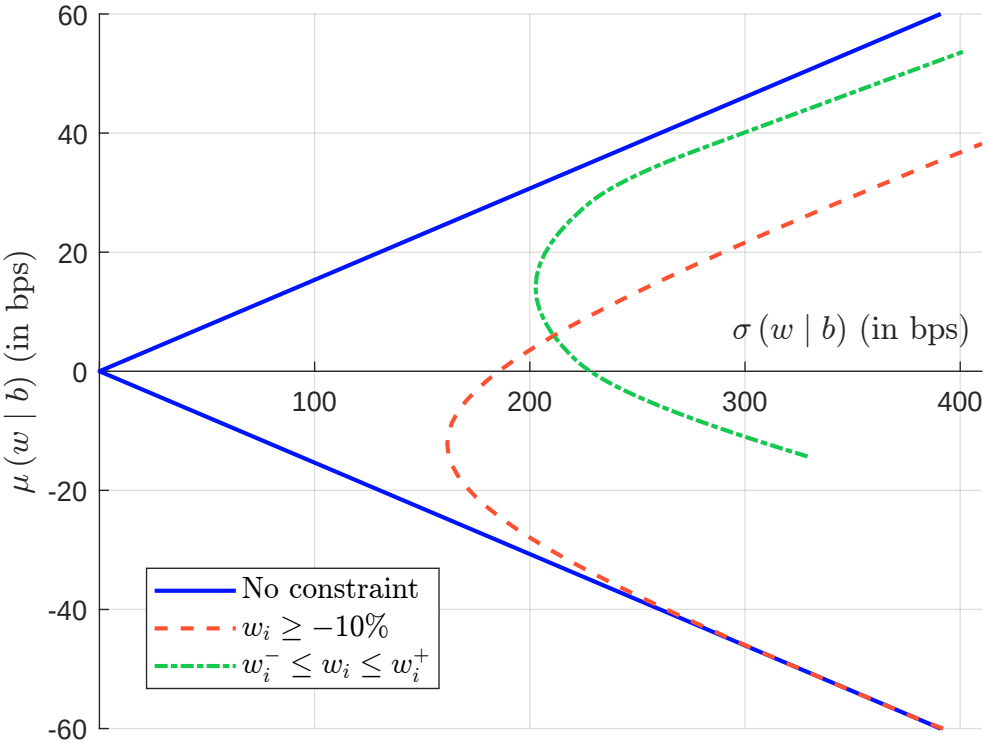


Figure 3.5: Tangency portfolio with respect to a benchmark (Example 10)

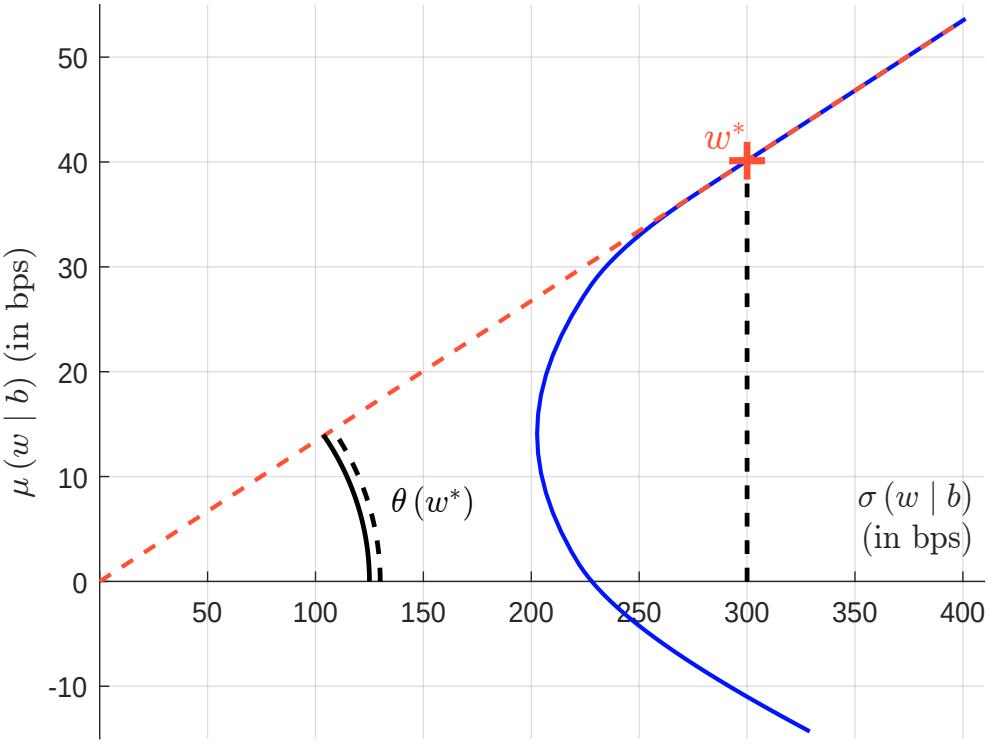

and:

$$\sigma^2(x \mid b) = (x-b)^\top \Sigma (x-b) = \alpha^2 \sigma^2(w \mid b)$$

We deduce that:

$$\mu(x \mid b) = \mathrm{IR}(w \mid b)\ \sigma(x \mid b)$$

It is the equation of a linear function between the tracking error volatility and the expected tracking error of the portfolio $x$. It implies that the efficient frontier is a straight line:

> "*If the manager is measured solely in terms of excess return performance, he or she should pick a point on the upper part of this efficient frontier. For instance, the manager may have a utility function that balances expected value added against tracking error volatility. Note that because the efficient set consists of a straight line, the maximal Sharpe ratio is not a usable criterion for portfolio allocation*" (Jorion, 2003, page 172).

If we add some other constraints to the portfolio optimization problem (3.11), the efficient frontier is no longer a straight line. In this case, one optimized portfolio dominates all other portfolios. It is the portfolio that belongs to the efficient frontier and the straight line that is tangent to the efficient frontier. It is also the portfolio that maximizes the information ratio.

Let us look at the previous efficient frontier when we impose lower and upper bounds (third case). When we combine it with the benchmark, we get the straight line shown in Figure 3.5 and the tangency portfolio $w^*$ is equal to $(46.56\%, 33.49\%, 39.95\%, -20.00\%)$.

### 3.1.2 ESG risk premium

We now analyze the impact of ESG investing on the CAPM. However, it is important to reiterate that the risk premium is the expected excess return that investors earn because they are exposed to systematic risk. Therefore, we need to distinguish between expected (or required) returns and historical (or realized) returns. Moreover, it is not very clear whether the risk premium is the long-term performance or a specific requirement of investors. This is the difference between the unconstrained risk premium $\pi_i$ and the implied risk premium $\tilde{\pi}_i$.

#### The Pástor-Stambaugh-Taylor model

In this section, we present the model developed by Pástor *et al.* (2021) (hereafter, PST model). It is a direct extension of the CAPM and has the advantage of emphasizing many intuitively stylized facts.

**Model settings** Pástor *et al.* (2021) consider an investment universe of $n$ assets corresponding to the stocks of $n$ firms. They assume that the asset excess returns $\tilde{R} = R - r = \left(\tilde{R}_1, \ldots, \tilde{R}_n\right)$ are normally distributed — $\tilde{R} \sim \mathcal{N}(\pi, \Sigma)$, and the firms produce social impact. Each firm has an ESG characteristic $\boldsymbol{\mathcal{G}}_i$, which is positive for *esg-friendly* (or *green*) firms and negative for *esg-unfriendly* (or *brown*) firms. This means that $\boldsymbol{\mathcal{G}}_i > 0$ induces positive social impacts, while $\boldsymbol{\mathcal{G}}_i < 0$ induces negative externalities on society. Consider an economy with a continuum of agents $(j = 1, 2, \ldots, \infty)$. We note $w_{i,j}$ the fraction of wealth invested by agent $j$ in stock $i$, and $w_j = (w_{1,j}, \ldots, w_{n,j})$ the allocation vector of agent $j$. The relationship between the initial and final wealth $W_j$ and $\tilde{W}_j$ is given by:

$$\tilde{W}_j = \left(1 + r + w_j^\top \tilde{R}\right) W_j$$

Pástor *et al.* (2021) assume that the economic agent $j$ has an exponential CARA utility function:

$$\boldsymbol{\mathcal{U}}\left(\tilde{W}_j, w_j\right) = -\exp\left(-\bar{\gamma}_j \tilde{W}_j - w_j^\top b_j W_j\right)$$

where $\bar{\gamma}_j$ is the absolute risk-aversion and $b_j = \varphi_j \boldsymbol{\mathcal{G}}$ is the vector of non-pecuniary benefits depending on the green intensity $\boldsymbol{\mathcal{G}}$ and the ESG preference coefficient $\varphi_j \geq 0$ of the economic agent.

**Optimal portfolio** The expected utility is equal to:

$$\begin{aligned}
\mathbb{E}\left[\boldsymbol{\mathcal{U}}\left(\tilde{W}_j, w_j\right)\right] &= \mathbb{E}\left[-\exp\left(-\bar{\gamma}_j \tilde{W}_j - w_j^\top b_j W_j\right)\right] \\
&= \mathbb{E}\left[-\exp\left(-\bar{\gamma}_j \left(1 + r + w_j^\top \tilde{R}\right) W_j - w_j^\top b_j W_j\right)\right] \\
&= -e^{-\bar{\gamma}_j (1+r) W_j} \mathbb{E}\left[\exp\left(-\bar{\gamma}_j w_j^\top W_j \left(\tilde{R} + \bar{\gamma}_j^{-1} b_j\right)\right)\right] \\
&= e^{-\bar{\Gamma}_j (1+r)} \mathbb{E}\left[\exp\left(-\bar{\Gamma}_j w_j^\top \left(\tilde{R} + \bar{\gamma}_j^{-1} b_j\right)\right)\right] \qquad (3.12)
\end{aligned}$$

where $\bar{\Gamma}_j = \bar{\gamma}_j W_j$ is the nominal risk aversion. We notice that $\tilde{R} + \bar{\gamma}_j^{-1} b_j \sim \mathcal{N}\left(\pi + \bar{\gamma}_j^{-1} b_j, \Sigma\right)$ and:

$$-\bar{\Gamma}_j w_j^\top \left(\tilde{R} + \bar{\Gamma}_j^{-1} b_j\right) \sim \mathcal{N}\left(-\bar{\Gamma}_j w_j^\top \left(\pi + \bar{\gamma}_j^{-1} b_j\right), \bar{\Gamma}_j^2 w_j^\top \Sigma w_j\right)$$

Using the mathematical expectation formula of the log-normal distribution[9], we deduce that:

$$\mathbb{E}\left[\boldsymbol{\mathcal{U}}\left(\tilde{W}_j, w_j\right)\right] = e^{-\bar{\Gamma}_j (1+r)} \exp\left(-\bar{\Gamma}_j w_j^\top \left(\pi + \bar{\gamma}_j^{-1} b_j\right) + \frac{1}{2} \bar{\Gamma}_j^2 w_j^\top \Sigma w_j\right)$$

The first-order condition is equal to:

$$-\bar{\Gamma}_j \left(\pi + \bar{\gamma}_j^{-1} b_j\right) + \bar{\Gamma}_j^2 \Sigma w_j = \mathbf{0}_n$$

Finally, Pástor *et al.* (2021) conclude that the optimal portfolio is:

$$w_j^\star = \Gamma_j \Sigma^{-1} \left(\pi + \gamma_j b_j\right) \qquad (3.13)$$

where $\Gamma_j = \bar{\Gamma}_j^{-1}$ and $\gamma_j = \bar{\gamma}_j^{-1}$ are the relative nominal and unitary risk-tolerance coefficients. This is the unconstrained optimal portfolio where asset returns include the green sentiment $\gamma_j b_j = \gamma_j \varphi_j \boldsymbol{\mathcal{G}}$.

**Remark 30** *We assume that $W_j = 1$. Since we have $\mathbf{1}_n^\top w_j = 1$, $w_j^\top r = r$ and $\bar{\Gamma}_j = \bar{\gamma}_j$, we deduce that:*

$$\begin{aligned}
-\ln \mathbb{E}\left[\boldsymbol{\mathcal{U}}\left(\tilde{W}_j, w_j\right)\right] &= \bar{\gamma}_j (1 + r) + \bar{\gamma}_j w_j^\top \left(\pi + \bar{\gamma}_j^{-1} b_j\right) - \frac{1}{2} \bar{\gamma}_j^2 w_j^\top \Sigma w_j \\
&\propto w_j^\top \left(\pi + r \mathbf{1}_n + \bar{\gamma}_j^{-1} b_j\right) - \frac{1}{2} \bar{\gamma}_j w_j^\top \Sigma w_j \\
&= w_j^\top \left(\mu + \bar{\gamma}_j^{-1} b_j\right) - \frac{1}{2} \bar{\gamma}_j w_j^\top \Sigma w_j
\end{aligned}$$

*Maximizing expected utility is then equivalent to solving the classical Markowitz QP problem:*

$$\begin{aligned}
w_j^\star(\gamma_j) &= \arg\min \frac{1}{2} w_j^\top \Sigma w_j - \gamma_j w_j^\top \mu' \\
&\text{s.t.} \quad \mathbf{1}_n^\top w_j = 1
\end{aligned}$$

*where $\gamma_j = \bar{\gamma}_j^{-1}$ is the relative risk tolerance and $\mu' = \mu + \gamma_j b_j$ is the vector of modified expected returns reflecting the ESG sentiment of the economic agent regarding the social impact of firms.*

[9] See Appendix A.2.1 on page 1061.

**Example 11** *We consider a universe of $n$ risky assets, where $n$ is an even number. The risk-free rate $r$ is set at 3%. We assume that the Sharpe ratio of these assets is the same and equal to 20%. The volatility of asset $i$ is equal to $\sigma_i = 0.10 + 0.20\, e^{-n^{-1}\lfloor 0.5i \rfloor}$. The correlation between asset returns is constant: $\mathbb{C} = \mathbb{C}_n(\rho)$. The social impact of firms is given by the vector $\boldsymbol{\mathcal{G}}$. If $\boldsymbol{\mathcal{G}}$ is not specified, it is equal to the cyclic vector $(+1\%, -1\%, +1\%, \ldots, +1\%, -1\%)$. This implies that half of the firms (green firms) have a positive social impact while the others (brown firms) have a negative impact.*

We consider the case where $n = 6$ and $\rho = 25\%$, and we assume that we cannot be short the assets. We calibrate the risk-tolerance parameter $\gamma$ so that the long-only optimized portfolio of the non-ESG investor has a volatility of 20%. We find $\gamma = 1.5456$ and obtain the results reported in Table 3.4. We verify that the optimized portfolio depends on the ESG preference coefficient $\varphi$. We consider a second set of ESG characteristics: $\boldsymbol{\mathcal{G}} = (10\%, 5\%, 2\%, 3\%, 25\%, 30\%)$. Since $\boldsymbol{\mathcal{G}}_i > 0$, we can assume that this investment universe has been filtered to retain only the best-in-class issuers and to implement an ESG selection strategy. Again, we measure the impact of $\varphi$ on the optimized portfolios. In Figure 3.6, we show the efficient frontier when the investment universe consits of 20 assets. We verify that the expected returns of the efficient frontier are reduced when ESG preferences are taken into account, and this reduction depends on the ESG preference coefficient $\varphi$. We also find that all of these efficient frontiers start at the same point, since the global minimum variance portfolio is not affected by the investor's ESG preferences.

Table 3.4: Mean-variance optimized portfolios with ESG preferences (Example 11, $n = 6$, $\rho = 25\%$)

| | $\boldsymbol{\mathcal{G}} = (1\%, -1\%, 1\%, -1\%, 1\%, -1\%)$ | | | | $\boldsymbol{\mathcal{G}} = (10\%, 5\%, 2\%, 3\%, 25\%, 30\%)$ | | | |
|---|---|---|---|---|---|---|---|---|
| $\varphi$ | 0.00% | 1.00% | 5.00% | 50.00% | 0.00% | 0.50% | 1.00% | 2.00% |
| $w_1^\star$ | 44.97% | 48.87% | 58.65% | 67.48% | 44.97% | 46.83% | 28.69% | 0.00% |
| $w_2^\star$ | 44.97% | 41.06% | 19.60% | 0.00% | 44.97% | 37.06% | 9.17% | 0.00% |
| $w_3^\star$ | 5.03% | 9.82% | 21.75% | 32.52% | 5.03% | 0.00% | 0.00% | 0.00% |
| $w_4^\star$ | 5.03% | 0.25% | 0.00% | 0.00% | 5.03% | 0.00% | 0.00% | 0.00% |
| $w_5^\star$ | 0.00% | 0.00% | 0.00% | 0.00% | 0.00% | 0.83% | 16.62% | 21.09% |
| $w_6^\star$ | 0.00% | 0.00% | 0.00% | 0.00% | 0.00% | 15.28% | 45.53% | 78.91% |
| $\mu(w^\star)$ | 8.33% | 8.33% | 8.27% | 8.22% | 8.33% | 8.23% | 7.79% | 7.43% |
| $\sigma(w^\star)$ | 20.00% | 20.09% | 20.07% | 21.56% | 20.00% | 19.33% | 16.70% | 19.17% |
| $\mathrm{SR}(w^\star \mid r)$ | 0.27 | 0.27 | 0.26 | 0.24 | 0.27 | 0.27 | 0.29 | 0.23 |

**Remark 31** *In this numerical example, the impact of ESG preferences is small because the assets have similar financial characteristics: the same Sharpe ratio and the same cross-correlation values. This explains why the optimized portfolios are different, but their Sharpe ratios are very close. Nevertheless, the expected return is always lower when implementing an ESG strategy*[10].

**Risk premium** The total market wealth $W$ is equal to $\int W_j \,\mathrm{d}j$. Let $\omega_j = W_j/W$ be the market share of economic agent $j$. The amount $W_{i,j}$ invested in stock $i$ is equal to $W_{i,j} = w_{i,j}^\star W_j = w_{i,j}^\star \omega_j W$. The total dollar amount invested in stock $i$ is then equal to

$$W_i = \int_j W_{i,j} \,\mathrm{d}j = \int_j w_{i,j}^\star \omega_j W \,\mathrm{d}j$$

[10] In the following, we will see that this is not always the case, as it depends on the sign of the aggregate ESG preference $w_m^\top \boldsymbol{\mathcal{G}}$ where $w_m$ is the market portfolio.

Figure 3.6: Efficient frontier with ESG preferences (Example 11, $n = 20$, $\rho = 25\%$)

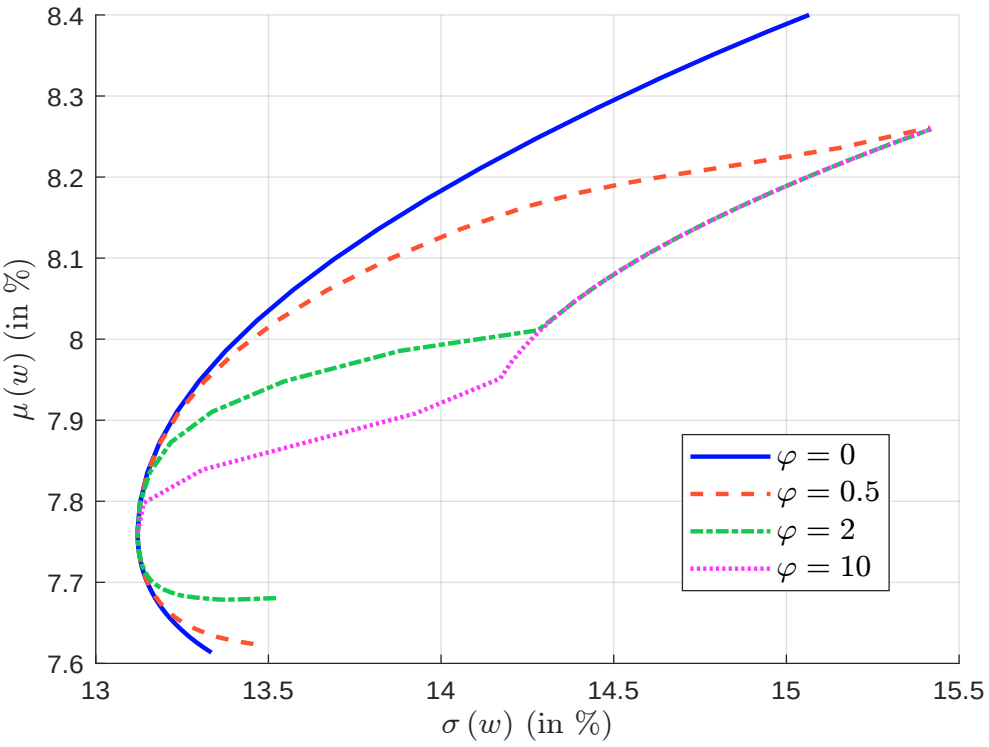


Let $w_m = (w_{1,m}, \ldots, w_{n,m})$ be the market portfolio. We have:

$$w_{i,m} = \frac{W_i}{W} = \int_j w_{i,j}^\star \omega_j \, \mathrm{d}j$$

and $\int_j \omega_j \, \mathrm{d}j = 1$. Pástor *et al.* (2021) deduce that the market clearing condition satisfies:

$$\begin{aligned} w_m &= \int_j \omega_j w_j^\star \, \mathrm{d}j \\ &= \int_j \omega_j \Gamma_j \Sigma^{-1} \left(\pi + \gamma_j b_j\right) \mathrm{d}j \\ &= \int_j \omega_j \Gamma_j \Sigma^{-1} \left(\pi + \gamma_j \varphi_j \boldsymbol{\mathcal{G}}\right) \mathrm{d}j \\ &= \left(\int_j \Gamma_j \omega_j \, \mathrm{d}j\right) \Sigma^{-1} \pi + \left(\int_j \omega_j \Gamma_j \psi_j \, \mathrm{d}j\right) \Sigma^{-1} \boldsymbol{\mathcal{G}} \end{aligned}$$

where $\psi_j = \gamma_j \varphi_j$. Let $\Gamma_m = \int_j \Gamma_j \omega_j \, \mathrm{d}j$ and $\psi_m = \Gamma_m^{-1} \left(\int_j \omega_j \Gamma_j \psi_j \, \mathrm{d}j\right)$ be the average risk tolerance and the weighted average of the ESG preferences. The expression for the market portfolio is then equal to:

$$w_m = \Gamma_m \Sigma^{-1} \pi + \Gamma_m \psi_m \Sigma^{-1} \boldsymbol{\mathcal{G}}$$

We deduce that the asset risk premia are equal to:

$$\pi = \frac{1}{\Gamma_m} \Sigma w_m - \psi_m \boldsymbol{\mathcal{G}}$$

while the market risk premium is defined as:

$$\begin{aligned}\pi_m &= w_m^\top \pi \\ &= \frac{1}{\Gamma_m} w_m^\top \Sigma w_m - \psi_m w_m^\top \boldsymbol{\mathcal{G}} \\ &= \frac{1}{\Gamma_m} \sigma_m^2 - \psi_m \boldsymbol{\mathcal{G}}_m\end{aligned}$$

where $\sigma_m = \sqrt{w_m^\top \Sigma w_m}$ and $\boldsymbol{\mathcal{G}}_m = w_m^\top \boldsymbol{\mathcal{G}}$ are the volatility and green intensity (or greenness) of the market portfolio. On page 147 (see footnote b.), we have seen that $\pi_m^{\text{capm}} = \Gamma_m^{-1} \sigma_m^2$ is the risk premium derived from the CAPM. Since $\Gamma_m \geq 0$ and $\psi_m \geq 0$, Pástor *et al.* (2021) notice that:

- The risk premium including ESG sentiment is lower than the CAPM risk premium when the market's ESG intensity is positive:

$$\boldsymbol{\mathcal{G}}_m > 0 \Longrightarrow \pi_m \leq \pi_m^{\text{capm}}$$

- It is greater than the CAPM risk premium when the market ESG intensity is negative:

$$\boldsymbol{\mathcal{G}}_m < 0 \Longrightarrow \pi_m \geq \pi_m^{\text{capm}}$$

- The gap $\Delta\pi_m^{\text{esg}} := |\pi_m - \pi_m^{\text{capm}}|$ is an increasing function of market ESG sentiment $\psi_m$:

$$\psi_m \nearrow \Longrightarrow \Delta\pi_m^{\text{esg}} \nearrow$$

If we assume that $\boldsymbol{\mathcal{G}}_m \approx 0$, we have $\Gamma_m = \sigma_m^2 / \pi_m$ and:

$$\pi = \beta \pi_m - \psi_m \boldsymbol{\mathcal{G}} \tag{3.14}$$

because $\beta(w_m) = \left(w_m^\top \Sigma w_m\right)^{-1} \Sigma w_m$ is the vector of asset betas with respect to the market portfolio. This is the main result of Pástor *et al.* (2021). It follows that the alpha of asset $i$ is equal to:

$$\alpha_i = \pi_i - \beta_i \pi_m = -\psi_m \boldsymbol{\mathcal{G}}_i$$

Pástor *et al.* (2021) conclude that when $\psi_m > 0$, "*green stocks have negative alphas and brown stocks have positive alphas. Moreover, greener stocks have lower alphas.*"

**Example 12** *We consider Example 11. The market consists of two long-only investors ($j = 1, 2$): a non-ESG investor ($\varphi_1 = 0$) and an ESG investor ($\varphi_2 > 0$). We assume that they have the same risk tolerance $\gamma$. We note $W_1$ and $W_2$ their financial wealth, which is fully invested in the risky assets. We assume that $W_1 = W_2 = 1$.*

If the market is at equilibrium, we need to compute the market portfolio. If there is no short-selling constraint, we have seen that the weights of the tangency portfolio are equal to:

$$w^* = \frac{\Sigma^{-1}(\mu - r\mathbf{1}_n)}{\mathbf{1}_n^\top \Sigma^{-1}(\mu - r\mathbf{1}_n)}$$

We obtain $w^* = (15.04\%, 15.04\%, 16.65\%, 16.65\%, 18.31\%, 18.31\%)$. Since there is no short position, this is the market portfolio[11] without ESG preferences. It follows that the optimal portfolio $w_1^\star$ of the first economic agent is equal to $w^*$. Then, we deduce the risk-tolerance coefficient of this agent:

$$\gamma_1 = \frac{1}{\mathbf{1}_n^\top \Sigma^{-1}(\mu - r\mathbf{1}_n)} = 0.4558$$

[11] Otherwise, we must solve the Markowitz QP problem with the constraints $\mathbf{1}_n^\top w = 1$ and $w_i \geq 0$.

We can now compute the optimal portfolio of the second economic agent by assuming that $\gamma_2 = \gamma_1$ and considering the following optimization problem:

$$\begin{aligned} w_2^\star &= \arg\min \frac{1}{2} w^\top \Sigma w - \gamma_2 w^\top (\mu + \gamma_2 \varphi_2 \boldsymbol{\mathcal{G}}) \\ &\text{s.t.} \quad \begin{cases} \mathbf{1}_n^\top w = 1 \\ w \geq \mathbf{0}_n \end{cases} \end{aligned}$$

It is important to use the QP program and not the analytical formula, because the ESG-tilted returns $\mu' = \mu + \gamma_2 \varphi_2 \boldsymbol{\mathcal{G}}$ can be very different from the asset returns $\mu$. In this example, the long-only market portfolio is equal to the long/short tangency portfolio because we assume a uniform correlation of 25% and a constant Sharpe ratio of 20%. The ESG preference $\varphi_2$ combined with the greenness vector $\boldsymbol{\mathcal{G}}$ can dramatically change the Sharpe ratio of the assets when calculated with the ESG-tilted returns. We obtain $w_2^\star = (18.86\%, 11.22\%, 21.33\%, 11.97\%, 23.96\%, 12.65\%)$. The market portfolio is then equal to:

$$\begin{aligned} w_m &= \frac{W_1}{W} w_1^\star + \frac{W_2}{W} w_2^\star \\ &= (1 - \omega^{\text{esg}})\, w_1^\star + \omega^{\text{esg}}\, w_2^\star \end{aligned}$$

where $W = W_1 + W_2$ and $\omega^{\text{esg}}$ is the wealth share of ESG investors. If $W_1 = W_2 = 1$, we obtain $w_m = (16.95\%, 13.13\%, 18.99\%, 14.31\%, 21.13\%, 15.48\%)$, $\mu_m = 7.86\%$ and $\sigma_m = 14.93\%$. It follows that the beta values are $\beta = (1.15, 1.05, 1.04, 0.95, 0.95, 0.86)$. We deduce that the risk premia are $\pi = (5.58\%, 5.12\%, 5.06\%, 4.61\%, 4.62\%, 4.17\%)$. Finally, we conclude that the alpha vector expressed in bps is $\alpha = (-19.09, 26.19, -19.43, 25.84, -19.72, 25.55)$. A summary of these results is given in Table 3.5.

Table 3.5: Computation of alpha returns (Example 12, $n = 6$, $\rho = 25\%$)

| | Portfolio $w_1^\star$ | | | Portfolio $w_2^\star$ | | | | Portfolio $w_m$ | | | |
|---|---|---|---|---|---|---|---|---|---|---|---|
| $i$ | $w_i$ (in %) | $\beta_i$ | $\pi_i$ (in %) | $w_i$ (in %) | $\beta_i$ | $\pi_i$ (in %) | $\alpha_i$ (in bps) | $w_i$ (in %) | $\beta_i$ | $\pi_i$ (in %) | $\alpha_i$ (in bps) |
| 1 | 15.04 | 1.11 | 5.39 | 18.86 | 1.17 | 5.69 | −30 | 16.95 | 1.15 | 5.58 | −19 |
| 2 | 15.04 | 1.11 | 5.39 | 11.22 | 0.99 | 4.80 | 58 | 13.13 | 1.05 | 5.12 | 26 |
| 3 | 16.65 | 1.00 | 4.87 | 21.33 | 1.07 | 5.18 | −32 | 18.99 | 1.04 | 5.06 | −19 |
| 4 | 16.65 | 1.00 | 4.87 | 11.97 | 0.88 | 4.30 | 57 | 14.31 | 0.95 | 4.61 | 26 |
| 5 | 18.31 | 0.91 | 4.43 | 23.96 | 0.98 | 4.76 | −33 | 21.13 | 0.95 | 4.62 | −20 |
| 6 | 18.31 | 0.91 | 4.43 | 12.65 | 0.80 | 3.87 | 56 | 15.48 | 0.86 | 4.17 | 26 |

**Remark 32** *In Figure 3.7, we show the evolution of the alpha return $\alpha_i$ with respect to the market share $\omega^{\text{esg}}$ of ESG investors. It increases in absolute value because the deviation of the market portfolio including ESG preferences increases with $\omega^{\text{esg}}$. We note that $\alpha_1 \approx \alpha_3 \approx \alpha_5$ and $\alpha_2 \approx \alpha_4 \approx \alpha_6$ because of the specification of the exercise problem. When the Sharpe ratio of the assets is different and the correlation is not uniform, the alpha returns are more diffuse.*

**Interpretation of the results** As mentioned earlier, we need to distinguish between expected returns and realized returns. From a theoretical point of view, there is a scientific consensus that the risk premium of brown assets is positive, which implies that the risk premium of green assets

Figure 3.7: Evolution of alpha return relative to market share of ESG investors (Example 12, $n = 6$, $\rho = 25\%$)

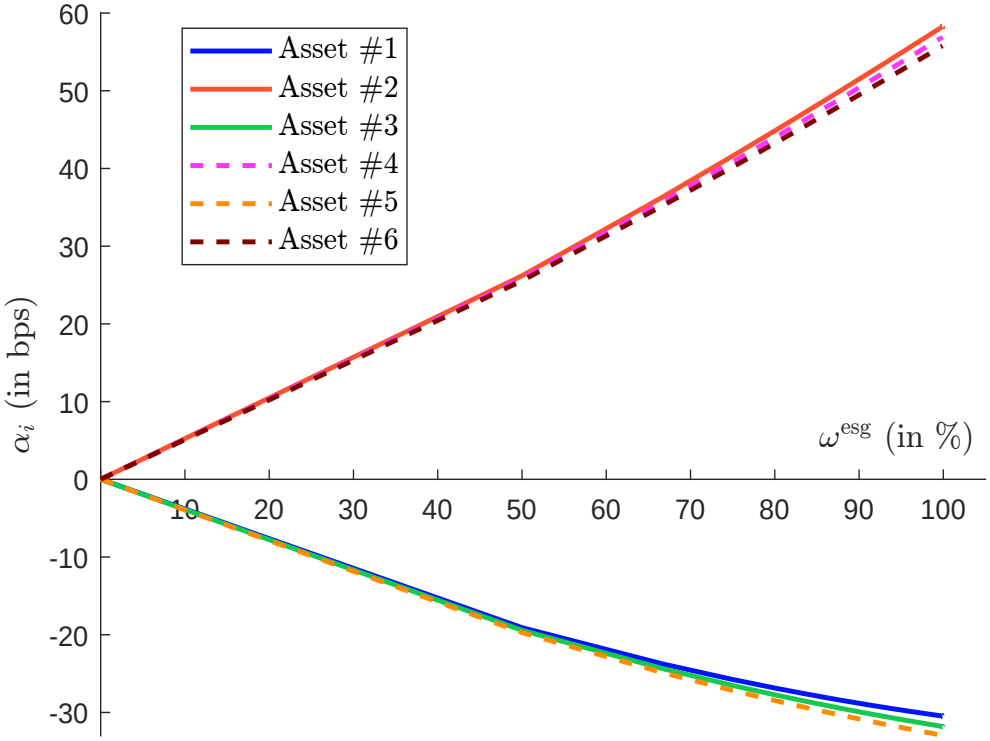


is negative (Zerbib, 2019; Ben Slimane *et al.*, 2020; Bolton and Kacperczyk, 2021). This is because there is a systematic market risk when investing in brown assets due to several factors, including carbon pricing, regulatory, reputational, asset stranding and climate hedging risks. Moreover, it is clear that high demand for green assets from ESG investors lowers their expected returns. However, we must be careful because the positive expected excess return of brown assets does not necessarily imply that the performance of green assets is lower than the performance of brown assets:

> "*In equilibrium, green assets have low expected returns because investors enjoy holding them and because green assets hedge climate risk. Green assets nevertheless outperform when positive shocks hit the ESG factor, which captures shifts in customers' tastes for green products and investors' tastes for green holdings.*" (Pástor *et al.*, 2021).

The important word in this quote is *equilibrium*, which means that green assets have low expected returns in the long run. In this case, investors need to earn an additional return to compensate for the risk they take by investing in brown assets. However, in the short run, when the market is not at equilibrium, green assets may outperform brown assets, especially when we observe a supply/demand imbalance.

We might ask, what does equilibrium mean? In fact, it refers to a certain long-term period. To quantify the long run more precisely, let us consider the one-factor risk model:

$$R_i - r = \alpha_i + \beta_i \left(R_m - r\right) + \varepsilon_i$$

where $R_m \sim \mathcal{N}\left(\mu_m, \sigma_m^2\right)$ is the stochastic market return, $\varepsilon_i \sim \mathcal{N}\left(0, \tilde{\sigma}_i^2\right)$ is the idiosyncratic risk and $\varepsilon_i \perp \varepsilon_j$. It follows that $(R_i, R_j)$ follows a bivariate Gaussian distribution:

$$\begin{pmatrix} R_i \\ R_j \end{pmatrix} = \mathcal{N}\left(\begin{pmatrix} \mu_i \\ \mu_j \end{pmatrix}, \begin{pmatrix} \sigma_i^2 & \sigma_{i,j} \\ \sigma_{i,j} & \sigma_j^2 \end{pmatrix}\right)$$

where $\mu_i = r + \alpha_i + \beta_i (\mu_m - r)$, $\sigma_i^2 = \beta_i^2 \sigma_m^2 + \tilde{\sigma}_i^2$ and $\sigma_{i,j} = \beta_i \beta_j \sigma_m^2$. We deduce that $R_i - R_j = \mathcal{N}\left(\mu_{i-j}, \sigma_{i-j}^2\right)$ where:

$$\mu_{i-j} = (\alpha_i - \alpha_j) + (\beta_i - \beta_j)(\mu_m - r)$$

and:

$$\sigma_{i-j}^2 = (\beta_i - \beta_j)^2 \sigma_m^2 + \tilde{\sigma}_i^2 + \tilde{\sigma}_j^2$$

Let us assume that the two assets have the same systematic risk: $\beta_i = \beta_j$. We obtain:

$$R_i - R_j = \mathcal{N}\left(\alpha_i - \alpha_j, \tilde{\sigma}_i^2 + \tilde{\sigma}_j^2\right)$$

In the standard CAPM, the alpha returns are equal to zero and we deduce that:

$$\Pr\{R_i < R_j\} = \frac{1}{2}$$

If two assets have the same systematic risk, the probability that one will underperform the other is 50%. Now let us take ESG preferences into account by assuming that asset $i$ is the green asset and asset $j$ is the brown asset. The one-year underperformance probability becomes:

$$p_u(\Delta\alpha) = \Pr\{R_i < R_j\} = \Phi\left(\frac{\alpha_j - \alpha_i}{\sqrt{\tilde{\sigma}_i^2 + \tilde{\sigma}_j^2}}\right) > \frac{1}{2}$$

because we have $\Delta\alpha = \alpha_j - \alpha_i > 0$. We can extend this formula to a holding period longer than one year. If we assume that the dynamics of asset returns are Brownian motions, we get:

$$p_u(\Delta\alpha, t) = \Phi\left(\frac{(\alpha_j - \alpha_i)\sqrt{t}}{\sqrt{\tilde{\sigma}_i^2 + \tilde{\sigma}_j^2}}\right)$$

where $t$ is the holding period. Using this formula, we can find the holding period to achieve a given underperformance probability $p_u$:

$$t(\Delta\alpha, p_u) = \frac{\left(\tilde{\sigma}_i^2 + \tilde{\sigma}_j^2\right)}{(\alpha_j - \alpha_i)^2} \Phi^{-1}(p_u)^2$$

In Figure 3.8, we show the relationship between $\Delta\alpha$ and the underperformance probability $p_u(\Delta\alpha, t)$ for several values of the holding period[12]. For plausible values of $\Delta\alpha$ (less than 200 bps), we see that the probability for a one-year holding period is less than 55%. It increases to 70% for a ten-year period, which is not very high. It follows that the values of $t(\Delta\alpha, p_u)$ are very high at the asset level. Let us now consider the same exercise at the portfolio level. We consider an equally-weighted portfolio of 500 green assets and 500 brown assets. Results are given in the bottom/right panel. If the alpha difference is 40 bps, the probability of underperformance is 90% over two years.

[12] We assume a typical value of 10% for the idiosyncratic volatility: $\tilde{\sigma}_i = \tilde{\sigma}_j = 10\%$.

Figure 3.8: Impact of alpha returns on underperformance probability

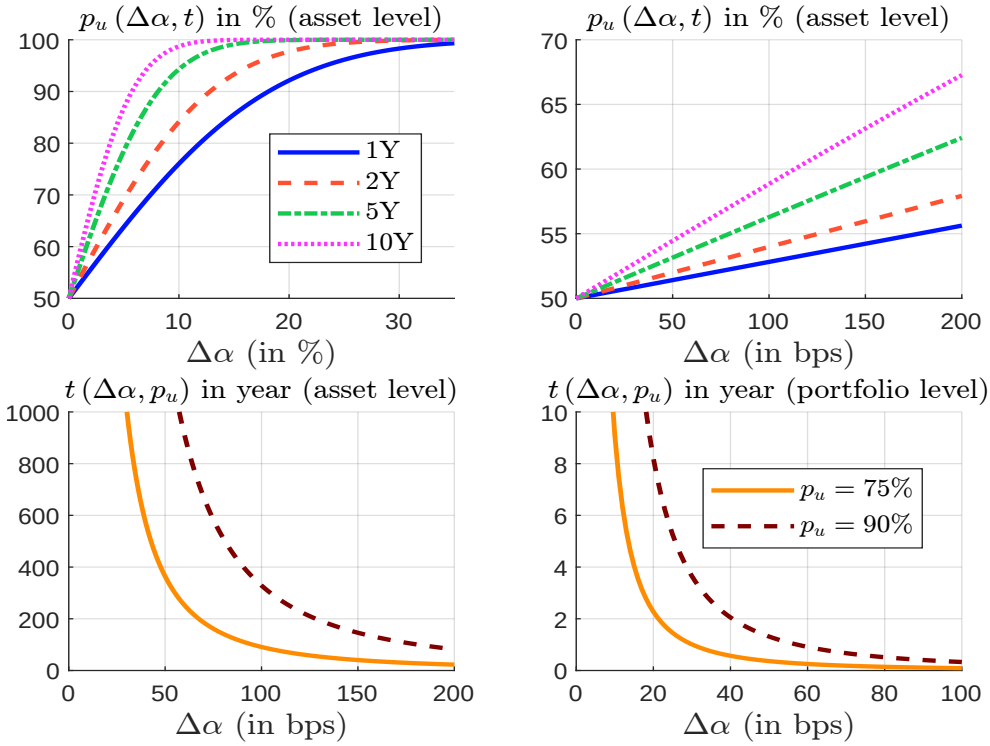


**Remark 33** *All these results show that the term equilibrium refers to long holding periods. At the asset level, alpha returns require at least ten years to observe a significant difference. At the portfolio level, a three-year holding period is required for alpha returns to materialize.*

One might ask whether the PST model accounts for the ESG risk premium or whether it is better suited to assess the green risk premium. In fact, the sustainable characteristic of the firm $i$ is measured by a non-random metric $\boldsymbol{\mathcal{G}}_i$. For instance, $\boldsymbol{\mathcal{G}}_i$ may correspond to the carbon footprint or the green intensity[13] of the firm. If we apply this model with ESG characteristics, $\boldsymbol{\mathcal{G}}_i$ is the ESG score $\boldsymbol{\mathcal{S}}_i$ of the firm. In this case, the assumption that all investors have the same view on the ESG score is a strong hypothesis. In particular, we have already seen that there is a large divergence between ESG scoring models (Berg *et al.*, 2022). In this context, the original formulation of the PST model is certainly better suited to assess the climate risk premium than the ESG risk premium.

### Extension of the model

**ESG uncertainty** The previous problem is addressed by Avramov *et al.* (2022) (hereafter, ACLT model), who analyze the impact of ESG score uncertainty on the ESG risk premium. They assume that ESG scores are stochastic and may be correlated with asset excess returns:

$$\begin{pmatrix} \tilde{R} \\ \boldsymbol{\mathcal{S}} \end{pmatrix} \sim \mathcal{N}\left( \begin{pmatrix} \pi \\ \mu_s \end{pmatrix}, \begin{pmatrix} \Sigma & \Sigma_{\pi,s} \\ \Sigma_{s,\pi} & \Sigma_s \end{pmatrix} \right)$$

where $\tilde{R}$ and $\boldsymbol{\mathcal{S}}$ are the random vectors of excess returns and ESG scores, respectively. It follows that $\tilde{b}_j = \varphi_j \boldsymbol{\mathcal{S}}$ is stochastic and not constant. Using Equation (3.12), we deduce that the expected

[13] Measured, for example, by the green revenue share.

utility of the economic agent $j$ is equal to:

$$\mathbb{E}\left[\boldsymbol{\mathcal{U}}\left(\tilde{W}_j, w_j\right)\right] = e^{-\bar{\Gamma}_j(1+r)}\mathbb{E}\left[\exp\left(-\bar{\Gamma}_j w_j^\top\left(\tilde{R}+\psi_j\boldsymbol{\mathcal{S}}\right)\right)\right]$$

where $\psi_j = \gamma_j\varphi_j$. Since we have $\tilde{R}+\psi_j\boldsymbol{\mathcal{S}} \sim \mathcal{N}\left(\breve{\mu}_j, \breve{\Sigma}_j\right)$ where $\breve{\mu}_j = \pi + \psi_j\mu_s$ and $\breve{\Sigma}_j = \Sigma + \psi_j^2\Sigma_s + 2\psi_j\Sigma_{\pi,s}$, a new expression for the expected utility is:

$$\mathbb{E}\left[\boldsymbol{\mathcal{U}}\left(\tilde{W}_j, w_j\right)\right] = e^{-\bar{\Gamma}_j(1+r)}\exp\left(-\bar{\Gamma}_j w_j^\top\breve{\mu}_j + \frac{1}{2}\bar{\Gamma}_j^2 w_j^\top\breve{\Sigma}_j w_j\right)$$

The first-order condition is equal to $-\bar{\Gamma}_j\breve{\mu}_j + \bar{\Gamma}_j^2\breve{\Sigma}_j w_j = 0$, which means that the optimal portfolio is:

$$w_j^\star = \Gamma_j\breve{\Sigma}_j^{-1}\tilde{\mu}_j = \Gamma_j\breve{\Sigma}_j^{-1}\left(\pi+\psi_j\mu_s\right)$$

This is exactly the same expression as in Equation (3.13) where the asset covariance matrix $\Sigma$ is replaced by the augmented covariance matrix $\breve{\Sigma}_j$ and the greenness vector $\boldsymbol{\mathcal{G}}$ is equal to the vector $\mu_s$ of expected ESG scores. Avramov *et al.* (2022) introduce the matrix $\Omega_j = \breve{\Sigma}_j^{-1} - \Sigma^{-1}$ and rewrite the optimal solution as follows:

$$w_j^\star = \underbrace{\Gamma_j\Sigma^{-1}\left(\pi+\psi_j\mu_s\right)}_{\text{PST solution}} + \underbrace{\Gamma_j^{-1}\Omega_j\left(\pi+\psi_j\mu_s\right)}_{\text{ESG uncertainty}}$$

Thus, the optimal portfolio consists of two components. The first is the optimal portfolio of the PST model. The second component is another portfolio due to the uncertainty in the ESG scores. The two portfolios have the same expression, except that the second portfolio depends on the matrix $\Omega_j$ rather than the covariance matrix $\Sigma$. Using market clearing conditions, Avramov *et al.* (2022) derive the CAPM-like relationship:

- If there is no ESG uncertainty ($\boldsymbol{\mathcal{S}} = \mu_s$ and $\Sigma_s = \mathbf{0}_{n,n}$), the vector of risk premia is given by:

$$\begin{aligned}\pi^{\text{esg}} &= \beta\pi_m - \psi_m\left(\mu_s - \beta\bar{\boldsymbol{\mathcal{S}}}_m\right)\\ &= \pi^{\text{capm}} - \psi_m\left(\mu_s - \beta\bar{\boldsymbol{\mathcal{S}}}_m\right)\end{aligned}$$

  where:

$$\begin{cases}\pi_m = \dfrac{1}{\Gamma_m}\sigma_m^2 - \psi_m\bar{\boldsymbol{\mathcal{S}}}_m\\ \sigma_m^2 = w_m^\top\Sigma w_m\\ \beta = \dfrac{\Sigma w_m}{w_m^\top\Sigma w_m}\\ \bar{\boldsymbol{\mathcal{S}}}_m = w_m^\top\mu_s\end{cases}$$

  Here, $\pi_m$, $\sigma_m$ and $\bar{\boldsymbol{\mathcal{S}}}_m$ are the risk premium, volatility and ESG score of the market portfolio $w_m$, and $\beta$ is the vector of beta coefficients. $\Gamma_m$ and $\psi_m$ are the aggregate risk tolerance and ESG preference across the investors:

$$\begin{cases}\Gamma_m = \dfrac{\int_j \omega_j\Gamma_j\,\mathrm{d}j}{\int_j\omega_j\,\mathrm{d}j} = \int_j\omega_j\Gamma_j\,\mathrm{d}j\\ \psi_m = \dfrac{\int_j\omega_j\Gamma_j\psi_j\,\mathrm{d}j}{\int_j\omega_j\Gamma_j\,\mathrm{d}j} = \dfrac{\int_j\omega_j\Gamma_j\psi_j\,\mathrm{d}j}{\Gamma_m}\end{cases}$$

  The authors retrieve the formula (3.14) when the market is ESG neutral[14].

[14] Pástor *et al.* (2021) assume that $\boldsymbol{\mathcal{G}}_m = 0$ and find that $\pi = \beta\pi_m - \psi_m\boldsymbol{\mathcal{G}}$.

- If there is uncertainty in the ESG scores ($\boldsymbol{\mathcal{S}} \neq \mu_s$ and $\Sigma_s \neq \mathbf{0}_{n,n}$), the vector of risk premia will be:

$$\begin{aligned}\breve{\pi}^{\text{esg}} &= \breve{\beta}\breve{\pi}_m - \psi_m\left(\breve{\mu}_s - \breve{\beta}\breve{\boldsymbol{\mathcal{S}}}_m\right)\\ &= \beta\pi_m + \left(\breve{\beta} - \beta\right)\pi_m - \psi_m\left(\breve{\mu}_s - \breve{\beta}\breve{\boldsymbol{\mathcal{S}}}_m\right)\end{aligned}$$

where $\beta$ and $\psi_m$ are the previously defined values and:

$$\begin{cases}\breve{\pi}_m = \dfrac{1}{\Gamma_m}\breve{\sigma}_m^2 - \psi_m\breve{\boldsymbol{\mathcal{S}}}_m\\ \breve{\sigma}_m^2 = w_m^\top\breve{\Sigma}_m w_m\\ \breve{\beta} = \dfrac{\breve{\Sigma}_m w_m}{w_m^\top\breve{\Sigma}_m w_m}\\ \breve{\mu}_s = \dfrac{\Psi_m\mu_s}{\psi_m}\\ \breve{\boldsymbol{\mathcal{S}}}_m = w_m^\top\tilde{\mu}_s\end{cases}$$

Here, $\breve{\pi}_m$, $\breve{\sigma}_m$ and $\breve{\boldsymbol{\mathcal{S}}}_m$ are the risk premium, volatility and ESG score of the market portfolio $w_m$, $\breve{\beta}$ is the vector of effective beta coefficients, and $\breve{\mu}_s$ is the vector of modified average ESG scores. These quantities depend on $\breve{\Sigma}_m$ and $\Psi_m$:

$$\begin{cases}\breve{\Sigma}_m = \left(\dfrac{\int_j \omega_j\Gamma_j\breve{\Sigma}_j^{-1}\,\mathrm{d}j}{\Gamma_m}\right)^{-1}\\ \Psi_m = \left(\int_j \omega_j\Gamma_j\breve{\Sigma}_j^{-1}\,\mathrm{d}j\right)^{-1}\int_j \omega_j\Gamma_j\breve{\Sigma}_j^{-1}\psi_j\,\mathrm{d}j\end{cases}$$

The relationship $\breve{\pi}^{\text{esg}} = \breve{\beta}\breve{\pi}_m - \psi_m\left(\breve{\mu}_s - \breve{\beta}\breve{\boldsymbol{\mathcal{S}}}_m\right)$ obtained with ESG uncertainty is very close to the equilibrium formula $\pi^{\text{esg}} = \beta\pi_m - \psi_m\left(\mu_s - \beta\bar{\boldsymbol{\mathcal{S}}}_m\right)$ obtained without ESG uncertainty. In fact, ESG uncertainty changes the risk perception of investors. Therefore, the ESG-tilted covariance matrix $\breve{\Sigma}_j = \Sigma + \psi_j^2\Sigma_s + 2\psi_j\Sigma_{\pi,s}$ is no longer equal to the asset covariance matrix $\Sigma$. It impacts the quantities related to the market portfolio.

To better understand the impact of ESG uncertainty on alpha returns, Avramov *et al.* (2022) consider the special case where agents have homogeneous preferences ($\bar{\gamma}_j = \bar{\gamma}$, $\varphi_j = \varphi$) and the same wealth ($W_j = 1$), the covariance matrix of ESG scores is diagonal ($\Sigma_s = \text{diag}\left(\sigma_{1,s}^2 \ldots, \sigma_{n,s}^2\right)$) and returns are independent of ESG scores ($\Sigma_{\pi,s} = \mathbf{0}_{n,n}$). They deduce that $\Gamma_m = \gamma$, $\psi_m = \psi = \gamma\varphi$, $\breve{\Sigma}_m = \Sigma + \psi^2\Sigma_s$, $\Psi_m = \psi I_n$, $\breve{\sigma}_m^2 = \sigma_m^2 + \psi^2\sigma_s^2$, $\sigma_m^2 = w_m^\top\Sigma w_m$, $\sigma_s^2 = w_m^\top\Sigma_s w_m$, $\breve{\mu}_s = \mu_s$ and $\breve{\boldsymbol{\mathcal{S}}}_m = w_m^\top\mu_s$. The vector of the effective beta is equal to:

$$\begin{aligned}\breve{\beta} &= \frac{\sigma_m^2}{\breve{\sigma}_m^2}\beta + \psi^2\frac{\sigma_s^2}{\breve{\sigma}_m^2}\beta_s\\ &= \beta + \psi^2\frac{\sigma_s^2}{\breve{\sigma}_m^2}\left(\beta_s - \beta\right)\end{aligned}$$

where:

$$\beta_s = \frac{\Sigma_s w_m}{\sigma_s^2}$$

Avramov *et al.* (2022) find that:

$$\begin{aligned}
\breve{\alpha}^{\text{esg}} &= \breve{\pi}^{\text{esg}} - \beta\pi_m \\
&= \psi^2 \frac{\sigma_s^2}{\breve{\sigma}_m^2}(\beta_s - \beta)\pi_m - \psi_m\left(\mu_s - \left(\beta + \psi^2\frac{\sigma_s^2}{\breve{\sigma}_m^2}(\beta_s - \beta)\right)\breve{\boldsymbol{\mathcal{S}}}_m\right) \\
&= \psi^2 \frac{\sigma_s^2}{\breve{\sigma}_m^2}(\beta_s - \beta)\left(\pi_m + \psi_m\breve{\boldsymbol{\mathcal{S}}}_m\right) - \psi_m\left(\mu_s - \beta\breve{\boldsymbol{\mathcal{S}}}_m\right)
\end{aligned}$$

If we consider the asset $i$, we obtain:

$$\beta_{i,s} = w_{i,m}\frac{\sigma_{i,s}^2}{\sigma_s^2}$$

$\beta_{i,s}$ increases with the volatility $\sigma_{i,s}$ of the score $\boldsymbol{\mathcal{S}}_i$. We deduce that:

$$\frac{\partial\,\breve{\alpha}_i^{\text{esg}}}{\partial\,\sigma_{i,s}} > 0$$

This implies that alpha increases with ESG uncertainty. The authors also examine the impact of ESG uncertainty on demand and test the model using the standard deviations from ESG rating agencies as a proxy for ESG uncertainty. Their conclusion is as follows:

> "*In equilibrium, the market premium increases and demand for stocks declines under ESG uncertainty. In addition, the CAPM alpha and effective beta both rise with ESG uncertainty and the negative ESG-alpha relation weakens.*" Avramov *et al.* (2022, page 642).

**Example 13** *Consider an investment universe with four assets. Their expected returns are* 5%, 6%, 7% *and* 8%, *while their volatilities are* 15%, 20%, 30% *and* 30%. *The correlation matrix of asset returns is given by the following matrix:*

$$\mathbb{C} = \begin{pmatrix} 100\% & & & \\ 10\% & 100\% & & \\ 40\% & 60\% & 100\% & \\ 50\% & 40\% & 80\% & 100\% \end{pmatrix}$$

*The risk-free return is set to* 2%. *The average ESG scores are* $+3\%$, $-2\%$, $+1\%$ *and* $-1\%$, *respectively, while the standard deviation of ESG score is the same for all assets and is* 20%. *We assume that the long-only investor's ESG preference* $\varphi$ *is equal to* 0.50 *while his risk tolerance corresponds to the market risk tolerance.*

We begin by calculating the market risk tolerance $\gamma_m = \left(\mathbf{1}_n^\top\Sigma^{-1}(\mu - r\mathbf{1}_n)\right)^{-1} = 0.4654$ and the market portfolio weights:

$$w_m = \gamma_m\Sigma^{-1}(\mu - r\mathbf{1}_n) = \begin{pmatrix} 50.08\% \\ 49.98\% \\ -22.52\% \\ 23.47\% \end{pmatrix}$$

Then we consider the following optimization problem:

$$\begin{aligned}
w^\star(\psi, \mu_s, \Sigma_s) &= \arg\min \frac{1}{2}w^\top\left(\Sigma + \psi^2\Sigma_s\right)w - \gamma_m(\mu + \psi\mu_s) \\
&\text{s.t.} \quad \begin{cases} \mathbf{1}_n^\top w = 1 \\ w \geq \mathbf{0}_n \end{cases}
\end{aligned}$$

where $\Sigma_s = 4\% \times I$, $\mu_s = (3\%, -2\%, 1\%, -1\%)$ and $\psi = \gamma_m \varphi = 0.4954 \times 0.50 = 0.2327$. To decompose the risk premium of the long-only ESG investor, we compute the long-only portfolio $w^\star(0, \mathbf{0}_n, \mathbf{0}_{n,n})$, the long-only portfolio without ESG uncertainty $w^\star(\psi, \mu_s, \mathbf{0}_{n,n})$ and the long-only portfolio with ESG uncertainty $w^\star(\psi, \mu_s, \Sigma_s)$. For each portfolio, we compute the beta coefficient $\beta(w^\star(\psi, \mu_s, \Sigma_s) \mid w_m)$ with respect to the market portfolio. We derive the risk premium $\pi(w^\star(\psi, \mu_s, \Sigma_s)) = \beta(w^\star(\psi, \mu_s, \Sigma_s) \mid w_m) \cdot \pi_m$ where $\pi_m = \mu(x_m) - r$. We get the following decomposition:

$$\begin{aligned}
\pi(w^\star(\psi, \mu_s, \Sigma_s)) &= \underbrace{\pi(w_m)}_{\text{market risk premium}} + \\
&\quad \underbrace{\pi(w^\star(0, \mathbf{0}_n, \mathbf{0}_{n,n})) - \pi(w_m)}_{\text{long-only alpha}} + \\
&\quad \underbrace{\pi(w^\star(\psi, \mu_s, \mathbf{0}_{n,n})) - \pi(w^\star(0, \mathbf{0}_n, \mathbf{0}_{n,n}))}_{\text{ESG score alpha}} + \\
&\quad \underbrace{\pi(w^\star(\psi, \mu_s, \Sigma_s)) - \pi(w^\star(\psi, \mu_s, \mathbf{0}_{n,n}))}_{\text{ESG uncertainty alpha}}
\end{aligned}$$

The optimal weights and risk statistics are given in Tables 3.6 and 3.7. We have:

$$\pi(w^\star(\psi, \mu_s, \Sigma_s)) = 3.74\% - 0.96 \text{ bps} - 19.80 \text{ bps} + 5.41 \text{ bps} = 3.50\%$$

In this example, the cost of the long-only constraint is $-0.96$ bps, the ESG score alpha is $-19.80$ bps, while the ESG uncertainty alpha is 5.41 bps.

Table 3.6: Weights of optimized portfolios (Example 13)

| Asset | $w_m$ | $w^\star(0, \mathbf{0}_n, \mathbf{0}_{n,n})$ | $w^\star(\psi, \mu_s, \mathbf{0}_{n,n})$ | $w^\star(\psi, \mu_s, \Sigma_s)$ |
|---|---|---|---|---|
| #1 | 50.08% | 52.00% | 64.03% | 61.87% |
| #2 | 48.98% | 39.65% | 31.51% | 32.05% |
| #3 | −22.52% | 0.00% | 0.00% | 0.00% |
| #4 | 23.47% | 8.35% | 4.47% | 6.09% |

Table 3.7: Risk statistics of optimized portfolios (Example 13)

| Portfolio | $\mu(w)$ | $\sigma(w)$ | $\beta(w \mid w_m)$ | $\pi(w)$ | $\boldsymbol{\mathcal{S}}(w)$ |
|---|---|---|---|---|---|
| $w_m$ | 5.74% | 13.20% | 1.0000 | 3.74% | 0.06% |
| $w^\star(0, \mathbf{0}_n, \mathbf{0}_{n,n})$ | 5.65% | 13.33% | 0.9743 | 3.65% | 0.68% |
| $w^\star(\psi, \mu_s, \mathbf{0}_{n,n})$ | 5.45% | 12.86% | 0.9214 | 3.45% | 1.25% |
| $w^\star(\psi, \mu_s, \Sigma_s)$ | 5.50% | 12.99% | 0.9358 | 3.50% | 1.15% |

**Risk factor model** In the capital asset pricing model, the asset return $R_i$ satisfies the one-factor risk model:

$$R_i - r = \alpha_i + \beta_i (R_m - r) + \varepsilon_i$$

where $\alpha_i = 0$, $\beta_i$ is the CAPM beta of asset $i$, $R_m \sim \mathcal{N}(\mu_m, \sigma_m^2)$ is the market return, $\varepsilon_i \sim \mathcal{N}(0, \tilde{\sigma}_i^2)$ is the residual. Moreover, we have $\varepsilon_i \perp R_m$ and $\varepsilon_i \perp \varepsilon_j$. In matrix form, we obtain:

$$R = r + \beta (R_m - r) + \varepsilon$$

where $R \sim \mathcal{N}(\mu, \Sigma)$, $\varepsilon = (\varepsilon_1, \ldots, \varepsilon_n) \sim \mathcal{N}(\mathbf{0}_n, D)$ and $D = \operatorname{diag}\left(\tilde{\sigma}_1^2, \ldots, \tilde{\sigma}_n^2\right)$. We deduce that:

$$\mu = \mathbb{E}[R] = r + \beta(\mu_m - r)$$

or:

$$\pi = \mu - r = \beta\pi_m$$

It follows that:

$$R - \mu = \beta(R_m - \mu_m) + \varepsilon$$

Therefore, the expression of the covariance matrix is:

$$\begin{aligned}
\Sigma &= \mathbb{E}\left[(R-\mu)(R-\mu)^\top\right] \\
&= \mathbb{E}\left[(\beta(R_m-\mu_m)+\varepsilon)(\beta(R_m-\mu_m)+\varepsilon)^\top\right] \\
&= \mathbb{E}\left[\beta(R_m-\mu_m)(R_m-\mu_m)\beta^\top + \varepsilon\varepsilon^\top + 2\beta(R_m-\mu_m)\varepsilon^\top\right] \\
&= \sigma_m^2\beta\beta^\top + D
\end{aligned}$$

When we introduce ESG preferences, we obtain a two-factor model:

$$R = r + \beta(R_m - r) + \beta_{\text{esg}} R_{\text{esg}} + \varepsilon$$

where $R \sim \mathcal{N}(\mu, \Sigma)$, $R_m \sim \mathcal{N}\left(\mu_m, \sigma_m^2\right)$ is the market return, $\varepsilon = (\varepsilon_1, \ldots, \varepsilon_n) \sim \mathcal{N}(\mathbf{0}_n, D)$ and $D = \operatorname{diag}\left(\tilde{\sigma}_1^2, \ldots, \tilde{\sigma}_n^2\right)$. Here, $R_{\text{esg}} \sim \mathcal{N}\left(\mu_{\text{esg}}, \sigma_{\text{esg}}^2\right)$ is the return of the ESG portfolio $w_{\text{esg}} \propto \Sigma^{-1}\mu_s$, which is a zero-beta strategy(Pástor *et al.*, 2021):

$$\beta^\top w_{\text{esg}} = 0$$

This is why we assume that $R_{\text{esg}} \perp R_m$ and $R_{\text{esg}} \perp \varepsilon$. We deduce that:

$$\mu = r + \beta(\mu_m - r) + \beta_{\text{esg}}\mu_{\text{esg}}$$

or:

$$\pi = \beta\pi_m + \beta_{\text{esg}}\mu_{\text{esg}}$$

For the covariance matrix, we obtain:

$$\Sigma = \sigma_m^2\beta\beta^\top + \sigma_{\text{esg}}^2\beta_{\text{esg}}\beta_{\text{esg}}^\top + D$$

Even if the ESG portfolio has a zero return ($\mu_{\text{esg}} = 0$), we see that it can have a big impact on the structure of the covariance matrix.

**Remark 34** *The CAPM and ESG coefficients $\beta_i$ and $\beta_{i,\text{esg}}$ do not have the same status. In fact, we generally assume that $\beta_i \geq 0$. Otherwise, the asset risk premium is negative: $\pi_i = \beta_i\pi_m$. Moreover, the CAPM average beta $\bar{\beta}$ is close to 1 because the beta of the market portfolio is equal to 1:*

$$\begin{aligned}
\beta(w_m) = 1 &\Leftrightarrow \frac{w_m^\top \Sigma w_m}{w_m^\top \Sigma w_m} = 1 \\
&\Leftrightarrow w_m^\top \frac{\Sigma w_m}{w_m^\top \Sigma w_m} = 1 \\
&\Leftrightarrow \sum_{i=1}^n w_{i,m}\beta_i = 1
\end{aligned}$$

*In practice, we assume that* $\beta_i \in [0,3]$ *in the stock market. This is not the case for ESG beta because the ESG factor is a zero-beta long/short portfolio. This means that* $\beta_{i,\text{esg}}$ *can be positive or negative. In practice, the ESG factor*[15] *is constructed so that* $\beta_{i,\text{esg}} \in [-1,1]$.

To measure the impact of ESG on the covariance matrix, we compare the one-factor and two-factor models. The expression for the asset variance is respectively $\sigma_i^2\,(\text{capm}) = \sigma_m^2\beta_i^2 + \tilde{\sigma}_i^2$ for the one-factor model and $\sigma_i^2\,(\text{esg}) = \sigma_m^2\beta_i^2 + \sigma_{\text{esg}}^2\beta_{i,\text{esg}}^2 + \tilde{\sigma}_i^2$ for the two-factor model. We deduce that:

$$\sigma_i^2\,(\text{esg}) - \sigma_i^2\,(\text{capm}) = \sigma_{\text{esg}}^2\beta_{i,\text{esg}}^2 \geq 0$$

Theoretically, the introduction of the ESG factor increases asset volatility. This is because a new risk is priced in by the market. From a practical point of view, the impact may be lower:

$$\sigma_i^2\,(\text{esg}) - \sigma_i^2\,(\text{capm}) \leq \sigma_{\text{esg}}^2\beta_{i,\text{esg}}^2$$

because the idiosyncratic volatility can be reduced in the two-factor model. In fact, we can assume that the ESG factor may capture some of the CAPM residual risk. If we focus on the correlation, we obtain:

$$\rho_{i,j}\,(\text{esg}) = \frac{\sigma_m^2\beta_i\beta_j + \sigma_{\text{esg}}^2\beta_{i,\text{esg}}\beta_{j,\text{esg}}}{\sigma_i\,(\text{esg})\,\sigma_j\,(\text{esg})}$$

and:

$$\rho_{i,j}\,(\text{esg}) - \rho_{i,j}\,(\text{capm}) = \underbrace{\left(\frac{1}{\sigma_i\,(\text{esg})\,\sigma_j\,(\text{esg})} - \frac{1}{\sigma_i\,(\text{capm})\,\sigma_j\,(\text{capm})}\right)\sigma_m^2\beta_i\beta_j}_{\text{negative}} + \underbrace{\frac{\sigma_{\text{esg}}^2\beta_{i,\text{esg}}\beta_{j,\text{esg}}}{\sigma_i\,(\text{esg})\,\sigma_j\,(\text{esg})}}_{\text{not signed}}$$

We have two effects:

1. As asset volatilities increase, the contribution of the CAPM covariance factor $\beta_i\beta_j$ in the two-factor model decreases.
2. The second component depends on the sign of the two ESG beta coefficients. If $\beta_{i,\text{esg}}$ and $\beta_{j,\text{esg}}$ are both positive or negative, the contribution is positive, otherwise it is negative. This means that the ESG factor increases the correlation between ESG-friendly (or green) assets. The correlation also increases between ESG-unfriendly (or brown) assets. However, the correlation between a green asset and a brown asset decreases.

**Example 14** *We consider an investment universe consisting of five assets. Their market betas are* 0.9, 0.8, 1.2, 0.7 *and* 1.3, *respectively, while their specific volatilities are* 4%, 12%, 5%, 8% *and* 5%. *The volatility of the market portfolio is* 25%. *As for the ESG factor, we have* $\sigma_{\text{esg}} = 10\%$, *while the ESG sensitivity values are set to* $-0.5$, 0.7, 0.2, 0.9 *and* $-0.3$.

The covariance matrices are reported in Tables 3.8 and 3.9. We verify that the asset volatilities have increased with the two-factor model: $\sigma_i\,(\text{esg}) > \sigma_i\,(\text{capm})$. We notice that most of correlations have decreased except for the cross-correlation $\rho_{2,4}$ between the second and fourth assets. These assets have the largest ESG sensitivities: $\beta_{2,\text{esg}} = 0.7$ and $\beta_{4,\text{esg}} = 0.9$. The cross-correlation $\rho_{1,5}$ is not reduced even through we have $\beta_{1,\text{esg}} = -0.5$ and $\beta_{5,\text{esg}} = -0.3$. In fact, the product $\beta_{1,\text{esg}}\beta_{5,\text{esg}}$

Table 3.8: CAPM covariance matrix (Example 14)

| Asset | $\sigma_i$ (in %) | $\rho_{i,j}$ (in %) | | | | |
|---|---|---|---|---|---|---|
| #1 | 22.85 | 100.00 | 84.43 | 97.12 | 89.54 | 97.31 |
| #2 | 23.32 | 84.43 | 100.00 | 84.58 | 77.99 | 84.75 |
| #3 | 30.41 | 97.12 | 84.58 | 100.00 | 89.71 | 97.49 |
| #4 | 19.24 | 89.54 | 77.99 | 89.71 | 100.00 | 89.89 |
| #5 | 32.88 | 97.31 | 84.75 | 97.49 | 89.89 | 100.00 |

Table 3.9: Two-factor covariance matrix (Example 14)

| Asset | $\sigma_i$ (in %) | $\rho_{i,j}$ (in %) | | | | |
|---|---|---|---|---|---|---|
| #1 | 23.39 | 100.00 | 72.85 | 93.27 | 70.18 | 96.61 |
| #2 | 24.35 | 72.85 | 100.00 | 82.72 | 79.84 | 78.23 |
| #3 | 30.48 | 93.27 | 82.72 | 100.00 | 83.87 | 96.28 |
| #4 | 21.24 | 70.18 | 79.84 | 83.87 | 100.00 | 77.24 |
| #5 | 33.02 | 96.61 | 78.23 | 96.28 | 77.24 | 100.00 |

is no large enough to compensate for the increase in volatilities: $\sigma_1(\text{esg}) - \sigma_1(\text{capm}) = 54$ bps and $\sigma_5(\text{esg}) - \sigma_5(\text{capm}) = 14$ bps.

We consider the portfolio $w = \vartheta\Sigma^{-1}\eta$ where $\eta$ is a $n \times 1$ vector and $\vartheta = 1/\left(\mathbf{1}_n^\top\Sigma^{-1}\eta\right)$ is the scalar such that $\mathbf{1}_n^\top w = 1$. Using results in Box 3.3, we deduce that:

$$\begin{aligned} w &= \vartheta D^{-1}\eta - \vartheta M^{-1}\eta \\ &= \vartheta D^{-1}\eta - \vartheta\omega_1\tilde{\beta}\tilde{\beta}^\top\eta - \vartheta\omega_2\tilde{\beta}_{\text{esg}}\tilde{\beta}_{\text{esg}}^\top\eta + \vartheta\omega_3\left(\tilde{\beta}_{\text{esg}}\tilde{\beta}^\top + \tilde{\beta}\tilde{\beta}_{\text{esg}}^\top\right)\eta \\ &= \underbrace{\vartheta\left(D^{-1} - \omega_1\tilde{\beta}\tilde{\beta}^\top\right)\eta}_{\text{capm}} + \underbrace{\vartheta\left(\omega_3\tilde{\beta}_{\text{esg}}\tilde{\beta}^\top + \omega_3\tilde{\beta}\tilde{\beta}_{\text{esg}}^\top - \omega_2\tilde{\beta}_{\text{esg}}\tilde{\beta}_{\text{esg}}^\top\right)\eta}_{\text{esg}} \end{aligned} \tag{3.15}$$

Therefore, we can derive analytical formulas for GMV ($\eta = \mathbf{1}_n$), MVO ($\eta = \gamma\mu$) and tangency ($\eta = \mu - r\mathbf{1}_n$) portfolios. For instance, if we look at the minimum variance portfolio, Roncalli *et al.* (2020) show that:

$$\omega_{i,\text{gmv}} = \frac{\sigma^2(\omega_{\text{gmv}})}{\tilde{\sigma}_i^2}\max\left(1 - \frac{\beta_i}{\beta^\star} - \frac{\beta_{i,\text{esg}}}{\beta_{\text{esg}}^\star}, c\right)$$

where $c = -\infty$ if there is no constraint and $c = 0$ if there is no short selling. Since the mean of the beta coefficients is close to one, $\beta^\star$ is positive, implying that the asset weight is a decreasing function of the asset beta. Therefore, the minimum variance portfolio is a low beta strategy. The effect of the ESG factor is more complex because the mean of the ESG beta coefficients is close to zero, implying that the threshold $\beta_{\text{esg}}^\star$ can be positive or negative. We conclude that the asset weight can be a decreasing or increasing function of the ESG betas.

**Example 15** *Consider an investment universe with five assets. Their market betas are* 0.7, 0.8, 0.9, 1.2 *and* 1.5, *respectively, while their specific volatilities are* 10%, 8%, 3%, 5% *and* 4%. *The volatility of the market portfolio is* 25%. *As for the ESG factor, we have* $\sigma_{\text{esg}} = 10\%$, *while the ESG sensitivity values are set to* $-0.5$, $-0.7$, $-0.5$, 0.9 *and* 1.3.

[15] Because the ESG factor is long/short, we can always scale its volatility by leveraging or deleveraging.

Box 3.3: One-factor and two-factor precision matrices

In portfolio optimization, several variables (weights, risk premium, etc.) are expressed in terms of the inverse of the covariance matrix, which is called the precision matrix. In the case of the one-factor model, we apply the Sherman-Morrison-Woodbury formula[a] with $A = D$ and $u = v = \sigma_m \beta$, and we obtain:

$$\Sigma^{-1} = D^{-1} - \frac{\sigma_m^2}{1 + \sigma_m^2 \tilde{\beta}^\top \beta} \tilde{\beta} \tilde{\beta}^\top$$

where $\tilde{\beta}_i = \beta_i / \tilde{\sigma}_i^2$.

For the two-factor model, we use the generalized Sherman-Morrison-Woodbury formula with $A = D$, $u_1 = v_1 = \sigma_m \beta$ and $u_2 = v_2 = \sigma_{\text{esg}} \beta_{\text{esg}}$. It follows that the inverse of the covariance matrix is equal to:

$$\Sigma^{-1} = D^{-1} - D^{-1} U S^{-1} V^\top D^{-1}$$

where $U = V = \begin{pmatrix} \sigma_m \beta & \sigma_{\text{esg}} \beta_{\text{esg}} \end{pmatrix}$ and:

$$S = \begin{pmatrix} 1 + \sigma_m^2 \beta^\top D^{-1} \beta & \sigma_m \sigma_{\text{esg}} \beta^\top D^{-1} \beta_{\text{esg}} \\ \sigma_m \sigma_{\text{esg}} \beta^\top D^{-1} \beta_{\text{esg}} & 1 + \sigma_{\text{esg}}^2 \beta_{\text{esg}}^\top D^{-1} \beta_{\text{esg}} \end{pmatrix}$$

Roncalli *et al.* (2020) show that:

$$\Sigma^{-1} = D^{-1} - M^{-1}$$

where:

$$M^{-1} = \omega_1 \tilde{\beta} \tilde{\beta}^\top + \omega_2 \tilde{\beta}_{\text{esg}} \tilde{\beta}_{\text{esg}}^\top - \omega_3 \left( \tilde{\beta}_{\text{esg}} \tilde{\beta}^\top + \tilde{\beta} \tilde{\beta}_{\text{esg}}^\top \right)$$

and:

$$\begin{cases} \tilde{\beta}_i = \beta_i / \tilde{\sigma}_i^2 \\ \tilde{\beta}_{i,\text{esg}} = \beta_{i,\text{esg}} / \tilde{\sigma}_i^2 \\ \omega_0 = 1 + \sigma_m^2 \tilde{\beta}^\top \beta + \sigma_{\text{esg}}^2 \tilde{\beta}_{\text{esg}}^\top \beta_{\text{esg}} + \sigma_m^2 \sigma_{\text{esg}}^2 \left( \left( \tilde{\beta}^\top \beta \right) \left( \tilde{\beta}_{\text{esg}}^\top \beta_{\text{esg}} \right) - \left( \tilde{\beta}^\top \beta_{\text{esg}} \right)^2 \right) \\ \omega_1 = \omega_0^{-1} \sigma_m^2 \left( 1 + \sigma_{\text{esg}}^2 \tilde{\beta}_{\text{esg}}^\top \beta_{\text{esg}} \right) \\ \omega_2 = \omega_0^{-1} \sigma_{\text{esg}}^2 \left( 1 + \sigma_m^2 \tilde{\beta}^\top \beta \right) \\ \omega_3 = \omega_0^{-1} \sigma_m^2 \sigma_{\text{esg}}^2 \left( \tilde{\beta}^\top \beta_{\text{esg}} \right) \end{cases}$$

[a] See Appendix A.1.1 on page 1046.

Tables 3.10 and 3.11 show the weights of the GMV and long-only MV portfolios and compare the allocation between the one-factor and two-factor models. If we consider Example 14, adding the ESG factor increases (resp. decreases) the weights of assets with negative (resp. positive) values of $\beta_{i,\text{esg}}$. The reason lies in the fact that the threshold $\beta_{\text{esg}}^\star$ is positive. In the case of Example 15, $\beta_{\text{esg}}^\star$ is equal to $-3.5677$ for the GMV portfolio and $-7.5752$ for the long-only MV portfolio. The relationship between $\beta_{i,\text{esg}}$ and $\omega_{i,\text{gmv}}$ becomes more complex. Indeed, the long exposure condition is $\beta_i / \beta^\star + \beta_{i,\text{esg}} / \beta_{\text{esg}}^\star \leq 1$. If $\beta_i \leq \beta^\star$, $\omega_{i,\text{gmv}}$ may be positive if $\beta_{i,\text{esg}}$ is greater than the bound

$\beta^{\star}_{\text{esg}}\left(1-\beta_i/\beta^{\star}\right)$, which is negative. Therefore, both positive and negative values of $\beta_{i,\text{esg}}$ can lead to a long exposure. If $\beta_i \geq \beta^{\star}$, the bound is positive and only an asset with a positive ESG sensitivity has a positive weight.

Table 3.10: Minimum variance portfolios (Example 14)

| Asset | $\beta_i$ | $\beta_{i,\text{esg}}$ | One-factor | | Two-factor | |
|---|---|---|---|---|---|---|
| | | | GMV | MV | GMV | MV |
| #1 | 0.90 | −0.50 | 147.33% | 0.00% | 166.55% | 33.54% |
| #2 | 0.80 | 0.70 | 24.67% | 9.45% | 21.37% | 1.46% |
| #3 | 1.20 | 0.20 | −49.19% | 0.00% | −58.80% | 0.00% |
| #4 | 0.70 | 0.90 | 74.20% | 90.55% | 65.06% | 64.99% |
| #5 | 1.30 | −0.30 | −97.01% | 0.00% | −94.18% | 0.00% |
| $\sigma(w)$ | | | 11.45% | 19.19% | 11.54% | 20.40% |
| $\beta(w)$ | | | 0.1913 | 0.7095 | 0.1954 | 0.7686 |
| $\beta_{\text{esg}}(w)$ | | | 0.2965 | 0.8811 | 0.0674 | 0.4274 |
| $\beta^{\star}$ | | | 1.0972 | 0.8307 | 1.0906 | 0.8667 |
| $\beta^{\star}_{\text{esg}}$ | | | | | 19.7724 | 9.7394 |

Table 3.11: Minimum variance portfolios (Example 15)

| Asset | $\beta_i$ | $\beta_{i,\text{esg}}$ | One-factor | | Two-factor | |
|---|---|---|---|---|---|---|
| | | | GMV | MV | GMV | MV |
| #1 | 0.70 | −0.50 | 26.21% | 66.96% | 57.34% | 73.46% |
| #2 | 0.80 | −0.70 | 32.17% | 33.04% | 19.57% | 26.54% |
| #3 | 0.90 | −0.50 | 166.32% | 0.00% | 10.31% | 0.00% |
| #4 | 1.20 | 0.90 | −7.55% | 0.00% | 130.35% | 0.00% |
| #5 | 1.50 | 1.30 | −117.15% | 0.00% | −117.58% | 0.00% |
| $\sigma(w)$ | | | 8.10% | 19.69% | 17.21% | 20.47% |
| $\beta(w)$ | | | 0.0899 | 0.7330 | 0.4513 | 0.7265 |
| $\beta_{\text{esg}}(w)$ | | | −2.7786 | −0.5661 | −0.8306 | −0.5531 |
| $\beta^{\star}$ | | | 1.1664 | 0.8462 | 1.0505 | 0.9227 |
| $\beta^{\star}_{\text{esg}}$ | | | | | −3.5677 | −7.5752 |

**Remark 35** *The previous examples illustrate that the global minimum variance portfolio can have a positive or negative ESG beta. In fact, it depends on the correlation between the CAPM betas and the ESG betas. In general, the GMV portfolio has a positive ESG beta if there is a negative correlation between $\beta_i$ and $\beta_{i,\text{esg}}$.*

If market risk and ESG factors are uncorrelated, we can assume that[16] $\beta^{\top}\beta_{\text{esg}} \approx 0$. If we consider mean-variance optimized portfolios, Equation (3.15) becomes:

$$w = \vartheta\left(D^{-1} - \omega_1\tilde{\beta}\tilde{\beta}^{\top} - \omega_2\tilde{\beta}_{\text{esg}}\tilde{\beta}_{\text{esg}}^{\top}\right)\mu$$

[16]Otherwise, it means that green assets are generally associated with high beta assets if $\beta^{\top}\beta_{\text{esg}} \gg 0$ or low beta assets if $\beta^{\top}\beta_{\text{esg}} \ll 0$.

We deduce that:

$$w_i \propto \omega_\eta \frac{\mu_i}{\tilde{\sigma}_i^2} - \omega_\beta \frac{\beta_i}{\tilde{\sigma}_i^2} - \omega_{\beta_{\text{esg}}} \frac{\beta_{i,\text{esg}}}{\tilde{\sigma}_i^2}$$

where:

$$\begin{cases} \omega_\eta = 1 + \sigma_m^2 \tilde{\beta}^\top \beta + \sigma_{\text{esg}}^2 \tilde{\beta}_{\text{esg}}^\top \beta_{\text{esg}} \geq 0 \\ \omega_\beta = \sigma_m^2 \left(1 + \sigma_{\text{esg}}^2 \tilde{\beta}_{\text{esg}}^\top \beta_{\text{esg}}\right) \sum_{j=1}^n \frac{\beta_j \mu_j}{\tilde{\sigma}_j^2} \geq 0 \\ \omega_{\beta_{\text{esg}}} = \sigma_{\text{esg}}^2 \left(1 + \sigma_m^2 \tilde{\beta}^\top \beta\right) \sum_{j=1}^n \frac{\beta_{j,\text{esg}} \mu_j}{\tilde{\sigma}_j^2} \leqslant 0 \end{cases}$$

We deduce that $w_i$ is an increasing function of $\mu_i$ and a decreasing function of $\beta_i$ and $\tilde{\sigma}_i$. Like the minimum variance portfolio, $w_i$ can be a decreasing or increasing function of $\beta_{i,\text{esg}}$ because $\omega_{\beta_{\text{esg}}}$ can be positive or negative.

### 3.1.3 ESG efficient frontier

Pedersen *et al.* (2021) propose an extension of the Markowitz optimization model to include ESG preferences (hereafter, the PFP model). Although the model settings are similar, the PFP model differs slightly from the PST model by focusing more on the efficient frontier.

#### Model settings

The investment universe consists of $n$ assets. We have $\tilde{R} = R - r \sim \mathcal{N}(\pi, \Sigma)$. The assets have an ESG score given by $\boldsymbol{\mathcal{S}} = (\boldsymbol{\mathcal{S}}_1, \ldots, \boldsymbol{\mathcal{S}}_n)$. Let $w = (w_1, \ldots, w_n)$ be the investor's portfolio. His initial wealth is $W$ whereas his terminal wealth is given by $\tilde{W} = \left(1 + r + w^\top \tilde{R}\right) W$. The model uses the mean-variance utility function, which is tilted by the ESG score of the portfolio:

$$\begin{aligned} \boldsymbol{\mathcal{U}}\left(\tilde{W}, w\right) &= \mathbb{E}\left[\tilde{W}\right] - \frac{\bar{\gamma}}{2} \text{var}\left(\tilde{W}\right) + \zeta\left(\boldsymbol{\mathcal{S}}(w)\right) W \\ &= \left(1 + r + w^\top \pi - \frac{\bar{\gamma}}{2} w^\top \Sigma w + \zeta\left(w^\top \boldsymbol{\mathcal{S}}\right)\right) W \end{aligned}$$

where $\zeta$ is a function that depends on the investor. Optimizing the utility function is equivalent to finding the mean-variance-esg optimized portfolio:

$$\begin{aligned} w^\star &= \arg\max w^\top \pi - \frac{\bar{\gamma}}{2} w^\top \Sigma w + \zeta\left(w^\top \boldsymbol{\mathcal{S}}\right) \\ &\text{s.t.} \quad \mathbf{1}_n^\top w = 1 \end{aligned}$$

Let $\sigma(w) = \sqrt{w^\top \Sigma w}$ and $\boldsymbol{\mathcal{S}}(w) = w^\top \boldsymbol{\mathcal{S}}$. The optimization problem can be decomposed as follows:

$$w^\star = \arg\left\{\max_{\bar{\boldsymbol{\mathcal{S}}}} \left\{\max_{\bar{\sigma}} \left\{\max_{w} \left\{f(w; \pi, \Sigma, \boldsymbol{\mathcal{S}}) \text{ s.t. } w \in \Omega\left(\bar{\sigma}, \bar{\boldsymbol{\mathcal{S}}}\right)\right\}\right\}\right\} \tag{3.16}$$

where:

$$f(w; \pi, \Sigma, \boldsymbol{\mathcal{S}}) = w^\top \pi - \frac{\bar{\gamma}}{2} \sigma^2(w) + \zeta\left(\boldsymbol{\mathcal{S}}(w)\right)$$

and:

$$\Omega = \left\{w \in \mathbb{R}^n : \mathbf{1}_n^\top w = 1, \sigma(w) = \bar{\sigma}, \boldsymbol{\mathcal{S}}(w) = \bar{\boldsymbol{\mathcal{S}}}\right\}$$

**The optimal portfolio**

We consider the first optimization subproblem, which is a $\sigma - \boldsymbol{\mathcal{S}}$ problem:

$$w^\star\left(\bar{\sigma}, \bar{\boldsymbol{\mathcal{S}}}\right) = \arg\max w^\top \pi \quad \text{s.t.} \quad \begin{cases} \mathbf{1}_n^\top w = 1 \\ \sigma(w) = \sqrt{w^\top \Sigma w} = \bar{\sigma} \\ \boldsymbol{\mathcal{S}}(w) = w^\top \boldsymbol{\mathcal{S}} = \bar{\boldsymbol{\mathcal{S}}} \end{cases}$$

Pedersen *et al.* (2021) rewrite the last two equations as $w^\top \Sigma w - \bar{\sigma}^2 = 0$ and $w^\top\left(\boldsymbol{\mathcal{S}} - \bar{\boldsymbol{\mathcal{S}}}\mathbf{1}_n\right) = 0$ because[17] $\mathbf{1}_n^\top w = 1$. Therefore, the Lagrange function is:

$$\mathcal{L}(w; \lambda_1, \lambda_2) = w^\top \pi + \lambda_1\left(w^\top \Sigma w - \bar{\sigma}^2\right) + \lambda_2\left(w^\top\left(\boldsymbol{\mathcal{S}} - \bar{\boldsymbol{\mathcal{S}}}\mathbf{1}_n\right)\right)$$

The first-order condition is:

$$\frac{\partial\, \mathcal{L}(w; \lambda_1, \lambda_2)}{\partial\, w} = \pi + 2\lambda_1 \Sigma w + \lambda_2\left(\boldsymbol{\mathcal{S}} - \bar{\boldsymbol{\mathcal{S}}}\mathbf{1}_n\right) = \mathbf{0}_n$$

We deduce that the optimal portfolio is given by:

$$w = -\frac{1}{2\lambda_1}\Sigma^{-1}\left(\pi + \lambda_2\left(\boldsymbol{\mathcal{S}} - \bar{\boldsymbol{\mathcal{S}}}\mathbf{1}_n\right)\right)$$

The second constraint $w^\top\left(\boldsymbol{\mathcal{S}} - \bar{\boldsymbol{\mathcal{S}}}\mathbf{1}_n\right) = 0$ implies that:

$$\begin{aligned}
(*) \quad &\Leftrightarrow \quad \left(\boldsymbol{\mathcal{S}} - \bar{\boldsymbol{\mathcal{S}}}\mathbf{1}_n\right)^\top \frac{1}{2\lambda_1}\Sigma^{-1}\left(\pi + \lambda_2\left(\boldsymbol{\mathcal{S}} - \bar{\boldsymbol{\mathcal{S}}}\mathbf{1}_n\right)\right) = 0 \\
&\Leftrightarrow \quad \lambda_2 = -\frac{\left(\boldsymbol{\mathcal{S}} - \bar{\boldsymbol{\mathcal{S}}}\mathbf{1}_n\right)^\top \Sigma^{-1}\pi}{\left(\boldsymbol{\mathcal{S}} - \bar{\boldsymbol{\mathcal{S}}}\mathbf{1}_n\right)^\top \Sigma^{-1}\left(\boldsymbol{\mathcal{S}} - \bar{\boldsymbol{\mathcal{S}}}\mathbf{1}_n\right)} \\
&\Leftrightarrow \quad \lambda_2 = \frac{\bar{\boldsymbol{\mathcal{S}}}\left(\mathbf{1}_n^\top \Sigma^{-1}\pi\right) - \boldsymbol{\mathcal{S}}^\top \Sigma^{-1}\pi}{\boldsymbol{\mathcal{S}}^\top \Sigma^{-1}\boldsymbol{\mathcal{S}} - 2\bar{\boldsymbol{\mathcal{S}}}\left(\mathbf{1}_n^\top \Sigma^{-1}\boldsymbol{\mathcal{S}}\right) + \bar{\boldsymbol{\mathcal{S}}}^2\left(\mathbf{1}_n^\top \Sigma^{-1}\mathbf{1}_n\right)} \\
&\Leftrightarrow \quad \lambda_2 = \frac{C_{1,\pi}\bar{\boldsymbol{\mathcal{S}}} - C_{s,\pi}}{C_{s,s} - 2C_{1,s}\bar{\boldsymbol{\mathcal{S}}} + C_{1,1}\bar{\boldsymbol{\mathcal{S}}}^2}
\end{aligned}$$

where $C_{x,y}$ is the compact notation for $x^\top \Sigma^{-1} y$ — $C_{1,\pi} = \mathbf{1}_n^\top \Sigma^{-1}\pi$, $C_{s,\pi} = \boldsymbol{\mathcal{S}}^\top \Sigma^{-1}\pi$, $C_{s,s} = \boldsymbol{\mathcal{S}}^\top \Sigma^{-1}\boldsymbol{\mathcal{S}}$, $C_{1,s} = \mathbf{1}_n^\top \Sigma^{-1}\boldsymbol{\mathcal{S}}$ and $C_{1,1} = \mathbf{1}_n^\top \Sigma^{-1}\mathbf{1}_n$. Using the first constraint $w^\top \Sigma w - \bar{\sigma}^2 = 0$, we deduce that:

$$\begin{aligned}
\bar{\sigma}^2 &= -\frac{1}{2\lambda_1} w^\top \Sigma \Sigma^{-1}\left(\pi + \lambda_2\left(\boldsymbol{\mathcal{S}} - \bar{\boldsymbol{\mathcal{S}}}\mathbf{1}_n\right)\right) \\
&= -\frac{1}{2\lambda_1}\left(w^\top \pi + \lambda_2 w^\top\left(\boldsymbol{\mathcal{S}} - \bar{\boldsymbol{\mathcal{S}}}\mathbf{1}_n\right)\right) \\
&= -\frac{1}{2\lambda_1} w^\top \pi \\
&= \frac{1}{4\lambda_1^2}\pi^\top \Sigma^{-1}\left(\pi + \lambda_2\left(\boldsymbol{\mathcal{S}} - \bar{\boldsymbol{\mathcal{S}}}\mathbf{1}_n\right)\right)
\end{aligned}$$

[17] This last constraint $\mathbf{1}_n^\top w = 1$ is not used in the sequel, implying that the fraction of wealth invested in the risk-free asset is equal to $w_r = 1 - \mathbf{1}_n^\top w$.

The first Lagrange coefficient is then equal to:

$$\begin{aligned}\lambda_1 &= -\frac{1}{2\bar{\sigma}}\sqrt{\pi^\top\Sigma^{-1}\pi + \lambda_2\left(\pi^\top\Sigma^{-1}\boldsymbol{\mathcal{S}} - \bar{\boldsymbol{\mathcal{S}}}\left(\pi^\top\Sigma^{-1}\mathbf{1}_n\right)\right)} \\ &= -\frac{1}{2\bar{\sigma}}\sqrt{C_{\pi,\pi} - \frac{\left(C_{1,\pi}\bar{\boldsymbol{\mathcal{S}}} - C_{s,\pi}\right)^2}{C_{s,s} - 2C_{1,s}\bar{\boldsymbol{\mathcal{S}}} + C_{1,1}\bar{\boldsymbol{\mathcal{S}}}^2}}\end{aligned}$$

where $C_{\pi,\pi} = \pi^\top\Sigma^{-1}\pi$. Pedersen *et al.* (2021) notice that the optimal portfolio is the product of the volatility $\bar{\sigma}$ and the vector $\varrho\left(\bar{\boldsymbol{\mathcal{S}}}\right)$:

$$\begin{aligned}w^\star\left(\bar{\sigma}, \bar{\boldsymbol{\mathcal{S}}}\right) &= -\frac{1}{2\lambda_1}\Sigma^{-1}\left(\pi + \lambda_2\left(\boldsymbol{\mathcal{S}} - \bar{\boldsymbol{\mathcal{S}}}\mathbf{1}_n\right)\right) \\ &= \bar{\sigma}\,\varrho\left(\bar{\boldsymbol{\mathcal{S}}}\right)\end{aligned}$$

where:

$$\varrho\left(\bar{\boldsymbol{\mathcal{S}}}\right) = \frac{1}{\lambda_1'}\Sigma^{-1}\left(\pi + \lambda_2\left(\boldsymbol{\mathcal{S}} - \bar{\boldsymbol{\mathcal{S}}}\mathbf{1}_n\right)\right)$$

and:

$$\lambda_1' = \sqrt{C_{\pi,\pi} - \frac{\left(C_{1,\pi}\bar{\boldsymbol{\mathcal{S}}} - C_{s,\pi}\right)^2}{C_{s,s} - 2C_{1,s}\bar{\boldsymbol{\mathcal{S}}} + C_{1,1}\bar{\boldsymbol{\mathcal{S}}}^2}}$$

**Example 16** *We consider an investment universe with four assets. Their expected returns are* 6%*,* 7%*,* 8% *and* 10%*, respectively, while their volatilities are* 15%*,* 20%*,* 25% *and* 30%*. The correlation matrix of the asset returns is given by the following matrix:*

$$\mathbb{C} = \begin{pmatrix} 100\% & & & \\ 20\% & 100\% & & \\ 30\% & 50\% & 100\% & \\ 40\% & 60\% & 70\% & 100\% \end{pmatrix}$$

*The risk-free rate is set to* 2%*. The ESG score vector is* $\boldsymbol{\mathcal{S}} = (3\%, 2\%, -2\%, -3\%)$*.*

We obtain $C_{1,\pi} = 2.4864$, $C_{s,\pi} = 0.0425$, $C_{s,s} = 0.1274$, $C_{1,s} = 1.9801$, $C_{1,1} = 64.1106$ and $C_{\pi,\pi} = 0.1193$. If we target $\bar{\sigma} = 20\%$ and $\bar{\boldsymbol{\mathcal{S}}} = 1\%$, we deduce that $\lambda_1 = -0.8514$ and $\lambda_2 = -0.1870$. The optimal portfolio is then:

$$w^\star\left(\bar{\sigma}, \bar{\boldsymbol{\mathcal{S}}}\right) = \begin{pmatrix} 59.31\% \\ 29.52\% \\ 21.76\% \\ 20.72\% \end{pmatrix}$$

It follows that the portfolio is leveraged since we have $w_r = 1 - \mathbf{1}_n^\top w = -31.31\%$. We verify that $\sqrt{w^\star\left(\bar{\sigma}, \bar{\boldsymbol{\mathcal{S}}}\right)^\top \Sigma w^\star\left(\bar{\sigma}, \bar{\boldsymbol{\mathcal{S}}}\right)} = 20\%$ and $\left(w^\star\left(\bar{\sigma}, \bar{\boldsymbol{\mathcal{S}}}\right)^\top \boldsymbol{\mathcal{S}}\right) \Big/ \left(\mathbf{1}_n^\top w^\star\left(\bar{\sigma}, \bar{\boldsymbol{\mathcal{S}}}\right)\right) = 1\%$. We also notice that:

$$\varrho\left(\bar{\boldsymbol{\mathcal{S}}}\right) = \begin{pmatrix} 2.9657 \\ 1.4759 \\ 1.0881 \\ 1.0358 \end{pmatrix}$$

and verify that $w^\star\left(\bar{\sigma}, \bar{\boldsymbol{\mathcal{S}}}\right) = \bar{\sigma}\,\varrho\left(\bar{\boldsymbol{\mathcal{S}}}\right)$. The portfolio is then leveraged when $\bar{\sigma} \geq 1/\left(\mathbf{1}_n^\top \varrho\left(\bar{\boldsymbol{\mathcal{S}}}\right)\right) = 17.75\%$.

**The Sharpe ratio of the optimal portfolio**

Let us rewrite the first-order condition as:

$$\begin{aligned}
(*) &\Leftrightarrow \pi + 2\lambda_1 \Sigma w + \lambda_2 \left(\boldsymbol{\mathcal{S}} - \bar{\boldsymbol{\mathcal{S}}} \mathbf{1}_n\right) = \mathbf{0}_n \\
&\Leftrightarrow w^\top \pi + 2\lambda_1 w^\top \Sigma w + \lambda_2 w^\top \left(\boldsymbol{\mathcal{S}} - \bar{\boldsymbol{\mathcal{S}}} \mathbf{1}_n\right) = \mathbf{0}_n \\
&\Leftrightarrow w^\top \pi + 2\lambda_1 \bar{\sigma}^2 = \mathbf{0}_n \\
&\Leftrightarrow \lambda_1 = -\frac{1}{2} \frac{w^\top \pi}{\bar{\sigma}^2} \\
&\Leftrightarrow \lambda_1 = -\frac{1}{2} \frac{\mathrm{SR}\left(w \mid r\right)}{\bar{\sigma}}
\end{aligned}$$

We deduce that the Sharpe ratio of the optimal portfolio $w^\star\left(\bar{\sigma}, \bar{\boldsymbol{\mathcal{S}}}\right)$ is equal to:

$$\mathrm{SR}\left(w^\star\left(\bar{\sigma}, \bar{\boldsymbol{\mathcal{S}}}\right) \mid r\right) = \sqrt{C_{\pi,\pi} - \frac{\left(C_{1,\pi}\bar{\boldsymbol{\mathcal{S}}} - C_{s,\pi}\right)^2}{C_{s,s} - 2C_{1,s}\bar{\boldsymbol{\mathcal{S}}} + C_{1,1}\bar{\boldsymbol{\mathcal{S}}}^2}} = \mathrm{SR}\left(\bar{\boldsymbol{\mathcal{S}}} \mid \pi, \Sigma, \boldsymbol{\mathcal{S}}\right)$$

Therefore, it depends on the asset parameters $\pi$, $\Sigma$, $\boldsymbol{\mathcal{S}}$, the investor's ESG objective $\bar{\boldsymbol{\mathcal{S}}}$, but not on the volatility target $\bar{\sigma}$.

Using Example 16, we deduce that the Sharpe ratio of the optimal portfolio $w^\star\left(20\%, 1\%\right)$ is equal to 0.3406. More generally, we verify that $\mathrm{SR}\left(w^\star\left(\bar{\sigma}, \bar{\boldsymbol{\mathcal{S}}}\right) \mid r\right)$ does not depend on the value of $\bar{\sigma}$. For instance, we have $\mathrm{SR}\left(w^\star\left(\bar{\sigma}, -3\%\right) \mid r\right) = 0.2724$, $\mathrm{SR}\left(w^\star\left(\bar{\sigma}, -2\%\right) \mid r\right) = 0.2875$, $\mathrm{SR}\left(w^\star\left(\bar{\sigma}, -1\%\right) \mid r\right) = 0.3052$, $\mathrm{SR}\left(w^\star\left(\bar{\sigma}, 0\%\right) \mid r\right) = 0.3242$, $\mathrm{SR}\left(w^\star\left(\bar{\sigma}, 1\%\right) \mid r\right) = 0.3406$, $\mathrm{SR}\left(w^\star\left(\bar{\sigma}, 2\%\right) \mid r\right) = 0.3443$, and $\mathrm{SR}\left(w^\star\left(\bar{\sigma}, 3\%\right) \mid r\right) = 0.3221$. In Figure 3.9, we show the relationship between the target value $\bar{\boldsymbol{\mathcal{S}}}$ and the Sharpe ratio $\mathrm{SR}\left(w^\star\left(\bar{\sigma}, \bar{\boldsymbol{\mathcal{S}}}\right) \mid r\right)$.

**The ESG-SR frontier**

Since the objective function is equal to:

$$\begin{aligned}
f\left(w^\star\left(\bar{\sigma}, \bar{\boldsymbol{\mathcal{S}}}\right); \pi, \Sigma, \boldsymbol{\mathcal{S}}\right) &= \left(\frac{w^\star\left(\bar{\sigma}, \bar{\boldsymbol{\mathcal{S}}}\right)^\top \pi}{\bar{\sigma}}\right) \bar{\sigma} - \frac{\bar{\gamma}}{2}\bar{\sigma}^2 + \zeta\left(\bar{\boldsymbol{\mathcal{S}}}\right) \\
&= \mathrm{SR}\left(\bar{\boldsymbol{\mathcal{S}}} \mid \pi, \Sigma, \boldsymbol{\mathcal{S}}\right) \bar{\sigma} - \frac{\bar{\gamma}}{2}\bar{\sigma}^2 + \zeta\left(\bar{\boldsymbol{\mathcal{S}}}\right)
\end{aligned}$$

the $\sigma$-problem becomes:

$$\max_{\bar{\sigma}} \left\{ \max_{w} \left\{ f\left(w; \pi, \Sigma, \boldsymbol{\mathcal{S}}\right) \text{ s.t. } w \in \Omega\left(\bar{\sigma}, \bar{\boldsymbol{\mathcal{S}}}\right) \right\} \right\} = \max_{\bar{\sigma}} \left\{ \mathrm{SR}\left(\bar{\boldsymbol{\mathcal{S}}} \mid \pi, \Sigma, \boldsymbol{\mathcal{S}}\right) \bar{\sigma} - \frac{\bar{\gamma}}{2}\bar{\sigma}^2 + \zeta\left(\bar{\boldsymbol{\mathcal{S}}}\right) \right\}$$

The first-order condition is $\mathrm{SR}\left(\bar{\boldsymbol{\mathcal{S}}} \mid \pi, \Sigma, \boldsymbol{\mathcal{S}}\right) - \bar{\gamma}\bar{\sigma} = 0$ or $\bar{\sigma} = \bar{\gamma}^{-1} \mathrm{SR}\left(\bar{\boldsymbol{\mathcal{S}}} \mid \pi, \Sigma, \boldsymbol{\mathcal{S}}\right)$, and we have:

$$\begin{aligned}
f\left(w^\star\left(\bar{\sigma}, \bar{\boldsymbol{\mathcal{S}}}\right); \pi, \Sigma, \boldsymbol{\mathcal{S}}\right) &= \bar{\gamma}^{-1} \mathrm{SR}^2\left(\bar{\boldsymbol{\mathcal{S}}} \mid \pi, \Sigma, \boldsymbol{\mathcal{S}}\right) - \frac{1}{2}\bar{\gamma}^{-1} \mathrm{SR}^2\left(\bar{\boldsymbol{\mathcal{S}}} \mid \pi, \Sigma, \boldsymbol{\mathcal{S}}\right) + \zeta\left(\bar{\boldsymbol{\mathcal{S}}}\right) \\
&= \frac{1}{2}\bar{\gamma}^{-1}\left(\mathrm{SR}^2\left(\bar{\boldsymbol{\mathcal{S}}} \mid \pi, \Sigma, \boldsymbol{\mathcal{S}}\right) + 2\bar{\gamma}\zeta\left(\bar{\boldsymbol{\mathcal{S}}}\right)\right)
\end{aligned}$$

We conclude that the $\boldsymbol{\mathcal{S}}$-problem becomes:

$$\boldsymbol{\mathcal{S}}^\star = \arg\max_{\bar{\boldsymbol{\mathcal{S}}}} \left\{ \mathrm{SR}^2\left(\bar{\boldsymbol{\mathcal{S}}} \mid \pi, \Sigma, \boldsymbol{\mathcal{S}}\right) + 2\bar{\gamma}\zeta\left(\bar{\boldsymbol{\mathcal{S}}}\right) \right\} \tag{3.17}$$

Figure 3.9: Relationship between $\bar{\boldsymbol{\mathcal{S}}}$ and $\mathrm{SR}\left(\bar{\boldsymbol{\mathcal{S}}} \mid \pi, \Sigma\right)$

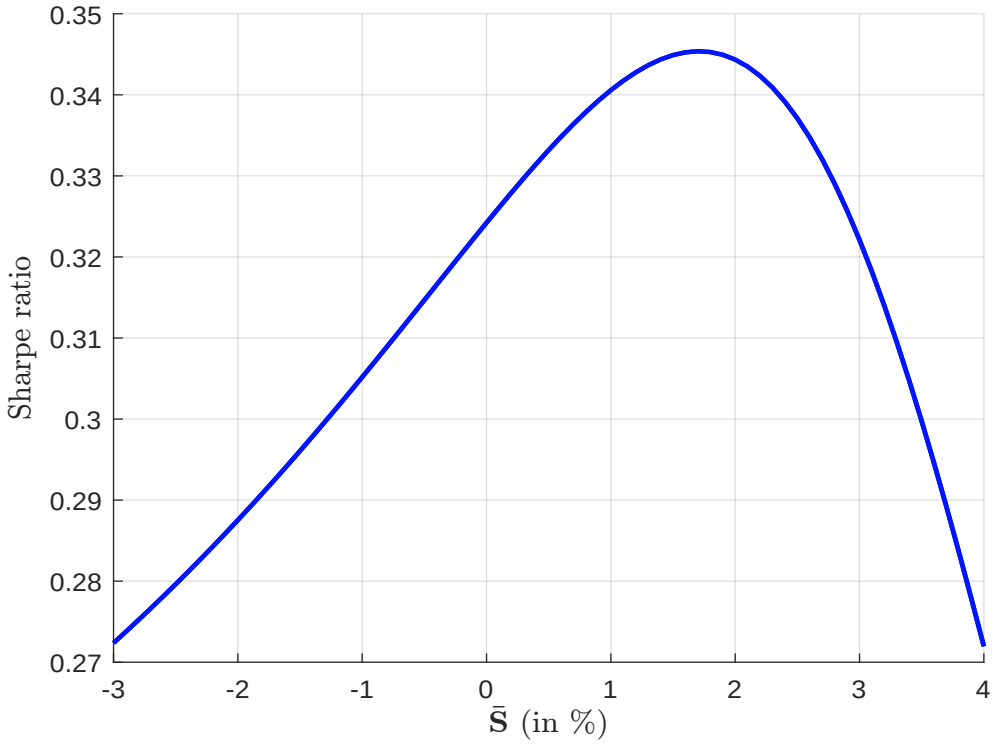


and the optimal portfolio is:

$$w^\star = w^\star\left(\sigma^\star, \boldsymbol{\mathcal{S}}^\star\right)$$

where $\boldsymbol{\mathcal{S}}^\star$ is the solution of the $\boldsymbol{\mathcal{S}}$-problem and $\sigma^\star = \bar{\gamma}^{-1}\,\mathrm{SR}\left(\boldsymbol{\mathcal{S}}^\star \mid \pi, \Sigma, \boldsymbol{\mathcal{S}}\right)$. Pedersen *et al.* (2021) distinguish three groups of investors:

- Type-U or ESG-unaware investors have no ESG preferences and do not use the information of ESG scores;
- Type-A or ESG-aware investors have no ESG preferences, but use ESG scores to update their views on risk premia;
- Type-M or ESG-motivated investors have ESG preferences, which means that they would like to have a high ESG score.

Type-U investors hold the same portfolio, which is the standard tangency portfolio calculated without the information of ESG scores:

$$w_U^\star = \frac{\Sigma^{-1}\pi}{\mathbf{1}_n^\top \Sigma^{-1}\pi}$$

Type-A investors choose the optimal portfolio with the highest Sharpe ratio. This is equivalent to setting $\zeta\left(s\right) = 0$ in Equation (3.17) and we note $\boldsymbol{\mathcal{S}}_A^\star$ the optimal ESG score. Finally, type-M investors choose an optimal portfolio on the ESG-SR efficient frontier that has an ESG score greater than the optimal ESG score: $\boldsymbol{\mathcal{S}}_M^\star \geq \boldsymbol{\mathcal{S}}_A^\star$. In this case, we have $\mathrm{SR}\left(\boldsymbol{\mathcal{S}}_M^\star \mid \pi, \Sigma, \boldsymbol{\mathcal{S}}\right) \leq \mathrm{SR}\left(\boldsymbol{\mathcal{S}}_A^\star \mid \pi, \Sigma, \boldsymbol{\mathcal{S}}\right)$. Therefore, type-M investors reduce their Sharpe ratio to achieve a better ESG score. While the optimal portfolio is the same for all type-A investors, it is different for two type-M investors who do not have the same risk-aversion coefficient $\bar{\gamma}$ and the same ESG utility function $\zeta\left(s\right)$.

Figure 3.10: Optimal portfolio for type-U investors (Example 16)

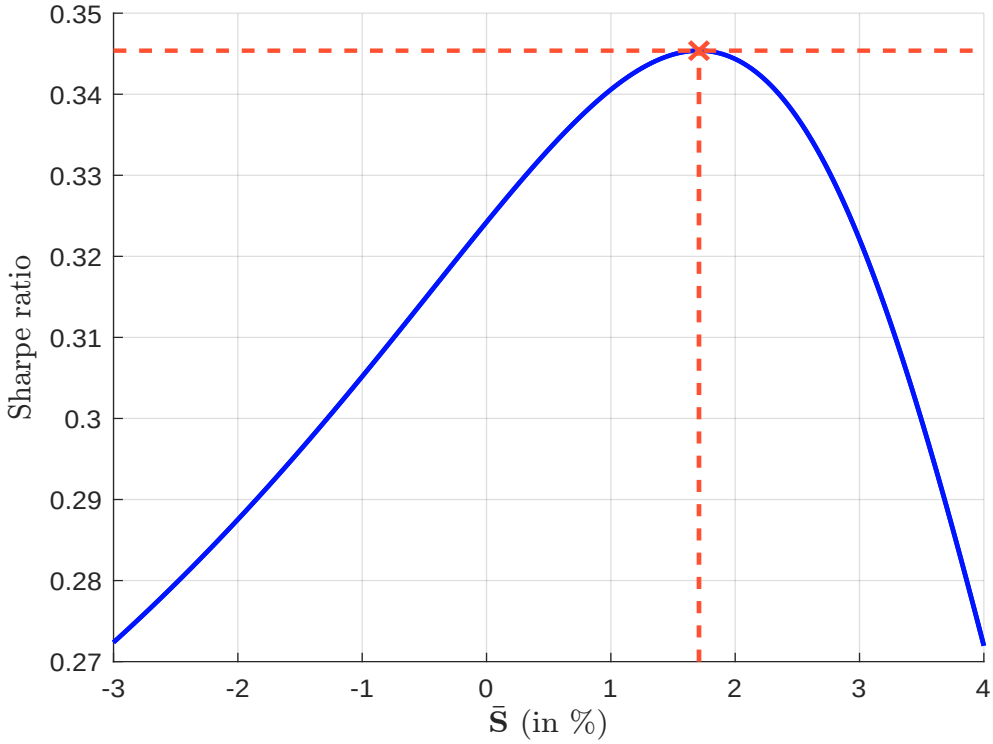


Figure 3.11: Optimal portfolio for type-A investors (Example 16)

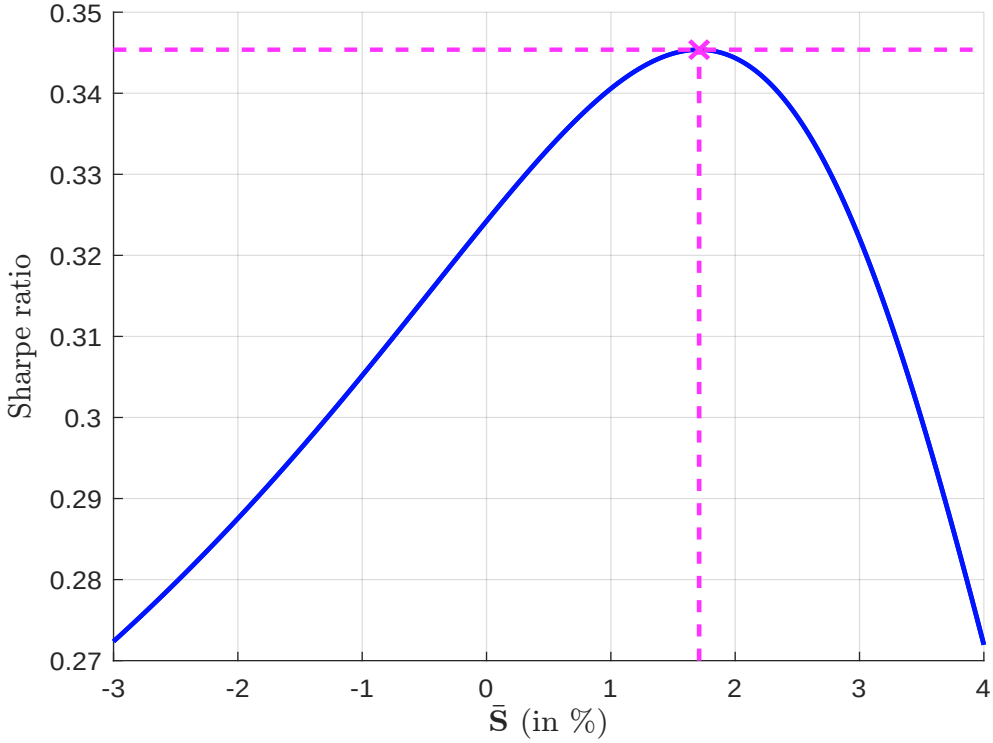

Figure 3.12: Optimal portfolio for type-M investors when $\zeta(s) = s$ (Example 16)

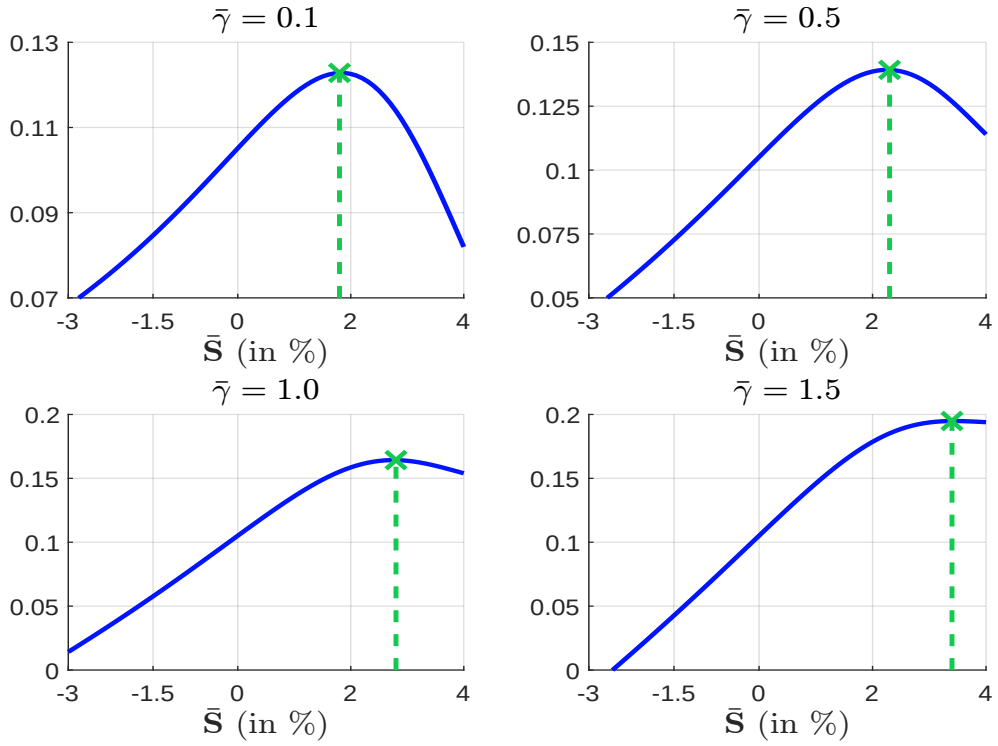


Figure 3.13: Optimal portfolio for type-M investors when $\zeta(s) = 0.2\sqrt{\max(s, 0)}$ (Example 16)

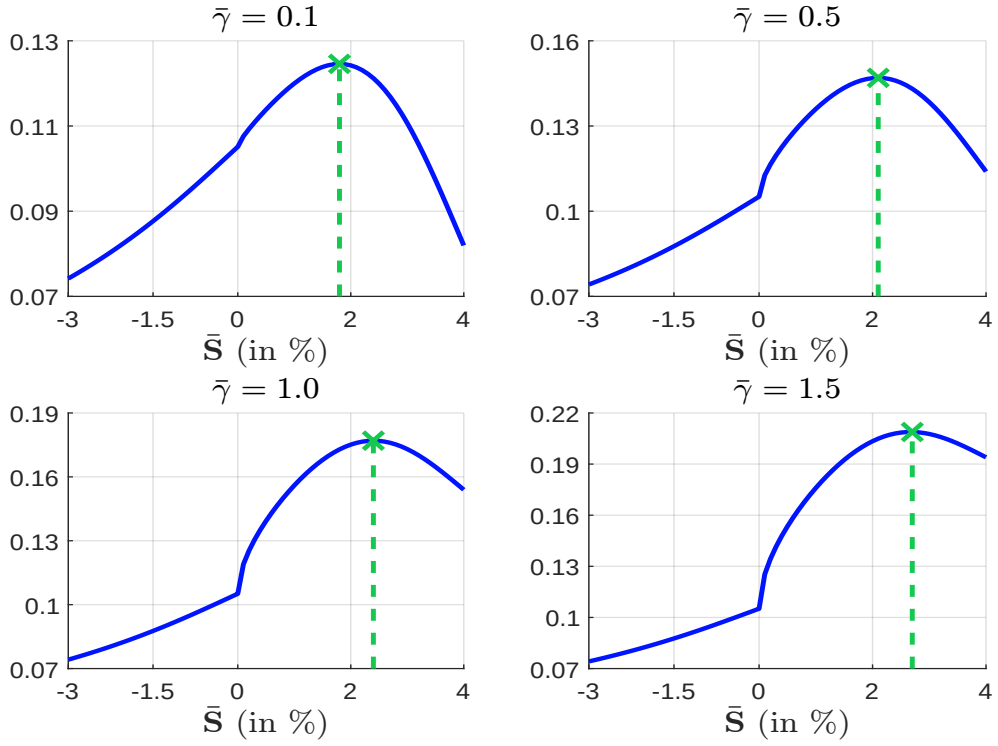

We consider Example 16. We compute the optimal portfolio for type-U investors. In this case, the previous analysis is not necessarily since the optimal portfolio is the traditional tangency portfolio. In the case of type-A investors, we need to find the portfolio that corresponds to the maximum Sharpe ratio of the ESG-SR efficient frontier (Figure 3.11). For type-M investors, we first calculate the function $\xi\left(\bar{\boldsymbol{\mathcal{S}}}\right)$:

$$\xi\left(\bar{\boldsymbol{\mathcal{S}}}\right) = \mathrm{SR}^2\left(\bar{\boldsymbol{\mathcal{S}}} \mid \pi, \Sigma, \boldsymbol{\mathcal{S}}\right) + 2\bar{\gamma}\zeta\left(\bar{\boldsymbol{\mathcal{S}}}\right)$$

The optimal portfolio then corresponds to the optimal ESG score that maximizes $\xi\left(\bar{\boldsymbol{\mathcal{S}}}\right)$. Two examples are provided in Figures 3.12 and 3.13. Results are summarized in Table 3.12. For instance, if $\bar{\gamma} = 1.5$ and $\zeta(s) = 0.2\sqrt{\max(s, 0)}$, the optimal portfolio is $w_M^\star = (107.2\%, 66.0\%, 6.5\%, -7.9\%)$ and its Sharpe ratio is 0.332. This portfolio has an ESG score of 2.7%.

Table 3.12: Optimal portfolios (Example 16)

| Statistics | Type-U | Type-A | Type-M | | | | | |
|---|---|---|---|---|---|---|---|---|
| | | | $\zeta(s) = s$ | | | $\zeta(s) = 0.2\sqrt{\max(s,0)}$ | | |
| $\bar{\gamma}$ | | | 0.500 | 1.000 | 1.500 | 0.500 | 1.000 | 1.500 |
| $\boldsymbol{\mathcal{S}}(w^\star)$ | 0.017 | 0.017 | 0.023 | 0.028 | 0.034 | 0.021 | 0.024 | 0.027 |
| $\sigma(w^\star)$ | 0.139 | 0.100 | 0.682 | 0.329 | 0.203 | 0.687 | 0.339 | 0.221 |
| $\mathrm{SR}(w^\star \mid r)$ | 0.345 | 0.345 | 0.341 | 0.329 | 0.305 | 0.343 | 0.339 | 0.332 |
| $w_1^\star$ | 0.524 | 0.378 | 3.028 | 1.623 | 1.090 | 2.900 | 1.542 | 1.072 |
| $w_2^\star$ | 0.289 | 0.208 | 1.786 | 1.009 | 0.718 | 1.673 | 0.919 | 0.660 |
| $w_3^\star$ | 0.120 | 0.086 | 0.383 | 0.073 | −0.056 | 0.464 | 0.169 | 0.065 |
| $w_4^\star$ | 0.067 | 0.048 | −0.012 | −0.144 | −0.178 | 0.106 | −0.035 | −0.079 |
| $w_r^\star$ | 0.000 | 0.280 | −4.184 | −1.562 | −0.574 | −4.143 | −1.596 | −0.718 |

**Impact on asset returns**

Pedersen *et al.* (2021) use the previous framework to analyze the dynamics of asset prices. They show that the impact of ESG depends strongly on the relative proportions of the three types of investors. Let $\omega^U$, $\omega^A$ and $\omega^M$ be the wealth shares of type-U, type-A and type-M investors, respectively. The authors assume that the security dividend payoff is given by the vector $\upsilon = (\upsilon_1, \ldots, \upsilon_n)$ and depends on the ESG scores:

$$\mathbb{E}[\upsilon \mid \boldsymbol{\mathcal{S}}] = \hat{\mu} + \theta\left(\boldsymbol{\mathcal{S}} - \boldsymbol{\mathcal{S}}_m\right)$$

where $\boldsymbol{\mathcal{S}}_m$ is the ESG score of the market portfolio and the parameter $\theta$ determines how informative ESG scores are of future profits. In particular, $\theta = 0$ if ESG scores are not informative. Otherwise, we can expect $\theta > 0$, implying that firms with better ESG scores are more profitable on average. Pedersen *et al.* (2021) derive the following propositions:

- If $\omega^U = 1$ and $\omega^A = \omega^M = 0$, then the unconditional expected returns are given by the CAPM:

  $$\mathbb{E}[R_i] - r = \beta_i\left(\mathbb{E}[R_m] - r\right)$$

  but conditional expected returns depend on the ESG scores:

  $$\mathbb{E}[R_i \mid \boldsymbol{\mathcal{S}}] - r = \beta_i\left(\mathbb{E}[R_m] - r\right) + \theta\frac{\boldsymbol{\mathcal{S}}_i - \boldsymbol{\mathcal{S}}_m}{P_i}$$

  where $P_i$ is the price of asset $i$. Two assets with the same beta do not necessarily have the same conditional risk premium.

- If $\omega^A = 1$ and $\omega^U = \omega^M = 0$, then the informational value of ESG scores is fully incorporated into asset prices, and we have:

$$\mathbb{E}\left[R_i \mid \boldsymbol{\mathcal{S}}\right] - r = \tilde{\beta}_i \left(\mathbb{E}\left[R_m \mid \boldsymbol{\mathcal{S}}\right] - r\right)$$

  where $\tilde{\beta}_i$ is the ESG-adjusted beta coefficient.

- If $\omega^M = 1$ and $\omega^U = \omega^A = 0$, then the conditional expected return is given by:

$$\mathbb{E}\left[R_i \mid \boldsymbol{\mathcal{S}}\right] - r = \tilde{\beta}_i \left(\mathbb{E}\left[R_m \mid \boldsymbol{\mathcal{S}}\right] - r\right) + \lambda_2 \left(\boldsymbol{\mathcal{S}}_i - \boldsymbol{\mathcal{S}}_m\right)$$

The best case for an ESG investor is $\omega^U = 1$ and $\omega^A = \omega^M = 0$ when all other investors are ESG-unaware. The adjustment of market prices then depends on the growth of type-A and type-M investors. More generally, negative and/or positive alpha returns are explained by asymmetric information, supply/demand imbalances and trading motivations. Therefore, there is no obvious conclusion:

> "*If all types of investors exist, then several things can happen. If a security has a higher ESG score, then, everything else equal, its expected return can be higher or lower. A higher ESG score increases the demand for the stock from type-M investors, leading to a higher price and, therefore, a lower required return [...] Companies with poor ESG scores that are down-weighted by type-M investors will have lower prices and higher cost of capital. [...] Furthermore, the force that can increase the expected return is that the higher ESG could be a favorable signal of firm fundamentals, and if many type-U investors ignore this, the fundamental signal perhaps would not be fully reflected in the price [...] A future increase in ESG investing would lead to higher prices for high-ESG stocks [...]. If these flows are unexpected (or not fully captured in the price for other reasons), then high-ESG stocks would experience a return boost during the period of this repricing of ESG. If these flows are expected, then expected returns should not be affected.*" (Pedersen *et al.*, 2021).

In this context, it is difficult to predict whether ESG investments will outperform or underperform in the short run, as it depends on many factors. In particular, the PST and PFP models use the efficient market hypothesis (EMH), which implies that asset prices must reflect all available information. For instance, as seen above, one consequence of EMH is that expected returns will not be affected if ESG investment flows are expected. In the real world, this type of assumption is difficult to verify because we know that asset prices do not react instantaneously. Assuming that the dynamics of asset prices depend only on unexpected events in the short run also limits the validity of the theoretical analysis. In the end, asset prices are driven by trading orders, regardless of the real motivations of investors. These motivations may be rational or irrational, related to fundamental or extra-financial information, etc. Moreover, the PST and PFP models consider a specific trading strategy that mimics the ESG integration strategy as defined on page 42. The previous results do not necessarily hold when we consider[18] a worst-in-class exclusion strategy, a best-in-class selection strategy, or an ESG momentum strategy. For all these reasons, the performance of ESG investing remains a hotly debated topic in the investment community. Nevertheless, these models are very useful because they provide a normative framework and help make sense of the chaos of empirical results.

[18] See for instance Zerbib (2022).

## 3.2 Empirical results

As noted above, the body of empirical research on the performance of ESG investing is impressive. However, there is no obvious consensus because there are so many factors to consider. First, ESG investing has evolved over the last thirteen years. The data are not the same — most of them didn't exist ten years ago — the practice of ESG scoring has definitely changed over time, the use of ESG considerations is new to many investors, etc. Backtesting an ESG strategy over a long history does not make sense. Second, we cannot assume that the relationship between ESG and performance is static (positive or negative). Rather, we must accept that the relationship between ESG and performance is dynamic. Sometimes ESG can create performance, and sometimes it does not. It was the case in the past, it will be the case in the future. This is because the relationship depends primarily on the investment and trading flows of investors. Third, the performance of ESG investing depends on portfolio implementation. This is not the same as considering an exclusion filter, adding an ESG score to an existing asset picking model, implementing a selection screen, etc. Finally, the relationship is different because it depends on the country, asset class, security universe, ESG definition, etc. Let us illustrate this with a few examples. When we talk about ESG performance, are we talking about the global ESG score or one of the pillars E, S and G? Are we talking about specific securities such as green bonds? Are we talking about American, European, Japanese or EM assets? As the questions can be multiplied endlessly, let us focus more on the why rather than the whether. Why has ESG investing created or destroyed value for a given investment universe over a given period of time?

### 3.2.1 Equity markets

The relationship between ESG and performance has been extensively studied in equity markets. According to Coqueret (2022, Sections 4.2-4.5, pages 51-66), we can classify them into four categories: (1) ESG improves performance, (2) ESG does not impact performance, (3) ESG is financially detrimental and (4) it depends on many factors. According to Friede *et al.* (2015), the first category dominates the others:

> "*[...] The results show that the business case for ESG investing is empirically very well founded. Roughly 90% of studies find a nonnegative ESG–CFP relation. More importantly, the large majority of studies reports positive findings. We highlight that the positive ESG impact on CFP appears stable over time. Promising results are obtained when differentiating for portfolio and non-portfolio studies, regions, and young asset classes for ESG investing such as emerging markets, corporate bonds, and green real estate.*" (Friede *et al.*, 2015, page 2010).

In fact, their results are not obvious to accept because the concept of corporate financial performance covers many dimensions and is not limited to financial performance in the stock market. For instance, CFP can also refer to the cost of capital (El Ghoul *et al.*, 2011). In addition, a large proportion of these studies focus on the G pillar (Gompers *et al.*, 2003) or use some proxy variables other than ESG scores or ratings (Edmans, 2011). We can also find many studies whose conclusion is more neutral or negative (Barnett and Salomon, 2006; Fabozzi *et al.*, 2008; Hong and Kacperczyk, 2009; Johnson *et al.*, 2009; Capelle-Blancard and Monjon, 2014; Matos, 2020).

Since these various publications, a consensus has emerged among professionals. Like other investment styles, ESG investing has its ups and downs, and the relationship between ESG and performance is not straightforward and depends on many factors. Understanding these factors is the key challenge for investors, rather than having a set of strong predetermined beliefs.

### Simulated results

Below we summarize the results obtained by Bennani *et al.* (2018) and Drei *et al.* (2019), who analyzed the impact of ESG on three equity portfolio management approaches: active management, passive management, and factor investing.

**Sorted portfolios** Bennani *et al.* (2018) use the Amundi scoring system. For each company and each date, they access the global ESG score and its three components E, S and G. The scores are normalized sector by sector to obtain a $z$-score shape, which means that they have a range roughly between $-3$ and $+3$. This also means that the scores are sector-neutral and are distributed as a standard Gaussian probability distribution.

Box 3.4: The method of characteristic-sorted portfolios

Portfolio sorting was popularized by Fama and French (1993) to test the impact of characteristics in asset pricing and to identify profitable investment strategies. The idea is to sort individual assets into portfolios with respect to a given variable. If each portfolio has roughly the same number of constituents and differs only in the level of the sorting variable, then differences in performance can be attributed to the impact of the sorting variable. Typically, each portfolio is equally or value weighted to maximize diversification. In the univariate case, the most popular approach is the quintile method, where the breakpoints for the sorting variable correspond to the 20th, 40th, 60th and 80th percentiles.

Table 3.A: An illustrative example

| Asset | $\mathcal{S}_i$ | Rank | $Q_i$ | Weight |
|---|---|---|---|---|
| #1 | −0.3 | 6 | $Q_3$ | +50% |
| #2 | 0.2 | 5 | $Q_3$ | +50% |
| #3 | −1.0 | 7 | $Q_4$ | +50% |
| #4 | 1.5 | 3 | $Q_2$ | +50% |
| **#5** | −2.9 | 10 | $Q_5$ | +50% |
| #6 | 0.8 | 4 | $Q_2$ | +50% |
| #7 | −1.4 | 8 | $Q_4$ | +50% |
| **#8** | 2.3 | 2 | $Q_1$ | +50% |
| **#9** | 2.8 | 1 | $Q_1$ | +50% |
| **#10** | −2.2 | 9 | $Q_5$ | +50% |

Consider the example above, where the sorting variable is an ESG score. Since we have 10 assets, each sorted portfolio has two assets. Portfolio $Q_1$ corresponds to the highest scores, while Portfolio $Q_5$ corresponds to the lowest scores. We obtain $Q_1 = (\#8, \#9)$, $Q_2 = (\#4, \#6)$, $Q_3 = (\#1, \#2)$, $Q_4 = (\#3, \#7)$ and $Q_5 = (\#5, \#10)$.

To construct the active management strategy, the authors use the sorting portfolio method. Each quarter, they rank the stocks according to their ESG score, and create five quintile portfolios[19]. Portfolio $Q_1$ corresponds to the 20% best-ranked stocks while Portfolio $Q_5$ corresponds to the 20% worst-rated stocks. The selected stocks are then equally weighted and each portfolio is invested on the first trading day of the quarter and held for three months. Quarterly rebalancing is performed to limit turnover.

[19] Given a universe of stocks, each portfolio then consits of 20% of assets.

Figure 3.14: Annualized return of ESG-sorted portfolios (MSCI North America, global score)

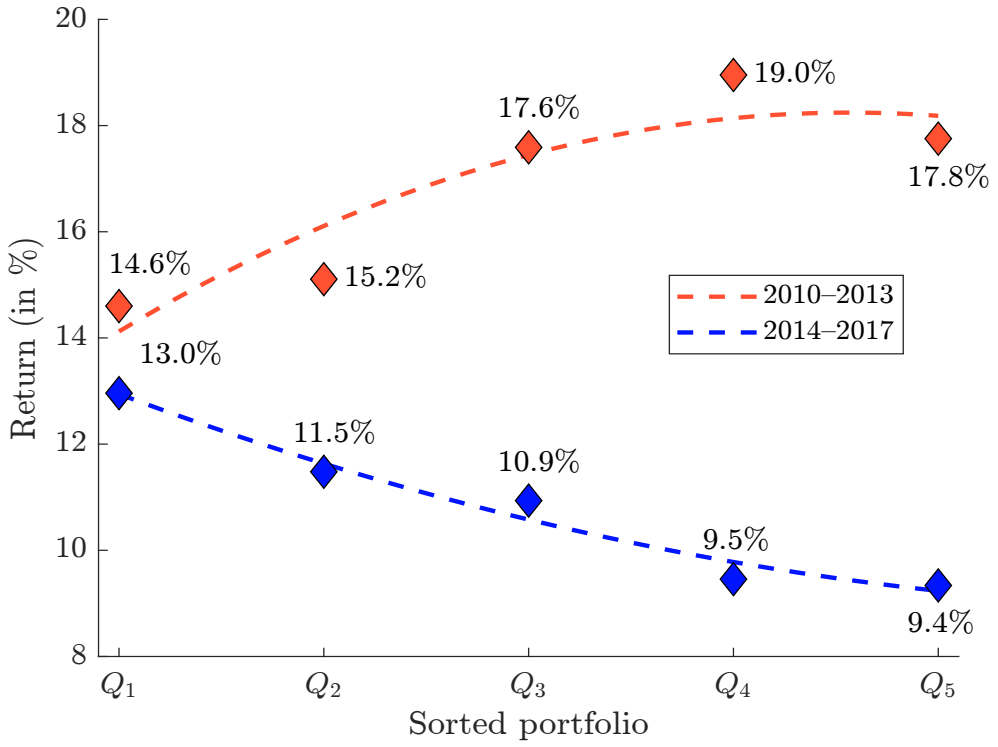


Source: Bennani *et al.* (2018).

They consider five investment universes using the following MSCI indexes: North America, EMU, Europe-ex-EMU, Japan and World. For each universe and each quintile portfolio, they calculate gross performance excluding transaction costs. Analyzing the results, the authors observe a break during the study period 2010–2017. Typically, the first half of the period is less favorable for ESG screening than the second half. In Figure 3.14, we report their results for North American stocks. Over the period 2010–2013, Portfolio $Q_1$ has a gross return of 14.6%, while Portfolio $Q_5$ has a gross return of 17.8%. We observe an increasing function between return and quintile. During this period, the best-in-class stocks underperformed worst-in-class stocks. The story is different if we focus on the period 2014–2017. Portfolio $Q_1$ shows a performance of 13.0%, while Portfolio $Q_5$ shows a performance of 9.4%. Clearly, the best-in-class stocks outperformed the worst-in-class stocks during this second period. Looking at individual pillars, Bennani *et al.* (2018) obtained very similar results in Figure 3.15. E, S and G stock picking has a negative impact on performance between 2010 and 2013, while the impact of E, S and G stock picking on performance is positive between 2014 and 2017. During the 2014–2017 period, environmental screening produces the best result, followed by governance scoring. However, for the governance component, the performance difference between Portfolios $Q_1$, $Q_2$, $Q_3$ and $Q_4$ is not significant. Only Portfolio $Q_5$ significantly underperforms, meaning that the worst-rated stocks are penalized, but the best-rated stocks are not necessarily rewarded.

These results clearly show that active ESG management was penalized during the period 2010–2013, while it generated excess performance between 2014 and 2017. In the case of the Eurozone, the conclusion is the same for the global ESG score, and its three components. For example, Portfolio $Q_1$ generated a return of 8.6%, while Portfolio $Q_5$ generated a return of 10.0% between 2010 and

Figure 3.15: Annualized return of ESG-sorted portfolios (MSCI North America, individual pillars)

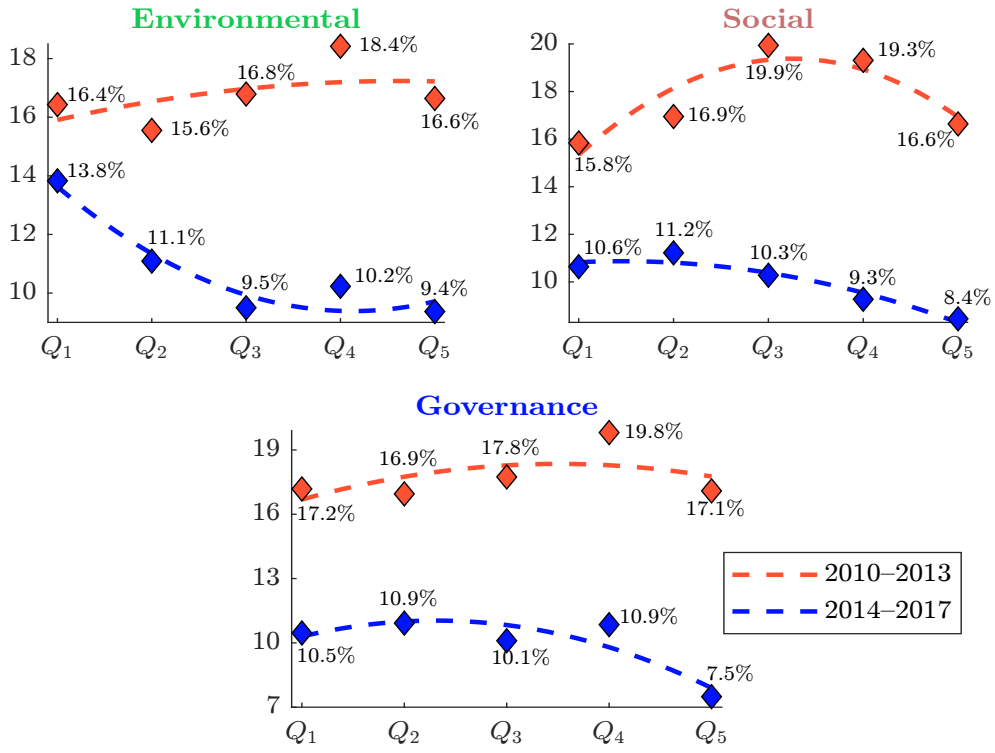


Source: Bennani *et al.* (2018).

2013 (Figure 3.16). On the contrary, the performance for the period 2014–2017 was 14.7% and 7.5% for Portfolios $Q_1$ and $Q_5$, respectively. Thus, the first period is characterized by a U-shape, while, in the second period, the best-in-class stocks significantly outperformed the worst-in-class stocks. Note that the performance difference mainly affects Portfolios $Q_1$ and $Q_5$, but not Portfolios $Q_2$, $Q_3$ and $Q_4$, implying that worst-in-class stocks are penalized and best-in-class stocks are rewarded. Looking at each individual pillar, governance is the most discriminating component (Figure 3.17). The difference between the $Q_1$ and $Q_5$ portfolios exceeds 7% in the last period. For the E score, we observe a U-shaped behavior between 2010 and 2013. Since 2014, the relationship between the quintile portfolios and their returns is clearly decreasing. It is less impressive than for the G score, but it affects all portfolios[20]. The integration of the social pillar is the least convincing.

For the other investment universes, the results are more heterogeneous. In the case of the Europe-ex-EMU universe, the ESG integration is country specific, which means that the performance is highly dependent on the overweight or underweight of each country. For example, the G screen largely overweights UK stocks when considering a $Q_1 - Q_5$ long/short portfolio. On the contrary, E or S screens favor Swedish stocks. The case of Japan is puzzling. In fact, ESG screening was less favorable in the period 2014–2017. If we consider the universe of the MSCI World index, the results are similar to those obtained for North America and the Eurozone. These different results are summarized in Table 3.13, where we have reported the impact of ESG screening on the returns of sorted portfolios. Again, the results illustrate the contrast between the two periods. In summary, Bennani *et al.* (2018) concluded that the relationship between performance and ESG is

[20]For the G score, the difference mainly concerns the $Q_1$ and $Q_5$ portfolios, and less so the median portfolios.

Figure 3.16: Annualized return of ESG-sorted portfolios (MSCI EMU, global score)

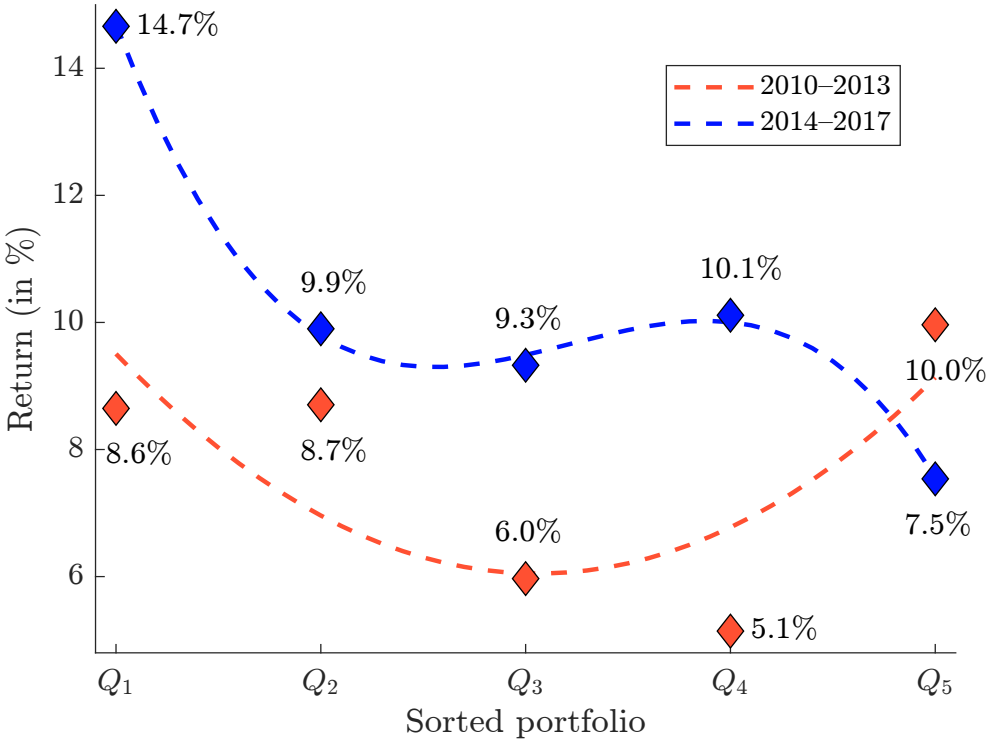


Source: Bennani *et al.* (2018).

Figure 3.17: Annualized return of ESG-sorted portfolios (MSCI EMU, individual pillars)

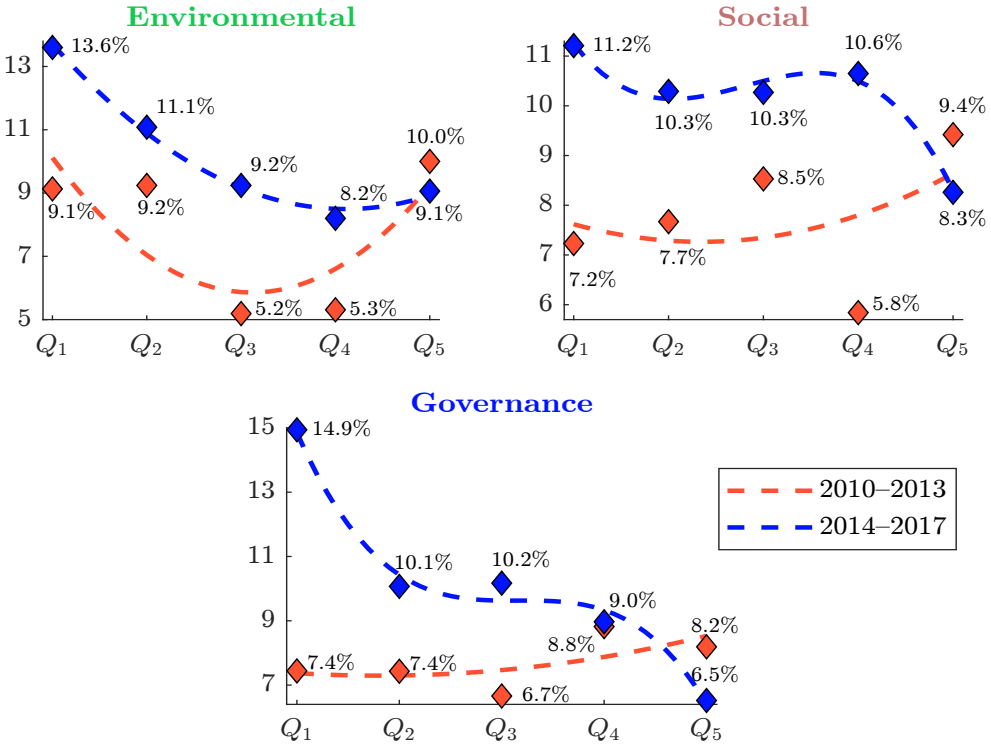


Source: Bennani *et al.* (2018).

time-varying and depends on several factors, particularly region and ESG pillar. They also found that some investment universes have ESG country biases, which implies that the relationship between performance and ESG cannot be analyzed. This is the case for the MSCI Europe-ex-EMU index, but such bias is not excluded for the MSCI World index.

Table 3.13: Impact of ESG screening on sorted portfolio returns (2010–2017)

| Period | Pillar | North America | EMU | Europe-ex-EMU | Japan | World |
|---|---|---|---|---|---|---|
| 2010–2013 | ESG | −− | − | **0** | + | **0** |
| | E | − | **0** | + | − | **0** |
| | S | − | − | **0** | − | − |
| | G | − | **0** | + | **0** | + |
| 2014–2017 | ESG | ++ | ++ | **0** | − | + |
| | E | ++ | ++ | − | + | ++ |
| | S | + | + | **0** | **0** | + |
| | G | + | ++ | **0** | + | ++ |

Source: Bennani *et al.* (2018).

The study by Drei *et al.* (2019) is an update of the analysis of Bennani *et al.* (2018) considering the recent period 2018–2019. They use exactly the same data, the same investment universes and the same methodology. Their main results are reported in Figures 3.18 and 3.19.

Box 3.5: Computing the performance of long/short portfolios

Let $w_{\mathcal{L}ong}$ and $w_{\mathcal{S}hort}$ be the long and short portfolios, respectively. We note $R_t(w)$ the annualized return of Portfolio $w$ between $t-1$ and $t$. The performance of the long/short portfolio $w_{\mathcal{L}ong} - w_{\mathcal{S}hort}$ satisfies the following definition:

$$(1 + R_t(w_{\mathcal{L}ong})) = (1 + \alpha_t(w_{\mathcal{L}ong} - w_{\mathcal{S}hort}))(1 + R_t(w_{\mathcal{S}hort}))$$

where $\alpha_t(w_{\mathcal{L}ong} - w_{\mathcal{S}hort})$ is the alpha return of $w_{\mathcal{L}ong} - w_{\mathcal{S}hort}$. We deduce that:

$$\alpha_t(w_{\mathcal{L}ong} - w_{\mathcal{S}hort}) = \frac{R_t(w_{\mathcal{L}ong}) - R_t(w_{\mathcal{S}hort})}{1 + R_t(w_{\mathcal{S}hort})} \tag{3.18}$$

Looking at the $Q_1 - Q_5$ long-short portfolios in North America (Figure 3.18) and the Eurozone (Figure 3.19), we can see the evolution of ESG integration and its pillars in both markets. In the 2010–2013 period, sustainable investors were penalized, as shown by the negative return of the $Q_1 - Q_5$ long-short portfolios. In the 2014–2017 period, after the radical break in ESG integration, ESG investing gained momentum and delivered positive returns across all pillars on both sides of the Atlantic. However, after eight years of parallel development, Drei *et al.* (2019) observed a contradictory trend in ESG investing between North America and the Eurozone between 2018 and 2019. Indeed, the latter period is characterized by a squeeze in alpha returns on all dimensions in North America, and even a loss on the E pillar. This loss is important because it is the first long-short portfolio with a negative return since the 2014 ESG turning point in these two investment universes. Moreover, we observe a decline in the performance of the S and G pillars during the period 2018–2019. Looking at the global ESG score, its performance remains positive but is divided

Figure 3.18: Annualized return of long/short $Q_1 - Q_5$ sorted portfolios (MSCI North America)

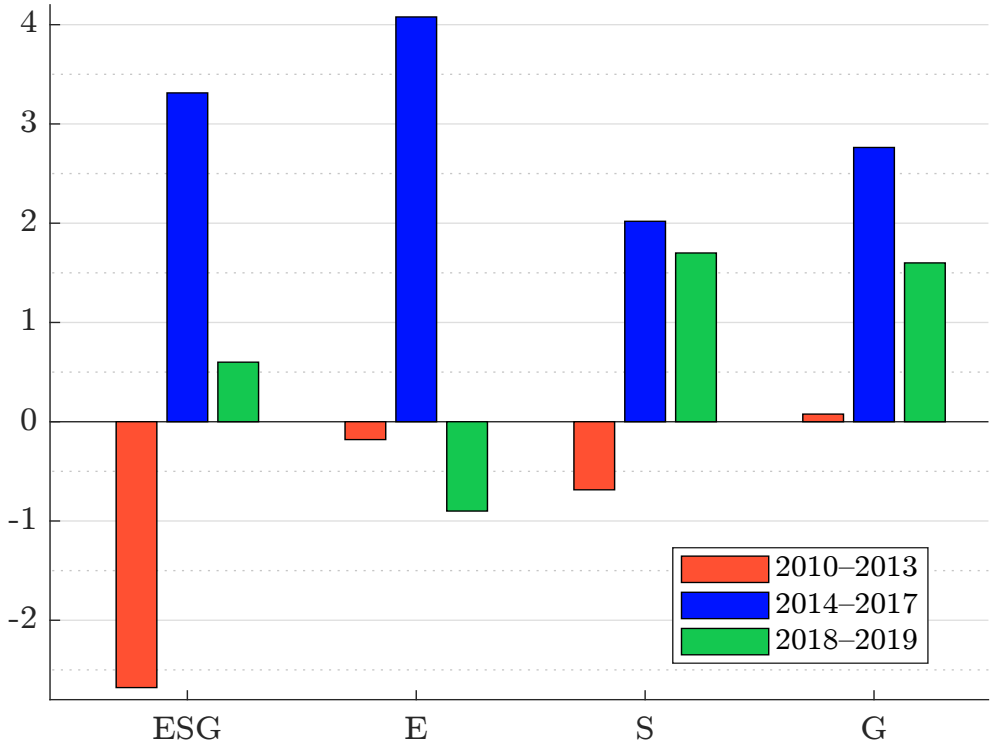


Source: Drei *et al.* (2019).

Figure 3.19: Annualized return of long/short $Q_1 - Q_5$ sorted portfolios (MSCI EMU)

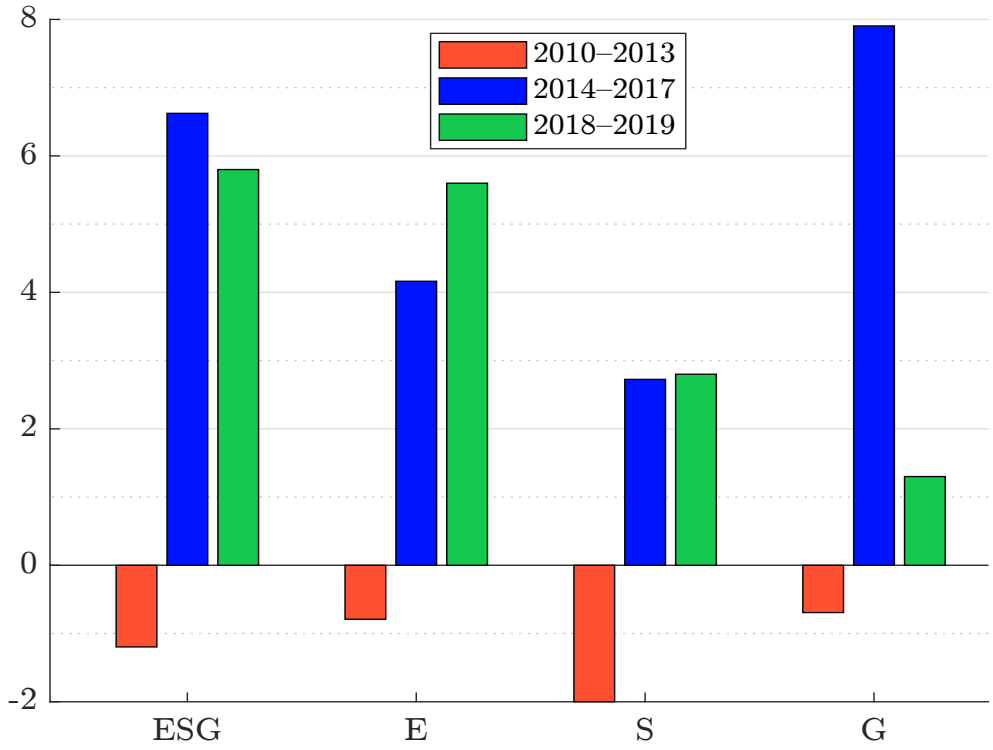


Source: Drei *et al.* (2019).

by a factor of six compared to the period 2014–2017. On the Eurozone side, the verdict is more positive. All long-short portfolio returns are positive. In the period 2018–2019, the E and S pillars generate even stronger returns compared to the previous period. The decline in the G long-short portfolio return can be partly attributed to a mean-reversion effect after an extraordinary period of impressive performance[21]. Drei *et al.* (2019) concluded that the period 2018–2019 is in line with the previous period for the Eurozone investment universe as the two periods post an annualized return around 6% in the case of the global ESG score.

How can these different results be explained? Bennani *et al.* (2018) assumed that two main effects contributed to ESG performance from 2014 to 2017: the selection effect of ESG screening and the demand effect of ESG assets. The selection effect refers to the direct impact of extra-financial information on stock prices. By taking into account other risk dimensions, the ESG investor can select companies that are better managed from a social, environmental and governance perspective, or avoid companies with extra-financial weaknesses. The idea is that sooner or later these extra-financial risks will have a financial impact on the company's performance. The second effect is related to the balance between supply and demand. In fact, a stock price is the equilibrium between supply and demand for that stock. Bennani *et al.* (2018) found that ESG investment flows that have been observed since 2014 have largely contributed to the good performance of ESG investments over the period 2014–2017, while the contribution of the selection effect is marginal. How to explain the 2014 break? In November 2013, the Norwegian Sovereign Wealth Fund adopted a new responsible investment policy (Dimson *et al.*, 2013). At about the same time, we observe a strong mobilization of the largest European institutional investors (APG, PGGM, ERAFP, FRR, etc.), which are massively invested in European and American equities[22]. The good performance of ESG investing in the period 2014–2017 is mainly explained by the portfolio rebalancing of these tier-one European institutional investors. The 2018–2019 period is different. Indeed, this first mobilization has been followed by a further mobilization of mid-sized (or tier-two) European institutional investors, while the involvement of US investors remains weak. Nevertheless, this second wave of investors has a low exposure to North American equities. The transatlantic divide observed between 2018 and 2019 is then mainly explained by the strategic asset allocation of these tier-two institutional investors. They rebalanced their portfolios, but the trading operations mainly concerned European stocks and not American stocks. A first explanation for the American setback can then be found in these engagement differences between European and American investors. In addition to these two effects (selection and supply/demand balance), Drei *et al.* (2019) suggest that a third factor may contribute to ESG performance: the political and regulatory environment. The poor performance of the E pillar in the US may be explained by the announced withdrawal of the United States from the Paris Climate Agreement and some changes at the US Environmental Protection Agency (EPA). More generally, another justification for the transatlantic divide could be the public policy of the Trump administration in terms of its ESG roadmap.

**Remark 36** *The original idea of the Amundi Investment Institute studies (Bennani et al., 2018; Drei et al., 2019) was to frequently update the empirical relationship between ESG and performance. However, the first study showed that there are country biases that are difficult to control for. Therefore, the second study focused on the investment universe of the MSCI North America and EMU indexes and considered the empirical relationship between ESG and performance to be monotonic. For instance, if the relationship is positive, we must observe* $R_t(Q_1) \geq R_t(Q_2) \geq R_t(Q_3) \geq R_t(Q_4) \geq R_t(Q_5)$*, while a negative relationship implies* $R_t(Q_1) \leq R_t(Q_2) \leq R_t(Q_3) \leq R_t(Q_4) \leq R_t(Q_5)$.

[21] In fact, the annualized return was 7.9% between 2014 and 2017, compared to just 1.3% for the period 2018–2019.

[22] For instance, the Norwegian Sovereign Wealth Fund had an exposure to US equities greater than that of the three largest US pension funds (CalPERS, CalSTRS and NYSCRF).

Figure 3.20: The monotonic assumption of the ESG-performance relationship

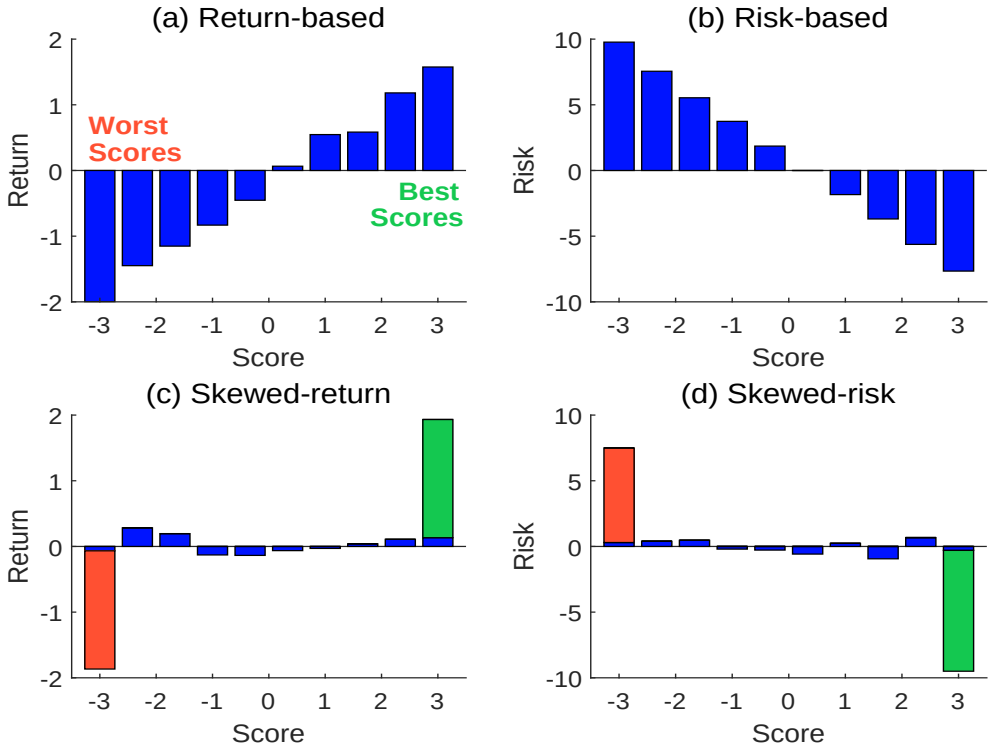


*More generally, there are some patterns we need to observe in order to interpret the results. Some of them are shown in Figure 3.20. For example, the implementation of an ESG exclusion strategy has a return-based rationale if the relationship is positive or if portfolio $Q_5$ underperforms the other quintile portfolios. Similarly, the implementation of an ESG selection strategy has a return-based rationale if the relationship is positive or if portfolio $Q_1$ outperforms the other quintile portfolios. However, Drei et al. (2019) noticed that most of the monotonous relationships observed during the period 2010–2017 were no longer valid between 2018 and 2019. For instance, they found that $R_t(Q_1) \geq R_t(Q_5)$ for the global ESG score in the Eurozone, but they also found that $R_t(Q_4) \geq R_t(Q_1)$, which is a puzzling result. This ranking disorder goes beyond the binary outcome in where $Q_1 \succ Q_5$ holds or does not. Drei et al. (2019) argue that this puzzle marks the emergence of new ESG investment strategies. The $Q_1 - Q_5$ approach is representative of a static view of ESG scores, where the best-in-class stocks remain best-in-class and the worst-in-class stocks remain worst-in-class, while playing the intermediate quintiles, especially the fourth quintile, seems to be associated with the ESG momentum strategy (Figure 3.21) and a dynamic view of ESG scores. In the period 2018–2019, ESG strategies have become more complex, which may explain the ranking disorder. This finding is consistent with the results reported by GSIA (2019). In its 2018 investment review, the organization documents that the most common way to participate in sustainable investing (as measured by assets under management allocated to each strategy) is to implement negative screening, but this approach is closely followed by ESG integration and corporate engagement strategies. Similarly, Eurosif (2018) found similar results a year earlier, stating that "the main strategy is exclusion, but in the last two years the growth rate of this strategy slowed down. In contrast, best-in-class and ESG integration have had a high growth rate." Investment strategies based on the dynamics of ESG ratings do not clearly correspond to negative or positive screening, but are more related to ESG integration. In this approach, an improvement in an extra-financial criterion can lead to portfolio rebalancing, just as we observe*

*for financial metrics. The convergence between the extra-financial approach and traditional security analysis certainly increases the focus on the dynamics and momentum of ESG ratings, and not just their static level. In this context, the analysis of the relationship between the performance of ESG investments and the static level of ESG scores is certainly outdated.*

Figure 3.21: How to play ESG momentum?

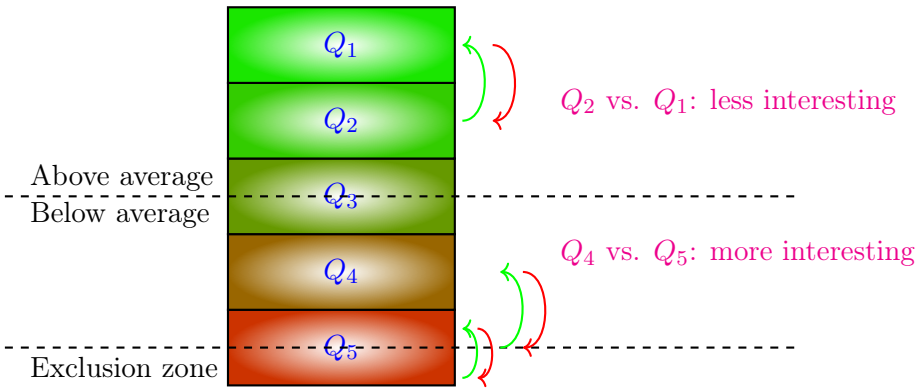


**Optimized portfolios** Many institutional investors implement ESG policies through passive management. In this case, they use two techniques: exclusion and optimization. The first approach consists of reducing the universe of the stock index by excluding the worst-rated stocks and then applying a capitalization-weighted scheme to construct the investment portfolio. The second approach is to improve the score of the investment portfolio with respect to the score of the benchmark portfolio, while controlling the tracking error risk. The first solution can be approximated using the second method, which means that optimized portfolios can be used to simulate the performance of passive ESG management (Bennani *et al.*, 2018; Drei *et al.*, 2019).

**Remark 37** *Let us compare the ESG-optimized approach with the ESG-sorting method. We note* $\mathbf{F}$ *the probability distribution of the score* $\boldsymbol{\mathcal{S}}$*. Portfolio* $Q_1$ *corresponds to best-in-class stocks* $\left\{i \in Q_1 \Leftrightarrow \boldsymbol{\mathcal{S}}_i \geq \mathbf{F}^{-1}(80\%)\right\}$*, while Portfolio* $Q_5$ *corresponds to worst-in-class stocks* $\left\{i \in Q_5 \Leftrightarrow \boldsymbol{\mathcal{S}}_i \leq \mathbf{F}^{-1}(20\%)\right\}$*. Also the weights are uniform:* $w_i(Q_j) = (5n)^{-1}$ *where* $n$ *is the total number of assets in the investment universe. In the case of the ESG-optimized approach, we have* $w^\star(\gamma) = \Sigma^{-1}(\gamma\boldsymbol{\mathcal{S}} + \Sigma b)$*, which implies that* $w_i^\star(\gamma) = b_i + \gamma\left(\Sigma^{-1}\boldsymbol{\mathcal{S}}\right)_i$*. Therefore, the benchmark weights are tilted by the inverse of the covariance matrix times the vector of ESG scores. For example, assuming the covariance matrix is diagonal and* $\boldsymbol{\mathcal{S}}_i \sim \mathcal{N}(0,1)$*, we obtain:*

$$w_i^\star(\gamma) = b_i + \gamma\frac{\boldsymbol{\mathcal{S}}_i}{\sigma_i^2}$$

*A positive score increases the benchmark weight, while* $\gamma$ *controls the discrepancy. If* $\gamma = 0$*, the optimal portfolio is the benchmark. If* $\gamma$ *tends to* $+\infty$*, the optimal weight is proportional to the score divided by the variance. When we add the long-only constraint, the optimization problem selects the stocks such that the ratio* $\boldsymbol{\mathcal{S}}_i/\sigma_i^2$ *is greater than a threshold that depends on the parameter* $\gamma$*. We can then calculate the value of* $\gamma$ *to retrieve the stock selection*[23] *given by portfolios* $Q_1$*,* $Q_1 + Q_2$*, etc. Therefore ESG-optimized and ESG-sorting approaches are related and generally produce similar results.*

[23] See Exercise 3.4.1 on page 227.

Box 3.6: ESG-optimized portfolios

Let $b$ be the benchmark, $\boldsymbol{\mathcal{S}}$ the vector of ESG scores and $\Sigma$ the covariance matrix. We consider the following optimization problem:

$$w^\star(\gamma) = \arg\min \frac{1}{2}\sigma^2(w \mid b) - \gamma \boldsymbol{\mathcal{S}}(w \mid b)$$

where $\sigma^2(w \mid b) = (w-b)^\top \Sigma (w-b)$ and $\boldsymbol{\mathcal{S}}(w \mid b)$ are the ex-ante tracking error variance and ESG excess score of portfolio $w$ relative to benchmark $b$. Since we have:

$$\boldsymbol{\mathcal{S}}(w \mid b) = (w-b)^\top \boldsymbol{\mathcal{S}} = \boldsymbol{\mathcal{S}}(w) - \boldsymbol{\mathcal{S}}(b)$$

we get the following optimization function:

$$w^\star(\gamma) = \arg\min \frac{1}{2} w^\top \Sigma w - w^\top (\gamma \boldsymbol{\mathcal{S}} + \Sigma b)$$

The ESG-variance efficient frontier is defined by the parametric curve $\left(\sigma^2(w^\star(\gamma) \mid b), \boldsymbol{\mathcal{S}}(w^\star(\gamma) \mid b)\right)$ with $\gamma \geq 0$. The QP form is given by $Q = \Sigma$ and $R = \gamma \boldsymbol{\mathcal{S}} + \Sigma b$. If we target an ESG excess score, for instance $\boldsymbol{\mathcal{S}}(w \mid b) \geq \Delta \boldsymbol{\mathcal{S}}^\star$, we set $\gamma = 0$ and add the inequality constraint $\boldsymbol{\mathcal{S}}^\top w \geq \boldsymbol{\mathcal{S}}(b) + \Delta \boldsymbol{\mathcal{S}}^\star$. The QP form is given by $Q = \Sigma$, $R = \Sigma b$, $C = -\boldsymbol{\mathcal{S}}^\top$ and $D = -(\boldsymbol{\mathcal{S}}(b) + \Delta \boldsymbol{\mathcal{S}}^\star)$. If we use the traditional long-only constraint ($\mathbf{1}_n^\top w = 1$ and $w_i \geq 0$), we have $A = \mathbf{1}_n^\top$, $B = 1$ and $w^- = \mathbf{0}_n$.

Figure 3.22 shows the ESG-variance efficient frontier estimated by Bennani *et al.* (2018). It represents the relationship between excess score and tracking error volatility for the MSCI World universe. For example, improving the score[24] of the index portfolio by 0.5 implies accepting a tracking error of 32 bps on average, and an excess score of 1.0 leads to a tracking error of 85 bps. Using risk attribution analysis, the authors also show that the governance pillar generates more tracking error than the environmental and social pillars[25]. These results imply that ESG passive management requires taking on significant tracking error risk relative to capitalization-weighted benchmarks.

Figure 3.24 shows the performance of ESG-optimized portfolios with respect to excess score. We see that the integration of ESG into passive management reduced the performance between 2010 and 2013, while it improved the annualized return between 2014 and 2017. For instance, an excess score of 1.0 resulted in an excess return of −34 bps in the first period and +45 bps in the second period. We also note that the relationship between excess score and excess return is not necessarily monotonic. For instance, targeting an excess score of 1.5 instead of 1.0 reduces the excess return from 45 bps to 19 bps in the second period. This is most likely due to the diversification effect. In fact, by increasing the excess score, we reduce the number of positions in the invested portfolios. There is a threshold at which the gains from ESG screening are offset by the losses from diversification reduction. Looking at the individual pillars, Bennani *et al.* (2018) draw the same conclusions that they have found for active management. For the MSCI World universe, all pillars destroyed value between 2010 and 2013, except for the environmental pillar, for which the results are neutral or slightly positive. This is particularly true for the governance pillar, whose underperformance is

[24] We recall that these studies use $z$-scores, which means that the range is between −3 and +3.

[25] On average, optimized portfolios with the G score have 50% more tracking error than those with E and S scores (see Figure 3.23).

Figure 3.22: Efficient frontier of ESG-optimized portfolios (MSCI World, 2010–2017, global score)

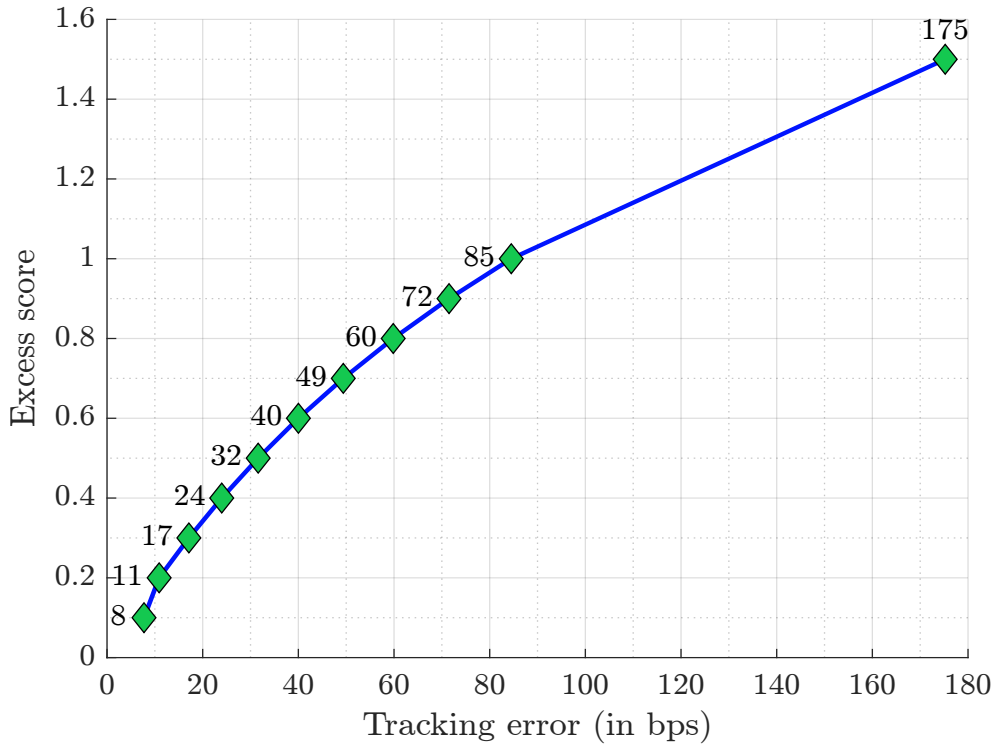


Source: Bennani *et al.* (2018).

Figure 3.23: Efficient frontier of ESG-optimized portfolios (MSCI World, 2010–2017, individual pillars)

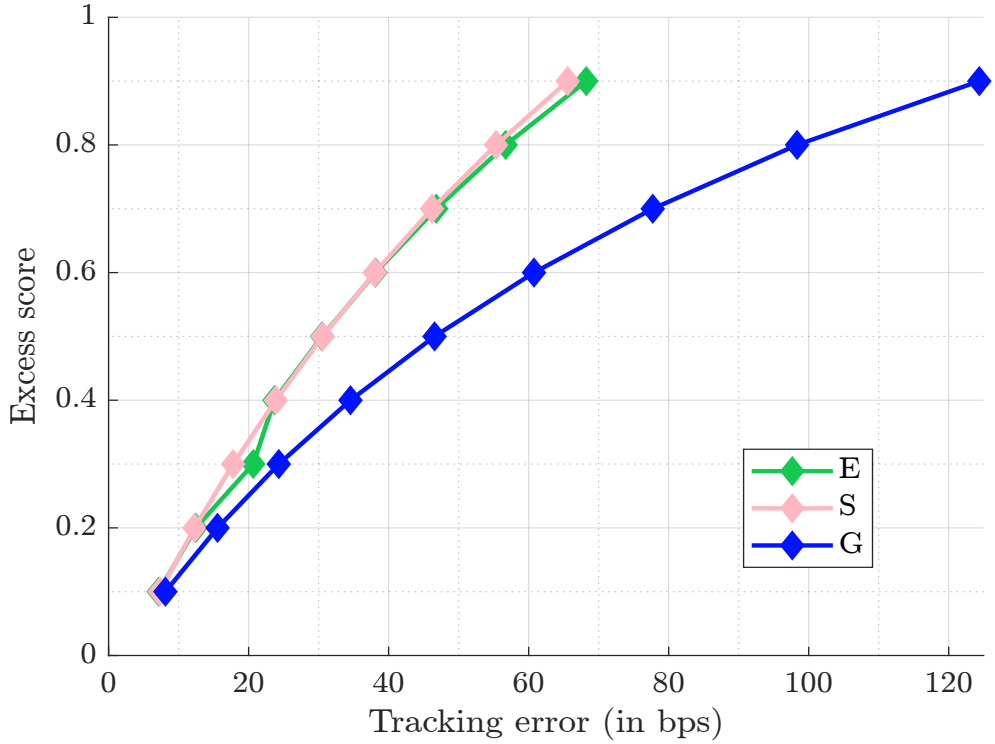


Source: Bennani *et al.* (2018).

Figure 3.24: Annualized excess return of ESG-optimized portfolios (MSCI World, 2010–2017, global score)

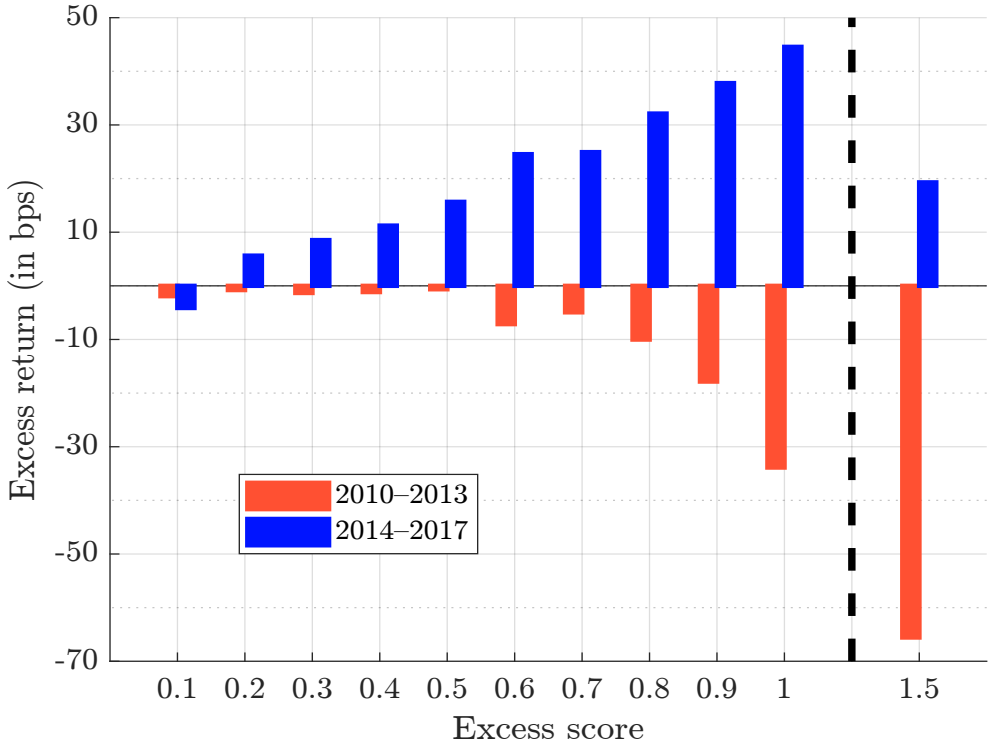


Source: Bennani *et al.* (2018).

Figure 3.25: Annualized excess return of ESG-optimized portfolios (MSCI World, 2010–2013, individual pillars)

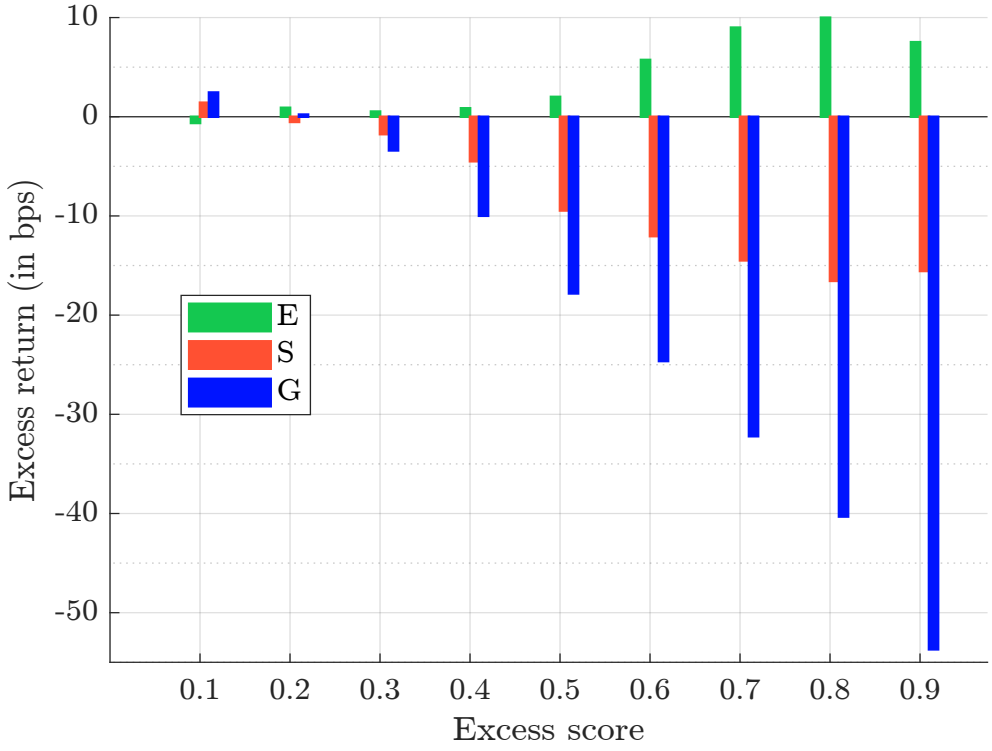


Source: Bennani *et al.* (2018).

Figure 3.26: Annualized excess return of ESG-optimized portfolios (MSCI World, 2014–2017, individual pillars)

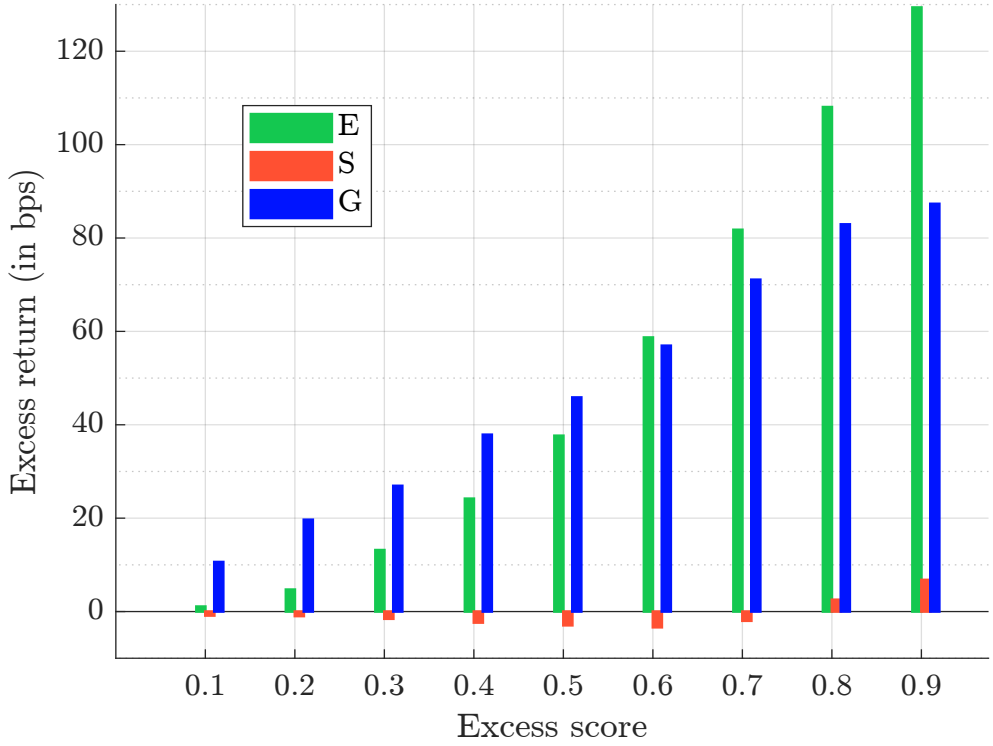


Source: Bennani *et al.* (2018).

Figure 3.27: Annualized excess return in bps of ESG-optimized portfolios (MSCI North America and EMU, 2010–2017)

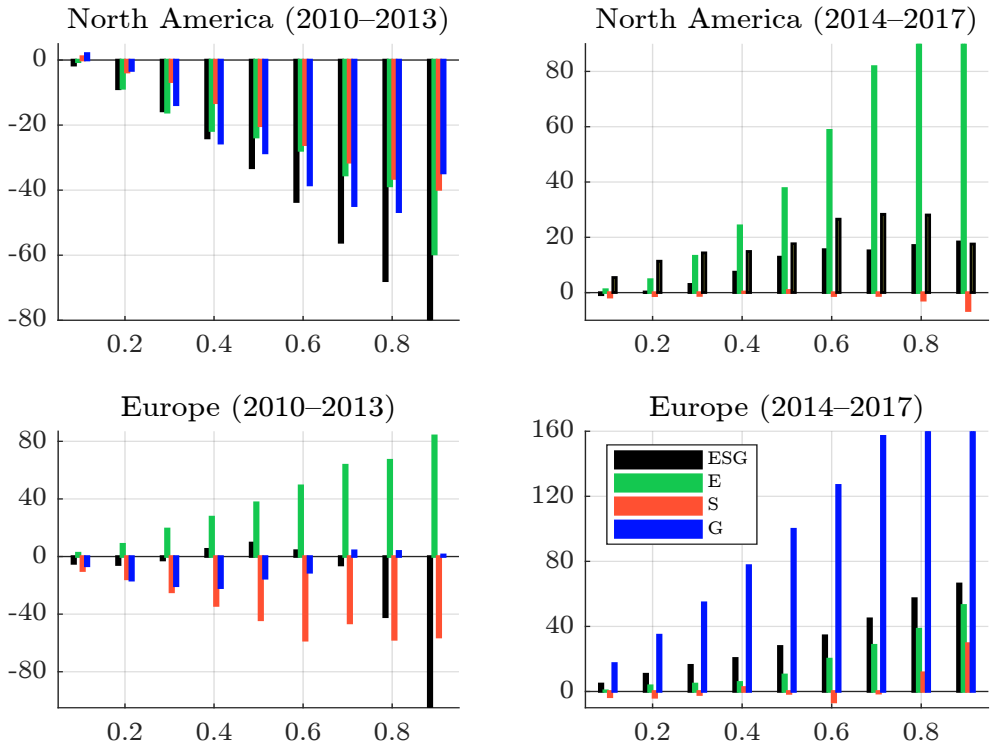


Source: Bennani *et al.* (2018).

about two to three times greater than the underperformance of the overall ESG score (Figure 3.25). For the period 2014–2017, the story changes. Every score generates outperformance, except for the social pillar (Figure 3.26). If we look at the North America and Europe investment universes[26], the performance of the optimized portfolios is in line with the performance of the stock-picking portfolios (Figure 3.27). Over the period 2010–2013, only the E score would have generated outperformance in Europe. In this region, the authors found that the performance of the ESG score was also neutral when targeting low tracking error risk (less than 60 bps) or low excess score (less than 0.8). In all other cases, we observe a negative excess return, especially in North America. Between 2014 and 2017, we obtain opposite results. All scores generate outperformance, except for the social pillar. The results are more significant in Europe than in North America. To sum up, the two big winners between 2014 and 2017 were the environmental pillar in North America and the governance pillar in Europe.

The updated study by Drei *et al.* (2019) has confirmed most of the results found by Bennani *et al.* (2018), in particular the trade-off between excess score and tracking error risk, and the reversal phenomenon of the ESG-performance relationship, which is negative when a high excess score is targeted. This reversal phenomenon is most likely due to the diversification effect. Indeed, by increasing the excess score, we reduce the number of positions held in the managed portfolio. There is therefore a threshold at which the gains from ESG screening are offset by the losses from reduced diversification. Since the relationship between quintile portfolios and performance is not monotonic, Drei *et al.* (2019) find that the performance of ESG-optimized portfolios is less impressive between 2018 and 2019 than between 2014 and 2017. Therefore, they observe a decrease in the maximum excess return. Focusing on the Eurozone investment universe, where the loss of diversification is reached more quickly than in North America, they conclude that "*optimized portfolios generate worse results (except for the social pillar)*" and, more generally, that "*risk-return profiles are less interesting than before.*" Therefore, the dynamic view of ESG investing implies that the performance of ESG-optimized portfolios will not necessarily be in line with the performance of $Q_1 - Q_5$ sorted portfolios due to the impact of the other sorted portfolios, particularly the fourth quintile portfolio.

**A new risk factor?** Previously, we saw that the long/short $Q_1 - Q_5$ strategy generated positive alpha between 2014 and 2019, while ESG investing has penalized ESG investors between 2010 and 2013. When we talk about alpha generation, we generally refer to factor investing. In fact, factor investing makes the difference between the financial performance of systematic factors and the financial performance of specific factors. Put another way, factor investing makes the difference between alpha and beta returns. In factor investing, the beta (or systematic) factors correspond to the common risk factors that explain a significant portion of the cross-section of stock returns. As ESG changes the landscape of asset management, we may ask whether ESG has become a new risk factor that needs to be integrated into a factor investing framework, or whether it remains an alpha strategy. To answer this question, Roncalli (2020b) uses the single-factor model:

$$R_{i,t} = \alpha_{i,j} + \beta_{i,j}\mathcal{F}_{j,t} + \varepsilon_{i,t}$$

where $R_{i,t}$ is the return of stock $i$ at time $t$, $\mathcal{F}_{j,t}$ is the value of the $j^{\text{th}}$ common risk factor at time $t$ and $\varepsilon_{i,t}$ is the idiosyncratic risk. The coefficients $\alpha_{i,j}$ and $\beta_{i,j}$ are estimated using ordinary least squares. For each stock, we compute the coefficient of determination:

$$\mathfrak{R}^2_{i,j} = 1 - \frac{\operatorname{var}(\varepsilon_{i,t})}{\operatorname{var}(R_{i,t})}$$

[26] Bennani *et al.* (2018) have merged Eurozone and Europe-ex-EMU stocks into the same investment universe because tracking error optimization forces the portfolio to be more or less country-neutral.

We then calculate the average proportion of return variance explained by the common factor: $\bar{\mathfrak{R}}_j^2 = \frac{1}{n}\sum_{i=1}^n \mathfrak{R}_{i,j}^2$. We consider the standard factors derived from a factor investing framework: size, value, momentum, low-volatility and quality. These factors $\mathcal{F}_{j,t}$ are constructed using the Fama-French method of sorted portfolios. Contrary to the academic literature, a long-only framework is used, which is the common approach of institutional investors. This means that the factors correspond to $Q_1$ portfolios or best-in-class stocks. We also consider the traditional market factor, which corresponds to the capitalization-weighted portfolio. All analyses use weekly returns. Results are shown in Table 3.14. We read these figures as follows: between 2010 and 2013, the market risk factor explains 40.8% of the dispersion of North American stock returns, this figure is 39.3% if we consider the size factor, and so one. We find that ESG is a strong contender as a stand-alone factor, competing with the market risk factor. On average, since 2014, the market risk factor explains 28.6% of the cross-section variance, while the ESG factor has an explanatory power of 27.4% in North America. In the Eurozone, these figures are 36.3% and 35.3%, respectively. Moreover, ESG has more explanatory power than the other risk factors in both North America and the Eurozone over the two periods: 2010–2013 and 2014–2019.

Table 3.14: Results of cross-section regression with long-only risk factors (single-factor linear regression model, average $\mathfrak{R}^2$)

| Factor | North America | | Eurozone | |
|---|---|---|---|---|
| | 2010–2013 | 2014–2019 | 2010–2013 | 2014–2019 |
| Market | 40.8% | 28.6% | 42.8% | 36.3% |
| Size | 39.3% | 26.1% | 37.1% | 23.3% |
| Value | 38.9% | 26.7% | 41.6% | 33.6% |
| Momentum | 39.6% | 26.3% | 40.8% | 34.1% |
| Low-volatility | 35.8% | 25.1% | 38.7% | 33.4% |
| Quality | 39.1% | 26.6% | 42.4% | 34.6% |
| ESG | 40.1% | 27.4% | 42.6% | 35.3% |

Source: Roncalli (2020b).

We now consider a multi-factor model:

$$R_{i,t} = \alpha_i + \sum_{j=1}^m \beta_{i,j}\mathcal{F}_{j,t} + \varepsilon_{i,t}$$

where $m$ is the number of risk factors. In this approach, we compare the CAPM, the standard five-factor model based on size, value, momentum, low-volatility and quality risk factors, and the six-factor model, which consists of adding the ESG factor to the universe of the five alternative risk factors. In Table 3.15, we verify that the five-factor model increases the proportion of systematic risk relative to the CAPM. For example, the CAPM and the 5F model explain 28.6% and 38.4%, respectively, of the cross-section variance in North America in the second period. Adding the ESG factor has a small impact between 2014 and 2019: 39.7% versus 38.4% in North America and 45.8% versus 45.0% in the Eurozone. This means that the ESG factor does not significantly improve the five-factor model. However, if we apply statistical significance tests to the six-factor model, we find that ESG is statistically significant in the Eurozone, but not in North America. We can conclude that ESG may be a risk factor in the Eurozone but not in North America.

Table 3.15: Results of cross-section regression with long-only risk factors (multi-factor linear regression model, average $\mathfrak{R}^2$)

| Model | North America | | Eurozone | |
|---|---|---|---|---|
| | 2010–2013 | 2014–2019 | 2010–2013 | 2014–2019 |
| CAPM | 40.8% | 28.6% | 42.8% | 36.3% |
| 5F model | 46.1% | 38.4% | 49.5% | 45.0% |
| 6F model (5F + ESG) | 46.7% | 39.7% | 50.1% | 45.8% |

Source: Roncalli (2020b).

The previous results may be disturbing. Indeed, cross-section regressions show that ESG is a very good single factor, but the added value of ESG in a multi-factor framework is limited. The difference between the two approaches is the cross-correlation between the risk factors included in the cross-section multi-factor regression. To better understand these results, Roncalli (2020b) considers a factor picking (or factor selection) approach. This approach is similar to the multi-factor approach, but a lasso penalized regression is used instead of the traditional least squares regression:

$$\left\{\hat{\alpha}_i, \hat{\beta}_{i,1}, \ldots, \hat{\beta}_{i,m}\right\} = \arg\min \left\{\frac{1}{2}\operatorname{var}(\varepsilon_{i,t}) + \lambda \left\|\beta_i\right\|_1\right\}$$

The advantage is that we can control the factor intensity of the multi-factor portfolio. This gives us a factor selection procedure. Starting with a low factor intensity ($\lambda \approx \infty$), we can determine which risk factor is the most important. We then increase the factor intensity to establish an order among the risk factors. When the factor intensity reaches 100% ($\lambda = 0$), we get the same results as before with the linear regression. The results are shown in Figures 3.28 and 3.29 for the period 2014–2019. In North America, we see that quality is the first selected factor, followed by ESG, momentum, value and finally low-volatility. Therefore, ESG is the second factor in North America. Thus, ESG should be an important factor when constructing a multi-factor portfolio. However, we observe that as we increase the factor intensity, the ESG beta first increases and then decreases. When the factor intensity reaches 100%, ESG represents a low exposure. Therefore, part of the ESG exposure has been replaced by exposure to other risk factors. This means that ESG has a high contribution in a low-diversified portfolio, but is somewhat redundant in an already well-diversified portfolio. In the case of the Eurozone, the situation is different. ESG is the first factor selected and remains an important factor even if we increase the factor intensity. For example, it is more important than momentum and low-volatility.

These different results (single-factor, multi-factor and factor picking) show that ESG investing remains an alpha strategy in North America. It may have generated outperformance, but the ESG risk factor cannot explain the dispersion of stock returns better than the standard five-factor risk model. This means that adding ESG to a multi-factor portfolio that is already well diversified adds very little value. This is clearly the definition of an alpha strategy. On the contrary, we find that ESG is a significant factor in a Eurozone multi-factor portfolio. We can then improve the diversification of multi-factor portfolios by including an ESG risk factor. Thus, in the Eurozone, an ESG strategy seems to be more of a beta strategy than an alpha strategy.

**Remark 38** *These last observations can be linked to the development of factor investing, for example low-volatility and quality risk factors (Roncalli, 2017). Low-volatility strategies have been around for many years, but they really took off in the asset management industry between 2003 and 2004, following the dot.com bubble. Initially, low-volatility strategies were viewed as alpha strategies. After the 2008 Global Financial Crisis, they were massively implemented and thus became beta strategies.*

Figure 3.28: Factor picking (MSCI North America, 2014–2019, global score)

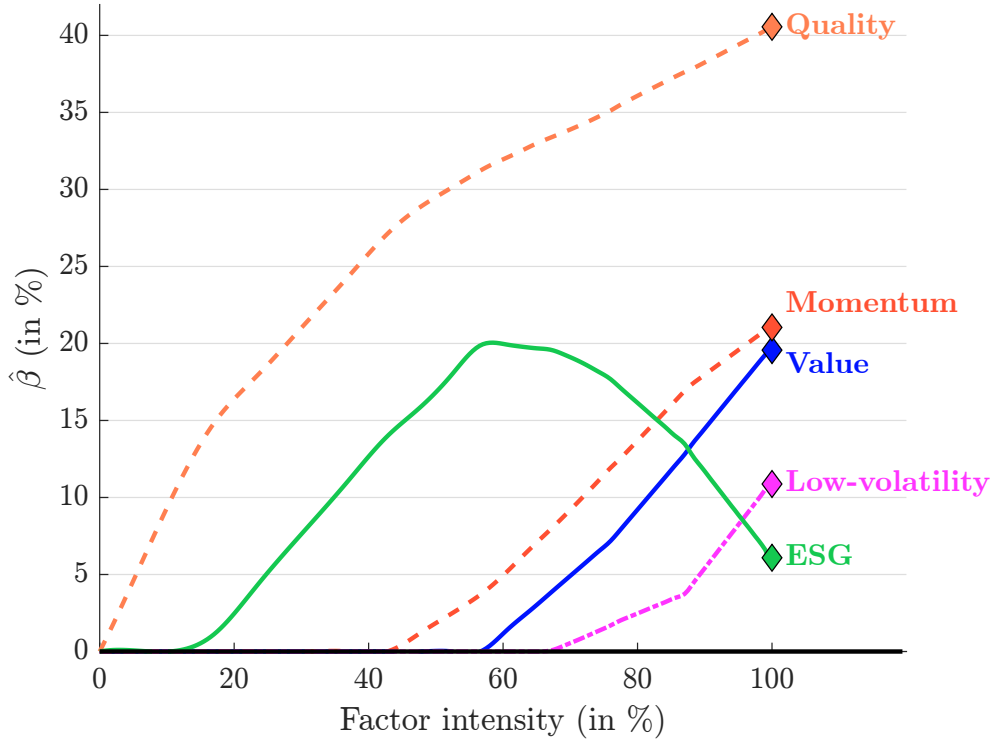


Source: Roncalli (2020b).

Figure 3.29: Factor picking (MSCI EMU, 2014–2019, global score)

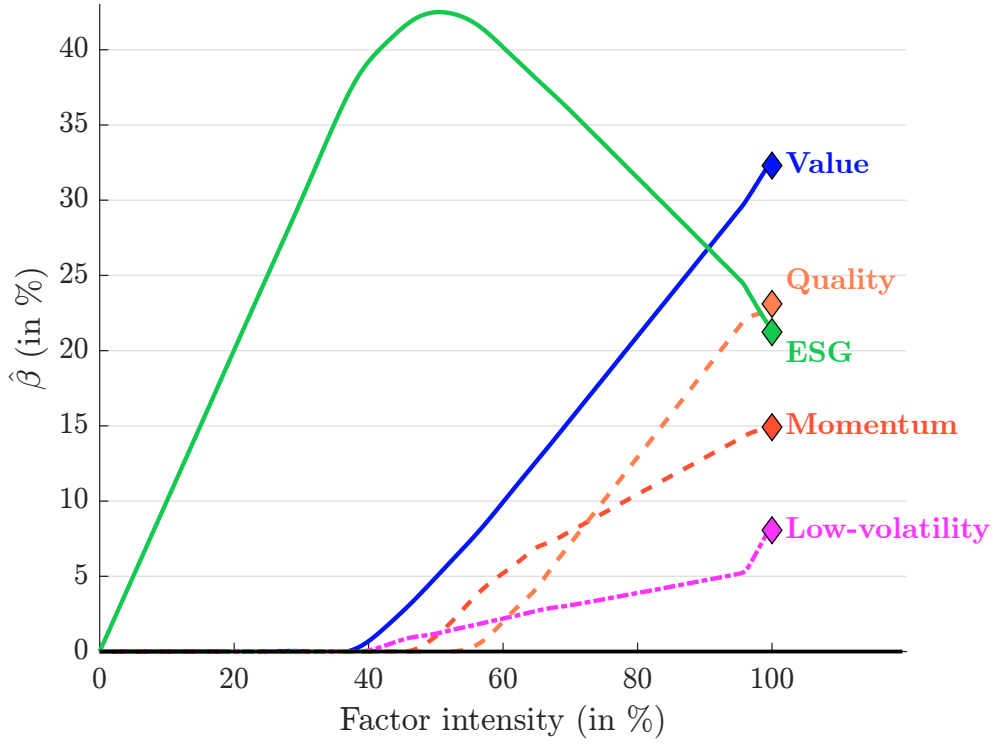


Source: Roncalli (2020b).

*The case of the quality anomaly is similar. This shows that there is no clear boundary between alpha and beta. When an alpha strategy is massively invested, it has enough impact on the structure of asset prices to become a risk factor. The alpha/beta status of ESG strategies is related to investment flows. Indeed, an alpha strategy becomes a common market risk factor when it represents a significant portion of investment portfolios and explains the cross-section dispersion of asset returns. This may explain why ESG is more of a risk factor in the Eurozone than in North America.*

Table 3.16: Performance of ESG equity indexes (MSCI World, 2010–2023)

| Year | Return (in %) | | | Alpha (in bps) | |
|---|---|---|---|---|---|
| | CW | ESG | SRI | ESG | SRI |
| 2010 | 11.8 | 10.7 | 10.6 | −109 | −114 |
| 2011 | −5.5 | −5.4 | −5.5 | 12 | 2 |
| 2012 | 15.8 | 14.5 | 13.2 | −135 | −258 |
| 2013 | 26.7 | 27.6 | 27.4 | 89 | 71 |
| 2014 | 4.9 | 4.9 | 3.9 | −6 | −102 |
| 2015 | −0.9 | −1.1 | −1.6 | −23 | −71 |
| 2016 | 7.5 | 7.3 | 7.7 | −26 | 18 |
| 2017 | 22.4 | 21.0 | 23.6 | −142 | 124 |
| 2018 | −8.7 | −7.8 | −6.7 | 94 | 199 |
| 2019 | 27.7 | 28.2 | 29.8 | 48 | 209 |
| 2020 | 15.9 | 15.3 | 19.9 | −61 | 396 |
| 2021 | 21.8 | 24.7 | 27.0 | 288 | 523 |
| 2022 | −18.1 | −19.6 | −22.5 | −143 | −436 |
| 2023 | 23.8 | 25.4 | 27.8 | 161 | 404 |
| 3Y | 7.3 | 8.0 | 8.0 | 67 | 70 |
| 5Y | 12.8 | 13.2 | 14.4 | 39 | 157 |
| 7Y | 10.7 | 11.0 | 12.3 | 25 | 161 |
| 10Y | 8.6 | 8.7 | 9.5 | 11 | 93 |

### Equity indexes

Another way to illustrate the time-varying nature of ESG investment performance is to analyze the annualized returns of equity indexes. In Table 3.16, we compare the MSCI World capitalization-weighted index (CW) with the MSCI World ESG Leaders and SRI indexes[27]. For each index, we report the annualized return in % and also calculate the alpha in bps relative to the CW parent index. For instance, the 2022 return was −18.1% for the MSCI World index (CW), −19.6% for the MSCI World ESG Leaders index and −22.5% for the MSCI World SRI index. The alpha of the ESG and SRI indexes is therefore negative, at −143 and −436 bps, respectively. Over the past fourteen years, the benchmark index has outperformed the ESG index eight times and the SRI index only five times. The 3Y, 5Y, 7Y and 10Y annualized returns are higher for the ESG and SRI indexes than for the CW index. These results clearly show that ESG investing can generate alpha in some periods. Moreover, the relative performance depends on the construction of the ESG index. In fact, we do not observe the same patterns between ESG Leaders and SRI indexes.

[27] "*MSCI ESG Leaders indexes target companies that have the highest ESG-rated performance in each sector of the parent index. MSCI SRI indexes are designed to track the performance of companies with high ESG ratings. They use a best-in-class selection approach to target the top 25% companies in each sector according to their MSCI ESG Ratings*" (www.msci.com/our-solutions/indexes/esg-indexes).

In Table 3.17, we confirm that the performance of ESG investments depends on several factors. For instance, the region has a significant impact. The MSCI EMU SRI Index has generated positive alpha every year between 2015 and 2021, with an average of 393 bps per year. For the MSCI EM ESG Leaders Index, the period of euphoria is between 2010 and 2017 with an average alpha of 423 bps per year. The choice of ESG scoring model is another factor. In fact, if we look at the S&P 500 ESG Index, it has a positive alpha in 2014, 2020 and 2022, while the MSCI USA ESG Leaders Index has a negative alpha in these years (19 vs. −49 bps in 2014, 138 vs. −251 bps in 2020 and 43 vs. −73 bps in 2022).

Figure 3.30: Alpha return of ESG equity indexes (in bps)

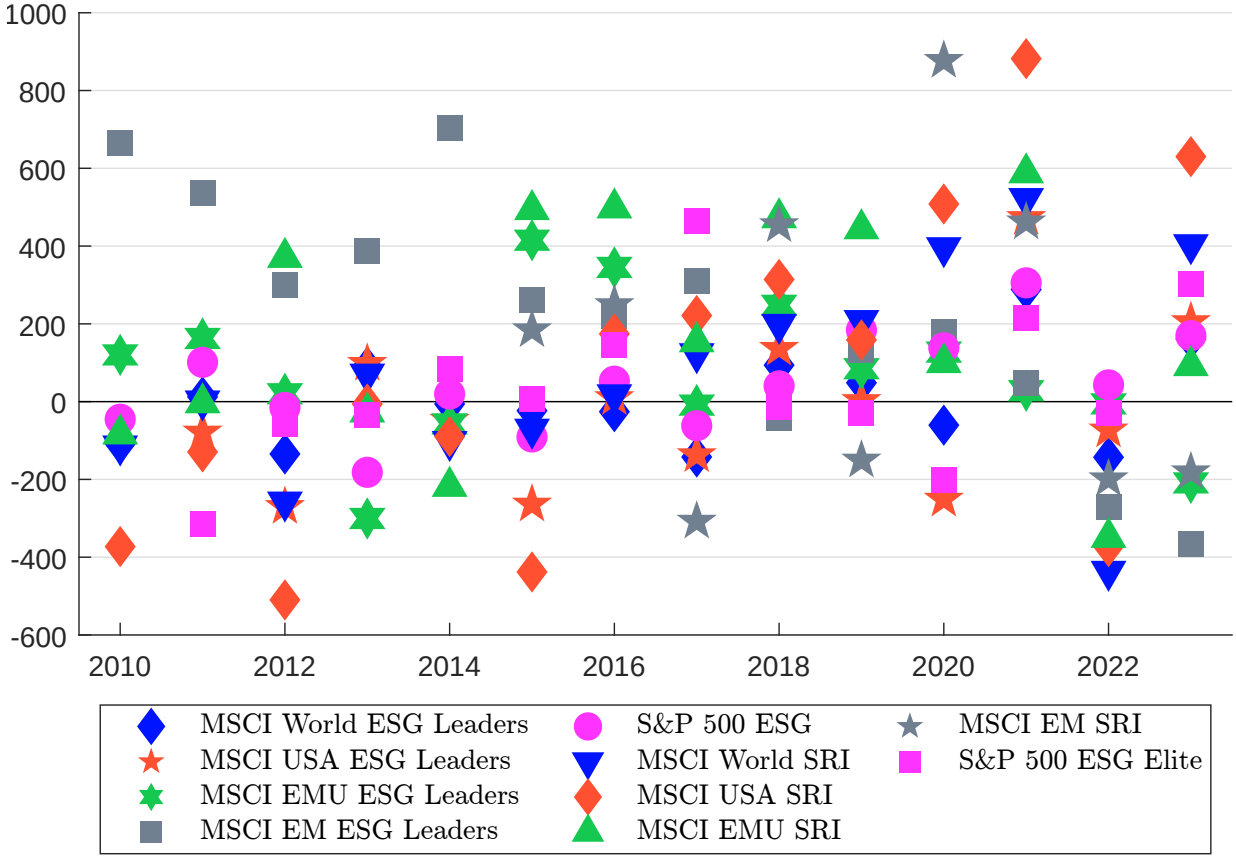


Source: MSCI, Factset & Author's calculations.

In Figure 3.30, we have plotted the distribution of alpha returns of ESG equity indexes over time. This illustrates perfectly that "*ESG investing has its good times and its bad times.*" While ESG indexes massively underperform CW indexes in 2022, they also massively outperform in 2021. The underperformance in 2022 is mainly due to the Russian war in Ukraine and the energy shock. In 2023, seven of the ten ESG indexes have positive alpha. The average alpha of the ten ESG indexes is 1.81% in 2020, 3.81% in 2021, −1.84% in 2022 and 1.21% in 2023. From 2010 to 2013, the average alpha is 82 bps per year. We retrieve the two-period results obtained by Bennani *et al.* (2018), where the average annual alpha is only 12 bps from 2010 to 2015 and 129 bps from 2016 to 2023. Curiously, the alpha is not negative in the first period. Moreover, the average alpha is negative only for the years 2012 and 2022, suggesting that ESG investing has had more good times than bad over the past fourteen years.

Table 3.17: Performance of ESG equity indexes

| Year | MSCI USA | | | | | MSCI EMU | | | | | MSCI EM | | | S&P 500 | | |
|---|---|---|---|---|---|---|---|---|---|---|---|---|---|---|---|---|
| | Return | | | Alpha | | Return | | | Alpha | | Return | | Alpha | Return | | Alpha |
| | CW | ESG | SRI | ESG | SRI | CW | ESG | SRI | ESG | SRI | CW | ESG | ESG | CW | ESG | ESG |
| 2010 | 14.8 | | 11.0 | | −373 | 2.4 | 3.6 | 1.6 | 120 | −83 | 18.9 | 25.5 | 665 | 14.4 | 13.9 | −45 |
| 2011 | 1.4 | 0.6 | 0.1 | −79 | −129 | −14.9 | −13.3 | −14.9 | 162 | −3 | −18.4 | −13.1 | 536 | 1.5 | 2.5 | 101 |
| 2012 | 15.3 | 12.6 | 10.2 | −270 | −510 | 19.3 | 19.5 | 23.0 | 20 | 371 | 18.2 | 21.2 | 299 | 15.2 | 15.1 | −15 |
| 2013 | 31.8 | 32.8 | 31.7 | 98 | −6 | 23.4 | 20.4 | 23.1 | −301 | −27 | −2.6 | 1.3 | 386 | 31.5 | 29.7 | −182 |
| 2014 | 12.7 | 12.2 | 11.8 | −49 | −90 | 4.3 | 3.7 | 2.1 | −57 | −218 | −2.2 | 4.8 | 703 | 13.0 | 13.2 | 19 |
| 2015 | 0.7 | −2.0 | −3.7 | −264 | −438 | 9.8 | 14.0 | 14.7 | 415 | 493 | −14.9 | −12.3 | 262 | 0.7 | −0.2 | −91 |
| 2016 | 10.9 | 11.0 | 12.6 | 10 | 174 | 4.4 | 7.8 | 9.4 | 345 | 498 | 11.2 | 13.4 | 221 | 11.2 | 11.8 | 53 |
| 2017 | 21.2 | 19.8 | 23.4 | −137 | 221 | 12.5 | 12.4 | 14.0 | −9 | 154 | 37.3 | 40.4 | 309 | 21.1 | 20.5 | −62 |
| 2018 | −5.0 | −3.7 | −1.9 | 137 | 314 | −12.7 | −10.2 | −8.0 | 248 | 472 | −14.6 | −15.0 | −42 | −4.9 | −4.5 | 40 |
| 2019 | 30.9 | 30.9 | 32.5 | 2 | 159 | 25.5 | 26.3 | 29.9 | 85 | 444 | 18.4 | 19.8 | 134 | 30.7 | 32.5 | 184 |
| 2020 | 20.7 | 18.2 | 25.8 | −251 | 508 | −1.0 | 0.3 | 0.0 | 127 | 100 | 18.3 | 20.1 | 178 | 17.8 | 19.1 | 138 |
| 2021 | 26.5 | 31.2 | 35.3 | 473 | 882 | 22.2 | 22.4 | 28.0 | 28 | 588 | −2.5 | −2.1 | 48 | 28.2 | 31.2 | 305 |
| 2022 | −19.8 | −20.6 | −23.6 | −73 | −373 | −12.5 | −12.5 | −16.0 | −6 | −349 | −20.1 | −22.8 | −270 | −18.5 | −18.1 | 43 |
| 2023 | 26.5 | 28.5 | 32.8 | 205 | 630 | 18.8 | 16.7 | 19.7 | −209 | 92 | 9.8 | 6.2 | −367 | 25.7 | 27.4 | 170 |
| 3Y | 8.7 | 10.2 | 11.2 | 159 | 251 | 8.3 | 7.7 | 8.8 | −58 | 51 | −5.1 | −7.1 | −199 | 9.5 | 11.1 | 156 |
| 5Y | 15.2 | 15.7 | 18.0 | 53 | 284 | 9.5 | 9.6 | 10.8 | 7 | 130 | 3.7 | 2.9 | −77 | 15.1 | 16.7 | 158 |
| 7Y | 12.9 | 13.3 | 15.7 | 41 | 281 | 6.4 | 6.9 | 8.4 | 47 | 192 | 5.0 | 4.7 | −30 | 12.8 | 13.9 | 109 |
| 10Y | 11.4 | 11.3 | 12.9 | −5 | 152 | 6.4 | 7.4 | 8.4 | 101 | 209 | 2.7 | 3.7 | 103 | 11.4 | 12.1 | 72 |

Source: MSCI, Factset & Author's calculations.

### 3.2.2 Fixed-income markets

Compared to equity markets, there are few studies analyzing the impact of ESG screening on fixed-income markets. For example, Menz (2010) examined the relationship between the valuation of Euro corporate bonds and corporate social responsibility and concluded that "*CSR has apparently not yet been incorporated into the pricing of corporate bonds.*" Similarly, a neutral or slightly positive effect of socially responsible investing was found by Derwall and Koedijk (2009) when they compared the performance of SRI and conventional bond funds. This overall neutrality, sometimes associated with a lack of maturity in the integration of ESG information into the bond market, was also highlighted by Goldreyer *et al.* (1999), Bauer *et al.* (2005) and Cortez *et al.* (2009). In the CAPM approach, active management performance is captured by measuring the alpha. However, Lin *et al.* (2019) constructed industry and credit-rating controlled quintile portfolios and found no significant evidence that ESG factors contribute to positive alpha in the bond market. On the contrary, Oikonomou *et al.* (2014) found that corporate social performance is rewarded in the corporate debt market. Results of Leite and Cortez (2016) are slightly positive, but highly country-specific. For example, they conclude that "*French SRI bond funds match the performance of their conventional peers, German funds slightly outperform and UK funds significantly underperform conventional funds.*" Polbennikov *et al.* (2016) also found a slight outperformance of high ESG-rated bonds over low ESG-rated bonds after controlling for different risk exposures. More recently, Gerard (2019) and Pereira *et al.* (2019) found no relationship between ESG and performance in corporate bond markets.

#### Simulated results

There are three main reasons why the relationship between ESG and bond returns may differ from the relationship between ESG and equity returns:

1. The first is ESG sensitivity. In fact, ESG criteria are very important to a shareholder because ESG risks can affect long-term business risk and have a strong impact on the value of equity. In the case of a bondholder, his main objective is to manage default risk, which is more of a short-term risk. Therefore, the concept of active ownership does not really apply to fixed-income instruments. For example, the absence of voting rights dramatically reduces the impact of engagement policies when ESG investors focus on the bond market. From a theoretical perspective, it is generally accepted that shareholders are more sensitive to ESG factors than bondholders. This may explain the lower integration of ESG in fixed-income markets. Other factors may also explain the difference in ESG sensitivity. For example, equity prices react faster and more strongly than bond prices to negative events, news flows and market sentiment, while bond prices are mainly driven by long-term fundamentals. In addition, the difference in liquidity between the two markets and the buy-and-hold strategy imply that bonds are traded less frequently than stocks. In this context, investors may feel that fixed-income markets do not price in ESG issues.

2. The second is the impact of ESG investment flows. In the case of equities, they put upward pressure on share prices. In the case of bonds, we see two effects. Investment flows can obviously affect the dynamics of credit spreads and then put pressure on bond prices, but they also have an impact on the primary market by reducing or increasing the coupon. ESG investment flows then have an impact on carry, and a high ESG score generally implies a reduction in carry due to the supply/demand balance.

3. The third reason is related to the correlation between ESG ratings and credit ratings. Some extra-financial information is already incorporated into credit ratings. In a bond investment

universe, the conditional probability distribution of ESG scores then differs from the unconditional probability distribution of ESG scores. In most cases, we distinguish between IG and HY bonds. Since we observe a positive correlation between ESG and credit ratings, it follows that there are more worst-in-class issuers in the HY universe than in the IG universe. So we observe a bias in the ESG scores, which are no longer sector-neutral in fixed-income markets. Moreover, the average ESG score is certainly not zero. It is positive for IG bonds and negative for HY bonds[28].

These various reasons explain why ESG scoring is more integrated in equity portfolio management, while ESG integration in bond portfolio management is generally limited to exclusions. Moreover, the development of pure ESG securities has generally led to a segmentation in the construction of bond portfolios. On the one hand, we find a core portfolio, which corresponds to a global aggregate fixed-income strategy and uses minimum ESG criteria without really promoting ESG analysis. On the other hand, a satellite portfolio is invested in green and sustainability bonds with the aim of implementing an impact investing strategy.

Figure 3.31: Probability density function of ESG scores

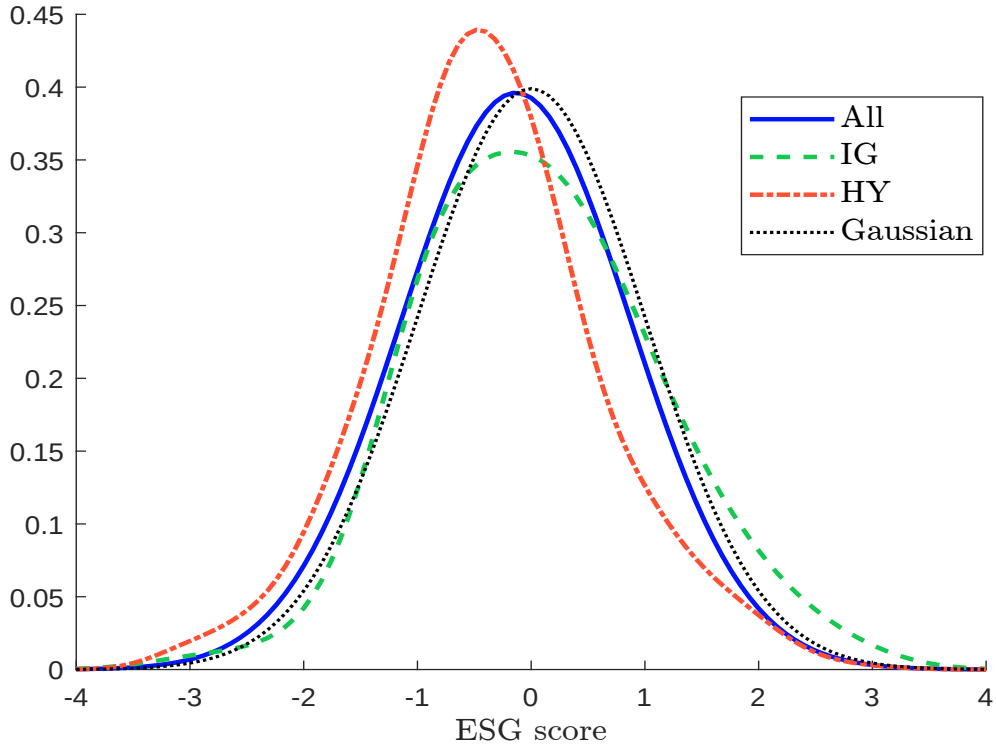


Source: Ben Slimane *et al.* (2019b).

**Sorted portfolios** Ben Slimane *et al.* (2019b) has applied the sorted and optimized approach of Bennani *et al.* (2018) to the universe of bonds from the Intercontinental Exchange Bank of America Merrill Lynch large cap investment grade corporate bond index. The study period is from January 2010 to August 2019. Each month, the bonds are ranked according to their ESG score and five

[28] In Figure 3.31, we show the estimated density function of Amundi ESG $z$-scores within the IG and HY universes. The empirical standard deviation of the $z$-scores is equal to 1.01 regardless of the bond universe. On the contrary, we find that the empirical mean is equal to 0.02 and $-0.38$ for IG and HY bonds, respectively.

quintile portfolios are created. Portfolio $Q_1$ corresponds to the 20% best-ranked bonds, whereas portfolio $Q_5$ corresponds to the 20% worst-rated bonds. By construction, the sorted portfolios are sector-neutral. However, the authors do some clustering because some sectors are small. Sorted portfolios are then constructed using the same weighting structure as the benchmark, with the selected bonds equally weighted within a sector. In addition, each portfolio is rebalanced on a monthly basis, meaning that the portfolio is invested on the first trading day of the month and held for the entire month. In Figure 3.32, we show the difference in returns between the best-in-class portfolio and the worst-in-class portfolio. We use two performance measures. Total return (TR) corresponds to the mark-to-market return of the portfolio, including bond price changes and coupon effects. Credit return or excess return (ER) is the return above the total return of a risk-matched basket of government bonds or interest rate swaps, thus neutralizing the interest rate and yield curve risk and isolating the portion of performance due solely to credit and optionality risks. Focusing on the total return measure, all $Q_1 - Q_5$ EUR-denominated portfolios had a positive performance over both the 2010–2013 and 2014–2019 periods. Looking at the credit return measure, ESG and (S) long/short portfolios had negative performance before 2014, while all portfolios had a positive performance in the second period. Looking at the universe of USD-denominated investment grade corporate bonds, the worst-in-class portfolio generally outperformed the best-in-class portfolio between 2010 and 2013, with the exception of the governance pillar.

Figure 3.32: Annualized return in bps of the long short $Q_1 - Q_5$ strategy (IG, 2010–2019)

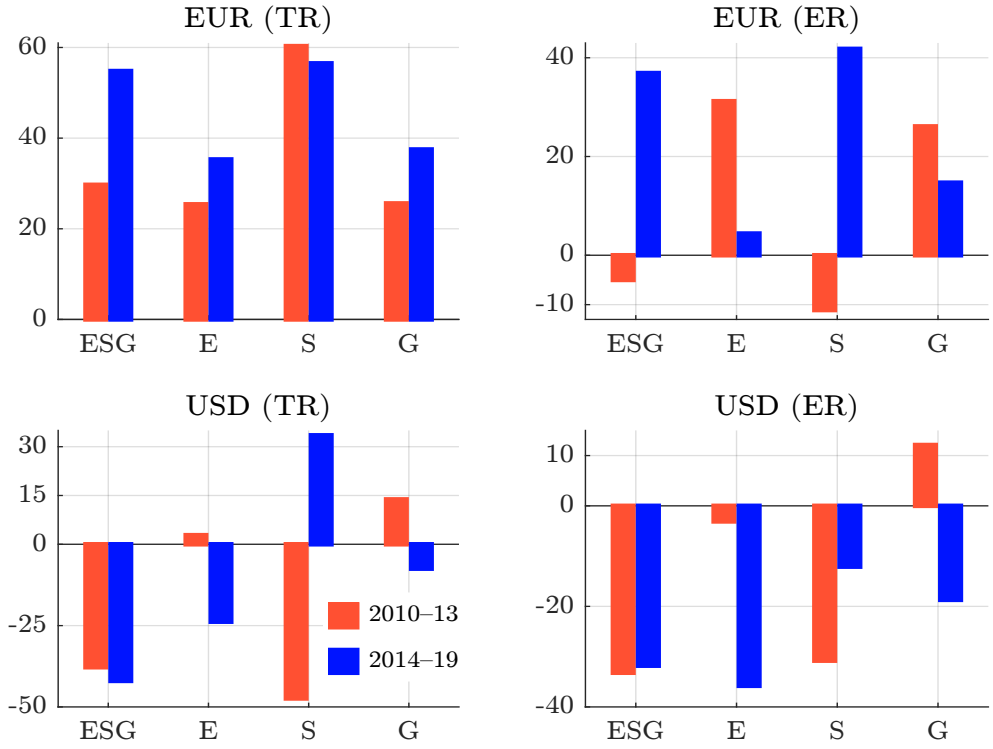


Source: Ben Slimane *et al.* (2019b).

We can draw the following conclusions from the previous results. First, the quintile portfolios show some strong bias in terms of duration risk. Therefore, the results based on credit return measures are not consistent with those based on total return measures. Second, these results confirm that the period 2014–2019 has generated better performance in terms of ESG investing, but only

for EUR-denominated corporate bonds. For USD-denominated corporate bonds, the performance remains negative. Finally, we need to be careful about the feasibility of capturing ESG alpha. For instance, if we consider the long/short strategy $Q_1 - Q_5$, the credit return is equal to 36.8 bps in the second period. We can decompose this ESG alpha into the long leg and the short leg. In Figure 3.33, we report the raw performance of sorted portfolios. The carry statistics in bps are:

| Period | $Q_1$ | $Q_5$ | $Q_1 - Q_5$ |
|---|---|---|---|
| 2010–2013 | 175 | 192 | −17 |
| 2014–2019 | 113 | 128 | −15 |

Therefore, the positive credit return of the long/short $Q_1 - Q_5$ cannot be explained by the carry exposure. It is due to the mark-to-market component and the dynamics of credit spreads and bond prices. This implies that an ESG strategy has a short carry position. On the one hand, buy-and-hold ESG investors may suffer from this structural exposure, but they can increase the credit risk of their buy-and-hold portfolio to compensate for the lower carry. On the other hand, active ESG investors can only outperform if they are able to rebalance their portfolio. Liquidity issues in the corporate bond market are then a barrier to generating ESG alpha in the fixed-income universe. In particular, when we impose turnover constraints on the construction of the previously simulated portfolios, we observe a decrease in the alpha return.

Figure 3.33: Annualized credit return in bps of ESG sorted portfolios (EUR IG, 2010–2019)

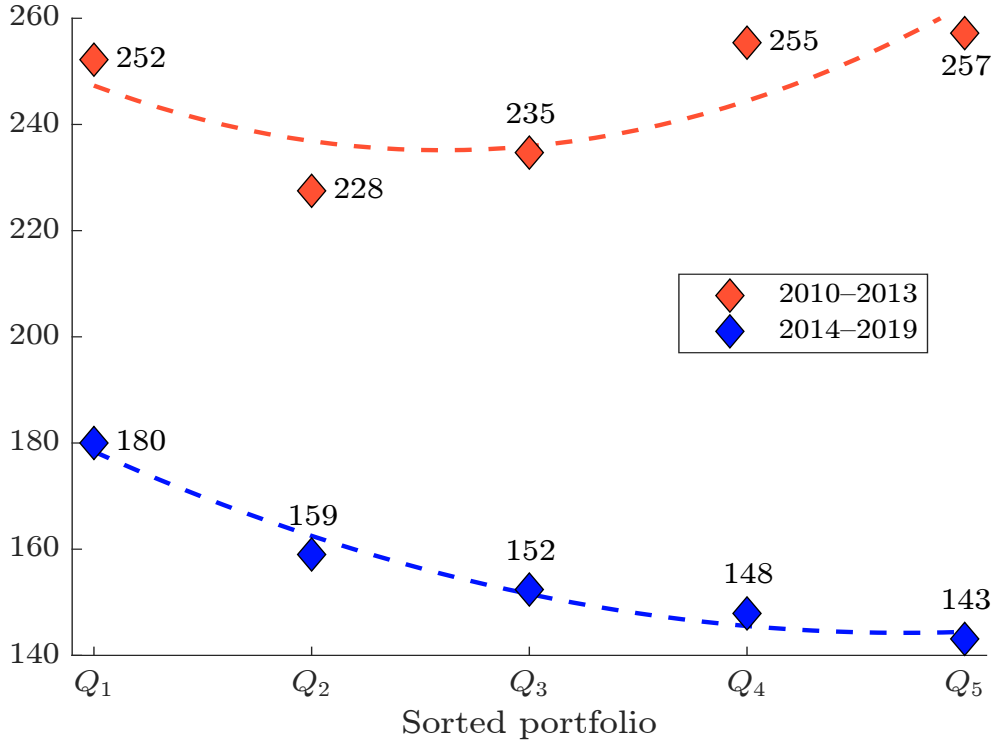


Source: Ben Slimane *et al.* (2019b).

**Remark 39** *The above results suggest that the annualized credit return may not be the most appropriate measure to compare the performance of ESG and business-as-usual investments. The Sharpe ratio or a risk-adjusted measure using the duration-times-spread factor may be more relevant.*

**Optimized portfolios** In the sorted portfolios, there is no control over duration or credit spread. Therefore, it is difficult to know whether the alpha return is explained by the ESG scoring or by the duration/spread bias. In fact, the sorted portfolio methodology is not really relevant when applied to the fixed-income universe. A better method is to consider the optimization approach, where the portfolio manager imposes some constraints on the active risk he can take with respect to the benchmark index. Ben Slimane *et al.* (2019b) define the active risk measure as the weighted average of duration risk and credit risk (see Box 3.7). They then implement an optimization program that consists of minimizing active risk while controlling the ESG excess score of the tilted portfolios. Starting from an ESG excess score of zero, they gradually increase the ESG score of the optimized portfolio until it reaches one. They find that the relationship between the ESG excess score and the ex-post tracking error volatility is approximately linear. On average, targeting an excess score of one requires accepting a tracking error of 25 bps.

Using the ICE (BofAML) Large Cap IG EUR Corporate Bond index, Figures 3.34 and 3.35 show the impact of ESG integration on the excess credit return of optimized portfolios for the periods 2010–2013 and 2014–2019. In the first period, the excess return of ESG-optimized portfolios is negative, meaning that ESG investors were penalized. This is particularly true when optimized portfolios targeted high excess scores. For example, an ESG excess score of +1 resulted in an underperformance of −35 bps per year. In the second period, we observe a small positive outperformance, which peaks at +4 bps when the ESG tilt is set to +1. We also observe that the relationship between the ESG excess score and the excess credit return is increasing. Looking at the individual pillars, the E, S and G optimized portfolios underperform over the period 2010–2013. Among the three pillars, environmental is the best pillar and its excess return falls to −22 bps when the target excess score is set to +1. Governance is the worst pillar and its excess return reaches −49 bps for the same tilt. After 2014, excess returns range from −3 to +9 bps. Social is the winning pillar and shows significant outperformance, peaking at +9 bps. The most recent period is then more favorable for ESG investors than before 2014.

If we look at the universe of USD investment grade corporate bonds, the results are different from those for EUR-denominated corporate bonds. ESG investing did not generate positive alpha over the entire 2010–2019 period (see Figures 3.36 and 3.37). However, the significant underperformance in the period 2010–2013 has been dramatically reduced since 2014. For example, the excess return is close to zero for the social pillar between 2014 and 2019. Another interesting observation is the behavior of the governance pillar. In many academic studies, the link between ESG and corporate financial performance is through the governance transmission channel. The results of Ben Slimane *et al.* (2019a) show that the governance pillar is not necessarily the most important factor and that investing in bonds with a good governance score is not fundamentally better than using the other pillars.

**Remark 40** *The authors wonder whether the transatlantic divide really concerns the currency of the bonds issued or whether it is more of a regional issue. For example, a EUR-denominated bond can be issued by a European company, but also by a company based outside Europe. Similarly, a USD-denominated bond can be issued by an American company, but also by a company based outside America. Ben Slimane et al. (2019b) calculated the contribution of the different regions (Europe, North America and others) to credit return. They found that Europe had a systematic positive contribution, while North America had a systematic negative contribution, regardless of the currency (EUR and USD). Therefore, this transatlantic divide shows that ESG investing was a source of outperformance when it came to IG bonds of European issuers, but a source of underperformance when it came to IG bonds of American issuers.*

Figure 3.34: Annualized excess return in bps of ESG optimized portfolios (EUR IG, 2010–2013)

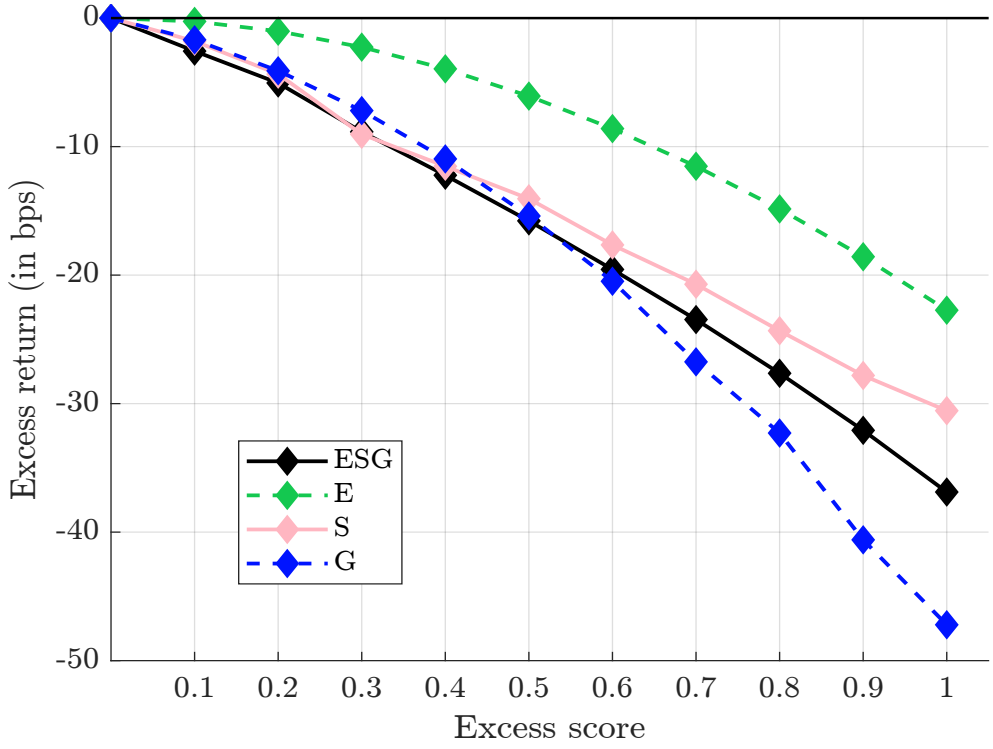


Figure 3.35: Annualized excess return in bps of ESG optimized portfolios (EUR IG, 2014–2019)

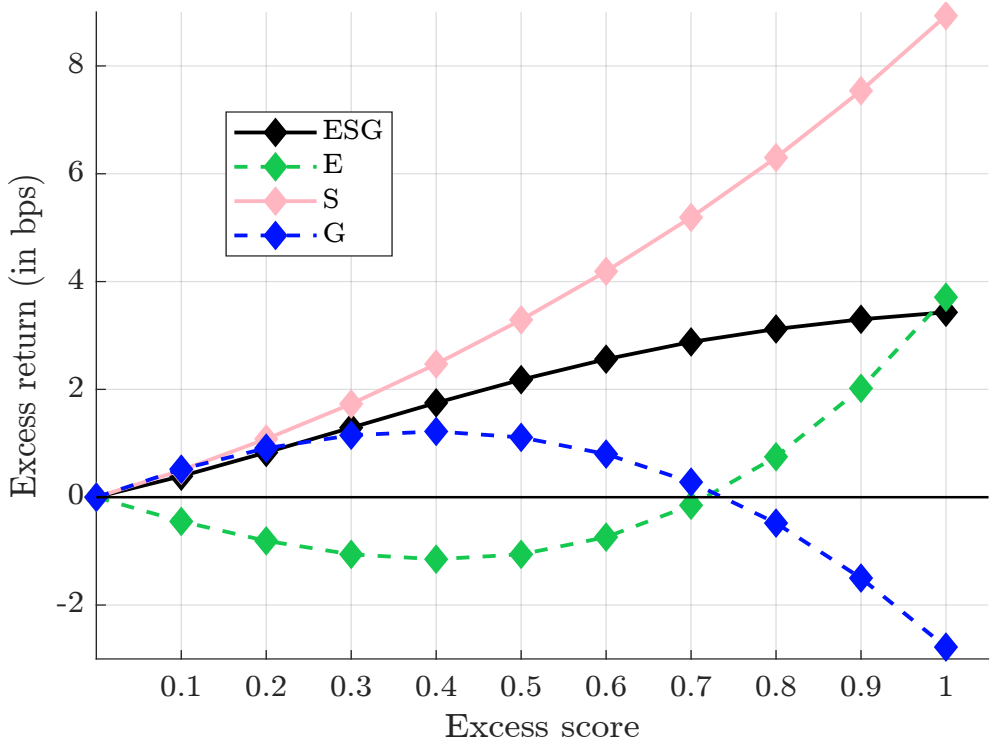


Source: Ben Slimane *et al.* (2019b).

Figure 3.36: Annualized excess return in bps of ESG optimized portfolios (USD IG, 2010–2013)

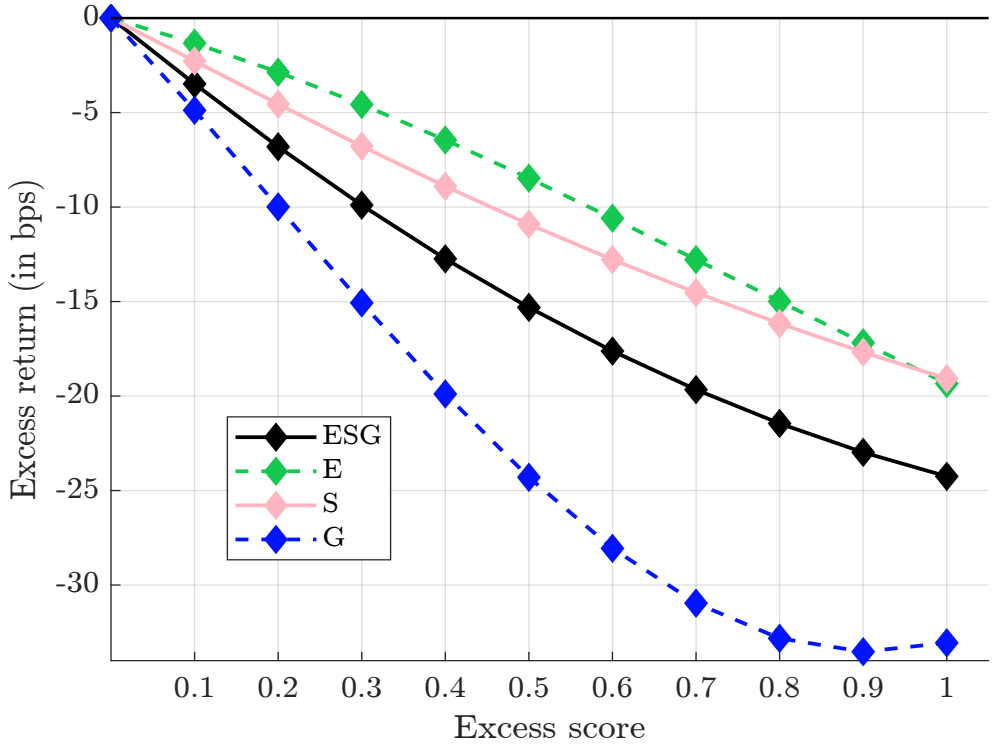


Figure 3.37: Annualized excess return in bps of ESG optimized portfolios (USD IG, 2014–2019)

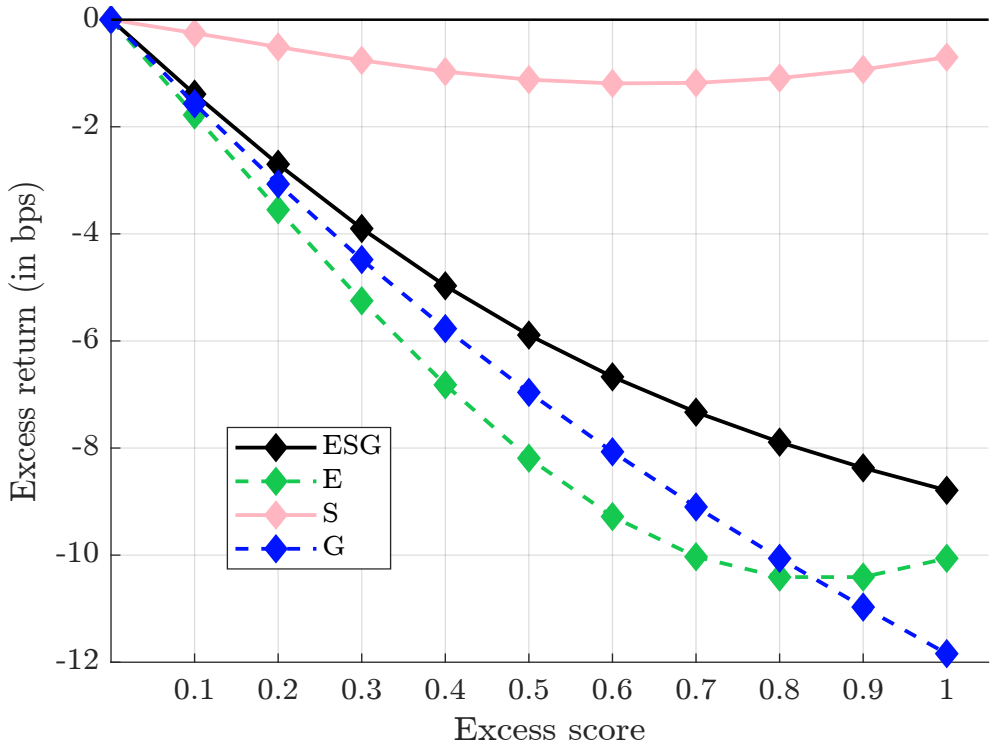


Source: Ben Slimane *et al.* (2019b).

Box 3.7: Building an optimized ESG portfolio in the fixed-income universe

The ESG score of the portfolio $w = (w_1, \ldots, w_n)$ is the weighted average of the individual scores: $\boldsymbol{\mathcal{S}}(w) = \sum_{i=1}^{n} w_i \boldsymbol{\mathcal{S}}_i$. If we consider a benchmark $b = (b_1, \ldots, b_n)$, we deduce that the ESG excess score of portfolio $w$ relative to benchmark $b$ is equal to:

$$\boldsymbol{\mathcal{S}}(w \mid b) = \sum_{i=1}^{n} (w_i - b_i) \boldsymbol{\mathcal{S}}_i = \boldsymbol{\mathcal{S}}(w) - \boldsymbol{\mathcal{S}}(b)$$

When we use $z$-scores, we observe that $\boldsymbol{\mathcal{S}}(b) \approx 0$ because there is no reason for a capitalization-weighted index to have a positive or negative ESG score. In general, it is a neutral ESG portfolio. On the contrary, an ESG portfolio $w$ aims to have a better ESG score than the benchmark: $\boldsymbol{\mathcal{S}}(w \mid b) > 0$. Of couse, when building an ESG-optimized portfolio, there is a trade-off between the ESG excess score $\boldsymbol{\mathcal{S}}(w \mid b)$ and the active or tracking risk $\mathcal{R}(w \mid b)$ relative to the benchmark. For example, if the active risk is zero, the ESG excess score will be zero. If we consider a high ESG score (*e.g.*, greater than 1.5), we must also take a high active risk. Therefore, the optimization problem becomes:

$$w^\star(\gamma) = \arg\min \frac{1}{2}\mathcal{R}(w \mid b) - \gamma \boldsymbol{\mathcal{S}}(w \mid b)$$

If $\gamma$ is set to zero, the optimized portfolio $w^\star(0)$ is the benchmark portfolio $b$. If $\gamma$ is set to infinity, the optimized portfolio $w^\star(\infty)$ is the bond with the highest $z$-score. The parameter $\gamma$ can then be calibrated to target a given excess score $\mathcal{S}^\star$. The problem is the choice of the tracking risk metric. In the case of bonds, we generally use two measures. First, we can track the modified duration of the sectors. It follows that the modified duration risk of portfolio $w$ relative to benchmark $b$ is:

$$\mathcal{R}_{\text{MD}}(w \mid b) = \sum_{j=1}^{n_S} \left( \left( \sum_{i \in \boldsymbol{\mathcal{S}}ector(j)} w_i \,\text{MD}_i \right) - \left( \sum_{i \in \boldsymbol{\mathcal{S}}ector(j)} b_i \,\text{MD}_i \right) \right)^2$$

where $n_S$ is the number of sectors and $\text{MD}_i$ is the modified duration of bond $i$. An alternative is to use the DTS risk measure:

$$\mathcal{R}_{\text{DTS}}(w \mid b) = \sum_{j=1}^{n_S} \left( \left( \sum_{i \in \boldsymbol{\mathcal{S}}ector(j)} w_i \,\text{DTS}_i \right) - \left( \sum_{i \in \boldsymbol{\mathcal{S}}ector(j)} b_i \,\text{DTS}_i \right) \right)^2$$

where $\text{DTS}_i$ is the duration-times-spread (DTS) factor of bond $i$. We can also define a hybrid approach where the risk measure is an average of the MD and DTS active risks:

$$\mathcal{R}(w \mid b) = \mathcal{R}_{\text{MD}}(w \mid b) + \mathcal{R}_{\text{DTS}}(w \mid b)$$

In fact, we can interpret $\mathcal{R}_{\text{MD}}(w \mid b)$ as a mesure of interest rate risk and $\mathcal{R}_{\text{DTS}}(w \mid b)$ as a measure of credit risk, while $\mathcal{R}(w \mid b)$ is an integrated measure of both interest rate and credit risk.

Table 3.18: Performance of ESG bond indexes

| Year | FTSE WGBI | | | FTSE EGBI | | | Bloomberg Euro Aggregate Corporate | | | | | | |
|---|---|---|---|---|---|---|---|---|---|---|---|---|---|
| | Return | | Alpha | Return | | Alpha | Return | | | | Alpha | | |
| | CW | ESG | ESG | CW | ESG | ESG | CW | SRI | S-SRI | ESG-S | SRI | S-SRI | ESG-S |
| 2010 | 4.61 | 4.31 | −30 | 0.61 | 4.14 | 353 | 3.07 | 2.93 | 2.96 | | −13 | −10 | |
| 2011 | 6.35 | 7.05 | 69 | 3.41 | 7.31 | 391 | 1.49 | 1.17 | 1.43 | | −32 | −5 | |
| 2012 | 1.65 | 3.06 | 141 | 10.65 | 7.39 | −326 | 13.59 | 13.99 | 12.96 | | 40 | −63 | |
| 2013 | −4.00 | −2.95 | 105 | 2.21 | −1.40 | −362 | 2.37 | 2.49 | 2.36 | | 12 | −1 | |
| 2014 | −0.48 | −0.22 | 26 | 13.19 | 11.44 | −175 | 8.40 | 8.31 | 8.49 | | −8 | 10 | |
| 2015 | −3.57 | −4.85 | −128 | 1.65 | 0.39 | −126 | −0.56 | −0.59 | −0.50 | −0.59 | −3 | 6 | −3 |
| 2016 | 1.60 | 1.02 | −59 | 3.20 | 4.00 | 81 | 4.73 | 4.60 | 4.44 | 4.60 | −13 | −29 | −13 |
| 2017 | 7.49 | 8.16 | 67 | 0.15 | −0.47 | −62 | 2.41 | 2.47 | 2.48 | 2.47 | 6 | 6 | 6 |
| 2018 | −0.84 | −1.41 | −57 | 0.88 | 1.65 | 78 | −1.25 | −1.12 | −1.11 | −1.12 | 13 | 14 | 13 |
| 2019 | 5.90 | 5.56 | −34 | 6.72 | 4.45 | −227 | 6.24 | 6.01 | 5.92 | 6.01 | −24 | −32 | −24 |
| 2020 | 10.11 | 10.90 | 79 | 5.03 | 4.11 | −92 | 2.77 | 2.69 | 2.70 | 2.52 | −8 | −7 | −25 |
| 2021 | −6.97 | −7.15 | −17 | −3.54 | −3.76 | −21 | −0.97 | −0.96 | −0.99 | −0.99 | 1 | −2 | −2 |
| 2022 | −18.26 | −20.00 | −173 | −18.52 | −19.06 | −54 | −13.65 | −13.62 | −13.48 | −13.48 | 3 | 16 | 17 |
| 2023 | 5.19 | 5.69 | 50 | 7.90 | 6.32 | −158 | 8.19 | 8.16 | 8.00 | 7.99 | −3 | −18 | −20 |
| 3Y | −7.18 | −7.75 | −57 | −5.34 | −6.09 | −74 | −2.56 | −2.55 | −2.56 | −2.56 | 0 | 0 | 0 |
| 5Y | −1.39 | −1.67 | −29 | −1.01 | −2.07 | −106 | 0.20 | 0.15 | 0.13 | 0.11 | −6 | −7 | −10 |
| 7Y | −0.09 | −0.29 | −20 | −0.58 | −1.32 | −74 | 0.31 | 0.29 | 0.28 | 0.26 | −1 | −2 | −4 |
| 10Y | −0.31 | −0.62 | −31 | 1.32 | 0.59 | −74 | 1.44 | 1.40 | 1.41 | | −3 | −3 | |

| Year | Bloomberg US Corporate | | | | | | | Bloomberg Global High Yield | | | | |
|---|---|---|---|---|---|---|---|---|---|---|---|---|
| | Return | | | | Alpha | | | Return | | | Alpha | |
| | CW | SRI | S-SRI | ESG-S | SRI | S-SRI | ESG-S | CW | SRI | SUS | SRI | SUS |
| 2019 | | | | | | | | 2.30 | 2.20 | | −9 | |
| 2020 | | | | | | | | 5.73 | 6.49 | 6.67 | 76 | 94 |
| 2021 | −1.04 | −1.55 | 9.56 | 2.34 | −51 | 1 060 | 338 | 2.53 | 0.92 | 0.48 | −161 | −205 |
| 2022 | −15.76 | −15.12 | −1.10 | −13.86 | 64 | 1 467 | 190 | −11.05 | −13.07 | −12.58 | −202 | −153 |
| 2023 | 8.52 | 8.44 | | | −8 | | | 13.66 | 14.14 | 13.59 | 48 | −7 |

Source: FTSE, Bloomberg & Author's calculations.

### Bond indexes

In Table 3.18, we compare the annualized returns of some well-known bond indexes (FTSE World Government Bond Index or WGBI, FTSE EMU Government Bond Index or EGBI, Bloomberg Euro Aggregate Corporate Total Return Index, Bloomberg US Corporate Total Return Index and Bloomberg Global High Yield Total Return Index) with the annualized returns of their ESG counterparts[29]. The results for bond indexes are close to those for equity indexes. Indeed, ESG investing has its ups and downs. However, we find that the results are less balanced than before. It seems that ESG investing generates positive alpha less often in the bond market, even in the case of European bonds (Figure 3.38). In fact, the main reason is that ESG bond indexes have less carry because they have better credit ratings[30].

Figure 3.38: Alpha returns of European ESG bond indexes (in bps)

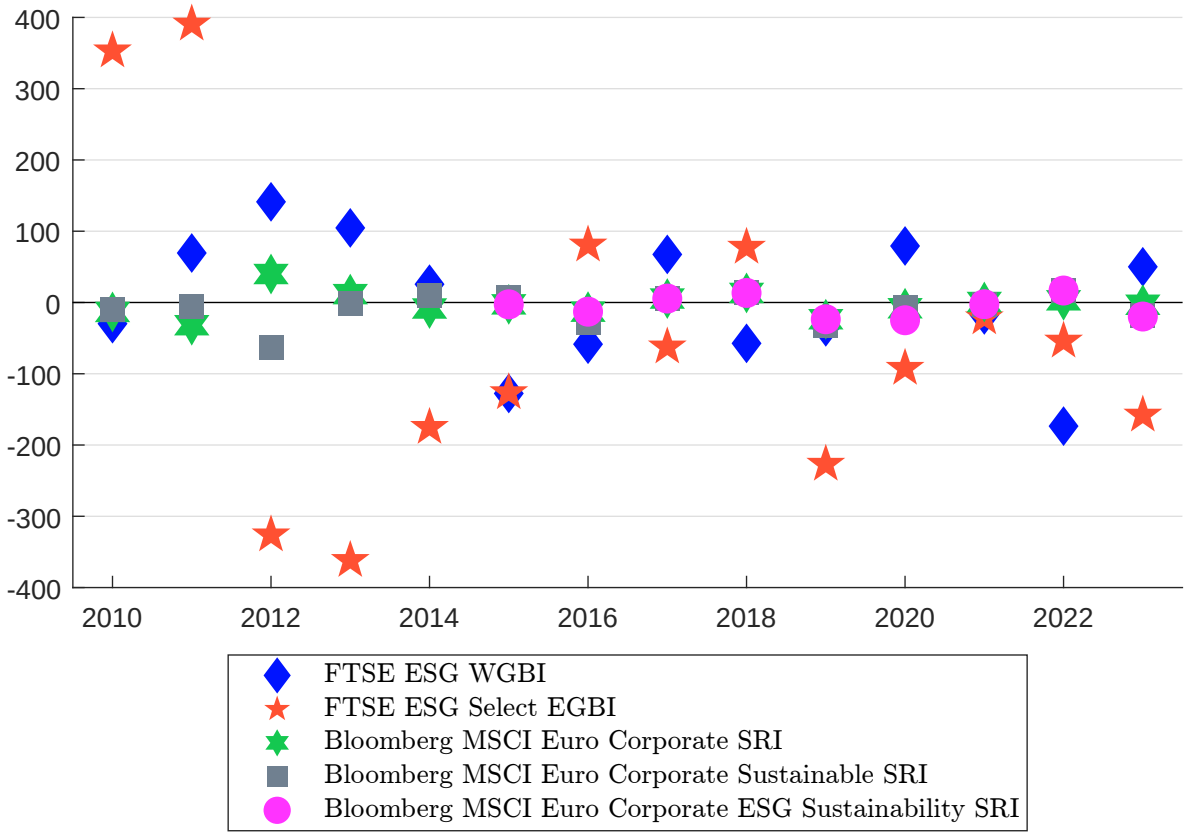


Source: FTSE, Bloomberg & Author's calculations.

[29]For the FTSE WGBI and EGBI, we use the FTSE ESG World Government Bond and FTSE ESG Select EMU Government Bond indexes. For the Bloomberg Euro Aggregate Corporate TR Index, we use the MSCI Euro Corporate SRI TR Index (SRI), the Bloomberg MSCI Euro Corporate Sustainable SRI TR Index (S-SRI), and the Bloomberg MSCI Euro Corporate ESG Sustainability SRI (ESG-S). For the Bloomberg Euro Aggregate Corporate TR Index, we use the MSCI Euro Corporate SRI TR Index (SRI), the Bloomberg MSCI Euro Corporate Sustainable SRI TR Index (S-SRI), and the Bloomberg MSCI Euro Corporate ESG Sustainability SRI (ESG-S). For the Bloomberg US Corporate TR Index, the comparison is done to the Bloomberg MSCI US Corporate SRI Select Index (SRI), the Bloomberg MSCI US Corporate Sustainability SRI Index (S-SRI) and the Bloomberg MSCI US Corporate ESG Sustainability SRI (ESG-S). Finally, the Bloomberg Global High Yield Total Return Index is compared to the Bloomberg MSCI Global High Yield SRI Index (SRI) and the Bloomberg MSCI Global High Yield Sustainability Index (SUS).

[30]The relationship between ESG and credit ratings is explored on page 213.

## 3.3 Cost of capital

While the previous two sections focused on the impact of ESG investing on returns, here we focus on the cost of capital. The cost of capital is the cost to a company of financing its operations. It represents the required rate of return that investors expect to receive for providing capital to the company, whether in the form of debt or equity. It is therefore the minimum rate of return that a company must achieve to justify its investments. The cost of capital has two components. The cost of debt is the interest rate a company pays on its borrowed funds, while the cost of equity is the return on equity investors require to compensate them for the risk they take by investing in the company's stock. In general, the weighted average cost of capital (WACC) is the most common method of determining a company's total cost of capital, taking into account the proportional weight of debt and equity in its capital structure:

$$\mathcal{WACC} = \frac{E}{E+D}\mathcal{C}_E + \frac{D}{E+D}\mathcal{C}_D\,(1-\tau_c)$$

where $\mathcal{WACC}$ is the weighted average cost of capital, $\mathcal{C}_E$ is the cost of equity, $\mathcal{C}_D$ is the cost of debt, $E$ is the market value of the firm's equity, $D$ is the market value of the firm's debt, and $\tau_c$ is the corporate tax rate.

The question is whether there is a relationship between ESG investing and the cost of capital. In fact, we can assume that there are several channels, at least two. The first is that the extra-financial information contained in ESG scores is value-added information that helps distinguish best-in-class companies from worst-in-class companies in terms of corporate financial performance. In this context, companies with higher ESG scores must have a lower cost of capital. The second channel is again the supply/demand balance between issuers and investors. The preference of ESG investors is to finance issuers with higher ESG scores, implying that ESG investors require a lower cost of capital for best-in-class companies than non-ESG investors. To answer the previous question, we postulate a relationship between the cost of capital and some ESG metrics. In general, we use linear regression:

$$y_{i,t} = \alpha + \underbrace{\beta x_{i,t}}_{\text{ESG metric}} + \underbrace{\sum_{k=1}^{n_z} \gamma_k z_{i,t}^{(k)}}_{\text{Control variables}} + \varepsilon_{i,t} \tag{3.19}$$

where $y_{i,t}$ is the endogenous variable that depends on the cost of capital of company $i$ at time $t$, $x_{i,t}$ is the ESG metric and $z_{i,t}^{(k)}$ is a set of control variables. The previous model can be extended to multiple ESG metrics and we obtain the following multi-factor regression model:

$$y_{i,t} = \alpha + \underbrace{\sum_{j=1}^{n_x} \beta_j x_{i,t}^{(j)}}_{\text{ESG variables}} + \underbrace{\sum_{k=1}^{n_z} \gamma_k z_{i,t}^{(k)}}_{\text{Control variables}} + \varepsilon_{i,t} \tag{3.20}$$

To test that the cost of capital is a decreasing function of the ESG variable $x_{i,t}^{(j)}$, we assume that $\beta_j < 0$. The choice of the dependent variable, the ESG variables, and the control variables is important and varies across studies.

### 3.3.1 Cost of equity

Sharfman and Fernando (2008) is a landmark study in the area of whether CSR performance has an impact on a company's cost of capital. Using a sample of 267 S&P 500 companies, the authors test three hypotheses:

$\mathcal{H}_1$ The higher the level of environmental risk management, the lower the firm's cost of debt capital for a given level of debt.

$\mathcal{H}_2$ The higher the level of environmental risk management, the lower the cost of equity capital.

$\mathcal{H}_3$ The higher the level of environmental risk management, the lower the firm's weighted average cost of capital.

The cost of equity capital is estimated using the CAPM:

$$\mathcal{C}_E = r + \beta\,(\mu_m - r)$$

where $\pi_m = \mu_m - r$ is the market risk premium, $r$ is the risk-free return and $\beta$ is the systematic risk coefficient (firm's beta with respect to the market portfolio). The cost of debt is estimated using the firm's marginal cost of borrowing from the Bloomberg Financial dataset. The ESG variable is the level of environmental risk management, which is given by an environmental score from the ESG rating agency KLD[31]. Finally, Sharfman and Fernando (2008) use three control variables, which are the firm's financial leverage, the logarithm of market capitalization, and industry membership (dummy variables). The linear regression is then:

$$y_{i,t} = \alpha + \beta \boldsymbol{\mathcal{S}}_{i,t} + \gamma_1 L_{i,t} + \gamma_2 M_{i,t} + \gamma_3 I_{i,t} + \varepsilon_{i,t}$$

where $y_{i,t}$ is one of the cost of capital measures ($\mathcal{C}_E$, $\mathcal{C}_D$ and $\mathcal{WACC}$), $(L_{i,t}, M_{i,t}, I_{i,t})$ are the three control variables, and $\boldsymbol{\mathcal{S}}_{i,t}$ is the environmental score. Sharfman and Fernando (2008) found that $\hat{\beta}$ has a positive sign for $\mathcal{C}_D$ and a negative sign for $\mathcal{C}_E$ and $\mathcal{WACC}$. They concluded that the level of environmental risk management increases the cost of debt and decreases the cost of equity and the weighted average cost of capital.

Another seminal study is El Ghoul *et al.* (2011), who test the relationship on a larger investment universe: 12 915 observations representing 2 809 unique firms between 1992 and 2007. They use four different models to estimate the cost of equity[32]: Claus-Thomas, Gebhardt-Lee-Swaminathan, Ohlson-Juettner-Nauroth, and Easton. The control variables include the stock's beta, size (log of total assets), book-to-market ratio, leverage (ratio of total debt to market value of equity), average long-run growth forecast, and dispersion of analyst forecasts. For the ESG variables, they use a large panel of KLD scores: (1) community, (2) diversity, (3) employee relations, (4) environment, (5) human rights and (6) product. They also consider an aggregate score, the CSR score, which is the sum of the community, diversity, employee relations, environment, human rights, and product characteristics scores. In addition to these ESG variables, they also construct controversial dummy variables related to alcohol, gambling, tobacco, firearms, military and nuclear activities. The univariate regression analysis is performed on the aggregate CSR score. El Ghoul *et al.* (2011) found that the average cost of equity for firms with a high CSR score is 56 basis points lower than for firms with a low CSR score. These results suggest that firms with better CSR scores have significantly lower cost of equity capital. They then conduct a multivariate regression analysis including the six dimensions of KLD social performance. They find that the employee relations, environmental policy, and product strategy dimensions contribute to lower firms' cost of equity, while the other three dimensions (community, diversity, and human rights) do not. In terms of controversies, they confirm the findings of Hong and Kacperczyk (2009) that the tobacco and nuclear power industries have higher equity financing costs.

[31] See page 26 for more details on KLD.
[32] The cost of equity formulas are described in Box 3.8.

Box 3.8: Cost of equity measurement

The cost of equity is the "*expected rate of return that the market requires in order to attract funds to a particular investment*" (Pratt and Grabowski, 2008). There are several ways to calculate it. One approach is to calculate the expected return $\mathbb{E}[R_t]$ of the stock from an asset pricing model (*e.g.*, CAPM, Fama-French model) and use $\mathbb{E}[R_t]$ as a proxy for $\mathcal{C}_E$. The second approach is to use a valuation model, such as the discounted cash flow (DCF) model or the dividend discount model (DDM). Recall that the price of a financial asset is the expected value of the stochastic discounted value of the cash flow leg. Under some assumptions (Roncalli, 2020a, chapter 3), we can show that:

$$P(t) = \sum_{t_m > t} B(t, t_m)\, \mathbb{E}[\mathrm{CF}(t_m) \mid \mathcal{F}_t]$$

where $\mathcal{F}_t$ is the filtration under the risk-neutral probability measure $\mathbb{Q}$, $B(t, t_m)$ is the discount factor for the maturity date $t_m$ and $\{\mathrm{CF}(t_m), t_m \geq t\}$ is the stream of stochastic cash flows. Let $\varrho$ be the constant discount rate such that:

$$P(t) = \sum_{t_m > t} \frac{\mathbb{E}[\mathrm{CF}(t_m) \mid \mathcal{F}_t]}{(1+\varrho)^{(t_m - t)}}$$

In the case of stocks, $\mathrm{CF}(t)$ is the earnings or dividends per share, and $\mathcal{C}_E$ is then equal to the discount rate $\varrho$. Below are some common formulas for calculating the cost of equity:

- In the CAPM, the cost of equity is equal to the expected rate of return:

$$\mathcal{C}_E = r + \beta(\mu_m - r) \tag{3.21}$$

  where $\pi_m = \mu_m - r$ is the market risk premium, $r$ is the risk-free rate and $\beta$ is the beta of the stock return relative to the market portfolio return. Once we have assumed a value for $\pi_m$, we can easily calculate $\mathcal{C}_E$ using the estimated beta coefficient.

- The Gordon growth model uses the dividend discount model and assumes that $\mathrm{DPS}(t_m) = (1+g)^{(t_m - t)}\, \mathrm{DPS}(t)$ is the dividend per share at time $t_m$ and $g$ is the growth rate. We deduce that:

$$P(t) = \sum_{t_m = t+1}^{\infty} \frac{\mathrm{DPS}(t_m)}{(1+\varrho)^{(t_m - t)}} = \mathrm{DPS}(t) \sum_{t_m = t+1}^{\infty} \frac{(1+g)^{(t_m - t)}}{(1+\varrho)^{(t_m - t)}} = \mathrm{DPS}(t)\, \frac{1+g}{\varrho - g}$$

  Since $\mathrm{DPS}(t+1) = (1+g)\,\mathrm{DPS}(t)$, we conclude that:

$$\mathcal{C}_E := \varrho = g + \mathrm{EDY} \tag{3.22}$$

  where $\mathrm{EDY} = \mathrm{DPS}(t+1)/P(t)$ is the expected one-year ahead dividend yield.

- The previous model can be extended by considering expected cash flows instead of dividends up to time $t^\star$ and assuming a period of constant growth after $t^\star$:

$$P(t) = \sum_{t_m = t+1}^{t^\star} \frac{\mathrm{CF}(t_m)}{(1+\varrho)^{(t_m - t)}} + \frac{(1+g)\,\mathrm{CF}(t^\star)}{(\varrho - g)\,(1+r)^{(t^\star - t)}} \tag{3.23}$$

Box 3.8: Cost of equity measurement (continued)

- Claus and Thomas (2001) develop a residual income model by assuming that $\text{CF}(t+n) = \text{EPS}(t+n) - \varrho\,\text{BPS}(t+n-1)$ and $\text{BPS}(t+n) = \text{BPS}(t+n-1) + \text{EPS}(t+n) - \text{DPS}(t+n)$ where $\text{EPS}(t+n)$, $\text{BPS}(t+n)$ and $\text{DPS}(t+n)$ are expected $n$-year ahead earnings per share, book value per share and dividend per share, respectively. By assuming a dividend policy, for example $\text{DPS}(t+n) = \delta\,\text{EPS}(t+n)$ where $\delta \geq 0$ is the dividend payout ratio, we can calculate all quantities and find the numerical solution $\varrho$ of the following equation:

$$P(t) = \text{BPS}(t) + \sum_{t_m=t+1}^{t^\star} \frac{\text{CF}(t_m)}{(1+\varrho)^{(t_m-t)}} + \frac{(1+g)\,\text{CF}(t^\star)}{(\varrho-g)\,(1+r)^{(t^\star-t)}} \tag{3.24}$$

- The model defined by Gebhardt *et al.* (2001) is close to the one proposed by Claus and Thomas (2001). We have:

$$P(t) = \text{BPS}(t) + \sum_{t_m=t+1}^{t^\star} \frac{(\text{ROE}(t_m) - \varrho)\,\text{BPS}(t_m-1)}{(1+\varrho)^{(t_m-t)}} + \frac{(\text{ROE}(t^\star+1) - \varrho)\,\text{BPS}(t^\star)}{\varrho\,(1+\varrho)^{(t^\star-t)}} \tag{3.25}$$

  where $\text{ROE}(t+n)$ is the expected return on equity and $\text{BPS}(t+n)$ is the expected book value per share satisfying the recurrence relationship $\text{BPS}(t+n) = \text{BPS}(t+n-1) + \text{EPS}(t+n) - \text{DPS}(t+n)$.

- Ohlson and Juettner-Nauroth (2005) suggest valuing stocks using the following formula:

$$P(t) = \frac{\text{EPS}(t+1)}{\varrho} + \frac{\text{EPS}(t+2) - \text{EPS}(t+1) - \varrho\,(\text{EPS}(t+1) - \text{DPS}(t+1))}{\varrho\,(\varrho-g)}$$

  where $\text{EPS}(t+n)$ and $\text{DPS}(t+n)$ are the expected $n$-year ahead earnings per share and dividends per share. Gode and Mohanram (2003) show that the cost of equity is equal to:

$$\mathcal{C}_E = A + \sqrt{A^2 + \frac{\text{EPS}(t+1)}{P(t)}\,(g'-g)} \tag{3.26}$$

  where $A = \frac{1}{2}\left(g + \frac{\text{DPS}(t+1)}{P(t)}\right)$ and $g' = \frac{\text{EPS}(t+2) - \text{EPS}(t+1)}{\text{EPS}(t+1)}$. If $g' = g$, we retrieve the cost of capital in the Gordon model:

$$\mathcal{C}_E = 2A = g + \frac{\text{DPS}(t+1)}{P(t)}$$

- Using the model by Ohlson and Juettner-Nauroth (2005), Easton (2004) assumes that $g = 0$:

$$P(t) = \frac{\text{EPS}(t+2) + \varrho\,\text{DPS}(t+1) - \text{EPS}(t+1)}{\varrho^2} \tag{3.27}$$

Since the publication of these two seminal articles[33], much research has been done to confirm or refute these findings. A comprehensive review can be found in Coqueret (2022). In most cases, academics find a negative relationship between extra-financial risks and the cost of equity (Ng and Rezaee, 2015; Gupta, 2018; Albuquerque *et al.*, 2019). However, there are a few studies that conclude that there is no relationship or a weak relationship (Humphrey *et al.*, 2012; Gregory *et al.*, 2014). Focusing on the most recent studies, the vast majority suggest that a good ESG score reduces the cost of equity, but there are some differences across the three pillars (Gonçalves *et al.*, 2022; Khanchel and Lassoued, 2022; Ramirez *et al.*, 2022). There is strong evidence that the relationship is negative for the E and G pillars, but not necessarily for the S pillar. For the environmental pillar, the carbon footprint measures used by investors also show such a negative relationship (Trinks *et al.*, 2022).

### 3.3.2 Cost of debt

The cost of debt is the effective interest rate that a company pays on its debt. It represents the cost to the company of borrowing funds through debt instruments such as bonds, loans, or lines of credit. There are several ways to measure it, but the most popular are the yield to maturity and credit spread for bonds, the marginal cost of borrowing for loans and lines of credit, and the credit rating. We have already seen that Sharfman and Fernando (2008) found a positive relationship between environmental risk management scores and the cost of debt. This finding is confirmed by Menz (2010), who examined the relationship between the valuation of Euro corporate bonds and corporate social responsibility (CSR) and concluded that "*CSR has apparently not yet been incorporated into the pricing of corporate bonds*". This overall neutrality, sometimes associated with a lack of maturity in the integration of ESG information into the bond market, has also been highlighted by Izzo and Magnanelli (2012).

On the contrary, Oikonomou *et al.* (2014) found that corporate social performance is rewarded in the corporate bond market. These authors use a procedure similar to the one described on page 209. They consider three dependent variables: the credit spread, the credit rating, and a dummy variable indicating whether the bond is speculative grade or not. The ESG variables are again several KLD scores. The control variables are divided into three categories: firm characteristics (firm size, interest coverage ratio, leverage, liquidity, market-to-book ratio, return on assets, research and development intensity, speculative dummy), bond characteristics (amount issued, convexity, duration, maturity) and sector characteristics (sector fixed effects). Bauer and Hann (2010), Attig *et al.* (2013), and Cooper (2015) also find a negative relationship between CSR and the cost of debt. Focusing on the most recent research, empirical studies generally conclude that firms with higher ESG scores benefit from lower cost of debt relative to firms with weaker ESG scores (Eliwa *et al.*, 2021; Raimo *et al.*, 2021; Apergis *et al.*, 2022).

Let us now see how we calculate the cost of debt in detail. According to Ben Slimane *et al.* (2019a), a typical linear regression model would look like this:

$$\ln s_{i,t} = \alpha_t + \beta \boldsymbol{\mathcal{S}}_{i,t} + \gamma_{md} \operatorname{MD}_{i,t} + \sum_{k=1}^{n_{\boldsymbol{\mathcal{S}}ector}} \gamma_{sector}(k)\, \boldsymbol{s}_{i,t}(k) + \sum_{k=1}^{n_{\mathcal{R}ating}} \gamma_{rating}(k)\, \mathcal{R}_{i,t}(k) + \varepsilon_{i,t} \tag{3.28}$$

where $s_{i,t}$ is the yield spread of bond $i$ at time $t$, $\boldsymbol{\mathcal{S}}_{i,t}$ is the ESG score, $\operatorname{MD}_{i,t}$ is the modified duration, $\boldsymbol{s}_{i,t}(k)$ is the dummy variable associated with the $k^{\text{th}}$ sector, $\mathcal{R}_{i,t}(k)$ is the dummy variable associated

[33] These are not the first two studies on the relationship between ESG and the cost of equity capital. For example, Skaife *et al.* (2004) and Derwall and Verwijmeren (2007) already showed that good governance reduces the cost of equity capital. Unfortunately, these two studies were never published.

Figure 3.39: Average ESG score by credit rating category (2010–2019)

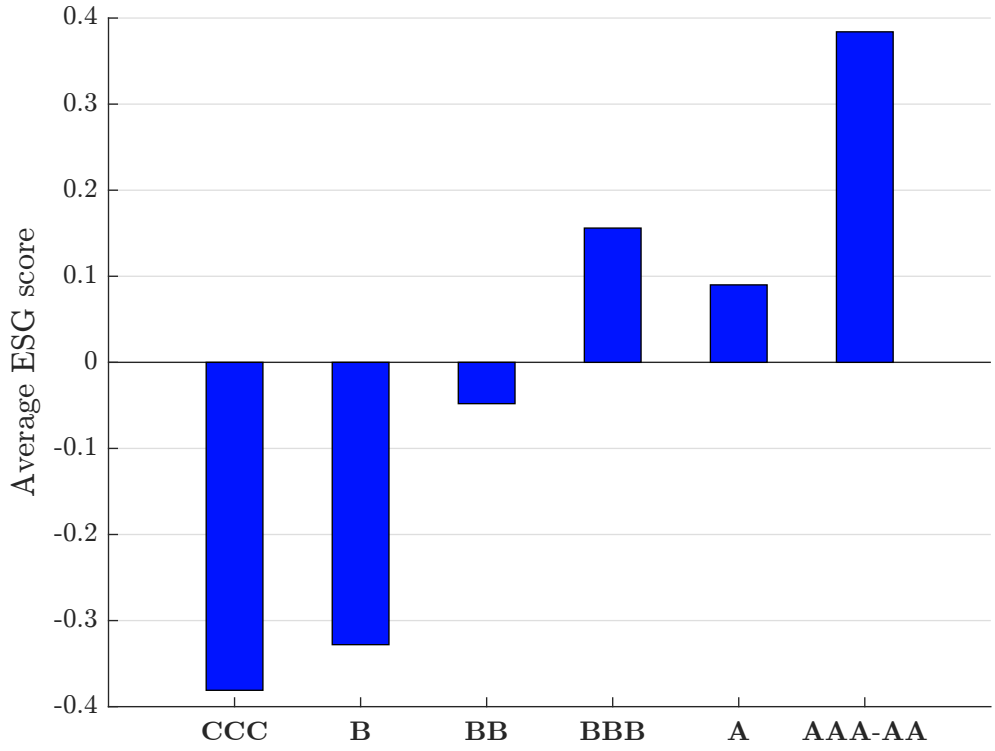


Source: Ben Slimane *et al.* (2019b, Figure 11, page 17).

with the $k^{\text{th}}$ rating and $\varepsilon_{i,t} \sim \mathcal{N}\left(0, \sigma^2\right)$. In this regression model, the control variables are modified duration and ratings (bond characteristics) and sectors (firm characteristics). It is important to include explanatory variables for the rating because there is a positive relationship between ESG ratings and credit ratings. To illustrate, Figure 3.39 shows the average ESG score by rating class[34]. Therefore, bonds with a good credit rating have a better ESG score than bonds with a poor credit rating. We reiterate that the ESG $z$-scores are between $-3$ and $+3$, which means that the mean of the ESG scores is zero while the standard deviation is one (Table 3.19). A Student's $t$-test shows that ESG scores by rating are statistically different from zero, except for the BB credit rating. ESG ratings and credit ratings are not independent. This is normal as rating agencies also include extra-financial risks in their credit ratings.

Table 3.19: ESG score relative to credit rating (2010–2019)

| Rating | Mean | Median | Stdev | Skewness | $t$-statistic |
|---|---|---|---|---|---|
| AA | 0.384 | 0.452 | 1.058 | −0.020 | 3.266 |
| A | 0.090 | 0.088 | 1.056 | 0.011 | 1.676 |
| BBB | 0.156 | 0.101 | 0.997 | 0.122 | 3.945 |
| BB | −0.048 | −0.109 | 1.002 | 0.131 | −0.795 |
| B | −0.328 | −0.414 | 0.957 | 0.196 | −4.534 |
| CCC | −0.381 | −0.394 | 1.095 | 0.129 | −2.525 |
| All ratings | 0.046 | 0.000 | 1.031 | 0.092 | 1.804 |

Source: Ben Slimane *et al.* (2019a, Table 11, page 22).

[34] We use the Amundi ESG $z$-scores for the period 2010–2019.

Table 3.20: Results of the panel data regression model (EUR IG corporate bonds, 2010–2019)

| | 2010–2013 | | | | 2014–2019 | | | |
|---|---|---|---|---|---|---|---|---|
| | ESG | E | S | G | ESG | E | S | G |
| $\mathfrak{R}^2$ (in %) | 60.0 | 59.4 | 59.5 | 60.3 | 66.3 | 65.0 | 65.2 | 64.6 |
| $\Delta\mathfrak{R}^2$ (in %) | 0.6 | 0.0 | 0.2 | 1.0 | 4.0 | 2.6 | 2.9 | 2.3 |
| $\hat{\beta}$ (in %) | −4.8 | −1.1 | −2.1 | −6.7 | −8.9 | −7.9 | −7.6 | −7.7 |
| $t$-statistic | −31.7 | −7.3 | −15.6 | −38.8 | −123.9 | −98.4 | 103.9 | −91.8 |

Source: Ben Slimane *et al.* (2019b, Table 2, page 18).

In Table 3.20, we report the results for the EUR IG universe obtained by Ben Slimane *et al.* (2019b). The coefficient of determination $\mathfrak{R}^2$ calculates the explanatory power of the model. It is relatively high at around 60% while the number of observations is around 192 000! We can also see that it has increased by an average of 6% over the period 2014–2019. The excess contribution represents the difference in $\mathfrak{R}^2$ between the regression with ESG score and the regression without ESG score. We observe that this excess contribution becomes significant after 2014. For example, it is +4.0% for the ESG score. Testing that the ESG score has a significant impact on the yield spread is equivalent to accepting the null hypothesis $\mathcal{H}_0 : \beta < 0$. For the ESG score and the period 2010–2013, we have $\hat{\beta} = -4.8\%$ and a $t$-statistic of −31.7. We therefore accept the null hypothesis. We also report the results for the three pillars E, S and G. All estimated betas are negative and significant at the 99% confidence level. The negative relationship between the score and the yield spread has also increased over the 2014–2019 period.

Table 3.21: Results of the panel data regression model (USD IG corporate bonds, 2010–2019)

| | 2010–2013 | | | | 2014–2019 | | | |
|---|---|---|---|---|---|---|---|---|
| | ESG | E | S | G | ESG | E | S | G |
| $\mathfrak{R}^2$ (in %) | 52.7 | 52.8 | 52.8 | 53.4 | 60.6 | 60.5 | 60.3 | 60.9 |
| $\Delta\mathfrak{R}^2$ (in %) | 0.0 | 0.2 | 0.2 | 0.7 | 0.3 | 0.2 | 0.0 | 0.7 |
| $\hat{\beta}$ (in %) | −0.3 | 2.7 | 2.6 | −7.5 | −3.7 | −3.1 | −0.0 | −6.3 |
| $t$-statistic | −2.1 | 19.3 | 20.6 | −43.0 | −47.7 | −39.6 | −0.4 | −73.2 |

Source: Ben Slimane *et al.* (2019b, Table 3, page 18).

If we look at the universe of USD IG corporate bonds, we get the results shown in Table 3.21. First, we see that the excess $\mathfrak{R}^2$ is low even for the most recent period. Second, only the G pillar has a negative sign in the first period. This is not the case for the most recent period. Indeed, the relationship between the score and the yield spread is negative and significant, except for the S pillar. Nevertheless, the relationship for USD IG corporate bonds is weaker that observed for EUR IG corporate bonds. These results illustrate that we can obtain a significant negative beta with a quasi zero variation of $\mathfrak{R}^2$. Therefore, we have to be careful in concluding that a negative value of $\beta$ implies a lower cost of debt.

The next step is to calculate the cost of debt, which is equal to the expected yield spread[35]:

$$\mathcal{C}_D = \mathbb{E}\left[s_i\right]$$

[35]We omit here the yield to maturity of the non-defaultable bond. This is not a problem as we generally analyze the cost of debt in terms of difference.

Using Equation (3.28), we get:

$$\mathcal{C}_D = \mathcal{C}_D\left(\text{MD}_i, \boldsymbol{s}_i, \mathcal{R}_i\right) \mathcal{C}_D\left(\boldsymbol{\mathcal{S}}_i\right)$$

where:

$$\mathcal{C}_D\left(\text{MD}_i, \boldsymbol{s}_i, \mathcal{R}_i\right) = \exp\left(\hat{\alpha} + \hat{\gamma}_{md}\,\text{MD}_i + \hat{\gamma}_{sector}\left(\boldsymbol{s}_i\right) + \hat{\gamma}_{rating}\left(\mathcal{R}_i\right) + \frac{1}{2}\hat{\sigma}^2\right)$$

and:

$$\mathcal{C}_D\left(\boldsymbol{\mathcal{S}}_i\right) = \exp\left(\hat{\beta}\,\boldsymbol{\mathcal{S}}_i\right)$$

The previous expression defines the cost of debt as the product of two factors. The first factor $\mathcal{C}_D\left(\text{MD}_i, \boldsymbol{s}_i, \mathcal{R}_i\right)$ is related to the control variables, while the second factor $\mathcal{C}_D\left(\boldsymbol{\mathcal{S}}_i\right)$ measures the impact of the ESG score. If the score is zero, $\mathcal{C}_D\left(\boldsymbol{\mathcal{S}}_i\right) = 1$ and $\mathcal{C}_D = \mathcal{C}_D\left(\text{MD}_i, \boldsymbol{s}_i, \mathcal{R}_i\right)$. In Figure 3.40, we show the relationship between the ESG score and the cost of debt when the base value is $\mathcal{C}_D\left(\text{MD}_i, \boldsymbol{s}_i, \mathcal{R}_i\right) = 4\%$. Very quickly, the impact of the ESG score is significant even if $\hat{\beta}$ is equal to $-1\%$. Suppose two companies issue two bonds with the same characteristics (same maturity, same sector, same rating), but they have two different ESG scores, then the difference in terms of cost of debt is equal to:

$$\Delta\mathcal{C}_D = \bar{\mathcal{C}}_D\left(e^{\hat{\beta}\boldsymbol{\mathcal{S}}_1} - e^{\hat{\beta}\boldsymbol{\mathcal{S}}_2}\right)$$

where $\bar{\mathcal{C}}_D$ is the average cost of debt (or the cost of debt if the ESG score is zero). For example, if one company has an ESG score of $-2$ and another company has an ESG score of $+1$, the difference in cost of debt is[36] 36 bps if $\hat{\beta} = -3\%$ and $\bar{\mathcal{C}}_D = 4\%$.

Figure 3.40: Relationship between ESG score and cost of debt ($\bar{\mathcal{C}}_D = 4\%$)

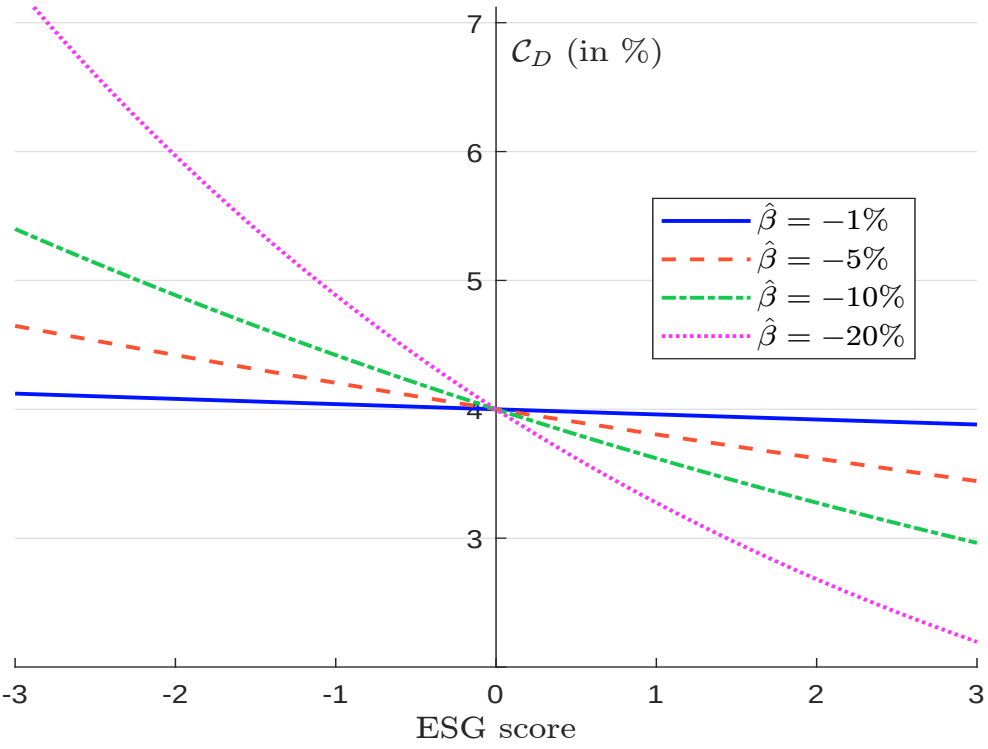


[36] We have $\Delta\mathcal{C}_D = 4\% \times \left(\exp\left(2 \times 3\%\right) - \exp\left(-1 \times 3\%\right)\right) = 0.0036$.

**Remark 41** *This methodology has been used by Ben Slimane et al. (2019a). For EUR IG corporate bonds, they found that one unit of ESG score implies an average reduction in yield spread of 9 bps after neutralizing the effects of credit rating, duration and sector. This means that the difference in the yield spread between a best-in-class company and a worst-in-class company is 31 bps on average. For USD IGs, the spread is 15 bps, which is half the spread observed for EUR IGs.*

### 3.3.3 The case of sovereign issuers

ESG rating agencies provide extra-financial information that may seem completely different from the financial information provided by credit rating agencies. However, the opposition between extra-financial and fundamental analysis is more complicated than it sounds, as we have seen in the case of corporate bonds. Rather than opposing each other, ESG and credit analysis can be seen as complementary. This is even more true in the case of sovereign risk, because a country's creditworthiness is highly dependent on its economic growth, political environment, willingness to pay its debts, social stability, etc., and we can easily relate these factors to ESG pillars. In fact, there is a large body of economic literature that examines the interrelationship between sovereign credit risk, economic development, environmental resources, social welfare, and governance (Alesina *et al.*, 1996). For example, country risk and sovereign credit risk are interrelated and highly dependent on political risk, which can be measured by governance (and social) indicators. In the academic literature, many research articles have been written to compare economic growth between two regions. Known as "*A Tale of Two Countries*", they generally highlight how institutions, governance, and political uncertainties affect economic development and financial performance (Lucas, 1993; Henry and Miller, 2009). Similarly, we can relate country risk to some social issues such as education, social infrastructure, democratic institutions, social inequality, etc. Finally, the environmental pillar also plays an important role due to climatic conditions, natural resources, water stress or climate change. These extra-financial risks affect not only a country's economy, but also its funding cost[37].

To assess the impact of sustainability on sovereign borrowing costs, analyses have often been conducted using either E, S, and G scores or the global ESG score. For example, Crifo *et al.* (2017) and Capelle-Blancard *et al.* (2019) found that countries with higher ESG ratings face lower bond yield spreads. However, there is no consensus in the literature on the "*winning pillar*". On the one hand, Capelle-Blancard *et al.* (2019) found that the environmental pillar is not priced in, while governance is more important than social in reducing borrowing costs. On the other hand, Martellini and Vallée (2016) found a negative relationship between environmental rating and bond yield spread. However, many studies focus mainly on developed markets. Using a larger set of countries, Dudás and Naffa (2020) found a negative relationship between ESG rating and cost of debt, highlighting the time-varying importance of ESG factors in their results, as well as the different effects across country income groups. In fact, they demonstrated the increasing importance of the environmental pillar in recent years, although the social and governance pillars remain the most important drivers of sovereign risk premia, except for low-income countries where some environmental variables dominate. Regarding the social pillar alone, Semet (2020) showed that income inequality tends to increase sovereign yield spreads, although the effect may be peculiar to developed countries. Martellini and Vallée (2016) also reported that a good social rating is associated with a reduction in emerging market bond spreads. Working with CDS spreads on a sample of developed and emerging markets, Hübel (2022) finds that higher ESG ratings are associated with lower CDS spreads. He also highlights that governance has a greater impact on a sovereign's short-term creditworthiness than the environmental and social pillars that are priced into longer-term CDS.

[37] Semet *et al.* (2021) provide a literature review on these various topics.

Semet *et al.* (2021) uses data from Verisk and supplements it with databases from the World Bank and the United Nations. In total, they test 269 ESG indicators across 26 themes, of which 100 are related to the environmental pillar, 83 to the social pillar and 86 to the governance pillar. The 26 themes are:

- **E** biodiversity, climate change, commitment to environmental standards, energy mix, natural hazard, natural hazard outcome, non-renewable energy resources, temperature, water management;
- **S** civil unrest, demographics, education, gender, health, human rights, income, labour market standards, migration, water and electricity access;
- **G** business environment and R&D, governance effectiveness, infrastructure and mobility, international relations, justice, national security, political stability.

On the financial data side, they consider generic 10 year government bond yields from Bloomberg and Eikon-Datastream, while macroeconomic variables are extracted from the IMF and World Bank databases. The analysis covers the period 2015-2020 and 67 countries. Using the pooling method, they estimate the following baseline model[38]:

$$\begin{aligned}\ln(s_{i,t}+1\%) &= \underset{(0.1349)}{1.9477^{***}} + \underset{(0.0125)}{0.0838^{***}} g_{i,t} + \underset{(0.0065)}{0.0524^{***}} \pi_{i,t} - \underset{(0.0007)}{0.0006} d_{i,t} - \\ &\quad \underset{(0.0054)}{0.0332^{***}} ca_{i,t} + \underset{(0.0082)}{0.0275^{***}} ra_{i,t} - \underset{(0.0012)}{0.0166^{***}} \mathcal{R}_{i,t} + \varepsilon_{i,t} \end{aligned} \tag{3.29}$$

where $s_{i,t}$ is the bond yield spread of country $i$ at time $t$, $g_{i,t}$ corresponds to the growth rate of the gross domestic product, the inflation variable $\pi_{i,t}$ refers to the percentage change of the consumer price index, the debt variable $d_{i,t}$ measures the ratio between the gross debt and the GDP of the country, $ca_{i,t}$ is the current account balance in percent of GDP, $ra_{i,t}$ corresponds to the reserve adequacy and $\mathcal{R}_{i,t}$ is a composite credit score computed as the average credit rating from three credit rating agencies (S&P, Moody's and Fitch). The baseline model has a total $\mathfrak{R}_c^2$ of 70% and can be interpreted as the result of fundamental analysis.

The previous model can be cast in Models (3.19) and (3.20) by setting $y_{i,t} = \ln(s_{i,t}+1\%)$ and $\sum_{k=1}^{6} \gamma_k z_{i,t}^{(k)} = \gamma_1 g_{i,t} + \gamma_2 \pi_{i,t} + \gamma_3 d_{i,t} + \gamma_4 ca_{i,t} + \gamma_5 ra_{i,t} + \gamma_6 \mathcal{R}_{i,t}$. Since the list of the 269 ESG variables is large, Semet *et al.* (2021) first performs a single-factor analysis using linear regression (3.19) and selects the ESG variables that have an estimated value $\hat{\beta}$ that is significant at the 99% confidence level. They find 184 significant variables. In Table 3.22, we report the seven most relevant variables by pillar. $\Delta\mathfrak{R}_c^2$ indicates the difference in $\mathfrak{R}_c^2$ between the regression with the ESG variable and the regression without the ESG variable. For example, the most relevant variable is freedom of assembly, which adds 8.74% of explanatory variable, which means that the coefficient of determination $\mathfrak{R}_c^2$ of the linear regression with the 7 variables is 78.74%. We recall that $\mathfrak{R}_c^2$ is 70% for the baseline model with the six control variables.

This single-factor analysis shows that all 26 ESG themes selected represent metrics that have an impact on determining a country's creditworthiness, confirming that investors integrate extra-financial criteria into bond pricing. However, some themes are more relevant than others (Table 3.23). For example, three themes that have been extensively studied and highlighted by academics as important factors for their impact on the cost of sovereign debt are less relevant. These are income, education, and political stability.

[38] Below each estimate $\hat{\gamma}_k$, the corresponding standard error $\sigma(\hat{\gamma}_k)$ is reported in parentheses.

Table 3.22: The 7 most relevant variables of the single-factor analysis by pillar

| Pillar | Theme | Variable | $\Delta\mathfrak{R}^2_c$ |
|---|---|---|---|
| E | Climate change | Climate change vulnerability (acute) | 5.51% |
| | Climate change | Climate change exposure (extreme) | 4.80% |
| | Water management | Agricultural water withdrawal | 4.02% |
| | Climate change | Climate change sensitivity (acute) | 3.95% |
| | Biodiversity | Biodiversity threatening score | 3.53% |
| | Climate change | Climate change exposure (acute) | 3.39% |
| | Climate change | Climate change vulnerability (average) | 3.11% |
| S | Human rights | Freedom of assembly | 8.74% |
| | Human rights | Extent of arbitrary unrest | 8.04% |
| | Human rights | Extent of torture and ill treatment | 7.63% |
| | Labour market standards | Severity of working time violations | 7.21% |
| | Labour market standards | Forced labour violations (extent) | 6.10% |
| | Labour market standards | Child labour (extent) | 5.83% |
| | Migration | Vulnerability of migrant workers | 5.83% |
| G | National security | Severity of kidnappings | 6.80% |
| | Business environment and R&D | Ease of access to loans | 6.77% |
| | Infrastructure and mobility | Roads km | 6.45% |
| | Business environment and R&D | Capacity for innovation | 5.65% |
| | Business environment and R&D | Ethical behaviour of firms | 5.37% |
| | National security | Frequency of kidnappings | 5.27% |
| | Infrastructure and mobility | Physical connectivity | 4.94% |

Source: Semet *et al.* (2021, Section 3.3, pages 12-24).

Table 3.23: Summary of the single-factor analysis

| Relevance | E | S | G |
|---|---|---|---|
| High | Temperature<br>Climate change<br>Natural hazard outcome | Labour market standards<br>Human rights<br>Migration | Infrastructure and mobility<br>National security<br>Justice |
| Low | Water management<br>Energy mix | Income<br>Education<br>Water and electricity access | Political stability |

Source: Semet *et al.* (2021).

The statistical analysis shows that the 184 significant variables are highly correlated, especially variables within a given theme. These colinearity problems and the large number of explanatory variables do not allow the construction of a multivariate regression model. Therefore, the authors perform a lasso regression with the 184 variables in order to keep the 7 more meaningful variables per pillar in a multivariate framework. The results are presented below in order of importance:

- E total GHG emissions (non-renewable energy resources), biodiversity threatening score (biodiversity), severe storm hazard (high extreme) (natural hazard), temperature change (temperature), fossil fuel intensity of the economy (non-renewable energy resources), drought hazard (high extreme) (natural hazard), Paris Agreement (commitment to environmental standards);

(S) vulnerability of migrant workers (migration), projected population change (5 years) (demographics), frequency of civil unrest incidents (civil unrest), index of labor standards (labor market standards), right to join trade unions (protection) (labor market standards), food import security (human rights), average monthly wage (income);

(G) exporting across borders (cost) (international relationships), ethical behaviour of firms (business environment and R&D), severity of kidnappings (national security), capacity for innovation (business environment and R&D), physical connectivity (infrastructure and mobility), air transport departures (infrastructure and mobility), rail lines km (infrastructure and mobility).

Note that these selected variables are not necessarily the same as the selected variables in Table 3.22. The reason is that the multi-factor regression model takes into account the correlation patterns between the ESG variables. Therefore, it may be interesting to combine two or three ESG variables with lower explanatory power than to keep the best ESG variable. Finally, Semet *et al.* (2021) obtain the multi-factor model shown in Table 3.24. In addition to the six control variables, 7 ESG variables are significant in explaining the sovereign yield spread. Moreover, they have the right sign, which means that a higher value of these ESG variables reduces the cost of debt of countries. In terms of explanatory power, the coefficient of determination $\mathfrak{R}_c^2$ of this integrated model is 83.5%. The difference $\Delta\mathfrak{R}_c^2$ from the baseline model is then 13.5%.

Table 3.24: Final multi-factor model of sovereign bond yields

| Variable | $\hat{\beta}$ | $t$-student | $p$-value |
|---|---|---|---|
| Intercept $\alpha$ | 2.834 | 15.72*** | 0.00 |
| GDP growth $g_{i,t}$ | 0.017 | 1.37 | 0.17 |
| Inflation $\pi_{i,t}$ | 0.048 | 6.64*** | 0.00 |
| Debt ratio $d_{i,t}$ | −0.001 | −1.71* | 0.08 |
| Current account balance $ca_{i,t}$ | −0.012 | −2.45** | 0.01 |
| Reserve adequacy $ra_{i,t}$ | 0.005 | 0.74 | 0.45 |
| Rating score $\mathcal{R}_{i,t}$ | −0.013 | −9.08*** | 0.00 |
| Exporting across borders (cost) | $4.05e^{-4}$ | 4.11*** | 0.00 |
| Severe storm hazard (absolute high extreme) | −0.015 | −1.66* | 0.09 |
| Capacity for innovation | −0.004 | −4.99*** | 0.00 |
| Ethical behavior of firms | −0.061 | −2.79*** | 0.00 |
| Temperature change | −0.149 | −3.50*** | 0.00 |
| Severity of kidnappings | −0.032 | −4.25*** | 0.00 |
| Drought hazard (absolute high extreme) | $3.33e^{-8}$ | 2.60*** | 0.00 |

Source: Semet *et al.* (2021, Table 29, page 64).

While the single analysis shows that (S) and (G) variables are more important than (E) variables, the multi-factor analysis when the three pillars are combined shows a different picture. In fact, governance and environmental issues dominate social issues in a multivariate framework. However, this analysis does not take into account the heterogeneity of the 67 countries in terms of economic development. Semet *et al.* (2021) repeat the analysis by distinguishing between high-income and middle-income countries.

Focusing on high-income countries, the authors select the 21 most important ESG variables using the same lasso procedure as in the global analysis above. Figure 3.41 shows the pillar importance of these 21 factors. The graph shows that the winning pillar for the high-income group is the (E)

Figure 3.41: ESG pillar importance for high-income countries

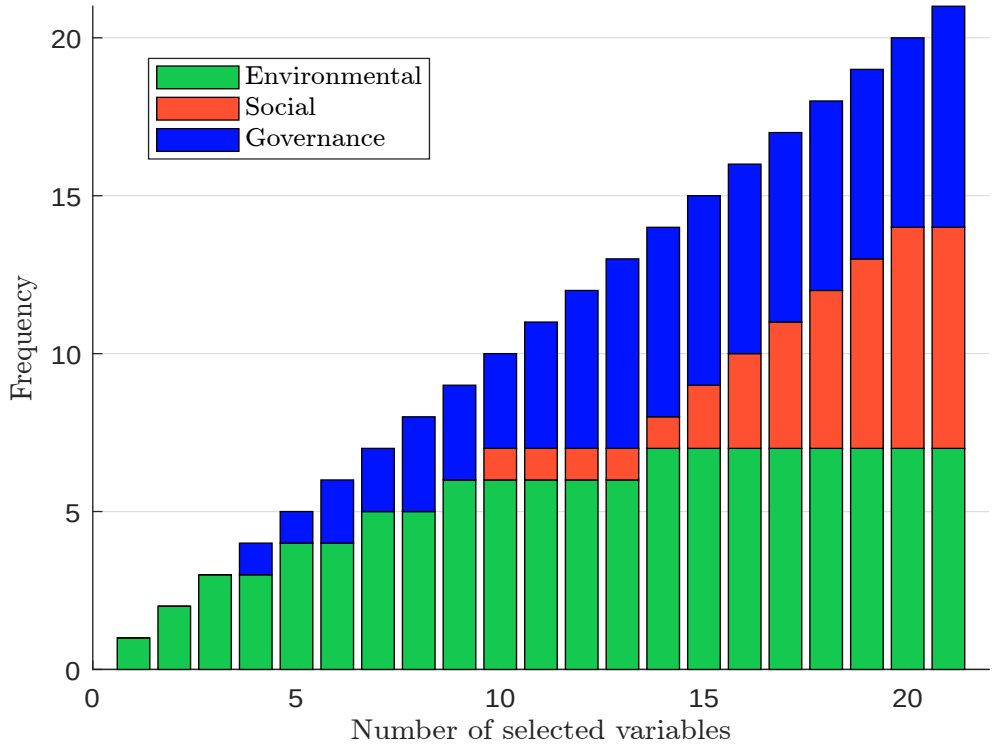


Source: Semet *et al.* (2021, Figure 11, page 40).

pillar. For example, if we had to choose only 9 indicators to explain the variation in government bond yields while controlling for economic effects, we would choose 3 governance indicators over 6 environmental indicators. The full set of environmental indicators is included in the model when the number of selected variables reaches 14 out of 21. The G pillar is also relevant for the sample of high-income countries. The first governance indicator selected in the model ranks fourth. Finally, we see that the S pillar is lagging behind, with none of the social indicators remaining in the list of seven variables. As a result, none of the social indicators seems to be relevant in explaining sovereign yield spreads in high-income countries. Given the set of indicators used in this analysis, these results suggest that environmental and governance issues dominate the ESG landscape in bond pricing. In Table 3.25, we present the first ten variables selected for the high-income group. The first ESG variable selected is the fossil fuel intensity of the economy. This result provides evidence of market integration of transition risk. The next two variables included in the model, temperature change and average annual cooling degree days, have odd curvatures that make them difficult to interpret. The fourth variable selected measures innovation capacity. This result suggests that countries that invest in R&D are rewarded by the market. This is the most critical governance indicator in the ESG landscape for sovereign bonds issued by high-income countries. The fifth and sixth selected variables are heat stress from the temperature theme and the severity of kidnappings, which can be understood as a proxy for a safe environment. Thus, national security is important to investors and ranks as the second most important issue in the governance pillar for high-income countries. Finally, the threat to biodiversity is also included in the model. This result suggests that the loss of biodiversity is under scrutiny by investors. Countries that act to preserve biodiversity may be rewarded with lower bond yield spreads.

Table 3.25: The most relevant variables of the multi-factor analysis (high-income vs. middle-income analysis)

| Category | Rank | Pillar | Variable |
|---|---|---|---|
| High income countries | 1 | E | Fossil fuel intensity of the economy |
| | 2 | E | Temperature change |
| | 3 | E | Cooling degree days annual average |
| | 4 | G | Capacity for innovation |
| | 5 | E | Heat stress (future) |
| | 6 | G | Severity of kidnappings |
| | 7 | E | Biodiversity threatening score |
| | 8 | G | Efficacy of corporate boards |
| | 9 | E | Total GHG emissions |
| | 10 | S | Significant marginalized group |
| Middle income countries | 1 | E | Tsunami hazard |
| | 2 | E | Transport infrastructure exposed to natural hazards |
| | 3 | G | Severity of kidnappings |
| | 4 | S | Discrimination based on LGBT status |
| | 5 | G | Air transport departures |
| | 6 | G | Exporting across borders (cost) |
| | 7 | S | Index of labour standards |
| | 8 | S | Vulnerability of migrant workers |
| | 9 | E | Paris Agreement |
| | 10 | G | Military expenditure (% of GDP) |

Source: Semet *et al.* (2021).

For the middle income group, the importance of the pillars is shown in Figure 3.42. We can clearly see the perfect balance between the pillars, as each colored bar gradually increases along a similar path. For example, if we only need to select 9 variables, we will take 3 from the E pillar, 3 from the S pillar, and 3 from the G pillar. In Table 3.25 we present the first ten variables selected for the middle income group found by Semet *et al.* (2021). The first indicator entered into the model is tsunami hazard, which represents the most significant physical risk to the creditworthiness of middle-income countries[39]. The second variable included in the model is transportation infrastructure exposed to natural hazards. Transportation disruptions caused by natural hazards can paralyze a country for months. Based on these two environmental indicators, we observe a gap between the two income groups. While the yields of high-income countries are sensitive to measures taken to address climate change, the yields of middle-income countries are more sensitive to the occurrence of extreme weather events and resilience to natural hazards. The third indicator selected by the lasso is the severity of kidnapping, the only metric common to both middle-income and high-income groups. It confirms the dominance of national security in the ESG landscape. The first social variable to enter the model is ranked fourth and measures the extent of discrimination based on a country's LGBT status. It reflects a fair integration of human rights in the country. The fifth variable selected is air travel. This would suggest that countries that

[39]The burden of tsunami hazard is borne mainly by countries in the Pacific and South Asian regions, where a significant proportion of middle-income countries are located.

rely on air travel as a means of exchange may face a higher risk of transition in the future. The sixth variable is the cost of exporting across borders. For middle-income countries, the lower the cost of exporting a container across borders, the lower the rate of return. This is a measure of a country's trade efficiency. The seventh variable is a labor standards index. Fair labor conditions are thus scrutinized by investors, reflecting an important ESG element for middle-income countries. We can also argue that labor rights violations in middle-income countries can lead to civil unrest and political violence, which can weaken creditworthiness.

Figure 3.42: ESG pillar importance for middle-income countries

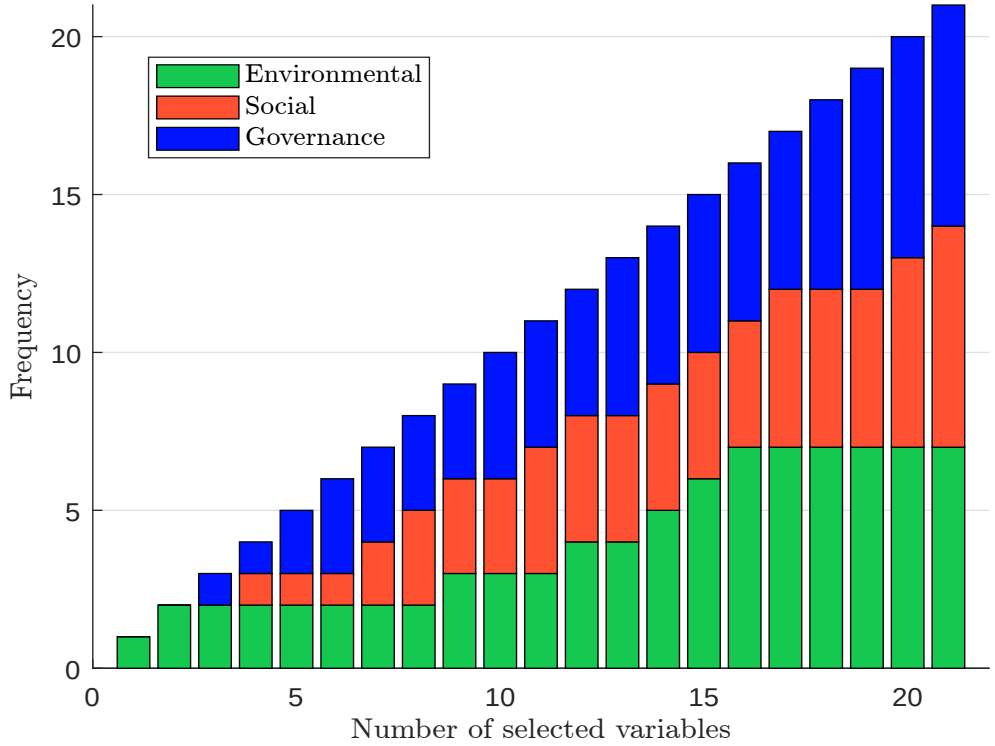


Source: Semet *et al.* (2021, Figure 13, page 43).

On page 213, we saw that ESG ratings and credit ratings are correlated when we look at companies. There is no reason why this should be any different when looking at countries. The rationale is as follows. We can assume that although rating agencies focus on financial criteria to assess a country's creditworthiness, they may inherently assess ESG performance as it can have a material impact on a country's solvency. Thus, extra-financial indicators could complement financial criteria in assessing a country's creditworthiness. This suggests that credit risk analysis cannot be separated from ESG considerations, thus invalidating the dichotomy between fundamental and extra-financial analysis. It could therefore be argued that social progress, environmental mitigation or governance effectiveness are cardinal factors in a country's creditworthiness. Semet *et al.* (2021) explores this issue by inferring credit ratings solely from extra-financial criteria to determine which ESG indicators are priced in by credit ating agencies. They model the probability $p_{i,t}$ of a country to be rated upper-grade by a logistic model:

$$p_{i,t} = \Pr\{\mathcal{R}_{i,t} \in \mathcal{UG}\} = \mathbf{F}\left(\beta_0 + \sum_{j=1}^{n_x} \beta_j x_{i,t}^{(j)}\right) \tag{3.30}$$

where $\mathcal{UG}$ is the set of upper grading ratings (from AAA to A−), $\mathcal{R}_{i,t}$ is the rating of country $i$ at

time $t$, $\mathbf{F}(z) = \dfrac{e^z}{1+e^z}$ is the cumulative function of the logistic distribution, and $x_{i,t}^{(j)}$ is the $j^{\text{th}}$ selected ESG variable. The coefficients $\beta_j$ are estimated using the maximum likelihood method. If the predicted probability $\hat{p}_{i,t}$ is greater than 50%, the country is classified in the upper-grade category. More specifically, Semet *et al.* (2021) use the following correspondence:

| Category | Rating | Probabilty range |
|---|---|---|
| Upper-grade | AAA | 83% – 100% |
| | AA | 67% – 82% |
| | A | 50% – 66% |
| Lower-grade | BBB | 39% – 49% |
| | BB | 29% – 38% |
| | B | 11% – 28% |
| | CCC | 0% – 10% |

For each pillar, the authors perform a lasso-logistic analysis to determine which seven indicators are more relevant in predicting a country's credit rating. They find the following variables[40]:

- **E** biodiversity threatening score, climate change vulnerability (average), domestic regulatory framework, energy self-sufficiency, wastewater treatment index, water import security (average), water intensity of the economy;
- **S** base pay/value added per worker, basic food stuffs net imports per person, food import security, health expenditure per capita, mean years of schooling of adults, public dissatisfaction with water quality, urban population change (5 years);
- **G** customs efficiency, enforcing a contract (time), getting electricity (time), government effectiveness index, paying tax (process), R&D expenditure (% of GDP), venture capital availability.

The coefficient of determination $\mathfrak{R}^2$ is 49.1%, 65.6% and 67.9% for the pillars **E**, **S** and **G**, respectively.

Combining the set of significant ESG indicators from the three pillars yields the results shown in Table 3.26. The parameters are reported in odds format ($\hat{\theta}_j = \exp\left(\hat{\beta}_j\right)$), while the $t$-student and $p$-value statistics correspond to the raw parameters $\hat{\beta}_j$. When the three pillars are mixed together, we note that the coefficient of determination increases significantly and reaches 91.1%. We also observe that some variables do not remain significant. In fact, only five (respectively seven) variables are statistically significant at 1% (respectively 5%). The environmental indicators disappear, confirming the weak power of the **E** pillar to predict sovereign ratings. These results confirm that governance and social dimensions are certainly at the forefront of rating agencies' analysis. We find that the indicator assessing (1) the average years of schooling of adults is particularly relevant to the analysis, as it has the highest $t$-student. The other important dimensions are (2) access to electricity, (3) urban population change, (4) availability of venture capital, and (5) food import security.

Figure 3.43 shows the model accuracy in predicting credit ratings for each rating group. Semet *et al.* (2021) note that the accuracy of the **G** pillar in predicting ratings is higher than that of the **E** or **S** pillars. They also note the perfect accuracy of the models in predicting sovereign ratings for the highest rating (AAA and AA), while BBB is the most difficult rating to predict.

[40] 5 variables are not significant at the 99% confidence level: energy self-sufficiency, wastewater treatment index, water intensity of the economy, customs efficiency and R&D expenditure (% of GDP).

Table 3.26: Estimated logistic model with the ESG selected variables

| Pillar | Variable | $\hat{\theta}_j$ | $t$-student | $p$-value |
|---|---|---|---|---|
| E | Domestic regulatory framework | 2.881 | 1.44 | 0.14 |
| | Climate change vulnerability (average) | 0.275 | −1.17 | 0.24 |
| | Water import security (average) | 0.717 | −0.50 | 0.61 |
| | Biodiversity threatening score | 1.029 | 0.14 | 0.88 |
| S | Health expenditure per capita | 0.998 | −1.10 | 0.26 |
| | Public dissatisfaction with water quality | 1.332 | 1.41 | 0.15 |
| | Mean years of schooling of adults | 68.298 | 3.37*** | 0.00 |
| | Base pay/value added per worker | 0.000 | −1.07 | 0.28 |
| | Urban population change (5 years) | 3.976 | 2.95*** | 0.00 |
| | Basic food stuffs net imports per person | 0.990 | −2.07** | 0.03 |
| | Food import security | 0.803 | −2.59*** | 0.00 |
| G | Government effectiveness index | 1.751 | 2.37** | 0.01 |
| | Venture capital availability | 1.099 | 2.93*** | 0.00 |
| | Enforcing a contract (time) | 0.999 | −0.31 | 0.75 |
| | Paying tax (process) | 0.846 | −1.47 | 0.14 |
| | Getting electricity (time) | 0.882 | −2.95*** | 0.00 |

Source: Semet *et al.* (2021).

Figure 3.43: Prediction accuracy of the logistic model

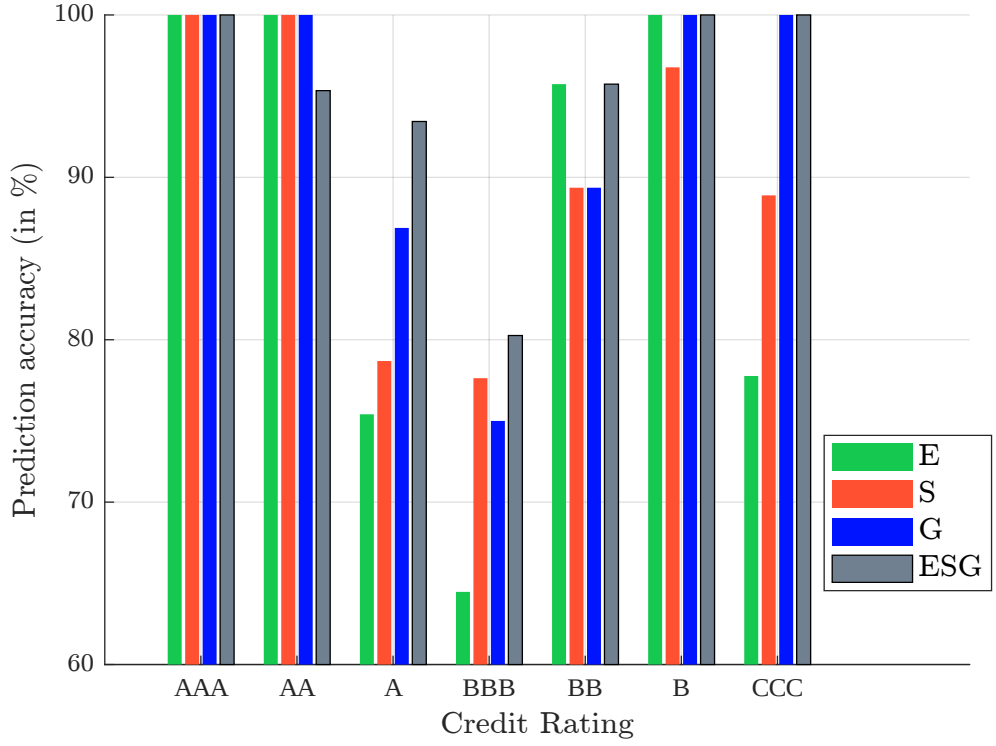


Source: Semet *et al.* (2021, Figure 13, page 43).

Table 3.27: Summary of the results found by Semet *et al.* (2021)

| What is directly priced in by the market? | What is indirectly priced in by credit rating agencies? |
|---|---|
| E ≻ G ≻ S | G ≻ S ≻ E |
| Significant market-based ESG indicators | ≠ Relevant CRA-based ESG indicators |
| • High-income countries<br>Transition risk ≻ Physical risk<br>• Middle-income countries<br>Physical risk ≻ Transition risk | E metrics are second-order variables:<br>• Environmental standards<br>• Water management<br>• Biodiversity<br>• Climate change |
| S matters for middle-income countries, especially for Gender inequality, Working conditions and Migration | Education, Demographics and Human rights are prominent indicators for the S pillar |
| National security, Infrastructure and mobility and International relationships are the relevant G metrics | Government effectiveness, Business environment and R&D dominate the G pillar |
| Fundamental analysis: $\mathfrak{R}_c^2 \approx 70\%$<br>Extra-financial analysis: $\Delta\mathfrak{R}_c^2 \approx 13.5\%$ | Accuracy $> 95\%$<br>AAA, AA, B, CCC ≻ A ≻ BB ≻ BBB |

Table 3.27 summarizes the results of Semet *et al.* (2021). The three pillars are not equally important when looking at the sovereign bond pricing. In fact, G and E dominate S. By refining the analysis to separate high- and middle-income countries, they conclude that environmental issues are indeed at the forefront of investors' concerns when assessing sovereign risk. However, they find a divergence between the two income groups. While sovereign yields in high-income countries are more related to the transition risk of climate change, they are more sensitive to the physical risk of climate change in middle-income countries. For high-income countries, S is chosen well after E and G. For middle-income countries, S is as important as G. They conclude that "*improvements in the identified ESG metrics induce lower borrowing costs for the sovereign issuer, but the importance of each pillar is a function of the country's level of development.*" Their analysis also shows that credit rating agencies integrate several classic S and G dimensions that are well documented in the academic literature. The authors point out that the set of metrics selected to predict ratings differs significantly from the set used to explain bond yields. This suggests that "*the market selects ESG metrics that are not already embedded in credit ratings to avoid double counting.*"

## 3.4 Exercises

### 3.4.1 Equity portfolio optimization with ESG scores

We consider the CAPM model:

$$R_i - r = \beta_i (R_m - r) + \varepsilon_i$$

where $R_i$ is the return of asset $i$, $R_m$ is the return of the market portfolio $w_m$, $r$ is the risk-free asset, $\beta_i$ is the beta of asset $i$ with respect to the market portfolio and $\varepsilon_i$ is the idiosyncratic risk of asset $i$. We have $R_m \perp \varepsilon_i$ and $\varepsilon_i \perp \varepsilon_j$. We note $\sigma_m$ the volatility of the market portfolio. Let $\tilde{\sigma}_i$, $\mu_i$ and $\boldsymbol{\mathcal{S}}_i$ be the idiosyncratic volatility, expected return and ESG score of asset $i$, respectively. We use a universe of 6 assets with the following parameter values:

| Asset $i$ | 1 | 2 | 3 | 4 | 5 | 6 |
|---|---|---|---|---|---|---|
| $\beta_i$ | 0.10 | 0.30 | 0.50 | 0.90 | 1.30 | 2.00 |
| $\tilde{\sigma}_i$ (in %) | 17.00 | 17.00 | 16.00 | 10.00 | 11.00 | 12.00 |
| $\mu_i$ (in %) | 1.50 | 2.50 | 3.50 | 5.50 | 7.50 | 11.00 |
| $\boldsymbol{\mathcal{S}}_i$ | 1.10 | 1.50 | 2.50 | −1.82 | −2.35 | −2.91 |

and $\sigma_m = 20\%$. The risk-free return $r$ is set to 1% and the expected return of the market portfolio $w_m$ is $\mu_m = 6\%$.

1. We assume that the CAPM is valid.
   (a) Compute the vector $\mu$ of expected returns.
   (b) Compute the covariance matrix $\Sigma$. Deduce the volatility $\sigma_i$ of asset $i$ and find the correlation matrix $\mathbb{C} = (\rho_{i,j})$ between asset returns.
   (c) Compute the tangency portfolio $w^*$. Calculate $\mu(w^*)$ and $\sigma(w^*)$. Deduce the Sharpe ratio and ESG score of the tangency portfolio.
   (d) Compute the beta coefficient $\beta_i(w^*)$ of the six assets with respect to the tangency portfolio $w^*$, and the implied expected return $\tilde{\mu}_i$:
   $$\tilde{\mu}_i = r + \beta_i(w^*)(\mu(w^*) - r)$$
   (e) Deduce the market portfolio $w_m$. Comment on the results.
2. We consider long-only portfolios and we also impose a minimum threshold $\boldsymbol{\mathcal{S}}^\star$ for the portfolio's ESG score:
   $$\boldsymbol{\mathcal{S}}(w) = w^\top \boldsymbol{\mathcal{S}} \geq \boldsymbol{\mathcal{S}}^\star$$
   (a) Let $\gamma$ be the risk tolerance. Write the mean-variance optimization problem.
   (b) Find the QP form of the MVO problem.
   (c) Compare the efficient frontier when (1) there is no ESG constraint ($\boldsymbol{\mathcal{S}}^\star = -\infty$), (2) we impose a positive ESG score ($\boldsymbol{\mathcal{S}}^\star = 0$) and (3) the minimum threshold is set to 0.5 ($\boldsymbol{\mathcal{S}}^\star = 0.5$). Comment on these results.
   (d) For each previous cases, find the tangency portfolio $w^*$ and the corresponding risk tolerance $\gamma^*$. Then compute $\mu(w^*)$, $\sigma(w^*)$, $\mathrm{SR}(w^* \mid r)$ and $\boldsymbol{\mathcal{S}}(w^*)$. Comment on these results.

(e) Draw the relationship between the minimum ESG score $\boldsymbol{\mathcal{S}}^\star$ and the Sharpe ratio $\mathrm{SR}(w^* \mid r)$ of the tangency portfolio.

(f) We assume that the market portfolio $w_m$ is the tangency portfolio when $\boldsymbol{\mathcal{S}}^\star = 0.5$.

i. Compute the beta coefficient $\beta_i(w_m)$ and the implied expected return $\tilde{\mu}_i(w_m)$ for each asset. Then derive the alpha return $\alpha_i$ of asset $i$. Comment on these results.

ii. Consider the equally-weighted portfolio $w_{\text{ew}}$. Compute its beta coefficient $\beta(w_{\text{ew}} \mid w_m)$, its implied expected return $\tilde{\mu}(w_{\text{ew}})$ and its alpha return $\alpha(w_{\text{ew}})$. Comment on these results.

3. The investor's goal is twofold. He wants to manage the tracking error risk of his portfolio relative to the benchmark $b = (15\%, 20\%, 19\%, 14\%, 15\%, 17\%)$ and have a better ESG score than the benchmark. However, this investor faces a long-only constraint because he cannot leverage his portfolio and he cannot short the assets.

(a) What is the ESG score of the benchmark?

(b) Assume the investor's portfolio is $w = (10\%, 10\%, 30\%, 20\%, 20\%, 10\%)$. Compute the excess score $\boldsymbol{\mathcal{S}}(w \mid b)$, the expected excess return $\mu(w \mid b)$, the tracking error volatility $\sigma(w \mid b)$ and the information ratio $\mathrm{IR}(w \mid b)$. Comment on these results.

(c) Same question with the portfolio $w = (10\%, 15\%, 30\%, 10\%, 15\%, 20\%)$.

(d) In the following, we assume that the investor does not have a return objective. In fact, the investor's objective is to improve the ESG score of the benchmark and to control the tracking error volatility. Let $\gamma$ be the risk tolerance. Give the corresponding esg-variance optimization problem.

(e) Find the matrix form of the corresponding QP problem.

(f) Plot the esg-variance efficient frontier $(\sigma(w^\star \mid b), \boldsymbol{\mathcal{S}}(w^\star \mid b))$ where $w^\star$ is an optimal portfolio.

(g) Find the optimal portfolio $w^\star$ when we target a given tracking error volatility $\sigma^\star$. The values of $\sigma^\star$ are 0%, 1%, 2%, 3% and 4%.

(h) Find the optimal portfolio $w^\star$ when we target a given excess score $\boldsymbol{\mathcal{S}}^\star$. The values of $\boldsymbol{\mathcal{S}}^\star$ are 0, 0.1, 0.2, 0.3 and 0.4.

(i) We want to compare the efficient frontier obtained in Question 3.f with the efficient frontier when we implement a best-in-class selection or a worst-in-class exclusion. The selection strategy consists of investing only in the three best ESG assets, while the exclusion strategy implies no exposure to the worst ESG asset. Plot the three efficient frontiers. Comment on these results.

(j) What minimum tracking error volatility must the investor accept to implement the best-in-class selection strategy? Give the corresponding optimal portfolio.

# Chapter 4

# Sustainable Financial Products

In the introduction, we saw that the market for ESG investments reached approximately $30 trillion in 2022, according to the Global Sustainable Investment Alliance (GSIA, 2023). This figure represents all ESG investments managed by asset owners and managers, regardless of the type or format of the investment. Therefore, a large portion of these investments represent assets managed internally by asset owners or private mandates given by institutional investors to asset managers. In this chapter, we focus on sustainable financial products that are distributed through public investment vehicles in the financial markets. These investments fall into three main families of financial products. The first category corresponds to sustainable mutual funds. While mutual funds are well defined from a legal perspective, sustainable mutual funds are more of a category within the mutual fund industry. This means that there is no official definition of a sustainable mutual fund. Therefore, the market for sustainable mutual funds will vary from one investment research firm to another. The second category is the market for sustainable securities, such as green bonds or social bonds. This category is better defined than the previous one. It is now the main instrument used by governments and corporations to finance the transition to a low-carbon economy. Finally, the third category is an extension of the first when the assets under management are not listed public securities. This is the market of sustainable real assets, broadly speaking, assets that do not correspond to public equities and bonds. This category consists of four main categories: sustainable private equity, sustainable private debt, sustainable infrastructure and sustainable real assets.

## 4.1 ESG mutual funds

A mutual fund is an investment vehicle that pools money from many investors to invest in a portfolio of securities such as stocks, bonds, money market instruments, or a combination of these assets. These funds are managed by investment management firms, called asset managers, who make investment decisions on behalf of the fund's investors. Asset managers receive a mandate to manage the portfolio from asset owners (*e.g.*, retail clients, banking networks, insurance companies, or institutional investors) in exchange for a management fee. In order to meet the heterogeneous objectives of different investors, asset managers highly structure and specialize mutual funds. The categories depend on the asset class, and we distinguish equity funds, bond funds, money market funds, balanced funds, etc. Another important criterion is the region in which the fund manager invests. For example, investors can buy an equity fund that specializes in European stocks, American stocks, or stocks of a particular country (*e.g.*, French stocks, Spanish stocks, Indian stocks). Other criteria may be used to classify mutual funds, such as the level of active risk relative to a benchmark. For example, the objective of an index fund is to replicate a benchmark index, while the objective of

an actively managed fund is to generate positive alpha relative to a benchmark. If the investment strategy is complex, involves the use of leverage or short selling, or invests in less liquid assets, the fund is generally restricted to accredited investors and is referred to as a hedge fund or alternative investment fund. Because of these different capabilities, the potential for misalignment between investor and fund manager, and mis-selling issues, mutual funds are highly regulated. This is also the case for ESG funds in Europe with the sustainable finance disclosure regulation (SFDR). In other countries, regulation of ESG funds is more heterogeneous or non-existent because the status of ESG funds has not yet been defined.

### 4.1.1 Regulation

#### Sustainable finance disclosure regulation

The SFDR has already been introduced in section 1.4.3 on page 36. We reiterate that all products must be classified as falling under either Article 6, 8 or 9:

| Article 6 | Article 8 | Article 9 |
|---|---|---|
| These funds do not integrate or promote sustainability factors in their investment decisions. This means that they can invest in assets regardless of their ESG practices. They do not face ESG constraints. Article 6 is the default category. It can be seen as the traditional investment approach before the advent of ESG. | These funds integrate environmental, social and governance factors into their investment decisions. This means that their investment policy depends on some ESG criteria. For example, they may exclude some assets from their investment universe because of their poor extra-financial score. However, financial performance remains the primary objective of these funds, ahead of sustainability. | These funds have sustainable investing as their primary objective. Like Article 8 funds, they incorporate ESG criteria. The difference is that they allocate capital based on the impact of these assets on the development of economic sustainability. In simple terms, these funds can be assimilated to the impact investing category of the ESG strategy classification. |

To maintain their Article 9 designation, funds must meet three requirements on an ongoing basis:

1. Positive impact
   The fund's investments must actively contribute to a specific environmental or social objective. This objective should be consistent with the overall objectives of the fund and pursued through a clear and transparent investment strategy.

2. Do no harm
   The fund must carefully assess and mitigate any potential negative social or environmental impacts of the companies in which it invests.

3. Strong governance
   Companies in the fund's portfolio must demonstrate strong governance practices. This ensures accountability and ethical behavior by the companies in which the fund invests.

While the social objective was originally included in the definition of Article 9 funds, this objective has lost momentum. It now seems that it cannot be the primary objective of an Article 9 fund, certainly because the social taxonomy has not yet been developed. Clearly, the environment is the primary objective of Article 9 funds, as evidenced by the pre-contractual disclosure in Box 4.1.

Box 4.1: Pre-contractual information disclosure for the Article 9 financial products

- What is the sustainable investment objective of this product?
  - How does this product measure that the sustainable investment objective will be met?
  - What investments are not sustainable, what is their purpose and are there any minimum environmental or social safeguards?
- Has a reference benchmark been designated for the purpose of ensuring consistency with the sustainable investment objective of the product and how the consistency is monitored?
  - How does the benchmark used differ from a relevant broad market index?
- What type of investments does this product make and what is the minimum proportion of sustainable investments?
  - What are the objectives of the sustainable investments?
  - How is significant harm to the environment and people avoided by the sustainable investments made?
- What is the minimum proportion of EU Taxonomy-aligned investments?
- Does this product commit to consider the most significant negative impacts of its investments on the environment and people (principal adverse impacts)?
- Does this product aim to decrease the greenhouse gas (GHG) emissions from the activities the product invests in?
  - What is the greenhouse gas emission reduction target of the product?
  - Is the greenhouse gas emission reduction target of the product compatible with the objective to limit global warming to 1.5°C?

Source: ESMA (2023) & https://www.esma.europa.eu/document/final-report-draft-rts-review-pai-and-financial-product-disclosures-sfdr-delegated.

According to Morningstar (2024b, Exhibit 11, page 15), the largest Article 9 fund is Nordea 1 – Global Climate and Environment Fund with €9.1 bn in assets under management as of December 2023. To understand the sustainability objective of the fund, we can analyze the ESG report and the SFDR report[1]. In the latter report, we can read:

- The fund will make at least 85% sustainable investments with an environmental objective in economic activities that qualify and do not qualify as environmentally sustainable under the EU taxonomy.
- The fund invests a minimum proportion of 2% of its total investments in activities that meet the technical criteria defined in the EU taxonomy.
- A fundamental bottom-up research process identifies companies with significant future cash

[1]Both reports are available at www.nordea.lu/en/professional/fund/climate-expertise.

Figure 4.1: Reclassification of Article 6, 8 and 9 funds

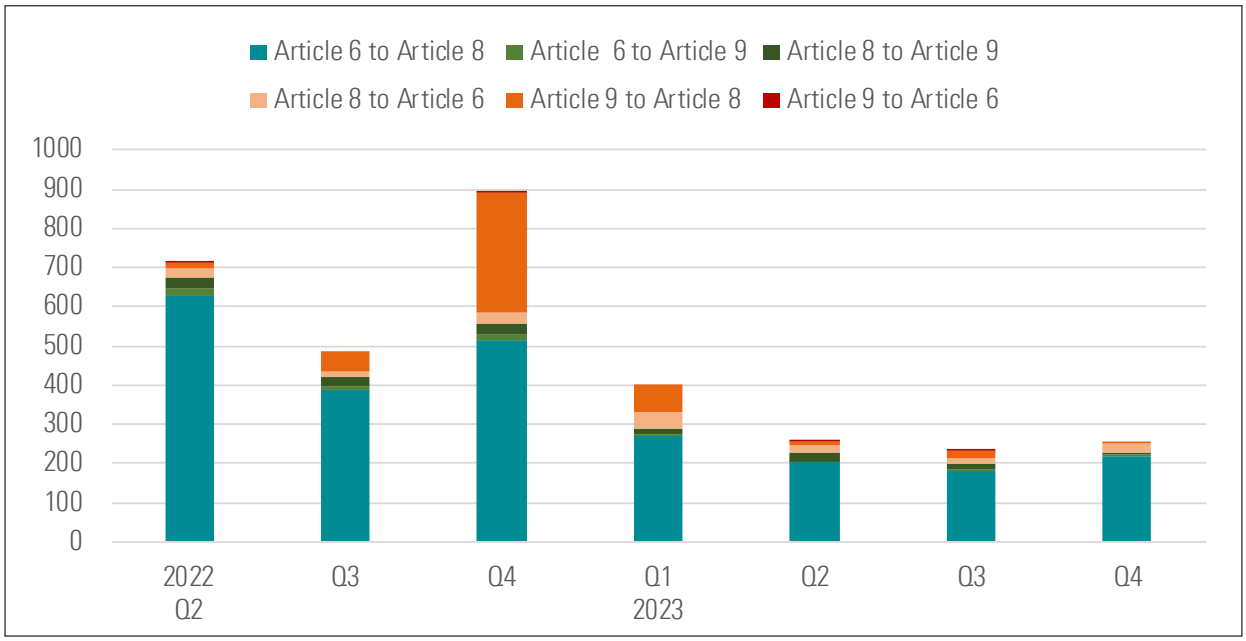


Source: Morningstar (2024b, Exhibit 8d, page 13).

flows from their contribution to environmental solutions such as resource efficiency, environmental protection and alternative energy solutions.

- Companies that are materially involved in the following activities are excluded from the investment universe: Pornography, Alcohol, Conventional weapons, Coal, Gambling, Natural gas, Nuclear weapons, Oil, Arctic drilling and oil sands, Tobacco and Controversial Weapons.
- The fund uses the Paris Aligned Fossil Fuel Policy (PAFF) developed by Nordea Asset Management to identify companies with credible transition plans.

Morningstar (2024b, Exhibit 10, page 14) considers that the largest Article 8 fund is Flossbach von Storch SICAV – Multiple Opportunities with €24.9 bn in assets under management as of December 2023. In the SFDR report[2], we can read:

- The fund promotes environmental or social characteristics, but does not have a sustainable investment objective.
- Social and environmental exclusion criteria are implemented, while an engagement policy is implemented as part of the investment strategy.

These two examples show that the main difference between Article 8 and Article 9 funds is the fund management process. Most Article 8 funds only implement asset exclusion based on some ESG criteria, while most Article 9 funds also implement a selection process based on green intensity and carbon footprint criteria. However, this distinction is somewhat theoretical as the classification is not always obvious. This explains why we see an ongoing reclassification of European funds. According to Morningstar (2024b, page 12), 256 funds changed their SFDR status in the last quarter of 2023: "*The majority of funds (218) moved to Article 8 from Article 6, while three upgraded to*

[2]It is available at www.flossbachvonstorch.ch/en/funds/LU0945408952.

*Article 9 from Article 6, and eight funds moved to Article 9 from Article 8. Meanwhile, four funds downgraded to Article 8 from Article 9.*". In Figure 4.1, we reproduce the history of quarterly reclassifications calculated by Morningstar (2024b). There are two important stylized facts. First, many mutual funds are upgraded from Article 6 to Article 8 each quarter. Second, we observe a wave of downgrades from Article 9 to Article 8 between the third quarter of 2022 and the first quarter of 2023. This period of voluntary reclassifications begins in July 2022, when the European Commission provided additional guidance to Article 9 funds as part of the SFDR. The key point emphasized that only funds that meet 100% sustainable criteria can qualify under Article 9. However, the definition and criteria for sustainable investments remained unclear. Fears of greenwashing and a misunderstanding of the original SFDR explain this wave of downgrades. Even today, the definition of sustainable investments is left to the discretion of the asset manager, although certain guidelines have been published and specified in the Regulatory Technical Standards[3] (ESMA, 2023). In Box 4.2, we have reported on Nordea Asset Management's definition of sustainable investment, which can be found in the pre-contractual SFDR document for the Nordea 1 – Global Climate and Environment Fund. We can compare this definition with the Pictet Asset Management's definition of sustainable investment, which can be found in the pre-contractual SFDR document for the Pictet Water Fund[4] (Box 4.3). While these two definitions use common guidelines, they are not strictly equivalent. Each asset manager is therefore free to interpret what constitutes a sustainable investment. For example, unlike Article 8 products, Article 9 funds must ensure that many of the companies in which they invest are aligned with the EU taxonomy. However, the percentage of alignment may vary from one asset manager to another.

**Minimum proportion of sustainable investments** Figure 4.2 shows the distribution of minimum sustainable investment percentages for Article 8 and Article 9 funds[5]. The two distributions are very different, as almost all Article 8 funds have a minimum sustainable investment percentage below 60%, while almost all Article 9 funds have a minimum sustainable investment percentage above 70%. About 35% of Article 8 funds report a minimum sustainable investment of 0%, while about 45% of Article 9 funds report a minimum sustainable investment of over 90%. These are the two most common frequencies. Curiously, 1% of Article 9 funds report a minimum sustainable investment of 0%.

**Principal adverse sustainability impacts** Initially, the EU identified 64 adverse impact indicators to be calculated and reported (18 mandatory and 46 voluntary). In the latest version of the SFDR, there are 74 indicators, of which 20 are mandatory. Below we report on the comprehensive list of indicators, which can be found in ESMA (2023, pages 91-120). Several distinctions can be made. First, we can distinguish between indicators applicable to investments in investee companies, sovereigns and supranationals, and real estate assets. Second, we can distinguish between climate and environmental indicators and social indicators. Third, we can distinguish between mandatory (principal adverse impacts) and voluntary indicators. Count statistics are given in Table 4.1. 77% of the indicators concern companies. While mandatory environmental indicators are more important than mandatory social indicators, the opposite is true for voluntary indicators. Some (S) indicators can be classified as (G) indicators. This is for example the case for indicators 12 (gender diversity of

[3] The term "*sustainable investment*" appears 272 times in the Final Report on draft Regulatory Technical Standards, but it is never defined.

[4] According to Morningstar (2024b, Exhibit 11, page 15), the Pictet Water Fund is the third largest Article 9 fund with €8.1 bn in assets under management as of December 2023.

[5] The x-label 0 corresponds to 0%, the label 10 corresponds to 0.1-9.9%, the label 20 corresponds to 10-19.9%, while the label 100 corresponds to 90-100%.

Box 4.2: Nordea Asset Management's definition of sustainable investment

"*We take into consideration the regulatory framework for sustainable finance, as well as proprietary investment methodologies, to ensure that sustainable investments can be identified, invested in and measured. In order to select sustainable investments, we apply three tests. The investment should pass all three tests to qualify as a sustainable investment.*

- *Step 1: Good governance test — a company needs to have sufficient processes in place related to the four good governance topics specified by the SFDR: sound management structures, employee relations, remuneration of staff and tax compliance, and must not be subject to significant controversies related to any of these topics.*
- *Step 2: Do no significant harm test — a company or an issuer cannot perform negatively on selected principal adverse impact (PAI) indicators. Principal adverse impacts are the most significant negative impacts of investment decisions on sustainability factors relating to environmental, social and employee matters, respect for human rights, anticorruption and antibribery matters. The thresholds defining negative outliers and poor performance vary for each PAI indicator.*
- *Step 3: Environmental or Social Contribution — NAM's proprietary process applies a pass/fail criteria on contribution to one or more of the UN SDGs or one or more of the environmental objectives in the EU Taxonomy, with a 20% threshold. Contribution may be measured on the proportion of revenue that can be linked to the above objectives. For sectors where capital expenditure or operating expenses or other relevant activity measures are more relevant, these will be used. Bonds that are issued under ICMA or equivalent frameworks (labelled bonds) are considered sustainable if their adherence under the relevant standard has been verified by an approved external auditor.*"

Source: https://www.nordeaassetmanagement.com/responsible-investment.

Box 4.3: Pictet Asset Management's definition of sustainable investment

"*Pictet Asset Management uses a proprietary reference framework as well as the objectives of the EU Taxonomy to define sustainable investments. Sustainable investments are calculated on a pass/fail basis including labelled bonds(where relevant to the asset class),and securities from issuers with minimum 20% exposure (as measured by revenue, EBIT, enterprise value or similar metrics) to economic activities that contribute to environmental or social objectives. In the absence of an EU social taxonomy, Pictet has developed a proprietary social taxonomy framework. The framework is based on the Report on Social Taxonomy published by the EU Platform on Sustainable Finance in 2022. Eligible activities are defined as socially beneficial goods and services that substantially contribute to one of the following three social objectives: (1) inclusive and sustainable communities, (2) adequate living standards and well-being for end users and (3) decent work. Whilst the fund includes achieving a positive environmental or social objective, its investment policy does not target specifically investments with climate change mitigation and climate change adaptation objectives as defined by the technical screening criteria of the Taxonomy Regulation.*"

Source: https://am.pictet/en/uk/institutional/funds.

Figure 4.2: Distribution of minimum sustainable investment percentages (Article 8 vs. Article 9 funds, December 2023)

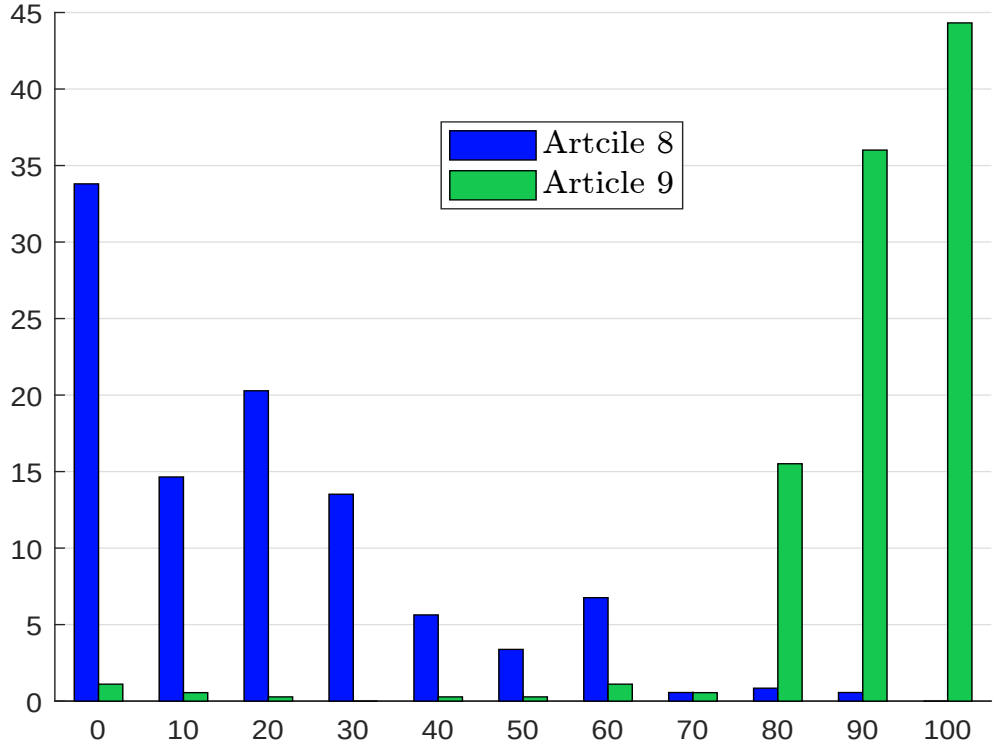


Source: Morningstar (2024b, Exhibit 23, page 27 & Exhibit 26, page 30).

management and supervisory boards), 13 (non-cooperative tax jurisdictions) and 52 (excessive CEO pay ratio). Most indicators are measured using a single metric, with the exception of indicators 1, 26, 35, 39 and 51. For each negative sustainability indicator, the fund must report on the current impact, the impact over the past year, and the actions taken, actions planned, and targets set for the next reporting period. In addition to these quantitative indicators, we also note three qualitative indicators that describe policies for identifying and prioritizing the most significant negative impacts on sustainability factors, engagement policies, and references to international standards. A fourth and final qualitative indicator is a historical comparison of the quantitative indicators over the life of the fund. The general idea is to show the overall sustainability trend of the product.

Table 4.1: Number of indicators in the SFDR

| | | Corporates | Sovereigns | Real estate assets | Total |
|---|---|---|---|---|---|
| Mandatory | E | 9 | 1 | 2 | 12 |
| | S | 7 | 1 | 0 | 8 |
| | Total | 16 | 2 | 2 | 20 |
| Voluntary | E | 17 | 1 | 5 | 23 |
| | S | 21 | 4 | 0 | 25 |
| | G | 3 | 3 | 0 | 6 |
| | Total | 41 | 8 | 5 | 54 |
| Total | | 57 | 10 | 7 | 74 |

Source: ESMA (2023) & Author's calculations.

### Climate and other environment-related indicators

- Greenhouse gas emissions
  1. GHG emissions
     - Scope 1 GHG emissions of investee companies expressed in tonnes of $CO_2$ equivalent
     - Scope 2 GHG emissions of investee companies emissions expressed in tonnes of $CO_2$ equivalent
     - Scope 3 GHG emissions of investee companies expressed in tonnes of $CO_2$ equivalent
     - Total GHG emissions of investee companies expressed in tonnes of $CO_2$ equivalent
  2. Carbon footprint
     - Total GHG emissions expressed per million EUR invested
  3. GHG intensity of investee companies
     - GHG emissions per million EUR of revenue of investee companies
  4. Exposure to companies active in the fossil fuel sector
     - Share of investments in companies active in the fossil fuel sector
  5. Share of non-renewable energy consumption and production
     - Share of non-renewable energy consumption and non-renewable energy production of investee companies from non-renewable energy sources compared to renewable energy sources, expressed as share of total energy intensity
  6. Energy consumption intensity per high impact climate sector
     - Energy consumption in MWh per million EUR of revenue of investee companies, per high impact climate sector
- Biodiversity
  7. Activities negatively affecting biodiversity-sensitive areas
     - Share of investments in investee companies with sites/operations located in or near to biodiversity-sensitive areas where activities of those investee companies negatively affect those areas
- Water
  8. Pollution of water
     - Tonnes of pollution emitted into water generated by investee companies per million EUR invested
- Waste
  9. Hazardous waste ratio
     - Tonnes of hazardous waste generated by investee companies per million EUR invested

### Indicators for social and employee, respect for human rights, anti-corruption and anti-bribery matters

- Social and employee matters
  10. Non-respect of OECD Guidelines for Multinational Enterprises or the UN Guiding Principles including the principles and rights set out in the eight fundamental conventions identified in the ILO Declaration and the International Bill of Human Rights
      - Share of investments in investee companies that have been involved in non-respect of the OECD Guidelines for Multinational Enterprises, the UN Guiding Principles, including the principles and rights set out in the eight fundamental conventions identified in the ILO Declaration and the International Bill of Human Rights
  11. Unadjusted gender pay gap between female and male employees
      - Average gender pay gap between female and male employees of investee companies
  12. Management and supervisory board gender diversity
      - Average ratio of female to male management and supervisory board members in investee companies, expressed as a percentage of all board members

13. Amount of accumulated earnings in non-cooperative tax jurisdictions applying to investee companies where the total consolidated revenue on their balance sheet date for each of the last two consecutive financial years exceeds a total of EUR 750 M
    - Amount of accumulated earnings at the end of the relevant financial year from investee companies where the total consolidated revenue on their balance sheet date for each of the last two consecutive financial years exceeds total of EUR 750M in jurisdictions that appear on the revised EU list of non-cooperative jurisdictions for tax purposes
14. Exposure to controversial weapons
    - Share of investments in investee companies involved in the manufacture or selling of controversial weapons
15. Exposure to companies active in the cultivation and production of tobacco
    - Share of investments in investee companies active in the cultivation and production of tobacco
16. Share of employees of investee companies earning less than the adequate wage
    - Average percentage of employees in investee companies earning less than the adequate wage

### Indicators applicable to investments in sovereigns and supranationals

- Environmental

17. Sovereign GHG intensity
    - GHG intensity of investee countries as a ratio of investee country's PPP-adjusted GDP

- Social

18. Investee countries subject to social violations
    - Investments in investee countries subject to social violations from international treaties and conventions, United Nations principles and where applicable national laws or principles

### Indicators applicable to investments in real estate assets

- Fossil fuels

19. Exposure to fossil fuels through real estate assets
    - Share of investments in real estate assets involved in the extraction, storage, transport, trade or manufacture of fossil fuels

- Energy efficiency

20. Exposure to energy inefficient real estate assets
    - Share of investments in energy inefficient real estate assets

### Other indicators for principal adverse impacts on sustainability factors

- Description of policies to identify and prioritise principal adverse impacts on sustainability factors (Article 7)
- Engagement policies (Article 8)
- References to international standards (Article 9)
- Historical comparison (Article 10)

### Additional climate and other environment-related indicators

### Climate and other environment-related indicators

- Emissions
  21. Emissions of inorganic pollutants
      - Tonnes of inorganic pollutants equivalent per million EUR invested
  22. Emissions of air pollutants
      - Tonnes of air pollutants equivalent per million EUR invested
  23. Emissions of ozone-depleting substances
      - Tonnes of ozone-depleting substances equivalent per million EUR invested
  24. Investments in companies without carbon emission reduction initiatives
      - Share of investments in investee companies without carbon emission reduction initiatives aimed at aligning with the Paris Agreement
- Energy performance
  25. Breakdown of energy consumption by type of non-renewable sources of energy
      - Share of energy from non-renewable sources used by investee companies broken down by each non-renewable energy source
- Water, waste and material emissions
  26. Water usage and recycling
      - Average amount of water consumed by the investee companies (in cubic meters) per million EUR of revenue of investee companies
      - Weighted average percentage of water recycled and reused by investee companies
  27. Investments in companies without water management policies
      - Share of investments in investee companies without water management policies
  28. Exposure to areas of high water stress
      - Share of investments in investee companies with sites located in areas of high water stress without a water management policy
  29. Investments in companies producing pesticides and other agrochemical products
      - Share of investments in investee companies the activities of which fall under Division 20.2 of Annex I to Regulation (EC) No 1893/2006
  30. Land degradation, desertification, soil sealing
      - Share of investments in investee companies the activities of which cause land degradation, desertification or soil sealing
  31. Investments in companies without sustainable land/agriculture practices or policies
      - Share of investments in investee companies, the activities of which involve land/agricultural activities without sustainable land/agriculture practices or policies
  32. Investments in companies without sustainable oceans/seas practices or policies
      - Share of investments in investee companies, the activities of which involve oceans, seas, coasts or inland water activities without sustainable oceans/seas practices or policies
  33. Non-recycled waste ratio
      - Tonnes of non-recycled waste generated by investee companies per million EUR invested
  34. Radioactive waste ratio
      - Tonnes radioactive waste generated by investee companies per million EUR invested
  35. Natural species and protected areas
      - Share of investments in investee companies whose operations affect threatened species
      - Share of investments in investee companies without a biodiversity protection policy covering operational sites owned, leased, managed in, or adjacent to, a protected area or an area of high biodiversity value outside protected areas

36. Deforestation
    - Share of investments in companies without a policy to address deforestation

- Green securities

37. Share of corporate debt securities not issued under Union legislation on environmentally sustainable bonds
    - Share of securities in investments not issued under Union legislation on environmentally sustainable bonds

### Indicators applicable to investments in sovereigns and supranationals

- Green securities

38. Share of sovereign and supranational debt securities not issued under Union legislation on environmentally sustainable bonds
    - Share of bonds not issued under Union legislation on environmentally sustainable bonds

### Indicators applicable to investments in real estate assets

- Greenhouse gas emissions

39. Real estate GHG emissions
    - Scope 1 GHG emissions generated by real estate assets expressed in tonnes of $CO_2$ equivalent
    - Scope 2 GHG emissions generated by real estate assets expressed in tonnes of $CO_2$ equivalent
    - Scope 3 GHG emissions generated by real estate assets expressed in tonnes of $CO_2$ equivalent
    - Total GHG emissions generated by real estate assets expressed in tonnes of $CO_2$ equivalent

- Energy consumption

40. Energy consumption intensity
    - Energy consumption in GWh of owned real estate assets per square meter

- Waste

41. Waste production in operations
    - Share of real estate assets not equipped with facilities for waste sorting and not covered by a waste recovery or recycling contract

- Resource consumption

42. Raw materials consumption for new construction and major renovations
    - Share of raw building materials (excluding recovered, recycled and biosourced) compared to the total weight of building materials used in new construction and major renovations

- Biodiversity

43. Land artificialisation
    - Share of non-vegetated surface area (surfaces that have not been vegetated in ground, as well as on roofs, terraces and walls) compared to the total surface area of the plots of all assets

### Additional indicators for social and employee, respect for human rights, anti-corruption and anti-bribery matters

### Indicators applicable to investments in investee companies

- Social and employee matters

  44. Investments in companies without workplace accident prevention policies or management systems
      - Share of investments in investee companies without a workplace accident prevention policy or management system
  45. Rate of recordable work-related accidents
      - Rate of recordable work-related accidents in investee companies
  46. Number of days lost to work-related injuries, accidents, ill health and fatalities
      - Number of workdays lost to work-related injuries, accidents, ill health or fatalities of investee companies
  47. Low coverage of collective bargaining agreements
      - Share of employees in investee companies not covered by collective bargaining agreements
  48. Lack of a supplier code of conduct
      - Share of investments in investee companies without any supplier code of conduct (against unsafe working conditions, child labour and forced labour)
  49. Lack of grievance/complaints handling mechanism related to employee matters
      - Share of investments in investee companies without a grievance/complaints handling mechanism related to employee matters
  50. Insufficient whistleblower protection
      - Share of investments in entities without policies on the protection of whistleblowers
  51. Incidents of discrimination and incidents of discrimination related to any type of discrimination leading to monetary and non-monetary sanctions in investee companies
      - Number of incidents of discrimination
      - Number of incidents of discrimination related to any type of discrimination leading to monetary and non-monetary sanctions in investee companies
  52. Excessive CEO pay ratio
      - Ratio within investee companies of the annual total compensation for the highest compensated individual to the median annual total compensation for all employees (excluding the highest-compensated individual)
  53. Excessive use of non-guaranteed-hour employees in investee companies
      - Share of non-guaranteed hour employees in investee companies as share of total employees
  54. Excessive use of temporary contract employees in investee companies
      - Share of temporary contract employees in investee companies as share of total employees
  55. Excessive use of non-employee employees in investee companies
      - Share of non-employee employees in investee companies as share of total employees
  56. Insufficient employment of persons with disabilities within the workforce
      - Share of persons with disabilities within the workforce of investee companies

- Human Rights

  57. Lack of processes and compliance mechanisms to monitor compliance with OECD Guidelines for Multinational Enterprises or the UN Guiding principles, including the principles and rights set out in the eight fundamental conventions identified in the ILO Declaration and the International Bill of Human Rights
      - Share of investments in investee companies without policies to monitor compliance with or grievance/complaints handling mechanisms to address violations of the OECD Guidelines for Multinational Enterprises or the UN Guiding principles, including the principles and rights set out in the eight fundamental conventions identified in the ILO Declaration and the International Bill of Human Rights
  58. Lack of human rights policies

    - Share of investments in entities without human rights policies

59. Lack of processes and measures for preventing trafficking in human beings
    - Share of investments in investee companies without policies against trafficking in human beings
60. Operations and suppliers at significant risk of incidents of child labour
    - Share of investments in investee companies exposed to operations and suppliers at significant risk of incidents of child labour in terms of geographic areas and/ or type of operation
61. Operations and suppliers at significant risk of forced or compulsory labour
    - Share of investments in investee companies exposed to operations and suppliers at significant risk of incidents of forced or compulsory labour in terms of geographic areas and / or the type of operation
62. Number of identified cases of severe human rights issues and incidents
    - Number of cases of severe human rights issues and incidents connected to investee companies
63. Lack of remediation mechanism for affected communities relating to the operations of the investee companies
    - Share of investments in investee companies without remediation mechanism for stakeholders materially affected by the operations of the investee companies
64. Lack of remediation handling mechanism for consumers/end-users of the investee company
    - Share of investments in investee companies without remediation mechanism for consumers/end-users of the investee companies

- Anti-corruption and anti-bribery

65. Lack of anti-corruption and anti-bribery policies
    - Share of investments in entities without policies on anti-corruption and anti-bribery consistent with the United Nations Convention against Corruption
66. Lack of action taken to address breaches of standards of anti-corruption and anti-bribery
    - Share of investments in investee companies with no action taken to address breaches in procedures and standards of anti-corruption and anti-bribery
67. Convictions and fines for violation of anti-corruption and anti-bribery laws
    - Share of investments in investee companies with convictions or fines for violations of anti-corruption and anti-bribery laws

### Indicators applicable to investments in sovereigns and supranationals

- Social

68. Average income inequality score
    - The distribution income and economic inequality among the participant in a particular economy including a quantitative indicator explained in the explanation column
69. Average freedom of expression score
    - Measuring the extent to which political and civil society organisations can operate freely including a quantitative indicator explained in the explanation column
70. Average human rights performance
    - Measure of the average human right performance of investee countries using a quantitative indicator explained in the explanation column

- Human rights

71. Average corruption score
    - Measure of the perceived level of public sector corruption using a quantitative indicator explained in the explanation column

- Governance

72. Investments in non-cooperative tax jurisdictions

    - Investments in jurisdictions on the EU list of non-cooperative jurisdictions for tax purposes

73. Average political stability score
    - Measure of the likelihood that the current regime will be overthrown by the use of force using a quantitative indicator explained in the explanation column

74. Average rule of law score
    - Measure of the level of corruption, lack of fundamental rights, and the deficiencies in civil and criminal justice using a quantitative indicator explained in the explanation column

These 74 indicators can be thought of as the metrics of an ESG scoring system, as defined in Figure 2.7 on page 66. Since we have seen that ESG metrics are noisy, we might wonder if the same is true for PAI metrics. We recall that disclosure of these indicators is mandatory for financial market participants and financial products. In fact, disclosure at the fund level appears to be rare. Indeed, looking at the 20 largest Article 9 funds as of December 2023 (Morningstar, 2024b, Exhibit 11, page 15), we found only two funds with a comprehensive PAI report available on the fund's website. These are Nordea 1 – Global Climate and Environment Fund and Handelsbanken Global Index Criteria Fund. Table 4.2 shows the figures for these two funds for the 20 mandatory principal adverse impacts. The case of financial market participants is easier because we generally found the PAI report on their website[6]. For example, we have reported on the PAI report of 6 asset managers in Table 4.2. Several comments can be made. First, the report concerns the legal entity and not the asset manager. For example, the report of Amundi Luxembourg covers all the Amundi funds located in Luxembourg, but not the Amundi funds located in Ireland, France, Germany, Austria, etc. Second, there are few indicators for which we observe consistent figures across reports. This may be the case for the eleventh indicator (gender pay gap). It is certainly not the case for greenhouse gas intensity, non-renewable energy share[7], energy consumption intensity[8], biodiversity impact, etc. For example, the GHG intensity of Amundi Luxembourg and AXA IM Paris are 286.9 and 1 109 $tCO_2e/€$ mn, respectively. The share of non-renewable energy is 0.83% (production) for JP Morgan AM Europe and 80.99% (consumption and production) for Schroder IM Europe. Emissions to water are 0.00 and 256.2 $t/€$ mn for BlackRock Ireland and Amundi Luxembourg, respectively. A third comment is that these large differences can only be explained by asset managers using different approaches or databases. For instance, the GHG intensity by Amundi Luxembourg includes Scope 1, 2 and 3 first-tier upstream GHG emissions, while this by AXA IM Paris considers a comprehensive coverage of Scope 3 upstream and downstream GHG emissions. Mirova's PAI report provides two GHG intensity figures: 3 317, $tCO_2e/€$ mn (without double counting correction) and 796, $tCO_2e/€$ mn (with double counting correction). These examples show that we are still a long way from harmonising measures between investors. Yet these 20 metrics are the most frequently encountered.

**Remark 42** *As far as the voluntary indicators are concerned, each financial market participant is spoilt for choice among the 54 remaining indicators. However, two of them are very often chosen by FMPs:*

*24. Investments in companies without carbon emission reduction initiatives*

*58. Lack of human rights policies*

[6] The PAI report is generally called "*statement on principal adverse impacts of investment decisions on sustainability factors*".

[7] If there are two numbers, the first measures the share of non-renewable energy consumption, while the second measures the share of non-renewable energy production. If there is only one number, there is no distinction between consumption and production.

[8] If there are two numbers, they represent the minimum and maximum intensity across all NACE sectors. If there is only one number, it corresponds to the weighted average of all NACE sectors.

Table 4.2: Statement on principal adverse impacts of investment decisions on sustainability factors

| Indicator | AXA IM Paris July 2023 | Amundi Luxembourg June 2023 | BlackRock Ireland June 2023 | DWS GmbH 2023 | JP Morgan AM Europe June 2023 | Schroder IM Europe June 2023 | Nordea 1 GCE Fund Q4 2023 | Handelsbanken GIC Fund 2023 |
|---|---|---|---|---|---|---|---|---|
| 1. Total GHG emissions | 60887445 | 16688741 | 233064529 | 117087045 | 88112702 | 41176662 | 739486 | 1773122 |
| 2. Carbon footprint | 497 | 91.6 | 271 | 489.4 | 221 | 374.77 | 83.3 | 305.33 |
| 3. GHG intensity | 1 109 | 286.9 | 597 | 1 087.9 | 864 | 1 014.03 | 290.5 | 860.39 |
| 4. Fossil fuel exposure (corporates) | 5.43% | 11.7% | 9% | 17.07% | 1.2% | 6.59% | 8.1% | 2.64% |
| 5. Non-renewable energy share | 60.01% | 77.7/64.2% | 64/60% | 75.15% | 0.97/0.83% | 80.99% | 77.6% | 68.24/15.14% |
| 6. Energy consumption intensity | 0.15-3.80 | 0.2/2.6 | 0.7 | 0.21-14.26 | 0-1.39 | 29.22 | 2.4 | 0.17/1117 |
| 7. Impact on biodiversity | 4.86% | 0.0% | 2% | 0.08% | 1.12% | 0.06% | 0.0% | 4.73% |
| 8. Emissions to water | 0.02 | 256.2 | 0 | 238.59 | 1.57 | 2.29 | 0.1 | 0.25 |
| 9. Hazardous waste | 5.72 | 22.6 | 57 | 8.29 | 2.64 | 3.52 | 0.4 | 33.36 |
| 10. Non-respect for human rights | 0.07% | 0.7% | 10% | 0.17% | 0.03% | 1.03% | 0.0% | 0.0% |
| 11. Gender pay gap | 14.87% | 9.6% | 15% | 14.27% | 8.29% | 12.74% | 6.7% | 15.13% |
| 12. Board gender diversity | 36% | 29.4% | 32% | 32.94% | 4.92% | 35.39% | 33.0% | 30.35% |
| 13. Non-cooperative tax jurisdictions | | | | | | | | |
| 14. Exposure to controversial weapons | 0% | 0.0% | <0.01% | 0% | 0.01% | 0% | 0.0% | 0.04% |
| 15. Tobacco exposure | | | | | | | | |
| 16. Lack of adequate wage | | | | | | | | |
| 17. Sovereign GHG intensity | 387 | 451.6 | 51 | 294.7 | 32.01 | 362.68 | | |
| 18. Country social violations | 1 | 8 | 4 | 6 | 1 | 2 | | |
| 19. Fossil fuel exposure (real estate) | | 0% | 0% | | | | | |
| 20. Energy-inefficient real estate | | 44.90% | 0% | | | | | |

Source: Asset managers' websites & Author's calculations.

### UK sustainability disclosure requirements

On 28 November 2023, the Financial Conduct Authority (FCA) published its final rules on sustainability disclosure requirements (SDRs) and investment labels (Policy Statement PS23/16). PS23/16 includes[9]:

- An anti-greenwashing rule for all firms authorised by the FCA to reinforce that sustainability-related claims must be fair, clear and not misleading.
- Rules on the naming and marketing of investment products to ensure that the use of sustainability-related terms is accurate.
- Four labels to help consumers navigate the investment product landscape and increase consumer confidence.
- Consumer-facing information to provide consumers with better, more accessible information to help them understand the key sustainability features of a product.
- Detailed information targeted at institutional investors and consumers seeking more information in pre-contractual, ongoing product-level, and entity-level disclosures.
- Requirements for distributors to ensure that product-level information (including labels) is made available to consumers.

The current UK SDRs only apply to UK domiciled funds, but may be extended in the future to cover overseas funds, such as UCITS funds. They will come into force between May 2024 and December 2026.

With the creation of the sustainability labels, UK funds will now be divided into three categories: (1) sustainability labeled funds that use one of the four labels; (2) unlabeled ESG funds that are marketed as ESG funds; and (3) non-ESG funds that are not marketed as ESG funds. The four voluntary sustainability labels are:

1. Sustainability Focus funds invest in assets that are environmentally or socially sustainable, determined by a robust, evidence-based standard of sustainability.
2. Sustainability Improvers funds invest in assets that have the potential to become more sustainable over time, determined by their potential to meet a robust, evidence-based standard of sustainability over time.
3. Sustainability Impact funds seek to achieve a predefined, positive, measurable environmental and/or social impact.
4. Sustainability Mixed Goals funds invest in assets that meet or have the potential to meet a robust, evidence-based standard for sustainability, and/ or invest with an aim to achieve positive impact.

To qualify for one of the four labels, a product must meet both general and specific criteria. The five general criteria are (1) sustainability objectives, (2) investment policy and strategy, (3) key performance indicators, (4) resources and governance, and (5) stewardship. Products must seek to achieve positive environmental and/or social outcomes as part of their investment objectives

[9]The link is www.fca.org.uk/publication/policy/ps23-16.pdf.

and disclose any potential negative outcomes[10]. At least 70% of the product's assets should be aligned with its sustainability objective, based on a robust, evidence-based standard. Firms must define KPIs to track progress toward sustainability goals. Firms must also have adequate resources, governance and organizational arrangements to support their sustainability objectives and outline their stewardship strategy to support their sustainability objectives, detailing expected activities and outcomes.

**Remark 43** *The SDRs can be seen as the UK version of the EU SFDR. However, they differ in terms of reporting, as the SDR endorses the ISSB reporting framework, which implies a single materiality approach rather than a double materiality approach.*

### Other regulations

With the exception of the UK SRDs, there are no equivalent regulations for financial products outside the European Union. In fact, most regulations relate to green taxonomies[11] and corporate ESG disclosures. Asset managers must then comply with these disclosure reports, but not the financial products and investment funds. Below is a list of the few initiatives in other countries.

**United States** On September 20, 2023, the SEC introduced new rules aimed at preventing the misleading use of ESG terms in mutual fund names and combating greenwashing. These rules update the Investment Company Act's "*Names Rule*" to ensure that fund names accurately reflect their investment strategies. Previously, funds were required to invest at least 80% of their assets in the areas suggested by their names. The new rules extend this requirement to ESG strategies, ensuring that fund names have a clear and established meaning. This extension will avoid situations where funds technically meet the 80% rule, but their remaining holdings contradict their names, for example a fund labeled *fossil fuel free* that holds fossil fuel investments in its remaining 20%.

**Japan** On March 2023, the Financial Services Agency of Japan issued new guidelines[12] for ESG investment funds: Comprehensive Guidelines for Supervision of Financial Instruments Business Operators, etc. Again, the aim of these guidelines is to combat greenwashing. They provide instructions and standards for the supervision of financial instruments business operators, including securities firms, investment advisors and other entities involved in the financial services industry in Japan. The guidelines cover compliance requirements, risk management, customer protection and market integrity. For example, funds that don't follow these guidelines are not allowed to use ESG-related terms such as "*green*" or "*sustainable*" in their names.

**Malaysia** On February 2023, the Securities Commission of Malaysia released a revised version of the Guidelines for Sustainable and Responsible Investment Funds, which sets out the reporting and disclosure requirements for a fund to qualify as a Sustainable and Responsible Investment (SRI) fund and an ASEAN Sustainable and Responsible Fund (SRF). SRI funds are now required to invest at least two-thirds of their net asset value in securities that meet their SRI policies and strategies. They are also encouraged to have a clear strategy for achieving their policies, such as ESG integration, ethical and faith-based investing, impact investing, etc.

[10] However, this does not mean that the SDRs adopt the DNSH principle.

[11] For example, green taxonomies are already active in Bangladesh, China, Colombia, Indonesia, Japan, Malaysia, Mexico, Norway, Russia, Singapore, South Africa, South Korea, and Thailand, while some 20 other countries are developing similar frameworks (*e.g.*, Brazil, Canada, India, Turkey, and the United Kingdom).

[12] The English version can be downloaded from `https://www.fsa.go.jp/common/law/guide/kinyushohin_eng.pdf`.

### 4.1.2 Sustainable labels

A label refers to a designation given to a particular type of product and is used to indicate certain characteristics or features of the product to help investors understand its nature and the risks associated with it. When applied to sustainable finance, an ESG label indicates that the products meet certain environmental, social or governance criteria. However, many products fall into this category. For example, Article 8 and 9 funds have an ESG stamp, but Article 8 and 9 cannot be considered as two SFDR labels because the classification of the fund is decided by the fund itself, so it is a self-designation. A label implies an external authority that certifies that the product complies with the sustainability rules of the label.

Figure 4.3: The jungle of sustainability labels

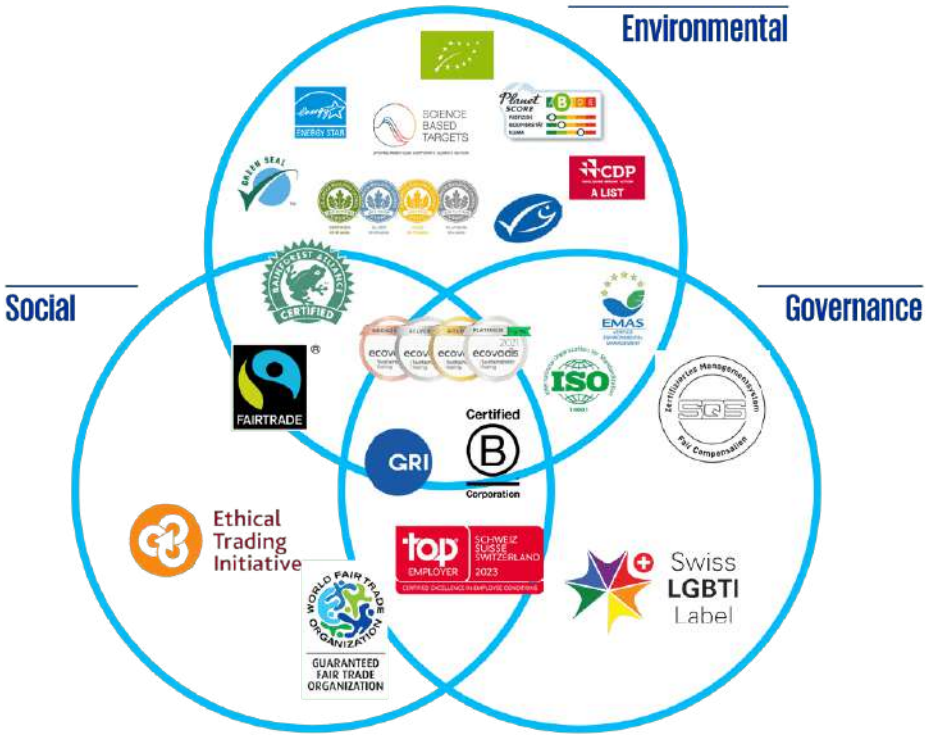


Source: www.kpmg.com/ch/en/home/insights/2023/03/sustainability-eco-label.html.

According to Ecolabel Index[13] and Standards Map[14], there are approximately hundreds labels in the world related to ESG or environmental considerations. This large number raises the question of how companies and people can navigate what KPMG[15] calls the "*jungle of sustainability and eco-labels*". This is especially true for consumers, who have a choice of many labels without knowing their characteristics, but who ultimately trust them (Testa *et al.*, 2015). In the financial sector, the problem is less significant because there are fewer players. For example, according to Megaeva *et al.* (2021, 2023), there are nine major labels in Europe with published and public criteria (Table 4.3).

[13]More than 400 eco-labels can be found at www.ecolabelindex.com/ecolabels.

[14]The website www.standardsmap.org/en/identify lists ESG labels according to several dimensions: SDGs, sector, sustainability themes, etc.

[15]KMPG (2023). Sustainability Standards and Labels: Navigating the Jungle. *Report*, October, 16 pages.

Table 4.3: Main sustainable labels

| | Name | website | Type | Country | Sponsor |
|---|---|---|---|---|---|
| | FNG-Siegel | www.fng-siegel.org | ESG | Austria, Germany, Switzerland | FNG: Forum Nachhaltige Geldanlagen |
| | Label Greenfin | www.ecologie.gouv.fr/label-greenfin | Green | France | French government |
| | Label ISR | www.lelabelisr.fr | ESG | France | French government |
| | LuxFLAG Climate Finance | www.luxflag.org/labels//climate-finance | ESG | Luxembourg | LuxFLAG |
| | LuxFLAG Environment | www.luxflag.org/labels/environment | ESG | Luxembourg | LuxFLAG |
| | LuxFLAG ESG | www.luxflag.org/labels/esg | ESG | Luxembourg | LuxFLAG |
| | LuxFLAG Microfinance | www.luxflag.org/labels/microfinance | ESG | Luxembourg | LuxFLAG |
| | Nordic Swan Ecolabel | www.nordic-swan-ecolabel.org | Green | Nordics | Nordic Council |
| | Towards Sustainability | www.towardssustainability.be | Green | Belgium | Febelfin |
| | Umweltzeichen | www.umweltzeichen.at | ESG | Austria | Austrian government |

### Greenwashing issues

The concept of labels is closely related to the issue of greenwashing, which can be defined as follows:

- "*The creation or propagation of an unfounded or misleading environmentalist image*" (Oxford English Dictionary)
- "*Behaviour or activities that make people believe that a company is doing more to protect the environment than it really is*" (Cambridge Dictionary)
- "*A term (combining green and whitewash) that environmentalists use to describe the activity (for example by corporate lobby groups) of giving a positive public image to practices that are environmentally unsound*" (Oxford Reference)
- "*The act or practice of making a product, policy, activity, etc. appear to be more environmentally friendly or less environmentally damaging than it really is*" (Merriam-Webster Dictionary)

Therefore, greenwashing is any activity by a company or organization that is intended to make people think that it cares about the environment, even if its actual business is actually harmful to the environment. For example, a common form of greenwashing is to publicly claim a commitment to the environment while quietly lobbying to avoid regulation.

Figure 4.4: A typology of firms based on environmental performance and communication

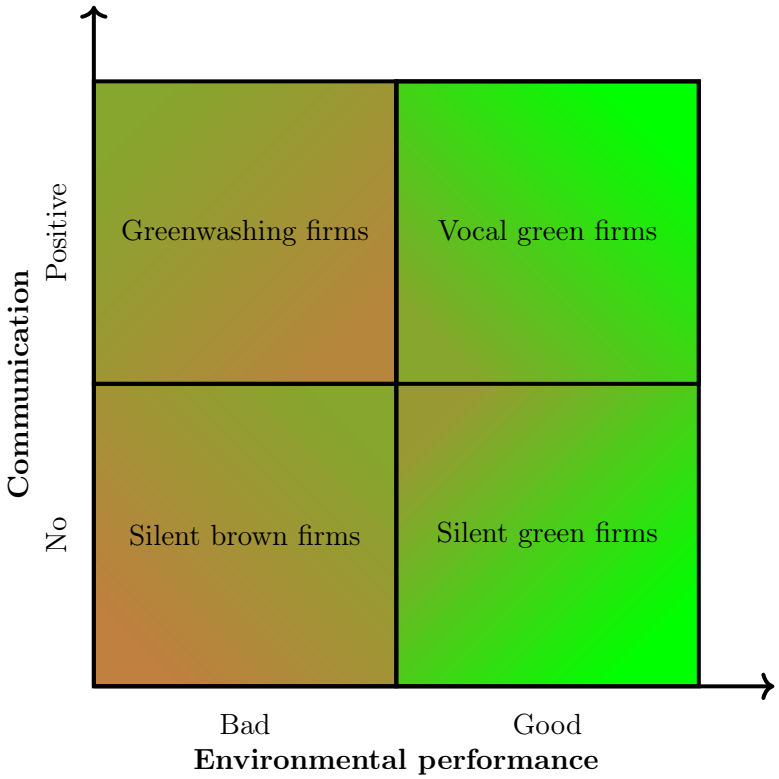


Source: Delmas and Burbano (2011, Figure 1, page 67).

According to Delmas and Burbano (2011), "*a greenwashing firm engages in two behaviors simultaneously: poor environmental performance and positive communication about its environmental*

*performance*" (Figure 4.4) and there are two ways by which a non-greenwashing firm can become a greenwashing firm:

- "*First, a vocal firm can alter its environmental performance.*"
- "*Second, a brown firm can alter communication about its environmental performance.*"

However, a firm's environmental performance is relatively fixed and changes very smoothly. Therefore, greenwashing is mainly explained by the communication axis. In this context, Delmas and Burbano (2011) identify four drivers of greenwashing:

1. Market external drivers: consumer demand, investor demand, and competitive pressure;
2. Non-market external drivers: lax and uncertain regulatory environment, and activist, NGO and media monitoring;
3. Individual psychological drivers: optimistic bias, narrow decision framing, and hyperbolic intertemporal discounting;
4. organizational drivers: firm characteristics, incentive structure and culture, effectiveness of intra-Firm communication, and organizational inertia.

Greenwashing does not only concern firms, but also products and services. This is why Delmas and Burbano (2011) distinguish two types of greenwashing: firm-level greenwashing and product-level greenwashing.

Figure 4.5: Count of unique entities with at least one ESG risk incident linked to both environmental footprint and misleading communication

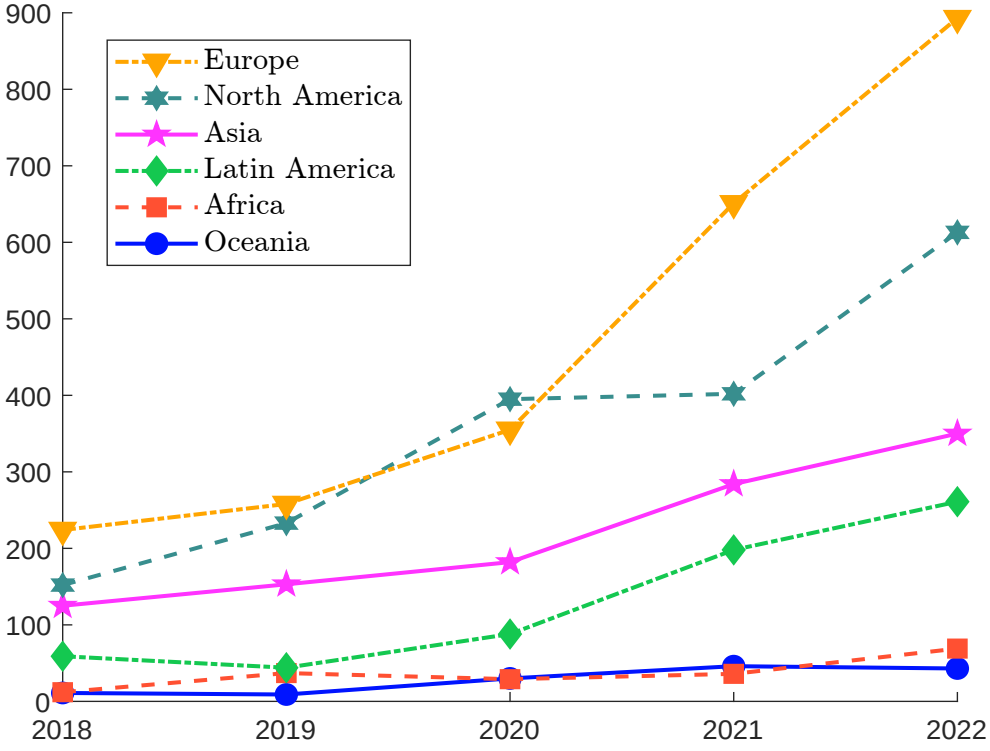


Source: RepRisk (2023, Figure 2).

RepRisk (2023) has developed a methodology to capture greenwashing events through the intersection of two ESG groups: an environmental issue (or controversy) and a misleading communication. From September 2018 to September 2023, RepRisk listed 4 237 risk incidents linked to ESG pillars and misleading communication broken down as follows: 30.1% for environmental risk events, 36.4% for environmental and social risk events, 26.3% for social risk events and 7.1% for governance risk events. In Figure 4.5, we show the evolution of greenwashing by region. We note that the risk of greenwashing has accelerated in Europe and North America. Table 4.4 gives the breakdown of sectors when considering greenwashing events related to climate change, GHG emissions, and global pollution. The sectors most exposed to greenwashing risk are oil and gas, banking and financial services, utilities and industrials and construction.

Table 4.4: Breakdown of sectors linked to climate greenwashing (in %)

| Sector | 2018-2022 | 2023 |
|---|---|---|
| Banking and financial services | 13.1 | 15.5 |
| Food and beverage | 9.2 | 8.2 |
| Industrials and construction | 8.1 | 9.5 |
| Mining | 5.0 | 3.9 |
| Oil and gas | 26.1 | 19.3 |
| Retail, personal, and household goods | 7.7 | 6.8 |
| Travel and airlines | 5.4 | 9.7 |
| Utilities | 11.6 | 10.0 |
| Other | 13.7 | 17.2 |

Source: RepRisk (2023, Figure 3).

When applied to the financial sector, greenwashing refers to "*a practice whereby sustainability-related statements, declarations, actions, or communications do not clearly and fairly reflect the underlying sustainability profile of an entity, a financial product, or financial services. This practice may be misleading to consumers, investors, or other market participants*" (EBA, 2023, page 12). Again, greenwashing can involve a financial institution, such as an asset owner or manager (entity-level greenwashing), an investment vehicle, such as a mutual fund (product-level greenwashing), or a financial service, such as an advisory agreement (service-level greenwashing). There are also two types of greenwashing risk:

- Explicit and intentional greenwashing
  Explicit greenwashing involves deliberately misleading consumers by making false or exaggerated claims about a product's environmental benefits. Financial institutions typically engage in explicit greenwashing to gain a competitive advantage in the marketplace.

- Unintentional greenwashing
  Financial institutions may unintentionally misrepresent the environmental attributes of their products due to incomplete or inaccurate information, biased metrics and data, or lack of precise regulations. Unintentional greenwashing can occur despite a company's sincere commitment to sustainability because of the multiple interpretations of ESG dimensions.

An example of intentional greenwashing is DWS Group, which has been accused of misleading investors by marketing its funds as greener than they actually were. The story began when former head of sustainability Desiree Fixler said the company was struggling with its environmental, social and governance investment strategy and claimed it was not giving investors an accurate picture. In

October 2023, DWS agreed to pay a $19 million fine to settle the charges in the US[16]. In Germany, investigation is still ongoing. An example of unintentional greenwashing is the wave of reclassifications from Article 9 to Article 8 that will occur at the end of 2022. The main reason is that the definition of Article 9 was not precise. In 2022, the publication of new SFDR regulatory technical standards led many asset managers to voluntarily downgrade funds from Article 9 to Article 8 in order to meet the new minimum requirements. So if the regulation is too vague, the risk of unintentional greenwashing increases.

In fact, it is extremely difficult to identify greenwashing at the corporate level. It is not always black and white. In the financial sector, most examples involve the banking industry and the financing of the fossil fuel industry (EBA, 2023; RepRisk, 2023). But they also help finance the transition to a low-carbon economy and renewable energy. Of course, banks will communicate publicly about its green activities, not its brown activities. Does that mean they are involved in greenwashing? Again, this is a matter of balance and interpretation. Another reason for this difficulty is that there are several shades or forms of greenwashing. Planet Tracker identifies six types of greenwashing activities[17]:

1. "*Greencrowding is built on the belief that you can hide in a crowd to avoid discovery; it relies on safety in numbers. If sustainability policies are being developed, it is likely that the group will move at the speed of the slowest.*

2. *Greenlighting occurs when company communications (including advertisements) spotlight a particularly green feature of its operations or products, however small, in order to draw attention away from environmentally damaging activities being conducted elsewhere.*

3. *Greenshifting is when companies imply that the consumer is at fault and shift the blame on to them.*

4. *Greenlabelling is a practice where marketers call something green or sustainable, but a closer examination reveals that their words are misleading.*

5. *Greenrinsing refers to when a company regularly changes its ESG targets before they are achieved.*

6. *Greenhushing refers to the act of corporate management teams under-reporting or hiding their sustainability credentials in order to evade investor scrutiny.*"

In theory, product-level greenwashing is easier to detect when the rules of the game are clear and well-defined. For example, the minimum requirements for Article 9 funds are now better defined, but there is still a lot of room for interpretation. Moreover, the status of Article 8 and 9 funds is based on the asset manager's self-declaration. In this context, Article 8 and 9 funds cannot be considered a label, as a label requires a comprehensive set of criteria and certification by an external auditor. These two features are the real added value of a label and a way to avoid greenwashing, as it is not the fund that decides on its status, but an external authority. Certification is then central to having a label. For example, we cannot talk about CTB and PAB labels because even if there is a comprehensive set of criteria, there is no certification process. We have a similar situation with the Green Bond Principles, which are a set of recommendations, not mandatory rules. However, it is extremely difficult to launch a green bond without external verification and possible certification by an organization like the Climate Bonds Initiative (CBI).

[16]This is the largest greenwashing penalty ever imposed by the SEC on an asset manager.
[17]Source: www.planet-tracker.org/wp-content/uploads/2023/01/Greenwashing-Hydra-3.pdf.

### ESG labels

In the following we describe the different European labels. The underlying idea is not to give a comprehensive presentation, because it is relatively complex to list all the criteria, minimum requirements and also guidelines of each label. This task has already been done by Megaeva *et al.* (2021, 2023). The goal is to give a broad overview of the different labels and to have an idea about the main differences between them. In particular, there are two types of labels: those that use a pass-or-fail system and those that use a grading or bonus point system. In the first case, all requirements are mandatory and must be met at all times to qualify for the label. In the second case, each requirement is assigned a score, and the total score must exceed a minimum threshold.

**Umweltzeichen Ecolabel (Austria)** The Austrian eco-label (UZ 49) for sustainable financial products was established by the Austrian government in 2004 and is the oldest financial eco-label in Europe[18]. Certification is carried out by the Federal Ministry for Climate Protection (BMK), while the Austrian consumer association (VKI) is responsible for the development and administration of the UZ guidelines. The Austrian label is a pass-or-fail system for financial products in the financing sector (*e.g.*, green bonds, sustainable savings products, current accounts and green loans) and a point system for investment products with portfolio characteristics (*e.g.*, mutual funds). The maximum score is 66 for equity funds, 55 for bond funds, and 35 for real estate funds. The minimum threshold is set at 75% of the maximum total score. All criteria are listed in Chapter 2 of the guidelines. Below is a breakdown of the scores by fund category:

| Section | Title | Equity | Bond | Real estate | Bonus |
|---|---|---|---|---|---|
| 2.3.1 | Selection criteria | 30 | 33 | 18 | |
| 2.3.2 | Implementation of Selection criteria | 22 | 10 | 12 | |
| 2.3.4 | Degree of selection investment universe | 5 | 5 | 5 | |
| 2.3.5 | Requirements EU taxonomy | | | | 10% |
| 2.3.6 | Engagement | 9 | 7 | 0 | |
| 2.3.7 | Bonus section | | | | 3% |
| | Total | 66 | 55 | 35 | |

In addition, the fund must comply with mandatory criteria relating to exclusion, research process, transparency, investment fund business, compliance, and information and declaration. Exclusions relate to business sectors (nuclear energy, fossil fuels, weapons and armaments, genetic engineering and tobacco) and business practices (UN Global Compact).

**Label ISR (France)** Label ISR is an ESG label sponsored by the French government and certified by one of three external auditors: Afnor Certification, EY France and Deloitte. It was introduced in 2016 and covers equity, bond and real estate funds. It can be considered the successor of the ISR label launched by Novethic in 2009 and suspended in 2016 due to the existence of this new label. A first revision took place in 2020. The third revision came into force in March 2024. In previous versions of Label ISR, the exclusion policy was decided by the fund. With the new version, there is an explicit list of exclusions based on social criteria (*e.g.*, controversial weapons, UN Global Compact, tobacco), environmental criteria (*e.g.*, thermal coal, fossil fuels) or governance criteria (*e.g.*, any company domiciled in a country on the Financial Action Task Force (FATF) blacklist or greylist). In addition to exclusions, the label offers asset managers two options:

[18]The latest version of the labeling guidelines is available at www.umweltzeichen.at/en/products/sustainable-finance. It corresponds to the Austrian Ecolabel Guideline UZ 49, Sustainable Financial Products, Version 6.0 of January 1st, 2024.

1. They can reduce their ESG investable universe by 30% compared to the fund's original investment universe. This reduction involves eliminating the 30% of investments with the lowest ESG scores, along with any exclusions imposed by the fund.

2. Alternatively, they can ensure that the average weighted ESG score of the portfolio is significantly higher than that of the original investment universe. Under this option, the average weighted ESG score of the portfolio must never fall below the weighted ESG score of the fund's original investment universe or benchmark index, even after excluding the 30% of investments with the worst ESG scores and any exclusions imposed by the fund.

**LuxFLAG ESG (Luxembourg)** LuxFLAG (Luxembourg Finance Labelling Agency) is a non-profit association created in Luxembourg in July 2006 by seven founding partners to support sustainable finance including the Association of the Luxembourg Fund Industry (ALFI), the European Investment Bank, the Luxembourg Stock Exchange and the Government of Luxembourg. The LuxFLAG ESG label is launched in May 2014 and is a pass-or-fail system. It requires 100% of the portfolio to be screened against one of the ESG strategies. It has a standard exclusion policy and requires the fund to integrate at least 3 investment strategies into the investment process. The certification process is conducted by a LuxFlag committee dedicated to the label.

**FNG-Siegel (Germany)** Forum Nachhaltige Geldanlagen (FNG) is the Sustainable Investment Forum (SIF) in the German-speaking countries (Germany, Austria and Switzerland). It launched the FNG-Siegel, also known as the FNG label, in 2015. It is a grading system, but it also includes some mandatory criteria and minimum requirements. Exclusions are related to weapons, nuclear energy, fossil fuels and UN Global Compact. The weighting of the grading system for the different categories is as follows:

| Category | Weighting |
|---|---|
| Institutional credibility | 10% |
| Product standards | 20% |
| Selection strategy | 35% |
| Dialogue strategy | 25% |
| ESG key performance indicators | 10% |
| Total score | 100% |

The label grades awarded are Basic for scores up to 24.99%, One Star for scores between 25% and 49.99%, Two Star for scores between 50% and 69.99%, and Three Star for scores of 70.00% or higher. Prior to 2021, the certification was managed as a third-party funded project at the chair of Professor Timo Busch in Hamburg. Since 2021, the evaluation process has been delegated to the non-profit scientific association F.I.R.S.T., which is responsible for the FNG label certifications, and the university spin-off Advanced Impact Research (AIR).

**Towards Sustainability (Belgium)** In 2019, the Federation of the Belgian Financial Sector (Febelfin) developed a new ESG label called Towards Sustainability. It is now managed by the Central Labelling Agency (CLA), a non-profit association incorporated under Belgian law. The label is a pass-or-fail system. To qualify for the label, a sustainable financial portfolio must employ the following four strategies: ESG integration, normative screening, exclusion[19], and an additional core strategy. The first three strategies ensure that the portfolio does not finance activities that cause

[19]Exclusions include weapons, tobacco, coal, unconventional oil and gas, and lagging electric utilities.

significant harm to sustainability factors. The additional strategy either reinforces ESG principles or aligns with the portfolio's sustainability objectives. These strategies may vary in their approach: a) best-in-class/universe selection, b) theme-based sustainability investing, c) impact investing, d) the objective of outperforming a benchmark on one or more ESG indicators, e) any other strategy approved by the CLA that results in the selection of more sustainable issuers. In addition to the required minimum of four ESG strategies, the non-technical portion of the portfolio must also meet minimum requirements for greenhouse gas intensity, gender diversity, sustainable investments, and corporate engagement and shareholder activism. For the different strategies (the first three DNSH strategies and the next five additional strategies), the CLA clearly defines the eligibility criteria for compliance. For example, a sustainability themed investing strategy selects investments based on one or more clearly defined themes as outlined by recognized frameworks endorsed by the CLA, such as the EU Taxonomy, the SDGs, the EU Green Bond Standard, the ICMA Social Bond Principles, and others. It must also meet at least one of the following criteria:

- At least 70% of the portfolio's assets are related to the selected theme(s). A company is considered related to a theme if it derives at least 50% of its revenues from activities related to that theme.
- At least 50% of the total portfolio is allocated to economic activities that contribute to the selected theme.
- The portfolio uses a best-in-universe approach, targeting the top 25% of the highest rated issuers based on an appropriate ESG rating relevant to the theme.
- The portfolio qualifies as an SFDR Article 9 portfolio and includes sustainability themed investments as part of its strategy.

### Green labels

Previous labels have a clear ESG focus. Below we present European eco-labels that aim to support the transition to a low-carbon economy. For comparison with the SFDR framework, green labels are the equivalent of Article 9 funds, while ESG labels are the equivalent of Article 8 funds. However, the comparison stops here as we recall that the SFDR is not a label.

**Nordic Swan (Nordic countries)** The Nordic Swan label was established in 1989 by the Nordic Council of Ministers as a voluntary labeling scheme for the Nordic countries of Denmark, Finland, Iceland, Norway and Sweden. According to its website[20], "*it is today the official Ecolabel of the Nordic countries, supported by all Nordic governments and the most recognised environmental label in the region. The goal is to enable consumers and professional buyers to choose the environmentally best goods and services by giving an effective tool to help companies develop more sustainable products and services.*" The Nordic Swan covers 58 different product groups, from alternative dry cleaning to windows and exterior doors. For financial products, the category corresponds to Investment Funds and Investment Products 101. It includes equity funds, bond funds, balanced funds and investment products. Funds must meet requirements within four different sustainability strategies:

- Exclude the worst companies and industries in coal, oil, gas, nuclear, tobacco, weapons, and non-compliance with international standards.

[20]The address of the web site is www.nordic-swan-ecolabel.org.

- Include more sustainable companies by rewarding companies with strong sustainability performance from an ESG and EU taxonomy perspective. The criteria also pay particular attention to sectors with high greenhouse gas emissions and/or high risk of biodiversity impact.
- Exercise active ownership by engaging with companies where there is uncertainty as to whether they will meet international standards if the company is not divested.
- Disclose all holdings in the portfolio and publish an annual sustainability report.

The Nordic Swan label is an ESG grading system with extra points for environmental focus. It is therefore both an ESG label and a green label. Out of a maximum of 14 and 11 points for equity and bond funds respectively, a minimum of 6 points for equity funds and 5 points for bond funds is required to obtain the Nordic Swan label. Below is the weighting scheme for equity funds:

| Section | Title | Points |
|---|---|---|
| Inclusion criteria | EU Taxonomy alignment | 6 |
| Inclusion criteria | Enhanced analysis and inclusion | 2 |
| Active ownership | Systematic and targeted engagement | 3 |
| Active ownership | Regular voting | 3 |

For example, the portfolio alignment with the EU taxonomy is calculated using the formula:

$$\boldsymbol{\mathcal{G}} = \sum_{i=1}^{n} w_i \cdot \min\left(\frac{\boldsymbol{\mathcal{GT}}_i + \boldsymbol{\mathcal{GC}}_i + \boldsymbol{\mathcal{GO}}_i}{T_i}, 1\right)$$

where $w_i$ is the weight of holding $i$ in the portfolio, $\boldsymbol{\mathcal{GT}}_i$ is the green turnover of company $i$ in the last year, $\boldsymbol{\mathcal{GC}}_i$ is the highest annual green capex of company $i$ in the last 3 years, $\boldsymbol{\mathcal{GO}}_i$ is the highest annual green opex of company $i$ in the last 3 years and $T_i$ is the turnover of company $i$ in the last year. The number of points is 1 if $\boldsymbol{\mathcal{G}} \geq 5\%$, 2 if $\boldsymbol{\mathcal{G}} \geq 10\%$, 3 if $\boldsymbol{\mathcal{G}} \geq 20\%$, 4 if $\boldsymbol{\mathcal{G}} \geq 30\%$, 5 if $\boldsymbol{\mathcal{G}} \geq 40\%$ and 6 if $\boldsymbol{\mathcal{G}} \geq 50\%$.

**LuxFLAG Environment (Luxembourg)** Launched in July 2011, the LuxFLAG Environment label requires a portfolio of investments in environmentally related sectors[21] representing at least 75% of the fund's total assets. A company is considered to be an environmental company if its turnover in environment-related sectors is at least 20% of its total turnover. The portfolio allocation in environmental companies, weighted by the proportion of each company's turnover in environment-related sectors, must be at least 33%. A second green label, the LuxFLAG Climate Finance label, was introduced in September 2016. This label is more stringent than the Environment label. For example, funds must be classified as Article 9 SFDR products to qualify for this label.

**Label Greenfin (France)** The Greenfin label is a public certification program launched in 2015 by the French Ministry of Ecological Transition and Territorial Cohesion. Its aim is to channel investments into environmental and energy projects that support a sustainable future. Like the French ISR label, the certification is guaranteed by three external auditors: Novethic, EY France and Afnor Certification. The activities eligible for the Greenfin label are initially based on the Climate Bond Initiative's taxonomy and cover 8 themes:

[21] Environmentally related sectors are defined in relation to a globally recognized classification system such as the FTSE Environmental Markets Classification System or the HSBC Climate Change Structure.

1. Energy: solar energy, wind energy, nuclear energy, bioenergy, hydraulic energy, geothermal energy, other renewable energies, energy distribution and management, energy storage, carbon capture, services;

2. Building: low carbon buildings, energy efficiency, energy capture systems, services;

3. Circular economy: technologies and products, services, waste energy valorization, existing fossil fuels energy valorization, waste management;

4. Industry: energy-efficient products, energy-efficient systems and processes, co-generation, tri-generation, etc., waste heat recovery, reduction of GHGs not linked to energy production, reduction of pollution, eco-efficient industrial processes, services, organic agro-food industry;

5. Transport: freight and railway transport system, urban rail transport system, electric vehicles, hybrid vehicles, alternative fuel vehicles, bus rapid transit, maritime transport, bicycle transport, biofuels, aviation biofuel, transport logistics;

6. Information and communications technology: data centres running on renewable energies, low-carbon facilities, products and technologies running on smart grid, substitution technologies;

7. Agriculture & forestry: organic agriculture, sustainable agriculture, forestry activities emitting less carbon and linked to carbon sequestration, low GHG emission agriculture, sequestering carbon and climate resilient;

8. Adaptation: water adaptation, infrastructures.

Each activity has a detailed description and some eligibility criteria. Three issuer pockets are then defined based on the weight of environmental activities in their revenues: Type I issuers are companies that generate more than 50% of their revenues from environmental activities; Type II issuers are companies that generate between 10% and 50% of their revenues from environmental activities; Type III issuers are companies that generate less than 10% of their revenues from environmental activities. Funds investing in private equities and bonds must have an allocation to Type I issuers of at least 75%. Funds investing in public equities must have an allocation of at least 75% in Type I and Type II issuers, with at least 20% in Type I issuers.

In addition to the previous allocation restrictions, the Greenfin label requires the exclusion of three categories of issuers: companies developing new projects for the exploration, extraction or transportation of coal, oil, gas and fossil fuels; companies deriving more than 5% of their revenues from the fossil fuel value chain; companies deriving 30% or more of their revenues from some energy-related activities that generate significant greenhouse gas emissions, such as storage and landfill without greenhouse gas capture or incineration without energy recovery.

### EU Ecolabel

The EU Ecolabel, established in 1992, is a European Union label for green products and services. It can be seen as the equivalent of the Nordic Swan label for the countries of the European Union. As of March 2024, 95 758 products and services have been awarded the EU Ecolabel and 2 743 licenses have been granted to companies. In January 2018, the HLEG final report proposed the creation of an EU-wide label for green investment funds[22]. Since then, several proposals for an EU Ecolabel for retail financial products have been made but never adopted. The current status of

[22] See Chapter 1, page 31.

the EU Ecolabel for green funds is therefore uncertain, as we don't know whether the European Commission is not satisfied with the latest version or whether the European Commission does not want to create this label. In its first versions (Kofoworola *et al.*, 2019), the EU Ecolabel was based on the pocket approach and was close to the Greenfin label system: the first pocket includes companies that generate more than 50% of their revenues from green activities; the second pocket corresponds to companies that generate between 20% and 50% of their revenues from green activities; the third pocket includes companies that generate less than 20% of their revenues from green activities. At least 60% of the portfolio value must be invested in the first and second pockets, with at least 20% invested in the first pocket. In its latest version (Konstantas *et al.*, 2021), the EU Ecolabel is based on a green intensity approach and is close to the Nordic Swan label system. For equity funds, the greenness of the portfolio is defined as:

$$\boldsymbol{\mathcal{G}} = \sum_{i=1}^{n} w_i \left( \frac{3}{5} \boldsymbol{\mathcal{GRS}}_i + \frac{2}{5} \max \left( \boldsymbol{\mathcal{GC}}_i^{5\mathrm{Y}}, \boldsymbol{\mathcal{GR}}_i^{5\mathrm{Y}} \right) \right)$$

where $w_i$ is the weight of holding $i$ in the portfolio, $\boldsymbol{\mathcal{GRS}}_i$ is the green revenue share of company $i$ in the last year, $\boldsymbol{\mathcal{GC}}_i$ is the cumulative green capex (in %) of company $i$ over the last 5 years and $\boldsymbol{\mathcal{GR}}_i$ is the estimated green revenue growth for the next 5 years. The minimum requirement is $\boldsymbol{\mathcal{G}} \geq 40\%$. For bond funds, at least 50% of the portfolio must be invested in green bonds. The latest version of the EU Ecolabel also includes other criteria, notably ESG exclusions and the quality of the engagement policy.

Figure 4.6: The EU Ecolabel logo

### 4.1.3 The market of ESG funds

Analyzing the ESG fund market requires a definition of an ESG fund. Again, we are faced with the question of what an ESG fund is. We therefore consider three types of analysis. The first analysis looks only at labeled funds, the second analysis focuses on Article 8 and 9 funds, and the third analysis looks at sustainable funds. By construction, the first and second analyses can only be carried out for European mutual funds, as there is no equivalent outside the European Union. For the third analysis, we have to rely on the definition of a sustainable fund provided by a third-party data provider. In this last case, we decided to use Morningstar, which is known as a reference in the mutual fund industry.

### Labeled European funds

According to Novethic's annual report, there are 2 733 European funds with an ESG label, with a total of 1 307 billion euros in assets under management (Table 4.5). This represents about 7% of the European mutual fund market. More than 75% of these funds are Article 8, with the remainder being Article 9. Two labels dominate the market: France's ISR label and Belgium's Towards Sustainability. They represent 66.8% of the number of funds and 80.8% of assets under management. We note that some funds have several labels. In fact, if we add up the first column of the table, we obtain a total of 3 183 funds. The difference between 3 183 and 2 733 funds represents the double counting due to multiple labels. 333 funds have at least two labels, but some funds have three or four labels. The green-labeled funds are a small fraction, representing 5.9% of funds and 2.5% of assets under management.

Table 4.5: Overview of European sustainable labels as of 31 July 2023

| Label | Number of funds | Multiple labels | AUM € bn | No. of funds (in %) | AUM (in %) |
|---|---|---|---|---|---|
| Label ISR | 1 354 | 205 | 783 | 42.54% | 47.83% |
| FNG-Siegel | 291 | 39 | 94 | 9.14% | 5.74% |
| LuxFLAG ESG | 246 | 43 | 112 | 7.73% | 6.84% |
| LuxFLAG Microfinance | 28 | 1 | 4 | 0.88% | 0.24% |
| Towards Sustainability | 771 | 492 | 539 | 24.22% | 32.93% |
| Umweltzeichen | 304 | 192 | 64 | 9.55% | 3.91% |
| Nordic Swan | 60 | 8 | 18 | 1.89% | 1.10% |
| LuxFLAG Environment | 9 | 1 | 1 | 0.28% | 0.06% |
| Label Greenfin | 120 | 23 | 22 | 3.77% | 1.34% |
| Total | 2 733 | 333 | 1 307 | | |

Source: Menif *et al.* (2023), `www.novethic.fr` & Author's calculations.

According to Brito-Ramos *et al.* (2024a,b), labeled funds, especially those with multiple labels, are often recognized as top ESG funds by private rating providers. Government labels and multiple labels are associated with higher ESG ratings for equity funds. These labeled funds also tend to be more compliant with Article 9 of the SFDR and often include ESG terminology in their names. In addition, once a fund has received the label, it attracts additional flows compared to otherwise comparable funds. These results confirm the resilience of labeled funds in 2022. In fact, while the European mutual fund market experienced a global outflow of €273 bn in 2022, labeled funds attracted €28 bn during the same period (EFAMA, 2023a; Menif *et al.*, 2023).

### Article 8 and 9 European investment funds

To analyze the market for Article 8 and 9 funds, we use two sources. The first is Morningstar (2024b), a commercial data provider. The second is EFAMA (2023b), the European Fund and Asset Management Association. The main difference between the two studies is that in the latter case the data collection is based on surveys of EFAMA member associations. Typically, EFAMA's

Box 4.4: UCITS and alternative investment funds

UCITS (Undertakings for Collective Investment in Transferable Securities) are investment funds that can be marketed to investors throughout the European Union. They meet specific regulatory standards designed to ensure investor protection and liquidity. UCITS funds can invest in a variety of assets, such as equities, bonds and derivatives, and must comply with diversification rules and leverage limits.

Alternative investment funds (AIFs), on the other hand, encompass a broader range of investment funds that fall outside the scope of UCITS regulation. They can include hedge funds, private equity funds, real estate funds and other alternative investments. AIFs are subject to the Alternative Investment Fund Managers Directive (AIFMD), which imposes rules on fund managers to enhance transparency and investor protection. AIFs may use leverage and short positions and are generally less liquid. While UCITS funds offer daily liquidity, AIFs may offer daily, weekly, monthly or quarterly liquidity (ESMA, 2024).

results are more comprehensive because they theoretically provide more complete coverage of the AIF market, while Morningstar's results are more focused on the UCITS market. This explains why EFAMA found that Article 8 and 9 funds represented €6.78 tn at the end of 2022, while Morningstar found total assets under management of €5.2 tn at the end of 2023. By the end of 2022, Article 8 and Article 9 funds represent 45% and 2.4% of the European fund market, respectively (Table 4.6). The progress between Q1 2021 and Q4 2022 is impressive for Article 8 funds, as their market share was only 25% in the first quarter of 2021. The progress of Article 9 funds is less significant due to the wave of reclassifications between July and December 2022. These figures are higher than Morningstar's (Table 4.7), which certainly reflects the differences between UCITS and AIFs. Indeed, we can assume that alternative funds, especially hedge funds, need fewer constraints, including ESG and climate constraints, to limit the impact on their financial performance.

Table 4.6: Market share of SFDR funds (UCITS and AIFs)

| Period | Article 6 | Article 8 | Article 9 |
|---|---|---|---|
| Q1 2021 | 72.7% | 25.0% | 2.3% |
| Q4 2022 | 52.6% | 45.0% | 2.4% |

Source: EFAMA (2023b, pages 2 and 4) & Author's calculations.

Table 4.7: Number of funds and breakdown of assets under management at the end of 2023

| Statistics | Article 6 | Article 8 | Article 9 |
|---|---|---|---|
| Number of funds | 52.5% | 43.4% | 4.0% |
| Assets under management | 41.0% | 55.5% | 3.5% |

Source: Morningstar (2024b, Exhibits 6a-6b, pages 8 and 9).

Table 4.8 shows the SFDR Article 8 and Article 9 market by country of domicile. The first two columns present the domestic market share of Article 8 and Article 9 funds by country of domicile. The next two columns provide the breakdown of Article 8 funds by country of domicile. The last column gives the market share by country at European market level (UCITS and AIF). Take Luxembourg, for example. On average, 53.8% and 4.3% of funds domiciled in Luxembourg are Article 8 and Article 9 funds respectively. The assets under management of Article 8 funds domiciled in Luxembourg amount to €2 194 billion, representing 34.09% of Article 8 funds in Europe. For

Article 9 funds domiciled in Luxembourg, these figures are €175.4 billion and 51.36% respectively. To have a basis for comparison, we note that the market share of funds domiciled in Luxembourg is 30.50% at the European level. We conclude that Article 8 and 9 funds are over-represented in the Nordic countries (Finland, Norway and Sweden), France, Luxembourg and the Netherlands. Conversely, Article 8 and 9 funds are under-represented in Germany, Ireland and Spain.

Table 4.8: The SFDR Article 8 and Article 9 market by country of domicile

| Country | Domestic breakdown | | Article 8 market | | Article 9 market | | Market share |
|---|---|---|---|---|---|---|---|
| | Article 8 | Article 9 | in € bn | in % | in € bn | in % | by country (in %) |
| Austria | | 2.5 | 77.0 | 1.20 | 5.0 | 1.46 | 1.21 |
| Belgium | 65.6 | 5.2 | 120.0 | 1.86 | 9.6 | 2.81 | 1.11 |
| Croatia | 36.9 | 0.3 | 1.0 | 0.02 | 0.0 | 0.00 | 0.02 |
| Denmark | 40.3 | 2.5 | 114.0 | 1.77 | 7.1 | 2.08 | 1.71 |
| Finland | 87.0 | 10.4 | 120.0 | 1.86 | 14.4 | 4.22 | 0.84 |
| France | 50.3 | 3.4 | 903.0 | 14.03 | 61.3 | 17.95 | 12.71 |
| Germany | 15.8 | 0.2 | 410.0 | 6.37 | 5.0 | 1.46 | 15.71 |
| Greece | 3.9 | | 0.5 | 0.01 | 0.0 | 0.00 | 0.08 |
| Hungary | 2.3 | | 0.5 | 0.01 | 0.0 | 0.01 | 0.14 |
| Ireland | 36.1 | 0.9 | 1 015.0 | 15.77 | 24.4 | 7.14 | 22.15 |
| Italy | 26.1 | 2.0 | 89.0 | 1.38 | 6.9 | 2.02 | 2.07 |
| Liechtenstein | 55.8 | 3.0 | 39.0 | 0.61 | 2.1 | 0.61 | 0.43 |
| Luxembourg | 53.8 | 4.3 | 2 194.0 | 34.09 | 175.4 | 51.36 | 30.50 |
| Malta | 1.0 | 0.1 | 0.2 | 0.00 | 0.0 | 0.01 | 0.12 |
| Netherlands | | 1.7 | 662.0 | 10.29 | 12.9 | 3.78 | 4.69 |
| Norway | 65.2 | 4.3 | 103.0 | 1.60 | 6.7 | 1.96 | 0.96 |
| Poland | 0.8 | 0.1 | 0.5 | 0.01 | 0.1 | 0.03 | 0.35 |
| Portugal | 47.7 | 0.3 | 14.0 | 0.22 | 0.1 | 0.03 | 0.18 |
| Slovakia | 5.1 | | 0.5 | 0.01 | 0.0 | 0.00 | 0.05 |
| Slovenia | 2.6 | | 0.1 | 0.00 | 0.0 | 0.00 | 0.03 |
| Spain | 31.1 | 0.8 | 100.0 | 1.55 | 2.7 | 0.79 | 1.96 |
| Sweden | 95.6 | 1.6 | 473.0 | 7.35 | 7.8 | 2.28 | 3.00 |
| Total | | | 6 436.3 | 100.00 | 341.5 | 100.00 | 100.00 |

Source: EFAMA (2023a,b) & Author's calculations.

In Tables 4.9 and 4.10, we list the 20 largest Article 8 and 9 funds as of the end of 2023, according to Morningstar (2024b). For each fund, we provide the name, category, assets under management in billions of euros, and whether the fund is active or passive. Among the top 20 Article 8 funds, we find 2 bond funds, 9 equity funds, 5 multi-asset funds, and 4 real estate funds. Three of the equity funds are sector-specific. Only one fund is passive. Among the top 20 Article 9 funds, we find 4 bond funds and 16 equity funds, of which 7 are sector-specific. Three funds are passive. On average, equity funds represent 50% of Article 8 funds and 70% of Article 9 funds.

The study by Becker *et al.* (2022) shows that EU funds directly affected by the SFDR became demonstrably more sustainable after its announcement. This suggests that the regulation is effective in directing investment towards greener options. In addition, the study finds that post-SFDR, investors prefer funds with a stronger ESG focus, resulting in increased capital allocation to these funds. SFDR has driven a significant portion of investment flows over the past two years, a conclusion shared by Morningstar (2024b).

Table 4.9: The 20 largest Article 8 funds (as of end 2023)

| Name | Category | AUM | Passive |
|---|---|---|---|
| Flossbach von Storch SICAV - Multiple Opportunities | Allocation | 24.9 | |
| Morgan Stanley Global Brands Fund | Global Equity | 20.5 | |
| AB FCP I - American Income Portfolio | US Fixed Income | 20.2 | |
| DWS Top Dividende | Global Equity | 19.5 | |
| Fidelity Funds - Global Technology Fund | Technology Sector | 18.6 | |
| Deka-ImmobilienEuropa | Real Estate | 18.5 | |
| JPMorgan Global Income Fund | Allocation | 17.5 | |
| hausInvest | Real Estate | 17.3 | |
| UniImmo: Deutschland | Real Estate | 16.7 | |
| UniImmo: Europa | Real Estate | 14.8 | |
| DWS Concept Kaldemorgen | Allocation | 14.0 | |
| iShares MSCI USA ESG Enhanced ETF | US Equity | 13.3 | ✓ |
| DWS VermÃűgensbildungsfonds I | Global Equity | 13.0 | |
| AB FCP I - Global High Yield Portfolio | Global Fixed Income | 12.9 | |
| Mercer Multi Asset Growth Fund | Allocation | 12.6 | |
| BlackRock World Healthscience Fund | Healthcare Sector | 11.9 | |
| Flossbach von Storch - Multiple Opportunities II | Allocation | 11.9 | |
| Swedbank Robur Technology | Technology Sector | 11.9 | |
| Morgan Stanley Global Opportunity Fund | Global Equity | 11.6 | |
| Pictet - Global Megatrend Selection | Global Equity | 11.3 | |

Source: Morningstar (2024b, Exhibit 10, page 14).

Table 4.10: The 20 largest Article 9 funds (as of end 2023)

| Name | Category | AUM | Passive |
|---|---|---|---|
| Nordea 1 - Global Climate and Environment Fund | Global Equity | 9.1 | |
| Handelsbanken Global Index Criteria | Global Equity | 8.7 | ✓ |
| Pictet-Water | Thematic Equity | 8.1 | |
| Pictet - Global Environmental Opportunities | Global Equity | 7.4 | |
| BlackRock Global Funds - Sustainable Energy Fund | Energy Sector | 6.1 | |
| Handelsbanken USA Index Criteria | US Equity | 4.9 | ✓ |
| Mirova Global Sustainable Equity Fund | Global Equity | 4.7 | |
| Pictet - Clean Energy Transition | Energy Sector | 4.6 | |
| Handelsbanken Norden Index Criteria | Europe Equity | 3.9 | ✓ |
| BNP Paribas Funds Aqua | Thematic Equity | 3.7 | |
| BNP Paribas Aqua | Thematic Equity | 3.6 | |
| RobecoSAM Smart Energy Equities | Energy Sector | 3.4 | |
| RobecoSAM Sustainable Water Equities | Thematic Equity | 3.2 | |
| DPAM L - Bonds Emerging Markets Sustainable | EM Fixed Income | 3.2 | |
| BNP Paribas Funds Climate Impact | Global Equity | 2.8 | |
| AB SICAV I - Sustainable Global Thematic Portfolio | Global Equity | 2.8 | |
| Impact ES Actions Europe | Europe Equity | 2.5 | |
| Goldman Sachs Green Bond | Europe Fixed Income | 2.4 | |
| Goldman Sachs - Green Bond | Europe Fixed Income | 2.4 | |
| Candriam Sustainable Bond Euro Corporate | Europe Fixed Income | 2.3 | |

Source: Morningstar (2024b, Exhibit 11, page 15).

### Sustainable funds

The previous section dealt with the SFDR market, which is a purely European market. To get a global view, we need to use criteria other than Article 8, Article 9 or even ESG labels. However, this type of exercise is not straightforward as there is no definition of what an ESG fund is and comparisons between countries and regions are not straightforward. How do we compare an ESG fund domiciled in China, the US, Canada, Singapore, Sweden or Italy? This is why we need to turn to an external data provider. In general, asset managers use three main databases to analyze sustainable investment funds: Broadridge (www.broadridge.com), LSEG Lipper (www.lseg.com) and Morningstar (www.morningstar.com). However, we must be careful because each data provider uses its own definition of sustainable funds, so the numbers are not comparable across data providers. For example, our calculations show that European mutual fund assets under management (excluding money market funds) are €7.3 tn if we use the Broadridge Responsible Investment funds category, €5.8 tn if we use the Morningstar Article 8 & 9 funds category, and €2.5 tn if we use the Morningstar sustainable funds category. In the following, we will use the latter database because it is the more restrictive one.

Box 4.5: Morningstar's definition of the global universe of sustainable funds

"*The global sustainable fund universe encompasses open-end funds and ETFs that, by prospectus or other regulatory filings, claim to focus on sustainability, impact, or environmental, social, and governance factors. Our universe of sustainable funds is based on intentionality rather than holdings. For example, a portfolio can score well on ESG metrics such as the Morningstar Sustainability Rating, but if ESG issues are not the focus of the fund's investment strategy, it will not be included in our universe. To identify intentionality, we relied on a combination of fund names (a strong indicator of intentionality) and information found in fund documents. The fund's documents should contain enough details to leave no doubt that ESG concerns figure prominently in the security-selection and portfolio construction process. The global sustainable fund universe does not contain the growing number of funds often referred to as ESG integrated funds, which formally consider ESG criteria in the investment process and engage with portfolio holdings but do not make ESG considerations the focus of the investment process. Furthermore, the global sustainable fund universe doesn't include funds that employ limited exclusionary screens [...] We however include ESG-screened passive funds in our universe as, typically for these, the exclusions are the sole purpose of the strategy. Finally, the global sustainable fund universe excludes money market funds, feeder funds, and funds of funds to avoid double counting and inflating flows and assets.*" (Morningstar, 2024a, page 43).

According to Morningstar (2024a), there are around 7 500 sustainable funds in the world with a total of $3 trillion in assets under management (Table 4.11). 84% of these assets are in Europe, 11% in the US and 5% in the rest of the world. The average fund size is $500 million in Europe and the US, which is five times the average size of sustainable funds in Asia and Oceania. The market share of sustainable funds continues to grow, with inflows into sustainable funds of $161 billion in 2022 and $63 billion in 2023. However, there is a contrast between the US and the other regions, as we observe net redemptions in the US in 2022 and 2023.

In Table 4.12, we show the top asset managers by sustainable fund assets. Morningstar (2024a) provides the top 20 for different categories (overall, actively managed and passively managed) and different regions (global, Europe and US). We note that the sustainable asset management industry

Table 4.11: Global sustainable fund statistics (as of December 2023)

| Region | Funds | | AUM | | Fund size |
|---|---|---|---|---|---|
| | # | in % | $ bn | in % | $ mn |
| Europe | 5 433 | 72.59 | 2 492 | 83.99 | 459 |
| United States | 647 | 8.64 | 324 | 10.92 | 501 |
| Asia ex-Japan | 595 | 7.95 | 62 | 2.09 | 104 |
| Australasia | 263 | 3.51 | 33 | 1.11 | 125 |
| Japan | 235 | 3.14 | 25 | 0.84 | 106 |
| Canada | 312 | 4.17 | 31 | 1.04 | 99 |
| Total | 7 485 | 100.00 | 2 967 | 100.00 | 396 |

Source: Morningstar (2024a, Exhibit 1, page 2) & Author's calculations.

Table 4.12: Top asset managers by sustainable fund assets (in $ bn)

| Firm | Global | | | Europe | | | United States | | |
|---|---|---|---|---|---|---|---|---|---|
| | Total | Active | Passive | Total | Active | Passive | Total | Active | Passive |
| BlackRock | 318.1 | 46.8 | 271.3 | 256.8 | 41.5 | 215.3 | 59.2 | 5.5 | 53.7 |
| UBS | 164.7 | 66.0 | 98.7 | 164.2 | 65.6 | 98.5 | | | |
| Amundi | 161.0 | 84.1 | 76.9 | 164.0 | 76.3 | 87.7 | 8.5 | 8.5 | |
| DWS | 93.1 | 56.0 | 37.2 | 89.7 | 57.4 | 32.2 | 5.2 | 4.9 | 0.3 |
| BNP Paribas | 85.8 | 54.4 | 31.4 | 85.8 | 54.4 | 31.4 | | | |
| Swisscanto | 84.0 | 52.3 | 31.7 | 84.0 | 52.3 | 31.7 | | | |
| Natixis | 74.5 | 72.0 | 2.5 | 73.8 | 71.3 | 2.5 | | | |
| Nordea | 57.2 | 57.2 | | 57.2 | 57.2 | | | | |
| Pictet | 49.7 | 49.7 | | 49.7 | 49.7 | | | | |
| Vanguard | 47.2 | 2.8 | 44.4 | | | 13.1 | 30.5 | 1.4 | 29.0 |
| Allianz GI | 46.6 | 46.6 | | 46.7 | 46.7 | | | | |
| Parnassus | 39.3 | 39.3 | | | | | 39.3 | 39.3 | |
| Eaton Vance | 34.7 | 25.0 | 9.7 | | | | | | |
| Royal London | 34.7 | 28.6 | 6.1 | 34.7 | 28.6 | 6.1 | | | |
| Calvert | | | | | | | 34.7 | 25.0 | 9.7 |
| Eurizon | 34.2 | 34.2 | | 34.3 | 34.3 | | | | |
| Goldman Sachs | 34.2 | 34.1 | 0.1 | 30.7 | 30.6 | 0.1 | | | |
| Handelsbanken | 33.8 | 4.8 | 29.0 | 36.2 | 5.5 | 30.7 | | | |
| AXA | 33.4 | 33.4 | | 32.9 | 32.9 | | | | |
| KBC | 33.2 | 33.2 | | 33.2 | 33.2 | | | | |
| Union Investment | 33.0 | 33.0 | | 37.7 | 37.7 | | | | |
| Deka | | | | 30.7 | 26.9 | 3.8 | | | |
| Robeco | | 27.4 | | 27.3 | 27.3 | | | | |
| Vontobel | | 27.3 | | 27.2 | 27.2 | | | | |
| Schroders | | 26.2 | | | | | | | |
| Candriam | | | | | 26.1 | | | | |
| State Street | | | 24.2 | | | 21.5 | | | 2.0 |
| Northern Trust | | | 22.6 | | | 20.6 | | | 2.0 |
| Nuveen/TIAA | | | 5.6 | | | | 21.7 | 16.2 | 5.6 |

Source: Morningstar (2024a, Exhibit 1, page 2) & Author's calculations.

is dominated by European asset managers such as UBS, Amundi, DWS, BNP Paribas, Swisscanto, Natixis, Nordea and Pictet. Two US managers, BlackRock and Vanguard, are in the top 10 due to their size in the ETF market. We also note the presence of two small US managers that have been leaders in responsible investing for 40 years (Parnassus and Calvert). As of December 2023, they managed $46.5 bn and $37.5 bn in total assets, respectively, with 85% and 93% in the Morningstar sustainable fund category. Table 4.12 also shows that the ranking is dominated by asset managers with a large passive management business. However, some purely active managers have also developed a sustainable fund business, such as Nordea, Pictet, Eurizon, Robeco and Vontobel. The big difference between Europe and the US is not only the size of the sustainable market, but also its structure. In Europe, the 20th largest asset manager has more than $27 billion in sustainable funds, compared to less than $3 billion in the US. The cumulative market share of the top 20 asset managers is 86.5% in the US, but only 56% in Europe (Figure 4.7). This means that many other asset managers have more than $10 billion in European sustainable funds, while they manage few assets in US sustainable funds. The US market for sustainable funds is therefore highly concentrated among a few players, whereas in Europe it is more atomistic. In other words, the sustainable fund business is a niche in the US, whereas it is mainstream in Europe.

Figure 4.7: Cumulative market share in % of the top 20 asset managers in the sustainable funds market

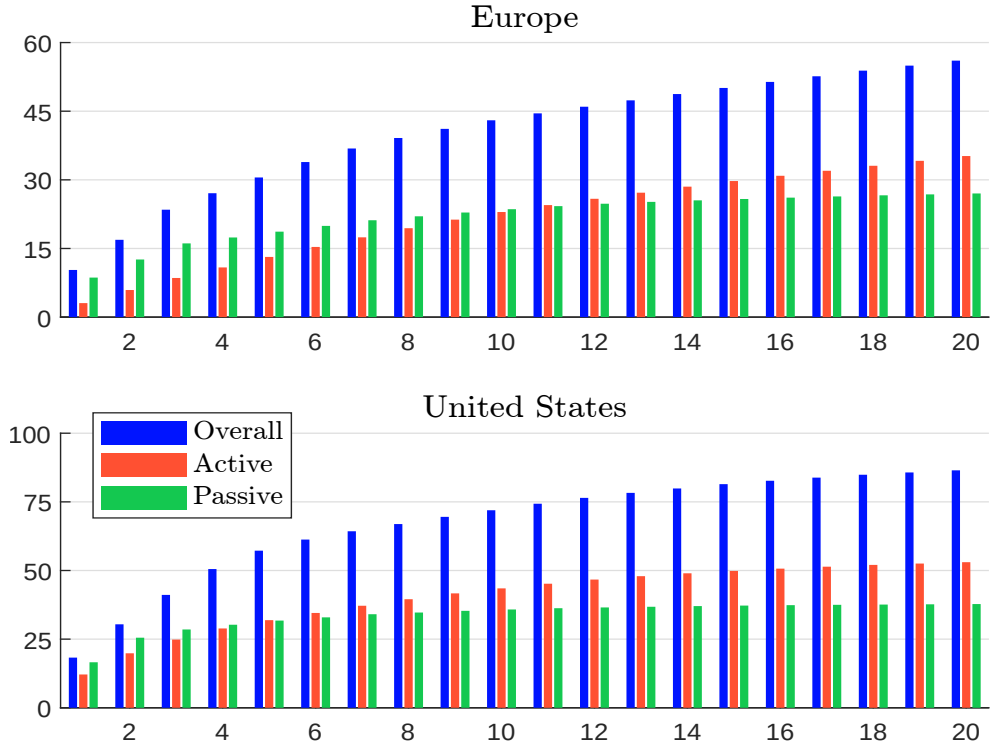


Source: Morningstar (2024a) & Author's calculations.

The previous analysis can be complemented by another Morningstar analysis dedicated to climate funds (Morningstar, 2023). Again, Morningstar uses several criteria to identify this sub-category of sustainable funds, notably name and investment policy. They group them into five strategies: low carbon, climate transition, green bonds, climate solutions and clean technology. As of June 2023, they found 1 407 climate-related open-end funds and ETFs, representing $534 billion or almost 20% of the global sustainable funds market. This market is again dominated by Europe (84% of assets),

Table 4.13: Largest climate funds (As of June 2023)

| Country | Name | Category | AUM ($ bn) |
|---|---|---|---|
| Europe | ACS Climate Transition World Equity Fund | Climate Transition | 12.8 |
| | iShares MSCI USA ESG Enhanced ETF | Climate Transition | 12.2 |
| | Nordea 1 Global Climate and Environment Fund | Climate Solutions | 10.8 |
| | Blackrock ACS World ESG Equity Tracker Fund | Low Carbon | 10.2 |
| | Pictet Global Environmental Opportunities | Climate Solutions | 8.4 |
| | Handelsbanken Global Index Criteria | Climate Transition | 8.0 |
| | iShares Environment & Low Carbon Tilt Real Estate | Low Carbon | 7.9 |
| | Blackrock ACS World Low Carbon Equity Tracker Fund | Low Carbon | 7.5 |
| | BlackRock Sustainable Energy Fund | Clean Technology | 7.3 |
| | Amundi MSCI USA SRI PAB | Climate Transition | 6.3 |
| United States | iShares Global Clean Energy ETF | Clean Technology | 4.2 |
| | Impax Global Environmental Markets Fund | Climate Solutions | 2.4 |
| | iShares Climate Conscious & Transition MSCI USA ETF | Climate Transition | 2.2 |
| | Xtrackers MSCI USA Climate Action Equity ETF | Climate Transition | 2.2 |
| | Invesco Solar ETF | Clean Technology | 2.1 |
| | First Trust NASDAQ Clean Edge Green Energy Index Fund | Clean Technology | 1.6 |
| | iShares Paris-Aligned Climate MSCI USA ETF | Climate Transition | 1.5 |
| | BlackRock U.S. Carbon Transition Readiness ETF | Climate Transition | 1.5 |
| | TIAA-CREF Social Choice Low Carbon Equity Fund | Low Carbon | 1.2 |
| | GMO Climate Change Fund | Clean Technology | 1.0 |
| China | Orient Secs Green Energy Car Alloc | Climate Solutions | 2.3 |
| | Huatai-PB CSI Photovoltaic Industry ETF | Clean Technology | 2.3 |
| | ABC-CA New Energy Theme Hybrid Fund | Clean Technology | 2.1 |
| | ChinaAMC New Energy Fund | Clean Technology | 2.0 |
| | TianHong CSI Photovoltaic Industry Idx | Clean Technology | 1.9 |
| | China Universal New Eneg Car Ind Index LOF | Climate Solutions | 1.9 |
| | ChinaAMC CSI New En Car Ind ETF | Climate Solutions | 1.6 |
| | Fullgoal China Secs New Energy Vehicles | Climate Solutions | 1.5 |
| | Cinda New Energy Ind Stk Fd | Clean Technology | 1.3 |
| | E Fund Pro-Environment Alloc | Climate Solutions | 1.1 |
| Japan | iShares MSCI Japan Climate Action ETF | Climate Transition | 0.818 |
| Taiwan | Cathay Global Autonomous and Electric Vehicles ETF | Climate Solutions | 0.808 |
| Australia | Russell Investments Low Carbon Global Shares Fund | Low Carbon | 0.611 |
| Australia | Russell Invest. Low Carbon Global Shares Fund AUDH | Low Carbon | 0.559 |
| Canada | Fidelity Climate Leadership Fund | Climate Transition | 0.400 |
| Canada | Desjardins SocieTerra Cleantech Fund | Clean Technology | 0.340 |
| Australia | State Street Climate ESG International Equity Fund | Low Carbon | 0.243 |
| South Korea | NH-Amundi Century Enterprise Green Korea Equity | Climate Solutions | 0.240 |
| Japan | NZAM ETF S&P/JPX Carbon Efficient Index | Low Carbon | 0.236 |
| Australia | SPDRÂő S&P World ex Australia Carbon Control Fund | Low Carbon | 0.217 |

Source: Morningstar (2023, Exhibits 14, 19, 24 & 30, pages 17, 23, 27 & 32).

followed by China (8.5%), the US (5.9%), Australia (0.5%), Canada (0.5%), South Korea (0.3%), Taiwan (0.3%) and Japan (0.2%). The largest climate funds by region are reported in Table 4.13. It is worth noting that Europe is more focused on low-carbon and climate transition strategies, while China is more focused on climate solutions and clean technology strategies, and the US is more focused on climate transition and clean technology strategies. Morningstar (2023, page 11) found the following asset class breakdown: 82.4% in equity funds, 12% in bond funds and 5.1% in multi-asset funds. Another interesting result is the large share of climate transition ETFs in Europe, which is due to the popularity of CTB/PAB benchmarks (Morningstar, 2023, page 18).

## 4.2 Green and social bonds

Alongside traditional investment vehicles that incorporate ESG criteria, we can find a category of securities that is entirely dedicated to sustainable finance. These are specific sustainable debt instruments. The two best known assets are green bonds and social bonds, but the list of sustainable fixed-income assets is much longer: sustainable bonds, transition bonds, sustainable-linked bonds, green loans, green notes, green ABCP notes, etc. Table 4.14 shows the segmentation of the sustainable bond market. According to CBI (2024c), the cumulative total GSS+ issuance stands at \$5.5 tn at the end of 2023, of which \$4.4 tn (80%) was found to be aligned. About 99% comes from GSS assets (Figure 4.8). The breakdown is as follows: 65% for green bonds, 18% for social bonds and 17% for sustainability bonds. The market is dominated by DM issuers (about 60%), with the remainder being two-thirds EM and one-third supranational.

Table 4.14: Sustainable fixed-income market

| Theme | | Label | Format |
|---|---|---|---|
| GSS+ | GSS | Green | Use of proceeds |
| | | Social | Use of proceeds |
| | | Sustainability | Use of proceeds |
| | Transition | Sustainability-Linked | Entity KPI-linked |
| | | Transition | Use of proceeds |

Source: CBI (2024c).

Figure 4.8: Issuance of GSS securities (in \$ bn)

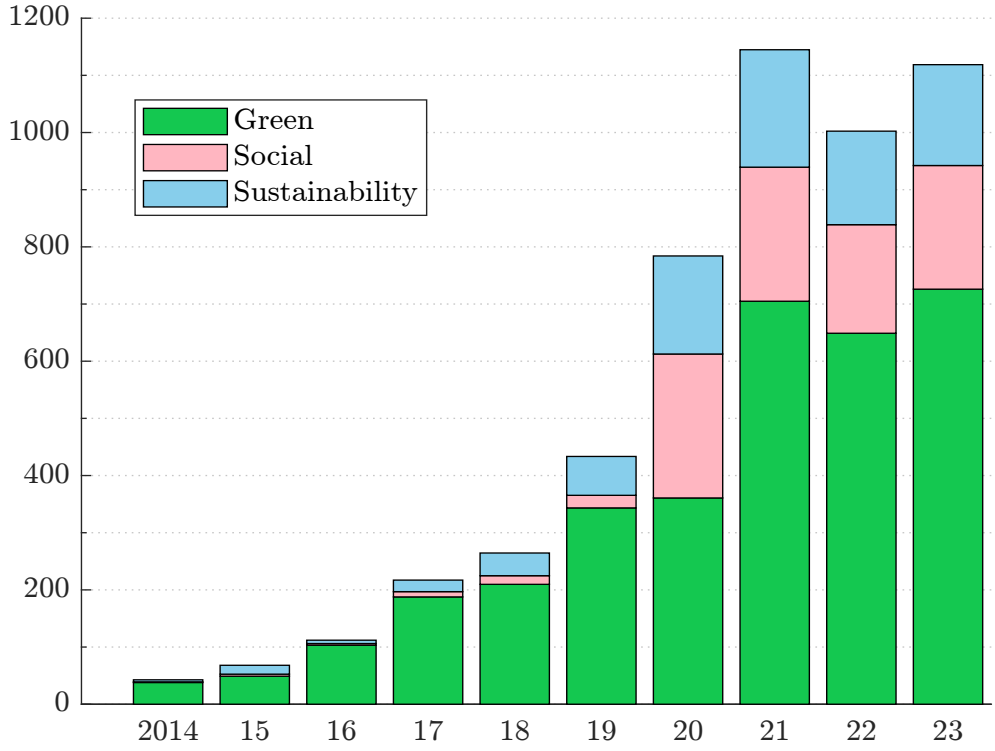


Source: https://www.climatebonds.net/market/data.

### 4.2.1 Green bonds

#### Definition

Green bonds are fixed-income securities that finance investments with an environmental objective. They differ from regular bonds in that they are labeled green by the issuer or an external third party, and there is a commitment to use the proceeds to finance green projects. However, there is no legally binding definition of a green bond. Most of market participants[23] have then adopted the definition of the GBP framework[24]:

> "*Green bonds are any type of bond instrument where the proceeds or an equivalent amount will be exclusively applied to finance or re-finance, in part or in full, new and/or existing eligible green projects and which are aligned with the four core components of the Green Bond Principles (GBP).*" (ICMA, 2021a, page 3).

The four core components of the GBP are:

1. Use of proceeds
2. Process for project evaluation and selection
3. Management of proceeds
4. Reporting

The use of proceeds (or funds) should be directed to eligible green projects, *e.g.*, renewable energy, energy efficiency, pollution prevention (greenhouse gas control, soil remediation, waste recycling), sustainable management of living natural resources (sustainable agriculture, sustainable forestry, restoration of natural landscapes), conservation of terrestrial and aquatic biodiversity (protection of coastal, marine and watershed environments), clean transport, sustainable water management, climate change adaptation, circular economy and eco-efficient products, green buildings. With respect to the project evaluation and selection process, the green bond issuer should clearly communicate the environmental sustainability objectives, the eligible projects and the related eligibility criteria. The third component deals with the management of the proceeds and includes the tracking of the "*balance sheet*" and the allocation of funds[25]. It also recommends an external audit by a third party. Finally, reporting must be based on the following pillars: transparency, description of projects, amounts allocated and expected impacts, qualitative performance indicators and quantitative performance measures[26].

**Remark 44** *The GBP is not the only framework for green bonds. The other popular guidelines are:*

- *China Green Bond Principles*[27] *(PBOC, CBIRC, July 2022)*
- *Climate Bonds Standard*[28] *(CBI, 2019)*
- *ASEAN Green Bond Standards*[29] *(ACMF, 2018)*

[23] According to IFC (2020, page 5), the Green Bond Principles are supported by 95% of issuers.
[24] The first version of the Green Bond Principles was published in January 2014.
[25] Proceeds should be credited to a sub-account.
[26] Here are some examples: energy capacity, electricity generation, GHG emissions reduced/avoided, number of people given access to clean power, decrease in water use, reduction in the number of cars required, etc.
[27] They replace China's Green Bond Standards published by PBOC in 2015.
[28] The first version is released in November 2011. A new version has been published in February 2024 (CBI, 2024a).
[29] The first version is published in 2017.

- *EU Green Bond Standard*[30]

*All these guidelines are based on a common framework and are closed to the GBP. The CBI approach, which also uses the GBP, is perhaps more comprehensive and provides more detail on how to issue a green bond*[31].

Green debt instruments can be issued in different formats. They differ in terms of collateral, recourse process in case of default, etc. For instance, the most common instrument is the green regular or "*Use of Proceeds*" bond (UoP bond), which has the same credit rating as a conventional bond, because bondholders have recourse to all the assets of the bond issuer. In the case of a green revenue bond, the collateral for the debt comes from the cash flows of the revenue streams collected by the issuer. A green project bond is a bond dedicated to a specific green project, meaning that the recourse process only affects the assets associated with the project. Green loans are loans that finance green projects and can be secured or unsecured. These four instruments (regular bond, revenue bond, project bond and green loan) are called asset-linked bond structures because they are linked to a specific asset/project. Asset-backed bond structures consist of securitization and covered bonds. Both involve a group of projects. Securitized bonds can use ABS/MBS/CLO/CDO securitization structures, while covered bonds are German debt instruments (Pfandbriefe) that use a dual recourse process based on the issuer and the cover pool[32].

The certification process (or external review) is an important step in the issuance of green bonds, as it is related to the issue of greenwashing. We recall that the GBP are voluntary process guidelines. They recommend that issuers engage an external review provider to obtain a pre-issuance assessment of the green project and an external auditor to obtain a post-issuance validation of the funding management. Certainly, the most popular form of external review is the second party opinion or SPO (IFC, 2020, page 19). In this case, the issuer's objective is to obtain a "*green bond label*" or the approval of its green project by a competent and independent body that is recognized by financial markets and investors. For instance, Ehlers and Packer (2017) and IFC (2020) list the following forms of green bond certification[33]:

- Second party opinion from ESG rating agencies (ISS, Sustainalytics, Vigeo-Eiris);
- Certification by green bond specialists (CBI, CICERO, DNV);
- Green bond assessment by statistical rating agencies (Moody's, S&P).

**Some examples**

The climate-related bond market began in 2001 with the issuance of a revenue bond (known as the solar bond) by the City of San Francisco. The goal was to finance 140 acres of solar panels that could power homes and commercial buildings with renewable energy. A second step was reached in 2007 when the European Investment Bank (EIB) issued the world's first Climate Awareness Bond (CAB) to finance renewable energy and energy efficiency projects. Finally, in 2008, the World Bank and the

[30] The proposal for a regulation on European green bonds has been released in 2021. It is based on four key requirements: (1) taxonomy-alignment; (2) transparency on how the bond proceeds are allocated through detailed reporting requirements; (3) all European green bonds must be checked by an external reviewer; (4) external reviewers must be supervised by the ESMA.

[31] See also the Green Bond Handbook published by IFC (2020).

[32] Investors may have recourse to the issuer, but if the issuer is unable to pay its debt, then bondholders gain recourse to the cover pool.

[33] Ehlers and Packer (2017) added green bond indexes as a fourth form of certification, as inclusion in a green bond index is a market recognition that the bond is green.

Swedish bank SEB created the first green bond for a group of Scandinavian institutional investors. Since then, the green bond market has grown rapidly. The amount issued has increased from less than \$3 bn in 2013 to more than \$700 bn in 2023. According to Baker *et al.* (2022), 2013 and 2014 marked the development of the green bond market. For instance, the first corporate green bonds were issued by the French utility EDF (\$1.8 bn) and the Swedish real estate company Vasakronan (\$120 bn). Toyota launched the automobile industry's first asset-backed green bond in 2014 (\$1.75 bn), while the Commonwealth of Massachusetts successfully completed the first municipal green bond in 2013 (\$100 mn). The development of sovereign green bonds begins with the issuance of Poland in December 2016 (\$1 bn) and France[34] in January 2017 (\$10 bn).

According to CBI (2022), the largest corporate issuers in 2021 were China Three Gorges (\$7.2 bn), Iberdrola (\$3.3 bn), CTP (\$3 bn), Ardagh (\$2.8 bn), Engie (\$2.6 bn), Ford Motor (\$2.5 bn), EDP (\$2.4 bn), State Grid Corporation of China (\$2.4 bn), Mondelez International (\$2.4 bn) and Liberty Global (\$2.3 bn). In 2022, the largest corporate issuer was again China Three Gorges (\$5.1 bn), followed by Orsted (\$4 bn), Iberdrola (\$3.1 bn), Honda Motor (\$2.8 bn), Volkswagen (\$2.6 bn), E.ON (\$2.6 bn), EDP (\$2.4 bn), General Motors (\$2.3 bn), RWE (\$2.1 bn) and Huaneng Lancang River Hydropower (\$2.3 bn). These figures lag far behind those of sovereign issuers and financial corporations. According to CBI (2023), the top three issuers in 2022 were the European Union (\$26 bn), the EIB (\$14.5 bn) and Germany (\$14.3 bn).

**Remark 45** *Post-issuance management of a green bond can be an issue. For example, the Mexico City Airport Trust issued \$6 bn of green bonds in 2016 and 2017 to finance the construction of a new airport. It complied with ICMA GBP and received a second party opinion from Sustainalytics, as well as green bond assessments from rating agencies Moody's and S&P. However, in October 2018, the new Mexican government announced a halt to the construction of the airport and launched a buyback package capped at \$1.8 bn.*

### The green bond market

**Statistics** From 2007 to the first half of 2022, CBI estimate that a total of 10 800 green bonds have been issued in the world[35]. The geographic repartition is the following: 52% in North America, 23% in Europe, 17% in Asia-Pacific and 8% in the rest of the world (including supranational entities). The distribution of deal size is highly skewed. Indeed, 70% of green bonds have a notional less than \$100 mn, whereas 3.2% of them have a deal size greater than \$1 bn. If we focus on the number of issuers, we obtain the following top five ranking[36]: 500 in US, 404 in China, 156 in Japan, 104 in Sweden and 63 in Norway. If we analyze the amount issued, the size of the green bond market is roughly equal to \$1.9 tn. In Figures 4.9 and 4.10, we have reported the issuance and notional outstanding (or cumulative issuance) by market type and region from 2014 to 2023. The market is lead by Europe (46%), followed by Asia-Pacific[37] (25%) and North America (20%). The issuance of green bonds mainly concerns four sectors: energy, buildings, transport and water. They represent 88% of the market (Figure 4.11). An analysis by issuer type shows the market is approximately balanced between financials (development banks and financial corporates), governement/sovereign issuers (including government-backed entities, local governments and states) and non-financial corporations (Figure 4.12).

[34] Green OAT 1.75% 25 June 2039.

[35] This number is skewed because Fannie Mae has been a very frequent issuer of relatively small green MBS deals (less than \$100 mn).

[36] The number of green bond issuers in France and Germany is respectively equal to 58 and 50.

[37] China represents more than 50% of the Asia-Pacific green bond market.

Figure 4.9: Issuance and notional outstanding of green debt by market type

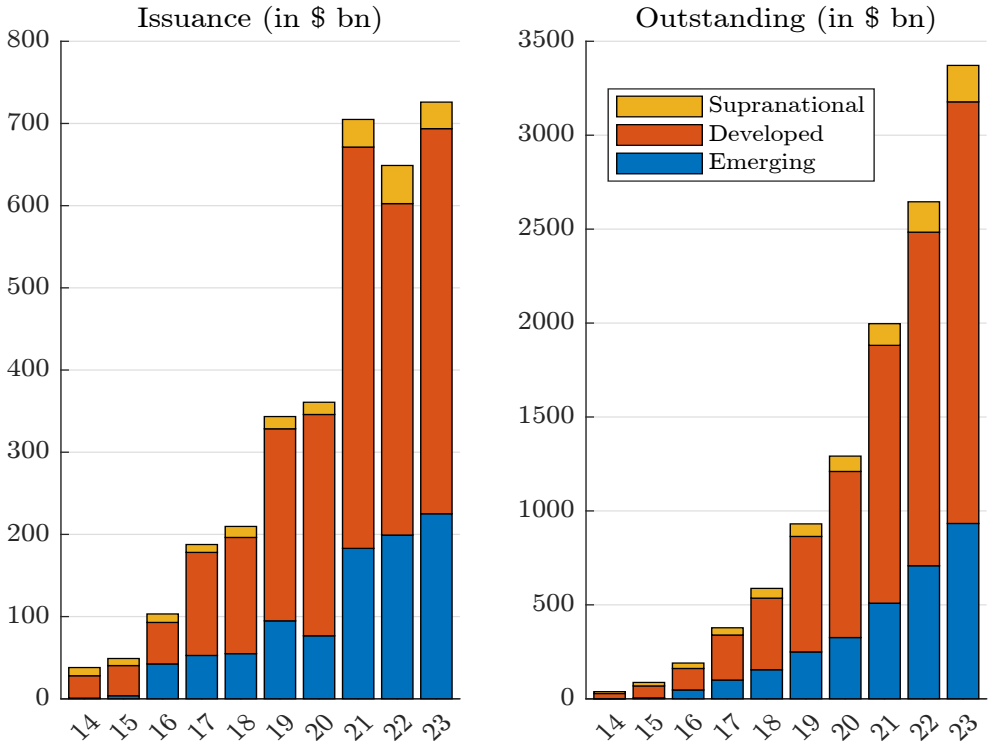


Figure 4.10: Issuance and notional outstanding of green debt by region

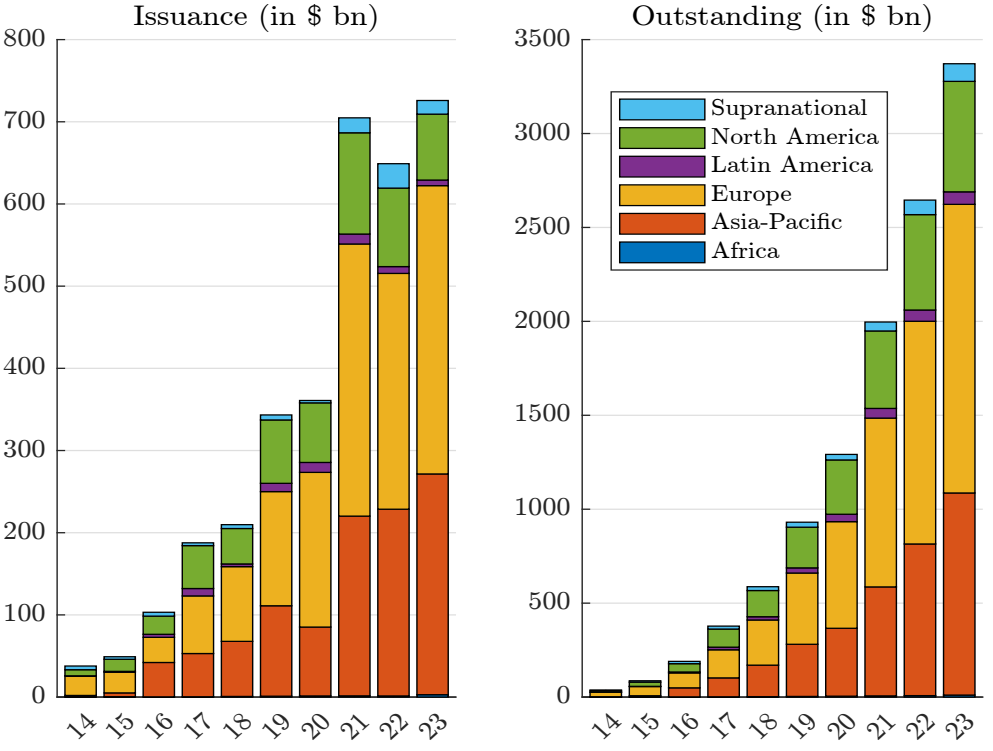


Source: https://www.climatebonds.net/market/data.

Figure 4.11: Issuance and notional outstanding of green debt by use of proceeds

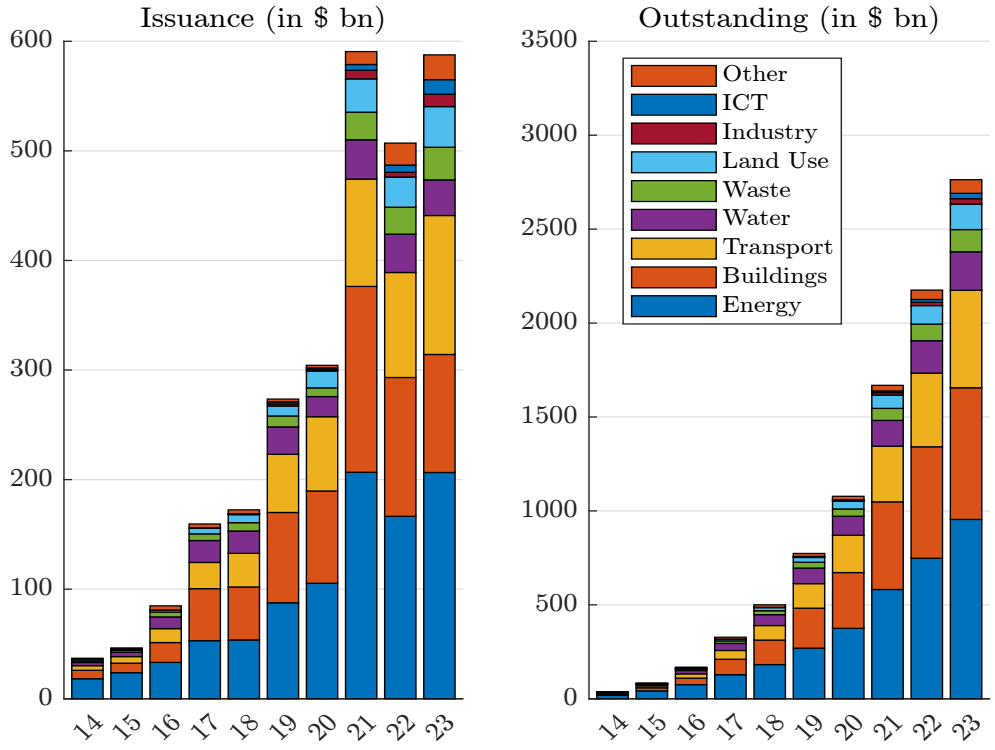


Figure 4.12: Issuance and notional outstanding of green debt by issuer type

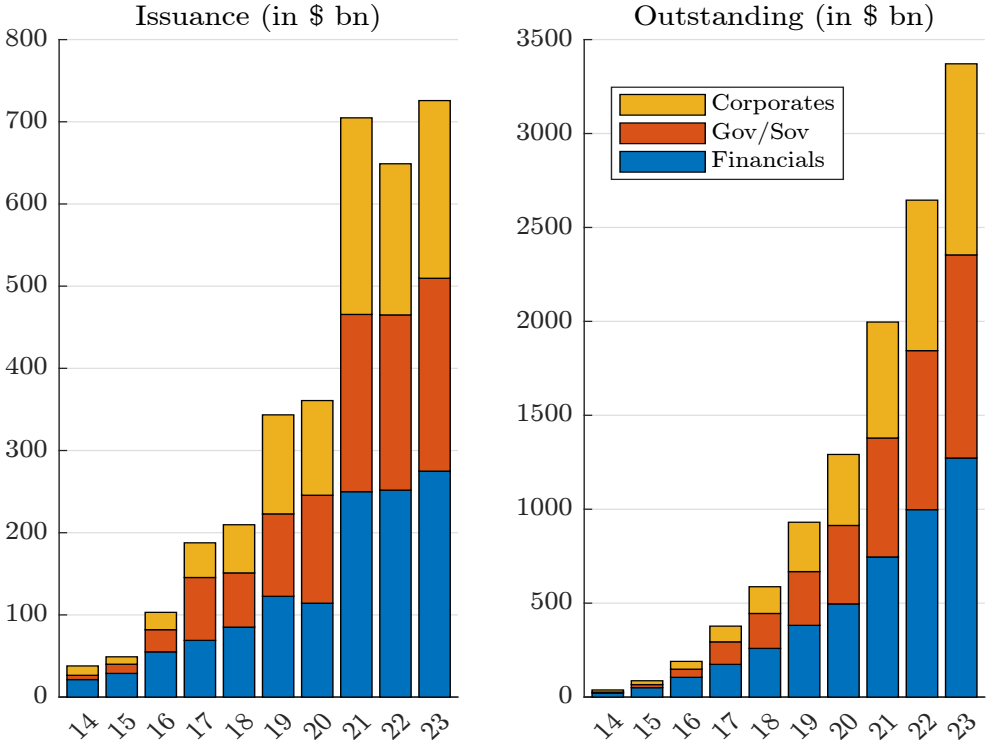


Source: https://www.climatebonds.net/market/data.

**How to invest in green bonds** There are several ways to invest in green bonds. We can consider a mutual fund (active management), an ETF (passive management) or a direct investment[38]. Here are some examples of active investment funds: Allianz IG green bond fund, Amundi RI impact green bonds, AXA WF ACT green bonds, BNP Paribas green bond, Calvert green bond fund, Mirova global green bond fund, TIAA-CREF green bond fund. In addition to these investment vehicles, institutional investors can also invest in some closed-end funds: Amundi planet emerging green one, Conservation fund green bonds, Foresight Italian green bond fund, etc. However, the largest investments in green bonds are made through passive management, particularly ETFs: Franklin Liberty green bond, iShares global green bond, Lyxor green bond, VanEck Vectors green bond, Xtrackers corporate green bond, etc. In this case, the ETF uses a green bond index such as:

- Bloomberg MSCI Global Green Bond Index (global green bonds)
- S&P Green Bond Index (global green bonds)
- Solactive Green Bond Index (global green bonds)
- ChinaBond China Climate-Aligned Bond Index (chinese green bonds)
- SSE Green Corporate Bond Index and SSE Green Bond Index (green bonds listed on the Shanghai Stock Exchange)
- ICE BofA Green Index (global green bonds)

### The economics of green bonds

**Rationale for issuing green bonds** Green bonds are very different from ESG portfolios and funds because the objective is to finance a specific green project. Therefore, the decision to invest in a green bond goes beyond CSR or SRI values (Maltais and Nykvist, 2020). From an issuer's perspective, it is a signal and a visible confirmation of the company's participation in the green economy (Flammer, 2021; Daubanes *et al.*, 2021). From an investor's perspective, it is a relatively easy way to implement an impact investing programme. In addition, green bonds are more climate-related than ESG-related assets. They are heavily involved in financing the climate transition. For example, the issuance of sovereign green bonds is generally presented as a response to climate change. Looking at the NextGenerationEU program of green bonds, the objective of the European Commission is to "*achieve the goal of climate neutrality by 2050.*" Denmark issued its first green bond in January 2022 and the funds will be used to "*support the production of renewable energy sources and the green transition of the transport sector.*" The success of the Republic of the Philippines is explained as the strong recognition and confidence of investors to "*achieving sustainable development and mitigating climate change, notably the pledge to reduce our greenhouse gas emissions by 75% by 2030.*" Therefore, a green bond is a signaling tool to show that governments and companies are responding to climate change[39]. This is the main conclusion of Caroline Flammer's research:

> [...] "*I show that investors respond positively to the issuance announcement, a response that is stronger for first-time issuers and bonds certified by third parties. The issuers improve their environmental performance post-issuance (i.e., higher environmental ratings and lower $CO_2$ emissions) and experience an increase in ownership by long-term and*

[38] Only the largest institutional investors have access to the primary market for green bonds. Nevertheless, they can trade green bonds in the secondary market.

[39] For example, we observe a high issuance activity just before and during the organization of a Conference of Parties (COP) to the UNFCCC.

> *green investors. Overall, the findings are consistent with a signaling argument — by issuing green bonds, companies credibly signal their commitment toward the environment.*" (Flammer, 2021, page 499)

From an economic point of view, green bonds can be seen as a second-best instrument in the absence of a global carbon pricing scheme (carbon tax), which is the Pigovian solution to the carbon externality (Ehlers and Packer, 2017; Daubanes *et al.*, 2021; Baker *et al.*, 2022). From this perspective, green bonds are the answer to the question of net-zero financing:

> "*Capital spending on physical assets for energy and land-use systems in the net-zero transition between 2021 and 2050 would amount to about* $275 *trillion, or* $9.2 *trillion per year on average, an annual increase of as much as* $3.5 *trillion from today*" (McKinsey, 2022, page viii).

This figure of $3.5 trillion is roughly equal to 1/2 of global corporate profits, 1/4 of total tax revenues, or 4.1% of world GDP. Thus, the gap between current and expected green investment is huge. Of course, green bonds help finance the climate transition, but they are a partial solution representing less than $800 mn of investment. Therefore, the second-best instrument is not currently the solution to climate change.

The last observation raises the question of whether the green bond market is driven by supply or demand. If green bonds are a second-best solution, then we should see more supply. The problem is that there seems to be no economic incentive other than green signaling. In this case, the temptation is to conclude that the green bond market is driven by the demand for green assets. It is true that we observe systematic oversubscription when a green bond is issued. We have already seen that the issuance of the European Commission in October 2021 was oversubscribed 11 times. Such events are not uncommon. For example, the Italian green BTP in December 2020 was oversubscribed 9 times, the German green bond in September 2020 was oversubscribed more than 5 times, and so on. Due to this supply/demand imbalance, we could expect that green and conventional bonds from the same issuer to be priced differently, even if the green and conventional bonds have the same characteristics (same coupon, same maturity, same seniority, same payment schedule). In particular, we expect a large negative premium for the green bond relative to the conventional bond. Below, we will see that the difference is relatively low, which is a market anomaly. In Section 8.3 on page 750, we will learn that a global and fair carbon tax implies a strong distortion of economic profitability across companies and sectors. On the contrary, green bond policies have little impact, which means that green bonds are not really a second-best instrument. They help capture investment flows and finance the climate transition because of the huge demand from investors, but the cost of greening the economy remains relatively high because they have little impact on negative carbon externalities, adverse selection and moral hazard. In this context, the development of green bonds is disappointing if the goal is to fight climate change and drastically reduce carbon emissions. Nevertheless, the development of green bonds is also positive because it contributes to the emergence and diffusion of green sentiment (Brière and Ramelli, 2021).

**Estimation of the greenium** The green bond premium (or greenium) is the difference in pricing between green bonds and regular bonds. Financial theory tells us that the yield of a bond depends on its characteristics (maturity, cash flow schedule, coupon rate, seniority, liquidity), the term structure of interest rates and the default risk of the bond issuer (Roncalli, 2020a, pages 131-136). Therefore, if we compare the yield of a green bond with the yield of a regular bond issued by the same issuer, the difference should be zero if the two bonds have the same characteristics or if they are twin bonds

(Box 4.6). In practice, this is usually not the case. Mathematically, the greenium is defined as:

$$\boldsymbol{g} = y\,(\text{GB}) - y\,(\text{CB}) \tag{4.1}$$

where $y\,(\text{GB})$ is the yield (or return) of the green bond and $y\,(\text{CB})$ is the yield (or return) of the conventional twin bond[40]. Let $s = y - y^\star$ be the difference between the yield with default risk and the yield without default risk. Another expression for the greenium is:

$$\begin{aligned} \boldsymbol{g} &= s\,(\text{GB}) - s\,(\text{CB}) + \underbrace{y^\star\,(\text{GB}) - y^\star\,(\text{CB})}_{\approx 0} \\ &\approx s\,(\text{GB}) - s\,(\text{CB}) \end{aligned} \tag{4.2}$$

So we can also define the greenium as the spread difference between the green bond and the conventional bond.

Box 4.6: Green twin bonds

The twin bond concept was introduced by the Federal Republic of Germany in 2020. The idea is that investors in German green bonds can exchange their holdings for a conventional German government bond with the same maturity and coupon at any time, but not vice versa. The aim is to increase the marketability of green bonds and improve the liquidity of the green bond market. The ability to compare two bonds from the same issuer with an equivalent maturity and coupon provides a direct measure of the greenium.

Table 4.A: German twin bonds (as of December 2023)

| Bond | Maturity | Coupon | Outstanding | Isin |
|---|---|---|---|---|
| 2020 (2030) Bund | 15/08/2030 | 0.00% | €9.50 bn | DE0001030708 |
| Bobl | 10/10/2025 | 0.00% | €8.50 bn | DE0001030716 |
| 2021 (2050) Bund | 15/08/2050 | 0.00% | €11.00 bn | DE0001030724 |
| 2021 (2031) Bund | 15/08/2031 | 0.00% | €9.00 bn | DE0001030732 |
| Bobl | 15/10/2027 | 1.30% | €9.00 bn | DE0001030740 |
| 2023 (2053) Bund | 15/08/2053 | 1.80% | €6.50 bn | DE0001030757 |
| 2023 (2033) Bund | 15/02/2033 | 2.30% | €7.25 bn | DE000BU3Z005 |

On 3 September 2020, the 10-year German green bond with a coupon of 0.00% was priced 1 basis point below the 10-year conventional German bond. On 19 January 2022, Denmark issued a 10-year green bond with the same maturity, interest payment dates and coupon rate as its 2031 conventional bond. The effective yield of the green bond was 5 basis points below the twin conventional bond. As of December 2023, Germany issued a total of 7 twins for a total amount of €60.75 billion.

**Remark 46** *The concept of bond yield (or bond return) is relatively complex because there is no single way to calculate the financial return of a bond. We generally use the yield to maturity, but we can also use the credit spread if we prefer to measure excess return. Another popular measure is the current yield, which is the next coupon value divided by the current market price of the bond.*

[40] This means that the conventional bond has the same characteristics as the green bond.

Box 4.7: Bond pricing

We assume that the bond pays coupons $C(t_m)$ with fixing dates $t_m$ and the notional $N$ (or the par/face value) at maturity date $T$. The cash flow scheme is reported in Figure 4.A. Knowing the yield curve, the price of the bond without default risk at time $t$ satisfies the following relationship (Roncalli, 2020a, Equation 3.2):

$$P_t + AC_t = \sum_{t_m \geq t} C(t_m) B_t(t_m) + N B_t(T)$$

where $B_t(t_m)$ is the discount factor at time $t$ for the maturity date $t_m$ and $AC_t$ is the accrued coupon. $P_t + AC_t$ is called the *dirty price* while $P_t$ refers to the *clean price*. The yield to maturity of the bond is the discount rate that gives its market price:

$$\sum_{t_m \geq t} C(t_m) e^{-(t_m - t)y} + N e^{-(T-t)y} = P_t + AC_t$$

Figure 4.A: Cash flows of a bond without default risk

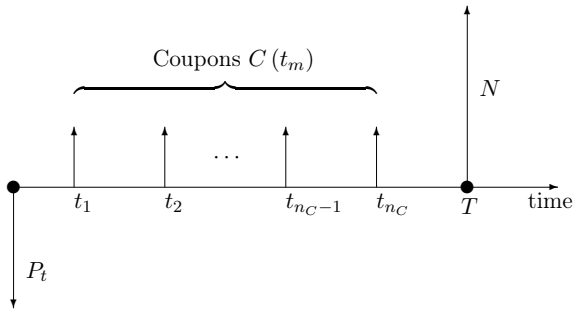


By introducing the credit risk of the issuer, the cash flows may be different because the issuer may default at the time $\boldsymbol{\tau} < T$ (Figure 4.B). Roncalli (2020a, Equation 3.3) shows that:

$$P_t + AC_t = \sum_{t_m \geq t} C(t_m) B_t(t_m) \mathbf{S}_t(t_m) + N B_t(T) \mathbf{S}_t(T) + \mathcal{R} N \int_t^T B_t(u) f_t(u) \, \mathrm{d}u$$

where $\mathcal{R}$ is the recovery rate, $\mathbf{S}_t(u)$ is the survival function at time $u$ and $f_t(u)$ the associated density function. The yield to maturity of the defaultable bond is computed in exactly the same way as without default risk. The credit spread $s = y - y^\star$ is then defined as the difference between the yield to maturity $y$ with default risk and the yield to maturity $y^\star$ without default risk.

Figure 4.B: Cash flows of a bond with default risk

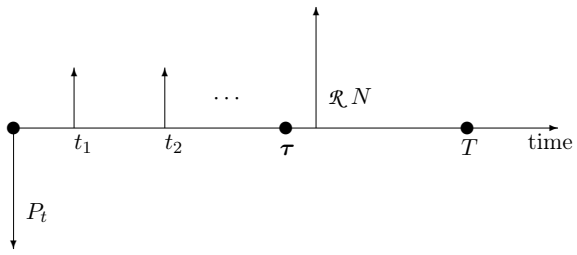

**Example 17** *We consider a 10-year green bond* $\mathrm{GB}_1$ *whose current price is* 91.35*. The corresponding conventional twin bond is a 20-year regular bond whose remaining maturity is exactly ten years and whose price is* 90.07*. We assume that the two bonds have the same coupon level*[41]*, which is equal to* 4%*.*

Let us consider Example 17. The computation of the yield to maturity[42] gives $y\,(\mathrm{GB}) = 5\%$ and $y\,(\mathrm{CB}) = 5.169\%$. We deduce that the greenium is equal to $-16.9$ bps. If we evaluate the bond return with the current yield, we have $y\,(\mathrm{GB}) = 4/91.35 = 4.379\%$ and $y\,(\mathrm{CB}) = 4/90.07 = 4.441\%$. In this case we get $g = -6.2$ bps. Note that the two measures are different even though the greenium is negative in both cases.

Figure 4.13: Greenium in bps of the German green bond (DBR 0% 15/08/2030)

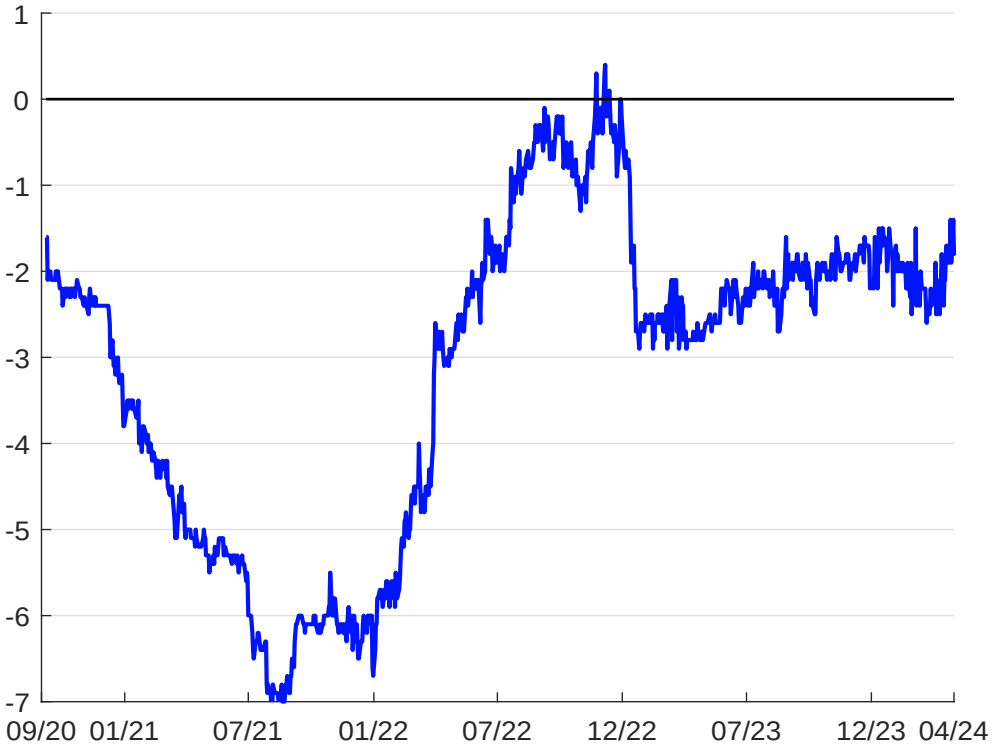


Source: Bloomberg (2024) & Author's calculations.

In the case of twin bonds, we can easily calculate the greenium since the green and regular bonds have exactly the same characteristics and are issued on the same date. In Figure 4.13, we show the dynamics of the greenium for the German Bund 0% 15/08/2030. This analysis comes from the research study by Pástor *et al.* (2022). We observe that the greenium is always almost negative since the inception date (08/09/2020). On average, the greenium is equal to $-3.12$ bps. Its range is between $-7$ and $+1$ bps. Another illustration of the greenium is provided by Zerbib (2019), who analyzed the perpetual 5.5 year callable green hybrid bond issued by Iberdrola on 14 November 2017:

[41] This assumption is not realistic because the regular bond was issued 10 years before the green bond. In this case, we expect that the coupon of the regular bond was different than the coupon of the green bond.

[42] We solve the equation $\sum_{t=1}^{10} 4e^{-ty} + 100e^{-10y} = P$ where $P = 91.35$ for the green bond and $P = 90.07$ for the conventional bond.

> "*At the beginning of the day, the coupon price was estimated at* 2.2%–2.375%. *The issue was quickly oversubscribed to* 3.3 *billion euros (compared to the initial offering of 1 billion euros), and the final coupon was eventually priced at* 1.875%, i.e., 5 *bps below the conventional benchmark.*" (Zerbib, 2019).

In both cases (German and Iberdrola bonds), we must distinguish between the greenium observed in the primary market (when the bonds are issued) and the greenium priced in the secondary market (when the bonds are traded). In the primary market, a negative greenium means that the investor has bought a green bond with a coupon lower than the coupon of the conventional bond. In the secondary market, a negative greenium means that the investor bought a green bond at a higher price than the market price of the conventional bond. Let $c$ be the coupon rate. Mathematically, we have $c\,(\text{GB}) \leq c\,(\text{CB})$ in the first case and $P_t\,(\text{GB}) \geq P_t\,(\text{CB})$ in the second case.

Estimating the greenium is a difficult task. First of all, we have to distinguish between primary and secondary markets. Most academic studies concern the secondary market because there are few observations to calculate the greenium in the primary market. Indeed, in the latter case, we can only have one observation per green bond (the day the green bond is issued). Nevertheless, the different academic studies generally estimate a negative greenium between 5 and 15 bps on the primary market (Ehlers and Packer, 2017; Gianfrate and Peri, 2019; Fatica *et al.*, 2021; Kapraun *et al.*, 2021; Löffler *et al.*, 2021; Baker *et al.*, 2022). These results confirm the professional consensus that the greenium is negative and significant at the issuance date. However, the persistence of the negative greenium in the secondary market is an issue and an open debate. We observe two opposing sides: those who think that the negative greenium persists and remains statistically significant, and those who think that the negative greenium disappears. For instance, Zerbib (2019) found a greenium of −2 bps for EUR and USD global bonds from July 2013 to December 2017. While they measured a greenium of −18 bps in the primary market, the estimates of Gianfrate and Peri (2019) are respectively −11, −13 and −5 bps for three trading dates[43]. In general, when academics estimate the greenium in both the primary and secondary markets, they find that the discount premium is higher at the issuance date. However, some academic studies find that the greenium in the secondary market is zero and statistically insignificant for municipal bonds (Larcker and Watts, 2020) and corporate bonds (Tang and Zhang, 2020; Flammer, 2021).

The second issue in estimating the greenium is the definition of the bond yield spread. For example, we can choose the effective yield, the spread to worst, etc. In general, we observe a small difference. For example, in the case of the German Bund 0% 15/08/2030, the average difference between the spread to worst and the effective yield is equal to 0.5 bps. Also we note that the greenium is different for two green bonds from the same issuer. An example is shown in Figure 4.14 with the German twin bonds. The last issue is the estimation method. According to Ben Slimane *et al.* (2020), there are two main approaches:

1. The bottom-up matching approach is to calculate the yield differential at the bond level. This means that we compare the green bond of an issuer with a synthetic conventional bond of the same issuer that has the same characteristics in terms of currency, seniority and duration (Zerbib, 2019). This matching method can be relaxed by considering a conventional bond from another issuer in the same country and sector and with the same rating (Flammer, 2021).

2. The top-down replication approach consists of calculating the yield differential at the portfolio level. The idea is to look at a diversified portfolio of green bonds and replicate it with a portfolio of conventional bonds. The aim of the replication process is to avoid biases in terms

[43] They are 10 January, 7 July and 14 December 2017.

Figure 4.14: Greenium for 4 German twin bonds (in bps)

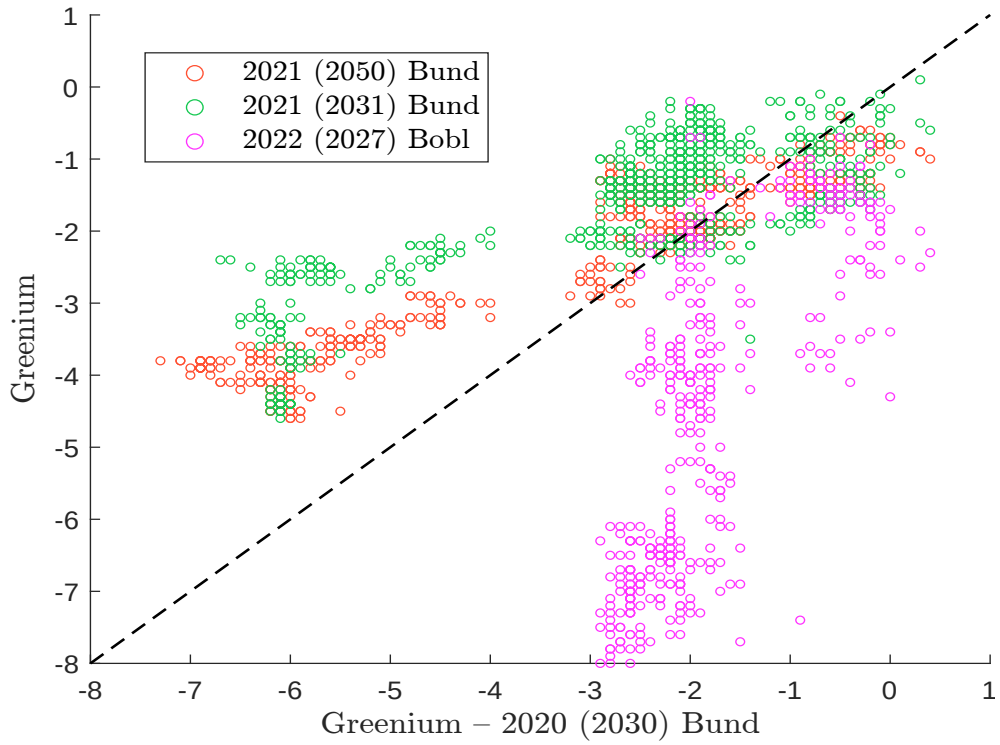


Source: Bloomberg (2024) & Author's calculations.

of currency, sector, credit rating, maturity, etc. Therefore, the greenium is the difference between the yield of the green bond portfolio and the yield of the replication portfolio.

In the bottom-up approach, we first filter all the conventional bonds that have the same issuer, the same currency, and the same seniority as the green bond GB. Then, we select the two closest conventional bonds $\text{CB}_1$ and $\text{CB}_2$ in terms of modified duration:

$$\left|\text{MD}\left(\text{GB}\right) - \text{MD}\left(\text{CB}_j\right)\right|_{j\neq 1,2} \geq \sup_{j=1,2} \left|\text{MD}\left(\text{GB}\right) - \text{MD}\left(\text{CB}_j\right)\right|$$

Finally, we perform the linear interpolation/extrapolation of the two yields $y\left(\text{CB}_1\right)$ and $y\left(\text{CB}_2\right)$ such that the modified duration of the synthetic conventional bond $\text{CB}^\star$ is exactly equal to the modified duration of the green bond. For example, assuming that $\text{MD}\left(\text{CB}_1\right) \leq \text{MD}\left(\text{CB}_2\right)$, the yield of the synthetic conventional bond is:

$$y\left(\text{CB}^\star\right) = y\left(\text{CB}_1\right) + \frac{\text{MD}\left(\text{GB}\right) - \text{MD}\left(\text{CB}_1\right)}{\text{MD}\left(\text{CB}_2\right) - \text{MD}\left(\text{CB}_1\right)} \left(y\left(\text{CB}_2\right) - y\left(\text{CB}_1\right)\right)$$

This calculation is done for each green bond $\text{GB}_i$ and the greenium is equal to the average of the yield difference:

$$\boldsymbol{g} = \frac{1}{n}\sum_{i=1}^{n} \left(y\left(\text{GB}_i\right) - y\left(\text{CB}_i^\star\right)\right)$$

**Example 18** *Let us consider a green bond with a modified duration of 8 years. Its yield return is equal to* 132 *bps. We can surround the green bond with two conventional bonds with modified durations of* 7 *and* 9.5 *years. The yields are* 125 *and* 148 *bps, respectively. The interpolated yield is equal to:*

$$y\,(\text{CB}) = 125 + \frac{8-7}{9.5-7}\,(148-125) = 134.2 \text{ bps}$$

*It follows that the greenium is equal to* $-2.2$ *bps:*

$$\boldsymbol{g} = 132 - 134.2 = -2.2 \text{ bps}$$

In the top-down approach proposed by Fender *et al.* (2019), we consider a portfolio $w = (w_1, \ldots, w_n)$ of $n$ green bonds. Then, we perform a clustering analysis by considering the 4-uplets (currency $\times$ sector $\times$ credit quality $\times$ maturity). Let $(C_h, S_j, R_k, M_l)$ be an observation for the 4-uplet (*e.g.*, EUR, Financials, AAA, 1Y-3Y). We calculate its weight:

$$\omega_{h,j,k,l} = \sum_{i \in (C_h, S_j, R_k, M_l)} w_i$$

The greenium is then defined as the weighted excess yield:

$$\boldsymbol{g} = \sum_{h,j,k,l} \omega_{h,j,k,l} \left( y_{h,j,k,l}\,(\text{GB}) - y_{h,j,k,l}\,(\text{CB}) \right)$$

where $\omega_{h,j,k,l}$ is the weight of the cluster $(C_h, S_j, R_k, M_l)$ in the green bond portfolio, $y_{h,j,k,l}\,(\text{GB})$ is the yield of the cluster in the green bond portfolio and $y_{h,j,k,l}\,(\text{CB})$ is the yield of the cluster in the benchmark portfolio. In general, this approach is applied to a green bond index, implying that the green bond portfolio is the green bond index and the benchmark portfolio is the parent bond index.

Table 4.15: Average greenium (in bps) relative to currency

| Year | All currencies | EUR | USD | Non-EUR |
|---|---|---|---|---|
| 2019 | −2.2 | −1.3 | −4.5 | −3.3 |
| 2020 | −2.3 | −2.0 | −3.2 | −2.6 |
| 2021 | −2.8 | −2.2 | −4.1 | −3.5 |
| 2022 | −3.7 | −3.5 | −5.5 | −3.9 |
| 2023 | −2.5 | −2.0 | −5.1 | −3.2 |
| 2019-2023 | −2.8 | −2.3 | −4.7 | −3.3 |

Source: Ben Slimane *et al.* (2023a, Table 2, page 14).

Figure 4.15 shows the evolution of the greenium (expressed in bps) calculated by Ben Slimane *et al.* (2023a) using the bottom-up approach. On average, it is negative and equal to −2.8 bps. The 95% confidence interval corresponds to the range −4.3 to −1.3 bps. Note that the greenium highly depends on the currency. On average, the greenium of USD-denominated bond is larger than the greenium of EUR-denominated bond (−4.7 vs −2.3 bps). The probability that the greenium in EUR is below −4.5 bps is less than 1%. On the contrary, this probability is higher than 50% for the greenium in USD. The correlation between EUR and USD premia varies over time and is not very high in absolute terms. For instance, it is equal to 17.2% since 2020. These differences do not only concern currencies, but also sectors, maturities, regions and ratings. For example, the greenium is not statistically significant for many sectors. Ben Slimane *et al.* (2020) also found that the volatility of green bond portfolios is lower than the volatility of conventional bond portfolios, implying that green and conventional bonds have identical Sharpe ratios over the last five years. In summary, we can assume that the greenium is slightly negative, but the magnitude is relatively small.

Figure 4.15: Evolution of the greenium with respect to the currency denomination (in bps)

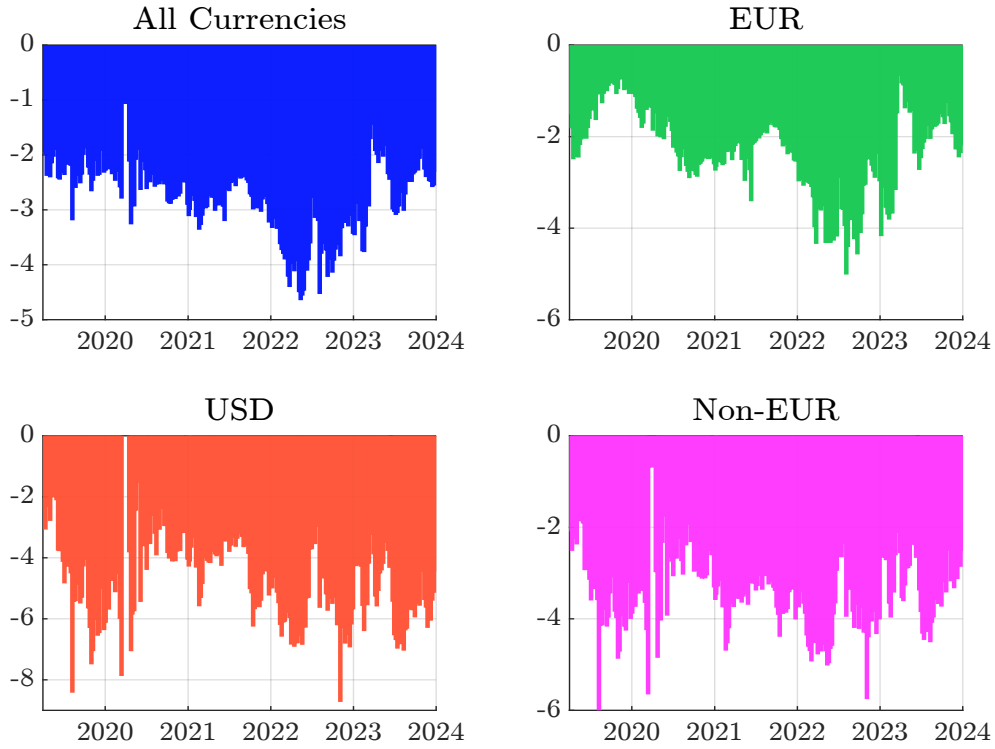


Source: Ben Slimane *et al.* (2023a, Figure 11, page 15).

**Remark 47** *To illustrate the sensitivity to the different characteristics, we consider the largest common pool of issuer types, i.e., agencies and sovereigns (AS), corporates (CORP), financials (FIN) and supranationals (SN). Table 4.16 shows the evolution of the greenium taking into account these four types of issuers. We notice a more pronounced greenium for corporate issuers. Besides the type of issuer, another important dimension is the currency of the bonds*[44]*. The case of sovereigns, supranationals and agencies (SSA) is also shown in Table 4.16. Again, the greenium is larger for green bonds denominated in dollars or other currencies than euros.*

Table 4.16: Average greenium (in bps) relative to issuer category

| Issuer | Currency | 2019 | 2020 | 2021 | 2022 | 2023 | 2019-2023 |
|---|---|---|---|---|---|---|---|
| AS | AC | −1.2 | −1.8 | −2.2 | −2.5 | −2.0 | −2.0 |
| CORP | | −3.9 | −3.9 | −3.8 | −7.2 | −2.9 | −4.5 |
| FIN | | −0.8 | −1.4 | −2.7 | −1.4 | −2.8 | −2.0 |
| SN | | −4.9 | −2.5 | −2.2 | −1.6 | −1.2 | −2.2 |
| SSA | AC | −2.4 | −2.0 | −2.2 | −2.3 | −1.8 | −2.1 |
| | EUR | −1.2 | −1.2 | −1.2 | −2.2 | −0.8 | −1.3 |
| | Non-EUR | −3.2 | −2.6 | −3.0 | −2.4 | −2.9 | −2.8 |

Source: Ben Slimane *et al.* (2023a, Table 4, page 17).

[44]The symbol AC stands for all currencies.

### 4.2.2 Social bonds

#### Definition

In the mid-2010s, the concept of green bonds was expanded to include social objectives. In January 2015, the first social bond was issued by the Spanish Instituto de Credito to support the financing of SMEs in economically depressed regions of Spain. In September 2015, Kutxabank issued the first social covered bond, the proceeds of which were used to finance and subsidize social housing projects in the Basque region. Since 2015, the framework for social bonds has evolved, but it is now a copy/paste version of the framework for green bonds. For example, the definition of a social bond is exactly the same as that of a green bond:

> "*Social Bonds are any type of bond instrument where the proceeds, or an equivalent amount, will be exclusively applied to finance or re-finance in part or in full new and/or existing eligible social projects and which are aligned with the four core components of the Social Bond Principles (SBP).*" (ICMA, 2021b, page 3).

Again, the four core components are the use of proceeds, the process for project evaluation and selection, the management of proceeds, and the reporting. The eligible social project must address or alleviate the specific social problem and, if possible, focus on a target population. Projects are usually part of social milestones such as:

- Basic infrastructure: access to affordable basic infrastructure (clean drinking water, sewerage, sanitation, transportation and energy);
- Basic services: access to basic services (health, health care, vocational training, education, and financial services);
- Affordable housing: access to affordable housing;
- Employment: reducing unemployment and increasing support for microfinance programs and the creation of small and medium-sized enterprises;
- Food security: access to safe, nutritious and sufficient food; resilient agricultural practices; food loss and waste;
- Empowerment: reducing inequalities in income, gender, resources, opportunities and assets.

The use of proceeds also introduces the concept of target population, which means that the goal of a social bond is defined by both a social project category and a target population. Examples of target populations include: (1) those living below the poverty line, (2) excluded and/or marginalized populations and/or communities, (3) persons with disabilities, (4) migrants and/or displaced persons, (5) the undereducated, (6) the underserved due to lack of quality access to essential goods and services, (7) the unemployed, (8) women and/or sexual and gender minorities, (9) the aging population and vulnerable youth, and (10) other vulnerable groups, including as a result of natural disasters. The target population confirms the positive social impact of the investment. To define impact reporting, ICMA provides a set of KPIs closely linked to the SDGs. Some examples are the number of hospital beds, the number of patients benefiting from health care or medical treatment, the percentage of underserved renters, the number of textbooks and educational materials provided, the number of people given access to financial services, and the percentage of people with disabilities employed (ICMA, 2021b). However, social impact reporting often suffers from a large amount of qualitative and intangible information that can be difficult to understand.

Box 4.8: Examples of social project categories and target populations

- Instituto de Crédito Oficial (Spanish state-owned bank, March 2020)
  "*The Social Bond proceeds under ICO's Second — Floor facilities will be allocated to loans to finance small, medium and micro enterprises with an emphasis on employment creation or employment retention in: (1) specific economically underperforming regions of Spain; (2) specific municipalities of Spain facing depopulation; (3) regions affected by a natural disaster. [...] The target populations are SMEs in line with European Union's standards.*"

- Pepper Money (non-bank lender in Australia and New Zealand, April 2022)
  "*The positive social impact of a Pepper Money eligible social project derives from its direct contribution to improving access to financial services and socio-economic empowerment, by using proprietary systems to make flexible loan solutions available to applicants who are not served by traditional banks. [...] Pepper Money is seeking to achieve positive social outcomes for a target population of Australians that lack access to essential financial services and experience inequitable access to and lack of control over assets. Pepper Money directly aims to address the positive social outcome of home ownership for borrowers who may have complexity in their income streams, gaps in their loan documentation or have adverse credit history. Traditionally, this cohort has been underserved by banks that rely on inflexible algorithmic loan application processing.*"

- Danone (French multinational food-products corporation, March 2018)
  "*The eligible project categories are: (1) research & innovation for advanced medical nutrition (target populations: infants, pregnant women, patients and elderly people with specific nutritional needs), (2) social inclusiveness (target poputions: farmers, excluded and/or marginalised populations and/or communities, people living under the poverty line, rural communities in developing countries), (3) responsible farming and agriculture (target populations: milk producers, farmers), etc.*"

- Korian (European care group, October 2021)
  "*The proceeds of any instrument issued under the framework will be used [...] to provide services, solutions, and technologies that will enable Korian to meet at least one of its social objectives: (1) to increase and improve long-term care nursing home capacity for dependent older adults; (2) to increase and improve medical capacity for people in need of medical support; (3) to increase and improve access to alternative, nonmedical services, technologies, and housing solutions that facilitate the retention of older adults' autonomy; and (4) to improve the daily provision of care to and foster a safer living environment for its patients. [...] Furthermore, Korian's target populations are older adults, which Korian defines as being over 65 years of age, and those who are dependent on others for some degree of care, which is defined by the health authorities or insurance system of the respective country.*"

- JASSO (Japan Student Services Organization, July 2022)
  "*The social project categories concern the financing of the 'Category 2 Scholarship Loans' (interest-bearing scholarship loans that have to be repaid) while the target population is made up of students with financial difficulties.*"

Source: Collected from the websites of the organizations.

### The social bond market

As of December 2023, 1 030 entities have issued more than 7 800 social bonds in fifty countries (CBI, 2024c). In addition to its smaller size, the social bond market differs from the green bond market in many ways. First, supranational issuers are more prevalent, with a cumulative market share of about 18% (Figure 4.16). Second, Europe and North America are less represented in the social bond market (respectively 33% and 11.9% versus 45.6% and 17.4% in the green bond market), while the share of Asian issuers is close to 35% (Figure 4.17). Third, the majority of social bond issuance is led by governments and sovereign entities, accounting for about 68% of the market (Figure 4.18). The breakdown of this figure is as follows: 58% for government-backed entities, 6.5% for local governments, and 3.1% for central governments. Corporates represent less than 10% of the social bond market, while their market share is more than 30% for green bonds. This market segmentation occurred between 2019 and 2020, when the market share of government and sovereign issuers increased sixfold, mainly due to the launch of the European SURE program. As a result, the social bond market is dominated by developed countries, and the majority of social bonds are denominated in euros (around 39% of the market). Finally, the structure of the bonds differs from that of green bonds, with a shorter maturity and a lower notional amount (CBI, 2024c).

Figure 4.16: Issuance and notional outstanding of social bonds by market

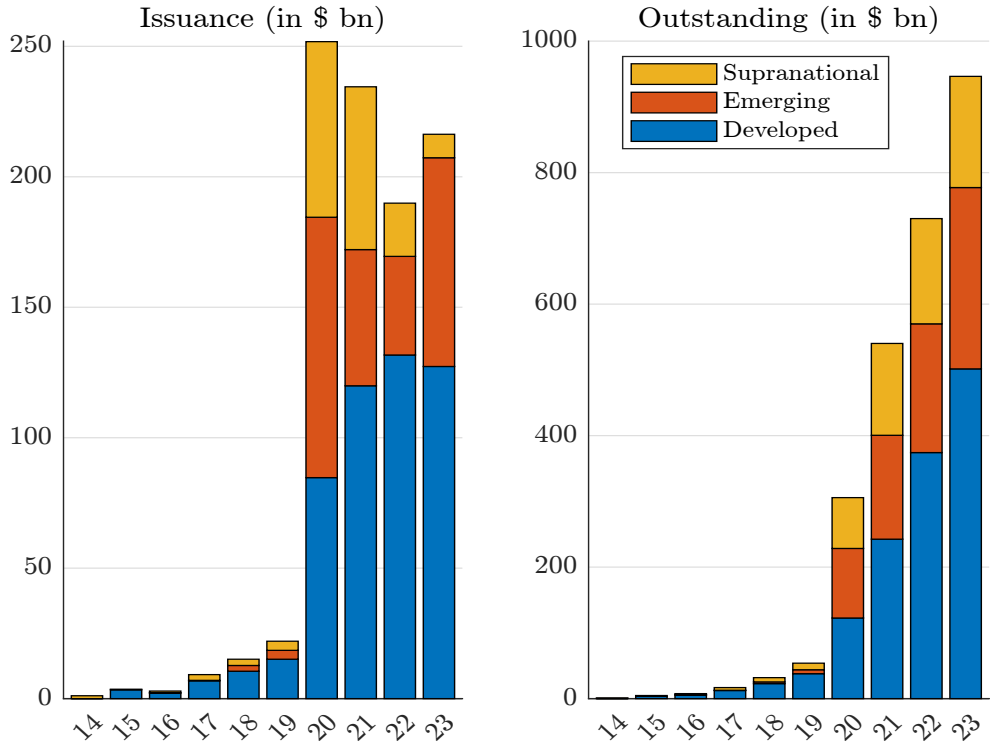


Source: https://www.climatebonds.net/market/data.

Ben Slimane *et al.* (2023a) find that the social bond premium, *i.e.*, the difference between the yield on social bonds and the yield on conventional bonds, is zero and not significant. They also find that there is no correlation between the green premium and the social bond premium. In fact, a large part of the social bond market can be seen as a restructuring of public social debt (unemployment benefits, pensions, etc.) and the financing of social infrastructure (schools, hospitals, etc.) and is not related to social projects to achieve a low-carbon economy.

Figure 4.17: Issuance and notional outstanding of social bonds by region

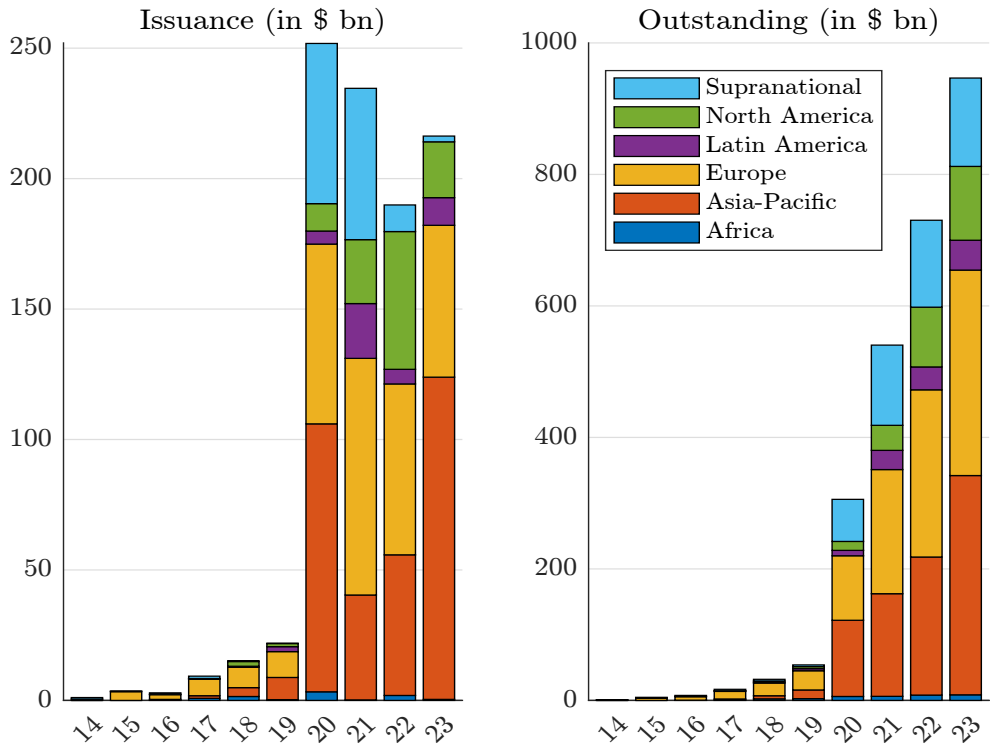


Source: https://www.climatebonds.net/market/data.

Figure 4.18: Issuance and notional outstanding of social bonds by type of issuer

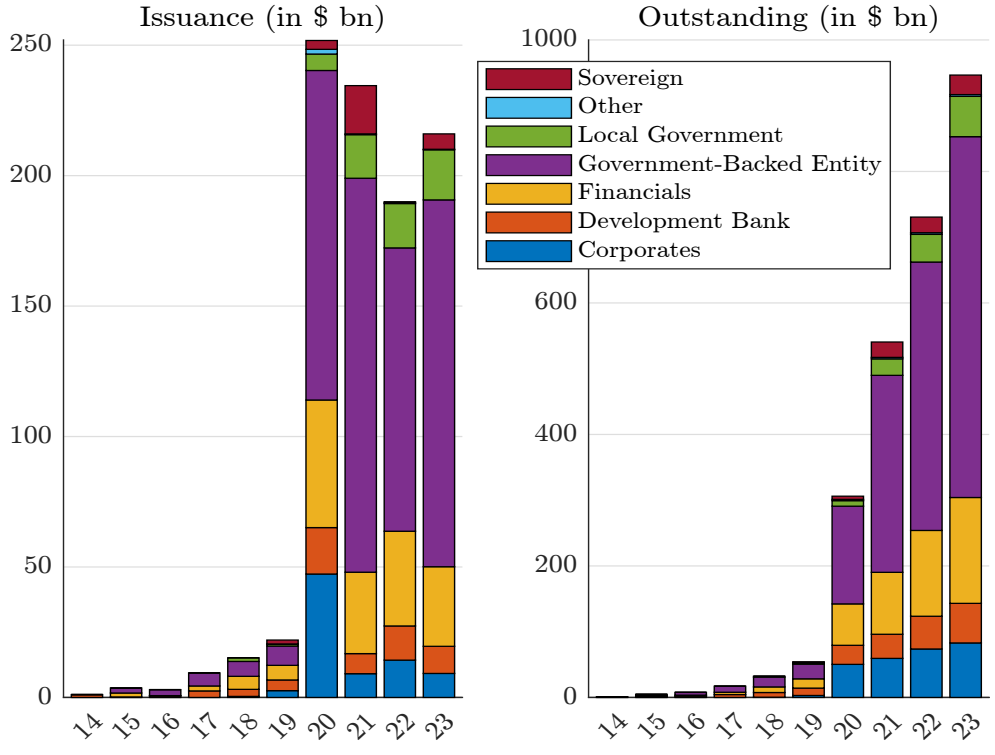


Source: https://www.climatebonds.net/market/data.

### 4.2.3 Other sustainability-related instruments

#### Sustainability bonds

Sustainability bonds are debt instruments issued to finance projects or activities that have both positive environmental and social impacts. The idea is that some social projects can have environmental co-benefits and vice versa. Sustainability bonds are aligned with the four core components of both the GBP and SBP. One example is the Series 2021 sustainability bonds issued by the American Museum of Natural History. The environmental objective is to partially finance the Gilder Center (green buildings), while the social objectives are to expand access to critical science education, and promote biocultural diversity and research. The social benefits accrue to target populations that include K-12 STEM education shortage areas and the general public.

According to CBI (2024c), the cumulative issuance of sustainability bonds reaches $870 billion at the end of December 2023. However, we observe a decline in issuance. 2021 was the peak year with $205.4 billion of issuance. In 2022 and 2023 this figure is close to $170 billion. The top 5 countries are the US, France, South Korea, Japan and Germany. Nearly half of sustainability bonds are issued by development banks, 25% by governments or related entities, and the remainder is split evenly between financial institutions and corporates.

#### Sustainability-linked bonds

A sustainability-linked bond (SLB) is a sustainability bond (green/social) plus a step-up coupon if the sustainability KPI is not met. Thus, an SLB belongs to the family of forward-looking performance-based instruments. The financial characteristics of the bond depend on whether the issuer meets pre-defined ESG objectives. These objectives are:

1. measured through predefined Key Performance Indicators (KPIs);
2. assessed against predefined Sustainability Performance Targets (SPTs).

Let us give some examples. In September 2019, ENEL issued a general purpose SDG linked bond based on SDGs 7 (affordable and clean energy), 13 (climate action), 9 (industry, innovation and infrastructure) and 11 (sustainable cities and communties). The KPI is installed renewable energy capacity RIC as of 31 December 2021, while the SPT is equal to 55%. If the SDG 7 target is not achieved[45] — RIC $< 55\%$, ENEL will have to pay a one-time step-up coupon of 25 bps. On April 2022, the independent report prepared by KPMG certifies that "*the percentage of installed renewable capacity as of 31 December 2021 is equal to* 57.5%." Since 2019, Enel has issued other sustainability-linked bonds[46] and is one of the largest SLB issuers.

On 18 February 2021, H&M issued an 8.5-year sustainability-linked bond[47] for a notional amount of €500 mn. The annual coupon rate is 25 bps and the objectives to be achieved by 2025 are:

$\text{KPI}_1$ Increase the share of recycled materials used to 30% ($\text{SPT}_1$);

$\text{KPI}_2$ Reduce emissions from the Group's own operations (Scope 1+2) by 20% with 2017 as a baseline ($\text{SPT}_2$);

$\text{KPI}_3$ Reduce Scope 3 emissions from fabric production, garment manufacturing, raw materials and upstream transportation by 10% using 2017 as a baseline ($\text{SPT}_3$).

[45] As of 30 June 2019, the KPI was equal to 45.9%
[46] See https://www.enel.com/investors/investing/sustainable-finance/sustainability-linked-finance.
[47] See https://hmgroup.com/investors/sustainability-linked-finance.

The global step-up rate is equal to:

$$\begin{aligned} r &= 40\% \times \mathbb{1}\{\text{KPI}_1 < \text{SPT}_1\} + \\ &\quad 20\% \times \mathbb{1}\{\text{KPI}_2 > \text{SPT}_2\} + \\ &\quad 40\% \times \mathbb{1}\{\text{KPI}_3 > \text{SPT}_3\} \end{aligned}$$

If the three targets are met, the step-up rate will be zero and no step-up coupon will be paid. Otherwise, H&M will pay a step-up coupon proportional to the step-up rate, which may be 20% ($\text{KPI}_2$ is not achieved), 40% ($\text{KPI}_1$ or $\text{KPI}_3$ is not achieved), 60% ($\text{KPI}_2$ is not achieved, and $\text{KPI}_1$ or $\text{KPI}_3$ is not achieved), 80% ($\text{KPI}_1$ and $\text{KPI}_3$ are not achieved) or 100% ($\text{KPI}_1$, $\text{KPI}_2$ and $\text{KPI}_3$ are not achieved). The H&M sustainability-linked bond attracted a lot of interest as it was 7.6 times oversubscribed.

According to Berrada *et al.* (2022), "*the SLB market has grown strongly since its inception. [...] Bloomberg identifies a total of 434 outstanding bonds flagged as 'sustainability-linked' as of February 2022. In contrast, in 2018, there was only a single SLB. The amount raised through the single 2018 SLB issue was $0.22 bn, whereas the total amount raised through all SLBs issued in 2021 was approximately $160 bn.*" These authors also found that the vast majority of SLB issues are exclusively E issues (65%) or a combination of E, S and G issues (17%) or E and G issues (3%). The other combinations are marginal (less than 1% each). They also found that the most common KPI is GHG emissions (40%), followed by the issuer's global ESG score (14%).

A more recent study was conducted by the Climate Bonds Initiative (CBI, 2024b). As of 30 November 2023, the key figures of the SLB market are as follows: $279 bn in issuance, 768 SLB bonds, 469 issuers, average bond size of $364 mn. Enel dominates the top ten issuers with $31.1 bn of issuance, followed by the Republic of Chile ($9.2 bn), Teva Pharmaceutical Industries ($7.5 bn), Eni ($5.2 bn) and Enbridge ($5.1 bn). SLBs have between one and four KPIs, with one being the most common, used by 59% of bonds. 65% of KPIs relate to climate change, 7.5% to product governance, 5% to diversity, equity and inclusion, and 3.5% to circular economy. Step-up coupons are the financial mechanism that dominates the current SLB market, appearing in 58% of SLBs and representing 78% of the amount issued. In this case, they provide a reward to bondholders in the form of a higher coupon if the issuer misses its targets. The average step-up coupon per target is 24.8 bps. Step-down coupons are rare (less than 7% of SLBs and 4% of amount issued). In this case, the coupon is canceled or reduced if the targets are met. In addition to step-up and step-down coupons, another financial tool is the redemption premium. With this mechanism, the issuer compensates by paying an additional amount if it decides to redeem the bond before maturity or at maturity. The redemption premium mechanism is used by 20% of SLBs representing 10% of the issued amount. The Climate Bonds Initiative study is very critical of the KPIs chosen by SLB issuers, their performance and their reporting:

> "*Three aspects linked to poor reporting are highlighted: failure to explain reasons for changes in performance, lack of clarity around data restatements (especially GHG emissions), and inconsistencies in issuer disclosure. [...] The market shows heterogeneous performance, with a relatively even split of outcomes. Within the sample, 31% of SLBs and 34% of the amount issued have all KPIs off track [...] Of the SLBs sampled, 12% have targets currently met, almost all of which with observation dates up to 2025. Within these, the later the observation date, the less ambitious the targets are likely to be. [...] As well as target ambition, target feasibility varies widely. Some issuers have targets that are only a slight improvement versus the baseline or have even already been met at issuance (i.e., highly feasible). If these targets also lack ambition (below 2°C in the case of GHG targets), they are clear examples of greenwashing.*" (CBI, 2024b, page 4).

**Transition bonds**

They are financial instruments designed to support the transition of an issuer that currently has significant carbon emissions. These bonds are typically used to finance projects such as renewable energy development, energy efficiency improvements, and other projects aimed at transitioning to a lower carbon economy. The ultimate goal of the bond issuer is always to reduce its carbon emissions. For example, transition bonds can be used to convert diesel-powered ships to natural gas or to implement carbon capture and storage. At the end of 2023, the cumulative issuance of transition bonds is $12.7 billion, or 0.3% of the GSS+ market. The world's first sovereign climate transition bond was issued by the Japanese government on 14 February 2024. The total amount of $11 billion is divided into several tranches and the proceeds will be used to finance the country's Green Transformation Program.

## 4.3 Sustainable alternative assets

Private assets refer to an asset class in which securities, such as stocks and bonds, are traded directly between investors and issuers, without the intermediation of public exchanges. Private assets cover a wide range of investments, including private equity, venture capital and private debt. Real assets refer to an asset class that includes investments in physical assets such as infrastructure, natural resources[48] and real estate. Therefore, real assets are tangible or physical assets whose value is linked to their physical characteristics rather than their financial characteristics. Investors generally assume that private assets and real assets form a single asset class known as alternative assets or private markets. In fact, the line between private and real assets is not always clearly defined. For example, real estate can be classified as a private asset. The common characteristics are that alternative assets are often illiquid and less regulated, require a longer investment horizon than public market investments, and have fewer disclosure requirements than public markets. Because the alternative investment market is less regulated, it is more difficult to obtain a global view of its size and components. In what follows, we use two data providers, Prequin and PitchBook, to assess the market for sustainable alternative assets[49].

Table 4.17: Breakdown of private markets AUM (as of June 2023)

| Asset class | North America | Europe | Asia | Other regions | World |
|---|---|---|---|---|---|
| Buyout | 18.2% | 7.6% | 2.9% | 0.7% | 29.5% |
| Venture capital | 8.2% | 1.6% | 9.9% | 0.9% | 20.6% |
| Growth | 4.8% | 1.0% | 3.9% | 0.7% | 10.5% |
| Other | 1.8% | 0.0% | 0.3% | 0.0% | 2.2% |
| Private debt | 8.0% | 3.4% | 0.9% | 0.7% | 12.9% |
| Real estate | 7.5% | 2.9% | 1.7% | 0.6% | 12.8% |
| Infrastructure & natural resources | 5.5% | 3.7% | 1.2% | 1.1% | 11.5% |
| Private equity | 33.1% | 10.3% | 17.0% | 2.4% | 62.8% |
| Private assets | 41.0% | 13.7% | 17.9% | 3.1% | 75.7% |
| Real assets | 13.1% | 6.6% | 2.9% | 1.7% | 24.3% |
| Total | 54.1% | 20.3% | 20.8% | 4.8% | 100.0% |

Source: Prequin database, McKinsey (2024, Exibit 6, page 12) & Author's calculations.

[48] Natural resources are materials or substances that occur naturally on Earth. Prequin considers five main categories: (1) Agriculture & Farmland, (2) Energy, (3) Metals & Mining, (4) Timberland, and (5) Water.

[49] Readers unfamiliar with alternative investments may wish to consult the free Alternatives 101 educational program at www.preqin.com/academy.

Box 4.9: Glossary of private equity terms

- The *buyout* strategy focuses on the majority acquisition of established private companies, typically with significant debt financing.
- *Distressed debt* refers to loans and borrowings associated with debtors that are experiencing financial or operational distress, default or bankruptcy.
- *Dry powder* is the available or unused capital that a private equity firm has at its disposal to make new investments. It represents the amount of capital that has been committed by limited partners but not yet committed to investments. It then measures the ability of the fund to make acquisitions or new investments.
- *Exit* refers to the process of divesting or selling the investments made by the private equity firm. It represents the point at which the firm seeks to realize its investment and generate returns for its investors.
- *Final closing* is the end of fundraising and the last time new investors are accepted into closed-end funds. It is then the final stage in which all necessary legal, financial and administrative processes are completed.
- *Fundraising* is the process of raising capital from investors for a newly formed fund. It ends with the final closing.
- The *general partner* (GP) is the partner with unlimited liability in a limited partnership. It is responsible for managing the fund and making investment decisions. It can be thought of as the fund manager.
- The *internal rate of return* (IRR) measures the profitability and performance of an investment over time. It represents the annualized rate of return that an investment is expected to earn based on its cash flows, including both cash inflows and outflows.
- *Leverage* increases the level of investment through borrowing and derivatives.
- A *leveraged buyout* is a technique in which a company is acquired with a significant amount of debt, often using the assets of the acquired company as collateral.
- A *limited partner* (LP) is a partner with limited liability in a partnership. It defines an investor in a private equity fund who provides capital but does not participate in the day-to-day management of the fund.
- The *liquidation phase* refers to the stage in the life of a fund when, at the end of the fund's life, the remaining assets are sold to liquidate the fund and distribute the proceeds to investors.
- *Venture capital* (VC) is a form of private equity investment that focuses on early-stage, high-growth companies with significant growth potential.
- *Vintage* refers to the year in which a fund begins investing its capital. It's an important metric used to evaluate a fund's performance and compare it to its peers.

According to McKinsey (2024), assets under management in private markets reached $13.1 trillion by June 2023. Table 4.17 shows the breakdown of private markets AUM. The order of magnitude is 7.6% for $1 trillion. The market is dominated by North America with a market share of 54.1%. Europe and Asia have a similar market size, each representing 20% of the market. Buyout strategy is the largest category, followed by venture capital. Private equity (*i.e.*, buyout, venture capital growth and other[50]) represents 62.8% of private markets. If we add private debt, we get a figure of 75.7% for private assets. The remaining 24.3% is real assets, with 12.8% in real estate and 11.5% in infrastructure and natural resources.

Data providers typically distinguish between private ESG funds and impact investing funds. For example, Prequin (2023) and PitchBook (2024) separate these two investment universes in their annual reports. Focusing on private ESG funds, Prequin (2023) found that total capital raised grow from $29.4 billion in 2020 to $92.0 billion in 2022. Since 2014, cumulative assets under management in private ESG markets have reached $300 billion. The market is dominated by private equity ESG buyout funds, which account for 50% of assets. Infrastructure is the second category that raises ESG capital, while venture capital, private debt, real estate and natural resources are more marginal ESG strategies (Prequin, 2023, Figure 1.3, page 6). Regionally, Europe leads the market with more than 70% of the market share, followed by North America and Asia. Prequin (2023) estimates that Article 8 funds have dominated the fundraising landscape, but Article 9 funds are gaining momentum. Focusing on impact investing funds, Prequin (2023) suggests that this market is 60% smaller than the market for private ESG funds. Regionally, the market is dominated by North America and Europe, which account for 95% of fundraising:

> "*ESG integration and regulations are more developed in Europe than other regions but impact investment strategies are more concentrated in North America. Rather than looking at when capital was secured, examining fund vintages from 2013 shows that European funds have dominated ESG integration fundraising, securing 76% of the global aggregate. However, among impact funds, North America funds of comparable vintages lead, accounting for 53% of capital raised.*" (Prequin, 2023, page 12).

One of the main reasons for this is that the market for impact investing funds is dominated by venture capital funds, particularly those specializing in renewable energy projects such as wind and solar. As a result, a large amount of assets are being invested in cleantech, a trend that has been stimulated by the 2022 Inflation Reduction Act in the United States (Prequin, 2023, page 12).

PitchBook's annual report on ESG in alternative investments also breaks out the private ESG fund market and the impact fund market. Figure 4.19 shows the evolution of total GP PRI signatories. PitchBook (2024) indicates that the number of new GPs publicly committing to ESG through the Principles for Responsible Investment increases significantly in 2020 and 2021. However, they observe a decline in 2022 and 2023. By December 2023, there are 2 503 GP signatories. This represents about 10% of global GPs. PitchBook (2024) questions the momentum of ESG in the private markets and sees a slowdown that may be explained by the ESG backlash in the US and the proliferation of greenhushing. The analysis of Article 8 funds shows a divergence from the global private fund market. Like Prequin (2023), PitchBook (2024) finds that more than 60% of assets are invested in private equity (buyouts) and infrastructure (see Table 4.18). Venture capital funds are underrepresented in Article 8 funds due to their small size and the ESG characteristics of these investments. Indeed, the primary objective of start-up companies is to survive from a financial point of view, which means that sustainability issues are not their main concern.

[50] This includes turnaround, private investment in public equity, balanced, hybrid funds, and funds with unspecified strategy (McKinsey, 2024).

Figure 4.19: GP PRI signatories

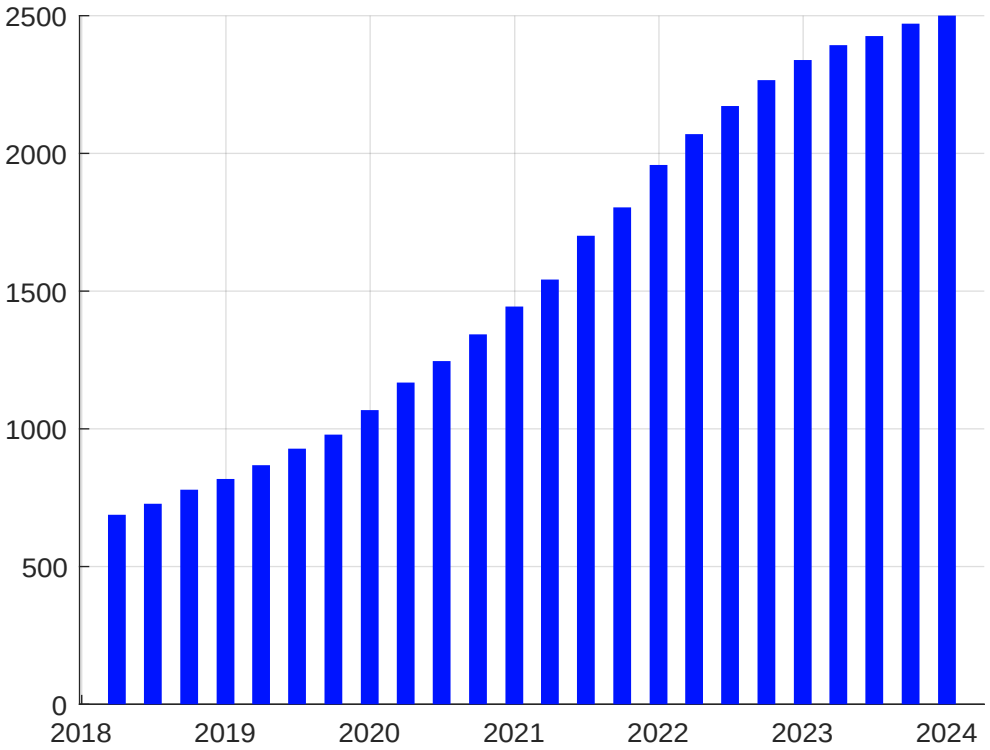


Source: PitchBook (2024, page 2) & https://pitchbook.com.

Table 4.18: Strategy representation among Article 8 funds (as of December 2023)

| Category | Article 8 funds | | Private markets | |
|---|---|---|---|---|
| | Number of funds | Capital raised | Number of funds | Capital raised |
| Private equity (buyout) | 25.80% | 34.50% | 21.92% | 37.62% |
| Venture capital | 14.60% | 4.40% | 46.49% | 15.96% |
| Private debt | 20.50% | 16.80% | 7.08% | 14.46% |
| Real estate | 23.20% | 14.20% | 12.60% | 12.34% |
| Real assets* | 12.60% | 29.90% | 4.16% | 9.69% |

*Real assets = infrastructure & natural resources.

Source: PitchBook (2024, page 6) & Author's calculations.

Table 4.19: Strategy representation among impact investing funds (as of December 2023)

| Category | Impact funds | | Private markets | |
|---|---|---|---|---|
| | Number of funds | Capital raised | Number of funds | Capital raised |
| Private equity (buyout) | 21.90% | 14.49% | 21.92% | 37.62% |
| Venture capital | 40.18% | 7.03% | 46.49% | 15.96% |
| Private debt | 7.16% | 6.26% | 7.08% | 14.46% |
| Real estate | 5.80% | 3.93% | 12.60% | 12.34% |
| Real assets* | 20.55% | 66.96% | 4.16% | 9.69% |

*Real assets = infrastructure & natural resources.

Source: PitchBook (2024), https://pitchbook.com & Author's calculations.

Figure 4.20: Assets under management of impact investing funds (in $ bn)

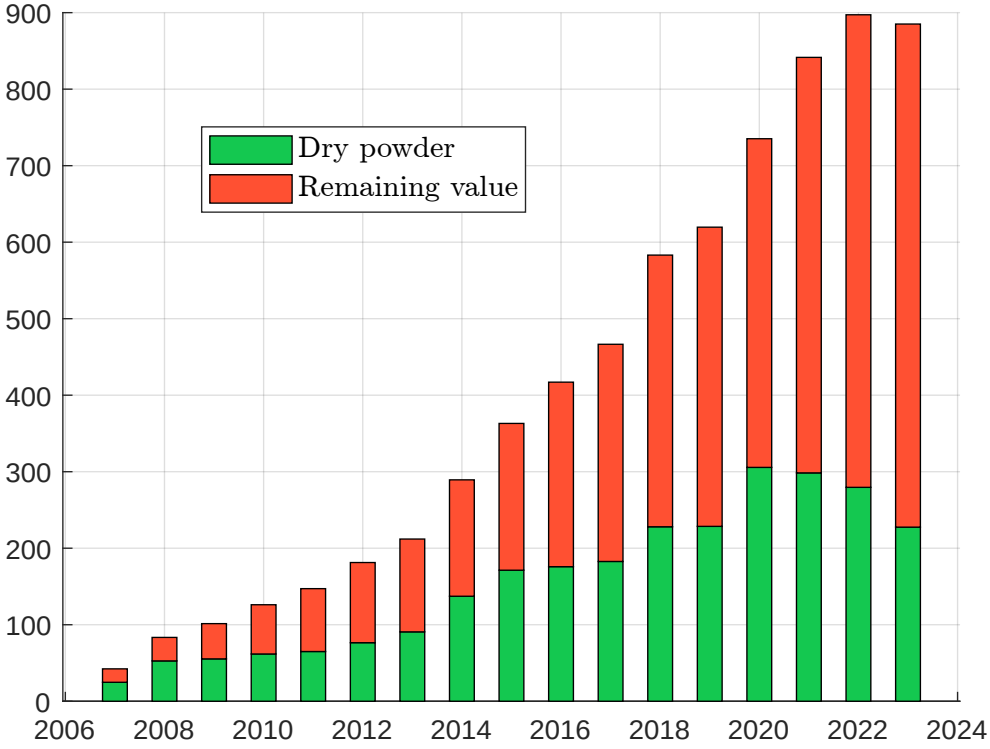


Source: PitchBook (2024), https://pitchbook.com & Author's calculations.

Table 4.20: Top 10 impact investing firms by capital raised (as of December 2023)

| Investor | Location | Aggregate capital (in $ bn) | Number of impact funds |
|---|---|---|---|
| Brookfield Corporation | Ontario, Canada | 61.40 | 6 |
| Global Infrastructure Partners | New York, US | 55.62 | 7 |
| Macquarie Asset Management | Australia | 37.78 | 13 |
| Kohlberg Kravis Roberts | New York, US | 36.48 | 7 |
| EQT | Stockholm, Sweden | 35.61 | 4 |
| China Development Bank | Beijing, China | 30.00 | 2 |
| Stonepeak | New York, US | 29.72 | 5 |
| Actis | England, UK | 28.63 | 37 |
| Copenhagen Infrastructure Partners | Denmark | 21.22 | 7 |
| I Squared Capital | Miami, US | 18.31 | 2 |
| Total | | 354.76 | 90 |

Source: PitchBook (2024, page 11).

Focusing on impact investing funds, PitchBook (2024) finds a decline in assets under management in 2023 (Figure 4.20). This trend is confirmed by fundraising numbers, which peak in 2022 at $150 billion raised by 213 funds. In 2023, fundraising drops dramatically to $44 billion for only 107 funds. We are very far from the 248 funds in 2021 and $111 billion in capital raised. In Table 4.20, we report the top 10 impact investing firms. Some of them are big names in the private markets such as KKR, EQT Partners or Brookfield Corporation. Others are infrastructure-focused GPs such as Global Infrastructure Partners, Macquarie and Copenhagen Infrastructure Partners.

### 4.3.1 ESG private equity and debt funds

According to Eccles *et al.* (2023), sustainability considerations are less common in private equity firms than in traditional asset management. Of course, PE firms have always been sensitive to governance issues because it is a core element in structuring a private equity firm. Indeed, GPs want to be involved in the management of the company, or at least have influence on the board, in order to deliver performance. By contrast, environmental and social issues have never been a core element of the private equity industry and have come relatively late to this market. However, PE firms have many advantages over traditional asset managers when it comes to implementing ESG and sustainability policies:

> "*Private equity's business model gives it clear advantages over investors in public equities when it comes to implementing a sustainability agenda. A PE firm has virtual control of its portfolio companies from an ownership and governance perspective, even when it doesn't own 100% of a company: It has one or more representatives on the board and a strong influence on who else serves. It has access to any information it wants about both financial and sustainability performance — whereas investors in public companies see only what the company reports. Finally, the firm determines executive compensation and can fire a CEO who is not delivering.*" (Eccles *et al.*, 2023)

The time horizon of GPs and LPs is much longer than that of asset managers and public market investors because most of their investments are illiquid. They are active long-term investors in the sense that they both invest for the long term and must actively manage their portfolios. By active, we do not mean asset trading, dynamic asset allocation, or portfolio rebalancing. In this specific case, active management means that portfolio construction is driven entirely by asset selection and a bottom-up approach. Top-down portfolio construction is secondary and, in most cases, nonexistent. However, since 2020 and the pandemic crisis, we have seen a shift in the private equity industry. More and more private equity firms are adopting ESG criteria and offering ESG funds. In fact, there are some structural reasons to believe that the ESG practices of the private equity industry will follow those of the asset management industry:

> "*Three forces are pushing ESG in the industry. First, ESG is becoming more important to limited partners and their beneficiaries. The largest asset owners — among them pension and sovereign wealth funds — are increasingly concerned about the system-level effects of climate change and inequality. [...] The second force pushing ESG in the industry derives from the belief of many LPs and GPs that it will be essential if private equity is to continue delivering its historically high returns. [...] The third force is portfolio companies' increasing recognition of the importance of ESG issues. The reasons are unsurprising: a changing zeitgeist reflected in the preferences of employees and customers; growing awareness of the significance of climate change; social expectations regarding diversity, equity, and inclusion; pressure from large public companies to which*

*the portfolio companies are suppliers; awareness of the sustainability focus in publicly listed companies; opportunities to boost their own value through sustainability; and increasing regulation.*" (Eccles *et al.*, 2023)

These reasons are not specific to PE firms and can apply to any asset owner or manager. Most limited partners are the institutional investors we encounter in the asset management industry. Asset allocation for these investors is not simply a matter of allocating equity and fixed income to public securities. These asset owners also invest heavily in alternative assets. Figure 4.21 shows the evolution of institutional allocations to alternative assets. In 2014, private markets represented 17.3% of the allocation, while in 2023 it is 27%. This represents growth of 56% over nine years, or 5% per year. This increase has been at the expense of equity and fixed-income allocations.

Figure 4.21: Allocation of institutional investors to alternative assets (in %)

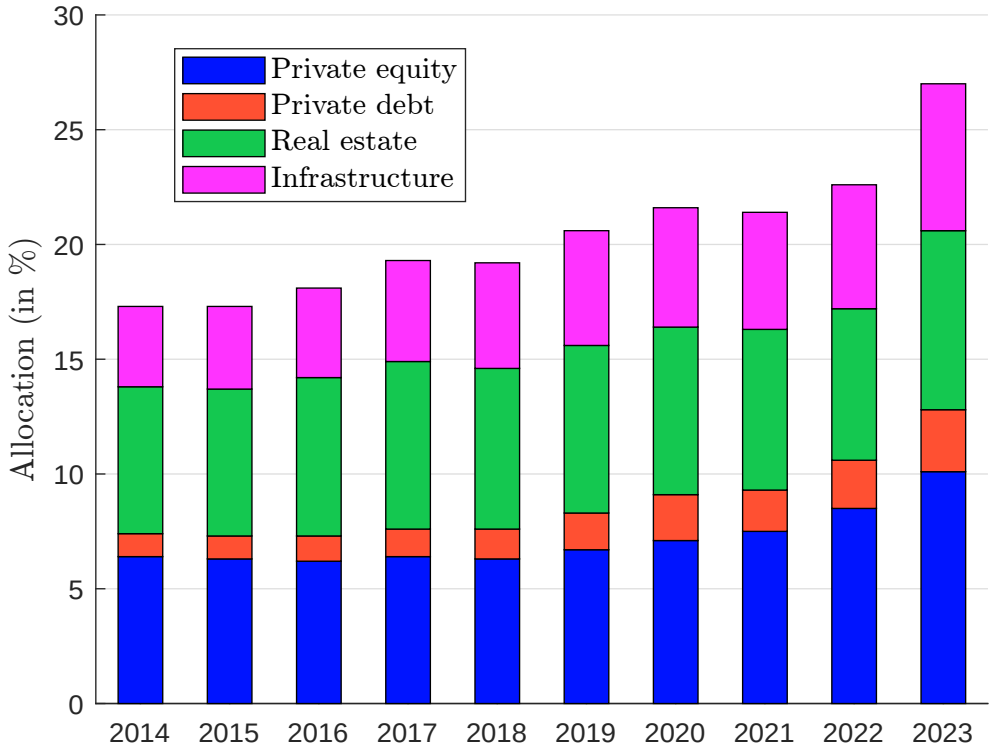


Source: McKinsey (2024, Exibit 7, page 13).

This level of ESG progress in private equity is illustrated by the launch of the ESG Data Convergence Initiative (EDCI) in 2021. At the height of the Covid-19 lockdown, CalPERS and Carlyle hosted a video conference with a small group of GPs and LPs to discuss the challenges they faced with ESG data. Despite the proliferation of ESG frameworks and rating providers, there was still no standardized, meaningful, performance-based data from private companies. The conversation evolved from sharing concerns to creating an action plan. In September 2021, the founding members, led by CalPERS and Carlyle as inaugural co-chairs, announced the launch of the initiative. Membership is now open to private debt firms, investment advisors and ESG data platforms. Since then, the EDCI has grown significantly, with more than 425 GPs and LPs now participating. The Steering Committee is currently chaired by Carlyle and CPP Investments. It also includes 7 LPs: APG, AlpInvest Partners, CalPERS, PGGM, Pictet, PSP Investments and StepStone Group and 7 GPs: Apollo Global Management, Cinven, CVC, EQT AB, PAG, Permira and TowerBrook.

Using data points collected by EDCI from approximately 185 GPs and 4 300 PE portfolio companies, BCG (2023b) has produced a report to understand how private markets currently compare to public markets on a variety of topics. One of the key findings is that PE firms have been more successful in driving decarbonization in larger portfolio companies than in smaller ones. A second finding is that private companies lag behind public companies in their use of renewable energy. Overall, the median private company that used at least some renewable energy sources 27% of its energy from renewable sources, compared to 36% for public companies. On social issues, private companies lag behind their public counterparts in some areas, particularly gender and minority diversity on their boards, but they can outperform on other measures, such as job creation. When it comes to work-related injuries, there are no clear differences between private and public companies. Curiously, the proportion of women on management teams in private companies was 5% higher than in public companies.

PRI (2019b, 2023) has produced two guides for incorporating ESG into private equity and private debt. These guides are very similar to those we find for listed equities and bonds. However, there are two key differences. The first is engagement, which is theoretically more efficient in private markets because of the weight of the GP on the board and in management. The second is due diligence, which must be adapted because private companies are not subject to public disclosure requirements. Therefore, they have less experience and less staff to fill out the ESG questionnaire. The due diligence questionnaire must then be adjusted to focus on the most important ESG criteria.

### 4.3.2 Sustainable infrastructure

Infrastructure refers to the long-lived physical structures and networks that are essential to the functioning of a society and its economy. These assets provide critical services that support daily life and economic activity. It can include a wide range of structures and networks, such as:

- Economic infrastructure: industrial parks, manufacturing facilities, shipping terminals, etc.
- Energy: power plants, electricity grids, oil and gas pipelines, refineries, storage facilities, renewable energy facilities, wind farms, etc.
- Other utilities: water and wastewater systems, waste management systems, telecommunications networks, etc.
- Social infrastructure: schools, hospitals, prisons, etc.
- Transportation: roads, bridges, railways, airports, ports, public transit systems, etc.

The European Commission defines green infrastructure as "*a strategically planned network of natural and semi-natural areas with other environmental features, designed and managed to deliver a wide range of ecosystem services, while also enhancing biodiversity*". Green infrastructure is implemented in a variety of sectors, from the energy sector through energy transmission infrastructure, and the water sector through natural water retention measures or sustainable urban drainage systems, to the urban landscape with street trees to help sequester carbon or green roofs to help regulate the temperature of buildings. In general, sustainable infrastructure falls into three main categories:

1. Net-zero infrastructure refers to the structures needed to achieve a low-carbon economy. It focuses primarily on the development of green electricity, the construction of electricity grids, and the storage of electricity.

2. Climate-resilient infrastructure refers to the construction or renovation of infrastructure, such as transportation and buildings, to withstand and adapt to the impacts of climate change, particularly extreme weather events, sea level rise, temperature increases, changes in precipitation patterns, and other physical risks.

3. Green infrastructure refers to a network of natural and engineered systems that provide environmental and social benefits in urban and rural environments. It's essentially the use of nature-based solutions to address challenges traditionally addressed with concrete and steel. It includes green roofs and walls, rain gardens and bioswales, permeable pavements, urban forests and greenways, and wetlands.

The first category is clearly a response to the transition risk component of climate risk, while the second category is more of a response to the physical risk component. The third category encompasses both dimensions and is also related to resource degradation and biodiversity loss. However, sustainable infrastructure is not limited to Pillar (E). According to PRI (2024), it must also mobilize Pillar (S). For example, we know that the infrastructure sector has many issues related to safety, working conditions, human rights and health. Therefore, ESG criteria must include labor standards and working conditions, including in the supply chain; land rights and indigenous rights; and diversity, equity and inclusion.

Box 4.10: An example of an ESG agency specializing in real assets: GRESB

GRESB, which stands for Global Real Estate Sustainability Benchmark, is a mission-driven, industry-led organization that provides actionable and transparent environmental, social and governance (ESG) data to the financial markets. They collect, validate, score and independently benchmark ESG data to provide business intelligence, engagement tools and regulatory reporting solutions for investors, asset managers and the broader industry. GRESB was established in the Netherlands in 2009 and consists of an independent foundation and a certified B-Corp. The GRESB Foundation focuses on the development, approval and administration of the GRESB Standards, while GRESB BV conducts ESG assessments and provides related services to GRESB members.

GRESB provides methodologies and frameworks to measure the ESG performance of individual assets and portfolios based on self-reported data to assess their alignment with the Sustainable Development Goals, the Paris Climate Agreement, and key international reporting frameworks. The data and scores are used to create industry ESG benchmarks: (1) real estate benchmark, (2) real estate development benchmark, (3) infrastructure fund benchmark, and (4) infrastructure asset benchmark. In addition, GRESB publishes the global aggregate benchmark data each year, showing the state of ESG in the real assets industry. This consists of two reports, one dedicated to real estate and one dedicated to infrastructure. The results of the 2023 report are available for download at `www.gresb.com/nl-en/gresb-public-results`.

As of December 2023, the GRESB benchmark database includes 784 real estate funds, 2 084 real estate assets, 172 infrastructure funds and 685 infrastructure assets. For example, it includes 29 airports (*e.g.*, Auckland, Brussels, Gatwick, Glasgow, Sydney), 65 road companies (*e.g.*, A63 Bordeaux Hendaye, APRR, Yongin Seoul Expressway), 27 social infrastructure (*e.g.*, Barts Hospital, Domus Social Housing Ltd, Hospital de Parla), etc.

Source: `www.gresb.com/nl-en`.

### 4.3.3 Sustainable real estate

The real estate sector emits significant amounts of $CO_2$ through building operations, building materials, and construction. Action is needed to be taken in the construction of new buildings, but also in the renovation of existing buildings. For existing buildings, it is very important to reduce energy consumption, eliminate emissions from energy and refrigerants, and reduce or eliminate the use of fossil fuels. This is done by improving equipment such as insulation, ventilation, and the use of renewable energy, as well as optimizing operations by installing GHG monitors or adjusting temperature settings. New construction must be energy and carbon efficient, taking into account new and clean technologies. In both cases (renovation and new construction), certification is an important indicator of what constitutes a green building (PRI, 2022c). It is widely used in the real estate industry and real estate funds. This is particularly true for new buildings, especially in Europe, where regulations require them to be in line with the European Commission's decarbonization policy and comply with the Energy Performance of Buildings Directive (EPBD).

This explains the strong momentum of sustainable real estate funds, which typically target multiple sectors and countries with a specific allocation to reach net zero by 2050. Unlike infrastructure, which is more difficult to monitor and evaluate, the carbon footprint of real estate is easier to assess. Below is a list of some of the tools used by real estate funds:

- *Accounting and Reporting of GHG Emissions from Real Estate Operations* developed by PCAF, CRREM and GRESB, www.crrem.eu/accounting-and-reporting-of-ghg-emissions
- *CRREM Risk Assessment Reference Guide* prepared by the Institute for Real Estate Economics (Austria) in collaboration with the University of Ulster, GRESB BV, University of Alicante and Tilburg University, www.crrem.eu/tool/reference-guide
- *CRREM Risk Assessment Tool* with updated CRREM-SBTi Aligned Decarbonization Pathways, www.crrem.eu/tool
- *EU Building Stock Observatory (BSO)* under the umbrella of the EU Commission to monitor the implementation of the Energy Performance of Buildings Directive (EPBD), https://energy.ec.europa.eu/topics/energy-efficiency/energy-efficient-buildings_en
- *PCAF European Building Emission Factor Database*, https://building-db.carbonaccountingfinancials.com/login.php
- *SBTi Buildings Guidance and Tool* developed by the Science Based Targets initiative, www.sciencebasedtargets.org/sectors/buildings
- *US Commercial Buildings Energy Consumption Survey (CBECS) database* developed by the US Energy Information Administration (EIA), https://www.eia.gov/consumption/commercial
- *US Residential Energy Consumption Survey (RECS) database* developed by the US Energy Information Administration (EIA), https://www.eia.gov/consumption/residential

In Europe, sustainable real estate funds mostly follow the CRREM (Carbon Risk Real Estate Monitor) path, targeting 1.5°C/2°C using a Paris-aligned decarbonization pathway per country and building type, ranging from office buildings to retail stores and hotels.

# Chapter 5

# Impact Investing

Impact investing is not ESG investing. That is, the two investment approaches are different. Perhaps it is more accurate to say that ESG investing is not impact investing. This is certainly the consensus of asset owners and managers who believe that impact investing is part of ESG investing. In fact, we saw in Chapter 1 that impact investing is one of the seven categories of ESG strategies. However, many investors believe that impact investing is a special animal in the sustainable finance ecosystem and should not be compared to ESG selection, ESG integration and other ESG strategies, with the possible exception of the second category dedicated to norms-based screening (Figure 1.15 on page 43). This second category is also known as the values strategy, and it is no coincidence that we can associate impact investing and values. In her Presidential Address at the American Finance Association (AFA) Annual Meeting in New Orleans on January 7, 2023, Lara Starks discussed the differences between investors' and managers' motivations for considering sustainable finance. Her presentation was titled *Value versus Values* and focused on the preferences of sustainable investors:

> "*For some investors, ESG decision making is driven by values, that is by preferences — in particular non-pecuniary preferences [...] For other investors and managers, ESG decision making is driven by financial value, that is, by a firm's risk and return opportunities. [...] Clear identification may be complicated by the fact that ESG investing can also be motivated by a combination of values and value.*" (Starks, 2023, pages 1838-1839).

In Figure 5.1 we reproduce the Venn diagram created by Laura Starks on the range of ESG approaches. Impact investing is unique in that it is driven primarily by values, not value. One could argue that norms-based screening is a similar strategy, but it is not. In fact, it is an exclusion strategy and is widely used by ESG investors because it has become mandatory if investors want to put an ESG stamp on their investments. In contrast, impact investing is a niche strategy. To understand the difference, we need to distinguish between investing WITH impact and investing FOR impact. Investing WITH impact means that impact considerations in the investment process come after financial return considerations (values after value), while investing FOR impact means that impact considerations in the investment process come before financial return considerations (values before value). This is why impact investing was first developed by philanthropic foundations. Investing FOR impact is a narrow segment of sustainable finance. In contrast, investing WITH impact can be claimed by virtually all ESG strategies. Using an ESG score, managing with a climate risk measure, applying an exclusion list, or engaging and voting have an impact on companies and the world, but they are not impact investing. Precisely, the first section of this chapter is devoted to the definition and scope of impact investing, to be clear about what it is and what it is not. This is followed by two sections on the SDGs and the impact investing market. Finally, we look at the biodiversity in a final section to illustrate the differences between investing WITH and FOR impact.

Figure 5.1: Values versus value in investment approaches

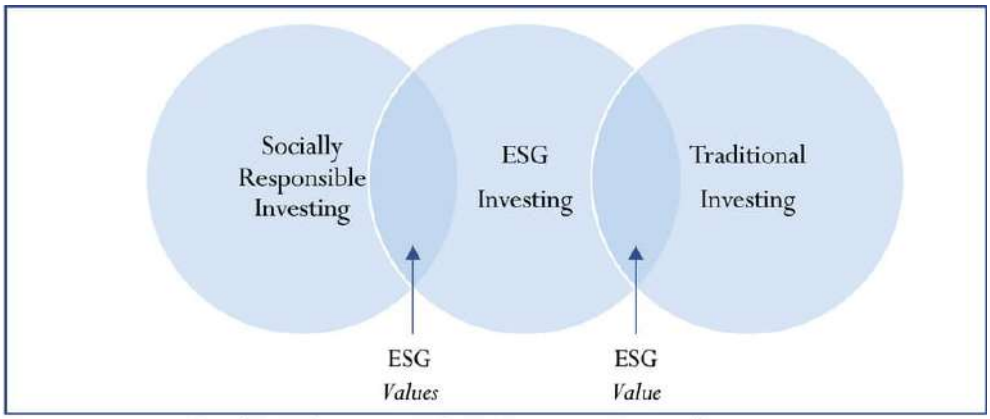


Panel A. *Values* versus *Value* in Investment Approaches

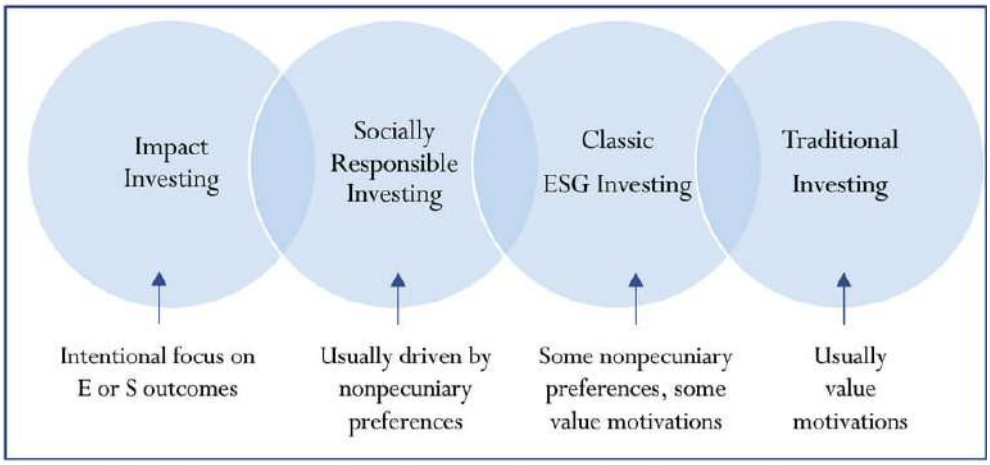


Panel B. *Values* versus *Value* in Investment Approaches: Investor Preferences

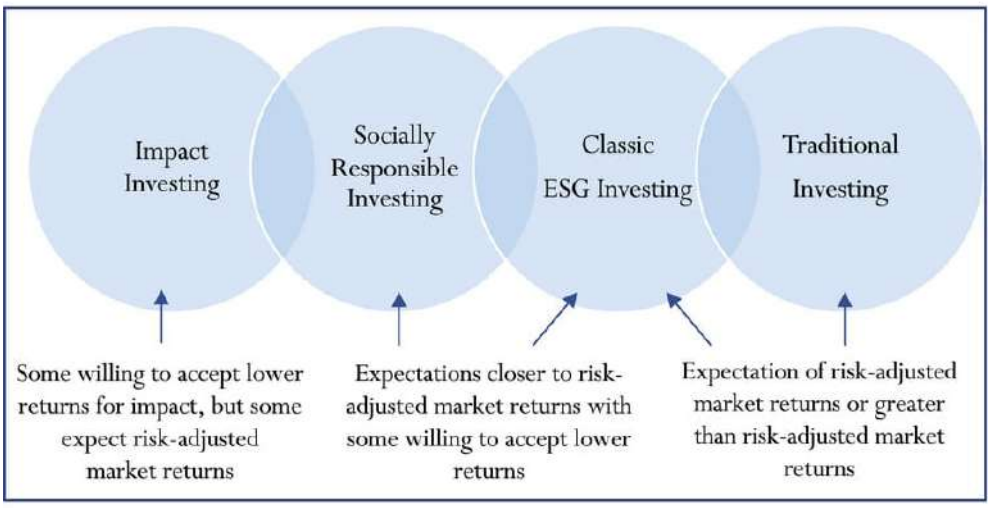


Panel C *Values* versus *Value* in Investment Approaches: Expected Returns

This figure illustrates a Venn diagram for the spectrum of investment approaches. Panel A shows the interlap between SRI, ESG, and traditional investing; Panel B shows the typical investor preferences related to the approaches; and Panel C shows the typical expected returns across the approaches.

Source: Starks (2023, Figure 1, page 1840).

## 5.1 Definition

Impact investing refers to "*investments with the intention to generate positive, measurable social and environmental impact alongside a financial return*" (GIIN, 2021, page 4). This is the definition of the Global Impact Investing Network. But the GIIN adds that the impact investing market must provide capital to address the world's most pressing challenges in areas such as sustainable agriculture, renewable energy, conservation, microfinance, and affordable and accessible basic services such as housing, health care, and education. The GIIN argues that the practice of impact investing is further defined by four core characteristics: "*(1) Intentionality: an investor's intention to have a positive social or environmental impact through investments is essential to impact investing; (2) Range of return expectations and asset classes: impact investments target financial returns that range from below market (sometimes called concessionary) to risk-adjusted market rate, and can be made across asset classes, including but not limited to cash equivalents, fixed income, venture capital, and private equity; (3) Investment with return expectations: impact investments are expected to generate a financial return on capital or, at minimum, a return of capital; (4) Impact measurement and management: a hallmark of impact investing is the commitment of the investor to measure and report the social and environmental performance and progress of underlying investments, ensuring transparency and accountability while informing the practice of impact investing and building the field.*"

These various elements provided by the GIIN to define impact investing call for several comments. First, the definition clearly indicates that the primary goal of impact investing is to generate a non-pecuniary return, and that financial performance is secondary. Therefore, the investor's preferences are not to maximize a risk-adjusted performance measure that is biased toward some sustainable non-pecuniary benefits. The optimization problems defined in Chapter 2 (the Pástor-Stambaugh-Taylor model and the Pedersen-Fitzgibbons-Pomorski model) are not valid in the case of impact investing. Investor preferences are more likely to maximize non-pecuniary benefits, subject to a minimum acceptable rate of return. Utility functions are different in the two cases, and a mean-variance framework is not valid when considering impact investing. We generally assume that the impact investor has no financial benchmark and that his expected return is below the market. Second, the investment universe of the impact investor is small compared to the investment universe of a traditional or ESG investor. In the eighties and nineties, impact investing was primarily focused on health care, education and microfinance for minorities and communities. At that time, the concept of social impact investing (or social investing) was very close to philanthropy: philanthropy involved giving money to charitable causes without expecting a financial return, while social impact investing involved giving money to social causes with the expectation of a minimal financial return. Since the 2000s, social impact investing has included other motivations beyond purely social issues, particularly environmental issues. It has become simply impact investing, which embraces both social and environmental considerations. The third comment relates to the second core feature devoted to asset classes. The GIIN identifies four asset classes: cash equivalents, fixed income, venture capital, and private equity. Cash equivalents and fixed income refer to short- and long-term debt instruments in both public and private markets. Venture capital and private equity are two forms of investment in unlisted companies. Private assets are then largely targeted by impact investors, while public assets are mainly represented by debt and fixed income instruments. This excludes public equity and the market for listed companies. Why can't buying shares in a public company be considered an impact investment? Certainly because buying public shares has no social or environmental impact from the investor's perspective. To better understand this lack of impact, we need to develop the last comment related to the fourth core characteristic: the measurement of impact. In fact, an investment can only be considered an impact investment if we can measure the

impact. This may seem trivial, but it is not. Consider the case of buying public stock. By definition, the investor has bought these shares from another investor. This new investor cannot measure social or environmental impact just because some shares have changed hands. Or he must buy enough shares to take control of the public company and change the way it does business. In contrast, the investor who funds a new hospital or a new school can measure the impact of that investment directly in terms of the number of additional hospital beds in the country or the number of children who benefit from that school. In both of these examples, the impact is measured as the difference between a KPI before and after the investment. This implies that the KPI has increased with this investment. The concept of additionality (supplementary benefit) is then essential when talking about impact investing. Consider an investor who has the choice of buying a forest or planting a new one. In the first case, the forest area does not change. Strictly speaking, this is not an impact investment. In the second case, the forest area has increased. This can be an impact investment.

### 5.1.1 Impact investing frameworks

#### The intentionality-additionality-measurability framework

From a practitioner's perspective, the four core characteristics are generally not obvious to apply and are replaced by other frameworks. For example, France Invest & FIR (2021) propose a framework based on three dimensions:

1. Intentionality
   The intention of the investment to contribute to the generation of a measurable social or environmental benefit

2. Additionality
   The positive impact that would not have occurred without this specific investment

3. Measurability
   The process of measuring the social and/or environmental impact of investments

Intentionality is the critical element of an impact investing framework because it often determines whether an investment is an impact investment or not. The investor's primary intention is to create social or environmental impact from an ex ante perspective. It cannot be an investment for other purposes[1]. For example, replacing an investment in the MSCI World Index with an investment in the MSCI World PAB Index is not an impact investment. This is also the case with many investment vehicles that are built using a top-down approach. In other words, the investor starts with the intention of funding or participating in a social or environmental project. For institutional investors whose investments are driven by strategic asset allocation, this can be an issue. They need to clearly separate which investments are impact and which are not. The fact that they are making assumptions about expected returns, volatilities and correlations, even for impact investments, can be challenging. This is easier for charities, philanthropic foundations or endowments that do not have liabilities to manage. By construction, impact intention precedes the investment decision. If it's the other way around, it's not impact investing, for example, claiming positive impacts after they have been generated. Impact could not be a by-product of the investment. To better assess intentionality[2], France Invest & FIR (2021) then suggest to define three characteristics: the impact thesis (and the link to the SDGs), the impact strategy and its implementation and the appropriate governance (Table 5.1).

[1] Of course, performance and returns remain important, but they are not the defining factor of an impact investment.
[2] In Table 5.2, we have listed some questions to answer that help assess the three dimensions.

Table 5.1: The 9 core characteristics of the intentionality-additionality-measurability framework

| Intentionality | Additionality | Measurability |
|---|---|---|
| • Thesis | • Coverage | • Metrics |
| • Strategy | • Time horizon | • Transparency |
| • Governance | • Commitment | • Remuneration |

The second dimension is additionality. It is sometimes referred to as contribution, but the latter concept is less demanding. In fact, we can think of all ESG strategies as contributing to society and participating in a better world. For example, some authors argue that they create market signals and encourage the adoption of better sustainable practices. However, the concept of additionality requires a distinction between individual and collective contributions, tangible and hypothetical outcomes, and realized and expected benefits. In Table 5.2 we list some questions that can help assess the additionality of an investment. One question in particular is important:

What would happen if the investment were not made?

If the answer is nothing or very little, then the investment is not an impact investment. A typical example is investing in publicly traded stocks that have no problem accessing capital, even if the company has a social or environmental impact, such as pharmaceutical companies or renewable energy companies. In this case, there are two main reasons: (1) if we don't fund the company, someone else will; (2) shares and capital are two different things in a public market. In contrast, most microfinance investments are considered impact investments because the borrowers have limited access to the debt market. Similarly, many impact investments are directed to private equity and private debt markets because companies in these sectors are typically young and in need of capital. It is also easier to claim additionality when investing in projects related to the labor market, education, food security, personal care services, and poor countries. In addition, additionality needs to be evaluated and defined in terms of two key characteristics: coverage and time horizon. Indeed, the negative and positive externalities of an investment may be different in the short and long term. For example, investments in R&D projects may have low additionality in the short term but high potential additionality in the long term, *e.g.*, funding a new vaccine R&D project. Portfolio coverage is also important. Ideally, additionality should cover 100% of the impact portfolio assets. Finally, engagement is the third factor to consider when assessing additionality. Impact investors need to be active, not passive, in their engagement with investee company managers to ensure alignment on maximizing impact and additionality.

The last dimension is more traditional in the ESG investment framework, as it relates to measurability and reporting. For example, the SFDR and CSRD regulations can help define impact metrics, but generally impact investors use specific and recognized reporting tools[3] designed for impact investing reporting, such as the IRIS+ system. A typical example of impact metrics is the number of MWh of electricity produced annually by a new wind farm and the equivalent of $CO_2$ emissions avoided. These metrics and KPIs should be transparent, can be quantitative or qualitative, and must be used for reporting as well as for managing the project or company. They are therefore both reporting outputs and management inputs. In the latter case, they are used for decision making and

[3]These are discussed in Section 5.1.4 on page 320.

Table 5.2: Questions to assess intentionality, additionality and measurability

**Intentionality**

What specific impact goal(s) does the investment seek to achieve?

- What are the ex-ante impact goals?
- How do the impact goals contribute to the UN SDGs?
- How does the investment policy support the impact goals?
- Does the impact cover the entire investment?
- What governance supports the achievement of the impact goals (impact committee, scientific committee, etc.)?

**Additionality**

What would happen if this investment were not made?

- Do the recipients of the funding typically have difficulty obtaining funding?
- Does the investment horizon allow for the long-term viability of the enterprise/project?
- What is the commitment to working with investee managers to achieve impact, and if so, how is it implemented?
- What initiatives are in place to support the impact of the investment beyond direct engagement with investees?

**Measurability**

How will impact and progress towards the goal(s) be measured?

- What is the impact reporting methodology?
- What are the impact KPIs?
- How are these impact KPIs used to inform decision-making?
- How are these impact indicators used to engage companies in the portfolio?
- What is the frequency of impact reporting?

compensation. Indeed, it is important that both investor performance and investee remuneration are linked to the metrics used for impact reporting. We see that this last dimension is related to the first two and cannot be defined once intentionality and additionality are established. In fact, the three dimensions are not independent and it is important to ensure coherence between them (Figure 5.2).

Figure 5.2: Links between intentionality, additionality and impact measurement

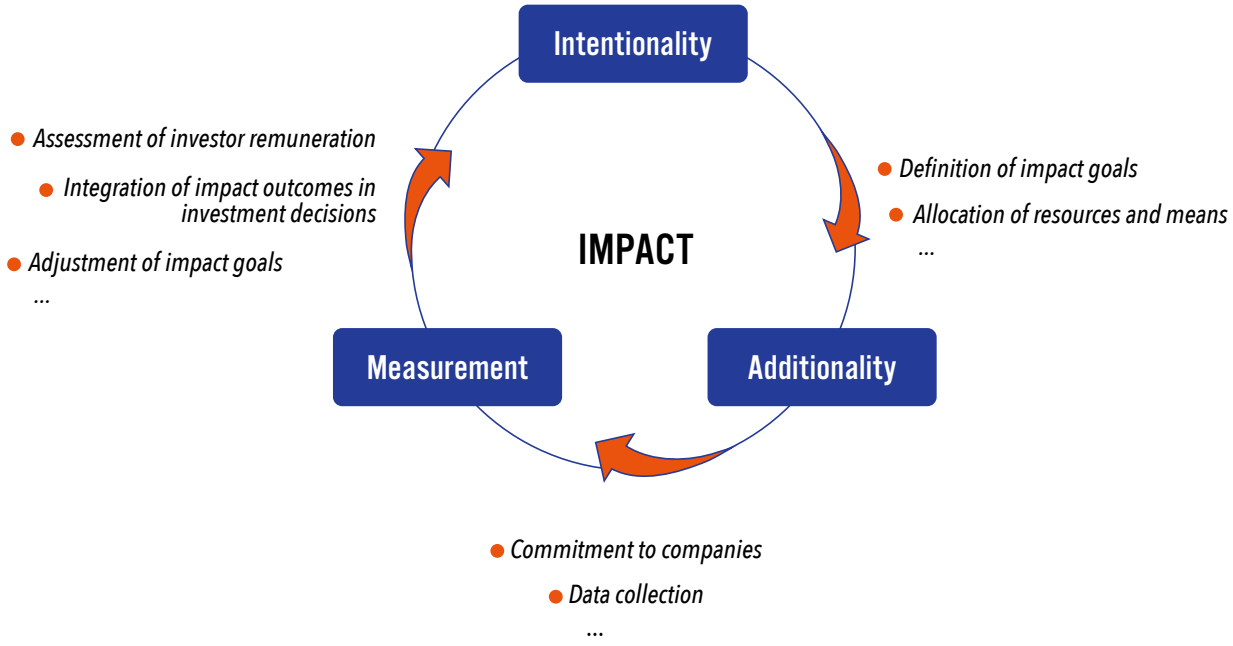


Source: France Invest & FIR (2021, Chart 1, page 4).

The distinction between impact investing and other ESG strategies needs to be clear, because too often impact investing is a repackaging of the latter. Negative screening and norms-based screening cannot be considered as impact investing, because the intention and the motivation of these strategies is not to generate positive impact. Investors do not want to invest in these companies because of moral values or because they want to avoid sustainability and financial risks. Similarly, best-in-class selection and ESG integration are not impact investing strategies because they are incompatible with the additionality property. In fact, they do not satisfy the coverage and commitment properties. By definition, voting is far from impact investing because materiality and measurability are difficult to assess. Moreover, the principle of individual attribution of additionality is not established. Finally, there may be some confusion between impact investing and sustainability themed investing. Indeed, some impact investing products or funds are also thematic products or funds. Therefore, in some cases, there is overlap between these two strategies.

### Other frameworks

The intentionality-additionality-measurement framework is not the only approach. Investors also use other methodologies, which can be divided into two main categories: (1) non-specialized and general frameworks, and (2) dedicated impact investing frameworks. For example, they may use the PRI reporting standards and the UN SDGs, which were not designed for this specific purpose. In 2018, the PRI supplemented its standards with a dedicated framework, the Impact Investing Market Map,

to identify mainstream impact investing companies and investments (PRI, 2018b). The following is a non-exhaustive list of dedicated impact investing frameworks[4]:

- The 5 dimensions of impact were developed by the Impact Management Principle (IMP) and incorporated into Impact Frontiers[5];
- The Operating Principles for Impact Management (OPIM) were launched in 2019, led by the International Finance Corporation (IFC) in partnership with a group of peer institutions. It is now a division of the GIIN[6];
- The Compass was developed by the GIIN and is a methodology for comparing and assessing impact;
- The B Impact Assessment is a system for B-Corp certification. It is a tool developed by B Lab to assess a company's impact on its employees, community, environment, and customers. After completing the assessment, companies go through a review process and companies that score a minimum of 80 out of 200 points are certified as B-Corps[7];
- The Theory of Change (ToC) in impact investing is a framework that explains how and why a desired change is expected to occur in a particular context (Jackson, 2013). It describes the path from initial inputs and activities to expected long-term outcomes and impacts, and articulates the assumptions and mechanisms that link investments to social or environmental benefits[8].

According to the French National Advisory Board (NAB), the most common frameworks used by French impact investors are[9] the Principles for Responsible Investment (61%), followed by the SDG Impact Standards (33%), the French Sustainable Finance Institute's rating grid (26%), the 5 dimensions of impact (26%), the Theory of Change (24%), and the B Impact Assessment (18%). In Germany[10], impact investors use their own framework (52%), the EU Taxonomy (41%), the Sustainable Development Goals (40%), the Principles for Responsible Investment (38%), GIIN's IRIS+ (36%), the 5 dimensions of impact (33%), OPIM (26%), the GIIN Compass (19%) and the B Impact Assessment (7%). Below, we describe two approaches that complement the intentionality-additionality-measurement framework.

**Impact management project (IMP)** From 2016 to 2018, the Impact Management Project (IMP) convened a community of 3 000 practitioners (companies and investors) and a network of 13 organizations, including PRI, OECD, and UNEP, to build a global consensus on how to measure,

[4]We exclude regional and country initiatives such as IMP+ACT and the Impact Investing Institute in the UK (www.impactinvest.org.uk) or the Sustainable Finance Institute's rating grid in France (www.institutdelafinancedurable.com).

[5]The norms can be found at https://impactfrontiers.org/norms/five-dimensions-of-impact.

[6]The dedicated website is www.impactprinciples.org.

[7]A Benefit Corporation, or B-Corp, is a type of for-profit company that includes a positive impact on society, employees, the community and the environment as one of its legally defined goals, in addition to profit. Benefit corporations are legally recognized in several countries (*e.g.*, Belgium and the Netherlands) and several states in the United States. The French and Italian equivalents of benefit corporations are '*entreprises à mission*' and '*Società Benefit*' respectively.

[8]There is not one framework, but several approaches proposed by GIIN, IMP, GSG Impact, etc.

[9]Source: NAB France (2023), Overview of the French Impact Investment Market 2023, *Report*, December, 20 pages, www.franceinvest.eu.

[10]Source: Bundesinitiative Impact Investing (2022), Impact Investing in Germany 2022 Marktstudie, *Report*, October, 48 pages, www.bundesinitiative-impact-investing.org.

Table 5.3: The five dimensions of impact (Impact Management Project)

| Impact dimension | | Impact questions |
|---|---|---|
| 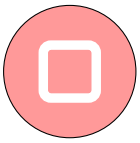 | What | What tells us what outcome the enterprise is contributing to, whether it is positive or negative, and how important the outcome is to stakeholders |
| 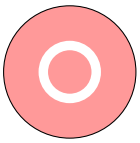 | Who | Who tells us which stakeholders are experiencing the outcome and how underserved they are in relation to the outcome |
| | How much | How Much tells us how many stakeholders experienced the outcome, what degree of change they experienced, and how long they experienced the outcome |
| 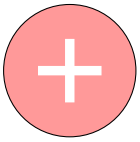 | Contribute | Contribution tells us whether an enterprise's and/or investor's efforts resulted in outcomes that were likely better than what would have occurred otherwise |
| | Risk | Risk tells us the likelihood that impact will be different than expected |

Source: www.impactfrontiers.org/norms/five-dimensions-of-impact.

improve, and disclose positive and negative impacts. The resulting consensus (or '*norms*') provide a framework for understanding how companies and investors impact people and the planet. These resources migrated to Impact Frontiers in 2021. The five dimensions of the framework are shown in Table 5.3. These dimensions are What, Who, How Much, Enterprise Contribution and Impact Risk. Each dimension is then defined by a set of characteristics and data categories. For example, the How Much dimension has 3 data categories:

1. Scale: the number of individuals experiencing the outcome, *e.g.*, 1 450 individuals;
2. Depth: the degree of change experienced by the stakeholder. Depth is calculated by analyzing the change that has occured between the '*outcome level at baseline*' (Who) and the '*outcome level in period*' (What), *e.g.*, 20% increase in outcome relative to baseline;
3. Duration: the time period for which the stakeholder experiences the outcome, *e.g.*, 24 months.

The mapping to the previous framework is not obvious. It is tempting to align intentionality with what and who, additionality with how much and contribution, and measurability with risk. However, the reporting dimension is missing or less present, probably because it is a framework for assessing positive and negative impacts and not fully dedicated to impact investing. Furthermore, impact is considered from the perspective of the company, not the investor. This also explains why intentionality is not at the heart of this framework.

**Operating principles for impact management (OPIM)** The Operating Principles for Impact Management outline an end-to-end process consisting of five main elements: strategy, origination and structuring, portfolio management, exit, and independent verification. Each element has its own set of principles. In total, there are nine principles that serve as the foundational components of an effective impact management system. These Principles are based on two core concepts: (1) core elements of a robust impact management system; and (2) transparency of signatories' alignment with the Principles. The nine principles are described in Figure 5.3 and more details on each principle can be found at www.impactprinciples.org.

Figure 5.3: The nine operating principles for impact management (OPIM)

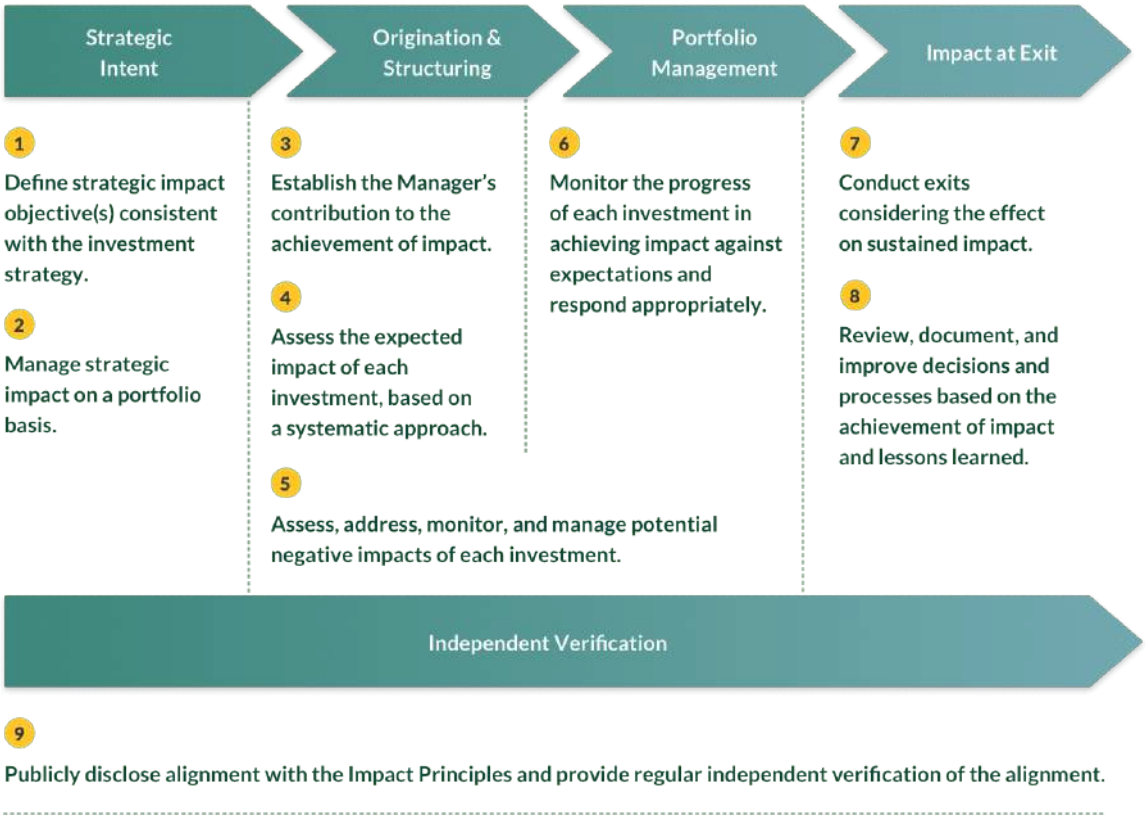


Source: www.impactprinciples.org.

The process for adopting the Principles is similar to the PRI. In fact, an investor wishing to use the OPIM must become a signatory and meet certain obligations. To do so, the investor must submit a letter of commitment, disclose total and covered assets under management, pay registration and filing fees, and publish an annual disclosure statement. The disclosure statement details compliance with the Principles and includes independent verification reports. As of the end of June 2024, there are 181 signatories in 40 countries representing $539 billion in covered assets. Signatories managing more than $10 billion under the Principles are the International Finance Corporation (Multilateral, $92.1 bn), the European Bank for Reconstruction and Development (Multilateral, $61.9 bn), the European Investment Bank (Multilateral, $43.3 bn), the US International Development Finance Corporation (US, $35.1 bn), the Multilateral Investment Guarantee Agency (Multilateral, $31.3), IDB Invest (Multilateral, $21.0), Brookfield Global Transition Fund (US, $15 bn), The Rise Fund (US, $15.0 bn), FMO (Netherlands, $14.1 bn), DEG (Germany, $11.4), BlackRock (US, $10.4) and BentallGreenOak (Canada, $10.1 bn).

### 5.1.2 Historical perspectives

#### The practitioner's corner

Contrary to what we can read on the Internet (*e.g.*, Wikipedia), the term '*impact investing*' did not appear for the first time in 2005 or 2007. It was used in the 1990s and perhaps earlier, and was associated with ethical investing, community investing, or philanthropic investing:

> "*Portfolio screening is by far the most prevalent approach [...] The second SRI approach, targeted investing, may hold greater promise for minority media, particularly for small local firms. Also known as* community investing *or* high-impact investing*, this method seeks out opportunities where relatively small capital investment can generate substantial social returns. Unlike portfolio screening, there is usually no demand that returns match or beat a specific benchmark.*" (Kurtz, 1999, page 685).

However, it is true that the term impact investing was popularized by the Rockefeller Foundation in the late 2000s. According to Höchstädter and Scheck (2015), the term impact investing was extensively discussed and largely adopted in October 2007 when investors and philanthropic organizations were invited to a Bellagio meeting organized by the Rockefeller Foundation[11]. In addition, Antony Bugg-Levine, who was a managing director at the Rockefeller Foundation from 2007 to 2011, has been instrumental in popularizing the term impact investing. In November 2010, he participated in the first comprehensive research study conducted by J.P. Morgan and the Rockefeller Foundation (O'Donohoe *et al.*, 2010). In June 2011, he also co-authored with Jed Emerson[12], Executive Vice President of ImpactAssets[13], the book *Impact Investing: Transforming How We Make Money While Making a Difference* (Bugg-Levine and Emerson, 2011). In September 2009, the Rockefeller Foundation, the United States Agency for International Development and other participants also launched the Global Impact Investing Network ("the GIIN") to accelerate the development of a more effective impact investing industry.

Figure 5.4: The Rockefeller Foundation

The philanthropic sector has been instrumental in developing and structuring the impact investing market. This is because the philanthropic sector has long experience in this area, as venture philanthropy has been developed since the 1970s. Venture philanthropy can be seen as the application of concepts and techniques from venture capital to the management of philanthropic goals (Letts *et al.*, 1997). In 2012, the OECD launched the Network of Foundations Working for Development (netFWD), a group of foundations and philanthropic leaders committed to optimizing the

[11] The Bellagio Center, located in Bellagio, Italy, is a prestigious retreat operated by the Rockefeller Foundation.

[12] Jed Emerson is known as the creator of the blended value proposition, which is another name for impact investing (Emerson, 2003).

[13] ImpactAssets was founded in 2010 as a spin-off of Calvert Impact Capital.

impact of philanthropy in development with three main axes: education, gender, and health. All of these initiatives have given rise to the term philanthropic capitalism. Another group of investors that has been key to the development of the impact investing market are Development Finance Institutions (DFIs). According to OECD, "*DFIs are specialised development banks or subsidiaries set up to support private sector development in developing countries. They are usually majority-owned by national governments and source their capital from national or international development funds or benefit from government guarantees. This ensures their creditworthiness, which enables them to raise large amounts of money on international capital markets and provide financing on very competitive terms.*" We generally distinguish two types of DFIs:

- Bilateral DFIs are typically owned and primarily funded by a single national government and focus on development projects in developing countries that align with the foreign policy and economic interests of the owning country[14];
- Multilateral DFIs are owned and funded by a consortium of national governments and operate on a broader international scale, supporting development projects that promote global or regional development goals[15].

The weight of DFIs in impact investing is significant. For example, if we look at the signatories of the Operating Principles for Impact Management (OPIM), the breakdown as of June 2024 is as follows:

| | Bilateral DFIs | Multilateral DFIs | Other signatories | Total |
|---|---|---|---|---|
| Number of investors | 17 | 8 | 142 | 167 |
| Covered assets (in $ bn) | 100.5 | 252.3 | 187.0 | 539.9 |
| Covered assets (in %) | 18.6% | 46.7% | 34.6% | 100% |

The 25 DFIs represent approximately 65% of the $539 billion in covered assets, while the 142 other signatories, including some major investors such as Brookfield Asset Management, BlackRock, UBS Group, Zurich Insurance Group and Amundi, represent less than 35%. The International Finance Corporation is arguably the most influential and active DFI in impact investing. It is one of the five institutions of the World Bank. The other four are the International Bank for Reconstruction and Development (IBRD), the International Development Association (IDA), the Multilateral Investment Guarantee Agency (MIGA), and the International Centre for Settlement of Investment Disputes (ICSID). While the IBRD lends to governments of middle-income and creditworthy low-income countries and the IDA provides highly concessional financing to governments of the poorest countries, the IFC provides loans, guarantees, equity, advisory and project development services, and mobilizes capital from other sources to increase private sector investment in developing countries. As such, IFC is responsible for supporting and financing private companies in the developing world with two overarching goals: reducing extreme poverty (SDG 1) and promoting shared prosperity (SDG 10). This positioning explains IFC's important role in impact investing. In addition to its massive direct investments, IFC has established OPIM and promoted blended finance with several innovations in deal structuring.

[14]The main bilateral DFIs include OeEB (Austria), BIO (Belgium), BMI-SBI (Belgium), FinDev Canada (Canada), IFU (Denmark), Finnfund (Finland), AFD/Proparco (France), KfW/DEG (Germany), CDP/SIMEST (Italy), FMO (Netherlands), Norfund (Norway), SOFID (Portugal), COFIDES (Spain), Swedfund (Sweden), SIFEM (Switzerland), CDC Group (United Kingdom) and the US International Development Finance Corporation (United States).

[15]The main multilateral DFIs include AFDB (African Development Bank), ADB (Asian Development Bank), EBRD (European Bank for Reconstruction and Development), EIB (European Investment Bank), IDB (Inter-American Development Bank), IFC (International Finance Corporation) and ISDB (Islamic Development Bank).

Box 5.1: Blended finance and impact investing

In simple terms, blended finance is the combination of public and private capital to finance projects in developing countries with social/environmental impacts. There are many variations on this definition[a]:

- "*Blended finance is the use of catalytic capital from public or philanthropic sources to increase private sector investment in sustainable development.*" (Convergence).
- "*Blended finance is the strategic use of public finance for the mobilization of additional private finance towards sustainable development in developing countries. The most significant value of blended finance transactions is the ability to unlock funding for investments in areas that are not well funded. These investment segments are typically seen as 'too risky' for low-risk-seeking investors, or returns are not commensurate with risk for risk-seeking investors.*" (World Economic Forum).
- "*Blending involves the strategic use of a limited amount of grant resources to catalyse additional financing for development projects. Grants are often combined with loans, equity, beneficiary resources or other forms of financing, with the aim of de-risking projects and making them bankable. Blending allows partners to get the most out of their grant resources and enhance their overall development impact.*" (European Investment Bank).

Each definition complements the simple one by highlighting some aspects of blending finance. For example, blending finance acts as a catalyst, helping to initiate or increase the scale of private investment that might not otherwise have taken place. In effect, this approach aims to fill financing gaps for projects or sectors in developing countries that private and traditional investors consider too risky or not profitable enough. In addition, these projects must contribute to the achievement of a number of sustainable development goals. In fact, blended finance differs from a traditional investment partnership or co-investment approach. In these cases, all investors take the same risk and receive the same financial return, but blended finance is not based on a mutual fund or club deal structure. Public investors take more risk than private investors or improve their risk/return profile to attract the private sector to finance the project. According to Flammer *et al.* (2024), blending can take the form of a concessional loan (with a below-market interest rate), a junior equity tranche, a risk management provision (including credit enhancement), or performance-based incentives. In order to achieve this type of blending, the deal must adopt a structuring approach. A typical example is a pay-through structure where the junior tranche is held by the public investors and the senior tranche is held by the private investors (Roncalli, 2020a, page 139). In this context, blending finance acts as a leverage of the funds provided by the public investors. For example, if the junior tranche corresponds to 20% of the first losses and \$1 billion of capital, the leverage ratio is equal to 5, meaning that this structure has mobilized \$5 billion of capital, of which \$4 billion comes from the private sector. By definition, blended finance is part of impact investing, as the objective of the investment is to finance projects with social or environmental benefits. For public investors, blended finance ticks all the boxes: intentionality, additionality and measurability. This is not the case for private investors, who bear only part of the risk.

[a] These definitions can be found at `www.convergence.finance`, `www.weforum.org` and `www.eib.org`.

Alongside philanthropic investors and development finance institutions, private equity investors have historically been the third category that has driven impact investing. This is expected given that impact investing began in the private equity and debt markets. This makes this market very different from the traditional ESG investment market. In fact, traditional asset managers have only recently embraced the concept of impact investing, whereas they have been implementing ESG investing for a long time. Not surprisingly, impact investing has its roots in the United States, the largest market and a pioneer in private equity and private debt. In 2011, ImpactAssets began compiling an annual list of the top 50 fund managers engaged in impact investing. Since then, the list has been revised annually through 2024. Below we reproduce the list from 2011. We note that most of the fund managers are active in private equity (34 fund managers) and private debt (25 fund managers). The first appearance of the public equity asset class in the Impact Assets 50 was in 2012, with 5 fund managers. This asset class peaked in 2018 with 7 fund managers. However, public assets (cash, public debt and public equity) remain far behind private assets (private debt, private equity and real estate), which represent at least 80% of the fund managers in the Impact Assets 50 list. This confirms the importance of real assets and their fund managers.

Table 5.4: Impact Assets 50 list in 2011

| Fund | Cash | Commodities | Private Debt | Private Equity | Public Debt | Public Equity | Real Estate |
|---|---|---|---|---|---|---|---|
| Absolute Portfolio Management | | | | ✓ | | | |
| Accion | | | ✓ | | | | |
| Acumen Capital Partners LLC | | | ✓ | | | | |
| Bamboo Finance | | ✓ | ✓ | | | | |
| BAML Capital Access Funds Management, LLC | | | ✓ | | | | |
| Beartooth Capital | | | | | | | ✓ |
| BlueOrchard Finance Ltd | | ✓ | ✓ | | | | |
| Bridges Fund Management Ltd | | | ✓ | | | | |
| Calvert Impact | | ✓ | | | | | |
| City Light Capital | | | ✓ | | | | |
| Community Investment Partners | | | | ✓ | | | |
| Core Innovation Capital | | | ✓ | | | | |
| Creation Investments Capital Management, LLC | | | ✓ | | | | |
| Developing World Markets | | ✓ | ✓ | | | | |
| E+Co | | ✓ | ✓ | | | | |
| EcoEnterprises Fund | | ✓ | ✓ | | | | |
| EKO Asset Management Partners, LLC | | | ✓ | | | | |
| Elevar Equity | | | ✓ | | | | |
| EnerTech Capital | | | ✓ | | | | |
| Equator Capital Partners | | | ✓ | | | | |
| Global Partnerships | | ✓ | | | | | |
| Good Capital | | ✓ | ✓ | | | | |
| Grassroots Capital Management Corp, PBC | | ✓ | ✓ | | | | |
| Habitat for Humanity International | | ✓ | | | | | |

*Continued on next page*

Table 5.4: Impact Assets 50 list in 2011

*Continued from previous page*

| Fund | Cash | Commodities | Private Debt | Private Equity | Public Debt | Public Equity | Real Estate |
|---|---|---|---|---|---|---|---|
| IGNIA | | | | ✓ | | | |
| Incofin Investment Management | | | ✓ | ✓ | | | |
| LeapFrog Investments | | | | ✓ | | | |
| Living Cities Inc. | | | ✓ | | | | |
| Lumni | | | ✓ | ✓ | | | |
| The Lyme Timber Company LLC | | | | | | | ✓ |
| Media Development Investment Fund, Inc. | | | ✓ | ✓ | | | |
| MicroVest Capital Management, LLC | | | ✓ | ✓ | | | |
| Mindful Investors | | | | ✓ | | | |
| Minlam Asset Management | | | ✓ | | | | |
| Murex Investments | | | | ✓ | | | |
| Nonprofit Finance Fund | | | ✓ | | | | |
| Pacific Community Ventures | | | | ✓ | | | |
| Partners for the Common Good | | | ✓ | | | | |
| Public Radio Capital | | | ✓ | | | | |
| Renewal2 | | | | ✓ | | | |
| Root Capital | | | ✓ | | | | |
| RSF Social Finance | ✓ | | ✓ | | | | |
| Sarona Asset Management | | | | ✓ | | | |
| Satori Capital | | | | ✓ | | | |
| Shared Interest | | | ✓ | | | | |
| SJF Ventures | | | | ✓ | | | |
| Small Enterprise Assistance Funds | | | ✓ | ✓ | | | |
| SustainVC | | | | ✓ | | | |
| Symbiotics SA | | | ✓ | | | | |
| Triodos Investment Management | | | ✓ | ✓ | | | |
| Total | 1 | 0 | 25 | 34 | 2 | 0 | 2 |

Source: https://impactassets.org/ia50.

The role of institutional investors has been fundamental to the development of ESG investing. However, with the exception of non-profits and foundations that see impact investing as an effective way to align their investments with their values, impact investing remains a niche sector for other institutional investors, particularly pension funds and insurance companies (Wood, 2013). For example, in 2022, impact investing accounted for less than 0.3% of ESG strategies (Table 1.11 on page 48). However, this is the figure calculated by the Global Sustainable Investment Alliance, which is primarily an institutional investor platform. There are several reasons for this lack of mobilization around impact investing. Impact investing requires more resources and knowledge than ESG investing, which can be quickly implemented by purchasing external ESG ratings. Impact investing is a specialized market by nature, with no mainstream investment vehicles. Another reason is the perception by institutional investors that the risk behind impact investing is higher than the risk

behind other traditional investments[16] (*e.g.*, liquidity risk, credit risk). There is one segment of the impact investing market where institutional investors have a massive presence. This is blended finance. But this is understandable because it is strongly supported by public investors such as DFIs and MDBs and the asset managers who structure the investment project. They do not invest directly in the projects.

Figure 5.5: Global Impact Investing Network

The impact investing ecosystem is complex, with many organizations dedicated to this market. The most prominent is the GIIN, a non-profit organization. Since its inception and under the leadership of its charismatic CEO, Amit Bouri, the GIIN has played a leading role in advancing the field of impact investing. In particular, the organization has developed and hosts a number of tools and resources to help investors navigate the impact investing landscape:

- Impact Reporting and Investment Standards (IRIS), which provides a common language and framework for measuring and reporting on the social and environmental impact of investments;
- GIIN Benchmarks, which allow investors to measure the impact performance of their investments relative to the market, peer groups and against the scale of the social and/or environmental challenge;
- GIIN COMPASS is a methodology for comparing and assessing impact that aims to standardize the components and process of impact performance analysis at the aggregate investment, fund or portfolio level;
- Operating Principles for Impact Management (OPIM) is a framework for investors to implement their impact management systems, ensuring that impact considerations are integrated throughout the investment lifecycle.

Today, the GIIN has more than 400 members in 50 countries[17]. The GIIN also publishes a number of reports and surveys on impact investing. In addition to the GIIN, many other organizations are involved in impact investing, such as ImpactAssets or Impact Europe.

### The academic's corner

Academics have also been involved in studying impact investing. However, they have been less prolific in this area compared to other aspects of sustainable finance, perhaps because this market is not easily accessible and data is not readily available. Moreover, they may use the term '*impact*

[16] See the blog of Laure Wessemius-Chibrac published in November 2023 at www.impacteurope.net/insights/unlocking-institutional-resources.

[17] We can find them at https://thegiin.org/members.

*investing*' in a broader sense that does not fit the framework of intentionality, additionality, and measurability[18]. Höchstädter and Scheck (2015) provides a first survey of academics' and practitioners' understanding of impact investing[19] and concludes that the heterogeneity of definitions is less pronounced than expected. However, this conclusion is not shared by Agrawal and Hockerts (2021). For these authors, the terminology has changed over time to be more accurate today. They also note that some academic articles make a distinction between impact investing, socially responsible investing, social impact bonds, microfinance and venture philanthropy, while others do not. The paper by Chiappini *et al.* (2023) analyzes 196 academic papers published over the years 2011–2021 on impact investing and seeks to answer the following research questions: (1) What are the research trends in impact investing? (2) What are the most relevant and emerging topics? (3) What are the directions for future research? They first note that 75% of the articles have been published since 2018, while the years 2011–2015 show less than 6 publications per year. The most common keyword in these 196 articles is social impact bond (99 articles), far ahead of social enterprise (17 articles). According to Chiappini *et al.* (2023), the most cited article in 2021 was *Private Finance for Public Goods: Social Impact Bonds by* Warner (2013). Since then, it has been largely surpassed by *Impact Investing* by Barber *et al.* (2021), which is the most influential paper on impact investing in the last 5 years. The articles published by academics prior to 2021 are organized around three basic themes:

1. Impact investing as a source of funding for high-impact social enterprises
2. Theoretical drivers and issues related to the marketization/financialization of public services
3. The practice of social impact bonds

It is only recently that the issue of performance and risk in impact investing has attracted the attention of academics, particularly since the publication of Barber *et al.* (2021) and Geczy *et al.* (2021). Before 2021, it was common to say that the financial return of impact investments was below the market[20], but without knowing exactly the magnitude between impact investments and traditional investments. Hand *et al.* (2021) collect seven published studies on the financial performance of impact investing for the GIIN: one academic study (Barber *et al.*, 2021) and six industry reports[21] (one from the IFC, two from Cambridge Associates and three from Symbiotics). Results are highly dependent on the market, methodology and data used. For example, IFC's private equity portfolio achieved a public market equivalent (PME) of 1.15, indicating that the portfolio outperformed a comparable public index by 15% over its lifetime. Similarly, the portfolio achieved a PME of 1.30 relative to the MSCI Emerging Market Index. Conversely, Barber *et al.* (2021) found that impact funds had an average internal rate of return (IRR) of 3.7% (with a median of 6.4%), compared to an average IRR of 11.6% (with a median of 7.4%) for impact-agnostic funds. Using random utility/willingness-to-pay (WTP) models, the authors estimated that investors accept 2.5 to 3.7 percentage points lower IRRs for impact funds. Heeb *et al.* (2023) conduct an experiment to assess the willingness-to-pay for $CO_2$ emission reductions with a panel of 527 experienced private investors and 125 high-net-worth impact investors. They show that investors have a significant

[18] An example of this is the famous paper *The Impact of Impact Investing* (Berk and van Binsbergen, 2024). The authors study the impact of divestment on the cost of capital and conclude that "*our results suggest that to have impact, instead of divesting, socially conscious investors should invest and exercise their rights of control to change corporate policy.*" Based on our definition, this paper focuses more on exclusion policy and ESG strategies than on impact investing. The next section, Investing WITH Impact vs. Investing FOR Impact, will clarify this.

[19] The comprehensive survey on socially responsible investments written by Renneboog *et al.* (2008) makes no mention of impact investing.

[20] Kurtz (1999) already mentioned on page 686 that the expected return of impact funds must be below market.

[21] We can find them at `www.ifc.org/en/insights-reports`, `www.cambridgeassociates.com/insights/sustainable-impact-investing` and `www.symbioticsgroup.com/publications`.

WTP for sustainable investments, but do not pay significantly more for more impact, for example when emission reductions are multiplied by a factor of 10. They also find that there is no significant difference between private investors and impact investors. Of course, these results relate to carbon reduction impacts and cannot be generalized to social and other environmental impacts, but they are still of interest to financial professionals.

Box 5.2: Willingness-to-pay (WTP)

Willingness-to-pay (WTP) is a measure of the maximum amount an individual is willing to pay for a good or service. It reflects the value an individual places on that good or service. The calculation of WTP depends on the context and can involve different methods (Breidert, 2006). The most common approaches are survey methods (*e.g.*, contingent valuation, conjoint analysis), experimental methods (*e.g.*, simulated experiment, auction), market data analysis (*e.g.*, hedonic price), or econometric models (*e.g.*, demand estimation, discrete choice model). The hedonic price technique assumes that the price $P$ of a good is a function of its attributes $X_1, X_2, \ldots, X_m$:

$$P = \beta_0 + \sum_{j=1}^{m} \beta_j X_j + \varepsilon$$

The WTP for the attribute $X_j$ can be calculated as:

$$\text{WTP} = \frac{\partial P}{\partial X_j} = \beta_j$$

In discrete choice models, willingness-to-pay can be derived from the (random) utility function of good $i$:

$$\boldsymbol{\mathcal{U}}_i = \alpha + \beta P_i + \sum_{j=1}^{m} \gamma_j X_{i,j} + \varepsilon_i$$

We have:

$$\text{WTP} = \frac{\partial P_i}{\partial X_{i,j}} = \frac{\partial \boldsymbol{\mathcal{U}}_i / \partial X_{i,j}}{\partial \boldsymbol{\mathcal{U}}_i / \partial P_i} = \frac{\gamma_j}{\beta}$$

Barber *et al.* (2021) assume that the utility function of investor $i$, facing a binary choice of whether to invest in fund $j$, is given by:

$$\boldsymbol{\mathcal{U}}_{i,j} = \alpha_i + \beta \mathbb{E}[R_j] + \sum_{j=1}^{m} \gamma_j X_j + \sum_{j=1}^{m'} \gamma'_j X_{i,j} + \delta_i \mathbb{I}_j + \varepsilon_i$$

where $\mathbb{E}[R_j]$ is the expected return for fund $j$, $X_j$ is a set of fund characteristics (*e.g.*, region, sector, fund size), $X_{i,j}$ is a set of investor characteristics and $\mathbb{I}_j$ is a dummy variable equal to one if fund $j$ is an impact fund and zero otherwise. Therefore, the WTP for impact for investor $i$ is:

$$\text{WTP} = \frac{\partial \mathbb{E}[R_j]}{\partial \mathbb{I}_j} = \frac{\partial \boldsymbol{\mathcal{U}}_{i,j} / \partial \mathbb{I}_j}{\partial \boldsymbol{\mathcal{U}}_{i,j} / \partial \mathbb{E}[R_j]} = \frac{\delta_i}{\beta}$$

### 5.1.3 Investing FOR impact vs. investing WITH impact

For a long time, there was no distinction between investing for impact and investing with impact. By the 2010s, the two terms were interchangeable and had the same meaning. For example, in 2013, the Swiss impact investing firm Obviam AG and the bank Morgan Stanley published two reports *Investing For Impact* and *Investing With Impact*, but the content and themes were the same (Martin, 2013). In 2018, the European Venture Philanthropy Association[22] clarifies "*the distinction between investing* with *impact, where impact is a secondary dimension of investing alongside financial return, and investing* for *impact, a segment where impact is the key dimension driving investment decisions.*" (Gianoncelli *et al.*, 2019, page 3). Investing for and with impact lies between the two extremes of the ESG spectrum: traditional philanthropy and SRI. On the one hand, investing for impact puts the social purpose organization (SPO) or social project and its beneficiaries at the center. On the other hand, investing with impact must guarantee a financial return that is competitive with the market. The degree of intentionality and the active risk taken by investors help to differentiate between *for* and *with*.

Figure 5.6: The impact ecosystem spectrum

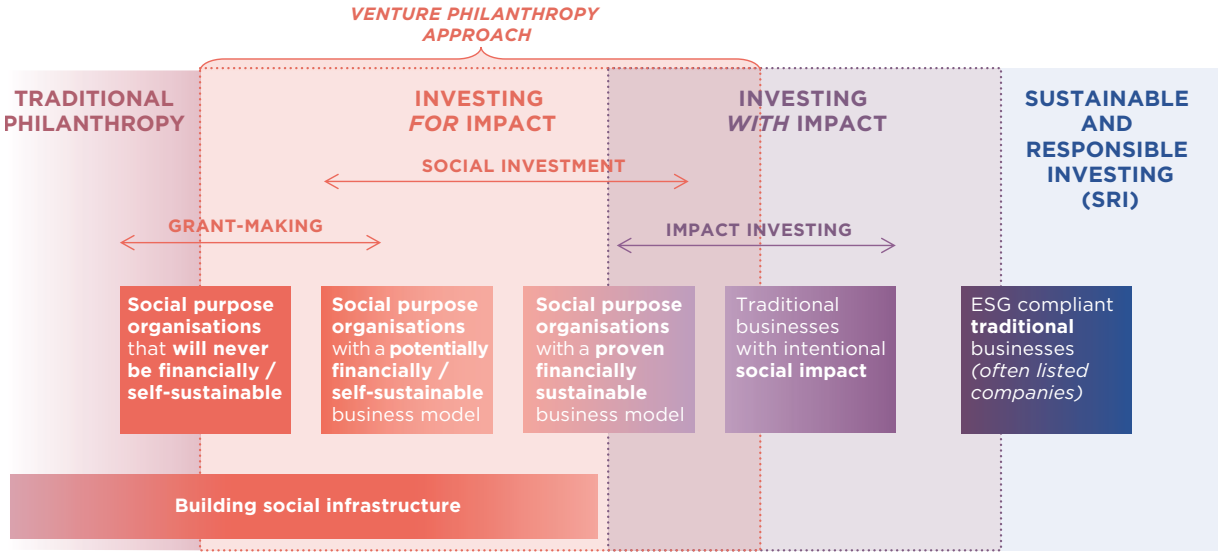


Source: Gianoncelli *et al.* (2019, Figure 13, page 44).

Figure 5.6 reproduces the impact ecosystem spectrum developed by Gianoncelli *et al.* (2019). The difference between *for* and *with* comes from the nature of the enterprises or projects to be financed, which must have a social purpose. Table 5.5 outlines some characteristics of these two types of investors, according to the EVPA. Investors with impact are in fact traditional investors who invest in conventionnal companies, use a market benchmark and want to have a positive impact on society. The market risk of their investments and their management approach are very similar to those of their other investments. A typical example is an asset owner who has converted his investment in the S&P 500 Index into the S&P 500 Climate PAB Index. This decision has a positive impact on society, so it is an investment with impact.

[22] The European Venture Philanthropy Association (EVPA), a non-profit organization based in Brussels, was founded in November 2003 by a group of European venture capitalists to apply the skills developed in the venture capital industry to the charity sector. In 2023, the EVPA becomes Impact Europe (`www.impacteurope.net`).

Table 5.5: The roles of investors *for* and *with* impact

| Investors FOR Impact | Investors WITH Impact |
|---|---|
| • Support innovative solutions to pressing societal problems<br>• Take risks that traditional investors are unwilling to take<br>• Provide in-depth non-financial support and technical assistance | • Need to guarantee some financial return alongside social impact<br>• Invest in proven solutions and/or organizations with viable business models<br>• Have access to large pools of resources and scale proven business models |

The motivation and the risks taken by investors for impact are different. Their goal is to finance the development of companies with a social and solidarity vocation, with the aim of ensuring that vulnerable populations benefit from the services provided by these companies. If these companies are very attractive from a financial perspective, or if they have no difficulty attracting capital, it is not an impact investment. A typical example is an investment in a global pharmaceutical or multinational food company, such as Pfizer or Danone. The financing of Moderna in 2010 or Aspire Food Group in 2013 could be considered an investment for impact. Figure 5.7 presents the charter of investors *for* impact and its 10 principles developed by EVPA members and 65 experts.

Figure 5.7: The charter of investors *for* impact

Source: Gianoncelli *et al.* (2019, page 85).

The terminology of investing for impact and investing with impact is close to a new impact investing framework developed by Busch *et al.* (2021), who suggests distinguishing between impact-aligned investments and impact-generating investments. They justify this new framework as follows:

> "*Practitioners and academics have been using different terms to describe investments in the sustainability context. The latest inflationary term is impact investments — investments that focus on real-world changes in terms of solving social challenges and/or mitigating ecological degradation. At the core of this definition is an emphasis on transformational changes. However, the term impact investment is often used interchangeably for any investment that incorporates environmental, social, and governance (ESG) aspects. In the latter instance, achieving transformational change is not the main purpose of such investments, which therefore carries the risk of impact washing (akin to green washing). To offer (re-)orientation from an academic perspective, we derive a new typology of sustainable investments. This typology delivers a precise definition of what impact investments are and what they should cover.*" (Busch *et al.*, 2021, page 1).

The typology is presented in Table 5.6. The authors justify this typology because they believe that intentionality is not objective and additionality is difficult to prove. They define 4 categories of sustainable investments: ESG-screened, ESG-managed, impact-related and impact-generated. The first category corresponds to investments that incorporate a minimum of ESG considerations, typically exclusion criteria. The second category applies exclusion criteria and another approach to ESG pre-investment decision making, such as norms-based screening, best-in-class, ESG integration or thematic funds. The third and fourth categories correspond to impact investments. These two categories require the use of at least one of the post-investment decision approaches, such as voting and engagement. For impact-aligned investments, materiality and impact are assessed through benchmark analysis or level of SDG alignment and can be done ex-post. For impact-generating investments, materiality must be assessed and measured ex-ante to quantify the expected impact. We have two comments on this topology. The first relates to thematic funds, as the distinction between thematic funds and impact investing is often unclear. Indeed, some thematic funds can be classified as impact investing. The second comment concerns voting. Unlike engagement, it is not obvious that voting creates impact and is seen as an active contribution.

This typology has been adapted and adopted by Eurosif (Busch *et al.*, 2024). There are some important changes. For example, the first two categories have been renamed Basic ESG and Advanced ESG. Documentation has been removed, while the Materiality dimension has become Performance Measurement. Finally, the dimensions Ambition Level and Investment Focus have been added. The new typology is shown in Table 5.7. Certainly the most important change is the introduction of the term '*investor contribution*' in place of '*investor impact*'. Investor contribution is[23] "*the contribution that the investor makes to enable enterprises (or intermediary investment managers) to achieve impact.*" In this topology, investors need to assess the extra-financial performance of the two impact categories by measuring company impact. They also need to measure their contribution in the case of impact-generating investments. Finally, this framework is closely related to investing *for* and *with* impact. Impact-aligned does not imply active contribution from the investor; it can be seen as investing with impact. Impact-generating, on the other hand, involves active contribution and greater engagement from the investor, aligning more with investing for impact. Whatever the framework, this duality between *with* and *for* or *aligned* and *generating* needs to be taken into account when we want to classify and define impact investing.

[23] This definition comes from the impact investing framework developed by the Impact Management Principle (IMP), which is described on page 304.

Table 5.6: A typology of sustainable investments

| | ESG-screened | ESG-managed | Impact-Aligned | Impact-Generating |
|---|---|---|---|---|
| Objective (underlying strategic purpose of the investment) | Mitigation of ESG-related risks and/or ethical considerations | Systematic reflection on ESG-related risks and opportunities | Address social and environmental challenges and goals | Actively contributing to social and environmental solutions and transformations |
| Materiality (measurement of tangible real-world parameters) | Materiality not addressed, *i.e.*, no further detailed description of approach or outputs | Materiality not measured, *i.e.*, only basic description of approach or outputs | Proof of materiality through the assessment of outputs via benchmark analysis or SDG alignment | Proof of materiality through the measurement of expected and generated impact |
| General approach (applied investment appraisal) | Any consideration of E, S, or G factors in investment appraisals; typically focusing on exclusion criteria | Comprehensive set of exclusion criteria; at least one further pre-investment decision approach$^{\star}$ is applied | Comprehensive set of exclusion criteria; sophisticated combination of pre- and post-investment$^{\dagger}$ decision approaches | Focus on impact generation by providing additional capital, incorporating forward-looking targets and/or post-investment$^{\dagger}$ decision approaches |
| Documentation (efforts to increase transparency) | No detailed documentation | Basic description and ideally external verification | Detailed description and external verification | Detailed description and external measurement of impact achievements |

$^{\star}$Pre-investment decision approaches: exclusions, norms-based screening, best-in-class, ESG integration, thematic funds.

$^{\dagger}$Post-investment decision approaches: voting, engagement.

Source: Busch *et al.* (2021, Table 1, page 7).

Table 5.7: Methodology for market studies on sustainability-related investments

| | **Basic ESG** | **Advanced ESG** | **Impact-Aligned** | **Impact-Generating** |
|---|---|---|---|---|
| Investment objective | Integration of ESG factors | Systematic analysis & incorporation of ESG factors | Align with positive impacts on environment and/or society | Measurable contribution to positive real-world impacts |
| Investment approach | Binding negative or positive screening | Binding negative & positive screening ($\leq$ 80% of initial universe investable) | Binding negative & positive screening for assets with positive impact | Exclude non-transformable activities & use stewardship or provide new capital to assets to generate measurable positive impact |
| Performance Measurement | | Measurement of ESG performance | Measurement of company impact | Measurement of company impact & investor contribution |
| Ambition level | Low | Moderate | Medium | High |
| Investment focus | | | Double materiality | |

Source: Busch *et al.* (2024).

### 5.1.4 Impact measurement

The issue of measurement is central to impact investing. It is one of the three dimensions of the intentionality-additionality-measurability framework, it corresponds to the How much and Contribute dimensions of the IMP framework, and it is also essential in the FOR or WITH approach. In addition, we need to distinguish between two types of impact:

1. The impact of the company, project or investee[24];
2. The contribution of the investor.

#### General formula

The investor impact $\mathbb{I}_j^{(\text{investor})}(t)$ for metric $j$ is then equal to:

$$\mathbb{I}_j^{(\text{investor})}(t) = \sum_{i=1}^{n} c_i^{(\text{investor})} \mathbb{I}_{i,j}(t) \tag{5.1}$$

where $\mathbb{I}_{i,j}(t)$ is the impact measure of project $i$ for metric $j$ and $c_i^{(\text{investor})}$ is the investor's contribution to project $i$. In some special cases, we may use a specific contribution $c_{i,j}^{(\text{investor})}$ that depends on metric $j$. To compute the investor's impact, we must first collect the impact metrics measured at the project level.

Table 5.8: Impact data (Example 19)

| Project | Investor contribution | Avoided $CO_2$ emissions | Amount of renewable energy | Number of additional jobs | Number of new homes built |
|---|---|---|---|---|---|
| 1 | 10% | 1 700 | 1 300 | 300 | |
| 2 | 5% | 1 500 | 650 | 100 | |
| 3 | 20% | 700 | 1 150 | 75 | |
| 4 | 50% | 5 000 | | 150 | 5 000 |
| 5 | 12% | 3 200 | | 510 | 15 000 |

**Example 19** *Consider an investor who has established an infrastructure fund in Africa that specializes in clean energy and housing. The investor's portfolio has financed three energy projects (two solar farms and one wind farm) and the construction of new homes in two countries. The impact data is reported above.*

For the avoided $CO_2$ emissions, we have:

$$\begin{aligned}\mathbb{I}_{\text{avoided}}^{(\text{investor})}(t) &= 0.10 \times 1\,700 + 0.05 \times 1\,500 + 0.20 \times 700 + 0.50 \times 5\,000 + 0.12 \times 3\,200 \\ &= 3\,269\end{aligned}$$

These five projects have avoided 3 269 $tCO_2e$ emissions. Similarly, the investor's portfolio has helped generate 392.5 MWh/year of renewable energy, created 183 jobs, and built 4 300 new homes.

Figure 5.8 presents two examples of impact reporting. Panel (a) displays data for Useroles, taken from the Mirova Energy Transition Infrastructure Impact Report 2023. The Useroles wind farm was developed and built by WKN France in the Burgundy-Franche-Comté region of the Côte d'Or. It is operational since 2019. Panel (b) provides figures for the BlueOrchard Microfinance Fund as of

[24] In the following, we will use project as a generic term for company and investee.

December 2023, taken from its Annual Impact Report 2023. Panel (a) therefore illustrates an impact report of a project, while Panel (b) illustrates an impact report of an investment. Note that the two reports are different in terms of the impact theme. The first report is based on environmental metrics, while the second report is based on financial inclusion. This means that the impact report is adapted to the investment strategy, which is normal. However, we also note that the Useroles wind farm report has a social component with an estimated 50 jobs supported and 100% women on board. In fact, the study of several impact reports shows that there is always a social aspect, even when the investment is in renewable energy. The opposite is not true.

Figure 5.8: Impact reporting

(a) (b)

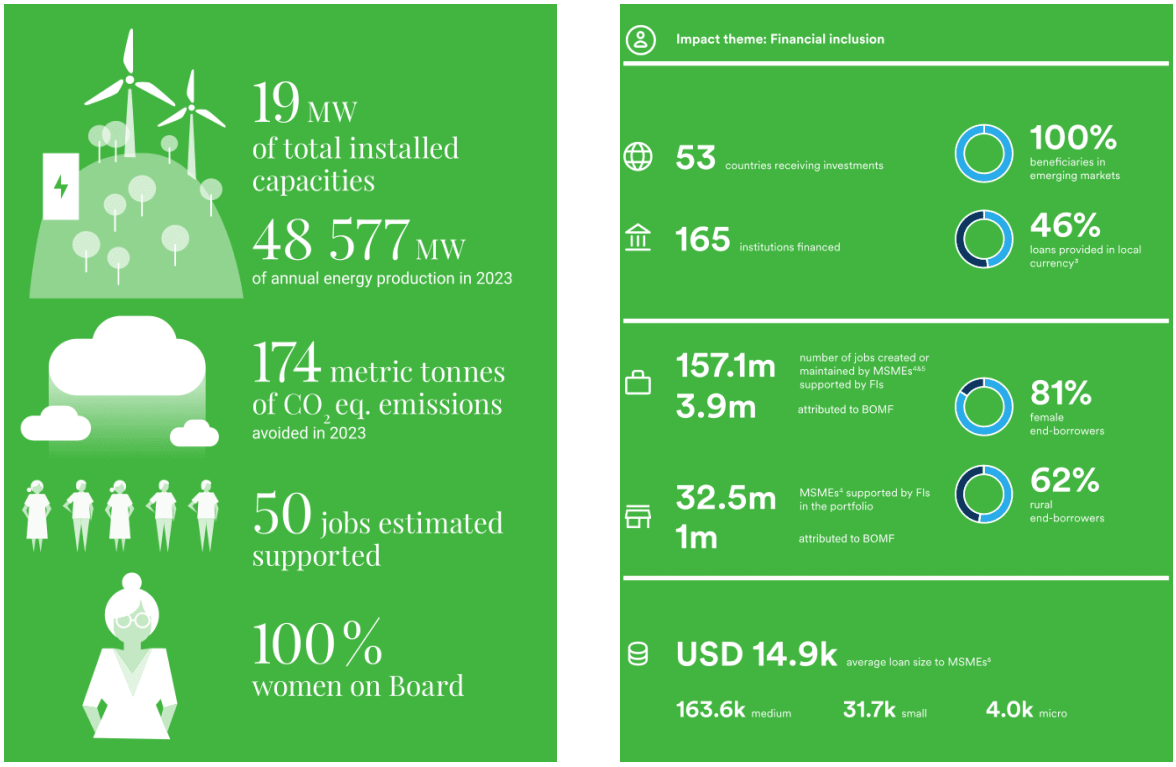


Useroles BlueOrchard Microfinance fund

Source: www.mirova.com & https://www.blueorchard.com/products/blueorchard-microfinance-fund-bomf.

Calculating $\mathbb{I}_j^{(\text{investor})}(t)$ requires defining the impact of the project $\mathbb{I}_{i,j}(t)$. At the same time, there is a large literature on calculating impact and causality, and few resources when applied to impact investing[25]. There are several ways to calculate $\mathbb{I}_{i,j}(t)$. We can use discretionary methods or more scientific and technical methods (GDN, 2021, page 24). Regarding the later, So and Staskevicius (2015) group them into four categories: expected return (social return on investment or SROI, social cost benefit analysis), theory of change (logic model), mission alignment methods (social value criteria, scorecards) and experimental methods (randomized controlled trial or RCT, historical baseline, pre/post assessment, regression discontinuity design, difference in differences).

[25]Nevertheless, we can cite Reeder and Colantonio (2013), So and Staskevicius (2015), Mishra (2018), EIB (2021) and GDN (2021).

Certainly the most used approach is the pre-post comparison:

$$\mathbb{I}_{i,j}(t) = \text{KPI}_{i,j}(t) - \text{KPI}_{i,j}(t-h)$$

This method compares the pre-investment KPI at time $t-h$ and the post-investment KPI at time $t$. For example, consider a company that had 20 employees five years ago and now has 150 employees. The number of additional jobs is:

$$\mathbb{I}_{i,j}(t) = 150 - 20 = 130$$

Another approach is to use a benchmark:

$$\mathbb{I}_{i,j}(t) = \text{KPI}_{i,j}(t) - \text{KPI}^{\star}_{i,j}(t)$$

where $\text{KPI}^{\star}_{i,j}(t)$ is the benchmarked KPI. For example, the benchmark may be a control group. In the case of microfinance, a typical control group is the set of microenterprises that do not benefit from microfinance support. A third method is to use randomized controlled trials:

$$\mathbb{I}_{i,j}(t) = \frac{1}{n'} \sum_{i'=1}^{n'} \left(\text{KPI}_{i,j}(t) - \text{KPI}_{i',j}(t)\right)$$

where $i' \in \mathcal{C}$ and $\mathcal{C}$ is the control group that serves as the baseline against which the impact of the investment is compared. The idea is to randomly select projects in the control group and compare the KPI of project $i$ with the KPI of the selected projects.

Box 5.3: Microeconomic impact assessment of the EIB's support for small businesses in the EU

The EIB Group supports access to finance for SMEs through commercial banks with the aim of promoting business performance, job creation and investments that increase productivity and competitiveness. This support is provided through multi-beneficiary intermediated loans, which benefit SMEs in two main ways:

1. Lower financing costs or longer loan maturities
   Financial intermediaries pass on the EIB's advantageous funding conditions to SMEs, resulting in lower financing costs or longer loan maturities. This improves the profitability of SMEs, leading to increased investment and job creation.

2. Improving access to credit
   EIB funding helps to ease credit constraints for SMEs, especially during economic downturns. By broadening the funding base of banks, the EIB enables them to lend to more companies with viable projects that might otherwise struggle to secure financing.

The EIB's Economics Department evaluated the benefits of intermediated lending to EU SMEs using quasi-experimental methods, comparing supported SMEs with similar unsupported firms. The results showed that EIB-supported loans led to a 4-6% increase in employment and an 8-14% increase in fixed assets for recipient firms. Smaller or younger firms experienced even larger positive employment and investment effects.

Source: EIB (2021, pages 20-21).

Figure 5.9: Impact on employment of EIB-supported lending to small and medium-sized enterprises

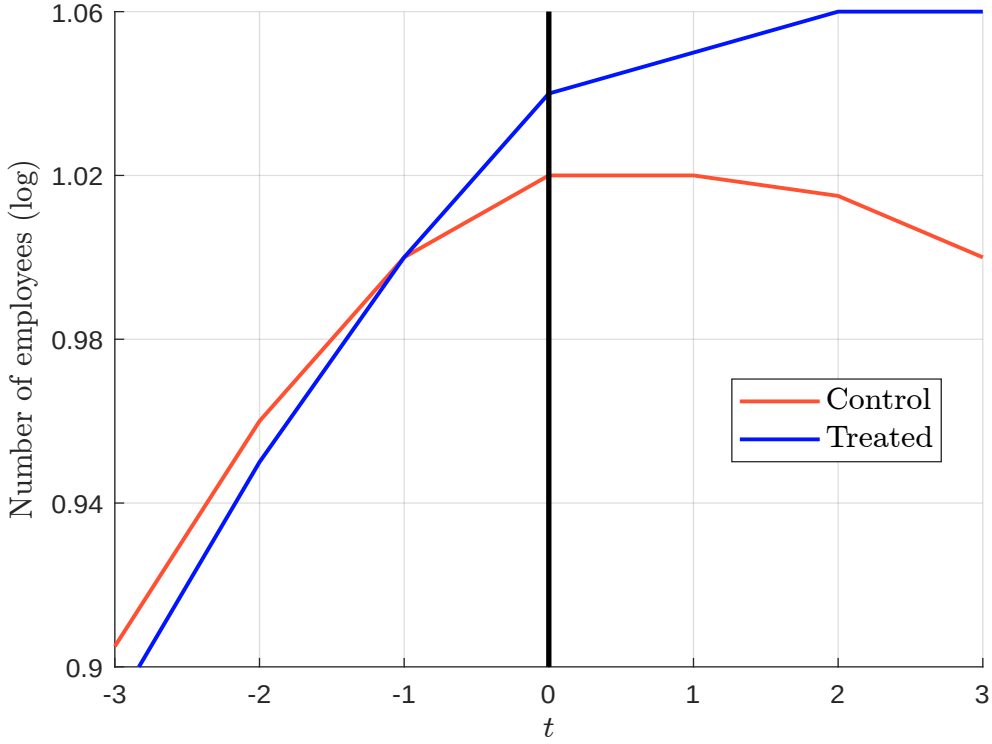


Performance of EIB loan beneficiaries (Treated) against the comparison group (Control) in the three years before and after the loan allocation, which takes place in year $t = 0$.

Source: EIB (2021, Figure 12, page 21).

Another issue in the calculation of $\mathbb{I}_j^{(\text{investor})}(t)$ is the determination of the investor's contribution $c_i^{(\text{investor})}$ to project $i$. It is rare that a project is fully supported by one investor, most of the time several investors participate in the financing of the project and not always at the same time and in the same phases. For example, a renewable energy project is typically divided into three main phases: development, construction, operation. Each phase is assigned an allocation key that represents a percentage of the total project value. Suppose the allocation key is 20%, 30%, and 50%, respectively, and the investor owns 10% of a company that participated in 60% of the development phase and 30% of another company that participated in 40% of the operation phase. In this case, the investor's contribution to the project is:

$$c_i^{(\text{investor})} = 10\% \times 60\% \times 20\% + 30\% \times 40\% \times 50\% = 1.2\% + 6\% = 7.2\%$$

If the project generates 1 000 MWh, the impact of the investor is:

$$\mathbb{I}_{i,j}(t) = 7.2\% \times 1\,000 = 72\,\text{MWh}$$

**Remark 48** *The allocation to project phases is a difficult task. It is common in private equity, but not in public equity. Moreover, there may be some issues of double counting, which is a real problem in the case of impact investing when we refer to the dimension of additionality. Let us take the previous example and assume that the renewable energy project is operated by a listed company. The listed company may report that it generates* 1 000 MWh*, while the impact allocation for the operational phase is only* 500 MWh*.*

### Impact measurement tools

There are really no standards that have emerged for impact reporting. Comparing two reports is not easy, especially if the two impact funds have two different impact investment focuses (Table 5.9). For example, we cannot compare Blue Ocean, Financial Inclusion and Agriculture & Forestry impact funds because the impact metrics are so different.

Table 5.9: Impact investment focus

| | |
|---|---|
| • Affordable housing & community development | • Place-based impact & local economic resilience |
| • Arts and culture preservation | • Media, technology & mobile |
| • Clean technology, alternative energy & climate change | • Microfinance, low-income financial services & micro-insurance |
| • Demographic-based impact | • Natural resources & conservation |
| • Diversity, equity and inclusion | • Nutrition, health & wellness |
| • Education | • Racial equity and justice |
| • Fair trade | • Small/medium business development |
| • Global health | • Sustainable agriculture |
| • Job creation and workforce development | • Water, sanitation and hygiene (WASH) |

Source: ImpactAssets (2024), https://impactassets.org/ia-50.

This is less true when we look at impact funds with the same focus. For example, here are five well-known financial inclusion (or microfinance) funds:

- BlueOrchard Microfinance Fund (BOMF), www.blueorchard.com/products/blueorchard-microfinance-fund-bomf
- Triodos Microfinance Fund, www.triodos-im.com/funds/triodos-microfinance-fund
- ResponsAbility Global Micro and SME Finance Fund, www.responsability.com/en/investment-products/responsability-global-micro-and-sme-finance-fund
- MicroVest Capital Management, www.microvestfund.com/impact-reports
- EIB Financial Inclusion Fund, www.eib.org/en/publications/financial-inclusion-fund

We find that these five impact reports use similar metrics, such as number of beneficiaries, female borrowers, rural borrowers, SMEs supported, number of jobs created or saved, average loan size, etc. However, beyond these common metrics, there are some differences in the information available, such as portfolio holdings, maturity statistics, location, etc.

In fact, there is no equivalent to TCFD reporting or SFDR in impact investing. For each impact topic, we need to find a reporting framework that fits the themes of the fund. For example, for water, sanitation and hygiene (WASH) and biodiversity, the Climate Disclosure Standards Board has published two application guidelines for disclosure (CDSB, 2021a,b). The most popular framework

for general topics is IRIS+. It can be found at https://iris.thegiin.org. There are more than 500 metrics available. To navigate, a system of filters is provided with the following sections[26]: Impact Category, SDGs, Joint Impact Indicators, Dimensions of Impact, Operational Impact, Product Service Impact, Focus, Investment Lens and Financials. Within each section, we can select one or more items. For example, the Impact Category section has 18 items: Agriculture, Air, Biodiversity & Ecosystems, Climate, Diversity & Inclusion, Education, Employment, Energy, Financial Services, Health, Real Estate, Land, Oceans & Coastal Zones, Pollution, Waste, Water, Cross Category and Infrastructure. The Dimensions of Impact section corresponds to the IMP framework and there are 7 items: What, Who, How Much Scale, How Much Depth, How Much Duration, Contribution Depth and Risk. The Focus section has two elements: Environmental and Social. If we filter on the impact category Biodiversity and Ecosystems and the focus Environmental, we get the following metrics: Biodiversity Assessment (OI5929), Biodiversity Footprint (PI6887), Critical Marine Habitats (OI3846), Forest Management Plan (OI2622), Indigenous Rights and Stewardship Practices (OI6482), Land Directly Controlled: Cultivated (OI1674), Marine Area Directly Controlled: Total (OI7876), Pesticide Hazard Classification Type (OI7394), Species Abundance (PI8027), Species: Total (PI7728) and Threatened Species Policy (OI1618). Each metric has a code, a reporting format (*e.g.*, decimal, percentage, text), a metric type, a metric level, an IRIS metric citation, usage guidance, a list of impact categories and themes, a list of SDG goals and targets, and a metric history. For example, code II6610 corresponds to the value of investments in communities historically marginalized on the basis of race and/or ethnicity[27]. The reporting format is decimal, and the list of impact categories and themes includes diversity and inclusion (gender lens, racial equity lens), financial services (financial inclusion), real estate (affordable quality housing, green buildings), and water (water, sanitation, and hygiene WASH).

## 5.2 Sustainable Development Goals

The Sustainable Development Goals have already been introduced in Chapter 1 on page 19. The SDGs are a set of 17 global objectives established by the United Nations to address critical issues such as poverty, inequality, climate change and environmental degradation by 2030. Impact investing always refers to the SDGs, which are ubiquitous in impact reporting. For example, below we report on the SDGs addressed by the BlueOrchard Microfinance Fund (BOMF).

Figure 5.10: SDGs addressed by the BlueOrchard Microfinance Fund (BOMF)

Source: www.blueorchard.com/products/blueorchard-microfinance-fund-bomf.

[26] The direct link is https://iris.thegiin.org/metrics.

[27] "*This metric is intended to capture the amount of capital managed by the organization that is invested into communities in which a majority (51%) of individuals are from groups historically marginalized due to race and/or ethnicity as defined locally.*" (source: https://iris.thegiin.org/metric/5.3/ii6610.

### 5.2.1 Where we stand with the SDGs

At first glance, the 17 SDGs may seem like a list of different goals. However, they are highly interconnected. For example, Johan Rockström argued that all sustainable development goals are directly or indirectly related to sustainable and healthy food. Therefore, it is common to group the SDGs into a few clusters. For example, the 5Ps framework groups the SDGs into five key areas:

1. People: SDG 1 (no poverty), SDG 2 (zero hunger), SDG 3 (good health and well-being), SDG 4 (quality education), SDG 5 (gender equality);
2. Planet: SDG 6 (clean water and sanitation), SDG 13 (climate action), SDG 14 (life below water), SDG 15 (life on land);
3. Prosperity: SDG 7 (affordable and clean energy), SDG 8 (decent work and economic growth), SDG 9 (industry, innovation and infrastructure), SDG 10 (reduced inequality), SDG 11 (sustainable cities and communities), SDG 12 (responsible consumption and production);
4. Peace: SDG 16 (peace, justice, and strong institutions);
5. Partnership: SDG 17 (partnerships for the goals).

Another famous grouping model is the SDG wedding cake, which is a visual representation to show the interconnectedness of the SDGs (Figure 5.11). The cake is represented by several layers stacked on top of each other. The bottom layer represents the biosphere, which is the foundation for all life on Earth. It includes elements such as clean water, healthy ecosystems, and biodiversity (SDGs 6 & 13-15). The middle layer represents society, whose goals focus on human needs and social

Figure 5.11: The SDG wedding cake

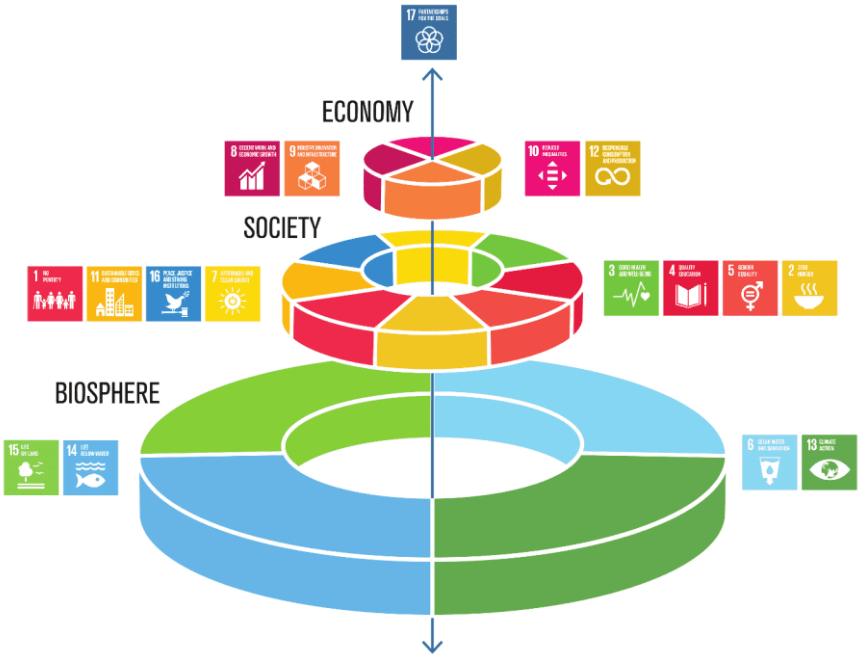


Source: www.stockholmresilience.org.

well-being (SDGs 1-5, 7, 11 & 16). The top layer represents the economy and consists of goals focused on economic growth and industry (SDGs 8-10 & 12). SDG 17 (partnerships for the goals) is shown alone and outside of the three-layer structure because of its unique role and the importance of cooperation between countries in promoting inclusive development (Gupta and Vegelin, 2016).

The data for the 231 unique indicators can be found at `https://unstats.un.org/sdgs/dataportal`. There are four approaches to analyzing them, corresponding to 4 different tags: Global Database, Country Profile, SDG Analytics, and Advanced Access through an API. The first tag is used to compare countries on selected indicators. For example, the indicator 1.1.1 measures the proportion of the population living below the international poverty line by sex, age, employment status and geographic location (urban/rural). It includes two variables. `SI_POV_DAY1` corresponds to the proportion of the population below the international poverty line (%), while `SI_POV_EMP1` corresponds to the employed population below the international poverty line, by sex and age (%). The screenshot of the indicator selection window for all countries and the year 2020 is shown in Figure 5.12. The Country Profiles window helps track progress toward global sustainability goals.

Figure 5.12: SDG indicator selection window

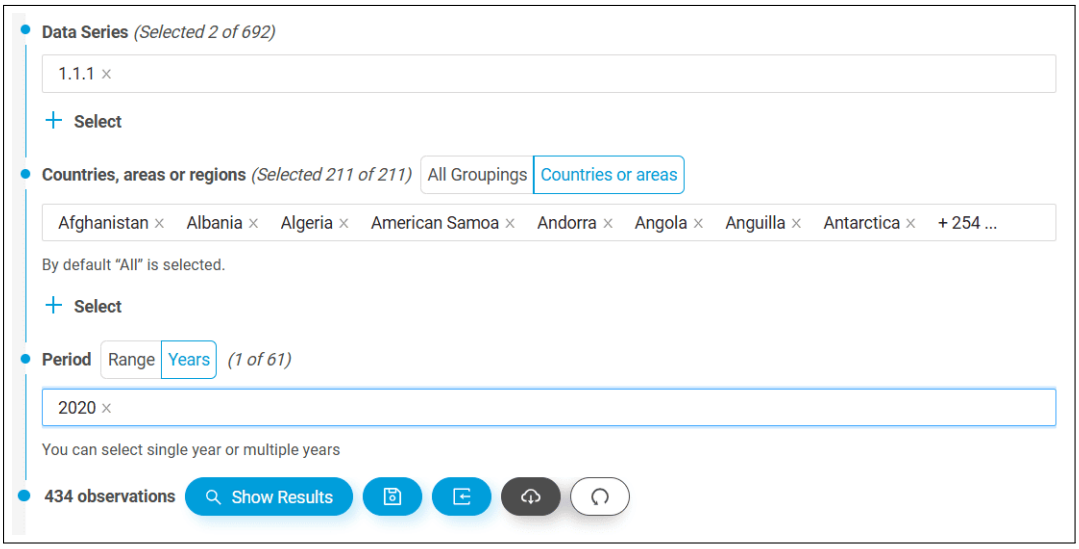


Since 2016, this SDG data has been analyzed annually by the United Nations, which produces a report to track the world's progress. The 2023 report comes to a pessimistic conclusion about achieving the SDGs by 2030:

> "*Halfway to the deadline for the 2030 Agenda, the SDG Progress Report shows we are leaving more than half the world behind. Progress on more than 50 per cent of targets of the SDGs is weak and insufficient; on 30 per cent, it has stalled or gone into reverse. These include key targets on poverty, hunger and climate. Unless we act now, the 2030 Agenda could become an epitaph for a world that might have been.*" (United Nations, 2023, page 2).

The 2023 report highlights significant setbacks in achieving the SDGs due to the climate crisis, the war in Ukraine, economic difficulties, and the lingering effects of the COVID-19 pandemic. Here are some examples:

- Extreme poverty has increased, reversing decades of progress. Projections indicate that 575 million people will remain impoverished by 2030, and only one-third of countries will have

halved their national poverty levels by then. The COVID-19 pandemic has contributed significantly to this setback. In 2020, 97 million more people were living on less than $2.15 a day compared to pre-pandemic levels, bringing the total number of people living in extreme poverty to 724 million.

- More than 600 million people worldwide are projected to be hungry in 2030. Nearly 2.4 billion people, or one in three, were moderately or severely food insecure in 2021. The prevalence of undernourishment increased from 7.9% in 2019 to 9.2% in 2021. Conflicts, economic shocks, and climate change worsened food security, with food prices increasing by 30% in 2021.

- Education gaps are widening, with 84 million children expected to be out of school by 2030 and 300 million students lacking basic numeracy and literacy skills by that year. In low-income countries, 40% of children of primary school age lack basic reading skills.

- Gender inequality persists, with 56% of countries lacking anti-discrimination laws for women. At the current rate, it will take 300 years to end child marriage, 286 years to close gaps in legal protection and eliminate discriminatory laws, and 140 years to achieve equal representation in workplace leadership. In 2020, women made up 40% of the global workforce but held only 28% of managerial positions, 25% of women aged 15-49 experienced physical or sexual violence by an intimate partner, and one in five young women were married before their 18th birthday.

- Global temperatures have risen by 1.1°C and may reach or exceed 1.5°C by 2035.

Despite these challenges, there have been notable improvements:

- Significant reductions in child mortality have been achieved, with 146 out of 200 countries on track to meet the under-5 mortality target. Effective HIV treatment has reduced AIDS-related deaths by 52% since 2010.

- The global population with access to electricity rose from 87% in 2015 to 91% in 2021. Renewable energy capacity in developing countries reached a record 268 watts per capita in 2021. Despite progress, 759 million people still lack electricity, and 675 million people still live in the dark.

- Internet access expanded by 66%, reaching 5.3 billion people in 2022.

On average, the UN estimates that 15% of the 231 indicators are on track, 48% are moderately or severely off track, and 37% are stagnant or regressing. The breakdown by SDG is shown in Figure Figure 5.13, Panel (b). Some goals face a contrasting picture, with a high proportion of both on-track and off-track indicators, such as SDG 12 (responsible consumption and production) and SDG 14 (life below water). Some goals show a negative and doomed picture, such as SDG 1 (no poverty), SDG 4 (quality education), SDG 6 (clean water and sanitation), SDG 8 (decent work and economic growth), SDG 13 (climate action), and SDG 16 (peace, justice and strong institutions).

The United Nations does not publish country-by-country analysis, but SDG country profiles are available at `https://unstats.un.org/sdgs/dataportal`. Another way to access the country profile is to look at the annual report written by Sachs *et al.* (2024), which uses the same SDG data from the United Nations. The advantage of this report is that the authors aggregate all SDG information data to calculate average scores and indices by SDG, country or region in full transparency, as defined in a detailed methodological paper (Lafortune *et al.*, 2018). Moreover, the raw data from the United Nations and the scores and indices from Sachs *et al.* (2024) are

Figure 5.13: Progress assessment for the 17 SDGs based on assessed targets, 2023 or latest data

(a) World-level progress

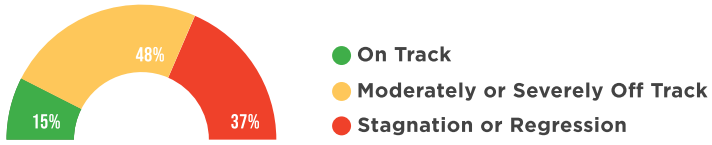


(b) Overall progress by SDG in %

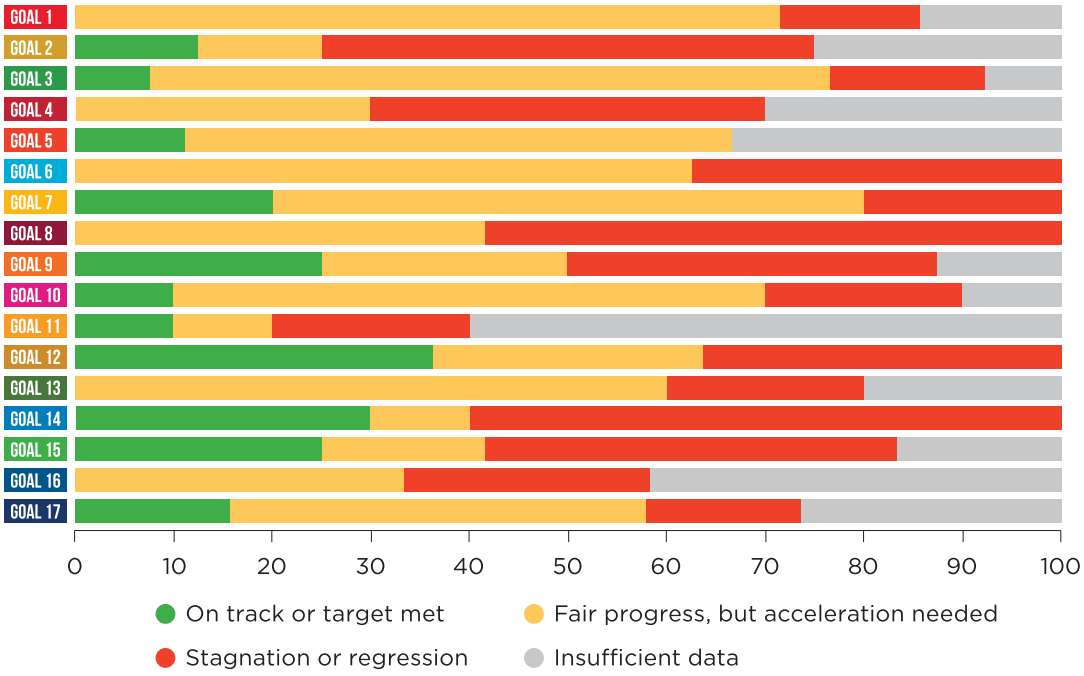


Source: United Nations (2023, pages 8 & 11).

freely available at https://dashboards.sdgindex.org. Two examples of SDG country profiles are available in Figures 5.14 and 5.15, and correspond to those published in the Sustainable Development Report 2024. The website offers an interactive interface and more information on each country. In addition to the SDG level and trend scores for the 69 goals calculated using the 231 unique indicators, the authors also produce two synthetic scores:

- The SDG index (or overall score) measures overall progress toward achieving all 17 SDGs. The score can be interpreted as a percentage of SDG achievement. A score of 100 indicates that all SDGs have been achieved. Therefore, the difference between 100 and a country's SDG index score is the distance, in percentage points, that must be overcome to reach optimum SDG performance.

- The spillover index assesses a country's spillover effects. Indeed, each country's actions can have a positive or negative impact on the ability of other countries to achieve the SDGs. The spillover index aggregates such spillovers along three dimensions: environmental and social impacts embodied in trade, economic and financial, and security. A higher score means that a country is causing more positive spillovers and fewer negative ones.

Figure 5.14: SDR country profile (Finland, 2024)

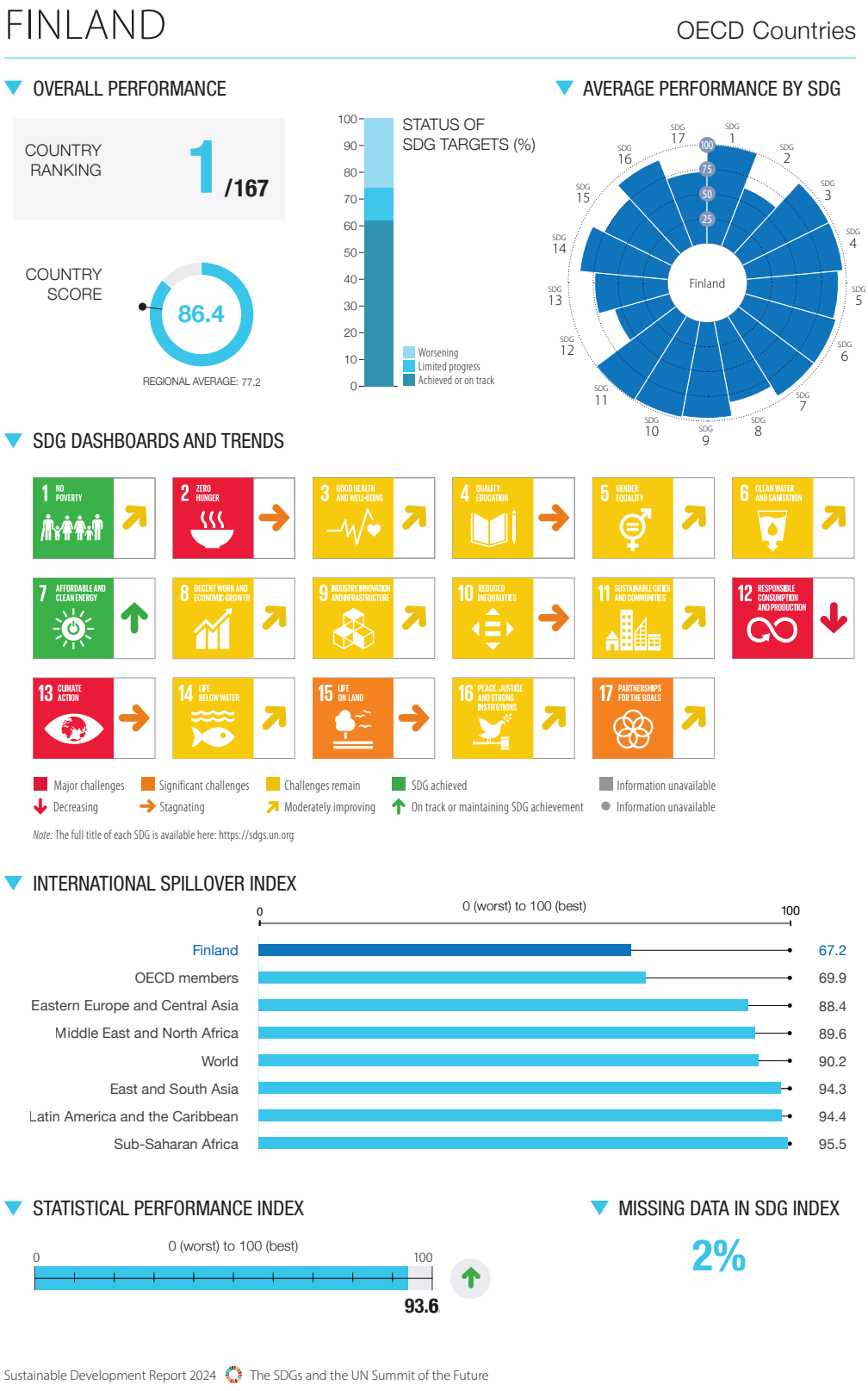

Figure 5.15: SDR country profile (South Sudan, 2024)

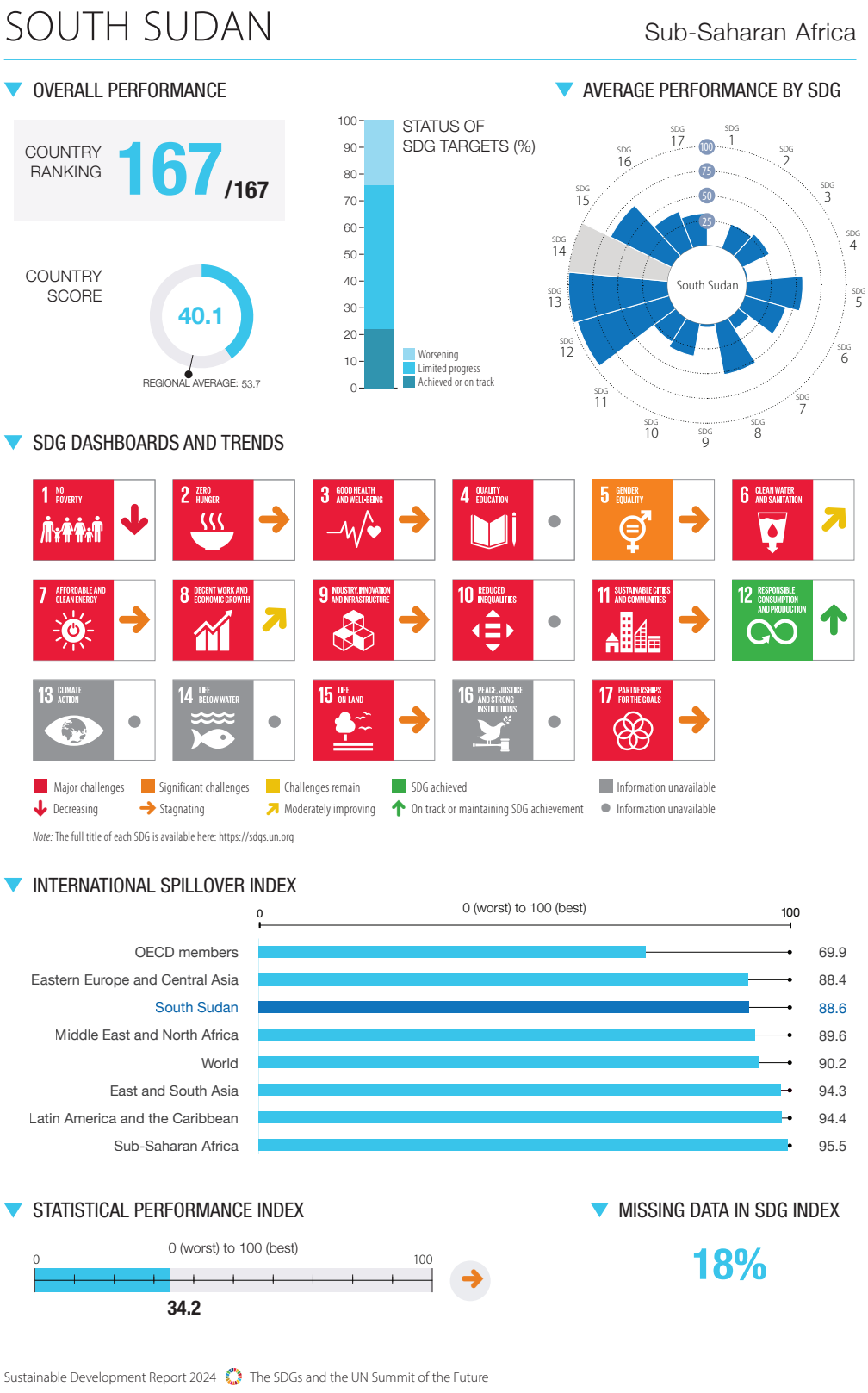

The top five countries with the highest SDG index scores are Finland (86.35), Sweden (85.7), Denmark (85), Germany (83.45), and France (82.76), while the bottom five countries[28] are South Sudan (40.14), Central African Republic (44.21), Chad (45.07), Somalia (45.42), and Yemen (46.87). In terms of the spillover index, the top five countries are Sierra Leone (98.71), Madagascar (98.67), Zambia (98.33), Maldives (97.67) and Malawi (97.44), while the bottom five countries are Singapore (28.49), Luxembourg (42.53), Qatar (43.33), Cyprus (44.61) and Switzerland (45.30). It is interesting to note that the two rankings are very different. In particular, we observe that poor countries have both a low SDG index and a high spillover index, while the opposite is true for rich countries. This illustrates the principle of '*do no significant harm*'. For example, rich countries can import goods from poor countries, which means that some of the consumption-based greenhouse gas emissions are outside the rich countries. Figure 5.16 shows the scatter plot between the SDG score and the spillover score for the 167 countries. In particular, we observe that a high SDG index is correlated with a low spillover index. On average, we obtain a Spearman correlation of $-61\%$ between the two series. The red curve corresponds to the fitted second-order polynomial regression:

$$\text{Spillover}_i = -16.57 + 4.06 \times \text{SDG}_i - 0.0374 \times \text{SDG}_i^2 + \varepsilon_i$$

This negative relationship, especially for countries with high SDG scores, calls into question the global equilibrium. Does it mean that in order to achieve all the SDGs, a country must necessarily have a negative impact on other countries? The answer is complex. But it highlights the special status of SDG 17. The global achievement of the SDGs requires a global and strong partnership between countries, because sustainable development cannot be achieved in a fragmented world.

Figure 5.16: Relationship between the SDG index and the Spillover index

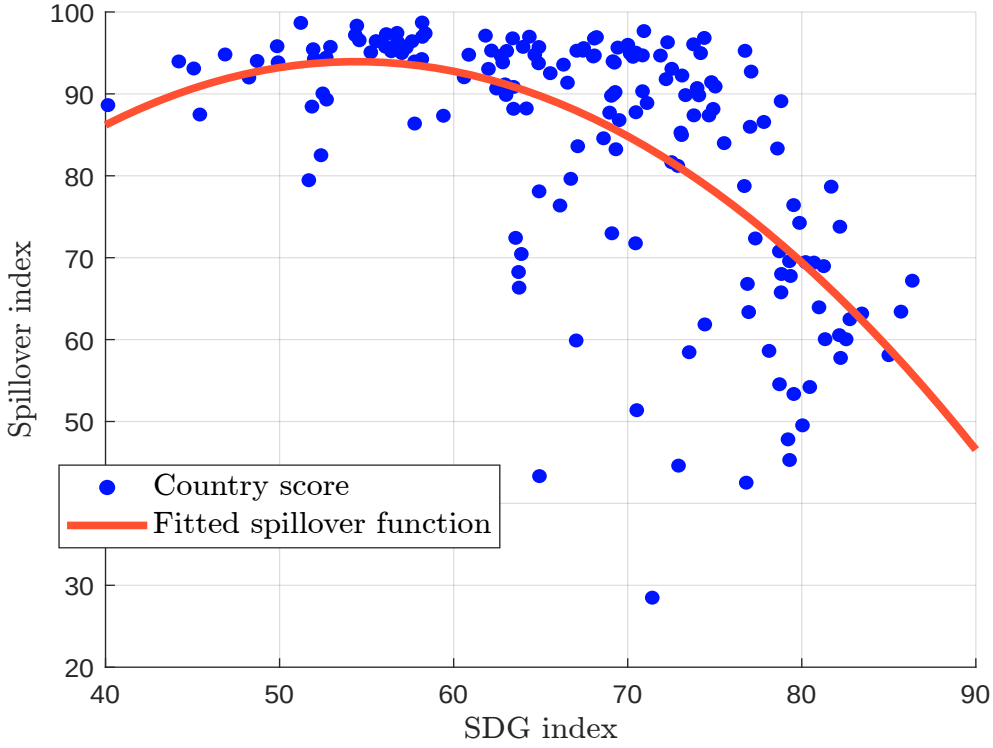


[28] To minimize bias due to missing data, the authors do not calculate the overall SDG index score and rank for countries with missing data on more than 20% of the indicators. Of the 193 UN member states, 167 countries are then scored and ranked.

### 5.2.2 SDGs and impact investing

Although the SDG framework and indicators were designed for countries rather than companies, ESG investors have swiftly adopted this framework to align their investments with the SDGs. We can find several mapping tables between the 17 SDGs and the three ESG pillars. For example, Khaled *et al.* (2021) suggests mapping SDGs 2-3, 6-9, 11-15, and 17 to the E dimension, SDGs 1-5, 8, 10, 12, and 16-17 to the S dimension, and SDGs 5, 12, and 17 to the G dimension. Below we visualize the mapping we propose in Table 1.5 on page 20, which is very close to the mapping recommended by the private bank Berenberg[29] in 2018.

Table 5.10: Aligning SDGs with ESG

[29]Source: Berenberg (2018). Understanding the SDGs in Sustainable Investing. *Report*, December, 27 pages, www.berenberg.de.

In fact, it is common for investors, funds, market studies, or special reports on impact investing to make a systematic reference to the SDGs. In Figure 5.10 on page 325, we have already seen that the BlueOrchard Microfinance Fund has five SDGs. Another example is the impact report of the 13 funds managed by Triodos Investment Management, one of the largest and most prominent impact investors in the world. All 13 reports[30] make extensive use of the SDGs. So do the reports produced by Phenix Capital, one of the leading data providers in impact investing. Below, we highlight the five most important SDGs considered by German impact investors.

Figure 5.17: Investors' view of the top 5 SDGs in Germany

51.3% 51.3% 50.0% 31.6% 30.3%

Source: Bundesinitiative Impact Investing (2022) (see Footnote 10 on page 304).

The SDGs are not only the responsibility of countries, but also of all stakeholders in society, including businesses. The challenges addressed by the SDGs are global and interconnected, affecting everyone and requiring cooperation across all sectors. For example, challenges such as SDG 5 on gender equality and SDG 13 on climate action are particularly relevant to businesses, as they are critical components of sustainable finance and ESG rating systems. In addition, other challenges directly affect companies, particularly those related to the economy. Goals such as SDG 8 on decent work and economic growth, SDG 9 on industry, innovation and infrastructure, and SDG 12 on responsible consumption and production are essential to business operations. Businesses therefore have a strategic role to play, alongside governments and civil society, in achieving the SDGs (Schramade, 2017; Mio *et al.*, 2020). To conduct business in alignment with the SDGs, companies and governments need investors and financial support. The investment needed to achieve the SDGs is substantial, necessitating the creation of specialized financial channels and investment vehicles. In particular, foreign direct investment (FDI) is generally insufficient (Zhan and Santos-Paulino, 2021). This concerns both horizontal FDI, when a company invests in the same type of business in a foreign country as it does in its home country, and vertical FDI, when a company invests in a different stage of production in the same industry, either upstream or downstream. Blended finance or public-private financing mechanisms are another approach to contribute to the SDGs (Sachs *et al.*, 2019). However, the leverage between private and public capital seems to be insufficient:

> "*Each $1 of MDB and DFI invested mobilises on average $0.75 of private finance for developing countries, but this falls to $0.37 for low-income countries. Expectations that blended finance can bridge the SDG financing gap are unrealistic: 'billions to billions' is more plausible than 'billions to trillions'.*" (Attridge and Engen, 2019, page 11).

Impact investing is a third approach to contributing to the SDGs, but we need to distinguish between two types of use of the SDG landmark:

- The SDGs are used to channel the capital, and the real motivation is to finance economic growth and improve the social situation in poor countries. In this case, the SDGs are really at the heart of the investment. This is the case with many microfinance funds, for example.

[30] The impact reports can be found at www.triodos-im.com/impact-report/2023.

- The SDGs are more often used to indicate that the investment is related to this framework, but the motivation is not necessarily to finance economic growth and improve social conditions in poor countries. For example, many climate impact funds invest in green bonds in developed countries. The SDG logos are then used, such as SDG 7 on affordable and clean energy, SDG 11 on sustainable cities and communities, and SDG 13 on climate action.

Therefore, references to the SDGs do not always imply impact investing, but impact investing is generally presented within an SDG framework.

### 5.2.3 SDG funds

The concept of an SDG investment fund does not exist in a standardized form, as there are different ways to use the SDG framework. However, we must acknowledge that many funds refer to SDGs, and it is common to hear a fund described as an SDG fund, similar to how some funds are labeled as ESG funds or climate funds. As with the latter two examples, there is no clear definition of what constitutes an SDG fund, although the term has been adopted by the European regulator (Balitzky and Mosson, 2024). In fact, there is no official or regulatory definition. An SDG fund is simply an investment fund that aims to align its portfolio with the SDGs. By adopting this definition, the door is open to interpretations of what an SDG fund is and is not. Again, by using the term SDG in its name, an investment is considered to be an SDG fund. For example, we can point to some public-private partnerships, such as the UN Joint SDG Fund and the Danish SDG Investment Fund. There are also private investment vehicles. Robeco, for example, has 10 SDG funds[31]: (1) Euro SDG Credits (pioneering SDG framework for credit portfolios), (2) Euro SDG Short Duration Bonds (applying Robeco's proprietary SDG framework across the euro bond market with a short maturity), (3) Global SDG Credits (select companies that contribute positively to the SDGs while aiming to outperform over the full credit cycle), (4) Global SDG Engagement Equities (actively targeting impact and financial returns), (5) Global SDG Equities (actively contributing towards meeting the SDGs), (6) QI Global SDG and Climate Beta Equities (systematically investing for global equity returns with significant sustainability improvements), (7) QI Global SDG and Climate Conservative Equities (systematically investing in low volatility stocks and a high sustainability profile), (8) QI Global SDG and Climate Multi-Factor Credits (systematic approach to credits with significant sustainability improvements), (9) SDG Credit Income (targeting a consistent level of income by investing in companies that contribute to the SDGs) and (10) SDG High Yield Bonds (benefiting from a long-term quality approach pays off in high yield bonds).

The ESMA report uses a general definition:

> "*SDG funds are funds stating to contribute towards achieving the SDGs.*" (Balitzky and Mosson, 2024, pages 4-5).

To identify SDG funds, Balitzky and Mosson (2024) first look at all funds domiciled in the EEA that mention the SDGs in their regulatory communications. Using NLP techniques, they find SDG-related terms in the fund's legal name, strategy (from the Morningstar prospectus), and KIID/KID. After a manual screening, the authors identify a sample of 289 SDG funds. They find that the size of SDG funds reaches €74 bn in September 2023, but the increase is mainly due to the launch of many SDG funds between September 2020 and October 2021. Since then, we observe a stagnation or decline in the SDG fund market. The authors construct a sample of non-SDG funds and compare the characteristics of the two samples in terms of exposure to the UN Global Compact, PAI metrics, and SDG scores. Balitzky and Mosson (2024, page 3) conclude that their results show that "*SDG*

[31] Source: www.robeco.com/en-int/glossary/sustainable-investing/sdg-funds.

*funds do not significantly differ from non-SDG counterparts or ESG peers regarding their alignment with the United Nations SDGs.*" An important comparison concerns the SDG index of SDG and non-SDG funds. For each SDG dimension, the authors then calculate the weighted average SDG score of countries, with the weights proportional to the sovereign debt invested by the funds. The overall SDG score is 74 for SDG funds, compared to 64 for non-SDG funds. This means that SDG funds are more aligned than non-SDG funds. However, the authors note that this relatively better performance does not hold systematically across all SDG dimensions. Figure 5.18 shows the average SDG score per SDG dimension. In the case of SDG 12 (responsible consumption and production) and SDG 13 (climate action), non-SDG funds outperform SDG funds.

Figure 5.18: Sovereign performance per SDG

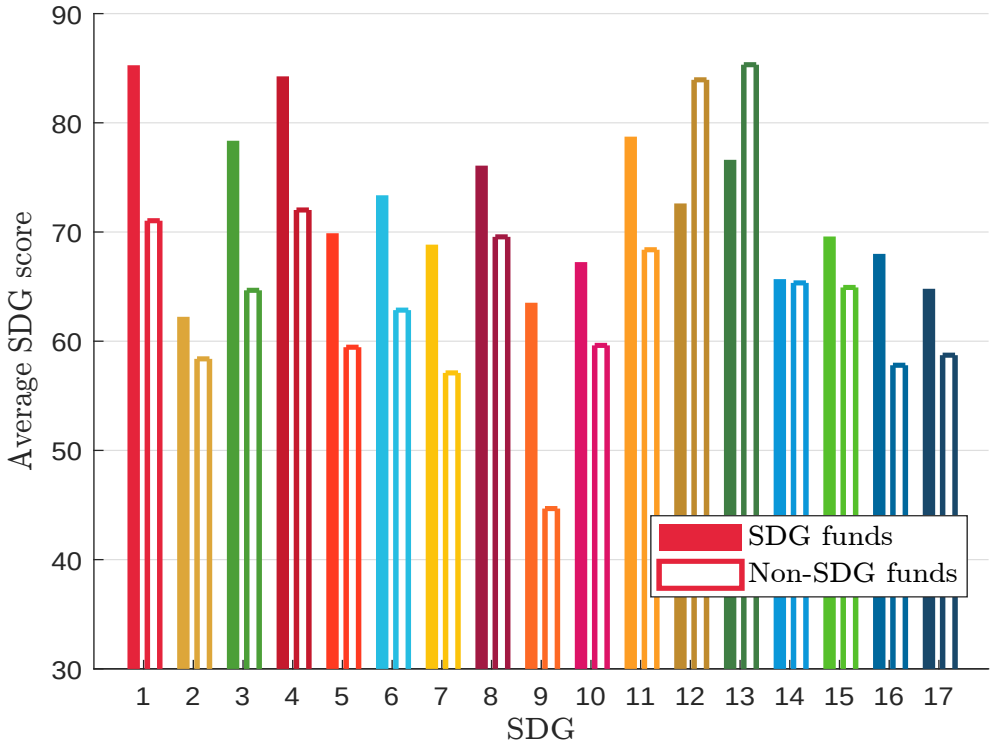


Source: Balitzky and Mosson (2024, Chart 10, page 12).

The previous comparison exercise raises the question of how to calculate the alignment of an SDG fund. Let $\mathbb{I}_i$ be the SDG index of country $i$ and $w_{i,j}$ be the weight of country $i$ in fund $j$. The SDG index for fund $j$ is then the weighted average given below:

$$\mathbb{I}_j = \sum_{i=1}^{n} w_{i,j}\mathbb{I}_i \tag{5.2}$$

It is generally assumed that the SDG index $\mathbb{I}_j$ measures the level of SDG alignment of fund $j$. Therefore, we can introduce a preference ordering:

$$j \succ j' \Leftrightarrow \mathbb{I}_j \geq \mathbb{I}_{j'} \tag{5.3}$$

This means that fund $j$ is more aligned than fund $j\prime$ if and only if fund $j$ has a better SDG index. The previous analysis can be done at the global level or for some SDG dimensions.

**Example 20** *We consider three SDG funds that hold sovereign debt or have country exposures, as described in Table 5.11. Amounts are in millions of dollars. For example, SDG Fund #1 has $25.9 million of exposure to Bangladesh, $10.3 million to Honduras, and $19.7 million to Haiti. SDG Fund #2 invests primarily in developed countries, while SDG Fund #3 combines investments in both developed and developing countries. For each country, we provide the SDG and spillover indexes calculated by Sachs et al. (2024).*

Table 5.11: SDG data and country exposures for three SDG funds (Example 20)

| Country | SDG index | Spillover index | Fund #1 | Fund #2 | Fund #3 |
|---|---|---|---|---|---|
| Denmark | 85.00 | 58.10 | | 100.1 | 65.8 |
| France | 82.76 | 62.49 | | 356.8 | 25.6 |
| Australia | 76.88 | 66.80 | | 211.3 | |
| Morocco | 70.85 | 94.70 | | | 56.5 |
| Bangladesh | 64.35 | 96.98 | 25.9 | | |
| Honduras | 62.00 | 93.05 | 10.3 | | |
| Nigeria | 54.58 | 96.55 | | | 12.3 |
| Haiti | 52.68 | 94.43 | 19.7 | | |

The SDG index for Fund #1 is equal to:

$$\mathbb{I}_1^{\text{SDG}} = \frac{25.9 \times 64.35 + 10.3 \times 62.00 + 19.7 \times 52.68}{25.9 + 10.3 + 19.7} = 59.80$$

For the spillover index, we get:

$$\mathbb{I}_1^{\text{Spillover}} = \frac{25.9 \times 96.98 + 10.3 \times 93.05 + 19.7 \times 94.43}{25.9 + 10.3 + 19.7} = 95.36$$

Finally, the results for the three SDG funds are:

| Score | Fund #1 | Fund #2 | Fund #3 |
|---|---|---|---|
| $\mathbb{I}_j^{\text{SDG}}$ | 59.80 | 81.24 | 77.32 |
| $\mathbb{I}_j^{\text{Spillover}}$ | 95.36 | 63.20 | 74.66 |

We obtain the following ranking:

$$\mathbb{I}_2^{\text{SDG}} \geq \mathbb{I}_3^{\text{SDG}} \geq \mathbb{I}_1^{\text{SDG}} \Rightarrow \text{Fund}_2 \succ \text{Fund}_3 \succ \text{Fund}_1$$

This means that Fund #2 is the most SDG-aligned of the three SDG funds. However, this result is completely absurd. In reality, it is more impactful to invest in countries like Bangladesh, Honduras, and Haiti than it is to invest in Denmark, France, and Australia. In other words, SDG alignment is not the right metric for impact investing. For example, investing in a country with an SDG index of 100% would result in zero SDG impact, as the country cannot further improve its SDG score because all sustainable development goals have already been achieved. Conversely, investing in a poor country with a low SDG score can have a significant impact. Thus, effective impact investing targets low SDG scores, not high ones. Therefore, the preference ordering defined in Equation (5.3) is completely wrong. If we look at the spillover index instead of the SDG index, Fund #1 has a better score. All these results raise the question of the SDG investor's utility function. Going back to the ESMA study, the fact that SDG funds have a higher SDG index score than non-SDG funds (74 vs. 64) is not necessarily a positive conclusion.

As mentioned above, the SDGs were created and defined for countries, not for companies. For example, we don't know how a company can contribute to indicator 1.2.2 (proportion of population living in multidimensional poverty) of SDG 1 (end poverty in all its forms everywhere). Nevertheless, several ESG rating agencies have developed scores for corporate SDG alignment since 2020:

- In September 2020, MSCI introduced the MSCI SDG Alignment Tool, designed to offer investors a comprehensive view of a company's overall contribution — both positive and negative — towards achieving each of the 17 SDGs.
- In March 2021, Factset announced the launch of the Truvalue Labs SDG Monitor, which allows investors to see the alignment of companies around the world with the SDGs in real time.
- Sustainalytics' impact metrics is a set of company-level metrics that provide investors with useful measures of companies' environmental and social impact. The metrics are aligned to Sustainalytics' proprietary impact framework and the UN SDGs.
- ISS developed the SDG Impact Rating to provide a comprehensive and detailed view of a company's overall SDG impact, as well as across all 17 SDGs, and to better understand the issuer's performance relative to its industry peers.
- In August 2021, Moody's launched SDG Alignment Screening, a data solution to help investors integrate the SDGs into SDG-aligned investment strategies, funds, indexes and reporting.
- Etc.

These SDG ratings and scores are used by asset owners and managers to create SDG funds, SDG investment strategies, etc. For example, on January 9, 2024, S&P Dow Jones Indices announced the launch of two new sustainability indexes: the S&P 500 SDG Index and the S&P Global LargeMidCap SDG Index. The S&P 500 SDG Index tracks large-cap US equities, while the S&P Global LargeMidCap SDG Index tracks a broad range of market capitalizations across developed and emerging markets. S&P Dow Jones Indices worked with Impact Cubed to develop these indices, using their methodology to evaluate companies based on their revenue-generating activities and community engagement[32].

To illustrate corporate SDG alignment, we consider the MSCI approach (MSCI, 2024), which is among the most widely used by professionals. The MSCI SDG alignment methodology assesses each company's alignment with the 17 SDGs using a numerical score ($-10$ to 10) and a categorical assessment (strongly aligned to strongly misaligned). It does not provide an aggregate company-level score. The evaluation includes:

1. SDG net alignment score and assessment: overall alignment with each SDG;
2. SDG product alignment score and assessment: alignment of the company's products and services with each SDG;
3. SDG operational alignment score and assessment: alignment of the company's operations with each SDG.

[32]The methodology behind the construction of the S&P SDG Indices, as well as the underlying data used, can be found at www.spglobal.com/spdji/en/education/article/introducing-the-sp-sustainable-development-goals-indices.

Figure 5.19: Example of the SDG net alignment assessment of a food retail company (MSCI)

Source: MSCI (2024, Exhibit 3, page 7).

Each company then receives a total of 51 scores and 51 corresponding assessments (17 net alignment + 17 product alignment + 17 operational alignment). The assessment is based on the score $\mathcal{S}$, categorized as: strongly aligned if $\mathcal{S} > 5$, aligned if $2 < \mathcal{S} \leq 5$, neutral if $-2 < \mathcal{S} \leq 2$, misaligned if $-10 < \mathcal{S} \leq -2$, and strongly misaligned if $\mathcal{S} = -10$. For example, if the SDG product alignment score for a company is $\mathcal{S} = 6$, then the company is considered strongly aligned for the product dimension. The SDG net alignment score is the average of its SDG product alignment score and SDG operational alignment score, unless one of the two scores is $-10$, in which case the net alignment score is $-10$:

$$\mathcal{S}^{\text{net}} = \begin{cases} \dfrac{\mathcal{S}^{\text{product}} + \mathcal{S}^{\text{operational}}}{2} & \text{if } \min\left(\mathcal{S}^{\text{product}}, \mathcal{S}^{\text{operational}}\right) > -10 \\ -10 & \text{if } \min\left(\mathcal{S}^{\text{product}}, \mathcal{S}^{\text{operational}}\right) = -10 \end{cases}$$

Criteria for a score of $-10$ in product or operational alignment are generating more than 50% of revenue from products/services with negative SDG impacts, or involvement in significant (red flag) controversies related to an SDG. Figure 5.19 shows an example of the SDG net alignment assessment of a food retailer, which can be found in MSCI (2024).

Table 5.12: SDG product alignment score aggregation

| Product alignment | | Score contribution |
|---|---|---|
| Positive alignment (% of revenue) | $> 50\%$ | $+10$ |
| | $25 - 50\%$ | $+7$ |
| | $10 - 25\%$ | $+5$ |
| | $5 - 10\%$ | $+3$ |
| | $0 - 5\%$ | $+1$ |
| Negative alignment (% of revenue) | $0 - 5\%$ | $-1$ |
| | $5 - 10\%$ | $-3$ |
| | $10 - 25\%$ | $-5$ |
| | $25 - 50\%$ | $-7$ |
| | $> 50\%$ | $-10$ |

Source: MSCI (2024, Exhibit 4, page 9).

To calculate the SDG product alignment score, MSCI (2024) determines the percentage of revenue that is positively aligned with the SDG and the percentage of revenue that is negatively aligned with the SDG. For each of the SDGs, they define a list of products and services with positive and negative impacts. For example, in the case of SDG 13 (climate action), revenue from services with positive impacts comes from alternative energy, including hydropower, demand-side management, smart grid, and turbine manufacturing for alternative energy and hydropower, while revenue from services with negative impacts comes from electricity generation from fossil fuels, oil and gas exploration and production, or coal mining, and fossil fuel turbines. Then they use the score aggregation method shown in Table 5.12. For example, if a utility company has 55% of its revenue from solar power generation, 20% of its revenue from coal power generation, and 25% of its revenue from water management, it has a positive alignment of 55% and a negative alignment of 20% with respect to SDG 13. The product alignment score for this company is $10 - 3 = 7$. Because this score is greater than 5, this company is considered to be strongly aligned with SDG 13. If the revenue split is not 55%/20%/25%, but 20%/55%/25%, the score is not $3 - 10 = -7$, but $-10$, because the positive impact cannot offset the negative impact. This means that a company with a negative impact score of $-10$ has a global score of $-10$ and is considered strongly misaligned.

Table 5.13: SDG operational alignment score aggregation

| | Operational alignment | Score contribution |
|---|---|---|
| Positive impact | Policies aligned with the SDG | +1 each |
| | Initiatives aligned with the SDG | +1 each |
| | Targets aligned with the SDG | +1 each |
| Negative impact | Involvement in operations with adverse impact | −1 each |
| | Any red flag controversies | −10 |
| | 3 or more orange flag controversies | −7 |
| | 7 or more yellow flag controversies | −7 |
| | 1 or 2 orange flag controversies | −5 |
| | 5 or 6 yellow flag controversies | −5 |
| | 3 or 4 yellow flag controversies | −3 |
| | 1 or 2 yellow flag controversies | −1 |
| Performance metrics | Improving trend | +2 |
| | Worsening trend | −2 |

Source: MSCI (2024, Exhibit 5, page 12).

The assessment of SDG positive and negative operational impacts is based on evidence from publicly disclosed company data. Each aligned policy, practice or target gains 1 point. Each engagement in operations with negative impacts loses 1 point. In addition, controversies contribute to the SDG negative operational impact score, which ranges from 0 to −10 based on the frequency and severity of incidents. This score uses the MSCI ESG controversy methodology to categorize controversies as red, orange, and yellow flags. Finally, the SDG operational alignment score takes into account a company's performance metrics, which are either positive or negative depending on the trend over the past three years. These performance metrics include energy consumption, carbon emissions, female employment, and employee injury rates. The method of aggregating the scores is shown in Table 5.13. Consider the case of SDG 5 (gender equality). The metrics indicating positive impact include programs for workforce diversity and diversity policies, a percentage of women in the workforce, executive management, and senior management all exceeding 20%, a percentage of women on the board exceeding 30%, and a minimum of one woman sits on the board. Metrics indicating negative impact involve controversies related to labor (such as gender discrimination, gender harassment, forced labor in operations or supply chains, and employee or labor discrimination in operations or supply chains) and customer discrimination. Finally, performance metrics include the trend in the growth of the percentage of women employees in the workforce over the past three years and the trend in the growth of the percentage of women in senior management.

The presentation of the MSCI approach highlights that corporate SDG alignment is based on two main components: revenue breakdown and controversies. Other SDG methodologies also rely on these two components. Notably, the country dimension is completely absent from these methodologies. For example, companies are considered aligned with SDG 2 (zero hunger) if their revenue comes from nutrition and sustainable agriculture. This concept of SDG 2 for corporate alignment differs significantly from the broader SDG 2 objectives. A company operating in a wealthy country with 100% of its revenues from sustainable agriculture is seen as strongly aligned with SDG 2. However, its actual contribution to the UN SDGs is negligible. Therefore, we must be cautious with corporate SDG alignment as it is easy to fall into SDG washing (Heras-Saizarbitoria *et al.*, 2022). While the use of SDG logos is helpful for visualizing the SDG themes behind impact investing, it is dangerous to take this further because companies are not countries.

## 5.3 The market of impact investing

In the following analysis, we examine the impact investing market from two perspectives. First, we assess the size of the market by analyzing statistics on assets under management. Second, we examine the different products that make up the impact investing market, including specialized investment vehicles such as social impact bonds, blended finance structured funds, and specialized investment funds such as blue and microfinance funds.

### 5.3.1 Market size

#### Total size

Estimating the size of the impact investing market is challenging due to the large proportion of direct investments, particularly those made by charities or philanthropic investors. However, we have three specialized sources that can provide an approximation of the size of the market. In October 2022, the GIIN estimated that more than 3 000 public and private organizations were managing $1.164 trillion in impact investing AUM globally as of December 2021 (Hand *et al.*, 2022). In a subset of 1 289 organizations, the average impact investment portfolio is $485 million, while the median is $62.5 million. This shows that a few large organizations manage high AUM in impact investing, implying that most organizations have relatively small allocations to impact investing. The geographic breakdown of impact AUM is 55% in Europe, 37% in North America, 3% in Africa, 2.5% in Asia and 1% in Latin America.

A second source for estimating the size of the market is the impact investing reports published by PitchBook (2023, 2024). There are several statistics available in the Excel file provided by PitchBook. To understand the different metrics, consider the following identity:

$$\text{Cumulative capital raised} + \text{Mark-to-market} + \text{Termination value} = \text{Dry powder} + \text{Remaining value}$$

where cumulative capital raised is the total amount of money committed by investors to the funds, mark-to-market reflects any appreciation or depreciation of the investments based on their current market price, termination value is the value realized from exited investments[33], dry powder is the uninvested portion of the capital raised (the capital available for future investments), and remaining value is the current value of the investments still held by the funds, including the mark-to-market value of those investments. We can simplify this equation because the right side is equal to the current assets under management:

$$\text{Dry powder} + \text{Remaining value} = \text{Current AUM}$$

Figure 5.20 shows the assets under management per year and their decomposition between dry powder and remaining value. As of June 30, 2023, the AUM is $885 billion, with a significant portion, 26%, not yet deployed and classified as dry powder. Fundraising activity can be measured in two ways: the number of funds launched and the capital raised during the year. These metrics are given in Figure 5.21, while the cumulative statistics since 2007 are shown in Figure 5.22. Between 2007 and 2023, 2 292 impact investing funds have been launched, raising a total of $1.05 trillion in capital. Of this capital, 47.2% has been raised in North America, 34.6% in Europe, 11.1% in Asia, and 7.1% in the rest of the world. Table 5.14 shows the breakdown of fundraising activity by strategy since 2007. While private equity and venture capital dominate the traditional ESG investing market in alternative assets, real assets account for two-thirds of the capital raised in impact investing for

[33] This is the cash or other value received when investments are sold or otherwise exited.

Figure 5.20: Size of the impact investing market (AUM in $ bn, PitchBook impact database)

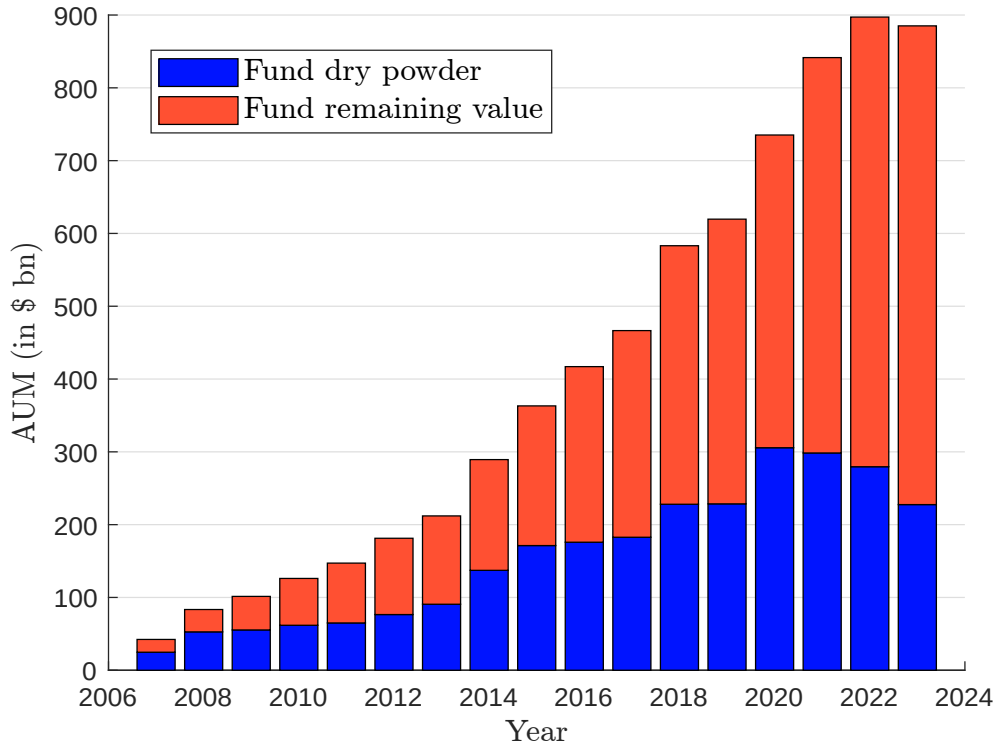


Source: PitchBook (2023, page 5), https://pitchbook.com & Author's calculations.

both public and private assets. According to the PitchBook database, most impact investments are made in private markets. In addition to the 67% allocated to real assets, private equity represents 21.5% of the capital raised, and real estate accounts for 3.9%. Furthermore, a significant portion of the debt strategy also pertains to private markets (Table 5.14).

Table 5.14: Strategy representation of impact investing (as of December 2023, PitchBook impact database)

| Strategy | Fund count | Capital raised |
|---|---|---|
| Private equity (buyout) | 21.90% | 14.49% |
| Venture capital | 40.18% | 7.03% |
| (Private) debt | 7.16% | 6.26% |
| Real estate | 5.80% | 3.93% |
| Real assets* | 20.55% | 66.96% |
| Other | 4.41% | 1.33% |

*Real assets = infrastructure & natural resources.

Source: PitchBook (2023), https://pitchbook.com & Author's calculations.

**Remark 49** *We observe a high dispersion in fund size. For example, the median fund size is $147.9 million in Europe, $63.8 million in North America, and $70.0 million in the rest of the world, while the average fund size is $633.0 million, $563.7 million, and $468.7 million, respectively. This high skew is mainly due to the large size of infrastructure funds. The dispersion is highest in Europe, where the top 10% of funds start at $1.6 billion, while the bottom 10% is $16.9 million.*

Figure 5.21: Fundraising activity (PitchBook impact database)

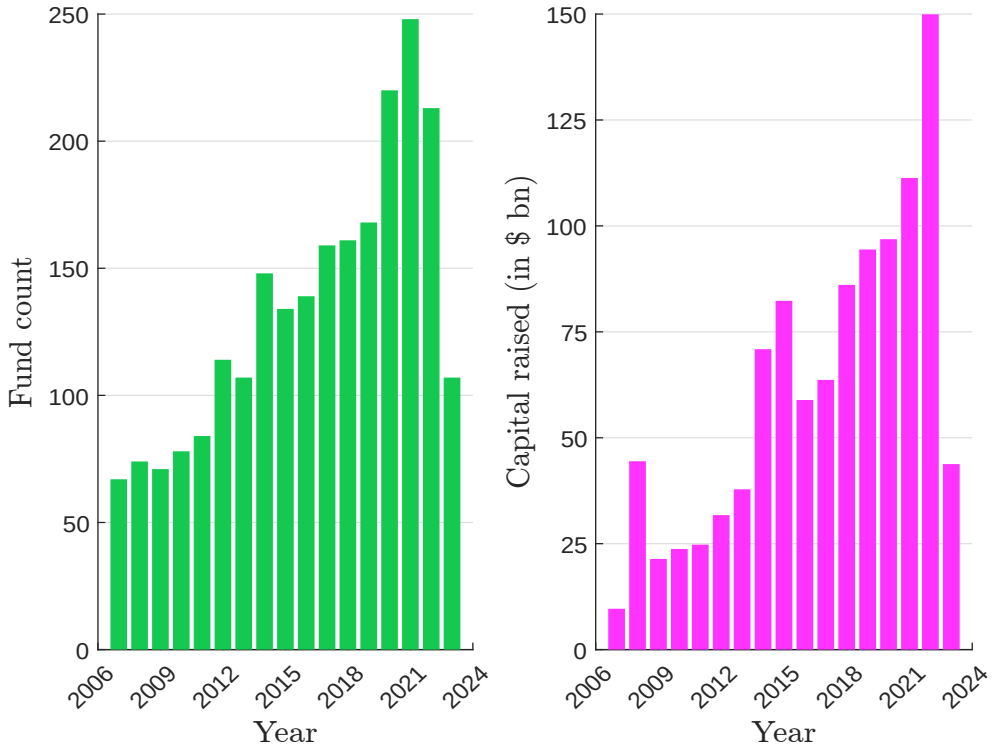


Source: PitchBook (2023, page 5), https://pitchbook.com & Author's calculations.

Figure 5.22: Cumulative fundraising (PitchBook impact database)

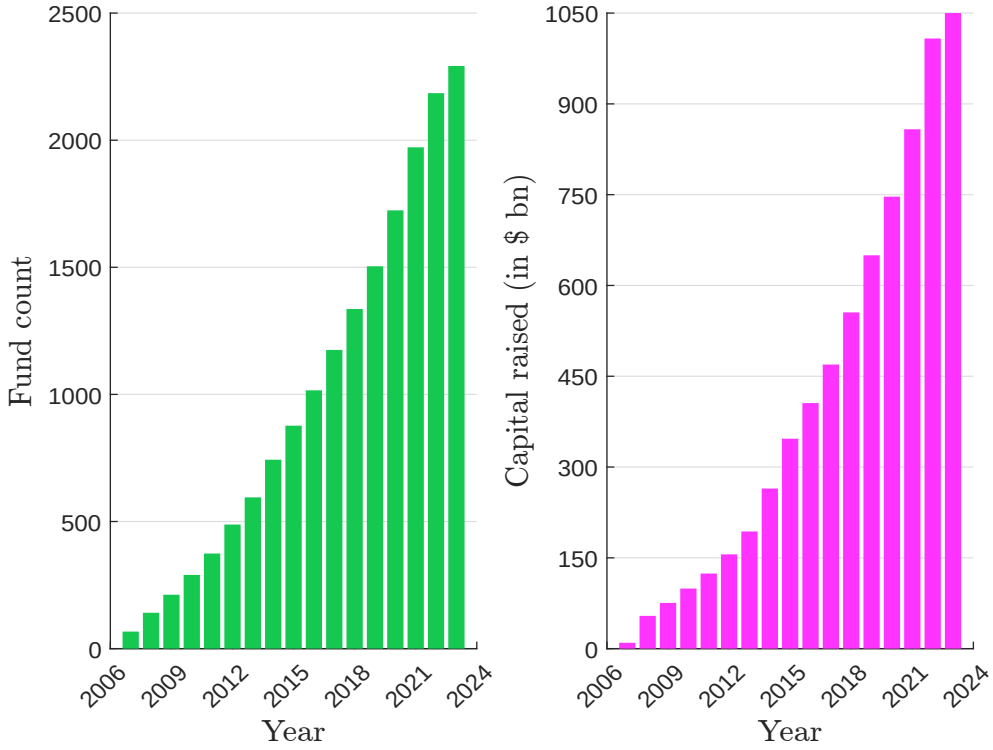


Source: PitchBook (2023, page 5), https://pitchbook.com & Author's calculations.

The third specialized source is the Phenix impact database, developed by the Phenix Capital Group. According to Phenix Capital (2024a), €589 billion has been allocated to more than 2 600 impact investing funds, which are managed by approximately 1 100 asset managers. The distribution of assets under management by strategy differs from the PitchBook database. In fact, we have the following breakdown: 48% private equity (buyout and venture capital), 22% real assets (including real estate), 13% private debt, 3% public debt, 9% public equity, and 4% other. Figure 5.23 shows the evolution of the capital raised between 2014 and 2023. We observe a significant increase in the rate of capital growth until 2020, followed by a notable slowdown starting in 2021. This deceleration is also reflected in the PitchBook impact database. Interestingly, this phenomenon coincides with a period of intense discussion and popularization of impact investing among asset managers.

Figure 5.23: Cumulative capital raised in € bn (Phenix impact database)

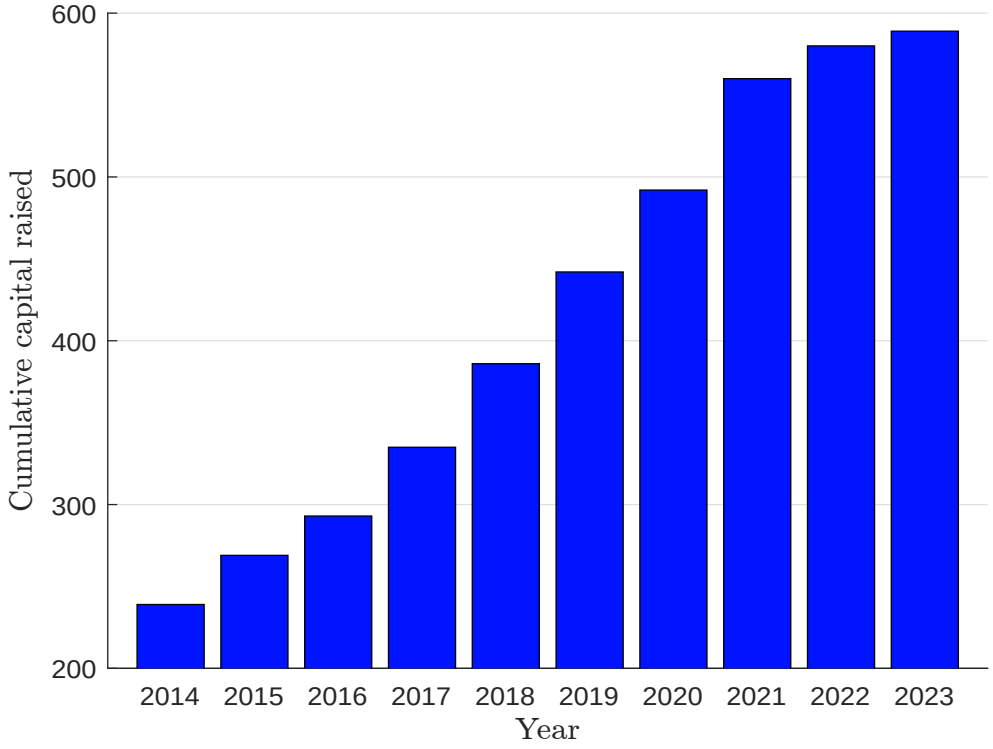


Source: Phenix Capital (2024a, page 16).

One interesting piece of information from the impact reports published by Phenix is the SDGs targeted by impact funds. Figure 5.24 shows Phenix's mapping of the SDGs to the themes commonly used by impact investing practitioners. This enables Phenix to count the number of funds targeting each SDG. The results are shown in Table 5.15. For instance, across all investment funds, SDG 7 (affordable and clean energy) is the most targeted goal, followed by SDG 9 (industry, innovation and infrastructure) and SDG 3 (good health and well-being). This ranking varies significantly by asset class. In private equity, impact funds predominantly target SDG 3 (good health and well-being) and SDG 2 (zero hunger), while in private debt, they focus on SDG 1 (no poverty) and SDG 5(gender equality). This is because private equity impact funds invest primarily in the healthcare and food sectors, whereas private debt impact funds are dominated by microfinance funds. In the case of real assets, the two most targeted goals are SDG 7 (affordable and clean energy) and SDG 11 (sustainable cities and communities) because of the importance of infrastructure in this asset class.

Figure 5.24: Phenix Capital Group's mapping of the SDGs to the themes commonly used by impact investing practitioners

Source: www.phenixcapitalgroup.com/sustainable-development-goals-impact-investing-themes.

Table 5.15: Most targeted SDGs (Phenix impact database)

| Rank | All Funds | Private Equity | Private Debt | Real Assets | Public Equity | Public Debt |
|---|---|---|---|---|---|---|
| 1 | SDG 7 | SDG 3 | SDG 1 | SDG 7 | SDG 7 | SDG 11 |
| 2 | SDG 9 | SDG 2 | SDG 5 | SDG 11 | SDG 3 | SDG 7 |
| 3 | SDG 3 | SDG 9 | SDG 7 | SDG 15 | SDG 9 | SDG 13 |
| 4 | SDG 2 | SDG 7 | SDG 2 | SDG 2 | SDG 12 | SDG 12 |
| 5 | SDG 11 | SDG 12 | SDG 8 | SDG 12 | SDG 11 | SDG 14 |

Source: Phenix Capital (2024a).

The situation in public markets differs from that in private markets. While there are some similarities between public and private equities, the same is not true for public and private debt. For example, public equity impact funds primarily target SDG 7 (affordable and clean energy) and SDG 3 (good health and well-being), which are also major goals for private equity impact funds. However, only one SDG (affordable and clean energy) is common among the top five SDGs targeted by both public equity impact funds and private equity impact funds.

**Remark 50** *These three specialized data sources provide three different pictures of the impact investing market. However, there are some similarities between them. First, the GIIN report is primarily based on data from Phenix Capital Group and Pitchbook. Second, while the size of the market differs from provider to provider (especially GIIN vs. Phenix), the three databases show the same trend in terms of capital growth. The growth of impact investing is more important through 2020 than from 2021.*

### Regional size

In addition to these global reports, there are also regionally focused impact investing reports. Here are a few examples:

1. *Estimating and Describing the UK Impact Investing Market*, published by EY and the Impact Investing Institute in March 2022;
2. *The African Investing for Impact Barometer*, published by RisCura in April 2022;
3. *Impact Investing in Germany 2022*, published by Bundesinitiative Impact Investing in October 2022;
4. *Accelerating Impact: Main Takeaways from the First Harmonised European Impact Investment Market Sizing Exercise*, published by EVPA in December 2022;
5. *Overview of the French Impact Investment Market 2023*, published by FAIR in November 2023;
6. *2023 in Retrospect: India Impact Investment Trends*, published by Impact Investors Council in May 2024;
7. *Impact Investing in Africa: A 2024 Analytical Map*, published by FERDI in June 2024;

Below we report the size estimated by each study for the corresponding region:

| Study | 1 | 2 | 3 | 4 | 5 | 6 | 7 |
|---|---|---|---|---|---|---|---|
| Region | UK | Africa | Germany | Europe | France | India | Africa |
| Reporting year | 2020 | 2021 | 2022 | 2022 | 2022 | 2023 | 2024 |
| AUM (in bn) | £58 | $72.6 | €38.9 | €80 | €14.8 | $2.9 | $25 |

These figures fall significantly short of the $1.164 trillion in impact investing assets under management (AUM) estimated by the GIIN (Hand *et al.*, 2022). According to the EVPA, the size of the impact investing market in Europe is around €80 billion, while the GIIN estimates it to be over $500 billion globally. One reason for the discrepancy is that a significant portion of the AUM in the GIIN study corresponds to publicly traded assets. Another factor is that most assets are self-reported. However, it is reasonable to conclude that the true size of the impact investing market is probably less than $500 billion and certainly not more than $1 trillion.

### 5.3.2 Market products

Another way to gain a clearer understanding of the impact investing market is to examine specific investment products. This approach can shed light on why there are such significant discrepancies in market size estimates, particularly when listed assets are included. In fact, the question of market size is closely related to the distinction made at the beginning of this chapter: investing WITH impact versus investing FOR impact. The analysis of specific products will help to clarify this distinction.

#### Social impact bonds

There is no single definition of social impact bonds (SIB), as they come in many different forms. Depending on the country and structure, they may also be referred to as pay-for-success bonds, social outcomes contracts (SOC), pay-for-benefit bonds, payment-by-results (PBR) instruments, development impact bonds, or simply impact bonds. However, they share certain common characteristics, most notably that they belong to the category of outcome-based financial contracts in which investors provide up-front capital to finance social programs and are repaid only if the desired outcomes are achieved. Typically, social impact bonds work through a partnership between the public sector, private investors, and service providers to address social issues such as homelessness, education, criminal justice, and public health. There are two major types of impact bonds. Domestic impact bonds are those where the outcome payer is the government representing the citizen target group. In contrast, development impact bonds (DIB) involve an external organization, such as an aid agency, as the outcome payer rather than the government.

In 2009, UK Prime Minister Gordon Brown committed the government to developing social outcomes contracts. At the same time, Social Finance, a London-based charity, developed the concept of social impact bonds and defined the SIB mechanism as follows:

> "*Social Impact Bonds are based on a commitment from government to use a proportion of the savings that result from improved social outcomes to reward non-government investors that fund the early intervention activities. Social Impact Bonds are based on a contract negotiated with government that includes clear definitions of the success metric — for example, the 1 year reoffending rate for short-sentence offenders in a specified geographic area; the target population — for example, offenders aged over 18 leaving prison after a sentence of less than 12 months and returning to a specified geographic area; the value of success — the amount returned to investors for a given improvement in the social outcome, generally a proportion of the related savings to government. In order to effectively incentivise investors this needs to be tailored to each situation. For example, the value of success may increase as the reoffending rate falls in recognition of the fact that more difficult target groups require more expensive interventions. Once the contract is in place, investment is raised from non-government investors. This investment is used to finance a range of interventions to improve the target social outcome over the contract period (around 5 years). If the interventions are successful and the social outcomes improve, government pays investors a reward based on the pre-agreed payment schedule.*" (Social Finance, 2009, page 3).

Social Finance proposed using the SIB mechanism to reduce recidivism. In the 2000s, approximately 40 000 adults in the UK left prison each year after serving sentences of less than 12 months. These prison placements cost the taxpayer over £213 million annually. Despite this, adults serving short sentences received no formal support to help them successfully reintegrate into the community,

resulting in 73% of these offenders reoffending within two years of release. Social Finance's approach aimed to provide support that would reduce reoffending rates, lower costs for the government and society, and use these savings to finance the interventions, with returns paid to investors. In 2010, the project was approved and the first SIB pilot was implemented in HM Prison Peterborough. From September 2010 to June 2014, approximately 2 000 offenders released from prison received one year of individualized care and support from a variety of organizations to assist with housing, employment, and, if necessary, drug and alcohol treatment. With a budget of £5 million, the program aimed to reduce recidivism by 7.5%. It was funded by private investors and Social Finance, who were reimbursed by the Ministry of Justice and the Big Lottery Fund. The program ultimately exceeded expectations, achieving a 9% reduction in reoffending. It's a story that's been told around the world[34] and the subject of numerous works on SIBs.

Box 5.4: Outcomes-based contracting

Outcomes-based contracting (OBC) shifts the focus of public service contracting from activities and inputs to achieving measurable outcomes that positively impact service users. Traditional models, such as fee-for-service, pay providers for delivering specified services. In contrast, OBC links payments to the achievement of specific outcomes, incentivizing service providers to deliver results that improve the lives of users. OBC is a subset of results-based financing (RBF), of which impact bonds are a prominent example, in which private investors provide up-front capital for service delivery and are repaid only if the desired outcomes are achieved. The theoretical benefits of OBC include incentivizing positive behavior, managing risk by transferring responsibility to providers or investors, and potentially reducing the cost of public services while increasing their effectiveness. However, evidence on the effectiveness of OBC remains limited and sometimes contradictory, as most evaluations focus on service outcomes rather than the contracting mechanism itself.

Source: https://golab.bsg.ox.ac.uk/the-basics/outcomes-based-contracting.

Since the pilot in 2010, approximately 300 impact bonds have been launched globally. In August 2012, the first impact bond outside the UK was introduced in New York City, targeting a reduction in reoffending. By 2013, the first social impact bonds were launched in Australia, Germany, and the Netherlands. In 2014, Belgium and Canada saw their first SIBs, followed by Austria, India, Israel, Finland, Portugal, and Switzerland in 2015. Additionally, in February 2015, the first development impact bond was announced to support sustainable cocoa and coffee production within the indigenous Asháninka community in Peru. In 2016, the UK government and the University of Oxford established the Government Outcomes Lab (GO Lab), a research and policy center dedicated to exploring how governments can work with the private and social sectors to improve social outcomes. In particular, the GO Lab developed the impact bond dataset INDIGO[35], which serves as the primary source of information on social impact bonds (SIBs). As of July 2024, the INDIGO dataset contains 321 projects (or impact bonds), 37 funds, and 1 645 organizations. One project corresponds to one impact bond. For example, project INDIGO-POJ-0001 is the Proyecta Tu Futuro (Plan Your Future, Buenos Aires Youth Employability SIB), which aims to reduce youth unemployment in the city of Buenos Aires[36]. A fund is a basket of social projects. For example, fund INDIGO-FUND-0001 is

[34] A fuller description of the Peterborough Prison SIB pilot, including the investment and payment structure, can be found in Disley *et al.* (2011, 2016).

[35] The direct link to the dataset is https://golab.bsg.ox.ac.uk/knowledge-bank/indigo.

[36] The project focuses on vulnerable unemployed young citizens and vulnerable young citizens who have not com-

the Youth Engagement Fund launched by the United Kingdom[37]. An organization is a stakeholder in an impact bond or fund. The GO Lab distinguishes three types of organizations, both of which participate to achieve better outcomes for the target group:

- Outcome payers are the commissioners. They identify social problems, specify payable outcomes that must be achieved to address those problems, and pay for the outcomes that are achieved.
- Service providers work with the target population to achieve the outcomes specified by the outcome payer and receive payments based on the achievement of specified outcomes.
- Investors provide upfront funding to the service provider to finance the project and are repaid based on the achievement of specified outcomes.

For example, organization INDIGO-ORG-0001 is Sheffield Futures, which is a youth charity. For a given impact bond or fund, we have the list of organizations participating in the project. For example, there are 14 organizations participating in the Buenos Aires Youth Employability SIB[38].

According to the INDIGO database, there are 296 social impact bonds (SIBs) with a total capital raised exceeding $760 million. The median size of these bonds is relatively small, at $1.2 million. Approximately 2.6 million people benefit from these impact projects, although the median number of service users is only 500. This suggests that most social impact bonds are highly targeted to specific groups. Around 40% of SIBs have matured and been completed, while 60% are still active. In terms of policy areas, employment and training is the most common focus, followed by health and wellbeing, child and family welfare, and homelessness. The SIB market is led by the UK, followed by the US, Portugal, Japan, and the Netherlands. However, the market's growth has slowed in recent years, particularly after the COVID-19 crisis, as illustrated by the number of social impact bonds initiated each year, shown in Table 5.16.

Table 5.16: Number of social impact bonds per start year

| Year | # | Year | # | Year | # |
|---|---|---|---|---|---|
| 2010 | 1 | 2015 | 24 | 2020 | 35 |
| 2011 | 1 | 2016 | 26 | 2021 | 22 |
| 2012 | 13 | 2017 | 41 | 2022 | 14 |
| 2013 | 7 | 2018 | 47 | 2023 | 9 |
| 2014 | 9 | 2019 | 36 | 2024 | 1 |

Source: https://golab.bsg.ox.ac.uk/knowledge-bank/indigo/impact-bond-dataset-v2.

**Remark 51** *There are few resources devoted to the theoretical aspects of SIB design, except for the work of Chowdhry et al. (2019).*

pleted high school. The intervention will provide weekly workshops on soft skills training, employment support, orientation and placement in companies. The intervention aims to help the participant to find and keep a job and to graduate from high school (if the participant has not yet graduated).

[37]The Youth Engagement Fund aims to support disadvantaged young people to participate and succeed in education or training in order to improve their employability, reduce their long-term dependency on benefits, and reduce their likelihood of offending. The UK government aims to provide funding through social impact bonds and will only pay out if projects deliver positive outcomes.

[38]They are Social Finance UK, AMIA, Fundacion Forge, Fundacion Pescar, Fundacion Reciduca, Acrux Partners, Beccar Varela Law Firm, Fundacion Alimentaris, Government of the City of Buenos Aires, Banco Ciudad de Buenos Aires, Banco Galicia, IRSA Propiedades Comerciales, Organizacion Roman, and the Inter-American Development Bank.

### Blue funds

A blue bond works similarly to a green or social bond, but with a specific focus on ocean and sea protection. Blue bonds are typically issued by governments, supranational organizations or development banks to support initiatives and finance projects that promote the conservation and sustainable use of ocean and water resources. In September 2023, ICMA, together with ADB, IFC, UNEP FI and UN Global Compact, developed a global practitioner's guide for bonds to finance the sustainable blue economy (SBE). It is a preliminary version of the Blue Bond Principles. According to this guide, funds raised through blue bonds are typically used to support eight typical activities (ICMA, 2023, Table 1, pages 6-7):

1. Coastal climate adaptation and resilience (climate change adaptation): Projects that support ecological and community resilience and adaptation to climate change including using nature-based solutions;

2. Marine ecosystem management, conservation, and restoration (terrestrial and aquatic biodiversity): Projects that manage, conserve, and restore the health of coastal and marine ecosystems[39];

3. Sustainable coastal and marine tourism: Projects that improve the environmental sustainability of coastal and marine tourism

4. Sustainable marine value chains (environmentally sustainable management of living natural resources and land use): Projects that improve the environmental sustainability of marine value chains:

   (a) Sustainable marine fisheries management
   (b) Sustainable aquaculture operations (algae, bivalves, fish, and seagrass)
   (c) Seafood supply chain sustainability

5. Marine renewable energy (renewable energy): Projects that increase contribution of marine and offshore renewable energy to energy mix and renewable energy projects that support other SBE sectors while safeguarding the marine environment. These include offshore wind (both fixed and floating installations), wave, tidal, floating solar and ocean thermal energy conversion;

6. Marine pollution (pollution prevention and control/sustainable water and wastewater management/circular economy adapted products, production technologies and processes): Projects that prevent, control, and reduce waste from entering the coastal and marine environments[40]:

   (a) Wastewater management
   (b) Solid waste management
   (c) Resource efficiency and circular economy (waste prevention and reduction)
   (d) Non-point source pollution management

7. Sustainable ports (clean transportation): Projects that increase environmental performance and sustainability of port functions and infrastructure;

[39] Projects must be within the marine environment or within 100 km of the coast.

[40] For wastewater management, projects must be within 100 km of the coast. For solid waste management, projects must be within 50 km of the coast or a river that drains to the ocean. For non-point source pollution management, projects must be within 200 km of the coast or within 50 km of rivers (and their tributaries) that flow to the ocean.

8. Sustainable marine transport (clean transportation): Projects that involve increasing environmental performance and sustainability of maritime transportation.

Blue bonds are a key component of blue finance, a broad term for investments aimed at supporting projects that protect oceans and improve water management. Other instruments in blue finance include blue loans and blue funds. More broadly, blue finance aligns with the concept of the blue economy, a term introduced by Belgian economist Gunter Pauli[41]. In 2015, Hoegh-Guldberg *et al.* (2015) estimated that the value of blue economy assets, including energy production, mining, tourism, maritime transportation, aquaculture, fisheries, and more, is more than $24 trillion[42]. These assets generate annual revenues of approximately $2.5 trillion. If considered as a national economy, the blue economy would rank as the world's seventh largest, surpassing both Brazil and Italy in GDP, just behind the United Kingdom. However, the blue economy faces significant risks as natural assets deteriorate, including declines in fisheries, habitats, and marine species. This has driven the emergence of the sustainable blue economy and the growth of blue finance.

In 2018, Seychelles became the first country to issue a blue bond, known as the Seychelles blue bond. The World Bank assisted in developing this 10-year bond, which raised $15 million[43] with the goal of expanding marine protected areas, enhancing governance of priority fisheries, and fostering the development of Seychelles' blue economy through the financing of sustainable fishing practices and marine conservation initiatives. The Seychelles blue bond is partially guaranteed by a $5 million guarantee from the World Bank and further supported by a $5 million concessional loan from the Global Environment Facility (GEF) which will partially cover interest payments for the bond. The Seychelles blue bond is an example of a use of proceeds (UOP) bond, a common term in green bond terminology. However, blue bond issuance can also take other forms. One such form is a debt-for-nature (DFN) swap, a financial arrangement in which a portion of a country's debt is forgiven or reduced in exchange for commitments to invest in marine conservation and sustainable management. In 2023, Ecuador completed the world's largest debt-for-nature swap (the Galapagos blue bond). Although it did not significantly reduce the government's overall debt, it allows Ecuador to direct savings toward conservation efforts in the Galapagos Islands. Credit Suisse led the transaction, facilitating a buyback of approximately $656 million in external bonds. The deal was supported by a blue bond, rated *Aa2* by Moody's due to a $85 million guarantee from the Inter-American Development Bank[44]. While the transaction reduced Ecuador's debt by approximately 1.6%, it is expected to generate $323 million for Galapagos marine conservation through 2041. Because the blue bond market is new, it is less mature than the green or social bond markets:

> "*Between 2018 and 2022, 26 blue bond transactions took place, amounting to a total value of $5 billion, with a 92% CAGR between those years. Currently, blue bonds represent less than 0.5% of the sustainable debt market. The use of proceeds has mostly focused on waste management, biodiversity, and sustainable fisheries, but also ranges across other areas of the sustainable blue economy. Only two-thirds of blue bond issuers report on impact metrics, providing further opportunity to add detail and rigor. We draw comparisons to the more mature green bond market and conclude that a lack of standardized definitions, metrics, and expertise by issuers and investors are significant barriers to the blue bond market.*" (Bosmans and de Mariz, 2023, page 1).

[41] See his book on the blue economy (Pauli, 2010).

[42] This estimate includes $6.9 trillion in direct ocean output, $5.2 trillion from shipping lanes, $7.8 trillion from productive coastlines, and $4.3 trillion from carbon absorption assets.

[43] The investors were Calvert Impact Capital, Nuveen, and Prudential Financial.

[44] The *Aa2* rating of the Galapagos blue bond is 16 notches above Ecuador's sovereign rating. The blue bond offers a coupon of 5.645% compared to the 17% to 26% yield on Ecuadorian government bonds.

As of July 2024, there are 41 blue bonds in circulation, 17 of which were issued in 2023. A key challenge for the growth of this market is that it primarily involves small island developing states, which often require technical assistance to issue blue bonds, implement projects and establish credibility with investors (Thompson, 2022; March *et al.*, 2023). Table 5.17 provides examples of blue bonds. It is important to note that blue bonds are issued not only by governments and multilateral development banks but also by corporations, such as Mowi, a seafood company, and Ørsted, an energy company.

Table 5.17: Some examples of blue bonds

| Year | Type | Amount (in $ mn) | Bond name |
|---|---|---|---|
| 2018 | UOP | 15 | Seychelles blue bond |
| 2018 | DFN | 21 | Seychelles debt-for-nature swap |
| 2019 | UOP | 220 | Nordic-Baltic blue bond I (Nordic Investment Bank) |
| 2020 | UOP | 220 | MOWI green bond |
| 2020 | UOP | 150 | Nordic-Baltic blue bond II (Nordic Investment Bank) |
| 2020 | UOP | 940 | Bank of China blue bond |
| 2021 | UOP | 300 | ADB Australia/NZ blue bond |
| 2021 | DFN | 365 | Belize debt-for-nature swap |
| 2022 | UOP | 385 | Bahamas blue bond |
| 2022 | DFN | 150 | Barbados debt-for-nature swap |
| 2023 | UOP | 3.5 | Cabo Verde marine & ocean-based blue bond (International Investment Bank) |
| 2023 | DFN | 656 | Galapagos debt-for-nature swap (Ecuador) |
| 2023 | UOP | 150 | Indonesia blue bond (Republic of Indonesia) |
| 2023 | UOP | 100 | Ørsted blue bond |
| 2023 | UOP | 50 | Bank of Ayudhya blue bond (Thailand) |
| 2023 | DFN | 500 | Gabon debt-for-nature swap |

Source: Author's research.

Blue funds are investment funds that focus on the blue economy. While they can invest in blue bonds, this market remains relatively small. As a result, they also allocate capital to other securities, such as public and private equities or private debt instruments. The Phenix impact database currently has 164 blue funds, representing less than 6% of the impact funds. However, we observe a high growth over the last ten years (Figure 5.25). The fund distribution is as follows: 50% private equity vehicles, 23.8% public debt funds and 15.9% public equity funds (Phenix Capital, 2024c, page 14). The primary investors in blue funds are foundations (20%), corporations (17%), and family offices (16%), with pension funds representing less than 10% of the investor base.

When we map these funds to the SDGs, we find that there are only 18 funds that focus solely on SDG 14 (life below water). In most cases, these blue funds also target other additional SDGs, such as SDG 6 (clean water and sanitation) and SDG 7 (affordable and clean energy). The total capital raised by blue funds is estimated to be €45 billion, while the total capacity for new investments over the next few years is approximately €13 billion (Phenix Capital, 2024c, page 10). These amounts fall far short of the $174.52 billion per year needed for ocean health (Johansen and Vestvik, 2020).

**Remark 52** *More recently, Ocean 14 Capital raised* €200 *mn for its first SDG 14 fund while Denmark's Navigare Capital is targeting* $650 *mn for its sustainable shipping fund. In November 2023, T Rowe Price and the IFC announced a partnership to launch a blue fund with a target size of* $425 *mn.*

Figure 5.25: Cumulative number of funds targeting the blue ocean economy

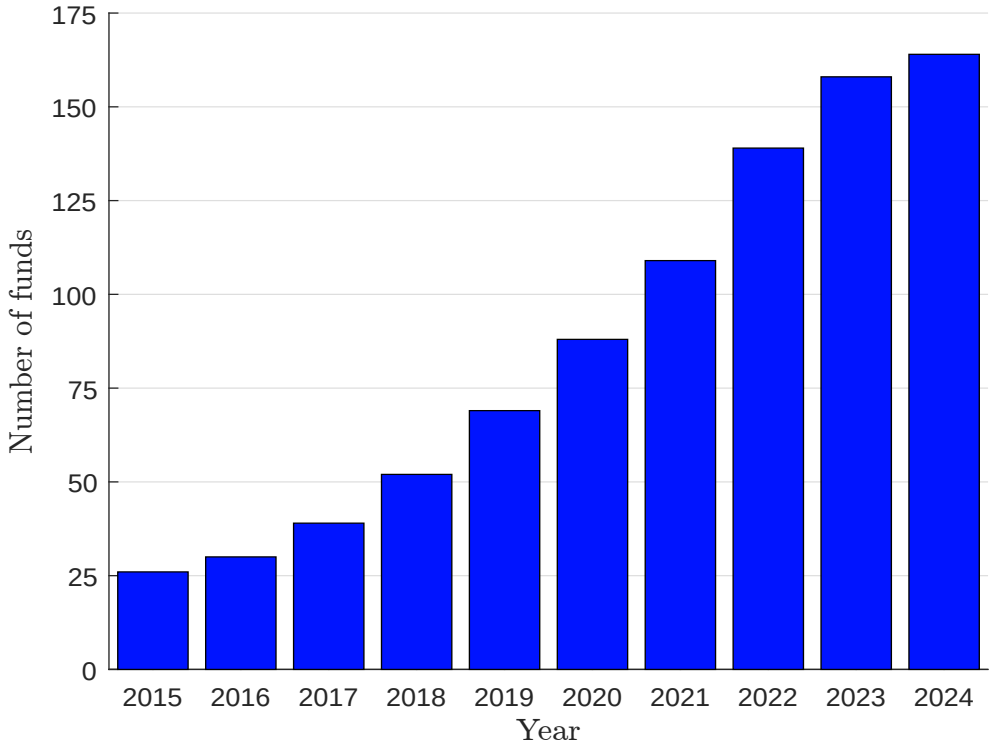


Source: Phenix Capital (2024c, page 11) & Author's calculations.

### Structured blended finance funds

Blended finance was previously introduced on page 309. It's an investment strategy that combines public[45] or philanthropic and private capital to fund projects in emerging and frontier markets. But blended finance goes beyond simple co-investment. Consider a mutual fund with both public institutions and private investors, such as pension funds or insurance companies. This fund may look like blended finance, but it's not. In this case, public and private investors have equal status, and the fund could exist without public participation. True blended finance involves situations where the investment product would not be possible without public involvement. Therefore, the participation of public investors is essential to the product's creation, with a clear distinction between the roles of public and private investors. A key feature of blended finance is its ability to catalyze and leverage private investment by addressing projects that are too risky to be financed by private capital alone. Due to issues such as asymmetric information, moral hazard, and low returns relative to the risks taken, many sustainable projects struggle to attract private investors. Blended finance helps overcome these barriers by ensuring that the risk sharing between private and public investors is not equal. The core idea is that public institutions assume a significant portion of the risk to encourage private capital participation. This differentiated risk-sharing is achieved through structured products, which are central to blended finance. For example, Convergence, the global network for blended finance network, defines it as follows:

> "*Blended finance is a structuring approach that allows organizations with different objectives to invest alongside each other while achieving their own objectives (whether*

[45] In this section, we use the term public investor in a broader sense to include, for example, development finance institutions (DFIs) and multilateral development banks (MDBs).

> *financial return, social impact, or a blend of both). The main investment barriers for private investors addressed by blended finance are (i) high perceived and real risk and (ii) poor returns for the risk relative to comparable investments. Blended finance creates investable opportunities in developing countries which leads to more development impact. Blended finance is not an investment approach, instrument, or end solution. It is also different from impact investing. Impact investing is an investment approach, and impact investors often participate in blended finance structures.*" (Convergence, 2024, https://www.convergence.finance/blended-finance).

Blended finance differs from impact investing for two main reasons. First, impact investing is a broader concept that encompasses a wider range of investment strategies and cannot be reduced to blended finance alone. Second, private investors do not always fit the criteria for impact investing, as they may not be willing to take the same level of risk or prioritize impact as public investors. However, it's important to note that many blended finance deals do indeed qualify as impact investments because of their explicit focus on achieving positive social or environmental outcomes. Therefore, when assessing the nature of a blended finance transaction, it's important to distinguish between the specific deal or project and the motivations of the individual investors involved.

Blended finance belongs to the family of structured finance (structured products, securitization, tranching, credit enhancement). According to Convergence (2024, page 12), there are four main typical blended finance structures:

- Concessional capital
  Public or philanthropic investors provide funds at below-market rates within the capital structure to reduce the overall cost of capital or to provide an additional layer of protection for private investors. The goal is to change the risk/return profile of the investment.

- Credit enhancing
  Public or philanthropic investors provide credit enhancement through guarantees or insurance against specific risks, such as political instability or natural disasters. The purpose of credit enhancing is to reduce the perceived risk of an investment, making it more attractive to private investors.

- Technical assistance facility (TAF)
  Transaction is associated with a grant-funded technical assistance facility that can be utilized pre- or post-investment to strengthen commercial viability and developmental impact. The purpose is to transfer knowledge to the owners of the project in order to make it successful. In practice, a technical assistance facility refers to a dedicated pool of human and capital resources that provide expertise, training, and advisory services to support the successful implementation of projects in developing markets.

- Design-stage grants
  Transaction design or preparation is funded by grants (including project preparation or design-stage grants). Therefore, they correspond to non-repayable funds provided in the early stages of a project to support its planning, structuring and preparation, or to cover the initial costs of project design to ensure that the project is viable and sustainable.

The distinction between the first two categories is somewhat arbitrary. Both categories aim to mitigate investment risk[46] or modify the risk-return profile. Within these categories, blended finance

[46] For example, credit enhancement can be used to obtain a better credit rating.

Box 5.5: Tranching technique and collateralized debt obligation

A collateralized debt obligation (CDO) is a pay-through ABS structure whose securities are bonds linked to a series of tranches. In the example below, there are 4 types of bonds, whose return depends on the loss of the corresponding tranche (equity, mezzanine, senior and super senior). Each tranche is characterized by an attachment point $A$ and a detachment point $D$. In our example, we have:

| Tranche | Equity | Mezzanine | Senior | Super senior |
|---|---|---|---|---|
| $A$ | 0% | 15% | 25% | 35% |
| $D$ | 15% | 25% | 35% | 100% |

The protection buyer of the tranche $[A, D]$ pays the protection seller a coupon rate on the outstanding principal amount of the tranche. In return, the protection buyer receives the protection leg, which is the loss on the tranche. However, the losses are subject to a payment priority, which is as follows:

- The equity tranche is the most risky security, which means that the first losses will hit this tranche alone until the cumulative loss reaches the detachment point;
- When the portfolio loss is greater than the detachment point of the equity tranche, the equity tranche ceases to exist and the protection seller of the mezzanine tranche will pay the next losses to the protection buyer of the mezzanine tranche;
- The protection buyer of a tranche pays the coupon from the inception of the CDO until the death of the tranche, *i.e.*, when the cumulative loss is greater than the detachment point of the tranche;

Figure 5.A: Structure of a collateralized debt obligation

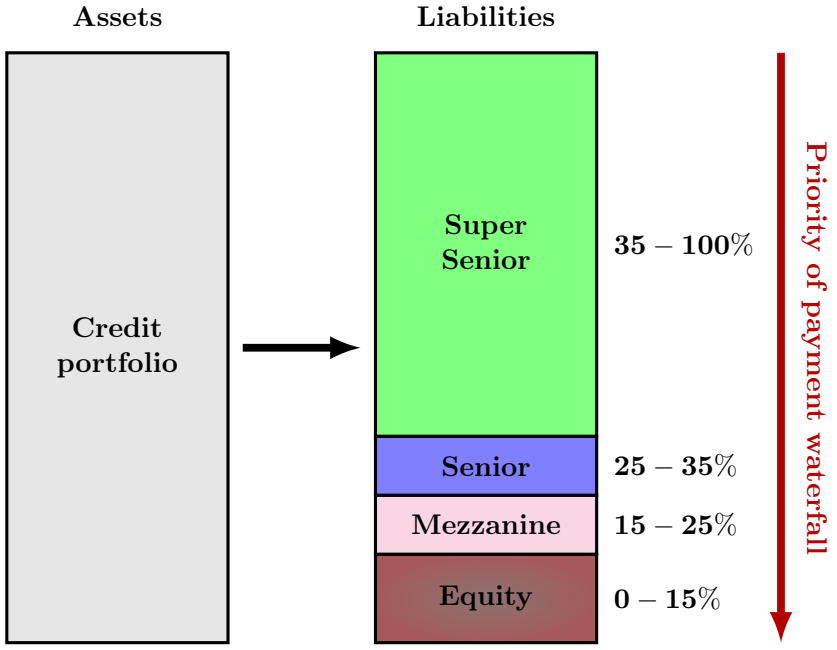


Source: Roncalli (2020a, pages 155-156).

can offer concessional loans, use tranching techniques to create a junior/mezzanine/senior liability structure, propose subordinated loans, provide junior equity, and offer first-loss guarantees. Similarly, the difference between the last two categories is somewhat arbitrary. Both categories focus on ensuring the success of the project. For example, public organizations may provide technical experts to assist with project development or financial experts to assess the project's potential to attract private investors.

Certainly, the most best-known blended finance products are based on the tranching technique that has gained popularity through credit securitization, asset-backed securities, and collateralized debt obligations (see Box 5.5). The concept of tranching involves creating multiple risk/return profiles from a single collateral pool of assets. In the case of a portfolio of defaultable loans, the senior tranche would offer a lower return compared to the equity tranche because the credit risk of the senior tranche is lower than that of the equity tranche. When applied to blended finance, the collateral pool could consist of a portfolio of projects, a basket of green bonds, or a set of credit loans. An example of a tranched product is the European Energy Efficiency fund (eeef), a Luxembourg-based alternative investment fund focused on financing energy efficiency, small-scale renewable energy and clean urban transport projects[47]. These projects typically involve municipalities, public authorities and public-private partnerships. The eeef provides a range of financial instruments, including equity, debt and mezzanine financing, and may use concessional capital. A summary of the eeef investment structure is shown in Figure 5.26.

Figure 5.26: The eeef investment structure

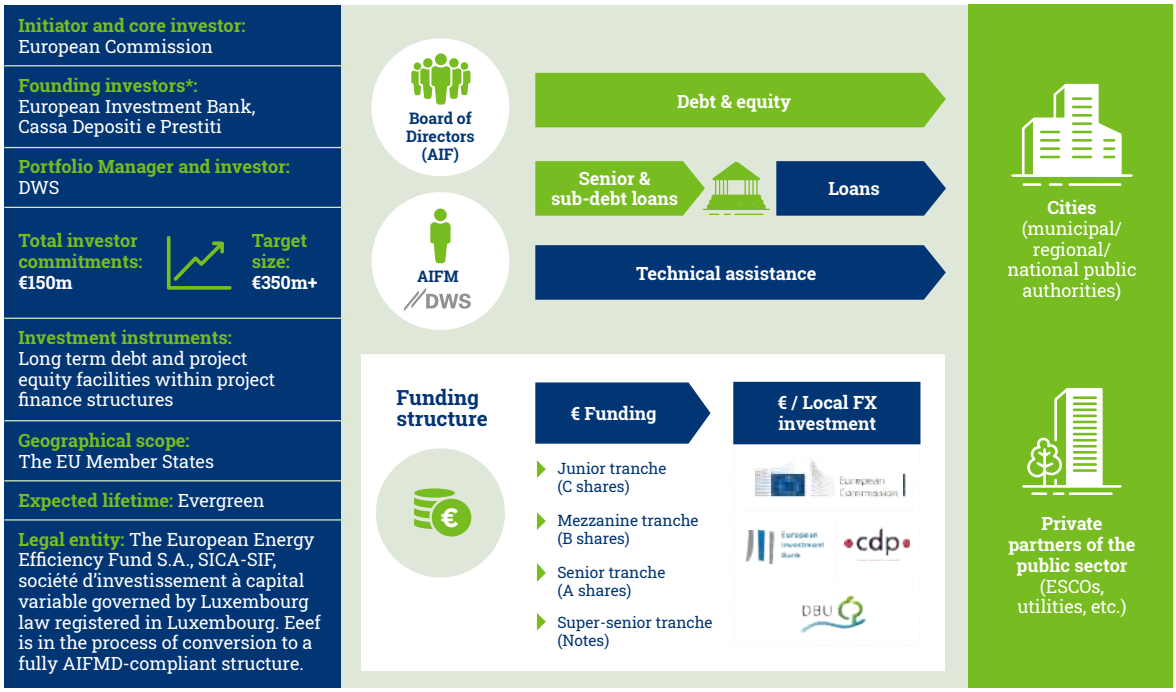


Source: Eurosif (2021, Figure 7, page 26).

Another example of a tranching product is the AP EGO fund (Amundi Planet Emerging Green One), a joint creation of Amundi and the IFC (Bolton *et al.*, 2020). The fund invests in emerging market (EM) green bonds in both primary and secondary markets and is structured as a CDO fund,

[47]The fund's website is `www.eeef.lu`.

with the IFC providing credit enhancement to mitigate specific investor risks. The senior tranche accounts for 90% of the fund's portfolio, with the remaining 10% split between the first-loss junior tranche (6.25%) and the mezzanine tranche (3.75%). The AP EGO fund is currently the largest EM green bond fund. This innovative fund aims to address two key challenges that have prevented financiers from scaling up infrastructure investment in emerging markets: first, how to mitigate sovereign credit risk in these regions, and second, how to generate sufficient supply of EM green bonds to meet demand from institutional investors in developed markets.

Let us see how a tranching product of blended finance works. To do this, we use part of the mathematical framework for pricing a CDO tranche (Roncalli, 2020a, page 157). Given an investment portfolio of $n$ bonds, the cumulative loss of the portfolio at time $t$ is equal to:

$$L_t = \sum_{i=1}^{n} N_i \cdot (1 - \mathcal{R}_i) \cdot \mathbb{1}\{\boldsymbol{\tau}_i \leq t\}$$

where $N_i$, $\mathcal{R}_i$ and $\boldsymbol{\tau}_i$ are the nominal amount, the recovery rate and the default time of bond $i$. The loss of tranche $[A, D]$ is given by:

$$L_t^{[A,D]} = (L_t - A) \cdot \mathbb{1}\{A \leq L_t \leq D\} + (D - A) \cdot \mathbb{1}\{L_t > D\}$$

where $A$ and $D$ are the attachment and detachment points expressed in \$. The outstanding notional amount of the tranche is therefore:

$$N_t^{[A,D]} = (D - A) - L_t^{[A,D]}$$

This notional amount is then reduced by the loss of the tranche. At inception date $t = 0$, $N_t^{[A,D]}$ is equal to the tranche thickness $D - A$. At the fixing date $t$, we have:

$$N_t^{[A,D]} = \begin{cases} D - A & \text{if} \quad L_t \leq A \\ D - L_t & \text{if} \quad A \leq L_t \leq D \\ 0 & \text{if} \quad L_t > D \end{cases}$$

We now define the income of each tranche. The gain between two fixing dates $t - 1$ and $t$ is equal to:

$$\Delta\Pi_t = \sum_{i=1}^{n} \boldsymbol{c}_i \cdot N_i \cdot \mathbb{1}\{\boldsymbol{\tau}_i > t\}$$

where $\boldsymbol{c}_i$ is the (fixed) coupon paid by bond $i$ between $t - 1$ and $t$. The cumulative profit generated by the portfolio at time $t$ is then equal to $\Pi_t = \Pi_{t-1} + \Delta\Pi_t$ where $\Pi_0 = 0$. At this stage, we need to define the revenue sharing policy between the different tranches:

$$\Delta\Pi_t^{[A,D]} = \varphi^{[A,D]}(\Delta\Pi_t)$$

In general, the gain for tranche $[A, D]$ depends on the total income $\Delta\Pi_t$ of the portfolio and the pricing formula $\varphi^{[A,D]}$. The cumulative profit of tranche $[A, D]$ is then $\Pi_t^{[A,D]} = \Pi_{t-1}^{[A,D]} + \Delta\Pi_t^{[A,D]}$ where $\Pi_0^{[A,D]} = 0$. We deduce that the cumulative return of the tranche is equal to:

$$R_t^{[A,D]} = \frac{\Pi_t^{[A,D]} - L_t^{[A,D]}}{D - A}$$

This is the difference between the income and the loss of the tranche. Finally, the average return is $\bar{R}_t^{[A,D]} = \frac{1}{t} R_t^{[A,D]}$.

**Example 21** *Consider a simple blended finance fund where the junior and senior tranches account for 20% and 80% of the investment, respectively. The total fund size is \$500 million, invested equally in 100 emerging market (EM) green bonds. We assume that these green bonds are homogeneous, each paying an annual coupon of 10%. The recovery rate is set to zero. To define the income distribution policy, the senior tranche receives an annual coupon of 4% until the junior tranche is exhausted, while the junior tranche receives the remaining income generated by the bond portfolio. Finally, the maturity of the fund is set at ten years.*

Let us apply the previous mathematical framework to this example. For the junior tranche, the attachment and detachment points are 0 and \$100 mn. For the senior tranche, the attachment and detachment points are \$100 mn and \$500 mn. We have $N_i = \$5$ mn, $\mathcal{R}_i = 0$ and $\boldsymbol{c}_i = 10\%$. Let $n_t^{\boldsymbol{\tau}} = \sum_{i=1}^{n} \mathbb{1}\{\boldsymbol{\tau}_i \leq t\}$ be the cumulative number of defaults. We deduce that[48]:

$$\begin{cases} L_t = \sum_{i=1}^{100} 5 \times (1-0) \times \mathbb{1}\{\boldsymbol{\tau}_i \leq t\} = 5n_t^{\boldsymbol{\tau}} \\ L_t^{(\text{junior})} = \min\left(5n_t^{\boldsymbol{\tau}}, 100\right) \\ L_t^{(\text{senior})} = \max\left(5n_t^{\boldsymbol{\tau}} - 100, 0\right) \end{cases}$$

The outstanding notional amount of the junior tranche is:

$$N_t^{(\text{junior})} = 100 - L_t^{(\text{junior})} = \max\left(100 - 5n_t^{\boldsymbol{\tau}}, 0\right)$$

For the senior tranche, we get:

$$N_t^{(\text{senior})} = 400 - L_t^{(\text{senior})} = \min\left(500 - 5n_t^{\boldsymbol{\tau}}, 400\right)$$

The income generated by the bond portfolio is:

$$\Delta\Pi_t = \sum_{i=1}^{100} 10\% \times 5 \times \mathbb{1}\{\boldsymbol{\tau}_i > t\} = 0.5\left(100 - n_t^{\boldsymbol{\tau}}\right)$$

The maximum annual income is \$50 mn. If there are 20 defaults, $\Delta\Pi_t = \$40$ mn is sufficient to pay the guaranteed income for the senior tranche, which is equal to $400 \times 4\% = \$16$ mn. We deduce that:

$$\Delta\Pi_t^{(\text{senior})} = \varphi^{(\text{senior})}\left(\Delta\Pi_t\right) = 16 \times \mathbb{1}\{n_t^{\boldsymbol{\tau}} \leq 20\} + \Delta\Pi_t \times \mathbb{1}\{n_t^{\boldsymbol{\tau}} > 20\}$$

and:

$$\Delta\Pi_t^{(\text{junior})} = \varphi^{(\text{junior})}\left(\Delta\Pi_t\right) = \Delta\Pi_t - \Delta\Pi_t^{(\text{senior})} = \left(\Delta\Pi_t - 16\right) \times \mathbb{1}\{n_t^{\boldsymbol{\tau}} \leq 20\}$$

We have all the formulas to perform a simulation of the blended finance fund.

Table 5.18 shows the results for three different scenarios. In the first scenario, the number of annual defaults over the ten-year period is 0, 1, 1, 0, 2, 1, 0, 1, 1, and 1. In this low-risk scenario, the total performance of the fund over the ten-year period is 8.80%. The junior tranche returns 28% and the senior tranche returns 4%. However, this scenario is considered unrealistic due to the low number of defaults relative to the 10% coupon level. The second scenario is more realistic, with an average annual default rate of 4.10%. In this scenario, the junior tranche pays 1.00% while the senior tranche pays 3.92%. The third scenario shows that the senior tranche can exceed a return of 4%. This is because the junior tranche is exhausted after four years, leaving the senior tranche exposed to credit risk from the fourth year onward. However, because fewer defaults occur between years four and ten, the senior tranche benefits from the high yield of green bonds and the lower default rate. As a result, the senior tranche achieves a return of 5.14% over the life of the fund.

Table 5.18: Simulation of the blended finance fund

| | $t$ | $n_t^{\mathcal{T}}$ | $L_t$ | $L_t^{(\text{junior})}$ | $L_t^{(\text{senior})}$ | $\Delta\Pi_t$ | $\Delta\Pi_t^{(\text{junior})}$ | $\Delta\Pi_t^{(\text{senior})}$ | $\Pi_t$ | $\Pi_t^{(\text{junior})}$ | $\Pi_t^{(\text{senior})}$ | $\bar{R}_t$ | $\bar{R}_t^{(\text{junior})}$ | $\bar{R}_t^{(\text{senior})}$ |
|---|---|---|---|---|---|---|---|---|---|---|---|---|---|---|
| Scenario #1 | 1 | 0 | 0.0 | 0.0 | 0.0 | 50.0 | 34.0 | 16.0 | 50.0 | 34.0 | 16.0 | 10.00% | 34.00% | 4.00% |
| | 2 | 1 | 5.0 | 5.0 | 0.0 | 49.5 | 33.5 | 16.0 | 99.5 | 67.5 | 32.0 | 9.45% | 31.25% | 4.00% |
| | 3 | 2 | 10.0 | 10.0 | 0.0 | 49.0 | 33.0 | 16.0 | 148.5 | 100.5 | 48.0 | 9.23% | 30.17% | 4.00% |
| | 4 | 2 | 10.0 | 10.0 | 0.0 | 49.0 | 33.0 | 16.0 | 197.5 | 133.5 | 64.0 | 9.38% | 30.88% | 4.00% |
| | 5 | 4 | 20.0 | 20.0 | 0.0 | 48.0 | 32.0 | 16.0 | 245.5 | 165.5 | 80.0 | 9.02% | 29.10% | 4.00% |
| | 6 | 5 | 25.0 | 25.0 | 0.0 | 47.5 | 31.5 | 16.0 | 293.0 | 197.0 | 96.0 | 8.93% | 28.67% | 4.00% |
| | 7 | 5 | 25.0 | 25.0 | 0.0 | 47.5 | 31.5 | 16.0 | 340.5 | 228.5 | 112.0 | 9.01% | 29.07% | 4.00% |
| | 8 | 6 | 30.0 | 30.0 | 0.0 | 47.0 | 31.0 | 16.0 | 387.5 | 259.5 | 128.0 | 8.94% | 28.69% | 4.00% |
| | 9 | 7 | 35.0 | 35.0 | 0.0 | 46.5 | 30.5 | 16.0 | 434.0 | 290.0 | 144.0 | 8.87% | 28.33% | 4.00% |
| | 10 | 8 | 40.0 | 40.0 | 0.0 | 46.0 | 30.0 | 16.0 | 480.0 | 320.0 | 160.0 | 8.80% | 28.00% | 4.00% |
| Scenario #2 | 1 | 6 | 30.0 | 30.0 | 0.0 | 47.0 | 31.0 | 16.0 | 47.0 | 31.0 | 16.0 | 3.40% | 1.00% | 4.00% |
| | 2 | 10 | 50.0 | 50.0 | 0.0 | 45.0 | 29.0 | 16.0 | 92.0 | 60.0 | 32.0 | 4.20% | 5.00% | 4.00% |
| | 3 | 16 | 80.0 | 80.0 | 0.0 | 42.0 | 26.0 | 16.0 | 134.0 | 86.0 | 48.0 | 3.60% | 2.00% | 4.00% |
| | 4 | 20 | 100.0 | 100.0 | 0.0 | 40.0 | 24.0 | 16.0 | 174.0 | 110.0 | 64.0 | 3.70% | 2.50% | 4.00% |
| | 5 | 25 | 125.0 | 100.0 | 25.0 | 37.5 | 0.0 | 37.5 | 211.5 | 110.0 | 101.5 | 3.46% | 2.00% | 3.82% |
| | 6 | 30 | 150.0 | 100.0 | 50.0 | 35.0 | 0.0 | 35.0 | 246.5 | 110.0 | 136.5 | 3.22% | 1.67% | 3.60% |
| | 7 | 32 | 160.0 | 100.0 | 60.0 | 34.0 | 0.0 | 34.0 | 280.5 | 110.0 | 170.5 | 3.44% | 1.43% | 3.95% |
| | 8 | 36 | 180.0 | 100.0 | 80.0 | 32.0 | 0.0 | 32.0 | 312.5 | 110.0 | 202.5 | 3.31% | 1.25% | 3.83% |
| | 9 | 40 | 200.0 | 100.0 | 100.0 | 30.0 | 0.0 | 30.0 | 342.5 | 110.0 | 232.5 | 3.17% | 1.11% | 3.68% |
| | 10 | 41 | 205.0 | 100.0 | 105.0 | 29.5 | 0.0 | 29.5 | 372.0 | 110.0 | 262.0 | 3.34% | 1.00% | 3.92% |
| Scenario #3 | 1 | 4 | 20.0 | 20.0 | 0.0 | 48.0 | 32.0 | 16.0 | 48.0 | 32.0 | 16.0 | 5.60% | 12.00% | 4.00% |
| | 2 | 7 | 35.0 | 35.0 | 0.0 | 46.5 | 30.5 | 16.0 | 94.5 | 62.5 | 32.0 | 5.95% | 13.75% | 4.00% |
| | 3 | 10 | 50.0 | 50.0 | 0.0 | 45.0 | 29.0 | 16.0 | 139.5 | 91.5 | 48.0 | 5.97% | 13.83% | 4.00% |
| | 4 | 20 | 100.0 | 100.0 | 0.0 | 40.0 | 24.0 | 16.0 | 179.5 | 115.5 | 64.0 | 3.98% | 3.88% | 4.00% |
| | 5 | 24 | 120.0 | 100.0 | 20.0 | 38.0 | 0.0 | 38.0 | 217.5 | 115.5 | 102.0 | 3.90% | 3.10% | 4.10% |
| | 6 | 27 | 135.0 | 100.0 | 35.0 | 36.5 | 0.0 | 36.5 | 254.0 | 115.5 | 138.5 | 3.97% | 2.58% | 4.31% |
| | 7 | 29 | 145.0 | 100.0 | 45.0 | 35.5 | 0.0 | 35.5 | 289.5 | 115.5 | 174.0 | 4.13% | 2.21% | 4.61% |
| | 8 | 30 | 150.0 | 100.0 | 50.0 | 35.0 | 0.0 | 35.0 | 324.5 | 115.5 | 209.0 | 4.36% | 1.94% | 4.97% |
| | 9 | 33 | 165.0 | 100.0 | 65.0 | 33.5 | 0.0 | 33.5 | 358.0 | 115.5 | 242.5 | 4.29% | 1.72% | 4.93% |
| | 10 | 34 | 170.0 | 100.0 | 70.0 | 33.0 | 0.0 | 33.0 | 391.0 | 115.5 | 275.5 | 4.42% | 1.55% | 5.14% |

Figure 5.27: Probability density function of the average returns $\bar{R}_{10}$, $\bar{R}_{10}^{(\text{junior})}$ and $\bar{R}_{10}^{(\text{senior})}$ (in %)

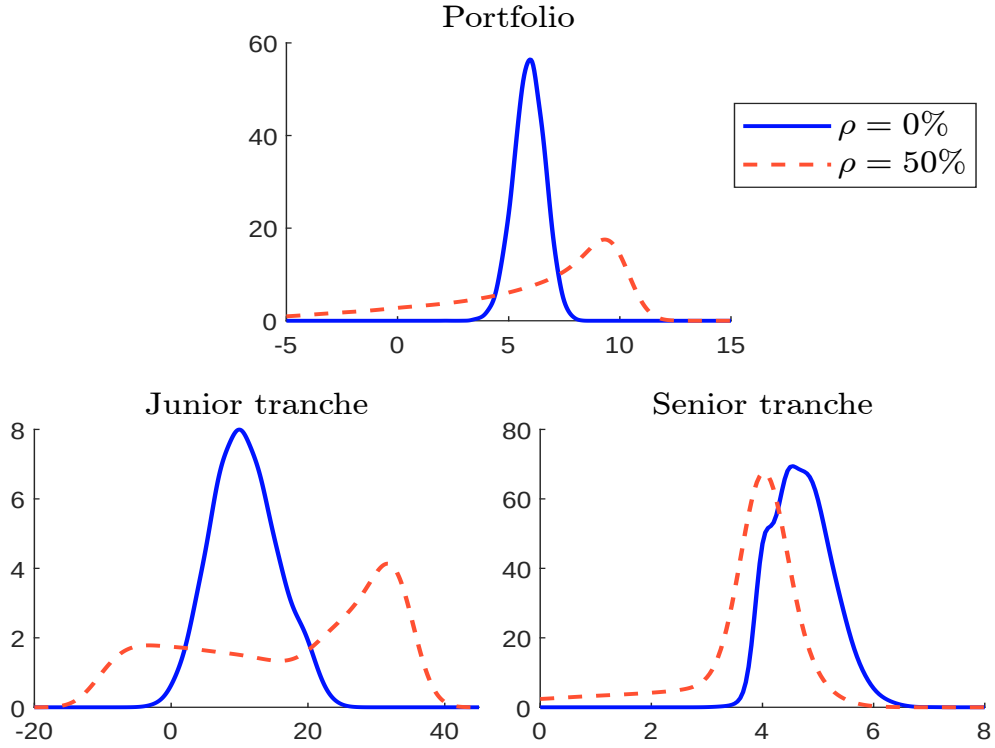


In practice, the fund manager performs Monte Carlo simulations to calibrate the income-sharing policy and to discuss with public and private investors the risk/return profile of each tranche. Assuming exponential default times with an intensity of 300 bps and correlated by a Gaussian copula with uniform correlation $\rho$, Figure 5.27 illustrates the results of 20 000 Monte Carlo simulations[49]. For the overall portfolio, an expected average return of 5.9% is observed, independent of $\rho$. However, the probability distribution of returns is significantly affected by $\rho$. In particular, the density function of $\bar{R}_t$ is left-skewed when $\rho = 50\%$. The expected average return of the junior tranche is 10.7% when $\rho = 0\%$ and increases to 16.8% when $\rho = 50\%$. While a high correlation between default times improves the junior tranche's performance, it also increases its risk since the probability of a negative return becomes more significant[50]. Conversely, the expected average return of the senior tranche decreases from 4.7% to 3.2% as $\rho$ increases from 0% to 50%. This indicates that a higher correlation between default times can negatively impact the performance of the senior tranche.

[48] In the following we use the following properties: $\min(a,b) \pm c = \min(a \pm c, b \pm c)$, $\max(a,b) \pm c = \max(a \pm c, b \pm c)$, $-\min(a,b) = \max(-a,-b)$ and $-\max(a,b) = \min(-a,-b)$. We deduce that $a - \min(b,c) = a + \max(-b,-c) = \max(a-b, a-c)$ and $a - \max(b,c) = a + \min(-b,-c) = \min(a-b, a-c)$.

[49] In this Monte Carlo exercise, the default times $(\boldsymbol{\tau}_1, \ldots, \boldsymbol{\tau}_n)$ are simulated with the following algorithm. First we simulate the Gaussian vector $(x_1, \ldots, x_n)$ with $x_i = \sqrt{\rho}\,\varepsilon_0 + \sqrt{1-\rho}\,\varepsilon_i$ where $(\varepsilon_0, \varepsilon_1, \ldots, \varepsilon_n)$ are $n+1$ independent normal random variates $\mathcal{N}(0,1)$. The simulated values of the Gaussian copula are then $(u_1, \ldots, u_n)$ with $u_i = \Phi(x_i)$. Finally, the simulated default times are generated using the inverse of the probability integral transform: $\boldsymbol{\tau}_i = -\ln(1-u_i)/\lambda_i$ where $\lambda_i = 300$ bps is the intensity parameter of the exponential distribution.

[50] Below is the probability of observing negative performance:

| | Portfolio | Junior | Senior |
|---|---|---|---|
| $\rho = 0\%$ | 0.0% | 0.3% | 0.0% |
| $\rho = 50\%$ | 11.4% | 19.1% | 8.7% |

Figure 5.28: Growth of blended finance activities

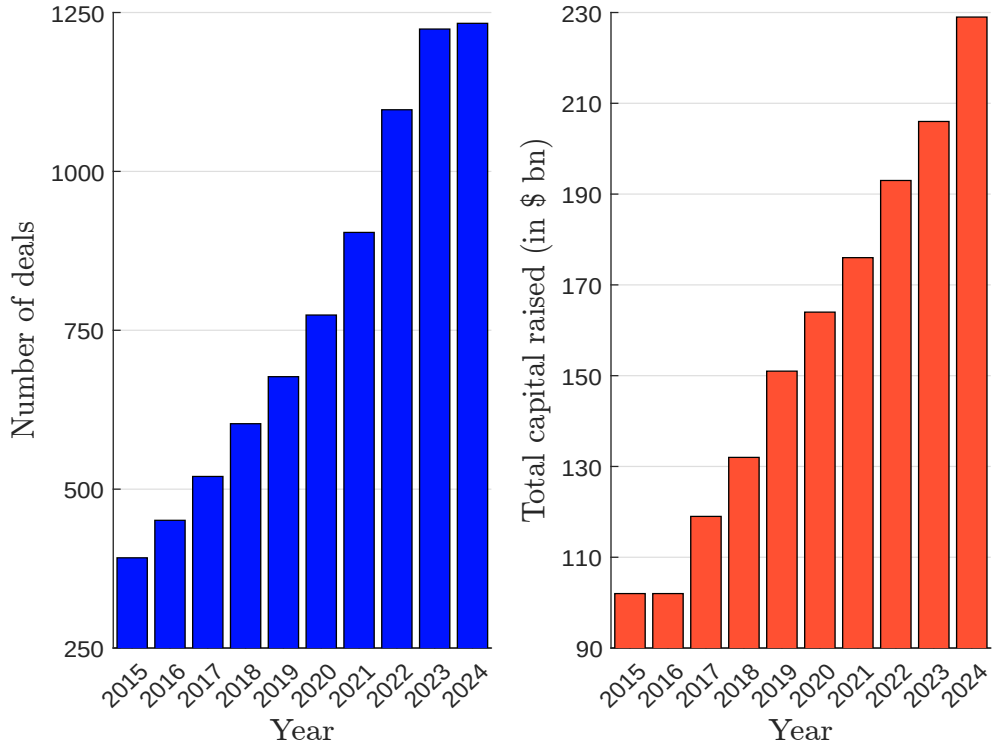


Source: Convergence (2024), www.convergence.finance/blended-finance & Author's calculations.

Convergence (2024) reports that blended finance has mobilized $230 billion for sustainable development in developing countries by June 2024 (Figure 5.28). This figure represents 1 200 transactions with a median deal size of $64 million. While most transactions (70%) are concessional loans, enhancing credit and technical assistance account for 25% each. Geographically, sub-Saharan Africa dominates the market with 50% of transactions, followed by Asia (27%) and Latin America (17%). However, the market is skewed towards smaller deals, with 35% of transactions under $25 million and only 15% exceeding $250 million. In terms of sectors, energy, financial services, and agriculture each account for more than 20% of blended finance transactions. In terms of investors, Convergence (2024) notes that 65% of blended finance investors are from the private sector, but the majority have only participated in one blended finance transaction. The public and philanthropic sectors represent 19% and 16% of investors, respectively. The most active public investors are the International Finance Corporation (IFC), the Netherlands Development Finance Company (FMO), the US International Development Finance Corporation (DFC), the US Agency for International Development (USAID), and the European Investment Bank (EIB), while the top philanthropic investors include the Shell Foundation, the Bill & Melinda Gates Foundation, the Omidyar Network, Oikocredit, and the Rockefeller Foundation.

### Microfinance funds

The most emblematic product in the impact investing universe is undoubtedly the microfinance fund. A microfinance fund is a financial vehicle that provides capital and other financial services to low-income individuals and businesses, often in developing countries. The goal of microfinance funds is to help these groups access financial resources that they might not otherwise be able to

obtain from traditional banks due to a lack of credit history, collateral or debt market structure. As a result, microfinance funds typically provide microloans, which are small amounts of capital. They focus on amounts in the thousands rather than millions of dollars.

Figure 5.29: SDGs targeted by microfinance

Microfinance funds are part of the microfinance ecosystem, which is a complex and large financial system that includes traditional banks[51], microfinance institutions (MFIs), non-banking financial companies, philanthropic investors, etc. Microfinance has an important role to play in advancing several of the SDGs. The key SDGs targeted by microfinance are:

- SDG 1 No Poverty
  Microfinance can help individuals and businesses escape poverty by giving them access to credit, savings and other financial services. This can enable them to start or grow their businesses, increase their incomes, create jobs and improve their livelihoods.
- SDG 2 Zero Hunger
  Microfinance can support smallholder farmers and food producers by providing them with loans to purchase seeds, fertilizers and equipment. This can help them increase agricultural productivity and food security. This is particularly important in rural areas where hunger is more prevalent.
- SDG 5 Gender Equality
  Microfinance institutions often focus on women, who are disproportionately affected by poverty and exclusion from financial systems. This can help them start their own businesses, become financially independent, and participate more fully in the economy.
- SDG 8 Decent Work and Economic Growth
  Microfinance can promote decent work and economic growth by providing individuals and businesses with the financial resources they need to create jobs and generate income. This can contribute to economic development and improved living standards.
- SDG 10 Reduced Inequality
  Microfinance can help reduce inequalities by providing financial services to marginalized groups, including the poor, women and rural communities, who often lack access to traditional banking services.

According to the World Bank's Global Financial Inclusion (Global Findex) Database 2021, approximately 1.4 billion adults worldwide remain unbanked or excluded from formal banking services[52]. The majority of the unbanked population is concentrated in developing regions, particularly in sub-Saharan Africa, South Asia, and parts of Latin America and Southeast Asia. Two segments of the

[51] For example, the reader can consult the 2024 Microfinance Social Performance Report, supported by BNP Paribas, available at https://group.bnpparibas/uploads/file/2024_bnp_paribas_microfinance_social_report.pdf.
[52] Source: www.worldbank.org/en/publication/globalfindex.

population are particularly affected. Women and people living in rural areas are more likely to be unbanked than men and people living in urban areas. This explains the importance of SDG 5 and SDG 10 in microfinance.

According to the *MicroFinance Global Strategic Business Report*, the global microfinance market was valued at approximately $224.6 billion in 2023. Projections indicate substantial growth, reaching $506.0 billion by 2030, with an annual growth rate of 12.3% during this period. These estimates are slightly higher than those reported by ATLAS, which valued the total market at $182.7 billion in 2022, serving 173 million borrowers[53]. Based on these figures, the average microfinance loan size in ATLAS's data was approximately $1 050. Data on microfinance funds is more difficult to obtain. However, we can use the classification of private debt funds in the Phenix impact database to assess this market:

> "*Private debt, also known as private credit, are loans made to companies that are not provided by banks or public markets. These private market investments can range in size and scale and be implemented in different forms, such as direct lending*[54]*, mezzanine finance*[55]*, and microcredit*[56]." (Phenix Capital, 2023, pages 6 & 31).

As explained by Phenix Capital (2024d, page 6), the private debt sector is often too small to qualify for loans from banks or public markets, but too large for microfinance organizations. As a result, the average loan size in microfinance funds is higher than in MFIs.

Table 5.19: Frequency of private debt funds per targeted region

| Region | Africa | Asia | Latam | Europe | Middle East | North America | Oceania |
|---|---|---|---|---|---|---|---|
| Frequency (in %) | 30.7 | 23.9 | 20.8% | 19.5 | 4.1 | 13.7 | 1.8 |

Source: Phenix Capital (2024d, page 12) & Author's calculations.

According to Phenix Capital (2024d), the estimated size of the private debt impact fund market is € 50 billion, with 394 funds managed by 218 asset managers. Of these funds, 70% are focused on emerging markets. Africa accounts for more than 30% of fund investments, followed by Asia, Latin America and Europe with approximately 20% each. A key difference between developed and emerging markets lies in the types of impact metrics used by private debt impact funds. Funds investing in developed markets prioritize (E) metrics more, allocating 70% to them and 30% to (S) metrics. In contrast, funds investing in emerging markets emphasize social metrics more, with a breakdown of 57% (S) metrics and 43% (E) metrics. Foundations, philanthropic investors, and development finance institutions are the primary sources of funding for private debt impact funds. Microfinance asset managers are specialized and distinct from the traditional asset management industry. Leading examples include BlueOrchard Finance (Switzerland), ResponsAbility Investments AG (Switzerland), Triodos Investment Management (Netherlands), Symbiotics (Switzerland), Oikocredit (Sweden), Incofin IM (Belgium), Developing World Markets (United States), Finance in Motion (Germany), Triple Jump (Netherlands), MicroVest Capital Management (United States) and Regmifa (Regional MSME Investment Fund for Sub-Saharan Africa).

[53] Source: www.atlasdata.org & *Impact Finance Barometer 2023* (www.convergences.org/publications).

[54] A specialised form of private debt, in which loans are made to middle-market companies. It is the private debt strategy with lower risk, achieved by using collateral.

[55] A specialised form of financing in which loans are subordinated to banks, with no collateral. It is the most equity-like form of private debt.

[56] A common form of microfinance, characterised by small loans to individuals or small companies.

## 5.4 An example with the biodiversity risk

Biodiversity has become an important issue in the ESG financial community in recent years. For example, the SFDR's mandatory principal adverse impact indicator on biodiversity (PAI 7) requires companies to disclose activities that negatively impact biodiversity sensitive areas[57], the sixth economic objective of the EU green taxonomy is the protection and restoration of biodiversity and ecosystems[58] while the ESRS E4 category of the CSRD is named biodiversity and ecosystems[59]. In this context, where biodiversity is an important issue in sustainable finance regulations, it was obvious that investors wanted to develop biodiversity products or manage investments with respect to biodiversity risks and they have done so. And this is certainly just the beginning. When we talk about biodiversity, the two words that come to mind are risk and impact. It's easy to take the shortcut that an investment that takes biodiversity into account is an investment with impact, but does that mean it falls into the category of impact investing? Generally not, because there is a significant difference between investing in assets that carry biodiversity risks and investing with the goal of having a positive impact on biodiversity. To understand this distinction between investing with impact and investing for impact, it is important to first define what biodiversity really means[60].

Box 5.6: Edward O. Wilson

Edward O. Wilson (1929–2021) was a renowned American biologist, naturalist, ecologist, and entomologist. He is widely regarded as one of the greatest natural scientists of our time and is often referred to as the father of biodiversity. He received his B.S. and M.S. in biology from the University of Alabama and his Ph.D. in biology from Harvard University in 1955. The author of more than 400 scientific articles from 1950 to 2005, he has written numerous influential books, including *The Theory of Island Biogeography* (1967), *Sociobiology* (1975), *On Human Nature* (1979), and *The Diversity of Life* (1992), which have had a profound impact on the fields of biology and ecology. In 1988, he co-edited the first book on biodiversity with Frances Peter.

Figure 5.B: Cover of the book *Tales from the Ant World*

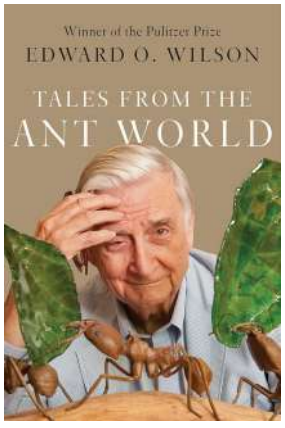


[57] See Section 1.4.3 on page 36 and Table 1.8 on page 38.
[58] See Section 1.4.1 on page 33.
[59] See Section 1.4.5 on page 39.
[60] This section is based on the textbook *Biodiversity: An Introduction* written by Kevin Gaston and John Spicer and the scientific book *Conservation Biology for All* edited by Navjot Sodhi and Paul Ehrlich. *Essentials of Conservation Biology* by Richard Primack is another reference book, but it is more advanced and technical.

### 5.4.1 Definition

We have already talked about biodiversity in Chapter 2, between the pages 62 and 65. Biodiversity, or biological diversity, refers to the variety and variability of life on Earth in all its many manifestations. According to Gaston and Spicer (2004), it is a broad, unifying concept that encompasses all forms, levels, and combinations of natural variation at all levels of biological organization. For example, it includes genetic diversity within species, the diversity of species in different habitats, and the diversity of ecosystems themselves. In other words, biodiversity encompasses all living organisms, from the smallest bacteria to the largest mammals, and the complex relationships and interactions among them. In addition, biodiversity is essential to the health of ecosystems, providing critical services such as air and water purification, crop pollination, climate regulation and food production.

**Remark 53** *In the scientific world, biodiversity is generally associated with conservation biology, the scientific discipline dedicated to understanding and preserving biodiversity and protecting ecosystems. This field emerged in response to the rapid loss of biodiversity due to human activities such as habitat destruction, pollution, and climate change. Biodiversity and conservation biology are therefore closely related, which is why many master's programs use both the term biodiversity and conservation biology.*

#### Key components of biodiversity

There are several ways to assess and measure biodiversity. In general, we consider three building blocks:

1. Genetic diversity
   This refers to the variety of genes within a species, such as different varieties of rice. Genetic diversity is essential for the survival and adaptability of species, allowing them to evolve in response to changing conditions.

2. Organismal (or species) diversity
   This refers to the variety of species in a given area or ecosystem. It includes the number of different species (species richness), the relative abundance of each species (species evenness), and variation in the distribution of species in space (beta diversity or species density). A greater number of species indicates greater biodiversity and generally contributes to more resilient ecosystems that are able to maintain their functionality after environmental changes.

3. Ecological (or ecosystem) diversity
   This refers to the variety of ecosystems in a region, including different habitats, biological communities, and ecological processes. Ecosystem diversity includes forests, grasslands, wetlands, deserts, marine environments, etc. This element is essential for maintaining the range of ecological processes that support life, such as nutrient cycling, energy flow, and climate regulation.

In Table 5.21 we reproduce the different elements of the three building blocks, which are organized in nested hierarchies with higher and lower order elements (Gaston, 2010, pages 27-32). Some elements are specific to a given building block, *e.g.*, nucleotides belong to the genetic diversity cluster, while other elements may be shared by two or three building blocks, *e.g.*, individuals belong to both the genetic diversity and species diversity clusters. In addition to these three building blocks, we can consider other dimensions of biodiversity, such as functional diversity[61] or temporal diversity[62].

[61] Functional diversity refers to the range of different functions or roles that species play within an ecosystem.

[62] Temporal diversity refers to changes in biodiversity over time, including seasonal variations, successional changes in ecosystems, and long-term evolutionary processes.

Table 5.20: Elements of biodiversity

| Ecological diversity | Genetic diversity | Organismal diversity |
|---|---|---|
| Biogeographic realms | | Domains or Kingdoms |
| Biomes | | Phyla |
| Provinces | | Families |
| Ecoregions | | Genera |
| Ecosystems | | Species |
| Habitats | | Subspecies |
| Populations | Populations | Populations |
| | Individuals | Individuals |
| | Chromosomes | |
| | Genes | |
| | Nucleotides | |

Source: Heywood (1995) & Gaston (2010, Table 2.1, page 27).

**Genetic diversity** Genetic (or genomic) diversity can be assessed at different structural levels: nucleotides, genes, or chromosomes. Thus, we can measure genetic diversity by nucleotide[63] differences, allelic diversity (average number of alleles per locus), gene diversity or polymorphism (proportion of polymorphic loci[64] across the genome), and heterozygosity[65].

Figure 5.30: Nucleotides, genes, and chromosomes

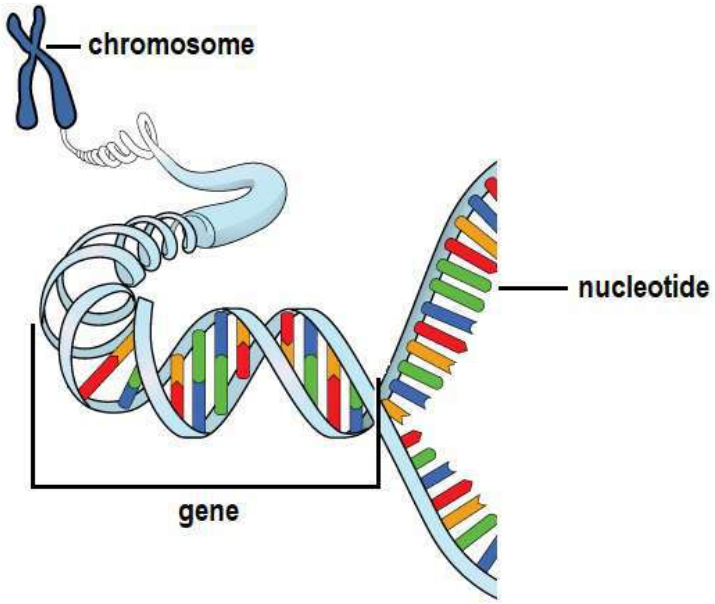


Source: blog.myheritage.com/2018/02/dna-basics-chapter-3-dna-expression.

[63]For example, adenine (A), cytosine (C), guanine (G), and thymine (T) are the four types of nucleotides that make up DNA.

[64]At a polymorphic locus, two or more different alleles exist within a population. For example, the ABO blood group system is determined by a polymorphic locus on chromosome 9, where multiple alleles (A, B, and O) exist, resulting in different blood types. The four basic ABO phenotypes are A, B, AB, and O.

[65]If an individual has two identical alleles at a given locus, they are said to be homozygous for that gene. If they have two different alleles, they are heterozygous.

Box 5.7: Ploidy and the number of chromosomes

Ploidy is the number of sets of chromosomes in the nucleus of a cell. Ploidy varies from species to species and can even vary within the same species. A haploid cell has only one set of chromosomes, while cells with two, three, four, etc. complete sets of chromosomes are called diploid, triploid, tetraploid, and so on. The haploid number of chromosomes is called $n$, while $2n$ and $kn$ are the diploid and $k$-ploid numbers of chromosomes, respectively. For example, humans are diploid because human cells contain two copies of each chromosome. Since humans have two copies of 23 chromosomes, the haploid number of chromosomes is $n = 23$, while the diploid number of chromosomes is $2n = 46$. The total number of chromosomes is $kn$, where $k$ is the ploidy of the cell. In the case of humans, the total number of chromosomes is then 46. Most organisms on Earth are diploid, so the reported number of chromosomes is generally the diploid number. There are some exceptions. For example, Mycoplasma, Escherichia coli (E. coli), and most bacteria are haploid organisms. Human gametes (sperm in males and egg in females) are also haploid because they are reproductive cells that contain half the number of chromosomes. This means that the number of chromosomes in the sperm or egg is $n = 23$, not $2n = 46$. In honey bees, the diploid queen has 32 chromosomes ($2n = 32$). The drones (male bees) are entirely derived from the queen (they are formed from unfertilized eggs), which means that the haploid drones have 16 chromosomes ($n = 16$). Female worker bees, on the other hand, are derived from the mother and a father, so they are diploid organisms with 32 chromosomes ($2n = 32$). A common example of a polyploid organism is the potato:

> "*Common cultivated potato varieties include tetraploid ($4n = 48$) with a basic chromosome number of 12, while there are cultivated species at the diploid ($2n = 24$) to pentaploid ($5n = 60$) levels. The triploid and pentaploid cultivated species are grown only on highland plateaus and slopes of the Andes, but diploid cultivated species are grown more widely and also used for breeding tetraploid varieties.*" (Watanabe, 2015, page 53).

To measure genetic diversity, we can look at the number of genes. However, we must be careful because genes can be divided into several categories based on their functions. For example, we generally distinguish between protein-coding genes, which encode instructions for the synthesis of proteins; non-coding genes, which produce RNA molecules that do not encode proteins but play an essential role in regulating gene expression and cellular processes; and pseudogenes, which are inactive copies of protein-coding genes. A more complex measure is genome size, also called C-value. The C-value is the amount of DNA contained in a haploid set of chromosomes. It is typically measured in picograms (pg) or base pairs (bp). A base pair is the basic unit of DNA sequence and corresponds to two nucleotides that combine to form the DNA double helix. The conversion between C-value and base pairs uses the following correspondence: 1 picogram is equal to 978 Mbp (million base pairs). For example, Gaston (2010, page 28) reports that the genome size of eukaryotic organisms (animals, plants, fungi, and many unicellular organisms) varies enormously, with C-values ranging from 0.0023 pg (or 2.25 million base pairs) for the parasitic microsporidium *Encephalitozoon intestinalis* to 1 400 pg (or 1.369 trillion base pairs) for the free-living amoeba *Chaos chaos*.

For a given organism, the number of genes and the C-value may vary from one measurement to another. They depend on the sample, the measurement instrument, the data size, etc. Therefore, most numbers are revised over time as data collection becomes more complete. Consider the human genome. Twenty years ago, Taft and Mattick (2003) wrote: "*Until recently, the estimated number of*

*protein-coding genes in the human genome was predicted to range from as low as 40 000 to as high as 120 000. However, it is now apparent that humans have no more than 30 000 protein-coding genes, similar to other vertebrates such as the mouse and pufferfish*". An important step in the sequencing of the human genome was taken in 2001 with the publication *The Sequence of the Human Genome* by Venter *et al.* (2001) in Science. They estimated 2.91 billion base pairs and 26 588 protein-coding genes. Since 2001, we have made great progress in sequencing the human genome, and the most recent published papers converge on some common numbers. Nurk *et al.* (2022) performed a new sequencing of the human genome and compared it to the previous reference studies performed by Schneider *et al.* (2017). Here are the results:

| Statistics | GRCH38 | T2T-CHM13 |
|---|---|---|
| Base pairs (Gbp) | 2.92 | 3.05 |
| Number of genes | 60 090 | 63 494 |
| Number of protein-coding genes | 19 890 | 19 969 |
| % of repeats | 51.89 | 53.94 |

where GRCH38 is the genomic database used by Schneider *et al.* (2017) and T2T-CHM13 is the genomic database used by Nurk *et al.* (2022). We can conclude that the human genome has 3 billion base pairs and the number of genes is 20 000. For many other organisms, the uncertainty in the number of base pairs and genes is more important because there are not enough resources (human and capital) to sequence their genomes with sophisticated instruments. Therefore, we may prefer to use the third metric of genetic diversity, the number of chromosomes, which is a more stable measure. For example, humans have exactly 46 chromosomes[66], while a mouse has exactly 40 chromosomes.

Table 5.21: Genetic diversity of some organisms

| Organism | C-value (in pg) | Base pairs (in Mbp) | Genes ($\times 10^3$) | Chromosomes ($2n$ or $kn$) |
|---|---|---|---|---|
| Mycoplasma (bacterium) | | 0.580 | 0.45 – 0.70 | 1* |
| Haemophilus influenzae (bacterium) | | 1.8 | 1.750 | 1* |
| Escherichia coli (bacterium) | | 4.6 | 4 – 5 | 1* |
| Drosophila melanogaster (fruit fly) | 0.17 | 180 | 13 – 17 | 8 |
| Arabidopsis thaliana (mustard plant) | 0.14 | 135 | 27 | 10 |
| Caenorhabditis elegans (nematode) | 0.10 | 100 | 21 | 12 |
| Saccharomyces cerevisiae (yeast) | 0.02 | 12 | 6 | 16 |
| Zea mays (corn) | 2.30 | 2 300 | 32 – 40 | 20 |
| Oryza sativa (rice) | 0.40 | 430 | 32 – 50 | 24 |
| Musmusculus (mouse) | 2.60 | 2 700 | 20 – 25 | 40 |
| Rattus norvegicus (brown rat) | 2.75 | 2 700 | 20 – 25 | 42 |
| Homo sapiens (human) | 3.20 | 3 050 | 20 | 46 |
| Solanum tuberosum (tetraploid potato) | 3.50 | 3 400 | 39 – 45 | 48* |
| Fragaria ananassa (octoploid strawberry) | 2.50 | 2 500 | 35 – 45 | 56* |
| Canis lupus familiaris (dog) | 2.80 | 2 800 | 20 | 78 |
| Agrodiaetus shahrami (butterfly) | 0.75 | 750 | 12 – 14 | 100 – 268* |
| Ophioglossum reticulatum (polyploid fern) | 6.25 | 6 200 | 30 – 50 | 1 440* |

Source: Author's research.

[66]This is not always true. Some humans have 47 chromosomes (trisomy), while others have 45 chromosomes (monosomy).

Table 5.21 shows the genetic diversity of some organisms. The first column gives the scientific name of the organism and indicates the family. Then we have the C-value calculated in pg, the genome size expressed in million base pairs, and the number of (protein-coding) genes. The last column is the number of chromosomes. The symbol * indicates that the cells are not diploid. The fern *Ophioglossum reticulatum* is the organism with the highest number of chromosomes. Interestingly, the number of chromosomes in butterflies can vary greatly from species to species. Most butterfly species have between 28 and 100 chromosomes. For example, common butterflies such as the Monarch (*Danaus plexippus*) have 30 chromosomes. Some species may have as few as 20 chromosomes or as many as 268 chromosomes, such as some *Agrodiaetus* butterflies.

Figure 5.31: Blue Morpho butterfly

Source: www.color-meanings.com/colorful-butterflies.

**Species diversity** Organismal diversity can be assessed at different levels, but the most common is species diversity. Individuals represent the first level. They are grouped into populations, which form the second level of organismal diversity. Individuals and populations are also the two last levels of genetic diversity. Finally, populations are grouped into species. Defining a species is not straightforward (De Queiroz, 2007). In common language, species refer to a group of organisms that share certain physical or morphological characteristics. For example, we might say that butterflies form a species. However, this is not true from a biological standpoint. According to *Nature*[67], "*a biological species is a group of organisms that can reproduce with one another in nature and produce fertile offspring. Species are defined by the fact that they are reproductively isolated from other groups, meaning that organisms within one species cannot successfully reproduce with those of another species.*" For example, butterflies belong to families, not species. Some well-known butterfly species include the Monarch (*Danaus plexippus*) and the Blue Morpho (*Morpho menelaus*). Phylogenetics is another widely used approach to classifying organisms into species. A phylogenetic species is defined as the smallest group of organisms that share a common ancestor and can be distinguished by unique genetic or physical characteristics. Species are then grouped into genera (singular: genus), genera are assembled into families, families into phyla, and so on, progressing through higher taxonomic levels. The principal ranks in modern biological taxonomies are domain, kingdom, phylum (or division), class, order, family, genus, and species. For example, humans are classified as *Homo sapiens*, a species within the genus *Homo*. The *Homo* genus includes *Homo sapiens*

[67]Source: https://www.nature.com/scitable/definition/species-312.

(the only surviving species today) and several extinct species, such as *Homo neanderthalensis*, *Homo erectus*, and *Homo habilis*. Homo belongs to the *Hominidae* family, also known as the great apes. This family also includes chimpanzees, bonobos, and gorillas. Humans are further classified into the *Primates* order, the *Mammalia* class, the *Chordata* phylum, the *Animalia* kingdom, and the *Eukarya* domain. Readers can explore the species taxonomic tree on specialized websites[68].

In 1988, Robert May published a landmark article in Science: *How Many Species are There on Earth?* This article does not answer the question in the title. Why not? Because he didn't have enough information at the time to make a confident estimate. May (1988) preferred to review the different kinds of information scientists need to produce an answer that isn't just a guess. Thirty-five years later, can we give an accurate answer? In fact, not as many scientific articles suggest:

> "*In 2010, Robert May pointed out an embarrassing truth about modern science*[69]*. Even as we invest huge amounts of time, money, and effort to find life on other planets, we still do not know how much life (i.e., how many species) is on our own. Although 'do not know' might sound like hyperbole, estimates have ranged wildly, from 2 million to 3 trillion.*" (Wiens, 2023, page 1).

The current reference paper on this topic is Mora *et al.* (2011), who estimated 8.7 million (±1.3 million standard error) eukaryotic species worldwide, of which 2.2 million (±0.18 million SE) are marine. The decomposition of their estimates is shown in Table 5.22. This result contrasts with the 1.5 or 2 million of species catalogued in current databases, suggesting that many species remain to be discovered. However, these figures continue to be challenged by new research, most of which puts the number of species on Earth at around 11 million, not excluding the possibility that there are at least one billion species on Earth (Larsen *et al.*, 2017).

Table 5.22: Currently catalogued and predicted total number of species on Earth and in the ocean

| Species | Earth | | | Ocean | | |
|---|---|---|---|---|---|---|
| | Catalogued | Predicted | ± SE | Catalogued | Predicted | ± SE |
| Eukaryotes | 1 233 500 | 8 740 000 | 1 300 000 | 193 756 | 2 210 000 | 182 000 |
| Animalia | 953 434 | 7 770 000 | 958 000 | 171 082 | 2 150 000 | 145 000 |
| Chromista | 13 033 | 27 500 | 30 500 | 4 859 | 7 400 | 9 640 |
| Fungi | 43 271 | 611 000 | 297 000 | 1 097 | 5 320 | 11 100 |
| Plantae | 215 644 | 298 000 | 8 200 | 8 600 | 16 600 | 9 130 |
| Protozoa | 8 118 | 36 400 | 6 690 | 8 118 | 36 400 | 6 690 |
| Prokaryotes | 10 860 | 10 100 | 3 630 | 653 | 1 320 | 436 |
| Archaea | 502 | 455 | 160 | 1 | 1 | 0 |
| Bacteria | 10 358 | 9 680 | 3 470 | 652 | 1 320 | 436 |
| Total | 1 244 360 | 8 750 000 | 1 300 000 | 194 409 | 2 210 000 | 182 000 |

Source: Mora *et al.* (2011, Table 2, page 5).

[68] The two most popular are `www.ncbi.nlm.nih.gov/taxonomy`, developed by the NCBI (National Center for Biotechnology Information), and `www.fws.gov/explore-taxonomic-tree`, provided by the FWS (US Fish & Wildlife Service).

[69] Here is the abstract of Robert May's paper:

> "*If some alien version of the Starship Enterprise visited Earth, what might be the visitors' first question? I think it would be: How many distinct life forms — species — does your planet have? Embarrassingly, our best-guess answer would be in the range of 5 to 10 million eukaryotes (never mind the viruses and bacteria), but we could defend numbers exceeding 100 million, or as low as 3 million.*" (May, 2010, page 41).

Table 5.23: Exploring the taxonomy classification tree

| Kingdom | Phylum | Class | Order | Family | Genus | Species | Vernacular name |
|---|---|---|---|---|---|---|---|
| Animalia | 34 | 109 | 704 | 10 119 | 164 366 | 1 551 595 | Animals |
| | Arthropoda | Insecta | 43 | 1 738 | 89 273 | 994 767 | Insects |
| | Arthropoda | Insecta | Lepidoptera | Nymphalidae | Morpho | Morpho menelaus | Blue morphos |
| | Chordata | Mammalia | Carnivora | Phocidae | 14 | 19 | True seals |
| | Chordata | Mammalia | Carnivora | Phocidae | Phoca | Phoca largha | Large seals |
| | Chordata | Mammalia | Carnivora | Phocidae | Phoca | Phoca vitulina | Common seals |
| | Chordata | Mammalia | Primates | 16 | 83 | 528 | Primates |
| | Chordata | Mammalia | Primates | Hominidae | Homo | Homo sapiens | Humans |
| | Mollusca | Gastropoda | Stylommatophora | Helicidae | Helix | Helix pomatia | Escargots |
| Archaea | 2 | 13 | 16 | 27 | 112 | 377 | |
| | Crenarchaeota | Thermoprotei | Thermoproteales | Thermoproteaceae | Caldivirga | Caldivirga maquilingensis | |
| Bacteria/Monera | 29 | 51 | 115 | 297 | 1 996 | 9 980 | Bacteria |
| | Firmicutes | Bacilli | Bacillales | Bacillaceae | Bacillus | Bacillus anthracis | B. anthracis |
| | Pseudomonadota | Gammaproteobacteria | Enterobacterales | Enterobacteriaceae | Escherichia | Escherichia coli | E. coli |
| Chromista | 13 | 58 | 200 | 1 101 | 7 248 | 61 900 | |
| | Foraminifera | 5 | 22 | 435 | 4 016 | 49 654 | |
| Fungi | 12 | 61 | 274 | 1 086 | 12 778 | 155 869 | |
| | Basidiomycota | Agaricomycetes | 23 | 148 | 1 875 | 40 825 | |
| | Basidiomycota | Agaricomycetes | Agaricales | Amanitaceae | Amanita | Amanita phalloides | Death caps |
| | Basidiomycota | Agaricomycetes | Boletales | Boletaceae | Boletus | Boletus edulis | Ceps |
| Plantae | 9 | 44 | 256 | 1 079 | 21 463 | 385 774 | Plants |
| | Tracheophyta | Liliopsida | Liliales | Liliaceae | Tulipa L. | 96 | Tulips |
| | Tracheophyta | Magnoliopsida | Fabales | Fabaceae | Phaseolus | Phaseolus vulgaris | Common bean |
| | Tracheophyta | Magnoliopsida | Rosales | Rosaceae | 110 | 8 147 | Roses |
| | Tracheophyta | Magnoliopsida | Solanales | Solanaceae | 102 | 2 808 | |
| | Tracheophyta | Magnoliopsida | Solanales | Solanaceae | Capsicum | Capsicum annuum | Pimientos |
| | Tracheophyta | Magnoliopsida | Solanales | Solanaceae | Solanum | Solanum lycopersicum | Tomatos |
| | Tracheophyta | Magnoliopsida | Solanales | Solanaceae | Solanum | Solanum tuberosum | Potatos |
| Protozoa | 10 | 41 | 74 | 227 | 1 090 | 2 659 | Protozoans |
| | Choanozoa | Ichthyosporea | Eccrinida | Amoebidiidae | Amoebidium | Amoebidium parasiticum | |

For each taxon, we indicate the parent nodes of the tree on the left and the number of taxa on the right. For example, *Insecta* belongs to the phylum *Arthropoda* in the kingdom *Animalia* and includes 43 orders, 1 738 families, 89 273 genera, and 994 767 species.

Source: Catalogue of Life, www.catalogueoflife.org.

**Ecological diversity** The third element of biodiversity is ecosystems. Again, there are several levels of ecological diversity. Populations, which are also part of genetic and organismal diversity, are the first level. Populations are grouped into habitats. The other three levels are ecosystems, ecoregions, and provinces. Then we find the biomes, which are large-scale ecosystems characterized by similar climatic conditions, vegetation, and wildlife. We generally distinguish between terrestrial and aquatic biomes. Terrestrial biomes include boreal forests (taiga), chaparral (Mediterranean climate), deserts, savannas, temperate forests, temperate grasslands, tropical rainforests, and tundra. Aquatic biomes include freshwater biomes such as wetlands and marine biomes such as oceans, coral reefs and mangroves. The highest level of ecological diversity corresponds to biogeographic realms, which are the broadest divisions of the Earth's land surface delineated by natural barriers such as oceans, deserts, and mountain ranges. Olson *et al.* (2001) defined eight realms: Australasia, Antarctic, Afrotropic, Indo-Malaya, Nearctic, Neotropic, Oceania and Palearctic.

Figure 5.32: The 867 terrestrial ecoregions of Olson *et al.* (2001)

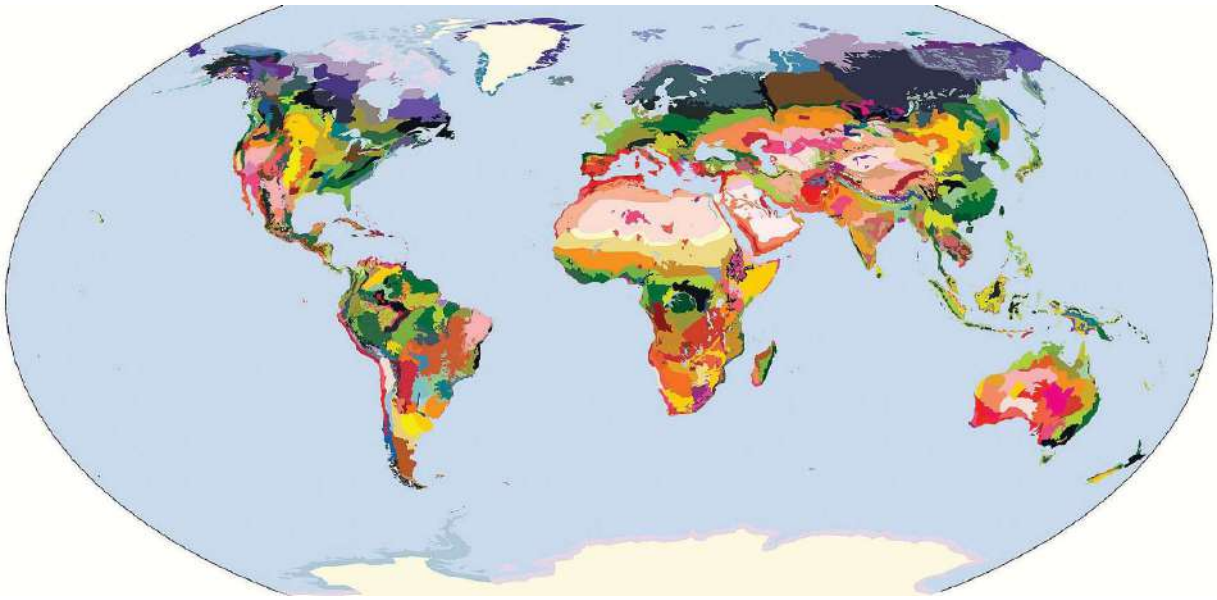

Source: Olson *et al.* (2001, Figure 2, page 935).

In general, ecoregions are the most common level at which ecological diversity is assessed. The World Wide Fund for Nature (WWF) describes them as biogeographic units, which are "*defined as relatively large units of land or water containing a distinct assemblage of natural communities sharing a large majority of species, dynamics, and environmental conditions.*" Most current world ecoregion maps[70] are based on the seminal work of Olson *et al.* (2001), who defined 867 distinct ecoregions (Figure 5.32). Among these ecosystems, Olson and Dinerstein (2002) identified 238 priority ecoregions for protection (142 terrestrial, 53 freshwater, and 43 marine). This research has been used extensively by the WWF and the International Union for Conservation of Nature (IUCN) to define protected areas[71]. The 2001 study was recently updated by Dinerstein *et al.* (2017), which

[70]See, for example, the maps available at `https://ecoregions.appspot.com` and `https://www.oneearth.org/bioregions`.

[71]IUCN has developed a system of protected area management categories to define, record and classify the wide variety of specific goals and concerns in categorizing protected areas and their objectives. The six categories are: strict nature reserve and wilderness area (Cat. I), national park (Cat. II), natural monument or feature (Cat. III), habitat or species management area (Cat. IV), protected landscape or seascape (Cat. V), and protected area with

now has a list of 846 terresterial ecoregions. A more recent study used a different mapping approach and identified 431 global ecosystems (Sayre *et al.*, 2020). By conducting a global gap analysis of the representation of these ecosystems in protected areas, the authors showed that most natural and semi-natural ecosystems are inadequately protected, with protection rates of less than 20%.

### Biodiversity loss (and gain)

Regardless of the element of biodiversity (genetic, organismal or ecological), most figures show that the loss of biodiversity is significant and has accelerated over the past 50 years. However, such a message is not really clear. Indeed, we can first ask ourselves what biodiversity loss is, how it is measured, and is the current figure really significant? For example, the second chapter of Gaston and Spicer (2004) is devoted to the temporal dynamics of biodiversity and illustrates that biodiversity has fluctuated over geological time scales, such as millions of years. This long-term perspective shows that changes in biodiversity are a natural part of Earth's history and makes it difficult to understand whether current trends represent an exceptional crisis or a continuation of these natural cycles.

Figure 5.33: Genus diversity during the Phanerozoic era

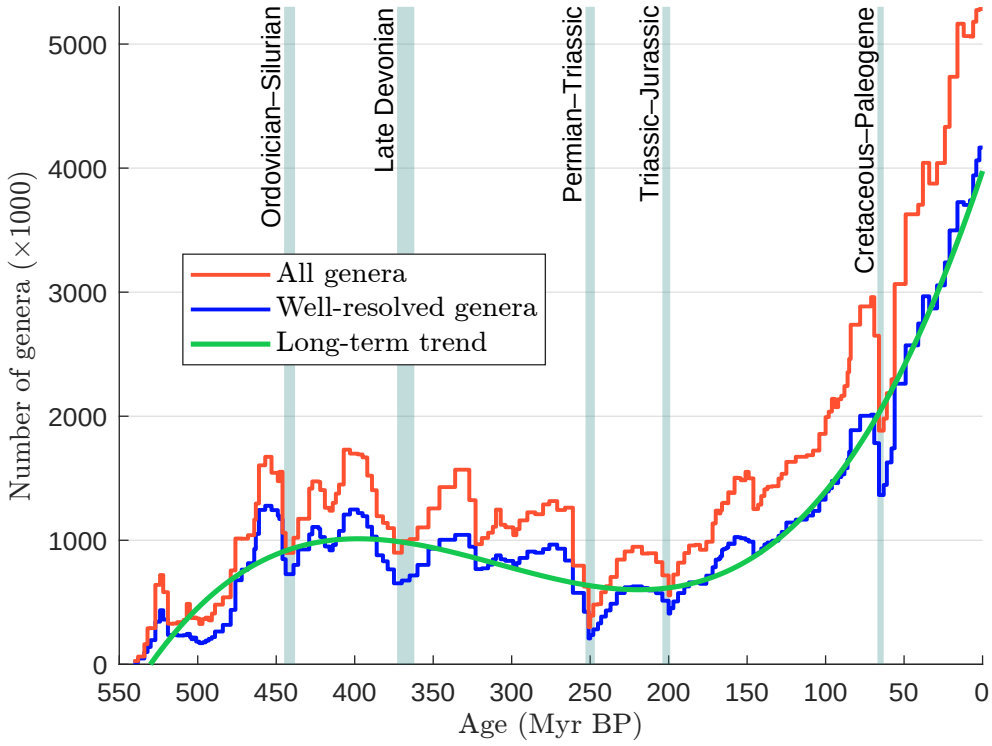


Source: Rohde and Muller (2005, Figure 1, page 208) & Supplementary Tables (www.nature.com/articles/nature03339).

The evolution of biodiversity over time is typically represented by a Sepkoski curve, which plots the number of genera over time. Although this is a simple metric, it is difficult to calculate due to

sustainable use of natural resources (Cat. VI). For example, in France, Les Landes de Gascogne is managed under IUCN category VI of protected areas, while Le Parc du Mercantour is managed under IUCN category II. Readers can explore protected areas and other effective area-based conservation measures (OECMs) at www.protectedplanet.net.

the complexity of data collection. Joseph John Sepkoski devoted much of his career to building a database of marine animal families and genera. This dataset, used extensively in numerous publications, was released in 2002 after Sepkoski's death (Sepkoski, 2002). Figure 5.33 shows the Sepkoski curve generated by Rohde and Muller (2005). The three series shown are: the total number of known genera of marine animals from Sepkoski's catalog[72], the total number of well-defined genera (*i.e.*, known genera excluding those with single occurrences or poorly dated records), and the long-term trend estimated using a third-order polynomial fitted to the data. First, we observe that the number of genera has fluctuated continuously throughout the Phanerozoic. About 500 million years ago, the number of genera was estimated at 370 000, while today it exceeds 5 million. Second, the increase in the number of genera was not linear. Genus diversity increased about 400 million years ago, then declined until about 200 million years ago, after which it increased dramatically. In the present era, genus diversity is higher than at any time in Earth's history. Finally, while the long-term trend is clear, there are numerous discontinuities with a frequency of about one million years. In particular, we observe several sharp declines known as extinction events or mass extinctions.

**Speciation, extinction and the birth-death model** The number of species on Earth results from a balance between two evolutionary processes: speciation (the formation of new species) and extinction[73]. When speciation rates exceed extinction rates, the number of species increases. Conversely, when extinction rates exceed speciation rates, the number of species decreases. Both processes can occur naturally or be influenced by external factors. In fact, the processes of birth and death apply not only to individuals and populations, but also to higher levels of biological classification, such as species. For example, *Homo sapiens* appeared about 300 000 years ago, while *Australopithecus* disappeared about 1.9 million years ago. Similarly, dinosaurs became extinct about 65 million years ago, illustrating that species extinction is a natural process that can occur without human intervention. Thus, we generally recognize that each species and subspecies has a finite lifespan:

> "*Like all species, plants, mammals, and birds have been subject to extinction as a fundamental part of evolution. Indeed, only about 2–4% of all the species that have ever lived during the 600 million years of the fossil record still survive today. Looking at the fossil record, it can be said that invertebrate species and mammals have had an average life span of 5–10 and 1–2 million years, respectively.*" (Mace, 1998).

Even as some species disappear, new species continue to appear. This process of species formation is called speciation or diversification (Gaston and Spicer, 2004, Section 2.3.2, page 31). Speciation most often occurs when populations of the same species become geographically isolated. Over time, these populations evolve independently, accumulating genetic changes that can eventually lead to the emergence of distinct species. As these genetic differences increase, individuals from the two populations may no longer be able to interbreed or produce fertile offspring. A classic example of this phenomenon is donkeys and horses. Both belong to the same family (*Equidae*) and genus (*Equus*), but are classified as separate species. Donkeys (*Equus africanus asinus*) are a subspecies of the African wild ass (*Equus africanus*), while domestic horses (*Equus ferus caballus*) are a subspecies of the wild horse (*Equus ferus*). Although donkeys and horses can interbreed, their offspring are usually sterile[74], meaning they cannot reproduce. This sterility occurs because donkeys have 62

[72]The Sepkoski database can be found at `https://strata.geology.wisc.edu/jack`.

[73]Extinction refers to the complete disappearance of a species from the Earth, while extirpation refers to the disappearance of a species from a particular region, but the species continues to exist in other regions.

[74]The offspring of a female horse and a male donkey is a mule, while the offspring of a male horse and a female donkey is a hinny.

Figure 5.34: Rates of origination and extinction during the Phanerozoic era

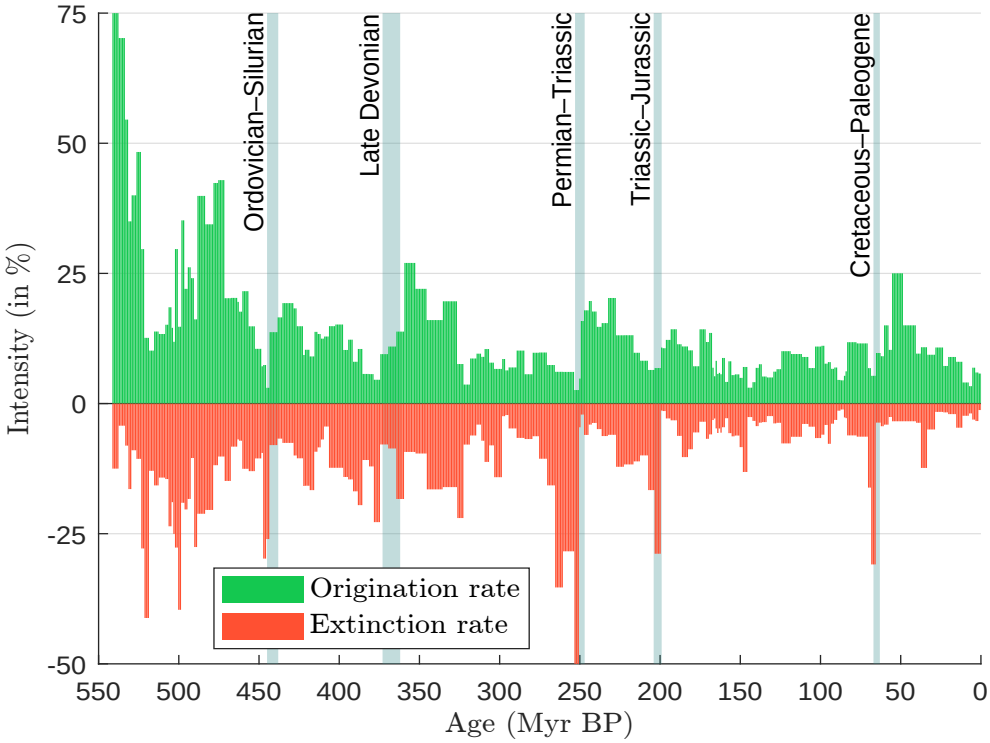


Source: Rohde and Muller (2005) & Author's calculations.

Figure 5.35: Net diversification rate during the Phanerozoic era

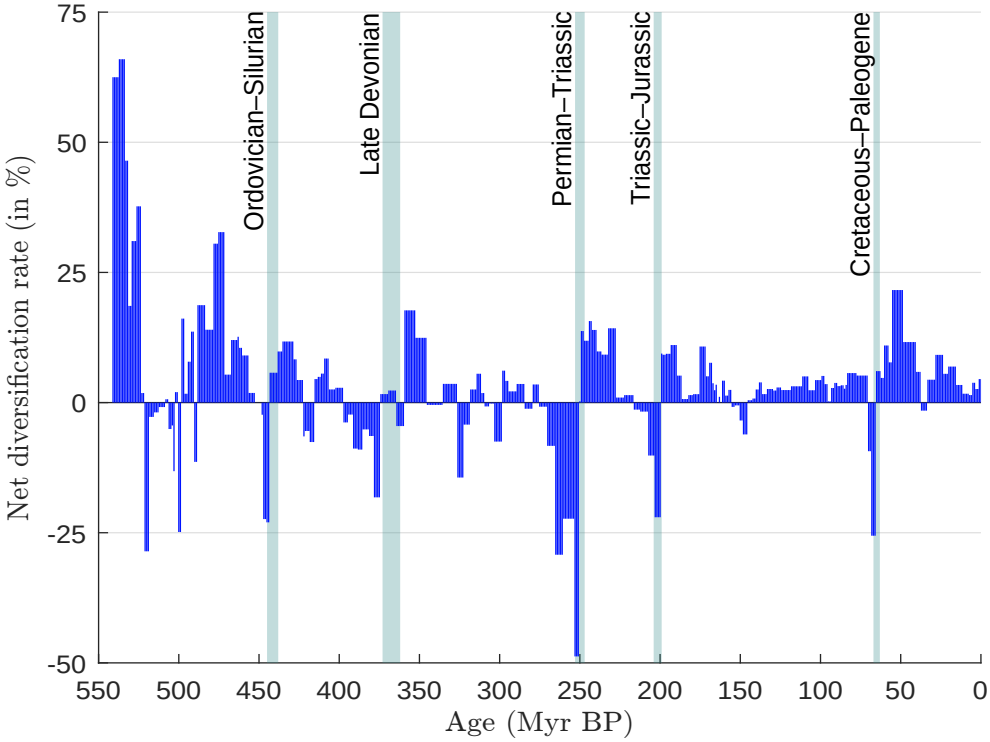


Source: Rohde and Muller (2005) & Author's calculations.

chromosomes while horses have 64, resulting in offspring with 63 chromosomes. In fact, donkeys, horses and zebras share a common ancestor, but diverged for various reasons. According to Carbone *et al.* (2006), zebras and donkeys split about 0.9 million years ago, while their common ancestor diverged from the horse about 2 million years ago.

The number of species $N(t)$ at time $t+1$ can be expressed as:

$$N(t+1) = N(t) + \Delta N^{+}(t+1) - \Delta N^{-}(t+1)$$

where $\Delta N^{+}(t+1)$ and $\Delta N^{-}(t+1)$ are the number of new species and extinct species between $t$ and $t+1$. In continuous time, this equation becomes:

$$\frac{\mathrm{d}N(t)}{\mathrm{d}t} = \frac{\mathrm{d}N^{+}(t)}{\mathrm{d}t} - \frac{\mathrm{d}N^{-}(t)}{\mathrm{d}t}$$

Dividing both sides by $N(t)$ gives:

$$\underbrace{\frac{\mathrm{d}N(t)}{N(t)\,\mathrm{d}t}}_{\delta(t)} = \underbrace{\frac{\mathrm{d}N^{+}(t)}{N(t)\,\mathrm{d}t}}_{\lambda(t)} - \underbrace{\frac{\mathrm{d}N^{-}(t)}{N(t)\,\mathrm{d}t}}_{\mu(t)}$$

The growth rate $\delta(t)$ is the difference between the origination (or speciation) rate $\lambda(t)$ and the extinction rate $\mu(t)$:

$$\delta(t) = \lambda(t) - \mu(t) \tag{5.4}$$

$\delta(t)$ is also called the net diversification rate. Here, $\lambda(t)$, $\mu(t)$ and $\delta(t)$ are assumed to be instantaneous rates. Given two dates $t_1$ and $t_2$, we can compute the cumulative rates $\lambda(t_1,t_2) = \int_{t_1}^{t_2} \lambda(t)\,\mathrm{d}t$, $\mu(t_1,t_2) = \int_{t_1}^{t_2} \mu(t)\,\mathrm{d}t$, and $\delta(t_1,t_2) = \int_{t_1}^{t_2} \delta(t)\,\mathrm{d}t$. We derive the average rate by dividing the cumulative rate by the time interval. For example, the average net diversification rate is equal to:

$$\bar{\delta}(t_1,t_2) = \frac{\delta(t_1,t_2)}{t_2-t_1} = \frac{1}{t_2-t_1}\int_{t_1}^{t_2} \delta(t)\,\mathrm{d}t$$

In Figures 5.34 and 5.35, we report the origination, extinction, and net diversification rates calculated by Rohde and Muller (2005) from the Sepkoski database. For example, the range of the net diversification rate $\delta(t_1,t_2)$ is between $-49\%$ and $+66\%$. However, these numbers are difficult to compare because they represent time periods ranging from one million years to seven million years.

The previous remark indicates that we need to normalize the extinction (and other) rates. These rates can be expressed as a percentage per decade, century, or millennium. For long-term trends based on fossil records, we typically express them as a percentage per million years. For example, if the extinction rate $\mu$ is constant and equals 1% per century, this is equivalent to an extinction rate of:

$$\mu = \frac{1\%}{1 \text{ century}} = \frac{1\%}{100 \text{ years}} = 0.01\% \text{ per year}$$

If we assume that the speciation rate is zero, then the number of surviving species follows an exponential survival function:

$$S(t) = \frac{N(t)}{N_0} = e^{-\mu t} \tag{5.5}$$

We deduce that the lifespan (or average lifetime) of species is the inverse of the extinction rate:

$$\tau = \frac{1}{\mu}$$

For example, if the extinction rate of a genus is 0.1% per millennium, we obtain:

$$\tau = \frac{1000 \text{ years}}{0.1\%} = 10^6 \text{ years (or 1 million years)}$$

The lifespan of this genus is then one million years. Pimm *et al.* (1995) introduced a new metric $\eta$ for assessing extinction rates. They use the number of extinctions (E) per million species per year (MSY) or E/MSY. The relationship between $\eta$, $\mu$ and $\tau$ is then:

$$\eta = 10^6 \mu = \frac{10^6}{\tau}$$

For example, if $\mu$ is 0.1% per millennium, we get:

$$\eta = \frac{0.1\%}{10^3 \text{ years}} \times 10^6 = \frac{10^{-3}}{10^3 \text{ years}} \times 10^6 = 1 \text{ E/MSY}$$

If there are 1 million species, the number of extinctions per year would be one. Because scientists use these three metrics $\eta$, $\mu$, and $\tau$ interchangeably to assess extinction rates, it is crucial to understand their definitions and how to convert one metric to another.

**Remark 54** *We consider the previous example where the extinction rate of a genus equals* 1% *per century or* 0.01% *per year. We get:*

$$\mu = \frac{1\%}{1 \text{ century}} = \frac{1\%}{10^2 \text{ years}} \times \frac{10^6}{10^6} = 10\,000\% \text{ per million years}$$

*This example shows that we must be careful with conversion formulas because they ignore the compound effect. Using Equation 5.5, we deduce that*[75]*:*

$$\mu^\star = -\frac{1}{t} \ln \left( \frac{N(t)}{N_0} \right) = -\frac{1}{t} \ln \left( 1 - \frac{N_0 - N(t)}{N_0} \right) = -\frac{1}{t} \ln \left( 1 - \frac{N^+(t)}{N_0} \right)$$

*where $N^+(t)$ is the number of extinctions between 0 and $t$. This formula was proposed by Spalding and Hull (2021) to calculate the extinction rate for long timescales.*

**Example 22** *We consider three datasets with different species:*

| *Species* | $N_0$ | $\Delta N^+$ | $\Delta N^-$ | $\Delta t$ |
|---|---|---|---|---|
| *Birds* | 5 000 | 7 | 5 | 10 *years* |
| *Insects* | 75 000 | 25 | 50 | 3 *centuries* |
| *Plants* | $10^6$ | $30 \times 10^3$ | $15 \times 10^3$ | 1 *millennium* |

*where $N_0$ is the number of species at the beginning of the period, and $\Delta N^+$ and $\Delta N^-$ are the number of new and dead species during the period $\Delta t$.*

The calculated values of $\lambda$, $\mu$, and $\delta$ are shown in the table below. For example, the net diversification rate for the bird species is 0.004% per year, or 4% per millennium. In this example, it is better to use a longer time unit (millennium instead of year) because of the magnitude of the rates.

| Species | $\lambda$ | $\mu$ | $\delta$ | $\lambda$ | $\mu$ | $\delta$ |
|---|---|---|---|---|---|---|
| | (in % per year) | | | (in % per millenium) | | |
| Birds | 0.01400 | 0.01000 | 0.00400 | 14.00 | 10.00 | 4.00 |
| Insects | 0.00011 | 0.00022 | −0.00011 | 0.11 | 0.22 | −0.11 |
| Plants | 0.00300 | 0.00150 | 0.00150 | 3.00 | 1.50 | 1.50 |

[75] To distinguish the logarithmic approach from the arithmetic approach, we use the symbol $\mu^\star$ instead of $\mu$. We also define $\tau^\star = 1/\mu^\star$ and $\eta^\star = 10^6 \mu^\star = 10^6/\tau^\star$.

We now focus on the extinction rate and calculate this metric with different units. $\mu(0, \Delta t)$ is the cumulative extinction rate. For the bird and plant species, it is equal to:

$$\mu_{\text{bird}}(0, \Delta t) = \frac{5}{5\,000} = 0.1\%$$

and:

$$\mu_{\text{plant}}(0, \Delta t) = \frac{15 \times 10^3}{10^6} = 1.5\%$$

These two rates cannot be directly compared because the time periods over which the extinction rate is assessed are very different (10 years versus 1 millennium). Therefore, it is important to normalize. The extinction rate $\mu$ is then expressed in % per year. We can also calculate the extinction rate $\mu^\star$ using the previous logarithmic formula. These two extinction rates can then be converted in lifetime (expressed in years) and E/MSY. Numerical results are given below:

| Species | $\mu(0, \Delta t)$ (in %) | $\mu$ (in % per year) | $\mu^\star$ | $\tau$ (in years) | $\tau^\star$ | $\eta$ (in E/MSY) | $\eta^\star$ |
|---|---|---|---|---|---|---|---|
| Birds | 0.10000 | 0.01000 | 0.01401 | 10 000 | 7 138 | 100.0 | 140.1 |
| Insects | 0.06667 | 0.00022 | 0.00011 | 450 000 | 899 850 | 2.2 | 1.1 |
| Plants | 1.50000 | 0.00150 | 0.00305 | 66 667 | 32 831 | 15.0 | 30.5 |

Several observations can be made. First, the figures for $\mu(0, \Delta t)$ cannot be compared directly due to their lack of normalization. We observe extinction rates of 0.1%, 0.07% and 1.5% for birds, insects, and plants, respectively, but these values correspond to different time periods: ten years, three centuries, and one millennium. Second, the results obtained using the arithmetic approach differ from those using the logarithmic approach. Finally, the lifetime and E/MSY figures are probably the easiest to interpret. For example, among one million species, we observe 100, 2.2, and 15 extinctions per year for birds, insects, and plants.

**Background extension rate** The background extension rate is the normal or typical extension rate that has occurred over the past 500 million years. By normal, we mean the long-term rate at which species would go extinct in the absence of human presence. Thus, most estimates use data up to 1 500 AD. In a brief communication, Simpson (1952) estimated the average duration of a species to be between 0.5 and 5 million years. This was one of the first publications on the subject. For marine invertebrates, Valentine (1970) estimated the average lifetime to be between 5 and 10 million years. The publication of Van Valen (1973) marked a turning point and generated considerable controversy. In this influential paper, the author introduced the concept of Van Valen's Law, which states that extinction rates within a given taxonomic group remain constant over time. To explain this pattern, he proposed the Red Queen hypothesis, which suggests that species must constantly evolve to keep up with competitors and predators. This ongoing evolutionary *arms race* results in a constant extinction rate. Van Valen (1973, Table 1) calculated the background extinction rate for 20 families, 38 genera, and 3 species. His results satisfy the following coherent inequalities:

$$\tau_{\text{family}} \geq \tau_{\text{genus}} \geq \tau_{\text{species}}$$

We report some of his estimates[76] in Table 5.24. The work of Pimm *et al.* (1995) was a major milestone in the study of background extinction rates. Based on an analysis of 11 studies, they estimated

[76] Van Valen (1973) used the macarthur (ma) measure to define the lifespan of species. One macarthur is the rate of extinction given a half-life of 500 years. Since the figures reported by Van Valen are expressed in micromacarthurs ($\mu$ma), we estimate the lifespan in million years using the following formula: $\tau = 500/(\mu \ln 2)$ where $\mu$ is the extinction rate in $\mu$ma.

Table 5.24: Estimates of the background extension rate $\bar{\eta}$

| Taxonomy | $\tau$ (in myr) | $\eta$ (in E/MSY) | Source |
|---|---|---|---|
| All species | $1-10$ | $0.10-1.00$ | Pimm *et al.* (1995) |
| All species | 1.0 | 0.10 | De Vos *et al.* (2015) |
| All fossil groups | $0.5-5$ | $0.20-2.00$ | Simpson (1952) |
| Marine fossil groups | $7.4-20$ | $0.05-0.13$ | Raup and Sepkoski (1982) |
| Marine invertebrates | $5-10$ | $0.10-0.20$ | Valentine (1970) |
| Cetacea (genus) | 3.61 | 0.277 | Van Valen (1973) |
| Devonian & Cenozoic bivalves | $6.5-9.7$ | $0.10-0.15$ | Valentine (1970) |
| Silurian graptolites | $2.0-3.0$ | $0.33-0.50$ | Rickards (1977) |
| Diatoms | 8.02 | 0.125 | Van Valen (1973) |
| Dinoflagellata | 13.12 | 0.076 | Van Valen (1973) |
| Foraminifera (planktonic) | 7.21 | 0.139 | Van Valen (1973) |
| Foraminifera (genus) | 24.04 | 0.042 | Van Valen (1973) |
| Foraminifera (family) | 72.13 | 0.014 | Van Valen (1973) |
| Arthropods | $1.07-11.11$ | $0.090-0.934$ | De Vos *et al.* (2015) |
| Chordates | $1.71-15.63$ | $0.064-0.586$ | De Vos *et al.* (2015) |
| Mammals | 0.56 | 1.800 | Barnosky *et al.* (2011) |
| Mammals & birds | $0.55-4.80$ | $0.208-1.818$ | Loehle and Eschenbach (2012) |
| Mammals | $9.80-43.48$ | $0.023-0.102$ | De Vos *et al.* (2015) |
| Mammals | 0.50 | 2.000 | Ceballos *et al.* (2015) |
| Mollusca | $0.60-7.41$ | $0.135-1.672$ | De Vos *et al.* (2015) |
| Primates (genus) | 3.28 | 0.305 | Van Valen (1973) |
| Reptilia (family) | 24.05 | 0.042 | Van Valen (1973) |
| Plants | $2.84-18.87$ | $0.053-0.352$ | De Vos *et al.* (2015) |
| Plants | $7.69-20.00$ | $0.050-0.130$ | Gray (2019) |

the background rate $\bar{\eta}$ to be between 0.1 and 1 E/MSY. Since then, the 1 E/MSY benchmark has been widely adopted in many mass extinction studies. However, it's important to note that this benchmark can vary depending on the specific species or taxonomic group being considered. For example, Barnosky *et al.* (2011) proposed a benchmark of 1.8 E/MSY for mammals. De Vos *et al.* (2015) conducted a comprehensive study across different taxa (arthropods, chordates, mammals, mollusca, and plants) and suggested that the lower bound of the Pimm *et al.* (1995) estimate is a more appropriate benchmark, namely $\bar{\eta} = 0.1$ E/MSY.

**Mass extinction** A mass extinction is a widespread and rapid decline in Earth's biodiversity (genetic or species diversity), during which a substantial proportion of the planet's species disappear over a relatively short period of time — typically thousands to millions of years, which is short on the geologic time scale. The characterization of an extinction event is then determined using calculated extinction rates. Mathematically, we have:

$$[t_1, t_2] \text{ is an extinction event period} \Leftrightarrow \mu(t_1, t_2) \geq \mu^\star \text{ and } \bar{\eta}(t_1, t_2) \gg \bar{\eta} \tag{5.6}$$

where $\mu(t_1, t_2)$ is the (total) extinction rate expressed in % during the period $[t_1, t_2]$, $\bar{\eta}(t_1, t_2)$ is the mean extinction rate expressed in E/MSY, $\mu^\star$ is a threshold value and $\bar{\eta}$ is the background rate. For example, $\mu^\star = 30\%$ means that 30% of species must disappear between times $t_1$ and $t_2$ for the period $[t_1, t_2]$ to be characterized as an extension event. Although there is no consensus on the threshold,

scientists generally use a minimum of 30% for species and 15% for families to characterize a mass extinction.

Using fossil data records, Raup and Sepkoski (1982) demonstrated that four mass extinctions in the marine realm — occurring in the late Ordovician, Permian, Triassic, and Cretaceous periods — had extinction rates that were statistically significantly higher than background rate levels. However, this was not the case for a fifth extinction event in the Devonian. Benton (1995) used a new database that included both marine and continental fossil records and examined 22 extinction events. His results showed that extinction rates can be very different for marine and continental organisms. The study of Bambach (2006) identifies eighteen extinctions and comes to the same conclusion:

> "*A review of different methods of tabulating data from the Sepkoski database reveals 18 intervals during the Phanerozoic have peaks of both magnitude and rate of extinction that appear in each tabulating scheme. These intervals all fit Sepkoski's definition of mass extinction. However, they vary widely in timing and effect of extinction, demonstrating that mass extinctions are not a homogeneous group of events.*" (Bambach, 2006, page 127).

For this reason, paleontologists often use a scale to categorize mass extinction events, distinguishing between[77]:

- Small extinction events: Relatively minor events that do not drastically alter biodiversity;
- Pulse events: More pronounced extinctions that can significantly impact certain taxonomic groups;
- The '*Big Five*' extinctions: The five major mass extinctions in Earth's history that resulted in a significant loss of biodiversity.

The Big Five extinctions are those identified by Raup and Sepkoski (1982). For each event, we report below some figures[78] on the total extinction rate[79] and the possible causes:

1. Ordovician-Silurian mass extinction — LOME (445–443 Myr BP)
   About 27% of all families, 57% of all genera and 85% of all species became extinct. It is generally assumed that the cause is climate change (global cooling) and volcanic activity, which affect the chemistry of the atmosphere and oceans and $CO_2$ sequestration.

[77]For more informations and illustrations, the reader can consult Chapter 7 of Primack (2014) for detailed information on extinction with a lot of numbers and examples.

[78]Following the terminology of Algeo and Shen (2024), we use the following abbreviations for the five major mass extinctions: LOME for Late Ordovician, LDME for Late Devonian, EPME for end-Permian, ETME for end-Triassic and ECME for end-Cretaceous mass extinctions. Other commonly used abbreviations include: O-S for Ordovician-Silurian, L-D for Late Devonian, P-T for Permian-Triassic, T-J for Triassic-Jurassic, K-Pg for Cretaceous-Paleogene (previously called K-T for Cretaceous-Tertiary) extinctions. It's important to note that a mass extinction period can be characterized by multiple extinction events. According to Benton (1995), the Big Five extinctions can be further broken down as follows: 1 event for LOME (Ashgillian), 2 events for LDME (Givetian-Frasnian & Famennian), 3 events for EMPE (Ufimian, Kazanian-Tatarian & Tatarian), 3 events for ETME (Carnian, Norian-Rhaetian & Rhaetain) and 2 events for ECME (Cenomanian & Maastrichtian).

[79]These figures come from the Wikipedia page (`https://en.wikipedia.org/wiki/Extinction_event`) and are based on the book of Benton (2015). These estimates should be treated with caution, as they may vary from study to study. For example, Barnosky *et al.* (2011) estimated extinction rates for genera and species to be 57% and 86% for LOME, 35% and 75% for LDME, 56% and 96% for EPME, 47% and 80% for ETME, and 40% and 76% for ECME, respectively. However, we observe that the order of magnitude is the same in most studies.

2. Late Devonian mass extinction — LDME (372–359 Myr BP)
   About 19% of all families, 35-50% of all genera and 75% of all species became extinct. The cause is generally thought to be climate change (global cooling followed by global warming) and the removal of global $CO_2$.

3. Permian-Triassic extinction or '*The Great Dying*' — EPME (252–251 Myr BP)
   About 57% of marine families, 84% of marine genera, 81% of all marine species and 90% of terrestrial vertebrate species became extinct. The cause is generally thought to be climate change (global warming) and volcanic activity (massive volcanic eruptions in Siberia).

4. Triassic-Jurassic extinction — ETME (200–201 Myr BP)
   About 23% of all families, 48% of all genera (20% of marine families and 55% of marine genera) and 70-75% of all species became extinct. It is generally thought to be caused by volcanic activity (massive volcanic eruptions in the Central Atlantic Magmatic Province) and sea level changes.

5. Cretaceous-Paleogene extinction — ECME (66 Myr BP)
   About 17% of all families, 47% of all genera and 75% of all species became extinct. The Cretaceous extinction is marked by the disappearance of the Dinausores. It is generally assumed that the cause is an asteroid impact followed by widespread environmental disruption, including tsunamis, forest fires, and climate change.

We find that the causes, while diverse, are related to a small number of natural phenomena:

> "*Every mass extinction has both an ultimate cause, i.e., the trigger that leads to various climato-environmental changes, and one or more proximate cause(s), i.e., the specific climato-environmental changes that result in elevated biotic mortality. With regard to ultimate causes, strong cases can be made that bolide (i.e., meteor) impacts, large igneous province eruptions and bioevolutionary events have each triggered one or more of the Phanerozoic Big Five mass extinctions, and that tectono-oceanic changes have triggered some second-order extinction events. [...] With regard to proximate mechanisms, most extinctions are related to either carbon-release or carbon-burial processes, the former being associated with climatic warming, ocean acidification, reduced marine productivity and lower carbonate* $\delta^{13}$C *values, and the latter with climatic cooling, increased marine productivity and higher carbonate* $\delta^{13}$C *values.*" (Algeo and Shen, 2024, page 1).

The leading hypothesis for the fifth mass extinction is the impact of a large asteroid that struck the Earth near the Yucatán Peninsula in Mexico, forming the Chicxulub crater (Schulte *et al.*, 2010). The asteroid, estimated to be 10 to 15 kilometers in diameter, released an immense amount of energy, equivalent to billions of nuclear bombs. This catastrophic impact caused massive earthquakes, tsunamis, and forest fires. In addition, the impact likely caused a '*nuclear winter*' as a massive plume of debris and vaporized rock was ejected into the atmosphere and spread globally. This debris blocked sunlight, leading to a drastic cooling of the planet, reduced photosynthesis, and a collapse of food chains. While the asteroid impact hypothesis is widely accepted, other factors such as climate change and volcanic activity may also have contributed to the Cretaceous-Paleogene mass extinction. Interestingly, this extinction paved the way for the rise of mammals, including humans, as it wiped out the dinosaurs that had previously dominated the planet. As shown in Figure 5.34 on page 376, biodiversity tends to rebound significantly after each mass extinction. Although biodiversity loss is generally followed by strong gains, this recovery occurs on the paleontological timescale of millions of years.

Box 5.8: IUCN Red List of Threatened Species

Founded in 1964, the International Union for Conservation of Nature (IUCN) is responsible for maintaining and updating the IUCN Red List of Threatened Species. It is now considered the world's most comprehensive source of information on the global extinction status of animals, fungi and plants. They correspond to three kingdoms in organismal diversity or modern biological taxonomy, the other two being protista (single-celled eukaryota) and monera (single-celled prokaryota). IUCN (2012) assesses the risk status of a species according to the following A-E criteria: (A) population size reduction (population decline measured over the longer of 10 years or 3 generations, trend), (B) geographic range (extent of occurrence, area of occupancy), (C) small population size and decline (number of mature individuals, trend), (D) very small or restricted population (number of mature individuals, number of locations), and (E) quantitative analysis (probability of extinction). The Red List divides then species into nine categories:

- Not Evaluated (NE) & Data Deficient (DD)
  A taxon is NE if it has not yet been evaluated against the criteria. NE species are not published in the IUCN Red List. A taxon is DD if there is insufficient information to make a direct or indirect assessment of its risk of extinction based on its distribution and/or population status. A taxon in this category may be well studied and its biology well understood, but adequate data on abundance and/or distribution are lacking.

- Least Concern (LC) & Near Threatened (NT)
  A taxon is LC if it has been assessed against the Red List criteria and is not considered CR, EN, VU or NT. A taxon is NT if it has been evaluated against the criteria, but does not currently qualify as CR, EN, or VU, but is close to or is likely to qualify for a threatened category in the near future.

- Vulnerable (VU), Endangered (EN) & Critically Endangered (CR)
  A taxon is VU (EN or CR, respectively) if the best available evidence indicates that it meets any of the criteria A to E for VU and is therefore considered to be at high (very high or extremely high, respectively) risk of extinction in the wild.

- Extinct in the Wild (EW)
  A taxon is EW if it is known to survive only in cultivation, captivity, or as a naturalized population (or populations) far outside its historical range. A taxon is presumed to be EW if exhaustive surveys in known and/or expected habitats at appropriate times (diurnal, seasonal, annual) throughout its historical range have failed to record an individual. Surveys should be conducted over a period of time appropriate to the life cycle and life form of the taxon.

- Extinct (EX)
  A taxon is EX when there is no reasonable doubt that the last individual has died. A taxon is presumed EX when exhaustive surveys in known and/or expected habitat at appropriate times (diurnal, seasonal, annual) throughout its historical range have failed to record an individual. Surveys should be conducted over a period of time appropriate to the life cycle and life form of the taxon.

**The Holocene extinction, the Anthropocene extinction or the sixth mass extinction?** At the October 1991 symposium *The Visions of a Sustainable World* at Caltech, Edward O. Wilson warned that "*we are now in the midst of a sixth extinction spasm, the greatest since the one that closed the age of the dinosaurs 66 million years ago.*" In 1995, Richard Leakey published the book *The Sixth Extinction*, which popularized the term in the scientific community (Leakey and Lewin, 1995). Since then, numerous research papers have been published (Pimm and Brooks, 2000; Wake and Vredenburg, 2008; Barnosky *et al.*, 2011; Dirzo *et al.*, 2014; Ceballos *et al.*, 2015; Cowie *et al.*, 2022). However, it was Elizabeth Kolbert's book *The Sixth Extinction: An Unnatural History*, which won the Pulitzer Prize in 2015, that introduced the term to the general public (Kolbert, 2014).

There is no doubt that the extinction rate observed since 1500 AD is largely higher than the background rate, as demonstrated by Pimm *et al.* (1995, page 347) ("*recent extinction rates are 100 to 1 000 times their pre-human levels in well-known, but taxonomically diverse groups from widely different environments*"), and De Vos *et al.* (2015, page 452) ("*current extinction rates are 1 000 times higher than natural background rates of extinction and future rates are likely to be 10 000 times higher*"). This is true for both terrestrial and marine extinctions (Ceballos *et al.*, 2017; Del Monte-Luna *et al.*, 2023). This is why we can speak of a Holocene extinction. There is also no doubt that this extinction event is due to humans, leading to the concept of Anthropocene extinction or defaunation (Dirzo *et al.*, 2014). However, it is still difficult to definitively classify our current epoch as the sixth mass extinction. While we meet the criterion for the elevated background extinction rate based on relation (5.6), we have yet to confirm the condition $\mu(t_1, t_2) \geq \mu^\star$. Therefore, there is no scientific research that claims that more than 75% of all marine and terrestrial vertebrate species have become extinct in the last five centuries or in the last 10 000 years. We do not really know. Moreover, a mass extinction is usually followed by a period of intense species origination. Therefore, it is difficult to say that the sixth mass extinction has already occurred (Barnosky *et al.*, 2011). The majority of scientists prefer to argue that "*we are either entering or in the midst of the sixth great mass extinction*" (Wake and Vredenburg, 2008).

Why are we talking about the sixth mass extinction? Because the number of species that have become extinct in the last few centuries is so large, these extinctions are due to human activities, and we do not expect these extinctions to stop in the next few years with population growth and deforestation. The trends are dramatic and we are clearly facing a biodiversity crisis. These facts are extensively documented in the research cited above, as well as in the monumental 1148-page report by the Intergovernmental Science-Policy Platform on Biodiversity and Ecosystem Services (IPBES, 2019).

The stylized facts about current extinction rates are based on the IUCN Red List of Threatened Species (Box 5.8). As of September 2024, the current Red List database contains 163 040 species whose extinction risk has been assessed. For each species, we can obtain the assessment report by using the search query `https://www.iucnredlist.org/search`. For example, the figures for the snow leopard are available at `www.iucnredlist.org/species/22732/50664030`. We learned that the snow leopard species (*Panthera uncia*) was assessed in November 2016. Panthera uncia is currently listed as VU (Vulnerable), whereas in 2008 it was listed as EN (Endangered). Much more information can be found in its assessment card[80].

[80] The snow leopard belongs to the following taxonomic classification tree: Animalia (kingdom), Chordata (phylum), Mammalia (class), Carnivora (order), Felidae (family), Panthera (genus), and Panthera uncia (species). The number of mature individuals is estimated to be between 2 710 and 3 386, with a decreasing population trend. It is found in Asia, including Afghanistan, Bhutan, China, India, Kazakhstan, Kyrgyzstan, Mongolia, Nepal, Pakistan, the Russian Federation, Tajikistan, and Uzbekistan. The Panthera uncia inhabits altitudes between 500 and 5 800 meters. Its home range is estimated to be about 2.8 million km$^2$ and its generation length is approximately 7.54 years. Additionally, a list of threats and conservation actions has been documented.

Figure 5.36: Number of extinct species since 1500 AD

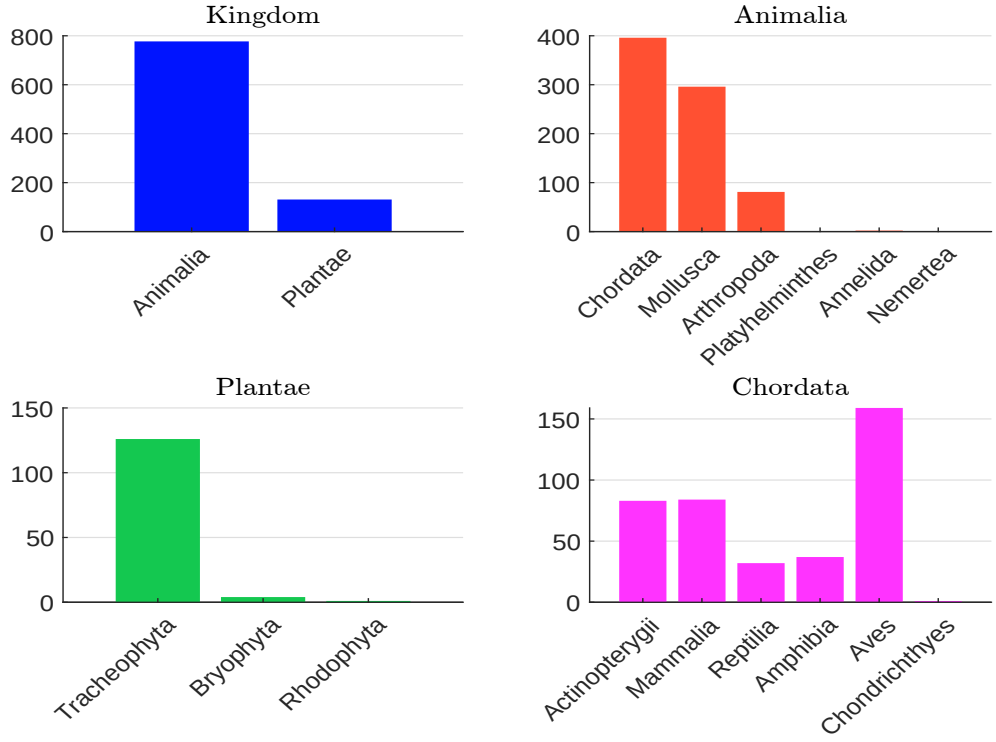


Source: IUCN (2024a), www.iucnredlist.org & Author's calculations.

Among the 163 040 species evaluated, 908 are extinct, with the following distribution: 85.6% from Animalia and 14.4% from Plantae (Table 5.25). This corresponds to an extinction rate of 0.56%. Most of these extinct species belong to four phyla: Chordata, Mollusca, Arthropoda, and Tracheophyta (Figure 5.36). Within the Chordata phylum, the class Aves (birds) is the most represented, followed by Mammalia, Actinopterygii (ray-finned fishes), Amphibia, and Reptilia. In the Mollusca phylum, most extinct species are in the class Gastropoda, with the remainder in Bivalvia. In the Tracheophyta phylum, the class Magnoliopsida is the most dominant. Some examples of extinct species are the Dodo, the Splendid Poisson Frog, the Floreana Giant Tortoise, the St Helena Olive, the Stringwood and the Galapagos Amaranth.

Table 5.25 shows the breakdown of the 163 040 evaluated species according to the IUCN Red List categories. There are 81 species classified as Extinct in the Wild (EW), with a balanced distribution between Animalia and Plantae. Examples of EW species include the Spix's Macaw, the Polynesian Tree Snail, the Golden Skiffia, the Yellow Fatu, the Superb Cyanea, and Wood's Cycad. A similar distribution between Animalia and Plantae is observed for Critically Endangered (CE) species, but their number is much larger, totaling 10 031 species. Examples include the Hainan Gibbon, the Golden Line Fish, the Gomera Stick Grasshopper, the Didymous Chamomile, the French Grass, and the Hawaiian Gardenia.

According to IUCN (2024b), the number of threatened species (TH) is defined as follows:

$$\text{TH} = \text{EW} + \text{CR} + \text{EN} + \text{VU}$$

It is usually expressed in %:

$$\text{TH}\,(\%) = \frac{\text{TH}}{\text{TOT} - \text{EX} - \text{DD}} = \frac{\text{EW} + \text{CR} + \text{EN} + \text{VU}}{\text{TOT} - \text{EX} - \text{DD}}$$

Table 5.25: Statistics of the IUCN Red List database

| Kingdom | Animalia | Chromistra | Fungi | Plantae | Total |
|---|---|---|---|---|---|
| Extinct | 777 | | | 131 | 908 |
| Extinct in the Wild | 36 | | | 45 | 81 |
| Critically Endangered | 4 067 | 4 | 45 | 5 915 | 10 031 |
| Endangered | 6 426 | 1 | 105 | 11 477 | 18 009 |
| Vulnerable | 7 165 | 1 | 178 | 9 937 | 17 281 |
| Conservation Dependent | 18 | | | 114 | 132 |
| Near Threatened | 5 149 | | 66 | 4 203 | 9 418 |
| Least Concern | 51 689 | | 240 | 33 373 | 85 302 |
| Data Deficient | 15 895 | 12 | 160 | 5 811 | 21 878 |
| Total | 91 222 | 18 | 794 | 71 006 | 163 040 |

Source: IUCN (2024a), www.iucnredlist.org & Author's calculations.

Table 5.26: Number of species assessed and number of threatened species by major group of organisms

| Taxon | Clade | Number of species | Evaluated species # | Evaluated species % | Threatened species # | Threatened species % |
|---|---|---|---|---|---|---|
| Vertebrates | Mammals | 6 701 | 5 983 | 89.3% | 1 338 | 22.4% |
| | Birds | 11 195 | 11 195 | 100.0% | 1 354 | 12.1% |
| | Reptiles | 12 162 | 10 309 | 84.8% | 1 844 | 17.9% |
| | Amphibians | 8 744 | 8 011 | 91.6% | 2 873 | 35.9% |
| | Fishes | 36 863 | 27 972 | 75.9% | 3 927 | 14.0% |
| | Subtotal | 75 665 | 63 470 | 83.9% | 11 336 | 17.9% |
| Invertebrates | Insects | 1 053 578 | 12 718 | 1.2% | 2 415 | 19.0% |
| | Molluscs | 86 859 | 9 111 | 10.5% | 2 451 | 26.9% |
| | Crustaceans | 90 531 | 3 213 | 3.5% | 747 | 23.2% |
| | Corals | 5 623 | 831 | 14.8% | 252 | 30.3% |
| | Arachnids | 95 894 | 774 | 0.8% | 272 | 35.1% |
| | Velvet Worms | 222 | 11 | 5.0% | 9 | 81.8% |
| | Horseshoe Crabs | 4 | 4 | 100.0% | 2 | 50.0% |
| | Others | 157 543 | 1 090 | 0.7% | 174 | 16.0% |
| | Subtotal | 1 490 254 | 27 752 | 1.9% | 6 322 | 22.8% |
| Plants | Mosses | 21 925 | 327 | 1.5% | 181 | 55.4% |
| | Ferns and Allies | 11 800 | 821 | 7.0% | 321 | 39.1% |
| | Gymnosperms | 1 113 | 1 059 | 95.1% | 451 | 42.6% |
| | Flowering Plants | 369 000 | 68 704 | 18.6% | 26 367 | 38.4% |
| | Green Algae | 13 960 | 17 | 0.1% | 0 | 0.0% |
| | Red Algae | 7 523 | 78 | 1.0% | 9 | 11.5% |
| | Subtotal | 425 321 | 71 006 | 16.7% | 27 329 | 38.5% |
| Fungi | Mushrooms, etc. | 156 313 | 794 | 0.5% | 328 | 41.3% |
| | Brown Algae | 4 683 | 18 | 0.4% | 6 | 33.3% |
| | Subtotal | 160 996 | 812 | 0.5% | 334 | 41.1% |
| | Total | 2 152 236 | 163 040 | 7.6% | 45 321 | 27.8% |

Source: IUCN (2024b, Table 1a), www.iucnredlist.org & Author's calculations.

where TOT is the total number of species assessed[81]. We deduce that:

$$\text{TH} = 81 + 10\,031 + 18\,009 + 17\,281 = 45\,402$$

In Table 5.26 we reproduce the calculations that can be found in IUCN (2024b, Table 1a). In this case, the number of threatened species does not include the EW category, which means that:

$$\text{TH}^\star = 10\,031 + 18\,009 + 17\,281 = 45\,321$$

The percentage of threatened species is 27.8%. Excluding the clades with low population numbers, we conclude that two categories are particularly threatened: Amphibians and flowering plants with a threat rate of 35.9% and 38.4% respectively. Figure 5.37 shows the evolution of the number of threatened species over time. Over the past 24 years, the number of threatened species has increased by 310%, which corresponds to an annual growth rate of 6.1%. This graph is widely cited and can be found in numerous publications on the current biodiversity crisis. However, caution is needed. A significant part of this trend is due to the fact that the database has become more comprehensive over time. For instance, the IUCN Red List aims to assess 260 000 species and reassess 142 000 of those already assessed by 2030. Naturally, the number of threatened species will rise as the database's coverage increases. For this reason, we have included the proportion of threatened species in Figure 5.38. Since 2010, this proportion has remained stable at around 30%.

However, the previous observation could not hide the fact that the current biodiversity crisis is real and serious, and that we may be in a sixth mass extinction period. There are so many facts that demonstrate this critical situation (Barnosky *et al.*, 2011; Ceballos *et al.*, 2015; Cowie *et al.*, 2022). A major challenge in addressing the current biodiversity crisis is the concept of '*extinction debt*' (Kuussaari *et al.*, 2009; Figueiredo *et al.*, 2019). This refers to the delayed extinction of species following environmental changes such as habitat loss, fragmentation or degradation. Despite these threats, species may persist for years, decades, or even centuries before succumbing to extinction. This lag creates a debt, where species are essentially doomed, but survive temporarily in their environment. Therefore, extension debt is related to habitat loss and relaxation time:

> "*The idea that species can initially survive habitat change but later become extinct without any further habitat modification has a long history. It was first conceptualized in island biogeography (MacArthur and Wilson, 1967) and further elaborated by Jared Diamond, who introduced the term relaxation time as the delay of expected extinctions after habitat loss. According to theoretical predictions and supporting empirical data, the relaxation time increases with increasing patch area and with decreasing isolation. A second root stems from metapopulation modeling. Tilman et al. (1994) introduced the term extinction debt and considered the order of extinctions in relation to competitive dominance [...] The concept of extinction debt is related to relaxation time but specifies the number or proportion of extant species predicted to become extinct as the species community reaches a new equilibrium after an environmental perturbation.*" (Kuussaari *et al.*, 2009, page 565).

[81] Sometimes the IUCN gives a lower and an upper bound for the estimated percentage of threatened species:

$$\text{LB}\,(\%) \leq \text{TH}\,(\%) \leq \text{UB}\,(\%)$$

where:

$$\text{LB}\,(\%) = \frac{\text{TH}}{\text{TOT} - \text{EX}} = \frac{\text{EW} + \text{CR} + \text{EN} + \text{VU}}{\text{TOT} - \text{EX}}$$

and:

$$\text{UB}\,(\%) = \frac{\text{TH}}{\text{TOT} - \text{EX}} = \frac{\text{EW} + \text{CR} + \text{EN} + \text{VU} + \text{DD}}{\text{TOT} - \text{EX}}$$

Figure 5.37: Number of species in the threatened categories (CR, EN, and VU)

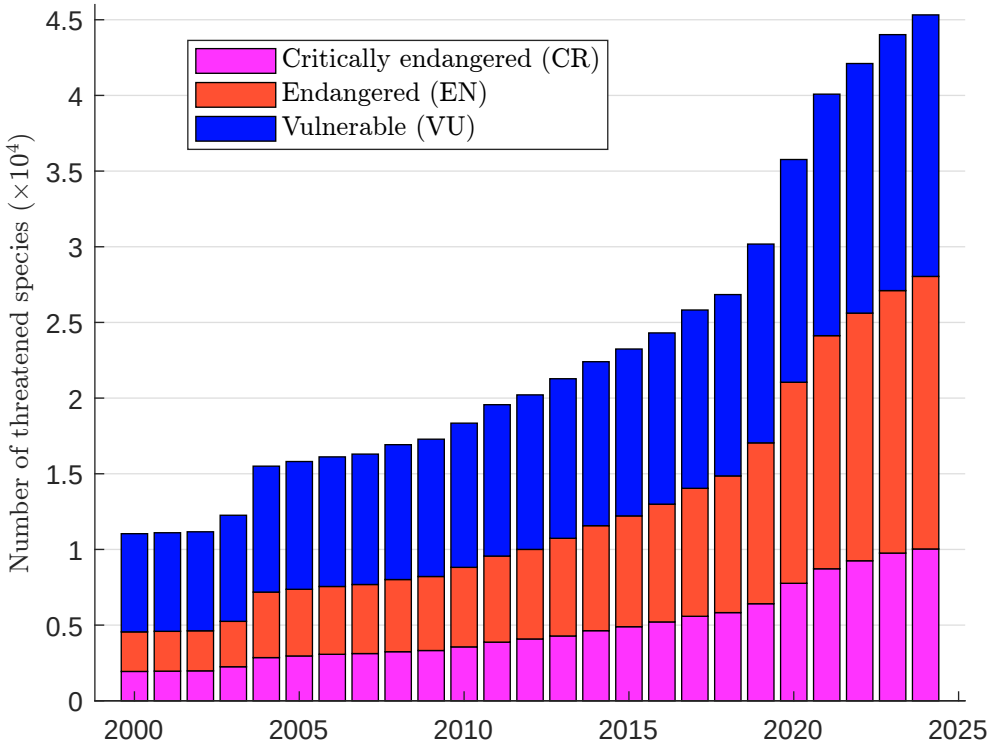


Source: IUCN (2024b, Tables 1.b & 2), www.iucnredlist.org & Author's calculations.

Figure 5.38: Percentage of species in the threatened categories (CR, EN, and VU)

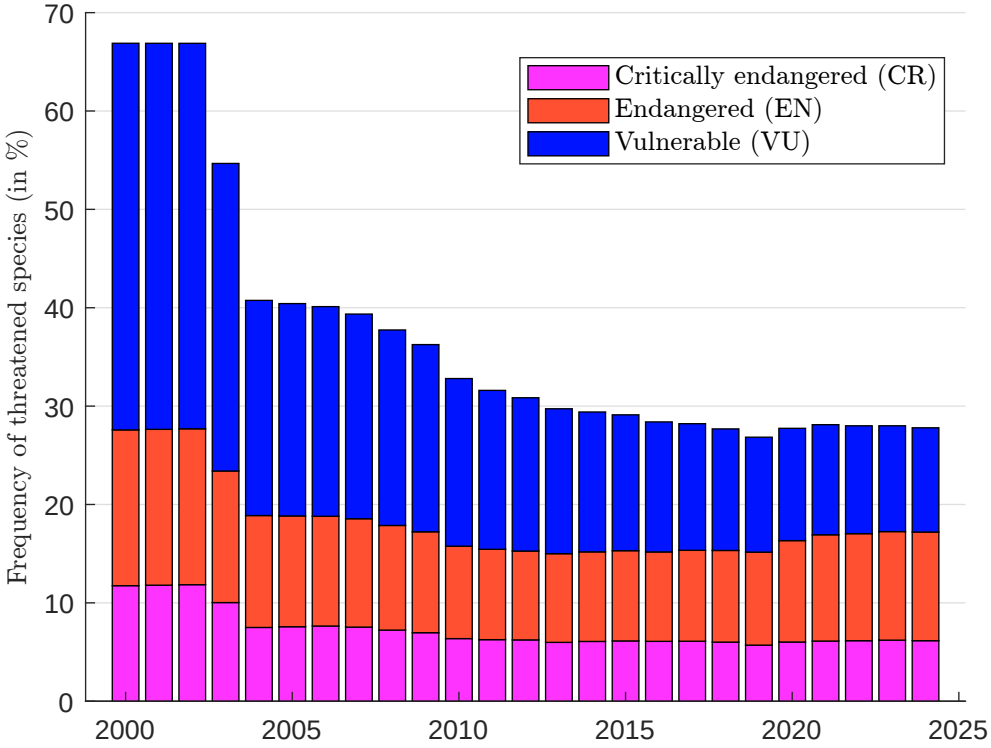


Source: IUCN (2024b, Tables 1.b & 2), www.iucnredlist.org & Author's calculations.

The issue of habitat loss is explored on page 432, while the issue of relaxation time[82] can be described as follows. Kuussaari *et al.* (2009, Glossary, page 564) defined the equilibrium (or stable) state in an ecological community when the number of species does not change because the local extinction rate is equal to the local origination rate. The relaxation time scale is then the time to reach a new equilibrium. Assessing the extinction debt for a given species involves estimating whether the species will eventually go extinct and, if so, determining the likely time of extinction. Kuussaari *et al.* (2009, Box 1, page 567) outline five main approaches for evaluating extinction debt:

- Detection of extinction debt using past and present habitat characteristics;
- Estimating extinction debt by comparing present-day stable and unstable landscapes;
- Estimating extinction debt based on past and present species richness and habitat characteristics;
- Tracking extinction debt based on time series data;
- Evaluating extinction debt for single species using empirical population data and spatially explicit modeling.

The survey of empirical studies on extinction debt by Kuussaari *et al.* (2009, Table 1, page 568) found inconsistencies across these approaches. For instance, studies using the first approach typically conclude that amphibians are subject to extinction debts, while studies using the second approach often suggest that amphibians are not subject to extinction debts. However, empirical evidence consistently suggests that forest birds, primates, wood-living fungi, and forest beetles are likely to have extinction debts.

In Halley *et al.* (2016b), it is assumed that the remaining habitat area is reduced from $A_0$ to $A$, leading to a corresponding decline in species richness to a new value $S(t)$ at time $t$. The equation governing species loss is given by:

$$\frac{\mathrm{d}S(t)}{\mathrm{d}t} = \lambda(t) - \mu(t) S(t) \tag{5.7}$$

where $\lambda(t)$ is the origination rate and $\mu(t)$ is the extinction date. The remaining habitat contains a (constant) number $N(t)$ of individuals, which is proportional to the area $A$ and the density $\rho$ of individuals per unit area: $N(t) = \rho A$. Let $n(t) = N(t)/S(t)$ be the average population size per species. At time $t = 0$, we have $n = N_0/S_0 = \rho A/S_0$ where $S(0) = S_0$ is the initial species richness. The authors further assumed that the extinction rate is described by:

$$\mu(t) = kn(t)^{-\alpha} = k\left(\frac{S(t)}{N(t)}\right)^{\alpha}$$

Therefore, Equation (5.7) becomes:

$$\frac{\mathrm{d}S(t)}{\mathrm{d}t} = \lambda(t) - k\left(\frac{S(t)}{\rho A}\right)^{\alpha} S(t) = \lambda(t) - \frac{k}{n^{\alpha} S_0^{\alpha}} S(t)^{\alpha+1} \tag{5.8}$$

The numerical solution can be easily found when the origination rate $\lambda(t)$ is specified. In the case of extinction debt, we can assume that $\lambda(t) = 0$ and the solution is[83]:

$$S(t) = S_0\left(1 + \frac{k\alpha}{n^{\alpha}} t\right)^{-1/\alpha} \tag{5.9}$$

[82] The concept of relaxation time is used extensively in equilibrium temperature modeling (see pages 671 and 683) and bifurcation theory (see page 692).

[83] This is derived from the known solution of the differential equation $x'(t) = -bx(t)^{\alpha+1}$ with initial condition $x(0) = x_0$, which is $x(t) = \left(\alpha b t + x_0^{-\alpha}\right)^{-1/\alpha}$.

Figure 5.39 shows the evolution of the relative species richness for various values of $\alpha$ with fixed parameters $A = 500$, $k = 0.20$, $\rho = 0.90$ and $S_0 = 100$. As the value of $\alpha$ approaches 0, the solution converges to the exponential model, which assumes species richness is independent of population size. In this case we have $S(t) = S_0 e^{-kt}$. When $\alpha$ approaches 1, we obtain the neutral model, where species richness remains constant over time: $S(t) = S_0$. In the other cases $\alpha \in (0, 1)$, the extinction curve follows a hyperbolic trajectory. To understand the effect of time, Halley *et al.* (2016b) examine the case $\alpha = 0.5$ and show that the extinction debt is inversely proportional to the square of time:

$$S(t) = \frac{S_0}{\left(1 + \frac{k}{2\sqrt{n}}t\right)^2} \sim \frac{2S_0}{k^2}t^{-2}$$

Extinction debt is typically quantified by the relaxation time $\tau$, which represents the time required for species richness to decrease by half. Solving the equation $S(t) = S_0/2$ gives the following solution:

$$S_0\left(1 + \frac{k\alpha}{n^\alpha}\tau\right)^{-1/\alpha} = \frac{S_0}{2} \Leftrightarrow \tau = (2^\alpha - 1)\frac{n^\alpha}{k\alpha} \propto n^\alpha$$

In the previous example, $\tau$ is equal to 4.2, 8.8 and 18.6, respectively.

Figure 5.39: Relative species richness and relaxation time

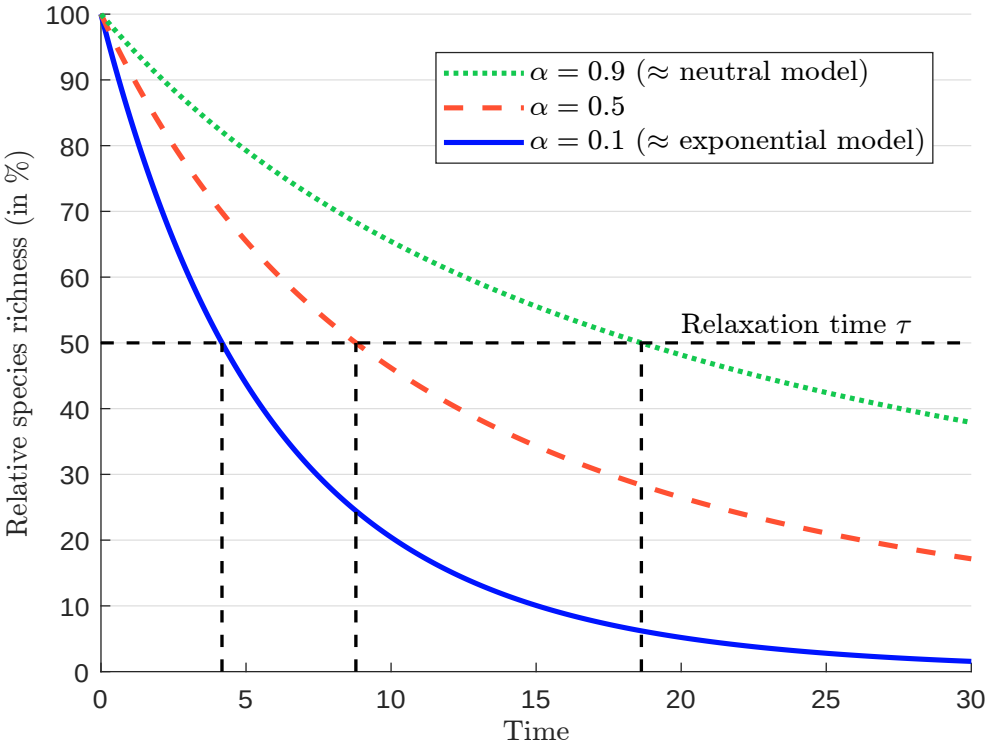


The previous analysis assumes no speciation, which means that the equilibrium species richness $\bar{S} = \lim_{t\to\infty} S(t)$ ultimately approaches zero. To get a more realistic model, we now introduce a constant origination rate: $\lambda(t) = \lambda$. The equilibrium state $\bar{S}$ is reached when the rate of change in species richness becomes zero:

$$\frac{\mathrm{d}S(t)}{\mathrm{d}t} = 0 \Leftrightarrow \lambda - \frac{k}{n^\alpha S_0^\alpha}\bar{S}^{\alpha+1} = 0 \Leftrightarrow \bar{S} = \left(\frac{\lambda n^\alpha S_0^\alpha}{k}\right)^{1/(\alpha+1)}$$

This is the value of the steady state after the reduction of the area to $A$. Before reducing the area, the steady state $\bar{S}_0$ satisfies the following equation:

$$\lambda - \frac{k}{n_0^\alpha \bar{S}_0^\alpha} \bar{S}_0^{\alpha+1} = 0 \Leftrightarrow \bar{S}_0 = \left( \frac{\lambda (\rho A_0)^\alpha}{k} \right)^{1/(\alpha+1)}$$

because the original habitat area was $A_0$ and $n_0 = \rho A_0 / \bar{S}_0$. In Figure 5.40 we illustrate the transition from one steady state to another. We use the following parameters: $A_0 = 1000$, $A = 500$, $k = 0.10$, $\alpha = 0.5$, $\rho = 10$ and $\lambda = 5\%$. Initially, at time $t = -1000$ years, we consider two starting values for species richness: $S(-1000) = 15$ and $S(-1000) = 12$. Both trajectories converge to the steady state value $\bar{S}_0 = 13.572$. At time $t = 0$, we reduce the available habitat by 50%, causing the species richness to shift to a new steady state $\bar{S}_0 = 10.772$. However, it takes time, and the transition between the two equilibria is not instantaneous. It is gradual, resulting in what is known as an extinction debt. The key challenge is to determine whether we are in the early or late stages of this extinction debt process.

Figure 5.40: Extinction debt and steady state

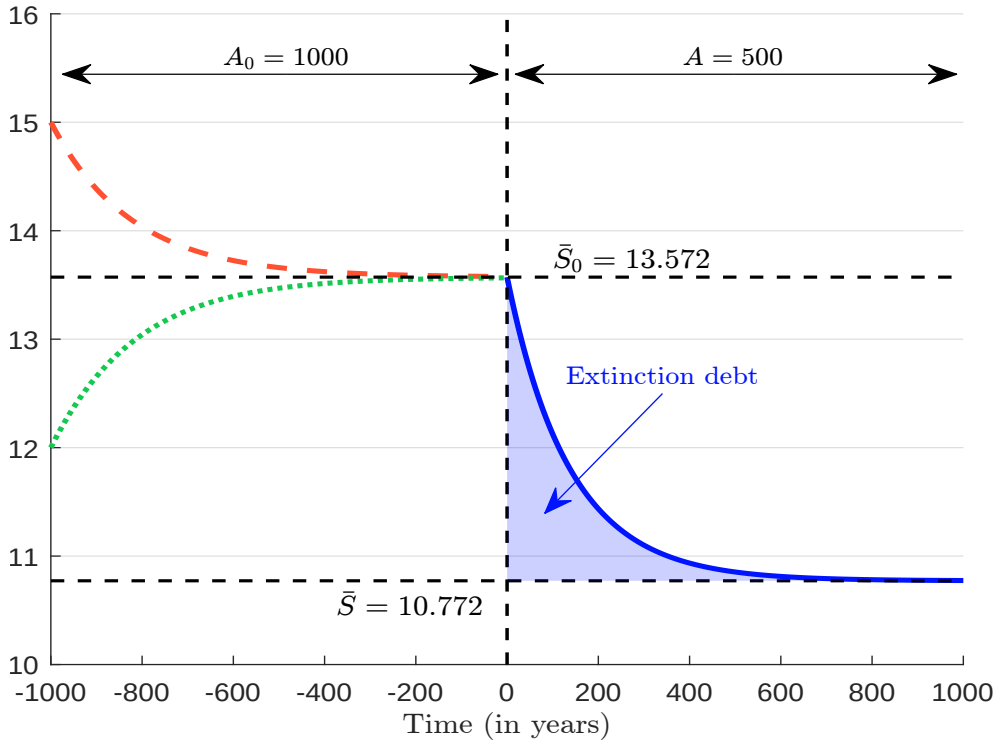


**Remark 55** *The modeling of extinction debt, particularly in relation to the current biodiversity crisis, has generated extensive research. Notable contributions include the work of Tilman et al. (1994), Hanski and Ovaskainen (2002, 2003), and more recently, Spalding and Hull (2021) with the pulse event model (Box 5.9).*

Box 5.9: The Spalding-Hull pulse model

Spalding and Hull (2021) extended the constant birth-death model by introducing extinction pulses:

$$\mu^{(\text{pulse})}(t) = \mu_0 - \sum_{k=1}^{n^{(\text{pulse})}} \omega_k^{(\text{pulse})} \ln\left(1 - A_k^{(\text{pulse})}\right) f_k\left(t - t_k^{(\text{pulse})}\right)$$

where $\mu_0$ is the background rate, $n^{(\text{pulse})}$ is the number of pulses, $\omega_k^{(\text{pulse})}$, $A_k^{(\text{pulse})}$ and $t_k^{(\text{pulse})}$ are the scaling factor, the fraction of species removed and the date of the $k^{\text{th}}$ extinction pulse event, and $f_k(x)$ is the probability density function. For example, Spalding and Hull (2021) used the Gaussian single pulse model:

$$\mu^{(\text{pulse})}(t) = \mu_0 - \omega^{(\text{pulse})} \frac{\ln\left(1 - A^{(\text{pulse})}\right)}{\sigma\sqrt{2\pi}} \exp\left(-\frac{1}{2}\left(\frac{t - t^{(\text{pulse})}}{\sigma}\right)^2\right)$$

where $\sigma$ is the standard deviation controlling the pulse duration. We deduce that:

$$\begin{aligned}
\mathcal{E}(t) &= \frac{1}{\Delta t}\int_t^{t+\Delta t} \mu^{(\text{pulse})}(s)\ \mathrm{d}s \\
&= \mu_0(s) - \frac{\omega^{(\text{pulse})} \ln\left(1 - A^{(\text{pulse})}\right)}{\Delta t}\left(\Phi\left(\frac{t + \Delta t - t^{(\text{pulse})}}{\sigma}\right) - \Phi\left(\frac{t - t^{(\text{pulse})}}{\sigma}\right)\right)
\end{aligned}$$

Using the following parameters: $\mu_0 = 0.1\,\text{E/MSY}$, $\omega = 10^5$, $A^{(\text{pulse})} = 30\%$, $\sigma = 120$ years, and $t^{(\text{pulse})} = 2100$ years AD, we obtain the results given in Figure 5.C.

Figure 5.C: Illustration of the Spalding-Hull pulse model

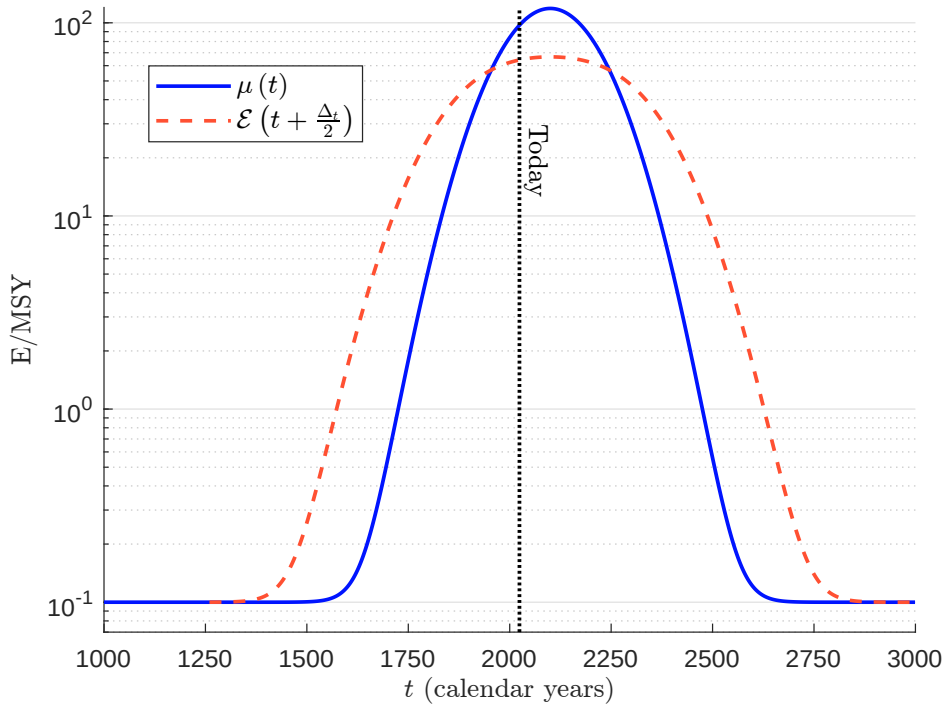

### Biodiversity hotspot

A biodiversity hotspot is a region of the world that is both rich in plant and animal species and highly threatened by human activities. Specifically, it is characterized by the following two criteria:

- Exceptional levels of endemism: The region must have at least 1 500 species of vascular plants that are endemic, meaning that they are found nowhere else on Earth;
- High levels of habitat loss: The region must have lost at least 70% of its original natural vegetation, typically due to human activities such as deforestation, agriculture, or urbanization.

The term biodiversity hotspot was coined by Norman Myers, who identified 10 geographic regions as conservation priorities (Myers, 1988). This list has been updated twice by Norman Myers: 18 hotspots in 1990 and 25 hotspots in 2000 (Myers, 1990; Myers *et al.*, 2000). New publications have updated this list several times (Mittermeier *et al.*, 2011). The last update is done by Noss *et al.* (2015), who included the North American Coastal Plain. Today we recognize 36 biodiversity hotspots (Figure 5.41).

Figure 5.41: The 36 biodiversity hotspots

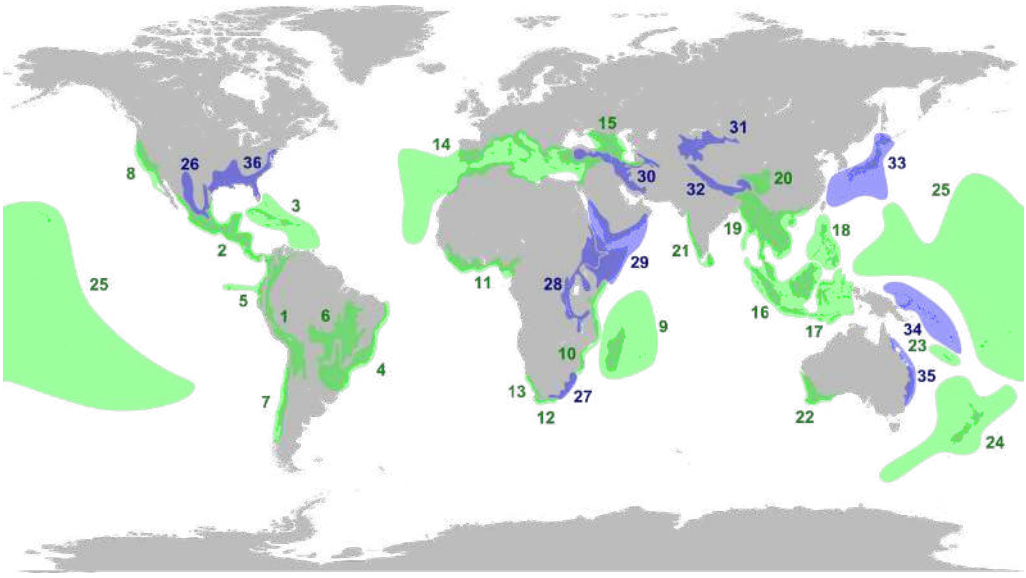


The 25 original biodiversity hotspots identified by Myers *et al.* (2000) are in green, while the added eleven regions are in blue. The 36 regions are (1) Tropical Andes, (2) Mesoamerica, (3) Caribbean Islands, (4) Atlantic Forest, (5) Tumbes-Chocó-Magdalena, (6) Cerrado, (7) Chilean Winter Rainfall-Valdivian Forests, (8) California Floristic Province, (9) Madagascar and the Indian Ocean Islands, (10) Coastal Forests of Eastern Africa, (11) Guinean Forests of West Africa, (12) Cape Floristic Region, (13) Succulent Karoo, (14) Mediterranean Basin, (15) Caucasus, (16) Sundaland, Indonesia and Nicobar islands of India, (17) Wallacea of Indonesia, (18) Philippines, (19) Indo-Burma, Bangladesh, India and Myanmar, (20) Mountains of Southwest China, (21) Western Ghats and Sri Lanka, (22) Southwest Australia, (23) New Caledonia, (24) New Zealand, (25) Polynesia-Micronesia, (26) Madrean pine-oak woodlands, (27) Maputaland-Pondoland-Albany, (28) Eastern Afromontane, (29) Horn of Africa, (30) Irano-Anatolian, (31) Mountains of Central Asia, (32) Eastern Himalaya, (33) Japan, (34) East Melanesian Islands, (35) Eastern Australian temperate forests, and (36) North American Coastal Plain.

Source: upload.wikimedia.org/wikipedia/commons/9/93/Biodiversity_Hotspots.svg.

These biodiversity hotspots cover only 2.5% of the Earth's land surface, but support more than half of the world's endemic plant species. As shown in Figure 5.41, many of these hotspots are concentrated around the tropics. Biodiversity is unevenly distributed across the Earth's surface, a pattern known as the biodiversity gradient. This concept refers to the variation in species diversity across geographic regions, often along specific environmental gradients. The most common example is the latitudinal biodiversity gradient, which describes how species richness generally increases as one moves from the poles toward the equator (Willig *et al.*, 2003). As noted by Gaston and Spicer (2004, Section 3.4, pages 71-85), it is hard to explain this phenomenon[84], understand the causes and draw general conclusions.

In fact, biodiversity hotspots are often characterized by a high extinction debt because they frequently host species that are on a delayed extinction pathway due to past habitat destruction. These regions are at high risk of losing species in the future, even if no additional habitat loss occurs. The existence of an extinction debt makes conservation efforts in hotspots particularly urgent, as many species may already be committed to extinction. Fragmentation and isolation in these areas exacerbate the problem by weakening the long-term survival chances of species. Therefore, unless immediate action is taken, biodiversity hotspots may face significant hidden biodiversity loss and a substantial extinction debt.

### 5.4.2 Ecosystem functions and services

#### Definition

Ecosystem functions are natural processes, such as nutrient cycling, while ecosystem services are the benefits humans derive from these processes, such as food:

> "*In our increasingly technological society, people give little thought to how dependent they are on the proper functioning of ecosystems and the crucial services for humanity that flow from them. Ecosystem services are* "the conditions and processes through which natural ecosystems, and the species that make them up, sustain and fulfill human life" *(Daily, 1997, page 3); in other words,* "the set of ecosystem functions that are useful to humans" *(Kremen, 2005, page 468). Although people have been long aware that natural ecosystems help support human societies, the explicit recognition of "ecosystem services" is relatively recent (Mooney and Ehrlich, 1997).*" (Sekercioglu, 2010, page 45).

Sekercioglu (2010) classified ecosystem services into 6 categories: (1) climate and biogeochemical cycles (climate stability, air purification, UV protection), (2) regulation of the hydrological cycle (drought mitigation, flood mitigation, water purification), (3) soils and erosion (detoxification and decomposition of wastes, soil formation and soil fertility), (4) biodiversity and ecosystem function (ecosystem goods), (5) mobile linkages (pollination, seed dispersal), and (7) nature's remedies for emerging diseases (medicine, pest control). For his part, Gaston and Spicer (2004, Chapter 4) made the distinction between direct-use and indirect-use values of ecosystem services. The direct-use

[84] Gaston and Spicer (2004, pages 72 and 73) highlights four key features of the latitudinal biodiversity gradient:

- Persistence: The latitudinal gradient has been a consistent feature throughout much of Earth's history;
- Equatorial Peak: The peak of biodiversity often occurs slightly off-center from the equator;
- Asymmetry: The gradient often shows an asymmetric pattern, with a steeper increase from northern regions toward the equator and a more gradual decrease from the equator to southern regions;
- Steepness variation: The steepness of the gradient can vary considerably among taxonomic groups. For example, butterflies are more tropical than birds.

value describes the role of biological resources in consumption or production and mainly concerns commodities such as food, medicine and industrial materials. This category also includes biological control, recreational use (*e.g.*, hunting and fishing), and ecotourism. Indirect-use values are more related to ecosystem functions such as atmospheric regulation, climate regulation, hydrological regulation, nutrient cycling, pest control, photosynthesis, pollination, and soil formation and maintenance.

One of the first classifications of ecosystem services was developed by Millennium Ecosystem Assessment (2005, Table 1, page 7 & Box 3.1, page 50). They distinguished 4 families: supporting, provisioning, regulating and cultural services. However, they emphasized the main role of supporting ecosystem services (nutrient cycling, soil formation, primary production), which is essential for the other three ecosystem services[85]. In other words, without supporting ecosystem services, there is no life. The major report of IPBES (2019, Glossary, page 1031) adopted a different classification based on three categories: material (corresponding to provisioning services), regulating (corresponding to the merger of supporting and regulating services), non material (corresponding to cultural services). This three-category system has also been adopted by ENCORE (2024) and TNFD (2023, page 28), which distinguish between (1) provisioning, (2) regulation and maintenance, and (3) cultural services. However, the categorization between the last three systems changes relatively when we consider the Level 2 system[86]. Below is a list of the different ecosystem services described in the 4 classification systems:

1. Aesthetic and cultural services

    - Aesthetic, symbolic and spiritual values (nature inspires creativity, provides spiritual connections, and contributes to cultural identity)
    - Cultural and spiritual significance (many ecosystems have deep cultural, historical or spiritual significance for local communities and indigenous peoples)
    - Educational, scientific and research services (biodiversity provides opportunities for scientific study and learning)
    - Recreational opportunities and tourism (forests, parks and other natural areas provide opportunities for recreation and tourism)
    - Visual amenity services (non-material benefits that contribute to well-being, emotional satisfaction, and cultural enrichment)

2. Provisioning services

    - Energy (natural processes by which ecosystems produce energy such as biomass, solar energy capture, and fossil fuels)
    - Food and feed (agriculture, biomass supply, fisheries, plants, animals, seafood, and livestock)
    - Genetic resources (biodiversity provides genetic material essential for breeding crops and livestock, and developing new technologies)

[85] Provisioning services include food, freshwater, timber, wood, fiber, fuel, and genetic resources; regulating services include the regulation of climate, floods, disease, water quality, and waste management; and cultural services include recreation, aesthetic enjoyment, education, and spiritual fulfillment.

[86] In the case of ENCORE, the classification system is described in the two CSV files of the 2024 zipped database: `ENCORE knowledge base/Encore files/02. Ecosystem services definition.csv` and `ENCORE knowledge base/Encore files/08. Ecosystem services and ecosystem components.csv`. A comparison of the three systems (IPBES, ENCORE and TNFD) can be found in NGFS (2024, Table 1, page 45).

- Medicinal and biochemical resources (many medicines and pharmaceutical products are derived from natural compounds found in biodiversity)
- Raw materials (timber, fuel wood, minerals, fibers, and other natural resources)
- Water supply (clean water for drinking, irrigation, and industrial use)

3. Regulating services

- Air quality regulation (ecosystems filter pollutants from the air, improving air quality)
- Climate regulation (forests absorb carbon dioxide and help regulate global temperatures)
- Waste detoxification and decomposition (natural decomposition of organic matter, natural ability to detoxify harmful chemicals and pollutants)
- Erosion control (vegetation helps stabilize soils, reducing erosion and preventing landslides)
- Hazard and extreme event regulation (flood, storm, rainfall)
- Pest and disease control (natural predators and parasites help regulate populations of harmful organisms)
- Pollination and seed dispersal (bees, birds, insects, and other pollinators allow many plants to reproduce)
- Water purification (freshwater, wetlands, and forests filter pollutants from water)

4. Supporting services

- Habitat creation and maintenance (habitats are the natural environments in which organisms live, grow, and reproduce; they form the basis of ecosystems by providing the resources necessary for species to thrive)
- Nutrient cycling (the movement of nutrients through ecosystems, essential for plant growth and productivity)
- Photosynthesis (plants convert solar energy into chemical energy, producing oxygen and forming the base of the food chain)
- Primary production (the production of organic material by plants and algae forms the foundation of ecosystems)
- Soil formation and fertility (the breakdown of rocks and organic matter to create soil)
- Water cycle regulation (ecosystems play an important role in regulating the water cycle, from evaporation to precipitation)

Rather than examining all of these ecosystem services, we focus on two of them (pollination and food) to illustrate the importance of ecosystem functions. We also develop the concept of natural capital, which is essential for valuing these ecosystem services.

### Natural capital

Ecosystem services are derived from natural capital, which can be defined as the world's stock of natural assets, including geology, soil, air, water, and all living things. The concept of natural capital in biodiversity is generally attributed to David Pearce, an environmental economist, with his work on the economics of sustainable development (Pearce, 1988). However, the concept itself draws on earlier ideas in ecological economics[87]. For example, the underlying idea of natural capital can be

[87] For a historical perspective on natural capital in economics, the reader can refer to Åkerman (2003) and Missemer (2018).

found in the extension of input-output models[88] proposed by Daly (1968), who argued that biology and economics are not two separate sciences but need to be integrated:

> "*The purpose of this essay is to bring together some of the more salient similarities between biology and economics and to argue that, far from being superficial, these analogies are profoundly rooted in the fact that the ultimate subject matter of biology and economics is* one, *viz.*, the life process." (Daly, 1968, page 392).

However, the concept was really popularized by Robert Costanza in 1997 and his seminal paper on the valuation of ecosystem services and natural capital (Costanza *et al.*, 1997). The definition of natural capital has remained largely consistent since Pearce (1988), for whom natural capital is "*the set of all environmental assets*". Costanza and Daly (1992) used the stock-flow model to define capital as a stock that provides a flow of valuable goods or services into the future. In this context, natural capital and natural income are simply the stock and flow components, respectively, of natural resources. Today, natural capital is broadly recognized as the stock of environmental assets and ecosystem services that provide goods and services to humans and life. The challenge, once this definition is accepted, is to determine the full extent of these assets and services and to value them accurately.

Table 5.27: Total value of annual ecosystem services in 1997 (1995 price levels)

| Biome | Area (in ha $\times 10^6$) | Value (in \$/ha/yr) | Total value (in \$ bn/yr) | Breakdown (in %) |
|---|---|---|---|---|
| Marine | 36 302 | 577 | 20 949 | 63.0 |
| Open ocean | 33 200 | 252 | 8 381 | 25.2 |
| Coastal | 3 102 | 4 052 | 12 568 | 37.8 |
| Terrestrial | 15 323 | 804 | 12 319 | 37.0 |
| Forest | 4 855 | 969 | 4 706 | 14.1 |
| Grassland & meadow | 3 898 | 232 | 906 | 2.7 |
| Wetland | 330 | 14 785 | 4 879 | 14.7 |
| Lake & river | 200 | 8 498 | 1 700 | 5.1 |
| Desert | 1 925 | | | |
| Tundra | 743 | | | |
| Ice & rock | 1 640 | | | |
| Cropland | 1 400 | 92 | 128 | 0.4 |
| Urban | 332 | | | |
| Total | 51 625 | | 33 268 | 100.0 |

Source: Costanza *et al.* (1997, Table 2, page 256) & Author's calculations.

The publication of Costanza *et al.* (1997) marked a milestone in the valuation of natural capital. They estimated that the value of ecosystem services was in the range of \$16–\$54 trillion per year, with an average of \$33 tn/yr in 1995. Given that world GDP was \$28 trillion per year, ecosystems would represent 1.2 times the economic value created by humans (Pearce, 1998). The positive reception of the paper published in *Nature* was largely supported by the scientific community, although we can find some criticism of the methodology, the total figure of \$33 tn/yr and the applicability to environmental policy. However, the impact of the paper has been profound, leading to further research on ecosystem service valuation.

[88] See Section 8.4.2 on page 819.

The natural capital $\mathcal{K}$ is the sum of the natural capital $\mathcal{K}_{i,j}$ for $n$ biomes and $m$ ecosystem services:

$$\mathcal{K} = \sum_{i=1}^{n} \sum_{j=1}^{m} \mathcal{K}_{i,j} \tag{5.10}$$

We can assume that the value of a biome's ecosystem service is proportional to its area:

$$\mathcal{K}_{i,j} = A_i V_{i,j} \tag{5.11}$$

where $A_i$ is the area of biome $i$ (in hectares) and $V_{i,j}$ is the monetary value of ecosystem service $j$ (in dollars per hectare per year). Therefore, $\mathcal{K}_{i,j}$ and $\mathcal{K}$ are expressed in dollars per year. From Equation (5.10), we deduce that:

$$\mathcal{K} = \sum_{i=1}^{n} \mathcal{K}_i^{(\text{biome})} = \sum_{j=1}^{m} \mathcal{K}_j^{(\text{service})} \tag{5.12}$$

where $\mathcal{K}_i^{(\text{biome})} = \sum_{j=1}^{m} A_i V_{i,j} = A_i \sum_{j=1}^{m} V_{i,j}$ and $\mathcal{K}_j^{(\text{service})} = \sum_{i=1}^{n} A_i V_{i,j}$. To calculate $\mathcal{K}_{i,j}$ or $V_{i,j}$, Costanza *et al.* (1997) estimated the willingness-to-pay of individuals for ecosystem services. For example, if a 10-hectare forest provides \$500 per year in market benefits for raw materials and \$250 per year in non-market benefits for aesthetic services, the total value of ecosystem services for that forest would be \$750 per year or \$75 $\text{ha}^{-1}\text{yr}^{-1}$. In Table 5.27, we report the values of annual ecosystem services for the different biomes estimated by Costanza *et al.* (1997). Of the \$33 tn, 63% comes from marine biomes and 37% from terrestrial biomes. In the case of marine biomes, both open ocean and coastal areas make a significant contribution, the former because of its large area (33 200 ha), the latter because of its high unit value (\$4 052 $\text{ha}^{-1}\text{yr}^{-1}$). In the case of terrestrial biomes, forest and wetland are the two main contributors, the former because of its large area (4 855 ha), the latter because of its high unit value (\$14 785 $\text{ha}^{-1}\text{yr}^{-1}$). Table 5.28 shows the breakdown of the \$33 tn in terms of the 17 ecosystem services examined by the authors. 51.3% comes from nutrient cycling, followed by cultural services at 9.1%, waste treatment at 6.8%, and disturbance regulation at 5.3%.

The previous study has been updated in 2014 using the same methodology, but with a more comprehensive approach to estimate the unit value $V_{i,j}$. In fact, the unit values in Costanza *et al.* (2014) are based on the TEEB valuation database developed by Van der Ploeg and de Groot (2010), which collected 1 310 value estimates from 320 publications. An analysis of this database can be found in De Groot *et al.* (2012), who selected 665 unit values. For example, using 2007 price levels, they estimate that the mean value of coral reefs is \$352 249 $\text{ha}^{-1}\text{yr}^{-1}$, while the mean value of open oceans is only \$491 $\text{ha}^{-1}\text{yr}^{-1}$. Other interesting figures are: \$193 845 $\text{ha}^{-1}\text{yr}^{-1}$ for coastal wetlands, \$25 682 $\text{ha}^{-1}\text{yr}^{-1}$ for coastal wetlands, \$5 264 $\text{ha}^{-1}\text{yr}^{-1}$ for tropical forests, \$4 267 $\text{ha}^{-1}\text{yr}^{-1}$ for lakes and rivers, etc. We report the calculations made by Costanza *et al.* (2014) for the year 2011 in Table 5.29. The authors estimated 4 total values of natural capital by considering both 1997 and 2011 figures. Using 2007 price levels[89], they obtained \$45.9 tn/yr when considering 2011 biome areas and unit values, \$41.6 tn/yr when considering 2011 biome areas and 1997 unit values, \$145 tn/yr when considering 1997 biome areas and 2011 unit values, and \$124.8 tn/yr when considering 2011 biome areas and unit values. These different figures can be used to assess changes in biome areas and the effect of updated unit values. They concluded that changes in global land use have resulted in a loss of ecosystem services ranging from \$4.3 to \$20.2 tn/yr.

[89]The 1997 study used 1995 prices to calculate unit values. To convert them to 2007 prices, we need to multiply them by a factor of 1.38.

Table 5.28: Average global value of annual ecosystem services in 1997 (1995 price levels)

| # | Ecosystem service | Ecosystem functions | Value (in $ bn/yr) | Breakdown (in %) |
|---|---|---|---|---|
| 1 | Gas regulation | Regulation of atmospheric chemical composition | 1 341 | 4.0 |
| 2 | Climate regulation | Regulation of global temperature, precipitation, and other biologically mediated climatic processes at global or local levels | 684 | 2.1 |
| 3 | Disturbance regulation | Capacitance, damping, and integrity of ecosystem response to environmental fluctuations | 1 779 | 5.3 |
| 4 | Water regulation | Regulation of hydrological flows | 1 115 | 3.4 |
| 5 | Water supply | Storage and retention of water | 1 692 | 5.1 |
| 6 | Erosion control and sediment retention | Retention of soil within an ecosystem | 576 | 1.7 |
| 7 | Soil formation | Soil formation processes | 53 | 0.2 |
| 8 | Nutrient cycling | Storage, internal cycling, processing, and acquisition of nutrients | 17 075 | 51.3 |
| 9 | Waste treatment | Recovery of mobile nutrients and removal or breakdown of excess or xenic nutrients and compounds | 2 277 | 6.8 |
| 10 | Pollination | Movement of floral gametes | 117 | 0.4 |
| 11 | Biological control | Trophic-dynamic regulations of populations | 417 | 1.3 |
| 12 | Refugia | Habitat for resident and transient populations | 124 | 0.4 |
| 13 | Food production | That portion of gross primary production extractable as food | 1 386 | 4.2 |
| 14 | Raw materials | That portion of gross primary production extractable as raw materials | 721 | 2.2 |
| 15 | Genetic resources | Sources of unique biological materials and products | 79 | 0.2 |
| 16 | Recreation | Providing opportunities for recreational activities | 815 | 2.4 |
| 17 | Cultural | Providing opportunities for non-commercial uses | 3 015 | 9.1 |
| | Total | | 33 268 | 100.0 |

Source: Costanza *et al.* (1997, Table 2, page 256) & Author's calculations.

Table 5.29: Changes in annual ecosystem services between 1997 and 2011

| | Area (in hectare) | | Unit values (in $/ha/yr) | | Total value (in $/yr) | | | | |
|---|---|---|---|---|---|---|---|---|---|
| Price levels | | | 2007 | 2007 | 1995 | 2007 | 2007 | 2007 | 2007 |
| Area | 1997 | 2011 | | | 1997 | 1997 | 2011 | 1997 | 2011 |
| Unit values | | | 1997 | 2011 | 1997 | 1997 | 1997 | 2011 | 2011 |
| Marine | 36 302 | 36 302 | 796 | 1 368 | 20.9 | 28.9 | 29.5 | 60.5 | 49.7 |
| Open Ocean | 33 200 | 33 200 | 348 | 660 | 8.4 | 11.6 | 11.6 | 21.9 | 21.9 |
| Coastal | 3 102 | 3 102 | 5 592 | 8 944 | 12.6 | 17.3 | 18.0 | 38.6 | 27.7 |
| Terrestrial | 15 323 | 15 323 | 1 109 | 4 901 | 12.3 | 17.0 | 12.1 | 84.5 | 75.1 |
| Forest | 4 855 | 4 261 | 1 338 | 3 800 | 4.7 | 6.5 | 4.7 | 19.5 | 16.2 |
| Grassland | 3 898 | 4 418 | 321 | 4 166 | 0.9 | 1.2 | 1.4 | 16.2 | 18.4 |
| Wetland | 330 | 188 | 20 404 | 140 174 | 4.9 | 6.7 | 3.4 | 36.2 | 26.4 |
| Lake & river | 200 | 200 | 11 727 | 12 512 | 1.7 | 2.3 | 2.3 | 2.5 | 2.5 |
| Cropland | 1 400 | 1 672 | 126 | 5 567 | 0.1 | 0.2 | 0.2 | 7.8 | 9.3 |
| Urban | 332 | 352 | | 6 661 | | | | 2.2 | 2.3 |
| Total | 51 625 | 51 625 | | | 33.3 | 45.9 | 41.6 | 145.0 | 124.8 |
| Difference | | | | | | | −4.3 | | −20.2 |

Source: Costanza *et al.* (2014, Table 3, page 156) & Author's calculations.

Figure 5.42: World map with the different ecosystem types and the calculated values of their ecosystem services (in US dollars per hectare per year)

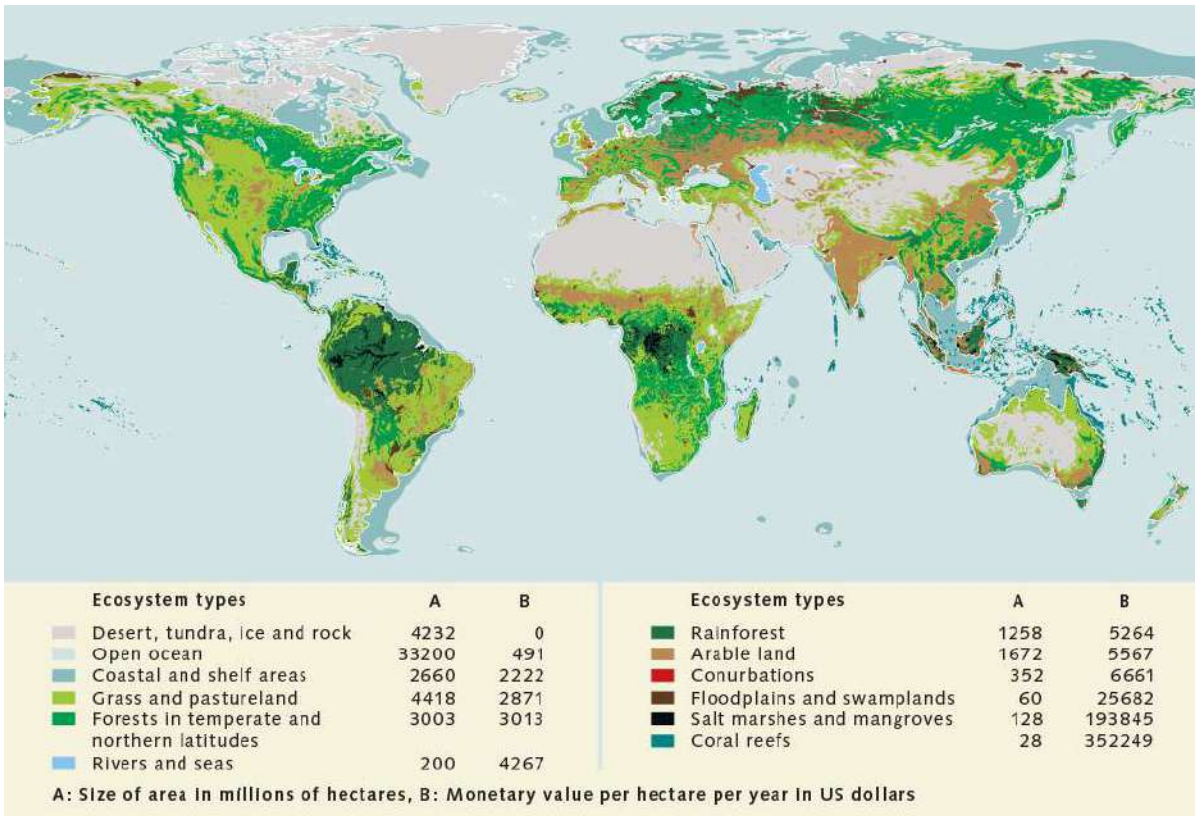


Source: World Ocean Review (2015, Figure 1.12, page 27).

**Remark 56** *Since 1997, the valuation of ecosystem services has been widely adopted by scientists, organizations and policy makers*[90] *(Hein et al., 2020; Legesse et al, 2022). The following are some of the frameworks, projects and initiatives for the valuation of ecosystem services*[91]*: System of Environmental-Economic Accounting (SEEA), Common International Classification of Ecosystem Services (CICES), The Economics of Ecosystems and Biodiversity (TEEB), Natural Capital Accounting and Valuation of Ecosystem Services (NCAVES).*

Box 5.10: The System of Environmental-Economic Accounting (SEEA)

The System of Environmental-Economic Accounting (SEEA), endorsed by the United Nations, is a framework that integrates economic and environmental data to provide a comprehensive view of the interactions between the economy and the environment, and the stocks and flows of environmental assets. It establishes common concepts, definitions, classifications, and accounting rules, to enable the production of internationally comparable statistics and accounts. The SEEA framework follows an accounting structure similar to the System of National Accounts (SNA), ensuring coherence with traditional economic accounting practices. The SEEA is modular, with each module addressing a specific topic. The SEEA central framework develops the rules and guidelines for measuring the relationship between the environment and the economy, focusing on three key areas: environmental flows (changes in natural assets), stocks of environmental assets (measurement of natural assets) and economic activity related to the environment (monetary economic flows related to natural assets). The four main modules are:

- Ecosystem accounting (SEEA EA) with 4 types of accounts: ecosystem extent accounts, ecosystem condition accounts, ecosystem services flow accounts (physical and monetary), and monetary ecosystem asset accounts;
- Agriculture, forestry and fisheries with two types of accounts: flow accounts and asset accounts (both physical and monetary);
- SEEA-Energy with two types of accounts: flow accounts and asset accounts (both physical and monetary);
- SEEA-Water with three types of accounts: physical flow accounts, physical asset accounts and economic accounts.

In addition, four other modules have been developed on air emissions, environmental activities, land and material flow accounts. Examples of SEEA accounts can be found at `seea.un.org/content/projects`.

In January 2020, the World Economic Forum published a series of reports aimed at "*providing pathways for business to be part of the transition to a nature-positive economy*". In particular, World Economic Forum (2020a) estimated that $44 trillion of economic value creation — more than half of global GDP — is moderately or highly dependent on nature[92]. Among the 163 economic

[90] World maps of ecosystem valuation, such as Figure 5.42, are very common in academic and policy publications.

[91] The corresponding websites are `seea.un.org`, `www.cices.eu`, `www.teebweb.org`, and `seea.un.org/home/natural-capital-accounting-project`.

[92] The exact figures are $31 tn or 37% of the world GDP for moderately dependent industries and $13 tn or 15% of the world GDP for highly dependent industries.

sectors considered in the study, construction ($4 tn), agriculture ($2.5 tn), and food and beverages ($1.4 tn) are the three largest industries most dependent on nature. The impact on secondary and tertiary sectors can also be significant through their supply chains. This publication was followed by several public studies in 2021 showing how GDP creation is strongly linked to biodiversity[93]. These reports consistently highlight that the link between GDP and biodiversity is currently poorly understood, while the economic and financial risks posed by biodiversity loss are enormous.

**Pollination service**

Pollination is the process by which pollen is transferred from the male part of a flower (the anther) to the female part (the stigma) of the same or another flower. This is a crucial step in the reproductive cycle of many plants, as it leads to the production of seeds and fruits. There are two main types of pollination:

1. Self-pollination, in which pollen from one flower is transferred to the stigma of the same flower. For example, many crops and fruit trees are self-pollinating, including aubergines, barley, beans, cauliflower, lentils, lettuce, olives, onions, peppers, potatoes, soybeans, tomatoes, rice, and wheat;

2. Cross-pollination, when pollen is transferred from the anther of one flower to the stigma of a flower on another plant of the same species. Examples include apples, blackberries, blackcurrants, broccoli, carrots, cacao, daffodils, lavender, pears, plums, pumpkins, raspberries, strawberries, and tulips.

We also distinguish three methods of cross-pollination:

1. Abiotic pollination involves natural transport phenomena such as wind, water, and rain. Examples of wind-pollinated plants include conifers, grasses, and many trees.

2. Biotic pollination requires living pollinators to move pollen from one flower to another. Most pollinators are insects (ants, beetles, bees, butterflies, flies, wasps and moths), but some are vertebrates (bats, birds, *e.g.*, honeyeaters and hummingbirds).

3. Hand pollination (also known as mechanical or human pollination) is a technique in which humans manually transfer pollen from the male to the female plant. Examples of plants that are commonly hand pollinated include corn, cucumbers, melons, vanilla, and zucchini.

These classifications are only theoretical. Most plants are pollinated in more than one way. For example, a self-pollinating species may also be pollinated by animals or by hand. Similarly, 100% of apples are not 100% animal pollinated. Olhnuud *et al.* (2022) showed that the animal-dependent pollination rate varies from species to species (*e.g.*, Gala vs. Golden apple) and from region to region (*e.g.*, Asia vs. Europe).

By analyzing data of 137 single crops and 115 commodity[94] crops provided by FAO, Klein *et al.* (2007) identified 124 major crops (57 single crops and 67 commodity crops) used for human food with significant annual production, representing 99% of total world food production. They

[93] We can cite Dasgupta (2021), OECD (2021) and Svartzman *et al.* (2021) among others.

[94] A single crop refers to a specific plant species. A commodity, on the other hand, represents a group of different crop species. For instance, the fresh vegetables category as defined by the FAO includes 21 distinct crops, such as celery and rhubarb. Similarly, other commodity categories include fresh fruits (15 crops, including litchi and pawpaw), fresh tropical fruits (17 crops, including guava and passion fruit), roots and tubers (8 crops, such as yam bean and topinambur), and pulses (6 crops, including guar bean and velvet bean).

Box 5.11: The story of the original vanilla bean

The Chinantla Forest is considered the birthplace of vanilla, and the vanilla plant, or vine, is native to Mexico. There, the vines grew and flourished without the help of humans. Wild vanilla is naturally pollinated by melipona bees and small hummingbirds found only in Mexico. Before 1850, all vanilla beans came from the forests of Mexico, and France was the number one importer of the '*black flower*'. The Aztecs, and the Mayans before them, believed that the scent of vanilla could help them communicate with the gods and had long mastered the fermentation techniques needed to cure the beans. They cultivated '*tlilxotchitl*' or black flowers so that the flavors could be combined with cocoa and coffee. In 1521, Cortés was the first European to bring the dark pods or beans back to Charles Quint. Vanilla beans first arrived in France in 1664. Later, Louis XIV fell in love with the taste of vanilla and wanted vanilla beans to be grown on the island of Réunion, then known as Bourbon Island. But until the mid-19th century, vanilla beans were still only made in Mexico. Although the technique of curing the beans was known, pollination of the flower was not. In 1836 and 1841, Charles Morren, a Belgian botanist, and Edmond Albius, a slave on Réunion Island discovered how to bypass bee pollination by manually pollinating vanilla flowers. Soon after, vanilla plants were exported by the French to plantations in Tahiti, Madagascar, Mauritius, Réunion Island, and the Comoros.

Text reproduced from www.epices-roellinger.com.

estimated that 70% of these major crops depend on animal pollination (87 crops), 23% do not rely on animal pollination (28 crops), while 7% have not been evaluated (9 crops). Despite this, in terms of global production in 2004, these three categories contributed 35%, 60%, and 5%, respectively. This is because the four largest crops (sugar cane, corn, wheat, and rice) do not require animal pollination, but represented more than 50% of global crop production in 2004. Klein *et al.* (2007) also created a classification of the pollination dependence of different crops. They considered a crop to be pollinator dependent if animal pollination is required to increase the quantity and/or quality of fruits or seeds directly consumed by humans. Alternatively, a crop is considered non-dependent if it is pollinated either abiotically (wind) or autogamously (self-fertilizing). They created five categories:

1. Essential
   Animal pollinators are essential for most varieties, otherwise we observe a reduction in production of more than 90%, comparing experiments with and without animal pollinators;

2. High
   Animal pollinators are strongly needed (40 to less than 90% reduction);

3. Modest
   Animal pollinators are clearly beneficial (10 to less than 40% reduction);

4. Little
   Some evidence suggests that animal pollinators are beneficial (greater than 0 to less than 10% reduction);

5. No increase
   No increase in production with animal pollination.

Table 5.30 shows the classification found by Klein *et al.* (2007, Supplemental Material 2) (103 crops) and updated by Aizen *et al.* (2019, Appendix S1) (11 additional crops).

Table 5.30: How dependent are foods on pollinator insects?

| | |
|---|---|
| No dependency | Yields are not affected by pollinators |
| | Cereals: barley, maize, millet, oats, rice, rye, sorghum, wheat |
| | Roots and tubers: carrots, cassava, potatoes, sweet potatoes |
| | Legumes including chickpeas, lentils, peas |
| | Fruit and veg including bananas, grapes, lettuce, pepper, pineapples |
| | Sugar crops: sugar beet, sugar cane |
| | Also includes areca nuts, asparagus, broccoli, cabbages, castor oil seed, cauliflower, chicory roots, dates, garlic, hazelnuts, jojoba seeds, leeks, olives, onions, pistachios, quinoa, spinach, taro, triticale, walnuts, yams |
| Little dependency | Yield reduction of 0% to 10% without pollinators |
| | Fruits and veg including lemons, limes, oranges, papayas, tomatoes |
| | Oilcrops including linseed, palm oil, poppy seed, safflower seed |
| | Legumes including beans (dry & green), cow peas, pigeon peas |
| | Groundnuts |
| | Also includes bambara beans, chillies, clementines, grapefruit, mandarins, persimmons, string beans, tangerines |
| Modest dependency | Yield reduction of 10% to 40% without pollinators |
| | Oilcrops including mustard seed, rapeseed, sesame, sunflower seed |
| | Soybeans |
| | Fruits including currants, egglant, figs, gooseberries, strawberries |
| | Coconuts and okra |
| | Coffee beans |
| | Also includes broad beans, chestnut, karite nuts, seed cotton |
| High dependency | Yield reduction of 40% to 90% without pollinators |
| | Fruits including apples, apricots, blueberries, cherries, cranberries, guavas, mangoes, nectarines, peaches, plums, pears, raspberries |
| | Nuts including almonds, cashew nuts, kola nuts |
| | Avocados |
| | Also includes anise, badian, buckwheat, coriander, cucumber, fennel, nutmeg |
| Essential | Yield reduction greater than 90% without pollinators |
| | Fruits including kiwi, melons, pumpkins, watermelons |
| | Cocoa beans |
| | Brazil nuts |
| | Also includes quinces, vanilla |

Source: Klein *et al.* (2007, Supplemental Material 2), Aizen *et al.* (2019, Appendix S1), https://ourworldindata.org/pollinator-dependence & icons taken from https://icons8.com/icons.

Box 5.12: Who are animal pollinators?

Bees are the most important group of animal pollinators. There are an estimated 20 000 species of bees (family *Apidae*), but only nine species of honey bees are recognized and form the genus *Apis* (*Apidae; Apinae; Apini; Apis*). The Western honey bee (*Apis mellifera*) is the most common honey bee and the one most often domesticated for honey production. The other species are *Apis andreniformis*, *Apis cerana* (Asiatic honey bee), *Apis dorsata* (Giant honey bee), *Apis florea* (Little honey bee), *Apis koschevnikovi*, *Apis laboriosa* (Himalayan honey bee), *Apis nigrocincta* and *Apis nuluensis*. We generally distinguish between honey bees that are managed by humans and wild bees. There are many species in the latter category, but the most important are Bumble bees (*Apidae; Apinae; Bombini*), Carpenter bees (*Apidae; Xylocopinae*), Stingless bees (*Apidae; Apinae; Meliponini*), and solitary bees such as sand bees (family *Andrenidae; Andreninae; Andrena*) or nomad bees (*Apidae; Nomadinae; Nomadini; Nomada*). Bees are generally attracted to yellow (and blue) flowers.

Non-bee insects also play a significant role in global crop pollination. For instance, Rader *et al.* (2016) found that approximately 40% of visits to crop flowers are made by non-bee insects. In fact, butterflies and moths (order *Lepidoptera*) are the second most important group of animal pollinators. Other insects that contribute to pollination include ants (family *Formicidae*), beetles (order *Coleoptera*), and flies (order *Diptera*). In the case of ants, pollination typically occurs in low-growing flowers positioned close to the stem. Examples of ant-pollinated plants include small's stonecrop (*Diamorpha smallii*), alpine nailwort (*Paronychia pulvinata*), and cascade knotweed (*Polygonum cascadense*). Butterflies have excellent color vision, which explains why they are attracted to red, orange, yellow, blue and purple flowers. Moths, on the other hand, prefer pale or white flowers because they tend to come out at night.

The primary pollinators of cacao are tiny flies from the families of biting midges (*Ceratopogonidae*, including the genus *Forcipomyia*) and, to a lesser extent, gall midges (*Cecidomyiidae*). These small flies, sometimes only a few millimeters long, are uniquely suited to pollinate cacao because the reproductive parts of cacao flowers are very small (less than 2 mm) and complex, with structures that make them difficult for larger insects to access.

In addition to insect pollinators, vertebrate pollinators also participate in the reproductive success of plants, especially tropical plants (Ratto *et al.*, 2018). Bird pollinators include hummingbirds (*Trochilidae*), sunbirds (*Nectariniidae*), honeycreepers (*Meliphagidae*), and some parrots. Birds are generally attracted to red, orange, and yellow flowers. Some known bird-pollinated plants include hibiscus, eucalyptus, and some orchids. Bats, like moths, prefer pale or white flowers. They are involved in the pollination of mango, banana, durian, guava, and agave (used to make tequila). While rodents and reptiles are less common vertebrate pollinators, they can still contribute to the reproduction of certain plants.

It is very difficult to estimate the contribution of each species to pollination. However, it is generally accepted that managed honey bees provide 50–75% of agricultural pollination, while wild bees and other pollinators account for the remaining 25–50% (Garibaldi *et al.*, 2013; IPBES, 2016).

Source: www.fs.usda.gov/managing-land/wildflowers/pollinators/who-are-the-pollinators & www.cacaopollination.com/cacao-pollinators.

Using the previous classification, Aizen *et al.* (2009) estimated that the direct reduction in total agricultural production in the absence of animal pollination would be 5% for developed regions and 8% for developing regions. These figures are based on the production deficit in volume, calculated as:

$$D_t^{(\text{volume})} = \frac{\sum_{i=1}^n P_{i,t} - \sum_{i=1}^n P_{i,t}\left(1-\delta_i\right)}{\sum_{i=1}^n P_{i,t}} = \frac{\sum_{i=1}^n P_{i,t}\delta_i}{\sum_{i=1}^n P_{i,t}} = \sum_{i=1}^n w_{i,t}\delta_i \tag{5.13}$$

where $n$ is the number of crops, $P_{i,t}$ is the volume production in metric tonnes of crop $i$ in year $t$, $w_{i,t}$ is the weight of crop $i$ in the total agricultural production, $\delta_i$ is the dependency rate, which is equal to 0% for crops that are not dependent on animal pollinators and 100% for crops that are completely dependent on animal pollinators[95]. Aizen *et al.* (2009) also calculated the percentage increase in area needed to compensate for the production deficit:

$$A_t^{(\text{compensation})} = \frac{\sum_{i=1}^n \frac{A_{i,t}}{1-\delta_i} - \sum_{i=1}^n A_{i,t}}{\sum_{i=1}^n A_{i,t}} = \frac{\sum_{i=1}^n A_{i,t}\frac{\delta_i}{1-\delta_i}}{\sum_{i=1}^n A_{i,t}} = \sum_{i=1}^n w_{i,t}\frac{\delta_i}{1-\delta_i} \tag{5.14}$$

where $A_{i,t}$ is the cultivated area (in hectares) of crop $i$ in year $t$ and $\left(1-\delta_i\right)^{-1} A_{i,t}$ is the area needed to produce $P_{i,t}$ in the absence of pollination[96]. They found that area compensation is 15% in developed regions and 42% in developing regions. Another interesting finding is that production deficit and area compensation have generally increased over time. These different results are mainly explained by the fact that human diets have changed over time and that human diets today are more diversified than fifty years ago, with more vegetables and fruits being consumed. In addition, the low figures for production deficit are mainly due to the importance of cereals in the human diet, while the high figures for area compensation are mainly due to the greater area needed to cultivate crops that depend on animal pollination, *e.g.*, apples, avocados, cocoa, mangoes, peaches. In terms of volume and metric tonnes, the production yield of the first category is higher than that of the second. However, it's worth considering whether a volume-based analysis is the most appropriate approach to assess the importance of pollinators. For example, 1 kg of wheat and 1 kg of tomatoes provide different nutritional values, suggesting that volume alone may not accurately reflect their contribution to human well-being. Eilers *et al.* (2011) conducted a similar analysis using the same data and methodology but focused on the nutritional value of crops instead of volume. Let $V_{j,t}^{(\text{nutritional})}$ be the total amount of nutrient $j$ in year $t$. We have:

$$V_{j,t}^{(\text{nutritional})} = \sum_{i=1}^n V_{i,j}^{(\text{nutritional})} P_{i,t}\left(1-R_i\right) \tag{5.15}$$

where $V_{i,j}^{(\text{nutritional})}$ is the amount of nutrient $j$ in a metric tonne of crop $i$, $P_{i,t}$ is the volume production in tonnes of crop $i$ in year $t$, and $R_i$ is the proportion of crop $i$ that is not consumed by humans due to inedible parts, such as pits, stems, or shells. We can decompose $V_{j,t}^{(\text{nutritional})}$ into three components: $V_{j,t}^{(1)} = \sum_{i=1}^n \mathbb{1}\left\{\delta_i = 0\right\} \cdot V_{i,j}^{(\text{nutritional})} P_{i,t}\left(1-R_i\right)$ is the nutritional value of pollinator-independent crops; $V_{j,t}^{(2)} = \sum_{i=1}^n \mathbb{1}\left\{\delta_i > 0\right\} \cdot \left(1-\delta_i\right) V_{i,j}^{(\text{nutritional})} P_{i,t}\left(1-R_i\right)$ is the nutritional value of pollinator-dependent crops due to abiotic and self-pollination; $V_{j,t}^{(3)} = \sum_{i=1}^n \mathbb{1}\left\{\delta_i > 0\right\} \cdot \delta_i V_{i,j}^{(\text{nutritional})} P_{i,t}\left(1-R_i\right)$ is the nutritional value of pollinator-dependent crops attributed to animal pollination alone. Results are shown in Table 5.31, where the key metric to

[95] Aizen *et al.* (2009) used the following values for $\delta_i$: 0%, 5%, 25%, 65% and 95% for no, little, modest, high and essential dependency classes.

[96] We assume that production is proportional to area: $P_{i,t} \propto A_{i,t}$.

consider is $V_{j,t}^{(3)}$ (last column). In terms of energy (calories) and protein, about 80% of the human diet comes from pollinator-independent crop production. The proportion attributed to crop production dependent on animal pollination is low, at less than 3%. Similar figures are observed for minerals, except for fluoride and calcium, where the proportions attributed to animal pollination are 19.83% and 9.11%, respectively. The most significant effects of animal pollination are observed for vitamins[97], especially vitamin A (41.03%), carotene (about 40%), certain forms of vitamin E (about 20%) and vitamin C (19.64%). We conclude that animal pollination has a significant impact on human diets by contributing to nutritional diversification, particularly at the vitamin level.

Table 5.31: Proportion in % of nutrients derived from pollinator-independent and pollinator-dependent crops

| Nutrient | | $V_{j,t}^{(1)}$ | $V_{j,t}^{(2)}$ | $V_{j,t}^{(3)}$ |
|---|---|---|---|---|
| Macro-nutrients | Energy | 78.83 | 18.59 | 2.58 |
| | Protein | 83.43 | 13.57 | 3.00 |
| | Fat | 26.02 | 66.98 | 7.00 |
| Vitamins | A | 28.71 | 30.26 | 41.03 |
| | $\beta$-carotene | 27.44 | 34.19 | 38.37 |
| | $\alpha$-carotene | 32.25 | 29.83 | 37.92 |
| | $\beta$-cryptoxanthin (carotene) | 0.77 | 56.99 | 42.24 |
| | Lycopene (carotene) | 0.00 | 56.67 | 43.33 |
| | Lutein & Zeaxanthin (carotene) | 94.05 | 3.92 | 2.03 |
| | E ($\alpha$-tocopherol) | 63.73 | 28.94 | 7.33 |
| | E ($\beta$-tocopherol) | 0.63 | 72.50 | 26.87 |
| | E ($\gamma$-tocopherol) | 32.92 | 52.66 | 14.42 |
| | E ($\delta$-tocopherol) | 14.87 | 62.50 | 22.63 |
| | K | 71.55 | 19.28 | 9.17 |
| | C | 6.99 | 73.37 | 19.64 |
| | B1 (Thiamin) | 95.29 | 4.00 | 0.71 |
| | B2 (Riboflavin) | 97.66 | 1.92 | 0.42 |
| | B3 (Niacin) | 89.46 | 8.93 | 1.61 |
| | B5 (Pantothenic acid) | 87.57 | 9.34 | 3.09 |
| | B6 | 97.93 | 1.58 | 0.49 |
| | B9 (Folate) | 55.49 | 37.19 | 7.32 |
| Minerals | Calcium | 42.40 | 48.49 | 9.11 |
| | Iron | 70.66 | 23.14 | 6.20 |
| | Magnesium | 88.50 | 9.06 | 2.44 |
| | Phosphorus | 89.06 | 8.72 | 2.22 |
| | Potassium | 72.74 | 20.93 | 6.33 |
| | Sodium | 87.18 | 8.63 | 4.19 |
| | Zinc | 91.80 | 6.54 | 1.66 |
| | Copper | 80.92 | 15.21 | 3.87 |
| | Mangan | 93.87 | 4.94 | 1.19 |
| | Selenium | 97.46 | 1.97 | 0.57 |
| | Fluoride | 45.57 | 34.60 | 19.83 |

Source: Eilers *et al.* (2011, Table 1, page 2011).

[97]Vitamin A is essential for vision, vitamin C is a powerful antioxidant and vital for collagen production, vitamin E plays a role in immune function, and carotenes act as precursors to vitamin A.

Another interesting figure is that 308 000 out of a total of 352 000 flowering plants are partially or totally pollinated by animals, which represents a proportion of 87.5% (Ollerton *et al.*, 2011). These species, known as angiosperms (*Angiospermae*), include many fruit trees and flowers such as roses and tulips. While the primary benefits of these species are food and medicine, they also provide secondary benefits such as reducing pest populations and improving soil and water quality. Another important service is the enhancement of rural aesthetics and the provision of cultural and visual amenities (Wratten *et al.*, 2012; Dicks *et al.*, 2021). Without bees and butterflies, the world would not be the same, and many blue, orange, pink, purple, red, violet and yellow flowers would disappear, as these pollinators are essential for their reproduction. The loss of these vibrant flowers would have a significant impact on the beauty of natural landscapes.

Figure 5.43: Trend in the number of bee colonies (1961–2022)

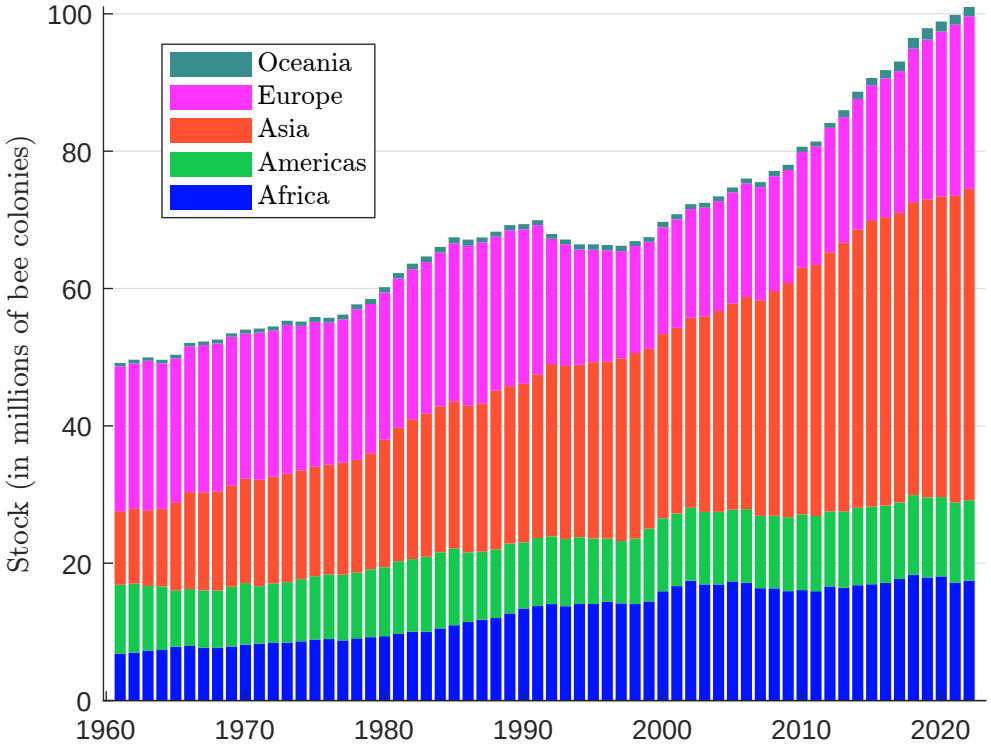


Source: www.fao.org/faostat/en/#data/QCL & Author's calculations.

Potts *et al.* (2010) alerted the scientific community and policy makers to the global decline of pollinators and its potential impact on human well-being:

> "*Pollinators are a key component of global biodiversity, providing vital ecosystem services to crops and wild plants. There is clear evidence of recent declines in both wild and domesticated pollinators, and parallel declines in the plants that rely upon them.*" (Potts *et al.*, 2010, page 345).

It is challenging to accurately define pollinator decline, as data can sometimes initially be contradictory. For example, Potts *et al.* (2010) reported declines in honey bee populations in the United States (59% loss of colonies between 1947 and 2005) and Central Europe (25% loss of colonies between 1985 and 2005). Globally, however, the number of managed honey bee colonies has increased over the past six decades. From 1965 to 2015, production of pollinator-dependent crops has increased by 300% (IPBES, 2016, page XXI). This increase is mainly due to the growing presence

Table 5.32: Regional distribution of managed honey bee colonies (in millions)

| Region | Stock (in million colonies) | | | | Growth (in %) | |
|---|---|---|---|---|---|---|
| | 1961 | 1980 | 2000 | 2022 | 1961–2022 | 2000–2022 |
| Europe | 21.10 | 21.42 | 15.55 | 25.12 | 19.1 | 61.6 |
| Western Europe | 3.76 | 3.35 | 2.45 | 3.55 | −5.5 | 45.3 |
| Northern Europe | 0.44 | 0.40 | 0.27 | 0.64 | 45.6 | 138.3 |
| Eastern Europe | 14.02 | 13.71 | 7.36 | 10.66 | −24.0 | 44.8 |
| Southern Europe | 2.87 | 3.95 | 5.47 | 10.27 | 257.3 | 87.6 |
| Americas | 10.02 | 10.03 | 10.62 | 11.71 | 16.9 | 10.2 |
| Northern America | 5.85 | 4.75 | 3.22 | 3.40 | −41.9 | 5.5 |
| Central America | 2.26 | 2.80 | 2.19 | 2.68 | 18.5 | 22.3 |
| Caribbean | 0.23 | 0.32 | 0.28 | 0.40 | 72.5 | 45.8 |
| South America | 1.67 | 2.16 | 4.94 | 5.23 | 212.4 | 6.0 |
| Africa | 6.85 | 9.37 | 15.92 | 17.46 | 155.1 | 9.7 |
| Asia | 10.70 | 18.61 | 26.82 | 45.34 | 323.6 | 69.1 |
| Oceania | 0.51 | 0.76 | 0.80 | 1.36 | 168.7 | 70.9 |
| World | 49.17 | 60.20 | 69.71 | 101.00 | 105.4 | 44.9 |

Source: www.fao.org/faostat/en/#data/QCL & Author's calculations.

of fruits in human diets (such as tropical and seasonal fruits). However, many pollinator species are listed as vulnerable, endangered or critically endangered on the IUCN Red List. In fact, we need to distinguish between managed honey bees and other animal pollinators. According to FAO statistics[98], the number of managed bee colonies has doubled between 1961 and 2022 (Figure 5.43). In 1961, there were 49.2 million colonies, while today there are more than 100 million (Table 5.32). Most of this growth has occurred in Asia (+324%), Africa (+155%), Southern Europe (+257%) and South America (+212%). Below is a regional breakdown of colony numbers:

| Year | Europe | America | Africa | Asia | Oceania |
|---|---|---|---|---|---|
| 1961 | 42.9% | 20.4% | 13.9% | 21.8% | 1.0% |
| 2022 | 24.9% | 11.6% | 17.3% | 44.9% | 1.3% |

Asia now accounts for 45% of the global market, followed by Europe with 25%. Three regions have experienced a decline in honey bee populations over the last sixty years: North America (−41.9%), Eastern Europe (−24.0%), and Western Europe (−5.5%). However, in the past 20 years, they have reversed this trend, showing positive growth. The current problem is not the decline of honey bee colonies, but the dramatic decline of insects worldwide. For example, Hallmann *et al.* (2017) measured a decline in total flying insect biomass of more than 75 percent over 27 years in 63 German protected areas. Sánchez-Bayo and Wyckhuys (2019) estimate that 40% of the world's insect species could become extinct in the next few decades. The case of butterflies, for example, is dramatic, as shown by Warren *et al.* (2021), who studied the status of butterflies in the United Kingdom, the Netherlands, and Belgium:

> "*[...] In the United Kingdom, 8% of resident species have become extinct, and since 1976 overall numbers declined by around 50%. In the Netherlands, 20% of species have become extinct, and since 1990 overall numbers in the country declined by 50%. Distribution*

[98] The data can be obtained from the FAO website: www.fao.org/faostat/en/#data/QCL. Select the domain *Crops and livestock products*, then the item *Live Animals/Bees* and the element *Stocks*.

> *trends showed that butterfly distributions began decreasing long ago, and between 1890 and 1940, distributions declined by 80%. In Flanders (Belgium), 20 butterflies have become extinct (29%), and between 1992 and 2007 overall numbers declined by around 30%. A European Grassland Butterfly Indicator from 16 European countries shows there has been a 39% decline of grassland butterflies since 1990. The 2010 Red List of European butterflies listed 38 of the 482 European species (8%) as threatened and 44 species (10%) as near threatened [...].*" (Warren *et al.*, 2021, page 1).

According to Butterfly Conservation[99], 80% of butterfly species have declined in abundance or distribution since the 1970s. In the United States, the situation is even worse than in Europe, where some butterfly species have experienced declines of up to 2% per year in the recent period (Thogmartin *et al.*, 2017; Wepprich *et al.*, 2019). In fact, the decline of wild bees and other pollinators cannot be compensated by an increase in honeybees because they play different roles in crop pollination and do not visit plants in the same way or at the same time (Rader *et al.*, 2016). Therefore, crop yield and quality depend on pollinator biodiversity.

The drivers and risks associated with pollinator decline have been extensively reviewed in the 2016 report of the Intergovernmental Science-Policy Platform on Biodiversity and Ecosystem Services (IPBES). A summary can be found in Potts *et al.* (2016). According to IPBES (2016, Chapter 2, pages 30–149), there are five main drivers of change in pollination networks:

1. Land use and its change ("*It is well established that habitat loss and degradation [...] affect pollinator diversity, abundance and richness. These changes can negatively affect community stability, pollination networks and the survival and evolutionary potential of pollinator and plant species.*")

2. Pesticides, GMOs, veterinary medicines and pollutants ("*It is clear that pollinators may be exposed to a wide range of pesticides in both agricultural and urban environments. The risk posed by pesticides is driven by a combination of the toxicity (hazard) and the level of exposure; [...] Insecticides are toxic to insect pollinators and their exposure, and thus the risk posed, is increased if, for example, labels do not provide use information to minimise pollinator exposure or the label is not complied with by the pesticide applicator.*")

3. Pollinator diseases and pollinator management ("*Bee management is a global and complex driver of pollinator loss. Spreading of diseases by managed honey bees and bumble bees into wild bee species has been shown to present a threat to some wild species and populations.*")

4. Invasive alien species ("*Invasive predators can directly kill pollinators or disrupt pollinator communities and associated pollination systems, whilst invasive pollinators can outcompete or transmit diseases to native pollinator species or simply be accommodated in the existing pollinator assemblage.*")

5. Climate change ("*Many plant and pollinator species have moved their ranges, altered their abundance, and shifted their seasonal activities in response to observed climate change over recent decades.*")

Using this classification, Dicks *et al.* (2021) conducted a formal expert elicitation process to assess the regional and global importance of these drivers. Results are presented in Table 5.33. Globally, land cover and management are the most important drivers of pollinator decline, followed by pesticide

[99] See the latest report *The State of the UK's Butterflies 2022*, available at www.butterfly-conservation.org/state-of-uk-butterflies-2022.

Table 5.33: Assessment of the importance of the top eight drivers of pollinator decline

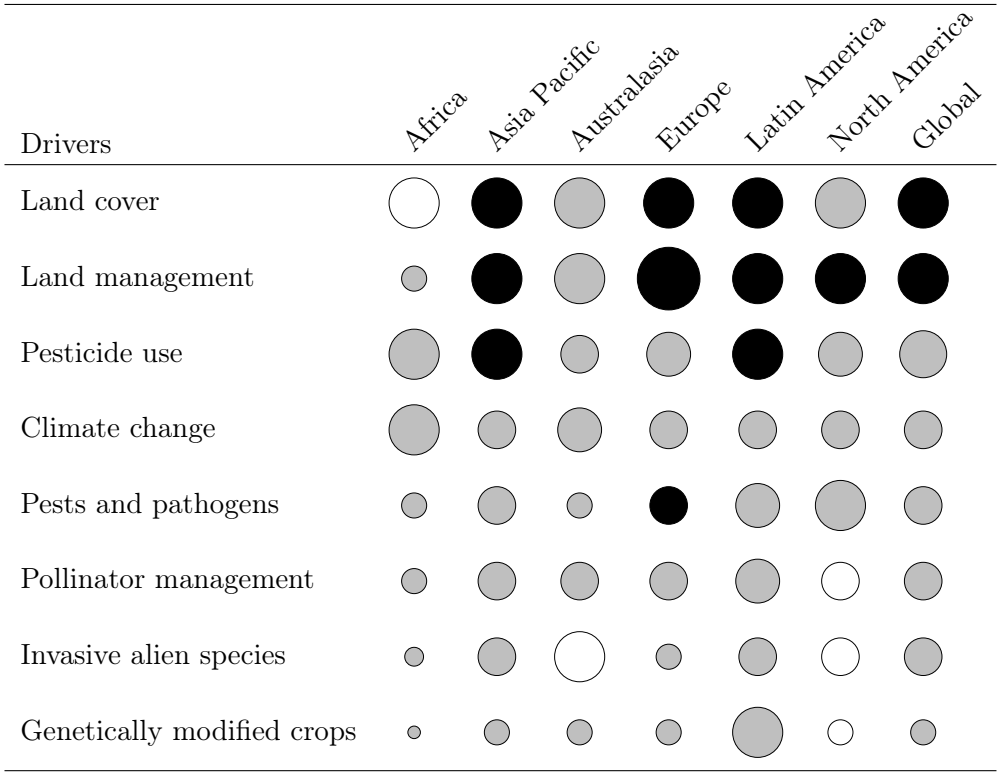


The circle size is proportional to the importance score between 1 (not important) and 4 (the most important). The circle color corresponds to the confidence score: ● = well established, ◯ = established but incomplete, and ○ = inconclusive.

Source: Dicks *et al.* (2021, Figure 2, page 1457 & Supplementary Table 2).

use. Climate change, pests and pathogens, pollinator management and invasive alien species are also important, but to a lesser extent, and contribute equally. GMOs are the least important driver. However, there are some strong differences between regions. Pesticide use is very important in Asia Pacific and Latin America. In Europe and North America, land management is the most important issue. The impact of these changes can be divided into two main categories:

- Impact on food production (pollination deficits, yield instability, honey production, food security, wild fruit availability, managed pollinators)

- Impact on biocultural diversity (wild pollinator and plant diversity, aesthetic and cultural values)

Although we have some estimates of these risks, it is currently difficult to predict the future trajectory of pollination ecosystem services and the consequences for human quality of life. The conclusion of Dicks *et al.* (2021) summarized perfectly what science can say about this issue: "*Despite extensive research on pollinator decline, our analysis reveals considerable scientific uncertainty about what this means for human society.*" Regarding the impact on food production, the future is not entirely bleak, especially with the potential for hand pollination and advancements in robotic pollination. The impact on biocultural diversity is more complex and harder to address.

### Food and feed service

There are several ways to look at food and feed[100] in the context of biodiversity. Food biodiversity refers to the diversity of plants, animals and other organisms used for human consumption. It can be analyzed from two main perspectives. From a production perspective, food biodiversity describes the supply of food in terms of volume (*e.g.*, tonnes produced). From a consumption perspective, it describes the demand for food in terms of nutrient intake, such as calories, proteins, vitamins and minerals. Additional approaches can be explored, such as comparing farmed foods to wild foods, examining the diversity of local versus global food systems, or exploring sustainable versus conventional agricultural practices.

The main source of food is agriculture, which involves food production managed by humans. Historically, wild foods were the sole component of human diets. Today, the proportion of food production attributed to wild foods is relatively small compared to agricultural sources, although it continues to play an important role in certain communities, particularly for indigenous peoples, in certain regions, and in some rural areas[101]. Therefore, in the following we will only consider non-wild foods for which data have been collected by the FAO since 1961 and are freely available for more than 245 countries.

**Food production** World production of primary crops reached 9.61 billion tonnes in 2022 (Table 5.34). Since 1961, this figure has been multiplied by a factor of 3.78, representing an annual growth rate of 2.2% over the past sixty years. Cereals and sugar crops account for 31.8% and 22.7% of global production, respectively, while fruits, roots and tubers, and vegetables each contribute approximately 10%. In Table 5.34 we have also reported the top 20 crops by production. We see that sugar cane has the largest share, accounting for 20% of global primary crop production. In second place is maize with 12.11%. This is followed by wheat (8.41%), rice (8.08%), and oil palm (4.42%). The top five crops account for more than 50% of total production, the top 10 for about 70%, and the top 20 for more than 80%. This indicates a high concentration of production in a small number of crops. In Figure 5.44, we present the Lorenz curve for the 162 crops in the FAO database. The graph confirms the previous findings and highlights the high concentration, as 10% of the crops account for 80% of the total production volume. Moreover, this lack of diversity is the same in 2022 as it was in 1961, but this does not mean that the structure of crop production has not changed. In fact, we observe that the market shares are very different between 1961 and 2022. For example, potatoes represented 10.7% of total production in 1961, but only 3.9% today. The shares of corn, oil palm fruits, soybeans, onions, cucumbers, yams, and rapeseed have increased significantly, while the shares of sugar beets, barley, and sweet potatoes have experienced notable declines. Figure 5.45 illustrates the evolution of harvested area over the past sixty years. Between 1961 and 2022, cropland expanded by 51.6%, though this growth was uneven. The period before 2000 saw an annual growth rate of 0.5%, while after 2000, this rate accelerated to 1% per year. As a result, the overall 278% increase in crop production during this period was largely due to productivity gains and shifts in production structure. In Table 5.34, we report crop yield, which is defined as the ratio between production (expressed in tonnes) and harvested area (expressed in hectares). Yield has increased for all crops, on average by a factor of 2.49. We notice that fruits have a better yield than staples. All these factors explain the dynamics of world crop production.

[100] Food is for human consumption, while feed is for animals.

[101] In the early 1990s, it was estimated to be less than 10% worldwide. However, reliable data are lacking. In the European Union, according to Schulp *et al.* (2014), the amount of wild foods collected is very small compared to total food, and the economic and nutritional value of wild foods is a few thousandths of the total consumption. However, wild foods provide an important cultural ecosystem service, as a wide variety of game (38 species), mushrooms (27

Table 5.34: World production of primary crops

| Crop | Production (in billion tonnes) | | | | | 1961 breakdown | | 2022 breakdown | | Yield (in t/ha) | |
|---|---|---|---|---|---|---|---|---|---|---|---|
| | 1961 | 1980 | 2000 | 2020 | 2022 | (in %) | (% cum.) | (in %) | (% cum.) | 1961 | 2022 |
| Primary crops | 2.54 | 4.02 | 6.14 | 9.38 | 9.61 | 100.00 | | 100.00 | | 2.61 | 6.49 |
| Cereals | 0.88 | 1.55 | 2.06 | 3.00 | 3.06 | 34.58 | | 31.84 | | 1.35 | 4.18 |
| Fruit | 0.22 | 0.40 | 0.68 | 1.07 | 1.10 | 8.87 | | 11.44 | | 7.62 | 14.09 |
| Oil crops | 0.07 | 0.15 | 0.32 | 0.66 | 0.68 | 2.90 | | 7.06 | | 0.33 | 1.01 |
| Pulses, Roots and Tubers | 0.50 | 0.56 | 0.75 | 0.96 | 1.00 | 19.56 | | 10.44 | | 4.45 | 6.02 |
| Sugar crops | 0.61 | 1.00 | 1.50 | 2.13 | 2.18 | 24.02 | | 22.73 | | 38.16 | 71.61 |
| Vegetables | 0.20 | 0.29 | 0.69 | 1.15 | 1.17 | 7.79 | | 12.21 | | 9.34 | 20.13 |
| Other | 0.06 | 0.06 | 0.15 | 0.41 | 0.41 | 2.28 | | 4.29 | | | |
| Sugar cane | 0.45 | 0.73 | 1.25 | 1.88 | 1.92 | 17.66 | 17.66 | 20.00 | 20.00 | 50.27 | 73.67 |
| Maize (corn) | 0.21 | 0.40 | 0.59 | 1.16 | 1.16 | 8.09 | 25.75 | 12.11 | 32.11 | 1.94 | 5.72 |
| Wheat | 0.22 | 0.44 | 0.59 | 0.76 | 0.81 | 8.77 | 34.52 | 8.41 | 40.52 | 1.09 | 3.69 |
| Rice | 0.22 | 0.40 | 0.60 | 0.77 | 0.78 | 8.50 | 43.02 | 8.08 | 48.60 | 1.87 | 4.70 |
| Oil palm fruit | 0.01 | 0.03 | 0.12 | 0.42 | 0.42 | 0.54 | 43.56 | 4.42 | 53.02 | 3.77 | 14.15 |
| Potatoes | 0.27 | 0.24 | 0.32 | 0.37 | 0.37 | 10.67 | 54.23 | 3.90 | 56.92 | 12.22 | 21.07 |
| Soya beans | 0.03 | 0.08 | 0.16 | 0.36 | 0.35 | 1.06 | 55.29 | 3.63 | 60.55 | 1.13 | 2.61 |
| Cassava, fresh | 0.07 | 0.12 | 0.18 | 0.31 | 0.33 | 2.81 | 58.10 | 3.44 | 63.99 | 7.40 | 10.31 |
| Other vegetables, fresh n.e.c. | 0.06 | 0.09 | 0.21 | 0.29 | 0.30 | 2.46 | 60.55 | 3.10 | 67.09 | 8.42 | 14.53 |
| Sugar beet | 0.16 | 0.27 | 0.25 | 0.25 | 0.26 | 6.33 | 66.88 | 2.72 | 69.81 | 23.17 | 60.77 |
| Tomatoes | 0.03 | 0.05 | 0.11 | 0.19 | 0.19 | 1.09 | 67.97 | 1.94 | 71.74 | 16.43 | 37.84 |
| Barley | 0.07 | 0.16 | 0.13 | 0.16 | 0.15 | 2.86 | 70.83 | 1.61 | 73.36 | 1.33 | 3.29 |
| Bananas | 0.02 | 0.04 | 0.07 | 0.13 | 0.14 | 0.88 | 71.71 | 1.41 | 74.76 | 10.65 | 22.75 |
| Onions and shallots | 0.01 | 0.02 | 0.05 | 0.11 | 0.11 | 0.55 | 72.26 | 1.15 | 75.91 | 11.68 | 18.54 |
| Watermelons | 0.02 | 0.03 | 0.08 | 0.10 | 0.10 | 0.70 | 72.96 | 1.04 | 76.95 | 9.13 | 34.27 |
| Apples | 0.02 | 0.03 | 0.06 | 0.09 | 0.10 | 0.67 | 73.64 | 1.00 | 77.95 | 9.91 | 19.86 |
| Cucumbers and gherkins | 0.01 | 0.01 | 0.04 | 0.09 | 0.09 | 0.38 | 74.01 | 0.99 | 78.94 | 9.43 | 43.56 |
| Yams | 0.01 | 0.01 | 0.04 | 0.08 | 0.09 | 0.33 | 74.34 | 0.92 | 79.85 | 7.23 | 8.49 |
| Rape or colza seed | 0.00 | 0.01 | 0.04 | 0.07 | 0.09 | 0.14 | 74.48 | 0.91 | 80.76 | 0.57 | 2.18 |
| Sweet potatoes | 0.10 | 0.14 | 0.14 | 0.09 | 0.09 | 3.87 | 78.36 | 0.90 | 81.66 | 7.35 | 11.92 |

Source: www.fao.org/faostat/en/#data/QCL & Author's calculations.

Figure 5.44: Lorenz curve of world crop production

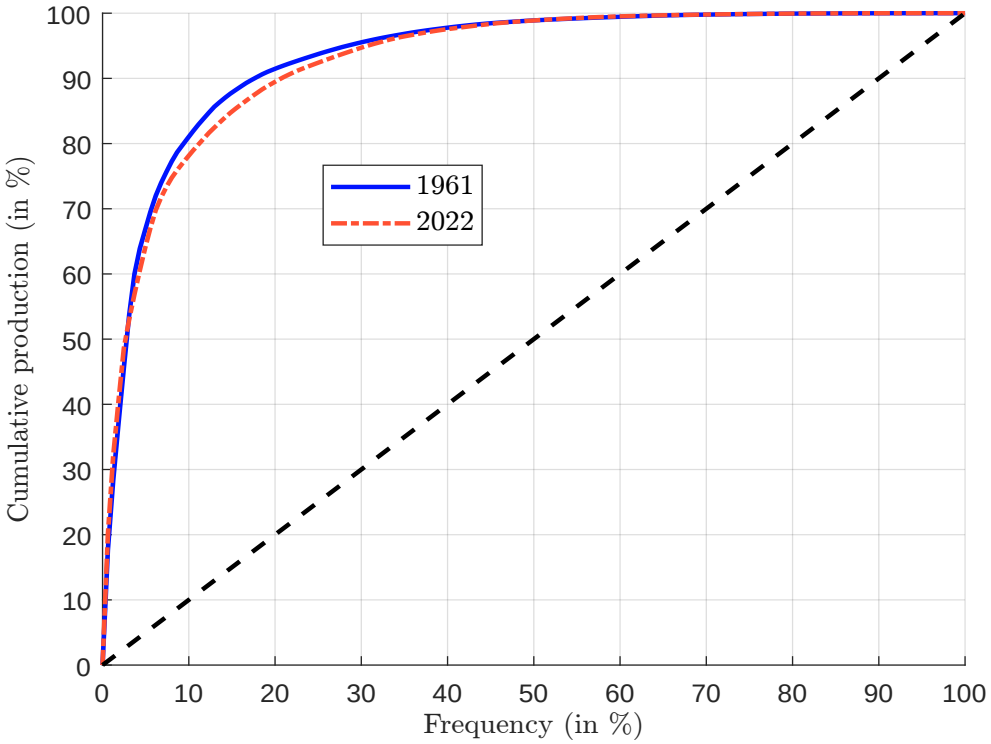


Source: www.fao.org/faostat/en/#data/QCL & Author's calculations.

Figure 5.45: Harvested area for crop production

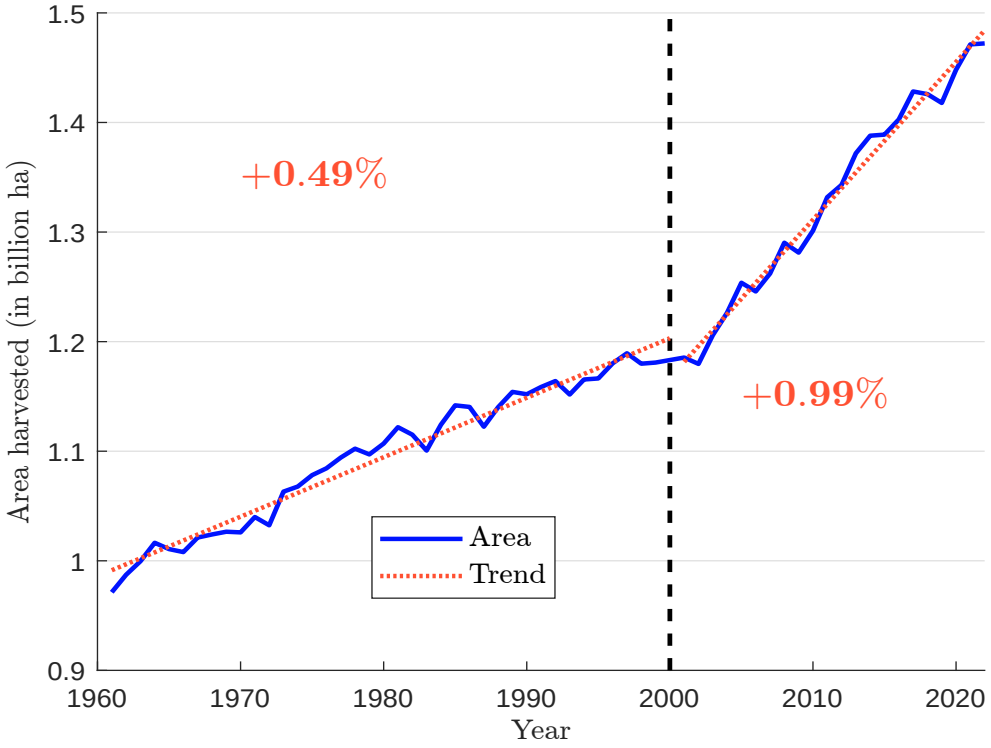


Source: www.fao.org/faostat/en/#data/QCL & Author's calculations.

We now look at livestock production (Table 5.35). Like crops, livestock has experienced remarkable growth: +1 456% for poultry meat, +517% for eggs, +395% for pork meat, etc. However, the magnitude of the production volume is not the same. In fact, we get a total of less than 1.4 billion tonnes, smaller compared to the 9.6 billion tonnes of crop production.

Table 5.35: World production of primary livestock (in million tonnes)

| Livestock | 1961 | 1970 | 1980 | 1990 | 2000 | 2010 | 2020 | 2021 | 2022 | Growth |
|---|---|---|---|---|---|---|---|---|---|---|
| Eggs | 15 | 20 | 27 | 37 | 55 | 69 | 93 | 93 | 93 | 517% |
| Milk | 344 | 392 | 466 | 542 | 579 | 725 | 921 | 941 | 930 | 170% |
| Meat | 71 | 101 | 137 | 180 | 232 | 294 | 339 | 355 | 361 | 405% |
| Beef & Buffalo | 29 | 40 | 47 | 55 | 58 | 67 | 74 | 75 | 76 | 165% |
| Pork | 25 | 36 | 53 | 70 | 89 | 108 | 108 | 121 | 123 | 395% |
| Poultry | 9 | 15 | 26 | 41 | 69 | 99 | 135 | 136 | 139 | 1 456% |
| Sheep & Goat | 6 | 7 | 7 | 10 | 11 | 14 | 16 | 16 | 17 | 176% |
| Other | 3 | 3 | 4 | 4 | 4 | 6 | 6 | 6 | 6 | 106% |

Source: www.fao.org/faostat/en/#data/QCL & Author's calculations.

The remarkable growth in primary crops and livestock can be attributed to three key factors: expansion of cultivated area (although we have seen that only one-third of this growth is due to this factor), the adoption of intensive agricultural practices, and the increased use of inputs such as fertilizers and pesticides. Fertilizer use has increased sixfold in the last sixty years, while pesticide use has doubled between 1990 and 2022 (Table 5.36).

Table 5.36: Agricultural use of inputs (fertilizers and pesticides)

| Input | 1961 | 1980 | 2000 | 2020 | 2022 | 1961 | 1980 | 2000 | 2020 | 2022 |
|---|---|---|---|---|---|---|---|---|---|---|
| | Agricultural use (in million tonnes) | | | | | Use par area of cropland (in kg/ha) | | | | |
| Fertilizer | 31.0 | 116.6 | 135.2 | 201.7 | 185.4 | 20.8 | 76.8 | 85.9 | 123.5 | 113.1 |
| Nitrogen | 11.5 | 60.6 | 81.0 | 114.7 | 108.1 | 7.6 | 39.6 | 51.3 | 69.6 | 65.4 |
| Phosphate | 10.9 | 31.8 | 32.5 | 47.8 | 41.9 | 7.5 | 21.4 | 21.0 | 29.8 | 26.0 |
| Potash | 8.6 | 24.2 | 21.7 | 39.3 | 35.5 | 5.7 | 15.8 | 13.7 | 24.1 | 21.7 |
| Pesticide | | | 2.2 | 3.4 | 3.7 | | | 1.5 | 2.2 | 2.4 |

Source: www.fao.org/faostat/en/#data/RFN, www.fao.org/faostat/en/#data/RP & Author's calculations.

**Remark 57** *The figures presented in this paragraph can be analyzed at the country or regional level. In this case, we observe large differences between regions of the world, for example between the Americas and Africa, or between developed and developing countries (FAO, 2023b).*

**Food consumption** Table 5.37 shows the food supply[102] per capital and per day for the different regions of the world. In general, food supply is assessed along three primary dimensions: energy intake, protein intake, and fat intake. In 2022, the global average daily per capita intake was 2 985 kilocalories of energy[103], 92 grams of protein, and 87 grams of fat. Over the past sixty years, these figures have increased by 36%, 51%, and 81%, respectively. However, these averages mask

species), and vascular plants (81 species) are collected and consumed by more than 100 million EU citizens.

[102]Food supply measures the amount available for consumption at the end of the supply chain and does not include consumption waste.

[103]In the context of nutrition, 1 Calorie (with a capital C) is used as a shorthand for 1 kilocalorie (kcal).

Table 5.37: Food supply per capital per day (energy, protein & fat)

| Region | Energy (in Cal/capita/day) | | | Protein ( in g/capita/day) | | | Fat ( in g/capita/day) | | |
|---|---|---|---|---|---|---|---|---|---|
| | 1961 | 1990 | 2022 | 1961 | 1990 | 2022 | 1961 | 1990 | 2022 |
| Africa | 1 993 | 2 291 | 2 567 | 53 | 59 | 66 | 40 | 47 | 56 |
| Eastern Africa | 1 989 | 1 925 | 2 263 | 56 | 50 | 59 | 29 | 32 | 47 |
| Middle Africa | 2 018 | 1 847 | 2 312 | 49 | 45 | 46 | 36 | 44 | 41 |
| Northern Africa | 1 920 | 2 851 | 3 142 | 53 | 78 | 91 | 38 | 60 | 74 |
| Southern Africa | 2 603 | 2 755 | 2 713 | 70 | 73 | 79 | 58 | 64 | 91 |
| Western Africa | 1 909 | 2 199 | 2 644 | 46 | 52 | 65 | 46 | 49 | 57 |
| Americas | 2 559 | 2 953 | 3 392 | 77 | 82 | 104 | 78 | 97 | 135 |
| Northern America | 2 873 | 3 447 | 3 881 | 95 | 107 | 122 | 110 | 138 | 177 |
| Central America | 2 180 | 2 796 | 3 173 | 59 | 73 | 94 | 48 | 69 | 101 |
| Caribbean | 1 992 | 2 390 | 2 828 | 47 | 57 | 75 | 42 | 65 | 78 |
| South America | 2 329 | 2 599 | 3 111 | 63 | 65 | 95 | 49 | 73 | 118 |
| Asia | 1 805 | 2 414 | 2 944 | 47 | 61 | 93 | 25 | 49 | 78 |
| Central Asia | | | 3 169 | | | 103 | | | 104 |
| Eastern Asia | 1 594 | 2 564 | 3 361 | 44 | 69 | 124 | 18 | 56 | 95 |
| Southern Asia | 2 014 | 2 242 | 2 584 | 52 | 54 | 72 | 30 | 40 | 62 |
| South-eastern Asia | 1 836 | 2 178 | 2 880 | 40 | 48 | 80 | 27 | 41 | 69 |
| Western Asia | 2 501 | 3 273 | 3 128 | 76 | 93 | 93 | 57 | 84 | 101 |
| Europe | 3 041 | 3 367 | 3 471 | 90 | 104 | 112 | 89 | 125 | 140 |
| Eastern Europe | 3 100 | 3 360 | 3 375 | 95 | 105 | 109 | 73 | 108 | 121 |
| Northern Europe | 3 176 | 3 214 | 3 402 | 91 | 96 | 113 | 131 | 134 | 141 |
| Southern Europe | 2 838 | 3 469 | 3 519 | 82 | 107 | 116 | 72 | 136 | 149 |
| Western Europe | 3 016 | 3 374 | 3 615 | 89 | 103 | 113 | 113 | 149 | 162 |
| Oceania | 3 021 | 3 139 | 3 101 | 100 | 105 | 101 | 108 | 126 | 128 |
| Australasia | 3 060 | 3 188 | 3 417 | 103 | 109 | 115 | 111 | 129 | 152 |
| Melanesia | 2 534 | 2 547 | 2 314 | 54 | 65 | 66 | 60 | 86 | 66 |
| Micronesia | 2 424 | 2 622 | 2 937 | 51 | 64 | 86 | 116 | 94 | 126 |
| Polynesia | 2 239 | 2 683 | 2 959 | 55 | 77 | 107 | 73 | 107 | 117 |
| World | 2 196 | 2 621 | 2 985 | 61 | 70 | 92 | 48 | 67 | 87 |

Source: www.fao.org/faostat/en/#data/FBS, www.fao.org/faostat/en/#data/FBSH & Author's calculations.

significant differences between regions. For example, fat intake is currently only 41 g/capita/day in Middle Africa, while it reaches 177 g/capita/day in North America. These differences are even more pronounced when we look at countries. Figure 5.46 shows the dispersion of food supply for the 200 countries included in the FAO database. We can see that the dispersion has not decreased since 1961, in fact it has increased! Countries with the lowest average energy intake include Burundi, Lesotho, Somalia, Haiti, and Madagascar, while those with the highest energy intake are Israel, the United States, Ireland, Belgium, and Turkey. For protein intake, the lowest levels are found in the Democratic Republic of the Congo, Madagascar, Burundi, Somalia, and Mozambique, while Iceland, Israel, Ireland, Mongolia, and Montenegro have the highest. In terms of fat intake, Burundi, DR Congo, Madagascar, Rwanda, and Cambodia rank the lowest, while Belgium, Austria, the United States, Israel, and Germany rank the highest. This reflects economic disparities, but also some of the dietary habits of the countries with the highest levels. The vegetal/animal structure of the human diet also has an impact (Table 5.38). In fact, protein intake from animal sources has increased over the past sixty years, while the contribution of animal products to fat intake has decreased.

Figure 5.46: Country dispersion of food supply

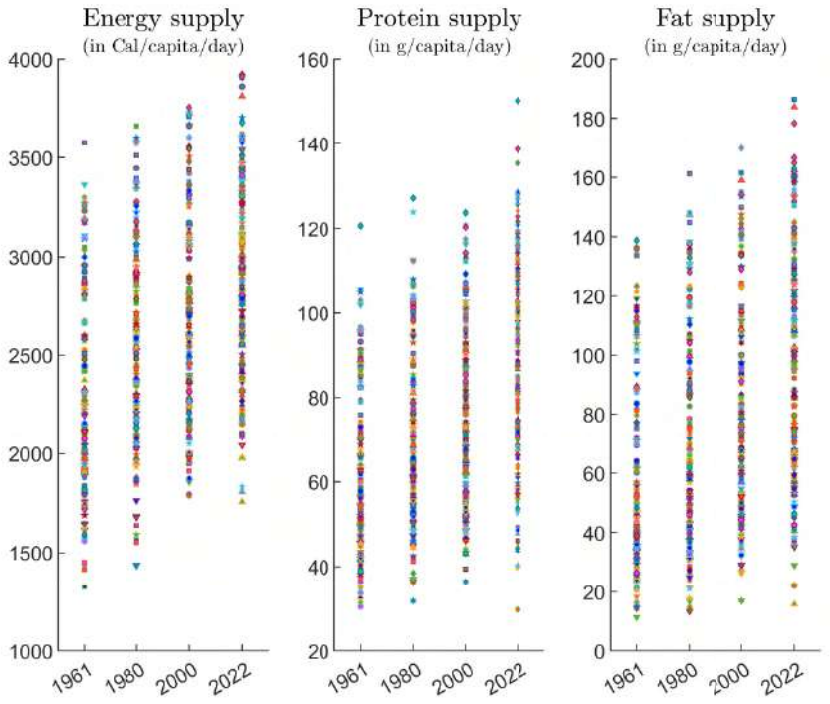


Source: www.fao.org/faostat/en/#data/FBS, www.fao.org/faostat/en/#data/FBSH & Author's calculations.

Table 5.38: Split of food supply between vegetal and animal products

| Food | 1961 | | | 2022 | | |
|---|---|---|---|---|---|---|
| Origin | Energy | Protein | Fat | Energy | Protein | Fat |
| Vegetal | 1 858 | 41.80 | 22.80 | 2 460 | 53.45 | 51.33 |
| Animal | 338 | 19.66 | 24.72 | 525 | 38.08 | 35.98 |
| Total | 2 196 | 61.46 | 47.52 | 2 945 | 91.52 | 87.31 |

Source: www.fao.org/faostat/en/#data/FBS, www.fao.org/faostat/en/#data/FBSH & Author's calculations.

**Food security** Biodiversity is closely linked to food security, as it provides the foundation for resilient and sustainable food systems. This interconnectedness has several dimensions. Moreover, the concept of double materiality is highly relevant, as biodiversity impacts food production, while food and agricultural production also has a significant impact on biodiversity. In this context, it is challenging to classify and list all the dimensions. Therefore, we will focus on a few key dimensions that are essential for food security. The first dimension is the genetic diversity of crops and livestock. Below is an excerpt from the press release of the FAO 2019 biodiversity assessment publication (FAO, 2019):

> "*Less biodiversity means that plants and animals are more vulnerable to pests and diseases. Compounded by our reliance on fewer and fewer species to feed ourselves, the increasing loss of biodiversity for food and agriculture puts food security and nutrition at risk.*" (José Graziano da Silva, FAO Director-General, 22 February 2019, Rome).

Many crop species are no longer cultivated because production is concentrated on the most profitable crops. Over time, this has led to an industrial selection of species, resulting in the homogenization and globalization of the human diet. In this context, we are more vulnerable when a species faces problems such as disease. Here are some examples:

- Irish potato famine (1845–1852)
  The main cause was the infection of potato crops by the potato blight (caused by the fungus-like microorganism *Phytophthora infestans*). This blight led to one million deaths and caused the mass emigration of another million people. The severity of the disease was largely due to Ireland's dependence on a single crop, the potato.

- Coffee leaf rust outbreak in Sri Lanka (1860–1890)
  Coffee leaf rust (CLR) is a disease of the coffee plant caused by the fungus *Hemileia vastatrix*. In the 1860s, coffee production was an important resource for Sri Lanka, but the outbreak of coffee leaf rust destroyed the coffee industry in the region and led to a shift to tea cultivation.

- Panama disease in bananas (1950s)
  Panama disease, caused by the fungus *Fusarium oxysporum*, infects banana plants and nearly eradicated the Gros Michel variety in the 1950s. This led to its replacement with the Cavendish variety, which now faces a similar threat from a new strain of the disease.

- Southern corn leaf blight in the United States (1970)
  Southern corn leaf blight is a disease of corn caused by the plant pathogen *Bipolaris maydis* (Race O, Race C, and Race T). The 1970 epidemic in the USA was triggered by the widespread use of Texas male sterile cytoplasm corn, which made 90% of hybrid crops susceptible to the newly emerged Race T pathogen. This outbreak, which began in the southern U.S. and spread rapidly in the north, destroyed approximately 15% of corn production.

- Wheat stem rust Ug99 in Africa (1998–present)
  Ug99 is a strain of wheat stem rust caused by the fungus *Puccinia graminis*. It was first identified in 1998 and has spread to several countries in Africa and the Middle East. It poses a significant threat to global wheat production due to the high susceptibility of many wheat varieties.

- Citrus greening disease in Florida (2005–present)
  Citrus greening disease, caused by *Liberibacter bacteria*, affects citrus plants and exists in three forms: a heat-tolerant Asian type and heat-sensitive African and American types. First identified in 1929 and reported in southern China in 1943, the disease has severely impacted citrus production in the United States, particularly in Florida, where orange production has declined by more than 50% since 2005.

These diseases highlight the risks of focusing on one or a few crop species. In fact, reliance on a limited number of crop species increases the vulnerability of agriculture to disease. When a single pathogen targets a widely grown crop, such as Panama disease in bananas or Southern corn leaf blight in maize, the impact can be catastrophic, causing widespread losses. Biodiversity is then essential for building resilience to future outbreaks. Coffee is a typical example. According to Davis *et al.* (2019), coffee production is concentrated in a small number of coffee species. In particular, Arabica (*Coffea arabica*) and Robusta (*Coffea canephora*) account for 60% and 40% of traded coffee, respectively, leaving little room for other species. Arabica coffee has been cultivated for at least several hundred years, which is not the case with Robusta, which was first cultivated in the mid-1800s. Robusta coffee went from being a minor African crop to a major global commodity in only

about 150 years, and Davis *et al.* (2019) concluded that "*Robusta coffee provides a good example of how a (relatively) newly discovered wild species has transformed a globally important crop.*" One of the main reasons for its success is its resistance to coffee leaf rust. Of the 124 known coffee species worldwide, their conservation status according to the IUCN extinction risk classification is as follows: 13 are Critically Endangered (CR); 40 are Endangered (EN); 22 are Vulnerable (VU); 9 are Near Threatened (NT); 26 are Least Concern (LC); 14 are Not Evaluated (NE) or Data Deficient (DD). This means that 75% of coffee species are threatened with extinction (Davis *et al.*, 2019, Figure 1, page 2). Therefore, coffee production is at significant risk if existing diseases[104] become more severe or if new diseases emerge, as the number of alternative species that could potentially replace today's Arabica or Robusta varieties has declined over the past century.

The previous example deals with intraspecific diversity (for example, the different types of coffee in the genus *Coffea*), but biodiversity loss is also related to interspecific diversity (for example, the different crops in the clade *Mesangiospermae*). While intraspecific diversity of the food supply has declined in recent times, interspecific diversity has increased with the diversification of diets and trade in commodities, especially in developed countries. Many people now eat exotic fruits, fish and vegetables that would not have been available less than a century ago. Agricultural specialization and the diversity of human diets explain the growth of agricultural trade. Table 5.39 shows that the export share of most crops and commodities has increased. For example, avocado exports represented less than 1% of production in 1961, compared to more than 35% of production in 2021. FAO statistics show that the largest increases (more than 30% between 1961 and 2021) are for cherries, coconut oil, cranberries, kiwi, lentils, mustard seeds, natural honey, olive oil, peas, quinoa, and soybeans. Looking at OECD statistics, the largest increases (+20% between 1990 and 2023) are for edible fish meals, skim milk powder, soybeans, and sugar. Agricultural trade is a resilient factor in food security, but it also reveals the vulnerability of some countries that have specialized in the most profitable crops.

Box 5.13: Founder crops

The concept of "*founder crops*" was introduced by Zohary and Hopf (1988). The authors proposed that eight plant species were first domesticated by early farming communities, laying the foundation of early Neolithic agriculture in Southwest Asia (the Fertile Crescent region of the Near East) around 10 500 years BP. These crops are thought to form the basis of modern agriculture in Europe, Southwest Asia, South Asia, and North Africa. The original founder crops included three cereals (emmer wheat, einkorn wheat, and barley), four pulses (lentil, pea, chickpea, and bitter vetch), and flax.

Subsequent research has suggested that many other species could also be considered as founder crops. This list has been extended for various regions and may include rice and foxtail millet in the Yangtze and Yellow River valleys (about 9 500 years BP), maize, squash, and common bean in southwest Mexico (5 300 years BP), potato, quinoa, and common bean in the Central Andes (5 100 years BP), as well as goosefoot, sunflower, and squash in the Eastern United States (5 100 years BP).

[104] There are many coffee diseases that can be classified into four main categories: bacterial diseases, fungal diseases, root diseases, and viral diseases. Here are some examples: anthracnose (*Colletotrichum*), bacterial blight of coffee (*Pseudomonas syringae*), black rot (*Koleroga noxia*), brown eye spot (*Cercospora coffeicola*), cercospora leaf spot (*Cercospora coffeicola*), coffee leaf rust (*Hemileia vastatrix*), coffee berry disease (*Colletotrichum kahawae*), coffee ringspot virus (*Brevipalpus phoenicis*), coffee wilt disease (*Fusarium xylarioides*), root-knot nematode disease (*Meloidogyne*).

Table 5.39: Share of world crop production exported (in %)

| | Crop | 1961 | 2021 | Crop | 1961 | 2021 |
|---|---|---|---|---|---|---|
| FAO statistics | Apples | 9.4 | 8.8 | Olive oil | 14.9 | 66.2 |
| | Apricots | 5.0 | 8.6 | Onions and shallots | 2.0 | 9.1 |
| | Avocados | 0.2 | 36.3 | Oranges | 16.3 | 10.0 |
| | Bananas | 16.6 | 19.3 | Peaches and nectarines | 6.0 | 7.0 |
| | Barley | 9.9 | 30.0 | Peas | 4.0 | 48.7 |
| | Blueberries | 36.9 | 39.7 | Persimmons | 0.4 | 14.0 |
| | Cauliflowers | 6.4 | 6.1 | Pineapples | 2.8 | 12.7 |
| | Cherries | 2.9 | 35.2 | Pomelos | 10.3 | 11.0 |
| | Coconut oil | 21.1 | 80.6 | Potatoes | 1.0 | 3.8 |
| | Cranberries | 0.0 | 50.9 | Quinoa | 0.0 | 68.8 |
| | Cucumbers | 1.5 | 3.5 | Sesame seeds | 11.0 | 32.2 |
| | Dates | 14.0 | 19.1 | Soybeans | 15.5 | 43.2 |
| | Eggplants | 0.2 | 1.1 | Spinach | 0.3 | 1.1 |
| | Kiwi fruit | 0.0 | 36.4 | Strawberries | 5.4 | 11.1 |
| | Lentils | 6.5 | 67.5 | Tomatoes | 3.9 | 4.4 |
| | Maize | 6.8 | 16.2 | Vanilla | 73.8 | 91.6 |
| | Mustard seeds | 19.3 | 53.8 | Watermelons | 0.9 | 4.7 |
| | Natural honey | 11.0 | 42.3 | Wheat | 17.8 | 25.9 |
| | Commodity | 1990 | 2023 | Commodity | 1990 | 2023 |
| OECD statistics | Beef meat | 9.2 | 18.2 | Pork meat | 1.9 | 8.7 |
| | Butter | 10.0 | 7.8 | Poultry meat | 8.5 | 11.2 |
| | Cheese | 4.0 | 13.6 | Pulses | 10.5 | 19.8 |
| | Cotton | 24.2 | 36.5 | Rice | 3.4 | 10.1 |
| | Edible fish meals | 44.7 | 67.6 | Roots and tubers | 7.3 | 7.8 |
| | Eggs | 2.6 | 1.6 | Sheep meat | 12.2 | 9.0 |
| | Fish | 15.4 | 23.0 | Skim milk powder | 26.4 | 57.9 |
| | Fresh dairy products | 0.0 | 0.1 | Soybeans | 26.6 | 45.1 |
| | Maize | 12.8 | 15.3 | Sugar | 9.8 | 36.8 |
| | Oilseed meals | 24.2 | 24.5 | Vegetable oils | 24.3 | 37.2 |
| | Other coarse grains | 7.7 | 14.0 | Wheat | 19.4 | 24.1 |
| | Other oilseeds | 15.2 | 13.6 | Whole milk powder | 45.9 | 49.9 |

Source: www.fao.org/faostat/en/#data/QCL, www.fao.org/faostat/en/#data/TCL, https://data-explorer.oecd.org & Author's calculations.

A typical example of crop expansion is maize (Pollan, 2007; Hartigan, 2017). In 2022, maize (*Zea mays*) was the world's most widely produced grain crop (1.16 billion tonnes, covering the second-largest cultivated area (203.5 million hectares) and achieving the highest grain yield (5.72 tonnes per hectare). Today, maize appears in a wide range of foods, including candy corn, corn dogs, corn flakes, corn soup, cornstarch, corn tortillas, cornbread, polenta, popcorn, tamales, and more. This proliferation is especially noticeable in the Americas. For instance, Maize is the focus of the documentary film *King Corn*, which was released in October 2007. The film explores the trend of increased corn production and its impact on American society. However, maize has not always been the dominant crop that "*has conquered the world*." Native to Central America, maize was introduced to Europe in the early 16$^{\text{th}}$ century following Christopher Columbus's voyages to the Americas. Initially brought to Spain by explorers returning from the New World, maize gradually

spread across southern Europe, the Mediterranean, and eventually to Africa and Asia. Its global spread was largely due to its adaptability to different climates and soil conditions. Figure 5.47 illustrates the expansion of maize in world agriculture. The first panel shows the area harvested. In 1961, this was 105.6 million hectares — less than the area cultivated for rice (115.4 million hectares) and wheat (204.2 million hectares). By 2022, the area cultivated for maize is nearly equal to that of wheat and surpasses that of rice. Maize production has accelerated since 2000, driven by a significant expansion of harvested area and the introduction of genetically modified (GMO) maize varieties. One of the key issues with maize production is its substitution effect on the supply of other crops. In particular, the primary use of maize is not for direct human consumption but as animal feed. Using FAO statistics, we report below the breakdown of maize use[105]:

| Year | Animal feed | Human food | Losses | Seed | Processing | Other uses |
|---|---|---|---|---|---|---|
| 2010 | 55.3% | 13.6% | 3.5% | 0.7% | 5.7% | 21.2% |
| 2022 | 60.4% | 11.4% | 5.2% | 0.7% | 5.8% | 16.5% |

60% of maize is used as animal feed, mainly for poultry and cattle. Direct human consumption accounts for only 11% of total production, which is less than the *other uses* category. In fact, a significant portion of maize (between 10% and 20%) is processed to produce ethanol, a biofuel used primarily in gasoline blends.

Figure 5.47: Area harvested, production and yield of cereal crops

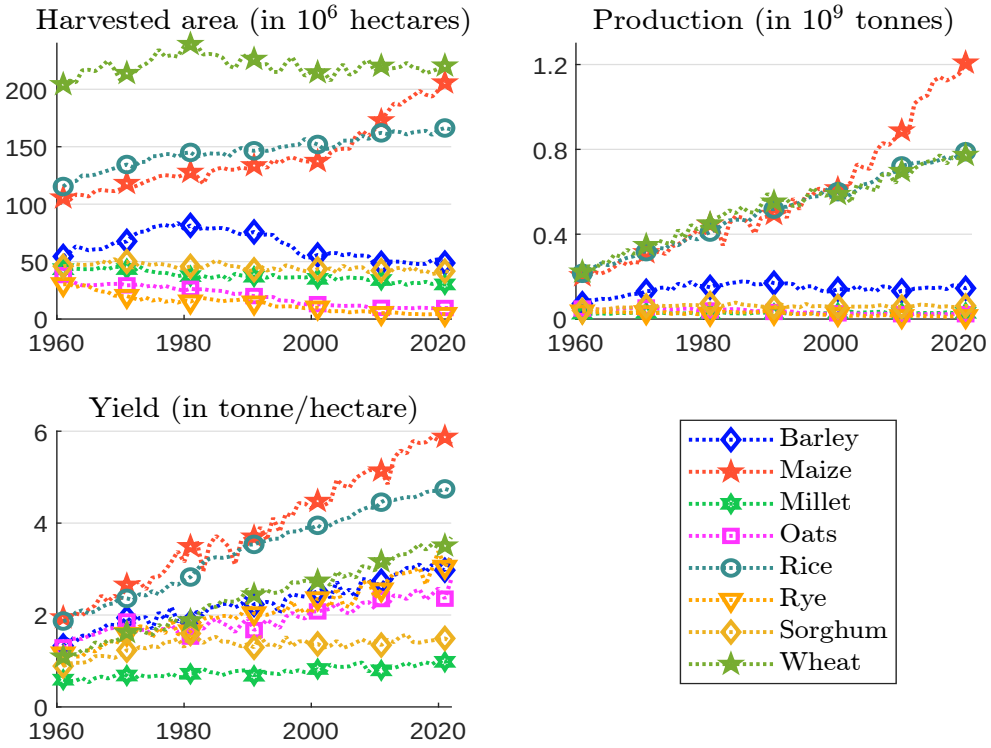


Source: www.fao.org/faostat/en/#data/QCL & Author's calculations.

The previous issue relates to the Earth's capacity to provide all necessary ecosystem functions without compromising others. Here, the *Do No Significant Harm* (DNSH) concept plays a crucial

[105] We first calculate the net supply quantity with the following equations: Supply quantity = Production + Imports − Exports − Stock variation. Then, we use the following decomposition: Supply quantity = Feed + Seed + Losses + Processing + Other uses (non-food) + Tourist consumption + Residuals + Food.

role. But it's not just a matter of choosing one ecosystem service over another. Instead, we see a global deterioration of ecosystem services when examining the ecological footprint and the Earth's biocapacity. The ecological footprint, introduced by Wackernagel and Rees (1996), measures the rate at which we consume resources and produce waste compared to the rate at which nature can regenerate those resources and absorb waste. This metric balances the demand for ecosystem services against their supply. On the demand side, the ecological footprint assesses the use of productive land areas, and quantifies the ecological assets required by a population or product to produce the resources it consumes and to absorb its wastes. On the supply side, biocapacity measures the productivity of ecological assets (such as cropland, grazing land, forests, fisheries, and built-up areas). Both metrics are expressed in global hectares, either for a region or per capita, allowing for meaningful comparisons across regions.

Figure 5.48: Global ecological footprint and biocapacity (in global hectares per capita)

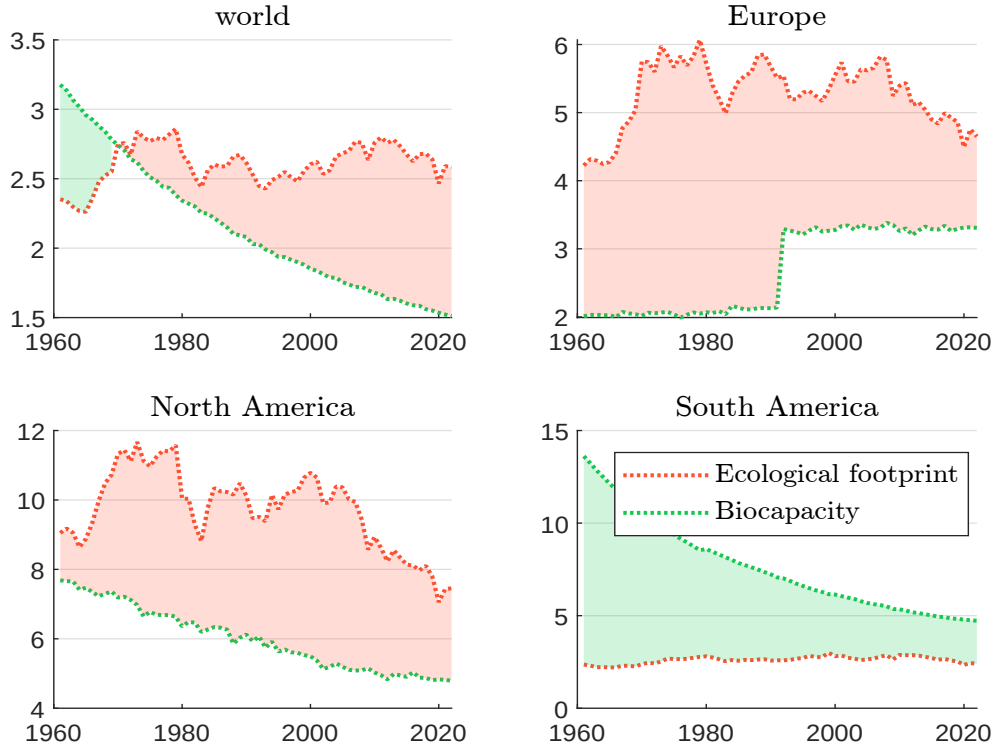


Source: https://data.footprintnetwork.org & Author's calculations.

Figure 5.48 shows the global ecological footprint when considering the various ecological assets. If the ecological footprint exceeds biocapacity, the region has a biocapacity deficit (red area); otherwise, it has a biocapacity reserve (green area). Before 1970, global biocapacity was greater than the ecological footprint, but since then, a biocapacity deficit has emerged. This shift has occurred because, while the per capita ecological footprint has remained relatively constant, the per capita biocapacity has declined, as the Earth's resources are finite. There are significant regional differences. South America's biocapacity balance has declined over time but remains positive, while Europe has experienced a biocapacity deficit for many years. If we focus specifically on the ecosystem service of cropland (Figure 5.49), we see different regional trends. In Asia, Europe, and South America, both demand and supply per capita have increased. However, the biocapacity balance remains positive in South America, is negative but significantly reduced in Europe, and is negative and increasing in Asia. In North America, the biocapacity reserve has remained roughly constant since 2000.

Figure 5.49: Cropland ecological footprint and biocapacity (in global hectares per capita)

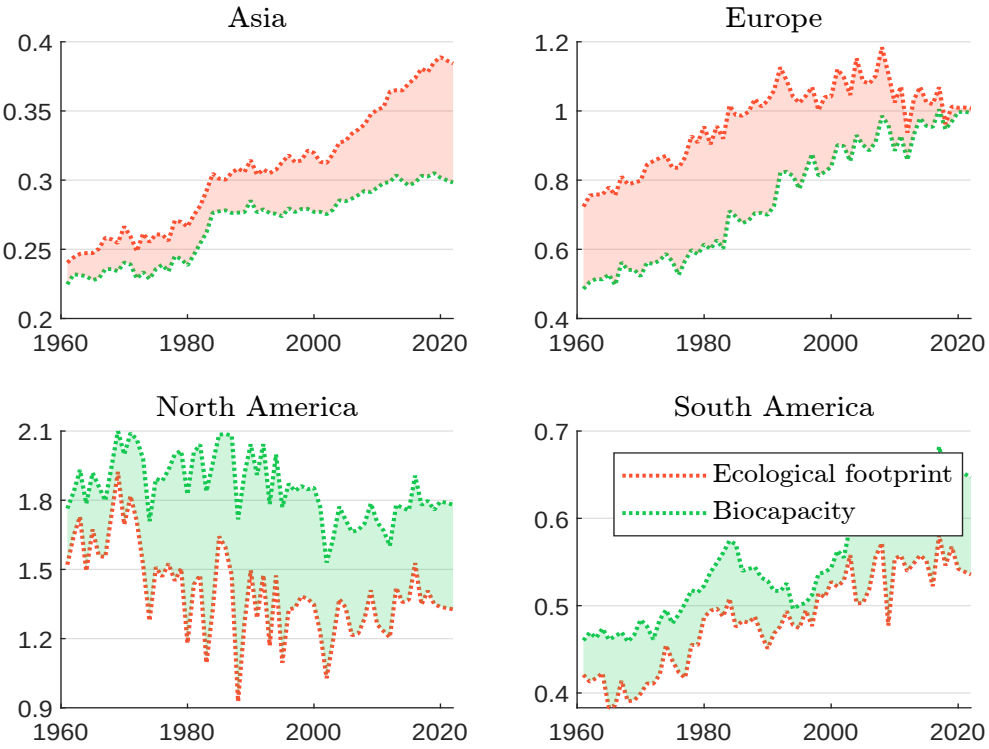


Source: https://data.footprintnetwork.org & Author's calculations.

In addition to food diversity, a second important dimension of food security is the Earth's capacity to feed the planet, or 8.2 billion people. The FAO uses several measures to assess food insecurity. One of the main metrics is the prevalence of (severe/moderate) food insecurity. Let $X$ and $R$ be the random variables for energy intake and energy requirement, respectively, with a joint probability distribution $\mathbf{F}(x, r)$. Sukhatme (1961, Equation 1, page 466) defines the prevalence of undernourishment as the probability that intake is less than requirement:

$$\text{PoU} = \Pr\{X < R\} = \iint \mathbb{1}\{x < r\} \cdot \mathrm{d}\mathbf{F}(x, r) = \iint_{x<r} f(x, r)\, \mathrm{d}x\, \mathrm{d}r \tag{5.16}$$

where $f(x, r)$ is the bivariate density function of $(X, R)$. The non-parametric estimator of PoU is the empirical frequency:

$$\text{PoU} = \frac{1}{n} \sum_{i=1}^{n} \mathbb{1}\{x_i < r_i\}$$

where $n$ denotes the population size and $(x_i, r_i)$ are the observed intake and requirement values for individual $i$. Another approach assumes a parametric density function $f(x, r; \theta)$, estimates the vector of parameters $\theta$, and calculates $\text{PoU} = \iint_{x<r} f\left(x, r; \hat{\theta}\right) \mathrm{d}x\, \mathrm{d}r$. Both statistical methods require a sample $(x_i, r_i)$ of energy intake and requirement values. However, in practice, determining an individual's exact energy requirement is challenging. Therefore, the FAO approximates the prevalence of undernourishment as follows:

$$\text{PoU} = \Pr\{X < r_L\} = \int_{x<r_L} f_x(x)\, \mathrm{d}x = \mathbf{F}_x(r_L) \tag{5.17}$$

where $\mathbf{F}_x(x)$ is the cumulative distribution function of energy intake, often called dietary energy consumption (DEC), and $r_L$ is a cut-off point representing the minimum requirement, also known as the minimum dietary energy requirement (MDER)[106]. The univariate approach is valid when applied to a homogenous group such that $\sigma(R) \approx 0$. Therefore PoU is calculated at the group level (*e.g.*, sex $\times$ age) and then aggregated across the different groups in a population. It is commonly accepted that $X \sim \mathcal{LN}(\mu_x, \sigma_x^2)$. The calibration of the parameters $\mu_x$ and $\sigma_x$ is done by matching the first two statistical moments of $X$. Let $\mu(X)$ and $\text{CV}(X) = \sigma(X)/\mu(X)$ be the empirical mean[107] and the coefficient of variation of $X$, respectively. Since we have $\mu(X) = \exp\left(\mu_x + \frac{1}{2}\sigma_x^2\right)$ and $\text{CV}^2(X) = \exp(\sigma_x^2) - 1$, we deduce that:

$$\begin{cases} \mu_x = \ln \mu(X) - \dfrac{1}{2}\ln\left(\text{CV}^2(X) + 1\right) \\ \sigma_x = \sqrt{\ln\left(\text{CV}^2(X) + 1\right)} \end{cases}$$

According to FAO (2024a), the minimum energy requirement $m_i$ by sex and age group is calculated by estimating the basal metabolic rate (BMR) and multiplying it by the ideal weight for a healthy person in that sex/age group. These ideal weights are derived from the body mass index (BMI) reference tables published by the World Health Organization (WHO). The minimum energy requirement is then adjusted using a physical activity level (PAL) coefficient. Finally, the cut-off point is obtained as the weighted average of the minimum energy requirements: $r_L = \sum_{i=1}^{n} f_i m_i$ where $f_i$ is the frequency of individuals in sex/age group $i$ within the population.

**Remark 58** *While the estimation of $\mu(X)$ is simply the empirical mean, the estimation of $\text{CV}(X)$ is more complex. According to Naiken (2002), the coefficient of variation is assumed to have two components:*

$$\text{CV}^2(X) = \text{CV}^2(X \mid Y) + \text{CV}^2(X \mid R)$$

*where $\text{CV}(X \mid Y)$ is the coefficient of variation of $X$ due to income dispersion and $\text{CV}(X \mid R)$ is the coefficient of variation of $X$ due to energy requirement. In general, $\text{CV}(X \mid R)$ is assumed to be constant and equal to 20%.*

**Example 23** *We assume[108] that the average dietary energy consumption (ADEC) $\mu(X)$ is 2 589 kcal/capita/day, the coefficient of variation $CV(X)$ is 0.27, the minimum dietary energy requirement (MDER) $r_L$ is 1 803 kcal/capita/day and the average dietary energy requirement (ADER) is 2 333 kcal/capita/day.*

We first calibrate the log-normal distribution of the dietary energy consumption. The estimated values of the parameters are:

$$\sigma_x = \sqrt{\ln(0.27^2 + 1)} = 0.2653$$

[106] This approximation is suggested in Sukhatme (1961, Equation 4, page 473). See also Exercise 5.5.1 on page 564 for a comparison between the bivariate and univariate distribution approaches.

[107] The mean dietary energy consumption is given by:

$$\mu(X) = \frac{1}{365}\left(\frac{1}{N}\sum_{i=1}^{m} Q_i C_i\right)$$

where $Q_i$ is the amount (in kg) of food product $i$ consumed annually by the population, $C_i$ is the energy density (in Calories/kg) of food product $i$, and $N$ is the population size. The term $\sum_{i=1}^{m} Q_i C_i$ represents the total calories consumed by the population in one year, while $\mu(X)$ is the average number of calories per capita per day. We recall that food available for human consumption is equal to the total food supply (production + imports − exports − changes in stocks) minus animal feed minus seeds minus other non-human uses minus waste.

[108] These figures are those obtained from the FAO in the case of India in 2022.

and:

$$\mu_x = \ln(2\,589) - \frac{0.2653^2}{2} = 7.8238$$

We can then deduce that the prevalence of undernourishment is 10.91%:

$$\text{PoU} = \Pr\{X < 1803\} = \Phi\left(\frac{\ln(1\,803) - 7.8238}{0.2653}\right) = 0.1091$$

Figure 5.50 shows the probability distribution of the dietary energy consumption $X$, the MDER and the prevalence of undernourishment. We also report the values of ADER and ADEC, which measure the average dietary energy requirement and consumption. In this case, we observe that ADER < ADEC, which is the normal situation.

Figure 5.50: Dietary energy consumption and prevalence of undernourishment (India, 2022)

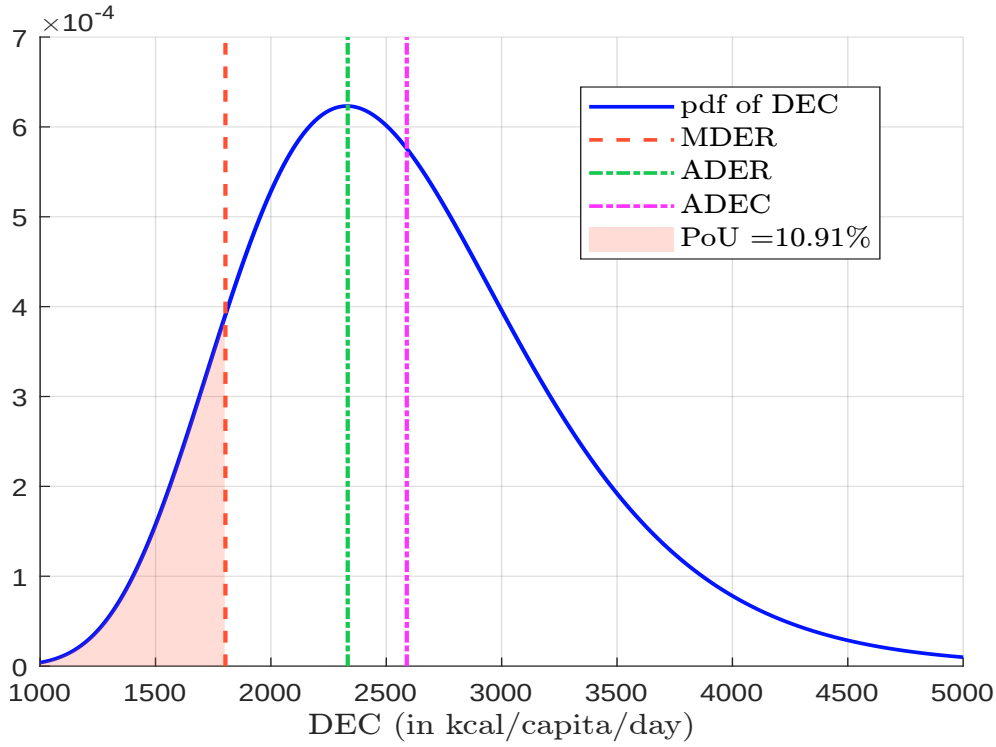


Source: www.fao.org/faostat/en/#data/FS & Author's calculations.

Figure 5.51 shows the evolution of several statistics from 2000 to 2022. The first panel compares ADEC, ADER and MDER. As expected, the average and minimum dietary energy requirements are relatively stable. On average, ADER is equal to 2 360 kcal/capita/year, while MDER is equal to 1 820 kcal/capita/year. On the contrary, the average dietary energy consumption is increasing over time at the global level. It is now close to 3 000 kcal/capita /year. However, these global figures hide some large differences between countries, as some countries have experienced large declines in recent years. In fact, we observe that the prevalence of undernourishment has decreased from 2000 to 2019, but it is increasing since 2020. As a result, the number of undernourished people is currently around 730 million. Figure 5.52 highlights this wide variability across countries. Average dietary energy consumption ranges from 1 834 Calories per capita per day in Somalia to 3 912 Calories in the USA. Somalia also has the highest prevalence of undernourishment, at 51% in 2022. The suite of

Figure 5.51: Prevalence of undernourishment and number of undernourished people (World)

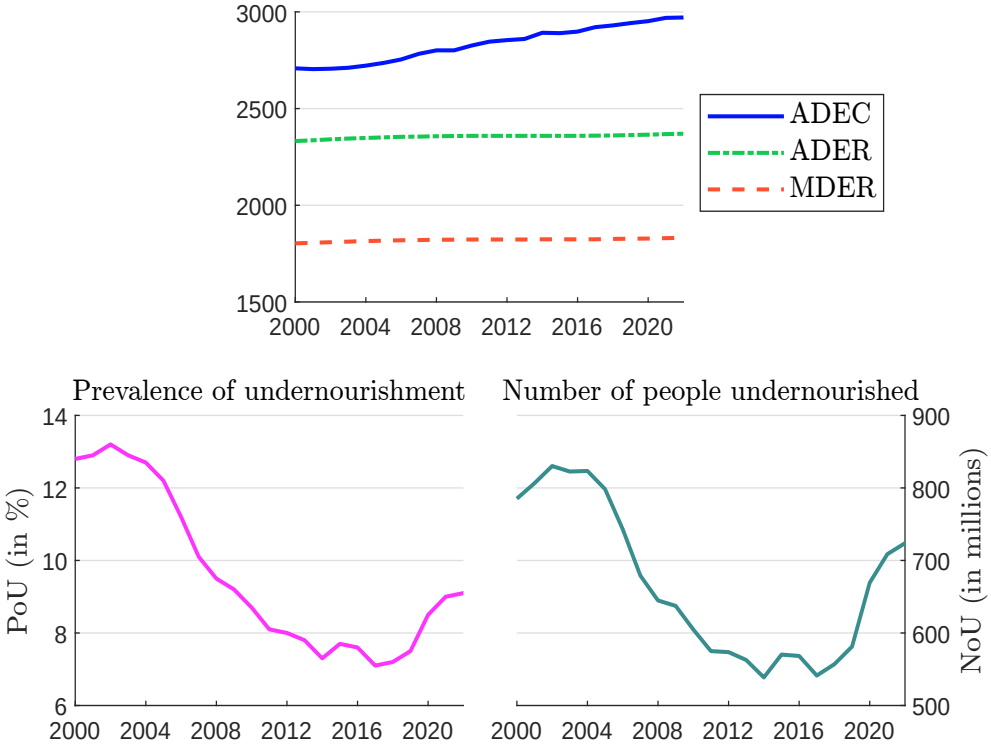


Source: www.fao.org/faostat/en/#data/FS & Author's calculations.

Figure 5.52: Histogram of food insecurity indicators (country level, 2022)

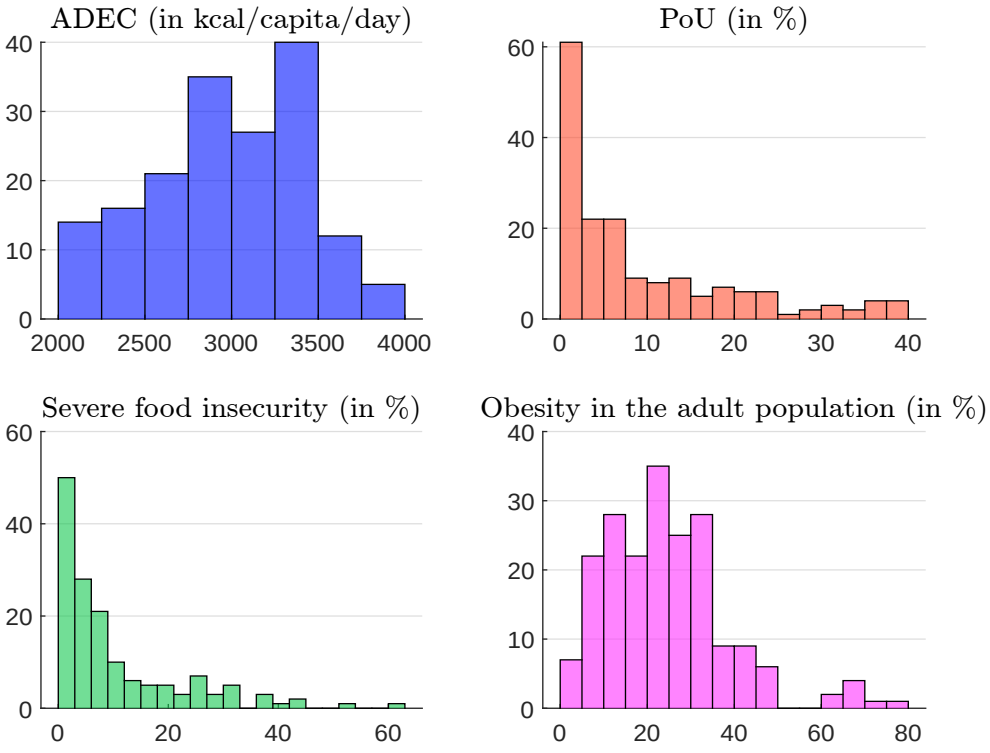


Source: www.fao.org/faostat/en/#data/FS & Author's calculations.

food security indicators on the FAOSTAT website includes many other statistics on food insecurity. For example, the bottom panels of Figure 5.52 show the prevalence of severe food insecurity in the total population and the prevalence of obesity in adults (18 years and older). Other indicators are presented in table 5.40 for the different regions of the world.

Table 5.40: Food security indicators by region (2022)

| Indicator | Africa | Asia | Europe | North America | Oceania | South America | World |
|---|---|---|---|---|---|---|---|
| MDER (kcal/capita/day) | 1 736 | 1 831.0 | 1 931 | 1 962 | 1 871 | 1 856 | 1 832 |
| ADER (kcal/capita/day) | 2 237 | 2 369.0 | 2 505 | 2 554 | 2 424 | 2 403 | 2 370 |
| ADEC (kcal/capita/day) | 2 578 | 2 917.0 | 3 467 | 3 882 | 3 104 | 3 104 | 2 971 |
| Prevalence of undernourishment | 19.9 | 8.2 | | | 7.1 | 6.6 | 9.1 |
| People undernourished (million) | 284.1 | 386.5 | | | 3.2 | 43.9 | 723.8 |
| Severe food insecurity | | | | | | | |
| Total population | 21.7 | 9.7 | 1.8 | 0.9 | 9.3 | 11.0 | 10.8 |
| Rural adult population | 23.5 | 10.4 | 1.7 | 0.8 | 2.8 | 13.5 | 12.2 |
| Town adult population | 22.2 | 10.9 | 1.9 | 0.7 | 4.0 | 12.9 | 11.5 |
| Urban adult population | 19.8 | 8.3 | 1.8 | 1.2 | 3.0 | 9.6 | 9.3 |
| Male adult population | 20.8 | 8.6 | 1.7 | 0.7 | 8.5 | 9.6 | 9.1 |
| Female adult population | 21.3 | 9.9 | 1.9 | 1.2 | 8.3 | 12.0 | 10.2 |
| Total population (million) | 309.0 | 459.2 | 13.3 | 3.5 | 4.2 | 72.5 | 861.7 |
| Male adults (million) | 87.9 | 157.2 | 6.4 | 1.0 | 1.5 | 23.7 | 277.7 |
| Female adults (million) | 92.0 | 177.6 | 7.8 | 1.9 | 1.4 | 31.2 | 311.9 |
| Water services | | | | | | | |
| Safely managed drinking water | 33.0 | 76.0 | 93.0 | 97.0 | | 75.0 | 73.0 |
| Basic drinking water | 66.0 | 95.0 | 98.0 | 100.0 | | 98.0 | 91.0 |
| Sanitation services | | | | | | | |
| Safely managed sanitation | 26.0 | 59.0 | 79.0 | 96.0 | 73.0 | 49.0 | 57.0 |
| Basic sanitation | 36.0 | 86.0 | 97.0 | 100.0 | 80.0 | 90.0 | 81.0 |
| Children under 5 years | | | | | | | |
| Affected by wasting | 5.8 | 9.3 | | 0.2 | | 1.4 | 6.8 |
| Who are stunted | 30.0 | 22.3 | 4.0 | 3.6 | 22.0 | 11.5 | 22.3 |
| Who are overweight | 4.9 | 5.1 | 7.3 | 8.2 | 16.8 | 8.6 | 5.6 |
| Affected by wasting (million) | 12.2 | 31.6 | | | | 0.7 | 45.0 |
| Who are stunted (million) | 63.1 | 76.6 | 1.4 | 0.7 | 0.8 | 5.7 | 148.1 |
| Who are overweight (million) | 10.2 | 17.7 | 2.6 | 1.7 | 0.6 | 4.2 | 37.0 |
| Obesity | | | | | | | |
| Adult population | 16.2 | 10.4 | 21.4 | 40.3 | 29.5 | 29.9 | 15.8 |
| Adult population (million) | 123.9 | 353.9 | 129.0 | 119.2 | 9.6 | 141.4 | 880.7 |

All statistics are expressed in %, except those whose units are indicated.

Source: www.fao.org/faostat/en/#data/FS & Author's calculations.

**Remark 59** *As discussed in Section 2.1.1 on page 54, food security encompasses many dimensions and issues. Here, we focus on two critical aspects: genetic diversity and the capacity to feed the global population. In a fragmented world, a third important dimension is each country's dependence on external sources for its food supply.*

### 5.4.3 Biodiversity threats and risks

Primack (2014) categorizes different threats to biodiversity into three main clusters: (1) extinction, (2) habitat destruction, fragmentation, degradation, and global climate change, and (3) overexploitation, invasive species, and disease. Sodhi and Ehrlich (2010) consider a similar list of biodiversity risks but groups them differently: (1) extinction, (2) habitat loss and fragmentation, (3) overexploitation, (4) invasive species, (5) climate change, and (6) fire. In reality, these factors often interact with each other, amplifying their combined effects. Moreover, it is important to distinguish between biodiversity threats and biodiversity risks:

- Biodiversity threats are the specific drivers or causes of biodiversity loss. They are external factors that contribute directly or indirectly to biodiversity loss by impacting species, habitats, and ecosystems. For example, invasive species can severely disrupt an ecosystem and therefore constitute a threat to biodiversity.
- Biodiversity risks refer to the potential consequences of biodiversity loss due to these threats. Specifically, biodiversity risks encompass the likelihood and severity of negative impacts on human life and ecosystem functions. For example, the emergence of new diseases as a result of ecosystem disturbances is a biodiversity risk.

The distinction between biodiversity threats and biodiversity risks is not always clear. For example, habitat loss is a threat because it directly reduces biodiversity and disrupts ecosystems. But it is also a risk because activities such as agriculture and land-use change contribute to further habitat loss. Similarly, pollution can be both a threat and a risk to biodiversity. It is a direct factor in biodiversity loss, but it can also result from that loss. In this context, the boundary between threats and risks to biodiversity can be somewhat artificial. Furthermore, these different threats are often interrelated, and the same is true of risks. In addition, feedback loops can complicate the distinction between the two concepts. For instance, habitat fragmentation may reduce biodiversity, but the resulting loss of biodiversity may in turn exacerbate further habitat fragmentation. According to Wilson (1989), the central cause of biodiversity risk is the destruction of natural ecosystems by human beings. He identified five major threats: habitat destruction, overexploitation, pollution, global climate change and invasion by introduced species. He argued that these five causes are driven by underlying social conditions, in particular increased per capita consumption, rapid population growth and unsound economic policies. Since this seminal paper on biodiversity loss, these key elements have been extensively studied and documented by scientists, showing that the Earth's ecosystems are dominated by humans (Vitousek *et al.*, 1997), and that humans are ultimately the cause of the current biodiversity crisis. Land-use change is undoubtedly the greatest threat (Sala *et al.*, 2000), while the decline in species richness is the most visible risk.

The possibility of a sixth mass extinction (Late Quaternary Mass Extinction or LQME), has been raised before[109]. According to Algeo and Shen (2024), the LQME differs from previous extinctions because it is driven by technological advances, particularly those that have allowed humans to exert widespread influence over the Earth's climate and ecosystems. The extinction process occurred in phases. In the first phase (50 Kyr BP–1750 AD), overhunting and the loss of top predators led to the extinction of many large animal species, especially after human expansion into new regions such as Australasia and the Americas. The first phase is characterized by limited global impacts (less than 1% of species loss) but significant ecosystem impacts. The current phase (1750 AD to present) is driven by habitat loss as humans convert land for agriculture and urbanization, with invasive species and climate change also contributing to species loss. The current phase is characterized by current

[109] See the section on page 384 dedicated to the LQME.

Figure 5.53: Stages of the Late Quaternary mass extinction

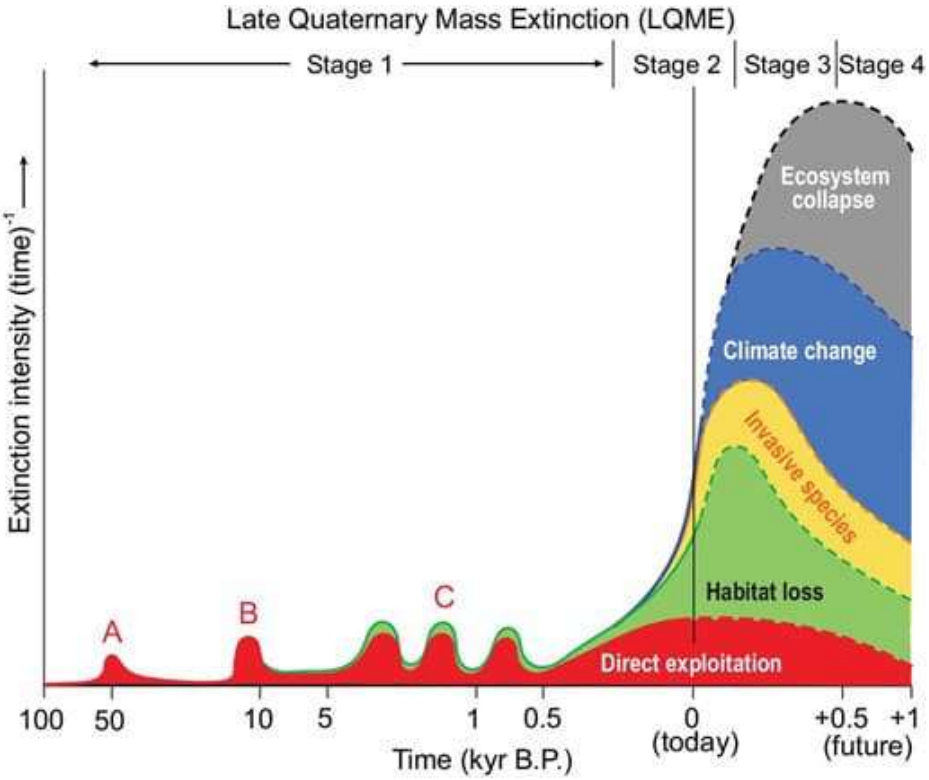


Stage 1 (from ∼ 50 to 0.25 ka), characterized by direct exploitation of species, comprised megafaunal extinctions in (A) Australasia, (B) the Americas and (C) the Indo-Pacific region. Stage 2 (from ∼ 0.25 ka to the near future) is dominated by extinctions due to habitat loss. Stages 3 and 4 (future, timeline speculative) will be marked by climate change and ecosystem collapse, respectively, as the dominant proximate causes of extinction, while invasive species will play a supporting role during Stages 2 to 4.

Source: Algeo and Shen (2024, Figure 5, page 11).

losses of 1–2% of total biodiversity, but the extinction rate is about 1 000 times the background extinction rate. Algeo and Shen (2024) suggest that the near future phase will be dominated by climate change, which will become the primary driver of biodiversity loss, while they estimate that the final phase could lead to widespread ecosystem collapse. In this case, the final phase could be characterized by a rapid and extensive loss of biodiversity, comparable to Earth's largest historical extinction events. Figure 5.53 illustrates this worst-case scenario of the sixth mass extinction.

**Remark 60** *World Economic Forum (2020b) published the New Nature Economy Report to address the growing threats posed by biodiversity loss and the current biodiversity crisis to economies and businesses worldwide. The report emphasizes that biodiversity decline is not only an environmental issue but also a significant economic risk. The report outlines 15 major threats to biodiversity and identifies 15 critical transitions across three socio-economic systems. These threats are linked to issues such as habitat loss, overexploitation, and pollution, which pose not only risks to human welfare but also substantial risks to our economic systems. The proposed transitions aim to reduce nature-related risks while unlocking economic opportunities, potentially generating $10 trillion in economic value and creating 395 million jobs by 2030.*

Box 5.14: New Nature Economy Report II (World Economic Forum, 2020)

In 2000, the World Economic Forum issued an alarming report on the impact of business on biodiversity and biodiversity on business (double materiality). This report highlights three key socio-economic systems: (1) food, land and ocean use, (2) infrastructure and the built environment, and (3) energy and extractives. These systems contribute 12%, 40% and 23% of global GDP, respectively, and employ 40%, 18% and 16% of the world's workforce. They also exert the greatest pressure on biodiversity, with 80% of threatened and near-threatened species at risk from activities in these sectors, and 72% affected by the food, land and ocean use sector alone. The WEF estimates that over half of the global GDP (around $44 trillion in economic value) relies heavily or moderately on natural resources. It also identifies 15 major pressing business-related threats to nature:

- Food, land and ocean use: (1) annual and perennial non-timber crops, (2) logging and wood harvesting, (3) livestock farming and ranching, (4) invasive non-native/alien species/diseases, (5) fire and fire suppression, (6) agricultural and forestry effluents, (7a) water management/use*, (8) fishing and aquatic resources;
- Infrastructure and the built environment: (9) housing and urban areas, (10) tourism and recreational areas, (11) domestic and urban wastewater, (12) roads and railroads, (13) commercial and industrial areas, (14) industrial and military effluents;
- Energy and extractives: (15) mining and quarrying, (7b) dams*.

In a similar way, the WEF identities 15 key socio-economic transitions needed to tackle the nature crisis:

- Food, land and ocean use: (1) ecosystem restoration and avoided expansion, (2) productive and regenerative agriculture, (3) healthy and productive ocean, (4) sustainable management of forests, (5) planet-compatible consumption, (6) transparent and sustainable supply chains;
- Infrastructure and the built environment: (7) densification of the urban environment, (8) nature-positive built environment design, (9) planet-compatible urban utilities, (10) nature as infrastructure, (11) nature-positive connecting infrastructure;
- Energy and extractives: (12) circular and resource efficient models, (13) nature-positive metals and minerals extraction, (14) sustainable materials supply chains, (15) nature-positive energy transition.

*Dams and water management/use are treated as separate threats because they involve different economic activities.

Box 5.14: New Nature Economy Report II (continued)

The capital investment required to implement these fifteen transitions accross the three systems is approximately $2.7 trillion per year, which the following breakdown: 16% for the six transitions related to food, land and ocean use, 64% for the five transitions related to infrastructure and the built environment, and 31% for the four transitions related to energy and extractives. However, implementing these transitions could generate $10 trillion in business opportunities and create approximately 400 million jobs by 2030. Among these, the food, land, and ocean use system is expected to yield the greatest socio-economic benefits.

Table 5.C: Key figures of the New Nature Economy Report II

| System | Description | Share of threatened species impacted | Threats | Total business opportunities by 2030 | Total jobs by 2030 | Annualized investment costs (2020–2030) |
|---|---|---|---|---|---|---|
| | Food, land and ocean use | 72% | 8 | $3 565 bn | 191 mn | $440 bn |
| | Infrastructure and the built environment | 29% | 6 | $3 015 bn | 117 mn | $1 430 bn |
| 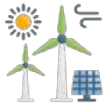 | Energy and extractives | 18% | 2 | $3 530 bn | 87 mn | $840 bn |
| | Total† of the three socio-economic systems | 79% | 15 | $10 110 bn | 395 mn | 2 710 bn |

†Because some species are affected by more than one of the three systems, the percentage of species impacted by all systems is less than the sum of the percentages impacted by each individual system. The total number of threats is also 15 because water management/use and dams are considered as a single threat.

Source: World Economic Forum (2020b, pages 8-16).

Figure 5.54: Habitat loss vs. fragmentation vs. degradation

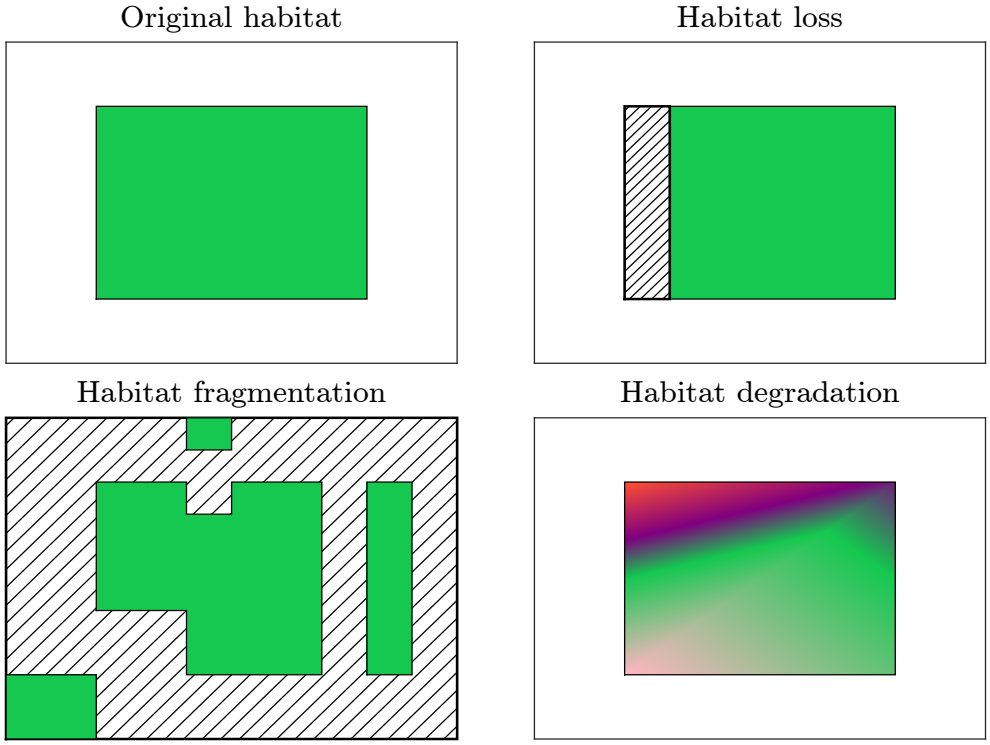


**Habitat loss, fragmentation and degradation**

Habitat loss, fragmentation, and degradation is the largest cause of biodiversity loss and the primary threat leading to species extinction. Written in the singular form, this sentence suggests that these three processes are interconnected or form a single, overarching factor. However, it's important to distinguish between them:

- Habitat loss occurs when a natural habitat is completely removed, destroyed, or converted to another use, resulting in the disappearance of species that previously lived there. For example, deforestation — transforming a forest into cropland or an urban area — is a typical case of habitat loss. This process is the most severe form of habitat disruption, because it eliminates the existing living space and is often irreversible.

- Habitat fragmentation occurs when a large, continuous habitat is divided into smaller, isolated patches by human-made structures. Building highways through a forest, for instance, is a typical example of habitat fragmentation. Fragmentation creates habitat islands that may be too small to support the original populations, increasing the risk of species decline or extinction.

- Habitat degradation is the process by which the quality of a habitat is damaged or reduced, making it less suitable for the species that live there. Factors such as pollution, water contamination, water stress, climate change or invasive species often contribute to degradation. In such cases, species may become endangered as their populations decline or suffer from poor health.

In summary, loss is the total elimination of a habitat, fragmentation is the breaking up of a habitat into smaller habitats, and degradation is the decline in habitat quality (Figure 5.54). The dis-

tinction between these three concepts and the definition of habitat fragmentation were popularized by Fahrig (2003). In her research, Lenore Fahrig challenges common perceptions of habitat fragmentation. She argues that while habitat loss typically has detrimental effects on biodiversity, the effects of fragmentation itself[110] are more nuanced. In particular, fragmentation can sometimes have neutral or even potentially beneficial consequences for some species by creating more diverse landscape configurations that increase habitat heterogeneity and enhance dispersal opportunities (Fahrig, 2017):

> "*I found 118 studies reporting 381 significant responses to habitat fragmentation independent of habitat amount. Of these responses, 76% were positive. Most significant fragmentation effects were positive, irrespective of how the authors controlled for habitat amount, the measure of fragmentation, the taxonomic group, the type of response variable, or the degree of specialization or conservation status of the species or species group. [...] Thus, although 24% of significant responses to habitat fragmentation were negative, I found no conditions in which most responses were negative. Authors suggest a wide range of possible explanations for significant positive responses to habitat fragmentation: increased functional connectivity, habitat diversity, positive edge effects, stability of predator-prey/host-parasitoid systems, reduced competition, spreading of risk, and landscape complementation.*" (Fahrig, 2017, page 1).

This conclusion contrasts sharply with the findings of Haddad *et al.* (2015), who reported very negative impacts:

> "*We conducted an analysis of global forest cover to reveal that 70% of remaining forest is within 1 km of the forest's edge, subject to the degrading effects of fragmentation. A synthesis of fragmentation experiments spanning multiple biomes and scales, five continents, and 35 years demonstrates that habitat fragmentation reduces biodiversity by 13 to 75% and impairs key ecosystem functions by decreasing biomass and altering nutrient cycles.*" (Haddad *et al.*, 2015, page 1).

These conflicting results have fueled a lively debate in the journal *Biological Conservation*, reflected in two contrasting publications: *Is Habitat Fragmentation Good for Biodiversity?* (Fletcher *et al.*, 2018) and *Is Habitat Fragmentation Bad for Biodiversity?* (Fahrig *et al.*, 2019). To this day, the debate remains open, especially when we consider human pressures and matrix conditions[111] (Ramírez-Delgado *et al.*, 2022).

**Theory of island biogeography** This theory (known as TIB) was proposed by MacArthur and Wilson (1967) to explain the factors that influence biodiversity on islands. They emphasised the importance of studying islands because they are less complex and more common than larger ecosystems, meaning that research can be easily replicated. Their theory describes how the size of an island and its distance from the mainland affect the balance between immigration and extinction rates of species. This balance ultimately determines an equilibrium, or the number and types of species an island can support. An illustration is provided in Figure 5.55. Two key elements characterize the theory of island biogeography. First, the distance from the mainland measures the isolation of the island. Indeed, islands closer to the mainland have more species because they are easier for species

[110] We generally speak of fragmentation '*per se*', *i.e.*, fragmentation independent of habitat loss.

[111] In the context of biodiversity, the matrix condition refers to the quality and characteristics of the landscape that surrounds habitat patches or fragements. It's essentially the non-habitat environment that separates discrete areas of suitable habitat.

to reach, receive colonizers more frequently, and so on. Second, the size of the island determines species richness. Larger islands support greater species diversity because they offer more diverse habitats, contain more resources, and so forth. Specifically, MacArthur and Wilson (1967) proposed that the immigration rate[112] $\lambda(t)$ decreases with the number of species present and the isolation of the island (first panel in Figure 5.55), while the extinction rate $\mu(t)$ increases with the number of species present but decreases with the size of the island (second panel in Figure 5.55). Equilibrium occurs when immigration and extinction rates are equal, implying that the net diversification rate is zero: $\delta(t) = \lambda(t) - \mu(t) = 0$ (third panel in Figure 5.55).

Figure 5.55: Theory of island biogeography

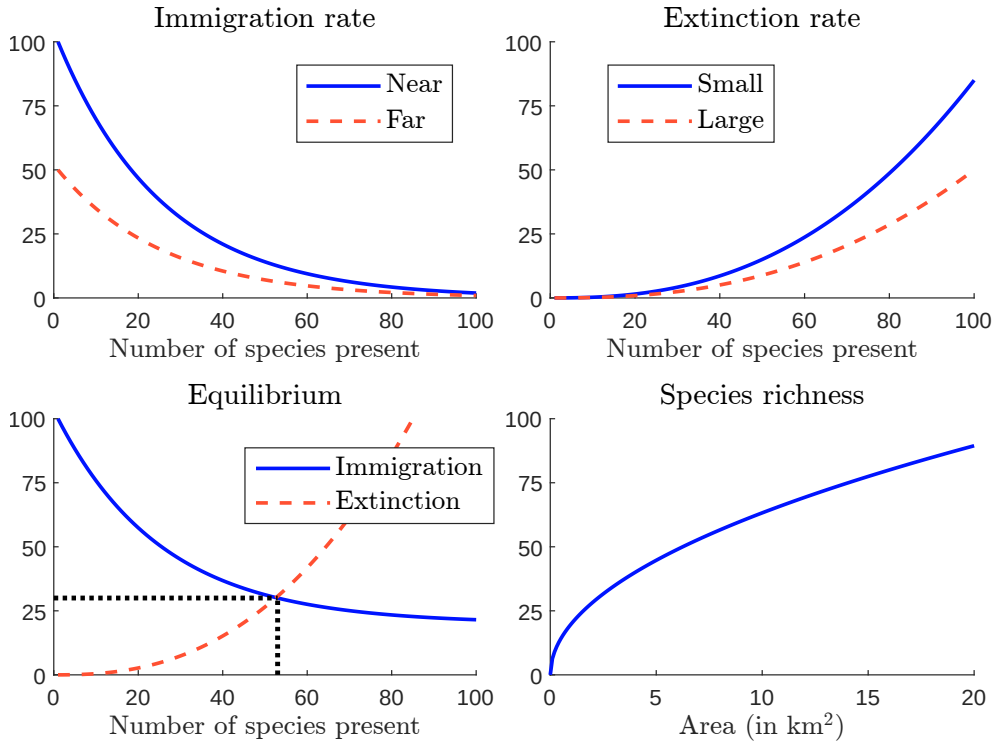


**Species-area relationship** The previous equilibrium model is often associated with the species-area relationship (SAR). Since extinction dynamics are influenced by the size of an island, an increase in island size shifts the equilibrium point to the right on the immigration-extinction diagram, indicating higher species richness. However, the rate of increase in species richness is generally slower than the rate of increase in area[113] (fourth panel in Figure 5.55). This reflects "*an ecological version of the law of diminishing returns*" (Lomolino, 2001): as area increases, each additional unit of area contributes proportionally less to species diversity. Certainly, the most famous species-area relationship is the power model originally formulated by Arrhenius (1921):

$$S = cA^z \tag{5.18}$$

where $S$ is species richness, $c$ is a constant, $A$ is the area of the island and $z$ is the slope of the log-log $A$–$S$ curve. Typical values of $z$ are between 0.15 and 0.35. If the areas of the original and

[112] In the theory of island biogeography, the immigration rate corresponds to the origination rate in the birth-death model.

[113] See Exercise 5.5.2 on page 566 for a mathematical derivation of the species-area relationship from the theory of island biogeography.

current habitats are $A_0$ and $A$, respectively, we obtain the following survival function:

$$\frac{S}{S_0} = \left(\frac{A}{A_0}\right)^z$$

This equation is used by Pimm *et al.* (1995) to calibrate species loss due to habitat loss:

$$\mathcal{L}oss_{species} = 1 - (1 - \mathcal{L}oss_{habitat})^z \tag{5.19}$$

Assuming $z = 0.25$, Pimm *et al.* (1995, page 349) found that 50% of habitat loss should reduce the number of species by 15.91%, while 90% of habitat loss leads to 43.77% of species loss (Table 5.41).

Table 5.41: Species loss $\mathcal{L}oss_{species}$

| $z$ | $\mathcal{L}oss_{habitat}$ | | | | | |
|---|---|---|---|---|---|---|
| | 0.00% | 25.00% | 50.00% | 75.00% | 90.00% | 100.00% |
| 0.05 | 0.00% | 1.43% | 3.41% | 6.70% | 10.87% | 100.00 |
| 0.10 | 0.00% | 2.84% | 6.70% | 12.94% | 20.57% | 100.00% |
| 0.25 | 0.00% | 6.94% | 15.91% | 29.29% | 43.77% | 100.00% |
| 0.35 | 0.00% | 9.58% | 21.54% | 38.44% | 55.33% | 100.00% |

While ecologists are nearly unanimous in accepting the principles of the species-area relationship[114], they do not always agree on the specific form it should take. An alternative to Equation (5.18) is the exponential model proposed by Gleason (1922):

$$S = c + z \ln(A) \tag{5.20}$$

These two models (power and exponential) were extensively studied in the seminal review by Connor and McCoy (1979). The authors provided a comprehensive and critical analysis of the species-area curve, arguing that many estimated SAR curves could be explained by statistical sampling effects rather than underlying biological mechanisms. Therefore, they emphasized the importance of distinguishing between ecological drivers (*e.g.*, habitat diversity, island biogeography) and statistical drivers (*e.g.*, sampling bias, incomplete sampling, inappropriate statistical methods) of SAR. By examining 100 datasets, they showed that the value of $z$ varies across scales and contexts (*e.g.*, small versus large areas) and concluded that the species-area relationship is not a fixed law but rather a complex, context-dependent pattern. This variation depends on specific ecological settings, taxonomic groups, and geographic regions. In particular, they noted that the parameters $c$ and $z$ estimated for one island or archipelago cannot be reliably applied to another island or archipelago. Furthermore, reducing the species-area relationship to a function of a single variable with two parameters fails to account for several second-order factors, such as elevation, latitude, and the density of small- and large-bodied species. Nevertheless, the search for the best species-area relationship model has continued to fascinate researchers since the publication of Connor and McCoy's paper in 1979. While it is impossible to cite all of the subsequent studies, some have significantly shaped this field. For instance, the default value of $z = 0.25$ for the power model is largely due to the influential

[114]The relationship between species and area is considered to be a fundamental ecological principle:

> "*It is common, perhaps axiomatic, to refer to the species-area relationship as one of ecology's few laws [...]. According to a very broad consensus of ecologists, the pattern has two principal features: 1) species richness of a given taxon increases with the area sampled, and 2) the rate of increase slows for the larger islands or patches of habitat.*" (Lomolino, 2001, page 1).

book by Rosenzweig (1995). Similarly, Tjørve (2003) made an important contribution by organizing a comparison of 14 statistical models to identify the best-fitting SAR model. More recently, Dengler (2009) and Triantis *et al.* (2012) reviewed 23 and 20 functions, respectively, and concluded that no single function universally outperforms all others. However, they emphasized that the power model often provides the best fit and remains a robust choice when it does not. Triantis *et al.* (2012) also identified three other simple models that can rival the power model for certain datasets: the linear model ($S = c + zA$), the exponential model ($S = c + z\ln(A)$), and the Kobayashi model ($S = c\ln(1 + zA)$).

Figure 5.56: Analyzing the species-area relationship in Mediterranean islands

(a) Tyrrhenian islands (b) Aegean islands

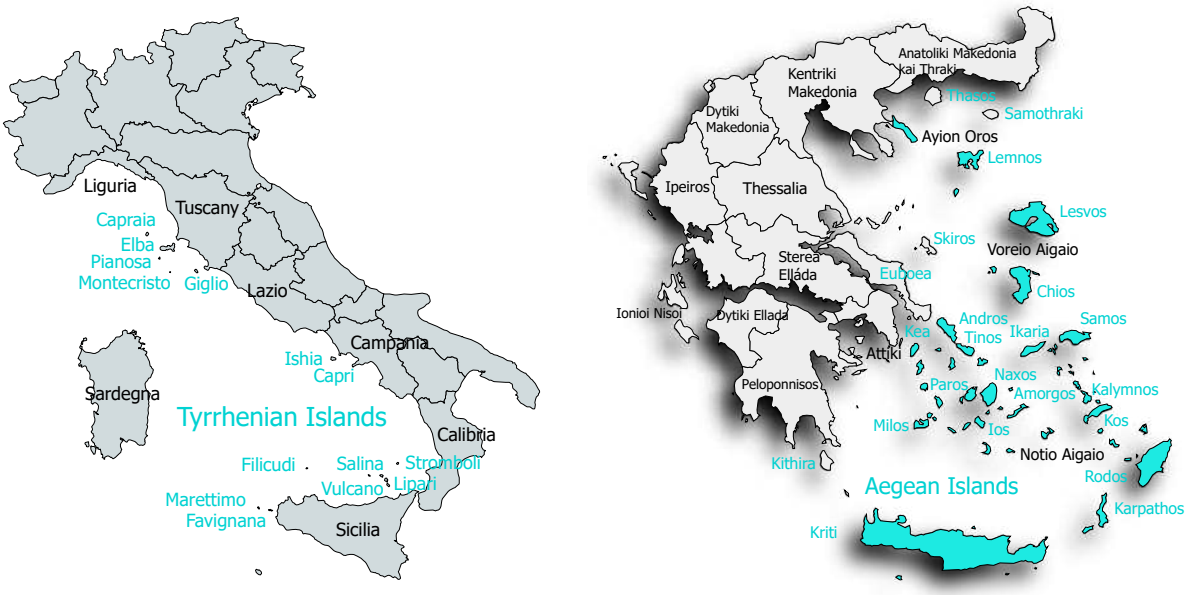


Source: Fattorini *et al.* (2017, Figure 1), created with www.paintmaps.com.

Let us now examine an empirical application to understand how the species-area relationship is estimated. For this purpose, we consider the study[115] by Fattorini *et al.* (2017). The authors estimated the SAR curves for two groups of Mediterranean islands: the Tyrrhenian Islands, located in Italy, and the Aegean Islands, located between Greece and Turkey. In Figure 5.56, we present the Tyrrhenian islands with areas larger than $10\,\text{km}^2$ and the Aegean islands with areas exceeding $100\,\text{km}^2$. The Tyrrhenian islands are mainly located off the western coast of Italy, near regions such as Tuscany, Lazio, Campania, Calabria, and Sicily. The dataset includes 47 islands, with the largest being Elba ($223\,\text{km}^2$) and the smallest being Scoglietto di Portoferraio ($24.9\,\text{m}^2$). The Aegean Sea is known for its multitude of islands, the total number of which is estimated to be around 6 000. However, the dataset contains only 127 islands, with the largest being Rodos ($1\,401\,\text{km}^2$) and the smallest being Petallidi ($6\,000\,\text{m}^2$). The results for various taxonomic groups (centipedes, isopods, land snails, reptiles and tenebrionid beetles) are given in Table 5.42 and Figure 5.57. Fattorini *et al.* (2017) found that $z$ varies between 0.141 and 0.308, while $c$ varies between 2.716 and 12.274 species per $\text{km}^2$. According to the authors, these results "*demonstrate the importance of comparing SARs either of different groups within the same area, or of the same group in different areas.*"

[115] The advantage of this study is that the dataset is relatively small, and the results are easily reproducible since the data are freely available on the paper's webpage: onlinelibrary.wiley.com/doi/abs/10.1111/jbi.12874.

Table 5.42: Estimated values of $c$, $z$, and $S$ for different area values $A$

| Islands | Species | $c$ | $z$ | Area $A$ (in km$^2$) | | | | | |
|---|---|---|---|---|---|---|---|---|---|
| | | | | 0.01 | 0.10 | 1 | 10 | 100 | 1 000 |
| Tyrrhenian | Centipedes | 6.281 | 0.308 | 1.52 | 3.09 | 6.28 | 12.77 | 25.94 | 52.73 |
| | Isopods | 9.226 | 0.262 | 2.76 | 5.05 | 9.23 | 16.87 | 30.83 | 56.36 |
| | Land snails | 12.274 | 0.225 | 4.35 | 7.31 | 12.27 | 20.61 | 34.59 | 58.08 |
| | Reptiles | 3.357 | 0.141 | 1.75 | 2.43 | 3.36 | 4.64 | 6.43 | 8.89 |
| | Tenebrionids | 8.610 | 0.270 | 2.48 | 4.62 | 8.61 | 16.03 | 29.85 | 55.59 |
| Aegean | Centipedes | 3.864 | 0.243 | 1.26 | 2.21 | 3.86 | 6.76 | 11.83 | 20.70 |
| | Isopods | 9.354 | 0.203 | 3.67 | 5.86 | 9.35 | 14.93 | 23.82 | 38.02 |
| | Land snails | 9.572 | 0.184 | 4.10 | 6.27 | 9.57 | 14.62 | 22.34 | 34.12 |
| | Reptiles | 2.716 | 0.278 | 0.75 | 1.43 | 2.72 | 5.15 | 9.77 | 18.53 |
| | Tenebrionids | 4.055 | 0.268 | 1.18 | 2.19 | 4.05 | 7.52 | 13.93 | 25.82 |

Source: Fattorini *et al.* (2017, Table 1).

Figure 5.57: SAR curves in Tyrrhenian and Aegean islands

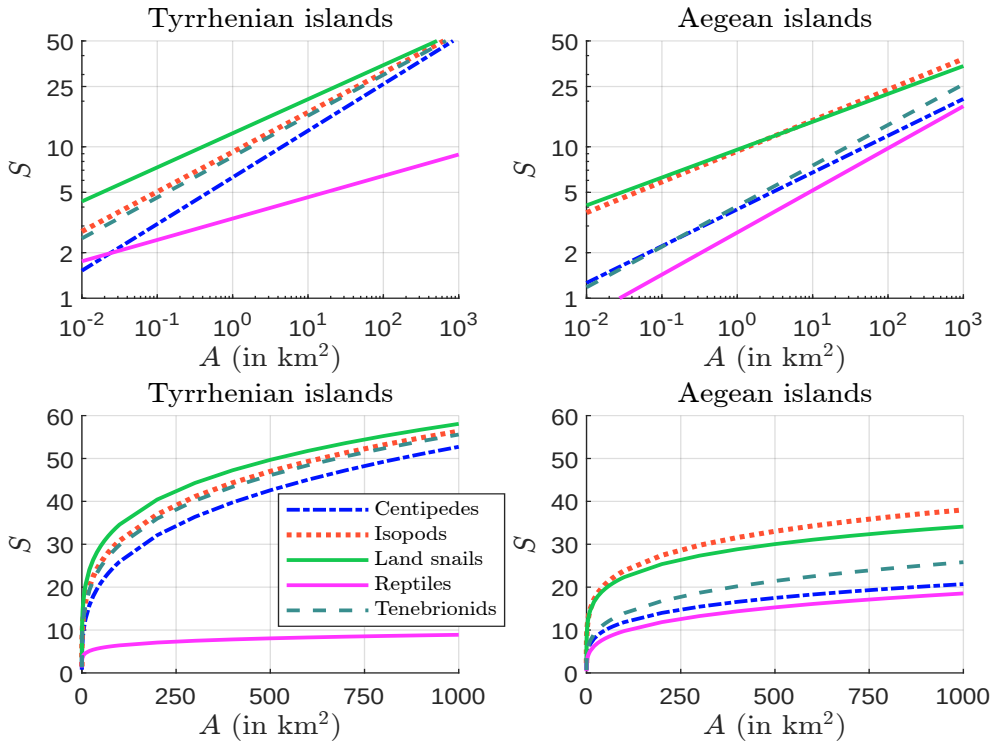


Source: Fattorini *et al.* (2017) & Author's calculations.

**Example 24** *Table 5.43 shows the data used by Fattorini et al. (2017, Appendix S1) to estimate the SAR curve of land snail species in the Tyrrhenian Islands. The area $A$ is expressed in* $\text{km}^2$.

Table 5.43: Number of species of land snails in the Tyrrhenian islands

| Island | $A$ | $S$ | Island | $A$ | $S$ | Island | $A$ | $S$ |
|---|---|---|---|---|---|---|---|---|
| Alicudi | 5.000 | 11 | Filicudi | 9.000 | 20 | Montecristo | 10.430 | 18 |
| Argentarola | 0.012 | 4 | Formica di Grosseto | 0.145 | 5 | Panarea | 3.380 | 22 |
| Basiluzzo | 0.270 | 11 | Giannutri | 2.390 | 19 | Pianosa | 10.410 | 28 |
| Capraia | 19.000 | 18 | Giglio | 21.000 | 35 | Salina | 26.000 | 25 |
| Cerboli | 0.051 | 8 | Gorgona | 2.270 | 24 | Stromboli | 12.000 | 18 |
| Elba | 223.000 | 50 | Lipari | 37.000 | 28 | Vulcano | 21.000 | 13 |

Source: Fattorini *et al.* (2017, Appendix S1).

Since the equation $S = cA^z$ is equivalent to $\ln(S) = \ln(c) + z\ln(A)$, the species-area relationship is generally estimated using the log-log regression model:

$$Y_i = \beta^\top X_i + \varepsilon_i$$

where $i = 1, \ldots, n$, $n$ is the number of observations, $S_i$ and $A_i$ are the number of species and the area of the $i^{\text{th}}$ observation, $Y_i = \ln(S_i)$, $X_i = \begin{pmatrix} 1 & \ln(A_i) \end{pmatrix}$, $\beta = \begin{pmatrix} \ln(c) \\ z \end{pmatrix}$ and $\varepsilon_i \sim N\left(0, \sigma_\varepsilon^2\right)$ is the noise process. We have:

$$\begin{aligned}
\hat{\beta} &= \left(X^\top X\right)^{-1} X^\top Y \\
&= \begin{pmatrix} n & \sum_{i=1}^n \ln(A_i) \\ \sum_{i=1}^n \ln(A_i) & \sum_{i=1}^n \ln^2(A_i) \end{pmatrix}^{-1} \begin{pmatrix} \sum_{i=1}^n \ln(S_i) \\ \sum_{i=1}^n \ln(A_i)\ln(S_i) \end{pmatrix} \\
&= \begin{pmatrix} 18 & 24.5506 \\ 24.5506 & 141.5006 \end{pmatrix}^{-1} \begin{pmatrix} 50.6670 \\ 93.3758 \end{pmatrix} \\
&= \begin{pmatrix} 2.5084 \\ 0.2247 \end{pmatrix}
\end{aligned}$$

We deduce that $\hat{c} = \exp\left(\hat{\beta}_1\right) = 12.285$ and $\hat{z} = \hat{\beta}_2 = 0.225$. In Table 5.44, we compare the figures presented in the research paper (columns $c$ and $z$) and our estimates (columns $\hat{\beta}_1$, $\exp\left(\hat{\beta}_1\right)$ and $\hat{\beta}_2$). We get the same values for $z$ and very close values for $c$, the difference being due to rounding.

Table 5.44: Comparison of SAR values: research paper results vs. our estimates

| Species | Tyrrhenian islands | | | | | | Aegean islands | | | | | |
|---|---|---|---|---|---|---|---|---|---|---|---|---|
| | $n$ | $c$ | $z$ | $\hat{\beta}_1$ | $e^{\hat{\beta}_1}$ | $\hat{\beta}_2$ | $n$ | $c$ | $z$ | $\hat{\beta}_1$ | $e^{\hat{\beta}_1}$ | $\hat{\beta}_2$ |
| Centipedes | 32 | 6.281 | 0.308 | 1.837 | 6.275 | 0.308 | 43 | 3.864 | 0.243 | 1.352 | 3.865 | 0.243 |
| Isopods | 28 | 9.226 | 0.262 | 2.221 | 9.216 | 0.262 | 43 | 9.354 | 0.203 | 2.236 | 9.360 | 0.203 |
| Land snails | 18 | 12.274 | 0.225 | 2.508 | 12.285 | 0.225 | 65 | 9.572 | 0.184 | 2.258 | 9.567 | 0.184 |
| Reptiles | 28 | 3.357 | 0.141 | 1.212 | 3.360 | 0.141 | 56 | 2.716 | 0.278 | 1.001 | 2.720 | 0.277 |
| Tenebrionids | 46 | 8.610 | 0.270 | 2.153 | 8.607 | 0.270 | 32 | 4.055 | 0.268 | 1.417 | 4.125 | 0.265 |

Source: Fattorini *et al.* (2017, Table 1) & Author's calculations.

We have seen how the species-area relationship can be used to measure the effect of habitat loss, *i.e.*, when area $A$ is reduced. Hanski *et al.* (2013) suggested reformulating Equation (5.18) to account for habitat fragmentation. Let $\varphi$ be the degree of fragmentation. The authors introduce the function $P(\varphi)$, which measures the fraction of the species that are expected to persist when the degree of fragmentation of $A$ is given by $\varphi$ and assume that $P(\varphi) = e^{-b\varphi}$ where $b$ is a parameter. We have $P(0) = 1$ and $P(\infty) = 0$. We deduce that the species-area relationship becomes:

$$S = cA^z P(\varphi) = cA^z e^{-b\varphi} \tag{5.21}$$

If the initial area $A_0$ is reduced to $A$, we have:

$$\frac{S}{S_0} = \left(\frac{A}{A_0}\right)^z e^{-b(\varphi-\varphi_0)}$$

where $\varphi_0$ is the degree of fragmentation of $A_0$. We deduce that:

$$\mathcal{L}oss_{\text{species}} = 1 - (1 - \mathcal{L}oss_{\text{habitat}})^z \, e^{-b\,\Delta_{\text{frag}}} \tag{5.22}$$

where $\Delta_{\text{frag}} = \varphi - \varphi_0$ is the variation in the fragmentation. When $\varphi = \varphi_0$, we retrieve Equation (5.20).

**Example 25** *We assume that* $c = 10$, $z = 0.25$ *and* $b = 0.10$. *We consider two initial landscapes, each with an initial area* $A_0$ *equal to* $100\,\text{km}^2$. *The first landscape is unfragmented* ($\varphi_0 = 0$), *while the second landscape is fragmented* ($\varphi_0 = 0.50$). *Both landscapes experience a habitat loss of* 50%. *In the first landscape, this habitat reduction is accompanied by habitat fragmentation* ($\varphi = 0.50$), *while in the second landscape we observe an improvement in habitat quality* ($\varphi = 0.25$).

We obtain the following results:

| Landscape | #1 | #2 |
|---|---|---|
| $S_0$ | 31.6228 | 30.0805 |
| $S$ | 25.2946 | 25.9349 |
| $\mathcal{L}oss_{\text{species}}$ | 20.01% | 13.78% |

Normally, the impact of habitat loss alone on the species loss is $0.50^{0.25}$, or 15.91%. However, the species loss is higher in the first landscape because habitat fragmentation has increased. In contrast, the species loss is lower in the second landscape because the fragmentation has increased.

**Species distribution, sampling and endemics-area curve** The species-area relationship describes the impact of area size on the number of species. It is a simple two-parameter model and may be limited in its ability to capture the effects of habitat loss on species richness and biodiversity. In particular, it overlooks important aspects of biodiversity such as species evenness and abundance[116]. It also ignores the spatial distribution of species and sampling effects. In this section, we explain these two effects, show how sampling affects the species-area relationship, and define species loss more precisely by introducing the endemics-area relationship.

[116] Abundance refers to the total number of individuals per species or in an ecosystem, while evenness is the degree to which individuals are evenly distributed across species.

**Species abundance models** We consider a region or community[117] with $S$ species. For each species $i$, the number of individuals is denoted by $n_i$. The species abundance can be described by a traditional frequency distribution table[118]:

| Species | 1 | 2 | $\cdots$ | $i$ | $\cdots$ | $S$ |
|---|---|---|---|---|---|---|
| Frequency | $n_1$ | $n_2$ | | $n_i$ | | $n_S$ |

Another approach is to calculate the species abundance distribution (SAD), which summarizes the number of species by their abundance (McGill *et al.*, 2007):

| Number of individuals | 1 | 2 | $\cdots$ | $j$ | $\cdots$ | $n^+$ |
|---|---|---|---|---|---|---|
| Number of species | $s(1)$ | $s(2)$ | | $s(j)$ | | $s(n^+)$ |

where $s(j)$ is the number of species with $j$ individuals, and $n^+ = \max n_i$ is the maximum number of individuals found in any single species in the community. Mathematically, we have:

$$s(j) = \sum_{i=1}^{S} \mathbb{1}\{n_i = j\}$$

The two representations — the frequency table and the species abundance distribution — then convey the same information about the structure of the community. However, it is not possible to retrieve the exact value of $n_i$ from the SAD. This is because individual species are not identified in the SAD, unlike in the frequency table, where species are explicitly listed.

**Example 26** *We consider a community consisting of* 25 *species and* 407 *individuals, distributed across a region of* $2\,\text{km}^2$. *The abundances of the* 25 *species are as follows:* $2, 10, 13, 2, 1, 5, 25, 17, 1, 4, 28, 117, 23, 10, 13, 1, 4, 3, 10, 5, 7, 70, 10, 25, 1$.

There are four species with only one individual, so $s(1) = 4$. Similarly, $s(2) = 2$ because there are two species with two individuals each. For $s(3)$, we have $s(3) = 1$, as only one species has three individuals, and so on. Finally, we get the resulting species abundance distribution:

| $j$ | 1 | 2 | 3 | 4 | 5 | 7 | 10 | 13 | 17 | 23 | 25 | 28 | 70 | 117 |
|---|---|---|---|---|---|---|---|---|---|---|---|---|---|---|
| $s(j)$ | 4 | 2 | 1 | 2 | 2 | 1 | 4 | 2 | 1 | 1 | 2 | 1 | 1 | 1 |

We confirm that the total abundance is exactly 407 individuals[119]. In practice, the label $j$ is omitted when $s(j) = 0$ (McGill *et al.*, 2007). However, when the number of species is large, the species abundance distribution can become highly atomic or fragmented, with many values of $s(j) = 1$. To address this, it is important to group the number of individuals into classes. We have $s(\mathcal{C}_c) = \sum_{j \in (\mathcal{C}_c)} s(j)$ where $\mathcal{C}_c$ represents the $c^{\text{th}}$ grouping class. Here is an example where we group species whose number of individuals is greater than 5:

| $\mathcal{C}_c$ | 1 | 2 | 3 | 4 | 5 | 6–10 | 11–25 | 26–50 | 51–100 | 100–117 |
|---|---|---|---|---|---|---|---|---|---|---|
| $s(\mathcal{C}_c)$ | 4 | 2 | 1 | 2 | 2 | 5 | 6 | 1 | 1 | 1 |

[117] A community is the total set of species in an ecosystem.

[118] It is called the rank-abundance distribution when $n_i$ are sorted (in ascending or descending order).

[119] We have the following property:

$$\sum_{j=1}^{\infty} s(j) \cdot j = \sum_{i=1}^{S} n_i = n$$

There are five species with an abundance of 6 to 10 individuals, six species with an abundance of 11 to 25 individuals, and so on. According to McGill *et al.* (2007, page 996), another way to illustrate the relative abundance and diversity of species within a community is to use a rank-abundance diagram (RAD), which is a graphical representation used in ecology to provide insights into species richness and species evenness. On the $x$-axis, species are ranked according to their abundance, from most abundant (rank 1) to least abundant (rank $S$), while on the $y$-axis, we plot relative abundance, that is the proportion of individuals belonging to each species. Mathematically, we calculate the order statistics of the set $\{n_1, \ldots, n_S\}$:

$$\underset{\mathcal{R}_S}{n_{1:S}} \leq \underset{\mathcal{R}_{S-1}}{n_{2:S}} \leq \cdots \leq \underset{\mathcal{R}_k}{n_{S-k+1:S}} \leq \cdots \leq \underset{\mathcal{R}_1}{n_{S:S}}$$

We then assign the rank $\mathcal{R}_k$ to the order statistic $n_{S-k+1:S}$. The relative abundance $f_k$ associated with $\mathcal{R}_k$ is defined as $f_k = \dfrac{n_{S-k+1:S}}{n} = \dfrac{n_i}{n}$ where index $i$ is the solution to the equation $n_i = n_{S-k+1:S}$. By construction we have $f_1 = \dfrac{\max n_i}{n}$ and $f_S = \dfrac{\min n_i}{n}$. Looking at the previous example, we get the following rank-abundance distribution:

| $k$ | 1 | 2 | 3 | 4, 5 | 6 | 7 | 8, 9 | $\cdots$ | 19 | 20, 21 | 22–25 |
|---|---|---|---|---|---|---|---|---|---|---|---|
| $i$ | 12 | 22 | 11 | 7, 24 | 13 | 8 | 3, 15 | | 18 | 1,4 | 5, 9, 16, 25 |
| $n_i$ | 117 | 70 | 28 | 25 | 23 | 17 | 13 | $\cdots$ | 3 | 2 | 1 |
| $f_k$ (in %) | 28.75 | 17.20 | 6.88 | 6.14 | 5.65 | 4.18 | 3.19 | | 0.74 | 0.49 | 0.25 |

Species 12 ranks first and represents 28.75% of the total abundance of the community. It is followed by species 22 and 11, whose relative abundance is 17.20% and 6.88%, respectively.

In 1949–1951, Robert H. Whittaker studied plant community composition in the Siskiyou Mountains to understand variation across environmental gradients. He developed the concept of diversity partitioning. His work, published in 1960, led to extensive data analyses and contributed significantly to the study of community structure (Whittaker, 1960). Since 2022, the data are freely available at `https://doi.org/10.6084/m9.figshare.19661094.v3` (Whittaker *et al.*, 2022). We use the tree data CSV file, which contains 2 078 observations with the following information:

- The first column represents the sample number, corresponding to one of the 359 sampling locations;
- The second column lists the species name;
- The third column gives the number of individuals of each species in the sample;
- The fourth column indicates the number of large individuals with a diameter at breast height[120] (DBH) greater than 30 inches (76.2 cm).

For each species, we pooled the data from the 359 sampling sites. We obtain the abundance of 59 tree species. The five most represented trees are *Lithocarpus densiflorus*, *Quercus chrysolepis*, *Abies concolor*, *Pseudotsuga menziesii* and *Chrysolepis chrysophylla*. Their abundance is 8 439, 4 207, 4 172, 3 725 and 1 886, respectively. The species abundance distribution is shown in Figures 5.58 and 5.59. The species abundance curve is constructed with classes of length 50. Most of these classes have one or two species, except for the first three classes: 22 species for the first class (between 1 and 50 individuals), 7 species for the second class (between 51 and 100 individuals), and 3 species for the third class (between 101 and 150 individuals).

[120] In the United States, DBH refers to the diameter of the tree measured 4.5 feet above the ground.

Figure 5.58: Species abundance curve (Preston plot)

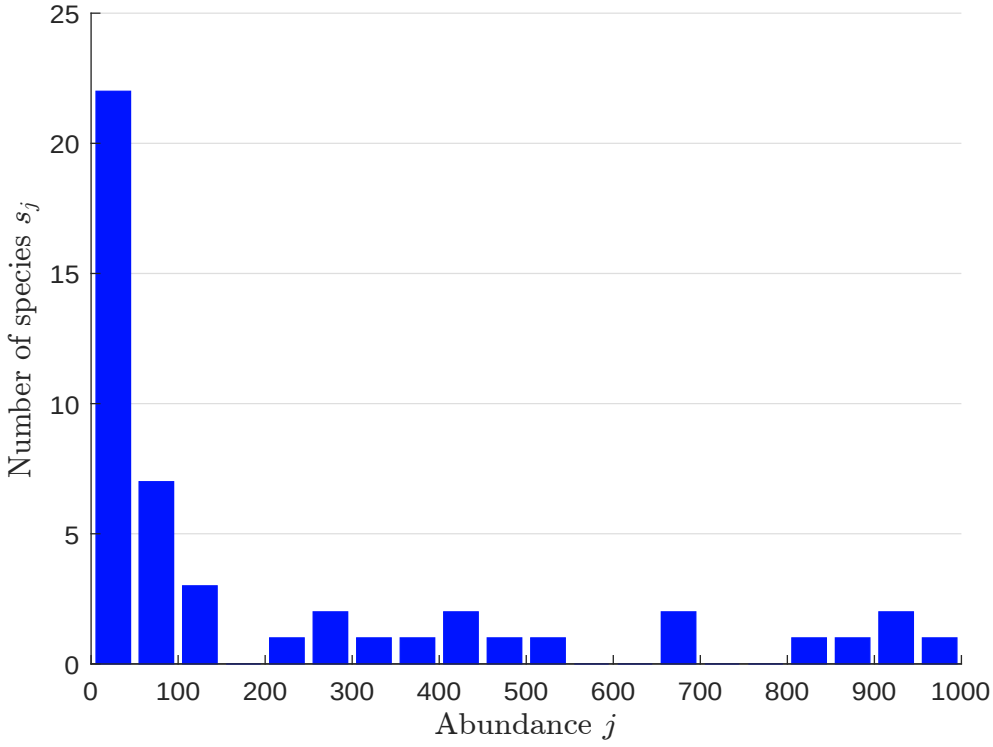


Figure 5.59: Rank-abundance curve (Whittaker plot)

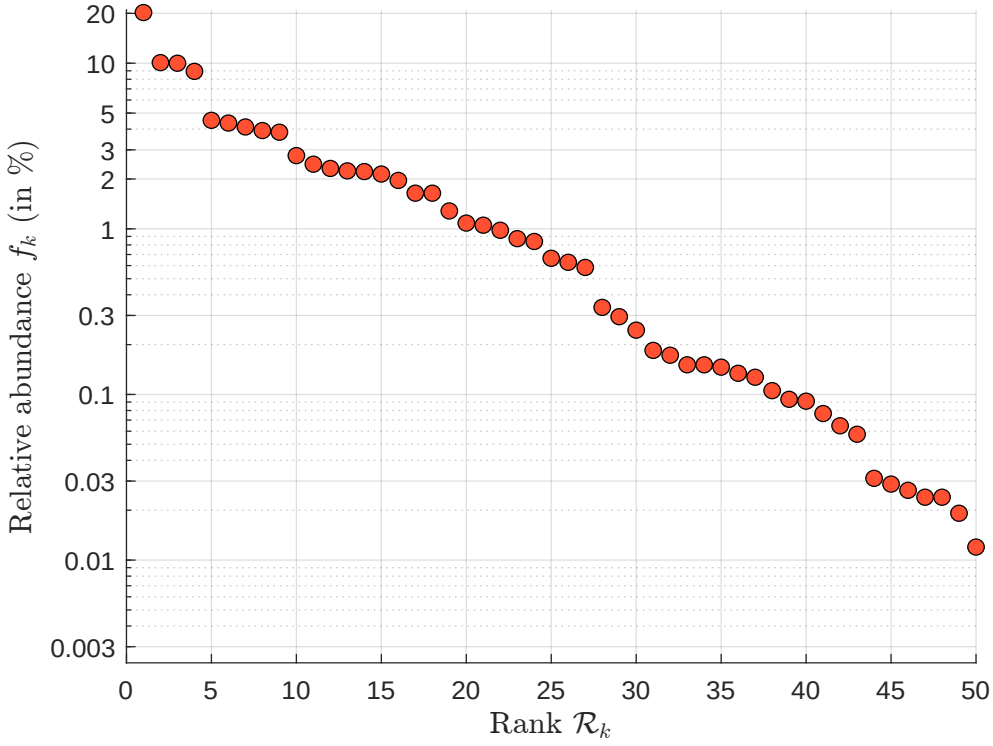

Figure 5.60: Barro Colorado Island (Panama)

There are many ways to plot a species abundance distribution. The species abundance curve (also called a frequency histogram) and the rank-abundance curve (Whittaker, 1965) are just a few examples. Other methods include the species rarefaction curve, the empirical cumulative distribution function (ECDF), the $k$-dominance plot, and the Robbins curve, among others (Matthews and Whittaker, 2015). Moreover, the axes of these graphs can be linear, but they are often transformed using $\log_2$ or $\log_{10}$ functions to better display the variability in the shape of the species abundance distribution. One particularly famous plot was proposed by Preston (1948), who popularized the use of a frequency histogram with $\log_2$-based classes along the $x$-axis. In this approach, the number of species is grouped into intervals of $2^k$ (*e.g.*, 1, 2, 4, 8, 16, 32, 64, etc.), called octaves. Using Example 26, we obtain the following results[121]:

| Octave $k$ | 1 | 2 | 3 | 4 | 5 | 6 | 7 |
|---|---|---|---|---|---|---|---|
| $\mathcal{C}_k$ | 1 | 2–3 | 4–7 | 8–15 | 16–31 | 32–63 | 64–127 |
| $s\,(k)$ | 4 | 3 | 5 | 6 | 5 | 0 | 2 |

We now consider another community ecology dataset, the Barro Colorado Island (BCI) data, which was established by the Smithsonian Tropical Research Institute (STRI) and studied to understand the dynamics of tropical forest vegetation. The data contain 50 contiguous 1-ha plots and record tree species identity, spatial coordinates, size measurements, and environmental variables. Periodic censuses have been conducted every five years since 1980 until 2015. Such analysis and data collection has been done in many other regions of the world, especially in South America. In Figure 5.61 we show the species abundance distribution of the tropical forest tree dataset[122] compiled by Condit *et al.* (2002). This dataset includes 100 plots from Barro Colorado Island in Panama, the Yasuni National Park in Ecuador and the Manu Biosphere Reserve in Peru. The histogram shows that many species are found in the first octaves. Preston (1948) proposed that species abundances

[121] The general formula for the range of each octave $k$ is $2^{k-1}$ to $2^k - 1$. The first octave contains the species with one individual, the second octave contains the species with two and three individuals, the third octave contains the species with four to seven individuals, and so on.

[122] The `conditwebtable.xls` file is available at `www.science.org/doi/abs/10.1126/science.1066854`.

in natural communities follow a log-normal distribution. When the logarithm of species abundances forms a bell-shaped curve, this pattern suggests that most species are moderately abundant, with fewer species being either extremely rare or extremely common. In some cases, when the positive skew of the log-normal distribution is very pronounced, the number of species decreases logarithmically with abundance, indicating that most species have only a few individuals. Preston (1948) further concluded that because many species in an ecological community are rare, they are often not observed in traditional ecological surveys[123]. This means that traditional sampling methods tend to underestimate total species richness, because rare species are likely to be missed in small samples.

Figure 5.61: Species abundance distribution of tropical forest trees

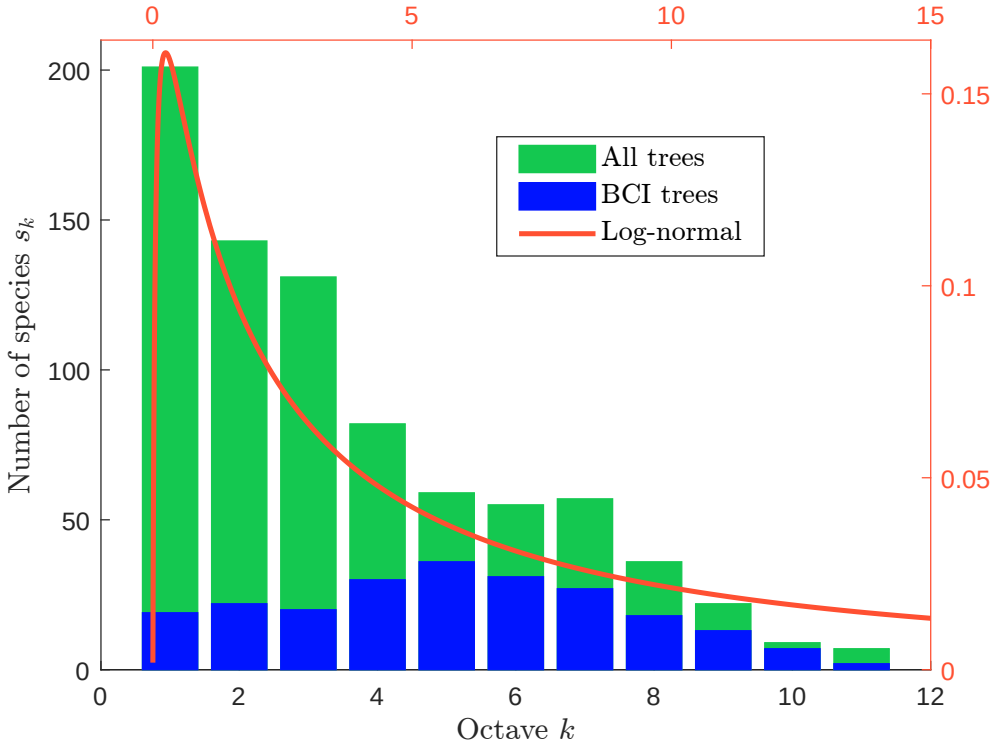


Empirical analysis of the number of species has led to the formulation of several probability models of species abundance. In 1932, Isao Motomura developed the resource (or niche) preemption model, which assumes that one species preempts a fraction $\kappa \in (0,1)$ of the resource, a second species the same fraction $\kappa$ of the remaining resource $(1-\kappa)$, and so on. Assuming that the abundance of species $i$ is proportional to its share of the resource, *i.e.*, $(1-\kappa)^{i-1}\kappa$, we obtain the geometric rank-abundance model[124]:

$$n_i = \frac{n\kappa\,(1-\kappa)^{i-1}}{1-(1-\kappa)^S} \tag{5.23}$$

where $S$ is the number of species and $n$ is the total number of individuals. Another approach was proposed by Fisher *et al.* (1943), who developed a model where the number of species is derived

[123] This concept is often called the '*invisible fraction*' in ecology.

[124] The scaling factor ensures that the sum of the individuals equals the total abundance:

$$\sum_{i=1}^{S} n_i = \frac{n\kappa}{1-(1-\kappa)^S}\sum_{i=1}^{S}(1-\kappa)^{i-1} = \frac{n\kappa}{1-(1-\kappa)^S}\cdot\frac{1-(1-\kappa)^S}{1-(1-\kappa)} = n$$

from the limiting form of the negative binomial distribution $\mathcal{NB}(r,p)$, excluding zero observations. They demonstrated that the expected number of species with exactly $j$ individuals is given by:

$$s(j) = \alpha \frac{x^j}{j} \tag{5.24}$$

where $x = (1-p)^{-1} p \in (0,1)$, $p$ is the success probability of the negative binomial distribution, and $\alpha$ is a scaling factor that depends on the parameters $r$ and $p$. Since the total expected number of species is $S = \sum_{j=1}^{\infty} s(j) = -\alpha \ln(1-x)$ and the total expected number of individuals is $n = \sum_{j=1}^{\infty} s(j) \cdot j = \sum_{j=1}^{\infty} \alpha x^j = \alpha x / (1-x)$, the parameters of the log-series distribution $\mathcal{LS}(\alpha, x)$ can be determined by solving the following system of equations[125]:

$$\begin{cases} S = \alpha \ln\left(1 + \dfrac{n}{\alpha}\right) \\ x = \dfrac{n}{\alpha + n} \end{cases} \tag{5.25}$$

In chronological order, the third and fourth important SAD models are the log-normal model of Preston (1948), seen earlier on page 443, and the broken-stick model formulated by MacArthur (1957). In the log-normal model, the probability that a species has $j$ individuals is given by $\Pr\{X = j\}$ where $X \sim \mathcal{LN}(\mu, \sigma^2)$. In practice, $j$ is discrete rather than continuous. Considering the disjoint intervals $\left[j - \frac{1}{2}, j + \frac{1}{2}\right]$, we get[126]:

$$s_j = S \frac{\Phi\left(\sigma^{-1}\left(\ln\left(j + \frac{1}{2}\right) - \mu\right)\right) - \Phi\left(\sigma^{-1}\left(\ln\left(j - \frac{1}{2}\right) - \mu\right)\right)}{1 - \Phi\left(\sigma^{-1}\left(\ln\left(\frac{1}{2}\right) - \mu\right)\right)} \tag{5.26}$$

By construction we have $\sum_{j=1}^{\infty} s_j = S$. To calibrate $\mu$ and $\sigma$, we can fit the first moment — $\frac{n}{S} = e^{\mu + \frac{1}{2}\sigma^2}$ (or use the discrete version $\sum_{j=1}^{\infty} s_j \cdot j = n$ — or we can estimate $\mu$ and $\sigma$ using the method of maximum likelihood. The broken-stick model assumes that the total resources (or individuals) available in a community are divided randomly among species, leading to a characteristic pattern of abundances. The community is represented as a stick of fixed length, the stick is broken into $S$ segments at $S-1$ randomly chosen points, and the lengths of the resulting segments are proportional to the abundances of the $S$ species — they follow a uniform distribution. The $i^{\text{th}}$ largest segment corresponds to a specific harmonic expectation based on the number of breaks. The abundance of the $i^{\text{th}}$ species is then given by $n_i = \frac{n}{S} \sum_{k=i}^{S} \frac{1}{k}$. May (1975) demonstrated that the corresponding species abundance distribution is:

$$s(j) = \frac{S}{n}(S-1)\left(1 - \frac{j}{n}\right)^{S-2} \tag{5.27}$$

[125] However, this approach ignores the distribution of the number of individuals $(n_1, n_2, \ldots, n_S)$. This means that two communities with the same number of species, the same total abundance, but different distributions of individuals among species will have the same species abundance distribution. To overcome this limitation, it is preferable to estimate the parameters $x$ using the maximum likelihood method with the following probability mass function: $\Pr\{N = j\} = -\frac{x^j}{j \ln(1-x)}$ where $N$ is the random variable representing the abundance of a species. Once the parameter $x$ is estimated, the parameter $\alpha$ can be calculated as it serves as a scaling factor to fit the total number of species $S$.

[126] The normalization factor is needed because the support of the log-normal distribution is $(0, +\infty)$, while in this case we use the support $\left(\frac{1}{2}, +\infty\right)$.

where $j \in [0, S]$. We verify that the total number of species is exactly equal to $S$[127]. Figure 5.25 illustrates the four distributions when the number of species is $S = 15$ and the total abundance is $n = 80$. For the geometric model, the parameter $\kappa$ is set to 0.50. The parameters of the log-series model are determined by solving Equation (), yielding $\alpha = 5.450$ and $x = 0.936$. In the case of the log-normal model, we set $\sigma = 1$, which implies $\mu = \ln\left(\frac{80}{15}\right) - 0.5 \times 1^2 = 1.174$. The broken-stick model is already parameterized using $n$ and $S$. The calibration of the parameters can be improved if the rank-abundance distribution $(n_1, \ldots, n_S)$ or the species abundance distribution $(s(1), \ldots, s(n^+))$ is known, by using the method of maximum likelihood. However, this approach is applicable only for the first three models.

Figure 5.62: Species abundance models

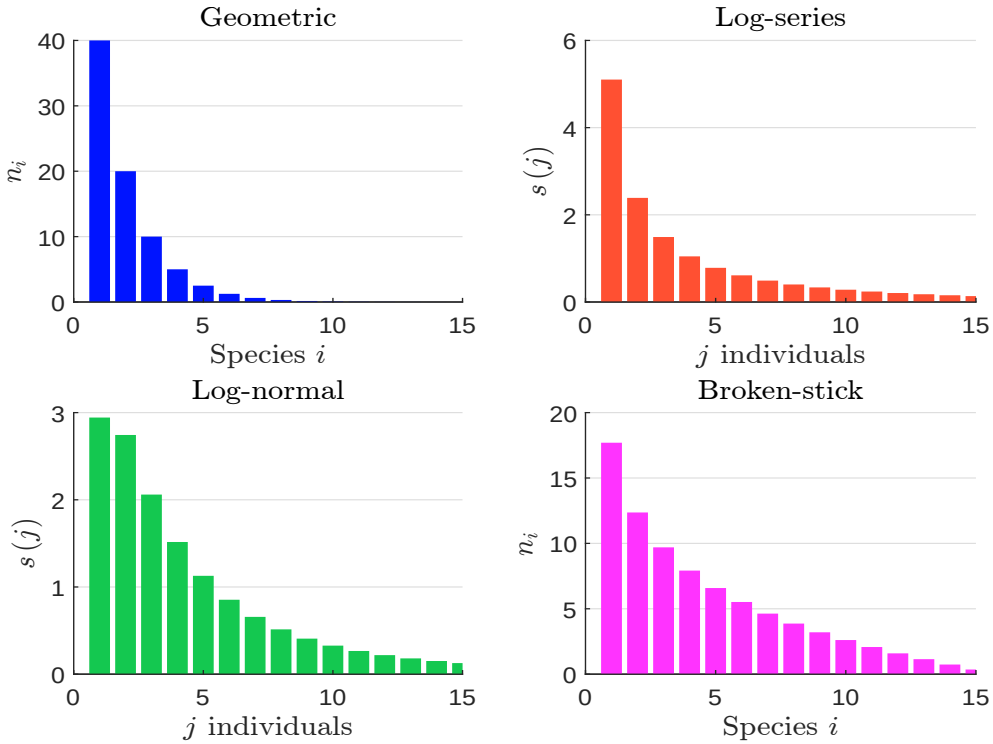


**Sampling** The species accumulation curve (SAC) is a graphical representation that illustrates how the number of observed species in a particular environment increases with additional sampling effort. It is also referred to as the species discovery curve or the collector's curve. The $x$-axis represents the sampling effort, such as the number of samples, individuals, cells, or plots surveyed, while the $y$-axis represents the cumulative number of species recorded. Let $n_i(s)$ be the number of

[127] Specifically, we have:

$$\int_0^n s(j)\,\mathrm{d}j = S(S-1)\int_0^n \left(1-\frac{j}{n}\right)^{S-2}\frac{\mathrm{d}j}{n}$$

Using the change of variable $u = \frac{j}{n}$, we obtain the desired result:

$$\int_0^n s(j)\,\mathrm{d}j = S(S-1)\int_0^1 (1-u)^{S-2}\,\mathrm{d}u = S(S-1)\left[-\frac{(1-u)^{S-1}}{S-1}\right]_0^1 = S$$

individuals of species $i$ recorded in the $s^{\text{th}}$ sample. The SAC function is defined as:

$$\text{SAC}(m) = \sum_{i=1}^{S} \mathbb{1}\left\{\sum_{s=1}^{m} n_i(s) \geq 1\right\}$$

where $m \leq m_s$ is the number of samples, and $m_s$ is the total number of samples available. $\text{SAC}(m)$ counts the number of species present in the $m$ samples. When a sample represents an individual, $\text{SAC}(m)$ is the expected number of species among $m$ individuals selected at random. Hurlbert (1971, Equation (13), page 581) shows that[128]:

$$\text{SAC}(m) = \sum_{i=1}^{S}\left(1 - \frac{\binom{n-n_i}{m}}{\binom{n}{m}}\right)$$

where $n_i$ is the abundance (number of individuals) of the $i^{\text{th}}$ species and $n$ is the total abundance of the community. In this case, the species accumulation curve is often referred to as the species rarefaction curve. In the Barro Colorado Island census, the database contains 21 457 trees and 225 species, located in 50 1-ha plots. For each plot, the species and the number of individuals per species are recorded. Figure 5.63 shows the distribution of individual trees across the 50 plots. The species rarefaction curve is given in Figure 5.64. In addition to the theoretically expected number of species, the 95% confidence interval is also reported.

Figure 5.63: Number of individuals per plot (BCI trees)

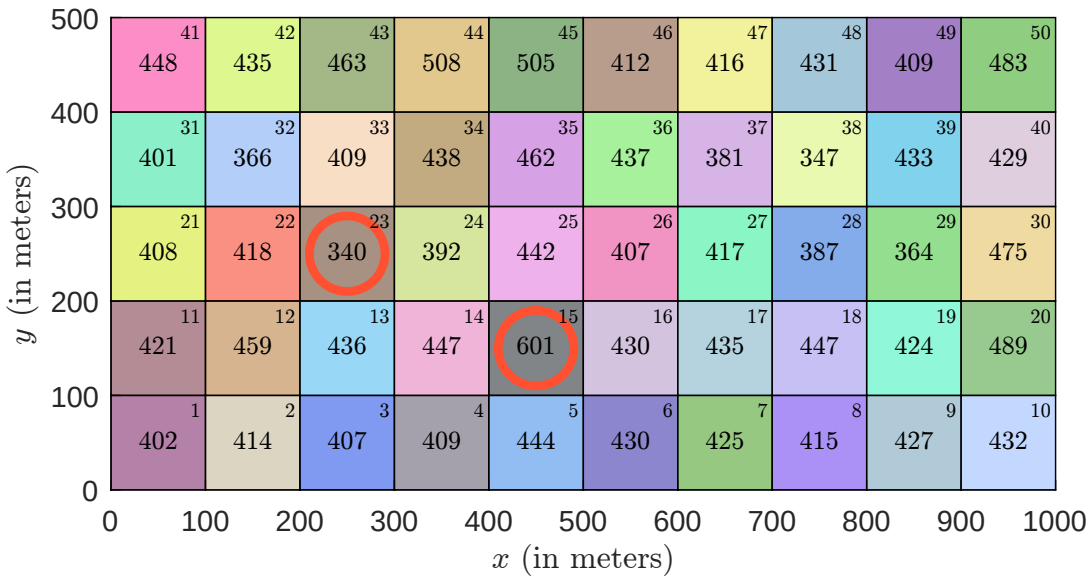


More generally, the species accumulation curve is represented as the parametric curve $(\text{SAC}(1), \ldots, \text{SAC}(m_s))$, where the sample set at iteration $m$ is constructed by adding one sample to the set used in the previous iteration $m-1$, selected from the $m_s - m + 1$ remaining samples. Thus, the species accumulation curve is sensitive to the order in which the $m_s$ samples are arranged. For

[128] The binomial coefficient $\binom{n-n_i}{m}$ is zero when $m > n - n_i$.

Figure 5.64: Species accumulation curve (BCI trees)

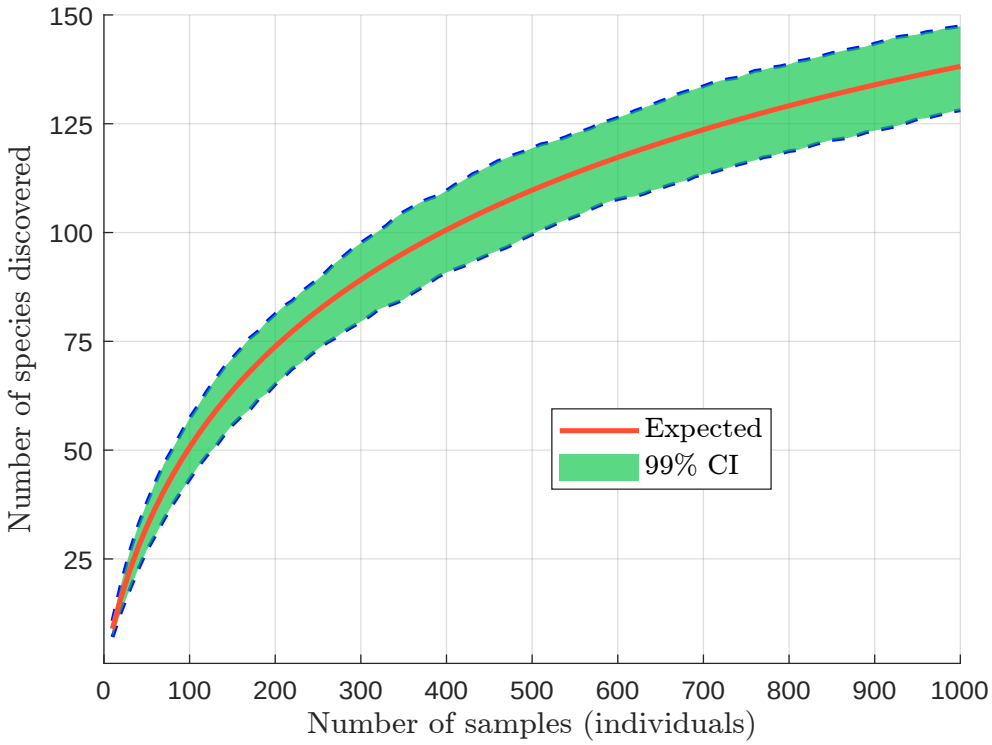


instance, samples may be ordered by size, either from smallest to largest or vice versa. Alternatively, the historical order of sampling, from first to last, may be considered. Considering the BCI dataset, we discover 77 tree species if we start by sampling the 11th plot, and 109 tree species if the first sample is the 39th plot (Figure 5.65). To eliminate the sensitivity of the results to the ordering of the samples, we can use a third approach, which consists of generating random permutations of the entire sample set $(1, \ldots, m_s)$, computing the SAC function for each permutation, and performing a Monte Carlo simulation. By repeating this process $r$ times and averaging the resulting curves, a more robust estimate of the species accumulation curve can be obtained. Figure 5.66 shows the species accumulation curve for trees in the Barro Colorado Island census. The mean curve (in red) is estimated using the Monte Carlo method with 1 000 replications. The 99% confidence interval is also shown in green.

The previous estimator of the species accumulation curve has some bias because it does not account for the underestimation of rare species. To address this problem, more sophisticated approaches are often used, in particular the estimators developed by Anne Chao. The *Chao1* estimator is a non-parametric method for estimating species richness from abundance data (Chao, 1984). It uses the frequency of rare species (singletons and doubletons) in the dataset to estimate the likely number of undetected species. The *Chao2* estimator is a variant of *Chao1* designed for use with presence-absence data across multiple samples (Chao, 1987). Instead of focusing on individual counts, it examines how often species are detected in different samples. The formula for this estimator is as follows:

$$S_{\text{Chao2}}(m_s) = S_{\text{obs}}(m_s) + \frac{(m_s - 1)}{m_s}\left(\frac{q_1(q_1 - 1)}{2(q_2 + 1)}\right)$$

where $S_{\text{obs}}(m_s) = \text{SAC}(m_s)$ is the total number of species observed in the set of $m_s$ samples, $q_m$ is the number of species present in exactly $m$ samples — $q_1$ and $q_2$ are then the number of singleton

Figure 5.65: Number of species per plot (BCI trees)

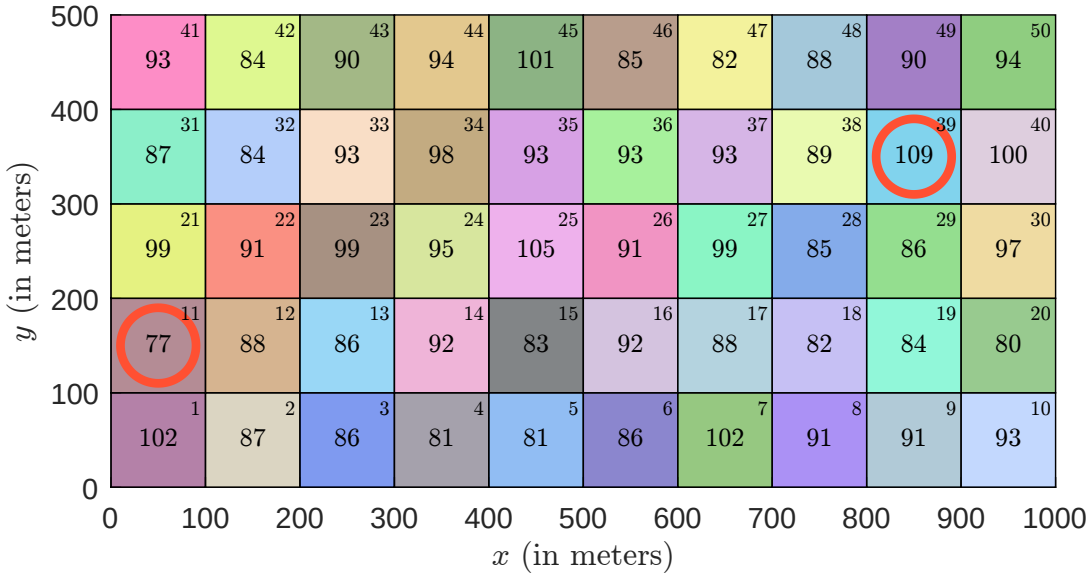


Figure 5.66: Species accumulation curve (BCI trees)

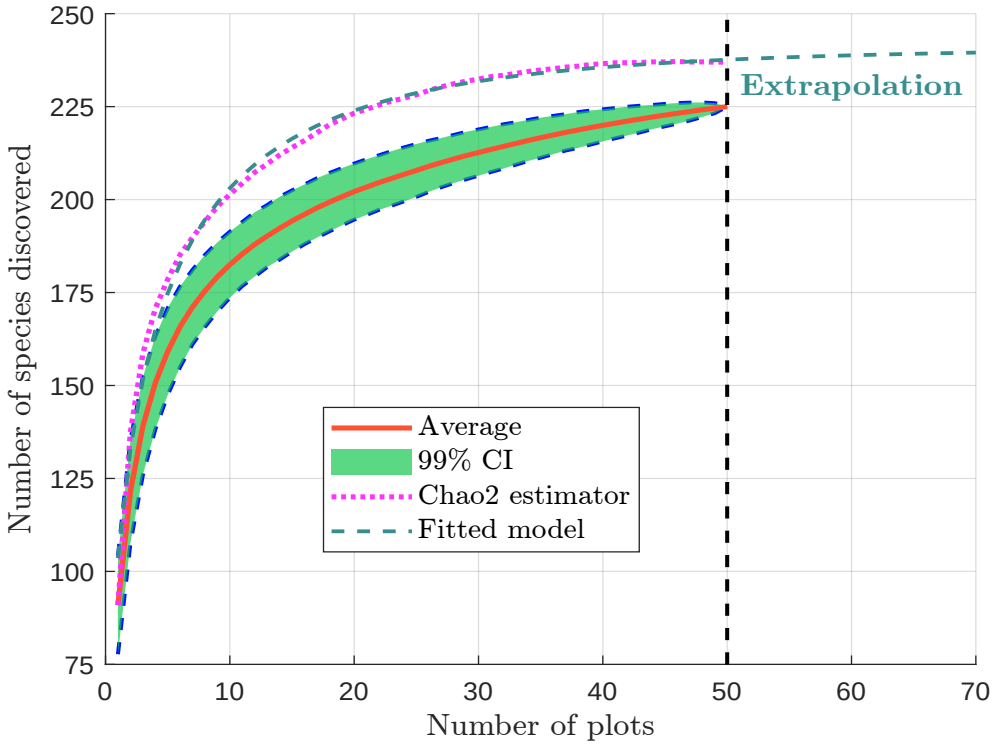

and doubleton species. In Figure 5.66 we have added the *Chaos2* estimator to compare with the traditional empirical estimator. In this case, the number of tree species for the 50 ha patch is estimated to be 237 instead of 225.

The species accumulation curve is widely used to estimate the number of species in a region larger than the sampled area. This approach, known as extrapolation, was popularized by Robert K. Colwell in numerous published research papers (Colwell and Coddington, 1994; Gotelli and Colwell, 2001; Colwell *et al.*, 2004) . For example, Cazzolla Gatti *et al.* (2022) used this method to estimate the number of tree species on Earth. They first fitted a log-series model, then estimated the species accumulation curve, corrected it with the *Chao2* estimator, and finally extrapolated it by considering the lower 95% confidence bound. Their results indicate that there are 73 271 tree species globally, with the following distribution: 11 874 in Africa, 16 262 in Eurasia, 11 129 in North America, 31 110 in South America, and 8 232 in Oceania. Returning to the BCI tree database, we assume that the number of species follows the exponential model: $\text{SAC}(m) = \theta_1\left(1-\exp\left(-\theta_2 m^{\theta_3}\right)\right)$. Using the species accumulation curve, we fit the parameters $(\theta_1, \theta_2, \theta_3)$ using the method of non-linear least squares. We find $\hat{\theta}_1 = 241.064$, $\hat{\theta}_2 = 0.562$ and $\hat{\theta}_3 = 0.517$. Since the 50 plots corresponds to 50 hectares, we would need to sample $15.6 \times 100 = 1\,560$ plots to cover the entire area of Barro Colorado Island, which spans $15.6\,\text{km}^2$. We estimate that there are about 241 different tree species[129], suggesting that 16 species remain to be discovered in the island (Figure 5.66).

**Species-area relationship vs. endemics-area relationship** We consider a region (or area) $A$ where the total number of species and the number of individuals per species are known exactly to be $S$ and $n_i$. The species-area relationship can be expressed as the equality: $\text{SAR}(A) = S$. Our goal is to determine the expected number of species $S_a$ of a subregion (or subarea) $a$ contained within the larger region $A$. Assuming random placement of individuals within the area, we can show that the species-area relationship becomes[130]:

$$\text{SAR}(a) = S_a = S - \sum_{i=1}^{S}\left(1-\frac{a}{A}\right)^{n_i}$$

where $n_i$ is the number of individuals of species $i$ in region $A$. We define two types of endemism as follows:

- Global endemism: A species is globally endemic to $A$ if it is found exclusively in region $A$ and nowhere else.
- Local endemism: A species is locally endemic to $a$ if it occurs exclusively in subarea $a$ and not in the complementary area $A - a$.

Under the assumption of random placement, the endemics-area relationship (EAR) is[131]:

$$\text{EAR}(a) = E_a = \sum_{i=1}^{S}\left(\frac{a}{A}\right)^{n_i}$$

where $E_a$ is the expected number of species endemic to the subregion $a$. In Table 5.45, we report the expressions for $\text{SAR}(a)$ and $\text{EAR}(a)$ under different models (He and Legendre, 2002; Green and

[129] We have:

$$\text{SAC}(1\,560) = \hat{\theta}_1\left(1-\exp\left(-\hat{\theta}_2 \times 1\,560^{\hat{\theta}_3}\right)\right) \approx 241$$

[130] The proof is given in Question 1 of Exercise 5.5.3 on page 568.

[131] The proof is given in Question 2 of Exercise 5.5.3 on page 568.

Table 5.45: Species-area and endemics-area relationships for various species abundance models

| Model | Specification | SAR $(a)$ | EAR $(a)$ |
|---|---|---|---|
| Random placement | $n_i$ is known | $S_a = S - \sum_{i=1}^{S} \left(1 - \frac{a}{A}\right)^{n_i}$ | $E_a = \sum_{i=1}^{S} \left(\frac{a}{A}\right)^{n_i}$ |
| Most even | $n_i = \frac{n}{S}$ | $S_a = S\left(1 - \left(1 - \frac{a}{A}\right)^{\frac{n}{S}}\right)$ | $E_a = S\left(\frac{a}{A}\right)^{\frac{n}{S}}$ |
| Most uneven | $n_{i<S} = 1, n_S = n - S + 1$ | $S_a = 1 + (S-1)\frac{a}{A} - \left(1 - \frac{a}{A}\right)^{n-S+1}$ | $E_a = (S-1)\frac{a}{A} + \left(\frac{a}{A}\right)^{n-S+1}$ |
| Geometric | $n_i = \frac{n\kappa(1-\kappa)^{i-1}}{1-(1-\kappa)^S}$ | | |
| Mixed even-uneven | $n_{i\leq s} = 1,\ n_{i>s} = \frac{n-s}{S-s}$ | $S_a = s\frac{a}{A} + (S-s)\cdot \left(1 - \left(1 - \frac{a}{A}\right)^{\frac{n-s}{S-s}}\right)$ | $E_a = S - s\left(1 - \frac{a}{A}\right) - (S-s)\left(1 - \left(\frac{a}{A}\right)^{\frac{n-s}{S-s}}\right)$ |
| Random placement | $s(j)$ is known | $S_a = S - \sum_j s_j \left(1 - \frac{a}{A}\right)^j$ | $E_a = \sum_j s_j \left(\frac{a}{A}\right)^j$ |
| Log-series | $s(j) = \alpha\frac{x^j}{j}$ | $S_a = \alpha \ln\left(1 + \frac{x}{1-x}\frac{a}{A}\right)$ | $E_a = -\alpha \ln\left(1 - x\frac{a}{A}\right)$ |
| Broken-stick | $s(j) = \frac{S}{n}(S-1)\left(1 - \frac{j}{n}\right)^{S-2}$ | $S_a = \frac{S\ln\left(1 - \frac{a}{A}\right)}{\ln\left(1 - \frac{a}{A}\right) - \frac{S}{n}}$ | $E_a = -\frac{S^2}{n\ln\left(\frac{a}{A}\right) - S}$ |
| Truncated negative binomial distribution | $s(j) = \frac{\Gamma(\gamma+j)}{\Gamma(j+1)\Gamma(\gamma)} \cdot \frac{\phi^j}{(1+\phi)^{\gamma+j} - (1+\phi)}$ | $S_a = \frac{S\left(1 - \left(1 + \phi\frac{a}{A}\right)^{-\gamma}\right)}{1 - (1+\phi)^{-\gamma}}$ | $E_a = S\frac{\left(1 + \phi\left(1 - \frac{a}{A}\right)\right)^{-\gamma} - (1+\phi)^{-\gamma}}{1 - (1+\phi)^{-\gamma}}$ |

$n_i$ is the number of individuals of species $i$, $s_j$ is the number of species with $j$ individuals, $\alpha$ and $x$ are the parameters of the log-series model, $\kappa$ is the resource preemption parameter, and $\gamma$ and $\phi$ are the shape and scale parameters of the TNBD model.

Source: He and Legendre (2002, Table 1, page 1187), Green and Ostling (2003, Table 1, page 3091) & Author's calculations.

Ostling, 2003). According to He and Hubbell (2011), the expected number of species lost due to the loss of area $a$ can be calculated as:

$$\mathcal{L}oss\,(a \mid A) = S_A - S_{A-a} = S - \left(S - \sum_{i=1}^{S}\left(1 - \frac{A-a}{A}\right)^{n_i}\right) = \sum_{i=1}^{S}\left(\frac{a}{A}\right)^{n_i} = E_a$$

Thus, $E_a$ can be interpreted as the number of species lost if habitat area $a$ is destroyed. This gives the following identity:

$$\text{SAR}\,(A) = \text{SAR}\,(A-a) + \text{EAR}\,(a)$$

which states that the number of species in region $A$ is equal to the sum of the species found in subregion $A-a$ and the species locally endemic in subregion $a$.

He and Legendre (2002) used the tree dataset from the Pasoh Forest Reserve in Malaysia. The research area consists of a 50-ha plot ($500 \times 1000$ m), established in 1986 and resurveyed several times between 1990 and 2016. The 1987 survey recorded 335 356 individual stems and 814 tree species. He and Legendre (2002) calibrated several species abundance models[132]. Figure 5.67 shows the estimated species-area relationship for each model compared to the empirical species-area relationship derived from the recorded data. We observe that the empirical curve lies between the broken-stick and geometric models. The endemics-area relationship is plotted in Figure 5.68. We restrict the analysis to surface areas larger than 1 ha because $\text{EAR}\,(a) \approx 0$ when $a \approx 0$. This is not the case for the function $\text{SAR}\,(a)$. As noted by He and Hubbell (2011), there is an asymmetry between the two curves. In fact, it is easier to discover a species quickly when exploring a patch, whereas the extinction of a species requires the destruction of a large proportion of the patch. He and Hubbell (2011) concluded that species-area relationships always overestimate extinction rates due to habitat loss:

> "*Here we show that extinction rates estimated from the SAR are all overestimates. [...] These overestimates are due to the false assumption that the sampling problem for extinction is simply the reverse of the sampling problem for the SAR. The area that must be added to find the first individual of a species is in general much smaller than the area that must be removed to eliminate the last individual of a species. Therefore, on average, it takes a much greater loss of area to cause the extinction of a species than it takes to add the species on first encounter, except in the degenerate case of a species having a single individual. [...] Only in a very special and biologically unrealistic case, when all species are randomly and independently distributed in space, is it possible to derive the EAR from the SAR.*" (He and Hubbell, 2011, page 368).

In this context, the choice of the power-law model can create some bias. Recall that $S_A = cA^z$. We can deduce that $S_{A-a} = c\,(A-a)^z$ and $E_a = S_A - S_{A-a} = cA^z - c\,(A-a)^z$. It follows that:

$$\mathcal{L}oss_{species} = \frac{E_a}{S_A} = 1 - \frac{(A-a)^z}{A^z} = 1 - (1 - \mathcal{L}oss_{habitat})^z \tag{5.28}$$

We retrieve Equation (5.19) on page 435. At first glance, it seems that the approach based on the endemics-area relationship is coherent with the species-area relationship. In fact, the issue lies in the calibration of the endemics-area curve, which generally produces a value of $z$ smaller than

[132] The estimated parameters are $\kappa = 0.009927$ for the geometric model, and $\alpha = 100.3014$ and $x = 0.999701$ for the log-series model. The other models are completely determined by the number of individuals ($n = 335\,356$) and the number of species ($S = 814$).

Figure 5.67: Species-area relationship (Pasoh Forest Reserve)

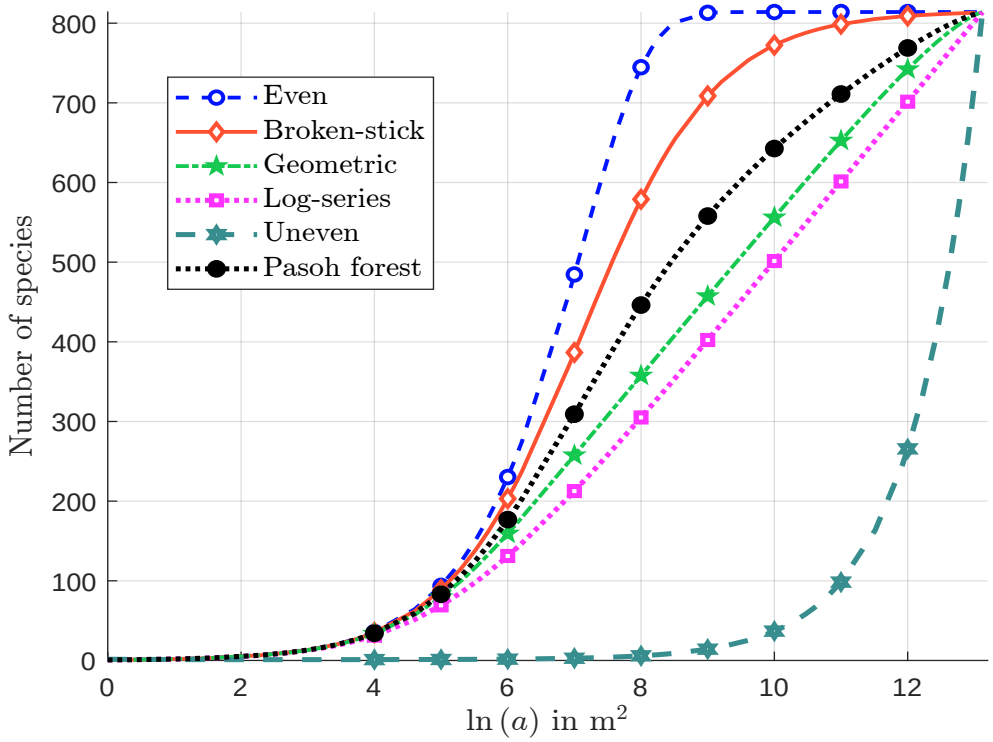


Source: He and Legendre (2002, Figure 2a, page 1191) & Author's calculations.

Figure 5.68: Endemics-area relationship (Pasoh Forest Reserve)

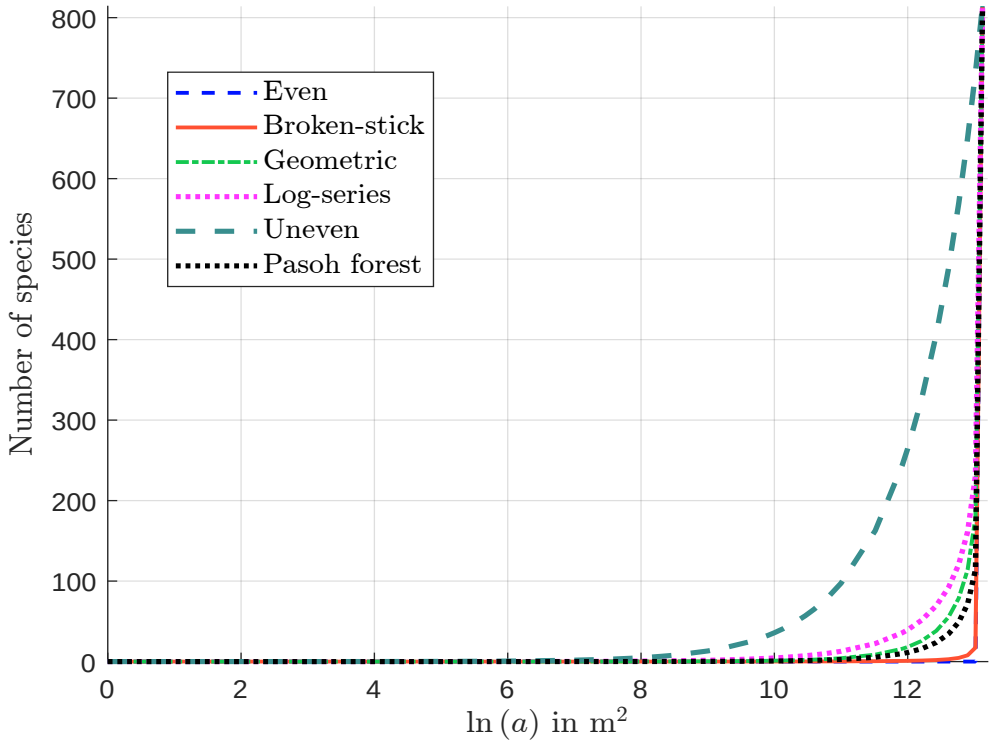


Source: Green and Ostling (2003, Figure 1a, page 3093) & Author's calculations.

Figure 5.69: Comparison of species-area and endemics-area curves (Barro Colorado Island)

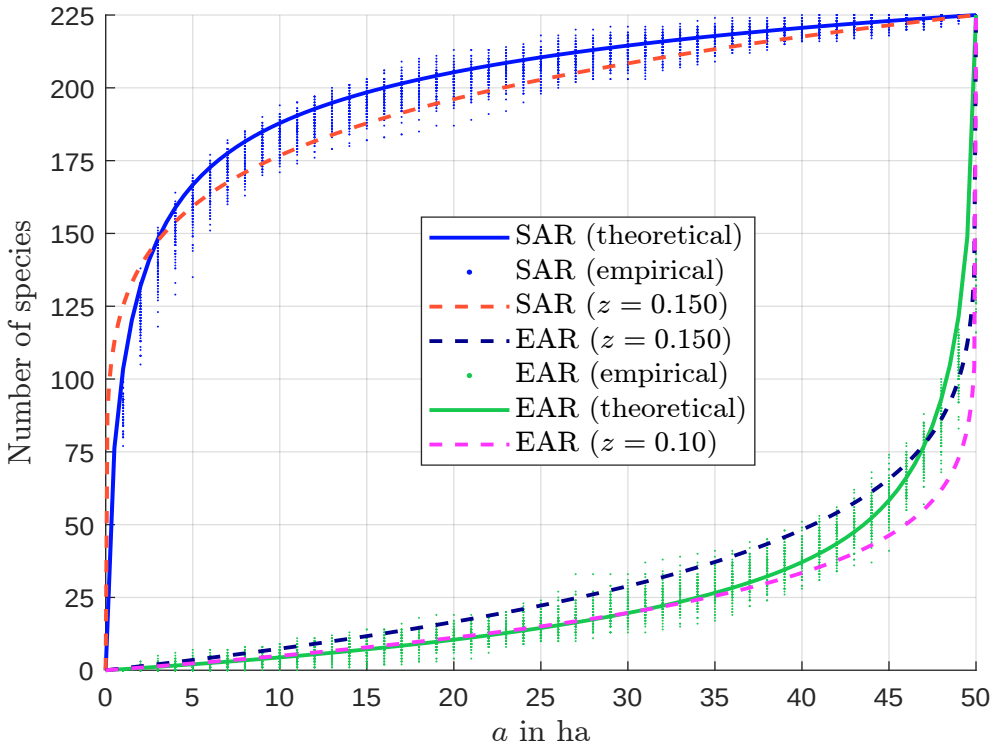


Source: He and Hubbell (2011, Figure S1) & Author's calculations.

the value obtained with the species-area curve. As a result, we deduce that the extinction rate is overestimated:

$$\mathcal{L}oss_{species} = 1 - (1 - \mathcal{L}oss_{habitat})^{z_{\text{EAR}}} \leq 1 - (1 - \mathcal{L}oss_{habitat})^{z_{\text{SAR}}}$$

To illustrate this bias, He and Hubbell (2011) considered nine datasets, including those from the Barro Colorado Island and the Pasoh Forest, and found that $z_{\text{EAR}} \leq z_{\text{SAR}}$ in all cases. For example, for the Pasoh Forest Reserve, they found $z_{\text{EAR}} = 0.0536$ and $z_{\text{SAR}} = 0.124$. Figure 5.69 shows the empirical and theoretical SAR and EAR curves, along with the calibrated power-law models. We verify that $\mathcal{L}oss_{species}$ is overestimated when $z_{\text{SAR}}$ is used instead of $z_{\text{EAR}}$. On page 435 we estimate that 50% of habitat loss should reduce the number of species by 15.91%, while 90% of habitat loss leads to 43.77% of species loss because we use the value $z_{\text{SAR}} = 0.25$ suggested by Pimm *et al.* (1995). If we consider a value of $z_{\text{EAR}} = 0.10$, which is the median value obtained by He and Hubbell (2011), 50% of habitat loss should reduce the number of species by 6.70%, while 90% of habitat loss leads to 20.57% of species loss (Table 5.41, page 435). The numbers are quite different.

**Remark 61** *Censuses of tree data are abundant and valuable for studying relationships between habitat and species richness. Many of these datasets (including those from Barro Colorado Island and the Pasoh Forest Reserve) are available at* `http://ctfs.si.edu/datarequest`*, the data portal of ForestGEO (Forest Global Earth Observatory). ForestGEO is a global network dedicated to the study of forests and their ecosystems. Hosted by the Smithsonian Institution, it is one of the most comprehensive forest monitoring programs in the world. The network includes 78 forest research sites in the Americas, Africa, Asia, Europe, and Oceania, that monitor the growth and survival of approximately 7 million trees representing nearly 13 000 species.*

Box 5.15: Forest definitions adopted by major international environmental and forestry organizations

- United Nations Food and Agriculture Organization (2000)
  Land with tree crown cover (or equivalent stocking level) of more than 10% and an area of more than 0.5 ha. Trees should be able to reach a minimum height of 5 m at maturity *in situ*.
- United Nations Framework Convention on Climate Change (2002)
  Minimum area of 0.05–1.0 ha of land with tree crown cover (or equivalent stocking level) of more than 10–30% with trees that have the potential to reach a minimum height of 2–5 m at maturity *in situ*.
- United Nations Convention on Biological Diversity
  Land area of more than 0.5 ha, with a tree canopy cover of more than 10%, which is not primarily under agriculture or other specific non-forest land use.
- United Nations Convention to Combat Desertification (2000)
  Dense canopy with multi-layered structure including large trees in the upper story.
- International Union of Forest Research Organizations (2002)
  Land area with a minimum 10% tree crown coverage (or equivalent stocking level), or formerly having such tree cover and that is being naturally or artificially regenerated or that is being afforested.

Source: Chazdon *et al.* (2016, Box 1, page 542).

**Forest loss** Among the various types of habitat loss, forests are particularly important because they are biodiversity hotspots, home to numerous endemic species. These ecosystems provide essential services, including climate regulation, water cycle maintenance, and soil stabilization. In addition, forests are complex, interconnected networks where species are highly interdependent. Loss of forest habitat can trigger trophic cascades, destabilizing entire ecological systems by disrupting some fundamental biological relationships. However, the concept of forest loss is somewhat vague and requires a clear definition of what constitutes a forest and what does not. According to the Oxford English Dictionary, a forest is defined as "*a large area of land that is thickly covered with trees*", while the Cambridge Dictionary defined it as "*a large area of land covered with trees and plants, usually larger than a wood*". However, despite its common usage, there is no universally agreed-upon definition of the word forest. The concept of a forest extends far beyond a simple description of tree coverage and must encompass various dimensions of biodiversity, particularly when aiming to measure ecosystem functions or address key aspects of forest conservation biology (Zalles *et al.*, 2024). For instance, these aspects include forest loss, degradation, afforestation, reforestation, and other related processes. In Box 5.15, we report the forest definitions of five international organizations collected by Chazdon *et al.* (2016). While the definition depends on the purpose and the organization, the FAO definition is the most widely used globally. The FAO definition is practical because it uses measurable parameters such as tree height, canopy cover, and area. Here is the latest version used for the 2025 FRA[133]:

[133] A forest is defined by the presence of trees and the absence of dominant non-forest land uses. It includes young or regenerating areas that are expected to reach a height of 5 meters and a canopy cover of 10%. Forests also include mangroves, shelterbelts, bamboo, palms, and specialty plantations such as rubber and cork oak. Protected areas, forest infrastructure and abandoned shifting cultivation areas with tree regeneration are included. Agricultural tree

> "*Land spanning more than 0.5 hectares with trees higher than 5 meters and a canopy cover of more than 10 percent, or trees able to reach these thresholds in situ. It does not include land that is predominantly under agricultural or urban land use.*" (FAO, 2023a, Section 1a, page 7).

Another success factor is that data on forest status and trends are easily available thanks to the Global Forest Resources Assessment (FRA), which is collected and published by the FAO every five years[134].

Figure 5.70: Proportion and distribution of global forest area by climatic domain in 2020

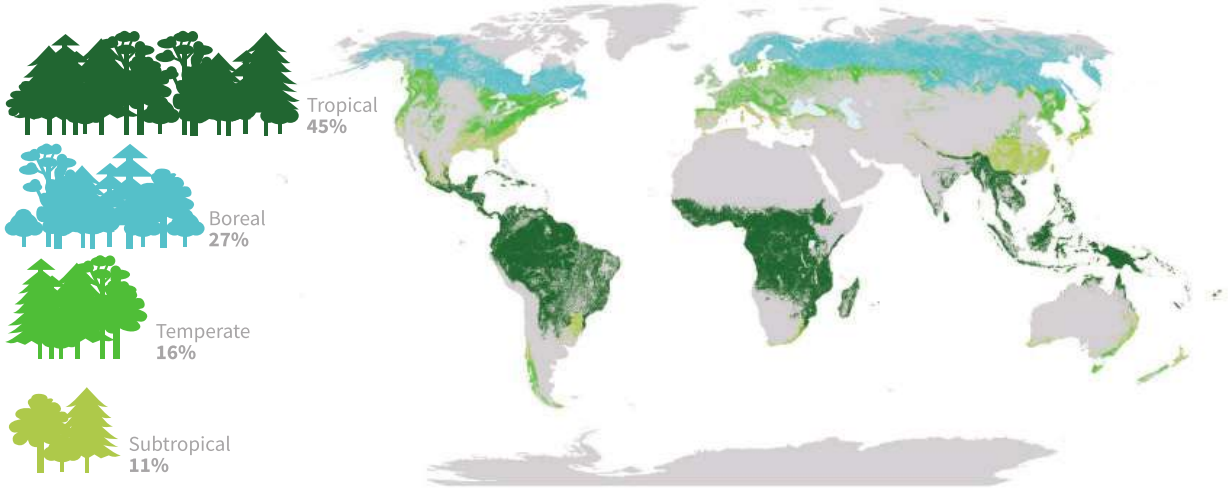


Source: FAO (2020, page 1).

According to FAO (2020), the world has a total forest area of 4.06 billion hectares, which represents 31% of the total land area. This area corresponds to 0.52 ha per person. Tropical forests[135] account for 45% of the world's forests, followed by boreal forests (27%), temperate forests (16%) and subtropical forests (11%), while polar forests account for less than 1% (Figure 5.70). More than 50% of the world's forests are located in just five countries: Russia, Brazil, Canada, the United States and China. In Table 5.46, we present the forest area of the top 20 countries, changes by decade, the distribution of the world's forest area in 2020, and the proportion of primary forest[136] in 2020. For instance, Brazil had 589 million hectares of forest in 1990, which decreased to 497 million hectares in 2020. The country experienced forest area losses of 6.42%, 7.17%, and 2.92% between 1990–2000, 2000–2010, and 2010–2020, respectively. In 2020, Brazil accounted for 12.24% of the world's forest area, and 43.53% of its forests were classified as primary forests. Figure 5.71 shows the percentage of land area covered by forests. Globally, forests cover 31.1% of the total land area, but there are significant differences between countries. Seven countries have more than 90% of their land area covered by forest: Suriname (97.41%), French Guiana (97.36%), Guyana (93.55%),

systems such as orchards, fruit plantations and agroforestry with crops are excluded.

[134]The FRA website is `www.fao.org/forest-resources-assessment` while the FRA data are available at `https://fra-data.fao.org/assessments/fra/2020`.

[135]The climatic groups are defined as follows: tropical (all months without frost; in marine areas above 18°C), subtropical (eight months or more above 10°C), temperate (four to eight months above 10°C), boreal (up to three months above 10°C) and polar (all months below 10°C).

[136]Primary forests are old-growth natural forests that have been largely undisturbed by human activity and have retained their original biodiversity and ecological processes.

Table 5.46: Forest area (top 20 countries and six world regions)

| Country/region | Value (in million ha) | | | | Variation by decade (in %) | | | Geographical distribution | | Primary forest |
|---|---|---|---|---|---|---|---|---|---|---|
| | 1990 | 2000 | 2010 | 2020 | 2000 | 2010 | 2020 | in % | Cumulated | in % |
| Russia | 809 | 809 | 815 | 815 | 0.04 | 0.72 | 0.02 | 20.09 | 20.09 | 31.30 |
| Brazil | 589 | 551 | 512 | 497 | −6.42 | −7.17 | −2.92 | 12.24 | 32.32 | 43.53 |
| Canada | 348 | 348 | 347 | 347 | −0.14 | −0.14 | −0.11 | 8.55 | 40.87 | 59.13 |
| United States of America | 302 | 304 | 309 | 310 | 0.36 | 1.71 | 0.35 | 7.63 | 48.50 | 24.31 |
| China | 157 | 177 | 201 | 220 | 12.64 | 13.34 | 9.65 | 5.42 | 53.92 | 5.21 |
| Australia | 134 | 132 | 130 | 134 | −1.54 | −1.72 | 3.44 | 3.30 | 57.22 | |
| Congo (DRC) | 151 | 144 | 137 | 126 | −4.47 | −4.68 | −8.03 | 3.11 | 60.33 | 65.59 |
| Indonesia | 119 | 101 | 100 | 92 | −14.56 | −1.60 | −7.55 | 2.27 | 62.60 | 48.56 |
| Peru | 76 | 75 | 74 | 72 | −1.51 | −1.66 | −2.32 | 1.78 | 64.38 | |
| India | 64 | 68 | 69 | 72 | 5.71 | 2.82 | 3.83 | 1.78 | 66.16 | 21.76 |
| Angola | 79 | 78 | 72 | 67 | −1.96 | −7.14 | −7.69 | 1.64 | 67.80 | 40.15 |
| Mexico | 71 | 68 | 67 | 66 | −3.13 | −2.10 | −1.87 | 1.62 | 69.42 | 48.77 |
| Colombia | 65 | 63 | 61 | 59 | −3.42 | −3.07 | −2.74 | 1.46 | 70.88 | |
| Bolivia | 58 | 55 | 53 | 51 | −4.68 | −3.66 | −4.24 | 1.25 | 72.13 | |
| Venezuela | 52 | 49 | 48 | 46 | −5.53 | −3.35 | −2.68 | 1.14 | 73.27 | 97.06 |
| Tanzania | 57 | 54 | 50 | 46 | −6.48 | −6.93 | −8.42 | 1.13 | 74.40 | 62.32 |
| Zambia | 47 | 47 | 47 | 45 | −0.76 | −0.76 | −4.03 | 1.10 | 75.50 | |
| Mozambique | 43 | 41 | 39 | 37 | −5.05 | −5.38 | −5.72 | 0.91 | 76.40 | |
| Papua New Guinea | 36 | 36 | 36 | 36 | −0.33 | −0.27 | −0.89 | 0.88 | 77.29 | |
| Argentina | 35 | 33 | 30 | 29 | −5.19 | −9.48 | −5.43 | 0.70 | 77.99 | |
| Africa | 743 | 710 | 676 | 637 | −4.41 | −4.79 | −5.82 | 15.68 | 15.68 | 19.30 |
| Asia | 585 | 587 | 611 | 623 | 0.34 | 4.01 | 1.92 | 15.34 | 31.03 | 13.79 |
| Europe | 994 | 1 002 | 1 014 | 1 017 | 0.80 | 1.17 | 0.34 | 25.07 | 56.09 | 25.22 |
| North and Central America | 755 | 752 | 754 | 753 | −0.39 | 0.24 | −0.20 | 18.54 | 74.64 | 41.62 |
| Oceania | 185 | 183 | 181 | 185 | −0.89 | −1.26 | 2.34 | 4.56 | 79.20 | 1.41 |
| South America | 974 | 923 | 870 | 844 | −5.24 | −5.69 | −2.98 | 20.80 | 100.00 | 35.38 |
| World | 4 236 | 4 158 | 4 106 | 4 059 | −1.85 | −1.24 | −1.15 | 100.00 | 200.00 | 26.61 |

Source: FAO (2020), https://fra-data.fao.org/assessments/fra/2020, & Author's calculations.

Figure 5.71: Percentage of land area covered by forest, by country (2020)

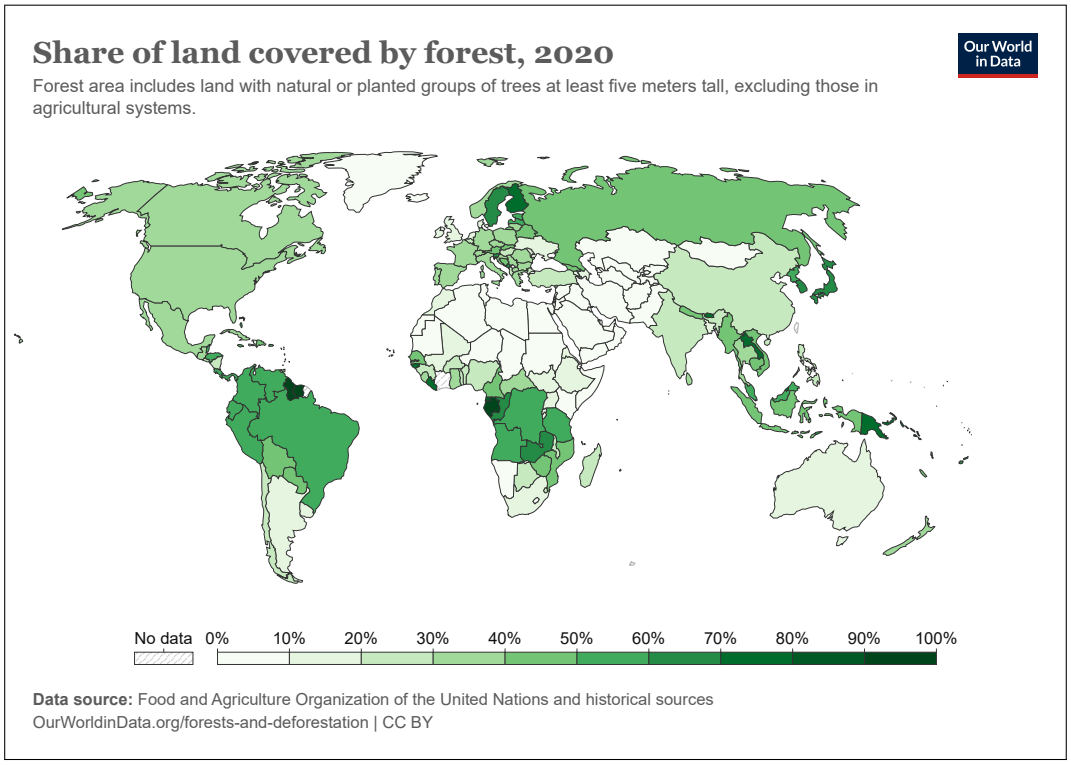


Source: Our World in Data, https://ourworldindata.org/forest-area.

Figure 5.72: Distribution of global forest area (2020)

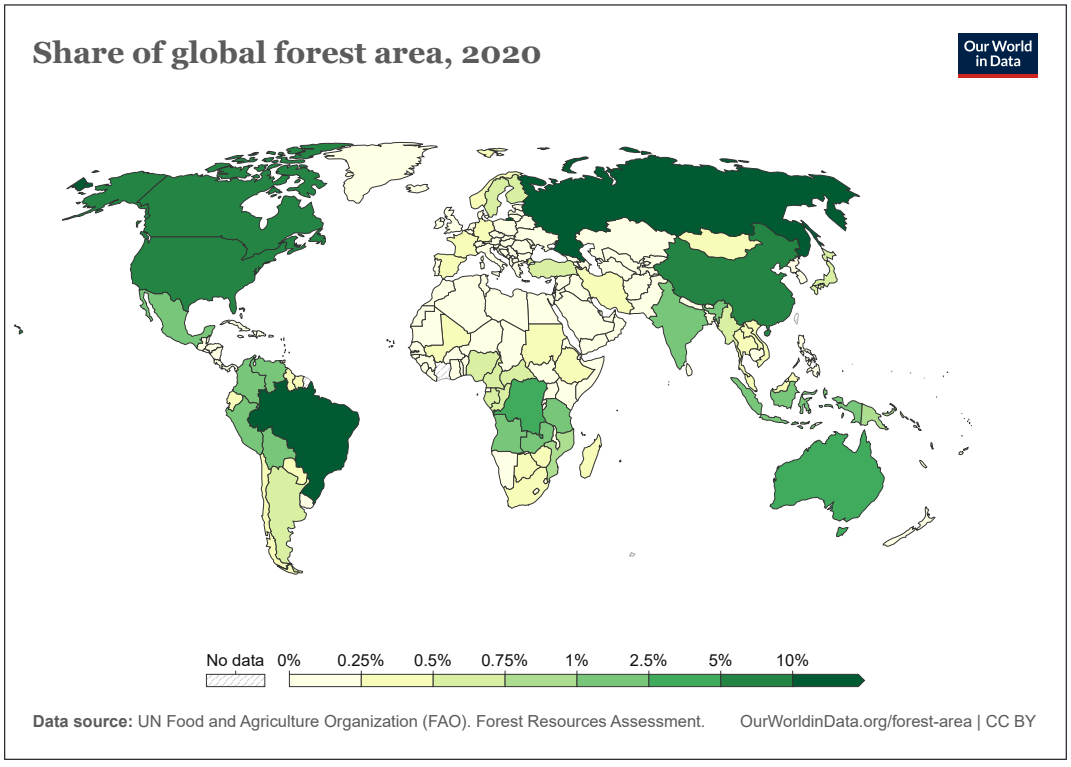


Source: Our World in Data, https://ourworldindata.org/forest-area.

Micronesia (92.03%), Gabon (91.32%), Solomon Islands (90.14%), and Palau (90.02%). Some of the world's largest countries also have a significant proportion of their land area covered by forest. For example, Russia (49.78%), China (23.34%), the United States (33.87%), Canada (38.15%), and Brazil (59.42%) all have significant forest cover. Conversely, other large countries have relatively low forest cover, such as Argentina (10.44%), Kazakhstan (1.28%), and Algeria (0.82%). Among the largest European countries (those with a land area of more than 20 million hectares), forest cover also varies widely. Most of these countries have at least 30% forest cover, including Belarus (43.19%), Germany (32.73%), Spain (37.17%), Finland (73.74%), France (31.51%), Italy (32.52%), Norway (40.05%), Poland (30.97%), Romania (30.12%) and Sweden (68.69%). However, some countries fall below this threshold, such as Ukraine (16.73%) and the United Kingdom (13.19%).

Table 5.47 presents some key forest characteristics. Globally, 17% of forests are located in protected areas, representing more than 700 million hectares. Among the six world regions, South America has the highest proportion of forests in protected areas (30.5%), followed by Africa (24.8%). Natural (regenerative) forests account for 92.4% of the global forest area, while 7.2% consists of planted forests. In addition, the majority of the world's forests are publicly owned (71.5%), compared to 21.7% under private ownership, with the remainder classified as unknown. Public ownership predominates in all regions, especially in Europe (88.2%), largely due to Russia, where 100% of forests are publicly owned.

We have seen that the world lost 177 million hectares of forest between 1990 and 2020. Focusing on the period 2015–2020, the annual forest loss was about 5 million hectares. This figure, representing the net change, is the difference between the forest expansion rate and the deforestation rate. In Table 5.47, we present these two statistics together with the reforestation rate, all expressed in 1 000 hectares per year. For some countries, data on forest expansion, deforestation, and reforestation[137] are missing (*e.g.*, the United States, Australia, Congo, Angola), which introduces bias into the global rates. However, estimates from FAO (2020, page 4) indicate that the annual net loss of 5 million hectares is the result of a deforestation rate of 10 million hectares per year offset by a forest expansion rate of 5 million hectares per year. Although there is a declining trend in forest loss in the short term, the average rate of forest loss has accelerated in the long term. In fact, between the invention of agriculture and the beginning of the Industrial Revolution, we lost 2% of forest area every 5 000 years. Since 1700, as shown in Table 5.48, this rate has accelerated, especially since 1950.

The GFA dataset is not dedicated to the study of forest loss, although it contains a lot of information on this topic. To obtain information at a higher resolution than regional and country levels, and at a higher frequency than the 5-year period (for example, to obtain statistics on the Amazon rainforest on quarterly basis), other sources of information are available:

- The Global Forest Review (GFR) is an initiative of the World Resources Institute (WRI) that provides data, analysis and insight on the world's forests (`https://research.wri.org/gfr/global-forest-review`). It serves as a resource for tracking the state of the world's forests, understanding deforestation trends, and evaluating forest conservation efforts. GFR uses many datasets derived from geospatial data and maps.

- Global Forest Watch (GFW) is an online platform, available at `www.globalforestwatch.org` and developed by the World Resources Institute (WRI), that provides near real-time

[137] Forest expansion refers to the growth of forest on land previously used for other purposes, involving a change of land use from non-forest to forest. It includes both afforestation (planting of trees on land that was not previously forested) and natural expansion of forests. Deforestation is the conversion of forested land to other land uses, whether this change is caused by human activities or by natural processes. Reforestation is the reestablishment of forest on land that is still classified as forest, typically through planting or deliberate seeding. Unlike forest expansion, it does not involve a change in land use.

Table 5.47: Forest characteristics, ownership and annual change (top 20 countries and six world regions)

| Country/region | Forest area ($10^6$ ha) | Protected (%) | Regenerative (%) | Planted (%) | Private ownership (%) | Public ownership (%) | Expansion ($10^3$ ha/year) | Deforestation ($10^3$ ha/year) | Reforestation ($10^3$ ha/year) | Coverage (%) | Net change ($10^3$ ha/year) |
|---|---|---|---|---|---|---|---|---|---|---|---|
| Russia | 815 | 2.3 | 97.7 | 2.3 | 0.0 | 100.0 | 76 | 0 | 945 | 100.0 | 76 |
| Brazil | 497 | 30.1 | 97.7 | 2.3 | 44.2 | 55.8 | 243 | 1 696 | 257 | 100.0 | −1 453 |
| Canada | 347 | 8.5 | 94.8 | 5.2 | 8.2 | 91.4 | 0 | 38 | 427 | 100.0 | −38 |
| United States of America | 310 | 10.2 | 91.1 | 8.9 | 58.1 | 41.9 | | | 691 | 0.0 | −60 |
| China | 220 | 13.8 | 61.5 | 38.5 | 41.3 | 58.7 | 2 070 | 133 | 273 | 100.0 | 1 937 |
| Australia | 134 | 18.0 | 98.2 | 1.8 | 32.3 | 67.0 | | | | 0.0 | 182 |
| Congo (DRC) | 126 | 19.3 | 100.0 | 0.0 | 0.0 | 100.0 | | | | 0.0 | −1 101 |
| Indonesia | 92 | 56.2 | 95.1 | 4.9 | 1.1 | 91.2 | 71 | 650 | 7 | 100.0 | −579 |
| Peru | 72 | 31.6 | 98.5 | 1.5 | 16.0 | 84.0 | 6 | 179 | | 100.0 | −173 |
| India | 72 | 19.4 | 81.6 | 18.4 | 18.5 | 81.5 | 935 | 668 | | 100.0 | 266 |
| Angola | 67 | 2.8 | 98.8 | 1.2 | 0.0 | 100.0 | | | 0 | 0.0 | −555 |
| Mexico | 66 | | 99.8 | 0.2 | 79.3 | 3.6 | 38 | 166 | 159 | 100.0 | −128 |
| Colombia | 59 | 21.0 | 99.3 | 0.7 | 30.4 | 66.0 | 1 | 199 | 497 | 100.0 | −199 |
| Bolivia | 51 | 24.5 | 99.9 | 0.1 | 0.1 | 99.9 | 4 | 243 | 3 | 100.0 | −239 |
| Venezuela | 46 | 98.6 | 97.1 | 2.9 | 2.3 | 97.7 | 18 | 108 | 4 | 100.0 | −90 |
| Tanzania | 46 | 62.3 | 98.8 | 1.2 | 7.3 | 4.1 | 5 | 474 | 27 | 100.0 | −469 |
| Zambia | 45 | 71.0 | 99.9 | 0.1 | 6.4 | 26.2 | 2 | 190 | 4 | 100.0 | −188 |
| Mozambique | 37 | 41.4 | 99.8 | 0.2 | 0.2 | 99.8 | 28 | 267 | 2 | 100.0 | −239 |
| Papua New Guinea | 36 | 3.8 | 99.8 | 0.2 | 99.9 | 0.1 | 0 | 34 | 0 | 99.4 | −34 |
| Argentina | 29 | 6.7 | 95.0 | 5.0 | 4.4 | 0.0 | 30 | 135 | 17 | 100.0 | −105 |
| Africa | 637 | 24.8 | 98.2 | 1.8 | 5.5 | 71.4 | 404 | 2 149 | 353 | 44.0 | −3 969 |
| Asia | 623 | 21.9 | 78.2 | 21.7 | 21.6 | 76.8 | 3 477 | 1 922 | 1 221 | 118.2 | 1 316 |
| Europe | 1 017 | 4.9 | 91.3 | 7.4 | 9.1 | 88.2 | 255 | 69 | 1 593 | 56.0 | 331 |
| North and Central America | 753 | 9.5 | 93.7 | 6.2 | 35.2 | 60.5 | 79 | 372 | 1 322 | 84.2 | −348 |
| Oceania | 185 | 15.7 | 97.1 | 2.6 | 47.2 | 52.2 | 16 | 40 | 56 | −15.0 | 163 |
| South America | 844 | 30.5 | 97.6 | 2.4 | 31.9 | 61.6 | 460 | 2 962 | 947 | 100.9 | −2 481 |
| World | 4 059 | 17.3 | 92.4 | 7.2 | 21.7 | 71.5 | 4 691 | 7 514 | 5 492 | 56.6 | −4 987 |

Source: FAO (2020), https://fra-data.fao.org/assessments/fra/2020, & Author's calculations.

Table 5.48: Distribution of habitable land on Earth (excluding glaciers and deserts)

| Time | Forests | Cropland | Grazing land | Wild grassland and shrubs | Urban and built-up land |
|---|---|---|---|---|---|
| 10 000 years ago | 57% | | | 42% | |
| 5 000 years ago | 55% | | 1% | 44% | |
| 1700 | 52% | 3% | 6% | 38% | |
| 1900 | 48% | 8% | 16% | 27% | |
| 1950 | 44% | 12% | 31% | 12% | 1% |
| 2020 | 37% | 16% | 31% | 14% | 2% |

Source: Our World in Data, https://ourworldindata.org/forest-area & Author's calculations

monitoring of global forest change. It uses advanced satellite technology, big data, and open access to empower users to monitor forests and take action against deforestation.

- Academic studies are extensively documented on specific regions and provide high-level analysis of data provided by GFA, GFR, GFW and other datasets. They may include a new way of observing forests, for example using satellite imagery[138], an in-depth analysis of forms of forest degradation[139], etc.

According to the Global Forest Review, the top 10 countries with the highest global tree cover loss between 2001 and 2023 are Russia (83.7 Million hectares or Mha), Brazil (68.9 Mha), Canada (57.5 Mha), the United States (47.9 Mha), Indonesia (30.8 Mha), the Democratic Republic of Congo (19.7 Mha), China (12.1 Mha), Malaysia (9.2 Mha), Australia (9 Mha), and Bolivia (8 Mha). However, tree cover loss does not always equate to deforestation. In some cases, such as commercial forestry, tree cover loss is temporary because forests are allowed to regrow after harvesting. This is particularly true in countries such as Russia and Canada, which have a permanent tree cover loss rate of 0%. Similarly, the United States, China and Australia have permanent loss rates of less than 5%. In contrast, countries such as Indonesia, Malaysia and Bolivia have permanent tree cover loss rates of more than 80%, indicating significant deforestation. Brazil and the Democratic Republic of the Congo fall between these two extremes, with permanent forest loss rates of 71% and 35%, respectively. Together, these 10 countries are responsible for 71% of the global tree cover loss of 488 Mha between 2001 and 2023. Curtis *et al.* (2018) propose a classification of forest loss into five main drivers (Box 5.16). Forestry accounts for 32% of global forest loss between 2001 and 2023, followed by shifting agriculture and wildfires, each contributing 23%. Commodity-driven deforestation accounts for 21%, while urbanization is responsible for less than 1%. According to the Global Forest Review, the drivers of forest loss vary significantly from one region to another (Figure 5.73). While commodity-driven deforestation is the leading cause of forest loss in Latin America and Southeast Asia, its impact is minimal in other regions, which are dominated by wildfires and forestry, with the exception of Africa, where 95% of forest loss is attributed to shifting agriculture.

The Global Forest Review also provides many interesting figures for understanding deforestation. For example, we learn that seven commodities account for 57% of all agricultural-related tree cover

[138]Three notable examples are the studies by Hansen *et al.* (2013b) and Potapov *et al.* (2022), which use a dataset of land cover at a 30-meter spatial resolution derived from NASA's Landsat program, and the study by Lesiv *et al.* (2022), which is based on a dataset of forest management practices at a 100-meter resolution for the year 2015, derived from the European Space Agency's PROBA-V satellite imagery program.

[139]See for example Lapola *et al.* (2023), who studied four primary disturbances contributing to Amazon forest degradation: timber extraction, fire (sometimes used for land clearing, which can escape control and damage surrounding forests), edge effects (resulting from deforestation and habitat fragmentation), and extreme drought.

Box 5.16: Drivers of forest loss

- Forestry
  Large-scale forestry operations in managed forests or tree plantations where future regrowth is likely. Regrowth may occur through natural regeneration or tree planting.
- Commodity-driven deforestation
  Long-term permanent conversion of forest and shrubland to non-forest land for commodity production, including agriculture, mining, or oil and gas production.
- Wildfire
  Burning of vegetation without visible human conversion or agricultural activity afterward. Some of these fires occur naturally, but others are set by humans. In humid tropical forests, fires are not natural to the ecosystem and are almost always set by humans, usually to clear land for agriculture.
- Shifting agriculture
  Agricultural practices in which forests are cleared, used for agricultural production for a few years, and then temporarily abandoned to allow trees to regrow. Shifting agriculture involves many different types of smallholder farming practices.
- Urbanization
  Permanent conversion of forests to human settlements for the expansion and intensification of existing urban centers.

Source: Curtis *et al.* (2018, pages 1108-1109).

Figure 5.73: Drivers of tree cover loss by region (2001–2023)

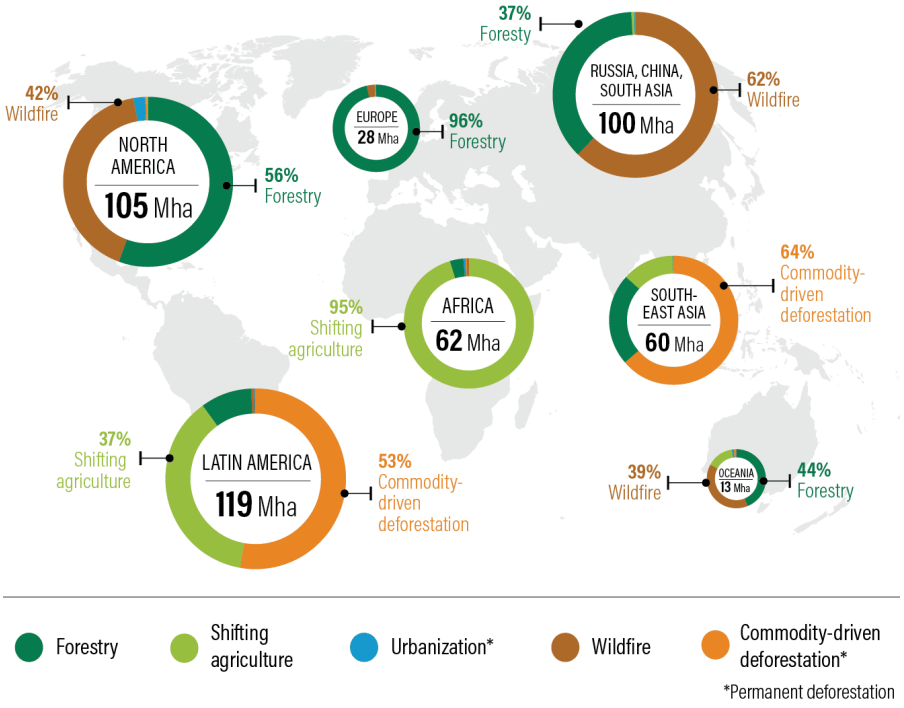


Source: https://research.wri.org/gfr/global-forest-review.

loss between 2001 and 2015, with cattle (pasture use) alone accounting for 36%, followed by oil palm (8%), soy (6.5%) and cocoa (2%). As mentioned earlier, forest loss and deforestation are major drivers of biodiversity loss[140], but forest degradation also plays a significant role in this process. In particular, the detrimental consequences of forest degradation have been highlighted by Barlow *et al.* (2016) and Watson *et al.* (2018), who showed that the impact of degradation can equal that of deforestation in some regions. However, the concept of forest degradation is not easy to define and requires a multi-dimensional analysis:

> "*Forest degradation is broadly defined as a reduction in the capacity of a forest to produce ecosystem services such as carbon storage and wood products as a result of anthropogenic and environmental changes. [...] There is, however, no generally recognized way to identify a degraded forest because perceptions of forest degradation vary depending on the cause, the particular goods or services of interest, and the temporal and spatial scales considered. [...] the types of degradation can be represented using five criteria that relate to the drivers of degradation, loss of ecosystem services and sustainable management, including: productivity, biodiversity, unusual disturbances, protective functions, and carbon storage.*" (Thompson *et al.*, 2013, page 1).

Among the 11 indicators proposed by Thompson *et al.* (2013, Table 1, page 3), the Global Forest Review has selected three approaches to measure forest degradation and forest disturbance:

1. Forest area experiencing a partial (more than 20% and less than 90%) loss of tree canopy cover;
2. Tree cover extent experiencing tree cover loss due to fire;
3. Intact forest landscapes that can no longer be considered intact due to evidence of human disturbance.

Their results are as follows[141]. Between 2001 and 2012, 185 Mha of forest experienced a partial reduction in tree canopy cover, representing 5% of the global forest area, with 85% of this occurring in tropical forests. Additionally, 113 Mha of tree cover loss was associated with fire between 2001 and 2023, accounting for 2.8% of the global forest area. Lastly, 155 Mha of forest area classified as intact in 2000 could no longer be considered intact by 2020, representing 4% of the global forest area.

### Invasive species

An invasive species is a non-native (or alien) species (plants, animals, or microorganisms) that is intentionally or accidentally introduced into a new environment and poses a threat to native species and biodiversity. The main characteristics of invasive species are:

- Non-native
  Invasive species are plants and animals that live in areas where they do not naturally exist. However, not all non-native species are invasive. For instance, corn is not native to Europe but is not considered an invasive species.

[140] For example, Betts *et al.* (2017) examined how deforestation affects biodiversity in different landscapes. They found that deforestation significantly increased the likelihood of species being listed as threatened, upgraded to higher threat categories, or experiencing population declines. Crucially, "*these risks were disproportionately high in relatively intact landscapes; even minimal deforestation had severe consequences for vertebrate biodiversity loss.*" In contrast, in already fragmented landscapes, the effects of forest loss were less pronounced.

[141] Source: https://research.wri.org/gfr/forest-condition-indicators/forest-degradation.

- Rapid spread
  Invasive species tend to reproduce and grow very quickly because they lack natural predators in the new environment.

- Harmful effects
  Invasive species often outcompete native species for resources, take over habitats, and disrupt native ecosystems.

These three characteristics are typically assessed to determine whether a species is invasive[142]. In addition, invasive species are usually introduced with (intentional or accidental) human assistance (Simberloff *et al.*, 2013). One of the greatest challenges is managing alien invasions because eradication of established invaders is rare and post-invasion control is difficult (Mack *et al.*, 2000).

Many countries have developed their own taxonomy of invasive alien species (IAS). For example, the National Invasive Species Information Center (NISIC), established in 2005 under the US Department of Agriculture (USDA), manages the website `www.invasivespeciesinfo.gov`, which lists invasive species in the United States. As of December 2024, 194 species are reported to be invasive in the United States. In alphabetical order, the first invasive species listed[143] is the African clawed frog (*Xenopus laevis*), which is native to Africa. It was introduced to California in 1968 and imported for laboratory research and the pet trade. This species negatively impacts native amphibian and fish populations. The $107^{m}$*athrmth* invasive species on the list is kudzu (*Pueraria montana*), which is native to Asia. It was introduced to the USA in the late 1800s as an ornamental plant and for erosion control. Kudzu vine outcompetes native species and disrupts ecosystems. In the European Union, invasive alien species are controlled by EU Regulation 1143/2014, which contains a set of measures to be taken throughout the EU in relation to invasive alien species. In addition, the European Union has established a list of 88 regulated invasive alien species[144] (47 animal species and 41 plant species). Here are some examples of invasive species: Egyptian goose (*Alopochen aegyptiaca*), western mosquitofish (*Gambusia affinis*), fox squirrel (*Sciurus niger*), tropical fire ant (*Solenopsis geminata*), African clawed frog (*Xenopus laevis*), Senegal tea plant (*Gymnocoronis spilanthoides*), floating pennywort (*Hydrocotyle ranunculoides*), water primrose (*Ludwigia grandiflora*), kudzu vine (*Pueraria montana*). At the global level, the Global Invasive Species Database (GISD) is a free, online, searchable source of information on alien and invasive species that negatively impact biodiversity. However, this database was developed in 2000 and is no longer maintained in the 2020s.

The previous examples focus on invasive animal and plant species. However, invasive species can also include infectious diseases and microorganisms. For example, Berger *et al.* (1998) studied the devastating effects of the amphibian chytrid fungus (*Batrachochytrium dendrobatidis*) and its impact on amphibian mortality and population decline. While these authors suggested that environmental factors such as climate change and habitat modification were responsible for the spread of the fungus, Weldon *et al.* (2004) found that "*Africa was the origin of amphibian chytrid and that the international trade in Xenopus laevis frogs, which began in the mid-1930s, was the means of dissemination.*" Although the chytrid fungus is not a traditional invasive species in the sense of an animal or plant, it is an example of an invasive pathogen that has had a devastating impact on native amphibian populations. Another example is the *Pseudogymnoascus destructans* fungus that causes white-nose syndrome, a fatal disease that has killed millions of bats in North America (Blehert *et al.*, 2009). This fungus is thought to have originated in Europe, where local bats evolved resistance. It

[142] For instance, IPBES (2023, page 76) estimates that 37 000 species are established aliens, but only 5 250 are invasive alien species.
[143] The list is available at `www.invasivespeciesinfo.gov/species-profiles-list`.
[144] They are listed in the 187-page report *An Introduction to the Invasive Alien Species of Union Concern*, published by the European Commission in 2022.

was introduced to North America by humans and has since become an invasive pathogen for native bats in North America.

Primack (2014, pages 226-237) and Simberloff (2010, pages 131-142) report numerous striking cases of invasive species. For example, the introduction of predatory snakes has led to a decline in bird populations on several small islands. Simberloff (2010, page 136) notes that predators have often been intentionally introduced as biological control agents for specific target species, but in some cases these predators have also attacked non-target species and driven them to extinction:

> "*One of the worst such disasters was the introduction of the rosy wolf snail (Euglandina rosea), native to Central America and Florida, to many Pacific islands to control the previously introduced giant African snail (Achatina fulica). The predator not only failed to control the targeted prey (which grows to be too large for the rosy wolf snail to attack it) but caused the extinction of over 50 species of native land snails [...] The small Indian mongoose, implicated as the sole cause or a contributing cause in the extinction of several island species of birds, mammals, and frogs, was deliberately introduced to all these islands as a biological control agent for introduced rats [...] The mosquitofish (Gambusia affinis) from Mexico and Central America has been introduced to Europe, Asia, Africa, Australia, and many islands for mosquito control. Its record on this score is mixed [...] However, it preys on native invertebrates and small fishes and in Australia is implicated in extinction of several fish species.*" (Simberloff, 2010, page 137).

Biological control is one of the reasons for the introduction of alien species, the other three being European colonization (birds, mammals, and fish for food), agriculture (including horticulture and aquaculture), and accidental transport (especially rats, snakes, and insects) (Primack, 2014, page 226). Among the regions most affected by invasive species, New Zealand is a special case. Non-native predators kill over 25 million native birds annually, and many native land species have already been lost, including sixty bird species, three frog species, seven vascular plants, and numerous invertebrates. Currently, more than 3 000 native land species are either threatened or endangered. In July 2016, the New Zealand government launched the *Predator Free 2050* initiative[145], which aims to completely eradicate certain introduced predators by the year 2050. The goals of Predator Free 2050 are ambitious, seeking to restore New Zealand's ecosystems to a state where native species can thrive without the constant threat of introduced predators. The initiative targets three primary groups of invasive species:

1. Mustelids: stoats (*Mustela erminea*), ferrets (*Mustela furo*), and weasels (*Mustela nivalis*).
2. Rats: ship rats (*Rattus rattus*), Norway rats (*Rattus norvegicus*), and kiore (*Rattus exulans*).
3. Possums: brushtail possums (*Trichosurus vulpecula*).

In 2024, New Zealand's Department of Conservation published the biennial progress report (2021–2023) to evaluate progress toward the seven interim targets. One target was achieved[146], four are on track to be achieved by 2025, and two will not be met[147]. New Zealand's situation is far from unique. In fact, many islands — especially those in the Pacific — face similar challenges (Simberloff, 2010).

[145] Documents on the strategy, implementation plan, and progress report are available at `www.doc.govt.nz/nature/pests-and-threats/predator-free-2050`.

[146] This relates to Goal 1 ("*By 2025, we will increase by 1 million hectares (compared with 2016) the area of New Zealand mainland where predators are suppressed, through Predator Free 2050 project*").

[147] This relates to Goal 3 ("*By 2025, we will have eradicated all mammalian predators from New Zealand's uninhabited offshore islands*") and Goal 4 ("*By 2025, we will have developed a breakthrough science solution that would be capable of eradicating at least one small mammal predator from the New Zealand mainland*").

The isolation of island habitats favors the evolution of endemic species, but this same isolation also makes these species exceptionally vulnerable to the threats posed by invasive species:

> "*Because they evolved in the absence of selective pressures from mammalian grazers and predators, many endemic island plants and animals have evolutionarily lost or never developed defenses against these enemies and often lack a fear of them. Many island plants do not produce the bad-tasting, tough vegetative tissue that discourages herbivores, nor do they have the ability to resprout rapidly following damage. Some birds have lost the power of flight and simply build their nests on the ground.*" (Primack, 2014, pages 228-229).

This vulnerability of endemic species helps explain why invasive alien species have contributed to 60% of recent species extinctions, of which 90% occurred on islands[148] (IPBES, 2023).

Figure 5.74: Average annual cost of invasive species (in 2017 $ mn)

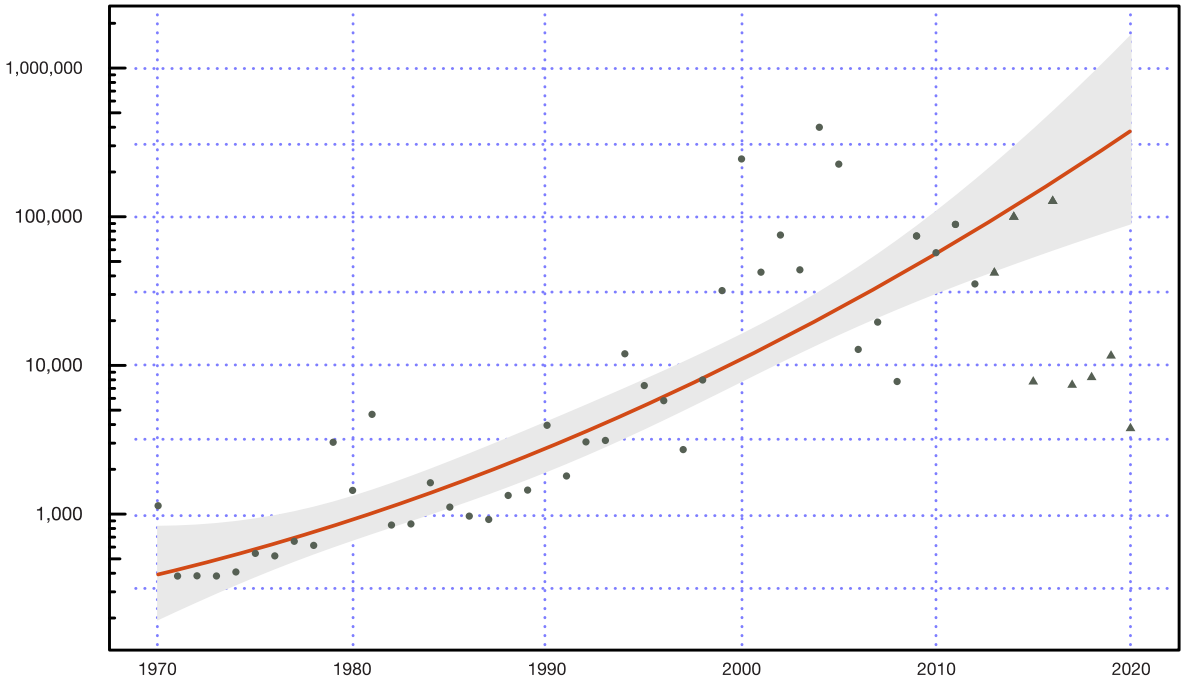


Source: IPBES (2023, figure 4.25, page 455).

Using the methodology and database developed by Diagne *et al.* (2021), IPBES (2023) estimated that the global annual economic cost of biological invasions amounted to $423 billion in 2019. Of these costs, 92% are due to the negative impacts of invasive alien species on nature's contribution to people or quality of life, while only 8% are related to the management of biological invasions. A significant proportion of these costs are attributed to reductions in food supply (66%), followed by impacts on human health, livelihoods, and water security. Notably, these costs have been observed to quadruple every decade (Figure 5.74). Over the past 50 years (1970–2019), the cumulative economic costs of biological invasions amount to $1.738 trillion when considering only the most reliable data (observed and high reliability). When potential and low-reliability costs are included, the total rises to $11.633 trillion (IPBES, 2023, Box 4.13, page 456).

[148] According to IPBES (2023, Figure SPM 3), 218 invasive alien species have caused 1 215 local extinctions of native species.

### Pollution

According to the IPBES glossary, "*pollution is the introduction of contaminants into the natural environment that cause adverse change*". This is a general definition that can lead to different interpretations. If we refer to the UN Data glossary, pollution is the "*presence of substances and heat in environmental media (air, water, land) whose nature, location, or quantity produces undesirable environmental effects*" and is the "*activity that generates pollutants*". A pollutant or contaminant is a substance present in concentrations that can harm organisms (humans, plants, and animals) or exceed an environmental quality standard. In this context, concentration is a critical factor, as pollution is typically associated with quantities that excess thresholds, leading to a reduction in quality of life. We generally distinguish between point source and non-point source pollution:

- Point source pollution comes from a single, identifiable source, such as a pipe, drain, or specific location. It is easier to monitor and control because the source is clearly identified.
- Non-point source pollution comes from multiple diffuse sources rather than a single point of origin. It is often carried into water bodies by rainfall, snowmelt, or runoff.

It's impossible to give an exact number of pollutants in the world because many pollutants can undergo chemical reactions to form different compounds in the environment, creating secondary pollutants, and new chemical compounds are constantly being created by industrial processes. Nevertheless, we can categorize pollutants in three main ways:

- By source:
  - Natural pollutants occur without human intervention, such as volcanic eruptions, forest fires, and natural decomposition processes;
  - Anthropogenic pollutants result from human activities, including industrial emissions, vehicle exhaust, and agricultural practices;
- By chemical composition:
  - Organic pollutants contain carbon-based compounds, such as pesticides, petroleum products, and plastic waste;
  - Inorganic pollutants lack carbon in their structure, including heavy metals (such as mercury and lead), mineral acids, and inorganic salts;
- Through environmental persistence:
  - Persistent pollutants remain in the environment for long periods of time without breaking down, such as certain pesticides, heavy metals, and some industrial chemicals;
  - Non-persistent pollutants break down relatively quickly through natural processes, such as many biological wastes and some air pollutants.

**Types of biodiversity pollution** Because there is a wide range of contaminants[149], pollution can also be divided into different categories. The eight major types of pollution are listed below:

[149]For example, the European Chemicals Agency has registered 26 865 unique chemical substances that can be placed on the European Economic Area market by companies with a valid registration as of November 2024 (https://echa.europa.eu/information-on-chemicals). In the United States, the non-confidential portion of EPA's Toxic Substances Control Act (TSCA) Inventory contains 86 770 chemicals, of which 42 377 are active as of May 2024 (www.epa.gov/tsca-inventory).

1. Air pollution
   According to the WHO glossary, "*air pollution is contamination of the indoor*[150] *or outdoor*[151] *environment by any chemical, physical or biological agent that modifies the natural characteristics of the atmosphere*". It can harm living organisms, damage the natural environment, or degrade air quality. Pollutants can be in the form of solid particles, liquid droplets, or gases, and can be either natural (such as volcanic ash) or man-made (such as industrial emissions). Air pollutants can be classified as particulate matter (such as $PM_{2.5}$, $PM_{10}$, ultrafine particles, and dust), primary pollutants (those emitted directly into the atmosphere, such as carbon monoxide CO, nitrogen oxides $NO_x$, and sulfur dioxide $SO_2$), and secondary pollutants (those formed in the air through chemical reactions, such as acid rain, aerosols and ozone $O_3$). Air pollution measurement is the assessment of air quality, or the concentration of pollutants in the air. This is done using ground-based stations or satellite-based monitoring (remote sensing). Measurements are typically expressed in terms of concentration (*e.g.*, milligrams per cubic meter) or parts per million/billion by volume (ppmv/ppbv).

2. Biological pollution
   Biological pollution refers to the introduction of harmful or invasive living organisms into an ecosystem where they do not occur naturally. It includes invasive species, the spread of pathogens, and biologically active agents (such as some genetically modified organisms (GMOs) or antibiotic-resistant microbes). Biological pollution often intersects with air, chemical, and water pollution. For example, nutrient runoff from fertilizers (chemical pollution) creates conditions for harmful algal blooms (biological pollution). Similarly, cholera is an example of biological pollution, because it involves the contamination of water with a pathogenic microorganism, the bacterium *Vibrio cholerae*.

3. Chemical pollution
   Chemical pollution refers to the release of harmful chemical substances into the environment — air, water, soil, or living organisms — causing adverse effects on ecosystems. Consequently, chemical pollution is often a component of other pollution categories: air pollution, plastic pollution, soil pollution, and water pollution. Given its significant impact and the serious challenges it poses to humanity, governments and the UN Environment Assembly (UNEA) are planning to establish a global intergovernmental science-policy panel on chemicals, waste, and pollution prevention. The number of chemical pollutants is unknown because there is no comprehensive inventory of chemical substances. However, Wang *et al.* (2020) estimated that more than 350 000 chemicals and chemical mixtures have been produced and synthesized by humans. Moreover, the global use of chemicals is expected to increase by 70% between 2020 and 2030 (Naidu *et al.*, 2021, page 2), with the largest growth anticipated in China, which is projected to account for nearly 50% of the global chemical market by 2030. Of course, not all chemicals are harmful and dangerous, but a large proportion are. For example, the European Environment Agency (EEA) estimates that about 60% of the total volume consumed in Europe is hazardous to health, and that 8% of deaths can be attributed to hazardous chemicals[152]. It is not easy to find a universally accepted classification of hazardous chemicals in the context of biodiversity. However, in the context of industrial activities, the Globally Harmonized System

[150] Contamination of the air inside a home or building, often caused by cooking, smoking, or poor ventilation. According to González-Martín *et al.* (2021), more than 5 million people die each year from diseases caused by indoor air pollution. The problem of exposure to indoor air pollution is growing as people spend more time indoors. In Europe, for example, people spend 90% of their time indoors.

[151] Pollution in the open air, often from industrial or vehicular sources.

[152] Source: `www.eea.europa.eu/en/topics/in-depth/chemicals`.

Box 5.17: Silent Spring by Rachel Carson (1962)

Silent Spring[a] is a landmark environmental book published in 1962 by Rachel Carson. It's considered one of the most influential environmental books ever written and is widely credited with launching the modern environmental movement. The book documents the harmful effects of pesticides on the environment and wildlife. Carson focused particularly on DDT, which was widely used after World War II. She showed how these chemicals not only harmed pests, but also accumulated in ecosystems, harming wildlife and humans. The book faced fierce opposition from the chemical industry, but captured widespread public attention and sparked debates about environmental health and the unregulated use of chemicals. It led to the eventual ban of DDT in the United States in 1972 and inspired stricter pesticide regulations worldwide.

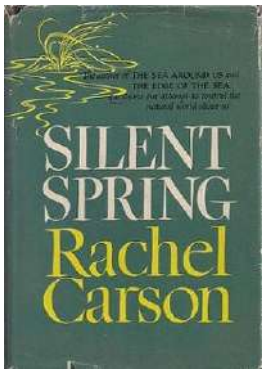


[a]The title refers specifically to the absence of birdsong in spring, traditionally a time when birds sing and nature comes back to life after winter.

of Classification and Labelling of Chemicals (GHS) is an internationally recognized system for classifying and communicating the hazards of chemical substances and mixtures. The GHS defines a set of nine hazard classes, such as flammables, oxidizers, corrosives, and acute toxins, and divides each class into categories based on the severity of the hazard (Table 5.49). Another approach to classifying hazardous chemicals is by the source of contamination. This classification helps to understand the origin of these chemicals and their potential impact on the environment:

- Industrial emissions
  These are chemicals released into the environment during industrial processes such as manufacturing, chemical production, and power generation. Common pollutants from industrial emissions include volatile organic compounds (VOCs), heavy metals (mercury, lead), persistent organic pollutants (POPs), and solvents, which can contaminate air, water, and soil.
- Agricultural runoff
  Agricultural activities contribute significantly to chemical pollution, especially through runoff of pesticides, herbicides, fertilizers (containing nitrates and phosphates), and animal waste. These chemicals are often washed into rivers and lakes when it rains, contaminating the water and harming aquatic life.

Table 5.49: Globally harmonized system of classification and labelling of chemicals (GHS) pictogram for hazardous substances

GHS01: Explosive

GHS02: Flammable

GHS03: Oxidizing

GHS04: Compressed gas

GHS05: Corrosive

GHS06: Fatal or toxic

GHS07: Low level toxicity

GHS08: Serious health hazard

GHS09: Hazardous to the environment

Source: https://unece.org/transport/dangerous-goods/ghs-pictograms.

- Household and municipal waste
  Household products, including cleaning products (containing solvents and disinfectants), pharmaceuticals, personal care products, paints, batteries, and plastics, contribute to pollution when disposed of improperly. Wastewater from homes and businesses can carry contaminants such as detergents, synthetic chemicals, and pharmaceuticals into sewage systems, which are not always fully treated before being released into the environment.
- Petroleum products
  Oil spills and runoff from petroleum-related activities are also sources of chemical pollutants. Petroleum products such as gasoline, diesel, and oils, can have a devastating effect on aquatic ecosystems, because they are toxic to marine life and persist in the environment for long periods of time.
- Transportation emissions
  Road vehicles, aircraft, and ships, especially those powered by fossil fuels, emit harmful pollutants such as nitrogen oxides ($NO_x$), sulfur dioxide ($SO_2$), carbon monoxide (CO), and particulate matter (PM) into the air. These pollutants contribute to air quality problems, acid rain, and human respiratory illnesses. Additionally, the particulate matter can affect soil and water quality.

An alternative to the previous classification is to divide hazardous chemicals into four categories[153]: conventional pollutants, heavy metals, persistent organic pollutants, and emerging

[153]In both classifications, a chemical may belong to more than one category.

contaminants. Conventional pollutants typically refer to pollutants that have been recognized and regulated for many years (*e.g.*, CO, $NO_x$, $SO_2$, PM). Heavy metals are a group of metallic elements that have a relatively high density and are toxic to humans and wildlife even at low concentrations. In biodiversity, a density greater than $5\,g/cm^3$ is used to define them. Examples of heavy metals hazardous to human health[154] include arsenic (As), cadmium (Cd), chromium (Cr), lead (Pb), and mercury (Hg). According to the Stockholm Convention on Persistent Organic Pollutants, POPs "*are organic chemical substances, that is, they are carbon-based. They possess a particular combination of physical and chemical properties such that, once released into the environment, they remain intact for exceptionally long periods of time (many years); they become widely distributed throughout the environment as a result of natural processes involving soil, water and, most notably, air; they accumulate in the living organisms including humans, and are found at higher concentrations at higher levels in the food chain; and they are toxic to both humans and wildlife.*" When this international environmental treaty was signed in 2001, 12 POPs were recognized and classified into 3 categories: pesticides (aldrin, chlordane, DDT, dieldrin, endrin, heptachlor, hexachlorobenzene HCB, mirex, toxaphene), industrial chemicals (hexachlorobenzene HCB, polychlorinated biphenyls PCB), and by-products (hexachlorobenzene HCB, polychlorinated dibenzo-p-dioxins PCDD and polychlorinated dibenzofurans PCDF, polychlorinated biphenyls PCB). The Stockholm Convention has been revised several times. As of December 2024, there are 32 POPs. The last category concerns emerging contaminants, which are chemical substances that are not commonly monitored or regulated, pose potential risks, and may be persistent. Examples of emerging contaminants include pharmaceuticals and personal care products (PPCP), endocrine-disrupting chemicals (EDC), micro and nanoplastics, antibiotic-resistant genes (ARG), among others (Wang *et al.*, 2024, Table 1, page 4). The challenge with emerging contaminants is tracking these substances and assessing the potential risks posed by novel chemical mixtures. For example, Escher *et al.* (2020) reported that "*the number of new chemicals is rising, with the Chemical Abstract Service Registry growing from 20 million to 156 million chemicals between 2002 and 2019*", which equates to approximately 20 000 new chemical products being synthesized every day.

4. Light pollution
   Light pollution is the presence of unwanted, excessive, misdirected, or obtrusive artificial light that interferes with the natural environment. It occurs when artificial lighting disrupts the natural darkness of the night[155], affecting processes such as wildlife migration, reproduction, and feeding. It is often the result of poor lighting design, over-illumination, or the scattering of light in the atmosphere. Only recently has light pollution been widely recognized as a significant threat to biodiversity and a growing environmental concern (Hölker *et al.*, 2010). Although the full effects of light pollution are not yet known, we now have a better understanding of how it affects ecosystems, species, and human health[156]. Some well-known examples

[154] Note that some metals are essential to human health in trace amounts, meaning that they are necessary for proper biological functions and play critical roles in enzymes, metabolism, immune functions, protein synthesis, etc. Typical examples include calcium (Ca), copper (Cu), iron (Fe), potassium (K), magnesium (Mg), and zinc (Zn). However, even essential metals can be toxic in excess.

[155] Longcore and Rich (2004) distinguished between '*astronomical light pollution*', which obscures the view of the night sky, and '*ecological light pollution*', which alters the natural light regime in terrestrial and aquatic ecosystems.

[156] See the special issue *Light Pollution* (Volume 380, Issue 6650) published by *Science* on June 16, 2023. Below is the introduction to this special issue:

> "*For most of history, the only lights made by humans were naked flames. Daily life was governed by the times of sunrise and sunset, outdoor nighttime activities depended on the phase of the Moon, and viewing the stars was a common and culturally important activity. Today, the widespread deployment of outdoor*

Box 5.18: Persistent organic pollutants

According to the Stockholm Convention on Persistent Organic Pollutants (Annex D, pages 74-75, 2023 version), the assessment of POPs focuses on four key properties[a]:

- Persistence
  The chemical must resist degradation by environmental processes and persist in the environment for long periods of time. In particular, its half-life must be greater than 2 months (60 days) in water or 6 months (180 days) in soil/sediment.
- Bioaccumulation
  The chemical must accumulate in the tissues of living organisms, and increases in concentration as it moves up the food chain (biomagnification). In particular, its bio-concentration factor (BCF) is greater than 5 000 or its log $K_{\text{ow}}$ ($n$-octanol-water partition coefficient) is greater than 5.
- Potential for long-range environmental transportation
  The chemical can travel long distances through air and water, affecting ecosystems far from its original source. In particular, its half-life in air must be greater than 2 days, which is equivalent to a distance of 690 km, assuming an average wind speed of 4 m/s (Scheringer *et al.*, 2012, page 384).
- Adverse effects
  The chemical has a significant level of toxicity or ecotoxicity.

Below we report figures of different chemicals, which has been collected by Scheringer *et al.* (2012, Supporting material):

| CAS | Chemical | Half-life | log $K_{\text{ow}}$ | Transportation | Toxicity |
|---|---|---|---|---|---|
| 50-29-3 | DDT | 289 | 6.85 | 3.11 | Yes |
| 53-19-0 | Mitotane | 130 | 5.87 | 2.46 | Yes |
| 57-74-9 | Chlordane | 1 440 | 6.24 | 2.12 | Yes |
| 95-94-3 | Tetrachlorobenzene | 86 | 4.61 | 130 | Yes |
| 118-74-1 | Hexachlorobenzene | 229 | 5.79 | 158 | Yes |
| 307-43-7 | Perflubrodec | 5 670 | 7.91 | $10^6$ | Yes |
| 307-45-9 | Perfluorodecane | 7 960 | 7.51 | $10^6$ | No |
| 2172-49-8 | Propionyl chloride | 192 | 6.45 | 2.13 | Yes |
| 3182-02-3 | Dichlorophenyl | 344 | 6.08 | 2.35 | Yes |
| 13947-96-1 | Trichloromethyl | 213 | 4.86 | 198 | Yes |
| 25267-15-6 | Polychloropinene | 4 410 | 8.09 | 10.80 | No |
| 27753-52-2 | Nonabrombiphenyl | 2 060 | 11.77 | 439 | Yes |

By applying the screening criteria of persistence, bioaccumulation, long-range transport potential and toxicity to a set of 93 144 organic chemicals, they identified 510 chemicals that exceed all four criteria and can be considered potential POPs. They also estimated that the number of potential POPs ranges from 190 (lower bound) to 1 200 (upper bound) chemicals.

[a] Source: www.pops.int.

include disorientation of sea turtles, bird migration, insect disruption, human sleep disturbance, metabolic disorders, and increased risk of some cancers (Walker *et al.*, 2020). Recently, Anderson *et al.* (2024) estimated that the annual loss of ecosystem service value due to light pollution is $3.4 trillion, which is about 3% of the total global value of ecosystem services and 3% of global GDP.

5. Noise pollution
   Noise pollution refers to unwanted, disturbing, or excessive[157] sounds that negatively affect the health and well-being of humans, animals, and the environment. It typically results from human activities and disrupts natural auditory environments. The emergence of noise pollution as a biodiversity threat precedes that of light pollution, with research studies dating back to the 1990s. However, as with light pollution, much remains to be learned about its full extent and long-term consequences. To date, the impacts of noise pollution are evident in both human health — such as hearing loss, sleep disturbance, mental health issues, and cognitive impairments — and wildlife — where it disrupts communication, leads to habitat abandonment, and interferes with pollination processes. Among these effects, marine noise pollution is a well-documented issue (Di Franco *et al.*, 2020; Solé *et al.*, 2023) because fish rely on sound for essential activities such as mating calls, territorial defense, predator alerts, and navigation during migration. Underwater communication is vital to their survival, but can be severely disrupted by shipping traffic, sonar noise and other anthropogenic sounds.

6. Plastic pollution
   Plastic pollution is the accumulation of plastic materials and particles in the environment. Plastics are a wide range of synthetic or semi-synthetic materials made from polymers derived from fossil fuels such as natural gas or petroleum. In general, plastic pollutants are categorized by size as nano-, micro-, or macro-debris. Plastics pose a critical environmental threat to wildlife through multiple mechanisms: direct physical harm through suffocation and entanglement, and chemical toxicity through leaching. A particularly insidious threat comes from micro-plastics — fragments smaller than 5 mm — which are readily ingested by both marine and terrestrial organisms. These particles not only accumulate throughout the food chain, but also act as vectors for concentrated toxins and pollutants. When ingested, they can trigger cascading health effects, compromising animals' immune systems, disrupting endocrine function and impairing reproductive capabilities, ultimately threatening species survival rates. Plastic pollution is pervasive and highly persistent in the environment due to slow natural degradation processes. This explains its widespread presence in diverse ecosystems around the world, including deserts, farms, mountaintops, oceans, and even Arctic snow (MacLeod *et al.*, 2021). Furthermore, plastic emissions are increasing and are projected to continue rising, even under optimistic waste reduction scenarios. Figure 5.75 shows the evolution of global thermoplastic production[158] since 1950 and its projections to 2050. In 1950 the production

*electric lighting means that the night is no longer dark for most people — few can see the Milky Way from their homes. Outdoor lighting has many legitimate uses that have benefited society. However, it often leads to illumination at times and locations that are unnecessary, excessive, intrusive, or harmful: light pollution.*" (Smith *et al.*, 2023).

[157] Unwanted sound refers to any unpleasant or disruptive noise. Disturbing sounds interfere with daily activities like sleeping, working, or communicating. Excessive sounds are those that are too loud or too frequent.

[158] It is difficult to obtain reliable figures on global plastics production because the definition of plastics is not standardized and because of double counting in production statistics. Thermoplastics are a type of plastic that becomes soft and malleable when heated and hardens when cooled. They account for about 85% of all plastics produced worldwide. The other major category of plastics is thermosets, which, unlike thermoplastics, cannot be

Figure 5.75: Global production of thermoplastics with projections, 1950–2050 (in Mt)

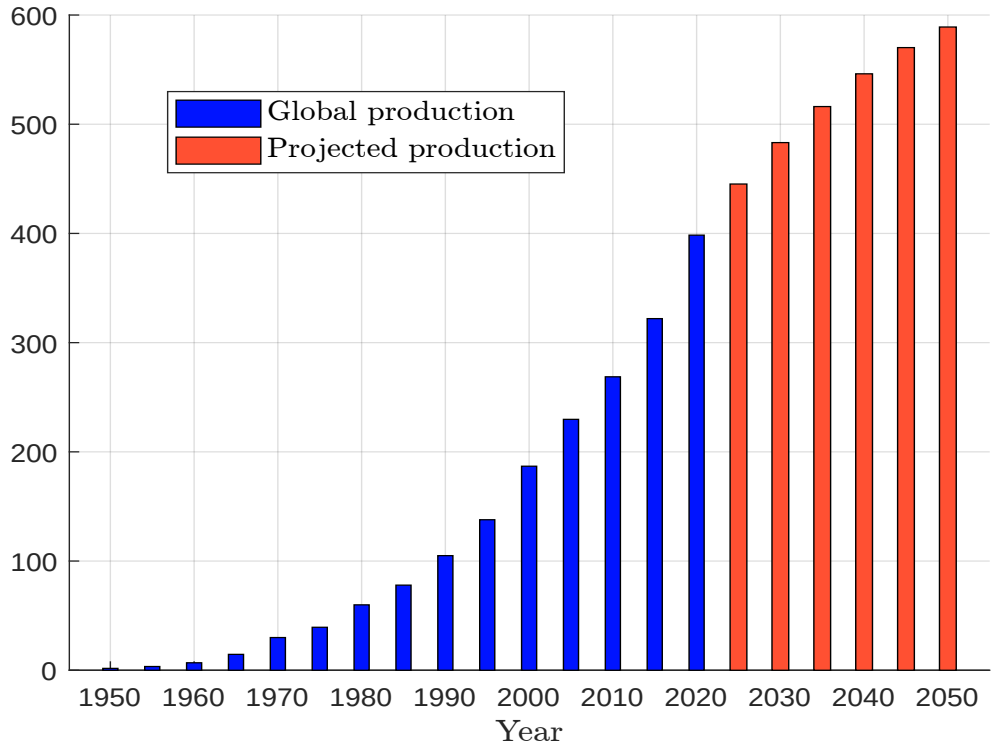


Source: www.iea.org/data-and-statistics/charts/production-of-key-thermoplastics-1980-2050.

was less than 2 million tonnes, in 2023 it was 414 million tonnes, and we expect a production of 590 million tonnes in 2050. The expected annual growth rate over the next 30 years is 1.3% — lower than the 4.6% annual growth observed over the past three decades, but still significant. This indicates that plastics production will continue to grow, making the search for solutions to establish a circular economy an ongoing and critical discussion. According to OECD (2022), approximately 25% of plastic waste is mismanaged, with a small fraction (less than 1%) eventually being transported into the oceans. This has led to the formation of garbage patches[159]. One of the best-known plastic accumulation zones is the Great Pacific Garbage Patch (GPGP), located in the subtropical waters between California and Hawaii. This patch covers an area of approximately 1.6 million square kilometers — comparable to the size of Mongolia or Iran. A study by Lebreton *et al.* (2018) estimated that at least 79 000 tonnes (ranging between 45 000 and 129 000 tonnes) of marine plastics are currently floating within the GPGP. Notably, over 75% of the mass of the GPGP consists of debris larger than 5 centimeters, with discarded fishing nets accounting for at least 46% of the total. While microplastics make up only 8% of the total mass, they account for a staggering 94% of the estimated 1.8 trillion (ranging from 1.1 to 3.6 trillion) pieces of plastic floating in the region. About 1 600 rivers are responsible for 80% of marine plastic pollution, which is estimated to be between 0.8 and 2.7 million tonnes of plastic waste discharged into the oceans annually (Meijer *et al.*, 2021). The top 10 plastic-emitting rivers are Pasig (Philippines), Tullahan (Philippines), Ulhas (India), Klang (Malaysia), Meycauayan (Philippines), Pampanga (Philip-

remelted once formed.

[159]Vast gyres of marine debris created by ocean currents and the increasing influx of plastic pollution from human activities

pines), Libmanan (Philippines), Ganges (India), Rio Grande de Mindanao (Philippines), and Agno (Philippines) (Meijer *et al.*, 2021, Table S5). As a result[160], Asia accounts for 81% of marine plastic pollution, followed by Africa (8%), South America (5.5%) and North America (4.5%).

7. Soil pollution
   Soil pollution (or soil contamination) is the presence or accumulation of toxic substances, harmful chemicals, salts, pathogens, or other contaminants in soil that adversely affect soil quality, reduce soil fertility, and pose risks to human health and ecosystems. The most common sources of soil pollution are industrial activities (*e.g.*, chemical pollutants, heavy metals, radioactive contaminants), agricultural practices (*e.g.*, soil degradation and the use of fertilizers, pesticides and herbicides), waste disposal and mining (*e.g.*, petroleum hydrocarbons, solvents). The impacts of soil pollution are many, but the most important are health risks, food security[161], ecosystem degradation and habitat loss. A typical example of soil pollution is the use of nitrogen-based products (*e.g.*, ammonium nitrate, ammonium sulfate) commonly found in fertilizers and pesticides. Stevens *et al.* (2004) and Clark and Tilman (2008) conducted extensive studies on the long-term effects of chronic, low-level nitrogen deposition in prairie grasslands. Their research showed that even modest nitrogen inputs significantly reduced plant species diversity over time by favoring nitrogen-tolerant species, ultimately disrupting ecological balance. These findings were further supported by Bobbink *et al.* (2010), whose comprehensive synthesis of the effects of nitrogen deposition on terrestrial plant diversity showed that excessive nitrogen inputs fundamentally alter soil chemistry. Their work showed that this change creates conditions that favor fast-growing species while reducing overall biodiversity in different ecosystems.

8. Water pollution
   Water pollution is the contamination of water bodies (*e.g.*, rivers, lakes, oceans, groundwater, and streams) by harmful substances that degrade water quality and make water unsafe for drinking, swimming, agriculture, and other uses. It occurs when pollutants such as chemicals, waste, or microorganisms are discharged into water systems without adequate treatment to remove harmful compounds. Water pollution also includes thermal (or heat) pollution, which occurs when hot water is discharged from industrial processes, raising water temperatures. This increase in temperature depletes oxygen levels and disrupts species adapted to cooler environments. This example shows that water pollution is not a single phenomenon, but comes in many forms. The same is true for other types of pollution. This diversity presents a challenge in accurately measuring pollution. For water pollution in particular, there are several ways to measure it. The five most common are: (1) pH level, which measures the acidity or alkalinity of water (normal readings range from 6.5 to 8.5); (2) biological oxygen demand (BOD), which measures the amount of oxygen required by microorganisms to break down organic matter (high BOD indicates high levels of organic pollution because microorganisms require more oxygen); (3) turbidity, which measures the presence of suspended solids such as silt, clay, or organic matter (high turbidity can harm aquatic organisms and block sunlight needed for photosynthesis); (4) dissolved oxygen (DO), which measures the amount of dissolved oxygen in

[160]The top 15 countries contributing to marine plastic pollution are the Philippines, India, Malaysia, China, Indonesia, Brazil, Vietnam, Bangladesh, Thailand, Nigeria, Turkey, Cameroon, Sri Lanka and Guatemala.

[161]For example, Zhang *et al.* (2015) emphasized that soil contamination by heavy metals is a major concern in China, posing a significant risk to food safety and public health. They found that 10.18% of farmland soils in China are polluted with heavy metals, primarily cadmium (Cd), mercury (Hg), copper (Cu), and Nickel (Ni). Furthermore, approximately 13.86% of grain production in China is potentially contaminated with heavy metals.

the water (low levels indicate organic pollution or high nutrient loading, which leads to oxygen depletion); and (5) nitrate and phosphate levels (excessive nutrients lead to eutrophication, which causes algal blooms and oxygen depletion). However, this list is far from exhaustive. For example, Syeed *et al.* (2023) list a total of 69 water quality parameters (6 biological indicators, 10 physical indicators, and 53 chemical indicators[162]) as represented in Figure 5.76.

Figure 5.76: Taxonomy of the 69 water quality parameters along their natural factors (biological, physical, chemical)

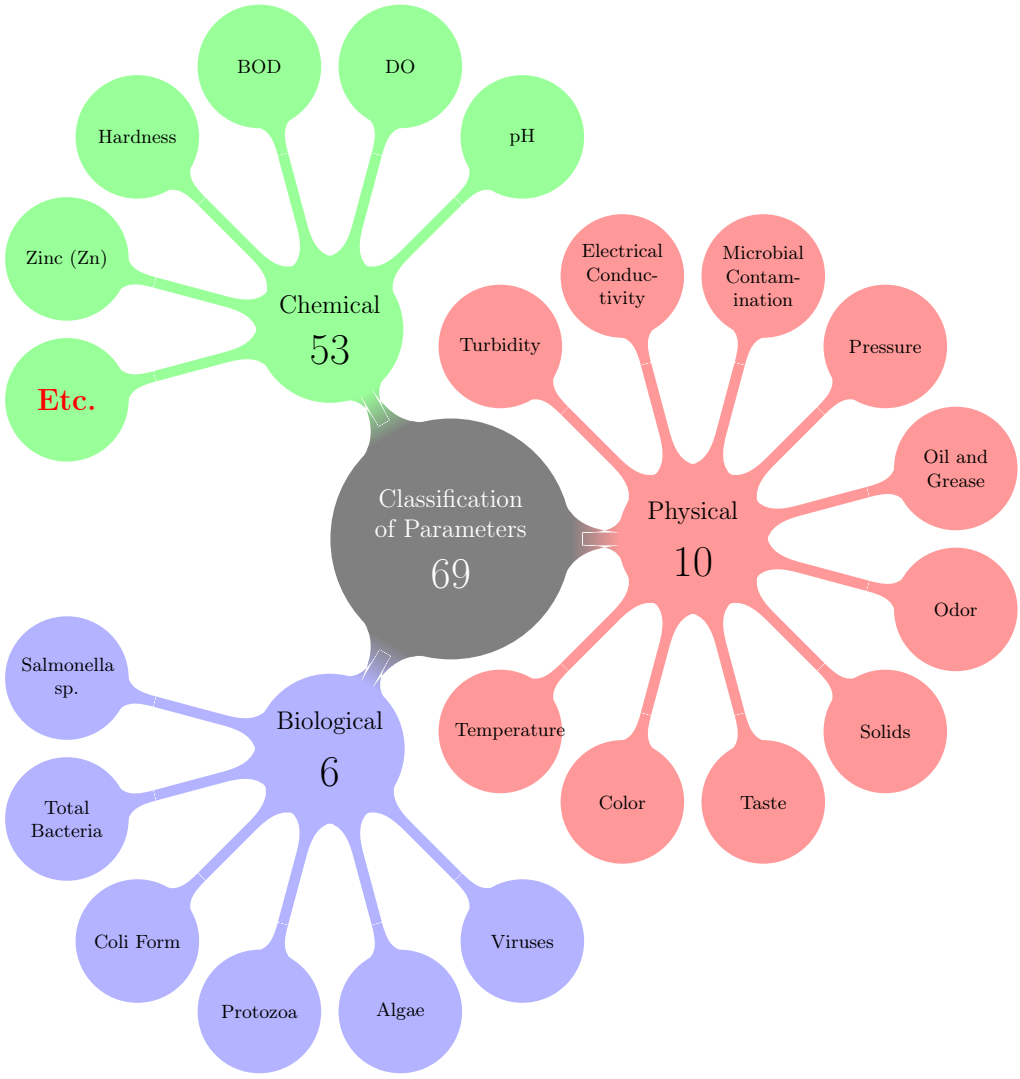


Source: Syeed *et al.* (2023, Figure 5, page 7).

[162]The 53 chemical measures are pH, total dissolved solid (TDS), oxidation-reduction potential (ORP), dissolved oxygen (DO), ammonia ($NH_3$), colored dissolved organic matter, Sulphide ($S^{2-}$), chemical oxygen demand (COD), biochemical oxygen demand (BOD), chloride ($Cl^-$), nitrate ($NO_3^-$), salinity, tryptophan ($C_{11}H_{12}N_2O_2$), bicarbonate ($NaHCO_3$), alkalinity ($HCO_3^-$), total hardness as $CaCO_3$, arsenic (As), zinc (Zn), phosphate ($PO_4^{3-}$), chlorine (Cl), fluoride ($F^-$), aluminum (Al), chromium (Cr), copper (Cu), iron (Fe), nitrogen (N) total, potassium (K), organic matter by $KMnO_4$, barium (Ba), carbonate ($HCO_3^-$), chromium hexavalent (Cr(VI)), hydrocarbons ($C_nH_{2n+2}$), sulfate ($SO_4^{2-}$), hydrogen sulphide as $H_2S$, beryllium (Be), dissolved organic carbon (DOC), silver (Ag), phosphorus (P), carbon tetrachloride ($CCl_4$), iodine (I), tin (Sn), Boron (B), manganese (Mn), mercury (Hg), nickel (Ni), selenium (Se), lead (Pb), cyanide ($CN^-$), pesticides, nitrogen (N), cadmium (Cd), calcium (Ca) and sodium (Na).

Box 5.19: Environmental toxicology and ecotoxicology

The study and assessment of pollution impacts fall under the disciplines of environmental toxicology and ecotoxicology. Environmental toxicology primarily focuses on how toxic substances — such as pollutants, chemicals, heavy metals, and pesticides — affect humans, animals, plants, and other living organisms. It also investigates the mechanisms by which these contaminants enter the environment, their distribution, and how they are metabolized or eliminated by organisms. Ecotoxicology, while closely related, is more concerned with studying pollution at the ecosystem level rather than focusing on individual organisms. It examines how contaminants affect populations, communities, and ecological processes. Despite this distinction, there is considerable overlap between the two fields. For instance, two foundational textbooks *Environmental Toxicology* (Wright and Welbourn, 2002) and *Fundamentals of Ecotoxicology* (Newman, 2019) cover substantially similar content and concepts.

**Dose-response relationship** The dose-response model[163] describes how the amount of a contaminant (dose) affects health or environmental outcomes (response). Toxicologists use this model to understand how different doses of pollutants cause different levels of harm.

Figure 5.77: Sigmoidal dose-response curve

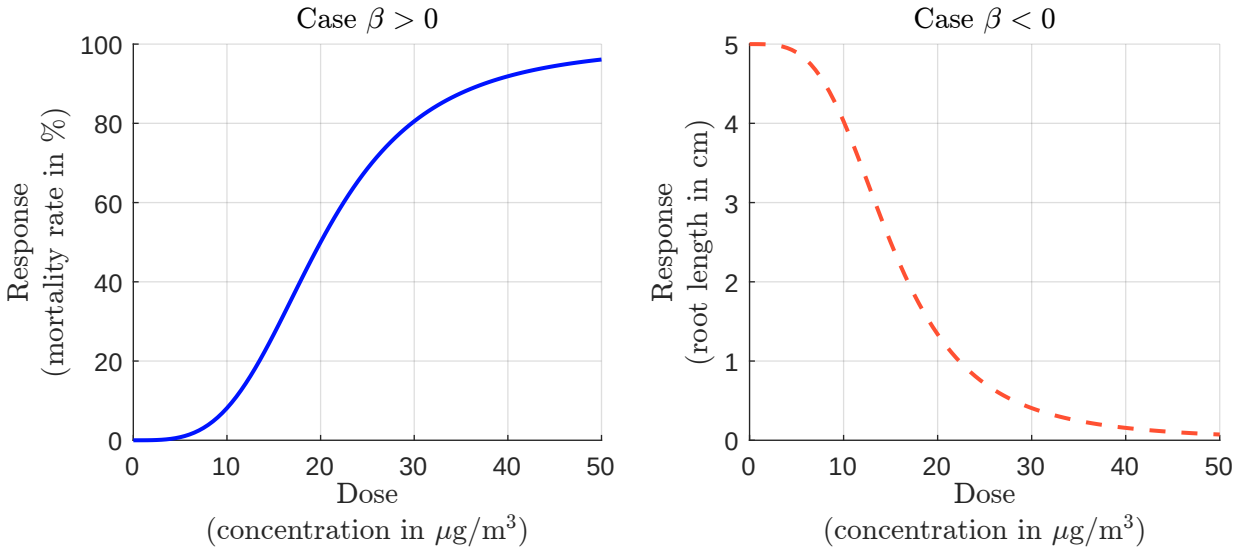


Figure 5.77 shows a typical dose-response curve, with the applied dose plotted on the $x$-axis and the observed response plotted on the $y$-axis. The curve is generally sigmoidal in shape and can be classified into two distinct forms depending on the nature of the response:

- Increasing response
  In this form, the response increases with the concentration of the substance. For example, mortality rates may increase with increasing levels of air, soil, or water pollution.

[163] In the scientific literature, this relationship is also known as the concentration-response relationship or exposure-response relationship. The World Health Organization (WHO) and the European Environment Agency (EEA) use the term concentration-response function (CRF).

- Decreasing response
  In this form, the response decreases with increasing concentration. For example, physical characteristics such as production levels, weight, or height may decrease in response to increasing levels of air, soil, or water pollution.

According to Ritz *et al.* (2015), the (generalized) log-logistic function is the most commonly dose-response model[164]:

$$y = f\left(x; \alpha, \beta, y_{\min}, y_{\max}\right) = y_{\min} + \frac{y_{\max} - y_{\min}}{1 + \exp\left(-\beta\left(\ln\left(x\right) - \ln\left(\alpha\right)\right)\right)} = y_{\min} + \frac{y_{\max} - y_{\min}}{1 + \left(\frac{x}{\alpha}\right)^{-\beta}} \tag{5.29}$$

where $x \geq 0$ is the concentration rate of the dose, $y \in (y_{\min}, y_{\max})$ is the response, $\alpha > 0$ is the scale parameter, and $\beta \in \mathbb{R}$ is the shape parameter. If $\beta > 0$, the dose-response curve is increasing, otherwise it is decreasing[165]. The second popular function is the log-normal model:

$$y = y_{\min} + \left(y_{\max} - y_{\min}\right) \Phi\left(\beta \ln\left(\frac{x}{\alpha}\right)\right) \tag{5.30}$$

Ritz (2010, Table 1, page 226) listed another class of dose-response model based on the Weibull distribution[166]:

$$y = y_{\min} + \left(y_{\max} - y_{\min}\right) \exp\left(-\left(\frac{x}{\alpha}\right)^{\beta}\right) \tag{5.32}$$

The three previous classes of models ignore the hormesis phenomenon, where a substance or environmental factor produces opposite effects at low and high doses. Specifically, the substance may have a stimulatory effect at low doses, while the same substance becomes toxic at high doses. To account for hormesis, a popular approach is to include a bump term in the log-logistic model:

$$y = y_{\min} + \frac{y_{\max} - y_{\min} + \gamma g\left(x\right)}{1 + \left(\frac{x}{\alpha}\right)^{-\beta}} \tag{5.33}$$

where $\gamma \geq 0$ and $g\left(x\right)$ is the bump function. In the Brain-Cousens model, $g\left(x\right) = x$, whereas in the Cedergreen-Ritz-Streibig model, $g\left(x\right) = \exp\left(-x^{-\eta}\right)$ (Cedergreen *et al.*, 2005). Figure 5.78 shows the different dose-response models and the biological phenomenon of hormesis. The parameters are $\alpha = 20$, $\beta = -3.5$, $y_{\min} = 0$, $y_{\max} = 5$. The Brain-Cousens model uses $\gamma = 0.2$, while the parameters of the Cedergreen-Ritz-Streibig model are $\gamma = 3$ and $\eta = 0.4$. An example of hormesis in biodiversity toxicology is provided by Eze *et al.* (2021), who analyzed 15 plant species to assess their tolerance to diesel fuel toxicity. The dose-response analysis showed that increasing diesel fuel concentrations in soil generally resulted in a consistent decrease in biomass for 13 species. However, the study found that hydrocarbons had a statistically significant hormetic effect on alfalfa (*Medicago sativa*), where low concentrations of diesel fuel stimulated growth, but higher concentrations resulted in a decrease in biomass. Carbon monoxide and oxygen are other examples of hormesis. Similarly, radiation hormesis refers to the hypothesis that low doses of ionizing radiation may induce beneficial biological effects, such as enhanced DNA repair mechanisms or improved immune system function. However, while the concept of radiation hormesis is intriguing and has supporting data, it remains controversial, particularly in public health and regulatory contexts (Calabrese and Mattson, 2017).

[164] The log-logistic probability distribution corresponds to $y_{\min} = 0$, $y_{\max} = 1$ and $\beta > 0$.

[165] The increasing dose-response curve in Figure 5.77 was generated using the following set of parameters: $\alpha = 20$, $\beta = 3.5$, $y_{\min} = 0$ and $y_{\max} = 100$. The decreasing dose-response curve uses $\alpha = 15$, $\beta = -3.5$, $y_{\min} = 0$ and $y_{\max} = 5$.

[166] This model is called Weibull-1 and generates an increasing response. To model a decreasing response, we consider the Weibull-2 function:

$$y = y_{\min} + \left(y_{\max} - y_{\min}\right)\left(1 - \exp\left(-\left(\frac{x}{\alpha}\right)^{\beta}\right)\right) \tag{5.31}$$

Figure 5.78: Hormesis biological phenomenon

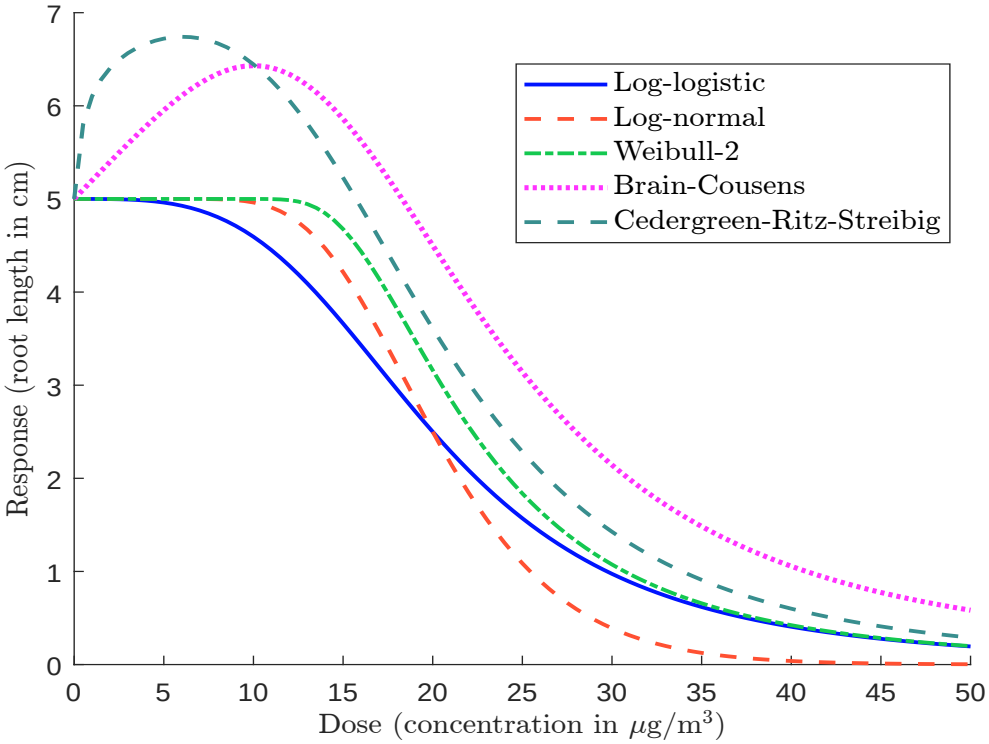


It is clear that a dose-response model can be thought of as a nonlinear regression model, where the dependent variable $y$ represents the response or effect, and the independent variable $x$ is the dose or concentration. In general, different types of response are distinguished: (1) continuous response (measures a continuous variable, such as biomass); (2) binary response (measures the presence or absence of a specific event, such as dead/alive); (3) time-to-response (measures the time it takes for a response to occur after exposure to a dose, such as the time to onset of toxicity after exposure to a chemical); (4) discrete or categorical response (the response falls into one of several ordered categories, such as none, mild, moderate, or severe effects). From a dose-response model where the response is the percentage of individuals who respond to a given dose of a drug, we can calculate the statistic $\text{ED}_p$, which is the dose required to achieve the desired therapeutic effect in $p\%$ of the population. When $p = 50\%$, we obtain the median effective dose, $\text{ED}_{50}$, which is the dose of the drug that produces the therapeutic response in 50% of the population. $\text{ED}_{50}$ is a standard statistic in pharmacology. By analogy, we can define the median toxic dose $\text{TD}_{50}$ and the median lethal dose $\text{LD}_{50}$, which represent the dose at which 50% of the population will experience a specific toxic effect or die, respectively. When the dose refers to the concentration of a pollutant or chemical, we use the terms half-maximal effective concentration $\text{EC}_{50}$ or half-lethal concentration $\text{LC}_{50}$ instead. In the log-logistic and log-normal models, the median effective concentration corresponds to the parameter $\alpha$ of the function[167]:

$$y = \frac{y_{\max} + y_{\min}}{2} \Leftrightarrow x = \text{EC}_{50} = \alpha$$

[167]Notice that $\frac{y_{\max} + y_{\min}}{2} = y_{\min} + \frac{y_{\max} - y_{\min}}{2}$. This implies that $\left(\frac{x}{\alpha}\right)^{-\beta} = 1$ in the case of the log-logistic model and $\Phi\left(\beta \ln\left(\frac{x}{\alpha}\right)\right) = \frac{1}{2}$ in the case of the log-normal model.

This result is not surprising because dose-response curves are related to the famous Hill equation[168] (Goutelle *et al.*, 2008):

$$E = E_0 + (E_{\max} - E_0)\frac{[C]^n}{\mathrm{EC}_{50}^n + [C]^n}$$

where $E$ is the effect produced by the drug/agonist at concentration $[C]$, $E_0$ is the baseline response, $E_{\max}$ is the maximum effect, $\mathrm{EC}_{50}$ is the concentration that produces half the maximum effect, and $n$ is the Hill coefficient (or the slope of the curve).

Figure 5.79: Threshold concentration

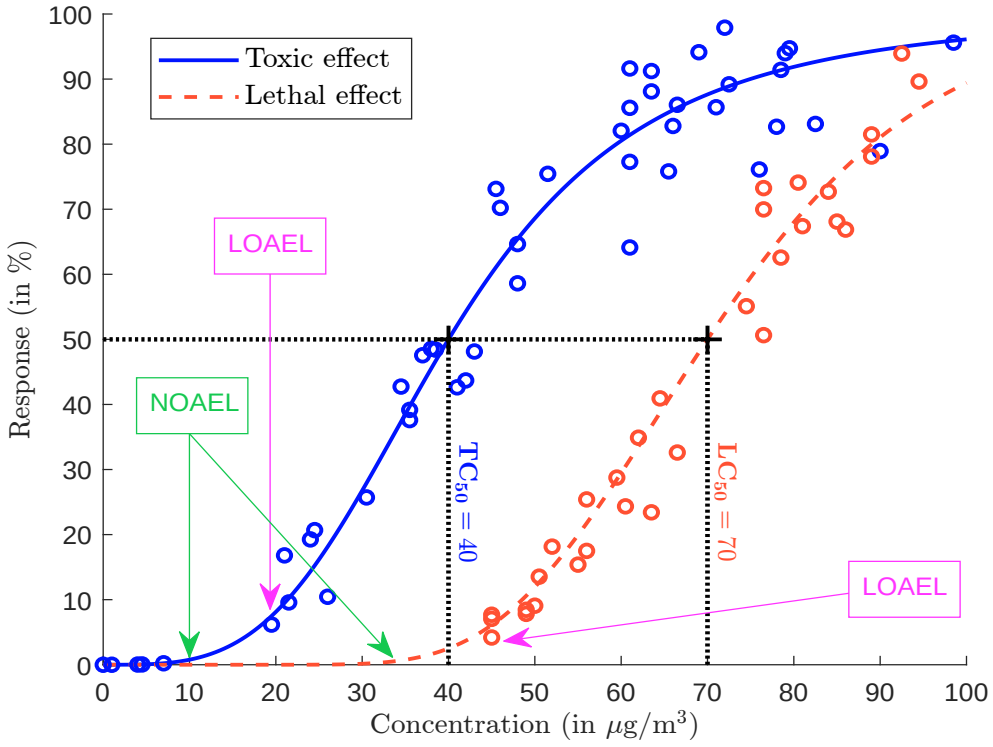


Because dose-response curves help identify relationships between exposure levels and effects, they are widely used to set safe exposure limits (threshold concentrations) to prevent adverse health outcomes in humans and adverse effects on the environment. For instance, the World Health Organization has developed a dose-response framework to measure the risk of chemicals on health (World Health Organization, 2009). Similarly, in 2021, the US Environmental Protection Agency (EPA) published tabulated dose-response assessments for both chronic and acute exposures to air pollutants[169]. The European Union has long used dose-response curves linking traffic noise to annoyance and sleep disturbance to inform and shape public policy on noise pollution mitigation. To understand how thresholds and safe exposure limits are set, let's examine the dose-response curves in

[168] We have:

$$\frac{E - E_0}{E_{\max} - E_0} = \frac{1}{1 + \left(\frac{[C]}{\mathrm{EC}_{50}}\right)^{-n}}$$

and we identify the parameters of the log-logistic dose-response model: $\alpha = \mathrm{EC}_{50}$, $\beta = n$, $y_{\min} = E_0$, and $y_{\max} = E_{\max}$.

[169] Tables with values for long-term (chronic) inhalation and oral exposure and values for short-term (acute) inhalation exposure are available at www.epa.gov/fera/dose-response-assessment-assessing-health-risks-associated-exposure-hazardous-air-pollutants.

Figure 5.79. The figure shows two functions: one that measures toxicity and another that measures mortality. From these curves, we can determine critical values including $TC_{50}$ and $LC_{50}$, as well as two key regulatory statistics:

- NOAEL (no observed adverse effect level) represents the highest dose or concentration at which no adverse effects are observed. This metric is fundamental to establishing maximum safe exposure levels for humans and ecosystems, as it indicates the threshold below which a substance demonstrates no harmful effects.
- LOAEL (lowest observed adverse effect level) is the lowest dose or concentration at which adverse effects are first observed. This measure helps policymakers identify the point at which a substance begins to pose a risk.

Figure 5.79 illustrates NOAEL and LOAEL values for both toxic and lethal effects. For toxicity, the data shows a NOAEL of $10\,\mu g/m^3$ and a LOAEL of $20\,\mu g/m^3$, suggesting a potential threshold concentration of $10\,\mu g/m^3$. In contrast, if mortality alone is considered, the threshold concentration could be set as high as $40\,\mu g/m^3$. In practice, the setting of threshold concentrations involves several considerations. While theoretical best practice suggests using the NOAEL as the threshold, regulatory agencies often default to the LOAEL. To ensure adequate protection for vulnerable populations — including children, elderly individuals, and those with pre-existing health conditions — authorities often apply safety factors to these baseline values. The final threshold concentration is then calculated by dividing either the NOAEL or LOAEL by the appropriate safety factor.

**Remark 62** *In the case of pollution, safe exposure limits are set primarily in terms of toxic effects. In the case of medicine and pharmacology, agencies use both therapeutic effects, toxic effects, and lethal effects, i.e., there is a trade-off between benefits and risks.*

**Application to air quality standards** The previous framework has been extensively used to set air quality standards. In 2000, the World Health Organization published a report entitled "*Guidelines for Air Quality*". This report has been updated twice, in 2006 and 2021 (World Health Organization, 2006, 2021). The purpose of these reports is to provide recommended limits for key air pollutants to protect public health. The methodology is based on the concentration-response function (CRF), which is another term for the dose-response relationship. In Table 5.50, we present the WHO air quality guidelines (AQG), which represent the concentration levels of pollutants below which adverse health effects are expected to be minimal (World Health Organization, 2021). For example, the AQG level for particulate matter[170] $PM_{2.5}$ is $5\,\mu g/m^3$ on an annual basis. We have also included air quality standards for several regions and countries (Brazil, China, EU, India, US, and Switzerland), which generally correspond to the limit values established to protect human health. For a long time, air quality standards in Europe were governed by Directive 2008/50/EC. Since October 2024, the EU has introduced a new directive (2024/2881) that sets limit values for the year 2030. It is important to note that the limit values depend on the time period, but they can also vary depending on the objective. For example, there are different limits for the protection of human health, vegetation, and ecosystems. In the United States, limits are set under the Clean Air Act, which was last amended in 1990. For some pollutants, two separate standards are set: primary standards (which focus on protecting the health of sensitive populations, such as asthmatics, children, and the elderly) and

[170] Particulate matter consists of microscopic particles of solid or liquid substances suspended in the air. They are generally divided into three categories. Inhalable coarse particles, designated $PM_{10}$, are particles with a diameter of $10\,\mu m$ or less. Fine particles, designated $PM_{2.5}$, are particles with a diameter of $2.5\,\mu m$ or less. Finally, ultrafine particles (UFP) are particles with a diameter of $100\,nm$ or less.

Table 5.50: Air quality standards (limit values for the protection of human health)

| Pollutant | Symbol | Unit | Period | WHO | EU | | US | China | India | Brazil | Switzerland |
|---|---|---|---|---|---|---|---|---|---|---|---|
| | | | | 2021 | 2008 | 2030 | 1990 | 2012 | 2009 | 1990 | 2024 |
| Particulate matter | $PM_{2.5}$ | $\mu g/m^3$ | Annual | 5 | 25 | 10 | 9/15 | 15/35 | 40 | | 10 |
| | | | 24-hour | 15 | | 25 | 35 | 35/75 | 60 | | |
| | $PM_{10}$ | | Annual | 15 | 40 | 20 | | 40/70 | 60 | | 20 |
| | | | 24-hour | 45 | 50 | 45 | 150 | 50/150 | 100 | | 50 |
| Ozone | $O_3$ | $\mu g/m^3$ | Peak-season | 60 | | | | | | | |
| | | | 8-hour | 100 | 120 | 120 | 137 | 100/160 | 100 | | |
| Nitrogen dioxide | $NO_2$ | $\mu g/m^3$ | Annual | 10 | 40 | 20 | 100 | 40 | 30/40 | 100 | 30 |
| | | | 24-hour | 25 | | 50 | | 80 | 80 | | 80 |
| | | | 1-hour | 200 | 200 | 200 | 188 | 200 | | 190/320 | |
| Sulfur dioxide | $SO_2$ | $\mu g/m^3$ | Annual | | | 20 | 26 | 20/60 | 20/50 | 40/80 | 30 |
| | | | 24-hour | 40 | 125 | 50 | | 50/150 | 80 | 100/365 | 100 |
| | | | 1 hour | | 350 | 350 | 196 | 150/500 | | | |
| | | | 10-minute | 500 | | | | | | | |
| Carbon monoxide | CO | $mg/m^3$ | 24-hour | 4 | | 4 | | 4 | | | 8 |
| | | | 8-hour | 10 | 10 | 10 | 10 | | 2 | 10 | |
| | | | 1-hour | 35 | | | 40 | 10 | 4 | 40 | |
| | | | 15-minute | 100 | | | | | | | |
| Lead | Pb | $\mu g/m^3$ | Annual | 0.5 | 0.5 | 0.5 | | 0.5 | 0.5 | | |
| | | | 3-month | | | | 0.15 | | | | |
| Amonia | $NH_3$ | $\mu g/m^3$ | Annual | | | | | | 100 | | |
| Arsenic | As | $ng/m^3$ | Annual | 6.6 | 6 | 6 | | | 6 | | |
| Benzene | $C_6H_6$ | $\mu g/m^3$ | Annual | 1.7 | 5 | 3.4 | | | 5 | | |
| Benzo[a]pyrene | BaP | $ng/m^3$ | Annual | 0.12 | | 1 | | 1 | 1 | | |
| Cadmium | Cd | $ng/m^3$ | Annual | 5 | 5 | 5 | | | | | |
| Nickel | Ni | $ng/m^3$ | Annual | 25 | 20 | 20 | | | 20 | | |
| Total suspended particles | TSP | $\mu g/m^3$ | Annual | | | | | 80/200 | | 60/80 | |

Source: World Health Organization (2021, Tables 0.1 & 0.2, pages xvii-xviii), Directive 2008/50/EC (https://eur-lex.europa.eu/eli/dir/2008/50/oj), EU Directive 2024/2881 (https://eur-lex.europa.eu/eli/dir/2024/2881/oj), NAAQS Table (www.epa.gov/criteria-air-pollutants/naaqs-table), www.transportpolicy.net/topic/air-quality-standards (Brazil, China and India), Switzerland OAPC (www.fedlex.admin.ch/eli/cc/1986/208_208_208) & Author's calculations.

secondary standards (which focus on protecting the welfare of the public, including animals, crops, vegetation, and buildings). In China, India, and Brazil, air quality standards may also include two separate limits. The first generally applies to special regions, such as national parks and protected areas, while the second applies to all other areas.

**Remark 63** *Similar figures are established for other quality standards (e.g., noise pollution, soil pollution, water pollution), but they are less comprehensive than those for air quality*[171].

**Air quality index** An air quality index (AQI) is a standardized system used to communicate air quality to the public in an understandable way. It provides a single number that indicates the level of air pollution and its potential impact on health. The concept of air quality indices was first developed by academics in the 1950s and later adopted by environmental agencies, typically at the federal, provincial, or municipal level, in the 1960s and 1970s (Ott and Thorn, 1976; Ott, 1978). The first country-wide AQI systems were introduced in Canada (1970) and the United States (1976), followed by several European countries in the 1980s. Today, most countries have established their own air quality index systems. While these systems share some common features and have become more consistent over time, they are still not uniform. They often differ in the pollutants measured, the critical thresholds used, and, most importantly, the scales on which their indices are reported, making cross-country comparisons difficult. For example, Canada's AQI scale ranges from 1 to 10+, while China's ranges from 0 to 500. In Europe, the index typically ranges from 0 to 100+, and in Australia from 0 to 200+. These variations highlight the difficulties of harmonizing AQI systems across regions, despite their common goal of informing and protecting public health. The World Health Organization has published numerous guidelines to harmonize standards and reduce disparities between countries. However, we are still far from a single global AQI system. Nevertheless, several initiatives are helping to compare air quality indices across countries. One of the most prominent is the World Air Quality Index project (`aqicn.org` and `waqi.info`), which collects data from government monitoring stations in over 100 countries.

Although there is no globally harmonized AQI system, the one developed by the US EPA is undoubtedly one of the most widely used and has served as a model for many other countries' AQI frameworks. For example, the US AQI system is also used by the World Air Quality Index project. The US AQI is calculated based on five key pollutants: carbon monoxide (CO), nitrogen dioxide ($NO_2$), ground-level ozone ($O_3$), particulate matter ($PM_{10}$ and $PM_{2.5}$), and sulfur dioxide ($SO_2$). For each pollutant, a sub-index is calculated based on its concentration:

$$I_j = I_{j,\text{low}} + \left( \frac{[C_j] - [C_j]_{\text{low}}}{[C_j]_{\text{high}} - [C_j]_{\text{low}}} \right) (I_{j,\text{high}} - I_{j,\text{low}}) \tag{5.34}$$

where $j$ represents the pollutant, $[C_j]$ is the concentration of the pollutant in the air, $[C_j]_{\text{low}}$ and $[C_j]_{\text{high}}$ are the breakpoints for the concentration range, and $I_{j,\text{low}}$ and $I_{j,\text{high}}$ are the sub-index values corresponding to the low and high breakpoints, respectively. The overall Air Quality Index (AQI) is then calculated as the maximum of the sub-indices for all pollutants:

$$\text{AQI} = \max_j I_j$$

[171] In Canada, these figures are available on the CCME website (`https://ccme.ca/en/summary-table`), where users can select a chemical and obtain the following limits: Water Quality Guidelines for the Protection of Agriculture; Sediment Quality Guidelines for the Protection of Aquatic Life; Soil Quality Guidelines for the Protection of Environmental and Human Health; Tissue Residue Quality Guidelines for the Protection of Wildlife Consumers of Aquatic Biota; Groundwater Quality Guidelines for the Protection of Environmental and Human Health.

Table 5.51: US AQI categories

| Category | AQI band | Levels of concern | Daily AQI color |
|---|---|---|---|
| 1 | 0 to 50 | Good | Green |
| 2 | 51 to 100 | Moderate | Yellow |
| 3 | 101 to 150 | Unhealthy for sensitive groups | Orange |
| 4 | 151 to 200 | Unhealthy | Red |
| 5 | 201 to 300 | Very unhealthy | Purple |
| 6 | 301 and higher | Hazardous | Maroon |

Source: US EPA (2024, Tables 1 and 5, paged 3–12).

Since the highest breakpoint is typically 500, each sub-index is mapped to a score between 0 and 500. Once calculated, the sub-index is assigned to one of six categories, each represented by a specific color that indicates the health risk posed by the level of air pollution (Table 5.51). For instance, if the sub-index is less than 50, the category is good and the color is green, meaning that air quality is satisfactory, air pollution poses little or no risk, and it's great to be active outside. If the sub-index is between 101 and 150, members of sensitive groups may experience health effects and need to limit outdoor activity, while the general public is less likely to be affected.

To understand how the air quality index is calculated, we consider an example with particulate matter $PM_{2.5}$. Below we report the breakpoints $[C_j]_{\text{low}}$ and $[C_j]_{\text{high}}$ for the concentration range, and the values $I_{j,\text{low}}$ and $I_{j,\text{high}}$ of the corresponding AQI band[172]:

| AQI category | 1 | 2 | 3 | 4 | 5 | 6 |
|---|---|---|---|---|---|---|
| $[C_j]_{\text{low}}$ (in µg/m$^3$) | 0.0 | 9.1 | 35.5 | 55.5 | 125.5 | 225.5 |
| $[C_j]_{\text{high}}$ (in µg/m$^3$) | 9.0 | 35.4 | 55.4 | 125.4 | 225.4 | 500.4 |
| $I_{j,\text{low}}$ | 0 | 51 | 101 | 151 | 201 | 301 |
| $I_{j,\text{high}}$ | 50 | 100 | 150 | 200 | 300 | 500 |

Suppose we have a 24-hour $PM_{2.5}$ value of 27.4 µg/m$^3$. This value falls into the second AQI category, those concentration values that are above 9.1 and below 35.4. Applying Equation (5.34) gives:

$$I_{PM_{2.5}} = 51 + \left(\frac{27.4 - 9.1}{35.4 - 9.1}\right)(100 - 51) = 85.0951$$

A 24-hour $PM_{2.5}$ value of 27.4 µg/m$^3$ then corresponds to an air quality index of 85. Figure 5.80 shows the piecewise function (5.34) applied to particulate matter $PM_{2.5}$ and the corresponding AQI colors.

Figure 5.81 illustrates the AQI levels for particulate matter $PM_{2.5}$ in 2024 across four cities: New Delhi, Beijing, Paris, and Montreal. The data show significant disparities in air quality between these cities. In particular, New Delhi experienced 175 days with an AQI above 150, compared to 41 days in Beijing. In contrast, the maximum AQI value observed in Paris and Montreal was 113 and 104, respectively. In 2024, the average AQI values for these cities were 164 (New Delhi), 91 (Beijing), 49 (Paris), and 31 (Montreal). This indicates that Paris was more polluted than Montreal, as Paris had 136 days with an AQI above 50, while Montreal reported only 44 such days.

[172]Source: US EPA (2024, Table 6, page 14).

Figure 5.80: US air quality index for particulate matter $PM_{2.5}$

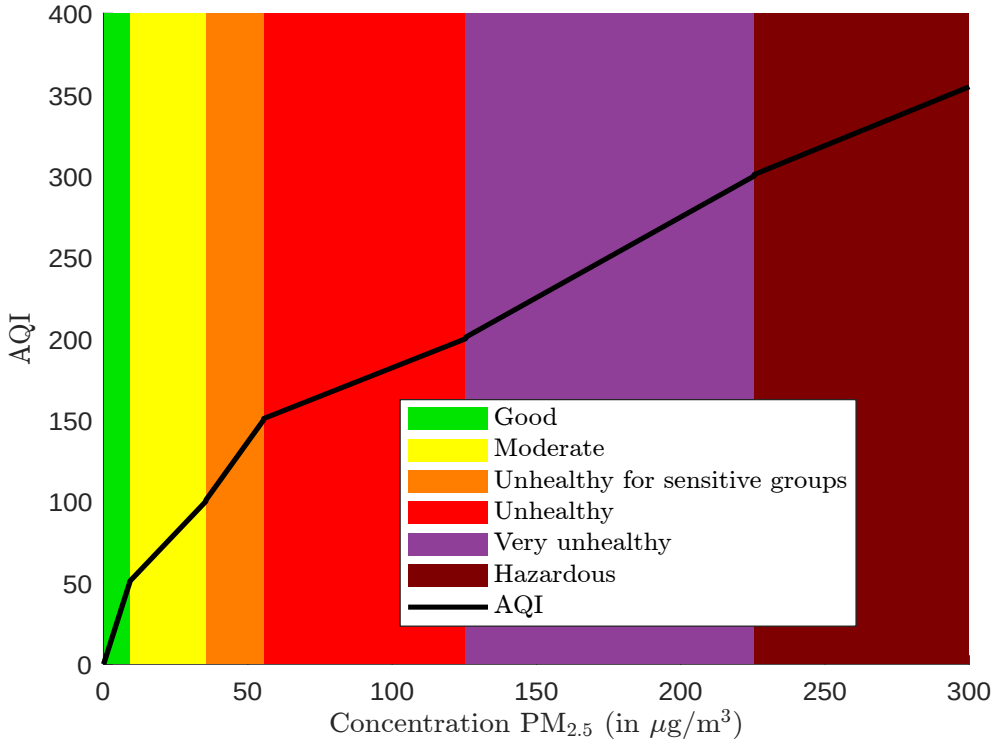


Source: US EPA (2024) & Author's calculations.

Figure 5.81: 2024 AQI $PM_{2.5}$ values in New Delhi, Beijing, Paris, and Montreal

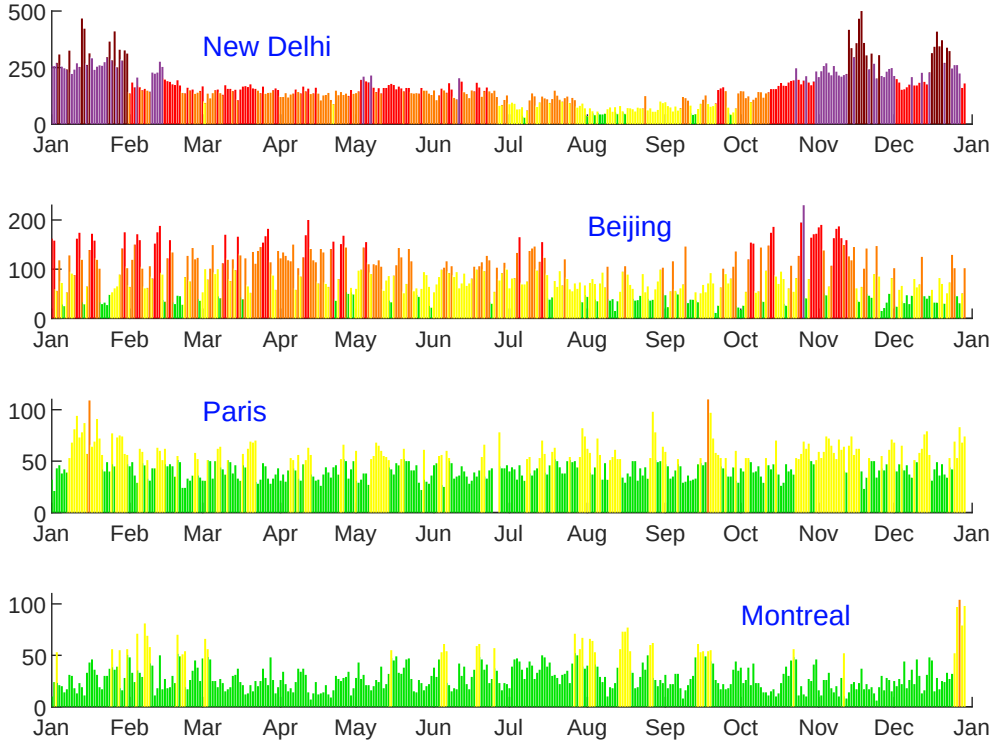


Source: World Air Quality Index (WAQI), https://aqicn.org/data-platform & Author's calculations.

**The cost of pollution** Measuring the costs of pollution is a complex challenge for several reasons. The first difficulty lies in defining what is meant by the term '*cost*'. Pollution does not result in a single type of cost, but rather a wide range of impacts, including health-related costs, lost productivity, damage to infrastructure and property, ecosystem degradation, reduced crop yields, resource depletion, and cleanup efforts. Identifying and categorizing these diverse costs is a fundamental step that adds to the complexity of the task. The second challenge is how to estimate these costs. Measuring the economic impact of pollution requires making assumptions and building statistical models. Results can vary widely depending on the methods and assumptions used, underscoring the importance of careful model selection in producing reliable estimates. A third major obstacle is the availability and relevance of data. Pollution measurements are often incomplete or inconsistent across countries because some countries lack the infrastructure to monitor certain pollutants. In addition, global coverage of pollutants is far from comprehensive. For example, particulate matter $PM_{2.5}$ is the most widely measured pollutant in the world, but reliable data on other types of pollution, such as soil, water, noise, and light pollution, remain scarce. This lack of comprehensive data makes it particularly difficult to assess the global impacts of these less-studied forms of pollution. Given these complexities, our discussion will focus primarily on two key issues: the health impacts and the economic costs associated with air pollution.

**Health impacts** The health effects of pollution are well documented in the scientific literature. However, air pollution is the most extensively studied topic, followed by water and plastic pollution. We estimate that 70% to 85% of health impact studies focus on air pollution. Research on water and plastic pollution each accounts for approximately 7% to 13%, while studies on soil and noise pollution make up about 2% to 4% each. Chemical pollution[173] represents around 1%, and light and biological pollution each account for less than 1%.

Table 5.52: Human health effects of pollution

| Health impact | Air | Biological | Chemical | Light | Noise | Plastic | Soil | Water |
|---|---|---|---|---|---|---|---|---|
| Cancer | ✓ | | ✓ | | | ✓ | ✓ | ✓ |
| Cardiovascular problems | ✓ | | ✓ | | ✓ | | | |
| Cognitive development | ✓ | ✓ | ✓ | | | | | |
| Endocrine disruption | | | ✓ | | | ✓ | ✓ | ✓ |
| Food contamination | | ✓ | | | | ✓ | ✓ | ✓ |
| Hearing loss | | | | | ✓ | | | |
| Infectious diseases | | ✓ | | | | | ✓ | ✓ |
| Mental health | ✓ | | ✓ | ✓ | ✓ | | | |
| Neurological effects | ✓ | | ✓ | | | | | |
| Physical development | ✓ | | ✓ | | | | | ✓ |
| Poisoning | ✓ | ✓ | ✓ | | | ✓ | ✓ | ✓ |
| Respiratory problems | ✓ | ✓ | ✓ | | | ✓ | | |
| Skin problems | ✓ | ✓ | | | | | | ✓ |
| Sleep disruption | ✓ | | | ✓ | ✓ | | | |

Source: Author's research.

In Table 5.52 we summarize the different effects of the eight pollution categories on human health. Most scientific studies typically look at only a subset of pollution types and health categories. For example, consider the famous study by the *Lancet* Commission on Pollution and Health (Landrigan

[173]The underrepresentation of chemical pollution stems from its overlap with air, soil, and water pollution.

Table 5.53: Global estimated pollution-attributable deaths (in millions) in 2019

| Pollution type | Female | Male | Total | in % |
|---|---|---|---|---|
| Total air pollution | 2.92 | 3.75 | 6.67 | 74.0 |
| Household air | 1.13 | 1.18 | 2.31 | 25.6 |
| Ambient particulate | 1.70 | 2.44 | 4.14 | 45.9 |
| Ambient ozone | 0.16 | 0.21 | 0.37 | 4.1 |
| Total water pollution | 0.73 | 0.63 | 1.36 | 15.1 |
| Unsafe sanitation | 0.40 | 0.36 | 0.76 | 8.4 |
| Unsafe source | 0.66 | 0.57 | 1.23 | 13.7 |
| Total occupational pollution | 0.22 | 0.65 | 0.87 | 9.7 |
| Carcinogens | 0.07 | 0.28 | 0.35 | 3.9 |
| Particulates | 0.15 | 0.37 | 0.52 | 5.8 |
| Lead pollution | 0.35 | 0.56 | 0.90 | 10.0 |
| Total pollution | 3.92 | 5.09 | 9.01 | 100.0 |

Source: Fuller *et al.* (2022).

*et al.*, 2018). The *Lancet* Commission has divided the pollutome (*i.e.*, the totality of all forms of pollution that have the potential to harm human health) into three zones:

- "*Zone 1 includes well established pollution-disease pairs, for which there are robust estimates of their contributions to the global burden of disease. The associations between ambient air pollution and noncommunicable disease are the prime example.*
- *Zone 2 includes the emerging effects of known pollutants, where evidence of causation is building, but associations between exposures and disease are not yet fully characterised and the burden of disease has not yet been quantified. Examples include associations between* $PM_{2.5}$ *air pollution and diabetes, pre-term birth, and diseases of the central nervous system, including autism in children, and dementia in the elderly. [...]*
- *Zone 3 includes new and emerging pollutants, most of them chemical pollutants whose effects on human health are only beginning to be recognised and are not yet quantified. [...] This zone includes developmental neurotoxicants; endocrine disruptors; new classes of pesticides such as the neonicotinoids; chemical herbicides such as glyphosate and nano-particles; and pharmaceutical wastes.*" (Landrigan *et al.*, 2018, page 11).

Focusing on Zone 1, the *Lancet* Commission estimated[174] that pollution is the leading environmental cause of disease and premature death, responsible for 9 million deaths in 2015 — 15.6% of the global 54.75 million deaths — disproportionately affecting the poor, vulnerable, and children in low- and middle-income countries (more than 90% of pollution-related deaths). These figures have been updated for 2019 using the same set of pollution types[175]. Fuller *et al.* (2022) found that the global

[174]The data used by the *Lancet* Commission (and many other international bodies studying pollution) come from the Global Burden of Disease (GBD) study, which is both a comprehensive research program and a database designed to quantify the impact of diseases, injuries, and risk factors on the health of populations worldwide. Initiated by the World Health Organization (WHO) in 1990, it is now managed by the Institute for Health Metrics and Evaluation (IHME) at the University of Washington. Data and results can be downloaded from https://vizhub.healthdata.org/gbd-results.

[175]The study covers the pollution related to the contamination of air by fine particulate matter ($PM_{2.5}$); ozone; sulfur and nitrogen oxides; freshwater pollution; contamination of the ocean by mercury, nitrogen, phosphorus, plastic, and petroleum waste; and poisoning of the land by lead, mercury, pesticides, industrial chemicals, electronic waste, and radioactive waste.

figure of 9 million deaths remains unchanged, accounting for one in six global deaths (Table 5.53). While deaths from poverty-related pollution (household air and water) have decreased, deaths from modern pollution sources (ambient air and chemicals such as lead) have increased by 7% since 2015 and 66% since 2000. Pollution — especially air pollution, which accounts for about 75% of pollution-related deaths each year — is now the leading risk factor for morbidity and mortality. It is on a par with smoking and far ahead of malnutrition, drug and alcohol use, HIV, and road traffic injuries (Fuller *et al.*, 2022, Figure 1, page 536).

The differences in air pollution-related deaths between regions and countries are significant. Figure 5.82 shows the proportion of deaths attributable to air pollution in 2021. The top five countries are North Korea (30.7%), Solomon Islands (27.3%), Vanuatu (23.4%), Bangladesh (22.2%), and Myanmar (21.2%), while the bottom five countries are Finland (0.8%), Sweden and Iceland (1%), and Canada, Estonia, and Norway (1.2%). The figures for China and India are 20.1% and 18.5% respectively. In South Asia, more than 18% of deaths are due to air pollution, compared with less than 2% in North America. There is also a significant difference between low-income countries (13.6%) and high-income countries (3.3%).

Figure 5.82: Share of deaths attributed to air pollution (2021)

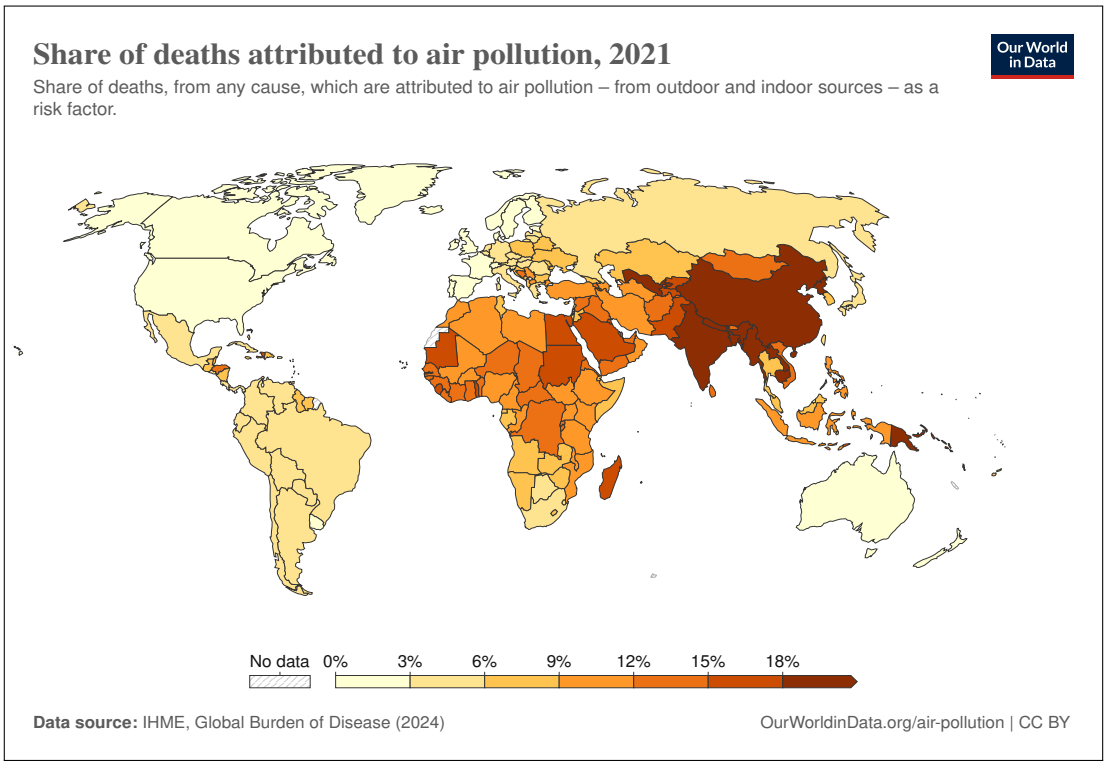


Source: Our World in Data, https://ourworldindata.org/air-pollution.

A significant number of deaths attributed to pollution from unsafe water sources are concentrated in Africa, India, and Southeast Asia[176]. The top five countries with the highest proportion of such deaths are Chad (7.0%), South Sudan (6.6%), Niger (5.3%), Somalia (4.1%), and Kiribati (4.0%). In sub-Saharan Africa, 2.5% of deaths are related to unsafe water sources, compared with 0% in North America and Europe. Again, the difference between low-income countries (2.3%) and high-income countries (0%) is large.

[176]Source: Our World in Data, https://ourworldindata.org/grapher/share-deaths-unsafe-water.

Box 5.20: Non-monetary value of health impacts

The Global Burden of Disease (GBD) defines three non-monetary values of health effects:

- Years of life lost (YLL)
  The YLL measures the burden of premature mortality. For an individual, it is calculated by comparing the age at which a person dies and the standard life expectancy. For example, if a person in a population dies at the age of 50 and the standard life expectancy is 75, the years of life lost are 25. For a homogeneous population we have:
  $$\text{YLL} = \sum_{i=1}^{n} \text{YLL}_i = \sum_{i=1}^{n} (L_i - L^\star)$$
  where $L_i$ is the age of the deceased, $L^\star$ is the standard life expectancy of the polution and $n$ is the number of deaths.

- Years lost/lived with disability (YLD)
  The YLD measures the burden of living with a health condition that causes disability or reduced quality of life but does not result in death. For an individual, it is calculated as the product of the disability weight (DW) and the average duration of the condition. The disability weight is a value between 0 (for perfect health) and 1 (equivalent to death) that reflects the severity of the health condition. For a population and a given disease, the YLD is calculated as the sum of individual YLD values, which is the number of cases of the disease multiplied by the disability weight of the disease and the average duration of the disease.

- Disability-adjusted life years (DALY)
  The DALY is the sum of YLL and YLD. It provides a single, comprehensive measure of health loss because it is a combined measure of both premature mortality and non-fatal health loss.

Another interesting study is the World Bank report, which uses data from the Global Burden of Disease[177] 2019, but focuses only on particulate matter $PM_{2.5}$, both outdoor (ambient air pollution) and indoor (household air pollution, *i.e.*, the use of fuels for cooking and heating). Global pollution exposure to ambient $PM_{2.5}$ was $43\,\mu g/m^3$ in 2019 compared to the WHO recommended level of $5\,\mu g/m^3$. World Bank (2022, page xiii) distinguishes two types of costs:

1. Death and premature mortality;
2. Morbidity due to illness and disability.

For premature deaths, World Bank (2022) reported that 6.45 million premature deaths in 2019 were attributed to exposure to $PM_{2.5}$ pollution. $PM_{2.5}$ was responsible for about 8.1% of global mortality. Globally, 64.2% of all $PM_{2.5}$ deaths were due to ambient air pollution (outdoor pollution), while 35.8% were due to household air pollution from the use of solid fuels (indoor pollution). About 95% of these deaths occurred in low- and middle-income countries, with 27.7% in China, 24.6% in India, 3.6% in Pakistan, 3.1% in Nigeria, and 2.9% in Indonesia. In terms of morbidity, World Bank (2022) estimated that air pollution has caused 21 million years lived with disability (YLD) and 93 billion days lived with illness (DLI) in 2019. The YLD figures are calculated by the Global Burden

[177] This is the same data used by Fuller *et al.* (2022) (see Footnote 174 on page 487).

of Disease (GBD) using the methodology described in Box 5.20, while the DLI figures are estimated by the World Bank using this formula:

$$\text{DLI} = \frac{365 \times \text{YLD}}{\text{DW}}$$

where DW is the disability weight. The breakdown of the morbidity impact is shown in Table 5.54. Type 2 diabetes accounts for 33% of days lived with illness, COPD (chronic obstructive pulmonary disease) for 24%, stroke for 11%, cataracts for 12%, ischaemic heart disease (IHD) for 18%, and low respiratory infections (LRI) for 1%.

Table 5.54: Global burden of morbidity from $PM_{2.5}$ exposure in 2019

| Disease | YLD | | DLI | | DW |
|---|---|---|---|---|---|
| | (in mn) | (in %) | (in bn) | (in %) | (in %) |
| Type 2 diabetes | 6.653 | 31.34 | 30.252 | 32.52 | 8.03 |
| COPD | 5.831 | 27.47 | 22.780 | 24.49 | 9.34 |
| Stroke | 5.028 | 23.68 | 10.497 | 11.29 | 17.48 |
| Cataracts | 2.143 | 10.10 | 11.370 | 12.22 | 6.88 |
| IHD | 1.248 | 5.88 | 16.654 | 17.90 | 2.74 |
| LRI | 0.198 | 0.93 | 1.214 | 1.31 | 5.95 |
| Lung cancer | 0.099 | 0.47 | 0.214 | 0.23 | 16.92 |
| Neonatal disorders | 0.019 | 0.09 | 0.035 | 0.04 | 20.32 |
| Other | 0.008 | 0.04 | 0.000 | 0.00 | |
| Total | 21.229 | 100.00 | 93.016 | 100.00 | 8.33 |

Source: World Bank (2022, Table 3.6, page 22) & Author's calculations.

Understanding the health effects of pollution remains a complex and multifaceted challenge for researchers and policy makers. While significant progress has been made in certain areas, such as the study of the effects of particulate matter, many other forms of pollution remain poorly understood. $PM_{2.5}$ has been the subject of extensive scientific investigation due to its well-documented and profound effects on human health. A substantial body of literature, including the seminal work of Pope and Dockery (2006), has elucidated the biological mechanisms by which $PM_{2.5}$ contributes to a range of adverse health outcomes, such as cardiovascular and respiratory disease. Subsequent studies, such as those by Lelieveld *et al* (2015) and Thangavel *et al.* (2022), have expanded our understanding, highlighting the risk factors associated with long-term exposure to this pollutant and its contribution to global mortality. Despite this progress, our knowledge of the health effects of other forms of pollution is less comprehensive, leaving significant gaps in our understanding. Research conducted by the *Lancet* Commission has highlighted areas known as Zone 2 and Zone 3, which include emerging and less studied pollutants. These zones represent critical frontiers in pollution research that require further exploration and scientific investigation. For example, soil contamination by heavy metals such as lead and mercury has long been recognized as a public health concern, but its broader impacts on ecosystems and human health need to be better understood. Similarly, the effects of black carbon, a component of soot produced by incomplete combustion of fossil fuels and biomass, are increasingly understood to have both direct and indirect health effects. Another prominent example is glyphosate, a widely used herbicide that has generated considerable public and scientific debate. While some studies suggest potential health risks (Van Bruggen *et al.*, 2018), such as links to cancer or endocrine disruption, others argue that these findings remain inconclusive due to methodological limitations and conflicting evidence. This controversy underscores the broader challenge of assessing the health effects of complex chemical exposures,

particularly in the absence of robust long-term studies. Moreover, the health effects of pollution are not limited to morbidity and mortality. Impacts on other dimensions of health must also be considered, such as cognitive and physical development, mental health, skin conditions, and more. Addressing these broader dimensions is critical to developing a comprehensive understanding of how pollution affects human well-being.

**Global economic costs** Estimating the economic costs of pollution poses significant challenges due to complex methodological issues and considerable data uncertainty. The time horizon is particularly important, as the inclusion of long-term costs yields very different results than the analysis of short-term impacts. Consequently, the following results should be interpreted with considerable caution. When examining such estimates, orders of magnitude and relative rankings tend to be more reliable indicators than absolute figures. This explains the considerable variation in results among the scientific research publications on this topic. In the following, we focus mainly on two reports: *Quantifying the Economic Costs of Air Pollution from Fossil Fuels* (Myllyvirta, 2020) and *The Global Health Cost of $PM_{2.5}$ Air Pollution: A Case for Action Beyond 2021* (World Bank, 2022). But there are other reports that can be used. For example, the *Lancet* Commission estimated that welfare losses due to pollution are more than $4.6 trillion per year, or 6.2% of global economic output, and that 81.5% of these economic losses are due to ambient air pollution and household air pollution, with the remainder explained by lead exposure (9.8%) and water pollution (8.7%) (Landrigan *et al.*, 2018, Table 5, page 487). These figures already give an idea of the global economic cost of pollution.

Myllyvirta (2020) proposes a simple method for estimating the economic cost of pollution. He divides the impacts of pollution into various health and economic outcomes. A common health outcome of air pollution is premature death, but pollution also causes other health issues such as childhood asthma, preterm births, illnesses, or disabilities, as well as economic outcomes like work absences or productivity losses. The total cost is calculated as the sum of the economic costs of these different health and economic outcomes:

$$\mathcal{C} = \sum_{j=1}^{m} \mathcal{C}_j = \sum_{j=1}^{m} n_j c_j$$

where $m$ is the number of health or economic outcomes, $n_j$ is the number of cases of the $j^{\text{th}}$ outcome, and $c_j$ is the average unit cost of the $j^{\text{th}}$ outcome. Consider the example of a hypothetical country. If the average unit cost of a lost workday is $150 and pollution is responsible for 2.5 million lost workdays, the pollution-related cost of lost workdays is $2.5 \times 10^6 \times 150 = \$375$ mn. If the average unit cost of a preterm birth (including initial hospitalization and long-term health effects) is $30 000 and pollution is responsible for 2 000 preterm births, the pollution-related cost of preterm birth is $30 \times 10^3 \times 2\,000 = \$60$ mn. The total cost of these two health and economic outcomes is then $435 million. Using published concentration-response functions (to estimate $n_j$) and unit costs by country (to assess $n_j$), and considering six health and economic outcomes, Myllyvirta (2020) estimated that air pollution from fossil fuels resulted in a global economic cost equivalent to 3.3% of GDP in 2018:

> "*The economic costs of air pollution from fossil fuels are estimated at $2.9 trillion in 2018, or 3.3% of global GDP [...] An estimated 4.5 million people died in 2018 due to exposure to air pollution from fossil fuels. On average, each death was associated with a loss of 19 years of life. [...] Fossil fuel $PM_{2.5}$ pollution was responsible for 1.8 billion days of work absence, 4 million new cases of child asthma and 2 million preterm births, among other health impacts that affect healthcare costs, economic productivity and welfare.*" (Myllyvirta, 2020, page 2).

The distribution of this total cost is as follows: 84% is attributed to adult deaths, followed by disability due to chronic diseases (7%), sick leave (3.5%), preterm births (3.15%), child deaths (1.75%), and asthma (0.6%). The global figure of 3.3% masks disparities between countries, as shown in Table 5.55. China has the highest costs (6.6% of GDP), followed by Bulgaria and Hungary (6.0% of GDP). On the contrary, Brazil and Spain have low costs, less than 2% of their GDP. However, these figures do not reflect the full reality. In fact, by measuring costs by GDP, the analysis favors high-income countries because of their high GDP. Myllyvirta (2020) provided the economic cost of air pollution per capita. In this case, the country with the highest costs is Luxembourg ($2 600 per capita), followed by the US ($1 900 per capita), Switzerland ($1 900 per capita), Austria ($1 700 per capita) and Germany ($1 700 per capita). Interestingly, the cost in France is $800 per capita.

Table 5.55: Economic costs of air pollution from fossil fuels (% of GDP, 2018)

| | Country | Cost | | Country | Cost |
|---|---|---|---|---|---|
| | China | 6.6% | | Bulgaria | 6.0% |
| | Hungary | 6.0% | | Ukraine | 5.8% |
| | Serbia | 5.8% | | Belarus | 5.4% |
| | India | 5.4% | | Romania | 5.3% |
| | Bangladesh | 5.1% | | Moldova | 5.0% |
| | Poland | 4.9% | | Russia | 4.1% |
| | Germany | 3.5% | | South Korea | 3.4% |
| | USA | 3.0% | | Japan | 2.5% |
| | UK | 2.3% | | France | 2.0% |
| | Spain | 1.7% | | Brazil | 0.8% |

Source: Myllyvirta (2020, page 6) & Centre for Research on Energy and Clean Air (CREA).

The report of the World Bank focuses only on the particulate matter $PM_{2.5}$, and distinguishes two types of cost: (1) death and premature mortality and (2) morbidity due to illness and disability. The economic cost of premature deaths is estimated using the approach based on the value of statistical life (VSL), while the economic cost of morbidity is estimated by the years lost with disability (YLD) (see Box 5.21). The global economic cost of mortality and morbidity was estimated at $8.1 trillion, or 6.1% of global GDP in 2019, with the following breakdown: 85% from premature mortality and 15% from morbidity. Low- and middle-income countries bear a disproportionate share of these costs, accounting for more than 90% of the global health burden of $PM_{2.5}$ pollution. The most affected regions are South Asia, and East Asia and Pacific, with costs equivalent to 10.3% and 9.3% of GDP, respectively (Table 5.56). Table 5.57 lists the top three countries in each region ranked by percentage of GDP. For example, China ranks first in East Asia & Pacific (EAP) with an economic cost equivalent to 12.9% of GDP. In Europe, Serbia is the leading country with a cost of 18.9% of GDP. Table 5.58 provides the top 15 countries in terms of absolute cost in billions of dollars. For each country, we also indicate the breakdown between outdoor and indoor pollution, and the proportion attributed to mortality and morbidity. For instance, China has a total cost of $3 029 billion, of which 79% arises from outdoor pollution, and 12% is attributed to morbidity.

Table 5.56: Annual cost of health damages from $PM_{2.5}$ by region (% of GDP, 2019)

| Region | Outdoor | Indoor | Mortality | Morbidity | Total |
|---|---|---|---|---|---|
| East Asia and Pacific (EAP) | 7.3% | 2.0% | 8.1% | 1.2% | 9.3% |
| Europe and Central Asia (ECA) | 4.4% | 0.2% | 4.0% | 0.6% | 4.6% |
| Latin America and Carribean (LAC) | 2.7% | 0.7% | 2.9% | 0.5% | 3.4% |
| Middle Easth and North Africa (MNA) | 5.5% | 0.0% | 4.7% | 0.8% | 5.5% |
| North America (NA) | 1.7% | 0.0% | 1.3% | 0.4% | 1.7% |
| South Asia (SA) | 5.9% | 4.3% | 8.3% | 2.0% | 10.3% |
| Sub-Saharan Africa (SSA) | 3.6% | 2.4% | 5.2% | 0.8% | 6.0% |
| Low-income countries | 1.3% | 4.6% | 5.0% | 0.9% | 5.9% |
| Lower-middle-income countries | 5.4% | 3.6% | 7.5% | 1.5% | 9.0% |
| Upper-middle-income countries | 7.1% | 1.8% | 7.8% | 1.1% | 8.9% |
| High-income non OECD countries | 4.3% | 0.2% | 4.0% | 0.5% | 4.5% |
| High-income OECD | 2.8% | 0.0% | 2.3% | 0.5% | 2.8% |

Source: World Bank (2022, Figures 3.13 & 3.14, pages 20 & 21) & Author's calculations.

Table 5.57: Annual cost of health damages from $PM_{2.5}$ by country (% of GDP, 2019)

| Region | Top 1 country | | Top 2 country | | Top 3 country | |
|---|---|---|---|---|---|---|
| EAP | China | 12.9% | Papua New Guinea | 12.0% | Myanmar | 11.4% |
| ECA | Serbia | 18.9% | Bulgaria | 16.3% | North Macedonia | 15.9% |
| LAC | Barbados | 8.8% | Haiti | 8.1% | Trinidad/Tobago | 7.8% |
| MNA | Egypt | 8.6% | Morocco | 7.3% | Tunisia | 6.5% |
| NA | USA | 1.7% | Canada | 1.2% | | |
| SA | India | 10.6% | Nepal | 10.2% | Pakistan | 8.9% |
| SSA | Burkina Faso | 9.1% | Mali | 9.1% | Central African Republic | 8.7% |

Source: World Bank (2022, Table 3.5, page 21).

Table 5.58: Annual cost of health damages from $PM_{2.5}$ by country in 2019 (Top 15)

| Country | Total (in $ bn) | Total (in % of GDP) | Outdoor (in %) | Indoor (in %) | Mortality (in %) | Morbidity (in %) |
|---|---|---|---|---|---|---|
| China | 3 029 | 12.9 | 79 | 21 | 88 | 12 |
| India | 1 022 | 10.6 | 60 | 40 | 81 | 19 |
| United States | 373 | 1.7 | 100 | 0 | 78 | 22 |
| Russia | 241 | 5.7 | 97 | 3 | 91 | 9 |
| Indonesia | 220 | 6.6 | 56 | 44 | 85 | 15 |
| Japan | 210 | 3.8 | 100 | 0 | 82 | 18 |
| Germany | 178 | 3.8 | 100 | 0 | 81 | 19 |
| Turkey | 134 | 5.8 | 99 | 1 | 85 | 15 |
| Italy | 132 | 5.0 | 99 | 1 | 83 | 17 |
| Poland | 127 | 9.8 | 91 | 9 | 86 | 14 |
| South Korea | 114 | 5.1 | 100 | 0 | 83 | 17 |
| Egypt | 105 | 8.6 | 100 | 0 | 87 | 13 |
| Mexico | 104 | 4.0 | 78 | 22 | 84 | 16 |
| Saudi Arabia | 96 | 5.7 | 100 | 0 | 89 | 11 |
| Pakistan | 94 | 8.9 | 48 | 52 | 82 | 18 |

Source: World Bank (2022, Table A.3, page 40) & Author's calculations.

Box 5.21: A basic economic model of pollution costs

Dechezleprêtre *et al.* (2019) consider a classical output function that uses capital and labor as factors of production, but also incorporates pollution as an additional variable: $Y = F(K, L, P)$, where $Y$ is economic output, $K$ is capital, $L$ is labor, and $P$ is pollution. The labor input $L$ can be expressed as $L = N \cdot A_L \cdot T_L$ where $N$ is the workforce size (or the population), $A_L$ is labor productivity, $T_L = \tau - \varsigma$ is the time individuals spend working, which is the difference between the total endowment of labor time $\tau$ and sick time $\varsigma$. It is assumed that all three variables ($N$, $A_L$, and $\varsigma$) depend on the pollution $P$. Consequently, the output function can be rewritten as:

$$Y = F\left(K, N(P) A_L(P) \left(\tau - \varsigma(P)\right), P\right)$$

From this, we deduce the derivative of the logarithm of output with respect to pollution:

$$\frac{\mathrm{d} \ln Y}{\mathrm{d} P} = \frac{\partial \ln Y}{\partial \ln L} \frac{\partial \ln L}{\partial P} + \frac{\partial \ln Y}{\partial P} = \epsilon_L \frac{\partial \ln L}{\partial P} + \frac{\partial \ln Y}{\partial P}$$

where $\varepsilon_L \geq 0$ is the elasticity of output with respect to labor. Breaking this down further:

$$\frac{\mathrm{d} \ln Y}{\mathrm{d} P} = \epsilon_L \left( \frac{\partial \ln N}{\partial P} + \frac{\partial \ln A_L}{\partial P} + \frac{\partial \ln\left(\tau - \varsigma(P)\right)}{\partial P} \right) + \frac{\partial \ln Y}{\partial P}$$

Expanding the third term:

$$\frac{\partial \ln\left(\tau - \varsigma(P)\right)}{\partial P} = -\frac{1}{\tau - \varsigma(P)} \frac{\partial \varsigma(P)}{\partial P} = -\frac{\varsigma(P)}{\tau - \varsigma(P)} \frac{\partial \ln \varsigma(P)}{\partial P}$$

Substituting this into the equation and introducing the notation $\theta = \dfrac{\varsigma}{\tau - \varsigma}$, which represents the ratio of sick time to effective labor time, we get:

$$\frac{\mathrm{d} \ln Y}{\mathrm{d} P} = \epsilon_L \underbrace{\left( \frac{\partial \ln N}{\partial P} + \frac{\partial \ln A_L}{\partial P} - \theta \frac{\partial \ln \varsigma(P)}{\partial P} \right)}_{\text{Pollution-related labor impact}} + \frac{\partial \ln Y}{\partial P}$$

This equation can be expressed in the following compact form:

$$\beta_P = \epsilon_L \beta_{L,P} + \beta_{L,P}$$

Therefore, pollution has an indirect impact on output through the labor factor, which operates through three dimensions:

1. Pollution increases mortality, reducing the size of labor force: $\dfrac{\partial \ln N}{\partial P} < 0$.
2. Pollution increases morbidity, decreasing labor productivity: $\dfrac{\partial \ln A_L}{\partial P} < 0$.
3. Pollution increases morbidity, leading to more work absences: $\frac{\partial \ln \varsigma(P)}{\partial P} > 0$.

Box 5.21: A basic economic model of pollution costs (Continued from previous page)

The labor-related impact of pollution also depends on the labor-output elasticity. A higher value of $\epsilon$ results in a higher cost of pollution, especially in labor-intensive industries (Graff Zivin and Neidell, 2013). Consequently, the labor-related impact of pollution is always negative: $\epsilon_L \beta_{L,P} \leq 0$. In contrast, the direct impact of pollution on output can be either positive or negative: $\beta_{L,P} = \dfrac{\partial \ln Y}{\partial P} \lessgtr 0$. When pollution levels are low, increasing pollution can have a positive impact because GDP is boosted by an increase in energy supply. However, when pollution levels are very high, increasing pollution has a negative impact due to the negative externalities (*e.g.*, infrastructure damage, reduced agricultural yields, water stress) that affect the production system. Therefore, the direct relationship follows a bell curve: $\beta_{L,P}$ is initially positive, but becomes negative as pollution increases. The aggregation of these two effects is not straightforward. While $\beta_P$ may be positive when pollution levels are low, it is certain to become negative when pollution levels are high.

**Economic costs in Europe** Studying the economic costs of air pollution in Europe is particularly valuable because of the availability of more reliable and comprehensive data. This allows researchers to consider additional pollutants beyond $PM_2.5$, such as heavy metals (*e.g.*, arsenic) and organic pollutants (*e.g.*, benzene). They can also examine trends in economic costs over time and assess the impact of policy regulations on air quality and associated costs. For instance, Dechezleprêtre *et al.* (2019) estimated that a $1\,\mu g/m^3$ increase in $PM_{2.5}$ concentration leads to a 0.8% reduction in real GDP within the same year. Notably, 95% of this impact is attributed to a decline in output per worker, which can result from higher absenteeism or reduced labor productivity. Since $PM_{2.5}$ pollution in Europe has decreased by $0.2\mu g/m^3$ per year since 2000, reducing air pollution could increase real GDP by 1.6% per decade. Thus, this study shows that reducing air pollution generates economic growth through improved labor productivity.

More recently, Mejino-López and Oliu-Barton (2024) studied the allocation of EU funds among member states and the cost-effectiveness of European air pollution policies. Using the results of Dechezleprêtre *et al.* (2019), they estimated the costs of particulate matter $PM_{2.5}$ as follows[178]:

$$\mathcal{C} = \beta_P \cdot ([C] - \mathrm{AQG})^+ \cdot \mathrm{GDP} = 0.8\% \cdot \max\left([C]_{\mathrm{PM}_{2.5}} - 5\,\mu g/m^3, 0\right) \cdot \mathrm{GDP}$$

On a global basis, they found that costs have declined since 2014, but remain at high levels:

> "*Despite significant progress, air pollution still causes €600 billion in losses each year in the European Union — equal to 4% of its annual GDP. These costs stem from productivity losses such as increased absenteeism, the reduction of in-job productivity and harm to ecosystems. Air pollution costs are disproportionately high in eastern Europe and Italy, where losses are projected to remain above 6% of GDP until 2030. The EU's 10% most-polluted regions suffer 25% of the burden of mortality attributable to air pollution.*" (Mejino-López and Oliu-Barton, 2024, page 1).

The large differences between countries are shown in Figure 5.83. For each country, Mejino-López and Oliu-Barton (2024) calculated the cost of air pollution for three seven-year periods[179]: 2014–2020,

[178] Since we have $\beta_P = \Delta \ln Y / \Delta P$, we deduce that $\Delta Y = \beta_P \cdot \Delta P \cdot Y$.

[179] For the 2024–2030 period, they used World Bank projections of GDP and extrapolated $PM_{2.5}$ concentrations based on linear regressions.

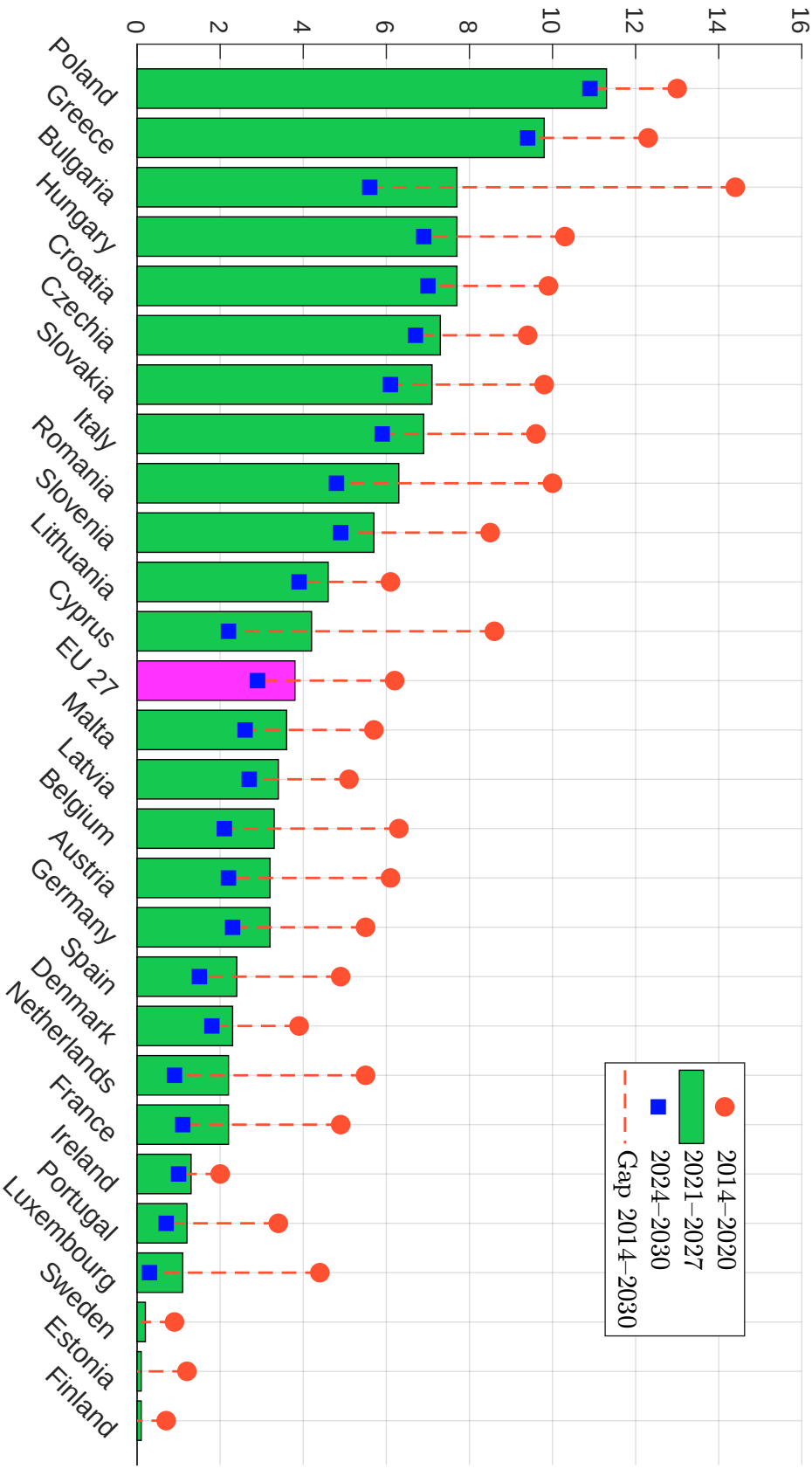


Figure 5.83: Estimated cost of air pollution by country (in % of GDP)

Source: Mejino-López and Oliu-Barton (2024, Figure 10, page 17).

2021–2027, and 2024–2030. Some countries, such as Bulgaria, Romania, Cyprus, Belgium, and the Netherlands have dramatically reduced air pollution when considering the gap 2014–2030. However, there are still some air pollution hotspots in Europe. Considering the 234 EU regions, Mejino-López and Oliu-Barton (2024) identified 16 hotspots: 5 in Bulgaria, 4 in Poland, 2 in Romania, and 1 each in Czechia, Croatia, and Hungary. These hotspots represent 7% of the EU population, but concentrate 14% of air pollution mortality.

EEA (2024a) uses a different methodology to estimate the economic costs of pollution. The analysis focuses on industrial facilities in Europe[180] and considers the following groups of pollutants:

- Main air pollutants: particulate matter ($PM_{2.5}$, $PM_{10}$), sulfur dioxide ($SO_2$), ammonia ($NH_3$), nitrogen oxides ($NO_x$), and non-methane volatile organic compounds (NM VOC);
- Greenhouse gases (GHG): carbon dioxide ($CO_2$), methane ($CH_4$) and nitrous oxide ($N_2O$);
- Heavy metals: arsenic (As), cadmium (Cd), chromium VI (Cr), lead (Pb), mercury (Hg), and nickel (Ni);
- Organic pollutants: 1,3 butadiene, benzene, formaldehyde, polycyclic aromatic hydrocarbons, dioxins and furans.

The study examines only air pollution and estimates the external costs of these facilities, taking into account both health effects (mortality and morbidity) and non-health effects (damage to buildings, crops, and forests). Health effects for the main pollutants are quantified using concentration-response functions and unit costs based on the value of a statistical life (VSL) and the value of life year (VOLY). For greenhouse gases, negative externalities are assessed by calculating the marginal abatement cost of carbon emissions required to meet the Paris Agreement targets. The results, broken down by country, are presented in Table 5.59. EEA (2024a) estimates that the economic costs associated with the value of a statistical life and the value of a life year are 2.23% and 1.39% of GDP, respectively, for the EU-27. The most affected countries are Bulgaria, Poland, Greece, Romania and Estonia, while the top five Member States with facilities contributing the highest external costs are Germany, Poland, Italy, France and Spain. Table 5.60 shows the amount of negative externalities in millions of euro. In 2012, the costs for the EU-27 were 326.5 and 536.7 billion euros, depending on the approach (VOLY vs. VSL). In 2021, these figures become 219.4 and 352.7 billion euros, representing a decrease of 32.8% and 34.3% of total external costs, respectively. During the period 2012-2021, the cumulative externalities were 2.7 and 4.3 trillion euros, respectively.

We see that heavy metals and organic pollutants are responsible for less than 5% of the economic costs, and these costs are mainly concentrated on lead, followed by cadmium and mercury. For the group of major air pollutants, sulfur dioxide and nitrogen oxides are the main contributors. EEA (2024a) also finds that 129 facilities (out of about 9 400 facilities) are responsible for about 50% of the total damage caused by air emissions:

> "*It is worth noting that half (25) of the 50 most polluting facilities in 2021 were thermal power stations, with most of them located in Germany (nine) and Poland (six). Twenty-three of these 25 plants burn lignite or hard coal as their main fuel.*" (EEA, 2024a, page 10).

[180] The study is based on the European Pollutant Release and Transfer Register (E-PRTR) dataset, a comprehensive database established under European Union Regulation 166/2006 to provide public access to environmental data from large industrial facilities across Europe. E-PRTR contains data reported annually by more than 30 000 industrial facilities in the EU, Iceland, Liechtenstein, Norway, Serbia, Switzerland and the United Kingdom from 65 economic activities and covers 91 pollutants, including emissions to air, water and land as well as waste transfers.

Table 5.59: External costs of air pollution (2021)

| | Country | Relative cost | | Breakdown of external costs | |
|---|---|---|---|---|---|
| | | VOLY/GDP | VSL/GDP | VOLY | VSL |
| | Austria | 0.71% | 1.07% | 1.43% | 1.34% |
| | Belgium | 1.59% | 2.68% | 3.96% | 4.16% |
| | Bulgaria | 7.87% | 16.11% | 2.77% | 3.53% |
| | Croatia | 1.72% | 2.89% | 0.50% | 0.52% |
| | Cyprus | 2.89% | 3.02% | 0.34% | 0.22% |
| | Denmark | 0.47% | 0.64% | 0.78% | 0.66% |
| | Estonia | 3.35% | 3.75% | 0.52% | 0.36% |
| | Finland | 2.12% | 2.36% | 2.63% | 1.82% |
| | France | 0.68% | 1.07% | 8.39% | 8.25% |
| | Germany | 1.54% | 2.63% | 27.41% | 29.19% |
| | Greece | 2.93% | 4.76% | 2.63% | 2.67% |
| | Hungary | 2.21% | 4.27% | 1.69% | 2.03% |
| | Ireland | 0.50% | 0.62% | 1.06% | 0.82% |
| | Italy | 1.06% | 1.79% | 9.35% | 9.87% |
| | Latvia | 0.69% | 1.05% | 0.11% | 0.11% |
| | Luxembourg | 0.35% | 0.65% | 0.13% | 0.15% |
| | Netherlands | 1.37% | 1.91% | 5.81% | 5.03% |
| | Poland | 5.63% | 8.68% | 16.06% | 15.43% |
| | Portugal | 1.67% | 2.18% | 1.77% | 1.45% |
| | Romania | 2.47% | 4.55% | 2.96% | 3.38% |
| | Slovenia | 1.76% | 2.99% | 0.46% | 0.48% |
| | Spain | 1.07% | 1.77% | 6.40% | 6.58% |
| | Sweden | 1.07% | 1.18% | 2.86% | 1.95% |
| | EU-27 | 1.39% | 2.23% | | |

Source: EEA (2024b, Figure 4.2, Tables 4.2 & 4.3, pages 31–34), Author's calculations & icons taken from https://icons8.com/icons.

Table 5.60: External costs of air pollution in €mn (2021)

| Pollutants | 2012 | 2021 | Cumulative | 2021 Breakdown |
|---|---|---|---|---|
| Main air (VOLY) | 119 042 | 59 728 | 834 066 | $SO_2$: 45.3%, $NO_x$: 41.1%, $NH_3$: 7.5%, $PM_{10}$: 5.0%, NM VOC: 1.2% |
| Main air (VSL) | 329 152 | 193 056 | 2 426 585 | $SO_2$: 45.7%, $NO_x$: 40.5%, $NH_3$: 7.7%, $PM_{10}$: 5.0%, NM VOC: 1.0% |
| GHG | 193 641 | 150 657 | 1 728 224 | $CO_2$: 94.5%, $CH_4$: 4.9%, $N_2O$: 0.6% |
| Heavy metals | 13 803 | 8 924 | 120 622 | Pb: 79.6%, Cd: 15.9%, Hg: 3.2%, As: 1.3%, Cr(VI): 0.1%, Ni: 0.0% |
| Organic | 66 | 69 | 1 071 | Dioxins: 82.6%, B(a)P: 15.9%, Benzene: 1.4% |
| Total (VOLY) | 326 553 | 219 378 | 2 683 984 | GHG: 68.7%, Main air: 27.2%, Heavy metals: 4.1%, Organic: 0.0% |
| Total (VSL) | 536 663 | 352 707 | 4 276 503 | Main air: 54.7%, GHG: 42.7%, Heavy metals: 2.5%, Organic: 0.0% |

Source: EEA (2024b, Table 4.1, Figures 4.4–4.7, pages 28 & 35–37) & Author's calculations.

The technical report contains an interesting analysis of marginal damage costs (MDC) for different pollutants and countries. The MDC represents the monetary value of the damage caused by emitting one additional tonne of a specific pollutant into the environment. For the main air pollutants, the average marginal costs for 2019, expressed in 2021 thousand euros per kg of pollutant emitted into the air, are as follows[181]:

| Pollutant | $NO_x$ | $SO_2$ | $PM_{10}$ | $PM_{2.5}$ | NM VOC | $NH_3$ |
|---|---|---|---|---|---|---|
| MDC (VOLY) | 15.4 | 16.2 | 51.5 | 86.5 | 1.8 | 19.0 |
| MDC (VSL) | 43.0 | 38.3 | 141.1 | 237.1 | 4.5 | 52.3 |

while for heavy metals and organic compounds they find these values:

| Pollutant | Arsenic | Cadmium | Chromium VI | Lead | Mercury |
|---|---|---|---|---|---|
| MDC | 10.3 | 253.1 | 0.7 | 45.2 | 16.8 |
| Pollutant | Nickel | 1,3 Butadiene | Benzene | B(a)P | Dioxins |
| MDC | 0.02 | 0.00 | 0.00 | 1.4 | 132 600 |

We read these numbers as follows. One additional tonne of $NO_x$ emitted to the air induces an additional cost of 15 400 euros in the VOLY method, while one additional tonne of $PM_{2.5}$ emitted to the air induces an additional cost of 237 100 euros in the VSL method. The pollutant with the highest marginal damage cost is dioxins with an MDC of 132.6 million euro per kg.

**Remark 64** *Although the EEA report is certainly one of the most comprehensive, well-documented and data-driven studies of the economic costs of air pollution, it also shows that this is a complex task and that there are many uncertainties about these costs. Key assumptions include the specification of concentration-response functions and the modelling of $PM_{2.5}$ impacts. In addition, this report is far from exhaustive as it does not include some important activities that do not correspond to industrial installations. For example, the industrial facilities reported in the E-PRTR database cover*

[181] Source: EEA (2024a, Tables 3.1 & 3.4, pages 26 & 27).

*49% of $SO_x$ and 48% of mercury, but only 3% of $PM_{10}$ and 10% of lead. Furthermore, the study only analyses outdoor pollution and does not consider indoor pollution, in particular the impact of emissions on workers inside the facilities.*

Box 5.22: Monetary economic value of health impacts

In Box 5.21 on page 494, we have defined three non-monetary measures of health impact: years of life lost (YLL), years lived with disability (YLD) and disability-adjusted life years (DALY). To assess economic costs, we need to convert these physical measures into monetary ones. Some standard approaches are described below.

- The quality-adjusted life year (QALY) is a unit of measurement that combines both the quantity and quality of life lived into a single index. One QALY represents one year of perfect health, and zero QALYs represent one year of death. It can be used to evaluate the benefits of a policy[a]:

$$\text{QALY} = \text{Years of Life Gained} \times \text{Average Quality of Life Weight}$$

  This approach is called linear because it is equivalent to directly summing the annual quality of life weights:

$$\text{QALY} = \sum_{u=t}^{T} Q(u)$$

  where $T$ is the maximum time horizon and $Q(t) \in [0,1]$ is the quality life of weight at time $t$. According to Hammitt (2023, Equation 2.5), a non-linear approach is to calculate the quality-adjusted life expectancy (QALE)[b]:

$$\text{QALE} = \frac{1}{S(t)} \int_t^T e^{-\varrho(u-t)} \mathbf{S}(u)\, \mathbb{E}[Q(u)]\, \mathrm{d}u$$

  where $\mathbf{S}(t)$ is the survival function at time $t$, $\varrho$ is the discount rate and $\mathbb{E}[Q(t)]$ is the expected quality weight.

- The value of a statistical life (VSL) is the economic value placed on the benefit of avoiding a death. It is not the value of an individual's life *per se*, but rather a measure of society's collective willingness to pay for small reductions in mortality risk. As such, the VSL is closely related to the concept of willingness-to-pay. The VSL is based on the amount of money that individuals are willing to pay for a given reduction in the risk of premature death. Several approaches are used to estimate VSL, including revealed preferences (*e.g.*, wage premiums for risky jobs) and stated preferences (*e.g.*, surveys asking about risk reduction choices). Hammitt (2023) mathematically defines the VSL as follows:

$$\text{VSL} = \frac{v}{\Delta L}$$

  where $v$ is the monetary value of the risk reduction and $\Delta L$ is the expected number

[a] When we want to evaluate the cost of a disease, we replace Years of Life Gained by Years of Life Lost.
[b] $T$ can be set to $\infty$, since $S(\infty) = 0$.

Box 5.22: Monetary economic value of health impacts (Continued from previous page)

of lives saved. For example, if workers in an industry are paid an additional \$1 000 per year to face a 1 in 10 000 increased risk of death, the VSL can be calculated as $\text{VSL} = \frac{1\,000}{1/10\,000} = \$10\,\text{mn}$. In this example, the VSL is \$10 million, reflecting the monetary value associated with risk reductions that collectively save one statistical life. In the case of the economic costs of air pollution, EEA (2024b, page 19) used a VSL of €4.2 million — for infant mortality, it is set to €6.5 million.

- The value per statistical life year (VSLY) — or the value of a life year (VOLY) — is equal to the value of a statistical life divided by the remaining expected life years Hammitt (2023, Equation 2.10):

$$\text{VSLY} = \frac{\text{VSL}}{\frac{1}{\mathbf{S}(t)} \int_t^T e^{-\varrho(u-t)} \mathbf{S}(u)\, \mathrm{d}u}$$

  It represents the economic value of extending the life of a population by one additional year. Using the previous example, if the average remaining expected life in the industry is 40 years, $\text{VSLY} = \frac{\$10\,\text{mn}}{40} = \$250\,000$. In the case of air pollution, EEA (2024b, page 19) used a VOLY of €111 470, which means that the remaining expected life years used for this study is 37.68 years.

- VSL, VSLY, and VOLY are not available for all countries, as their computation requires extensive data and statistical resources. These metrics are generally well documented for OECD countries, the United States, and Europe, where data availability and research capacity are higher. For other countries, country-specific figures can be estimated by adjusting a baseline statistic using a transfer function, as described by Hammitt and Robinson (2011) and Viscusi and Masterman (2017):

$$\text{VSL}_c = \text{VSL}_b \left( \frac{(Y/N)_c}{(Y/N)_b} \right)^{\epsilon}$$

  where $\text{VSL}_c$ is the country-specific VSL, $\text{VSL}_b$ is the baseline VSL, $(Y/N)$ is the GDP per capita and $\epsilon$ is the income elasticity of VSL, which captures how VSL scales with income. For high-income countries, $\epsilon$ is typically less than 1, reflecting the diminishing marginal utility of income. For low-income countries, $\epsilon \geq 1$ because the value of risk reduction increase more sharply as income rises[a].

Other approaches are available, but most are less popular than QALY and VSL, with the exception of willingness-to-pay[b] and cost of illness (COI). COI includes direct medical costs (medical care, hospitalization), direct non-medical costs (transportation to medical care, home modification), and indirect costs (loss of productivity and income).

[a] In very poor countries, each additional dollar has extremely high utility for basic consumption. This makes people relatively less willing to trade income for risk reduction.

[b] Willingness-to-pay is defined in Box 5.2 on page 314.

### Overexploitation and resource extraction

Overexploitation is the practice of harvesting renewable resources faster than they can be replenished. This unsustainable practice often leads to significant declines in species populations, ecosystem degradation, evolutionary consequences, and in some cases, extinction. It commonly occurs through activities such as overfishing, in which fish stocks are harvested at a rate that exceeds their ability to reproduce; deforestation, in which timber is harvested at a rate that exceeds forest regeneration; hunting and poaching, characterized by the excessive killing of animals for food, sport, or trade; and illegal wildlife trade, including the poaching of animals for their body parts or the pet trade, such as the ivory and rhino horn markets. The concept of overexploitation can also be applied to natural resources such as minerals (*e.g.*, phosphorus and rare earth elements) and fossil fuels (*e.g.*, oil and natural gas). Even if they are not expected to become extinct by 2100, many natural resources will face problems as high-grade deposits are rapidly depleted and easily accessible deposits become increasingly scarce. Cobalt and zinc are typical examples.

Overexploitation is neither a new nor a recent phenomenon. It has existed throughout history, with varying degrees of severity in different contexts:

> "*Although there is considerable variation in detail, there is remarkable consistency in the history of resource exploitation: resources are inevitably overexploited, often to the point of collapse or extinction.*" (Ludwig *et al.*, 1993, page 17).

Peres (2010) highlights numerous examples of overexploitation that underscore the profound impact of human activities on wildlife. One notable pattern is the extinction of large-bodied vertebrates, which has been largely attributed to human overhunting and overkilling in the post-Pleistocene. Evidence suggests that humans historically shifted their hunting practices from larger to smaller animals after depleting populations of larger species. Large animals are particularly attractive targets because their size provides a greater yield of meat, hides, and bones, making them economically valuable. However, these species often have slower reproductive rates, characterized by longer gestation periods and fewer offspring per birth. This makes it difficult for their populations to recover from significant declines caused by hunting or habitat destruction. As large species declined or went extinct, humans increasingly relied on hunting smaller animals to meet their needs. This pattern — overhunting of large animals followed by a shift to smaller species — has been documented across regions and historical periods. Svenning *et al.* (2021, Figure 1, page 3) found that among terrestrial mammals, only 11 of 57 species of megaherbivores (mean adult body mass greater than 1 000 kg) survived to 1 000 AD:

| Status | *Cetartiodactyla* | *Cingulata* | *Diprotodontia* | *Litopterna* | *Notoungulata* | *Rhinocerotidae* | *Pilosa* | *Elephantidae* | *Proboscidea* | Total |
|---|---|---|---|---|---|---|---|---|---|---|
| Survivor | 4 | | | | | 4 | | 3 | | 11 |
| Extinct | 4 | 4 | 1 | 2 | 3 | 4 | 16 | 7 | 5 | 46 |

Survivors include three species of elephant, four species of rhinoceros, the common hippopotamus, the giraffe, and two species of cattle. The extinct species include seven species of elephant, four species of rhinoceros, one species of hippopotamus, the mastodon, etc. Ripple *et al.* (2019) studied the threats to megafauna, which are large vertebrate species. They considered all species weighing more than 100 kg for mammals, ray-finned fish, and cartilaginous fish, and all species weighing more than 40 kg for amphibians, birds, and reptiles. They found that the proportion of threatened

species was significantly higher among megafauna than among all vertebrates (58.6% vs. 21.3%). Furthermore, 70% of megafauna species have declining populations, with birds and amphibians being particularly affected (100% of species in these groups have declining populations), followed by cartilaginous fish (89.7%) and ray-finned fish (83.8%). Focusing on specific species, Ripple *et al.* (2019) identified various threats to megafauna. They concluded that harvesting of megafauna for human consumption[182] is the single most important threat across all classes studied (Table 5.61), far outweighing other factors. Harvesting is a threat in more than 95% of cases, while invasive species and habitat development are threats in less than 40% of cases. Interestingly, climate change was found to be a threat in less than 20% of cases.

Table 5.61: Current threats to megafauna

| | Megafauna | $n$ | Animal husbandry | Climate | Cropping | Development | Harvesting | Invasives | Pollution | Transportation |
|---|---|---|---|---|---|---|---|---|---|---|
| | Cartilaginous fish | 38 | 3% | 11% | | 13% | 100% | | 13% | 8% |
| | Mammals | 73 | 53% | | 61% | 56% | 98% | 54% | | 51% |
| | Ray-finned fish | 29 | | | | 14% | 100% | 31% | 40% | 28% |
| | Reptiles | 20 | | 40% | 25% | 40% | 90% | 65% | | 25% |

Source: Ripple *et al.* (2019, Figure 2, page 5).

As explained by Peres (2010), overexploitation can lead to the rapid collapse of species. In some cases, just a few years or decades are sufficient, and it does not necessarily take centuries or millennia for a species to become nearly extinct. One of the best known examples is the North American buffalo (*Bison bison*), which experienced a dramatic collapse in less than 40 years:

> "*Prior to European exploration and settlement of North America, the buffalo or American bison inhabited vast stretches of the continent. [...] At its greatest moment, the total numbers for the continent may have been as high as 25 to 30 million before white settlement. On the Great Plains, where the bison were most suited and most plentiful, its population is estimated to have been 20 million as late as 1800. Even by 1850, substantially more than 10 million bison roamed the plains. Yet, by 1890, these plains held just 1 000 bison.*" (Lueck, 2002, page 609).

After 1890, the story of the American bison took a more hopeful turn, thanks to conservation efforts. A few individuals established small herds on private ranches to preserve the species. The US government protected a small population of wild bison in Yellowstone, providing an important sanctuary. Laws were also passed prohibiting the hunting of bison. Over time, through the combined efforts of individuals, conservation groups, and the government, the bison population began to recover. Today, bison are no longer endangered. There are approximately 400 000 bison in North America, but most are managed as livestock on private ranches. In fact, only about 30 000 are wild bison[183].

[182] The unsustainable hunting of wild animals for food is called the bushmeat crisis.

[183] Source: https://bisoncentral.com/bison-by-the-numbers.

Box 5.23: The Tragedy of the Commons

Published in Science in 1968, *The Tragedy of the Commons* by Garrett Hardin is a seminal essay that explores the conflict between individual interests and the common good in the context of shared resources. The article focuses on how individuals, acting in their own self-interest, can deplete or degrade shared resources (referred to as '*commons*'), even when it is not in the collective best interest to do so. Hardin (1968) illustrates this dilemma with a hypothetical example of a shared pasture (the commons) where each herder individually benefits by adding more cattle to the pasture. Each herder reasons that adding one more animal will bring him personal gain, while the negative consequences (overgrazing) are shared by all users of the commons. Therefore, from an individual perspective, it's rational to add more animals. However, if every herder follows this logic, the collective overuse of the pasture leads to its destruction, as the resources become insufficient to sustain the community. This illustrates the dilemma of individual gain versus collective ruin.

The essay applies this principle to various domains, including national parks, pollution, and environmental issues. It had a profound and far-reaching impact across multiple fields, influencing academic thought, public policy, and environmental management. However, the article has also faced significant criticism. For instance, Nobel laureate Elinor Ostrom provided empirical evidence demonstrating that communities can often self-organize to manage commons effectively, challenging the assumption that the tragedy is inevitable. More recently, the concept of the tragedy of the commons has resonated with contemporary challenges such as climate change. It has been extensively revisited, notably inspiring the idea of the '*tragedy of the horizon*' (Carney, 2015), which highlights the short-term focus of financial markets and policy-making in addressing long-term environmental risks.

Beyond species extinction, overexploitation occurs in other areas and can take different forms. One important form is the depletion and impoverishment of natural resources. We often think of excessive logging for timber, overgrazing by livestock, and unsustainable harvesting of medicinal plants, all of which involve the depletion of plants that reduce soil fertility and lead to erosion. However, natural resource depletion also includes other essential resources such as water, minerals, and energy resources. In this context, IPBES provides a highly critical assessment of resource extraction:

> "*Extraction of living biomass and nonliving materials is increasing as both populations and per capita consumption increased sixfold from 1970 to 2010, while the demand for materials used in construction and industry quadrupled during that time. [...] Materials for construction and industry increased 4-fold, with the most dramatic increases for lower-middle (7-fold) and upper-middle income countries (11-fold) and the Asia and the Pacific region (10-fold for whole region) and, generally, the growing economies. The use of biomass, fossil fuels, metal ores and non-metallic minerals doubled from 2005 (26.3 billion tons) to 2015 (46.4 billion tons), growing an annual rate of 6.1%.*" (IPBES, 2019, page 121).

The root causes of overexploitation lie in the expanding size and growth of the human population, coupled with rising standards of living. These driving forces are described by various terms, such as '*the scale of the human enterprise*' (Ehrlich, 1995; Gaston and Spicer, 2004), '*the great acceleration*' (Steffen *et al.*, 2015a), and others. Collectively, they underscore the profound impact of human activities on the planet's natural systems.

**An example with freshwater** Overexploitation of water resources includes both the overdrawing of groundwater from aquifers for irrigation or consumption, and the unsustainable use of surface water, such as river diversions and lake exploitation. Figure 5.84 shows the annual freshwater withdrawals measured in trillion $m^3$. We observe four main periods. From 1900 to 1950, the trend is relatively slow. Then there is a sharp acceleration in freshwater withdrawals until 1980, followed by a first slowdown from 1980 to 2010 and a second slowdown since 2010. This graph illustrates '*The Great Acceleration*' described by Steffen *et al.* (2015a), which refers to the dramatic, rapid increase in human activity and its profound impact on Earth's systems that began after World War II.

Figure 5.84: Global freshwater withdrawals (in trillion $m^3$ per year)

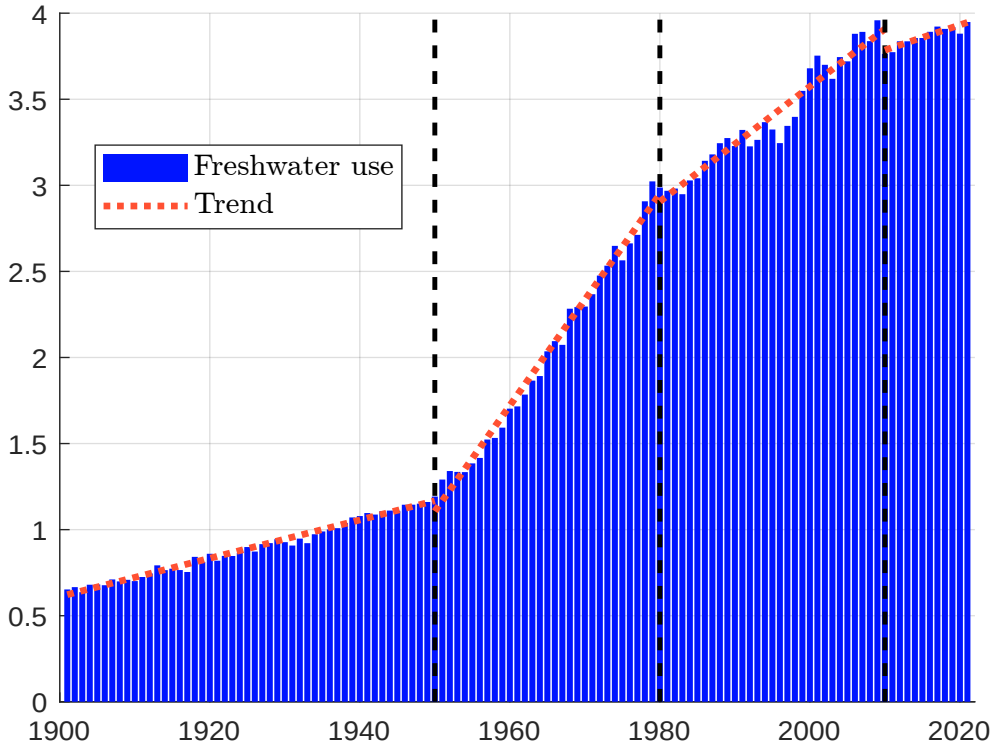


Source: Flörke *et al.* (2013), Steffen *et al.* (2015a), https://databank.worldbank.org/source/world-development-indicators & Author's calculations.

Freshwater resources and withdrawals are unevenly distributed. In Table 5.62, we report several statistics for different countries: (1) the total annual freshwater withdrawals in billion cubic meters in 2000, (2) the total annual freshwater withdrawals in billion cubic meters in 2021, (3, 4, 5) the distribution among agriculture, industry, and domestic use, (6) the renewable internal freshwater resources[184] in billion cubic meters in 2021, (7) the renewable internal freshwater resources per capita, and (8) the water stress. The total volume of renewable freshwater resources worldwide is approximately 42.8 trillion cubic meters, with more than 50% concentrated in just seven countries: Brazil, Canada, China, India, Indonesia, Russia, and the United States. Some countries have very limited renewable freshwater resources. For instance, Egypt, Libya, and Saudi Arabia each have less than 2 billion cubic meters of freshwater resources, despite their large land areas. These disparities

[184]Renewable internal freshwater resource flows measure the total volume of freshwater generated by natural processes within a country's borders. This includes water from precipitation (rain, snow) that contributes to rivers, lakes, and groundwater but excludes any water that flows in from other countries.

Table 5.62: Freshwater withdrawals by country

| Country | Total | | Agriculture | Industry | Domestic | Renewable resources | Renewable per capita | Water stress |
|---|---|---|---|---|---|---|---|---|
| | 2000 | 2021 | 2021 | | | 2021 | | |
| | (in bn $m^3$) | | (in %) | | | (in bn $m^3$) | (in $m^3$) | (in %) |
| Algeria | 5.6 | 9.8 | 63.8 | 1.8 | 34.4 | 11 | 251 | 137.9 |
| Argentina | 30.4 | 37.7 | 73.9 | 10.6 | 15.5 | 292 | 6 444 | 10.5 |
| Australia | 21.7 | 11.4 | 67.8 | 18.1 | 14.0 | 492 | 19 155 | 4.6 |
| Bangladesh | | 35.9 | 87.8 | 2.1 | 10.0 | 105 | 626 | 5.7 |
| Brazil | 56.1 | 67.3 | 61.3 | 14.5 | 24.2 | 5 661 | 27 015 | 1.5 |
| Canada | 41.9 | 36.3 | 11.4 | 74.2 | 14.4 | 2 850 | 74 530 | 3.7 |
| China | 550.9 | 568.5 | 62.1 | 17.7 | 20.1 | 2 813 | 1 992 | 41.5 |
| Congo (DRC) | 0.6 | 0.7 | 10.5 | 21.5 | 68.0 | 900 | 9 077 | 0.2 |
| Egypt | 57.0 | 77.5 | 79.2 | 7.0 | 13.9 | 1 | 9 | 141.2 |
| France | 32.7 | 24.7 | 13.9 | 64.3 | 21.7 | 200 | 2 948 | 21.6 |
| Gabon | 0.1 | 0.1 | 29.0 | 10.1 | 60.9 | 164 | 69 003 | 0.5 |
| Germany | 44.9 | 25.8 | 4.2 | 54.3 | 41.5 | 107 | 1 286 | 35.4 |
| Iceland | 0.2 | 0.3 | 0.1 | 71.1 | 28.7 | 170 | 456 351 | 0.4 |
| India | 610.4 | 647.5 | 90.4 | 2.2 | 7.4 | 1 446 | 1 022 | 66.5 |
| Indonesia | 113.3 | 222.6 | 85.2 | 4.1 | 10.7 | 2 019 | 7 294 | 29.7 |
| Iran | 88.5 | 93.0 | 92.2 | 1.2 | 6.6 | 128 | 1 453 | 81.3 |
| Italy | 45.1 | 33.6 | 50.2 | 22.7 | 27.1 | 182 | 3 086 | 29.6 |
| Kazakhstan | 21.0 | 24.6 | 62.7 | 18.5 | 18.8 | 64 | 3 259 | 34.1 |
| Korea, Rep. | 27.7 | 29.2 | 58.9 | 16.4 | 24.6 | 65 | 1 253 | 85.2 |
| Libya | 4.3 | 5.7 | 83.2 | 4.8 | 12.0 | 1 | 98 | 817.1 |
| Madagascar | 13.4 | 13.5 | 95.9 | 1.2 | 2.9 | 337 | 11 350 | 11.3 |
| Malaysia | 5.6 | 6.7 | 45.6 | 29.9 | 24.5 | 580 | 16 918 | 3.4 |
| Mexico | 68.2 | 89.9 | 75.7 | 9.5 | 14.8 | 409 | 3 204 | 45.0 |
| Netherlands | 8.4 | 7.9 | 1.0 | 73.5 | 25.5 | 11 | 627 | 16.1 |
| Nigeria | 10.3 | 12.5 | 44.2 | 15.8 | 40.1 | 221 | 1 011 | 9.7 |
| Pakistan | 172.6 | 264.2 | 94.0 | 0.8 | 5.3 | 55 | 230 | 162.1 |
| Philippines | | 89.0 | 76.2 | 13.4 | 10.3 | 479 | 4 235 | 27.2 |
| Qatar | 0.2 | 0.2 | 33.3 | 4.3 | 62.4 | 0 | 22 | 431.0 |
| Russia | 75.9 | 64.8 | 28.8 | 44.8 | 26.5 | 4 312 | 29 790 | 4.1 |
| Saudi Arabia | 19.7 | 23.4 | 81.6 | 5.4 | 13.1 | 2 | 78 | 974.2 |
| South Africa | 12.7 | 20.9 | 61.3 | 21.2 | 17.4 | 45 | 728 | 66.9 |
| Spain | 36.1 | 29.0 | 65.3 | 19.0 | 15.7 | 111 | 2 345 | 43.3 |
| Sudan | | 26.9 | 96.2 | 0.3 | 3.5 | 4 | 83 | 118.7 |
| Ukraine | 18.3 | 9.5 | 31.0 | 40.9 | 28.1 | 55 | 1 244 | 12.3 |
| United Kingdom | 12.5 | 8.4 | 14.0 | 12.0 | 74.0 | 145 | 2 163 | 14.4 |
| United States | 473.5 | 444.4 | 39.7 | 47.2 | 13.1 | 2 818 | 8 487 | 28.2 |
| Viet Nam | 71.8 | 81.9 | 94.8 | 3.7 | 1.5 | 359 | 3 633 | 18.1 |
| World | 3 679.8 | 3 948.7 | 71.6 | 15.1 | 13.1 | 42 809 | 5 429 | |

Source: https://databank.worldbank.org/source/world-development-indicators.

are even more pronounced when considering renewable internal freshwater resources per capita. For example, Canada has more than 70 000 $m^3$ of freshwater per capita, while Egypt has less than 10 $m^3$. In addition, a worrying downward trend in available freshwater resources has been observed (Figure 5.85). Over the past 60 years, the global volume of renewable internal freshwater resources has declined by about 60%. In India, this decline is even more severe, approaching 70%. This downward trend is primarily driven by high withdrawal rates. Globally, about 4 trillion cubic meters of freshwater are withdrawn each year. Agriculture is the largest contributor, accounting for 71% of total withdrawals, followed by industry at 15%. Domestic use accounts for 13% of total withdrawals worldwide. However, domestic water use has grown much faster than agricultural and industrial use, increasing sevenfold over the past 50 years. In some countries, domestic freshwater use accounts for more than 40% of total withdrawals, such as in many African countries, as well as in Germany and the United Kingdom. In Table 5.62, we also report the ratio of total freshwater withdrawals to total renewable freshwater resources, referring specifically to internal freshwater resources. This ratio is commonly known as water stress. Water stress is considered high when the ratio exceeds 75% and critical when it exceeds[185] 100%. We observe that some countries are experiencing critical water stress, including Algeria, Egypt, Libya, Pakistan, Qatar, Saudi Arabia, and Sudan. In fact, as of 2021, there are 25 countries with water stress levels exceeding 75%.

Figure 5.85: Renewable internal freshwater resources per capita (base 100 in 1961)

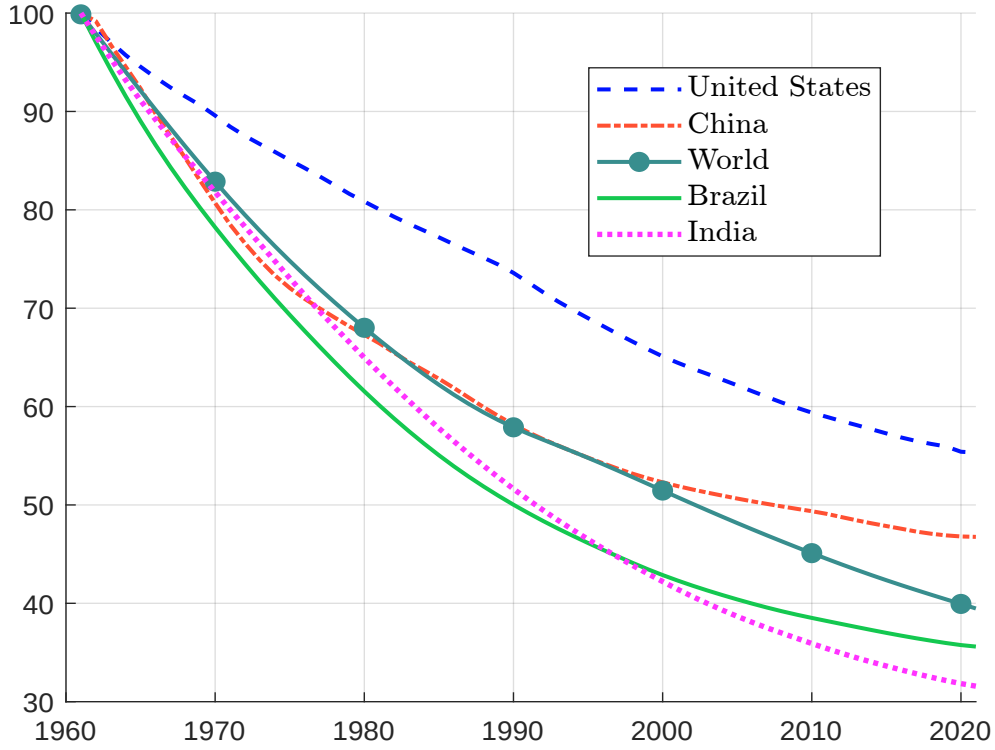


Source: https://databank.worldbank.org/source/world-development-indicators & Author's calculations.

[185] A water stress level greater than 100% means that a country is withdrawing more freshwater annually than the total amount of renewable internal freshwater resources. This indicates overexploitation of additional water sources beyond what is naturally replenished within the country. For example, a country may rely on non-renewable groundwater, external freshwater resources that originate outside its borders and flow in through rivers and lakes (*e.g.*, the Nile and the Danube), or desalination, which involves the conversion of seawater into freshwater (*e.g.*, in Qatar and Saudi Arabia).

**Mathematical models of population and resource ecology with harvesting** Historically, the Malthusian growth model is considered the first mathematical population model. In this case, the population growth rate is constant:

$$\frac{\mathrm{d}N(t)}{\mathrm{d}t} = \delta N(t)$$

where $N(t)$ is the number of individuals, $N(t_0) = N_0$ is the initial population size and $\delta = \lambda - \mu$ is the difference between the birth rate and the death/mortality rate. Malthus (1798) believed that the population tends to grow exponentially[186], whereas he believed that food production and other resources increase at a linear rate due to the finite nature of land and labor. Therefore, Malthus predicted that the world would eventually face a crisis where resources would not be sufficient to support the growing population. However, his conclusions were later criticized by Verhulst (1838), who highlighted the role of the law of diminishing returns. Verhulst provided numerous examples demonstrating that population growth is inherently limited and cannot continue indefinitely. To model this, he proposed that population size follows the nonlinear differential equation:

$$\frac{\mathrm{d}N(t)}{\mathrm{d}t} = \delta N(t) - \varphi(N(t))$$

By considering the specific case where $\varphi(x) = \eta x^2$, Verhulst derived the well-known logistic population model:

$$N(t) = \frac{\delta N_0 e^{\delta(t-t_0)}}{\delta + \eta N_0 \left(e^{\delta(t-t_0)} - 1\right)}$$

This model illustrates how population growth slows as it approaches a finite carrying capacity, offering a more realistic depiction of population dynamics compared to Malthus' original exponential growth predictions. In the 1920s, mathematician Vito Volterra introduced a class of population dynamics models describing multiple species competing for the same food or resources, or interacting as predators and prey (Volterra, 1928). During the same period, biophysicist Alfred Lotka independently developed similar equations to analyze predator-prey interactions (Lotka, 1925). These equations are now known as the Lotka-Volterra equations and form a pair of first-order nonlinear differential equations:

$$\begin{cases} \dfrac{\mathrm{d}x(t)}{\mathrm{d}t} = ax(t) - bx(t)\,y(t) \\ \dfrac{\mathrm{d}y(t)}{\mathrm{d}t} = cx(t)\,y(t) - dy(t) \end{cases} \tag{5.35}$$

where $x(t)$ is the prey population, $y(t)$ is the predator population, $a$ is the intrinsic growth rate of the prey (in the absence of predators), $b$ is the predation rate coefficient, $c$ is the reproduction rate of predators per prey consumed, and $d$ is the natural mortality rate of predators. These three models (Malthus, Verhulst, and Lotka-Volterra) form the basis for modeling population and resource dynamics with harvesting.

In the following, $x(t)$ represents the size of a population, the amount of a resource or the biomass stock of a species in a finite environment. When the stock $x(t)$ is small, the size of the environment has no impact, and $x(t)$ can grow at an exponential rate $\delta$, also known as the intrinsic growth rate. However, beyond a certain threshold, the density of the stock or population becomes too high to sustain the growth rate, and the regenerative rate of the stock decreases. This suggests the existence of a threshold $\kappa$ at which $x(t)$ remains constant. Therefore, we assume that the stock variation is determined by the product of three factors: the constant intrinsic growth rate $\delta$ (or

[186] The solution of the differential equation is an exponential curve: $N(t) = N_0 e^{\delta(t-t_0)}$.

biotic potential), the regenerative rate[187] $\xi(t) = \dfrac{\kappa - x(t)}{\kappa}$ (or biotic resistance), which depends on the distance between the current stock $x(t)$ and the threshold $\kappa$ which is called the carrying capacity, and the current stock $x(t)$. This results in the following differential equation:

$$\frac{\mathrm{d}x(t)}{\mathrm{d}t} = \delta\left(\frac{\kappa - x(t)}{\kappa}\right)x(t)$$

This model corresponds to the logistic model formulated by Verhulst (1838), where $\eta = \delta/\kappa$. We deduce that the solution is:

$$x(t) = \frac{\kappa N_0 e^{\delta(t-t_0)}}{\kappa + N_0\left(e^{\delta(t-t_0)} - 1\right)}$$

We verify that $x(t)$ tends asymptotically to $\kappa$ as $t \to \infty$. This model can be easily modified by considering exploitation:

$$\frac{\mathrm{d}x(t)}{\mathrm{d}t} = \delta x(t)\left(1 - \frac{x(t)}{\kappa}\right) - h(x(t))$$

where $h(x(t))$ is the harvest, catch or removal rate. This model has been considered by Gordon (1954) and Schaefer (1954) in the case of fisheries management. The maximum sustainable yield (MSY) is the largest harvest rate of a renewable resource that can be sustained indefinitely without causing the population to decline. The sustainable harvest rate is given by:

$$h(x(t)) = \delta x(t)\left(1 - \frac{x(t)}{\kappa}\right)$$

The maximum value of $h(x)$ is reached when $h'(x) = 0$ or $\delta\left(1 - \dfrac{x}{\kappa}\right) - \delta\dfrac{x}{\kappa} = 0$. We deduce that the maximum sustainable yield is achieved when the stock is at half the carrying capacity: $x(t) = \dfrac{\kappa}{2}$. We deduce that:

$$\text{MSY} := \max h(x(t)) = h\left(\frac{\kappa}{2}\right) = \frac{\delta}{4}\kappa$$

Figure 5.86 shows the function $g(x) = \delta x\left(1 - \dfrac{x}{\kappa}\right) - h$ when $\delta = 30\%$, $\kappa = 200$ and $h = \epsilon \cdot \text{MSY}$. The stability analysis demonstrates that the number of stable equilibria depends on the harvest rate[188]. If $h = 0$, we have a stable equilibrium at $x^\star = \kappa$ and an unstable equilibrium at $x^\star = 0$. If $0 < h < \dfrac{\delta}{4}\kappa$, the two equilibria lie between 0 and $\kappa$. Among them, only the equilibrium $x^\star = \dfrac{\delta\kappa + \sqrt{\delta\kappa(\delta\kappa - 4h)}}{2\delta}$ is stable. If $h = \text{MSY} = \dfrac{\delta}{4}\kappa$, the equilibrium at $x^\star = \dfrac{\kappa}{2}$ is unstable. Indeed, if $x(t) > x^\star$, $\dfrac{\mathrm{d}x(t)}{\mathrm{d}t} < 0$

[187] The regenerative rate $\xi(t)$ is positive if $x(t) < \kappa$, zero at $x(t) = \kappa$, and negative if $x(t) < \kappa$. In the latter case, the stock is declining because the population density is too high to sustain it.

[188] We obtain a second order polynomial:

$$\frac{\mathrm{d}x(t)}{\mathrm{d}t} = g(x) = 0 \Leftrightarrow -\delta x^2 + \delta\kappa x - h\kappa = 0$$

We have $\Delta = \delta\kappa(\delta\kappa - 4h)$. If $h > \text{MSY}$, then there is no root and $\dfrac{\mathrm{d}x(t)}{\mathrm{d}t} < 0$. It follows that $x(t)$ converges to the stable equilibrium $x_1^\star = 0$. If $h = \text{MSY}$, there is a root: $x' = \kappa/2$. Therefore, we have two stable equilibria: $x_1^\star = 0$ and $x_2^\star = \kappa/2$. If $h < \text{MSY}$, we have $\sqrt{\Delta} < \delta\kappa$ and there are two roots: $x' = \left(\delta\kappa - \sqrt{\Delta}\right)/(2\delta)$ and $x'' = \left(\delta\kappa + \sqrt{\Delta}\right)/(2\delta)$. Therefore, we have two stable equilibria $x_1^\star = 0$ and $x_3^\star = \left(\delta\kappa + \sqrt{\Delta}\right)/(2\delta)$ and one unstable equilibrium $x_2^\star = \left(\delta\kappa - \sqrt{\Delta}\right)/(2\delta)$.

Figure 5.86: Stability analysis of the logistic model with harvesting

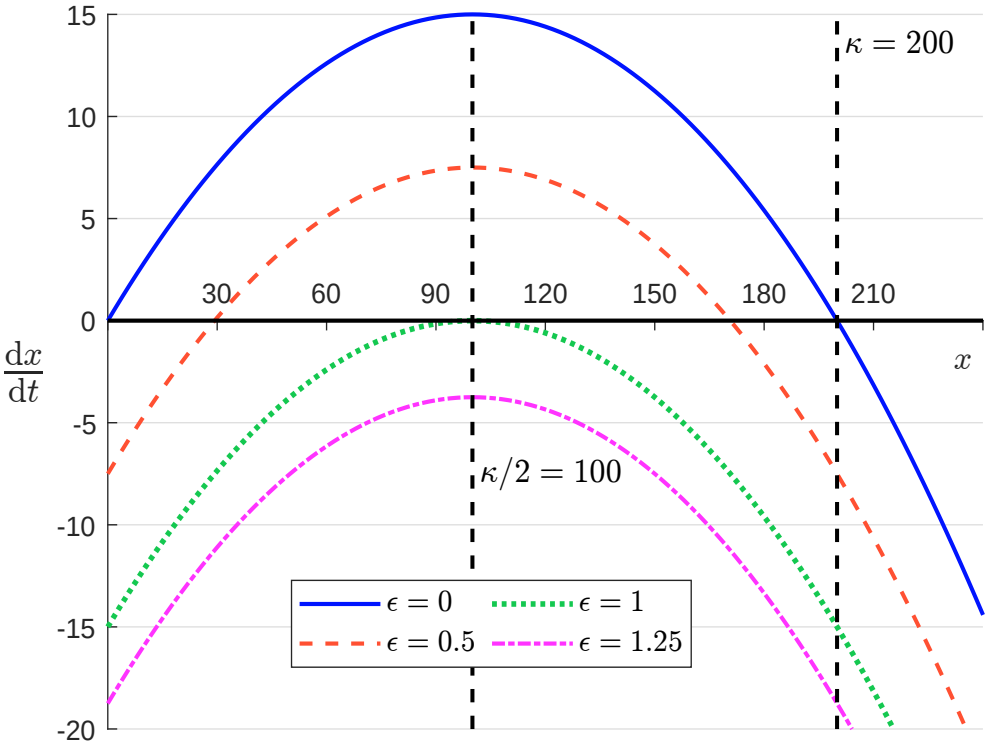


and $x(t)$ tends toward $x^\star$, but if $x(t) < x^\star$, $\frac{dx(t)}{dt} < 0$ and $x(t)$ tends to 0. Finally, if $h >$ MSY, $x(t)$ tends asymptotically to 0. These results are summarized in Table 5.63. In Figure 5.87, we have simulated the model with three different starting values $x_0$ and four values of the parameter $\epsilon$. This shows the stability of each equilibrium. In particular, when $h =$ MSY, we obtain an equilibrium at $x^\star = \kappa/2$ only when the initial stock is already larger than the equilibrium.

Table 5.63: Sign table of $\frac{dx(t)}{dt}$

| $x$ | $0$ | $\frac{\delta\kappa - \sqrt{\delta\kappa(\delta\kappa - 4h)}}{2\delta}$ | | | $\frac{\kappa}{2}$ | $\frac{\delta\kappa + \sqrt{\delta\kappa(\delta\kappa - 4h)}}{2\delta}$ | | | $\kappa$ | | $\infty$ |
|---|---|---|---|---|---|---|---|---|---|---|---|
| $h = 0$ | 0 | + | + | + | + | + | + | + | 0 | − | − |
| $0 < h < \frac{\delta}{4}\kappa$ | − | − | 0 | + | + | + | 0 | − | − | − | − |
| $h = \frac{\delta}{4}\kappa$ | − | − | − | − | 0 | − | − | − | − | − | − |
| $h > \frac{\delta}{4}\kappa$ | − | − | − | − | − | − | − | − | − | − | − |

Figure 5.87: Simulation of the logistic model with harvesting

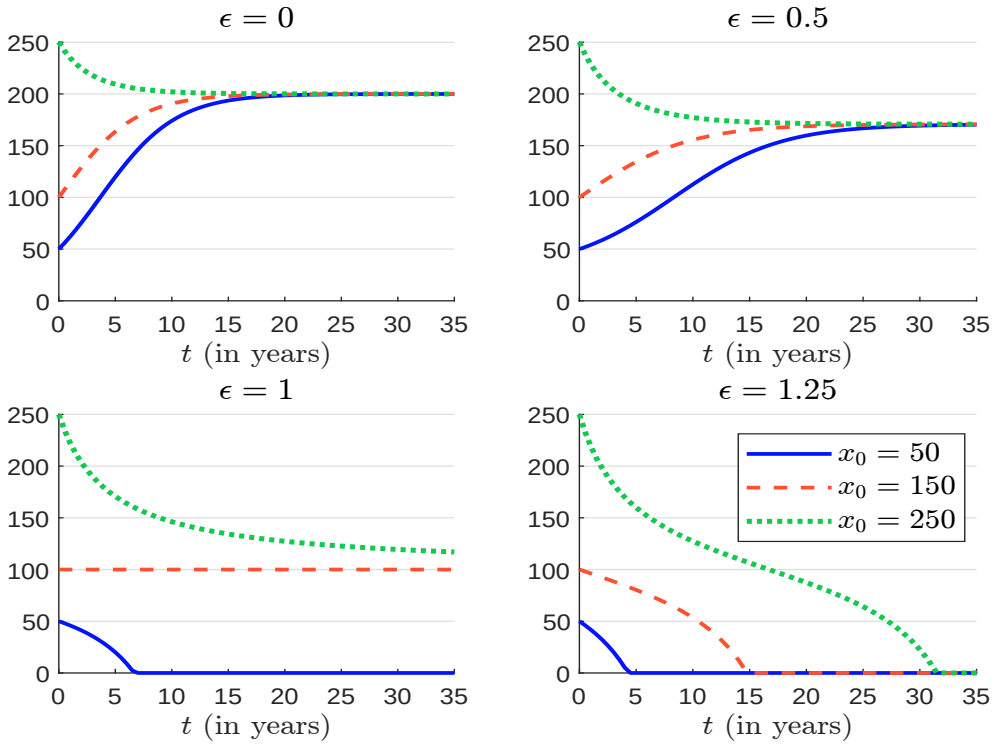


Figure 5.88: Equilibrium $x^\star$ and harvest rate $h$

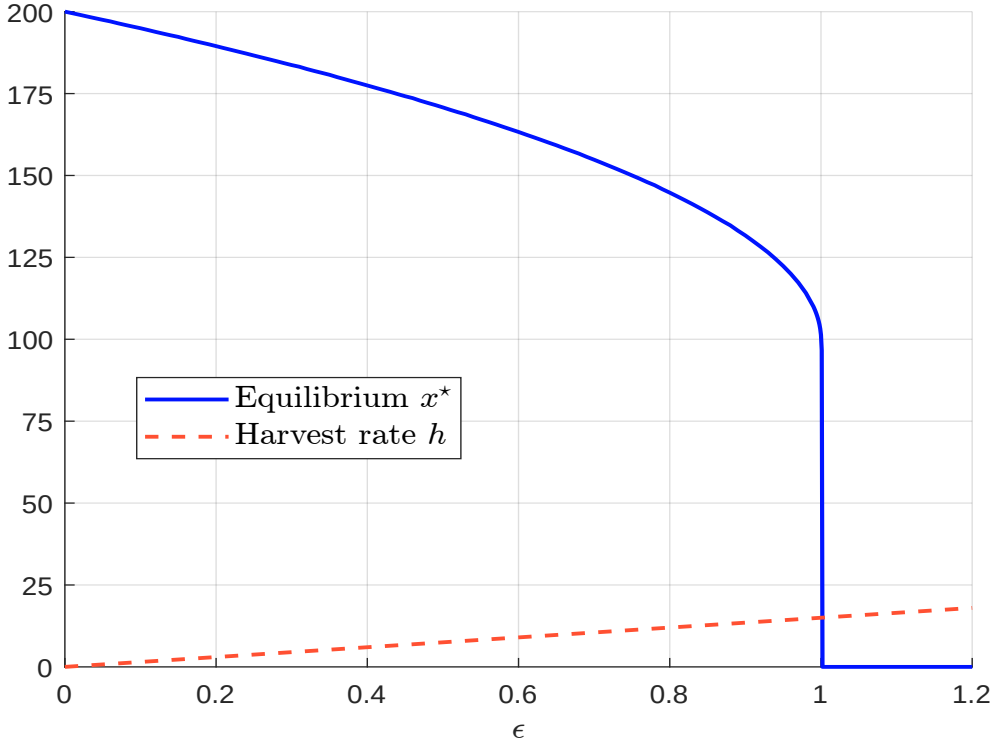

Figure 5.88 illustrates the equilibrium $x^\star$ and the harvest rate $h$ as a function of the coefficient $\epsilon$. By construction, $x^\star$ decreases with respect to $\epsilon$. When $\epsilon = 1$ or $h = \text{MSY}$, we verify that the equilibrium is unstable, indicating that $h = \text{MSY}$ is indeed a critical and undesirable harvest rate. To prevent overexploitation, it is essential that the absolute harvest rate remains below the maximum sustainable yield. Consequently, the relative harvest rate, defined as the ratio of the absolute harvest rate to the carrying capacity, must be less than one quarter of the intrinsic growth rate:

$$\eta = \frac{h}{\kappa} < \eta^\star = \frac{\delta}{4}$$

For example, if $\delta = 30\%$ per year, then $\eta^\star = 7.5\%$, meaning that the relative harvest rate must be less than 7.5% per year. Conversely, if $\delta = 2\%$, the relative harvest rate must be much lower, less than 0.5% per year ($\eta^\star = 0.5\%$). Here are some typical values for various species:

- Fish species
  In general, small and fast growing fish species such as sardines and anchovies can have rates of 100% or higher, while large and slow growing fish species such as sharks and tuna often have rates below 10%. Many commercial fish species, such as cod and haddock, have intrinsic growth rates between 10% and 50% per year.

- Mammals
  Large mammals such as whales and elephants typically have low rates (5%–20% per year) because they reproduce slowly and have long gestation periods, while small mammals such as rodents and rabbits can have higher rates (50%–200% per year), reflecting their ability to reproduce rapidly.

- Bacteria
  Bacteria can have very high intrinsic growth rates, sometimes doubling several times a day. For example, Escherichia coli (E. coli) can have rates of 20+ per day under optimal conditions.

Because large, slow-growing animals (such as many large fish species and mammals) have low intrinsic growth rates, they are highly vulnerable to overharvesting.

Table 5.64: Proportion in % of remaining buffalo under different harvest rate assumptions

| | $\eta$ (in %) | 1.00 | 2.00 | 3.00 | 4.00 | 4.10 | 4.20 | 4.30 | 4.40 |
|---|---|---|---|---|---|---|---|---|---|
| $t$ | 10 years | 93.55 | 86.81 | 79.77 | 72.40 | 71.65 | 70.89 | 70.12 | 69.36 |
| | 20 years | 90.88 | 80.64 | 68.95 | 55.35 | 53.85 | 52.34 | 50.79 | 49.22 |
| | 30 years | 89.71 | 77.32 | 61.63 | 40.10 | 37.45 | 34.68 | 31.78 | 28.74 |
| | 40 years | 89.18 | 75.41 | 55.85 | 21.32 | 16.04 | 10.18 | 3.62 | 0.00 |

Consider the dramatic collapse of the American buffalo. Suppose the intrinsic growth rate is 10% per year (Lueck, 2002; Jolles, 2007), and the initial buffalo population is at its carrying capacity ($x_0 = \kappa$). Table 5.64 shows the proportion of the remaining buffalo population under different relative harvest rate assumptions after 10, 20, 30, and 40 years.

- If the relative harvest rate $\eta$ is 1%, the remaining buffalo population after 10, 20, 30, and 40 years is 93.6%, 90.9%, 89.7%, and 89.2%, respectively.

- If the relative harvest rate is 4%, these figures decrease to 72.4%, 55.4%, 40.1%, and 21.3%.

- At a relative harvest rate of 4.4%, the buffalo population is completely wiped out (0% remaining) after 40 years.

The previous model can be extended in several directions (Quinn and Deriso, 1999). Gilpin *et al.* (1976) introduced a parameter $\theta \geq 0$ to control the asymmetry of the growth curve:

$$\frac{\mathrm{d}x(t)}{\mathrm{d}t} = \delta x(t)\left(1 - \left(\frac{x(t)}{\kappa}\right)^{\theta}\right) - h(x(t))$$

In this formulation, $\theta$ allows the inflection point of the growth curve to vary between 0 and $\kappa$. When $\theta < 1$ (resp. $\theta > 1$), the maximum growth occurs for $x(t) < \kappa/2$ (resp. $x(t) < \kappa/2$). The case $\theta < 1$ is generally observed when resources are limited. Another extension is to consider different parameterizations of the harvest function. According to Begon and Townsend (2021), the three most popular functions $h(x)$ are:

1. Fixed quota (or constant catch) management
   This specifies a predetermined, fixed number of animals that can be harvested. In this case, $h(x) = q$ is a constant, corresponding to the case we have already studied.

2. Fixed proportion harvesting
   This specifies a proportion $e$ of animals that can be harvested, rather than a specific number:

   $$h(x) = ex$$

   where $e$ is the exploitation rate expressed as a percentage.

3. Fixed escapement (or constant escapement rule)
   This specifies not the number of animals to be harvested, but rather the number of animals to remain unharvested. In this approach, harvest occurs only when the population exceeds a threshold $x_{\min}$, ensuring a minimum escapement:

   $$h(x) = e(x - x_{\min})^{+}$$

Figure 5.89 shows the impact of the parameter $\theta$ and different harvesting management strategies on population size[189]. We note that the parameter $\theta$ has a significant impact when a fixed quota is used, whereas its effect is less pronounced under fixed proportion harvesting. In the latter case, the population dynamics follow the equation:

$$\frac{\mathrm{d}x(t)}{\mathrm{d}t} = (\delta - e)x(t) - \delta\frac{x(t)^2}{\kappa}\left(\frac{x(t)}{\kappa}\right)^{\theta-1}$$

Here, the term $x(t)^2/\kappa$ has a greater magnitude than $(x(t)/\kappa)^{\theta-1}$, particularly when $\theta \geq 1$. We also observe that fixed escapement is the safest exploitation approach, as it ensures that $x^\star > x_{\min}$ — the limit case is obtained as $e \to \infty$.

Overexploitation can also be studied using a second class of multi-species models based on the Lotka-Volterra formulation. In the two-dimensional case, the system is given by:

$$\begin{cases} \dfrac{\mathrm{d}x(t)}{\mathrm{d}t} = ax(t) - bx(t)y(t) - h_x(x(t), y(t)) \\ \dfrac{\mathrm{d}y(t)}{\mathrm{d}t} = cx(t)y(t) - dy(t) - h_y(x(t), y(t)) \end{cases}$$

[189] The intrinsic growth rate $\delta$ is set to 30%, while $x_0$ and $\kappa$ are both equal to 100.

Figure 5.89: Impact of the harvest function and the inflection point

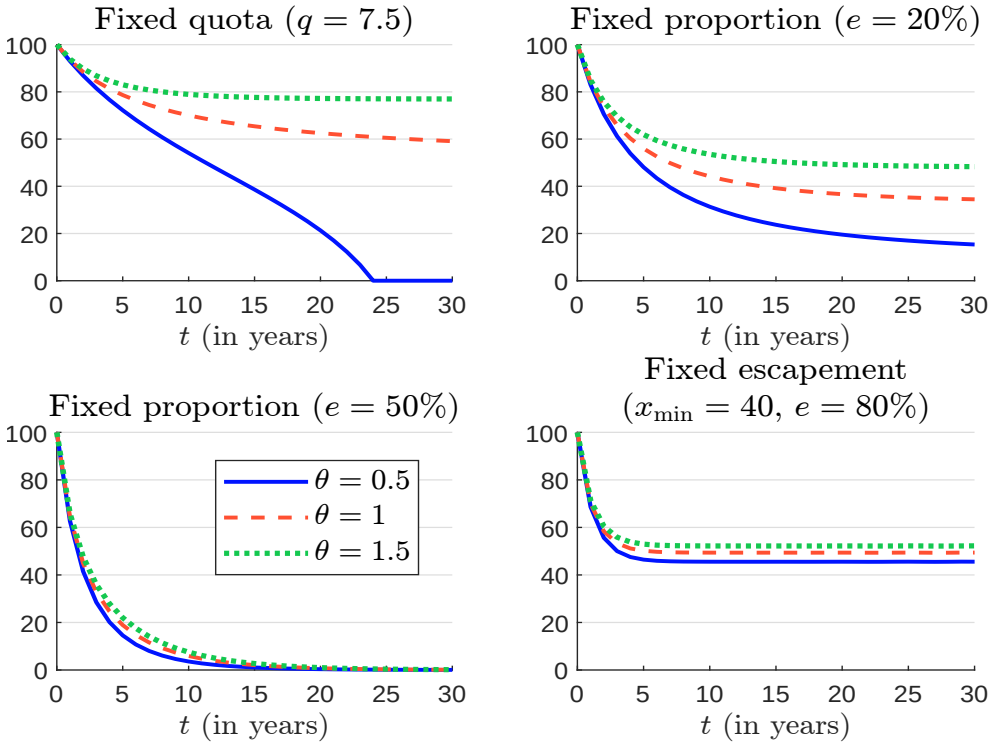


where $h_x(x, y)$ and $h_{x,y}(y)$ are the harvest functions of the prey and predator species, respectively. The classical Lotka-Volterra model is obtained by setting $h_x(x) = h_y(y) = 0$. This model has been extensively studied in both population dynamics modeling and the mathematical field of nonlinear systems, because it can be linked to the theory of deterministic chaos (characterized by sensitive dependence on initial conditions, strange attractors, and bifurcations). We can show that the classical Lotka-Volterra model has an unstable equilibrium at $(0, 0)$ and a stable equilibrium at $\left(\frac{d}{c}, \frac{a}{b}\right)$. Let us assume that $a = 2$, $b = 3$, $c = 2$ and $d = 4$. Figure 5.90 shows the solutions $x(t)$ and $y(t)$ when the initial biomass values are $x_0 = 0.5$ and $y_0 = 1.5$ tonnes. Since there are initially too many predators and not enough prey, the predator population declines in the first phase. This allows the prey population to recover and reproduce, leading to an increase in prey biomass. In the second phase, as the prey population grows, the predators have more food available and begin to increase in number. Ultimately, this predator-prey system generates cyclical dynamics, as illustrated by the vector field analysis of the dynamical system (Figure 5.91). In this example, the cycle lasts 2.70 years. Figure 5.92 shows the phase portrait of the Lotka-Volterra model[190], depicting the orbits or limit cycles generated by the system of differential equations.

[190] We have:

$$\frac{\mathrm{d}y}{\mathrm{d}x} = \frac{cxy - dy}{ax - bxy}$$

It follows that $(ax - bxy)\,\mathrm{d}y = (cxy - dy)\,\mathrm{d}x$. Dividing by $xy$, we get $c\,\mathrm{d}x - d\frac{\mathrm{d}x}{x} + b\,\mathrm{d}y - a\frac{\mathrm{d}y}{y} = 0$. We deduce that the solution is:

$$cx - d\ln x + by - a\ln y = C \tag{5.36}$$

where $C$ is a constant. The phase portrait is the set of solutions $(x, y)$ that satisfy Equation (5.36) for a given value of $C$.

Figure 5.90: Simulation of the Lotka-Volterra model ($a = 2$, $b = 3$, $c = 2$, $d = 4$)

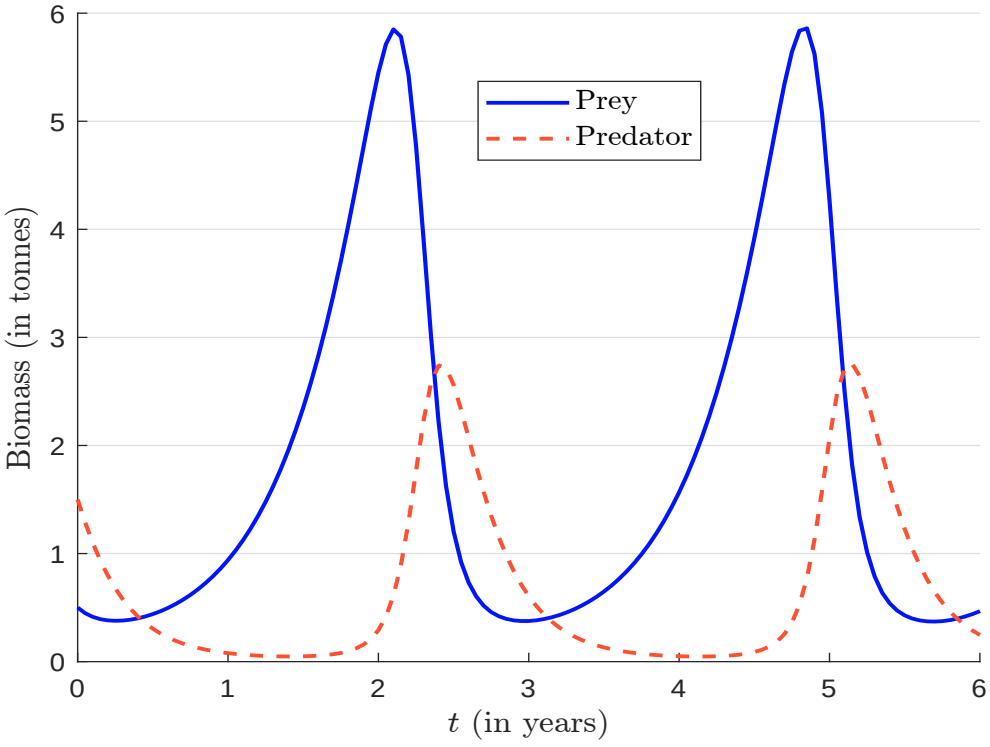


Figure 5.91: Vector field representation of the Lotka-Volterra model ($a = 2$, $b = 3$, $c = 2$, $d = 4$)

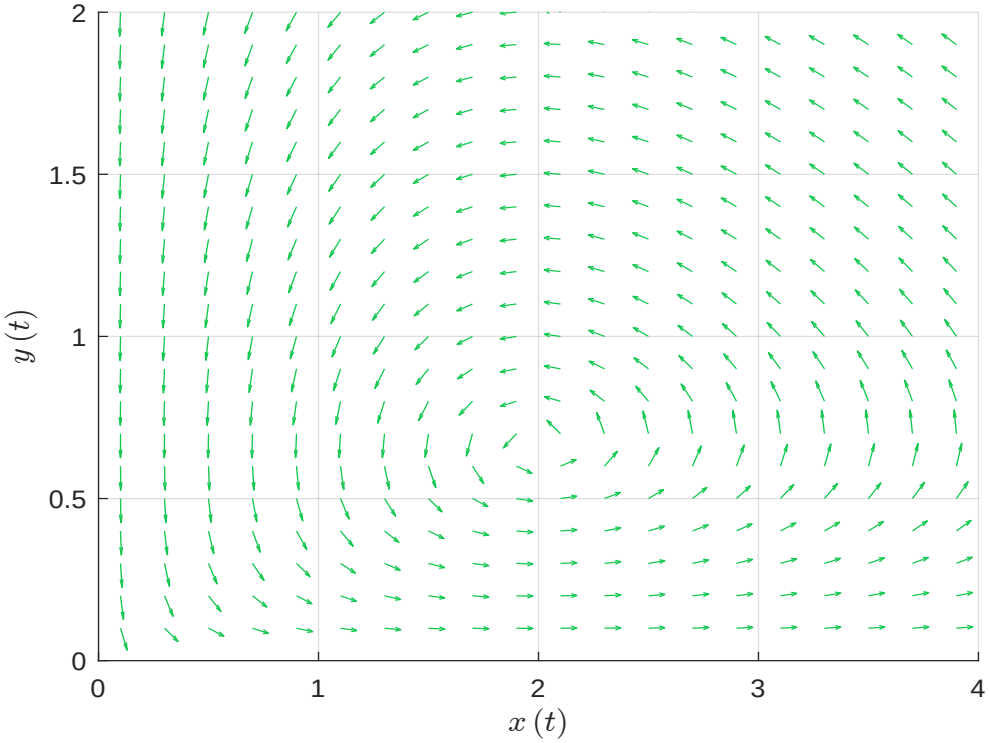

Figure 5.92: Phase portrait of the Lotka-Volterra model ($a = 2$, $b = 3$, $c = 2$, $d = 4$)

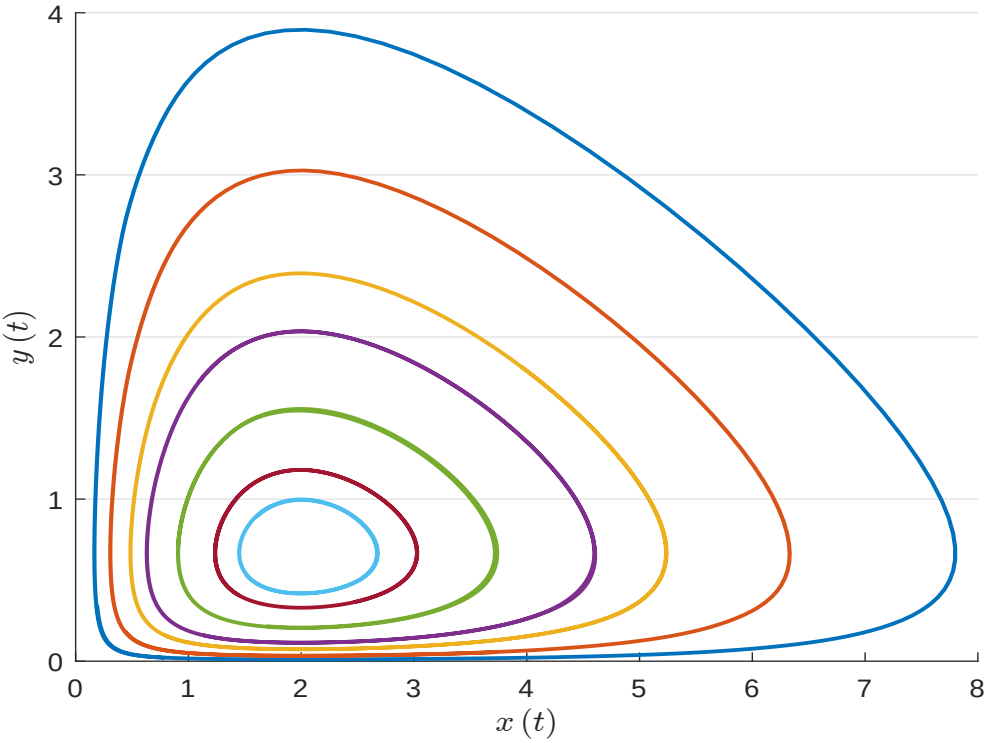


Figure 5.93: Simulation of the Lotka-Volterra model with harvesting ($a = 2$, $b = 3$, $c = 2$, $d = 4$, $e_y = 5$, $y_{\min} = 1$)

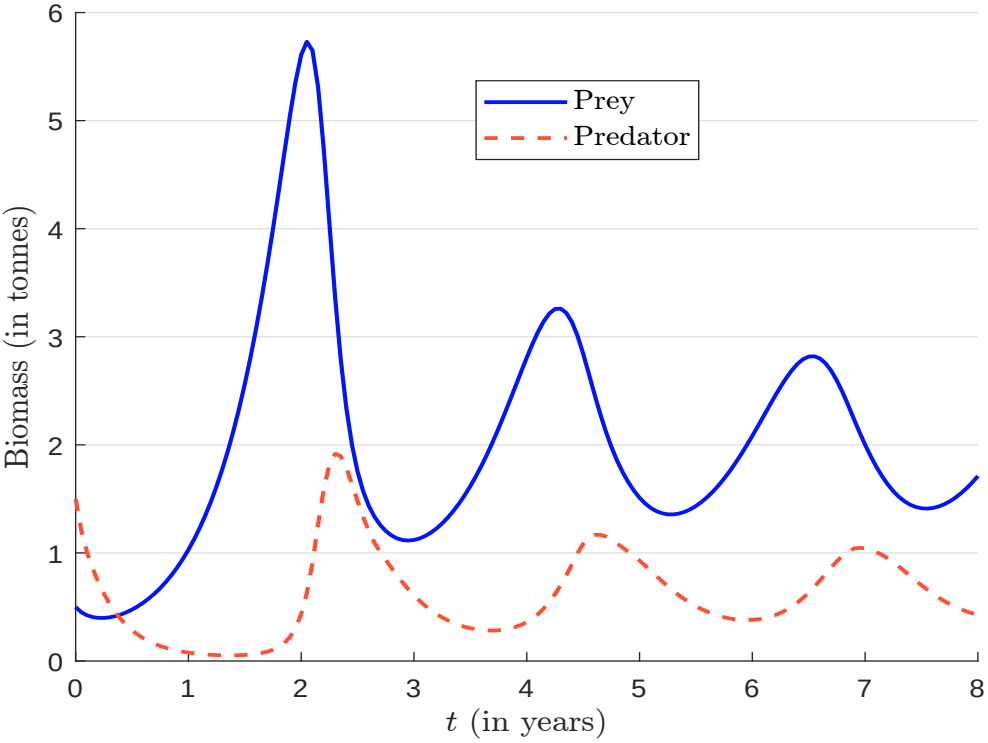

Now let us consider exploitation. There are many ways to specify the harvest functions $h_x(x,y)$ and $h_y(x,y)$. If we aim to protect the prey species, we can set $h_x(x,y) = 0$ and $h_y(x,y) = e_y(y - y_{\min})^+$, where $e_y$ is the exploitation rate of the predator species above the threshold $y_{\min}$. This leads to a dynamic in which the biomass of both prey and predator species becomes more stable (Figure 5.93). Another approach is to protect the prey species when its population falls below a threshold $x_{\min}$. In this case, for example, we can define the harvest function as $h_y(x,y) = e_y y(x_{\min} - x)^+$.

**Remark 65** *The Lotka-Volterra model can also be used to study the impact of invasive species, which can be considered as another form of overexploitation. In this context, $x$ represents the native species, while $y$ represents the invasive species (Roques et al., 2015).*

After its publication, the Lotka-Volterra model was rapidly extended in many directions. In reviewing these developments, Solomon (1949) introduced the concepts of functional and numerical responses:

1. The '*functional response*' describes how the predation rate (*i.e.*, the number of prey consumed per predator) varies with prey density. It quantifies the efficiency of individual predators in capturing and consuming prey.

2. The '*numerical response*' describes how predator population density changes in response to prey density. It reflects the total population-level effect of prey availability on predator numbers, including factors such as predator consumption, reproduction and migration, but excluding natural mortality.

From a mathematical point of view, we can write:

$$\begin{cases} \dfrac{\mathrm{d}x(t)}{\mathrm{d}t} = \delta(t)\,x(t) - f(x(t), y(t))\,y(t) \\ \dfrac{\mathrm{d}y(t)}{\mathrm{d}t} = g(x(t), y(t))\,y(t) - \mu(t)\,y(t) \end{cases}$$

where $\delta(t)$ is the growth rate of the prey species, $f(x,y)$ is the functional response, $g(x,y)$ is the numerical response, and $\mu(t)$ is the mortality rate of the predator species. The classical Lotka-Volterra model is obtained by setting $\delta(t) = a$, $f(x,y) = bx$, $g(x,y) = cx$ and $\mu(t) = d$. In the late 1950s, Holling (1959a,b) conducted a comprehensive review of predation theory and proposed a classification of predation models based on the form of their functional responses. These types describe how predation rate varies with prey density:

- Type I (linear)
  Predation rate increases linearly with prey density until a maximum is reached. This simple, though somewhat unrealistic, model assumes that predators can process prey immediately upon encounter. It's often used in simplified models.

- Type II (decelerating)
  Predation rate still increases with prey density, but the rate of increase slows as prey becomes more abundant. This reflects factors such as predator handling time (the time it takes to consume each prey item) or satiation (when the predator becomes full).

- Type III (sigmoidal)
  Predation rate follows a sigmoidal curve, *i.e.*, a slow initial increase at low prey densities, followed by an accelerated increase at moderate densities, and finally saturation at high densities.

This pattern often results from more complex predator behavior, such as learning, improved search efficiency, or the presence of prey refugia. It suggests that predators initially struggle to find or handle prey, but become more efficient over time.

Since Holling's publication, a fourth type has been added. Type IV responses are not monotonic. They increase to a maximum rate and decrease for higher values of x. The decrease can be explained by resource toxicity or predator confusion (Gentleman *et al.*, 2003). These responses can be found for some bacterial processes. Below, we give some examples of functional responses:

| Type | I | II | III | IV |
|---|---|---|---|---|
| $f(x,y)$ | $cx$ | $\frac{\alpha x}{\beta + x}$ | $\frac{\alpha x^2}{\beta + x^2}$ | $\frac{\alpha x}{\beta + x + \gamma x^2}$ |

These responses are illustrated[191] in Figure 5.94. Type II responses are the most well-known, as they are associated with the Michaelis-Menten-Monod equation.

Figure 5.94: Holling functional responses

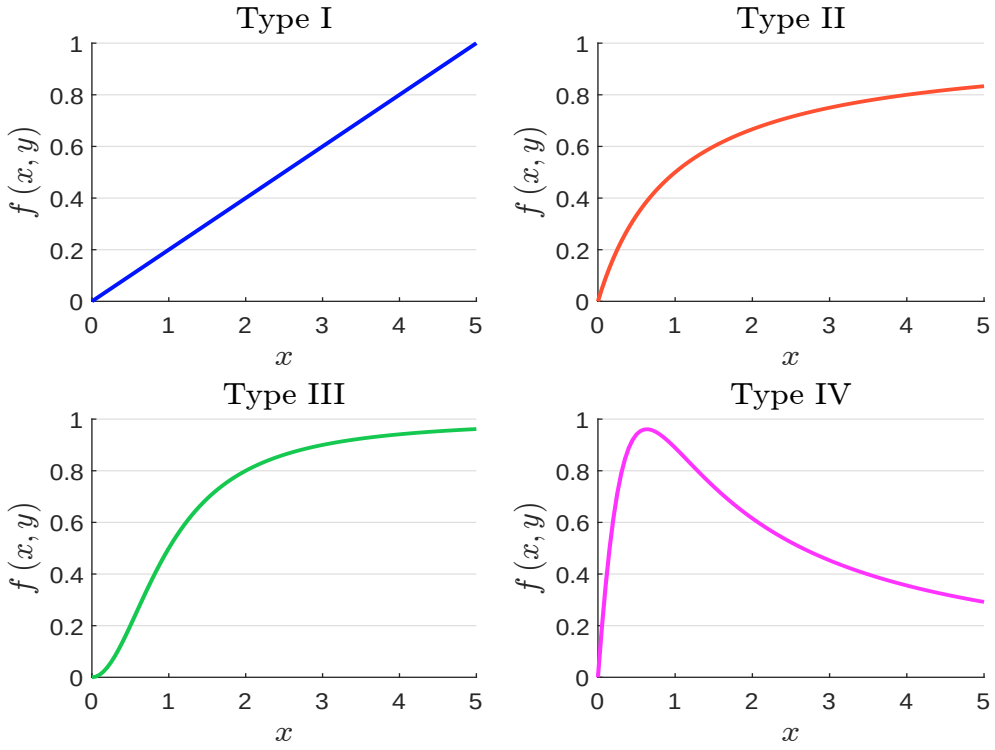


Tanner (1975) used the Holling Type II functional response and assumed that both prey and predator populations follow a logistic growth model. This leads to the Holling-Tanner predator-prey model:

$$\begin{cases} \dfrac{\mathrm{d}x(t)}{\mathrm{d}t} = \delta x(t)\left(1 - \dfrac{x(t)}{\kappa}\right) - \dfrac{\alpha x(t)}{\beta + x(t)} y(t) \\ \dfrac{\mathrm{d}y(t)}{\mathrm{d}t} = \sigma y(t)\left(1 - \dfrac{y(t)}{\gamma x(t)}\right) \end{cases}$$

[191] We have used the following parameters: $c = 0.2$ (type I), $\alpha = \beta = 1$ (types II and III), $\alpha = 4$, $\beta = 1$ and $\gamma = 2.5$ (type IV).

where $x(t)$ is the prey population and $y(t)$ is the predator population. Here, the carrying capacity of the predator population is related to the size of the prey population: $\kappa_y = \gamma x(t)$. The interpretation of the parameters is the following: $\delta$ is the intrinsic growth rate of the prey, $\kappa$ is the carrying capacity of the prey, $\alpha$ is the maximum predation rate, $\beta$ is the half-saturation constant that determines how prey abundance affects predation, $\sigma$ is the intrinsic growth rate of the predators, and $\gamma$ is the maximum predator-prey ratio. This model is more complex than the single logistic growth model because it can have four critical points[192]. Figure 5.95 shows the simulation[193] of the Holling-Tanner predator-prey model when the initial values are $x_0 = 8$ and $y_0 = 5.5$, and the parameters are $\delta = 10\%$, $\kappa = 100$, $\alpha = 4$, $\beta = 20$, $\sigma = 20\%$, and $\gamma = 10\%$.

Figure 5.95: Simulation of the Holling-Tanner predator-prey model

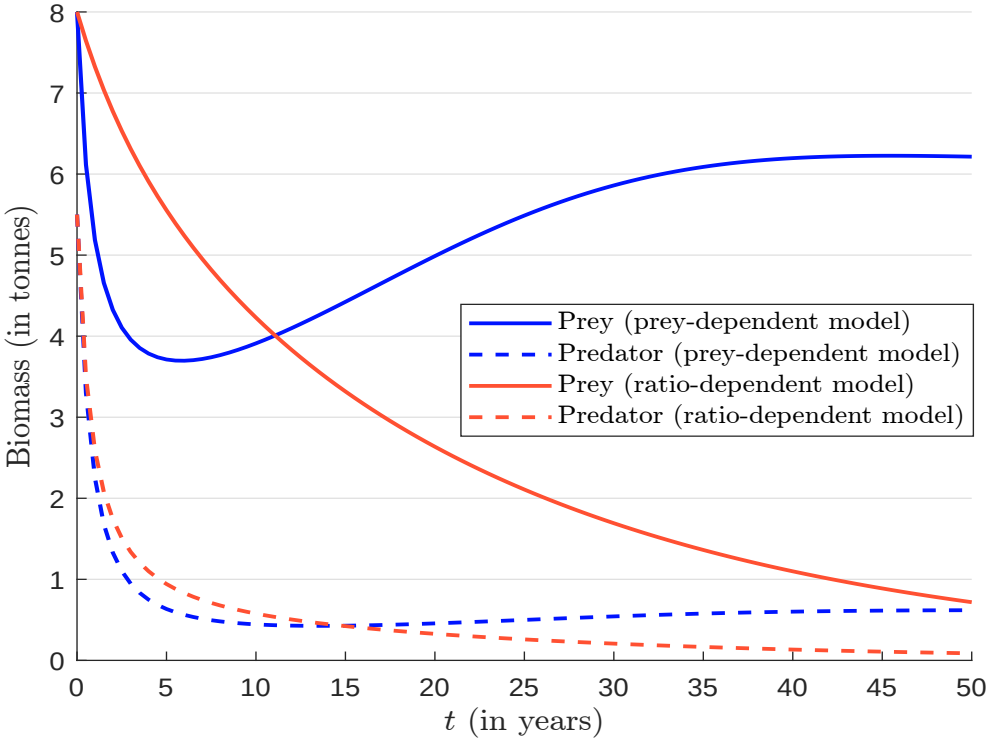


Previous functional responses depend only on the prey population. In a seminal paper, Arditi and Ginzburg (1989) challenge the traditional view of predator-prey interactions in which the predator's consumption rate depends solely on prey density. They propose an alternative approach in which

[192]The stability analysis implies that:

$$\frac{\mathrm{d}y(t)}{\mathrm{d}t} = 0 \Leftrightarrow y(t) = 0 \wedge y(t) = \gamma x(t)$$

and:

$$\frac{\mathrm{d}x(t)}{\mathrm{d}t} = 0 \Leftrightarrow \delta x(\kappa - x)(\beta + x) - \alpha\gamma\kappa x^2 = 0$$

We can show that there can be four equilibria: $(0,0)$, $(\kappa,0)$, $(x_-, \gamma x_-)$ and $(x_+, \gamma x_+)$ where:

$$x_\pm = \frac{(\delta\kappa - \delta\beta - \alpha\gamma\kappa) \pm \sqrt{(\delta\kappa - \delta\beta - \alpha\gamma\kappa)^2 + 4\beta\delta^2\kappa}}{2\delta}$$

[193]It corresponds to the blue curve.

the predator's consumption rate depends on the ratio of prey to predator densities, introducing the concept of ratio-dependent predation $r = x/y$:

$$f(x, y) = \frac{\alpha r}{\beta + r} = \frac{\alpha x}{\beta y + x}$$

In prey-dependent models (Holling type II), when prey is rare, predation is still significant. In ratio-dependent models, when prey is rare relative to predators, predation decreases dramatically, which is more realistic in nature. Figure 5.95 shows the effect of using a ratio-dependent model instead of a prey-dependent model[194].

**Remark 66** *The introduction of harvesting in the Holling-Tanner predator-prey model is the same as in the Lotka-Volterra model. We can then derive the equilibria (Diz-Pita and Otero-Espinar, 2021), analyze the effects of harvesting policy and define the maximum sustainable yield (Ghosh and Kar, 2013; Kar and Ghosh, 2013).*

While predator-prey models describe interactions in which one species benefits at the expense of another, competition models describe interactions in which both species suffer from their coexistence due to competition for shared resources such as food, space, or other ecological resources (Polis *et al.*, 1989). The most well-known competition model is the Lotka-Volterra multi-species competition model, which is mathematically similar to the predator-prey model but with negative interactions for both species (Case and Gilpin, 1974):

$$\frac{\mathrm{d}x_i(t)}{\mathrm{d}t} = \delta_i x_i(t) \left(1 - \frac{\sum_{j=1}^{n} \omega_{i,j} x_j(t)}{\kappa_i}\right) \tag{5.37}$$

where $i = 1, \ldots, n$ is the species index, $n$ is the number of species, $\delta_i$ and $\kappa_i$ are the intrinsic growth rate and the carrying capacity of species $i$, and $\omega_{i,j} \geq 0$ is the competition coefficient (how much species $j$ affects species $i$). Another interference competition model consists in considering that each species is a prey for the other species. In this case, we consider a multi-species logistic growth model and include Lotka-Volterra penalties:

$$\frac{\mathrm{d}x_i(t)}{\mathrm{d}t} = \delta_i x_i(t) \left(1 - \frac{x_i(t)}{\kappa_i}\right) - \sum_{j \neq i} \alpha_{i,j} x_i(t) x_j(t) \tag{5.38}$$

where $\alpha_{i,j} \geq 0$ is the coefficient of interaction between species $i$ and $j$. More generally, interference competition models combine the logistic growth model and Holling functional responses:

$$\frac{\mathrm{d}x_i(t)}{\mathrm{d}t} = \delta_i x_i(t) \left(1 - \frac{x_i(t)}{\kappa_i}\right) - \sum_{j \neq i} f_{i,j}(x_1(t), \ldots, x_n(t)) x_j(t) \tag{5.39}$$

Model (5.38) is a special case of model (5.39) when we use a Holling type I linear response: $f_{i,j}(x_1, \ldots, x_n) = \alpha_{i,j} x_i$. For Holling type II responses, we can write:

$$f_{i,j}(x_1, \ldots, x_n) = \frac{\alpha_{i,j} x_i}{\beta_{i,j} + x_i}$$

These different models can exhibit chaotic behavior, even in low dimension. For instance,

[194] We use exactly the same parameters and initial values as in the classical Holling-Tanner prey-dependent model. The blue curves correspond to the prey-dependent model, while the red curves correspond to the ratio-dependent model.

Box 5.24: Symbiosis and interspecific interactions

The term symbiosis, derived from Greek roots meaning '*together*'and '*living*', describes a close and long-term biological interaction between two different organisms. An ecological community includes all the populations of different species that coexist in a given area. The interactions between these species are called interspecific interactions. They can be categorized as positive (+), negative (−), or neutral (0) based on their effects on the species involved (Polis *et al.*, 1989). There are seven broad types of symbiosis:

1. Amensalism (−/0)
   One species is harmed and the other is unaffected, often through the release of a chemical compound.

2. Commensalism (+/0)
   One species benefits while the other remains unaffected. A classic example is barnacles that attach themselves to whales for transportation, gaining a mobile habitat while the whale remains indifferent.

3. Competition (−/−)
   Both species are negatively affected by the limited availability of shared resources such as food, water, or nesting sites. For example, the swift fox (*Vulpes velox*) and coyotes (*Canis latrans*) competing for the same resources may both experience reduced reproductive success (Kitchen *et al.*, 1999).

4. Mutualism (+/+)
   Both species benefit from the interaction. A common example is the relationship between bees and flowers, where bees receive food (nectar) and flowers receive pollination assistance.

5. Neutralism (0/0)
   Neither species is affected by the interaction. Although theoretically possible, true neutralism is difficult to prove definitively in complex ecosystems. For example, a butterfly and a snake living in the same habitat may appear neutral.

6. Parasitism (+/−)
   One species (the parasite) benefits at the expense of the other (the host). Ticks that feed on the blood of a mammal are an example of this relationship, where the tick gains nourishment while the host experiences potential harm and irritation.

7. Predation (+/−)
   One species (the predator) benefits by killing and consuming the other (the prey). A lion hunting a zebra is a clear example of predation.

Vano *et al.* (2006) studied model (5.37) with four species and the following parameters: $\delta = (1.00, 0.72, 1.53, 1.27)$, $\kappa = (10, 10, 10, 10)$ and:

$$\Omega = (\omega_{i,j}) = \begin{pmatrix} 1 & 1.09 & 1.52 & 0 \\ 0 & 1 & 0.44 & 1.36 \\ 2.33 & 0 & 1 & 0.47 \\ 1.21 & 0.51 & 0.35 & 1 \end{pmatrix}$$

They showed that the chaotic attractor of this dynamical system corresponds to homoclinic orbits (Figure 5.96).

Figure 5.96: Phase portrait of the Lotka-Volterra four-species competition model

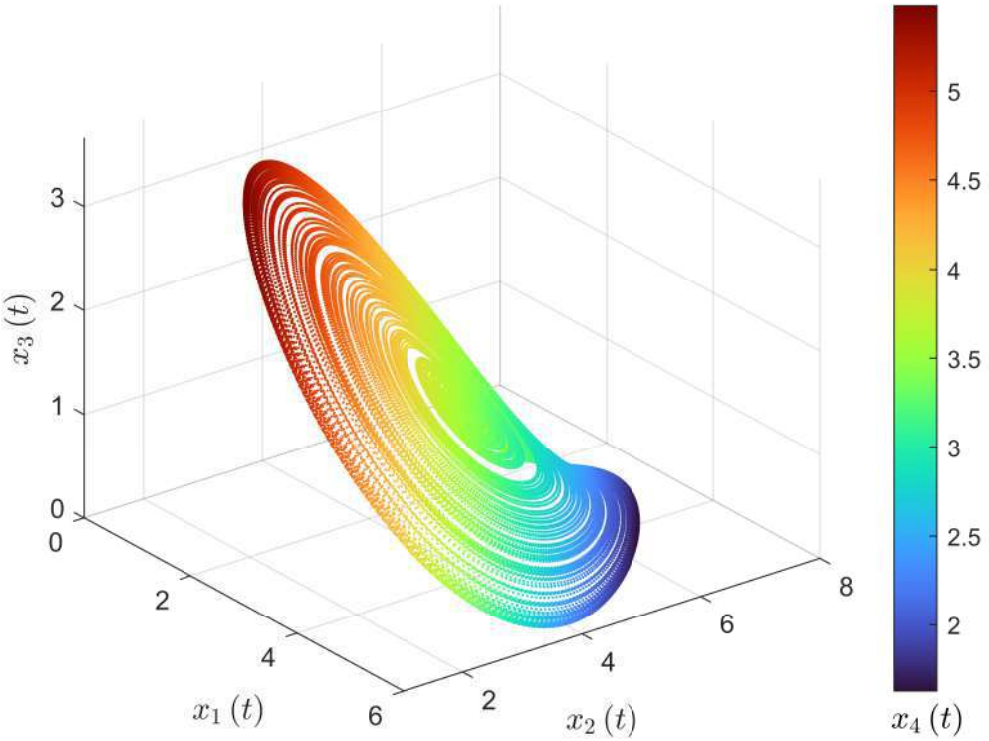


Source: Vano *et al.* (2006, Figure 3, page 2386).

A second family of competition models explicitly introduces a set of resources. One of the first explicit resource competition models was proposed by MacArthur and Levins (1964). This model has been extensively used and extended by Robert MacArthur in several research papers and is now known as MacArthur consumer-resource model (Chesson, 1990). In MacArthur (1970), the model is formulated as follows:

$$\begin{cases} \dfrac{\mathrm{d}x_i(t)}{\mathrm{d}t} = \beta_i x_i(t) \left( \displaystyle\sum_{j=1}^{m} \alpha_{i,j} \omega_j y_j(t) \right) - \mu_i x_i(t) \\ \dfrac{\mathrm{d}y_j(t)}{\mathrm{d}t} = \delta_j y_j(t) \left( 1 - \dfrac{y_j(t)}{\kappa_j} \right) - \displaystyle\sum_{i=1}^{n} \alpha_{i,j} x_i(t) \end{cases}$$

where $x_i(t)$ represents the population density of species $i$, $y_j(t)$ represents the population density of resource $j$ (*e.g.*, food resources), $\beta_i$ is a conversion factor that translates resource consumption into per capita growth rate, $\alpha_{i,j}$ is the rate at which species $i$ captures resource $j$, $\omega_j$ is the value of a unit of resource $j$ to the consumer (*e.g.*, caloric energy), $\mu_i$ is the mortality rate of species $i$, and $\delta_j$ is the intrinsic growth rate of resource $j$. A variant of the MacArthur model assumes that resource availability depends on three factors: supply, depletion and consumption. In this case, we

Box 5.25: Robert H. MacArthur

Despite his tragically short life (1930–1972), Robert MacArthur was one of the most influential ecologists of the 20th century (Fretwell, 1975; Brown, 1999). He received his Ph.D. from Yale University in 1957 under the direction of G. E. Hutchinson and was a professor at the University of Pennsylvania and Princeton University. He is known for developing the theory of island biogeography, the study of limiting similarity (niche theory), consumer-resource theory, and his contributions to the complexity-stability debate. According to Brown (1999), "*MacArthur's influence stems not only from his substantial and frequently cited published works but also from his direct personal interactions and collaborations with contemporary scientists, especially young people*". He had a significant influence on his co-authors, all of whom went on to brilliant careers: Martin L. Cody, Joseph Hurd Connell, Jared Mason Diamond, Henry Stainken Horn, George Evelyn Hutchinson, James R. Karr, Peter Hubert Klopfer, Richard Levins, Robert McCredie May, Harry Frederick Recher, Eric Rodger Pianka, Michael L. Rosenzweig, and Edward Osborne Wilson.

obtain the following Lotka-Volterra competition model with externally supplied resources (Cui *et al.*, 2024):

$$\begin{cases} \dfrac{\mathrm{d}x_i(t)}{\mathrm{d}t} = \beta_i x_i(t)\left(\sum_{j=1}^{m}\alpha_{i,j}\omega_j y_j(t)\right) - \mu_i x_i(t) \\ \dfrac{\mathrm{d}y_j(t)}{\mathrm{d}t} = \kappa_j - \varrho_j y_j(t) - \left(\sum_{i=1}^{n}\alpha_{i,j}x_i(t)\right) y_j(t) \end{cases}$$

where $\kappa_j$ is the supply of resource $j$, $\varrho_j$ is the natural depletion or decay rate of resource $j$, and $\alpha_{i,j}$ is the rate at which species $i$ consumes resource $j$. Along with Robert MacArthur, David Tilman is another prolific researcher on competition models and their impact on community structure. In his book, Tilman (1982) used the following general formulation:

$$\begin{cases} \dfrac{\mathrm{d}x_i(t)}{\mathrm{d}t} = f_i(y_1(t),\ldots,y_m(t))\,x_i(t) - \mu_i(t)\,x_i(t) \\ \dfrac{\mathrm{d}y_j(t)}{\mathrm{d}t} = g_j(y_j(t)) - \sum_{i=1}^{n}\alpha_{i,j}(y_1(t),\ldots,y_m(t))\,f_i(y_1(t),\ldots,y_m(t))\,x_i(t) \end{cases}$$

where $f_i(y_1,\ldots,y_m)$ is the growth function of consumer $i$, $\mu_i(t)$ is the mortality rate function of consumer $i$, $g_j(y_j)$ is the growth function of resource $j$, and $\alpha_{i,j}(y_1,\ldots,y_m)$ is the conversion factor function from resource $j$ to consumer $i$. The MacArthur consumer-resource model and the Lotka-Volterra competition model with externally supplied resources are both special cases of Tilman's general model[195].

[195]The MacArthur consumer-resource model is obtained by setting $f_i(y_1,\ldots,y_m) = \beta_i\sum_{j=1}^{m}\alpha_{i,j}\omega_j y_j$, $\mu_i(t) = \mu_i$,

The competitive exclusion principle (or Gause's law) states that two species competing for exactly the same resource cannot stably coexist indefinitely. One will outcompete the other. For coexistence to occur, the species must occupy slightly different niches or use resources differently (niche theory). This traditional interpretation of competitive exclusion and niche theory has been challenged by much research. In fact, although there are many examples where the traditional interpretation is valid[196], there are also many examples where multiple competitive species can coexist[197]. Moreover, Armstrong and McGehee (1980) demonstrated that under certain conditions, multiple species can coexist with fewer resources in a Lotka-Volterra model of multi-species competition. In fact, the relationship between biodiversity and competition is more complex, as demonstrated by Chesson (1990), who examined the processes that allow multiple species to coexist within the same ecological community and addressed the apparent paradox of high biodiversity despite competitive interactions. He categorized mechanisms that promote species coexistence into two primary types: equalizing mechanisms (which reduce average fitness differences between species, minimizing competitive inequalities) and stabilizing mechanisms (which increase negative intraspecific interactions relative to interspecific interactions, promoting coexistence by ensuring that species limit their own population growth more than they limit that of others). He also emphasized that environmental variability, both spatial and temporal, can facilitate coexistence. It follows that competition and harvesting are not equivalent. It is not obvious that competition dramatically reduces biodiversity, which is not the case with harvesting. However, the effects of harvesting strategies in multi-species consumer-resource metapopulations are not well known. For example, Strevens and Bonsall (2011) found that certain harvesting strategies, particularly fixed proportion harvesting, resulted in larger regional population sizes, fewer local extinctions, and higher yields compared to unharvested metapopulations. This counterintuitive result suggests that increasing local mortality through specific harvesting methods can increase overall population sizes — a phenomenon referred to as the '*hydra effect*'. However, as Abrams (2009) points out, there is little empirical evidence for hydra effects in nature. Thus, there is a gap between previous theoretical and empirical results.

**Overexploitation in aquatic systems** In the early 2000s, several important research papers alerted the scientific community to the threat of overfishing and the potential collapse of marine ecosystems. Jackson *et al.* (2001) examined how historical overfishing had led to the degradation and collapse of coastal ecosystems over time. Using a variety of historical data — including archaeological records, historical documents, and paleoecological studies — the authors described how the removal of top predators and key species (*e.g.*, sharks, sea otters, cod, oysters) through overfishing could trigger cascading effects throughout the food web, leading to shifts in the abundance and distribution of other species. For example, the loss of large predators led to an increase in prey species, which in turn overgrazed habitats. In addition, the destruction of habitat-forming species (*e.g.*, oyster

$g_j(y_j) = \delta_j y_j\left(1-\kappa_j^{-1}y_j\right)$, and $\alpha_{i,j}(y_1,\ldots,y_m) = \left(\beta_i\sum_{j=1}^m \alpha_{i,j}\omega_j y_j\right)^{-1}\alpha_{i,j}$. For the Lotka-Volterra competition model with externally supplied resources, the generic functions for the resources are $g_j(y_j) = \kappa_j - \varrho_j y_j$, and $\alpha_{i,j}(y_1,\ldots,y_m) = \left(\beta_i\sum_{j=1}^m \alpha_{i,j}\omega_j y_j\right)^{-1}\alpha_{i,j}y_j$.

[196] A famous example is the competition between the flour beetles *Tribolium castaneum* and *Tribolium confusum* (Park, 1962; Pointer *et al.*, 2021).

[197] A well-known example that challenges the competitive exclusion principle is the plankton paradox, first described by Hutchinson (1961). In aquatic ecosystems, numerous species of phytoplankton coexist despite competing for a limited number of resources such as light, nitrogen, and phosphorus. According to the principle of competitive exclusion, only a few dominant species should survive because they would outcompete the others. In natural environments, however, dozens of phytoplankton species coexist in the same habitat. A second well-known example was described by MacArthur (1958), who studied five species of warblers (small songbirds) coexisting in the same forest areas and apparently feeding on the same insects. This apparent contradiction of competitive exclusion led to the development of the theory of niche differentiation.

reefs, seagrass beds, corals) led to a decline in biodiversity and ecosystem functions. Pauly *et al.* (2002) introduced the concept of '*fishing down marine food webs*', where fisheries increasingly target smaller, lower trophic level species as larger predatory fish become scarce. The authors emphasized that without significant intervention, global fisheries would continue to decline, putting marine biodiversity at risk. Pauly *et al.* (2005) built on these themes and expanded the discussion of the consequences of overfishing for marine ecosystems and global food security:

> "*With the development of industrial fishing, and the resulting invasion of the refuges previously provided by distance and depth, our interactions with fisheries resources have come to resemble the wars of extermination that newly arrived hunters conducted 40 000–50 000 years ago in Australia, and 12 000–13 000 years ago against large terrestrial mammals in North America.*" (Pauly *et al.*, 2005, page 5).

Another milestone was reached with the publication of empirical research by Myers and Worm (2003) and Worm *et al.* (2006) in *Nature* and *Science*. Myers and Worm (2003) defined the following biomass time-trend model:

$$N_i(t) = N_i(0)\left((1-\varphi_i)\,e^{-r_i(t-t_0)} + \varphi_i\right)$$

where $N_i(t)$ is the biomass at time $t$, $N_i(0)$ is the initial biomass before industrialized exploitation, $r_i$ is the rate of decline and $\varphi_i$ is the fraction of the community that remains at equilibrium as $t \to \infty$. Using large predator biomass data from nine oceanic ecosystems (tropical/subtropical/temperate $\times$ Atlantic/Indian/Pacific) and four shelf ecosystems (Gulf of Thailand, South Georgia, Southern Grand Banks, and Saint Pierre Banks), they estimated the coefficients $\hat{r}_i$ and $\hat{\varphi}_i$ by using the method of maximum likelihood, and the parameters of the nonlinear mixed-effects models assuming that $r_i \sim \mathcal{N}(\mu_r, \sigma_r^2)$ and $\varphi_i \sim \mathcal{N}(\mu_\varphi, \sigma_\varphi^2)$. Figure 5.97 shows the results for the global region and three specific regions[198]. The authors concluded that industrialized fisheries typically reduce community biomass by 80% within 15 years of exploitation, and that the biomass of large predatory fishes is now only about 10% of pre-industrial levels. Worm *et al.* (2006) "*analyzed local experiments, long-term regional time series, and global fisheries data to test how biodiversity loss affects marine ecosystem services across temporal and spatial scales.*" They found that "*rates of resource collapse increased and recovery potential, stability, and water quality decreased exponentially with declining diversity.*" They emphasized that their findings highlight the societal consequences of the ongoing erosion of biodiversity, which appears to be accelerating globally. Moreover, they expressed serious concern about this trend, as their regression model predicted the global collapse of all commercially

[198] Below, we report the estimated values found by Myers and Worm (2003, Table 1, page 281):

| Region | $\hat{r}_i$ | $\hat{\mu}_r$ | $\hat{\varphi}_i$ | $\hat{\mu}_\varphi$ |
|---|---|---|---|---|
| Tropical Atlantic | 16.6 | 16.7 | 12.1 | 11.9 |
| Subtropical Atlantic | 12.9 | 13.0 | 8.1 | 8.3 |
| Temperate Atlantic | 21.4 | 20.3 | 4.7 | 5.3 |
| Tropical Indian | 9.2 | 9.5 | 17.6 | 16.8 |
| Subtropical Indian | 6.5 | 6.8 | 8.2 | 9.2 |
| Temperate Indian | 30.7 | 27.7 | 5.5 | 6.3 |
| Tropical Pacific | 12.1 | 12.4 | 15.5 | 14.9 |
| Subtropical Pacific | 12.8 | 13.5 | 23.5 | 21.5 |
| Temperate Pacific | 20.8 | 20.4 | 8.2 | 8.5 |
| Gulf of Thailand | 25.6 | 22.2 | 9.3 | 9.8 |
| South Georgia | 166.6 | 30.8 | 20.9 | 16.0 |
| Southern Grand Banks | 4.0 | 5.7 | 0.0 | 10.0 |
| Saint Pierre Banks | 5.1 | 6.3 | 2.7 | 7.9 |
| Global | | 16.0 | | 10.3 |

fished taxa by the mid-21st century (specifically, by 2048). Some newspapers and journalists have focused on this figure, interpreting it as a prediction that "*the oceans will be empty by 2048*". For example, this claim was mentioned in the controversial documentary *Seaspiracy*, which premiered on Netflix in 2021.

Figure 5.97: Time trends of community biomass in oceanic and shelf ecosystems

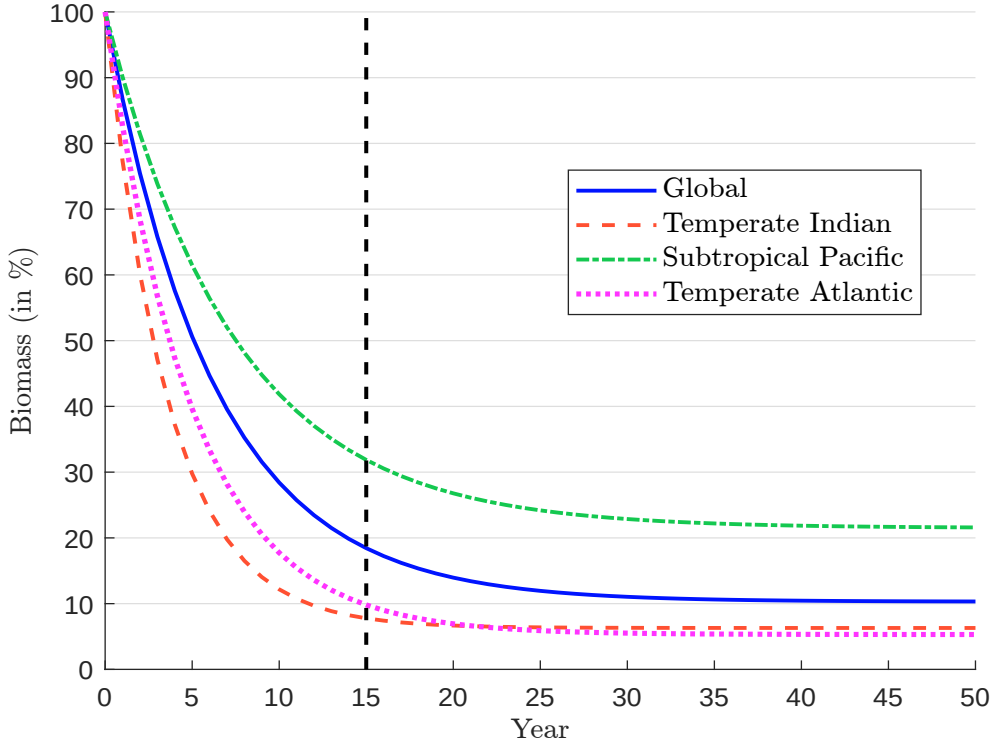


Source: Myers and Worm (2003, Figure 1, page 280) & Author's calculations.

As Boris Worm later explained, this period marked the peak of pessimism. Indeed, Worm's study was not the only one with a gloomy outlook — many studies in the 2000s warned that the collapse of global fisheries could become a reality. Thurstan *et al.* (2010) analyzed annual demersal fish landings from bottom trawls in the United Kingdom from 1889 to 2007 (Figure 5.98). Their results showed a dramatic decline in the commercial productivity of fisheries, with landings per unit of fishing power falling by 94% over the past 118 years. Another well-known example is the collapse of the Atlantic cod fishery in eastern Canada (Myers *et al.*, 1997). According to Schijns *et al.* (2021), "*the fishery for Northern Atlantic cod (Gadus morhua) off Newfoundland and Labrador, Eastern Canada, presents the most spectacular case of an exploited stock crashed in a few decades by an industrial bottom trawl fishery under a seemingly sophisticated management regime after half a millennium of sustainable fishing. The fishery, which had generated annual catches of 100 000 to 200 000 tonnes from the beginning of the 16th century to the 1950s, peaked in 1968 at 810 000 tonnes, followed by a devastating collapse and closure 24 years later.*" Figure 5.99 illustrates the evolution of cod harvests in eastern Canada. We observe a continuous increase throughout the 18th and 19th centuries, with a sharp acceleration in the 20th century, especially after 1960. Schijns *et al.* (2021) estimated the maximum sustainable yield at 380 000 tonnes, a level well below the harvest volumes recorded between 1960 and 1990. We have also reported the estimated stock levels in Figure 5.99, which

Figure 5.98: Fish catch in the United Kingdom

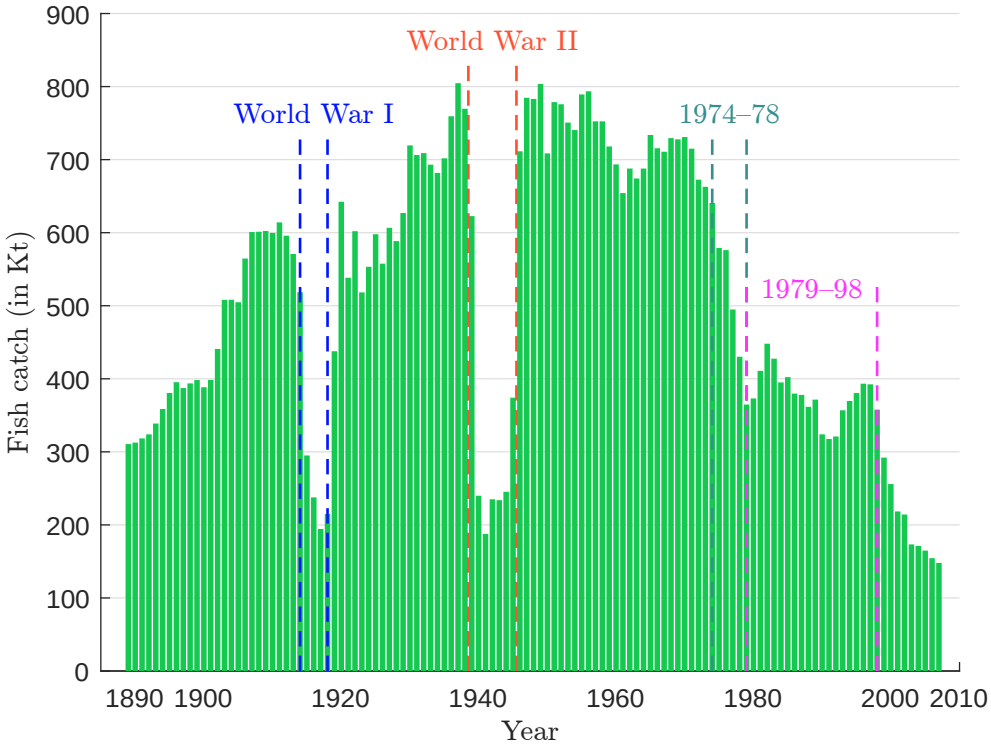


Source: Thurstan *et al.* (2010, Figure 1a, page 2) & `www.ourworldindata.org/fish-and-overfishing`.

Figure 5.99: Northern code catch in eastern Canada

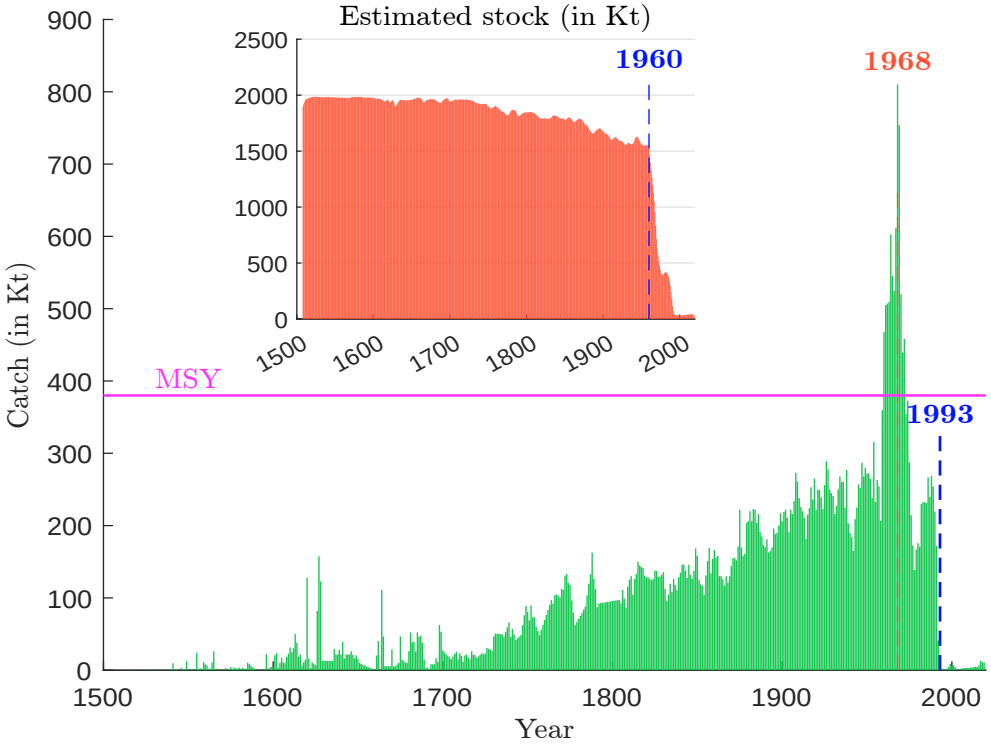


Source: Schijns *et al.* (2021, Figure 1, page 2679) & Author's calculations.

clearly shows the abrupt collapse in just thirty years[199]. On July 2, 1992, the Canadian government announced a moratorium on cod fishing. Originally intended to be a temporary two-year ban to allow the northern cod population to recover, the moratorium has effectively become permanent, as cod stocks have shown very limited signs of recovery even after more than 30 years. This decision had a devastating impact on coastal communities that depended on the fishery, resulting in the loss of approximately 30 000 jobs — one of the largest mass layoffs in Canadian history. Other notable examples of fishery collapses and management challenges include the Californian Pacific sardine collapse (which reached its lowest point in the mid-1950s), the Peruvian anchoveta crisis (1972-1973, triggered by an El Niño event combined with overfishing), the overexploitation of orange roughy (beginning in the 1980s, particularly severe in New Zealand and Australia), the significant decline of Pacific bluefin tuna (throughout the 20th century), and the Namibian sardine collapse (late 1960s to early 1970s). In some cases, however, these species have shown signs of recovery.

Figure 5.100: Global seafood production in Mt (1960–2022)

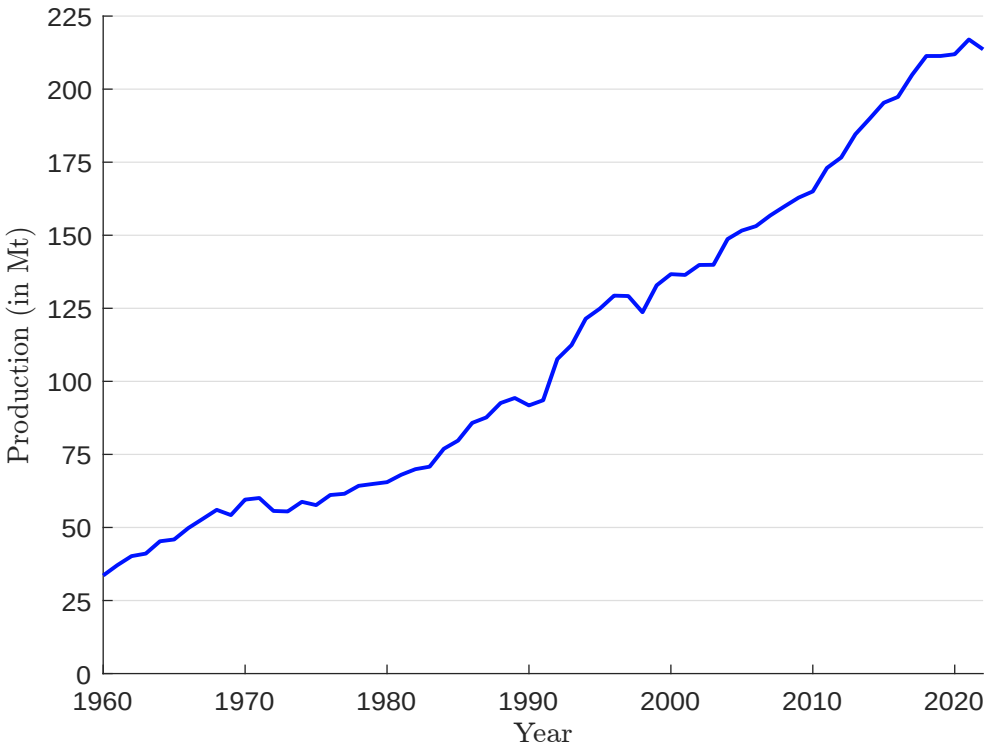


Source: https://databank.worldbank.org/source/world-development-indicators & Author's calculations.

To better understand the current sustainability of fisheries in the world, we refer to the FAO report on world fisheries and aquaculture. According to FAO (2024b), fish production (including algae production) reached a new record high, with a total production[200] of 223.2 million tonnes (Figure 5.100). Of this production, 89% is used for human consumption, equivalent to an estimated 20.7 kg

[199]The biomass stock is estimated using the discrete version of the logistic growth population model with harvest:

$$x(t+1) = x(t) + \delta x(t)\left(1 - \frac{x(t)}{\kappa}\right) - h(t)$$

where $x(t)$ is the biomass stock in year $t$, $\delta$ is the intrinsic growth rate, $\kappa$ is the carrying capacity and $h(t)$ is the fish harvest in year $t$.

[200]63% of this production is finfish, 17% algae, 11% molluscs and 8% crustaceans.

per capita, while the remainder is mainly used for fishmeal and fish oil. The FAO estimates that 61.8 million people are employed in the primary production sector. In sixty years, fish production has increased by a factor of more than 5, while the growth rate between 1960 and 2022 is 2.98%. These figures can be explained by two factors: an increase in the world's population and an increase in the share of seafood in the human diet.

Figure 5.101: Global capture fisheries and aquaculture in Mt (1960–2022)

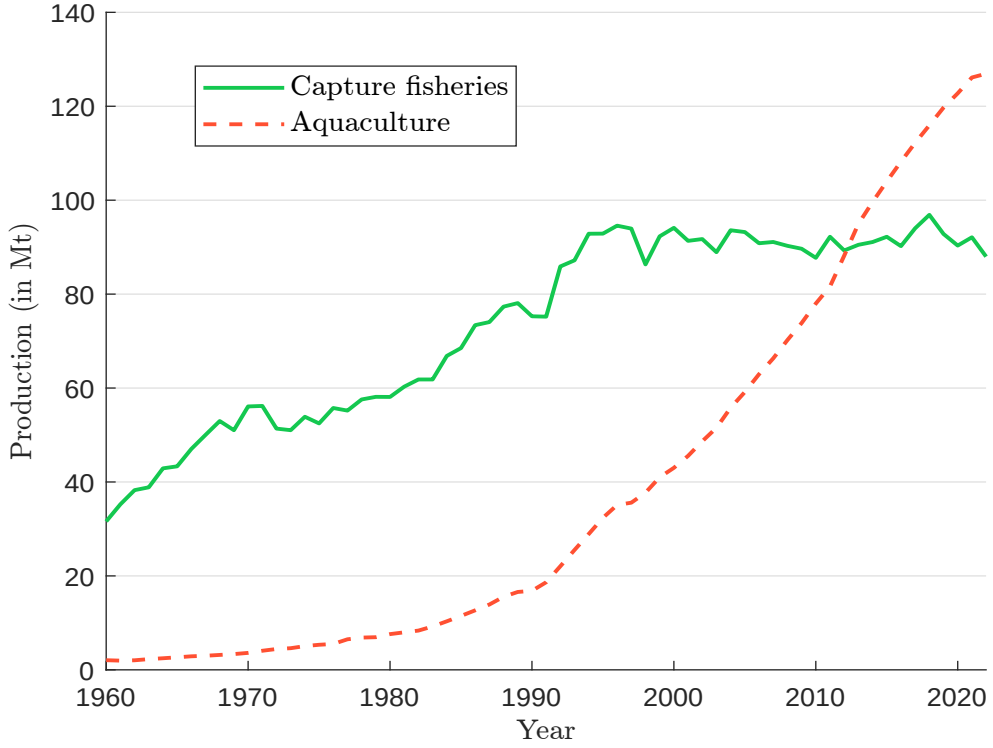


Source: https://databank.worldbank.org/source/world-development-indicators & Author's calculations.

An annual growth rate of 3% means a multiplication factor of 19 over one century and 369 over two centuries! In this context, it is understandable that some people predict that sooner or later the oceans will be empty. However, if we examine the components of the production, namely capture fisheries and aquaculture[201], we observe two distinct phases (Figure 5.101):

- From 1960 to 1990, production growth was driven primarily by capture fisheries.
- Since 1990, capture fisheries have remained constant, while aquaculture has experienced impressive growth.

In 1960, capture fisheries accounted for 95% of seafood production, while today aquaculture contributes about 60% of total seafood production. As a result, fish production has shifted from an industry based on the capture of wild fish to one based on aquaculture. Table 5.65 shows seafood

[201] Here are the definitions used by the FAO. Capture fisheries production measures the volume of fish catches landed by a country for all commercial, industrial, recreational and subsistence purposes. Aquaculture is understood to mean the farming of aquatic organisms including fish, molluscs, crustaceans and aquatic plants. Aquaculture production specifically refers to output from aquaculture activities, which are designated for final harvest for consumption. Total fisheries production measures the volume of aquatic species caught by a country for all commercial, industrial, recreational and subsistence purposes. The harvest from mariculture, aquaculture and other kinds of fish farming is also included.

Table 5.65: Fisheries production by country (1960–2022)

| | Country | 1960 | 1980 | 2000 | 2010 | 2020 | 2022 |
|---|---|---|---|---|---|---|---|
| | | Capture fisheries production | | | | | |
| | World (in Mt) | 31.6 | 58.1 | 94.1 | 87.7 | 90.3 | 88.0 |
| Top 10 (in %) | China | 7.0 | 5.4 | 15.8 | 17.2 | 14.9 | 15.0 |
| | Indonesia | 2.2 | 2.8 | 4.4 | 6.1 | 7.7 | 8.4 |
| | India | 3.5 | 3.6 | 4.0 | 5.4 | 5.2 | 6.3 |
| | Peru | 11.1 | 4.7 | 11.3 | 4.9 | 6.3 | 6.1 |
| | Russia | 0.0 | 0.0 | 4.3 | 4.6 | 5.6 | 5.7 |
| | United States | 8.6 | 6.4 | 5.1 | 5.0 | 4.7 | 4.8 |
| | Vietnam | 1.4 | 0.8 | 1.7 | 2.6 | 3.9 | 4.1 |
| | Japan | 18.7 | 17.3 | 5.5 | 4.8 | 3.6 | 3.4 |
| | Chile | 1.1 | 5.0 | 4.8 | 3.5 | 2.4 | 3.1 |
| | Norway | 4.4 | 4.4 | 3.1 | 3.2 | 2.9 | 3.0 |
| | | Aquaculture production | | | | | |
| | World (in Mt) | 2.0 | 7.6 | 43.0 | 78.0 | 122.8 | 126.9 |
| Top 10 (in %) | China | 46.8 | 40.8 | 69.2 | 61.3 | 57.4 | 59.4 |
| | Indonesia | 3.9 | 3.0 | 2.3 | 8.0 | 12.1 | 11.5 |
| | India | 2.2 | 4.8 | 4.5 | 4.9 | 7.0 | 8.1 |
| | Vietnam | 1.8 | 1.3 | 1.2 | 3.5 | 3.8 | 4.1 |
| | Bangladesh | 2.4 | 1.2 | 1.5 | 1.7 | 2.1 | 2.2 |
| | Philippines | 3.0 | 4.4 | 2.6 | 3.3 | 1.9 | 1.9 |
| | Norway | 0.1 | 0.1 | 1.1 | 1.3 | 1.2 | 1.3 |
| | Egypt | 0.2 | 0.2 | 0.8 | 1.2 | 1.3 | 1.2 |
| | Chile | 0.0 | 0.0 | 1.0 | 0.9 | 1.2 | 1.2 |
| | Myanmar | 0.0 | 0.0 | 0.2 | 1.1 | 0.9 | 0.9 |
| | | Total production | | | | | |
| | World (in Mt) | 33.6 | 65.5 | 136.7 | 165.0 | 211.9 | 213.6 |

Source: https://databank.worldbank.org/source/world-development-indicators & Author's calculations.

production by country across different decades[202]. In 1960, fish production was led by Japan, Peru, China, and the United States, with production shares of 18.6%, 10.4%, 9.5%, and 8.4%, respectively. These countries were followed by Norway (4.1%), India (3.5%), the United Kingdom (3.0%), Canada (2.8%), Spain (2.7%), South Africa (2.6%), Germany (2.3%), France (2.3%), Indonesia (2.3%), and Iceland (1.9%). In 2022, seafood production had become dominated by China with a production share of 41.5%, followed by Indonesia (10.3%), India (7.4%), Vietnam (4.1%), Peru (2.6%), Russia (2.5%), Bangladesh (2.2%), the United States (2.2%), Norway (2.0%), and Chile (2.0%). This represents a complete transformation of global seafood production over sixty years. For example, in 2022, former major producers had dropped significantly in rank: Japan (13th, 1.83%), Spain (23rd, 0.51%), Canada (25th, 0.41%), France (30th, 0.34%), and Germany (54th, 0.10%). Today, 70% of production is located in Asia, while South America, Europe, Africa and North America represent 9%, 9%, 7% and 3%, respectively. We also observe a long-term upward trend in per capita consumption of aquatic food products. Between 1961 and 2021, consumption rises from 9.1 kg to 20.6 kg per person, an average annual increase of about 1.4%. The growth in fish production can then be attributed equally to demographic expansion and changes in dietary preferences.

[202]These figures differ from previous ones because they exclude some forms of algae production.

FAO (2024b) assesses the sustainability of fisheries by comparing the biomass stock $x(t)$ with the maximum sustainable yield (MSY) and defines three categories:

| Category | Overfished | Maximally sustainably fished | Underfished |
|---|---|---|---|
| $\frac{x(t)}{\text{MSY}}$ | $[0, 0.8[$ | $[0.8, 1.2]$ | $]1.2, +\infty)$ |
| Unsustainable | ✓ | | |
| Sustainable | | ✓ | ✓ |

The FAO analysis shows that the proportion of fishery stocks within biologically sustainable levels declined from 94% in 1974 to 62% in 2021[203]. This means that 38% of fishery stocks are not sustainable. This figure masks a large discrepancy between the 15 major FAO fishing regions[204]. Indeed, four areas have more than 50% of their fish stocks at unsustainable levels: the eastern central Atlantic (51.3%), the northwest Pacific (56%), the Mediterranean and Black Sea (62.5%), and the southeast Pacific (66.7%). In contrast, four areas have more than 75% of fisheries stocks that are sustainable: the eastern central Pacific (84.2%), the northeast Atlantic (79.4%), the northeast Pacific (76.5%), and the southwest Pacific (75.9%). According to FAO (2024b, Figure 20, page 45), three distinct patterns emerge:

1. Areas with a continuously increasing trend in landings since 1950
   This group includes four areas: the eastern central Atlantic, the eastern and western Indian Ocean, and the western central Pacific.

2. Areas with landings oscillating around a globally stable value since 1990, associated with the dominance of pelagic, short-lived species
   This group includes three areas: the northwest, northeast and eastern central Pacific.

3. Areas with an overall declining landing trend following historical peaks
   This group includes the remaining eight regions.

With fisheries production expected to increase by 10% over the next decade, FAO has proposed a process to achieve this goal and improve sustainability: the *FAO Blue Transformation Roadmap 2022–2030*. This roadmap focuses on three main pillars: expanding sustainable aquaculture, improving fisheries management, and strengthening value chains and market access (FAO, 2022). Since we have reached a limit in terms of harvesting wild fish, the growth of fisheries production would be mainly through aquaculture. It is also important to improve fisheries management. For example, there is an urgent need to reduce discards or bycatch:

> "*Discards, or discarded catch is that portion of the total organic material of animal origin in the catch, which is thrown away, or dumped at sea for whatever reason. It does not include plant materials and post-harvest waste such as offal. The discards may be dead, or alive.*" (Pérez Roda *et al.*, 2019, page 1).

This happens for various reasons, such as the fish are too small or young, they're not the target species, the fish have low commercial value, the catch exceeds the storage capacity of the vessel, the fish are damaged, etc. Precise estimates of global fish discards are difficult to obtain, but approximate

[203] Each fishery stock is weighted equally in this assessment. When the stocks are weighted by the volume of landings, the 62% figure increases to 77%.

[204] These are the Atlantic (eastern central, northeast, northwest, southeast, southwest, western central), the Indian Ocean (eastern, western), the Mediterranean and Black Sea, and the Pacific (eastern central, northeast, northwest, southeast, southwest, western central).

Figure 5.102: Estimated fish discards in Mt (1950–2018)

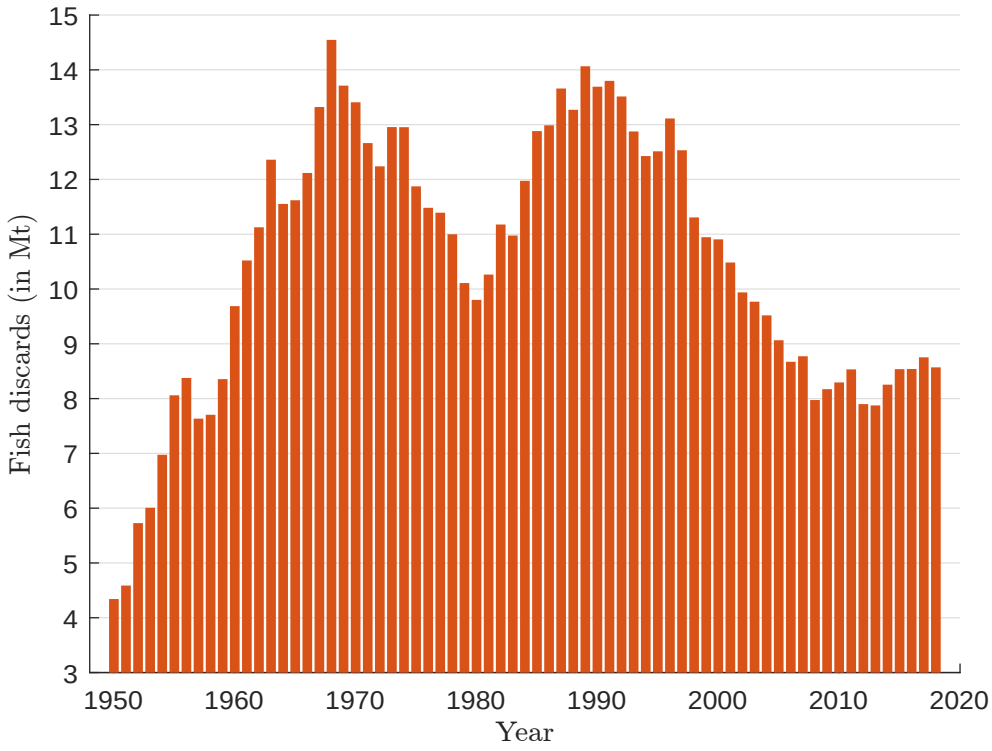


Source: FishStat & www.ourworldindata.org/grapher/fish-discards.

values are available. Zeller *et al.* (2018) estimated that discards increased from 5 million tonnes per year in the early 1950s to a peak of 18.8 million tonnes in 1989, before declining to less than 10 million tonnes per year in recent years. This represented 10–20% of the total fish catch until 2000 and now represents less than 10% of the total annual catch. Similarly, Pérez Roda *et al.* (2019) estimated that annual discards averaged 9.1 million tonnes between 2010 and 2014, representing 10.8% of the total annual catch during this period. From a regional perspective, the northwest Pacific and northeast Atlantic together accounted for 39% of global discards. Among fisheries, those targeting crustaceans had the highest discard rates. In fact, the problem is not just bycatch, but fish waste in general. For example, Coppola *et al.* (2021) report that about two thirds of the total amount of fish is discarded. This explains why fish and seafood products provide about 1% of the total calories in the human diet at the global level. However, fish remains an important source of essential nutrients, providing omega-3 fatty acids, vitamins (A, B12 and D) and minerals such as iron (Fe), iodine (I), zinc (Zn) and calcium (Ca), which are essential for human health. Moreover, many local communities rely heavily on fisheries for their livelihoods. In this global context, the call of Worm *et al.* (2009) to rebuild global fisheries remains highly relevant (Duarte *et al.*, 2020).

**Remark 67** *To go further, the most prominent fisheries databases*[205] *include the FAO FishStat database, now called FishStatJ (data on fish production, trade and consumption), the RAM Legacy Stock Assessment database (a global compilation of detailed stock assessment data), and Sea Around Us (a research initiative that provides global fisheries catch reconstructions, including estimates of illegal, unreported and unregulated fishing).*

[205]The websites are www.fao.org/fishery/en/statistics/software/fishstatj, www.ramlegacy.org and www.seaaroundus.org.

**Overexploitation in tropical forests** By definition, overexploitation in tropical forest ecosystems is related to deforestation and habitat degradation. However, we need to distinguish between the two concepts: deforestation and overexploitation (Wilkie *et al.*, 2011). According to Peres (2010), overexploitation of tropical forests involves three main issues:

- Timber extraction refers to the process of harvesting trees for commercial purposes, such as logging for wood, paper, and construction materials;
- Tropical forest vertebrates have been hunting in tropical forests for over 100 000 years, but their consumption increased during the 20th century;
- Non-timber forest products are biological resources such as plants and raw materials.

Rice *et al.* (1997) questioned the feasibility and effectiveness of sustainable forest management in tropical regions. They argued that sustainable logging in tropical forests is often ineffective because it yields less timber than conventional logging. Empirical studies support this (Pearce *et al.*, 2003). Another important challenge is the lack of financial incentives for loggers to harvest at sustainable levels and invest in forest regeneration, as economic principles suggest that trees should be harvested when their volume growth rate falls below the prevailing interest rate (Peres, 2010). Delaying harvesting beyond this point entails an opportunity cost, as profits from immediate harvesting could be reinvested elsewhere for higher returns. Reynolds and Peres (2006) used a study of Bolivian mahogany by Raymond Gullison to illustrate this problem. Despite legal restrictions, trees as small as 40 cm in diameter were harvested — well below the legal limit — because at this size, mahogany trees grow in volume at a rate of 4% per year, and their market value increases at about 1% per year due to rising timber prices, while Bolivia's real interest rates averaged 17% in the mid-1990s. This significant gap between tree growth rates and high interest rates creates strong economic pressure to harvest trees as soon as they have market value, rather than waiting for them to mature.

Let us formalize the opportunity cost problem. If we denote by $\Delta p$ and $\Delta v$ the annual changes in timber prices and tree volume relative to a reference age $t_0$, the market value $W(t)$ of the trees is given by:

$$W(t) = p(t)\, v(t) = p_0 v_0 (1+\Delta p)^{t-t_0} (1+\Delta v)^{t-t_0}$$

where $p_0$ and $v_0$ are the price level and the volume of trees at age $t_0$. Now assume that trees are harvested at age $\tau \leq t$ and the proceeds are invested at the risk-free rate $r$. The resulting wealth conditional on this harvest is equal to:

$$W(t \mid \tau \leq t) = p(\tau)\, v(\tau) (1+r)^{t-\tau}$$

The economic objective is to maximize the conditional wealth $W(t \mid \tau \leq t)$ or to find the optimal harvest age $\tau$ that maximizes the return. Figure 5.103 illustrates the economic problem with the following assumptions: $t_0 = 20$ years, $p_0 = \$500/\text{m}^3$, $v_0 = 2\,\text{m}^3$, $\Delta p = 1\%$ and $\Delta v = 4\%$. If the tree is harvested at age 20, the income is $W(20) = 500 \times 2 = \$1\,000$. If the harvest is delayed by 30 years, the income increases to $W(50) = \left(500 \times 1.01^{30}\right) \times \left(2 \times 1.04^{30}\right) = \$4\,371.6$. Now suppose the interest rate is 3%, the income from logging at age 20 and reinvesting would be $W(50 \mid \tau = 20) = 1\,000 \times 1.03^{30} = \$2\,427.3$. Since $W(50 \mid \tau = 20) < W(50)$, there is a financial gain from waiting another 30 years before harvesting. However, if the interest rate is 7%, we have $W(50 \mid \tau = 20) =$

Figure 5.103: Opportunity cost of logging in tropical forests

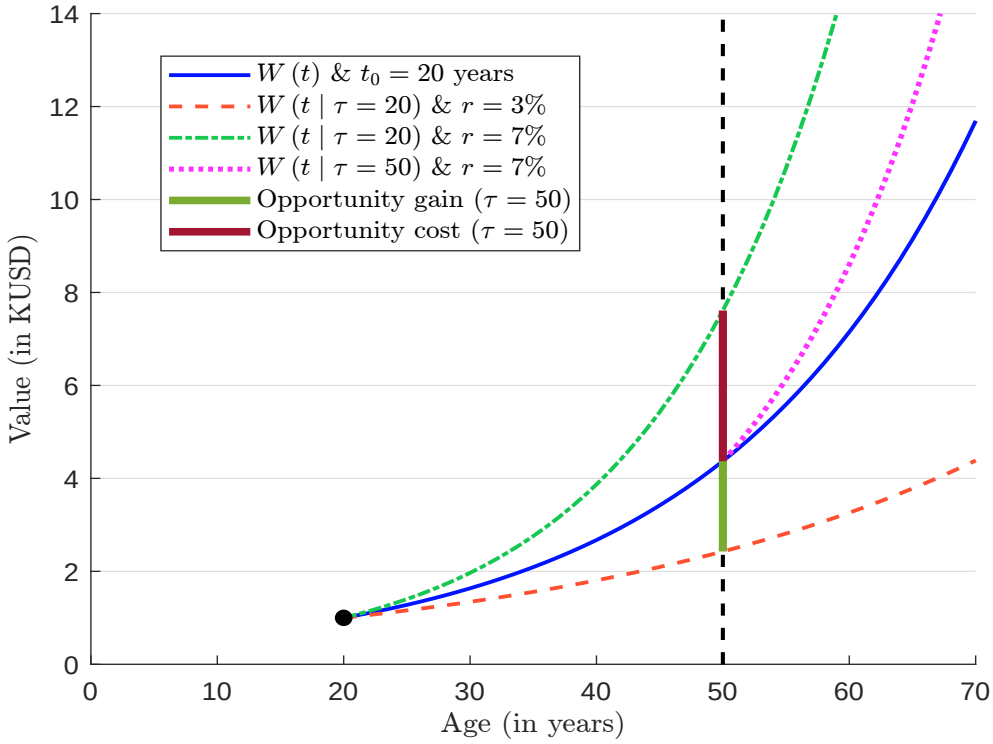


$1\,000 \times 1.07^{30} = \$7\,612.3$. This implies a significant opportunity cost for delaying the harvest[206]. In general, there is an opportunity cost when the interest rate is relatively high, especially when $r \geq \Delta p + \Delta v$. According to Rice *et al.* (1997), there is no economic solution to this problem, and they suggest that protected areas are the only viable way to manage tropical forests sustainably. Twenty-five years later, the debate about selective logging and its impact on biodiversity remains open (Bicknell *et al.*, 2015; Burivalova *et al.*, 2021).

Hunting wild animals is a practice with deep historical roots, initially driven by the basic need for food. Today, food security in developed countries rarely depends on hunting. Conversely, it remains a vital source of food in many developing countries. In addition to providing food for personal consumption, hunting can be an important source of income for hunters and their families. In these cases, harvested animals are sold not only for food but also for other purposes, such as the production of leather goods and medicinal products. There is much evidence of overexploitation over the last fifty years, especially as the trade of wild animals has increased. This has two major consequences. First, hunting of wild animals causes biodiversity loss. For example, Peres and Palacios (2007) provided a meta-analysis of changes in population density for 30 species of mammals, birds, and reptiles in 101 forest sites. Populations declined by up to 75% in more intensively hunted areas compared to less intensively hunted areas. Of the 30 species studied, 22 declined significantly at high levels of hunting. As expected, body size significantly influenced the magnitude of changes

[206] This opportunity cost is underestimated because two harvests could occur within 50 years. Therefore, the opportunity cost is given by:

$$\mathcal{C} = \underbrace{W(50 \mid \tau = 20)}_{\text{Income from 1st harvest}} + \underbrace{W(30 \mid \tau = 20)}_{\text{Income from 2nd harvest}} + \underbrace{W(10)}_{\text{3rd tree at age 10}} - \underbrace{W(50)}_{\text{Tree at age 50}}$$

Box 5.26: The bushmeat crisis

Bushmeat is the meat of wild animals that are hunted for food (Nasi *et al.*, 2008; Fa *et al.*, 2002). The meat is either eaten by the hunter or sold to make money. In the media, the term bushmeat is generally used to refer to the illegal hunting of protected animals in Africa. This includes various species such as antelopes, monkeys, rodents and other wild animals. Bushmeat has historically been a vital protein source in parts of Africa, Latin America and South Asia. In remote rural areas of West and Central Africa, it constitutes 80–90% of animal protein intake. While subsistence hunting by local communities isn't the main conservation issue, growing commercial demand is problematic. The market for bushmeat is now increasingly driven by urban consumers and diaspora communities, leading to unsustainable harvesting in several African regions.

Estimating the global impact of bushmeat harvesting is challenging. However, according to Nasi *et al.* (2011), "*the harvest of animals such as tapir, duikers, deer, pigs, peccaries, primates and larger rodents, birds and reptiles [...] represents around 6 million tonnes of animals extracted yearly [...] with an estimated yearly extraction rate in the Congo Basin of 4.5 million tonnes.*". While more than 1 000 animal species are affected by bushmeat hunting, Ripple *et al.* (2016) estimated that approximately 300 of these terrestrial mammal species are threatened with extinction. This also means that the majority of mammal species (70%) are not listed as threatened on the IUCN Red List.

The term '*bushmeat crisis*' refers to this paradox: the need for local people to hunt wild animals to improve their food security and well-being, while at the same time this practice has a significant negative impact on biodiversity. In this context, trade-offs and dilemmas are more difficult to resolve, as the study by Cawthorn and Hoffman (2015) shows.

in abundance, with large-bodied species declining faster in overhunted areas. Considering the 12 most hunted species, mean total biomass decreased almost elevenfold from 980 kg/km$^2$ in unhunted areas to only 89 kg/km$^2$ in highly hunted areas (Peres, 2010, page 111). The second consequence is the threat to the food security of local populations that depend on wildlife hunting. Indeed, hunting has become more sophisticated, systematic, and industrialized. For example, several studies indicate that African bushmeat has become an organized luxury market in African urban centers and restaurants (Gluszek *et al.*, 2021), as well as in Europe (Gombeer *et al.*, 2021), with porcupines, pangolins, antelopes, and snakes being the most sought-after products. For instance, Chaber *et al.* (2023) estimate that an average of 3.9 tonnes of bushmeat is smuggled through Brussels Airport each month. While the wildlife trade provides short-term financial benefits to hunters and their families, most do not make significant profits. Moreover, the ongoing loss of biodiversity today means food insecurity for these families in the future (Nasi *et al.*, 2011).

Another way to understand the impact of overexploitation on biodiversity loss is the growth of trafficking in protected species of wild fauna and flora. According to Traffic (`www.traffic.org`), "*the illegal trade in wild species is one of the most profitable criminal activities in the world, estimated to be worth up to $23 billion each year.*" The UNODC (United Nations Office on Drugs and Crime) published the third edition of the World Wildlife Crime Report in 2024. This report shows that despite two decades of concerted action at the international and national levels and the entry into force in 1975 of CITES (the Convention on International Trade in Endangered Species of Wild Fauna and Flora), wildlife trafficking continues worldwide. Moreover, the report estimates that "*wildlife crime is interconnected with the activities of large and powerful organized crime groups operating*

Box 5.27: Operation Thunder 2024

On 4 February 2025, INTERPOL announced that nearly 20 000 live animals, all endangered or protected species, were seized in a global operation against wildlife and forestry trafficking networks jointly coordinated by INTERPOL and the World Customs Organization (WCO). *Operation Thunder 2024* took place in 138 countries between 11 November and 6 December 2024. Authorities arrested 365 suspects and identified six transnational criminal networks suspected of trafficking in animals and plants protected by the Convention on International Trade in Endangered Species of Wild Fauna and Flora (CITES). In addition to live animals, participating countries seized hundreds of thousands of protected animal parts and derivatives, trees, plants, marine life and arthropods. Timber cases represented the most significant seizures, occurring primarily in maritime container shipments, while most other seizures took place at airports and postal hubs. More than 100 companies involved in the trade of protected species were also identified. Significant seizures included:

- 134 tonnes of timber headed to Asia via ocean freight (Indonesia);
- 41 tonnes of exotic timber headed to Asia via ocean freight (Kenya);
- 4 472 kg of pangolin scales (Nigeria);
- 6 500 live songbirds discovered during a vehicle inspection at the Syrian border (Turkey);
- 5 193 live red-eared slider turtles concealed in passenger suitcases arriving from Malaysia at Chennai Airport (India);
- 3 700 protected plants intercepted en route from Ecuador (Peru);
- 8 rhino horns found in a suspect's luggage while transiting from Mozambique to Thailand (Qatar);
- One tonne of sea cucumbers, considered a seafood delicacy, smuggled from Nicaragua (United States);
- 973 kg of dried shark fins originating from Morocco seized at the airport (Hong Kong);
- 8 tigers, aged between two months and two years, discovered in a suspected illegal breeding facility (Czech Republic);
- 846 pieces of reticulated python skin, from the world's longest snake species, concealed onboard a ship (Indonesia).

Source: INTERPOL (2025), https://www.interpol.int/News-and-Events.

*in some of the most fragile and diverse ecosystems from the Amazon to the Golden Triangle*[207]." UNDOC (2024, page 46) reports that from 2015 to 2021, more than 140 000 seizures of wildlife products were made in 162 countries, involving 4 000 different species. Analysis of seizure records shows that coral pieces were the most common item found in the illegal wildlife trade, accounting for 16% of the total number of seizures. Other seizures included crocodiles (9%), elephants (6%), bivalves and carnivores (5% each), parrots and cockatoos (4%), orchids (4%), and many other species. Figure 5.104 illustrates the most affected species based on the standardized seizure index, which serves as a proxy for the market value of the seized goods. In this case, seizures of rhinos (29%) rank first, followed by pangolins (28%) and elephants (15%).

Figure 5.104: Percentage share by species group aggregated by standardized seizure index (2015–2021)

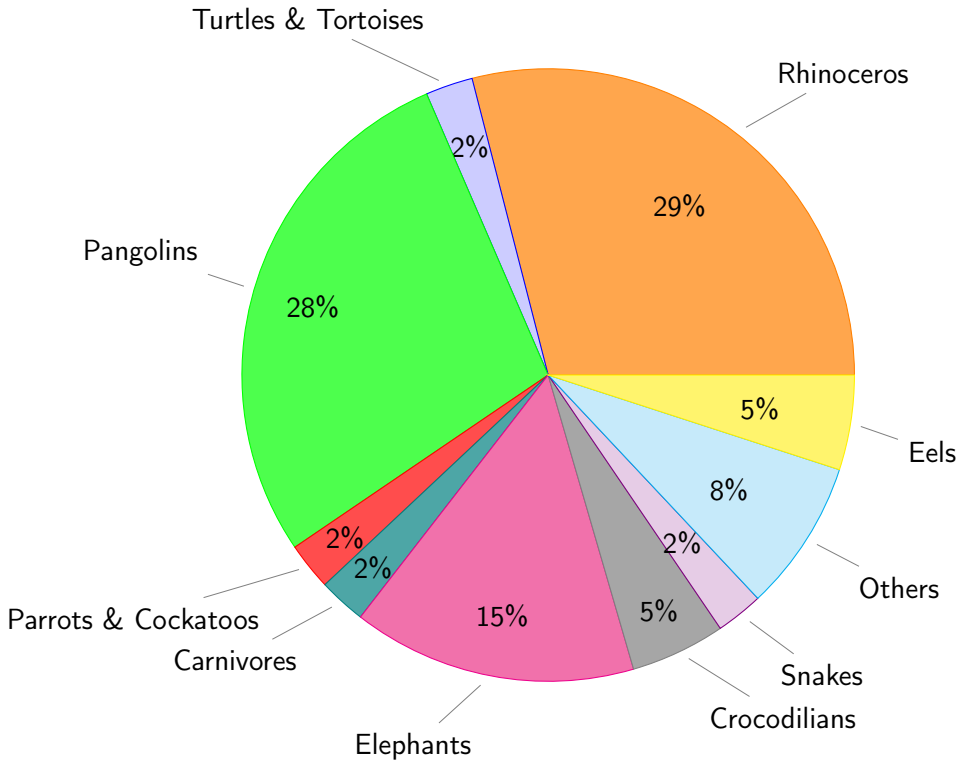


Source: UNDOC (2024, Figure 2.3, page 63).

The case of the rhinoceros is emblematic, as hunting has had a devastating impact on rhinoceros populations, pushing several species to the brink of extinction since 1900. The number of black rhinos declined by over 95% from around 100 000 in 1960 to fewer than 2 500 in the 1990s due to hunting and poaching. Although conservation efforts have helped, they remain critically endangered with only about 6 200 animals recorded in 2021. White rhinos were nearly extinct, with the southern population falling to fewer than 100 individuals in the early 20th century. They have been saved by rigorous conservation and breeding programs. As of 2021, there are approximately 16 000 individuals. In contrast, the northern white rhino has virtually disappeared, with only two females remaining in 2021. Indian rhinos were reduced to less than 100 individuals in 1900 due to hunting, but have since

[207] The Golden Triangle refers to a mountainous region in Southeast Asia where the borders of Thailand, Laos and Myanmar meet.

recovered thanks to conservation efforts and now number around 4 000. Javan and Sumatran rhinos were already rare in 1900, but continued to decline due to hunting and habitat loss, and both species now number fewer than 100 individuals. In Figure 5.105, we show the evolution of the number of rhinos in the world. We observe that only three of the six species are really significant, and that the recovery since 1990 is mainly due to the expansion of the white rhino in southern Africa[208].

Figure 5.105: Number of rhinoceros in the world (1960–2021)

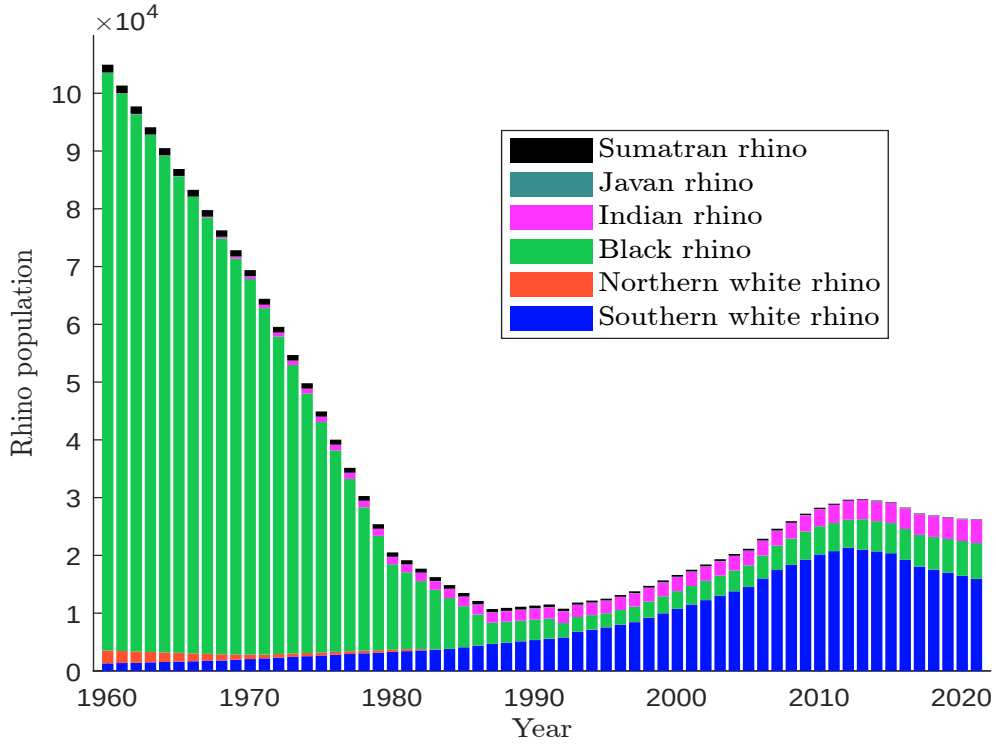


Source: www.ourworldindata.org/rhino-populations & Author's calculations.

Two decades ago, Bengis *et al.* (2004) and Kruse *et al.* (2004) raised concerns about the growing risk of zoonotic pandemics and the role of biodiversity loss, particularly deforestation and habitat alteration. Zoonoses are diseases transmissible from animals to humans caused by pathogens — viruses, bacteria, fungi, or parasites — that circulate naturally in animal populations[209]. In a landmark study, Taylor *et al.* (2001) analyzed 1 415 human pathogenic species and found that 61% were zoonotic. Since then, the emergence of new diseases and pandemics, many of which are linked or suspected to be linked to the wildlife trade, has underscored these concerns. Examples include avian influenza (H5N1), COVID-19, Ebola, H1N1 influenza, MERS, SARS, and Zika. In addition, research has established or strongly suggested a zoonotic origin for diseases such as bubonic plague, chikungunya, dengue fever, HIV/AIDS, Lyme disease, the 1918 Spanish flu, salmonellosis, and rabies. It is also now widely accepted that hunting and the bushmeat trade have become important factors in the transmission of zoonotic diseases (Hilderink and De Winter, 2021). The case of SARS-CoV-2 (COVID-19) is emblematic. While many hypotheses were initially proposed, it is now widely accepted that bats and pangolins likely played a role as reservoirs or intermediate hosts in the transmission of the virus (Zhang *et al.*, 2021). However, Bernstein *et al.* (2022) identified three key

[208] As of 2021, the numbers of rhinoceros are as follows: 15 940 southern white rhinos, 2 northern white rhinos, 6 195 black rhinos, 4 014 Indian rhinos, 76 Javan rhinos, and 41 Sumatran rhinos.
[209] The list of major zoonotic diseases can be found in Rahman *et al.* (2020).

areas for pandemic prevention: regulation of wildlife trade and hunting, mitigation of agricultural intensification and expansion, and conservation of tropical forests. The study also estimated that the cost of primary pandemic prevention measures is significantly less than the economic and human losses caused each year by emerging viral zoonoses.

The overexploitation of tropical forests is not limited to timber and wild animals. According to Peres (2010), it also includes plant products such as fruits, nuts, oil seeds, latex, resins, gums, medicinal plants, spices, dyes, ornamental plants, and raw materials such as firewood, climbing palms, bamboo, and rattan. Palm oil is a prominent example, and wild orchids are another[210].

**Remark 68** *More generally, overexploitation can be a threat to many natural resources, including fossil fuels, metal ores, non-metallic minerals, limestone and sand (IPBES, 2019).*

#### Climate change

The case of climate change is examined in detail in Part 2 of this Handbook. For example, Chapter 8 explains the concept and economic implications of climate change, while Chapter 12 discusses the physical risk of climate change. Climate change and biodiversity are inextricably linked. A rise in temperature, more intense precipitation, and an increase in natural disasters will naturally affect biodiversity. Animals such as butterflies, insects and birds are typical examples. Similarly, climate change has significant impacts on many aspects of non-animal biodiversity, including agriculture, forests, freshwater ecosystems and soil health.

### 5.4.4 Biodiversity measurement

Measuring biodiversity is essential for governments, regions, municipalities, companies, financial institutions and investors for two primary reasons. First, they operate within regulatory frameworks that increasingly require biodiversity risk monitoring[211]. Second, they must make decisions that either affect or are affected by biodiversity, a concept known as double materiality. For example, a company's corporate social responsibility strategy must include a biodiversity dimension, project financing should consider the potential for biodiversity loss, and governments need biodiversity metrics to develop effective conservation strategies and policies. Similar to ESG and climate risk assessment, measuring biodiversity risk requires the collection of relevant data. This data is then used within standardized methodologies to calculate biodiversity metrics, such as mean species abundance. In addition, a variety of commercial and open source solutions are available to assess biodiversity risk at various scales, including geospatial points, regional, national, and company-specific levels.

#### Essential biodiversity variables

Measuring biodiversity is complex due to its multifaceted nature and numerous dimensions. Moreover, even when focusing on a single dimension, data availability is often limited. However, these data are critical for assessing progress towards biodiversity goals. Mace and Baillie (2007) emphasized the importance of developing effective biodiversity indicators that are relevant to policy objectives and simple enough to facilitate comparisons between regions and countries. They discussed the distinction between pressures, status and responses, and called for urgent action to define a set of biodiversity indicators that are truly relevant for measuring biodiversity risks. Nearly twenty years

[210] According to UNODC (2024), the five most trafficked plant species are cedar and other sapindales, rosewood, agarwood and other myrtales, golden chicken fern, and orchids. Palm oil is not listed in CITES.

[211] This is discussed further in the following section on biodiversity governance and regulation.

later, significant progress has been made, but biodiversity measurement remains a challenge due to the lack of consistent and clear indicators. The article by Mace and Baillie was written in the context of the 2010 Biodiversity Target adopted by the Convention on Biological Diversity (CBD), whose objective was to "*halt the loss of biological diversity at all levels by the year 2010.*" The monitoring of progress was defined with respect to 22 headline indicators[212]. In fact, a number of these indicators were vague, for example the indicators (8) Ecological footprint and related concepts, (10) Trends in invasive alien species and (15) Incidence of human-induced ecosystem failure.

Table 5.66: EBV classes and names

| # | EBV class | EBV theme |
|---|---|---|
| 1 | Genetic composition | Genetic diversity (richness and heterozygosity), genetic differentiation (number of genetic units and genetic distance), effective population size, inbreeding |
| 2 | Species populations | Species distributions, species abundances |
| 3 | Species traits | Morphology, physiology, phenology, movement, reproduction |
| 4 | Community composition | Community abundance, taxonomic/phylogenetic diversity, trait diversity, interaction diversity |
| 5 | Ecosystem functioning | Primary productivity, ecosystem phenology, ecosystem disturbances |
| 6 | Ecosystem structure | Live cover fraction, ecosystem distribution, ecosystem vertical profile |

Source: https://geobon.org/ebvs/what-are-ebvs.

The lack of clear indicators led Pereira *et al.* (2013) to introduce the concept of essential biodiversity variables (EBVs), with the aim of establishing a standardized framework for monitoring biodiversity change worldwide:

> "*Despite progress in digital mobilization of biodiversity records and data standards, there is insufficient consistent national or regional biodiversity monitoring and sharing of such information. Along with inadequate human and financial resources, a key obstacle is the lack of consensus about what to monitor. Many initiatives collect data that could be integrated into an EBV global observation network, though important gaps remain. Different organizations and projects adopt diverse measurements, with some important biodiversity dimensions, such as genetic diversity, often missing.*" (Pereira *et al.*, 2013, page 277).

The essential biodiversity variables are maintained by the Group on Earth Observations Biodiversity Observation Network[213] (GEO BON). Table 5.66 shows the 6 EBV classes and the associated EBV themes[214]. Schmeller *et al.* (2018) proposed to focus on the eight candidate EBVs given in Table 5.67. Many other indicators have been proposed by the scientific community, the latest and most promising indicators are certainly the remote sensing geospatial patterns measured by satellites (Skidmore *et al.*, 2021). All these indicators can be used to build a biodiversity scoring system. However, the lack of consensus and standardization remains an obstacle to biodiversity monitoring.

[212]For instance, the first three indicators were (1) Trends in extent of selected biomes, ecosystems, and habitats, (2) Trends in abundance and distribution of selected species and (3) Coverage of protected areas.

[213]The website is www.geobon.org, while the EBV datasets are available at https://portal.geobon.org/datasets.

[214]Here are some examples of EBV indicators promoted by GEO-BON: Biodiversity Habitat Index (BHI), Genetic Diversity Indicator (GDI), Global Ecosystem Restoration Index (GERI), Local Biodiversity Intactness Index (LBII),

Table 5.67: Eight essential biodiversity variables (Schmeller *et al.*, 2018)

| Indicator | Definition |
|---|---|
| Abundance | Abundance is the number of individuals of a species within a local population. |
| Allelic diversity | Allelic diversity is the average number of alleles per locus in a population of a given species. |
| Body mass | Body mass scaled by body size, or the body mass index (BMI), indicates the condition and energy reserves of animals. |
| Ecosystem heterogeneity | Ecosystem heterogeneity describes the amount of variability in space and time of ecosystems. |
| Phenology | Phenology is defined as annually recurring life-cycle events, such as the timing of migration or flowering. |
| Range dynamics | Range dynamics are changes in species distributions through time, space and shape. This EBV is derived from the species distribution EBV for detecting critical ecological change early. |
| Size at first reproduction | Size at first reproduction is the individual body size (length) reached by an organism at the time when its first reproduction occurs. |
| Survival rates | Survival rate is the average probability that an organism will stay alive between two time points. |

Source: Schmeller *et al.* (2018).

### Biodiversity metrics

We have already mentioned the Living Planet Index and the Red List Index[215]. These indices focus on the extinction risk of species, and the better geographic resolution we have is the country. Below we present alternative simple measures of biodiversity that are available at higher resolutions.

**Mean species abundance (MSA)** Mean species abundance is one of the most popular biodiversity indicators because it is easy to understand and has been widely popularized by GLOBIO (`www.globio.info`). Let $n_i$ be the abundance of species $i$ in an area $A$, $n_i^\star$ be the abundance of species $i$ in a reference state, and $S_A$ be the number of native species in the area. The MSA of area $A$ is calculated as follows:

$$\text{MSA} = \frac{1}{S_A} \sum_{i=1}^{S_A} \min\left(\frac{n_i}{n_i^\star}, 1\right)$$

By construction we have $\text{MSA} \in [0, 1]$. An MSA of 1 corresponds to an undisturbed area, while a low MSA value indicates a highly disturbed area, where many native species have disappeared or experienced significant population declines. Consider the example illustrated in Figure 5.106. There are four native species in the reference area. In the disturbed area, the parrots have disappeared and have been replaced by rodents. The MSA is then calculated as follows:

$$\text{MSA} = \frac{1}{4}\left(\frac{0}{2} + \frac{2}{4} + \frac{3}{4} + \frac{1}{2}\right) = 43.75\%$$

Protected Area Representativeness & Connectedness indices (PARC), Invasive Alien Species Rate (IAS), Species Habitat Index (SHI), Species Protection Index (SPI), and Species Status Information Index (SSII).

[215] See Chapter 2 on pages 62–64.

Figure 5.106: Computation of the MSA

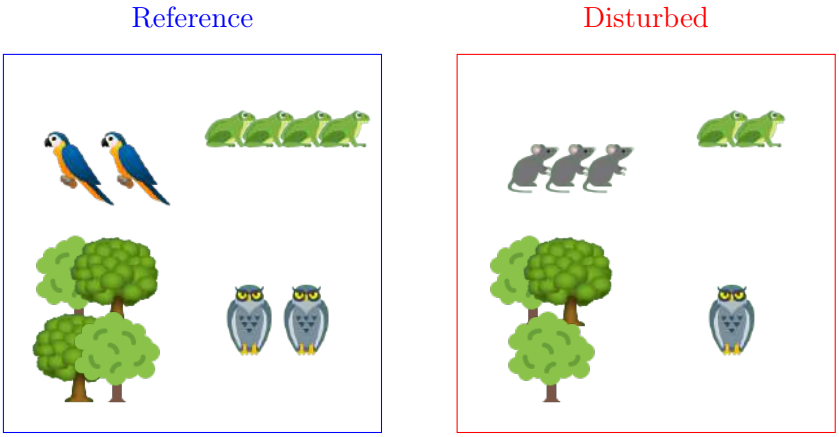


In GLOBIO, the MSA is calculated for different pressures: land use, climate change, roads, nitrogen deposition, hunting. An overall MSA is calculated by combining the MSA of the different pressures (Alkemade *et al.*, 2009):

$$\text{MSA} = \prod_{j=1}^{p} \text{MSA}_{(j)}$$

where $\text{MSA}_{(j)}$ is the MSA for pressure $j$ and $p$ is the number of pressures (between 1 and 5). According to Schipper *et al.* (2020), the contribution of pressure $j$ to biodiversity loss is equal to:

$$C_{(j)} = \frac{\left(1 - \text{MSA}_{(j)}\right)}{\sum_{j=1}^{p}\left(1 - \text{MSA}_{(j)}\right)}\left(1 - \text{MSA}\right)$$

where $1 - \text{MSA}_{(j)}$ is the biodiversity loss for pressure $j$.

Figure 5.107 shows global MSA values for the year 2015. Notably, MSA values approach one in polar regions and deserts. This pattern requires careful interpretation because the MSA does not measure biodiversity richness, but rather the intactness of biodiversity relative to an undisturbed reference state (Schipper *et al.*, 2020). In naturally species-poor ecosystems such as deserts, tundra, and polar regions, where reference biodiversity is already low, even limited human disturbance results in high MSA values. This reflects minimal deviation from the natural state rather than high biodiversity. In essence, when the reference biodiversity of a region is naturally low, the potential for biodiversity loss is limited, resulting in MSA values close to one in these ecosystems despite their relatively low species richness. This illustrates an important characteristic of the MSA metric: it quantifies the relative preservation of native ecological communities rather than absolute biodiversity.

**Remark 69** *Since the release of the first version of GLOBIO in 2000, the model has been improved and enriched over the years. Three extensions of GLOBIO have been developed to cover additional relevant aspects of nature. GLOBIO-ES models changes in global ecosystem services by assessing current conditions, trends and future scenarios of nature's benefits to humans, such as food, water, climate regulation, soil health and health support. GLOBIO-Aquatic models the health of freshwater ecosystems by quantifying biodiversity (MSA) and water quality (algal blooms) based on human pressures such as land use, flow alteration, eutrophication and temperature. GLOBIO-Species models how human pressures affect the distribution and population size of individual vertebrate species, enabling the calculation of biodiversity indicators such as the RLI and LPI metrics to track progress towards biodiversity goals.*

Figure 5.107: Mean species abundance values for 2015 (GLOBIO 4)

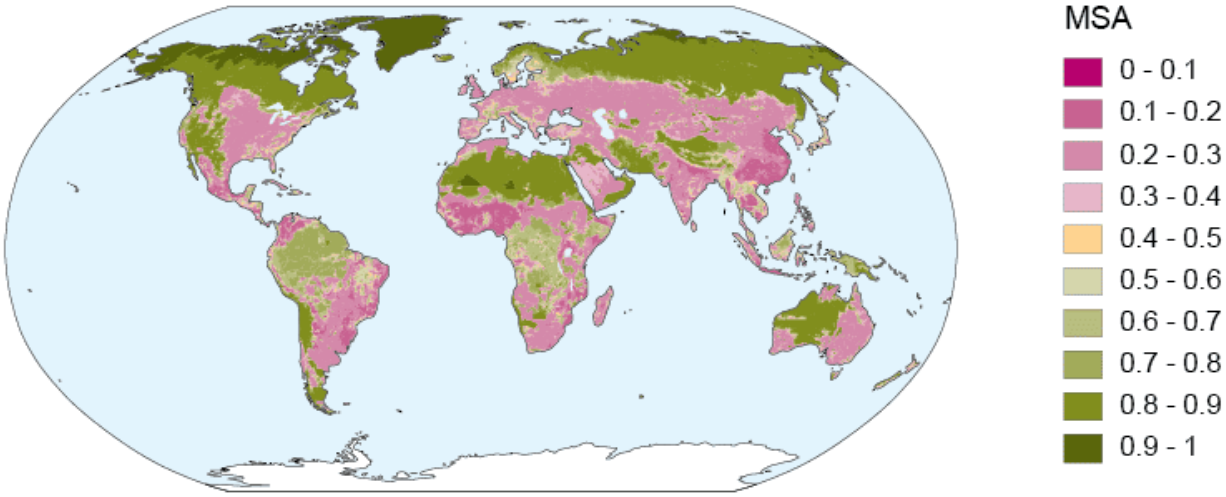


Source: Schipper *et al.* (2020, Figure 4(a), page 766).

**Potentially disappeared fraction (PDF)** The potentially disappeared fraction is a metric used to assess the biodiversity loss due to environmental change, particularly human activities such as pollution, habitat destruction, and climate change. Originally developed by Müller-Wenk (1998), it has been widely used in life cycle assessment (LCA) models to evaluate the environmental footprint of products and activities. PDF represents the fraction of species that have disappeared or are expected to disappear from a region due to environmental pressures such as land use, climate change, or pollution[216]. The PDF of area $A$ is:

$$\text{PDF} = \frac{S_0 - S_A}{S_0} = \frac{1}{S_0} \sum_{j=1}^{S_0} \mathbb{1}\{j \notin A\}$$

where $S_0$ is the undisturbed species richness of $A$, $S_A$ is the current species richness of $A$, and $j$ is the species index. PDF equals zero if no species disappear (no biodiversity loss), while PDF equals one if all species in the considered ecosystem disappear (total biodiversity loss). PDF is equal to 25% for the area shown in Figure 5.106, because 25% of the species in this area have disappeared (parrot species have disappeared, while frogs, trees, and owls remain).

The PDF approach has been popularized by the ReCIPe LCA model (Goedkoop *et al.*, 2008), which provides characterization factors (CFs) that translate human interventions in the environment (emissions, resource use, land use) into potential impacts on biodiversity, often expressed as PDF values. More complex approaches have been developed to calculate PDFs and CFs, such as the model of Kuipers *et al.* (2021), which uses the species-area relationship and defines new characterization factors[217]. The unit PDF.m$^2$.yr is often used. It represents the potential area (in square meters) where all species are potentially lost per year. For instance, 10 PDF.m$^2$.yr means that 10 m$^2$ has lost all its species during a year.

[216] We have already encountered the PDF measure when studying the species-area relationship. The PDF measure is a generalization of the metric $\mathcal{L}oss_{species}$ when the pressures are not limited to habitat loss (see Equation (5.19) on page 435).

[217] CF and PDF values can be found in the Supplementary Data available online (Tables S2 and S3).

**Biodiversity intactness index (BII)** A biodiversity intactness index is a metric that aims to measure how much of a region's natural biodiversity remains, despite human impacts. For instance, if we measure intactness at the species level, we can define the BII from the PDF:

$$\text{BII} = 1 - \text{PDF}$$

Scholes *et al.* (2005) proposed the following empirical estimator of the biodiversity intactness index:

$$\text{BII} = \frac{\sum_i \sum_j \sum_k S_{i,j} A_{j,k} I_{i,j,k}}{\sum_i \sum_j \sum_k R_{i,j} A_{j,k}} \tag{5.40}$$

where $i$ is the taxon index, $j$ is the ecosystem index, $k$ is the land use index, $S_{i,j}$ is the species richness of taxon $i$ in ecosystem $j$, $A_{j,k}$ is the area of land use $k$ in ecosystem $j$, and $I_{i,j,k}$ is the population impact or relative population of taxon $i$ (compared to the reference state) under land use $k$ in ecosystem $j$. We generally assume that $I_{i,j,k} \leq 1$, but there may be special situations where the population has increased, meaning that $I_{i,j,k}$ may be greater than 1. At first glance, Formula (5.40) seems complex, but it is simply a weighted average of the various population impacts:

$$\text{BII} = \sum_i \sum_j \sum_k w_{i,j,k} I_{i,j,k}$$

where $w_{i,j,k} = \dfrac{S_{i,j} A_{j,k}}{\sum_i \sum_j \sum_k R_{i,j} A_{j,k}}$ and the sum of weights is equal to one — $\sum_i \sum_j \sum_k w_{i,j,k} = 100\%$. If there is only one ecosystem and one land use, Formula (5.40) reduces to the weighted average of the population impacts where the weights are proportional to the species richness $S_i$ of taxon $i$. For example, assuming there are three taxonomic groups (birds, mammals, and plants), the species richness is 100 bird species, 50 mammal species, 200 plant species, and the population impacts are 50%, 80%, and 90%, respectively, we get:

$$\text{BII} = \frac{100 \times 50\% + 50 \times 80\% + 200 \times 90\%}{100 + 50 + 200} = \frac{270}{350} = 77.14\%$$

Table 5.68: Biodiversity intactness index in % of tropical forests (2001–2012)

| Region | Metric | ISO code | | | | | | | |
|---|---|---|---|---|---|---|---|---|---|
| | | ARG | BOL | BRA | CHL | COL | CUB | PER | PRY |
| South America | 2001 BII | 48.3 | 72.8 | 82.7 | 14.6 | 81.2 | 18.0 | 88.2 | 58.2 |
| | 2012 BII | 46.4 | 71.2 | 80.7 | 16.1 | 80.0 | 19.3 | 87.5 | 53.0 |
| | Change (in %) | −3.8 | −2.2 | −2.4 | 10.2 | −1.4 | 7.8 | −0.8 | −8.9 |
| | | CIV | CMR | COD | COG | GAB | LBR | SLE | TGO |
| Africa | 2001 BII | 57.0 | 79.7 | 84.2 | 89.7 | 87.9 | 72.6 | 60.2 | 58.7 |
| | 2012 BII | 41.9 | 79.3 | 83.2 | 88.8 | 87.3 | 72.8 | 57.2 | 57.7 |
| | Change (in %) | −26.4 | −0.5 | −1.2 | −1.1 | −0.7 | 0.3 | −4.9 | −1.8 |
| | | CHN | KHM | IDN | IND | LAO | MYS | THA | VNM |
| South Asia | 2001 BII | 38.6 | 41.2 | 75.8 | 13.3 | 64.5 | 79.6 | 31.0 | 39.5 |
| | 2012 BII | 36.4 | 34.5 | 70.4 | 13.0 | 61.3 | 70.5 | 29.7 | 38.2 |
| | Change (in %) | −5.5 | −16.2 | −7.1 | −1.5 | −4.9 | −11.4 | −4.2 | −3.4 |

Source: De Palma *et al.* (2021), https://doi.org/10.5519/5wriutqz & Author's calculations.

The calculation of the biodiversity intactness index requires the collection of population impacts for different pressures and taxa. Data sets can be found on various websites such as www.nhm.ac.uk/our-science/services/data/biodiversity-intactness-index.html. In Table 5.68 we report the values of the biodiversity intactness index in tropical forests calculated by De Palma *et al.* (2021) between 2001 and 2012. We find high heterogeneity even within the same region. For example, Peru had a BII of 88% in 2012, while it was only 19% in Argentina. Côte d'Ivoire experienced the largest decline (−26%), while the intactness of biodiversity in Chile improved by 10% between 2011 and 2012.

**Species threat abatement and restoration (STAR)** The species threat abatement and restoration (STAR) metric is a global framework designed to quantify and guide efforts to reduce biodiversity loss. It measures the potential contribution of specific conservation actions (reducing pressure on species and restoring habitats) to improving the status of threatened species. According to Mair *et al.* (2021), for a given location $i$ and a given threat $j$, the STAR threat-abatement score is calculated as a weighted average of the species IUCN Red List status:

$$T_{i,j} = \sum_{s=1}^{S} T_{i,j}^{(s)} = \sum_{s=1}^{S} \pi_{i,s} w_s c_{j,s}$$

where $\pi_{i,s} \in [0,1]$ is the current area of habitat (AOH) of species $s$ within location $i$ — expressed as a percentage of the current global AOH of the species, $w_s \in \{1,2,3,4\}$ is the IUCN Red List category weight[218] of species $s$, $c_{j,s}$ is the relative contribution of threat $j$ to the extinction risk of species $s$, and $S$ is the species richness at location $i$. The STAR restoration score for a given location $i$ and a given threat $j$ is calculated as:

$$R_{i,j} = \sum_{s=1}^{S} R_{i,j}^{(s)} = \sum_{s=1}^{S} \varphi_{i,s} w_s c_{j,s} m_{i,s}$$

where $\varphi_{i,s} \in [0,1]$ is the amount of restorable AOH for species $s$ at location $i$ — expressed as a percentage of the current global AOH of the species, and $m_{i,s} > 0$ is a multiplier appropriate for the habitat at location $i$ to discount restoration results — the default value is 29%. The scores $T_{i,j}$ and $R_{i,j}$ can be decomposed to obtain the contribution $T_{i,j}^{(s)}$ and $R_{i,j}^{(s)}$ of each species. By construction, the contributions are between 0 and 1, while the scores are between 0 and the species richness $S$. Below, we provide an example to compute $T_{i,j}$ and $R_{i,j}$ and their species contribution $T_{i,j}^{(s)}$ and $R_{i,j}^{(s)}$:

| Species | Red List | $w_s$ | $\pi_{i,s}$ | $c_{j,s}$ | $\varphi_{i,s}$ | $m_{i,s}$ | $T_{i,j}^{(s)}$ | $R_{i,j}^{(s)}$ |
|---|---|---|---|---|---|---|---|---|
| *Salmo salar* (salmon) | NT | 1 | 25% | 90% | 10% | 29% | 0.225 | 0.026 |
| *Phengaris teleius* (butterfly) | VU | 2 | 50% | 90% | 25% | 29% | 0.900 | 0.131 |
| *Conraua goliath* (frog) | EN | 3 | 80% | 80% | 25% | 29% | 1.920 | 0.174 |
| *Pericallis malvifolia* (magnolia) | CR | 4 | 75% | 80% | 20% | 29% | 2.400 | 0.186 |
| Total | | | | | | | 5.445 | 0.516 |

The site contains four species, each belonging to a different IUCN Red List category. Salmon occupy 25% of the habitat, indicating this is either a marine site or one with rivers. The threat contribution is high at 90%, meaning this threat is responsible for 90% of the extinction risk to salmon. Potential

[218] $w_s$ takes the values 1, 2, 3, and 4 for near threatened, vulnerable, endangered, and critically endangered, respectively.

habitat restoration is 10%, suggesting we can reduce extinction risk by that amount. This yields an absolute contribution of 0.225 for salmon, representing 4.1% of the total threat-abatement score. In contrast, magnolias represent 44% of the threat-abatement score due to two main factors: they cover a larger habitat area, and the species *Pericallis malvifolia* is classified as critically endangered on the IUCN Red List.

Figure 5.108: Global STAR threat-abatement score for amphibians, birds and mammals (at a 50-km grid cell resolution)

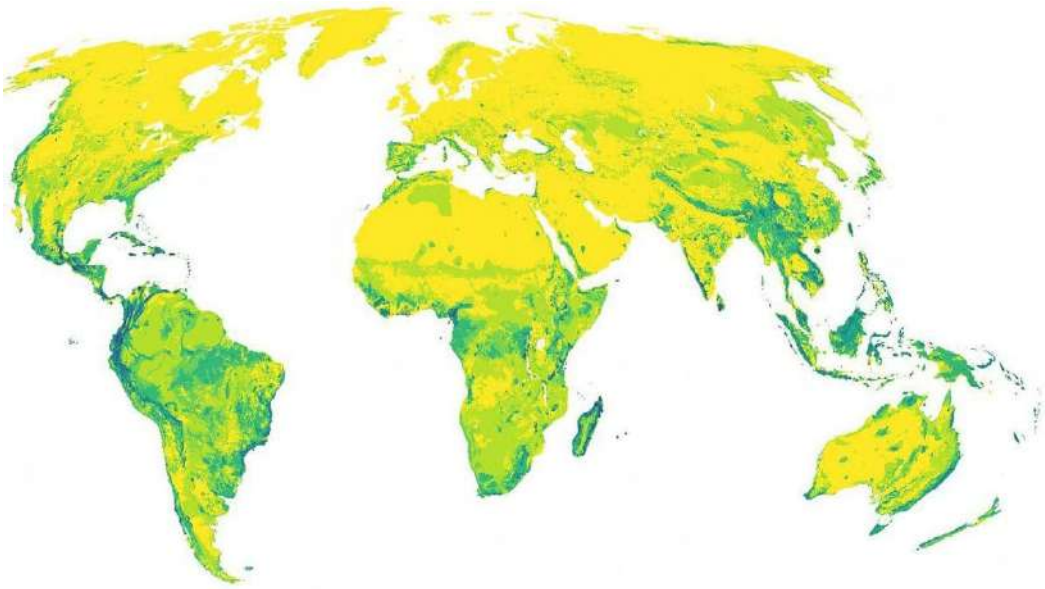

Source: Mair *et al.* (2021, figure 2).

Figure 5.108 illustrates the global STAR threat-abatement scores for amphibians, birds, and mammals as calculated by Mair *et al.* (2021). The color gradient ranges from yellow (low scores) to green (high scores). The distribution shows that biodiversity conservation priorities are geographically concentrated in some regions, particularly South America, South Asia, and southern Africa, suggesting that effective biodiversity risk management requires targeted approaches in these hotspots:

> "*While every nation can contribute towards halting biodiversity loss, Indonesia, Colombia, Mexico, Madagascar and Brazil combined have stewardship over 31% of total STAR values for terrestrial amphibians, birds and mammals. Among actions, sustainable crop production and forestry dominate, contributing 41% of total STAR values for these taxonomic groups. Key Biodiversity Areas cover 9% of the terrestrial surface but capture 47% of STAR values.*" (Mair *et al.*, 2021, page 836).

**Comparison of these methodologies** Which methodology is best? There is no definitive answer. First, in addition to the widely accepted approaches, there are numerous other valuable methodologies that receive less attention but provide important insights into biodiversity assessment. Second, these methodologies target different aspects of biodiversity — from species abundance and richness to density and ecosystem integrity — making direct comparisons problematic. Third, while all of these methodologies require substantial data inputs, they often present simplified perspectives by focusing on single dimensions of biodiversity. In particular, they focus primarily on species popula-

tions, which represent only one of the six essential biodiversity variables. This explains why these methods are so closely related (Rossberg, 2022; Rossberg *et al.*, 2023). Fourth, a major limitation of these approaches is their general failure to incorporate ecosystem services — a critical dimension for a comprehensive understanding of biodiversity and its relationship to human well-being.

### Commercial solutions

In addition to the established biodiversity measurement practices seen previously, a wide range of commercial approaches has emerged, offering diverse tools such as datasets, analytical software, calculation methods and comprehensive assessment services. In their Update Report 5 for the EU Business & Biodiversity Platform, De Ryck *et al.* (2024) documented 37 different approaches, indicating a significant increase in demand for biodiversity advisory services. However, concerns remain about the robustness and long-term viability of these tools. This pattern mirrors the evolution of ESG measurement, which has experienced rapid expansion followed by a period of consolidation. Critically, despite widespread agreement on the need for standardization and alignment, neither regulatory nor voluntary disclosure frameworks mandate specific measurement approaches. This is a significant barrier.

Table 5.69 provides an overview of available biodiversity assessment solutions. De Ryck *et al.* (2024) proposes a framework for evaluating these tools based on eight key criteria: business context, biodiversity pressures, level of ambition, scope, metrics, data requirements, implementation effort, and sector applicability. This framework allows companies to select methodologies that meet their specific needs and capabilities[219]. The landscape of biodiversity assessment tools varies widely in specialization — some are tailored to specific industries such as finance, mining or agriculture, while others are broadly applicable. These solutions also vary in their measurement granularity, with capabilities ranging from localized assessments (site or project level) to broader assessments (product, company or entire supply chain analysis). They also address different dimensions of biodiversity, including species diversity, habitat integrity, and ecosystem services, while accounting for different environmental pressures, such as land-use change, climate impacts, pollution sources, and the spread of invasive species. A critical criterion for selecting an approach is the scope of the solution, which defines the boundaries of what is included when measuring impacts and dependencies. These scopes can be categorized as follows[220]:

1. Scope 1: Impacts generated within the entity's control and other impacts directly caused by the entity during the assessment period;
2. Scope 2: Impacts resulting from the generation of non-fuel energy (electricity, steam, heat and cooling) for use at the site level, including impacts from land use change, fragmentation and related factors;
3. Scope 3
   (a) Scope 3 Upstream: Impacts that are a consequence of the company's activities, but are caused by sources not owned or controlled by the company within its upstream supply chain;
   (b) Scope 3 Downstream: Impacts that are a consequence of the company's activities, but are caused by sources not owned or controlled by the company within its downstream consumption and waste processes.

[219] See also Bailon *et al.* (2024) for a comparison of the different solutions.

[220] These scope definitions are based on the GHG Protocol and are analogous to the scope definitions used to measure GHG emissions (see Section 9.1.3 on page 878).

Table 5.69: List of commercial solutions for measuring biodiversity

| Sigle | Name | Sponsors | OS‡ |
|---|---|---|---|
| ABD Index | AgroBioDiversity Index | Alliance of Bioversity International, CIAT | |
| B-INTACT | Biodiversity Integrated Assessment Computation Tool | FAO | ✓ |
| BFFI | Biodiversity Footprint for Financial Institutions | ASN Bank, CREM, PRé Sustainability | ✓ |
| BFM | Biodiversity Footprint Methodology | Plansup | |
| BIA-GBS | Biodiversity Impact Analytics – Global Biodiversity Score | CDC Biodiversité, Carbon4 Finance | |
| BIAT | Biodiversity Impact Assessment Tool | ISS ESG | |
| BII | Biodiversity Intactness Index | Natural History Museum (UK) | |
| BIM | Biodiversity Impact Metric | Cambridge Institute for Sustainable Leadership | |
| BRF | Biodiversity Risk Filter | WWF | ✓ |
| CBF | Corporate Biodiversity Footprint | Iceberg Datalab | |
| ENCORE | Exploring Natural Capital Opportunities, Risks and Exposure | Global Canopy, UNEP FI, UNEP-WCMC | ✓ |
| GBS | Global Biodiversity Score | CDC Biodiversité | |
| GBSFI | Global Biodiversity Score for Financial Institutions | CDC Biodiversité | |
| GID | Global Impact Database | Impact Institute | |
| GIST NBS | Nature & Biodiversity Suite (BIGER/SLAM/DIRO 360) | GIST Impact | |
| IBAT | Integrated Biodiversity Assessment Tool | BirdLife International, Conservation International, IUCN, UNEP-WCMC | |
| InVEST | Integrated Valuation of Ecosystem Services and Trade-offs | Natural Capital Project | ✓ |
| MBFM | MSCI Biodiversity Footprint Metrics | MSCI | |
| NRP | Nature Risk Profile | S&P Global | |
| NVE | Nature Value Explorer | Flemish Institute for Technological Research | ✓ |
| PBF | Product Biodiversity Footprint | I Care | |

‡OS stands for Open Source.

Source: Bailon *et al.* (2024), De Ryck *et al.* (2024) & Author's research.

Comparison of biodiversity assessment solutions reveals a paradoxical landscape characterized by both significant uniformity and heterogeneity. On the one hand, there is considerable homogeneity in the basic approaches, with most methodologies primarily emphasizing metrics of species abundance and diversity. Many solutions are based on identical underlying data sets, which are simply presented through different interfaces or analytical frameworks. On the other hand, there is considerable heterogeneity in the maturity of these solutions. Established tools have been widely adopted by many institutions over long periods of time and have evolved into comprehensive, integrated platforms. Meanwhile, other solutions remain in earlier stages of development, functioning essentially as proofs of concept or experimental approaches with limited implementation history.

### 5.4.5 Biodiversity governance and regulation

Biodiversity risk, like climate risk, is subject to regulation, and its governance has evolved significantly in recent years. While the political agenda may lack clarity, its mere existence represents progress. In particular, the Conference of the Parties has recently received more media attention than in previous years.

#### Convention on Biodiversity (CBD)

The Convention on Biological Diversity was adopted at the 1992 Earth Summit in Rio de Janeiro and entered into force in 1993. The purpose of this international treaty is to address the global loss of biological diversity, with the following objectives:

1. The conservation of biological diversity;
2. The sustainable use of its components;
3. The fair and equitable sharing of the benefits arising out of the utilization of genetic resources.

Similar to the United Nations Framework Convention on Climate Change (UNFCCC), the Conference of the Parties (COP) serves as the governing body of the CBD, meeting every two years to make key decisions. Some of the major treaties and initiatives adopted under the CBD include:

- The International Coral Reef Initiative (1994, COP1, Bahamas), a partnership of nations and organizations to protect coral reefs;
- The Cartagena Protocol on Biosafety (2000), which regulates the international movement of living modified organisms to ensure biosafety;
- The Nagoya Protocol on Access and Benefit-Sharing (2010, COP10, Japan), which establishes a legal framework for the equitable sharing of benefits arising from the use of genetic resources, and adopts the Aichi Biodiversity Targets (2011–2020), which set 20 global targets for biodiversity conservation;
- The Pyeongchang Roadmap (2014, COP12, South Korea), which aims to accelerate global efforts to achieve the Aichi Biodiversity Targets;
- The Kunming-Montreal Global Biodiversity Framework, known as the GBF (2022, COP15), which includes the goal of protecting 30% of the Earth's land and marine areas by 2030 (the $30 \times 30$ target).

Table 5.70: Aichi Biodiversity Targets (2011–2020)

| | |
|---|---|
| Strategic Goal A | Address the underlying causes of biodiversity loss by mainstreaming biodiversity across government and society (Target 1–4) |
| Strategic Goal B | Reduce the direct pressures on biodiversity and promote sustainable use (Target 5–10) |
| Strategic Goal C | To improve the status of biodiversity by safeguarding ecosystems, species and genetic diversity (Target 11–13) |
| Strategic Goal D | Enhance the benefits to all from biodiversity and ecosystem services (Target 14–16) |
| Strategic Goal E | Enhance implementation through participatory planning, knowledge management and capacity building (Target 17–20) |
| Target 5 | By 2020, the rate of loss of all natural habitats, including forests, is at least halved and, where feasible, brought close to zero, and degradation and fragmentation are significantly reduced |
| Target 7 | By 2020 areas under agriculture, aquaculture and forestry are managed sustainably, ensuring conservation of biodiversity |
| Target 8 | By 2020, pollution, including from excess nutrients, has been brought to levels that are not detrimental to ecosystem function and biodiversity |
| Target 9 | By 2020, invasive alien species are identified, priority species are controlled or eradicated, and measures are in place to manage pathways to prevent their introduction and establishment |
| Target 11 | By 2020, at least 17% of terrestrial and inland water areas and 10% of coastal and marine areas are protected by well-connected systems of protected areas |
| Target 12 | By 2020, the extinction of known threatened species has been prevented, and their conservation status has been improved and maintained, especially for those species most in decline |
| Target 15 | By 2020, the resilience of ecosystems has been enhanced, including restoration of at least 15% of degraded ecosystems |
| Target 20 | By 2020, the goal is to significantly increase financial resources for effective implementation of the Strategic Plan for Biodiversity 2011–2020 |

Source: https://www.cbd.int/sp/targets.

**Aichi Biodiversity Targets** The Aichi targets are a set of 20 global biodiversity goals adopted at the 10th Conference of the Parties in Japan in 2010. These 20 targets are grouped into five strategic goals, as shown in Table 5.70. The overall objective is to reduce the rate of biodiversity loss, as reflected in some of the targets listed in Table 5.70. However, there is broad consensus that the world has failed to achieve any of the Aichi targets. Several factors have contributed to this failure. First, many of the targets are vague and lack clear, enforceable commitments, making it difficult to hold countries accountable. Enforcement mechanisms are limited, and the wording of many targets leaves room for interpretation. For example, Target 7 states that "*by 2020 areas under agriculture, aquaculture and forestry are managed sustainably, ensuring conservation of biodiversity.*" But what does that mean in practice? What specific actions should be taken? What metrics should be used to assess sustainability in these sectors? The lack of clear definitions and measurable indicators has weakened the impact of the targets. The second factor is inadequate funding, which creates a significant gap between what is needed and what is available for biodiversity conservation projects.

For example, Target 20 states that "*by 2020, at the latest, the mobilization of financial resources for effectively implementing the Strategic Plan for Biodiversity 2011–2020 from all sources, and in accordance with the consolidated and agreed process in the Strategy for Resource Mobilization, should increase substantially from the current levels.*" McCarthy *et al.* (2012) examined the financial costs of Targets 11 and 12, which relate to protected areas and extinction prevention. For Target 11, they estimated that protecting and effectively managing all terrestrial areas of global importance for bird conservation would cost $65.1 billion annually, and adding areas for other taxa would increase this to $76.1 billion annually. For Target 12, they estimated that reducing the risk of extinction of all globally threatened bird species by at least one IUCN Red List category would cost between $875 million and $1.23 billion, representing only 12% of current funding. In another study, by comparing actual expenditures with expected levels, Waldron *et al.* (2013) identified 40 severely underfunded countries, with the top five being Iraq, Djibouti, Angola, Kyrgyzstan, and Guyana. Most of the countries in this ranking are developing countries, with the exception of five developed countries: Finland, Iceland, France, Australia and Austria. More recently, the Paulson Institute, the Nature Conservancy, and the Cornell Atkinson Center for Sustainability conducted a comprehensive review of global biodiversity finance and concluded that there is a huge funding gap:

> "*This report determines that, in 2019, the total global annual flow of funds toward biodiversity protection amounted to approximately $124–143 billion per year against an estimated annual need of $722–967 billion to halt the decline in global biodiversity between now and 2030. Taken together, these figures reveal a biodiversity financing gap of $598–824 billion per year. [...] Significantly, this report shows that annual governmental expenditures on activities harmful to biodiversity in the form of agricultural, forestry, and fisheries subsidies — $274–542 billion per year in 2019 — are two to four times higher than annual capital flows toward biodiversity conservation.*" (Deutz *et al*, 2020, page 12).

Finally, the third factor contributing to the failure of the Aichi targets was the lack of government commitment, inadequate monitoring and reporting by the CBD, and low public awareness. These factors combined to weaken stakeholder engagement, resulting in limited societal pressure for action.

**Kunming-Montreal Global Biodiversity Framework** The failure of the Strategic Plan for Biodiversity 2011–2020 and its Aichi Biodiversity Targets created an urgent need for a more effective global approach. At CBD COP15 in December 2022, 192 countries responded by adopting the Kunming-Montreal Global Biodiversity Framework (GBF). This new framework aims to re-launch global biodiversity conservation efforts by addressing the gaps in national ambition and commitment, as well as previous initiatives. The GBF text is divided into several sections, the most important of which are Section F (2050 vision and 2030 mission), Section G (global goals for 2050) and Section H (global targets for 2030). According to Convention on Biological Diversity (2022), the vision of the Kunming-Montreal Global Biodiversity Framework is "*a world of living in harmony with nature where by 2050, biodiversity is valued, conserved, restored and wisely used, maintaining ecosystem services, sustaining a healthy planet and delivering benefits essential for all people.*" The four 2020 goals are to protect and restore (goal A), prosper with nature (goal B), share benefits fairly (goal C), and invest and collaborate (goal D). While the first three goals are easy to understand, the fourth goal is described as follows:

> "*Adequate means of implementation, including financial resources, capacity-building, technical and scientific cooperation, and access to and transfer of technology to fully implement the Kunming-Montreal Global Biodiversity Framework are secured and equitably accessible to all Parties, especially developing country Parties, in particular the*

Table 5.71: The 23 targets of the Kunming-Montreal Global Biodiversity Framework

| Target | Purpose |
|---|---|
| 1 | Plan and manage all areas to reduce biodiversity loss |
| 2 | Restore 30% of all degraded ecosystems — terrestrial, inland water, and marine and coastal ecosystems |
| 3 | Conserve 30% of land, waters and seas — protected areas and other effective area-based conservation measures |
| 4 | Halt species extinction, protect genetic diversity, and manage human-wildlife conflicts |
| 5 | Ensure sustainable, safe and legal harvesting and trade of wild species (reducing the risk of pathogen spillover) |
| 6 | Reduce the introduction of invasive alien species by 50% and minimize their impact — eradicating or controlling invasive alien species, especially in priority sites, such as islands |
| 7 | Reduce pollution to levels that are not harmful to biodiversity — (a) reducing excess nutrients lost to the environment by at least half, (b) reducing the overall risk from pesticides and highly hazardous chemicals by at least half, (c) preventing, reducing, and working towards eliminating plastic pollution |
| 8 | Minimize the impacts of climate change on biodiversity and build resilience |
| 9 | Manage wild species sustainably to benefit people |
| 10 | Enhance biodiversity and sustainability in agriculture, aquaculture, fisheries, and forestry |
| 11 | Restore, maintain and enhance nature's contributions to people |
| 12 | Enhance green spaces and urban planning for human well-being and biodiversity |
| 13 | Increase the sharing of benefits from genetic resources, digital sequence information and traditional knowledge |
| 14 | Integrate biodiversity in decision-making at every level |
| 15 | Businesses assess, disclose and reduce biodiversity-related risks and negative impacts |
| 16 | Enable sustainable consumption choices to reduce waste and overconsumption |
| 17 | Strengthen biosafety and distribute the benefits of biotechnology |
| 18 | Reduce harmful incentives by at least $500 billion per year, and scale up positive incentives for biodiversity |
| 19 | Mobilize $200 billion per year for biodiversity from all sources, including $30 billion through international finance |
| 20 | Strengthen capacity-building, technology transfer, and scientific and technical cooperation for biodiversity |
| 21 | Ensure that knowledge is available and accessible to guide biodiversity action |
| 22 | Ensure participation in decision-making and access to justice and information related to biodiversity for all |
| 23 | Ensure gender equality and a gender-responsive approach for biodiversity action |

Source: (Convention on Biological Diversity, 2022, pages 9–13).

> *least developed countries and small island developing States, as well as countries with economies in transition, progressively closing the biodiversity finance gap of $700 billion per year, and aligning financial flows with the Kunming-Montreal Global Biodiversity Framework and the 2050 Vision for biodiversity.*" (Convention on Biological Diversity, 2022, page 9).

Table 5.71 shows the 23 targets. At first glance, one might get the impression that the Kunming-Montreal targets are close to the Aichi targets. This is true, and we also note that some targets are always vague. However, if the official text is not technical, the CBD has done some work since its publication to be more precise. In fact, the guidelines for these targets, the indicators for monitoring progress and the national targets submitted to the CBD Secretariat are available on the website `www.cbd.int/gbf/targets`. For each target, we can find the following guidance notes prepared by the Secretariat:

A. Why is this target important?

B. Explanation of the target and its elements

C. Links to other elements of the Kunming-Montreal GBF, and other frameworks and processes

D. Guiding questions to national-setting

E. Indicators

F. Relevant resources that can assist implementation

Concerning indicators, they are split into three categories: headline indicators[221], component indicators and complementary indicators. For example, if we consider Target 6 on invasive alien species, there is one headline indicator (rate of invasive alien species establishment), three component indicators (rate of invasive alien species impact and rate of impact; rate of invasive alien species spread; number of invasive alien species introductions) and three complementary indicators (number of invasive alien species on national lists; trends in abundance, temporal occurrence and spatial distribution of non-indigenous species; Red List Index (impact of invasive alien species)).

A major challenge in implementing the Kunming-Montreal GBF is financing. Goal D of the GBF recognized a current biodiversity finance gap of $700 billion per year. To address this, Target 18 proposes to reduce incentives and subsidies that harm biodiversity by $500 billion per year by 2030,

[221] Here are all the headline indicators identified by the CBD Secretariat as of March 2025: 1.A.1 Red List of ecosystems; 1.A.2 Extent of natural ecosystems; 1.1 Per cent of land and seas covered by biodiversity-inclusive spatial plans; 2.2 Area under restoration; 3.1 Coverage of protected areas and OECMs; 4.A.3 Red list Index; 4.A.4 The proportion of populations within species with an effective population size $> 500$; 5.1 Proportion of fish stocks within biologically sustainable levels; 6.1 Rate of invasive alien species establishment; 7.1 Index of coastal eutrophication potential; 7.2 Pesticide environment concentration; 9.1 Benefits from the sustainable use of wild species; 9.2 Percentage of the population in traditional occupations; 10.1 Proportion of agricultural area under productive and sustainable agriculture; 10.2 Progress towards sustainable forest management; 11.B.1 Services provided by ecosystems; 12.1 Average share of the built-up area of cities that is green/blue space for public use for all; 13.C.1 Indicator on monetary benefits received; 13.C.2 Indicator on non-monetary benefits; 15.1 Number of companies reporting on disclosures of risks, dependencies and impacts on biodiversity; 18.1 Positive incentives in place to promote biodiversity conservation and sustainable use; 19.D.1 International public funding, including official development assistance for conservation and sustainable use of biodiversity and ecosystems; 19.D.2 Domestic public funding of conservation and sustainable use of biodiversity and ecosystems; 19.D.3 Private funding (domestic and international) of conservation and sustainable use of biodiversity and ecosystems; 21.1 Indicator on biodiversity information for monitoring the global biodiversity framework. The first number is the GBF target number. Note that headline indicators have not yet been identified for some targets.

while Target 19 specifies that at least $200 billion per year needs to be mobilized by 2030 to implement national biodiversity strategies. The latter target includes increasing financial resources from developed countries, providing development assistance to developing countries, leveraging private finance, promoting blended finance, encouraging impact funds, and promoting innovative schemes such as payments for ecosystem services, green bonds, biodiversity offsets and credits, and benefit-sharing mechanisms. As previously noted, Deutz *et al* (2020) estimated biodiversity funding at $124–143 billion per year in 2019, with the breakdown shown in Table 5.72. 57% and 20% are financed through domestic budgets and natural infrastructure, respectively. Green financial products, such as green bonds and nature-based solutions, account for less than 3%. Using the OECD's category of potential biodiversity subsidies, the authors estimated global harmful subsidies to be between $274 and $542 billion per year in 2019.

Table 5.72: Global biodiversity conservation financing in 2019 (in $ bn)

| Financial flows | Lower limit | Upper limit | Midpoint | Percentage |
|---|---|---|---|---|
| Domestic budgets and tax policy | 74.6 | 77.7 | 76.2 | 57.1% |
| Natural infrastructure | 26.9 | 26.9 | 26.9 | 20.2% |
| Biodiversity offsets | 6.3 | 9.2 | 7.8 | 5.8% |
| Sustainable supply chains | 5.5 | 8.2 | 6.8 | 5.1% |
| Official development assistance (ODA) | 4.0 | 9.7 | 6.8 | 5.1% |
| Green financial products | 3.8 | 6.3 | 5.0 | 3.8% |
| Philanthropy & conservation NGOs | 1.7 | 3.5 | 2.6 | 2.0% |
| Nature-based solutions & carbon markets | 0.8 | 1.4 | 1.1 | 0.8% |
| Total | 123.6 | 142.9 | 133.3 | 100.0% |

Source: Deutz *et al* (2020, Table 3.1, page 48).

Estimated funding needs are reported in Table 5.73. Croplands and protected areas account for 64% of total funding, while fisheries and forest conservation accounts for only 7% of total funding (about $60 billion per year). Deutz *et al* (2020) proposed nine financial and policy mechanisms to reduce the biodiversity financing gap. The optimistic estimate is a total positive financial flow of $632.5 billion, which is insufficient to close the gap (Table 5.74). While significant progress has been made since 2022 (establishment of the Global Biodiversity Framework Fund (GBFF), launch of the Cali Fund), we are still not on track to meet the 23 goals of the Kunming-Montreal Global Biodiversity Framework.

Table 5.73: Global biodiversity conservation funding needs (in $ bn)

| Funding needs | Lower limit | Upper limit | Midpoint | Percentage |
|---|---|---|---|---|
| Croplands | 315 | 420 | 367.5 | 43.5% |
| Protected areas | 149 | 192 | 170.5 | 20.2% |
| Rangelands | 81 | 81 | 81.0 | 9.6% |
| Urban environments | 73 | 73 | 73.0 | 8.6% |
| Invasive alien species | 36 | 84 | 60.0 | 7.1% |
| Coastal | 27 | 37 | 32.0 | 3.8% |
| Fisheries | 23 | 47 | 35.0 | 4.1% |
| Forests | 19 | 32 | 25.5 | 3.0% |
| Total | 722 | 967 | 844.5 | 100.0% |

Source: Deutz *et al* (2020, Figure 4.1, page 55).

Table 5.74: Estimated positive and negative flows to biodiversity conservation (in $ bn)

| Financial flows | 2019 | | 2030 | |
|---|---|---|---|---|
| | Lower limit | Upper limit | Lower limit | Upper limit |
| Harmful subsidy reform | −542.0 | −273.9 | −268.1 | 0.0 |
| Domestic budgets and tax policy | 74.6 | 77.7 | 102.9 | 155.4 |
| Natural infrastructure | 26.9 | 26.9 | 104.7 | 138.6 |
| Biodiversity offsets | 6.3 | 9.2 | 162.0 | 168.0 |
| Sustainable supply chains | 5.5 | 8.2 | 12.3 | 18.7 |
| Official development assistance (ODA) | 4.0 | 9.7 | 8.0 | 19.4 |
| Green financial products | 3.8 | 6.3 | 30.9 | 92.5 |
| Philanthropy & conservation NGOs | 1.7 | 3.5 | | |
| Nature-based solutions & carbon markets | 0.8 | 1.4 | 24.9 | 39.9 |
| Total | 123.6 | 142.9 | 445.7 | 632.5 |

Source: Deutz *et al* (2020, Figure 5.1, page 64).

### IPBES

Established in 2012, the Intergovernmental Science-Policy Platform on Biodiversity and Ecosystem Services (IPBES) is an international organization that assesses the state of the world's biodiversity and ecosystem services. It plays a similar role for biodiversity as the Intergovernmental Panel on Climate Change (IPCC) does for global warming. The current staff of the IPBES Secretariat is employed by UNEP and located in Bonn, Germany. In addition, about 2 900 experts participate or have participated in the work of IPBES. Its main functions are to provide comprehensive scientific assessments of the state of biodiversity and ecosystem services, to support policy development and implementation, and to identify key scientific information needed for policymakers. The organization has gained international recognition primarily through its influential assessment reports. As of March 2025, it has produced 13 assessment reports:

- Global reports
  - Global assessment report on biodiversity and ecosystem services (2019)
- Thematic reports
  - Pollinators, pollination and food production (2016)
  - Land degradation and restoration (2018)
  - Sustainable use of wild species (2022)
  - Invasive alien species and their control (2023)
  - Interlinkages among biodiversity, water, food and health (2024)
- Methodological reports
  - Scenarios and models of biodiversity and ecosystem services (2016)
  - The diverse values and valuation of nature (2022)
  - Underlying causes of biodiversity loss and the determinants of transformative change and options for achieving the 2050 Vision for Biodiversity (2024)

- Regional reports
  - Biodiversity and ecosystem services for Africa (2018)
  - Biodiversity and ecosystem services for the Americas (2018)
  - Biodiversity and ecosystem services for Asia and the Pacific (2018)
  - Biodiversity and ecosystem services for Europe and Central Asia (2018)

In addition, four new assessment reports will be published in the coming years: Impact and dependence of business on biodiversity and nature's contributions to people (2025); Monitoring biodiversity and nature's contributions to people (2026); Integrated biodiversity-inclusive spatial planning and ecological connectivity (2027); Second global assessment of biodiversity and ecosystem services (2028).

Figure 5.109: Some IPBES assessment reports

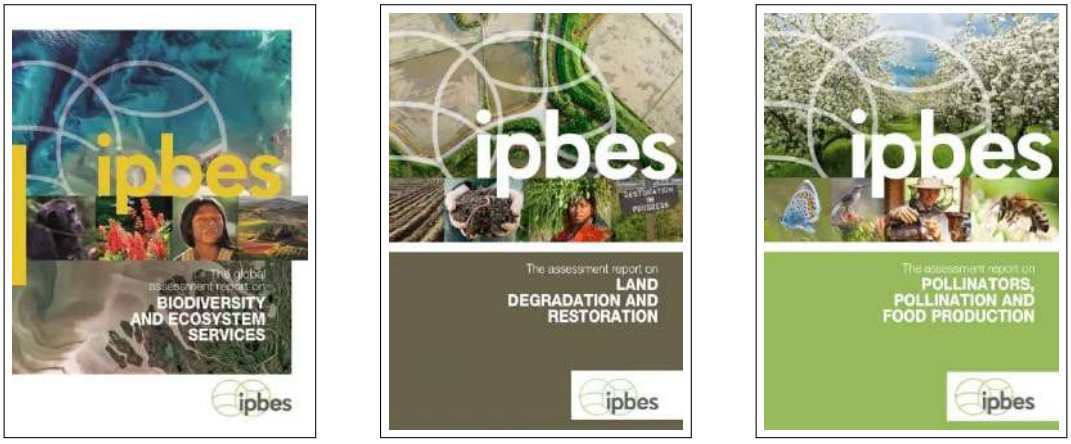


Source: IPBES & www.ipbes.net/assessing-knowledge.

### TNFD

The Taskforce on Nature-related Financial Disclosures is a global initiative to develop a framework for companies and financial institutions to report and act on nature-related risks and opportunities. Officially launched in 2021 by four founding organizations (Global Canopy, UNDP, UNEP FI and WWF), the TNFD differs from the TCFD in that it is not supported by the Financial Stability Board (FSB) or any other international regulatory body. Instead, it is a market-driven initiative supported by national governments, corporations and financial institutions. The 40 members of the Taskforce are senior executives from financial institutions (17), corporations (17) and market service providers (6). In April 2024, the ISSB and TNFD announced joint research projects on risks and opportunities related to nature and human capital. However, there are currently no plans to integrate the TNFD framework into the ISSB's sustainability standards (IFRS S1 and IFRS S2).

TNFD uses the same structure as TCFD, organized into four pillars: Governance, Strategy, Risk & impact management, and Metrics & targets. The TNFD framework is based on 14 recommended disclosures, 11 of which are carried over from the TCFD framework (Table 5.75). The three additional recommended disclosures are (3) engagement with indigenous peoples, local communities (IPLC) and affected stakeholders, (7) disclosure of the location of assets and activities in direct operations and, where possible, in the upstream/downstream value chain, and (9) identification and

assessment of nature-related dependencies in the upstream/downstream value chain. According to TNFD (2023), the framework is consistent with ISSB and GRI standards, and is aligned with Target 15 of the Kunming-Montreal GBF. In addition, the TNFD has developed guidance for some specific sectors (*e.g.*, aquaculture, beverages, metals and mining, chemicals) and the following biomes: tropical and sub-tropical forests, savannas and grasslands, intensive land-use systems, urban and industrial ecosystems, rivers and streams, and marine shelf. Two types of indicators are included in TNFD:

- A small set of core indicators (global core indicators applicable to all sectors and sector core indicators for each sector)
- A large set of additional disclosure and assessment indicators (optional)

In TNFD (2023), there are 14 global core indicators, including 9 indicators for nature-related dependencies and impacts (Table 5.76) and 5 indicators for nature-related risks and opportunities (Table 5.77). In addition, TNFD (2023) introduces several additional global and sector-specific indicators[222].

Table 5.75: The 14 recommended disclosures (TNFD, 2023)

| Pillar | # | Recommended Disclosure |
|---|---|---|
| Governance | 1 | Board oversight |
| | 2 | Management's role |
| | 3 | Human rights policies (IPLC) |
| Strategy | 4 | Risks and opportunities |
| | 5 | Impact on organization |
| | 6 | Resilience of strategy |
| | 7 | Locations of assets/activites/value chain |
| Risk management | 8 | Risk identification and assessment processes |
| | 9 | Dependencies in the value chain |
| | 10 | Risk management processes |
| | 11 | Integration into overall risk management |
| Metrics and targets | 12 | Nature-related metrics |
| | 13 | Metrics used to manage impacts and risks |
| | 14 | Nature-related targets |

Source: TNFD (2023) & https://tnfd.global.

As of October 2024, there are 502 TNFD adopters, including 318 corporations and 129 financial institutions. The majority are located in Asia (236) and Europe (183). These adopters represent $17.7 trillion in assets under management and $6.5 trillion in market capitalization.

### European biodiversity framework

The EU Biodiversity Strategy for 2030 was published in May 2020 and is part of the European Green Deal to tackle the ongoing biodiversity loss crisis. It replaces the Biodiversity strategy for 2020. The overall goal is to restore biodiversity and healthy ecosystems across the EU. Examples of quantitative targets include planting 3 billion trees by 2030, restoring 25 000 km of free-flowing rivers by removing barriers, increasing organic farming to 25% of agricultural land, and reducing

[222] These can be found in TNFD (2023, Annex 2, pages 89–99) and Section 3 of the various sector guidance documents.

Table 5.76: TNFD core global disclosure indicators for nature-related dependencies and impacts

| # | Indicator | Unit | GBF Targets |
|---|---|---|---|
| C1.0 | Total spatial footprint | $km^2$ | 1, 2, 5, 11 |
| C1.1 | Extent of land/freshwater/ocean-use change | $km^2$ | 1, 2, 5, 11 |
| C2.0 | Pollutants released to soil split by type | tonne | 7, 11 |
| C2.1 | Wastewater discharged | $m^3$ | 7, 11 |
| C2.2 | Waste generation and disposal | $m^3$ | 7, 11 |
| C2.3 | Plastic pollution | tonne | 7, 11 |
| C2.4 | Non-GHG air pollutants | $PM_{2.5}$, etc. | 7, 11 |
| C3.0 | Water withdrawal and consumption from areas of water scarcity | $m^3$ | 11 |
| C3.1 | Quantity of high-risk natural commodities sourced from land/ocean/freshwater | tonne | 5, 9, 11 |
| C4.0 | Measures against unintentional introduction of invasive alien species | | 6, 11 |
| C5.0 | Ecosystem condition | | 1, 2, 3, 4, 11 |
| C5.0 | Species extinction risk | | 1, 2, 3, 4, 11 |

Table 5.77: TNFD core global disclosure indicators for nature-related risks and opportunities

| # | Indicator |
|---|---|
| C7.0 | Value of assets, liabilities, revenue and expenses that are assessed as vulnerable to nature-related transition risks (total and proportion of total) |
| C7.1 | Value of assets, liabilities, revenue and expenses that are assessed as vulnerable to nature-related physical risks (total and proportion of total) |
| C7.2 | Description and value of significant fines/penalties received/litigation action in the year due to negative nature-related impacts |
| C7.3 | Amount of capital expenditure, financing or investment deployed towards nature-related opportunities, by type of opportunity, with reference to a government or regulator green investment taxonomy or third-party industry or NGO taxonomy, where relevant |
| C7.4 | Increase and proportion of revenue from products and services producing demonstrable positive impacts on nature with a description of impacts |

Table 5.78: Examples of TNFD additional global disclosure indicators

| # | Indicator |
|---|---|
| A2.3 | Light and noise pollution |
| A3.4 | Area used for the production of natural commodities |
| A3.5 | Use of wild species |
| A4.0 | Number/extent of unintentionally introduced species, varieties or strains |
| A7.0 | Value of write-offs and early retirements of assets due to nature-related risks |
| A8.4 | Capital expenditure on adaption due to nature-related physical risks |
| A20.0 | Proportion of sites that have active engagement with local stakeholders on nature-related issues |

Source: TNFD (2023, Tables 6–10, pages 83–99).

pesticide use by 50%. In June 2022, the European Commission also adopted a proposal for a Nature Restoration Law. EU member states will have to develop their national restoration plans by 2026 with the following objectives: restore at least 30% of habitats in poor condition by 2030, 60% by 2040, and 90% by 2050. Since then, two guidelines on forest and soil monitoring have been published in 2023. In the coming years, we can expect new biodiversity laws and regulations in the European Union, following the establishment of the EU Biodiversity Platform (EUBP) in 2022. The platform currently consists of 10 working groups addressing various biodiversity issues[223].

### 5.4.6 Investment approaches

While ESG and climate investing are now two mainstream investment approaches in asset management, the concept of biodiversity investing is relatively new. In fact, the term '*biodiversity finance*' is generally more appropriate, as it encompasses a broader range of financial instruments beyond investment practices. Nevertheless, the field of biodiversity investing is developing rapidly. For example, with the exception of BIOFIN, which was launched by UNDP in 2012 following the CBD COP10 in Nagoya in 2010, most of the major biodiversity-focused financial initiatives and alliances have been created more recently, particularly following the One Planet Summit or the CBD COP15 in 2022 (Table 5.79). This also explains why biodiversity investing is a relatively new topic for academics[224], as most of the existing literature is in the gray area (Hutchinson and Lucey, 2024).

Table 5.79: Biodiversity finance initiatives

| Acronym | Name | Website | Year |
|---|---|---|---|
| BCA | Biodiversity Credit Alliance | www.biodiversitycreditalliance.org | 2022 |
| BIOFIN | Biodiversity Finance Initiative | www.biofin.org | 2012 |
| BfN | Business for Nature | www.businessfornature.org | 2019 |
| FfB | Finance for Biodiversity Foundation | www.financeforbiodiversity.org | 2021 |
| NCIA | Natural Capital Investment Alliance | www.sustainable-markets.org | 2021 |
| NA 100 | Nature Action 100 | www.natureaction100.org | 2023 |

**Remark 70** *Biodiversity finance can include economic and financial instruments that are not related to the concepts of biodiversity investing. For example, most OECD research and publications on biodiversity finance focus on public finance, policy instruments such as taxes, subsidies or payments for ecosystem services.*

#### Financial instruments

The Global Biodiversity Framework considers that the private sector is essential to achieve the *2050 Vision for Biodiversity*, not just the public sector. For instance, the private sector is mentioned in several targets. Thus, Target 15 requires large companies and financial institutions to monitor, assess, and disclose biodiversity risks. Target 19 states that private resources must be mobilized by "*leveraging private finance, promoting blended finance, implementing strategies for raising new and additional resources, and encouraging the private sector to invest in biodiversity, including*

[223]These are (1) Working group on forests and nature; (2) Invasive alien species expert group; (3) Sub-group on monitoring and assessment; (4) Working group on green infrastructure; (5) Working group on invasive alien species; (6) Commission expert group on the birds and habitats directives; (7) Marine issues; (8) Reporting under the nature directives; (9) Expert group on the nature restoration regulation; (10) Working group on pollinators.

[224]Recent academic research on biodiversity investing includes Giglio *et al* (2023b), Flammer *et al* (2025), and Cherief *et al* (2025).

*through impact funds and other instruments*." To better understand biodiversity investing from the perspective of private investors, one approach is to list the different instruments that fit into this category. Here is a classification of the main instruments:

- Fixed-income instruments
  - Blue bonds

    *Definition* Debt securities designed to raise capital for marine and ocean conservation projects (*e.g.*, protecting marine biodiversity, restoring coastal ecosystems, financing sustainable fisheries)

    *Example* Seychelles Blue Bond (2018), which raised $15 million to support sustainable marine areas and fisheries
  - Debt-for-nature swaps

    *Definition* Financial transactions in which a portion of a country's debt is forgiven in exchange for environmental commitments

    *Example* Gabon debt-for-nature swap (2023), which restructured $500 million of debt to protect 30% of marine and forest ecosystems
  - Green and sustainable bonds

    *Definition* Debt instruments that target environmental projects and sustainable land use

    *Example* Colombia Biodiversity Bond (BBVA/IFC), which raised $50 million to finance projects focused on reforestation and wildlife habitat restoration
  - Natural capital bonds, nature performance bonds and conservation performance bonds

    *Definition* Bonds that directly finance the protection and restoration of natural capital, with returns linked to specific ecological performance metrics and biodiversity outcomes, or that monetize the value of ecosystem services and biodiversity

    *Example* Voluntary carbon credit-linked bonds, such as the IFC Forest Bond
  - Sustainability-linked bonds and pay-for-success financial instruments

    *Definition* Bonds whose financial characteristics can change based on the achievement of sustainability targets

    *Example* Rhino Bond (2022), issued by the World Bank ($150 million), where returns are linked to the growth of the black rhino population in Africa
- Market-based instruments
  - Biodiversity credits/offsets

    *Definition* Tradable units representing positive biodiversity outcomes (market mechanisms to promote biodiversity conservation)

    *Example* UK Biodiversity Net Gain (BNG) policy (developers must ensure a 10% net gain in biodiversity by funding conservation projects or purchasing biodiversity credits)
  - Nature-based insurance products

    *Definition* Insurance mechanisms to protect natural capital and ecosystem services

    *Example* Parametric insurance for coral reef protection in the Caribbean and Central America (provides insurance coverage for coastal infrastructure and triggers payouts for reef restoration after hurricanes)

  - Payments for ecosystem services (PES)

    *Definition* Schemes that provide financial incentives to landowners or communities to manage their land in a way that maintains or enhances ecosystem services

    *Example* Vittel (Nestlé Waters) offers PES to farmers in the Vosges mountains in France to maintain water quality

- Investment funds

  - Biodiversity impact funds

    *Definition* Specialized investment vehicles focused on biodiversity conservation

    *Example* The African Forestry Impact Platform (AFIP) managed by Norfund, which invests in sustainable forestry and conservation projects

  - Blended finance

    *Definition* Combines public and private capital to attract more capital to biodiversity projects

    *Example* The Land Degradation Neutrality (LDN) Fund initiated by the United Nations Convention to Combat Desertification (UNCCD) and Mirova, which finances the rehabilitation of degraded land

  - Conservation trust funds

    *Definition* Long-term financing mechanisms for conservation and sustainable development

    *Example* Bhutan Trust Fund for Environmental Conservation (BTFEC)

  - Private equity and venture capital funds

    *Definition* Investment funds focused on companies and technologies that support biodiversity

    *Example* Regeneration VC Fund

**The avoid-minimize-restore-offset approach**

To effectively integrate biodiversity into investment processes, it is essential to understand the mitigation hierarchy, a fundamental principle of conservation biology (Arlidge *et al*, 2018). The mitigation hierarchy is a structured framework to guide decision-making in managing environmental impacts. It prioritizes actions to avoid, minimize, restore, and offset negative impacts on biodiversity (Figure 5.110). Avoid prevents negative impacts on biodiversity before they occur. This step emphasizes avoiding environmentally harmful activities and encourages decision-makers to choose alternative actions or project designs that have no or minimal adverse effects on biodiversity. For example, this might involve selecting a project site that is not located in a critical habitat or a biodiversity hotspot. Minimize aims to reduce the impact of unavoidable harm to biodiversity as much as possible by decreasing the magnitude, duration and/or intensity of potential impacts when they cannot be avoided completely. An example is implementing construction practices that reduce habitat destruction, such as minimizing land clearing or avoiding key wildlife breeding seasons. Restore focuses on rehabilitating ecosystems that have been damaged by development activities. This can include replanting trees in areas affected by deforestation, restoring native vegetation, or rebuilding habitat structures to support local ecological systems. Finally, if residual impacts remain after avoid, minimize, and restore measures, offsets are used to compensate for the remaining losses. This involves creating or enhancing biodiversity elsewhere to achieve no net loss or a net gain in ecological value.

Figure 5.110: Mitigation hierarchy for nature conservation

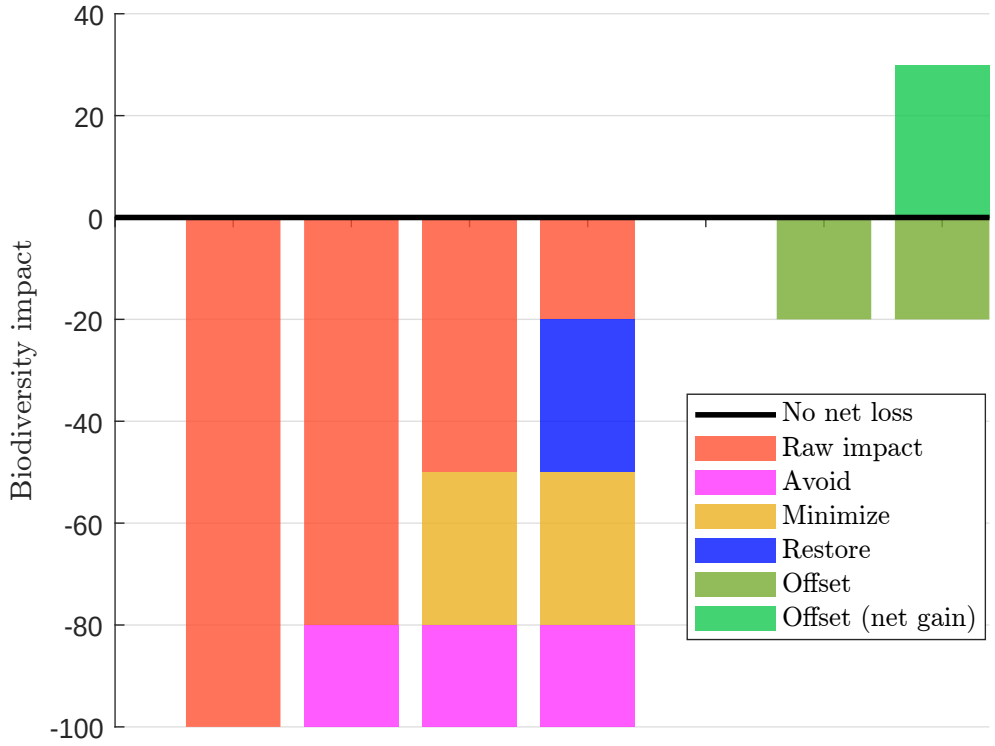


By construction, the mitigation hierarchy is an impact approach where we assess how companies and investments impact biodiversity. From a financial perspective, it is equally important to consider how companies and investments are affected by biodiversity loss. In this context, we can adopt a dependency approach based on four key risk dimensions: transition risk, physical risk, litigation risk and systemic risk. For instance, some sectors or companies are highly dependent on raw materials, soil productivity, or freshwater. As a result, loss of biodiversity can create physical risk directly or indirectly through the supply chain. Transitional risk can arise from new or emerging regulations and changes in consumer preferences. Litigation risk arises when companies face potential legal challenges related to environmental damage, failure to protect biodiversity, or non-compliance with environmental regulations. Such risks can result in significant financial penalties, reputational damage and lawsuits. The final category of risk is systemic risk, which affects companies indirectly. For example, they may be affected by severe pandemics that disrupt global ecosystems and economic systems. This dual perspective of biodiversity risk refers to the double materiality principle:

Double materiality principle

| | | |
|---|---|---|
| Dependency | $\Longleftarrow$ | How does biodiversity affect companies and investments? |
| Impact | $\Longrightarrow$ | How do companies and investments affect biodiversity? |

Applying the avoid dimension of the mitigation hierarchy to investments requires the adoption of negative screening and the establishment of exclusion criteria for issuers or projects that significantly harm biodiversity. The minimize dimension can be effectively implemented through best-in-class strategies or selective approaches that prioritize companies with stronger biodiversity practices. A key challenge in this dimension is the development and use of biodiversity metrics that appropriately

account for both sector-specific impacts and geographic contexts, as the importance of biodiversity varies widely across ecosystems. For the restore/offset dimension, the focus shifts to creating positive impacts. Traditional avoidance and minimization metrics prove inadequate here, as these final stages require the identification and selection of companies and projects that have a positive biodiversity footprint. This requires a different set of metrics that focus on restoration outcomes, additionality and measurable biodiversity gains. For example, an MSA metric is not relevant to this dimension. As a result, each progression through the hierarchy requires increasingly sophisticated measurement approaches, moving from harm reduction to positive contribution assessment.

Figure 5.111: Linking ESG investment strategies and biodiversity mitigation dimensions

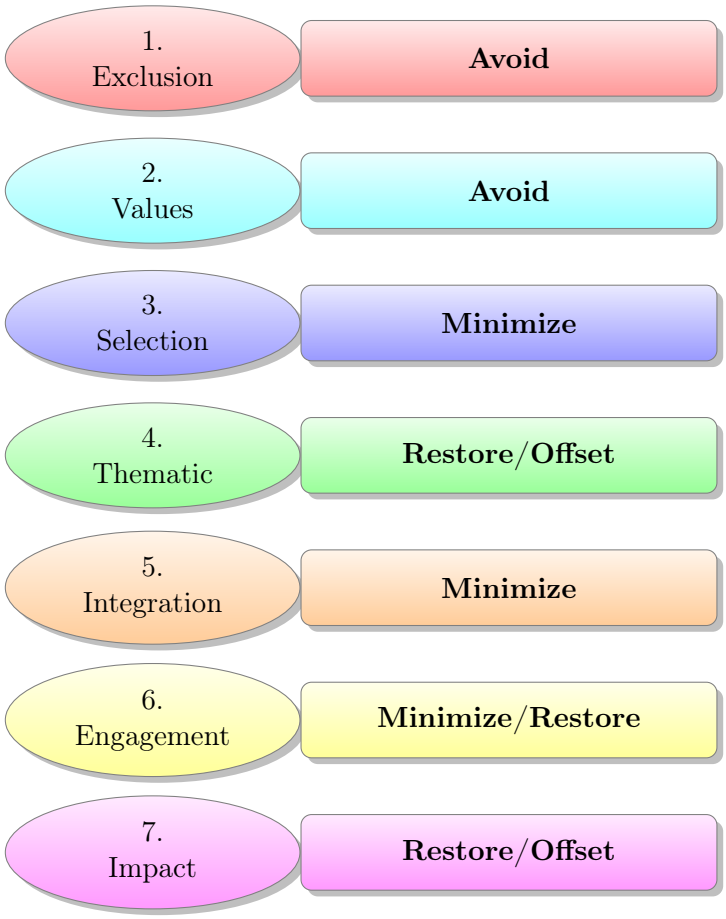


### The impact investing approach

According to Phenix Capital (2024b), the biodiversity impact fund landscape appears robust, with 1 080 biodiversity-related funds and a market size of €129 billion in open-end investment funds. At first glance, these figures appear substantial, especially when compared to the investment required to meet the targets of the GBF. However, a deeper analysis reveals a more nuanced picture. A striking 69% of these funds primarily address food-related needs rather than direct biodiversity conservation. When focusing specifically on funds targeting SDG 14 (life below water) and SDG 15 (life on land), the numbers drop to 162 and 278 impact funds, respectively. Real assets and private equity dominate these specialized sectors, accounting for 33% and 30% of these biodiversity-focused funds, respectively. However, the geographic and thematic distribution reveals significant gaps.

Only 11 real asset impact funds focus on timber and forests in Asia, 12 in Africa, and 26 in South America — regions that contain much of the world's remaining primary biodiversity. This creates a paradox. While the aggregate numbers suggest impressive financial mobilization for biodiversity, an examination of specific critical issues, such as forest conservation, reveals low investment volumes.

## 5.5 Exercises

### 5.5.1 Calculating the prevalence of undernourishment

Let $X$ and $R$ be the random variables representing energy intake and energy requirement, respectively.

1. We assume that the random vector $(X, R)$ follows a bivariate log-normal distribution: $(X, R) \sim \mathcal{LN}\left(\mu_x, \sigma_x^2, \mu_r, \sigma_r^2, \rho\right)$.

   (a) Find the probability distribution of $D = X/R$. Then, calculate the prevalence of undernourishment, denoted by $\text{PoU}^\star = \Pr\{X < R\}$.

   (b) Assume that $\mu_x = 7.50$, $\sigma_x = 0.20$, $\mu_r = 7.20$, and $\sigma_r = 0.05$. Plot the density functions of $X$ and $R$.

   (c) Plot the function of $\text{PoU}^\star$ as $\rho$ varies in the interval $[-1, 1]$. Comment on the results.

   (d) Compute the prevalence of undernourishment defined by $\text{PoU} = \Pr\{X < r_L\}$. Plot the relationship between $r_L$ and PoU when $r_L \in [1000, 1600]$.

   (e) Find the value of $r_L^\star$ such as $\text{PoU} = \text{PoU}^\star$. Calibrate the parameter $r_L^\star$ for the prevalence of undernourishment calculated in Question 1.c.

2. We want to calibrate the probability distribution function of $X$. We assume that $X \sim \mathcal{LN}\left(\mu_x, \sigma_x^2\right)$.

   (a) Give the first two moments of $X$. We will denote them by $\mu(X)$ and $\sigma^2(X)$.

   (b) Deduce the coefficient of variation $\text{CV}(X)$.

   (c) Find the moment estimators of $\mu_x$ and $\sigma_x$ from $\mu(X)$ and $\text{CV}(X)$.

   (d) We consider an hypothetical country with a population of 1 million and two food components (cereals and fruits/vegetables), whose the food balance sheet is as follows:

   | | Production | Imports | Exports | ΔStocks | Feed | Waste |
   |---|---|---|---|---|---|---|
   | #1 | 349 000 | 1 025 | 40 000 | −1 000 | 45 000 | 9 000 |
   | #2 | 50 000 | 9 010 | 1 000 | 6 000 | 500 | 500 |

   All the figures are expressed in tonnes. Calculate the food available for human consumption. Assuming that the average energy density is 3 500 and 500 Calories/kg for cereals and fruits/vegetables respectively, find the average dietary energy consumption $\mu(X)$ expressed in kcal/capita/day.

   (e) The average dietary energy consumption by household expenditure deciles are 1 650 (first decile), 1 985, 2 150, 2 350, 2 530, 2 550, 2 650, 2 750, 3 100 and 3 630 (last decile). Calculate the coefficient of variation $\text{CV}(X \mid Y)$. Check that $\mu(X \mid Y) = \mu(X)$. Assuming that $\text{CV}(X \mid R) = 0.20$, calculate $\text{CV}(X)$.

(f) Calibrate the parameters $\mu_x$ and $\sigma_x$ using the previous figures. What is the prevalence of undernourishment if we assume that $r_L = 1\,850$? Give an estimate of the number of undernourished people.

3. We seek to estimate the minimum dietary energy requirement.

(a) We recall that the body mass index (BMI) is expressed in $\text{kg}/\text{m}^2$ and is defined as the ratio of the weight (in kg) to the square of the height (in meter):

$$\text{BMI} = \frac{\text{weight}}{\text{height}^2}$$

The ideal value of BMI is 22. To define undernourished people, we assume that their weight is below a reference value:

$$\text{weight} \leq \text{weight}^\star$$

where:

$$\text{weight}^\star = \text{BMI}\,(p) \cdot \text{height}^2$$

where $p$ is a percentile value that depends on age. If the age is less than ten years, $p$ is set to 50%, while for individuals 10 years and older, it is set to 5%. Below, we give the values of $\text{BMI}\,(p)$ and the average height per age and sex:

| | Age | −3 | 3–10 | 10–18 | 18–30 | 30–60 | 60+ |
|---|---|---|---|---|---|---|---|
| $\text{BMI}\,(p)$ | Female | 15.5 | 15.5 | 17.0 | 17.5 | 17.5 | 17.5 |
| | Male | 15.5 | 15.5 | 17.0 | 18.5 | 18.5 | 18.5 |
| Height | Female | 0.80 | 1.20 | 1.55 | 1.60 | 1.60 | 1.60 |
| | Male | 0.88 | 1.24 | 1.58 | 1.72 | 1.72 | 1.72 |

Calculate the reference value $\text{weight}^\star$ per age and sex to determine the undernourishment.

(b) We assume that the basal metabolic rate (BMR) is given by the Schofield equation:

$$\text{BMR} = \alpha + \beta \cdot \text{weight}^\star$$

where $\alpha_j$ and $\beta_j$ are the estimates of the linear regression between weight and BMR:

| | Age | −3 | 3–10 | 10–18 | 18–30 | 30–60 | 60+ |
|---|---|---|---|---|---|---|---|
| $\alpha$ | Female | −31.1 | 485.9 | 692.6 | 486.6 | 845.6 | 658.5 |
| | Male | −30.4 | 504.3 | 658.2 | 692.2 | 873.1 | 587.7 |
| $\beta$ | Female | 58.317 | 20.315 | 13.384 | 14.818 | 8.126 | 9.082 |
| | Male | 59.512 | 22.706 | 17.686 | 15.057 | 11.472 | 11.711 |

Calculate the basal metabolic rate for each group.

(c) The minimum dietary energy requirement is equal to the physical activity level (PAL) times the basal metabolic rate:

$$\text{MDER} = \text{PAL} \cdot \text{BMR}$$

We assume that the population is on average lightly active, implying that PAL = 1.55. Calculate the minium dietary energy requirement for the different groups.

(d) We assume that the proportion of females and males is the same, while the distribution of the population by age is as follows:

| Age | −3 | 3–10 | 10–18 | 18–30 | 30–60 | 60+ |
|---|---|---|---|---|---|---|
| Frequency | 9.9% | 15% | 16% | 18% | 29% | 12.1% |

Calculate the minium dietary energy requirement of the population.

4. We want to calculate the depth of the food deficit:

$$\text{FD} = \int_{x<r_L} (\bar{r} - x)\, f_x(x)\, \mathrm{d}x$$

where $r_L$ is the minimum dietary energy requirement (MDER), $\bar{r}$ is the average dietary energy requirement (ADER), and $f_x(x)$ is the probability density function of the dietary energy consumption $X$.

(a) What is the interpretation of the indicator FD?

(b) Find the probabilistic expression of the indicator FD.

(c) Find the analytical value of FD when $X \sim \mathcal{LN}\left(\mu_x, \sigma_x^2\right)$.

(d) Calculate the depth of the food deficit in the case of Question 2 if we assume that the average dietary energy requirement is equal to 2 500 Calories per person per day.

### 5.5.2 Calculating the species-area relationship using the theory of island biogeography

1. We consider the model of island biogeography developed by Beaugrand *et al.* (2024). We denote species richness by $S(t)$. At the initial date $t_0$, we have $S(t_0) = S_0$ (we can assume that $S_0 = 0$). The authors assume the existence of a saturation date $t_s$, *i.e.*, the species richness cannot exceed a limit value:

$$0 \leq S(t) \leq S_s = S(t_s)$$

(a) Let $f(x) = ae^{b(x/c)^d}$ where $a > 0$, $c > 0$ and $d > 0$. The parameter $b$ can take two values: $-1$ or $+1$. We also assume that $0 \leq x \leq c$. In which case do we get a decreasing, increasing, concave and convex function?

(b) Let $\lambda(t)$ represent the immigration rate. We assume that:

$$\lambda(t) = \lambda_0 \frac{e^{-\left(\frac{S(t)}{S_s}\right)^{\beta_1 \lambda_0}} - e^{-1}}{1 - e^{-1}} \qquad \text{for } \lambda_0 \geq \lambda(t) \geq \lambda_s = \lambda(t_s)$$

where $\lambda_0 \geq 0$ is the initial immigration rate, and $\beta_1 > 0$ is a parameter. Prove that $\lambda(t)$ is a decreasing function of $S(t)$, with $\lambda(t_0) = \lambda_0$ and $\lambda(t_s) = 0$. Determine whether $\lambda(t)$ is a convex or concave function. Plot the function $\lambda(t)$ for the following parameter sets $(\lambda_0, \beta_1, S_s)$: $(1.0, 0.2, 200)$, $(1.0, 0.5, 200)$, $(1.0, 1.0, 200)$, and $(0.9, 2.0, 150)$. Analyze and comment on these results.

(c) Let $\mu^{\text{long}}(t)$ be the long-term extinction rate. We assume that:

$$\mu^{\text{long}}(t) = \mu_s \frac{e^{\left(\frac{S(t)}{S_s}\right)^{\beta_2 \mu_s}} - 1}{e^1 - 1} \qquad \text{for } \mu_0^{\text{long}} \leq \mu^{\text{long}}(t) \leq \mu_s = \mu^{\text{long}}(t_s)$$

where $\mu_s \geq 0$ is the extinction rate at the saturation date, and $\beta_2 > 0$ is a parameter. Prove that $\mu^{\text{long}}(t)$ is an increasing function of $S(t)$, with $\mu^{\text{long}}(t_0) = 0$ and $\mu^{\text{long}}(t_s) = \mu_s$. Determine whether $\mu^{\text{long}}(t)$ is a convex or concave function. Plot the function $\mu^{\text{long}}(t)$ for the following parameter sets $(\mu_s, \beta_2, S_s)$: $(1.0, 0.2, 200)$, $(1.0, 0.5, 200)$, $(1.0, 1.0, 200)$, and $(0.5, 2.0, 150)$. Analyze and comment on these results.

(d) Let $\mu^{\text{short}}(t)$ be the short-term extinction rate. We assume that:

$$\mu^{\text{short}}(t) = \beta_3 \lambda(t) e^{-\beta_4 S(t)} \qquad \text{for } \mu_0^{\text{short}} \geq \mu^{\text{short}}(t) \geq \mu_s^{\text{short}} = \mu^{\text{short}}(t_s)$$

where $\beta_3$ and $\beta_4$ are two positive parameters. Prove that $\mu^{\text{short}}(t)$ is a decreasing function of $S(t)$, with $\mu^{\text{short}}(t_0) \leq \beta_3 \lambda_0$ and $\mu^{\text{short}}(t_s) = 0$. Plot the function[225] $\mu^{\text{short}}(t)$ for the following parameter sets $(\beta_3, \beta_4, S_s)$: $(0.2, 0.02, 200)$, $(0.5, 0.02, 200)$, $(0.8, 0.02, 200)$, and $(1.0, 0.10, 150)$.

(e) Let $\mu(t) = \mu^{\text{short}}(t) + \mu^{\text{long}}(t)$ be the extinction rate. Show that $\mu(t_0) = \mu^{\text{short}}(t_0)$ and $\mu(t_s) = \mu_s$. Plot the function $\mu(t)$ for the following set of parameters: $\lambda_0 = 1$, $\beta_1 = 0.5$, $\mu_s = 1$, $\beta_2 = 2$, $\beta_3 = 0.70$, $\beta_4 = 0.01$, and $S_s = 200$. Comment on these results.

(f) The dynamics of species richness is governed by the following differential equation:

$$\frac{\mathrm{d}S(t)}{\mathrm{d}t} = \delta(t) = \lambda(t) - \mu(t)$$

What is the condition for $S(t)$ to reach an equilibrium? Illustrate and determine the equilibrium $S^\star$ using the set of parameters provided in Question 1.e.

(g) Under what conditions can two equilibria exist? Let $S_1^\star$ and $S_2^\star$ be the two equilibria, with $S_1^\star \leq S_2^\star$. Show that $S_1^\star$ is an unstable steady state, while $S_2^\star$ is a stable steady state. Deduce that there is a third equilibrium $S_0^\star$, with $S_0^\star \leq S_1^\star \leq S_2^\star$. Illustrate the three-equilibrium case with the following set of parameters: $\lambda_0 = 1$, $\beta_1 = 0.5$, $\mu_s = 1$, $\beta_2 = 2$, $\beta_3 = 1.70$, $\beta_4 = 0.02$, and $S_s = 200$.

(h) Using the two sets of parameters defined in Questions 1.e and 1.g, simulate the process $S(t)$ when the initial species richness $S_0$ is 0, 25, 30, 50 and 120, respectively. Comment on these results.

2. We aim to analyze the dynamics of the TIB steady state $S^\star$ under the assumption that there is no short-term extinction rate, meaning $\beta_3 = 0$ or $\mu^{\text{short}}(t) = 0$. The default parameter values are $\lambda_0 = 1$, $\beta_1 = 0.5$, $\mu_s = 1$, $\beta_2 = 1$, and $S_s = 200$.

(a) What is the impact of $\beta_2$ on the equilibrium $S^\star$? Compare the solutions for $\beta_2 = 0.2$, $\beta_2 = 1$, and $\beta_2 = 5$.

(b) Plot the relationship between $\beta_2$ and $S^\star$.

(c) What is the impact of $\mu_s$ on the equilibrium $S^\star$?

(d) Plot the relationship between $\mu_s$ and $S^\star$.

[225] We assume $\lambda_0 = 1.0$ and $\beta_1 = 0.5$ to define $\lambda(t)$.

(e) What conclusion can we draw about the relationship between the area $A$ and the equilibrium $S^\star$.

(f) We assume that the area $A$ (expressed in $\text{km}^2$) is related to the parameter $\beta_2$ as follows: $A = \beta_2^{0.75}$. A sampling of $\beta_2$ is taken between 0.01 and 5.00 with a step size of 0.01. Use nonlinear least squares to estimate the power model $S = cA^z$, the exponential model $S = c + z\ln(A)$, and the Kobayashi model $S = c\ln(1 + zA)$. Compare the TIB equilibrium $S^\star$ with the forecasts of the fitted models. Comment on these results.

### 5.5.3 Species abundance models

*Remark: This exercise was inspired by the research articles of Coleman (1981), and He and Legendre (2002).*

1. We consider an area (or an ecosystem) $A$ containing $S$ species. Let $n_i$ denote the abundance of the $i^{\text{th}}$ species and let $n = \sum_{i=1}^{S} n_i$ represent the total abundance in the area. We focus on a subarea $a \subseteq A$ and denote by $\tilde{S}_a$ the random variable representing the number of species in this subarea. We introduce the notation $S_a = \mathbb{E}\left[\tilde{S}_a\right]$ to represent the expected number of species in the subarea.

   (a) Let $p_i$ be the probability that species $i$ is present in the subarea $a$, and $\tilde{S}_i \sim \mathcal{B}(p_i)$ the random variable indicating its presence ($\tilde{S}_i = 1$) or its absence ($\tilde{S}_i = 0$). What is the probability distribution of $\tilde{S}_a$? Deduce the value of $S_a$. Application: Given $p = (p_1, \ldots, p_5) = (20\%, 30\%, 10\%, 65\%, 10\%)$, calculate $\tilde{S}_a$ and $S_a$.

   (b) We assume a random placement of the species within the area $A$. What is the probability of observing $k$ individuals of species $i$ in the subarea $a$? Show that:

$$\tilde{S}_i \sim \mathcal{PB}\left(p_i = 1 - \left(1 - \frac{a}{A}\right)^{n_i}\right)$$

   Find the value of $S_a$. Application: Given $(n_1, \ldots, n_5) = (10, 4, 25, 6, 8)$, $A = 10\,\text{km}^2$, and $a = 2\,\text{km}^2$, calculate $\tilde{S}_a$ and $S_a$.

   (c) Calculate $S_a$ for the following models:

   i. Most even model:

$$n_i = \frac{n}{S} \quad \text{for } i = 1, \ldots, S$$

   ii. Most uneven model:

$$n_i = 1 \quad \text{for } i < S \quad \text{and} \quad n_S = n - S + 1$$

   Calculate $\tilde{S}_a$ and $S_a$.

   iii. Mixed even-uneven model:

$$n_i = 1 \quad \text{for } i \leq s \quad \text{and} \quad n_i = \frac{n - s}{S - s} = n_{s+1} \text{ for } i > s$$

   iv. He-Gaston model:

$$p_i = 1 - \left(1 - \frac{a}{A}\right)\left(1 + \frac{n_i a}{\kappa_i A}\right)^{-\kappa_i}$$

   where $\kappa_i \in (-\infty, m_i) \cup [0, \infty)$ is a parameter which describes the spatial pattern of species $i$ and $m_i = n_i a/A$ is the mean density of species $i$ in the subarea $a$.

v. Broken-stick model[226]:

$$n_i = \frac{n}{S}\sum_{k=i}^{S}\frac{1}{k}$$

(d) The species abundance distribution is defined as the series $\{s(1), s(2), \ldots\}$ where $s(j)$ is the number of species with $j$ individuals. Show that:

$$S_a = S - \sum_j s(j)\left(1 - \frac{a}{A}\right)^j$$

Application: Calculate $S_a$ for the log-series distribution:

$$s(j) = \alpha\frac{x^j}{j}$$

where $\alpha$ is a parameter related to the total diversity and $x \in (0,1)$ is a parameter determining the relative abundance.

2. We say that the species is locally endemic to subarea $a \subseteq A$ if it is found exclusively in subarea $a$ and not in the complementary area $A - a$.

(a) Calculate the probability $\breve{p}_i$ of endemism of species $i$.

(b) What is the expected number $E_a$ of locally endemic species?

(c) Calculate $S_{A-a}$ and $E_{A-a}$ for the complementary area $A - a$. Deduce that:

$$S_{A-a} + E_a = S$$

(d) Show that:

$$0 \leq S_a + E_a \leq 2S$$

### 5.5.4 Valuation of risks to life and health

*Remark: This exercise was inspired by the research article by Hammitt (2023).*

Let $\tau$ be a survival time[227], whose survival function is $\mathbf{S}(t) = \Pr\{\tau > t\}$ and density function is $f(t) = -\partial\mathbf{S}(t)$. We have $\mathbf{S}(0) = 1$ and $\mathbf{S}(\infty) = 0$.

1. Assume that the individual is alive at time $t$. What is the conditional survival function $\mathbf{S}(u \mid t) = \Pr\{\tau > u \mid \tau > t\}$?

2. Show that the average length of life (or life expectancy) for an individual who is alive at time $t$ is given by:

$$\mathrm{LE}(t) = \mathbb{E}[\tau \mid \tau > t] = \frac{1}{\mathbf{S}(t)}\int_t^\infty \mathbf{S}(u)\,\mathrm{d}u$$

[226] Hint: Approximate the harmonic sum by $\ln\left(\frac{S}{i}\right)$, and replace the sum $\sum_{i=1}^{S}\left(1 - \frac{a}{A}\right)^{n_i}$ with its integral form.

[227] In mortality analysis, this is referred to as time-to-event or time-to-death.

3. Let $\varrho$ be the discount rate and $X(t)$ a payoff function. Following the seminal paper of Yaari (1965), we define the expected present value of the payoff, taking into account the future lifetime, as:
$$\mathbb{E}[X; t, \varrho] = \int_t^\infty e^{-\varrho(u-t)} \mathbf{S}(u \mid t) X(u) \, \mathrm{d}u$$
What is the rationale behind this formula?

4. The discounted remaining life expectancy is defined as the expected present value of the future lifetime:
$$\mathrm{LE}(t; \varrho) = \mathbb{E}[1; t, \varrho] = \frac{1}{\mathbf{S}(t)} \int_t^\infty e^{-\varrho(u-t)} \mathbf{S}(u) \, \mathrm{d}u$$
Shows that:
$$\mathrm{LE}(t; \varrho) \geq \mathrm{DLE}(t; \varrho) = \int_t^\infty e^{-\varrho(u-t)} (u-t) f(u \mid t) \, \mathrm{d}u$$
What is the interpretation of $\mathrm{DLE}(t; \varrho)$? Under which condition do we have equality?

5. Assume that the survival time follows an exponential distribution: $\tau \sim \mathcal{E}(\lambda)$. Derive the formulas for $\mathrm{LE}(t; \varrho)$ and $\mathrm{DLE}(t; \varrho)$? Comment on these results.

6. We assume that life expectancy is 70 years ($\mathbb{E}[\tau] = 70$). We consider two survival functions: $\tau \sim \mathcal{E}(\lambda)$ and $\tau \sim \mathcal{W}_{\text{eibull}}(a, b)$, where the survival function is defined as $\mathbf{S}(t) = \exp\left(-\left(\frac{x}{a}\right)^b\right)$.

   (a) Calibrate the parameters $\lambda$ and $a$ so that $b = 5$. Plot the survival functions $\mathbf{S}(t)$ and $\mathbf{S}(u \mid t = 50)$. Comment on these results.

   (b) We assume that $\varrho = 3\%$. Calculate $\mathrm{LE}(0; \varrho)$ and $\mathrm{DLE}(0; \varrho)$ if the survival time is exponential.

   (c) Assume that the survival time is Weibull distributed. Using numerical integration, plot the discounted life expectancy $\mathrm{LE}(t; \varrho)$ for $t \in [0, 100]$ and for different discount rates $\varrho$ (0%, 1%, 2%, 3% and 10%). Comment on these results.

7. We assume that the quality life weight $\hat{Q}(t)$ is a random variable between 0 and 1, and we note $Q(t) = \mathbb{E}\left[\hat{Q}(t)\right]$ its expected value. The quality-adjusted life expectancy (QALE) is defined as $\mathrm{QALE}(t; \varrho) = \mathbb{E}[Q(t); t, \varphi]$.

   (a) Give the formula of $\mathrm{QALE}(t; \varrho)$ when the function $Q(t)$ is constant.

   (b) Show that:
   $$\mathrm{QALE}(t; \varrho) \leq \mathrm{LE}(t; \varrho)$$

   (c) Consider the previously calibrated Weibull distribution. We assume that:
   $$Q_1(t) = \begin{cases} 1 & \text{if } t \leq t_1 \\ 1 - \kappa_1 \dfrac{(t - t_1)}{t_2 - t_1} & \text{if } t_1 \leq t \leq t_2 \\ 1 - \kappa_1 - \kappa_2 \dfrac{(t - t_2)}{t_3 - t_2} & \text{if } t_2 \leq t \leq t_3 \\ 1 - \kappa_1 - \kappa_2 & \text{if } t \geq t_3 \end{cases}$$

What is the rationale for this specification? We consider a second HRQL function:

$$Q_2(t) = \exp(-\kappa t)$$

Compare $\text{QALE}(t;\varrho)$ and $\text{LE}(t;\varrho)$ for the following set of parameters: $t_1 = 50$, $\kappa_1 = 10\%$, $t_2 = 70$, $\kappa_2 = 20\%$, $t_3 = 90$, and $\kappa = 2\%$.

8. Let $\mathcal{R}(t)$ be the impact on mortality risk. We use the convention that $\mathcal{R}(t)$ is positive if the impact is a risk reduction and negative if the impact is a risk increase. We define $\Delta L(t) = \mathcal{R}(t) \cdot \Delta t$ as the expected number of lives saved (or the decrease in the number of deaths) during the short time interval $\Delta t$. Hammitt (2023) also defines the increase in life expectancy as $\Delta\text{LE}(t) = \Delta L(t) \cdot \text{LE}(t;\varrho)$ and the increase in quality-adjusted life expectancy as $\Delta\text{QALE}(t) = \Delta L(t) \cdot \text{QALE}(t;\varrho)$. The monetary value $v$ of the risk reduction $\mathcal{R}(t)$ is the product of the value of a statistical life (VSL) and the expected number of lives saved. Similarly, $v$ can be expressed as the product of the value per statistical life year (VSLY) and the increase in life expectancy or as the product of the value per quality-adjusted life year (VQALY) and the increase in quality-adjusted life expectancy. Following Hammitt (2023), we have:

$$v = \text{VSL}(t) \cdot \Delta L(t) = \text{VSLY}(t) \cdot \Delta\text{LE}(t) = \text{VQALY}(t) \cdot \Delta\text{QALE}(t)$$

   (a) Find $\text{VSL}(t)$ and express $\text{VSLY}(t)$ and $\text{VQALY}(t)$ as functions of $\text{VSL}(t)$.

   (b) Hammitt (2023) considers persistent risk impact $\mathcal{I}(t)$ and defines the economic gain from risk reduction as:

$$\mathcal{G}(t;\varrho) = \frac{1}{\mathbf{S}(t)} \int_t^\infty e^{-\varrho(u-t)} \mathbf{S}(u)\, \text{VSL}(u)\, \mathcal{I}(u)\, \mathrm{d}u$$

   What is the interpretation of $\mathcal{G}(t;\varrho)$? Assume that $\mathcal{I}(t) = \mathcal{R}(t)$. What is the associated payoff function. Give the expression for the payoff function using $\text{VSLY}(t)$ or $\text{VQALY}(t)$.

   (c) What is the value of $\mathcal{G}(t;\varrho)$ if $\text{VSL}(t)$ and $\mathcal{I}(t)$ are assumed to be constant?

   (d) In the case of air pollution, the economic cost is sometimes estimated using the following formula:

$$\mathcal{C} = \text{VSLY} \cdot \text{YLL}$$

   What is the rationale for this formula?

   (e) Consider a numerical application using the previously calibrated Weibull distribution and the HRQL function $Q_1(t)$. Compute the values of $\text{LE}(t;\varrho)$ and $\text{QALE}(t;\varrho)$ for $t \in \{0, 40, 80\}$ and $\varrho \in \{0, 3\%\}$. Workers in an industry are paid an additional \$1 000 per year to face a 1 in 10 000 increased risk of death. Compute the value of a statistical life. Deduce the values of $\text{VSLY}(t)$ and $\text{VQALY}(t)$. What is the drawback of assuming a constant VSL regardless the worker's age. Therefore, we prefer to assume a constant $\text{VSLY}(t)$, equal to \$150 000. Deduce the values of $\text{VSL}(t)$ and $\text{VQALY}(t)$. Calculate the economic gain $\mathcal{G}(t;\varrho)$ of a policy that avoids 5 deaths among 100 000 people. Comment on these results.

# Chapter 6

# Engagement & Voting Policy

According to GSIA (2021), corporate engagement & shareholder action is one of the seven categories of ESG strategies. It is defined as "*employing shareholder power to influence corporate behaviour, including through direct corporate engagement (i.e., communicating with senior management and/or boards of companies), filing or co-filing shareholder proposals, and proxy voting that is guided by comprehensive ESG guidelines.*" While this category of ESG strategies goes by different names — engagement and voting on sustainability matters for Eurosif, active ownership for the PRI — the scope of ESG engagement is well defined. It refers to the process of interacting with companies to encourage them to adopt sustainable and socially responsible practices. This may involve discussing issues related to corporate social responsibility and the sustainability impact of the business with company management and board members, and working with them to develop and implement practices that are aligned with the shareholder's ESG principles. ESG engagement can be conducted by asset owners, asset managers, or organizations that seek to influence corporate behavior (*e.g.*, Climate Action 100+). However, the ultimate goal of ESG engagement is always to align companies' ESG practices with investors' ESG expectations. ESG engagement is often confused with the term ESG stewardship. In fact, ESG engagement is part of ESG stewardship, but the latter is a broader concept and refers to all the actions asset owners and managers take to encourage companies to adopt sustainable and socially responsible practices. Of course, engagement is the cornerstone of stewardship because shareholder engagement and voting are the most direct ways to influence companies. However, companies are also impacted when an investor implements ESG scoring or publishes its exclusion list. Increasingly, we see the term stewardship replacing the term engagement. For instance, the publication of ESG stewardship reports by asset owners and managers has replaced the publication of ESG engagement over the past three years. In February 2021, the PRI published the guide "*Stewardship*" on active ownership:

> "*It guides investors on how to implement the PRI's Principle 2, which sets out signatories' commitment to stewardship, stating: we will be active owners and incorporate ESG issues into our ownership policies and practices. [...] The PRI defines stewardship as the use of influence by institutional investors to maximise overall long-term value including the value of common economic, social and environmental assets, on which returns and clients' and beneficiaries' interests depend.*" (PRI, 2021a).

While ESG engagement and ESG stewardship are closely related concepts, ESG stewardship is generally interpreted by investors as their ESG policies, including rating models, strategies, organizations, etc. In this chapter, in a first section, we focus on active ownership and define the different forms of ESG shareholder activism. In a second section, we examine the voting policies of ESG investors.

## 6.1 Active ownership

### 6.1.1 Definition

From an ESG perspective, the terms active ownership, engagement and shareholder activism are interchangeable. Shareholder activism is certainly the term most often used by academics, while professionals prefer to talk about engagement and active ownership. A shareholder activist is a shareholder who uses his or her stake in a (listed) company to influence the board of directors and change the way the company is managed. For example, Gillan and Starks (2000) define active shareholders as "*investors who, dissatisfied with some aspect of a company's management or operations, try to bring about change within the company without a change in control.*" The changes may relate to the business model, strategy or ESG policies. Passive shareholders, on the other hand, are investors who own shares in the company but have no intention of influencing the company. When we refer to ESG engagement, the issues focus on sustainable and socially responsible practices.

Conflicts of interest between shareholders and management are well documented and central in the theory of the firm (Williamson, 1970; Jensen and Meckling, 1976). Indeed, shareholders and management may have different goals. In particular, the concept of "*managerial entrenchment*" refers to the tendency of managers to act in their own self-interest with a short-term time horizon rather than in the interests of shareholders, whose objective is to improve the long-term performance of the firm. In this context, managers may seek to maximize their own utility rather than the utility of shareholders, who are the owners of the firm. For example, managers have incentives to grow firms beyond optimal size because it increases their power, the resources under their control, and also their compensation (Murphy, 1985). Similarly, the separation of ownership and control, corporate social responsibility, and the definition of a corporate objective function can lead to a misalignment of preferences between shareholders and the board of directors (Jensen and Meckling, 1976). Therefore, active shareholders can serve as effective monitors of management behavior, especially when agency costs emerge[1] (Jensen, 1993) or negative externalities can generate large potential costs.

The debate about the separation of ownership and control is amplified when we introduce stakeholder theory (Freeman, 2004). In fact, there may be some conflict between shareholders and stakeholders because shareholders do not necessarily have ESG preferences. On page 3, we have already mentioned the debate between the classical shareholder theory and the stakeholder theory. For Friedman (1970), "*the social responsibility of business is to increase its profits.*" Nevertheless, the shareholder vs. stakeholder debate has changed over time as more and more investors, especially institutional investors, have now sustainability preferences. Moreover, corporate social responsibility has evolved quite spectacularly since the seminal publication of Bowen (1953) — see for instance Drucker (1954), Jones (1980), Mintzberg (1983), Drucker (1984), Wood (1991), Mitchell *et al.* (1997), Carroll (1999), Crowther and Aras (2008), Carroll and Shabana (2010), Jha and Cox (2015) and Yuan *et al.* (2020). It is now widely accepted that corporations also have social responsibilities. Peter Drucker summarizes it as follows: "*leaders in every single institution and in every single sector . . . have two responsibilities. They are responsible and accountable for the performance of their institutions, and that requires them and their institutions to be concentrated, focused, limited. They are responsible also, however, for the community as a whole.*" For corporations, this implies an unlimited liability clause with respect to their employees, their consumers, and society as a whole. One of the main objectives is then to minimize legal problems. This is especially true for negative

[1] The main reason for this is that internal control mechanisms are generally not designed to oversee the chief executive officer and senior managers of the company. Therefore, the board of directors is the only way to supervise the CEO and his or her actions. In some cases, this supervision is reversed, *i.e.*, the CEO supervises and controls the board of directors.

externalities on the environment caused by the company. This echoes the liability risks defined by Carney (2015):

> "*[...] the impacts that could arise tomorrow if parties who have suffered loss or damage from the effects of climate change seek compensation from those they hold responsible. Such claims could come decades in the future [...].*"

The current context is very different from the 1970s, when Milton Friedman wrote his famous article. Today, corporate social responsibility is no longer an option. However, this does not mean that there is complete alignment between management, shareholders and stakeholders.

### 6.1.2 The various forms of active ownership

According to Bekjarovski and Brière (2018), active ownership can take several forms:

1. Engage behind the scenes with management and the board;
2. Propose resolutions (shareholder proposals);
3. Vote (form coalition, express dissent, call back lent shares);
4. Voice displeasure publicly (in the media);
5. Initiate a takeover (acquire a sizable equity share);
6. Exit (sell shares, take an offsetting bet, divestment);

The first two approaches take the form of dialogue between investors and companies, involving direct communication with company management and board members to discuss ESG issues. This is particularly true for the first approach. It is also the case for the second approach, as resolutions are discussed prior to annual general meetings (AGMs). The third approach can be considered one of the financial obligations of investors. This is certainly the most common way to participate in the life of a company once a year. The last three approaches take the form of an action or reaction if investors do not agree with the company's sustainability policy or the results of the AGM. We generally find all of these six approaches (except initiating a takeover) in the engagement/sustainability/stewardship reports of asset owners and managers (Figure 6.1).

**Remark 71** *The first five approaches are complementary, while exit corresponds to a non-return situation. In the latter case, the engagement process between the investor and the company is terminated as the investor is no longer a shareholder of the company.*

#### Engage behind the scenes

Twenty years ago, meetings between management and a company's board of directors were rare. In addition to public meetings following earnings announcements, communication between investors and investee companies typically took the form of a morning breakfast where a selection of equity or credit analysts were invited to meet with a company representative, usually the chief financial officer (CFO). This has changed over time, particularly with the development of extra-financial analysis. Today, private communication between ESG investors and companies has become very common. Engage behind the scenes refers to any meetings or actions taken by the active shareholder to better understand the ESG strategy of companies and to challenge companies on specific sustainability issues:

Figure 6.1: Example of engagement/sustainability/stewardship reports

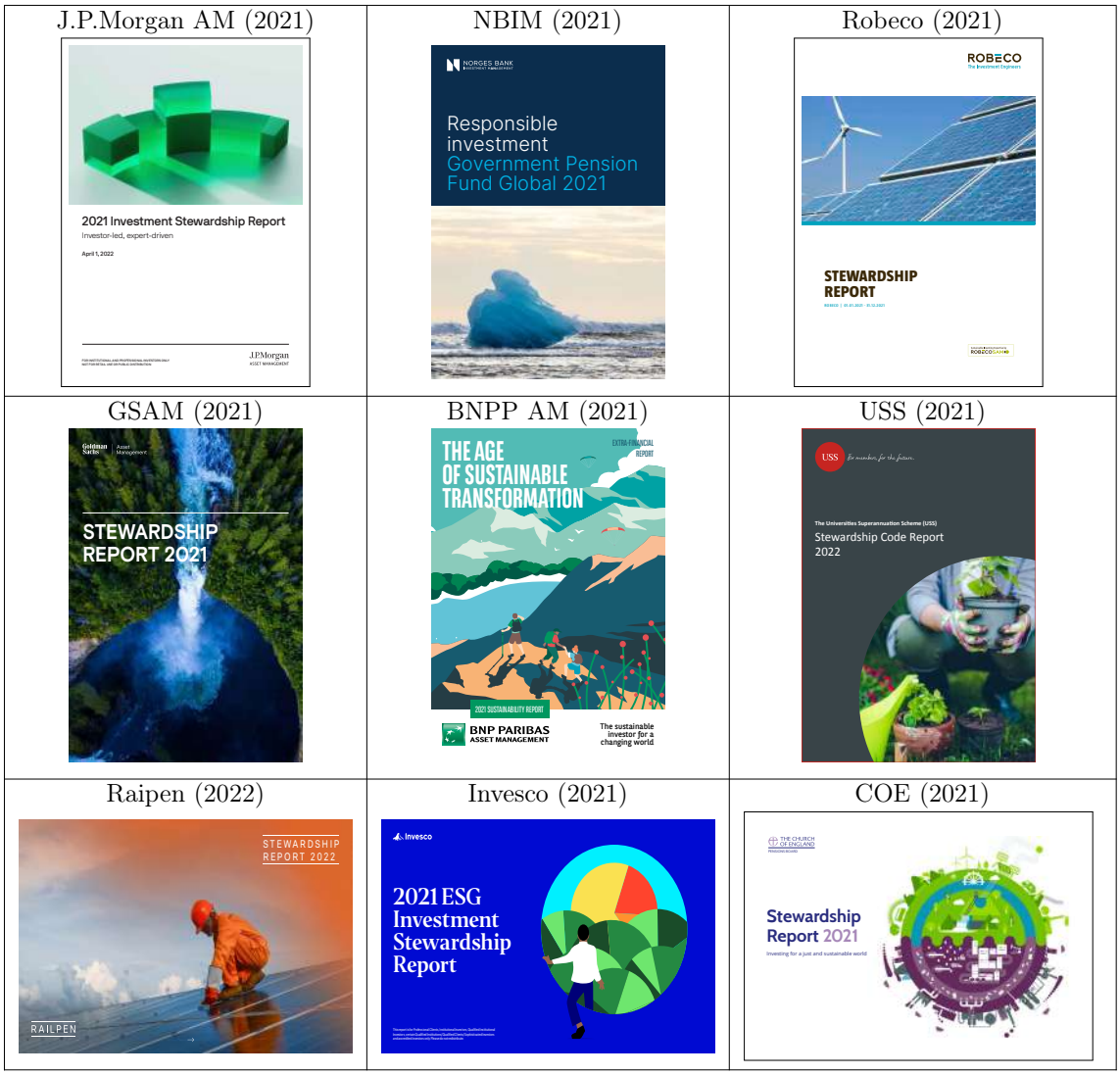


Source: Corporate websites.

> "*Behind the curtain engagement involves private communication between activist shareholders and the firm's board or management, that tends to precede public measures such as vote, shareholder proposals and voice. In a sense, the existence of other forms of public activism can be taken as a signal that behind the scene engagements were unsuccessful. When it comes to environmental and social issues, writing to the board or management is a common method though which shareholders can express concern and attempt to influence corporate policy behind the curtain; alternatively, face to face meetings with management or non-executive directors are a more common behind the scene engagement method when it comes to governance.*" (Bekjarovski and Brière, 2018, page 10)

In fact, we can group these face-to-face meetings and more formal exchanges (letters and position statements) into three families:

1. Ongoing engagement, where the goal for investors is to explain their ESG policies and gather

information from the company. For instance, they may encourage companies to adopt ESG best practices, alert companies to ESG risks, or better understand sector-specific ESG challenges;

2. Engagement for influence (or protest), where the goal is to express dissatisfaction with respect to specific ESG issues, make recommendations to the company and measure/control companies' ESG progress;

3. Pre-AGM engagement, where the goal is to discuss with companies any resolution items that the investor may vote against.

For many years, engage behind the scenes was very informal, relying primarily on ESG analysts. This is no longer the case. Most investors now have an engagement process in place, generally based on three steps. The first step is to create an engagement list of a few issues. The idea is to focus on the most important issues, not to cover everything. Second, each engagement item is screened to identify the most serious cases. Finally, engagement can begin with the targeted companies. As noted in PRI (2019c), formalizing policies and processes is important, but the ultimate goal of active ownership is to achieve results. Therefore, investors need to track their engagement. The different stages are:

- Issues are brought to the attention of the company;
- Issues are acknowledged by the company;
- The company develops a strategy to address the issues;
- The company implements changes and the issues are resolved;
- The company does not resolve the issues and the engagement fails.

**Remark 72** *Although investors claim that transparency is the cornerstone of their stewardship and engagement practices, most of them never publish the list of companies and issues they target. Sometimes they provide anonymous examples in their engagement reports.*

It is very difficult to obtain public statistics about the engagement behind the scenes and its evolution. For instance, McCahery *et al.* (2016) found that "63% *of the respondents state that, in the past five years, they have engaged in direct discussions with management, and* 45% *have had private discussions with a company's board outside of management's presence*", but these results are based on a survey of 143 respondents relative to 3 300 invitations sent between December 2012 and July 2013. More recently, the study by Barko *et al.* (2022) is based on a proprietary database provided by a large European asset manager. We can always find figures from stewardship and engagement reports, but it gives a partial view of this topic. For example, Amundi (French asset manager, €2 064 tn in assets under management) reports 2 334 engagements in 2021 with the following breakdown by ESG theme[2]: dialogue to foster a stronger voting exercise and a sounder corporate governance (1 033), transition to a low-carbon economy (547), strong governance for sustainable development (287), social cohesion through the protection of direct and indirect employees (222), preservation of natural capital (165) and product, client, societal responsibility (80). The first category corresponds to the 2021 pre-AGM dialogue statistics, which means that the Amundi corporate governance team had dialogue with 1 033 issuers in 2021. The 2 334 engagements can be broken down into 397 soft engagements, 904 active engagements, 654 voting alerts and 379 pre-AGM dialogues. Amundi also states that it engaged with 1 364 individual companies in 2021. A second example of asset managers

[2]Source: Amundi (2022), 2021 Engagement Report, https://about.amundi.com/esg-documentation.

Figure 6.2: Difference between stewardship and engagement reports

Amundi Stewardship Report (2021)

Amundi Engagement Report (2021)

Source: Amundi corporate website, https://about.amundi.com/esg-documentation.

is Robeco, which is a Dutch asset manager with €200.7 bn in assets under management at the end of 2021. They reported 270 engagement cases[3] (79 environmental issues, 76 social issues, 52 governance issues, 35 SDG issues and 28 global controversial issues), while the number of engagement activities was 942 including 393 conference calls, 402 written correspondence, and 4 physical meetings. In terms of asset owners, PGGM (Dutch pension fund with €293.5 bn in assets under management at the end of 2021) reported 154 corporate engagements in its 2021 integrated annuel report[4]. A second example of asset owners is the Norway's sovereign wealth fund, which managed €1.24 tn at the end of 2021. They held a total of 2 628 meetings with 1 163 companies[5], and they had written communications with 486 companies in 2021. They also gave the breakdown by topic[6]: E climate change (797), circular economy (190), biodiversity (48), ocean sustainability (18), etc.; S children's rights (40), data privacy (34), customer interests (129), etc.; G effective boards (267), compensation (183), shareholder protection (68), etc. These four examples concern large investors, but smaller investors also communicate about their engagement policies. Platypus Asset Management, an Australian boutique firm with $5 bn in assets under management, conducted 66 one-on-one meetings on ESG issues in 2021. Their 2021 engagement report[7] is very transparent as they list the date of each meeting, the name of the company, the ESG issue, and a summary of the meeting[8].

[3]Source: Robeco (2022), Active Ownership Report Q4 2021, www.robeco.com/en-int/sustainable-investing/influence.

[4]Source: PGGM (2022), 2021 Integrated Annual Report, www.pggm.nl/en/integrated-report.

[5]Source: NBIM (2022), Government Pension Fund Global 2021 — Responsible Investment, www.nbim.no/en/publications/reports/2021/responsible-investment-2021.

[6]The total is greater than 2 628 because several topics can be discussed during a meeting.

[7]Source: Platypus Asset Management (2022), Engagement Report 2021, www.platypusassetmanagement.com.au/~/media/platypus/documents/media/engagement-report.ashx.

[8]For instance, on 9 June 2021, they met with FPH on general governance. Here is the summary: "*Discussed Fisher and Paykel's approach to ESG including carbon — embodied emissions, very impressive science-based reduction*

**Propose resolutions**

According to the SEC (Securities Exchange Act Rule 14a-8, §240), "*a shareholder proposal or resolution is a recommendation or requirement that the company and/or its board of directors take action, which the shareholder intend to present at a meeting of the company's shareholders. The proposal should state as clearly as possible the course of action that the shareholder believes the company should follow. If the proposal is placed on the company's proxy card, the company must also provide in the form of proxy means for shareholders to specify by boxes a choice between approval or disapproval, or abstention.*" Generally, shareholder resolutions are presented to management. Nevertheless, not all proposals submitted to management are necessarily accepted. In the US, if a company wants to exclude a shareholder proposal, it can write a letter to the SEC explaining that the proposal violates one or more conditions of SEC Rule 14a-8 (Matsusaka *et al.*, 2021). Shareholder resolutions may be excluded because of procedural requirements[9] or substantive bases[10]. Then, the SEC may or may not accept the exclusion. If the SEC accepts the exclusion, the company receives a "*no-action*" letter, indicating that the SEC will take no action if the company omits the proposal from the proxy statement[11]. Other countries have different rules for submitting and approving shareholder proposals. In France, Germany and the United Kingdom, shareholders can submit a resolution to the company if they own at least 5% of the capital. This threshold is 2.5% in Italy, 0.33% in the Netherlands and 3% in Spain. If shareholders organize jointly, the rule is the same in France, Germany, Italy and the Netherlands. In Spain, there is no provision for shareholders to organize jointly. In the UK, they must represent 100 shareholders and have an investment of at least £10,000.

A shareholder resolution can be seen as an escalation in the context of failed engagement or lack of responsiveness by the company. It is a way for investors to publicly demonstrate that they are not satisfied with management. However, even if the resolution is approved by a majority of shareholders, its implementation may be an issue. In the US, for instance, shareholder resolutions are not binding. This is not the case in Europe, but the management of the company can always delay implementation or consider partial implementation. In this context, shareholder resolutions are seen more as a negative signal or a dissent sent to the company and the market, especially if they receive media coverage and attention. Nevertheless, shareholder resolutions that are voted on

*targets including Scope 3, dovetails nicely with focus on product quality/need to scrutinise supply chain. The CEO is focused on emissions and potential cost impact of the transition on the business. Also discussed gender diversity and modern slavery.*"

[9]The procedural requirements are described in Rules 14a-8(b)-(h): proponent must have continuously held shares worth $2 000 or 1% of the company's value for at least one year prior submitting the proposal and must continue to hold them through the date of the meeting; proponent may submit only one proposal per meeting; proposal and supporting statement may not exceed 500 words; proposal must be submitted at least 120 days before the proxy statement is mailed; proponent or representative must be present at the meeting (Matsusaka *et al.*, 2021, Table 1).

[10]The thirteen substantive bases are described in Rule 14a-8(i): improper subject for action under state law; will cause the company to violate state, federal, or foreign law to which it is subject; proposal and supporting statement are materially false or misleading; relates to redress of a personal claim or grievance, or be designed to provide a benefit to proponent that is not shared by the other shareholders at large; relates to operations that account for less than 5 percent of company assets or sales; company lacks the power to implement; deals with ordinary business operations; would disqualify a director candidate, remove a director from office, question competence of director or nominee, seek to include specific nominee, or otherwise affect the outcome of director election; conflicts with company's own proposal; company has already substantially implemented proposal; substantially duplicates another proposal; deals with substantially the same subject as another proposal from previous years that received (specified) low support from shareholders; relates to specific amounts of dividends (Matsusaka *et al.*, 2021, Table 1).

[11]On page 3, we saw that shareholders organized resolutions against the production of napalm during the Vietnam War. For example, the Medical Committee for Human Rights filed a shareholder proposal in 1969 to force the Dow Chemical Company to stop producing napalm. The SEC allowed Dow to exclude this shareholder proposal from its 1970 proxy voting, and so the proposal was not presented to shareholders at the 1970 annual general meeting.

are an exception. For example, below we report some figures[12] for companies in the Russell 3000 Index as of proxy season 2022 (from 1st June 2021 to 30 June 2022):

- 98% of proposals are submitted by management, while less than 2% are shareholder resolutions;
- Only 60% of shareholder resolutions are voted on; the other 40% are omitted, not filed, withdrawn or pending;
- The average number of shareholder proposals per company is about two;
- Proponents of shareholder resolutions are concentrated among a small number of investors or organizations (15 proponents were responsible of 75% of shareholder proposals);
- The breakdown of shareholder proposals voted in 2022 was as follows: 11% related to E issues, 41% related to S issues and 48% related to G issues.

These figures show that there are few shareholder proposals and that they are generally submitted by the same group of investors. In fact, many shareholder proposals that are filed to proxy voting are withdrawn following negotiations between shareholders and management before the annual general meeting[13]. Few investors therefore have a real experience of a shareholder resolution that is voted on at the AGM.

### Vote

In just five years, voting at annual general meetings has become the norm for ESG investors. It is now considered a fiduciary duty of asset owners and managers, and evidence that an investor is socially responsible. Today, voting decisions are scrutinized and analyzed by many associations and NGOs. For instance, new editions of the Voting Matters series published by ShareAction[14] are eagerly awaited by asset managers.

The voting landscape has evolved significantly in recent years, particularly in Europe. In the US, mutual funds have a long history of voting at shareholder meetings, as the SEC has always considered voting to be one of the most important fiduciary duties of mutual funds[15]. This explains why US mutual funds have a higher proportion of voting participation than European mutual funds. In fact, the ESG fad has changed in many different ways the activity of voting, which is now a priority from investors. First, the gap between asset owners and asset managers has has narrowed considerably, whereas the voting participation of asset managers was poor ten years ago (Brière *et al.*, 2020). Second, voting infrastructures have been more strongly developed in Europe, while they have existed in the US for many years. Nevertheless, the proxy advisory market is dominated by

[12] We use the reports of Rosati *et al.* (2022) and Tonello (2022).

[13] An example can be found in the 2021 Stewardship report of Robeco: "*At the end of 2020, we filed a shareholder resolution at ADM's 2021 shareholder meeting, asking the company to step up its efforts to eliminate deforestation in its soy supply chain. After several weeks of intense negotiations, spanning across multiple meetings with ADM's head of sustainability and corporate secretary, we managed to get the company to agree to most of our key requests and so we withdrew the proposal. Our achievement was to ensure that ADM published a revised no-deforestation policy, and committed to eliminate deforestation from all its supply chains by 2030.*" (Robeco, 2021, page 32). ADM is a company that specializes in food, pet and animal nutrition. Other examples can be found in the stewardship reports of Amundi, Candriam, Groupama Asset Management, etc.

[14] ShareAction is a UK-based registered charity that promotes responsible investment.

[15] You may consult the speech "*Every Vote Counts: The Importance of Fund Voting and Disclosure*" by the Commissioner Allison Herren Lee at the 2021 ICI Mutual Funds and Investment Management Conference (March 17, 2021, www.sec.gov/news/speech/lee-every-vote-counts).

Figure 6.3: Voting Matters series of ShareAction

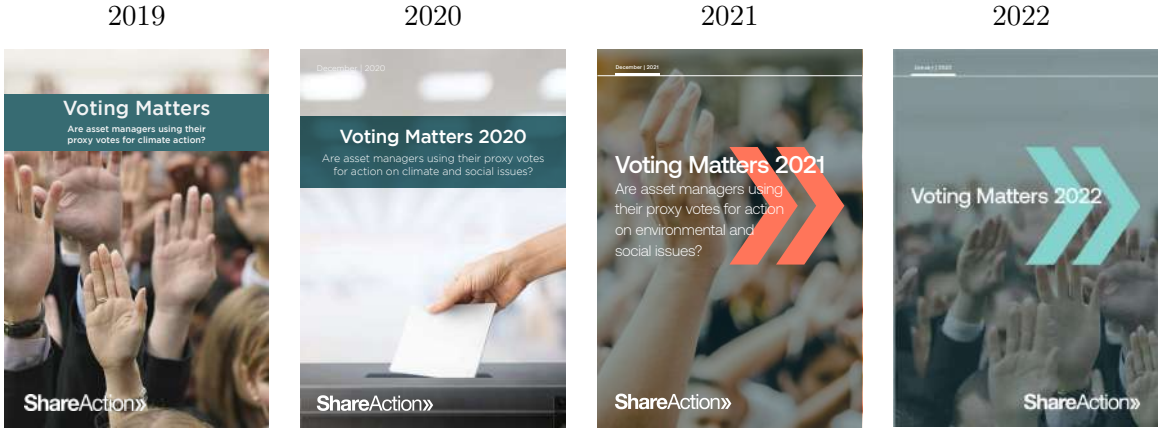


Source: https://shareaction.org.

two US proxy advisory firms[16] (Institutional Shareholder Services, or ISS, and Glass Lewis), which represent 97% of the market. Third, asset managers are under great pressure to vote if they want to be credible. Voting has become a central pillar of any responsible investment policy, and it is now part of the ESG credentials that asset owners use to select asset managers.

In 2002, the United Kingdom adopted legislation requiring companies to allow shareholders to have a mandatory but non-binding vote on executive compensation at each annual general meeting. This concept is called *say on pay*. According to Rosati *et al.* (2022), the results for the 2022 season showed an increasing in shareholder opposition on this issue. For instance, support for executive remuneration was 87% for Russell 3000 companies in 2022 compared to 89% in 2021. Norwegian Cruise Line Holdings was the worst performer, with only 15.4% of votes for. In Europe, we see the same phenomenon. In Germany, 25% of say on pay votes were contested. In France and Spain, the most controversial resolution was the remuneration policy proposal. For example, about 50% of say on pay resolutions in France received at least 10% of shareholder opposition. For comparison, the average support rate for management proposals is generally very high, exceeding 95%.

Say on climate is inspired by say on pay proposals. This initiative[17] was launched by hedge fund activist investor Chris Hohn through the Children's Investment Fund Foundation (CIFF) in 2020. It is supported by CIFF, CDP, ShareAction and the Australasian Centre for Corporate Responsibility (ACRR). More generally, a say on climate is any shareholder or management resolution on the company's climate strategy. If it is filed by the management, they expect that shareholders to vote for (shareholder approval of the climate strategy). If it is filed by shareholders, the resolution is against the company's climate strategy. In 2021, 26 companies[18] presented a climate strategy at their annual general meetings[19] and there were 88 climate-related shareholder proposals that were voted on (ISS Governance, 2022). The average support rate was 93% for resolutions filed by the company and 32.7% for resolutions proposed by shareholders.

[16] Their websites are www.issgovernance.com/solutions/proxy-voting-services and www.glasslewis.com.

[17] The website is www.sayonclimate.org.

[18] 19 were in Europe (3 in France, 5 in Spain, 1 in Switzerland and 10 in the United Kingdom), 3 in North America (1 in Canada and 2 in the United States), 3 in South Africa and 1 in Australia.

[19] In 2022, the number of companies increased and reached 36. Among them, we find seven oil and gas companies (BP, Equinor, Repsol, Santos, Shell, TotalEnergies, Woodside Petroleum).

As we have seen, there are few shareholder proposals per company. The number of voted shareholder proposals is even smaller. For instance, among the Russell 3000 companies, there were only 555 shareholder resolutions voted in 2022, or less than 1 resolution for 5 companies. In Figure 6.4, we have shown the average support rate. In 2022, it is less than 40% for governance issues and drops to 29% for environmental and social issues. Finally, the number of voted proposals received majority support is 82. This means that there was one shareholder resolution that was approved for 37 companies. Therefore, we can question the impact and effectiveness of voting. This explains that voting is another form of voice for many academics.

Figure 6.4: Average support rate of shareholder proposals (Russell 3000 companies)

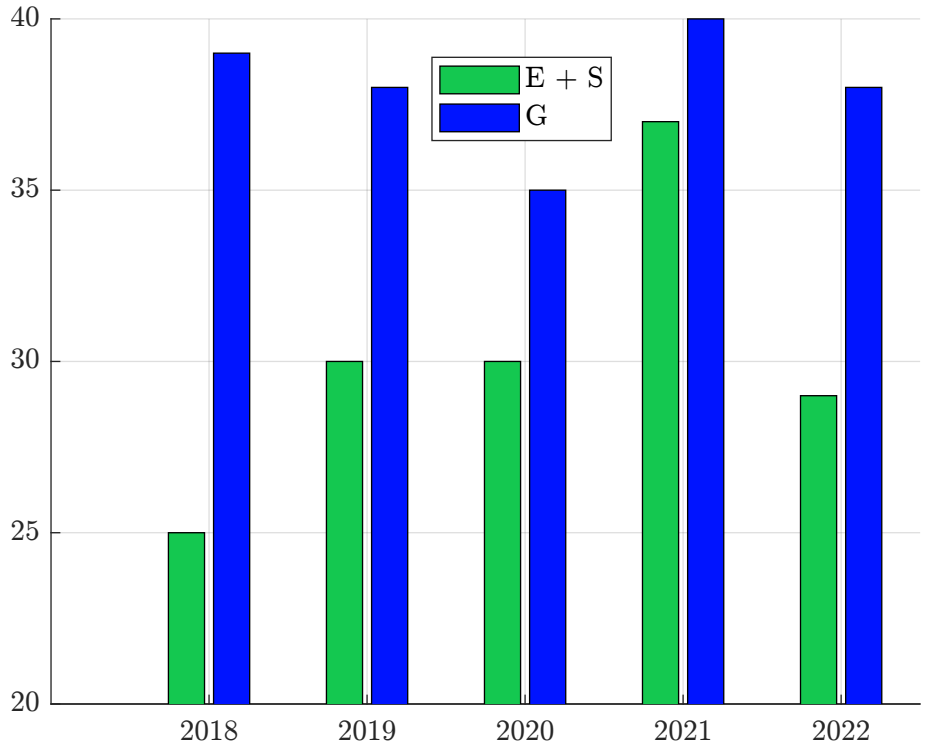


Source: PwC's Governance Insights Center (2022).

Focus on the year 2022 and the US, the main topics of shareholder proposals were emissions reduction targets and Scope 3 inclusion for the E pillar; diversity, civil rights and racial equity audits, human rights and employee harassment for the S pillar; and executive compensation and political lobbying for the G pillar (Rosati *et al.*, 2022). In Europe, most shareholder resolutions are about executive pay.

**Remark 73** *The voting behavior of asset managers is analyzed in Section 6.2.4 on page 597.*

### Voice

The term voice was popularized in 1970 by economist Albert Hirschman, when he published his book "*Exit, Voice, and Loyalty: Responses to Decline in Firms, Organizations, and States*". The book states that members of an organization have two main possible responses when they believe the organization is failing. They can exit (withdraw from the relationship) or they can voice (change the relationship by communicating the complaint). From a socio-economic perspective, exit is associated

Figure 6.5: Pass rate of shareholder proposals (Russell 3000 companies)

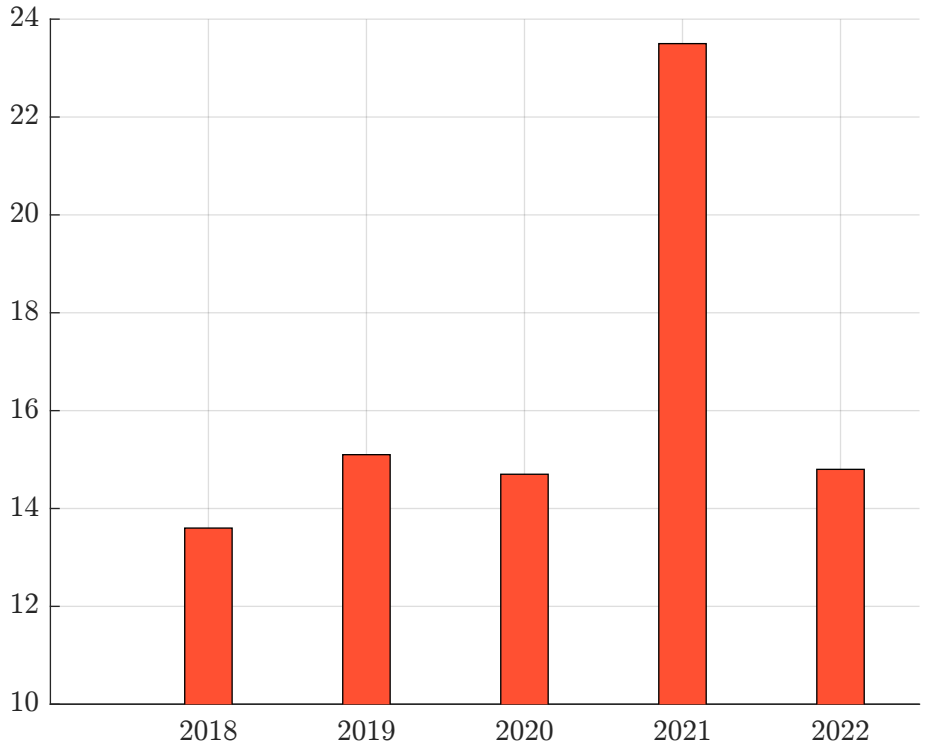


Source: Tonello (2022).

with Adam Smith's invisible hand, while voice is inherently political and can be confrontational. The exit-voice model of Hirschman (1970) can be applied to many situations: protest movements, migration, class actions, and even corporate governance (Kostant, 1999).

In the theory of shareholder activism, voice can refer to different forms of engagement, such as engage behind the scenes or propose resolutions (Edmans, 2014). In this chapter, voice refers to a situation in which the communication between activist shareholders and the company becomes public. Like resolution proposals, voice can be interpreted as a form of escalation. Indeed, the debate and the disagreement become public, which means that other stakeholders are informed and can participate, such as other shareholders, the media, politics and society. The company then faces the risk of being placed in the political spotlight and having to respond to public criticism and scrutiny. The situation can become uncomfortable for the company, especially if non-technical stakeholders (the media and society) focus on the issue.

According to McCahery *et al.* (2016), voice is rarely used by individual institutional investors. One reason is that public communication may be ineffective, justifying the prevalence of behind the scenes communication (Levit, 2019). However, the use of voice has increased in recent years due to two main factors. The first is that collaborative engagement between investors is now quite common, thanks to initiatives such as the PRI or Climate Action 100+. In this context, they require more transparency by tracking the progress of each member. For example, when signing up to the Climate Action 100+ initiative, investors are asked to nominate which focus companies they wish to engage with, and whether this is as a lead investor or a collaborating investor. The second factor is the increasing involvement of NGOs in the debate on engagement and greenwashing[20]. In this

[20]For instance, we can cite the following examples among others: As You Sow, Citizens' Climate Lobby, Climate

context, investors sometimes have to answer publicly to greenwashing suspicions or accusations for supporting and financing some companies that are considered by these NGOs to be harmful to the environment or human health. All these elements explain why the voice against companies, but also the voice against investors, has recently gained in importance.

### Initiate a takeover

Acquiring a large stake in a company is an aggressive form of shareholder activism. The underlying idea is to form a coalition with other large shareholders to obtain a board set and ultimately control the company's board. This strategy is typically implemented by activist hedge funds (Gantchev, 2013). In general, managers perceive activist events as a hostile act because their compensation and job security are threatened (Gantchev *et al.*, 2019). In most cases, this form of shareholder activism has a great impact on the company (change of business strategy, implementation of proposed solutions, etc.). However, it has never been used by ESG investors. Therefore, it is only motivated by financial underperformance and not by extra-financial issues.

### Exit

Exit refers to the process of selling investments in a particular company or industry. Divestment is a more general term that implies a significant reduction in exposure. In this case, we refer to a partial divestment, while an exit corresponds to a full divestment[21]. For example, investors may decide to divest from a company if they are not satisfied with its ESG performance, particularly if the company's policies implicate social issues or if it does not take sufficient action to address environmental concerns. Investors may also decide to divest from a sector such as fossil fuels or tobacco. The exit policy is therefore linked to two ESG investment strategies: exclusion and norms-based screening[22]. Nevertheless, divestment cannot be equated with these ESG strategies. In fact, the concept of divestment/exit implies that investors are currently invested in the company and decide to sell their participation because they disagree with the company's ESG policies. In this context, divestment is the ultimate engagement action, meaning that investors believe they cannot influence the company's behavior by staying invested. In this case, divestment is "*the final step in an escalation strategy*" (PRI, 2022a) and can be seen as a failure of engagement on the part of investors. When it concerns an industry, divestment may be motivated by high risks or low opportunities for the industry to transition to a more sustainable business model. For example, divestment from coal reserves or the mining sector can reduce the investors' exposure to the risk of stranded assets[23]. As we saw in the first chapter, exit can also be motivated by moral values. In this case, it is consistent with the norms-based screening strategy.

The case of the fossil fuel sector is certainly the most symbolic divestment issue. According to the Global Divestment Commitments Database, approximately 1 600 institutions[24] have committed to divest from fossil fuels as of January 2024. In Figure 6.6, we show the breakdown by type of organization. The top three categories are faith-based organizations, educational institutions, and philanthropic foundations, representing 63.50% of divesting institutions. They are followed by pension funds. Commitments fall into four categories: (1) thermal coal only, (2) coal and tar sands, (3) partial divestment from some but not all types of fossil fuel companies, (4) full divestment from

Alliance, Friends of the Earth, Fund Our Future, Oxfam, Reclaim Finance and Sunrise Movement.

[21] Nevertheless, we note that the two terms are often used interchangeably.

[22] These strategies are described on page 44.

[23] Stranded assets are discussed in Section 10.3 on page 944.

[24] Including Axa Insurance, La Banque Postale, Harvard University, the State of Maine, the Norwegian Sovereign Wealth Fund, and the University of Oxford.

Box 6.1: Case study: the Cambridge University endowment fund

In their research paper "To Divest or to Engage? A Case Study of Investor Responses to Climate Activism", Chambers *et al.* (2020) examined the interesting case of the Cambridge University endowment fund:

> "*A dilemma faced by an increasing number of investors is whether to divest from environmentally damaging businesses or whether to enter into a dialogue with them. This predicament now has its epicentre in Cambridge, England, where the ancient University of Cambridge faces great pressure from students and staff to respond to the threat of climate breakdown. Having already received two reports on its approach to responsible investment, the university has appointed a new chief investment officer (CIO) who, alongside University Council and the wider university community, needs to consider the question of whether to divest from or to engage with fossil-fuel firms.*"

This paper tells the story of the Cambridge fossil fuel divestment movement from 2012 to 2020. This includes the creation of the Positive Investment Cambridge group, the establishment of the Ethical Investment Working Group, the publication of several reports, many Zero Carbon Society petitions in favor of fossil fuel divestment, the formation of the Divestment Working Group, the activism of students and faculty staff, the involvement of many distinguished scholars, including prestigious professors (*e.g.*, astronomer Royal officer, Nobel laureate, chief scientific adviser, distinguished statisticians, Fields medalists, fellows of the Royal Academy and the Royal Society), etc. The research paper shows how the pressure on institutional investors to respond to climate activism can be accelerated. It concludes that "*investment professionals need to understand the forces for change*", "*a head-in-the-sand response is counter-productive*" and "*changes in investment policy should be evidence-based.*"

any fossil fuel company (thermal coal, oil, gas). Some investors are already "*fossil free*", meaning that they currently have no investments in fossil fuel companies and are committed to avoiding any fossil fuel investments in the future. The debate about fossil fuel divestment is tough, because it is not only an investor debate, but also a societal one. In Box 6.1, we report on the tense relationship between the two sides. We find that the decision to divest or not can be motivated by considerations other than rational evidence. Pressure from anti-fossil fuel movements may be one factor, fear of greenwashing another. Moreover, "*exit relaxes the tension between the activist and the board*" (Levit, 2019). In some ways, exit is a comfortable position. The investor can continue to communicate with the company, but the situation is completely different. Before the exit, the investor has to convince the company to move. After the exit, the company has to prove that it will change and convince the investor to come back. So the roles are reversed.

We have already seen that vote is a form of voice. For Admati and Pfleiderer (2009), exit is also a form of voice. Most academic studies show that the effects of exit are mixed because the costs of divestment can be high and its effectiveness is limited (Jahnke, 2019; Levit, 2019; Broccardo *et al.*, 2022; Edmans *et al.*, 2022). For some academics, the impact of divestment may also be negative:

> "*Large divestment campaigns are undertaken in part to depress share prices of firms that investors see as engaged in harmful activities. We show that, if successful, investors who divest earn lower and riskier returns than those that do not, leading them to control*

Figure 6.6: What kinds of institutions are divesting from fossil fuel?

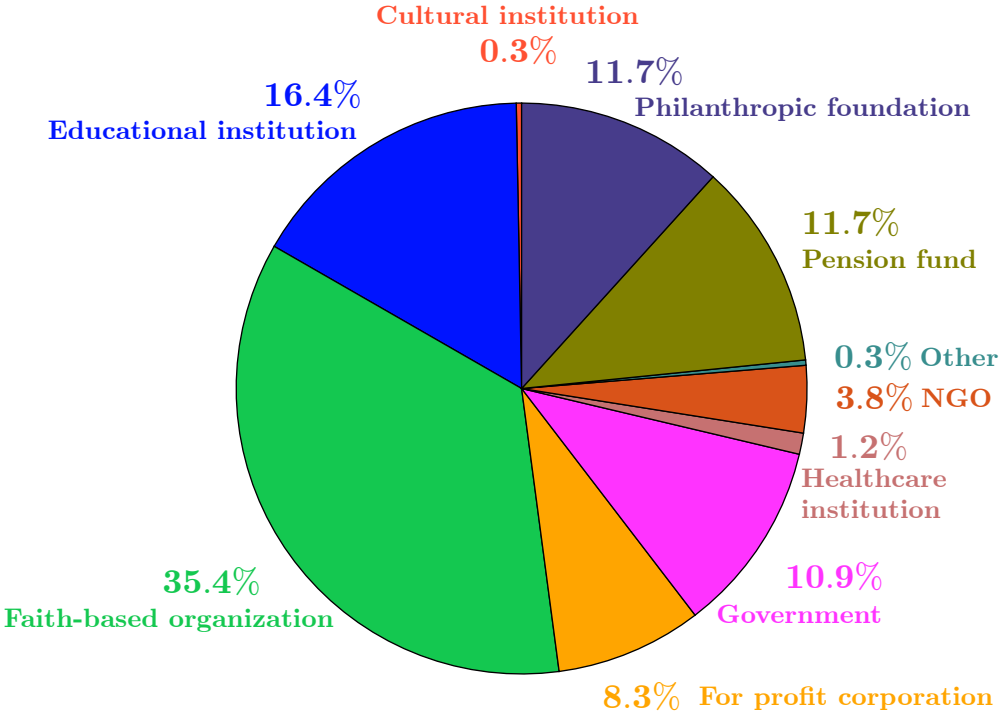


Source: https://divestmentdatabase.org.

> *a decreasing share of wealth over time. Divestment therefore has only a temporary price impact. Further, we show that, for standard managerial compensation schemes, divestment campaigns actually provide an incentive for executives to increase, not reduce, the harm that they create. Therefore, divestment is both counter-productive in the short run, and self-defeating in the long run.*" (Davies and Van Wesep, 2018, page 558).

In fact, we need to distinguish between the effects on the primary and secondary markets. In theory, divestment reduces the price of the company's shares on the secondary market, which means that expected returns increase. On the primary market, it leads to a higher cost of capital due to lower demand. Thus, the rationale for exit is the effect on the cost of capital. However, it is difficult to verify this effect empirically over the last 10 years. Academics are more unanimous when they examine the effect before exit. In fact, according to Edmans (2009), the threat of exit has more impact than divestment itself, and "*the power of loyalty relies on the threat of exit.*" Again, we see that voice and exit are complementary rather than mutually exclusive.

### 6.1.3 Individual versus collective engagement

Coordinating engagement efforts between different asset owners and managers can lead to several key benefits and increase efficiency compared to individual engagement (Gillan and Starks, 2000). The doctrine was established in 2018 by PRI (2018a, pages 16 and 17). According to this research, investors tend to prefer to engage with companies on ESG issues on an individual basis, as this allows for a more tailored approach to meet each investor's unique requirements. However, investors and companies also identified a potential downside to this approach in terms of cost and duplication of requests, particularly when multiple investors make similar requests. For example, during a controversy, investor demands may suddenly increase and become difficult for the company to manage.

Box 6.2: Case studies of fossil fuel divestment

Church of England Pensions Board

By the end of 2021, the CoE Pensions Board was responsible for nearly £3.7 bn of assets across three pension schemes. In July 2018, the General Synod of the Church of England voted on a motion to ensure that by 2023 CoE pension funds will have divested from fossil fuel companies that are not prepared to align with the goals of the Paris Agreement. In 2020, they engaged with 21 companies. At the end of the process, 12 companies were deemed to be making sufficient progress, while 9 companies were added to the list of restricted investments. These divestments totaled £32.23 mn.

Source: Church of England Pensions Board, Stewardship Report 2020.

The Universities Superannuation Scheme (USS)

The Universities Superannuation Scheme (USS) is the pension scheme for university staff in the UK. It manages about £90 bn. In 2020, USS undertook a review of the sectors in which the scheme invests. They concluded that, in several cases, the outcomes predicted by the market did not adequately take into account the potential financial impact of certain specific risks, including ESG. As a result, they excluded certain sectors: tobacco manufacturing; thermal coal mining (coal to be burned for electricity generation), specifically where they accounted for more than 25% of revenues; and certain controversial weapons. The first exclusion was announced in May 2020. Divestment from these sectors was completed two years later. According to Ethics for USS (a group of USS members committed to reforming USS and ensuring an investment strategy that protects the planet, respects human rights, invests responsibly, and provides good pensions), "*USS still has large investments in the industries responsible for the climate emergency [...], while they recognise that USS has made plans to decarbonize its investment portfolio.*" Ethics for USS estimates that "*USS continues to invest £570 mn in 48 leading fossil fuels companies*", and USS should expand its divestment policy "*to include other companies that have not committed to a credible path towards zero emissions.*"

Source: USS, Stewardship Code Report 2022 & https://divestuss.org.

In Table 6.1, we report the pros and cons of individual and collective forms of engagement. For investors, the advantages of collective engagement are:

- By combining their resources and voices, investors can put more pressure on companies to address their concerns.
- A unified stance from diverse investors sends a clear and consistent message to companies, creating a stronger signal.
- Collaboration saves time and resources for all participants and enhances the credibility of the engagement process.

However, collective engagement can be negative if investors are not aligned and investors have different requirements. It is therefore important that collective engagement is managed by a lead investor. We have seen that the two most prominent coordinated engagement initiatives are those of PRI and Climate Action 100+, but other notable initiatives include the Ceres Investor Network, the Institutional Investors Group on Climate Change (IIGCC), and the Net Zero Asset Managers initiative

(NZAM). Using a database of engagements provided by PRI, Dimson *et al.* (2021) discuss globally coordinated engagements by long-term shareholders to influence companies on environmental and social issues. It highlights a two-tier strategy involving lead and supporting investors as effective, leading to improved target performance and increased fund flows. Factors influencing leadership include higher stakes, geographic and cultural proximity, and the domestic presence of lead investors. The study also emphasizes the growing prevalence of these engagements, driven by institutional expertise and interest, and concludes that structured engagement strategies help achieve goals.

Table 6.1: Pros and cons of individual and collective forms of engagement

| | INDIVIDUAL INVESTOR ESG ENGAGEMENTS | | COLLECTIVE INVESTOR ESG ENGAGEMENTS | |
|---|---|---|---|---|
| | **Corporate Perceptions** | **Investor Perceptions** | **Corporate Perceptions** | **Investor Perceptions** |
| PROS | ▪ Face-to-face and one-to-one dialogues are effective to address multiple ESG issues.<br>▪ Avoidance of misrepresentation of ESG performance by third-parties.<br>▪ One-to-one interactions allow the building of trust, and long-term relationships, with investors. | ▪ Alignment of engagement goals with internal ESG and engagement policies.<br>▪ Strategic benefits of proactively addressing emerging ESG topics.<br>▪ Enables a strategic focus on corporate stocks with ambiguous ESG scores. | ▪ Larger, collective assets under management working together can give more leverage to internal corporate drives on ESG issues.<br>▪ Cost savings in terms of time spent with investors.<br>▪ Perceived higher ESG expertise of the investor group. | ▪ Higher power and influence through the collective assets under management.<br>▪ More relevant for systemic and marketplace issues, or if investors have 'thematic' engagement policies.<br>▪ Cost savings on monitoring. |
| CONS | ▪ Need to manage numerous, different investor requests.<br>▪ Redundancy in questions asked by multiple, individual investors.<br>▪ Costly and time consuming process, especially if ESG requests by multiple investors increase. | ▪ Potentially low shareholding insufficient to capture board-level attention.<br>▪ Limited resources that can be spent to maintain the continuity of engagement and/ or financial analyst engagement. | ▪ Lack of interest from investors for overall corporate ESG management activities, due to specific ESG thematic focus.<br>▪ Higher coordination costs if investors fail to coordinate their efforts.<br>▪ Investors with no or too little shareholding may attend meetings. | ▪ Broad international focus that may not be coherent with national investment strategies.<br>▪ Possibility of free-riding.<br>▪ Time-consuming process if investor views are divergent. |

Source: PRI (2018a, Table 3).

### 6.1.4 The role of institutional investors

The impact of institutional investors[25] on corporate governance has been extensively studied by academics (Gillan and Starks, 2000; Appel *et al.*, 2016; Chen *et al.*, 2020). One of their conclusions is that the role of these investors in companies is growing. One reason is that institutional ownership has increased over time for two reasons. They manage more money than they used to, and they have

[25]Institutional investors include asset owners (endowments, insurance companies, pension funds, sovereign wealth funds) and asset managers (ETFs, hedge funds, mutual funds).

increased their allocation to equity markets. An history of institutional shareholder activism can be found in Gillan and Starks (2000). However, institutional active ownership has been accelerated by the issue of climate change (Krueger *et al.*, 2020), and the definition of fiduciary duty is at the heart of this issue. This is especially true for pension funds. Even the ETF industry has been affected by the active ownership phenomenon. In particular, we can cite the article of Appel *et al.* (2016): Passive Investors, Not Passive Owners[26]. Today, we can say that engagement has become a pillar of the investment process for these institutional investors.

To illustrate the importance of institutional investors, we look at several examples. Below, we list Apple's top 5 institutional investors based on the company's 2023 annual report[27]:

| # | Investor | Stock outstanding |
|---|---|---|
| 1 | Vanguard | 8.36% |
| 2 | Blackrock | 6.30% |
| 3 | Berkshire Hathaway | 5.80% |
| 4 | State Street | 3.66% |
| 5 | Fidelity Investments | 1.90% |

According to `www.techopedia.com`, "*Apple's initial institutional shareholders are not clearly documented, but by delving into the company's proxy filings from 1994, we can gain some insight. As of November 30, 1994, the only institutional shareholder listed was the Capital Group. This company [...] held a significant stake in Apple at that time. Their holdings amounted to 11.84 million shares, which constituted 9.8% of Apple's total outstanding stock. By 2010, Blackrock and Fidelity Investment had become key Apple shareholders, with Blackrock holding 5.50% and Fidelity 5.04% of the total stock. However, by late 2015, Vanguard Group emerged as Apple's largest shareholder [...] Berkshire Hathaway became one of Apple's biggest shareholders in 2020.*" In general, we can find the shareholding structure of companies in their annual reports. Thus, in 2023, institutional investors own 83% of General Electric, 78% of Danone and Sanofi, 77% of Goldman Sachs, 75% of Total, 70% of McDonald, 65% of Coca-Cola, 58% of Ford Motor Company and 51% of ENI. This ratio depends very much on the history of the company, as some companies may be mainly owned by the founder, a government, a family or private investors. For instance, 43% of Tesla is owned by private investors, including Elon Musk, who is Tesla's largest individual shareholder with a 12.93% stake. LVMH's capital structure is dominated by the Arnaud family group (48.2%), followed by foreign institutional investors (38.2%) and French institutional investors (7.3%).

According to Medina *et al.* (2022), institutional investors[28] account for approximately 43% of global market capitalization in 2020 followed by the corporations (11%), the public sector (10%) and strategic individuals (9%). Other free-float investors include direct retail investors, corporations and institutional investors whose holdings are below the disclosure thresholds. They represent 27% of global market capitalization. However, these global figures mask a wide variation across countries. The share of institutional investors varies from a negligible percentage in Bulgaria, Lithuania and Saudi Arabia to more than 60% in Iceland, the United Kingdom and the United States (Table 6.2). The total holdings of the 50 largest institutional investors in the stock market increased by 80% between 2007 and 2019. In 2020, they represented 27% of the equity market capitalization. If we look at companies in investable indexes, institutional ownership is even larger. In fact, institutional

[26]The study concludes that "*passive mutual funds influence firms' governance choices, resulting in more independent directors, removal of takeover defenses, and more equal voting rights.*"

[27]Source: `www.techopedia.com/largest-apple-shareholder`.

[28]The following percentages are underestimated as they only include institutional investors whose holdings are public because they are above the disclosure thresholds.

Table 6.2: Ownership by investor category as share of market capitalisation (in %, December 2020)

| Country | Corporation | Public sector | Strategic individual | Institutional | Other free-float | Non-domestic Total | Non-domestic % Instit. |
|---|---|---|---|---|---|---|---|
| Argentina | 25 | 17 | 17 | 10 | 31 | 10 | 42 |
| Australia | 5 | 2 | 6 | 27 | 60 | 16 | 80 |
| Austria | 21 | 23 | 6 | 23 | 27 | 15 | 56 |
| Belgium | 26 | 3 | 7 | 35 | 29 | 33 | 70 |
| Brazil | 29 | 10 | 8 | 27 | 26 | 17 | 57 |
| Bulgaria | 75 | 2 | 9 | 1 | 13 | 0 | 0 |
| Canada | 6 | 4 | 4 | 46 | 40 | 23 | 88 |
| Chile | 54 | 1 | 13 | 12 | 20 | 6 | 24 |
| China | 12 | 29 | 18 | 11 | 30 | 3 | 50 |
| Colombia | 32 | 35 | 3 | 16 | 14 | 6 | 43 |
| Croatia | 57 | 17 | 5 | 10 | 11 | 1 | 2 |
| Denmark | 10 | 10 | 2 | 36 | 42 | 27 | 93 |
| Estonia | 35 | 17 | 14 | 11 | 23 | 7 | 58 |
| Finland | 5 | 17 | 9 | 31 | 38 | 21 | 88 |
| France | 20 | 6 | 14 | 27 | 33 | 21 | 70 |
| Germany | 15 | 7 | 10 | 30 | 38 | 23 | 72 |
| Greece | 25 | 11 | 14 | 16 | 34 | 14 | 44 |
| Hong Kong | 22 | 11 | 19 | 18 | 30 | 15 | 27 |
| Hungary | 21 | 5 | 6 | 32 | 36 | 26 | 74 |
| Iceland | 9 | 1 | 7 | 66 | 17 | 16 | 94 |
| India | 33 | 12 | 11 | 22 | 22 | 13 | 57 |
| Indonesia | 43 | 17 | 10 | 8 | 22 | 8 | 30 |
| Ireland | 6 | 8 | 4 | 49 | 33 | 48 | 92 |
| Israel | 19 | 1 | 19 | 31 | 30 | 14 | 74 |
| Italy | 13 | 11 | 11 | 29 | 36 | 25 | 81 |
| Japan | 22 | 3 | 6 | 30 | 39 | 15 | 79 |
| Korea | 23 | 10 | 10 | 18 | 39 | 15 | 83 |
| Lithuania | 27 | 43 | 10 | 2 | 18 | 2 | 6 |
| Mexico | 19 | 2 | 34 | 20 | 25 | 13 | 45 |
| Netherlands | 20 | 3 | 4 | 40 | 33 | 37 | 67 |
| New Zealand | 6 | 19 | 5 | 20 | 50 | 16 | 84 |
| Norway | 10 | 29 | 9 | 30 | 22 | 18 | 72 |
| Poland | 17 | 14 | 14 | 35 | 20 | 19 | 53 |
| Portugal | 37 | 13 | 10 | 22 | 18 | 21 | 54 |
| Romania | 30 | 28 | 2 | 16 | 24 | 7 | 21 |
| Russia | 18 | 31 | 17 | 11 | 23 | 10 | 45 |
| Saudi Arabia | 2 | 87 | 2 | 1 | 8 | 1 | 50 |
| Slovenia | 14 | 34 | 0 | 8 | 44 | 7 | 47 |
| South Africa | 20 | 15 | 3 | 31 | 31 | 19 | 56 |
| Spain | 13 | 7 | 16 | 25 | 39 | 24 | 67 |
| Sweden | 12 | 6 | 12 | 38 | 32 | 19 | 79 |
| Switzerland | 6 | 6 | 6 | 33 | 49 | 26 | 84 |
| Turkey | 38 | 25 | 9 | 9 | 19 | 5 | 15 |
| United Kingdom | 6 | 6 | 4 | 60 | 24 | 32 | 76 |
| United States | 3 | 3 | 6 | 68 | 20 | 11 | 69 |
| Total | 11 | 10 | 9 | 43 | 27 | | |

Source: Medina *et al.* (2022, Table A.1, page 47).

investors own 52% of the MSCI World and 77% of the MSCI USA (Medina *et al.*, 2022, Figure 4.3, page 33). In other countries, these figures are lower: 39% of the MSCI Europe, 31% of the MSCI Japan and 16% of the MSCI Emerging Markets.

Table 6.3: Major holders of Exxon Mobil Corporation (percentage and cumulative)

| # | Institutional investor | % | Cum. | Top mutual fund holders | % | Cum. |
|---|---|---|---|---|---|---|
| 1 | Vanguard | 9.80 | 9.80 | Vanguard Total Stock Market | 3.15 | 3.15 |
| 2 | Blackrock | 6.88 | 16.68 | Vanguard 500 Index Fund | 2.47 | 5.62 |
| 3 | State Street | 5.44 | 22.12 | SPDR Energy Select | 2.05 | 7.67 |
| 4 | Fidelity Investments | 3.71 | 25.83 | Fidelity 500 Index Fund | 1.19 | 8.86 |
| 5 | Geode Capital Management | 1.93 | 27.76 | SPDR S&P 500 ETF Trust | 1.16 | 10.02 |
| 6 | JP Morgan Chase | 1.55 | 29.31 | iShares Core S&P 500 ETF | 1.01 | 11.03 |
| 7 | Bank of America | 1.48 | 30.79 | Vanguard Value Index Fund | 0.84 | 11.87 |
| 8 | Morgan Stanley | 1.41 | 32.20 | Vanguard Institutional Index Fund | 0.67 | 12.54 |
| 9 | NBIM | 1.39 | 33.59 | Vanguard Dividend Appreciation | 0.58 | 13.12 |
| 10 | Northern Trust | 1.08 | 34.67 | Vanguard Energy Index Fund | 0.53 | 13.65 |

Source: `finance.yahoo.com/quote/XOM/holders`.

Table 6.4: Major holders of BP p.l.c. (percentage and cumulative)

| # | Institutional investor | % | Cum. | Top mutual fund holders | % | Cum. |
|---|---|---|---|---|---|---|
| 1 | State Street | 0.78 | 0.78 | DFA International Core Equity | 0.13 | 0.13 |
| 2 | Fisher Asset Management | 0.68 | 1.46 | Vanguard Energy Fund | 0.12 | 0.25 |
| 3 | Arrowstreet Capital | 0.65 | 2.11 | John Hancock Mutual Fds III | 0.12 | 0.37 |
| 4 | Acadian Asset Management | 0.61 | 2.72 | Vanguard Growth and Income Fund | 0.09 | 0.46 |
| 5 | Morgan Stanley | 0.48 | 3.20 | T. Rowe Price Real Assets Trust | 0.08 | 0.54 |
| 6 | Dimensional Fund Advisors | 0.43 | 3.63 | T. Rowe Price Real Assets Trust I | 0.08 | 0.62 |
| 7 | Blackrock | 0.39 | 4.02 | T. Rowe Price New Era Fund | 0.07 | 0.69 |
| 8 | Wellington Management | 0.37 | 4.39 | T. Rowe Price Real Assets Fund | 0.07 | 0.76 |
| 9 | Boston Partners | 0.32 | 4.71 | DFA International Value Series | 0.06 | 0.82 |
| 10 | Goldman Sachs | 0.32 | 5.03 | BlackRock Basic Value Fund | 0.05 | 0.87 |

Source: `finance.yahoo.com/quote/BP/holders`.

There is also a large dispersion among companies in the same industry. In Tables 6.3 and 6.4 we report on the major shareholders of Exxon Mobil Corporation and BP p.l.c. and find that the capital structure is completely different. These two companies operate in the oil and gas sector. The top 10 institutional investors control almost 35% of Exxon, while they control only 5% of BP. On average, with the rise of passive management, ownership of listed companies tends to be concentrated among a small number of investors, particularly institutional investors. For example, the top three institutional investors own 23.50% of US listed companies. These figures are 22.60% in the United Kingdom, 21.70% in Denmark and 20.10% in the Netherlands (Medina *et al.*, 2022, Table A.3, page 49). In the United States, the top three institutional investors are typically Vanguard, BlackRock, and State Street. These three asset managers dominate the market for passive management, giving rise to the concept of the "*Big Three*" (Fichtner *et al.*, 2017). Bebchuk and Hirst (2019) showed that "*the Big Three have quadrupled their collective ownership stake in S&P 500 companies over the past two decades; [...] they collectively cast an average of about 25% of the votes at S&P 500 companies.*" Extrapolating from past trends, the Big Three could cast 40% of the votes at S&P 500 companies within two decades. The authors concluded that "*voting in most significant public companies will come to be dominated by the future Giant Three.*" Azar *et al.* (2021) examined the influence of the

Big Three in reducing corporate carbon emissions worldwide. By analyzing their engagement with individual companies, the study found that they focus on large companies with high $CO_2$ emissions and significant ownership stakes. It also found a negative relationship between Big Three ownership and subsequent carbon emissions among MSCI index constituents, which strengthens over time as these institutions publicly commit to addressing ESG issues. This example shows that institutional investors have significant engagement and voting power, and they can certainly influence companies.

### 6.1.5 Performance of active ownership

Previously, we have seen that institutional investors have a lot of power to engage with companies and to vote. However, we may wonder whether active ownership has a real impact on companies. Measuring the performance and success of active ownership is not an easy task. Certainly, the most famous research on these issues is the study conducted by Dimson *et al.* (2015):

> "*We analyze an extensive proprietary database of corporate social responsibility engagements with US public companies from 1999–2009. Engagements address environmental, social, and governance concerns. Successful (unsuccessful) engagements are followed by positive (zero) abnormal returns. Companies with inferior governance and socially conscious institutional investors are more likely to be engaged. Success in engagements is more probable if the engaged firm has reputational concerns and higher capacity to implement changes. Collaboration among activists is instrumental in increasing the success rate of environmental/social engagements. After successful engagements, particularly on environmental/social issues, companies experience improved accounting performance and governance and increased institutional ownership.*" (Dimson *et al.*, 2015, page 3225).

Two measures of performance are then used: the stock market reaction to engagements (or cumulative abnormal returns around initial engagements) and the company's post-engagement ESG performance (or post-engagement ESG score/rating). This initial publication has been followed by a few studies that have at least partially confirmed these results (Grewal *et al.*, 2016). However, we must be cautious about these academic conclusions for several reasons. First, as we saw earlier, there are different forms of engagement, and some of them, such as behind-the-scenes engagement, are not public. In this case, it is not possible to assess their performance. Second, the different forms of engagement are usually employed by different investors at the same time. How can the impact of one form be disentangled from that of another? For example, most shareholder resolutions do not receive majority support. However, Grewal *et al.* (2016) found that they can have an impact. We may wonder whether this is just because shareholders have proposed a resolution or whether it is due to other forms of engagement, particularly engage behind the scenes, voice or exit. A third reason is that the results of most theoretical models are very sensitive and can lead to different conclusions depending on the framework. In particular, equilibria are very fragile (Gollier and Pouget, 2022) or can be multiple (Levit *et al.*, 2024). These models emphasize that multiple factors are at play, meaning that each engagement is unique. This is also the view of professionals who engage with companies. The success of the engagement depends not only on the investors, but also to a large extent on the management of the company, the shareholder structure and the country. Investors have the impression that it's case-by-case and that we can't generalize, especially since there's a lot of survivor bias. In fact, investors communicate a lot about their successes, but there are many unsuccessful cases that are not known and not in databases. The final reason is that different forms of engagement do not have the same impact. For example, the performance of exit is generally considered to be negative. The same conclusion applies to voting, since most shareholder resolutions never receive a majority.

## 6.2 ESG voting

According to PRI (2021b), voting is the most important pillar of an engagement policy and a powerful tool in the stewardship toolkit. Over the years, voting has become an integral part of many ESG investment policies. In this section, we introduce the voting process and how proxy voting works. We also discuss the voting principles that define a voting policy. Finally, we present the current landscape of ESG voting with statistics on asset managers and asset owners.

### 6.2.1 Voting process

Each country has its own voting process. Nevertheless, they share some common ground. According to NBIM (2020), they typically include the following steps:

- *"The company sets the agenda for the annual shareholder meeting;*
- *The custodian confirms the identity of the shareholders and the number of shares eligible for voting — often for a specific date ahead of the meeting (record date);*
- *Shareholders receive the meeting materials from the company (may be before or after the record date);*
- *Shareholders procuring proxy advisory services receive voting recommendations;*
- *Shareholders instruct the custodian on how to vote, often through a proxy voting service provider, within a deadline ahead of the shareholder meeting (cut-off date);*
- *Voting takes place at the shareholder meeting;*
- *Shareholders receive confirmation from the service provider that their voting instructions have been carried out.*"

### 6.2.2 Proxy voting

Proxy voting is a process by which a shareholder of a company authorizes another party, known as a proxy, to attend the annual general meeting (AGM) and vote on his or her behalf. This allows shareholders who are unable or unwilling to attend the meeting to participate in the decision-making process. This may be for a variety of reasons, including that the shareholder is unable to attend the meeting in person or prefers to have someone with more expertise or aligned interests vote on his or her behalf. Proxy voting is very common in the asset management industry because asset managers generally do not have the resources to attend thousands of shareholder meetings. Therefore, they hire a proxy firm to do the job.

According to Larcker *et al.* (2018), the proxy voting market is dominated by two firms:

- Institutional Shareholder Services (ISS)
  Founded in 1985, ISS is the world's largest proxy advisory firm, providing recommendations on more than 40 000 shareholder meetings each year. They provide research, analysis, and voting recommendations on a wide range of corporate governance issues, including executive compensation, board composition, and environmental and social responsibility (ESG) proposals. The firm employs 3 000 employees across 25 global locations in 15 countries and serves approximately 3 400 clients. It is owned by Deutsche Börse Group.

- Glass Lewis
  Founded in 2003, Glass Lewis is the second largest proxy advisory firm in the world, advising on more than 30 000 shareholder meetings annually in over 100 countries. Similar to ISS, they provide research, analysis and voting recommendations on various corporate governance issues to influence the decisions of institutional investors. The firm employs 380 employees and serves approximately 1 300 investors. It is owned by Peloton Capital Management, a private equity firm, and Stephen Smith, a financial services entrepreneur.

As of 2021, Shu (2024) estimates that ISS and Glass Lewis collectively control approximately 90% of the US market. The other major players in the US are Egan-Jones Proxy Services and Broadbridge/ProxyVote. However, ISS and Glass Lewis are global players with a strong presence in Europe. They have also acquired many local players such as Proxinvest in France (Glass Lewis) or Nordic Investor Services in Sweden (ISS).

Figure 6.7: The two largest proxy advisory firms

According to many academic studies, proxy voting has many drawbacks and controversies (Davis and Kim, 2007; Larcker *et al.*, 2018; Malenko *et al.*, 2021; Bernard *et al.*, 2023). The main criticism is that proxy voting implies homogeneity of votes for two main reasons. The first is that most investors follow the recommendations of the proxy advisor, resulting in a high correlation among institutional votes (Shu, 2024). The second is that the market is highly concentrated. These two reasons mean that there is a lack of diversity in voting. As a result, we may face a situation where it is difficult to distinguish the votes of ESG and non-ESG mutual funds or the votes of two different investors. The similarity between the votes has led to the emergence of the concept of robo-voting. Strictly defined, robo-voting is the phenomenon whereby an investor or a mutual fund automatically adopts the voting recommendations of its proxy advisor. This practice has been facilitated by the emergence of online voting platforms, which allow proxy advisors to pre-fil these platforms with their recommended votes, making the process more streamlined for investors and funds. In a broader sense, robo-voting involves investors closely following the recommendations of proxy firms, with minimal adjustments made only to demonstrate a degree of independent decision-making. According to Matsusaka and Shu (2024), the phenomenon of robo-voting is underestimated, but it applies mainly to small investors and index funds.

**Remark 74** *Proxy voting and proxy advisory firms are regulated by the SEC. In July 2020, the SEC adopted rule amendments regarding proxy advisory services, reaffirming that they constitute a solicitation under the federal proxy rules. They clarified that the omission of certain information could violate antifraud provisions and introduced more disclosure and procedural requirements for proxy advisors to maintain exemptions from the federal proxy rules. The goal was to provide more transparent, accurate and complete information to investors using proxy advisory services. However, in July 2022, the Securities and Exchange Commission adopted rule amendments that rescinded significant portions of the 2020 rules.*

### 6.2.3 Defining a voting policy

A voting policy refers to the guidelines or principles that institutional investors, such as mutual funds, pension funds, or other entities with significant ownership stakes in publicly traded companies, use to guide their decisions when voting on corporate matters at shareholder meetings. These voting policies outline the criteria and considerations that investors use to evaluate proposals made by companies, such as the election of directors, executive compensation plans, mergers and acquisitions, corporate governance practices, environmental and social responsibility initiatives, and other matters that may affect shareholder value. The terms "*voting policy*", "*proxy voting guidelines*" or "*voting principles*" are interchangeable. In Figure 6.8, we show four different voting policies from two asset managers (DWS and Vanguard) and two asset owners (Ontario Teachers' pension plan and New York City pension funds).

Figure 6.8: Voting policy

Source: Corporate websites.

An example of the structure of a voting policy is shown in Box 6.3. In most cases, a proxy voting policy is articulated around the same components. For instance, Vanguard identifies four pillars: (1) board composition and effectiveness, (2) board oversight of strategy and risk, (3) executive compensation, and (4) shareholder rights. BlackRock defines its proxy voting policy around the following themes: (1) boards and directors, (2) auditors and audit-related issues, (3) capital structure proposals, (4) mergers, acquisitions, transactions and other special situations, (5) executive compensation, (6) material sustainability risks and opportunities, (7) general corporate governance issues, and (8) shareholder protection. The voting policy of DWS has nive components: (1) board, (2) management and board remuneration, (3) audit related agenda items, (4) financial accounts, use of profits and share capital related items, (5) say on climate and shareholder decarbonisation proposals, (6) statutes & legal structure agenda items, (7) market for control, (8) related-party transactions and (9) shareholder proposals. For the asset owner Ontario Teachers' pension plan, five issues are important: (1) board composition, (2) compensation, (3) corporate structure and capital management, (4) takeover protections and (5) shareholder rights and shareholder proposals. These examples illustrate the recurrence of certain elements, including boards, compensation, auditing, and shareholder rights, while sustainability, ESG and climate issues depend on the institutional investor. Voting guidelines are generally descriptive, but they also include some quantitative constraints. Here are two examples: (1) "*CalSTRS generally supports poison pills that are applied equitably to all shareholders, have at least 20% trigger threshold and have a sunset provision of no more than three*

Box 6.3: Amundi voting guidelines (structure of the voting policy)

1. Shareholders' rights: "*A corporate governance regime must protect and facilitate the exercise of shareholders' rights and ensure fair treatment of all shareholders, including minority and foreign shareholders.*"
   - General meeting organization
   - Voting rights and shareholder retention
   - Anti-takeover measures
   - Overall balance and transparency (payment of a responsible dividend, discharge of directors, choice and remuneration of auditors, regulated agreements)
   - Relocations and change of listing
2. Boards, committees and governing bodies: "*While the board is accountable to the company and its shareholders, it must also take due account of other stakeholders and respect their interests, in particular those of employees, creditors, clients and suppliers.*"
   - Quality of corporate governance information (quality of comply or explain on governance, board responsiveness)
   - Composition and balance of the board (independence, audit committee, nomination committee, remuneration committee)
   - A clear distribution of powers to forestall conflicts of interest
   - Functioning of the board
   - Attendance fees and remuneration of non-executive directors
3. Financial structure: "*With regard to shareholders' rights, [...] cumulative capital increases should not represent more than 60% of share capital.*"
   - Share issues without preferential subscription rights
   - Share issuance with preferential subscription rights
   - Mergers, acquisitions, demergers and other restructuring projects
   - Repurchase of own shares
   - Employee share ownership
4. Remuneration policy
   - General principles on executive remuneration
   - Balance of remuneration and value sharing
   - Transparency and remuneration report
   - Stock option and performance share plans
   - Severance pay
   - Pension plans
   - Exceptional remunerations (discretionary Power)
5. Environmental and Social issues
   - Natural capital preservation and the energy transition (say on climate)
   - Social cohesion
   - Board responsibility on environmental and social issues
   - Shareholder proposals

Source: Amundi (2024), Voting Policy 2024, about.amundi.com.

*years. CalSTRS believes that all poison pills should be approved by shareholders within 12 months or the next shareholder meeting, whichever comes first.*"; (2) "*Fidelity generally will support employee stock purchase plans if the minimum stock purchase price is equal to or greater than 85% (or at least 75% in the case of non-US companies where a lower minimum stock purchase price is equal to the prevailing best practices in that market) of the stock's fair market value and the plan constitutes a reasonable effort to encourage broad based participation in the company's stock.*"

### 6.2.4 Statistics about ESG voting

In this section, we analyze the behavior of investors in voting on ESG resolutions. In the case of asset managers, we use the annual reports published by ShareAction. The most recent report covered the 2023 proxy season and was published in January 2024 (Figure 6.9). For asset owners, data is more difficult to find. We use various surveys and supplement the assessment by studying the engagement reports of some pension funds. As a result, we don't have a true picture of asset owners' ESG voting.

Figure 6.9: 2023 Voting Matters

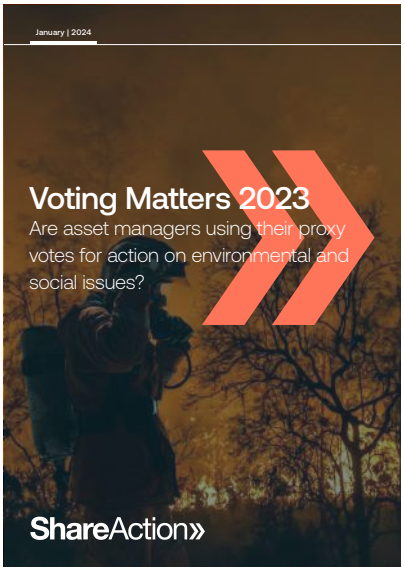


Source: https://shareaction.org.

#### Asset managers

ShareAction launched the Voting Matters series in 2019. At that time, the report examined how the largest asset managers voted on shareholder resolutions related to climate change (ShareAction, 2019). In 2020 and 2021, the analysis was expanded to include the S pillar in addition to the E pillar (ShareAction, 2020, 2021). The 2022 edition also analyzes shareholder-filed governance resolutions that directly relate executive compensation and political spending policies to environmental and social issues (ShareAction, 2023). Finally, the 2023 edition adds the lobbying dimension to the E and S pillars (ShareAction, 2024). To better understand the difference between the three categories, we list the sub-themes for each pillar:

- Environmental: biodiversity, climate change financing, climate change lobbying, climate change reporting, climate change strategy, climate change targets, plastics and packaging, pollution, sustainability pay metrics, water;

- Social: civil and social rights, diversity and discrimination, human rights, labour rights, public health, sustainability pay metrics;
- Lobbying: congruency of political spending, lobbying payments and policy, political contributions.

After merging the five datasets and cleaning the data[29], we obtain a database with 85 unique asset managers with the following frequencies: 35 in 2019, 54 in 2020, 65 in 2021, 68 in 2022 and 69 in 2023. There is only 25 asset managers[30], which are present every year. The scores calculated by ShareAction were based on 65 selected shareholder proposals in 2019, 102 in 2020, 146 in 2021, 252 in 2022 and 257 in 2023. In Table 6.5, we report some statistics of the selected shareholder resolutions. Let $s_j$ be the support rate of resolution $j$. The resolution has majority support if $s_j \geq 50\%$. For instance, of the 64 shareholder resolutions in 2019[31], only three received majority support, implying a success rate of 4.7%. For the period 2019–2022, this success rate is about 15%. It drops dramatically in 2023 due to the ESG backlash in the US. We have also reported the 10%, 25%, 75% and 90% percentiles[32]. The interquartile range is between 12% and 43%. Finally, we notice that the average support rate is higher for environmental resolutions than for social resolutions.

Table 6.5: Statistics of success rate shareholder resolutions

| Year | | 2019 | 2020 | 2021 | 2022 | 2023 |
|---|---|---|---|---|---|---|
| Number of resolutions | | 64 | 102 | 144 | 249 | 261 |
| Resolutions with majority support | | 3 | 15 | 29 | 37 | 8 |
| Success rate (in %) | | 4.7 | 14.7 | 20.1 | 14.9 | 3.1 |
| Average support rate (in %) | | 28.2 | 29.9 | 32.9 | 29.9 | 23.2 |
| Percentile of support rate (in %) | 10% | 6.5 | 9.2 | 7.2 | 9.4 | 8.2 |
| | 25% | 17.0 | 13.1 | 12.0 | 13.5 | 13.1 |
| | 75% | 37.7 | 42.6 | 42.8 | 40.3 | 31.6 |
| | 90% | 41.8 | 55.2 | 81.2 | 57.6 | 37.6 |
| Average support rate (in %) | E | 28.2 | 35.8 | 41.8 | 31.6 | 22.2 |
| | S | | 24.5 | 28.8 | 27.4 | 22.4 |

Source: ShareAction (2019, 2020, 2021, 2023, 2024) & Author's calculations.

For each asset manager, the support rate is calculated as:

$$\text{support rate} = \frac{\#\{\text{for}\}}{\#\{\text{for} + \text{against} + \text{abstention} + \text{dit-not-vote} + \text{split-vote}\}}$$

In Table 6.6, we calculate the average support rate for shareholder resolutions using two methods. The arithmetic mean is the simple average across all asset managers, while the contribution of each asset manager is proportional to its assets under management for the weighted mean. We observe that the arithmetic mean of the support rates increases continuously since 2019 when we consider the overall score and the S pillar. This is not the case for the E pillar for which we observe a lower

[29] Notably, some asset managers have merged or changed their name.

[30] They are APG AM, AXA IM, Abrdn, Allianz GI, Amundi AM, BNP PAM, BlackRock, Capital Group, DWS, Fidelity Investments, Generali Insurance AM, Goldman Sachs AM, HSBC Global AM, Invesco, J.P. Morgan AM, Legal & General, M&G IM, Ninety One, Northern Trust AM, SSGA, Schroders, T. Rowe Price, UBS AM, Vanguard, and Wellington Management.

[31] Some resolutions are excluded from the analysis because we don't have all the numbers.

[32] See Figure 6.10 for the empirical histogram.

Figure 6.10: Histogram (in %) of support rates

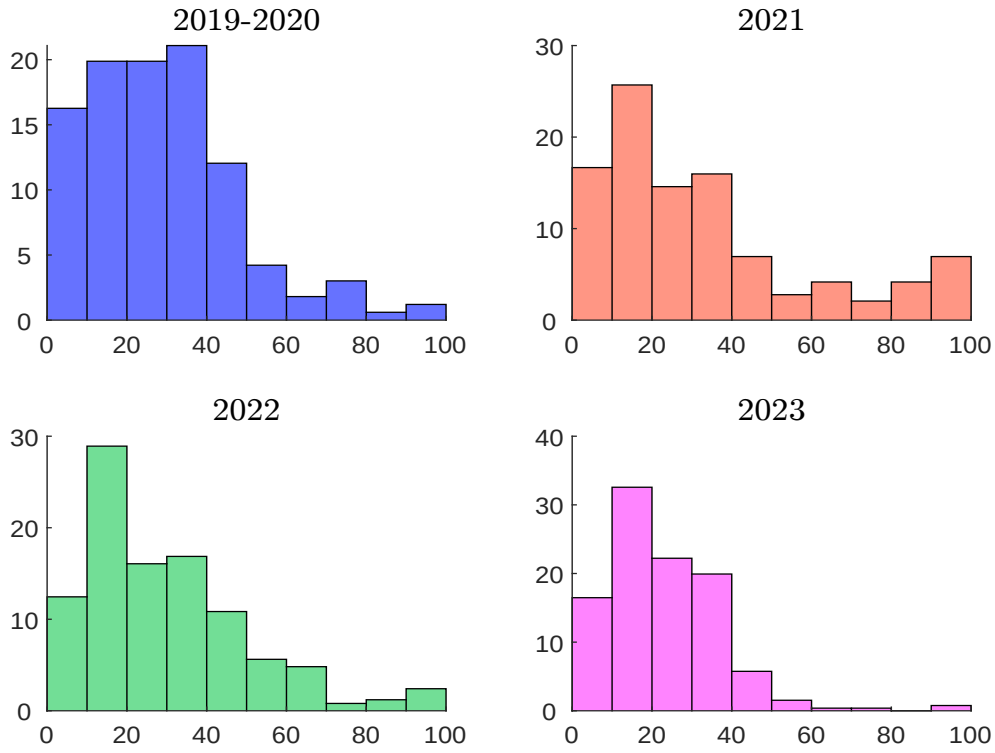


Source: ShareAction (2019, 2020, 2021, 2023, 2024) & Author's calculations.

value in 2022 and 2023 compared to 2021. Moreover, the value of 65% that we found in 2022 for the total score is due to the introduction of the pay & politics topic. We also note the high support for the lobbying pillar in 2023. If we focus on the weighted average, the figures are lower. For instance, the average support in 2023 is 39.8% instead of 65.2%. This means that the largest asset managers vote less in favor of shareholder proposals than the others.

Table 6.6: Average support rate in % for ESG resolutions

| Topic | Method | 2019 | 2020 | 2021 | 2022 | 2023 |
|---|---|---|---|---|---|---|
| Overall | Arithmetic | 45.8 | 57.4 | 58.9 | 65.0 | 65.2 |
| | Weighted | 32.7 | 42.1 | 47.6 | 46.5 | 39.8 |
| Environment | Arithmetic | 45.8 | 61.0 | 66.0 | 64.8 | 64.0 |
| | Weighted | 32.7 | 44.7 | 55.8 | 48.8 | 39.8 |
| Social | Arithmetic | | 53.3 | 55.2 | 62.7 | 64.3 |
| | Weighted | | 39.0 | 43.7 | 44.3 | 39.0 |
| Pay & politics | Arithmetic | | | | 71.5 | |
| | Weighted | | | | 47.8 | |
| Lobbying | Arithmetic | | | | | 69.9 |
| | Weighted | | | | | 42.1 |

Source: ShareAction (2019, 2020, 2021, 2023, 2024) & Author's calculations.

Figure 6.11: Arithmetic average support rate in % per region and year

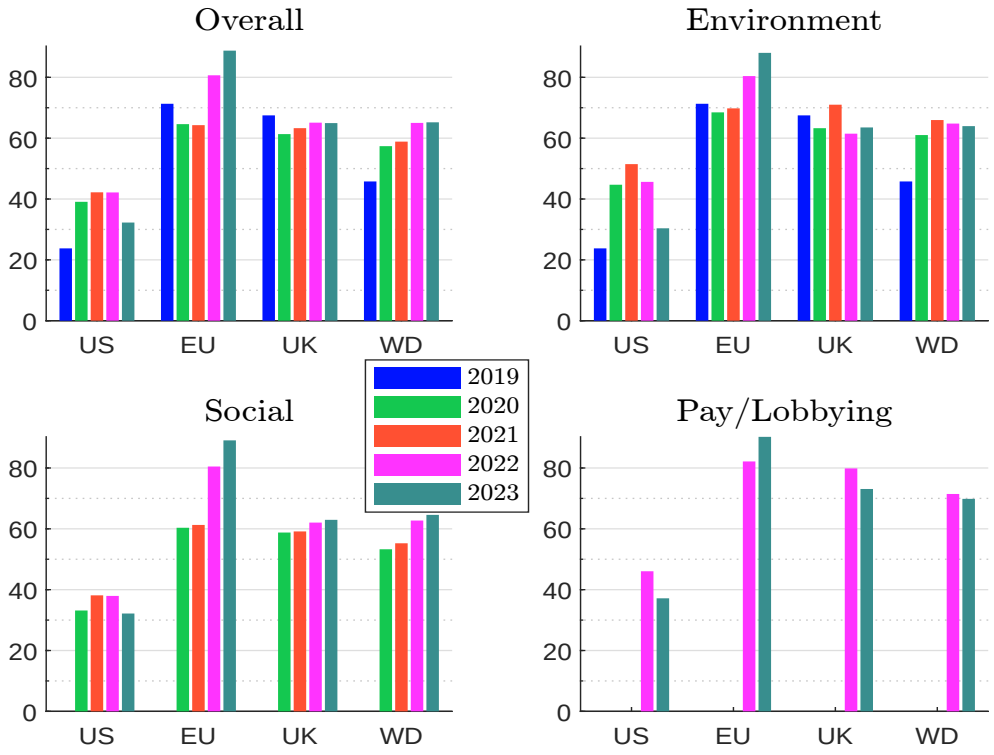


Source: ShareAction (2019, 2020, 2021, 2023, 2024) & Author's calculations.

Figure 6.12: Weighted average support rate in % per region and year

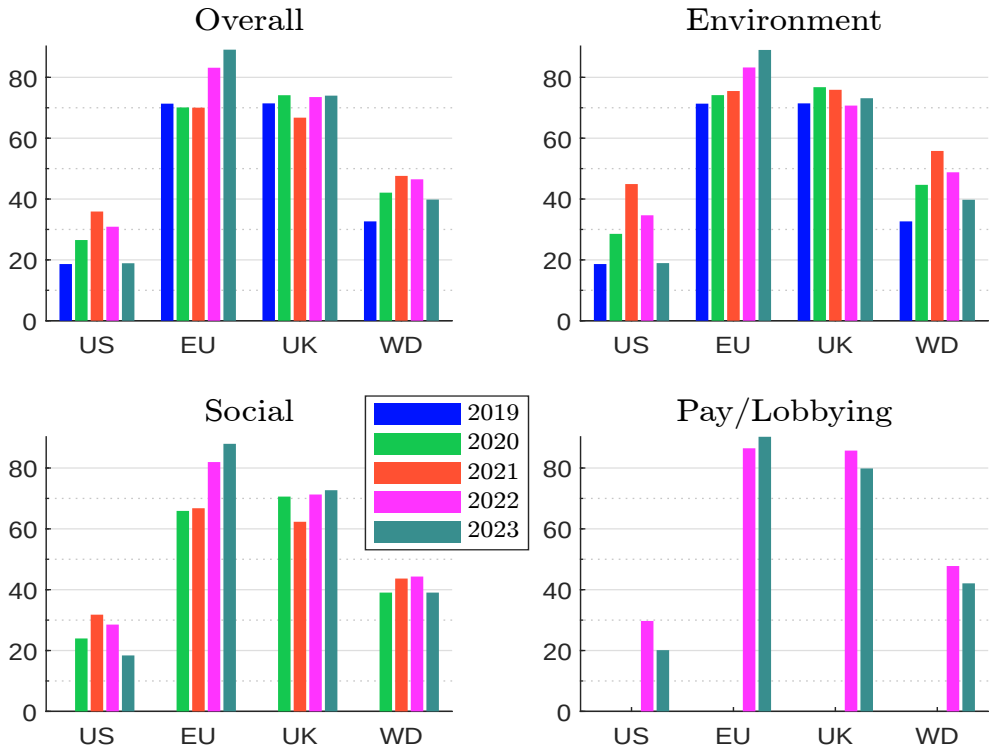


Source: ShareAction (2019, 2020, 2021, 2023, 2024) & Author's calculations.

If we perform a regional analysis (Figures 6.11 and 6.12), we observe the following facts. British and European[33] asset managers have similar voting patterns. Their level of support is significantly higher than in the US. Nevertheless, US asset managers improve their ESG voting policy in 2020 and 2021, which explains the increase in the overall score for the world. In 2022 and 2023, the increase in the European support is offset by the American setback.

Table 6.7: Best performers (2022, overall)

| Rank | Name | Country | AUM | Overall | E | S | Pay |
|---|---|---|---|---|---|---|---|
| 1 | Achmea IM | Netherlands | 251 | 100 | 100 | 100 | 100 |
| 1 | Impax AM | UK | 56 | 100 | 100 | 100 | 100 |
| 3 | BNP PAM | France | 761 | 99 | 97 | 100 | 100 |
| 3 | MN | Netherlands | 193 | 99 | 97 | 100 | 100 |
| 5 | Candriam | Luxembourg | 180 | 98 | 97 | 99 | 100 |
| 6 | PGGM | Netherlands | 331 | 97 | 93 | 100 | 97 |
| 7 | Man | UK | 149 | 96 | 98 | 94 | 98 |
| 8 | Robeco | Netherlands | 228 | 95 | 94 | 94 | 100 |
| 9 | Aviva Investors | UK | 363 | 93 | 88 | 96 | 100 |
| 10 | Amundi AM | France | 2 348 | 93 | 93 | 92 | 98 |
| 11 | Nordea AM | Finland | 333 | 91 | 93 | 89 | 90 |
| 12 | Aegon AM | Netherlands | 466 | 90 | 85 | 94 | 90 |
| 13 | Federated Hermes | UK | 672 | 89 | 88 | 87 | 90 |
| 14 | Pictet AM | Switzerland | 284 | 88 | 85 | 90 | 91 |
| 15 | Legal & General | Switzerland | 1 923 | 86 | 84 | 84 | 98 |

Source: ShareAction (2023) & Author's calculations.

Table 6.8: Worst performers (2022, overall)

| Rank | Name | Country | AUM | Overall | E | S | Pay |
|---|---|---|---|---|---|---|---|
| 59 | Goldman Sachs AM | US | 2 218 | 35 | 56 | 24 | 24 |
| 60 | Baillie Gifford | UK | 455 | 31 | 29 | 29 | 45 |
| 61 | SSGA | US | 4 140 | 29 | 30 | 31 | 22 |
| 62 | BlackRock | US | 10 014 | 24 | 28 | 24 | 15 |
| 63 | T. Rowe Price | US | 1 642 | 17 | 26 | 11 | 18 |
| 64 | Fidelity Investments | US | 4 520 | 17 | 23 | 19 | 2 |
| 65 | Vanguard | US | 8 274 | 10 | 12 | 9 | 9 |
| 66 | Dimensional Fund Advisors | US | 679 | 4 | 6 | 5 | 0 |
| 67 | Santander AM | Spain | 220 | 4 | 0 | 5 | 6 |
| 68 | Walter Scott & Partners | UK | 95 | 3 | 0 | 6 | 0 |

Source: ShareAction (2023) & Author's calculations.

In Tables 6.7 and 6.8, we report the ranking of the top fifteen and the bottom ten asset managers when considering the 2022 total score[34]. Two asset managers receive a score of 100%: Achmea IM and Impax AM Group. The top 15 rankings are dominated by asset managers based in the Netherlands, the UK and France, while seven American asset managers are in the bottom 10.

[33] This includes the following countries: Finland, France, Germany, Italy, Luxembourg, the Netherlands, Spain, Sweden, and Switzerland.

[34] For each row, we show the rank, the name, the country, the assets under management (in $ billion), and the 2022 score expressed as a percentage.

Table 6.9: Ranking of the 25 largest asset managers (2022, overall)

| Rank 2022 | Name | Country | AUM 2022 | Overall | | | | | Environment | | | | Social | | | | Pay | Lobbying |
|---|---|---|---|---|---|---|---|---|---|---|---|---|---|---|---|---|---|---|
| | | | | 2019 | 2020 | 2021 | 2022 | 2023 | 2020 | 2021 | 2022 | 2023 | 2020 | 2021 | 2022 | 2023 | 2022 | 2023 |
| 22 | BlackRock | US | 10 014 | 7 | 12 | 40 | 24 | 8 | 11 | 53 | 28 | 9 | 12 | 34 | 24 | 8 | 15 | 7 |
| 25 | Vanguard | US | 8 274 | 8 | 14 | 26 | 10 | 3 | 15 | 38 | 12 | 5 | 12 | 20 | 9 | 2 | 9 | 2 |
| 23 | Fidelity Investments | US | 4 520 | 9 | 31 | 29 | 17 | 16 | 20 | 23 | 23 | 12 | 44 | 33 | 19 | 21 | 2 | 12 |
| 21 | SSGA | US | 4 140 | 26 | 35 | 32 | 29 | 23 | 40 | 42 | 30 | 29 | 29 | 27 | 31 | 20 | 22 | 16 |
| 18 | J.P. Morgan AM | US | 2 742 | 7 | 43 | 37 | 37 | 23 | 51 | 50 | 43 | 26 | 34 | 31 | 25 | 11 | 53 | 41 |
| 16 | Capital Group | US | 2 716 | 5 | 8 | 28 | 45 | 8 | 12 | 26 | 37 | 8 | 4 | 31 | 47 | 11 | 58 | 0 |
| 2 | Amundi AM | France | 2 348 | 66 | 89 | 93 | 93 | 98 | 91 | 97 | 93 | 100 | 88 | 90 | 92 | 96 | 98 | 100 |
| 20 | Goldman Sachs AM | US | 2 218 | 37 | 45 | 47 | 35 | 5 | 48 | 57 | 56 | 7 | 43 | 40 | 24 | 2 | 24 | 5 |
| 3 | Legal & General | UK | 1 923 | 82 | 96 | 77 | 86 | 92 | 96 | 87 | 84 | 89 | 95 | 73 | 84 | 92 | 98 | 100 |
| 24 | T. Rowe Price | US | 1 642 | 5 | 22 | 31 | 17 | 6 | 27 | 44 | 26 | 9 | 17 | 25 | 11 | 4 | 18 | 2 |
| 15 | Invesco | US | 1 611 | 34 | 37 | 37 | 47 | 39 | 52 | 51 | 54 | 35 | 19 | 28 | 37 | 37 | 61 | 52 |
| 12 | Morgan Stanley IM | US | 1 566 | | | 55 | 64 | 58 | | 59 | 64 | 51 | | 53 | 65 | 62 | 63 | 65 |
| 14 | Wellington Management | US | 1 426 | 10 | 51 | 44 | 48 | 29 | 62 | 60 | 63 | 31 | 39 | 37 | 41 | 26 | 36 | 33 |
| 7 | Northern Trust AM | US | 1 348 | 21 | 70 | 60 | 83 | 77 | 79 | 68 | 83 | 69 | 59 | 57 | 78 | 80 | 96 | 93 |
| 13 | Nuveen AM | US | 1 271 | 62 | 63 | 56 | 59 | | 71 | 76 | 57 | | 56 | 48 | 52 | | 79 | |
| 8 | UBS AM | Switzerland | 1 216 | 90 | 79 | 75 | 83 | 82 | 91 | 72 | 84 | 82 | 67 | 75 | 80 | 82 | 87 | 82 |
| 4 | DWS | Germany | 1 055 | 74 | 66 | 85 | 86 | 86 | 66 | 92 | 86 | 89 | 65 | 80 | 80 | 77 | 100 | 98 |
| 10 | AXA IM | France | 1 009 | 79 | 71 | 55 | 73 | 75 | 85 | 72 | 69 | 76 | 55 | 45 | 68 | 65 | 95 | 95 |
| 6 | Schroders | UK | 991 | 56 | 62 | 73 | 85 | 83 | 63 | 78 | 81 | 84 | 60 | 70 | 87 | 81 | 87 | 83 |
| 17 | AllianceBernstein | US | 779 | | | | 43 | 33 | | | 40 | 16 | | | 39 | 42 | 60 | 55 |
| 5 | Allianz GI | Germany | 766 | 89 | 81 | 77 | 86 | 85 | 89 | 81 | 80 | 83 | 73 | 76 | 91 | 86 | 85 | 93 |
| 1 | BNP PAM | France | 761 | 48 | 72 | 98 | 99 | 96 | 65 | 96 | 97 | 95 | 80 | 99 | 100 | 97 | 100 | 94 |
| 19 | Columbia Threadneedle | US | 754 | | | | 37 | 55 | | | 43 | 50 | | | 25 | 54 | 53 | 67 |
| 9 | Manulife IM | Canada | 723 | | | | 75 | 84 | | | 77 | 85 | | | 68 | 78 | 89 | 93 |
| 11 | APG AM | Netherlands | 721 | 72 | 70 | 59 | 72 | 87 | 80 | 65 | 89 | 96 | 59 | 56 | 57 | 76 | 83 | 94 |

Source: ShareAction (2019, 2020, 2021, 2023, 2024) & Author's calculations.

Focusing on the largest asset managers, we obtain the 2022 rankings shown in Table 6.9. For each row, we report the rank according to the 2022 total score, the name, the country, the assets under management (in $ billion) as of December 2022, the total score expressed as a percentage for the five reporting years (2019 to 2023). We also report the thematic scores (environmental, social, pay & politics and lobbying). In this case, the six best performers are BNP Paribas Asset Management, Amundi, Legal & General, DWS, Allianz GI and Schroders (two UK, two French and two German asset managers respectively). We also note that some asset managers have improved significantly. For example, BNP PAM's score improves from 48% in 2019 to 99% in 2022. For Northern Trust AM, we have 21% in 2019 versus 83% in 2022. If we look at the four largest US asset managers, they improve their scores between 2019 and 2021, but they support fewer resolutions in 2022 than in 2021. In 2023, their scores are even worse. This is certainly explained by political pressure and the anti-ESG movement in the US[35]. If we extend the analysis to the 85 managers in the database, we get the dynamics shown in Figure 6.13. Overall, the trends are upward, although we note some setbacks, especially in the US.

Figure 6.13: Evolution of the support rate in % per asset manager

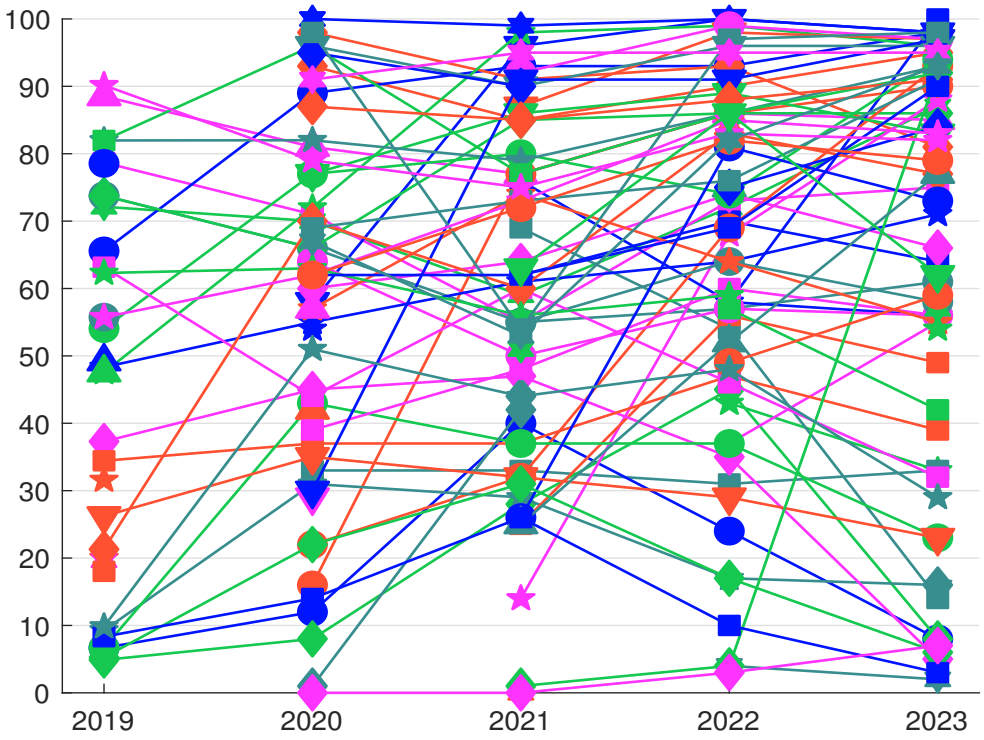


Source: ShareAction (2019, 2020, 2021, 2023, 2024) & Author's calculations.

According to ShareAction (2023), the main findings of the 2022 report are the following:

1. "*49 additional resolutions would have received majority support if the largest asset managers had voted in favour of them.*

2. *Voting performance has been stagnant in the US and the UK compared to 2021, while European asset managers have shown a large improvement.*

[35]See footnote 65 on page 30.

3. *Asset managers across the board are hesitant to back action-oriented resolutions, which would have the most transformative impact on environmental and social issues.*"

These trends are confirmed in the 2023 report with a decline in support for key environmental and social shareholder resolutions. In 2023, only 3% of the resolutions assessed were passed, down from 21% in 2021, with the four largest asset managers showing significant declines in support. However, there are pockets of progress, particularly in Europe, where legislative requirements appear to have improved voting performance. Some asset managers have consistently supported resolutions and also voted against directors on environmental and social grounds. Although many asset managers have made net-zero commitments, they often fail to back these up with action when it comes to voting. Greenwashing remains prevalent, with weak excuses such as claims that resolutions are too prescriptive. Some asset managers, including members of the Climate Action 100+, fail to adequately address climate change concerns.

Table 6.10: Statistics on Say on Climate resolutions

| Resolution | 2022 | | | | 2023 | | | |
|---|---|---|---|---|---|---|---|---|
| sponsor | # | Avg. | Min. | Max. | # | Avg. | Min. | Max. |
| Shareholder | 6 | 21.98% | 1.00% | 46.50% | 6 | 19.68% | 16.60% | 24.40% |
| Management | 30 | 89.17% | 51.00% | 99.90% | 11 | 90.83% | 69.70% | 98.60% |

In addition to the previous analysis, the 2022 and 2023 ShareAction reports include statistics on say on climate resolutions (Table 6.10). These are resolutions in which shareholders express their approval or disapproval of the company's global climate strategy. In 2022, of the 36 resolutions selected, only six were submitted by shareholders asking the company to hold an annual advisory vote on the company's climate plan. The remaining thirty resolutions were sponsored by the management. The shareholder- and management-sponsored proposals received an average of 21.98% and 89.17%, respectively. The range is between 1% and 46.5% for shareholder-sponsored resolutions, while it is between 51% and 99.9% for management-sponsored resolutions. In 2023, the results are similar, but the number of say on climate filed by management has been divided by 3.

Box 6.4: Case studies: Barclays, EDF and Woodside Energy say on climate resolutions

Electricité de France or EDF (French energy company) filed a management-sponsored say on climate resolution at its AGM on 12 May. The group's climate transition plan to achieve carbon neutrality by 2050 was approved by 99.1%.

The management of Barclays (UK bank) filed a Say on Climate resolution at the 2022 AGM on 4 May. They asked for approval of Barclays' climate strategy, targets and progress. Despite the plan's shortcomings on coal, the result was 80.8% for and 19.2% against. According to some NGOs, some asset managers prefer to vote 'for' in the hope that the company will improve its plan and return next year with an upgraded climate resolution.

Woodside Energy Group Ltd. (Australian energy company) filed a say on climate resolution at its 2022 AGM on 19 May. Management asked for approval of its climate report. The support rate was 51.03%, meaning that 48.97% of the company's shareholders voted against its climate transition plan. These disappointing results may force management to submit a new resolution in 2023, with a high risk of failure, or discourage management from submitting new Say on Climate resolutions in future years.

**Asset owners**

The comprehensive ShareAction report for asset managers has no equivalent for asset owners. As a result, we do not have global statistics on ESG voting by asset owners. To go further, one of the difficulties is having a clear view of the universe of asset owners. Each year, the Thinking Ahead Institute publishes a report listing the world's largest asset owners. Table 6.11 shows the top 50. According to Thinking Ahead Institute (2023), an asset owner has five qualifying characteristics:

1. "*Works directly for a defined group of beneficiaries/savers/investors as the manager of their assets in a fiduciary capacity under delegated responsibility;*
2. *Works with a sponsoring entity (government affiliate, company or not for profit);*
3. *Works within explicit law and possesses an implicit societal license to operate because of its societal trust and legitimacy;*
4. *Delivers mission specific outcomes to beneficiaries and stakeholders in the form of various payments or benefits into the future;*
5. *Employs a business model that combines a governance budget (resources and processes) and a risk budget (reflecting the mix of financial assets that delivers on the mission).*"

The ranking in Table 6.11 considers three types of asset owners: pension funds (PF), sovereign wealth funds (SWF) and outsourced chief investment officers (OCIO). A pension fund is a type of investment fund established by an employer, union, or government agency to provide retirement benefits for employees. The primary purpose of a pension fund is to accumulate assets over time through contributions from both the employer and the employees, and through the investment performance of the fund's investments. The goal is to generate returns that will pay future retirement benefits. A general distinction is made between public and private pension funds. A key difference between an asset manager and a pension fund is that the latter must meet liability targets. A sovereign wealth fund is a state-owned investment fund typically established by a government. These funds are created to manage and invest a country's excess reserves or revenues, often derived from commodities such as oil, natural gas, or other exports. The goal is to accumulate wealth for future generations. Unlike pension funds, SWFs do not necessarily have liabilities to meet. An outsourced chief investment officer, or OCIO, is essentially a third-party firm that an asset owner hires to manage its investment portfolio. As such, OCIOs are asset managers or advisory firms. The CIO delegation can take several forms: investment policy, strategic asset allocation, tactical asset allocation, reporting, due diligence, asset management, etc. In addition to PFs, SWFs and OCIOs, the other two categories of asset owners are foundations and endowments, and insurance companies. As a result, it is sometimes difficult to distinguish between asset owners and asset managers. In fact, many insurance companies also have an asset management business with both internal assets from the insurance business and external assets from other clients. This is typically the case with AXA IM or Allianz GI. This is also the case for public investment platforms (PIF), which are institutional investors that manage and invest a pool of capital from various depositors or funds. For example, the three leading asset owners in the Netherlands (APG, PGGM and MN Services) are considered public investment platforms because they manage the assets of several pension funds. In a sense, they are also asset managers. For this reason, they are also included in the Voting Matters series. According to Thinking Ahead Institute (2023), the three largest asset owners are the Government Pension Investment Fund (GPIF), Norges Bank Investment Management (NBIM) and China Investment Corporation (CIC).

Asset owners are at the forefront of many climate change and sustainability initiatives. For example, the PRI was created thanks to the founding asset owners. The Net Zero Asset Owner

Table 6.11: 50 largest asset owners in the world (Thinking Ahead Institute, 2023)

| # | Name | Country | Assets (in $ bn) | Fund type | Sigle |
|---|---|---|---|---|---|
| 1 | Government Pension Investment Fund | Japan | 1 449 | PF | GPIF |
| 2 | Norges Bank Investment Management | Norway | 1 250 | SWF | NBIM |
| 3 | China Investment Corporation | China | 1 149 | SWF | CIC |
| 4 | SAFE Investment Company | China | 1 034 | SWF | SAFE |
| 5 | Abu Dhabi Investment Authority | United Arab Emirates | 831 | SWF | ADIA |
| 6 | Kuwait Investment Authority | Kuwait | 769 | SWF | KIA |
| 7 | National Pension Service | South Korea | 706 | PF | NPS |
| 8 | GIC Private Limited | Singapore | 690 | SWF | GIC |
| 9 | Federal Retirement Thrift | US | 690 | PF | TSP |
| 10 | Public Investment Fund | Saudi Arabia | 620 | SWF | PIF |
| 11 | Algemene Pensioen Groep | Netherlands | 490 | PF | APG |
| 12 | California Public Employees | US | 432 | PF | CalPERS |
| 13 | Qatar Investment Authority | Qatar | 425 | SWF | QIA |
| 14 | Canada Pension Plan | Canada | 421 | PF | CPP |
| 15 | Central Provident Fund | Singapore | 407 | PF | CPF |
| 16 | National Social Security Fund | China | 347 | PF | NSSF |
| 17 | Mercer | US | 338 | OCIO | |
| 18 | Temasek Holdings | Singapore | 298 | SWF | |
| 19 | Caisse de dépôt et placement du Québec | Canada | 297 | PF | CDPQ |
| 20 | California State Teachers | US | 290 | PF | CalSTRS |
| 21 | Mubadala Investment Company | United Arab Emirates | 276 | SWF | Mubadala |
| 22 | Goldman Sachs | US | 247 | OCIO | GS |
| 23 | Stichting Pensioenfonds Zorg en Welzijn | Netherlands | 243 | PF | PGGM |
| 24 | New York State Common | US | 233 | PF | NYSCRF |
| 25 | Investment Corporation of Dubai | United Arab Emirates | 233 | SWF | ICD |
| 26 | New York City Retirement | US | 228 | PF | NYCERS |
| 27 | Employees Provident Fund | Malaysia | 228 | PF | EPF |
| 28 | Local Government Officials | Japan | 207 | PF | PAL |
| 29 | MN Services N.V. | Netherlands | 207 | PF | MN |
| 30 | BlackRock | US | 197 | OCIO | |
| 31 | Bureau of Labor Funds | Taiwan | 195 | PF | BLF |
| 32 | Public Service Pension Investment Board | Canada | 185 | PF | PSP |
| 33 | Florida State Board | US | 183 | PF | SBA |
| 34 | Ontario Teachers | Canada | 182 | PF | OTPP |
| 35 | AON | US | 178 | OCIO | AON |
| 36 | AustralianSuper | Australia | 176 | PF | |
| 37 | Public Investment Corporation | South Africa | 176 | SWF | PIC |
| 38 | Texas Teachers | US | 173 | PF | TRS |
| 39 | Turkey Wealth Fund | Turkey | 171 | SWF | TWF |
| 40 | Korea Investment Corporation | South Korea | 169 | SWF | KIC |
| 41 | British Columbia Investment | Canada | 169 | PF | BCI |
| 42 | Future Fund Management Agency | Australia | 165 | SWF | |
| 43 | Willis Towers Watson | US | 165 | OCIO | WTW |
| 44 | Employees' Provident | India | 159 | PF | EPFO |
| 45 | Australian Retirement Trust | Australia | 158 | PF | ART |
| 46 | Abu Dhabi Developmental Company | United Arab Emirates | 157 | SWF | ADQ |
| 47 | Washington State Investment Board | US | 155 | PF | WSIB |
| 48 | State Street Global Advisors | US | 153 | OCIO | SSGA |
| 49 | Russell Investments | US | 152 | OCIO | |
| 50 | Russian National Wealth Fund | Russia | 148 | SWF | NWF |

Source: www.thinkingaheadinstitute.org/research-papers/the-asset-owner-100-2023.

Alliance (NZAOA) is the first initiative to emerge from the various net zero groups. Asset owners also launched the One Planet Sovereign Wealth Funds[36] (OPSWF) in 2017 and the Paris Aligned Asset Owners commitment[37] in 2019. As leaders in the global sustainability movement, we can expect asset owners to be ahead of the curve compared to asset managers when it comes to engaging and voting with companies.

Climate Votes has published two research studies on asset owner voting practices. In the first study, they analyze the direct climate voting activities of the 46 asset owners that are part of the NZAOA, as well as the (proxy) voting practices reported in their 2019 PRI transparency reports (Cojoianu *et al.*, 2021). To do so, they compare the climate voting behavior of NZAOA members and other PRI members that are not members of the NZAOA, and find that:

> "*Our research reveals that between April 2009 to September 2021, asset owners that are now members of the NZAOA were more likely to vote in favour of climate action at Annual General Meetings (AGMs) of companies than the non-NZAOA peer group. This is an indicator that investors that joined the NZAOA in its first two years were early adopters of strong climate voting policies. However, when we analysed the voting pattern of NZAOA members and their non member peer group, we found that after becoming an NZAOA member, the NZAOA group's increase in pro-climate voting is not statistically different to the increase of the non-NZAOA peer group during the same time period. This is an indicator that joining the Alliance may be a recognition of existing voting practice, not an accelerator of that practice.*" (Cojoianu *et al.*, 2021, page 5).

Furthermore, their research shows that there is a lack of transparency regarding the voting records of NZAOA members as reported in their most recent PRI reports. In fact, only a small fraction of NZAOA members have publicly available records of their climate-related voting decisions made directly by them. Climate Votes releases a second study in January 2023 using the votes of 73 NZAOA in 2022. Among the different findings, Chin *et al.* (2023) observed that NZAOA members tend to vote in favor of climate-related proposals more often than their counterparts outside the group. However, it was noted that NZAOA members rarely take the initiative to sponsor such proposals themselves. Additionally, during the 2022 proxy season, NZAOA members did not consistently lead the way in supporting proposals aimed at ending the financing of new fossil fuel extraction. On the positive side, Alliance members often diverged from proxy advisor recommendations on climate resolutions in 2022, voting for them twice as often as Glass Lewis recommended.

An analysis of the voting practices of the largest pension funds reveals two groups. A first group where voting is not encouraged to influence. For example, on the GPIF website, we can read that "*GPIF itself does not exercise voting rights and instead entrusts its external asset managers with the exercise of voting rights in order to avoid having a direct influence on corporate management.*" A second group where voting is encouraged to influence. For example, on the CalPers website, we can read that "*as a long-term shareowner, we view proxy voting as one of the primary tools to influence a company's operations and corporate governance practices. That's why it's important for shareowners like us to vote our proxies based on the full understanding of publicly available information.*" So, as with asset managers, we can find asset owners who are very transparent and where we have access to their voting records, as well as asset owners where information is not available.

[36] The six founding members are ADIA, KIC, New Zealand Superannuation Fund (NZ Super Fund), NBIM, PIF and QIA.

[37] The website is `www.parisalignedassetowners.org`.

# Chapter 7

# Extra-financial Accounting


## 7.1 Historical perspectives

## 7.2 Single vs. double materiality

## 7.3 Environmental accounting

### 7.3.1 National environmental accounts

### 7.3.2 Corporate environmental accounts

## 7.4 Sustainability accounting

### 7.4.1 Social issues

### 7.4.2 Governance factors

# Part II

# Climate Risk

# Chapter 8

# The Physics and Economics of Climate Change

This second part focuses on the financial and economic implications of climate change. It is more technical than ESG because modeling climate risks is more complex than processing extra-financial data. Before presenting climate risk measures, analyzing transition and physical risks, optimizing portfolios with climate metrics, and managing risk, we need to have a minimum background on climate change. Three dimensions are important to consider: the fundamentals of climate change, the ecosystem, and the impact on the economy. It has taken a long time to understand the phenomenon of global warming and to accept the idea that humans are responsible for the increasing temperature anomaly since the industrial revolution. The fact that the global temperature at the earth's surface changes is not new and has been the case since the earth was formed. What is new, however, is that the temperature has changed so rapidly in just a century or two. In general, it has taken several thousand years to observe a change in temperature. In the first section, we explain how and why it has been possible to observe such an abrupt change. We present simple energy balance models to define three important physical concepts of climate change: the concept of radiative forcing, the estimation of equilibrium climate sensitivity, and the definition of tipping points. Awareness of the impacts of climate change has led governments to take, or attempt to take, action. The creation of the IPCC and the publication of its assessment reports have contributed greatly to the dissemination of scientific knowledge on climate change at the political and societal levels. The Earth Summit held in Rio de Janeiro in 1992 was a major step in politicizing climate change and popularizing this issue as a global problem for the world. It has been reinforced by the annual organization of the Conferences of the Parties. Today, we are in a climate change ecosystem where regulations can have a major impact on the business and strategy of companies. As we have not yet solved the problem, we can expect the regulatory environment to play an even greater role in the economy. Incorporating climate risk into economic models is not straightforward because the accepted economic models were developed before the 1980s, when climate change was not considered a problem outside a few aware people and scientific circles. Integrated assessment models are complex systems that focus on environmental or socio-economic issues and integrate information from economics, climate science, energy and agriculture. They emerged in the early 1980s and are now the main tools for evaluating climate policies and understanding the long-term impacts of climate change on the economy. They are central to defining climate scenarios and are widely used by the financial community, including central banks and regulators. The second major family of economic-climate models are extended versions of input-output models. Simpler than integrated assessment models, they are used to conduct sectoral analysis and measure consumption-based carbon footprints.

## 8.1 Awareness of climate change impacts

In this section, we review some important dates in climate science, from the discovery of the greenhouse effect in the early nineteenth century to the evidence of global warming in the late eighties. We will then examine natural and anthropogenic climate change. In particular, we will ask: Are human activities responsible for global warming? Finally, we will present some physical climate models that help to understand climate dynamics and the balance of greenhouse gas emissions.

### 8.1.1 Scientific evidence of global warming

#### The greenhouse effect

The greenhouse effect is the natural warming of the Earth that occurs when gases in the atmosphere trap heat from the sun that would otherwise escape into space (Figure 8.1). Without the greenhouse effect, the average temperature on Earth would be −18 degrees Celsius instead of the +15 degrees Celsius it is today.

Figure 8.1: Diagram showing how the greenhouse effect works

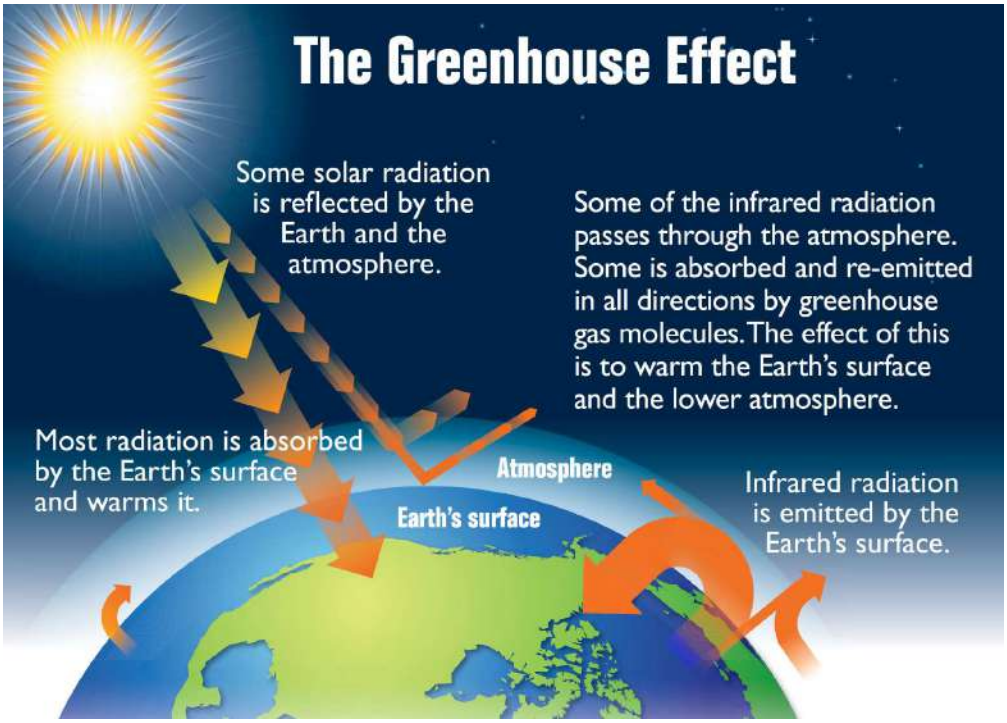


Source: US EPA (2012), https://energyeducation.ca/encyclopedia/Greenhouse_effect.

The founding text of the greenhouse effect is a French scientific publication written by Joseph Fourier in 1824: *Remarques générales sur les températures du globe terrestre et des espaces planétaires*[1]. Using some theoretical mathematical models he had developed earlier, Fourier (1824) calculated that the Earth should not be as warm as it is, given its distance from the sun and its size. He then defined the various sources of heat on the Earth's surface:

> "*The heat of the Earth's surface derives from three sources, which must first be distinguished:*

[1] *General Remarks on Global and Planetary Temperatures.*

1. *The Earth is heated by the sun's rays, whose uneven distribution produces the diversity of climates.*
2. *The Earth's temperature depends on the common temperature of planetary spaces, as it is exposed to the irradiation of the innumerable stars that surround the solar system on all sides.*
3. *The earth has retained within its mass some of the primitive heat it contained when the planets were formed.*"

He showed that the third effect is not significant and that the heat on the Earth's surface comes mainly from the sun (first factor). He distinguished luminous heat[2] ("*chaleur lumineuse*") and dark radiant heat[3] ("*chaleur rayonnante obscure*"), and explained that the difference between the two types of heat is due to the presence of the atmosphere. Joseph Fourier also referred to the work of the Swiss physicist and geologist Horace Bénédict de Saussure. In 1774, Saussure found that exposing a dark box with a pane of glass to the sun increased the temperature inside the box by several degrees compared to the temperature outside in the shade. He named this phenomenon "*l'effet de serre*" (the greenhouse effect in English). For Joseph Fourier, the interposition of the atmosphere is responsible for this greenhouse effect and is the factor that keeps the planet warmer because "*heat in the state of light meets with less resistance in penetrating the air than in returning to the air when it is converted into non-luminous heat.*"

Pouillet (1838) developed a pyrheliometer to measure the solar irradiance at the surface as a function of the atmospheric air mass. He found that the solar constant $S_0$ is equal to 1 230 $Wm^{-2}$, while the current estimate is about 1 368 $Wm^{-2}$. He also estimated the temperature in space to be −142°C. In fact, the temperature in space approaches absolute zero (or −273°C). According to NASA[4], it can reach 120°C during the lunar day at the moon's equator and drop to −130°C at night. At the moon's poles, temperatures can drop even lower, reaching −250°C. Like Joseph Fourier, Claude Pouillet explained that the greater absorption of the sun's rays and the relatively small variations in temperature were mainly due to the atmospheric stratum.

John Tyndall's work marks a new milestone. As an experienced mountaineer with a passion for glacier formation and melting, he studied climate-induced changes in the ice caps. In 1859, Tyndall showed that water vapor has a high heat absorption capacity. He went on to show that carbon dioxide and other gases could also absorb and radiate heat. Tyndall was not only interested in theory and equations, he also carried out many experiments to calculate the heat capacity of many gases using a measuring device based on thermopile technology. He realized the implications of his findings for climate change[5]:

> "*De Saussure, Fourier, Pouillet, and Hopkins regard this interception of the terrestrial rays as exercising the most important influence on climate. Now if, as the above experiments indicate, the chief influence be exercised by the aqueous vapour, every variation of this constituent must produce a change of climate. Similar remarks would apply to the carbonic acid diffused through the air; while an almost inappreciable admixture of any of the hydrocarbon vapours would produce great effects on the terrestrial rays and produce corresponding changes of climate. It is not therefore necessary to assume alterations in the density and height of the atmosphere, to account for different amounts of heat being preserved to the earth at different times; a slight change in its variable*

[2]This corresponds to the ultra-violet light.
[3]This corresponds to the thermal infrared radiation.
[4]See https://science.nasa.gov/mission/lro.
[5]Carbonic acid was the historical name given to $CO_2$ in the nineteenth century.

> *constituents would suffice for this. Such changes in fact may have produced all the mutations of climate which the researches of geologists reveal. However this may be, the facts above cited remain; they constitute true causes, the* extent *alone of the operation remaining doubtful.*" (Tyndall, 1861, pages 28-29).

Tyndall is the first scientist to prove that greenhouse gases exist and are responsible for the greenhouse effect.

In fact, Tyndall was not the first to discover the existence of greenhouse gases. Three years earlier, in 1856 and 1857, the American scientist Eunice Newton Foote had published two research papers with experiments showing that water vapor and carbon dioxide absorb heat from solar radiation. However, her work was forgotten until it was rediscovered by Raymond Sorenson in 2011. Foote's work led to debates about the paternity of greenhouse gases (Ortiz and Jackson, 2022).

Figure 8.2: The pioneers of the greenhouse effect

Joseph Fourier
(1766–1830)

Eunice Newton Foote
(1819–1888)

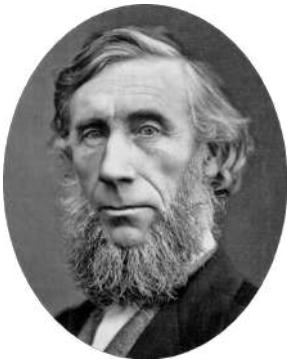

John Tyndall
(1820–1893)

Svante Arrhenius
(1859–1927)

Svante Arrhenius was the first scientist to calculate the effect of a change in atmospheric $CO_2$ on ground temperature. Svante Arrhenius (1859–1927) was a renowned Swedish chemist who won the Nobel Prize[6] in Chemistry in 1903 for his ionic dissociation theory. In 1896, he argued that variations in atmospheric carbon dioxide could significantly affect the Earth's heat balance. Making extensive use of the empirical works of Knut Ångström, Alexander Buchan, F. Paschen, Charles Pouillet, and especially the data collected by Samuel Pierpont Langley, he came to the following conclusion:

> "*We may now inquire how great the variation of the carbonic acid in the atmosphere be to cause a given change of the temperature. [...] Thus if the quantity of carbonic acid increases in geometric progression, the augmentation of the temperature will increase nearly in arithmetic progression.*" (Arrhenius, 1896, Section IV, pages 265-267).

This rule has often been interpreted to mean that a doubling of the $CO_2$ concentration leads to an increase in the average global temperature of about 5°C. This is the first time that an estimate of

[6] Arrhenius was involved in the establishment of the Nobel Institute from 1901, when he was elected a member of the Royal Swedish Academy of Sciences. From that year he was a member of the Nobel Committee for Physics and also for Chemistry. When the Nobel Institute for Physical Research was established in Stockholm in 1905, he was appointed rector of the Institute, a position he held until 1927. Svante Arrhenius is credited with many stories and intrigues about the awarding or not of the Nobel Prize, including the conflicts he had with Paul Ehrlich (theory of immunology) and Dmitri Mendeleev (periodic table of elements).

climate sensitivity has been calculated[7]. In the final section, devoted to the geological consequences, his calculations showed that:

> "*One may now ask, How much the carbonic acid vary according to our figures, in order that the temperature should attain the same values as in the Tertiary and Ice ages respectively? A simple calculation shows that the temperature of the Arctic regions would rise about* 8°C *to* 9°C*, if the carbonic acid increased* 2.5 *or* 3 *times its present value. In order to get the temperature of the ice age between the 40th and 50th parallels, the carbonic acid in the air should sink to* 0.62–0.55 *of present value (lowering the temperature* 4°C–5°C*).*" (Arrhenius, 1896, Section V, page 268).

The last part of the article is remarkable. He discussed the work of his friend and colleague Arvid Hogborm (1857–1940) on the influence of natural carbon dioxide cycles on the Earth's ice ages. In particular, he argued that these cycles were a much better explanation of climate change on a geological scale than the theory of James Croll (1821–1890), who assumed that it was due to the variations in the Earth's orbit[8]. He also discussed the impact of human activity on the concentration of $CO_2$ in the atmosphere, and in particular the impact of coal mining and production.

While Arrhenius studied only the heat absorption capacity of $CO_2$, Tyndall calculated the heat power of several gases: water vapor, carbon dioxide, oxygen, nitrogen, hydrogen, nitrous oxide, etc. However, Tyndall assumed that water vapor was the main contributor to the greenhouse effect and that the effect of carbon dioxide was negligible. We now know that this is not true. Since the 1970s, many scientific studies have been carried out to investigate the other greenhouse gases and their effects on the environment and global warming. Ozone has received much attention (World Meteorological Organization, 1982), followed by chlorofluorocarbons or CFCs (Ramanathan, 1975), nitrates and sulfates. The survey of Ramanathan *et al.* (1985) summarizes the state of scientific knowledge in the 1980s. It was at this point that a number of scientists began to reintroduce methane as a growing threat to climate change. For example, Kvenvolden (1988) analyzed the process of permafrost warming and methane release from gas hydrates and possible destabilization in the Arctic.

Table 8.1: List of greenhouse gases

| Greenhouse gas | Formula | Kyoto Protocol |
|---|---|---|
| Water vapor | $H_2O$ | |
| Carbon dioxide | $CO_2$ | ✓ |
| Methane | $CH_4$ | ✓ |
| Nitrous oxide | $N_2O$ | ✓ |
| Ozone | $O_3$ | |
| | Fluorinated or F-gases | |
| Sulfur hexafluoride | $SF_6$ | ✓ |
| Nitrogen trifluoride | $NF_3$ | ✓ |
| Chlorofluorocarbons | CFCs (CFC-11, CFC-12, etc.) | |
| Hydrofluorocarbons | HFCs (HFC-23, HFC-32, etc.) | ✓ |
| Hydrochlorofluorocarbons | HCFCs (HCFC-12, etc.) | |
| Perfluorocarbons | PFCs ($CF_4$, $C_2F_6$, etc.) | ✓ |

[7]Climate sensitivity measures the global temperature increase that will occur in response to a doubling of atmospheric $CO_2$ concentrations compared to pre-industrial levels.

[8]Today it is accepted that the two theories co-exist and explain the phenomenon of global glaciation (Hays *et al.*, 1976; Delmas *et al.*, 1980).

### Global warming

The discovery of the greenhouse effect implies that the temperature of the Earth depends on the concentration of greenhouse gases in the atmosphere. It does not mean that we are observing a global warming of the Earth, and even less that this global warming is due to human activities. For that, we need to show that the concentration of greenhouse gases has recently increased due to human influence. We also need to calculate the net effect of each gas. For example, the loss of ozone that we have observed in the lower stratosphere has a cooling effect on the Earth's surface, while the increase in ozone that has occurred in the troposphere has a warming effect on the Earth's surface.

Guy Stewart Callendar was a British steam engineer. In 1938, he linked the increased burning of fossil fuels to rising global temperatures. He compiled weather data and estimated a global temperature increase of about 0.25°C over the last fifty years. He also showed that the concentration of $CO_2$ in the atmosphere had increased by 10% during the same period, and he argued that this rising carbon dioxide content of the atmosphere was due to the burning of fossil fuels. Thus was born the "*Callendar Effect*", which links global warming to man's artificial production of carbon dioxide:

> "*By fuel combustion man has added about 150 000 million tons of carbon dioxide to the air during the past half century. The author estimates from the best available data that approximately three quarters of this has remained in the atmosphere. The radiation absorption coefficients of carbon dioxide and water vapour are used to show the effect of carbon dioxide on sky radiation. From this the increase in mean temperature, due to the artificial production of carbon dioxide, is estimated to be at the rate of* 0.003°C *per year at the present time. The temperature observations at zoo meteorological stations are used to show that world temperatures have actually increased at an average rate of* 0.005°C *per year during the past half century.*" (Callendar, 1938, page 223).

Guy Stewart Callendar, however, thought that this was not a bad thing. Like Svante Arrhenius[9], he believed that higher temperatures would be beneficial to civilization:

> "*In conclusion it may be said that the combustion of fossil fuel [...] is likely to prove beneficial to mankind in several ways, besides the provision of heat and power. For instance the above mentioned small increases of mean temperature would be important at the northern margin of cultivation, and the growth of favourably situated plants is directly proportional to the carbon dioxide pressure [...] In any case the return of the deadly glaciers should be delayed indefinitely.*" (Callendar, 1938, page 236).

According to Archer and Pierrehumbert (2011) (Table 8.1), three major research papers were written in the fifties. First, from 1956, the Canadian physicist Gilbert Norman Plass published a series of papers on the absorption of infrared radiation. His work confirmed that more carbon dioxide

[9]Thirty years earlier, in his book *Worlds in the Making: The Evolution of the Universe*, Arrhenius argued that a rise in global temperature could be beneficial to agriculture, providing more food for the world's population:

> "*We often hear lamentations that the coal stored up in the earth is wasted by the present generation without any thought of the future, and we are terrified by the awful destruction of life and property which has followed the volcanic eruptions of our days. We may find a kind of consolation in the consideration that here, as in every other case, there is good mixed with the evil. By the influence of the increasing percentage of carbonic acid in the atmosphere, we may hope to enjoy ages with more equable and better climates, especially as regards the colder regions of the earth, ages when the earth will bring forth much more abundant crops than at present, for the benefit of rapidly propagating mankind.*" (Arrhenius, 1908, Chapter II, page 63).

Box 8.1: The collected papers on global warming by David Archer and Raymond Pierrehumbert (1800–1980)

- 1824
  On the Temperatures of the Terrestrial Sphere and Interplanetary Space (Fourier)
- 1861
  On the Absorption and Radiation of Heat by Gases and Vapours, and on the Physical Connexion of Radiation, Absorption, and Conduction (Tyndall)
- 1896
  On the Influence of Carbonic Acid in the Air upon the Temperature of the Ground (Arrhenius)
- 1938
  The Artificial Production of Carbon Dioxide and its Influence on Temperature (Callendar)
- 1956
  The Influence of the $15\mu$ Carbon-dioxide Band on the Atmospheric Infra-red Cooling Rate (Plass)
- 1957
  Carbon Dioxide Exchange Between Atmosphere and Ocean and the Question of an Increase of Atmospheric $CO_2$ during the Past Decades (Revelle and Suess)
- 1958
  Distribution of Matter in the Sea and Atmosphere: Changes in the Carbon Dioxide Content of the Atmosphere and Sea due to Fossil Fuel Combustion (Bolin and Eriksson)
- 1960
  The Concentration and Isotopic Abundances of Carbon Dioxide in the Atmosphere (Keeling)
- 1967
  Thermal Equilibrium of the Atmosphere with a Given Distribution of Relative Humidity (Manabe and Wetherald)
- 1969
  The Effect of Solar Radiation Variations on the Climate of the Earth (Budyko)
  A Global Climatic Model Based on the Energy Balance of the Earth-Atmosphere System (Sellers)
- 1970
  Is Carbon Dioxide from Fossil Fuel Changing Man's Environment? (Keeling)
- 1972
  Man-Made Carbon Dioxide and the Greenhouse Effect (Sawyer)
- 1975
  The Effects of Doubling the $CO_2$ Concentration on the Climate of a General Circulation Model (Manabe and Wetherald)
- 1977
  Changes of Land Biota and Their Importance for the Carbon Cycle (Bolin)
  Neutralization of Fossil Fuel $CO_2$ by Marine Calcium Carbonate (Broecker and Takahashi)
- 1979
  Carbon Dioxide and Climate: A Scientific Assessment (Charney, Arakawa, Baker *et al.*)

Source: Archer and Pierrehumbert (2011).

Box 8.2: The collected papers on global warming by David Archer and Raymond Pierrehumbert (1980–2005)

- 1984
  Climate Sensitivity: Analysis of Feedback Mechanisms (Hansen, Lacis, Rind *et al.*)
- 1985
  Evidence From Polar Ice Cores for the Increase in Atmospheric $CO_2$ in the Past Two Centuries (Neftel, Moor, Oeschger and Stauffer)
- 1986
  Global Temperature Variations Between 1861 and 1984 (Jones, Wigley and Wright)
- 1987
  Vostok Ice Core Provides 160,000-Year Record of Atmospheric $CO_2$ (Barnola, Raynaud, Korotkevich and Lorius)
- 1990
  Observational Constraints on the Global Atmospheric $CO_2$ Budget (Tans, Fung and Takahashi)
- 1991
  Abrupt Deep-Sea Warming, Palaeoceanographic Changes and Benthic Extinctions at the End of the Palaeocene (Kennett and Stott)
- 1992
  Effects of Fuel and Forest Conservation on Future Levels of Atmospheric Carbon Dioxide (Walker and Kasting)
- 1995
  Climate Response to Increasing Levels of Greenhouse Gases and Sulphate Aerosols (Mitchell, Johns, Gregory and Tett)
- 1999
  Northern Hemisphere Temperatures During the Past Millennium: Inferences, Uncertainties, and Limitations (Mann, Bradley and Hughes)
- 2000
  Acceleration of Global Warming Due to Carbon-Cycle Feedbacks in a Coupled Climate Model (Cox, Betts, Jones, Spall and Totterdell)
  Reduced Calcification of Marine Plankton in Response to Increased Atmospheric $CO_2$ (Riebesell, Zondervan, Rost *et al.*)
- 2002
  Surface Melt-Induced Acceleration of Greenland Ice-sheet Flow (Zwally, Abdalati, Herring *et al.*)
- 2003
  Anthropogenic Carbon and Ocean pH (Caldeira and Wickett)
- 2004
  Contribution of Stratospheric Cooling to Satellite-Inferred Troposphoric Temperature Trends (Fu, Johanson, Warren and Seidel)
- 2005
  Earth's Energy Imbalance: Confirmation and Implications (Hansen, Nazarenko, Ruedy *et al.*)

Source: Archer and Pierrehumbert (2011).

would have a warming effect and showed that: (1) a doubling of $CO_2$ would warm the planet by 3.6°C; (2) halving the amount of $CO_2$ would reduce the surface temperature by 3.8°C; (3) human activities have increased the concentration of $CO_2$ in the atmosphere at a rate of 30% per century; (4) this increase implies a warming of 1.1°C per century (Plass, 1956, pages 152-153). Secondly, Revelle and Suess (1957) showed that the average lifetime of a $CO_2$ molecule in the atmosphere before it is dissolved in the ocean is of the order of 10 years. The resistance to atmospheric carbon dioxide being absorbed by the surface layer of the ocean is known as the "*buffer factor*" or "*Revelle factor*". They concluded that most of the $CO_2$ released by artificial fuel combustion since the beginning of the industrial revolution must have been absorbed by the oceans. However, they felt that the exponential increase in industrial fuel combustion could pose a problem in the future and dramatically increase atmospheric $CO_2$. The mechanism of the ocean's buffering capacity was explored in a third research paper by Bolin and Eriksson (1958), who developed a dynamic model of atmosphere-ocean interactions with respect to $CO_2$. They estimated that the upper ocean must have absorbed less than 10% of fossil fuel emissions and acted as a barrier to the transport of $CO_2$ to the deep ocean. They concluded that if industrial production continues to rise, atmospheric $CO_2$ is likely to increase by 25% by the end of the century. In addition to the impact of $CO_2$ on ocean acidification, they highlighted the impact of land use and biosphere:

> "*Because of the small buffering effect of the sea it seems likely that the biosphere on land may play a more important role for the changes actually occurring in the atmosphere due to the release of $CO_2$ by combustion than previously believed.*" (Bolin and Eriksson, 1958, page 130).

In Revelle and Suess (1957), the authors concluded that "*present data on the total amount of $CO_2$, in the atmosphere, on the rates and mechanisms of $CO_2$, exchange between the sea and the air and between the air and the soils, and on possible fluctuations in marine organic carbon, are insufficient to give an accurate base line for measurement of future changes in atmospheric $CO_2$.*" Several initiatives were launched in the 1950s, particularly in Scandinavia. However, the data collected were extremely noisy and the $CO_2$ measurements were not stable. Roger Revelle invited Charles David Keeling to join the Scripps Institution of Oceanography (SIO) in 1956. Keeling received his Ph.D. in chemistry from Northwestern University in 1953 and was a postdoctoral fellow in geochemistry at CalTech until 1956, where he developed a stable instrument capable of measuring carbon dioxide in atmospheric samples. He decided to install his equipment in Antarctica (Little America), California (La Jolla) and on the Mauna Loa volcano in Hawaii and started collecting carbon dioxide samples in 1958. In 1960, he published a first report and tabulated the monthly average concentrations of atmospheric $CO_2$ at the three stations. He concluded that there were strong seasonal variations in $CO_2$ levels in the northern hemisphere (La Jolla, California and Mauna Loa, Hawaii), and a small but persistent increase in concentration was found in Antarctica (Keeling, 1960, page 200). In 1961, he presented new data showing a steady increase in $CO_2$ levels and introduced the famous "*Keeling curve*", a measurement of atmospheric carbon dioxide concentration made at Mauna Loa since 1958 (Keeling, 1978). The data was collected by Keeling until his death in 2005, and then by his son. The current version of the Keeling curve is shown in Figure 8.3. In March 1958, the $CO_2$ concentration was equal to 315.71 ppm[10] or 611.8 mg/m$^3$. The limit of 400 ppm was reached in February 2015. In June 2023, the measure was 423.39 ppm or 820.5 mg/m$^3$.

In the 1960s, a small number of scientists developed simple mathematical models of the planet's climate system. After completing his PhD at the University of Tokyo in 1959, Syukuro Manabe

[10]One part per million (ppm) denotes one part per $10^6$ parts. It is equal to $10^{-6}$. So one milliliter of gas in 1 000 liters of air would be 1 ppm.

Figure 8.3: Keeling curve: monthly mean $CO_2$ concentration in Mauna Loa (1958–2023)

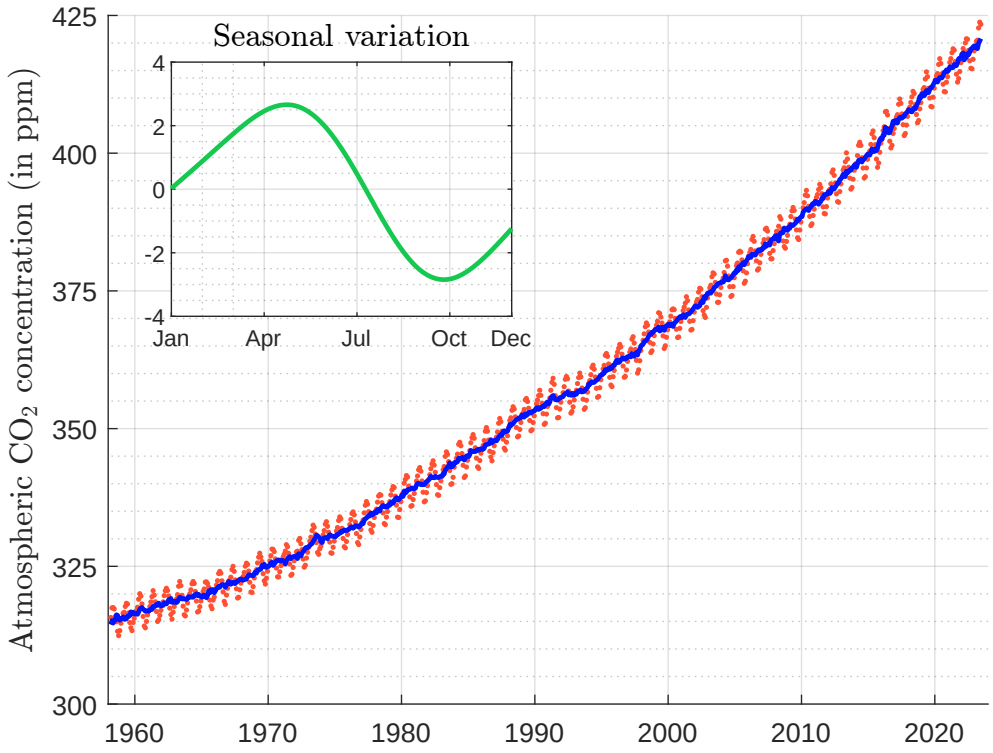


Source: Keeling *et al.* (2001) and https://scrippsco2.ucsd.edu.

went to the United States to work at the National Oceanographic and Atmospheric Administration (NOAA). Together with co-authors, Manabe published several research papers in 1961, 1964 and 1965 to develop a climate model. With the help of computer simulations, Manabe and Wetherald (1967) were able to obtain a first, but basic, model for predicting temperature by incorporating the hydrologic cycle (convective adjustment, feedback effect of water vapor, distribution of humidity, cloudiness). They found that as the concentration of carbon dioxide in the atmosphere increases, the temperature at the Earth's surface and in the troposphere rises, while it falls in the stratosphere. They also estimated the climate sensitivity to be between 1.3°C and 2.3°C. Manabe continued his research in the seventies and eighties. He and Kirk Bryan developed a general circulation model (GCM) and published the results in 1969. Manabe and Wetherald later used this original model to simulate the first three-dimensional experiment to test the idea of global warming. Their results were published in 1975.

In 2021, Syukuro Manabe and Klaus Hasselmann were awarded the Nobel Prize for their work on climate models. Klaus Hasselmann is a German oceanographer. He is known for his stochastic prediction model of climate change (Hasselmann, 1976; Frankignoul and Hasselmann, 1977). In fact, weather and climate forecasting has a long history, beginning with the book of Richardson (1922). However, it was the development of digital computers that accelerated the science of weather forecasting. Using the pioneering ENIAC computer and with the help of John von Neumann, Jules Charney and his team created a two-dimensional weather simulation model (Charney *et al.*, 1950), but the first general circulation model (GCM) is generally attributed to Phillips (1956). A GCM is a mathematical representation of the interactions between the components of the climate system (atmosphere, land surface, ocean and sea ice). In addition to the works of Manabe and Hasselmann,

we can also cite the research of Mikhail Budyko (1920–2001) and William Sellers (1928–2014), who introduced energy balance models[11] and warned of how positive and negative feedbacks (*i.e.*, loops of mutually reinforcing effects) could amplify human impacts on the global climate. In particular, Budyko (1969) and Sellers (1969) developed two models of catastrophic ice-albedo feedbacks. Today, these feedback loops are fully integrated into GCMs, and dozens of teams around the world use sophisticated GCM models and supercomputers to predict weather and climate change[12]. Another milestone was the Charney Report, *Carbon Dioxide and Climate: A Scientific Assessment*, prepared for the American Academy of Sciences, whose conclusions were presented to President Carter in 1979. On July 23-27, 1979, Jule Charney formed a study group to "*assess the scientific basis for projection of possible future climatic changes resulting from man-made releases of carbon dioxide into the atmosphere*" (Charney *et al.*, 1979, page iv). The study group had 13 members, including eminent scientists Akio Arakawa, Bert Bolin, Henry Stommel, etc. The report examined the results of five global climate models that simulate the climatic response to an increase in atmospheric CO2: three by Manabe and his colleagues at NOAA's Geophysical Fluid Dynamics Laboratory and two by James Hansen and his colleagues at NASA's Goddart Institute for Space Studies. The report estimated a climate sensitivity of 3°C, with an error of ±1.5°C.

Figure 8.4: The fathers of the concept of global warming

Guy Stewart Callendar (1898–1964) | Roger Revelle (1909–1991) | Charles David Keeling (1928–2005) | Wallace Broecker (1931–2019)

The term "*global warming*" was popularized by Broecker (1975). Wallace Broecker was a famous American geochemist and the author of more than 500 scientific articles and many books. His works on the role of the ocean in climate change, the global ocean circulation map, radiocarbon dating, etc. are considered the foundation of carbon cycle science. While the term global warming appears less than 10 times before 1975, many research papers will use the term extensively after Broecker's publication. Between 1975 and 1980, more than 2 500 scientific articles made reference to global warming. In the 1980s, Broecker and other scientists warned politicians about the dangers of climate change. In 1984, for example, Broecker testified at the Congressional hearing on climate change, declaring that carbon dioxide was the number one long-term environmental problem. On

[11] Scientists distinguish between Energy Balance Models (EBM), Earth System Models of Intermediate Complexity (EMIC), and General Circulation Models (GCM), from the simplest to the most complex. However, the distinction between these climate models is generally not obvious.

[12] Nowadays, GCMs are generally classified into three types of families: (1) Atmospheric General Circulation Model (AGCM), (2) Oceanic General Circulation Model (OGCM), and (3) Atmosphere-Ocean General Circulation Model (AOGCM).

June 23, 1988, James Hansen was invited to another Congressional hearing on climate change[13], organized by Senator Al Gore, and stated[14]:

> "*Mr. Chairman and committee members, thank you for the opportunity to present the results of my research on the greenhouse effect which has been carried out with my colleagues at the NASA Goddard Institute for Space Studies. I would like to draw three main conclusions. Number one, the earth is warmer in 1988 than at any time in the history of instrumental measurements. Number two, the global warming is now large enough that we can ascribe with a high degree of confidence a cause and effect relationship to the greenhouse effect. And number three, our computer climate simulations indicate that the greenhouse effect is already large enough to begin to affect the probability of extreme events such as summer heat waves.*"

So in the late eighties, climate change began to become a political issue. In 1988, the United Nations Environment Programme (UNEP) and the World Meteorological Organization (WMO) established the Intergovernmental Panel on Climate Change (IPCC) to provide policy makers with regular scientific assessments of climate change, its impacts and potential future risks, and to recommend options for adaptation and mitigation. Twenty years later, the IPCC and Al Gore were awarded the 2007 Nobel Peace Prize.

**Remark 75** *The reader who wants to go further and delve into the history of climate change research will find a vast amount of material and references on the website developed by Weart (2023): https://history.aip.org/climate/index.htm. The PDF version of the contents has more than 350 pages. Among the thirty sections, the most interesting are: Introduction and Summary, The Carbon Dioxide Greenhouse Effect, Roger Revelle's Discovery, General Circulation Models of Climate, and Past Climate Cycles: Ice Age Speculations.*

### 8.1.2 From the Holocene to the Anthropocene?

#### Definition

The Anthropocene is a proposed geological epoch that dates from the beginning of significant human impacts on Earth's geology and ecosystems, including but not limited to human-induced climate change. The Earth was formed 4.6 billion years ago. Its history can be traced using the geologic time scale (GTS) shown in Figure 8.5. Earth's history is divided into five subdivisions: eon, era, period, epoch, and age. The first three eons (Hadean, Archean and Proterozoic) can be grouped into a supereon called the Precambrian (covering the first 4 billion years). The Phanerozoic runs from the Cambrian to the present. We are in the Cenozoic era, Quaternary period, Holocene epoch and Meghalayan age. It is on the scale of ages that the question of the transition from the Holocene to the Anthropocene is currently being asked.

According to Lewis (2015), the term Anthropocene was popularized by Paul Crutzen[15] and Eugene Stoermer[16] in 2000 (Crutzen and Stoermer, 2000). In 2009, the Anthropocene Working

[13] Other scientists attended this congressional hearing, notably future lead authors for chapters of IPCC reports: Syukuro Manabe, Michael Oppenheimer, Professor at Princeton University, and William Moomaw, Professor at Tufts University.

[14] Source: https://babel.hathitrust.org/cgi/pt?id=uc1.b5127807, pages 39-41.

[15] Paul Crutzen (1933–2021) was awarded the 1995 Nobel Prize in Chemistry for his work in atmospheric chemistry, and in particular for his efforts to study the formation and decomposition of atmospheric ozone.

[16] Eugene Stoermer (1934–2012) was a professor of biology who specialized in the study of freshwater species and diatoms.

Figure 8.5: Geologic time scale

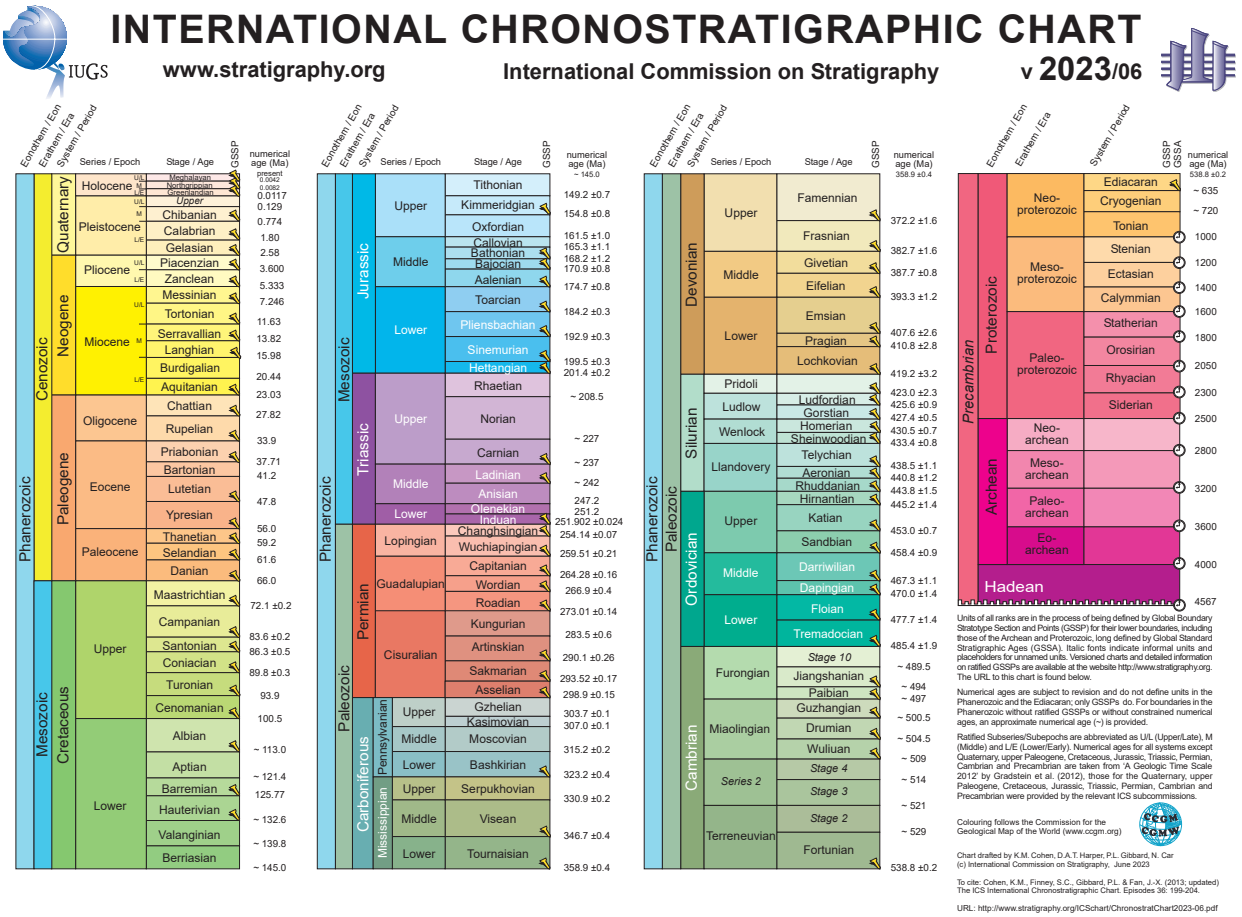


Source: International Commission on Stratigraphy (2023), https://stratigraphy.org/chart.

Group (AWG) was established as part of the quaternary stratigraphy subcommission[17], a constituent body of the International Commission on Stratigraphy (ICS). In 2019, the AWG agreed to submit a formal proposal to the ICS to establish the Anthropocene epoch, but the Anthropocene has not yet been ratified by the ICS. Indeed, the definition of the Anthropocene as a geological epoch rather than a geological event remains controversial and difficult. For example, scientists do not agree on the starting point of this epoch, known as the Global Stratotype Section and Point or GSSP. Lewis (2015) listed nine potential start dates[18]: (1) Megafauna extinction, 50 000–10 000 yr BP; (2) Origin of farming, ∼11 000 yr BP, (3) Extensive farming, ∼8 000 yr BP to present (4) Rice production, 6 500 yr BP to present; (5) Anthropogenic soils, ∼3 000–500 yr BP; (6) New-old world collision, 1 492–1 800; (7) Industrial Revolution, 1 760 to present; (8) Nuclear weapon detonation, 1 945 to present; (9) Persistent industrial chemicals, ∼1 950 to present. In 2016, the AWG proposed that the Anthropocene began in the 1950s, while in 2023 it chose Crawford Lake in Ontario, Canada, to best capture the geological impact of the Anthropocene. According to Waters *et al.* (2016), the effects of human impact are diverse and of different types. They listed several lines of evidence: the

[17]The AWG website is http://quaternary.stratigraphy.org/working-groups/anthropocene.

[18]In the calendar marking system, BP is "*Before Present*", while BC is "*Before Christ*". According to standard practice, the present is set to 1950 Anno Domini (AD).

alteration of sedimentary processes, the altered geochemical signatures in recent sediments and ice, the radiogenic signatures and radionuclides in sediments and ice, the carbon cycle evidence from ice cores, the climate change and rates of sea level change since the end of the last ice age, and the loss of biodiversity. However, the debate about the status of the Anthropocene is reignited by the publication of Gibbard *et al.* (2022):

> "*Over the course of the last decade the concept of the Anthropocene has become widely established within and beyond the geoscientific literature but its boundaries remain undefined. Formal definition of the Anthropocene as a chronostratigraphical series and geochronological epoch following the Holocene, at a fixed horizon and with a precise global start date, has been proposed, but fails to account for the diachronic nature of human impacts on global environmental systems during the late Quaternary. By contrast, defining the Anthropocene as an ongoing geological* event *more closely reflects the reality of both historical and ongoing human-environment interactions, encapsulating spatial and temporal heterogeneity, as well as diverse social and environmental processes that characterize anthropogenic global changes. Thus, an Anthropocene Event incorporates a substantially wider range of anthropogenic environmental and cultural effects, while at the same time applying more readily in different academic contexts than would be the case with a rigidly defined Anthropocene Series/Epoch.*" (Gibbard *et al.*, 2022, page 395).

It is certainly too early to consider a new era explained by human activity, but it remains relevant that human activity has an impact on climate.

### Geological history of the climate

**Precambrian and the age of early life** The Earth's climate patterns change naturally on time scales ranging from decades to millions of years[19]. During the Hadean eon (4.6–4.0 Gyr BP), the planet was characterized by volcanism and asteroid impacts. It was very hot, with temperatures certainly averaging around 80°C. The Moon was formed during this period. The Archean eon (4.0–2.5 Gyr BP) is the period when life on Earth began and oceans probably formed. Carbon dioxide emissions were abundant, and this high concentration probably gave rise to the greenhouse effect. The surface temperature decreased and may have been between 0°C and 40°C (Catling and Zahnle, 2020). The Proterozoic eon lasted from 2.5 billion to 540 million years ago. This was a time of oxygen accumulation in the Earth's atmosphere. The temperature history of the Proterozoic is controversial. There is evidence that the first glaciations occurred during the Proterozoic. However, the average temperature during the Proterozoic is estimated to have been between 10°C and 30°C.

Table 8.2: Units of time

| Symbol | Definition | (in year) | Symbol | Name |
|---|---|---|---|---|
| Kyr/kyr | Thousand/Kilo years | $10^3$ | ka | Kiloannus |
| Myr/myr | Mega/Million years | $10^6$ | Ma | Megaannus |
| Gyr/byr | Giga/Billion years | $10^9$ | Ga | Gigaannus |

To estimate temperatures during the Precambrian, scientists use indirect methods, including geochemical proxies (chemical properties of rocks and minerals), paleontological studies (type and distribution of fossils and sedimentary rocks), and general circulation models. One of the most

[19] in Table 8.2, report the two time units commonly used in geology (yr vs. a, *e.g.*, Gyr vs. Ga).

Box 8.3: Faint young Sun paradox & Snowball Earth hypothesis

The faint young Sun paradox describes the apparent contradiction between observations of liquid water early in Earth's history and the astrophysical expectation that the Sun's output during the Archean eon would be only 75% as intense as it is today. If the Sun was fainter when the Earth was young, we might expect the Earth to be completely frozen, but there is evidence for the presence of liquid water on the Earth's surface at that time (Feulner, 2012). Many explanations have been proposed: ammonia, methane, reduced albedo, tidal heating, etc. However, the most credible assumption is the high concentration of carbon dioxide during this period of weaker solar radiation:

> "*[...] we argue that the faint young Sun problem for Earth has essentially been solved. Unfrozen Archean oceans were likely maintained by higher concentrations of $CO_2$, consistent with the latest geological proxies, potentially helped by additional warming processes. This reinforces the expected key role of the carbon cycle for maintaining the habitability of terrestrial planets.*" (Charnay *et al.*, 2020, page 1).

Other curious events during the Precambrian are the Proterozoic glaciations. The Snowball Earth hypothesis proposes that the planet's surface was completely or nearly completely frozen during these icehouse climates, especially between 750 and 550 Ma (Hoffman *et al.*, 1998; Hoffman and Schrag, 2002). The Snowball Earth hypothesis can be explained by a runaway ice-albedo feedback. Albedo is the fraction of sunlight reflected back into space by a surface. For example, ice and snow have a high albedo, which means they reflect a lot of sunlight. As more ice and snow cover the Earth's surface, more sunlight is reflected back into space, causing the Earth to cool. This cooling leads to more ice and snow formation, which further cools the Earth, and so on. This is the runaway ice-albedo feedback. This hypothesis is currently a topic of debate among scientists, with alternative explanations also presented in the academic literature, including the high-obliquity hypothesis and the volcanic ash hypothesis. The high-obliquity hypothesis suggests that during a glacial period, the Earth had a much larger axial tilt than it does today[a]. The result would have been a decrease in the amount of solar radiation reaching the poles and an increase in the amount of solar radiation absorbed at the equator. As a result, glaciers would have melted at the equator and ice caps would have formed at the poles. The volcanic ash hypothesis suggests that volcanic ash filled the Earth's atmosphere, resulting in a cooling effect caused by the blocking of sunlight.

[a] This explanation refers to the Milankovitch cycles, which are variations in the Earth's orbit around the Sun that affect the amount of sunlight the planet receives. The main cycles concern the shape of the Earth's ellipsoid orbit (eccentricity), the axial tilt or angle of the Earth's axis (obliquity), and the direction of the Earth's axis of rotation (precession).

common methods is the clumped isotope thermometer, which is based on the analysis of the isotopic composition of certain molecules, such as carbonate minerals. For example, we can use the ratio of the two carbon isotopes $^{12}C$ and $^{13}C$ in carbonate rocks to infer the temperature at which the rocks formed. Its definition is:

$$\delta^{13}C = 1000 \times \left( \frac{^{13}C}{^{12}C}_{\text{sample}} \Big/ \frac{^{13}C}{^{12}C}_{\text{standard}} - 1 \right) \tag{8.1}$$

The unit of $\delta^{13}$C is parts per thousand[20] (per mil or ‰). Databases of $\delta^{13}$C can be found in the permanent repository ClumpDB[21] or scientific journals that publish research papers on geological temperatures. Below we consider the Precambrian Marine Carbonate Isotope Database (PMCID) provided by Shields and Veizer (2002), which can be downloaded from `https://earthref.org/ERDA/48`. The PMCID is a compilation of strontium, carbon, and oxygen isotope compositions of about 10 000 marine carbonate rocks of Archean to Ordovician age (between 3 800 Ma and 450 Ma), and includes data from 150 published articles and books. In Figure 8.6, we have reproduced the graph of the evolution of the carbon isotopes of marine carbonate obtained by Shields and Veizer (2002). We observe a high variation of $\delta^{13}$C, which indicates that the temperatures on Earth have varied a lot during the Precambrian. This also implies a large uncertainty in the estimates, and we must be careful with the figures calculated for this period.

Figure 8.6: Carbon isotopic evolution of marine carbonate

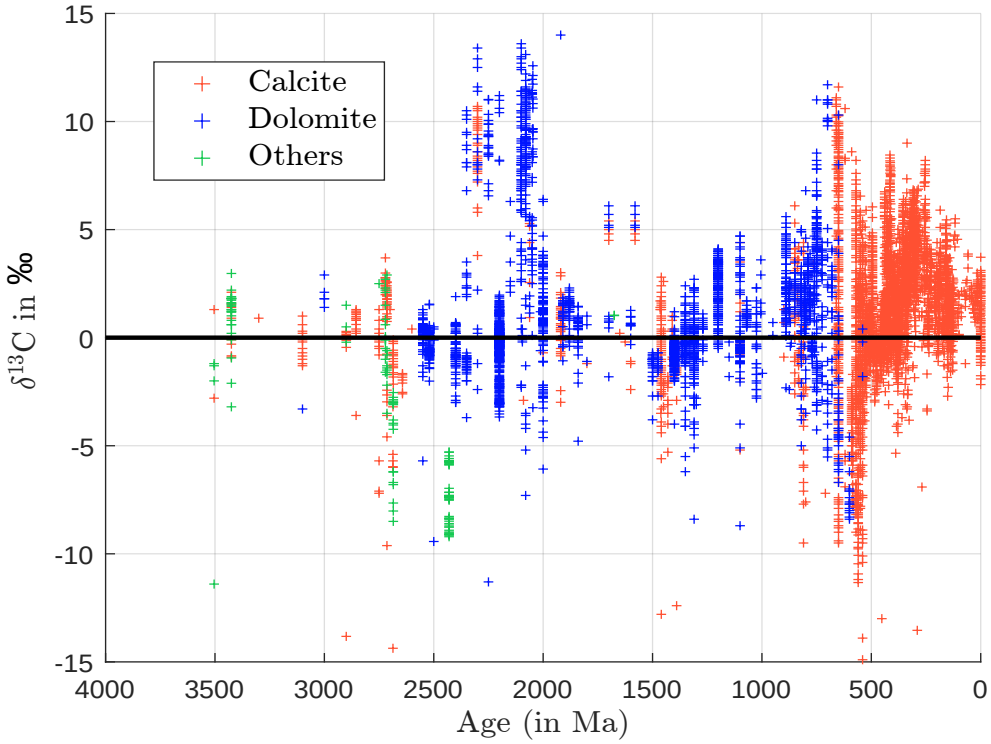


Source: Shields and Veizer (2002, Figure 2, page 5) & `https://earthref.org/ERDA/48`.

Another controversy is the Snowball Earth hypothesis presented in Box 8.3. How do we explain the massive perturbations in the carbon cycle during the Proterozoic (Figure 8.7), and how do we explain the snow and glaciers on all continents between 750 Ma and 550 Ma, when they seem to have been near the equator? Again, we must be careful because there may be multiple answers and a combination of factors. Moreover, it is difficult to imagine the time when we refer to the palaeoclimate, because the magnitude of these periods is so different from what we have experienced or learned in history, even if we consider the last 3500 years, which corresponds to the first written records. To better understand that these developments are very long, we generally use a tool called the cosmic calendar (Figure 8.8). This is a scale that maps the 13.8 billion year age of the universe

[20] The standard for $\delta^{13}$C is the Pee Dee Belemnite (PDB), which has a ratio $\frac{^{13}\text{C}}{^{12}\text{C}}$ equal to 0.011238.

[21] The web address is `www.earthchem.org/communities/clumpdb`.

Figure 8.7: Neoproterozoic carbon isotope data compilation

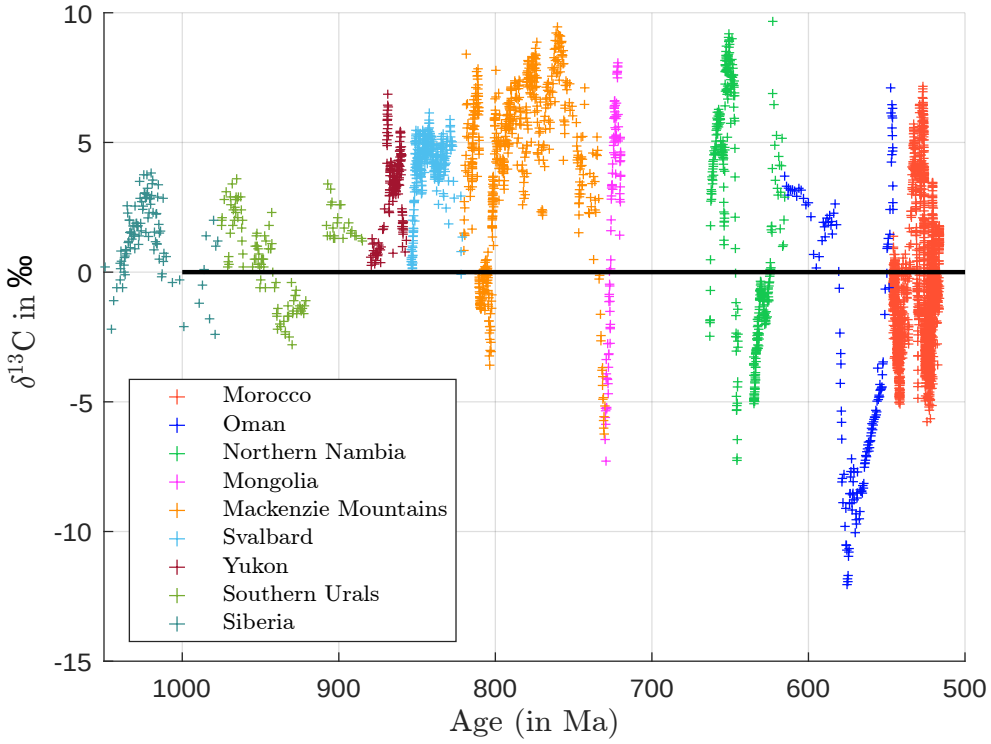


Source: Cox *et al.* (2016, Figure 2, page 90).

Figure 8.8: Cosmic calendar

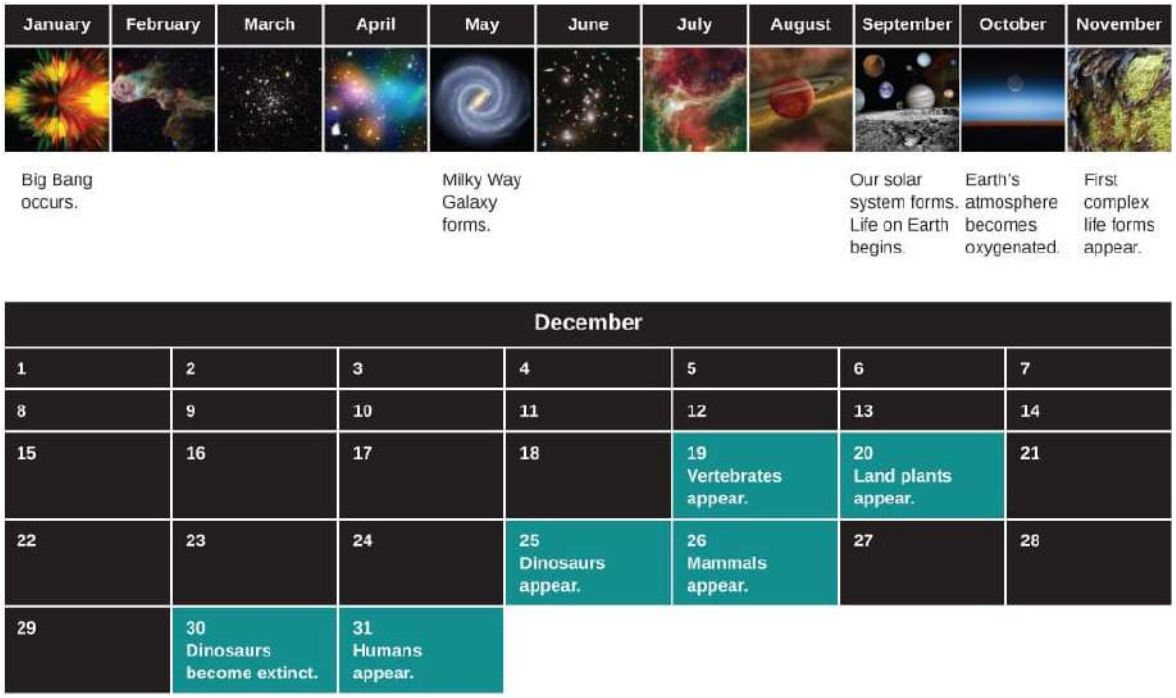


Source: https://courses.lumenlearning.com/suny-astronomy/chapter/a-conclusion-and-a-beginning.

to a single year to make it more intuitive for educational purposes. On this scale, the Big Bang took place at midnight on January 1, and the present time is mapped to midnight on December 31. The time in days is then equal to:

$$t_{\text{days}} = \left(1 - \frac{t_{\text{Ga}}}{13.797}\right) \times 365 \text{ days}$$

According to Sagan (1986), the Precambrian period begins on September 14 and ends on December 17. The first primates appear on December 29 and humans on December 31 at 22:30. They invent agriculture at 23:59:20. The invention of writing is at 23:59:45, and the voyage of Christopher Columbus takes place in the last second at 23:59:59. Modern human civilization then occurs in the last twenty minutes.

Box 8.4: Temperature scales

Three different scales are commonly used to measure temperature: Celsius, Kelvin, and Fahrenheit. Their symbols are °C, K, and °F, respectively. The Fahrenheit scale was developed by the German physicist Gabriel Fahrenheit in 1724. The Fahrenheit scale is defined by two fixed points: 32°F for the freezing point of water at sea level and 212°F for the boiling point of water at sea level. The interval between these two points is divided into 180 steps. The Celsius scale was developed by the Swedish astronomer Anders Celsius in 1742. This scale divides the interval between the two fixed points into 100 steps. The Celsius scale is also known as the centigrade scale. Finally, the Kelvin scale, developed by Lord Kelvin in 1848, is a modification of the Celsius scale in which 0 K is absolute zero. The relationships between the Celsius and Kelvin scales are $\mathcal{T}_{\circ\text{C}} = \mathcal{T}_{\text{K}} - 273.15$ and $\mathcal{T}_{\text{K}} = \mathcal{T}_{\circ\text{C}} + 273.15$. For Celsius and Fahrenheit, we have $\mathcal{T}_{\circ\text{C}} = \frac{5}{9}(\mathcal{T}_{\circ\text{F}} - 32)$ and $\mathcal{T}_{\circ\text{F}} = \frac{9}{5}\mathcal{T}_{\circ\text{F}} + 32$. Absolute zero is −273.15°C, 0 K and −459.67°F, implying that $\mathcal{T} \geq -273.15$°C, $\mathcal{T} \geq 0$ K, and $\mathcal{T} \geq -459.67$°F. The melting point (at standard pressure) is obtained at temperatures of 0°C, 273.15 K and 32°F, while the boiling point of water corresponds to temperatures of 100°C, 373.15 K and 212°F.

**Palaeoclimate during the Phanerozoic** Studying the climate of the Phanerozoic eon is generally easier than studying the Precambrian, because this period, which begins 541 million years ago, is characterized by a more abundant and diverse fossil record. In addition, we can use other materials, such as ice cores and ocean sediments. Figure 8.9 shows the global picture of temperature evolution during the Phanerozoic[22]. It was produced in 2014 by Glen Fergus, who has done a remarkable job of collecting data from a dozen published research papers[23]. It shows several episodes of hothouse scenarios and glacial cycles. The average temperature range compared to today is between −6°C and +15°C. The graph is divided into five panels. The first panel corresponds to the Palaeozoic (Cambrian, Ordovician, Silurian, Devonian, Mississippian, Pennsylvanian and Permian) and Mesozoic (Triassic, Jurassic and Cretaceous) eras. It covers the period from 541 Ma to 66 Ma. The second panel corresponds to a part of the Tertiary period and includes the Paleocene, Eocene, Oligocene and Miocene epochs (from 66 Ma to 5.3 Ma). The third and fourth panels show the average temperature of the Pliocene and Pleistocene. The Quaternary, which begins at 2.6 Ma BP, is characterised by many glaciations, while the Holocene is marked by an increase in temperature.

[22] Scientists use the Celsius, Kelvin and Fahrenheit scales indifferently. That is why we have given their definition in Box 8.4.

[23] We have removed some data from the original figure.

Figure 8.9: Earth temperature since 500 Myr BP (°C vs. 1960–1990 average)

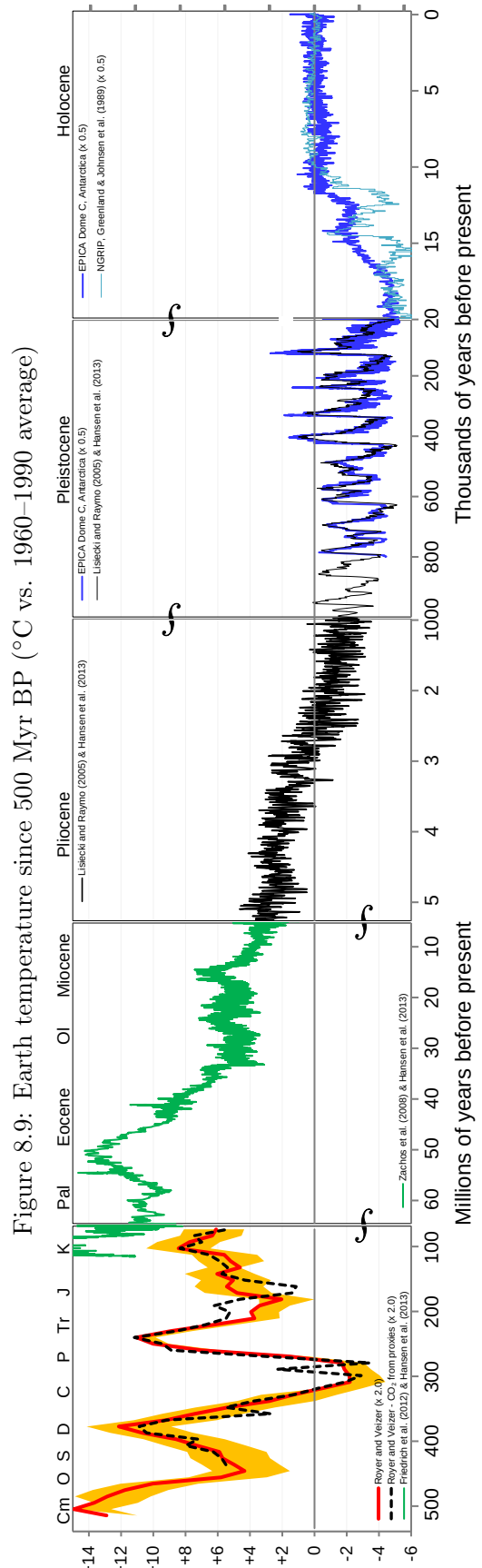


This shows estimates of global average surface air temperature over the 540 Myr of the Phanerozoic eon, since the first major proliferation of complex life forms on our planet. A major achievement of the last 30 years of climate science has been the production of a large set of actual measurements of temperature history (from physical proxies), replacing much of the earlier geological induction (*i.e.*, informed guesses). The graph shows selected proxy temperature estimates. Because many proxy temperature reconstructions indicate local rather than global temperature – or ocean rather than air temperature – considerable approximation may be involved in deriving these global temperature estimates. As a result, the relativities of some of the estimates plotted are approximate, especially the early ones. Surface air temperature is plotted as anomalies (differences) from the average over the reference interval 1960–1990 (which is about 14°C).

Time is plotted forward to the present, taken as 2015 CE. It connects five separate linearly scaled segments, expanding by about an order of magnitude at each vertical break. The first segment groups the Cambrian (C), Ordovician (O), Silurian (S), Devonian (D), Carboniferous (C), Permian (P), Triassic (Tr), Jurassic (J), and Cretaceous (K). The first break is at the Mesozoic-Cenozoic boundary (~65 Myr ago). This is the K-T boundary (called Cretaceous-Paleogene) where the dinosaurs became extinct. The second segment groups the Paleocene, Eocene, OLigocene, and Miocene. The second break is at the Miocene-Pliocene boundary (~5.3 Myr ago). The last three segments are Pliocene, Pleistocene, and Holocene. The last two breaks are at 1 Myr BP and 20 kyr BP.

Source: Glen Fergus (2014), `en.wikipedia.org/wiki/File:All_palaeotemps.png` & `https://gergs.net/all_palaeotemps-2.`

Let us know how these temperatures are estimated. To do this, we need to go back to the scientific history of climate change presented in section 8.1.1. Paleoclimate research began in the 1950s with several advances: radiocarbon dating with carbon 14, analysis of deep-sea cores and marine sediments, drilling of ice cores in Greenland and Antarctica, etc. Whichever method we use, we need two modelling tools: an age dating model and a formula that converts the calculated metric into a temperature, because the latter is not observed.

The history of ice core science is studied in Langway (2008) (2008) and Jouzel (2013). One of the first attempts to explore the interior of an ice sheet was made by Ernst Sorge during the Alfred Wegener Expedition to Eismitte in central Greenland from July 1930 to August 1931. Using a 15-meter deep pit, he investigated the individual limits of annual snow accumulation. Between 1949 and 1952, the first ice cores were extracted separately by three international research teams at depths of between 100 and 150 meters, but the quality of the ice cores was poor. With several initiatives (Site 2, Byrd Station and Little America), the period 1957–1958 is generally considered to be the starting point of ice core research (Jouzel, 2013). A new step was achieved in 1961, when the first ice core longer than 1 000 meters was taken at Camp Century. Since then, many projects have been carried out[24], but the most famous remains the ice-core drilling in Vostock, Antarctica (Petit *et al.*, 1999). Indeed, the depth record is held by the Vostock station, where scientists have drilled to a depth of 3 770 meters. In fact, it is very difficult to go beyond this figure because we reach the surface of oceans or lakes. In addition, the bottom of the ice core at very deep depths is modified by the water at the ocean surface and does not contain any palaeoclimate information.

Table 8.3: Recovered deep and very deep ice cores

| Greenland | | | Antarctica | | |
|---|---|---|---|---|---|
| Site 2 | 1956 | 305 m | Byrd Station | 1957–1958 | 307 m |
| Site 2 | 1957 | 411 m | Little America | 1958–1959 | 264 m |
| Camp Century | 1961–1966 | 1387 m | Byrd Station | 1966–1968 | 2164 m |
| Dye 3 | 1971 | 372 m | Vostock | 1990–1998 | 3623 m |
| Milcent | 1973 | 398 m | Dome Fuji | 1994–1997 | 2503 m |
| Crete | 1974 | 405 m | Vostock | 2005–2007 | 3658 m |
| Dye 3 | 1979–1981 | 2037 m | Dome Fuji | 2003–2007 | 3035 m |
| GRIP | 1989–1992 | 3029 m | Dome C | 1999–2005 | 3270 m |
| GISP 2 | 1989–1993 | 3057 m | Kohnen Station | 2001–2006 | 2774 m |
| NGRIP | 1996–2004 | 3090 m | WAIS | 2006–2011 | 3405 m |

Source: Langway (2008, Appendix A).

Analysis of trapped air bubbles in ice cores provides a direct record of the composition of the atmosphere at the time the ice formed. For example, we can measure the concentrations of greenhouse gases such as carbon dioxide and methane in the air bubbles to reconstruct past climate conditions. However, these measurements are not very robust and scientists prefer to use indirect measures. Dansgaard's seminal paper in 1964 discussed methods based on stable isotopes (Dansgaard, 1964). He defined the relative deviation $\delta$ of the heavy isotope content as follows:

$$\delta = 1000 \times \left( \frac{R_{\text{sample}} - R_{\text{standard}}}{R_{\text{standard}}} \right) \tag{8.2}$$

[24]In Table 8.3, we have listed some of these projects and the corresponding depth of the drilling. The locations of the projects are shown in Figures 8.10 and 8.11.

Figure 8.10: Greenland deep drilling sites

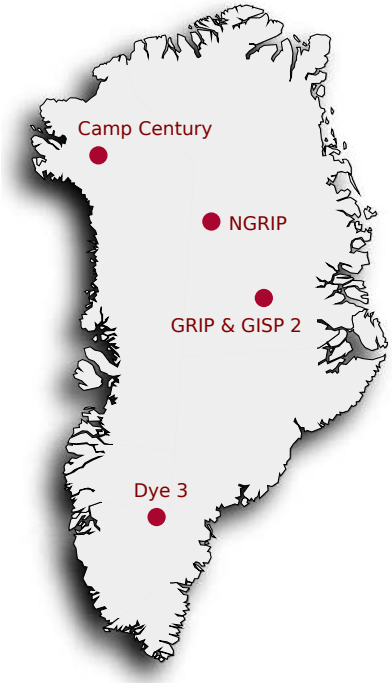


Source: Langway (2008, Appendix A), created with paintmaps.com.

Figure 8.11: Antarctica deep drilling sites

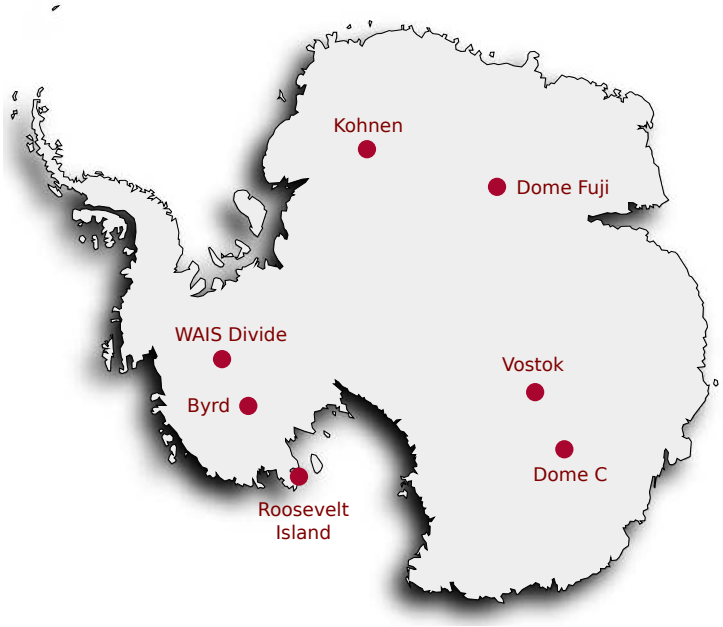


Source: Langway (2008, Appendix A), created with paintmaps.com.

Box 8.5: Isotopes of chemical elements

Isotopes are atoms of the same element. They have the same number of protons but differ in the number of neutrons. To write the symbol for an isotope, we use the standard AZE notation[a] ${}^{A}_{Z}\mathrm{E}$, where E is the chemical symbol for the element, $A$ is the atomic mass number (the total number of protons and neutrons in the nucleus of the atom) and $Z$ is the atomic number (the number of protons in the nucleus of the atom). For example, hydrogen has seven isotopes: ${}^{1}_{1}\mathrm{H}$ (protium), ${}^{2}_{1}\mathrm{H}$ or D (deuterium), ${}^{3}_{1}\mathrm{H}$ or T (tritium), ${}^{4}_{1}\mathrm{H}$, ${}^{5}_{1}\mathrm{H}$, ${}^{6}_{1}\mathrm{H}$, and ${}^{7}_{1}\mathrm{H}$. We also distinguish between stable and unstable isotopes. Stable isotopes have a stable nucleus and the forces holding the protons and neutrons together are strong enough to prevent the nucleus from decaying. The most stable isotopes have a neutron to proton ratio close to one. Unstable (or radioactive) isotopes have an unstable nucleus and they can decay into other elements. The most frequent isotope of an element is called the major (or principal) isotope. In the case of hydrogen, protium and deuterium are the two stable isotopes and protium is the main isotope, accounting for about 99.98% of all occurring hydrogen atoms. In addition to these two isotopes, five other isotopes of hydrogen are unstable. The table below lists the stable and unstable isotopes of hydrogen, carbon, oxygen and uranium. The main isotope and its abundance are also given.

| Element | Stable isotopes | Unstable isotopes | Major isotope |
|---|---|---|---|
| Hydrogen | ${}^{1}_{1}\mathrm{H}$ and ${}^{2}_{1}\mathrm{H}$ | ${}^{3}_{1}\mathrm{H}$ – ${}^{7}_{1}\mathrm{H}$ | Protium (99.98%) |
| Carbon | ${}^{12}_{6}\mathrm{C}$ and ${}^{13}_{6}\mathrm{C}$ | ${}^{8}_{6}\mathrm{C}$ – ${}^{11}_{6}\mathrm{C}$ and ${}^{14}_{6}\mathrm{C}$ – ${}^{22}_{6}\mathrm{C}$ | Carbon-12 (98.90%) |
| Oxygen | ${}^{16}_{8}\mathrm{O}$ and ${}^{18}_{8}\mathrm{O}$ | ${}^{17}_{8}\mathrm{O}$ and ${}^{19}_{8}\mathrm{O}$ – ${}^{27}_{8}\mathrm{O}$ | Oxygen-16 (99.76%) |
| Uranium | | ${}^{232}_{92}\mathrm{U}$ – ${}^{242}_{92}\mathrm{U}$ | Uranium-238 (99.27%) |

A heavy isotope is an isotope of an element that has more neutrons than the most abundant isotope. In general, heavy isotopes are more stable, and can have different chemical properties. The heavy isotopes of the previous elements are ${}^{2}_{1}\mathrm{H}$, ${}^{13}_{6}\mathrm{C}$, ${}^{18}_{8}\mathrm{O}$ and ${}^{238}_{92}\mathrm{U}$.

[a] We generally simplify the notation with ${}^{A}\mathrm{E}$ because all the isotopes of the same element have the same atomic number.

where $R$ is the absolute content. $\delta$ is measured in ‰. This is the general form of Equation (8.1) given on page 627, if we replace the ratio of the carbon isotope by $R$. As the chemical formula of water is $\mathrm{H_2O}$, climate reconstruction from ice cores is based on the analysis of hydrogen and oxygen. In the case of hydrogen, the common isotope is ${}^{1}\mathrm{H}$, while the heavy isotope is ${}^{2}\mathrm{H}$ (also called the deuterium or D). The ratio $R$ is then $\frac{{}^{2}\mathrm{H}}{{}^{1}\mathrm{H}}$ and the relative variation is written as $\delta\mathrm{D}$. In the case of oxygen, the common isotope is ${}^{16}\mathrm{O}$, while the heavy isotope is ${}^{18}\mathrm{O}$. The ratio $R$ is then $\frac{{}^{18}\mathrm{O}}{{}^{16}\mathrm{O}}$ and the relative variation is written as $\delta^{18}\mathrm{O}$. To compute $\delta\mathrm{D}$ and $\delta^{18}\mathrm{O}$, we need the standard values of ${}^{2}\mathrm{H}/{}^{1}\mathrm{H}$ and ${}^{18}\mathrm{O}/{}^{16}\mathrm{O}$. Using the standard mean ocean water (SMOW), they are equal to 0.00015576 and 0.0020052. Dansgaard (1964) assumed that the isotopic fractionation of water implies that $\delta\mathrm{D} = (8.1 \pm 0.1)\,\delta^{18}\mathrm{O} + (11 \pm 1)$ at equilibrium[25]. More generally, Merlivat and Jouzel (1979) showed that the relationship is linear: $\delta\mathrm{D} = s\,\delta^{18}\mathrm{O} + d$ where the slope $s$ and the deuterium excess $d$ may depend on several factors: temperature, latitude, humidity, etc.

[25] This relationship has already been established by Craig (1961), who found that $\delta\mathrm{D} = 8.0\,\delta^{18}\mathrm{O} + 10$. It is known as the meteroic water line.

Figure 8.12: Part of an ice core at WAIS Divide Field Camp

Source: Eli Duke, Antarctica: WAIS Divide Field Camp (Flickr), www.flickr.com/photos/80547277@N00/9518403333.

The aim of ice core analysis is to estimate the temperature function $t \longmapsto \mathcal{T}(t)$ with respect to the time age $t$. The raw analysis provides two measurements: the depth $d$ of the ice core drilling and the isotope ratio measure $\delta$, which is calculated using an instrument called an isotope ratio mass spectrometer (IRMS). We therefore observe the isotope function $d \longmapsto \delta(d)$. To obtain the temperature function, we proceed in two steps:

1. First, we transform the depth $d$ of the ice core drilling into the time age $t$:

$$t = \varphi_t(d)$$

2. We then estimate the temperature $\mathcal{T}$ associated with the isotope ratio $\delta(d)$:

$$\mathcal{T} = \varphi_{\mathcal{T}}(\delta(d))$$

Combining the two previous equations gives the desired parametric function $t \longmapsto \mathcal{T}(t)$. To illustrate the temperature reconstruction, we consider the research of Petit *et al.* (1999), who estimated the climate and atmospheric history of the past 420 000 years using the Vostok ice cores. To do this, we download the file `deutnat-noaa.txt` from https://www.ncei.noaa.gov/access/paleo-search/study/2453. Below we report a sample of this dataset:

```
# Vostok - Isotope and Gas Data and Temperature Reconstruction
#------------------------------------------------------------------------
#                World Data Service for Paleoclimatology, Boulder
#                                    and
#                     NOAA Paleoclimatology Program
#             National Centers for Environmental Information (NCEI)
#------------------------------------------------------------------------
```

```
[...]

#--------------------
# Variables format: Short_name <tab>
what, material, error, units, seasonality, data_type, detail,
method, data_format, additional_information
#  Note: the Short_name does not require a PaST term.
#
## depth_m    depth, , , meter, , ice cores;
              climate reconstructions, , , N,
## ice_ageBP  ice age, , , calendar year before present, , ice cores;
              climate reconstructions, , , N, GT4 chronology
## deltaD     delta 2H, bulk ice, , per mil SMOW, , ice cores, interpolated,
              isotope ratio mass spectrometry, N,
## deltaTS   surface temperature, delta 2H, , degree Celsius, annual, ice cores;
              climate reconstructions, anomalized, , N, linear regression; anomaly from recent
#
#--------------------
# Data:
# Data lines follow (have no #)
# Data line format - tab-delimited text, variable short name as header
# Missing_Values:
depth_m ice_ageBP deltaD deltaTS
   0        0   -438.0   0.00
   1       17   -438.0   0.00
   2       35   -438.0   0.00
   3       53   -438.0   0.00
   4       72   -438.0   0.00
   5       91   -438.0   0.00
   6      110   -438.0   0.00
   7      129   -438.0   0.00
   8      149   -442.9  -0.81
   9      170   -437.9   0.02
  10      190   -435.8   0.36
  11      211   -443.7  -0.95
  12      234   -449.1  -1.84
  13      258   -444.6  -1.09
  14      281   -442.5  -0.75
  15      304   -439.3  -0.22
  16      327   -440.9  -0.48
  17      351   -442.5  -0.75
  18      375   -436.6   0.23
  19      397   -430.0   1.33
  20      420   -435.9   0.35

[...]

3300   416872   -430.8   1.36
3301   417419   -430.3   1.43
3302   417969   -430.4   1.40
3303   418526   -431.1   1.27
3304   419095   -433.0   0.94
3305   419682   -435.5   0.51
3306   420281   -435.2   0.54
3307   420888   -436.4   0.32
3308   421507   -437.3   0.15
3309   422135   -437.6   0.08
3310   422766   -436.6   0.23
```

This dataset has four variables: depth $d$ (meter), age $t$ (yr BP), deuterium isotope ratio $\delta$D (‰) and surface temperature $\Delta T$ (°C). We have included the first 20 observations and the last 10 observations. Note that the measurement is made at every meter of the ice core. For example, the $11^{\text{th}}$ observation corresponds to a depth of 10 meters and the authors have calculated a deuterium isotope ratio $\delta$D of $-435.8$‰. Using an age dating model[26], this depth corresponds to an age of 190 years BP. Using a climate model[27], the authors obtained a surface temperature variation $\Delta\mathcal{T}$ of 0.36 degrees Celsius. In the first panel of Figure 8.13, we plot the function $d \longmapsto \delta\mathrm{D}(d)$. The maximum depth is 3 310 meters while $\delta\mathrm{D}(d)$ varies between $-500$‰ and $-400$‰. Several peaks and cycles are observed. The results of the age dating model are shown in the second panel. When the depth is less than 2 000 meters, we have a linear relationship between $d$ and the age $t$. Beyond this threshold, the function is convex. The mapping between $\delta$D and $\Delta\mathcal{T}$ depends on the model chosen. In our case, we use a linear function $\Delta\mathcal{T} = 78.2361 + 0.1794 \times \delta\mathrm{D}$, which is shown in the third panel. This gives the relationship between depth $d$ and temperature $\Delta\mathcal{T}$ in the fourth panel. Finally, the temperature function $t \longmapsto T(t)$ is shown in Figure 8.14. In Petit *et al.* (1999), this corresponds to panel b (isotopic temperature of the atmosphere) of Figure 3 on page 431.

Figure 8.13: Isotopic reconstruction of Vostok ice cores

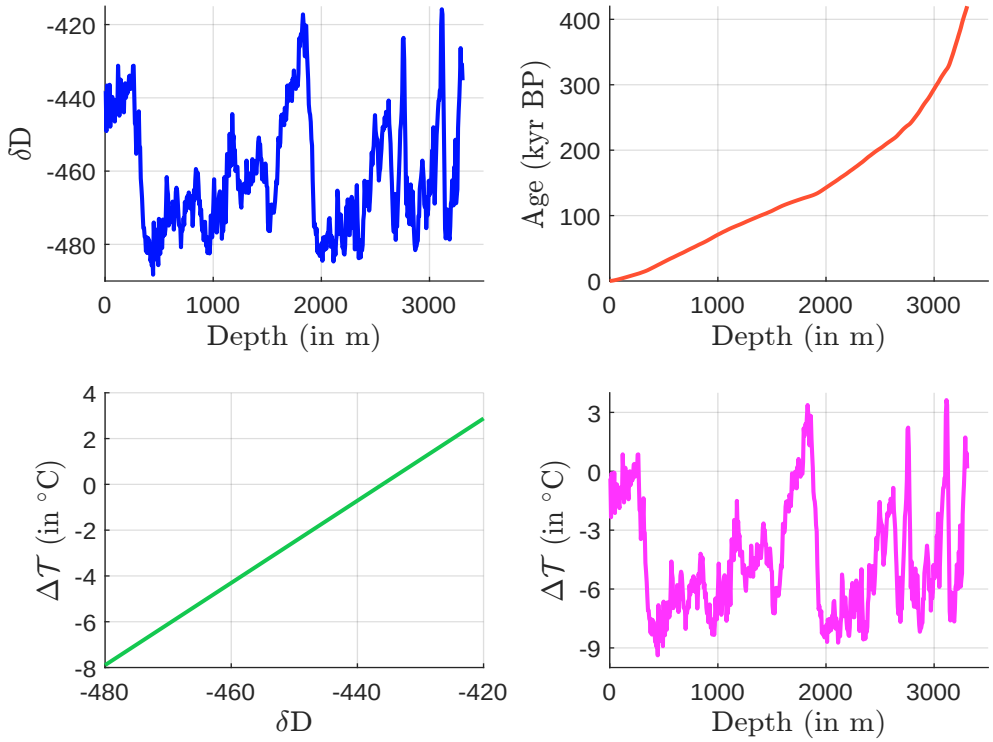


Source: Petit *et al.* (1999), https://www.ncei.noaa.gov/access/paleo-search/study/2453 & Author's calculations.

**Remark 76** *Other variables can be found in the dataset. For example, we report the gas concentration of $CH_4$ (in ppbv or parts per billion by volume) and $CO_2$ (in ppmv or parts per million by volume) and also the isotope ratio $\delta^{18}$O in Figure 8.15.*

[26] See Parrenin *et al.* (2007) for a review of the construction of the time scale with a focus on the EDC3 chronology, the importance of age markers and the mapping process.

[27] Described in the second section on page 431 of the article.

Figure 8.14: Temperature reconstruction of Vostok ice cores

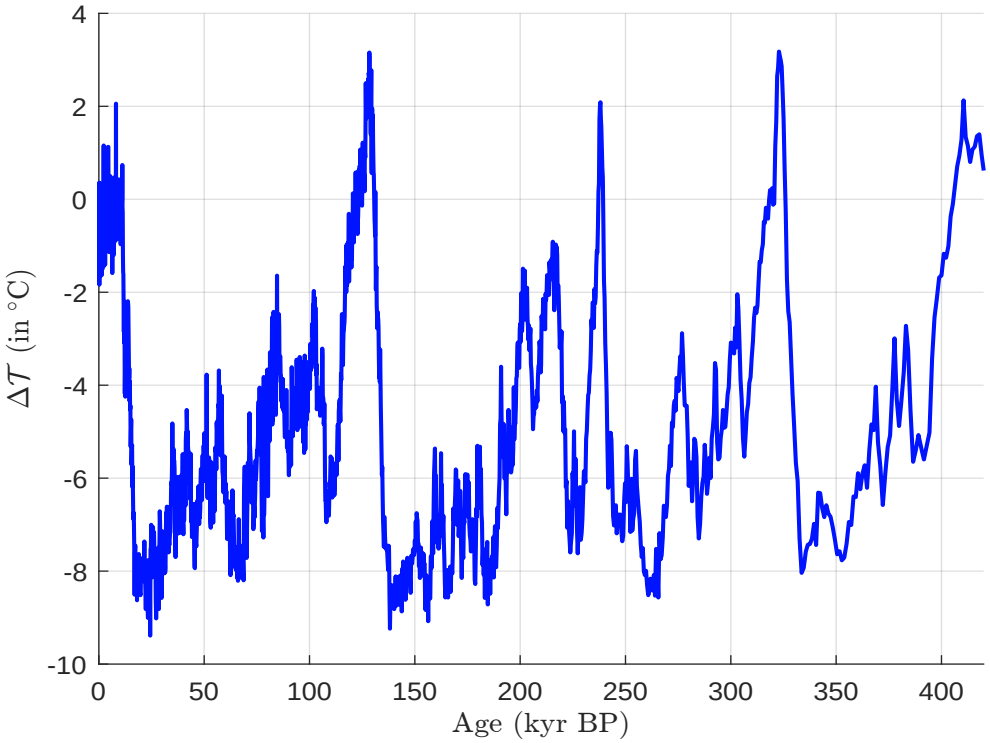


Source: Petit *et al.* (1999) & https://www.ncei.noaa.gov/access/paleo-search/study/2453.

Figure 8.15: Gas concentration of Vostok ice cores

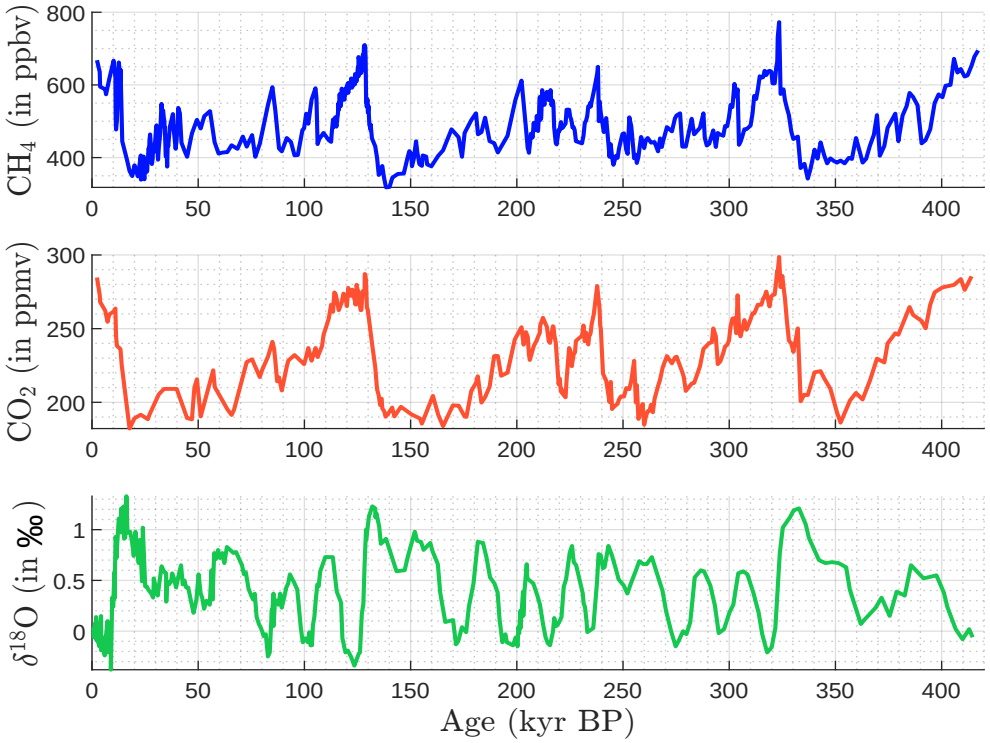


Source: Petit *et al.* (1999) & https://www.ncei.noaa.gov/access/paleo-search/study/2453.

In addition to ice cores, the previous analysis can be applied to rocks, lake and ocean sediments, and tree rings. Let's go back to Figure 8.9 and look at the different scientific references used to calculate the Earth's temperature since 500 Myr BP:

- The works of Royer *et al.* (2004) are related to the works of Veizer *et al.* (1999) and Veizer *et al.* (2000). Veizer *et al.* (1999) collected a total of 2 128 calcitic and phosphatic shells, mainly brachiopods with some conodonts and belemnites, and measured their $^{87}Sr/^{86}Sr$, $\delta^{13}C$ and $\delta^{18}O$ values. It is a statistical study where the authors calculated correlograms, trends and performed a factor analysis to show that the $^{87}Sr/^{86}Sr$, $\delta^{13}C$ and $\delta^{18}O$ system is driven by three factors: the first two are tectonic factors while the third is a biologically mediated redox balance of carbon and sulfur cycles. In 2000, Jàn Veizer and two co-authors used the previous database to write a controversial paper entitled "*Evidence for decoupling of atmospheric $CO_2$ and global climate during the Phanerozoic eon*". In particular, they concluded:

  > "*[...] our data conflict with a temperature reconstruction using an energy balance model that is forced by reconstructed atmospheric carbon dioxide concentrations. The results can be reconciled if atmospheric carbon dioxide concentrations were not the principal driver of climate variability on geological timescales for at least one-third of the Phanerozoic eon, or if the reconstructed carbon dioxide concentrations are not reliable.*" (Veizer *et al.*, 2000, page 698).

  The research by Dana Royer and his co-authors consisted of examining the dataset and the reconstructed temperature curve, and proposing a new reconstructed curve by applying a correction based on seawater pH:

  > "*Recent studies have purported to show a closer correspondence between reconstructed Phanerozoic records of cosmic ray flux and temperature than between $CO_2$ and temperature. The role of the greenhouse gas $CO_2$ in controlling global temperatures has therefore been questioned.[...] We explore the possible influence of seawater pH on the $\delta^{18}O$ record and find that a pH-corrected record matches the glacial record much better. Periodic fluctuations in the cosmic ray flux may be of some climatic significance, but are likely of second-order importance on a multimillion-year timescale.*" (Royer *et al.*, 2004, page 4).

- In 2004, the North Greenland Ice Core Project (NGRIP) members published an article in *Nature*, with two main contributions. First, they extensively studied the late Eemian period, which is the last interglacial period which began about 130 000 years ago and ended about 115 000 years ago. They revealed a previously unrecognised warm period initiated by an abrupt climate warming about 115 000 years ago, before glacial conditions had fully developed North Greenland Ice Core Project members (2004, pages 2-3). Second, they observed significant regional climate differences when analyzing ice cores from northern (NGRIP) and central (GRIP/GISP 2) Greenland regions, and suggested that "*the extent of ice in the Northern Hemisphere modulated the latitudinal temperature gradients in Greenland*" North Greenland Ice Core Project members (2004, page 1).

- The research carried out by Lisiecki and Raymo (2005) is remarkable. They studied the LR04 database, which contains over 38 000 individual $\delta^{18}O$ measurements from 57 ocean drilling sites[28]. Benthic $\delta^{18}O$ records are a climate proxy used to reconstruct past ocean temperatures (and also ice volume). Benthic foraminiferal calcite is the calcium carbonate material that

[28] Most of them were in the Atlantic Ocean, a few in the Pacific Ocean and even fewer in the Asian Ocean.

makes up the shells of benthic foraminifera, tiny organisms that live on the ocean floor. The calcium carbonate incorporates oxygen from the seawater, and the ratio $\delta^{18}O$ in foraminiferal shells depends on the temperature of the seawater when the shell was formed. Cooler water has higher $\delta^{18}O$ values, while warmer water has lower $\delta^{18}O$ values. The authors used various alignment and stacking techniques to synchronise the 57 time series. They were then able to derive a graphical correlation and create a unique series showing the common pattern of the 38 000 individual $\delta^{18}O$ measurements.

- The data labelled EPICA Dome C, Antarctica correspond to those calculated by Jouzel *et al.* (2007). A preliminary version of these data was published three years earlier (EPICA community members, 2004). This article focused on the comparison of the deuterium isotope ratio $\delta D$ between the Vostok and Dome C ice cores. The article by Jouzel *et al.* (2007) went further by converting the $\delta D$ data into a temperature record[29]. They also found that the combined effects of the precession and obliquity Milankovitch cycles drove the dynamics of the ice ages, implying that climate variability over the past 800 000 years cannot be explained by the radiative forcing of $CO_2$ and $CH_4$ alone.

- James Zachos and his co-authors have collected several sources of data (Zachos *et al.*, 2001, 2008). They have used similar data to those studied by Lisiecki and Raymo (2005), but they have included both the isotope ratios $\delta^{13}C$ and $\delta^{18}O$. By crossing these two pieces of information, they deduced the partial pressure of carbon dioxide[30] $pCO_2$ in the ocean over the past 65 million years. Another important contribution of these papers is the consideration of feedbacks and new estimates of climate sensitivity.

- Friedrich *et al.* (2012) compiled a new dataset of benthic foraminifera $\delta^{13}C$ and $\delta^{18}O$ ratios for the middle to late Cretaceous, spanning 55 million years. They highlighted the role of ocean circulation in greenhouse Earth episodes. For example, they showed that:

  1. "*There was widespread formation of bottom waters with temperatures above* 20°C *during the Cretaceous hothouse world*;
  2. *These bottom waters filled the North Atlantic and probably originated as thermocline or intermediate waters in the tropical oceans*;
  3. *The interbasin* $\delta^{13}C$ *gradient was unusually large during the Cretaceous hot greenhouse, probably because the North Atlantic sills prevented the free exchange of waters in the deep basin*;
  4. *The hot greenhouse ended when the Equatorial Atlantic Gateway opened sufficiently to flood the deep North Atlantic with relatively cool polar waters formed in the Southern Ocean.*"

  According to this study, plate tectonic movements are then an important factor for understanding the temperature dynamics during the Mesozoic, because they have influenced the circulation of warm and cold waters.

- Hansen *et al.* (2013a) proposed a simplified model to investigate the state dependence of climate sensitivity, sea level and atmospheric $CO_2$ through the Cenozoic. Their basic idea is

[29] The original data from Jouzel *et al.* (2007) can be accessed at `www.ncei.noaa.gov/access/paleo-search/study/6080` (file `edc3deuttemp2007.txt`). To obtain all the EPICA Dome C published data (80 files), the reader can explore the directory `ftp.ncdc.noaa.gov/pub/data/paleo/icecore/antarctica/epica_domec`.

[30] $pCO_2$ is a measure of the amount of carbon dioxide dissolved in a gas or liquid. It is measured in ppm or ppmv (parts per million by volume).

to estimate Cenozoic sea level and temperature from empirical data, filtering the data with minimal assumptions and modelling. In fact, the paper contains only five equations. For example, the equation for the lower ocean temperature is:

$$\mathcal{T}_{\mathrm{LO}} = \begin{cases} 5 - 8\left(\dfrac{\delta^{18}\mathrm{O} - 1.75}{3}\right) & \text{if } \delta^{18}\mathrm{O} < 3.25 \\ 1 - 4.4\left(\dfrac{\delta^{18}\mathrm{O} - 3.25}{3}\right) & \text{otherwise} \end{cases}$$

while the surface air temperature is equal to $\mathcal{T}_{\mathrm{AT}} = 2\mathcal{T}_{\mathrm{LO}} + 12.25$ during the Pleistocene. The relationship between the oxygen isotope ratio $\delta^{18}\mathrm{O}$, the deep ocean temperature $\mathcal{T}_{\mathrm{LO}}$ and the atmospheric temperature $\mathcal{T}_{\mathrm{AT}}$ is shown in Figure 8.16. Their results are very impressive, especially Figures 2c and 6, which compare the raw estimates of sea level and global mean surface temperature anomalies with the fitted estimates calculated with the equations. In Figure 8.16 we can see that the atmospheric temperature varies between 9.35°C and 14.37°C. This illustrates how an impact of ±3°C can have a large effect on the Earth's climate.

Figure 8.16: Relationship between $\delta^{18}\mathrm{O}$, $\mathcal{T}_{\mathrm{LO}}$ and $\mathcal{T}_{\mathrm{AT}}$ during the Pleistocene

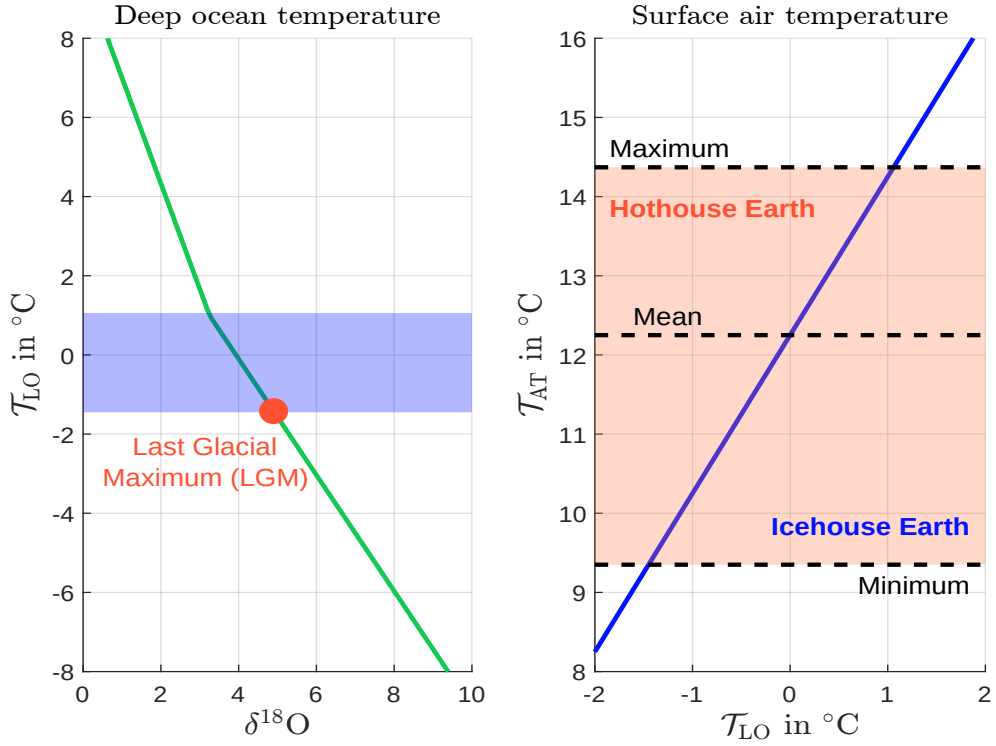


A comparison of Figure 8.14 with Figure 8.15 shows a high correlation between $CO_2$ concentration and temperature. But we also see that there is a high correlation when we look at the $CH_4$ concentration. If we consider a longer period, these correlations are lower. For example, we report the temporal evolution of atmospheric $CO_2$ reconstructed by Foster *et al.* (2017). Using a sample of 1 500 estimated atmospheric $CO_2$, they have performed a Loess regression. Their results for the last 420 million years are shown in Figure 8.17. Comparison with Figure 8.9 suggests that the evolution of $CO_2$ and $\Delta\mathcal{T}$ may be asynchrone in some periods, because $CO_2$ is not the only explanatory factor.

Figure 8.17: Evolution of the atmospheric $CO_2$ during the last 420 million years

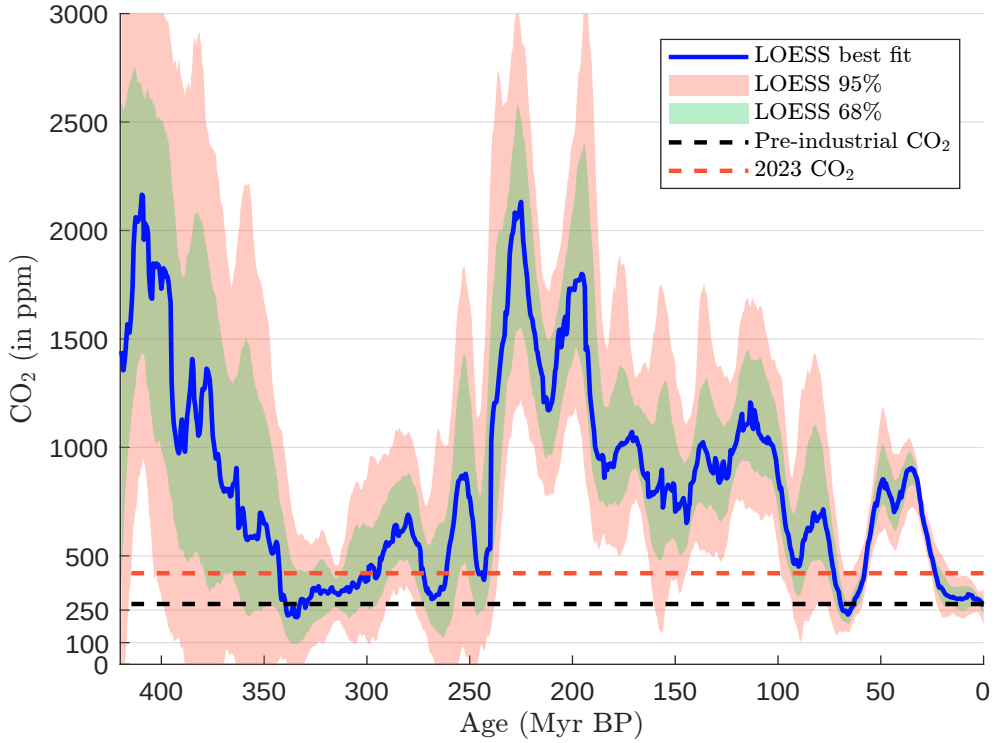


Source: Foster *et al.* (2017, Figure 1, page 3) & Supplementary Data 2 (www.nature.com/articles/ncomms14845).

### Anthropogenic factors of climate change

The term "*anthropogenic*" is derived from the Greek words "*anthropos*" (human) and "*genesis*" (origin) and refers to anything caused or influenced by human activity. This includes both direct and indirect impacts, such as climate change, pollution, deforestation, and biodiversity loss. In this section, we examine the human impact on climate change since the beginning of the Industrial Revolution, which is assumed to have occurred in 1760. First, we examine the temperature anomaly, then we consider anthropogenic greenhouse gas emissions, and finally we discuss the planetary boundaries framework. Chapter 12 on page 1033, on physical risks, complements this section and extends the analysis to other climate impacts such as flooding, sea-level rise, hurricanes, wildfires, heat waves, and agricultural productivity.

**Temperature anomaly** We define the temperature anomaly at time $t$ as the difference between the temperature at time $t$ and the temperature for a reference period:

$$\Delta\mathcal{T}(t) = \mathcal{T}(t) - \mathcal{T}_{\mathfrak{Base}}$$

where $\mathcal{T}_{\mathfrak{Base}}$ is the reference temperature. It is generally the average of the temperature of the reference period:

$$\mathcal{T}_{\mathfrak{Base}} = \frac{\sum_{j\in\mathfrak{Base}} \mathcal{T}(j)}{n_{\mathfrak{Base}}}$$

For example, the reference temperature can be the average temperature of the 20th century (from 1901 to 2000) or the pre-industrial period. In Figure 8.18, we report the global temperature anomaly

obtained with the HadCRUT5 database[31]. The reference period for the calculation of $\mathcal{T}_{\mathfrak{Base}}$ is 1961–1990. The blue circle corresponds to the annual average, while the red line is the 10-year moving average. For each year, we have also provided the 95% confidence interval with a black vertical line. In 2023, the temperature anomaly was +1.04°C with a 95% confidence interval between 0.97°C and 1.10°C, while the 10-year moving average was 0.86°C. Since 1975 there has been a clear upward trend. If we estimate the linear trend between 1975 and 2023, we get the dashed black line. A simple projection gives the following forecasts: +1.43°C in 2050, +1.93°C in 2075 and +2.42°C in 2100.

Figure 8.18: Global average land-ocean temperature anomaly relative to 1961–1990 average

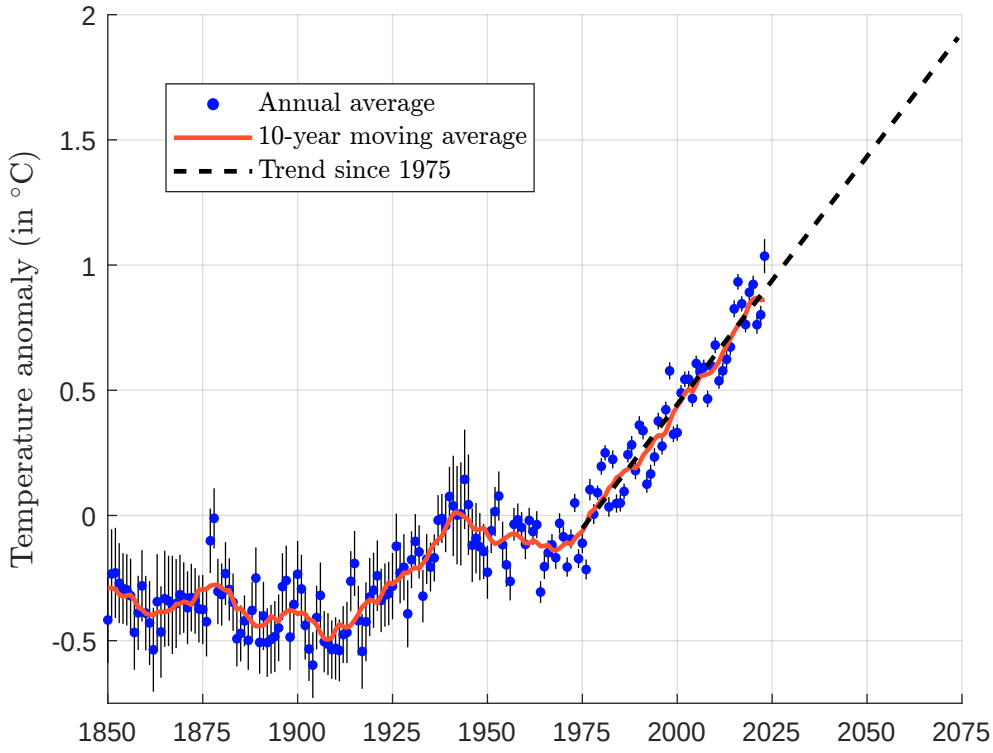


Source: Morice *et al.* (2021) & https://www.metoffice.gov.uk/hadobs/hadcrut5.

The previous analysis is a global picture. In fact, the temperature anomaly is calculated for a given location defined by a latitude, a longitude and an altitude. Let $\Delta\mathcal{T}_i(t)$ be the temperature anomaly for location $i$. The calculation of the temperature anomaly for a region is the weighted average of all locations belonging to the region grid:

$$\Delta\mathcal{T}_{\mathcal{R}egion}(t) = \sum_{i \in \mathcal{G}rid(\mathcal{R}egion)} w_i \cdot \Delta\mathcal{T}_i(t)$$

where $w_i$ is the weight of location $i$. So we can calculate the temperature for a country, a continent and even a hemisphere. In Figure 8.19, we show the temperature anomaly for the northern and southern hemispheres, calculated by Morice *et al.* (2021), using a regular 5° latitude by 5° longitude grid of the Earth. In fact, the global temperature anomaly shown in Figure 8.18 is just the simple average of the northern and southern hemisphere temperature anomalies shown in Figure 8.19. We can see that the temperature in the northern hemisphere has risen faster than in the southern

[31] This database is produced and maintained by the Met Office Hadley Centre, which is also responsible for many other datasets that can be found at https://www.metoffice.gov.uk/hadobs.

Figure 8.19: Average land-ocean temperature anomaly in the northern and southern hemispheres relative to the 1961–1990 average

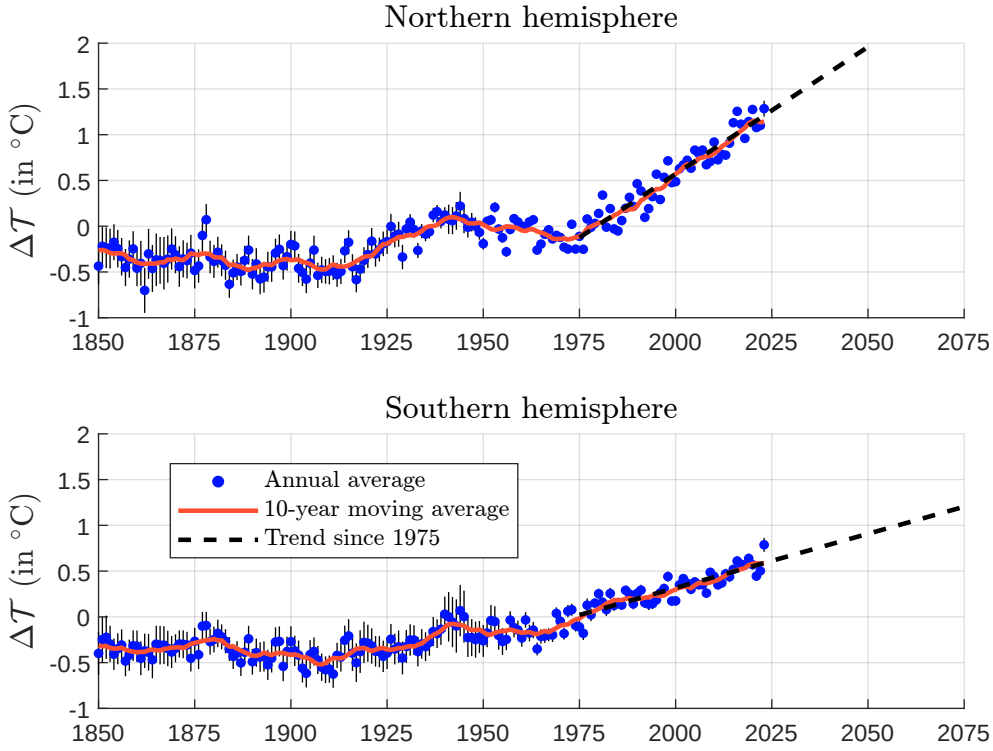


Source: Morice *et al.* (2021) & https://www.metoffice.gov.uk/hadobs/hadcrut5.

hemisphere. The slope of the trend since 1975 is +2.78°C per century for the northern hemisphere, which is higher than the slope of +1.18°C per century for the southern hemisphere. We therefore project a temperature anomaly of +3.35°C degrees and +1.50°C degrees respectively by 2100. All these results are summarized in Table 8.4.

Table 8.4: Linear projection of land-ocean temperature anomaly (in °C)

| Year | HadCRUT5 | | | NOAAGlobalTemp v5.1 | | |
|---|---|---|---|---|---|---|
| | Global | Northern | Southern | Global | Northern | Southern |
| 2050 | 1.4336 | 1.9595 | 0.9078 | 1.4576 | 1.9894 | 0.9247 |
| 2075 | 1.9288 | 2.6540 | 1.2035 | 1.9185 | 2.6715 | 1.1642 |
| 2100 | 2.4239 | 3.3486 | 1.4992 | 2.3795 | 3.3536 | 1.4038 |
| Slope | 0.0198 | 0.0278 | 0.0118 | 0.0184 | 0.0273 | 0.0096 |

Source: https://www.ncei.noaa.gov/access/monitoring/global-temperature-anomalies/anomalies, https://www.metoffice.gov.uk/hadobs/hadcrut5 & Author's calculations.

The previous figures were obtained using the HadCRUT5 dataset, which is based on several historical datasets, models, and reanalyses. A reanalysis is a process that combines historical weather observations with a computer model to produce a consistent and complete record of past weather conditions. This is necessary because historical records are not available in a grid. Reanalysis then allows the creation of a homogeneous database of temperature records for a given grid and time period. However, the temperature records depend on the database. Below we list five land-ocean

gridded temperature datasets, their web addresses, and the scientific reference that explains how these temperature records were calculated:

1. Berkeley Earth, `berkeleyearth.org/data` (Rohde and Hausfather, 2020);
2. ERA5, `cds.climate.copernicus.eu/cdsapp#!/dataset/reanalysis-era5-single-levels` (Hersbach *et al.*, 2020);
3. HadCRUT5, `www.metoffice.gov.uk/hadobs/hadcrut5` (Morice *et al.*, 2021);
4. GISTEMP v4, `data.giss.nasa.gov/gistemp` (Lenssen *et al*, 2019);
5. NOAAGlobalTemp v5.1, `www.ncei.noaa.gov/products/land-based-station/noaa-global-temp` (Vose *et al.*, 2021).

A comparison of these datasets shows a high degree of consistency between the estimates, but we must be careful because it also shows that the results can be different, especially if we look at specific locations (*e.g.*, a point on the grid or a country) rather than global locations.

Table 8.5: Linear projection of land and ocean temperature anomalies (in °C)

| Year | Global | | Northern | | Southern | |
|---|---|---|---|---|---|---|
| | Land | Ocean | Land | Ocean | Land | Ocean |
| 2050 | 2.4212 | 1.0238 | 2.8388 | 1.3482 | 1.4719 | 0.7972 |
| 2075 | 3.2386 | 1.3243 | 3.8176 | 1.8061 | 1.9222 | 0.9875 |
| 2100 | 4.0560 | 1.6247 | 4.7964 | 2.2641 | 2.3725 | 1.1779 |
| Slope | 0.0327 | 0.0120 | 0.0392 | 0.0183 | 0.0180 | 0.0076 |

Source: NOAAGlobalTemp v5.1 & Author's calculations.

We look at NOAAGlobalTemp v5.1 and display the land-ocean temperature anomaly in Figure 8.20. Note that the time series are very close to those plotted in Figures 8.18 and 8.19. The correlation between HadCRUT and NOAAGlobalTemp is 99.04% for the global surface, 99.27% for the northern hemisphere, and 97.74% for the southern hemisphere. Figure 8.20 also shows the decomposition of the land-ocean temperature into land and ocean temperatures. It can be seen that the temperature anomalies are more important for the land surface than for the ocean surface, implying that global warming is more important for the land than for the oceans. This is especially true in the northern hemisphere. We have calculated the trend[32] as before and reported the estimates in Tables 8.4 and 8.5. By the end of this century, the projected land temperature anomaly is +4.06°C for the world, 4.80°C for the northern hemisphere and 2.37°C for the southern hemisphere.

The discrepancy between the northern and southern hemispheres is even more pronounced when we look at countries. To illustrate this, we look at the temperature anomalies[33] on land as calculated by the FAO. As before, we calculate the trend with the temperature anomalies between 1975 and 2022 by country and project the trend to 2100. The results are shown in Figure 8.21. The range is from 0.64°C to 7.63°C. According to these results, Greenland and Russia[34] will be most affected, followed by Europe, Canada and the Middle East.

[32]The base period used by the NOAA model is different and is 1901–2000. To reconcile the two datasets, we need to adjust the HadCRUT5 data to have the same reference period as the NOAA data. This is equivalent to adding 0.10°C, 0.06°C, and 0.14°C degrees to the global surface, northern hemisphere, and southern hemisphere temperature anomalies of the HadCRUT5 data, respectively.

[33]We filter the database at `https://www.fao.org/faostat/en/#data/ET` using the item meteorological year and the element temperature change.

[34]For Russia and the countries of the former Soviet Union, historical data start in 1992 and may explain an overestimation of the trend.

Figure 8.20: Average temperature anomaly (land-ocean, land and ocean)

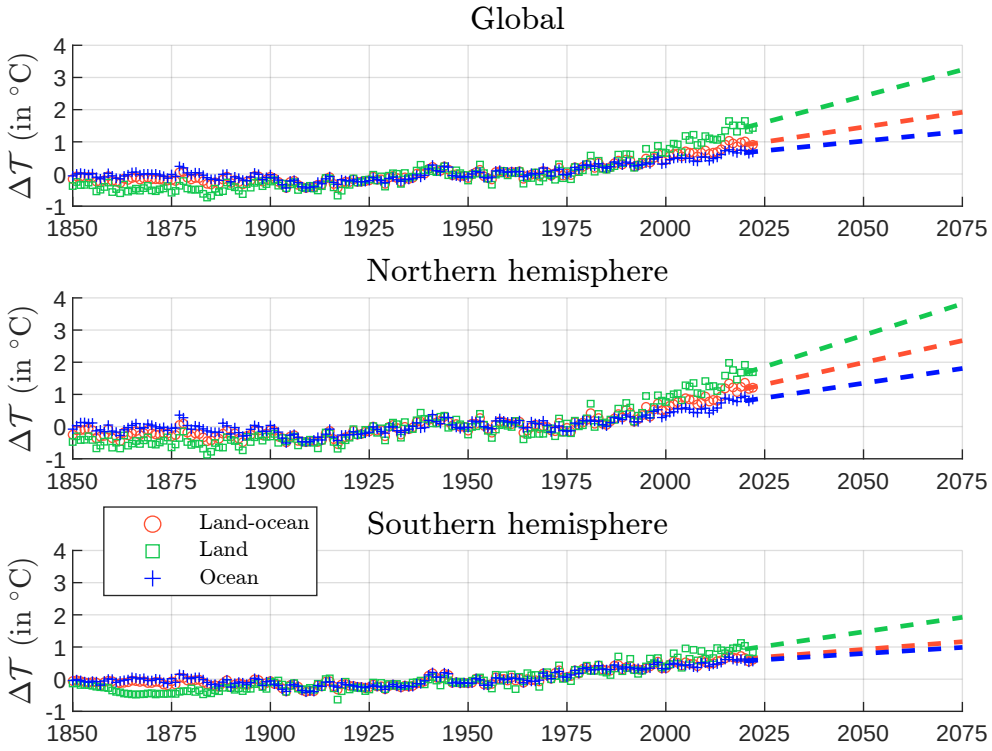


Source: Vose *et al.* (2021) & https://www.ncei.noaa.gov/access/monitoring/global-temperature-anomalies/anomalies.

Figure 8.21: Projection of temperature anomaly by 2100 (in °C)

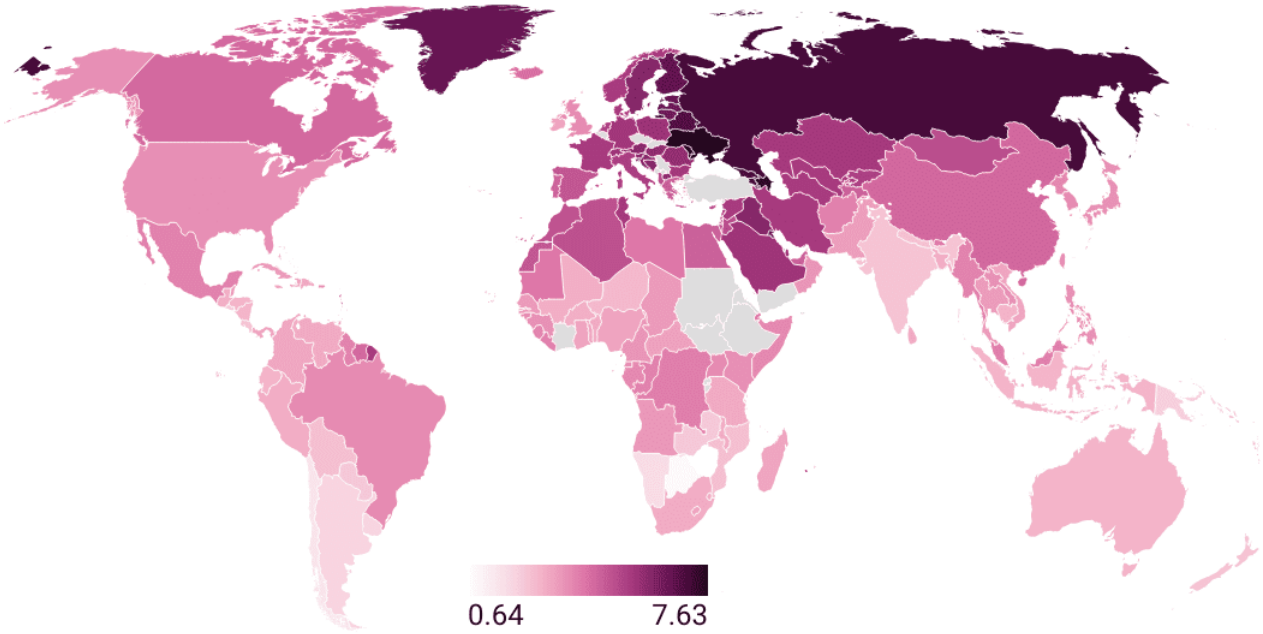


Source: https://www.fao.org/faostat/en/#data/ET & Author's calculations (created by Datawrapper).

**Anthropogenic GHG emissions** In order to study anthropogenic greenhouse gas emissions, we need to introduce some definitions and clarify some concepts of the global greenhouse gas budget. Let us first consider anthropogenic carbon dioxide emissions. According to Friedlingstein *et al.* (2022), the global carbon budget has five main components:

1. Fossil fuel combustion and oxidation from all energy and industrial processes, including cement production and carbonation;
2. Emissions from land-use change;
3. The growth rate of atmospheric $CO_2$ concentration;
4. The uptake of $CO_2$ by the oceans (ocean sink);
5. The uptake of $CO_2$ by the land (land sink).

These components are denoted $\mathcal{CE}_{\text{Industry}}$, $\mathcal{CE}_{\text{Land}}$, $\mathcal{CE}_{\text{AT}}$, $\mathcal{CS}_{\text{Ocean}}$, $\mathcal{CS}_{\text{Land}}$ respectively. From a theoretical point of view, we have the following identity:

$$\mathcal{CE}_{\text{AT}} = \underbrace{(\mathcal{CE}_{\text{Industry}} + \mathcal{CE}_{\text{Land}})}_{\text{Positive emissions}} - \underbrace{(\mathcal{CS}_{\text{Ocean}} + \mathcal{CS}_{\text{Land}})}_{\text{Negative emissions}}$$

As Friedlingstein *et al.* (2022) explained, this equality is not verified because of imperfect spatial and temporal data coverage, estimation errors and omission of minor terms. The authors therefore defined the estimated budget imbalance, which measures the mismatch between estimated emissions and estimated changes in the atmosphere, land and oceans:

$$\mathcal{CB}_{\text{Imbalance}} = \mathcal{CE}_{\text{Industry}} + \mathcal{CE}_{\text{Land}} - (\mathcal{CE}_{\text{AT}} + \mathcal{CS}_{\text{Ocean}} + \mathcal{CS}_{\text{Land}})$$

In the database provided by the authors[35], they split the carbon emissions $\mathcal{CE}_{\text{Industry}}$ into gross industrial emissions excluding carbonation minus cement carbonation sink[36]: $\mathcal{CE}_{\text{Industry}} = \mathcal{CE}^{\star}_{\text{Industry}} - \mathcal{CS}_{\text{Cement}}$.

In 2021, the authors estimate the following figures expressed in gigatonnes of carbon: $\mathcal{CE}^{\star}_{\text{Industry}} = 10.13$, $\mathcal{CE}_{\text{Land}} = 1.08$, $\mathcal{CE}_{\text{AT}} = 5.23$, $\mathcal{CS}_{\text{Ocean}} = 2.88$, $\mathcal{CS}_{\text{Land}} = 3.45$, $\mathcal{CS}_{\text{Cement}} = 0.23$, and $\mathcal{CB}_{\text{Imbalance}} = -0.58$. Expressed in gigatonnes of $CO_2$ we obtain: $\mathcal{CE}^{\star}_{\text{Industry}} = 37.12$, $\mathcal{CE}_{\text{Land}} = 3.94$, $\mathcal{CE}_{\text{AT}} = 19.14$, $\mathcal{CS}_{\text{Ocean}} = 10.55$, $\mathcal{CS}_{\text{Land}} = 12.64$, $\mathcal{CS}_{\text{Cement}} = 0.84$, and $\mathcal{CB}_{\text{Imbalance}} = -2.12$. Anthropogenic $CO_2$ emissions are therefore 36.28 $GtCO_2$ for industrial processes ($\mathcal{CE}_{\text{Industry}}$) and 3.94 $GtCO_2$ for land-use change. Since the total is 40.22 $GtCO_2$, 26.23% and 31.43% of the total anthropogenic $CO_2$ emissions have been absorbed by oceans and land, respectively, while 47.60% remain in the atmosphere. In Figure 8.22, we show the evolution of $\mathcal{CE}_{\text{Industry}}$ and $\mathcal{CE}_{\text{Land}}$. While carbon dioxide emissions from land-use change are relatively stable, carbon dioxide emissions from

[35]The full data set can be found at https://www.icos-cp.eu and https://globalcarbonbudgetdata.org. The main variables are available at https://globalcarbonbudget.org/wp-content/uploads/Global_Carbon_Budget_2022v1.0.xlsx. Carbon emissions are expressed in billion tonnes of carbon per year (GtC/yr). To convert these figures to billion tonnes of carbon dioxide ($GtCO_2$/yr), we multiply them by $\frac{44.011}{12.011}$ or 3.664. In fact, the atomic mass of carbon is 12.011 g/mol, and the atomic mass of oxygen is 15.999 g/mol. The molecular weight of $CO_2$ is therefore $12.011 + 2 \times 15.999 = 44.011$ g/mol.

[36]Cement carbonation sink is a natural process in which concrete absorbs carbon dioxide from the atmosphere. This process occurs when the calcium hydroxide in cement reacts with carbon dioxide in the air to form calcium carbonate:

$$Ca(OH)_2 + CO_2 \longrightarrow CaCO_3 + H_2O$$

Figure 8.22: Annual $CO_2$ emissions (in $GtCO_2$)

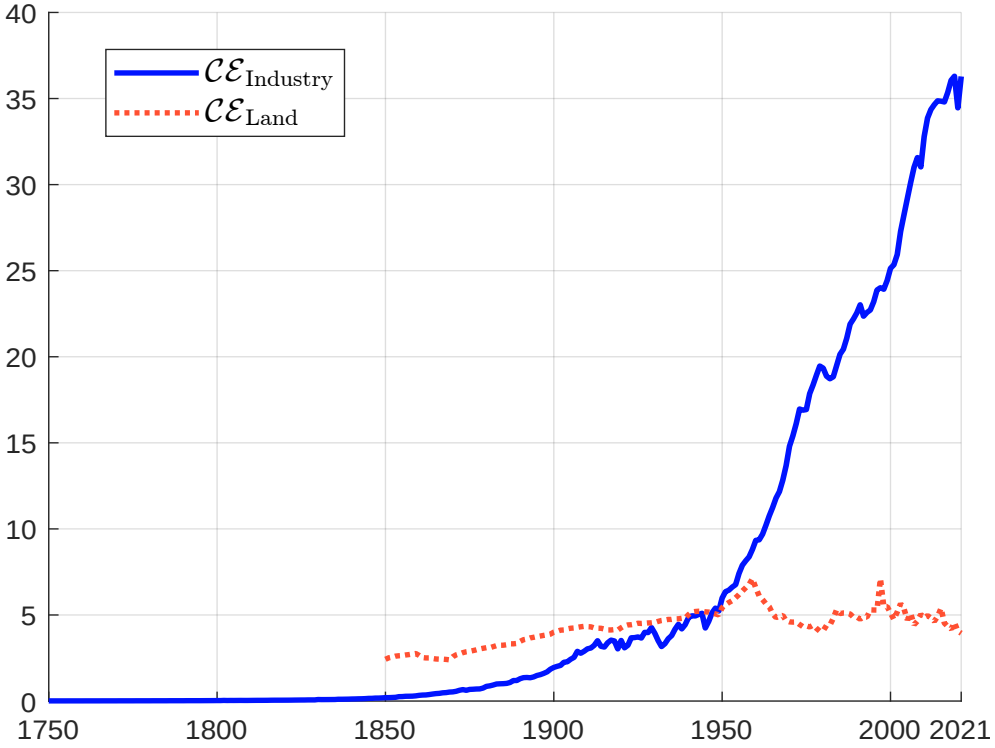


Source: Friedlingstein *et al.* (2022), https://globalcarbonbudget.org & Author's calculations.

Figure 8.23: Cumulative $CO_2$ emissions and carbon sinks (in $GtCO_2$)

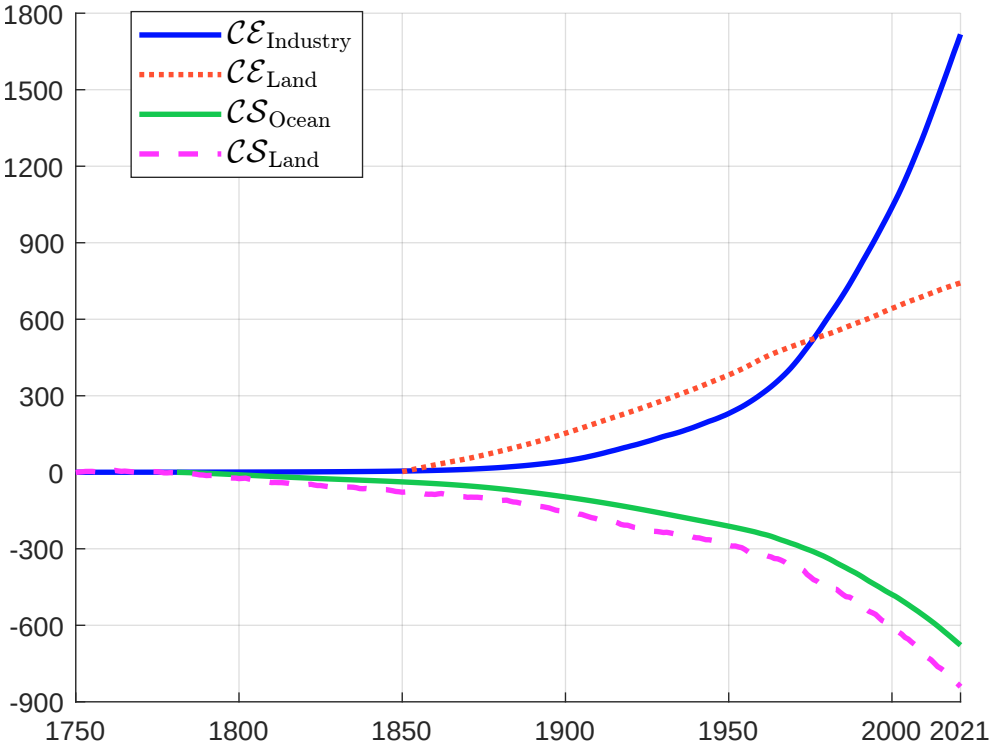


Source: Friedlingstein *et al.* (2022), https://globalcarbonbudget.org & Author's calculations.

Figure 8.24: Cumulative $CO_2$ budget imbalance in atmosphere (in $GtCO_2$)

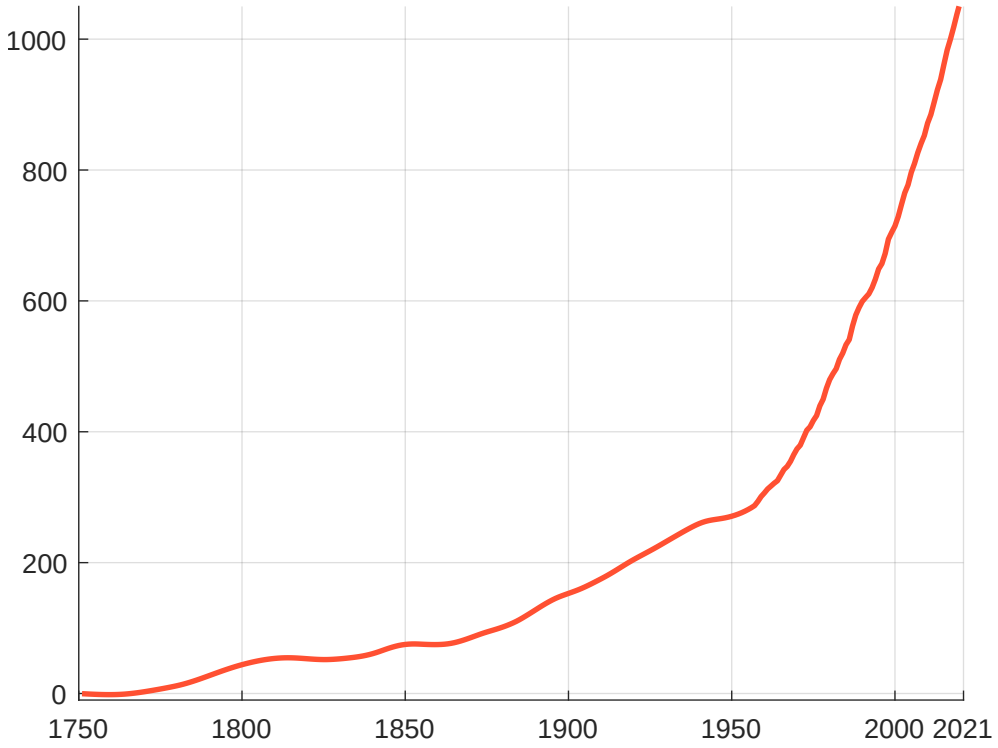


Source: Friedlingstein *et al.* (2022), `https://globalcarbonbudget.org` & Author's calculations.

industrial processes are growing faster since 1950. Looking at cumulative $CO_2$ emissions, we get Figure 8.23. We also show the negative emissions due to the two carbon sinks. From 1750, industrial processes and land-use change have emitted a total of 1 717 and 742 $GtCO_2$, respectively, and ocean and land sinks have absorbed a total of 678 and 841 $GtCO_2$, respectively. We can then calculate the cumulative $CO_2$ emissions remaining in the atmosphere in Figure 8.24. From 1750 to 2021, the net balance is 1 076 $GtCO_2$ of anthropogenic emissions. Friedlingstein *et al.* (2022) defined the airbone fraction as the ratio of the atmospheric $CO_2$ growth rate to total anthropogenic emissions. For the period 1750–2021, this ratio is equal to:

$$\text{AF} = \frac{\mathcal{CE}_{\text{AT}}}{\mathcal{CE}_{\text{Industry}} + \mathcal{CE}_{\text{Land}}} = \frac{1\,076}{1\,717 + 742} = 43.8\%$$

This means that 43.8% of anthropogenic emissions have not been absorbed by natural carbon sinks. The authors concluded that:

> "*The observed stability of the airborne fraction over the 1960–2020 period indicates that the ocean and land $CO_2$ sinks have on average been removing about 55% of the anthropogenic emissions.*" (Friedlingstein *et al.*, 2022, page 4834).

Let us now look at the contribution of different energy sources. Table 8.6 shows the breakdown of anthropogenic $CO_2$ emissions between coal, oil, gas, cement, flaring[37], and others. In 1850,

[37] Gas flaring is the burning of the natural gas associated with oil extraction. This gas is often burned because it is not economically feasible to collect and transport it. The top five flaring countries are Russia, Iraq, Iran, the United States, and Nigeria.

Table 8.6: Breakdown of anthropogenic $CO_2$ emission by energy source (in %)

| | Energy | 1850 | 1900 | 1950 | 1975 | 2000 | 2020 |
|---|---|---|---|---|---|---|---|
| Annual $CO_2$ emissions | Coal | 100.00 | 95.85 | 65.10 | 34.74 | 36.18 | 40.11 |
| | Oil | 0.00 | 3.55 | 26.79 | 47.64 | 40.42 | 33.23 |
| | Gas | 0.00 | 0.60 | 6.09 | 13.17 | 18.61 | 20.38 |
| | Cement | 0.00 | 0.00 | 1.13 | 1.99 | 2.87 | 4.33 |
| | Flaring | 0.00 | 0.00 | 0.81 | 2.18 | 1.05 | 1.12 |
| | Other | 0.00 | 0.00 | 0.08 | 0.29 | 0.86 | 0.83 |
| Cumulative $CO_2$ emissions | Coal | 100.00 | 97.58 | 85.24 | 63.49 | 50.00 | 46.29 |
| | Oil | 0.00 | 2.05 | 12.13 | 27.43 | 35.10 | 35.02 |
| | Gas | 0.00 | 0.37 | 2.15 | 6.88 | 11.72 | 14.52 |
| | Cement | 0.00 | 0.00 | 0.40 | 1.17 | 1.77 | 2.56 |
| | Flaring | 0.00 | 0.00 | 0.03 | 0.87 | 1.03 | 1.06 |
| | Other | 0.00 | 0.00 | 0.06 | 0.16 | 0.39 | 0.55 |

Source: Friedlingstein *et al.* (2022), https://globalcarbonbudget.org & Author's calculations.

Figure 8.25: Energy source breakdown of anthropogenic cumulative $CO_2$ (in %)

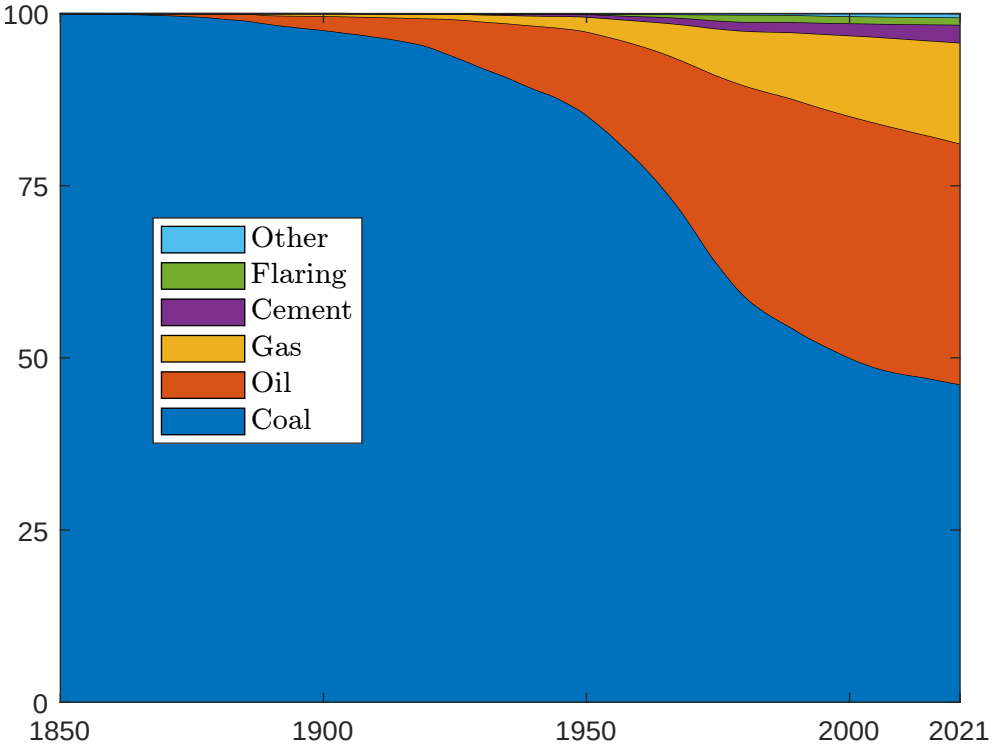


Source: Friedlingstein *et al.* (2022), https://globalcarbonbudget.org & Author's calculations.

100% of carbon emissions came from coal. Then we started burning oil, and later gas. Today, coal still accounts for 40% of current carbon emissions, while oil and gas account for 33% and 20%, respectively. The evolution of the distribution of cumulative $CO_2$ by energy source shows that the share of coal has decreased while the share of oil and gas has increased over the last century (Figure 8.25). In total, 46% of cumulative $CO_2$ emissions are due to coal, followed by oil and gas at 35% and 15%, respectively.

We also look at the breakdown of $CO_2$ emissions by region and country. The results are shown in Figures 8.26 to 8.29. Europe and North America have long been the main contributors, but Asia is now the world's largest $CO_2$ emitter. The country analysis shows that the top five emitters are China, India, Japan, Russia and the United States.

Box 8.6: Kaya identity

In the early seventies, the IPAT equation was proposed to describe the factors of the human impact on the environment (Chertow, 2000):

$$I = P \times A \times T$$

where $I$ is the level of human impact on climate, $P$ is the population, $A$ is the affluence[a] and $T$ is the technology. In the 1990s, this equation was supplanted by the Kaya identity, which states:

$$\text{Anthropogenic } CO_2 \text{ emissions} = \text{Population} \times \frac{\text{GDP}}{\text{Population}} \times \frac{\text{Energy}}{\text{GDP}} \times \frac{CO_2 \text{ emissions}}{\text{Energy}}$$

Using the notations of Kaya and Yokobori (1997), this identity is generally expressed as[b]:

$$F = P \times \frac{G}{P} \times \frac{E}{G} \times \frac{F}{E}$$

Therefore, the key drivers of anthropogenic $CO_2$ emissions include four main factors: the population (demographics), the GDP per capita (economics), the energy intensity of the GDP (engineering) and the carbon intensity (physics). Over the last century, we have observed that the first two factors have increased while the third factor has decreased. Looking into the future, we can expect these trends to continue. Decarbonizing the economy therefore means drastically reducing the carbon intensity of the energy supply. For example, if $P \nearrow 30\%$, $G/P \nearrow 20\%$, $E/G \searrow 15\%$, the carbon intensity must decrease by 32.6% to not increase the level of carbon emissions and decrease by 62.3% to reduce the carbon emissions by two.

[a] The affluence represents the average consumption of each person in the population. A common proxy for measuring affluence is the GDP per capita or the wealth per capita.

[b] See for instance Davis and Caldeira (2010).

The Kaya identity was popularised by Raupach *et al.* (2007). It is a mathematical equation for understanding the factors that explain $CO_2$ emissions (Box 8.6). According to this identity, the four drivers of emissions are population growth, GDP per capita, energy intensity (quantity of energy consumed per unit of GDP) and carbon intensity (amount of $CO_2$ emitted per unit of energy consumed). In Figure 8.30, we plot the $CO_2$ per unit energy ($kgCO_2$ per kWh), the energy per GDP (kWh per dollar), the $CO_2$ per GDP ($kgCO_2$ per dollar of GDP) and the GDP per capita (1000

Figure 8.26: Share of $CO_2$ emissions by region (in % of total)

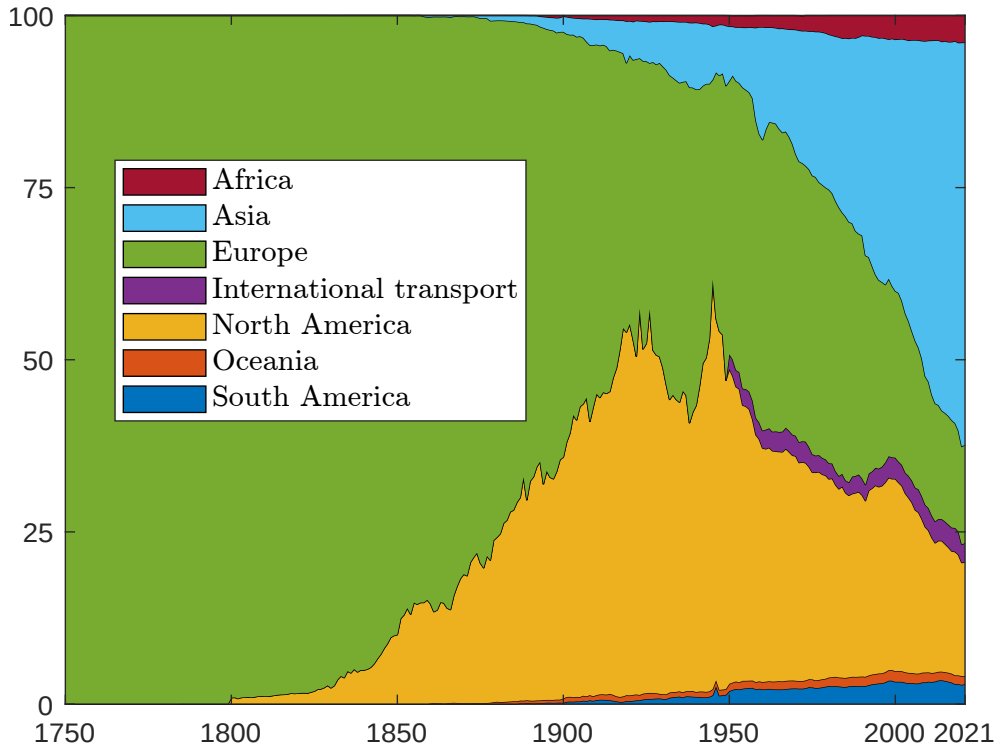


Source: Friedlingstein *et al.* (2022), https://globalcarbonbudget.org & https://github.com/owid/co2-data.

Figure 8.27: Share of cumulative $CO_2$ emissions by region (in % of total)

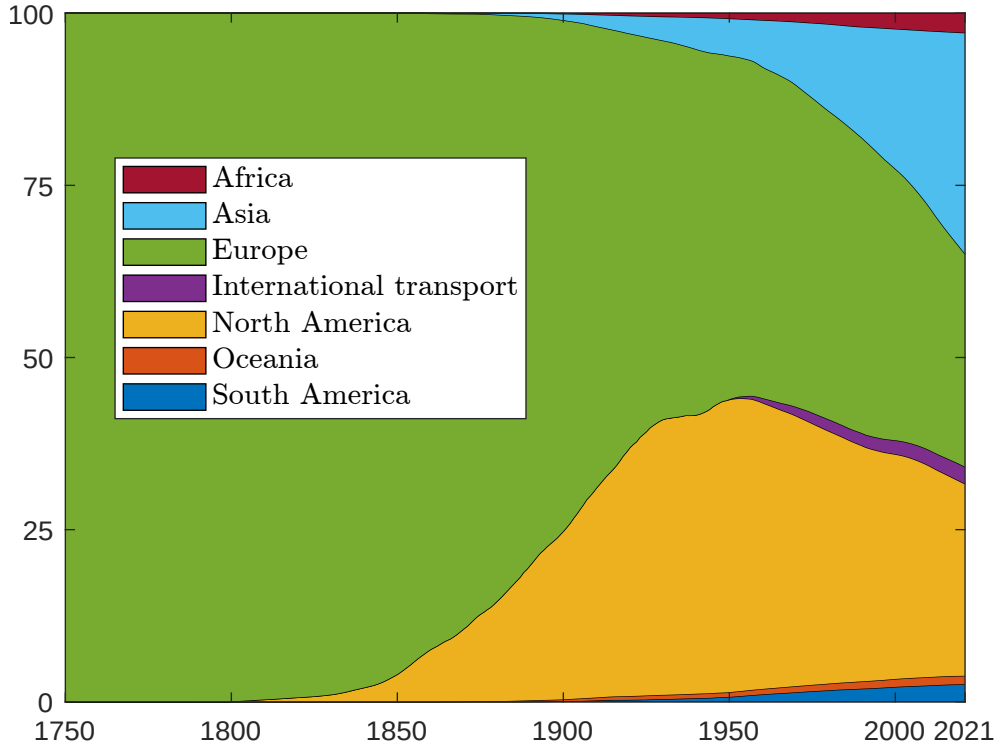


Source: Friedlingstein *et al.* (2022), https://globalcarbonbudget.org & https://github.com/owid/co2-data.

Figure 8.28: Share of $CO_2$ emissions by country (in % of total)

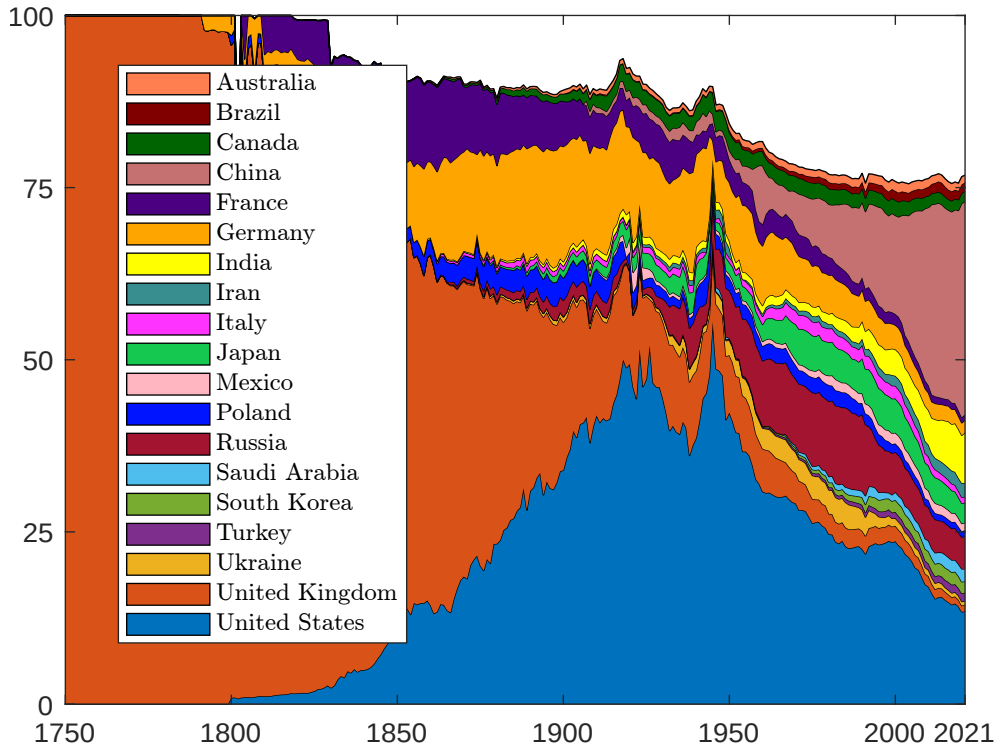


Source: Friedlingstein *et al.* (2022), https://globalcarbonbudget.org & https://github.com/owid/co2-data.

Figure 8.29: Share of cumulative $CO_2$ emissions by country (in % of total)

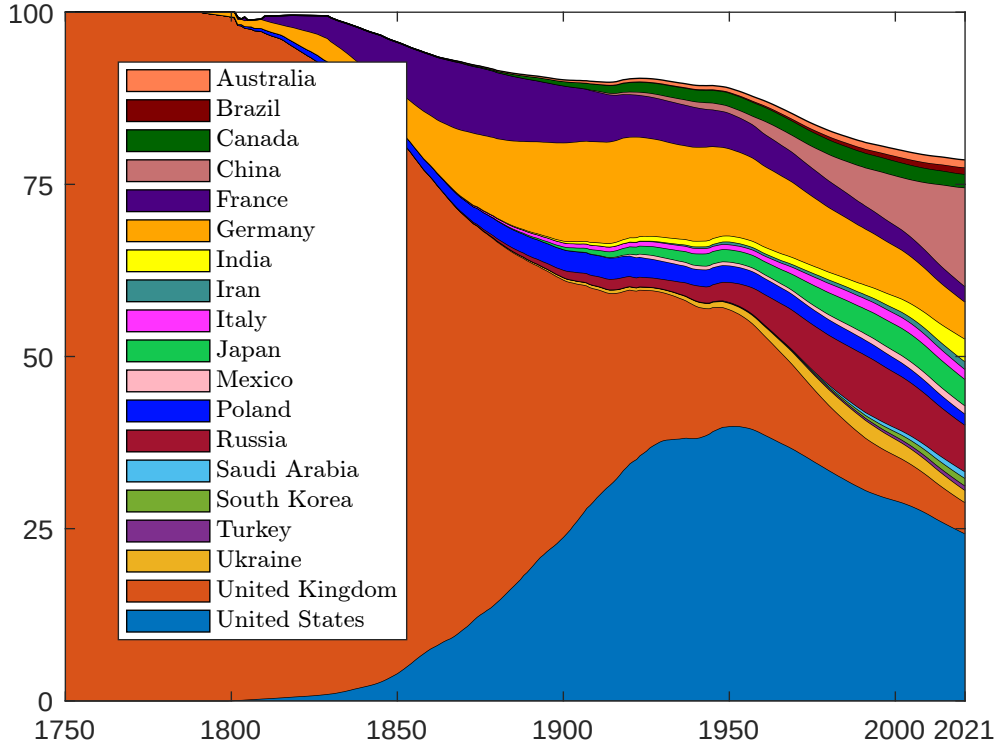


Source: Friedlingstein *et al.* (2022), https://globalcarbonbudget.org & https://github.com/owid/co2-data.

Figure 8.30: Key drivers of the Kaya identity

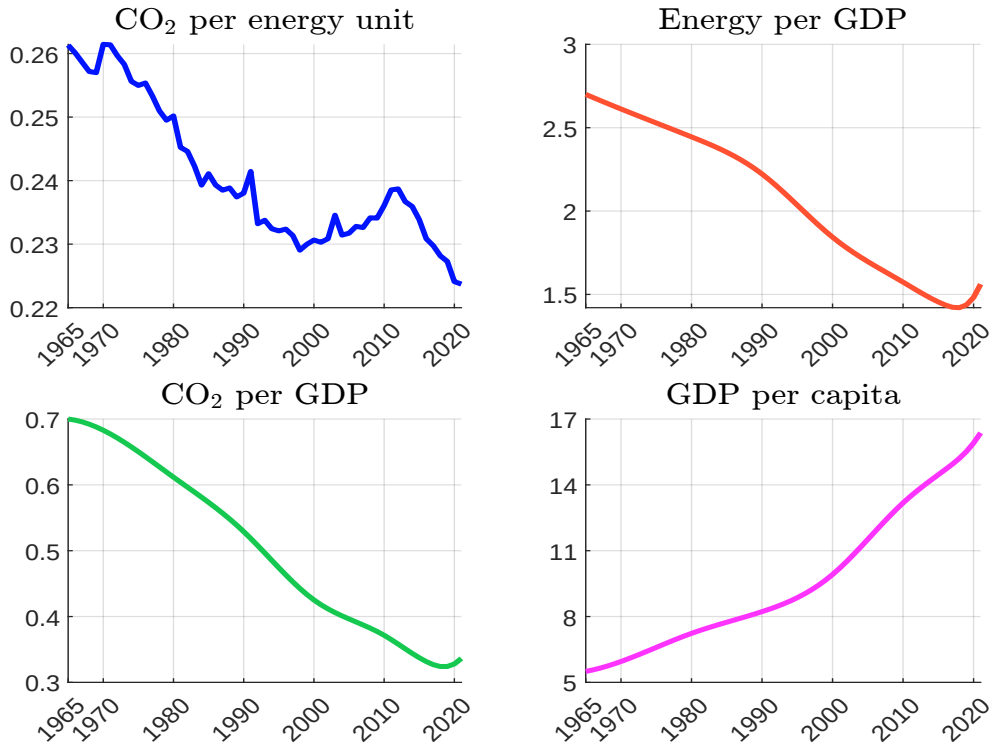


Source: Friedlingstein *et al.* (2022), https://globalcarbonbudget.org & https://github.com/owid/co2-data.

Figure 8.31: $CO_2$ emissions per capita (in $tCO_2$ per person)

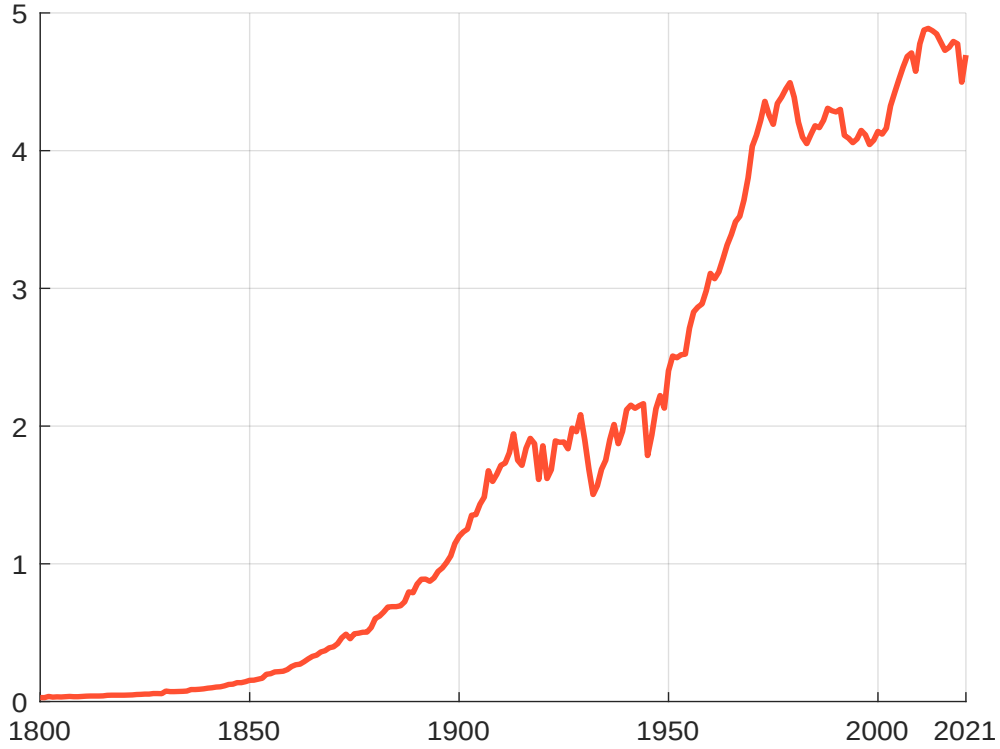


Source: Friedlingstein *et al.* (2022), https://globalcarbonbudget.org & https://github.com/owid/co2-data.

dollars per person). The first three measures fall, but GDP per capita does not. As people get richer, they consume more goods and services and emit more $CO_2$. This is the main driver of $CO_2$ emissions. This can be summarised by the trend in $CO_2$ per capita in Figure 8.31. We observe five periods: a continuous increase between 1800 and 1913, a flattening out between 1914 and 1945, a new increase between 1946 and 1979, a slight decrease between 1980 and 1999, and an upward trend again since 2000. Today, we produce about 5 tonnes of $CO_2$ per person.

Figure 8.32: GHG emissions (in $GtCO_2e$)

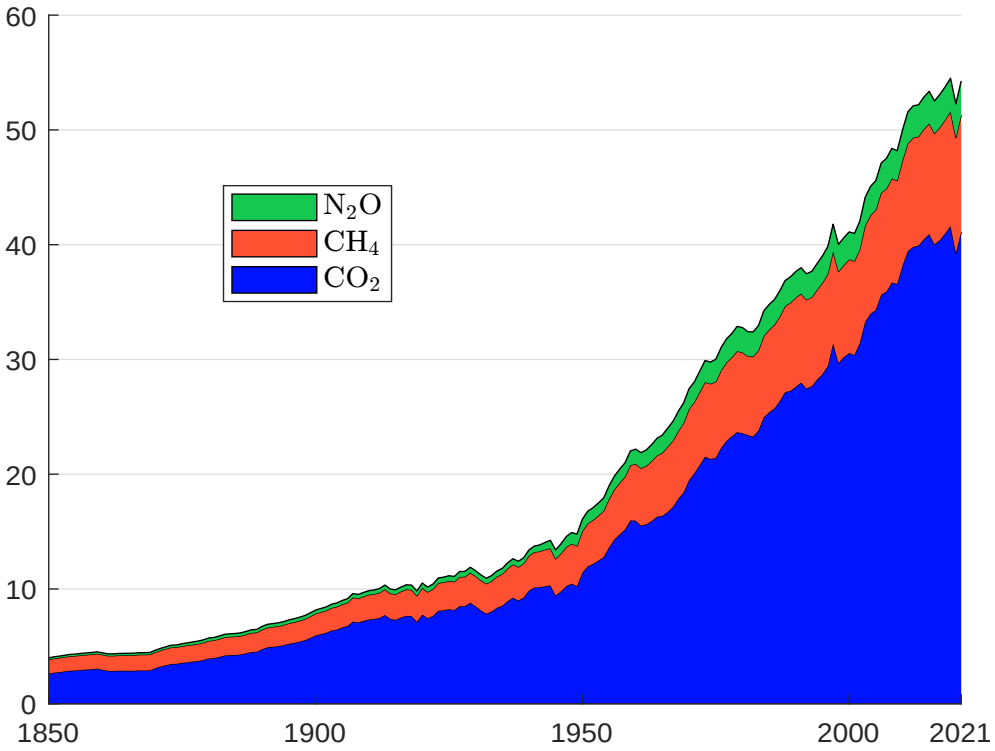


Source: Jones *et al.* (2023), https://zenodo.org/records/7636699#.ZFCy4exBweZ & Author's calculations.

The above analysis can be extended to other GHG emissions such as methane and nitrous oxide emissions. For each gas, it is important to specify the scope (*e.g.*, including or excluding land-use change and forestry). Using the data set calculated by Jones *et al.* (2023), we plot the evolution of greenhouse gas emissions[38] since 1850 and their decomposition into $CO_2$, $CH_4$ and $N_2O$ in Figure 8.32. GHG emissions include both industrial and land-use change sources. For the year 2021, Jones *et al.* (2023) estimated the following figures: 41.12 $GtCO_2$ for carbon dioxide, 10.18 $GtCO_2e$ for methane and 2.97 $GtCO_2e$ for nitrous oxide. The repartition is then 75.8%, 18.8% and 5.5%.

Table 8.7: 2021 greenhouse gas emissions (in $GtCO_2e$)

| $CH_4$ | | | $CO_2$ | | | $N_2O$ | | |
|---|---|---|---|---|---|---|---|---|
| $\mathcal{CE}_{\text{Industry}}$ | $\mathcal{CE}_{\text{Land}}$ | $\mathcal{CE}_{\text{Total}}$ | $\mathcal{CE}_{\text{Industry}}$ | $\mathcal{CE}_{\text{Land}}$ | $\mathcal{CE}_{\text{Total}}$ | $\mathcal{CE}_{\text{Industry}}$ | $\mathcal{CE}_{\text{Land}}$ | $\mathcal{CE}_{\text{Total}}$ |
| 6.23 | 3.95 | 10.18 | 37.11 | 4.00 | 41.12 | 0.79 | 2.18 | 2.97 |
| (61.2%) | (38.8%) | (18.8%) | (90.3%) | (9.7%) | (75.8%) | (26.7%) | (73.3%) | (5.5%) |

Source: Jones *et al.* (2023), https://zenodo.org/records/7636699#.ZFCy4exBweZ & Author's calculations.

[38] To calculate the $CO_2$ equivalent of $CH_4$ and $N_2O$, we use a global warming potential of 27.9 and 273 (see Section 9.1.1 on page 870.).

**Planetary boundaries** In addition to climate change, the impact of human activity on the Earth system affects many other issues. They can be summarised in terms of planetary boundaries, a concept developed by Rockström *et al.* (2009). We can define planetary boundaries as a normative framework for setting limits to the impact of human activities on the Earth system. Beyond these boundaries, the environment may no longer be able to regulate itself and the Earth system may leave the Holocene period of stability during which human society developed. The planetary boundaries framework has been updated twice, in 2015 (Steffen *et al.*, 2015b) and 2023 (Richardson *et al.*, 2023). We report the details of the current framework in Table 8.8 and Box 8.7. For each critical Earth process system, Richardson *et al.* (2023) defined a set of control variables and associated metrics. The baseline metric $m_{1750}$ corresponds to the pre-industrial Holocene base value. The planetary boundary is defined by a threshold $m_{\text{Boundary}}$, while $m_{\text{Upper}}$ indicates the upper end of the increasing risk. Finally, $m_{2023}$ is the current value of the control variable. If we assume that the risk increases with the metric, we have $m_{1750} \leq m_{\text{Boundary}} \leq m_{\text{Upper}}$. If $m_{2023} \geq m_{\text{Boundary}}$, the boundary is exceeded. If $m_{2023} \geq m_{\text{Upper}}$, this indicates a high risk. According to Richardson *et al.* (2023), six of the nine planetary boundaries have been crossed (Figure 8.33). They are climate change, biodiversity loss, biogeochemical flows, land-use change, freshwater change, and novel entities. The ocean acidification planetary boundary can be reached in a few years, while atmospheric aerosol loading and stratospheric ozone depletion are not at risk.

Figure 8.33: Planetary boundaries

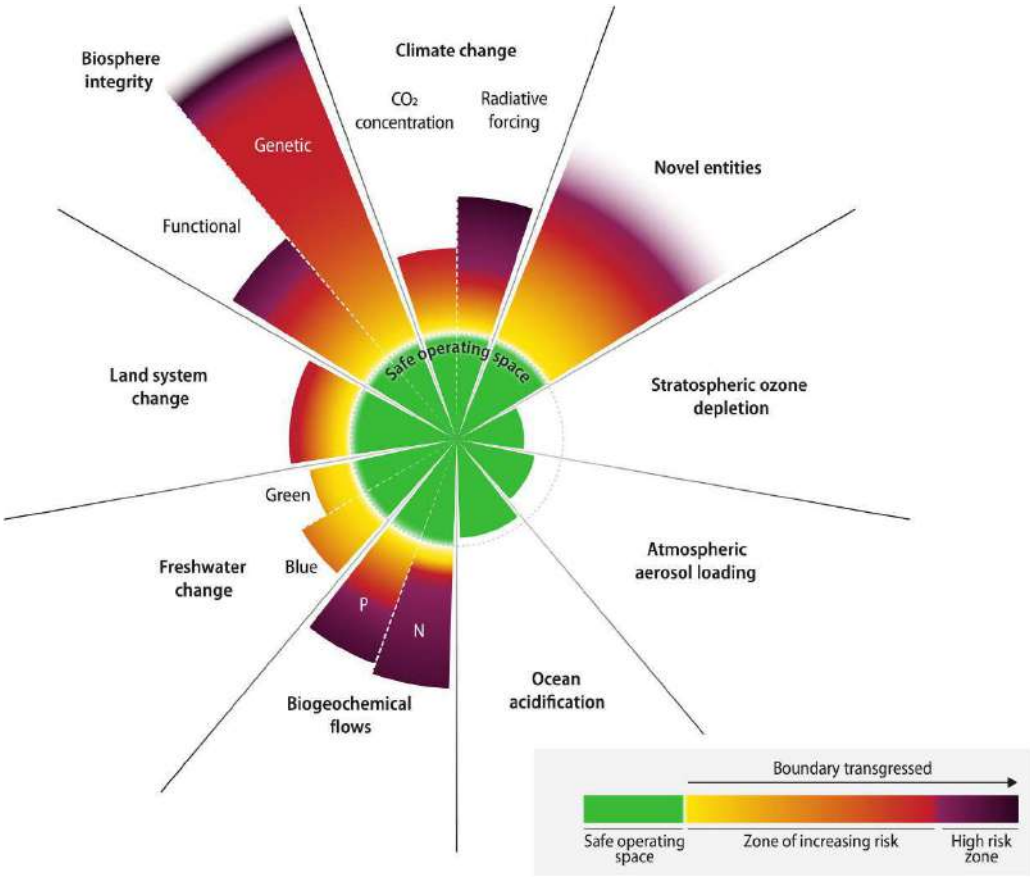


Source: Richardson *et al.* (2023, Figure 1, page 4).

Table 8.8: Current status of planetary boundaries

| No | Earth process system | Control variable | $m_{1750}$ | $m_{\text{Boundary}}$ | $m_{\text{upper}}$ | $m_{2023}$ | Crossed |
|---|---|---|---|---|---|---|---|
| 1 | Climate change | Atmospheric $CO_2$ concentration (ppm) | 280 | 350 | 450 | 417 | ✓ |
| | | Atmospheric radiative forcing ($W/m^2$) | 0 | 1.0 | 1.5 | 2.91 | ✓ |
| 2 | Biodiversity loss | Genetic diversity (E/MSY) | 1 | 10 | 100 | $> 100$ | ✓ |
| | | Functional integrity (% HANPP) | 1.9 | 10 | 20 | 30 | ✓ |
| 3 | Stratospheric ozone depletion | Stratospheric $O_3$ concentration (DU) | 290 | 276 | 261 | 284.6 | |
| 4 | Ocean acidification | Carbonate ion concentration ($\Omega_{\text{arg}}$) | 3.44 | 2.752 | 2.75 | 2.8 | |
| 5 | Biogeochemical flows | Phosphate flow (TgP/yr) – global | 0 | 11 | 100 | 22.6 | ✓ |
| | | Phosphate flow (TgP/yr) – regional | 0 | 6.2 | 11.2 | 17.5 | ✓ |
| | | Nitrogen flow (TgN/yr) | 0 | 62 | 82 | 190 | ✓ |
| 6 | Land-use change | Area of forested land (%) – global | 100 | 75 | 54 | 60 | ✓ |
| | | % area remaining – tropical | 100 | 85 | 60 | 58.6 | ✓ |
| | | % area remaining – temperate | 100 | 50 | 30 | 41.1 | ✓ |
| | | % area remaining – boreal | 100 | 85 | 60 | 63.5 | ✓ |
| 7 | Freshwater change | Blue water (%) | 9.4 | 10.2 | 50 | 18.2 | ✓ |
| | | Green water (%) | 9.8 | 11.1 | 50 | 15.8 | ✓ |
| 8 | Atmospheric aerosol loading | Inter-hemispheric difference (AOD) | 0.03 | 0.10 | 0.25 | 0.076 | |
| 9 | Novel entities | Synthetic chemicals (%) | 0 | 0 | NA | $> 0$ | ✓ |

Source: Richardson *et al.* (2023, Table 1, pages 4-5).

Box 8.7: Planetary boundaries defined by Richardson *et al.* (2023, Table 1, pages 4-5)

The planetary boundaries for climate change are defined by two control variables. First, the atmospheric $CO_2$ concentration $\mathcal{CC}_{\text{AT}}$ must be less than 280 ppm. Second, the total anthropogenic radiative forcing at the top of the atmosphere must be less than $+1.0\ \text{W/m}^2$. For biodiversity loss, there are again two targets. The genetic diversity target implies less than 10 extinctions per million species-years (E/MSY). Functional integrity measures the amount of energy produced by photosynthesis (net primary production or NNP). The control variable is herbivore-adjusted net primary production (HANPP), which is the amount of energy available to herbivores after plants have been consumed. The variation in HANPP must be less than 10% of the pre-industrial Holocene NPP. Stratospheric ozone depletion is measured by the stratospheric $O_3$ concentration $\mathcal{CC}_{\text{O}_3}$ or the total amount of ozone in a vertical column through the atmosphere (Dobson units or DU). The limit is $\mathcal{CC}_{\text{O}_3} \leq 276$ DU, which is 5% less than the pre-industrial level. For ocean acidification, the authors use the carbonate ion concentration $\left[\text{CO}_3^{2-}\right]$, which is a measure of the amount of dissolved carbonate ions in seawater. The control variable is the average global surface ocean saturation state with respect to aragonite $\Omega_{\text{arag}} = \dfrac{\left[\text{CO}_3^{2-}\right]}{\kappa_{sp}}$ where $\kappa_{sp}$ is the solubility product constant of aragonite. The limit $\Omega_{\text{arag}}$ is set to 80% of the pre-industrial Holocene baseline ($\Omega_{\text{arag}} = 3.44$). Biogeochemical flows reflect anthropogenic disturbances to the phosphorus (P) and nitrogen (N) cycles. The P cycle is assessed both globally (P flow from freshwater systems to the ocean) and regionally (P flow from fertilizers to erodible soils). The global limit is set at 11 Tg phosphorus per year, while the regional limit is set at 6.2 Tg phosphorus per year. Perturbation of the N cycle is measured by industrial and intentional nitrogen fixation. Its limit is set at 62 Tg nitrogen per year. The sixth Earth system process is assessed with both global (*e.g.*, deforestation, agriculture and urbanization) and biome-specific (*e.g.*, transformation of forests, grasslands, savannas, and deserts) land system changes. The global figure is calculated as the area of forest as a percentage of the original forest cover, while the biome figure is the area of forest as a percentage of the potential forest (% remaining area). The limits are 75% for the global figure, 85% for the tropical biome, 50% for the temperate biome and 85% for the boreal biome. Freshwater change is divided into blue water and green water. Blue water refers to surface water available for human use, while green water refers to water stored in the soil and vegetation (*i.e.*, water available to plants). The blue water control variable is the 95th percentile of global land area with deviations greater than the pre-industrial period, and its limit is set at 10.2%. The green water metric is the percentage of land area with deviations from pre-industrial variability. The pre-industrial Holocene baseline is 9.8%, and the limit is 11.1%. The eighth Earth system process is the atmospheric aerosol loading, the control variable is the inter-hemispheric difference in aerosol optical depth[a] (AOD), and the limit is 0.1 mean annual inter-hemispheric difference. The final planetary boundary concerns novel entities such as industrial chemicals, pesticides, microplastics, nanoparticles, nuclear waste and genetically modified organisms (GMO). The associated control variable is the percentage of synthetic chemicals released into the environment without adequate safety testing. This ninth planetary boundary is not well defined, because it is difficult to collect data on.

[a] AOD measures the amount of light absorbed by aerosols in the atmosphere. The inter-hemispheric difference in AOD is the difference between the average AOD in the Northern Hemisphere and the average AOD in the Southern Hemisphere.

### 8.1.3 The physics of climate change

In this section, energy and forcing are two interchangeable terms, meaning that $F_{\text{solar}} := \boldsymbol{\mathcal{E}}_{\text{solar}}$, $F_{\text{thermal}} := \boldsymbol{\mathcal{E}}_{\text{infrared}}$, etc. Moreover, we have made extensive use of Hartmann's Handbook on Climate Physics, particularly chapters 2, 3 and 10 (Hartmann, 2016).

#### Simple energy balance models

The Earth's temperature is closely related to its energy balance, which is the balance between the energy it receives from the Sun and the energy it emits:

> "*Temperature [...] is a measure of the energy contained in the movement of molecules. Therefore, to understand how the temperature is maintained, one must consider the energy balance that is formally stated in the first law of thermodynamics. The basic global energy balance of Earth is between energy coming from the Sun and energy returned to space by Earth's radiative emission. The generation of energy in the interior of Earth has a negligible influence on its energy budget.*" (Hartmann, 2016, page 25).

The first law of thermodynamics, also known as the law of conservation of energy, is a principle of physics which states that energy cannot be created or destroyed, it can only be transferred or converted from one form to another. This means that the total amount of energy in a closed system is conserved.

**Basics** To calculate the Earth's temperature, we need three basic tools of physics. They are the total solar irradiance, the Stefan-Boltzmann law and the emission temperature of a planet.

**Total solar irradiance** According to Hartmann (2016, page 29), the total amount of electromagnetic energy emitted by the Sun, also called the solar luminosity is $L_\odot = 3.828 \times 10^{26}$ watts. Using the first law of thermodynamics, the amount of energy emitted by any sphere with the Sun at its centre should be equal to the total energy flux from the Sun. Total solar irradiance (TSI) is defined as:

$$S_d = \frac{L_\odot}{4\pi d^2} \tag{8.3}$$

where $d$ is the distance of the sphere from the Sun in meters. For the Earth, the distance is between 147.1 and 152.1 million kilometers because the Earth's orbit around the Sun is not a perfect circle. Using a mean value of 149.6 million kilometers, we get:

$$S_0 = \frac{3.828 \times 10^{26}}{4\pi \left(149.6 \times 10^9\right)^2} = 1372.11 \text{ W/m}^2$$

A direct measurement by astrophysicists gives 1368 W/m$^2$ and we use this number in the sequel.

**Stefan-Boltzmann law** The Stefan-Boltzmann law describes the relationship between the total amount of radiation $\boldsymbol{\mathcal{E}}$ emitted by a body and its temperature $\mathcal{T}$:

$$\boldsymbol{\mathcal{E}} = \varepsilon\sigma\mathcal{T}^4 \tag{8.4}$$

where $\varepsilon \in [0, 1]$ is the emissivity of the body and $\sigma = 5.67 \times 10^{-8}$ W/m$^2$K$^{-4}$ is the Stefan-Boltzmann constant. For an ideal black body, we have $\varepsilon = 1$ and Equation (8.4) is related to the

Planck distribution[39] $B_\nu$ (or the intensity of the black body radiation):

$$\begin{aligned}\boldsymbol{\mathcal{E}} &= \pi \int_0^\infty B_\nu(\nu, \mathcal{T})\, \mathrm{d}\nu \\ &= \frac{2\pi^5 k^4}{15c^2h^3}\mathcal{T}^4 \\ &= \sigma\mathcal{T}^4\end{aligned}$$

where $h$ is Planck's constant, $c$ is the speed of light in a vacuum and $k$ is Boltzmann's constant.

Box 8.8: Planck radiation law and spectral density of electromagnetic radiation

In physics, Planck's law describes the spectral distribution of electromagnetic radiation emitted by a black body in thermal equilibrium at a given temperature. The expression for the spectral density function is:

$$B_\nu(\nu, \mathcal{T}) = \frac{2h\nu^3}{c^2} \frac{1}{\exp\left(\dfrac{h\nu}{k\mathcal{T}}\right) - 1}$$

where $h = 6.62607015 \times 10^{-34}\,\mathrm{J\,Hz^{-1}}$ is Planck's constant, $c = 299\,792\,458\,\mathrm{m\,s^{-1}}$ is the speed of light in a vacuum, $k = 1.380649 \times 10^{-23}\,\mathrm{J\,K^{-1}}$ is Boltzmann's constant, $\mathcal{T}$ is the temperature measured in Kelvin, and $\nu$ is the frequency in hertz. Alternatively, the law can be written in terms of the wavelength $\lambda$ expressed in meters:

$$\lambda = \frac{c}{\nu} \qquad \left(\sim \frac{\mathrm{m\,s^{-1}}}{\mathrm{Hz}} = \mathrm{m}\right)$$

We deduce that:

$$B_\lambda(\lambda, \mathcal{T}) = \frac{2hc^2}{\lambda^5} \frac{1}{\exp\left(\dfrac{hc}{\lambda k\mathcal{T}}\right) - 1}$$

Since we have $\dfrac{\mathrm{J\,Hz^{-1}m\,s^{-1}}}{\mathrm{m\,J\,K^{-1}K}} = 1$ and $\dfrac{\mathrm{J\,Hz^{-1}}\left(\mathrm{m\,s^{-1}}\right)^2}{\mathrm{m}^5} = \mathrm{J\,s^{-1}m^{-2}m^{-1}} = \mathrm{W\,m^{-2}m^{-1}}$, the unit of $B_\lambda(\lambda, \mathcal{T})$ is $\mathrm{W/m^2\,m^{-1}}$. In Figure 8.34, we show the spectral density for two values of temperature. We also show the visible spectrum, which is the band of the electromagnetic spectrum that is visible to the human eye. The electromagnetic spectrum also includes ultraviolet and infrared wavelengths. We use the following classification: UV (less than 380 nm), visible (380 nm to 780 nm), and infrared (greater than 780 nm). The temperature has a high impact on emitted radiations, since the spectral density is completely different for $\mathcal{T} = 5\,000\,\mathrm{K}$ and $\mathcal{T} = 3\,000\,\mathrm{K}$. Now let us illustrate the difference between solar and terrestrial radiation. In Figure 8.35, we scale the spectral density of the Earth's surface by a factor of $2.6 \times 10^6$ so that the two peaks are at the same level. Note that the spectrum of sunlight is shortwave radiation, while the spectrum of the Earth's surface is longwave radiation. We also see that the atmosphere is mainly transparent to a large part of the visible spectrum.

[39] The Planck distribution describes the probability of a photon being emitted with a particular energy.

Figure 8.34: Spectral density function $B_\lambda(\lambda, \mathcal{T})$ (in $10^{12}\,\mathrm{W/m^2\,m^{-1}}$)

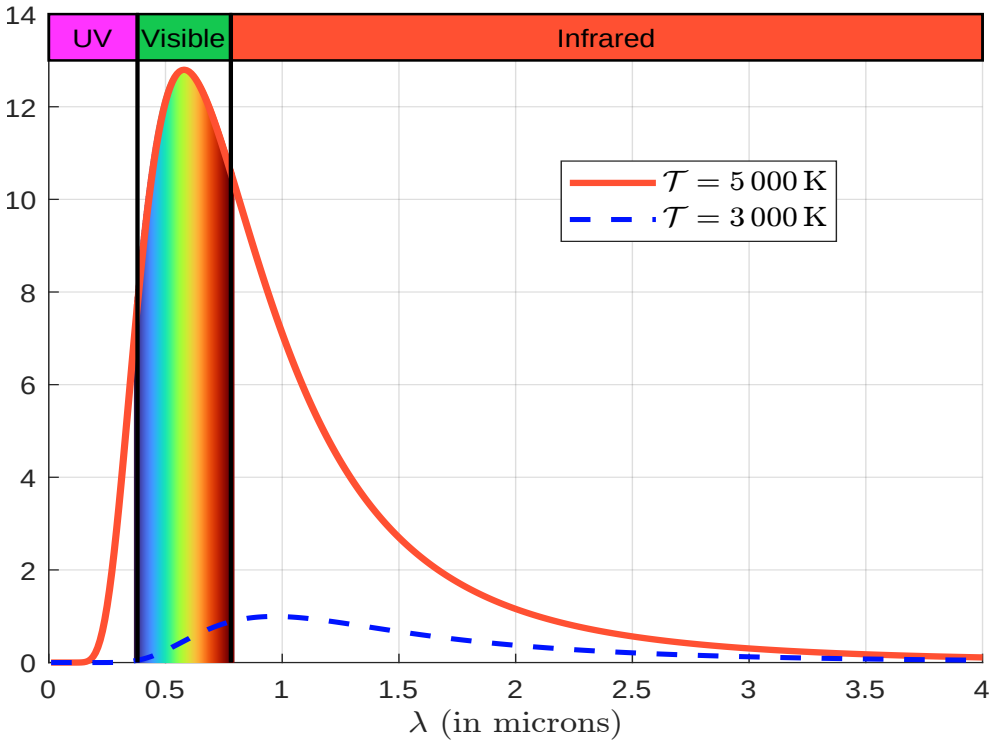


Figure 8.35: Comparison of the radiation spectra of sunlight and the Earth's surface (in $10^{12}\,\mathrm{W/m^2\,m^{-1}}$)

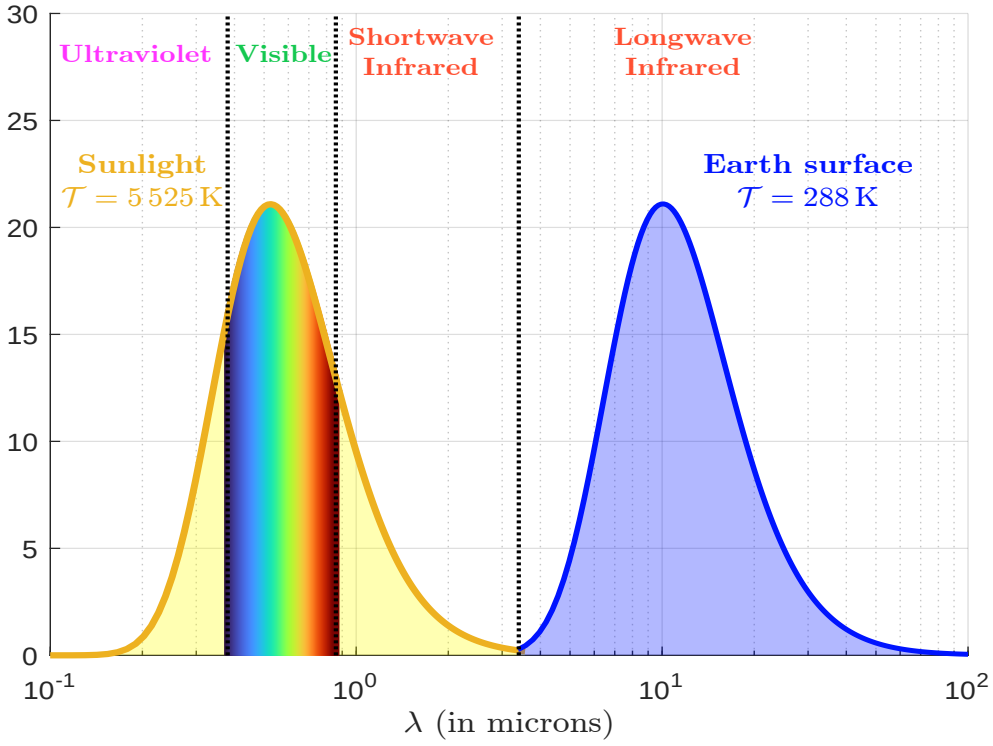

**Effective temperature of stars** Since the radius of the Sun $R_\odot$ is about 696 342 kilometers, the solar irradiance at the photosphere[40] is equal to:

$$S_\odot = \frac{L_\odot}{4\pi R_\odot^2} = \frac{3.828 \times 10^{26}}{4\pi \left(696\,342 \times 10^3\right)^2} = 62\,822\,741 \text{ W/m}^2$$

If we assume that the sun is a perfect black body[41], then we have:

$$\sigma \mathcal{T}_\odot^4 = S_\odot \Leftrightarrow \mathcal{T}_\odot = \sqrt[4]{\frac{S_\odot}{\sigma}}$$

The numerical calculation gives:

$$\mathcal{T}_\odot = \sqrt[4]{\frac{62\,822\,741}{5.67 \times 10^{-8}}} = 5\,769 \text{ K}$$

This effective temperature is slightly overestimated compared to a direct physical measurement. The previous analysis can be extended to other stars. Let $R_{\text{star}}$ be the stellar radius of the star. Since we have $L_{\text{star}} = 4\pi R_{\text{star}}^2 S_{\text{star}}$ and $S_{\text{star}} = \boldsymbol{\mathcal{E}} = \sigma \mathcal{T}^4$, we get:

$$\mathcal{T}_{\text{star}} = \sqrt[4]{\frac{L_{\text{star}}}{4\pi R_{\text{star}}^2 \sigma}} \tag{8.5}$$

$\mathcal{T}_{\text{star}}$ is defined as the temperature of a black body radiating the same amount of energy per unit area as the star. It may differ from the actual temperature of a star, which depends on its kinetic energy.

**Zero-order model of the atmosphere** Let us see how the effective temperature of the Earth is calculated.

**Incoming solar radiation** The incoming solar radiation is equal to:

$$F_{\text{solar}} = \frac{1}{4}\left(1 - \alpha_p\right) S_0$$

where $\alpha_p$ is the planetary albedo, which measures the amount of reflected sunlight. For example, $\alpha_p$ is equal to zero for a perfect black body, and one for a perfect white body. The ratio $\frac{1}{4}$ comes from the fact that no point on the planet receives the sun's energy continuously during a full day. This is particularly true at night, but also during the day, as the point is not necessarily at the sun's zenith. On average, we can show that a point on the planet receives $\frac{1}{4}$ of the solar energy, which is the ratio of the projected area of the sphere ($\mathcal{A}rea = \pi r^2$) divided by the surface area of the sphere ($\mathcal{A}rea = 4\pi r^2$). This incoming solar radiation is illustrated in Figure 8.36.

In the case of the Earth, we have $\alpha_p \approx 0.29$ (Stephens *et al.*, 2015, page 141). We deduce that:

$$F_{\text{solar}} = \frac{1}{4}\left(1 - 0.29\right) \times 1\,368 = 242.82 \text{ W/m}^2$$

To get an idea of how much energy is involved, consider a room with a surface area of $x$ square meters and receiving an energy $\boldsymbol{\mathcal{E}}$ expressed in watts. The radiation per square meter received by

[40] This is the visible surface of the Sun.

[41] In fact, the emissivity of the sun is $\varepsilon = 0.96$.

Figure 8.36: Incoming solar radiation

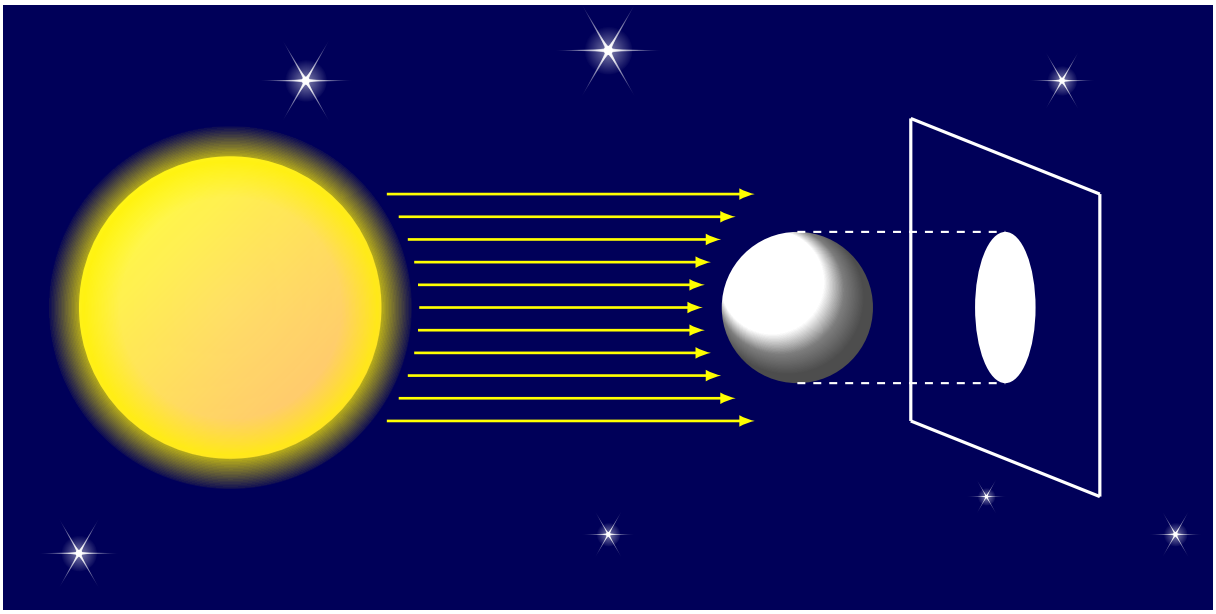

this room is equal to $\mathcal{E}/x$. If the room receives the same equivalent solar radiation $F_{\text{solar}}$, the energy must be equal to:

$$\mathcal{E} = x \cdot F_{\text{solar}}$$

Using a standard 200 watt lamp, we can calculate the number of lamps required to achieve the same equivalent solar radiation. The results are shown below:

| $x$ (in $m^2$) | 1 | 5 | 10 | 20 | 50 | 100 |
|---|---|---|---|---|---|---|
| $\mathcal{E}$ (in watts) | 242.8 | 1 214 | 2 428 | 4 856 | 12 141 | 24 282 |
| # lights | 1.2 | 9 | 12 | 24 | 61 | 121 |

For a room of 20 $m^2$, we need 24 lights.

**Effective temperature of the Earth** The Earth receives the incoming solar radiation $F_{\text{solar}}$, while the black body radiation is given by the Stefan-Boltzmann law. The schematic energy flow diagram is given in Figure 8.37. We deduce that:

$$\sigma \mathcal{T}_e^4 = \frac{1}{4}(1-\alpha_p) S_0 \Leftrightarrow \mathcal{T}_e = \sqrt[4]{\frac{(1-\alpha_p) S_0}{4\sigma}}$$

The numerical calculation gives:

$$\begin{aligned} \mathcal{T}_e &= \sqrt[4]{\frac{(1-0.29) \times 1\,368}{4 \times 5.67 \times 10^{-8}}} \\ &= 255.81\,\text{K} \\ &= 255.81°\text{C} - 273.15°\text{C} \\ &= -17.34°\text{C} \end{aligned}$$

The effective temperature of the Earth is then close to $-17.34°$C. Without greenhouse gases, the surface temperature of the Earth should be equal to the effective temperature. However, we observe

$$\mathcal{T}_s \approx +15°\text{C} \gg \mathcal{T}_e \approx -17°\text{C}$$

Figure 8.37: Zero-order model

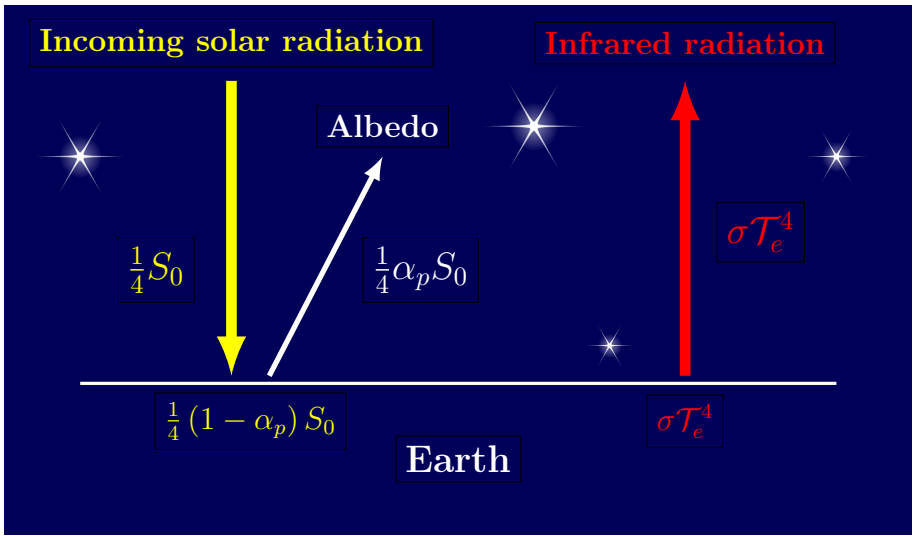


To explain this difference of 32°C, we need to introduce the greenhouse effect.

**Impact of the greenhouse effect** To illustrate the greenhouse effect, Hartmann (2016) proposed to include an atmosphere in the global energy balance. He assumed that the atmosphere is a black body for terrestrial radiation but transparent to solar radiation:

> "*Since solar radiation is mostly visible and near infrared, and Earth emits primarily thermal infrared radiation, the atmosphere may affect solar and terrestrial radiation very differently. [...] Since the atmospheric layer absorbs all of the energy emitted by the surface below it and emits like a blackbody, the only radiation emitted to space is from the atmosphere in this model.*" (Hartmann, 2016, pages 32-32).

From Figure 8.38, we can deduce that the energy balance for the Earth's surface is:

$$F_{\text{solar}} + \sigma\mathcal{T}_{\text{a}}^4 = \sigma\mathcal{T}_s^4$$

while the radiation balance for the atmosphere verifies:

$$\sigma\mathcal{T}_s^4 = 2\sigma\mathcal{T}_{\text{a}}^4$$

It follows that:

$$F_{\text{solar}} + \sigma\mathcal{T}_{\text{a}}^4 = 2\sigma\mathcal{T}_{\text{a}}^4$$

or[42]:

$$F_{\text{solar}} = \sigma\mathcal{T}_{\text{a}}^4 = \sigma\mathcal{T}_{\text{e}}^4$$

We conclude that:

$$\begin{cases} \mathcal{T}_{\text{a}} = \mathcal{T}_{\text{e}} \\ \mathcal{T}_s = \sqrt[4]{2}\mathcal{T}_{\text{e}} \end{cases}$$

[42] We use the fact that the effective temperature $\mathcal{T}_{\text{e}}$ is defined by the relation $\sigma\mathcal{T}_e^4 = \frac{1}{4}(1-\alpha_p)S_0 := F_{\text{solar}}$.

Using the previous numerical values, we obtain:

$$\begin{cases} \mathcal{T}_{\mathrm{a}} = 255.81\,\mathrm{K} = -17.34°\mathrm{C} \\ \mathcal{T}_s = 304.22\,\mathrm{K} = 31.07°\mathrm{C} \end{cases}$$

We find that the surface temperature is warmer than the observed global mean surface temperature. This is because the assumption that the atmosphere absorbs all the heat radiated from the surface is not true.

Figure 8.38: Zero-order model with greenhouse effect

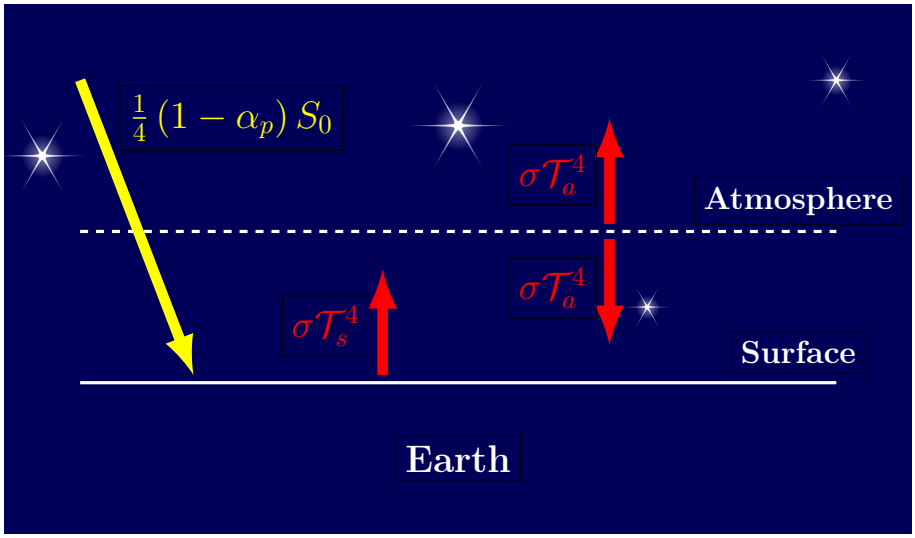


Another way to illustrate the greenhouse effect is to estimate the reflection parameter $\gamma_p$, which measures the net thermal radiation of the atmosphere with respect to the black body energy (Dommenget, 2022). We deduce that the balance $\boldsymbol{\mathcal{E}}_{\mathrm{net}}$ is:

$$\boldsymbol{\mathcal{E}}_{\mathrm{net}} = F_{\mathrm{solar}} - \sigma\mathcal{T}_s^4 - \gamma_p\sigma\mathcal{T}_s^4$$

Solving the equation $\boldsymbol{\mathcal{E}}_{\mathrm{net}} = 0$ gives:

$$\gamma_p = 1 - \frac{F_{\mathrm{solar}}}{\sigma\mathcal{T}_s^4} = 1 - \frac{(1-\alpha_p)\,S_0}{4\sigma\mathcal{T}_s^4}$$

Using a surface temperature of 15°C, we get $\gamma_p = 0.3788$. This means that only 62% of the infrared radiation goes into space and 38% stays on the surface.

**Multi-layer model of the atmosphere** Let us now consider the energy balance when we have two layers. This extension is motivated by the simplifying assumption that an atmosphere can be represented as a single black body:

> "*A layer of atmosphere that is almost opaque for longwave radiation can be crudely approximated as a blackbody that absorbs all terrestrial radiation that is incident upon it and emits like a blackbody at its temperature. For an atmosphere with a large infrared optical depth, the radiative transfer process can be represented with a series of blackbodies arranged in vertical layers. Two layers centered at 0.5 km and 2.0 km altitudes provide a simple approximation for Earth's atmosphere.*" (Hartmann, 2016, page 71).

Figure 8.39: Two-layer model

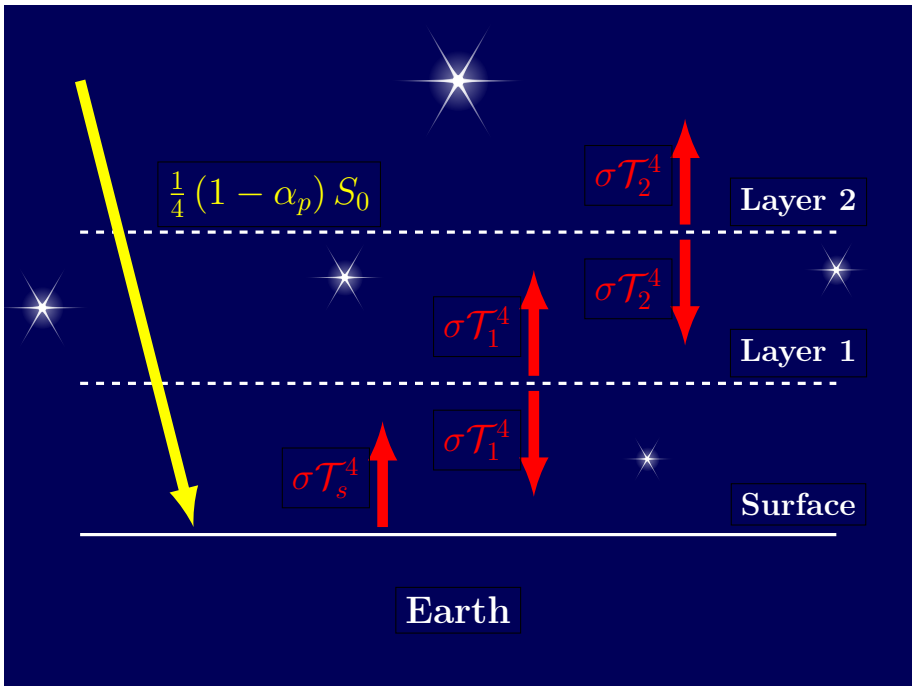


If we assume that the atmospheric layers are transparent to solar radiation, we have the schematic energy flow diagram shown in Figure 8.39. We have:

$$\begin{cases} F_{\text{solar}} + \sigma\mathcal{T}_1^4 = \sigma\mathcal{T}_s^4 \\ \sigma\mathcal{T}_2^4 + \sigma\mathcal{T}_s^4 = 2\sigma\mathcal{T}_1^4 \\ \sigma\mathcal{T}_1^4 = 2\sigma\mathcal{T}_2^4 \end{cases}$$

By replacing $F_{\text{solar}}$ by $\sigma\mathcal{T}_e^4$ and dividing the equations by $\sigma$, we get:

$$\begin{cases} \mathcal{T}_s^4 = 3\,\mathcal{T}_{\text{e}}^4 \\ \mathcal{T}_1^4 = 2\,\mathcal{T}_{\text{e}}^4 \\ \mathcal{T}_2^4 = 1\,\mathcal{T}_{\text{e}}^4 \end{cases}$$

The solution is then equal to:

$$\begin{cases} \mathcal{T}_s = \sqrt[4]{3}\,\mathcal{T}_{\text{e}} = 336.67\,\text{K} = 63.52°\text{C} \\ \mathcal{T}_1 = \sqrt[4]{2}\,\mathcal{T}_{\text{e}} = 304.22\,\text{K} = 31.07°\text{C} \\ \mathcal{T}_2 = \sqrt[4]{1}\,\mathcal{T}_{\text{e}} = 255.81\,\text{K} = -17.34°\text{C} \end{cases}$$

It is easy to generalize these results to the multi-layer atmosphere layer. Let $n$ be the total number of layers and $\mathcal{T}_k$ be the temperature at layer $k$. We have:

$$\begin{cases} \mathcal{T}_s = \mathcal{T}_0 = \sqrt[4]{n+1}\,\mathcal{T}_{\text{e}} \\ \mathcal{T}_k = \sqrt[4]{n+1-k}\,\mathcal{T}_{\text{e}} \qquad \text{for } k = 0, 1, \ldots, n \end{cases} \tag{8.6}$$

The multi-layer model is important because the atmosphere cannot be considered as a homogeneous black body. If this were true, the temperature of the atmosphere would be the same regardless of altitude. In reality, we observe that the temperature is highest at the Earth's surface and decreases

Table 8.9: Layers of the Earth's atmosphere

| Index | Layer | Altitude (in Km) |
|---|---|---|
| 1 | Troposphere | 12 |
| 2 | Stratosphere | 50 |
| 3 | Mesosphere | 80 |
| 4 | Thermosphere | 500 |
| 5 | Exosphere | 6 200 |

as we move towards the vacuum of space. This explains why the Earth's atmosphere is generally divided into five layers based on temperature and composition, as shown in Table 8.9. The solution of the multi-layer model given in Equation (8.6) satisfies the property that the temperature decreases with the layer index:

$$\frac{\partial \mathcal{T}_k}{\partial k} = -\frac{1}{4}(n+1-k)^{-3/4}\,\mathcal{T}_{\mathrm{e}} \leq 0$$

Let $z$ be the altitude in km. Since $z$ is an increasing function of the layer index $k$, we deduce from the previous property that:

$$\frac{\partial \mathcal{T}(z)}{\partial z} \leq 0$$

With this simple multi-layer model, we then showed that temperature is a decreasing function of altitude, that the Earth is warmer at the surface, and that the global temperature surface depends on the multi-layer structure of the atmosphere. So it also depends on the composition of the atmosphere, because that is the main determinant of the structure of the atmosphere. However, the previous multi-layer model is not realistic because the estimated temperatures are far from the observed mean temperatures.

**Emissivity model of the atmosphere** The previous model is too simple for several reasons. The first reason is that the real atmosphere is not opaque. This means that it is more of a gray body than a black body. In addition to radiation, energy is also transported by convection[43]. Therefore, we cannot ignore the effect of emissivity.

We consider the one-layer model described in Figure 8.38, and introduce the emissivity $\varepsilon$ of the atmosphere (Figure 8.40). The energy balance equilibrium becomes:

- The balance at the top of the atmosphere is:

$$F_{\text{solar}} - (1-\varepsilon)\,\sigma\mathcal{T}_s^4 - \varepsilon\sigma\mathcal{T}_a^4 = 0$$

- The balance of the atmosphere is:

$$\varepsilon\sigma\mathcal{T}_s^4 - 2\varepsilon\sigma\mathcal{T}_a^4 = 0$$

- The balance at the surface is:

$$F_{\text{solar}} + \varepsilon\sigma\mathcal{T}_a^4 - \sigma\mathcal{T}_s^4 = 0$$

The first equation is equivalent to:

$$(1-\varepsilon)\,\sigma\mathcal{T}_s^4 + \varepsilon\sigma\mathcal{T}_a^4 = F_{\text{solar}} = \sigma\mathcal{T}_e^4$$

[43] Another important missing factor is ocean transportation.

Figure 8.40: One-layer model with atmospheric emissivity

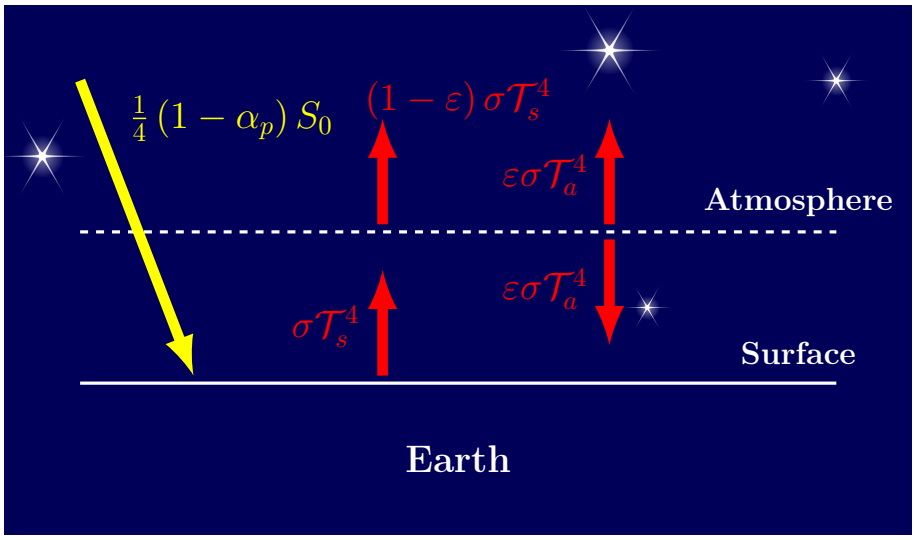


Using the second equation, it follows that:

$$\sigma\mathcal{T}_e^4 = (1-\varepsilon)\,\sigma\mathcal{T}_s^4 + \frac{1}{2}\varepsilon\sigma\mathcal{T}_s^4 = \left(1-\frac{1}{2}\varepsilon\right)\mathcal{T}_s^4$$

Finally, we conclude that[44]:

$$\mathcal{T}_s = \sqrt[4]{\frac{2}{2-\varepsilon}}\mathcal{T}_e$$

and:

$$\mathcal{T}_a = \sqrt[4]{\frac{1}{2-\varepsilon}}\mathcal{T}_e$$

The relationship between atmospheric emissivity $\varepsilon$ and temperature ($\mathcal{T}_s$ and $\mathcal{T}_a$) is shown in Figure 8.41. It is an increasing function. Therefore, for a given temperature $\mathcal{T}_s^\star$, we can find the unique value of the emissivity:

$$\varepsilon^\star = 2 - 2\left(\frac{\mathcal{T}_e}{\mathcal{T}_s^\star}\right)^4$$

Since $\mathcal{T}_s^\star \approx 15°\text{C}$, the emissivity of the atmosphere is 78%. This model then predicts an atmospheric temperature of $-30.8°\text{C}$.

**Remark 77** *More generally, the Earth's energy balance is the sum of net shortwave radiation and net longwave radiation (Liang et al., 2019):*

$$\mathcal{E}_{\text{net}} = \underbrace{\mathcal{E}_{\text{down}}^{\text{short}} - \mathcal{E}_{\text{up}}^{\text{short}}}_{\textit{Net shortwave}} + \underbrace{\mathcal{E}_{\text{down}}^{\text{long}} - \mathcal{E}_{\text{up}}^{\text{long}}}_{\textit{Net longwave}}$$

*where* $\mathcal{E}_{\text{down}}^{\text{short/long}}$ *is shortwave/longwave downward radiation and* $\mathcal{E}_{\text{up}}^{\text{short/long}}$ *is shortwave/longwave upward radiation. In the previous model, we have* $\mathcal{E}_{\text{net}}^{\text{short}} = \frac{1}{4}(1-\alpha_p)\,S_0$ *and* $\mathcal{E}_{\text{net}}^{\text{long}} = \varepsilon\sigma\mathcal{T}_a^4 - \sigma\mathcal{T}_s^4$. *Using more realistic assumptions, we get the Earth's energy balance shown in Figure 8.42. This type of representation was popularized by Kiehl and Trenberth (1997) and Trenberth et al. (2009).*

[44] We also check that the third equation is satisfied.

Figure 8.41: Relationship between atmospheric emissivity and temperature

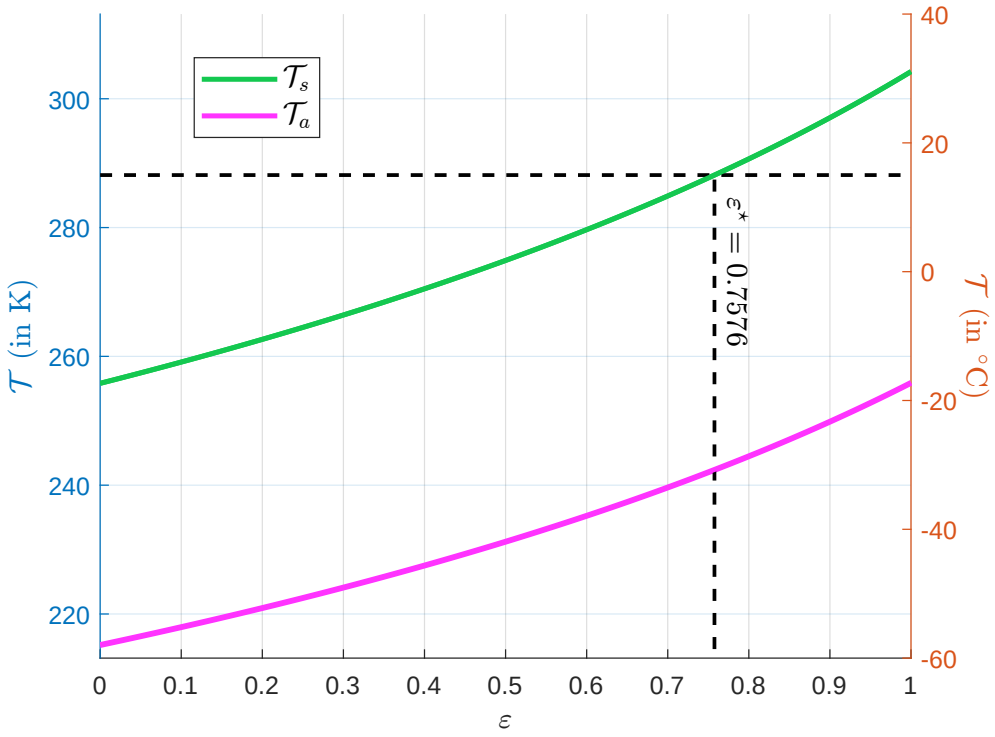


Figure 8.42: Earth's Energy Budget

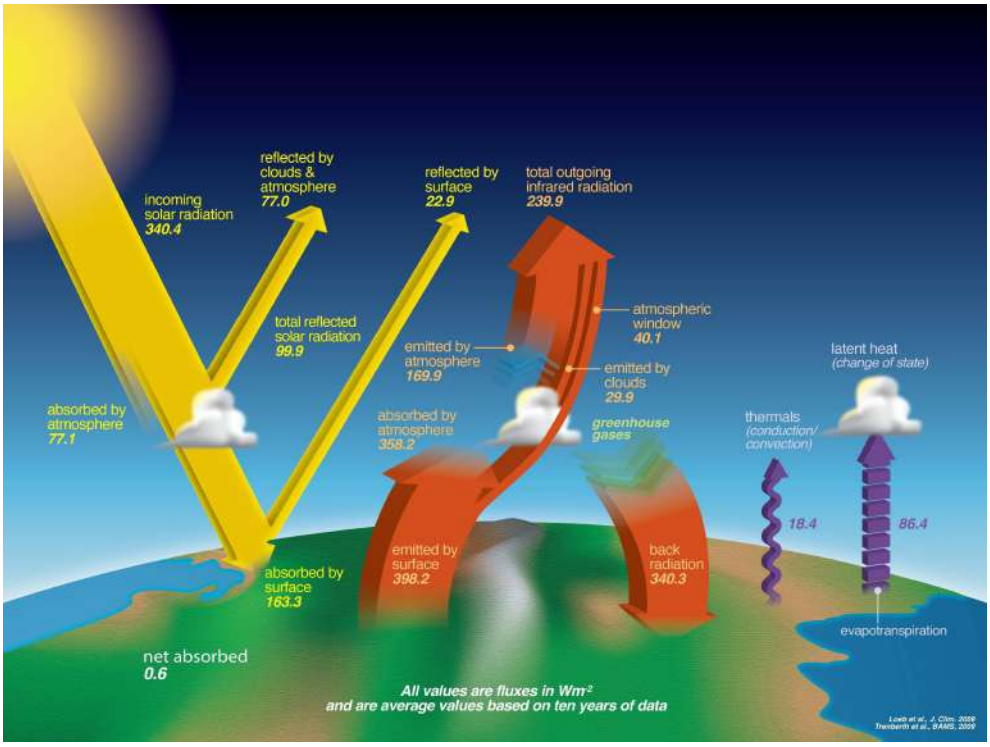


Source: NASA, https://mynasadata.larc.nasa.gov/basic-page/earths-energy-budget.

### Climate sensitivity and feedback

**Specific heat capacity** The specific heat capacity $c$ of a substance is the heat capacity $C$ of the substance divided by the mass of the substance:

$$c = \frac{C}{M} = \frac{1}{M}\frac{\Delta \mathcal{E}}{\Delta \mathcal{T}} \tag{8.7}$$

where $\Delta\mathcal{E}$ is the amount of heat required to raise the temperature of the substance by $\Delta\mathcal{T}$. Here, $M$ is the mass of the substance in kilograms (kg), $\Delta\mathcal{E}$ is the change in energy in joules (J), $\Delta\mathcal{T}$ is the change in temperature in Kelvin (K) and $c$ is the specific heat capacity in joules per kilogram per Kelvin ($\mathrm{J\,kg^{-1}\,K^{-1}}$). For example, the specific heat capacity of water is $4\,186\,\mathrm{J\,kg^{-1}\,K^{-1}}$. From Equation (8.7), we deduce that:

$$\Delta \mathcal{E} = Mc\,\Delta \mathcal{T} \tag{8.8}$$

In this case, the amount of energy required to raise the temperature of $1\,\mathrm{m^3}$ of water by 10°C is equal to:

$$\Delta \mathcal{E} = 10^3 \times 4\,186 \times 10 = 4\,186\,000\,\mathrm{J}$$

The specific heat capacity of air is about $1\,000\,\mathrm{J\,kg^{-1}\,K^{-1}}$, while the mass of the atmosphere is $5.148 \times 10^{18}$ kg. Therefore, the amount of energy required to raise the temperature of the atmosphere by 1°C is:

$$\begin{aligned} \Delta \mathcal{E} &= \left(5.148 \times 10^{18}\,\mathrm{kg}\right) \times \left(1\,000\,\mathrm{J\,kg^{-1}\,K^{-1}}\right) \times 1\,\mathrm{K} \\ &= 5.148 \times 10^{21}\,\mathrm{J} \end{aligned}$$

We can also write Equation (8.7) as follows:

$$\Delta \mathcal{T} = \frac{\Delta \mathcal{E}}{Mc} \tag{8.9}$$

This equation gives the change in temperature for a change in energy. For example, adding 1 000 joules of energy to one liter of water will increase its temperature by about 0.239°C:

$$\Delta \mathcal{T} = \frac{1000}{1 \times 4\,186} = 0.239$$

Equations (8.7)–(8.9) can be modified by scaling the mass $M$ of the substance to standardize the required energy $\Delta\mathcal{E}$. A possible scaling factor can be the surface area:

$$m = \frac{M}{\mathcal{A}rea}$$

and we get:

$$\Delta \mathcal{E} = mc\,\Delta \mathcal{T} \tag{8.10}$$

For the atmosphere, we have:

$$m = \frac{M}{\mathcal{A}rea} = \frac{5.148 \times 10^{18}\,\mathrm{kg}}{510.0645 \times 10^6 \times 10^6\,\mathrm{m^2}} = 1.0093 \times 10^4\,\mathrm{kg\,m^{-2}}$$

because the radius $r$ of the Earth is 6 371 km and the surface of the Earth is approximately $\mathcal{A}rea = 4\pi r^2 = 510.0645$ million $\mathrm{km^2}$. In some climate modeling textbooks, Equation (8.10) is expressed using other formulas for the mass of the atmosphere per unit area. For example, $m$ can be replaced

by the product of height $h$ and density $\rho$, or by the ratio of pressure $p$ to gravitational acceleration $g$. However, all these quantities are equivalent because we have:

$$m = h\rho = \left(8.2 \times 10^3\,\mathrm{m}\right) \times \left(1.225\,\mathrm{kg\,m^{-3}}\right) = 1.0045 \times 10^3\,\mathrm{kg\,m^{-2}}$$

and:

$$m = \frac{p}{g} = \frac{101\,325\,\mathrm{Pa}}{9.81\,\mathrm{m\,s^{-2}}} = \frac{101\,325\,\mathrm{m^{-1}\,kg\ s^{-2}}}{9.81\,\mathrm{m\,s^{-2}}} = 1.0329 \times 10^4\,\mathrm{kg\,m^{-2}}$$

where $h = 8.2\,\mathrm{km}$ is the height of the atmosphere[45], $\rho = 1.225\,\mathrm{kg\,m^{-3}}$ is the density of the atmosphere, $p = 101\,325\,\mathrm{Pa}$ is the standard atmospheric pressure at sea level on Earth, and $g = 9.81\,\mathrm{m\,s^{-2}}$ is the acceleration due to gravity at the Earth's surface. Therefore, we obtain the following equivalent formulas:

$$mc\,\Delta\mathcal{T} = h\rho c\,\Delta\mathcal{T} = \frac{p}{g}c\,\Delta\mathcal{T} = \Delta\boldsymbol{\mathcal{E}}$$

**Radiative relaxation timescale** We transform Equation (8.10) into a differential equation:

$$mc\frac{\mathrm{d}\mathcal{T}}{\mathrm{d}t} = \frac{\mathrm{d}\boldsymbol{\mathcal{E}}}{\mathrm{d}t}$$

We consider a black body. At the equilibrium, we have:

$$F_{\text{solar}} - \sigma\mathcal{T}^4 = 0$$

We deduce that:

$$\begin{aligned}\boldsymbol{\mathcal{E}} &= F_{\text{solar}} - \sigma\mathcal{T}^4\\ &= \sigma\mathcal{T}_e^4 - \sigma\mathcal{T}^4\end{aligned}$$

Let us assume that $\mathcal{T} = \mathcal{T}_e + \Delta\mathcal{T}$. It follows that:

$$mc\frac{\mathrm{d}\Delta\mathcal{T}}{\mathrm{d}t} = -4\sigma\mathcal{T}_e^3\Delta\mathcal{T}$$

because:

$$\frac{\partial}{\partial\Delta\mathcal{T}}\left(\sigma\mathcal{T}_e^4 - \sigma\mathcal{T}^4\right) = -4\sigma\mathcal{T}_e^3$$

Let $\tau_e$ be the radiative relaxation timescale defined as:

$$\tau_e = \frac{mc}{4\sigma\mathcal{T}_e^3}$$

We have:

$$\begin{cases}\dfrac{\mathrm{d}\Delta\mathcal{T}}{\mathrm{d}t} = -\dfrac{1}{\tau_e}\Delta\mathcal{T}\\ \Delta\mathcal{T}\left(0\right) = \Delta\mathcal{T}_0\end{cases}$$

The solution of this ordinary differential equation is well-known and we get:

$$\Delta\mathcal{T}\left(t\right) = \exp\left(-\frac{t}{\tau_e}\right)\Delta\mathcal{T}_0$$

[45]The height of the atmosphere depends on the choice of layer. Here we consider the troposphere, which is the lowest layer of the atmosphere at the polar regions.

$\Delta\mathcal{T}(t)$ gives the impulse response of an initial temperature shock of $\Delta\mathcal{T}_0$. Because $\tau_e > 0$, we conclude that the system is stable:

$$\lim_{t\to\infty} \Delta\mathcal{T}(t) = 0$$

We note that the equation for $\Delta\mathcal{T}(t)$ describes an exponential survival function with parameter $\tau_e^{-1}$. We deduce that the radiative relaxation timescale $\tau_e$ is the mean lifetime.

Using the previously obtained values for the atmosphere ($m = 1.0093 \times 10^4\,\mathrm{kg\,m^{-2}}$, $c = 1\,000\,\mathrm{J\,kg^{-1}\,K^{-1}}$ and $\mathcal{T}_e = 255.81\,\mathrm{K}$), the radiative relaxation timescale is equal to 31 days[46]:

$$\begin{aligned}
\tau_e &= \frac{\left(1.0093 \times 10^4\,\mathrm{kg\,m^{-2}}\right) \times \left(1\,000\,\mathrm{J\,kg^{-1}\,K^{-1}}\right)}{4 \times \left(5.67 \times 10^{-8}\,\mathrm{W\,m^{-2}\,K^{-4}}\right) \times \left(255.81\,\mathrm{K}\right)^3} \\
&= 2\,658\,427\,\mathrm{J\,W^{-1}} \\
&= \frac{2\,658\,427\,\mathrm{s}}{24 \times 3\,600\,\mathrm{s}} \\
&= 30.77\,\mathrm{days}
\end{aligned}$$

Figure 8.43 shows the impulse response function for $\Delta\mathcal{T}_0 = +1°\mathrm{C}$. We check that the effect of the initial shock disappears after a period of a few weeks. However, the memory of the temperature perturbation depends strongly on the effective temperature $\mathcal{T}_e$, as illustrated in the second panel of Figure 8.43. This explains why a temperature shock does not have the same effect all over the terrestrial globe, *e.g.*, in the polar regions or in the equatorial regions.

Figure 8.43: Impulse response function for $\Delta\mathcal{T}_0 = +1°\mathrm{C}$ and a black body

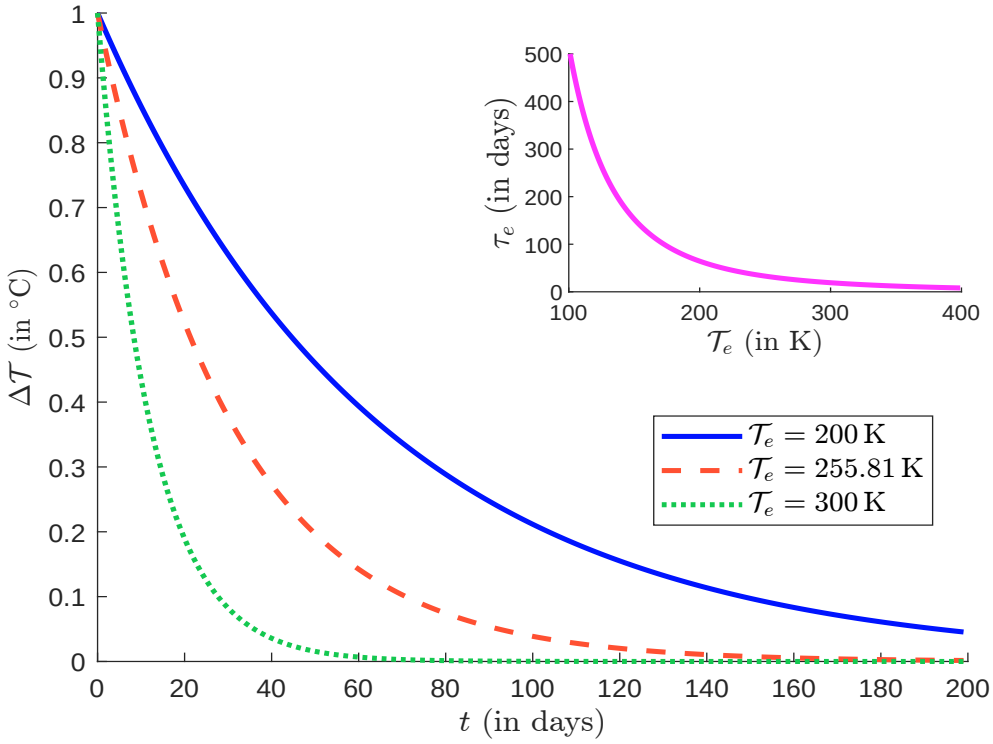


[46] We use the fact that $\mathrm{J\,W^{-1}} = \mathrm{s}$.

Figure 8.44: Impulse response function for $\Delta\mathcal{T}_0 = +1°\text{C}$ and a gray body

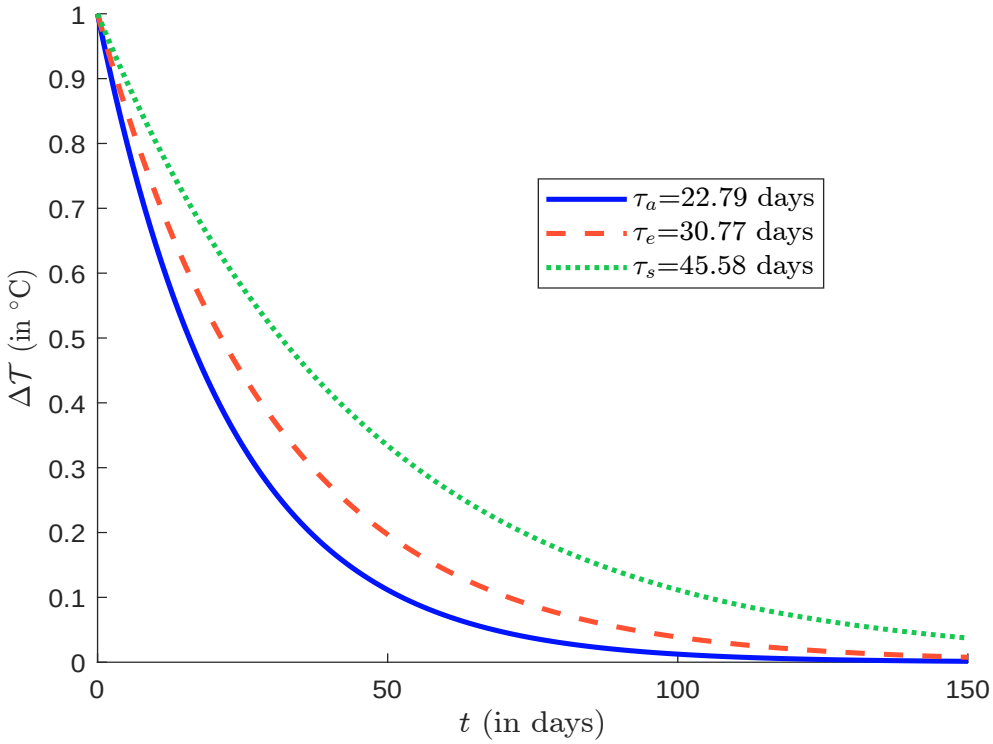


Now consider the case of a gray body and the one-layer model with emissivity. On page 668, we found that:

$$\sigma\mathcal{T}_e^4 = (2-\varepsilon)\,\sigma\mathcal{T}_a^4 = \left(\frac{2-\varepsilon}{2}\right)\sigma\mathcal{T}_s^4$$

We deduce that:

$$mc\frac{\mathrm{d}\mathcal{T}_a}{\mathrm{d}t} = \frac{\mathrm{d}}{\mathrm{d}t}\left(\sigma\mathcal{T}_e^4 - (2-\varepsilon)\,\sigma\mathcal{T}_a^4\right)$$

and:

$$mc\frac{\mathrm{d}\mathcal{T}_s}{\mathrm{d}t} = \frac{\mathrm{d}}{\mathrm{d}t}\left(\sigma\mathcal{T}_e^4 - \left(\frac{2-\varepsilon}{2}\right)\sigma\mathcal{T}_s^4\right)$$

Using the same reasoning as above, we obtain:

$$\begin{cases} \Delta\mathcal{T}_a(t) = \exp\left(-\dfrac{t}{\tau_a}\right)\Delta\mathcal{T}_0 \\ \Delta\mathcal{T}_s(t) = \exp\left(-\dfrac{t}{\tau_s}\right)\Delta\mathcal{T}_0 \end{cases}$$

where:

$$\tau_a = \frac{mc}{4\,(2-\varepsilon)\,\sigma\mathcal{T}_e^3} \qquad \text{and} \qquad \tau_s = \frac{mc}{2\,(2-\varepsilon)\,\sigma\mathcal{T}_e^3}$$

We consider an emissivity value of 65%, and find that $\tau_a = 22.79$ and $\tau_s = 45.58$ days. The corresponding impulse response functions are given in Figure 8.44. Although these calculations are rough and approximate[47], they clearly show that the response at the Earth's surface is not the same as in the different layers of the atmosphere.

[47] In fact, it is not realistic to use the same value for $m$, $c$ and $\mathcal{T}_e$.

**Mathematical definition of climate sensitivity and feedback** Before giving the mathematical expression of these two concepts, here is how Hartman introduces them in his book:

> "*[...] Climate forcing is a change to the climate system that can be expected to change the climate. Examples would be doubling the $CO_2$, increasing the total solar irradiance (TSI) by 2%, introducing volcanic aerosols into the stratosphere, etc. Climate forcings are usually quantified in terms of how many* $\mathrm{W/m^2}$ *they change the energy balance when imposed. For example, instantaneously doubling the $CO_2$ changes the energy balance at the top of the atmosphere by about* $4\,\mathrm{W/m^2}$*. A feedback process is a response of the climate system to surface warming that then alters the energy balance in such a way as to change the temperature response to the forcing. A positive feedback makes the forced response bigger, and a negative feedback makes it smaller. Classic examples of positive feedbacks are ice-albedo feedback and water-vapor feedback. When it warms, ice melts, and this reduces Earth's albedo and causes further warming. When it cools, ice grows, and this increases Earth's albedo, causing further cooling [...].*" (Hartmann, 2016, page 294).

Mathematically, we assume that some extra energy $\Delta F$ is added to the system. $\Delta F$ is called the radiative forcing and is measured in $\mathrm{W/m^2}$. The climate response is generally measured as the change in the surface temperature $\Delta \mathcal{T}_s$. The climate sensitivity is defined as:

$$\phi := \frac{\Delta \mathcal{T}_s}{\Delta F}$$

Using differential notation, we have:

$$\phi := \frac{\mathrm{d}\mathcal{T}_s}{\mathrm{d}F}$$

implying that:

$$\mathrm{d}\mathcal{T}_s = \phi\,\mathrm{d}F$$

Following Hartmann (2016, page 295), we assume that the perturbation $\mathrm{d}F$ depends on the temperature $\mathcal{T}_s$ and some exogenous factors $x_i$:

$$\mathrm{d}F = \frac{\partial F}{\partial \mathcal{T}_s}\mathrm{d}\mathcal{T}_s + \sum_{i=1}^{n} \frac{\partial F}{\partial x_i}\mathrm{d}x_i$$

We conclude that:

$$\left(1 - \phi \frac{\partial F}{\partial \mathcal{T}_s}\right)\mathrm{d}\mathcal{T}_s = \phi \sum_{i=1}^{n} \frac{\partial F}{\partial x_i}\mathrm{d}x_i$$

We then get a feedback mechanism, because the temperature dynamics depend on the factors $x_i$, but also on the temperature response.

Let us apply this framework to the one-layer model with emissivity. At the equilibrium, we have $\boldsymbol{\mathcal{E}} = 0$ where:

$$\begin{aligned}\boldsymbol{\mathcal{E}} &= F_{\text{solar}} - \left(\frac{2-\varepsilon}{2}\right)\sigma\mathcal{T}_s^4 \\ &= \frac{1}{4}(1-\alpha_p)\,S_0 - \left(\frac{2-\varepsilon}{2}\right)\sigma\mathcal{T}_s^4\end{aligned}$$

The first-order Taylor Series expansion of $\boldsymbol{\mathcal{E}} = 0$ gives:

$$\Delta\boldsymbol{\mathcal{E}} = \frac{1}{4}(1-\alpha_p)\,\Delta S_0 - \frac{1}{4}S_0\Delta\alpha_p + \frac{1}{2}\sigma\mathcal{T}_s^4\Delta\varepsilon - 4\left(\frac{2-\varepsilon}{2}\right)\sigma\mathcal{T}_s^3\Delta\mathcal{T}_s$$

Remember that each perturbation $\Delta y$ depends on the temperature $\mathcal{T}_s$ and some exogenous factors $x_i$:

$$\Delta y = \frac{\partial y}{\partial \mathcal{T}_s}\Delta \mathcal{T}_s + \sum_{i=1}^{n}\frac{\partial y}{\partial x_i}\Delta x_i$$

We have:

$$\begin{aligned}\Delta \boldsymbol{\mathcal{E}} &= \frac{1}{4}(1-\alpha_p)\,\Delta S_0 - \frac{1}{4}S_0\left(\frac{\partial \alpha_p}{\partial \mathcal{T}_s}\Delta \mathcal{T}_s + \sum_{i=1}^{n}\frac{\partial \alpha_p}{\partial x_i}\Delta x_i\right) + \\ &\quad \frac{1}{2}\sigma \mathcal{T}_s^4\left(\frac{\partial \varepsilon}{\partial \mathcal{T}_s}\Delta \mathcal{T}_s + \sum_{i=1}^{n}\frac{\partial \varepsilon}{\partial x_i}\Delta x_i\right) - 4\left(\frac{2-\varepsilon}{2}\right)\sigma \mathcal{T}_s^3 \Delta \mathcal{T}_s\end{aligned}$$

We deduce that[48]:

$$\Delta \boldsymbol{\mathcal{E}} = \lambda \Delta \mathcal{T}_s + \sum_{i=0}^{n}\Delta F_i \tag{8.11}$$

where $\Delta F_0 := \Delta F_{\text{solar}} = \frac{1}{4}(1-\alpha_p)\,\Delta S_0$,

$$\Delta F_i = \left(-\frac{1}{4}S_0\frac{\partial \alpha_p}{\partial x_i} + \frac{1}{2}\sigma \mathcal{T}_s^4\frac{\partial \varepsilon}{\partial x_i}\right)\Delta x_i \qquad \text{for } i \geq 1$$

and:

$$\lambda = -\frac{1}{4}S_0\frac{\partial \alpha_p}{\partial \mathcal{T}_s} + \frac{1}{2}\sigma \mathcal{T}_s^4\frac{\partial \varepsilon}{\partial \mathcal{T}_s} - 4\left(\frac{2-\varepsilon}{2}\right)\sigma \mathcal{T}_s^3$$

Since $\Delta \boldsymbol{\mathcal{E}}$ and $\Delta F_i$ are measured in $\mathrm{W/m^2}$ and $\Delta \mathcal{T}_s$ is measured in Kelvin, we deduce that $\lambda$ is measured in $\mathrm{W\,m^{-2}\,K^{-1}}$. As before, we transform $\Delta \boldsymbol{\mathcal{E}}$ into $\Delta \mathcal{T}_s$ by considering the heat capacity $c$ expressed in $\mathrm{W\,m^{-2}\,K^{-1}\,s}$. Then Equation (8.11) becomes:

$$c\frac{\mathrm{d}\Delta \mathcal{T}_s}{\mathrm{d}t} = \lambda \Delta \mathcal{T}_s + \Delta F \tag{8.12}$$

where $\Delta F = \sum_{i=0}^{n} F_i$. The climate feedback parameter $\lambda$ can be positive or negative, and we have the following mathematical properties:

- If $\lambda > 0$, the system is unstable;
- If $\lambda < 0$, the system is stable and the equilibrium is reached when:

$$\Delta \mathcal{T}_s = \Delta \mathcal{T}_s^{\star} = -\frac{\Delta F}{\lambda} = -\phi \Delta F \tag{8.13}$$

We see that the climate feedback parameter can be decomposed into three components:

$$\lambda = \lambda_0 + \lambda_{\alpha_p} + \lambda_{\varepsilon}$$

where:

1. $\lambda_0$ is the Planck feedback or the black body response:

$$\lambda_0 = -4\left(\frac{2-\varepsilon}{2}\right)\sigma \mathcal{T}_s^3$$

[48] $\lambda = \phi^{-1}$ is the inverse of the climate sensitivity parameter $\phi$ defined by Hartmann (2016).

2. $\lambda_{\alpha_p}$ is the surface albedo feedback:

$$\lambda_{\alpha_p} = -\frac{1}{4} S_0 \frac{\partial \alpha_p}{\partial \mathcal{T}_s}$$

3. $\lambda_\varepsilon$ is the emissivity feedback:

$$\lambda_\varepsilon = \frac{1}{2} \sigma \mathcal{T}_s^4 \frac{\partial \varepsilon}{\partial \mathcal{T}_s}$$

Since $\varepsilon < 1$, the Planck feedback is negative, meaning that it stabilizes the climate and counteracts global warming. In fact, as the Earth warms, it emits more thermal radiation into space, and this increased longwave radiation acts as a natural cooling mechanism. Conversely, as the Earth cools, it emits less thermal radiation into space, and this decreased longwave radiation acts as a natural warming mechanism. Earlier we found that $\varepsilon = 0.78$. So the estimate of $\lambda_0$ is[49]:

$$\begin{aligned} \lambda_0 &= -4\left(\frac{2-0.78}{2}\right) \times \left(5.67 \times 10^{-8}\right) \times (273.15+15)^3 \\ &= -3.310\,\mathrm{W\,m^{-2}\,K^{-1}} \end{aligned}$$

The sign of the surface albedo feedback depends on the sign of $\frac{\partial \alpha_p}{\partial \mathcal{T}_s}$. Two main factors play a role in determining $\alpha_p$:

> "*The albedo of the planet for solar radiation is primarily determined by the clouds and surface, with the main variable component of the latter being the ice/snow cover.*" (Hansen *et al.*, 1984, page 166).

The feedback is positive for the ice-albedo mechanism because $\frac{\partial \alpha_p}{\partial \mathcal{T}_s} < 0$. In fact, decreased temperature leads to increased sea ice and snow cover. This increases the albedo and decreases the absorption of shortwave radiation. This mechanism is satisfied globally, but we observe a lot of regional and seasonal variation (Stephens *et al.*, 2015). If the Earth were completely covered in ice, its albedo $\alpha_p$ would be about 84%, meaning it would reflect most of the sunlight that hits it. On the other hand, if the Earth were covered by a dark green forest canopy, the albedo would be about 14% and most of the sunlight would be absorbed[50]. This explains why the ice-albedo feedback is greatest in the polar regions (Goosse *et al.*, 2018). Cloud albedo feedback occurs because changes in cloud cover, cloud altitude or cloud properties affect the amount of reflected shortwave radiation. This feedback can be either positive or negative, depending on the specific change. The overall effect is a positive feedback (IPCC, 2021, Chapter 7, page 926). According to IPCC AR6, the value of the global surface albedo feedback is estimated to be $0.35\,\mathrm{W\,m^{-2}\,K^{-1}}$, with a 90% confidence interval from 0.10 to $0.60\,\mathrm{W\,m^{-2}\,K^{-1}}$ (IPCC, 2021, Chapter 7, page 971). This means that:

$$\frac{\partial \alpha_p}{\partial \mathcal{T}_s} = -\frac{4\lambda_{\alpha_p}}{S_0} = -\frac{4 \times 0.35}{1368} = -1.023 \times 10^{-3}$$

[49] For comparison, the most recent estimate is $-3.22\,\mathrm{W\,m^{-2}\,K^{-1}}$, while the 90% confidence interval is from $-3.4$ to $-3.0\,\mathrm{W\,m^{-2}\,K^{-1}}$ (IPCC, 2021, Chapter 7, page 968).

[50] Source: https://earthobservatory.nasa.gov/images/84499/measuring-earths-albedo.

Box 8.9: Ice-albedo feedback modeling

We have seen that the surface albedo feedback is equal to $\lambda_{\alpha_p} = -\frac{1}{4} S_0 \frac{\partial \alpha_p}{\partial \mathcal{T}_s}$. So we need to parameterize the temperature dependence of the albedo. If we assume that $\alpha_p = f_{\text{albedo}}(\mathcal{T}_s)$, then we get $\lambda_{\alpha_p} = -\frac{1}{4} S_0 f'_{\text{albedo}}(\mathcal{T}_s)$. For example, Sellers (1969) suggested:

$$\alpha_p = \begin{cases} b(\phi) - 0.009\mathcal{T}_s & \text{if } \mathcal{T}_s \leq 283.16\,\text{K} \\ b(\phi) - 2.548 & \text{if } \mathcal{T}_s \geq 283.16\,\text{K} \end{cases}$$

where $b(\phi)$ is an estimated coefficient that depends on the latitude $\phi$. Sellers (1969) found $b(\phi) \in [2.798, 2.992]$. Below, we show the function $b(\phi)$ with respect to the spherical coordinate $\phi$. On average we have $\overline{b(\phi)} = 2.8811$. We deduce that:

$$\lambda_{\alpha_p} = \frac{1}{4} \times 1\,368 \times 0.009 = 3.078\,\text{W}\,\text{m}^{-2}\,\text{K}^{-1}$$

It is obvious that this positive feedback has been overestimated. The reason is that snow and sea ice cover about 10% of the Earth's surface. Therefore, we get $\lambda_{\alpha_p} \approx 0.3\,\text{W}\,\text{m}^{-2}\,\text{K}^{-1}$.

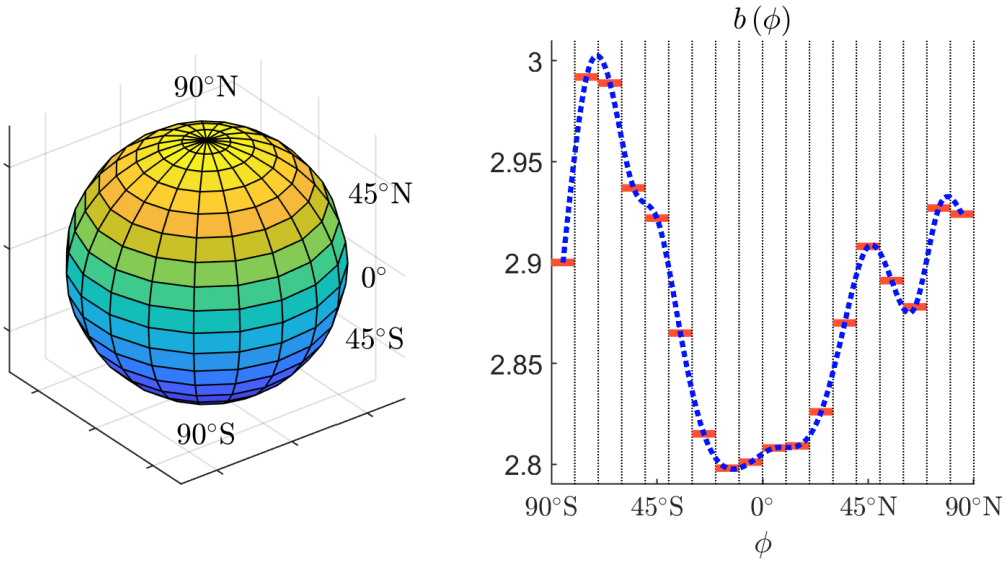


Budyko (1969) proposed another famous ice-albedo model, assuming that the land and oceans are completely covered by snow and sea ice when the temperature is below a threshold $\mathcal{T}_{\text{cold}}$, and that the planet is free of ice and snow when the temperature is above another threshold $\mathcal{T}_{\text{warm}}$:

$$\alpha_p = \begin{cases} \alpha_{\text{cold}} & \text{if } \mathcal{T}_s \leq \mathcal{T}_{\text{cold}} \\ \alpha_{\text{warm}} + (\alpha_{\text{cold}} - \alpha_{\text{warm}}) \left( \dfrac{\mathcal{T}_{\text{warm}} - \mathcal{T}_s}{\mathcal{T}_{\text{warm}} - \mathcal{T}_{\text{cold}}} \right)^{\eta} & \text{if } \mathcal{T}_{\text{cold}} \leq \mathcal{T}_s \leq \mathcal{T}_{\text{warm}} \\ \alpha_{\text{warm}} & \text{if } \mathcal{T}_s \geq \mathcal{T}_{\text{warm}} \end{cases}$$

where $\eta \geq 1$. It follows that:

$$\lambda_{\alpha_p}(\mathcal{T}_s) = \frac{1}{4} \eta S_0 (\alpha_{\text{cold}} - \alpha_{\text{warm}}) \frac{(\mathcal{T}_{\text{warm}} - \mathcal{T}_s)^{\eta-1}}{(\mathcal{T}_{\text{warm}} - \mathcal{T}_{\text{cold}})^{\eta}} \cdot \mathbb{1}\{\mathcal{T}_{\text{cold}} \leq \mathcal{T}_s \leq \mathcal{T}_{\text{warm}}\}$$

Using the values $\alpha_{\text{cold}} = 0.7$, $\mathcal{T}_{\text{cold}} = 260\,\text{K}$, $\alpha_{\text{warm}} = 0.3$, $\mathcal{T}_{\text{warm}} = 295\,\text{K}$ and $\eta = 2$, we get $\lambda_{\alpha_p}(282\,\text{K}) = 2.90\,\text{W}\,\text{m}^{-2}\,\text{K}^{-1}$, $\lambda_{\alpha_p}(288\,\text{K}) = 1.56\,\text{W}\,\text{m}^{-2}\,\text{K}^{-1}$ and $\lambda_{\alpha_p}(293\,\text{K}) = 0.45\,\text{W}\,\text{m}^{-2}\,\text{K}^{-1}$.

The third feedback is the change in emissivity, which is the sum of several components:

$$\lambda_\varepsilon = \lambda_{\text{water vapor}} + \lambda_{\text{lapse rate}} + \lambda_{\text{cloud longwave}} + \dots$$

The water vapor feedback, also known as the specific humidity feedback, is the most important positive and destabilizing feedback. It can be described as follows:

> "*[...] As the temperature increases, the amount of water vapor in saturated air increases. Since water vapor is the principal greenhouse gas, increasing water vapor content will increase the greenhouse effect of the atmosphere and raise the surface temperature even further.*" (Hartmann, 2016, page 297).

The mechanism behind water vapor feedback is related to the thermodynamics of moist (or humid) air in the atmosphere. Water molecules move freely between the liquid and vapor phases, and the equilibrium depends on the water vapor saturation $e_s$. The relationship between $e_s$ and temperature is given by the Clausius-Clapeyron equation:

$$\frac{\mathrm{d}e_s}{\mathrm{d}\mathcal{T}_s} = \frac{1}{(\alpha_{\text{vapor}} - \alpha_{\text{liquid}})\,\mathcal{T}_s} = \frac{L_{\text{vapor}} e_s}{R_{\text{vapor}} \mathcal{T}_s^2}$$

where $\alpha_{\text{vapor}}$ is the specific volume of the vapor phase, $\alpha_{\text{liquid}}$ is the specific volume of the liquid phase, $R_{\text{vapor}}$ is the gas constant of water vapor and $L_{\text{vapor}}$ is the specific latent heat of evaporation of water. If we rearrange this equation, we obtain the following relationship:

$$\frac{\mathrm{d}e_s}{e_s} = \left(\frac{L_{\text{vapor}}}{R_{\text{vapor}} \mathcal{T}_s}\right) \frac{\mathrm{d}\mathcal{T}_s}{\mathcal{T}_s} = \varphi \frac{\mathrm{d}\mathcal{T}_s}{\mathcal{T}_s}$$

According to (Hartmann, 2016, page 298), $\varphi \approx 20$, which means that a 1% change in temperature is associated with a 20% change in saturation humidity. This means that a 20% change in saturation humidity causes a change in temperature of $1\% \times (273.15 + 15) \approx 2.9\,\text{K}$. According to IPCC AR6, the value $\lambda_{\text{water vapor}}$ of the water vapor feedback is assessed to be $1.85\,\text{W}\,\text{m}^{-2}\,\text{K}^{-1}$ (IPCC, 2021, Chapter 7, page 969). The lapse rate mechanism describes the relationship between temperature and altitude in the atmosphere (Colman and Soden, 2021, page 13):

$$\Gamma = -\frac{\partial \mathcal{T}}{\partial z} \in \left[4\,\text{K}\,\text{km}^{-1}, 10\,\text{K}\,\text{km}^{-1}\right]$$

where $z$ is the altitude in kilometers. On average, the lapse rate is about 6.5°C per kilometer. This means that the temperature is not uniform throughout the atmosphere. According to IPCC (2021, Chapter 7, page 969), "*the warming is larger in the upper troposphere than in the lower troposphere [...] leading to a larger radiative emission to space and therefore a negative feedback*" and the average value of $\lambda_{\text{lapse rate}}$ is $-0.50\,\text{W}\,\text{m}^{-2}\,\text{K}^{-1}$. The case of cloud feedbacks is more complicated because it involves several mechanisms: (1) high cloud altitude, (2) tropical high cloud amount, (3) subtropical marine low cloud, (4) land cloud, (5) midlatitude cloud amount, (6) extratropical cloud optical depth, and (7) Arctic cloud. According to IPCC AR6, the value $\lambda_{\text{cloud}}$ of the net cloud feedback is estimated to be $0.42\,\text{W}\,\text{m}^{-2}\,\text{K}^{-1}$ (IPCC, 2021, Chapter 7, page 974). One of the difficulties is to decompose the cloud feedback into shortwave and longwave feedbacks, since the global surface albedo feedback already includes shortwave cloud mechanisms. Assuming that 2/3 of the cloud feedback is longwave radiation, we get:

$$\lambda_\varepsilon \approx 1.85 - 0.50 + \frac{2}{3} \times 0.42 = 1.63\,\text{W}\,\text{m}^{-2}\,\text{K}^{-1}$$

Finally, we can compute the total feedback parameter by summing the Planck feedback, the surface albedo feedback, and the emissivity feedback:

$$\begin{aligned}\lambda &= \lambda_0 + \lambda_{\alpha_p} + \lambda_\varepsilon \\ &= -3.31 + 0.35 + 1.63 \\ &= -1.33\,\mathrm{W\,m^{-2}\,K^{-1}}\end{aligned}$$

This value is obtained with a simple one-layer model with emissivity. It is relatively close to the average climate feedback parameter calculated with more complex models. However, using global climate models, we can assess the uncertainty in the climate feedback parameter. In this case, we consider the parameter $\lambda$ as a Gaussian random variable $\tilde{\lambda} \sim \mathcal{N}\left(\mu_\lambda, \sigma_\lambda^2\right)$. As before, we can decompose the feedback as a sum of individual feedbacks:

$$\tilde{\lambda} = \sum_{i=1}^{n} \tilde{\lambda}_i$$

where $\tilde{\lambda}_i \sim \mathcal{N}\left(\mu_i, \sigma_i^2\right)$. Assuming that the individual feedbacks are independent, we have:

$$\begin{cases} \mu_\lambda = \sum_{i=1}^{n} \mu_i \\ \sigma_\lambda = \sqrt{\sum_{i=1}^{n} \sigma_i^2} \end{cases}$$

Table 8.10: Parameters $\mu_i$ and $\sigma_i$ of feedback parameters

| Feedback mechanism | $\mu_i$ | $\sigma_i$ | Shortwave |
|---|---|---|---|
| High-cloud altitude | +0.20 | 0.10 | |
| Tropical marine low cloud | +0.25 | 0.16 | |
| Tropical anvil cloud area | −0.20 | 0.20 | |
| Land cloud amount | +0.08 | 0.08 | |
| Middle-latitude marine low-cloud amount | +0.12 | 0.12 | |
| High-latitude low-cloud optical depth | +0.00 | 0.10 | ✓ |
| Planck feedback | −3.20 | 0.10 | ✓ |
| Water vapor + lapse rate | +1.15 | 0.15 | |
| Surface albedo | +0.30 | 0.15 | ✓ |
| Total cloud | +0.45 | 0.33 | |
| Stratospheric | +0.00 | 0.10 | |
| Atmospheric composition changes | +0.00 | 0.15 | |
| Climate feedback parameter | −1.30 | 0.44 | |

Source: (Sherwood *et al.*, 2020, Table 1, page 18).

In Table 8.10, we report the estimated value of $\mu_i$ and $\sigma_i$ for individual climate feedbacks calculated by Sherwood *et al.* (2020, Table 1, page 18). The estimation process is based on multiple lines of evidence, including historical observations, general circulation models, and theory. The first part of the table lists the parameters for the individual cloud feedbacks. Their corresponding probability density functions are shown in Figure 8.45. Using this modeling framework, we can compute the probability that the feedback is positive:

$$\Pr\left\{\tilde{\lambda}_i \geq 0\right\} = 1 - \Phi\left(-\frac{\mu_i}{\sigma_i}\right)$$

Figure 8.45: Probability density function of individual cloud feedbacks

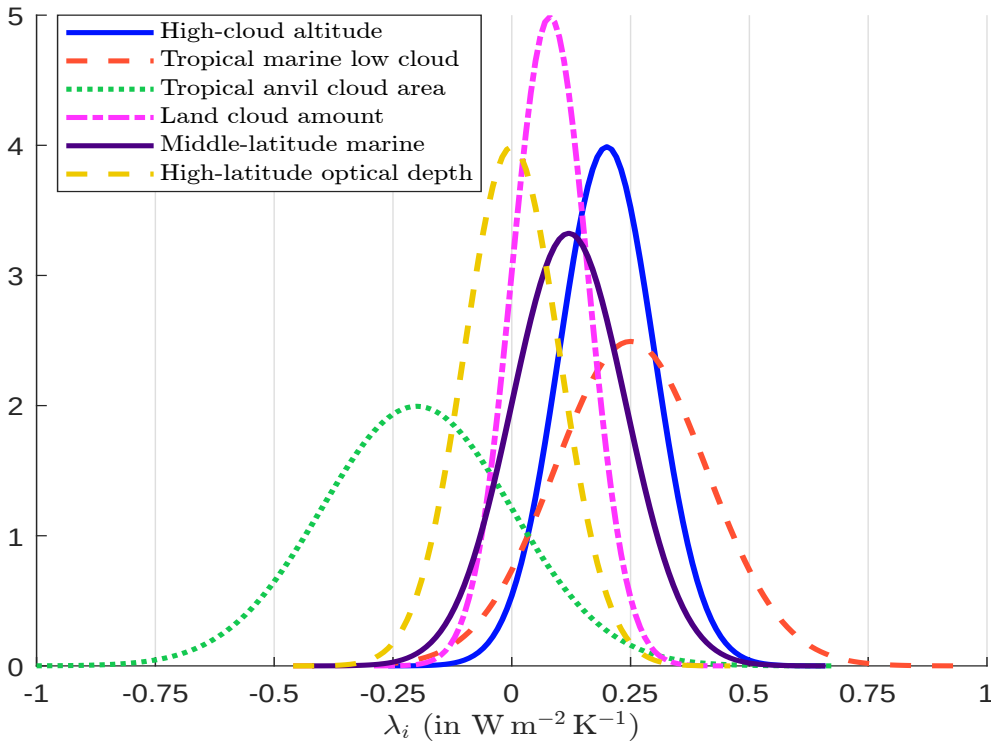


Figure 8.46: Probability density function of positive feedbacks

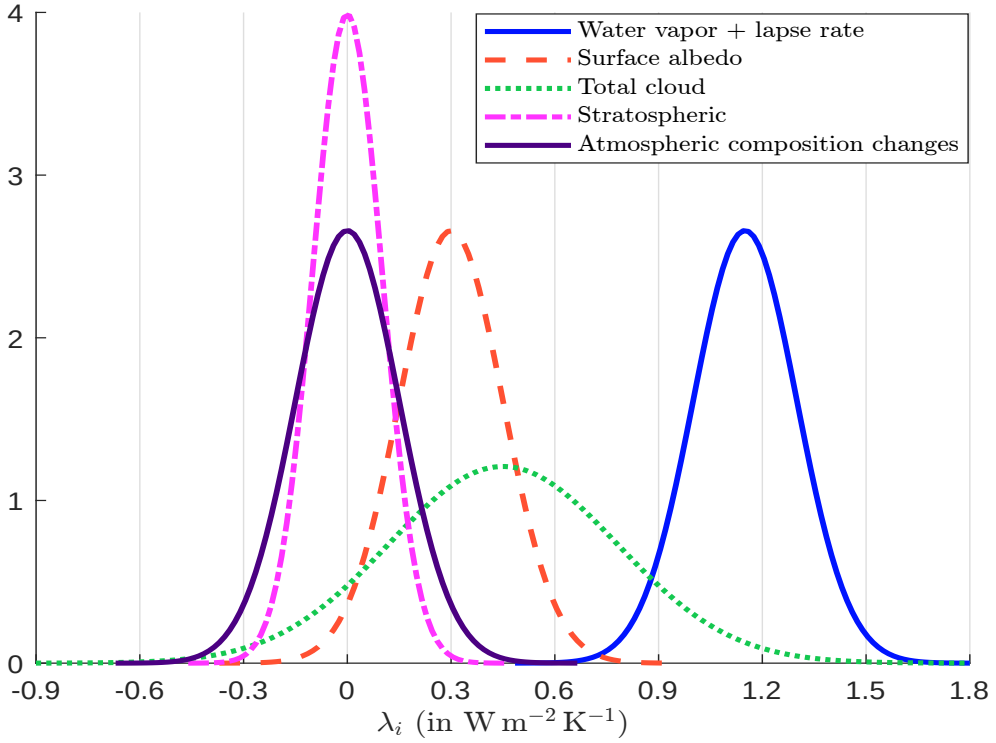

Figure 8.47: Comparison of $\tilde{\lambda}_{\text{Planck}}$ and $\tilde{\lambda}_{\text{positive}}$

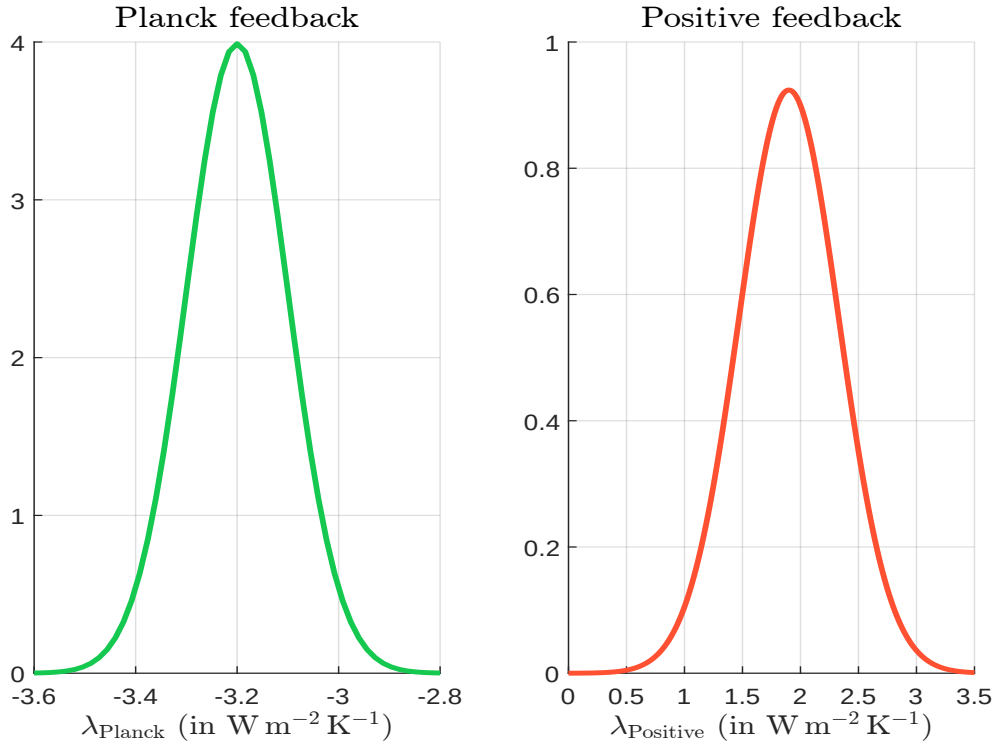


or the confidence interval at the $\alpha$ confidence level: $[\mu_i - c_\alpha \sigma_i, \mu_i + c_\alpha \sigma_i]$ where $c_\alpha = \Phi^{-1}((1+\alpha)/2)$. In IPCC AR6, the confidence intervals of $\tilde{\lambda}_i$ are called *likely* and *very likely* ranges and correspond to $\alpha = 66\%$ and $\alpha = 90\%$, respectively[51]. Using the parameters of the individual cloud feedbacks, we can infer the distribution of the total cloud feedback. We have:

$$\mu_{\text{total cloud}} = 0.20 + 0.25 - 0.20 + 0.08 + 0.12 + 0.00 = 0.45\,\text{W m}^{-2}\,\text{K}^{-1}$$

and:

$$\sigma_{\text{total cloud}} = \sqrt{0.10^2 + 0.16^2 + 0.20^2 + 0.08^2 + 0.12^2 + 0.10^2} = 0.3262\,\text{W m}^{-2}\,\text{K}^{-1}$$

These are the numbers obtained by Sherwood *et al.* (2020). We now plot the probability density functions of the five main positive feedback components in Figure 8.46 and aggregate them into a single feedback. We have:

$$\mu_{\text{positive}} = 1.15 + 0.30 + 0.45 + 0.00 + 0.00 = 1.90\,\text{W m}^{-2}\,\text{K}^{-1}$$

and:

$$\sigma_{\text{positive}} = \sqrt{0.15^2 + 0.15^2 + 0.33^2 + 0.10^2 + 0.15^2} = 0.4317\,\text{W m}^{-2}\,\text{K}^{-1}$$

The aggregated positive feedback is shown in Figure 8.47 and can be compared to the Planck feedback. Finally, Sherwood *et al.* (2020) aggregated all the positive and negative feedbacks to obtain the climate feedback parameter: $\tilde{\lambda} \sim \mathcal{N}(\mu_\lambda, \sigma_\lambda^2)$ where $\mu_\lambda = -1.30\,\text{W m}^{-2}\,\text{K}^{-1}$ and $\sigma_\lambda = 0.44\,\text{W m}^{-2}\,\text{K}^{-1}$. The probability density function of $\tilde{\lambda}$ is given in Figure 8.48. The probability that the climate feedback is positive is small[52], less than 1%.

[51] $c_\alpha$ is equal to 0.95 and 1.65.

[52] We have:

$$\Pr\left\{\tilde{\lambda} \geq 0\right\} = \Pr\left\{\frac{\tilde{\lambda} - \mu_\lambda}{\sigma_\lambda} \geq -\frac{\mu_\lambda}{\sigma_\lambda}\right\} = 1 - \Phi\left(-\frac{\mu_\lambda}{\sigma_\lambda}\right) = 1 - \Phi\left(\frac{1.30}{0.44}\right) = 0.16\%$$

Figure 8.48: Probability density function of the climate feedback parameter

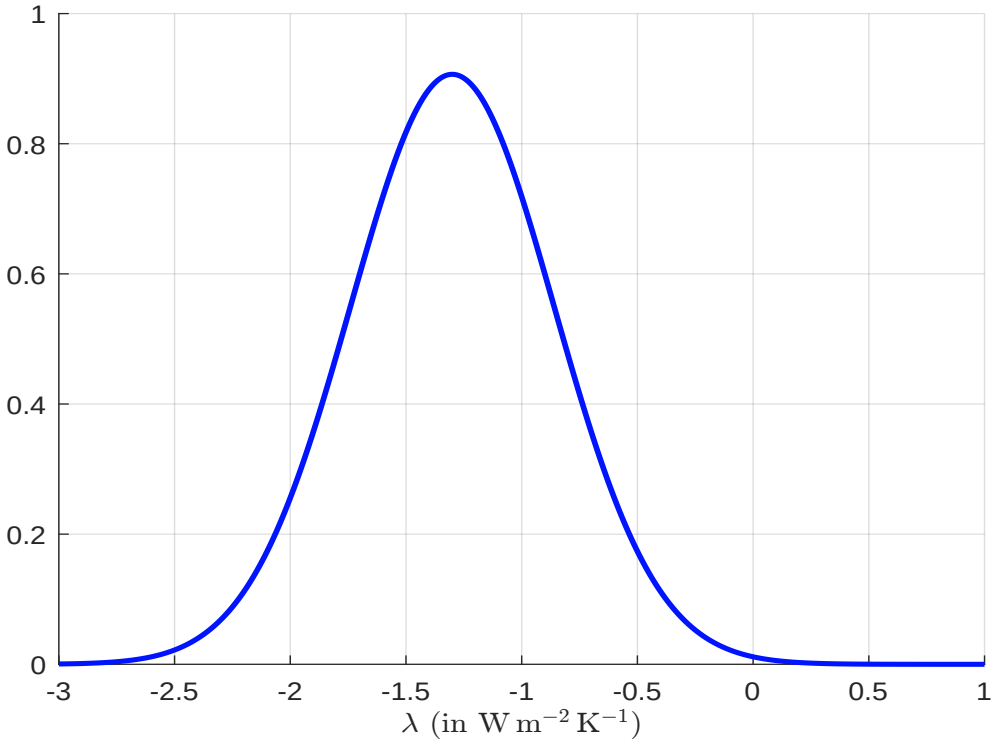


**Equilibrium climate sensitivity (ECS)** We recall that the definition of equilibrium is given by Equation (8.13):

$$\Delta\mathcal{T}_s^\star = -\frac{\Delta F}{\lambda} = -\phi\Delta F$$

Therefore, we can calculate the effect of a specific value of radiative forcing $\Delta F$ on temperature change. In particular, Earth's equilibrium climate sensitivity (ECS) is the long-term global mean surface temperature change due to a specific value of radiative forcing corresponding to a doubling of $CO_2$ in the atmosphere (Jeevanjee, 2023). We have:

$$\text{ECS} := \Delta\mathcal{T}_{2\times CO_2} = -\frac{\Delta F_{2\times CO_2}}{\lambda}$$

where ECS (or $\Delta\mathcal{T}_{2\times CO_2}$) is the equilibrium climate sensitivity, $\lambda$ is the climate sensitivity parameter and $\Delta F_{2\times CO_2}$ is the radiative forcing resulting from a doubling of the atmospheric carbon dioxide concentration.

**Stochastic equilibrium temperature modeling** Let us assume that $\Delta F = 4\,\text{W/m}^2$ and $\lambda = -1.33\,\text{W m}^{-2}\,\text{K}^{-1}$. The equilibrium warming is then equal to 3°C:

$$\Delta\mathcal{T}_s^\star = -\frac{4\,\text{W/m}^2}{-1.33\,\text{W m}^{-2}\,\text{K}^{-1}} = 3.0075\,\text{K}$$

Remember that the dynamics of the temperature change is given by the ordinary differential equation:

$$c\frac{\mathrm{d}\Delta\mathcal{T}_s}{\mathrm{d}t} = \lambda\Delta\mathcal{T}_s + \Delta F$$

We assume that the solution has the following form:

$$\Delta\mathcal{T}_s(t) = e^{At}B + C$$

We deduce that:

$$\frac{\mathrm{d}\Delta\mathcal{T}_s}{\mathrm{d}t} = Ae^{At}B = A\left(\Delta\mathcal{T}_s(t) - C\right)$$

The identification of the parameters results in:

$$\begin{cases} A = \dfrac{\lambda}{c} \\ -AC = \dfrac{\Delta F}{c} \\ B + C = \Delta\mathcal{T}_s(0) \end{cases}$$

The solutions are then $A = c^{-1}\lambda$,

$$C = -\frac{\Delta F}{Ac} = -\frac{\Delta F}{\lambda} = \Delta\mathcal{T}_s^\star$$

and:

$$B = \Delta\mathcal{T}_s(0) - C = \Delta\mathcal{T}_s(0) - \Delta\mathcal{T}_s^\star$$

Finally, we conclude that:

$$\Delta\mathcal{T}_s(t) = \exp\left(-\frac{t}{\tau}\right)\left(\Delta\mathcal{T}_s(0) - \Delta\mathcal{T}_s^\star\right) + \Delta\mathcal{T}_s^\star \tag{8.14}$$

where:

$$\tau = -\frac{c}{\lambda} \tag{8.15}$$

Again, we obtain that the equation for $\Delta\mathcal{T}_s(t)$ describes an exponential survival function with parameter $\tau^{-1}$. Using a specific heat capacity of $c = 4\times10^8\,\mathrm{J\,m^{-2}\,K^{-1}}$, we get[53]:

$$\tau = -\frac{c}{\lambda} = -\frac{4\times10^8\,\mathrm{J\,m^{-2}\,K^{-1}}}{-1.33\,\mathrm{W\,m^{-2}\,K^{-1}}} = \frac{4\times10^8\,\mathrm{W\,m^{-2}\,K^{-1}\,s}}{1.33\,\mathrm{W\,m^{-2}\,K^{-1}}} = 3.0075\times10^8\,\mathrm{s}$$

The relaxation time $\tau$ of the climate system is then equal to 3 480.92 days or 9.53 years[54]. Due to the exponential distribution, $\tau$ is also the mean lifetime. The computation of the half-life[55] gives $t_{1/2} = \tau\ln(2) = 6.61$ years. Considering that the initial state is $\Delta\mathcal{T}_s(0) = 0$, the dynamics of $\Delta\mathcal{T}_s(t)$ when $\Delta F = 4\,\mathrm{W/m^2}$ and $\lambda = -1.33\,\mathrm{W\,m^{-2}\,K^{-1}}$ is shown in Figure 8.49. We check that the system converges to the equilibrium: $\lim_{t\to\infty}\Delta\mathcal{T}_s(t) = \Delta\mathcal{T}_s^\star = 3.0075°\mathrm{C}$.

The previous analysis assumes that the climate feedback parameter is certain. In fact, it is stochastic, which means that the equilibrium temperature and the temperature dynamics are stochastic. If $\tilde{\lambda}\sim\mathcal{N}\left(\mu_\lambda,\sigma_\lambda^2\right)$, the equilibrium temperature is equal to:

$$\Delta\widetilde{\mathcal{T}}_s^\star = -\frac{\Delta F}{\tilde{\lambda}} = \frac{1}{\xi}$$

[53] We have $\mathrm{J\,m^{-2}\,K^{-1}} = \mathrm{J\,s^{-1}\,m^{-2}\,K^{-1}\,s} = \mathrm{W\,m^{-2}\,K^{-1}\,s}$.

[54] We scale $\tau$ by $24\times3\,600$ seconds to get the relaxation time expressed in days and assume that one year is 362.25 days.

[55] Since we have:

$$\Delta\mathcal{T}_s(t) - \Delta\mathcal{T}_s^\star = \exp\left(-\frac{t}{\tau}\right)\left(\Delta\mathcal{T}_s(0) - \Delta\mathcal{T}_s^\star\right)$$

the half-life $t_{1/2}$ is defined as the solution of the equation $\exp\left(-\dfrac{t_{1/2}}{\tau}\right) = \dfrac{1}{2}$.

Figure 8.49: Surface temperature dynamics after a radiative forcing of $4\,\mathrm{W/m^2}$ ($\lambda = -1.33\,\mathrm{W\,m^{-2}\,K^{-1}}$)

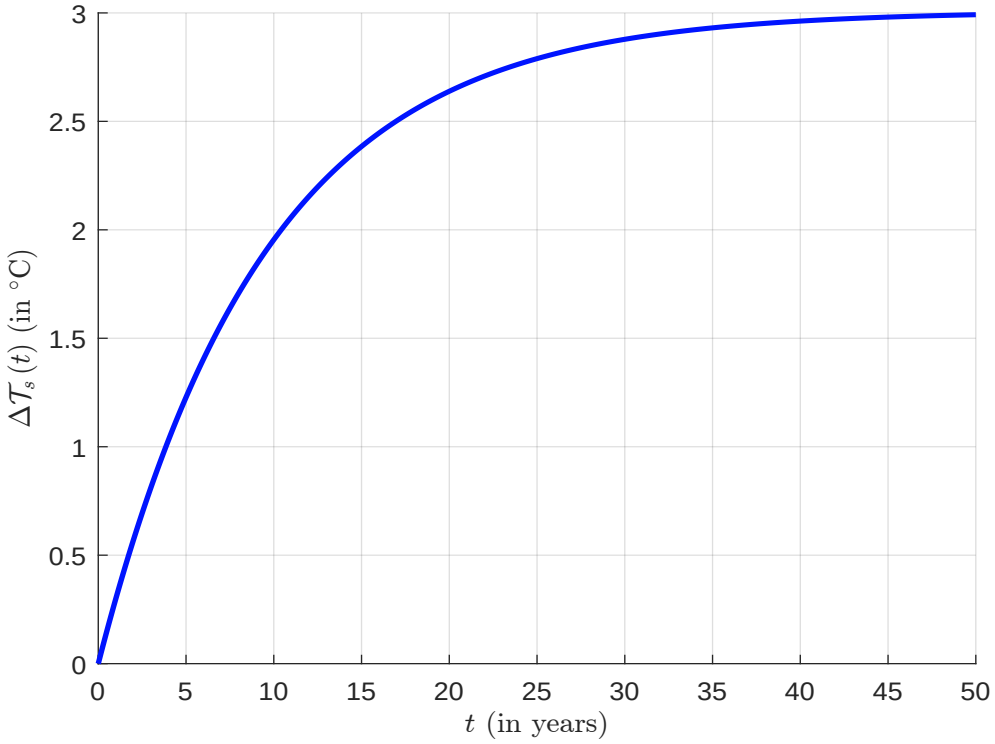


Figure 8.50: Probability density function of the equilibrium temperature ($\Delta F = 4\,\mathrm{W/m^2}$, $\mu_\lambda = -1.30\,\mathrm{W\,m^{-2}\,K^{-1}}$ and $\sigma_\lambda = 0.44\,\mathrm{W\,m^{-2}\,K^{-1}}$)

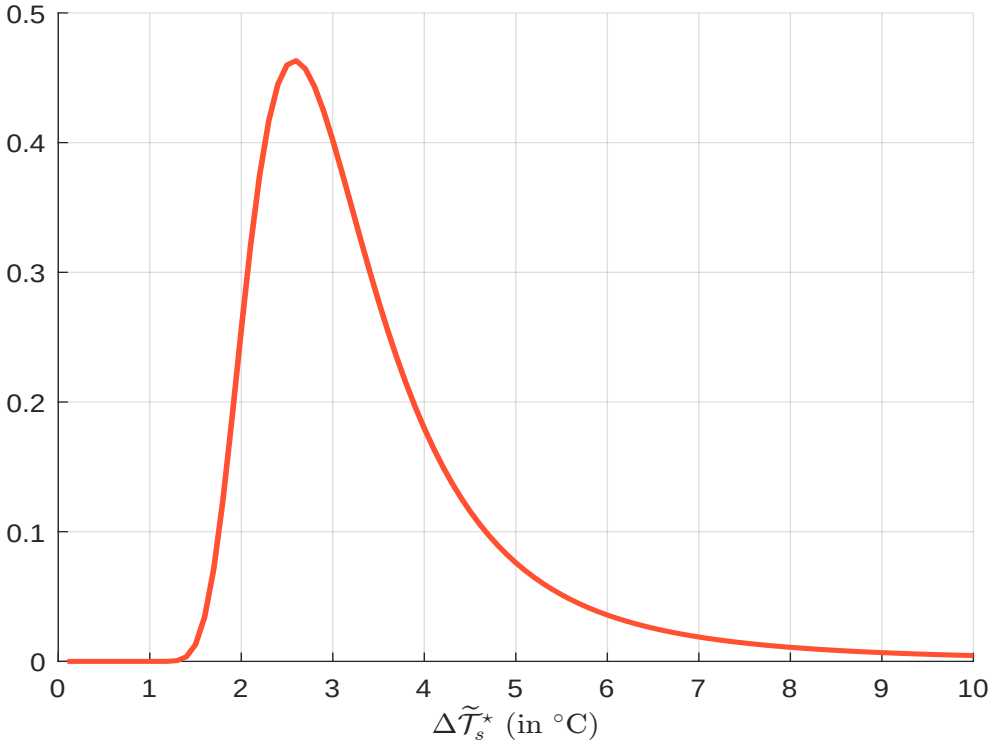

Figure 8.51: Probability density function of the relaxation time ($\mu_\lambda = -1.30\,\mathrm{W\,m^{-2}\,K^{-1}}$ and $\sigma_\lambda = 0.44\,\mathrm{W\,m^{-2}\,K^{-1}}$)

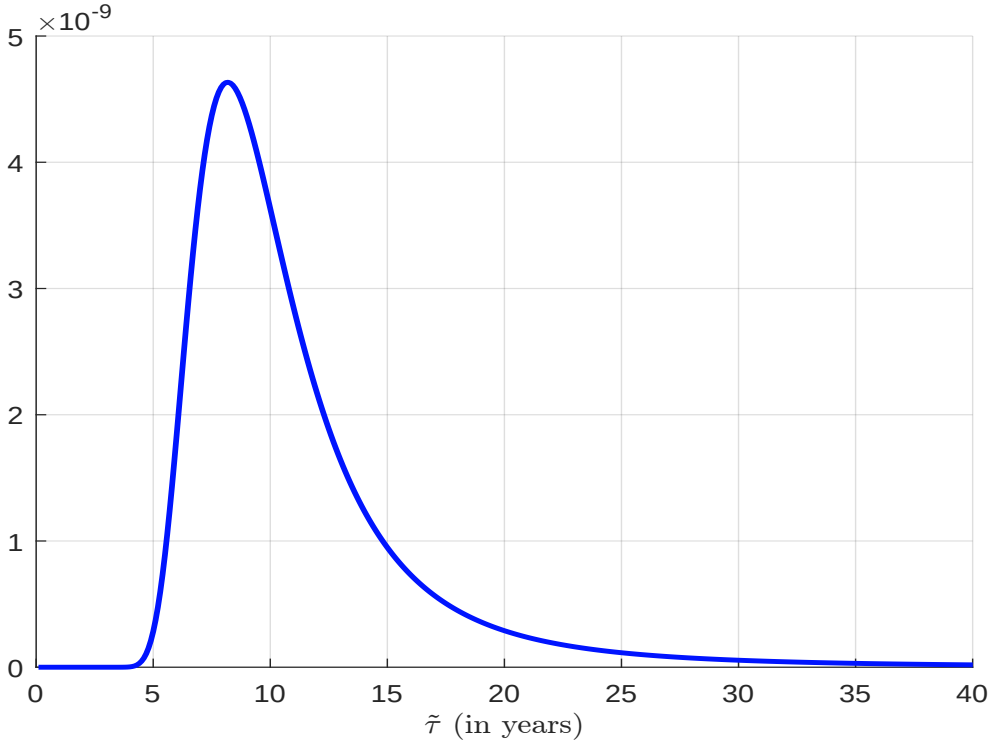


Figure 8.52: Monte Carlo simulation of the surface temperature dynamics after a radiative forcing of $4\,\mathrm{W/m^2}$ ($\mu_\lambda = -1.30\,\mathrm{W\,m^{-2}\,K^{-1}}$ and $\sigma_\lambda = 0.44\,\mathrm{W\,m^{-2}\,K^{-1}}$)

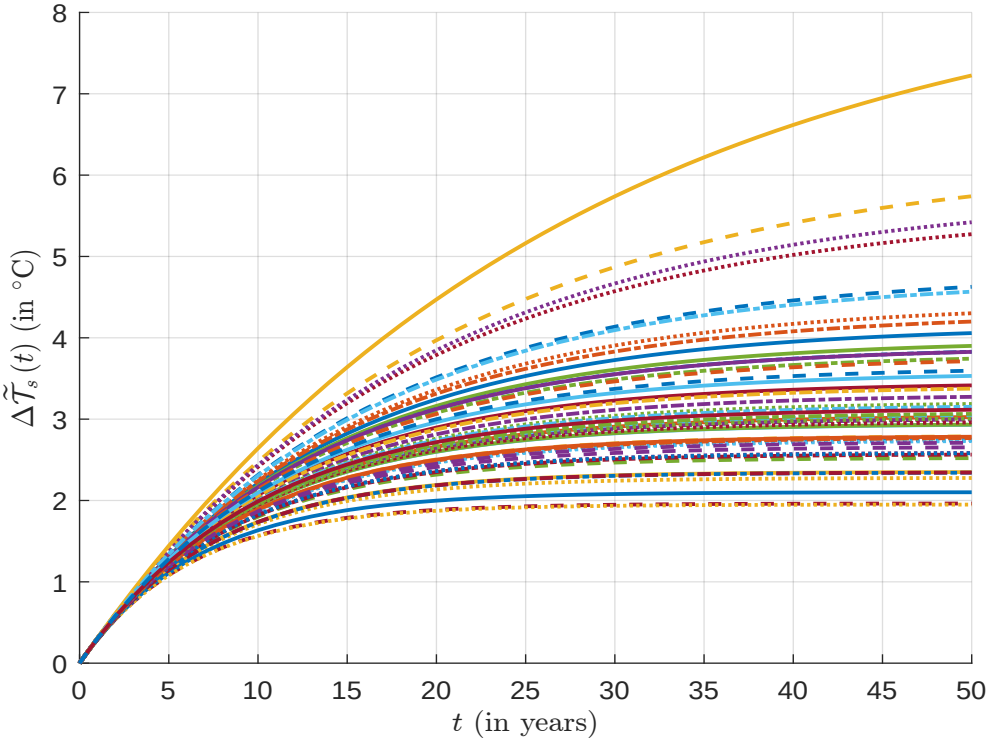

where:

$$\xi = -\frac{\tilde{\lambda}}{\Delta F} \sim \mathcal{N}\left(\mu_\xi, \sigma_\xi^2\right) \equiv \mathcal{N}\left(-\frac{\mu_\lambda}{\Delta F}, \frac{\sigma_\lambda^2}{\Delta F^2}\right)$$

We deduce that $\Delta\widetilde{\mathcal{T}}_s^\star$ follows a reciprocal normal distribution, and its probability density function is[56]:

$$f(x) = \frac{1}{\sigma_\xi x^2 \sqrt{2\pi}} e^{-\frac{1}{2}\left(\frac{x^{-1}-\mu_\xi}{\sigma_\xi}\right)^2}$$

Using the previous calibration of the climate feedback parameter $\tilde{\lambda} \sim \mathcal{N}\left(-1.30, 0.44^2\right)$, Figure 8.50 shows the probability density function of the equilibrium temperature when the radiative forcing is equal to $4\,\mathrm{W/m^2}$. The distribution of $\Delta\widetilde{\mathcal{T}}_s^\star$ is right skewed and has an excess of kurtosis. Using numerical integration, we compute the cumulative distribution function and the exceedance probability:

| Temperature $\theta$ | 2°C | 3°C | 4°C | 5°C | 7°C | 10°C |
|---|---|---|---|---|---|---|
| $\Pr\left\{\Delta\widetilde{\mathcal{T}}_s^\star \geq \theta\right\}$ | 94.26% | 52.86% | 24.61% | 12.63% | 4.73% | 1.88% |

The probability of observing an equilibrium temperature greater than 4°C and 7°C is close to 25% and 5%, respectively. Therefore, there is a high uncertainty in $\Delta\mathcal{T}_s^\star$ when we introduce the random nature of the climate feedback. The uncertainty of $\lambda$ also concerns the dynamics of $\Delta\mathcal{T}_s(t)$. Indeed, the mean lifetime becomes random and follows a reciprocal normal distribution:

$$\tilde{\tau} = -\frac{c}{\tilde{\lambda}} \sim \mathcal{RN}\left(-\frac{\mu_\lambda}{c}, \frac{\sigma_\lambda^2}{c}\right)$$

Figure 8.51 shows the probability distribution of $\tilde{\tau}$ when $\tilde{\lambda} \sim \mathcal{N}\left(-1.33, 0.44^2\right)$. Finally, we consider a Monte Carlo exercise and simulate 50 random paths of the surface temperature in Figure 8.51.

**Equilibrium climate sensitivity estimation** According to IPCC (2021, Chapter 7, page 926), the total anthropogenic ERF[57] over the industrial era (1750–2019) is $2.72\,\mathrm{W/m^2}$, the contribution of anthropogenic greenhouse gas emissions is $3.84\,\mathrm{W/m^2}$ and the combined effect of all radiative feedbacks (including Planck feedback) is estimated to be $-1.16\,\mathrm{W/m^2}$. Thus, the best estimate of the ECS is 3°C. The likely range is 2.5°C to 4°C (with a probability of 66%), and the very likely range is 2°C to 5°C (with a probability of 90%).

Figure 8.53 reproduces the IPCC graph showing the change in effective radiative forcing (ERF) from 1750 to 2019 by contributing forcing agents. The total anthropogenic effective radiative forcing is divided into six categories: carbon dioxide, other well-mixed greenhouse gases (methane, nitrous oxide, and halogens), ozone, stratospheric water vapor, albedo, contrails & aviation-induced cirrus, and aerosols (aerosol-cloud and aerosol-radiation). The contributions of $CO_2$, $CH_4$ and $N_2O$ are 79.41%, 19.9% and 17.3% of the total ERF, respectively. They are partially compensated by three negative contributors (aerosol-cloud, aerosol-radiation and land use). In Table 8.11, we report the evolution of these contributing forcings. In 2019, the total anthropogenic effective radiative forcing is $2.72\,\mathrm{W/m^2}$ and has increased by 29.3% over the last decade. The natural ERF due to volcanic activity and solar variations is $0.118\,\mathrm{W/m^2}$. We deduce that the total ERF, which is the sum of anthropogenic and natural ERF, is equal to $2.838\,\mathrm{W/m^2}$ in 2019. It has been multiplied by a factor of 4.85 in the last 70 years.

[56] We apply the theorem of variable change, which is explained on page 1064.

[57] Effective radiative forcing (ERF) is a measure of the change in radiative flux at the top of the atmosphere and does not include the Planck feedback.

Figure 8.53: Anthropogenic effective radiative forcing (ERF) from 1750 to 2019 by contributing forcing agents

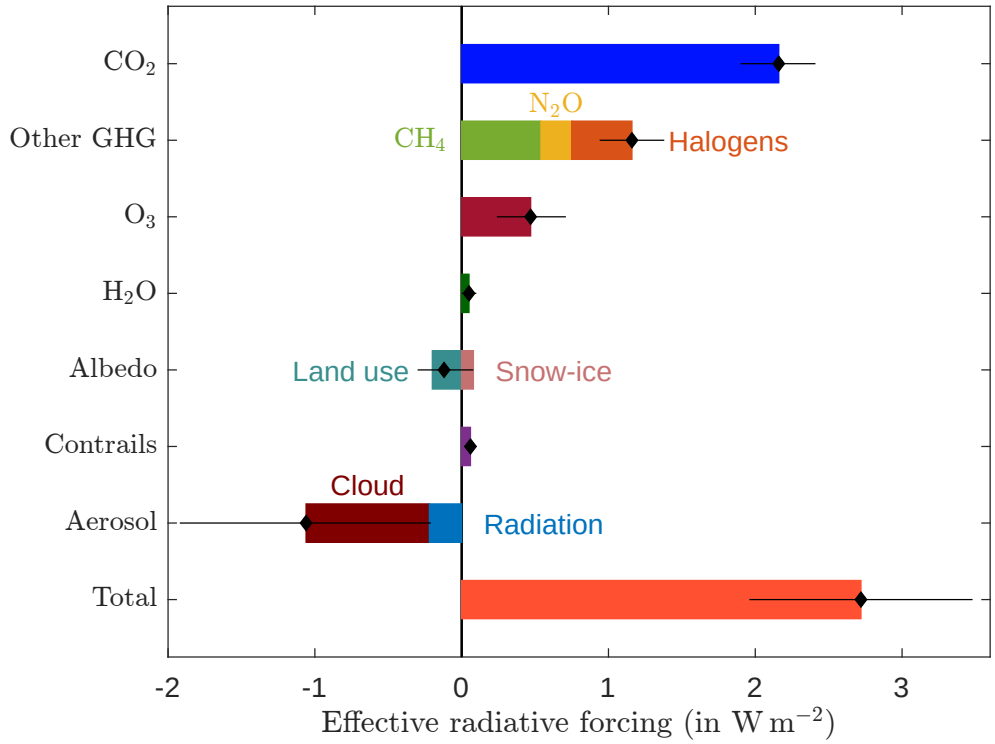


Source: (IPCC, 2021, Figure 7.6, Chapter 7, page 959) & https://www.ipcc.ch/report/ar6/wg1/figures/chapter-7/figure-7-6.

Table 8.11: Effective radiative forcing from 1750 to 2019

| Forcing agent | 1800 | 1850 | 1900 | 1950 | 2000 | 2010 | 2019 |
|---|---|---|---|---|---|---|---|
| $CO_2$ | 0.070 | 0.140 | 0.346 | 0.648 | 1.561 | 1.854 | 2.156 |
| $CH_4$ | 0.025 | 0.049 | 0.119 | 0.245 | 0.509 | 0.518 | 0.544 |
| $N_2O$ | 0.004 | 0.007 | 0.032 | 0.069 | 0.157 | 0.181 | 0.208 |
| Other GHG | 0.000 | 0.000 | 0.000 | 0.010 | 0.375 | 0.392 | 0.408 |
| $O_3$ | 0.015 | 0.030 | 0.081 | 0.167 | 0.399 | 0.443 | 0.474 |
| $H_2O$ (stratospheric) | 0.002 | 0.005 | 0.011 | 0.022 | 0.047 | 0.048 | 0.050 |
| Contrails | 0.000 | 0.000 | 0.000 | 0.005 | 0.039 | 0.044 | 0.058 |
| Aerosol | −0.018 | −0.078 | −0.346 | −0.708 | −1.221 | −1.266 | −1.058 |
| Black carbon on snow | 0.002 | 0.006 | 0.020 | 0.032 | 0.069 | 0.085 | 0.080 |
| Land use | −0.011 | −0.031 | −0.084 | −0.144 | −0.194 | −0.197 | −0.200 |
| Total (anthropogenic) | 0.089 | 0.128 | 0.179 | 0.346 | 1.739 | 2.103 | 2.720 |
| Volcanic | 0.183 | 0.194 | 0.198 | 0.182 | 0.175 | 0.137 | 0.140 |
| Solar | −0.043 | 0.008 | −0.037 | 0.057 | 0.110 | −0.008 | −0.022 |
| Total (natural) | 0.140 | 0.202 | 0.160 | 0.239 | 0.285 | 0.129 | 0.118 |
| Total | 0.229 | 0.330 | 0.339 | 0.585 | 2.025 | 2.232 | 2.838 |

Source: (IPCC, 2021, Figure 7.6, Chapter 7, page 959) & https://www.ipcc.ch/report/ar6/wg1/figures/chapter-7/figure-7-6.

**Remark 78** *The previous decomposition based on radiative sources can be complemented by an attribution based on GHG emissions. For example, Panel (a) in Figure 8.54 shows the global and annual mean ERF attributed to emitted compounds over the period 1750–2019 based on AerChemMIP simulations (Thornhill et al., 2021), while the emissions-based contributions to GSAT change are estimated in Panel (b).*

Figure 8.54: Contribution to effective radiative forcing (ERF) (a) and global mean surface air temperature (GSAT) change (b) from component emissions between 1750 to 2019 based on CMIP6 models

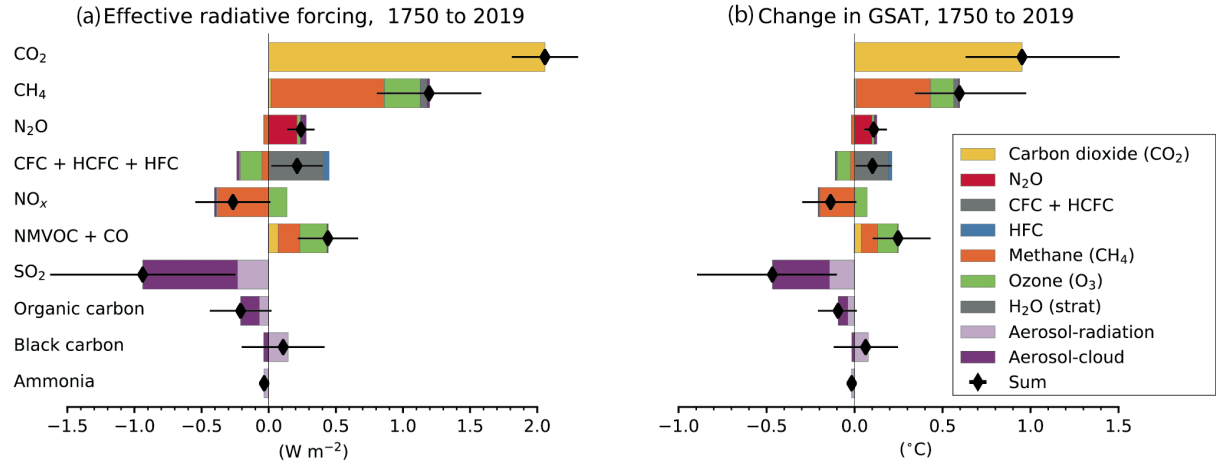


Source: (IPCC, 2021, Figure 6.12, Chapter 6, page 854) & https://www.ipcc.ch/report/ar6/wg1/figures/chapter-6/figure-6-12.

We now have all the information we need to calculate the equilibrium climate sensitivity. Using the parameters from Sherwood *et al.* (2020) $\lambda \sim \mathcal{N}\left(-1.30, 0.44^2\right)$ and $\Delta F_{2\times CO_2} \sim \mathcal{N}\left(4.00, 0.30^2\right)$, we get:

$$\begin{aligned} \text{ECS} &= -\frac{\Delta F_{2\times CO_2}}{\lambda} \\ &= -\frac{\mathcal{N}\left(4.00, 0.30^2\right)}{\mathcal{N}\left(-1.30, 0.44^2\right)} \\ &= \mathcal{NRD}\left(-4.00, 0.30^2, -1.30, 0.44^2\right) \end{aligned}$$

where $\mathcal{NRD}$ is the normal ratio distribution defined on page 1065. The probability density function of ECS is shown in Figure 8.55 and the exceedance probability is given below:

| Temperature $\theta$ | 2°C | 3°C | 4°C | 5°C | 7°C | 10°C |
|---|---|---|---|---|---|---|
| $\Pr\{\text{ECS} \geq \theta\}$ | 93.24% | 52.79% | 24.92% | 12.85% | 4.81% | 1.91% |

Therefore, we have a probability about 25% to observe a global warming greater than 4°C. In Figure 8.55, we compare the probability distribution when $\Delta F_{2\times CO_2}$ is constant and the probability distribution when $\Delta F_{2\times CO_2}$ is stochastic. This means comparing $\mathcal{RN}\left(\frac{1.30}{4.00}, \frac{0.44^2}{4.00^2}\right)$ and $\mathcal{NRD}\left(-4.00, 0.30^2, -1.30, 0.44^2\right)$. We conclude that the feedback uncertainty is the main contributor to the ECS uncertainty.

Figure 8.55: Probability density function of the equilibrium climate sensitivity ($\Delta F = +4.00\,\mathrm{W/m^2}$, $\sigma(\Delta F) = 0.30\,\mathrm{W/m^2}$, $\mu_\lambda = -1.30\,\mathrm{W\,m^{-2}\,K^{-1}}$ and $\sigma_\lambda = 0.44\,\mathrm{W\,m^{-2}\,K^{-1}}$)

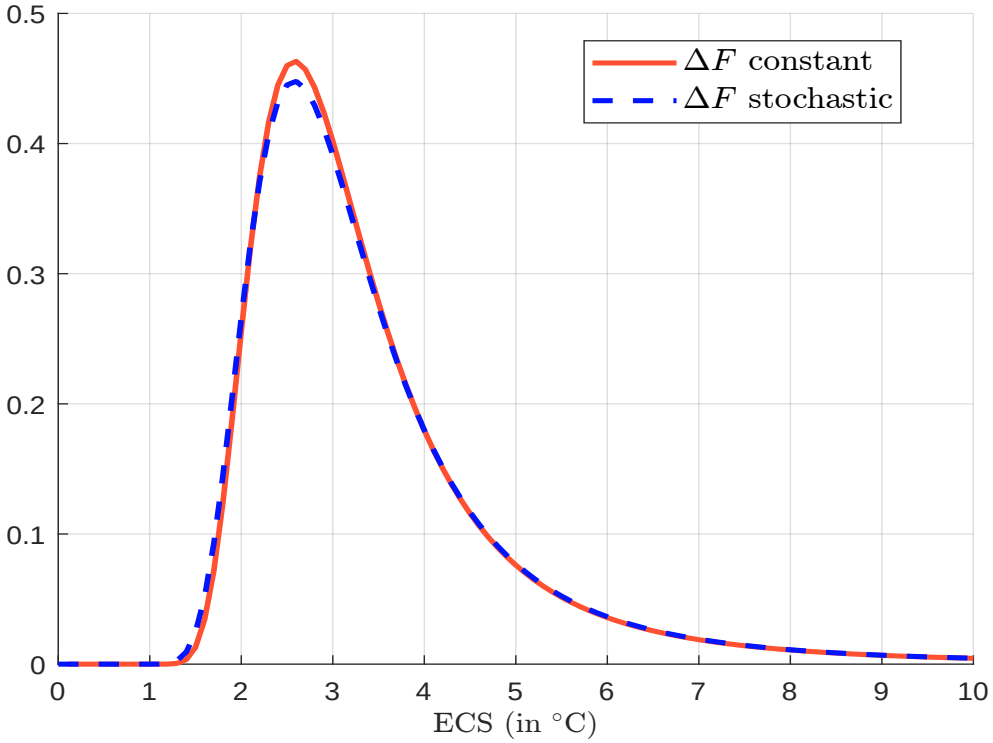


### Instability, tipping point and chaos

**An example of unstable equilibrium** We combine the Budyko model presented on page 677 with the one-layer model with emissivity. At equilibrium, we have:

$$\mathcal{E} = \frac{1}{4}\left(1 - \alpha_p\left(T_s\right)\right) S_0 - \left(\frac{2-\varepsilon}{2}\right)\sigma \mathcal{T}_s^4 = 0$$

where[58]:

$$\alpha_p\left(\mathcal{T}_s\right) = \begin{cases} \alpha_{\text{cold}} & \text{if } \mathcal{T}_s \leq \mathcal{T}_{\text{cold}} \\ \alpha_{\text{warm}} + \left(\alpha_{\text{cold}} - \alpha_{\text{warm}}\right)\left(\dfrac{\mathcal{T}_{\text{warm}} - \mathcal{T}_s}{\mathcal{T}_{\text{warm}} - \mathcal{T}_{\text{cold}}}\right)^{\eta} & \text{if } \mathcal{T}_{\text{cold}} \leq \mathcal{T}_s \leq \mathcal{T}_{\text{warm}} \\ \alpha_{\text{warm}} & \text{if } \mathcal{T}_s \geq \mathcal{T}_{\text{warm}} \end{cases}$$

In the first panel of Figure 8.56 we plot the albedo function $\alpha_p\left(\mathcal{T}_s\right)$ when $\eta$ is set to 3. The second panel shows the two forcing functions:

$$\begin{cases} F_{\text{solar}}\left(\mathcal{T}_s\right) = \dfrac{1}{4}\left(1 - \alpha_p\left(\left(\mathcal{T}_s\right)\right)\right) S_0 \\ F_{\text{blackbody}}\left(\mathcal{T}_s\right) = \left(\dfrac{2-\varepsilon}{2}\right)\sigma \mathcal{T}_s^4 \end{cases}$$

We then compare the net forcing function $F_{\text{solar}}\left(\mathcal{T}_s\right) - F_{\text{blackbody}}\left(\mathcal{T}_s\right)$ to the equation $\mathcal{E}\left(\mathcal{T}_s\right) = 0$

[58] We use the values $\alpha_{\text{cold}} = 0.7$, $\mathcal{T}_{\text{cold}} = 260\,\mathrm{K}$, $\alpha_{\text{warm}} = 0.3$ and $\mathcal{T}_{\text{warm}} = 295\,\mathrm{K}$.

Figure 8.56: Equilibrium states of the Budyko ice-albedo model

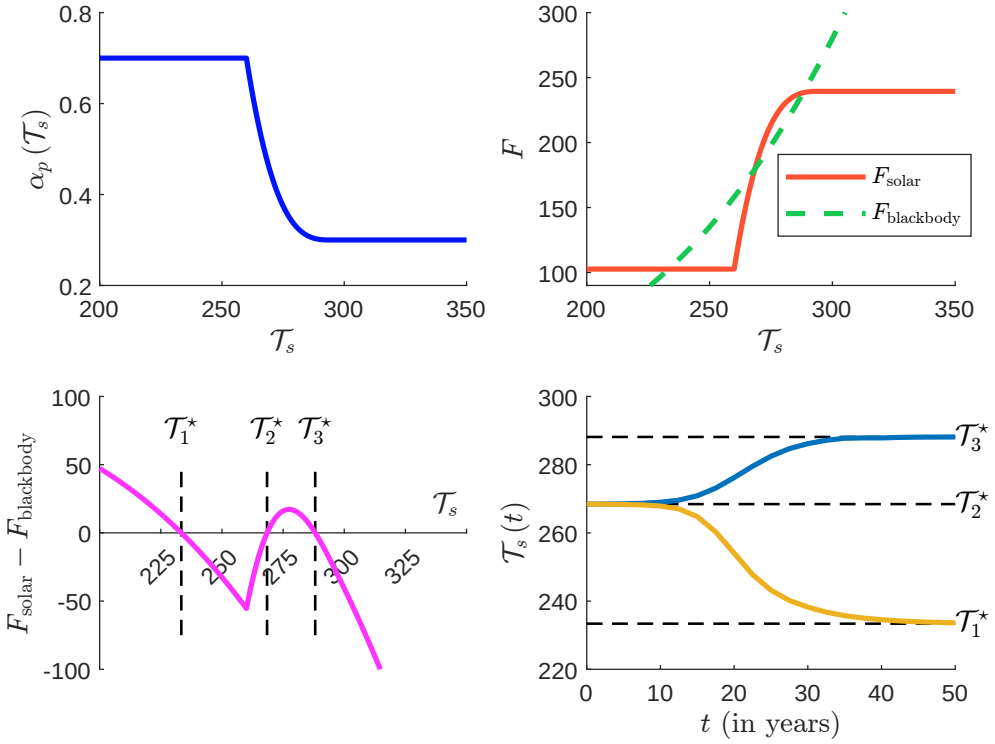


in the third panel. We can see graphically that there are three equilibrium states. By solving the equation $F_{\text{solar}}(\mathcal{T}_s) - F_{\text{blackbody}}(\mathcal{T}_s) = 0$ with a bisection algorithm, we find that the three equilibria are $\mathcal{T}_1^\star = 233.38\,\text{K}$, $\mathcal{T}_2^\star = 268.43\,\text{K}$, and $\mathcal{T}_3^\star = 288.13\,\text{K}$. To see if the equilibria are stable, we compute the total feedback:

$$\lambda(\mathcal{T}_s) = \lambda_0(\mathcal{T}_s) + \lambda_{\alpha_p}(\mathcal{T}_s)$$

where:

$$\lambda_0(\mathcal{T}_s) = -4\left(\frac{2-\varepsilon}{2}\right)\sigma\mathcal{T}_s^3$$

and:

$$\lambda_{\alpha_p}(\mathcal{T}_s) = \frac{1}{4}\eta S_0(\alpha_{\text{cold}} - \alpha_{\text{warm}})\frac{(\mathcal{T}_{\text{warm}} - \mathcal{T}_s)^{\eta-1}}{(\mathcal{T}_{\text{warm}} - \mathcal{T}_{\text{cold}})^{\eta}} \cdot \mathbb{1}\{\mathcal{T}_{\text{cold}} \leq \mathcal{T}_s \leq \mathcal{T}_{\text{warm}}\}$$

The results are shown below:

| State | Temperature | | $\lambda_0(\mathcal{T}_s)$ | $\lambda_{\alpha_p}(\mathcal{T}_s)$ | $\lambda(\mathcal{T}_s)$ |
|---|---|---|---|---|---|
| $\mathcal{T}_1^\star$ | 233.38 K | −39.77°C | −1.76 | 0.00 | −1.76 |
| $\mathcal{T}_2^\star$ | 268.43 K | −4.72°C | −2.68 | 6.75 | +4.08 |
| $\mathcal{T}_3^\star$ | 288.13 K | 14.98°C | −3.31 | 0.45 | −2.86 |

We conclude that $\mathcal{T}_1^\star$ and $\mathcal{T}_3^\star$ are two stable equilibria because $\lambda$ is negative, but $\mathcal{T}_2^\star$ is an unstable equilibrium. This means that if the climate system is in equilibrium $\mathcal{T}_2^\star$, any perturbation will cause instability and the temperature will not return to that equilibrium. To illustrate this instability, we consider the dynamics of the temperature:

$$c\frac{\mathrm{d}\mathcal{T}_s}{\mathrm{d}t} = F_{\text{solar}}(\mathcal{T}_s) - F_{\text{blackbody}}(\mathcal{T}_s) + \Delta F$$

where $c = 4 \times 10^8\,\mathrm{J\,m^{-2}\,K^{-1}}$ is the heat capacity and $\Delta F$ is the perturbation. We assume that the system is in equilibrium $\mathcal{T}_s(0) = \mathcal{T}_2^\star$. We introduce a small perturbation $\Delta F = +0.1\,\mathrm{W/m^2}$ and solve the above ordinary differential equation numerically. The solution is reported in the fourth panel of Figure 8.56. In this case, we have:

$$\lim_{t\to\infty} \mathcal{T}_s(t) = \mathcal{T}_3^\star$$

If the perturbation $\Delta F = -0.1\,\mathrm{W/m^2}$, we get:

$$\lim_{t\to\infty} \mathcal{T}_s(t) = \mathcal{T}_1^\star$$

We check that $\mathcal{T}_2^\star$ is an unstable equilibrium. The previous analysis concerns the sensitivity to the initial conditions. We can also consider the sensitivity to the parameters. For example, we can show that there is only one solution if $\eta < 1.9235$, while there are three solutions if $\eta > 1.9236$. Furthermore, there exists a parameter $\eta \in [1.9235, 1.9236]$ such that we get two solutions. This type of analysis is called bifurcation analysis.

**Tipping point definition** The concept of a tipping point emerged from stability analysis and bifurcation. The term was popularized in 2000 by Malcolm Gladwell in his book "*The Tipping Point: How Little Things Can Make a Big Difference*", which explored the concept in sociological change. In climate change, it was popularized in the late 2000s by Lenton *et al* (2008). In common parlance, a tipping point is a change. When applied to climate change, the term usually has a negative connotation and is generally associated with a change that could have devastating consequences for human society. However, when we look at scientific publications on climate change, a tipping point is a neutral mathematical concept. For example, here are the definitions adopted by Timothy Lenton and IPCC:

> "*The term tipping point commonly refers to a critical threshold at which a tiny perturbation can qualitatively alter the state or development of a system.*" (Lenton *et al*, 2008, page 1786).
>
> "*A climate tipping point occurs when a small change in forcing triggers a strongly nonlinear response in the internal dynamics of part of the climate system, qualitatively changing its future state.*" (Lenton, 2011, page 201).
>
> "*Tipping points refer to critical thresholds in a system that, when exceeded, can lead to a significant change in the state of the system, often with an understanding that the change is irreversible.*" (IPCC, 2018, page 262).
>
> In climate, a tipping point is "a *hypothesized critical threshold when global or regional climate changes from one stable state to another stable state. The tipping point event may be irreversible.*" (IPCC, 2021, page 1463).

In fact, these scientific definitions contrast with the content of these scientific publications, because a tipping point generally announces catastrophic events (Kemp *et al.*, 2022). For example, the term "*climate endgame*" refers to a hypothetical scenario in which climate change becomes catastrophic for human civilization and seems to be the Ten Plagues of Egypt with a series of super disasters: collapse of ecosystems, mass extinctions, global food shortages, water scarcity, etc.

**Bifurcation theory** Lenton (2011, Figure 2, page 203) gives a heuristic interpretation of the global warning when approaching a bifurcation point with a ball in a landscape of valleys and mountains. In Figures 8.57-8.59 we use an analogous story where the valleys represent stable attractors and the ball represents the state of the system. Figure 8.57 shows a stable equilibrium corresponding to the green ball. If the ball moves away from the equilibrium, but not too far, it will return to the equilibrium. This situation corresponds to the two red balls. This illustrates a reversible behavior where the system can retrace its path and return to its initial state. Figure 8.58 shows a red ball representing a tipping point. In fact, this equilibrium is unstable and corresponds to a bifurcation point, since the red ball cannot remain in this position indefinitely. If the system is initially at the red ball and is then slightly perturbed by a small disturbance, it will move toward the green balls and settle there. However, it is unpredictable which direction the red ball will take. It depends on many parameters. The red arrows represent the transitions between equilibria and indicate the direction between the tipping point and a stable equilibrium. Figure 8.59 shows the new position of the ball after it has moved to the left valley. Again the ball is in equilibrium. However, when it leaves this equilibrium, it cannot return to its initial position as shown in 8.59. In fact, the system has changed because part of the mountain has filled the valley. Instead, there is a new valley, but it's higher than the old one. Therefore, when the green ball leaves its equilibrium, it can move to the position represented by the yellow ball, but it cannot reach the position represented by the grey ball because it no longer exists.

To present the bifurcation theory of one-dimensional dynamical systems, we use chapters 2 and 3 of the classic textbook on bifurcation theory and chaos by Strogatz (2015). We consider the dynamical system of the form:

$$\frac{\mathrm{d}x}{\mathrm{d}t} = f(x, \mu)$$

where $\mu$ is the parameter set. We look at the mathematical properties of the system by analyzing the trajectories (or flows[59]) of $x(t)$. If $f(x, \mu) > 0$, then $x$ increases with time, while if $f(x, \mu) < 0$, then $x$ decreases with time. A fixed point $x^\star$ is then a value of $x$ such that the system does not change with time, *i.e.*, $f(x^\star, \mu) = 0$. Let $x = x^\star + \Delta x$ where $\Delta x$ is small. We have:

$$\begin{aligned}
\frac{\mathrm{d}x}{\mathrm{d}t} &= f(x^\star + \Delta x, \mu) \\
&= f(x^\star, \mu) + \frac{\partial f(x^\star, \mu)}{\partial x}\Delta x + O\left(\Delta x^2\right) \\
&= f(x^\star, \mu) + \lambda \Delta x + \mathcal{O}\left(\Delta x^2\right)
\end{aligned}$$

where $\lambda$ is the feedback of the system. Since we have:

$$\frac{\mathrm{d}x}{\mathrm{d}t} = \frac{\mathrm{d}(x^\star + \Delta x)}{\mathrm{d}t} = \frac{\mathrm{d}\Delta x}{\mathrm{d}t}$$

and:

$$f(x^\star + \Delta x, \mu) \approx f(x^\star, \mu) + \lambda \Delta x = \lambda \Delta x$$

We deduce that:

$$\frac{\mathrm{d}\Delta x}{\mathrm{d}t} = \lambda \Delta x$$

If $\lambda > 0$, then any small perturbation of the fixed point grows exponentially, while if $\lambda < 0$, then any small perturbation of the fixed point decays exponentially. In the first case the fixed point is

[59] A flow is used here as a synonym for a trajectory, and corresponds to a vector field that gives the direction and magnitude of the trajectory.

Figure 8.57: Stable equilibria

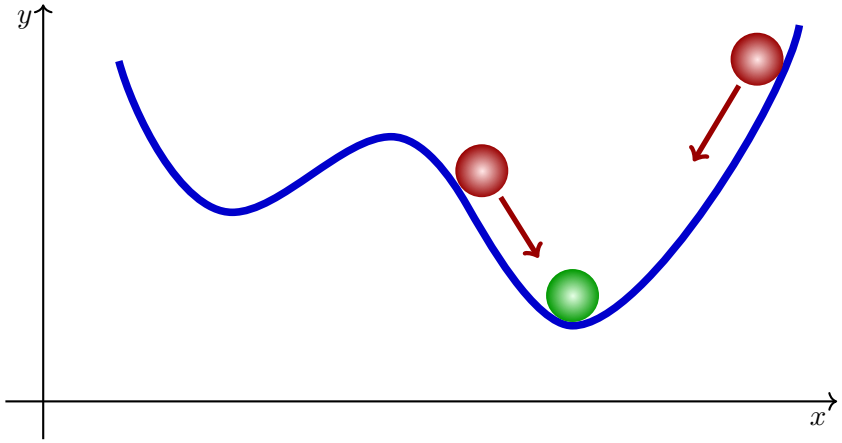


Figure 8.58: Unstable equilibrium

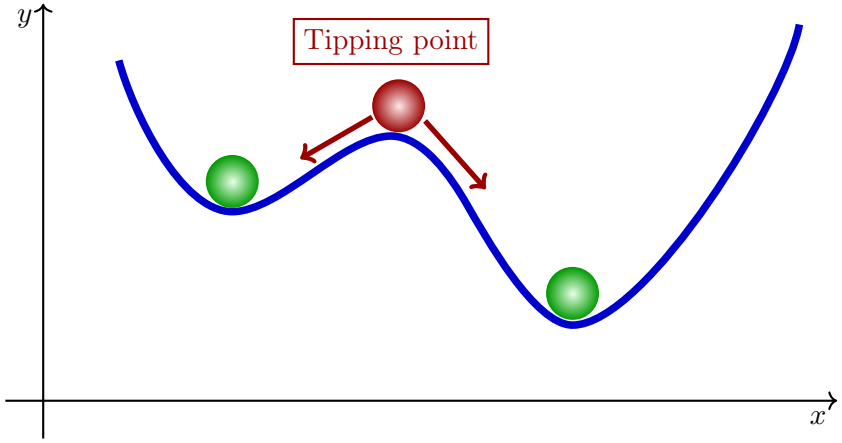


Figure 8.59: Irreversible tipping point

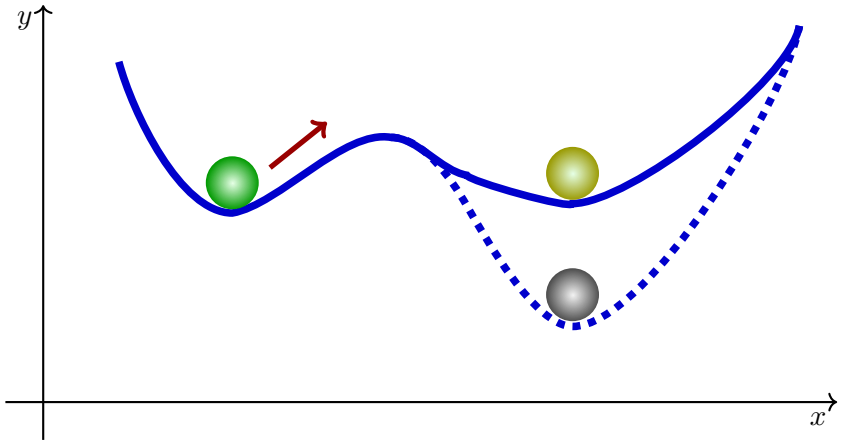

unstable, in the second case it is stable. When $\lambda = 0$, we need to study the second derivative of $f(x, \mu)$ to conclude. We also note that the relaxation timescale is equal to:

$$\tau = \frac{1}{|\partial_x f(x^\star, \mu)|}$$

**Example 27** *Consider the dynamical system* $\frac{\mathrm{d}x}{\mathrm{d}t} = x^2 + \mu$. *We have* $\partial_x f(x, \mu) = 2x$. *The fixed points are solutions of the equation* $x^2 = -\mu$. *If* $\mu > 0$, *there are no fixed points. If* $\mu = 0$, *the fixed point is* $x^\star = 0$ *and is not stable. If* $\mu < 0$, *there are two fixed points.* $x_1^\star = -\sqrt{-\mu}$ *is stable while* $x_2^\star = \sqrt{-\mu}$ *is unstable.*

The stability analysis evaluates the behavior of $f(x^\star + \varepsilon, \mu)$ and checks if the point $x^\star + \Delta x$ converges to the point $x^\star$. We can consider a second approach to stability where we evaluate the behavior of $f(x^\star, \mu + \varepsilon)$, *i.e.*, we apply the perturbation not directly to $x$ but to the control parameter $\mu$. In particular, we say that the value $\mu^\star$ is a bifurcation value if $f(x, \mu^\star)$ is not structurally stable. In the previous example, the dynamical system exhibits a bifurcation that occurs at $\mu = 0$. This type of bifurcation is called a saddle-node or fold bifurcation, because fixed points are created or destroyed. The first panel of Figure 8.60 shows the bifurcation diagram of the system. As $\mu$ increases, the distance between the stable and unstable fixed points decreases, and the equilibria are destroyed when $\mu$ is strictly positive. Following Strogatz (2015), other types of bifurcation are also common. A transcritical bifurcation occurs when fixed points exchange stability for a critical value of $\mu$. For example, the system $\frac{\mathrm{d}x(t)}{\mathrm{d}t} = \mu x - x^2$ has a transcritical bifurcation at $\mu = 0$ (second panel of Figure 8.60). A pitchfork bifurcation occurs when the system is unchanged and exhibits symmetry when $x = -x$. There are two forms of pitchfork bifurcation:

1. In a supercritical pitchfork bifurcation, a stable fixed point becomes unstable at a critical value of $\mu$. A canonical example is:
$$\frac{\mathrm{d}x}{\mathrm{d}t} = \mu x - x^3$$
The corresponding bifurcation diagram is shown in the third panel of Figure 8.60. We observe that $\mu = 0$ is a supercritical pitchfork bifurcation.

2. In a subcritical pitchfork bifurcation, an unstable fixed point becomes stable at a critical value of $\mu$. A canonical example is:
$$\frac{\mathrm{d}x}{\mathrm{d}t} = \mu x + x^3 - x^5$$
The corresponding bifurcation diagram is shown in the fourth panel of Figure 8.60. Let $\mu^\star = -0.25$ be the first value of $\mu$ that exhibits fixed points. When $\mu < \mu^\star$, there is a stable fixed point at $x^\star = 0$ because $\partial_x f(x^\star, \mu) < 0$. When $\mu = \mu^\star$, two new equilibria are created. When $\mu^\star < \mu \leq 0$, there are five fixed points. Three of these are stable equilibria. When $\mu > 0$, the stable equilibrium $x^\star = 0$ is destroyed and jumps to the stable branches or becomes unstable.

In bifurcation theory, hysteresis refers to a phenomenon where the behavior of the system depends on the history of its past states. For example, consider the previous subcritical pitchfork bifurcation and suppose the system is at equilibrium $x^\star = 0$. If we increase $\mu$, the system jumps to one of the stable branches. If we decrease $\mu$, the system does not return to its past equilibrium, but stays on the stable branch. However, if we decrease $\mu$ even more, the system jumps to its past equilibrium $x^\star = 0$ when $\mu$ reaches $\mu^\star = -0.25$. Therefore, the path of the system has formed a hysteresis loop.

Figure 8.60: Bifurcation diagram

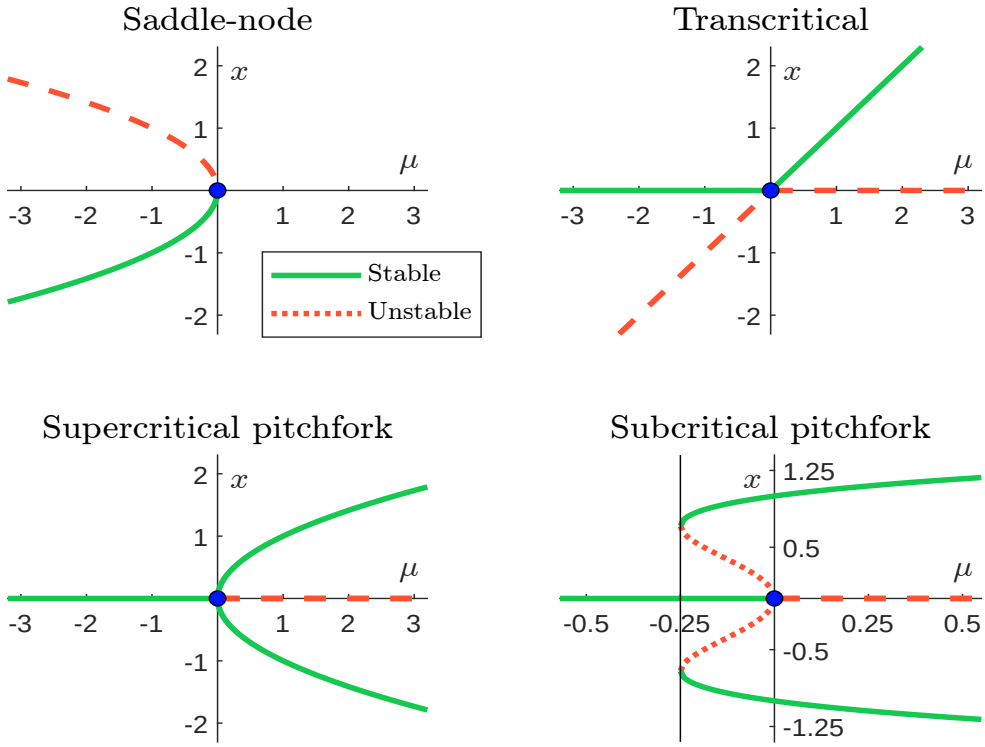


**Remark 79** *Chaos theory is closely related to bifurcation theory because chaos theory is primarily concerned with the behavior of dynamical systems that are highly sensitive to initial conditions. Since chaos is synonymous with disorder, a deterministic chaotic system exhibits aperiodic long-term behavior that appears to be random. These include strange attractors, feedback loops, limit cycles, self-similarity, fractals, butterfly effects, irregular oscillations, etc. The most famous chaotic models are the Hénon map, the Lorenz system, the logistic map, and the Rössler attractor described in Box 8.10.*

Let us return to the Budyko ice-albedo model described on page 689. Using the default values $S_0 = 1\,368\,\mathrm{W/m^2}$, $\varepsilon = 78\%$, $\eta = 3$, $\alpha_{\text{cold}} = 0.7$, $\mathcal{T}_{\text{cold}} = 260\,\mathrm{K}$, $\alpha_{\text{warm}} = 0.3$ and $\mathcal{T}_{\text{warm}} = 295\,\mathrm{K}$, we have obtained three fixed points: $\mathcal{T}_1^\star = 233.38\,\mathrm{K}$, $\mathcal{T}_2^\star = 268.43\,\mathrm{K}$, and $\mathcal{T}_3^\star = 288.13\,\mathrm{K}$. $\mathcal{T}_1^\star$ and $\mathcal{T}_3^\star$ were stable, while $\mathcal{T}_3^\star$ was unstable. To perform the bifurcation analysis of the Budyko ice-albedo model, we consider the range $\mathcal{T}_s \in [200\,\mathrm{K}, 300\,\mathrm{K}]$ and divide the range into ten intervals. Using the bisection algorithm, we solve the equation for each interval of $\mathcal{T}_s$ and each value of the parameter of interest:

$$\frac{1}{4}\left(1 - \alpha_p\left(\left(\mathcal{T}_s\right)\right)\right) S_0 - \left(\frac{2-\varepsilon}{2}\right)\sigma\mathcal{T}_s^4 = 0$$

We collect all fixed points $\{\mathcal{T}_1^\star, \mathcal{T}_2^\star, \ldots\}$. For each fixed point we calculate the feedback:

$$\lambda\left(\mathcal{T}_s\right) = \frac{1}{4}\eta S_0\left(\alpha_{\text{cold}} - \alpha_{\text{warm}}\right)\frac{\left(\mathcal{T}_{\text{warm}} - \mathcal{T}_s\right)^{\eta-1}}{\left(\mathcal{T}_{\text{warm}} - \mathcal{T}_{\text{cold}}\right)^{\eta}} \cdot \mathbb{1}\left\{\mathcal{T}_{\text{cold}} \leq \mathcal{T}_s \leq \mathcal{T}_{\text{warm}}\right\} - 4\left(\frac{2-\varepsilon}{2}\right)\sigma\mathcal{T}_s^3$$

We perform this analysis for a given range of the parameter of interest and plot the fixed points $\{\mathcal{T}_1^\star, \mathcal{T}_2^\star, \ldots\}$ against the parameter of interest. We also use a solid green line if the fixed point is stable or $\lambda\left(\mathcal{T}_s\right) < 0$, and a dashed red line otherwise. Results are shown in Figure 8.61, when the

Box 8.10: Rössler chaotic model

The Rössler model is a system of ordinary differential equations that exhibits chaotic dynamics (Rössler, 1976). It has become one of the most studied and widely used examples of a chaotic system. The Rössler equations are given by:

$$\begin{cases} \dfrac{\mathrm{d}x(t)}{\mathrm{d}t} = -(y(t) + z(t)) \\ \dfrac{\mathrm{d}y(t)}{\mathrm{d}t} = x(t) + ay(t) \\ \dfrac{\mathrm{d}z(t)}{\mathrm{d}t} = b + x(t)z(t) - cz(t) \end{cases}$$

where $a$, $b$ and $c$ are three parameters that control the behavior of the system. The Rössler attractor is a three-dimensional surface described by $(x(t), y(t), z(t))$. The attractor is very sensitive to the initial conditions $(x(0), y(0), z(0))$ and the set of parameters $(a, b, c)$. Below we plot the attractor in the first panel and the bifurcation diagram of $x(t)$ with respect to each parameter in the other three panels. We assume that the initial condition is $(x(0), y(0), z(0)) = (1, 1, 0)$ and the parameters[a] are $a = 0.2$, $b = 0.2$ and $c = 5.7$. We check that the dynamic system $(x(t), y(t), z(t))$ does not necessarily converge to a fixed point and is highly sensitive to the parameters. While the Rössler model is deterministic, its behavior is unpredictable like a stochastic model.

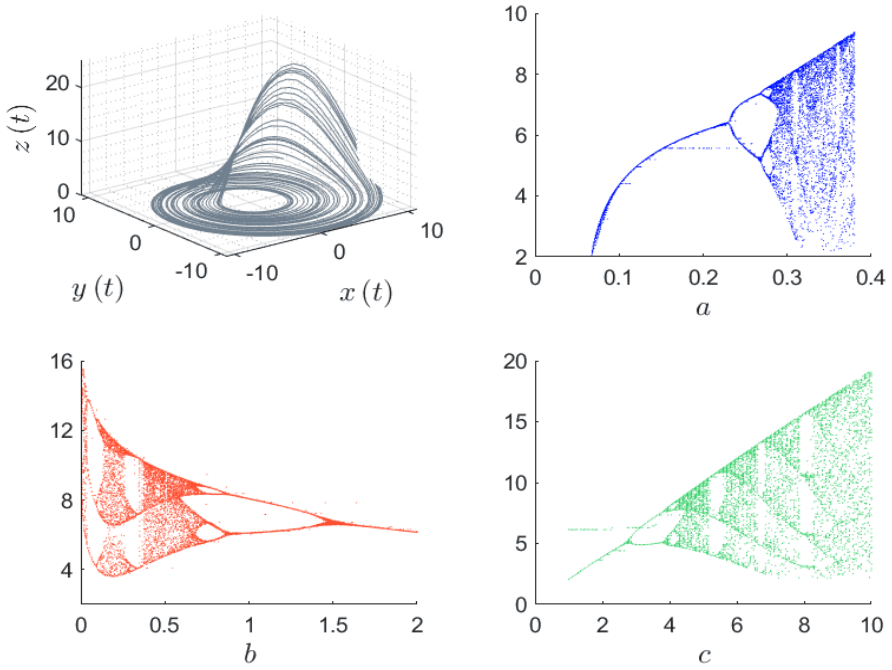


[a]For the bifurcation diagram of $a$, we set $b = 2$.

parameters of interest are $\eta$, $\varepsilon$, $S_0$ and $\alpha_{\text{cold}}$. We can make several remarks. First, we note that we can have one, two, or three fixed points, meaning that there is at least one equilibrium and no more than three equilibria for a set of parameters. Second, one of these fixed points is stable and it always generates a saddle-node bifurcation since two new equilibria are created. Third, the unstable fixed point is always between the two stable fixed points. Figure 8.62 shows the relaxation timescale of the different equilibria:

$$\tau = \frac{c}{|\lambda(\mathcal{T}_s)|}$$

Figure 8.61: Bifurcation of the Budyko ice-albedo model

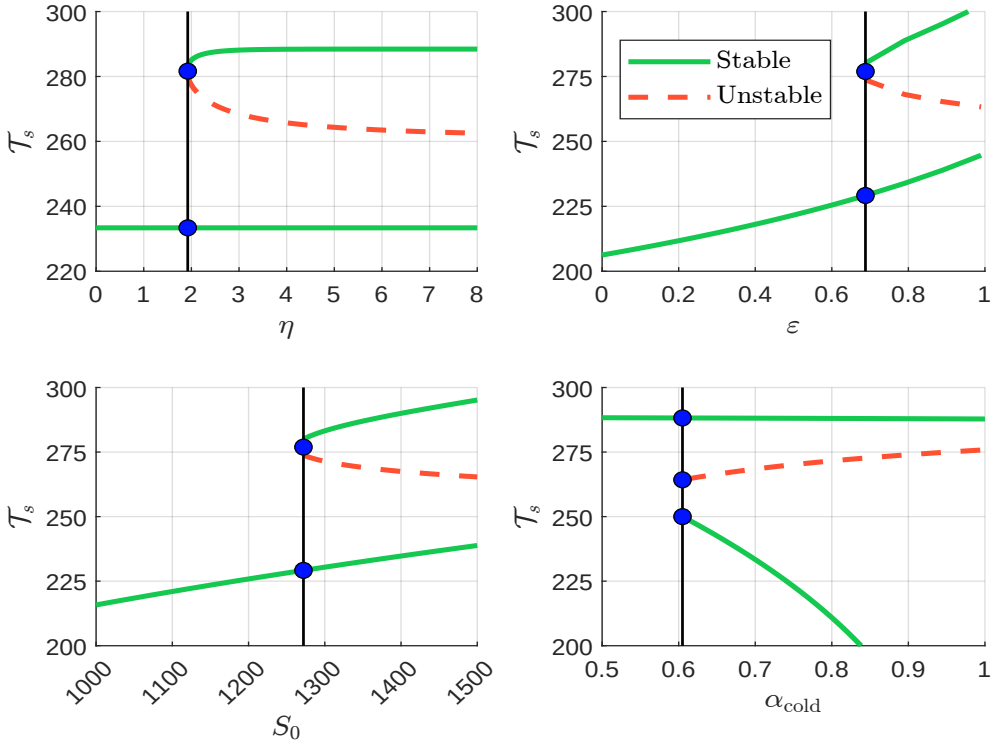


Figure 8.62: Relaxation timescale of the Budyko ice-albedo model (in years)

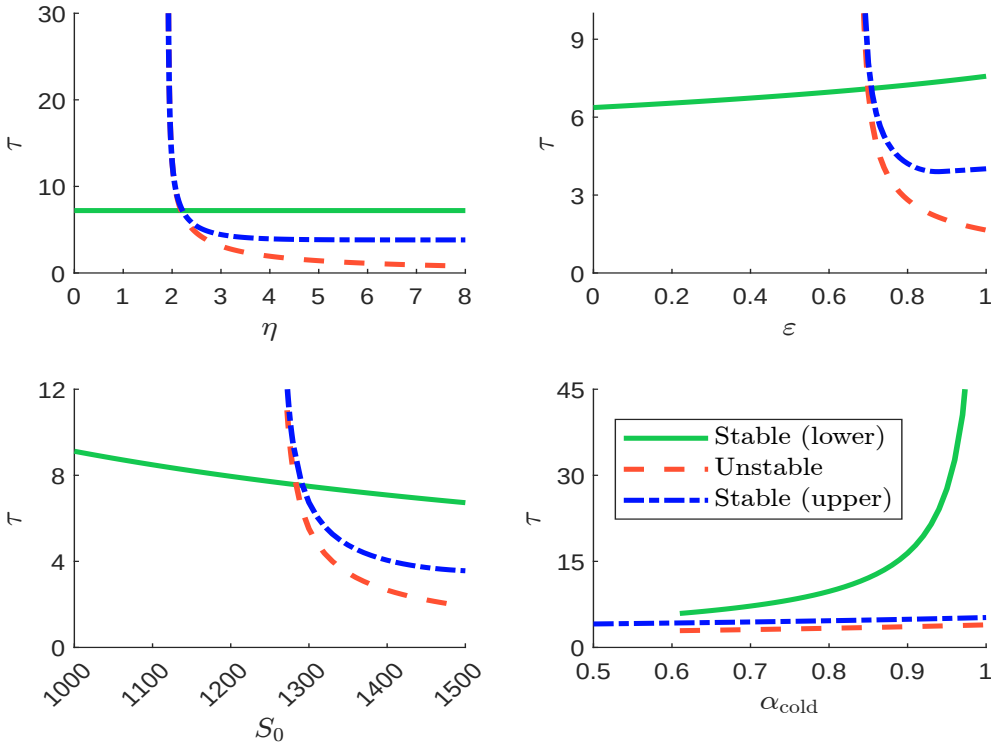

where $c = 4 \times 10^8 \, \mathrm{J\,m^{-2}\,K^{-1}}$ is the heat capacity. $\tau$ is expressed in years. Note that $\tau$ is less than 50 years, which is not realistic. In fact, the framework we have used to model the ice-albedo feedback is very simplistic and far from reality.

Figure 8.63: Bifurcation and overshooting tipping points

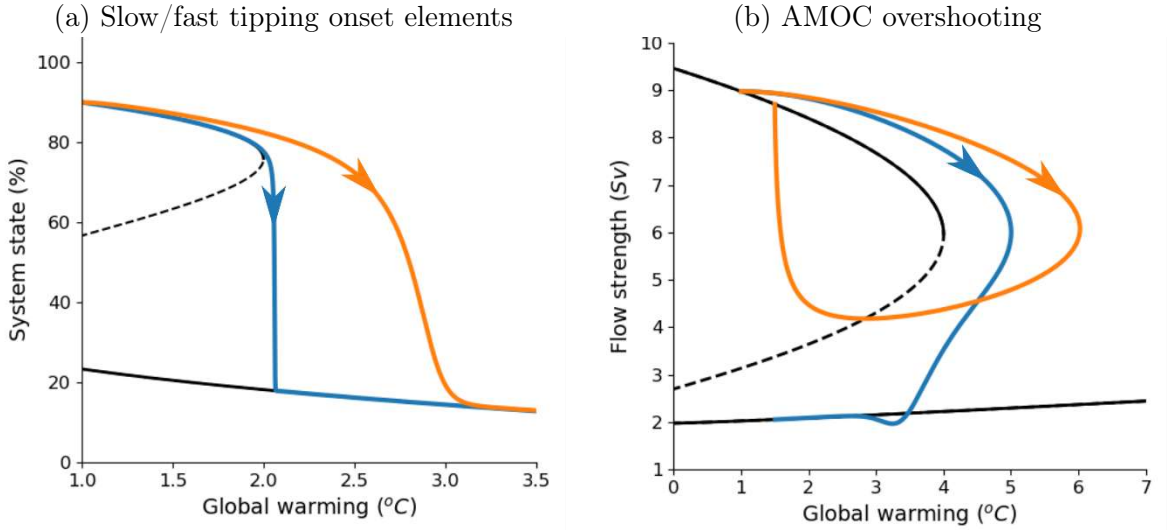


Source: Ritchie *et al.* (2021, Figures 1c & 3c, pages 518 & 520) & https://www.nature.com/articles/s41586-021-03263-2.

The Budyko ice-albedo model produces a relatively classical bifurcation where equilibria are created or destroyed at a bifurcation point. To obtain a more complex bifurcation diagram, we need to use a higher dimensional model or nonlinear feedback relationships. In Figure 8.63 we show two examples calculated by Ritchie *et al.* (2021). The first panel compares slow and fast overshooting tipping points and the importance of the radiative timescale[60]. The blue curve represents a rapidly overshooting tipping point system, such as the dieback of the Amazon forest, while the orange curve shows that the transition can take a long time even after we have passed the tipping point, such as the collapse of the Atlantic meridional overturning circulation (AMOC). This means that some tipping points may have already been reached, but we will not see their effects until the next century or millennium. The second panel shows the behavior of the AMOC when implementing an overshoot[61]. Two different trajectories are considered, one with a small overshoot and long recovery time (blue curve) and one with a large overshoot and short recovery time (orange curve). Contrary to expectations, the small overshoot leads to a persistent collapse of the AMOC, while the large overshoot allows a recovery. The resilience of the AMOC in this second scenario can be explained by the rapid reversal of global warming.

[60] Here is the description of the figure provided by the authors: "*System state vs. global warming for the fast onset tipping element (blue) and slow onset tipping element (orange). Both systems have a desired state, which is the upper solid black curve and represent contemporary conditions. An undesired stable state, given by the lower solid black curve, coexists with the desired state for warming levels below the 2°C threshold, separated by an unstable state (black dashed curve). Above the threshold, only the undesired equilibrium state remains.*" (Ritchie *et al.*, 2021, page 518).

[61] This figure shows the flow strength of the AMOC against global warming for short long and large fast overshoots: "*The blue curve is a small and long overshoot, while the orange curve is a much larger yet quick overshoot. An AMOC on state (upper solid black curve) and an AMOC off state (lower solid black curve) both coexist for warming levels below the threshold of 4°C and are separated by an unstable state (black dashed curve). Above the threshold only the AMOC off state remains.*" (Ritchie *et al.*, 2021, page 520).

**Climate tipping elements** Lenton *et al* (2008) introduced the term "*tipping element*" to describe large-scale components of the Earth system that may pass a tipping point. They identified 9 climate tipping elements: (1) Arctic sea ice, (2) Greenland ice sheet, (3) West Antarctic ice sheet, (4) Atlantic thermohaline circulation, (5) El Niño Southern Oscillation (ENSO), (6) Indian summer monsoon, (7) Sahara/Sahel and West African monsoons, (8) Amazon rainforest, and (9) boreal forest. They added to this list other candidate tipping elements that did not meet all the criteria for a tipping point: (10) Antarctic bottom water, (11) tundra, (12) permafrost, (13) marine methane hydrates, (14) ocean anoxia, and (15) Arctic ozone. The above short list of climate tipping elements has evolved over time (Lenton, 2011; Steffen *et al.*, 2018; Lenton *et al*, 2019). Today, there is a consensus on the most important tipping points, which has been published by Armstrong McKay *et al.* (2022). We report this short list in Table 8.12, while Figure 8.64 shows their location on the Earth.

Figure 8.64: Geographical distribution of global and regional tipping elements

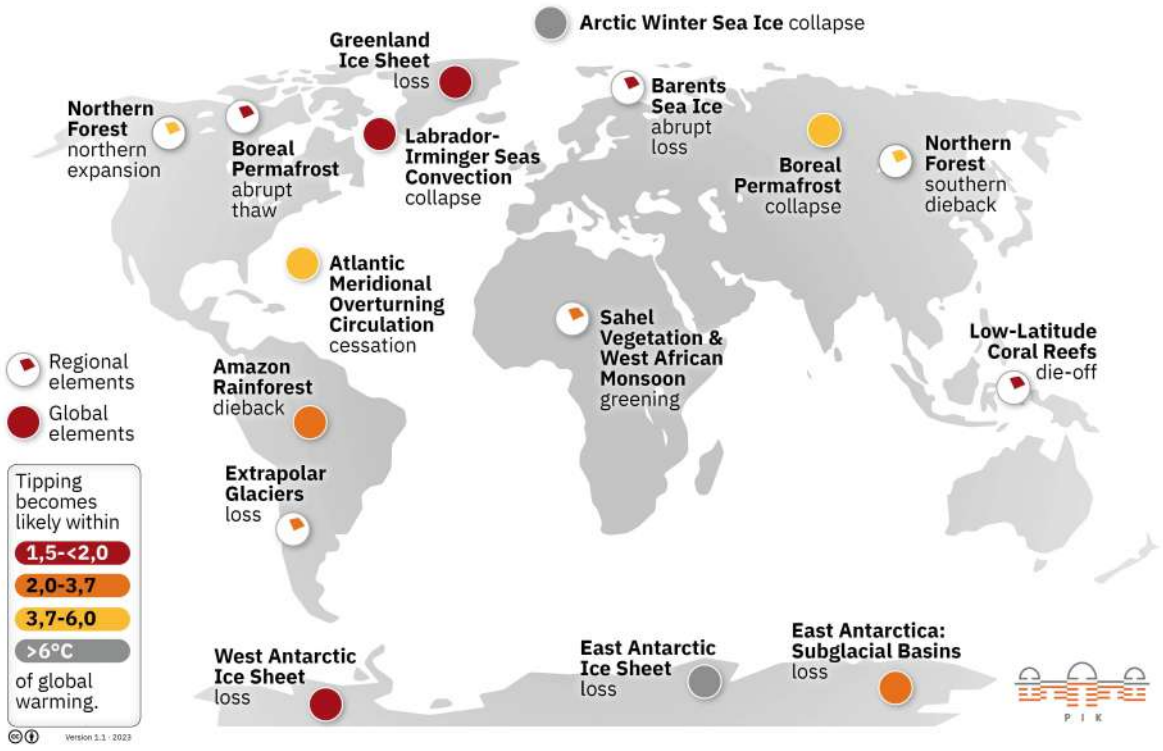


Source: Armstrong McKay *et al.* (2022) & `https://www.pik-potsdam.de/en/output/infodesk/tipping-elements`.

Armstrong McKay *et al.* (2022) distinguish 9 global core and 7 regional impact tipping elements that affect the cryosphere, ocean-atmosphere, and biosphere. For each climate tipping point, they estimate the threshold $\theta$, the timescale $\tau$ and the maximum impact $\delta$. This means that the tipping point is reached when the temperature anomaly is greater than $\theta$. The result is a new equilibrium that induces a temperature change of $\delta$ after $\tau$ years:

$$\Delta\mathcal{T}_s(0) \geq \theta \Rightarrow \text{tipping point} \Rightarrow \Delta\mathcal{T}_s(\tau) = \delta$$

For example, if $\theta = +1°\text{C}$, $\tau = 50$ years and $\delta = 0.2°\text{C}$, the tipping point is crossed when the temperature increase is 1°C. The new equilibrium will be reached after 50 years with a supplementary temperature increase of 0.2°C. The plausible range of these estimates is given in parentheses.

Table 8.12: Threshold, timescale, and impact estimates for the global and regional tipping elements

| Category | # | Climate tipping element | Tipping point | Threshold | | Timescale | | Maximum impact | |
|---|---|---|---|---|---|---|---|---|---|
| Global | 1 | Greenland ice sheet | collapse | 1.5°C | (0.8–3.0) | 10 kyr | (1–15) | 0.13°C | (0.5–3.0) |
| | 2 | West Antarctic ice sheet | collapse | 1.5°C | (1.0–3.0) | 2 kyr | (0.5–13) | 0.05°C | (1.0) |
| | 3 | Labrador-Irminger seas | collapse | 1.8°C | (1.1–3.8) | 10 yr | (5–50) | −0.50°C | (-3.0) |
| | 4 | East Antarctic subglacial basins | collapse | 3.0°C | (2.0–6.0) | 2 kyr | (0.5–10) | 0.05°C | |
| | 5 | Amazon rainforest | dieback | 3.5°C | (2.0–6.0) | 100 yr | (50–200) | 0.20°C | (0.4–2.0) |
| | 6 | Boreal permafrost | collapse | 4.0°C | (3.0–6.0) | 50 yr | (10–300) | 0.40°C | |
| | 7 | AMOC | collapse | 4.0°C | (1.4–8.0) | 50 yr | (15–300) | −0.50°C | (-4/-10) |
| | 8 | Arctic winter sea ice | collapse | 6.3°C | (4.5–8.7) | 20 yr | (10–100) | 0.60°C | (0.6–1.2) |
| | 9 | East Antarctic ice sheet | collapse | 7.5°C | (5.0–10.0) | > 10 kyr | | 0.60°C | (2.0) |
| Regional | 10 | Low-latitude coral reefs | die-off | 1.5°C | (1.0–2.0) | 10 yr | | | |
| | 11 | Boreal permafrost | abrupt thaw | 1.5°C | (1.0–2.3) | 200 yr | (100–300) | 0.04°C | |
| | 12 | Barents sea ice | abrupt loss | 1.6°C | (1.5–1.7) | 25 yr | | | |
| | 13 | Mountain glaciers | loss | 2.0°C | (1.5–3.0) | 200 yr | (50–1000) | 0.08°C | |
| | 14 | Sahel and West African monsoon | greening | 2.8°C | (2.0–3.5) | 50 yr | (10–500) | | |
| | 15 | Boreal forest (southern) | die-off | 4.0°C | (1.4–5.0) | 100 yr | (50+) | −0.18°C | (-0.5/-2) |
| | 16 | Boreal forest (northern) | expansion | 4.0°C | (1.5–7.2) | 100 yr | (40+) | 0.14°C | (0.5–1.0) |

Source: Armstrong McKay *et al.* (2022, Table 1, page 3).

Below is a list of the different tipping elements and some explanations of the mechanism behind them:

1. The Greenland ice sheet is the second largest ice sheet in the world. It covers 80% of the surface of Greenland. Its melting would increase sea level rise, possibly up to 7.4 meters, accelerate ocean acidification, and have a potentially positive feedback effect on climate change (Shepherd *et al.*, 2020).

2. The West Antarctic ice sheet is a large ice sheet in Antarctica. It sits on a bedrock that is mostly below sea level and has formed a deep subglacial basin due to the weight of the ice sheet, which can be up to 4 kilometers thick in places. Its collapse could raise global sea levels, possibly up to 3 meters (Alley *et al.*, 2015).

3. The Labrador and Irminger seas are located in the subpolar North Atlantic, between Canada, Greenland and Iceland. These seas are characterized by cold and salty waters that generate deep convection. This deep convection and the regulation of ocean salinity influence the circulation of the Atlantic meridional overturning circulation (AMOC). The collapse of the deep convection system in the Labrador and Irminger seas would affect the overall circulation in the North Subpolar Gyre (Chafik *et al.*, 2022).

4. East Antarctic subglacial basins are large, ice-filled depressions in the bedrock adjacent to the East Antarctic ice sheet. They also serve as reservoirs for meltwater. Certain subglacial basins, such as Wilkes, Aurora, and Recovery, are more susceptible to a situation called marine ice sheet instability (MISI). As the ice shelf at the edge of the ice sheet retreats, warm ocean water can flow into the deeper basin, further destabilizing the ice shelf. This process can create a self-perpetuating cycle of ice melt and ice shelf retreat (Stokes *et al.*, 2022).

5. The Amazon rainforest, also known as the Amazon jungle or Amazonia, is the largest rainforest in the world. It spans nine countries: Brazil, Peru, Colombia, Ecuador, Bolivia, Venezuela, Guyana, Suriname, and French Guiana. It contains the largest and most biodiverse area of tropical rainforest in the world. The Amazon rainforest acts as a massive carbon sink, absorbing and storing vast amounts of carbon dioxide through the process of photosynthesis. If the forest were to be subject to widespread deforestation or degradation, the stored carbon could be released back into the atmosphere, contributing to increased greenhouse gas concentrations. The Amazon also plays a critical role in the Earth's water cycle, influencing regional and global weather patterns. Its dense vegetation effectively captures rainwater and slowly releases it into streams and rivers, helping to maintain stable water levels, prevent flooding, and provide a steady source of fresh water (Gatti *et al.*, 2021).

6. Boreal permafrost is a permanently frozen layer of soil and rock that underlies much of the world's boreal forest. It is found in Siberia, Alaska, Northern Canada, and the Tibetan Plateau. Permafrost forms when the soil temperature remains below 0°C for at least two consecutive years. Boreal permafrost contains large amounts of organic carbon stored in the form of dead plant material that could not decompose due to the cold temperatures. It is also one of the largest reservoirs of methane. Rising temperatures may cause the boreal permafrost to thaw, releasing large amounts of carbon and methane into the atmosphere (Schuur *et al.*, 2015).

7. The Atlantic meridional overturning circulation (AMOC) is a large, complex system of ocean currents that transports warm water from the tropics to the North Atlantic and cold water from the North Atlantic to the subtropics. It is also known as the Gulf Stream system. A weakening

of the AMOC could have complex and regionally specific effects on temperatures. On a global scale, it could result in less warm water reaching higher latitudes, leading to cooler sea surface temperatures in the North Atlantic and warmer temperatures in the Southern Hemisphere (Liu *et al.*, 2017).

8. Arctic winter sea ice is the maximum extent of sea ice that forms in the Arctic Ocean during the winter months. It helps to regulate global temperatures by reflecting sunlight back into space. This albedo reflection helps to cool the Arctic. As sea ice melts, more sunlight is absorbed by the ocean, causing a further warming trend[62]. However, the impact of the albedo effect remains controversial (Bathiany *et al.*, 2016).

9. The East Antarctic ice sheet is the largest and thickest ice sheet on Earth. A complete collapse would raise the global sea levels by 50 meters. However, the East Antarctic ice sheet is generally considered to be more stable than the West Antarctic ice sheet, due to its higher elevation and more remote location (Stokes *et al.*, 2022).

10. Low-latitude coral reefs occur in the Atlantic, Indian, and Pacific Oceans, most notably in the Philippines, Indonesia, and Australia. They require warm, sunny weather and unpolluted water. Therefore, coral reefs can be affected by climate change, although their impact on climate change is more limited (Descombes *et al.*, 2015).

11. We have already seen that the boreal permafrost is a global tipping element, but it is also a regional tipping element. In fact, an abrupt thaw of the boreal permafrost would have devastating consequences for the region, affecting infrastructure (roads, buildings, transportation), the environment (flooding, forests, vegetation), and living conditions and health (Hjort *et al.*, 2022).

12. Barents sea ice is found in the Barents sea, an arm of the Arctic Ocean between Norway and Russia. The sea ice forms during the winter months and melts during the summer months. This regional tipping element is strongly related to two global tipping elements: Labrador-Irminger seas and AMOC (Moore *et al.*, 2022).

13. Mountain glaciers are large masses of ice that form on mountains at high altitudes. They are formed from compacted snow that has accumulated over many years. The melting of mountain glaciers would have a major regional impact on human life (Carey, 2010).

14. The West African monsoon is a seasonal wind pattern that affects the Sahel, bringing moisture from the Atlantic Ocean during the rainy season and drying out the region during the dry season. It is responsible for the region's agriculture and supports the livelihoods of millions of people. Changes in rainfall can affect vegetation, agriculture and people (Pausata *et al.*, 2020).

15. The boreal forest, also known as the taiga, is a biome that surrounds the Arctic region. Countries with significant areas of boreal forest include Canada, Russia, Sweden, Norway and Finland. The southern edge of the boreal forest is the boundary between the boreal forest and temperate forests or grasslands. The risk could be an abrupt die-off (Venäläinen *et al.*, 2020).

16. The northern edge of the boreal forest is typically found at higher latitudes, closer to the Arctic Circle. The change could be an abrupt expansion into a tundra forest characterised by treeless landscapes and permafrost (Girona *et al.*, 2023).

[62]Moreover, the warming Arctic has the potential to release methane from permafrost.

Almost all the climate tipping elements induce a temperature increase, except Labrador-Irminger seas, AMOC and the southern edge of the boreal forest. We also find some large differences in timescale (between 10 years and more than 10 000 years) and impact. According to Armstrong McKay *et al.* (2022), the Greenland and West Antarctic ice sheets have certainly passed their tipping points, and other tipping points such as the die-off of tropical coral reefs and boreal permafrost are close to crossing their threshold.

### Cascading tipping points and climate domino effects

**Mathematical framework of coupling tipping points** Based on an original idea by Brummitt *et al.* (2015), Klose *et al.* (2020) assumes that the climate tipping elements follow an ordinary differential equation with a double fold bifurcation:

$$\frac{\mathrm{d}x_i}{\mathrm{d}t} = f_i\left(x_i, \mu_i\right) = \frac{\alpha_i x_i - \beta_i x_i^3 + \mu_i}{\tau_i} \tag{8.16}$$

where $x_i$ is the $i^{\text{th}}$ tipping element, $\tau_i$ is the timescale, $\alpha_i > 0$ and $\beta_i > 0$ are two fixed parameters[63] and $\mu_i$ is the bifurcation parameter. Note that the cubic equation $f_i\left(x_i, \mu_i\right) = 0$ has three roots (real and complex). The feedback is equal to:

$$\lambda = \frac{\partial f_i\left(x_i, \mu_i\right)}{\partial x_i} = \frac{\alpha_i - 3\beta_i x_i^2}{\tau_i} \tag{8.17}$$

Since our system is a special case of an ODE with a RHS term which is a cubic polynomial, we can use the results given in Box 8.11. Comparing with the form of $f_i\left(x_i, \mu_i\right)$, we have $a = -\beta_i/\tau_i$, $b = 0$, $c = \alpha_i/\tau_i$, and $d = \mu_i/\tau_i$. Substituting these values into the expression for the discriminant, we get:

$$\Delta_i = \frac{4\beta_i\alpha_i^3 - 27\beta_i^2\mu_i^2}{\tau_i^4}$$

The number of stable equilibria depends on the discriminant $\Delta_i \propto 4\alpha_i^3 - 27\beta_i\mu_i^2$. If $\Delta_i < 0$ or $4\alpha_i^3 < 27\beta_i\mu_i^2$ there is one stable equilibrium, while if $\Delta > 0$ or $4\alpha_i^3 > 27\beta_i\mu_i^2$ there two stable equilibria[64]. Therefore, the bifurcation occurs when $\Delta_i = 0$ or:

$$\mu_i = \pm\sqrt{\frac{4\alpha_i^3}{27\beta_i}}$$

Figure 8.65 shows the bifurcation diagram of the system when[65] $\alpha_i = \beta_i = 1$. If $\mu_i$ is strongly negative, there is only one stable equilibrium. A first bifurcation occurs at $\mu_i = -\sqrt{\frac{4}{27}}$ and two more equilibria are created, one stable and another one unstable. Then two equilibria are destroyed when $\mu_i$ reaches the value $\sqrt{\frac{4}{27}}$ and $x_i^\star = -\sqrt{\frac{1}{3}}$. They are the lower stable equilibrium and the middle unstable equilibrium. Only the upper equilibrium remains when $\mu_i$ is greater than $\sqrt{\frac{4}{27}}$.

[63] According to Klose *et al.* (2020), $\alpha_i$ corresponds to the distance between the upper and lower layers of stable equilibria of the cusp, while $\beta_i$ controls the strength of the nonlinearity in the system.

[64] Since $-\beta_i < 0$, the graph of the cubic function $f_i\left(x_i, \mu_i\right)$ shows that the function is decreasing, then increasing and then decreasing. If we note that $x_{i,1}^\star$, $x_{i,2}^\star$, and $x_{i,3}^\star$ are the roots of $f_i\left(x_i, \mu_i\right) = 0$ with $x_{i,1}^\star \leq x_{i,2}^\star \leq x_{i,3}^\star$, we deduce that $f_i'\left(x_{i,1}^\star, \mu_i\right) \leq 0$, $f_i'\left(x_{i,2}^\star, \mu_i\right) \geq 0$, and $f_i'\left(x_{i,3}^\star, \mu_i\right) \leq 0$.

[65] Note that the bifurcation diagram does not depend on the timescale $\tau_i$.

Box 8.11: First-order ODE with a cubic polynomial

Consider the following ordinary differential equation (ODE):

$$\frac{\mathrm{d}x}{\mathrm{d}t} = f(x) = ax^3 + bx^2 + cx + d$$

where $f(x)$ is a general cubic polynomial. The discriminant of the general cubic equation $f(x) = 0$ is:

$$\Delta = 18abcd - 4b^3d + b^2c^2 - 4ac^3 - 27a^2d^2$$

and the first derivative is:

$$f'(x) = 3ax^2 + 2bx + c$$

The stability of the equilibria depends on the sign of the discriminant $\Delta$ and the sign of the derivative $f'(x)$:

1. Stable equilibria
   If $\Delta > 0$, the ODE can have three distinct real roots. In this case, the equilibrium points can be classified based on the sign of $f'(x)$ at each root. If $f'(x)$ is negative for all three roots, then all equilibrium points are stable.

2. Saddle equilibria
   If $\Delta < 0$, the ODE can have one real root and two complex conjugate roots. The real root corresponds to a saddle equilibrium point.

3. Unstable equilibria
   If $\Delta = 0$, the ODE can have a repeated real root. Stability depends on higher order derivatives.

Let $\alpha_i = \beta_i = 1$ and $\mu_i = 0.5$. We assume that the current state of the system is $x_i(0) = -1$. Figure 8.13 shows the convergence of $x_i(t)$ to equilibrium for three values of the timescale. Whatever the value of $\tau_i$, we have $\lim_{t\to\infty} x_i(t) = 1.1915$. The equilibrium is reached in seven years when $\tau_i = 1$, while we need more than 70 years when $\tau_i = 10$. In the case $\tau_i = 10$, convergence to equilibrium takes between 300 and 400 years.

To introduce the cascading effects between the tipping elements, Brummitt *et al.* (2015) and Klose *et al.* (2020) assume that $x_i$ depends on the other tipping elements $x_j$ with $j \neq i$:

$$\frac{\mathrm{d}x_i}{\mathrm{d}t} = f_i(x_i, \mu_i) + c_i(x_{-i}) = g_i(x_1, \ldots, x_n, \mu_i)$$

where $c_i(x_{-i})$ is the coupling function. In particular, they study the linear case where $c_i(x_{-i}) = \tau_i^{-1} \sum_{j\neq i} \gamma_{i,j} x_j$ and $\gamma_{i,j}$ measures the influence of subsystem $x_j$ on subsystem $x_i$. Therefore, Equation (8.16) becomes:

$$\frac{\mathrm{d}x_i}{\mathrm{d}t} = \frac{\alpha_i x_i - \beta_i x_i^3 + \mu_i + \sum_{j\neq i} \gamma_{i,j} x_j}{\tau_i} \tag{8.18}$$

We may wonder how the coupling function affects the tipping points. For example, in the two-dimensional case we have:

$$\begin{cases} \dfrac{\mathrm{d}x_1}{\mathrm{d}t} = \dfrac{\alpha_1 x_1 - \beta_1 x_1^3 + \mu_1 + \gamma_{1,2} x_2}{\tau_1} \\ \dfrac{\mathrm{d}x_2}{\mathrm{d}t} = \dfrac{\alpha_2 x_2 - \beta_2 x_2^3 + \mu_2 + \gamma_{2,1} x_1}{\tau_2} \end{cases}$$

Several coupling models can be distinguished:

Figure 8.65: Double fold bifurcation

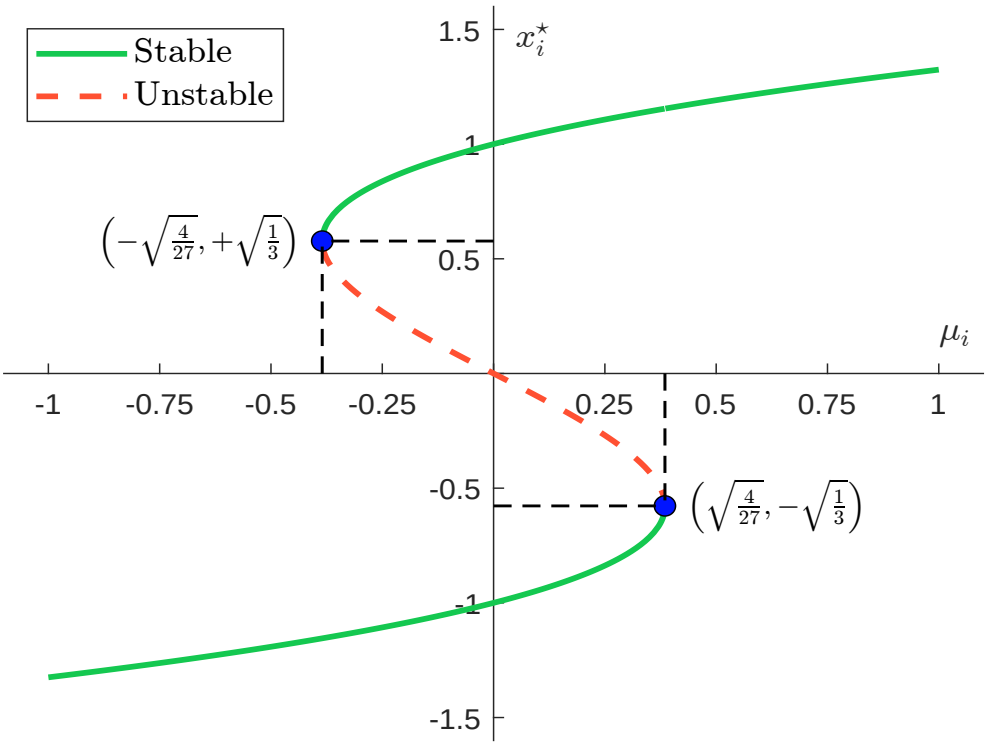


Source: Klose *et al.* (2020, Figure 1, page 3).

Figure 8.66: Convergence to the equilibrium

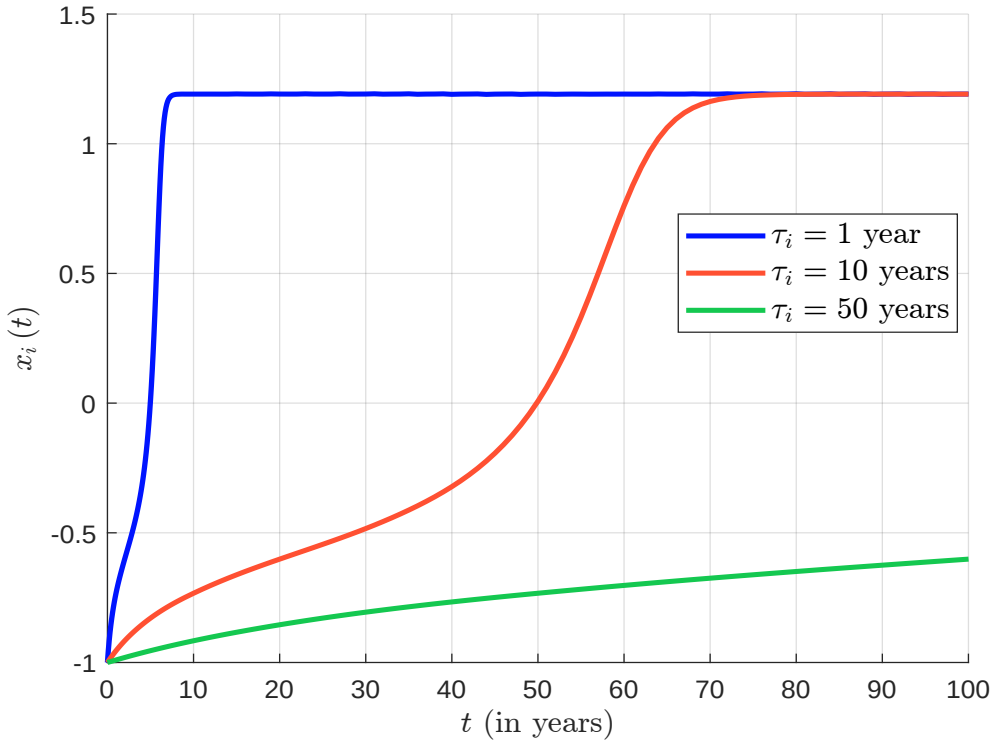

- If $\gamma_{1,2} = \gamma_{2,1} = 0$, then the two subsystems are uncoupled and the previous analysis remains valid.
- If $\gamma_{1,2} = 0$ and $\gamma_{2,1} \neq 0$, then the first subsystem drives the second subsystem ($x_1 \longrightarrow x_2$). We obtain a master-slave system with linear coupling (Brummitt *et al.*, 2015, Section 2.2, pages 3-5). For the first subsystem, we have $\Delta_1 = \dfrac{4\beta_1\alpha_1^3 - 27\beta_1^2\mu_1^2}{\tau_1^4}$, which means that we obtain the same results as in the uncoupled case. Assuming that $x_1$ is at the equilibrium $x_1^\star$, the discriminant for the second subsystem becomes:

$$\begin{aligned}\Delta_2 &= \frac{4\beta_2\alpha_2^3 - 27\beta_2^2\left(\mu_2 + \gamma_{2,1}x_1^\star\right)^2}{\tau_2^4} \\ &\propto 4\alpha_2^3 - 27\beta_2\left(\mu_2 + \gamma_{2,1}x_1^\star\right)^2\end{aligned}$$

  $\Delta_2$ then depends on the bifurcation parameter $\mu_2$, the coupling strength $\gamma_{2,1}$ and the equilibrium $x_1^\star$. If $\Delta_2 < 0$ or $4\alpha_2^3 < 27\beta_2\left(\mu_2 + \gamma_{2,1}x_1^\star\right)^2$ there is one stable equilibrium, while if $\Delta_2 > 0$ or $4\alpha_2^3 > 27\beta_2\left(\mu_2 + \gamma_{2,1}x_1^\star\right)^2$ there two stable equilibria. Therefore, the bifurcation occurs when:

$$\begin{aligned}\Delta_2 = 0 &\Leftrightarrow 4\alpha_2^3 - 27\beta_2\left(\mu_2 + \gamma_{2,1}x_1^\star\right)^2 = 0 \\ &\Leftrightarrow \mu_2 = -\gamma_{2,1}x_1^\star \pm \sqrt{\frac{4\alpha_2^3}{27\beta_2}}\end{aligned}$$

  As noted by Brummitt *et al.* (2015), the saddle-node bifurcation of the slave subsystem now depends on the equilibrium $x_1^\star$ of the master subsystem and the coupling strength $\gamma_{2,1}$. Therefore, we have to distinguish three cases: $\mu_1 \leq \mu_1^- = -\sqrt{\dfrac{4\alpha_1^3}{27\beta_1}}$, $\mu_1 \geq \mu_1^+ = \sqrt{\dfrac{4\alpha_1^3}{27\beta_1}}$, and $\mu_1^- \leq \mu_1 \leq \mu_1^+$.
- If $\gamma_{1,2} \neq 0$ and $\gamma_{2,1} \neq 0$, then the two subsystems are dependent. We can get complex equilibria with the possibility of loops and hysteresis effects.

We consider the previous example $\alpha_i = \beta_i = \tau_i = 1$ and assume that $\gamma_{1,2} = 0$ and $\gamma_{2,1} = 0.10$. We have a master-slave system ($x_1 \longrightarrow x_2$). In the case of uncoupling, the stable equilibrium is equal to $x_2^\star = -0.8376$ if we consider the lower branch and $\mu_2 = 0.25$. Let us assume that the equilibrium for the first subsystem is $x_1^\star = 5$. Therefore, the second system moves to the new equilibrium[66] $x_2^\star = 1.2626$. Previously, the equilibrium $x_2^\star$ was a function of the bifurcation parameter $\mu_2$: $x_2^\star = h\left(\mu_2 \mid \alpha_2, \beta_2\right)$. Now it also depends on the equilibrium $x_1^\star$:

$$x_2^\star = h\left(\mu_2, x_1^\star \mid \alpha_2, \beta_2\right)$$

For example, we have $x_2^\star = h\left(0.25, -10 \mid 1, 1\right) = -1.2626$. If $x_1^\star = 6$, we get three solutions: $-1.1429$, $0.4289$ and $0.7140$. All these solutions are shown in Figure 8.67. This implies that one subsystem can jump from one (stable) equilibrium to another equilibrium because the state of the other subsystem changes. In Figure 8.68, we represent all the solutions of the slave subsystem $x_2^\star = h\left(\mu_2, x_1^\star \mid \alpha_2, \beta_2\right)$ with respect to $\mu_2$ and $x_1^\star$. The first and third panels correspond to the stable lower and upper branches, while the second panel shows the unstable solutions.

[66] We solve the equation $x_2 - x_2^3 + (0.25 + 0.10 \times 5) = 0$.

Figure 8.67: Master-slave bifurcation

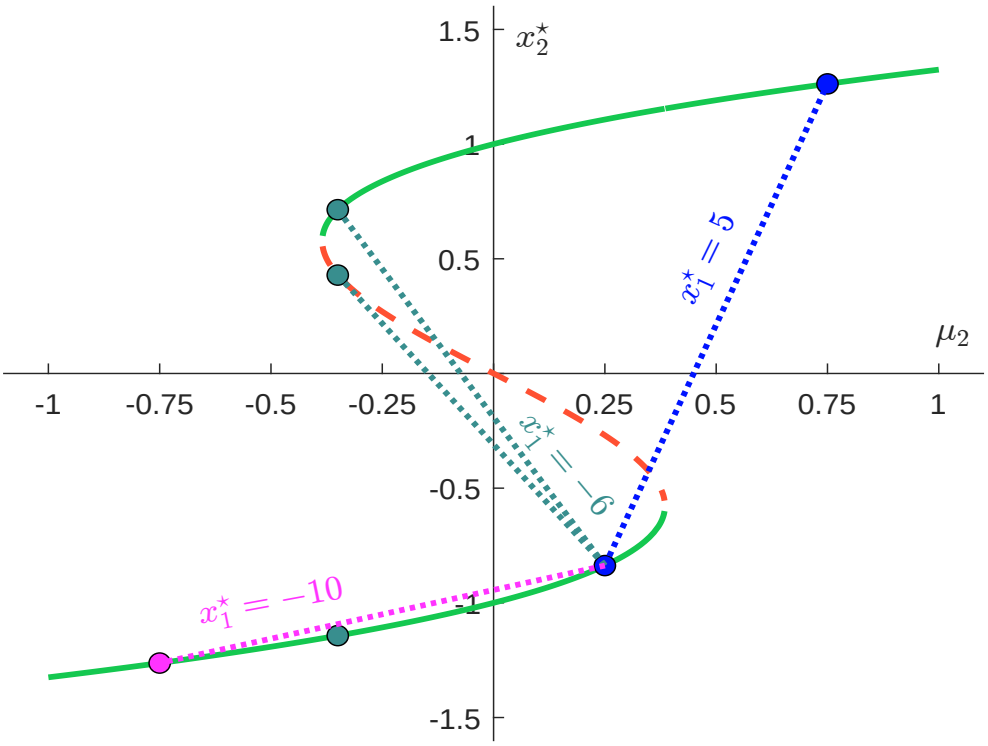


Source: Klose *et al.* (2020, Figure 2, page 6).

Figure 8.68: Equilibria of the slave subsystem

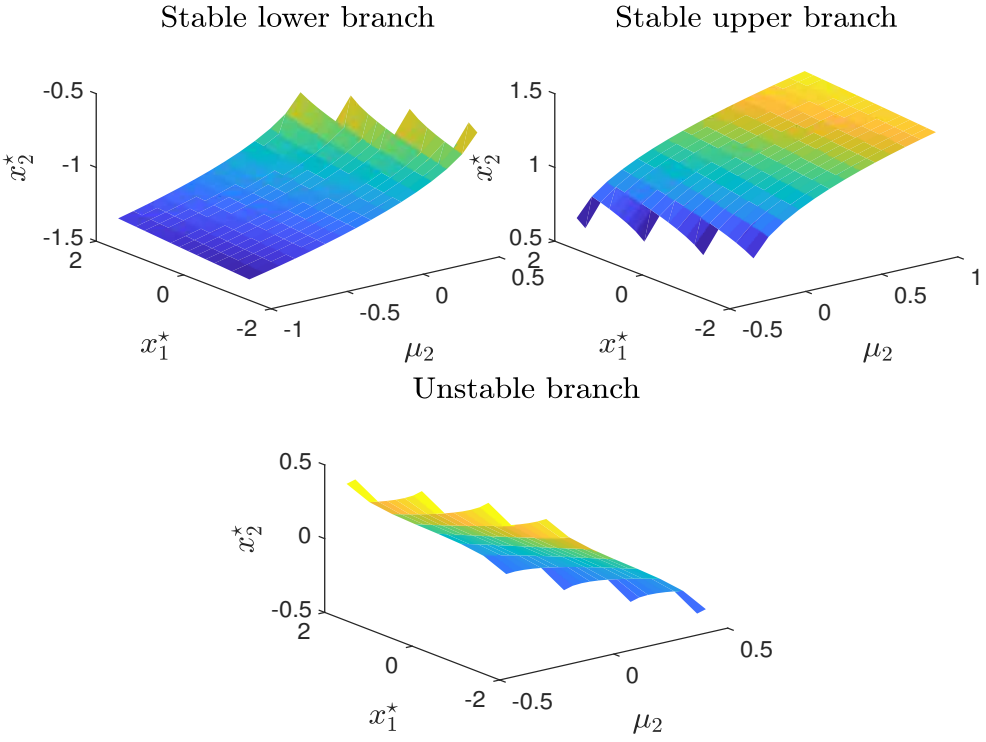

We can extend the previous analysis to the three-dimensional case to illustrate the concept of cascading tipping points. Brummitt *et al.* (2015) analyzed the following master-slave-slave system ($x_1 \longrightarrow x_2 \longrightarrow x_3$):

$$\begin{cases} \dfrac{\mathrm{d}x_1}{\mathrm{d}t} = \dfrac{\alpha_1 x_1 - \beta_1 x_1^3 + \mu_1}{\tau_1} \\ \dfrac{\mathrm{d}x_2}{\mathrm{d}t} = \dfrac{\alpha_2 x_2 - \beta_2 x_2^3 + \mu_2 + \gamma_{2,1} x_1}{\tau_2} \\ \dfrac{\mathrm{d}x_3}{\mathrm{d}t} = \dfrac{\alpha_3 x_3 - \beta_3 x_3^3 + \mu_3 + \gamma_{3,2} x_2}{\tau_3} \end{cases}$$

In particular, they showed that:

> "*Regime shifts can spread in two ways in this system $x_1 \longrightarrow x_2 \longrightarrow x_3$: First, if all three systems are sufficiently close to their tipping points, then a cascade of regime shifts can occur, one causing the next. The second way is more novel: if the intermediate system $x_2$ is relatively far from its tipping point whereas $x_1$ and $x_3$ are close to their tipping points, then the sequence of regime shifts can hop over the intermediate system $x_2$. That is, a regime shift in the master subsystem can nudge the intermediate system $x_2$ enough to trigger a regime shift in the third system $x_3$ but not so much that $x_2$ undergoes a regime shift.*" (Brummitt *et al.*, 2015, page 5).

**An application with Greenland and West Antarctic ice sheets, AMOC and Amazon rainforest** Using the previous framework developed by Brummitt *et al.* (2015) and Klose *et al.* (2020), Wunderling *et al.* (2021) analyze the dynamics of four tipping climate elements, namely (1) Greenland ice sheet, (2) West Antarctic ice sheet (WAIS), (3) the AMOC and (4) the Amazon rainforest (Figure 8.69). The dynamics of the tipping elements are defined as:

$$\frac{\mathrm{d}x_i}{\mathrm{d}t} = \frac{1}{\tau_i}\left(x_i - x_i^3 + \sqrt{\frac{4}{27}}\frac{\Delta\mathcal{T}_s}{\Delta\mathcal{T}_i^\star} + \frac{\gamma}{10}\sum_{j\neq i} s_{i,j}\,(x_j + 1)\right)$$

where $\Delta\mathcal{T}_s$ is the variation of the global mean surface temperature, $\Delta\mathcal{T}_i^\star$ is the critical temperature anomaly to reach a tipping point, $\gamma$ is the overall interaction strength and $s_{i,j}$ is the coupling strength between $x_i$ and $x_j$. Using the previous notations, we have $\alpha_i = 1$, $\beta_i = 1$, $\mu_i = \sqrt{\frac{4}{27}}\frac{\Delta T_s}{\Delta T_i^\star} + \frac{\gamma}{10}\sum_{j\neq i} s_{i,j}$ and $\gamma_{i,j} = \frac{\gamma}{10}s_{i,j}$.

Table 8.13: Parameters of the cascading model

| | Tipping element | Greenland | WAIS | AMOC | Amazon rainforest |
|---|---|---|---|---|---|
| | $\Delta\mathcal{T}_i^\star$ (in °C) | $0.8 - 3.2$ | $0.8 - 5.5$ | $3.5 - 6.0$ | $3.5 - 4.5$ |
| $s_{i,j}$ | Greenland | | $+10$ | $+10$ | |
| | WAIS | $+2$ | | $\pm 3$ | |
| | AMOC | $-10$ | $+1.5$ | | $\pm 2 - \pm 4$ |
| | Amazon rainforest | | | | |

Source: Wunderling *et al.* (2021, pages 608 and 610).

To better understand the model, we report the magnitude of $\Delta\mathcal{T}_i^\star$ and the values of $s_{i,j}$ used by Wunderling *et al.* (2021). For example, the critical temperature $\Delta\mathcal{T}_1^\star$ for the Greenland ice sheet is between 0.8°C and 3.2°C, which is close to the range estimated by Armstrong McKay *et al.* (2022)

Figure 8.69: Interactions between climate tipping elements and their roles in tipping cascades

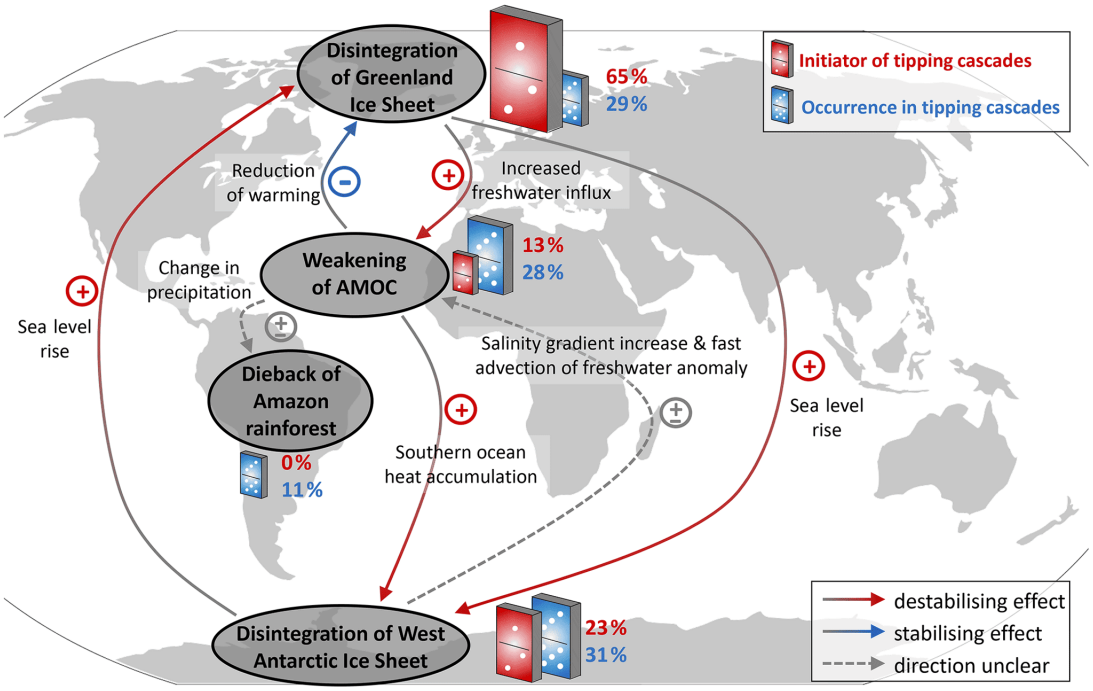


Source: Wunderling *et al.* (2021, Figure 1, page 603) & https://esd.copernicus.org/articles/12/601/2021.

(see Table 8.12 on page 700). The results of the Monte Carlo simulation exercise are presented in Table 8.14. Wunderling *et al.* (2021) found that tipping occurs in 61% of all simulations under the assumption of 2°C global warming. The split between single tipping and cascading tipping differs with respect to the global strength $\gamma$. In particular, when $\gamma$ is equal to one, the authors observed two-element cascades in 21% of all MC simulations, three-element cascades in 15% of all MC simulations, and there is a 4% chance of observing a full cascade phenomenon. They concluded that "*the interactions tend to destabilize the network of tipping elements*", even under the assumption that the Paris Agreement is respected.

Table 8.14: Share of tipping events

| $\gamma$ | Cascade size | | | |
|---|---|---|---|---|
| | 1 | 2 | 3 | 4 |
| 1.00 | 22% | 21% | 15% | 3% |
| 0.75 | 26% | 18% | 14% | 2% |
| 0.50 | 31% | 15% | 14% | 1% |
| 0.25 | 42% | 13% | 6% | |
| 0.10 | 56% | 5% | | |
| 0.00 | 61% | | | |

Source: Wunderling *et al.* (2021, Table 3, page 611).

**Remark 80** *This section on the physics of climate change provides a basic overview of the mechanisms behind climate change. It may be supplemented by Section 12.1 on Chapter 12 of Physical Risk Modeling, which is a comprehensive presentation of general circulation models.*

## 8.2 The ecosystem of climate change

The climate change ecosystem is relatively complex and involves many third parties. In this section, we focus on three types of actors: the scientific community, the Conference of the Parties, and regulators.

### 8.2.1 Scientists

#### Intergovernmental Panel on Climate Change

As mentioned above, the United Nations Environment Programme (UNEP) and the World Meteorological Organization (WMO) established the Intergovernmental Panel on Climate Change (IPCC) in 1988. The members of the IPCC are then governments (95 as of January 2024), not scientists, academic institutions, or NGOs. Its original mandate was to "*prepare a comprehensive review and recommendations on the state of knowledge of the science of climate change, the social and economic impacts of climate change, and possible response strategies and elements for inclusion in a possible future international climate convention.*" The first IPCC Assessment Report (AR) was published in 1990. It consists of a synthesis report (March 1990, 180 pages), followed by three working group reports: Scientific Assessment of Climate Change (June 1990, 414 pages), Impacts Assessment of Climate Change (July 1990, 296 pages), and the IPCC Response Strategies (October 1990, 332 pages). This first report presented scientific evidence that underscored the urgency of addressing climate change through international cooperation and was a catalyst for the creation of the United Nations Framework Convention on Climate Change (UNFCCC), the international treaty to reduce global warming. Among its findings, the report concludes that under a business-as-usual emissions scenario, the global mean temperature is likely to increase by about 0.3°C per decade.

Table 8.15: List of IPCC Chairs

| Date | Name | Country | Occupation |
|---|---|---|---|
| 1988–1997 | Bert Bolin | Sweden | Meteorologist |
| 1997–2002 | Robert T. Watson | UK | Chemist |
| 2002–2015 | Rajendra Kumar Pachauri | India | Engineer |
| 2015 | Ismail A.R. Elgizouli | Sudan | Civil servant |
| 2015–2024 | Hoesung Lee | South Korea | Economist |

This first report already reflected the structure of the IPCC, which is organized around three working groups led by two co-chairs. These three IPCC Working Groups are:

- Working Group I (WGI)
  Assesses the scientific aspects of the climate system that underpin past, present and future climate change.

- Working Group II (WGII)
  Assesses climate change impacts, adaptation options and vulnerabilities on human and natural systems.

- Working Group III (WGIII)
  Focuses on mitigation of climate change, assessment of methods to limit and reduce greenhouse gas emissions, and removal of greenhouse gases from the atmosphere.

Table 8.16: List of IPCC Assessment Reports

| Date | Symbol | Title of the report | website |
|---|---|---|---|
| 1990 | FAR/AR1 | First IPCC Assessment Report | www.ipcc.ch/reports/?rp=ar1 |
| 1995 | SAR/AR2 | Second Assessment Report | www.ipcc.ch/reports/?rp=ar2 |
| 2001 | TAR/AR3 | Third Assessment Report | www.ipcc.ch/reports/?rp=ar3 |
| 2007 | AR4 | Fourth Assessment Report | www.ipcc.ch/reports/?rp=ar4 |
| 2014 | AR5 | Fifth Assessment Report | www.ipcc.ch/reports/?rp=ar5 |
| 2023 | AR6 | Sixth Assessment Report | www.ipcc.ch/reports/?rp=ar6 |

The composition of the working groups reflects the task assigned, *e.g.*, the first working group has a majority of physicists, while we find more economists in the third working group. The three working groups are more or less independent, but the results of the second working group must be coordinated with the results of the first working group, while the analysis of the third working group must be consistent with the stylized facts found by the first and second working groups. This explains why the WGI report is published first, followed by the WGII report, and then the WGIII report. Finally, the synthesis is published later. For example, the WGI contribution to the Sixth Assessment Report (Climate Change 2021: The Physical Science Basis, 2 409 pages) was published on 9 August 2021, the WGII contribution (Climate Change 2022: Impacts, Adaptation and Vulnerability, 3 068 pages) on 28 February 2022, and the WGIII contribution (Climate Change 2022: Mitigation, 2 042 pages) on 4 April 2022. The synthesis report (Climate Change 2023: Synthesis Report, 186 pages) was released on 20 March 2023 to inform the 2023 Global Stocktake under the United Nations Framework Convention on Climate Change (UNFCCC).

Figure 8.70: Climate Change 2023: Synthesis Report (AR6)

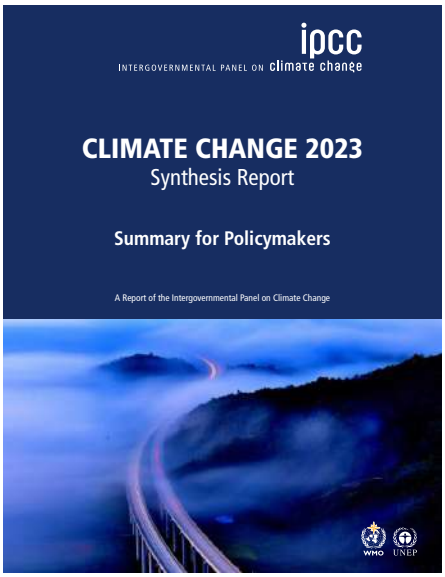


The process for publishing IPCC reports[67] is relatively complex and well standardized (IPCC, 1999). Authors are selected through an extensive process in which candidates submit detailed CVs. Selection is a collaborative effort involving governments, observer organizations and the scientific community. The aim is to form author teams that represent different scientific, technical and socio-

[67]In addition to publishing assessment reports, the IPCC also publishes special reports, the most prominent of which is the Special Report on Global Warming of 1.5°C (IPCC, 2018).

economic perspectives, and to ensure a balanced mix of experts from different regions and from both developed and developing countries. The idea is to avoid bias towards any particular nation or group and ensures that issues relevant to different regions receive appropriate attention in the reports. Chapter teams consist of coordinating lead authors, lead authors, and review editors. The Bureau of each IPCC Working Group selects scientists for these roles from the pool of nominated experts. For the Sixth Assessment Report, 782 experts were selected as chapter authors from some 2 827 nominations (Table 8.17). Once teams of authors are formed, each team must synthesize the scientific evidence on a given topic. This means that the IPCC does not conduct its own research, run its own models, or make its own measurements of climate or weather phenomena. It uses existing research that has been published in scientific journals and other relevant publications. For example, the Sixth Assessment Report contains more than 65 000 citations (Table 8.17). Once the first-order draft is prepared by the authors based on the existing literature in scientific journals and other relevant publications, it is reviewed by experts. After expert review of the first-order draft, the author teams prepare a second-order draft of the report, taking into account the review comments received. This second draft and an initial policy summary are then reviewed again by experts and governments. The review comments are incorporated into a final draft, which is then reviewed only by governments. For example, there were 61 513, 124 235, and 13 889 review comments for the first-order, second-order, and final drafts of the Sixth Assessment Report, respectively (Table 8.17). A plenary session with governments is then organized to accept the underlying final report and approve the policy summary line by line.

Table 8.17: Statistics of the Sixth Assessment Report

| Working Group | WGI | WGII | WGIII |
|---|---|---|---|
| Author team (Lead Authors, Review Editors) | 234 | 270 | 278 |
| Review comments | | | |
| First order draft (experts) | 23 462 | 16 348 | 21 703 |
| Second order draft (experts and governments) | 51 387 | 40 293 | 32 555 |
| Final draft (governments) | 3 158 | 5 777 | 4 954 |
| Number of citations | 14 000 | 34 000 | 18 000 |

The AR6 Synthesis Report (Summary for Policymakers) is relatively long (more than 40 pages), but the three main conclusions are as follows:

1. Unequivocal human influence
   The report reaffirms that human activities are unequivocally causing climate change. The evidence is now overwhelming, and it is highly likely that human influence has been the dominant cause of the observed warming since the mid-20th century. The report states that global surface temperatures have reached 1.1°C above pre-industrial levels.

2. Widespread and intensifying impacts
   The report emphasizes that climate change is already having a profound impact on the planet, affecting ecosystems, human health, and infrastructure. These impacts are projected to worsen in the future, even with moderate warming.

3. Urgency of mitigation and adaptation
   The report underscores the urgency of taking action to address climate change. Limiting global warming to 1.5°C will require rapid and far-reaching changes in energy systems, food production and land management. These changes are possible and would bring significant environmental and human health benefits.

### Climate research institutions

We reiterate that the IPCC does not conduct research on climate change. It uses scientists (academic professors, experts, etc.) working in climate research centers, universities and non-academic institutions[68] (*e.g.*, international bodies, intergovernmental organizations). Climate research institutes and university research centers are then an important component, as they provide most of the climate experts. Table 8.18 contains a list of some well-known climate research institutions, but the list is unofficial, non-exhaustive, far from complete, and expresses the personal views and biases of the author. In this list, we have excluded climate research centers that are part of universities. However, the distinction between an independent research center and a university research center is not always clear. For example, the Scripps Institution of Oceanography (SIO) is considered independent, while it is affiliated with the University of California San Diego (UCSD). These climate research institutions can then be a governmental organization (GO), a non-governmental organization (NGO), an international non-governmental organization (INGO), foundations, etc. Moreover, the scope of climate research institutions is not always easy to define. For example, do we include the Chinese Academy of Sciences or just the Institute of Atmospheric Physics of the Chinese Academy of Sciences? Do we include the Institut Pierre-Simon Laplace or the most famous of the ten research centers of the IPSL, the Laboratoire des Sciences du Climat et de l'Environnement (LSCE)? Once this selection is made, we find that the US largely dominates climate research. The most prominent institutions are GISS, NCAR, and NOAA in the United States, and IAP, IIASA, IPSL, MOHC, NIES, and PIK outside the United States.

Box 8.12: National Center for Atmospheric Research (NCAR)

The National Center for Atmospheric Research is a federally funded research and development center managed by the University Corporation for Atmospheric Research (UCAR) and funded by the National Science Foundation (NSF). NCAR was established in 1960, and its founding director was Walter Orr Roberts. Its headquarters are located in Boulder, Colorado. NCAR's annual budget was $173 million in 2017. The center is organized into eight laboratories with approximately 1 500 members. Notable scientists include or were Guy Brasseur, Clara Deser, Brant Foote, Marika M. Holland, Paul R. Julian, Jean-Francois Lamarque, David M. Lawrence, Gerald A. Meehl, Joanne Simpson, Kevin E. Trenberth, Warren M. Washington, and Tom M. L. Wigley.

Box 8.13: Potsdam Institute for Climate Impact Research (PIK)

The Potsdam Institute for Climate Impact Research is a government-funded research institute in Potsdam, Germany. It was founded in 1991 by Hans Joachim Schellnhuber, who is now Director of IIASA. With a network of about 400 researchers, PIK's mission is to address scientific issues in the fields of climate risks and sustainable development. The current directors of the institute are Ottmar Edenhofer, who also serves as chief economist, and Johan Rockström, former director of the Stockholm Resilience Center. In 2022, the Institute received about 13.3 million euros in institutional funding. Additional project funding from external sources amounted to approximately 18.2 million euros. The institute boasts many renowned researchers, including Elmar Kriegler, Christoph Müller, Ottmar Edenhofer, Alexander Popp, Stefan Rahmstorf and Johan Rockström.

[68] Examples of non-academic institutions include the International Energy Agency (IEA), the Energy Transitions Commission (ETC), the World Meteorological Organization (WMO), and the Organization for Economic Cooperation and Development (OECD).

Table 8.18: Some well-known climate research institutions

| Symbol | Climate research institutions | Country | Website |
|---|---|---|---|
| AARI | Arctic and Antarctic Research Institute | Russia | www.aari.ru |
| ARC | Australian Research Council Centre of Excellence for Climate Extremes | Australia | climateextremes.org.au |
| AWI | Alfred Wegener Institute for Polar and Marine Research | Germany | www.awi.de |
| CCCma | Canadian Centre for Climate Modelling and Analysis | Canada | www.canada.ca |
| CICERO | Center for International Climate and Environmental Research | Norway | www.cicero.oslo.no |
| CIMA | Centro de Investigaciones del Mar y la Atmósfera | Argentina | www.cima.fcen.uba.ar |
| CIRED | Centre international de recherche sur l'environnement et le développement | France | www.centre-cired.fr |
| CSIC | Spanish National Research Council | Spain | www.csic.es |
| CSIRO | Commonwealth Scientific and Industrial Research Organisation | Australia | www.csiro.au |
| CMCC | Euro-Mediterranean Center on Climate Change | Italy | www.cmcc.it |
| CNRS | French National Centre for Scientific Research | France | www.cnrs.fr |
| GISS | NASA Goddard Institute for Space Studies | US | www.giss.nasa.gov |
| IAP | Institute of Atmospheric Physics Chinese Academy of Sciences | China | english.iap.cas.cn |
| IIASA | International Institute for Applied Systems Analysis | Austria | www.iiasa.ac.at |
| IITM | Indian Institute of Tropical Meteorology | India | www.tropmet.res.in |
| IPSL | Institut Pierre-Simon Laplace (LSCE) | France | www.ipsl.fr |
| INECC | National Institute of Ecology and Climate Change | Mexico | www.gob.mx/inecc |
| JAMSTEC | Japan Agency for Marine-Earth Science and Technology | Japan | www.jamstec.go.jp |
| MOHC | Met Office Hadley Centre for Climate Science and Services | UK | www.metoffice.gov.uk |
| MPIM | Max Planck Institute for Meteorology | Germany | www.mpimet.mpg.de |
| NCAR | National Center for Atmospheric Research | US | ncar.ucar.edu |
| NERC | Natural Environment Research Council | UK | www.ukri.org/councils/nerc |
| NIES | National Institute for Environmental Studies | Japan | www.nies.go.jp |
| NOAA | National Oceanic and Atmospheric Administration | US | www.noaa.gov |
| NREL | National Renewable Energy Laboratory | US | www.nrel.gov |
| PBL | PBL Netherlands Environmental Assessment Agency | Netherlands | www.pbl.nl |
| PCMDI | Program for Climate Model Diagnosis & Intercomparison (LLNL) | US | www.pcmdi.llnl.gov |
| PIK | Potsdam Institute for Climate Impact Research | Germany | www.pik-potsdam.de |
| PNNL | Pacific Northwest National Laboratory | US | www.pnnl.gov |
| REKLIM | Helmholtz Climate Initiative Regional Climate | Germany | www.reklim.de |
| SEI | Stockholm Environment Institute | Sweden | www.sei.org |
| SIO | Scripps Institution of Oceanography | US | www.scripps.ucsd.edu |
| SMHI | Rossby Centre of the Swedish Meteorological and Hydrological Institute | Sweden | www.smhi.se |
| SPREP | Secretariat of the Pacific Regional Environment Programme (PCCC) | Samoa | www.sprep.org |
| WHOI | Woods Hole Oceanographic Institution | US | www.whoi.edu |

Source: Author's research.

Box 8.14: International Institute for Applied Systems Analysis (IIASA)

The International Institute for Applied Systems Analysis is an independent international research institute located in Laxenburg near Vienna, Austria. IIASA was founded by a charter signed on October 4, 1972 by representatives of the Soviet Union, the United States, and ten other countries from the Eastern and Western blocs. IIASA brings together experts from various fields to study complex issues such as climate change, energy, and sustainable development. In 2022, IIASA's annual budget was 24.4 million euros, of which just under half came from the Institute's national and regional member organizations (Austria, Brazil, China, Egypt, Finland, Germany, India, Iran, Israel, Japan, South Korea, Norway, Russia, Slovakia, Sub-Saharan Africa, Sweden, Ukraine, United Kingdom, United States, Vietnam). IIASA has about 500 researchers from 50 countries. Since December 2023, the Director General is Hans Joachim Schellnhuber. Among the researchers who work, have worked or have visited the research center, we can mention George Dantzig, Shinichiro Fujimori, Petr Havlìk, Leonid Kantorovich, Tjalling Koopmans, Nebojsa Nakicenovic, William D. Nordhaus, Michael Obersteiner, Howard Raiffa, Keywan Riahi, Joeri Rogelj and Thomas Schelling.

Box 8.15: National Oceanic and Atmospheric Administration (NOAA)

The National Oceanic and Atmospheric Administration is an agency of the United States Department of Commerce (DOC) responsible for monitoring and managing the nation's weather, climate, and oceans. NOAA was established in 1970. The scope of NOAA is vast: weather forecasting, oceanography, fisheries management, satellite operations. As a result, it employs 12 000 people worldwide, while the number of NOAA scientists and engineers is about 6 500. The Office of Oceanic and Atmospheric Research (OAR) is the primary research arm of NOAA. It is responsible for conducting a wide range of research on the Earth's atmosphere, oceans, and coasts. One of OAR's goals is to understand the causes and effects of climate change. The most prominent affiliated research center is the Geophysical Fluid Dynamics Laboratory (GFDL), a joint program of Princeton University and NOAA. GFDL researchers include Thomas L. Delworth, Larry W. Horowitz, Thomas R. Knutson, Vaishali Naik, and Venkatachalam Ramaswamy.

Box 8.16: Institut Pierre-Simon Laplace (IPSL)

The Institut Pierre-Simon Laplace is a French university research institute that brings together 10 laboratories with about 1 500 members. The institute was founded in 1991 by Gérard Mégie, and one of its directors was Jean Jouzel from 2001 to 2008. The 10 laboratories are (1) the Centre d'Enseignement et de Recherche en Environnement Atmosphérique (CEREA), (2) Géosciences Paris-Sud (GEOPS), (3) the Laboratoire Atmosphères, Milieux, Observations spatiales (LATMOS), (4) the team TASQ of the Laboratoire d'Études du Rayonnement et de la Matière en Astrophysique et Atmosphères (LERMA), (5) the Laboratoire Inter-universitaire des Systèmes Atmosphériques (LISA), (6) the Laboratoire de Météorologie Dynamique (LMD), (7) the Laboratoire d'Océanographie et du Climat Expérimentation et Approches Numériques (LOCEAN), (8) the Laboratoire des Sciences du Climat et de l'Environnement (LSCE), (9) the research center Milieux Environnementaux, Transferts et Interactions dans les hydrosystèmes et les Sols (METIS), and (10) the team Surface & Réservoirs of the Laboratoire de Géologie de l'ENS. IPSL is placed under the supervision of Centre National de la Recherche Scientifique (CNRS), Sorbonne Université (SU), Université Versailles Saint-Quentin (UVSQ), École Polytechnique, Commissariat à l'Énergie Atomique et aux Énergies Alternatives (CEA), Institut de Recherche pour le Développement (IRD) and École Nationale des Ponts et ChaussÃľes (ENPC). Researchers include Sandrine Bony, Laurent Bopp, Olivier Boucher, Pascale Braconnot, Philippe Ciais, Jean Jouzel, Pierre Friedlingstein, Valérie Masson-Delmotte, Robert Vautard, and Nicolas Viovy.

The picture of climate research centers would not be complete without mentioning university research, which does most of the work on the subject. However, compiling a list of top universities is a complex task for many reasons: the number of universities is very large; sometimes there are several research centers working on climate risks within the same university; the prominence of a research center may depend on the leadership of an emblematic individual or on the strength of a collaborative team, etc. Nevertheless, we can agree on a restrictive list of academic institutions.

To get a better idea of the leading universities and scientists influencing the climate change debate, we use Reuters 2021 Hot List ranking of top climate scientists. The list can be found at www.reuters.com/investigates/section/climate-change-scientists. The Hot List identifies the 1 000 most influential scientists using three rankings based on climate change research. The rankings take into account the number of published papers, citations by peers, and public reach through social and mainstream media. All data comes from Dimensions[69], Digital Science's academic research portal, which has been tracking academic research since 1988. The first ranking focuses on the number of climate-related papers published by each scientist, requiring at least one citation. The second ranking uses Dimensions' Field Citation Ratio to measure influence among peers in different scientific fields. The third ranking uses Dimensions' Altmetric Attention Score to assess a paper's public reach and influence outside the academic community. The final score for each scientist is the sum of these rankings, with lower scores indicating greater overall influence. In Table 8.19, we report the top 30 climate scientists on the Reuters Hot List. While this list is not perfect and has some limitations, including a potential bias toward prolific scientists and a reliance on titles and abstracts that may miss some relevant studies, it provides very consistent and informative results about the top climate scientists. The top five names are:

- Keywan Riahi, who is the Director of the Energy, Climate and Environment (ECE) Program at the International Institute for Applied Systems Analysis (IIASA) and one of the principal developers of the Representative Concentration Pathway (RCP) and Shared Socio-economic Pathway (SSP) concepts.
- Anthony A. Leiserowitz, Professor at Yale University, who studies public perceptions of climate change.
- Pierre Friedlingstein, who holds the Chair in Mathematical Modeling of the Climate System at the University of Exeter and coordinates the annual publication of the Global Carbon Budget.
- Detlef P. Van Vuuren, who is Professor at Utrecht University, Project Leader of the IMAGE Integrated Assessment Team at PBL Netherlands Environmental Assessment Agency, and one of the main developers of the Representative Concentration Pathway (RCP) and Shared Socio-economic Pathway (SSP) concepts.
- James E. Hansen, who is considered one of the world's most influential climate scientists and was the director of NASA Goddard Institute for Space Studies from 1981 to 2013.

All of these scientists (except Anthony A. Leiserowitz) have more than 100 000 citations according to Google Scholar. As mentioned above, the list has several biases. The most important is that it favors younger authors. In fact, there are more researchers working on climate change today than 20 or 30 years ago. And newer publications tend to cite more recent research because of the scientific standards of publication. This explains why Nobel laureates Klaus Hasselmann and Syukuro Manabe are ranked 639 and 755 respectively, and a leading researcher like Raymond Pierrehumbert is missing

[69]The website is www.dimensions.ai.

Table 8.19: Top 30 climate scientists on the Reuters Hot List

| Rank | Name | Gender | Institution | Location |
|---|---|---|---|---|
| 1 | Keywan Riahi | M | International Institute for Applied Systems Analysis | Austria |
| 2 | Anthony A. Leiserowitz | M | Yale University | United States |
| 3 | Pierre Friedlingstein | M | University of Exeter | United Kingdom |
| 4 | Detlef Peter Van Vuuren | M | Utrecht University | Netherlands |
| 5 | James E. Hansen | M | Columbia University | United States |
| 6 | Petr Havlìk | M | International Institute for Applied Systems Analysis | Austria |
| 7 | Edward Wile Maibach | M | George Mason University | United States |
| 8 | Josep G. Canadell | M | Commonwealth Scientific and Industrial Research Organisation | Australia |
| 9 | Sonia Isabelle Seneviratne | F | ETH Zurich | Switzerland |
| 10 | Mario Herrero | M | Commonwealth Scientific and Industrial Research Organisation | Australia |
| 11 | David B. Lobell | M | Stanford University | United States |
| 12 | Carlos Manuel Duarte | M | King Abdullah University of Science and Technology | Saudi Arabia |
| 13 | Kevin E. Trenberth | M | National Center for Atmospheric Research | United States |
| 14 | Stephen A. Sitch | M | University of Exeter | United Kingdom |
| 14 | Glen P. Peters | M | Center for International Climate and Environmental Research | Norway |
| 16 | Ove I. Hoegh-Guldberg | M | University of Queensland | Australia |
| 17 | Richard Arthur Betts | M | Met Office | United Kingdom |
| 18 | Michael G. Oppenheimer | M | Princeton University | United States |
| 18 | William Neil Adger | M | University of Exeter | United Kingdom |
| 20 | William Wai Lung Cheung | M | University of British Columbia | Canada |
| 21 | Christopher B. Field | M | Stanford University | United States |
| 23 | Shinichiro Fujimori | M | Kyoto University | Japan |
| 23 | Elmar Kriegler | M | Potsdam Institute for Climate Impact Research | Germany |
| 25 | Yadvinder Singh Malhi | M | University of Oxford | United Kingdom |
| 26 | Ken Caldeira | M | Carnegie Institution for Science's Department of Global Ecology | United States |
| 27 | Chris D. Thomas | M | University of York | United Kingdom |
| 28 | Stéphane Hallegatte | M | World Bank | United States |
| 28 | Andy P. Haines | M | London School of Hygiene & Tropical Medicine | United Kingdom |
| 30 | Michael Obersteiner | M | International Institute for Applied Systems Analysis | Austria |
| 40 | Philippe Ciais | M | Laboratoire des Sciences du Climat et de l'Environnement | France |
| 75 | Pete Smith | M | University of Aberdeen | United Kingdom |
| 164 | Richard S. J. Tol | M | VU Amsterdam | Netherlands |
| 173 | William D. Nordhaus | M | Yale University | United States |
| 240 | Phil D. Jones | M | University of East Anglia | United Kingdom |
| 338 | Filippo Giorgi | M | International Centre for Theoretical Physics | Italy |
| 639 | Klaus Hasselmann | M | Max Planck Institute for Meteorology | Germany |
| 755 | Syukuro Manabe | M | Princeton University | United States |

Source: Reuters (2021), www.reuters.com/investigates/special-report/climate-change-scientists-list.

from the list[70]. The list is also biased towards researchers from large teams involved in collaborative projects. There is no distinction between lead and secondary authors. In fact, writing a theoretical research paper alone is not on the same level as signing a research article with 100 other researchers. A third bias is that the number of citations and the market impact of a researcher increases with the number of peers involved in the research field. This explains why economist Richard S. J. Tol and Nobel laureate William D. Nordhaus are ranked only 164th and 173rd, respectively, despite their massive impact on several climate change issues (integrated assessment model, social cost of carbon, carbon tax, economic cost of climate change).

Table 8.20: Top 20 climate research institutions on the Reuters Hot List

| Institution | Count | Location |
|---|---|---|
| Potsdam Institute for Climate Impact Research (PIK) | 14 | Germany |
| University of Reading | 13 | United Kingdom |
| Institute of Atmospheric Physics (CAS) | 13 | China |
| Utrecht University | 12 | Netherlands |
| Met Office (MOHC) | 12 | United Kingdom |
| National Center for Atmospheric Research (NCAR) | 11 | United States |
| Columbia University | 10 | United States |
| ETH Zurich | 10 | Switzerland |
| Laboratoire des Sciences du Climat et de l'Environnement (IPSL) | 10 | France |
| International Institute for Applied Systems Analysis (IIASA) | 9 | Austria |
| University of Melbourne | 9 | Australia |
| University of Leeds | 9 | United Kingdom |
| Geophysical Fluid Dynamics Laboratory (NOAA) | 9 | United States |
| Max Planck Institute for Meteorology (MPIM) | 9 | Germany |
| Pacific Northwest National Laboratory (PNNL) | 8 | United States |
| Lamont-Doherty Earth Observatory (Columbia University) | 8 | United States |
| Massachusetts Institute of Technology | 8 | United States |
| University of Washington | 8 | United States |
| Wageningen University & Research | 8 | Netherlands |
| University of Tokyo | 8 | Japan |
| University of Bremen | 8 | Germany |

Source: Reuters (2021), www.reuters.com/investigates/special-report/climate-change-scientists-list.

Despite these biases in individual rankings, the Reuters Hot List can be used to assess global rankings and the importance of research institutions on an aggregate basis. In Table 8.20 we have counted the number of scientists present in the top 1000 by research center. Not surprisingly, PIK, IAP, MOHC, NCAR, IPSL, IIASA, MPIM and PNNL are among the top 20 climate research institutions. When we group the scientists by location, the United States largely dominates the

[70] In 2015, Carbon Brief conducted a survey to nominate the most influential climate change papers of all time. To do this, they asked all coordinating lead authors, lead authors, and review editors of the IPCC's AR5 report to nominate three papers from any time in history. The question asked was: "*What do you consider to be the three most influential papers in the field of climate change?*". The IPCC scientists' top choice for the most influential climate change paper of all time was the seminal paper *Thermal Equilibrium of the Atmosphere with a Given Distribution of Relative Humidity* by Manabe and Wetherald (1967), followed ex aequo by *Atmospheric Carbon Dioxide Variations at Mauna Loa Observatory, Hawaii* by Keeling *et al.* (1976) and *Robust Responses of the Hydrological Cycle to Global Warming* by Held and Soden (2006). However, despite the innovative and pioneering nature of these research, these papers are only cited 2 212, 1 157, and 4 763 times, respectively, according to Google Scholar as of January 1, 2024.

Table 8.21: Top 15 country on the Reuters Hot List

| Country | Count | Frequency | Cumulative |
|---|---|---|---|
| United States | 292 | 29.3% | 29.3% |
| United Kingdom | 112 | 11.3% | 40.6% |
| Germany | 91 | 9.1% | 49.7% |
| China | 87 | 8.7% | 58.5% |
| Australia | 74 | 7.4% | 65.9% |
| France | 40 | 4.0% | 69.9% |
| Netherlands | 39 | 3.9% | 73.9% |
| Canada | 37 | 3.7% | 77.6% |
| Japan | 30 | 3.0% | 80.6% |
| Switzerland | 28 | 2.8% | 83.4% |
| Spain | 22 | 2.2% | 85.6% |
| Italy | 20 | 2.0% | 87.6% |
| Norway | 13 | 1.3% | 88.9% |
| Denmark | 12 | 1.2% | 90.2% |
| South Korea | 12 | 1.2% | 91.4% |
| Austria | 10 | 1.0% | 92.4% |

Source: Reuters (2021), www.reuters.com/investigates/special-report/climate-change-scientists-list.

Figure 8.71: Location of the top 1000 climate scientists

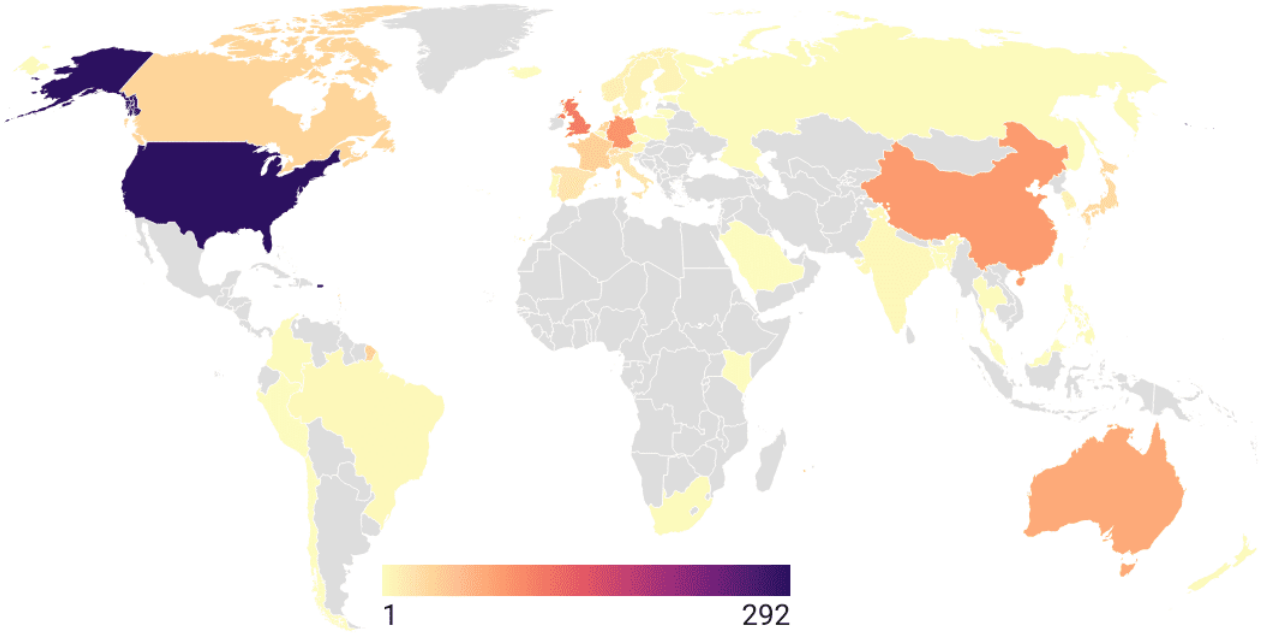


Source: Source: Reuters (2021), www.reuters.com/investigates/special-report/climate-change-scientists-list & Author's calculations (created by Datawrapper).

world of climate change science with 292 scientists in the top 1000 (Table 8.21). This is followed by the United Kingdom (112 scientists) and Germany (91 scientists). These 3 countries account for nearly 50% of the scientists on the Reuters Hot List[71]. In fact, the top 1000 scientists on the Reuters Hot List are located in a small number of countries, as shown in Figure 8.71.

The Reuters Hot List already provides some insight into the most important universities involved in the climate change debate. The University of Reading, Utrecht University, Columbia University and ETH Zurich are among the top 10. For a more complete picture, we look at the annual tables compiled by *Nature*. We cannot filter on climate change because it is too restrictive. The closer category is Earth & Environmental Sciences, and the results are shown in Tables 8.22 and 8.23. These rankings reflect the size of the university or the institution. The larger the university, the better the ranking. These rankings are dominated by American and Chinese institutions. Outside these two countries, the top five institutions[72] are Helmholtz Association of German Research Centers (Germany), CNRS (France), ETH Zurich (Switzerland), University of Cambridge (UK) and University of Queensland (Australia).

### Scientific journals

We cannot end this section without mentioning scientific journals, which play an important role in the dissemination of research and in the reputation of researchers. In addition to general scientific journals (Nature, Nature Communications, Science, Science Advances, American Economic Journal, Proceedings of the National Academy of Sciences, etc.), we find more specialized journals. Below is a non-exhaustive list of the most prestigious journals, classified by research topic:

- Atmospheric and Environmental Sciences
  Atmospheric Chemistry and Physics; Bulletin of the American Meteorological Society; Climate Dynamics; Climate in the Past; Earth System Dynamics; Earth System Science Data; Earth's Future; Environmental Research Letters; Journal of Advances in Modeling Earth Systems; Journal of Climate; Journal of Geophysical Research: Atmospheres; Geophysical Research Letters; Geoscientific Model Development; Global Change Biology; Journal of the Atmospheric Sciences; npj Climate and Atmospheric Science; Quarterly Journal of the Royal Meteorological Society; Reviews of Geophysics; Tellus.

- Climate change
  WIREs Climate Change; Climatic Change; Current Climate Change Reports; Global Environmental Change; Global and Planetary Change; Nature Climate Change; Nature Sustainability.

- Economics
  Climate Change Economics; Climate Policy; Ecological Economics; Environmental and Resource Economics; Environmental Modeling & Assessment; Journal of Environmental Economics and Management; Resource and Energy Economics; Review of Environmental Economics and Policy.

[71] Note that five scientists were not affiliated with an institution at the time of the Reuters Hot List, so the frequency is calculated as the number of scientists divided by 995, not 1 000.

[72] The other non-Chinese and non-US institutions ranked in the 2023 annual tables are (in descending order): University of Toronto (Canada), University of Oxford (UK), University of Tokyo (Japan), Utrecht University (Netherlands), Imperial College London (ICL), United Kingdom (UK), Max Planck Society (Germany), JAMSTEC (Japan), Leibniz Association (Germany), Spanish National Research Council (Spain), National Institute of Geophysics and Volcanology (Italy), Tohoku University (Japan), Monash University (Australia), Institute of Research for Development (France), University of Oslo (Norway), University of Leeds, (UK), University of Alberta (Canada), Curtin University (Australia), University of British Columbia (Canada), Technical University of Denmark (Denmark), McGill University (Canada), University of Bergen (Norway), and Stockholm University (Sweden).

Table 8.22: Top 30 leading institutions in Earth & Environmental Sciences (Nature index, 2016 ranking)

| Institution | 2016 | 2017 | 2018 | 2019 | 2020 | 2021 | 2022 | 2023 |
|---|---|---|---|---|---|---|---|---|
| Chinese Academy of Sciences (CAS), China | 1 | 1 | 1 | 1 | 1 | 1 | 1 | 1 |
| Helmholtz Association of German Research Centres, Germany | 2 | 2 | 2 | 2 | 2 | 2 | 2 | 3 |
| French National Centre for Scientific Research (CNRS), France | 3 | 4 | 4 | 3 | 3 | 3 | 3 | 6 |
| National Aeronautics and Space Administration (NASA), United States of America (USA) | 4 | 3 | 3 | 5 | 4 | 6 | 6 | 9 |
| Swiss Federal Institute of Technology Zurich (ETH Zurich), Switzerland | 5 | 5 | 6 | 4 | 5 | 5 | 5 | 10 |
| U.S. Geological Survey (USGS), United States of America (USA) | 6 | 9 | 8 | 12 | 7 | 9 | 17 | 31 |
| University of Colorado Boulder (CU-Boulder), United States of America (USA) | 7 | 10 | 9 | 7 | 14 | 20 | 22 | 26 |
| University of California, Berkeley (UC Berkeley), United States of America (USA) | 8 | 19 | 12 | 9 | 17 | 18 | 15 | 24 |
| Stanford University, United States of America (USA) | 9 | 8 | 13 | 22 | 9 | 15 | 14 | 20 |
| California Institute of Technology (Caltech), United States of America (USA) | 10 | 6 | 5 | 8 | 12 | 7 | 8 | 15 |
| National Oceanic and Atmospheric Administration (NOAA), United States of America (USA) | 11 | 7 | 7 | 14 | 8 | 8 | 18 | 17 |
| Columbia University in the City of New York (CU), United States of America (USA) | 12 | 12 | 16 | 11 | 11 | 13 | 23 | 22 |
| University of Washington (UW), United States of America (USA) | 13 | 11 | 10 | 10 | 10 | 17 | 21 | 21 |
| University of California, San Diego (UC San Diego), United States of America (USA) | 14 | 14 | 18 | 26 | 32 | 24 | 10 | 29 |
| The University of Tokyo (UTokyo), Japan | 15 | 15 | 20 | 23 | 20 | 31 | 29 | 50 |
| Peking University (PKU), China | 16 | 16 | 19 | 13 | 19 | 11 | 7 | 4 |
| The University of Texas at Austin (UT Austin), United States of America (USA) | 17 | 13 | 14 | 15 | 21 | 27 | 32 | 27 |
| The University of Queensland (UQ), Australia | 18 | 57 | 62 | 37 | 43 | 26 | 35 | 36 |
| Nanjing University (NJU), China | 19 | 18 | 11 | 6 | 6 | 4 | 4 | 2 |
| Massachusetts Institute of Technology (MIT), United States of America (USA) | 20 | 21 | 17 | 20 | 22 | 23 | 24 | 32 |
| University of Minnesota (UMN), United States of America (USA) | 21 | 45 | 22 | 47 | 39 | 41 | 68 | 52 |
| University of California, Los Angeles (UCLA), United States of America (USA) | 22 | 17 | 15 | 21 | 29 | 28 | 26 | 23 |
| University of Maryland, College Park (UMCP), United States of America (USA) | 23 | 32 | 55 | 40 | 53 | 66 | 77 | 80 |
| Woods Hole Oceanographic Institution (WHOI), United States of America (USA) | 24 | 34 | 50 | 30 | 37 | 51 | 56 | 67 |
| The Pennsylvania State University (Penn State), United States of America (USA) | 25 | 27 | 29 | 25 | 25 | 30 | 28 | 56 |
| University of Michigan (U-M), United States of America (USA) | 26 | 20 | 23 | 35 | 27 | 35 | 50 | 73 |
| University of Toronto (U of T), Canada | 27 | 38 | 34 | 29 | 34 | 34 | 40 | 40 |
| Georgia Institute of Technology (Georgia Tech), United States of America (USA) | 28 | 50 | 27 | 72 | 55 | 76 | 36 | |
| National Institute of Geophysics and Volcanology (INGV), Italy | 29 | 35 | 45 | 69 | | 97 | 88 | 77 |
| Princeton University, United States of America (USA) | 30 | 67 | 42 | 44 | 46 | 47 | 52 | 43 |

Source: Nature (2023), www.nature.com/nature-index/annual-tables.

Table 8.23: Top 30 leading institutions in Earth & Environmental Sciences (Nature index, 2023 ranking)

| Institution | 2016 | 2017 | 2018 | 2019 | 2020 | 2021 | 2022 | 2023 |
|---|---|---|---|---|---|---|---|---|
| Chinese Academy of Sciences (CAS), China | 1 | 1 | 1 | 1 | 1 | 1 | 1 | 1 |
| Nanjing University (NJU), China | 19 | 18 | 11 | 6 | 6 | 4 | 4 | 2 |
| Helmholtz Association of German Research Centres, Germany | 2 | 2 | 2 | 2 | 2 | 2 | 2 | 3 |
| Peking University (PKU), China | 16 | 16 | 19 | 13 | 19 | 11 | 7 | 4 |
| University of Chinese Academy of Sciences (UCAS), China | | 77 | 24 | 18 | 13 | 10 | 9 | 5 |
| French National Centre for Scientific Research (CNRS), France | 3 | 4 | 4 | 3 | 3 | 3 | 3 | 6 |
| Sun Yat-sen University (SYSU), China | | | | 65 | 42 | 19 | 13 | 7 |
| Tongji University, China | 60 | 43 | 43 | 17 | 15 | 12 | 16 | 8 |
| National Aeronautics and Space Administration (NASA), United States of America (USA) | 4 | 3 | 3 | 5 | 4 | 6 | 6 | 9 |
| Swiss Federal Institute of Technology Zurich (ETH Zurich), Switzerland | 5 | 5 | 6 | 4 | 5 | 5 | 5 | 10 |
| Zhejiang University (ZJU), China | | 75 | 73 | 53 | 36 | 40 | 25 | 11 |
| University of Science and Technology of China (USTC), China | 74 | 39 | 31 | 16 | 16 | 16 | 20 | 12 |
| China University of Geosciences (CUG), China | | 44 | 37 | 31 | 18 | 14 | 19 | 13 |
| China Meteorological Administration (CMA), China | 100 | 95 | 70 | 54 | 23 | 25 | 27 | 14 |
| California Institute of Technology (Caltech), United States of America (USA) | 10 | 6 | 5 | 8 | 12 | 7 | 8 | 15 |
| Ministry of Natural Resources (MNR), China | | | | 75 | 59 | 44 | 38 | 16 |
| National Oceanic and Atmospheric Administration (NOAA), United States of America (USA) | 11 | 7 | 7 | 14 | 8 | 8 | 18 | 17 |
| Tsinghua University, China | 53 | 36 | 30 | 28 | 26 | 21 | 12 | 18 |
| Southern University of Science and Technology (SUSTech), China | | | | | | 72 | 47 | 19 |
| Stanford University, United States of America (USA) | 9 | 8 | 13 | 22 | 9 | 15 | 14 | 20 |
| University of Washington (UW), United States of America (USA) | 13 | 11 | 10 | 10 | 10 | 17 | 21 | 21 |
| Columbia University in the City of New York (CU), United States of America (USA) | 12 | 12 | 16 | 11 | 11 | 13 | 23 | 22 |
| University of California, Los Angeles (UCLA), United States of America (USA) | 22 | 17 | 15 | 21 | 29 | 28 | 26 | 23 |
| University of California, Berkeley (UC Berkeley), United States of America (USA) | 8 | 19 | 12 | 9 | 17 | 18 | 15 | 24 |
| Wuhan University (WHU), China | | | 95 | 55 | 58 | 67 | 42 | 25 |
| University of Colorado Boulder (CU-Boulder), United States of America (USA) | 7 | 10 | 9 | 7 | 14 | 20 | 22 | 26 |
| The University of Texas at Austin (UT Austin), United States of America (USA) | 17 | 13 | 14 | 15 | 21 | 27 | 32 | 27 |
| Harbin Institute of Technology (HIT), China | | | 67 | 48 | 54 | 45 | 49 | 28 |
| University of California, San Diego (UC San Diego), United States of America (USA) | 14 | 14 | 18 | 26 | 32 | 24 | 10 | 29 |
| Nanjing University of Information Science and Technology (NUIST), China | | | | 100 | 77 | 49 | 46 | 30 |

Source: Nature (2023), www.nature.com/nature-index/annual-tables.

- Energy
  Energy and Environmental Science; Energy Economics; Energy Journal; Energy Policy; Energy Studies Review; Journal of Cleaner Production.

- Specialized topics
  Arctic, Antarctic, and Alpine Research; Artic Ice Journal; Cryosphere; Frontiers in Earth Science: Cryospheric Science; Polar Science; Quaternary Science Reviews; Water Research.

**Remark 81** *In this section, we do not examine some organizations that can have a major impact on the scientific debate on climate change and transition. Among them, the most important and influential is certainly the International Energy Agency (IEA), an autonomous intergovernmental organization based in Paris, founded in 1974, that provides policy advice, analysis and data on the entire global energy sector (www.iea.org). Its famous reports (World Energy Outlook, Net Zero by 2050) have a considerable impact and a large audience in the general media. Another example is the Energy Transitions Commission (ETC), an international think tank focused on economic growth and climate change mitigation (www.energy-transitions.org). More regional organizations can also have a local impact. For example, the Institute for Climate Economics (I4CE) is a registered non-profit organization founded by the French National Bank, Caisse des Dépôts, and the French Development Agency (AFD). It provides policy analysis on climate change mitigation and adaptation (www.i4ce.org). All of these organizations participate in the public debate and provide accessible research, surveys and databases that are of great interest in understanding current climate risk issues.*

### 8.2.2 Conferences of the Parties

#### Earth Summit

In June 1972, the United Nations held its first conference on the global environment (United Nations Conference on the Human Environment) in Stockholm and established the United Nations Environment Programme (UNEP) to coordinate responses to environmental issues within the United Nations system. Over the next 20 years, UNEP organized several conferences and participated in several initiatives, including the establishment of the Intergovernmental Panel on Climate Change (IPCC). In June 1992, a major achievement of UNEP was the organization of a conference in Rio de Janeiro, Brazil, to address the challenges of environment and development. Known as the United Nations Conference on Environment and Development (UNCED) or the Earth Summit, it was one of the largest UN conferences ever held, with the participation of 175 governments and more than 1 000 non-governmental organizations. It is considered a great success with several outcomes:

- The Rio Declaration on Environment and Development was signed by more than 170 countries and consists of 27 principles to guide countries in future sustainable development. The first principle declares that "*human beings are at the centre of concerns for sustainable development and are entitled to a healthy and productive life in harmony with nature*", while the eighth principle states that in order "*to achieve sustainable development and a higher quality of life for all people, States should reduce and eliminate unsustainable patterns of production and consumption and promote appropriate demographic policies*" (United Nations, 1992a).

- The Forest Principles (also known as the Rio Forest Principles) is a non-legally binding document that makes several recommendations for the conservation and sustainable development of forests. The second principle declares that "*States have the sovereign and inalienable right to utilize, manage and develop their forests in accordance with their development needs and level of socio-economic development [...] including the conversion of such areas for other uses*

*within the overall socio-economic development plan and based on rational land-use policies. Forest resources and forest lands should be sustainably managed to meet the social, economic, ecological, cultural and spiritual needs of present and future generations*" (United Nations, 1992b).

- Agenda 21, the third document drafted since 1989 and adopted at the 1992 Earth Summit, is a non-binding, comprehensive plan of action for sustainable development. Its original goal was to achieve numerous sustainable development goals by the year 2000 or earlier[73]. Agenda 21 is divided into four main sections:

  1. Social and economic dimensions
     This section focuses on promoting sustainable development through poverty eradication, sustainable consumption and production patterns, sustainable demography, promoting human health conditions, and integrating environment and development in decision-making.
  2. Conservation and management of resources for development
     This section focuses on protecting the atmosphere, managing land resources, combating deforestation, managing fragile ecosystems, conserving biodiversity, protecting oceans, managing freshwater resources, and controlling toxic chemicals and wastes (hazardous, solid, and radioactive).
  3. Strengthening the role of major groups
     This section emphasizes the importance of involving all sectors of society in sustainable development, including women, children, indigenous peoples, non-governmental organizations, local authorities, workers and their trade unions, business and industry, the scientific and technological community and farmers.
  4. Means of implementation
     This section outlines the financial resources, technology transfer and capacity building needed to implement Agenda 21.

  In fact, Agenda 21 anticipated the Sustainable Development Goals (SDGs) and laid the groundwork for addressing environmental and sustainable development. In a sense, the SDGs are a reaffirmation of Agenda 21, reiterating the commitment to sustainable development made in Agenda 21.

- The so-called Rio Conventions

  – The United Nations Framework Convention on Climate Change (UNFCCC) was adopted in 1992 and entered into force in 1994. The UNFCCC is the first legally binding international agreement on climate change. The main objective of the UNFCCC is to stabilize greenhouse gas concentrations at a level that would prevent dangerous anthropogenic interference with the climate system. It recognizes the importance of sustainable development and acknowledges the different responsibilities and capabilities of nations in addressing climate change.
  – The Convention on Biological Diversity (CBD) was adopted in 1992 and entered into force in 1993. The main objective of the CBD is to promote the conservation of biological diversity, the sustainable use of its components and the fair and equitable sharing of the benefits derived from genetic resources. It recognizes the intrinsic value of biodiversity and its critical role in maintaining ecosystem stability and supporting human well-being.

[73] The number 21 in Agenda 21 refers to the 21st century.

  - The United Nations Convention to Combat Desertification (UNCCD) was adopted in 1994 and entered into force in 1996. The main objective of the UNCCD is to combat desertification and land degradation in arid, semi-arid and dry sub-humid areas, particularly in Africa. It recognizes the importance of promoting sustainable land management practices, restoring degraded ecosystems, and encouraging the active participation of local communities in combating desertification in order to achieve land degradation neutrality.

- The launch of the UNEP Finance Initiative (UNEP FI), which works with banks, insurers and investors to create a sustainable finance sector.

### United Nations Framework Convention on Climate Change (UNFCCC)

The UNFCCC is the international treaty (or a convention[74]) adopted at the Earth Summit. It consists of 26 articles and two annexes. The objective of the UNFCCC is defined in Article 2:

> "*The ultimate objective of this Convention and any related legal instruments that the Conference of the Parties may adopt is to achieve, in accordance with the relevant provisions of the Convention, stabilization of greenhouse gas concentrations in the atmosphere at a level that would prevent dangerous anthropogenic interference with the climate system. Such a level should be achieved within a time-frame sufficient to allow ecosystems to adapt naturally to climate change, to ensure that food production is not threatened and to enable economic development to proceed in a sustainable manner.*" (United Nations, 1992d, page 9).

The commitments are set out in Article 4. The principle of common but differentiated responsibilities recognizes that all countries have a common responsibility to address climate change, but acknowledges that developed countries should take the lead because of their historical contributions to greenhouse gas emissions and their greater financial and technological capabilities. The Convention therefore distinguishes between three types of Parties: Annex I Parties, Annex II Parties, and Non-Annex I Parties. All Parties (including Non-Annex I Parties) must publish national inventories of anthropogenic emissions and implement climate change mitigation programs (Article 4.1). Annex I Parties are subject to more stringent obligations than Non-Annex I Parties. In particular, Annex I Parties are required to adopt national policies and take appropriate measures to mitigate climate change by limiting their anthropogenic emissions of greenhouse gases and to report on the steps taken to return to their 1990 emission levels (Article 4.2). Annex I Parties are industrialized countries that were members of the OECD in 1992 and countries with economies in transition[75]. Annex II Parties are a subset of Annex I Parties and correspond to developed countries. In addition to the commitments in Articles 4.1 and 4.2, they have specific financial responsibilities as described in Article 4.3. They must provide additional financial resources, including for technology transfer, to meet the costs of developing countries and some specific vulnerable countries. The full list of this last category is given in Article 4.3.8, including small island countries, countries with low-lying coastal areas, etc. These countries are either located in areas that are particularly vulnerable to the effects of climate change or have economies that are heavily dependent on climate-sensitive sectors.

[74] A United Nations convention is a formal, legally binding international agreement that is negotiated and approved by representatives of the participating countries.

[75] In 1992, Annex I Parties were Australia, Austria, Belarus*, Belgium, Bulgaria*, Canada, Czechoslovakia*, Denmark, European Economic Community, Estonia*, Finland, France, Germany, Greece, Hungary*, Iceland, Ireland, Italy, Japan, Latvia*, Lithuania*, Luxembourg, Netherlands, New Zealand, Norway, Poland*, Portugal, Romania*, Russian Federation*, Spain, Sweden, Switzerland, Turkey, Ukraine*, United Kingdom of Great Britain and Northern Ireland, United States of America. The symbol * indicated countries in transition.

Table 8.24: Chronological list of the meetings of the Conference of the Parties

| Year | COP | CMP | CMA | City | Country | Treaty |
|---|---|---|---|---|---|---|
| 1992 | | | | Rio de Janero | Brazil | Convention |
| 1995 | 1 | | | Berlin | Germany | |
| 1996 | 2 | | | Geneva | Switzerland | |
| 1997 | 3 | | | Kyoto | Japan | Kyoto Protocol |
| 1998 | 4 | | | Buenos Aires | Argentina | |
| 1999 | 5 | | | Bonn | Germany | |
| 2000 | 6-1 | | | The Hague | Netherlands | |
| 2001 | 6-2 | | | Bonn | Germany | |
| 2001 | 7 | | | Marrakech | Morocco | |
| 2002 | 8 | | | New Delhi | India | |
| 2003 | 9 | | | Milan | Italy | |
| 2004 | 10 | | | Buenos Aires | Argentina | |
| 2005 | 11 | 1 | | Montreal | Canada | |
| 2006 | 12 | 2 | | Nairobi | Kenya | |
| 2007 | 13 | 3 | | Bali | Indonesia | |
| 2008 | 14 | 4 | | Poznań | Poland | |
| 2009 | 15 | 5 | | Copenhagen | Denmark | |
| 2010 | 16 | 6 | | Cancún | Mexico | |
| 2011 | 17 | 7 | | Durban | South Africa | |
| 2012 | 18 | 8 | | Doha | Qatar | |
| 2013 | 19 | 9 | | Warsaw | Poland | |
| 2014 | 20 | 10 | | Lima | Peru | |
| 2015 | 21 | 11 | | Paris | France | Paris Agreement |
| 2016 | 22 | 12 | 1-1 | Marrakech | Morocco | |
| 2017 | 23 | 13 | 1-2 | Bonn | Germany | |
| 2018 | 24 | 14 | 1-3 | Katowice | Poland | |
| 2019 | 25 | 15 | 2 | Madrid | Spain | |
| 2021 | 26 | 16 | 3 | Glasgow | United Kingdom | |
| 2022 | 27 | 17 | 4 | Sharm El Sheikh | Egypt | |
| 2023 | 28 | 18 | 5 | Dubai | United Arab Emirates | |
| 2024 | 29 | 19 | 6 | Baku | Azerbaijan | |

To assist in the implementation of the UNFCCC and to give it life, a Conference of the Parties is established (Article 7):

> "*The Conference of the Parties, as the supreme body of this Convention, shall keep under regular review the implementation of the Convention and any related legal instruments that the Conference of the Parties may adopt, and shall make, within its mandate, the decisions necessary to promote the effective implementation of the Convention.*" (United Nations, 1992d, Article 7.2, page 17).

The list of Conferences of the Parties is given in Table 8.24. These annual conferences take place every year, except for 2020 due to the COVID-19 pandemic, and focus primarily on negotiations and debates to assess progress toward the goal of limiting climate change. Occasionally, COPs result in new agreements and treaties, often aimed at refining targets, establishing guidelines, or creating legally binding treaties such as the Kyoto Protocol or the Paris Agreement. A critical aspect of these

meetings is the assessment of each party's contributions to climate change mitigation and adaptation efforts. COPs are attended by representatives of governments and observer organizations, such as non-governmental organizations (NGOs), charities, and advocacy groups. The first COP was held in Berlin in April 1995, and the last in Dubai in December 2023. According to Oberthür and Ott (1995), 4 000 delegates, including more than 2 000 journalists, 200 observer organizations, 117 UNFCCC member countries and 50 observer states, followed the proceedings in Berlin, while there were more than 100 000 delegates in Dubai[76] (97 372 on-site and 3 074 virtual-only attendees).

### Kyoto Protocol

At the first COP in Berlin in April 1995, Parties recognised that the voluntary approach of the UNFCCC was a shortcoming and that there was a need for a more formal, comprehensive and binding approach to implementing the Convention. The Berlin Mandate sets the stage for new negotiations to establish quantitative targets and specific deadlines. In addition, the IPCC published the Synthesis Report of the Second Assessment Report (SAR) in October 1995 and the Revised 1996 IPCC Guidelines for National Greenhouse Gas Inventories. The negotiations started at COP1 continued at COP2 in Geneva, Switzerland, in 1996, but it was the intensive negotiations at COP3 in Kyoto, Japan, that led to the adoption of the Kyoto Protocol on 11 December 1997 (Oberthür and Ott, 1999). After a complex ratification process, it entered into force on 16 February 2005. As of 1 January 2024, there are currently 192 Parties to the Kyoto Protocol. The Protocol's first commitment period started in 2008 and ended in 2012. At COP18 in Doha, Qatar, a second commitment extended the first one from 2013 to 2020. In fact, there is no third commitment period for the Kyoto Protocol. In order to follow up the specific commitments of the Kyoto Protocol, a new Conference of the Parties was created: the Conference of the Parties serving as the Meeting of the Parties to the Kyoto Protocol or CMP. In fact, the CMP takes place during the same period as the COP and can be seen as parallel sessions of the COP dedicated to the Kyoto Protocol. The same mechanism will be created for the Paris Agreement in 1995. The CMA, or the Conference of the Parties serving as the Meeting of the Parties to the Paris Agreement, oversees the implementation of the Paris Agreement and corresponds to other parallel sessions of the COP. Table 8.24 summarises the chronology of events and the history of the COP, CMP and CMA.

Unlike the original UNFCCC international treaty, the Kyoto Protocol introduces quantified commitments to limit or reduce greenhouse gas (GHG) emissions from 1990 levels[77] for the five-year period 2008–2012. These targets are listed in Table 8.25. The Kyoto Protocol also defines the list of greenhouse gases to be measured (Table 8.26). New commitments and a new scope of greenhouse gases will be adopted at COP18 in 2012 (Tables 8.26 and 8.27). To meet their targets, countries must first implement national measures as part of a coherent climate policy. However, the Kyoto Protocol also provides them with an additional tool in the form of three market-based mechanisms:

- International Emissions Trading (EIT)
- Clean Development Mechanism (CDM)
- Joint Implementation (JI)

The EIT is a form of carbon emissions trading that allows countries to reduce their emissions by buying or selling emission allowances. Each Annex B Party[78] is allocated a number of Assigned Amount

[76] The list is available at https://unfccc.int/documents/634503.

[77] Some countries have a base year earlier than 1990.

[78] Annex B Parties to the Kyoto Protocol are Annex I Parties to the UNFCCC minus Belarus and Turkey, plus Liechtenstein and Monaco.

Table 8.25: Quantified first commitment under the Kyoto Protocol to limit or reduce emissions (% of base year)

| $\mathcal{R}$ | Country |
|---|---|
| +10% | Iceland |
| +8% | Australia |
| +1% | Norway |
| 0% | New Zealand, Russian Federation, Ukraine |
| −5% | Croatia |
| −6% | Canada, Hungary, Japan, Poland |
| −7% | United States of America |
| −8% | Austria, Belgium, Bulgaria, Czech Republic, Denmark, Estonia, European Community, Finland, France, Germany, Greece, Ireland, Italy, Latvia, Liechtenstein, Lithuania, Luxembourg, Monaco, Netherlands, Portugal, Romania, Slovakia, Slovenia, Spain, Sweden, Switzerland, United Kingdom of Great Britain and Northern Ireland |

Source: UNFCCC (1997, Annex B, page 24).

Table 8.26: List of greenhouse gases under the Kyoto Protocol and the Doha Amendment

| Greenhouse gas | Symbol | Kyoto Protocol | Doha Amendment |
|---|---|---|---|
| Carbon dioxide | $CO_2$ | ✓ | ✓ |
| Methane | $CH_4$ | ✓ | ✓ |
| Nitrous oxide | $N_2O$ | ✓ | ✓ |
| Hydrofluorocarbons | HFCs | ✓ | ✓ |
| Perfluorocarbons | PFCs | ✓ | ✓ |
| Sulphur hexafluoride | $SF_6$ | ✓ | ✓ |
| Nitrogen trifluoride | $NF_3$ | | ✓ |

Source: UNFCCC (1997, Annex A, page 22) & UNFCCC (2012, Article 1.B, page 4).

Table 8.27: Quantified second commitment under the Kyoto Protocol (Doha Amendment) to limit or reduce emissions (% of base year)

| $\mathcal{R}$ | Country |
|---|---|
| −0.5% | Australia |
| −5% | Kazakhstan |
| −12% | Belarus |
| −16% | Liechtenstein, Norway, Switzerland |
| −20% | Austria, Belgium, Bulgaria, Croatia, Cyprus, Czech Republic, Denmark, Estonia, European Union, Finland, France, Germany, Greece, Hungary, Iceland, Ireland, Italy, Latvia, Lithuania, Luxembourg, Malta, Norway, Poland, Portugal, Romania, Slovakia, Slovenia, Spain, Sweden, United Kingdom of Great Britain and Northern Ireland |
| −22% | Monaco |
| −24% | Ukraine |

Source: UNFCCC (2012, Article 1.A, pages 1-2).

Units (AAUs), which represent its allowed emissions for the Kyoto Protocol's commitment period. Parties that exceed their emission targets can sell their surplus AAUs to Parties that have difficulty meeting their targets. A central registry tracks the transfer of AAUs between parties. The European Union Emissions Trading Scheme (EU ETS) is the largest EIT program. The Clean Development Mechanism (CDM) allows Annex B Parties to implement emission reduction projects in developing countries. If certified, such projects can generate marketable Certified Emission Reduction (CER) credits that can be used to calculate Kyoto targets. The third market-based mechanism, known as Joint Implementation, allows Annex B Parties to obtain Emission Reduction Units (ERUs) from an emission reduction project in another Annex B Party, which can be used to calculate Kyoto targets.

The Kyoto Protocol has been extensively studied by economists (Böhringer, 2003). For example, in June 1999, the Energy Journal published a special and complete issue on the Kyoto Protocol (Weyant and Hill, 1999). Some famous economists such as William Nordhaus and Richard Tol participated in the issue (Nordhaus and Boyer, 1999; Tol, 1999). An overview of the economic literature up to the year 2002 can be found in Böhringer (2003). The economic questions concern the efficiency of quotas versus taxes, the rationality of a partially cooperative solution, the credibility of sanctions, the uncertainty of abatement costs, the cost-benefit analysis, and the negative externalities of the Kyoto Protocol. Most of the academic conclusions are negative about the Kyoto Protocol. For example, Nordhaus and Boyer (1999) wrote that "*[...] the benefit-cost ratio of the Kyoto Protocol is 1/7. Additionally, the emissions strategy is highly cost-ineffective, with the global temperature reduction achieved at a cost almost 8 times the cost of a strategy which is cost-effective in terms of where and when efficiency.*" Tol (1999) concluded that "*[...] the agreements of the Kyoto Protocol are not readily reconciled with economic rationality.*" In the introduction and overview to the special issue of the Energy Journal, John Weyant and Jennifer Hill summarized the findings of the 13 articles and 390 pages as follows:

> "*Despite these considerable uncertainties, a number of common results and insights emerge from the set of model results considered here. First, meeting the requirements of the Kyoto Protocol will not stop economic growth anywhere in the world, but it will not be free either. In most Annex I countries, significant adjustments will need to be undertaken and costs will need to be paid. Second, unless care is taken to prevent it, the sellers of international emissions rights (dominantly the Russian Federation in the case of Annex I trading, and China and India in the case of global trading) may be able to exercise market power raising the cost of the Protocol to the other Annex I countries. Third, meaningful global trading probably requires that the non-Annex I countries take on emissions targets; without them accounting and monitoring (even Annex I monitoring and enforcement may be quite difficult) becomes almost impossible. Finally, it appears that the emissions trajectory prescribed in the Kyoto Protocol is neither optimal in balancing the costs and benefits of climate change mitigation, nor cost effective in leading to stabilization of the concentration of carbon dioxide at any level above about 500 ppmv.*" (Weyant and Hill, 1999, page xliv)

As economists have pointed out, one of the issues is the monitoring of the Kyoto Protocol. Another issue is the actual impact of the Kyoto Protocol. The Kyoto Protocol required each country to ratify the agreement. The EU and its member states ratified the Protocol in 2002, Russia ratified the Protocol in 2004, but the US never ratified the Protocol. Canada withdrew from the Kyoto Protocol in 2011. In addition, Canada, Japan, New Zealand, Russia, and the United States did not participate in the second commitment of the Kyoto Protocol. Therefore, we have to question the success of the Kyoto Protocol because it has mainly affected the European Union and Australia. On

the European Union's website[79], we can read that total EU emissions, excluding Cyprus and Malta, which have no target, were 23.5 $GtCO_2e$ for the period 2008–2012. This represents a reduction of about 19% below base year levels, excluding additional reductions from carbon sinks (LULUCF) and international credits. For the second commitment (2013–2020), we can read in January 2024 that the EU countries are on track...

### Paris Climate Agreement

The Paris Climate Agreement is another international UNFCCC treaty on climate change, adopted at COP21 in Paris in December 2015 and entered into force in November 2016. It can be seen as a successor to the Kyoto Protocol, particularly its second commitment to go one step further. Indeed, as we have already seen, while the Kyoto Protocol is generally seen as a major political achievement on climate change, it has had little impact because it only applies to Annex I Parties and most non-European major emitting countries, with the exception of Australia, did not participate in the Doha Amendment. However, there are a number of important differences between the Kyoto Protocol and the Paris Agreement:

- The ultimate goal of the Paris Agreement is more precise than the Kyoto Protocol. In fact, it aims to "*strengthen the global response to the threat of climate change, in the context of sustainable development and efforts to eradicate poverty, including by: (a) Holding the increase in the global average temperature to well below* 2°C *above pre-industrial levels and pursuing efforts to limit the temperature increase to* 1.5°C *above pre-industrial levels, recognizing that this would significantly reduce the risks and impacts of climate change; (b) Increasing the ability to adapt to the adverse impacts of climate change and foster climate resilience and low greenhouse gas emissions development, in a manner that does not threaten food production; and (c) Making finance flows consistent with a pathway towards low greenhouse gas emissions and climate-resilient development.*" (UNFCCC, 2015, Article 2.1, page 2).

- In the Kyoto Protocol, targets are set top-down and are mandatory. The Paris Agreement takes a bottom-up approach, with each Party deciding on its own Nationally Determined Contribution (NDC), meaning that a country can change its contribution to the global objective. Furthermore, the definition of a NDC is left to the discretion of each country, but countries are expected to make them increasingly ambitious over time.

- The Paris Agreement is global and applies to all Parties to the UNFCCC, while the Kyoto Protocol only covers industrialized countries (or Annex I Parties). As of January 2024, 195 of the 198 members of the UNFCCC are Parties to the Agreement. Three UNFCCC members have not ratified the agreement: Iran, Libia and Yemen.

- The timeframe also varies, with countries submitting their NDCs every few years and generally every five years. For example, some countries have already submitted their updates twice.

In summary, the Kyoto Protocol was a more prescriptive and legally binding treaty than the Paris Agreement, which is more flexible, global, and based on voluntary action by countries.

As noted in Schleussner *et al.* (2016), the Paris Agreement is the first international treaty to set a global long-term temperature goal. Although the Paris Agreement has its roots in the COP15 in Copenhagen, Denmark, which in turn is influenced by the IPCC AR4, it is clear that the Paris Agreement is strongly influenced by the IPCC AR5, whose synthesis report is completed in November

[79] The website is https://climate.ec.europa.eu/eu-action/international-action-climate-change.

2014 (IPCC, 2014b). But the full rationale of the Paris Agreement will come later, with the famous IPCC publication of Global Warming of 1.5°C in 2018:

> *[...] Five years ago, the IPCC's Fifth Assessment Report provided the scientific input into the Paris Agreement, which aims to strengthen the global response to the threat of climate change by holding the increase in the global average temperature to well below* 2°C *above pre-industrial levels and to pursue efforts to limit the temperature increase to* 1.5°C *above pre-industrial levels. [...] This Report responds to the invitation for IPCC to provide a Special Report in 2018 on the impacts of global warming of* 1.5°C *above pre-industrial levels and related global greenhouse gas emission pathways' contained in the Decision of the 21st Conference of Parties of the United Nations Framework Convention on Climate Change to adopt the Paris Agreement. [...] The IPCC accepted the invitation in April 2016, deciding to prepare this Special Report on the impacts of global warming of* 1.5°C *above pre-industrial levels and related global greenhouse gas emission pathways, in the context of strengthening the global response to the threat of climate change, sustainable development, and efforts to eradicate poverty.* (IPCC, 2018, pages v and 4).

SR15 is the IPCC publication that had the greatest impact on politicians and media. It strengthened the legitimacy of the Paris Agreement, because after this publication, politicians could not say they did not know. But it also illustrates the ambiguous relationship between science and politics, because SR15 can be seen as serving the Paris Agreement (Livingston and Rummukainen, 2020). As noted by Jewell and Cherp (2020) and Cointe and Guillemot (2023), the initial skepticism of the 1.5°C target has given way to ownership and acceptance[80], but the political and scientific feasibility of the 1.5°C target remains an issue. In fact, it's rare to find politicians or scientists who actually believe that the 1.5 degree target is achievable. The front page of *The Economist* at COP27 is not so ironic. Still, having an ambitious but surely unattainable goal ultimately helps us move forward.

Figure 8.72: The Economist, Say goodbye to 1.5°C, November 5, 2022

[80] For example, Cointe and Guillemot (2023) interviewed one of the SR15 authors who said "*honestly, as a scientist, I thought it was a bad idea to produce a report on* 1.5°C*, but in fact, after having done so, I think it was a good idea. So, even though it was very much driven by political motivation, I think that there was still an intuition behind it that was quite powerful.*"

To understand what a Nationally Determined Contribution is, we can consult the NDC Registry at https://unfccc.int/NDCREG. The first thing to note is that each NDC has its own format and may contain different information. For example, if we look at the first Party, Afghanistan, the NDC is an 8-page document with the following executive summary:

| | |
|---|---|
| Base year | 2005 |
| Target years | 2020 to 2030 |
| Contribution type | Conditional |
| Sectors | Energy, natural resource management, agriculture, waste management and mining |
| Gases covered | Carbon dioxide ($CO_2$), methane ($CH_4$), and nitrous oxide ($N_2O$) |
| Target | There will be a 13.6% reduction in GHG emissions by 2030 compared to a business-as-usual (BAU) 2030 scenario, conditional on external support |
| Financial needs | Total: \$17.405 bn<br>Adaptation: \$10.785 bn + Mitigation: \$6.62 bn (2020–2030) |

If we look at the second Party, Albania, the NDC is documented in a 145-page report with no executive summary. The last Party is Zimbabwe, and the updated submission is a 56-page report. It contains a table summarizing the changes from the intended (or original) NDC. We report the excerpt on the emissions reduction target below:

- 2015 INDC
  - Business-as-usual (BAU) scenario
    "*The INDC BAU baseline focused solely on per capita energy emissions. Zimbabwean per capita energy emissions were projected to be* 1.06 $tCO_2e$ *in 2020,* 2.57 $tCO_2e$ *in 2025 and* 3.31 $tCO_2e$ *in 2030 under business-as-usual.*"
  - Emission reduction target
    "*The INDC emission reduction target was a* 33% *reduction in energy-related emissions per capita compared to BAU by 2030, conditional on international support. In the mitigation scenario, energy-related emissions per capita were projected to be* 2.21 $tCO_2e$ *in 2030.*"
- 2021 Revised NDC
  - Business-as-usual (BAU) scenario
    "*Updated to include all IPCC sectors. National total emissions in the base data period ranged between* 25.24 $MtCO_2e$ *in 2011 and* 41.66 $MtCO_2e$ *in 2015. Emissions in 2017 were* 35.84 $MtCO_2e$. *National total emissions per capita in the base data period ranged between* 2.03 $tCO_2e$ *in 2011 and* 2.98 $tCO_2e$ *in 2015. Emissions per capita in 2017 were* 2.45 $tCO_2e$. *The NDC revision process incorporated impacts of COVID-19 on emissions trends and macroeconomic parameters, including GDP, which fed into the updated baseline.*"
  - Emission reduction target
    "*The updated target is a* 40% *reduction in economy-wide GHG emissions per capita compared to BAU by 2030, conditional on international support. In the mitigation scenario, economy-wide emissions per capita are projected to be* 2.3 $tCO_2e$ *in 2030.*"

There is no official NDC database that can be used to compare different targets across countries. The most comprehensive unofficial database is the IGES NDC Database (IGES, 2022). Unfortunately, the last updated version was October 2022. The alternative is to use the databases of

Climate Watch (www.climatewatchdata.org/ndcs-explore) or the German Development Institute (https://klimalog.idos-research.de/ndc). The different NDCs can be classified into the following categories: mitigation, scope (GHG & sectors), implementation period, conditionality, financial needs, technology needs, market mechanisms, adaptation, climate policy, transparency and information.

In Table 8.28 we report the NDC reduction rate for the 45 largest GHG emitters in the world. For each NDC, we give the value of the reduction rate, the base year, the target year and the type of reduction. For example, China's climate commitment is to reduce carbon dioxide emissions per GDP by 65% from 2005 levels by 2030, as this is a carbon intensity reduction or CIR type. In April 2021, when the United States rejoined the Paris Agreement after withdrawing from it under the Trump administration, the Biden administration commits to reducing greenhouse gas emissions by 50% from 2005 levels by 2030, as this is an absolute emissions reduction or AER type. Indonesia submits an updated NDC in 2021, committing to reduce its GHG emissions by 31.89% unconditionally and 43.20% conditionally by 2030 compared to a business as usual (BAU) pathway. This means that Indonesia will implement climate policies that would reduce GHG emissions by 32% in 2030 compared to a situation where it does not implement these climate policies. It is therefore a relative emissions reduction or RER type. Several observations can be made. First, as mentioned above, climate pledges are not homogeneous. Most developed countries have an absolute emissions reduction or AER commitment, while developing countries express their commitments in terms of intensity reduction (per GDP) or in relation to a business-as-usual scenario (RER type). In the case of the European Union countries, their climate commitment is aligned with the Fit for 55 package. Therefore, all EU countries commit to reducing their GHG emissions by 55% in 2030 compared to 1990 levels (AER type). The second observation concerns the conditionality of the climate pledges for developing countries. In Table 8.28 we only report unconditional commitments, as conditional commitments depend on financial support from developed countries. The third observation is the definition of the RER type when it does not assume a business-as-usual scenario. For example, Saudi Arabia aims to avoid 278 $MtCO_2e$ of GHG emissions per year by 2030, with 2019 as the base year for this NDC, while South Africa's annual GHG emissions would be in the range of 350-420 $MtCO_2e$ in 2030. We have transformed these NDCs using a proxy reduction rate relative to a base year of 2020.

Will these NDCs be enough to meet the Paris Agreement target? Academics agree that the answer is no. In fact, academics have identified two main reasons:

1. The first reason is that the NDCs are not ambitious enough, which means that even if the climate pledges are met, the temperature anomaly will not stay below 2°C, much less if the target is 1.5°C;

2. The second reason is that some NDCs are not credible compared to the recent carbon emission trend of some countries and the lack of means to implement these NDCs.

For example, here is the abstract of Liu and Raftery (2021):

> "*[...] we find that the probabilities of meeting their nationally determined contributions for the largest emitters are low, e.g.,* 2% *for the USA and* 16% *for China. On current trends, the probability of staying below* 2°C *of warming is only* 5%*, but if all countries meet their nationally determined contributions and continue to reduce emissions at the same rate after 2030, it rises to* 26%*. If the USA alone does not meet its nationally determined contribution, it declines to* 18%*. To have an even chance of staying below* 2°C*, the average rate of decline in emissions would need to increase from the* 1% *per*

Table 8.28: 2022 GHG emissions and NDCs of top emitting countries

| Rank | Country | (1) | (2) | (3) | (4) | (5) | (6) | (7) | (8) | (9) | (10) |
|---|---|---|---|---|---|---|---|---|---|---|---|
| 1 | China | 15 685 | 29.16 | 29.16 | 10.95 | 0.61 | 35.62 | 65 | 2005 | 2030 | CIR |
| 2 | United States | 6 017 | 11.19 | 40.35 | 17.90 | 0.28 | −10.01 | 50 | 2005 | 2030 | AER |
| 3 | India | 3 943 | 7.33 | 47.68 | 2.79 | 0.39 | 38.85 | 45 | 2005 | 2030 | CIR |
| 4 | Russia | 2 580 | 4.80 | 52.48 | 17.99 | 0.64 | 14.90 | 30 | 1990 | 2030 | AER |
| 5 | Brazil | 1 310 | 2.44 | 54.91 | 6.05 | 0.40 | 11.27 | 50 | 2005 | 2030 | AER |
| 6 | Indonesia | 1 241 | 2.31 | 57.22 | 4.47 | 0.36 | 50.00 | 32 | BAU | 2030 | RER |
| 7 | Japan | 1 183 | 2.20 | 59.42 | 9.41 | 0.23 | −10.85 | 46 | 2013 | 2030 | AER |
| 8 | Iran | 952 | 1.77 | 61.19 | 11.20 | 0.70 | 17.94 | | | | |
| 9 | Mexico | 820 | 1.52 | 62.71 | 5.99 | 0.33 | 6.64 | 22 | BAU | 2030 | RER |
| 10 | Saudi Arabia | 811 | 1.51 | 64.22 | 22.64 | 0.45 | 30.84 | 34 | 2020 | 2030 | RER |
| 11 | Germany | 784 | 1.46 | 65.68 | 9.49 | 0.17 | −16.68 | 55 | 1990 | 2030 | AER |
| 12 | Canada | 757 | 1.41 | 67.09 | 19.79 | 0.40 | 4.22 | 40 | 2005 | 2030 | AER |
| 13 | International Shipping | 751 | 1.40 | 68.48 | | | 7.17 | | | | |
| 14 | South Korea | 726 | 1.35 | 69.83 | 14.01 | 0.31 | 7.79 | 40 | 2018 | 2030 | AER |
| 15 | Turkey | 688 | 1.28 | 71.11 | 8.09 | 0.24 | 61.73 | 21 | BAU | 2030 | RER |
| 16 | Australia | 571 | 1.06 | 72.17 | 21.98 | 0.43 | −5.06 | 43 | 2005 | 2030 | AER |
| 17 | Pakistan | 546 | 1.02 | 73.19 | 2.53 | 0.42 | 36.49 | 15 | BAU | 2030 | RER |
| 18 | South Africa | 535 | 0.99 | 74.18 | 8.91 | 0.66 | −9.11 | 40 | 2020 | 2030 | RER |
| 19 | Vietnam | 489 | 0.91 | 75.09 | 4.88 | 0.44 | 58.37 | 9 | BAU | 2030 | RER |
| 20 | Thailand | 464 | 0.86 | 75.95 | 6.67 | 0.37 | 8.76 | 20 | BAU | 2030 | RER |
| 21 | France | 430 | 0.80 | 76.75 | 6.50 | 0.14 | −16.37 | 55 | 1990 | 2030 | AER |
| 22 | United Kingdom | 427 | 0.79 | 77.54 | 6.27 | 0.14 | −28.29 | 68 | 1990 | 2030 | AER |
| 23 | International Aviation | 426 | 0.79 | 78.34 | | | −8.38 | | | | |
| 24 | Nigeria | 408 | 0.76 | 79.09 | 1.88 | 0.38 | 11.08 | 20 | BAU | 2030 | RER |
| 25 | Poland | 401 | 0.75 | 79.84 | 10.62 | 0.29 | −4.13 | 55 | 1990 | 2030 | AER |
| 26 | Italy | 395 | 0.73 | 80.57 | 6.70 | 0.15 | −21.62 | 55 | 1990 | 2030 | AER |
| 27 | Argentina | 383 | 0.71 | 81.29 | 8.27 | 0.37 | 10.60 | 10 | 2020 | 2030 | RER |
| 28 | Egypt | 378 | 0.70 | 81.99 | 3.55 | 0.27 | 19.16 | 33 | BAU | 2030 | RER |
| 29 | Iraq | 368 | 0.68 | 82.67 | 8.41 | 0.90 | 75.42 | | | | |
| 30 | Malaysia | 354 | 0.66 | 83.33 | 10.50 | 0.37 | 26.48 | 45 | 2005 | 2030 | CIR |
| 31 | Kazakhstan | 332 | 0.62 | 83.95 | 17.33 | 0.65 | 3.50 | 15 | 1990 | 2030 | AER |
| 32 | Spain | 329 | 0.61 | 84.56 | 7.08 | 0.17 | −13.07 | 55 | 1990 | 2030 | AER |
| 33 | Taiwan | 308 | 0.57 | 85.13 | 12.86 | 0.19 | 1.57 | | | | |
| 34 | United Arab Emirates | 295 | 0.55 | 85.68 | 29.33 | 0.42 | 31.21 | 31 | BAU | 2030 | RER |
| 35 | Algeria | 284 | 0.53 | 86.21 | 6.38 | 0.57 | 36.01 | 7 | BAU | 2030 | RER |
| 36 | Bangladesh | 281 | 0.52 | 86.73 | 1.62 | 0.26 | 29.87 | 7 | BAU | 2030 | RER |
| 37 | Philippines | 265 | 0.49 | 87.22 | 2.35 | 0.27 | 50.56 | 3 | BAU | 2030 | RER |
| 38 | Uzbekistan | 227 | 0.42 | 87.65 | 6.67 | 0.79 | 9.25 | 35 | 2010 | 2030 | CIR |
| 39 | Colombia | 216 | 0.40 | 88.05 | 4.23 | 0.27 | 18.88 | 51 | BAU | 2030 | RER |
| 40 | Ukraine | 209 | 0.39 | 88.43 | 4.84 | 0.55 | −47.32 | 65 | 1990 | 2030 | AER |
| 41 | Qatar | 195 | 0.36 | 88.80 | 67.38 | 0.74 | 41.86 | 25 | BAU | 2030 | RER |
| 42 | Ethiopia | 192 | 0.36 | 89.15 | 1.63 | 0.66 | 53.40 | 14 | BAU | 2030 | RER |
| 43 | Venezuela | 170 | 0.32 | 89.47 | 4.99 | 1.02 | −35.03 | 20 | BAU | 2030 | RER |
| 44 | Myanmar | 169 | 0.31 | 89.78 | 3.04 | 0.76 | 42.10 | | | | |
| 45 | Kuwait | 168 | 0.31 | 90.10 | 37.96 | 0.80 | 35.24 | 7 | BAU | 2035 | RER |
| | Total | 53 786 | | | 6.76 | 0.39 | 14.46 | | | | |

(1) GHG emissions in 2022 in $MtCO_2e$, (2) share in %, (3) cumulative share in %, (4) GHG emissions per capita in 2022 in $tCO_2e$, (5) GHG emissions per GDP in 2022 in $kgCO_2e$, (6) GHG emissions growth between 2010 and 2022 in %, (7) NDC reduction rate, (8) base year (BAU = business-as-usual), (9) target year, (10) mitigation type (AER = absolute emissions reduction, CIR = carbon intensity reduction, RER = relative emissions reduction).

Source: Crippa *et al.* (2023), https://edgar.jrc.ec.europa.eu/report_2023, IGES (2022), https://unfccc.int/NDCREG & Author's calculations.

> *year needed to meet the nationally determined contributions, to* 1.8% *per year.*" (Liu and Raftery, 2021, page 1).

More recently, Meinshausen *et al.* (2022) and Wang *et al.* (2023) are more optimistic about the 2°C pathway when all conditional climate pledges from developing countries are included in the analysis. However, the 1.5°C target still appears unrealistic, with Wang *et al.* (2023) estimating that there is still an emissions gap of 10-15 $GtCO_2e$ by 2030 to follow the 1.5°C pathway. Ahead of COP28 in Dubai, the UNFCCC Secretariat has produced two reports to inform Parties to the CMA that national climate action plans remain insufficient to limit global temperature rise to 1.5°C and meet the goals of the Paris Agreement (UNFCCC, 2023a,b). The second report states:

> "*Full implementation of all latest NDCs is estimated to lead to a* 5.3% *(*2.3%-8.2%*) emission reduction by 2030 relative to the 2019 level; while implementation of all latest NDCs excluding any conditional elements is estimated to result in* 1.4% *higher emissions in 2030 than in 2019 (ranging from* 1.5% *lower to* 4.2% *higher).*" (UNFCCC, 2023b, Article I.11, page 5).

In Table 8.28 we have reported for each country the GHG emissions in 2022 in $MtCO_2e$ and also the corresponding share in % of total emissions. It can be seen that GHG emissions are concentrated in a few countries and regions. In 2022, China accounts for 29.16% of total GHG emissions, followed by the US, India, Russia and Brazil with contributions of 11.19%, 7.33%, 4.80% and 2.44% respectively. The cumulative share of the top five countries then amounts to almost 55% of total GHG emissions, while more than 75% of GHG emissions are concentrated in 18 countries and the international shipping. The European Union (27 countries) has a share of 6.67% in 2022. In this context, it is clear that the 1.5°C target is not in the hands of the Europeans, who were the backbone of the Kyoto Protocol and made a significant contribution to the signing of the Paris Agreement. Using the EDGAR database[81], we calculate the growth of GHG emissions since 1990 and plot its evolution for some developed countries (Figure 8.73) and developing countries (Figure 8.74). It is interesting to see the heterogeneity of emissions trajectories between the US and the EU, between China and Russia, etc. For example, the European Union has dramatically reduced its emissions since 1990 and Japan more recently, while the United States is close to 1990 levels and Canada has sharply increased its GHG emissions during this period. Nevertheless, all these countries have experienced a trajectory below the global trajectory of GHG emissions. If we look at the top developing countries, they generally have a trajectory above the global trajectory, with the exception of Russia. This is particularly true for China and India.

To understand the drivers of the emissions growth, we can again use a Kaya decomposition[82]. For example, we can consider a simplified approach where emissions are driven by population:

$$\text{GHG emissions} = \text{Population} \times \frac{\text{GHG emissions}}{\text{Population}}$$

or by GDP:

$$\text{GHG emissions} = \text{GDP} \times \frac{\text{GHG emissions}}{\text{GDP}}$$

Figure 8.75 shows the scatter plot of per capita GHG emissions between 1990 and 2002. On a global basis, this ratio is relatively stable between 6 and 7 $tCO_2e$ per capita (black circle). On average, the number of countries that have increased this intensity measure is roughly equal to the number

[81] The link is https://edgar.jrc.ec.europa.eu.
[82] The Kaya identity is defined in Box 8.6 on page 651.

Figure 8.73: Growth of greenhouse gas emissions in % for developed countries (base year = 1990)

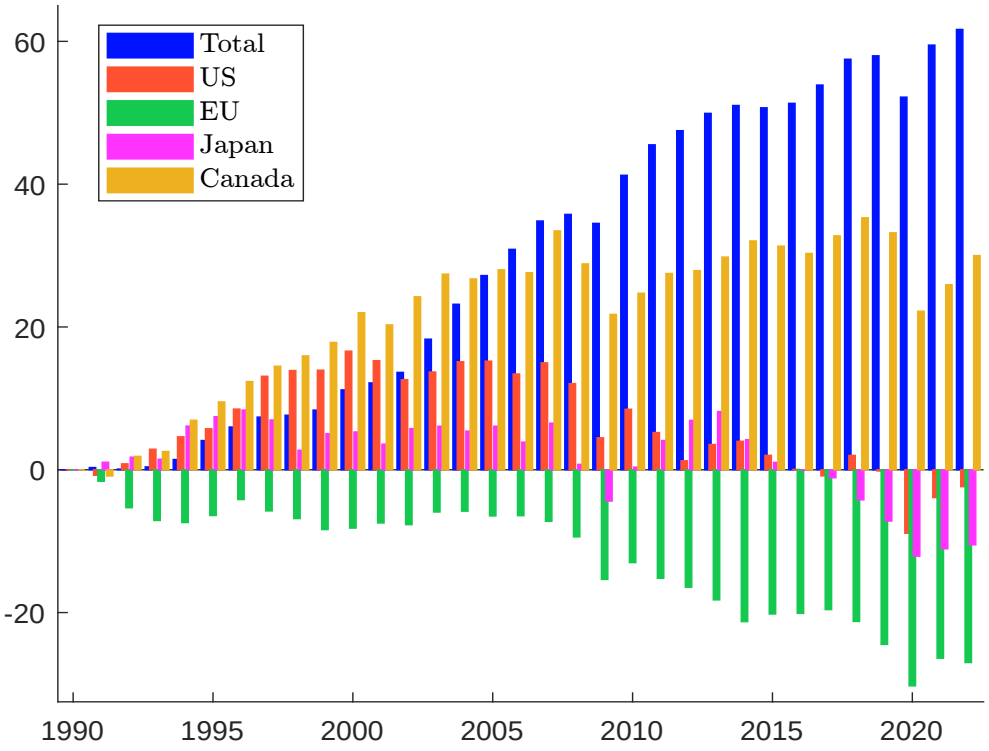


Figure 8.74: Growth of greenhouse gas emissions in % for developing countries (base year = 1990)

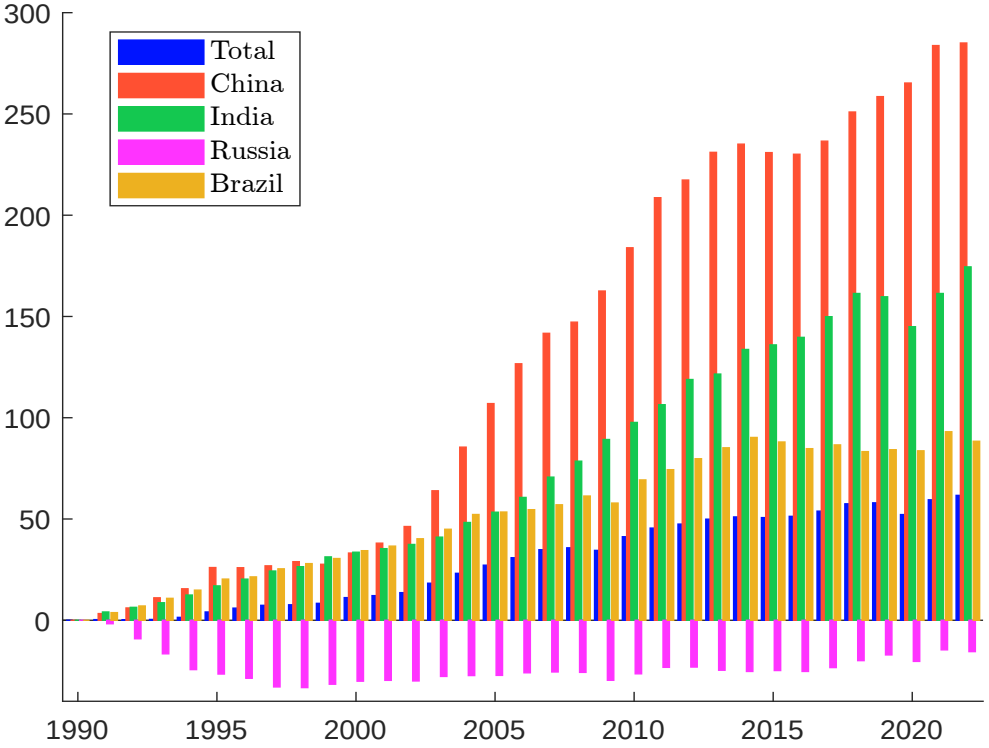

Figure 8.75: Per capita GHG emissions (1990 vs. 2022)

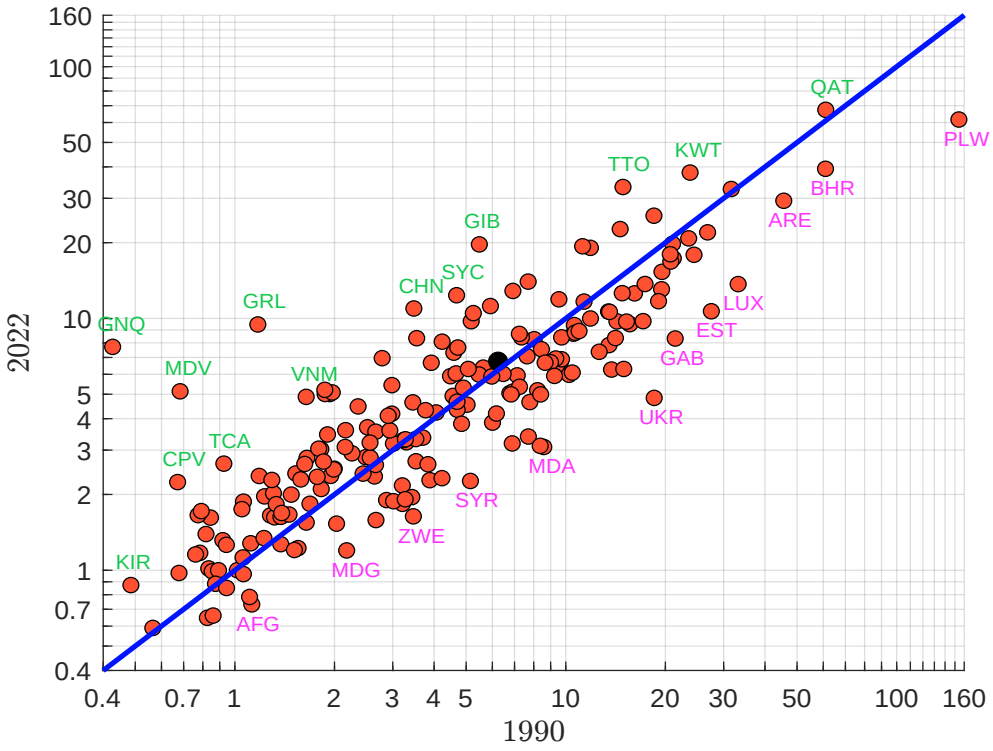


Figure 8.76: GHG emissions per GDP (1990 vs. 2022)

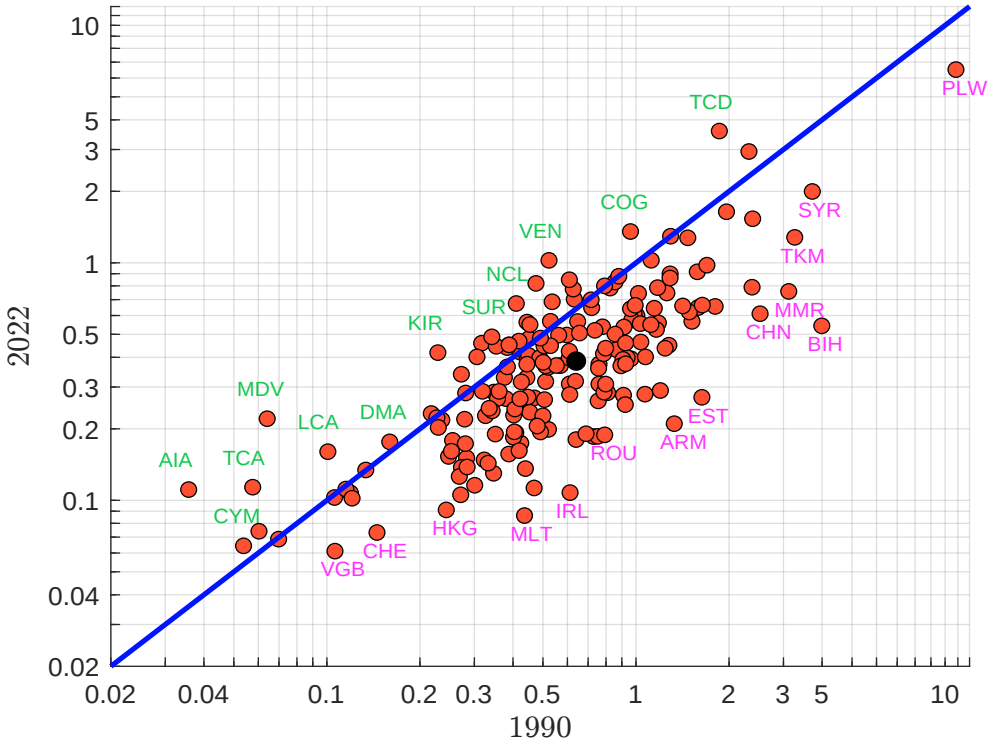

of countries that have decreased it. In fact, this ratio is not interesting for projecting the evolution of GHG emissions because it is difficult to control. A better decomposition is to use the per capita approach, as shown in Figure 8.76. On average, it was equal to 0.69 $\text{kgCO}_2\text{e}$ per \$ of GDP in 1990. It is now equal to 0.39 $\text{kgCO}_2\text{e}$ per \$ of GDP in 2022. The countries with the highest reduction rate are Bosnia and Herzegovina (86%), Armenia (84%), Estonia (83%), Ireland (82%) and Malta (80%). China reduced its emissions per GDP by 76% to a level of 0.61. Peters *et al.* (2017) proposed to use another Kaya identity to track the Paris Agreement NDCs:

$$\text{GHG emissions} = \text{GDP} \times \frac{\text{Energy}}{\text{GDP}} \times \frac{\text{GHG emissions}}{\text{Energy}}$$

This simplified Kaya decomposition shows that the achievement of NDCs depends on three factors: the GDP growth of the economy, its energy intensity and its emission intensity. As explained by Peters *et al.* (2017), energy intensity is difficult to manage because it is highly dependent on the economy of the country. Therefore, the only way to curb GHG emissions is to improve emission intensity, which needs to be reduced by a factor greater than GDP growth.

**Remark 82** *To track government climate action and progress towards the Paris Agreement goals, we can use the Climate Action Tracker, an independent scientific project that collects and measures this information (Figure 8.77). As of 1 January 2024, CAT tracks 39 countries and the EU covering around 85% of global emissions.*

Figure 8.77: The CAT thermometer

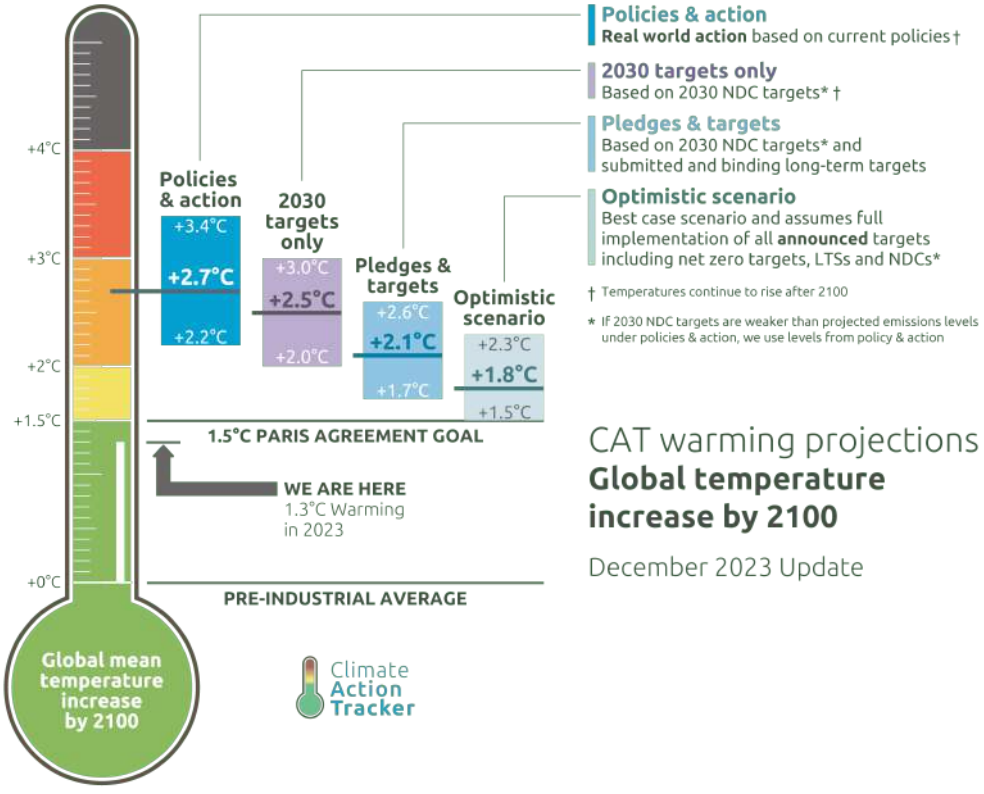


Source: Climate Action Tracker (2023), https://climateactiontracker.org.

### 8.2.3 Regulation policies

A comprehensive presentation of national climate change regulations around the world would take too much time, as the number of regulations today is huge and has increased dramatically since 2015 and the signing of the Paris Agreement. In this section, we only illustrate the impact of the UNFCCC and COPs at the country or regional level. In addition, we do not list all regulations affecting the financial sector, as these have already been presented in chapters 1 and 4. For example, it is clear that SFDR, CSRD and the EU Taxonomy are European regulations related to COP21.

#### United States

The US Environmental Protection Agency (EPA) is an independent agency of the US government, established in 1970. It is responsible for protecting the environment and enforcing standards under a variety of environmental laws. Here are some examples of regulations implemented or proposed by the EPA since 2020:

- An 85% reduction in the production and consumption of hydrofluorocarbons over the next 15 years, beginning in 2021;
- Vehicle emissions standards, including stricter GHG emissions standards for cars and light trucks beginning in 2023;
- Aviation GHG standards for commercial aircraft and large business jets;
- Renewable Fuel Standard (RFS) program, a federal program that requires a certain amount of renewable fuel to be blended into transportation fuel each year[83];
- Regulation of power plant emissions through the Acid Rain Program (ARP) and Mercury and Air Toxics Standards (MATS).

These new regulations complement existing regulations such as the Clean Air Act (CAA) of 1970, the federal law that regulates air emissions from stationary and mobile sources, including power plants, factories, and vehicles. In August 2022, the United States passed the Inflation Reduction Act (IRA). One of its goals is to support clean energy development, including investments in solar, wind, and geothermal power, as well as energy efficiency and grid modernization. In December 2023, the EPA issued a new methane rule to reduce methane emissions from oil and natural gas operations. In 2022 and 2023, some states also increased their renewable portfolio standards (RPS), which are mandates to increase energy production from renewable sources such as wind, solar, biomass, and geothermal[84].

**Remark 83** *At the financial level, the Securities and Exchange Commission (SEC) has taken steps to improve climate-related disclosures for public companies. In March 2022, the SEC proposed a new climate disclosure rule that is aligned with the TCFD framework and is similar in approach to the European CSRD/ESRS and the IFRS sustainability disclosure standards (ISSB). As of January 2024, the SEC has not finalized the proposed rule and no timeline has been provided. In fact, the proposed rule is controversial, with some critics arguing that it would be too costly to comply with.*

[83] Under the RFS, EPA sets annual renewable fuel volume targets, measured in Renewable Volume Obligations (RVOs), for four categories of renewable fuel: cellulosic biofuel, biomass-based diesel, advanced biofuel, and total renewable fuel.

[84] In the United States, this is known as the Renewable Electricity Standard (RES).

### European Union

In December 2019, the European Commission announced the European Green Deal, a framework and roadmap to make Europe the first climate neutral continent. The European Green Deal includes a wide range of initiatives to tackle the challenges of climate change, halt environmental degradation, promote sustainable growth and ensure a just transition. The goal set out in the European Green Deal has been translated into law in the European Climate Law, which was formally adopted by the EU Council in June 2021. The objective of the European Climate Law is to set the long-term direction for achieving the 2050 climate neutrality target across all policy areas in a socially equitable and cost-effective manner, and includes the following components:

- Set a 2030 target to reduce net greenhouse gas emissions by at least 55% compared to 1990 levels;
- Establish a system to monitor progress and take further action if necessary;
- Establish the European Scientific Advisory Board on Climate Change to provide independent scientific advice;
- Define the EU-wide greenhouse gas emission reduction path for 2030–2050;
- Provide predictability for investors and other economic actors;
- Ensure that the transition to climate neutrality is irreversible;
- Commit to negative emissions after 2050.

In July 2021, the European Commission presented the Fit for 55 package, which aims to meet the first quantitative target of the European Climate Change Law, namely to reduce Europe's net greenhouse gas emissions by at least 55% by 2030 (Figure 8.78). The package consists of several legislative proposals. As of 1 January 2024, 12 proposals have been adopted[85]:

1. Reform of the emissions trading system (ETS, April 2023)
   The EU emissions trading system tackles climate change by putting a price on carbon emissions. Companies operating in certain sectors must buy allowances each year to cover their greenhouse gas emissions. These allowances are limited in number and decrease each year, providing a financial incentive to reduce emissions. To prevent certain industries from being disadvantaged by carbon leakage (the shifting of emissions to unregulated areas), they receive free allowances to maintain their competitiveness. The EU ETS covers around 40% of total emissions produced in the EU and has significantly reduced emissions from covered sectors by 41% since its launch in 2005. It covers around 10 000 companies in sectors such as electricity and heat production, energy-intensive industries (including oil refineries, steel production, cement, glass and paper manufacturing) and commercial aviation for flights within the European Economic Area. The reform extends the scope of the EU ETS to maritime transport and increases the 2030 emission reduction target from 43% to 62% compared to the 2005 baseline. This implies a faster reduction in the emissions cap, with an annual reduction of 4.3% between 2024 and 2027 and 4.4% between 2028 and 2030, compared to the current rate of 2.2%. As a result, fewer allowances will be available on the market between 2024 and 2030. In addition, there are plans to gradually phase out free allowances for certain sectors, coinciding with the introduction of the carbon border adjustment mechanism (CBAM).

[85] All the information below has been taken from the European Council website (Figure 8.79). By clicking on each icon, we can access an infographic explaining the content of a particular regulation. The text of each bullet point is a plain language version of each infographic.

Figure 8.78: European Commission communication on the European Green Deal, 14 July 2021

Source: European Commission (2021), https://twitter.com/EU_Commission/status/1415289818565816321.

2. New emissions trading system for building and road transport fuels (April 2023)
   A new emissions trading system, known as ETS 2, has been set up to regulate $CO_2$ emissions from fuel combustion in buildings, road transport and other additional sectors (small industries). The main objectives are to stimulate investment in building renovation and to promote low-emission mobility. ETS 2 is due to start in 2027. Unlike the existing EU ETS, ETS 2 will use a cap-and-trade mechanism that focuses on upstream emissions, targeting fuel suppliers rather than end users such as households or vehicle owners. The emissions cap for ETS 2 aims to achieve a 42% reduction by 2030 compared to 2005 levels.

3. Social climate fund (April 2023)
   It is estimated that more than 34 million people in the EU live in energy poverty. In addition, the implementation of the new emissions trading system for buildings, road transport and other sectors may indirectly affect certain new categories of individuals and businesses. The main objective of the social climate fund is to mitigate energy poverty and improve access to low-emission mobility and transport in the EU. Revenues from the sale of allowances under the ETS 2 are allocated to the social climate fund. Member States can use the fund to support vulnerable households, small businesses and transport users through various measures and investments aimed at improving energy efficiency in buildings, renovating buildings, decarbonizing heating and cooling systems, promoting low-emission mobility and transport, and providing temporary and limited direct income support.

4. Revision of the effort sharing regulation (ESR, March 2023)
   The effort sharing regulation sets targets for each Member State to reduce greenhouse gas emissions from several economic sectors that currently account for about 60% of total EU emissions[86]: agriculture, buildings, road transport, small industry and waste. With the introduction of the Fit for 55 package, the buildings and road transport sectors will be covered by both the ESR and ETS 2. Under the updated regulations, the EU aims to achieve a 40% reduction in greenhouse gas emissions from the ESR sectors by 2030 compared to 2005 levels, an increase from the previous target of 29%. To achieve this, the revised effort sharing regulation sets new binding 2030 targets for each Member State and sets annual national emission limits leading progressively to these national 2030 targets[87]. It also introduces a number of flexibilities to help Member States meet their targets[88].

5. Revision of the regulation on land use, forestry and agriculture (LULUCF, March 2023)
   The LULUCF regulation, adopted in 2018, requires EU Member States to ensure that emissions from land use, land-use change, and forestry are offset by equivalent removals in the period 2021–2030 (the "*no debit*" rule). Activities covered by the rules include those related to land use and forestry, which can occur in areas such as grasslands, agricultural land, and forests. Carbon sequestration is the process by which forests and land absorb $CO_2$, with EU forests currently absorbing nearly 10% of the EU's total annual greenhouse gas emissions. The new rules include an increased carbon sequestration target of 310 $MtCO_2e$ by 2030, compared to the current target[89] of 225 $MtCO_2e$. Binding targets for Member States are based on recent

[86] The remaining 40% of GHG emissions are covered by the EU ETS.

[87] Table 8.29 shows the national reduction targets by 2030 under the ESR. It compares the original 2018 levels with the revised 2023 levels. For example, Austria's original target was to reduce GHG emissions by 36%. The revised target is now 48%.

[88] There are 3 flexibility rules: (1) if a country emits less than its annual limit, it can use part of the surplus in the following year; (2) if a country emits more than its annual allocation, it can borrow from the following year's allocation; (3) countries can buy and sell surplus allocations among themselves.

[89] In 2019, net carbon removals in the EU were already 195 $MtCO_2e$, with the following breakdown: −329.4 forest,

Table 8.29: National reduction targets under the ESR (revised 2023 vs. original 2018)

| Country | 2018 | 2023 | Country | 2018 | 2023 | Country | 2018 | 2023 |
|---|---|---|---|---|---|---|---|---|
| Austria | 36.0% | 48.0% | France | 37.0% | 47.5% | Malta | 19.0% | 19.0% |
| Belgium | 35.0% | 47.0% | Germany | 38.0% | 50.0% | Netherlands | 36.0% | 48.0% |
| Bulgaria | 0.0% | 10.0% | Greece | 16.0% | 22.7% | Poland | 7.0% | 17.7% |
| Croatia | 7.0% | 16.7% | Hungary | 7.0% | 17.7% | Portugal | 17.0% | 28.7% |
| Cyprus | 24.0% | 32.0% | Ireland | 30.0% | 42.0% | Romania | 2.0% | 12.7% |
| Czechia | 14.0% | 26.0% | Italy | 33.0% | 43.7% | Slovakia | 12.0% | 22.7% |
| Denmark | 39.0% | 50.0% | Latvia | 6.0% | 17.0% | Slovenia | 15.0% | 27.0% |
| Estonia | 13.0% | 24.0% | Lithuania | 9.0% | 21.0% | Spain | 26.0% | 37.7% |
| Finland | 39.0% | 50.0% | Luxembourg | 40.0% | 50.0% | Sweden | 40.0% | 50.0% |

Source: European Commission (2023), https://climate.ec.europa.eu/eu-action/effort-sharing-member-states-emission-targets.

removal levels and the potential for further increases. The accounting rules are simplified and a two-phase approach is introduced, with phase 1 maintaining the current system until 2025 and phase 2 introducing a new EU-level target for net removals by 2030.

6. Revised regulation on $CO_2$ emissions from new cars and vans (March 2023)
   Cars and vans are responsible for around 15% of the EU's total $CO_2$ emissions. To address this, the proposed regulation increases the $CO_2$ emission reduction targets for 2030 and sets a new 100% target for 2035. This means that all new cars and vans put on the EU market after 2035 would be zero-emission vehicles. The proposed agenda for $CO_2$ emission reductions for new cars and vans is as follows:

   (a) 2021–2024: limit value of 95 $gCO_2$/km for cars and 147 $gCO_2$/km for vans;

   (b) 2025–2029: 15% reduction for both cars and vans (resulting in 81 $gCO_2$/km for cars and 125 $gCO_2$/km for vans);

   (c) 2030–2034: 55% reduction for cars and 50% for vans (resulting in 43 $gCO_2$/km for cars and 73.5 $gCO_2$/km for vans);

   (d) 2035+: 100% reduction for both cars and vans (resulting in 0 $gCO_2$/km).

   In addition to the transition to zero-emission vehicles and cleaner air, this regulation aims to strengthen the technological leadership and competitiveness of the EU automotive industry[90]

7. Carbon border adjustment mechanism (CBAM, April 2023)
   The carbon border adjustment mechanism is a tool to address carbon leakage, where industries with high GHG emissions relocate production outside the EU to areas with less stringent climate policies. CBAM works by requiring EU importers to purchase CBAM allowances for products manufactured outside the EU to offset the price advantage resulting from the lack of ETS allowances. This mechanism aligns with the EU's goal of climate neutrality by working alongside the EU ETS to promote emission reductions in high-emitting industries inside and

+41.1 cropland, +44.4 settlement, +13.1 grassland, +1.7 other land, +16.9 wood products, +16.9 wetlands and +0.4 other.

[90]The EU automotive industry accounts for more than 7% of the EU's GDP, provides 12.7 million jobs or 6.6% of all jobs in the EU, is the world's second largest producer of motor vehicles after China, and is the largest research and development sector in the EU.

outside the EU. It also encourages other countries to adopt carbon pricing policies. Initially, the CBAM will cover sectors with high emissions and a high risk of carbon leakage, including iron and steel, cement, fertilizers, aluminum, electricity, hydrogen production, and certain products upstream and downstream of these sectors. Over time, the scope of the CBAM will be expanded to include additional sectors.

8. Renewable energy directive (RED III, October 2023)
In 2009, the first renewable energy directive (RED I) set a minimum target of 20% for the use of renewable energy by 2020. This target was exceeded, with nearly 22% of energy consumed in the EU coming from renewable sources in 2021. Building on this achievement, RED II was introduced in 2018, aiming for a 32% share of renewable energy by 2030. In October 2023, the European Council adopted the third iteration of the EU Renewable Energy Directive (RED III), setting a target of 42.5% renewable energy by 2030. This new target will nearly double the EU's share of renewable energy compared to 2020. In addition, RED III sets specific sectoral targets for 2030:

   (a) Buildings: Target of 49% renewable energy;

   (b) Industry: Increase the use of renewable energy by 1.6% per year;

   (c) Hydrogen in industry: Target 42% from renewable fuels of non-biological origin (60% by 2035);

   (d) Heating and cooling: Increase the use of renewable energy by 0.8% per year until 2026, followed by an annual increase of 1.1% until 2030;

   (e) Transport: Member States have the option of either reducing the emission intensity of transport fuels by 14.5% or ensuring that the share of renewable energy in transport is at least 29%; In addition, the combination of advanced biofuels and renewable fuels of non-biological origin should reach 5.5%, with at least 1% coming from renewable fuels of non-biological origin (mainly hydrogen).

9. Energy efficiency directive (EED, July 2023)
The EU energy efficiency directive has led to significant energy savings of nearly one-third compared to 2007 consumption projections for 2030. The revised legislation makes it mandatory for the EU as a whole to reduce final energy consumption. Specifically, the new target requires a mandatory 11.7% reduction in EU final energy consumption by 2030 compared to 2020 projections. This builds on the previous achievement of an average reduction of 29% (compared to 2007 estimates for 2030). In particular, the previous targets aimed at a 32.5% reduction in both primary and final consumption. The revised strategy introduces two new targets: an indicative target of a 40.6% reduction in primary consumption and a mandatory target of a 38% reduction in final consumption. Member States will also have to step up their energy savings efforts between 2024 and 2030, with an average annual saving of 1.49% in final energy consumption, rising to 1.9% by 2030. Key sectors such as buildings, transport and industry will be targeted for energy savings. The public sector will contribute by reducing final consumption by 1.9% per year, excluding public transport and the armed forces, and by renovating buildings to improve energy performance at a rate of 3% per year.

10. Alternative fuels infrastructure regulation (AFIR, July 2023)
The aim of the AFIR is to ensure that there is sufficient infrastructure for cars, trucks, ships and planes to charge or refuel with alternative fuels such as hydrogen or liquefied methane. This infrastructure should be well distributed across the Union to alleviate concerns about

limited range. Although currently only about 5% of the total fleet, there are over 13.4 million alternative fuel cars and vans in the EU and it is estimated that this could increase tenfold by 2050. The expected changes will affect road transport, ports and airports. For road transport, charging stations will be installed every 60 kilometers on major roads for vehicles under 3.5 tonnes by 2025 and for heavier trucks by 2030. These stations will increase their capacity annually to accommodate the growing number of registered vehicles. For trucks over 3.5 tonnes, there will be two charging stations per secure parking area by 2027, increasing to four by 2030. Charging stations will also be installed in urban areas, with exceptions for low-traffic roads. Hydrogen refuelling stations will be installed every 200 kilometers on major roads by 2030, with at least one in every urban area. Each station will be able to provide 1 tonne of hydrogen per day at 700 bar pressure. Liquefied methane refuelling stations will be strategically located along major roads to facilitate the use of methane-powered vehicles across the EU. In ports, at least 90% of container and passenger ships in the busiest seaports will have access to shore-side electricity. Most inland waterway ports will have shore-side electricity by 2030. For airports, electricity will be available for all aircraft stands near terminals by 2025 and for all remote stands by 2030. Exceptions may be made for remote stands at airports with less than 10 000 flights per year.

11. ReFuelEU aviation regulation (October 2023)
    The ReFuelEU aviation regulation is a new legislation aimed at reducing emissions from aviation, which currently accounts for 14.4% of EU transport emissions (2018 data). The regulation requires aviation fuel suppliers at EU airports to gradually increase the proportion of sustainable fuels they distribute, with a particular focus on synthetic fuels. The mandatory minimum share of sustainable aviation fuels will start at 2% in 2025, rising to 6% in 2030, 20% in 2035, 34% in 2040 and 42% in 2045. The ultimate goal is to reach 70% by 2050. It also requires EU airports to develop the necessary infrastructure for the delivery, storage and refuelling of sustainable aviation fuels. In addition, the regulation includes the implementation of an EU labeling system to inform consumers about the environmental performance of flights. This system is designed to empower consumers to make informed choices and encourage the uptake of greener flight options.

12. FuelEU maritime regulation (July 2023)
    Like the ReFuelEU aviation regulation, the FuelEU maritime regulation is a new regulation for ships over 5 000 gross tonnes calling at European ports[91] (with exceptions such as fishing vessels). The objective is to reduce the GHG intensity of the energy used on board by 2% in 2025, 6% in 2030, 14.5% in 2035, 31% in 2040 and 62% in 2045. The ultimate goal is to achieve 80% by 2050.

In addition to these 12 adopted proposals, three new proposals have already been provisionally agreed by the co-legislators:

- Energy performance of buildings directive (EPBD)
  Buildings in the EU are significant energy consumers, accounting for 40% of final energy consumption and 36% of energy-related GHG emissions, with around 75% of existing buildings inefficient and in need of major renovation. New regulations require all new public buildings to be zero emission by 2028, followed by all new construction by 2030. Existing buildings will also see significant changes. Non-residential buildings will have to meet minimum energy

[91] Ships over 5 000 gross tonnes represent 55% of all ships and are responsible for 90% of $CO_2$ emissions from the maritime sector, which accounts for 13.5% of EU transport emissions (2018 data).

standards set by Member States, with targets to improve the energy performance of 16% of the worst performing buildings by 2030 and 26% by 2033. Similarly, residential buildings will be required to achieve a 16% reduction in energy consumption by 2030 and a 20-22% reduction by 2035, primarily through renovation of the least efficient buildings, with the ultimate goal of achieving zero emissions from all buildings by 2050. Exceptions will be made for certain building types, such as historic buildings and those used for religious activities. In addition, the use of solar energy will be expanded, with requirements for solar panels in new construction and incentives for retrofitting existing buildings. The EU also plans to provide financial incentives and administrative support to facilitate these transformative efforts.

- EU methane regulation for the energy sector
  Globally, 60% of methane emissions are caused by human activities, with wetlands, agriculture, energy and waste activities, in descending order of importance, being the main sources. The new EU regulations include several key measures: (1) implementing robust procedures for measuring and reporting methane emissions in the energy sector, including independent audits and the establishment of public inventories for inactive wells and coal mines; (2) requiring leak detection and repair to reduce emissions within the EU, as well as limiting methane releases at energy production facilities through measures such as venting and flaring, and requiring Member States to adopt mitigation plans; (3) addressing energy imports by requiring the tracking of emissions associated with imported energy.

- Updated EU rules to decarbonise gas markets and promote hydrogen
  Renewable and low-carbon gases refer to gaseous fuels that have a reduced carbon footprint compared to fossil fuels. Renewable gases, derived from organic sources such as biogas and biomethane, or from non-biological renewable sources using electricity, such as renewable hydrogen and synthetic methane, offer environmentally sustainable alternatives. Low carbon gases, while not derived from renewable energy, emit at least 70% fewer greenhouse gas emissions over their life cycle than fossil natural gas. The proposed hydrogen and decarbonized gas market package aims to revise and introduce new regulations to reduce the carbon impact of the gas market. The aim is to phase out fossil natural gas and promote the introduction of renewable and low-carbon gases in the EU by 2030 and beyond. Key objectives of the new rules include: creating a hydrogen market with a target of 40 gigawatts of renewable hydrogen electrolyser capacity and 10 million tonnes of renewable hydrogen production by 2030; integrating renewable and low-carbon gases into the existing gas grid; ensuring consumer engagement and protection through simplified processes for switching energy suppliers; and increasing security of supply while limiting dependence on gas imports from Russia and Belarus through increased cooperation and restrictions.

**Remark 84** *One proposal did not materialise. The European Commission originally tabled a proposal to revise the Energy Taxation Directive (ETD) as part of the Fit for 55 package. The ETD entered into force in 2003 and sets the framework for the taxation of energy products used as electricity, motor and aviation fuels and most heating fuels. The reforms announced in July 2021 should include the introduction of tax rates, expressed in euros per gigajoule, based on the environmental impact of energy products rather than their volume, and a broadening of the tax base to include energy contents and processes that were previously excluded. To be adopted, the proposal requires unanimity in the European Council after consultation of the European Parliament and the European Economic and Social Committee. In November 2023, the European Council concluded that the positions of delegations remained divergent on several key issues and that the reform of the Energy Taxation Directive was abandoned.*

Figure 8.79: What is included in the Fit for 55 package?

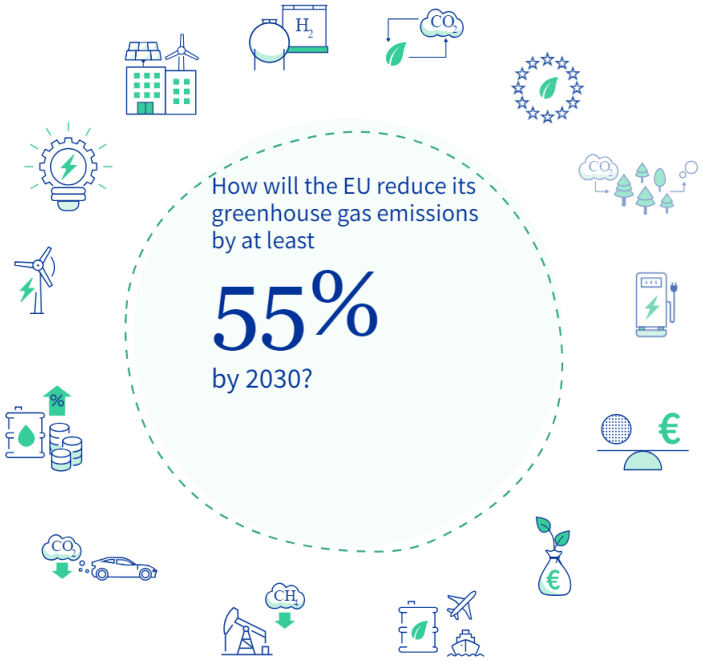


Source: European Council (2024), https://www.consilium.europa.eu/en/policies/green-deal/fit-for-55-the-eu-plan-for-a-green-transition.

### France

EU regulations apply to each EU member state, but each EU member state also has its own climate-related regulations and policies. One of the problems is that it is sometimes difficult to distinguish between national regulations that simply mirror an EU regulation and national regulations that fall outside the scope of the EU regulation. This is because a European regulation transposed into national law often combines several pieces of European legislation. Here are some examples from France:

- Energy Transition Act of 2015 (Loi relative à la transition énergétique pour la croissance verte du 17 août 2015)
- Energy and Climate Act of 2019 (Loi relative à l'énergie et au climat du 8 novembre 2019)
- Mobility Orientation Act of 2019 (Loi d'orientation des mobilités du 24 décembre 2019)
- Anti-Waste Act for a Circular Economy of 2020 (Loi relative à la lutte contre le gaspillage et à l'économie circulaire du 10 février 2020)
- National low carbon strategy (Stratégie nationale bas-carbone du 21 avril 2020 or SNBC)
- Climate and Resilience Act of 2021 (Loi climat et résilience du 22 août 2021)
- Environnemental Regulation (Réglementation environnementale RE2020)

The Energy Transition Act provides France with specific targets and action plans to implement the Paris Climate Agreement. Initially introduced in 2015 as a unique French regulation, its significance

expanded with the European Union's adoption of the Paris Agreement. Consequently, the Act now aligns with the EU's objectives regarding the Paris Climate Agreement. The national low carbon strategy (SNBC) is the roadmap of France to reduce its GHG emissions. It details the targets and instruments for each of the sectors concerned: buildings, agriculture, transport, forest wood and soils, energy production and industry. Again, it can be seen as a mix of several regulations that make up the Fit for 55 package. The RE2020 environmental regulation will come into force on 1 January 2022. As it can be seen as a proper French law on climate change, it borrows many elements from EU legislation on buildings.

### Germany

Germany has enacted several important climate change-related laws and regulations to promote environmental sustainability and reduce greenhouse gas emissions. Here are some of the most important laws and regulations with their German equivalents[92]:

- Klimaschutzgesetz (climate change act)
  Introduced in 2019, this law establishes binding targets for reducing greenhouse gas emissions in Germany, with the aim of achieving climate neutrality by 2050. The legislation specifies annual $CO_2$ reduction targets and emission limits for all sectors, with ongoing monitoring to facilitate corrective action if necessary.

- Klimaschutzprogramm 2030 (climate action programme 2030)
  The Klimaschutzprogramm 2030, a key component of the Germany climate change act, focuses on achieving the 2030 emission reduction targets and serves as Germany's contribution to the Fit for 55 package. Some key measures include the implementation of a national emissions trading system for smaller emitters, financial incentives for energy-efficient building renovation, subsidies for the purchase of electric vehicles and the development of charging infrastructure, and a coal phase-out plan with a 2038 deadline for the end of coal-fired power generation.

- Erneuerbare-Energien-Gesetz (EEG or renewable energy sources act)
  The Erneuerbare-Energien-Gesetz promotes renewable electricity generation to reduce greenhouse gas emissions and achieve energy independence. Enacted in 2000 and regularly updated to reflect market changes and technological advances, the EEG prioritizes the integration of renewable energy sources such as wind, solar, biomass, hydropower, and geothermal into the national grid. Key elements include feed-in tariffs (which guarantee fixed prices for electricity generated from renewable sources), priority grid access, grid expansion and modernization, and financing mechanisms.

- Energieeinsparverordnung (EnEV or energy saving ordinance)
  The Energieeinsparverordnung sets minimum energy performance standards for both new and existing buildings to reduce their energy consumption and associated greenhouse gas emissions. Key aspects of the EnEV include energy performance standards for insulation, heating systems, ventilation, and the use of renewable energy sources. It also includes provisions for energy certification, energy audits and technical standards.

- Energiewirtschaftsgesetz (EnWG or energy industry act)
  The Energiewirtschaftsgesetz regulates the energy sector. Enacted in 1935 and extensively revised over the years, the EnWG governs various aspects of energy production, distribution and consumption with the goal of ensuring a reliable, affordable and sustainable energy supply.

[92]Source: www.bundesregierung.de/breg-de/schwerpunkte/klimaschutz.

### United Kingdom

The Climate Change Act 2008 is the cornerstone of the UK's strategy for tackling climate change. It mandates the reduction of carbon dioxide and other greenhouse gas emissions. The Act sets out a comprehensive framework for achieving these targets and underlines the UK's commitment to urgent international action on climate change. Key features of the Climate Change Act include setting a target to significantly reduce the UK's greenhouse gas emissions by 2050; establishing the Committee on Climate Change (CCC) to provide an evidence-based and independent assessment of emissions targets; a commitment to reduce greenhouse gas emissions to at least 100% below 1990 levels (net zero) by 2050, including emissions from the devolved administrations; the implementation of legally binding carbon budgets to limit greenhouse gas emissions over five-year periods, with advice from the CCC on appropriate levels; and the production of a UK climate change risk assessment (CCRA) every five years to assess current and future climate risks and opportunities, accompanied by a national adaptation programme (NAP) in response. In addition, the Climate Change Levy (CCL) is a tax on the use of energy in industry, commerce and the public sector. The CCL is paid either at the main rates for electricity, gas and solid fuels such as coal, lignite, coke and petroleum coke, or at the carbon price support (CPS) rates for gas, LPG, coal and other solid fossil fuels to encourage industry to use low carbon technology to generate electricity. The UK has its own emissions trading scheme and an equivalent European-style CBAM mechanism is planned to be implemented by 2027.

### Other countries

There are many climate change-related laws around the world. For example, the Climate Change Laws of the World database[93], developed in collaboration with the Grantham Research Institute at LSE and the Sabin Center at Columbia Law School, contains more than 5 000 laws, policies, and UNFCCC submissions from every country. Below are some key regulations for some other countries:

- Australia: national greenhouse and energy reporting scheme (2007), emissions reduction fund (2014), safeguard mechanism (2015), renewable energy target scheme (2021), national climate resilience and adaptation strategy (2021–2025).

- Canada: Canadian environmental protection act (1999), pan-Canadian framework on clean growth and climate change (2016), greenhouse gas pollution pricing act (2018), Canadian net-zero emissions accountability act (2021), clean fuel standard (2022).

- China: renewable energy law (2005), energy conservation law (2007), carbon emissions trading management regulations (2021), 14$^{\text{th}}$ five-year plan for green development (2021–2025).

- India: national action plan on climate change (2008), energy conservation act (2001), renewable energy sources act (2015), national programme on climate change & human health (2019), green hydrogen/ammonia policy (2022).

- Japan: act on promotion of global warming countermeasures (1998), energy conservation act (1979), climate change adaptation act (2018), green growth strategy through achieving carbon neutrality in 2050 (2021), renewable energy act (2022).

[93]The website is https://climate-laws.org.

## 8.3 Integrated assessment models

Integrated assessment models (IAMs) can be defined as approaches that link main features of society and economy with the biosphere and atmosphere into a common modeling framework. They generally couple a macroeconomic model with a climate risk model in order to simulate the economic impacts of climate change. IAMs are used by policy markers to analyze the economic cost of climate change and the impact of climate action. According to Nordhaus (2017b), the most important applications are:

1. Making projections of economic variables (*e.g.*, GDP) that take into account global warming;
2. Calculating the impacts of alternative assumptions;
3. Tracing the effects and estimating the costs and benefits of alternative climate policies;
4. Estimating the uncertainty of future economic pathways.

For instance, the US government uses three IAMs to estimate the social cost of greenhouse gases, that is the value of avoiding one tonne of GHG emissions (IWG, 2021). These models are Dynamic Integrated Climate and Economy (DICE), Climate Framework for Uncertainty, Negotiation, and Distribution (FUND) and Policy Analysis of the Greenhouse Gas Effect (PAGE). The number of IAMs has grown rapidly, especially these last years with the increasing awareness of scientists to take into account climate change into economic modeling. Already in the late 1990s, Kelly and Kolstad (1999) count 21 major integrated assessment models. Today, current IAMs may be very complex and integrate social dimensions (*e.g.*, inequality, education, health, food security), industry dimensions (*e.g.*, sectors, infrastructure, rare earth elements), biodiversity dimensions (*e.g.*, species, ecosystem, food), etc. In this section, we first present the DICE model, which is certainly one of the simplest IAMs, but also the most famous. Even if DICE is a highly stylized reference point, it is an excellent educational tool for understanding the economics and physics of IAMs.

### 8.3.1 The DICE model

There are many versions of DICE. William Nordhaus began to develop DICE with a simple energy/climate model in the 1970s (Nordhaus, 1977). The current format of the model can already be found in Nordhaus (1992). Since this publication in *Science*, William Nordhaus has multiplied the research projects on DICE. Some of them were published in academic journals, others in many books[94], but most of them were unpublished. In what follows, we use the presentation and the notations of Nordhaus and Sztorc (2013), which corresponds to the user's manual of the DICE 2013R software. We also extensively refer to the comprehensive survey of Le Guenedal (2019).

#### The 2013 model

DICE uses a standard neoclassical model of economic growth known as the Ramsey-Cass-Koopmans model. It is an extension of the Solow model when the saving rate is not constant but endogenous. The social planner maximizes then the welfare utility function and determines the optimal path of saving rates to increase global consumption in the future. Nordhaus introduces the impact of climate change as a negative externality that hurts the economy and the output. In order to mitigate the cost

[94]The most famous are *Managing the Global Commons: The Economics of Climate Change* (1994), *A Question of Balance: Weighing the Options on Global Warming Policies* (2008), *The Climate Casino: Risk, Uncertainty, and Economics for a Warming World* (2013) and *The Spirit of Green* (2021).

of climate physical risks, the social planner can increase climate investments via a control variable on climate transition risks. Therefore, the general equilibrium depends on two decision variables: the saving rate and the climate control variable.

**Production and consumption functions** Nordhaus and Sztorc (2013) assume that the gross production $Y(t)$ is given by the Cobb-Douglas function:

$$Y(t) = A(t) K(t)^{\gamma} L(t)^{1-\gamma}$$

where $A(t)$ is the total productivity factor (or technological progress), $K(t)$ is the capital input and $L(t)$ is the labor input. The parameter $\gamma \in ]0,1[$ measures the elasticity of the capital factor:

$$\gamma = \frac{\partial \ln Y(t)}{\partial \ln K(t)} = \frac{\partial Y(t)}{\partial K(t)} \frac{K(t)}{Y(t)}$$

Traditional economic models do not make the distinction between the production $Y(t)$ and the net output $Q(t)$ because we have the identity $Y(t) = Q(t)$. Nevertheless, physical and transition climate risks generate losses:

$$Q(t) = \Omega_{\text{climate}}(t) Y(t) \leq Y(t)$$

where $\Omega_{\text{climate}}(t) \in ]0,1[$ is the loss percentage of the production. $Q(t)$ is then the net output when taking into account negative externalities of climate change. The saving rate $s(t)$ is assumed to be time-dependent and is a control variable. Using the classical identities $Q(t) = C(t) + I(t)$ and $I(t) = s(t) Q(t)$ where $I(t)$ is the investment, the expression of the consumption $C(t)$ is then equal to:

$$\begin{aligned} C(t) &= (1 - s(t)) Q(t) \\ &= (1 - s(t)) \Omega_{\text{climate}}(t) A(t) K(t)^{\gamma} L(t)^{1-\gamma} \end{aligned} \tag{8.19}$$

In order to introduce the time dependence and complete the economic model, the authors assume that the dynamics of the state variables are:

$$\begin{cases} A(t) = (1 + g_A(t)) A(t-1) \\ K(t) = (1 - \delta_K) K(t-1) + I(t) \\ L(t) = (1 + g_L(t)) L(t-1) \end{cases} \tag{8.20}$$

where $g_A(t)$ is the growth rate of the technological progress, $\delta_K$ is the depreciation rate of the capital stock and $g_L(t)$ is the growth rate of the labor factor. The two growth rates $g_A(t)$ and $g_L(t)$ decline over time, implying that:

$$g_A(t) = \frac{1}{1 + \delta_A} g_A(t-1)$$

and:

$$g_L(t) = \frac{1}{1 + \delta_L} g_L(t-1)$$

where $\delta_A \geq 0$ and $\delta_L \geq 0$.

**Example 28** *The world population was equal to 7.725 billion in 2019 and 7.805 billion in 2020. At the beginning of the 1970s, we estimate that the annual growth rate was equal to 2.045%. According to the United Nations, the global population could surpass 10 billion by 2100.*

In 2020, the annual growth rate was equal to:

$$g_L(2020) = \frac{L(2020)}{L(2019)} - 1 = \frac{7.805}{7.725} - 1 = 1.036\%$$

Since we have $g_L(t) = \left(\frac{1}{1+\delta_L}\right)^{t-t_0} g_L(t_0)$, we deduce that:

$$\delta_L = \left(\frac{g_L(t_0)}{g_L(t)}\right)^{1/(t-t_0)} - 1$$

An estimate of $\delta_L$ is then:

$$\delta_L = \left(\frac{g_L(1970)}{g_L(2020)}\right)^{1/30} - 1 = 2.292\%$$

In Figure 8.80, we report the dynamics of the labor input $L(t)$ by assuming that $L(2020) = 7.805$, $g_L(2020) = 1.036\%$ and $\delta_L = 2.292\%$. We estimate that the global population could reach 11.4 billion by 2100. In order to measure the sensitivity to the model parameters, we have also estimated the world population when $\delta_L$ is equal to 1.50% and 3.25%. The range is 10.5 and 12.6 billion at the end of this century.

Figure 8.80: Evolution of the labor input $L(t)$

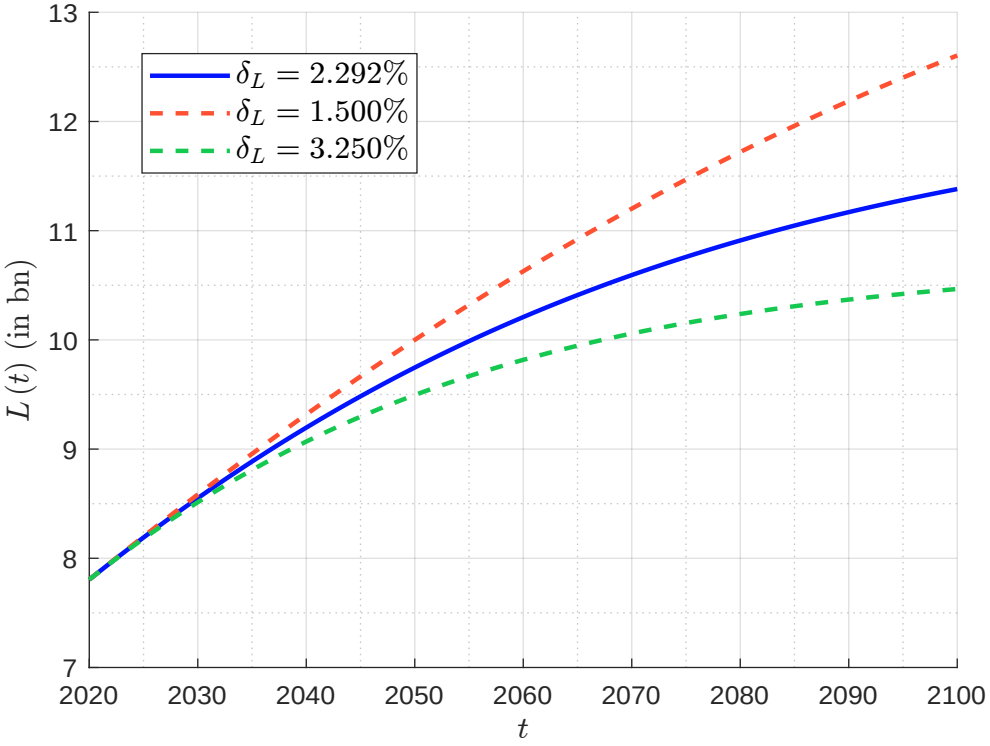


In Figure 8.81, we compare the different probabilistic projections, which are computed by the Department of Economic and Social Affairs (DESA) of the United Nations[95]. We notice that the previous calibration is close to the median estimation. Of course, we can use these data in order to better calibrate the DICE model. For instance, if we have a time series of $g_L(t)$, we can estimate $\delta_L$

[95] The data source are available at https://population.un.org/wpp.

Figure 8.81: Projection of the world population

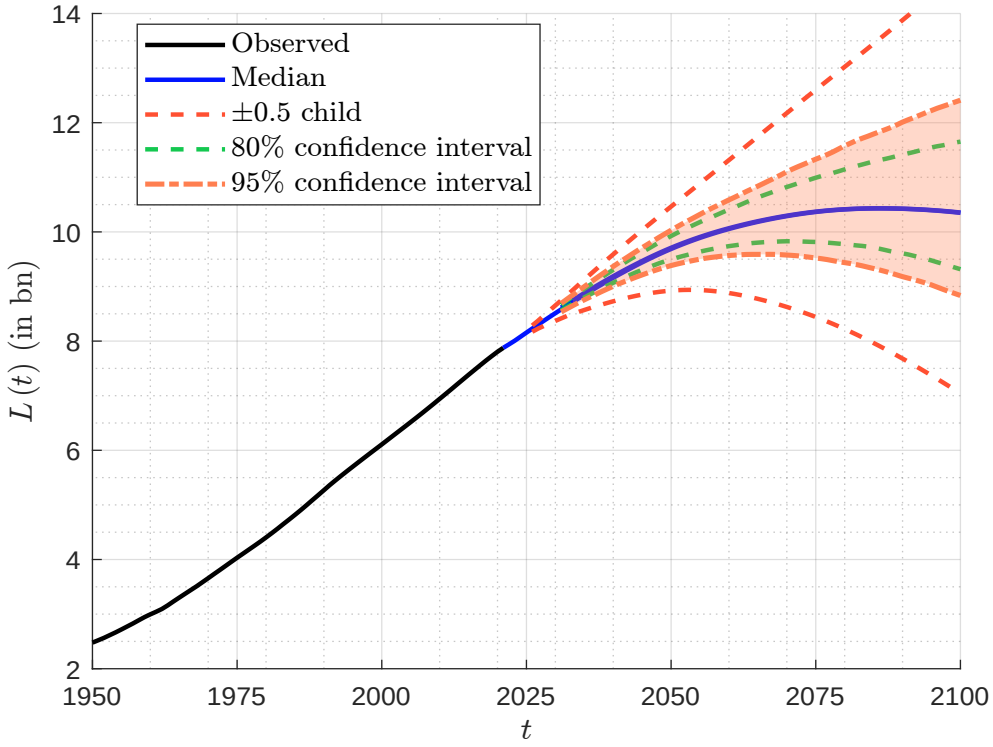


Source: United Nations (2022), World Population Prospects, https://population.un.org/wpp.

Figure 8.82: Population growth rate

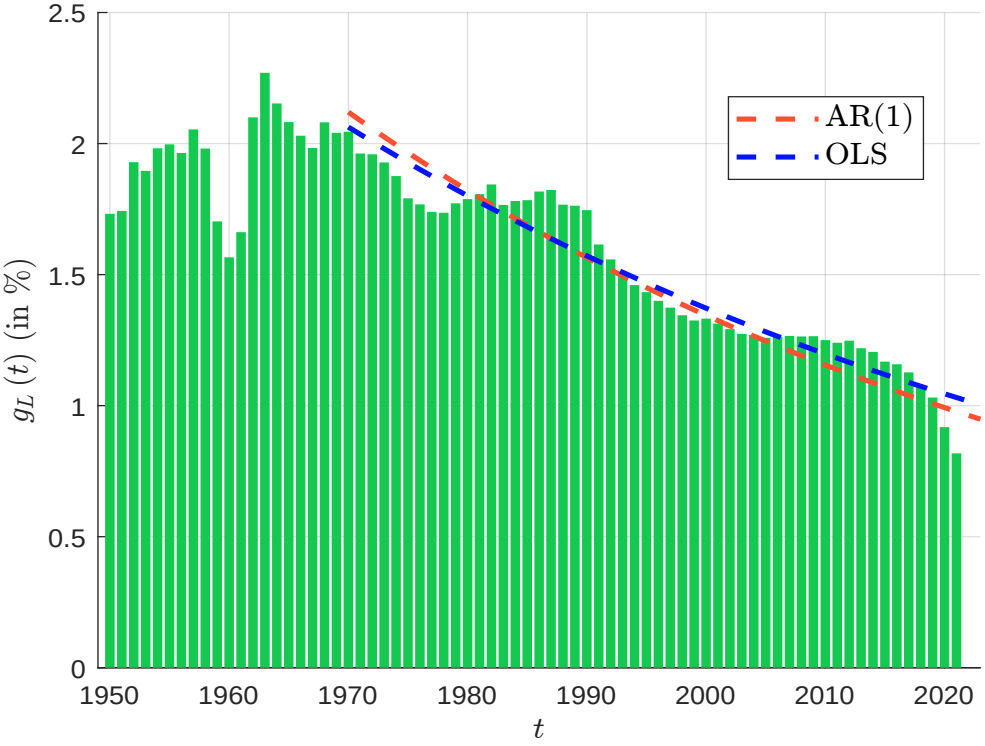


Source: United Nations (2022), https://population.un.org/wpp & Author's calculations.

by considering the AR(1) process: $g_L(t) = \phi g_L(t-1) + \varepsilon(t)$. We have $\hat{\delta}_L = \left(1 - \hat{\phi}\right)/\hat{\phi}$. Another method consists in using the following relationship:

$$g_L(t) = \left(\frac{1}{1+\delta_L}\right)^{t-t_0} g_L(t_0)$$

We deduce that $\ln g_L(t) = \ln g_L(t_0) - (t-t_0)\ln(1+\delta_L)$. We can then estimate the parameter $\delta_L$ by considering the linear regression: $\ln g_L(t) = \beta_0 + \beta_1(t-t_0) + \varepsilon(t)$. It follows that $\hat{\delta}_L = e^{-\hat{\beta}_1} - 1$. Using the historical population growth rates between 1970 and 2021 provided by the United Nations (Figure 8.82), we obtain $\hat{\phi} = 0.985$, $\hat{\beta}_0 = 0.724$ and $\hat{\beta}_1 = -0.014$. The estimated value of $\delta_L$ is then equal to 1.529% for the AR(1) process and 1.369% for the log-linear model. In Figure 8.82, we observe a high decline of the population growth rate in the last years, since the last value $g_L(2021)$ was equal to 0.82%.

Table 8.30: Average productivity growth rate (in %)

| Country | 1960–1970 | 1970–1980 | 1980–1990 | 1990–2000 | 2000–2010 | 2010–2020 |
|---|---|---|---|---|---|---|
| AUS | 1.02 | 0.07 | −0.23 | 1.02 | 0.36 | 0.13 |
| BRA | 2.39 | 2.05 | −1.04 | −1.12 | −0.17 | −1.63 |
| CAN | 2.18 | 0.38 | −0.25 | 0.21 | −0.21 | 0.40 |
| CHN | −0.03 | −0.06 | −0.04 | −0.41 | 2.24 | −0.35 |
| FRA | 3.59 | 1.63 | 1.12 | 0.61 | −0.11 | 0.02 |
| DEU | 2.33 | 1.63 | 0.75 | 1.52 | 0.01 | 0.74 |
| IND | 2.37 | −1.22 | 1.06 | 1.04 | 0.70 | 1.89 |
| ITA | 3.71 | 1.66 | −0.19 | −0.20 | −1.32 | −0.34 |
| JPN | 4.05 | 0.77 | 1.09 | −0.22 | −0.15 | 0.69 |
| ZAF | 2.37 | 0.30 | −0.84 | −1.11 | 0.50 | −1.20 |
| GBR | 0.50 | 0.72 | 0.75 | 0.42 | 0.12 | 0.08 |
| USA | 1.00 | 0.42 | 0.46 | 0.73 | 0.65 | 0.56 |

Source: Penn World Table 10.01 (Feenstra *et al.*, 2015) & Author's calculations.

Concerning the total factor productivity (TFP), also called the multifactor productivity (MFP), Nordhaus and Sztorc (2013) estimated that $g_A(2010) = 1.53\%$ and $\delta_A = 0.12\%$. If we would like to recalibrate these figures, there are currently four main databases that provide TFP/MFP statistics[96]: the OECD Productivity Statistics, the EUKLEMS–INTANProd database, the Conference Board Total Economy Database, and the Penn World Table (PWT), which is certainly the most known framework among economists (Feenstra *et al.*, 2015). We use this last database and consider a sample of twelve countries. The TFP index is reported in Figure 8.83. We notice a high discrepancy between countries and also between periods (see Table 8.30). Based on these statistics, $g_A(2020)$ is closer to 0.75% if we include developing countries. If we assume that the TFP growth rate has been divided by a factor $d$ in $n$ years, we have $\delta_A = \sqrt[n]{d} - 1$. Some examples of the growth rate path $g_A(t)$ are given in Figure 8.84.

For the investment $I(t)$, the capital stock $K(t)$ and the gross output $Y(t)$, we can use the previous databases such as the Penn World Table, or the investment and capital stock dataset (ICSD)

[96] We can download them at www.oecd.org/sdd/productivity-stats, https://euklems-intanprod-llee.luiss.it, www.conference-board.org/data/economydatabase/total-economy-database-productivity and www.rug.nl/ggdc/productivity/pwt.

Figure 8.83: Total factor productivity index (base 100 = 1960)

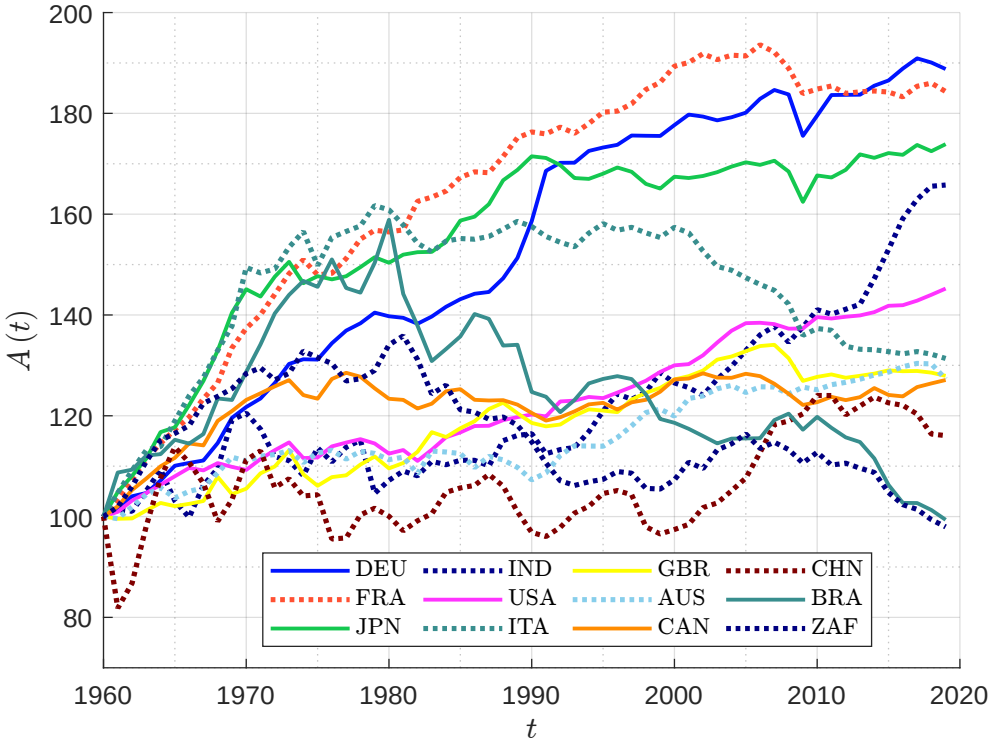


Source: Penn World Table 10.01 (Feenstra *et al.*, 2015) & Author's calculations.

Figure 8.84: Dynamics of the TFP growth rate

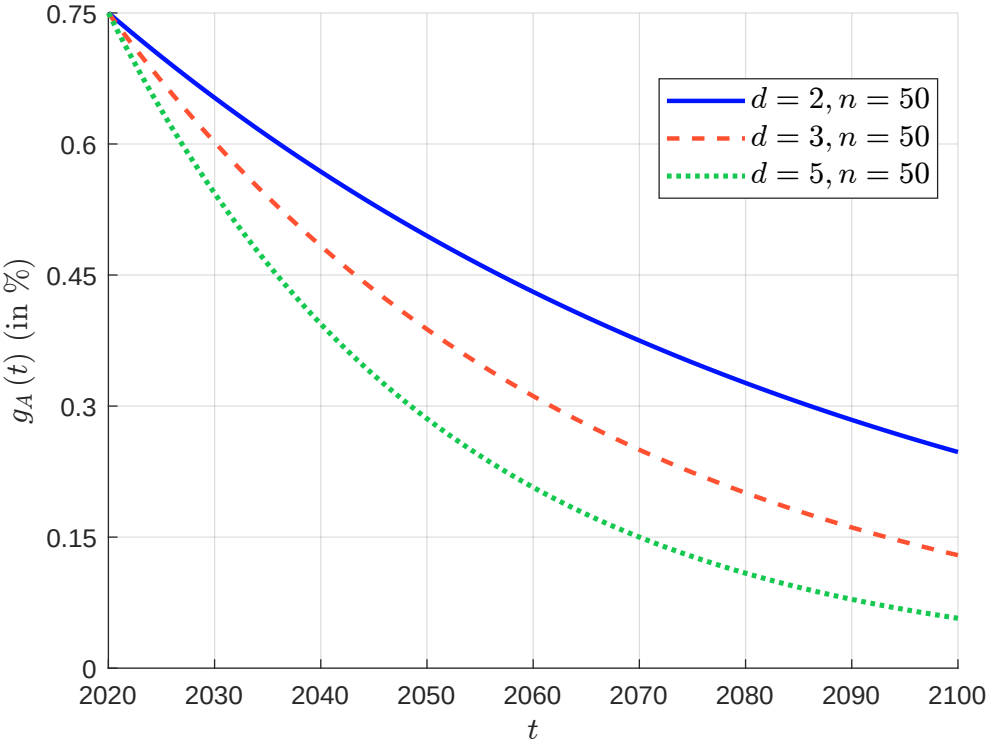

of the International Monetary Fund[97]. We have reported the evolution of the variables[98] in Figure 8.85. In 2019, we obtain $I(2019) = \$30.625$ tn, $K(2019) = \$318.773$ tn and $Y(2019) = \$124.418$ tn. We have also calculated the annual depreciation rate[99]:

$$\delta_K(t) = \frac{K(t-1) - K(t) + I(t)}{K(t-1)}$$

and we obtain $\delta_K(2019) = 6.25\%$. We have now all the elements to calibrate the initial value of $A(t)$. For that, we assume that $\gamma$ takes the typical value of 0.30 and we obtain:

$$A(2019) = \frac{Y(t)}{K(t)^{\gamma} L(t)^{1-\gamma}} = \frac{124.418}{318.773^{0.30} \times 7.725^{0.70}} = 5.276$$

We can now solve the macroeconomic model in the absence of climate change effects. In this case, $\Omega_{\text{climate}}(t) = 1$ and $Q(t) = Y(t)$. By assuming that the saving rate $s(t)$ is constant[100], we obtain the simulations[101] in Figure 8.86. We recall that the variables $C(t)$, $I(t)$, $K(t)$ and $Y(t)$ are expressed in trillions of constant 2017 international dollars. If $s(t) = 25\%$, the GDP in 2100 would be equal to \$507.47 tn. It would be reduced to \$408.65 tn if $s(t) = 15\%$.

**Cost function of climate change** We have seen that the net output is reduced because of climate change. The survival function is given by:

$$\Omega_{\text{climate}}(t) = \Omega_D(t)\,\Omega_\Lambda(t) = \frac{1}{1 + D(t)}(1 - \Lambda(t))$$

where $D(t) \geq 0$ is the climate damage function (physical risk) and $\Lambda(t) \geq 0$ is the mitigation or abatement cost (transition risk). The costs $D(t)$ result from natural disasters and climatic events, such as wildfires, storms, and floods, whereas the costs $\Lambda(t)$ are incurred from reducing GHG emissions and result from policy for financing the transition to a low-carbon economy. Nordhaus and Sztorc (2013) assume that $D(t)$ depends on the atmospheric temperature $\mathcal{T}_{\text{AT}}(t)$:

$$D(t) = \psi_1 \mathcal{T}_{\text{AT}}(t) + \psi_2 \mathcal{T}_{\text{AT}}(t)^2$$

where $\psi_1 \geq 0$ and $\psi_2 \geq 0$ are two parameters. $\mathcal{T}_{\text{AT}}(t)$ measures the global mean surface temperature and corresponds to the temperature increase in °C from 1900. Therefore, $\mathcal{L}_D(t) = 1 - \Omega_D(t) = 1 - (1 + D(t))^{-1}$ represents the fraction of net output that is lost because of the global warming. For the abatement cost function, the authors consider that it depends on the control variable $\mu(t)$:

$$\Lambda(t) = \theta_1(t)\,\mu(t)^{\theta_2}$$

where $\theta_1(t) \geq 0$ and $\theta_2 \geq 0$ are two parameters. For the emission-control rate, we have $\mu(t) \in [0, 1]$. Finally, we deduce that the global impact of climate change is equal to:

$$\Omega_{\text{climate}}(t) = \frac{1 - \theta_1(t)\,\mu(t)^{\theta_2}}{1 + \psi_1 \mathcal{T}_{\text{AT}}(t) + \psi_2 \mathcal{T}_{\text{AT}}(t)^2} \tag{8.21}$$

[97] The database is available at `https://data.imf.org`.

[98] $I(t)$ is the sum of the general government investment (variable `igov_rppp`), the private investment (variable `ipriv_rppp`) and public-private partnership investment (variable `ippp_rppp`); $K(t)$ is the sum of general government capital stock (variable `kgov_rppp`), private capital stock (variable `kpriv_rppp`) and public-private partnership capital stock (variable `kppp_rppp`); $Y(t)$ corresponds to the gross domestic product (variable `gdp_rppp`). All the variables are expressed in trillions of constant 2017 international dollars.

[99] Since the trajectory of $\delta_K(t)$ is erratic, we have preferred to report the 3-year moving average of $\delta_K(t)$.

[100] We recall that $s(t)$ is a control variable.

[101] We use the following initial values: $L(2019) = 7.725$ bn, $g_L = 1\%$, $\delta_L = 1.5\%$, $I(2019) = \$30.625$ tn, $K(2019) = \$318.773$ tn, $\delta_K = 6.25\%$, $A(2019) = 5.276$, $g_A(2019) = 0.75\%$, $\delta_A = 0.12\%$, $\gamma = 0.30$ and $Y(2019) = \$124.418$ tn.

Figure 8.85: Historical estimates of $I(t)$, $K(t)$, $Y(t)$ and $\delta_K(t)$

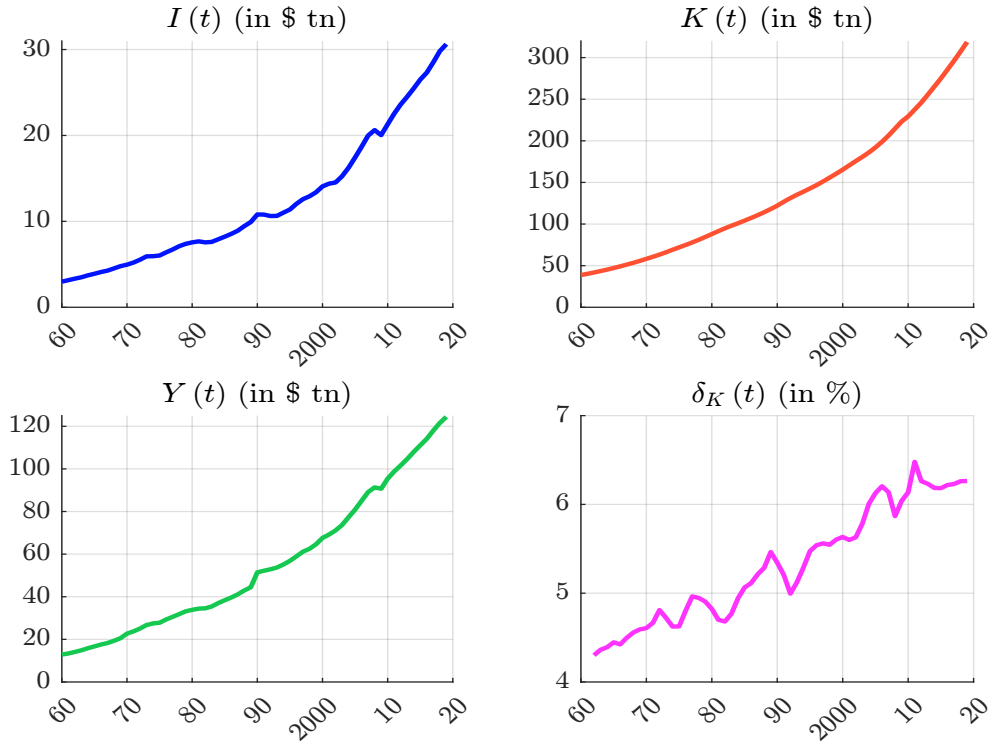


Source: IMF Investment and Capital Stock Dataset (2021) & Author's calculations.

Figure 8.86: Simulation of the DICE macroeconomic module

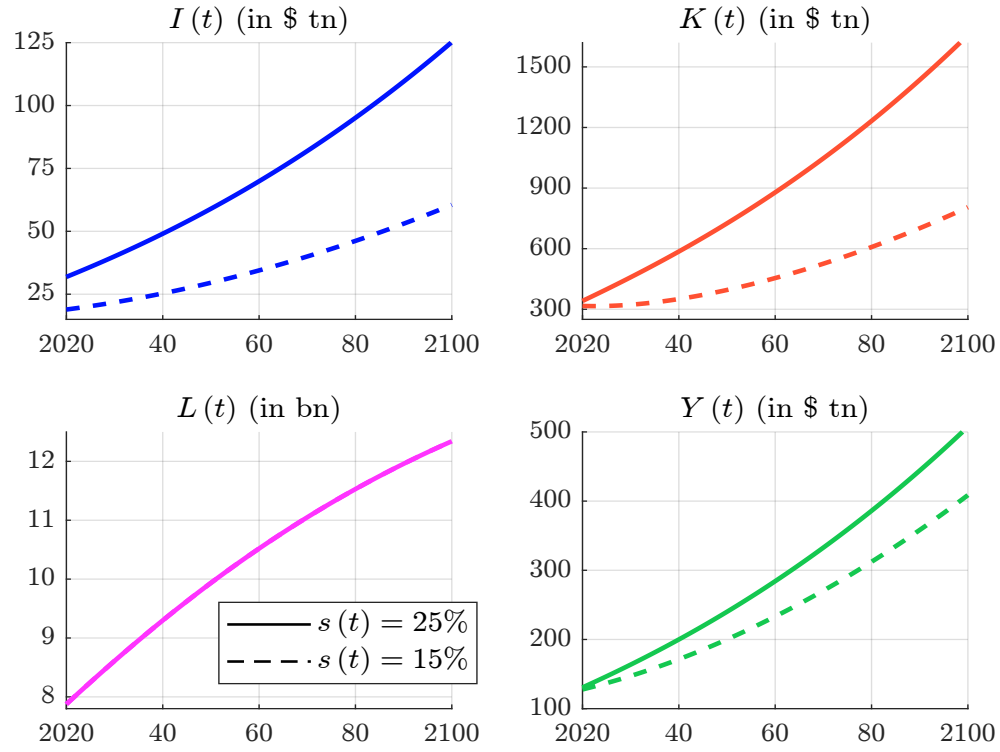

We notice that $\Omega_{\text{climate}}(t)$ depends on two variables: the atmospheric temperature $\mathcal{T}_{\text{AT}}(t)$ and the control variable $\mu(t)$. In the DICE model, $\mathcal{T}_{\text{AT}}(t)$ is a state variable while $\mu(t)$ is a decision variable. $\Omega_{\text{climate}}(t)$ is a then a decreasing function of $\mathcal{T}_{\text{AT}}(t)$ and $\mu(t)$ and we have the following properties:

$$\begin{cases} \Omega_{\text{climate}}(t) = 1 \Leftrightarrow \mathcal{T}_{\text{AT}}(t) = 0 \wedge \mu(t) = 0 \\ \lim\limits_{\mathcal{T}_{\text{AT}}(t)\to\infty} \Omega_{\text{climate}}(t) = 0 \\ \lim\limits_{\mu(t)\to 1} \Omega_{\text{climate}}(t) = \dfrac{1-\theta_1(t)}{1+\psi_1\mathcal{T}_{\text{AT}}(t)+\psi_2\mathcal{T}_{\text{AT}}(t)^2} \end{cases}$$

Nordhaus and Sztorc (2013) used $\psi_1 = 0$ and $\psi_2 = 2.67 \times 10^{-3}$ for the specification of $D(t)$. In Figure 8.87, we have represented the corresponding loss function $\mathcal{L}_D(\mathcal{T}_{\text{AT}}) := \mathcal{L}_D(t) = 1 - \Omega_D(t)$ as a function of the temperature increase $\mathcal{T}_{\text{AT}}$. For instance, we obtain $\mathcal{L}_D(1°\text{C}) = 0.27\%$, $\mathcal{L}_D(2°\text{C}) = 1.06\%$, $\mathcal{L}_D(5°\text{C}) = 6.26\%$ and $\mathcal{L}_D(10°\text{C}) = 21.07\%$ (dashed green line). We may think that these figures are underestimated in 2023. Already, fifteen years ago, the magnitude of these losses has created a scientific debate among economists. For instance, Hanemann (2008) found a higher loss function if the temperature reaches 2.5°C. Indeed, he estimated an annual loss of \$113 bn in the US versus \$28 bn for Nordhaus and Boyer (2000) (base year = 1990). Therefore, we can show that the parameter $\psi_2$ must take the value $1.135 \times 10^{-3}$ to obtain the ratio 113/28:

$$D(t) = 11.35 \times 10^{-3} \times \mathcal{T}_{\text{AT}}(t)^2$$

In a series of research papers (Weitzman, 2009, 2010, 2012), Martin Weitzman investigated several functional forms of the climate damage function. Using a stochastic modeling of the temperature $\mathcal{T}_{\text{AT}}$, Weitzman (2012) estimated the following climate damage function:

$$D(t) = \left(\frac{\mathcal{T}_{\text{AT}}(t)}{20.46}\right)^2 + \left(\frac{\mathcal{T}_{\text{AT}}(t)}{6.081}\right)^{6.754}$$

The first term corresponds to the Nordhaus specification[102], whereas the second term corresponds to "*a tipping point where the damages function changes dramatically around the iconic global warming level of* 6°C" (Weitzman, 2012, page 235). If we fit the Hanemann damage function using the Weitzman function, we obtain an alternative specification with higher damage for low temperature increase:

$$D(t) = 1.35 \times 10^{-2} \times \mathcal{T}_{\text{AT}}(t)^2 + 6.0287 \times 10^{-7} \times \mathcal{T}_{\text{AT}}(t)^{7.5}$$

While the previous damage functions are based on the functional form $D(t) = \sum_{k=1}^{m} \psi_k \mathcal{T}_{\text{AT}}(t)^{\alpha_k}$, Weitzman (2009) suggested the exponential quadratic damage function[103]: $\Omega_D(t) = \exp\left(-\beta\mathcal{T}_{\text{AT}}(t)^2\right)$. Pindyck (2012) proposed then the following parameterization:

$$\Omega_D(t) = e^{-\beta'\mathcal{T}_{\text{AT}}(t)^2 G}$$

where $G \sim \mathbf{F}_G$ is a random variable that follows a displaced gamma distribution[104] $\mathcal{DG}(\alpha, \beta, \theta)$ where $\alpha = 4.5$, $\beta = 4.69 \times 10^{-5}$ and $\theta = -7.46 \times 10^{-5}$. Following Daniel *et al.* (2016), we set $\beta' = 13.97$ and $G = \mathbf{F}_G^{-1}(99.99\%)$. We have reported all these alternative loss functions[105] in Figure 8.87. We notice a high level of disagreement between these different research works (Howard and Sterner, 2017; Tol, 2022).

[102] We have $1/20.46^2 \approx 2.4 \times 10^{-3}$, which was the value used by Nordhaus (2008).
[103] See Pindyck (2013, page 867) and Wagner and Weitzman (2015).
[104] If $X \sim \mathcal{DG}(\alpha, \beta, \theta)$, then $X - \theta \sim \mathcal{G}(\alpha, \beta)$.
[105] We also include the piecewise function $D(t) = 0.011\mathcal{T}_{\text{AT}}(t) + \mathbb{1}\{\mathcal{T}_{\text{AT}}(t) > 3°\text{C}\} \cdot (0.036 - 0.011)(\mathcal{T}_{\text{AT}}(t) - 3°\text{C})$, which has been estimated by Newbold and Marten (2014).

Figure 8.87: Loss function due to climate damage costs

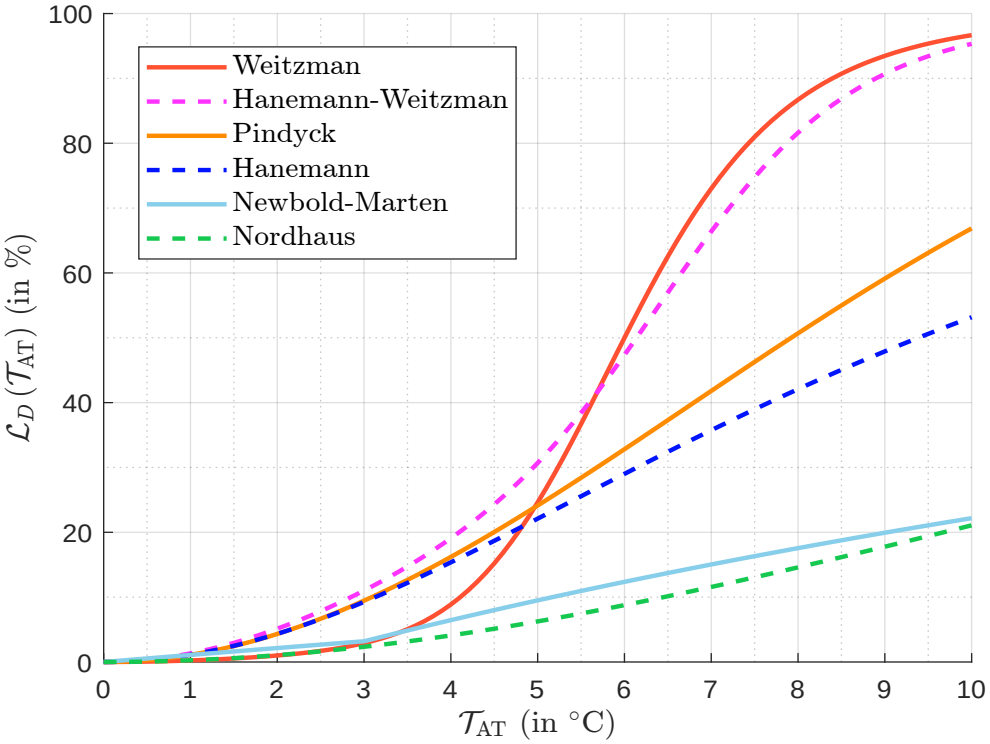


For the abatement cost function, Nordhaus (2018b) assumed that $\theta_1(t) = 0.0741 \times 0.98^{t-t_0}$ where $t_0$ is the base year of the abatement technology and $\theta_2 = 2.6$. The explanation is the following:

> "*The interpretation here is that at zero emissions for the first period* ($t = t_0$)*, abatement is 7.41% of output. That percentage declines at 2% per year. The abatement cost function is highly convex, reflecting the sharp diminishing returns to reducing emissions. [...] The model assumes the existence of a backstop technology, which is a technology that produces energy services with zero GHG emissions* ($\mu = 1$)*. The backstop price in 2020 is \$550 per ton of* $CO_2$e*, and the backstop cost declines at 0.5% per year. Additionally, it is assumed that there are no negative emissions technologies initially, but that negative emissions are available after 2150.*" (Nordhaus, 2018b, page 357).

Therefore, we can also define the cost of mitigation efforts as the following alternative form (Kellett *et al.*, 2019):

$$\theta_1(t) \propto p_b(t_0)(1-\delta_b)^{t-t_0}\sigma(t)$$

where $p_b(2020) = \$550/\text{tCO}_2\text{e}$, $\delta_b = 0.5\%$ and $\sigma(t)$ is the carbon intensity of economic activity, which is equal to the ratio of anthropogenic GHG emissions to economic output $Y(t)$. In Figure 8.88, we show the abatement cost function $\Lambda(t)$ for different values of the control rate $\mu(t)$, which is the second control variable with the saving rate $s(t)$.

**Remark 85** *There is a large literature on abatement costs, especially about the concept of marginal abatement cost (MAC). Since this concept is at the core of the transition risk (Gillingham and Stock, 2018) and is highly related to the carbon tax (Daniel et al., 2019), it will be developed in Section 10.2.2 on page 944.*

Figure 8.88: Abatement cost function

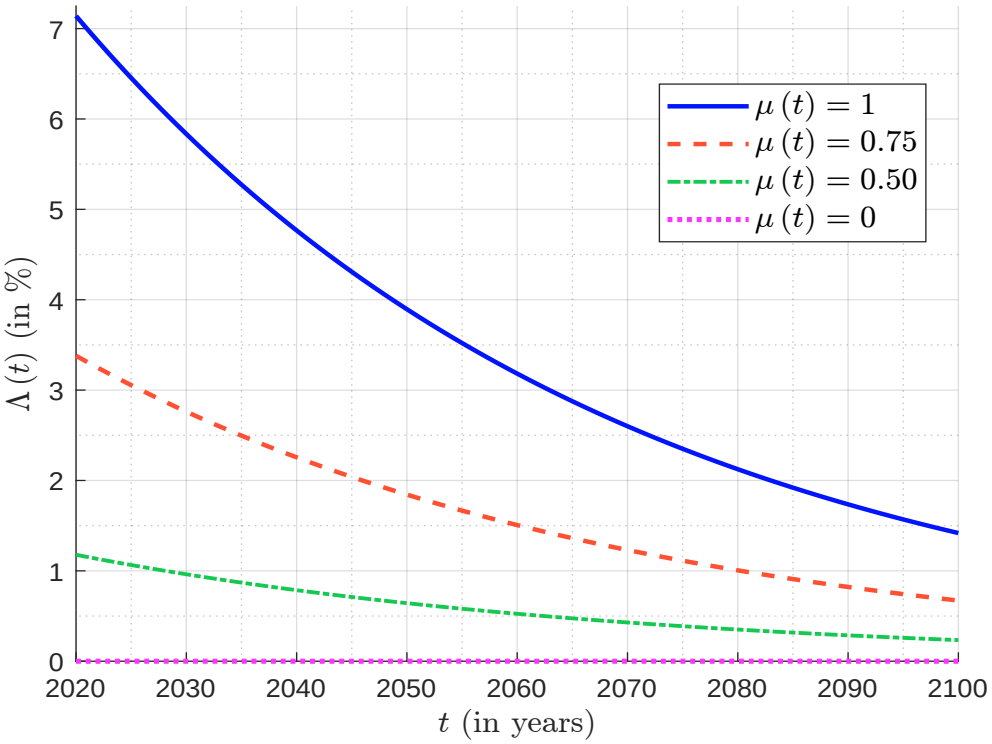


**Temperature modeling** We now turn to the physics of the DICE model. As noticed by Nordhaus (2017b), IAMs are "*highly simplified representations of complex economic and geophysical realities*", and can not compete with general circulation models[106] (GCM). Nevertheless, these models are based on basic physics of temperature forecasts, produce plausible temperature trajectories and "*do a reasonable job capturing uncertainty about the equilibrium climate sensitivity*" (Calel and Stainforth, 2017a, page 1202).

The GHG emissions $\mathcal{CE}(t)$ depends on the production $Y(t)$ and the land-use emissions $\mathcal{CE}_{\text{Land}}(t)$:

$$\begin{aligned}\mathcal{CE}(t) &= \mathcal{CE}_{\text{Industry}}(t) + \mathcal{CE}_{\text{Land}}(t) \\ &= (1-\mu(t))\sigma(t)Y(t) + \mathcal{CE}_{\text{Land}}(t)\end{aligned} \tag{8.22}$$

where $\sigma(t)$ is the impact of the production on GHG emissions. $\mathcal{CE}_{\text{Industry}}(t)$ corresponds to the anthropogenic emissions due to industrial activities. We have We have $\mathcal{CE}_{\text{Land}}(t) = (1-\delta_{\text{Land}})\mathcal{CE}_{\text{Land}}(t-1)$. The control variable $\mu(t)$ measures the impact of climate change mitigation policies:

$$\underbrace{\mathcal{CE}_{\text{Land}}(t)}_{\mu(t)=1} \leq \mathcal{CE}(t) \leq \underbrace{\sigma(t)Y(t) + \mathcal{CE}_{\text{Land}}(t)}_{\mu(t)=0}$$

$\mu(t) = 1$ corresponds to the case where mitigation policies have eliminated the effects of climate change, while $\mu(t) = 0$ indicates that no specific policy has been put in place. Since $\mu(t)$ is an endogenous variable, it must be viewed as an effort rate that the economy must bear to limit global

[106] They simulate general circulation of planetary atmosphere and oceans, using the Navier-Stokes equations on a rotating sphere and thermodynamic terms for energy sources (radiation, latent heat). They are used for weather forecasting, understanding the climate, and forecasting climate change.

warming. Concerning the ratio $\sigma(t)$, it measures the relationship between the carbon emissions due to industrial activities and the gross output in the absence of mitigation policies ($\mu(t) = 0$):

$$\sigma(t) = \frac{\mathcal{CE}(t) - \mathcal{CE}_{\text{Land}}(t)}{Y(t)} = \frac{\mathcal{CE}_{\text{Industry}}(t)}{Y(t)}$$

Therefore, it can be interpreted as an emission factor or the anthropogenic carbon intensity of the economy. This parameter is integrated into the model as follows:

$$\sigma(t) = (1 + g_\sigma(t))\sigma(t-1) \tag{8.23}$$

where:

$$g_\sigma(t) = \frac{1}{1+\delta_\sigma} g_\sigma(t-1)$$

and $\delta_\sigma$ is the decline rate of the GHG emissions growth.

Figure 8.89: Physical carbon pump

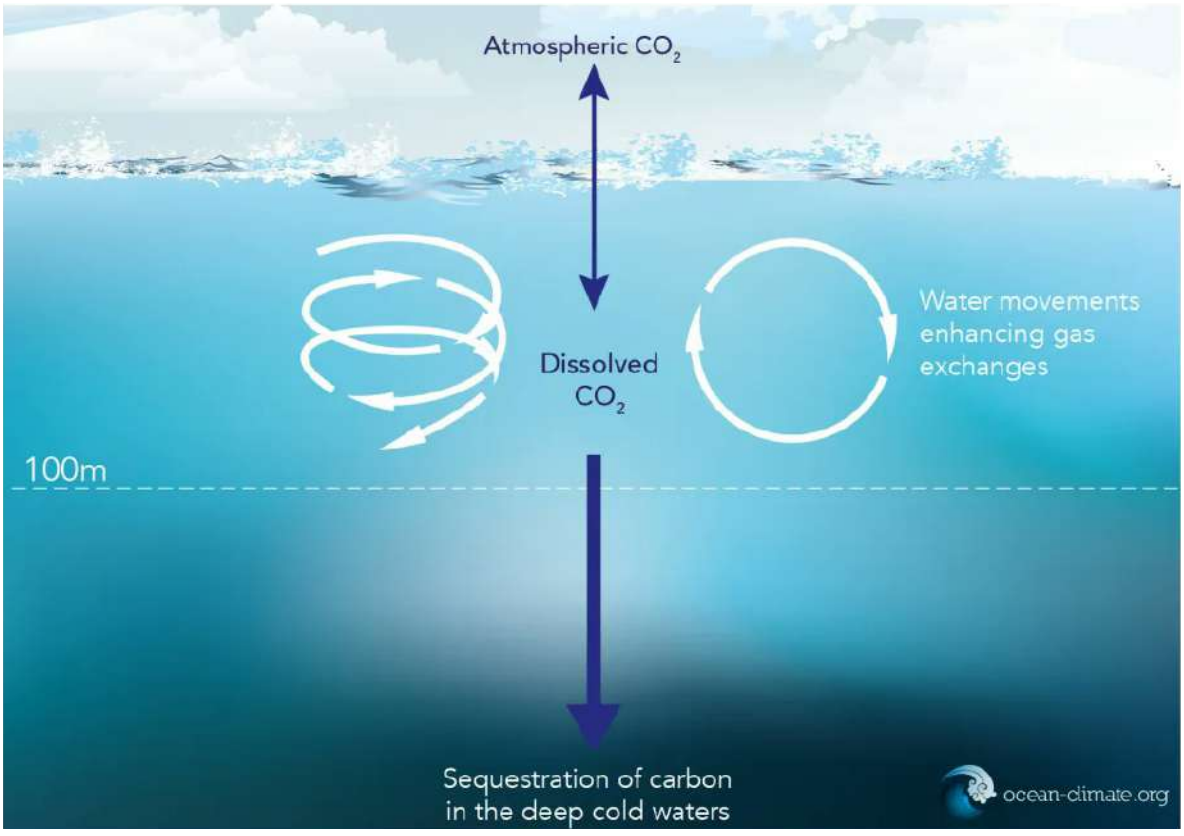


Source: ocean-climate.org.

In order to relate the carbon emissions $\mathcal{CE}(t)$ and the atmospheric temperature $\mathcal{T}_{\text{AT}}(t)$, the DICE model uses a reduced form of a general circulation model describing the evolution of GHG concentrations in three carbon-sink reservoirs: the atmosphere AT, the upper ocean UP and the deep (or lower) ocean LO. As we will see on page 1034, the ocean hold fifty times more $CO_2$ than the atmosphere. Indeed, a fraction of carbon from the atmosphere is absorbed by the upper ocean and transported by ocean circulation patterns. It is then stored in the deep ocean or re-radiated

from the upper ocean to the atmosphere influencing regional temperatures. The sequestration of carbon in the deep ocean depends on the temperature of cold waters, implying that a small part of the carbon stored in the deep ocean may return to the upper ocean. This physical carbon pump is illustrated in Figure 8.89. Taking into account this global heat transfer scheme, Nordhaus and Sztorc (2013) assume that the dynamics of carbon concentrations[107] are:

$$\begin{cases} \mathcal{CC}_{\text{AT}}(t) = \phi_{1,1}\mathcal{CC}_{\text{AT}}(t-1) + \phi_{1,2}\mathcal{CC}_{\text{UP}}(t-1) + \phi_1 \boldsymbol{\mathcal{CE}}(t) \\ \mathcal{CC}_{\text{UP}}(t) = \phi_{2,1}\mathcal{CC}_{\text{AT}}(t-1) + \phi_{2,2}\mathcal{CC}_{\text{UP}}(t-1) + \phi_{2,3}\mathcal{CC}_{\text{LO}}(t-1) \\ \mathcal{CC}_{\text{LO}}(t) = \phi_{3,2}\mathcal{CC}_{\text{UP}}(t-1) + \phi_{3,3}\mathcal{CC}_{\text{LO}}(t-1) \end{cases}$$

where $\phi_{i,j}$ represents the flow parameters between carbon-sink reservoirs[108], and $\phi_1$ is the mass percentage of carbon in $CO_2$. Let $\mathcal{CC} = (\mathcal{CC}_{\text{AT}}, \mathcal{CC}_{\text{UP}}, \mathcal{CC}_{\text{LO}})$ be the vector of the three-reservoir layers. The dynamics of $\mathcal{CC}$ is then a vector autoregressive process:

$$\mathcal{CC}(t) = \Phi_{\mathcal{CC}}\mathcal{CC}(t-1) + B_{\mathcal{CC}}\boldsymbol{\mathcal{CE}}(t) \tag{8.24}$$

where $B_{\mathcal{CC}} = (\phi_1, 0, 0)$ and:

$$\Phi_{\mathcal{CC}} = \begin{pmatrix} \phi_{1,1} & \phi_{1,2} & 0 \\ \phi_{2,1} & \phi_{2,2} & \phi_{3,2} \\ 0 & \phi_{3,2} & \phi_{3,3} \end{pmatrix}$$

The next step consists in linking accumulated carbon emissions in the atmosphere and global warming at the Earth's surface through increases in radiative forcing:

$$\mathcal{F}_{\text{RAD}}(t) = \frac{\eta}{\ln 2} \ln\left(\frac{\mathcal{CC}_{\text{AT}}(t)}{\mathcal{CC}_{\text{AT}}(1750)}\right) + \mathcal{F}_{\text{EX}}(t) \tag{8.25}$$

where $\mathcal{F}_{\text{RAD}}(t)$ is the change in total radiative forcing of GHG emissions since 1750 (expressed in $\text{W/m}^2$), $\eta$ is the temperature forcing parameter and $\mathcal{F}_{\text{EX}}(t)$ is the exogenous forcing. Finally, the climate system for temperatures is characterized by a two-layer system:

$$\begin{cases} \mathcal{T}_{\text{AT}}(t) = \mathcal{T}_{\text{AT}}(t-1) + \xi_1\left(\mathcal{F}_{\text{RAD}}(t) - \xi_2\mathcal{T}_{\text{AT}}(t-1) - \xi_3\left(\mathcal{T}_{\text{AT}}(t-1) - \mathcal{T}_{\text{LO}}(t-1)\right)\right) \\ \mathcal{T}_{\text{LO}}(t) = \mathcal{T}_{\text{LO}}(t-1) + \xi_4\left(\mathcal{T}_{\text{AT}}(t-1) - \mathcal{T}_{\text{LO}}(t-1)\right) \end{cases}$$

where $\mathcal{T}_{\text{AT}}(t)$ and $\mathcal{T}_{\text{LO}}(t)$ are respectively the mean surface temperature and the temperature of the deep ocean. This system of equations means that "*higher radiative forcing warms the atmospheric layer, which then warms the upper ocean, gradually warming the deep ocean*" (Nordhaus and Sztorc, 2013, page 17). The authors simplify the relationships by only considering a two-box model: the atmosphere and the upper ocean. According to Calel and Stainforth (2017a), $\xi_1$ measures the speed of adjustment parameter for atmospheric temperature, $\xi_2$ is the ratio of increased forcing from $CO_2$ doubling to the climate sensitivity, $\xi_3$ is the heat loss coefficient from atmosphere to oceans and $\xi_4$ is the heat gain coefficient by deep oceans. Let $\mathcal{T} = (\mathcal{T}_{\text{AT}}, \mathcal{T}_{\text{LO}})$ be the temperature vector. We have:

$$\mathcal{T}(t) = \Xi_{\mathcal{T}}\mathcal{T}(t-1) + B_{\mathcal{T}}\mathcal{F}_{\text{RAD}}(t) \tag{8.26}$$

where $B_{\mathcal{T}} = (\xi_1, 0)$ and:

$$\Xi_{\mathcal{T}} = \begin{pmatrix} 1 - \xi_1(\xi_2 + \xi_3) & \xi_1\xi_3 \\ \xi_4 & 1 - \xi_4 \end{pmatrix} = \begin{pmatrix} \xi'_{1,1} & \xi'_{1,2} \\ \xi'_{2,1} & \xi'_{2,2} \end{pmatrix}$$

[107] The carbon concentration is expressed in grams of carbon, and not in $gCO_2e$. The conversion is 12/44 or 0.2727 gC/g $CO_2$.

[108] By construction, we have $\sum_{i=1}^{3} \phi_{i,j} = 1$ for $j = 1, 2, 3$. $\phi_{i,i}$ is then the probability that a molecule remains in its carbon sink, while $\phi_{i,j}$ is the probability that a molecule stored in the carbon sink $j$ goes to the carbon sink $i$.

Box 8.17: Correspondence between DICE and the two-box model

We have previously seen that the two-box model of climate change is based on the heat diffusion between the atmosphere and the deep ocean:

$$\begin{cases} c_{\text{AT}} \dfrac{\mathrm{d}\mathcal{T}_{\text{AT}}(t)}{\mathrm{d}t} &= \mathcal{F}_{\text{RAD}}(t) - \lambda \mathcal{T}_{\text{AT}}(t) - \beta\left(\mathcal{T}_{\text{AT}}(t) - \mathcal{T}_{\text{LO}}(t)\right) \\ c_{\text{LO}} \dfrac{\mathcal{T}_{\text{LO}}(t)}{\mathrm{d}t} &= \beta\left(\mathcal{T}_{\text{AT}}(t) - \mathcal{T}_{\text{LO}}(t)\right) \end{cases}$$

where $c_{\text{AT}}$ is the effective heat capacity of the atmosphere (including the upper ocean and the land surface), $c_{\text{LO}}$is the effective heat capacity of the deep ocean, $\lambda$ is the feedback parameter and $\beta$ is the heat transfer coefficient between the upper and lower oceans. Using a forward Euler discretization, Calel and Stainforth (2017a) found that:

$$\begin{cases} \mathcal{T}_{\text{AT}}(t) &= \mathcal{T}_{\text{AT}}(t-1) + \dfrac{1}{c_{\text{AT}}}\left(\mathcal{F}_{\text{RAD}}(t-1) - \lambda \mathcal{T}_{\text{AT}}(t-1) - \right. \\ & \qquad \left. \beta\left(\mathcal{T}_{\text{AT}}(t-1) - \mathcal{T}_{\text{LO}}(t-1)\right)\right)\Delta t \\ \mathcal{T}_{\text{LO}}(t) &= \mathcal{T}_{\text{LO}}(t-1) + \dfrac{\beta}{c_{\text{LO}}}\left(\mathcal{T}_{\text{AT}}(t-1) - \mathcal{T}_{\text{LO}}(t-1)\right)\Delta t \end{cases}$$

where $\Delta t$ is the length of time step (expressed in seconds). Therefore, we have the following relationships[a]:

$$\begin{cases} \xi_1 = \dfrac{1}{c_{\text{AT}}}\Delta t \\ \xi_2 = \lambda \\ \xi_3 = \beta \\ \xi_4 = \dfrac{\beta}{c_{\text{LO}}}\Delta t \end{cases} \quad \text{and} \quad \begin{cases} \xi'_{1,1} = 1 - \dfrac{\lambda + \beta}{c_{\text{AT}}}\Delta t \\ \xi'_{1,2} = \dfrac{\beta}{c_{\text{AT}}}\Delta t \\ \xi'_{2,1} = \dfrac{\beta}{c_{\text{LO}}}\Delta t \\ \xi'_{2,2} = 1 - \dfrac{\beta}{c_{\text{LO}}}\Delta t \end{cases}$$

[a] Calel and Stainforth (2017a) noticed that the only difference is that the DICE model uses $\mathcal{F}_{\text{RAD}}(t)$ instead of $\mathcal{F}_{\text{RAD}}(t-1)$, which is not a problem if the time step is small.

Below, we report the parameter and initial values used by the 2013 version[109]:

- $t_0 = 2010$, $\Delta t = 5$ years;
- Equation (8.22): $\boldsymbol{\mathcal{CE}}(t_0) = 36.91$ $\text{GtCO}_2\text{e}$, $\mu(t_0) = 3.9\%$, $\sigma(t_0) = 0.5491$ $\text{GtCO}_2\text{e}/\$$ tn, $Y(t_0) = \$63.69$ tn, $\boldsymbol{\mathcal{CE}}_{\text{Industry}}(t_0) = 33.61$ $\text{GtCO}_2\text{e}$, $\delta_{\text{Land}} = 0.2$, and $\boldsymbol{\mathcal{CE}}_{\text{land}}(t_0) = 3.3$ $\text{GtCO}_2\text{e}$;
- Equation (8.23): $\sigma(t_0) = 0.5491$ $\text{GtCO}_2\text{e}/\$$ tn, $g_\sigma(t_0) = 1\%$ and $\delta_\sigma = 0.1\%$;
- Equation (8.24): $\mathcal{CC}_{\text{AT}}(t_0) = 830.4$, $\mathcal{CC}_{\text{UP}}(t_0) = 1\,527$, $\mathcal{CC}_{\text{LO}}(t_0) = 10\,010$, $\phi_1 = 0.2727$ $\text{gC}/\text{gCO}_2$, $\boldsymbol{\mathcal{CE}}(t_0) = 36.91$ $\text{GtCO}_2\text{e}$, and the carbon cycle diffusion matrix is equal to:

$$\Phi_{\mathcal{CC}} = \begin{pmatrix} 91.20\% & 3.83\% & 0 \\ 8.80\% & 95.92\% & 0.03\% \\ 0 & 0.25\% & 99.97\% \end{pmatrix}$$

[109] They can be found in Kellett *et al.* (2019, Table 2 & Appendices A and B).

- Equation (8.25): $\mathcal{F}_{\text{RAD}}(t_0) = 2.14$ W/m$^2$, $\eta = 3.8$ W/m$^2$, $\mathcal{CC}_{\text{AT}}(t_0) = 830.4$, $\mathcal{CC}_{\text{AT}}(1750) = 588$ GtC, $\mathcal{F}_{\text{EX}}(t)$ is the linear interpolation function between $\mathcal{F}_{\text{EX}}(t_0) = 0.25$ W/m$^2$ and $\mathcal{F}_{\text{EX}}(2100) = 0.70$ W/m$^2$ for $t \in [t_0, 2100]$, and is equal to $\mathcal{F}_{\text{EX}}(2100)$ for $t \geq 2100$;
- Equation (8.26): $\mathcal{T}_{\text{AT}}(t_0) = 0.8°$C, $\mathcal{T}_{\text{LO}}(t_0) = 0.0068°$C, $\xi_1 = 0.098$, $\mathcal{F}_{\text{RAD}}(t_0) = 2.14$ W/m$^2$, and the temperature diffusion matrix is given by[110]:

$$\Xi_{\mathcal{T}} = \begin{pmatrix} 86.30 & 0.8624 \\ 2.5 & 97.5 \end{pmatrix} \times 10^{-2}$$

From Equation (8.26), we can compute the steady-state temperatures:

$$\begin{aligned} \mathcal{T}(\infty) &= (I_2 - \Xi_{\mathcal{T}})^{-1} B_{\mathcal{T}} \mathcal{F}_{\text{RAD}}(\infty) \\ &= \frac{\mathcal{F}_{\text{RAD}}(\infty)}{\xi_2} \mathbf{1}_2 \\ &= \begin{pmatrix} 0.76316 \\ 0.76316 \end{pmatrix} \mathcal{F}_{\text{RAD}}(\infty) \end{aligned}$$

We deduce that:

$$\Delta\mathcal{T}_{\text{AT}}(\infty) = \frac{1}{\xi_2} \Delta\mathcal{F}_{\text{RAD}}(\infty) = 0.76316 \times \Delta\mathcal{F}_{\text{RAD}}(\infty)$$

A variation of $\pm 1$ W/m$^2$ implies a variation of $\pm 1°$C of the atmospheric temperature. Therefore, in order to limit global warming, we need to reduce radiative forcing and the carbon concentration $\mathcal{CC}_{\text{AT}}(t)$ in the atmosphere (Equation 8.25). This is done by emitting lower carbon emissions (Equation 8.24). In Figure 8.90, we show the impulse response analysis[111] by considering a reduction of one $GtCO_2e$. We notice that the carbon concentration in the atmosphere is reduced because the carbon is stored in the upper ocean and then in the deep ocean. To achieve carbon emissions reduction, we have three choices (Equation 8.22):

1. We can reduce the production $Y(t)$;
2. We can reduce the carbon intensity $\sigma(t)$ of industrial activities;
3. We can increase the mitigation effort $\mu(t)$ and accelerate the transition to a low-carbon economy;

In order to illustrate the climate module, we run Equations (8.22–8.26) with the parameter and initial values used by the 2013 version. For that, we need to define $Y(t)$ and $\mu(t)$, which are the two external variables of the temperature modeling system. By assuming that $Y(t) = Y(t_0)$ and $\mu(t) = \mu(t_0)$, we obtain the results in Table 8.31. If we consider the following functions $Y(t) = (1 + g_Y)^{t-t_0} Y(t_0)$ and $\mu(t) = \min\left(e^{g_\mu (t-t_0)} \mu(t_0), 1\right)$, the trajectories of $Y(t)$, $\mu(t)$, $\mathcal{T}_{\text{AT}}(t)$ and $\mathcal{T}_{\text{LO}}(t)$ those given in Figure 8.91. We observe that we can limit global warming if we limit the economic growth $g_Y$ or we dramatically increase the mitigation effort $\mu(t)$. The nightmare climate-economic scenario is obtained when the economic growth is high and there is no mitigation effort (Figure 8.92).

[110] We have $\xi_1 = 0.098$, $\xi_2 = 3.8/2.9$, $\xi_3 = 0.088$, and $\xi_4 = 0.025$ (Calel and Stainforth, 2017a, page 1203). The DICE model uses a 5-year time step. If we prefer to use $\Delta t = 1$ year, we have:

$$\Xi_{\mathcal{T}} = \begin{pmatrix} 97.2592 & 0.1725 \\ 0.5 & 99.5 \end{pmatrix} \times 10^{-2}$$

and $\xi_1 = 0.0196$ because $c_{\text{AT}} = 51.0204$, $c_{\text{LO}} = 17.6$, $\lambda = 1.3103$ and $\beta = 0.088$.

[111] Following Roncalli (2020a, page 646), the matrix of impulse responses after $t$ years is $\Phi_{\mathcal{CC}}^t$, while the matrix of cumulated responses is $I_3 + \sum_{k=1}^t \Phi_{\mathcal{CC}}^k$.

Figure 8.90: Impulse response analysis on carbon AT, LO, and UP concentrations ($\Delta\mathcal{CE} = -1$ GtCO$_2$e)

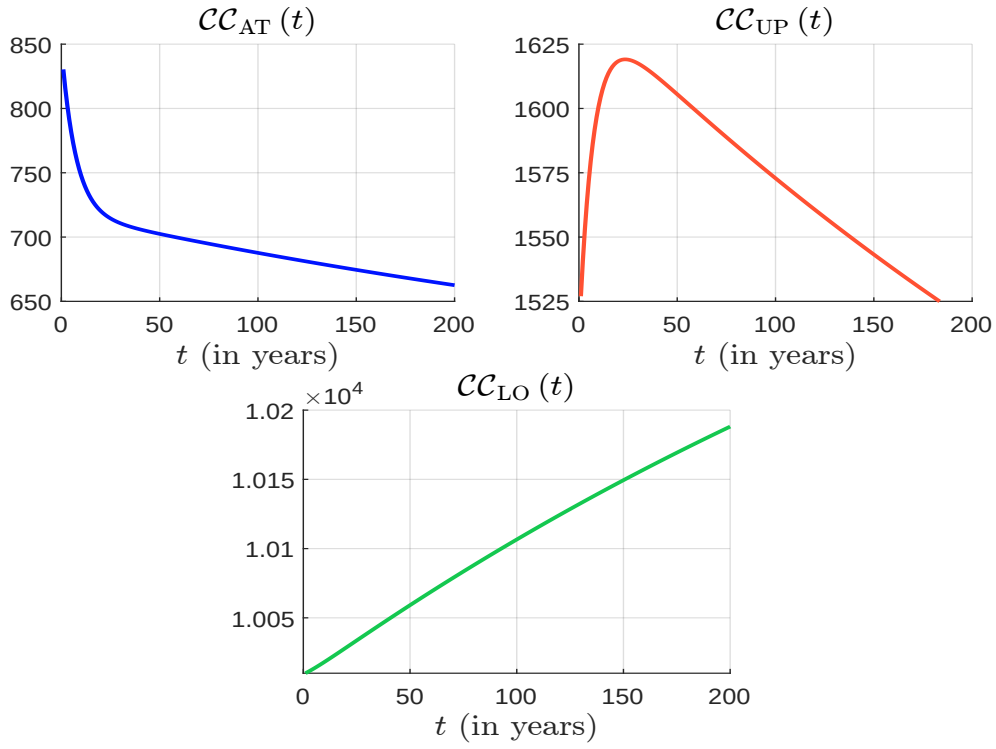


Table 8.31: Output of the DICE climate module ($Y(t) = Y(t_0)$, $\mu(t) = \mu(t_0)$)

| $t$ | $\mathcal{CE}(t)$ | $\sigma(t)$ | $\mathcal{CC}_{\text{AT}}(t)$ | $\mathcal{F}_{\text{RAD}}(t)$ | $\mathcal{T}_{\text{AT}}(t)$ | $\mathcal{T}_{\text{LO}}(t)$ |
|---|---|---|---|---|---|---|
| 2010 | 36.91 | 0.55 | 830.4 | 2.14 | 0.800 | 0.007 |
| 2015 | 36.25 | 0.55 | 825.7 | 2.14 | 0.900 | 0.027 |
| 2020 | 36.06 | 0.56 | 821.9 | 2.14 | 0.986 | 0.048 |
| 2025 | 35.97 | 0.57 | 818.9 | 2.14 | 1.061 | 0.072 |
| 2030 | 35.98 | 0.57 | 816.6 | 2.15 | 1.127 | 0.097 |
| 2035 | 36.05 | 0.58 | 814.9 | 2.16 | 1.186 | 0.122 |
| 2040 | 36.18 | 0.58 | 813.9 | 2.18 | 1.238 | 0.149 |
| 2045 | 36.36 | 0.59 | 813.3 | 2.20 | 1.286 | 0.176 |
| 2050 | 36.58 | 0.59 | 813.3 | 2.23 | 1.329 | 0.204 |
| 2055 | 36.82 | 0.60 | 813.6 | 2.26 | 1.370 | 0.232 |
| 2060 | 37.09 | 0.61 | 814.4 | 2.29 | 1.408 | 0.261 |
| 2065 | 37.39 | 0.61 | 815.4 | 2.32 | 1.445 | 0.289 |
| 2070 | 37.70 | 0.62 | 816.8 | 2.35 | 1.480 | 0.318 |
| 2075 | 38.02 | 0.62 | 818.4 | 2.39 | 1.514 | 0.347 |
| 2080 | 38.36 | 0.63 | 820.3 | 2.43 | 1.547 | 0.376 |
| 2085 | 38.71 | 0.64 | 822.4 | 2.46 | 1.580 | 0.406 |
| 2090 | 39.06 | 0.64 | 824.7 | 2.50 | 1.612 | 0.435 |
| 2095 | 39.43 | 0.65 | 827.1 | 2.55 | 1.645 | 0.464 |
| 2100 | 39.80 | 0.66 | 829.7 | 2.59 | 1.677 | 0.494 |

Figure 8.91: Simulation of the DICE climate module

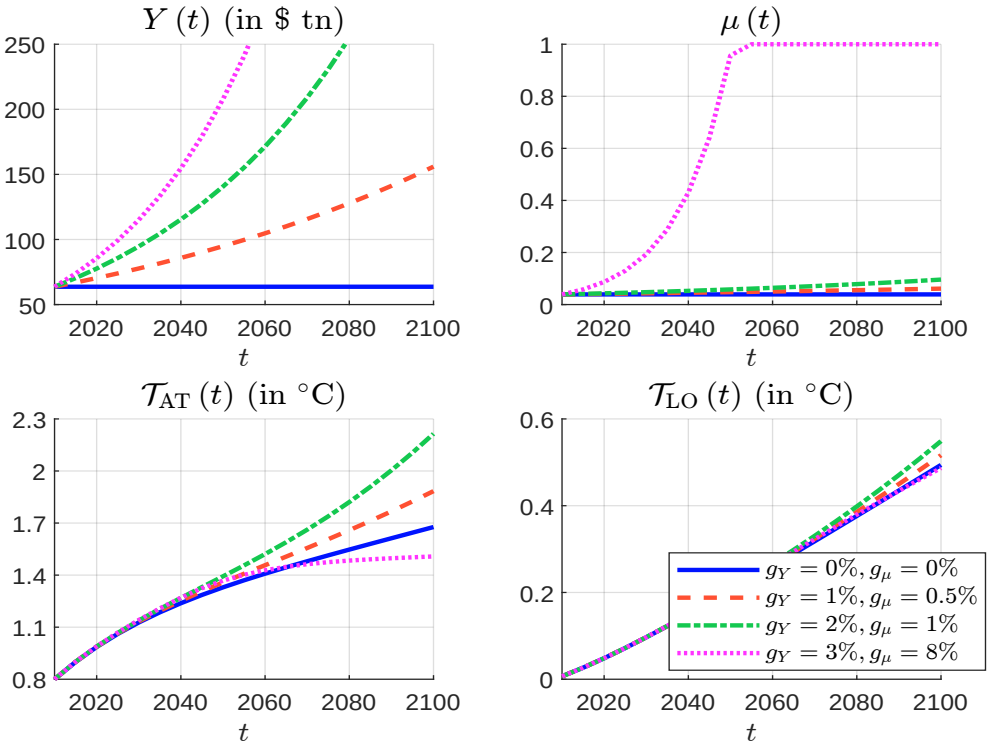


Figure 8.92: The nightmare climate-economic scenario ($g_Y = 0\%$, $\mu\,(t) = 0$)

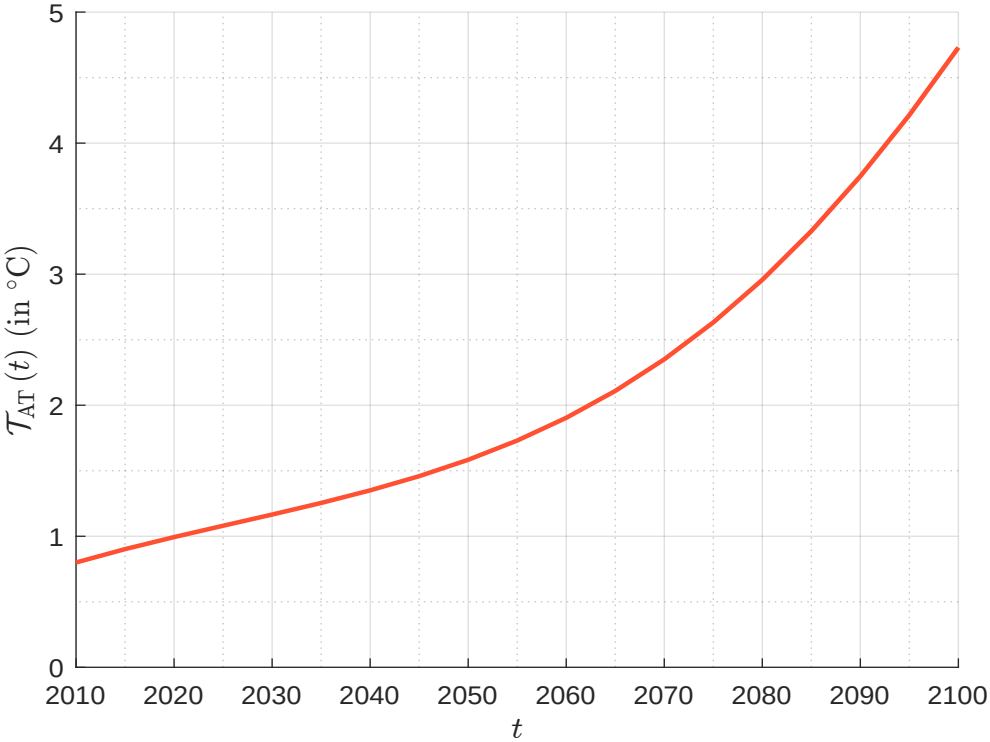

**Social welfare maximization** The last step of the DICE model is to define the social preferences and the objective function to optimize. The model assumes that the climate policy $\mu(t)$ is chosen to maximize the social welfare function $W$, which is the discounted sum of the generational utilities:

$$W(s(t), \mu(t)) = \sum_{t=t_0+1}^{T} \frac{L(t)\mathcal{U}(c(t))}{(1+\varrho)^{t-t_0}}$$

where $\varrho$ is the (generational) discount rate and $c(t) = C(t)/L(t)$ is the consumption per capita. $\mathcal{U}(c)$ is the CRRA utility function:

$$\mathcal{U}(c) = \frac{c^{1-\alpha} - 1}{1-\alpha}$$

where $\alpha \geq 0$ is the constant elasticity of marginal utility of consumption, which can be interpreted as the generational inequality aversion[112] in the context of the Ramsey-Cass-Koopmans model. When $\alpha$ is close to zero, there is low risk aversion to intergenerational inequality. When $\alpha$ is equal to one, the social welfare becomes egalitarian between generations. When $\alpha \to \infty$, we obtain an infinite total utility.

The optimal control problem is then given by:

$$\begin{aligned} (s^\star(t), \mu^\star(t)) &= \arg\max W(s(t), \mu(t)) \\ \text{s.t.} &\begin{cases} \text{Equations (8.19–8.26)} \\ \mu(t) \in [0,1] \\ s(t) \in [0,1] \end{cases} \end{aligned} \tag{8.27}$$

We reiterate that the optimization problem has two control variables: the saving rate $s(t)$ and the climate mitigation policy $\mu(t)$. The first control variable $s(t)$ is common to many economic models of optimal growth. It manages the substitution between the present consumption and the present investment, which determines the future consumption. The second control variable $\mu(t)$ is a new variable that manages the substitution between the present climate damages and the future climate damages. The two variables do not have the same status, because $s(t)$ is generally chosen by households, which is not the case of $\mu(t)$.

**Remark 86** *The 2013 version of the DICE model assumes that* $\alpha = 1.45$ *and* $\varrho = 1.5\%$.

### Social cost of carbon

Above, we have presented the mathematical objective function of the DICE model. Nevertheless, the final objective of the DICE model is not to estimate the optimal pathway of $\mu(t)$, which is a conceptual measure of the mitigation effort. The main goal is to compute the social cost of carbon, which is the central pillar in the cost benefit analysis of climate change policies:

> "*The most important single economic concept in the economics of climate change is the social cost of carbon (SCC). This term designates the economic cost caused by an additional tonne of carbon dioxide emissions or its equivalent. In a more precise definition, it is the change in the discounted value of economic welfare from an additional unit of COtwo-equivalent emissions. The SCC has become a central tool used in climate change policy, particularly in the determination of regulatory policies that involve greenhouse gas emissions.*" (Nordhaus, 2017a, page 1518).

[112] When $\alpha \to 1$, $\mathcal{U}(c) = \ln c$.

From a mathematical viewpoint, the social cost of carbon is then defined as:

$$\text{SCC}(t) = \frac{\dfrac{\partial W(t)}{\partial \mathcal{CE}(t)}}{\dfrac{\partial W(t)}{\partial C(t)}} = \frac{\partial C(t)}{\partial \mathcal{CE}(t)}$$

It is expressed in $\$/\text{tCO}_2$. This measure can be extended to other greenhouse gases. For instance, IWG (2021) also estimated this figure for the Methane and the Nitrous Oxide. They found a magnitude order of \$200 for $CO_2$, \$6 000 for $CH_4$, and \$70 000 for $N_2O$.

The DICE model can be applied to different scenarios. For instance, we can consider the baseline scenario ($\mu(t) = \mu(t_0)$), the optimal scenario (social welfare maximization) or the 2°C scenario ($\mathcal{T}_{\text{AT}}(t) \leq 2°\text{C}$). In Figures 8.93–8.96, we report the results found by Le Guenedal (2019) when we use the 2013 and 2016 versions of the model[113]. The difference between the two versions is mainly explained by the update of the parameter values (Kellett *et al.*, 2019, Table 2). With the 2013 version, the control variable $\mu(t)$ remains below one when considering the optimal scenario, the temperature $\mathcal{T}_{\text{AT}}(t)$ crosses 2°C around 2050 and the social cost of carbon is less than \$150 (Figure 8.93). With the 2016 version, the optimal scenario is a little bit different since we need to make more efforts in terms of mitigation and the SCC in greater than \$150 after 2050 (Figure 8.95). The 2°C scenario implies higher values of $\mu(t)$ and $\text{SCC}(t)$ for the 2013 version (Figure 8.94). Unfortunately, we observe that this scenario is no longer feasible with the 2016 version[114] (Figure 8.96).

Table 8.32: Global SCC under different scenario assumptions (in $\$/\text{tCO}_2$)

| Scenario | 2015 | 2020 | 2025 | 2030 | 2050 | CAGR |
|---|---|---|---|---|---|---|
| Baseline | 31.2 | 37.3 | 44.0 | 51.6 | 102.5 | 3.46% |
| Optimal | 30.7 | 36.7 | 43.5 | 51.2 | 103.6 | 3.54% |
| 2.5°C-max | 184.4 | 229.1 | 284.1 | 351.0 | 1 006.2 | 4.97% |
| 2.5°C-mean | 106.7 | 133.1 | 165.1 | 203.7 | 543.3 | 4.76% |

Source: Nordhaus (2017a, Table 1, page 1520).

In table 8.32, we report the SCC estimated for standard DICE models computed by Nordhaus (2017a). The baseline scenario corresponds to the current policy, while the optimal scenario is the given by the optimized control path (Equation 8.27). Under the baseline scenario assumption, the SCC value is $\$31.2/\text{tCO}_2$ in 2015 and reaches $\$102.5/\text{tCO}_2$ in 2050, implying a compound annual growth rate of 3.46%. The optimal scenario gives SCC figures that are very close to the baseline scenario. Nordhaus (2017a) also evaluated two alternative scenarios: the 2.5°C-max scenario constraints the temperature to be below 2.5°C, whereas the 2.5°C-mean imposes an average temperature of 2.5°C for the next 100 years. The impact of these two alternative scenarios is significant. In this case, the social cost of carbon can reach the value $\$1\,000/\text{tCO}_2$ in 2050.

**Remark 87** *The social cost of carbon is also known as the carbon tax, the carbon price or the shadow price of carbon emissions. Since it is one of the main policy tools to manage the transition risk, it will be extensively studied in Chapter 10.*

[113] These simulations are computed with the Matlab implementation of MPC-DICE, which replicates the functionality of the DICE-2013R/2016R model (Faulwasser *et al.*, 2018). The source code is available at `https://github.com/cmkellett/MPC-DICE`. These results can also be generated using the two other Maltab implementations provided by Kellett *et al.* (2016) and Lemoine (2020).

[114] See Nordhaus (2017b, page 17).

Figure 8.93: Optimal welfare scenario (DICE 2013R)

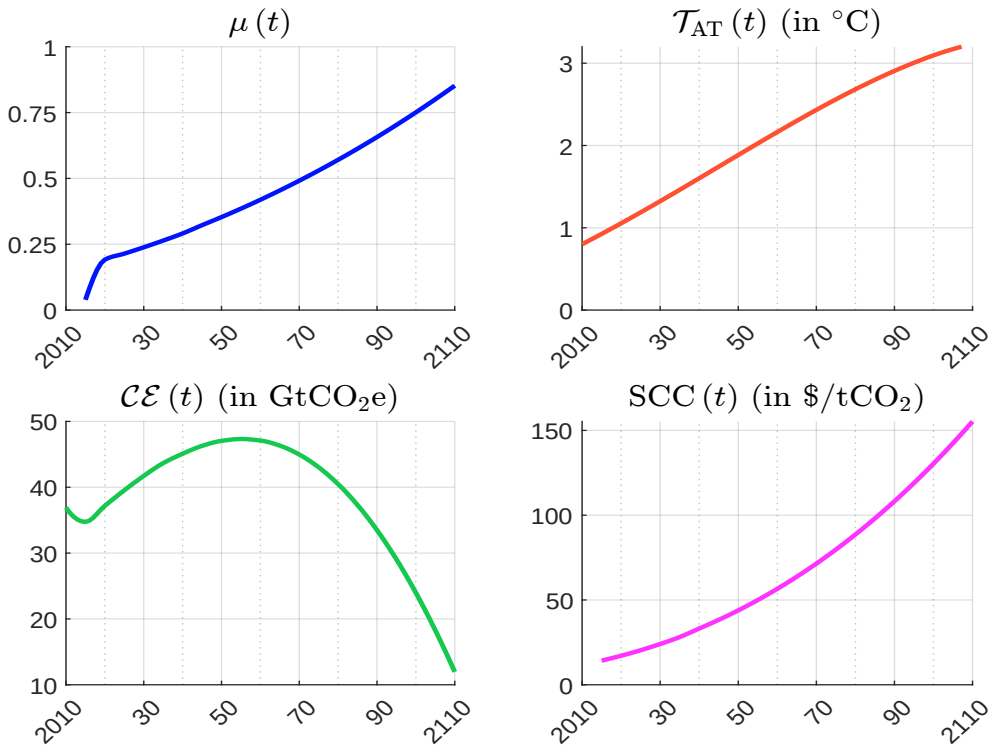


Source: Le Guenedal (2019).

Figure 8.94: 2°C scenario (DICE 2013R)

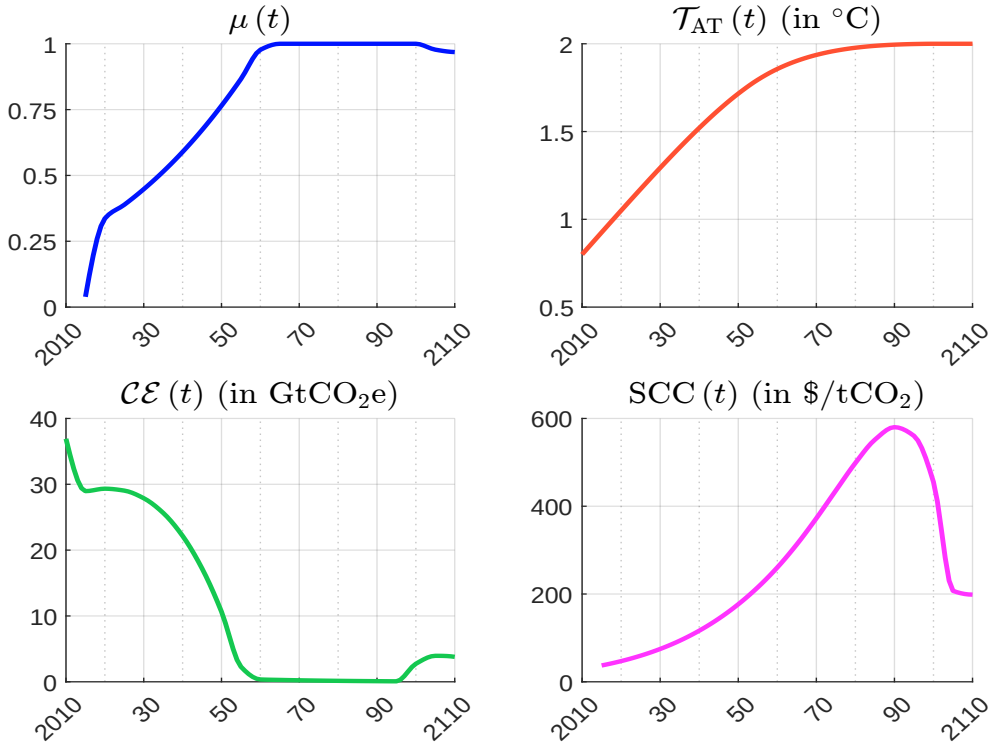


Source: Le Guenedal (2019).

Figure 8.95: Optimal welfare scenario (DICE 2016R)

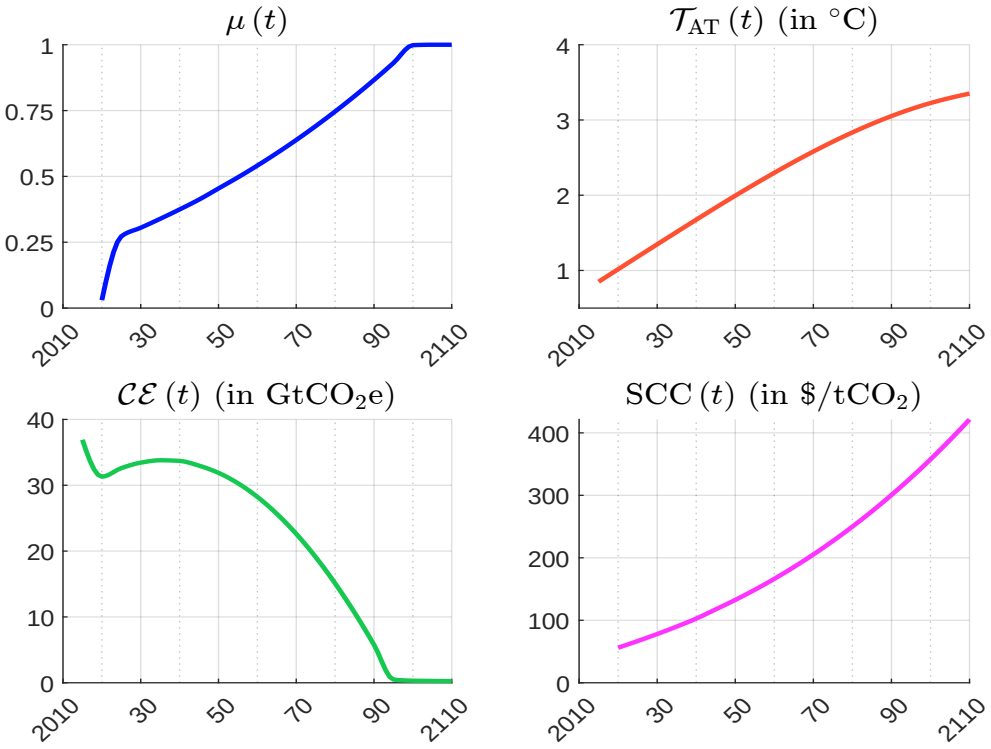


Source: Le Guenedal (2019).

Figure 8.96: 2°C scenario (DICE 2016R)

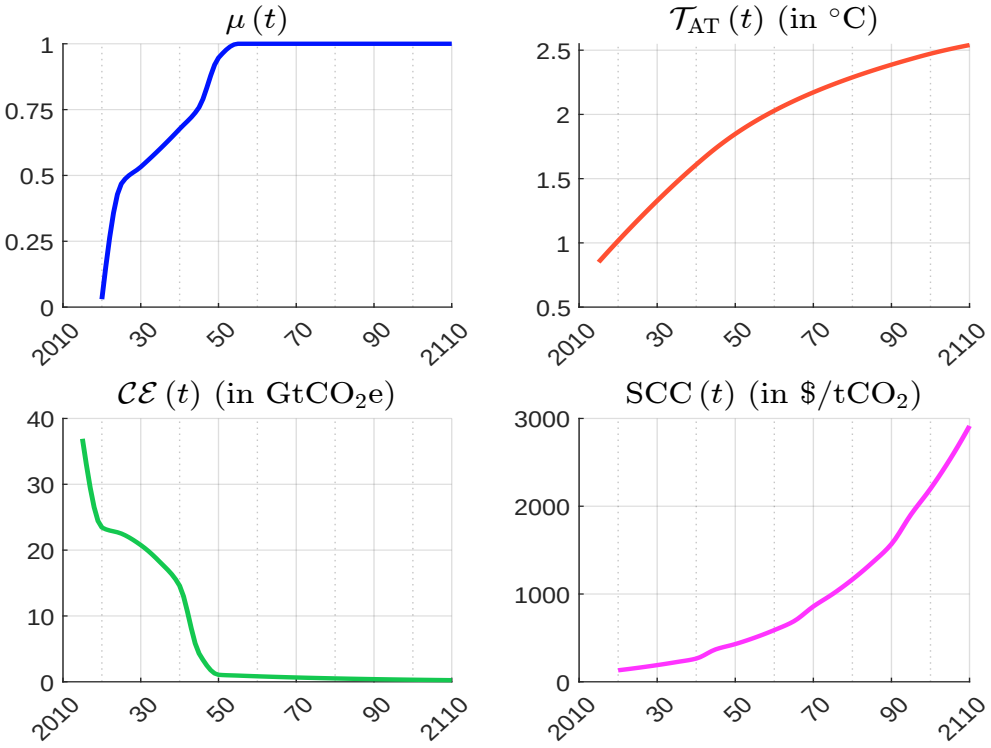


Source: Le Guenedal (2019).

### The Stern-Nordhaus controversy

In 2007, Nicholas Stern published a report called *The Economics of Climate Change: The Stern Review,* that was commissioned by the British government (Stern, 2007). The Stern Review called for sharp and immediate action to stabilize greenhouse gases because "*the benefits of strong, early action on climate change outweighs the costs.*" According to Weitzman (2007), the analysis supporting this conclusion is based on two main arguments. The first one concerns the high value of the discount rate, which is used by IAMs and the DICE model. The second argument is more ethical and related to the large uncertainty about the future of the world. Therefore, the Stern Review proposes to use $\varrho = 0.10\%$. The publication of the book has created turmoil in the scientific community, and many economists have participated to the debate. For instance, we can find dozens of reviews and critiques of the Stern Review that have been published in academic journals (*Journal of Economic Literature*, *Science*, *Energy Policy*, *Climate Change*, etc.).

Figure 8.97: Discounted value of \$10

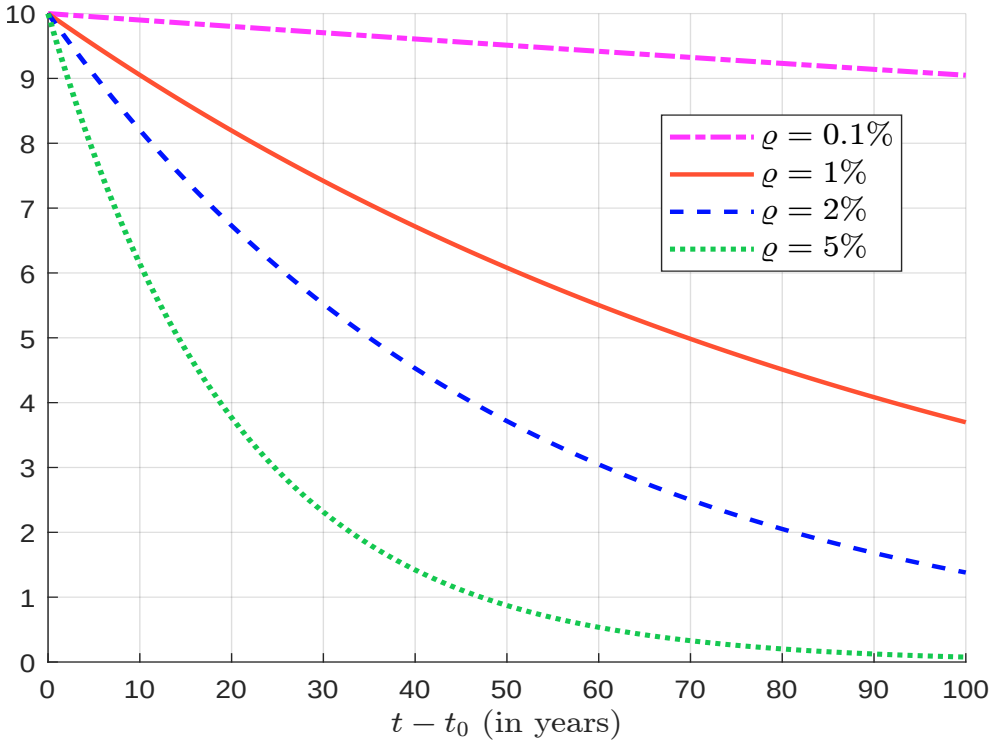


In order to illustrate the impact of $\varrho$, we report the discounted value of \$100 in Figure 8.97. Since the time horizon of the economic analysis is relatively long (greater or equal to 100 years), we obtain very different discounted values. For instance, if $\varrho$ is equal to 2% (or 0.1%), the well-being of someone 100yr from now would be valued 86% (or 10%) less than the well-being of someone living today (Hänsel *et al.*, 2020). In this context, it is obvious that $\varrho$ is certainly the most important parameter when computing the social cost of carbon.

The time (or generational) discount rate $\varrho$ used in the DICE model is also called the pure rate of time preference and is related to the Ramsey rule[115]:

$$r = \varrho + \alpha g_c$$

[115] See Box 8.18.

Box 8.18: The Ramsey rule

We consider the optimization problem[a]:

$$\begin{aligned} v\left(k\left(t\right)\right) &= \max_{c(t)} \int_0^\infty e^{-\varrho t} \boldsymbol{\mathcal{U}}\left(c\left(t\right)\right) \mathrm{d}t \\ &\text{s.t.} \quad \mathrm{d}k\left(t\right) = rk\left(t\right) \mathrm{d}t - c\left(t\right) \mathrm{d}t \end{aligned}$$

where $c\left(t\right) = C\left(t\right)/L\left(t\right)$ and $k\left(t\right) = K\left(t\right)/L\left(t\right)$ are the per capita consumption and capital, and $r$ is the real interest rate. The Bellman equation is:

$$\max_{c(t)} \left\{ \boldsymbol{\mathcal{U}}\left(c\left(t\right)\right) - \varrho v\left(k\left(t\right)\right) + \frac{\partial v\left(k\left(t\right)\right)}{\partial k}\left(rk\left(t\right) - c\left(t\right)\right) \right\} = 0$$

or:

$$\varrho v\left(k\left(t\right)\right) = \max_{c(t)} \left\{ \boldsymbol{\mathcal{U}}\left(c\left(t\right)\right) - v'\left(k\left(t\right)\right) c\left(t\right) \right\} + rk\left(t\right) v'\left(k\left(t\right)\right)$$

If we assume that the utility function is CRRA — $\boldsymbol{\mathcal{U}}\left(c\right) = c^{1-\alpha}/\left(1-\alpha\right)$, we obtain:

$$\max_{c} \left\{ \boldsymbol{\mathcal{U}}\left(c\right) - v'\left(k\right) c \right\} \Leftrightarrow v'\left(k\right) = \boldsymbol{\mathcal{U}}'\left(c\right) = c^{-\alpha}$$

implying that $c = v'\left(k\right)^{-1/\alpha}$ and:

$$\max_{c} \left\{ \boldsymbol{\mathcal{U}}\left(c\right) - v'\left(k\right) c \right\} = \frac{c^{1-\alpha}}{1-\alpha} - c^{1-\alpha} = \frac{\alpha}{1-\alpha} c^{1-\alpha} = \frac{\alpha}{1-\alpha} v'\left(k\right)^{-(1-\alpha)/\alpha}$$

The Bellman equation becomes then:

$$\varrho v\left(k\right) = \frac{\alpha}{1-\alpha} v'\left(k\right)^{-(1-\alpha)/\alpha} + rkv'\left(k\right)$$

We can verify that the optimal solution of the previous equation has the following expression:

$$v^\star\left(k\left(t\right)\right) = \left(\frac{\varrho - r\left(1-\alpha\right)}{\alpha}\right)^{-\alpha} \frac{k\left(t\right)^{1-\alpha}}{1-\alpha}$$

The optimal consumption is then equal to:

$$c^\star\left(t\right) = \left(\frac{\partial v^\star\left(k\left(t\right)\right)}{\partial k}\right)^{-1/\alpha} = \frac{\varrho - r\left(1-\alpha\right)}{\alpha} k\left(t\right)$$

It follows that:

$$\mathrm{d}k^\star\left(t\right) = rk^\star\left(t\right) \mathrm{d}t - c^\star\left(t\right) \mathrm{d}t = \left(r - \frac{\varrho - r\left(1-\alpha\right)}{\alpha}\right) k^\star\left(t\right) \mathrm{d}t = \underbrace{\frac{r-\varrho}{\alpha}}_{g_k} k^\star\left(t\right) \mathrm{d}t$$

In the Ramsey model, the optimal growth of capital is also equal to the optimal growth of consumption ($g_k = g_c$). Finally, we obtain the Ramsey rule:

$$g_c = \frac{\partial_t c\left(t\right)}{c\left(t\right)} = \frac{r-\varrho}{\alpha}$$

[a] This derivation of the Ramsey rule has been suggested by Peter Tankov.

where $r$ is the real interest rate, $g_c = \partial c(t)/c(t)$ is the growth rate of per capita consumption, and $\alpha$ is the consumption elasticity of the utility function (or the elasticity of substitution)[116]. The Ramsey rule can be interpreted as a condition for the optimality of intertemporal consumption choice. Therefore, $r$ can be interpreted as the consumption discount rate, *the social discount rate* or *the discount rate on goods* (Nordhaus, 2019). There are then two ways to use the Ramsey rule. From the previous relationship, we can deduce the optimal value of $\varrho$ from the historical estimates of $r$ and $g_C$: $\varrho = r - \alpha g_c$. For example, if the real interest rate is equal to 4%, $g_c = 2\%$ and $\alpha = 1$, we obtain $\varrho = 2\%$. Nordhaus (2019) justified the historical (or descriptive) approach as follows:

> "*This approach assumes that investments to slow climate change must compete with investments in other areas. The benchmark should therefore reflect the opportunity cost of investment. The descriptive approach yields a market rate of return in the neighborhood of 5% per year when risks are appropriately included.*"

According to Nordhaus (2007), the assumption $\varrho = 0.10\%$ is not consistent with historical observations, because this implies a low goods discount rate, around 1% per year, while the descriptive approach yields a market rate of return in the neighborhood of 5% per year. The first approach contrasts with the normative (or prescriptive) approach, which consists in fixing directly $\varrho$ for ethical reasons. This is the position of Stern and Taylor (2007), who claims that there are "*many reasons for thinking that market rates and other approaches that illustrate observable market behavior cannot be seen as reflections of an ethical response to the issues at hand. There is no real economic market that reveals our ethical decisions on how we should act together on environmental issues in the very long term. Most long-term capital markets are very thin and imperfect.*" In fact, as shown by Gollier (2010, 2013), the Ramsey rule is not always valid when the uncertainty on economic growth is high. In particular, there is no reason to use the same rate to discount environmental impacts and monetary benefits.

Table 8.33: Global SCC under different discount rate assumptions

| Discount rate | 2015 | 2020 | 2025 | 2030 | 2050 | CAGR |
|---|---|---|---|---|---|---|
| Stern | 197.4 | 266.5 | 324.6 | 376.2 | 629.2 | 3.37% |
| Nordhaus | 30.7 | 36.7 | 43.5 | 51.2 | 103.6 | 3.54% |
| 2.5% | 128.5 | 140.0 | 152.0 | 164.6 | 235.7 | 1.75% |
| 3% | 79.1 | 87.3 | 95.9 | 104.9 | 156.6 | 1.97% |
| 4% | 36.3 | 40.9 | 45.8 | 51.1 | 81.7 | 2.34% |
| 5% | 19.7 | 22.6 | 25.7 | 29.1 | 49.2 | 2.65% |

Source: Nordhaus (2017a, Table 1, page 1520).

In Table 8.33, we report the estimated values of SCC, which was obtained by Nordhaus (2017a) under different discount rate assumptions. We better understand the call for sharp and immediate action by Nicholas Stern, since the social cost of carbon was equal to \$197.4/tCO$_2$ in 2015 when the discount rate is set to 0.1%!

[116] Hänsel *et al.* (2020, page 783) interpret the parameter $\alpha$ as measuring intertemporal inequality aversion:

> "*Due to diminishing marginal utility, the idea is that an additional \$1 is worth more to a poor person than to a rich one. In a growing economy, citizens in the future will be richer and their lower marginal utility motivates discounting. Suppose the economy grows at 2%. People living in 100yr will be seven times richer. If inequality aversion is the only reason for discounting, if $\alpha = 1$ (or 1.45), which corresponds to the values of the median expert (Nordhaus), the value of \$1 in 100yr is only 14 (or 6) cents.*"

### 8.3.2 Other models

In Table 8.34, we report a short list of IAMs. For instance, Grubb *et al.* (2021) counts 28 major climate economic models[117]. They make the distinction between stylized simple IAMs and complex IAMs. While the purpose of the first category is focused on the optimal path of the economy based on policy optimization, the second category generally aims to evaluate the impact of a climate scenario or a given policy on the economy.

Table 8.34: Main integrated assessment models

| Model | Reference | Name |
|---|---|---|
| Stylized simple models | | |
| DICE | Nordhaus and Sztorc (2013) | Dynamic Integrated Climate-Economy |
| FUND | Anthoff and Tol (2014) | Climate Framework for Uncertainty, Negotiation and Distribution |
| PAGE | Hope (2011) | Policy Analysis of the Greenhouse Effect |
| Complex models | | |
| AIM/CGE | Fujimori *et al.* (2017) | Asia-Pacific Integrated Model/Computable General Equilibrium |
| GCAM | Calvin *et al.* (2019) | Global Change Assessment Model |
| GLOBIOM | Havlìk *et al.* (2018) | Global Biosphere Management Model |
| IMACLIM-R | Sassi *et al.* (2010) | Integrated Model to Assess Climate Change |
| IMAGE | Stehfest *et al.* (2014) | Integrated Model to Assess the Greenhouse Effect |
| MAGICC | Meinshausen *et al.* (2011) | Model for the Assessment of Greenhouse Gas Induced Climate Change |
| MAgPIE | Dietrich *et al.* (2019) | Model of Agricultural Production and its Impact on the Environment |
| MESSAGEix | Huppmann *et al.* (2019) | Model for Energy Supply Strategy Alternatives and their General Environmental Impact |
| REMIND | Aboumahboub *et al.* (2020) | REgional Model of INvestments and Development |
| WITCH | Bosetti *et al.* (2006) | World Induced Technical Change Hybrid |

Source: Grubb *et al.* (2021, Table A1, pages 24-26) & Author's research.

The FUND model is available at `www.fund-model.org`. A `Julia` implementation can be found at `https://github.com/fund-model/MimiFUND.jl`. The PAGE model requires Microsoft Excel and the `@RISK` Excel plug-in, but Moore *et al.* (2018) propose a `Julia` open-source implementation at `https://github.com/anthofflab/MimiPAGE2009.jl` and `http://anthofflab.berkeley.edu/MimiPAGE2009.jl/stable`. The AIM/CGE is hosted at `www-iam.nies.go.jp/aim/index.html`. The GCAM model is available at `http://jgcri.github.io/gcam-doc/index.html` (documentation and open-source code). GLOBIOM has been developed using `GAMS`[118]. The source code is not available, but a graphical user interface and a R interface is provided at `https://iiasa.`

[117] A more exhaustive list can be found in `www.iamcdocumentation.eu`, where a reference card is provided for each model.

[118] `GAMS` (General Algebraic Modeling System) is a high level modeling system for mathematical programming and optimization. It consists of a language compiler and a range of optimizer solvers, and requires a user license to be used (`www.gams.com`).

github.io/GLOBIOM. IMACLIM-R is not public. This is also the case of IMAGE, but we can download many data items, such as SSP scenario data, spatial data global land-use maps, scenario results and renewable energy data (www.pbl.nl/en/image/about-image). A compiled version of MAGGIC can be download at https://magicc.org. An online version is also available at https://live.magicc.org. The documentation of MAgPIE can be found at www.pik-potsdam.de/en/institute/departments/activities/land-use-modelling/magpie, while the link https://github.com/magpiemodel/magpie contains the model code and the R implementation. For MESSAGEix, the documentation is available at https://docs.messageix.org/en/stable, while the python programs can be found at https://github.com/iiasa/message_ix. The documentation of REMIND can be found at www.pik-potsdam.de/en/institute/departments/transformation-pathways/models/remind, while the link https://github.com/remindmodel/remind contains the R implementation. Finally, the website www.witchmodel.org is dedicated to the WITCH model. The code is open-source (https://github.com/witch-team/witchmodel), but requires a GAMS license.

### Stylized IAMs

Stylized integrated assessment models use the same structure as DICE (Figure 8.98). The FUND model has five main components: (1) population, production and income, (2) emissions, abatements and costs, (3) atmosphere and climate, (4) impacts (agriculture, forestry, water resources, energy consumption, sea level rise, ecosystems, human health, extreme weather, mortality), (5) optimization of the utility function, where the social welfare if a mixture of per capita income, damage of climate change and air pollution, and emission reduction costs Tol (1997). It also considers 16 regions. For its part, PAGE has two main modules (Hope, 2011; Moore *et al.*, 2018). Like the DICE model, the climate sensitivity is derived from a stylized GCM, but it explicitly introduces a sea level rise component and also considers $CH_4$ and $N_2O$ forcing cycles, and not only the $CO_2$ cycle[119]. The economic module has four components: (1) population, production and income, (2) damage costs, (3) climate policy action and (4) consumption utility maximization. It is also possible to perform a regional analysis[120].

Figure 8.98: Stylized integrated assessment models

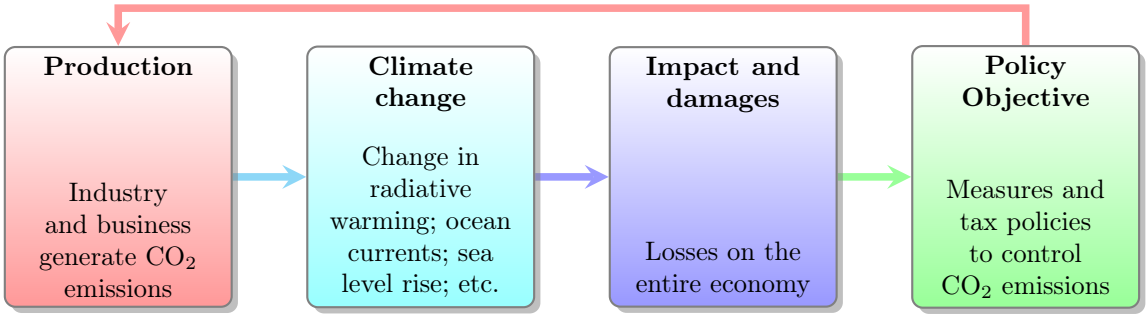


A comprehensive comparison of DICE, FUND and PAGE can be found in Diaz and Moore (2017a,b), and Rose *et al.* (2017a,b). It appears that parameter values and functional forms are not always the same (Diaz and Moore (2017a, Table 1, page 776), Rose *et al.* (2017b, Table S2, pages 2-5)), and damage estimates projected by the three models are dramatically different (Diaz

[119] We also find these additions in the FUND model

[120] The default regions are Africa, China, Europe, Latin America, other OECD countries, Russia, South-East Asia and the United States.

Figure 8.99: Histogram of the 150 000 US Government SCC estimates for 2020 with a 3% discount rate

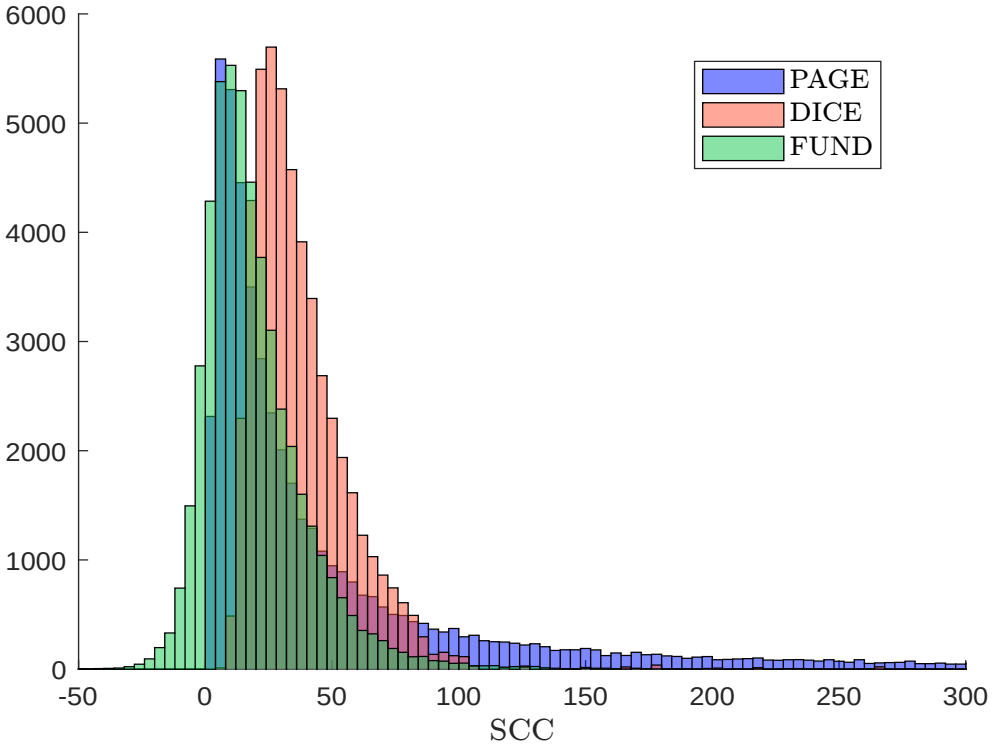


The figure combines the 50 000 2020 3% discount rate estimates from each of the three US Government models to illustrate their influence on the aggregate histogram that determines the official USG SCC for 2020 at 3%, which is equal to $42 (average) and $123 (95th percentile).

Source: (Rose *et al.*, 2017a, page 3).

and Moore, 2017a, Figure 2, page 777). In this context, the social cost of carbone reaches different levels depending on the model (Figure 8.99). In particular, Rose *et al.* (2017a) confirmed the ordering/raking PAGE $\succ$ DICE $\succ$ FUND that most academic studies have found when computing the social cost of carbon:

> "*We find significant variation in component-level behavior between models driven by model-specific structural and implementation elements, some resulting in artificial differences in results. These elements combine to produce model-specific tendencies in climate and damage responses that contribute to differences observed in SCC outcomes — producing PAGE SCC distributions with longer and fatter right tails and higher averages, followed by DICE with more compact distributions and lower averages, and FUND with distributions that include net benefits and the lowest averages.*" (Rose *et al.*, 2017a, page 1).

The previous stylized models have inspired many research projects and IAMs. This is especially true for DICE. For instance, the RESPONSE model of Pottier *et al.* (2015) and the ENTICE model of Popp (2004) are two variants of DICE. We can also mention the RICE model developed by Nordhaus and Yang (1996), which is a regional extension of the DICE framework with 12 regions. The RICE model introduces an important feature, which is the use of Negishi welfare weights with multiple countries. Those weights are given by the relationship $\omega_k(t) \propto 1/\mathcal{U}'(c_k(t))$ where $k$ is the

country index. In the case of the CRRA utility function $\boldsymbol{\mathcal{U}}(c) = c^{1-\alpha}/(1-\alpha)$, we obtain:

$$\omega_k(t) = \frac{c_k(t)^\alpha}{\sum_{k'=1}^{n_C} c_{k'}(t)^\alpha}$$

where $n_C$ is the number of countries. Then, the social welfare function becomes:

$$W(s_1(t), \ldots, s_{n_C}(t), \mu_1(t), \ldots, \mu_{n_C}(t),) = \sum_{k=1}^{n_C} \sum_{t=t_0+1}^{T} \omega_k(t) \frac{L_k(t) \boldsymbol{\mathcal{U}}(c_k(t))}{(1+\varrho_k)^{t-t_0}}$$

Negishi welfare weights are generally used to find a market equilibrium by optimising the weighted objective function (or Negishi social welfare function). However, these weights have been criticized to be inequitable, since the current wealth distribution would change. For instance, Stanton (2011) pointed out that the choice of weights are related to the regional inequality issue:

> "*In a global climate policy debate fraught with differing understandings of right and wrong, the importance of making transparent the ethical assumptions used in climate-economics models cannot be overestimated. [...] Negishi weights freeze the current distribution of income between world regions; without this constraint, IAMs that maximize global welfare would recommend an equalization of income across regions as part of their policy advice. With Negishi weights in place, these models instead recommend a course of action that would be optimal only in a world in which global income redistribution cannot and will not take place.*"

This question of regional inequality is central when considering climate change and the transition risk. For instance, Dennig *et al.* (2015) choose $\omega_k(t) = 1$ in their Nested Inequalities Climate-Economy (NICE) model, which is a direct extension of RICE, because they restrict consumption redistribution between regions.

### Complex IAMs

As their name suggest, complex IAMs are complex. While stylized simple IAMs are generally developed by one or two academics, complex IAMs are built by an institution with a big research team and are continuously improved and updated[121]. For that reason, it seems a pointless exercise to present one of them in details. For instance, GCAM has been developed at Pacific Northwest National Laboratory for over 30 years. The source code is today about 120 Mo, there are 910 CSV data files for a total of 230 Mo. Therefore, it is better to understand how they work and how they can be used. In Figure 8.100, we have reported the global structure of GCAM. In this type of complex models, the economic component is a small part of the structure. Furthermore, these big complex models are generally split into elementary complex models. In Figure 8.101, we have reported the structure of GLOBIOM. This model is specialized in agriculture, bioenergy and forestry. This model can communicate with MESSAGEix and other models as shown in Figure 8.102. With GCAM and MESSAGE, REMIND is another key complex IAM (Figure 8.103). Again, we notice that REMIND can be connected with MAgPIE, which is specialized in the land use. We also remark that it can take

[121] AIM/CGE, IMAGE, GCAM, IMACLIM-R, MESSAGE-GLOBIOM, REMIND-MAgPIE, WITCH are respectively hosted by the National Institute for Environmental Studies (NIES, Japan), the PBL Environmental Assessment Agency (Netherlands), the Pacific Northwest National Laboratory (PNNL, US), the Centre international de recherche sur l'environnement et le développement (CIRED, France), the International Institute for Applied Systems Analysis (IIASA, Austria), the Potsdam Institute for Climate Impact Research (PIK, Germany) and the European Institute on Economics and the Environment (RFF-CMCC-EIEE, Italy).

Figure 8.100: Linkages between the major systems in GCAM

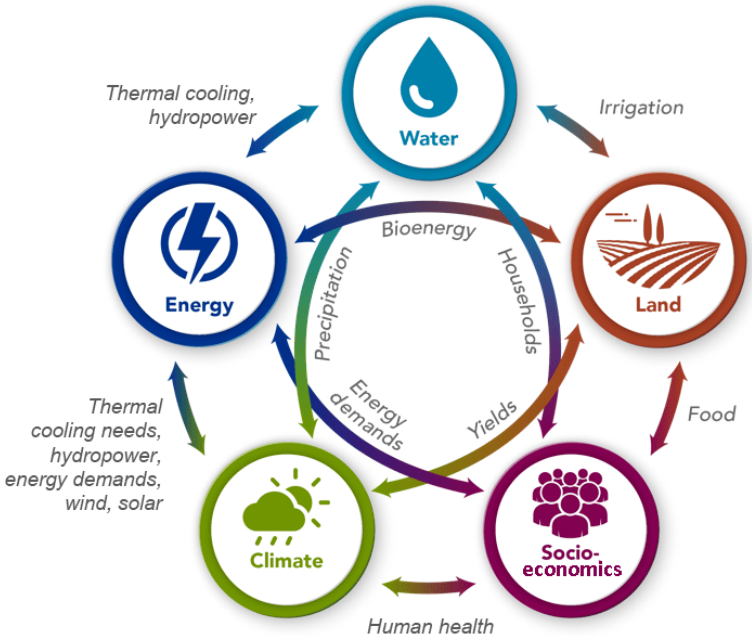


Source: Calvin *et al.* (2019).

Figure 8.101: The main land-use sectors of GLOBIOM

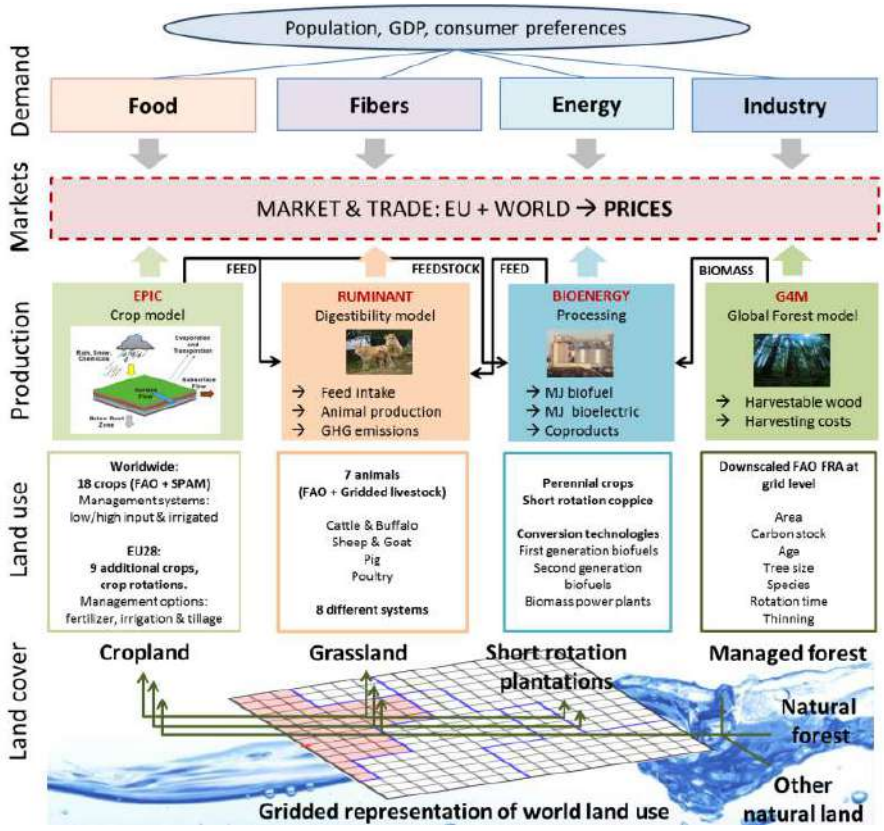


Source: https://iiasa.github.io/GLOBIOM.

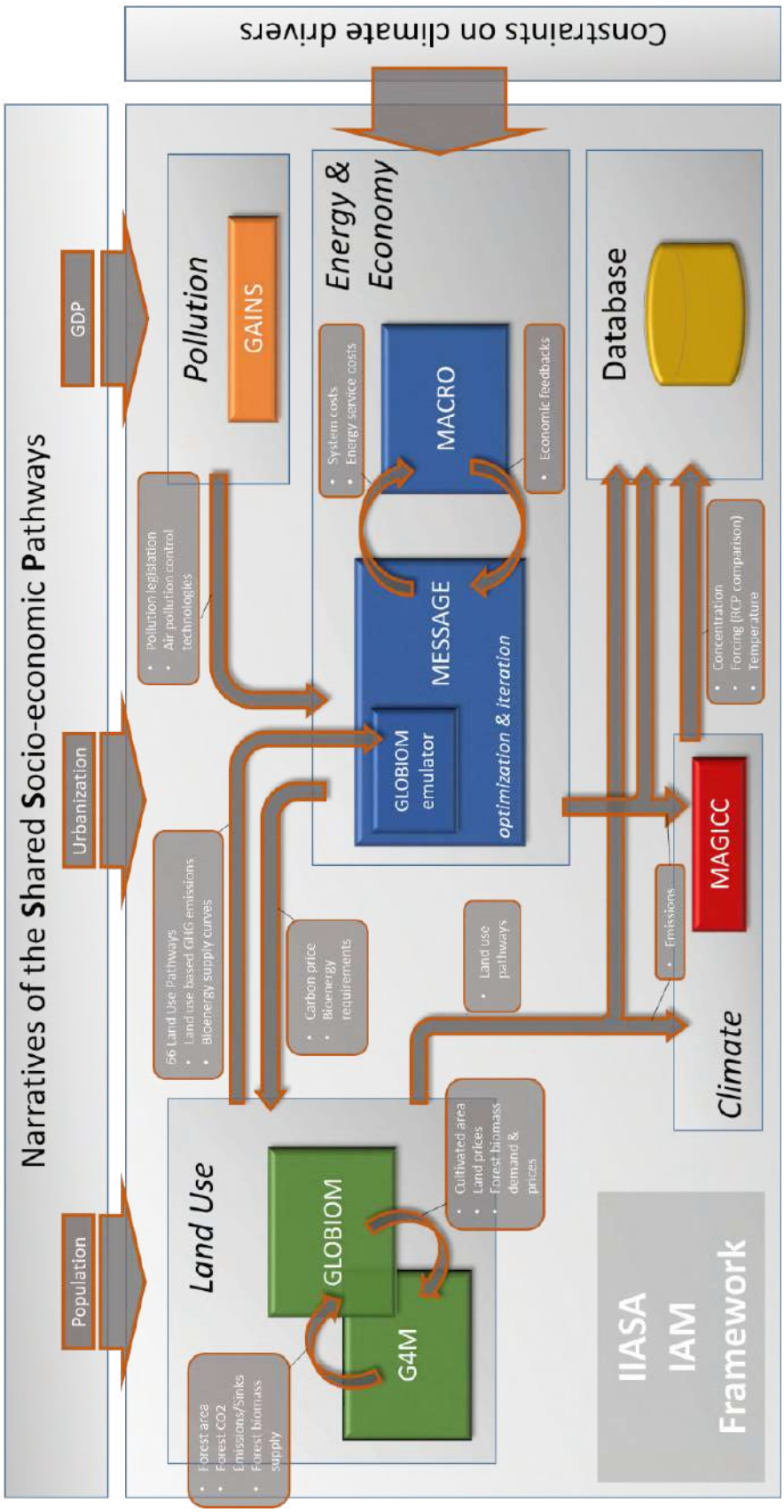


Figure 8.102: Overview of the IIASA IAM framework

Source: https://docs.messageix.org/projects/global/en/latest/overview/index.html.

Figure 8.103: The Remind-MAgPIE framework

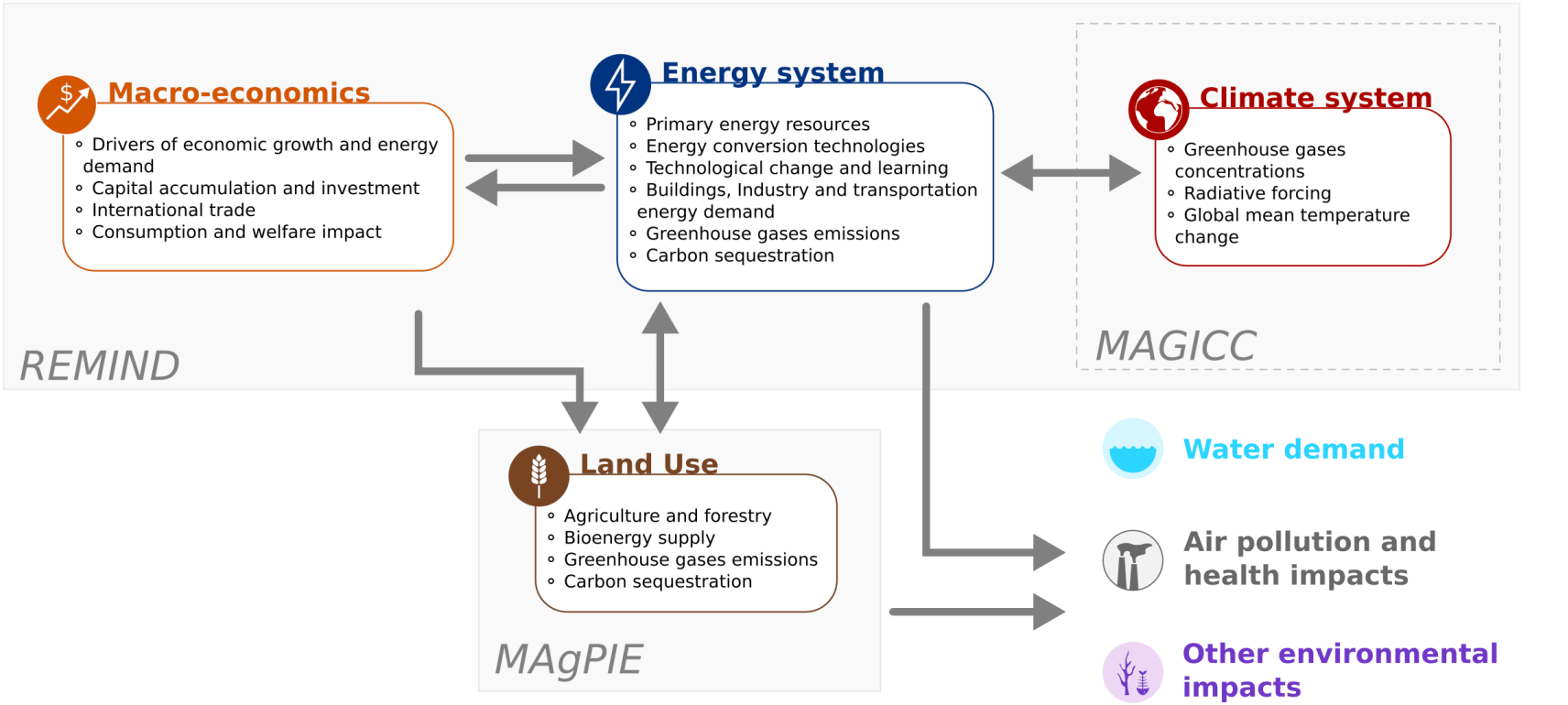


Source: www.pik-potsdam.de/en/institute/departments/transformation-pathways/models/remind.

input data from MAGICC, exactly like MESSAGEix, and it can also feed MAGICC with output data.

Even if these models can be used in an optimization mode, whose objective is to compute optimal paths and perform a cost benefit analysis, they are mainly exploited in order to evaluate a climate policy or to simulate climate/economic trajectories with respect to a given scenario. Like any models, even if they are extensively used by policy markers and the scientific community, they have often been criticised.

#### Criticisms of integrated assessment models

According to Pindyck (2017), "*IAM-based analyses of climate policy create a perception of knowledge and precision that is illusory and can fool policymakers into thinking that the forecasts the models generate have some kind of scientific legitimacy.*" In particular, Robert Pindyck considers that the most important flaws are the following:

- Certain inputs, such as the discount rate, are arbitrary, but they can have a big impact on the model outputs, such as the social cost of carbon;
- There is a lot of uncertainty about climate sensitivity and the temperature trajectory;
- Modeling damage functions is arbitrary, because we have little data to estimate the relationship between an increase in temperature and gross domestic product;
- IAMs are unable to consider tail risk, *i.e.*, a tipping point or the likelihood/possible impact of a catastrophic climate outcome.

In Table 8.35, we report another list of criticisms found by Gambhir *et al.* (2019). We can multiply this type of criticism, and it is relatively essay to do it. We know that all models have flaws and are a simplification of reality. Nevertheless, to repeat the words of George box, "*all models are wrong, but some are useful.*" For instance, we notice that Pindyck (2017) only referenced DICE, FUND and PAGE, while Gambhir *et al.* (2019) focused on complex IAMs. In both cases, criticisms are general and dot not concern a specific model. In this context, it is not always obvious to form an opinion on a model versus another one. For complex IAMs, it is almost impossible. As well, we notice that most comparative studies concern the stylized simple models.

### 8.3.3 Scenarios

As we have already explained, there are two ways to use IAMs: policy optimization and policy/scenario evaluation/simulation. In this section, we focus on the second approach, and more precisely on the scenario simulation. We distinguish two types of simulation outputs: shared socioeconomic pathways (SSPs) and macroeconomic pathways. Before presenting them, we briefly present climate scenarios, which are the input of the evaluation process.

Figure 8.104: Scenario evaluation

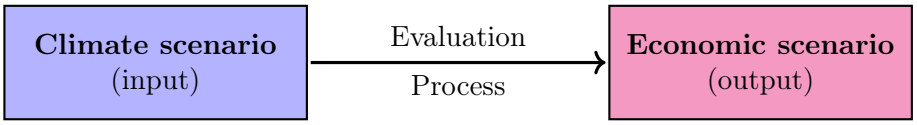

Table 8.35: Main integrated assessment models

| Criticism category | Example of specific criticism |
|---|---|
| Lack of transparency | Lack of documentation |
| Inappropriate input assumptions | Low share of solar PV in mitigation modelling exercises |
| Lack of clarity on model inputs versus outputs | Energy demand reduction as a result of model choice or modeler input? |
| Reliance of mitigation costs on baseline assumptions | Significant differences in costs of achieving mitigation |
| Inadequate representation of innovation processes | Spillover between low-carbon technologies |
| Lack of representation of behavioural and economic systems | Customer behavior changes |
| Lack of assessment of real-world feasibility | Feasibility of pathways given full consideration of social, political and technical barriers |
| Lack of interaction with other policy goals | Lack of consideration of mitigation pathways in light of other policy goals such as energy security |
| Lack of representation of fine temporal and geographical scale | Geographical dispersion of electricity systems |
| Over-reliance on negative emissions technologies | Unrealistically high levels of negative emissions technologies |

Source: Adapted from Gambhir *et al.* (2019, Table 1, page 10).

### Climate scenarios

It is important to understand the different climate scenarios that are used to simulate economic scenarios. In what follows, we focus on four main scenario databases:

- The representative concentration pathways (RCPs) that can be found in the IPCC AR5 (IPCC, 2013);
- The decarbonization pathway scenarios developed by the IEA (IEA, 2017);
- The 1.5°C scenarios proposed by the IPCC SR15 (IPCC, 2018) and the IEA (IEA, 2021);
- The new scenarios for the future published in the IPCC AR6 (IPCC, 2022).

**The RCP scenarios** A representative concentration pathway (RCP) is a greenhouse gas concentration trajectory adopted by IPCC (2013). The AR5 scenario database comprises 31 models and 1 184 scenarios. Among these different scenarios, four pathways have been selected to represent four reference scenarios:

1. RCP 2.6: GHG emissions start declining by 2020 and go to zero by 2100 (IMAGE);
2. RCP 4.5: GHG emissions peak around 2040, and then decline (MiniCAM);
3. RCP 6.0: GHG emissions peak around 2080, and then decline (AIM);
4. RCP 8.5: GHG emissions continue to rise throughout the 21st century (MESSAGE).

Figure 8.105: Total radiative forcing (in $W/m^2$)

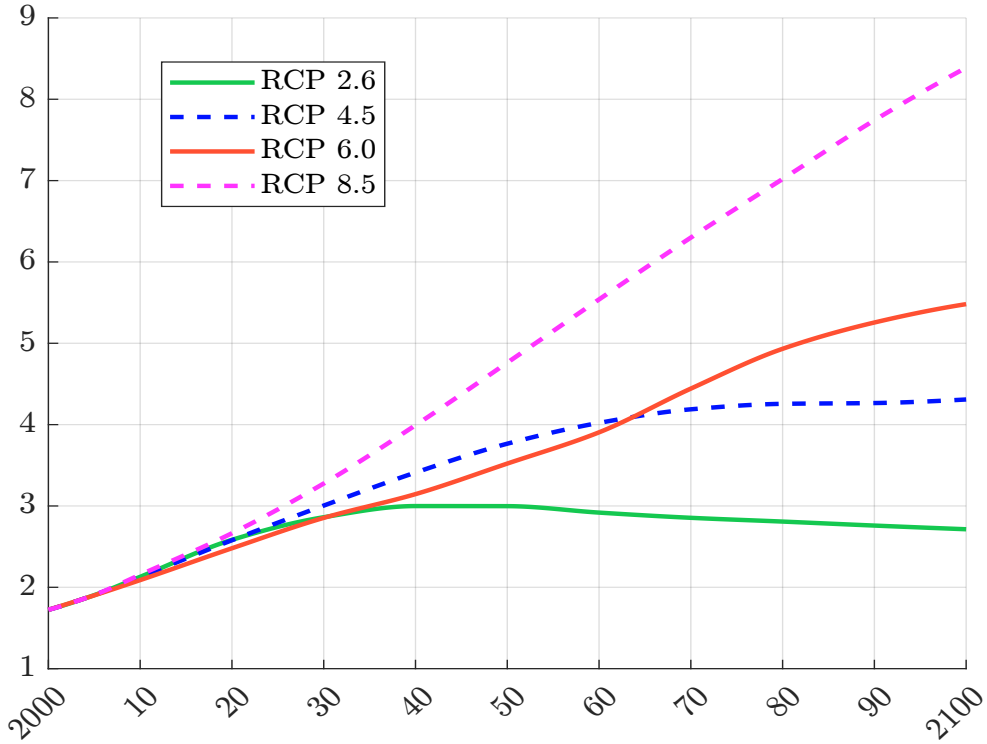


Source: https://tntcat.iiasa.ac.at/RcpDb.

Figure 8.106: Greenhouse gas concentration trajectory

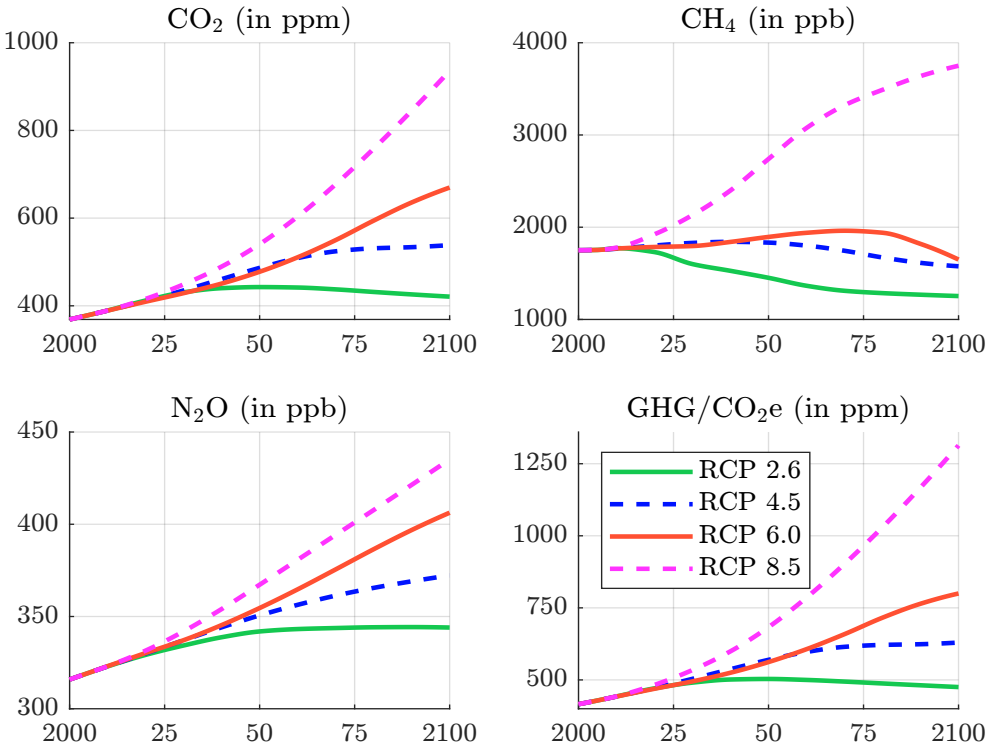


Source: https://tntcat.iiasa.ac.at/RcpDb.

Figure 8.107: Greenhouse gas emissions trajectory

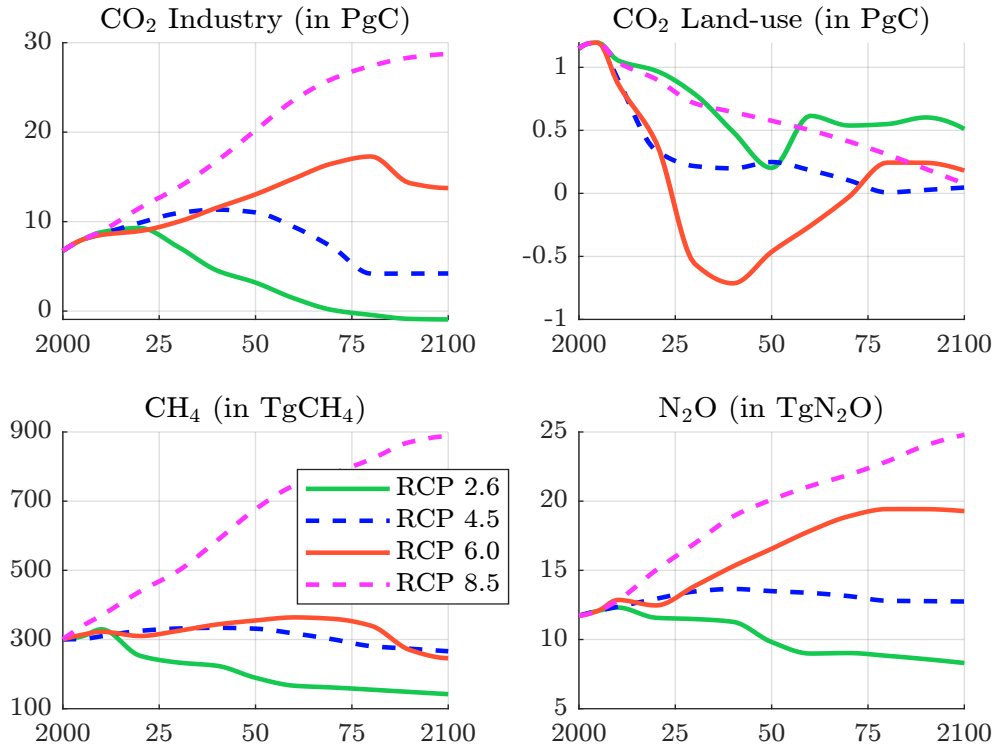


Source: https://tntcat.iiasa.ac.at/RcpDb.

Figure 8.108: Total GHG emissions trajectory (in $GtCO_2e$)

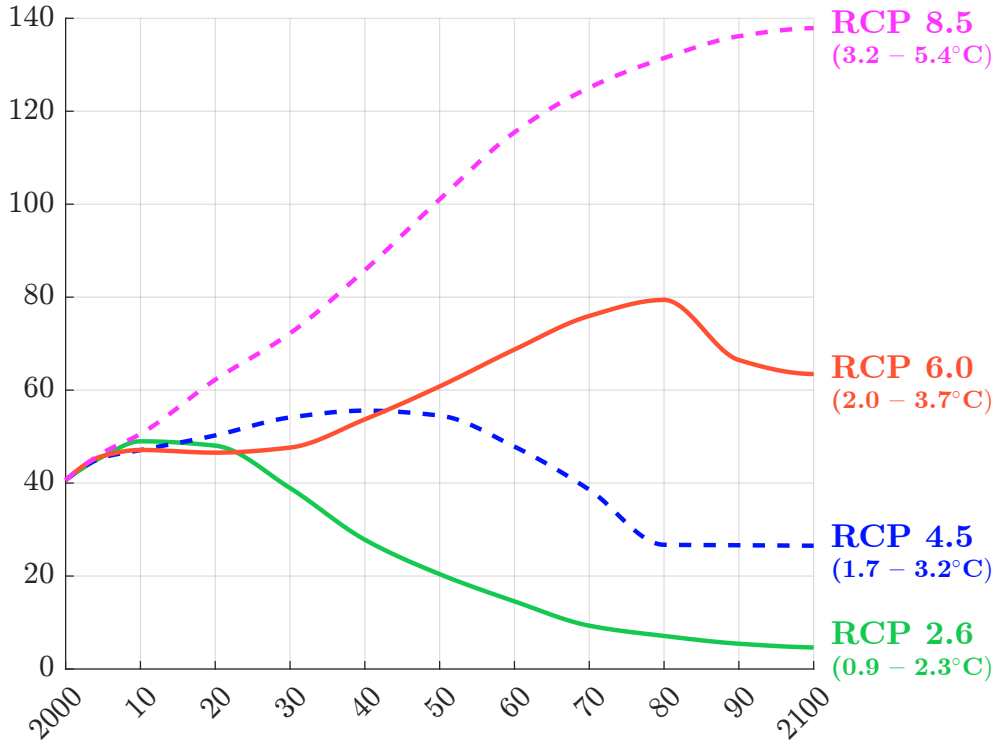


Source: https://tntcat.iiasa.ac.at/RcpDb.

The name of each scenario refers to the value of the radiative forcing by 2050 (Figure 8.105). Figure 8.106 shows the GHG concentration trajectory for $CO_2$, $CH_4$ and $N_2O$ gases. We also report the $CO_2e$ concentration, which is the aggregation of the several GHG concentrations. In Figure 8.107, we show the emissions trajectories for the three main greenhouse gases. For $CO_2$, we distinguish between two categories: industry and land-use change. Finally, we give the total GHG emissions[122] trajectories in Figure 8.107. We notice that the RCP scenario database do not provide a temperature scenario, because the relationship between GHG emissions and temperature depends on several factors. This is why we can only provide a temperature range for each RCP scenario (Figure 8.108).

**The IEA scenarios** As energy represents the largest portion of GHG emissions, the most common way to reduce global emissions is to impose a global shift in the energy supply or demand. To encourage this shifting, the international energy agency has developed energy pathways. These scenarios are not a forecast of the future but explore the different possibilities across the energy system. For instance, IEA (2017) presented three pathways for energy sector development to 2060. The reference technology scenario (RTS) was a baseline scenario that took into account existing climate-related commitments by countries, while the 2°C scenario (2DS) corresponded to a rapid decarbonisation pathway in line with international policy goals. The beyond 2°C scenario (B2DS) was a variant of the 2DS, where the energy sector reached carbon neutrality by 2060 to limit future temperature increases to 1.75°C by 2100. The previous three scenarios were replaced by two new scenarios in 2020. The sustainable development scenario (SDS) "*sets out the major changes that would be required to reach the key energy-related goals of the UN sustainable development agenda*", including a universal access to modern energy by 2030. This scenario is consistent with reaching net zero emissions by around 2070. The previous RTS scenario becomes the stated policies scenario (STEPS). Finally, the last edition of the IEA's Energy Technology Perspectives (ETP) only focuses on the NZE[123] and the announced pledges scenario (APS), which assumes that governments will meet all the climate-related commitments they have announced.

The international energy agency evaluates these different scenarios using its Global Energy and Climate (GEC) model[124]. This model covers 26 regions individually with dedicated bottom-up modelling for final energy demand, energy transformation and energy supply. Using assumptions on population, GDP, fossil fuel prices and ressources (crude oil, natural gas and steam coal), $CO_2$ prices, electricity and technology costs, the GEC model predicts primary energy demand and supply by sources (oil, coal, natural gas, nuclear, biomass and waste, hydro, geothermal, wind, solar, hydrogen), electricity generation and capacity, $CO_2$ and $CH_4$ emissions, investment needs and costs, and materials and critical minerals demand. For instance, we report the $CO_2$ emissions estimated in ETP 2017 in Figure 8.109. We notice that we can not achieve the degC2 scenario when considering the country commitments (RTS).

[122] They have been calculated as follows:

$$\begin{aligned}\text{Total GHG emissions in } GtCO_2e \;=\; & CO_2 \text{ emissions in PgC} \times \frac{44}{12} + \\ & CH_4 \text{ emissions in Tg} \times \frac{28}{1000} + \\ & N_2O \text{ emissions in Tg} \times \frac{265}{1000}\end{aligned}$$

This formula uses the AR5 GWP values (see Section 9.1.1 on page 870), the mass percentage of carbon in carbon dioxide, which is equal to $12/44 = 27.27\%$ (because carbon has an atomic mass of 12 and oxygen has an atomic mass of 16, implying that $CO_2$ has an atomic mass of 44), and the petagram/teragram conversion factor (1 Pg = 1000 Tg).

[123] See page 919.

[124] Its description is available at `www.iea.org/reports/global-energy-and-climate-model`.

Figure 8.109: Direct $CO_2$ emissions (in Gt)

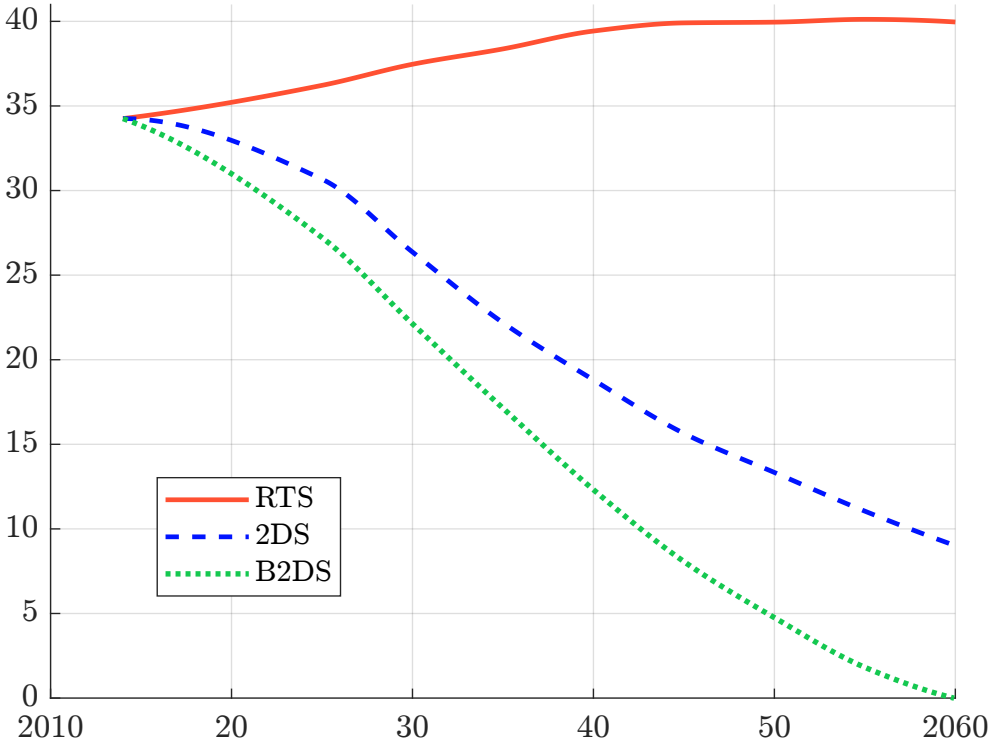


Source: IEA (2017, Figures 1.6 and 1.9).

**The 1.5°C scenarios** In 2018, IPCC issued a special report on the impacts of global warming of 1.5°C above pre-industrial levels and related global greenhouse gas emission pathways. According to the report, "*limiting global warming to* 1.5°C, *compared with* 2°C, *could reduce the number of people both exposed to climate-related risks and susceptible to poverty by up to several hundred million by 2050.*" While the goal of the climate Paris Agreement was to limit global temperature increase to well below 2°C, the IPCC reaffirms then that states must pursue efforts to limit the temperature increase to 1.5°C, because the cost-benefit analysis of the 1.5°C scenario versus 2°C scenario shows that we can reach some tipping points in the second scenario that will generate too much costs for the society, governments and people.

The IPCC SR15 database contains 177 scenarios computed with 24 models[125]. We filter the database in order to keep climate scenarios, whose explicit objective is 1.5°C or well below 2°C. We obtain 114 scenarios, whose CO2 emissions trajectory is reported in Figure 8.110. For each date, we estimate the mean and the standard deviation and compute the 50% and 95% confidence interval in Figure 8.111. We notice that the emissions are close to zero by 2050 on average. This is why the 11.5°C scenario is generally associated to the net zero emissions by 2050 (NZE) scenario. We must be careful because these figures correspond to expected values, meaning that there is a significant probability that the temperature increase can be greater than 1.5°C even if the scenario occurs. For instance, we have reported the global mean temperature of the 114 scenarios, which has been computed with the MAGICC 6 model (Figure 8.112). We observe that the temperature can be

[125] AIM/CGE (2.0 & 2.1), C-ROADS-5.005, GCAM 4.2, GENeSYS-MOD 1.0, IEA 2017 models (ETP & WEM), IMAGE (3.0.1 & 3.0.2), MERGE-ETL 6.0, MESSAGE (V.3, GLOBIOM & ix-GLOBIOM), POLES (ADVANCE, CD-LINKS & EMF33), REMIND (1.5 & 1.7), REMIND-MAgPIE (1.5 & 1.7-3.0), Shell World Energy Model 2018, and WITCH-GLOBIOM (3.1, 4.2 & 4.4).

Figure 8.110: IPCC 1.5°C scenarios of $CO_2$ emissions

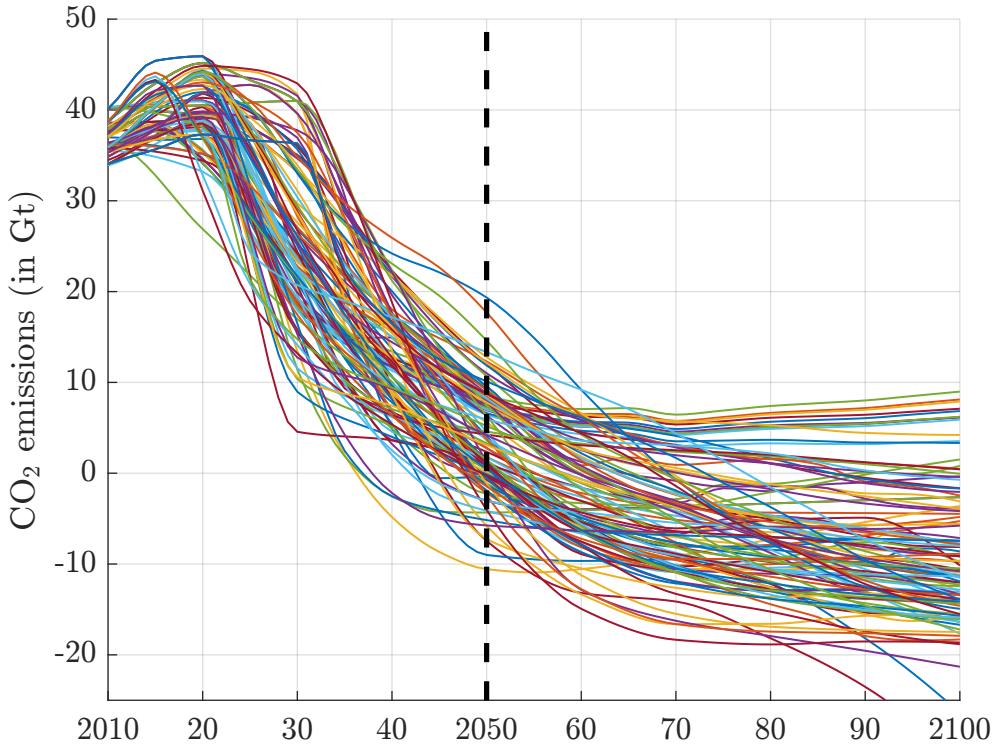


Source: https://data.ene.iiasa.ac.at/iamc-1.5c-explorer.

Figure 8.111: Confidence interval of the average IPCC 1.5°C scenario

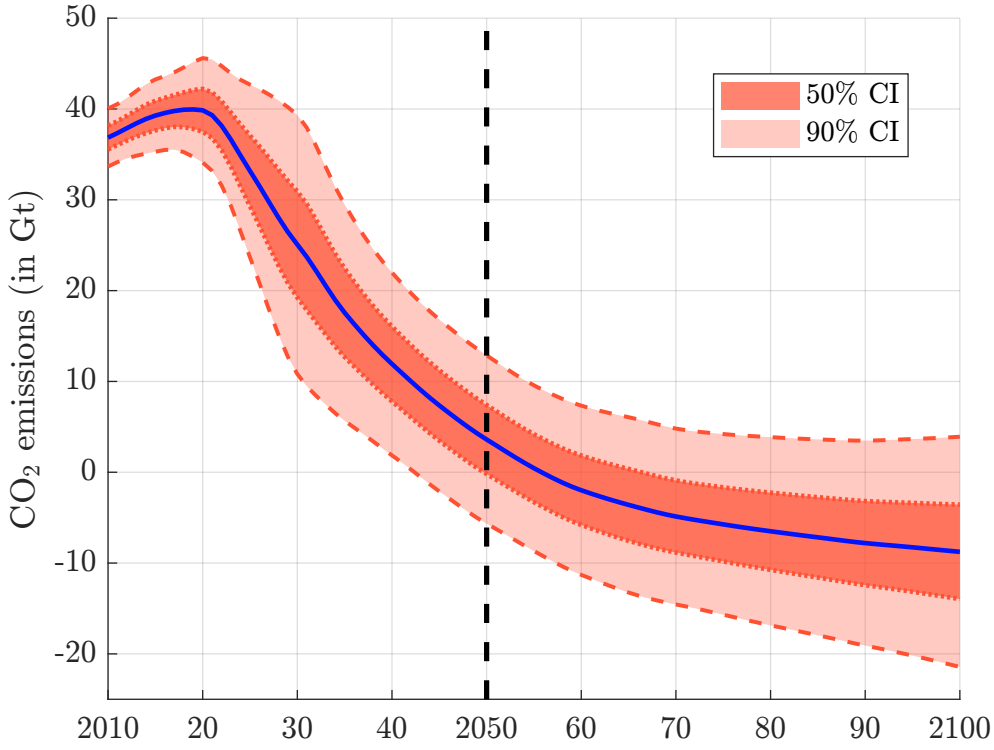


Source: https://data.ene.iiasa.ac.at/iamc-1.5c-explorer.

Figure 8.112: IPCC 1.5°C scenarios of the global mean temperature

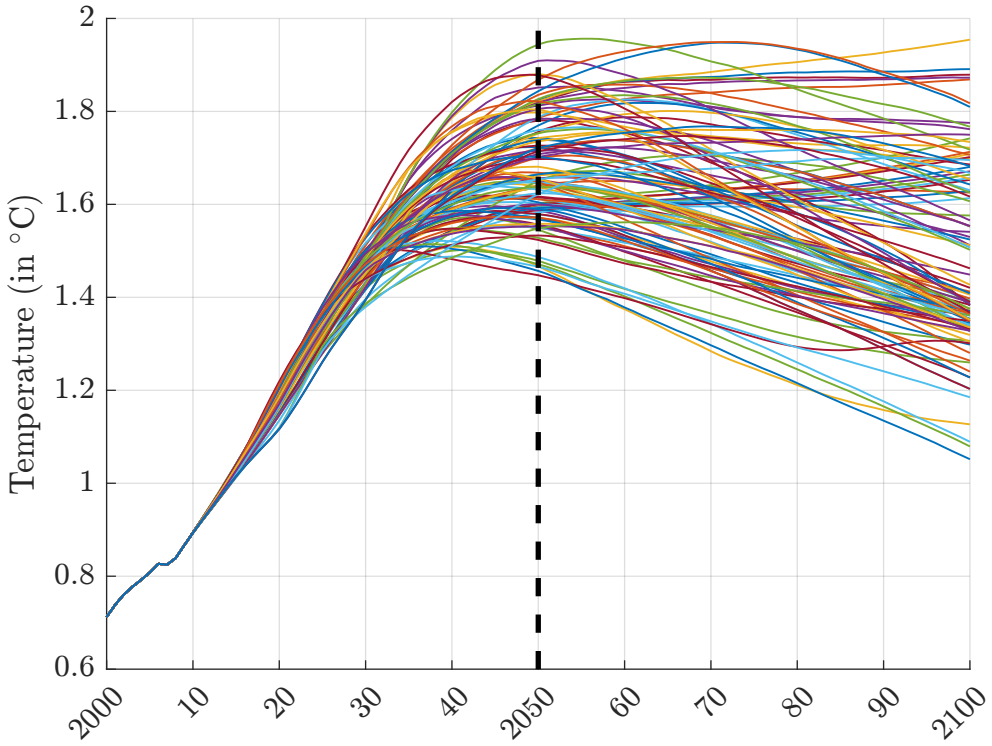


Source: https://data.ene.iiasa.ac.at/iamc-1.5c-explorer.

greater than 1.5°C by 2100, since only 56% of the 114 scenarios produce an expected temperature below this threshold. In Figures 8.113 and 8.114, we also give the evolution of the exceedance probabilities. We notice that the probability to observe a temperature greater than 1.5°C by 2050 is greater than 60%, while it is equal to only 15% if the threshold is 2°C.

**The AR6 scenarios** IPCC (2022) has updated the RCP scenarios. The new dataset[126] contains 188 models, 1 389 scenarios, 244 countries and regions, and 1 791 variables, which can be split into six main categories:

- Agriculture: agricultural demand, crop, food, livestock, production, etc.
- Capital cost: coal, electricity, gas, hydro, hydrogen, nuclear, etc.
- Energy: capacity, efficiency, final energy, lifetime, OM cost, primary/secondary energy, etc.
- GHG impact: carbon sequestration, concentration, emissions, forcing, temperature, etc.
- Natural resources: biodiversity, land cover, water consumption, etc.
- Socio-economic variables: capital formation, capital stock, consumption, discount rate, employment, expenditure, export, food demand, GDP, Gini coefficient, import, inequality, interest rate, investment, labour supply, policy cost, population, prices, production, public debt, government revenue, taxes, trade, unemployment, value added, welfare, etc.

For example, we have reported the distribution of some output variables on page 790.

[126] The amount of data is huge (3 Go).

Figure 8.113: Confidence interval of the exceedance probability $\Pr\{\mathcal{T} > 1.5°\text{C}\}$ (MAGICC 6)

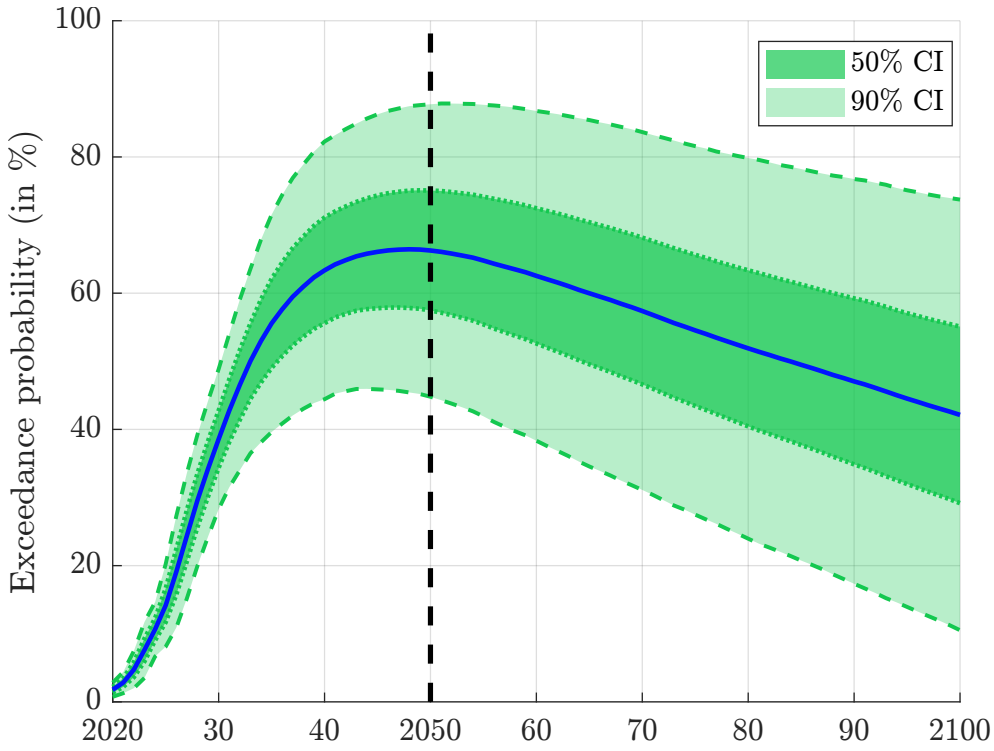


Source: https://data.ene.iiasa.ac.at/iamc-1.5c-explorer.

Figure 8.114: Confidence interval of the exceedance probability $\Pr\{\mathcal{T} > 2°\text{C}\}$ (MAGICC 6)

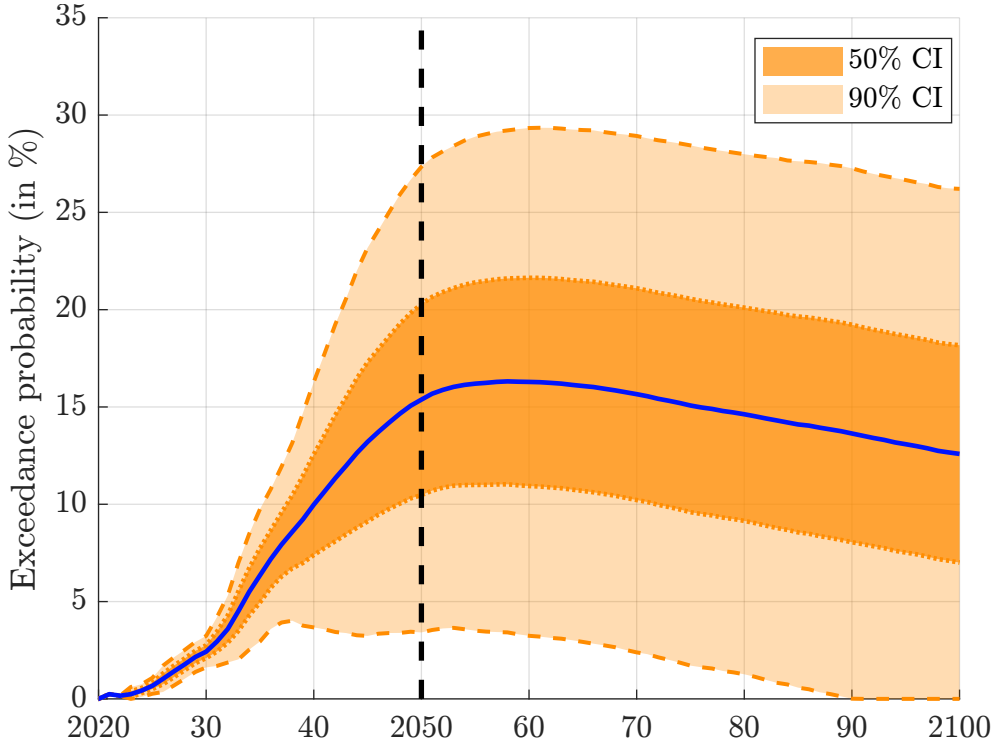


Source: https://data.ene.iiasa.ac.at/iamc-1.5c-explorer.

Figure 8.115: Histogram of some AR6 output variables by 2100

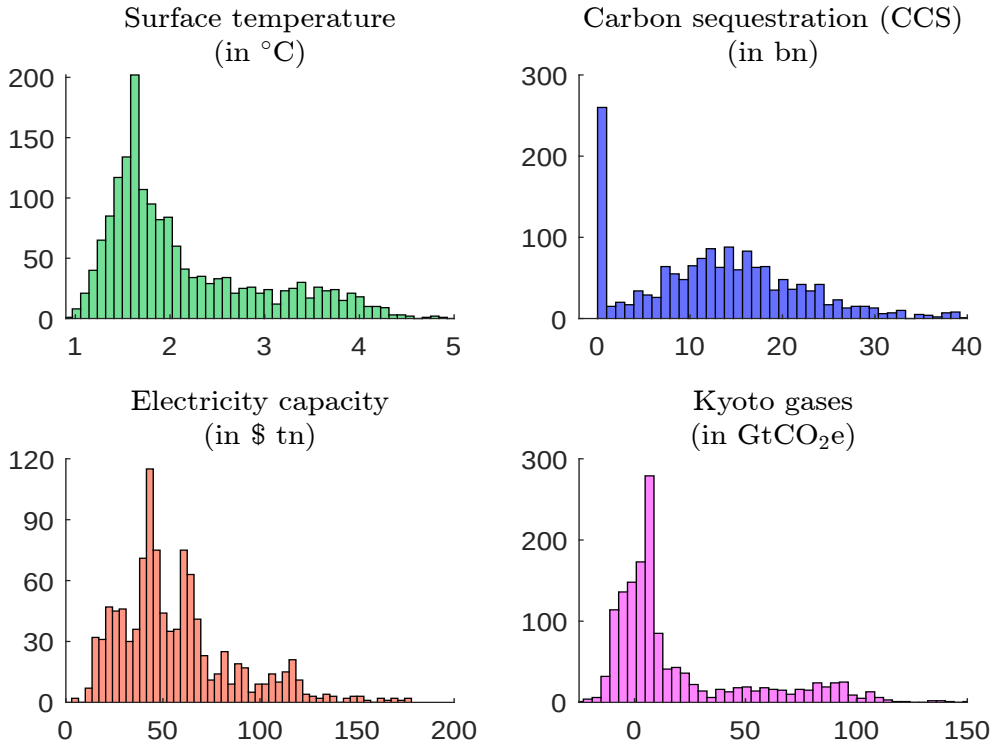


Source: https://data.ene.iiasa.ac.at/ar6.

Figure 8.116: Histogram of some AR6 output variables by 2100

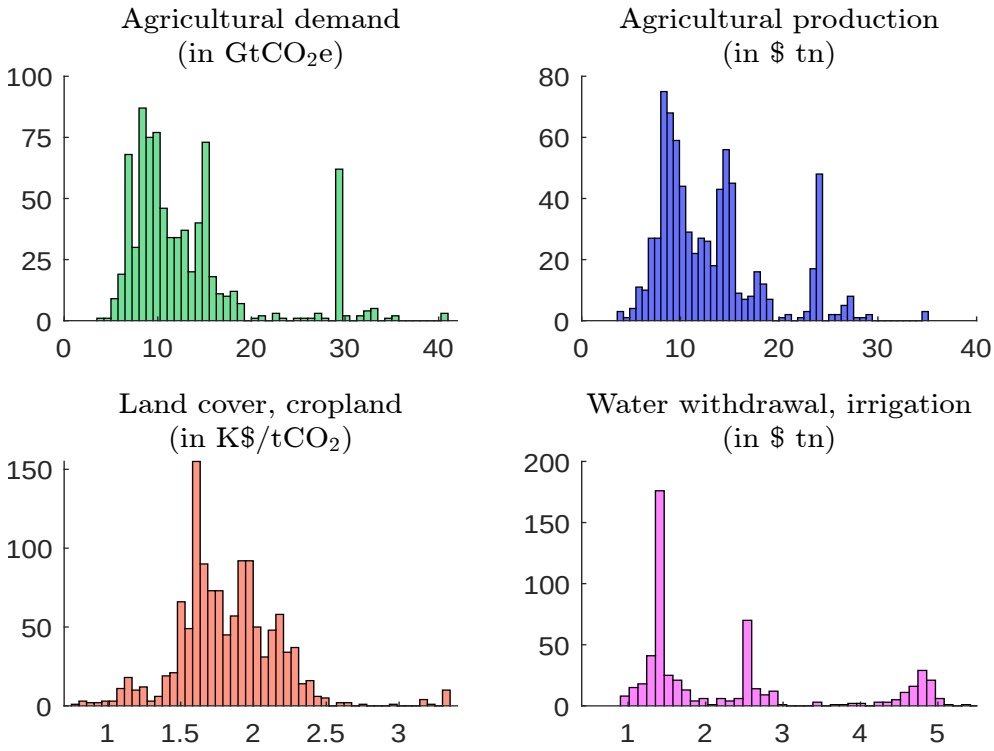


Source: https://data.ene.iiasa.ac.at/ar6.

### Shared socioeconomic pathways

Shared socioeconomic pathways are a set of five narrative scenarios proposed by O'Neill *et al.* (2014). These narratives describe alternative economic developments that are related to challenges for climate change adaptation and mitigation (Figure 8.117). According to (O'Neill *et al.*, 2014, page 389), "*the SSPs describe plausible alternative trends in the evolution of society and natural systems over the 21st century at the level of the world and large world regions; They consist of two elements: a narrative storyline and a set of quantified measures of development. SSPs are reference pathways in that they assume no climate change or climate impacts, and no new climate policies.*"

Figure 8.117: The shared socioeconomic pathways

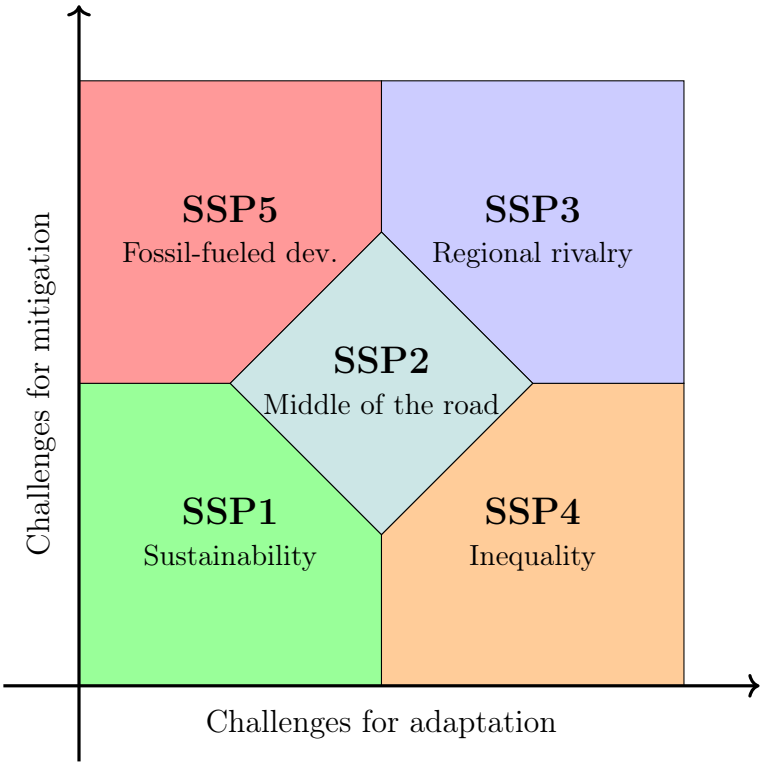


Source: O'Neill *et al.* (2017).

The concept of SSP is clarified in O'Neill *et al.* (2017):

> "*The SSP narratives [are] a set of five qualitative descriptions of future changes in demographics, human development, economy and lifestyle, policies and institutions, technology, and environment and natural resources. [...] Development of the narratives drew on expert opinion to (1) identify key determinants of the challenges [to mitigation and adaptation] that were essential to incorporate in the narratives and (2) combine these elements in the narratives in a manner consistent with scholarship on their interrelationships. The narratives are intended as a description of plausible future conditions at the level of large world regions that can serve as a basis for integrated scenarios of emissions and land use, as well as climate impact, adaptation and vulnerability analyses.*"

In particular, they described the five pathways and developed the narrative storyline for each of them (Figure 8.118). SSP1 and SSP2 corresponds to smooth scenarios, which are characterized by

Figure 8.118: The shared socioeconomic pathways

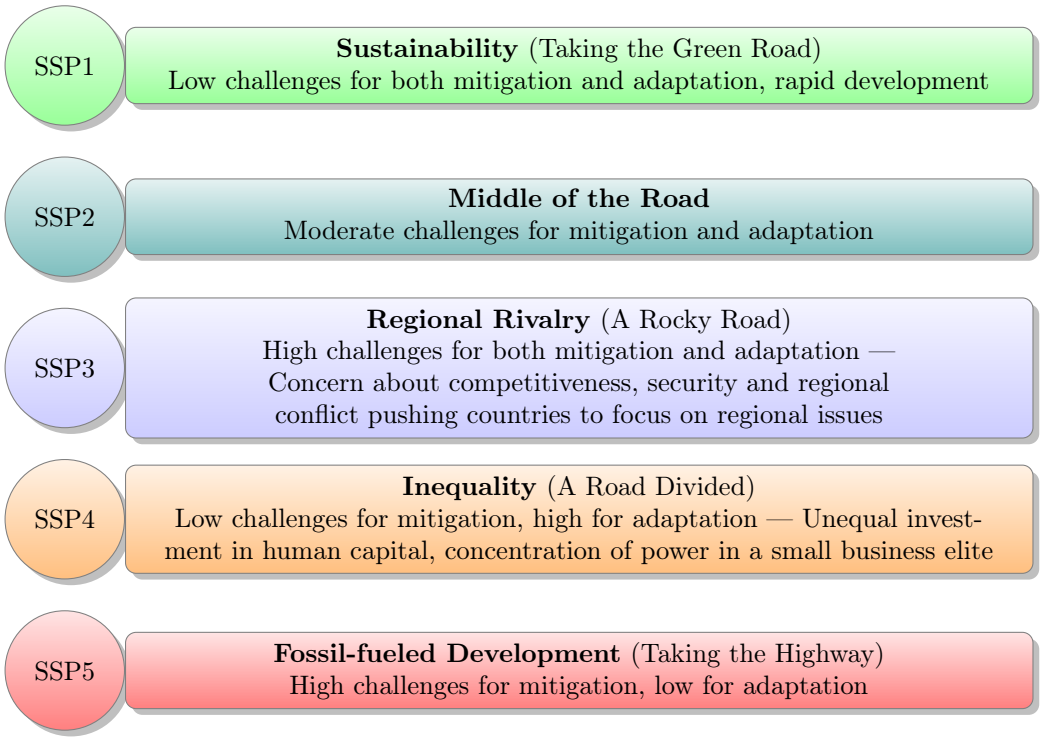


Source: O'Neill *et al.* (2017).

a relative easy transition toward a sustainable world. SSP1 implies a shift from historical patterns, less resource-intensive lifestyles, an improvement of natural resource efficiency and a global green growth strategy. SSP2 may be interpreted as a continuation of the economic development that was observed in the twentieth century. Emerging economies become rapidly developed and middle-income economies, global population growth is under control and moderate, but inequalities remains. SSP3 describes an increasingly individualist world with more nationalism and regional conflicts. In this situation, countries mainly focus on regional issues and less on international cooperation. This fragmented world implies high inequalities within and between countries. Inequality and poverty is also the central theme of SSP4, which corresponds to a multi-level society with a lot of issues (social cohesion, access to water, sanitation and health ware, education, etc). SSP5 corresponds to a high resilience of the economy, and consequently nothing is done to reduce inequalities and negative externalities. We observe that the SSPs can be related to ESG dimensions:

- **E** The mitigation/adaptation trade-off is obviously an environmental issue, but the SSPs encompass other environmental narratives, *e.g.*, land use, energy efficiency and green economy;
- **S** The social dimension is the central theme of SSPs, and concerns demography, wealth, inequality & poverty, health, education, employment, and more generally the evolution of society. This explains that SSPs and SDGs are highly interconnected;
- **G** Finally, the governance dimension is present though two major themes: international fragmentation or cooperation, and the political/economic system, including corruption, stability, rule of law, etc.

We notice that all these SSP themes can be found in a sovereign ESG framework[127].

While O'Neill *et al.* (2014) have introduced the concept of SSP and given a very broad definition, the analysis proposed by O'Neill *et al.* (2017) is purely qualitative and descriptive. In fact, the first broad quantification of SSPs is done by Riahi *et al.* (2017), who have generated the five narrative scenarios with the following IAMs:

- SSP1: IMAGE (PBL)
- SSP2: MESSAGE-GLOBIOM (IIASA)
- SSP3: AIM/CGE (NIES)
- SSP4: GCAM (PNNL)
- SSP5: REMIND-MAGPIE (PIK) and WITCH-GLOBIOM (FEEM)

Results obtained by these authors are summarized in Figures 8.119–8.122. We only focus on baseline scenarios and we group the indicators into four main categories. In Figure 8.119, the demography projection shows three main pathways: population decline (SSP1, SSP5), population stabilization (SSP2, SSP4) and population growth (SSP5). If we consider the economic growth projections, we obtain another kind of breakdown (Figure 8.120). SSP5 corresponds to the highest GDP projections. It is following by SSP1 and SSP2, while SSP4 and SSP3 are the two laggard scenarios. In the last panel, we have reported the GDP per primary energy ratio. It shows that SSP1 has the highest efficiency. The case of SSP3 is interesting since the improvement of the energy efficiency follows the economic growth beyond 2040.

Figures 8.121 and 8.122 give an overview of the environmental narratives. As expected, SSP1 and SSP5 are the two extreme scenarios if we focus on climate change (temperature and $CO_2$ emissions). If we consider the land use, the opposite scenario become SSP1 and SSP3. In SSP1, the forest increases while cropland and pasture decrease or are stable. In SSP3, the forest dramatically decreases and there is 50% more cropland by 2100. Another interesting SSP indicator is the urban share (first panel in Figure 8.122). The urbanization of the world continues, but at different paces. By the end of century, the projected rate of urbanization reaches 60% for SSP3, 80% for SSP3 and more than 90% for the other SSPs. O'Neill *et al.* (2014) explained that "*urbanization is constrained by slow economic growth and limited mobility across regions in SSP3, while urbanization is assumed to be rapid in both SSP1 and SSP5, which are associated with high income growth.*"

To illustrate inequality issues, we can conduct the previous at a regional/country level. For example, Figure 8.123 shows demography and GDP/Capita growth projections in Africa and Asia. It is obvious that these two regions will not have the same economic development even if they follow the same shared socioeconomic pathway. This is particular true for the SSP4 scenario, for which we observe a population growth in Africa and a population decline in Asia. The impact of SSP4 on the GDP growth is also large in Africa with respect to the SSP2 scenario. The relationship between income inequalities and SSPs has been extensively studied by Rao *et al.* (2019). Using their dataset, we report in Figure 8.123 the boxplots of the Gini coefficient by 2100 for 184 countries, and compare these values with the 2020 estimates. We notice that income inequality within a country decreases for SSP1, SSP2 and SSP5 scenarios[128], while it increases for SSP3 and SSP4. These results illustrate that inequalities across/within countries are important to understand the social cohesion dimension.

[127] See Section 2.1.1 on page 54.

[128] Nevertheless, we also observe that there are more outlier countries for these scenarios.

Figure 8.119: SSP demography projections

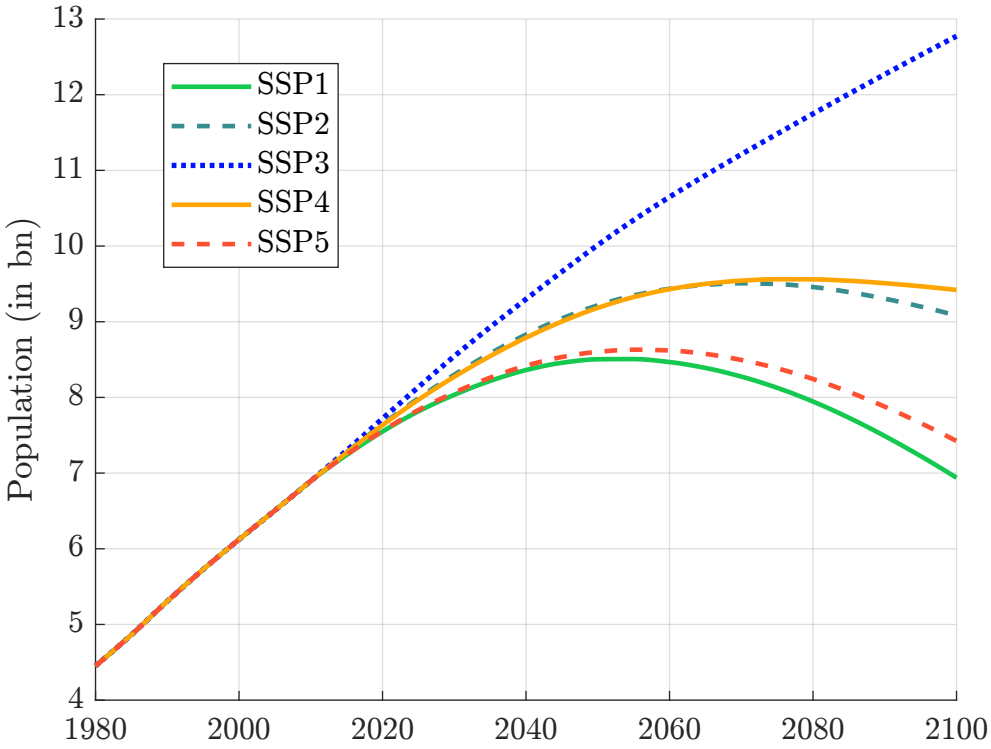


Source: https://tntcat.iiasa.ac.at/SspDb.

Figure 8.120: SSP economic projections

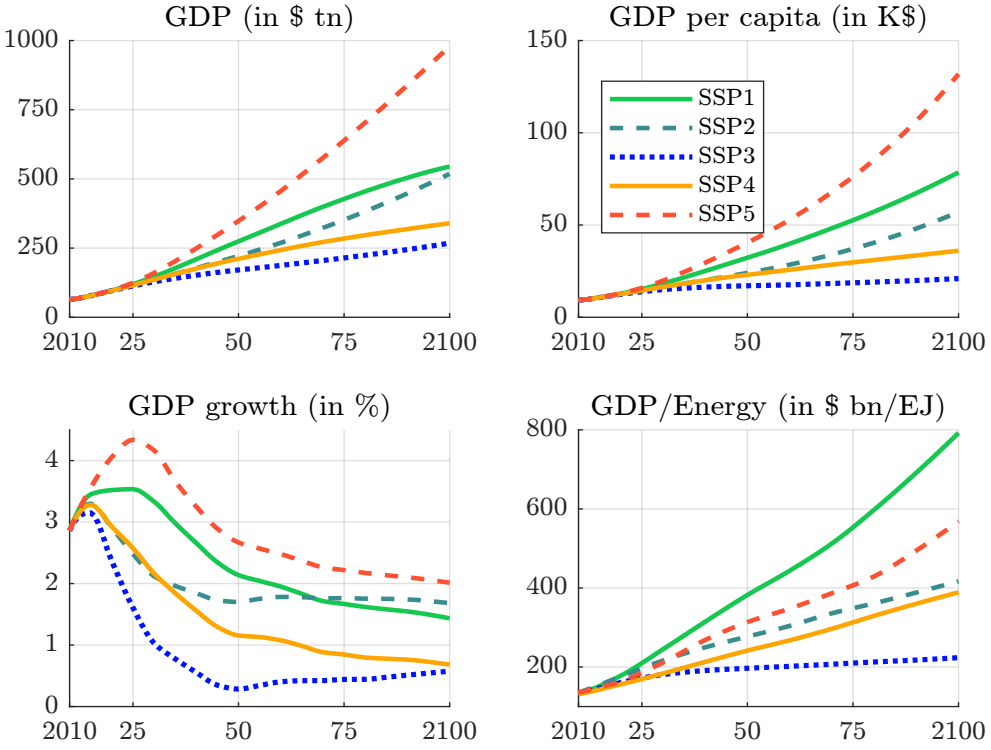


Source: https://tntcat.iiasa.ac.at/SspDb.

Figure 8.121: SSP environmental projections

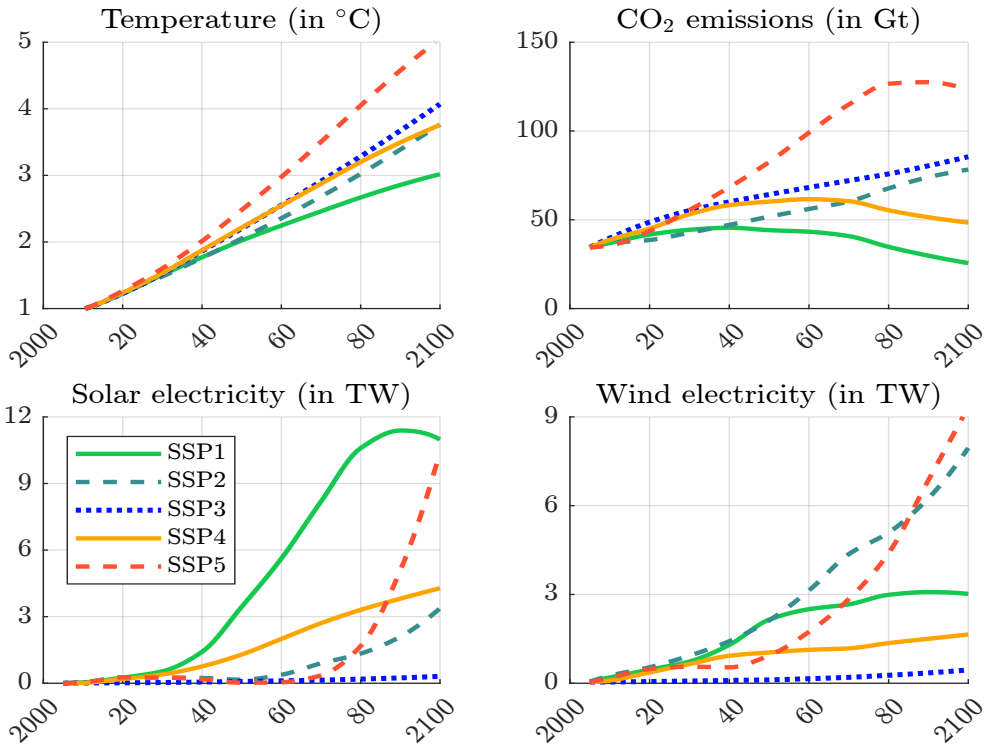


Source: https://tntcat.iiasa.ac.at/SspDb.

Figure 8.122: SSP land-use projections

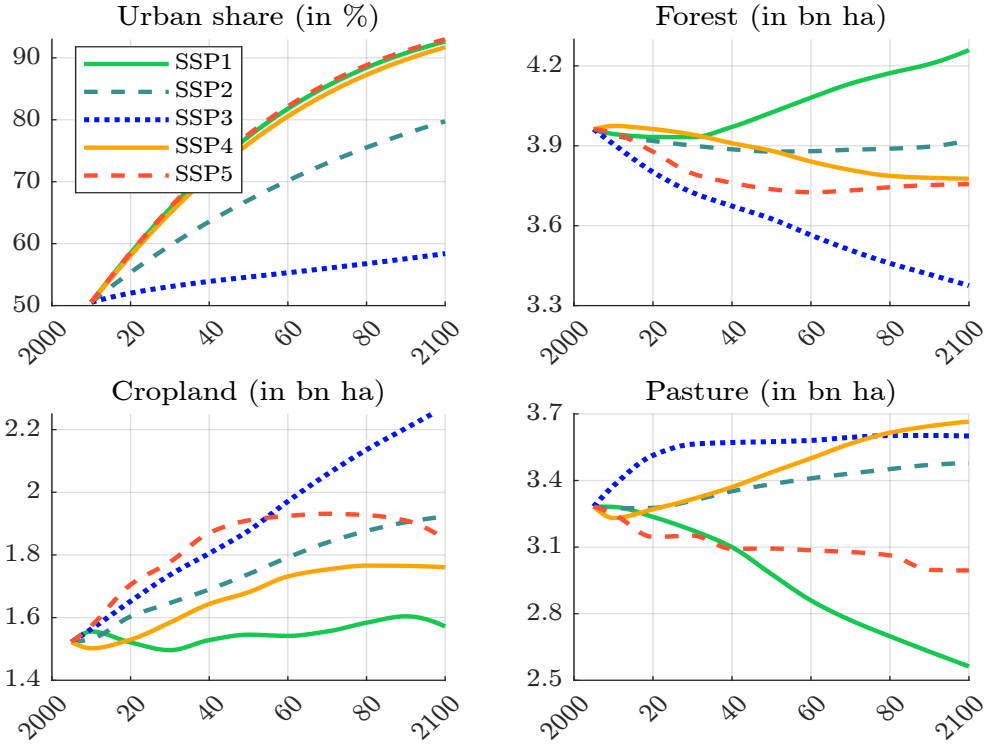


Source: https://tntcat.iiasa.ac.at/SspDb.

Figure 8.123: Example of SSP regional differences

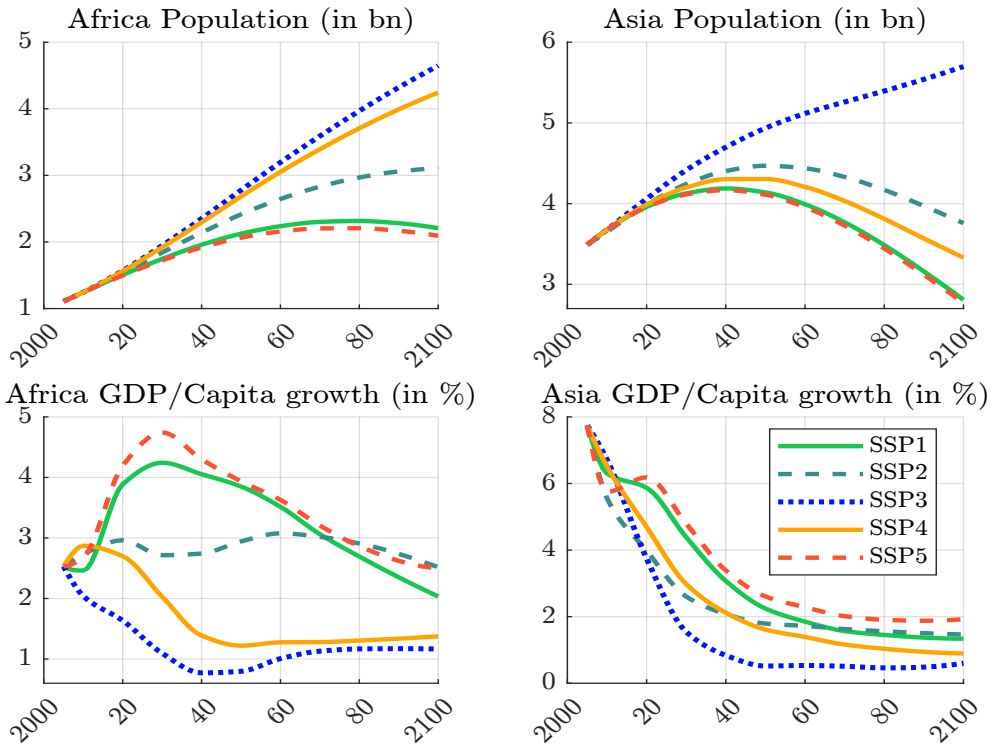


Source: https://tntcat.iiasa.ac.at/SspDb.

Figure 8.124: Gini coefficient projections by 2100

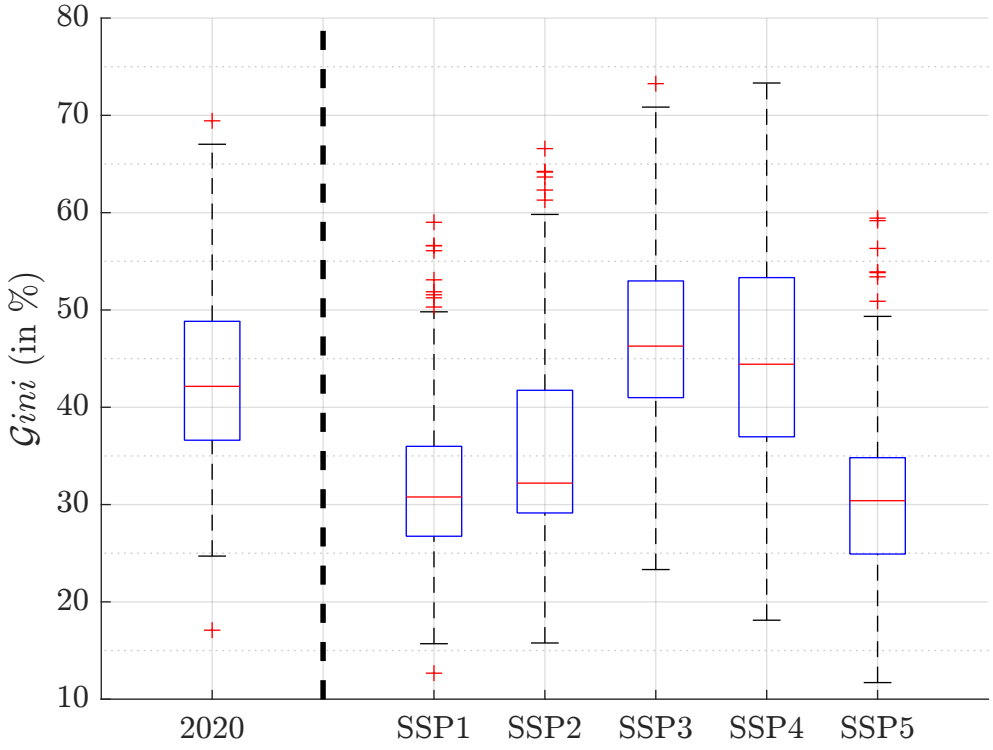


Source: https://tntcat.iiasa.ac.at/SspDb.

### Macroeconomic scenarios

The main objective of IAMs is to produce macroeconomic scenarios. For instance, the stylized simple models generate population, capital stock and GDP pathways, even though they are generally used only to compute the social cost of carbon. Indeed, these models are too simple to describe realistic economic scenarios. This is why these latter are simulated using complex IAMs. In the previous section dedicated to SSPs, we have already seen some output variables that are generated. In what follows, we focus on the NGFS scenarios, which have recently become a common standard. Today, the NGFS framework is an official tool that is used and recognized by central banks and supervisors, and also a reference point for financial institutions (investors, asset managers, and banks).

**NGFS scenarios framework** In 2020, the Network for Greening the Financial System (NGFS) has developed a set of scenarios for climate financial risk assessment[129]. The initial goal was to help central banks and supervisors exploring the possible impacts on the economy and the financial system. The NGFS scenarios framework consists in six scenarios located in the NGFS climate risk matrix given in Figure 8.125.

Figure 8.125: NGFS scenarios framework

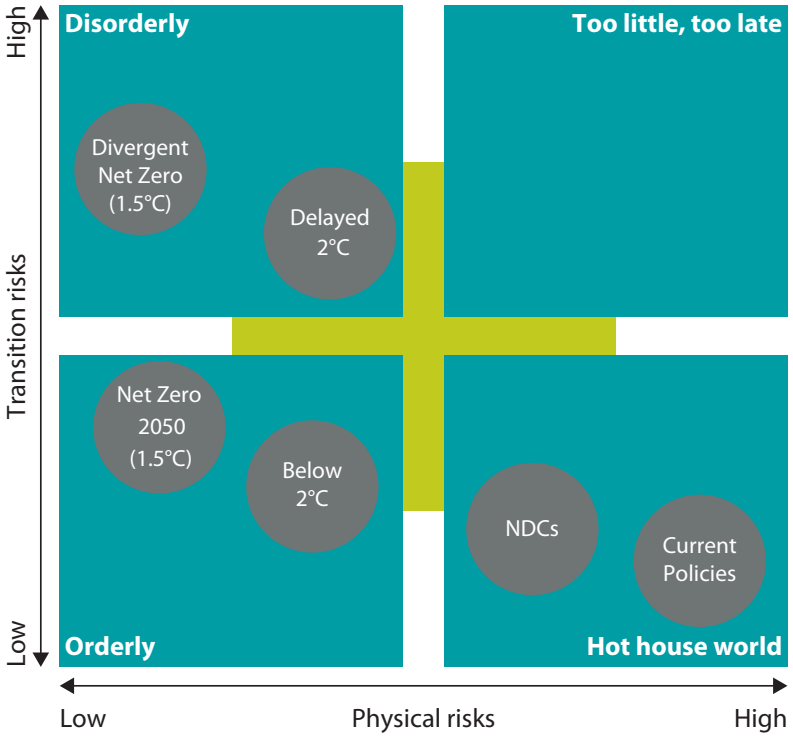


Source: Richters *et al.* (2022) & www.ngfs.net.

Below, we report the description of the six scenarios, which is done by NGFS (2022).

- Orderly scenarios assume climate policies are introduced early and become gradually more stringent. Both physical and transition risks are relatively subdued.

[129]The third version of these scenarios was released in September 2022.

#1 Net-zero 2050 limits global warming to 1.5°C through stringent climate policies and innovation, reaching global net zero $CO_2$ emissions around 2050. Some jurisdictions such as the US, EU, UK, Canada, Australia and Japan reach net zero for all GHGs.

#2 Below 2°C gradually increases the stringency of climate policies, giving a 67% chance of limiting global warming to below 2°C.

- Disorderly scenarios explore higher transition risk due to policies being delayed or divergent across countries and sectors. For example, carbon prices are typically higher for a given temperature outcome.

#3 Divergent net zero reaches net zero around 2050 but with higher costs due to divergent policies introduced across sectors leading to a quicker phase out of oil use.

#4 Delayed transition assumes annual emissions do not decrease until 2030. Strong policies are needed to limit warming to below 2°C. Negative emissions are limited.

- Hot house world scenarios assume that some climate policies are implemented in some jurisdictions, but globally efforts are insufficient to halt significant global warming. The scenarios result in severe physical risk including irreversible impacts like sea-level rise.

#5 Nationally determined contributions (NDCs) includes all pledged targets even if not yet backed up by implemented effective policies.

#6 Current policies assumes that only currently implemented policies are preserved, leading to high physical risks.

In what follows, we use the following acronyms NZ, B2D, DNZ, D2D, NDC, CP when we refer to these 6 scenarios. Table 8.36 shows the impact of climate risk on each scenario. For the physical risk, NGFS uses both chronic and acute impacts. Chronic risks[130] affect agriculture, labor productivity and natural capital. Acute risks or extreme weather events[131] implies destruction, economic losses, lower insurance cover and business disruption. Transition risk takes several forms: policy risk, technology risk and coordination risk. The climate transition pathways are generated by three IAMs: GCAM, MESSAGEix-GLOBIOM and REMIND-MAgPIE, while the economic variables are produced by the NiGEM macroeconomic model[132] in order to obtain harmonized metrics between scenarios and climate models. Moreover, a seventh scenario is produced by NiGEM without the IAM inputs and corresponds to the baseline (BSL) scenario, which does not take into account climate risk.

**Description of the database** The NGFS database[133] is entirely described in Richters *et al.* (2022). It contains three EXCEL files. `IAM_data` contains the data generated by the three IAM models, `Downscaled_data` are the energy data produced by the previous models at the country level, while `NiGEM_data` corresponds to the data generated by the NiGEM model. In what follows, we only consider this last file. In order to select data, we first must specify the model and the scenario. The baseline scenario is obtained with the NiGEM model. For the six climate scenarios, we must choose one integrated assessment model (GCAM, MESSAGEix-GLOBIOM
index[general]MESSAGE modelindex[general]GLOBIOM model or REMID-MAgPIE) and associate

[130] Such as increased temperatures, rising sea levels, ocean acidification and seasonal precipitation.
[131] Such as such as tropical cyclones, droughts, floods and wildfires.
[132] It is developed by the National Institute for Economic and Social Research (NIESR). A description can be found at `www.niesr.ac.uk/nigem-macroeconomic-model`.
[133] The economic scenarios can be downloaded at `https://data.ene.iiasa.ac.at/ngfs`.

Table 8.36: Physical and transition risk level of NGFS scenarios

| | | Physical risk | Transition risk | | | |
|---|---|---|---|---|---|---|
| **Category** | **Scenario** | **Policy ambition** | **Policy reaction** | **Technology change** | **Carbon dioxide removal** $^{-}$ | **Regional policy variation** $^{+}$ |
| Orderly | Net Zero 2050 | 1.4°C | Immediate and smooth | Fast change | Medium-high use | Medium variation |
| | Below 2°C | 1.6°C | Immediate and smooth | Moderate change | Medium-high use | Low variation |
| Disorderly | Divergent Net Zero | 1.4°C | Immediate but divergent across sectors | Fast change | Low-medium use | Medium variation |
| | Delayed Transition | 1.6 °C | Delayed | Slow / Fast change | Low-medium use | High variation |
| Hot house world | Nationally Determined Contributions (NDCs) | 2.6°C | NDCs | Slow change | Low-medium use | Medium variation |
| | Current Policies | 3°C + | Non-currente policies | Slow change | Low use | Low variation |

Lower risk, moderate risk and higher risk

Color coding indicates whether the characteristic makes the scenario more or less severe from a macro-financial risk perspective.

Source: NGFS (2022) & www.ngfs.net.

Table 8.37: NGFS database — Economic block

**Scenarios**

1. Net Zero 2050 (NZ)
2. Below 2°C (B2D)
3. Divergent Net Zero (DNZ)
4. Delayed Transition (DT)
5. Notionally Determined Contribution (NDC)
6. Current Policies (CP)
7. Baseline (BSL)

**Models**

- GCAM 5.3+ NGFS
- MESSAGEix-GLOBIOM 1.1-M-R12
- NiGEM NGFS v1.22
- REMIND-MAgPIE 3.0-4.4
- NiGEM NGFS v1.22 / Downscaling
  - GCAM 5.3+ NGFS
  - MESSAGEix-GLOBIOM 1.1-M-R12
  - REMIND-MAgPIE 3.0-4.4
- REMIND-MAgPIE 3.0-4.4
  - IntegratedPhysicalDamages (95th-high)
  - IntegratedPhysicalDamages (median)

**Energy variables**

- Coal price
- Gas price
- Oil price
- Quarterly consumption of coal
- Quarterly consumption of gas
- Quarterly consumption of non-carbon
- Quarterly consumption of oil
- Total energy consumption

**Economic variables**

- Central bank intervention rate
- Consumption (private sector)
- Domestic demand
- Effective exchange rate
- Equity prices
- Exchange rate
- Exports (goods and services excluding MTIC)
- Exports (goods and services)
- Government consumption
- Gross Domestic Product (GDP)
- Gross domestic income
- Gross operating surplus
- House prices (residential)
- Imports (goods and services excluding MTIC)
- Imports (goods and services)
- Inflation rate
- Investment (government)
- Investment (private sector)
- Long term interest rate
- Productivity (output per hour worked)
- Real personal disposable income
- Trend output for capacity utilisation
- Unemployment rate

it with the NiGEM model. Once the model and the scenario are chosen, we can filter the data by region and/or variable. We have reported the name of the variables in Table 8.37. They are of two types. Energy variables concern price and consumption of coal, gas, oil and non-carbon (or renewables/green energy). Economic variables cover production, consumption, income, investment, interest rates, inflation and unemployment.

**Empirical results** We report the impact of NGFS scenarios on GDP in Tables 8.38, 8.39 and 8.40 when the time horizon is set to 2050 and the region corresponds to the world. The results depend on the selected model. For instance, if we consider the B2D scenario and the chronic physical risk, the GDP impact is equal to −3.09% with GCAM, −2.05% with MESSAGEix and −2.24% with REMIND. For each table, the impact is related to the selected scenario and the selected risk. We notice that the largest loss is obtained with the combined risk (physical and transition), but there is no individual risk that dominates the other. For example, the chronic physical risk has more impact for the B2D, DT, NDC and NZ scenarios while the transition risk dominates for the DNZ scenario. We also observe that the impacts of physical and transition risks are almost additive when they are combined. Another interesting remark concerns the magnitude of the GDP loss. If we consider GCAM and REMIND, there is no obvious ranking in terms of scenario severity. This is not the case of the MESSAGEix model, which assumes that DNZ and DT are the two most severe scenarios, followed by four other scenarios.

Table 8.38: Impact of climate change on the GDP loss by 2050 (GCAM)

| Risk | B2D | CP | DNZ | DT | NDC | NZ |
|---|---|---|---|---|---|---|
| Chronic physical risk | −3.09 | −5.64 | −2.35 | −3.28 | −5.15 | −2.56 |
| Transition risk | −0.75 | | −3.66 | −1.78 | −0.89 | −0.88 |
| Combined risk | −3.84 | −5.64 | −6.00 | −5.05 | −6.03 | −3.44 |
| Combined + business confidence | | | −6.03 | −5.09 | | |

Source: https://data.ene.iiasa.ac.at/ngfs.

Table 8.39: Impact of climate change on the GDP loss by 2050 (MESSAGEix-GLOBIOM)

| Risk | B2D | CP | DNZ | DT | NDC | NZ |
|---|---|---|---|---|---|---|
| Chronic physical risk | −2.05 | −5.26 | −1.55 | −2.64 | −4.78 | −1.59 |
| Transition risk | −1.46 | | −10.00 | −10.77 | −1.39 | −3.26 |
| Combined risk | −3.51 | −5.26 | −11.53 | −13.37 | −6.16 | −4.84 |
| Combined + business confidence | | | −11.57 | −13.40 | | |

Source: https://data.ene.iiasa.ac.at/ngfs.

Table 8.40: Impact of climate change on the GDP loss by 2050 (REMIND-MAgPIE)

| Risk | B2D | CP | DNZ | DT | NDC | NZ |
|---|---|---|---|---|---|---|
| Chronic physical risk | −2.24 | −6.05 | −1.67 | −2.65 | −5.41 | −1.76 |
| Transition risk | −0.78 | | −3.01 | −1.95 | −0.33 | −1.46 |
| Combined risk | −3.02 | −6.05 | −4.68 | −4.59 | −5.73 | −3.21 |
| Combined + business confidence | | | −4.70 | −4.63 | | |

Source: https://data.ene.iiasa.ac.at/ngfs.

By using the MESSAGEix-GLOBIOM model and selecting the combined risk, we obtain the results per country and region in Table 8.41. On average, the GDP loss by 2050 is between −3.51% (current policies) and −13.37% (delayed transition). This large difference is also observed when we compare countries and region. For example, if we focus on the NZ scenario, the impact is negative and equal to −17.11% for Russia while it is positive for developing Europe, South Korea and Switzerland. Therefore, we conclude that there is a high heterogeneity between countries (see also Figures 8.126 and 8.127).

Table 8.41: Impact of climate change on the GDP loss by 2050 (MESSAGEix-GLOBIOM)

| Region | B2D | CP | DNZ | DT | NDC | NZ |
|---|---|---|---|---|---|---|
| Africa | −13.58 | −7.50 | −27.35 | −29.37 | −11.78 | −18.36 |
| Asia | −1.50 | −7.29 | −5.44 | −8.76 | −6.78 | −1.38 |
| Australia | −4.11 | −3.90 | −11.03 | −11.74 | −5.77 | −5.19 |
| Brazil | −4.43 | −5.92 | −13.15 | −15.90 | −6.67 | −6.65 |
| Canada | −1.02 | −2.37 | −15.07 | −18.12 | −4.33 | −4.87 |
| China | −2.33 | −4.97 | −5.13 | −6.73 | −4.67 | −2.76 |
| Developing Europe | −0.28 | −3.11 | −0.56 | −7.38 | −2.73 | 0.39 |
| Europe | −1.02 | −2.84 | −9.64 | −11.02 | −4.01 | −1.62 |
| France | −1.15 | −2.80 | −8.35 | −9.48 | −3.68 | −1.56 |
| Germany | −0.77 | −2.38 | −8.58 | −9.38 | −3.63 | −1.21 |
| India | −3.45 | −8.61 | −16.43 | −17.74 | −8.71 | −3.86 |
| Italy | −0.15 | −3.69 | −9.23 | −12.88 | −4.85 | −0.89 |
| Japan | −1.26 | −4.14 | −7.16 | −10.05 | −4.61 | −1.40 |
| Latam | −4.35 | −6.10 | −12.70 | −14.58 | −6.97 | −5.74 |
| Middle East | −9.97 | −7.98 | −22.03 | −21.96 | −10.28 | −15.24 |
| Russia | −12.18 | −2.26 | −23.46 | −23.80 | −7.54 | −17.11 |
| South Africa | −2.02 | −5.06 | −7.24 | −9.16 | −5.38 | −3.04 |
| South Korea | 0.11 | −3.49 | −3.23 | −7.57 | −3.33 | 0.12 |
| Spain | −2.41 | −3.81 | −12.49 | −12.89 | −5.41 | −3.30 |
| Switzerland | 2.32 | −2.25 | −9.47 | −10.35 | −2.18 | 2.30 |
| United Kingdom | −0.86 | −1.90 | −6.50 | −8.05 | −2.56 | −1.33 |
| United States | −2.67 | −4.38 | −15.37 | −17.66 | −6.31 | −4.36 |
| World | −3.51 | −5.26 | −11.53 | −13.37 | −6.16 | −4.84 |

Source: https://data.ene.iiasa.ac.at/ngfs.

The previous analysis can be extended to other economic variables. In Figure 8.128, we show the impact on inflation, unemployment, private investment, productivity, equity prices and public investment in the case of China. With respect to the baseline scenario, the delayed transition may induce more inflation (up to 6%) and unemployment (up to 0.8%) between 2030 and 2040, and less public and private investments. It may also strongly impact the equity market and the financial performance of stocks. Finally, the economy may be less productive. We have reported a similar analysis in the case of United States, France and United Kingdom in Figures 8.129, 8.130 and 8.131. Again, we notice that the impact on the economy depends on the country or region. Even if there is no winner for some scenarios, some countries will loose less than others. Climate change will then create new inequalities between regions. In particular, two regions seems to be especially vulnerable: Africa and the Middle East.

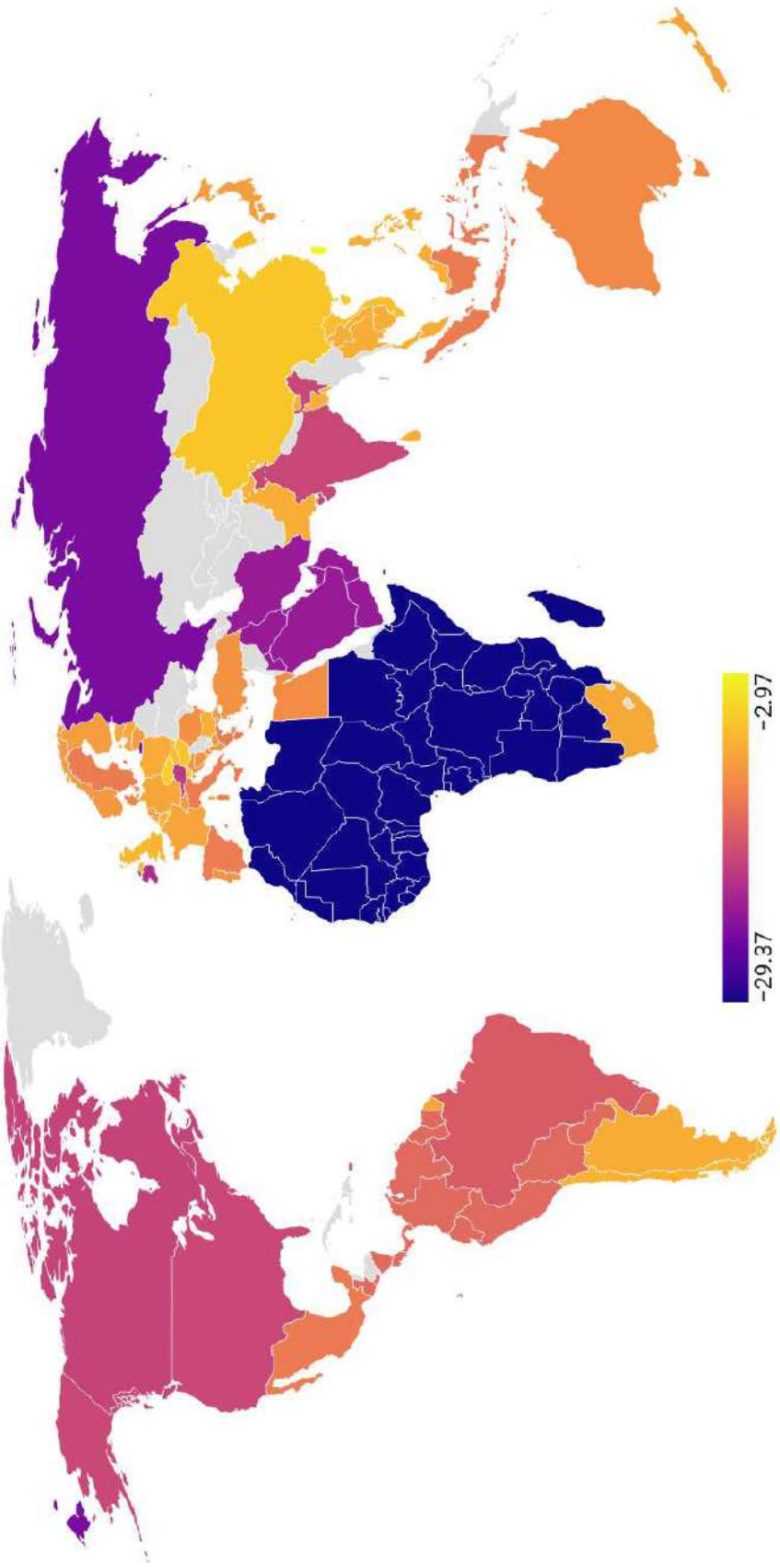


Figure 8.126: GDP impact by 2050 (% change from baseline) — Delayed transition scenario

Source: https://data.ene.iiasa.ac.at/ngfs & Author's calculations (created by Datawrapper).

Figure 8.127: GDP impact by 2050 (% change from baseline) — Net-zero 2050 scenario

Source: https://data.ene.iiasa.ac.at/ngfs & Author's calculations (created by Datawrapper).

Figure 8.128: Impact of climate scenarios on economics (% change from baseline) — China

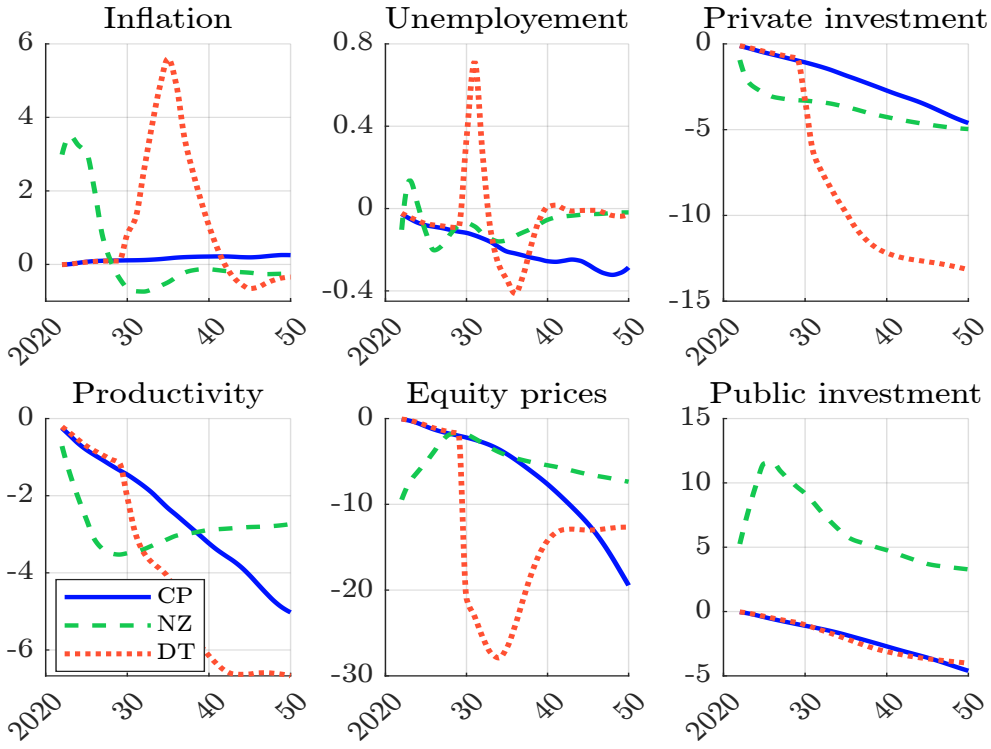


Source: https://data.ene.iiasa.ac.at/ngfs & Author's calculations.

Figure 8.129: Impact of climate scenarios on economics (% change from baseline) — United States

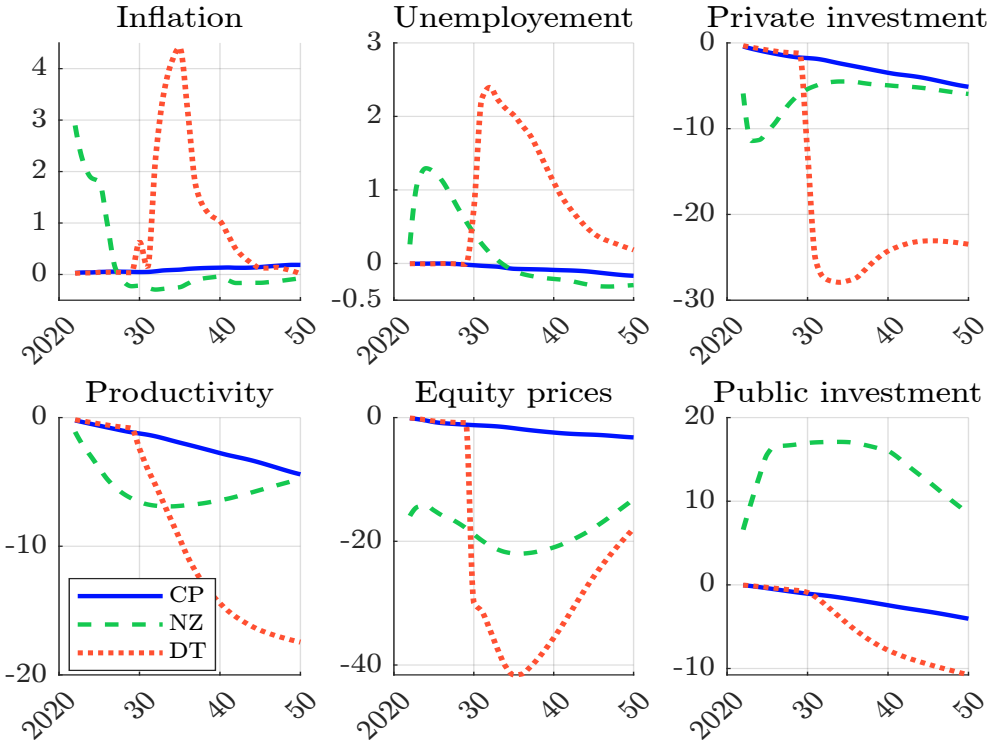


Source: https://data.ene.iiasa.ac.at/ngfs & Author's calculations.

Figure 8.130: Impact of climate scenarios on economics (% change from baseline) — France

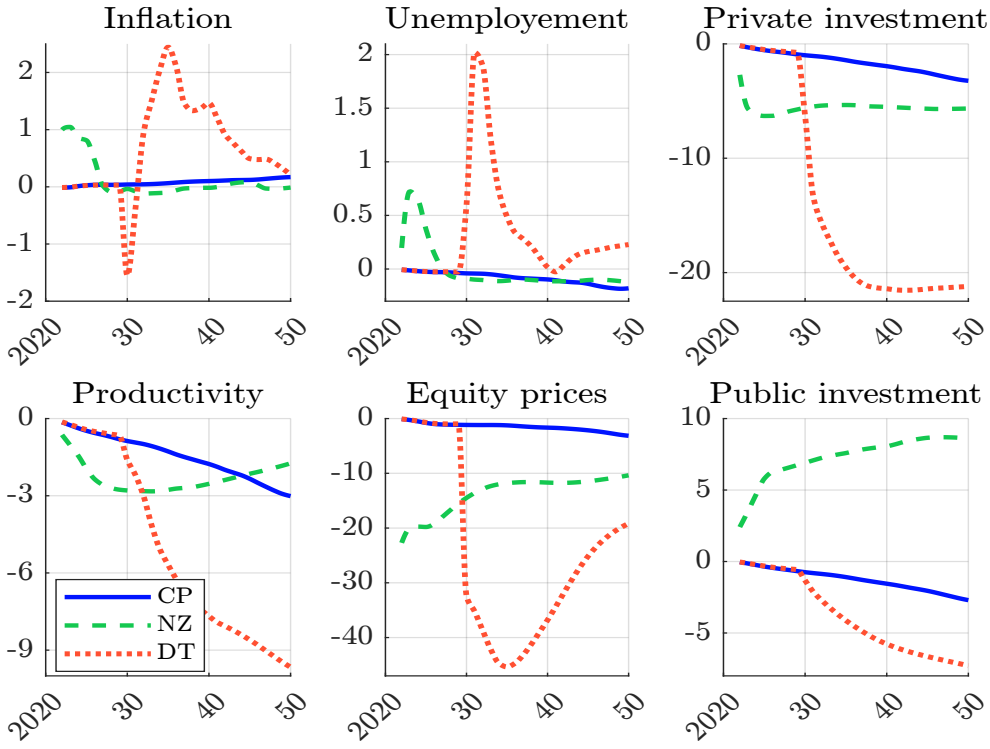


Source: https://data.ene.iiasa.ac.at/ngfs & Author's calculations.

Figure 8.131: Impact of climate scenarios on economics (% change from baseline) — United Kingdom

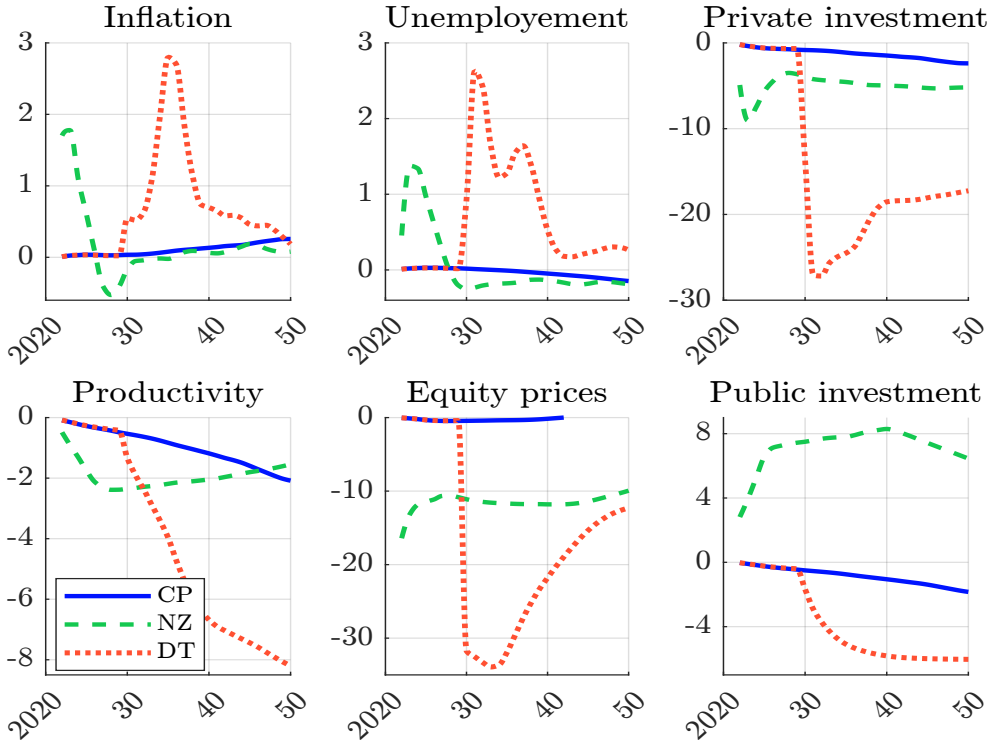


Source: https://data.ene.iiasa.ac.at/ngfs & Author's calculations.

## 8.4 Environmentally-extended input-output model

An input-output model is a mathematical tool that represents the macroeconomic relationships between different units or industries. It can be used to model the supply chain of a product, the sectoral structure of an economy, the production network of a country or the foreign exchange between regions. Most of these models are monetary in nature. When applied to economic transactions between different sectors, they can be used to calculate the contribution or value added of each sector to the final output of an economy. Environmentally-extended input-output (EEIO) analysis is an extension of the input-output framework to include environmental externalities such as pollution and greenhouse gas emissions. In particular, we can use EEIO models to estimate upstream Scope 3 emissions, define a stress testing framework or calculate the value-at-risk of a portfolio (Desnos *et al.*, 2023).

### 8.4.1 Input-output analysis

The input-output model was first introduced by Leontief (1936, 1941). It quantifies the interdependencies between different sectors in a single or multi-regional economy, based on the product flows between sectors (Miller and Blair, 2009). The underlying idea is to model the linkages between sectors and to describe the relationships from each of the producer/seller sectors to each of the purchaser/buyer sectors.

#### The demand-pull quantity model

Following Miller and Blair (2009), we consider $n$ different sectors and we note $Z_{i,j}$ the value of transactions from sector $i$ to sector $j$. We can interpret $Z_{i,j}$ in different ways:

1. It is the output that sector $i$ sells to sector $j$;
2. It is the input of sector $i$ required by sector $j$ for its production (or output).

Let $y_i$ be the final demand for products sold by sector $i$. This final demand is made up of the external sales to households, government purchases, and demand resulting from investment capacity and foreign trade. Then, the total production $x_i$ of sector $i$ is equal to:

$$\underbrace{x_i}_{\text{Supply}} = \underbrace{\sum_{j=1}^{n} Z_{i,j} + y_i}_{\text{Demand}} \tag{8.28}$$

In this equation, $x_i$ and $\sum_{j=1}^{n} Z_{i,j} + y_i$ are the supply and demand related to products of sector $i$, and $z_i = \sum_{j=1}^{n} Z_{i,j}$ represents intermediate demand. The interdependence relation between sectors is usually expressed as a ratio between $Z_{i,j}$ and $x_j$:

$$A_{i,j} = \frac{Z_{i,j}}{x_j}$$

Let $A = (A_{i,j}) = Z\,\mathrm{diag}\,(x)^{-1}$ be the input-output matrix of the technical coefficients $A_{i,j}$. In a matrix form, we have $x = Z\mathbf{1}_n + y$ and $Z \equiv A\,\mathrm{diag}\,(x) = A \odot x^\top$, and we deduce that:

$$x = Ax + y$$

where $x = (x_1, \ldots, x_n)$ and $y = (y_1, \ldots, y_n)$. Assuming that final demand is exogenous, technical coefficients are fixed and output is endogenous, we obtain:

$$x = (I_n - A)^{-1}\, y \tag{8.29}$$

$\boldsymbol{\mathcal{L}} = (I_n - A)^{-1}$ is known as the Leontief inverse (or multiplier) matrix and represents the amount of total output from sector $i$ that is required by sector $j$ to satisfy its final demand. Equation (8.29) describes a *demand-pull quantity* model.

**Example 29** *We consider the basic economy given below:*

| | | To | | | | Final | Total |
|---|---|---|---|---|---|---|---|
| | | Energy | Materials | Industrials | Services | Demand | Output |
| | | $Z$ | | | | $y$ | $x$ |
| From | Energy | 500 | 800 | 1 600 | 1 250 | 850 | 5 000 |
| | Materials | 500 | 400 | 1 600 | 625 | 875 | 4 000 |
| | Industrials | 250 | 800 | 2 400 | 1 250 | 3 300 | 8 000 |
| | Services | 100 | 200 | 800 | 4 375 | 7 025 | 12 500 |

*This basic economy has four sectors: energy, materials, industrials and services. In this economy, businesses in the energy sector buy* \$500 *of goods and services from other businesses in the energy sector,* \$500 *of goods and services from the materials sector,* \$250 *of goods and services from the industrials sector, and* \$100 *of goods and services from the services sector. The final demand for goods and services produced in the energy sector is equal to* \$850*, while the total output of this sector is equal to* \$5 000*.*

We deduce that the matrix of technical coefficients is equal to:

$$A = Z\,\mathrm{diag}\,(x)^{-1} = \begin{pmatrix} 10\% & 20\% & 20\% & 10\% \\ 10\% & 10\% & 20\% & 5\% \\ 5\% & 20\% & 30\% & 10\% \\ 2\% & 5\% & 10\% & 35\% \end{pmatrix}$$

It follows that the multiplier matrix is equal to:

$$\boldsymbol{\mathcal{L}} = (I_4 - A)^{-1} = \begin{pmatrix} 1.1881 & 0.3894 & 0.4919 & 0.2884 \\ 0.1678 & 1.2552 & 0.4336 & 0.1891 \\ 0.1430 & 0.4110 & 1.6303 & 0.3044 \\ 0.0715 & 0.1718 & 0.2993 & 1.6087 \end{pmatrix}$$

We verify that:

$$x = \boldsymbol{\mathcal{L}}y = \begin{pmatrix} 1.1881 & 0.3894 & 0.4919 & 0.2884 \\ 0.1678 & 1.2552 & 0.4336 & 0.1891 \\ 0.1430 & 0.4110 & 1.6303 & 0.3044 \\ 0.0715 & 0.1718 & 0.2993 & 1.6087 \end{pmatrix} \begin{pmatrix} 850 \\ 875 \\ 3\,300 \\ 7\,025 \end{pmatrix} = \begin{pmatrix} 5\,000 \\ 4\,000 \\ 8\,000 \\ 12\,500 \end{pmatrix}$$

Suppose we have a variation in final demand. From Equation (8.29), we obtain $\Delta x = \boldsymbol{\mathcal{L}}\Delta y$. For instance, an increase of \$10 in the final demand for services implies:

$$\Delta x = \boldsymbol{\mathcal{L}}\Delta y = \begin{pmatrix} 1.1881 & 0.3894 & 0.4919 & 0.2884 \\ 0.1678 & 1.2552 & 0.4336 & 0.1891 \\ 0.1430 & 0.4110 & 1.6303 & 0.3044 \\ 0.0715 & 0.1718 & 0.2993 & 1.6087 \end{pmatrix} \begin{pmatrix} 0 \\ 0 \\ 0 \\ 10 \end{pmatrix} = \begin{pmatrix} 2.8842 \\ 1.8907 \\ 3.0444 \\ 16.0872 \end{pmatrix}$$

This means that energy production increases by \$2.88, materials production increases by \$1.89, and so on.

### The cost-push price model

Let $m$ be number of primary inputs (*e.g.*, labor, capital, etc.). Let $V = (V_{k,j})$ be the value added matrix where $V_{k,j}$ represents the amount of primary input $k$ required to produce the output of sector $j$. Since the total input of each sector is equal to its total output, we have $x_j = \sum_{i=1}^{n} Z_{i,j} + \sum_{k=1}^{m} V_{k,j}$. Therefore, $v_j = \sum_{k=1}^{m} V_{k,j} = x_j - \sum_{i=1}^{n} Z_{i,j}$ represents the other expenditure of sector $j$ or the total primary inputs used in sector $j$. We have $v = (v_1, \ldots, v_n) = V^\top \mathbf{1}_m$. Let $p = (p_1, \ldots, p_n)$ and $\psi = (\psi_1, \ldots, \psi_m)$ be the vector of sector prices and primary inputs. $p_j$ and $\psi_k$ are then the prices per unit of sector $j$ and primary input $k$. As in the quantity model, the interdependence relationship between primary inputs and sectors is expressed as the ratio between $V_{k,j}$ and $x_j$:

$$B_{k,j} = \frac{V_{k,j}}{x_j}$$

We denote the input-output matrix of the technical coefficients by $B = (B_{k,j}) \equiv V \operatorname{diag}(x)^{-1}$. Following Gutierrez (2008), the value of the output must be equal to the value of its inputs:

$$\underbrace{p_j x_j}_{\text{Value of the output}} = \underbrace{\sum_{i=1}^{n} Z_{i,j} p_i + \sum_{k=1}^{m} V_{k,j} \psi_k}_{\text{Value of the inputs}}$$

We deduce that:

$$\begin{aligned} p_j &= \sum_{i=1}^{n} \frac{Z_{i,j}}{x_j} p_i + \sum_{k=1}^{m} \frac{V_{k,j}}{x_j} \psi_k \\ &= \sum_{i=1}^{n} A_{i,j} p_i + \sum_{k=1}^{m} B_{k,j} \psi_k \end{aligned}$$

In a matrix form, we get $p = A^\top p + B^\top \psi$. $v = B^\top \psi$ is the vector of value added ratios. Finally, the output prices are equal to:

$$p = \left(I_n - A^\top\right)^{-1} v \tag{8.30}$$

$\tilde{\boldsymbol{\mathcal{L}}} = \left(I_n - A^\top\right)^{-1}$ is known as the dual inverse matrix and represents the amount of costs from sector $j$ that are passed on to sector $i$. Equation (8.30) describes a *cost-push price* model. By adding the income identity[134], Gutierrez (2008) proposed the following complete version of the full basic input-output model:

$$\begin{cases} x = (I_n - A)^{-1} y \\ v = V^\top \mathbf{1}_m \\ v = B^\top \psi \\ p = \left(I_n - A^\top\right)^{-1} v \\ x^\top v = y^\top p \end{cases} \tag{8.31}$$

It mixes both the quantity and price models. In this system, $A$, $B$ and $V$ are the model parameters, $\psi$, $v$ and $y$ are the exogenous variables, and $x$ and $p$ are the endogenous variables. By changing the model parameters or the exogenous variables, we can measure the impacts $\Delta y$ and $\Delta v$ on the quantities and prices in the economy.

**Remark 88** *The previous analysis was derived for physical input-output tables, where flows are expressed in product units. However, the analysis remains valid when monetary input-output tables*

[134] Since the input-output analysis assumes an equilibrium model, the total value of the revenues $y^\top p$ is equal to the total value of costs $x^\top v$.

*are considered. The only difference is the calculation of the primary cost vector. In a monetary input-output analysis, $\psi$ is set by construction to $\mathbf{1}_m$, which means that $v = B^\top \mathbf{1}_m = (v_1/x_1, \ldots, v_n/x_n)$ and $p = \mathbf{1}_n$ (Miller and Blair, 2009, Section 2.6.3, pages 43-44).*

**Example 30** *We consider the previous basic economy. We assume that the value added is made up of two items: labour and capital. We have:*

| | | To | | | | Final | Total |
|---|---|---|---|---|---|---|---|
| | | Energy | Materials | Industrials | Services | Demand | Output |
| | | $Z$ | | | | $y$ | $x$ |
| From | Energy | 500 | 800 | 1 600 | 1 250 | 850 | 5 000 |
| | Materials | 500 | 400 | 1 600 | 625 | 875 | 4 000 |
| | Industrials | 250 | 800 | 2 400 | 1 250 | 3 300 | 8 000 |
| | Services | 100 | 200 | 800 | 4 375 | 7 025 | 12 500 |
| Value added | Labour | 3 000 | 800 | 1 000 | 3 000 | | |
| | Capital | 650 | 1 000 | 600 | 2 000 | | |
| | Income | 5 000 | 4 000 | 8 000 | 12 500 | | |

*The energy sector has a labour consumption of* \$3 000 *and a total output of* \$5 000*. By construction, the income of the sector is equal to the output of the sector. We deduce that the capital item (capital interest and net profit) is equal to* \$650*.*

We have:

$$V = \begin{pmatrix} 3\,000 & 800 & 1\,000 & 3\,000 \\ 650 & 1\,000 & 600 & 2\,000 \end{pmatrix}$$

and:

$$v = V^\top \mathbf{1}_2 = x - Z^\top \mathbf{1}_4 = \begin{pmatrix} 3\,650 \\ 1\,800 \\ 1\,600 \\ 5\,000 \end{pmatrix}$$

We deduce that:

$$B = \begin{pmatrix} 0.60 & 0.20 & 0.125 & 0.24 \\ 0.13 & 0.25 & 0.075 & 0.16 \end{pmatrix}$$

Since we have a monetary input-output table, the labour and capital costs are equal to the monetary unit, *i.e.*, one dollar ($\psi_1 = \psi_2 = 1$). It follows that:

$$v = B^\top \mathbf{1}_2 = \begin{pmatrix} 0.73 \\ 0.45 \\ 0.20 \\ 0.40 \end{pmatrix}$$

The interpretation is as follows. For the energy sector, intermediate consumption is 27% and value added is 73%. For the other three sectors, the value added ratios are 45%, 20% and 40% respectively. Finally, we obtain:

$$\tilde{\boldsymbol{\mathcal{L}}} = \left(I_n - A^\top\right)^{-1} = \begin{pmatrix} 1.1881 & 0.1678 & 0.1430 & 0.0715 \\ 0.3894 & 1.2552 & 0.4110 & 0.1718 \\ 0.4919 & 0.4336 & 1.6303 & 0.2993 \\ 0.2884 & 0.1891 & 0.3044 & 1.6087 \end{pmatrix}$$

and:

$$p = \tilde{\boldsymbol{\mathcal{L}}} v = \mathbf{1}_4$$

We check that the prices in a monetary input-output table are normalized to one dollar. In this basic economy, the total final demand $y^\top p$ is equal to \$12 050, which is equal to the total value added $x^\top v$. Suppose we have a variation in the labour/capital costs. From Equation (8.31), we obtain $\Delta p = \tilde{\boldsymbol{\mathcal{L}}} \Delta v$. For example, a 10% increase in costs in the energy sector means that the price of energy increases by 11.88%, the price of materials by 3.89%, and so on:

$$\Delta p = \tilde{\boldsymbol{\mathcal{L}}} \Delta v = \begin{pmatrix} 1.1881 & 0.1678 & 0.1430 & 0.0715 \\ 0.3894 & 1.2552 & 0.4110 & 0.1718 \\ 0.4919 & 0.4336 & 1.6303 & 0.2993 \\ 0.2884 & 0.1891 & 0.3044 & 1.6087 \end{pmatrix} \begin{pmatrix} 0.10 \\ 0.00 \\ 0.00 \\ 0.00 \end{pmatrix} = \begin{pmatrix} 11.88\% \\ 3.89\% \\ 4.92\% \\ 2.88\% \end{pmatrix}$$

The definition of a price index is:

$$\mathcal{PI} = \sum_{j=1}^{n} \alpha_j p_j = \alpha^\top p$$

where $\alpha = (\alpha_1, \ldots, \alpha_n)$ is the weights of the basket of items. We deduce that the inflation rate between two dates $t_0$ and $t_1$ is:

$$\pi = \frac{\mathcal{PI}(t_1) - \mathcal{PI}(t_0)}{\mathcal{PI}(t_0)} = \frac{\alpha^\top \left(I_n - A^\top\right)^{-1} \Delta v(t_0, t_1)}{\alpha^\top (I_n - A^\top)^{-1} v(t_0)}$$

We can simplify this formula because $p(t_0) = \left(I_n - A^\top\right)^{-1} v(t_0) = \mathbf{1}_n$ and $\mathbf{1}_n^\top \alpha = 1$. Finally, we have:

$$\pi = \alpha^\top \left(I_n - A^\top\right)^{-1} \Delta v \tag{8.32}$$

In general, we define two price indexes: the producer price index (PPI) where the basket weights are proportional to the output ($\alpha_j \propto x_j$) and the consumer price index (CPI) where the basket weights are proportional to the final demand ($\alpha_j \propto y_j$). In the latter case we obtain:

$$\text{CPI} = \frac{y^\top \left(I_n - A^\top\right)^{-1} \Delta v}{\mathbf{1}_n^\top y} = \frac{\Delta v^\top (I_n - A)^{-1} y}{\mathbf{1}_n^\top y} = \frac{\Delta v^\top x}{\mathbf{1}_n^\top y} = \frac{\sum_{j=1}^n x_j \Delta v_j}{\sum_{j=1}^n y_j}$$

Looking at the previous example, a 10% increase in energy costs will cause the producer price index to rise by 5.10% and the consumer price index by 4.15%.

### Mathematical properties

Since we have $\left(I_n - A^\top\right)^{-1} = \left((I_n - A)^\top\right)^{-1} = \left((I_n - A)^{-1}\right)^\top$, we deduce that $\tilde{\boldsymbol{\mathcal{L}}} = \boldsymbol{\mathcal{L}}^\top$. So we can study $\boldsymbol{\mathcal{L}}$ or $\tilde{\boldsymbol{\mathcal{L}}}$ indifferently, because they share the same properties. The matrix $\boldsymbol{\mathcal{L}}$ admits the following Neumann series:

$$\begin{aligned} \boldsymbol{\mathcal{L}} &= (I_n - A)^{-1} \\ &= I_n + A + A^2 + A^3 + \ldots \\ &= \sum_{k=0}^{\infty} A^k \end{aligned} \tag{8.33}$$

Box 8.19: Neumann series

A Neumann series is a mathematical series of the form $S := \sum_{k=0}^{\infty} T^k$ where $T$ is a bounded linear operator and $T^k = T^{k-1} \circ T = T \circ T^{k-1}$. If the Neumann series converges in the operator norm, then $\mathrm{Id} - T$ is invertible and its inverse is the Neumann series:

$$(\mathrm{Id} - T)^{-1} = S = \sum_{k=0}^{\infty} T^k$$

where Id is the identity operator. A sufficient condition is that the spectral radius of $T$ is less than one. If $A$ is an invertible matrix, we conclude that:

$$(I_n - A)^{-1} = \sum_{k=0}^{\infty} A^k$$

and $\lim_{k=0} \left\| A^k \right\| = 0$. This result generalizes the geometric series:

$$\frac{1}{1-x} = 1 + x + x^2 + \ldots \qquad \text{where } |x| < 1$$

Since $A$ is a doubly substochastic matrix[135], the eigendecomposition of $A$ is $A = V\Lambda V^{-1}$ where $V$ is the matrix of eigenvectors, $\Lambda = \mathrm{diag}\,(\lambda_1, \ldots, \lambda_n)$ and $|\lambda_i| \leq 1$. If we assume that $A$ is irreducible, the Perron-Frobenius theorem states that the spectral radius $\varrho\,(A)$ is strictly lower than 1 and corresponds to the largest positive eigenvalue $\lambda_1$. This implies that all the eigenvalues $\lambda_1 \geq \lambda_2 \geq \ldots \geq \lambda_n$ satisfies $|\lambda_i| < 1$. As we have $A^k = V\Lambda^k V^{-1}$, we deduce that $\lim_{k\to\infty} A^k = V\Lambda^k V^{-1} = \mathbf{0}_{n,n}$. The Neumann series $\sum_{k=0}^{\infty} A^k$ converges then to a finite matrix, which implies that the multiplier matrix $\boldsymbol{\mathcal{L}}$ is nonsingular.

From Equation (8.33), we deduce that $\boldsymbol{\mathcal{L}} \succeq I_n$ because $A^k \succeq \mathbf{0}_{n,n}$ for $k \geq 1$ (Property NN4 on page 1056). We also get the following decomposition:

$$\begin{aligned} x &= \sum_{k=0}^{\infty} A^k y \\ &= y + Ay + A^2 y + \ldots \\ &= \sum_{k=0}^{\infty} y_{(k)} \end{aligned}$$

where $y_{(0)} = y$ is the final demand (or zero-tier intermediate demand), $y_{(1)} = Ay$ is the first-tier intermediate demand, $y_{(2)} = A^2 y$ is the second-tier intermediate demand, and $y_{(k)} = A^k y$ is the $k^{\text{th}}$-tier intermediate demand. Furthermore, we have:

$$\frac{\partial\, x}{\partial\, y} = (I_n - A)^{-1} \equiv \boldsymbol{\mathcal{L}} \succeq I_n$$

We can better understand why the matrix $\boldsymbol{\mathcal{L}}$ is also called the multiplier matrix because it is an analogy to Keynesian consumption theory and the effect of a change in aggregate demand on the output.

[135] See Appendix A.1.4 on page 1056.

Table 8.42: Tier decomposition of the output (Example 29)

| | $k$ | 0 | 1 | 2 | 3 | 4 | 5 |
|---|---|---|---|---|---|---|---|
| $y_{(k)}$ | Energy | 850.0 | 1 622.5 | 1 066.0 | 630.8 | 362.1 | 205.2 |
| | Materials | 875.0 | 1 183.8 | 805.1 | 486.3 | 282.1 | 160.7 |
| | Industrials | 3 300.0 | 1 910.0 | 1 175.8 | 695.1 | 400.0 | 227.1 |
| | Services | 7 025.0 | 2 849.5 | 1 280.0 | 627.1 | 325.9 | 175.4 |
| $y_{(0:k)}$ | Energy | 850.0 | 2 472.5 | 3 538.5 | 4 169.2 | 4 531.3 | 4 736.5 |
| | Materials | 875.0 | 2 058.8 | 2 863.9 | 3 350.1 | 3 632.2 | 3 792.9 |
| | Industrials | 3 300.0 | 5 210.0 | 6 385.8 | 7 080.9 | 7 480.9 | 7 708.0 |
| | Services | 7 025.0 | 9 874.5 | 11 154.5 | 11 781.6 | 12 107.5 | 12 283.0 |

In Tables 8.42 and 8.43, we report the values of intermediate demand $y_{(k)}$ in the case of Example 29. It can be seen that the first-tier intermediate demand is larger than final demand when we look at the energy and materials sector. For instance, we have $y_{(1),1} = 1622.5$ but $y_{(0),1} = y_1 = 850$. In the case of industrials and services, we obtain the opposite effect. We also check that the $k$-tier intermediate demand converges to zero. We have also reported the cumulative demand of the first $k$ tiers: $y_{(0:k)} = \sum_{h=0}^{k} y_{(k)}$. This illustrates that $\lim_{k\to\infty} y_{(0:k)} = x$.

Table 8.43: Tier decomposition of the output (Example 29)

| | $k$ | 10 | 20 | 25 |
|---|---|---|---|---|
| $y_{(k)}$ | Energy | 11.45 | 0.03 | 0.00 |
| | Materials | 9.01 | 0.03 | 0.00 |
| | Industrials | 12.69 | 0.04 | 0.00 |
| | Services | 9.29 | 0.03 | 0.00 |
| $y_{(0:k)}$ | Energy | 4 985.42 | 4 999.96 | 5 000.00 |
| | Materials | 3 988.52 | 3 999.97 | 4 000.00 |
| | Industrials | 7 983.83 | 7 999.95 | 8 000.00 |
| | Services | 12 488.18 | 12 499.96 | 12 500.00 |

Since $y_{(k)}$ converges to $\mathbf{0}_n$, we can ask whether this convergence is monotone. In particular, do we check that $y_{(k)} \succeq y_{(k+1)}$? The answer to this question is no. In fact, we can easily find counterexamples. The reason is that $A^k \not\succeq A^{k+1}$. For instance, we have seen that $y_{(1),1} \geq y_{(0),1}$ in Example 29. Nevertheless, we observe empirically that the relation $y_{(k)} \succeq y_{(k+1)}$ is satisfied for $k \geq k^\star$. This means that for sufficiently large $k$, the contribution of the $k^{\text{th}}$ tier decreases with respect to $k$. A sufficient (but not necessary) condition is that $A^k \succeq A^{k+1}$ for $k = k^\star$. Let us assume that $A^k \succeq A^{k+1}$ holds for $k = k^\star$. Let us note $B = A^k$, $C = A^{k+1}$ and $D = A$. Property NN1 (Appendix A.1.4 on page 1056) implies that $BD \succeq CD$. This means that if $A^k \succeq A^{k+1}$, then $A^{k+1} \succeq A^{k+2}$. We conclude that if $A^k \succeq A^{k+1}$ for $k = k^\star$, then $A^k \succeq A^{k+1}$ for $k \geq k^\star$ and the relation $y_{(k)} \succeq y_{(k+1)}$ is satisfied for $k \geq k^\star$ if we assume that $y \succeq \mathbf{0}_n$.

**Remark 89** *Theoretically, the partial monotonicity property does not hold if some elements of final demand are negative. Empirically, we observe that the property is always satisfied because* $y_{(0:k)}$ *converges to* $\boldsymbol{\mathcal{L}}y$ *and the production is always positive:* $\boldsymbol{\mathcal{L}}y \equiv x \succeq \mathbf{0}_n$.

Looking again at our numerical example, we check that the monotonicity property $y_{(k)} \succeq y_{(k+1)}$ is satisfied for $k \geq 1$.

### Multi-regional input-output analysis

While an input-output table (IOT) usually covers only one region and tracks economic flows between sectors within that region, a multi-regional input-output table (MRIO) involves several regions. It includes national harmonized input-output tables and export and import data calculated within the same sectoral structure. The two best known MRIO databases are GTAP (global trade analysis project) and WIOD (world input-output database). They can be downloaded from `www.gtap.agecon.purdue.edu` and `www.rug.nl/ggdc/valuechain/wiod` respectively. The advantage of WIOD is that it is free, which is not the case with GTAP. However, the latest version is from November 2014. An alternative is to use the input-output tables provided by the OECD. The data can be found at `https://stats.oecd.org/Index.aspx?DataSetCode=IOTS`. Below we describe the WIOD table in order to understand the basic structure of an MRIO database.

We download the zipped file `WIOTS_in_EXCEL.zip` with the button `WIOT tables Excel` from `www.rug.nl/ggdc/valuechain/wiod/wiod-2016-release` and use the Excel binary spreadsheet `WIOT2014_Nov16_ROW.xlsb`, which is shown in Figure 8.132. This file contains the 2014 input-output table for 44 regions (28 EU countries, 15 other major countries and a global region corresponding to the rest-of-the-world aggregate) and 56 sectors. The list of countries and their ISO codes can be found in Table 8.45. ROW is the ISO code for the rest of the world. We also report the list of industries in Table 8.44. A comprehensive description of database can be found in Dietzenbacher *et al.* (2023) and Timmer *et al.* (2015). The structure of the database is:

| | $Z$<br>$(56 \times 44) \times (56 \times 44)$ | $y$<br>$(56 \times 44) \times (5 \times 44)$ | $x$<br>$(56 \times 44) \times 1$ |
|---|---|---|---|
| Sum | $1 \times (56 \times 44)$ | $1 \times (5 \times 44)$ | $\mathbf{0}_{1,1}$ |
| Value added | $V$<br>$6 \times (56 \times 44)$ | $6 \times (5 \times 44)$ | $\mathbf{0}_{6,1}$ |
| Output | $w$<br>$1 \times (56 \times 44)$ | $\mathbf{0}_{6,5\times44}$ | $\mathbf{0}_{1,1}$ |

We have five main blocks of matrices: $Z$, $y$, $x$, $V$ and $w$. First we have the matrix $Z$ with 2 464 rows and 2 464 columns. It shows the flows between all sectors for all countries. For instance, the first 56 rows correspond to the 56 sectors of Australia (AUS), the first 56 columns correspond to the 56 sectors of Australia (AUS), the next 56 columns correspond to the 56 sectors of Austria (AUT). The structure of $Z$ is then:

| | | To | | | | |
|---|---|---|---|---|---|---|
| | | AUS | AUT | $\cdots$ | USA | ROW |
| From | AUS | AUS $\longrightarrow$ AUS | AUS $\longrightarrow$ AUT | $\cdots$ | AUS $\longrightarrow$ USA | AUS $\longrightarrow$ ROW |
| | AUT | AUT $\longrightarrow$ AUS | AUT $\longrightarrow$ AUT | | AUT $\longrightarrow$ USA | AUT $\longrightarrow$ ROW |
| | $\vdots$ | $\vdots$ | | | | $\vdots$ |
| | ROW | ROW $\longrightarrow$ AUS | ROW $\longrightarrow$ AUT | $\cdots$ | ROW $\longrightarrow$ USA | ROW $\longrightarrow$ ROW |

The dimension of each submatrix $\mathcal{C}_i \longrightarrow \mathcal{C}_j$ is equal to $56 \times 56$. All the items are expressed in millions of dollars. For example, we read in Figure 8.132 that $Z_{1,1} = \$12\,924$ mn and $Z_{1,2} = \$112$ mn. This means that the sector *crop and animal production, hunting and related service activities* in Australia sells \$12.924 bn and \$112 mn of goods and services to this sector and the sector *forestry and logging* in Australia. Second, the matrix $y$ consists of five final demand items: (a) final consumption expenditure by households; (b) final consumption expenditure by non-profit organisations serving households (NPISH); (c) final consumption expenditure by government; (d)

Figure 8.132: World input-output database (November 2014)

| | A | B | C | D | E | F | G | H | I | J | K | L | M | N | O | P | Q | R | S |
|---|---|---|---|---|---|---|---|---|---|---|---|---|---|---|---|---|---|---|---|
| 1 | **Intercountry Input-Output Table** | | | | | | | | | | | | | | | | | | |
| 2 | 43 countries, in current prices | | | | | | | | | | | | | | | | | | |
| 3 | (industry-by-industry) | | | | A01 animal production, hunting and related service activities | A02 Forestry and logging | A03 Fishing and aquaculture | B Mining and quarrying | C10-C12 e of food products, beverages and tobacco products | C13-C15 e of textiles, wearing apparel and leather products | C16 e of wood and of products of wood and cork, except | C17 Manufactur e of paper and paper products | C18 Printing and reproductio n of recorded media | C19 Manufactur e of coke and refined petroleum products | C20 Manufactur e of chemicals and chemical products | C21 e of basic pharmaceu tical products and pharmaceu | C22 Manufactur e of rubber and plastic products | C23 Manufactur e of other non-metallic mineral products | C24 Manufactur e of basic metals |
| 4 | (millions of US$) | | | | | | | | | | | | | | | | | | |
| 5 | | | | | AUS | AUS | AUS | AUS | AUS | AUS | AUS | AUS | AUS | AUS | AUS | AUS | AUS | AUS | AUS |
| 6 | | | | | **c1** | **c2** | **c3** | **c4** | **c5** | **c6** | **c7** | **c8** | **c9** | **c10** | **c11** | **c12** | **c13** | **c14** | **c15** |
| 7 | A01 | oduction, hunting and related service activities | AUS | **r1** | 12 924 | 112 | 228 | 539 | 25 139 | 737 | 4 | 3 | 2 | 0 | 87 | 109 | 147 | 5 | 8 |
| 8 | A02 | Forestry and logging | AUS | **r2** | 83 | 201 | 0 | 17 | 3 | 0 | 1 431 | 0 | 5 | 0 | 161 | 30 | 25 | 1 | 1 |
| 9 | A03 | Fishing and aquaculture | AUS | **r3** | 19 | 0 | 19 | 4 | 316 | 23 | 0 | 0 | 0 | 0 | 0 | 0 | 0 | 1 | 1 |
| 10 | B | Mining and quarrying | AUS | **r4** | 116 | 1 | 6 | 4 492 | 332 | 6 | 30 | 50 | 21 | 10 760 | 551 | 25 | 50 | 611 | 11 722 |
| 11 | C10-C12 | od products, beverages and tobacco products | AUS | **r5** | 1 591 | 1 | 43 | 203 | 10 852 | 262 | 11 | 18 | 11 | 3 | 243 | 109 | 28 | 21 | 33 |
| 12 | C13-C15 | textiles, wearing apparel and leather products | AUS | **r6** | 42 | 1 | 3 | 92 | 67 | 66 | 7 | 7 | 13 | 1 | 29 | 12 | 22 | 22 | 22 |
| 13 | C16 | cture of articles of straw and plaiting materials | AUS | **r7** | 23 | 0 | 1 | 32 | 11 | 3 | 547 | 187 | 2 | 0 | 3 | 1 | 11 | 20 | 24 |
| 14 | C17 | Manufacture of paper and paper products | AUS | **r8** | 28 | 0 | 0 | 51 | 652 | 8 | 15 | 579 | 433 | 1 | 70 | 117 | 45 | 88 | 11 |
| 15 | C18 | Printing and reproduction of recorded media | AUS | **r9** | 65 | 0 | 1 | 239 | 87 | 5 | 9 | 67 | 404 | 1 | 22 | 24 | 15 | 30 | 37 |
| 16 | C19 | cture of coke and refined petroleum products | AUS | **r10** | 877 | 230 | 117 | 2 248 | 105 | 7 | 17 | 20 | 13 | 101 | 501 | 9 | 129 | 75 | 684 |
| 17 | C20 | ufacture of chemicals and chemical products | AUS | **r11** | 772 | 0 | 2 | 565 | 141 | 11 | 41 | 141 | 67 | 20 | 865 | 469 | 909 | 200 | 98 |
| 18 | C21 | cal products and pharmaceutical preparations | AUS | **r12** | 667 | 0 | 1 | 197 | 42 | 1 | 6 | 35 | 6 | 1 | 30 | 677 | 24 | 24 | 38 |
| 19 | C22 | Manufacture of rubber and plastic products | AUS | **r13** | 86 | 1 | 8 | 248 | 366 | 15 | 41 | 86 | 170 | 3 | 197 | 96 | 260 | 62 | 41 |
| 20 | C23 | facture of other non-metallic mineral products | AUS | **r14** | 29 | 0 | 1 | 138 | 248 | 1 | 45 | 7 | 4 | 1 | 64 | 67 | 21 | 1 349 | 125 |
| 21 | C24 | Manufacture of basic metals | AUS | **r15** | 44 | 0 | 2 | 628 | 48 | 4 | 28 | 24 | 13 | 3 | 22 | 12 | 32 | 89 | 3 079 |
| 22 | C25 | al products, except machinery and equipment | AUS | **r16** | 151 | 1 | 22 | 2 053 | 321 | 8 | 116 | 68 | 21 | 2 | 119 | 45 | 98 | 540 | 396 |
| 23 | C26 | re of computer, electronic and optical products | AUS | **r17** | 32 | 0 | 2 | 112 | 29 | 2 | 4 | 7 | 7 | 0 | 6 | 7 | 5 | 10 | 13 |
| 24 | C27 | Manufacture of electrical equipment | AUS | **r18** | 36 | 0 | 8 | 179 | 40 | 2 | 3 | 16 | 5 | 0 | 7 | 4 | 13 | 10 | 25 |
| 25 | C28 | anufacture of machinery and equipment n.e.c. | AUS | **r19** | 290 | 1 | 68 | 2 172 | 232 | 6 | 19 | 35 | 54 | 1 | 52 | 23 | 27 | 92 | 123 |
| 26 | C29 | ure of motor vehicles, trailers and semi-trailers | AUS | **r20** | 38 | 0 | 4 | 112 | 39 | 3 | 5 | 5 | 6 | 0 | 10 | 7 | 4 | 13 | 16 |
| 27 | C30 | Manufacture of other transport equipment | AUS | **r21** | 52 | 0 | 31 | 212 | 23 | 1 | 3 | 6 | 7 | 0 | 6 | 7 | 4 | 11 | 11 |
| 28 | C31_C32 | Manufacture of furniture; other manufacturing | AUS | **r22** | 18 | 0 | 1 | 56 | 30 | 3 | 17 | 9 | 5 | 0 | 10 | 5 | 8 | 12 | 17 |
| 29 | C33 | r and installation of machinery and equipment | AUS | **r23** | 0 | 0 | 0 | 0 | 0 | 0 | 0 | 0 | 0 | 0 | 0 | 0 | 0 | 0 | 0 |
| 30 | D35 | tricity, gas, steam and air conditioning supply | AUS | **r24** | 517 | 3 | 14 | 3 138 | 1 163 | 73 | 188 | 328 | 112 | 885 | 641 | 165 | 313 | 404 | 2 640 |
| 31 | E36 | Water collection, treatment and supply | AUS | **r25** | 900 | 0 | 1 | 170 | 213 | 6 | 10 | 99 | 16 | 4 | 48 | 89 | 30 | 56 | 211 |
| 32 | E37-E39 | tivities and other waste management services | AUS | **r26** | 82 | 0 | 1 | 29 | 59 | 3 | 4 | 4 | 8 | 0 | 10 | 5 | 9 | 26 | 52 |
| 33 | F | Construction | AUS | **r27** | 1 683 | 1 | 12 | 7 508 | 296 | 14 | 374 | 60 | 66 | 5 | 55 | 61 | 45 | 112 | 230 |

2014

Source: Dietzenbacher *et al.* (2023); Timmer *et al.* (2015) & `www.rug.nl/ggdc/valuechain/wiod`.

Table 8.44: List of industries/sectors in the 2014 WIOD table

| No. | Name |
|---|---|
| $\mathcal{S}_1$ | Accommodation and food service activities |
| $\mathcal{S}_2$ | Activities auxiliary to financial services and insurance activities |
| $\mathcal{S}_3$ | Activities of extraterritorial organizations and bodies |
| $\mathcal{S}_4$ | Activities of households as employers; undifferentiated goods- and services-producing activities of households for own use |
| $\mathcal{S}_5$ | Administrative and support service activities |
| $\mathcal{S}_6$ | Advertising and market research |
| $\mathcal{S}_7$ | Air transport |
| $\mathcal{S}_8$ | Architectural and engineering activities; technical testing and analysis |
| $\mathcal{S}_9$ | Computer programming, consultancy and related activities; information service activities |
| $\mathcal{S}_{10}$ | Construction |
| $\mathcal{S}_{11}$ | Crop and animal production, hunting and related service activities |
| $\mathcal{S}_{12}$ | Education |
| $\mathcal{S}_{13}$ | Electricity, gas, steam and air conditioning supply |
| $\mathcal{S}_{14}$ | Financial service activities, except insurance and pension funding |
| $\mathcal{S}_{15}$ | Fishing and aquaculture |
| $\mathcal{S}_{16}$ | Forestry and logging |
| $\mathcal{S}_{17}$ | Human health and social work activities |
| $\mathcal{S}_{18}$ | Insurance, reinsurance and pension funding, except compulsory social security |
| $\mathcal{S}_{19}$ | Land transport and transport via pipelines |
| $\mathcal{S}_{20}$ | Legal and accounting activities; activities of head offices; management consultancy activities |
| $\mathcal{S}_{21}$ | Manufacture of basic metals |
| $\mathcal{S}_{22}$ | Manufacture of basic pharmaceutical products and pharmaceutical preparations |
| $\mathcal{S}_{23}$ | Manufacture of chemicals and chemical products |
| $\mathcal{S}_{24}$ | Manufacture of coke and refined petroleum products |
| $\mathcal{S}_{25}$ | Manufacture of computer, electronic and optical products |
| $\mathcal{S}_{26}$ | Manufacture of electrical equipment |
| $\mathcal{S}_{27}$ | Manufacture of fabricated metal products, except machinery and equipment |
| $\mathcal{S}_{28}$ | Manufacture of food products, beverages and tobacco products |
| $\mathcal{S}_{29}$ | Manufacture of furniture; other manufacturing |
| $\mathcal{S}_{30}$ | Manufacture of machinery and equipment n.e.c. |
| $\mathcal{S}_{31}$ | Manufacture of motor vehicles, trailers and semi-trailers |
| $\mathcal{S}_{32}$ | Manufacture of other non-metallic mineral products |
| $\mathcal{S}_{33}$ | Manufacture of other transport equipment |
| $\mathcal{S}_{34}$ | Manufacture of paper and paper products |
| $\mathcal{S}_{35}$ | Manufacture of rubber and plastic products |
| $\mathcal{S}_{36}$ | Manufacture of textiles, wearing apparel and leather products |
| $\mathcal{S}_{37}$ | Manufacture of wood and of products of wood and cork, except furniture; manufacture of articles of straw and plaiting materials |
| $\mathcal{S}_{38}$ | Mining and quarrying |
| $\mathcal{S}_{39}$ | Motion picture, video and television programme production, sound recording and music publishing activities; programming and broadcasting activities |
| $\mathcal{S}_{40}$ | Other professional, scientific and technical activities; veterinary activities |
| $\mathcal{S}_{41}$ | Other service activities |
| $\mathcal{S}_{42}$ | Postal and courier activities |
| $\mathcal{S}_{43}$ | Printing and reproduction of recorded media |
| $\mathcal{S}_{44}$ | Public administration and defence; compulsory social security |
| $\mathcal{S}_{45}$ | Publishing activities |
| $\mathcal{S}_{46}$ | Real estate activities |
| $\mathcal{S}_{47}$ | Repair and installation of machinery and equipment |
| $\mathcal{S}_{48}$ | Retail trade, except of motor vehicles and motorcycles |
| $\mathcal{S}_{49}$ | Scientific research and development |
| $\mathcal{S}_{50}$ | Sewerage; waste collection, treatment and disposal activities; materials recovery; remediation activities and other waste management services |
| $\mathcal{S}_{51}$ | Telecommunications |
| $\mathcal{S}_{52}$ | Warehousing and support activities for transportation |
| $\mathcal{S}_{53}$ | Water collection, treatment and supply |
| $\mathcal{S}_{54}$ | Water transport |
| $\mathcal{S}_{55}$ | Wholesale and retail trade and repair of motor vehicles and motorcycles |
| $\mathcal{S}_{56}$ | Wholesale trade, except of motor vehicles and motorcycles |

gross fixed capital formation; (e) changes in inventories and valuables. The sum of these five items is then the aggregate final demand. Third, the vector $x$ corresponds to the output. For example, $x_1 = \$70\,292$ mn is the total production of the sector *crop and animal production, hunting and related service activities* in Australia. The fourth block matrix is $V$ and has six rows: (a) taxes less subsidies on products; (b) cif/fob adjustments on exports; (c) direct purchases abroad by residents; (d) purchases on the domestic territory by non-residents; (e) value added at basic prices; (f) international transport margins. Again, we can aggregate these six items to calculate a total value added. Finally, the last block is the row vector $w$. By construction, we have $w_j = x_j$. For example, we check that $w_1$ is equal to $\$70\,292$ mn with the following decomposition: the total intermediate consumption is equal to $\$39\,039$ mn while the total value added is equal to $502 + 0 + 0 + 0 + 30\,489 + 262 = \$31\,253$ mn.

Table 8.45: List of countries/regions in the 2014 WIOD table

| No. | ISO | Name | No. | ISO | Name |
|---|---|---|---|---|---|
| $\mathcal{C}_1$ | AUS | Australia | $\mathcal{C}_2$ | AUT | Austria |
| $\mathcal{C}_3$ | BEL | Belgium | $\mathcal{C}_4$ | BGR | Bulgaria |
| $\mathcal{C}_5$ | BRA | Brazil | $\mathcal{C}_6$ | CAN | Canada |
| $\mathcal{C}_7$ | CHE | Switzerland | $\mathcal{C}_8$ | CHN | China |
| $\mathcal{C}_9$ | CYP | Cyprus | $\mathcal{C}_{10}$ | CZE | Czech Republic |
| $\mathcal{C}_{11}$ | DEU | Germany | $\mathcal{C}_{12}$ | DNK | Denmark |
| $\mathcal{C}_{13}$ | ESP | Spain | $\mathcal{C}_{14}$ | EST | Estonia |
| $\mathcal{C}_{15}$ | FIN | Finland | $\mathcal{C}_{16}$ | FRA | France |
| $\mathcal{C}_{17}$ | GBR | United Kingdom | $\mathcal{C}_{18}$ | GRC | Greece |
| $\mathcal{C}_{19}$ | HRV | Croatia | $\mathcal{C}_{20}$ | HUN | Hungary |
| $\mathcal{C}_{21}$ | IDN | Indonesia | $\mathcal{C}_{22}$ | IND | India |
| $\mathcal{C}_{23}$ | IRL | Ireland | $\mathcal{C}_{24}$ | ITA | Italy |
| $\mathcal{C}_{25}$ | JPN | Japan | $\mathcal{C}_{26}$ | KOR | Republic of Korea |
| $\mathcal{C}_{27}$ | LTU | Lithuania | $\mathcal{C}_{28}$ | LUX | Luxembourg |
| $\mathcal{C}_{29}$ | LVA | Latvia | $\mathcal{C}_{30}$ | MEX | Mexico |
| $\mathcal{C}_{31}$ | MLT | Malta | $\mathcal{C}_{32}$ | NLD | Netherlands |
| $\mathcal{C}_{33}$ | NOR | Norway | $\mathcal{C}_{34}$ | POL | Poland |
| $\mathcal{C}_{35}$ | PRT | Portugal | $\mathcal{C}_{36}$ | ROU | Romania |
| $\mathcal{C}_{37}$ | RUS | Russian Federation | $\mathcal{C}_{38}$ | SVK | Slovakia |
| $\mathcal{C}_{39}$ | SVN | Slovenia | $\mathcal{C}_{40}$ | SWE | Sweden |
| $\mathcal{C}_{41}$ | TUR | Turkey | $\mathcal{C}_{42}$ | TWN | Taiwan |
| $\mathcal{C}_{43}$ | USA | United States of America | $\mathcal{C}_{44}$ | ROW | Rest-of-the-world |

In Figure 8.133 we plot the sparsity pattern of the input-output matrix, and only the values of $A_{i,j}$ greater than 5% are colored. We see that the density of the matrix is mainly within the country submatrices. Outside of these intra-country matrices, the input-output table is sparse except for a few countries: China, Germany, Russia, USA and the rest-of-the-world region.

Let us now analyze the Leontief matrix $\boldsymbol{\mathcal{L}} = (I - A)^{-1}$. In Figure 8.134, we perform the eigen-decomposition $A = V\Lambda V^{-1}$ and plot the spectrum of $A$. Figure 8.135 shows the Frobenius norm of the matrix $A^k$ for $k = 0, \ldots, 10$ and the Leontief matrix $\boldsymbol{\mathcal{L}}$. We find that the convergence of the Leontief matrix is achieved very fast since the Frobenius norm of $A^k$ is less than 1 after the third tier and 0.1 after the seventh tier.

Figure 8.133: Sparsity pattern of the input-output matrix $A$

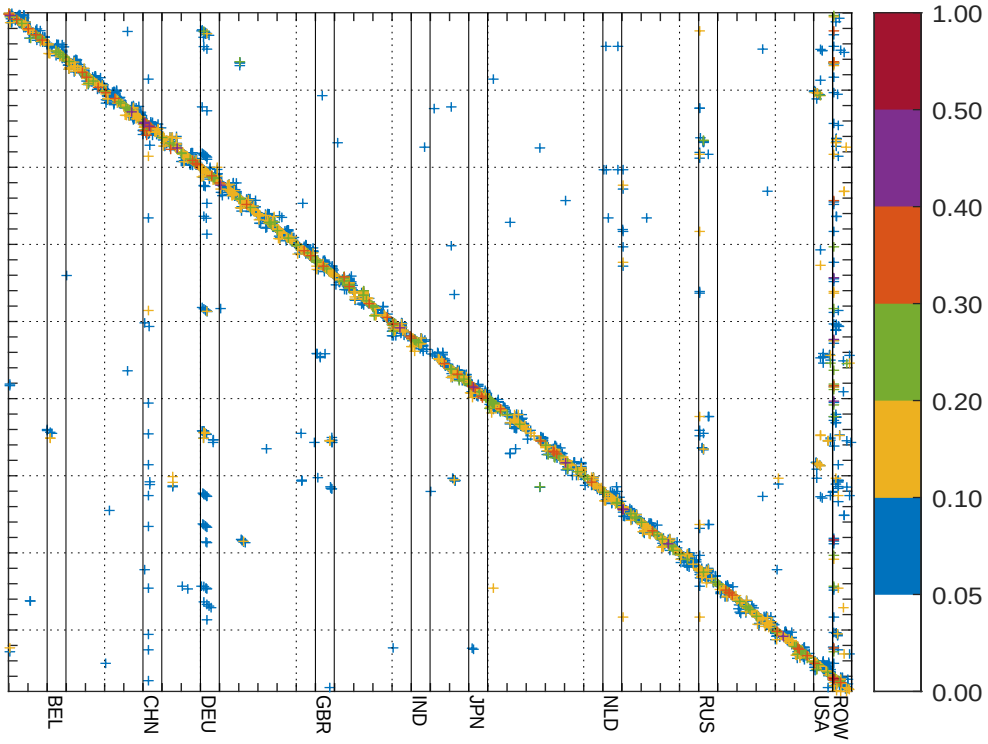


Figure 8.134: Spectrum of the matrix $A$

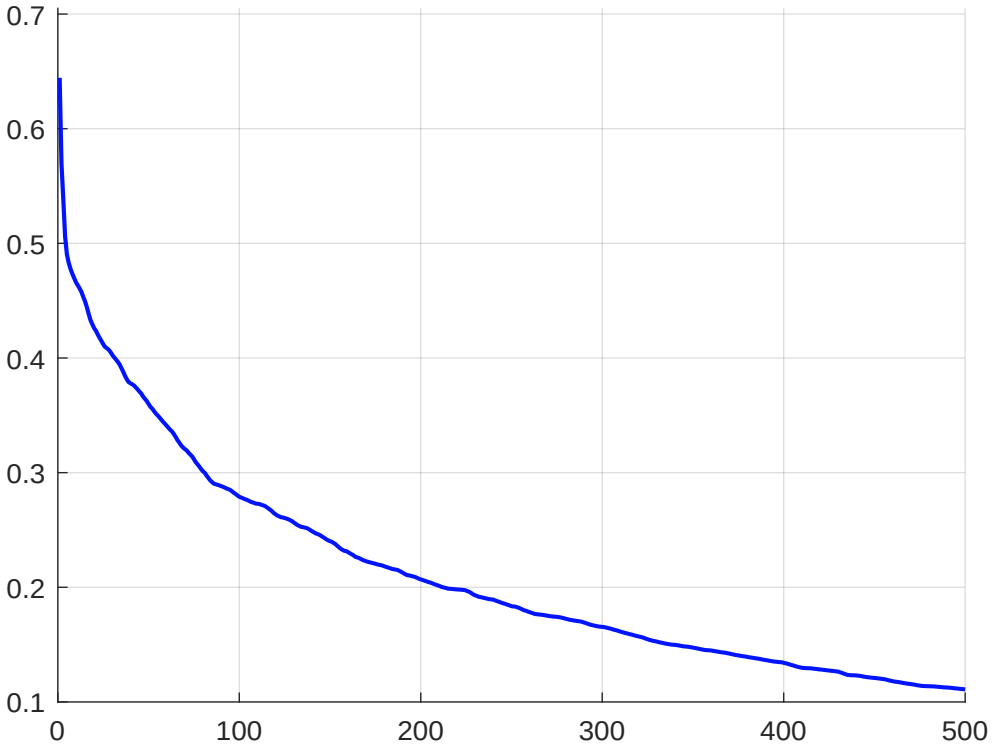

Figure 8.135: Frobenious norm of the matrix $A^k$

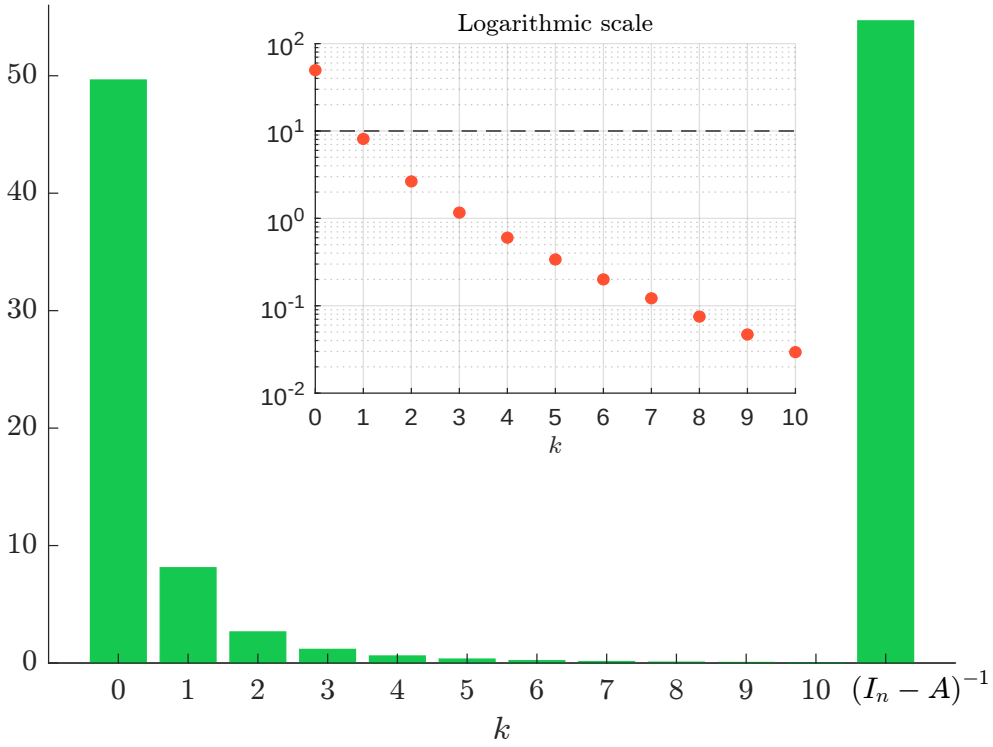


### 8.4.2 Application to environmental problems

In the late 1960s, several authors proposed linking economic and ecological systems using generalized input-output models. For example, Daly (1968) suggested extending the technical coefficients with additional rows/columns to reflect non-human sectors such as animals, plants, and bacteria, and non-living sectors such as the atmosphere, hydrosphere, and lithosphere. Leontief (1970) himself explained how externalities such as pollution could be incorporated into a basic input-output model. Since these first contributions, input-output analysis has been extended to many environmental problems[136].

#### Production-based vs. consumption-based inventory

To understand how input-output analysis can be used to measure carbon emissions, consider the mathematical problem of calculating the contribution of carbon emissions per product. Following Miller and Blair (2009), we denote by $C^{(x)} = \left(C^{(x)}_{g,j}\right)$ the pollution output matrix where $C^{(x)}_{g,j}$ is the total amount of the $g^{\text{th}}$ pollutant generated by the output of the $j^{\text{th}}$ sector. Similarly, we define $D^{(y)} = C^{(x)} \operatorname{diag}(x)^{-1} = \left(D^{(y)}_{g,j}\right)$ the matrix of direct impact coefficients where $D^{(y)}_{g,j} = c^{(y)}_{g,j}/x_j$ is the amount of the $g^{\text{th}}$ pollutant generated by 1\$ of the output of the $j^{\text{th}}$ sector. Let $\varpi = (\varpi_1, \ldots, \varpi_m)$ be the vector of pollution level. We have:

$$\varpi = D^{(x)}x = D^{(x)}(I_n - A)^{-1}y = D^{(y)}y$$

where $D^{(y)} = D^{(x)}(I_n - A)^{-1}$ is the pollutant multiplier matrix with respect to the final demand $y$. $D^{(y)}$ also measures the product carbon footprint (PCF). Since we have the following identity

[136] See Chapters 9 and 10 of Miller and Blair (2009).

$\varpi_g = \left(D^{(y)}y\right)_g = \sum_{j=1}^{n} D^{(y)}_{g,j} y_j$, we deduce that the total contribution of sector $j$ to the $g^{\text{th}}$ pollutant is equal to:

$$C^{(x)}_{g,j} = \frac{\partial\, \varpi_g}{\partial\, y_j} y_j = D^{(y)}_{g,j} y_j$$

Again, we can decompose the pollutant level according to the $k^{\text{th}}$ tier. We have:

$$\varpi = D^{(y)}y = \sum_{k=0}^{\infty} D^{(x)}A^k y = \sum_{k=0}^{\infty} \varpi_{(k)}$$

where $\varpi_{(0)} = D^{(x)}y$ is the pollutant level due to the final demand (or the zero-tier pollutant level), $\varpi_{(1)} = D^{(x)}Ay$ is the pollutant level due to the first-tier supply chain, and $\varpi_{(k)} = D^{(x)}A^k y$ is the $k^{\text{th}}$-tier pollutant level. The matrix $D^{(y)}_{(k)} = D^{(x)}A^k$ is called the $k^{\text{th}}$-tier multiplier matrix and satisfies the identity $D^{(y)} \equiv \sum_{k=0}^{\infty} D^{(y)}_{(k)}$.

**Example 31** *We consider three products, whose input-output table is given below:*

| | | To | | | Final demand | Total output |
|---|---|---|---|---|---|---|
| | | $P_1$ | $P_2$ | $P_3$ | $y$ | $x$ |
| From | $P_1$ | 100 | 300 | 100 | 500 | 1 000 |
| | $P_2$ | 250 | 150 | 200 | 1 600 | 2 000 |
| | $P_3$ | 25 | 200 | 75 | 200 | 500 |
| | Value added | 625 | 1 350 | 125 | | |
| | Total outlays | 1 000 | 2 000 | 500 | | |
| GHG | $CO_2$ | 50 | 20 | 5 | 75 | |
| | $CH_4$ | 3 | 1 | 0 | 4 | |

*Intermediate production of* \$100 *of* $P_1$, \$300 *of* $P_2$, *and* \$100 *of* $P_3$ *is required to produce* \$500 *of* $P_1$. *This environmentally-extended input-output table has two additional rows corresponding to the GHG emissions. For instance, the production of* $P_1$ *causes* 50 $\text{kgCO}_2$ *and* 3 $\text{kgCH}_4$.

The matrix of technical coefficients is equal to:

$$A = Z\,\text{diag}\,(x)^{-1} = \begin{pmatrix} 10.0\% & 15.0\% & 20.0\% \\ 25.0\% & 7.5\% & 40.0\% \\ 2.5\% & 10.0\% & 15.0\% \end{pmatrix}$$

It follows that the matrix of multipliers is equal to:

$$\boldsymbol{\mathcal{L}} = (I_3 - A)^{-1} = \begin{pmatrix} 1.1871 & 0.2346 & 0.3897 \\ 0.3539 & 1.2090 & 0.6522 \\ 0.0766 & 0.1491 & 1.2647 \end{pmatrix}$$

The direct impact matrix is equal to the GHG emissions divided by the output:

$$D^{(x)} = \begin{pmatrix} 50/1000 & 20/2000 & 5/500 \\ 3/1000 & 1/2000 & 0/500 \end{pmatrix} = \begin{pmatrix} 0.05 & 0.01 & 0.01 \\ 0.003 & 0.0005 & 0 \end{pmatrix}$$

The unit of $D^{(x)}$ is expressed in kilogram of the gas per dollar. For instance, the GHG intensities of the product $P_1$ are equal to 0.05 $kgCO_2/\$$ and 0.003 $kgCH_4/\$$. Finally, we obtain:

$$D^{(y)} = D^{(x)}\boldsymbol{\mathcal{L}} = \begin{pmatrix} 0.0637 & 0.0253 & 0.0387 \\ 0.0037 & 0.0013 & 0.0015 \end{pmatrix}$$

While $D^{(x)}$ corresponds to the production-based inventory, $D^{(y)}$ measures the carbon footprint from the perspective of the consumption-based inventory (Kitzes, 2013). This gives us the following decomposition:

$$C^{(y)} = \begin{pmatrix} 31.83 & 35.44 & 7.73 \\ 1.87 & 1.83 & 0.30 \end{pmatrix} \neq \begin{pmatrix} 50 & 20 & 5 \\ 3 & 1 & 0 \end{pmatrix} = C^{(x)}$$

We notice that the two contribution matrices are different. For instance, while the production of $P_1$ is responsible of 50 $kgCO_2$, the final consumption of $P_1$ is responsible of only 31.83 $kgCO_2$, meaning that 18.17 $kgCO_2$ are emitted by $P_1$ for the other two products. The difference between $C^{(x)}$ and $C^{(y)}$ depends on the structure of the matrix $A$ and the vector $y$. Let us apply a perturbation to the previous example. We assume that there is no final demand of $P_1$: $y_1 = 0$. For consistency, we also assume that the GHG emissions of Product $P_1$ are divided by two because the production is reduced by 50%. We find that:

$$C^{(y)} = \begin{pmatrix} 0 & 40.96 & 9.04 \\ 0 & 2.13 & 0.37 \end{pmatrix} \neq \begin{pmatrix} 25 & 20 & 5 \\ 1.5 & 1 & 0 \end{pmatrix} = C^{(x)}$$

The consumption-based contribution of $P_1$ is null because $P_1$ is manufactured for the other two products.

**Remark 90** *We can show that $C^{(x)} = C^{(y)}$ implies that $A$ is a diagonal matrix. We conclude that the supply chain and interconnectedness between sectors can lead to a misperception of the sectoral carbon footprint.*

The previous framework can be applied to many problems involving the calculation of carbon footprints. Miller and Blair (2009) examined three categories of EEIO analysis: generalized input-output, economic-ecological, and commodity-by-industry models. An overview of generalized input-output models can be found in Minx *et al.* (2009) and Wiedmann (2009). These models are commonly used to calculate the carbon footprint of nations, sectors, supply chains, etc., and to analyze the impact of foreign trade. The use of economic-ecological models is less popular, since it involves building an input-output table for ecological sectors (species, plants, etc.). Commodity-by-industry models are more studied because it is easier to collect data for the commodity sector.

### EEIO databases

The use of environmentally-extended input-output models requires credible database. Two EEIO databases dominate the market: Eora and Exiobase. According to `https://worldmrio.com`, the Eora global supply chain database uses more than 15 000 sectors across 190 countries, and contains about 2 700 environmental indicators covering GHG emissions, air pollution, energy use, water demand, land use, etc. Exiobase is a multi-regional environmentally-extended supply-use and input-output model with 44 countries, 163 industries, 200 products and 417 emission categories (`www.exiobase.eu`).

We consider the Exiobase data for the year 2022. To do this, we download the MRIO archive in industry by industry format (`IOT_2022_ixi.zip`) and the MRIO archive in product by product format (`IOT_2022_pxp.zip`) from the website: `https://zenodo.org/record/5589597`. Both archives

have the same structure. The economic input-output data are stored in the root of the archive, which contains four data files:

1. The $Z$ matrix (`Z.txt` — flow/transactions matrix)
2. The $A$ matrix (`A.txt` — direct requirements matrix)
3. The $y$ matrix (`y.txt` — final demand)
4. The $x$ vector (`x.txt` — gross/total output)

and four description files (`finaldemand.txt`, `industries.txt`, `products.txt` and `units.txt`). Exiobase provides also two set of extension data stored in the sub-folders `satellite` (uncharacterized stressors data — *e.g.*, $CO_2$ emissions, land use per category, etc.) and `impacts` (characterized stressors data — *e.g.*, total GWP100, total land use, etc.). The structure of the two sub-folders is the following:

- Factors of productions/stressors/impacts: `F.txt`
- Stressors/impacts of the final demand: `F_Y.txt`
- Direct stressor/impact coefficients: `S.txt`
- Stressor/impact coefficients of the final demand: `S_Y.txt`
- MRIO extension multipliers (total requirement factors of consumption): `M.txt`
- Consumption based accounts per sector: `D_cba.txt`
- Production based accounts per sector: `D_pba.txt`
- Consumption based accounts per region: `D_cba_reg.txt`
- Production based accounts per region: `D_pba_reg.txt`
- Import accounts per region: `D_imp_reg.txt`
- Export accounts per region: `D_exp_reg.txt`
- Absolute units of the stressor and impacts: `unit.txt`

Previously, we have given the detailed sectors in the WIOD database, which is a $56 \times 56$ industry by industry IOT. Exiobase is both a $163 \times 163$ industry by industry IOT and a $200 \times 200$ product by product IOT. The first fifteen products are listed here: paddy rice, wheat, cereal grains nec, vegetables, fruit, nuts, oil seeds, sugar cane and beet, plant-based fibers, crops nec, cattle, pigs, poultry, meat animals nec, animal products nec, raw milk, wool and silk-worm cocoons. In the impact sub-directory, we find measurement that concerns employment (in hour), GHG emissions (in GWP100), water consumption (in $Mm^3$), Nitrogen (in kg), land-use crop, forest, pasture (in $km^2$), etc. In the satellite sub-directory, we have similar information but in a disaggregated form. For instance, the employment item has seven categories: low-skilled male, low-skilled female, medium-skilled male, medium-skilled female, high-skilled male, high-skilled female, vulnerable.

### 8.4.3 Estimation of first-tier and indirect emissions

#### Basic formula

We assume that the carbon footprint is evaluated in $CO_2e$, which means that the input-output analysis considers only one pollutant, with all greenhouse gases being converted to the carbon based on their global warming potential. In this case, $D^{(x)}$ is a row vector of dimension $n$, and $D_j^{(x)}$ measures the direct emission intensity of sector $j$. We reiterate that the total emission intensities are equal to $D^{(y)} = D^{(x)}\boldsymbol{\mathcal{L}} = D^{(x)}(I_n - A)^{-1}$. $D^{(y)}$ is a row vector of dimension $n$, and $D_j^{(y)}$ measures the direct and indirect emission intensity of sector $j$. Using the usual notation $\boldsymbol{\mathcal{CI}}$ for the carbon intensity, we have[137]:

$$\begin{aligned}\boldsymbol{\mathcal{CI}}_{\text{total}} &= \boldsymbol{\mathcal{L}}^\top \boldsymbol{\mathcal{CI}}_1 \\ &= \left(I_n - A^\top\right)^{-1} \boldsymbol{\mathcal{CI}}_1 \\ &= \tilde{\boldsymbol{\mathcal{L}}}\, \boldsymbol{\mathcal{CI}}_1 \end{aligned} \tag{8.34}$$

where $\boldsymbol{\mathcal{CI}}_1 = \boldsymbol{\mathcal{CI}}_{\text{direct}}$ is the vector of direct carbon intensities and $\boldsymbol{\mathcal{CI}}_{\text{total}}$ is the vector of direct plus indirect carbon intensities. It follows that the indirect carbon intensities are given by:

$$\begin{aligned}\boldsymbol{\mathcal{CI}}_{\text{indirect}} &= \boldsymbol{\mathcal{CI}}_{\text{total}} - \boldsymbol{\mathcal{CI}}_1 \\ &= \left(\left(I_n - A^\top\right)^{-1} - I_n\right) \boldsymbol{\mathcal{CI}}_{\text{direct}} \end{aligned} \tag{8.35}$$

In particular, we can decompose $\boldsymbol{\mathcal{CI}}_{\text{indirect}}$ using the Neumann series:

$$\boldsymbol{\mathcal{CI}}_{\text{indirect}} = \underbrace{A^\top \boldsymbol{\mathcal{CI}}_1}_{\text{First-tier}} + \underbrace{\left(A^\top\right)^2 \boldsymbol{\mathcal{CI}}_1}_{\text{Second-tier}} + \ldots + \underbrace{\left(A^\top\right)^k \boldsymbol{\mathcal{CI}}_1}_{k^{th}\text{-tier}} + \ldots \tag{8.36}$$

and we have:

$$\boldsymbol{\mathcal{CI}}_{\text{total}} = \underbrace{\underbrace{\boldsymbol{\mathcal{CI}}_1}_{\text{Scope 1}}}_{\text{Direct intensities}} + \underbrace{\underbrace{A^\top \boldsymbol{\mathcal{CI}}_1}_{\text{First-tier}} + \underbrace{\left(A^\top\right)^2 \boldsymbol{\mathcal{CI}}_1}_{\text{Second-tier}} + \ldots + \underbrace{\left(A^\top\right)^k \boldsymbol{\mathcal{CI}}_1}_{k^{th}\text{-tier}} + \ldots}_{\text{Indirect intensities}} \tag{8.37}$$

Equations (8.34–8.37) are the core formulas of the consumption-based inventory approach and the calculation of indirect carbon intensities.

#### Illustration

Continuing with Example 30, let us assume that the carbon emissions, expressed in $ktCO_2e$, are as follows: 500 for the energy sector, 200 for the materials sector, 200 for the industrials sector and 125 for the services sector. We deduce that the vector of Scope 1 carbon intensities is equal to:

$$\boldsymbol{\mathcal{CI}}_1 = \text{diag}(x)^{-1} \boldsymbol{\mathcal{CE}}_1 = \begin{pmatrix} 500/5\,000 \\ 200/4\,000 \\ 200/8\,000 \\ 125/12\,500 \end{pmatrix} \times 10^3 = \begin{pmatrix} 100 \\ 50 \\ 25 \\ 10 \end{pmatrix}$$

[137] Because $D^{(x)} = \boldsymbol{\mathcal{CI}}_1^\top$ and $D^{(y)} = \boldsymbol{\mathcal{CI}}_{\text{total}}^\top$.

We multiply the carbon emissions by a factor of 1 000 to express carbon intensities[138] in $gCO_2e/\$$ or equivalently $tCO_2e/\$$ mn. Energy is the most polluting sector with 500 $ktCO_2e$, followed by materials and industrials with 200 $ktCO_2e$. Energy and services have respectively the highest and lowest carbon intensity, respectively 100 $tCO_2e/\$$ mn and 10 $tCO_2e/\$$ mn. We have:

$$\begin{aligned}
\boldsymbol{\mathcal{CI}}_{\text{total}} &= \tilde{\boldsymbol{\mathcal{L}}}\,\boldsymbol{\mathcal{CI}}_1 \\
&= \begin{pmatrix} 1.1881 & 0.1678 & 0.1430 & 0.0715 \\ 0.3894 & 1.2552 & 0.4110 & 0.1718 \\ 0.4919 & 0.4336 & 1.6303 & 0.2993 \\ 0.2884 & 0.1891 & 0.3044 & 1.6087 \end{pmatrix} \begin{pmatrix} 100 \\ 50 \\ 25 \\ 10 \end{pmatrix} \\
&= \begin{pmatrix} 131.49 \\ 113.69 \\ 114.62 \\ 61.99 \end{pmatrix}
\end{aligned}$$

We can then decompose $\boldsymbol{\mathcal{CI}}_{\text{total}}$ between $\boldsymbol{\mathcal{CI}}_{\text{direct}}$ and $\boldsymbol{\mathcal{CI}}_{\text{indirect}}$. Finally, we obtain we obtain the direct and indirect carbon intensities given in Table 8.46. While the Scope 1 carbon intensity of the energy sector is equal to 100 $tCO_2e/\$$ mn, its total carbon intensity is equal to 131.49 $tCO_2e/\$$ mn. The difference of 31.49 $tCO_2e/\$$ mn corresponds to the indirect emissions. In the case of the energy sector, direct and indirect emissions represent 76.05% and 23.95% of the total emissions, respectively. In fact, this sector has the lowest ratio of indirect carbon emissions. On the contrary, for the services sector, 83.87% of the total emissions are indirect.

Table 8.46: Direct and indirect carbon intensities

| Sector | $\boldsymbol{\mathcal{CI}}_1$ | $\boldsymbol{\mathcal{CI}}_{\text{total}}$ | $\boldsymbol{\mathcal{CI}}_{\text{direct}}$ | $\boldsymbol{\mathcal{CI}}_{\text{indirect}}$ | $\boldsymbol{\mathcal{CI}}_{\text{direct}}$ | $\boldsymbol{\mathcal{CI}}_{\text{indirect}}$ | $\frac{\boldsymbol{\mathcal{CI}}_{\text{total}}}{\boldsymbol{\mathcal{CI}}_1}$ |
|---|---|---|---|---|---|---|---|
| | (in $tCO_2e/\$$ mn) | | | | (in %) | | |
| Energy | 100.00 | 131.49 | 100.00 | 31.49 | 76.05% | 23.95% | 1.31 |
| Materials | 50.00 | 113.69 | 50.00 | 63.69 | 43.98% | 56.02% | 2.27 |
| Industrials | 25.00 | 114.62 | 25.00 | 89.62 | 21.81% | 78.19% | 4.58 |
| Services | 10.00 | 61.99 | 10.00 | 51.99 | 16.13% | 83.87% | 6.20 |

We denote by $\boldsymbol{\mathcal{CI}}_{(k)} = \left(A^\top\right)^k \boldsymbol{\mathcal{CI}}_1$ the indirect carbon intensity when considering the $k^{\text{th}}$ tier, and $\boldsymbol{\mathcal{CI}}_{(1-k)} = \sum_{h=1}^{k} \left(A^\top\right)^h \boldsymbol{\mathcal{CI}}_1$ the cumulative indirect carbon intensity for the first $k$ tiers. The results are shown in Table 8.47. For the services sector, the first and second tiers add 18.50 and 13.50 $tCO_2e/\$$ mn to the indirect carbon intensity, respectively. If we restrict the analysis to the first two tiers, the indirect carbon intensity is equal to 32. The tree presented in Figure 8.136 explains this computation[139]. To produce \$1 of services, we must purchase 0.10\$ of energy, \$0.05 of materials, and so on. It follows that the first-tier indirect carbon intensities for the services sector is equal to:

$$\begin{aligned}
\boldsymbol{\mathcal{CI}}_{(1)}(\mathcal{S}_4) &= 0.10 \times 100 + 0.05 \times 50 + 0.10 \times 25 + 0.35 \times 10 \\
&= 10 + 2.5 + 2.5 + 3.5 \\
&= 18.50
\end{aligned}$$

[138] Remember that the unit of carbon intensity is $tCO_2e/\$$ mn. When we divide by 1 million, we get an equivalent unit of $gCO_2e/\$$.

[139] To make the graph easier to read, we use the following correspondences: energy $\longleftarrow \mathcal{S}_1$, materials $\longleftarrow \mathcal{S}_2$, industrials $\longleftarrow \mathcal{S}_3$ and services $\longleftarrow \mathcal{S}_4$.

Figure 8.136: Upstream tree of the first- and second-tier rounds for the services sector

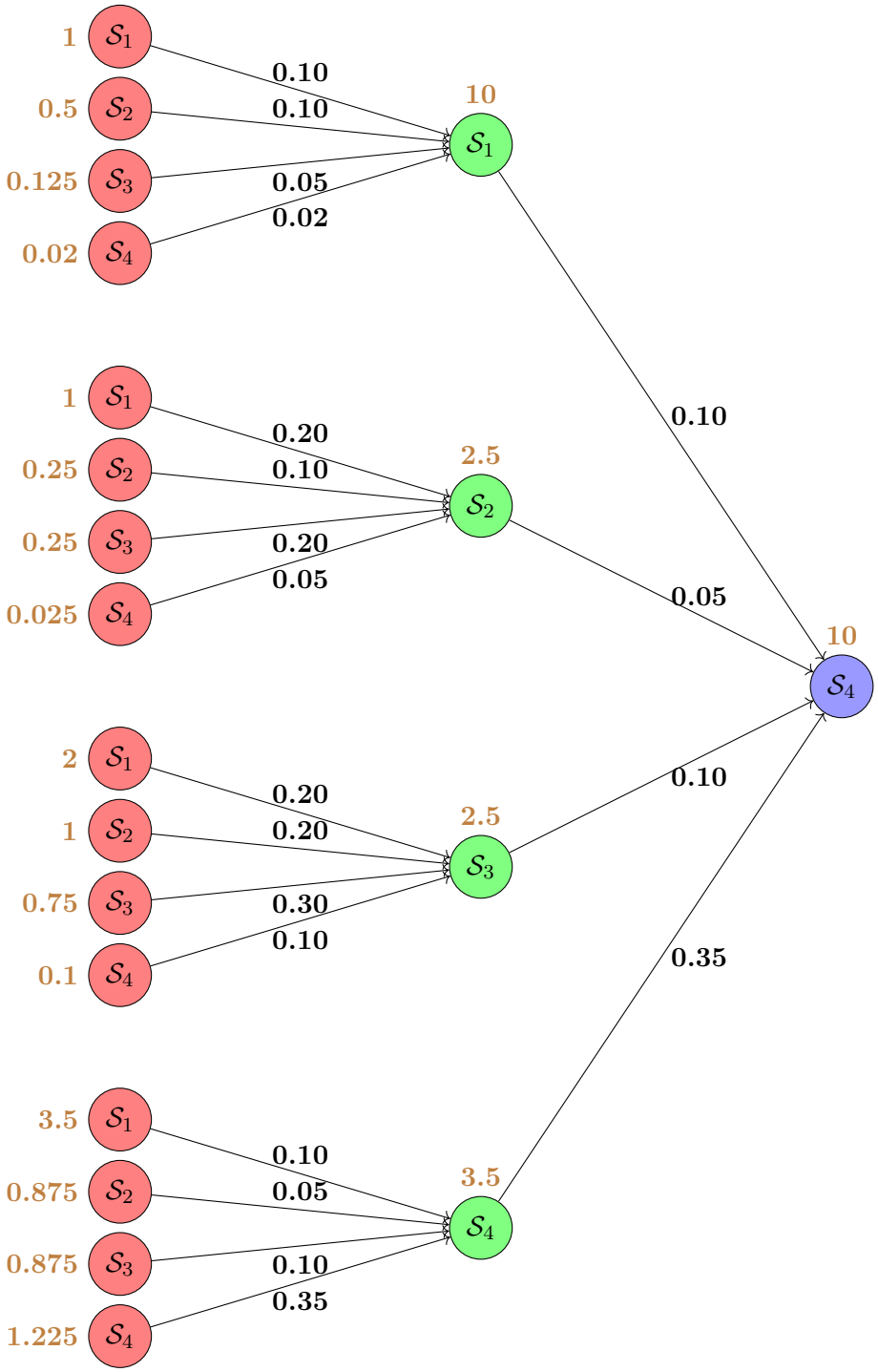

We can continue the analysis and consider the second tier. In fact, the companies involved in the first-tier round also purchase goods and services that generate new indirect emissions. We have:

$$\begin{aligned}
\boldsymbol{\mathcal{CI}}_{(2)}(\mathcal{S}_4) &= 0.10 \times \underbrace{(0.10 \times 100 + 0.10 \times 50 + 0.05 \times 25 + 0.02 \times 10)}_{\text{Indirect emissions from energy sector companies}} + \\
&\quad 0.05 \times \underbrace{(0.20 \times 100 + 0.10 \times 50 + 0.20 \times 25 + 0.05 \times 10)}_{\text{Indirect emissions from materials sector companies}} + \\
&\quad 0.10 \times \underbrace{(0.20 \times 100 + 0.20 \times 50 + 0.30 \times 25 + 0.10 \times 10)}_{\text{Indirect emissions from industrials sector companies}} + \\
&\quad 0.35 \times \underbrace{(0.10 \times 100 + 0.05 \times 50 + 0.10 \times 25 + 0.35 \times 10)}_{\text{Indirect emissions from services sector companies}} \\
&= 13.495
\end{aligned}$$

We can continue the analysis, and we verify that $\boldsymbol{\mathcal{CI}}_{(3)}(\mathcal{S}_4) = 8.45$, $\boldsymbol{\mathcal{CI}}_{(4)}(\mathcal{S}_4) = 4.98$, etc. Finally, the cumulative sum converges to $\boldsymbol{\mathcal{CI}}_{(1-\infty)}(\mathcal{S}_4) = 51.99$.

Table 8.47: Tier decomposition of carbon intensities

| | Sector | 1 | 2 | 3 | 4 | 5 | 10 | 15 | $\infty$ |
|---|---|---|---|---|---|---|---|---|---|
| $\boldsymbol{\mathcal{CI}}_{(k)}$ | Energy | 16.45 | 6.99 | 3.60 | 1.97 | 1.09 | 0.06 | 0.00 | 0.00 |
| | Materials | 30.50 | 14.97 | 8.13 | 4.47 | 2.48 | 0.14 | 0.01 | 0.00 |
| | Industrials | 38.50 | 22.79 | 12.58 | 6.96 | 3.88 | 0.21 | 0.01 | 0.00 |
| | Services | 18.50 | 13.50 | 8.45 | 4.98 | 2.86 | 0.16 | 0.01 | 0.00 |
| $\boldsymbol{\mathcal{CI}}_{(1-k)}$ | Energy | 16.45 | 23.44 | 27.04 | 29.02 | 30.11 | 31.41 | 31.48 | 31.49 |
| | Materials | 30.50 | 45.47 | 53.59 | 58.06 | 60.55 | 63.52 | 63.68 | 63.69 |
| | Industrials | 38.50 | 61.29 | 73.87 | 80.83 | 84.71 | 89.35 | 89.61 | 89.62 |
| | Services | 18.50 | 32.00 | 40.44 | 45.43 | 48.29 | 51.79 | 51.98 | 51.99 |

The previous analysis concerns the carbon intensity. To estimate total emissions, we simply multiply by the output and we have the following identities:

$$\frac{\boldsymbol{\mathcal{CE}}_{\text{total}}}{\boldsymbol{\mathcal{CE}}_1} = \frac{\boldsymbol{\mathcal{CI}}_{\text{total}}}{\boldsymbol{\mathcal{CI}}_1} \Leftrightarrow \boldsymbol{\mathcal{CE}}_{\text{total}} = \boldsymbol{\mathcal{CI}}_{\text{total}} \odot \frac{\boldsymbol{\mathcal{CE}}_1}{\boldsymbol{\mathcal{CI}}_1} = x \odot \boldsymbol{\mathcal{CI}}_{\text{total}} \tag{8.38}$$

Therefore, the indirect emissions are given by:

$$\boldsymbol{\mathcal{CE}}_{\text{indirect}} = \boldsymbol{\mathcal{CE}}_{\text{total}} - \boldsymbol{\mathcal{CE}}_{\text{direct}} = (\boldsymbol{\mathcal{CI}}_{\text{total}} - \boldsymbol{\mathcal{CI}}_1) \odot \frac{\boldsymbol{\mathcal{CE}}_1}{\boldsymbol{\mathcal{CI}}_1} \tag{8.39}$$

The breakdown of the total carbon emissions is provided in Table 8.48. We notice that indirect carbon emissions are double counted. Indeed, the total direct carbon emissions are equal to 1 025 $\text{ktCO}_2\text{e}$ and the indirect emissions add 1 779 $\text{ktCO}_2\text{e}$. Based on direct emissions, we have the following distribution: 49% for energy, 20% for materials, 20% for industrials and 12% for the sector of services. If we include the indirect emissions, we get a different picture. For instance, the services sector represents more than 25% of the total emissions because the direct emissions have been multiplied by a factor of 6.2, while the contribution of energy is now less than 25%.

**Remark 91** *It would be wrong to directly diffuse the carbon emissions instead of the carbon intensities:* $\boldsymbol{\mathcal{CE}}_{\text{total}} = \left(I_n - A^\top\right)^{-1} \boldsymbol{\mathcal{CE}}_1$. *Indeed, carbon emissions are not comparable from one sector to another sector, because they are not normalized and monetary input-output tables give the technical coefficients for \$1 of output from each sector.*

Table 8.48: Decomposition of carbon emissions

| Sector | $\mathcal{CE}_{\text{direct}}$ | $\mathcal{CE}_{\text{indirect}}$ (in $ktCO_2e$) | $\mathcal{CE}_{\text{total}}$ | $\mathcal{CE}_{\text{direct}}$ | $\mathcal{CE}_{\text{indirect}}$ (in %) | $\mathcal{CE}_{\text{total}}$ |
|---|---|---|---|---|---|---|
| Energy | 500 | 157.44 | 657.44 | 48.78 | 8.85 | 23.45 |
| Materials | 200 | 254.76 | 454.76 | 19.51 | 14.32 | 16.22 |
| Industrials | 200 | 716.97 | 916.97 | 19.51 | 40.30 | 32.70 |
| Services | 125 | 649.92 | 774.92 | 12.20 | 36.53 | 27.64 |
| Total | 1 025 | 1 779.10 | 2 804.10 | 100.00 | 100.00 | 100.00 |

**Upstream vs. downstream analysis**

The previous analysis is an output-based analysis. This is obvious if we look at Figure 8.136, which illustrates the impacts of requirement to produce \$1 in a sector. Once we have produced \$1 in a given sector, we may wonder how it is used by the value chain. In this case, we get an input-based analysis. In fact, instead of moving up the supply chain, we move down the value chain (Figure 8.137). Therefore, this approach is also known as downstream analysis while the output-based approach is known as upstream analysis.

To perform a downstream analysis, we must first define the technical coefficients for \$1 input (and not output):

$$\breve{A}_{i,j} = \frac{Z_{i,j}}{x_i}$$

$\breve{A}_{i,j}$ indicates the proportion of \$1 produced by sector $i$ that is used by sector $j$. We denote the matrix of input impacts by $\breve{A} = \left(\breve{A}_{i,j}\right) = \text{diag}\,(x)^{-1} Z$. We note that:

$$\breve{A}_{i,j} = \frac{Z_{i,j}}{x_j} \cdot \frac{x_j}{x_i} = A_{i,j} \cdot T_{i,j}$$

In a matrix form, we have $\breve{A} = A \odot T$ where $T = (T_{i,j}) = \left(x_i^{-1} x_j\right)$. Using the same reasoning as in the previous paragraphs, we can show that:

$$\boldsymbol{\mathcal{CI}}_{\text{total}}^{\text{down}} = \left(I_n - \breve{A}\right)^{-1} \boldsymbol{\mathcal{CI}}_1 \tag{8.40}$$

where $\boldsymbol{\mathcal{CI}}_{\text{total}}^{\text{down}}$ is the vector of downstream (direct plus indirect downstream) carbon intensities. It follows that the indirect downstream carbon intensities are given by:

$$\boldsymbol{\mathcal{CI}}_{\text{indirect}}^{\text{down}} = \boldsymbol{\mathcal{CI}}_{\text{total}}^{\text{down}} - \boldsymbol{\mathcal{CI}}_1 = \left(\left(I_n - \breve{A}\right)^{-1} - I_n\right) \boldsymbol{\mathcal{CI}}_{\text{direct}} \tag{8.41}$$

In particular, we can decompose $\boldsymbol{\mathcal{CI}}_{\text{indirect}}^{\text{down}}$ as follows:

$$\boldsymbol{\mathcal{CI}}_{\text{indirect}}^{\text{down}} = \underbrace{\breve{A}\boldsymbol{\mathcal{CI}}_1}_{\text{First-tier}} + \underbrace{\breve{A}^2\boldsymbol{\mathcal{CI}}_1}_{\text{Second-tier}} + \ldots + \underbrace{\breve{A}^k\boldsymbol{\mathcal{CI}}_1}_{k^{th}\text{-tier}} + \ldots$$

and we have:

$$\boldsymbol{\mathcal{CI}}_{\text{total}}^{\text{down}} = \underbrace{\underbrace{\boldsymbol{\mathcal{CI}}_1}_{\text{Scope 1}}}_{\text{Direct downstream}} + \underbrace{\underbrace{\breve{A}\boldsymbol{\mathcal{CI}}_1}_{\text{First-tier}} + \underbrace{\breve{A}^2\boldsymbol{\mathcal{CI}}_1}_{\text{Second-tier}} + \ldots + \underbrace{\breve{A}^k\boldsymbol{\mathcal{CI}}_1}_{k^{th}\text{-tier}} + \ldots}_{\text{Indirect downstream}}$$

Figure 8.137: Downstream tree of the first- and second-tier rounds for the services sector

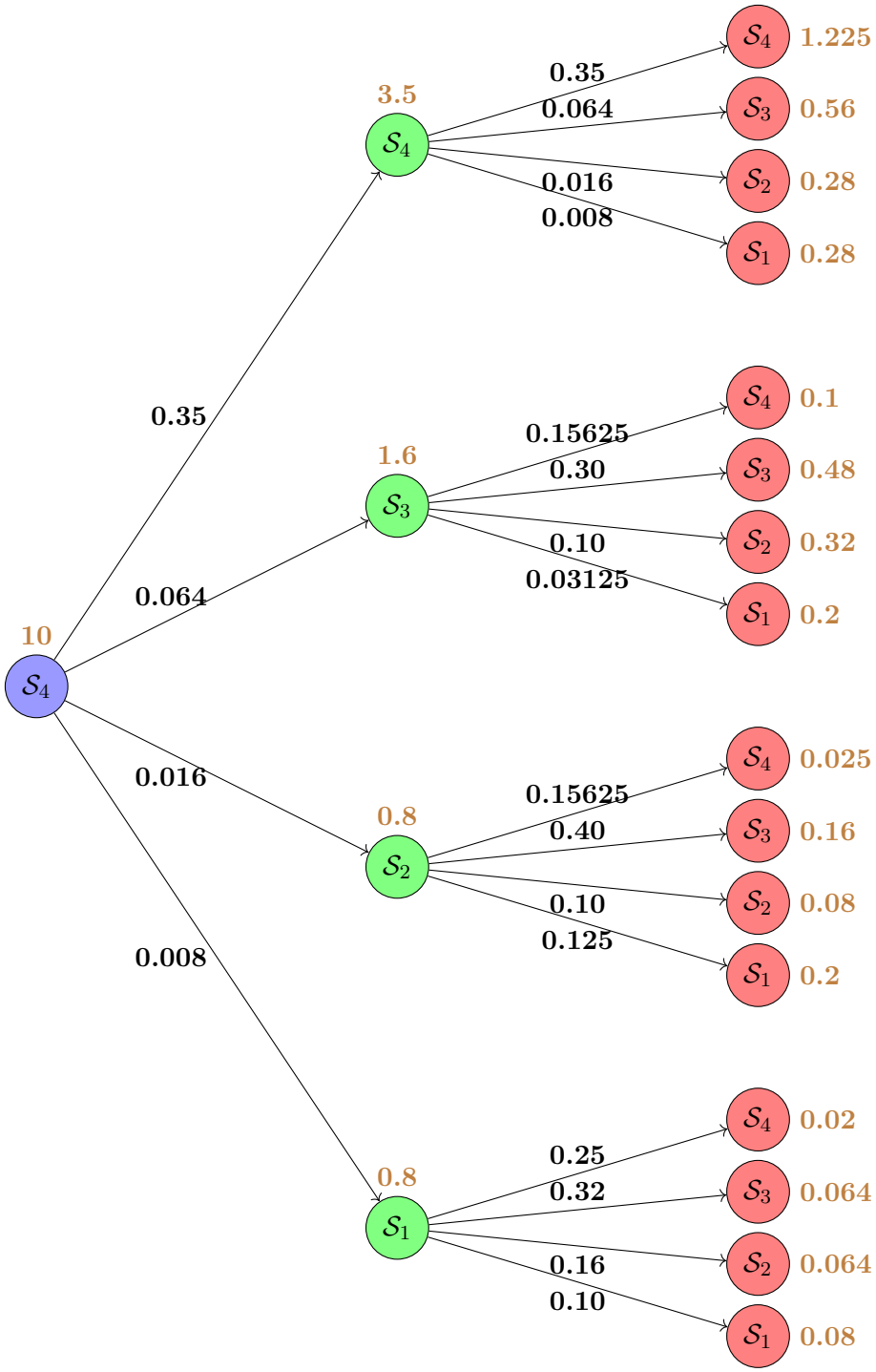

Again, we use the proportionality rule to calculate carbon emissions. We have:

$$\mathcal{CE}_{\text{total}}^{\text{down}} = \mathcal{CI}_{\text{total}}^{\text{down}} \odot \frac{\mathcal{CE}_1}{\mathcal{CI}_1}$$

and:

$$\mathcal{CE}_{\text{indirect}}^{\text{down}} = \mathcal{CE}_{\text{total}}^{\text{down}} - \mathcal{CE}_{\text{direct}}^{\text{down}} = \left(\mathcal{CI}_{\text{total}}^{\text{down}} - \mathcal{CI}_1\right) \odot \frac{\mathcal{CE}_1}{\mathcal{CI}_1}$$

Using our previous example, the downstream matrix $\breve{A}$ is equal to:

$$\begin{aligned}\breve{A} &= \text{diag}\,(x)^{-1}\, Z \\ &= \begin{pmatrix} 0.10000 & 0.16000 & 0.32000 & 0.25000 \\ 0.12500 & 0.10000 & 0.40000 & 0.15625 \\ 0.03125 & 0.10000 & 0.30000 & 0.15625 \\ 0.00800 & 0.01600 & 0.06400 & 0.35000 \end{pmatrix}\end{aligned}$$

We deduce the downstream multiplier matrix:

$$\breve{\mathcal{L}} = \begin{pmatrix} 1.18811 & 0.31149 & 0.78705 & 0.72104 \\ 0.20970 & 1.25525 & 0.86717 & 0.59085 \\ 0.08938 & 0.20550 & 1.63035 & 0.47568 \\ 0.02859 & 0.05497 & 0.19156 & 1.60872 \end{pmatrix}$$

In Tables 8.49, 8.50 and 8.51, we report the downstream carbon intensities and emissions. These figures can be compared with those obtained in the case of the upstream analysis (Tables 8.46, 8.47 and 8.48).

Table 8.49: Direct and indirect downstream carbon intensities

| Sector | $\mathcal{CI}_1$ | $\mathcal{CI}_{\text{total}}^{\text{down}}$ | $\mathcal{CI}_{\text{direct}}^{\text{down}}$ | $\mathcal{CI}_{\text{indirect}}^{\text{down}}$ | $\mathcal{CI}_{\text{direct}}^{\text{down}}$ | $\mathcal{CI}_{\text{indirect}}^{\text{down}}$ | $\frac{\mathcal{CI}_{\text{total}}^{\text{down}}}{\mathcal{CI}_1}$ |
|---|---|---|---|---|---|---|---|
| | (in $\text{tCO}_2\text{e}/\$$ mn) | | | | (in %) | | |
| Energy | 100.00 | 161.27 | 100.00 | 61.27 | 62.01% | 37.99% | 1.61 |
| Materials | 50.00 | 111.32 | 50.00 | 61.32 | 44.92% | 55.08% | 2.23 |
| Industrials | 25.00 | 64.73 | 25.00 | 39.73 | 38.62% | 61.38% | 2.59 |
| Services | 10.00 | 26.48 | 10.00 | 16.48 | 37.76% | 62.24% | 2.65 |

Table 8.50: Tier decomposition of downstream carbon intensities

| | Sector | 1 | 2 | 3 | 4 | 5 | 10 | 15 | $\infty$ |
|---|---|---|---|---|---|---|---|---|---|
| $\mathcal{CI}_{(k)}^{\text{down}}$ | Energy | 28.50 | 14.68 | 8.00 | 4.45 | 2.48 | 0.14 | 0.00 | 0.00 |
| | Materials | 29.06 | 14.39 | 7.92 | 4.39 | 2.45 | 0.13 | 0.01 | 0.00 |
| | Industrials | 17.19 | 10.00 | 5.54 | 3.09 | 1.72 | 0.09 | 0.01 | 0.00 |
| | Services | 6.70 | 4.14 | 2.44 | 1.40 | 0.79 | 0.04 | 0.00 | 0.00 |
| $\mathcal{CI}_{(1-k)}^{\text{down}}$ | Energy | 28.50 | 43.17 | 51.18 | 55.63 | 58.11 | 61.10 | 61.26 | 61.27 |
| | Materials | 29.06 | 43.45 | 51.37 | 55.76 | 58.21 | 61.15 | 61.31 | 61.32 |
| | Industrials | 17.19 | 27.19 | 32.73 | 35.82 | 37.54 | 39.61 | 39.72 | 39.73 |
| | Services | 6.70 | 10.84 | 13.27 | 14.67 | 15.46 | 16.43 | 16.48 | 16.48 |

We find that the results of the downstream analysis are different. While the energy and materials sectors have the lowest upstream indirect emissions, they have the highest downstream emissions.

This is due to the structure of the supply chain. Most of the output from the energy and materials sectors is destined to be used by the value chain to produce goods and services. In contrast, the industrials and services sectors require a lot of output from the value chain to produce goods and services directly. In this context, carbon emissions generally move downward for the energy and materials sectors, while they move upward for the industrials and services sectors. Finally, the indirect downstream emissions are equal to 1 075 $\text{ktCO}_2\text{e}$, while the indirect upstream emissions are equal to 1 779 $\text{ktCO}_2\text{e}$. To better understand the difference between the downstream and the upstream, we also plot the downstream tree of the first two tiers for the services sector in Figure 8.137. If we compare this tree with Figure 8.137, we see that the downstream trees grow to the right, while the upstream trees grow to the left.

Table 8.51: Decomposition of downstream carbon emissions

| Sector | $\boldsymbol{\mathcal{CE}}^{\text{down}}_{\text{direct}}$ | $\boldsymbol{\mathcal{CE}}^{\text{down}}_{\text{indirect}}$ (in $\text{ktCO}_2\text{e}$) | $\boldsymbol{\mathcal{CE}}^{\text{down}}_{\text{total}}$ | $\boldsymbol{\mathcal{CE}}^{\text{down}}_{\text{direct}}$ | $\boldsymbol{\mathcal{CE}}^{\text{down}}_{\text{indirect}}$ (in %) | $\boldsymbol{\mathcal{CE}}^{\text{down}}_{\text{total}}$ |
|---|---|---|---|---|---|---|
| Energy | 500 | 306.36 | 806.36 | 48.78 | 28.49 | 38.39 |
| Materials | 200 | 245.28 | 445.28 | 19.51 | 22.81 | 21.20 |
| Industrials | 200 | 317.83 | 517.83 | 19.51 | 29.55 | 24.65 |
| Services | 125 | 206.04 | 331.04 | 12.20 | 19.16 | 15.76 |
| Total | 1 025 | 1 075.50 | 2 100.50 | 100.00 | 100.00 | 100.00 |

**Remark 92** *As noted by Desnos et al. (2023), we must be careful with the upstream and downstream concepts of input-output analysis because they do not correspond to the upstream and downstream concepts of the GHG Protocol. There are several reasons for this. First, an input-output analysis does not distinguish between Scope 2 and Scope 3 emissions. Both are embedded in indirect emissions. Second, the GHG Protocol divides Scope 3 emissions into 8 upstream and 7 downstream categories. Downstream in the GHG Protocol refers to carbon emissions after goods and services have been produced. It includes their use by other sectors as well as final demand. Input-output analysis does not take into account downstream carbon emissions due to final demand (e.g., recycling or waste management). Thus, the downstream concept in input-output analysis is not consistent with the GHG Protocol definition. Third, we can see that there is a lot of double counting in the two analyses. For example, suppose that the matrix $A$ is diagonal. In this case, we can show that $\boldsymbol{\mathcal{CE}}^{\text{up}}_{\text{indirect}} = \boldsymbol{\mathcal{CE}}^{\text{down}}_{\text{indirect}}$. In this particular case, the upstream and downstream analyses refer to the same carbon emissions, and we do not really know whether these emissions are upstream or downstream in the value chain.*

### Mathematical properties

The mathematical properties derived in Section 8.4.1 on page 807 remain valid when we consider the upstream or downstream analysis of carbon intensities. Indeed, we reiterate that the properties require only that $A$ is a doubly substochastic matrix. This is also the case for the matrices $A^\top$ (upstream multiplier matrix $\tilde{\boldsymbol{\mathcal{L}}}$) and $\breve{A}$ (downstream multiplier matrix $\breve{\boldsymbol{\mathcal{L}}}$). In particular, since the carbon intensities are not negative, the partial monotony property is satisfied. This means that there exists an index $k^\star$ such that $\boldsymbol{\mathcal{CI}}_{(k)} \succeq \boldsymbol{\mathcal{CI}}_{(k+1)}$ for the upstream analysis and $\boldsymbol{\mathcal{CI}}^{\text{down}}_{(k)} \succeq \boldsymbol{\mathcal{CI}}^{\text{down}}_{(k+1)}$ for the downstream analysis.

We recall that $\boldsymbol{\mathcal{CI}}_{\text{total}} = \left(I_n - A^\top\right)^{-1} \boldsymbol{\mathcal{CI}}_1 = \sum_{k=0}^{\infty} \left(A^\top\right)^k \boldsymbol{\mathcal{CI}}_1 = \sum_{k=0}^{\infty} \boldsymbol{\mathcal{CI}}_{(k)}$. Let $w_{(k)}$ be the relative contribution vector of the $k^{\text{th}}$ tier. We have:

$$w_{(k),j} = \frac{\boldsymbol{\mathcal{CI}}_{(k),j}}{\sum_{h=0}^{\infty} \boldsymbol{\mathcal{CI}}_{(k),j}}$$

Box 8.20: Calculating the upstreamness index

Let $M$ be a square matrix of dimension $n \times n$. We have:

$$\frac{\partial\,(I_n - M)^{-1}}{\partial\, M} = (I_n - M)^{-1}\,(I_n - M)^{-1}$$

and:

$$\frac{\partial \sum_{k=0}^{\infty} M^k}{\partial\, M} = \sum_{k=0}^{\infty} kM^{k-1}$$

It follows that:

$$\begin{aligned}\sum_{k=0}^{\infty} kM^k &= M\sum_{k=0}^{\infty} kM^{k-1}\\ &= M\frac{\partial \sum_{k=0}^{\infty} M^k}{\partial\, M}\\ &= M\frac{\partial\,(I_n - M)^{-1}}{\partial\, M}\\ &= M\,(I_n - M)^{-1}\,(I_n - M)^{-1}\end{aligned}$$

Let $z$ be a vector. Since we have $(I_n - M)^{-1} z = \sum_{k=0}^{\infty} M^k z = \sum_{k=0}^{\infty} z_{(k)}$ with $z_{(k)} = M^k z$, we deduce that:

$$\sum_{k=0}^{\infty} k \cdot z_{(k)} = \left(\sum_{k=0}^{\infty} kM^k\right) z = M\,(I_n - M)^{-1}\,(I_n - M)^{-1}\,z$$

The upstreamness index of sector $j$ is then equal to:

$$\boldsymbol{\kappa}_j^{\text{up}} := \frac{\left(\sum_{k=0}^{\infty} k \cdot z_{(k)}\right)_j}{\left(\sum_{k=0}^{\infty} z_{(k)}\right)_j} = \frac{\left(M\,(I_n - M)^{-1}\,(I_n - M)^{-1}\,z\right)_j}{\left((I_n - M)^{-1}\,z\right)_j}$$

This expression is not exactly the formula proposed by Antràs *et al.* (2012), because they do not weight the tiers in the same way.

Following Antràs *et al.* (2012), we define the upstreamness index as the weighted average of the tiers with respect to their relative contributions:

$$\boldsymbol{\kappa}_j^{\text{up}} = \sum_{k=0}^{\infty} k \cdot w_{(k),j} = 0 \times \frac{\boldsymbol{\mathcal{CI}}_{(0),j}}{\boldsymbol{\mathcal{CI}}_{\text{total},j}} + 1 \times \frac{\boldsymbol{\mathcal{CI}}_{(1),j}}{\boldsymbol{\mathcal{CI}}_{\text{total},j}} + 2 \times \frac{\boldsymbol{\mathcal{CI}}_{(2),j}}{\boldsymbol{\mathcal{CI}}_{\text{total},j}} + \ldots = \frac{\left(\sum_{k=0}^{\infty} k \cdot \boldsymbol{\mathcal{CI}}_{(k)}\right)_j}{\left(\sum_{k=0}^{\infty} \boldsymbol{\mathcal{CI}}_{(k)}\right)_j}$$

In Box 8.20, we show that[140]:

$$\boldsymbol{\kappa}_j^{\text{up}} = \frac{\left(A^\top\left(I_n - A^\top\right)^{-2}\boldsymbol{\mathcal{CI}}_1\right)_j}{\left(\left(I_n - A^\top\right)^{-1}\boldsymbol{\mathcal{CI}}_1\right)_j}$$

[140] We set $M = A^\top$ and $M = \check{A}$, respectively.

and:

$$\boldsymbol{\kappa}_j^{\text{down}} = \frac{\left(\breve{A}\left(I_n - \breve{A}\right)^{-2}\boldsymbol{\mathcal{CI}}_1\right)_j}{\left(\left(I_n - \breve{A}\right)^{-1}\boldsymbol{\mathcal{CI}}_1\right)_j}$$

If we consider our previous example, we obtain the following results:

| | | Energy | Materials | Industrials | Services |
|---|---|---|---|---|---|
| $M = A$ | $z = y$ | 2.01 | 1.92 | 1.40 | 0.88 |
| $M = A^\top$ | $z = \boldsymbol{\mathcal{CI}}_1$ | 0.49 | 1.21 | 1.79 | 2.13 |
| $M = \breve{A}$ | $z = \boldsymbol{\mathcal{CI}}_1$ | 0.84 | 1.20 | 1.40 | 1.48 |

The upstreamness index of the energy sector is equal to 0.49, while its downstreamness index is equal to 0.84. In the case of the services sector, we obtain a higher upstreamness index ($\boldsymbol{\kappa}_4^{\text{up}} = 2.13$). This indicates that the generation of carbon emissions in this sector affects higher tiers.

### Comparison of upstream emissions between Exiobase, Trucost and WIOD

We report here some calculations made by Desnos *et al.* (2023). We recall that the total carbon intensity and emission vectors are equal to $\boldsymbol{\mathcal{CI}}_{\text{total}} = \left(I_n - A^\top\right)^{-1}\boldsymbol{\mathcal{CI}}_1$ and $\boldsymbol{\mathcal{CE}}_{\text{total}} = x \odot \boldsymbol{\mathcal{CI}}_{\text{total}}$. For the $k^{\text{th}}$ tier, the formulas become $\boldsymbol{\mathcal{CI}}_{(k)} = \left(A^\top\right)^k\boldsymbol{\mathcal{CI}}_1$ and $\boldsymbol{\mathcal{CE}}_{(k)} = x \odot \boldsymbol{\mathcal{CI}}_{(k)}$. The dimension of all these vectors is $n \times 1$, where $n$ is the number of countries times the number of industries. For Trucost, carbon emissions and intensities are directly available. Direct emissions from input-output models can be compared to Scope 1 emissions of Trucost, while the total emissions correspond to Scope 1 plus Scope 2 plus upstream Scope 3 emissions from Trucost. We can also compare the direct plus first-tier indirect emissions of Trucost with the first-tier cumulative emissions $\boldsymbol{\mathcal{CE}}_{(0-1)}$ calculated from input-output models.

If we want to aggregate the results such that $i \in \Omega$, we have:

$$\boldsymbol{\mathcal{CE}}_{\text{total}}(\Omega) = \sum_{i\in\Omega}\boldsymbol{\mathcal{CE}}_{\text{total},i} = \omega^\top\boldsymbol{\mathcal{CE}}_{\text{total}}$$

where $\omega = (\omega_i)$ is a vector of dimension $n \times 1$ with $\omega_i = 1$ if $i \in \Omega$ and $\omega_i = 0$ otherwise. We deduce that the carbon intensity of $\Omega$ is equal to:

$$\boldsymbol{\mathcal{CI}}_{\text{total}}(\Omega) = \frac{\sum_{i\in\Omega}\boldsymbol{\mathcal{CE}}_{\text{total},i}}{\sum_{i\in\Omega}x_i} = \frac{\sum_{i\in\Omega}x_i\boldsymbol{\mathcal{CI}}_{\text{total},i}}{\sum_{i\in\Omega}x_i} = \sum_{i\in\Omega}w_i\boldsymbol{\mathcal{CI}}_{\text{total},i}$$

where $w_i = \left(\sum_{j\in\Omega}x_j\right)^{-1}x_i$ is the weight of item $i$ in the set $\Omega$. The carbon intensity of $\Omega$ is then equal to its weighted average carbon intensity (WACI). These calculations also apply to $\boldsymbol{\mathcal{CE}}_{(k)}$, $\boldsymbol{\mathcal{CE}}_{(0:k)}$, $\boldsymbol{\mathcal{CI}}_{(k)}$ and $\boldsymbol{\mathcal{CI}}_{(0:k)}$.

We perform a global analysis by setting $\omega = \mathbf{1}_n$. In Table 8.52, we report the multiplication coefficients $m_{(k)} = \boldsymbol{\mathcal{CE}}_{(k)}/\boldsymbol{\mathcal{CE}}_1$ and $m_{(0-k)} = \boldsymbol{\mathcal{CE}}_{(0-k)}/\boldsymbol{\mathcal{CE}}_1$, and we also compute the contribution ratio $c_{(0-k)} = \boldsymbol{\mathcal{CE}}_{(0-k)}/\boldsymbol{\mathcal{CE}}_{\text{total}}$. For the WIOD table, the direct plus indirect emissions are 3.14 times the Scope 1 emissions, which means that the indirect emissions are more than twice the direct emissions. In the case of the Exiobase tables, the ratio $m_{(0-\infty)}$ is equal to 2.76 in 2014 and 2.75 in 2022. We note that the convergence is rapid, as more than 90% of the total emissions are located in the first five tiers.

Table 8.52: Ratio of upstream carbon emissions (global analysis)

| Tier | WIOD 2014 | | | Exiobase 2014 | | | Exiobase 2022 | | |
|---|---|---|---|---|---|---|---|---|---|
| | $m_{(k)}$ | $m_{(0-k)}$ | $c_{(0-k)}$ | $m_{(k)}$ | $m_{(0-k)}$ | $c_{(0-k)}$ | $m_{(k)}$ | $m_{(0-k)}$ | $c_{(0-k)}$ |
| 0 | 1.00 | 1.00 | 31.8% | 1.00 | 1.00 | 36.2% | 1.00 | 1.00 | 36.4% |
| 1 | 0.77 | 1.76 | 56.1% | 0.72 | 1.72 | 62.5% | 0.73 | 1.73 | 62.9% |
| 2 | 0.50 | 2.26 | 71.9% | 0.43 | 2.15 | 78.0% | 0.42 | 2.15 | 78.3% |
| 3 | 0.32 | 2.58 | 82.1% | 0.25 | 2.40 | 87.0% | 0.25 | 2.40 | 87.3% |
| 4 | 0.20 | 2.78 | 88.6% | 0.15 | 2.55 | 92.3% | 0.14 | 2.54 | 92.5% |
| 5 | 0.13 | 2.91 | 92.7% | 0.09 | 2.63 | 95.5% | 0.08 | 2.62 | 95.5% |
| 6 | 0.08 | 3.00 | 95.4% | 0.05 | 2.69 | 97.3% | 0.05 | 2.67 | 97.3% |
| 7 | 0.05 | 3.05 | 97.0% | 0.03 | 2.72 | 98.4% | 0.03 | 2.70 | 98.4% |
| 8 | 0.03 | 3.08 | 98.1% | 0.02 | 2.73 | 99.0% | 0.02 | 2.72 | 99.0% |
| 9 | 0.02 | 3.11 | 98.8% | 0.01 | 2.74 | 99.4% | 0.01 | 2.73 | 99.4% |
| 10 | 0.01 | 3.12 | 99.2% | 0.01 | 2.75 | 99.7% | 0.01 | 2.74 | 99.7% |
| $\infty$ | 0.00 | 3.14 | 100.0% | 0.00 | 2.76 | 100.0% | 0.00 | 2.75 | 100.0% |

Source: Desnos *et al.* (2023, Table 15, page 52).

Figure 8.138: Multiplication coefficient $m_{(0-1)}$ and $m_{(0-\infty)}$ (global analysis)

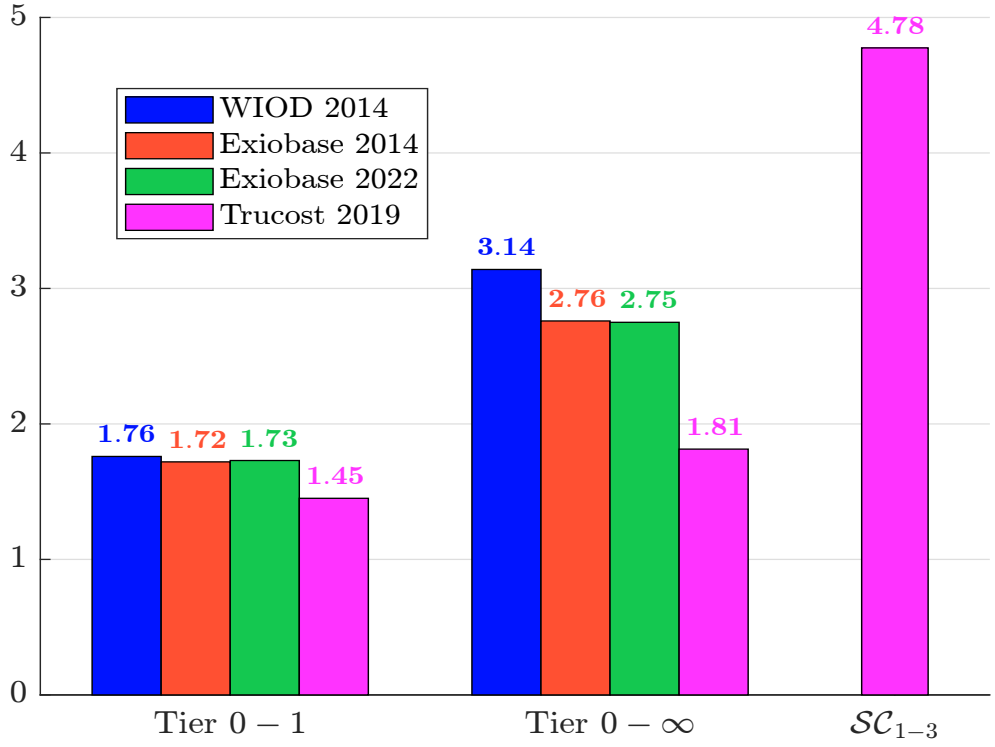


Source: Desnos *et al.* (2023, Figure 25, page 53).

In the case of Trucost, we can only compute $m_{(0-1)}$ and $m_{(0-\infty)}$. Results are shown in Figure 8.138. We notice that the multiplication coefficients obtained with Trucost are smaller than those computed with input-output models (1.45–1.54 versus 1.7 for the first tier). Nevertheless, the multiplication coefficient is very high when we integrate Scope 3 emissions since we obtain a value of 4.78 in 2019 and 6.75 in 2021.

Desnos *et al.* (2023) also suggested a country analysis[141]. They observed some large differences from one country to another. For instance, Figure 8.139 shows the multiplication coefficient $m_{(0-\infty)}$ of the different countries. The lowest value is obtained for the USA ($m_{(0-\infty)} = 2.19$), while the highest factor is observed for Switzerland ($m_{(0-\infty)} = 7.21$).

Figure 8.139: Multiplying coefficient $m_{(0-\infty)}$ (country analysis, WIOD 2014)

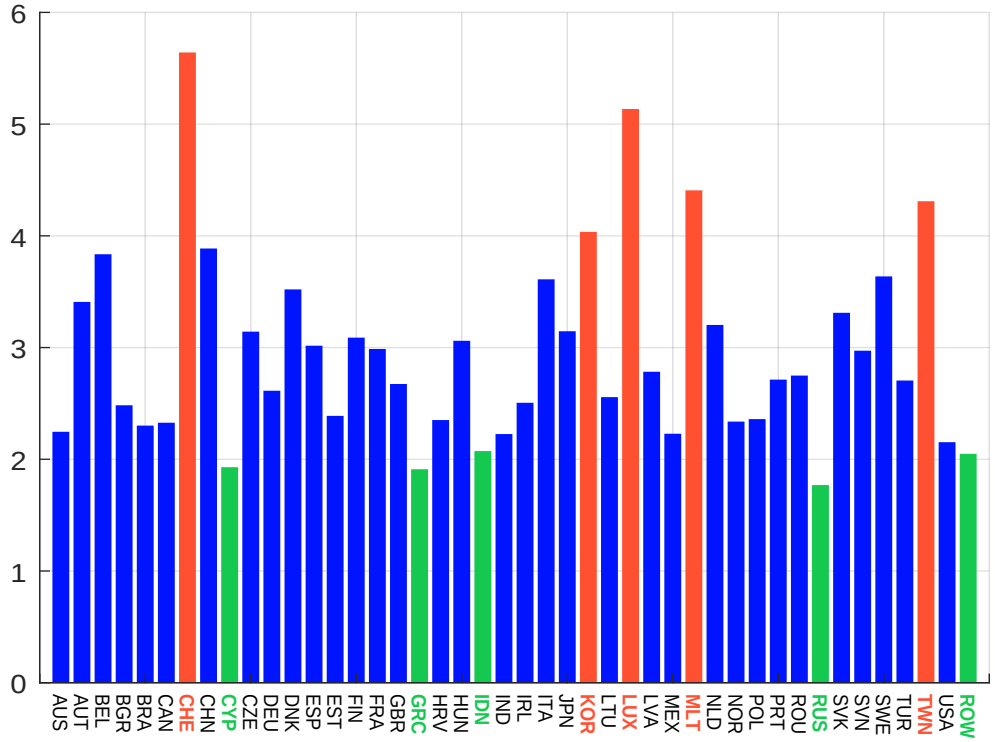


Source: Desnos *et al.* (2023, Figure 26, page 54).

Desnos *et al.* (2023) applied the previous framework to estimate the upstream of the MSCI World index. They first estimated the total carbon intensity of all issuers in the portfolio:

$$\boldsymbol{\mathcal{CI}}_{\text{total},i} = \boldsymbol{\mathcal{CI}}_{1,i}^{\text{reported}} + \boldsymbol{\mathcal{CI}}_{\text{indirect},i}^{\text{estimated}}$$

where $\boldsymbol{\mathcal{CI}}_{1,i}^{\text{reported}}$ is the Scope 1 carbon intensity reported by the issuer $i$ and $\boldsymbol{\mathcal{CI}}_{\text{indirect},i}^{\text{estimated}}$ is the estimated indirect carbon intensity. In the case of Trucost, they used the values estimated by the data provider. For the input-output databases, they used the formula $\boldsymbol{\mathcal{CI}}_{\text{indirect}}^{\text{estimated}} = \left(\left(I_n - A^\top\right)^{-1} - I_n\right)\boldsymbol{\mathcal{CI}}_{\text{direct}}$ and considered the row corresponding to the sector and the country of the issuer $i$. They then aggregated the carbon intensity of the MSCI World Index at the GICS level 1 sectors. The results are shown in Table 8.53 and Figure 8.140. The direct plus indirect intensity of

[141] In this case, $\omega_i = 1$ if $i$ belongs to the country and $\omega_i = 0$ otherwise.

the MSCI World Index is equal to 299 $tCO_2e/\$$ mn with Exiobase 2022, 281 $tCO_2e/\$$ mn with Trucost 2021 and 278 $tCO_2e/\$$ mn with WIOD 2014. The difference between the lowest and the highest value is then equal to 7.5%, which is a low figure. If we look at the GICS sectors, the differences are more significant, especially for consumer staples, energy and materials. For instance, the carbon intensity of the energy sector is equal to 757 $tCO_2e/\$$ mn with WIOD 2014 and 1 373 $tCO_2e/\$$ mn with Exiobase 2022. They also calculated the contribution of each sector to the carbon intensity of the MSCI World Index:

$$c_j(w) = \frac{\sum_{i \in \mathcal{S}_{ector_j}} w_i \cdot \mathcal{CI}_{\text{total},i}}{\sum_i w_i \cdot \mathcal{CI}_{\text{total},i}}$$

where $w$ is the vector of weights in the MSCI World Index and $c_j(w)$ is the contribution of the $j^{\text{th}}$ sector. In Table 8.54, we see some significant differences. This is true for the previously mentioned sectors (consumer staples, energy and materials), but also for consumer discretionary, health care and information technology.

Table 8.53: Direct + indirect carbon intensities of GICS sectors (MSCI World index, May 2023)

| Sector | Exiobase 2022 | Trucost 2021 | WIOD 2014 |
|---|---|---|---|
| Communication Services | 66 | 78 | 102 |
| Consumer Discretionary | 168 | 209 | 219 |
| Consumer Staples | 437 | 387 | 277 |
| Energy | 1 373 | 796 | 757 |
| Financials | 83 | 55 | 83 |
| Health Care | 108 | 120 | 167 |
| Industrials | 276 | 277 | 307 |
| Information Technology | 110 | 138 | 131 |
| Materials | 791 | 973 | 747 |
| Real Estate | 128 | 134 | 138 |
| Utilities | 1 872 | 1 833 | 1 889 |
| MSCI World | 299 | 281 | 278 |

Source: Desnos *et al.* (2023, Table 57, page 178).

Table 8.54: Breakdown of the portfolio intensity by GICS sector (MSCI World Index, May 2023)

| Sector | Exiobase 2022 | Trucost 2021 | WIOD 2014 |
|---|---|---|---|
| Communication Services | 1.5% | 1.9% | 2.5% |
| Consumer Discretionary | 5.9% | 7.8% | 8.4% |
| Consumer Staples | 11.6% | 10.9% | 7.9% |
| Energy | 22.9% | 14.1% | 13.6% |
| Financials | 4.2% | 2.9% | 4.5% |
| Health Care | 4.8% | 5.7% | 8.0% |
| Industrials | 10.2% | 10.8% | 12.1% |
| Information Technology | 7.5% | 10.0% | 9.6% |
| Materials | 11.7% | 15.3% | 11.9% |
| Real Estate | 1.1% | 1.2% | 1.2% |
| Utilities | 18.6% | 19.4% | 20.2% |

Source: Desnos *et al.* (2023, Table 21, page 62).

Figure 8.140: Total carbon intensity $\boldsymbol{\mathcal{CI}}_{\text{total}}$ by GICS sector (MSCI World Index, May 2023)

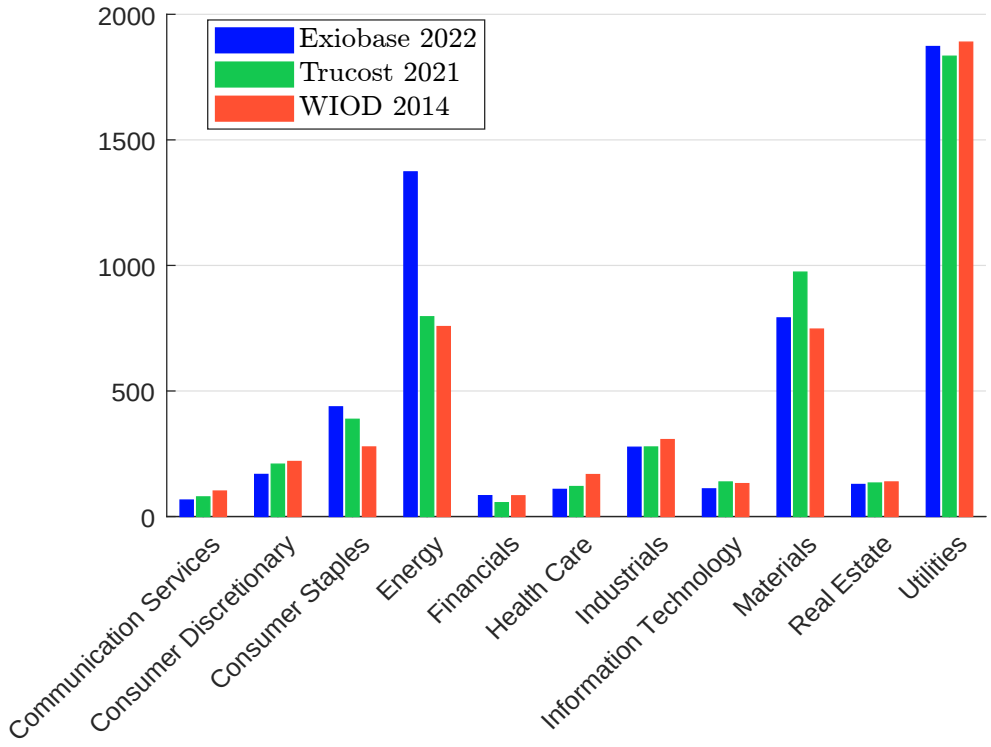


Source: Desnos *et al.* (2023, Figure 33, page 61).

### 8.4.4 Imported and exported carbon emissions

On page 819, we have analyzed the difference in carbon footprint when we use a production-based or consumption-based inventory. We can extend this framework by considering multiple regions. In this case, we can adjust a country's carbon footprint for imports and exports. For instance, it may be unfair to attribute the $CO_2$ emissions of a good to a country if that country exports 100% of that good to the rest of the world. The concept of imported and exported carbon emissions is then central when we would like to measuring a country's carbon footprint, which reflects the consumption and lifestyle choices of its citizens (Turner *et al.*, 2007; Wiedmann *et al.*, 2007). The groundbreaking research paper by Peters and Hertwich (2008) has been followed by a large number of studies[142]. They all conclude that there is a large bias when focusing on territorial emissions due to production.

#### Calculation of balanced emissions

Let's learn how to calculate the $CO_2$ embodied in international trade by using the input-output framework. We have:

- $y_{j,r}$ is the final demand of the $j^{\text{th}}$ sector and the $r^{\text{th}}$ region.
- $y = (y_1, \ldots, y_n)$ is the vector of final demand where $y_j = \sum_{r=1}^{p} y_{j,r}$ is the final demand of the $j^{\text{th}}$ sector.

[142]For example, we can cite the works of Davis and Caldeira (2010), Peters *et al.* (2011), Yamano and Guilhoto (2020), Lamb *et al.* (2021) and Friedlingstein *et al.* (2022).

- $C^{(x)} = \left(C^{(x)}_{g,j}\right)$ is the pollution output matrix where $C^{(x)}_{g,j}$ is the total amount of the $g^{\text{th}}$ pollutant generated by the output of the $j^{\text{th}}$ sector.
- $D^{(y)} = C^{(x)} \operatorname{diag}(x)^{-1} = \left(D^{(y)}_{g,j}\right)$ is the matrix of direct impact coefficients where $D^{(y)}_{g,j} = c^{(y)}_{g,j}/x_j$ is the amount of the $g^{\text{th}}$ pollutant generated by 1\$ of the output of the $j^{\text{th}}$ sector.
- $\varpi = (\varpi_1, \ldots, \varpi_m)$ is the vector of pollution level. We have:

$$\varpi = D^{(x)}x = D^{(x)}(I_n - A)^{-1}y = D^{(y)}y$$

where $D^{(y)} = D^{(x)}(I_n - A)^{-1}$ is the pollutant multiplier matrix with respect to the final demand $y$.

In the production-based approach, the total contribution of the $r^{\text{th}}$ to the $g^{\text{th}}$ pollutant is equal to:

$$C^{(x,r)}_g = \sum_{j \in r} C^{(x)}_{g,j} \tag{8.42}$$

In the consumption-based approach, we have the following identity:

$$\varpi_g = \left(D^{(y)}y\right)_g = \sum_{j=1}^{n} D^{(y)}_{g,j}y_j = \sum_{j=1}^{n} D^{(y)}_{g,j} \sum_{r=1}^{p} y_{j,r} = \sum_{r=1}^{p}\sum_{j=1}^{n} D^{(y)}_{g,j}y_{j,r}$$

we deduce that the total contribution of the $r^{\text{th}}$ region to the $g^{\text{th}}$ pollutant is equal to:

$$\begin{aligned} C^{(y,r)}_g &= \sum_{j=1}^{n} \frac{\partial \varpi_g}{\partial y_{j,r}} y_{j,r} \\ &= \sum_{j=1}^{n} D^{(y)}_{g,j}y_{j,r} \end{aligned} \tag{8.43}$$

**Example 32** *We consider two sectors ($\mathcal{S}_1$ and $\mathcal{S}_2$) and three regions ($\mathcal{R}_1$, $\mathcal{R}_2$ and $\mathcal{R}_3$), whose input-output table is given below:*

| | | $Z$ | | | | | | $y$ | | | $x$ |
|---|---|---|---|---|---|---|---|---|---|---|---|
| | | $\mathcal{R}_1$ | | $\mathcal{R}_2$ | | $\mathcal{R}_3$ | | $\mathcal{R}_1$ | $\mathcal{R}_2$ | $\mathcal{R}_3$ | |
| | | $\mathcal{S}_1$ | $\mathcal{S}_2$ | $\mathcal{S}_1$ | $\mathcal{S}_2$ | $\mathcal{S}_1$ | $\mathcal{S}_2$ | | | | |
| $\mathcal{R}_1$ | $\mathcal{S}_1$ | 100 | 300 | 10 | 10 | 20 | 0 | 500 | 200 | 25 | 1 165 |
| | $\mathcal{S}_2$ | 250 | 150 | 20 | 0 | 10 | 0 | 800 | 100 | 17 | 1 347 |
| $\mathcal{R}_2$ | $\mathcal{S}_1$ | 10 | 10 | 110 | 310 | 0 | 0 | 20 | 200 | 15 | 675 |
| | $\mathcal{S}_2$ | 20 | 20 | 80 | 25 | 15 | 20 | 0 | 200 | 5 | 385 |
| $\mathcal{R}_3$ | $\mathcal{S}_1$ | 10 | 5 | 8 | 3 | 40 | 7 | 5 | 25 | 50 | 153 |
| | $\mathcal{S}_2$ | 5 | 2 | 8 | 8 | 12 | 35 | 3 | 50 | 50 | 173 |
| $V$ | | 770 | 860 | 439 | 29 | 56 | 111 | | | | |
| $x$ | | 1 165 | 1 347 | 675 | 385 | 153 | 173 | | | | |
| GHG | $CO_2$ | 50 000 | 20 000 | 10 000 | 10 000 | 5 000 | 5 000 | | 100 000 | | |
| | $CH_4$ | 5 000 | 3 000 | 0 | 0 | 1 000 | 1 000 | | 10 000 | | |

*$Z$, $y$, $x$ and $V$ are expressed in \$ mn, while the GHG are calculated in tonne. Final demand is split between the three regions. For instance, $x_1$ is equal to \$1 165 mn, its intermediary demand is equal to $100+300+10+10+20+0$ or \$440 mn and its final demand is equal to \$725 mn with the following breakdown: 500 for the region $\mathcal{R}_1$, 200 for the region $\mathcal{R}_2$ and 25 for the region $\mathcal{R}_3$.*

If we take a production-based approach, $x_1$ and $x_2$ are in region $\mathcal{R}_1$, which means that this region is responsible for 70 000 $tCO_2$ and 8 000 $tCH_4$. Finally, we obtain the following distribution among the three regions:

| | Absolute | | | Relative | | |
|---|---|---|---|---|---|---|
| | $\mathcal{R}_1$ | $\mathcal{R}_2$ | $\mathcal{R}_3$ | $\mathcal{R}_1$ | $\mathcal{R}_2$ | $\mathcal{R}_3$ |
| $CO_2$ | 70 000 | 20 000 | 10 000 | 70% | 20% | 10% |
| $CH_4$ | 8 000 | 0 | 2 000 | 80% | 0% | 20% |

We have:

$$A = Z\,\text{diag}\,(x)^{-1} = \begin{pmatrix} 0.0858 & 0.2227 & 0.0148 & 0.0260 & 0.1307 & 0.0000 \\ 0.2146 & 0.1114 & 0.0296 & 0.0000 & 0.0654 & 0.0000 \\ 0.0086 & 0.0074 & 0.1630 & 0.8052 & 0.0000 & 0.0000 \\ 0.0172 & 0.0148 & 0.1185 & 0.0649 & 0.0980 & 0.1156 \\ 0.0086 & 0.0037 & 0.0119 & 0.0078 & 0.2614 & 0.0405 \\ 0.0043 & 0.0015 & 0.0119 & 0.0208 & 0.0784 & 0.2023 \end{pmatrix}$$

and:

$$\boldsymbol{\mathcal{L}} = (I_6 - A)^{-1} = \begin{pmatrix} 1.1674 & 0.2953 & 0.0454 & 0.0741 & 0.2450 & 0.0232 \\ 0.2848 & 1.1989 & 0.0586 & 0.0601 & 0.1663 & 0.0171 \\ 0.0482 & 0.0445 & 1.3705 & 1.1871 & 0.1893 & 0.1816 \\ 0.0351 & 0.0320 & 0.1817 & 1.2327 & 0.1927 & 0.1884 \\ 0.0167 & 0.0109 & 0.0263 & 0.0362 & 1.3706 & 0.0748 \\ 0.0101 & 0.0064 & 0.0280 & 0.0538 & 0.1442 & 1.2687 \end{pmatrix}$$

The direct impact matrix is equal to the GHG emissions divided by the output:

$$\begin{aligned} D^{(x)} &= \begin{pmatrix} 50\,000/1\,165 & 20\,000/1\,347 & 10\,000/675 & 10\,000/385 & 5\,000/153 & 5\,000/173 \\ 5\,000/1\,165 & 3\,000/1\,347 & 0/675 & 0/385 & 1\,000/153 & 1\,000/173 \end{pmatrix} \\ &= \begin{pmatrix} 42.9185 & 14.8478 & 14.8148 & 25.9740 & 32.6797 & 28.9017 \\ 4.2918 & 2.2272 & 0.0000 & 0.0000 & 6.5359 & 5.7803 \end{pmatrix} \end{aligned}$$

The unit of $D^{(x)}$ is expressed in tonnes of the gas per million dollars. The carbon intensity of the sector $\mathcal{S}_1$ in the region $\mathcal{R}_1$ is equal to 42.9185 $tCO_2$/\$ mn, while the methane intensity is equal to 4.2918 $tCH_4$/\$ mn. We have:

$$D^{(y)} = D^{(x)}\boldsymbol{\mathcal{L}} = \begin{pmatrix} 56.7948 & 32.5033 & 29.5091 & 56.4128 & 69.7564 & 47.9460 \\ 5.8121 & 4.0453 & 0.6591 & 0.9993 & 11.2142 & 7.9600 \end{pmatrix}$$

Using Equation (8.43), we finally obtain the following decomposition:

| | Absolute | | | Relative | | |
|---|---|---|---|---|---|---|
| | $\mathcal{R}_1$ | $\mathcal{R}_2$ | $\mathcal{R}_3$ | $\mathcal{R}_1$ | $\mathcal{R}_2$ | $\mathcal{R}_3$ |
| $CO_2$ | 55 483 | 35 935 | 8 582 | 55.5% | 35.9% | 8.6% |
| $CH_4$ | 6 235 | 2 577 | 1 188 | 62.4% | 25.8% | 11.9% |

In the consumption-based approach, the region $\mathcal{R}_1$ is responsible for 55.5% of carbon emissions, which is lower than the 70% figure obtained in the production-based approach. The second region sees a high increase in carbon emissions of 79.5%.

Let us now look at how the concept of imported and exported emissions is defined. In Table 8.55, we report the allocation of carbon emissions to intermediate and final uses. For intermediate consumption, the allocation to $Z_{i,j}$ is equal to:

$$\boldsymbol{\mathcal{CE}}_i\,(Z_{i,j}) = \frac{Z_{i,j}}{x_i} \cdot \boldsymbol{\mathcal{CE}}_i$$

while we have for the final consumption:

$$\mathcal{CE}_i\left(y_{i,r}\right) = \frac{y_{i,r}}{x_i} \cdot \mathcal{CE}_i$$

By construction, we verify the equality:

$$\sum_{j=1}^{n} \mathcal{CE}_i\left(Z_{i,j}\right) + \sum_{r=1}^{p} \mathcal{CE}_i\left(y_{i,r}\right) = \left(\sum_{j=1}^{n} \frac{Z_{i,j}}{x_i} + \sum_{r=1}^{p} \frac{y_{i,r}}{x_i}\right) \mathcal{CE}_i = \mathcal{CE}_i$$

Table 8.55: Allocation of carbon emissions to intermediate and final uses (production-based approach)

| | $Z$ | | | | | | $y$ | | | Total |
|---|---|---|---|---|---|---|---|---|---|---|
| | $\mathcal{R}_1$ | $\mathcal{R}_1$ | $\mathcal{R}_2$ | $\mathcal{R}_2$ | $\mathcal{R}_3$ | $\mathcal{R}_3$ | $\mathcal{R}_1$ | $\mathcal{R}_2$ | $\mathcal{R}_3$ | |
| $(\mathcal{S}_1, \mathcal{R}_1)$ | 4 292 | 12 876 | 429 | 429 | 858 | 0 | 21 459 | 8 584 | 1 073 | 50 000 |
| $(\mathcal{S}_2, \mathcal{R}_1)$ | 3 712 | 2 227 | 297 | 0 | 148 | 0 | 11 878 | 1 485 | 252 | 20 000 |
| $(\mathcal{S}_1, \mathcal{R}_2)$ | 148 | 148 | 1 630 | 4 593 | 0 | 0 | 296 | 2 963 | 222 | 10 000 |
| $(\mathcal{S}_2, \mathcal{R}_2)$ | 519 | 519 | 2 078 | 649 | 390 | 519 | 0 | 5 195 | 130 | 10 000 |
| $(\mathcal{S}_1, \mathcal{R}_3)$ | 327 | 163 | 261 | 98 | 1 307 | 229 | 163 | 817 | 1 634 | 5 000 |
| $(\mathcal{S}_2, \mathcal{R}_3)$ | 145 | 58 | 231 | 231 | 347 | 1 012 | 87 | 1 445 | 1 445 | 5 000 |
| Total | 9 143 | 15 992 | 4 926 | 6 000 | 3 050 | 1 760 | 33 884 | 20 488 | 4 757 | 100 000 |

From Table 8.55, we can aggregate the columns to obtain the regional carbon allocation (Table 8.56). For instance, the carbon allocation to sector $\mathcal{S}_1$ and region $\mathcal{R}_1$ is equal to:

$$4\,292 + 12\,876 + 21\,459 = 38\,627 \text{ tCO}_2$$

Table 8.56: Carbon allocation by region (production-based approach, column aggregation)

| | $\mathcal{R}_1$ | $\mathcal{R}_2$ | $\mathcal{R}_3$ | Total |
|---|---|---|---|---|
| $(\mathcal{S}_1, \mathcal{R}_1)$ | 38 627 | 9 442 | 1 931 | 50 000 |
| $(\mathcal{S}_2, \mathcal{R}_1)$ | 17 817 | 1 782 | 401 | 20 000 |
| $(\mathcal{S}_1, \mathcal{R}_2)$ | 593 | 9 185 | 222 | 10 000 |
| $(\mathcal{S}_2, \mathcal{R}_2)$ | 1 039 | 7 922 | 1 039 | 10 000 |
| $(\mathcal{S}_1, \mathcal{R}_3)$ | 654 | 1 176 | 3 170 | 5 000 |
| $(\mathcal{S}_2, \mathcal{R}_3)$ | 289 | 1 908 | 2 803 | 5 000 |
| Total | 59 018 | 31 415 | 9 567 | 100 000 |

Table 8.57: Carbon allocation by region (production-based approach, row aggregation)

| | $\mathcal{R}_1$ | $\mathcal{R}_2$ | $\mathcal{R}_3$ | Total |
|---|---|---|---|---|
| $\mathcal{R}_1$ | 56 444 | 11 224 | 2 332 | 70 000 |
| $\mathcal{R}_2$ | 1 632 | 17 107 | 1 261 | 20 000 |
| $\mathcal{R}_3$ | 943 | 3 084 | 5 973 | 10 000 |
| Total | 59 018 | 31 415 | 9 567 | 100 000 |

By aggregating the rows, we finally obtain the allocation given in Table 8.57. For example, the carbon allocation of goods produced in region $\mathcal{R}_1$ and consumed in region $\mathcal{R}_1$ is equal to:

$$3\,8627 + 17\,817 = 56\,444 \text{ tCO}_2$$

The carbon allocation of goods produced in region $\mathcal{R}_1$ and consumed in region $\mathcal{R}_2$ is equal to:

$$9\,442 + 1\,782 = 11\,224 \text{ tCO}_2$$

The row shows the allocation split of the emissions produced in a given region. The column shows the allocation split of the emissions consumed in a given region. For example, among the 70 000 $\text{tCO}_2$ emitted in region $\mathcal{R}_1$, 11 224 and 2 332 are exported in regions $\mathcal{R}_2$ and $\mathcal{R}_3$. Therefore, 56 444 $\text{tCO}_2$ remain in region $\mathcal{R}_1$. Since $\mathcal{R}_1$ also imports 1 632 $\text{tCO}_2$ from region $\mathcal{R}_2$ and 943 $\text{tCO}_2$ from region $\mathcal{R}_3$, the total carbon emissions allocated to region $\mathcal{R}_1$ is equal to 59 018 $\text{tCO}_2$. A summary of the allocation process is given below:

| | $\mathcal{R}_1$ | $\mathcal{R}_2$ | $\mathcal{R}_3$ | Total |
|---|---|---|---|---|
| Produced emissions | 70 000 | 20 000 | 10 000 | 100 000 |
| − Exported emissions | 13 556 | 2 893 | 4 027 | 20 475 |
| = Intermediate emissions | 56 444 | 17 107 | 5 973 | 79 525 |
| + Imported emissions | 2 574 | 14 308 | 3 593 | 20 475 |
| = Regional emissions | 59 018 | 31 415 | 9 567 | 100 000 |

By construction, exported emissions are equal to imported emissions at the aggregate level, but not at the regional level. In the case of region $\mathcal{R}_1$, we have the following results:

$$\underbrace{70\,000}_{\text{produced}} - \underbrace{13\,556}_{\text{exported}} + \underbrace{2\,574}_{\text{imported}} = \underbrace{59\,018}_{\text{allocated}} \neq \underbrace{55\,483}_{\text{consumed}}$$

Note that we do not get the previous figure of 55 483 $\text{tCO}_2$ emissions. The reason for this is that the above analysis is based on the tier-one decomposition and does not include the full value chain relationships.

Table 8.58: Carbon allocation by region (consumption-based approach, column aggregation)

| | $\mathcal{R}_1$ | $\mathcal{R}_2$ | $\mathcal{R}_3$ | Total | Produced emissions | EEIO correction |
|---|---|---|---|---|---|---|
| $(\mathcal{S}_1, \mathcal{R}_1)$ | 28 397 | 11 359 | 1 420 | 41 176 | 50 000 | −8 824 |
| $(\mathcal{S}_2, \mathcal{R}_1)$ | 26 003 | 3 250 | 553 | 29 806 | 20 000 | 9 806 |
| $(\mathcal{S}_1, \mathcal{R}_2)$ | 590 | 5 902 | 443 | 6 935 | 10 000 | −3 065 |
| $(\mathcal{S}_2, \mathcal{R}_2)$ | 0 | 11 283 | 282 | 11 565 | 10 000 | 1 565 |
| $(\mathcal{S}_1, \mathcal{R}_3)$ | 349 | 1 744 | 3 488 | 5 581 | 5 000 | 581 |
| $(\mathcal{S}_2, \mathcal{R}_3)$ | 144 | 2 397 | 2 397 | 4 938 | 5 000 | −62 |
| Total | 55 483 | 35 935 | 8 582 | 100 000 | 100 000 | 0 |

Table 8.59: Carbon allocation by region (consumption-based approach, row aggregation)

| | $\mathcal{R}_1$ | $\mathcal{R}_2$ | $\mathcal{R}_3$ | Total |
|---|---|---|---|---|
| $\mathcal{R}_1$ | 54 400 | 14 609 | 1 972 | 70 982 |
| $\mathcal{R}_2$ | 590 | 17 184 | 725 | 18 499 |
| $\mathcal{R}_3$ | 493 | 4 141 | 5 885 | 10 519 |
| Total | 55 483 | 35 935 | 8 582 | 100 000 |

In order to take into account the full value chain, we proceed as previously by considering the consumption-based emissions $D_{g,j}^{(y)} y_{j,r}$ instead of the production-based emissions $C_{g,j}^{(x)}$. We obtain

the results shown in Table 8.58. We can then compute the EEIO correction $cr_{g,j}^{(y)}$, which is defined by the following equation:

$$\sum_{r=1}^{p} D_{g,j}^{(y)} y_{j,r} = C_{g,j}^{(x)} + cr_{g,j}^{(y)}$$

For example, it is equal to $-8\,824$ $tCO_2$ for $(\mathcal{S}_1, \mathcal{R}_1)$. We then perform the row aggregation (Table 8.59), and we finally obtain the following allocation results:

| | $\mathcal{R}_1$ | $\mathcal{R}_2$ | $\mathcal{R}_3$ | Total |
|---|---|---|---|---|
| Produced emissions | 70 000 | 20 000 | 10 000 | 100 000 |
| + EEIO correction | 982 | −1 501 | 519 | 0 |
| = Consumed emissions | 70 982 | 18 499 | 10 519 | 100 000 |
| − Exported emissions | 16 582 | 1 315 | 4 634 | 22 530 |
| = Intermediate emissions | 54 400 | 17 184 | 5 885 | 77 470 |
| + Imported emissions | 1 083 | 18 751 | 2 697 | 22 530 |
| = Regional emissions | 55 483 | 35 935 | 8 582 | 100 000 |
| Net imported emissions | −14 517 | 15 935 | −1 418 | 0 |

We can define the concept of net imported emissions, which takes into account the EEIO correction, imported and exported emissions. It is the difference between the emissions due to consumption and the emissions due to production. In our example, $\mathcal{R}_1$ and $\mathcal{R}_3$ are net exporting regions, while $\mathcal{R}_2$ is a net importing region.

**Remark 93** *The previous formulas can be easily translated using the traditional notations. Let* $\boldsymbol{\mathcal{CI}}_1 = (\boldsymbol{\mathcal{CI}}_{1,1}, \ldots, \boldsymbol{\mathcal{CI}}_{n,1})$ *be the vector of carbon intensities evaluated in* $CO_2e$*, where* $\boldsymbol{\mathcal{CI}}_{j,1}$ *measures the direct emission intensity of sector* $j$*. The vector of consumption-based carbon intensities is equal to:*

$$\boldsymbol{\mathcal{CI}}^{(y)} = \tilde{\boldsymbol{\mathcal{L}}}\, \boldsymbol{\mathcal{CI}}_1 := \boldsymbol{\mathcal{CI}}_{\text{total}} \tag{8.44}$$

*Let* $y = (y_{j,r})$ *be the* $n \times p$ *matrix, where* $y_{j,r}$ *is the final demand of the* $j^{\text{th}}$ *sector and the* $r^{\text{th}}$ *region. We have:*

$$\boldsymbol{\mathcal{CE}}^{(y)} = \boldsymbol{\mathcal{CI}}^{(y)} \odot y \tag{8.45}$$

$\boldsymbol{\mathcal{CE}}^{(y)}$ *is the* $n \times p$ *matrix of carbon emissions. The consumption-based carbon emissions of the* $r^{\text{th}}$ *region is then equal to:*

$$\boldsymbol{\mathcal{CE}}^{(y,r)} = \mathbf{1}_n^\top \left( \boldsymbol{\mathcal{CE}}^{(y)} \mathbf{e}_r \right) \tag{8.46}$$

*while the imported and exported carbon emissions of the* $r^{\text{th}}$ *region are:*

$$\boldsymbol{\mathcal{CE}}_{\text{imported}}^{(y,r)} = \sum_{j \notin r} \left( \boldsymbol{\mathcal{CE}}^{(y)} \mathbf{e}_r \right)_j \tag{8.47}$$

*and:*

$$\boldsymbol{\mathcal{CE}}_{\text{exported}}^{(y,r)} = \sum_{j \in r} \sum_{k \neq r} \left( \boldsymbol{\mathcal{CE}}^{(y)} \mathbf{e}_r \right)_j \tag{8.48}$$

*Equations (8.44–8.48) are the basic formulas for calculating imported and exported carbon emissions. We can also easily define consumed, intermediate and net imported emissions and the EEIO correction at both the sectoral and regional levels.*

### Stylized facts

Figure 8.141 shows a global picture of carbon emissions embedded in trade, which can be found at https://ourworldindata.org/consumption-based-co2. The data are taken from the famous *Global Carbon Budget* (2022) report (Friedlingstein *et al.*, 2022). The exported (blue color) or imported (red color) emissions are normalized to domestic production emissions. For example, a value of 100% indicates a country whose imported emissions are equal to its domestic production emissions. We notice that the European countries and the United States are colored red, which means that they are net importers of $CO_2$. On the contrary, the BRICS countries[143] are net exporters of CO2, as are Australia, Canada and the Middle East region.

Figure 8.141: $CO_2$ emissions embedded in trade, 2020

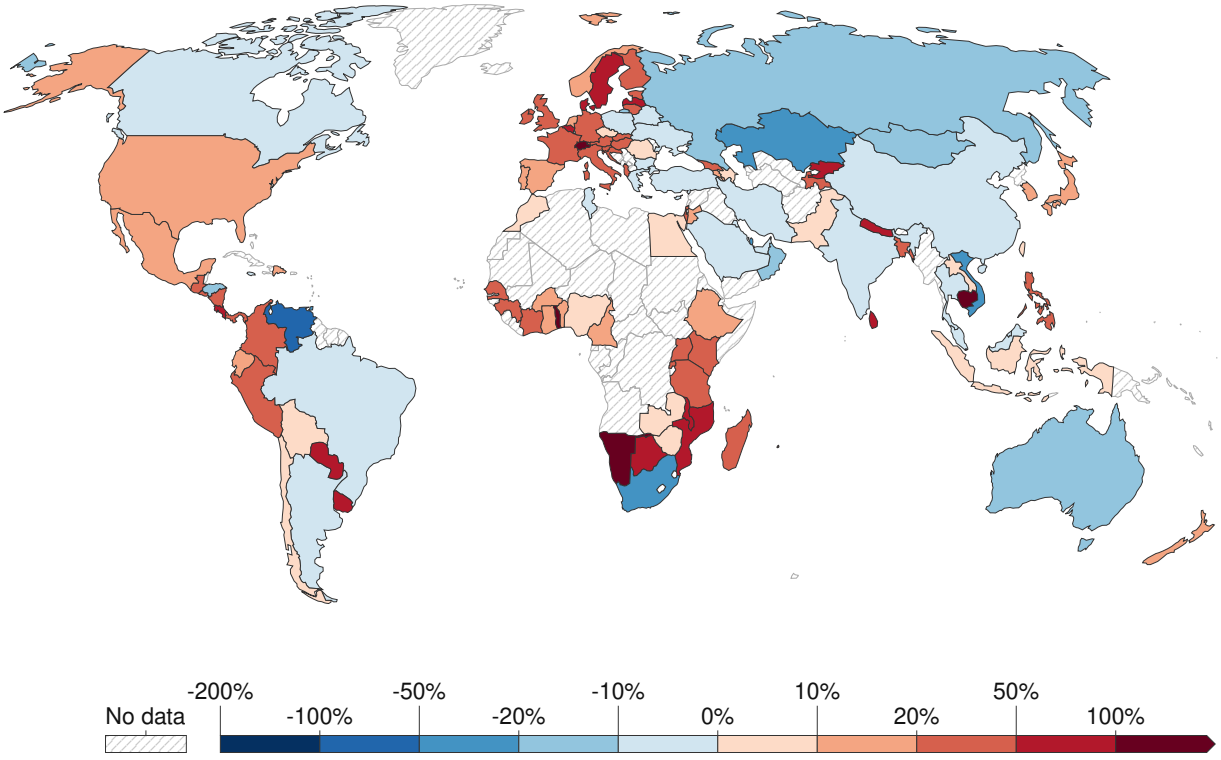


This is measured as emissions exported or imported as a percentage of domestic production emissions. Positive values (red) represent net importers of $CO_2$. Negative values (blue) represent net exporters of $CO_2$.

Source: https://ourworldindata.org/consumption-based-co2.

The OECD maintains a database of imported and exported $CO_2$ at www.oecd.org/industry/ind/carbondioxideemissionsembodiedininternationaltrade.htm. Calculations are detailed in Yamano and Guilhoto (2020). We use an updated version of these data, which can be obtained from the OECD statistics website[144]. In our case, we are interested in three variables:

- FD_CO2: CO2 emissions embodied in domestic final demand, by source country and industry;
- PROD_CO2: CO2 emissions based on production;

[143] Brazil, Russia, India, China and South Africa.
[144] The exact link is https://stats.oecd.org/Index.aspx?DataSetCode=IO_GHG_2021.

- BALCO2_FD: CO2 embodied in final demand, balance.

The first variable is the consumption-based emissions, the second variable is the production-based emissions, while the third variable is the difference between the previous two: BALCO2_FD = PROD_CO2 − FD_CO2. Using our notations, the GHG balance is equal to:

$$\mathcal{CE}^{(x-y,r)} = \mathcal{CE}^{(x,r)} - \mathcal{CE}^{(y,r)}$$

We can choose a specific industry or all activities (DTOTAL) and also the partner for the trade analysis. If the partner is WLD, we get the emissions of each country/region with respect to the world. If the partner is CHN, we obtain the emissions of each country/region with respect to China. In Table 8.60, we report the top importing and exporting countries. In 2018, the largest importer of carbon emissions is the United States, followed by Japan and Germany, while the largest exporter of carbon emissions is China, followed by Russia and South Africa. In the first case the GHG balance is negative, in the second case it is positive. In a sense, these rankings show a contrast between developed and emerging economies.

Table 8.60: Top importing and exporting countries by carbon emissions (in $MtCO_2e$, 2018)

| | | Top importers | | | | Top exporters | |
|---|---|---|---|---|---|---|---|
| Rank | ISO | Country | Balance | Rank | ISO | Country | Balance |
| 1 | USA | United States | −752.10 | 1 | CHN | China | 895.45 |
| 2 | JPN | Japan | −160.62 | 2 | RUS | Russian Federation | 343.48 |
| 3 | DEU | Germany | −128.73 | 3 | ZAF | South Africa | 122.47 |
| 4 | GBR | United Kingdom | −123.77 | 4 | IND | India | 106.10 |
| 5 | FRA | France | −111.65 | 5 | TWN | Chinese Taipei | 77.03 |
| 6 | ITA | Italy | −80.09 | 6 | SGP | Singapore | 62.19 |
| 7 | HKG | Hong Kong, China | −70.14 | 7 | KOR | Korea | 54.35 |
| 8 | CHE | Switzerland | −44.53 | 8 | CAN | Canada | 53.12 |
| 9 | PHL | Philippines | −40.49 | 9 | VNM | Viet Nam | 52.31 |
| 10 | SWE | Sweden | −29.67 | 10 | MYS | Malaysia | 46.52 |

Source: Yamano and Guilhoto (2020), https://stats.oecd.org & Author's calculations.

These rankings also show a divide between OECD and non-OECD countries. In Figure 8.142, we reproduce Figure 4-1 on page 24 of the OECD research report written by Yamano and Guilhoto (2020). The comparison between aggregate OECD and aggregate non-OECD production- and consumption-based emissions shows two different dynamics. For OECD countries, the long-term trend between 1995 and 2018 is quite stable. On the contrary, there is a general increase in emissions from non-OECD economies over the same period.

> "*These increases are in great part linked with the need of these countries to sustain their own development and to improve the quality of life of their population. A consequence being that many of these countries are important net exporters of $CO_2$ emissions as they develop a strong manufacturing base to meet the consumption needs of more developed nations. Despite increasing industrialisation, emissions per capita in non-OECD economies are still low compared to OECD countries*" (Yamano and Guilhoto, 2020, page 23).

Figure 8.142: Total production- and consumption-based $CO_2$ emitted by OECD and non-OECD countries (in $GtCO_2e$)

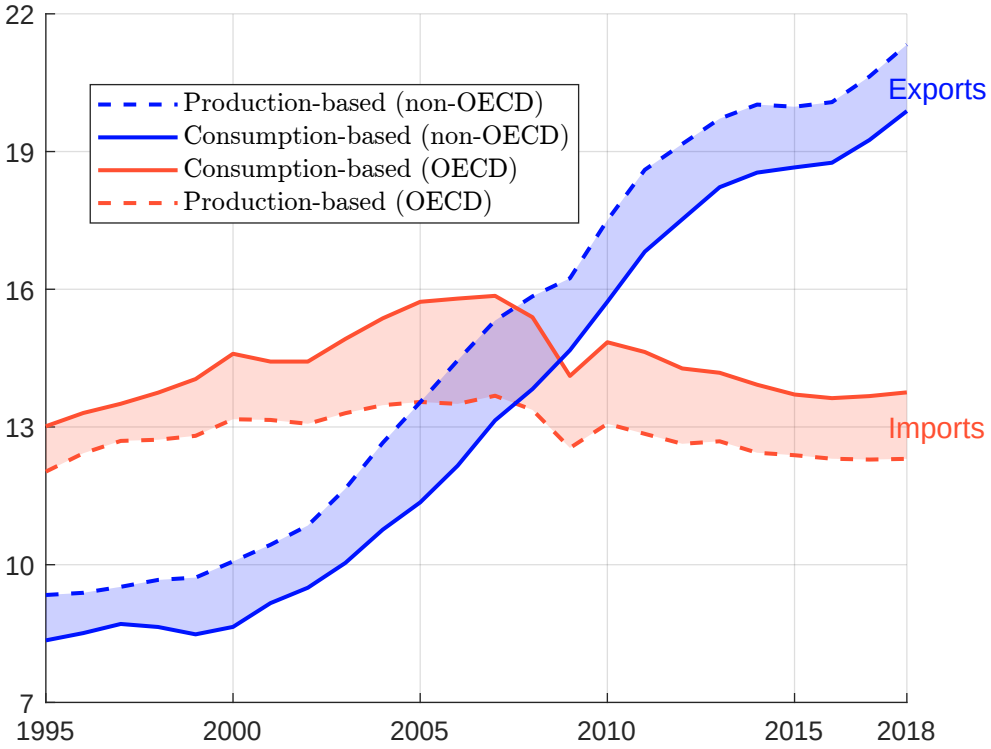


Source: Yamano and Guilhoto (2020), https://stats.oecd.org & Author's calculations.

Figure 8.143: Decomposition of OECD imported emissions (in $GtCO_2e$)

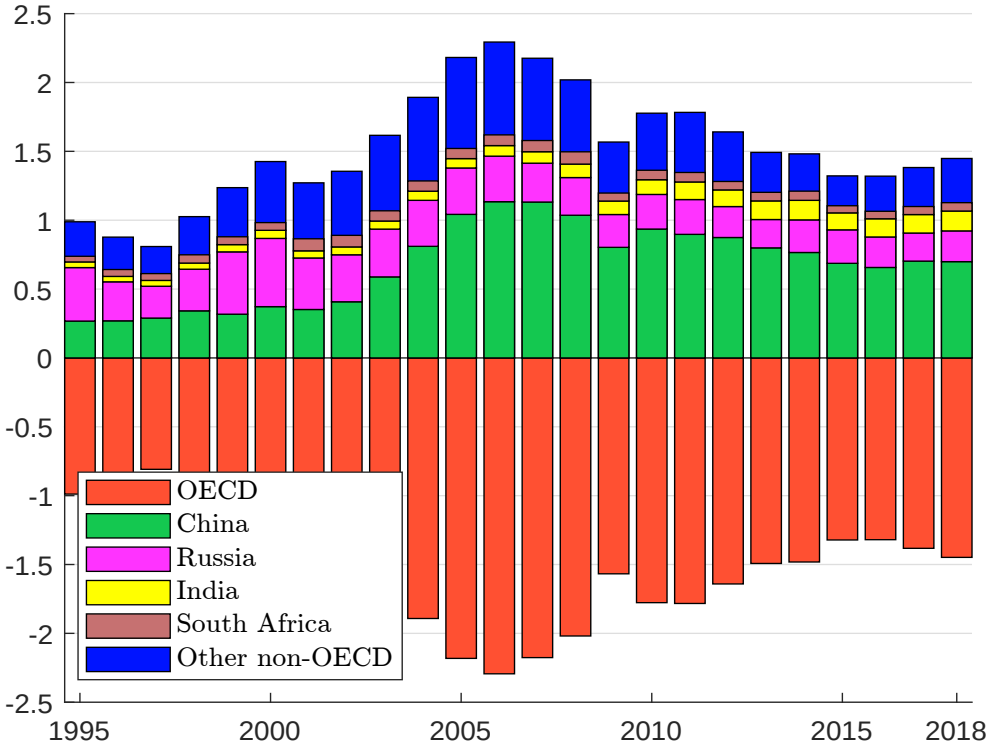


Source: Yamano and Guilhoto (2020), https://stats.oecd.org & Author's calculations.

Figure 8.144: Net exported emissions (in $MtCO_2e$)

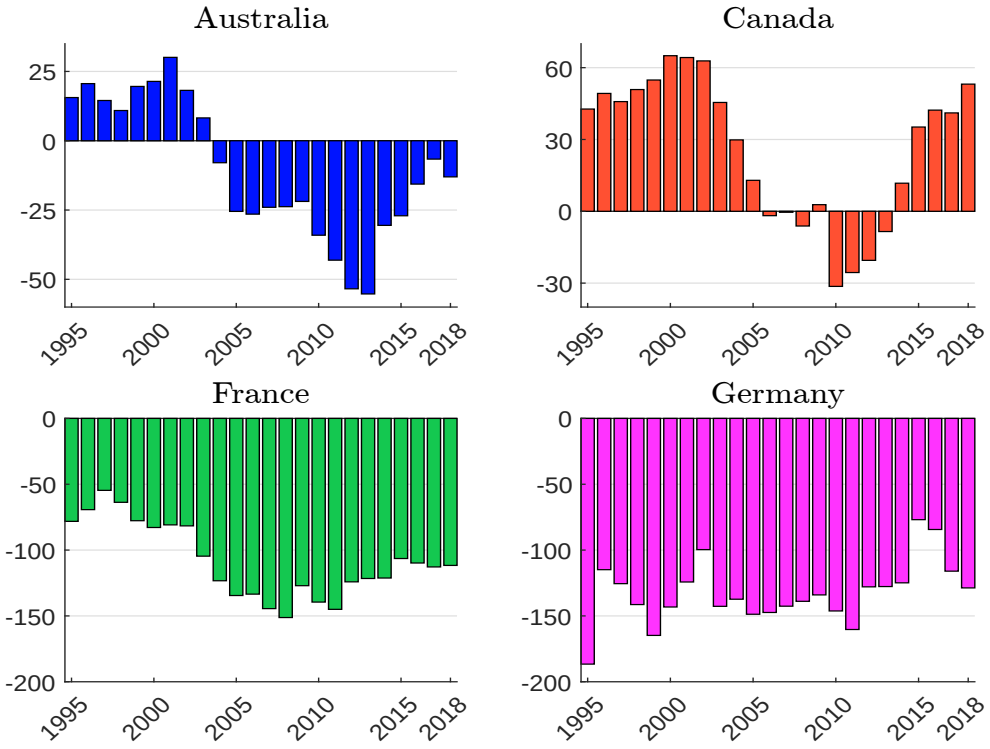


Source: Yamano and Guilhoto (2020), https://stats.oecd.org & Author's calculations.

Figure 8.145: Net exported emissions (in $MtCO_2e$)

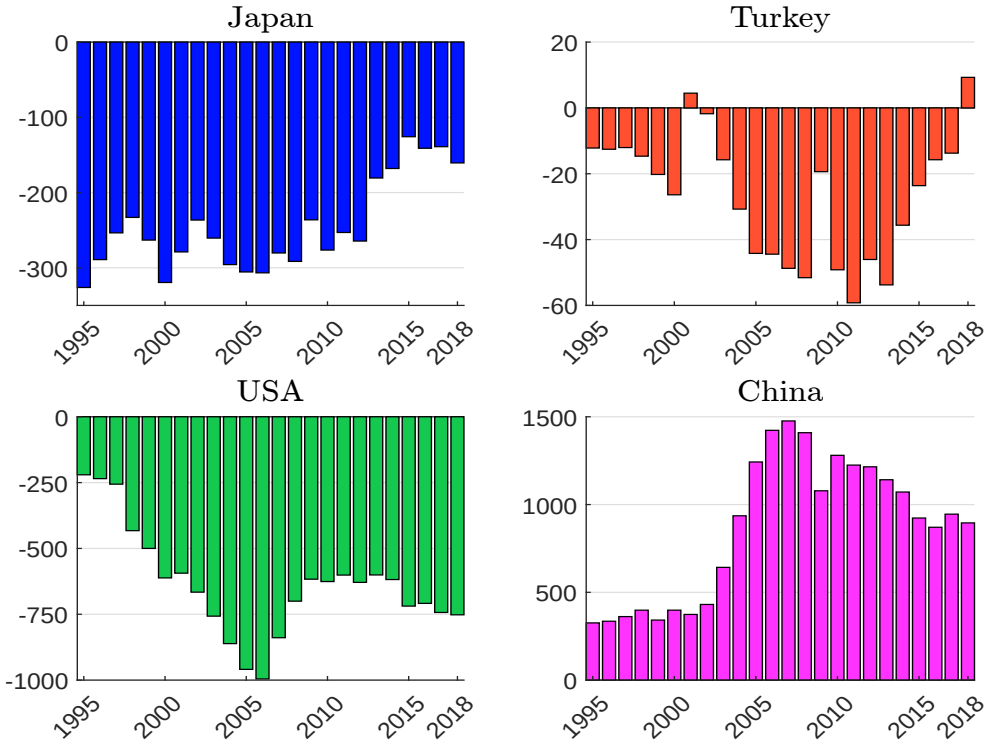


Source: Yamano and Guilhoto (2020), https://stats.oecd.org & Author's calculations.

Figures 8.144 and 8.145 show the evolution of net exported emissions for some countries. First, we see that they are highly time-varying. One reason for this is that the calculation is sensitive to the Leontief matrix of input-output analysis. Second, we observe different patterns across countries. For example, France and Germany are at similar levels in 2018, but this was not the case in 1995. Canada was a net exporter before 2005, a net importer between 2005 and 2015, and a net exporter again after 2015.

**Remark 94** *The calculation of imported and exported emissions depends on many factors, especially when using input-output analysis. Depending on the data source, we may find different results. For instance, Australia is a net exporter according to Figure 8.141 and a net importer according to Figure 8.144. According to Commissariat Général au Développement Durable (2020), France's carbon footprint is made up of* 45% *domestic emissions and* 55% *imported emissions. The estimated value of imported emissions is then more than* 350 $\text{MtCO}_2\text{e}$. *According to the OECD calculation, this figure is close to* 110 $\text{MtCO}_2\text{e}$. *These two examples illustrate the large uncertainty in the calculation of GHG emissions embodied in trade.*

### 8.4.5 Taxation, pass-through and price dynamics

To study the impact of taxation on production costs, we need to diffuse the carbon tax in the input-output economic model to account for the cascading effects through the value chain. The diffusion of the carbon tax depends on the assumption of the reaction function of suppliers and pass-through mechanisms.

#### Value added approach

By construction, a carbon tax affects the income of producers, who may react in different ways. We first consider a flexible price model and assume that they want to maintain their level of value added.

**Remark 95** *In the following, $p^-$ is the price vector before the carbon tax, while $p$ is the price vector including the tax effect.*

**Impact on production prices** The absolute amount of the carbon tax for sector $j$ is equal to:

$$T_{\text{direct},j} = \boldsymbol{\tau}_j \boldsymbol{\mathcal{CE}}_{1,j}$$

where $\boldsymbol{\tau}_j$ is the nominal carbon tax expressed in $\$/\text{tCO}_2\text{e}$ and $\boldsymbol{\mathcal{CE}}_{1,j}$ is the Scope 1 emissions of the sector. We deduce that the carbon tax rate is equal to:

$$t_{\text{direct},j} = \frac{T_{\text{direct},j}}{x_j} = \frac{\boldsymbol{\tau}_j \boldsymbol{\mathcal{CE}}_{1,j}}{x_j} = \boldsymbol{\tau}_j \boldsymbol{\mathcal{CI}}_{1,j}$$

Note that $t_{\text{direct},j}$ has no unit and is equal to the product of the tax and the Scope 1 carbon intensity. The input-output model implies that:

$$p_j x_j = \sum_{i=1}^{n} Z_{i,j} p_i + \sum_{k=1}^{m} V_{k,j} \psi_k + T_{\text{direct},j}$$

We deduce that:

$$p_j = \sum_{i=1}^{n} A_{i,j} p_i + \sum_{k=1}^{m} B_{k,j} \psi_k + t_{\text{direct},j} = \sum_{i=1}^{n} A_{i,j} p_i + \upsilon_j + t_{\text{direct},j}$$

It follows that:

$$p = \left(I_n - A^\top\right)^{-1} (\upsilon + t_{\text{direct}})$$

where $t_{\text{direct}} = (t_{\text{direct},1}, \ldots, t_{\text{direct},n})$ is the vector of direct tax rates. We recover the cost-push price model, where the vector $\upsilon$ of value added ratios is replaced by $\upsilon + t_{\text{direct}}$. It follows that the vector of price changes due to the carbon tax is equal to:

$$\Delta p = \left(I_n - A^\top\right)^{-1} t_{\text{direct}} \tag{8.49}$$

This result is obvious since Equation (8.30) implies that $\Delta p = \left(I_n - A^\top\right)^{-1} \Delta \upsilon$ and $\Delta \upsilon$ corresponds to the vector $t_{\text{direct}}$ of direct tax rates.

**Impact on the price index** The definition of a price index is:

$$\mathcal{PI} = \sum_{i=1}^{n} \alpha_i p_i = \alpha^\top p$$

where $\alpha = (\alpha_1, \ldots, \alpha_n)$ are the weights of the items in the basket. We deduce that the inflation rate is:

$$\pi = \frac{\Delta \mathcal{PI}}{\mathcal{PI}^-} = \frac{\mathcal{PI} - \mathcal{PI}^-}{\mathcal{PI}^-} = \frac{\alpha^\top \left(I_n - A^\top\right)^{-1} t_{\text{direct}}}{\alpha^\top \left(I_n - A^\top\right)^{-1} \upsilon}$$

We can simplify this formula because $p^- = \left(I_n - A^\top\right)^{-1} \upsilon = \mathbf{1}_n$ and $\mathbf{1}_n^\top \alpha = 1$. Finally, we have:

$$\pi = \alpha^\top \left(I_n - A^\top\right)^{-1} t_{\text{direct}} \tag{8.50}$$

**Computation of the total tax amount** The total tax cost is equal to:

$$T_{\text{total}} = x \odot \Delta p = x \odot \left(I_n - A^\top\right)^{-1} t_{\text{direct}} \tag{8.51}$$

while the direct tax cost is $T_{\text{direct}} = x \odot t_{\text{direct}}$. Since we have $x \succeq \mathbf{0}_n$ and $\left(I_n - A^\top\right)^{-1} \succeq I_n$ and using Hadarmard properties[145], then we conclude that the total tax cost is greater than the direct tax cost for all the sectors:

$$T_{\text{total},j} \geq T_{\text{direct},j}$$

Since the total cost to the economy is equal to $\mathcal{C}_{\text{total}} = \sum_{j=1}^{n} T_{\text{total},j} = x^\top \left(I_n - A^\top\right)^{-1} t_{\text{direct}}$, the tax incidence is then equal to:

$$\mathcal{TI} = \frac{\mathcal{C}_{\text{total}}}{\mathbf{1}_n^\top x} = \frac{x^\top \left(I_n - A^\top\right)^{-1} t_{\text{direct}}}{\mathbf{1}_n^\top x}$$

[145] Let $A$, $B$ and $C$ be three nonnegative matrices. If $B \preceq C$, then $A \odot B \preceq A \odot C$.

**Common mistakes in calculating total tax costs** In some research papers, we can find two formulas that seem to be intuitive:

$$T'_{\text{total}} = \left(I_n - A^\top\right)^{-1} T_{\text{direct}}$$

and:

$$T''_{\text{total}} = \boldsymbol{\tau} \odot \boldsymbol{\mathcal{CE}}_{\text{total}}$$

The two previous equations are generally wrong because the Hadamard and matrix products are not associative: $A \odot (BC) \neq (A \odot B) C$.

**Mathematical properties** Let us denote by $f(\boldsymbol{\tau})$ the function $f$ that depends on the vector $\boldsymbol{\tau} = (\boldsymbol{\tau}_1, \ldots, \boldsymbol{\tau}_n)$ of carbon taxes. Let $\lambda \geq 0$ be a positive scalar. The functions $\Delta p$, $\pi$, $T_{\text{total}}$, $\mathcal{C}_{\text{total}}$ and $\mathcal{TI}$ are homogeneous[146] and additive[147]. For instance, we have:

$$\Delta p(\lambda\boldsymbol{\tau}) = \left(I_n - A^\top\right)^{-1} t_{\text{direct}}(\lambda\boldsymbol{\tau}) = \lambda \left(I_n - A^\top\right)^{-1} t_{\text{direct}}(\boldsymbol{\tau}) = \lambda \Delta p(\boldsymbol{\tau})$$

If the tax is uniform $\boldsymbol{\tau} = \tau \mathbf{1}_n$, the vector of total tax amount is the product of the tax by the total emissions:

$$T_{\text{total}}(\tau \mathbf{1}_n) = \tau \boldsymbol{\mathcal{CE}}_{\text{total}}$$

The tax incidence for a given sector is then proportional to the direct plus indirect carbon emissions of the sector. At the global level, the tax incidence is equal to the carbon tax multiplied by the total carbon intensity of the world:

$$\mathcal{TI}(\tau \mathbf{1}_n) = \frac{\mathbf{1}_n^\top \tau \boldsymbol{\mathcal{CE}}_{\text{total}}}{\mathbf{1}_n^\top x} = \tau \boldsymbol{\mathcal{CI}}_{\text{total}}$$

**Illustration** Consider a variant of Example 29. Table 8.61 gives the values of $Z_{i,j}$, $y_j$, $x_j$ and $V_{1,j}$ in \$ mn. The carbon emissions are expressed in $\text{ktCO}_2\text{e}$, while the carbon intensities are expressed in $\text{tCO}_2\text{e}/\$$ mn. We have:

$$A = Z \operatorname{diag}^{-1}(x) = \begin{pmatrix} 0.10 & 0.20 & 0.20 & 0.10 \\ 0.10 & 0.10 & 0.20 & 0.05 \\ 0.05 & 0.20 & 0.30 & 0.10 \\ 0.02 & 0.05 & 0.10 & 0.35 \end{pmatrix}$$

and:

$$\tilde{\boldsymbol{\mathcal{L}}} = \left(I_4 - A^\top\right)^{-1} = \begin{pmatrix} 1.1881 & 0.1678 & 0.1430 & 0.0715 \\ 0.3894 & 1.2552 & 0.4110 & 0.1718 \\ 0.4919 & 0.4336 & 1.6303 & 0.2993 \\ 0.2884 & 0.1891 & 0.3044 & 1.6087 \end{pmatrix}$$

Then, we calculate the vector $v$ of value added ratios:

$$v = \begin{pmatrix} 3\,650/5\,000 \\ 1\,800/4\,000 \\ 1\,600/8\,000 \\ 5\,000/12\,500 \end{pmatrix} = \begin{pmatrix} 0.73 \\ 0.45 \\ 0.20 \\ 0.40 \end{pmatrix}$$

[146] This means that $f(\lambda\boldsymbol{\tau}) = \lambda f(\boldsymbol{\tau})$.
[147] We have $f(\boldsymbol{\tau} + \boldsymbol{\tau}') = f(\boldsymbol{\tau}) + f(\boldsymbol{\tau}')$.

Table 8.61: Environmentally extended monetary input-output table

| Sector | $Z$ | | | | $y$ | $x$ | $\mathcal{CE}_1$ | $\mathcal{CI}_1$ |
|---|---|---|---|---|---|---|---|---|
| Energy | 500 | 800 | 1 600 | 1 250 | 850 | 5 000 | 500 | 100 |
| Materials | 500 | 400 | 1 600 | 625 | 875 | 4 000 | 200 | 50 |
| Industrials | 250 | 800 | 2 400 | 1 250 | 3 300 | 8 000 | 200 | 25 |
| Services | 100 | 200 | 800 | 4 375 | 7 025 | 12 500 | 125 | 10 |
| Value added | 3 650 | 1 800 | 1 600 | 5 000 | | | | |
| Income | 5 000 | 4 000 | 8 000 | 12 500 | | | | |

We check that $p^- = \tilde{\boldsymbol{\mathcal{L}}} v = \mathbf{1}_4$. By construction, all the prices are standardized and equal to one in a monetary input-output model. We now introduce a differentiated carbon tax: $\boldsymbol{\tau}_1 = \$200/\text{tCO}_2\text{e}$ and $\boldsymbol{\tau}_2 = \boldsymbol{\tau}_3 = \boldsymbol{\tau}_4 = \$100/\text{tCO}_2\text{e}$. The direct tax costs are 100, 20, 20 and 12.5 million dollars for Energy, Materials, Industrials and Services respectively. We deduce that the vector of carbon tax rates is $t_{\text{direct}} = (2.00\%, 0.50\%, 0.25\%, 0.10\%)$. It follows that:

$$p = \left(I_n - A^\top\right)^{-1} (v + t_{\text{direct}}) = \begin{pmatrix} 1.0250 \\ 1.0153 \\ 1.0164 \\ 1.0091 \end{pmatrix}$$

If we assume that the basket of goods and services is $\alpha = (10\%, 20\%, 30\%, 40\%)$, the price index $\mathcal{PI}$ is 1.0141 while the inflation rate $\pi$ is 1.410%. Finally, we calculate the total tax cost and obtain the results shown in Table 8.62. The direct tax cost is multiplied by a factor of 2.8 when we consider the diffusion of the carbon tax. We check that $T_{\text{total}} \neq T'_{\text{total}} \neq T''_{\text{total}}$. Services is the most affected sector, followed by Industrials, Materials and Energy with impact ratios $T_{\text{total}}/T_{\text{direct}}$ of 9.1, 6.6, 3.1 and 1.3 respectively. In Table 8.63, we consider a uniform tax of $\$100/\text{tCO}_2\text{e}$. We check that $T_{\text{total}} = T''_{\text{total}}$ but $T_{\text{total}} \neq T'_{\text{total}}$.

Table 8.62: Total carbon costs (in $ mn) (differentiated tax)

| Sector | $T_{\text{direct}}$ | $T_{\text{total}}$ | $T'_{\text{total}}$ | $T''_{\text{total}}$ | $\mathcal{CE}_{\text{direct}}$ | $\mathcal{CE}_{\text{total}}$ |
|---|---|---|---|---|---|---|
| Energy | 100.00 | 125.15 | 125.92 | 131.49 | 500.00 | 657.44 |
| Materials | 20.00 | 61.05 | 74.41 | 45.48 | 200.00 | 454.76 |
| Industrials | 20.00 | 131.05 | 94.21 | 91.70 | 200.00 | 916.97 |
| Services | 12.50 | 113.54 | 58.82 | 77.49 | 125.00 | 774.92 |
| Sum | 152.50 | 430.79 | 353.36 | 346.15 | 1 025.00 | 2 804.10 |

Table 8.63: Total carbon costs (in $ mn) (uniform taxation)

| Sector | $T_{\text{direct}}$ | $T_{\text{total}}$ | $T'_{\text{total}}$ | $T''_{\text{total}}$ | $\mathcal{CE}_{\text{direct}}$ | $\mathcal{CE}_{\text{total}}$ |
|---|---|---|---|---|---|---|
| Energy | 50.00 | 65.74 | 66.51 | 65.74 | 500.00 | 657.44 |
| Materials | 20.00 | 45.48 | 54.94 | 45.48 | 200.00 | 454.76 |
| Industrials | 20.00 | 91.70 | 69.62 | 91.70 | 200.00 | 916.97 |
| Services | 12.50 | 77.49 | 44.40 | 77.49 | 125.00 | 774.92 |
| Sum | 102.50 | 280.41 | 235.47 | 280.41 | 1 025.00 | 2 804.10 |

### Mark-up pricing approach

**Theoretical framework** We consider a second approach proposed by Gemechu *et al.* (2014) and Mardones and Mena (2020). Mark-up pricing refers to a business strategy in which the suppliers determine the selling price by adding a fixed percentage to the cost of production. Let $p_j^-$ be the price before the introduction of the carbon tax. We define $\xi_j$ as the price factor induced by the carbon tax: $t_{\text{direct},j} = \xi_j p_j^-$. It follows that $p_j^- = \sum_{i=1}^n A_{i,j} p_i^- + \upsilon_j$ and[148]:

$$\begin{aligned} p_j &= \left(\sum_{i=1}^n A_{i,j} p_i + \upsilon_j\right) + t_{\text{direct},j} \\ &= \left(\sum_{i=1}^n A_{i,j} p_i + \upsilon_j\right) + \xi_j p_j^- \\ &= (1+\xi_j)\left(\sum_{i=1}^n A_{i,j} p_i + \upsilon_j\right) \end{aligned}$$

We deduce that:

$$\frac{p_j}{1+\xi_j} = \sum_{i=1}^n A_{i,j} p_i + \upsilon_j$$

and:

$$p_j\left(1 - \frac{\xi_j}{1+\xi_j}\right) = \sum_{i=1}^n A_{i,j} p_i + \upsilon_j$$

It follows that:

$$\begin{aligned} p_j &= \sum_{i=1}^n A_{i,j} p_i + \frac{\xi_j}{1+\xi_j} p_j + \upsilon_j \\ &= \sum_{i=1}^n A_{i,j} p_i + p_j\left(1 - \frac{1}{1+\xi_j}\right) + \upsilon_j \end{aligned}$$

In a matrix form, we have:

$$p = A^\top p + (I_n - D_\xi)\, p + \upsilon$$

where:

$$D_\xi = \text{diag}\left(\frac{1}{1+\xi_1}, \ldots, \frac{1}{1+\xi_n}\right)$$

Finally, we obtain:

$$p = \left(I_n - A_\xi^\top\right)^{-1} \upsilon$$

where $A_\xi = A + I_n - D_\xi$. Another expression is:

$$p = \tilde{\boldsymbol{\mathcal{L}}}_m \upsilon = \left(D_\xi - A^\top\right)^{-1} \upsilon \tag{8.52}$$

where $\tilde{\boldsymbol{\mathcal{L}}}_m = \left(D_\xi - A^\top\right)^{-1}$ is the mark-up inverse matrix. The vector of price variations is then:

$$\Delta p = \left(\tilde{\boldsymbol{\mathcal{L}}}_m - \tilde{\boldsymbol{\mathcal{L}}}\right) \upsilon \tag{8.53}$$

[148] We assume that $p_j \approx p_j^-$.

The expression of the price index is $\mathcal{PI} = \alpha^\top \left(D_\xi - A^\top\right)^{-1} \upsilon$ whereas the inflation rate is equal to $\pi = \alpha^\top \left(\tilde{\boldsymbol{\mathcal{L}}}_m - \tilde{\boldsymbol{\mathcal{L}}}\right) \upsilon$. From Equation (8.53), we also deduce the total tax cost:

$$T_{\text{total}} = x \odot \left(\tilde{\boldsymbol{\mathcal{L}}}_m - \tilde{\boldsymbol{\mathcal{L}}}\right) \upsilon \tag{8.54}$$

Note that the mark-up approach implies replacing the identity matrix $I_n$ with the diagonal matrix $D_\xi$ in the cost-push price model. Since we have $D_\xi \preceq I_n$, we deduce that $D_\xi^{-1} \succeq I_n$. Desnos *et al.* (2023) also showed that $\tilde{\boldsymbol{\mathcal{L}}}_m \succeq \tilde{\boldsymbol{\mathcal{L}}}$.

**Illustration** Considering the previous example, we have:

$$\tilde{\boldsymbol{\mathcal{L}}}_m = \left(D_\xi - A^\top\right)^{-1} = \begin{pmatrix} 1.2170 & 0.1730 & 0.1474 & 0.0735 \\ 0.4017 & 1.2650 & 0.4165 & 0.1740 \\ 0.5067 & 0.4398 & 1.6394 & 0.3021 \\ 0.2965 & 0.1919 & 0.3074 & 1.6121 \end{pmatrix}$$

In the case of differentiated taxation, we obtain:

$$p = \tilde{\boldsymbol{\mathcal{L}}}_m \upsilon = \begin{pmatrix} 1.0252 \\ 1.0154 \\ 1.0165 \\ 1.0091 \end{pmatrix}$$

The inflation rate $\pi$ is equal to 1.421% and the total carbon costs (in \$ mn) are 125.82, 61.53, 132.10 and 114.33. The global cost is then \$433.78 mn compared to \$430.79 mn in the value added approach.

### Pass-through integration

**Definition** According to RBB Economics (2014), "*cost pass-through describes what happens when a business changes the price of the production or services it sells following a change in the cost of producing them.*" Therefore, a pass-through rate is closely related to the supply and demand elasticity. This concept of price adjustment is extremely common in many fields of economics: exchange rates, imperfect competition and Cournot-Bertrand equilibria, product taxation and retail prices, inflation regimes, etc. In other words, pass-through is the ability of a sector or a company to pass costs through its supply chain. In general, this parameter ranges from 0%, where the entire amount is supported by the agent, to 100%, where the entire amount is passed on to customers. As this parameter depends on several factors, such as supply and demand elasticity, international trade exposure, market concentration, product homogeneity, etc., its estimation is not easy, which implies a large uncertainty about the tax incidence in a transition risk framework.

Pass-through strongly depends on the market structure and the supply-demand equilibrium. In Figure 8.146, we show different demand curves whose slope depends on the consumer response to different price levels. If the slope of the curve is steep, it suggests that an increase in price would lead to a marginal decrease in sales. This scenario represents inelastic demand, where consumer demand is relatively unchanged when the price moves up or down. Conversely, if the demand curve is flatter, an increase in price will result in a significant reduction in the quantity demanded. This situation represents elastic demand, where consumers are highly responsive to price changes. If the demand curve is linear, there is no curvature, which means that the rate of decline in demand remains

Figure 8.146: Demand curvature

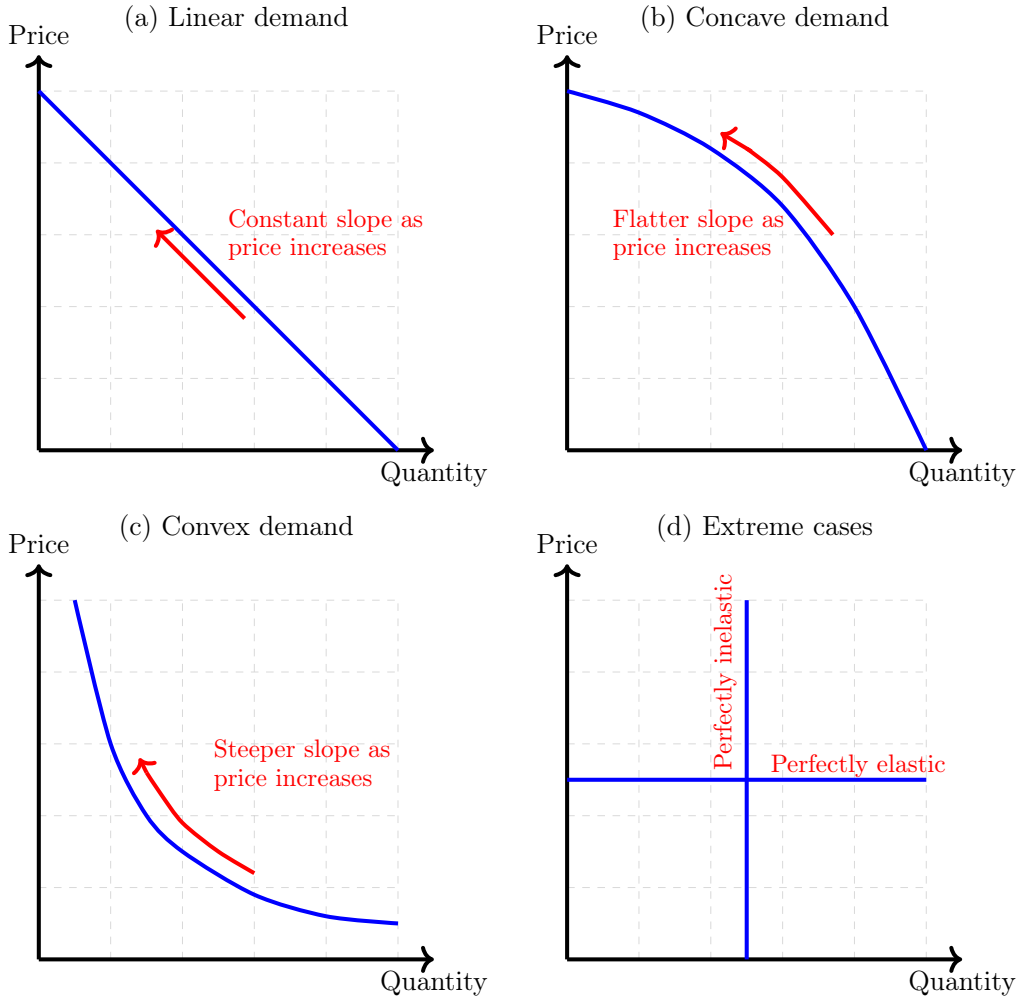


Source: RBB Economics (2014, Figure 2, page 16).

constant as the price increases (top/left panel in Figure 8.146). In situations where demand falls more sharply as the price rises, this type of demand is classified as concave to the origin (top/right panel in Figure 8.146). As prices rise in this scenario, the demand curve becomes increasingly flatter, indicating increased price sensitivity or greater elasticity. In this scenario, firms should absorb part of the cost, implying a relatively low pass-through rate. Finally, if the rate of decline in demand slows with each price increase, this type of demand curve is said to be convex to the origin. In this case, as prices escalate, the remaining demand becomes less sensitive to these price fluctuations (bottom/left panel of the figure). Firms can then pass on the costs and set a relatively high pass-through rate.

From an economic point of view, the specification of the pass-through depends on several factors. In the case of competition, the general formula for the pass-through rate $\phi$ is:

$$\phi = \frac{\mathrm{d}\, p}{\mathrm{d}\, \tau} = \frac{\text{price sensitivity of supply}}{\text{price sensitivity of supply} - \text{price sensitivity of demand}}$$

We deduce that $\phi \in [0, 100\%]$. In a monopolistic situation, the previous formula becomes:

$$\phi = \frac{1}{2 + \text{elasticity of the slope of inverse demand}}$$

Since the slope elasticity of inverse demand is negative, $\phi \geq 50\%$. We get similar results in oligopolistic situations. In monopolistic and oligopolistic situations, it can also be greater than 100% if demand is highly convex. In Table 8.64, we report some estimates of path-through rates.

Table 8.64: Pass-through rates (in %) for intensive sectors

| Sector | Rate |
|---|---|
| Electricity, gas and steam | 100% |
| Petroleum refining | 100% |
| Base metals | 78% |
| Mining | 78% |
| Waste/wastewater | 78% |
| Land transport | 78% |
| Fishery | 75% |
| Non-metallic minerals | 60% |
| Agriculture | 50% |
| Chemicals | 40% |
| Maritime transport | 30% |
| Aviation | 30% |
| Paper | 10% |

Source: Sautel *et al.* (2022, page 35).

**Analytical formula** We focus on the value added model, which is the most widely used approach in the academic literature. It is also the simplest model to introduce the pass-through mechanism. We have:

$$\Delta p = \tilde{\boldsymbol{\mathcal{L}}} \Delta v = \sum_{k=0}^{\infty} \left(A^{\top}\right)^k \Delta v = \sum_{k=0}^{\infty} \Delta p_{(k)}$$

where $\Delta p_{(k)} = \left(A^{\top}\right)^k \Delta v$ is the price impact at the $k^{\text{th}}$ tier. In fact, $\Delta p_{(k)}$ satisfies the following recurrence relation:

$$\begin{cases} \Delta p_{(k)} = A^{\top} \Delta p_{(k-1)} \\ \Delta p_{(0)} = \Delta v \end{cases}$$

If we consider the price $p_j$ of sector $j$, we have $\Delta p_{(0),j} = \Delta v_j$ and:

$$\Delta p_{(k),j} = \sum_{i=1}^{n} A_{i,j} \Delta p_{(k-1),i}$$

This representation helps to better understand the cascading effect of the carbon tax. In the zeroth round, it induces an additional cost $\Delta v_j$, which is fully passed on to the price $p_j$ of the sector. The new price is then $p_j + \Delta p_{(0),j} = p_j + \Delta v_j$. In the first round, sector $j$ faces new additional costs due to the price increase of intermediate consumption. We have $\Delta p_{(1),j} = \sum_{i=1}^{n} A_{i,j} \Delta p_{(0),i} = \sum_{i=1}^{n} A_{i,j} \Delta v_i$. The iteration process continues and we have $\Delta p_{(2),j} = \sum_{i=1}^{n} A_{i,j} \Delta p_{(1),i} = \sum_{i=1}^{n} \sum_{k=1}^{n} A_{i,j} A_{k,i} \Delta v_k$ at the second round.

Now let us introduce the pass-through mechanism. By definition, we have $\Delta p_{(0),j} = \phi_j \Delta v_j$ where $\phi_j$ denotes the pass-through rate of sector $j$. In the first round, we have:

$$\Delta p_{(1),j} = \sum_{i=1}^{n} A_{i,j} \left(\phi_i \Delta p_{(0),i}\right) = \sum_{i=1}^{n} A_{i,j} \left(\phi_i \Delta v_i\right)$$

More generally, the recurrence relation is:

$$\Delta p_{(k),j} = \sum_{i=1}^{n} A_{i,j} \boldsymbol{\phi}_i \Delta p_{(k-1),i}$$

Let $\boldsymbol{\phi} = (\boldsymbol{\phi}_1, \ldots, \boldsymbol{\phi}_n)$ and $\Phi = \operatorname{diag}(\boldsymbol{\phi})$ be the pass-through vector and matrix. The recurrence matrix form is:

$$\begin{cases} \Delta p_{(k)} = A^\top \Phi \Delta p_{(k-1)} \\ \Delta p_{(0)} = \Phi \Delta \upsilon \end{cases}$$

We deduce that:

$$\begin{aligned} \Delta p &= \sum_{k=0}^{\infty} \left(A^\top \Phi\right)^k \Phi \Delta \upsilon \\ &= \left(I_n - A^\top \Phi\right)^{-1} \Phi \Delta \upsilon \\ &= \tilde{\boldsymbol{\mathcal{L}}}(\boldsymbol{\phi}) \Delta \upsilon \end{aligned} \tag{8.55}$$

where $\tilde{\boldsymbol{\mathcal{L}}}(\boldsymbol{\phi}) = \left(I_n - A^\top \Phi\right)^{-1} \Phi$.

Since $A$ is a substochastic matrix and $\Phi$ is a positive diagonal matrix, we verify that $\boldsymbol{\phi}' \succeq \boldsymbol{\phi} \Rightarrow \tilde{\boldsymbol{\mathcal{L}}}(\boldsymbol{\phi}') \succeq \tilde{\boldsymbol{\mathcal{L}}}(\boldsymbol{\phi})$. The lower bound is then reached when $\boldsymbol{\phi} = \mathbf{0}_n$ while the upper bound is reached when $\boldsymbol{\phi} = \mathbf{1}_n$.

**Application to the carbon tax** Applying the previous analysis to the carbon tax, we have $\Delta \upsilon = t_{\text{direct}}$. In this case, the concept of total tax cost must be redefined because part of the cost is paid by producers and part by consumers. By consumers, we must understand the downstream of the value chain. We have:

$$\begin{aligned} T_{\text{producer}} &= x \odot (I_n - \Phi)\, t_{\text{direct}} \\ &= x \odot (\mathbf{1}_n - \boldsymbol{\phi}) \odot t_{\text{direct}} \\ &= (\mathbf{1}_n - \boldsymbol{\phi}) \odot T_{\text{direct}} \end{aligned}$$

and:

$$T_{\text{consumer}} = T_{\text{downstream}} = x \odot \tilde{\boldsymbol{\mathcal{L}}}(\boldsymbol{\phi})\, t_{\text{direct}}$$

We deduce that:

$$\begin{aligned} T_{\text{total}} &= T_{\text{producer}} + T_{\text{consumer}} \\ &= x \odot \left(I_n - \Phi + \tilde{\boldsymbol{\mathcal{L}}}(\boldsymbol{\phi})\right) t_{\text{direct}} \end{aligned}$$

If $\boldsymbol{\phi}_j = 100\%$, we have $\tilde{\boldsymbol{\mathcal{L}}}(\mathbf{1}_n) = \tilde{\boldsymbol{\mathcal{L}}}$ and $\Delta p = \tilde{\boldsymbol{\mathcal{L}}}\, t_{\text{direct}}$. This is the original approach. If $\boldsymbol{\phi}_j = 0\%$, we have $\tilde{\boldsymbol{\mathcal{L}}}(\mathbf{0}_n) = \mathbf{0}_{n,n}$, $\Delta p = \mathbf{0}_n$, $T_{\text{producer}} = T_{\text{direct}}$ but $T_{\text{consumer}} = \mathbf{0}_n$. The costs passed on to consumers (or the downstream of the value chain) are zero because the direct costs are initially absorbed by the producers.

**Remark 96** *The functions $\Delta p$, $\pi$, $T_{\text{total}}$, $\mathcal{C}_{\text{total}}$ and $\mathcal{TI}$ remain homogeneous and additive with respect to $\boldsymbol{\tau}$. We can also show that:*

$$\boldsymbol{\phi}' \succeq \boldsymbol{\phi} \Rightarrow T_{\text{total}}(\boldsymbol{\tau}, \boldsymbol{\phi}') \succeq T_{\text{total}}(\boldsymbol{\tau}, \boldsymbol{\phi})$$

*The effects of the tax is maximum when $\boldsymbol{\phi} = \mathbf{1}_n$ and minimum when $\boldsymbol{\phi} = \mathbf{0}_n$. If we consider a uniform pass-through, the total cost of the carbon tax is an increasing function of the pass-through rate.*

Figure 8.147: Producer and consumer cost contributions (uniform pass-through rate)

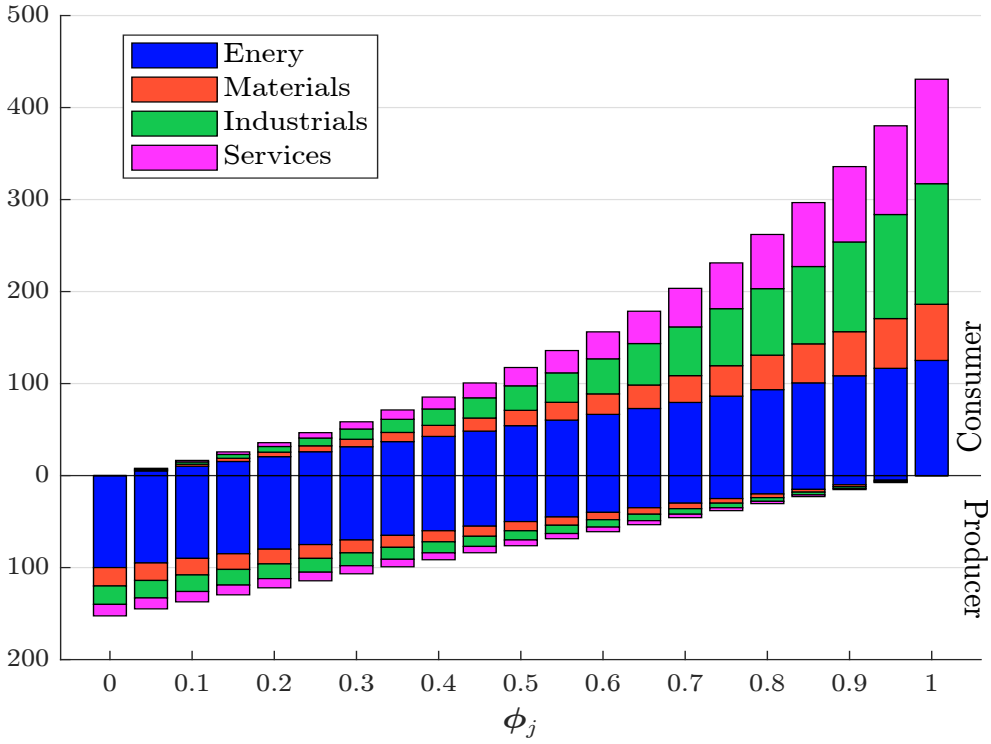


Figure 8.148: Producer and consumer cost contributions ($\phi_2 = \phi_3 = \phi_4 = 0\%$)

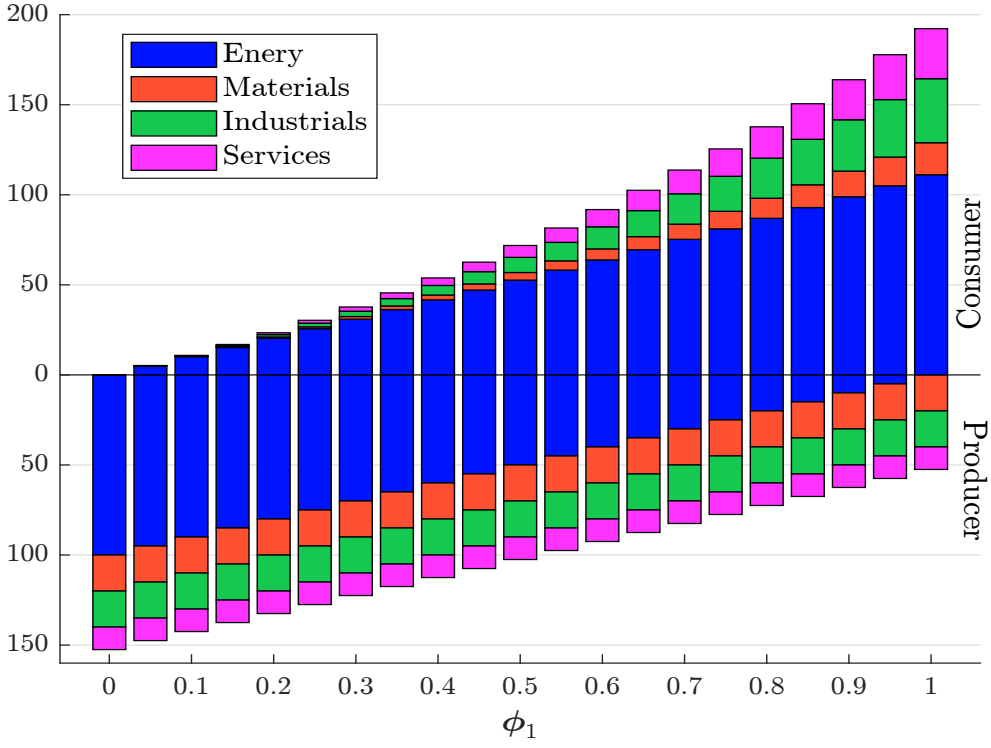

**Illustration** Continuing our example of differential taxation, let's assume that pass-through rates are uniform ($\boldsymbol{\phi}_1 = \boldsymbol{\phi}_2 = \boldsymbol{\phi}_3 = \boldsymbol{\phi}_4$). The evolution of the total cost is shown in Figure 8.147. When $\boldsymbol{\phi}_j = 0\%$, $T_{\text{total}}$ is equal to \$152.50 mn and is the lower bound. The upper bound is reached when $\boldsymbol{\phi}_j = 100\%$ and we get $T_{\text{total}} = \$430.79$ mn. We have also shown the contribution of each sector by distinguishing between direct and indirect costs. Figure 8.148 corresponds to the case where the Energy sector passes on the direct costs to the other sectors.

### Empirical results

There are many studies of carbon taxation and input-output models (Köppl and Schratzenstaller, 2023). In the following, we focus on two studies that have extensively examined the impact of pass-through rates on the economic cost of a carbon tax and its impact on inflation. We also produce new results by implementing a carbon tax of \$100/tCO$_2$e and differentiated pass-through rates.

**The study of Desnos *et al.* (2023)** The authors analyze the impact of a uniform tax $\boldsymbol{\tau}$ for all countries and a uniform pass-through rate $\boldsymbol{\phi}$ for all sectors. The direct cost $\mathcal{C}_{\text{direct}} = \sum_{j=1}^{n} T_{\text{direct}}$ and the total cost $\mathcal{C}_{\text{total}} = \sum_{j=1}^{n} T_{\text{total}}$ are shown in Figure 8.149. If the carbon tax is set at \$100/tCO$_2$e, the direct cost is \$4.8 tn, while the total cost is \$6.1 tn if $\boldsymbol{\phi} = 50\%$ and \$13.3 tn if $\boldsymbol{\phi} = 100\%$. These correspond to 2.8%, 3.6% and 7.8% of the world GDP respectively. If we apply a carbon tax of \$500/tCO$_2$e, these costs become \$24.2, \$30.4 and \$66.4 tn respectively. They show that the relationship between total costs and the pass-through parameter is cubic. They suggest the following approximation:

$$\frac{\mathcal{C}_{\text{total}}\left(\boldsymbol{\tau}, \phi \mathbf{1}_n\right)}{\mathcal{C}_{\text{direct}}\left(\boldsymbol{\tau}, \phi \mathbf{1}_n\right)} \approx 1 + m_{(1-\infty)}\phi^3$$

Therefore, a small error in pass-through rate estimate can lead to a large error in the cost estimate.

Desnos *et al.* (2023) then analyze the impact of the carbon tax on the inflation. To do this, they define two price indexes: the producer price index (PPI), where the basket weights are proportional to the output ($\alpha_j \propto x_j$) and the consumer price index (CPI), where the basket weights are proportional to the final demand ($\alpha_j \propto y_j$). Results are shown in Figure 8.150. Again, the inflation rate depends on the pass-through rate. For a carbon tax of \$500/tCO$_2$e and a pass-through rate of 100%, the PPI inflation rate is close to 40%, while the CPI inflation rate reaches 30%. These global figures are the result of a large discrepancy between country inflation rates. Figure 8.151 shows the world map of the country inflation rates for a uniform tax of \$100/tCO$_2$e. There are three factors (basket composition, value chain impact and direct carbon emissions of the country) that explain the dispersion of the inflation rates:

$$\pi = \underbrace{\alpha^\top}_{\text{Basket}} \cdot \underbrace{\tilde{\boldsymbol{\mathcal{L}}}\left(\boldsymbol{\phi}\right)}_{\text{Value chain}} \cdot \underbrace{t_{\text{direct}}}_{\text{Scope 1}}$$

Direct costs are the main contributor, followed by the impact of the downstream diffusion of the carbon tax. For example, Europe's low inflation rate is explained by its low direct emissions, but Europe is heavily penalized by its value chain. China is affected by both factors, while Russia's high inflation is mainly due to its direct emissions, as its value chain impact is among the lowest in the world.

Desnos *et al.* (2023) analyze a regional taxation scenario in which a carbon tax is imposed uniquely within a specific region of the world. This situation is likely to arise due to the lack of uniformity in carbon pricing. They first consider a uniform taxation across EU Member States, which is certainly the most likely scenario. In this scenario, a \$500/tCO$_2$e carbon tax with a 100% pass-through would result in a global cost of \$4.5 tn, of which \$4 tn would be borne by EU countries

Figure 8.149: World economic cost in $ tn (global analysis, uniform tax, Exiobase 2022)

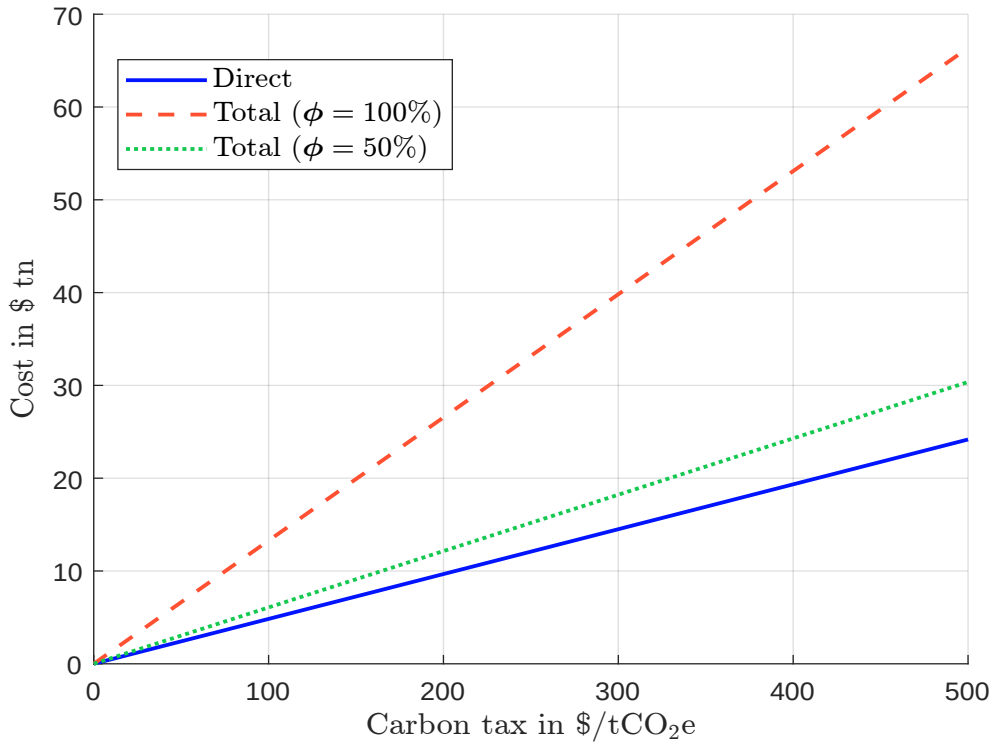


Source: Desnos *et al.* (2023, Figure 41, page 82).

Figure 8.150: World inflation rate in % (global analysis, uniform tax, Exiobase 2022)

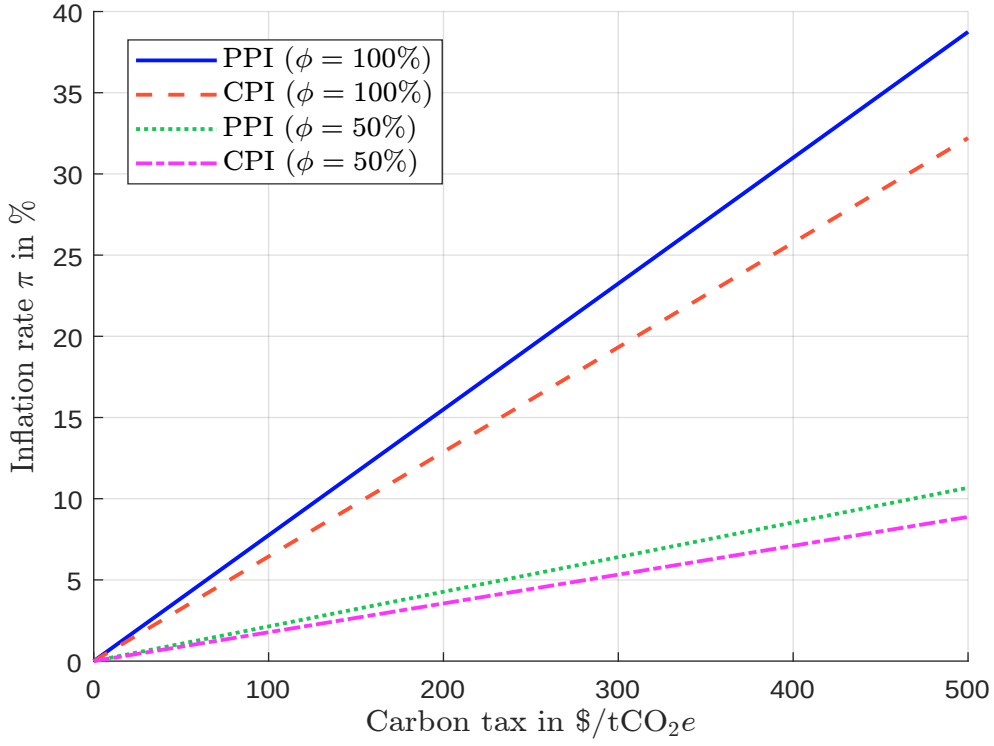


Source: Desnos *et al.* (2023, Figure 44, page 84).

Figure 8.151: Production inflation rate in % (global analysis, uniform tax, $\tau = \$100/tCO_2e$, $\phi = 100\%$, Exiobase 2022)

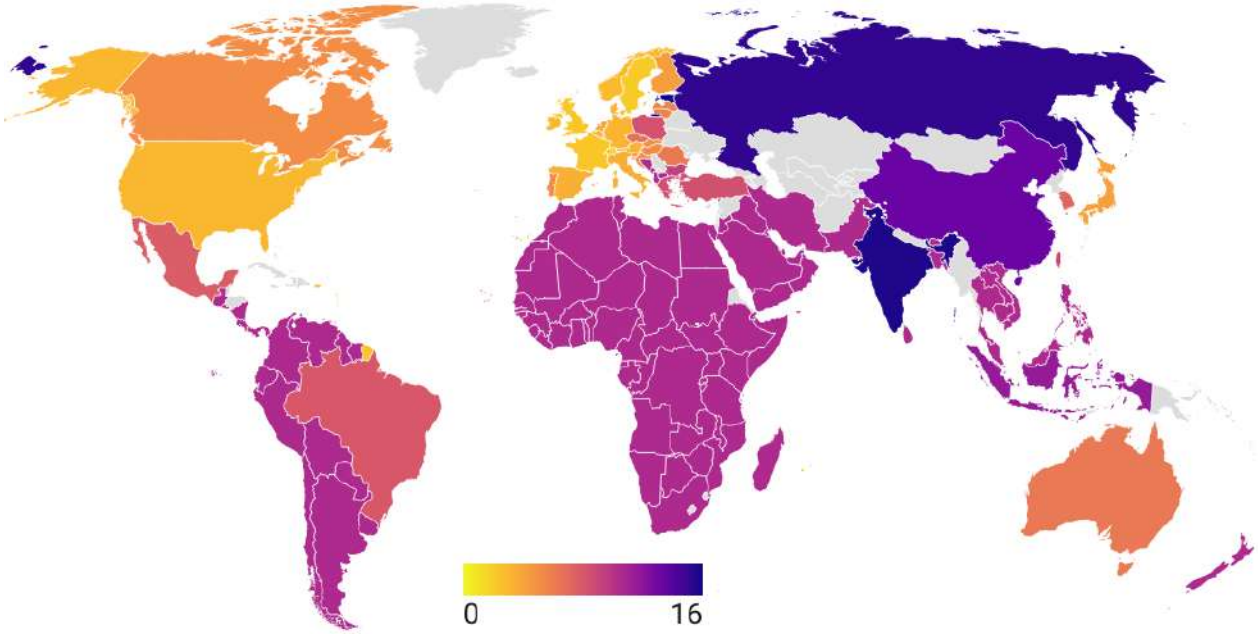


Source: Desnos *et al.* (2023, Figure 45, page 85).

and a \$0.5 tn by non-EU countries. If EU sectors absorb their increased costs by passing only 50% through the value chain, non-EU countries are less affected by carbon tax diffusion, and their costs fall from \$521 bn to \$54 bn. Moreover, the costs relative to GDP for EU sectors fall as they absorb the carbon tax, from 14% if they pass on the carbon tax in full to 8% if direct emitters bear half of the cost of the carbon tax. Among the EU countries, Germany is the most affected, followed by Poland and Italy (Figure 8.152).

Table 8.65: Domestic and foreign impacts (in \$ bn) of a regional tax (uniform taxation, $\phi = 100\%$, Exiobase 2022)

| Carbon tax | Domestic impact | | | Foreign impact | | |
|---|---|---|---|---|---|---|
| | EU | USA | China | EU | USA | China |
| $\$100/tCO_2e$ | 792 | 886 | 4 710 | 104 | 118 | 257 |
| $\$250/tCO_2e$ | 1 979 | 2 215 | 11 774 | 261 | 296 | 643 |
| $\$500/tCO_2e$ | 3 959 | 4 430 | 23 549 | 521 | 592 | 1 287 |

Source: Desnos *et al.* (2023, Tabke 30, page 91).

Table 8.65 shows the global foreign impact of a tax in the EU, US and China for three values of the carbon price. China always has the highest external impact, with a cost of \$1 287 bn for a $\$500/tCO_2e$ carbon price, while the EU's external impact is only \$521 bn. To better understand the winners and the losers, we report the fifteen largest countries affected by a carbon tax in Table 8.66. In this scenario, the tax is set at $\$100/tCO_2e$ and the pass-through parameter is set to 100%. When the tax is applied in the European Union, the rest-of-the-world region is most affected, accounting for 25.25% of the total costs supported by foreign countries. This is followed by China (23.62%),

Figure 8.152: Cost breakdown (EU, uniform tax, $\phi = 50\%$, Exiobase 2022)

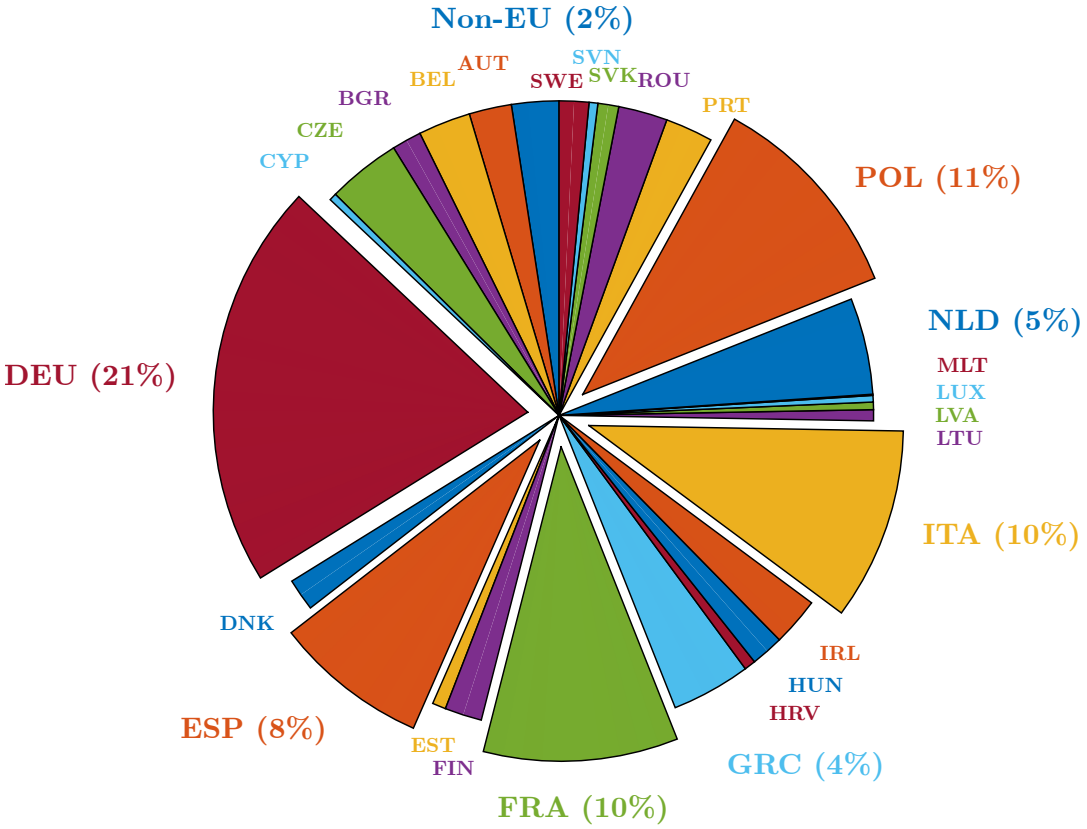


Source: Desnos *et al.* (2023, Figure 49, page 88).

Table 8.66: Fifteen most affected foreign countries (uniform tax, $\tau = \$100/tCO_2e$, $\phi = 100\%$, Exiobase 2022)

| Rank | EU tax | | US tax | | Chinese tax | |
|---|---|---|---|---|---|---|
| 1 | ROW | 25.25% | CHN | 24.74% | ROW | 36.89% |
| 2 | CHN | 23.62% | ROW | 18.60% | USA | 12.95% |
| 3 | USA | 11.45% | CAN | 9.35% | KOR | 8.87% |
| 4 | GBR | 8.77% | MEX | 8.51% | IND | 6.91% |
| 5 | CHE | 4.32% | KOR | 6.89% | JPN | 6.44% |
| 6 | KOR | 4.05% | JPN | 5.05% | DEU | 3.61% |
| 7 | IND | 3.67% | IND | 4.28% | MEX | 2.19% |
| 8 | JPN | 3.31% | DEU | 2.80% | FRA | 1.88% |
| 9 | TUR | 2.62% | BRA | 2.51% | GBR | 1.83% |
| 10 | TWN | 2.08% | GBR | 2.34% | BRA | 1.75% |
| 11 | CAN | 2.06% | FRA | 1.63% | IDN | 1.74% |
| 12 | RUS | 1.96% | TWN | 1.59% | CAN | 1.62% |
| 13 | BRA | 1.90% | IRL | 1.47% | ITA | 1.59% |
| 14 | MEX | 1.70% | ITA | 1.43% | AUS | 1.31% |
| 15 | NOR | 1.46% | NLD | 1.23% | TUR | 1.11% |

Source: Desnos *et al.* (2023, Table 31, page 91).

the United States (11.45%) and the United Kingdom (8.77%). This would also be the case with a Chinese tax, but it now represents more than 36% of the foreign costs. This is followed by the United States (12.95%), South Korea (8.87%) and India (6.91%). In the case of a US tax, China would be the most affected country with 24.74% of the total impact, followed by the rest-of-the-world region (18.60%), Canada (9.35%) and Mexico (8.51%). It is important to note that the US has strong trade relations with China, but also with other countries in the Americas (Canada, Mexico, Brazil). These results highlight the trade links between countries, and consequently, the potential exposure to a carbon tax. For example, if we focus on Turkey, it is highly linked to the EU, as it would be the $9^{th}$ country most affected by an EU carbon tax. It would also be affected by a Chinese tax, as it would be the $15^{th}$ most affected country. The impact would be smaller in the case of a US carbon tax. Similarly, we see the importance of Germany in the Chinese and US supply chain.

**The study of Sautel *et al.* (2022)** The analysis carried out by Sautel *et al.* (2022) uses the previous input-output framework. It focuses on France and considers a carbon tax of €250 per tonne of $CO_2$. The estimates are based on the WIOD database and default values of pass-through rates (see Table 8.64 on page 853). The conclusions are as follows:

> "*The total additional cost of introducing a price of* €250 *per tonne of* $CO_2$ *to be paid by French emitting installations is* €57.6 *billion, or about* 2.5 *points of GDP. Of this total,* €7 *billion corresponds to purchases by foreign operators and investments by French and foreign operators. [...] Of this* €50.3 *billion, French companies would ultimately bear* 57% *of the additional costs, or about* €28.7 *billion. The rest would be passed on to final demand, i.e.,* 21.6 *billion euros.*" (Sautel *et al.*, 2022, page 39).

**The study of Roncalli and Semet (2024)** It is common to assume that the pass-through rate follows a beta distribution, as it is a parameter between 0 and 1:

$$\phi \sim \mathcal{B}(\alpha, \beta)$$

Following Sautel *et al.* (2022), Desnos *et al.* (2023) considered four types of sectors with respect to price-demand elasticity (highly-elastic, high-elastic, medium-elastic and low-elastic), and used the expert-opinion values of the parameters $\alpha$ and $\beta$ given in Table 8.67. We give the mean, the standard deviation and the 95% range, and show the associated probability density functions in Figure 8.153. The first type is right-skewed, while the fourth type is left-skewed. The second and third types are more symmetric. Moreover, these four distribution functions are ordered since they verify the first-order stochastic dominance principle (Figure 8.154).

Table 8.67: Probabilistic characterization of the four pass-through types

| Statistic | | Highly-elastic | High-elastic | Medium-elastic | Low-elastic |
|---|---|---|---|---|---|
| Parameters | $\alpha$ | 3.0 | 4.0 | 14.0 | 12.0 |
| | $\beta$ | 12.0 | 6.0 | 6.0 | 0.6 |
| Moments | $\mu_\phi$ | 20% | 40% | 70% | 95% |
| | $\sigma_\phi$ | 10% | 15% | 10% | 6% |
| Range | $Q_\phi(2.5\%)$ | 5% | 14% | 49% | 79% |
| | $Q_\phi(97.5\%)$ | 43% | 70% | 87% | 100% |

Desnos *et al.* (2023) defined a mapping between the WIOD sectors and the four types of pass-through mechanisms. They used this classification to build a Monte Carlo Value-at-Risk engine[149].

[149] See Section 13.3 on page 1039.

Figure 8.153: Probability density function of pass-through rates

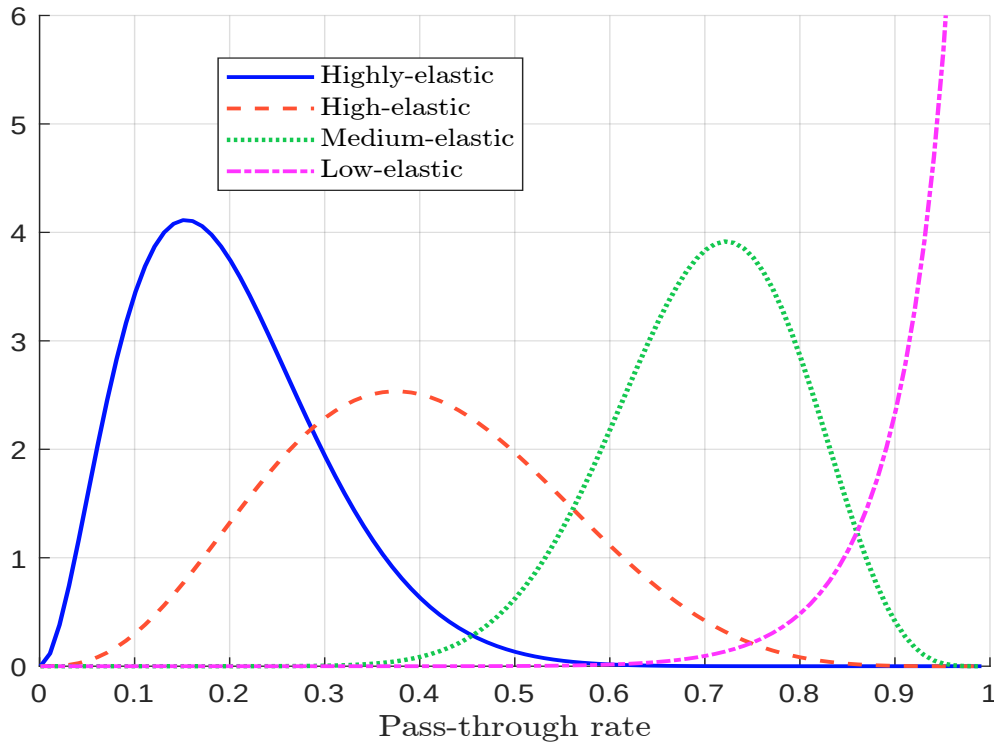


Figure 8.154: Probability density function of pass-through rates

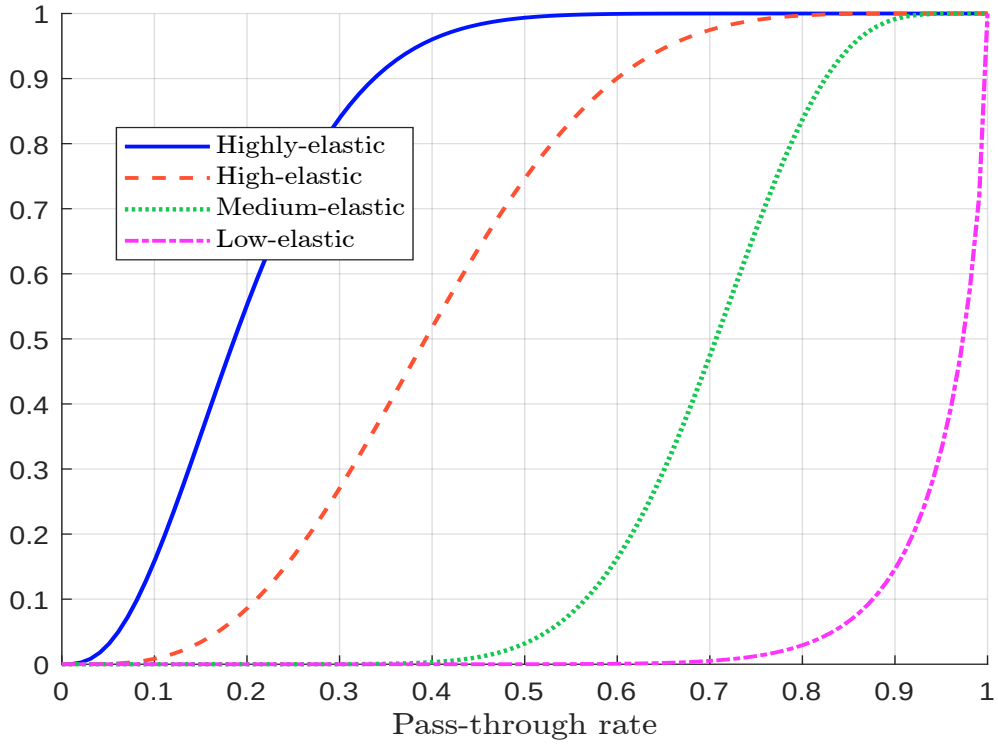

Roncalli and Semet (2024) use their classification to measure the impact of a \$100/tCO$_2$e carbon tax. They assume that the carbon tax is applied to a given region and compute the total cost vector as follows:

$$T_{\text{total}} = x \odot \left(I_n - \operatorname{diag}(\boldsymbol{\phi}) + \tilde{\boldsymbol{\mathcal{L}}}(\boldsymbol{\phi})\right) t_{\text{direct}}$$

They assume that the pass-through rate of the sector is constant and equal to the mean of the corresponding beta distribution: $\boldsymbol{\phi} = \mu_{\boldsymbol{\phi}}$. They decompose the total costs into what is paid by the producer and what is paid by the downstream value chain, including the final consumer:

$$\begin{cases} T_{\text{producer}} = x \odot (\mathbf{1}_n - \boldsymbol{\phi}) \odot t_{\text{direct}} \\ T_{\text{downstream}} = x \odot \tilde{\boldsymbol{\mathcal{L}}}(\boldsymbol{\phi})\, t_{\text{direct}} \end{cases}$$

They also consider a second decomposition between the direct costs of the carbon tax and the indirect costs due to the pass-through mechanism:

$$\begin{cases} T_{\text{direct}} = x \odot t_{\text{direct}} \\ T_{\text{indirect}} = T_{\text{total}} - T_{\text{direct}} = x \odot \left(\tilde{\boldsymbol{\mathcal{L}}}(\boldsymbol{\phi}) - \operatorname{diag}(\boldsymbol{\phi})\right) t_{\text{direct}} \end{cases}$$

By definition, government revenue is equal to the direct cost of the carbon tax:

$$R_{\text{government}} = T_{\text{direct}} = x \odot t_{\text{direct}}$$

All of the previous measures can be aggregated at a global level or at a country/regional level[150]. Inflation rates are calculated using the following formula:

$$\pi = \alpha^\top \Delta p = \alpha^\top \tilde{\boldsymbol{\mathcal{L}}}(\boldsymbol{\phi})\, t_{\text{direct}}$$

They distinguish between PPI and CPI inflation. In the first case, the basket weights $\alpha$ are defined with respect to the output vector, while in the second case they use the final demand vector: $\alpha_{\text{ppi}} = x / (\mathbf{1}_n^\top x)$ and $\alpha_{\text{cpi}} = y / (\mathbf{1}_n^\top y)$. If the analysis is conducted at the country/regional level, the weights are calculated using the country's output and final demand vectors.

In Table 8.68, we report the results of Roncalli and Semet (2024) when considering a uniform global carbon tax of \$100/tCO$_2$e. The cost and revenue figures are expressed as a percentage of GDP[151]. At the global level, the implementation of a uniform carbon tax affects GDP by 5.01% and generates revenue of 2.82%. The net cost would then be 2.18% of world GDP. While the government revenue is exactly the direct cost of the carbon tax, the net cost is the indirect cost of the carbon tax due to the pass-through mechanism. If we split the total cost between what is paid by the producer and what is paid by the downstream supply chain, including the final consumer, we find that of the 5.01% of the total cost, only 0.93% is paid by the producers, while 4.08% is paid by the value chain and consumers. This means that only 20% of the carbon tax is effectively borne by the producers themselves. Analysis at the regional level highlights economic disparities between countries. Overall, four countries have net costs above 3%. India is the most affected country with a net cost of 4.55% of GDP, followed by Russia (4.24%), China (4.03%) and Bulgaria (3.12%).

The previous results are not realistic because it is unlikely that common measures such as an international carbon pricing system will see the light of day. In this context, Roncalli and Semet (2024) propose to analyze the economic impact of the implementation of individual climate policies, in particular the implementation of an individual carbon tax in Europe, the United States and

[150] Let $S$ be a set of sectors. The aggregated costs and revenues are equal to $\mathcal{C} = \sum_{j \in S} T_j$ and $\mathcal{R} = \sum_{j \in S} R_j$.

[151] This means that we normalize these figures by the total output $\mathbf{1}_n^\top x$.

Table 8.68: Economic impact of a global carbon tax ($100/tCO$_2$e, Exiobase 2022)

| Region | Cost | | | | | | Revenue |
|---|---|---|---|---|---|---|---|
| | $\mathcal{C}_{\text{total}}$ | $\mathcal{C}_{\text{direct}}$ | $\mathcal{C}_{\text{indirect}}$ | $\mathcal{C}_{\text{producer}}$ | $\mathcal{C}_{\text{downstream}}$ | $\mathcal{C}_{\text{net}}$ | $\mathcal{R}_{\text{government}}$ |
| World | 5.01% | 2.82% | 2.18% | 0.93% | 4.08% | 2.18% | 2.82% |
| AUS | 4.63% | 2.93% | 1.70% | 0.81% | 3.82% | 1.70% | 2.93% |
| AUT | 2.08% | 0.91% | 1.17% | 0.30% | 1.77% | 1.17% | 0.91% |
| BEL | 1.77% | 0.94% | 0.82% | 0.44% | 1.33% | 0.82% | 0.94% |
| BGR | 7.07% | 3.94% | 3.12% | 0.89% | 6.18% | 3.12% | 3.94% |
| BRA | 5.22% | 3.78% | 1.44% | 2.01% | 3.21% | 1.44% | 3.78% |
| CAN | 3.74% | 2.25% | 1.49% | 0.57% | 3.17% | 1.49% | 2.25% |
| CHE | 0.75% | 0.30% | 0.45% | 0.16% | 0.59% | 0.45% | 0.30% |
| CHN | 7.47% | 3.44% | 4.03% | 1.21% | 6.26% | 4.03% | 3.44% |
| CYP | 5.05% | 3.94% | 1.11% | 2.49% | 2.56% | 1.11% | 3.94% |
| CZE | 4.47% | 2.13% | 2.34% | 0.44% | 4.03% | 2.34% | 2.13% |
| DEU | 1.99% | 1.10% | 0.89% | 0.35% | 1.64% | 0.89% | 1.10% |
| DNK | 1.47% | 0.98% | 0.49% | 0.54% | 0.93% | 0.49% | 0.98% |
| ESP | 2.25% | 1.15% | 1.11% | 0.41% | 1.84% | 1.11% | 1.15% |
| FIN | 2.80% | 1.36% | 1.44% | 0.36% | 2.44% | 1.44% | 1.36% |
| FRA | 1.39% | 0.79% | 0.60% | 0.35% | 1.04% | 0.60% | 0.79% |
| GBR | 1.53% | 0.88% | 0.65% | 0.33% | 1.20% | 0.65% | 0.88% |
| GRC | 6.39% | 4.61% | 1.78% | 2.52% | 3.87% | 1.78% | 4.61% |
| HRV | 3.57% | 2.18% | 1.38% | 0.89% | 2.67% | 1.38% | 2.18% |
| HUN | 3.41% | 1.83% | 1.58% | 0.61% | 2.80% | 1.58% | 1.83% |
| IDN | 7.85% | 5.53% | 2.31% | 2.08% | 5.77% | 2.31% | 5.53% |
| IND | 11.38% | 6.83% | 4.55% | 2.28% | 9.11% | 4.55% | 6.83% |
| IRL | 1.47% | 0.95% | 0.52% | 0.57% | 0.89% | 0.52% | 0.95% |
| ITA | 2.22% | 0.93% | 1.29% | 0.28% | 1.93% | 1.29% | 0.93% |
| JPN | 2.85% | 1.38% | 1.47% | 0.32% | 2.53% | 1.47% | 1.38% |
| KOR | 4.23% | 1.61% | 2.61% | 0.38% | 3.85% | 2.61% | 1.61% |
| LTU | 4.06% | 2.41% | 1.65% | 1.00% | 3.06% | 1.65% | 2.41% |
| LUX | 1.15% | 0.51% | 0.64% | 0.35% | 0.80% | 0.64% | 0.51% |
| LVA | 3.43% | 2.15% | 1.28% | 1.07% | 2.36% | 1.28% | 2.15% |
| MEX | 5.59% | 3.60% | 1.99% | 1.02% | 4.57% | 1.99% | 3.60% |
| MLT | 1.82% | 0.64% | 1.18% | 0.17% | 1.65% | 1.18% | 0.64% |
| NLD | 2.25% | 1.14% | 1.12% | 0.51% | 1.74% | 1.12% | 1.14% |
| NOR | 1.81% | 1.31% | 0.51% | 0.58% | 1.23% | 0.51% | 1.31% |
| POL | 5.84% | 3.44% | 2.40% | 0.98% | 4.86% | 2.40% | 3.44% |
| PRT | 3.77% | 2.13% | 1.64% | 0.70% | 3.07% | 1.64% | 2.13% |
| ROU | 4.10% | 2.19% | 1.91% | 0.69% | 3.42% | 1.91% | 2.19% |
| RUS | 12.79% | 8.55% | 4.24% | 1.44% | 11.34% | 4.24% | 8.55% |
| SVK | 3.29% | 1.62% | 1.66% | 0.42% | 2.87% | 1.66% | 1.62% |
| SVN | 2.79% | 1.51% | 1.28% | 0.47% | 2.32% | 1.28% | 1.51% |
| SWE | 1.21% | 0.59% | 0.62% | 0.21% | 1.00% | 0.62% | 0.59% |
| TUR | 5.78% | 3.73% | 2.05% | 1.39% | 4.39% | 2.05% | 3.73% |
| TWN | 5.16% | 2.21% | 2.95% | 0.75% | 4.41% | 2.95% | 2.21% |
| USA | 2.17% | 1.40% | 0.78% | 0.34% | 1.83% | 0.78% | 1.40% |
| ROW | 7.55% | 5.14% | 2.40% | 1.87% | 5.68% | 2.40% | 5.14% |

Source: Roncalli and Semet (2024, Table 1, page 16).

Table 8.69: Economic impact of a EU carbon tax ($100/tCO$_2$e, Exiobase 2022)

| Region | Cost | | | | | | Revenue |
|---|---|---|---|---|---|---|---|
| | $\mathcal{C}_{\text{total}}$ | $\mathcal{C}_{\text{direct}}$ | $\mathcal{C}_{\text{indirect}}$ | $\mathcal{C}_{\text{producer}}$ | $\mathcal{C}_{\text{downstream}}$ | $\mathcal{C}_{\text{net}}$ | $\mathcal{R}_{\text{government}}$ |
| World | 0.36% | 0.22% | 0.14% | 0.07% | 0.28% | 0.14% | 0.22% |
| BGR | 6.30% | 3.94% | 2.35% | 0.89% | 5.41% | 2.35% | 3.94% |
| GRC | 5.64% | 4.61% | 1.03% | 2.52% | 3.12% | 1.03% | 4.61% |
| POL | 5.21% | 3.44% | 1.77% | 0.98% | 4.24% | 1.77% | 3.44% |
| CYP | 4.86% | 3.94% | 0.92% | 2.49% | 2.37% | 0.92% | 3.94% |
| CZE | 3.90% | 2.13% | 1.76% | 0.44% | 3.46% | 1.76% | 2.13% |
| ROU | 3.60% | 2.19% | 1.41% | 0.69% | 2.91% | 1.41% | 2.19% |
| PRT | 3.28% | 2.13% | 1.15% | 0.70% | 2.58% | 1.15% | 2.13% |
| LTU | 3.22% | 2.41% | 0.82% | 1.00% | 2.22% | 0.82% | 2.41% |
| LVA | 3.11% | 2.15% | 0.96% | 1.07% | 2.05% | 0.96% | 2.15% |
| HRV | 2.88% | 2.18% | 0.70% | 0.89% | 1.99% | 0.70% | 2.18% |
| SVK | 2.72% | 1.62% | 1.09% | 0.42% | 2.30% | 1.09% | 1.62% |
| HUN | 2.70% | 1.83% | 0.87% | 0.61% | 2.08% | 0.87% | 1.83% |
| SVN | 2.38% | 1.51% | 0.87% | 0.47% | 1.91% | 0.87% | 1.51% |
| FIN | 2.27% | 1.36% | 0.91% | 0.36% | 1.91% | 0.91% | 1.36% |
| ESP | 1.82% | 1.15% | 0.68% | 0.41% | 1.41% | 0.68% | 1.15% |

Source: Roncalli and Semet (2024, Table 2, page 18).

Table 8.70: Economic impact of a US carbon tax ($100/tCO$_2$e, Exiobase 2022)

| Region | Cost | | | | | | Revenue |
|---|---|---|---|---|---|---|---|
| | $\mathcal{C}_{\text{total}}$ | $\mathcal{C}_{\text{direct}}$ | $\mathcal{C}_{\text{indirect}}$ | $\mathcal{C}_{\text{producer}}$ | $\mathcal{C}_{\text{downstream}}$ | $\mathcal{C}_{\text{net}}$ | $\mathcal{R}_{\text{government}}$ |
| World | 0.44% | 0.29% | 0.14% | 0.07% | 0.37% | 0.14% | 0.29% |
| USA | 1.96% | 1.40% | 0.57% | 0.34% | 1.62% | 0.57% | 1.40% |
| CAN | 0.18% | 0.00% | 0.18% | 0.00% | 0.18% | 0.18% | 0.00% |
| MEX | 0.18% | 0.00% | 0.18% | 0.00% | 0.18% | 0.18% | 0.00% |
| KOR | 0.07% | 0.00% | 0.07% | 0.00% | 0.07% | 0.07% | 0.00% |
| IRL | 0.06% | 0.00% | 0.06% | 0.00% | 0.06% | 0.06% | 0.00% |
| BRA | 0.05% | 0.00% | 0.05% | 0.00% | 0.05% | 0.05% | 0.00% |
| TWN | 0.04% | 0.00% | 0.04% | 0.00% | 0.04% | 0.04% | 0.00% |
| ROW | 0.04% | 0.00% | 0.04% | 0.00% | 0.04% | 0.04% | 0.00% |
| IND | 0.04% | 0.00% | 0.04% | 0.00% | 0.04% | 0.04% | 0.00% |
| NLD | 0.03% | 0.00% | 0.03% | 0.00% | 0.03% | 0.03% | 0.00% |
| GBR | 0.03% | 0.00% | 0.03% | 0.00% | 0.03% | 0.03% | 0.00% |
| NOR | 0.02% | 0.00% | 0.02% | 0.00% | 0.02% | 0.02% | 0.00% |
| BEL | 0.02% | 0.00% | 0.02% | 0.00% | 0.02% | 0.02% | 0.00% |
| JPN | 0.02% | 0.00% | 0.02% | 0.00% | 0.02% | 0.02% | 0.00% |
| CHN | 0.02% | 0.00% | 0.02% | 0.00% | 0.02% | 0.02% | 0.00% |

Source: Roncalli and Semet (2024, Table 3, page 18).

Table 8.71: Economic impact of a carbon tax in China ($100/tCO$_2$e, Exiobase 2022)

| Region | Cost | | | | | | Revenue |
|---|---|---|---|---|---|---|---|
| | $\mathcal{C}_{\text{total}}$ | $\mathcal{C}_{\text{direct}}$ | $\mathcal{C}_{\text{indirect}}$ | $\mathcal{C}_{\text{producer}}$ | $\mathcal{C}_{\text{downstream}}$ | $\mathcal{C}_{\text{net}}$ | $\mathcal{R}_{\text{government}}$ |
| World | 1.66% | 0.81% | 0.85% | 0.29% | 1.38% | 0.85% | 0.81% |
| CHN | 6.89% | 3.44% | 3.45% | 1.21% | 5.68% | 3.45% | 3.44% |
| ROW | 0.13% | 0.00% | 0.13% | 0.00% | 0.13% | 0.13% | 0.00% |
| KOR | 0.12% | 0.00% | 0.12% | 0.00% | 0.12% | 0.12% | 0.00% |
| MEX | 0.06% | 0.00% | 0.06% | 0.00% | 0.06% | 0.06% | 0.00% |
| IND | 0.05% | 0.00% | 0.05% | 0.00% | 0.05% | 0.05% | 0.00% |
| IDN | 0.05% | 0.00% | 0.05% | 0.00% | 0.05% | 0.05% | 0.00% |
| JPN | 0.04% | 0.00% | 0.04% | 0.00% | 0.04% | 0.04% | 0.00% |
| POL | 0.04% | 0.00% | 0.04% | 0.00% | 0.04% | 0.04% | 0.00% |
| CZE | 0.04% | 0.00% | 0.04% | 0.00% | 0.04% | 0.04% | 0.00% |
| HUN | 0.04% | 0.00% | 0.04% | 0.00% | 0.04% | 0.04% | 0.00% |
| TUR | 0.04% | 0.00% | 0.04% | 0.00% | 0.04% | 0.04% | 0.00% |
| CAN | 0.03% | 0.00% | 0.03% | 0.00% | 0.03% | 0.03% | 0.00% |
| BEL | 0.03% | 0.00% | 0.03% | 0.00% | 0.03% | 0.03% | 0.00% |
| SVK | 0.03% | 0.00% | 0.03% | 0.00% | 0.03% | 0.03% | 0.00% |
| AUS | 0.03% | 0.00% | 0.03% | 0.00% | 0.03% | 0.03% | 0.00% |

Source: Roncalli and Semet (2024, Table 4, page 19).

China. In Table 8.69, we observe that the implementation of a carbon tax within the EU member states will primarily affect the European economy since more than 95% of the total costs will fall on the countries of the European Union. In Tables 8.70 and 8.71, we report estimates for a US and a Chinese carbon tax, respectively. As in the case of the EU tax, the economic incidence of the carbon tax is almost entirely borne by the domestic economy. For the US, the total cost is less than 2% of GDP, while for China this figure reaches 6.89%. The two main trading partners of the United States, Canada and Mexico, will be indirectly affected by the tax by up to $5.5 bn and $3.7 bn, respectively, which is less than 0.2% of their respective GDP. Despite the limited cascading effect of the domestic carbon tax, the estimates illustrate the distortionary effects of an isolated climate policy. Finally, comparing the macroeconomic effects on a global scale, we see that the impact of an American or Chinese tax on world GDP is larger than that of a European tax. A Chinese carbon tax could induce a significant cost of 1.66% on the global economy, which is more than four times the total impact of a European tax.

In Table 8.72 and 8.73, we present the PPI and CPI values for the fifteen most affected countries, categorized according to different tax structures. With a uniform global tax of $100/tCO$_2$e, cost-push inflation reaches 4.08% worldwide, while escalating producer prices lead to a 3.53% increase in consumer prices worldwide. Focusing on the regional tax, inflation is mainly supported by the region that implements the carbon tax. This is especially true for the European and Chinese tax.

In summary, the introduction of a regional carbon tax creates a competitive distortion between the region introducing the tax and the rest of the world. Moreover, the introduction of a carbon tax leads to inflation. This is because path-through mechanisms amplify the price dynamics of the costs passed on by producers. The real benefits of a carbon tax are then challenging and are discussed in detail in Chapter 10.

Table 8.72: Producer price index ($\pi_{\text{ppi}}$) estimates ($100/tCO$_2$e, Exiobase 2022)

| Rank | Global tax | | EU tax | | US tax | | China tax | |
|---|---|---|---|---|---|---|---|---|
| | World | 4.08% | World | 0.28% | World | 0.37% | World | 1.38% |
| 1 | RUS | 11.34% | BGR | 5.41% | USA | 1.62% | CHN | 5.68% |
| 2 | IND | 9.11% | POL | 4.24% | CAN | 0.18% | ROW | 0.13% |
| 3 | CHN | 6.26% | CZE | 3.46% | MEX | 0.18% | KOR | 0.12% |
| 4 | BGR | 6.18% | GRC | 3.12% | KOR | 0.07% | MEX | 0.06% |
| 5 | IDN | 5.77% | ROU | 2.91% | IRL | 0.06% | IND | 0.05% |
| 6 | ROW | 5.68% | PRT | 2.58% | BRA | 0.05% | IDN | 0.05% |
| 7 | POL | 4.86% | CYP | 2.37% | TWN | 0.04% | JPN | 0.04% |
| 8 | MEX | 4.57% | SVK | 2.30% | ROW | 0.04% | POL | 0.04% |
| 9 | TWN | 4.41% | LTU | 2.22% | IND | 0.04% | CZE | 0.04% |
| 10 | TUR | 4.39% | HUN | 2.08% | NLD | 0.03% | HUN | 0.04% |
| 11 | CZE | 4.03% | LVA | 2.05% | GBR | 0.03% | TUR | 0.04% |
| 12 | GRC | 3.87% | HRV | 1.99% | NOR | 0.02% | CAN | 0.03% |
| 13 | KOR | 3.85% | SVN | 1.91% | BEL | 0.02% | BEL | 0.03% |
| 14 | AUS | 3.82% | FIN | 1.91% | JPN | 0.02% | SVK | 0.03% |
| 15 | ROU | 3.42% | AUT | 1.50% | CHN | 0.02% | AUS | 0.03% |

Source: Roncalli and Semet (2024, Table 5, page 20).

Table 8.73: Consumer price index ($\pi_{\text{cpi}}$) estimates ($100/tCO$_2$e, Exiobase 2022)

| Rank | Global tax | | EU tax | | US tax | | China tax | |
|---|---|---|---|---|---|---|---|---|
| | World | 3.53% | World | 0.48% | World | 0.27% | World | 1.15% |
| 1 | IDN | 6.75% | FRA | 5.95% | USA | 1.06% | CHN | 5.88% |
| 2 | CHN | 6.35% | CZE | 4.07% | MEX | 0.16% | ROW | 0.16% |
| 3 | FRA | 6.29% | HRV | 3.83% | CAN | 0.16% | KOR | 0.08% |
| 4 | IND | 5.98% | GRC | 3.59% | IRL | 0.05% | AUS | 0.07% |
| 5 | RUS | 5.72% | POL | 3.49% | BRA | 0.04% | IND | 0.07% |
| 6 | CZE | 4.63% | CYP | 3.32% | GBR | 0.04% | CAN | 0.07% |
| 7 | HRV | 4.42% | BGR | 3.16% | ROW | 0.04% | MEX | 0.06% |
| 8 | GRC | 4.35% | SVK | 2.80% | KOR | 0.03% | TUR | 0.05% |
| 9 | POL | 4.14% | MLT | 2.69% | IND | 0.03% | IDN | 0.04% |
| 10 | BGR | 3.89% | PRT | 2.58% | NOR | 0.03% | BRA | 0.04% |
| 11 | ROW | 3.82% | LUX | 2.30% | NLD | 0.03% | JPN | 0.04% |
| 12 | TWN | 3.73% | HUN | 2.20% | LUX | 0.03% | BEL | 0.04% |
| 13 | CYP | 3.57% | LTU | 2.11% | TWN | 0.02% | RUS | 0.04% |
| 14 | MLT | 3.38% | NLD | 2.11% | BEL | 0.02% | GRC | 0.04% |
| 15 | SVK | 3.36% | SVN | 1.90% | TUR | 0.02% | POL | 0.04% |

Source: Roncalli and Semet (2024, Table 6, page 21).

## 8.5 Exercises

# Chapter 9

# Climate Risk Measures

In this chapter, we list the various metrics that are helpful in assessing climate risk. We focus on traditional metrics related to the concept of carbon footprint. This concept seems easy to understand, but difficult to define precisely. In their seminal book on the ecological footprint, Wackernagel and Rees (1996) stated that "*the carbon footprint stands for a certain amount of gaseous emissions that are relevant to climate change and associated with human production or consumption activities.*" Wiedmann and Minx (2008, pages 2-4) listed several definitions found in the scientific literature and the grey literature (NGOs, consultants, data providers, etc.) between 1960 and 2007. They also proposed a definition of their own:

> "*The carbon footprint is a measure of the exclusive total amount of carbon dioxide emissions that is directly and indirectly caused by an activity or is accumulated over the life stages of a product.*" (Wiedmann and Minx, 2008, page 5).

Note that this definition includes only carbon dioxide emissions. The authors excluded methane, because they felt that it should be reserved for another measure, that could be called climate footprint. Furthermore, they pointed out that the carbon footprint should be measured physically in a unit of mass (*e.g.*, kg) and not converted into a land area unit (*e.g.*, ha). This digression shows that the concepts of climate risk measurement are very recent[1] and not necessarily clear and stable. In the first section, we will then discuss how to measure carbon emissions. In particular, we will distinguish the three scopes, define the carbon dioxide equivalent ($CO_2e$) unit based on global warming potential (GWP) values, and present some examples of carbon footprint calculations. We will examine some specific sectors, such as transportation and agriculture, and the two main approaches: activity-based and energy-based methods. In the second section, we will analyze the concept of carbon intensity, which is a normalization of the carbon emissions measure in order to compare countries, companies or portfolios. In the case of physical intensity ratios, total emissions are divided by physical quantities. For instance, it is common to measure the carbon footprint of transportation in terms of $kgCO_2e$ per kilometer traveled, while the carbon footprint of a country is typically measured in terms of $tCO_2e$ per capita. The second way to calculate carbon intensity is to use monetary quantities in the denominator. In the previous example, we can divide the total carbon emissions by the revenue generated by the transportation activity or the GDP of the country. Carbon intensity based on monetary units plays an important role in finance and especially in portfolio management. While carbon emissions and intensity are two static measures, in the third section we will develop some dynamic risk measures based on carbon budget and trend. Finally, the last section is dedicated to green intensity measures, whose objective is to assess the greenness of products, countries, companies or assets.

[1] The publication of this much cited research paper was only fifteen years ago.

## 9.1 Carbon emissions

Carbon footprint is a generic term used to define the total greenhouse gas (GHG) emissions caused by a given system, activity, company, country, or region. Greenhouse gases are made up of water vapor ($H_2O$), carbon dioxide ($CO_2$), methane ($CH_4$), nitrous oxide ($N_2O$), Ozone ($O_3$), etc. They absorb and emit radiation energy, causing the greenhouse effect. We remind that the greenhouse effect was a crucial factor for the development of human life on Earth. Indeed, without the greenhouse effect, the average temperature of Earth's surface would be about $-18°C$. With the greenhouse effect, the current temperature of Earth's surface is about $+15°C$. Nevertheless, the increasing concentration of some GHGs is an issue because it is a factor in global warming. It mainly concerns carbon dioxide, and to a lesser extent, methane and nitrous oxide.

### 9.1.1 Global warming potential

Carbon footprint is generally measured in carbon dioxide equivalent ($CO_2e$), which is a term for describing different GHGs in a common unit. In this framework, a quantity of GHG is expressed as $CO_2e$ by multiplying the GHG amount by its global warming potential (GWP):

$$\text{equivalent mass of } CO_2 = \text{mass of the gas} \times \text{gwp of the gas}$$

where the GWP of a gas is the amount of $CO_2$ that would warm the earth equally. Since the mass of the gas is expressed in kilogram and the GWP has no unit, the mass of $CO_2$ equivalent is also expressed in kilogram. For instance, the IPCC's $5^{\text{th}}$ assessment report has used the following rules (IPCC, 2014a): 1 kg of methane corresponds to 28 kg of $CO_2$ and 1 kg of nitrous oxide corresponds to 265 kg of $CO_2$. The definition of a common unit allows two companies to be compared properly. To compute the carbon footprint of a system that is made up of several gases, we apply the weighted sum formula:

$$m = \sum_{i=1}^{n} m_i \cdot \text{gwp}_i$$

where $m$ is the mass of $CO_2$ equivalent, $m_i$ and $\text{gwp}_i$ are the mass and the global warming potential of the $i^{\text{th}}$ gas, and $n$ is the number of gases. $m$ and $m_i$ have the same mass unit (eg., kilogram or kg, tonne or t, kilotonne or kt, megatonne or Mt, gigatonne or Gt). However, $m$ measures a mass of $CO_2$ equivalent. Therefore, it better to use the following units: $kgCO_2e$, $tCO_2e$, $ktCO_2e$, $MtCO_2e$ and $GtCO_2e$.

**Example 33** *We consider a company $A$ that emits* 3 017 *tonnes of* $CO_2$, 10 *tonnes of* $CH_4$ *and* 1.8 *tonnes of* $N_2O$. *For the company $B$, the GHG emissions are respectively equal to* 2 302 *tonnes of* $CO_2$, 32 *tonnes of* $CH_4$ *and* 3.0 *tonnes of* $N_2O$.

The mass of $CO_2$ equivalent for companies $A$ and $B$ is equal to:

$$m_A = 3017 \times 1 + 10 \times 28 + 1.8 \times 265 = 3\,774 \text{ tCO}_2\text{e}$$

and:

$$m_B = 2302 \times 1 + 32 \times 28 + 3.0 \times 265 = 3\,993 \text{ tCO}_2\text{e}$$

We notice that company $B$ emits more carbon emissions than company $A$ when they are measured in $CO_2$ equivalent. We can also compute the mass contribution of each gas:

$$c_i = \frac{m_i \cdot \text{gwp}_i}{m}$$

The mass decomposition is reported below:

| Company | Mass | Absolute contribution | | | Relative contribution | | |
|---|---|---|---|---|---|---|---|
| $A$ | 3 774 | 3 017 | 280 | 477 | 79.94% | 7.42% | 12.64% |
| $B$ | 3 993 | 2 302 | 896 | 795 | 57.65% | 22.44% | 19.91% |

The contribution of the carbon dioxide gas is equal to 79.94% for company $A$ and 57.65% for company $B$. Concerning methane gas, its contribution is respectively equal to 7.42% and 22.44%.

Box 9.1: Estimation of the global warming potential

According to IPCC (2007), GWP is defined as "*the cumulative radiative forcing, both direct and indirect effects, over a specified time horizon resulting from the emission of a unit mass of gas related to some reference gas.*" Since each gas differs in their capacity to absorb the energy (radiative efficiency) and how long it stays in the atmosphere (lifetime), its impact on global warming depends on these two factors. GWP is then a synthetic measure that combines radiative efficiency and lifetime.

The mathematical definition of the global warming potential is:

$$\text{gwp}_i(t) = \frac{\text{Agwp}_i(t)}{\text{Agwp}_0(t)} = \frac{\int_0^t RF_i(s)\,\mathrm{d}s}{\int_0^t RF_0(s)\,\mathrm{d}s} = \frac{\int_0^t A_i(s)\,\mathbf{S}_i(s)\,\mathrm{d}s}{\int_0^t A_0(s)\,\mathbf{S}_0(s)\,\mathrm{d}s} \tag{9.1}$$

where $A_i(t)$ is the radiative efficiency value of gas $i$ (or the radiative forcing increase per unit mass increase of gas $i$ in the atmosphere), $\mathbf{S}_i(t)$ is the decay function (or the fraction of gas $i$ remaining in the atmosphere after $t$ years following an incremental pulse of the gas) and $i = 0$ is the reference gas (e.g, $CO_2$). The radiative forcing $RF_i(t) = A_i(t)\,\mathbf{S}_i(t)$ is the product of the radiative efficiency and the decay function, whereas the absolute global warming potential $\text{Agwp}_i(t)$ is the cumulative radiative forcing of the gas $i$ between 0 and $t$. GWP is then the ratio between the cumulative radiative forcing of the gas and this of the reference gas. We also notice that it depends on the time horizon $t$.

It is generally accepted to describe the decay function (or impulse response function) by exponential functions (Joos *et al.*, 2013):

$$\mathbf{S}_i(t) = \sum_{j=1}^{m} a_{i,j} e^{-\lambda_{i,j} t} \tag{9.2}$$

where $\sum_{j=1}^{m} a_{i,j} = 1$. Once we have defined the radiative efficiency function $A_i(t)$ and the set of parameters $\{(a_{i,j}, \lambda_{i,j}), j = 1, \ldots, m\}$ of the impulse function, we compute Equation (9.1) using numerical integration. In the case where $A_i(t)$ and $A_0(t)$ are constant, we obtain:

$$\text{gwp}_i(t) = \frac{A_i \sum_{j=1}^{m} a_{i,j} \lambda_{i,j}^{-1} \left(1 - e^{-\lambda_{i,j} t}\right)}{A_0 \sum_{j=1}^{m} a_{0,j} \lambda_{0,j}^{-1} \left(1 - e^{-\lambda_{0,j} t}\right)}$$

In Box 9.1, we explain how GWP is computed. We notice that the global warming potential value depends on the time horizon. For instance, the relative warming impact of one molecule of a greenhouse gas is not the same at 20 years than 100 years. We also notice that the estimation of GWP implies to make some assumptions about the impulse response (or decay) function and the radiative efficiency value. Let us see how the value for methane has been obtained. IPCC (2013)

assumed that the radiative intensity is constant and used the following values[2]: $A_{CO_2} = 1.76 \times 10^{-18}$ and $A_{CH_4} = 2.11 \times 10^{-16}$. The impulse response functions were estimated by least squares and they found the following approximated curve:

$$\mathbf{S}_{CO_2}(t) = 0.2173 + 0.2240 \cdot \exp\left(-\frac{t}{394.4}\right) + 0.2824 \cdot \exp\left(-\frac{t}{36.54}\right) + 0.2763 \cdot \exp\left(-\frac{t}{4.304}\right)$$

and:

$$\mathbf{S}_{CH_4}(t) = \exp\left(-\frac{t}{12.4}\right)$$

These two decay functions are reported in Figure 9.1. We can interpret them as survival functions[3], meaning that the density function can be computed as $f_i(t) = -\partial_t \mathbf{S}_i(t)$.

Figure 9.1: Fraction of gas remaining in the atmosphere

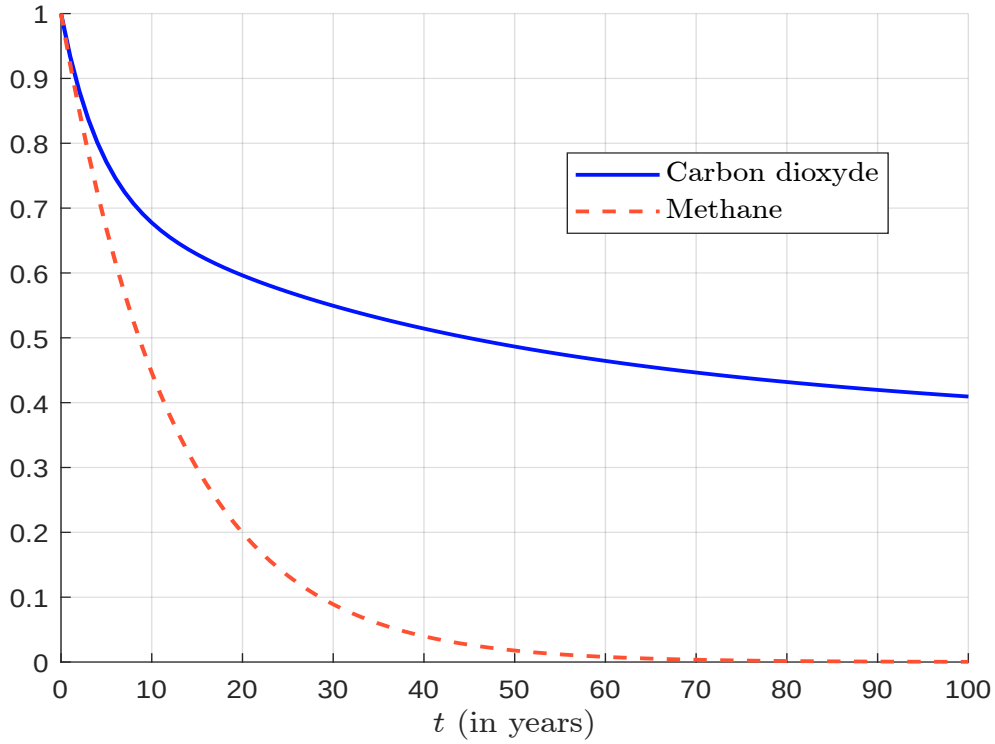


Source: Kleinberg (2020) & Author's calculations.

In the case of the exponential distribution $\mathcal{E}(\lambda)$, we have $\mathbf{S}_i(t) = e^{-\lambda t}$ and $f_i(t) = \lambda e^{-\lambda t}$ where $\lambda$ is the rate parameter. Let $\tau_i$ be random time that the gas remains in the atmosphere. We have $\mathbb{E}[\tau_i] = 1/\lambda$ for the exponential random time. The survival function of the $CH_4$ gas is exponential with a mean time equal to 12.4 years ($\lambda = 1/12.4$). In the case of the general formula (9.2), the probability density function is equal to:

$$f_i(t) = -\partial_t \mathbf{S}_i(t) = \sum_{j=1}^{m} a_{i,j} \lambda_{i,j} e^{-\lambda_{i,j} t}$$

[2]The unit is $W \cdot m^{-2} g^{-1}$.
[3]This is why we use the notation $\mathbf{S}(t)$.

Figure 9.2: Probability density function of the random time

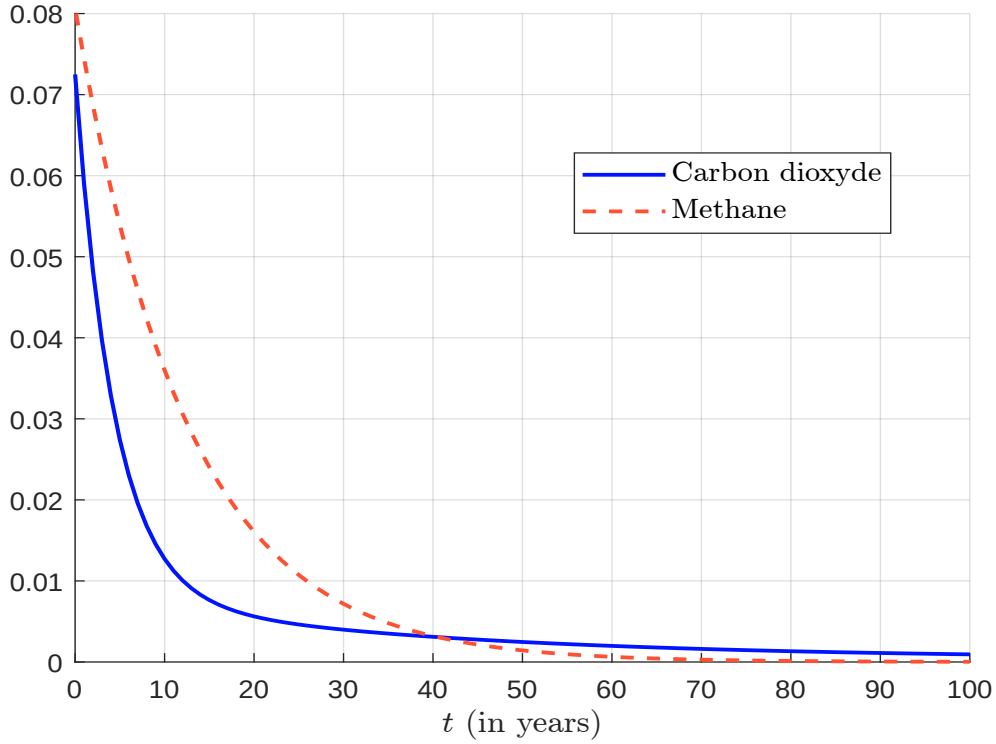


Source: Kleinberg (2020) & Author's calculations.

and the mean time $\mathcal{T}_i$ is given by:

$$\begin{aligned}\mathcal{T}_i := \mathbb{E}[\tau_i] &= \int_0^\infty s f_i(s)\,\mathrm{d}s \\ &= \sum_{j=1}^m a_{i,j} \int_0^\infty \lambda_{i,j} s e^{-\lambda_{i,j} s}\,\mathrm{d}s \\ &= \sum_{j=1}^m \frac{a_{i,j}}{\lambda_{i,j}}\end{aligned}$$

Another way to find this result is to notice that $f_i(t)$ is an exponential mixture distribution where $m$ is the number of mixture components, $\mathcal{E}(\lambda_{i,j})$ is the probability distribution associated with the $j^{\text{th}}$ component and $a_{i,j}$ is the mixture weight of the $j^{\text{th}}$ component. Therefore, we deduce that the mean time is equal to the weighted average of the mean times of the mixture components:

$$\mathcal{T}_i = \mathbb{E}[\tau_i] = \sum_{j=1}^m a_{i,j}\mathbb{E}[\tau_{i,j}] = \sum_{j=1}^m a_{i,j}\mathcal{T}_{i,j}$$

For the $CO_2$ gas, the exponential mixture distribution is defined by the following parameters:

| $j$ | 1 | 2 | 3 | 4 |
|---|---|---|---|---|
| $a_{i,j}$ | 0.2173 | 0.2240 | 0.2824 | 0.2763 |
| $\lambda_{i,j}$ $(\times 10^3)$ | 0.00 | 2.535 | 27.367 | 232.342 |
| $\mathcal{T}_{i,j}$ (in years) | $\infty$ | 394.4 | 36.54 | 4.304 |

We can now explain why the carbon dioxide stays longer in the atmosphere than the methane. When we compare the density functions of the two gases (Figure 9.2), we observe that the disappearance

probabilities are located before 50 years, since the probability to stay in the atmosphere after 50 years is less than 2%. For the $CO_2$ gas, we have roughly 50% that the molecule disappears and 50% that the molecule stays. In fact, we notice that one mixture component corresponds to a permanent state ($\lambda_{i,1} = 0$) with a weight of 21.73%. This explains that the $CO_2$ molecule can stay in the atmosphere, and we have $\mathbf{S}_{CO_2}(\infty) = 21.73\%$.

We compute $\text{Agwp}_{CO_2}(t)$ and $\text{Agwp}_{CH_4}(t)$ and report their values in Figure 9.3. Even if the methane has a much shorter atmospheric lifetime than the carbon dioxide, it absorbs much more energy — because of the value of $A_{CH_4}$ compared to the value of $A_{CO_2}$. Nevertheless, the absolute global warming potential is unbounded for COtwo because we have $\text{Agwp}_{CO_2}(\infty) = \infty$. For the methane, it reaches an upper bound, which corresponds to the ratio $A_{CH_4} \times \mathcal{T}_{CH_4} \propto 2.11 \times 12.4 = 26.164$. Therefore, $\text{gwp}_{CH_4}(t)$ is a decreasing function with respect to the time horizon (Figure 9.4). The instantaneous global warming potential of the methane is equal to:

$$\text{gwp}_{CH_4}(0) = \frac{A_{CH_4}}{A_{CO_2}} = \frac{2.11 \times 10^{-16}}{1.76 \times 10^{-18}} \approx 119.9$$

After 100 years, we obtain $\text{gwp}_{CH_4}(100) = 28.3853$, which is the value calculated by IPCC (2013, 2014a). Because of the persistant regime of the carbon dioxyde, we have $\text{gwp}_{CH_4}(\infty) = 0$. In fact, the global warming potential of $CO_2$ becomes greater than this of $CH_4$ when $t \geq 6\,382$ years.

The previous analysis shows that the estimation of the global warming potential involves significant scientific uncertainty. First, the choice of a 100-year time horizon is arbitrary, and any other choice will change the GWP value. Second, the survival function $\mathbf{S}_i(t)$ is estimated and based on empirical experiments. Third, we have assumed that the radiative efficiency $A_i(t)$ is constant and equal to the initial value $A_i(0)$. In this context, we can consider that $\text{gwp}_i(t)$ is stochastic or cannot be observed without any error. The GHG protocol considers the six gases listed in the Kyoto Protocol: carbon dioxide, methane, nitrous oxide, sulphur hexafluoride, hydrofluorocarbons, and perfluorocarbons. Table 9.1 gives their GWP values according to the different IPCC reports. We notice that they have continuously changed.

Table 9.1: GWP values for 100-year time horizon

| Name | Formula | AR2 | AR4 | AR5 | AR6 |
|---|---|---|---|---|---|
| Carbon dioxide | $CO_2$ | 1 | 1 | 1 | 1 |
| Methane | $CH_4$ | 21 | 25 | 28 | 27.9 |
| Nitrous oxide | $N_2O$ | 310 | 298 | 265 | 273 |
| Sulphur hexafluoride | $SF_6$ | 23 900 | 22 800 | 23 500 | 25 200 |
| Hydrofluorocarbons (HFC) | $CHF_3$ | 11 700 | 14 800 | 12 400 | 14 600 |
| | $CH_2F_2$ | 650 | 675 | 677 | 771 |
| | Etc. | | | | |
| Perfluorocarbons (PFC) | $CF_4$ | 6 500 | 7 390 | 6 630 | 7 380 |
| | $C_2F_6$ | 9 200 | 12 200 | 11 100 | 12 400 |
| | Etc. | | | | |

**Remark 97** *The GWP has been subjected to many criticisms because it does not directly measure the impact on the temperature and it is a single-pulse emission metric (Kleinberg, 2020). The alternative metric is the global temperature potential (GTP) proposed by Shine et al. (2005). While the GWP is a measure of the energy absorbed over a given time period, the GTP is a measure of the temperature change at the end of that time period. The adoption of the GTP is however extremely rare, because its calculation is complicated and it appeared after the Kyoto Protocol.*

Figure 9.3: Absolute global warming potential

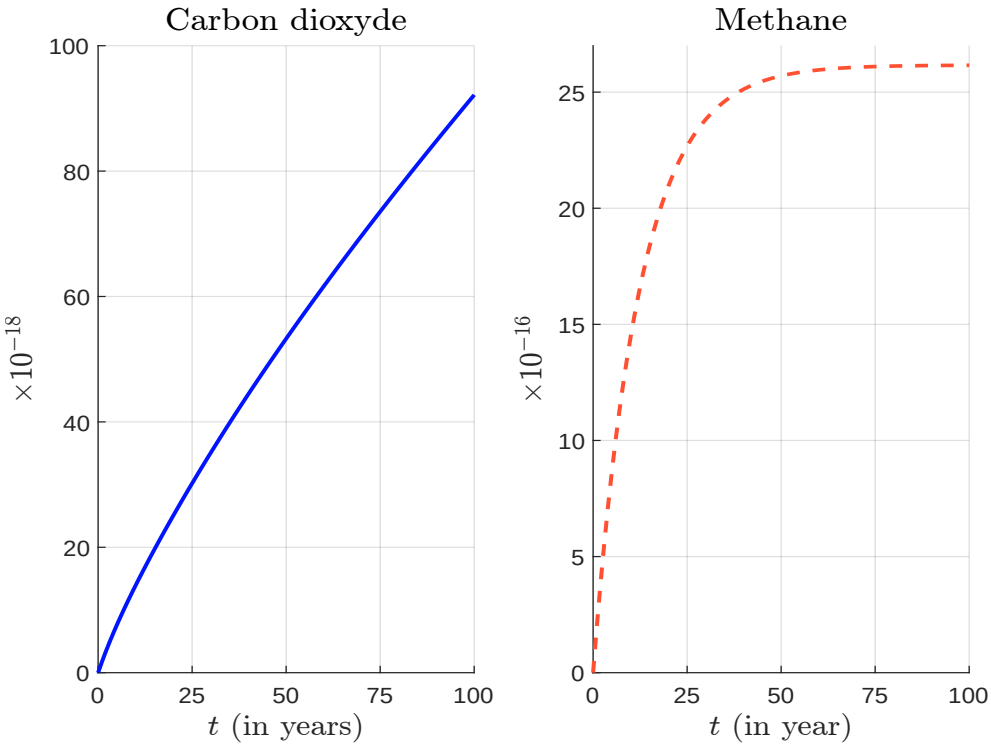


Source: Kleinberg (2020) & Author's calculations.

Figure 9.4: Global warming potential for methane

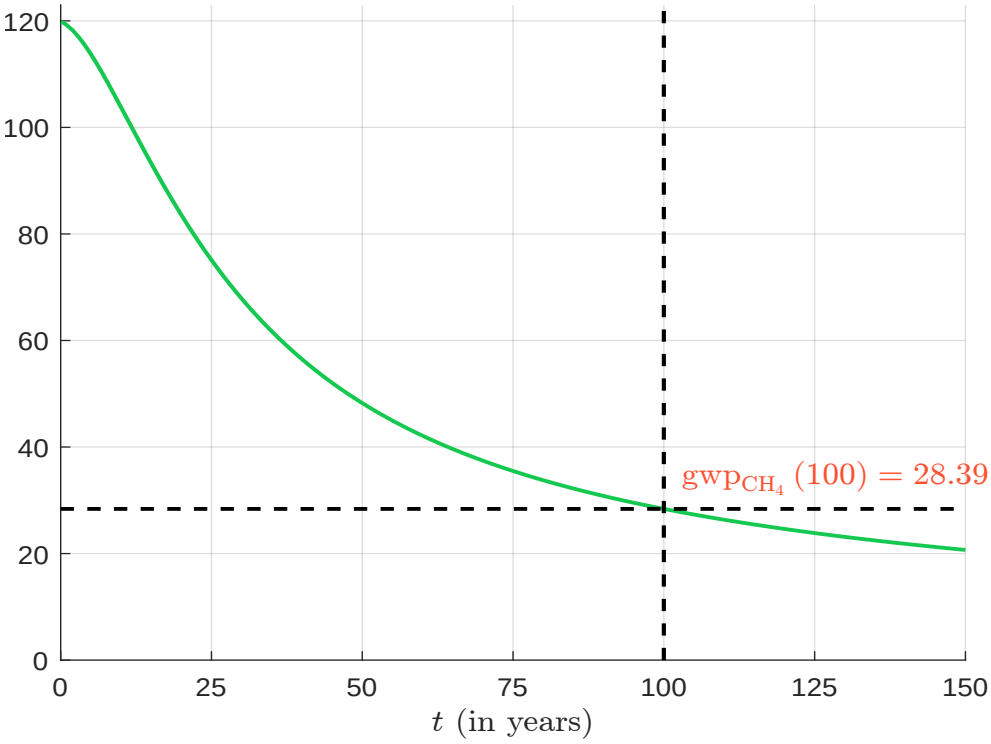


Source: Kleinberg (2020) & Author's calculations.

### 9.1.2 Consolidation accounting at the company level

Greenhouse gas accounting requires to define rules about what is reported and what is not reported. For instance, we have seen that the GHG protocol does not consider all greenhouse gases. In a similar way, the consolidation of GHG emissions (also named organizational boundary) follows specific principles, which are similar to those we can find in financial consolidation accounting. For corporate reporting, the GHG protocol distinguishes two approaches:

1. Equity share approach
2. Control approach

Under the first approach, a parent company must report carbon emissions of a subsidiary company according to its share of equity (or ownership ratio). This is the simplest accounting method. For example, if company $A$ owns 25% of company $B$, company $A$ have to take into account 25% of the company $B$'s GHG emissions. Under the second approach, it can use either the financial control method or the operational control method. The company financially controls an operation if it bears the majority risks and rewards of this operation[4], whereas it has operational control if it has the full authority to implement the operation. The control approach is based on the all-or-none principle: Company $A$ includes 100% of the company $B$'s GHG emissions if $A$ controls $B$, otherwise it includes 0%. In Table 9.2, we report the three accounting principles. By definition, the company has financial (and operational) control on group companies or subsidiaries. This explains that 100% of GHG emissions are consolidated. Associated and affiliated companies differ from the previous categories, because the company do not have the financial control. In this case, no GHG emissions are consolidated under the financial control method. Nevertheless, the company may have operational control, which explains that 100% of GHG emissions may be consolidated[5]. For joint ventures and partnerships, we apply the equity share principle for the financial control method, and we use the same rule than for associated and affiliated companies when we consider the financial control approach. Since the category fixed assets correspond to investments, the company receives dividends but has no control and GHG emissions are not consolidated. The same case applies to franchises because they are sperate legal entities and franchisers have no equity rights or control. In the opposite situation, the franchise is considered as a subsidiary.

Table 9.2: Percent of reported GHG emissions under each consolidation method

| Accounting categories | GHG accouting based on | | |
|---|---|---|---|
| | equity share | financial control | operational control |
| Wholly owned asset | 100% | 100% | 100% |
| Group companies/subsidiaries | Ownership ratio | 100% | 100% |
| Associated/affiliated companies | Ownership ratio | 0% | 0%/100% |
| Joint ventures/partnerships | Ownership ratio | Ownership ratio | 0%/100% |
| Fixed asset investments | 0% | 0% | 0% |
| Franchises | 0% | 0% | 0% |
| | Ownership ratio | 100% | 100% |

Source: GHG Protocol (2004, Table 1, page 19).

**Remark 98** *An illustration of the differences between the equity share and control approaches is given in GHG Protocol (2004) on pages 22 and 23. This concerns the Holland Industries Group.*

[4]For instance when the company has more than 50% voting rights.
[5]If the company has no operational control, GHG emissions are not consolidated.

**Example 34** *We report the organizational structure of company A in Figure 9.5. This industrial group has several subsidiaries, partnerships and joint ventures. For instance, Companies B and C are integrated to company A, implying that the latter has financial and operational control on them. Company D is in the same situation even if company A has not the majority of capital. Indeed, company A treats company D as a subsidiary in its financial accounts, because the remaining capital is diluted and they control the management. The participation in company E is an investment. Company C has two joint ventures. For company F, it owns 75% of the capital, while company G is held in equal proportion by company A and another partner. Finally, company H is affiliated to company D, which has no financial or operational control.*

Figure 9.5: Defining the organizational boundary of company $A$

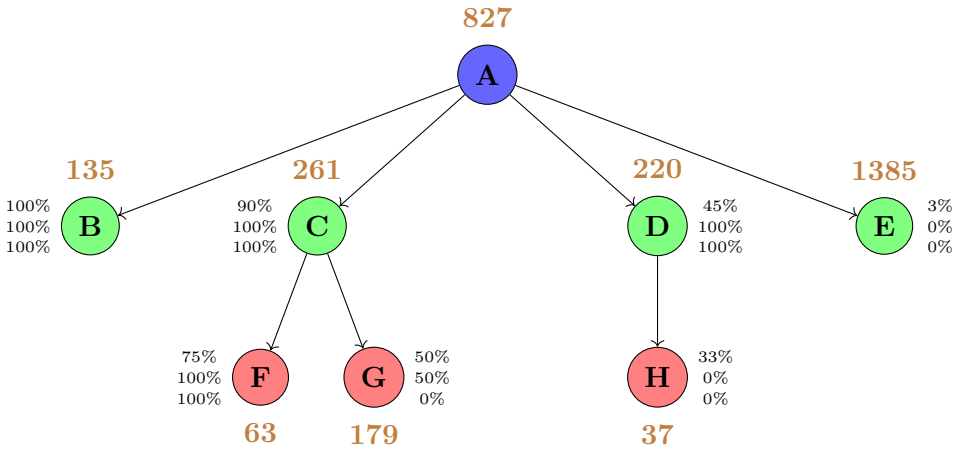


For each company, the brown number corresponds to the carbon emissions in $\text{tCO}_2\text{e}$. The three figures at the right or left of the node corresponds respectively to the equity share, the financial control and the operational control.

Computing the carbon emissions reported by company $A$ will depend on the accounting method. In the case of the equity share approach, we exclude the investment in company $H$ and obtain:

$$\begin{aligned}\mathcal{CE}_A &= 827 + 100\% \times 135 + 90\% \times 261 + 45\% \times 220 + 0\% \times 1\,385 + \\ &\quad 90\% \times 75\% \times 63 + 90\% \times 50\% \times 179 + 45\% \times 33\% \times 37 \\ &= 1\,424.4\,\text{tCO}_2\text{e}\end{aligned}$$

If we use the financial control approach, the reported carbon emissions become:

$$\begin{aligned}\mathcal{CE}_A &= 827 + 100\% \times 135 + 100\% \times 261 + 100\% \times 220 + 0\% \times 1\,385 + \\ &\quad 100\% \times 100\% \times 63 + 100\% \times 50\% \times 179 + 100\% \times 0\% \times 37 \\ &= 1\,595.50\,\text{tCO}_2\text{e}\end{aligned}$$

With the operational control approach, they are slightly different from above because of the treatment of company $G$:

$$\begin{aligned}\mathcal{CE}_A &= 827 + 100\% \times 135 + 100\% \times 261 + 100\% \times 220 + 0\% \times 1385 + \\ &\quad 100\% \times 100\% \times 63 + 100\% \times 0\% \times 179 + 100\% \times 0\% \times 37 \\ &= 1\,506.00\,\text{tCO}_2\text{e}\end{aligned}$$

Generally, an equity share of 50% or more induces a financial/operational control, which implies that 100% of carbon emissions are consolidated and reported by the parent company. By contrast, the consolidation factor may be equal to 0% if the parent company has no control, even in the case it has a significant equity share (*e.g.*, between 30% and 40%).

### 9.1.3 Scope 1, 2 and 3 emissions

The GHG Protocol corporate standard classifies a company's greenhouse gas emissions in three scopes[6]:

- Scope 1 denotes direct GHG emissions occurring from sources that are owned and controlled by the issuer.
- Scope 2 corresponds to the indirect GHG emissions from the consumption of purchased electricity, heat or steam.
- Scope 3 are other indirect emissions (not included in scope 2) of the entire value chain. They can be divided into two main categories[7]:
  - Upstream scope 3 emissions are defined as indirect carbon emissions related to purchased goods and services.
  - Downstream scope 3 emissions are defined as indirect carbon emissions related to sold goods and services.

Scope 1 emissions are also called direct emissions, whereas indirect emissions encompass both scope 2 and 3 GHG emissions. Unlike scope 1 and 2, scope 3 is an optional reporting category.

**Remark 99** *The GHG protocol defines "the operational boundary as the scope of direct and indirect emissions for operations that fall within a company's established organizational boundary. The operational boundary (scope 1, scope 2, scope 3) is decided at the corporate level after setting the organizational boundary. The selected operational boundary is then uniformly applied to identify and categorize direct and indirect emissions at each operational level. The established organizational and operational boundaries together constitute a company's inventory boundary."*

Before explaining in fine detail the different scopes and their computation, we report six examples of carbon footprint reporting in Table 9.3. We consider the CDP database, since most of companies reporting to CDP use the GHG protocol framework. The CDP reporting framework is based on a questionnaire (see Box 9.2 on page 880). We first notice all the figures are not calculated. This is normal since scope 3 is not mandatory in the GHG protocol framework. When the sub-category is empty, we don't know whether it is equal to zero or a missing value, meaning that the company has not the capacity or implemented the method to compute it. In the case of Amazon, the sub-category end-of-life treatment of sold products is equal to zero and not an empty case. A second remark concerns the definition of the scope 2, because there are two approaches: location-based and market-based. How to read this table? If we consider the first company Amazon, its scope 1 emissions are equal to 9.62 $MtCO_2e$. For the scope 2 emissions, they are equal to 9.02 $MtCO_2e$ when they are calculated with the location-based method or 5.27 $MtCO_2e$ when they are calculated

[6] The latest version of corporate accounting and reporting standard can be found at www.ghgprotocol.org/corporate-standard.

[7] The upstream value chain includes all activities related to the suppliers whereas the downstream value chain refers to post-manufacturing activities.

Table 9.3: Examples of CDP reporting (carbon emissions in $tCO_2e$, reporting year 2020)

| Scope | Category | Sub-category | Amazon | Danone | ENEL | Pfizer | Netflix | Walmart |
|---|---|---|---|---|---|---|---|---|
| 1 | | | 9 623 138 | 668 354 | 45 255 000 | 654 460 | 30 883 | 7 236 499 |
| 2 | Location-based (2a) | | 9 019 786 | 864 710 | 4 990 685 | 551 577 | 28 585 | 11 031 800 |
| | Market-based (2b) | | 5 265 089 | 479 210 | 7 855 954 | 542 521 | 141 | 9 190 337 |
| 3 | Upstream | Purchased goods and services | 16 683 423 | 19 920 918 | | 2 526 537 | 765 208 | 130 200 000 |
| | | Capital goods | 13 202 065 | | | 191 894 | 116 366 | 645 328 |
| | | Fuel and energy related activities | 1 248 847 | 283 764 | 1 061 268 | 203 093 | 12 287 | 3 327 874 |
| | | Upstream transportation and distribution | 8 563 695 | 321 558 | 112 358 | 723 558 | 64 693 | 342 577 |
| | | Waste generated in operations | 16 628 | 152 789 | 3 161 | 14 940 | | 869 927 |
| | | Business travel | 313 043 | | | 35 128 | 41 439 | 37 439 |
| | | Employee commuting | 306 033 | | | 48 414 | 19 116 | 3 500 000 |
| | | Upstream leased assets | 1 223 903 | | | 30 522 | 131 | |
| | Downstream | Downstream transportation and distribution | 2 785 676 | 1 627 090 | | 7 295 | | 5 099 |
| | | Processing of sold products | | | | | | |
| | | Use of sold products | 1 426 543 | 1 885 548 | 46 524 860 | | 952 | 32 211 000 |
| | | End-of-life treatment of sold products | 0 | 782 649 | | | | 130 |
| | | Downstream leased assets | | | | | 349 | 130 000 |
| | | Franchises | | | | | | |
| | | Investments | | | | 36 839 | | |
| Total | Scope 1 + 2a | | 18 642 924 | 1 533 064 | 50 245 685 | 1 206 037 | 59 468 | 18 268 299 |
| | Scope 1 + 2b | | 14 888 227 | 1 147 564 | 53 110 954 | 1 196 981 | 31 024 | 16 426 836 |
| | Scope 3 upstream | | 41 557 637 | 20 679 029 | 1 176 787 | 3 774 086 | 1 019 240 | 138 923 145 |
| | Scope 3 downstream | | 4 212 219 | 4 295 287 | 46 524 860 | 44 134 | 1 301 | 32 346 229 |
| | Scope 3 | | 45 769 856 | 24 974 316 | 47 701 647 | 3 818 220 | 1 020 541 | 171 269 374 |
| | Scope 1 + 2a + 3 | | 64 412 780 | 26 507 380 | 97 947 332 | 5 024 257 | 1 080 009 | 189 537 673 |
| | Scope 1 + 2b + 3 | | 60 658 083 | 26 121 880 | 100 812 601 | 5 015 201 | 1 051 565 | 187 696 210 |

Source: CDP database as of 01/07/2022 & Author's computation.

with the market-based method. The fifteen sub-categories of scope 3 emissions are not aggregated, and each item is filled separately. The last of part of the table (from Scope 1 + 2a to Scope 1 + 2a + 3 is not included in the CDP questionnaire. These figures are calculated by summing the different items.

Box 9.2: CDP questionnaire for corporates

In order to report to CDP, companies must fill the CDP questionnaire on climate change, which is available at www.cdp.net/en/guidance/guidance-for-companies in HTML, Word and PDF formats. The full questionnaire has 129 pages and 16 sections. Emissions methodology corresponds to section C5, while emissions data are reported in section C6 with the following breakdown: scope 1 emissions (§C6.1), scope 2 emissions (§C6.3), scope 3 emissions (§C6.5) and emissions intensities (§C6.10).

### Scope 1 emissions

According to GHG Protocol (2004, page 40)GHG-Protocol, once the inventory boundary has been established, "*companies generally calculate GHG emissions using the following steps: (1) Identify GHG emissions sources; (2) Select a GHG emissions calculation approach; (3) Collect activity data and choose emission factors; (4) Apply calculation tools and (5) Roll-up GHG emissions data to corporate level. The identification step helps to categorize the GHG emission sources.*" The identification step consists in categorizing the GHG emissions in the four main source categories:

1. Stationary combustion: combustion of fuels in stationary equipment (*e.g.*, boilers, turbines, heaters, incinerators);

2. Mobile combustion: combustion of fuels in transportation devices (*e.g.*, automobiles, trucks, trains, airplanes, boats);

3. Process emissions: emissions from physical or chemical processes (*e.g.*, cement manufacturing, petrochemical processing, aluminum smelting);

4. Fugitive emissions: intentional and unintentional releases as well as fugitive emissions (*e.g.*, such as equipment leaks, coal piles, wastewater treatment, cooling towers).

Concretely, the company lists all the activities that result in a GHG emission, and allocates them to the three scopes. Then, we apply an emission factor to each activity and each gas:

$$E_{g,h} = A_h \cdot \mathcal{EF}_{g,h}$$

where $A_h$ is the $h^{\text{th}}$ activity rate (also called activity data) and $\mathcal{EF}_{g,h}$ is the emission factor for the $h^{\text{th}}$ activity and the $g^{\text{th}}$ gas. $A_h$ can be measured in volume, weight, distance, duration, surface, frequency, etc. Since $E_{g,h}$ is expressed in tonne, $\mathcal{EF}_{g,h}$ is measured in tonne per activity unit. For instance, if $A_h$ is measured in hectare, $EF_{g,h}$ is measured in tonne per hectare. In fact, the emission factor is a coefficient that attempts to quantify how much of a greenhouse gas is released into the atmosphere by an activity that releases that gas[8]. For each gas, we calculate the total emissions:

$$E_g = \sum_{h=1}^{n_A} E_{g,h} = \sum_{h=1}^{n_A} A_h \cdot \mathcal{EF}_{g,h}$$

where $n_A$ is the number of activities. Finally, we estimate the carbon emissions by applying the right GWP and summing up all the gases:

$$\mathcal{CE} = \sum_{g=1}^{n_G} \text{gwp}_g \cdot E_g$$

where $n_G$ is the number of gases[9]. Therefore, the compact formula is:

$$\mathcal{CE} = \sum_{g=1}^{n_G} \text{gwp}_g \cdot \left( \sum_{h=1}^{n_A} A_h \cdot \mathcal{EF}_{g,h} \right)$$

The carbon footprint of the company can be split into activities:

$$\mathcal{CE} = \sum_{h=1}^{n_A} A_h \left( \sum_{g=1}^{n_G} \text{gwp}_g \cdot \mathcal{EF}_{g,h} \right) = \sum_{h=1}^{n_A} A_h \cdot \mathcal{EF}_h = \sum_{h=1}^{n_A} \mathcal{CE}_h$$

where $\mathcal{EF}_h$ and $\mathcal{CE}_h$ are the global emission factor and carbon emissions related to the $h^{\text{th}}$ activity. We can also aggregate several activities:

$$\mathcal{CE}_{\mathcal{A}} = \sum_{h \in \mathcal{A}} \mathcal{CE}_h = \sum_{h \in \mathcal{A}} A_h \cdot \mathcal{EF}_h$$

where $\mathcal{A}$ is the set of activities. It may happen that some emission factors are defined without a reference to a specific gas (*e.g.*, $CO_2$ or $CH_4$). In this case, the emission factor is a synthetic measure which already take into account the GWP of the gases:

$$\mathcal{EF}_h = \sum_{g=1}^{n_G} \text{gwp}_g \cdot \mathcal{EF}_{g,h}$$

[8] For example, how many kg of GHG are emitted by 1 kWh of natural gas?
[9] $n_G$ is equal to six in the GHG Protocol.

The expression of the carbon footprint becomes:

$$\mathcal{CE} = \sum_{h \in \mathcal{A}_1} A_h \left( \sum_{g=1}^{n_G} \text{gwp}_g \cdot \mathcal{EF}_{g,h} \right) + \sum_{h \in \mathcal{A}_2} A_h \cdot \mathcal{EF}_h$$

where $\mathcal{A}_1$ and $\mathcal{A}_2$ are the sets of activities without and with synthetic emission factors.

The choice of data inputs is codified by IPCC (2006, 2019):

- Tier 1 methods use global default emission factors;
- Tier 2 methods use country-level or region-specific emission factors;
- Tier 3 methods use directly monitored or site-specific emission factors.

We can find emission factors in several sources: IPCC Emission Factor Database (Box 9.3), National Inventory Reports[10] (NIRs), country emission factor databases[11], international agencies or academic publications. In the US, the emission factors are calculated by the Environmental Protection Agency (US EPA). In the UK, this is the National Atmospheric Emissions Inventory (NAEI) agency, which is in charge to define the emission factors. In France, the database is managed by ADEME (Agence de l'Environnement et de la Maîtrise de l'Energie) and contains about 5 300 validated emission factors. Generally, we can download these emission factors in an Excel or PDF file.

Let us see an example. We consider the GHG inventory document[12] published by Enel. The scope 1 is based on the following activities: (1) combustion of fossil fuels in electricity generation activities; (2) combustion of fossil fuels in generators used for electricity generation and distribution activities; (3) combustion of fossil fuels in vehicles under the Company's control; (4) combustion of fuels for heating offices and canteens; (5) $CH_4$ leakage in gas-fired thermoelectric power plants; (6) $SF_6$ losses in electricity generation and distribution activities; (7) HFCs gas losses from cooling systems; (8) $NF_3$ losses from the production of solar panels; (9) Transportation of fuel (LNG and coal) on vessels under own operational control and (10) $CH_4$ emissions from the decomposition of organic matter in hydroelectric basins. For the calculations, they use the parameter values of IPCC (2006) for emission factors and the GWP figures of IPCC (2014a). They obtained the following results in 2021 expressed in $ktCO_2e$:

| | $CO_2$ | $CH_4$ | $N_2O$ | $NF_3$ | $SF_6$ | HFCs | Total |
|---|---|---|---|---|---|---|---|
| Electricity power generation | 50 643.54 | 385.25 | 98.14 | 0.014 | 31.15 | 10.22 | 51 168.32 |
| Electricity distribution | 208.33 | 0.24 | 0.45 | | 111.62 | | 320.64 |
| Real estate | 79.87 | 0.22 | 1.24 | | | | 81.30 |
| Total | 50 931.72 | 385.71 | 99.83 | 0.014 | 142.77 | 10.22 | 51 750.26 |

The scope 1 emissions of Enel is then equal to 51.75 $MtCO_2e$. The contribution of $CO_2$ is the most important since it represents 98.4% of the total emissions, implying that the other gases have a small impact. In terms of activities, GHG emissions are mainly located in the electricity power generation. Buildings has a contribution of 0.2%.

[10] The NIR reports can be found at the UNFCCC website: https://unfccc.int/ghg-inventories-annex-i-parties/2021.

[11] Here are some websites: www.epa.gov/climateleadership/ghg-emission-factors-hub (US), https://naei.beis.gov.uk/data/ef-all (UK), https://bilans-ges.ademe.fr (France), www.dcceew.gov.au/climate-change/publications/national-greenhouse-accounts-factors-2021 (Australia), www.isprambiente.gov.it (Italy), https://publications.gc.ca/site/eng/9.911206/publication.html (Canada).

[12] Enel (2022). *Quantification and Reporting of Greenhouse Gas Emissions in Accordance with the Corporate GHG Protocol*. 12th April 2022, www.enel.com/investors/sustainability.

Box 9.3: IPCC emission factor database (EFDB)

The IPCC emission factor database[a] (EFDB) is a database on various parameters to be used in calculation of anthropogenic emissions by sources and removals by sinks of greenhouse gases. It contains the IPCC default data[b], and data from peer-reviewed journals and other publications including national inventory reports (NIRs). The database includes emission factors for five categories:

1. Energy (fuel combustion activities, fugitive emissions from fuels, carbon dioxide transport and storage);
2. Industrial processes and product use (mineral industry, chemical industry, metal industry, non-energy products from fuels and solvent use, electronics industry, product uses as substitutes for ozone depleting substances, other product manufacture and use, other);
3. Agriculture, forestry, and other land use (livestock, land, aggregate sources and non-CO2 emissions sources on land, other);
4. Waste (solid waste disposal, biological treatment of solid waste, incineration and open burning of waste, wastewater treatment and discharge, other)
5. Other (Indirect $N_2O$ emissions from the atmospheric deposition of nitrogen in $NO_x$ and $NH_3$, other)

Some figures of the library are given in Table 9.4. We notice that they may depend on the region and technical criteria. The unit is also important. For instance, if the emission factors are expressed in tCarbon/TeraJoule (tonne of carbon per terajoule energy), we multiply the emission factor $\boldsymbol{\mathcal{EF}}$ (in tC/TJ) by the energy consumption $C$ (in TJ) to obtain the carbon content (in tonnes of carbon). Since one tonne of $CO_2$ contains 0.2727 tonne of carbon, we then deduce that the $CO_2$ emissions are equal to $\dfrac{C \cdot \boldsymbol{\mathcal{EF}}}{0.2727}$ $tCO_2e$. In this case, the activity data corresponds to the energy consumption.

[a] The website is www.ipcc-nggip.iges.or.jp/EFDB.

[b] Revised 1996 IPCC Guidelines, IPCC Good Practice Guidance and Uncertainty Management in National Greenhouse Gas Inventories, IPCC Good Practice Guidance for Land Use, Land-Use Change and Forestry, 2006 IPCC Guidelines for National Greenhouse Gas Inventories and 2013 Supplement to the 2006 IPCC Guidelines for National Greenhouse Gas Inventories: Wetlands.

Table 9.4: Examples of emission factors (EFDB, IPCC)

| Category | Description | Gas | Region | Value | Unit |
|---|---|---|---|---|---|
| Iron and steel production | Integrated facility | $CO_2$ | Canada | 1.6 | t/tonne |
| | Electrode consumption from steel produced in electric arc furnaces | $CO_2$ | Global | 5.0 | kg/tonne |
| | Steel processing (rolling mills) | $N_2O$ | Global | 40 | g/tonne |
| Manufacture of solid fuels | Metallurgical coke production | $CO_2$ | Global | 0.56 | t/tonne |
| | | $CH_4$ | Global | 0.1 | g/tonne |
| Fuel combustion activities | Crude oil | $CO_2$ | Global | 20 | tCarbon/TeraJoule |
| | Natural gas | $CO_2$ | Global | 15.3 | tCarbon/TeraJoule |
| | Ethane | $CO_2$ | Global | 16.8 | tCarbon/TeraJoule |
| Integrated circuit or semiconductor | Semiconductor manufacturing (silicon) | $CF_4$ | Global | 0.9 | kg/$m^2$ |
| Cement production | Cement production | $CO_2$ | Global | 0.4985 | t/tonne |
| Horses | Enteric fermentation | $CH_4$ | Global | 18 | kg/head/year |
| | Manure management (annual average temperature is less than 15oC) | $CH_4$ | Developed countries | 1.4 | kg/head/year |
| | Manure management (annual average temperature is between 15oC and 25oc) | $CH_4$ | Developed countries | 2.1 | kg/head/year |
| Buffalo | Enteric fermentation | $CH_4$ | Global | 55 | kg/head/year |
| Poultry | Manure management (annual average temperature is less than 15oC) | $CH_4$ | Developed countries | 0.078 | kg/head/year |
| | Manure management (annual average temperature is between 15oC and 25oc) | $CH_4$ | Developed countries | 0.117 | kg/head/year |
| | Manure management (annual average temperature is greater than 25oC) | $CH_4$ | Developed countries | 0.157 | kg/head/year |
| | Manure management (annual average temperature is greater than 25oC) | $CH_4$ | Developing countries | 0.023 | kg/head/year |

Source: EFDB, www.ipcc-nggip.iges.or.jp/EFDB.

### Scope 2 emissions

Scope 2 is "*an indirect emission category that includes GHG emissions from the purchased or acquired electricity, steam, heat, or cooling consumed*" (GHG Protocol, 2015, page 34). There are then four forms of energy that are tracked in scope 2:

- Electricity
  People use electricity for operating machines, lighting, heating, cooling, electric vehicle charging, computers, electronics, public transportation systems, etc.
- Steam
  Industries use steam for mechanical work, heating, propulsion, driven turbines in electric power plants, etc.
- Heat
  Buildings use heat to control inside temperature and heat water, while the industrial sector uses heat for washing, cooking, sterilizing, drying, etc. Heat may be produced from electricity, solar heat processes or thermal combustion.
- Cooling
  It is produced from electricity or though the processes of forced air, conduction, convection, etc.

Scope 2 includes indirect emissions from generation only. For instance, the distribution of energy within a grid is tracked in scope 3. In Figures 9.6–9.9, we report the different cases that are illustrated in the GHG Protocol: if the consumed electricity comes from owned/operated equipment, no scope 2 emissions are reported (Figure 9.6); if the consumed electricity comes from a direct line transfer or the grid[13], the consumer of the energy reports the emissions in scope 2 (Figures 9.7 and (Figure 9.8); if some consumed electricity comes from the owned/operated equipment, and some is purchased from the grid, the operator (company $A$) has both scope 1 emissions from energy generation, and scope 3 emissions from energy purchased on the grid (Figure 9.9).

Figure 9.6: Energy production and consumption from owned/operated generation

Figure 9.7: Direct line energy transfer

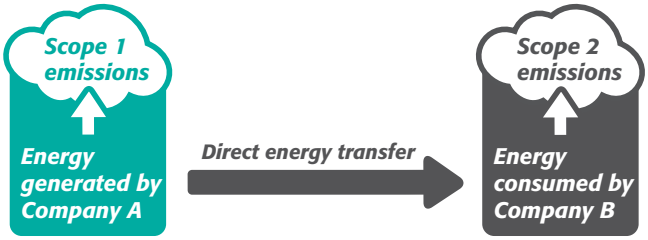


Source: GHG Protocol (2015, Figures 5.1 and 5.2, pages 35-36).

[13] A grid is "*a system of power transmission and distribution lines under the control of a coordinating entity or grid operator, which transfers electrical energy generated by power plants to energy users — also called a power grid.*" (CDP, 2022, page 8).

Figure 9.8: Electricity production on a grid

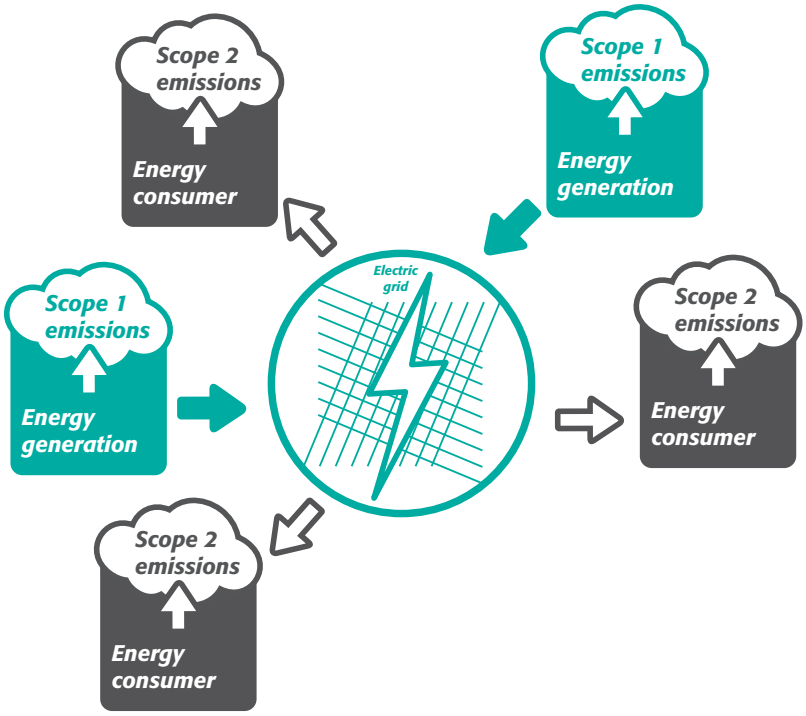


Source: GHG Protocol (2015, Figure 5.4, page 38).

Figure 9.9: Facility consuming both energy generated on-site and purchased from the grid

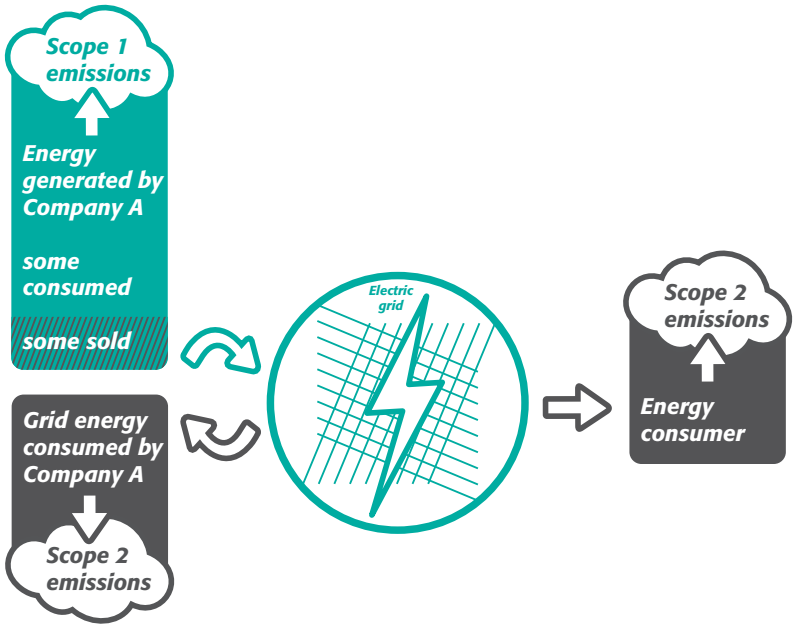


Source: GHG Protocol (2015, Figure 5.3, page 37).

Scope 2 emissions are calculated using activity data and emission factors[14] expressed in MWh and $tCO_2e/MWh$:

$$\mathcal{CE} = \sum_s A_s \cdot \mathcal{EF}_s$$

where $A_s$ is the amount of purchased electricity for the energy generation source $s$ and $\mathcal{EF}_s$ is the emission factor of the source $s$. The source can be an electricity supplier[15], a specific or country grid, a specific power station, etc.

**Remark 100** *A Megawatt-hour is the common billing unit for electrical energy delivered to consumers. 1 000 MWh is equivalent to 3.6 TeraJoule (TJ). The TJ unit is used by IPCC (2006) (see Table 9.4 on page 884). A third energy unit is also used to defined emissions factors in North America (Canada and the US) and the United Kingdom: the British thermal unit or Btu (1 Btu is equivalent to 1.0551 KJ or 0.2931 Wh).*

**Example 35** *We consider a company, whose electricity consumption is equal to* 2 000 *MWh per year. The electricity comes from two sources:* 60% *from a direct line with an electricity supplier (source* $S_1$*) and* 40% *from the country grid (source* $S_2$*). The emission factors are respectively equal to* 200 *and* 350 $gCO_2e/kWh$.

The electricity consumption from source $S_1$ is equal to $60\% \times 2\,000 = 1\,200$ MWh or 1 200 000 kWh. We deduce that the carbon emissions from this source is:

$$\mathcal{CE}(S_1) = \left(1.2 \times 10^6\right) \times 200 = 240 \times 10^6 \text{ } gCO_2e = 240 \text{ } tCO_2e$$

For the second source, we obtain:

$$\mathcal{CE}(S_2) = \left(0.8 \times 10^6\right) \times 350 = 280 \times 10^6 \text{ } gCO_2e = 280 \text{ } tCO_2e$$

We deduce that the scope 2 carbon emissions of this company is equal to 520 $tCO_2e$.

Let us consider again the GHG inventory report of Enel (page 882). We remind that the scope 1 emissions of Enel is equal to 51 750 265 $tCO_2e$. In the same document, we learn that the ratio between scope 1 emissions and the total electricity production is equal to 227 $gCO_2e/kWh$ (or 0.227 $tCO_2e/MWh$). We deduce that the 2021 electricity production of Enel is [16]:

$$A = \frac{51,750\,265}{0.227} = 227\,974\,735 \text{ MWh} = 228 \text{ TWh}$$

Two main methods are available for accounting scope 2 emissions:

- Location-based method
  In this approach, the company uses the average emission factor of the region or the country. For instance, if the electricity consumption is located in France, the company can use the emission intensity of the French energy mix;

[14] This approach is also known as the emission rate approach.

[15] The largest electricity companies are EDF, Enel, Engie, E.ON, Fortum, Marubeni, Siemens, State Grid Corporation of China, Tokyo Electric Power, and Uniper.

[16] In this example, we inverse the equation in order to estimate the activity data of an electricity supplier:

$$A = \frac{\mathcal{CE}}{\mathcal{EF}}$$

where $\mathcal{CE}$ is the scope 1 emissions of the utility company.

- Market-based method
  This approach reflects the GHG emissions from the electricity that the company has chosen in the market. This means that the scope 2 carbon emissions will depend on the scope 1 carbon intensity of the electricity supplier.

Under the market-based method, an emission factor is associated to each electricity contract. To be relevant, contacts must meet some quality criteria and concern some specific instruments: energy attribute certificates [17] (*e.g.*, RECs, GOs), power purchase agreements with energy generators and green electricity products.

Figure 9.10: Emission factor in $gCO_2e/kWh$ of electricity generation (European Union, 1990–1992)

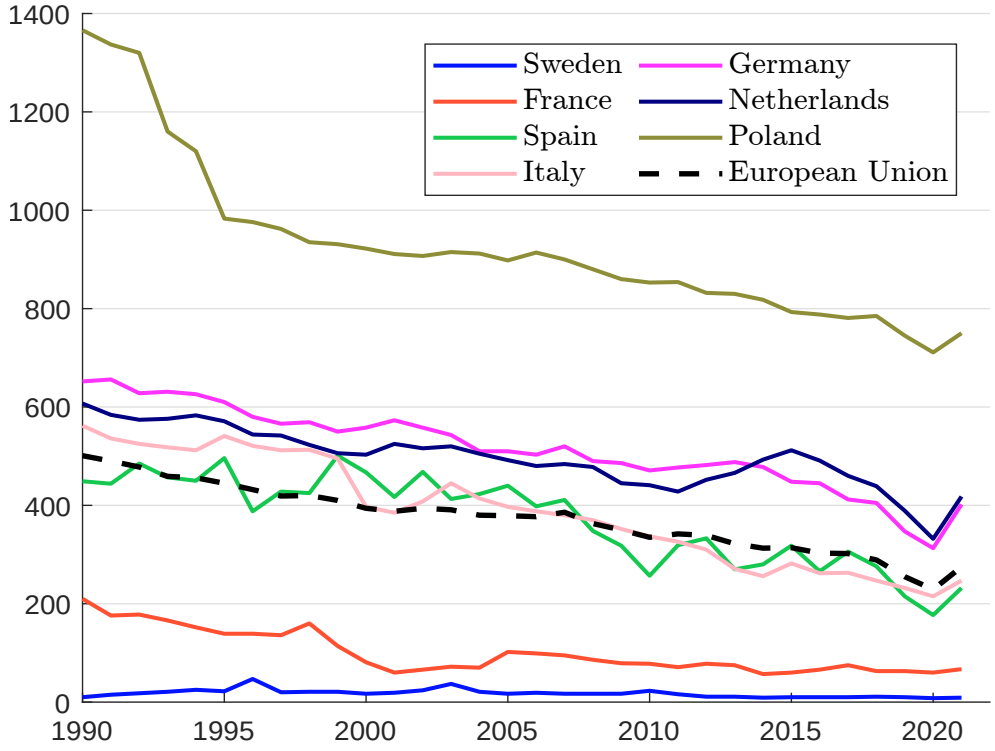


Source: European Environment Agency (2022), www.eea.europa.eu/data-and-maps & Author's calculations.

The location-based method depends on the emission factor of the regional, subnational or national grid. Its value highly depends on the energy mix and the grid infrastructure. For instance, we report the evolution of national emission factors of some European countries in Figure 9.10. We notice that they tend to decrease since thirty years and they differ from one country to another. On average, the emission factor is equal to 275 $gCO_2e/kWh$ in the European Union in 2021. The two extreme countries are Sweden (9 $gCO_2e/kWh$) and Poland (750 $gCO_2e/kWh$). The reason is that most of Sweden's electricity supply comes from hydropower and nuclear, while Poland produces 83% of its electricity from fossil fuels (and 72% from coal). Emission factors for several region and countries in the world are given in Table 9.5. We notice the high heterogeneity of the figures. The continent with the lowest value is South America (204 $gCO_2e/kWh$) while Asia has the largest emission factor (539 $gCO_2e/kWh$). Two countries which are geographically close may have different

[17] REC (or renewable energy certificate) is an energy attribute certificate used in Australia, Canada, India and the US, while GO (guarantee of origin) is an energy attribute certificate used in Europe.

emission factors. This is the case of France and Germany (58 vs. 354 $gCO_2e/kWh$), Canada and the US (128 vs. 380 $gCO_2e/kWh$), etc.

Table 9.5: Emission factor in $gCO_2e/kWh$ of electricity generation in the world

| Region | $\mathcal{EF}$ | Country | $\mathcal{EF}$ | Country | $\mathcal{EF}$ | Country | $\mathcal{EF}$ |
|---|---|---|---|---|---|---|---|
| Africa | 484 | Australia | 531 | Germany | 354 | Portugal | 183 |
| Asia | 539 | Canada | 128 | India | 637 | Russia | 360 |
| Europe | 280 | China | 544 | Iran | 492 | Spain | 169 |
| North America | 352 | Costa Rica | 33 | Italy | 226 | Switzerland | 47 |
| South America | 204 | Cuba | 575 | Japan | 479 | United Kingdom | 270 |
| World | 442 | France | 58 | Norway | 26 | United States | 380 |

Source: https://ourworldindata.org/grapher/carbon-intensity-electricity

**Example 36** *We consider a French bank, whose activities are mainly located in France and the Western Europe. Below, we report the energy consumption (in MWh) by country:*

| | | | | | | | |
|---|---|---|---|---|---|---|---|
| Belgium | 125 807 | France | 1 132 261 | Germany | 71 890 | Ireland | 125 807 |
| Italy | 197 696 | Luxembourg | 33 069 | Netherlands | 18 152 | Portugal | 12 581 |
| Spain | 61 106 | Switzerland | 73 148 | UK | 124 010 | World | 37 742 |

If we consider a Tier 1 approach, we can estimate scope 2 emissions of the bank by computing the total activity data and multiplying by the global emission factor. Since we have twelve sources, we obtain:

$$A = \sum_{s=1}^{12} A_s = 125\,807 + 1\,132\,261 + \ldots + 37\,742 = 2\,013\,269 \text{ MWh}$$

and:

$$\begin{aligned} \mathcal{CE} &= A \cdot \mathcal{EF}_{World} \\ &= \left(2\,013{,}269 \times 10^3\right) \times 442 \\ &= 889\,864\,898\,000 \text{ gCO}_2\text{e} \\ &= 889.86 \text{ ktCO}_2\text{e} \end{aligned}$$

Another Tier 1 approach is to consider the emission factor of the European Union, because the rest of the world represents less than 2% of the electricity consumption. Using $\mathcal{EF}_{EU} = 275$, we obtain $\mathcal{CE} = 553.65$ $ktCO_2e$. The third approach uses a Tier 2 method by considering the emission factor of each country. In this case, we have to collect the data. We use figures in Table 9.5 and the following emission factors: Belgium (143); Ireland (402); Luxembourg (68) and Netherlands (331). It follows that:

$$\begin{aligned} \mathcal{CE} &= \sum_{s=1}^{12} A_s \cdot \mathcal{EF}_s \\ &= \left(125\,807 \times 143 + 1\,132\,261 \times 58 + \ldots + 124\,010 \times 270 + 37\,742 \times 442\right) \times \frac{10^3}{10^9} \\ &= 278.85 \text{ ktCO}_2\text{e} \end{aligned}$$

We notice that the estimated scope 2 emissions of this bank are sensitive to the chosen approach.

The market-based accounting approach requires to track the electricity of each supplier. For that, the company can use reliable tracking systems (North American REC, European Energy Certificate System GO, International REC standard, TIGR registry) and supplier-based contactual instruments. This Tier 1 approach is based on contract-specific emission factors. Nevertheless, when they are not available, the company can use supplier-based average and residual mix emission factors.

**Example 37** *We consider a Norwegian company, whose current electricity consumption is equal to* 1 351 *Mwh.* 60% *of the electricity comes from the Norwegian hydroelectricity and the GO system guarantees that this green electricity emits* 1 $gCO_2e/kWh$.

If we assume that the remaining 40% of the electricity consumption comes from the Norwegian grid[18], the market-based scope 2 emissions of this company are equal to:

$$\begin{aligned} \mathcal{CE} &= \frac{10^6 \times 60\% \times 1 + 10^6 \times 40\% \times 26}{10^6} \\ &= 11 \text{ ktCO}_2\text{e} \end{aligned}$$

The market-based approach may reduce the scope 2 emissions when the company purchases green electricity. For instance, the emission factors in France are the following: 6 for nuclear, 418 for natural gas, 730 for fuel oil and 1 058 for coal. In Table 9.6, we have reported the life cycle emission factors for several technologies. Even if these figures depend on many parameters (vintage, country, etc.) and the ranges are relatively wide, we clearly observe an ordering. Wind, nuclear, hydro and solar electricity generates less GHG emissions than gas, fuel oil and coal.

Table 9.6: Emission factor in $gCO_2e$/KWh from electricity supply technologies (IPCC, 2014a; UNECE, 2022)

| Technology | Characteristic | IPCC | | UNECE | |
|---|---|---|---|---|---|
| | | Mean | Min–Max | Mean | Min–Max |
| Wind | Onshore | 11 | 7–56 | 12 | 8–16 |
| | Offshore | 12 | 8–35 | 13 | 13–23 |
| Nuclear | | 12 | 3–110 | 6 | |
| Hydro power | | 24 | 1–2200 | 11 | 6–147 |
| Solar power | CSP | 27 | 9–63 | 32 | 14–122 |
| | Rooftop (PV) | 41 | 26–60 | 22 | 9–83 |
| | Utility/Ground (PV) | 48 | 18–180 | 20 | 8–82 |
| Geothermal | | 38 | 6–79 | | |
| Biomass | Dedicated | 230 | 130–420 | | |
| Gas | CCUS | 169 | 90-370 | 130 | 92–221 |
| | Combined cycle | 490 | 410–650 | 430 | 403–513 |
| Fuel oil | | | 510–1170 | | |
| Coal | CCUS | 161 | 70–290 | 350 | 190–470 |
| | PC | 820 | 740–650 | 1 000 | 912–1095 |

CSP: concentrated solar power; PV: photovoltaic power; CCUS: carbon capture, use, and storage; PC: pulverized coal.

[18]The emission factor for Norway is 26 $gCO_2e$/kWh.

Let us consider again the example of Enel (page 882). They obtained the following figures (expressed in $ktCO_2e$):

| | Electricity purchased from the grid | Losses on the distribution grid | Total |
|---|---|---|---|
| Location-based | 1 336.67 | 2 966.52 | 4 303.18 |
| Market-based | 2 351.00 | 4 763.15 | 7 114.15 |

The first category derives from the generation of electricity purchased and consumed by Enel (electricity consumption taken from the network for civil use or for energy generation in thermoelectric and hydroelectric plants). The second category includes indirect emissions due to dissipated energy emissions from technical losses from Enel's distribution network and from the transmission system. We notice that this second category represented 67% and 69% of scope 2 emissions. Curiously, the market-based figure is greater than the location-based approach: 7.11 vs. 4.30 $MtCO_2e$.

We consider the CDP database and compare the location-based and market-based values for the year 2020. Statistics are reported in Table 9.7. Less than 1% of issuers have declared zero scope 2 carbon emissions with the location-based approach. This figure becomes 8.78% when we consider the market-based approach. 70% of issuers have greater location-based emissions than market-based emissions. About 10% have the same value, meaning that these issuers have certainly used the mix residual approach to compute the scope 2 emissions with the market-based approach. The mean variation ratio[19] is equal to +26.59%. This result is explained by the frequency asymmetry, but also by the fact that the variation is higher for issuers that have greater location-based emissions than market-based emissions (+43.29% vs. −22.04%).

Table 9.7: Statistics of CDP scope 2 emissions (2020)

| | $\mathcal{CE}_{\text{loc}} = 0$ | $\mathcal{CE}_{\text{loc}} = \mathcal{CE}_{\text{mkt}} = 0$ | $\mathcal{CE}_{\text{mkt}} = 0$ |
|---|---|---|---|
| Frequency | 0.89% | 0.39% | 8.78% |
| | $\mathcal{CE}_{\text{loc}} > \mathcal{CE}_{\text{mkt}}$ | $\mathcal{CE}_{\text{loc}} = \mathcal{CE}_{mkt}$ | $\mathcal{CE}_{\text{loc}} < \mathcal{CE}_{\text{mkt}}$ |
| Frequency | 70.43% | 9.48% | 20.09% |
| Mean variation ratio | +43.89% | 0.00% | −22.04% |

Source: CDP database as of 01/07/2022 & Author's computation.

### Scope 3 emissions

Scope 3 emissions are all the indirect emissions in the company's value chain, apart from indirect emissions which are reported in scope 2. They are divided into fifteen categories of emissions: eight upstream categories and seven downstream categories (Table 9.8). We report below their description as it appears in GHG Protocol (2011, Table 5.4, pages 34-37):

1. Purchased goods and services (not included in categories 2-8)
   Extraction, production, and transportation of goods and services purchased or acquired by the company;

2. Capital goods
   Extraction, production, and transportation of capital goods purchased or acquired by the company;

[19] The variation ratio is equal to $\dfrac{CE_{\text{loc}} - CE_{\text{mkt}}}{\max\left(CE_{\text{loc}}, CE_{\text{mkt}}\right)}$.

Table 9.8: The scope 3 carbon emissions categories

| Upstream | Downstream |
|---|---|
| 1. Purchased goods and services | 1. Downstream transportation and distribution |
| 2. Capital goods | 2. Processing of sold products |
| 3. Fuel and energy related activities | 3. Use of sold products |
| 4. Upstream transportation and distribution | 4. End-of-life treatment of sold products |
| 5. Waste generated in operations | 5. Downstream leased assets |
| 6. Business travel | 6. Franchises |
| 7. Employee commuting | 7. Investments |
| 8. Upstream leased assets | 8. Other downstream |
| 9. Other upstream | |

3. Fuel- and energy-related activities (not included in scope 1 or 2)
   Extraction, production, and transportation of fuels and energy purchased or acquired by the company;

4. Upstream transportation and distribution
   Transportation and distribution of products purchased by the company between the company's tier 1 suppliers and its own operations; Transportation and distribution services purchased by the company, including inbound logistics, outbound logistics (*e.g.*, sold products), and transportation and distribution between the company's own facilities;

5. Waste generated in operations
   Disposal and treatment of waste generated in the company's operations;

6. Business travel
   Transportation of employees for business-related activities;

7. Employee commuting
   Transportation of employees between their homes and their work sites;

8. Upstream leased assets
   Operation of assets leased by the company (lessee);

9. Downstream transportation and distribution
   Transportation and distribution of products sold by the company between the company's operations and the end consumer (if not paid for by the company);

10. Processing of sold products
    Processing of intermediate products sold by downstream companies (*e.g.*, manufacturers);

11. Use of sold products
    End use of goods and services sold by the company;

12. End-of-life treatment of sold products
    Waste disposal and treatment of products sold by the company at the end of their life;

13. Downstream leased assets
    Operation of assets owned by the company (lessor) and leased to other entities;

14. Franchises
    Operation of franchises reported by franchisor;

15. Investments
    Operation of investments (including equity and debt investments and project finance).

All these categories share the principle that there is no double counting of emissions between the scopes. For instance, the transport categories do not concern vehicles and facilities owned, controlled or operated by the company, because their GHG emissions are already reported in scope 1 and 2. This means that the transport of employees with a company's vehicle is reported in scope 1 and 2, but not in scope 3. On the contrary, the public transport of employees is reported in scope 3.

Table 9.9: Scope 3 emission factors for business travel and employee commuting (United States)

| Vehicle type | $CO_2$ (kg/unit) | $CH_4$ (g/unit) | $N_2O$ (g/unit) | Unit |
|---|---|---|---|---|
| Passenger car | 0.332 | 0.0070 | 0.0070 | vehicle-mile |
| Light-duty truck | 0.454 | 0.0120 | 0.0090 | vehicle-mile |
| Motorcycle | 0.183 | 0.0700 | 0.0070 | vehicle-mile |
| Intercity rail (northeast corridor) | 0.058 | 0.0055 | 0.0007 | passenger-mile |
| Intercity rail (other routes) | 0.150 | 0.0117 | 0.0038 | passenger-mile |
| Intercity rail (national average) | 0.113 | 0.0092 | 0.0026 | passenger-mile |
| Commuter rail | 0.139 | 0.0112 | 0.0028 | passenger-mile |
| Transit rail (subway, tram) | 0.099 | 0.0084 | 0.0012 | passenger-mile |
| Bus | 0.056 | 0.0210 | 0.0009 | passenger-mile |
| Air travel (short haul, $<$ 300 miles) | 0.207 | 0.0064 | 0.0066 | passenger-mile |
| Air travel (medium haul, 300-2300 miles) | 0.129 | 0.0006 | 0.0041 | passenger-mile |
| Air travel (long haul, $>$ 2300 miles) | 0.163 | 0.0006 | 0.0052 | passenger-mile |

These factors are intended for use in the distance-based method defined in the scope 3 calculation guidance. If fuel data are available, then the fuel-based method should be used.

Source: US EPA (2020), Table 10, www.epa.gov, `ghg-emission-factors-hub.xlsx`.

The computation of scope 3 emissions requires specific emission factors. For example, Table 9.9 gives their values for business travel (category 6) and employee commuting (category 7) in the US. In the same document, we can find other scope 3 emissions factors (categories 4, 5, 9 and 12). Collecting data is not an easy task since there is no available comprehensive database at the global level. Nevertheless, we can find documented databases at the sector level. For instance, AGRIBALYSE provides references data on the environmental impacts of agricultural and food products through a database built according to the life cycle analysis (LCA) methodology[20]. Other databases can be found in the GHG Protocol website (https://ghgprotocol.org/life-cycle-databases). The

[20]The web site is https://doc.agribalyse.fr.

GHG protocol has also developed several calculation tools (cross-sector, country-specific, sector-specific and cities). With Quantis, they also provide scope 3 evaluator (S3E), which is a free web-based tool[21].

Since it may be sometimes difficult to manipulate physical units, the organizations have also developed monetary emission factors, which are expressed in $kgCO_2e/k\$$ or $kgCO_2e/k€$. Some figures are reported in Table 9.10. For example, a business air travel, whose cost is equal to \$1 000, induces a scope 3 emissions of 1 970 $kgCO_2e$ according to the scope 3 evaluator tool.

Table 9.10: Examples of monetary scope 3 emission factors

| Category | S3E | ADEME | Category | S3E | ADEME |
|---|---|---|---|---|---|
| Agriculture | 2 500 | 2 300 | Air transport | 1 970 | 1 190 |
| Construction | 810 | 360 | Education | 310 | 120 |
| Financial intermediation | 140 | 110 | Health and Social Work | 300 | 500 |
| Hotels and restaurants | 560 | 320 | Rubber and plastics | 1 270 | 800 |
| Telecommunications | 300 | 170 | Textiles | 1 100 | 600 |

Source: Scope 3 Evaluator (S3E), https://quantis-suite.com/Scope-3-Evaluator & ADEME, https://bilans-ges.ademe.fr.

Ducoulombier (2021) highlights the importance of scope 3 emissions, but also the lack of data robustness. Since the reporting of these indirect emissions remains voluntary, we observe heterogenous data in the CDP database with scope 3 items that are partially or not calculated. In this context, most of ESG data providers estimate scope 3 upstream and downstream values using statistical model or environmentally-extended input-output (EEIO) framework[22]. This means that the reported scope 3 emissions are rarely used.

**Remark 101** *In order to distinguish the different scopes, we use the following notations:* $\boldsymbol{\mathcal{SC}}_1$ *for scope 1 emissions,* $\boldsymbol{\mathcal{SC}}_2$ *for scope 2 emissions and* $\boldsymbol{\mathcal{SC}}_3 = \boldsymbol{\mathcal{SC}}_3^{\text{up}} + \boldsymbol{\mathcal{SC}}_3^{\text{down}}$ *for scope 3 emissions, where* $\boldsymbol{\mathcal{SC}}_3^{\text{up}}$ *and* $\boldsymbol{\mathcal{SC}}_3^{\text{down}}$ *refer to upstream and downstream scope 3 emissions. The cumulative emissions are then denoted by* $\boldsymbol{\mathcal{SC}}_{1-2} = \boldsymbol{\mathcal{SC}}_1 + \boldsymbol{\mathcal{SC}}_2$, $\boldsymbol{\mathcal{SC}}_{1-3}^{\text{up}} = \boldsymbol{\mathcal{SC}}_1 + \boldsymbol{\mathcal{SC}}_2 + \boldsymbol{\mathcal{SC}}_3^{\text{up}}$ *and* $\boldsymbol{\mathcal{SC}}_{1-3} = \boldsymbol{\mathcal{SC}}_1 + \boldsymbol{\mathcal{SC}}_2 + \boldsymbol{\mathcal{SC}}_3$.

### 9.1.4 Carbon emissions of investment portfolios

There are two main methods for measuring the carbon footprint of an investment portfolio. The first method if the financed emissions approach. In this case, the investor calculates the carbon emissions that are financed across both equity and debt. Generally, we use EVIC to estimate the value of the enterprise. It is "*the sum of the market capitalization of ordinary and preferred shares at fiscal year end and the book values of total debt and minorities interests*" (TEG, 2019b). Let $W$ be the wealth invested in the company, the financed emissions are equal to:

$$\boldsymbol{\mathcal{CE}}(W) = \frac{W}{\text{EVIC}} \cdot \boldsymbol{\mathcal{CE}}$$

In the case of a portfolio $(W_1, \ldots, W_n)$ where $W_i$ is the wealth invested in company $i$, we have:

$$\boldsymbol{\mathcal{CE}}(W) = \sum_{i=1}^{n} \boldsymbol{\mathcal{CE}}_i(W_i) = \sum_{i=1}^{n} \frac{W_i}{\text{EVIC}_i} \cdot \boldsymbol{\mathcal{CE}}_i \tag{9.3}$$

[21] The tool is available at https://quantis-suite.com/Scope-3-Evaluator.
[22] This model is studied in Section 8.4 on page 807.

where $\text{EVIC}_i$ and $\boldsymbol{\mathcal{CE}}_i$ are the enterprise value and carbon emissions of company $i$. It follows that $\boldsymbol{\mathcal{CE}}(W)$ is expressed in $\text{tCO}_2\text{e}$.

A second method is to use the ownership approach (Le Guenedal and Roncalli, 2022). In this case, we break down the carbon emissions between the stockholders of the company. Equation (9.3) becomes:

$$\boldsymbol{\mathcal{CE}}(W) = \sum_{i=1}^{n} \frac{W_i}{\text{MV}_i} \cdot \boldsymbol{\mathcal{CE}}_i = \sum_{i=1}^{n} \varpi_i \cdot \boldsymbol{\mathcal{CE}}_i \tag{9.4}$$

where $\text{MV}_i$ is the market value of company $i$ and $\varpi_i$ is the ownership ratio of the investor. Let $W = \sum_{i=1}^{n} W_i$ be the portfolio value. The portfolio weight of asset $i$ is given by:

$$w_i = \frac{W_i}{W}$$

We deduce that:

$$\varpi_i = \frac{W_i}{\text{MV}_i} = \frac{w_i \cdot W}{\text{MV}_i}$$

and:

$$\boldsymbol{\mathcal{CE}}(W) = \sum_{i=1}^{n} \frac{w_i \cdot W}{\text{MV}_i} CE_i = W \left( \sum_{i=1}^{n} w_i \cdot \frac{\boldsymbol{\mathcal{CE}}_i}{\text{MV}_i} \right) = W \left( \sum_{i=1}^{n} w_i \cdot \boldsymbol{\mathcal{CI}}_i^{\text{MV}} \right)$$

where $\boldsymbol{\mathcal{CI}}_i^{\text{MV}}$ is the market value-based carbon intensity of company $i$:

$$\boldsymbol{\mathcal{CI}}_i^{\text{MV}} = \frac{\boldsymbol{\mathcal{CE}}_i}{\text{MV}_i}$$

Since $\boldsymbol{\mathcal{CE}}(W)$ is a linear function of $W$, the carbon footprint of the portfolio is generally computed with $W = \$1$ mn and is expressed in $\text{tCO}_2\text{e}$ (per \$ mn invested).

**Remark 102** *The second approach is valid only for equity portfolios. To compute the market value (or the total market capitalization), we use the following approximation:*

$$\text{MV} = \frac{\text{MC}}{\mathcal{FP}}$$

*where* MC *and* $\mathcal{FP}$ *are the free float market capitalisation and percentage of the company.*

**Example 38** *We consider a \$100 mn investment portfolio with the following composition:* \$63.1 *mn in company A,* \$16.9 *mn in company B and* \$20.0 *mn in company C. The data are the following:*

| Issuer | Market capitalization (in \$ bn) | | | Debt | $\mathcal{FP}$ | $\boldsymbol{\mathcal{SC}}_{1-2}$ |
|---|---|---|---|---|---|---|
| | 31/12/2021 | 31/12/2022 | 31/01/2023 | (in \$ bn) | (in %) | (in $\text{ktCO}_2\text{e}$) |
| $A$ | 12.886 | 10.356 | 10.625 | 1.112 | 99.8 | 756.144 |
| $B$ | 7.005 | 6.735 | 6.823 | 0.000 | 39.3 | 23.112 |
| $C$ | 3.271 | 3.287 | 3.474 | 0.458 | 96.7 | 454.460 |

As of 31 January 2023, the EVIC value for company $A$ is equal to:

$$\text{EVIC}_A = \frac{10\,356}{0.998} + 1\,112 = \$11\,489 \text{ mn}$$

We deduce that the financed emissions are equal to:

$$\boldsymbol{\mathcal{CE}}_A(\$63.1 \text{ mn}) = \frac{63.1}{11\,489} \times 756.144 = 4.153 \text{ ktCO}_2\text{e}$$

If we assume that the investor has no bond in the portfolio, we can use the ownership approach:

$$\varpi_A = \frac{63.1}{(10\,625/0.998)} = 59.2695 \text{ bps}$$

The carbon emissions of the investment in company $A$ is then equal to:

$$\mathcal{CE}_A(\$63.1 \text{ mn}) = 59.2695 \times 10^{-4} \times 756.144 = 4.482 \text{ ktCO}_2\text{e}$$

Finally, we obtain the following results[23]:

| | Financed emissions | Carbon emissions |
|---|---|---|
| Company A | 4.153 | 4.482 |
| Company B | 0.023 | 0.022 |
| Company C | 2.356 | 2.530 |
| Portfolio | 6.532 | 7.034 |

### 9.1.5 Statistics

In what follows, we use the analysis done by Barahhou *et al.* (2022). We consider the Trucost dataset of carbon emissions as of 01/06/2022 and analyze the distribution of carbon emissions in 2019 for around 15 000 companies. We prefer to use the year 2019 instead of the year 2020, because the covid-19 crisis had a significant impact on the carbon footprint. In Figure 9.11, we have reported the scope 1 and 2 carbon emissions per GICS sector. We notice that including scope 2 has a limited impact, except for some low-carbon sectors such as Consumer Services, Information Technology and Real Estate. In Table 9.11, we have calculated the breakdown of carbon emissions. Scope 1 and 2 emissions represent 17.6 $\text{GtCO}_2\text{e}$, and the most important sector contributors are Utilities (34.4%), Materials (31.4%), Energy (14.0%) and Industrials (10.0%). This means that these 4 strategic sectors explain about 90% of scope 1 and 2 carbon emissions.

Table 9.11: Breakdown (in %) of carbon emissions in 2019

| Sector | $\mathcal{SC}_1$ | $\mathcal{SC}_2$ | $\mathcal{SC}_{1-2}$ | $\mathcal{SC}_3^{\text{up}}$ | $\mathcal{SC}_3^{\text{down}}$ | $\mathcal{SC}_3$ | $\mathcal{SC}_{1-3}$ |
|---|---|---|---|---|---|---|---|
| Communication Services | 0.1 | 5.1 | 0.8 | 1.5 | 0.2 | 0.4 | 0.5 |
| Consumer Discretionary | 1.7 | 9.7 | 2.9 | 14.1 | 10.2 | 10.8 | 9.1 |
| Consumer Staples | 2.3 | 6.7 | 2.9 | 18.6 | 1.6 | 4.4 | 4.1 |
| Energy | 15.0 | 8.5 | 14.0 | 14.1 | 40.1 | 36.0 | 31.2 |
| Financials | 0.7 | 1.8 | 0.9 | 2.6 | 1.8 | 2.0 | 1.7 |
| Health Care | 0.3 | 1.7 | 0.5 | 2.6 | 0.2 | 0.6 | 0.6 |
| Industrials | 10.2 | 8.9 | 10.0 | 15.6 | 24.2 | 22.8 | 20.0 |
| Information Technology | 0.6 | 6.8 | 1.5 | 4.9 | 2.3 | 2.7 | 2.5 |
| Materials | 29.8 | 40.7 | 31.4 | 20.2 | 13.5 | 14.6 | 18.2 |
| Real Estate | 0.3 | 2.8 | 0.6 | 1.1 | 1.0 | 1.0 | 0.9 |
| Utilities | 39.0 | 7.3 | 34.4 | 4.7 | 4.8 | 4.8 | 11.2 |
| Total (in $\text{GtCO}_2\text{e}$) | 15.1 | 2.6 | 17.6 | 10.3 | 53.7 | 64.0 | 81.6 |

Source: Trucost (2022) & Barahhou *et al.* (2022).

[23]For the financed emissions, we use the data as of 31 December 2022 while the ownership ratio is based on the current data (as of 31 January 2023). In this example, the data as of 31 December 2021 are never used.

Figure 9.11: 2019 carbon emissions per GICS sector in $GtCO_2e$ (scope 1 & 2)

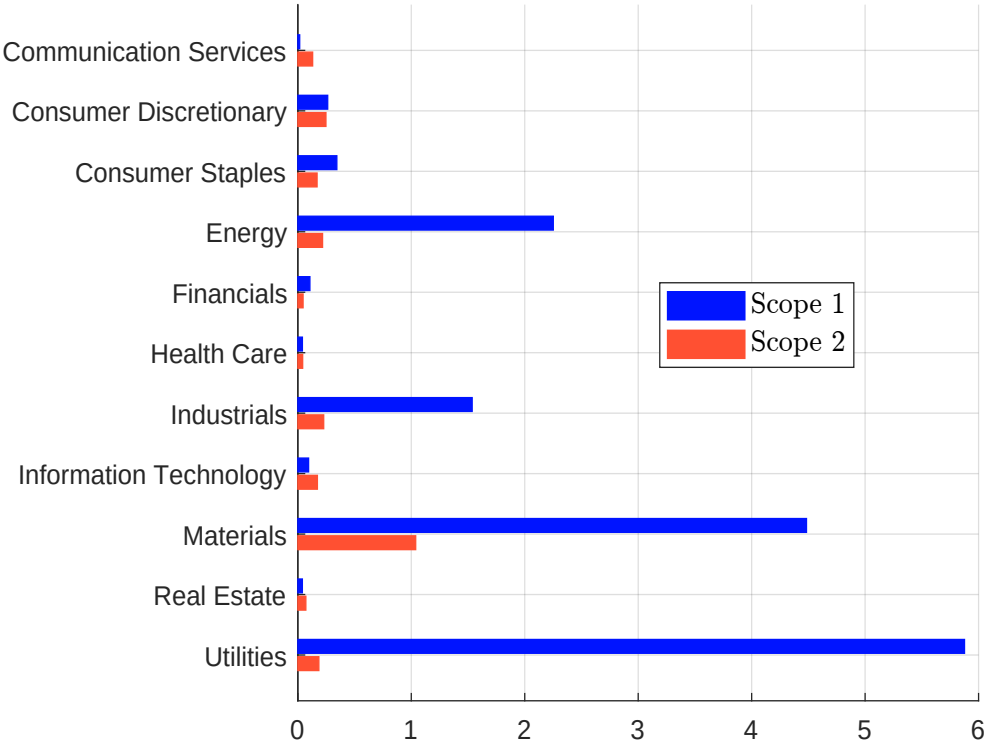


Source: Trucost (2022) & Barahhou *et al.* (2022).

Figure 9.12: 2019 carbon emissions per GICS sector in $GtCO_2e$ (scope 1, 2 & 3 upstream)

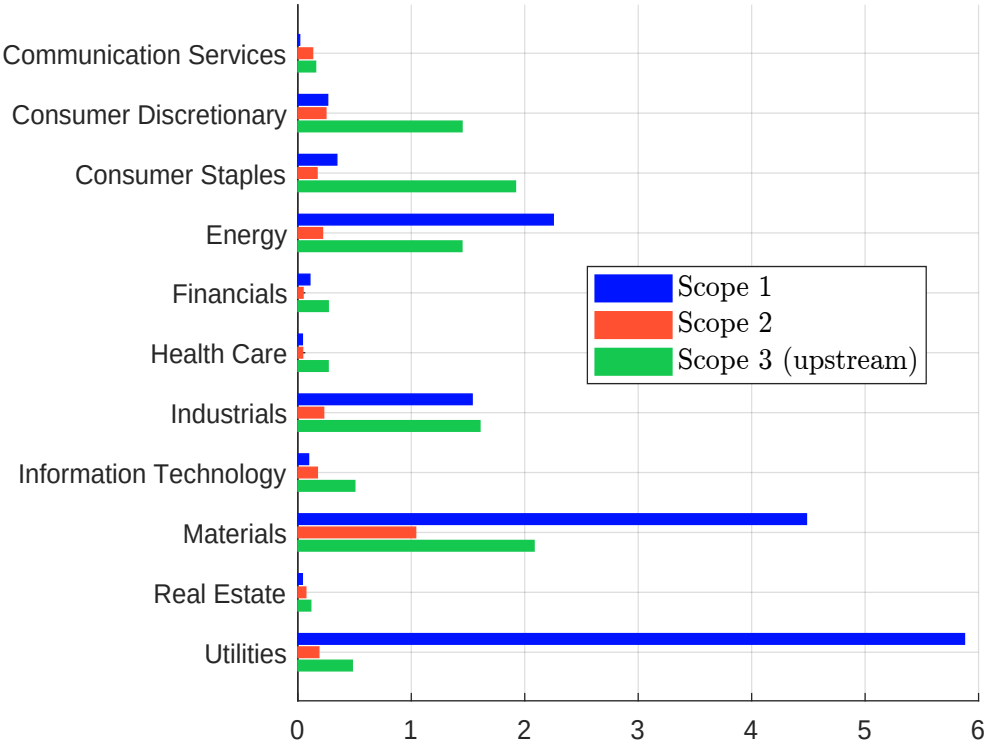


Source: Trucost (2022) & Barahhou *et al.* (2022).

Figure 9.13: 2019 carbon emissions per GICS sector in $GtCO_2e$ (scope 1, 2 & 3)

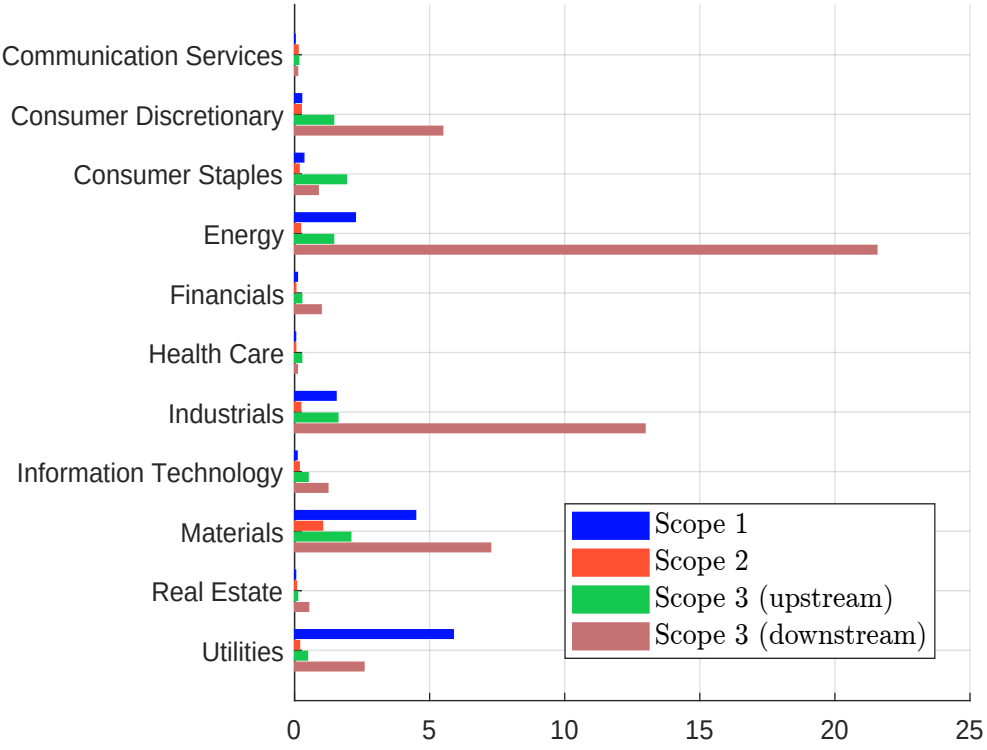


Source: Trucost (2022) & Barahhou *et al.* (2022).

In Figure 9.12, we observe that some sectors are highly impacted by the upstream scope 3 emissions. For instance, the ratio $\frac{\mathcal{SC}_3^{\text{up}}}{\mathcal{SC}_{1-2}}$ is greater than 2.5 for Consumer Discretionary, Consumer Staples and Health Care, and is close to 2 for Information Technology. Among the strategic sectors, Energy and Industrials are the most penalized whereas the upstream scope 3 emissions of Utilities is relatively small compared to its scope 1 emissions.

While the impact of the upstream scope 3 is significant, the impact of the downstream scope 3 is huge as demonstrated in Figure 9.13. Four sectors have very large downstream carbon emissions: Consumer Discretionary, Energy, Industrials and Materials. While Utilities has the most important contribution in terms of scope 1 and 2 since it represents 34.4% of carbon emissions, its contribution to scope 3 is relatively modest and is equal to 4.8%. Including or not scope 3, in particular the downstream carbon emissions, changes the whole picture of the breakdown between the sectors. Figure 9.14 is a visualisation of the sector contribution by considering the addition of several scopes. At each step, the contribution of Materials and Utilities decreases whereas it increases for Consumer Discretionary, Energy, Industrials and Information Technology. Among the most significant sectors[24], the behavior of Consumer Staples is singular since its contribution increases when adding scope 2 and upstream scope 3, but decreases when considering downstream scope 3.

**Remark 103** *When considering scope 3 emissions, double counting is a real issue. According to Table 9.11, the total carbon emissions is* 17.6 $GtCO_2e$ *for scope* $1+2$*, and* 81.6 $GtCO_2e$ *for scope* $1+2+3$*, while we estimate that the world emits about* 36 $GtCO_2e$ *per year.*

[24] They correspond to sectors that have a contribution greater than 2%.

Figure 9.14: Sector contribution in %

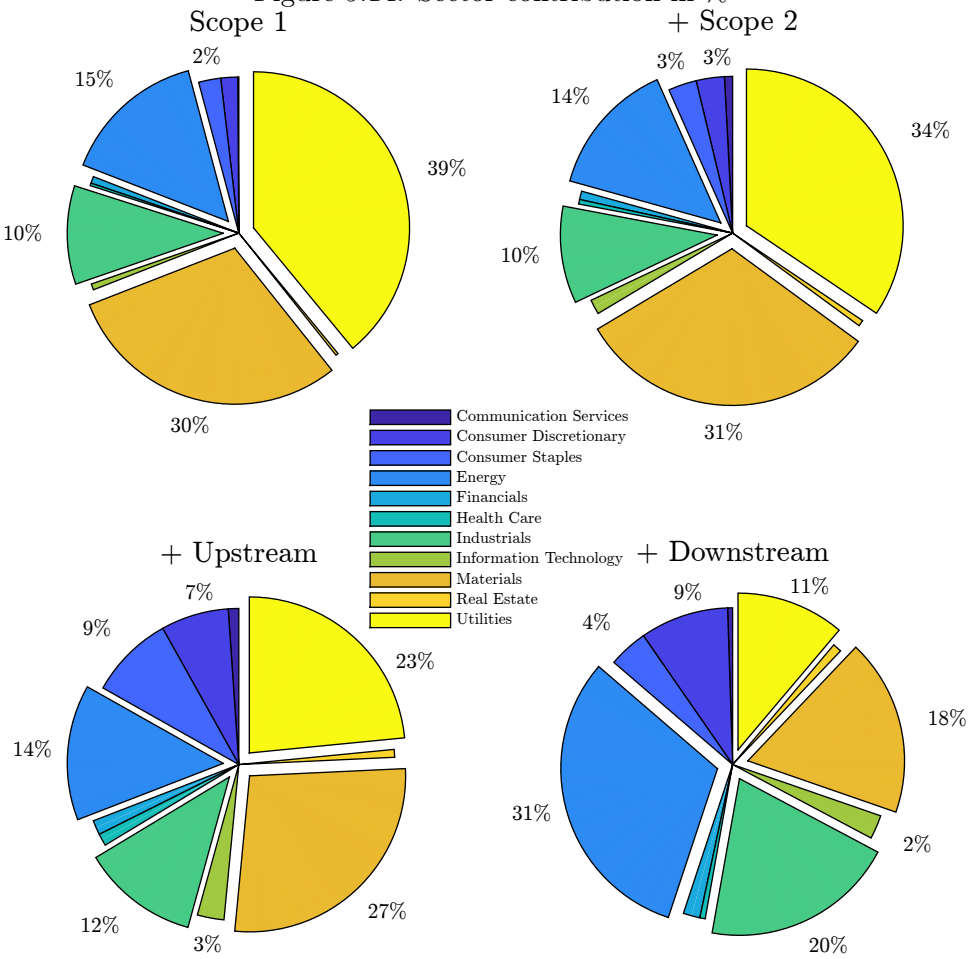


Source: Trucost (2022) & Barahhou *et al.* (2022).

In Figure 9.15, we draw the histogram of carbon emissions and indicate the 5% and 95% percentile values. We need to use a logarithmic scale, because the range is between some tonnes of $CO_2e$ to several dozen tonnes of $CO_2e$. This graph shows that it is difficult to compute the carbon footprint of a portfolio based on carbon emissions, because this metric is not homogeneous to the company size. This is why the carbon intensity metric is preferred in financial markets.

### 9.1.6 Negative emissions, avoided emissions, and carbon offsetting

Negative emissions, also known as carbon dioxide removal or CDR, is the process of removing $CO_2$ from the atmosphere. There are two main categories of negative emissions:

1. Natural climate solutions
   Examples include forest restoration and afforestation[25], reducing soil disturbance[26], etc.

[25] Afforestation is the process of creating a new forest (planting trees in an area where there was no forest in the past), while reforestation is the process of planting trees in areas where there was forest before.

[26] This is the practice of minimizing disturbance to the soil surface and structure, such as using minimum tillage or planting certain crops that protect the soil.

Figure 9.15: Histogram of 2019 carbon emissions (logarithmic scale, $tCO_2e$)

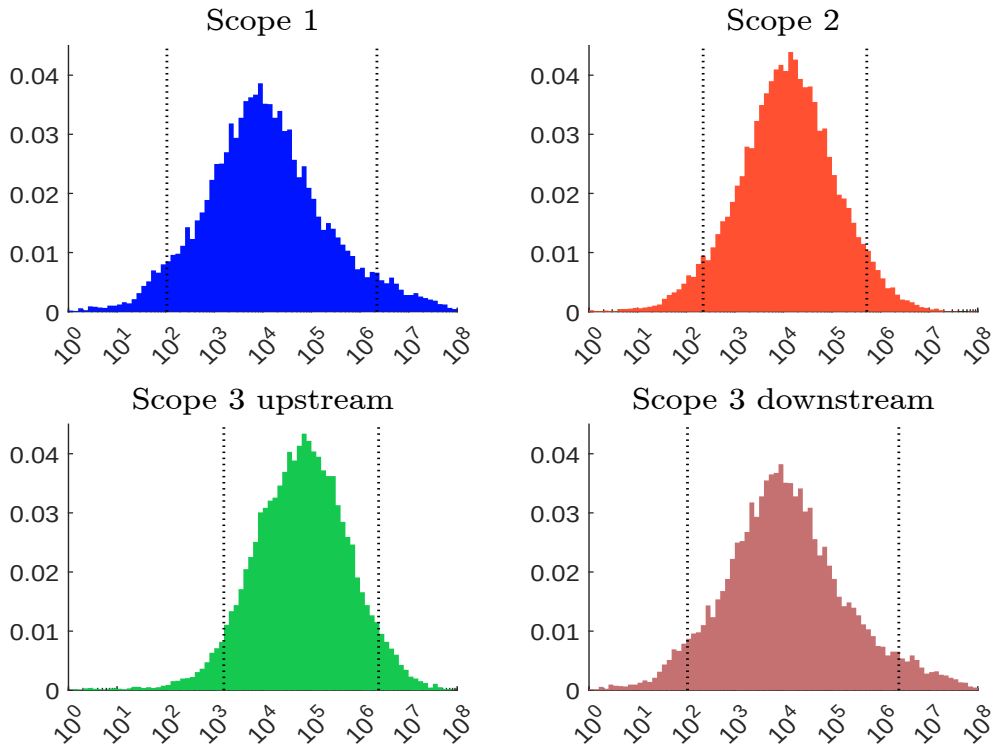


Source: Trucost (2022) & Barahhou *et al.* (2022).

2. Negative emission technologies
   Examples are direct air capture with carbon storage[27] (DACCS), bioenergy with carbon capture and storage[28] (BECCS), enhanced weathering[29], ocean fertilization[30], etc.

Tanzer and Ramírez (2019) gives a more formal definition of negative emissions by considering four minimum criteria for determining whether a technology induces negative emissions:

> "*[...] (1) Physical greenhouse gases are removed from the atmosphere. (2) The removed gases are stored out of the atmosphere in a manner intended to be permanent. (3) Upstream and downstream greenhouse gas emissions associated with the removal and storage process, such as biomass origin, energy use, gas fate, and co-product fate, are comprehensively estimated and included in the emission balance. (4) The total quantity of atmospheric greenhouse gases removed and permanently stored is greater than the total quantity of greenhouse gases emitted to the atmosphere.*" (Tanzer and Ramírez, 2019, page 1216)

In a series of three review papers, Jan Minx and his co-authors provided a comprehensive overview of negative emissions (Minx *et al.*, 2018; Fuss *et al.*, 2018; Nemet *et al.*, 2018). They emphasized

[27] This technology uses special filters to capture $CO_2$ directly from the air, while the captured $CO_2$ is then stored underground or used in other applications.

[28] This process involves capturing and storing the $CO_2$ emissions from burning biomass, such as wood or grasses.

[29] This process involves the application of finely ground minerals, such as olivine or basalt, to land surfaces. When these minerals react with atmospheric $CO_2$, they form harmless minerals and carbonates, trapping the carbon in a stable mineral form. The goal is to accelerate the natural process of weathering.

[30] This technology involves adding nutrients to the ocean, which can stimulate the growth of phytoplankton in the ocean, which then absorbs $CO_2$ through photosynthesis.

that the efficiency, capacity, and cost of different technologies vary widely. A typical example is direct air capture technology[31]. The rationale for the technology is presented in the book published by National Academies of Sciences, Engineering, and Medicine (2019). There are two general types of DAC processes: DAC with liquid solvents (L-DAC) and DAC with solid sorbents (S-DAC). In an L-DAC process, there are four stages: absorption, regeneration, purification and separation. Each phase involves a chemical reaction:

$$\begin{aligned} 2\,\mathrm{KOH} + \mathrm{CO_2} &\longrightarrow \mathrm{H_2O} + \mathrm{K_2CO_3} \\ \mathrm{CaO} + \mathrm{H_2O} &\longrightarrow \mathrm{Ca\,(OH)_2} \\ \mathrm{K_2CO_3} + \mathrm{Ca\,(OH)_2} &\longrightarrow 2\,\mathrm{KOH} + \mathrm{CaCO_3} \\ \mathrm{CaCO_3} &\longrightarrow \mathrm{CaO} + \mathrm{CO_2} \end{aligned}$$

The goal is to use the liquid solvent KOH to react with atmospheric carbon dioxide $CO_2$ to produce pure $CO_2$ and calcium oxide CaO. In an S-DAC process, solid materials or sorbents, such as porous polymers or metal-organic frameworks, are used to adsorb $CO_2$. The costs associated with DAC technology include the initial investment to build the DAC system (*e.g.*, air contractor, causticizer, calciner, and slaker), the price of solvents and sorbents, the electricity needs to perform the chemical reactions, and the cost of storage. The current price of removing a tonne of $CO_2$ is around \$1 000, which is high compared to the price of carbon traded on $CO_2$ markets. Another factor in assessing the relevance of DAC technologies is the measurement of carbon efficiency, which depends on the amount and carbon intensity of electricity used to remove atmospheric $CO_2$. Today, the carbon efficiency of the best DAC plans is less than 70%. This is, of course, the current situation and many improvements are expected in the coming years. For instance, IEA (2022) estimated that DAC costs could fall below \$100/t$CO_2$ by 2030.

Box 9.4: An example of DAC companies: Climeworks

Climeworks (https://climeworks.com) is a Swiss company founded in 2009 as a spin-off from ETH Zurich. It specializes in DAC technology and has established itself as a pioneer in this field with two other companies: Carbon Engineering (Canada) and Global Thermostat (USA). In September 2021, Climeworks inaugurates the world's first large-scale direct air capture and storage plant "*Orca*" in Iceland, with a capacity to capture 4 000 tonnes of $CO_2$ per year. The storage of $CO_2$ is carried out by the company Carbfix, which injects it deep underground, where it mineralizes and turns into stone. In June 2022, Climeworks announces a second, newest and largest direct air capture and storage facility, "*Mammoth*", also in Iceland. It will have a nominal $CO_2$ capture capacity of up to 36 000 tonnes per year when fully operational.

A related concept to negative emissions is avoided emissions, often incorrectly referred to as Scope 4 emissions. According to Russell (2023), "*comparative impacts are estimated as the difference between the total, attributional, life-cycle GHG inventories of a company's product (the assessed product) and an alternative (or reference) product that provides an equivalent function*":

$$\boldsymbol{\mathcal{AE}} = \boldsymbol{\mathcal{CE}}\,(\text{reference product}) - \boldsymbol{\mathcal{CE}}\,(\text{assessed product})$$

Avoided emissions can be positive ($\boldsymbol{\mathcal{AE}} \geq 0$) or negative ($\boldsymbol{\mathcal{AE}} < 0$). For example, an electric car emits $CO_2$, especially when we consider the life cycle of the batteries, but electric cars do not emit

[31] DAC and DACCS are two interchangeable terms because carbon storage is implicit in all carbon dioxide capture, use, and storage (CCUS) technologies.

greenhouse gases from burning gasoline. In this example, the reference product is the gasoline-powered car and the assessed product is the electric car, and we expect the avoided emissions to be positive. However, there are two issues in calculating avoided emissions. First, which car should we choose to represent the gasoline car or the reference product? Second, what is the use of the electric car? In fact, the avoided emissions depend on many factors, such as the carbon intensity of the electricity, recycling assumptions, etc.

In addition to negative emissions and avoided emissions, carbon offsetting includes a third concept: carbon credits. Carbon credits are transferable financial instruments that represent one tonne of carbon dioxide or another greenhouse gas. They are traded on carbon markets where companies, governments and individuals can buy and sell credits to meet their emission reduction targets. The price of carbon credits can vary depending on supply and demand, as well as the type of project and the region in which it is located. There are two main types of carbon credit systems:

- Cap-and-trade systems
  These systems place a limit on the total amount of GHG emissions that can be released from a given region or industry. Companies are allocated a certain number of carbon credits (emission allowances) and can buy or sell credits to meet their emissions targets. These government-regulated schemes make up the compliance carbon market.

- Voluntary carbon markets
  These markets are not regulated by the government, and companies can voluntarily buy carbon credits to offset their emissions. Voluntary carbon markets are often used to offset emissions from activities not covered by cap-and-trade systems. In this case, the avoided emissions from a carbon offset (*e.g.*, through the use of negative emission technologies) must be counted on the balance sheet of the buyer, not the seller, who is the developer of the project.

We can now give a precise definition of carbon offsetting. Carbon offsetting is when a company offsets its own carbon emissions by providing emission reductions outside of its own operations. This means that the company purchases a verified carbon credit in a voluntary carbon market that funds a negative emission project. Carbon offsetting does not involve avoided emissions because they concerns the company's own operations and are associated with a change in the company's business strategy. Carbon offsets also do not include carbon credits purchased in a cap-and-trade system because these carbon credits do not necessarily result in negative emissions. Because carbon offsetting involves reducing a company's carbon footprint, it is commonly associated with the race to net-zero emissions. However, we need to make a clear distinction between the two concepts. It is now accepted that some activities will continue to emit GHGs in 2050 due to a lack of carbon-free alternatives, even in the most stringent net-zero scenario. In such situations, carbon offsets must be used primarily by companies exposed to these hard-to-abate sectors, such as cement or airlines. In Figure 9.16 we reproduce the taxonomy of carbon offsets proposed by Allen *et al.* (2020). Based on our definition, only categories IV and V fall under the strict definition of carbon offsetting.

Allen *et al.* (2020) proposed a framework for assessing the relevance of carbon offsets to ensure that they contribute to a net-zero economy. The Oxford principles for net-zero aligned carbon offsetting are:

1. Cut emissions, use high quality offsets, and regularly revise offsetting strategy as best practice evolves
   Companies' first priority is to reduce their own emissions, not to purchase carbon offsets. If they do, they need to buy offsets that ensure environmental integrity, high standards and certification in line with accounting practices. The largest GHG offset programs are the Verified

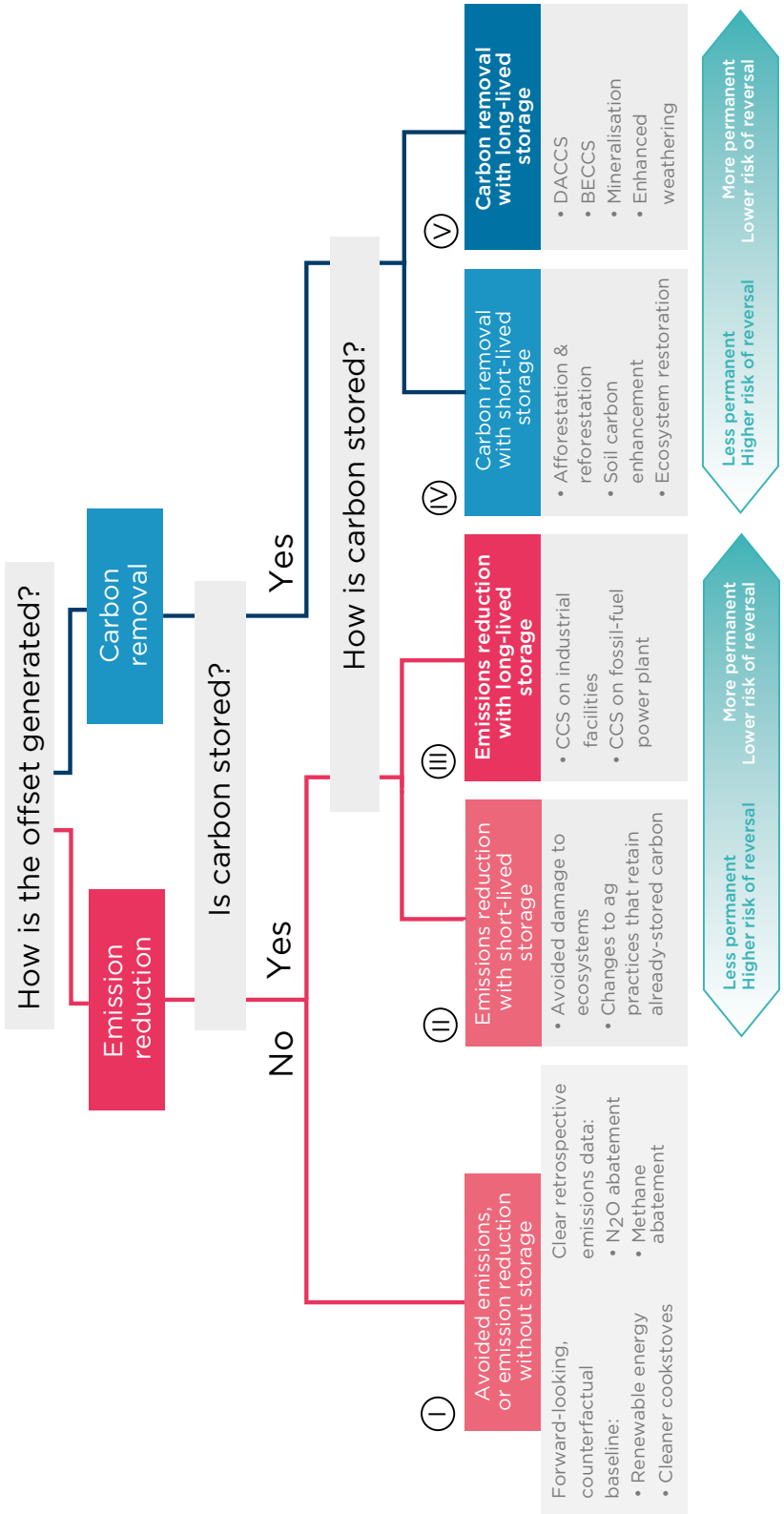


Figure 9.16: Taxonomy of carbon offsets

Source: Allen *et al.* (2020, Figure 1, page 7).

Carbon Standard (VCS) and the Gold Standard (GS). The status of projects that meet these standards can be tracked through official registries whose goal is to certify the ownership of each negative emissions project. Specifically, ownership is transferred to the buyer of the carbon credits and then canceled when the credits are sold. The purpose of registries is to ensure that negative emissions are not counted twice.

2. Shift to carbon removal offsetting
There is clearly an imbalance between the supply of certified negative emissions projects and the projects needed to achieve net zero in the long term. Creating demand for carbon removal offsets today will send the necessary market signal to increase supply. Figure 9.17 shows the size of the voluntary carbon market (VCM). It has been multiplied by two after 2019. According to Ecosystem Marketplace (2023b), the cumulative volume has reached 2.3 $GtCO_2e$ with a value of \$10 billion. This implies an average price of \$4.35 per tonne of $CO_2$. From 2021, the average price is more likely to be between \$7 and \$8 per tonne of $CO_2$. The market is largely dominated by renewable energy projects and forestry & land use. Since 2020, projects on household & community devices have also been promoted. Although developing, the voluntary carbon market remains relatively small and immature, with many intermediaries and few end users[32]. For example, the energy sector is the main buyer of voluntary carbon credits, accounting for more than 50% of the market. However, the market is expected to reach between \$10 billion and \$40 billion by 2030, up from a record \$2.1 billion in 2021 (BCG, 2023a).

Figure 9.17: Voluntary carbon market size by volume of traded carbon credits

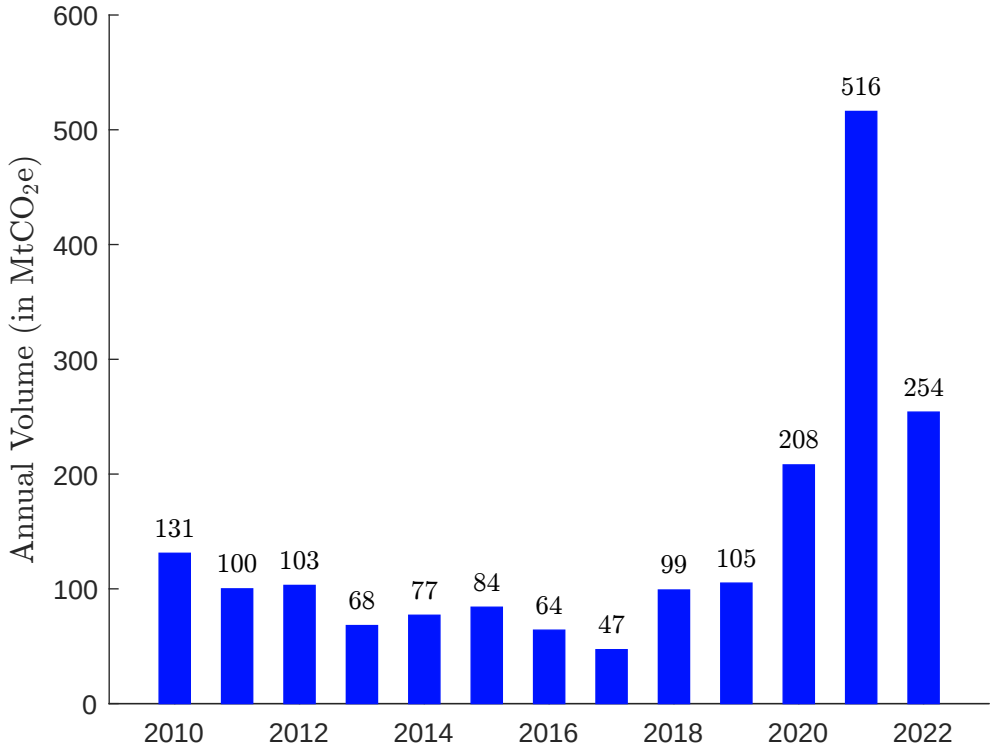


Source: Ecosystem Marketplace (2023b, Figure 2, page 8).

[32]In fact, it is concentrated in a few companies. According to Ecosystem Marketplace (2023a), the top 10 buyers in 2021 were Delta Air Lines, TotalEnergies, Shell, Volkswagen, Takeda Pharmaceuticals, Comcast, Diamondback Energy, La Poste, Telstra and Eni.

3. Shift to long-lived storage
   The issue of $CO_2$ storage and sequestration is an important one. As noted by Allen *et al.* (2020), "*short-lived storage involves methods that have a higher risk of being reversed over decades. Long-lived storage refers to methods of storing carbon that have a low risk of reversal over centuries to millennia, such as storing CO2 in geological reservoirs or mineralising carbon into stable forms. Short-lived storage offsets help buy time to reduce emissions and invest in long-lived storage, but they are not a long-term solution for achieving balance between sinks and sources.*" Measuring the efficiency of a technology is not straightforward and is highly dependent on the lifetime of the project (Terlouw *et al.*, 2021) and the system boundary. Figure 9.18 shows an example taken from Tanzer and Ramírez (2019). Chiquier *et al.* (2022) proposed to evaluate the efficiency of carbon dioxide removal by considering the amount of $CO_2$ stored (or removed) and the amount of $CO_2$ leaked (or emitted) over the supply chain:

$$\eta(t) = \frac{\mathrm{CO}_2^{\text{stored}}(t) - \mathrm{CO}_2^{\text{leaked}}(t)}{\mathrm{CO}_2^{\text{stored}}(t)}$$

   The metric $\eta(t)$ depends on the lifetime $t$ expressed in years. In general, it is a decreasing function of time $t$, which means that the efficiency is maximum at the beginning of the project. In the case of an afforestation/reforestation project implemented in 2020 in the UK, Chiquier *et al.* (2022) estimates $\eta(10) = 87.1\%$, $\eta(30) = 98.8\%$, $\eta(100) = 98.9\%$, and $\eta(1000) = 61.9\%$. Here, the CDR efficiency increases in the beginning because the forest establishment emits $CO_2$ and the trees are young. Then the trees grow and the efficiency is close to 100% between 30 and 100 years. In the long term, the efficiency decreases due to the risk of forest fires. A summary of key features for each CDR pathway is provided in Table 9.12.

Table 9.12: Summary of key features for each CDR pathway

| CDR | $\eta(100)$ | $\eta(1000)$ | Timing | Permanence |
|---|---|---|---|---|
| Afforestation | 63 to 99% | 31 to 95% | Decades | Very low |
| Reforestation | 63 to 99% | 31 to 95% | Decades | Very low |
| BECCS | 52 to 87% | 78 to 87% | Immediate to decades | High/very high |
| Biochar | 20 to 39% | −3 to 5% | Immediate | Low/very low |
| DACCS | −5 to 90% | −5 to 90% | Immediate | Very high |
| Enhanced weathering | 17 to 92% | 51 to 92% | Immediate to decades | High/very high |

Source: Chiquier *et al.* (2022, Table 1, page 4400).

4. Support the development of net-zero aligned offsetting
   The fourth principle is to promote carbon offsetting. To develop this market, companies can enter into long-term agreements, form sector-specific alliances, support the restoration and protection of natural and semi-natural ecosystems, and incorporate these principles into regulation.

Carbon accounting for negative emission technologies is still an open question (Brander *et al.*, 2021; Kaplan *et al.*, 2023). It is closely related to the issue of certification and credibility of CDR projects. Accounting for carbon offsets also challenges the economic incentives of these projects from the perspective of buyers of carbon credits. Microsoft's experience described in *Nature* is an interesting testimony from an end user and provides some insights to improve the ecosystem of negative emission technologies and carbon offsetting (Joppa *et al.*, 2021).

Figure 9.18: Perceived $CO_2$ emissions of a simplified steel production system when viewed from different system boundaries

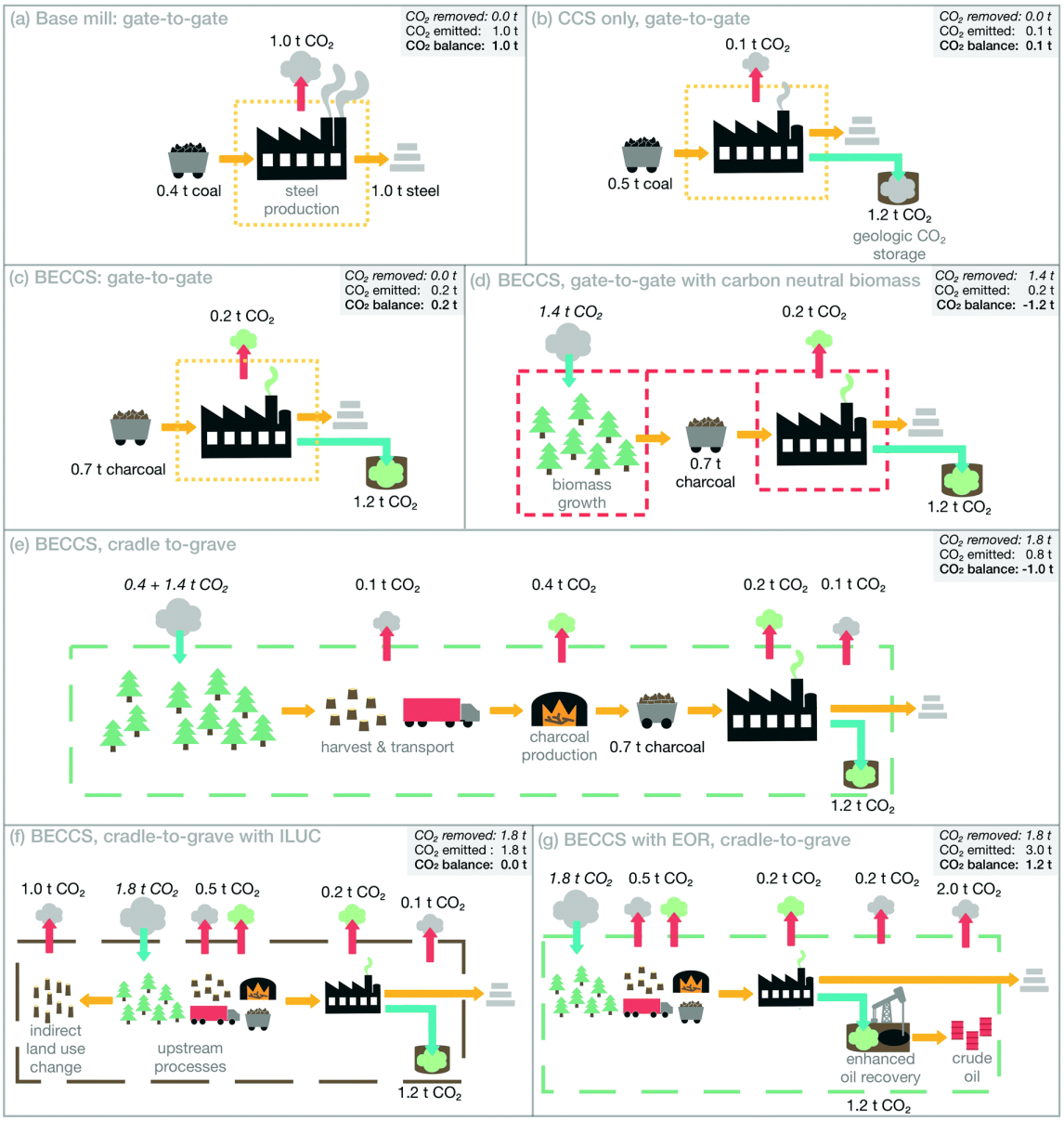


The dashed line in each sub-figure represents the system boundaries used to estimate the total $CO_2$ emissions in the upper right corner of each figure. The system design and numbers used are greatly simplified for illustrative purposes. (a-c) show the gate-to-gate $CO_2$ emissions of a steel mill, considering only the $CO_2$ produced at the mill itself for normal production (a), with the use of carbon capture and storage (b), and with the use of bioenergy with carbon capture and storage (c). (d) extends the system boundaries to include photosynthetic uptake of the exact amount of $CO_2$ released by combustion, assuming the charcoal is carbon neutral. (e) is a simplified cradle-to-grave system that includes in its boundaries the $CO_2$ absorbed by the wood that is lost in the charcoal production process, the $CO_2$ emissions from biomass harvesting and transportation, the $CO_2$ emissions from charcoal production, and the $CO_2$ emissions from $CO_2$ storage. (f) is a variant where biomass production has significant indirect land use change emissions. (g) is a variant where geological storage of $CO_2$ results in the production and combustion of fossil fuels whose $CO_2$ emissions exceed the $CO_2$ stored.

Source: Tanzer and Ramírez (2019, Figure 2, page 1214).

## 9.2 Carbon intensity

While carbon emissions measure the carbon footprint in an absolute value, the carbon intensity is a relative metric of the carbon footprint. The underlying idea is to normalize the carbon emissions by a size or activity unit. For instance, we can measure the carbon footprint of countries by $tCO_2e$ per capita, watching television by $CO_2e$ emissions per viewer-hour, washing machines by $kgCO_2e$ per wash, cars by $kgCO_2e$ per kilometer driven, companies by $ktCO_2e$ per \$1 mn revenue, etc. We distinguish two types of carbon intensity: carbon intensities whose activity units are physical and carbon intensities whose activity units are monetary.

### 9.2.1 Physical intensity ratios

The product carbon footprint (PCF) measures the relative carbon emissions of a product throughout its life cycle. This approach, which is called life cycle assessment (LCA), distinguishes two methods:

- Cradle-to-gate refers to the carbon footprint of a product from the moment it is produced (including the extraction of raw materials) to the moment it enters the store;
- In contrast, cradle-to-grave covers the entire life cycle of a product, including the use-phase and recycling.

Below, we report some examples of product carbon footprint computed by ADEME.

Table 9.13: Examples of product carbon footprint (in $kgCO_2e$ per unit)

| Product | Category | Cradle-to-gate | Cradle-to-grave |
|---|---|---|---|
| Screen | 21.5 inches | 222 | 236 |
| | 23.8 inches | 248 | 265 |
| Computer | Laptop | 156 | 169 |
| | Desktop | 169 | 189 |
| | High performance | 295 | 394 |
| Smartphone | Classical | 16 | 16 |
| | 5 inches | 33 | 32 |
| Oven | Built-in electric | 187 | 319 |
| | Professional (combi steamer) | 734 | 12 676 |
| Washing machine | Capacity 5kg | 248 | 468 |
| | Capacity 7kg | 275 | 539 |
| Shirt | Coton | 10 | 13 |
| | Viscose | 9 | 12 |
| Balloon | Football | 3.4 | 5.1 |
| | Basket-ball | 3.6 | 5.9 |

Source: Lhotellier *et al.* (2018, Annex 4, pages 212-215).

The previous analysis can be extended to corporate carbon footprint (CCF). For instance, we can measure the CCF of a cement manufacturer by the amount of GHG emissions per tonne of cement. In the airline sector, the main traffic metric is the revenue passenger kilometers (RPK), which is calculated by multiplying the number of paying passengers by the distance traveled. Therefore, the CCF of airlines can be measured by the amount of GHG emissions per RPK (Table 9.14).

Table 9.14: Physical carbon intensity per production unit

| Sector | Unit | Description |
|---|---|---|
| Transport sector (aviation) | $CO_2e$/RPK | Revenue passenger kilometers |
| Transport sector (shipping) | $CO_2e$/RTK | Revenue tonne kilometers |
| Industry (cement) | $CO_2e$/t cement | Tonne of cement |
| Industry (steel) | $CO_2e$/t steel | Tonne of steel |
| Electricity | $CO_2e$/MWh | Megawatt hour |
| Buildings | $CO_2e$/SQM | Square meter |

### 9.2.2 Monetary intensity ratios

From a financial point of view, it does not make sense to compare and aggregate the carbon emissions of a large cap company with the carbon emissions of a small cap company. Carbon intensity is then a more relevant metric. ESG analysts can then compare companies that belong to the same activity sector by using physical intensity ratios. For example, they can compare all the cement manufacturers, because they can normalize the carbon emissions by the volume of cement production. In a similar way, they can compare all the airline companies, because they can normalize the carbon emissions by the RPK metric. Nevertheless, the physical intensity ratios are not relevant when we consider a portfolio that is invested in several sectors. How to compare a cement-based carbon intensity with a RPK-based carbon intensity? How to aggregate the two metrics? Until now, nobody has the answer.

Therefore, portfolio managers will use monetary intensity ratios, which are defined as:

$$\mathcal{CI} = \frac{\mathcal{CE}}{Y}$$

where $\mathcal{CE}$ is the company's carbon emissions and $Y$ is a monetary variable measuring its activity. For instance, we can use revenues, sales, etc. to normalize carbon emissions:

- Revenue:
$$\mathcal{CI}^{\text{Revenue}} = \frac{\mathcal{CE}}{\text{Revenue}}$$
- Sales:
$$\mathcal{CI}^{\text{Sales}} = \frac{\mathcal{CE}}{\text{Sales}}$$
- Enterprise value including cash:
$$\mathcal{CI}^{\text{EVIC}} = \frac{\mathcal{CE}}{\text{EVIC}}$$
- Market value:
$$\mathcal{CI}^{\text{MV}} = \frac{\mathcal{CE}}{\text{MV}}$$

Even the previous carbon emission metrics based on EVIC and market value can be viewed as carbon intensity metrics.

If we consider the EVIC-based approach, the carbon intensity of the portfolio is given by:

$$\begin{aligned}
\boldsymbol{\mathcal{CI}}^{\text{EVIC}}(w) &= \frac{\boldsymbol{\mathcal{CE}}^{\text{EVIC}}(W)}{W} \\
&= \frac{1}{W}\sum_{i=1}^{n}\frac{W_i}{\text{EVIC}_i}\cdot\boldsymbol{\mathcal{CE}}_i \\
&= \sum_{i=1}^{n}\frac{W_i}{W}\cdot\frac{\boldsymbol{\mathcal{CE}}_i}{\text{EVIC}_i} \\
&= \sum_{i=1}^{n} w_i\cdot\boldsymbol{\mathcal{CI}}_i^{\text{EVIC}}
\end{aligned}$$

where $w = (w_1, \ldots, w_n)$ is the vector of portfolio weights. We notice that the carbon intensity satisfies the additivity property. In a similar way, we obtain:

$$\boldsymbol{\mathcal{CI}}^{\text{MV}}(w) = \sum_{i=1}^{n} w_i\cdot\boldsymbol{\mathcal{CI}}_i^{\text{MV}}$$

Let us now consider the revenue-based carbon intensity (also called the economic carbon intensity). We denote by $Y_i$ the revenue of issuer $i$. The carbon intensity of the portfolio becomes:

$$\boldsymbol{\mathcal{CI}}^{\text{Revenue}}(w) = \frac{\boldsymbol{\mathcal{CE}}(w)}{Y(w)}$$

where $\boldsymbol{\mathcal{CE}}(w)$ measures the carbon emissions of the portfolio:

$$\boldsymbol{\mathcal{CE}}(w) = \sum_{i=1}^{n} W_i\cdot\frac{\boldsymbol{\mathcal{CE}}_i}{\text{MV}_i} = W\sum_{i=1}^{n}\frac{w_i}{\text{MV}_i}\cdot\boldsymbol{\mathcal{CE}}_i$$

and $Y(w)$ is the total revenue of the portfolio:

$$Y(w) = \sum_{i=1}^{n} W_i\cdot\frac{Y_i}{\text{MV}_i} = W\sum_{i=1}^{n}\frac{w_i}{\text{MV}_i}\cdot Y_i$$

We deduce that:

$$\begin{aligned}
\boldsymbol{\mathcal{CI}}^{\text{Revenue}}(w) &= \frac{\sum_{i=1}^{n}\frac{w_i}{\text{MV}_i}\cdot\boldsymbol{\mathcal{CE}}_i}{\sum_{i=1}^{n}\frac{w_i}{\text{MV}_i}\cdot Y_i} \\
&= \sum_{i=1}^{n} w_i\cdot\omega_i\cdot\boldsymbol{\mathcal{CI}}_i^{\text{Revenue}}
\end{aligned}$$

where $\omega_i$ is the ratio between the revenue per market value of company $i$ and the weighted average revenue per market value of the portfolio:

$$\omega_i = \frac{\frac{Y_i}{\text{MV}_i}}{\sum_{k=1}^{n} w_k\cdot\frac{Y_k}{\text{MV}_k}}$$

Except when all the companies have the same revenue per market value ratio, we deduce that the revenue-based carbon intensity does not satisfy the additivity property since we have $\boldsymbol{\mathcal{CI}}^{\text{Revenue}}(w) \neq \sum_{i=1}^{n} w_i \cdot \boldsymbol{\mathcal{CI}}_i^{\text{Revenue}}$. In order to avoid this problem, we generally use the weighted average carbon intensity (WACI) of the portfolio:

$$\boldsymbol{\mathcal{CI}}^{\text{Revenue}}(w) = \sum_{i=1}^{n} w_i \cdot \boldsymbol{\mathcal{CI}}_i^{\text{Revenue}} \tag{9.5}$$

This method is the standard approach in portfolio management.

**Remark 104** *Carbon intensity is additive when we consider a given issuer:*

$$\begin{aligned}\boldsymbol{\mathcal{CI}}_i(\boldsymbol{\mathcal{SC}}_{1-3}) &= \frac{\boldsymbol{\mathcal{CE}}_i(\boldsymbol{\mathcal{SC}}_1) + \boldsymbol{\mathcal{CE}}_i(\boldsymbol{\mathcal{SC}}_2) + \boldsymbol{\mathcal{CE}}_i(\boldsymbol{\mathcal{SC}}_3)}{Y_i} \\ &= \boldsymbol{\mathcal{CI}}_i(\boldsymbol{\mathcal{SC}}_1) + \boldsymbol{\mathcal{CI}}_i(\boldsymbol{\mathcal{SC}}_2) + \boldsymbol{\mathcal{CI}}_i(\boldsymbol{\mathcal{SC}}_3)\end{aligned}$$

**Example 39** *We assume that* $\boldsymbol{\mathcal{CE}}_1 = 5 \times 10^6$ $\text{CO}_2\text{e}$, $Y_1 = \$0.2 \times 10^6$, $\text{MV}_1 = \$10 \times 10^6$, $\boldsymbol{\mathcal{CE}}_2 = 50 \times 10^6$ $\text{CO}_2\text{e}$, $Y_2 = \$4 \times 10^6$ *and* $\text{MV}_2 = \$10 \times 10^6$. *We invest* $W = \$10$ *mn.*

We deduce that:

$$\boldsymbol{\mathcal{CI}}_1 = \frac{5 \times 10^6}{0.2 \times 10^6} = 25.0 \text{ tCO}_2\text{e}/\$ \text{ mn}$$

and $\boldsymbol{\mathcal{CI}}_2 = 12.5$ $\text{tCO}_2\text{e}/\$$ mn. Since we have:

$$\begin{cases} \boldsymbol{\mathcal{CE}}(w) = W\left(w_1 \dfrac{\boldsymbol{\mathcal{CE}}_1}{\text{MV}_1} + w_2 \dfrac{\boldsymbol{\mathcal{CE}}_2}{\text{MV}_2}\right) \\ Y(w) = W\left(w_1 \dfrac{Y_1}{\text{MV}_1} + w_2 \dfrac{Y_2}{\text{MV}_2}\right) \\ \boldsymbol{\mathcal{CI}}(w) = w_1 \boldsymbol{\mathcal{CI}}_1 + w_2 \boldsymbol{\mathcal{CI}}_2 \end{cases}$$

We obtain the following results:

| $w_1$ | $w_2$ | $\boldsymbol{\mathcal{CE}}(w)$ $(\times 10^6\ \text{CO}_2\text{e})$ | $Y(w)$ $(\times \$10^6)$ | $\dfrac{\boldsymbol{\mathcal{CE}}(w)}{Y(w)}$ | $\boldsymbol{\mathcal{CI}}(w)$ |
|---|---|---|---|---|---|
| 0% | 100% | 50.00 | 4.00 | 12.50 | 12.50 |
| 10% | 90% | 45.50 | 3.62 | 12.57 | 13.75 |
| 20% | 80% | 41.00 | 3.24 | 12.65 | 15.00 |
| 30% | 70% | 36.50 | 2.86 | 12.76 | 16.25 |
| 50% | 50% | 27.50 | 2.10 | 13.10 | 18.75 |
| 70% | 30% | 18.50 | 1.34 | 13.81 | 21.25 |
| 80% | 20% | 14.00 | 0.96 | 14.58 | 22.50 |
| 90% | 10% | 9.50 | 0.58 | 16.38 | 23.75 |
| 100% | 0% | 5.00 | 0.20 | 25.00 | 25.00 |

We notice that the weighted average carbon intensity can be very different than the economic carbon intensity. Let us assume that we buy the two companies, implying that $W = \$20$ mn, $w_1 = 50\%$ and $w_2 = 50\%$. In this case, we obtain $\boldsymbol{\mathcal{CE}}(w) = 55 \times 10^6$ and $Y(w) = \$4 \times 10^6$. The economic carbon intensity is then equal to $55/4 = 13.10$ while the WACI is 18.75.

**Remark 105** *For sovereign issuers, the economic carbon intensity is measured in mega-tonnes of* $\text{CO}_2\text{e}$ *per million dollars of GDP while the physical carbon intensity unit is* $\text{tCO}_2\text{e}$ *per capita.*

### 9.2.3 Statistics

Some CCF values are provided in Table 9.15. These figures illustrate some issues in the computation of the carbon footprint at the issuer level. First, it is obvious that it is important to take into account scope 3 to have the real picture of the carbon footprint of an issuer. Indeed, we notice that some issuers have a low scope 1, because they have more or less outsourced the manufacturing of their products. Since a part of the production is located in upstream scope 3, we can not make a fair comparison between issuers if we only consider scope 1 and 2. We face a similar issue with the distribution of the products. The magnitude of some scope 3 carbon intensities raises also the question of their computation. Indeed, while scope 1 and 2 are mandatory to report, there is no obligation for a company to report its scope 3. Moreover, while there is one unique figure for scope 1 and 2 emissions in the CDP reporting files, scope 3 emissions are split into 15 categories, and it is extremely rare that a company reports all scope 3 categories. This explains that the frequency of estimated values is larger for scope 3.

Figure 9.19: Histogram of 2019 carbon intensities (logarithmic scale, $tCO_2e$/$ mn)

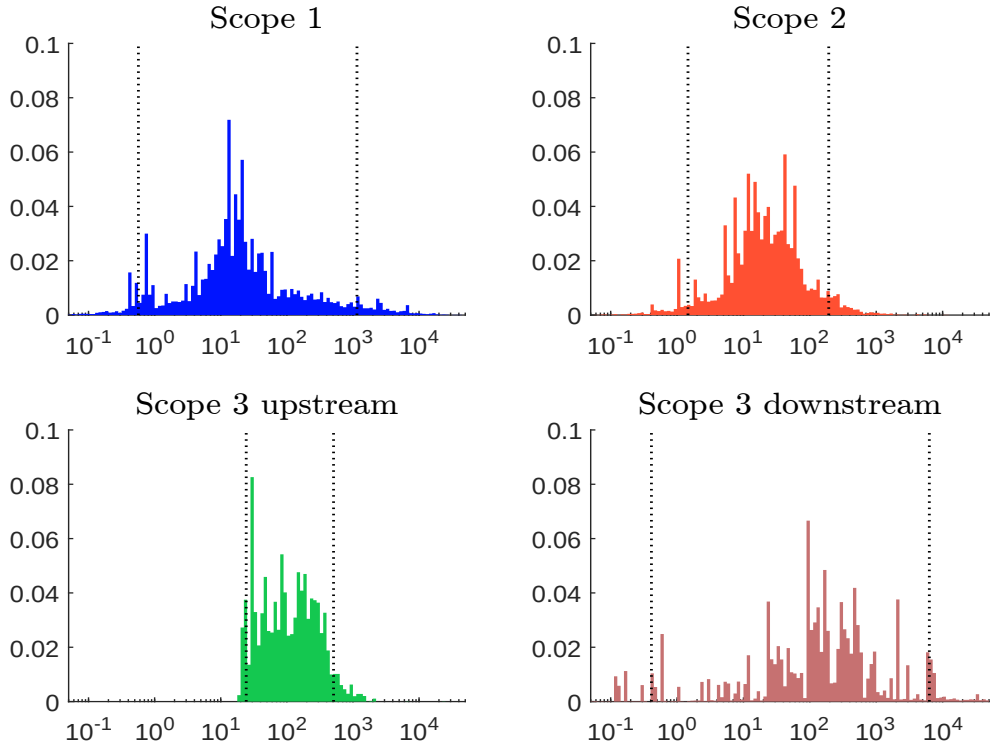


Source: Trucost (2022) & Barahhou *et al.* (2022).

In Figure 9.19, we show the distribution of carbon intensities. Since the range may be very large (from zero to several thousand), we use a logarithmic scale. Moreover, the dotted vertical lines indicate the $5^{\text{th}}$ and $95^{\text{th}}$ percentiles. We observe that the distribution support is very large for scope 1, 2 and 3 downstream. In this case, there are many extreme points with very low and very high carbon intensities. Therefore, we will see that it is relatively easy to reduce the carbon footprint of a portfolio. Now, if we focus on upstream scope 3, we obtain another story, because the range is not so large. Indeed, we do not have issuers with very low carbon intensity. Therefore, incorporating upstream scope 3 will change the nature of portfolio decarbonization, which will become more difficult.

Table 9.15: Examples of 2019 carbon emissions and intensities

| Company | Carbon emissions (in $tCO_2e$) | | | | Revenue | Intensity (in $tCO_2e$/$ mn) | | | |
|---|---|---|---|---|---|---|---|---|---|
| | $\mathcal{SC}_1$ | $\mathcal{SC}_2$ | $\mathcal{SC}_3^{\text{up}}$ | $\mathcal{SC}_3^{\text{down}}$ | (in $ mn) | $\mathcal{SC}_1$ | $\mathcal{SC}_2$ | $\mathcal{SC}_3^{\text{up}}$ | $\mathcal{SC}_3^{\text{down}}$ |
| Airbus | 576 705 | 386 674 | 12 284 183 | 23 661 432 | 78 899 | 7.3 | 4.9 | 155.7 | 299.9 |
| Allianz | 46 745 | 224 315 | 3 449 234 | 3 904 000 | 135 279 | 0.3 | 1.7 | 25.5 | 28.9 |
| Alphabet | 111 283 | 5 118 152 | 7 142 566 | | 161 857 | 0.7 | 31.6 | 44.1 | |
| Amazon | 5 760 000 | 5 500 000 | 20 054 722 | 10 438 551 | 280 522 | 20.5 | 19.6 | 71.5 | 37.2 |
| Apple | 50 549 | 862 127 | 27 624 282 | 5 470 771 | 260 174 | 0.2 | 3.3 | 106.2 | 21.0 |
| BNP Paribas | 64 829 | 280 789 | 1 923 307 | 1 884 | 78 244 | 0.8 | 3.6 | 24.6 | 0.0 |
| Boeing | 611 001 | 871 000 | 9 878 431 | 22 959 719 | 76 559 | 8.0 | 11.4 | 129.0 | 299.9 |
| BP | 49 199 999 | 5 200 000 | 103 840 194 | 582 639 687 | 276 850 | 177.7 | 18.8 | 375.1 | 2 104.5 |
| Caterpillar | 905 000 | 926 000 | 15 197 607 | 401 993 744 | 53 800 | 16.8 | 17.2 | 282.5 | 7 472.0 |
| Danone | 722 122 | 944 877 | 28 969 780 | 4 464 773 | 28 308 | 25.5 | 33.4 | 1 023.4 | 157.7 |
| Enel | 69 981 891 | 5 365 386 | 8 726 973 | 53 774 821 | 86 610 | 808.0 | 61.9 | 100.8 | 620.9 |
| Exxon | 111 000 000 | 9 000 000 | 107 282 831 | 594 131 943 | 255 583 | 434.3 | 35.2 | 419.8 | 2 324.6 |
| JPMorgan Chase | 81 655 | 692 299 | 3 101 582 | 15 448 469 | 115 627 | 0.7 | 6.0 | 26.8 | 133.6 |
| Juventus | 6 665 | 15 739 | 35 842 | 77 114 | 709 | 9.4 | 22.2 | 50.6 | 108.8 |
| LVMH | 67 613 | 262 609 | 11 853 749 | 942 520 | 60 083 | 1.1 | 4.4 | 197.3 | 15.7 |
| Microsoft | 113 414 | 3 556 553 | 5 977 488 | 4 003 770 | 125 843 | 0.9 | 28.3 | 47.5 | 31.8 |
| Nestle | 3 291 303 | 3 206 495 | 61 262 078 | 33 900 606 | 93 153 | 35.3 | 34.4 | 657.6 | 363.9 |
| Netflix | 38 481 | 145 443 | 1 900 283 | 2 192 255 | 20 156 | 1.9 | 7.2 | 94.3 | 108.8 |
| NVIDIA | 2 767 | 65 048 | 2 756 353 | 1 184 981 | 11 716 | 0.2 | 5.6 | 235.3 | 101.1 |
| PepsiCo | 3 552 415 | 1 556 523 | 32 598 029 | 14 229 956 | 67 161 | 52.9 | 23.2 | 485.4 | 211.9 |
| Pfizer | 734 638 | 762 840 | 4 667 225 | 133 468 | 51 750 | 14.2 | 14.7 | 90.2 | 2.6 |
| Roche | 288 157 | 329 541 | 5 812 735 | 347 437 | 64 154 | 4.5 | 5.1 | 90.6 | 5.4 |
| Samsung Electronics | 5 067 000 | 10 998 000 | 33 554 245 | 60 978 947 | 197 733 | 25.6 | 55.6 | 169.7 | 308.4 |
| TotalEnergies | 40 909 135 | 3 596 127 | 49 817 293 | 456 993 576 | 200 316 | 204.2 | 18.0 | 248.7 | 2 280.0 |
| Toyota | 2 522 987 | 5 227 844 | 66 148 020 | 330 714 268 | 272 608 | 9.3 | 19.2 | 242.6 | 1 213.2 |
| Volkswagen | 4 494 066 | 5 973 894 | 65 335 372 | 354 913 446 | 282 817 | 15.9 | 21.1 | 231.0 | 1 254.9 |
| Walmart | 6 101 641 | 13 057 352 | 40 651 079 | 32 346 229 | 514 405 | 11.9 | 25.4 | 79.0 | 62.9 |

Source: Trucost (2022) & Barahhou *et al.* (2022).

Table 9.16: Carbon intensity in $tCO_2e/\$$ mn per GICS sector and sector contribution in % (MSCI World, June 2022)

| Sector | $b_i$ (in %) | Carbon intensity | | | | Risk contribution | | | |
|---|---|---|---|---|---|---|---|---|---|
| | | $\mathcal{SC}_1$ | $\mathcal{SC}_{1-2}$ | $\mathcal{SC}_{1-3}^{\text{up}}$ | $\mathcal{SC}_{1-3}$ | $\mathcal{SC}_1$ | $\mathcal{SC}_{1-2}$ | $\mathcal{SC}_{1-3}^{\text{up}}$ | $\mathcal{SC}_{1-3}$ |
| Communication Services | 7.58 | 2 | 28 | 134 | 172 | 0.14 | 1.31 | 3.30 | 1.31 |
| Consumer Discretionary | 10.56 | 23 | 65 | 206 | 590 | 1.87 | 4.17 | 6.92 | 6.21 |
| Consumer Staples | 7.80 | 28 | 55 | 401 | 929 | 1.68 | 2.66 | 10.16 | 7.38 |
| Energy | 4.99 | 632 | 698 | 1 006 | 6 823 | 24.49 | 21.53 | 16.33 | 34.37 |
| Financials | 13.56 | 13 | 19 | 52 | 244 | 1.33 | 1.58 | 2.28 | 3.34 |
| Health Care | 14.15 | 10 | 22 | 120 | 146 | 1.12 | 1.92 | 5.54 | 2.12 |
| Industrials | 9.90 | 111 | 130 | 298 | 1 662 | 8.38 | 7.83 | 9.43 | 16.38 |
| Information Technology | 21.08 | 7 | 23 | 112 | 239 | 1.13 | 3.03 | 7.57 | 5.06 |
| Materials | 4.28 | 478 | 702 | 1 113 | 2 957 | 15.89 | 18.57 | 15.48 | 12.93 |
| Real Estate | 2.90 | 22 | 101 | 167 | 571 | 0.48 | 1.81 | 1.57 | 1.65 |
| Utilities | 3.21 | 1 744 | 1 794 | 2 053 | 2 840 | 43.47 | 35.59 | 21.41 | 9.24 |
| MSCI World | | 130 | 163 | 310 | 992 | | | | |
| MSCI World EW | | 168 | 211 | 391 | 1 155 | | | | |

Source: MSCI (2022), Trucost (2022) & Barahhou *et al.* (2022).

Let $b = (b_1, \ldots, b_n)$ be the weights of the assets that belong to a benchmark. Its weighted average carbon intensity is given by $\mathcal{CI}(b) = \sum_{i=1}^n b_i \cdot \mathcal{CI}_i$ where $\mathcal{CI}_i$ is the carbon intensity of asset $i$. If we focus on the carbon intensity for a given sector, we use the following formula:

$$\mathcal{CI}(\mathcal{S}ector_j) = \frac{\sum_{i \in \mathcal{S}ector_j} b_i \cdot \mathcal{CI}_i}{\sum_{i \in \mathcal{S}ector_j} b_i}$$

In Table 9.16, we report the carbon intensity of the MSCI World index and its sectors. We also compute the risk contribution of each sector as follows: $\mathcal{RC}(\mathcal{S}ector_j) = \left(\sum_{i \in \mathcal{S}ector_j} b_i \cdot \mathcal{CI}_i\right) / \mathcal{CI}(b)$. We obtain 130 $tCO_2e/\$$ mn for scope 1, 163 $tCO_2e/\$$ mn if we include scope 2, 310 $tCO_2e/\$$ mn if we add upstream scope 3, and finally 992 $tCO_2e/\$$ mn if we consider the full scope 3. We notice a large cap bias because the MSCI World equally-weighted portfolio shows higher figures. We also observe a high discrepancy between sectors. Low-carbon sectors are Communication Services, Financials, Health Care and Information Technology, whereas high-carbon sectors are Energy, Materials and Utilities. In terms of risk contribution, Consumer Services represents 7.58% of the nominal allocation, but only 0.14% of the carbon allocation if we consider scope 1. If we focus on the first two scopes, Utilities is the main contributor, followed by Energy and Materials. By including upstream scope 3 emissions, the contribution of Consumer Staples becomes significant. We also notice that the Utilities contribution has strongly been reduced whereas the Industrials contribution increases when we consider the three scopes.

**Remark 106** *The question of double-counting is less important when we consider carbon intensities, especially monetary measures. Indeed, the carbon intensity can be seen as a scoring system, and portfolio managers generally use carbon intensity in a relative way, and not in an absolute way. For instance, they do not target a given carbon intensity. Their goal is more reducing the carbon intensity relatively to a benchmark, without analyzing the absolute value of the benchmark itself. Moreover, the aggregation at the portfolio level is generally done thanks to the WACI measure, which indicates that the carbon intensity is more viewed as a score than a physical measure.*

## 9.3 Dynamic risk measures

In this section, we present the basics for building dynamic carbon metrics that are very useful when defining net-zero investment portfolios and assessing the decarbonization policy of issuers. The main tools are the carbon budget, the carbon trend and the carbon target. By combining these tools, we will be able to present the $\mathcal{PAC}$ framework which is the cornerstone of implied temperature ratings (ITR). It measures the participation, the ambition and the credibility of a company to reduce its carbon emissions.

### 9.3.1 Carbon budget

#### Definition

The carbon budget defines the amount of GHG emissions that a country, a company or an organization produces over the time period $[t_0, t]$. From a mathematical point of view, it corresponds to the signed area of the region bounded by the function $\boldsymbol{\mathcal{CE}}(t)$:

$$\boldsymbol{\mathcal{CB}}(t_0, t) = \int_{t_0}^{t} \boldsymbol{\mathcal{CE}}(s)\, \mathrm{d}s$$

The carbon budget can be computed with other functions than the carbon emissions. For instance, if the reference level is equal to $\boldsymbol{\mathcal{CE}}^{\star}(t)$ at time $t$, we obtain:

$$\boldsymbol{\mathcal{CB}}^{\star}(t_0, t) = \int_{t_0}^{t} \boldsymbol{\mathcal{CE}}^{\star}(s)\, \mathrm{d}s$$

Therefore, we can easily compute the excess (or net) carbon budget since we have:

$$\int_{t_0}^{t} \left(\boldsymbol{\mathcal{CE}}(s) - \boldsymbol{\mathcal{CE}}^{\star}(s)\right) \mathrm{d}s = \boldsymbol{\mathcal{CB}}(t_0, t) - \boldsymbol{\mathcal{CB}}^{\star}(t_0, t)$$

If the reference level is constant — $\boldsymbol{\mathcal{CE}}^{\star}(t) = \boldsymbol{\mathcal{CE}}^{\star}$, the previous formula becomes:

$$\int_{t_0}^{t} \left(\boldsymbol{\mathcal{CE}}(s) - \boldsymbol{\mathcal{CE}}^{\star}\right) \mathrm{d}s = \boldsymbol{\mathcal{CB}}(t_0, t) - \boldsymbol{\mathcal{CE}}^{\star}(t - t_0)$$

**Example 40** *In Table 9.17, we report the historical data of carbon emissions from 2010 to 2020. Moreover, the company has announced its carbon targets for the years until 2050.*

Table 9.17: Carbon emissions in $\mathrm{MtCO_2e}$

| $t$ | 2010 | 2011 | 2012 | 2013 | 2014 | 2015 | 2016 | 2017 |
|---|---|---|---|---|---|---|---|---|
| $\boldsymbol{\mathcal{CE}}(t)$ | 4.800 | 4.950 | 5.100 | 5.175 | 5.175 | 5.175 | 5.175 | 5.100 |
| $t$ | 2018 | 2019 | 2020 | 2025* | 2030* | 2035* | 2040* | 2050* |
| $\boldsymbol{\mathcal{CE}}(t)$ | 5.025 | 4.950 | 4.875 | 4.200 | 3.300 | 1.500 | 0.750 | 0.150 |

The asterisk * indicates that the company has announced a carbon target for this year.

We consider the carbon pathway given in Example 40 and report different carbon budgets in Figure 9.20. The first panel (top/left) corresponds to the carbon budget that was spent by the company from 2010 to 2020. The second panel (top/right) is the targeted carbon budget that is estimated or planned by the company for the period between 2020 and 2035. The last two panels (bottom/left and bottom/right) considers a constant reference level, which may be for example the

average target of the industry. If we assume that the reference level $\mathcal{CE}^\star$ is equal to 3 $MtCO_2e$ (bottom/left panel), we notice that the net carbon budget is the difference between two areas. From January 2020 to October 2030, the carbon emissions are greater than $\mathcal{CE}^\star$ and this period has a positive contribution to the carbon budget. On the contrary, the period from November 2030 to December 2035 has a negative contribution. On average, the net carbon budget is positive. In the case where the reference level $\mathcal{CE}^\star$ is equal to 4 $MtCO_2e$ (bottom/right panel), the excess carbon budget is negative.

Figure 9.20: Past, expected and net carbon budgets (Example 40)

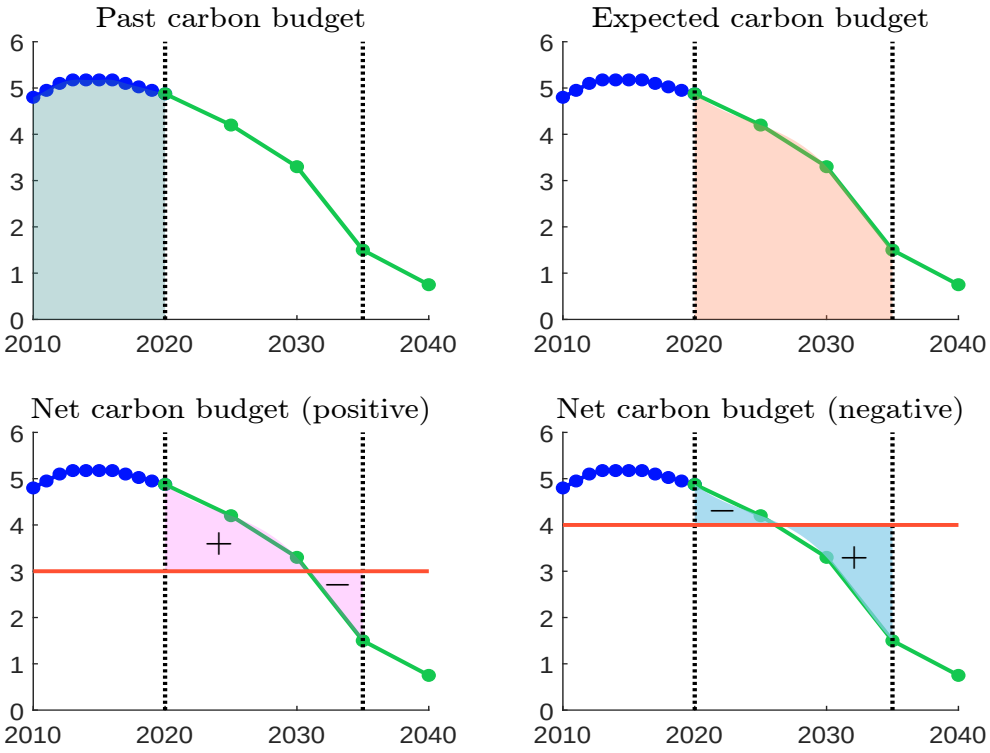


**Computation of the carbon budget (numerical solution)**

We consider the equally-spaced partition $\{[t_0, t_0 + \Delta t], \ldots, [t - \Delta t, t]\}$ of $[t_0, t]$. Let $m = \dfrac{t - t_0}{\Delta t}$ be the number of intervals. We set $\mathcal{CE}_k = \mathcal{CE}(t_0 + k\Delta t)$. The right Riemann approximation is:

$$\mathcal{CB}(t_0, t) = \int_{t_0}^{t} \mathcal{CE}(s)\, \mathrm{d}s \approx \sum_{k=1}^{m} \mathcal{CE}(t_0 + k\Delta t)\, \Delta t = \Delta t \sum_{k=1}^{m} \mathcal{CE}_k$$

If we use the left Riemann sum, we obtain:

$$\mathcal{CB}(t_0, t) \approx \Delta t \sum_{k=0}^{m-1} \mathcal{CE}_k$$

Finally, the midpoint rule is given by:

$$\mathcal{CB}(t_0, t) \approx \Delta t \sum_{k=1}^{m} \mathcal{CE}\left(t_0 + \frac{k}{2}\Delta t\right)$$

In the case of a yearly partition, the previous formulas are simplified since we have $\Delta t = 1$. For instance, the left Riemann sum becomes:

$$\mathcal{CB}(t_0, t) = \sum_{k=0}^{m-1} \mathcal{CE}_k = \mathcal{CE}(t_0) + \ldots + \mathcal{CE}(t-1)$$

If we consider Example 40, the carbon budget from 1st January 2010 to 1st January 2020 is equal to:

$$\begin{aligned}\mathcal{CB}(2010, 2020) &= 4.8 + 4.95 + 5.1 + 5.175 + 5.175 + 5.175 + 5.175 + 5.1 + 5.025 + 4.95 \\ &= 50.625 \text{ MtCO}_2\text{e}\end{aligned}$$

**Remark 107** *Instead of Riemann sums, we can use more sophisticated methods such as trapezoidal and Simpon's rules (Roncalli, 2020a, Section A.1.2.3, pages 1037-1041). We can also interpolate the carbon emissions with spline functions and then implement a Gaussian quadrature.*

### Computation of the carbon budget (analytical solution)

**Constant reduction rate** If we use a constant linear reduction rate $\mathcal{R}(t_0, t) = \mathcal{R}(t - t_0)$, we obtain the following analytical expression:

$$\mathcal{CB}(t_0, t) = \int_{t_0}^{t} (\mathcal{CE}(t_0) - \mathcal{R}(s - t_0))\, \mathrm{d}s = (t - t_0)\,\mathcal{CE}(t_0) - \frac{(t - t_0)^2}{2}\mathcal{R} \tag{9.6}$$

In the case of a constant compound reduction rate:

$$\mathcal{CE}(t) = (1 - \mathcal{R})^{(t-t_0)}\,\mathcal{CE}(t_0)$$

we obtain:

$$\begin{aligned}\mathcal{CB}(t_0, t) &= \mathcal{CE}(t_0) \int_{t_0}^{t} (1 - \mathcal{R})^{(s-t_0)}\, \mathrm{d}s \\ &= \mathcal{CE}(t_0) \left[\frac{(1 - \mathcal{R})^{(s-t_0)}}{\ln(1 - \mathcal{R})}\right]_{t_0}^{t} \\ &= \frac{(1 - \mathcal{R})^{(t-t_0)} - 1}{\ln(1 - \mathcal{R})}\mathcal{CE}(t_0)\end{aligned} \tag{9.7}$$

If we assume that $\mathcal{CE}(t) = e^{-\mathcal{R}(t-t_0)}\mathcal{CE}(t_0)$, we have:

$$\mathcal{CB}(t_0, t) = \mathcal{CE}(t_0) \left[-\frac{e^{-\mathcal{R}(s-t_0)}}{\mathcal{R}}\right]_{t_0}^{t} = \mathcal{CE}(t_0)\,\frac{\left(1 - e^{-\mathcal{R}(t-t_0)}\right)}{\mathcal{R}} \tag{9.8}$$

**Remark 108** *If the carbon emissions increase at a positive growth rate $g$, we set $\mathcal{R} = -g$.*

According to IPCC (2018), the probability that the temperature $\mathcal{T}$ remains below 1.5°C by 2050 depends on a carbon budget. They estimated that the remaining carbon budget $\mathcal{CB}(2019, t)$ is 580 $\text{GtCO}_2\text{e}$ for a 50% probability of limiting warming to 1.5°C, 420 $\text{GtCO}_2\text{e}$ for a 66% probability and 300 $\text{GtCO}_2\text{e}$ for a 83% probability. In Figure 9.21, we have computed $\mathcal{CB}(2019, t)$ by setting $\mathcal{CE}(2019) = 36$ $\text{GtCO}_2\text{e}$ and assuming a constant compound reduction rate $\mathcal{R}$. If nothing is done, the probability to reach 1.5°C by 2035 is close to 50% since we obtain $\mathcal{CB}(2019, 2035) = 571.41$ $\text{GtCO}_2\text{e}$. With a reduction rate of 7%, we have a probability of 65% to limit global warming to 1.5°C by 2050. This explains that many reduction targets are calibrated on this figure, for example the Paris aligned benchmarks (CTB and PAB).

Figure 9.21: Probability to reach 1.5°C

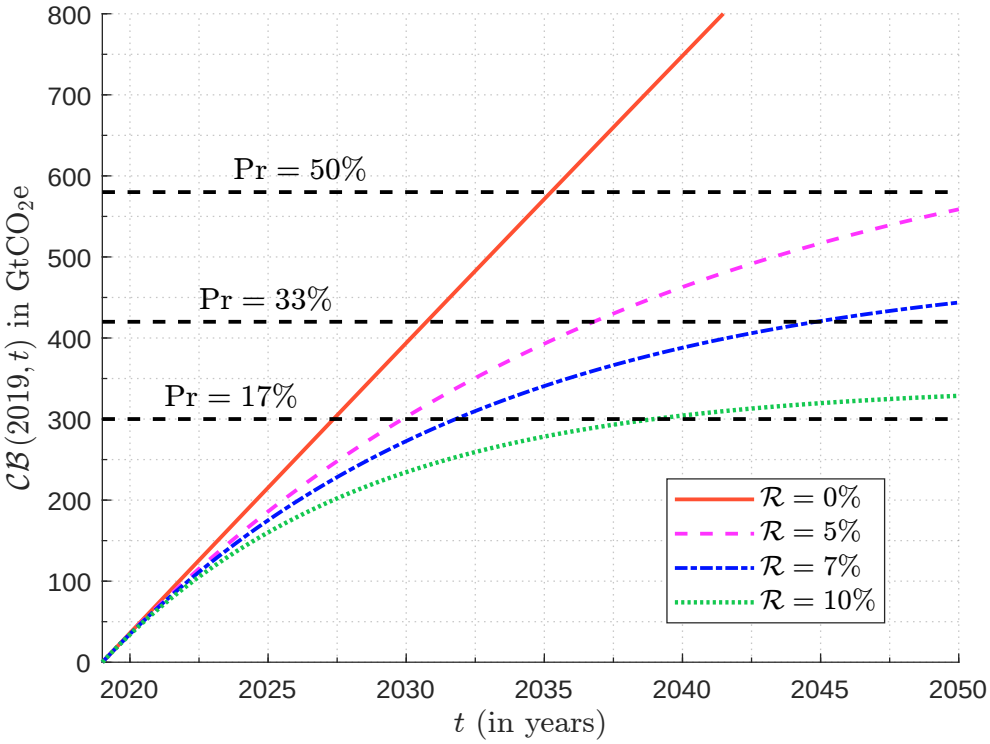


**Linear function** If we assume that $\boldsymbol{\mathcal{CE}}(t) = \beta_0 + \beta_1 t$, we deduce that:

$$\begin{aligned}\boldsymbol{\mathcal{CB}}(t_0,t) &= \int_{t_0}^{t} (\beta_0 + \beta_1 s)\,\mathrm{d}s \\ &= \left[\beta_0 s + \frac{1}{2}\beta_1 s^2\right]_{t_0}^{t} \\ &= \beta_0 (t - t_0) + \frac{1}{2}\beta_1 \left(t^2 - t_0^2\right) \end{aligned} \tag{9.9}$$

We can extend this formula to a piecewise linear function. We assume that $\boldsymbol{\mathcal{CE}}(t)$ is known for $t \in \{t_0, t_1, \ldots, t_m\}$ and $\boldsymbol{\mathcal{CE}}(t)$ is linear between two consecutive dates:

$$\boldsymbol{\mathcal{CE}}(t) = \boldsymbol{\mathcal{CE}}(t_{k-1}) + \frac{\boldsymbol{\mathcal{CE}}(t_k) - \boldsymbol{\mathcal{CE}}(t_{k-1})}{t_k - t_{k-1}}(t - t_{k-1}) \qquad \text{if } t \in [t_{k-1}, t_k]$$

We notice that this equation can be written as:

$$\boldsymbol{\mathcal{CE}}(t) = \underbrace{\frac{t_k}{t_k - t_{k-1}}\boldsymbol{\mathcal{CE}}(t_{k-1}) - \frac{t_{k-1}}{t_k - t_{k-1}}\boldsymbol{\mathcal{CE}}(t_k)}_{\beta_{0,k}} + \underbrace{\frac{\boldsymbol{\mathcal{CE}}(t_k) - \boldsymbol{\mathcal{CE}}(t_{k-1})}{t_k - t_{k-1}}}_{\beta_{1,k}} t$$

We deduce that:

$$\boldsymbol{\mathcal{CB}}(t_0,t) = \sum_{k=1}^{k(t)} \int_{t_{k-1}}^{t_k} \boldsymbol{\mathcal{CE}}(s)\,\mathrm{d}s + \int_{t_{k(t)}}^{t} \boldsymbol{\mathcal{CE}}(s)\,\mathrm{d}s$$

where $k(t) = \{\max k : t_k \leq t\}$. Using Equation (9.9), we conclude that[33]:

$$\mathcal{CB}(t_0, t) = \sum_{k=1}^{k(t)} \beta_{0,k}^{\star} (t_k - t_{k-1}) + \frac{1}{2} \sum_{k=1}^{k(t)} \beta_{1,k} \left(t_k^2 - t_{k-1}^2\right) + \beta_{0,k(t)+1} \left(t - t_{k(t)}\right) + \frac{1}{2} \beta_{1,k(t)+1} \left(t^2 - t_{k(t)}^2\right) \tag{9.10}$$

If we consider Example 40 and assume that the carbon emissions are linear between two consecutive years, the carbon budget from 1st January 2010 to 1st January 2020 is equal to 50.662 $MtCO_2e$, which is close to the value 50.625 $MtCO_2e$ obtained previously. When we consider the carbon targets, the Riemann sums are not appropriate because the targets are measured every five or ten years. Since the objective is that the company reduces continuously its carbon emissions, it is better to compute the carbon budget by assuming a piecewise linear function. In our example, we obtain $\mathcal{CB}(2020, 2035) = 53.437$ $MtCO_2e$with the following decomposition[34]: $\mathcal{CB}(2020, 2025) = 22.687$ $MtCO_2e$ (42.46%), $\mathcal{CB}(2025, 2030) = 18.750$ $MtCO_2e$ (35.09%) and $\mathcal{CB}(2030, 2035) = 12.000$ $MtCO_2e$ (22.46%). We also have $\mathcal{CB}(2020, 2050) = 63.562$ $MtCO_2e$, implying that the first period 2020–2035 represents 84.07% of the carbon emissions.

Table 9.18: IEA NZE scenario (in $GtCO_2e$)

| Sector | 2010 | 2011 | 2012 | 2013 | 2014 | 2015 | 2016 | 2017 | 2018 | 2019 |
|---|---|---|---|---|---|---|---|---|---|---|
| Electricity | 12.4 | 13 | 13.3 | 13.5 | 13.6 | 13.3 | 13.3 | 13.5 | 14 | 13.8 |
| Buildings | 2.89 | 2.81 | 2.78 | 2.9 | 2.84 | 2.87 | 2.91 | 2.95 | 2.98 | 3.01 |
| Transport | 7.01 | 7.13 | 7.18 | 7.37 | 7.5 | 7.72 | 7.88 | 8.08 | 8.25 | 8.29 |
| Industry | 8.06 | 8.47 | 8.57 | 8.71 | 8.78 | 8.71 | 8.56 | 8.52 | 8.72 | 8.9 |
| Other | 1.87 | 1.89 | 1.91 | 1.96 | 1.87 | 1.89 | 1.89 | 1.92 | 1.92 | 1.91 |
| Gross emissions | 32.2 | 33.3 | 33.7 | 34.4 | 34.5 | 34.5 | 34.5 | 35 | 35.9 | 35.9 |
| BECCS/DACCS | 0 | 0 | 0 | 0 | 0 | 0 | 0 | 0 | 0 | 0 |
| Net emissions | 32.2 | 33.3 | 33.7 | 34.4 | 34.5 | 34.5 | 34.5 | 35 | 35.9 | 35.9 |

| Sector | 2020 | 2025 | 2030 | 2035 | 2040 | 2045 | 2050 |
|---|---|---|---|---|---|---|---|
| Electricity | 13.5 | 10.8 | 5.82 | 2.12 | −0.08 | −0.31 | −0.37 |
| Buildings | 2.86 | 2.43 | 1.81 | 1.21 | 0.69 | 0.32 | 0.12 |
| Transport | 7.15 | 7.23 | 5.72 | 4.11 | 2.69 | 1.5 | 0.69 |
| Industry | 8.48 | 8.14 | 6.89 | 5.25 | 3.48 | 1.8 | 0.52 |
| Other | 1.91 | 1.66 | 0.91 | 0.09 | −0.46 | −0.82 | −0.96 |
| Gross emissions | 33.9 | 30.3 | 21.5 | 13.7 | 7.77 | 4.3 | 1.94 |
| BECCS/DACCS | 0 | −0.06 | −0.32 | −0.96 | −1.46 | −1.8 | −1.94 |
| Net emissions | 33.9 | 30.2 | 21.1 | 12.8 | 6.32 | 2.5 | 0.00 |

Source: IEA (2021, Figure 2.3, page 55).

[33] When $t$ belongs to the set $\{t_0, t_1, \ldots, t_m\}$, we can simplify this expression as follows:

$$\mathcal{CB}(t_0, t) = \sum_{k=1}^{k(t)} (\mathcal{CE}(t_{k-1}) t_k - \mathcal{CE}(t_k) t_{k-1}) + \frac{1}{2} \sum_{k=1}^{k(t)} (\mathcal{CE}(t_k) - \mathcal{CE}(t_{k-1})) (t_k + t_{k-1})$$

[34] We use the Chasles property of the Riemann integral:

$$\mathcal{CB}(t_0, t_2) = \int_{t_0}^{t_2} \mathcal{CE}(s)\, \mathrm{d}s = \int_{t_0}^{t_1} \mathcal{CE}(s)\, \mathrm{d}s + \int_{t_1}^{t_2} \mathcal{CE}(s)\, \mathrm{d}s = \mathcal{CB}(t_0, t_1) + \mathcal{CB}(t_1, t_2)$$

**Example 41** *We consider the net-zero emissions (NZE) scenario provided by the International Energy Agency (IEA, 2021). We remind that it is a normative scenario that shows a pathway for the global energy sector to achieve net-zero* $CO_2e$ *emissions by 2050. For each important sector, IEA gives the past trajectory of carbon emissions and the decarbonization pathway that could be achievable (Table 9.18). This net-zero scenario has been calibrated with a carbon budget of approximatively* 500 $GtCO_2e$.

Figure 9.22: $CO_2$ emissions by sector in the IEA NZE scenario (in $GtCO_2e$)

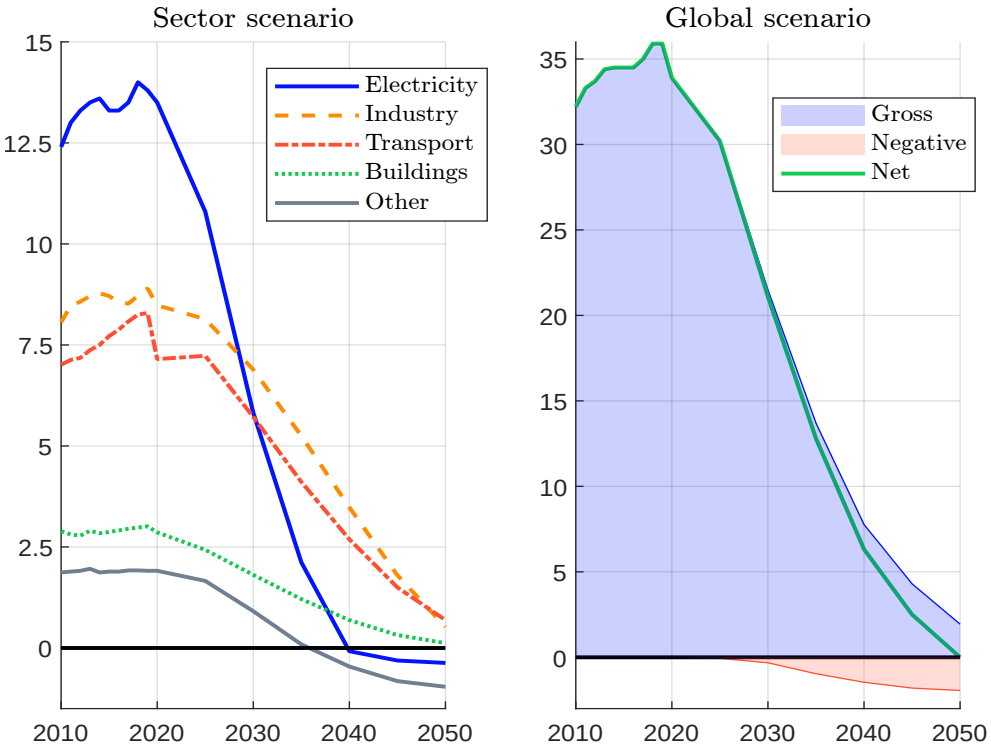


Source: IEA (2021) & Author's calculations.

In Figure 9.22, we show the decarbonization pathway of each sector and the global economy. We notice the importance of the technologies bioenergy with carbon capture and storage (BECCS) and direct air carbon capture with carbon storage (DACCS). Indeed, they will help to compensate the remaining 2 $GtCO_2e$ of carbon emissions. In Table 9.19, we have computed the carbon budget $\mathcal{CB}(2019, t)$ for each sector and the global system. We notice that the sectors Electricity, Industry and Transport represent about 85% of the global budget.

Table 9.19: Carbon budget in the IEA NZE scenario (in $GtCO_2e$)

| $t$ | Electricity | Buildings | Transport | Industry | Other | Gross emissions |
|---|---|---|---|---|---|---|
| 2025 | 74.4 | 50.2 | 43.7 | 16.2 | 10.8 | 195.4 |
| 2030 | 115.9 | 87.8 | 76.0 | 26.8 | 17.3 | 324.9 |
| 2040 | 140.9 | 140.0 | 117.6 | 39.1 | 18.8 | 466.6 |
| 2045 | 139.9 | 153.2 | 128.1 | 41.6 | 15.6 | 496.8 |
| 2050 | 138.2 | 159.0 | 133.6 | 42.7 | 11.2 | 512.4 |

Source: IEA (2021) & Author's calculations.

### 9.3.2 Carbon trend

#### Linear trend model

Le Guenedal *et al.* (2022) defined the carbon trend by considering the linear trend model:

$$\boldsymbol{\mathcal{CE}}(t) = \beta_0 + \beta_1 t + u(t) \tag{9.11}$$

where $u(t) \sim \mathcal{N}\left(0, \sigma_u^2\right)$. We estimate the parameters $\beta_0$ and $\beta_1$ with the least squares method and a sample of observations. Therefore, the projected carbon trajectory is given by:

$$\boldsymbol{\mathcal{CE}}^{\mathcal{T}rend}(t) = \widehat{\boldsymbol{\mathcal{CE}}}(t) = \hat{\beta}_0 + \hat{\beta}_1 t \tag{9.12}$$

Let $\{t_{\mathcal{F}irst}, t_{\mathcal{F}irst}+1, \ldots, t_{\mathcal{L}ast}\}$ be the set of observation dates. We interpret $\boldsymbol{\mathcal{CE}}^{\mathcal{T}rend}(t)$ as follows:

- If $t < t_{\mathcal{F}irst}$, $\boldsymbol{\mathcal{CE}}^{\mathcal{T}rend}(t)$ is the *back-calculated* value of carbon emissions before the first observation date (retropolation);
- If $t_{\mathcal{F}irst} \leq t \leq t_{\mathcal{L}ast}$, $\boldsymbol{\mathcal{CE}}^{\mathcal{T}rend}(t)$ is the *predicted* value of carbon emissions and can be compared with the *observed* value of carbon emissions (out-of-sample estimation);
- If $t > t_{\mathcal{L}ast}$, $\boldsymbol{\mathcal{CE}}^{\mathcal{T}rend}(t)$ is the *forecast* value of carbon emissions and could be compared with the *future* value of carbon emissions when this later will be available (out-of-sample estimation);

This model is very simple and the underlying idea is to extrapolate the past trajectory. Nevertheless, we can derive several metrics that are useful to compare the existing track record of the issuer with its willingness to really reduce its carbon emissions.

Equation (9.12) is not easy to interpret, because the intercept $\hat{\beta}_0$ corresponds to the estimated value $\widehat{\boldsymbol{\mathcal{CE}}}(0)$ at time $t = 0$. Then, it is convenient to use another base year $t_0$, implying that Equation (9.11) becomes:

$$\boldsymbol{\mathcal{CE}}(t) = \beta_0' + \beta_1'(t - t_0) + u(t) \tag{9.13}$$

In this case, the carbon trend is given by:

$$\boldsymbol{\mathcal{CE}}^{\mathcal{T}rend}(t) = \hat{\beta}_0' + \hat{\beta}_1'(t - t_0) \tag{9.14}$$

We can show that the two models (9.12) and (9.14) are equivalent and give the same value $\widehat{\boldsymbol{\mathcal{CE}}}(t)$. Indeed, we have the following relationships:

$$\begin{cases} \beta_0' = \beta_0 + \beta_1 t_0 \\ \beta_1' = \beta_1 \end{cases}$$

The new parameterization does not change the slope of the trend, but only the constant $\hat{\beta}_0'$ which is now equal to $\widehat{\boldsymbol{\mathcal{CE}}}(t_0)$.

**Remark 109** *The previous approach can be extended to the carbon intensity measure* $\boldsymbol{\mathcal{CI}}(t)$.

**Example 42** *In Table 9.20, we report the evolution of scope* $1+2$ *carbon emissions for company A.*

Table 9.20: Carbon emissions in $MtCO_2e$ (company $A$)

| Year | 2007 | 2008 | 2009 | 2010 | 2011 | 2012 | 2013 |
|---|---|---|---|---|---|---|---|
| $\mathcal{CE}(t)$ | 57.8 | 58.4 | 57.9 | 55.1 | 51.6 | 48.3 | 47.1 |
| Year | 2014 | 2015 | 2016 | 2017 | 2018 | 2019 | 2020 |
| $\mathcal{CE}(t)$ | 46.1 | 44.4 | 42.7 | 41.4 | 40.2 | 41.9 | 45.0 |

Using the carbon emissions given in Table 9.20, we obtain the following estimates[35]: $\hat{\beta}_0 = 2\,970.43$ and $\hat{\beta}_1 = -1.4512$. If we consider the regression model (9.13), the results become $\hat{\beta}'_0 = 57.85$ and $\hat{\beta}'_1 = -1.4512$ if the base year $t_0$ is set to 2007, and $\hat{\beta}'_0 = 38.99$ and $\hat{\beta}'_1 = -1.4512$ if the base year $t_0$ is set to 2020. We verify that all the figures are coherent:

$$\begin{aligned}\mathcal{CE}^{\mathcal{T}rend}(t) &= 38.99 - 1.4512 \times (t - 2020)\\ &= 2\,970.43 - 1.4512 \times t\end{aligned}$$

We notice that the trend model is more intuitive if we use the base year $t_0 = 2020$. The estimated carbon emissions is equal to 38.99 $MtCO_2e$ in 2020 and we observe a reduction of 1.4512 $MtCO_2e$ every year. For instance, the forecast value for the year 2025 is:

$$\mathcal{CE}^{\mathcal{T}rend}(2025) = 38.99 - 1.4512 \times 5 = 31.73 \text{ MtCO}_2\text{e}$$

We have reported the in-sample estimated values and out-of-sample forecast values in Figure 9.23. When $t$ is set to the year 2020, we observe that there is a gap between the observed value $\mathcal{CE}(t)$ and the estimated value $\widehat{\mathcal{CE}}(t)$ because $\mathcal{CE}(2020) = 45.0 \gg \widehat{\mathcal{CE}}(2020) = 38.99$. We deduce that the current carbon emissions are greater than the figure given by the trend, meaning that the company has made less effort in recent years compared to the past history. We can then rescale the trend model by imposing that the last value $\mathcal{CE}(t_{\mathcal{L}ast})$ is equal to the estimated value $\widehat{\mathcal{CE}}(t_{\mathcal{L}ast})$. We deduce that:

$$\hat{\beta}'_0 + \hat{\beta}'_1 (t_{\mathcal{L}ast} - t_0) = \mathcal{CE}(t_{\mathcal{L}ast}) \Leftrightarrow \hat{\beta}'_0 = \mathcal{CE}(t_{\mathcal{L}ast}) - \hat{\beta}'_1 (t_{\mathcal{L}ast} - t_0)$$

If $t_{\mathcal{L}ast} = t_0$, we obtain $\hat{\beta}'_0 = \mathcal{CE}(t_{\mathcal{L}ast})$. In our example, the rescaled model has the following expression:

$$\mathcal{CE}^{\mathcal{T}rend}(t) = 45 - 1.4512 \times (t - 2020)$$

In Figure 9.23, we verify that the rescaled model has the same slope as previously, but it is now coherent with the last observation of carbon emissions. In the sequel, we will always consider rescaled trend models, because they are more relevant.

### Log-linear trend model

Instead of a linear model, we can use a log-linear trend model:

$$\ln \mathcal{CE}(t) = \gamma_0 + \gamma_1 (t - t_0) + v(t) \tag{9.15}$$

where $v(t) \sim \mathcal{N}(0, \sigma_v^2)$. Again, we estimate the parameters $\gamma_0$ and $\gamma_1$ by ordinary least squares. Let $Y(t) = \ln \mathcal{CE}(t)$ be the logarithmic transform of the carbon emissions. We have:

$$\hat{Y}(t) = \hat{\gamma}_0 + \hat{\gamma}_1 (t - t_0)$$

[35] $\hat{\sigma}_u$ is equal to 2.5844.

Figure 9.23: Linear carbon trend (Example 42)

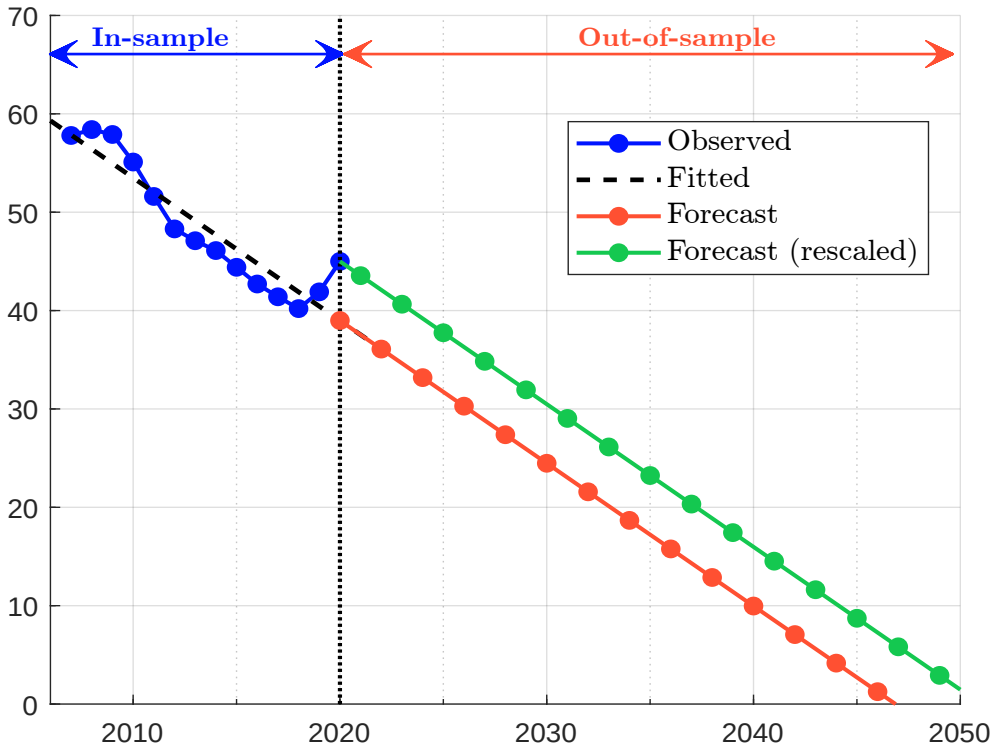


and:

$$\begin{aligned}\widehat{\mathcal{CE}}(t) &= \exp\left(\hat{Y}(t)\right)\\ &= \exp\left(\hat{\gamma}_0+\hat{\gamma}_1(t-t_0)\right)\\ &= \widehat{\mathcal{CE}}(t_0)\exp\left(\hat{\gamma}_1(t-t_0)\right)\end{aligned}$$

where $\widehat{\mathcal{CE}}(t_0)=\exp(\hat{\gamma}_0)$. The estimator (9.15) does not take into account the variance bias of log-linear models. Indeed, the correct value of the mathematical expectation is equal to[36]:

$$\begin{aligned}\mathbb{E}[\mathcal{CE}(t)] &= \mathbb{E}\left[e^{Y(t)}\right]\\ &= \mathbb{E}\left[\mathcal{LN}\left(\gamma_0+\gamma_1(t-t_0),\sigma_v^2\right)\right]\\ &= \exp\left(\gamma_0+\gamma_1(t-t_0)+\frac{1}{2}\sigma_v^2\right)\end{aligned}$$

Therefore, we obtain:

$$\begin{aligned}\widehat{\mathcal{CE}}(t) &= \exp\left(\hat{\gamma}_0+\hat{\gamma}_1(t-t_0)+\frac{1}{2}\hat{\sigma}_v^2\right)\\ &= \widehat{\mathcal{CE}}(t_0)\exp\left(\hat{\gamma}_1(t-t_0)\right)\end{aligned}$$

where $\widehat{\mathcal{CE}}(t_0)=\exp\left(\hat{\gamma}_0+\frac{1}{2}\hat{\sigma}_v^2\right)$. Again, we can rescale the trend model such that $\widehat{\mathcal{CE}}(t_{\mathcal{L}ast})=\mathcal{CE}(t_{\mathcal{L}ast})$. It follows that:

$$\hat{\gamma}_0+\frac{1}{2}\hat{\sigma}_v^2=\ln\mathcal{CE}(t_{\mathcal{L}ast})-\hat{\gamma}_1(t_{\mathcal{L}ast}-t_0)$$

[36] We remind that $\mathbb{E}[X]=\exp\left(\mu+\frac{1}{2}\sigma^2\right)$ if $X\sim\mathcal{LN}(\mu,\sigma^2)$ (see Section A.2.1 on page 1061).

If the base year $t_0$ is equal to the last year $t_{\mathcal{L}ast}$, the forecast value is equal to:

$$\mathcal{CE}^{\mathcal{T}rend}(t) = \mathcal{CE}(t_0)\exp(\hat{\gamma}_1(t - t_0)) \tag{9.16}$$

**Remark 110** *While the slope of the trend is measured in* $CO_2e$ *in the linear trend model, it is measured in* % *in the log-linear model. In fact, we estimate an absolute trend in the former model and a relative trend in the later model. From Equation (9.15), we have:*

$$\frac{\partial \mathcal{CE}(t)}{\partial t} = \frac{\exp(\gamma_0 + \gamma_1(t - t_0) + v(t))}{\partial t} = \gamma_1 \mathcal{CE}(t)$$

*We verify that the slope* $\gamma_1$ *is the relative variation of carbon emissions:*

$$\frac{\dfrac{\partial \mathcal{CE}(t)}{\partial t}}{\mathcal{CE}(t)} = \frac{\partial \ln \mathcal{CE}(t)}{\partial t} = \gamma_1$$

Using Example 42 and the 2020 base year, we obtain the following results: $\hat{\gamma}_0 = 3.6800$, $\hat{\gamma}_1 = -2.95\%$ and $\hat{\sigma}_v = 0.0520$. It follows that $\widehat{\mathcal{CE}}(2020)$ takes the value 39.65 $MtCO_2e$ without the correction of the variance bias and 39.70 $MtCO_2e$ with the correction of the variance bias. Using the parameterization (9.16), we compare the estimated log-linear trend with the estimated linear trend in Figure 9.24. We notice that the log-linear trend is convex and the future reduction rate of carbon emissions are less important than those obtained with the linear model.

Figure 9.24: Log-linear carbon trend (Example 42)

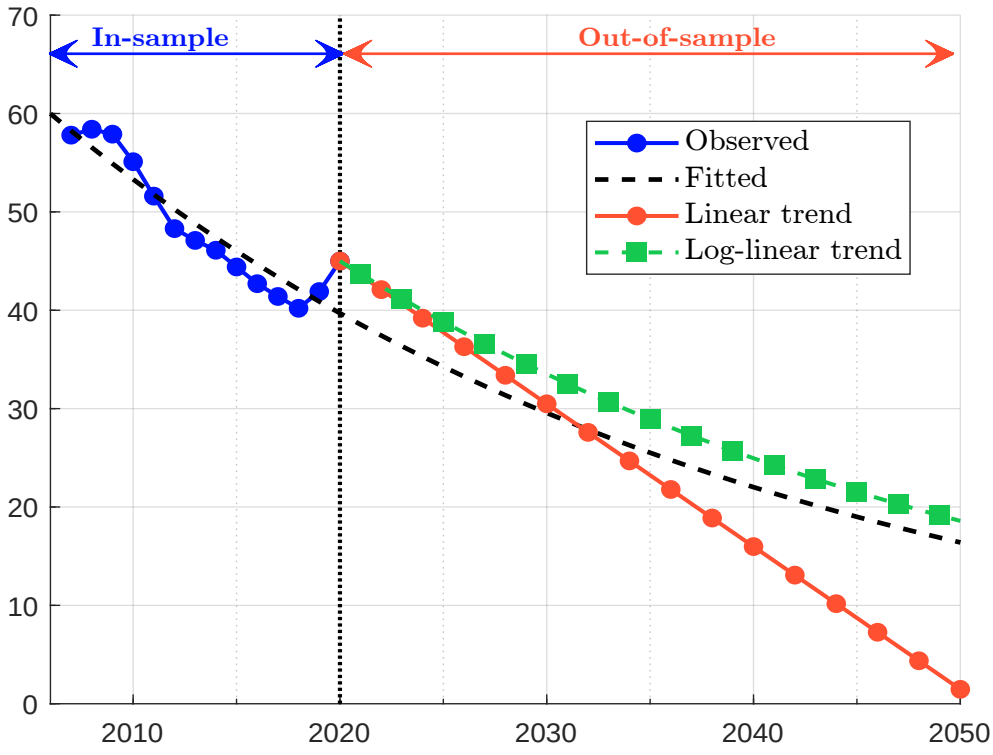

**Example 43** *We consider several historical trajectories of scope* 1 *carbon emissions:*

| # | 2010 | 2011 | 2012 | 2013 | 2014 | 2015 | 2016 | 2017 | 2018 | 2019 | 2020 |
|---|---|---|---|---|---|---|---|---|---|---|---|
| 1 | 10.0 | 11.1 | 10.5 | 12.5 | 13.0 | 14.8 | 16.0 | 16.5 | 17.0 | 17.5 | 19.8 |
| 2 | 10.0 | 10.2 | 10.5 | 11.0 | 10.8 | 10.8 | 13.0 | 12.5 | 13.5 | 13.6 | 13.6 |
| 3 | 10.0 | 9.9 | 9.5 | 9.0 | 9.3 | 8.8 | 8.7 | 8.5 | 9.0 | 8.0 | 8.2 |
| 4 | 10.0 | 9.5 | 9.0 | 9.0 | 8.3 | 8.1 | 7.7 | 6.5 | 7.0 | 6.1 | 6.2 |

For each historical trajectory, we estimate the two models and report the estimated trends in Figure 9.25. When the slope is positive, the log-linear trend is systematically above the linear trend in the long run ($t \to \infty$). When the slope is negative, we observe the oppositive phenomenon. In this last case, the linear trend $\widehat{\mathcal{CE}}(\infty)$ tends to $-\infty$ while the log-linear trend $\widehat{\mathcal{CE}}(\infty)$ tends to 0. The fact that carbon emissions are negative may be disturbing. From a theoretical viewpoint, it is not impossible because of the impact of negative emissions (due to negative emissions, carbon credits or carbon removal methods for instance). Nevertheless, it is extremely rare especially if we take into account scope 3 emissions. From a modeling viewpoint, it is then better to impose that carbon emissions are positive.

Figure 9.25: Log-linear vs. linear carbon trend (Example 43)

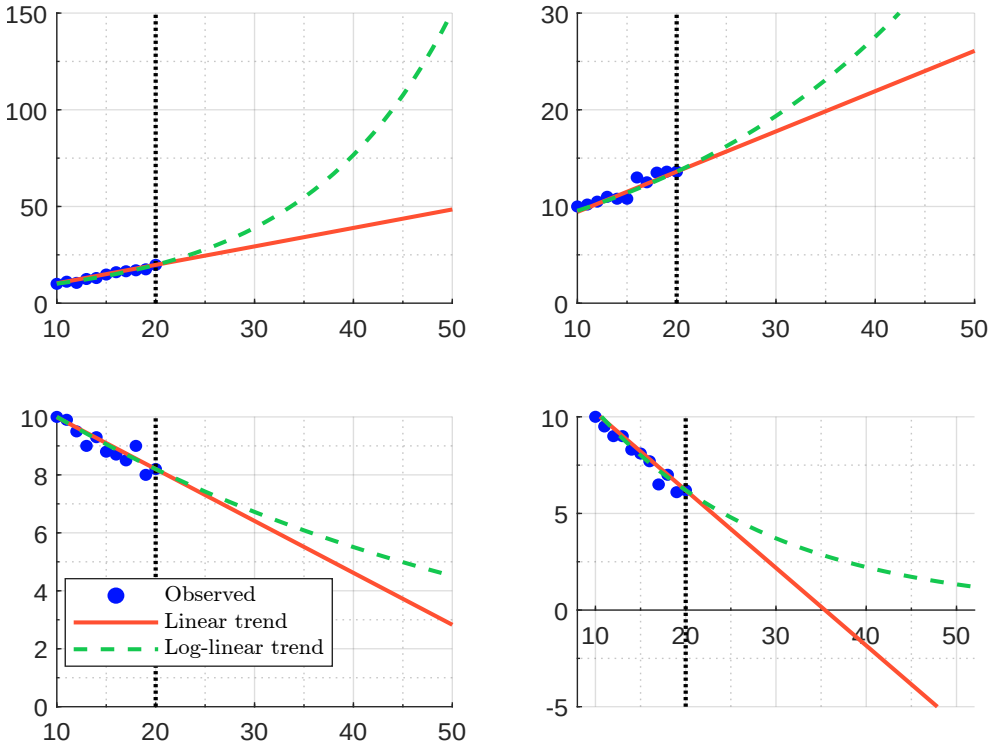


It seems then that the log-linear model is more relevant when the trend is negative. If we consider companies with a positive trend, the log-linear model may produce exploding carbon emissions. Let us compute the ratio of expected growth rates between $t_0$ and $t$. For the linear model, the expected growth rate is:

$$\frac{\widehat{\mathcal{CE}}(t) - \mathcal{CE}(t_0)}{\mathcal{CE}(t_0)} = \frac{\mathcal{CE}(t_0) + \hat{\beta}_1 (t - t_0) - \mathcal{CE}(t_0)}{\mathcal{CE}(t_0)} = \frac{\hat{\beta}_1 (t - t_0)}{\mathcal{CE}(t_0)}$$

while the log-linear model gives:

$$\frac{\widehat{\mathcal{CE}}(t) - \mathcal{CE}(t_0)}{\mathcal{CE}(t_0)} = \frac{\mathcal{CE}(t_0)\exp(\hat{\gamma}_1(t-t_0)) - \mathcal{CE}(t_0)}{\mathcal{CE}(t_0)} = \exp(\hat{\gamma}_1(t-t_0)) - 1$$

Therefore, the ratio of expected growth rates is proportional to:

$$\begin{aligned}
\frac{\exp(\hat{\gamma}_1(t-t_0)) - 1}{\hat{\beta}_1(t-t_0)} &\approx \frac{1}{\hat{\beta}_1(t-t_0)} \sum_{n=1}^{\infty} \frac{\hat{\gamma}_1^n (t-t_0)^n}{n!} \\
&= \frac{\hat{\gamma}_1}{\hat{\beta}_1} \sum_{n=0}^{\infty} \frac{\hat{\gamma}_1^n (t-t_0)^n}{(n+1)!} \\
&\approx \frac{\hat{\gamma}_1}{\hat{\beta}_1} \left(1 + \frac{1}{2}\hat{\gamma}_1(t-t_0) + \frac{1}{6}\hat{\gamma}_1^2(t-t_0)^2 + \frac{1}{24}\hat{\gamma}_1^3(t-t_0)^3 + \dots\right)
\end{aligned}$$

We deduce that the exploding effect cannot be avoided. This is why we must be very careful when we consider the log-linear model. One possible solution is to use the linear model when $\hat{\gamma}_1$ is greater than a threshold and the log-linear model otherwise. In Table 9.21, we compute the multiplication factor $M(\gamma_1, t) = e^{\gamma t}$ for different values of the growth rate $\gamma_1$ and different time horizon. For instance, if we target the year 2050, we have $t \approx 30$ years, we notice that carbon emissions are multiplied by a factor greater than 10 if the growth rate is 8%. Since there are many uncertainties about data collection and data computation, an historical growth rate of 8% may be explained by several factors:

- The company has really increased its carbon emissions by 8%;
- The company has underestimated its carbon emissions in the past and is more conservative today;
- The company has changed the reporting perimeter;
- Etc.

Applying a factor of 10 with a 30-year time horizon may then be not realistic. This is why we must be careful when estimating the carbon trend and analyze the outlier companies.

Table 9.21: Multiplication factor $M(\gamma_1, t)$

| $t$ | $\gamma_1$ | | | | | | | | | |
|---|---|---|---|---|---|---|---|---|---|---|
| (in years) | 1% | 2% | 3% | 4% | 5% | 6% | 7% | 8% | 9% | 10% |
| 1 | 1.01 | 1.02 | 1.03 | 1.04 | 1.05 | 1.06 | 1.07 | 1.08 | 1.09 | 1.11 |
| 5 | 1.05 | 1.11 | 1.16 | 1.22 | 1.28 | 1.35 | 1.42 | 1.49 | 1.57 | 1.65 |
| 10 | 1.11 | 1.22 | 1.35 | 1.49 | 1.65 | 1.82 | 2.01 | 2.23 | 2.46 | 2.72 |
| 15 | 1.16 | 1.35 | 1.57 | 1.82 | 2.12 | 2.46 | 2.86 | 3.32 | 3.86 | 4.48 |
| 20 | 1.22 | 1.49 | 1.82 | 2.23 | 2.72 | 3.32 | 4.06 | 4.95 | 6.05 | 7.39 |
| 25 | 1.28 | 1.65 | 2.12 | 2.72 | 3.49 | 4.48 | 5.75 | 7.39 | 9.49 | 12.18 |
| 30 | 1.35 | 1.82 | 2.46 | 3.32 | 4.48 | 6.05 | 8.17 | 11.02 | 14.88 | 20.09 |

**Remark 111** *The expected growth rate is related to the concept of carbon momentum that will be presented later on page 927.*

### Stochastic trend model

Following Roncalli (2020a), the linear trend model can be written as:

$$\begin{cases} y(t) = \mu(t) + u(t) \\ \mu(t) = \mu(t-1) + \beta_1 \end{cases}$$

where $u(t) \sim \mathcal{N}\left(0, \sigma_u^2\right)$. In this case, we have $y(t) = \beta_0 + \beta_1 t + u(t)$ where $\beta_0 = \mu(t_0) - \beta_1 t_0$. A way to introduce a stochastic trend is to add a noise $\eta(t)$ in the trend equation: $\mu(t) = \mu(t-1) + \beta_1 + \eta(t)$ where $\eta(t) \sim \mathcal{N}\left(0, \sigma_\eta^2\right)$. Let us now assume that the slope of the trend is also stochastic:

$$\begin{cases} y(t) = \mu(t) + u(t) \\ \mu(t) = \mu(t-1) + \beta_1(t-1) + \eta(t) \\ \beta_1(t) = \beta_1(t-1) + \zeta(t) \end{cases}$$

where $\zeta(t) \sim \mathcal{N}\left(0, \sigma_\zeta^2\right)$. This model is called the local linear trend (LLT) model (Roncalli, 2020a, page 653). Using the Kalman filter (KF), we can estimate both the stochastic trend $\mu(t)$ and the stochastic slope $\beta_1(t)$.

Let us come back to Example 42. We estimate the parameters $(\sigma_u, \sigma_\eta, \sigma_\zeta)$ by maximizing the Whittle log-likelihood function (Roncalli, 2020a, pages 686-687). We obtain $\hat{\sigma}_u = 0.7022$, $\hat{\sigma}_\eta = 0.7019$ and $\hat{\sigma}_\zeta = 0.8350$. We deduce that the standard deviation of the stochastic slope variation $\beta_1(t) - \beta_1(t-1)$ is equal to 0.8350 $\mathrm{MtCO_2e}$. This indicates that there is a high uncertainty in the trend computation. Then, we run the Kalman filter to estimate $\hat{\mu}(t)$ and $\hat{\beta}_1(t)$. In Table 9.22, we report these values and compare them with the estimates using the rolling least squares (RLS). We notice that the time-varying slope produced by the Kalman filter may be very different from the one produced by the method of least squares[37]. In particular, the magnitude of the variability is not the same. This is normal since the rolling least squares estimate a global slope from the beginning of the sample to time $t$ whereas the Kalman filter estimates a local slope for the period $[t-1, t]$. Therefore, $\hat{\beta}_i(t)$ is an estimator of the average slope in the case of the linear trend model and an estimator of the marginal slope in the case of the local linear trend model.

**Remark 112** *With the stochastic trend model, Le Guenedal et al. (2022) introduce the concept of carbon velocity, which measures the normalized slope change between $t-h$ and $t$:*

$$\boldsymbol{v}^{(h)}(t) = \frac{\hat{\beta}_1(t) - \hat{\beta}_1(t-h)}{h}$$

*The rationale for this measure is the following. A commitment to reduce carbon emissions implies a negative trend: $\hat{\beta}_1(t) < 0$. Nevertheless, it can take many years for a company to change the sign of the trend slope if it has a bad track record. Therefore, we can use the velocity to verify that the company is making significant efforts in the recent period. In this case, we must have $\boldsymbol{v}^{(h)}(t) < 0$ for low values[38] of $h$. In the case of the local linear trend model, we notice that the one-step velocity is equal to the innovation of the slope:*

$$\boldsymbol{v}^{(1)}(t) = \hat{\beta}_1(t) - \hat{\beta}_1(t-1) = \hat{\zeta}(t)$$

[37] For instance, we have $\hat{\beta}_1(2020) = -1.4512$ $\mathrm{MtCO_2e}$ with the least squares method and $\hat{\beta}_1(2020) = +1.7701$ $\mathrm{MtCO_2e}$ with the Kalman filter.

[38] Generally, $h$ is equal to 1, 2 or 3 years.

Table 9.22: Kalman filter estimation of the stochastic trend (Example 42)

| $t$ | $\mathcal{CE}(t)$ | $\hat{\beta}_1(t)$ (RLS) | $\beta_1(t)$ (KF) | $\mu(t)$ (KF) |
|---|---|---|---|---|
| 2007 | 57.80 | | 0.0000 | 57.80 |
| 2008 | 58.40 | | 0.2168 | 58.25 |
| 2009 | 57.90 | 0.0500 | −0.0441 | 58.00 |
| 2010 | 55.10 | −0.8600 | −1.3941 | 55.56 |
| 2011 | 51.60 | −1.5700 | −2.6080 | 52.01 |
| 2012 | 48.30 | −2.0200 | −3.1288 | 48.47 |
| 2013 | 47.10 | −2.0929 | −2.2977 | 46.82 |
| 2014 | 46.10 | −2.0321 | −1.5508 | 45.85 |
| 2015 | 44.40 | −1.9817 | −1.5029 | 44.38 |
| 2016 | 42.70 | −1.9406 | −1.5887 | 42.73 |
| 2017 | 41.40 | −1.8891 | −1.4655 | 41.36 |
| 2018 | 40.20 | −1.8329 | −1.3202 | 40.15 |
| 2019 | 41.90 | −1.6824 | 0.1339 | 41.41 |
| 2020 | 45.00 | −1.4512 | 1.7701 | 44.45 |

### Carbon momentum

Le Guenedal *et al.* (2022) define the long-term carbon momentum as the growth rate of carbon emissions. In the case of the linear trend model, we have:

$$\mathcal{CM}^{Long}(t) = \frac{\hat{\beta}_1(t)}{\mathcal{CE}(t)}$$

while it is directly equal to $\hat{\gamma}_1(t)$ in the case of the log-linear trend model:

$$\mathcal{CM}^{Long}(t) = \hat{\gamma}_1(t)$$

Le Guenedal *et al.* (2022) also define the short-term carbon momentum as the one-year carbon velocity:

$$\mathcal{CM}^{Short}(t) = \frac{\boldsymbol{v}^{(1)}(t)}{\mathcal{CE}(t)}$$

If we apply this concept to the log-linear model, we obtain $\mathcal{CM}^{Short}(t) = \boldsymbol{v}^{(1)}(t)$ where:

$$\boldsymbol{v}^{(h)}(t) = \frac{\hat{\gamma}_1(t) - \hat{\gamma}_1(t-h)}{h}$$

In the case of the stochastic trend model, we have $\mathcal{CM}^{Short}(t) = \hat{\zeta}(t)$.

**Remark 113** *Carbon momentum plays a key role when we will define net-zero investment portfolios, because it is highly related to the concept of self-decarbonization*[39].

[39] See Section 11.3 on page 991.

### Application

Table 9.23 and 9.24 gives some statistics about carbon momentum. It reproduces the results obtained by Barahhou *et al.* (2022) by considering the issuers of the MSCI World index. Since it is difficult to obtain at least 5-year historical data, we focus on the scopes $\mathcal{SC}_1$, $\mathcal{SC}_{1-2}$ and $\mathcal{SC}_{1-3}^{\text{up}}$, and we do not consider the scope $\mathcal{SC}_{1-3}$. If we use the linear trend model, the median value of $\mathcal{CM}^{\mathcal{L}ong}(t)$ is equal to 0% for scope 1, 1.6% when we include the scope 2, and 2.3% when we add the upstream scope 3. The carbon momentum is negative for only 29.4% of issuers when we consider $\mathcal{SC}_{1-3}^{\text{up}}$. This means that a majority of issuers have a positive carbon trend. For instance, about 10% of issuers have a carbon momentum greater than 10%! If we consider carbon intensity instead of carbon emission, we obtain another story. Indeed, issuers with a negative trend dominate issuers with a positive trend. Therefore, it is easier to build a self-decarbonized portfolio when we consider the carbon intensity measure. If we estimate the carbon momentum with the log-linear trend model, results are slightly different. For instance, 19.2% of issuers have a carbon momentum $\mathcal{SC}_{1-3}^{\text{up}}$ greater than 10% versus 8.0% with the linear trend model.

Table 9.23: Statistics (in %) of carbon momentum $\mathcal{CM}^{\mathcal{L}ong}(t)$ (MSCI World index, 1995 – 2021, linear trend)

| Statistics | Carbon emissions | | | Carbon intensity | | |
|---|---|---|---|---|---|---|
| | $\mathcal{SC}_1$ | $\mathcal{SC}_{1-2}$ | $\mathcal{SC}_{1-3}^{\text{up}}$ | $\mathcal{SC}_1$ | $\mathcal{SC}_{1-2}$ | $\mathcal{SC}_{1-3}^{\text{up}}$ |
| Median | 0.0 | 1.6 | 2.3 | −4.8 | −2.4 | −1.3 |
| Negative | 49.9 | 41.1 | 29.4 | 76.0 | 69.6 | 75.6 |
| Positive | 50.1 | 58.9 | 70.6 | 24.0 | 30.4 | 24.4 |
| $< -10\%$ | 23.4 | 15.8 | 5.8 | 36.0 | 25.0 | 5.7 |
| $< -5\%$ | 32.1 | 22.2 | 10.6 | 48.6 | 36.7 | 13.4 |
| $> +5\%$ | 22.9 | 27.5 | 23.6 | 6.2 | 7.3 | 2.7 |
| $> +10\%$ | 9.2 | 9.5 | 8.0 | 2.3 | 2.6 | 1.0 |

Source: Trucost database (2022) & Barahhou *et al.* (2022).

Table 9.24: Statistics (in %) of carbon momentum $\mathcal{CM}^{\mathcal{L}ong}(t)$ (MSCI World index, 1995 – 2021, log-linear trend)

| Statistics | Carbon emissions | | | Carbon intensity | | |
|---|---|---|---|---|---|---|
| | $\mathcal{SC}_1$ | $\mathcal{SC}_{1-2}$ | $\mathcal{SC}_{1-3}^{\text{up}}$ | $\mathcal{SC}_1$ | $\mathcal{SC}_{1-2}$ | $\mathcal{SC}_{1-3}^{\text{up}}$ |
| Median | −0.1 | 1.7 | 2.8 | −3.6 | −1.9 | −1.2 |
| Negative | 50.6 | 40.3 | 29.0 | 76.3 | 69.0 | 75.8 |
| Positive | 49.4 | 59.7 | 71.0 | 23.7 | 31.0 | 24.2 |
| $< -10\%$ | 13.6 | 8.0 | 2.8 | 20.8 | 12.3 | 2.1 |
| $< -5\%$ | 26.6 | 16.9 | 7.5 | 42.3 | 29.0 | 8.4 |
| $> +5\%$ | 29.8 | 35.9 | 37.1 | 9.0 | 10.1 | 4.0 |
| $> +10\%$ | 16.9 | 19.4 | 19.2 | 4.0 | 4.1 | 1.6 |

Source: Trucost database (2022) & Barahhou *et al.* (2022).

### 9.3.3 Participation, ambition and credibility for an alignment strategy

In this section, we define the three pillars that help to evaluate a company's alignment strategy with respect to a given climate scenario, *e.g.*, the net-zero emissions scenario. These three pillars are participation, ambition and credibility. They form the $\mathcal{PAC}$ framework, and they can be quantified using the tool of carbon budget.

#### Carbon target and decarbonization scenario

In addition to the historical pathway of carbon emissions, the $\mathcal{PAC}$ framework requires two other time series:

- The reduction targets announced by the company;
- The market-based sector scenario associated to the company that defines the decarbonization pathway.

Carbon reduction targets are defined by companies at a scope emissions level with different time horizons[40]. For instance, the issuer can commit to reduce its scope 1 emissions by 50% over a period of 20 years and its scope 3 emissions by 30% over a period of 10 years. Even if the time frame of carbon reduction targets goes to 60 years, most of reduction targets concern the next twenty years. In the CDP database, we observe that most targets are underway or new, and a large proportion of companies set targets to reduce emissions by less than 50% from their base year. We also notice that some targets are reported over multiple scopes[41] and we can have multiple release dates. Therefore, it is important to transform these heterogenous figures into a unique reduction pathway with one base year $t_0$:

$$\mathbb{CT} = \left\{ \boldsymbol{\mathcal{R}}^{\mathcal{T}arget}\left(t_0, t_k\right), k = 1, \ldots, n_T \right\}$$

where $n_T$ is the number of targets and $\boldsymbol{\mathcal{R}}^{\mathcal{T}arget}\left(t_0, t_k\right)$ is the reduction rate between $t_0$ and $t_k$ for the $k^{\text{th}}$ target.

Concerning the market-based scenario, we generally use sector scenarios provided by IPCC, IEA or IIASA. In some circumstances, we can take global scenarios, but only when we do not have the choice because there is no appropriate scenario for the sector. Again, the decarbonization scenario is defined as a set of reduction rates:

$$\mathbb{CS} = \left\{ \boldsymbol{\mathcal{R}}^{\mathcal{S}cenario}\left(t_0, t_k\right), k = 1, \ldots, n_S \right\}$$

where $n_S$ is the number of scenario data points. The reduction rate is calculated as follows:

$$\boldsymbol{\mathcal{R}}^{\mathcal{S}cenario}\left(t_0, t_k\right) = 1 - \frac{\boldsymbol{\mathcal{CE}}^{\mathcal{S}cenario}\left(t_k\right)}{\boldsymbol{\mathcal{CE}}^{\mathcal{S}cenario}\left(t_0\right)}$$

where $t_0$ is the base year and $\boldsymbol{\mathcal{CE}}^{S}\left(t_k\right)$ is the value of carbon emissions at time $t_k$ in the market-based scenario. For instance, if we consider the IEA NZE scenario (see Table 9.18 on page 918), we obtain the results given in Table 9.25. Carbon emissions have been floored at zero in order to verify that the reduction rate is always less than or equal to 100%. We notice that the Electricity sector must decarbonize very quickly: $-20\%$ in 2025, $-57\%$ in 2030 and $-84\%$ in 2035. The carbon emissions reduction of the Industry and Transport sectors is delayed and really begins after 2025. If we consider the global scenario, the reduction rate is set to 10% in 2025 and increases by 5% every year until 2035.

[40] Carbon reduction targets can be found in the CDP database.
[41] For instance, the target can concern only one scope, scope $1 + 2$ or all scopes.

Table 9.25: Reduction rates of the IEA NZE scenario (base year = 2020)

| Year | Electricity | Industry | Transport | Buildings | Other | Global |
|---|---|---|---|---|---|---|
| 2025 | 20.0 | 4.0 | −1.1 | 15.0 | 13.1 | 10.6 |
| 2030 | 56.9 | 18.8 | 20.0 | 36.7 | 52.4 | 36.6 |
| 2035 | 84.3 | 38.1 | 42.5 | 57.7 | 95.3 | 59.6 |
| 2040 | 100.0 | 59.0 | 62.4 | 75.9 | 100.0 | 77.1 |
| 2045 | 100.0 | 78.8 | 79.0 | 88.8 | 100.0 | 87.3 |
| 2050 | 100.0 | 93.9 | 90.3 | 95.8 | 100.0 | 94.3 |

Source: IEA (2021) & Author's calculations.

### Definition of the $\mathcal{PAC}$ framework

The $\mathcal{PAC}$ framework has been introduced by Le Guenedal *et al.* (2022) and is based on the relative positioning of three carbon trajectories: (1) the historical trajectory and its trend, (2) the carbon targets and (3) the decarbonization scenario. It helps to answer several operational questions.

1. First, is the trend of the issuer in line with the scenario? In this case, we would like to know if the company has already reduced its carbon emissions. While the reduction targets correspond to future intentions, the carbon trend measures the past efforts of the company.

2. Is the commitment of the issuer to fight climate change ambitious? In particular, we would like to know if the target trajectory is above, below or in line with the market-based scenario, which is appropriate for the sector of the issuer. This is an important topic, because achieving the net-zero emissions scenario can only be possible if there are no free riders.

3. Finally, a third question is critical and certainly the most important issue. Is the target setting of the company relevant and robust? Indeed, we may wonder if the target trajectory is a too ambitious promise and a form of greenwashing or, on the contrary, a plausible decarbonization pathway.

Therefore, the assessment of the company's targets has three dimensions or pillars: (historical) participation, ambition and credibility. They form the $\mathcal{PAC}$ framework.

**Example 44** *We consider again Example 42. Company A has announced the following targets:* $\boldsymbol{\mathcal{R}}^{\mathcal{T}arget}(2020, 2025) = 40\%$, $\boldsymbol{\mathcal{R}}^{\mathcal{T}arget}(2020, 2030) = 50\%$, $\boldsymbol{\mathcal{R}}^{\mathcal{T}arget}(2020, 2035) = 75\%$, $\boldsymbol{\mathcal{R}}^{\mathcal{T}arget}(2020, 2040) = 80\%$ *and* $\boldsymbol{\mathcal{R}}^{\mathcal{T}arget}(2020, 2050) = 90\%$. *Since company A is an utility corporation, we propose to use the IEA NZE scenario for the sector Electricity.*

We have reported the different pathways of company $A$ in Figure 9.26. We notice that the announced targets are below the carbon trend except in 2050. A comparison between the targets and the global scenario indicates that company $A$ is more ambitious than the average firm. Nevertheless, the comparison is less favorable when we consider the decarbonization scenario of the corresponding sector. In order to quantify the relative the relative positioning of these trajectories, we compute the carbon budgets with the different pathways. If we consider the time horizon 2035, the carbon budget of the targets is slightly lower than the carbon budget of the decarbonization scenario (388 vs. 407 $MtCO_2e$). This indicates a true ambition to reduce its carbon emissions in line with what the market expects. Nevertheless, we observe a high carbon budget based on the trend model (512 $MtCO_2e$). This questions the credibility of the targets, even if the company has done some efforts in the past.

Table 9.26: Comparison of carbon budgets (base year = 2020, Example 44)

| Year | Trend (linear) | Trend (log-linear) | Target | Scenario (global) | Scenario (electricity) |
|---|---|---|---|---|---|
| 2025 | 207 | 209 | 180 | 213 | 203 |
| 2030 | 377 | 390 | 304 | 385 | 341 |
| 2035 | 512 | 546 | 388 | 502 | 407 |
| 2040 | 610 | 680 | 439 | 573 | 425 |
| 2045 | 671 | 796 | 478 | 613 | 425 |
| 2050 | 697 | 896 | 506 | 634 | 425 |

**Assessment of the $\mathcal{PAC}$ pillars**

These three pillars depend on the carbon trajectories $\boldsymbol{\mathcal{CE}}(t)$, $\boldsymbol{\mathcal{CE}}^{\mathcal{T}rend}(t)$, $\boldsymbol{\mathcal{CE}}^{\mathcal{T}arget}(t)$ and $\boldsymbol{\mathcal{CE}}^{\mathcal{S}cenario}(t)$, where $\boldsymbol{\mathcal{CE}}(t)$ is the time series of historical carbon emissions, $\boldsymbol{\mathcal{CE}}^{\mathcal{T}rend}(t)$ and $\boldsymbol{\mathcal{CE}}^{\mathcal{T}arget}(t)$ are the estimated carbon emissions deduced from the trend model and the targets, and $\boldsymbol{\mathcal{CE}}^{\mathcal{S}cenario}(t)$ is the market-based decarbonization scenario. Generally, the participation only depends on the past observations and corresponds to the track record analysis of historical carbon emissions. The ambition compares the target trajectory on one side and the scenario or the trend on the other side. Indeed, we measure to what extent companies are willing to reverse their current carbon emissions and have objectives that match the scenario. Finally, we can measure the credibility of the targets by comparing the current trend of carbon emissions and the reduction targets or by analyzing the recent dynamics of the track record.

We note $t_{\mathcal{F}irst}$ as the first date, $t_{\mathcal{L}ast}$ as the last reporting date and $t_{\mathcal{S}cenario}$ as the target date of the decarbonization scenario. In Figure 9.27, we illustrate the underlying ideas of the $\mathcal{PAC}$ pillars. Let us consider the first three panels. They show the historical carbon emissions of different companies. It is obvious that the company in the top-left panel has a positive participation to slow global warming, whereas the participation of the company in the top-center panel is negative. In the top-right panel, we give three examples that are mixed. In this case, we do not observe a clear pattern: downward or upward trend of carbon emissions. Therefore, the company's participation can be measured by the metrics that are related to the carbon trend. The next three panels in Figure 9.27 illustrate the ambition pillar. In this case, we directly compare the carbon targets of the company and the market-based risk scenario. The companies belong to the same sector, implying that the decarbonization scenario is the same for the middle-left, middle-center and middle-right panels. The middle-left panel shows an ambitious company since its carbon targets are lower than the market-based scenario. In other words, the company has announced that it will make a greater effort than is expected by the market. On the contrary, the company in the middle-center panel is less ambitious, because it plans to reduce its carbon emissions at a slower pace. Finally, the middle-right panel presents two mixed situations. The first one concerns a company that has high ambitions at the beginning of the period $[t_{\mathcal{L}ast}, t_{\mathcal{S}cenario}]$ but it has not disclosed its ambitions for the end of the period. The company's ambition in the short term is then counterweighted by the absence of ambition in the long run. The second example is about a company that concentrates its ambition in the long run. These two examples question the true willingness of these companies to substantially reduce their carbon emissions. Finally, the credibility pillar is illustrated in the last three panels in Figure 9.27. In this case, we compare the carbon emissions trend and the targets communicated by the company. The bottom-left panel corresponds to a credible company, since it has announced more or less a reduction trajectory that is in line with what it has done in the

Figure 9.26: Carbon trend, targets and NZE scenario of company $A$

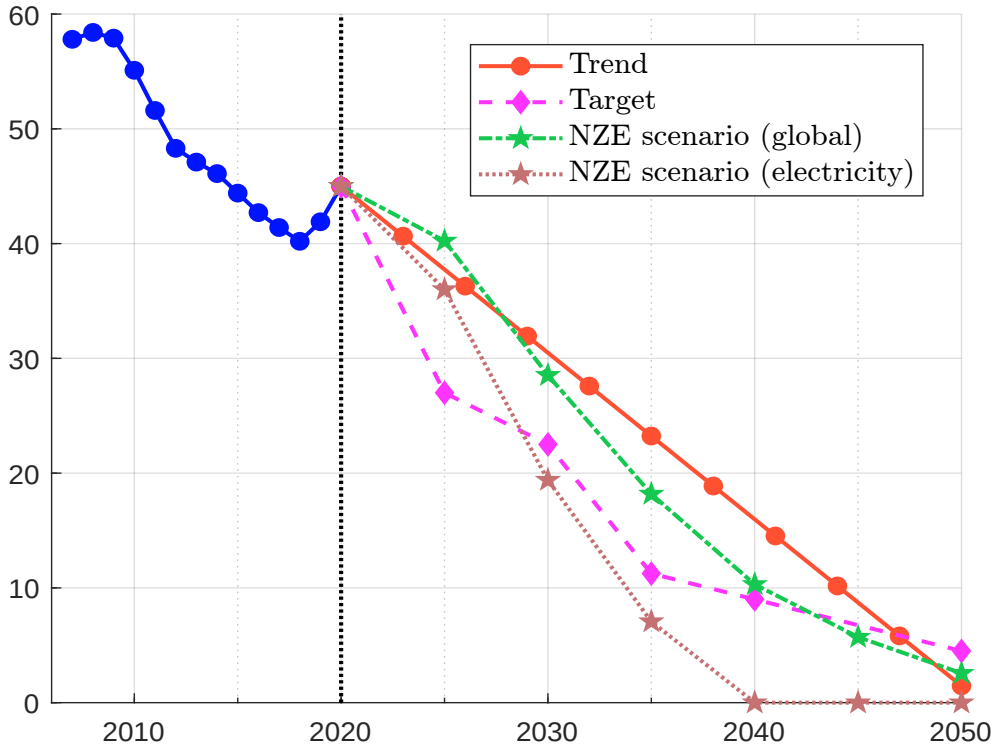


Source: IEA (2021) & Author's calculations.

past. This is not the case of the company in the bottom-center panel. Clearly, it has announced a reduction of its carbon emissions, but it has continuously increased them in the past. Again, the bottom-right panel presents a mixed situation. The company has announced a reduction trajectory that is not very far from the past trend, but there are two issues. The first one is that it has increased its carbon emissions in the short term, implying that we can have some doubts about the downward trend. The second issue is that it accelerates its objective of carbon emissions reduction at the end of the period $[t_{\mathcal{L}ast}, t_{\mathcal{S}cenario}]$ in order to meet the requirements of the market-based scenario, but its efforts are not very substantial in the short term.

### Temperature scoring system

Le Guenedal *et al.* (2022) derive many metrics to measure the three dimensions. They can be classified into four main families. The gap metrics measure the differences between two trajectories or carbon budgets[42]. The duration metrics calculate the time which is necessary to achieve a given objective[43]. The velocity metrics assess the short-term dynamics of the carbon emissions. Finally,

[42] An example is the difference between the trend budget and the scenario budget:

$$\mathcal{G}ap\left(t, t^{\mathcal{S}cenario}\right) = \mathcal{CB}^{\mathcal{T}rend}\left(t, t^{\mathcal{S}cenario}\right) - \mathcal{CB}^{\mathcal{S}cenario}\left(t, t^{\mathcal{S}cenario}\right)$$

[43] For instance, the trend duration is the time horizon for achieving zero carbon emissions:

$$\mathcal{D}^{\mathcal{T}rend} = \inf\left\{t : \mathcal{CE}^{\mathcal{T}rend}(t) \leq 0\right\}$$

Figure 9.27: Illustration of the participation, ambition and credibility pillars

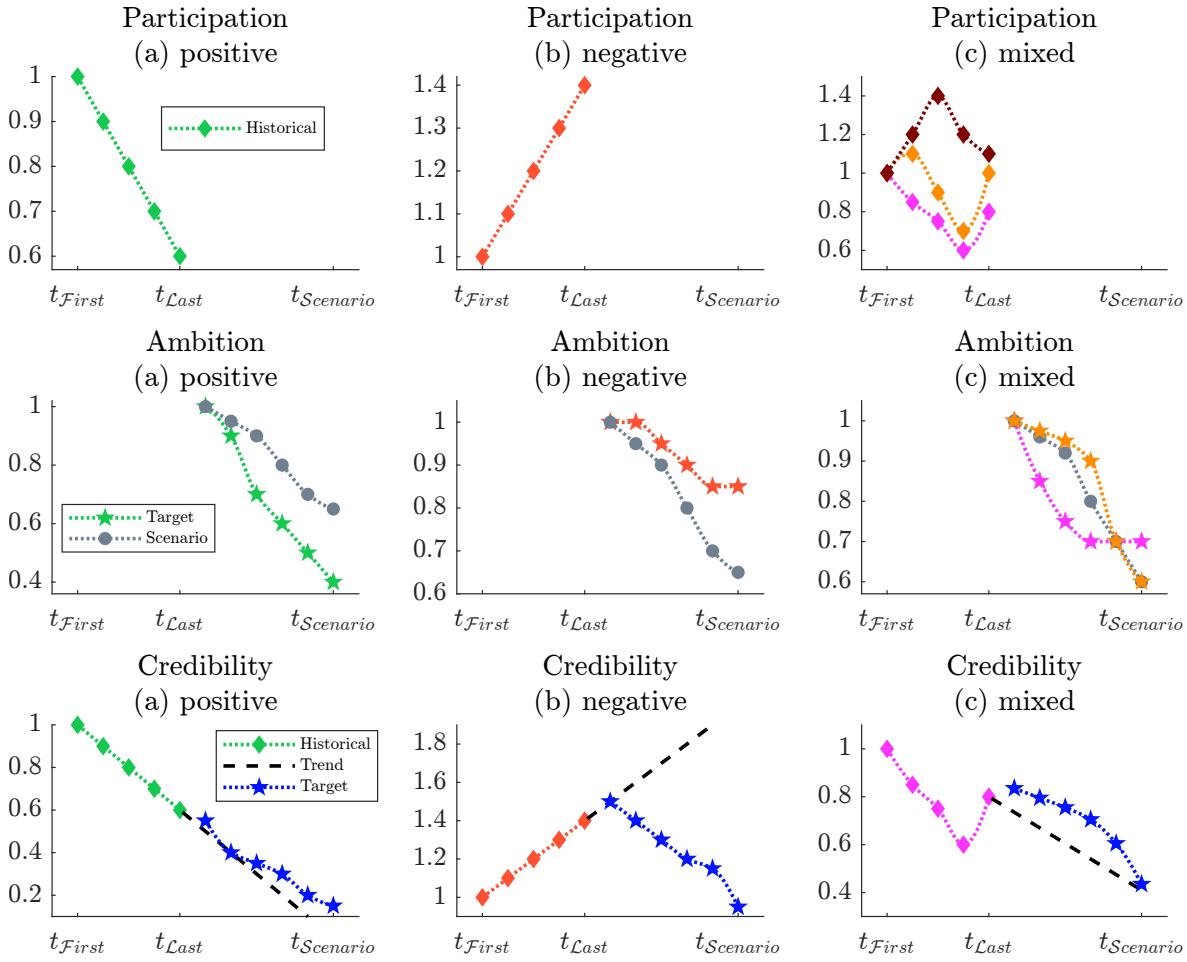


Source: Le Guenedal *et al.* (2022).

the last category computes the short-term reduction that the company must implement to satisfy the objective imposed by the market-based scenario[44]. Each pillar can then be studied using different metrics. Like the ESG risk, we can use a scoring system in order to analyze the $\mathcal{PAC}$ pillars and build three scores: the participation score $\mathcal{PS}_i$, the ambition score $\mathcal{AS}_i$ and the credibility score $\mathcal{CS}_i$. In Figure 9.28, we have represented several configurations of the $\mathcal{PAC}$ scoring system. If the three scores $\mathcal{PS}_i$, $\mathcal{AS}_i$ and $\mathcal{CS}_i$ are high and greater than 0.5 (which is the median value of a $q$-score), the company is both ambitious and credible and has already made some efforts to reduce its carbon emissions (Panel (a)). On the contrary, in Panel (b), we have a company, whose three scores are below the median. These two extreme cases are very frequent. Nevertheless, we can also obtain a more balanced scoring. For instance, Panel (c) corresponds to a company that has substantially reduced its past emissions but has announced weak reduction targets. Therefore, its ambition score is low, but its credibility score is high. It may be a company that does not talk a lot about its climate change policy, but its track record has demonstrated that it is committed. Finally, Panel (d) represents the scoring of a company with very high ambition, but it has continuously increased its carbon emissions in the past. Therefore, we can suspect a type of greenwashing. These examples

[44]The burn-out scenario refers to a sudden and violent reduction of carbon emissions such that the gap is equal to zero.

show that the three dimensions are correlated. For instance, we can assume a positive correlation between participation and credibility, and a negative correlation between ambition and credibility. Indeed, high credibility can only be obtained if participation is high or ambition is weak. Similarly, low credibility can be associated with excessively high ambition or weak participation, implying that the correlation between participation and credibility is unclear.

Figure 9.28: The $\mathcal{PAC}$ scoring system

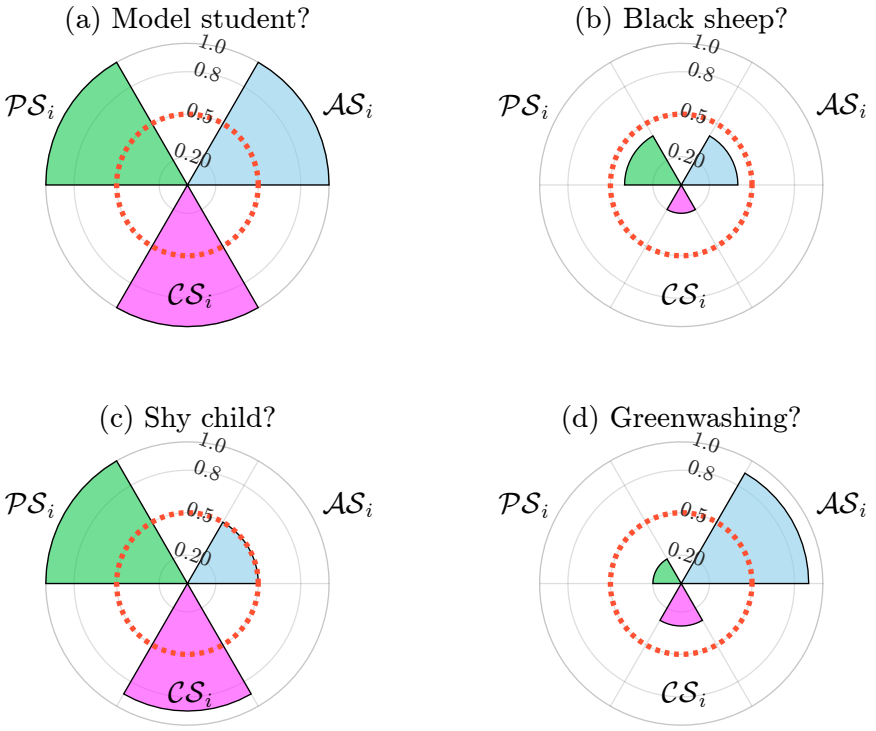


Source: Le Guenedal *et al.* (2022).

**Remark 114** *While the $\mathcal{PAC}$ framework is the backbone to analyze the decarbonization commitment of the company's climate strategy (like the ESG pillars for analyzing the extra-financial risks of the company), the $\mathcal{PAC}$ scoring system is similar to the ESG scoring system. Most of implied temperature ratings are based on the participation, ambition and credibility pillars*[45].

### 9.3.4 Illustration

We consider the analysis done by Le Guenedal *et al.* (2022). The base year is 2013 and they rebase the trajectories by the carbon emissions $\boldsymbol{\mathcal{CE}}$ (2013). The market-based scenario is the IEA NZE scenario. Company $B$ is a US based multinational technology conglomerate. Carbon emissions and targets are reported in Figure 9.29. Company $B$ is a particularly relevant example of the expectations from investors in the NZE context. Indeed, participation switched favorably after 2018 with a significant reduction in the scope 3 emissions from the use of sold products. The credibility is confirmed with the 2020 data point as the duration $\boldsymbol{\mathcal{D}}^{\mathcal{T}rend}$ drops under the duration of the NZE scenario. Figure 9.30 illustrates Company $C$ which is a major US airline. Its participation switched favorably in 2020. The credibility has not switched even with the significant drop in 2020, since the duration $\boldsymbol{\mathcal{D}}^{\mathcal{T}rend}$

[45] See Section 10.5.1 on page 945.

remains larger than the NZE time horizon. In fact, the reduction of $\mathcal{CE}$ (2020) sourced from both scope 1 and scope 3 emissions is related to the drop in activity due to the Covid-19 crisis. Company $D$ is a European multinational company which supplies industrial resources and services to various industries (Figure 9.31). The company has a clear ambition and has embraced the NZE context. However, the metrics indicate that in terms of participation, the trend has not been negative and has deteriorated in previous years. We stress here that although Company $D$ pays attention to its carbon intensity policy, it has not been active on the absolute carbon emissions level.

Figure 9.29: Carbon emissions, trend, targets and NZE scenario (Company $B$)

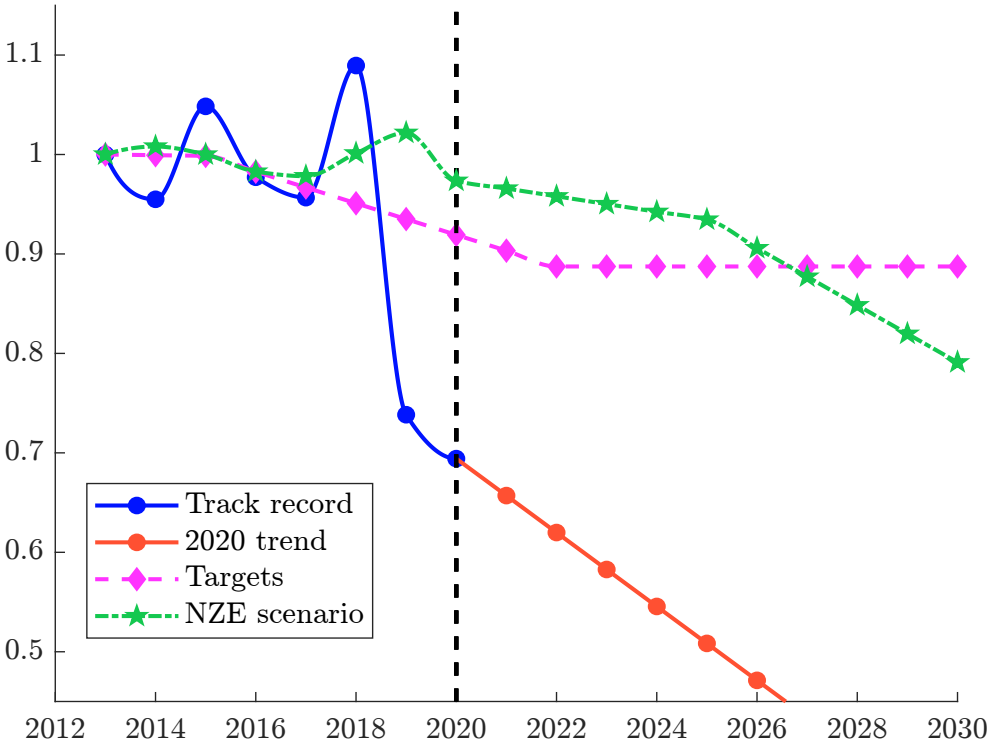


Source: CDP database (2021), IEA (2021) & Le Guenedal *et al.* (2022).

On a global basis, we observe an increase of carbon emissions between 2013 and 2019, and a plateau in 2020, which is probably due to emissions reduction related to the Covid-19 crisis (Figure 9.32). Carbon targets are in line with the NZE scenario until 2025. After this date, we clearly see that the targeted reduction rates are lower than the NZE required reduction rates. We notice that the reduction targets are more or less in line with the NZE scenario. However, and more strikingly, there is a huge gap between the upward trend between 2013 and 2020 and what has been announced by the companies. Figure 9.32 perfectly illustrates the interest of the $\mathcal{PAC}$ framework, since we observe inconsistencies between the ambition of these issuers on one side, and their participation and credibility on another side. The sector analysis is interesting, because we observe some large differences between the sectors in Figure 9.33. First, the trajectory of carbon emissions is highly dependent on the sector. Electricity is the sector that has been making the greatest effort whereas we observe a large increase in carbon emissions for the Industry sector. The impact of the Covid-19 pandemic on the transport sector is particularly striking. Second, there are small differences between the reduction targets, except for the Transport sector that is slightly less ambitious.

Figure 9.30: Carbon emissions, trend, targets and NZE scenario (Company $C$)

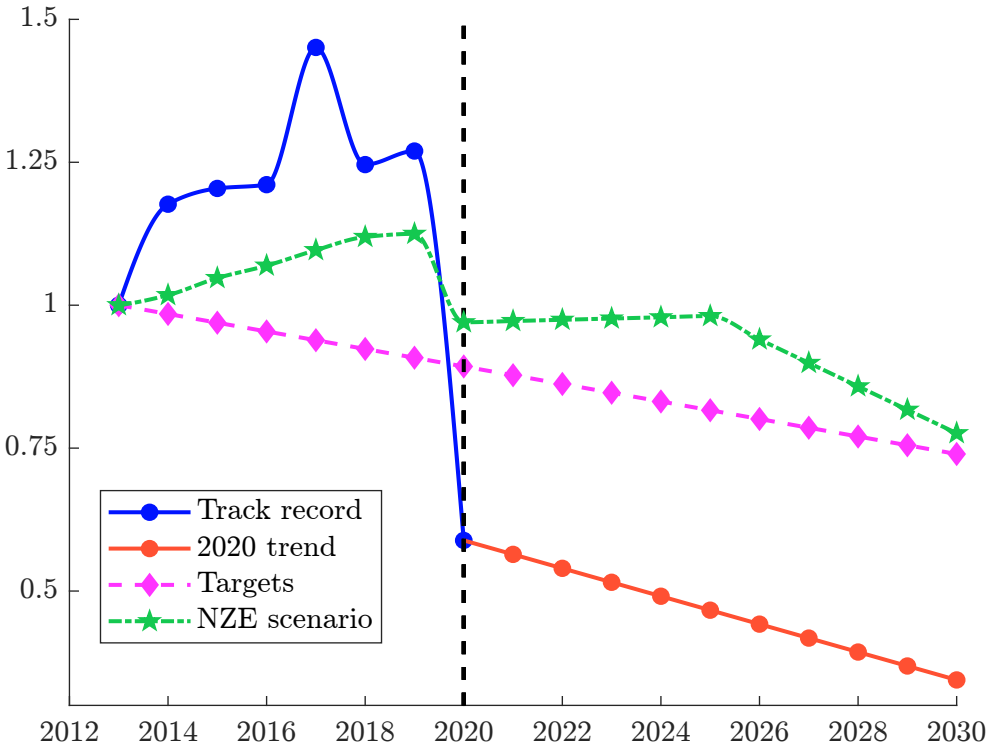


Source: CDP database (2021), IEA (2021) & Le Guenedal *et al.* (2022).

Figure 9.31: Carbon emissions, trend, targets and NZE scenario (Company $D$)

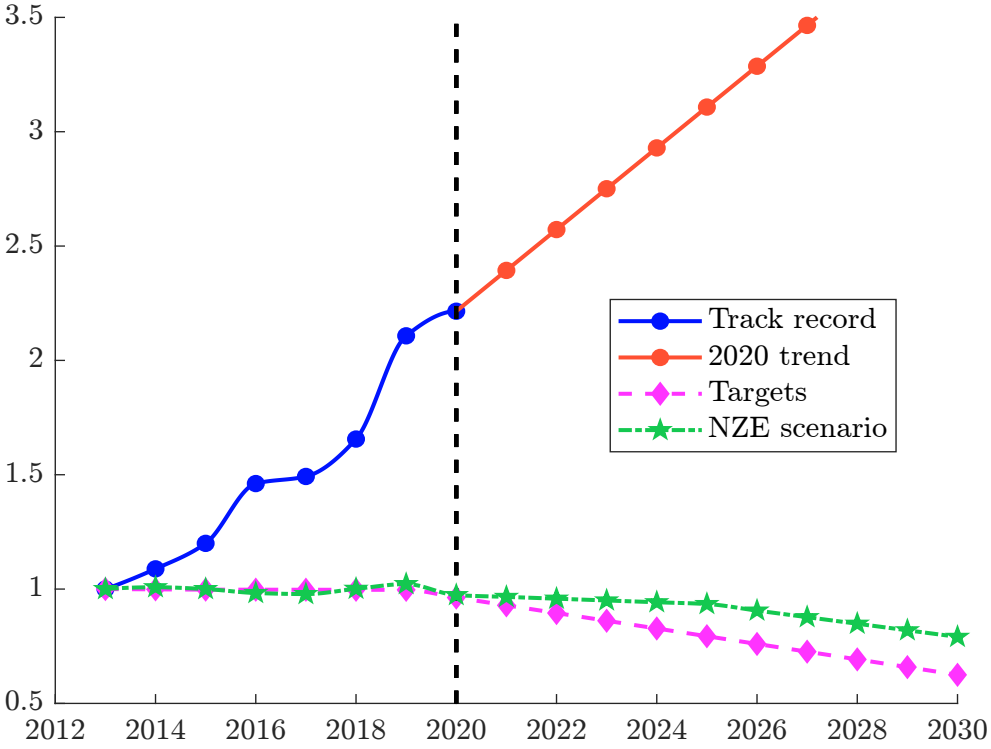


Source: CDP database (2021), IEA (2021) & Le Guenedal *et al.* (2022).

Figure 9.32: Carbon emissions, trend, targets and NZE scenario (median analysis, global universe)

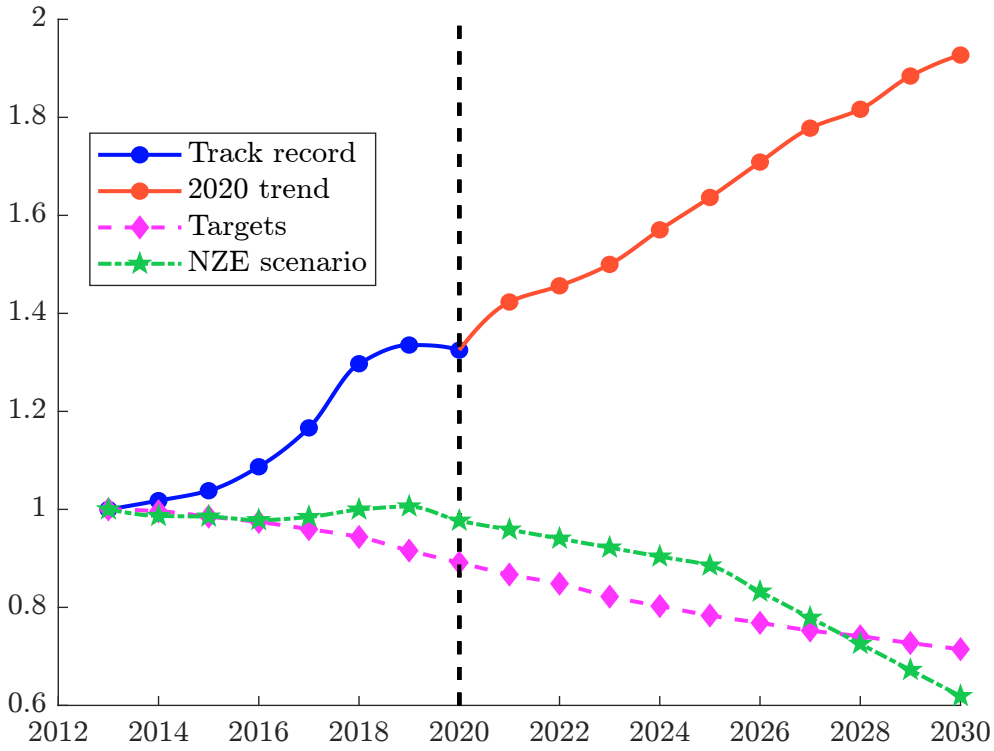


Source: CDP database (2021), IEA (2021) & Le Guenedal *et al.* (2022).

Figure 9.33: Carbon emissions, trend, targets and NZE scenario (median analysis, sector universe)

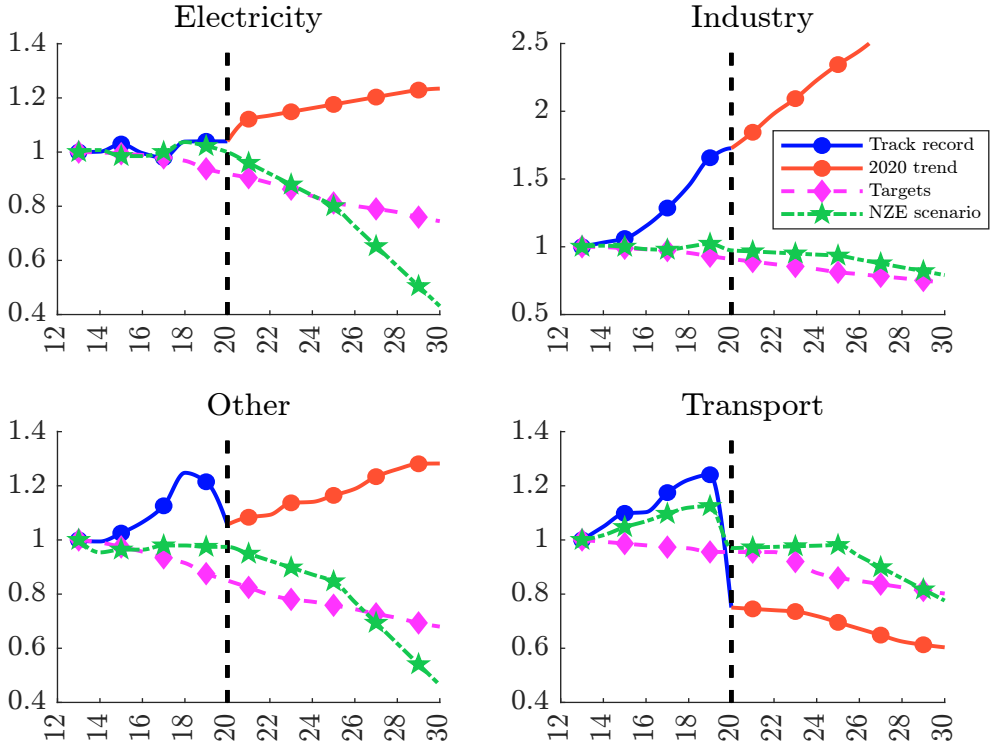


Source: CDP database (2021), IEA (2021) & Le Guenedal *et al.* (2022).

## 9.4 Greenness measures

Until now, we have focused on carbon metrics to measure the "*brownness*" of organizations or products. We now consider "*greenness*" measures, whose objective is to assess the positive contribution to limit global warming. In some sense, brownness and greenness measures are related. Nevertheless, we cannot deduce one measure from another one. Let us define the brown and green intensities of a company as the proportion of brown and green activities. We note them $\boldsymbol{\mathcal{BI}}$ and $\boldsymbol{\mathcal{GI}}$. By construction, we have $\boldsymbol{\mathcal{BI}} \in [0,1]$, $\boldsymbol{\mathcal{GI}} \in [0,1]$ and $0 \leq \boldsymbol{\mathcal{BI}} + \boldsymbol{\mathcal{GI}} \leq 1$. Most of the time, we have $\boldsymbol{\mathcal{BI}} + \boldsymbol{\mathcal{GI}} \neq 1$, meaning that we cannot deduce the green intensity from the brown intensity. While the carbon footprint is a well-defined concept, greenness is then more difficult to assess. In fact, it is a multi-faceted concept. For instance, if one company changes its business model so that its new products are carbon efficient, we can measure the company's greenness based on the avoided emissions generated by the change of the business model. For other companies, the greenness can be evaluated by estimating the R&D amount dedicated to green projects. Therefore, we observe a big difference between carbon and greenness metrics. Indeed, while it makes sense to compute the carbon footprint of all companies, the greenness may be indefinite for some companies, because they have no vocation to participate in the transition to a low-carbon economy. Therefore, Figure 9.34 illustrates that we cannot classifies all activities into these two categories, since there are many activities that are neither brown nor green. Some companies are then neutral and are not exposed to the green business. These remarks argue in favor of considering simple and homogeneous measures of greenness.

Figure 9.34: Brown and green activities at the company level

### 9.4.1 Green taxonomy

The purpose of a green taxonomy is to define what is green, and its objective is to inform investors about the greenness of their investments. Therefore, they can evaluate whether these levels satisfy or not their expectations. A green taxonomy is all the more important as we observe a strong development of green sentiment among investors (Brière and Ramelli, 2021). In this context, the investor may want to assess the proportion of his portfolio that is invested in environmentally sustainable assets. Therefore, a green taxonomy is necessary for both asset owners and managers.

The most famous example is the European green taxonomy, which has been already presented on page 33. We remind that the EU taxonomy for sustainable activities is "*a classification system, establishing a list of environmentally sustainable economic activities.*" These economic activities must have a substantive contribution to at least one of the following six environmental objectives: (1) climate change mitigation; (2) climate change adaptation; (3) sustainable use and protection of water and marine resources; (4) transition to a circular economy; (5) pollution prevention and control; (6) protection and restoration of biodiversity and ecosystem. Moreover, a business activity must also meet two other criteria to qualify as sustainable. First, the activity must do no significant

harm to the other environmental objectives (DNSH constraint) and second, it must comply with minimum social safeguards (MS constraint). Figure 9.35 summarizes the different steps.

Figure 9.35: EU taxonomy for sustainable activities

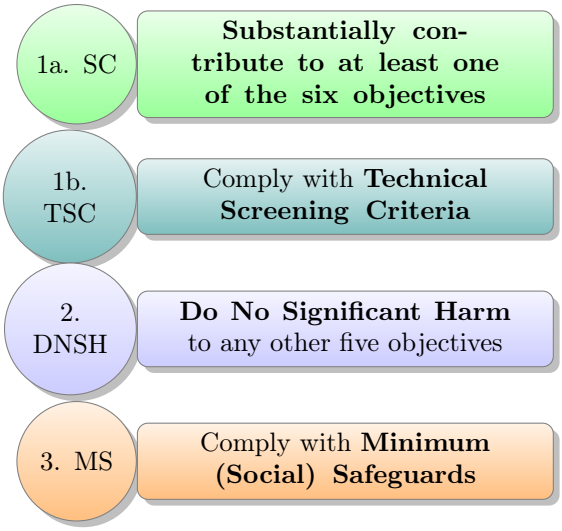


**Remark 115** *The EU taxonomy is not finalized and only concerns the first two objectives as of today (January 2023).*

### 9.4.2 Green revenue share

#### Relationship between the green intensity and the green revenue share

There are several ways to compute the green intensity. This is why we observe some significant differences between data providers. One method is to translate the 3-step approach of the EU taxonomy into the following equation:

$$\boldsymbol{\mathcal{GI}} = \frac{\mathcal{GR}}{\mathcal{TR}} \cdot (1 - \mathcal{P}) \cdot \mathbb{1}\left\{\boldsymbol{\mathcal{S}} \geq \boldsymbol{\mathcal{S}}^{\star}\right\}$$

where $\mathcal{GR}$ is the green revenue deduced from the six environmentally sustainable objectives, $\mathcal{TR}$ is the total revenue, $\mathcal{P}$ is the penalty coefficient reflecting the DNSH constraint, $\boldsymbol{\mathcal{S}}$ is the minimum safeguard score and $\boldsymbol{\mathcal{S}}^{\star}$ is the threshold. The first term is a proxy of the turnover KPI and corresponds to the green revenue share:

$$\boldsymbol{\mathcal{GRS}} = \frac{\mathcal{GR}}{\mathcal{TR}}$$

By construction, we have $0 \leq \boldsymbol{\mathcal{GRS}} \leq 1$. This measure is then impacted by the DNSH coefficient. If the penalty coefficient is equal to zero, the green activities of the issuer do not significantly harm the other objectives and we have $\boldsymbol{\mathcal{GI}} = \boldsymbol{\mathcal{GRS}}$. Otherwise, the green intensity satisfies $0 \leq \boldsymbol{\mathcal{GI}} = \boldsymbol{\mathcal{GRS}} \cdot (1 - \mathcal{P}) \leq \boldsymbol{\mathcal{GRS}}$. Finally, the indicator function $\mathbb{1}\left\{\boldsymbol{\mathcal{S}} \geq \boldsymbol{\mathcal{S}}^{\star}\right\}$ is a binary all-or-nothing variable. It is equal to one if the firm complies with minimum social safeguards. Otherwise, the green intensity is equal to zero if the firm doesn't pass this materiality test. It follows that an upper bound of the green intensity is the green revenue share since we have $\boldsymbol{\mathcal{GI}} \leq \boldsymbol{\mathcal{GRS}}$.

Box 9.5: EU green taxonomy

The EU taxonomy is described in the Delegated Act on the climate objectives of 4 June 2021. For each activity, three items are provided: the description of the activity, the technical screening criteria, and the DNSH compliance. Let us consider Transport of $CO_2$ (page 100 of the Delegated Act). We have the following information:

1. Description of the activity
   This concerns the transport of captured $CO_2$ via all modes; the construction and operation of $CO_2$ pipelines and retrofit of gas networks where the main purpose is the integration of captured $CO_2$. The economic activities in this category could be associated with several NACE codes, in particular F42.21 and H49.50. An economic activity in this category is an enabling activity.

2. Technical screening criteria
   This activity has a substantial contribution to climate change mitigation:

   (a) The $CO_2$ transported from the installation where it is captured to the injection point does not lead to $CO_2$ leakages above 0.5% of the mass of $CO_2$ transported.

   (b) The $CO_2$ is delivered to a permanent $CO_2$ storage site that meets the criteria for underground geological storage of $CO_2$ set out in Section 5.12 of this Annex; or to other transport modalities, which lead to permanent $CO_2$ storage site that meet those criteria.

   (c) Appropriate leak detection systems are applied and a monitoring plan is in place, with the report verified by an independent third party.

   (d) The activity may include the installation of assets that increase the flexibility and improve the management of an existing network.

3. Do no significant harm
   Three out of five categories are concerned: (2) climate change adaptation: the activity complies with the criteria set out in Appendix A to this Annex; (3) sustainable use and protection of water and marine resources: The activity complies with the criteria set out in Appendix B to this Annex. (4) transition to a circular economy: N/A; (5) pollution prevention and control: N/A; (6) protection and restoration of biodiversity and ecosystems: the activity complies with the criteria set out in Appendix D to this Annex.

This example shows that the revenues generated by the transport of $CO_2$ are not necessarily green, because the technical screening criteria imply that $CO_2$ leakages must be below 0.5% of the mass of $CO_2$ transported. We also observe that some criteria are generic while others are specific to an activity. For instance, the life cycle GHG emissions from the generation of electricity (whatever the electricity source) must be lower than 100 $gCO_2e$ per kWh. Some criteria also concern the activity efficiency. For example, the power density of the electricity generation facility must be above 5 Watt per $m^2$ for the hydropower sector.

Concerning the DNSH compliance criteria, they may for instance imply that the activity does use persistent organic pollutants, ether, mercury, substances that deplete the ozone layer, certain hazardous substances, etc. In a similar way, an environmental impact assessment (EIA) must be conducted for sites located near biodiversity-sensitive areas.

**Example 45** *We consider a company in the hydropower sector which has five production sites. Below, we indicate the power density efficiency, the GHG emissions, the DNSH compliance with respect to the biodiversity and the corresponding revenue:*

| Site | #1 | #2 | #3 | #4 | #5 |
|---|---|---|---|---|---|
| Efficiency (in Watt per $m^2$) | 3.2 | 3.5 | 3.3 | 5.6 | 4.2 |
| GHG emissions (in $gCO_2e$ per kWh) | 35 | 103 | 45 | 12 | 36 |
| Biodiversity DNSH compliance | ✓ | ✓ | ✓ | ✓ | |
| Revenue (in $ mn) | 103 | 256 | 89 | 174 | 218 |

The total revenue is equal to:

$$\mathcal{TR} = 103 + 256 + 89 + 174 + 218 = \$840 \text{ mn}$$

We notice that the fourth site does not pass the technical screening, because the power density is above 5 Watt per $m^2$. The second site does not also comply because it has a GHG emissions greater than 100 $gCO_2e$ per kWh. We deduce that the green revenue is equal to:

$$\mathcal{GR} = 103 + 89 + 218 = \$410 \text{ mn}$$

We conclude that the green revenue share is equal to 48.8%. According to the EU green taxonomy, the green intensity is lower because the last site is close to a biodiversity area and has a negative impact. Therefore, we have:

$$\boldsymbol{\mathcal{GI}} = \frac{103 + 89}{840} = 22.9\%$$

### Statistics

In Table 9.27, we report the descriptive statistics of green revenue share calculated by Barahhou *et al.* (2022) with the MSCI database. For each category[46], they have computed:

- The frequency $\mathbf{F}(x) = \Pr\{\boldsymbol{\mathcal{GRS}} > x\}$;
- The statistical quantile $\mathbf{Q}(\alpha) = \inf\{x : \Pr\{\boldsymbol{\mathcal{GRS}} \leq x\} \geq \alpha\}$;
- The arithmetic average $n^{-1}\sum_{i=1}^n \boldsymbol{\mathcal{GRS}}_i$ and the weighted mean $\boldsymbol{\mathcal{GRS}}(b) = \sum_{i=1}^n b_i \boldsymbol{\mathcal{GRS}}_i$ where $b_i$ is the weight of issuer $i$ in the MSCI ACWI IMI benchmark.

For instance, 9.82% of issuers have a green revenue share that concerns alternative energy. This figure becomes less than 1% if we consider a green revenue share greater than 50%. The average value is equal to 1.36% whereas the weighted value is equal to 0.77%. This indicates a small cap bias. For energy efficiency, the average is lower than the weighted mean, implying a bias towards big companies. If we consider the total green revenue share, 27.85% have a positive figure and only 3.17% have a figure greater than 50%. The 90% quintile is equal to 11.82%. Therefore, we notice a high positive skewness for the distribution. The green revenue share is then located in a small number of companies.

**Remark 116** *Barahhou et al. (2022) estimated that the green revenue share of the MSCI World index and the Bloomberg Global Investment Grade Corporate Bond index are respectively equal to 5.24% and 3.49% in June 2022. This is not a high figure, because the economy is today far to be green. These results are confirmed by Alessi and Battiston (2022), who estimated "a greenness of about 2.8% for EU financial markets" according to the existing EU green taxonomy*[47].

[46] The MSCI taxonomy uses 6 categories: (1) alternative energy, (2) energy efficiency, (3) green building, (4) pollution prevention and control, (5) sustainable agriculture and (6) sustainable water.

[47] This concerns the first two categories, which are the most important.

Table 9.27: Statistics in % of green revenue share (MSCI ACWI IMI, June 2022)

| Category | Frequency $\mathbf{F}(x)$ | | | | Quantile $\mathbf{Q}(\alpha)$ | | | | Mean | |
|---|---|---|---|---|---|---|---|---|---|---|
| | 0 | 25% | 50% | 75% | 75% | 90% | 95% | Max | Avg | Wgt |
| (1) | 9.82 | 1.47 | 0.96 | 0.75 | 0.00 | 0.00 | 2.85 | 100.00 | 1.36 | 0.77 |
| (2) | 14.10 | 1.45 | 0.65 | 0.31 | 0.00 | 1.25 | 6.12 | 100.00 | 1.39 | 3.50 |
| (3) | 4.84 | 1.68 | 1.02 | 0.31 | 0.00 | 0.00 | 0.00 | 100.00 | 1.16 | 0.51 |
| (4) | 4.79 | 0.30 | 0.10 | 0.06 | 0.00 | 0.00 | 0.00 | 99.69 | 0.32 | 0.22 |
| (5) | 1.00 | 0.39 | 0.20 | 0.09 | 0.00 | 0.00 | 0.00 | 98.47 | 0.26 | 0.10 |
| (6) | 4.75 | 0.28 | 0.11 | 0.05 | 0.00 | 0.00 | 0.00 | 99.98 | 0.29 | 0.14 |
| Total | 27.85 | 5.82 | 3.17 | 1.68 | 0.42 | 11.82 | 30.36 | 100.00 | 4.78 | 5.24 |

Source: MSCI (2022) & Barahhou *et al.* (2022).

### 9.4.3 Green capex

Curabitur tellus magna, porttitor a, commodo a, commodo in, tortor. Donec interdum. Praesent scelerisque. Maecenas posuere sodales odio. Vivamus metus lacus, varius quis, imperdiet quis, rhoncus a, turpis. Etiam ligula arcu, elementum a, venenatis quis, sollicitudin sed, metus. Donec nunc pede, tincidunt in, venenatis vitae, faucibus vel, nibh. Pellentesque wisi. Nullam malesuada. Morbi ut tellus ut pede tincidunt porta. Lorem ipsum dolor sit amet, consectetuer adipiscing elit. Etiam congue neque id dolor.

### 9.4.4 Other metrics

Nulla non mauris vitae wisi posuere convallis. Sed eu nulla nec eros scelerisque pharetra. Nullam varius. Etiam dignissim elementum metus. Vestibulum faucibus, metus sit amet mattis rhoncus, sapien dui laoreet odio, nec ultricies nibh augue a enim. Fusce in ligula. Quisque at magna et nulla commodo consequat. Proin accumsan imperdiet sem. Nunc porta. Donec feugiat mi at justo. Phasellus facilisis ipsum quis ante. In ac elit eget ipsum pharetra faucibus. Maecenas viverra nulla in massa.

## 9.5 Exercises

Chapter 10

# Transition Risk Modeling

## 10.1 A primer on the economic analysis of negative externalities

### 10.1.1 Optimal taxation

### 10.1.2 Economic theory of quotas

### 10.1.3 Game theory

**Cooperative solution**

**Non-cooperative solution**

**Coordinated solution**

### 10.1.4 Uncertainty

McKibbin and Wilcoxen (2002)

### 10.1.5 Irreversibility

### 10.1.6 Cost-benefit analysis versus option theory

## 10.2 Carbon tax and pricing

### 10.2.1 Mathematics of carbon tax

### 10.2.2 Abatement cost

### 10.2.3 Cap-and-trade

## 10.3 Stranded assets

## 10.4 Decarbonization pathway

### 10.4.1 Global analysis

### 10.4.2 Sector analysis

**Power and electricity**

**Hydrogen**

**Buildings**

**Mobility and transport**

**Materials**

**Industry**

**Water management**

**Waste management and circular economy**

## 10.5 Transition risk measures

### 10.5.1 Temperature rating modeling

## 10.6 Exercises

# Chapter 11

# Climate Portfolio Construction

With the 2015 Paris Agreement, the development of ESG investing, and the emergence of net-zero investment policies, climate risk is undoubtedly the most important issue and challenge for asset owners and managers today and in the coming years. Building portfolios to manage climate risk began in 2014, when asset owners AP4 and FRR worked with asset manager Amundi and index provider MSCI to define an investment strategy to help hedge climate risk (Andersson *et al.*, 2016). Together, they defined the concept of a low-carbon portfolio. The 2015–2020 period corresponds to the growth of ESG investing and the adoption of sustainable finance by many asset owners and managers. During this period, climate investing is part of ESG investing, and climate portfolio construction remains relatively marginal, essentially involving passive management. On the contrary, ESG investing has seen a major development with the adoption of ESG scores in active management. Since 2020, we have seen a new trend. The line between ESG investing and climate investing is becoming increasingly blurred, and the two issues are now separate. One of the reasons for this is the emergence of net-zero investment policies, which have profoundly changed the investment decisions of asset owners. This separation has accelerated with COP26. The proliferation of net zero alliances (GFANZ, NZAOA, NZAM, NZBA, etc.), the commitments made by financial institutions (asset managers, banks, pension funds, insurance companies, etc.), and the push for regulation[1] are all contributing to the shift from ESG investing to climate investing.

This chapter is dedicated to portfolio construction when we integrate climate risk measures. It is therefore closely related to Chapter 9, as we use carbon footprint and green footprint metrics. It is also related to Chapter 10 on transition risk, as the goal of climate investing is to reduce the transition risk of investment portfolios. Integrating physical risk is more complicated today, because we do not have the right metrics to assess physical risk at the corporate or security level. Finally, it is related to Chapter 2, which is dedicated to the impact of ESG investing on asset prices and portfolio returns, because we use the same tools and methodologies. We will therefore make extensive use of portfolio optimization. A comprehensive review of portfolio optimization is presented in the first section. We distinguish between allocations to equity and fixed income portfolios because they require two different approaches. The reason is that we generally measure equity risk in terms of volatility risk, while bond risk is multi-dimensional and must at least integrate duration and credit risk. The second section is a guide to building a low-carbon portfolio. While there are several approaches, the choice of Scope emissions is certainly the most important decision and has a major impact on asset allocation. Finally, the last section focuses on net-zero investing and lists many challenges to defining an investment portfolio that is aligned with a net-zero emissions scenario.

[1] Examples include the Net-Zero Industry Act of the European Commission, the work of the NGFS on climate scenarios, or the climate stress tests organized by the ECB.

## 11.1 Portfolio optimization in practice

Before studying portfolio allocation in the context of climate risk, we first begin to remind some basics about portfolio optimization. As mentioned by Perrin and Roncalli (2020), the success of mean-variance optimization is due to the appealing properties of the quadratic utility function, and it is easy to solve numerically quadratic programming problems[2]. This is why most of the portfolio allocation problems that we will encounter in this chapter will be cast into a QP problem, whose standard formulation is[3]:

$$\begin{aligned} x^\star &= \arg\min \frac{1}{2} x^\top Q x - x^\top R \\ &\text{s.t.} \begin{cases} Ax = B \\ Cx \leq D \\ x^- \leq x \leq x^+ \end{cases} \end{aligned} \tag{11.1}$$

where $x$ is a $n \times 1$ vector, $Q$ is a $n \times n$ matrix, $R$ is a $n \times 1$ vector, $A$ is a $n_A \times n$ matrix, $B$ is a $n_A \times 1$ vector, $C$ is a $n_C \times n$ matrix, $D$ is a $n_C \times 1$ vector, and $x^-$ and $x^+$ are two $n \times 1$ vectors. If $n_A = 0$, there is no equality constraints. Similarly, there is no inequality constraints if $n_C = 0$. If there is no lower bounds or/and upper bounds, this implies that $x^- = -\infty \cdot \mathbf{1}_n$ and $x^+ = \infty \cdot \mathbf{1}_n$. From a numerical viewpoint, QP solvers generally replace these bounds by $x^- = -c \cdot \mathbf{1}_n$ and $x^+ = c \cdot \mathbf{1}_n$ where $c$ is a large floating-point number[4] (*e.g.*, $c = 10^{200}$).

### 11.1.1 Equity portfolios

#### Basic optimization problems

We consider a universe of $n$ assets. We note $w$ the vector of portfolio weights. Let $\mu$ and $\Sigma$ be the vector of expected returns and the covariance matrix of asset returns. The long-only mean-variance optimization problem is given by:

$$\begin{aligned} w^\star &= \arg\min \frac{1}{2} w^\top \Sigma w - \gamma w^\top \mu \\ &\text{s.t.} \begin{cases} \mathbf{1}_n^\top w = 1 \\ \mathbf{0}_n \leq w \leq \mathbf{1}_n \end{cases} \end{aligned}$$

where $\gamma$ is the risk-tolerance coefficient, the equality constraint is the budget constraint ($\sum_{i=1}^n w_i = 1$) and the bounds correspond to the no short-selling restriction ($w_i \geq 0$). We recognize a QP problem where $Q = \Sigma$, $R = \gamma\mu$, $A = \mathbf{1}_n^\top$, $B = 1$, $w^- = \mathbf{0}_n$ and $w^+ = \mathbf{1}$. In this problem, we have one equality constraint ($n_A = 1$) and zero inequality constraint[5] ($n_C = 1$).

In many problems, we will have to manage the portfolio with respect to a benchmark. In this case, the objective function depends on the tracking error risk variance $\sigma^2(w \mid b) = (w - b)^\top \Sigma (w - b)$ where $b$ is the vector of benchmark weights. In Section 3.1.1 on page 148, we have seen that the tracking error optimization problem is defined as:

$$\begin{aligned} w^\star &= \arg\min \frac{1}{2} w^\top \Sigma w - w^\top (\gamma\mu + \Sigma b) \\ &\text{s.t.} \begin{cases} \mathbf{1}_n^\top w = 1 \\ \mathbf{0}_n \leq w \leq \mathbf{1}_n \end{cases} \end{aligned}$$

[2] See Appendix A.1.2 on page 1052.
[3] The objective function is a quadratic form and is noted $\mathcal{QF}(x; Q, R, \mathbf{0}_n)$.
[4] The largest finite floating-point number in IEEE double precision is equal to $\left(2 - 2^{-52}\right) \times 2^{1023}$.
[5] We do not take into account the bounds.

This is exactly the same QP problem as previously except that $R = \gamma\mu + \Sigma b$. If the objective of the portfolio manager is to minimize the tracking error risk, we obtain $R = \Sigma b$.

**Specification of the constraints**

We can extend the previous framework by considering more constraints. For instance, we consider a sector weight constraint:

$$s_j^- \leq \sum_{i \in \boldsymbol{\mathcal{S}}ector_j} w_i \leq s_j^+$$

We notice that:

$$\sum_{i \in \boldsymbol{\mathcal{S}}ector_j} w_i = \boldsymbol{s}_j^\top w$$

where $\boldsymbol{s}_j$ is the $n \times 1$ sector-mapping vector whose elements are $\boldsymbol{s}_{i,j} = \mathbb{1}\{i \in \boldsymbol{\mathcal{S}}ector_j\}$. We deduce that the sector constraint can be written as:

$$s_j^- \leq \sum_{i \in \boldsymbol{\mathcal{S}}ector_j} w_i \leq s_j^+ \Leftrightarrow \begin{cases} s_j^- \leq \boldsymbol{s}_j^\top w \\ \boldsymbol{s}_j^\top w \leq s_j^+ \end{cases} \Leftrightarrow \begin{cases} -\boldsymbol{s}_j^\top w \leq -s_j^- \\ \boldsymbol{s}_j^\top w \leq s_j^+ \end{cases}$$

It follows that the inequality constraint $Cw \leq D$ is defined by the following system:

$$\underbrace{\begin{pmatrix} -\boldsymbol{s}_j^\top \\ \boldsymbol{s}_j^\top \end{pmatrix}}_{C} w \leq \underbrace{\begin{pmatrix} -s_j^- \\ s_j^+ \end{pmatrix}}_{D}$$

In this case, $C$ is a $2 \times n$ matrix and $D$ is a $2 \times 1$ vector. The previous analysis can be extended when there are many sectors.

We denote by $\boldsymbol{\mathcal{S}}$ a vector of scores (*e.g.*, ESG scores) and we would like to impose that the (linear) score of the portfolio is greater than a threshold $\boldsymbol{\mathcal{S}}^\star$:

$$\sum_{i=1}^n w_i \boldsymbol{\mathcal{S}}_i \geq \boldsymbol{\mathcal{S}}^\star$$

The QP form of this constraint is:

$$-\boldsymbol{\mathcal{S}}^\top w \leq -\boldsymbol{\mathcal{S}}^\star$$

Let us now assume that we would like to apply this constraint to a sector. In this case, we have:

$$\begin{aligned} \sum_{i \in \boldsymbol{\mathcal{S}}ector_j} w_i \boldsymbol{\mathcal{S}}_i \geq \boldsymbol{\mathcal{S}}_j^\star &\Leftrightarrow \sum_{i=1}^n \mathbb{1}\{i \in \boldsymbol{\mathcal{S}}ector_j\} w_i \boldsymbol{\mathcal{S}}_i \geq \boldsymbol{\mathcal{S}}_j^\star \\ &\Leftrightarrow \sum_{i=1}^n \boldsymbol{s}_{i,j} w_i \boldsymbol{\mathcal{S}}_i \geq \boldsymbol{\mathcal{S}}_j^\star \\ &\Leftrightarrow \sum_{i=1}^n w_i \left(\boldsymbol{s}_{i,j} \boldsymbol{\mathcal{S}}_i\right) \geq \boldsymbol{\mathcal{S}}_j^\star \\ &\Leftrightarrow \left(\boldsymbol{s}_j \circ \boldsymbol{\mathcal{S}}\right)^\top w \geq \boldsymbol{\mathcal{S}}_j^\star \end{aligned}$$

where $a \circ b$ is the Hadamard product: $(a \circ b)_i = a_i b_i$. The QP form of the sector-specific score constraint is defined by $C = -\left(\boldsymbol{s}_j \circ \boldsymbol{\mathcal{S}}\right)^\top$ and $D = -\boldsymbol{\mathcal{S}}_j^\star$.

**Example 46** *We consider a capitalization-weighted equity index, which is composed of 8 stocks. The weights are equal to 23%, 19%, 17%, 13%, 9%, 8%, 6% and 5%. We assume that the stock volatilities are equal to 22%, 20%, 25%, 18%, 35%, 23%, 13% and 29%. The correlation matrix is given by:*

$$\mathbb{C} = \begin{pmatrix} 100\% & & & & & & & \\ 80\% & 100\% & & & & & & \\ 70\% & 75\% & 100\% & & & & & \\ 60\% & 65\% & 80\% & 100\% & & & & \\ 70\% & 50\% & 70\% & 85\% & 100\% & & & \\ 50\% & 60\% & 70\% & 80\% & 60\% & 100\% & & \\ 70\% & 50\% & 70\% & 75\% & 80\% & 50\% & 100\% & \\ 60\% & 65\% & 70\% & 75\% & 65\% & 70\% & 80\% & 100\% \end{pmatrix}$$

*The ESG score, carbon intensity and sector of the eight stocks are the following:*

| Stock | #1 | #2 | #3 | #4 | #5 | #6 | #7 | #8 |
|---|---|---|---|---|---|---|---|---|
| $\mathcal{S}$ | −1.20 | 0.80 | 2.75 | 1.60 | −2.75 | −1.30 | 0.90 | −1.70 |
| $\mathcal{CI}$ | 125 | 75 | 254 | 822 | 109 | 17 | 341 | 741 |
| $\mathcal{S}ector$ | 1 | 1 | 2 | 2 | 1 | 2 | 1 | 2 |

The objective function is minimizing the tracking error risk. We deduce that the equivalent QP problem is:

$$\begin{aligned} w^\star &= \arg\min \frac{1}{2} w^\top Q w - w^\top R \\ &\text{s.t.} \begin{cases} Aw = B \\ Cw \leq D \\ w^- \leq w \leq w^+ \end{cases} \end{aligned}$$

where[6]:

$$Q = \Sigma = \begin{pmatrix} 484.00 & 352.00 & 385.00 & 237.60 & 539.00 & 253.00 & 200.20 & 382.80 \\ 352.00 & 400.00 & 375.00 & 234.00 & 350.00 & 276.00 & 130.00 & 377.00 \\ 385.00 & 375.00 & 625.00 & 360.00 & 612.50 & 402.50 & 227.50 & 507.50 \\ 237.60 & 234.00 & 360.00 & 324.00 & 535.50 & 331.20 & 175.50 & 391.50 \\ 539.00 & 350.00 & 612.50 & 535.50 & 1225.00 & 483.00 & 364.00 & 659.75 \\ 253.00 & 276.00 & 402.50 & 331.20 & 483.00 & 529.00 & 149.50 & 466.90 \\ 200.20 & 130.00 & 227.50 & 175.50 & 364.00 & 149.50 & 169.00 & 301.60 \\ 382.80 & 377.00 & 507.50 & 391.50 & 659.75 & 466.90 & 301.60 & 841.00 \end{pmatrix} \times 10^{-4}$$

and:

$$R = \Sigma b = \begin{pmatrix} 3.74 \\ 3.31 \\ 4.39 \\ 3.07 \\ 5.68 \\ 3.40 \\ 2.02 \\ 4.54 \end{pmatrix} \times 10^{-2}$$

[6] We have $\Sigma_{i,j} = \mathbb{C}_{i,j}\sigma_i\sigma_j$.

We assume that the portfolio is long-only. It follows that $w^- = \mathbf{0}_8$ and $w^+ = \mathbf{1}_8$. To satisfy the budget constraint $\sum_{i=1}^8 w_i = 1$, we have a first linear equation $A_0 w = B_0$ where $A_0 = \mathbf{1}_8^\top$ and $B_0 = 1$. We consider three type of constraints:

- We impose a relative reduction of the benchmark carbon intensity:

$$\boldsymbol{\mathcal{CI}}(w) \leq (1 - \boldsymbol{\mathcal{R}})\, \boldsymbol{\mathcal{CI}}(b)$$

  where $\boldsymbol{\mathcal{R}}$ is the reduction rate. Since $\boldsymbol{\mathcal{CI}}(w) = \boldsymbol{\mathcal{CI}}^\top w$, we deduce the following inequality constraint $C_1 w \leq D_1$ where $C_1 = \boldsymbol{\mathcal{CI}}^\top$ and $D_1 = (1 - \boldsymbol{\mathcal{R}})\, \boldsymbol{\mathcal{CI}}(b)$.

- We impose an absolute increase of the benchmark ESG score:

$$\boldsymbol{\mathcal{S}}(w) \geq \boldsymbol{\mathcal{S}}(b) + \Delta\boldsymbol{\mathcal{S}}^\star$$

  Since $\boldsymbol{\mathcal{S}}(w) = \boldsymbol{\mathcal{S}}^\top w$, we deduce the following inequality constraint $C_2 w \leq D_2$ where $C_2 = -\boldsymbol{\mathcal{S}}^\top$ and $D_2 = -\left(\boldsymbol{\mathcal{S}}(b) + \Delta\boldsymbol{\mathcal{S}}^\star\right)$.

- We impose the sector neutrality of the portfolio meaning that:

$$\sum_{i \in \boldsymbol{\mathcal{S}}ector_j} w_i = \sum_{i \in \boldsymbol{\mathcal{S}}ector_j} b_i$$

  We note:

$$A_1 = \boldsymbol{s}_1^\top = \begin{pmatrix} 1 & 1 & 0 & 0 & 1 & 0 & 1 & 0 \end{pmatrix}$$

  and:

$$A_2 = \boldsymbol{s}_2^\top = \begin{pmatrix} 0 & 0 & 1 & 1 & 0 & 1 & 0 & 1 \end{pmatrix}$$

  We compute $B_1 = \boldsymbol{s}_1^\top b = \sum_{i \in \boldsymbol{\mathcal{S}}ector_1} b_i$ and $B_2 = \boldsymbol{s}_2^\top b = \sum_{i \in \boldsymbol{\mathcal{S}}ector_2} b_i$. The sector neutrality constraint can be written as:

$$\begin{pmatrix} A_1 \\ A_2 \end{pmatrix} w = \begin{pmatrix} B_1 \\ B_2 \end{pmatrix}$$

Let us now combine the different constraints. For that, we use the block matrix notation, which is particularly convenient when manipulating nested QP problems. The set #1 of constraint corresponds to the reduction of the carbon intensity, the set #2 corresponds to the ESG score improvement, the set #3 combines the two constraints and we add the sector neutrality in the set #4 of constraints.

| Set of constraints | Carbon intensity | ESG score | Sector neutrality | $A$ | $B$ | $C$ | $D$ |
|---|---|---|---|---|---|---|---|
| #1 | ✓ | | | $A_0$ | $B_0$ | $C_1$ | $D_1$ |
| #2 | | ✓ | | $A_0$ | $B_0$ | $C_2$ | $D_2$ |
| #3 | ✓ | ✓ | | $A_0$ | $B_0$ | $\begin{bmatrix} C_1 \\ C_2 \end{bmatrix}$ | $\begin{bmatrix} D_1 \\ D_2 \end{bmatrix}$ |
| #4 | ✓ | ✓ | ✓ | $\begin{bmatrix} A_0 \\ A_1 \\ A_2 \end{bmatrix}$ | $\begin{bmatrix} B_0 \\ B_1 \\ B_2 \end{bmatrix}$ | $\begin{bmatrix} C_1 \\ C_2 \end{bmatrix}$ | $\begin{bmatrix} D_1 \\ D_2 \end{bmatrix}$ |

We can now solve the QP problem with the right specification of matrices $A$, $B$, $C$ and $D$ for each set of constraints. Results are reported below for the following parameters[7]: $\boldsymbol{\mathcal{R}} = 30\%$ and $\Delta\boldsymbol{\mathcal{S}}^\star = 0.50$. We indicate the optimal weights $w^\star$, the tracking error volatility $\sigma(w^\star \mid b)$, the carbon intensity $\boldsymbol{\mathcal{CI}}(w^\star)$, the effective reduction rate[8] $\boldsymbol{\mathcal{R}}(w^\star \mid b)$, the ESG score $\boldsymbol{\mathcal{S}}(w^\star)$, the ESG score variation $\boldsymbol{\mathcal{S}}(w^\star) - \boldsymbol{\mathcal{S}}(b)$, the weights[9] $w^\star(\boldsymbol{\mathcal{S}}ector_1)$ and $w^\star(\boldsymbol{\mathcal{S}}ector_2)$ of sectors 1 and 2.

| | | Benchmark | Set #1 | Set #2 | Set #3 | Set #4 |
|---|---|---|---|---|---|---|
| Weights (in %) | $w_1^\star$ | 23.00 | 18.17 | 25.03 | 8.64 | 12.04 |
| | $w_2^\star$ | 19.00 | 24.25 | 14.25 | 29.27 | 23.76 |
| | $w_3^\star$ | 17.00 | 16.92 | 21.95 | 26.80 | 30.55 |
| | $w_4^\star$ | 13.00 | 2.70 | 27.30 | 1.48 | 2.25 |
| | $w_5^\star$ | 9.00 | 12.31 | 3.72 | 10.63 | 8.51 |
| | $w_6^\star$ | 8.00 | 11.23 | 1.34 | 6.30 | 10.20 |
| | $w_7^\star$ | 6.00 | 11.28 | 1.68 | 16.87 | 12.69 |
| | $w_8^\star$ | 5.00 | 3.15 | 4.74 | 0.00 | 0.00 |
| Statistics | $\sigma(w^\star \mid b)$ (in %) | 0.00 | 0.50 | 1.18 | 1.90 | 2.12 |
| | $\boldsymbol{\mathcal{CI}}(w^\star)$ | 261.72 | 183.20 | 367.25 | 183.20 | 183.20 |
| | $\boldsymbol{\mathcal{R}}(w^\star \mid b)$ (in %) | | 30.00 | −40.32 | 30.00 | 30.00 |
| | $\boldsymbol{\mathcal{S}}(w^\star)$ | 0.17 | 0.05 | 0.67 | 0.67 | 0.67 |
| | $\boldsymbol{\mathcal{S}}(w^\star) - \boldsymbol{\mathcal{S}}(b)$ | | −0.12 | 0.50 | 0.50 | 0.50 |
| | $w^\star(\boldsymbol{\mathcal{S}}ector_1)$ (in %) | 57.00 | 66.00 | 44.67 | 65.41 | 57.00 |
| | $w^\star(\boldsymbol{\mathcal{S}}ector_2)$ (in %) | 43.00 | 34.00 | 55.33 | 34.59 | 43.00 |

If we only reduce the carbon intensity, the tracking error cost is 50 bps. Nevertheless, the ESG score of the optimized portfolio is below the ESG score of the benchmark (0.05 vs. 0.17). If we improve the ESG score by 0.50, the tracking error cost is 118 bps. This optimal portfolio has a carbon footprint which is higher than this of the benchmark (367.25 vs. 261.72). If we combine the two constraints, the tracking error cost is close to 2%. We observe a reallocation between the sectors. For instance, sector 1 represents 65.41% of the portfolio while its weight is equal to 57% in the benchmark. Finally, the tracking error volatility of the optimal portfolio is equal to 2.12% when we add the sector neutrality constraint.

**Dealing with constraints on relative weights**

Let us assume that we would like to reduce the carbon footprint at the sector level. In this case, we denote by $\boldsymbol{\mathcal{CI}}(w; \boldsymbol{\mathcal{S}}ector_j)$ the carbon intensity of the $j^{\text{th}}$ sector within the portfolio $w$:

$$\boldsymbol{\mathcal{CI}}(w; \boldsymbol{\mathcal{S}}ector_j) = \sum_{i \in \boldsymbol{\mathcal{S}}ector_j} \tilde{w}_i \boldsymbol{\mathcal{CI}}_i$$

where $\tilde{w}_i$ is the normalized weight in the sector bucket:

$$\tilde{w}_i = \frac{w_i}{\sum_{k \in \boldsymbol{\mathcal{S}}ector_j} w_k}$$

[7] We have $B_1 = 0.57$, $B_2 = 0.43$, $D_1 = 183.2040$ and $D_2 = -0.6690$.

[8] We have:

$$\boldsymbol{\mathcal{R}}(w \mid b) = \frac{\boldsymbol{\mathcal{CI}}(b) - \boldsymbol{\mathcal{CI}}(w)}{\boldsymbol{\mathcal{CI}}(b)}$$

[9] We have:

$$w(\boldsymbol{\mathcal{S}}ector_j) = \sum_{i \in \boldsymbol{\mathcal{S}}ector_j} w_i = \boldsymbol{s}_j^\top w$$

Another expression of $\mathcal{CI}(w; \mathcal{S}ector_j)$ is:

$$\mathcal{CI}(w; \mathcal{S}ector_j) = \frac{\sum_{i \in \mathcal{S}ector_j} w_i \mathcal{CI}_i}{\sum_{i \in \mathcal{S}ector_j} w_i} = \frac{(\boldsymbol{s}_j \circ \mathcal{CI})^\top w}{\boldsymbol{s}_j^\top w}$$

If we consider the constraint $\mathcal{CI}(w; \mathcal{S}ector_j) \leq \mathcal{CI}_j^\star$, we obtain:

$$\begin{aligned}
(*) \quad &\Leftrightarrow \quad \mathcal{CI}(w; \mathcal{S}ector_j) \leq \mathcal{CI}_j^\star \\
&\Leftrightarrow \quad (\boldsymbol{s}_j \circ \mathcal{CI})^\top w \leq \mathcal{CI}_j^\star \left(\boldsymbol{s}_j^\top w\right) \\
&\Leftrightarrow \quad \left((\boldsymbol{s}_j \circ \mathcal{CI}) - \mathcal{CI}_j^\star \boldsymbol{s}_j\right)^\top w \leq 0 \\
&\Leftrightarrow \quad \left(\boldsymbol{s}_j \circ \left(\mathcal{CI} - \mathcal{CI}_j^\star\right)\right)^\top w \leq 0
\end{aligned} \tag{11.2}$$

The QP form is then $C = \left(\boldsymbol{s}_j \circ \left(\mathcal{CI} - \mathcal{CI}_j^\star\right)\right)^\top$ and $D = 0$. We remark that we obtain a classical reduction constraint where the vector of carbon intensities is replaced by the vector of deviations $\mathcal{CI} - \mathcal{CI}_j^\star$.

**Remark 117** *We have defined an absolute threshold $\mathcal{CI}_j^\star$, but we can implement a relative threshold by setting $\mathcal{CI}_j^\star = (1 - \mathcal{R}_j)\,\mathcal{CI}(b; \mathcal{S}ector_j)$.*

Let us consider again Example 46 on page 950. We would like to reduce the carbon footprint of the benchmark by 30% and impose the sector neutrality. In this case, the linear equality constraint $Aw = B$ is defined by:

$$A = \begin{pmatrix} 1 & 1 & 1 & 1 & 1 & 1 & 1 & 1 \\ 1 & 1 & 0 & 0 & 1 & 0 & 1 & 0 \\ 0 & 0 & 1 & 1 & 0 & 1 & 0 & 1 \end{pmatrix}$$

and:

$$B = \begin{pmatrix} 100\% \\ 57\% \\ 43\% \end{pmatrix}$$

For the linear inequality constraint $Cw \leq D$, we obtain:

$$C = \begin{pmatrix} 125 & 75 & 254 & 822 & 109 & 17 & 341 & 741 \end{pmatrix}$$

and:

$$D = 183.2040$$

The optimal solution is $w^\star = (21.54\%, 18.50\%, 21.15\%, 3.31\%, 10.02\%, 15.26\%, 6.94\%, 3.27\%)$. The tracking error volatility $\sigma(w^\star \mid b)$ is equal to 112 bps. We verify that the carbon intensity of $w^\star$ is equal to 183.20, which corresponds to a reduction rate of 30% compared to the carbon intensity of the benchmark — $\mathcal{CI}(b) = 261.72$. Nevertheless, we observe that the sector breakdown of the carbon footprint is the following:

$$\begin{cases} \mathcal{CI}(w^\star; \mathcal{S}ector_1) = 132.25 \\ \mathcal{CI}(w^\star; \mathcal{S}ector_2) = 250.74 \end{cases} \quad \text{versus} \quad \begin{cases} \mathcal{CI}(b; \mathcal{S}ector_1) = 128.54 \\ \mathcal{CI}(b; \mathcal{S}ector_2) = 438.26 \end{cases}$$

It follows that the 30% global reduction is explained by an increase of 2.89% of the carbon footprint for the first sector and a decrease of 42.79% of the carbon footprint for the second sector. We deduce that the decarbonization of this portfolio is only supported by the second sector. This is

why we impose that the first sector must reduce its carbon footprint by $\boldsymbol{\mathcal{R}}_1 = 20\%$. In this case, the inequality system becomes:

$$\begin{aligned} C &= \begin{pmatrix} \boldsymbol{\mathcal{CI}}^\top \\ \left(\boldsymbol{s}_1 \circ \left(\boldsymbol{\mathcal{CI}} - \left(1 - \boldsymbol{\mathcal{R}}_1\right)\boldsymbol{\mathcal{CI}}\left(b; \boldsymbol{\mathcal{S}}ector_1\right)\right)\right)^\top \end{pmatrix} \\ &= \begin{pmatrix} 125 & 75 & 254 & 822 & 109 & 17 & 341 & 741 \\ 22.1649 & -27.8351 & 0 & 0 & 6.1649 & 0 & 238.1649 & 0 \end{pmatrix} \end{aligned}$$

and:

$$D = \begin{pmatrix} 183.2040 \\ 0 \end{pmatrix}$$

Solving this new QP problem gives the following optimal portfolio:

$$w^\star = (22.70\%, 22.67\%, 19.23\%, 5.67\%, 11.39\%, 14.50\%, 0.24\%, 3.61\%)$$

The tracking error volatility $\sigma\left(w^\star \mid b\right)$ becomes 144 bps. We verify that the carbon intensity of $w^\star$ is equal to 183.20. Moreover, we obtain $\boldsymbol{\mathcal{CI}}\left(w^\star; \boldsymbol{\mathcal{S}}ector_1\right) = 102.84$ and $\boldsymbol{\mathcal{CI}}\left(w^\star; \boldsymbol{\mathcal{S}}ector_2\right) = 289.74$, *i.e.*, a reduction of 20% and 33.89% respectively.

### 11.1.2 Bond portfolios

#### Risk measure of a bond portfolio

There is a large consensus to use the historical volatility as a risk measure for an equity portfolio, even if it is not perfect and has many drawbacks. For instance, skewness and kurtosis risks are not taken into account, correlations are time-varying, we generally observe jumps in the time series of stock returns, volatility is heteroscedastic, etc. In the case of fixed-income portfolios, the historical volatility is not a relevant risk measure, because the bond volatility depends on duration, credit spread, liquidity, etc. Let us consider a zero-coupon bond, whose price and maturity date are $B\left(t, T\right)$ and $T$. Following Roncalli (2013, page 225), we have:

$$B_t\left(t, T\right) = e^{-(r(t)+s(t))(T-t)+L(t)}$$

where $r\left(t\right)$, $s\left(t\right)$ and $L\left(t\right)$ are the interest rate, the credit spread and the liquidity premium. We deduce that:

$$\begin{aligned} \mathrm{d}\ln B\left(t, T\right) &= -\left(T - t\right)\,\mathrm{d}r\left(t\right) - \left(T - t\right)\,\mathrm{d}s\left(t\right) + \mathrm{d}L\left(t\right) \\ &= -D\,\mathrm{d}r\left(t\right) - \left(D\,s\left(t\right)\right)\frac{\mathrm{d}s\left(t\right)}{s\left(t\right)} + \mathrm{d}L\left(t\right) \\ &= -D\,\mathrm{d}r\left(t\right) - \mathrm{DTS}\left(t\right)\frac{\mathrm{d}s\left(t\right)}{s\left(t\right)} + \mathrm{d}L\left(t\right) \end{aligned}$$

where $D = T - t$ is the remaining maturity (or duration) and $\mathrm{DTS}\left(t\right)$ is the duration-times-spread factor. If we assume that $r\left(t\right)$, $s\left(t\right)$ and $L\left(t\right)$ are independent, the risk of the defaultable bond is equal to:

$$\sigma^2\left(\mathrm{d}\ln B\left(t, T\right)\right) = D^2\sigma^2\left(\mathrm{d}r\left(t\right)\right) + \mathrm{DTS}\left(t\right)^2\sigma^2\left(\frac{\mathrm{d}s\left(t\right)}{s\left(t\right)}\right) + \sigma^2\left(\mathrm{d}L\left(t\right)\right)$$

It can then be decomposed into three components: an interest-rate risk component, a credit risk component and a liquidity risk component. In the case where the three volatility risks (interest rate, credit spread and liquidity) are constant, we obtain:

$$\sigma^2\left(\mathrm{d}\ln B\left(t, T\right)\right) = D^2\sigma_r^2 + \mathrm{DTS}\left(t\right)^2\sigma_s^2 + \sigma_L^2$$

We see that the bond risk depends not only on interest rate, credit and liquidity volatilities but it varies with respect to the duration and the level of the credit spread. Therefore, we confirm that the historical volatility of a bond price is not a relevant risk measure.

**Remark 118** *In the sequel, we do not consider the liquidity risk, since it is generally measured by proprietary liquidity scores (Ben Slimane and De Jong, 2017).*

### Basic optimization problems

In practice, the duration risk is measured using the modified duration (MD) metric. We have:

$$\mathrm{MD}(w) = \sum_{i=1}^{n} w_i \,\mathrm{MD}_i$$

The portfolio DTS is equal to:

$$\mathrm{DTS}(w) = \sum_{i=1}^{n} w_i \,\mathrm{DTS}_i$$

Generally, the construction of a bond portfolio uses the clustering approach. The bond universe is divided into clusters based on the currency, the sector, the credit quality and the maturity band. For instance, the cluster (EUR, Financials, AAA to A−, 1Y-3Y) corresponds to euro-denominated bonds from the financials sector, whose rating is greater than A− and the duration is between one and three years. A cluster is then a generalization of the sector concept. Nevertheless, we will continue to use the term sector instead of the term cluster in the sequel when we will build bond portfolios. Let $\mathrm{MD}_j(w)$ and $\mathrm{DTS}_j(w)$ be the MD and DTS contributions[10] of the $j^{\text{th}}$ sector. We have $\mathrm{MD}_j(w) = \sum_{i\in\mathcal{S}ector_j} w_i \,\mathrm{MD}_i$ and $\mathrm{DTS}_j(w) = \sum_{i\in\mathcal{S}ector_j} w_i \,\mathrm{DTS}_i$. Bond portfolio optimization consists in maximizing the expected carry of the portfolio under a set of numerous constraints:

$$\Omega = \left\{ j = 1, \ldots, n_{\mathcal{S}ector} : \mathrm{MD}_j(w) \approx \mathrm{MD}_j^\star, \mathrm{DTS}_j(w) \approx \mathrm{DTS}_j^\star \right\}$$

Therefore, the objective function of the optimization problem has the following form:

$$w^\star = \arg\min \frac{\varphi_{\mathrm{MD}}}{2} \sum_{j=1}^{n_{\mathcal{S}ector}} \left(\mathrm{MD}_j(w) - \mathrm{MD}_j^\star\right)^2 + \frac{\varphi_{\mathrm{DTS}}}{2} \sum_{j=1}^{n_{\mathcal{S}ector}} \left(\mathrm{DTS}_j(w) - \mathrm{DTS}_j^\star\right)^2 - \gamma \sum_{i=1}^{n} w_i \mathcal{C}_i \tag{11.3}$$

where $\varphi_{\mathrm{MD}} \geq 0$ and $\varphi_{\mathrm{DTS}} \geq 0$ indicate the relative weight of each risk component, $\mathcal{C}_i$ is the expected carry[11] of bond $i$ and $\gamma$ is the risk-tolerance coefficient. In order to solve this optimization problem, the goal is to transform Equation (11.3) into a QP problem:

$$\begin{aligned} w^\star &= \arg\min \mathcal{QF}(w; Q, R, c) \\ &\text{s.t.} \begin{cases} \mathbf{1}_n^\top w = 1 \\ \mathbf{0}_n \leq w \leq \mathbf{1}_n \end{cases} \end{aligned} \tag{11.4}$$

where $\mathcal{QF}(w; Q, R, c)$ is the quadratic form of the objective function.

[10] Be careful, they do not measure the MD and DTS of the sector, which are measured with relative weights within the sector.

[11] The expected carry of a bond corresponds to the carry of the bond plus its expected mark-to-market return minus the expected credit loss.

We use the properties of quadratic forms presented in Section A.1.3 on page 1054. We have[12]:

$$\begin{aligned}
\frac{1}{2}\left(\mathrm{MD}_j(w)-\mathrm{MD}_j^\star\right)^2 &= \frac{1}{2}\left(\sum\nolimits_{i\in\boldsymbol{\mathcal{S}}ector_j} w_i\,\mathrm{MD}_i-\mathrm{MD}_j^\star\right)^2\\
&= \frac{1}{2}\left(\sum_{i=1}^n \boldsymbol{s}_{i,j}w_i\,\mathrm{MD}_i-\mathrm{MD}_j^\star\right)^2\\
&= \frac{1}{2}\left(\sum_{i=1}^n \boldsymbol{s}_{i,j}\,\mathrm{MD}_i\,w_i\right)^2-w^\top\left(\boldsymbol{s}_j\circ\mathrm{MD}\right)\mathrm{MD}_j^\star+\frac{1}{2}\mathrm{MD}_j^{\star^2}\\
&= \mathcal{QF}\left(w;\mathcal{T}\left(\boldsymbol{s}_j\circ\mathrm{MD}\right),\left(\boldsymbol{s}_j\circ\mathrm{MD}\right)\mathrm{MD}_j^\star,\frac{1}{2}\mathrm{MD}_j^{\star^2}\right)
\end{aligned}$$

where $\mathrm{MD}=(\mathrm{MD}_1,\ldots,\mathrm{MD}_n)$ is the vector of modified durations. It follows that:

$$\frac{1}{2}\sum_{j=1}^{n_{\boldsymbol{\mathcal{S}}ector}}\left(\mathrm{MD}_j(w)-\mathrm{MD}_j^\star\right)^2=\mathcal{QF}\left(w;Q_{\mathrm{MD}},R_{\mathrm{MD}},c_{\mathrm{MD}}\right)$$

where:

$$\begin{cases}
Q_{\mathrm{MD}}=\displaystyle\sum_{j=1}^{n_{\boldsymbol{\mathcal{S}}ector}}\mathcal{T}\left(\boldsymbol{s}_j\circ\mathrm{MD}\right)\\
R_{\mathrm{MD}}=\displaystyle\sum_{j=1}^{n_{\boldsymbol{\mathcal{S}}ector}}\left(\boldsymbol{s}_j\circ\mathrm{MD}\right)\mathrm{MD}_j^\star\\
c_{\mathrm{MD}}=\dfrac{1}{2}\displaystyle\sum_{j=1}^{n_{\boldsymbol{\mathcal{S}}ector}}\mathrm{MD}_j^{\star^2}
\end{cases}$$

In a similar way, we have:

$$\frac{1}{2}\sum_{j=1}^{n_{\boldsymbol{\mathcal{S}}ector}}\left(\mathrm{DTS}_j(w)-\mathrm{DTS}_j^\star\right)^2=\mathcal{QF}\left(w;Q_{\mathrm{DTS}},R_{\mathrm{DTS}},c_{\mathrm{DTS}}\right)$$

where:

$$\begin{cases}
Q_{\mathrm{DTS}}=\displaystyle\sum_{j=1}^{n_{\boldsymbol{\mathcal{S}}ector}}\mathcal{T}\left(\boldsymbol{s}_j\circ\mathrm{DTS}\right)\\
R_{\mathrm{MD}}=\displaystyle\sum_{j=1}^{n_{\boldsymbol{\mathcal{S}}ector}}\left(\boldsymbol{s}_j\circ\mathrm{DTS}\right)\mathrm{DTS}_j^\star\\
c_{\mathrm{DTS}}=\dfrac{1}{2}\displaystyle\sum_{j=1}^{n_{\boldsymbol{\mathcal{S}}ector}}\mathrm{DTS}_j^{\star^2}
\end{cases}$$

where $\mathrm{DTS}=(\mathrm{DTS}_1,\ldots,\mathrm{DTS}_n)$ is the vector of DTS values. Since we have $-\gamma\sum_{i=1}^n w_i\mathcal{C}_i=\mathcal{QF}\left(w;\mathbf{0}_{n,n},\gamma\mathcal{C},0\right)$ where $\mathcal{C}=(\mathcal{C}_1,\ldots,\mathcal{C}_n)$ is the vector of expected carry values, we conclude that the function to optimize is:

$$\begin{aligned}
\mathcal{QF}\left(w;Q,R,c\right) &= \varphi_{\mathrm{MD}}\mathcal{QF}\left(w;Q_{\mathrm{MD}},R_{\mathrm{MD}},c_{\mathrm{MD}}\right)+\varphi_{\mathrm{DTS}}\mathcal{QF}\left(w;Q_{\mathrm{DTS}},R_{\mathrm{DTS}},c_{\mathrm{DTS}}\right)+\\
&\quad \mathcal{QF}\left(w;\mathbf{0}_{n,n},\gamma\mathcal{C},0\right)
\end{aligned}$$

[12] We remind that $\mathcal{T}(u)=uu^\top$.

where:

$$\begin{cases} Q = \varphi_{\text{MD}} Q_{\text{MD}} + \varphi_{\text{DTS}} Q_{\text{DTS}} \\ R = \gamma \mathcal{C} + \varphi_{\text{MD}} R_{\text{MD}} + \varphi_{\text{DTS}} R_{\text{DTS}} \\ c = \varphi_{\text{MD}} c_{\text{MD}} + \varphi_{\text{DTS}} c_{\text{DTS}} \end{cases}$$

We can extend the previous analysis when there is a benchmark. In this case, the threshold values $\text{MD}_j^\star$ and $\text{DTS}_j^\star$ are equal to the MD and DTS contributions of the benchmark: $\text{MD}_j^\star = \sum_{i \in \boldsymbol{\mathcal{S}ector}_j} b_i \,\text{MD}_i$ and $\text{DTS}_j^\star = \sum_{i \in \boldsymbol{\mathcal{S}ector}_j} b_i \,\text{DTS}_i$. The MD- and DTS-based tracking error variances are then equal to:

$$\mathcal{R}_{\text{MD}}(w \mid b) = \sigma_{\text{MD}}^2(w \mid b) = \sum_{j=1}^{n_{\boldsymbol{\mathcal{S}ector}}} \left( \sum\nolimits_{i \in \boldsymbol{\mathcal{S}ector}_j} (w_i - b_i) \,\text{MD}_i \right)^2$$

and:

$$\mathcal{R}_{\text{DTS}}(w \mid b) = \sigma_{\text{DTS}}^2(w \mid b) = \sum_{j=1}^{n_{\boldsymbol{\mathcal{S}ector}}} \left( \sum\nolimits_{i \in \boldsymbol{\mathcal{S}ector}_j} (w_i - b_i) \,\text{DTS}_i \right)^2$$

Generally, we also consider a third active risk component called the active share risk[13]:

$$\mathcal{R}_{\text{AS}}(w \mid b) = \sigma_{\text{AS}}^2(w \mid b) = \sum_{i=1}^{n} (w_i - b_i)^2$$

The basic optimization problem becomes:

$$\begin{aligned} w^\star &= \arg\min \frac{1}{2} \mathcal{R}(w \mid b) - \gamma \sum_{i=1}^{n} (w_i - b_i) \,\mathcal{C}_i \\ &\text{s.t.} \begin{cases} \mathbf{1}_n^\top w = 1 \\ \mathbf{0}_n \leq w \leq \mathbf{1}_n \end{cases} \end{aligned} \tag{11.5}$$

where the synthetic risk measure is equal to:

$$\mathcal{R}(w \mid b) = \varphi_{\text{AS}} \mathcal{R}_{\text{AS}}(w \mid b) + \varphi_{\text{MD}} \mathcal{R}_{\text{MD}}(w \mid b) + \varphi_{\text{DTS}} \mathcal{R}_{\text{DTS}}(w \mid b)$$

By using the properties $\mathcal{QF}(x - y; Q, R, c) = \mathcal{QF}\left(x; Q, R + Qy, \frac{1}{2} y^\top Q y + y^\top R + c\right)$, $\mathcal{T}(\boldsymbol{s}_j \circ \text{MD})\, b = (\boldsymbol{s}_j \circ \text{MD})(\boldsymbol{s}_j \circ \text{MD})^\top b = (\boldsymbol{s}_j \circ \text{MD})\,\text{MD}_j^\star$, $\mathcal{T}(\boldsymbol{s}_j \circ \text{DTS})\, b = (\boldsymbol{s}_j \circ \text{DTS})\,\text{DTS}_j^\star$, $b^\top \mathcal{T}(\boldsymbol{s}_j \circ \text{MD})\, b = \text{MD}_j^{\star^2}$ and $b^\top \mathcal{T}(\boldsymbol{s}_j \circ \text{DTS})\, b = \text{DTS}_j^{\star^2}$, we have:

$$\begin{cases} \frac{1}{2} \mathcal{R}_{\text{AS}}(w \mid b) = \mathcal{QF}(w; Q_{\text{AS}}(b), R_{\text{AS}}(b), c_{\text{AS}}(b)) \\ \frac{1}{2} \mathcal{R}_{\text{MD}}(w \mid b) = \mathcal{QF}(w; Q_{\text{MD}}(b), R_{\text{MD}}(b), c_{\text{MD}}(b)) \\ \frac{1}{2} \mathcal{R}_{\text{DTS}}(w \mid b) = \mathcal{QF}(w; Q_{\text{DTS}}(b), R_{\text{DTS}}(b), c_{\text{DTS}}(b)) \end{cases}$$

[13] The traditional definition of the active share is:

$$\text{AS}(w \mid b) = \frac{1}{2} \sum_{i=1}^{n} |w_i - b_i|$$

We prefer to use the $\mathcal{L}_2$-norm which is more tractable from a numerical viewpoint.

where $Q_{\text{AS}}(b) = I_n$, $R_{\text{AS}}(b) = b$, $c_{\text{AS}}(b) = \frac{1}{2}b^\top b$, $Q_{\text{MD}}(b) = Q_{\text{MD}}$, $R_{\text{MD}}(b) = Q_{\text{MD}}b = R_{\text{MD}}$, $c_{\text{MD}}(b) = \frac{1}{2}b^\top Q_{\text{MD}}b = c_{\text{MD}}$, $Q_{\text{DTS}}(b) = Q_{\text{DTS}}$, $R_{\text{DTS}}(b) = Q_{\text{DTS}}b = R_{\text{DTS}}$, and $c_{\text{DTS}}(b) = \frac{1}{2}b^\top Q_{\text{DTS}}b = c_{\text{DTS}}$. We conclude that Equation (11.5) becomes:

$$\begin{aligned} w^\star &= \arg\min \mathcal{QF}(w; Q(b), R(b), c(b)) \\ &\text{s.t.} \begin{cases} \mathbf{1}_n^\top w = 1 \\ \mathbf{0}_n \leq w \leq \mathbf{1}_n \end{cases} \end{aligned} \tag{11.6}$$

where[14]:

$$\begin{cases} Q(b) = \varphi_{\text{AS}}Q_{\text{AS}}(b) + \varphi_{\text{MD}}Q_{\text{MD}}(b) + \varphi_{\text{DTS}}Q_{\text{DTS}}(b) \\ R(b) = \gamma\mathcal{C} + \varphi_{\text{AS}}R_{\text{AS}}(b) + \varphi_{\text{MD}}R_{\text{MD}}(b) + \varphi_{\text{DTS}}R_{\text{DTS}}(b) \\ c(b) = \gamma b^\top\mathcal{C} + \varphi_{\text{AS}}c_{\text{AS}}(b) + \varphi_{\text{MD}}c_{\text{MD}}(b) + \varphi_{\text{DTS}}c_{\text{DTS}}(b) \end{cases}$$

**Remark 119** *We notice that the optimization problem (11.4) is a special case of the optimization problem (11.6) when $\varphi_{\text{AS}}$ and $b$ are set to 0 and $\mathbf{0}_n$.*

**Example 47** *We consider an investment universe of five bonds with the following characteristics: the benchmark is $b = (30\%, 25\%, 20\%, 15\%, 10\%)$; the modified durations (in years) are $\text{MD} = (3, 7, 6, 12, 2)$; the DTS values (in bps) are $\text{DTS} = (100, 250, 70, 400, 150)$; the carry vector (in bps) is $\mathcal{C} = (200, 300, 150, 250, 600)$; the first, third and fourth bonds belong to the first sector while the second and fourth bonds belong to the second sector. We assume that $\varphi_{\text{AS}} = 1$, $\varphi_{\text{MD}} = 1$, $\varphi_{\text{DTS}} = 0.001$ and $\gamma = 20\%$.*

We proceed by steps in order to obtain the final quadratic form. First, we first compute the modified duration and the duration-times-spread factor of the benchmark. We obtain $\text{MD}(b) = 5.85$ years and $\text{DTS}(b) = 181.50$ bps. The sector contributions are $\text{MD}_1(b) = 3.90$ and $\text{DTS}_1(b) = 104.00$ for sector $\boldsymbol{\mathcal{S}}ector_1$, and $\text{MD}_2(b) = 1.95$ and $\text{DTS}_2(b) = 77.50$ for sector $\boldsymbol{\mathcal{S}}ector_2$. The target values are then $\text{MD}_1^\star = 3.90$, $\text{MD}_2^\star = 1.95$, $\text{DTS}_1^\star = 104.00$ and $\text{DTS}_2^\star = 77.50$. Second, we compute the matrices $Q_{\text{MD}}$, $R_{\text{MD}}$, $c_{\text{MD}}$, $Q_{\text{DTS}}$, $R_{\text{DTS}}$, and $c_{\text{DTS}}$. Third, using the benchmark composition $b$, we deduce the matrices $Q_{\text{AS}}(b)$, $R_{\text{AS}}(b)$, $c_{\text{AS}}(b)$, $Q_{\text{MD}}(b)$, $R_{\text{MD}}(b)$, $c_{\text{MD}}(b)$, $Q_{\text{DTS}}(b)$, $R_{\text{DTS}}(b)$ and $c_{\text{DTS}}(b)$. Finally, we calculate the matrices $Q(b)$, $R(b)$ and $c(b)$. All these matrices are reported in Table 11.1 on page 959. If we compute $\mathcal{QF}(w_{\text{ew}}; Q(b), R(b), c(b))$ where $w_{\text{ew}}$ is the equally-weighted portfolio, we obtain $-7.37812$. Another way to check that we obtain the good results is to verify that $\mathcal{QF}(b; Q(b), R(b), c(b)) = 0$.

### Illustration

**Example 48** *We consider an investment universe of nine corporate bonds with the following characteristics:*

| Issuer | #1 | #2 | #3 | #4 | #5 | #6 | #7 | #8 | #9 |
|---|---|---|---|---|---|---|---|---|---|
| $b_i$ (in %) | 21 | 19 | 16 | 12 | 11 | 8 | 6 | 4 | 3 |
| $\boldsymbol{\mathcal{CI}}_i$ (in $\text{tCO}_2\text{e}/\$$ mn) | 111 | 52 | 369 | 157 | 18 | 415 | 17 | 253 | 900 |
| $\text{MD}_i$ (in years) | 3.16 | 6.48 | 3.54 | 9.23 | 6.40 | 2.30 | 8.12 | 7.96 | 5.48 |
| $\text{DTS}_i$ (in bps) | 107 | 255 | 75 | 996 | 289 | 45 | 620 | 285 | 125 |
| $\boldsymbol{\mathcal{S}}ector$ | 1 | 1 | 1 | 2 | 2 | 2 | 3 | 3 | 3 |

*We assume that the portfolio weights can not deviate too far from the benchmark and impose the following constraint: $0.25 \times b_i \leq w_i \leq 4 \times b_i$. We have $\varphi_{\text{AS}} = 100$, $\varphi_{\text{MD}} = 25$ and $\varphi_{\text{DTS}} = 0.001$.*

Table 11.1: Quadratic form (Example 47)

| $Q_{\text{AS}}(b) = Q_{\text{AS}}$ | | | | | $R_{\text{AS}}$ | $R_{\text{AS}}(b)$ | $c_{\text{AS}}$ | $c_{\text{AS}}(b)$ |
|---|---|---|---|---|---|---|---|---|
| 1 | 0 | 0 | 0 | 0 | 0.00 | 0.30 | | |
| 0 | 1 | 0 | 0 | 0 | 0.00 | 0.25 | | |
| 0 | 0 | 1 | 0 | 0 | 0.00 | 0.20 | 0.0000 | 0.1125 |
| 0 | 0 | 0 | 1 | 0 | 0.00 | 0.15 | | |
| 0 | 0 | 0 | 0 | 1 | 0.00 | 0.10 | | |
| $Q_{\text{MD}}(b) = Q_{\text{MD}}$ | | | | | $R_{\text{MD}}$ | $R_{\text{MD}}(b)$ | $c_{\text{MD}}$ | $c_{\text{MD}}(b)$ |
| 9 | 0 | 18 | 36 | 0 | 11.70 | 11.70 | | |
| 0 | 49 | 0 | 0 | 14 | 13.65 | 13.65 | | |
| 18 | 0 | 36 | 72 | 0 | 23.40 | 23.40 | 9.5062 | 9.5062 |
| 36 | 0 | 72 | 144 | 0 | 46.80 | 46.80 | | |
| 0 | 14 | 0 | 0 | 4 | 3.90 | 3.90 | | |
| $Q_{\text{DTS}}(b) = Q_{\text{DTS}}$ | | | | | $R_{\text{DTS}}$ | $R_{\text{DTS}}(b)$ | $c_{\text{DTS}}$ | $c_{\text{DTS}}(b)$ |
| 10000 | 0 | 7000 | 40000 | 0 | 10400 | 10400 | | |
| 0 | 62500 | 0 | 0 | 37500 | 19375 | 19375 | | |
| 7000 | 0 | 4900 | 28000 | 0 | 7280 | 7280 | 8411.1250 | 8411.1250 |
| 40000 | 0 | 28000 | 160000 | 0 | 41600 | 41600 | | |
| 0 | 37500 | 0 | 0 | 22500 | 11625 | 11625 | | |
| | | $Q(b)$ | | | $R(b)$ | | $c(b)$ | |
| 20.0 | 0.0 | 25.0 | 76.0 | 0.0 | 62.400 | | | |
| 0.0 | 112.5 | 0.0 | 0.0 | 51.5 | 93.275 | | | |
| 25.0 | 0.0 | 41.9 | 100.0 | 0.0 | 60.880 | | 70.530 | |
| 76.0 | 0.0 | 100.0 | 305.0 | 0.0 | 138.550 | | | |
| 0.0 | 51.5 | 0.0 | 0.0 | 27.5 | 135.625 | | | |

The objective is to reduce the carbon footprint of the benchmark and minimizing the tracking error risk. In this case, the carry vector $\mathcal{C}$ is set to the zero vector and the optimization problem is defined as:

$$\begin{aligned} w^{\star}(\boldsymbol{\mathcal{R}}) &= \arg\min \frac{1}{2} w^{\top} Q(b)\, w - w^{\top} R(b) \\ &\text{s.t.} \begin{cases} \mathbf{1}_9^{\top} w = 1 \\ \boldsymbol{\mathcal{CI}}^{\top} w \leq (1 - \boldsymbol{\mathcal{R}})\, \boldsymbol{\mathcal{CI}}(b) \\ \dfrac{b}{4} \leq w \leq 4b \end{cases} \end{aligned}$$

where $\boldsymbol{\mathcal{R}}$ is the reduction rate. Since the bonds are ordering by sectors, $Q(b)$ is a block diagonal matrix:

$$Q(b) = \begin{pmatrix} Q_1 & \mathbf{0}_{3\times 3} & \mathbf{0}_{3\times 3} \\ \mathbf{0}_{3\times 3} & Q_2 & \mathbf{0}_{3\times 3} \\ \mathbf{0}_{3\times 3} & \mathbf{0}_{3\times 3} & Q_3 \end{pmatrix} \times 10^3$$

where:

$$Q_1 = \begin{pmatrix} 0.3611 & 0.5392 & 0.2877 \\ 0.5392 & 1.2148 & 0.5926 \\ 0.2877 & 0.5926 & 0.4189 \end{pmatrix}, \qquad Q_2 = \begin{pmatrix} 3.2218 & 1.7646 & 0.5755 \\ 1.7646 & 1.2075 & 0.3810 \\ 0.5755 & 0.3810 & 0.2343 \end{pmatrix}$$

[14] We have $-\gamma \sum_{i=1}^{n} (w_i - b_i)\, \mathcal{C}_i = \mathcal{QF}(w; \mathbf{0}_{n,n}, \gamma\mathcal{C}, \gamma b^{\top}\mathcal{C})$.

Figure 11.1: Relationship between the reduction rate and the tracking risk (Example 48)

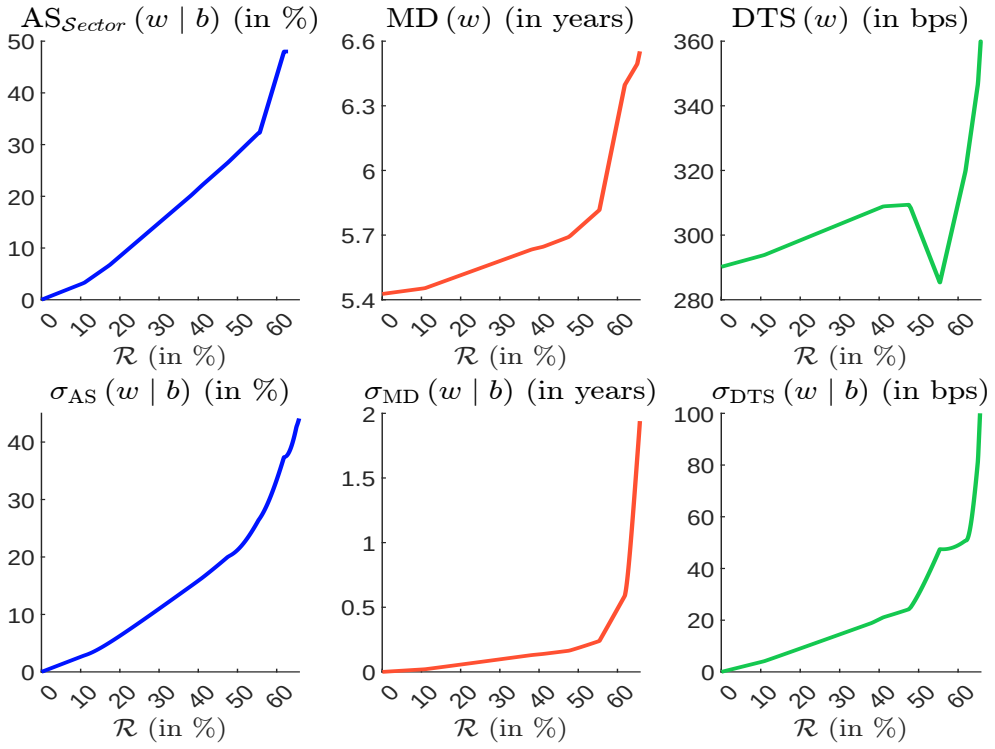


and:

$$Q_3 = \begin{pmatrix} 2.1328 & 1.7926 & 1.1899 \\ 1.7926 & 1.7653 & 1.1261 \\ 1.1899 & 1.1261 & 0.8664 \end{pmatrix}$$

The vector $R(b)$ is equal to $(2.2431, 4.3886, 2.4004, 6.2678, 3.7506, 1.2972, 2.3537, 2.1195, 1.4243) \times 10^2$. In Tables 11.2 and 11.3, we report the optimal weights and the risk statistics. Increasing the reduction rate implies to take more active risk in terms of active share, modified duration and duration-times-spread factor. For instance, if we target $\boldsymbol{\mathcal{R}} = 50\%$, the MD-based tracking risk is 2.4 months while the DTS-based tracking risk is 30.11 bps. The asset- and sector-based[15] active shares are respectively equal to 21.21% and 28.31%. In Figure 11.1, we show the relationship between the reduction rate and these different risk statistics. We notice that there is no solution to the optimization problem when $\boldsymbol{\mathcal{R}} \geq 65.73\%$.

Table 11.2: Weights in % of optimized bond portfolios (Example 48)

| Portfolio | #1 | #2 | #3 | #4 | #5 | #6 | #7 | #8 | #9 |
|---|---|---|---|---|---|---|---|---|---|
| $b$ | 21.00 | 19.00 | 16.00 | 12.00 | 11.00 | 8.00 | 6.00 | 4.00 | 3.00 |
| $w^\star(10\%)$ | 21.92 | 19.01 | 15.53 | 11.72 | 11.68 | 7.82 | 6.68 | 4.71 | 0.94 |
| $w^\star(30\%)$ | 26.29 | 20.24 | 10.90 | 10.24 | 16.13 | 3.74 | 9.21 | 2.50 | 0.75 |
| $w^\star(50\%)$ | 27.48 | 23.97 | 4.00 | 6.94 | 22.70 | 2.00 | 11.15 | 1.00 | 0.75 |

[15] The sector-based active share is defined as $\text{AS}_{\boldsymbol{\mathcal{S}}ector}(w \mid b) = \frac{1}{2}\sum_{j=1}^{n_{\boldsymbol{\mathcal{S}}ector}} \left|\sum_{i \in Sector_j}(w_i - b_i)\right|$.

Table 11.3: Risk statistics of optimized bond portfolios (Example 48)

| Portfolio | $\text{AS}_{\boldsymbol{\mathcal{S}ector}}$ (in %) | $\text{MD}(w)$ (in years) | $\text{DTS}(w)$ (in bps) | $\sigma_{\text{AS}}(w \mid b)$ (in %) | $\sigma_{\text{MD}}(w \mid b)$ (in years) | $\sigma_{\text{DTS}}(w \mid b)$ (in bps) | $\boldsymbol{\mathcal{CI}}(w)$ $\text{gCO}_2\text{e}/\$$ |
|---|---|---|---|---|---|---|---|
| $b$ | 0.00 | 5.43 | 290.18 | 0.00 | 0.00 | 0.00 | 184.39 |
| $w^\star$ (10%) | 3.00 | 5.45 | 293.53 | 2.62 | 0.02 | 3.80 | 165.95 |
| $w^\star$ (30%) | 14.87 | 5.58 | 303.36 | 10.98 | 0.10 | 14.49 | 129.07 |
| $w^\star$ (50%) | 28.31 | 5.73 | 302.14 | 21.21 | 0.19 | 30.11 | 92.19 |

### 11.1.3 Advanced optimization problems

In this section, we go beyond the previous approaches in order to solve more complex portfolio optimization problems. First, we consider the case of large bond universes when there are more than 10 000 bonds in the index. In this case, we generally use linear programming (LP) algorithms. Second, we show how to incorporate some standard nonlinear constraints in the QP/LP framework. Finally, we consider mathematical problems when the variable to optimize is not a vector of weights, but the numbers of shares. In particular, this last problem occurs when we would like to build an investible fixed-income portfolio.

#### Large bond universe

Quadratic problem algorithms are efficient when the dimension of the problem is relative small, say, when $n \leq 5\,000$. The issue is not the convergence of the algorithm, but more the manipulation of the Hessian matrix $Q$ of the quadratic form. Indeed, since $Q$ is a $n \times n$ matrix, we have to store $n^2$ floating-point numbers. For instance, $Q$ has 25 millions of elements when $n$ is equal to 5 000. In the case of bond portfolio optimization, we have seen that $Q$ is a block matrix with the following structure[16]:

$$Q = \begin{pmatrix} Q_1 & \mathbf{0}_{n_{(1)} \times n_{(2)}} & & \mathbf{0} \\ \mathbf{0}_{n_{(2)} \times n_{(1)}} & Q_2 & & \\ & & \ddots & \\ \mathbf{0} & & & Q_{n_{\boldsymbol{\mathcal{S}ector}}} \end{pmatrix}$$

where $Q_j$ is the $n_{(j)} \times n_{(j)}$ matrix associated to the $j^{\text{th}}$ sector and $n_{(j)}$ is the number of assets that belong to the $j^{\text{th}}$ sector. By construction, we have $\sum_{j=1}^{n_{\boldsymbol{\mathcal{S}ector}}} n_{(j)} = n$. Therefore, the number of non-zero entries is equal to:

$$\eta(Q) = \sum_{j=1}^{n_{\boldsymbol{\mathcal{S}ector}}} n_{(j)}^2 \ll n^2$$

Let us assume that the number of assets are equally distributed among the sectors; $n_{(j)} = n/n_{\boldsymbol{\mathcal{S}ector}}$. We obtain:

$$\eta(Q) = \sum_{j=1}^{n_{\boldsymbol{\mathcal{S}ector}}} \left(\frac{n}{n_{\boldsymbol{\mathcal{S}ector}}}\right)^2 = \frac{n^2}{n_{\boldsymbol{\mathcal{S}ector}}}$$

We deduce that $Q$ is a highly sparse matrix since the number of non-zero elements is a fraction of the full number of elements. If $n = 5\,000$ and $n_{\boldsymbol{\mathcal{S}ector}} = 10$, the number of non-zero elements is equal to 2.5 millions of elements. We reiterate that the bucket concept in bond portfolio optimization generalizes the sector concept. For instance, if we consider ten sectors, three currencies and five

[16] We assume that the bonds are ordered according to the sectors.

maturity bands, the number of buckets is equal to $10 \times 3 \times 5 = 150$. If $n = 5\,000$, the number of non-zero elements is approximatively equal to 167 000 of elements. This is equivalent to manipulate a dense matrix of dimension $409 \times 409$. It follows that portfolio optimization with large bond universe remains feasible by using sparse quadratic programming solvers.

As of 31/01/2023, the Bloomberg Global Aggregate Total Return Index has 28 799 securities, while the ICE BOFA Global Broad Market Index has 33 575 securities. For these two bond universes, we reach the limits of QP optimization from a numerical viewpoint. For instance, the number of non-zero entries is equal to more than 8 million floating-point numbers for the Hessian $Q$ matrix when $n$ is equal to 35 000 and we have 150 equally-distributed buckets. In the case where we only consider sectors as buckets, we have more than 120 million floating-point numbers for 10 equally-distributed sectors. Moreover, the number of bonds are generally concentrated in some sectors, *e.g.*, Financials. This explains that bond portfolio managers prefer to use another approach than the QP framework when performing portfolio optimization with such large investment universes.

Figure 11.2: Relationship between $\mathcal{L}_1$-norm $\mathcal{L}_2$-norm

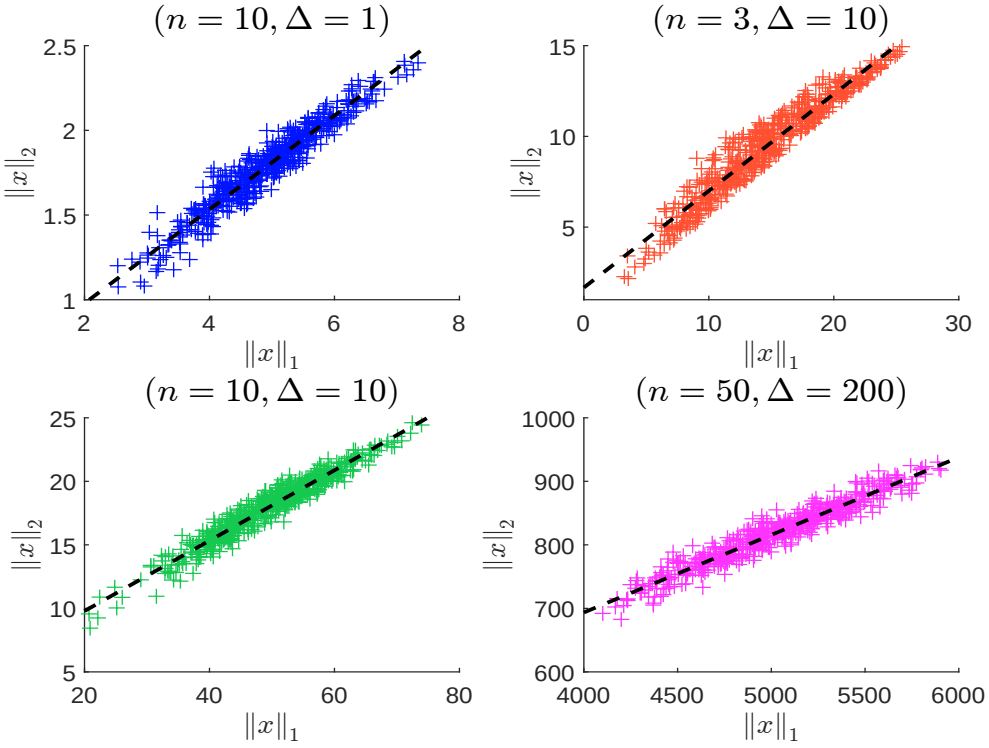


The underlying idea is to replace $\mathcal{L}_2$-norm risk measures by $\mathcal{L}_1$-norm risk measures. We recall that $f(x) = \sqrt{x^2} = |x|$ when $x$ is a scalar. In the general case where $x$ is a $n \times 1$ vector, we have $\|x\|_1 = \sum_{i=1}^n |x_i|$ and $\|x\|_2 = \sqrt{\sum_{i=1}^n x_i^2} = \sqrt{x^\top x}$. We notice that $\|x\|_2^2 \leq \sum_{i=1}^n |x_i| \sum_{i=1}^n |x_i| = \|x\|_1^2$ and $\|x\|_1^2 = \mathbf{1}_n^\top |x| \leq \|\mathbf{1}_n\|_2 \cdot \|x\|_2 \leq \sqrt{n}\,\|x\|_2$, implying that $\|x\|_2 \leq \|x\|_1 \leq \sqrt{n}\,\|x\|_2$. This means that there is not a simple relationship between the two norms. Nevertheless, if the vector $x$ is "*homogenous*", we can use the following approximation $\|x\|_2 \approx \beta_0 + \beta_1 \|x\|_1$ where $0 < \beta_1 \leq 1$. In Figure 11.2, we report the scatter plot of $(\|x\|_1, \|x\|_2)$ and the least square fitting model $\|x\|_2 = \hat{\beta}_0 + \hat{\beta}_1 \|x\|_1$ when $x_i$ is the random variate, whose probability distribution is $\mathbf{F}(x_i) = \Pr\left\{\mathcal{U}_{[0,1]} \leq \Delta^{-1} x_i\right\}$. The estimated values $\left(\hat{\beta}_0, \hat{\beta}_1\right)$ depend then on the dimension $n$ of the vector $x$ and the parameter $\Delta$.

We exploit the previous relationship and replace the synthetic risk measure by:

$$\mathcal{D}(w \mid b) = \varphi'_{\text{AS}}\mathcal{D}_{\text{AS}}(w \mid b) + \varphi'_{\text{MD}}\mathcal{D}_{\text{MD}}(w \mid b) + \varphi'_{\text{DTS}}\mathcal{D}_{\text{DTS}}(w \mid b)$$

where:

$$\begin{aligned}
\mathcal{D}_{\text{AS}}(w \mid b) &= \frac{1}{2}\sum_{i=1}^{n}|w_i - b_i| = \frac{1}{2}\|w - b\|_1 \\
\mathcal{D}_{\text{MD}}(w \mid b) &= \sum_{j=1}^{n_{\boldsymbol{\mathcal{S}}ector}}\left|\sum\nolimits_{i\in\boldsymbol{\mathcal{S}}ector_j}(w_i - b_i)\,\text{MD}_i\right| = \sum_{j=1}^{n_{\boldsymbol{\mathcal{S}}ector}}\|\boldsymbol{s}_j \circ (w - b) \circ \text{MD}\|_1 \\
\mathcal{D}_{\text{DTS}}(w \mid b) &= \sum_{j=1}^{n_{\boldsymbol{\mathcal{S}}ector}}\left|\sum\nolimits_{i\in\boldsymbol{\mathcal{S}}ector_j}(w_i - b_i)\,\text{DTS}_i\right| = \sum_{j=1}^{n_{\boldsymbol{\mathcal{S}}ector}}\|\boldsymbol{s}_j \circ (w - b) \circ \text{DTS}\|_1
\end{aligned}$$

The optimization problem becomes then:

$$\begin{aligned}
w^\star &= \arg\min \mathcal{D}(w \mid b) - \gamma\sum_{i=1}^{n}(w_i - b_i)\,\mathcal{C}_i \\
&\text{s.t.} \begin{cases} \mathbf{1}_n^\top w = 1 \\ \mathbf{0}_n \leq w \leq \mathbf{1}_n \end{cases}
\end{aligned} \tag{11.7}$$

Using the absolute value trick, we transform the nonlinear objective function into a linear function:

$$\begin{aligned}
w^\star &= \arg\min \frac{1}{2}\varphi'_{\text{AS}}\sum_{i=1}^{n}\tau_{i,w} + \varphi'_{\text{MD}}\sum_{j=1}^{n_{\boldsymbol{\mathcal{S}}ector}}\tau_{j,\text{MD}} + \varphi'_{\text{DTS}}\sum_{j=1}^{n_{\boldsymbol{\mathcal{S}}ector}}\tau_{j,\text{DTS}} - \gamma\sum_{i=1}^{n}(w_i - b_i)\,\mathcal{C}_i \\
&\text{s.t.} \begin{cases}
\mathbf{1}_n^\top w = 1 \\
\mathbf{0}_n \leq w \leq \mathbf{1}_n \\
|w_i - b_i| \leq \tau_{i,w} \\
\left|\sum_{i\in\boldsymbol{\mathcal{S}}ector_j}(w_i - b_i)\,\text{MD}_i\right| \leq \tau_{j,\text{MD}} \\
\left|\sum_{i\in\boldsymbol{\mathcal{S}}ector_j}(w_i - b_i)\,\text{DTS}_i\right| \leq \tau_{j,\text{DTS}} \\
\tau_{i,w} \geq 0, \tau_{j,\text{MD}} \geq 0, \tau_{j,\text{DTS}} \geq 0
\end{cases}
\end{aligned}$$

We notice that:

$$|w_i - b_i| \leq \tau_{i,w} \Leftrightarrow \begin{cases} w_i - \tau_{i,w} \leq b_i \\ -w_i - \tau_{i,w} \leq -b_i \end{cases}$$

and:

$$\begin{aligned}
(*) &\Leftrightarrow \left|\sum\nolimits_{i\in\boldsymbol{\mathcal{S}}ector_j}(w_i - b_i)\,\text{MD}_i\right| \leq \tau_{j,\text{MD}} \\
&\Leftrightarrow -\tau_{j,\text{MD}} \leq \sum\nolimits_{i\in\boldsymbol{\mathcal{S}}ector_j}(w_i - b_i)\,\text{MD}_i \leq \tau_{j,\text{MD}} \\
&\Leftrightarrow -\tau_{j,\text{MD}} + \sum\nolimits_{i\in\boldsymbol{\mathcal{S}}ector_j} b_i\,\text{MD}_i \leq \sum\nolimits_{i\in\boldsymbol{\mathcal{S}}ector_j} w_i\,\text{MD}_i \leq \tau_{j,\text{MD}} + \sum\nolimits_{i\in\boldsymbol{\mathcal{S}}ector_j} b_i\,\text{MD}_i \\
&\Leftrightarrow -\tau_{j,\text{MD}} + \text{MD}_j^\star \leq (\boldsymbol{s}_j \circ \text{MD})^\top w \leq \tau_{j,\text{MD}} + \text{MD}_j^\star \\
&\Leftrightarrow \begin{cases} (\boldsymbol{s}_j \circ \text{MD})^\top w - \tau_{j,\text{MD}} \leq \text{MD}_j^\star \\ -(\boldsymbol{s}_j \circ \text{MD})^\top w - \tau_{j,\text{MD}} \leq -\text{MD}_j^\star \end{cases}
\end{aligned}$$

We can now formulate problem (11.7) as a standard linear programming (LP) problem:

$$x^\star = \arg\min c^\top x \quad \text{s.t.} \quad \begin{cases} Ax = B \\ Cx \leq D \\ x^- \leq x \leq x^+ \end{cases} \tag{11.8}$$

where:

$$x = \begin{pmatrix} w \\ \tau_w \\ \tau_{\text{MD}} \\ \tau_{\text{DTS}} \end{pmatrix}$$

is a vector of dimension $n_x = 2 \times (n + n_{\boldsymbol{\mathcal{S}ector}})$. The vector $c$ is equal to:

$$c = \begin{pmatrix} -\gamma \mathcal{C} \\ \frac{1}{2}\varphi'_{\text{AS}} \mathbf{1}_n \\ \varphi'_{\text{MD}} \mathbf{1}_{n_{\boldsymbol{\mathcal{S}ector}}} \\ \varphi'_{\text{DTS}} \mathbf{1}_{n_{\boldsymbol{\mathcal{S}ector}}} \end{pmatrix}$$

The equality constraint is defined by $A = \begin{pmatrix} \mathbf{1}_n^\top & \mathbf{0}_n^\top & \mathbf{0}_{n_{\boldsymbol{\mathcal{S}ector}}}^\top & \mathbf{0}_{n_{\boldsymbol{\mathcal{S}ector}}}^\top \end{pmatrix}$ and $B = 1$. We also have:

$$Cx \leq D \Leftrightarrow \begin{pmatrix} I_n & -I_n & \mathbf{0}_{n,n_{\boldsymbol{\mathcal{S}ector}}} & \mathbf{0}_{n,n_{\boldsymbol{\mathcal{S}ector}}} \\ -I_n & -I_n & \mathbf{0}_{n,n_{\boldsymbol{\mathcal{S}ector}}} & \mathbf{0}_{n,n_{\boldsymbol{\mathcal{S}ector}}} \\ C_{\text{MD}} & \mathbf{0}_{n_{\boldsymbol{\mathcal{S}ector}},n} & -I_{n_{\boldsymbol{\mathcal{S}ector}}} & \mathbf{0}_{n_{\boldsymbol{\mathcal{S}ector}},n_{\boldsymbol{\mathcal{S}ector}}} \\ -C_{\text{MD}} & \mathbf{0}_{n_{\boldsymbol{\mathcal{S}ector}},n} & -I_{n_{\boldsymbol{\mathcal{S}ector}}} & \mathbf{0}_{n_{\boldsymbol{\mathcal{S}ector}},n_{\boldsymbol{\mathcal{S}ector}}} \\ C_{\text{DTS}} & \mathbf{0}_{n_{\boldsymbol{\mathcal{S}ector}},n} & \mathbf{0}_{n_{\boldsymbol{\mathcal{S}ector}},n_{\boldsymbol{\mathcal{S}ector}}} & -I_{n_{\boldsymbol{\mathcal{S}ector}}} \\ -C_{\text{DTS}} & \mathbf{0}_{n_{\boldsymbol{\mathcal{S}ector}},n} & \mathbf{0}_{n_{\boldsymbol{\mathcal{S}ector}},n_{\boldsymbol{\mathcal{S}ector}}} & -I_{n_{\boldsymbol{\mathcal{S}ector}}} \end{pmatrix} x \leq \begin{pmatrix} b \\ -b \\ \text{MD}^\star \\ -\text{MD}^\star \\ \text{DTS}^\star \\ -\text{DTS}^\star \end{pmatrix}$$

where $C_{\text{MD}}$ and $C_{\text{DTS}}$ are two $n_{\boldsymbol{\mathcal{S}ector}} \times n$ matrices, whose $(j,i)$-elements are $\boldsymbol{s}_{i,j}\,\text{MD}_i$ and $\boldsymbol{s}_{i,j}\,\text{DTS}_i$, $\text{MD}^\star = \left(\text{MD}_1^\star, \ldots, \text{MD}_{n_{\boldsymbol{\mathcal{S}ector}}}^\star\right)$ and $\text{DTS}^\star = \left(\text{DTS}_1^\star, \ldots, \text{DTS}_{n_{\boldsymbol{\mathcal{S}ector}}}^\star\right)$. Finally, the bounds are $x^- = \mathbf{0}_{n_x}$ and[17] $x^+ = \infty \cdot \mathbf{1}_{n_x}$.

**Remark 120** *In the case where there are additional constraints, they are cast into LP constraints using the following equivalence:*

$$\begin{cases} Aw = B \\ Cw \leq D \end{cases} \Leftrightarrow \begin{cases} \begin{pmatrix} A & \mathbf{0}_{n_A,n_x-n} \end{pmatrix} x = B \\ \begin{pmatrix} C & \mathbf{0}_{n_A,n_x-n} \end{pmatrix} x \leq D \end{cases}$$

**Remark 121** *While the dimension of the QP problem was $n$, the dimension of the LP problem is $2 \times (n + n_{\boldsymbol{\mathcal{S}ector}})$. This is not an issue since LP algorithms are efficient to solve optimization problems with million of decision variables.*

**Example 49** *We consider a toy example with four corporate bonds:*

| Issuer | #1 | #2 | #3 | #4 |
|---|---|---|---|---|
| $b_i$ (in %) | 35 | 15 | 20 | 30 |
| $\boldsymbol{\mathcal{CI}}_i$ (in $\text{tCO}_2\text{e}$/\$ mn) | 117 | 284 | 162.5 | 359 |
| $\text{MD}_i$ (in years) | 3.0 | 5.0 | 2.0 | 6.0 |
| $\text{DTS}_i$ (in bps) | 100 | 150 | 200 | 250 |
| $\boldsymbol{\mathcal{S}ector}$ | 1 | 1 | 2 | 2 |

*We would like to reduce the carbon footprint by 20%, and we set $\varphi'_{\text{AS}} = 100$, $\varphi'_{\text{MD}} = 25$ and $\varphi'_{\text{DTS}} = 1$.*

[17] We remark that the constraint $w \leq \mathbf{1}_n$ is already embedded into the linear equality constraint.

We have $n = 4$, $n_{\mathcal{S}ector} = 2$ and:

$$x = (\underbrace{w_1, w_2, w_3, w_4}_{w}, \underbrace{\tau_{w_1}, \tau_{w_2}, \tau_{w_3}, \tau_{w_4}}_{\tau_w}, \underbrace{\tau_{\text{MD}_1}, \tau_{\text{MD}_2}}_{\tau_{\text{MD}}}, \underbrace{\tau_{\text{DTS}_1}, \tau_{\text{DTS}_2}}_{\tau_{\text{DTS}}})$$

Since the vector $\mathcal{C}$ is equal to $\mathbf{0}_4$, we obtain:

$$c = (0, 0, 0, 0, 50, 50, 50, 50, 25, 25, 1, 1)$$

The equality system $Ax = B$ is defined by:

$$A = \begin{pmatrix} 1 & 1 & 1 & 1 & 0 & 0 & 0 & 0 & 0 & 0 & 0 & 0 \end{pmatrix}$$

and $B = 1$, while the inequality system $Cx \leq D$ is given by:

$$C = \left(\begin{array}{cccc:c:cccc} \multicolumn{4}{c:}{I_4} & -I_4 & \multicolumn{4}{c}{\mathbf{0}_{4,4}} \\ \hdashline \multicolumn{4}{c:}{-I_4} & -I_4 & \multicolumn{4}{c}{\mathbf{0}_{4,4}} \\ \hdashline 3 & 5 & 0 & 0 & & -1 & 0 & 0 & 0 \\ 0 & 0 & 2 & 6 & \mathbf{0}_{4,4} & 0 & -1 & 0 & 0 \\ -3 & -5 & 0 & 0 & & -1 & 0 & 0 & 0 \\ 0 & 0 & -2 & -6 & & 0 & -1 & 0 & 0 \\ \hdashline 100 & 150 & 0 & 0 & & 0 & 0 & -1 & 0 \\ 0 & 0 & 200 & 250 & \mathbf{0}_{4,4} & 0 & 0 & 0 & -1 \\ -100 & -150 & 0 & 0 & & 0 & 0 & -1 & 0 \\ 0 & 0 & -200 & -250 & & 0 & 0 & 0 & -1 \\ \hdashline 117 & 284 & 162.5 & 359 & \mathbf{0}_{1,4} & 0 & 0 & 0 & 0 \end{array}\right)$$

and:

$$D = (0.35, 0.15, 0.2, 0.3, -0.35, -0.15, -0.2, -0.3, 1.8, 2.2, -1.8, -2.2, 57.5, 115, -57.5, -115, 179)$$

The last row of $Cx \leq D$ corresponds to the carbon footprint constraint. Indeed, we have $\boldsymbol{\mathcal{CI}}(b) = 223.75$ tCO$_2$e/\$ mn and $(1 - \boldsymbol{\mathcal{R}})\boldsymbol{\mathcal{CI}}(b) = 0.80 \times 223.75 = 179.00$ tCO$_2$e/\$ mn. We can now solve the LP program, and we obtain the following solution: $w^\star = (47.34\%, 0\%, 33.3\%, 19.36\%)$, $\tau_w^\star = (12.34\%, 15\%, 13.3\%, 10.64\%)$, $\tau_{\text{MD}}^\star = (0.3798, 0.3725)$ and $\tau_{\text{DTS}}^\star = (10.1604, 0)$.

We consider Example 48 on page 958. By assuming that $\varphi'_{\text{AS}} = \varphi_{\text{AS}} = 100$, $\varphi'_{\text{MD}} = \varphi_{\text{MD}} = 25$ and $\varphi'_{\text{DTS}} = \varphi'_{\text{DTS}} = 0.001$, we obtain the results given in Table 11.4 and 11.5. By construction, these results differ from those obtained in 11.2 and 11.3 on page 960. However, we observe a consistency between the two solutions. In particular, the overweighting and underweighting directions are respected by the QP and LP algorithms.

Table 11.4: Weights in % of optimized bond portfolios (Example 48)

| Portfolio | #1 | #2 | #3 | #4 | #5 | #6 | #7 | #8 | #9 |
|---|---|---|---|---|---|---|---|---|---|
| $b$ | 21.00 | 19.00 | 16.00 | 12.00 | 11.00 | 8.00 | 6.00 | 4.00 | 3.00 |
| $w^\star\,(10\%)$ | 21.70 | 19.00 | 16.00 | 12.00 | 11.00 | 8.00 | 7.46 | 4.00 | 0.84 |
| $w^\star\,(30\%)$ | 34.44 | 19.00 | 4.00 | 11.65 | 11.98 | 6.65 | 7.52 | 4.00 | 0.75 |
| $w^\star\,(50\%)$ | 33.69 | 19.37 | 4.00 | 3.91 | 24.82 | 2.00 | 10.46 | 1.00 | 0.75 |

**Remark 122** *The linear programming approach is used by Barahhou et al. (2022) and Ben Slimane et al. (2023a) to implement portfolio alignment and net-zero investment policies*[18]*. The reason is that the investment universe of corporate bonds is too large to be manipulated by the QP algorithm.*

[18]See Section 11.2 on page 967 for using linear programming for decarbonized bond portfolios and Section 11.3 on page 991 for net-zero bond portfolios.

Table 11.5: Risk statistics of optimized bond portfolios (Example 48)

| Portfolio | $\text{AS}_{\mathcal{S}ector}$ (in %) | $\text{MD}(w)$ (in years) | $\text{DTS}(w)$ (in bps) | $\sigma_{\text{AS}}(w \mid b)$ (in %) | $\sigma_{\text{MD}}(w \mid b)$ (in years) | $\sigma_{\text{DTS}}(w \mid b)$ (in bps) | $\mathcal{CI}(w)$ $\text{gCO}_2\text{e}/\$$ |
|---|---|---|---|---|---|---|---|
| $b$ | 0.00 | 5.43 | 290.18 | 0.00 | 0.00 | 0.00 | 184.39 |
| $w^\star$ (10%) | 2.16 | 5.45 | 297.28 | 2.16 | 0.02 | 7.10 | 165.95 |
| $w^\star$ (30%) | 15.95 | 5.43 | 300.96 | 15.95 | 0.00 | 13.20 | 129.07 |
| $w^\star$ (50%) | 31.34 | 5.43 | 268.66 | 31.34 | 0.00 | 65.12 | 92.19 |

### Nonlinear constraints

A first idea to deal with nonlinear constraints is to use a general optimization solver, such as the sequential quadratic programming algorithm.However, this algorithm is not efficient when the dimension of the problem is large. In most cases, nonlinear constraints are standard in portfolio optimization. They concern the turnover, the transaction costs, the leverage limit, etc. Therefore, we can use the quadratic property of the objective function to solve the nonlinear constrained optimization problem. The underlying idea is to preserve the QP or LP structure of the problem by considering sequential optimization. Among the different algorithms, the most famous is the alternating direction method of multipliers[19] (ADMM), which can be used to solve many nonlinear portfolio optimization problems (Perrin and Roncalli, 2020). In particular, Lezmi *et al.* (2022) used it to solve multi-period portfolio allocation and some classes of net-zero optimization problems.

### Investible portfolios

The previous optimization problems are defined with respect to the unknown variable $w = (w_1, \ldots, w_n)$, where $w_i$ is the portfolio weight of Security $i$. In this approach, $w \in \mathbb{R}^n$ and the budget constraint is $\sum_{i=1}^n w_i = 1$. This type of problem falls under the umbrella of continuous portfolio optimization. In some cases, it does not make sense to define the portfolio allocation by considering continuous weights because the solution is far from investible. Therefore, the unknown variable becomes $q = (q_1, \ldots, q_n)$, where $q_i$ is the number of shares of Security $i$. Let $P_i$ be the price and $Q_i = q_i P_i$ be the tradable amount. In this approach, $q \in \mathbb{N}^n$ and the budget constraint is $\sum_{i=1}^n q_i P_i = \sum_{i=1}^n Q_i = \mathcal{A}$ where $\mathcal{A}$ is the investment amount. This type of problem falls under the umbrella of discrete portfolio optimization and can be solved using genetic algorithms (Ben Slimane, 2021) or mixed integer programming algorithms (Ben Slimane and Menchaoui, 2023).

Given an optimal solution $w^\star$, the amount invested in Security $i$ is equal to $Q_i = w_i^\star \mathcal{A}$. For some markets, $Q_i$ may be far from the optimal investible solution, which is equal to $q_i^\star P_i$. This is for example the case of corporate bonds[20]. Let us introduce some definitions. The minimum tradable lot size is the minimum order size that can be bought or sold for a bond, while the incremental lot size is the minimum multiple that must be added to the minimum tradable lot to buy or sell a bond. For example, if the minimum tradable lot size is 10 000 and the incremental lot size is 1 000, the order sizes are $Q = 10\,000 + 1\,000 \cdot k$ where $k \in \mathbb{N}$. For EUR and USD corporate bonds, the minimum tradable size is typically €100 000 and \$2 000, respectively. Suppose we want to invest 5% of a million euros in a security. If the lot size of the security is €540, we have the choice of buying 92 or 93 shares, that is €49 680 or €50 220. Both solutions are close to the desired amount of €50 000. If the minimum tradeable amount of the security is €100 000, we have the choice of investing 0 or €100 000. Both solutions are far from the desired amount of €50 000.

[19] The ADMM algorithm is described on page 1053.

[20] For equity and sovereign bond portfolios, it is common practice to use continuous portfolio optimization.

## 11.2 Portfolio decarbonization

The objective of portfolio decarbonization is to construct a portfolio $w$ with a low carbon metric, which is generally the carbon intensity. Most of the time, the fund manager needs a reference portfolio $b$ in order to measure the reduction $\mathcal{R}(w \mid b)$. This reference portfolio can be the capitalization-weighted benchmark of the investment universe, a model portfolio, the managed portfolio one year ago, etc. When an explicit objective is defined, portfolio decarbonization can be viewed as a portfolio management constraint:

$$\mathcal{CI}(w) \leq (1 - \mathcal{R})\,\mathcal{CI}(b)$$

In this case, the decarbonization issue is solved by using constrained portfolio optimization. This framework can be extended when the global decarbonization constraint is replaced by a set of sector-specific decarbonization constraints. At first sight, portfolio decarbonization is then an application of basic portfolio optimization. Nevertheless, there are many implementation differences that make the exercise more difficult than we can imagine. In particular, portfolio decarbonization is ultimately an exclusion process and can be put in the category of exclusion ESG strategies. In some sense, portfolio decarbonization is a disguised form of divestment, which impacts the worst-in-class issuers that have the higher carbon intensities.

### 11.2.1 Global reduction of the carbon footprint

#### Equity portfolios

Let $b$ be the reference portfolio (*e.g.*, a benchmark). The optimization problem is defined as:

$$w^\star = \arg\min \frac{1}{2}(w-b)^\top \Sigma (w-b) \quad \text{s.t.} \begin{cases} \mathbf{1}_n^\top w = 1 \\ w \in \Omega \\ \mathbf{0}_n \leq w \leq \mathbf{1}_n \\ \mathcal{CI}(w) \leq (1-\mathcal{R})\,\mathcal{CI}(b) \end{cases} \tag{11.9}$$

where $\mathcal{R}$ is the reduction rate and $w \in \Omega$ is a set of additional weight constraints (*e.g.*, weight or sector deviation). Therefore, we minimize the tracking error variance of the investment portfolio $w$ with respect to the reference portfolio $b$ by imposing a long-only constraint and reducing the carbon intensity of the benchmark. Since we both impose a constraint and minimize the tracking error risk, the portfolio $w$ has fewer stocks than the benchmark $b$. In fact, the number of stocks depends on several parameters: the reduction rate $\mathcal{R}$, the number $n$ of stocks in the benchmark and the covariance matrix. This implies that portfolio $w$ is less diversified than benchmark $b$. In order to explicitly control the number of removed stocks, Andersson *et al.* (2016) proposed a second portfolio decarbonization approach by eliminating the $m$ worst performing issuers in terms of carbon intensity.

Let $\mathcal{CI}_{i:n}$ be the order statistics of $(\mathcal{CI}_1, \ldots, \mathcal{CI}_n)$ such that:

$$\min \mathcal{CI}_i = \mathcal{CI}_{1:n} \leq \mathcal{CI}_{2:n} \leq \cdots \leq \mathcal{CI}_{i:n} \leq \cdots \leq \mathcal{CI}_{n:n} = \max \mathcal{CI}_i$$

The carbon intensity bound $\mathcal{CI}^{(m,n)}$ is defined as $\mathcal{CI}^{(m,n)} = \mathcal{CI}_{n-m+1:n}$ where $\mathcal{CI}_{n-m+1:n}$ is the $(n-m+1)$-th order statistic of $(\mathcal{CI}_1, \ldots, \mathcal{CI}_n)$. Eliminating the $m$ worst performing assets is equivalent to imposing the following constraint: $\mathcal{CI}_i \geq \mathcal{CI}^{(m,n)} \Rightarrow w_i = 0$. We then obtain the

following optimization problem:

$$
\begin{aligned}
w^\star &= \arg\min \frac{1}{2} (w-b)^\top \Sigma (w-b) \\
&\text{s.t.} \begin{cases} \mathbf{1}_n^\top w = 1 \\ w \in \Omega \\ \mathbf{0}_n \leq w \leq \mathbb{1}\left\{\boldsymbol{\mathcal{CI}} < \boldsymbol{\mathcal{CI}}^{(m,n)}\right\} \end{cases}
\end{aligned} \tag{11.10}
$$

Finally, a third method consists in re-weighting the remaining assets:

$$
w_i^\star = \frac{\mathbb{1}\left\{\boldsymbol{\mathcal{CI}}_i < \boldsymbol{\mathcal{CI}}^{(m,n)}\right\} \cdot b_i}{\sum_{k=1}^n \mathbb{1}\left\{\boldsymbol{\mathcal{CI}}_k < \boldsymbol{\mathcal{CI}}^{(m,n)}\right\} \cdot b_k} \tag{11.11}
$$

**Remark 123** *Problem (11.9) is called the "threshold" approach, whereas problems (11.10) and (11.11) are known as the "order-statistic" and "naive" approach.*

The QP form of problem (11.9) is: $Q = \Sigma$, $R = \Sigma b$, $A = \mathbf{1}_n^\top$, $B = 1$, $C = \boldsymbol{\mathcal{CI}}^\top$, $D = (1 - \boldsymbol{\mathcal{R}})\,\boldsymbol{\mathcal{CI}}(b)$, $w^- = \mathbf{0}_n$ and $w^+ = \mathbf{1}_n$. For problem (11.10), the matrices $C$ and $D$ vanishes and the upper bound becomes $w^+ = \mathbb{1}\left\{\boldsymbol{\mathcal{CI}} < \boldsymbol{\mathcal{CI}}^{(m,n)}\right\}$, which is a vector of zeros and ones.

**Example 50** *We consider a capitalization-weighted equity index, which is composed of eight stocks. Their weights are equal to* 20%, 19%, 17%, 13%, 12%, 8%, 6% *and* 5%. *The carbon intensities (expressed in* $\text{tCO}_2\text{e}/\$$ mn*) are respectively equal to* 100.5, 97.2, 250.4, 352.3, 27.1, 54.2, 78.6 *and* 426.7. *To evaluate the risk of the portfolio, we use the market one-factor model: the beta* $\beta_i$ *of each stock is equal to* 0.30, 1.80, 0.85, 0.83, 1.47, 0.94, 1.67 *and* 1.08, *the idiosyncratic volatilities* $\tilde{\sigma}_i$ *are respectively equal to* 10%, 5%, 6%, 12%, 15%, 4%, 8% *and* 7%, *and the estimated market volatility* $\sigma_m$ *is* 18%.

In order to solve the different optimization problems, we need to compute the covariance matrix:

$$
\Sigma = \beta\beta^\top \sigma_m^2 + D
$$

where $\beta$ is the vector of beta coefficients, $\sigma_m^2$ is the variance of the market portfolio and $D = diag\left(\tilde{\sigma}_1^2, \ldots, \tilde{\sigma}_n^2\right)$ is the diagonal matrix, whose elements are the idiosyncratic variances. The specification of the $D$ matrix in the optimization problem (11.9) also requires to compute the carbon intensity of the benchmark and we obtain $\boldsymbol{\mathcal{CI}}(b) = 160.57$ $\text{tCO}_2\text{e}/\$$ mn. We report the different results in Tables 11.6, 11.7 and 11.8. With the threshold approach, we can target a explicit value of the reduction rate. For instance, if $\boldsymbol{\mathcal{R}}$ is set to 10%, the tracking error volatility $\sigma(w^\star \mid b)$ is equal to 30 bps. In the case of the order-statistic approach, it is not possible to have an optimized portfolio, whose tracking error volatility is less than 37 bps. This figure is obtained when we exclude the eight stock, which has the largest carbon intensity. In this case, the reduction rate is equal to 9.62%. If we exclude the two assets that have the largest carbon footprint (asset #4 and #8), the tracking error volatility and the reduction rate are equal to 1.68% and 29.33%. If we use the order-statistic approach, it is then not possible to target an intermediary reduction rate, for instance 20% in our example. For a given value of $m$, the naive implies a lower reduction rate and a higher tracking risk compared to the order-statistic approach. For example, if $m$ is equal to 3, their values are respectively equal to 2.25% and 54.05% versus 3.04% and 51.26%. In Figure 11.3, we show the efficient decarbonization frontier which indicates the relationship between the reduction rate and

Table 11.6: Optimal decarbonization portfolios (Example 50, threshold approach)

| $\boldsymbol{\mathcal{R}}$ | 0 | 10 | 20 | 30 | 40 | 50 | $\boldsymbol{\mathcal{CI}}_i$ |
|---|---|---|---|---|---|---|---|
| $w_1^\star$ | 20.00 | 20.54 | 21.14 | 21.86 | 22.58 | 22.96 | 100.5 |
| $w_2^\star$ | 19.00 | 19.33 | 19.29 | 18.70 | 18.11 | 17.23 | 97.2 |
| $w_3^\star$ | 17.00 | 15.67 | 12.91 | 8.06 | 3.22 | 0.00 | 250.4 |
| $w_4^\star$ | 13.00 | 12.28 | 10.95 | 8.74 | 6.53 | 3.36 | 352.3 |
| $w_5^\star$ | 12.00 | 12.26 | 12.60 | 13.07 | 13.53 | 14.08 | 27.1 |
| $w_6^\star$ | 8.00 | 11.71 | 16.42 | 22.57 | 28.73 | 34.77 | 54.2 |
| $w_7^\star$ | 6.00 | 6.36 | 6.69 | 7.00 | 7.30 | 7.59 | 78.6 |
| $w_8^\star$ | 5.00 | 1.86 | 0.00 | 0.00 | 0.00 | 0.00 | 426.7 |
| $\sigma\left(w^\star \mid b\right)$ | 0.00 | 30.01 | 61.90 | 104.10 | 149.65 | 196.87 | |
| $\boldsymbol{\mathcal{CI}}\left(w\right)$ | 160.57 | 144.52 | 128.46 | 112.40 | 96.34 | 80.29 | |
| $\boldsymbol{\mathcal{R}}\left(w \mid b\right)$ | 0.00 | 10.00 | 20.00 | 30.00 | 40.00 | 50.00 | |

The reduction rate and weights are expressed in %, while the tracking error volatility is measured in bps.

Table 11.7: Optimal decarbonization portfolios (Example 50, order-statistic approach)

| $m$ | 0 | 1 | 2 | 3 | 4 | 5 | 6 | 7 | $\boldsymbol{\mathcal{CI}}_i$ |
|---|---|---|---|---|---|---|---|---|---|
| $w_1^\star$ | 20.00 | 20.40 | 22.35 | 26.46 | 0.00 | 0.00 | 0.00 | 0.00 | 100.5 |
| $w_2^\star$ | 19.00 | 19.90 | 20.07 | 20.83 | 7.57 | 0.00 | 0.00 | 0.00 | 97.2 |
| $w_3^\star$ | 17.00 | 17.94 | 21.41 | 0.00 | 0.00 | 0.00 | 0.00 | 0.00 | 250.4 |
| $w_4^\star$ | 13.00 | 13.24 | 0.00 | 0.00 | 0.00 | 0.00 | 0.00 | 0.00 | 352.3 |
| $w_5^\star$ | 12.00 | 12.12 | 12.32 | 12.79 | 13.04 | 14.26 | 18.78 | 100.00 | 27.1 |
| $w_6^\star$ | 8.00 | 10.04 | 17.14 | 32.38 | 74.66 | 75.12 | 81.22 | 0.00 | 54.2 |
| $w_7^\star$ | 6.00 | 6.37 | 6.70 | 7.53 | 4.73 | 10.62 | 0.00 | 0.00 | 78.6 |
| $w_8^\star$ | 5.00 | 0.00 | 0.00 | 0.00 | 0.00 | 0.00 | 0.00 | 0.00 | 426.7 |
| $\sigma\left(w^\star \mid b\right)$ | 0.00 | 0.37 | 1.68 | 2.25 | 3.98 | 4.04 | 4.30 | 15.41 | |
| $\boldsymbol{\mathcal{CI}}\left(w\right)$ | 160.57 | 145.12 | 113.48 | 73.78 | 55.08 | 52.93 | 49.11 | 27.10 | |
| $\boldsymbol{\mathcal{R}}\left(w \mid b\right)$ | 0.00 | 9.62 | 29.33 | 54.05 | 65.70 | 67.04 | 69.42 | 83.12 | |

The reduction rate, weights, and tracking error volatility are expressed in %.

Table 11.8: Optimal decarbonization portfolios (Example 50, naive approach)

| $m$ | 0 | 1 | 2 | 3 | 4 | 5 | 6 | 7 | $\boldsymbol{\mathcal{CI}}_i$ |
|---|---|---|---|---|---|---|---|---|---|
| $w_1^\star$ | 20.00 | 21.05 | 24.39 | 30.77 | 0.00 | 0.00 | 0.00 | 0.00 | 100.5 |
| $w_2^\star$ | 19.00 | 20.00 | 23.17 | 29.23 | 42.22 | 0.00 | 0.00 | 0.00 | 97.2 |
| $w_3^\star$ | 17.00 | 17.89 | 20.73 | 0.00 | 0.00 | 0.00 | 0.00 | 0.00 | 250.4 |
| $w_4^\star$ | 13.00 | 13.68 | 0.00 | 0.00 | 0.00 | 0.00 | 0.00 | 0.00 | 352.3 |
| $w_5^\star$ | 12.00 | 12.63 | 14.63 | 18.46 | 26.67 | 46.15 | 60.00 | 100.00 | 27.1 |
| $w_6^\star$ | 8.00 | 8.42 | 9.76 | 12.31 | 17.78 | 30.77 | 40.00 | 0.00 | 54.2 |
| $w_7^\star$ | 6.00 | 6.32 | 7.32 | 9.23 | 13.33 | 23.08 | 0.00 | 0.00 | 78.6 |
| $w_8^\star$ | 5.00 | 0.00 | 0.00 | 0.00 | 0.00 | 0.00 | 0.00 | 0.00 | 426.7 |
| $\sigma\left(w^\star \mid b\right)$ | 0.00 | 0.39 | 1.85 | 3.04 | 9.46 | 8.08 | 8.65 | 15.41 | |
| $\boldsymbol{\mathcal{CI}}\left(w\right)$ | 160.57 | 146.57 | 113.95 | 78.26 | 68.38 | 47.32 | 37.94 | 27.10 | |
| $\boldsymbol{\mathcal{R}}\left(w \mid b\right)$ | 0.00 | 8.72 | 29.04 | 51.26 | 57.41 | 70.53 | 76.37 | 83.12 | |

The reduction rate, weights, and tracking error volatility are expressed in %.

Figure 11.3: Efficient decarbonization frontier (Example 50)

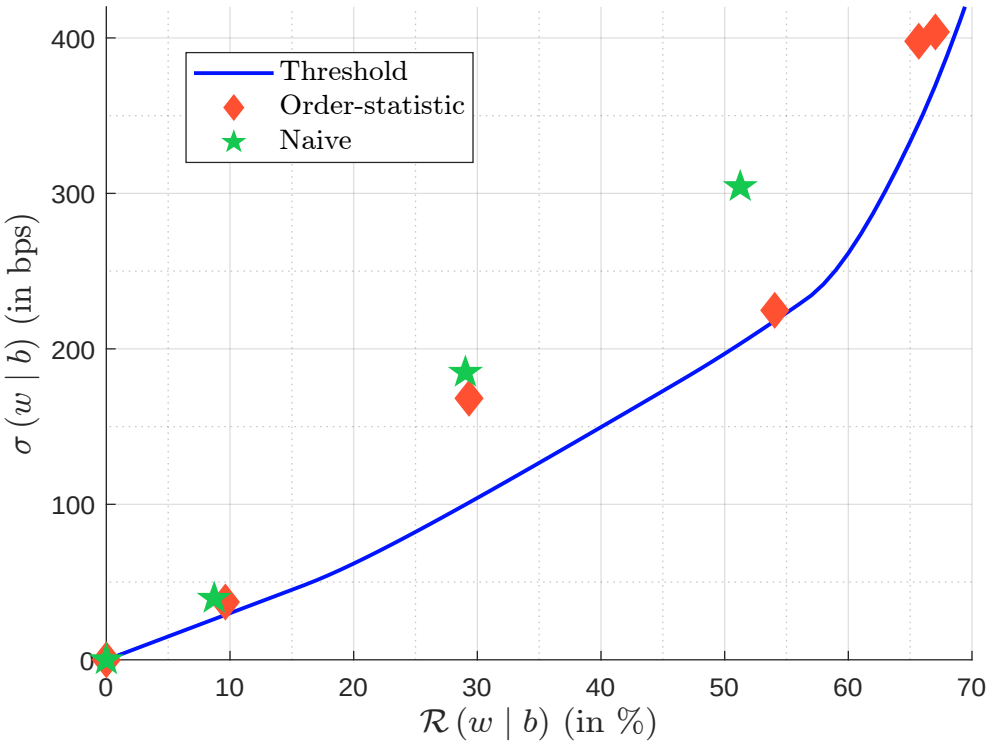


Figure 11.4: Efficient decarbonization frontier of the interpolated naive approach (Example 50)

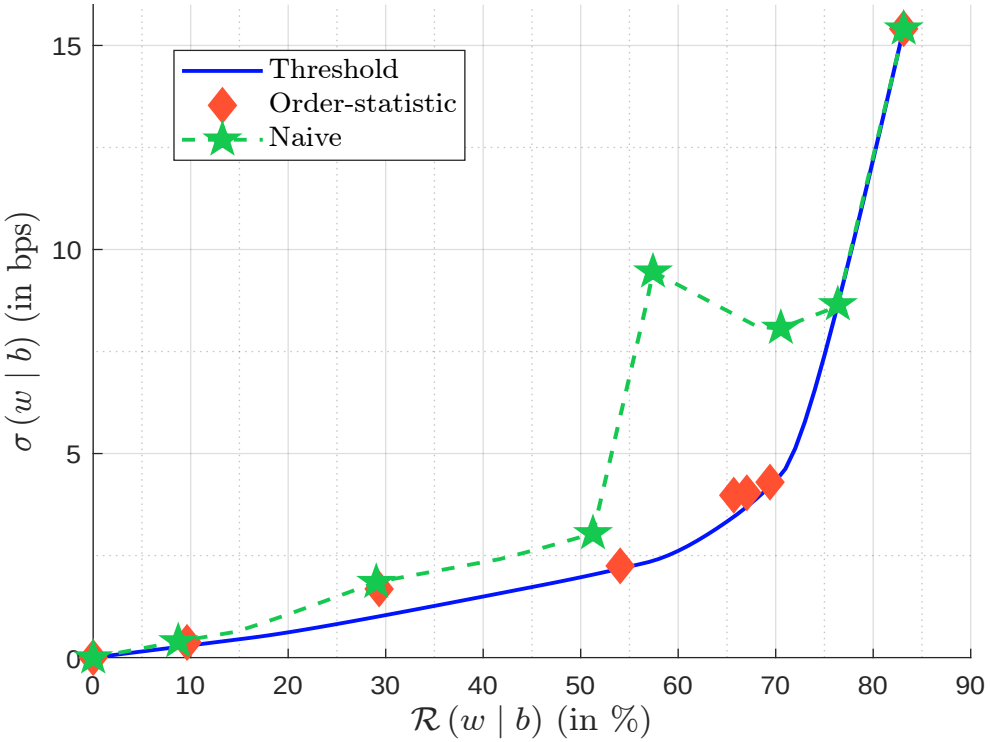

the tracking error volatility. In the case of the threshold approach, it is a continuous curve, which is not the case for the two other approaches.

In the case of the naive approach, we can extend the method to a given reduction rate $\boldsymbol{\mathcal{R}}$. Let us denote by $w^\star_{(m)}$ the optimal portfolio when we exclude $m$ assets. We consider the index $m$ such that[21]:

$$\boldsymbol{\mathcal{R}}\left(w^\star_{(m-1)} \mid b\right) \leq \boldsymbol{\mathcal{R}} \leq \boldsymbol{\mathcal{R}}\left(w^\star_{(m)} \mid b\right)$$

We define the portfolio $w^\star$ as the linear interpolation between $w^\star_{(m-1)}$ and $w^\star_{(m)}$:

$$w^\star = \alpha w^\star_{(m-1)} + (1-\alpha)\, w^\star_{(m)}$$

where:

$$\alpha = \frac{\boldsymbol{\mathcal{R}}\left(w^\star_{(m)} \mid b\right) - \boldsymbol{\mathcal{R}}}{\boldsymbol{\mathcal{R}}\left(w^\star_{(m)} \mid b\right) - \boldsymbol{\mathcal{R}}\left(w^\star_{(m-1)} \mid b\right)}$$

We deduce that:

$$\begin{aligned}
\boldsymbol{\mathcal{R}}\left(w^\star \mid b\right) &= 1 - \frac{w^{\star\top}\boldsymbol{\mathcal{CI}}}{b^\top \boldsymbol{\mathcal{CI}}} \\
&= 1 - \frac{\left(\alpha w^\star_{(m-1)} + (1-\alpha)\, w^\star_{(m)}\right)^\top \boldsymbol{\mathcal{CI}}}{b^\top \boldsymbol{\mathcal{CI}}} \\
&= (\alpha + (1-\alpha)) - \left(\alpha \frac{w^{\star\top}_{(m-1)}\boldsymbol{\mathcal{CI}}}{b^\top \boldsymbol{\mathcal{CI}}} + (1-\alpha)\frac{w^{\star\top}_{(m)}\boldsymbol{\mathcal{CI}}}{b^\top \boldsymbol{\mathcal{CI}}}\right) \\
&= \alpha \boldsymbol{\mathcal{R}}\left(w^\star_{(m-1)} \mid b\right) + (1-\alpha)\,\boldsymbol{\mathcal{R}}\left(w^\star_{(m)} \mid b\right) \\
&= \boldsymbol{\mathcal{R}}
\end{aligned}$$

In Figure 11.4, we report the efficient decarbonization frontier when we apply the interpolated naive method to Exercise. We notice that the tracking error volatility is not necessarily an increasing function of the reduction rate. This is certainly the main drawback of the naive approach. The monotonicity property is also not always satisfied when we consider the order-statistic approach[22].

### Bond portfolios

In the case of bond portfolios, we can use the same framework as equity portfolios except that we use the synthetic risk measure $\mathcal{R}(w \mid b)$ instead of the tracking error variance. We can implement the threshold or order-statistic approach, but the naive approach is not really appropriate since it may induce high deformation of the MD and DTS profiles.

**Example 51** *We consider a debt-weighted bond index, which is composed of eight bonds. Their weights are equal to* 20%, 19%, 17%, 13%, 12%, 8%, 6% *and* 5%. *The carbon intensities (expressed in* $tCO_2e/\$$ mn*) are respectively equal to* 100.5, 97.2, 250.4, 352.3, 27.1, 54.2, 78.6 *and* 426.7. *To evaluate the risk of the portfolio, we use the modified duration which is respectively equal to* 3.1, 6.6, 7.2, 5, 4.7, 2.1, 8.1 *and* 2.6 *years, and the duration-times-spread factor, which is respectively equal to* 100, 155, 575, 436, 159, 145, 804 *and* 365 *bps. There are two sectors. Bonds #1, #3, #4 and #8 belong to* $\boldsymbol{\mathcal{S}}ector_1$ *while Bonds #2, #5, #6 and #7 belong to* $\boldsymbol{\mathcal{S}}ector_2$.

Results are given in Tables 11.9 and 11.10. We see the impact of the decarbonization constraint on the modified duration or the DTS factor on the portfolio.

[21] We have $\boldsymbol{\mathcal{R}}\left(w^\star_{(0)}\right) = 0$ and $w^\star_{(0)} = b$.

[22] See Exercise 11.4.2 on page 1032.

Table 11.9: Optimal decarbonization portfolios (Example 51, threshold approach)

| $\boldsymbol{\mathcal{R}}$ | 0 | 10 | 20 | 30 | 40 | 50 | $\boldsymbol{\mathcal{CI}}_i$ |
|---|---|---|---|---|---|---|---|
| $w_1^\star$ | 20.00 | 21.62 | 23.93 | 26.72 | 30.08 | 33.44 | 100.5 |
| $w_2^\star$ | 19.00 | 18.18 | 16.98 | 14.18 | 7.88 | 1.58 | 97.2 |
| $w_3^\star$ | 17.00 | 18.92 | 21.94 | 22.65 | 16.82 | 11.00 | 250.4 |
| $w_4^\star$ | 13.00 | 11.34 | 5.35 | 0.00 | 0.00 | 0.00 | 352.3 |
| $w_5^\star$ | 12.00 | 13.72 | 16.14 | 21.63 | 33.89 | 46.14 | 27.1 |
| $w_6^\star$ | 8.00 | 9.60 | 10.47 | 10.06 | 7.21 | 4.36 | 54.2 |
| $w_7^\star$ | 6.00 | 5.56 | 5.19 | 4.75 | 4.11 | 3.48 | 78.6 |
| $w_8^\star$ | 5.00 | 1.05 | 0.00 | 0.00 | 0.00 | 0.00 | 426.7 |
| $\text{AS}_{\boldsymbol{\mathcal{S}}ector}$ | 0.00 | 6.87 | 15.49 | 24.07 | 31.97 | 47.58 | |
| $\text{MD}(w)$ | 5.48 | 5.49 | 5.45 | 5.29 | 4.90 | 4.51 | |
| $\text{DTS}(w)$ | 301.05 | 292.34 | 282.28 | 266.12 | 236.45 | 206.78 | |
| $\sigma_{\text{AS}}(w \mid b)$ | 0.00 | 5.57 | 12.31 | 19.82 | 30.04 | 43.58 | |
| $\sigma_{\text{MD}}(w \mid b)$ | 0.00 | 0.01 | 0.04 | 0.17 | 0.49 | 0.81 | |
| $\sigma_{\text{DTS}}(w \mid b)$ | 0.00 | 8.99 | 19.29 | 35.74 | 65.88 | 96.01 | |
| $\boldsymbol{\mathcal{CI}}(w)$ | 160.57 | 144.52 | 128.46 | 112.40 | 96.34 | 80.29 | |
| $\boldsymbol{\mathcal{R}}(w \mid b)$ | 0.00 | 10.00 | 20.00 | 30.00 | 40.00 | 50.00 | |

The reduction rate, weights, and active share metrics are expressed in %, the MD metrics are measured in years, and the DTS metrics are computed in bps.

Table 11.10: Optimal decarbonization portfolios (Example 51, order-statistic approach)

| $m$ | 0 | 1 | 2 | 3 | 4 | 5 | 6 | 7 | $\boldsymbol{\mathcal{CI}}_i$ |
|---|---|---|---|---|---|---|---|---|---|
| $w_1^\star$ | 20.00 | 20.83 | 24.62 | 64.64 | 0.00 | 0.00 | 0.00 | 0.00 | 100.5 |
| $w_2^\star$ | 19.00 | 18.60 | 18.13 | 21.32 | 3.32 | 0.00 | 0.00 | 0.00 | 97.2 |
| $w_3^\star$ | 17.00 | 17.79 | 26.30 | 0.00 | 0.00 | 0.00 | 0.00 | 0.00 | 250.4 |
| $w_4^\star$ | 13.00 | 14.53 | 0.00 | 0.00 | 0.00 | 0.00 | 0.00 | 0.00 | 352.3 |
| $w_5^\star$ | 12.00 | 12.89 | 13.96 | 6.00 | 36.57 | 41.27 | 41.27 | 100.00 | 27.1 |
| $w_6^\star$ | 8.00 | 9.74 | 11.85 | 0.00 | 60.11 | 58.73 | 58.73 | 0.00 | 54.2 |
| $w_7^\star$ | 6.00 | 5.62 | 5.15 | 8.03 | 0.00 | 0.00 | 0.00 | 0.00 | 78.6 |
| $w_8^\star$ | 5.00 | 0.00 | 0.00 | 0.00 | 0.00 | 0.00 | 0.00 | 0.00 | 426.7 |
| $\text{AS}_{\boldsymbol{\mathcal{S}}ector}$ | 0.00 | 5.78 | 19.72 | 49.00 | 76.68 | 80.00 | 80.00 | 88.00 | |
| $\text{MD}(w)$ | 5.48 | 5.52 | 5.54 | 4.77 | 3.27 | 3.17 | 3.17 | 4.70 | |
| $\text{DTS}(w)$ | 301.05 | 295.08 | 284.71 | 171.82 | 150.45 | 150.78 | 150.78 | 159.00 | |
| $\sigma_{\text{AS}}(w \mid b)$ | 0.00 | 5.73 | 17.94 | 50.85 | 66.96 | 68.63 | 68.63 | 95.33 | |
| $\sigma_{\text{MD}}(w \mid b)$ | 0.00 | 0.03 | 0.04 | 0.63 | 2.66 | 2.64 | 2.64 | 3.21 | |
| $\sigma_{\text{DTS}}(w \mid b)$ | 0.00 | 6.21 | 16.87 | 128.04 | 197.22 | 197.29 | 197.29 | 199.22 | |
| $\boldsymbol{\mathcal{CI}}(w)$ | 160.57 | 147.94 | 122.46 | 93.63 | 45.72 | 43.02 | 43.02 | 27.10 | |
| $\boldsymbol{\mathcal{R}}(w \mid b)$ | 0.00 | 7.87 | 23.74 | 41.69 | 71.53 | 73.21 | 73.21 | 83.12 | |

The reduction rate, weights and active share metrics are expressed in %, the MD metrics are measured in years, and the DTS metrics are computed in bps.

### 11.2.2 Sector-specific constraints

Sectors are very important in portfolio construction and allocation. For instance, performance attribution is generally done by distinguishing three components: sector allocation, asset selection and interaction effect. Since the goal of portfolio decarbonization is not to take active bets, this explains that most of allocation constraints concern sectors. Therefore, it is necessary to understand sector classification systems in asset management. In Box 11.1, we describe the GICS system, which is the most known and used sector taxonomy.

#### Sector scenario

The previous approach can be extended by considering one decarbonization scenario per sector instead of a global reduction rate:

$$\boldsymbol{\mathcal{CI}}(w; \boldsymbol{\mathcal{S}}ector_j) \leq (1 - \boldsymbol{\mathcal{R}}_j)\, \boldsymbol{\mathcal{CI}}(b; \boldsymbol{\mathcal{S}}ector_j)$$

for $j = 1, \ldots, n_{\boldsymbol{\mathcal{S}}ector}$. On page 953, we have seen that these constraints can be written as:

$$\left(\boldsymbol{s}_j \circ \left(\boldsymbol{\mathcal{CI}} - \boldsymbol{\mathcal{CI}}_j^\star\right)\right)^\top w \leq 0$$

where $\boldsymbol{\mathcal{CI}}_j^\star = (1 - \boldsymbol{\mathcal{R}}_j)\, \boldsymbol{\mathcal{CI}}(b; \boldsymbol{\mathcal{S}}ector_j)$. The QP form $Cw \leq D$ is then:

$$C = \begin{pmatrix} \left(\boldsymbol{s}_1 \circ \left(\boldsymbol{\mathcal{CI}} - \boldsymbol{\mathcal{CI}}_1^\star\right)\right)^\top \\ \vdots \\ \left(\boldsymbol{s}_j \circ \left(\boldsymbol{\mathcal{CI}} - \boldsymbol{\mathcal{CI}}_j^\star\right)\right)^\top \\ \vdots \\ \left(\boldsymbol{s}_{n_{\boldsymbol{\mathcal{S}}ector}} \circ \left(\boldsymbol{\mathcal{CI}} - \boldsymbol{\mathcal{CI}}_{n_{\boldsymbol{\mathcal{S}}ector}}^\star\right)\right)^\top \end{pmatrix}$$

and:

$$D = \begin{pmatrix} (1 - \boldsymbol{\mathcal{R}}_1)\, \boldsymbol{\mathcal{CI}}(b; \boldsymbol{\mathcal{S}}ector_1) \\ \vdots \\ (1 - \boldsymbol{\mathcal{R}}_j)\, \boldsymbol{\mathcal{CI}}(b; \boldsymbol{\mathcal{S}}ector_j) \\ \vdots \\ (1 - \boldsymbol{\mathcal{R}}_{n_{\boldsymbol{\mathcal{S}}ector}})\, \boldsymbol{\mathcal{CI}}(b; \boldsymbol{\mathcal{S}}ector_{n_{\boldsymbol{\mathcal{S}}ector}}) \end{pmatrix}$$

We can also apply these constraints on a subset of sectors and combine them with a global reduction constraint.

In Table 9.25 on page 930, we have seen that the reduction rates of the IEA NZE scenario depend on the sector. In particular, the Electricity sector must decarbonize itself faster than the other sectors. For 2030, using 2020 as the base year, the reduction rates are 56.9% for the Electricity sector, 18.8% for the Industry sector, 20.0% for the Transport sector, 36.7% for the Buildings sector and 52.4% for the other sectors. The global reduction rate is set to 36.6%. In Table 9.16 on page 913, we have reported the carbon intensity of the MSCI World index. It is equal to 163 $\text{tCO}_2\text{e}/\$$ mn if we consider the scope $1 + 2$ emissions. By 2030, we can then use the following global threshold:

$$\boldsymbol{\mathcal{CI}}^\star = (1 - \boldsymbol{\mathcal{R}})\, \boldsymbol{\mathcal{CI}}(b) = (1 - 0.366) \times 163 = 103.3 \text{ tCO}_2\text{e}/\$ \text{ mn}$$

If we use the sector scenarios, we first have to map the IEA sectors on to the GICS sectors. For instance, the Utilities sector corresponds to the Electricity sector. Since the carbon intensity of this sector is equal to 1 794 $\text{tCO}_2\text{e}/\$$ mn, we can use the following specific threshold:

$$\boldsymbol{\mathcal{CI}}_j^\star = (1 - \boldsymbol{\mathcal{R}}_j)\, \boldsymbol{\mathcal{CI}}(b; \boldsymbol{\mathcal{S}}ector_j) = (1 - 0.569) \times 1\,794 = 773.2 \text{ tCO}_2\text{e}/\$ \text{ mn}$$

Box 11.1: Global Industry Classification Standard (GICS)

The Global Industry Classification Standard (GICS) is an industry taxonomy developed in 1999 by MSCI and Standard & Poor's (S&P) and based on a 4-level structure:

| Level | 1 | 2 | 3 | 4 |
|---|---|---|---|---|
| Name | Sector | Industry group | Industry | Sub-industry |
| Code | AA | AABB | AABBCC | AABBCCDD |

GICS is used as a basis for S&P and MSCI market indexes. The level codes are generated using 2-, 4-, 6- and 8-number classifications, whose root (AA, BB, CC and DD) is a multiple of ten $(10, 20, \ldots, 90)$. For instance, the Energy sector has the following structure:

- Energy (1010)
  - Energy (1010)
    - Energy equipment & services (101010)
      - Oil & gas drilling (10101010): drilling contractors or owners of drilling rigs that contract their services for drilling wells;
      - Oil & gas equipment & services (10101020): manufacturers of equipment, including drilling rigs and equipment, and providers of supplies and services to companies involved in the drilling, evaluation and completion of oil and gas wells;
    - Oil, gas & consumable fuels (101020)
      - Integrated oil & gas (10102010): integrated oil companies engaged in the exploration & production of oil and gas;
      - Oil & gas exploration & production (10102020): companies engaged in the exploration and production of oil and gas not classified elsewhere;
      - Oil & gas refining & marketing (10102030): companies engaged in the refining and marketing of oil, gas and/or refined products;
      - Oil & gas storage & transportation (10102040): companies engaged in the storage and/or transportation of oil, gas and/or refined products;
      - Coal & consumable fuels (10102050): companies primarily involved in the production and mining of coal, related products and other consumable fuels related to the generation of energy.

The Energy sector has then one industry group, two industries and seven sub-industries. Here is the number of items per sector:

| Name | Sector | Industry Group | Industry | Sub-industry |
|---|---|---|---|---|
| Energy | 1 | 1 | 2 | 7 |
| Materials | 1 | 1 | 5 | 17 |
| Industrials | 1 | 3 | 14 | 27 |
| Consumer Discretionary | 1 | 4 | 10 | 27 |
| Consumer Staples | 1 | 3 | 6 | 12 |
| Health Care | 1 | 2 | 6 | 10 |
| Financials | 1 | 3 | 6 | 18 |
| Information Technology | 1 | 3 | 6 | 12 |
| Communication Services | 1 | 2 | 5 | 10 |
| Utilities | 1 | 1 | 5 | 6 |
| Real Estate | 1 | 2 | 10 | 17 |
| Total | 11 | 25 | 75 | 163 |

Finally, we report the level 3 classification in Tables 11.11 and 11.12.

Table 11.11: GICS level 3 classification (March 2023)

| Sector | | Industry Group | | Industry | |
|---|---|---|---|---|---|
| 10 | Energy | 1010 | Energy | 101010 | Energy Equipment & Services |
| | | | | 101020 | Oil, Gas & Consumable Fuels |
| 15 | Materials | 1510 | Materials | 151010 | Chemicals |
| | | | | 151020 | Construction Materials |
| | | | | 151030 | Containers & Packaging |
| | | | | 151040 | Metals & Mining |
| | | | | 151050 | Paper & Forest Products |
| 20 | Industrials | 2010 | Capital Goods | 201010 | Aerospace & Defense |
| | | | | 201020 | Building Products |
| | | | | 201030 | Construction & Engineering |
| | | | | 201040 | Electrical Equipment |
| | | | | 201050 | Industrial Conglomerates |
| | | | | 201060 | Machinery |
| | | | | 201070 | Trading Companies & Distributors |
| | | 2020 | Commercial & Professional Services | 202010 | Commercial Services & Supplies |
| | | | | 202020 | Professional Services |
| | | 2030 | Transportation | 203010 | Air Freight & Logistics |
| | | | | 203020 | Passenger Airlines |
| | | | | 203030 | Marine Transportation |
| | | | | 203040 | Ground Transportation |
| | | | | 203050 | Transportation Infrastructure |
| 25 | Consumer Discretionary | 2510 | Automobiles & Components | 251010 | Automobile Components |
| | | | | 251020 | Automobiles |
| | | 2520 | Consumer Durables & Apparel | 252010 | Household Durables |
| | | | | 252020 | Leisure Products |
| | | | | 252030 | Textiles, Apparel & Luxury Goods |
| | | 2530 | Consumer Services | 253010 | Hotels, Restaurants & Leisure |
| | | | | 253020 | Diversified Consumer Services |
| | | 2550 | Consumer Discretionary Distribution & Retail | 255010 | Distributors |
| | | | | 255030 | Broadline Retail |
| | | | | 255040 | Specialty Retail |
| 30 | Consumer Staples | 3010 | Consumer Staples Dist. & Retail | 301010 | Consumer Staples Distribution & Retail |
| | | 3020 | Food, Beverage & Tobacco | 302010 | Beverages |
| | | | | 302020 | Food Products |
| | | | | 302030 | Tobacco |
| | | 3030 | Household & Personal Products | 303010 | Household Products |
| | | | | 303020 | Personal Care Products |

Table 11.12: GICS level 3 classification (March 2023)

| Sector | | Industry Group | | Industry | |
|---|---|---|---|---|---|
| 35 | Health Care | 3510 | Health Care Equipment & Services | 351010 | Health Care Equipment & Supplies |
| | | | | 351020 | Health Care Providers & Services |
| | | | | 351030 | Health Care Technology |
| | | 3520 | Pharmaceuticals, Biotechnology & Life Sciences | 352010 | Biotechnology |
| | | | | 352020 | Pharmaceuticals |
| | | | | 352030 | Life Sciences Tools & Services |
| 40 | Financials | 4010 | Banks | 401010 | Banks |
| | | 4020 | Financial Services | 402010 | Financial Services |
| | | | | 402020 | Consumer Finance |
| | | | | 402030 | Capital Markets |
| | | | | 402040 | Mortgage Real Estate Investment Trusts (REITs) |
| | | 4030 | Insurance | 403010 | Insurance |
| 45 | Information Technology | 4510 | Software & Services | 451020 | IT Services |
| | | | | 451030 | Software |
| | | 4520 | Technology Hardware & Equipment | 452010 | Communications Equipment |
| | | | | 452020 | Technology Hardware, Storage & Peripherals |
| | | | | 452030 | Electronic Equipment, Instruments & Components |
| | | 4530 | Semiconductors & SC. Equip. | 453010 | Semiconductors & Semiconductor Equipment |
| 50 | Communication Services | 5010 | Telecommunication Services | 501010 | Diversified Telecommunication Services |
| | | | | 501020 | Wireless Telecommunication Services |
| | | 5020 | Media & Entertainment | 502010 | Media |
| | | | | 502020 | Entertainment |
| | | | | 502030 | Interactive Media & Services |
| 55 | Utilities | 5510 | Utilities | 551010 | Electric Utilities |
| | | | | 551020 | Gas Utilities |
| | | | | 551030 | Multi-Utilities |
| | | | | 551040 | Water Utilities |
| | | | | 551050 | Independent Power and Renewable Electricity Producers |
| 60 | Real Estate | 6010 | Equity Real Estate Investment Trusts (REITs) | 601010 | Diversified REITs |
| | | | | 601025 | Industrial REITs |
| | | | | 601030 | Hotel & Resort REITs |
| | | | | 601040 | Office REITs |
| | | | | 601050 | Health Care REITs |
| | | | | 601060 | Residential REITs |
| | | | | 601070 | Retail REITs |
| | | | | 601080 | Specialized REITs |
| | | 6020 | Real Estate Management & Dev. | 602010 | Real Estate Management & Development |

Table 11.13 shows the different sector thresholds for the different scope emissions. For that, we have assumed the following mapping between the GICS sectors and the IEA sectors: Communication Services → Other, Consumer Discretionary → Other, Consumer Staples → Other, Energy → Electricity, Financials → Other, Health Care → Other, Industrials → Industry, Information Technology → Other, Materials → Buildings, Real Estate → Buildings and Utilities → Electricity. This mapping is simplistic since the Industrials GICS sector is composed of three industry groups: capital goods, commercial & professional services and transportation. Therefore, we can obtain a more accurate mapping if we use the GICS level II classification.

Table 11.13: Carbon intensity and threshold in $tCO_2e/\$$ mn by GICS sector (MSCI World, 2030)

| Sector | $\mathcal{CI}(b;\mathcal{S}ector_j)$ | | | | $\mathcal{R}_j$ | $\mathcal{CI}_j^\star$ | | | |
|---|---|---|---|---|---|---|---|---|---|
| | $\mathcal{SC}_1$ | $\mathcal{SC}_{1-2}$ | $\mathcal{SC}_{1-3}^{\text{up}}$ | $\mathcal{SC}_{1-3}$ | (in %) | $\mathcal{SC}_1$ | $\mathcal{SC}_{1-2}$ | $\mathcal{SC}_{1-3}^{\text{up}}$ | $\mathcal{SC}_{1-3}$ |
| Communication Services | 2 | 28 | 134 | 172 | 52.4 | 1 | 13 | 64 | 82 |
| Consumer Discretionary | 23 | 65 | 206 | 590 | 52.4 | 11 | 31 | 98 | 281 |
| Consumer Staples | 28 | 55 | 401 | 929 | 52.4 | 13 | 26 | 191 | 442 |
| Energy | 632 | 698 | 1 006 | 6 823 | 56.9 | 272 | 301 | 434 | 2 941 |
| Financials | 13 | 19 | 52 | 244 | 52.4 | 6 | 9 | 25 | 116 |
| Health Care | 10 | 22 | 120 | 146 | 52.4 | 5 | 10 | 57 | 70 |
| Industrials | 111 | 130 | 298 | 1 662 | 18.8 | 90 | 106 | 242 | 1 350 |
| Information Technology | 7 | 23 | 112 | 239 | 52.4 | 3 | 11 | 53 | 114 |
| Materials | 478 | 702 | 1 113 | 2 957 | 36.7 | 303 | 445 | 704 | 1 872 |
| Real Estate | 22 | 101 | 167 | 571 | 36.7 | 14 | 64 | 106 | 361 |
| Utilities | 1 744 | 1 794 | 2 053 | 2 840 | 56.9 | 752 | 773 | 885 | 1 224 |
| MSCI World | 130 | 163 | 310 | 992 | 36.6 | 82 | 103 | 196 | 629 |

Source: MSCI (2022), Trucost (2022) & Author's calculations.

**Remark 124** *The mapping between the different classifications is not always obvious. Indeed, asset owners and managers generally use the Global Industry Classification System (GICS), while the European Union and the United Nations have their own classification systems: the Statistical Classification of Economic Activities in the European Community (NACE) and the International Standard Industrial Classification (ISIC). Le Guenedal et al. (2022) perform a mapping between the four classification systems: GICS, NACE, ISIC and IEA. At the more granular level, they obtain a perfect match only in 70% of cases.*

### Sector and weight deviation constraints

**Equity portfolio** If we consider problem (11.9), we notice that the set of weight constraints are $\Omega_0 \cap \Omega$. The first set of constraint $\Omega_0 = \left\{w : \mathbf{1}_n^\top w = 1, \mathbf{0}_n \leq w \leq \mathbf{1}_n\right\}$ is necessary to obtain a long-only portfolio, but is not sufficient to define a realistic portfolio because it can be concentrated in few number of assets. Therefore, portfolio managers and index providers generally impose some additional constraints to obtain a diversified portfolio:

1. To control the weight deviation between portfolio $w$ and benchmark $b$, we can use:

$$\Omega := \mathcal{C}_1\left(m_w^-, m_w^+\right) = \left\{w : m_w^- b \leq w \leq m_w^+ b\right\}$$

where $m_w^- \in [0, 1[$ and $m_w^+ \in [1, \infty[$. In this case, the portfolio's weight $w_i$ can only deviate from the benchmark's weight $b_i$ by lower and upper ratios $m_w^-$ and $m_w^+$. Typical figures are $m_w^- = 1/2$ and $m_w^+ = 2$.

2. Another approach consists in controlling the sector deviations. In this case, we can use a relative deviation allowance[23]:

$$\Omega := \mathcal{C}_2\left(m_s^-, m_s^+\right) = \left\{ \forall j : m_s^- \sum_{i \in \boldsymbol{\mathcal{S}}ector_j} b_i \leq \sum_{i \in \boldsymbol{\mathcal{S}}ector_j} w_i \leq m_s^+ \sum_{i \in \boldsymbol{\mathcal{S}}ector_j} b_i \right\}$$

where $m_s^- \in [0, 1[$ and $m_s^+ \in [1, \infty[$. Typical figures are $m_s^- = 1/2$, $m_s^+ = 2$ and $\delta_s^+ = 5\%$.

In the sequel, we define 4 sets of constraints: $\mathcal{C}_0$ imposes long-only constraints, $\mathcal{C}_1\left(m_w^-, m_w^+\right)$ adds stock weight constraints, $\mathcal{C}_2\left(m_s\right)$ adds sector relative allocation constraints with $m_s^- = 1/m_s$ and $m_s^+ = m_s$, and $\mathcal{C}_3\left(m_w^-, m_w^+, m_s\right) = \mathcal{C}_1\left(m_w^-, m_w^+\right) \cap \mathcal{C}_2\left(m_s\right)$ combines $\mathcal{C}_1$ and $\mathcal{C}_2$.

**Bond portfolio** In the case of bond portfolio optimization, the current problem is already highly constrained at the sector level, because the objective function controls MD and DTS tracking risks at the sector level. Therefore, we need to use another constraints $\Omega_0 \cap \Omega$, where the first set $\Omega_0 := \mathcal{C}_0 = \left\{w : \mathbf{1}_n^\top w = 1, \mathbf{0}_n \leq w \leq \mathbf{1}_n\right\}$ defines a long-only portfolio and the second set $\Omega$ controls the deviation of risk metrics between portfolio $w$ and benchmark $b$:

1. We can neutralize the modified duration at the portfolio level:

$$\Omega := \mathcal{C}_1' = \left\{w : \mathrm{MD}\left(w\right) = \mathrm{MD}\left(b\right)\right\} = \left\{ w : \sum_{i=1}^n \left(x_i - b_i\right) \mathrm{MD}_i = 0 \right\}$$

2. We can neutralize the duration-times-spread factor at the portfolio level:

$$\Omega := \mathcal{C}_2' = \left\{w : \mathrm{DTS}\left(w\right) = \mathrm{DTS}\left(b\right)\right\} = \left\{ w : \sum_{i=1}^n \left(x_i - b_i\right) \mathrm{DTS}_i = 0 \right\}$$

3. We can constraint the portfolio to have the same weight per maturity bucket as the benchmark:

$$\Omega := \mathcal{C}_3' = \left\{ w : \sum_{i \in \boldsymbol{\mathcal{B}}ucket_j} \left(x_i - b_i\right) = 0 \right\}$$

where $\boldsymbol{\mathcal{B}}ucket_j$ is the $j^{\text{th}}$ maturity bucket. Typical maturity buckets (expressed in years) are: 0–1, 1–3, 3–5, 5–7, 7–10 and 10+.

4. Instead of maturity buckets, we can consider rating categories:

$$\Omega := \mathcal{C}_4' = \left\{ w : \sum_{i \in \mathcal{R}_j} \left(x_i - b_i\right) = 0 \right\}$$

where $\mathcal{R}_j$ is the $j^{\text{th}}$ rating category. For investment grade bonds, typical rating categories are: AAA–AA (AAA, AA+, AA and AA−), A (A+, A and A−) and BBB (BBB+, BBB, BBB−).

[23] An alternative approach is to use an absolute deviation allowance:

$$\Omega = \left\{ \forall j : \left| \sum_{i \in \boldsymbol{\mathcal{S}}ector_j} \left(w_i - b_i\right) \right| \leq \delta_s^+ \right\}$$

where $\delta_s^+ \in [0, 1]$.

**HCIS constraint**

The CTB and PAB labels require that the exposure to sectors highly exposed to climate change is at least equal to the exposure in the investment universe. TEG (2019a) distinguishes two types of sectors:

1. High climate impact sectors (HCIS);

2. Low climate impact sectors (LCIS).

According to TEG (2019a), the first category is made up of "*sectors that are key to the low-carbon transition.*" They correspond to the following NACE classes: A. Agriculture, Forestry, and Fishing; B. Mining and Quarrying; C. Manufacturing; D. Electricity, Gas, Steam, and Air Conditioning Supply; E. Water Supply; Sewerage, Waste Management, and Remediation Activities; F. Construction; G. Wholesale and Retail Trade; Repair of Motor Vehicles and Motorcycles; H. Transportation and Storage; L. Real Estate Activities. Let $\mathcal{HCIS}(w) = \sum_{i \in \text{HCIS}} w_i$ be the HCIS weight of portfolio $w$. In order to comply with CTB and PAB labels, we must verify that:

$$\mathcal{HCIS}(w) \geq \mathcal{HCIS}(b) \tag{11.12}$$

TEG (2019b, Appendix B, pages 26-170) has published a mapping between the NACE classes and several sector classification structures: BICS (Bloomberg), GICS (MSCI and S&P), ICB (FTSE) and TRBC (Refinitiv). In the case of the GICS taxonomy, about 70% of sub-industries are classified as high climate impact sectors. The HCIS constraint has been criticized because this figure is very high. This would mean that almost all activities are critical for building a low-carbon economy. Therefore, only two sectors are classified in low climate impact sectors (Communication Services and Financials), but more than half of the Health Care and Information Technology sub-industries are viewed as high climate impact sectors. The original idea of the HCIS constraint was to continue financing the sectors that are essential for reaching a low-carbon economy (*e.g.*, Energy and Utilities) and at the same time promoting investments in green issuers instead of brown issuers in these sectors. Nevertheless, the constraint (11.12) is not very restrictive with this broad HCIS measure. Moreover, this constraint encourages substitutions between sectors or industries and not substitutions between issuers within a same sector. Therefore, the trade-off is not necessarily between green electricity and brown electricity, but for example between electricity generation and health care equipment.

In Table 11.14, we report the weight and the carbon intensity of each sector when applying the HCIS constraint to the MSCI World index. The carbon intensity of the MSCI World index is equal to 992 $\text{tCO}_2\text{e}/\$$ mn when we consider the scope $\boldsymbol{\mathcal{SC}}_{1-3}$ and 1 498 after the HCIS filter. We verify that the HCIS investment universe has a higher carbon intensity than the reference universe. Nevertheless, the HCIS universe represents 59.79% of the MSCI World index, which is a very high figure. This means that more than half of stocks have a high climate impact. This explains that the HCIS constraint is not really used in portfolio allocation. Indeed, it is difficult to justify that 70% of the Health Care sector, 50% of the Information Technology sector but 0% of the Financials sector are classified as high climate impact sectors.

### 11.2.3 Empirical results

We apply the previous framework to the MSCI World index and the ICE BofA Global Corporate index. The numerical results are those obtained by Barahhou *et al.* (2022).

Table 11.14: Weight and carbon intensity when applying the HCIS filter (MSCI World, June 2022)

| Sector | Index | HCIS | $\mathcal{SC}_1$ | | $\mathcal{SC}_{1-2}$ | | $\mathcal{SC}_{1-3}^{\text{up}}$ | | $\mathcal{SC}_{1-3}$ | |
|---|---|---|---|---|---|---|---|---|---|---|
| | $b_j$ | $b'_j$ | $\mathcal{CI}$ | $\mathcal{CI}'$ | $\mathcal{CI}$ | $\mathcal{CI}'$ | $\mathcal{CI}$ | $\mathcal{CI}'$ | $\mathcal{CI}$ | $\mathcal{CI}'$ |
| Communication Services | 7.58 | 0.00 | 2 | | 28 | | 134 | | 172 | |
| Consumer Discretionary | 10.56 | 8.01 | 23 | 14 | 65 | 31 | 206 | 189 | 590 | 462 |
| Consumer Staples | 7.80 | 7.80 | 28 | 28 | 55 | 55 | 401 | 401 | 929 | 929 |
| Energy | 4.99 | 4.99 | 632 | 632 | 698 | 698 | 1 006 | 1 006 | 6 823 | 6 823 |
| Financials | 13.56 | 0.00 | 13 | | 19 | | 52 | | 244 | |
| Health Care | 14.15 | 9.98 | 10 | 13 | 22 | 26 | 120 | 141 | 146 | 177 |
| Industrials | 9.90 | 7.96 | 111 | 132 | 130 | 151 | 298 | 332 | 1 662 | 1 921 |
| Information Technology | 21.08 | 10.67 | 7 | 12 | 23 | 30 | 112 | 165 | 239 | 390 |
| Materials | 4.28 | 4.28 | 478 | 478 | 702 | 702 | 1 113 | 1 113 | 2 957 | 2 957 |
| Real Estate | 2.90 | 2.90 | 22 | 22 | 101 | 101 | 167 | 167 | 571 | 571 |
| Utilities | 3.21 | 3.21 | 1 744 | 1 744 | 1 794 | 1 794 | 2 053 | 2 053 | 2 840 | 2 840 |
| MSCI World | 100.00 | 59.79 | 130 | 210 | 163 | 252 | 310 | 458 | 992 | 1 498 |

The weights are expressed in %. Column $b_j$ represents the sector weight in the benchmark, while column $b'_j$ indicates the sector weight when applying the HCIS filter. The carbon intensities are measured in $tCO_2e/\$$ mn. Column $\mathcal{CI}$ is the WACI measure of the sector, while column $\mathcal{CI}'$ takes into account the HCIS filter.

Source: MSCI (2022), Trucost (2022) & Author's calculations.

### Equity portfolios

In Table 11.13 on page 977, we have reported the carbon intensity of the MSCI World index and its sectors. We obtain 130 $tCO_2e/\$$ mn for scope $\mathcal{SC}_1$, 163 $tCO_2e/\$$ mn if we include scope 2, 310 $tCO_2e/\$$ mn if we add the upstream scope 3, and finally $992tCO_2e/\$$ mn if we consider the full scope $\mathcal{SC}_{1-3}$. We observe a high discrepancy between sectors. Low-carbon sectors are Communication Services, Financials, Health Care and Information Technology, whereas high-carbon sectors are Energy, Materials and Utilities. We foresee that decarbonizing a portfolio implies reducing the exposure to high-carbon sectors and increasing the exposure to low-carbon sectors. When imposing sector constraints, for instance sector neutrality, the trade-off will be between issuers of the same sector. In Figures 11.5 and 11.6, we show the empirical distribution of carbon intensities for each sector (logarithmic scale). Portfolio decarbonization consists in underweighting the issuers with high carbon intensities and overweigthing the issuers with high carbon intensities. The number of outliers or extreme cases depends on the scope. Therefore, portfolio decarbonization will be more or less difficult depending on the definition of scope emissions.

Barahhou *et al.* (2022) consider the basic optimization problem:

$$w^\star = \arg\min \frac{1}{2} (w-b)^\top \Sigma (w-b)$$
$$\text{s.t.} \begin{cases} \mathcal{CI}(w) \leq (1-\mathcal{R})\,\mathcal{CI}(b) \\ w \in \Omega_0 \cap \Omega \end{cases}$$

and measure the impact of constraints $\Omega_0 \cap \Omega$ on the tracking error volatility. Figure 11.7 corresponds to the $\mathcal{C}_0$ constraint. The tracking risk increases when we include scope 2 or upstream scope 3, whereas downstream scope 3 reduces it because of its large dispersion. Sector allocation is given in Table 11.15. We observe that portfolio decarbonization is a strategy that is long on Financials sector and short on Energy, Materials and Utilities sectors.

Figure 11.5: Boxplot of carbon intensity per sector (MSCI World, June 2022, scope $\mathcal{SC}_{1-2}$)

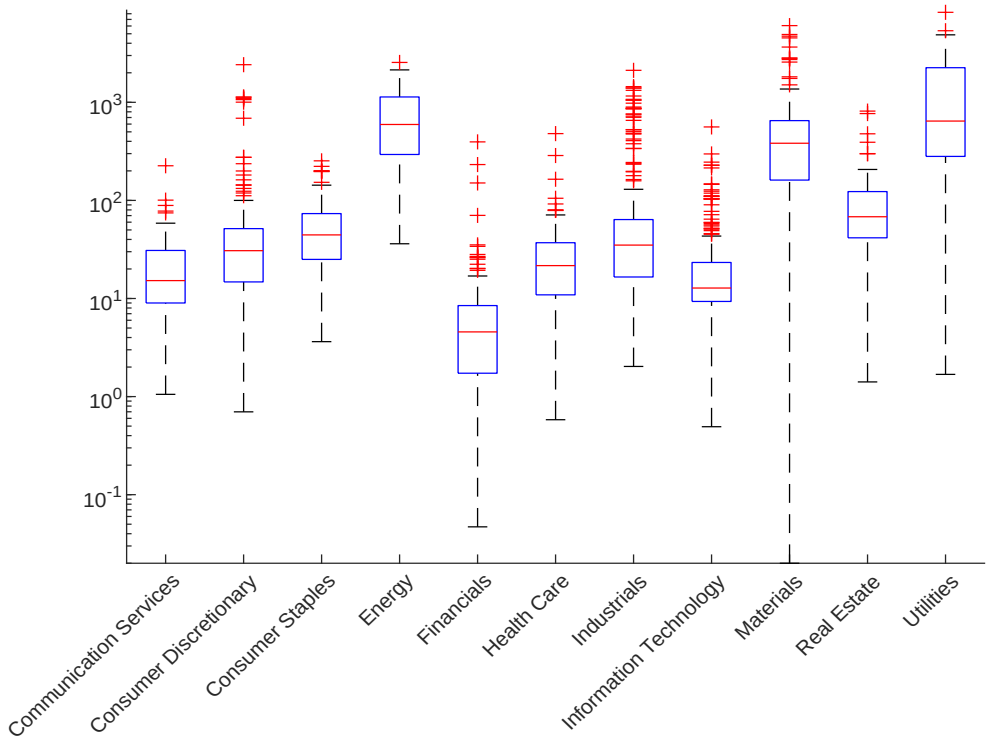


Source: MSCI (2022), Trucost (2022) & Barahhou *et al.* (2022).

Figure 11.6: Boxplot of carbon intensity per sector (MSCI World, June 2022, scope $\mathcal{SC}_{1-3}$)

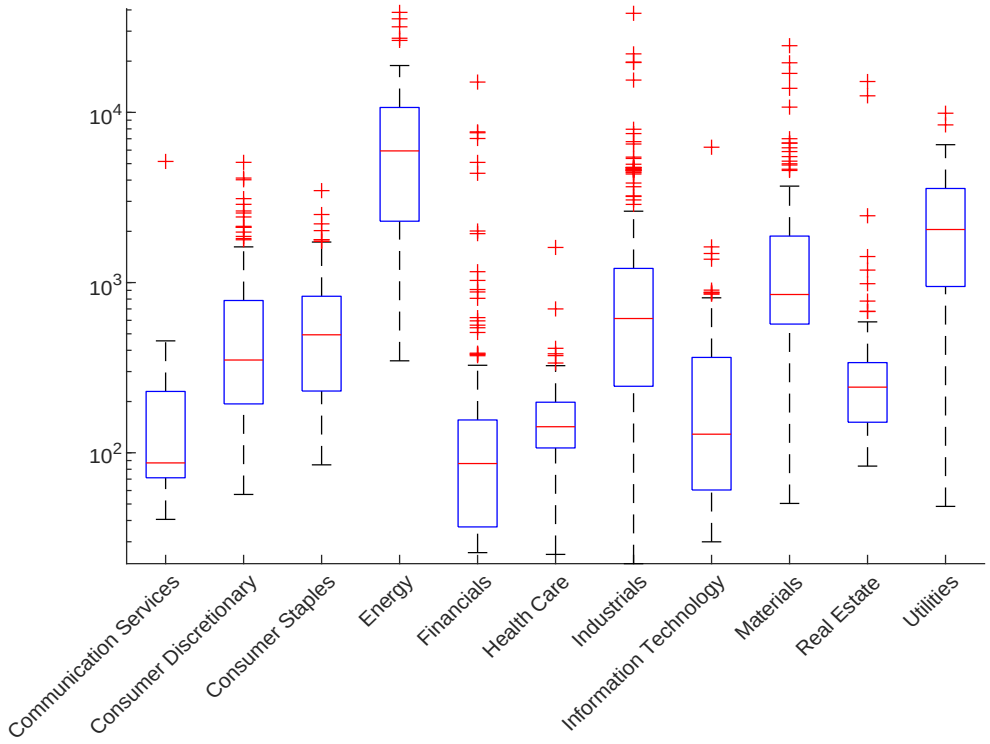


Source: MSCI (2022), Trucost (2022) & Barahhou *et al.* (2022).

Figure 11.7: Impact of the carbon scope on the tracking error volatility (MSCI World, June 2022, $\mathcal{C}_0$ constraint)

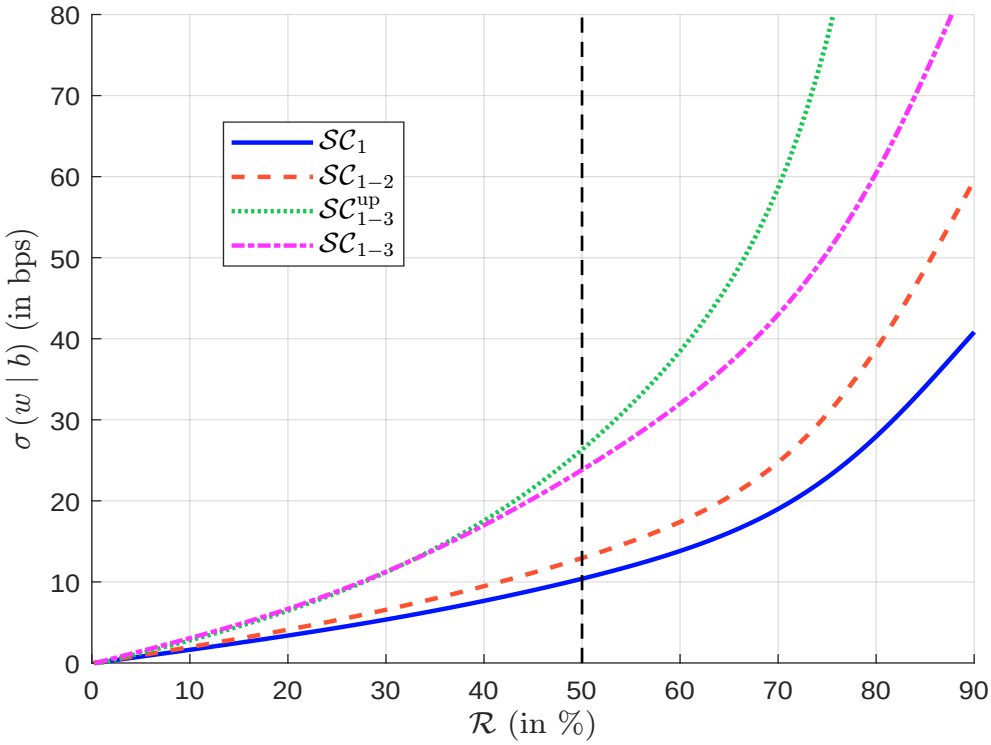


Source: MSCI (2022), Trucost (2022) & Barahhou *et al.* (2022).

Table 11.15: Sector allocation in % (MSCI World, June 2022, $\mathcal{C}_0$ constraint, scope $\boldsymbol{\mathcal{SC}}_{1-3}$)

| Sector | Index | Reduction rate $\boldsymbol{\mathcal{R}}$ | | | | | | |
|---|---|---|---|---|---|---|---|---|
| | | 30% | 40% | 50% | 60% | 70% | 80% | 90% |
| Communication Services | 7.58 | 7.95 | 8.15 | 8.42 | 8.78 | 9.34 | 10.13 | 12.27 |
| Consumer Discretionary | 10.56 | 10.69 | 10.69 | 10.65 | 10.52 | 10.23 | 9.62 | 6.74 |
| Consumer Staples | 7.80 | 7.80 | 7.69 | 7.48 | 7.11 | 6.35 | 5.03 | 1.77 |
| Energy | 4.99 | 4.14 | 3.65 | 3.10 | 2.45 | 1.50 | 0.49 | 0.00 |
| Financials | 13.56 | 14.53 | 15.17 | 15.94 | 16.90 | 18.39 | 20.55 | 28.62 |
| Health Care | 14.15 | 14.74 | 15.09 | 15.50 | 16.00 | 16.78 | 17.77 | 17.69 |
| Industrials | 9.90 | 9.28 | 9.01 | 8.71 | 8.36 | 7.79 | 7.21 | 6.03 |
| Information Technology | 21.08 | 21.68 | 22.03 | 22.39 | 22.88 | 23.51 | 24.12 | 24.02 |
| Materials | 4.28 | 3.78 | 3.46 | 3.06 | 2.56 | 1.85 | 1.14 | 0.24 |
| Real Estate | 2.90 | 3.12 | 3.27 | 3.41 | 3.57 | 3.72 | 3.71 | 2.51 |
| Utilities | 3.21 | 2.28 | 1.79 | 1.36 | 0.90 | 0.54 | 0.24 | 0.12 |

Source: MSCI (2022), Trucost (2022) & Barahhou *et al.* (2022).

If we impose the classical weight constraint $\mathcal{C}_1\left(1/3, 3\right)$, which is very popular in index portfolio management, we observe a high increase in the tracking error volatility (Panel 1, Figure 11.8). Moreover, we generally have no solution when $\boldsymbol{\mathcal{R}} > 60\%$. The issue comes from the lower bound, which is way to narrow. Indeed, portfolio decarbonization is an exclusion process. By imposing a lower bound, we then limit portfolio decarbonization. For instance, we obtain similar results between constraint $\mathcal{C}_1\left(0, 3\right)$ and constraint $\mathcal{C}_0$ (Panel 2, Figure 11.8). Nevertheless, we must be careful when choosing $m_w^+$, because a low value can lead to infeasible solutions. For instance, this is the case of constraint $\mathcal{C}_1\left(0, 1.25\right)$, as shown in Panel 4, Figure 11.8.

The impact of sector constraints is less important than the impact of weight constraints. For instance, constraint $\mathcal{C}_2\left(2\right)$ does not increase the tracking error volatility with respect to constraint $\mathcal{C}_0$ (Panel 1, Figure 11.9). If we impose sector neutrality (constraint $\mathcal{C}_2\left(1\right)$), we observe a small increase of the tracking risk. Indeed, for low reduction rates (less than 50%), the tracking error volatility remains below 40 bps (Panel 2, Figure 11.9). At first sight, it may be surprising that weight constraints are more binding than sector constraints. Indeed, we generally consider that the sector contribution is greater than the idiosyncratic contribution. Therefore, we expect that the inter-class dispersion largely dominates the intra-class variance. Nevertheless, this viewpoint is biased because it considers homogeneous sectors. In our case, we use level 1 of the GICS classification. The concept of sector is then very heterogeneous. Within a particular sector, we can have low-carbon and high-carbon issuers as we have seen in Figures 11.5 and 11.6.

The combination of weight and sectoral constraints is a more difficult exercise as shown in the bottom panels in Figure 11.9. This is why portfolio managers generally use less restrictive rules. Thus, $\mathcal{C}_3\left(0, 10, 2\right)$ constraint has became the standard approach in the ETF market when building climate benchmarks. As shown in Figure 11.10, the impact of this constraint is relatively low.

Figure 11.8: Impact of $\mathcal{C}_1$ constraint on the tracking error volatility (MSCI World, June 2022)

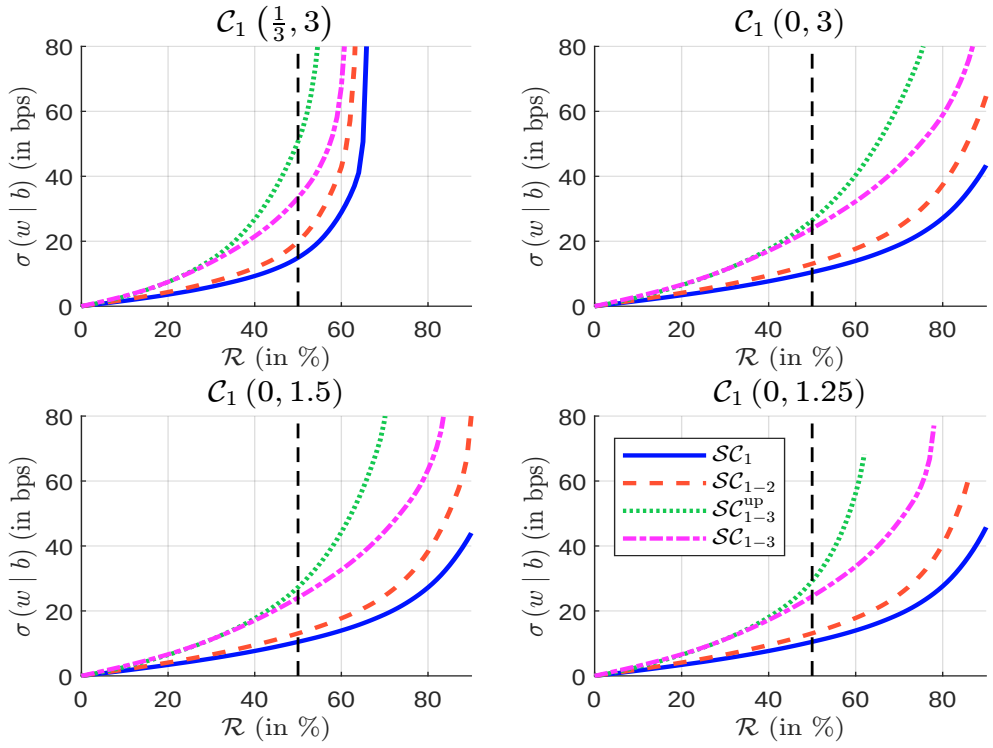


Source: MSCI (2022), Trucost (2022) & Barahhou *et al.* (2022).

Figure 11.9: Impact of $\mathcal{C}_2$ and $\mathcal{C}_3$ constraints (MSCI World, June 2022)

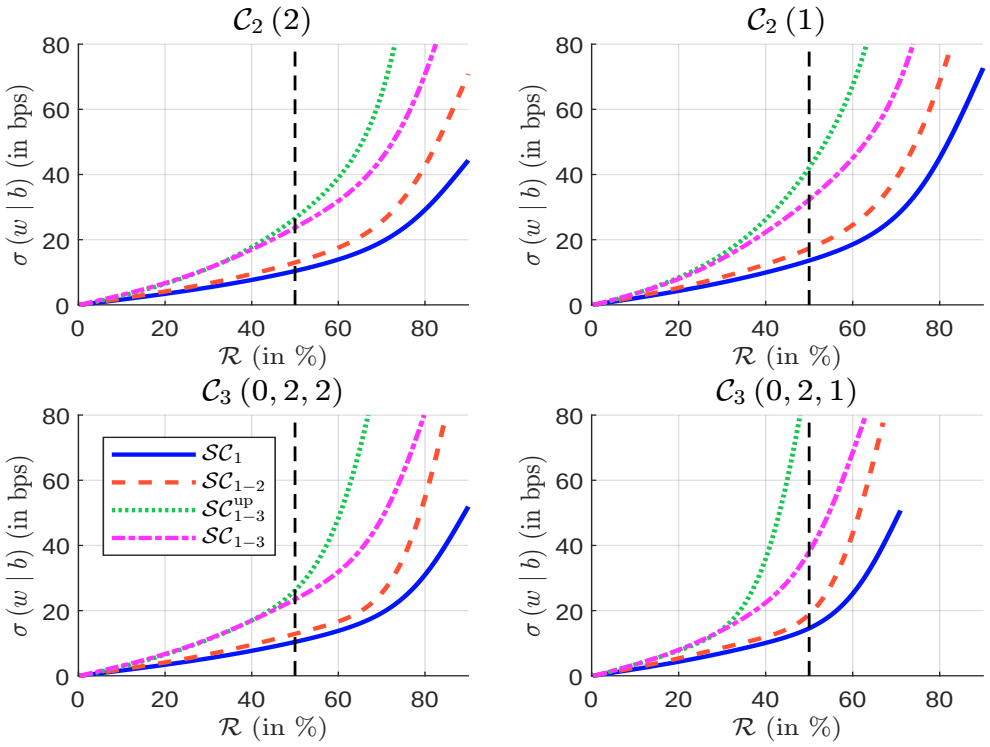


Source: MSCI (2022), Trucost (2022) & Barahhou *et al.* (2022).

Figure 11.10: Tracking error volatility with $\mathcal{C}_3\,(0, 10, 2)$ constraint (MSCI World, June 2022)

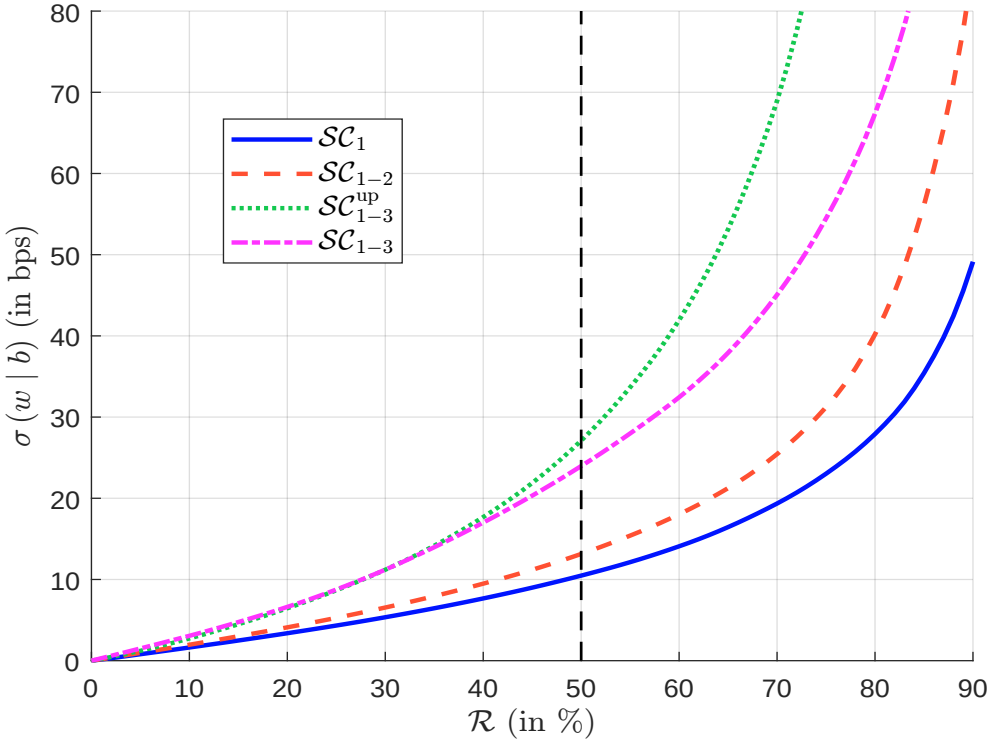


Source: MSCI (2022), Trucost (2022) & Barahhou *et al.* (2022).

The efficiency of the order-statistic and naive approaches depends on the distribution of carbon intensities. For instance, if the carbon intensity of the index is concentrated in one stock, then removing this stock reduces dramatically the carbon footprint of the portfolio. In Figure 11.11, we have reported the relative carbon footprint contribution of the $m$ worst performing assets:

$$\mathcal{CFC}^{(m,n)} = \frac{\sum_{i=1}^{n} \mathbb{1}\left\{\boldsymbol{\mathcal{CI}}_i \geq \boldsymbol{\mathcal{CI}}^{(m,n)}\right\} \cdot b_i \boldsymbol{\mathcal{CI}}_i}{\boldsymbol{\mathcal{CI}}(b)}$$

where $\boldsymbol{\mathcal{CI}}^{(m,n)} = \boldsymbol{\mathcal{CI}}_{n-m+1:n}$ is the $(n-m+1)$-th order statistic. By construction, $\mathcal{CFC}^{(m,n)}$ is an increasing function with respect to $m$ and we have the following properties: $\mathcal{CFC}^{(0,n)} = 0$ and $\mathcal{CFC}^{(n,n)} = 1$. The fifty worst performing stocks[24] represent respectively about 50% and 40% of $\boldsymbol{\mathcal{SC}}_1$ and $\boldsymbol{\mathcal{SC}}_{1-3}$ carbon intensities of the MSCI World index. The previous analysis can be extended by considering another metric to perform the rank ordering, for instance the absolute contribution of stock $i$:

$$\mathcal{CFC}^{(m,n)} = \frac{\sum_{i=1}^{n} \mathbb{1}\left\{\mathcal{CIC}_i \geq \mathcal{CIC}^{(m,n)}\right\} \cdot b_i \boldsymbol{\mathcal{CI}}_i}{\boldsymbol{\mathcal{CI}}(b)}$$

where $\mathcal{CIC}_i = b_i \boldsymbol{\mathcal{CI}}_i$ and $\mathcal{CIC}^{(m,n)} = \mathcal{CIC}_{n-m+1:n}$. In this approach, we do not consider $\boldsymbol{\mathcal{CI}}_i$ but the product $b_i \boldsymbol{\mathcal{CI}}_i$ to define the exclusion process. Results are given in Figure 11.12. The 50 worst performing stocks represent then 70% and 55% of $\boldsymbol{\mathcal{SC}}_1$ and $\boldsymbol{\mathcal{SC}}_{1-3}$ carbon intensities.

Figure 11.11: Carbon footprint contribution $\mathcal{CFC}^{(m,n)}$ in % (MSCI World, June 2022, first approach)

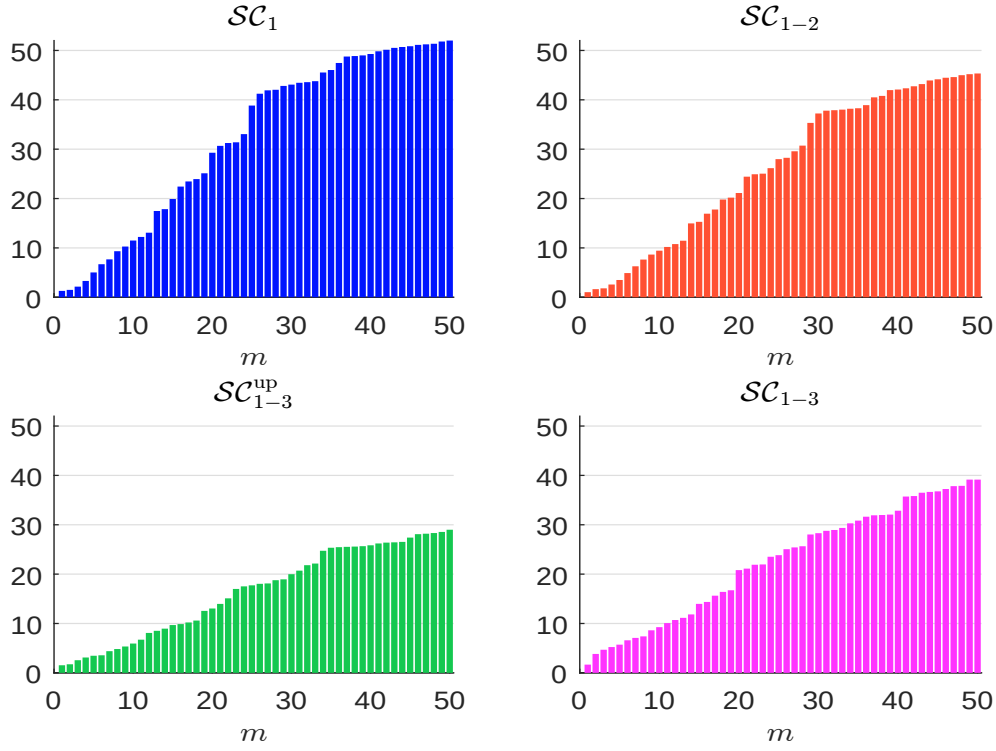


Source: MSCI (2022), Trucost (2022) & Author's calculations.

[24] The MSCI World index was composed of 1 513 stocks in June 2022.

Figure 11.12: Carbon footprint contribution $\mathcal{CFC}^{(m,n)}$ in % (MSCI World, June 2022, second approach)

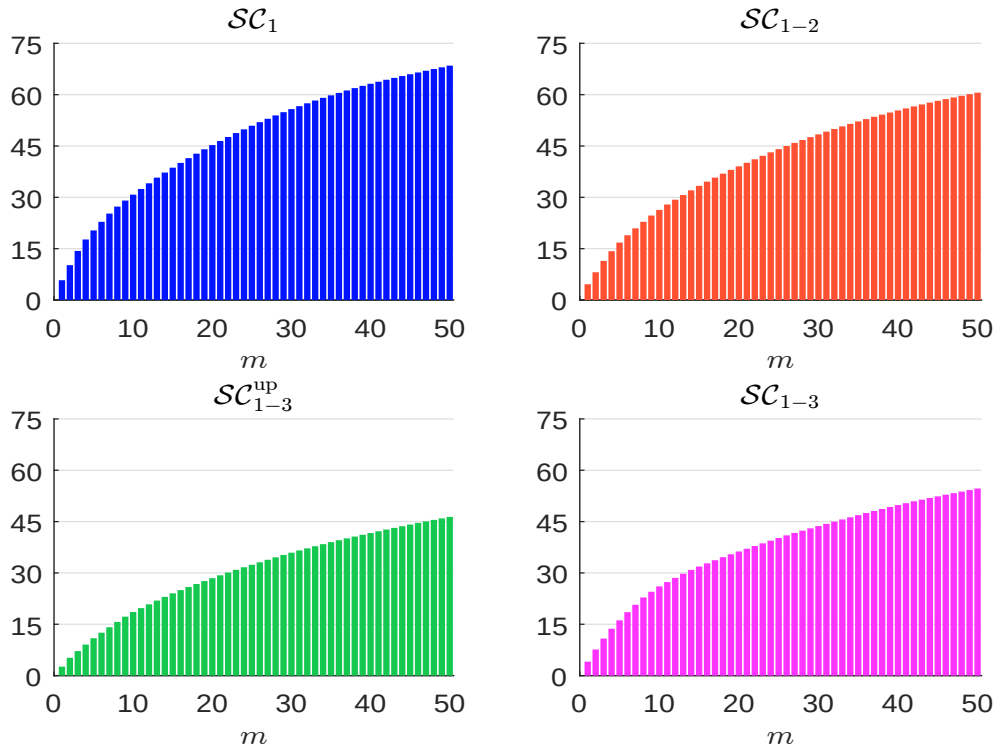


Source: MSCI (2022), Trucost (2022) & Author's calculations.

Table 11.16: Carbon footprint contribution $\mathcal{CFC}^{(m,n)}$ in % (MSCI World, June 2022, second approach, $\boldsymbol{\mathcal{SC}}_{1-3}$)

| Sector | $m$ | | | | | | | |
|---|---|---|---|---|---|---|---|---|
| | 1 | 5 | 10 | 25 | 50 | 75 | 100 | 200 |
| Communication Services | | | | | | 0.44 | 0.44 | 0.73 |
| Consumer Discretionary | | | | 0.78 | 1.37 | 2.44 | 2.93 | 4.28 |
| Consumer Staples | | 2.46 | 2.46 | 2.46 | 3.75 | 4.44 | 4.92 | 5.62 |
| Energy | | 9.61 | 17.35 | 23.78 | 29.56 | 31.78 | 33.02 | 33.89 |
| Financials | | | | | | 0.72 | 1.53 | 1.88 |
| Health Care | | | | | | | 0.21 | 0.37 |
| Industrials | | | 2.16 | 5.59 | 7.13 | 8.70 | 9.48 | 13.05 |
| Information Technology | | | | 0.98 | 1.58 | 1.94 | 2.15 | 3.30 |
| Materials | 4.08 | 4.08 | 4.08 | 5.81 | 7.31 | 8.81 | 9.59 | 10.75 |
| Real Estate | | | | | 0.77 | 0.77 | 0.77 | 0.85 |
| Utilities | | | | 0.81 | 3.20 | 3.89 | 5.24 | 7.98 |
| Total | 4.08 | 16.15 | 26.06 | 40.21 | 54.66 | 63.94 | 70.29 | 82.70 |

Source: MSCI (2022), Trucost (2022) & Author's calculations.

Table 11.17: Weight contribution $\mathcal{WC}^{(m,n)}$ in % (MSCI World, June 2022, second approach, $\boldsymbol{\mathcal{SC}}_{1-3}$)

| Sector | $b_j$ (in %) | $m$ = 1 | 5 | 10 | 25 | 50 | 75 | 100 | 200 |
|---|---|---|---|---|---|---|---|---|---|
| Communication Services | 7.58 | | | | | | 0.08 | 0.08 | 3.03 |
| Consumer Discretionary | 10.56 | | | | 0.58 | 1.79 | 2.44 | 4.51 | 5.89 |
| Consumer Staples | 7.80 | | 0.70 | 0.70 | 0.70 | 1.90 | 2.50 | 2.84 | 3.84 |
| Energy | 4.99 | | 1.71 | 2.25 | 2.96 | 3.62 | 3.99 | 4.33 | 4.65 |
| Financials | 13.56 | | | | | | 0.74 | 1.17 | 2.33 |
| Health Care | 14.15 | | | | | | | 0.95 | 1.34 |
| Industrials | 9.90 | | | 0.06 | 0.32 | 0.70 | 0.96 | 1.20 | 4.12 |
| Information Technology | 21.08 | | | | 0.16 | 4.70 | 8.42 | 8.78 | 11.62 |
| Materials | 4.28 | 0.29 | 0.29 | 0.29 | 0.47 | 0.88 | 1.10 | 1.40 | 1.87 |
| Real Estate | 2.90 | | | | | 0.05 | 0.05 | 0.05 | 0.23 |
| Utilities | 3.21 | | | | 0.31 | 0.86 | 1.04 | 1.31 | 2.33 |
| Total | | 0.29 | 2.71 | 3.30 | 5.49 | 14.50 | 21.32 | 26.63 | 41.24 |

Source: MSCI (2022), Trucost (2022) & Author's calculations.

In Table 11.16, we have reported the relative carbon intensity contribution $\mathcal{CFC}^{(m,n)}$ for several values of $m$. For example, one stock contributes to 4.08% of the $\boldsymbol{\mathcal{SC}}_{1-3}$ carbon intensity[25], while the fifty worst performing stocks have a contribution of 54.66%. Table 11.16 also shows the sector allocation of $\mathcal{CFC}^{(m,n)}$. We verify that the Energy sector is the most important contributor and represents about 50% on average when $m \leq 100$. In Table 11.17, we calculate the weight contribution:

$$\mathcal{WC}^{(m,n)} = \sum_{i=1}^{n} \mathbb{1}\left\{\mathcal{CIC}_i \geq \mathcal{CIC}^{(m,n)}\right\} \cdot b_i$$

We notice that the fifty worst performing stocks represent then 14.50% of the MSCI World index in terms of allocation, but 54.66% of its carbon footprint[26].

**Remark 125** *The previous figures highly depend on the scope definition and the ordering approach. For instance, if we consider scope* $\boldsymbol{\mathcal{SC}}_{1-2}$*, the fifty worst performing stocks represent then* 12.65% *of the MSCI World index in terms of allocation, but* 60.58% *of its carbon footprint. If we consider the first ordering approach based on the carbon intensity* $\boldsymbol{\mathcal{CI}}_i$ *and not the absolute contribution* $\mathcal{CIC}_i$*, the figures become respectively* 2.57% *and* 45.34%*.*

We implement the order-statistic optimization problem:

$$\begin{aligned} w^\star &= \arg\min \frac{1}{2}(w-b)^\top \Sigma (w-b) \\ &\text{s.t.} \begin{cases} \mathbf{1}_n^\top w = 1 \\ \mathbf{0}_n \leq w \leq w^{(m,n)} \end{cases} \end{aligned}$$

where the upper bound $w^{(m,n)}$ is equal to $\mathbb{1}\left\{\boldsymbol{\mathcal{CI}} < \boldsymbol{\mathcal{CI}}^{(m,n)}\right\}$ for the first ordering approach and $\mathbb{1}\left\{\mathcal{CIC} < \mathcal{CIC}^{(m,n)}\right\}$ for the second ordering approach[27]. We compare the optimization method

[25] We remind that the $\boldsymbol{\mathcal{SC}}_{1-3}$ carbon intensity of the MSCI World index is equal to 992 $tCO_2e/\$$ mn.
[26] If we consider the first approach, 3.21% of the allocation explains 39.15% of the carbon footprint.
[27] We have $\mathcal{CIC} = (\mathcal{CIC}_1, \ldots, \mathcal{CIC}_n)$ where $\mathcal{CIC}_i = b_i \boldsymbol{\mathcal{CI}}_i$.

Figure 11.13: Tracking error volatility (MSCI World, June 2022, $\boldsymbol{\mathcal{SC}}_{1-3}$, first ordering method)

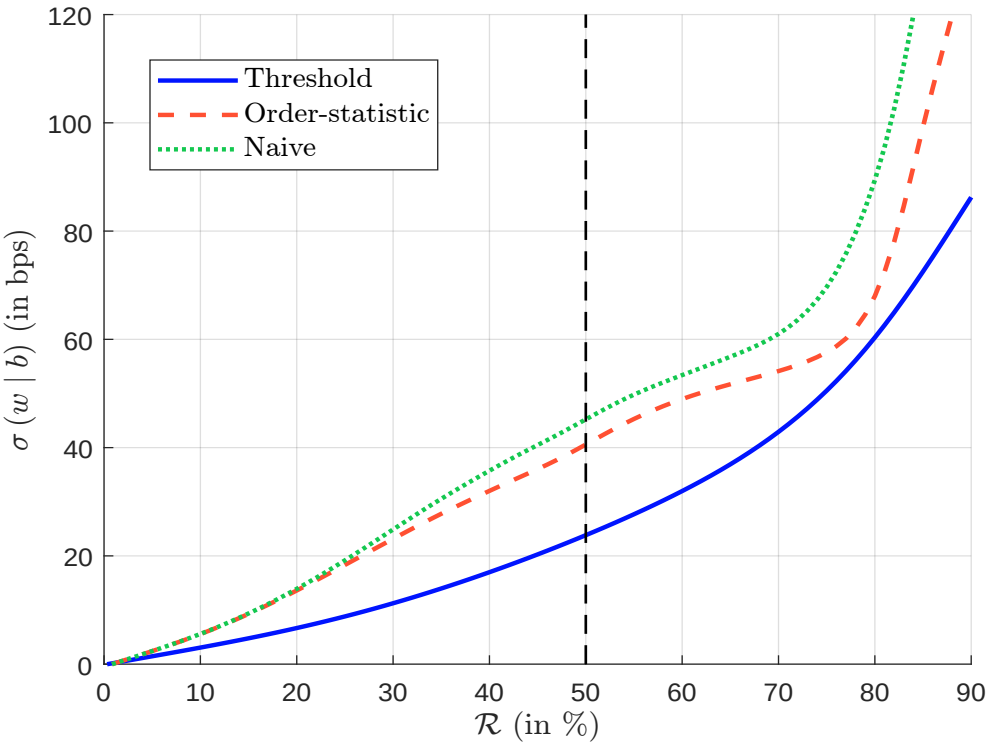


Source: MSCI (2022), Trucost (2022) & Author's calculations.

Figure 11.14: Tracking error volatility (MSCI World, June 2022, $\boldsymbol{\mathcal{SC}}_{1-3}$, second ordering method)

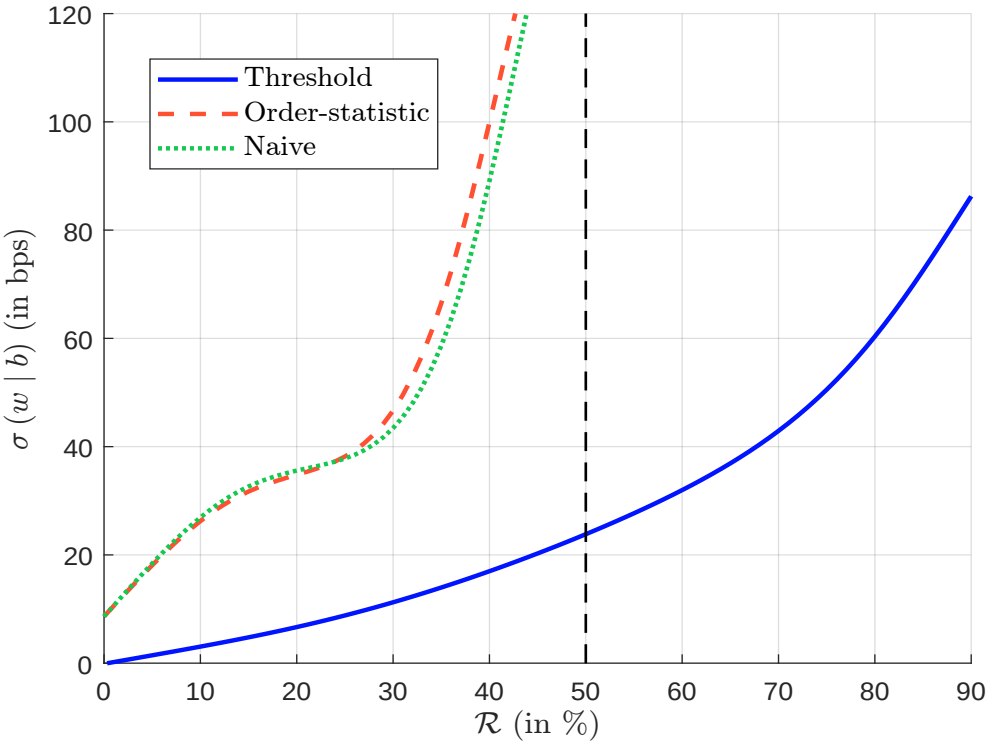


Source: MSCI (2022), Trucost (2022) & Author's calculations.

with the naive method:

$$w_i^\star = \frac{e_i b_i}{\sum_{k=1}^n e_k b_k}$$

where $e_i$ is defined as $\mathbb{1}\left\{\boldsymbol{\mathcal{CI}}_i < \boldsymbol{\mathcal{CI}}^{(m,n)}\right\}$ for the first ordering approach and $\mathbb{1}\left\{\mathcal{CIC}_i < \mathcal{CIC}^{(m,n)}\right\}$ for the second ordering approach. Results are given in Figures 11.13 and 11.14. Compared to the threshold method, the order-statistic and naive solutions are less efficient with a higher tracking error volatility. We also observe that the second ordering approach is not robust, because it may remove stocks, whose carbon intensity contribution is mainly explained by their weights.

### Bond portfolios

In the case of corporate bonds, Barahhou *et al.* (2022) solve the following optimization problem:

$$\begin{aligned} w^\star &= \arg\min \frac{1}{2}\sum_{i=1}^n |w_i - b_i| + 50 \sum_{j=1}^{n_{\boldsymbol{\mathcal{S}ector}}} \left| \sum_{i \in \boldsymbol{\mathcal{S}ector}_j} (w_i - b_i)\,\mathrm{DTS}_i \right| \\ \text{s.t.} &\begin{cases} \boldsymbol{\mathcal{CI}}(w) \leq (1-\boldsymbol{\mathcal{R}})\,\boldsymbol{\mathcal{CI}}(b) \\ w \in \mathcal{C}_0 \cap \mathcal{C}_1' \cap \mathcal{C}_3' \cap \mathcal{C}_4' \end{cases} \end{aligned}$$

We remind that $\mathcal{C}_1'$ constraint neutralizes the modified duration at the portfolio level, whereas $\mathcal{C}_3'$ and $\mathcal{C}_4'$ constraints requires the portfolio to have the same weights as the benchmark per maturity bucket and rating category. The tracking risk measures $\mathcal{D}_{\text{AS}}(w \mid b)$ and $\mathcal{D}_{\text{DTS}}(w \mid b)$ are reported in Figures 11.15 and 11.16. We observe that the tracking risk is low when we consider the DTS component, whereas it is significant when we focus on the active share component.

Table 11.18: Sector allocation in % (ICE Global Corp., June 2022, scope $\boldsymbol{\mathcal{SC}}_{1-3}$)

| Sector | Index | Reduction rate $\boldsymbol{\mathcal{R}}$ | | | | | | |
|---|---|---|---|---|---|---|---|---|
| | | 30% | 40% | 50% | 60% | 70% | 80% | 90% |
| Communication Services | 7.34 | 7.35 | 7.34 | 7.37 | 7.43 | 7.43 | 7.31 | 7.30 |
| Consumer Discretionary | 5.97 | 5.97 | 5.96 | 5.94 | 5.93 | 5.46 | 4.48 | 3.55 |
| Consumer Staples | 6.04 | 6.04 | 6.04 | 6.04 | 6.04 | 6.02 | 5.39 | 4.06 |
| Energy | 6.49 | 5.49 | 4.42 | 3.84 | 3.69 | 3.23 | 2.58 | 2.52 |
| Financials | 33.91 | 34.64 | 35.66 | 35.96 | 36.09 | 37.36 | 38.86 | 39.00 |
| Health Care | 7.50 | 7.50 | 7.50 | 7.50 | 7.50 | 7.50 | 7.52 | 7.48 |
| Industrials | 8.92 | 9.38 | 9.62 | 10.19 | 11.34 | 12.07 | 13.55 | 18.13 |
| Information Technology | 5.57 | 5.57 | 5.59 | 5.59 | 5.60 | 5.60 | 5.52 | 5.27 |
| Materials | 3.44 | 3.43 | 3.31 | 3.18 | 3.12 | 2.64 | 2.25 | 1.86 |
| Real Estate | 4.76 | 4.74 | 4.74 | 4.74 | 4.74 | 4.66 | 4.61 | 3.93 |
| Utilities | 10.06 | 9.89 | 9.82 | 9.64 | 8.52 | 8.04 | 7.92 | 6.88 |

Source: ICE (2022), Trucost (2022) & Barahhou *et al.* (2022).

Table 11.18 shows the sector allocation when considering scope $\boldsymbol{\mathcal{SC}}_{1-3}$. Like for equities, the decarbonization process is a strategy that is long on the Financials sector and short on Materials and Utilities sectors. Health care, Communication Services, Consumer Discretionary, and Information Technology weights are very close to their benchmark's. The case of the Industrials sector may be disturbing, but the deviation highly depends on the scope.

Figure 11.15: Impact of the carbon scope on the active share in % (ICE Global Corp., June 2022)

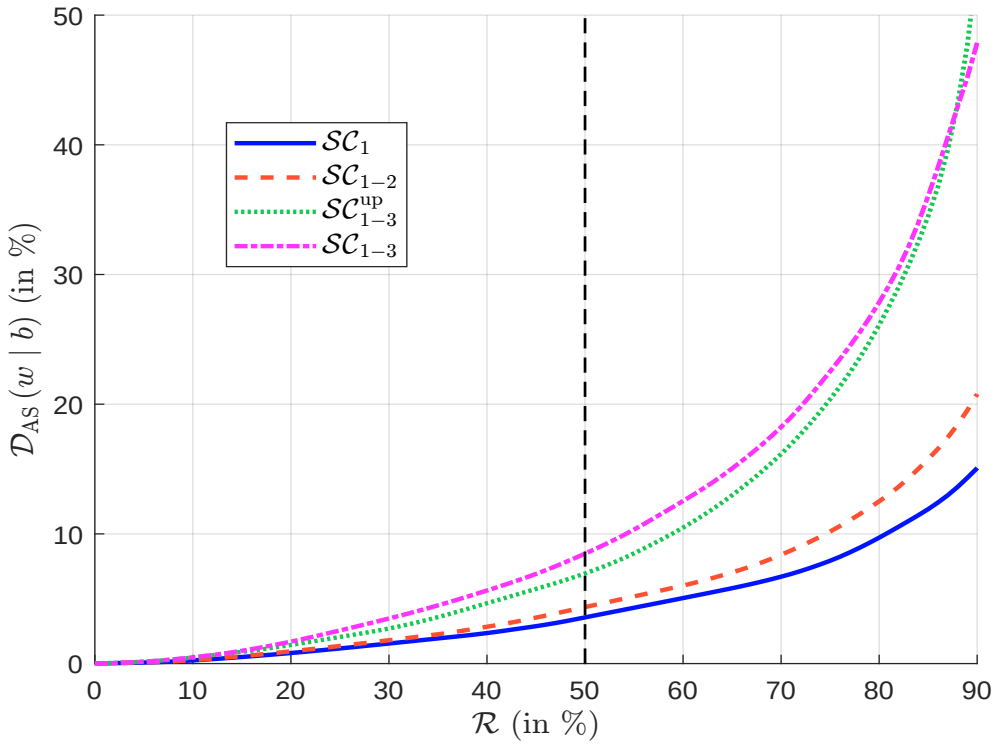


Source: ICE (2022), Trucost (2022) & Barahhou *et al.* (2022).

Figure 11.16: Impact of the carbon scope on the DTS risk in bps (ICE Global Corp., June 2022)

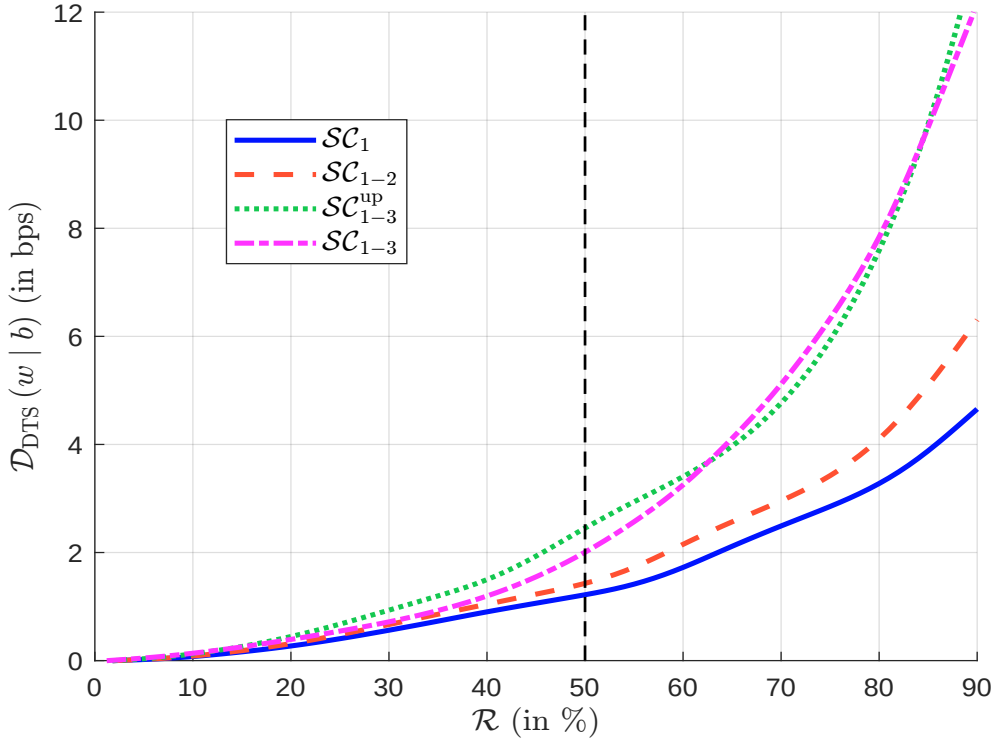


Source: ICE (2022), Trucost (2022) & Barahhou *et al.* (2022).

## 11.3 Net-zero investing

The emergence of net-zero emissions policies is one of the hottest topics in finance today. In particular, net-zero emissions policies have gained significant traction in recent years with the proliferation of net-zero alliances (GFANZ, NZAOA, NZAM, NZBA, etc.) and their commitments. This issue is significantly changing portfolio allocation and investment frameworks for both passive and active investors. Indeed, it implies that investors need to implement dynamic decarbonization pathways with continuous reference to business-as-usual benchmarks. In addition, a net-zero portfolio must be considered to finance the transition. The greenness or green intensity of the portfolio is therefore important. A net-zero investment policy therefore has two main dimensions: decarbonizing the portfolio and financing the transition. This means that net-zero investing is not only a carbon footprint issue, but also a green footprint issue.

According to Ben Slimane *et al.* (2023b), there are two approaches to implementing a net-zero investment policy. The integrated approach combines the decarbonization and financing dimensions in an allocation process that considers both carbon intensity for the decarbonization dimension and green intensity for the financing dimension. In the core-satellite strategy, the decarbonization dimension is managed within the core portfolio, while the objective of the satellite strategy is to finance the transition to a low-carbon economy.

### 11.3.1 Integrated approach

#### Choice of the decarbonization scenario

**The carbon emissions/intensity approach** A decarbonization scenario is defined as a function that relates a decarbonization rate to a time index $t$:

$$\begin{aligned} f &: \mathbb{R}^+ \longrightarrow [0,1] \\ &\quad t \longmapsto \boldsymbol{\mathcal{R}}(t_0, t) \end{aligned}$$

where $t_0$ is the base year and $\boldsymbol{\mathcal{R}}\left(t_0, t_0^-\right) = 0$. In general, we assume that $\boldsymbol{\mathcal{R}}(t_0, t)$ is a nondecreasing function of time $t$. When considering a decarbonization pathway, we need to distinguish between two different concepts: economic decarbonization and financial decarbonization. In the first case, the variable of interest is the level of carbon emissions, while in the second case we use carbon intensity. Figure 11.17 shows the Net-Zero Emissions by 2050 (NZE) scenario provided by the International Energy Agency[28]. This is a normative scenario based on a number of assumptions about the global energy sector. From this scenario, we can calculate the decarbonization path of the real economy and the different sectors. Figure 11.18 compares these with those used by the CTB and PAB benchmarks. It is clear that we are not comparing apples to apples. In fact, in the case of the real economy, carbon emissions $\boldsymbol{\mathcal{CE}}(t)$ are assumed to follow the following trajectory:

$$\boldsymbol{\mathcal{CE}}(t) = (1 - \boldsymbol{\mathcal{R}}(t_0, t))\, \boldsymbol{\mathcal{CE}}(t_0)$$

while we have for the PAB and CTB pathways:

$$\boldsymbol{\mathcal{CI}}(t) = (1 - \Delta\boldsymbol{\mathcal{R}})^{t-t_0} \left(1 - \boldsymbol{\mathcal{R}}^-\right) \boldsymbol{\mathcal{CI}}(t_0)$$

where $\Delta\boldsymbol{\mathcal{R}} = 7\%$ and $\boldsymbol{\mathcal{R}}^-$ takes the values 30% (CTB) and 50% (PAB) respectively (TEG, 2019a). By construction, the reduction path expressed in terms of carbon intensity must be lower than the

[28] This scenario has already been explored in Chapter 9 (see Figure 9.22 on page 919).

Figure 11.17: $CO_2$ emissions by sector in the IEA NZE scenario (in $GtCO_2e$)

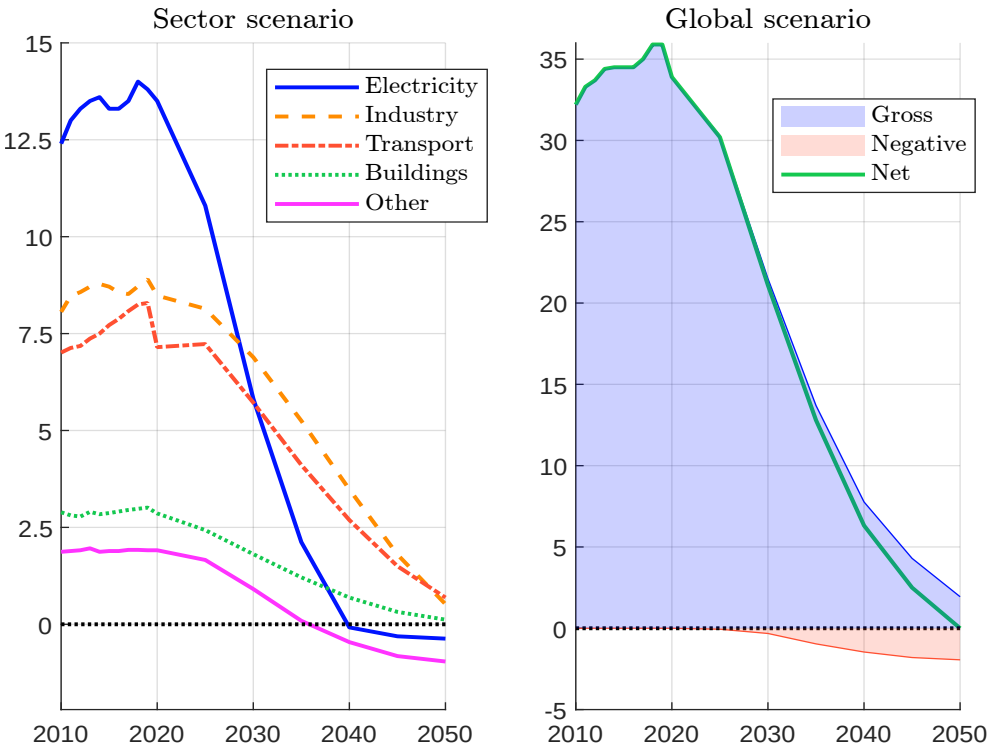


Source: IEA (2021).

Figure 11.18: IEA, NZAOA, CTB and PAB decarbonization pathways

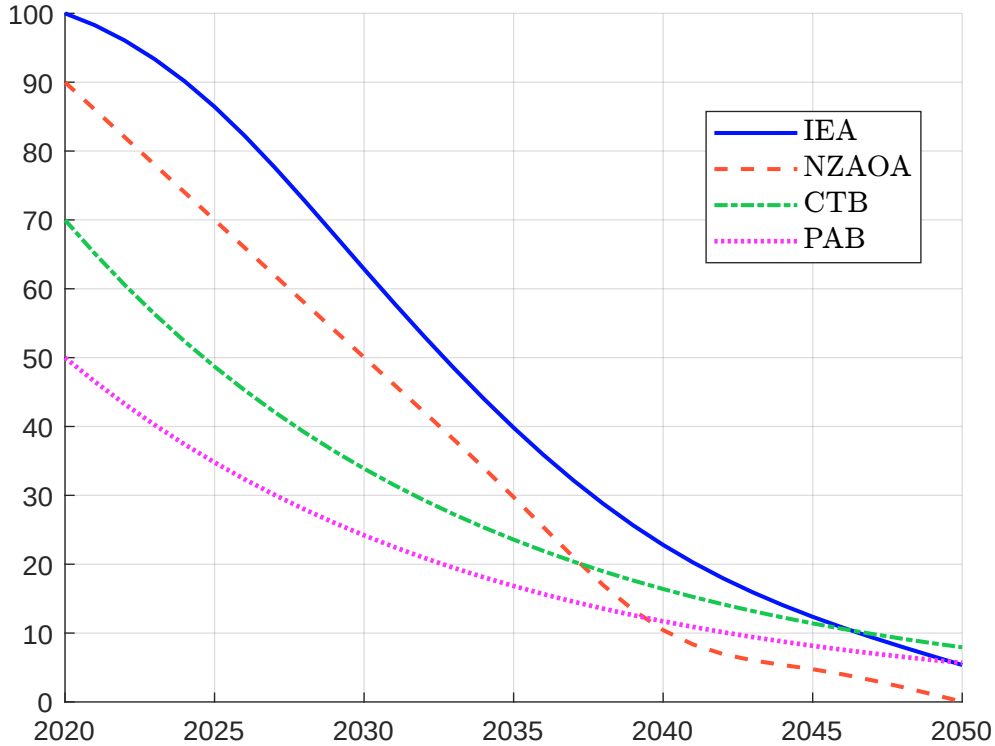

reduction path expressed in terms of carbon emissions. This observation raises the question of the magnitude of the reduction rate. Let us assume that the base date is 2020. The Paris aligned benchmarks imply a reduction rate of 65% by 2025 and 75% by 2030 (Table 11.19). This is much higher than the reduction rates proposed by the International Energy Agency, which are about 15% and 40% by 2025 and 2030 respectively. By comparison, the net-zero frameworks for asset owners propose a reduction rate of about 30% by 2025 and 50% by 2030. The NZAOA curve corresponds to this average asset owner trajectory.

Table 11.19: IEA, NZAOA, CTB and PAB decarbonization rates (baseline = 2020)

| Year<br>$\boldsymbol{\mathcal{R}}^-$<br>$\Delta\boldsymbol{\mathcal{R}}$ | CTB<br>30%<br>7% | PAB<br>50%<br>7% | NZE<br>IEA<br>Scenario | NZAOA<br>Average<br>Scenario |
|---|---|---|---|---|
| 2020 | 30.0% | 50.0% | 0.0% | 10.0% |
| 2021 | 34.9% | 53.5% | 1.7% | 14.0% |
| 2022 | 39.5% | 56.8% | 3.9% | 18.0% |
| 2023 | 43.7% | 59.8% | 6.7% | 22.0% |
| 2024 | 47.6% | 62.6% | 9.9% | 26.0% |
| 2025 | 51.3% | 65.2% | 13.6% | 30.0% |
| 2026 | 54.7% | 67.7% | 17.8% | 34.0% |
| 2027 | 57.9% | 69.9% | 22.3% | 38.0% |
| 2028 | 60.8% | 72.0% | 27.2% | 42.0% |
| 2029 | 63.6% | 74.0% | 32.1% | 46.0% |
| 2030 | 66.1% | 75.8% | 37.1% | 50.0% |
| 2035 | 76.4% | 83.2% | 60.2% | 70.3% |
| 2040 | 83.6% | 88.3% | 77.2% | 89.6% |
| 2045 | 88.6% | 91.9% | 87.6% | 95.2% |
| 2050 | 92.1% | 94.3% | 94.6% | 100.0% |

Source: Ben Slimane *et al.* (2023b).

The previous analysis considered a global path for the entire economy. However, Figure 11.17 shows that not all sectors are the same. In particular, three major sectors are affected (buildings, electricity and transportation), while some sectors are "*hard-to-abate*" such as materials, steel, cement, petrochemicals, etc. Therefore, a net-zero investment policy must focus on these sectors, which means that we must not spend too much effort on some sectors, such as health care or communication services. There is also a sequencing of decarbonization across sectors as shown in Figure 11.19. The order is as follows:

$$\text{Electricity} \succ \text{Buildings} \succ \text{Transport} \succ \text{Industry}$$

**The carbon budget approach** A different approach has been suggested by Bolton *et al.* (2022). The underlying idea is to consider the definition of a net-zero emissions scenario. In fact, a NZE scenario can be defined by a decarbonization pathway that satisfies the following constraints:

$$\begin{cases} \boldsymbol{\mathcal{CB}}(t_0, 2050) \leq \boldsymbol{\mathcal{CB}}^+ \text{ GtCO}_2\text{e} \\ \boldsymbol{\mathcal{CE}}(2050) \approx 0 \text{ GtCO}_2\text{e} \end{cases}$$

where $t_0$ is the base date and $\boldsymbol{\mathcal{CB}}^+$ is the maximum carbon budget. If we look at the SR15 results from IPCC (2018), we can set $t_0 = 2019$ and $\boldsymbol{\mathcal{CB}}^+ = 580\,\text{GtCO}_2\text{e}$, meaning that there is a 50%

Figure 11.19: Sectoral decarbonization pathways

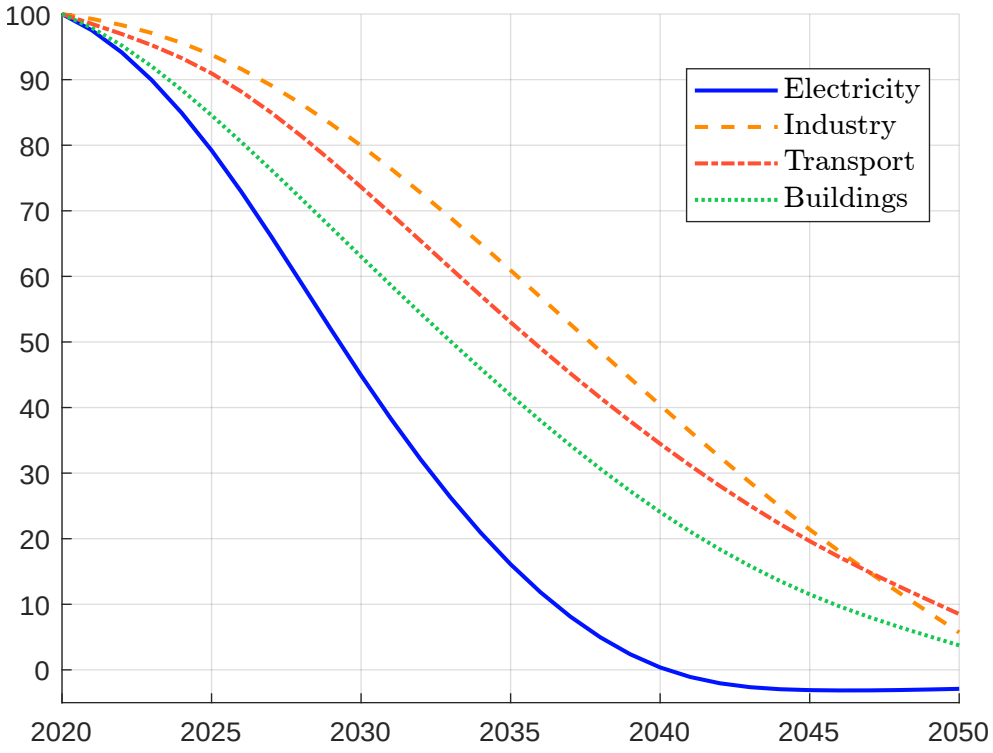


probability of limiting the global warning to 1.5°C. If we want to increase this probability, we can replace the maximum carbon budget $\boldsymbol{\mathcal{CB}}^+$ with a lower number, *e.g.*, 420 $\mathrm{GtCO_2e}$ for a 66% probability and 300 $\mathrm{GtCO_2e}$ for an 83% probability. Over the years, the budget constraint moves, especially if the economy's decarbonization path is not met.

Let us assume that carbon dioxide emissions follow the pathways of the CTB/PAB:

$$\boldsymbol{\mathcal{CE}}(t) = (1 - \Delta\boldsymbol{\mathcal{R}})^{t-t_0} \left(1 - \boldsymbol{\mathcal{R}}^-\right) \boldsymbol{\mathcal{CE}}(t_0)$$

Using Equation (9.7) on page 916, we obtain:

$$\boldsymbol{\mathcal{CB}}(t_0, t) = \left( \frac{(1 - \Delta\boldsymbol{\mathcal{R}})^{t-t_0} - 1}{\ln(1 - \Delta\boldsymbol{\mathcal{R}})} \right) \left(1 - \boldsymbol{\mathcal{R}}^-\right) \boldsymbol{\mathcal{CE}}(t_0) \tag{11.13}$$

By considering several values of $\boldsymbol{\mathcal{R}}^-$ and $\Delta\boldsymbol{\mathcal{R}}$, and assuming that $\boldsymbol{\mathcal{CE}}(2020) = 36\,\mathrm{GtCO_2e}$, we obtain the figures given in Table 11.20. For instance, the carbon budget $\boldsymbol{\mathcal{CB}}(2020, 2050)$ is equal to 308 $\mathrm{GtCO_2e}$ if $\boldsymbol{\mathcal{R}}^- = 30\%$ and $\Delta\boldsymbol{\mathcal{R}} = 7\%$.

Recall that carbon intensity $\boldsymbol{\mathcal{CI}}(t)$ is defined as the ratio of carbon emissions $\boldsymbol{\mathcal{CE}}(t)$ and the normalization variable $Y(t)$:

$$\boldsymbol{\mathcal{CI}}(t) = \frac{\boldsymbol{\mathcal{CE}}(t)}{Y(t)}$$

Let $\boldsymbol{\mathcal{R}}_{\boldsymbol{\mathcal{CI}}}(t_0, t)$ and $\boldsymbol{\mathcal{R}}_{\boldsymbol{\mathcal{CE}}}(t_0, t)$ be the reduction rates of carbon intensity and emissions between $t_0$ and $t$. We have the following relationship:

$$\boldsymbol{\mathcal{R}}_{\boldsymbol{\mathcal{CI}}}(t_0, t) = \frac{\boldsymbol{\mathcal{CI}}(t_0) - \boldsymbol{\mathcal{CI}}(t)}{\boldsymbol{\mathcal{CI}}(t_0)} = \frac{g_Y(t_0, t) + \boldsymbol{\mathcal{R}}_{\boldsymbol{\mathcal{CE}}}(t_0, t)}{1 + g_Y(t_0, t)}$$

Table 11.20: Carbon budget $\mathcal{CB}(2020, 2050)$ (in $GtCO_2e$) when defining the decarbonization pathway of carbon emissions

| $\mathcal{R}^-$ | | 0% | 10% | 20% | 30% | 50% | 75% |
|---|---|---|---|---|---|---|---|
| $\Delta\mathcal{R}$ | 5% | 551 | 496 | 441 | 386 | 276 | 138 |
| | 6% | 491 | 442 | 393 | 344 | 245 | 123 |
| | 7% | 440 | 396 | 352 | 308 | 220 | 110 |
| | 8% | 396 | 357 | 317 | 277 | 198 | 99 |
| | 9% | 359 | 323 | 287 | 251 | 180 | 90 |
| | 10% | 327 | 294 | 262 | 229 | 164 | 82 |

where $g_Y(t_0, t)$ is the growth rate of the normalization variable. Assuming that $g_Y(t_0, t) \geq 0$, we can show that the rate of reduction in carbon intensity is always greater than the rate of reduction in carbon emissions. In most cases, we assume that the annual growth rate of the normalization variable is constant: $Y(t) = (1 + g_Y) Y(t-1)$. We deduce that the compound growth rate is equal to $g_Y(t_0, t) = (1 + g_Y)^{t-t_0} - 1$.

Since we have $\mathcal{CE}(t) = Y(t)\,\mathcal{CI}(t)$, we obtain:

$$\begin{aligned}
\mathcal{CB}(t_0, t) &= \mathcal{CE}(t_0) \int_{t_0}^{t} (1 + g_Y(t_0, s))\,(1 - \mathcal{R}_{\mathcal{CI}}(t_0, s))\,\mathrm{d}s \\
&= \underbrace{(t - t_0)\,\mathcal{CE}(t_0)}_{\mathcal{CB}_1(t_0,t)} + \underbrace{\mathcal{CE}(t_0) \int_{t_0}^{t} g_Y(t_0, s)\,\mathrm{d}s}_{\mathcal{CB}_2(t_0,t)} - \\
&\quad \underbrace{\mathcal{CE}(t_0) \int_{t_0}^{t} (1 + g_Y(t_0, s))\,\mathcal{R}_{\mathcal{CI}}(t_0, s)\,\mathrm{d}s}_{\mathcal{CB}_3(t_0,t)}
\end{aligned}$$

We can divide the carbon budget into three components. The first component $\mathcal{CB}_1(t_0, t)$ corresponds to the total carbon emissions if nothing is done. The second component $\mathcal{CB}_2(t_0, t)$ corresponds to the additional carbon budget if the carbon intensity remains unchanged. The third component $\mathcal{CB}_3(t_0, t)$ is the carbon budget removed by the intensity reduction. If we assume that the annual growth rate of $Y(t)$ is constant and use the PAB/CTB formula for the intensity decarbonization pathway, we get:

$$\mathcal{CB}(t_0, t) = \frac{(1 + g_Y)^{t-t_0}\,(1 - \Delta\mathcal{R}_{\mathcal{CI}})^{t-t_0} - 1}{\ln(1 + g_Y) + \ln(1 - \Delta\mathcal{R}_{\mathcal{CI}})} \left(1 - \mathcal{R}^-_{\mathcal{CI}}\right) \mathcal{CE}(t_0) \tag{11.14}$$

Table 11.21 shows the effect of $g_Y$, $\mathcal{R}^-_{\mathcal{CI}}$ and $\Delta\mathcal{R}_{\mathcal{CI}}$ on the calculation of $\mathcal{CB}(2020, 2050)$ when $\mathcal{CE}(2020) = 36\,GtCO_2e$. If $g_Y = 0\%$, we get the previous results given in Table 11.20. When $g_Y > 0$, the estimated carbon budget is higher. For example, if $\mathcal{R}^-_{\mathcal{CI}} = 30\%$ and $\Delta\mathcal{R}_{\mathcal{CI}} = 7\%$, the carbon budget is equal to $540\,GtCO_2e$ if $g_Y = 5\%$ while it is equal to $308\,GtCO_2e$ if $g_Y = 0\%$. Therefore, we need to use a more aggressive decarbonization pathway for carbon intensity than for carbon emissions.

To satisfy a given carbon budget $\mathcal{CB}(t_0, t)$, we can calibrate a decarbonization pathway in terms of carbon emissions or in terms of carbon intensity. In the first case, we can approximate the integral by the finite sum:

$$\mathcal{CB}(t_0, t) \approx \sum_{t_i=t_0+1}^{t} \mathcal{CE}(t_i)$$

Table 11.21: Carbon budget $\mathcal{CB}(2020, 2050)$ (in $GtCO_2e$) when defining the decarbonization pathway of carbon intensity

| $\mathcal{R}^-_{\mathcal{CI}}$ | | 0% | 10% | 20% | 30% | 50% | 75% | 0% | 10% | 20% | 30% | 50% | 75% |
|---|---|---|---|---|---|---|---|---|---|---|---|---|---|
| | | $g_Y = 1\%$ | | | | | | $g_Y = 3\%$ | | | | | |
| $\Delta\mathcal{R}_{\mathcal{CI}}$ | 5% | 619 | 557 | 495 | 433 | 309 | 155 | 793 | 714 | 635 | 555 | 397 | 198 |
| | 6% | 547 | 493 | 438 | 383 | 274 | 137 | 691 | 622 | 553 | 484 | 346 | 173 |
| | 7% | 487 | 438 | 390 | 341 | 244 | 122 | 607 | 546 | 485 | 425 | 303 | 152 |
| | 8% | 436 | 392 | 349 | 305 | 218 | 109 | 536 | 482 | 429 | 375 | 268 | 134 |
| | 9% | 393 | 353 | 314 | 275 | 196 | 98 | 476 | 429 | 381 | 333 | 238 | 119 |
| | 10% | 356 | 320 | 285 | 249 | 178 | 89 | 426 | 383 | 341 | 298 | 213 | 107 |
| | | $g_Y = 5\%$ | | | | | | $g_Y = 10\%$ | | | | | |
| $\Delta\mathcal{R}_{\mathcal{CI}}$ | 5% | 1040 | 936 | 832 | 728 | 520 | 260 | 2245 | 2021 | 1796 | 1572 | 1123 | 561 |
| | 6% | 893 | 804 | 715 | 625 | 447 | 223 | 1859 | 1673 | 1487 | 1301 | 930 | 465 |
| | 7% | 772 | 695 | 618 | 540 | 386 | 193 | 1549 | 1394 | 1239 | 1084 | 774 | 387 |
| | 8% | 672 | 605 | 538 | 470 | 336 | 168 | 1299 | 1169 | 1039 | 909 | 649 | 325 |
| | 9% | 589 | 530 | 471 | 412 | 295 | 147 | 1096 | 987 | 877 | 767 | 548 | 274 |
| | 10% | 520 | 468 | 416 | 364 | 260 | 130 | 932 | 839 | 746 | 653 | 466 | 233 |

and choose a path $\{\mathcal{CE}(t_0+1), \ldots, \mathcal{CE}(t)\}$ that satisfies the carbon budget. We can also assume that $\mathcal{CE}(t) = (1-\Delta\mathcal{R}_{\mathcal{CE}})^{t-t_0}(1-\mathcal{R}^-_{\mathcal{CE}})\mathcal{CE}(t_0)$ and calibrate the parameters $(\mathcal{R}^-_{\mathcal{CE}}, \Delta\mathcal{R}_{\mathcal{CE}})$ such that they satisfy the inequality:

$$\frac{(1-\Delta\mathcal{R}_{\mathcal{CE}})^{t-t_0}-1}{\ln(1-\Delta\mathcal{R}_{\mathcal{CE}})}(1-\mathcal{R}^-_{\mathcal{CE}})\mathcal{CE}(t_0) \leq \mathcal{CB}(t_0,t)$$

We remark that:

$$\frac{(1-\Delta\mathcal{R}_{\mathcal{CE}})^{t-t_0}-1}{\ln(1-\Delta\mathcal{R}_{\mathcal{CE}})} \leq \frac{1}{1-\mathcal{R}^-_{\mathcal{CE}}}\frac{\mathcal{CB}(t_0,t)}{\mathcal{CE}(t_0)} \tag{11.15}$$

This means that the solution does not depend on the absolute value of the carbon budget, but on the ratio of the carbon budget to current emissions. In the second case, we assume that $g_Y$ is given and calibrate the parameters $(\mathcal{R}^-_{\mathcal{CI}}, \Delta\mathcal{R}_{\mathcal{CI}})$ in the same way:

$$\frac{(1-\Delta\mathcal{R}_{\mathcal{CI}})^{t-t_0}-1}{\ln(1+g_Y)+\ln(1-\Delta\mathcal{R}_{\mathcal{CI}})} \leq \frac{1}{(1+g_Y)^{t-t_0}(1-\mathcal{R}^-_{\mathcal{CI}})}\frac{\mathcal{CB}(t_0,t)}{\mathcal{CE}(t_0)} \tag{11.16}$$

**Example 52** *We want to reduce the carbon emissions by* 400% *from* $t_0 = 2020$ *to* $t = 2050$. *We assume that* $\mathcal{R}^-_{\mathcal{CE}} = \mathcal{R}^-_{\mathcal{CI}} = 0$ *and* $g_Y = 3\%$.

We have:

$$\frac{(t-t_0)\mathcal{CE}(t_0)}{\mathcal{CB}(t_0,t)} = 400\% \Leftrightarrow \frac{\mathcal{CB}(t_0,t)}{\mathcal{CE}(t_0)} = \frac{30}{4} = 7.5$$

because $t - t_0$ is equal to 30 years. The numerical solution to Equation (11.15) is $\Delta\mathcal{R}_{\mathcal{CE}} = 5.88\%$. It follows that:

$$\begin{aligned}(1-\Delta\mathcal{R}_{\mathcal{CE}}) = (1+g_Y)(1-\Delta\mathcal{R}_{\mathcal{CI}}) &\Leftrightarrow \Delta\mathcal{R}_{\mathcal{CI}} = 1-\left(\frac{1-\Delta\mathcal{R}_{\mathcal{CE}}}{1+g_Y}\right)\\ &\Leftrightarrow \Delta\mathcal{R}_{\mathcal{CI}} = 1-\left(\frac{1-5.88\%}{1+3\%}\right) = 8.62\%\end{aligned}$$

We check that this is the solution of Equation (11.16).

### Dynamic decarbonization and portfolio alignment

**General framework** While the decarbonization problem finds an optimal portfolio $w^\star(\boldsymbol{\mathcal{R}})$ with respect to a given reduction rate $\boldsymbol{\mathcal{R}}$, the alignment problem defines an optimal portfolio $w^\star(t)$ with respect to a given date $t$. Therefore, this second problem can be seen as a special case of the first problem, where we use the mapping function between the date $t$ and the reduction rate $\boldsymbol{\mathcal{R}}$. The inequality constraint $\boldsymbol{\mathcal{CI}}(w) \leq (1-\boldsymbol{\mathcal{R}})\,\boldsymbol{\mathcal{CI}}(b)$ becomes:

$$\boldsymbol{\mathcal{CI}}(t,w) \leq (1-\boldsymbol{\mathcal{R}}(t_0,t))\,\boldsymbol{\mathcal{CI}}(t_0,b(t_0)) \tag{11.17}$$

where $t_0$ is the base year, $\boldsymbol{\mathcal{R}}(t_0,t)$ is the decarbonization pathway of the NZE scenario and $\boldsymbol{\mathcal{CI}}(t_0,b(t_0))$ is the carbon intensity of the benchmark at time $t_0$. Portfolio alignment is the process of aligning the decarbonization rate of the portfolio $w^\star(t)$ with respect to the decarbonization pathway of the net-zero scenario. We have the following properties:

- Decarbonizing the aligned portfolio becomes easier over time as the benchmark decarbonizes itself:
$$\boldsymbol{\mathcal{CI}}(t,b(t)) \ll \boldsymbol{\mathcal{CI}}(t_0,b(t_0)) \qquad \text{for } t > t_0$$
- Decarbonizing the aligned portfolio becomes more difficult over time as the benchmark carbonizes itself:
$$\boldsymbol{\mathcal{CI}}(t,b(t)) \gg \boldsymbol{\mathcal{CI}}(t_0,b(t_0)) \qquad \text{for } t > t_0$$
- The aligned portfolio matches the benchmark portfolio if the benchmark is sufficiently decarbonized:
$$\boldsymbol{\mathcal{CI}}(t,b(t)) \leq (1-\boldsymbol{\mathcal{R}}(t_0,t))\,\boldsymbol{\mathcal{CI}}(t_0,b(t_0))$$

Since we have $\boldsymbol{\mathcal{CI}}(t,b(t)) = \sum_{i=1}^n \boldsymbol{\mathcal{CI}}_i(t)\,b_i(t)$, the decarbonization of a net-zero investment process is strongly influenced by two factors: changes in benchmark weights and changes in the carbon intensity of assets. In fact, we can imagine that the decarbonization process will become easier over time because the market capitalization of green assets will grow faster than the market capitalization of brown assets and/or because the global decarbonization of the world is well established and on the right track.

**Remark 126** *If we consider a carbon budget/emissions approach, we change the inequality constraint (11.17) by* $\boldsymbol{\mathcal{CE}}(t,w) \leq (1-\boldsymbol{\mathcal{R}}(t_0,t))\,\boldsymbol{\mathcal{CE}}(t_0,b(t_0))$ *or* $\boldsymbol{\mathcal{CB}}(t_0,t,w) \leq \boldsymbol{\mathcal{CB}}^\star(t_0,t)$ *where* $\boldsymbol{\mathcal{CB}}^\star(t_0,t)$ *is the carbon budget target at time* $t$*. In addition, we saw in the previous section that we can calibrate an intensity-based scenario from an emissions- or budget-based scenario.*

**Equity portfolios** Suppose the objective is to replicate a benchmark and to align the portfolio with a given scenario. The optimization problem becomes:

$$\begin{aligned} w^\star(t) &= \arg\min \frac{1}{2}(w-b(t))^\top \Sigma(t)\,(w-b(t)) \\ &\text{s.t.} \begin{cases} \boldsymbol{\mathcal{CI}}(t,w) \leq (1-\boldsymbol{\mathcal{R}}(t_0,t))\,\boldsymbol{\mathcal{CI}}(t_0,b(t_0)) \\ w \in \Omega_0 \cap \Omega \end{cases} \end{aligned} \tag{11.18}$$

where $\Omega_0 = \mathcal{C}_0 = \left\{w : \mathbf{1}_n^\top w = 1, \mathbf{0}_n \leq w \leq \mathbf{1}_n\right\}$ defines the long-only constraint and $\Omega$ is the set of additional constraints. Note that the benchmark $b(t)$, the covariance matrix $\Sigma(t)$, and the carbon intensity $\boldsymbol{\mathcal{CI}}(t,x)$ are functions of time $t$. This means that the data is updated each time we rebalance the portfolio[29].

[29] For example, at time $t+1$, the optimization problem depends on the data available at that time, not the data available at time $t$ in the past.

**Example 53** *We consider Example 50. We want to align the portfolio with respect to the CTB scenario. To compute the optimal portfolio* $w^\star(t)$ *where* $t = t_0 + h$ *and* $h = 0, 1, 2, ...$ *years, we assume that the benchmark* $b(t)$*, the covariance matrix* $\Sigma(t)$*, and the vector* $\boldsymbol{\mathcal{CI}}(t)$ *of carbon intensities do not change over time.*

First, we compute the mapping function between the time $t$ and the decarbonization rate $\boldsymbol{\mathcal{R}}(t_0, t)$:

$$\boldsymbol{\mathcal{R}}(t_0, t) = 1 - (1 - 30\%) \times (1 - 7\%)^h$$

We get $\boldsymbol{\mathcal{R}}(t_0, t_0) = 30\%$, $\boldsymbol{\mathcal{R}}(t_0, t_0 + 1) = 34.90\%$, $\boldsymbol{\mathcal{R}}(t_0, t_0 + 2) = 39.46\%$, and so on. Second, we solve the optimization problem (11.18) for the different values of time $t$. The results are shown in Table 11.22.

Table 11.22: Equity portfolio alignment (Example 53)

| $t$ | $b(t_0)$ | $t_0$ | $t_0+1$ | $t_0+2$ | $t_0+3$ | $t_0+4$ | $t_0+5$ | $t_0+10$ |
|---|---|---|---|---|---|---|---|---|
| $w_1^\star$ | 20.00 | 21.86 | 22.21 | 22.54 | 22.84 | 23.02 | 22.92 | 8.81 |
| $w_2^\star$ | 19.00 | 18.70 | 18.41 | 18.15 | 17.90 | 17.58 | 17.04 | 0.00 |
| $w_3^\star$ | 17.00 | 8.06 | 5.69 | 3.48 | 1.43 | 0.00 | 0.00 | 0.00 |
| $w_4^\star$ | 13.00 | 8.74 | 7.66 | 6.65 | 5.72 | 4.56 | 2.70 | 0.00 |
| $w_5^\star$ | 12.00 | 13.07 | 13.29 | 13.51 | 13.70 | 13.91 | 14.18 | 21.22 |
| $w_6^\star$ | 8.00 | 22.57 | 25.59 | 28.39 | 31.00 | 33.39 | 35.54 | 62.31 |
| $w_7^\star$ | 6.00 | 7.00 | 7.15 | 7.29 | 7.42 | 7.53 | 7.63 | 7.66 |
| $w_8^\star$ | 5.00 | 0.00 | 0.00 | 0.00 | 0.00 | 0.00 | 0.00 | 0.00 |
| $\sigma(w^\star \mid b(t))$ | 0.01 | 104.10 | 126.22 | 147.14 | 166.79 | 185.24 | 203.51 | 352.42 |
| $\boldsymbol{\mathcal{CI}}(t, w)$ | 160.57 | 112.40 | 104.53 | 97.22 | 90.41 | 84.08 | 78.20 | 54.40 |
| $\boldsymbol{\mathcal{R}}(w \mid b(t_0))$ | 0.00 | 30.00 | 34.90 | 39.46 | 43.70 | 47.64 | 51.30 | 66.12 |

The reduction rate and weights are expressed in %, while the tracking error volatility is measured in bps.

Instead of using the threshold approach, we can implement the order statistic or the naive approach when performing portfolio alignment. These approaches make sense because net-zero investing is an exclusion process, as shown by Barahhou *et al.* (2022). Examples of portfolio alignment based on order-statistic and naive approaches can be found in Jondeau *et al.* (2021), Bolton *et al.* (2022), and Ben Slimane *et al.* (2023b).

**Bond portfolios** For bonds, the tracking error volatility is replaced by the active risk function proposed by Barahhou *et al.* (2022):

$$\mathcal{D}(w \mid b) = \varphi \underbrace{\sum_{s=1}^{n_{Sector}} \left| \sum_{i \in s} (w_i - b_i) \, \mathrm{DTS}_i \right|}_{\text{DTS component}} + \underbrace{\frac{1}{2} \sum_{i \in b} |w_i - b_i|}_{\text{AS component}} + \underbrace{\mathbb{1}_{\Omega_{\mathrm{MD}}}(w)}_{\text{MD component}} \tag{11.19}$$

where $\mathrm{DTS}_i$ and $\mathrm{MD}_i$ are the duration-times-spread and modified duration factors, $\Omega_{\mathrm{MD}} = \{w : \sum_{i=1}^n (w_i - b_i) \, \mathrm{MD}_i = 0\}$ and $\mathbb{1}_\Omega(w)$ is the convex indicator function. The optimization problem becomes then:

$$\begin{aligned} w^\star(t) &= \arg\min \mathcal{D}(w \mid b(t)) \\ \text{s.t.} &\begin{cases} \boldsymbol{\mathcal{CI}}(t, w) \leq (1 - \boldsymbol{\mathcal{R}}(t_0, t)) \, \boldsymbol{\mathcal{CI}}(t_0, b(t_0)) \\ w \in \Omega_0 \cap \Omega \end{cases} \end{aligned} \tag{11.20}$$

Again, the benchmark $b(t)$ and the risk factors (modified duration, DTS, etc.) are functions of time $t$. To solve this mathematical problem, we transform it into a linear programming problem and use standard LP algorithms.

**Example 54** *We consider Example 51. We want to align the portfolio with respect to the CTB scenario. To compute the optimal portfolio $w^\star(t)$ where $t = t_0 + h$ and $h = 0, 1, 2, ...$ years, we assume that the benchmark, the modified duration and the duration-times-spread factors do not change over time.*

The corresponding LP problem is[30]:

$$\begin{aligned} x^\star &= \arg\min c^\top x \\ &\text{s.t.} \begin{cases} Ax = B \\ Cx \leq D \\ x^- \leq x \leq x^+ \end{cases} \end{aligned} \tag{11.21}$$

where $x = (w, \tau_w, \tau_{\text{DTS}})$ is a $18 \times 1$ vector. The $18 \times 1$ vector $c$ is equal to $\left(\mathbf{0}_8, \frac{1}{2}\mathbf{1}_8, \varphi\mathbf{1}_2\right)$. The equality constraint includes the convex indicator function $\mathbb{1}_{\Omega_{\text{MD}}}(w)$ and is defined by:

$$Ax = B \Leftrightarrow \begin{pmatrix} \mathbf{1}_8^\top & \mathbf{0}_8^\top & \mathbf{0}_2^\top \\ \text{MD}^\top & \mathbf{0}_8^\top & \mathbf{0}_2^\top \end{pmatrix} x = \begin{pmatrix} 1 \\ 5.476 \end{pmatrix}$$

The inequality constraints are:

$$Cx \leq D \Leftrightarrow \begin{pmatrix} I_8 & -I_8 & \mathbf{0}_{8,2} \\ -I_8 & -I_8 & \mathbf{0}_{8,2} \\ C_{\text{DTS}} & \mathbf{0}_{2,8} & -I_2 \\ -C_{\text{DTS}} & \mathbf{0}_{2,8} & -I_2 \\ \boldsymbol{\mathcal{CI}}(t)^\top & \mathbf{0}_{1,8} & 0 \end{pmatrix} x \leq \begin{pmatrix} b \\ -b \\ 192.68 \\ 108.37 \\ -192.68 \\ -108.37 \\ 160.574 \times (1 - \boldsymbol{\mathcal{R}}(t_0, t)) \end{pmatrix}$$

where:

$$C_{\text{DTS}} = \begin{pmatrix} 100 & 0 & 575 & 436 & 0 & 0 & 0 & 365 \\ 0 & 155 & 0 & 0 & 159 & 145 & 804 & 0 \end{pmatrix}$$

Finally, the bounds are $x^- = \mathbf{0}_{18}$ and $x^+ = \infty \cdot \mathbf{1}_{18}$. The solutions are shown in Table 11.23.

### Defining a net-zero investment policy

**General framework** As explained by Barahhou *et al.* (2022) and Ben Slimane *et al.* (2023b), net-zero investment policies must address two dimensions: portfolio alignment and financing the transition. Therefore, the set of constraints to be applied must include this second dimension:

$$\Omega = \Omega_{\text{alignment}} \cap \Omega_{\text{transition}}$$

where:

$$\Omega_{\text{alignment}} = \{w : \boldsymbol{\mathcal{CI}}(t, w) \leq (1 - \boldsymbol{\mathcal{R}}(t_0, t))\, \boldsymbol{\mathcal{CI}}(t_0, b(t_0))\}$$

[30] We use the LP framework and the transformation problem (11.8) defined on page 964.

Table 11.23: Bond portfolio alignment (Example 54)

| $t$ | $b(t_0)$ | $t_0$ | $t_0+1$ | $t_0+2$ | $t_0+3$ | $t_0+4$ | $t_0+5$ | $t_0+10$ |
|---|---|---|---|---|---|---|---|---|
| $w_1^\star$ | 20.00 | 20.00 | 20.00 | 20.00 | 13.98 | 17.64 | 16.02 | 5.02 |
| $w_2^\star$ | 19.00 | 13.99 | 17.79 | 19.00 | 19.00 | 19.00 | 19.00 | 19.00 |
| $w_3^\star$ | 17.00 | 25.43 | 20.96 | 17.78 | 17.00 | 13.64 | 11.65 | 4.61 |
| $w_4^\star$ | 13.00 | 0.00 | 0.00 | 0.00 | 0.00 | 0.00 | 0.00 | 0.00 |
| $w_5^\star$ | 12.00 | 28.97 | 30.71 | 35.84 | 43.52 | 48.80 | 53.33 | 71.37 |
| $w_6^\star$ | 8.00 | 8.00 | 8.00 | 5.67 | 6.46 | 0.92 | 0.00 | 0.00 |
| $w_7^\star$ | 6.00 | 3.61 | 2.53 | 1.70 | 0.04 | 0.00 | 0.00 | 0.00 |
| $w_8^\star$ | 5.00 | 0.00 | 0.00 | 0.00 | 0.00 | 0.00 | 0.00 | 0.00 |
| $\mathrm{AS}(w)$ | 0.00 | 25.40 | 22.68 | 24.62 | 31.52 | 36.80 | 41.33 | 59.37 |
| $\mathrm{MD}(w)$ | 5.48 | 5.48 | 5.48 | 5.48 | 5.48 | 5.48 | 5.48 | 5.48 |
| $\mathrm{DTS}(w)$ | 301.05 | 274.61 | 248.91 | 230.60 | 220.10 | 204.46 | 197.26 | 174.46 |
| $\mathcal{D}(w \mid b)$ | 0.00 | 0.39 | 0.49 | 0.60 | 0.72 | 0.85 | 0.99 | 1.57 |
| $\boldsymbol{\mathcal{CI}}(w)$ | 160.57 | 112.40 | 104.53 | 97.22 | 90.41 | 84.08 | 78.20 | 54.40 |
| $\boldsymbol{\mathcal{R}}(w \mid b)$ | 0.00 | 30.00 | 34.90 | 39.46 | 43.70 | 47.64 | 51.30 | 66.12 |

The reduction rate, weights, and active share metrics are expressed in %, the MD metrics are measured in years, and the DTS metrics are calculated in bps.

While specifying $\Omega_{\text{alignment}}$ is straightforward, specifying $\Omega_{\text{transition}}$ is more complex. Indeed, the goal of a net-zero investment policy is to participate in the transformation to a low-carbon economy. As explained in Chapter 15 of IPCC (2022), this transformation involves large programs of capital reallocation for the low-carbon transition. However, ensuring efficient capital allocation in line with climate targets is not an easy task. Therefore, the number of factors to define net-zero investments can be very large. Barahhou *et al.* (2022) considers three of them, which are:

1. The self-decarbonization of the portfolio;
2. The greenness of the portfolio;
3. The exclusion of net-zero "*enemies*" (free riders).

Therefore, we have:

$$\Omega_{\text{transition}} = \Omega_{\text{self-decarbonization}} \cap \Omega_{\text{greenness}} \cap \Omega_{\text{exclusion}}$$

**Self-decarbonization and endogeneity of the decarbonization pathway** In the context of a net-zero scenario, portfolio alignment is a dynamic approach to portfolio decarbonization. Most investors have solved this problem by considering a time-varying rate of carbon footprint reduction. In this case, the portfolio is periodically rebalanced to match the decarbonization pathway. This is what we have done in the previous paragraph. However, the decarbonization dimension of net-zero investing cannot be summarized by a sequence of decarbonization rates or a sequence of portfolio rebalancing. In fact, if net-zero investing consists of building successive independent portfolios, there is no mechanism that respects the endogenous aspect of the decarbonization pathway. In particular, if the time-varying decarbonization is due only to the rebalancing process, it is clear that the portfolio cannot claim to be net-zero. In fact, the endogenous aspect of the decarbonization pathway implies a self-decarbonization of the portfolio. Consider an example to illustrate the concept of self-decarbonization. Suppose the decarbonization rate at the beginning of year $t$ is 30%. For

the next year $t+1$, the goal is to achieve a decarbonization rate of 35%. Two extreme cases are considered below. In the first panel on the left, effective decarbonization of the portfolio at the end of the year is 25%, which means that the carbon footprint of the portfolio has increased. In this case, we need to rebalance the portfolio to reach the 35% level at the beginning of year $t+1$. This is the bad case because the self-decarbonization of the portfolio is zero. In the third panel on the right, the decarbonization rate of the portfolio is higher than 35% at the end of the year, which means that we do not need to rebalance the portfolio. This is the good case because the portfolio has decarbonized itself, meaning that the carbon footprint of the issuers in the portfolio is following a trajectory consistent with the net-zero scenario.

| | Bad case | Mixed case | Good case |
|---|---|---|---|
| Effective decarbonization | | | |
| at the beginning of the year $t$ | 30% | 30% | 30% |
| at the end of the year $t$ | 25% | 33% | 36% |
| Self-decarbonization | 0% | 3% | 6% |
| Relabancing requirement | 10% | 2% | 0% |

The previous example illustrates that we can always follow a decarbonization path by rebalancing the portfolio if it is composed of liquid assets, but this does not mean that the investment process is a net-zero investment policy. In particular, there are some financial businesses where it is difficult to rebalance the portfolio because the assets are not liquid, such as a portfolio of private equities, a portfolio of car insurance policies, or a portfolio of loans.

We therefore need to introduce an incentive mechanism to achieve a minimum level of self-decarbonization. The objective of the temperature ratings is precisely to assess an issuer's ability to adapt to a carbon emissions scenario. Implied temperature ratings can be seen as a synthetic scoring system based on the $\mathcal{PAC}$ framework (Le Guenedal *et al.*, 2022), which measures the (past) participation, ambition and credibility of the issuer[31]. As a temperature rating system is often perceived as a black box, we may consider a simplified approach that is more transparent. For example, we can use net-zero targets that have been approved and validated by a third party. Using a linear interpolation model, we can calculate the annual self-decarbonization rate of issuers and derive the self-decarbonization level of portfolios. This simple approach is limited for two reasons. First, the data is not homogeneous, as target dates and scopes may differ. Second, self-decarbonization cannot be calculated for issuers without a net-zero commitment or validation. Another approach is to focus on the first pillar, which is participation. In fact, participation is a technical term used to identify past self-decarbonization. This explains why carbon trends and carbon momentum measures are very important metrics for a net-zero investor. This is a way to introduce a dynamic approach to carbon footprints and move beyond current levels, which are a poor estimate of the issuer's finish line and an even poorer estimate of how quickly the issuer will get there.

Following Barahhou *et al.* (2022), we can specify the self-decarbonization constraint as follows:

$$\Omega_{\text{self-decarbonization}} = \{w : \boldsymbol{\mathcal{CM}}(t, w) \leq \boldsymbol{\mathcal{CM}}^{\star}(t)\}$$

where $\boldsymbol{\mathcal{CM}}(t, w)$ is the carbon momentum of the portfolio $w$ at time $t$ and $\boldsymbol{\mathcal{CM}}^{\star}(t)$ is the self-decarbonization minimum threshold. For example, if $\boldsymbol{\mathcal{CM}}^{\star}(t) = -3\%$, we expect to reduce the carbon footprint of the portfolio by 3% next year if the observed trend continues. By construction, carbon momentum is inherently a backward-looking approach to self-decarbonization that can be complemented by more forward-looking measures of self-decarbonization.

[31] See Section 9.3.2 on page 920.

**Green footprint** The second factor in the transition dimension is the greenness of the portfolio. In fact, to achieve a low-carbon economy by 2050, we need to reduce the carbon footprint, but we also need to improve the green intensity of the economy. This means that net-zero investing is not just a carbon footprint issue, it is also a green footprint issue, and these two concepts are different. The goal of the second factor is then to finance the transition to a low-carbon economy, or in other words, to reallocate capital investment to green activities. The greenness constraint can be written as follows:

$$\Omega_{\text{greenness}} = \{w : \boldsymbol{\mathcal{GI}}(t, w) \geq \boldsymbol{\mathcal{GI}}^{\star}(t)\}$$

where $\boldsymbol{\mathcal{GI}}(t, w)$ is the green intensity of the portfolio $w$ at time $t$ and $\boldsymbol{\mathcal{GI}}^{\star}(t)$ is the minimum threshold. In general, the absolute measure $\boldsymbol{\mathcal{GI}}^{\star}(t)$ is expressed as a relative value with respect to the benchmark:

$$\boldsymbol{\mathcal{GI}}^{\star}(t) = (1 + \boldsymbol{\mathcal{G}})\, \boldsymbol{\mathcal{GI}}(t, b(t))$$

where $\boldsymbol{\mathcal{G}}$ is the minimum growth value. For example, if $\boldsymbol{\mathcal{G}} = 100\%$, we want to improve the green footprint of the benchmark so that the green intensity of the portfolio is at least twice the green intensity of the benchmark[32].

**Remark 127** *Another approach is to use a greenness pathway* $\boldsymbol{\mathcal{GI}}^{\star}(t) = (1 + \boldsymbol{\mathcal{G}}(t_0, t))\, \boldsymbol{\mathcal{GI}}(t, b(t_0))$. *In this case,* $\Omega_{greenness}$ *and* $\Omega_{alignment}$ *are two symmetric constraints.*

The choice of green intensity is critical. In theory, we want to improve the future green footprint of the economy. Therefore, an appropriate measure would be a forward-looking metric. The ideal candidate is green capex because it measures current green investment. It is therefore a proxy for future green revenues. However, the scarcity and current robustness of green capex data is an obstacle. As a result, most investors prefer to use green revenue share.

**Net-zero exclusion policy** Any net-zero investment portfolio must include an exclusion policy, which may include sectors and/or issuers. Most asset owners and managers have a coal exclusion policy when implementing net-zero. Some may also include the fossil fuel sector. These sector exclusions are related to ESG exclusion strategies. As with ESG investing, investors also create an exclusion list of issuers. In some cases, the net-zero exclusion list is the same as the ESG exclusion list, but in most cases, the net-zero exclusion list is specific. The criteria can be the issuer's carbon emissions or intensity relative to the sector, but the most popular metric is the temperature score. For example, an issuer will often be excluded if its temperature score is above a cap threshold, such as 4 or 5 degrees Celsius. The rationale is to exclude issuers that are not willing to participate in the net-zero journey. In the same spirit as the temperature score, Barahhou *et al.* (2022) suggests excluding issuers whose carbon momentum is greater than a threshold $\boldsymbol{\mathcal{CM}}^{+}$:

$$\Omega_{\text{exclusion}} = \left\{w : \boldsymbol{\mathcal{CM}}_i \geq \boldsymbol{\mathcal{CM}}^{+} \Rightarrow w_i = 0\right\}$$

Again, the underlying rationale is to measure the willingness of issuers to follow a net-zero scenario, and to exclude issuers who have not played the game in the past. For example, if $\boldsymbol{\mathcal{CM}}^{+} = 10\%$, we exclude issuers that have recently increased their carbon footprint by more than 10%. On page 928 we have seen that the proportion of excluded issuers can be high, especially if we consider carbon emissions.

**Remark 128** *To manage the self-decarbonization of the portfolio or to define the exclusion list, it is better to use the long-term carbon momentum than the short-term carbon momentum.*

[32] $\boldsymbol{\mathcal{G}} = 100\%$ is the standard measure in the ETF market.

**Equity portfolios** The optimization problem (11.18) on page 997 becomes:

$$
\begin{aligned}
w^\star(t) &= \arg\min \frac{1}{2}(w - b(t))^\top \Sigma(t)(w - b(t)) \qquad (11.22)\\
\text{s.t.} &\begin{cases}
\boldsymbol{\mathcal{CI}}(t,w) \leq (1 - \boldsymbol{\mathcal{R}}(t_0,t))\,\boldsymbol{\mathcal{CI}}(t_0,b(t_0)) & \leftarrow \text{Alignment}\\
\boldsymbol{\mathcal{CM}}(t,w) \leq \boldsymbol{\mathcal{CM}}^\star(t) & \leftarrow \text{Self-decarbonization}\\
\boldsymbol{\mathcal{GI}}(t,w) \geq (1+\mathcal{G})\,\boldsymbol{\mathcal{GI}}(t,b(t)) & \leftarrow \text{Greenness}\\
0 \leq w_i \leq \mathbb{1}\left\{\boldsymbol{\mathcal{CM}}_i(t) \leq \boldsymbol{\mathcal{CM}}^+\right\} & \leftarrow \text{Exclusion}\\
w \in \Omega_0 \cap \Omega & \leftarrow \text{Other constraints}
\end{cases}
\end{aligned}
$$

We deduce that the quadratic form is $Q = \Sigma(t)$, $R = \Sigma(t)\,b(t)$, $A = \mathbf{1}_n^\top$, $B = 1$, $w^- = \mathbf{0}_n$, $w^+ = \mathbf{1}\left\{\boldsymbol{\mathcal{CM}}(t) \leq \boldsymbol{\mathcal{CM}}^+\right\}$ and:

$$
Cw \leq D \Leftrightarrow \begin{pmatrix} \boldsymbol{\mathcal{CI}}(t)^\top \\ \boldsymbol{\mathcal{CM}}(t)^\top \\ -\boldsymbol{\mathcal{GI}}(t)^\top \end{pmatrix} w \leq \begin{pmatrix} (1 - \boldsymbol{\mathcal{R}}(t_0,t))\,\boldsymbol{\mathcal{CI}}(t_0,b(t_0)) \\ \boldsymbol{\mathcal{CM}}^\star(t) \\ -(1+\mathcal{G})\,\boldsymbol{\mathcal{GI}}(t,b(t)) \end{pmatrix}
$$

Here, we assume that the carbon momentum function is a linear function:

$$
\boldsymbol{\mathcal{CM}}(t,w) = w^\top \boldsymbol{\mathcal{CM}}(t) = \sum_{i=1}^n w_i \boldsymbol{\mathcal{CM}}_i(t)
$$

where $\boldsymbol{\mathcal{CM}}(t) = (\boldsymbol{\mathcal{CM}}_1(t), \ldots, \boldsymbol{\mathcal{CM}}_n(t))$ is the carbon momentum vector.

**Remark 129** *In the previous optimization problem, the carbon momentum constraint can be replaced by a temperature constraint* $\boldsymbol{\mathcal{TS}}(t,w) \leq \boldsymbol{\mathcal{TS}}^\star(t)$ *where* $\boldsymbol{\mathcal{TS}}(t,w) = w^\top \boldsymbol{\mathcal{TS}}(t) = \sum_{i=1}^n w_i \boldsymbol{\mathcal{TS}}_i(t)$ *and* $\boldsymbol{\mathcal{TS}}_i(t)$ *is the temperature score of issuer* $i$*.*

Note that the aggregation of the carbon momentum or temperature score at the portfolio level uses the weighted average approach, as does the WACI formulation for carbon intensity. If we use long-term carbon momentum estimated with a linear trend model, we can perform an exact calculation of the carbon momentum at the portfolio level. Using the results in Box 11.2, we have:

$$
\begin{aligned}
\boldsymbol{\mathcal{CM}}(t,w) \leq \boldsymbol{\mathcal{CM}}^\star(t) &\Leftrightarrow \sum_{i=1}^n \tilde{w}_i \boldsymbol{\mathcal{CM}}_i(t) \leq \boldsymbol{\mathcal{CM}}^\star(t)\\
&\Leftrightarrow \sum_{i=1}^n \frac{w_i \boldsymbol{\mathcal{CI}}_i(t)}{\sum_{j=1}^n w_j \boldsymbol{\mathcal{CI}}_j(t)} \boldsymbol{\mathcal{CM}}_i(t) \leq \boldsymbol{\mathcal{CM}}^\star(t)\\
&\Leftrightarrow \sum_{i=1}^n w_i \boldsymbol{\mathcal{CI}}_i(t)\,\boldsymbol{\mathcal{CM}}_i(t) \leq \sum_{j=1}^n w_j \boldsymbol{\mathcal{CI}}_j(t)\,\boldsymbol{\mathcal{CM}}^\star(t)\\
&\Leftrightarrow \sum_{i=1}^n w_i \boldsymbol{\mathcal{CI}}_i(t)\,(\boldsymbol{\mathcal{CM}}_i(t) - \boldsymbol{\mathcal{CM}}^\star(t)) \leq 0\\
&\Leftrightarrow \sum_{i=1}^n w_i \zeta_i \leq 0
\end{aligned}
$$

where:

$$
\zeta_i = \boldsymbol{\mathcal{CI}}_i(t)\,(\boldsymbol{\mathcal{CM}}_i(t) - \boldsymbol{\mathcal{CM}}^\star(t))
$$

Box 11.2: Carbon momentum aggregation at the portfolio level

We recall that $\boldsymbol{\mathcal{CM}}_i^{\mathcal{L}ong}(t) = \dfrac{\hat{\beta}_{i,1}(t)}{\boldsymbol{\mathcal{CI}}_i(t)}$ where $i$ is the issuer, $\boldsymbol{\mathcal{CI}}_i(t)$ is the carbon intensity, and $\hat{\beta}_{i,1}(t)$ is the slope of the linear trend model:

$$\widehat{\boldsymbol{\mathcal{CI}}}_i(t) = \hat{\beta}_{i,0}(t) + \hat{\beta}_{i,1}(t)(t - t_0)$$

The carbon intensity of the portfolio is given by its weighted average: $\boldsymbol{\mathcal{CI}}(t,w) = \sum_{i=1}^n w_i \boldsymbol{\mathcal{CI}}_i(t)$. This follows:

$$\begin{aligned}
\widehat{\boldsymbol{\mathcal{CI}}}(t,w) &= \sum_{i=1}^n w_i \widehat{\boldsymbol{\mathcal{CI}}}_i(t) \\
&= \sum_{i=1}^n w_i \hat{\beta}_{i,0}(t) + \underbrace{\sum_{i=1}^n w_i \hat{\beta}_{i,1}(t)}_{\hat{\beta}_1(t,w)}(t - t_0)
\end{aligned}$$

where $\hat{\beta}_1(t,w) = \sum_{i=1}^n w_i \hat{\beta}_{i,1}(t)$. We deduce that:

$$\begin{aligned}
\boldsymbol{\mathcal{CM}}^{\mathcal{L}ong}(t,w) &= \frac{\hat{\beta}_1(t,w)}{\boldsymbol{\mathcal{CI}}(t,w)} \\
&= \frac{\sum_{i=1}^n w_i \hat{\beta}_{i,1}(t)}{\sum_{i=1}^n w_i \boldsymbol{\mathcal{CI}}_i(t)} \\
&= \frac{\sum_{i=1}^n w_i \boldsymbol{\mathcal{CI}}_i(t)\, \boldsymbol{\mathcal{CM}}_i^{\mathcal{L}ong}(t)}{\sum_{i=1}^n w_i \boldsymbol{\mathcal{CI}}_i(t)} \\
&= \sum_{i=1}^n \tilde{w}_i \boldsymbol{\mathcal{CM}}_i^{\mathcal{L}ong}(t)
\end{aligned}$$

where the adjusted weight $\tilde{w}_i$ is equal to:

$$\tilde{w}_i = \frac{w_i \boldsymbol{\mathcal{CI}}_i(t)}{\sum_{j=1}^n w_j \boldsymbol{\mathcal{CI}}_j(t)}$$

We see that $\boldsymbol{\mathcal{CM}}^{\mathcal{L}ong}(t,w) \neq \sum_{i=1}^n w_i \boldsymbol{\mathcal{CM}}_i^{\mathcal{L}ong}(t)$. This aggregation method is also valid at the sector level by using the weight of each issuer in its respective sector.

The formulation of the QP problem remains the same, but the inequality constraints are changed:

$$Cw \leq D \Leftrightarrow \begin{pmatrix} \boldsymbol{\mathcal{CI}}(t)^\top \\ \zeta^\top \\ -\boldsymbol{\mathcal{GI}}(t)^\top \end{pmatrix} w \leq \begin{pmatrix} (1 - \boldsymbol{\mathcal{R}}(t_0,t))\, \boldsymbol{\mathcal{CI}}(t_0, b(t_0)) \\ 0 \\ -(1 + \boldsymbol{\mathcal{G}})\, \boldsymbol{\mathcal{GI}}(t, b(t)) \end{pmatrix}$$

where $\zeta = (\zeta_1, \ldots, \zeta_n)$.

If we define the carbon momentum by considering the log-linear trend model, we get $\boldsymbol{\mathcal{CM}}_i^{\mathcal{L}ong}(t) = \hat{\gamma}_{i,1}(t)$. We cannot find an analytically exact formula $\hat{\gamma}_1(t,w)$ for the portfolio. Therefore, we use the weighted average approach:

$$\boldsymbol{\mathcal{CM}}(t,w) = \sum_{i=1}^n w_i \hat{\gamma}_{i,1}(t)$$

**Example 55** *We consider Example 53. The carbon momentum values are equal to* $-3.1\%$, $-1.2\%$, $-5.8\%$, $-1.4\%$, $+7.4\%$, $-2.6\%$, $+1.2\%$, *and* $-8.0\%$. *We measure the green intensity by the green revenue share. Its values are equal to* $10.2\%$, $45.3\%$, $7.5\%$, $0\%$, $0\%$, $35.6\%$, $17.8\%$ *and* $3.0\%$. *The net-zero investment policy imposes to follow the CTB decarbonization pathway with a self-decarbonization of* $3\%$, *and to improve the green intensity of the benchmark by* $100\%$.

The solutions of the QP optimization problem are shown in Table 11.24. The carbon momentum of the benchmark is $\boldsymbol{\mathcal{CM}}(t_0, b) = -1.66\%$, which is not enough to ensure a self-decarbonization of 3%. The green intensity of the benchmark is $\boldsymbol{\mathcal{GI}}(t_0, b) = 15.99\%$, which means that the green intensity target is 31.98%. If we consider the base date $t_0$, the solution has a lower carbon intensity than the target defined by the CTB decarbonization pathway, because the self-decarbonization and green intensity constraints imply a greater reduction in carbon footprint. We also note that there is no solution for the years $t_0 + 5$ and $t_0 + 10$.

Table 11.24: Net-zero equity portfolio (Example 55)

| $t$ | $b(t_0)$ | $t_0$ | $t_0+1$ | $t_0+2$ | $t_0+3$ | $t_0+4$ | $t_0+5$ | $t_0+10$ |
|---|---|---|---|---|---|---|---|---|
| $w_1^\star$ | 20.00 | 5.26 | 3.51 | 1.49 | 0.00 | 0.02 | | |
| $w_2^\star$ | 19.00 | 20.96 | 17.27 | 13.00 | 8.82 | 4.16 | | |
| $w_3^\star$ | 17.00 | 3.35 | 7.27 | 11.82 | 15.02 | 14.32 | | |
| $w_4^\star$ | 13.00 | 0.00 | 0.00 | 0.00 | 0.00 | 0.00 | No feasible | |
| $w_5^\star$ | 12.00 | 0.00 | 0.00 | 0.00 | 0.00 | 0.00 | solution | |
| $w_6^\star$ | 8.00 | 60.06 | 64.69 | 70.05 | 75.37 | 81.51 | | |
| $w_7^\star$ | 6.00 | 0.00 | 0.00 | 0.00 | 0.00 | 0.00 | | |
| $w_8^\star$ | 5.00 | 10.37 | 7.25 | 3.64 | 0.79 | 0.00 | | |
| $\sigma(w^\star \mid b(t))$ | 0.00 | 370.16 | 376.38 | 398.30 | 430.94 | 472.44 | | |
| $\boldsymbol{\mathcal{CI}}(t, w)$ | 160.57 | 110.85 | 104.53 | 97.22 | 90.41 | 84.08 | | |
| $\boldsymbol{\mathcal{R}}(w \mid b(t_0))$ | 0.00 | 30.96 | 34.90 | 39.46 | 43.70 | 47.64 | | |
| $\boldsymbol{\mathcal{CM}}(t, w)$ | −1.66 | −3.00 | −3.00 | −3.00 | −3.00 | −3.00 | | |
| $\boldsymbol{\mathcal{GI}}(t, w)$ | 15.99 | 31.98 | 31.98 | 31.98 | 31.98 | 31.98 | | |

The reduction rate, weights, carbon momentum and green intensity are expressed in %, while the tracking error volatility is measured in bps.

**Remark 130** *This example shows that there is not always a mathematical solution to the net-zero optimization problem when we stack many constraints. Moreover, even if there is a mathematical solution, it may not be investable due to poor liquidity or poor diversification. In this example, the net-zero portfolio is highly concentrated in the sixth asset. Of course, our example has only eight assets, so the net-zero portfolio can become concentrated very quickly. However, this drawback may be present if we also consider large equity universes such as the MSCI World. Therefore, there is a trade-off between the existence of the solution and the investability of the solution.*

**Bond portfolios** By introducing the transition constraints $\Omega_{\text{transition}}$, the optimization problem (11.20) becomes:

$$
\begin{aligned}
w^\star(t) \;=\; & \arg\min \mathcal{D}(w \mid b(t)) \\
& \text{s.t.} \begin{cases}
\boldsymbol{\mathcal{CI}}(t, w) \leq (1 - \boldsymbol{\mathcal{R}}(t_0, t))\, \boldsymbol{\mathcal{CI}}(t_0, b(t_0)) & \leftarrow \text{Alignment} \\
\boldsymbol{\mathcal{CM}}(t, w) \leq \boldsymbol{\mathcal{CM}}^\star(t) & \leftarrow \text{Self-decarbonization} \\
\boldsymbol{\mathcal{GI}}(t, w) \geq (1 + \boldsymbol{\mathcal{G}})\, \boldsymbol{\mathcal{GI}}(t, b(t)) & \leftarrow \text{Greenness} \\
0 \leq w_i \leq \mathbb{1}\left\{\boldsymbol{\mathcal{CM}}_i(t) \leq \boldsymbol{\mathcal{CM}}^+\right\} & \leftarrow \text{Exclusion} \\
w \in \Omega_0 \cap \Omega & \leftarrow \text{Other constraints}
\end{cases}
\end{aligned}
\tag{11.23}
$$

We get the same LP form except for the set of inequality constraints:

$$Cx \leq D \Leftrightarrow \begin{pmatrix} I_n & -I_n & \mathbf{0}_{n,n_{\mathcal{S}ector}} \\ -I_n & -I_n & \mathbf{0}_{n,n_{\mathcal{S}ector}} \\ C_{\text{DTS}} & \mathbf{0}_{n_{\mathcal{S}ector},n} & -I_{n_{\mathcal{S}ector}} \\ -C_{\text{DTS}} & \mathbf{0}_{n_{\mathcal{S}ector},n} & -I_{n_{\mathcal{S}ector}} \\ \boldsymbol{\mathcal{CI}}(t)^\top & \mathbf{0}_{1,n} & \mathbf{0}_{1,n_{\mathcal{S}ector}} \\ \boldsymbol{\mathcal{CM}}(t)^\top & \mathbf{0}_{1,n} & \mathbf{0}_{1,n_{\mathcal{S}ector}} \\ -\boldsymbol{\mathcal{GI}}(t)^\top & \mathbf{0}_{1,n} & \mathbf{0}_{1,n_{\mathcal{S}ector}} \end{pmatrix} x \leq \begin{pmatrix} b \\ -b \\ \text{DTS}^\star \\ -\text{DTS}^\star \\ (1-\boldsymbol{\mathcal{R}}(t_0,t))\,\boldsymbol{\mathcal{CI}}(t_0,b(t_0)) \\ \boldsymbol{\mathcal{CM}}^\star(t) \\ -(1+\boldsymbol{\mathcal{G}})\,\boldsymbol{\mathcal{GI}}(t,b(t)) \end{pmatrix}$$

and the upper bound: $x^+ = \left(\mathbb{1}\left\{\boldsymbol{\mathcal{CM}}(t) \leq \boldsymbol{\mathcal{CM}}^+\right\}, \infty \cdot \mathbf{1}_n, \infty \cdot \mathbf{1}_{n_{\mathcal{S}ector}}\right)$.

**Example 56** *We consider Example 54. The carbon momentum values are equal to* $-3.1\%$, $-1.2\%$, $-5.8\%$, $-1.4\%$, $+7.4\%$, $-2.6\%$, $+1.2\%$, *and* $-8.0\%$. *We measure the green intensity by the green revenue share. Its values are equal to* $10.2\%$, $45.3\%$, $7.5\%$, $0\%$, $0\%$, $35.6\%$, $17.8\%$ *and* $3.0\%$. *The net-zero investment policy imposes to follow the CTB decarbonization pathway with a self-decarbonization of* $2\%$, *and to improve the green intensity of the benchmark by* $100\%$.

The solutions of the LP optimization problem are shown in Table 11.25. Note that again there is no solution for some dates. In addition, compared to the net-zero equity portfolio exercise, we have changed the self-decarbonization target $\boldsymbol{\mathcal{CM}}^\star(t)$, which is equal to $-2\%$. Indeed, if we set $\boldsymbol{\mathcal{CM}}^\star(t) = -3\%$, we have no solution to the optimization problem even for the base date $t_0$.

Table 11.25: Net-zero bond portfolio (Example 56)

| $t$ | $b(t_0)$ | $t_0$ | $t_0+1$ | $t_0+2$ | $t_0+3$ | $t_0+4$ | $t_0+5$ | $t_0+10$ |
|---|---|---|---|---|---|---|---|---|
| $w_1^\star$ | 20.00 | 4.28 | 13.80 | 20.48 | 26.34 | 19.02 | | |
| $w_2^\star$ | 19.00 | 34.78 | 38.94 | 42.72 | 46.23 | 49.01 | | |
| $w_3^\star$ | 17.00 | 21.03 | 13.86 | 7.73 | 2.11 | 0.00 | | |
| $w_4^\star$ | 13.00 | 0.00 | 0.00 | 0.00 | 0.00 | 0.00 | No feasible | |
| $w_5^\star$ | 12.00 | 0.00 | 0.00 | 0.00 | 0.00 | 0.00 | solution | |
| $w_6^\star$ | 8.00 | 39.91 | 33.40 | 29.07 | 25.32 | 31.97 | | |
| $w_7^\star$ | 6.00 | 0.00 | 0.00 | 0.00 | 0.00 | 0.00 | | |
| $w_8^\star$ | 5.00 | 0.00 | 0.00 | 0.00 | 0.00 | 0.00 | | |
| AS $(w)$ | 0.00 | 51.72 | 45.34 | 45.27 | 50.89 | 53.98 | | |
| MD $(w)$ | 5.48 | 5.48 | 5.48 | 5.48 | 5.48 | 5.48 | | |
| DTS $(w)$ | 301.05 | 236.99 | 202.30 | 173.29 | 146.83 | 141.34 | | |
| $\mathcal{D}(w \mid b)$ | 0.00 | 0.87 | 0.95 | 1.09 | 1.28 | 1.48 | | |
| $\boldsymbol{\mathcal{CI}}(w)$ | 160.57 | 112.40 | 104.53 | 97.22 | 90.41 | 84.08 | | |
| $\boldsymbol{\mathcal{R}}(w \mid b)$ | 0.00 | 30.00 | 34.90 | 39.46 | 43.70 | 47.64 | | |
| $\boldsymbol{\mathcal{CM}}(t,w)$ | $-1.66$ | $-2.81$ | $-2.57$ | $-2.35$ | $-2.15$ | $-2.01$ | | |
| $\boldsymbol{\mathcal{GI}}(t,w)$ | 15.99 | 31.98 | 31.98 | 32.37 | 32.80 | 35.52 | | |

The reduction rate, weights, carbon momentum, green intensity and active share metrics are expressed in %, the MD metrics are measured in years, and the DTS metrics are calculated in bps.

### Empirical results

The following empirical results are taken from Barahhou *et al.* (2022) and Ben Slimane *et al.* (2023b). First, we examine the dynamic decarbonization of equity portfolios. In Figure 11.20, we show the relationship between time and tracking error volatility with respect to Scope emissions when

Figure 11.20: Tracking error volatility of dynamic decarbonized portfolios (MSCI World, June 2022, $\mathcal{C}_0$ constraint)

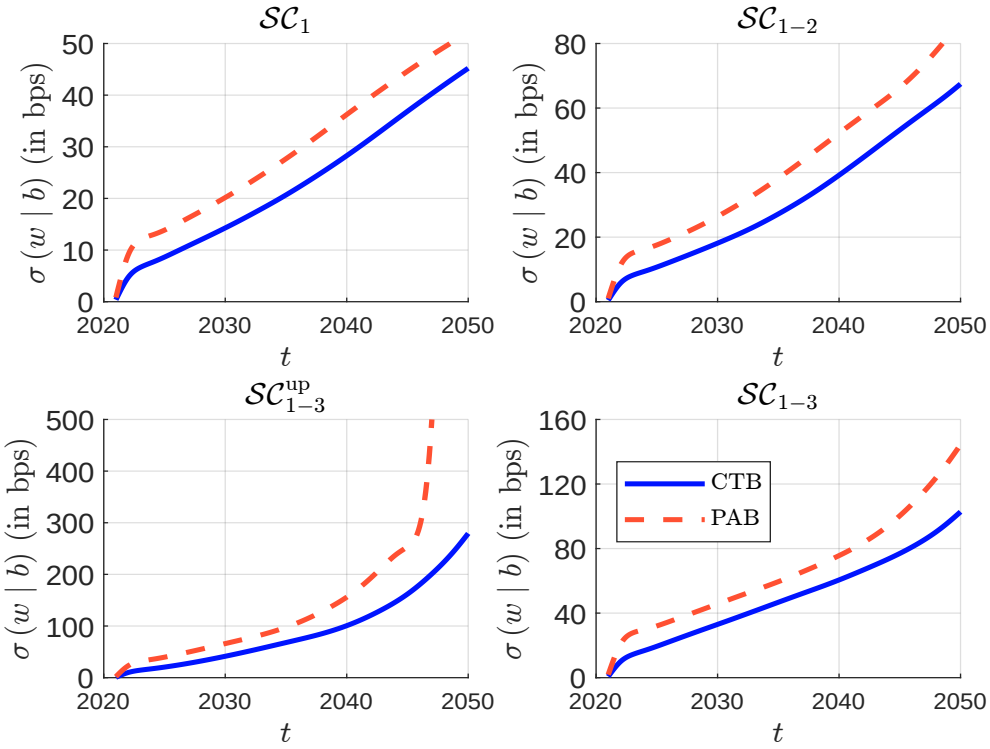


Figure 11.21: Tracking error volatility of dynamic decarbonized portfolios (MSCI World, June 2022, $\mathcal{C}_3(0, 10, 2)$ constraint)

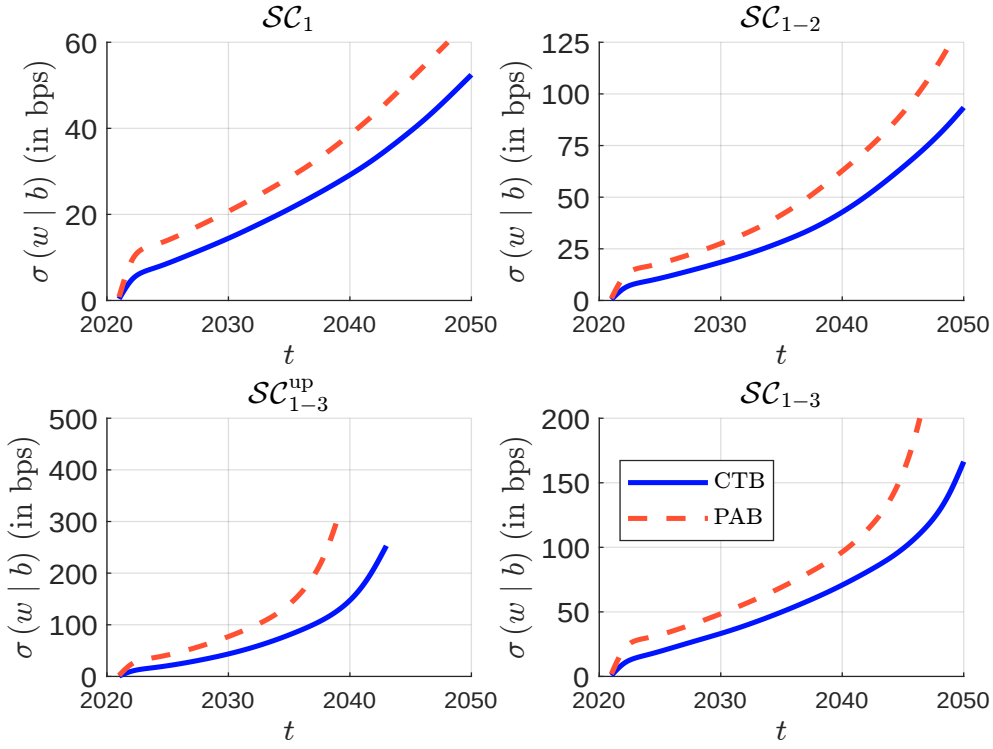


Source: MSCI (2022), Trucost (2022) & Barahhou *et al.* (2022).

considering the CTB and PAB decarbonization pathways and the MSCI World universe. Including Scope 3 has a significant impact on the tracking risk, especially when upstream Scope 3 emissions are considered. On average, the inclusion of Scope 3 results in a multiplication of the tracking error volatility by a factor of three. Barahhou *et al.* (2022) reported results considering the $\mathcal{C}_3(0,2,1)$ constraint, which imposes sector neutrality. They showed that the solution may not exist even before 2030 for the PAB decarbonization pathway. In order to have acceptable solutions, the ETF industry generally uses the $\mathcal{C}_3(0,10,2)$ constraint (Figure 11.21).

The previous analysis deals only with the decarbonization dimension. Barahhou *et al.* (2022) then introduced the transition dimension and solved the following optimization problem:

$$
\begin{aligned}
w^\star(t) &= \arg\min \frac{1}{2}(w-b(t))^\top \Sigma(t)(w-b(t)) \\
&\text{s.t.} \begin{cases}
\boldsymbol{\mathcal{CI}}(t,w) \leq (1-\boldsymbol{\mathcal{R}}(t_0,t))\,\boldsymbol{\mathcal{CI}}(t_0,b(t_0)) \\
\boldsymbol{\mathcal{CM}}(t,w) \leq \boldsymbol{\mathcal{CM}}^\star(t) \\
\boldsymbol{\mathcal{GI}}(t,w) \geq (1+\boldsymbol{\mathcal{G}})\,\boldsymbol{\mathcal{GI}}(t,b(t)) \\
w \in \mathcal{C}_0 \cap \mathcal{C}_3(0,10,2)
\end{cases}
\end{aligned}
$$

where $\boldsymbol{\mathcal{CM}}^\star(t) = -5\%$ and $\boldsymbol{\mathcal{G}} = 100\%$. In Figure 11.23, we plot the relationship between time $t$ and the tracking error volatility $\sigma(w^\star(t) \mid b(t))$, measured in bps, when considering the PAB decarbonization pathway[33]. We also report the decomposition between the decarbonization and transition dimensions. The results of these simulations clearly show that the transition dimension induces significant and additional costs. On average, we observe that the additional cost of the tracking error for the years 2022–2030 is 27, 25, 21 and 19 bps for Scopes $\boldsymbol{\mathcal{SC}}_1$, $\boldsymbol{\mathcal{SC}}_{1-2}$, $\boldsymbol{\mathcal{SC}}_{1-3}^{\text{up}}$ and $\boldsymbol{\mathcal{SC}}_{1-3}$, respectively. Moreover, there may be no solution to the optimization problem by 2050, especially if the carbon footprint is based on upstream/downstream Scope 3 emissions. Of course, all these results are very sensitive to the choice of the green multiplier $\boldsymbol{\mathcal{G}}$ and the carbon threshold $\boldsymbol{\mathcal{CM}}^\star$.

The previous results are valid for the MSCI World index, which is a large investment universe with more than 1 500 stocks. Let us focus on smaller investment universes by considering the MSCI EMU and USA indexes. The results are shown in Figures 11.24 and 11.25. The tracking error volatilities for smaller universes become larger in fewer years than for the MSCI World index, and we also fail to find solutions sooner. We could separate these results by putting the Scope 1 and 2 alignment on one side and Scope 3 on the other. Looking at Scopes 1 and 2, we see that in both universes the aligned portfolio breaks earlier than the MSCI World. However, even though the MSCI EMU universe is smaller than the MSCI USA universe, we can find solutions for a longer period of time. This is due to the distribution of green revenues and carbon dynamics, which are easier to reconcile with the intensity reduction constraint for the EMU. The inclusion of Scope 3 intensities paints a different picture. Although the EMU net-zero portfolios have lower tracking errors than the USA net-zero portfolios, larger universes tend to provide longer solutions. The fact that we are unable to align the EMU portfolio in terms of Scope 3 carbon intensities after 2040 therefore highlights the difficulty of portfolio alignment for a relatively small investment universe.

In practice, many constraints can be used to construct net-zero portfolios. We have seen above that the cost of tracking error can be significant and that the solution may not exist for long time horizons. Because the net-zero portfolio excludes some assets, it may be more concentrated than the benchmark. Therefore, we may face not only diversification risk, but also liquidity risk. These risks will be reduced as the economy decarbonizes in the coming years. However, we are not immune to

[33] To assess the impact of the weight/sector constraint $\mathcal{C}_3(0,10,2)$, we report the results based on the $\mathcal{C}_0$ constraint only in Figure 11.22.

Figure 11.22: Tracking error volatility of net-zero portfolios (MSCI World, June 2022, $\mathcal{C}_0$ constraint, $\boldsymbol{\mathcal{G}} = 100\%$, $\boldsymbol{\mathcal{CM}}^\star = -5\%$, PAB)

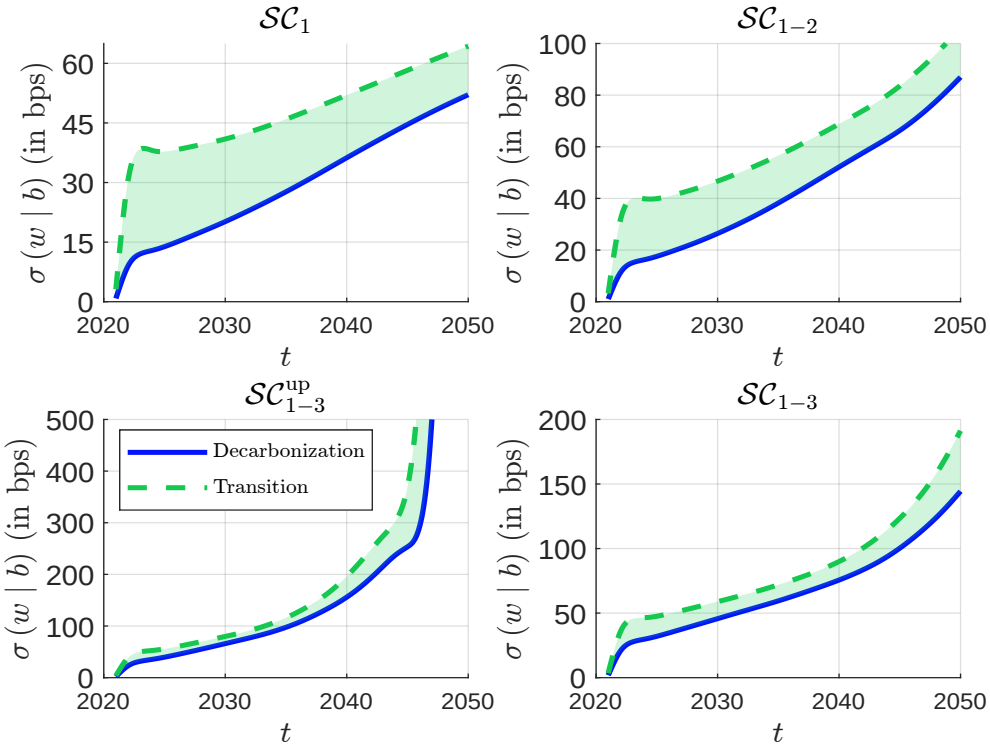


Figure 11.23: Tracking error volatility of net-zero portfolios (MSCI World, June 2022, $\mathcal{C}_3(0, 10, 2)$ constraint, $\boldsymbol{\mathcal{G}} = 100\%$, $\boldsymbol{\mathcal{CM}}^\star = -5\%$, PAB)

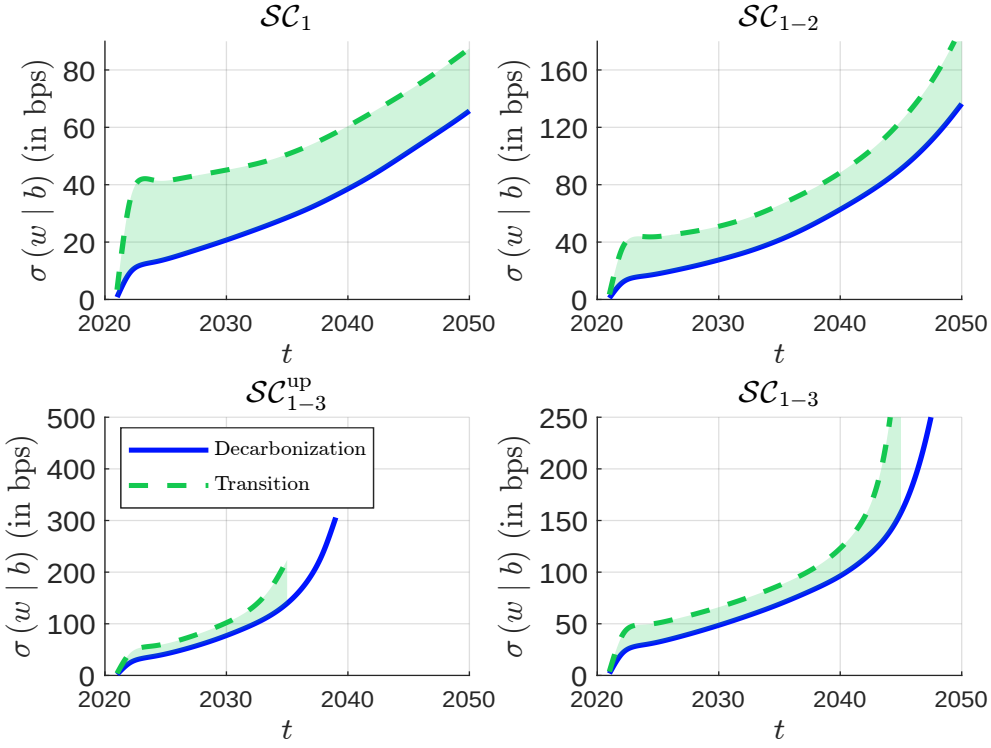


Source: MSCI (2022), Trucost (2022) & Barahhou *et al.* (2022).

Figure 11.24: Tracking error volatility of net-zero portfolios (MSCI EMU, June 2022, $\mathcal{C}_3\,(0, 10, 2)$ constraint, $\boldsymbol{\mathcal{G}} = 100\%$, $\boldsymbol{\mathcal{CM}}^\star = -5\%$, PAB)

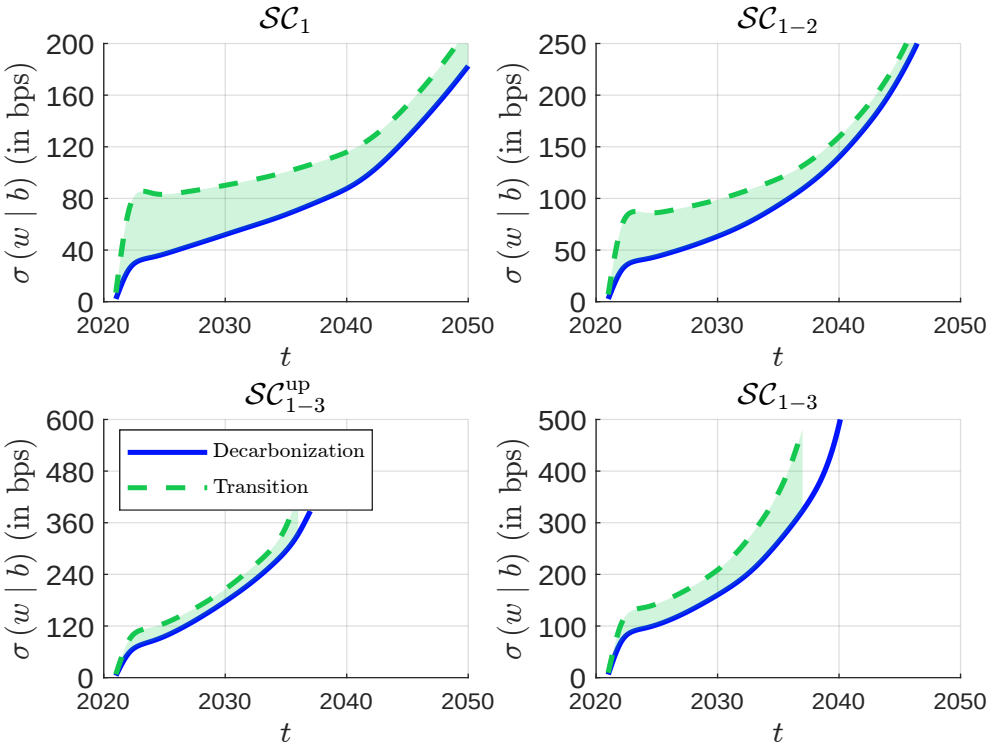


Figure 11.25: Tracking error volatility of net-zero portfolios (MSCI USA, Jun. 2022, $\mathcal{C}_3\,(0, 10, 2)$ constraint, $\boldsymbol{\mathcal{G}} = 100\%$, $\boldsymbol{\mathcal{CM}}^\star = -5\%$, PAB)

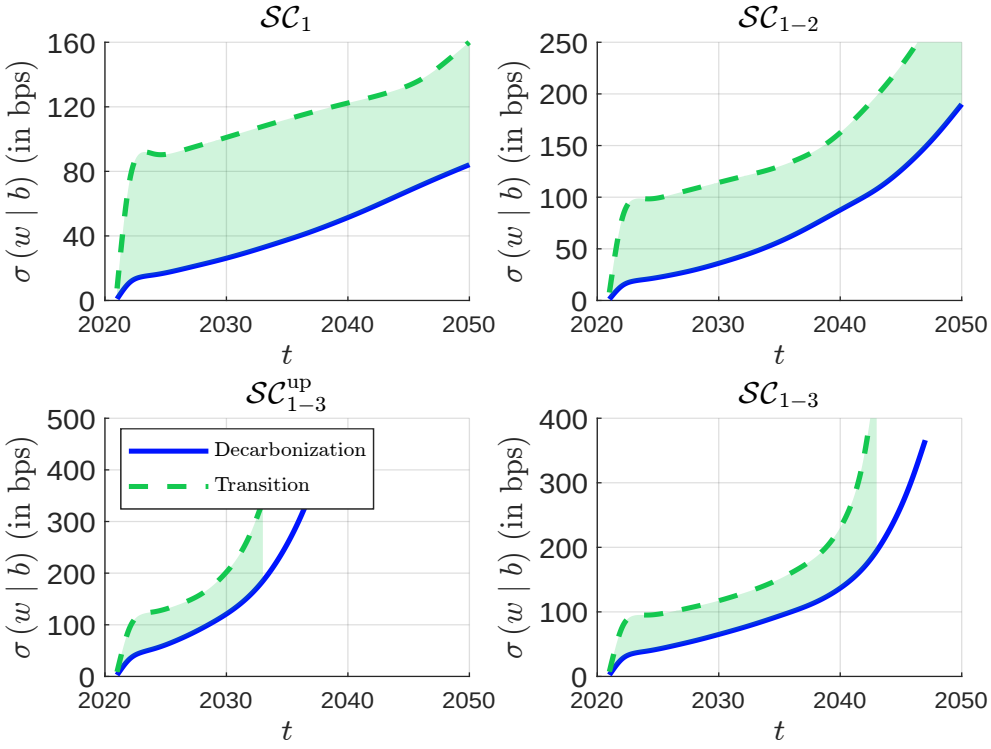


Source: MSCI (2022), Trucost (2022) & Barahhou *et al.* (2022).

the possibility that carbon emissions will continue to rise in the short term. In this case, solutions will be very sensitive to the gap between the carbon target of net-zero portfolios and the carbon footprint of the economy. To illustrate the shrinkage risk of the investment universe, we calculate the number of stocks selected per sector for each optimized portfolio and divide these figures by the corresponding number of stocks in the index[34]. In the case of Scope $\boldsymbol{\mathcal{SC}}_{1-3}$, the radar chart of these frequencies is shown in Figure 11.26. We observe that the investment universe is shrunk at the first date. The green area represents the removed part by 2030. With the exception of the communication services, financials, health care, information technology and real estate sectors, the investment in the other sectors is concentrated on few stocks. This shrinkage effect is also observed for small investment universes. By construction, the shrinkage of the investment universe worsens if we add other constraints. For instance, the impact of the momentum exclusion constraint is illustrated in Figure 11.27. In this case, we complete the set of constraints by the exclusion constraint $\{\boldsymbol{\mathcal{CM}}_i(t) \geq 0 \Rightarrow w_i = 0\}$, meaning that we exclude issuers with a positive carbon trend. We notice that the investment universe is highly reduced even from the first year. These results show that we cannot reduce the cost of net-zero investing to the cost of tracking risk. As seen above, there is also a cost of diversification risk. There is also a liquidity risk, as illustrated by Barahhou *et al.* (2022). Indeed, they showed that the repartition between large, mid and small caps changes. In some particular cases, they observed that the allocation to small- and micro-cap buckets increases over time.

Figure 11.26: Radar chart of investment universe shrinkage (MSCI World, June 2022, $\mathcal{C}_3(0, 10, 2)$ constraint, $\boldsymbol{\mathcal{G}} = 100\%$, $\boldsymbol{\mathcal{CM}}^\star = -5\%$, PAB, Scope $\boldsymbol{\mathcal{SC}}_{1-3}$)

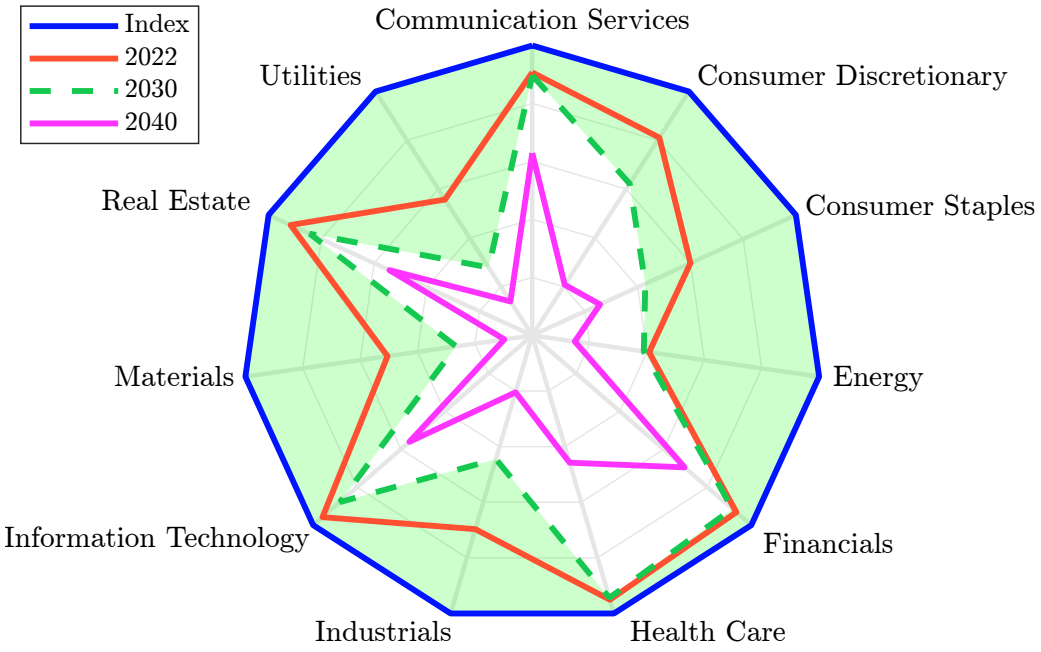


Source: MSCI (2022), Trucost (2022) & Barahhou *et al.* (2022).

[34]For example, if the frequency for the energy sector is 25%, this means that the optimized portfolio selected 25% of the energy stocks and removed 75% of the energy investment universe.

The results obtained by Barahhou *et al.* (2022) are based on simulations and do not take into account all the investment constraints that may be encountered in a net-zero portfolio, such as ESG constraints and the exclusion of some activities. Therefore, the estimated cost of tracking error risk can be viewed as a lower bound on the cost of real net-zero investing.

Figure 11.27: Impact of momentum exclusion on universe shrinkage (MSCI World, June 2022, $\mathcal{C}_3\,(0, 10, 2)$ constraint, $\boldsymbol{\mathcal{G}} = 100\%$, $\boldsymbol{\mathcal{CM}}^{\star} = -5\%$, PAB, Scope $\boldsymbol{\mathcal{SC}}_{1-3}$, $\boldsymbol{\mathcal{CM}}^{+} = 0\%$)

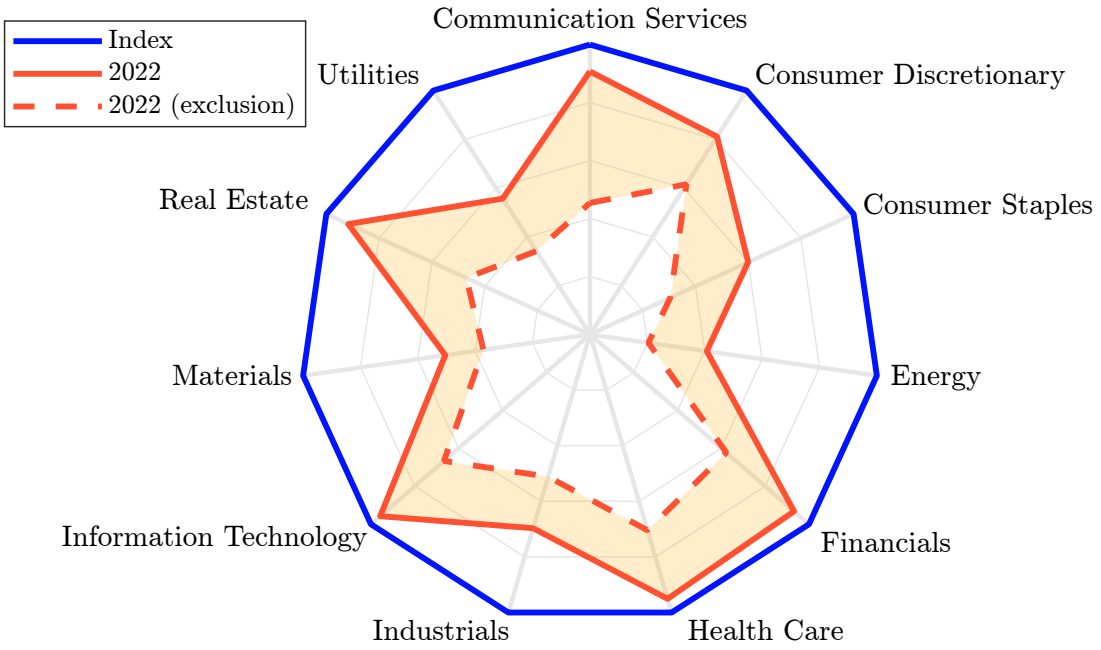


Source: MSCI (2022), Trucost (2022) & Barahhou *et al.* (2022).

We now turn to the case of corporate bonds. Using the CTB and PAB decarbonization scenarios, we get the results in Figures 11.28 and 11.29. The DTS risk is not significant and is less than 6 bps until 2030. This is not the case for the active share risk, which can reach 20% in 2030 for the PAB decarbonization pathway. When we include the transition constraints, the additional cost seems relatively low compared to what we have observed for equity investment universes. For example, Barahhou *et al.* (2022) found that the DTS tracking risk and active share increase by less than 1 bp and 1%, respectively, when $\boldsymbol{\mathcal{G}}$ is set to 100%. However, they found that the exclusion constraint can significantly increase costs. For example, requiring issuers to have a negative carbon momentum increases the tracking risk by 20% on average.

The case of government bonds is studied by Barahhou *et al.* (2023). As with corporate bonds, the integrated approach for sovereign bonds consists of several steps: (1) we need to define the decarbonization scenario at the country level; (2) we can assess the self-decarbonization of a country by considering the government's credible commitments and decarbonization plans towards a low-carbon economy; (3) a specific green intensity measure needs to measure the country's contribution to the climate transition and its greenness. Unlike corporate bonds, there are many options for choosing the net-zero scenario. We have already discussed some of them in Section 8.3.3 on page 781. We can choose between the IPCC scenarios, the NGFS scenarios, the IEA scenarios, etc. Barahhou *et*

Figure 11.28: Duration-times-spread cost of dynamically decarbonized portfolios (Global Corporate, June 2022)

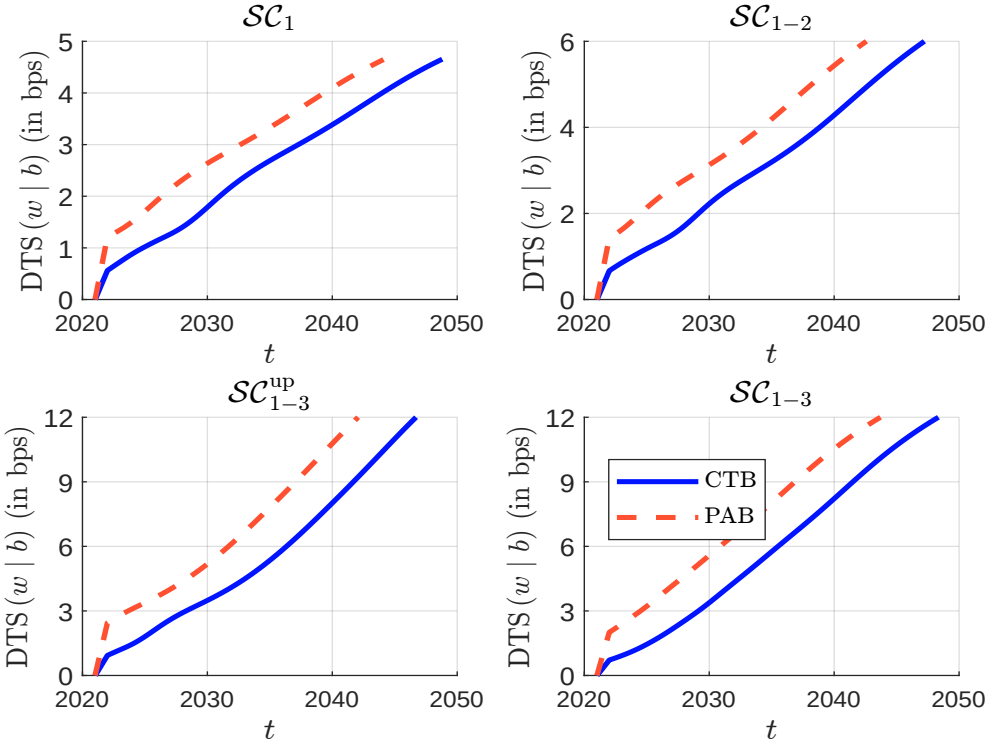


Figure 11.29: Active share of dynamically decarbonized portfolios (Global Corporate, June 2022)

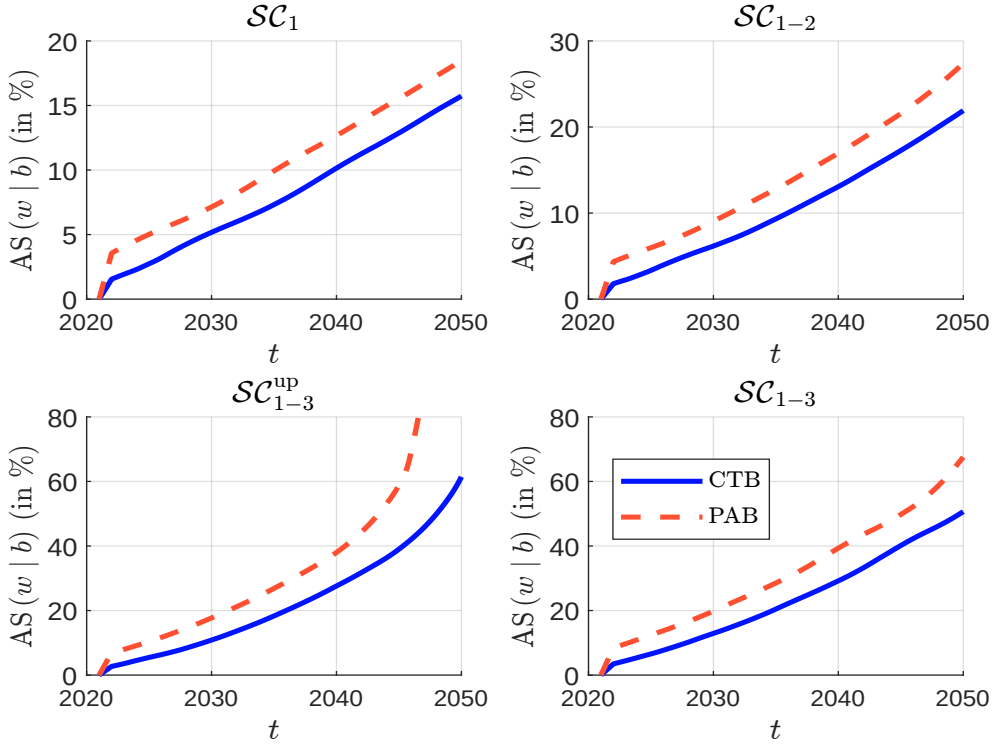


Source: ICE (2022), Trucost (2022) & Barahhou *et al.* (2022).

*al.* (2023) explained that the stated policies scenario (STEPS) and the announced pledges scenario (APS) cannot be used because they are not consistent with limiting global warming to 1.5°C. It is better to use the NZE scenarios from NGFS or IEA. Figure 11.30 shows the decarbonization pathway derived from the IEA NZE scenario (IEA, 2021, Figure 2.2, page 53). We distinguish between advanced economies, and emerging market and developing economies. Using 2020 as a baseline, the decarbonization pathways in terms of carbon emissions are similar for developed and developing countries. This is not the case when looking at carbon intensity, which corresponds to $CO_2$ emissions per capita.

Figure 11.30: IEA decarbonization pathways

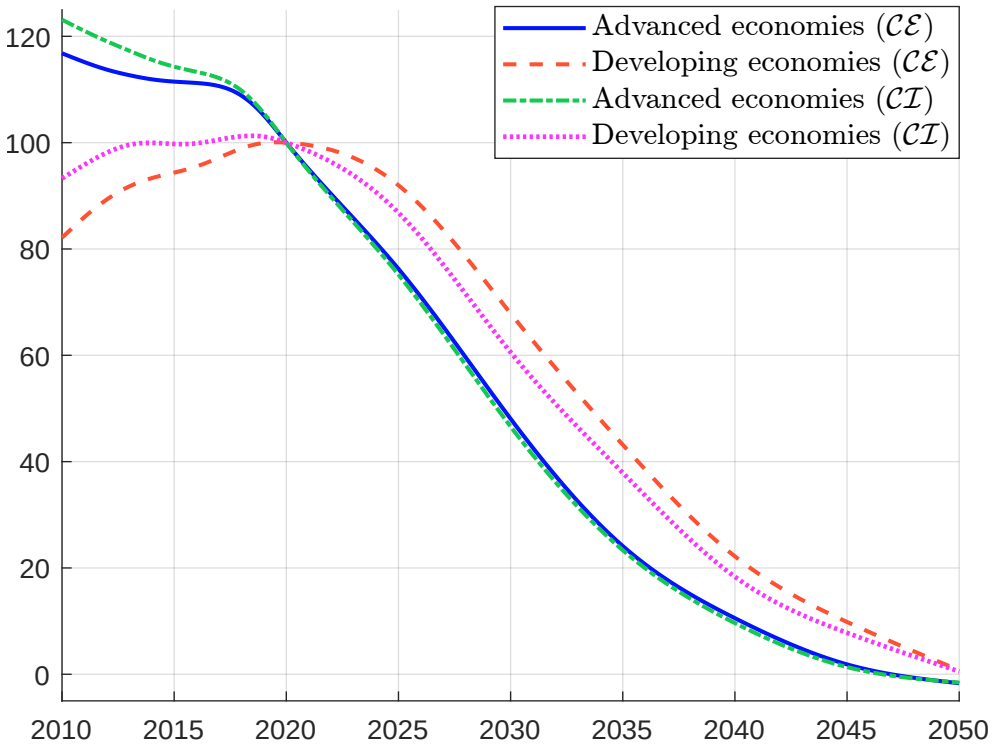


Choosing the scope of emissions and how to measure the carbon footprint is another important issue. As seen in Section 8.4.4 on page 836, we can define carbon emissions at the country level by considering a production-based or consumption-based inventory. If we prefer a carbon intensity measure, the normalization variable can be population, GDP, or public debt. Barahhou *et al.* (2023) showed that the distribution of carbon intensity metrics across countries is very different for these three measures. For the green footprint, they listed several metrics: government spending data[35] from the IEA, government spending on environmental protection[36] from the IMF's Climate Change Dashboard, the amount of green bonds issued, and environmental taxes[37] by country from the IMF's

[35]The website is https://www.iea.org/reports/government-energy-spending-tracker-2.

[36]This database contains the following seven time series: (1) Environmental protection expenditure, (2) Biodiversity and landscape protection expenditure, (3) Expenditure on environmental protection n.e.c., (4) Environmental protection R&D expenditure, (5) Pollution abatement expenditure, (6) Waste management expenditure and (7) Waste water management expenditure. The website for downloading the data is https://climatedata.imf.org/datasets/d22a6decd9b147fd9040f793082b219b_0/explore.

[37]This database contains the following five time series: (1) Environmental taxes, (2) Taxes on energy (including fuels for transport), (3) Taxes on pollution, (4) Taxes on resources and (5) Taxes on transport (excluding fuels for transport). The website for downloading the data is https://climatedata.imf.org/datasets/

Climate Change Dashboard. Using data on carbon emissions and commitments, they also derived four types of forward-looking metrics: (1) carbon trend, (2) nationally determined contribution (NDC), (3) NDC ambition, and (4) NDC fulfillment. In particular, Barahhou *et al.* (2023) defined two simple criteria:

- Commitments aligned with the NZE scenario (CAS) imply that countries have NDC target emissions that fall within a certain range around the value projected by the NZE scenario;
- Emissions on track with commitments (EOTC) indicate countries with historical trends in line with their NDC commitments.

These two metrics measure the ambition and credibility of the $\mathcal{PAC}$ framework. In Table 11.26, we report the CAS and EOTC statistics found by Barahhou *et al.* (2023). Only 6.6% of countries have sufficient ambition and credibility consistent with the NZE scenario, while about 70% of countries do not meet these two criteria.

Table 11.26: CAS and EOTC statistics on Bloomberg Global Aggregate Treasuries

| | | | | |
|---|---|---|---|---|
| CAS | ✓ | ✓ | | No criteria |
| EOTC | ✓ | | ✓ | met |
| Frequency | 6.6% | 23.3% | 0.7% | 69.5% |

Source: Barahhou *et al.* (2023, Figure 14, page 23).

Very quickly, there is no solution to the optimization problem after 2030, which means that the current ambitions of countries are not sufficient to build a net-zero sovereign bond portfolio in the long run. In Table 11.27, we report the authors' estimated first year of country exit for a given set of parameters and the GHG/GDP intensity metric. Some countries are removed from the portfolio in 2024 such as Canada, Indonesia, New Zealand and South Korea, but most of developed countries exit the portfolio in 2029. Changing the green constraint could delay the first year of exit by a year or two, but the problem is the constraint of the decarbonization pathway, which is impossible to manage after 2032.

Table 11.27: First year of country exit from the NZE investment portfolio (GHG/GDP intensity metric)

| | | | | | | | |
|---|---|---|---|---|---|---|---|
| Australia | 2025 | Finland | 2029 | Lithuania | 2025 | Romania | 2029 |
| Austria | 2029 | France | 2029 | Luxembourg | 2029 | Singapore | 2029 |
| Belgium | 2028 | Germany | 2029 | Mexico | 2029 | Slovakia | 2025 |
| Canada | 2024 | Hong Kong | 2029 | Malaysia | 2028 | Slovenia | 2028 |
| Chile | 2029 | Hungary | 2029 | Malta | 2029 | South Korea | 2024 |
| China | 2028 | Indonesia | 2024 | Netherlands | 2029 | Spain | 2028 |
| Colombia | 2029 | Ireland | 2029 | Norway | 2029 | Switzerland | 2029 |
| Cyprus | 2029 | Israel | 2029 | New Zealand | 2024 | Sweden | 2029 |
| Czechia | 2024 | Italy | 2029 | Peru | 2029 | Thailand | 2025 |
| Denmark | 2029 | Japan | 2029 | Poland | 2029 | United Kingdom | 2029 |
| Estonia | 2025 | Latvia | 2028 | Portugal | 2028 | United States | 2028 |

Source: Barahhou *et al.* (2023, Table 9, page 26).

`3fb1ed30d3394574b3145246846023b1_0/explore`.

Table 11.28: Country exclusion year by intensity metric

| Metric | GHG / GDP | GHG / Population | $CO_2$ (production) / GDP | $CO_2$ (consumption) / Population |
|---|---|---|---|---|
| China | 2028 | 2031 | 2027 | 2031 |
| France | 2029 | 2032 | 2027 | 2031 |
| Indonesia | 2024 | 2032 | 2024 | 2031 |
| Ireland | 2029 | 2030 | 2027 | 2030 |
| Japan | 2029 | 2032 | 2027 | 2031 |
| United States | 2028 | 2030 | 2026 | 2029 |
| United Kingdom | 2029 | 2032 | 2027 | 2031 |
| Sweden | 2029 | 2032 | 2027 | 2031 |

Source: Barahhou *et al.* (2023, Table 14, page 31).

The effect of the intensity metric is also significant. Table 11.28 shows when the country is removed from the NZE investment portfolio. We observe significant differences when we use GHG per GDP or GHG per capita. In addition, the use of a production-based or a consumption-based inventory also affects the results[38]. However, regardless of the metrics used, we generally found that a net-zero sovereign bond portfolio tended to overweight European countries.

The previous empirical results for equities, corporate bonds, and sovereign bonds suggest the following lessons. First, the solution is parameter and data sensitive. In particular, we need to be careful in choosing the carbon scope metric to assess the decarbonization rate. A net-zero investment policy only makes sense for a closed system. Therefore, Scope 3 emissions need to be taken into account to align a portfolio with a net-zero scenario. The problem is that we see a lack of data reliability on Scope 3 emissions today. Similarly, the solution is highly dependent on the green intensity target and the level of self-decarbonization we want to achieve. Then we have to be careful because there may be no solution to the optimization problem in the medium term. The question of no solution depends on the relative speed of the portfolio's decarbonization path relative to the economy's decarbonization path and the initial starting point. The second key finding is that portfolio alignment (or decarbonization) and net-zero construction lead to different solutions. In particular, decarbonizing a portfolio is easier than constructing a net-zero portfolio. We find that decarbonizing along CTB or PAB pathways never leads to exploding tracking errors by 2030. In fact, the real problem with decarbonization is the diversification and liquidity risk that an investor may face. These results are amplified when we add the transition dimension to the optimization program. In addition to higher tracking risk, there is no guarantee that there will always be a solution. Moreover, the introduction of the transition pillar highlights the difficulty of choosing an appropriate set of constraints for net-zero portfolios, as some metrics may be negatively correlated with others. Portfolio decarbonization is systematically a strategy that is long financial issuers and short energy, materials and utilities issuers. Therefore, we have a situation where the transition dimension of a decarbonized portfolio is weaker than that of the benchmark portfolio, as green solutions are also located in carbon-intensive sectors. It is therefore crucial to distinguish between issuers with a high carbon footprint that will not participate in the transition and those that will reduce their carbon emissions and find low-carbon solutions. The third key finding is that portfolio

[38] In this case, estimated metrics are generally available for $CO_2$ emissions than for all GHG emissions because consumption-based estimates are obtained with input-output analysis. In addition, it is traditionally accepted that the intensity measure uses GDP as the normalization variable for the production-based inventory, because it depends on national production, and the population for the consumption-based inventory, because it depends on population size.

decarbonization and alignment are two processes of exclusion. This means that it is quite impossible to achieve net-zero alignment without allowing the algorithm to exclude companies (or countries) from the benchmark. For example, the optimization program will generally not find a solution if it imposes non-zero lower bounds. As a result, some key players in the transition, such as energy and utility companies, unfortunately disappear. Furthermore, imposing sector neutrality can lead to similar problems in finding a solution. The final lesson is that it is easier to implement net-zero in bonds than in equities. At first glance, this result may seem surprising, since there is no reason why net-zero should affect the equity and bond markets differently. In fact, there are two possible explanations. First, the structure of equity and bond indexes is different, with the latter having a more balanced allocation across sectors and a high exposure to financial issuers. Second, bond indexes are strongly influenced by new fresh capital, while equity indexes are sticky to the stock of existing capital. This is because the primary bond market is very active, which implies a significant impact on the secondary market. Indeed, bonds mature and are replaced by new, greener bonds. The primary market then helps to achieve net-zero in bonds. This is not the case in the stock market, where IPOs and capital increases are only a small part of the secondary market. This means that portfolio holdings change faster for bond indexes than for equity indexes. Therefore, the greenness of bond indexes increases faster than the greenness of equity indexes. All of these factors suggests that the cost of implementing net-zero investments relative to traditional investments will be higher for equity portfolios than for bond portfolios, and that the bond market will benefit more quickly from the transition to a low-carbon economy.

### 11.3.2 Core-satellite approach

We have seen that the comprehensive integrated approach can sometimes be difficult to implement because today, on average, carbon intensities are positively correlated with green intensities. This means that the greenness of the economy is not necessarily found in companies with low carbon footprints. Therefore, a second approach has emerged that is easier to implement. It consists of adopting a core-satellite strategy, where decarbonization is applied to the core portfolio, while the objective of the satellite portfolio is to finance the transition to a low-carbon economy. In the financial literature, the core portfolio is called the net-zero decarbonization portfolio, while the satellite portfolio is called the net-zero contribution portfolio, but other terms are used, as shown in Table 11.29.

Table 11.29: The two building block approach

| Decarbonizing the portfolio | Financing the transition |
|---|---|
| • Net-zero decarbonization portfolio | • Net-zero contribution portfolio |
| • Net-zero transition portfolio | • Net-zero funding portfolio |
| • Dynamic low-carbon portfolio | • Net-zero transformation portfolio |

This is equivalent to splitting the problem into two sub-problems. The goal of the first sub-problem is to decarbonize and manage the carbon footprint of the investment. The goal of the second sub-problem is to contribute to increasing the green footprint of the economy. The two sub-problems are summarized in Table 11.30. The core portfolio is more of a top-down allocation process and exclusion strategy, where the central climate risk metric is carbon intensity. The satellite

portfolio is more of a bottom-up allocation process and asset selection strategy, where the central climate risk metric is green intensity. This approach also has the advantage of making the allocation between the two net-zero strategies clear. Of course, the allocation $\alpha(t)$ to the satellite can be dynamic and change over time as the world and economy progresses towards net-zero.

Table 11.30: The core-satellite approach

| Decarbonized portfolio | | Contribution portfolio |
|---|---|---|
| • Carbon intensity | | • Green intensity |
| • Decarbonization pathway | + | • Financing the transition |
| • Top-down approach | | • Bottom-up approach |
| • Portfolio construction | | • Security selection |
| • Net-zero carbon metrics | | • Net-zero transition metrics |
| $\mathbf{1-\alpha(t)}$ | | $\boldsymbol{\alpha(t)}$ |

### Core portfolio

The core portfolio is the largest part of the net-zero investment portfolio and the objective is to manage the decarbonization dimension. Therefore, only carbon metrics are used to assess the carbon footprint of the portfolio and its trajectory. If we write the alignment process in terms of portfolio optimization, a typical program for the equity bucket looks like this:

$$
\begin{aligned}
w^\star(t) &= \arg\min \frac{1}{2}(w - b(t))^\top \Sigma(t)(w - b(t)) \\
&\text{s.t.} \begin{cases} \boldsymbol{\mathcal{CI}}(t, w) \leq (1 - \boldsymbol{\mathcal{R}}(t_0, t))\, \boldsymbol{\mathcal{CI}}(t_0, b(t_0)) \\ \boldsymbol{\mathcal{CM}}(t, w) \leq \boldsymbol{\mathcal{CM}}^\star(t) \\ 0 \leq w_i \leq \mathbb{1}\left\{\boldsymbol{\mathcal{CM}}_i(t) \leq \boldsymbol{\mathcal{CM}}^+\right\} \\ w \in \Omega_0 \cap \Omega \end{cases}
\end{aligned} \tag{11.24}
$$

This is exactly the optimization problem defined in Equation (11.22), except that the green intensity constraints are removed because the green footprint is managed through the satellite portfolio. For the bond bucket, we get a similar optimization problem:

$$
\begin{aligned}
w^\star(t) &= \arg\min \mathcal{D}(w \mid b(t)) \\
&\text{s.t.} \begin{cases} \boldsymbol{\mathcal{CI}}(t, w) \leq (1 - \boldsymbol{\mathcal{R}}(t_0, t))\, \boldsymbol{\mathcal{CI}}(t_0, b(t_0)) \\ \boldsymbol{\mathcal{CM}}(t, w) \leq \boldsymbol{\mathcal{CM}}^\star(t) \\ 0 \leq w_i \leq \mathbb{1}\left\{\boldsymbol{\mathcal{CM}}_i(t) \leq \boldsymbol{\mathcal{CM}}^+\right\} \\ w \in \Omega_0 \cap \Omega \end{cases}
\end{aligned} \tag{11.25}
$$

In both cases, the implementation of the portfolio alignment process considers a global decarbonization scenario constraint, a self-decarbonization constraint, and an exclusion constraint. Ben Slimane *et al.* (2023b) also suggested that a number of specific sectoral decarbonization pathways can be considered, consistent with the International Energy Agency's sequencing principles. In particular, the issue of electricity is central to the net zero scenario. Electricity has to be green by 2035. From a financial perspective, this means that we will have to finance the transition of the power sector on

a massive scale. However, if we only implement a global decarbonization scenario, Ben Slimane *et al.* (2023b) noted that utility issuers are quickly excluded from the net-zero optimization program. The core net-zero portfolio invests in pure players that produce green power and doesn't give others time to transform their business models. This is not consistent with the goal of net-zero investing. Ben Slimane *et al.* (2023b) then proposed to constrain the optimization problem to follow the NZE scenario for the electricity sector. Using the results on page 952, the constraint to meet a reduction rate for a given sector $\boldsymbol{\mathcal{S}}ector_j$ can be expressed as:

$$\frac{\sum_{i=1}^n \mathbb{1}\left\{i \in \boldsymbol{\mathcal{S}}ector_j\right\} w_i \boldsymbol{\mathcal{CI}}_i}{\sum_{i=1}^n \mathbb{1}\left\{i \in \boldsymbol{\mathcal{S}}ector_j\right\} w_i} = \boldsymbol{\mathcal{CI}}\left(\boldsymbol{\mathcal{S}}ector_j, \boldsymbol{\mathcal{R}}_j\right)$$

where $\boldsymbol{\mathcal{CI}}\left(\boldsymbol{\mathcal{S}}ector_j, \boldsymbol{\mathcal{R}}_j\right)$ is the carbon intensity target for the given sector:

$$\boldsymbol{\mathcal{CI}}\left(\boldsymbol{\mathcal{S}}ector_j, \boldsymbol{\mathcal{R}}_j\right) = \left(1 - \boldsymbol{\mathcal{R}}_j\right) \frac{\sum_{i=1}^n \mathbb{1}\left\{i \in \boldsymbol{\mathcal{S}}ector_j\right\} b_i \boldsymbol{\mathcal{CI}}_i}{\sum_{i=1}^n \mathbb{1}\left\{i \in \boldsymbol{\mathcal{S}}ector_j\right\} b_i}$$

We deduce that:

$$\sum_{i=1}^n \mathbb{1}\left\{i \in \boldsymbol{\mathcal{S}}ector_j\right\} w_i \boldsymbol{\mathcal{CI}}_i = \boldsymbol{\mathcal{CI}}\left(\boldsymbol{\mathcal{S}}ector_j, \boldsymbol{\mathcal{R}}_j\right) \sum_{i=1}^n \mathbb{1}\left\{i \in \boldsymbol{\mathcal{S}}ector_j\right\} w_i$$

which is equivalent to the following constraint:

$$\sum_{i=1}^n \mathbb{1}\left\{i \in \boldsymbol{\mathcal{S}}ector_j\right\} w_i \left(\boldsymbol{\mathcal{CI}}_i - \boldsymbol{\mathcal{CI}}\left(\boldsymbol{\mathcal{S}}ector_j, \boldsymbol{\mathcal{R}}_j\right)\right) = 0 \Leftrightarrow \left(\boldsymbol{s}_j \circ \left(\boldsymbol{\mathcal{CI}}_i - \boldsymbol{\mathcal{CI}}_j^\star\right)\right)^\top w = 0$$

where $\boldsymbol{\mathcal{CI}}_j^\star = \boldsymbol{\mathcal{CI}}\left(\boldsymbol{\mathcal{S}}ector_j, \boldsymbol{\mathcal{R}}_j\right)$. Since this is a linear equation, the previous optimization problems with this constraint remain a QP or LP problem and can be solved easily. In Figures 11.31 and 11.32, we reproduce the tracking error volatility $\sigma\left(w \mid b\right)$ of equity portfolios and the active risk $\mathcal{D}\left(w \mid b\right)$ of bond portfolios when we impose the IEA NZE scenario for the electricity sector, $\boldsymbol{\mathcal{CM}}^\star = -3.5\%$ and $\boldsymbol{\mathcal{CM}}^+ = 10\%$, and we consider different NZE decarbonization scenarios (IEA, NZAOA, CTB and PAB). In these simulations, Ben Slimane *et al.* (2023b) found that if we allocate the tracking risk between the different constraints, the two most important contributors are the global decarbonisation pathway and the exclusion constraints, while the costs of self-decarbonisation and the specific electricity decarbonisation pathway are relatively low.

### Satellite portfolio

While the core portfolio aims to implement decarbonization policies, the satellite portfolio aims to finance the transition to a low-carbon economy and monitor green intensity. As the core-satellite approach is implemented in strategic asset allocation or multi-asset portfolios, the investment universe is diversified and typically consists of the following asset classes:

- Green, sustainability and sustainability-linked bonds
- Green stocks
- Green infrastructure
- Sustainable real estate

Figure 11.31: Tracking error volatility of decarbonized portfolios (MSCI World, December 2021, $\boldsymbol{\mathcal{CM}}^{\star} = -3.5\%$, $\boldsymbol{\mathcal{CM}}^{+} = 10\%$, IEA NZE electricity sector scenario)

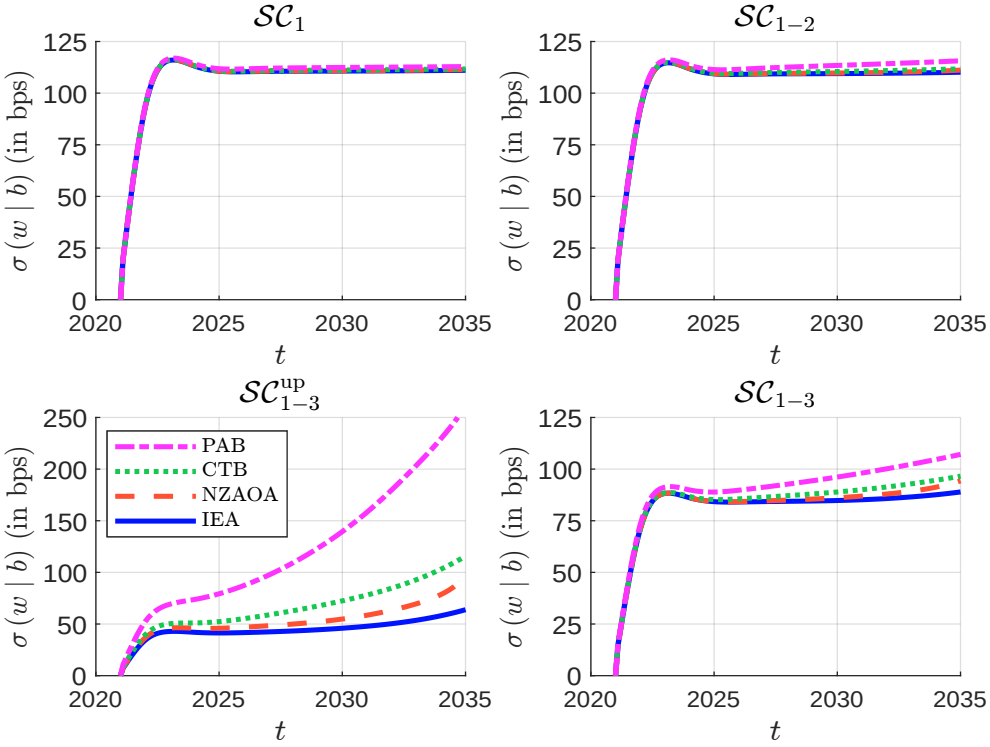


Figure 11.32: Active risk of decarbonized portfolios (Global Corporate, December 2021, $\boldsymbol{\mathcal{CM}}^{\star} = -3.5\%$, $\boldsymbol{\mathcal{CM}}^{+} = 10\%$, IEA NZE electricity sector scenario)

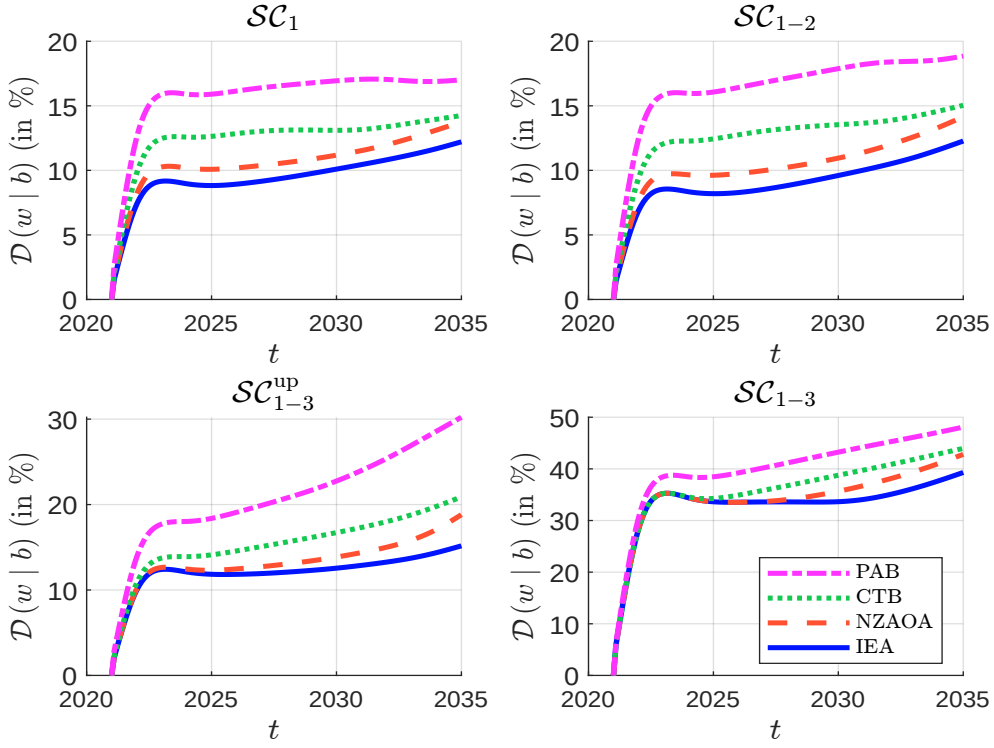


Source: Ben Slimane *et al.* (2023b).

Table 11.31: Main sub-industries of the net-zero satellite portfolio (GICS level 4)

| Code | Level 4 | Level 2 | Level 1 |
|---|---|---|---|
| 15102010 | Construction Materials | Materials | Materials |
| 15104010 | Aluminium | | |
| 15104020 | Diversified Metals & Mining | | |
| 15104025 | Copper | | |
| 15104040 | Precious Metals & Minerals | | |
| 15104045 | Silver | | |
| 15104050 | Steel | | |
| 20102010 | Building Products | Capital Goods | Industrials |
| 20103010 | Construction & Engineering | | |
| 20104010 | Electrical Components & Equipment | | |
| 20104020 | Heavy Electrical Equipment | | |
| 20106010 | Construction Machinery & Heavy Transportation Eqpt. | | |
| 20106015 | Agricultural & Farm Machinery | | |
| 20201050 | Environmental & Facilities Services | Commercial & Professional Services | |
| 20304010 | Rail Transportation | Transportation | |
| 20305010 | Airport Services | | |
| 20305020 | Highways & Railtracks | | |
| 20305030 | Marine Ports & Services | | |
| 25101010 | Automotive Parts & Equipment | Automobiles & Components | Consumer Discretionary |
| 25102010 | Automobile Manufacturers | | |
| 25201010 | Consumer Electronics | Consumer Durables & Apparel | |
| 25201030 | Homebuilding | | |
| 25201040 | Household Appliances | | |
| 30202010 | Agricultural Products | Services Food, Beverage & Tobacco | Consumer Staples |
| 55101010 | Electric Utilities | Utilities | Utilities |
| 55103010 | Multi-Utilities | | |
| 55104010 | Water Utilities | | |
| 55105020 | Renewable Electricity | | |
| 60201030 | Real Estate Development | Real Estate Management & Development | Real Estate |

Source: Ben Slimane *et al.* (2023b, Table 14, page 44).

The net-zero transition analysis on page 945 shows that the list of major sectors to be financed is relatively small. The mapping to level 4 of the GICS classification is shown in Table 11.31. In fact, we identify 29 sub-industries out of the 163 included in the GICS classification. Looking at the major sub-industries that can be included in the net-zero satellite portfolio, four of the eleven GICS sectors are over-represented, two are included, and the other five are excluded. The four over-represented sectors are Industrials, Materials, Consumer Discretionary and Utilities. The Industrials sector is divided into three industry groups: Capital Goods, which includes sub-industries related to machinery, equipment and construction; Transportation, where we look at how to improve public transportation systems and their infrastructure; and finally, Commercial & Professional Services, which includes the Environmental & Facilities Services sub-industry, which mainly covers waste management and pollution control. The Materials sector is characterized by the various materials used in the energy transition, such as aluminium, copper, steel, etc. The Consumer Discretionary sector is divided into two industry groups, Automobiles & Components, where we find auto manufacturers and auto parts, and Consumer Durables & Apparel, related to housing and appliances. Finally, the Utilities sectors will show different types of utilities needed for the transition, such as electric utilities, water utilities, or even renewable energy. Then we include two sub-industries that belong to the Consumer Staples and Real Estate sectors, respectively: agricultural products and real estate development. In summary, this means that not all sectors are represented. Figure 11.33 shows the four levels of the GICS classification[39] and indicates which sub-industry falls within the definition of the satellite investment universe.

**Remark 131** *It is clear that the GICS classification is not relevant when considering a net-zero investing framework. For example, there is no sector such as electricity storage, hydrogen storage, photovoltaic electricity generation, wind electricity generation, nuclear electricity generation in existing plants, etc. The NACE classification is more appropriate, and has the advantage to be in line with the EU green taxonomy. Nevertheless, GICS is the classification used by investors.*

**Green bonds** We look at the Bloomberg database of the GSS+ investment universe. For each bond, Bloomberg indicates whether it is a green, social, sustainability, sustainability-linked or conventional bond. Issue amounts are shown in Table 11.32. In 2022, 1 784 green bonds were issued for a total of \$531.6 bn. This represents 15% of the net-zero financing needs[40]. For the other categories, the amount to be issued in 2022 is equal to \$152.8 bn for social bonds, \$174.8 bn for sustainability bonds and \$144.3 bn for sustainability-linked bonds. As explained by Ben Slimane *et al.* (2023a), social bonds are not net-zero transition instruments, but more conventional bonds to finance social debt and social infrastructure. Therefore, if we look at a broad definition of the net-zero fixed income universe (green, sustainability and sustainability-linked bonds), we get a total of \$850.7 bn, which can be seen as the upper bound of current investment opportunities. This is less than 25% of the \$3.5 tn previously required to achieve net-zero.

In Figure 11.34 we compare the performance of the Bloomberg Global Green Bond index with the performance of the Bloomberg Global Aggregate index. We see that there is a high tracking risk. Between January 2014 and September 2023, the volatility of the tracking error is 2.7%. Several factors explain this high figure: sector allocation, duration, credit risk, etc. Investors must therefore accept a higher active risk for the satellite portfolio than for the core portfolio.

[39] It is described in Box 11.1 on page 974.
[40] On page 10.4.1 we saw that the net-zero funding requirement is equivalent to \$3.5 tn per year.

Figure 11.33: Narrow specification of the satellite investment universe

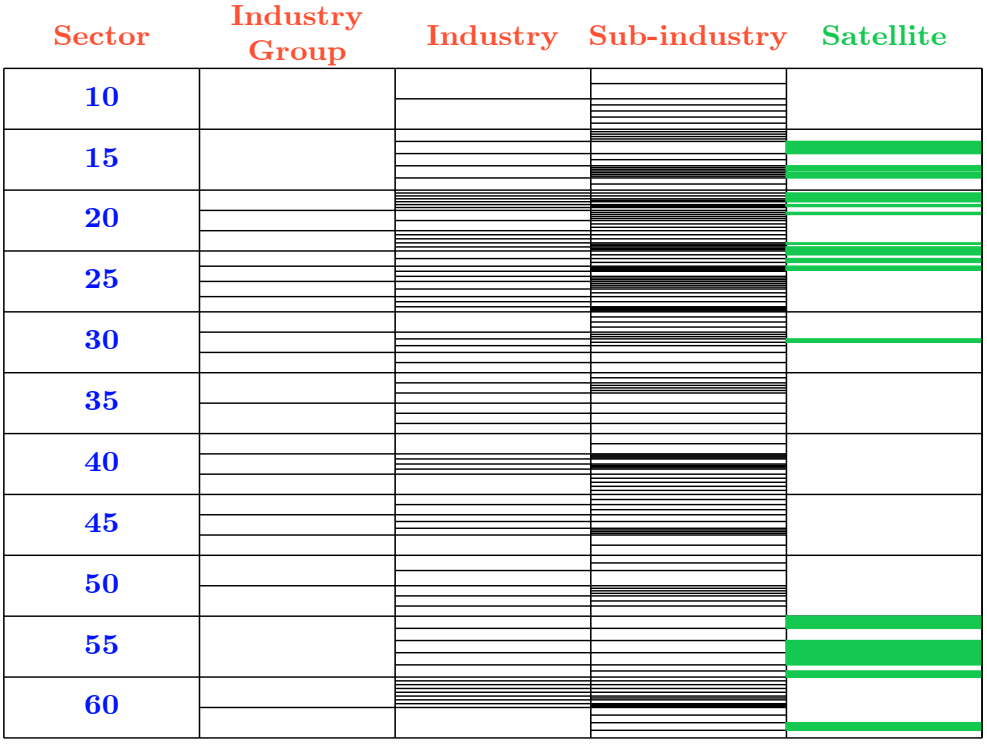


Source: Ben Slimane *et al.* (2023b, Figure 31, page 45).

Table 11.32: GSS+ bond issuance

| Year | Green | | Social | | Sustainability | | SLB | |
|---|---|---|---|---|---|---|---|---|
| | # | $ bn | # | $ bn | # | $ bn | # | $ bn |
| 2022 | 1 784 | 531.6 | 542 | 152.8 | 614 | 174.8 | 382 | 144.3 |
| 2021 | 1 971 | 686.1 | 554 | 242.1 | 646 | 233.2 | 343 | 161.5 |
| 2020 | 1 076 | 291.2 | 273 | 172.0 | 308 | 154.8 | 47 | 16.5 |
| 2019 | 877 | 268.0 | 99 | 22.2 | 333 | 85.2 | 18 | 8.9 |
| 2018 | 582 | 165.3 | 48 | 16.5 | 52 | 22.1 | 1 | 2.2 |
| 2017 | 472 | 160.9 | 46 | 11.8 | 17 | 9.2 | 1 | 0.2 |
| 2016 | 285 | 99.7 | 14 | 2.2 | 16 | 6.6 | 0 | 0.0 |

Source: Bloomberg (2023), GSS+ Instrument Indicator & Author's calculations.

Figure 11.34: Performance and duration of the Bloomberg Global Green Bond and Aggregate indexes

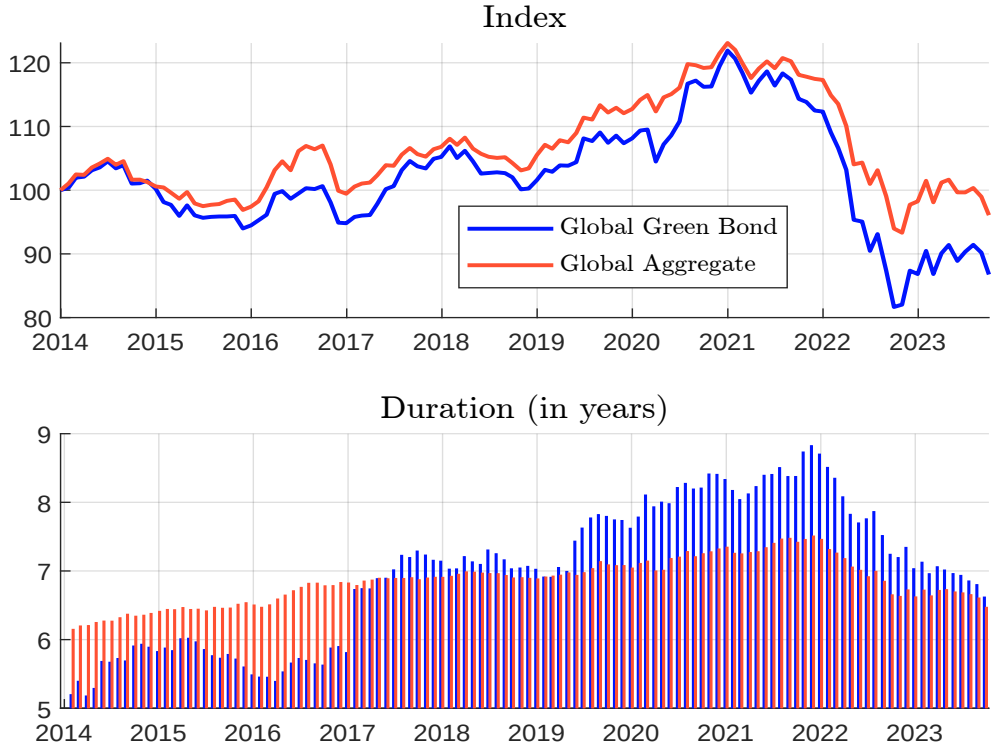


Source: Bloomberg (2023) & Author's calculations.

**Green stocks** We can invest in green stocks through thematic funds, which focus on a specific theme, or through an equity basket. In general, the second approach is used by equity managers, while the first is preferred by other fund managers, especially multi-asset managers. The emergence of economic, social and technological megatrends is strongly influencing the expansion of thematic funds. Some funds address the environmental challenge with a broader range of climate policies and solutions, investing only in companies with the best environmental practices and targets. These funds do not necessarily focus on net-zero transition. However, they generally include renewable energy stocks. Some more specific thematic funds have been developed to address net-zero issues such as clean energy, hydrogen, water management and future mobility. Figure 11.35 shows the performance of four thematic equity indexes: Bloomberg BioEnergy, Bloomberg Hydrogen, MSCI Future Mobility and MSCI New Energy. These indexes have a high risk of tracking error relative to the MSCI World index. On average, the tracking error volatility of the satellite equity portfolio is expected to be around 20%. The fund manager can also develop a stock-picking process related to the net-zero theme. In this case, he can build a screening based on green revenue share, green capex or green opex measures. More generally, the idea behind building a satellite equity portfolio with a basket of stocks is to select stocks according to a green intensity measure that can be aligned with the EU taxonomy.

**Green infrastructure** The European Commission[41] defines green infrastructure as "*a strategically planned network of natural and semi-natural areas with other environmental features, designed and managed to deliver a wide range of ecosystem services, while also enhancing biodiversity.*" Green

[41] https://environment.ec.europa.eu/topics/nature-and-biodiversity/green-infrastructure_en.

Figure 11.35: Performance and tracking error volatility of thematic equity indexes

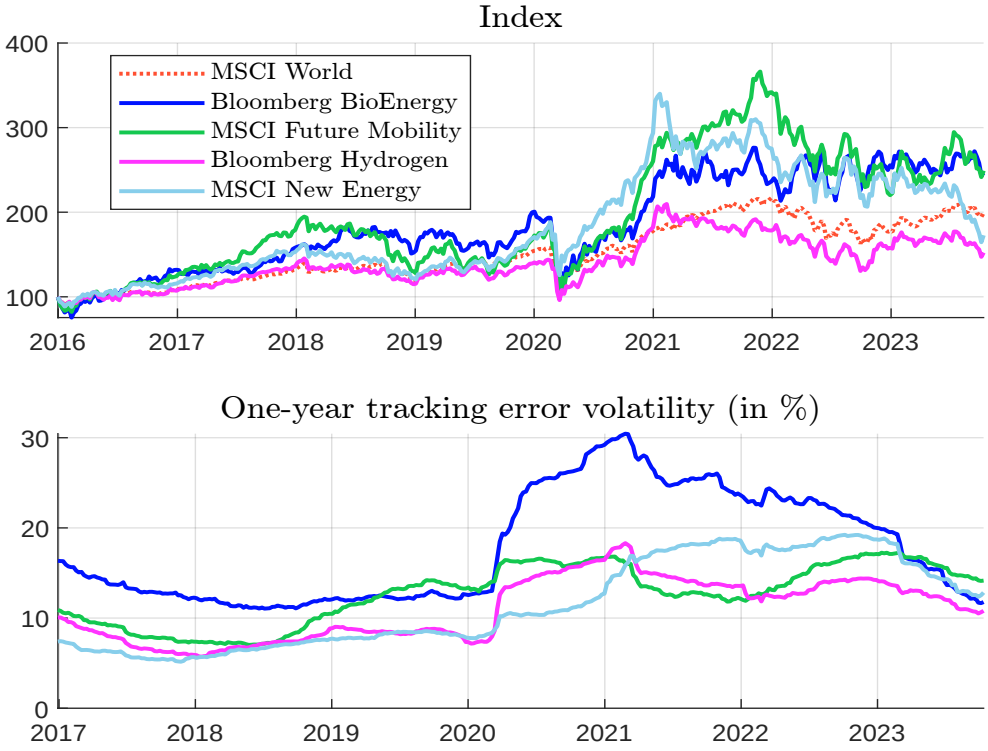


Source: Bloomberg (2023), MSCI (2023) & Author's calculations.

infrastructure is implemented in a variety of sectors, from energy through energy transmission infrastructure, water through natural water retention measures or sustainable urban drainage systems, to the urban landscape with street trees to help sequester carbon or green roofs to help regulate the temperature of buildings. The cost of implementing green infrastructure is in the identification, mapping, planning and creation of the infrastructure, but the environmental, economic and social benefits make it worthwhile. Funds that assess infrastructure needs are emerging in the market and typically invest in owners of sustainable infrastructure assets as well as companies that are leaders in infrastructure investment. In addition to infrastructure funds, investors are also considering direct investments such as green car parks, water infrastructure and flood defences.

**Sustainable real estate** The real estate sector emits significant amounts of $CO_2$ through building operations, building materials, and construction. Action is needed in the construction of new buildings, but also in the renovation of existing buildings. For existing buildings, it is very important to reduce energy consumption, eliminate emissions from energy and refrigerants, and reduce or eliminate the use of fossil fuels. This is done by improving equipment such as insulation, ventilation, and the use of renewable energy, as well as optimizing operations by installing GHG monitors or adjusting temperature settings. New construction must be energy and carbon efficient, taking into account new and clean technologies. Sustainable real estate funds have entered the market, typically targeting multiple sectors and countries with a specific allocation to achieve net-zero by 2050. They mostly follow the CRREM (carbon risk real estate monitor) pathway, targeting 1.5°C/2°C using a Paris-aligned decarbonization pathway per country and building type, ranging from office buildings to retail stores and hotels.

### Allocation process

In the following, we assume that the core-satellite portfolio is invested in stocks and bonds, but the inclusion of green infrastructure and sustainable real estate is straightforward.

**The stock/bond mix allocation** Let $\alpha_{\text{equity}}$ and $\alpha_{\text{bond}}$ be the proportions of stocks and bonds in the multi-asset portfolio. Let $\alpha^{\text{satellite}}$ be the weight of the satellite portfolio. The core allocation is given by the vector $\left(\alpha^{\text{core}}_{\text{equity}}, \alpha^{\text{core}}_{\text{bond}}\right)$, while the satellite allocation is defined by $\left(\alpha^{\text{satellite}}_{\text{equity}}, \alpha^{\text{satellite}}_{\text{bond}}\right)$. We have the following identities:

$$\begin{cases} \alpha_{\text{equity}} = \left(1-\alpha^{\text{satellite}}\right)\alpha^{\text{core}}_{\text{equity}} + \alpha^{\text{satellite}}\alpha^{\text{satellite}}_{\text{equity}} \\ \alpha_{\text{bond}} = \left(1-\alpha^{\text{satellite}}\right)\alpha^{\text{core}}_{\text{bond}} + \left(1-\alpha^{\text{satellite}}\right)\alpha^{\text{satellite}}_{\text{bond}} \end{cases} \tag{11.26}$$

In general, the fund manager targets a strategic asset allocation at the portfolio level, *i.e.*, the proportions $\alpha_{\text{equity}}$ and $\alpha_{\text{bond}}$ are given. For example, a defensive portfolio corresponds to a 20/80 constant mix strategy, while the 50/50 allocation is known as a balanced portfolio. Another famous allocation rule is the 60/40 portfolio, which is 60% in stocks and 40% in bonds. A first solution to Equation (11.26) is to maintain the same proportion of stocks and bonds in the core and satellite portfolios:

$$\begin{cases} \alpha^{\text{core}}_{\text{equity}} = \alpha^{\text{satellite}}_{\text{equity}} = \alpha_{\text{equity}} \\ \alpha^{\text{core}}_{\text{bond}} = \alpha^{\text{satellite}}_{\text{bond}} = \alpha_{\text{bond}} \end{cases}$$

However, this solution is not always satisfactory. In fact, the satellite portfolio generally has more bonds than the overall portfolio because the investment universe of green bonds is larger than the investment universe of green stocks. As a result, bonds are overweighted in the satellite portfolio. A second solution to Equation (11.26) is to calculate the proportion of bonds in the core portfolio relative to the proportion of bonds in the satellite portfolio:

$$\alpha^{\text{core}}_{\text{bond}} = \frac{\alpha_{\text{bond}} - \alpha^{\text{satellite}}\alpha^{\text{satellite}}_{\text{bond}}}{1-\alpha^{\text{satellite}}}$$

**Example 57** *We consider a 60/40 constant mix strategy. The satellite portfolio represents* 10% *of the net zero investments. We assume that the satellite portfolio has* 70% *exposure to green bonds.*

We have $\alpha_{\text{equity}} = 60\%$, $\alpha_{\text{bond}} = 40\%$, $\alpha^{\text{core}} = 90\%$, $\alpha^{\text{satellite}} = 10\%$ and $\alpha^{\text{satellite}}_{\text{bond}} = 70\%$. We deduce that:

$$\alpha^{\text{core}}_{\text{bond}} = \frac{0.40 - 0.10 \times 0.70}{1-0.10} = \frac{33}{90} = 36.67\%$$

The core allocation is then $(63.33\%, 36.67\%)$, while the satellite allocation is $(30\%, 70\%)$. We check that:

$$\begin{cases} \alpha_{\text{equity}} = 0.90 \times \left(1 - \dfrac{33}{90}\right) + 0.10 \times 0.30 = 60\% \\ \alpha_{\text{bond}} = 0.90 \times \dfrac{33}{90} + 0.10 \times 0.70 = 40\% \end{cases}$$

In Table 11.33, we report the values taken by $\alpha^{\text{core}}_{\text{bond}}$ when we target several constant mix strategies (60/40, 50/50, and 20/80). We assume that $\alpha^{\text{satellite}}_{\text{bond}}$ is set to 70% or 90% and consider several values of $\alpha^{\text{satellite}}$. For example, if green bonds account for 70% of the satellite portfolio's allocation and the satellite has a weight of 25%, the core portfolio's bond allocation must be set to 30% to achieve a 60/40 constant mix strategy.

Table 11.33: Calculating the bond allocation in the core portfolio ($\alpha_{\text{bond}}^{\text{core}}$ in %)

| Strategy | | 60/40 | | | 50/50 | | | 20/80 | | |
|---|---|---|---|---|---|---|---|---|---|---|
| $\alpha_{\text{bond}}^{\text{satellite}}$ | | 70.0 | 80.0 | 90.0 | 70.0 | 80.0 | 90.0 | 70.0 | 80.0 | 90.0 |
| $\alpha^{\text{satellite}}$ | 0% | 40.0 | 40.0 | 40.0 | 50.0 | 50.0 | 50.0 | 80.0 | 80.0 | 80.0 |
| | 1% | 39.7 | 39.6 | 39.5 | 49.8 | 49.7 | 49.6 | 80.1 | 80.0 | 79.9 |
| | 5% | 38.4 | 37.9 | 37.4 | 48.9 | 48.4 | 47.9 | 80.5 | 80.0 | 79.5 |
| | 10% | 36.7 | 35.6 | 34.4 | 47.8 | 46.7 | 45.6 | 81.1 | 80.0 | 78.9 |
| | 15% | 34.7 | 32.9 | 31.2 | 46.5 | 44.7 | 42.9 | 81.8 | 80.0 | 78.2 |
| | 20% | 32.5 | 30.0 | 27.5 | 45.0 | 42.5 | 40.0 | 82.5 | 80.0 | 77.5 |
| | 25% | 30.0 | 26.7 | 23.3 | 43.3 | 40.0 | 36.7 | 83.3 | 80.0 | 76.7 |

**Tracking error risk of the core-satellite portfolio** Let $w$, $w^{\text{core}}$, $w^{\text{satellite}}$, and $b$ be the core-satellite, core, satellite and benchmark portfolios, respectively. The return of the core-satellite portfolio is equal to:

$$\begin{aligned} R(w) &= \left(1-\alpha^{\text{satellite}}\right) \underbrace{\left(\alpha_{\text{equity}}^{\text{core}} R\left(w_{\text{equity}}^{\text{core}}\right) + \alpha_{\text{bond}}^{\text{core}} R\left(w_{\text{bond}}^{\text{core}}\right)\right)}_{\text{Core portfolio's return}} + \\ & \alpha^{\text{satellite}} \underbrace{\left(\alpha_{\text{equity}}^{\text{satellite}} R\left(w_{\text{equity}}^{\text{satellite}}\right) + \alpha_{\text{bond}}^{\text{satellite}} R\left(w_{\text{bond}}^{\text{satellite}}\right)\right)}_{\text{Satellite portfolio's return}} \end{aligned}$$

By construction, we have $\alpha_{\text{equity}}^{\text{core}} + \alpha_{\text{bond}}^{\text{core}} = 1$ and $\alpha_{\text{equity}}^{\text{satellite}} + \alpha_{\text{bond}}^{\text{satellite}} = 1$. The proportion invested in equities is equal to $\alpha_{\text{equity}} = \left(1-\alpha^{\text{satellite}}\right)\alpha_{\text{equity}}^{\text{core}} + \alpha^{\text{satellite}}\alpha_{\text{equity}}^{\text{satellite}}$ whereas the proportion invested in bonds is the complementary part ($\alpha_{\text{bond}} = 1 - \alpha_{\text{equity}}$). We deduce that:

$$R(w) = \tilde{\boldsymbol{\alpha}}^{\top} \tilde{\boldsymbol{R}}(w)$$

where $\tilde{\boldsymbol{R}}(w) = \left(R\left(w_{\text{equity}}^{\text{core}}\right), R\left(w_{\text{bond}}^{\text{core}}\right), R\left(w_{\text{equity}}^{\text{satellite}}\right), R\left(w_{\text{bond}}^{\text{satellite}}\right)\right)$ and:

$$\tilde{\boldsymbol{\alpha}} = \begin{pmatrix} \left(1-\alpha^{\text{satellite}}\right)\alpha_{\text{equity}}^{\text{core}} \\ \left(1-\alpha^{\text{satellite}}\right)\alpha_{\text{bond}}^{\text{core}} \\ \alpha^{\text{satellite}}\alpha_{\text{equity}}^{\text{satellite}} \\ \alpha^{\text{satellite}}\alpha_{\text{bond}}^{\text{satellite}} \end{pmatrix}$$

The benchmark portfolio's return is given by:

$$R(b) = \alpha_{\text{equity}} R\left(b_{\text{equity}}\right) + \left(1-\alpha_{\text{equity}}\right) R\left(b_{\text{bond}}\right)$$

Ben Slimane *et al.* (2023b) showed that:

$$\begin{aligned} R(b) &= \left(1-\alpha^{\text{satellite}}\right)\left(\alpha_{\text{equity}}^{\text{core}} R\left(b_{\text{equity}}\right) + \alpha_{\text{bond}}^{\text{core}} R\left(b_{\text{bond}}\right)\right) + \\ & \alpha^{\text{satellite}}\left(\alpha_{\text{equity}}^{\text{satellite}} R\left(b_{\text{equity}}\right) + \alpha_{\text{bond}}^{\text{satellite}} R\left(b_{\text{bond}}\right)\right) \end{aligned}$$

We deduce that:

$$R(b) = \tilde{\boldsymbol{\alpha}}^{\top} \tilde{\boldsymbol{R}}(b)$$

where $\tilde{\boldsymbol{R}}(b) = \left(R\left(b_{\text{Equity}}\right), R\left(b_{\text{bond}}\right), R\left(b_{\text{equity}}\right), R\left(b_{\text{bond}}\right)\right)$. The tracking error is defined as:

$$e = R(w) - R(b) = \tilde{\boldsymbol{\alpha}}^{\top}\left(\tilde{\boldsymbol{R}}(w) - \tilde{\boldsymbol{R}}(b)\right)$$

Let $\tilde{\boldsymbol{\Sigma}}(w \mid b)$ be the $4 \times 4$ covariance matrix of $\tilde{\boldsymbol{R}}(w) - \tilde{\boldsymbol{R}}(b)$. We conclude that the tracking error volatility of the core-satellite portfolio has the following expression:

$$\sigma(w \mid b) = \sqrt{\tilde{\boldsymbol{\alpha}}^\top \tilde{\boldsymbol{\Sigma}}(w \mid b)\, \tilde{\boldsymbol{\alpha}}} = \sqrt{(\tilde{\boldsymbol{\alpha}} \circ \tilde{\boldsymbol{\sigma}}(w \mid b))^\top \tilde{\boldsymbol{\rho}}(w \mid b)\, (\tilde{\boldsymbol{\alpha}} \circ \tilde{\boldsymbol{\sigma}}(w \mid b))}$$

where $\tilde{\boldsymbol{\rho}}(w \mid b)$ is the correlation matrix of $R(w) - R(b)$ and $\tilde{\boldsymbol{\sigma}}(w \mid b)$ is the vector of tracking error volatilities:

$$\tilde{\boldsymbol{\sigma}}(w \mid b) = \begin{pmatrix} \sigma\left(w_{\text{equity}}^{\text{core}} \mid b_{\text{equity}}\right) \\ \sigma\left(w_{\text{bond}}^{\text{core}} \mid b_{\text{bond}}\right) \\ \sigma\left(w_{\text{equity}}^{\text{satellite}} \mid b_{\text{equity}}\right) \\ \sigma\left(w_{\text{bond}}^{\text{satellite}} \mid b_{\text{bond}}\right) \end{pmatrix}$$

**Example 58** *The tracking error volatilities are* 2% *for the core equity portfolio,* 25 *bps for the core bond portfolio,* 20% *for the satellite equity portfolio, and* 3% *for the satellite bond portfolio. To define the correlation matrix* $\tilde{\boldsymbol{\rho}}(w \mid b)$*, we assume an* 80% *correlation between the two equity baskets, a* 50% *correlation between the two bond baskets, and a* 0% *correlation between the equity and bond baskets. We consider a 60/40 constant mix strategy. The satellite portfolio represents* 10% *of the net zero portfolio and has* 70% *exposure to green bonds.*

We compute the tracking error covariance matrix $\tilde{\boldsymbol{\Sigma}}(w \mid b)$ as follows: the tracking error variance for the core equity portfolio is $\tilde{\boldsymbol{\Sigma}}_{1,1}(w \mid b) = 0.02^2$, the tracking error variance for the satellite equity portfolio is $\tilde{\boldsymbol{\Sigma}}_{3,3}(w \mid b) = 0.20^2$, the tracking error covariance for the two core portfolios is $\tilde{\boldsymbol{\Sigma}}_{1,2}(w \mid b) = 0 \times 0.02 \times 0.0025$, the tracking error covariance for the core equity portfolio and the satellite equity portfolio is $\tilde{\boldsymbol{\Sigma}}_{1,3}(w \mid b) = 0.80 \times 0.02 \times 0.20$, and so on. Finally, we get:

$$\tilde{\boldsymbol{\Sigma}}(w \mid b) = \begin{pmatrix} 4 & 0 & 32 & 0 \\ 0 & 0.0625 & 0 & 0.375 \\ 32 & 0 & 400 & 0 \\ 0 & 0.375 & 0 & 9 \end{pmatrix} \times 10^{-4}$$

Since we have $\tilde{\boldsymbol{\alpha}} = (57\%, 33\%, 3\%, 7\%)$, we deduce that $\sigma(w \mid b) = 1.68\%$.

We consider several constant mix strategies with the same allocation within the core and satellite portfolios: $\alpha_{\text{equity}}^{\text{core}} = \alpha_{\text{equity}}^{\text{satellite}} = \alpha_{\text{equity}}$ and $\alpha_{\text{bond}}^{\text{core}} = \alpha_{\text{bond}}^{\text{satellite}} = \alpha_{\text{bond}}$. We assume that the tracking error volatilities are 2% for the core equity portfolio, 25 bps for the core bond portfolio, 20% for the satellite equity portfolio, and 3% for the satellite bond portfolio. We consider a lower and an upper bound on the correlation matrix $\tilde{\boldsymbol{\rho}}(w \mid b)$. For the lower bound, we set all cross-correlations to zero. For the upper bound, we assume an 80% correlation between the two equity baskets, an 80% correlation between the two bond baskets, and a 0% correlation between the equity and bond baskets. The results[42] are shown in Table 11.34 for three different values of $\alpha^{\text{satellite}}$. When the satellite weight is set to 20%, the tracking error volatility for the pure bond allocation is between 63 and 80 bps. For the 60/40 constant mix allocation, we obtain $\sigma(w \mid b) \in [2.60\%, 3.68\%]$, while for the pure equity allocation we have $\sigma(w \mid b) \in [4.31\%, 5.60\%]$. Ben Slimane *et al.* (2023b) estimated that the tracking error volatility of a net-zero core-satellite portfolio is currently around 3% for a 60/40 constant mix strategy.

[42] Defensive, balanced and dynamic portfolios correspond to 20/80, 50/50 and 80/20 constant mix strategies, respectively.

Table 11.34: Estimation of the tracking error volatility of the core-satellite portfolio (in %)

| | $\alpha^{\text{satellite}}$ | Bond | Defensive | Balanced | 60/40 | Dynamic | Equity |
|---|---|---|---|---|---|---|---|
| Lower bound | 10% | 0.38 | 0.62 | 1.36 | 1.62 | 2.15 | 2.69 |
| | 20% | 0.63 | 1.00 | 2.18 | 2.60 | 3.45 | 4.31 |
| | 30% | 0.92 | 1.43 | 3.11 | 3.71 | 4.93 | 6.16 |
| Upper bound | 10% | 0.53 | 1.18 | 2.16 | 2.49 | 3.15 | 3.80 |
| | 20% | 0.80 | 1.76 | 3.20 | 3.68 | 4.64 | 5.60 |
| | 30% | 1.07 | 2.34 | 4.24 | 4.87 | 6.13 | 7.40 |

**Dynamic allocation** The allocation between the core and satellite portfolios depends on the investment opportunities for the satellite portfolio. Today, we see a large imbalance between the supply of green assets and what is needed to finance the transition. Therefore, we can expect the allocation in the satellite portfolio to be small, but to increase in the future:

$$\frac{\partial \alpha^{\text{satellite}}(t)}{\partial t} \geq 0$$

The allocation $\alpha^{\text{satellite}}$ is then time-varying and must be revised periodically, *e.g.*, once a year.

## 11.4 Exercise

### 11.4.1 Equity and bond portfolio optimization with green preferences

We consider an investment universe of 8 issuers. In the table below, we report the carbon emissions $\boldsymbol{\mathcal{CE}}_{i,j}$ (in $ktCO_2e$) of these companies and their revenues $Y_i$ (in \$ bn), and we indicate in the last row whether the company belongs to sector $\boldsymbol{\mathcal{S}}ector_1$ or $\boldsymbol{\mathcal{S}}ector_2$:

| Issuer | #1 | #2 | #3 | #4 | #5 | #6 | #7 | #8 |
|---|---|---|---|---|---|---|---|---|
| $\boldsymbol{\mathcal{CE}}_{i,1}$ | 75 | 5 000 | 720 | 50 | 2 500 | 25 | 30 000 | 5 |
| $\boldsymbol{\mathcal{CE}}_{i,2}$ | 75 | 5 000 | 1 030 | 350 | 4 500 | 5 | 2000 | 64 |
| $\boldsymbol{\mathcal{CE}}_{i,3}$ | 24 000 | 15 000 | 1 210 | 550 | 500 | 187 | 30 000 | 199 |
| $Y_i$ | 300 | 328 | 125 | 100 | 200 | 102 | 107 | 25 |
| $\boldsymbol{\mathcal{S}}ector$ | 1 | 2 | 1 | 1 | 2 | 1 | 2 | 2 |

The benchmark $b$ of this investment universe is defined as:

$$b = (22\%, 19\%, 17\%, 13\%, 11\%, 8\%, 6\%, 4\%)$$

In what follows, we consider long-only portfolios.

1. We want to compute the carbon intensity of the benchmark.
   (a) Compute the carbon intensities $\boldsymbol{\mathcal{CI}}_{i,j}$ of each company $i$ for the scopes 1, 2 and 3.
   (b) Deduce the carbon intensities $\boldsymbol{\mathcal{CI}}_{i,j}$ of each company $i$ for the scopes $1+2$ and $1+2+3$.
   (c) Deduce the weighted average carbon intensity (WACI) of the benchmark if we consider the scope $1+2+3$.
   (d) We assume that the market capitalization of the benchmark portfolio is equal to \$10 tn and we invest \$1 bn.

i. Deduce the market capitalization of each company (expressed in \$ bn).

ii. Compute the ownership ratio for each asset (expressed in bps).

iii. Compute the carbon emissions of the benchmark portfolio[43] if we invest \$1 bn and we consider the scope $1+2+3$.

iv. Compare the (exact) carbon intensity of the benchmark portfolio with the WACI value obtained in Question 1.c.

2. We want to manage an equity portfolio with respect to the previous investment universe and reduce the weighted average carbon intensity of the benchmark by the rate $\boldsymbol{\mathcal{R}}$. We assume that the volatility of the stocks is respectively equal to 22%, 20%, 25%, 18%, 40%, 23%, 13% and 29%. The correlation matrix between these stocks is given by:

$$\rho = \begin{pmatrix} 100\% & & & & & & & \\ 80\% & 100\% & & & & & & \\ 70\% & 75\% & 100\% & & & & & \\ 60\% & 65\% & 80\% & 100\% & & & & \\ 70\% & 50\% & 70\% & 85\% & 100\% & & & \\ 50\% & 60\% & 70\% & 80\% & 60\% & 100\% & & \\ 70\% & 50\% & 70\% & 75\% & 80\% & 50\% & 100\% & \\ 60\% & 65\% & 70\% & 75\% & 65\% & 70\% & 60\% & 100\% \end{pmatrix}$$

(a) Compute the covariance matrix $\Sigma$.

(b) Write the optimization problem if the objective function is to minimize the tracking error risk under the constraint of carbon intensity reduction.

(c) Give the QP formulation of the optimization problem.

(d) $\boldsymbol{\mathcal{R}}$ is equal to 20%. Find the optimal portfolio if we target scope $1+2$. What is the value of the tracking error volatility?

(e) Same question if $\boldsymbol{\mathcal{R}}$ is equal to 30%, 50%, and 70%.

(f) We target scope $1+2+3$. Find the optimal portfolio if $\boldsymbol{\mathcal{R}}$ is equal to $20\%, 30\%$, 50% and 70%. Give the value of the tracking error volatility for each optimized portfolio.

(g) Compare the optimal solutions obtained in Questions 2.e and 2.f.

3. We want to manage a bond portfolio with respect to the previous investment universe and reduce the weighted average carbon intensity of the benchmark by the rate $\boldsymbol{\mathcal{R}}$. We use the scope $1+2+3$. In the table below, we report the modified duration $\text{MD}_i$ and the duration-times-spread factor $\text{DTS}_i$ of each corporate bond $i$:

| Asset | #1 | #2 | #3 | #4 | #5 | #6 | #7 | #8 |
|---|---|---|---|---|---|---|---|---|
| $\text{MD}_i$ (in years) | 3.56 | 7.48 | 6.54 | 10.23 | 2.40 | 2.30 | 9.12 | 7.96 |
| $\text{DTS}_i$ (in bps) | 103 | 155 | 75 | 796 | 89 | 45 | 320 | 245 |
| $\boldsymbol{\mathcal{S}}ector$ | 1 | 2 | 1 | 1 | 2 | 1 | 2 | 2 |

We remind that the active risk can be calculated using three functions. For the active share, we have:

$$\mathcal{R}_{\text{AS}}(w \mid b) = \sigma^2_{\text{AS}}(w \mid b) = \sum_{i=1}^{n} (w_i - b_i)^2$$

[43] We assume that the float percentage is equal to 100% for all the 8 companies.

We also consider the MD-based tracking error risk:

$$\mathcal{R}_{\mathrm{MD}}(w \mid b) = \sigma^2_{\mathrm{MD}}(w \mid b) = \sum_{j=1}^{n_{\boldsymbol{\mathcal{S}ector}}} \left( \sum\nolimits_{i \in \boldsymbol{\mathcal{S}ector}_j} (w_i - b_i) \, \mathrm{MD}_i \right)^2$$

and the DTS-based tracking error risk:

$$\mathcal{R}_{\mathrm{DTS}}(w \mid b) = \sigma^2_{\mathrm{DTS}}(w \mid b) = \sum_{j=1}^{n_{\boldsymbol{\mathcal{S}ector}}} \left( \sum\nolimits_{i \in \boldsymbol{\mathcal{S}ector}_j} (w_i - b_i) \, \mathrm{DTS}_i \right)^2$$

Finally, we define the synthetic risk measure as a combination of AS, MD and DTS active risks:

$$\mathcal{R}(w \mid b) = \varphi_{\mathrm{AS}} \mathcal{R}_{\mathrm{AS}}(w \mid b) + \varphi_{\mathrm{MD}} \mathcal{R}_{\mathrm{MD}}(w \mid b) + \varphi_{\mathrm{DTS}} \mathcal{R}_{\mathrm{DTS}}(w \mid b)$$

where $\varphi_{\mathrm{AS}} \geq 0$, $\varphi_{\mathrm{MD}} \geq 0$ and $\varphi_{\mathrm{DTS}} \geq 0$ indicate the weight of each risk. In what follows, we use the following numerical values: $\varphi_{\mathrm{AS}} = 100$, $\varphi_{\mathrm{MD}} = 25$ and $\varphi_{\mathrm{DTS}} = 1$. The reduction rate $\boldsymbol{\mathcal{R}}$ of the weighted average carbon intensity is set to 50% for the scope $1 + 2 + 3$.

(a) Compute the modified duration $\mathrm{MD}(b)$ and the duration-times-spread factor $\mathrm{DTS}(b)$ of the benchmark.

(b) Let $w_{\mathrm{ew}}$ be the equally-weighted portfolio. Compute[44] $\mathrm{MD}(w_{\mathrm{ew}})$, $\mathrm{DTS}(w_{\mathrm{ew}})$, $\sigma_{\mathrm{AS}}(w_{\mathrm{ew}} \mid b)$, $\sigma_{\mathrm{MD}}(w_{\mathrm{ew}} \mid b)$ and $\sigma_{\mathrm{DTS}}(w_{\mathrm{ew}} \mid b)$.

(c) We consider the following optimization problem:

$$\begin{aligned} w^\star &= \arg\min \frac{1}{2} \mathcal{R}_{\mathrm{AS}}(w \mid b) \\ &\text{s.t.} \begin{cases} \sum_{i=1}^n w_i = 1 \\ \mathrm{MD}(w) = \mathrm{MD}(b) \\ \mathrm{DTS}(w) = \mathrm{DTS}(b) \\ \boldsymbol{\mathcal{CI}}(w) \leq (1 - \boldsymbol{\mathcal{R}}) \boldsymbol{\mathcal{CI}}(b) \\ 0 \leq w_i \leq 1 \end{cases} \end{aligned}$$

Give the analytical value of the objective function. Find the optimal portfolio $w^\star$. Compute $\mathrm{MD}(w^\star)$, $\mathrm{DTS}(w^\star)$, $\sigma_{\mathrm{AS}}(w^\star \mid b)$, $\sigma_{\mathrm{MD}}(w^\star \mid b)$ and $\sigma_{\mathrm{DTS}}(w^\star \mid b)$.

(d) We consider the following optimization problem:

$$\begin{aligned} w^\star &= \arg\min \frac{\varphi_{\mathrm{AS}}}{2} \mathcal{R}_{\mathrm{AS}}(w \mid b) + \frac{\varphi_{\mathrm{MD}}}{2} \mathcal{R}_{\mathrm{MD}}(w \mid b) \\ &\text{s.t.} \begin{cases} \sum_{i=1}^n w_i = 1 \\ \mathrm{DTS}(w) = \mathrm{DTS}(b) \\ \boldsymbol{\mathcal{CI}}(w) \leq (1 - \boldsymbol{\mathcal{R}}) \boldsymbol{\mathcal{CI}}(b) \\ 0 \leq w_i \leq 1 \end{cases} \end{aligned}$$

Give the analytical value of the objective function. Find the optimal portfolio $w^\star$. Compute $\mathrm{MD}(w^\star)$, $\mathrm{DTS}(w^\star)$, $\sigma_{\mathrm{AS}}(w^\star \mid b)$, $\sigma_{\mathrm{MD}}(w^\star \mid b)$ and $\sigma_{\mathrm{DTS}}(w^\star \mid b)$.

[44] Precise the corresponding unit (years, bps or %) for each metric.

(e) We consider the following optimization problem:

$$\begin{aligned} w^\star &= \arg\min \frac{1}{2}\mathcal{R}(w \mid b) \\ &\text{s.t.} \begin{cases} \sum_{i=1}^n w_i = 1 \\ \boldsymbol{\mathcal{CI}}(w) \leq (1-\boldsymbol{\mathcal{R}})\,\boldsymbol{\mathcal{CI}}(b) \\ 0 \leq w_i \leq 1 \end{cases} \end{aligned}$$

Give the analytical value of the objective function. Find the optimal portfolio $w^\star$. Compute $\mathrm{MD}(w^\star)$, $\mathrm{DTS}(w^\star)$, $\sigma_{\mathrm{AS}}(w^\star \mid b)$, $\sigma_{\mathrm{MD}}(w^\star \mid b)$ and $\sigma_{\mathrm{DTS}}(w^\star \mid b)$.

(f) Comment on the results obtained in Questions 3.c, 3.d and 3.e.

(g) How to find the previous solution of Question 3.e using a QP solver?

4. We consider a variant of Question 3 and assume that the synthetic risk measure is:

$$\mathcal{D}(w \mid b) = \varphi_{\mathrm{AS}}\mathcal{D}_{\mathrm{AS}}(w \mid b) + \varphi_{\mathrm{MD}}\mathcal{D}_{\mathrm{MD}}(w \mid b) + \varphi_{\mathrm{DTS}}\mathcal{D}_{\mathrm{DTS}}(w \mid b)$$

where:

$$\begin{aligned} \mathcal{D}_{\mathrm{AS}}(w \mid b) &= \frac{1}{2}\sum_{i=1}^n |w_i - b_i| \\ \mathcal{D}_{\mathrm{MD}}(w \mid b) &= \sum_{j=1}^{n_{\boldsymbol{\mathcal{S}ector}}} \left| \sum\nolimits_{i \in \boldsymbol{\mathcal{S}ector}_j} (w_i - b_i)\,\mathrm{MD}_i \right| \\ \mathcal{D}_{\mathrm{DTS}}(w \mid b) &= \sum_{j=1}^{n_{\boldsymbol{\mathcal{S}ector}}} \left| \sum\nolimits_{i \in \boldsymbol{\mathcal{S}ector}_j} (w_i - b_i)\,\mathrm{DTS}_i \right| \end{aligned}$$

(a) Define the corresponding optimization problem when the objective is to minimize the active risk and reduce the carbon intensity of the benchmark by $\boldsymbol{\mathcal{R}}$.

(b) Give the LP formulation of the optimization problem.

(c) Find the optimal portfolio when $\boldsymbol{\mathcal{R}}$ is set to 50%. Compare the solution with this obtained in Question 3.e.

### 11.4.2 Monotonicity property of the order-statistic and naive approaches

Chapter 12

# Physical Risk Modeling

## 12.1 General circulation model

### 12.1.1 Carbon cycle

### 12.1.2 Greenhouse gas chemistry

### 12.1.3 Horizontal and vertical heat transport

### 12.1.4 Oceans

### 12.1.5 Carbon sinks

## 12.2 Statistical modeling of climate hazards

### 12.2.1 Chronic risk

### 12.2.2 Acute risk

## 12.3 Geolocation

### 12.3.1 Climate hazard location

### 12.3.2 Asset location

## 12.4 Applications

### 12.4.1 Cyclones and hurricanes

### 12.4.2 Drought

### 12.4.3 Floods

### 12.4.4 Extreme heat

### 12.4.5 Water stress

### 12.4.6 Wildfire

## 12.5 Exercises

Chapter 13

# Climate Stress Testing and Risk Management

## 13.1 Transmission channels

### 13.1.1 Direct and indirect transmission

### 13.1.2 Credit transmission channel

### 13.1.3 Market transmission channel

### 13.1.4 Systemic risk

## 13.2 Climate risk hedging

## 13.3 Climate value-at-risk

## 13.4 Climate stress testing

## 13.5 Exercises

# Conclusion

# Appendices

# Appendix A

# Technical Appendix

## A.1 Mathematical tools

### A.1.1 Linear algebra

#### Eigendecomposition

The value $\lambda$ is an eigenvalue of the $n \times n$ matrix $A$ if there exists a non-zero eigenvector $v$ such that we have $Av = \lambda v$. We denote $V$ the matrix composed of the $n$ eigenvectors. We have $AV = V\Lambda$ where $\Lambda = \text{diag}(\lambda_1, \ldots, \lambda_n)$ is the diagonal matrix of eigenvalues. We finally obtain the eigendecomposition of the matrix $A$:

$$A = V\Lambda V^{-1}$$

If $A$ is an hermitian matrix[1], then the matrix $V$ of eigenvectors is unitary. It follows that:

$$A = V\Lambda V^*$$

In particular, if $A$ is a symmetric real matrix, we obtain the following relationship[2]:

$$A = V\Lambda V^\top$$

#### Schur decomposition and matrix function

The Schur decomposition of the $n \times n$ matrix $A$ is equal to:

$$A = QTQ^* \tag{A.1}$$

where $Q$ is a unitary matrix and $T$ is an upper triangular matrix[3]. This decomposition is useful to calculate matrix functions.

Let us consider the matrix function in the space $\mathbb{M}$ of square matrices:

$$\begin{aligned} f: \quad & \mathbb{M} \longrightarrow \mathbb{M} \\ & A \longmapsto B = f(A) \end{aligned}$$

For instance, if $f(x) = \sqrt{x}$ and $A$ is positive, we can define the matrix $B$ such that:

$$BB^* = B^*B = A$$

[1] The square matrix $A$ is hermitian if it is equal to its own conjugate transpose $A^*$, implying that we have $A_{i,j} = \text{conj}\, A_{j,i}$;

[2] We have $A^\top = \left(V\Lambda V^{-1}\right)^\top = \left(V^{-1}\right)^\top \Lambda V^\top$. We deduce that $V^{-1} = V^\top$.

[3] $Q$ and $T$ are also called the transformation matrix and the Schur form of $A$.

$B$ is called the square root of $A$ and we note $B = A^{1/2}$. This matrix function generalizes the scalar-valued function to the set of matrices. Let us consider the following Taylor expansion:

$$f(x) = f(x_0) + (x - x_0) f'(x_0) + \frac{(x - x_0)^2}{2!} f''(x_0) + \dots$$

We can show that if the series converge for $|x - x_0| < \alpha$, then the matrix $f(A)$ defined by the following expression:

$$f(A) = f(x_0) + (A - x_0 I) f'(x_0) + \frac{(A - x_0 I)^2}{2!} f''(x_0) + \dots$$

converges to the matrix $B$ if $|A - x_0 I| < \alpha$ and we note $B = f(A)$. In the case of the exponential function, we have:

$$f(x) = e^x = \sum_{k=0}^{\infty} \frac{x^k}{k!}$$

We deduce that the exponential of the matrix $A$ is equal to:

$$B = e^A = \sum_{k=0}^{\infty} \frac{A^k}{k!}$$

In a similar way, the logarithm of $A$ is the matrix $B$ such that $e^B = A$ and we note $B = \ln A$.

Let $A$ and $B$ be two $n \times n$ square matrices. Using the Taylor expansion, Golub and Van Loan (2013) showed that $f\left(A^\top\right) = f(A)^\top$, $Af(A) = f(A) A$ and $f\left(B^{-1}AB\right) = B^{-1} f(A) B$. It follows that:

$$e^{A^\top} = \left(e^A\right)^\top$$

and:

$$e^{B^{-1}AB} = B^{-1} e^A B$$

If $AB = BA$, we can also prove that $Ae^B = e^B A$ and $e^{A+B} = e^A e^B = e^B e^A$.

**Remark 132** *There are different ways to compute numerically $f(A)$. For transcendental functions, we have:*

$$f(A) = Q f(T) Q^*$$

*where $A = QTQ^*$ is the Schur decomposition of $A$. Because $T$ is an upper diagonal matrix, $f(T)$ is also a diagonal matrix whose elements can be calculated with Algorithm 9.1.1 of Golub and Van Loan (2013). This algorithm is reproduced below*[4].

### Sherman-Morrison-Woodbury formula

Let $u$ and $v$ be two $n \times 1$ vectors and $A$ be an invertible $n \times n$ matrix. We can show that (Golub and Van Loan, 2013):

$$\left(A + uv^\top\right)^{-1} = A^{-1} - \frac{1}{1 + v^\top A^{-1} u} A^{-1} uv^\top A^{-1}$$

[4]For the exponential matrix, we may prefer to use the Pade approximation method, which is described in Algorithm 9.3.1 (scaling and squaring) of Golub and Van Loan (2013). See also the survey of Moler and Van Loan (2003).

**Algorithm 2** Schur-Parlett matrix function $f(A)$

Compute the Schur decomposition $A = QTQ^*$
Initialize $F$ to the matrix $\mathbf{0}_{n\times n}$
**for** $i = 1 : n$ **do**
  $f_{i,i} \leftarrow f(t_{i,i})$
**end for**
**for** $p = 1 : n-1$ **do**
  **for** $i = 1 : n-p$ **do**
    $j \leftarrow i + p$
    $s \leftarrow t_{i,j}(f_{j,j} - f_{i,i})$
    **for** $k = i+1 : j-1$ **do**
      $s \leftarrow s + t_{i,k}f_{k,j} - f_{i,k}t_{k,j}$
    **end for**
    $f_{i,j} \leftarrow s/(t_{j,j} - t_{i,i})$
  **end for**
**end for**
$B \leftarrow QFQ^*$
**return** $B$

Source: Golub and Van Loan (2013), page 519.

Batista and Karawia (2009) extended the SMW formula when the outer product is a sum:

$$\left(A + \sum_{k=1}^{m} u_k v_k^\top\right)^{-1} = A^{-1} - A^{-1}US^{-1}V^\top A^{-1}$$

where $U = \begin{pmatrix} u_1 & \cdots & u_m \end{pmatrix}$ and $V = \begin{pmatrix} v_1 & \cdots & v_m \end{pmatrix}$ are two $n \times m$ matrices, and $S = I_m + T$ and $T = (T_{i,j})$ are two $m \times m$ matrices where $T_{i,j} = v_i^\top A^{-1} u_j$. In the case $m = 2$, Roncalli *et al.* (2020) showed that the SMW formula becomes:

$$\left(A + u_1 v_1^\top + u_2 v_2^\top\right)^{-1} = A^{-1} - A^{-1}CA^{-1}$$

where:

$$C = \frac{\left(I_n - u_2 v_2^\top A^{-1}\right) u_1 v_1^\top + \left(I_n - u_1 v_1^\top A^{-1}\right) u_2 v_2^\top + u_1 v_2^\top A^{-1} u_2 v_1^\top + u_2 v_1^\top A^{-1} u_1 v_2^\top}{1 + \left(v_1^\top A^{-1} u_1\right)\left(v_2^\top A^{-1} u_2\right) + v_1^\top A^{-1} u_1 + v_2^\top A^{-1} u_2 - \left(v_2^\top A^{-1} u_1\right)\left(v_1^\top A^{-1} u_2\right)}$$

### A.1.2 Optimization

#### Bisection algorithm

The simplest algorithm to find the roots of the equation $f(x) = 0$ is the bisection algorithm. We assume that the function $f$ is continuous on the interval $[a, b]$, and $f(a)$ and $f(b)$ have oppositive signs: $f(a) f(b) < 0$. The underlying idea is to reduce the bracket by computing the midpoint $c = (a+b)/2$. If $f(a) f(c) < 0$, then the interval becomes $[a, c]$, otherwise it is equal to $[c, b]$. This step is repeated until the interval is sufficiently small. The absolute error is divided by 2 at each step so the method converges linearly. Let $c^\star$ be a root such that $f(c^\star) = 0$ and $c^\star \in [a, b]$. Let $c_{(k)}$ be the midpoint at the $k^{\text{th}}$ iteration. Then the difference between $c_{(k)}$ and $c^\star$ is bounded by $\left|c_{(k)} - c^\star\right| \leq 2^{-k}(b-a)$. For instance, after 10 iterations, we are sure that the interval has been divided by $2^{10} = 1024$. After 20 iterations, the interval is divided by $10^6$.

**Linear programming**

The canonical form of a linear program is:

$$\begin{array}{rcl} x^\star & = & \arg\max c^\top x \\ & \text{s.t.} & \left\{ \begin{array}{l} Sx \leq T \\ x \geq \mathbf{0}_n \end{array} \right. \end{array}$$

where $x$ is a $n \times 1$ vector, $c$ is a $n \times 1$ vector, $S$ is a $n_S \times n$ matrix, and $T$ is a $n_S \times 1$ vector. A minimization linear programming (LP) problem can be cast into a maximization LP problem because $\min c^\top x \equiv \max -c^\top x$. A maximization LP problem is in standard form if it is written as:

$$\begin{array}{rcl} x^\star & = & \arg\max c^\top x \\ & \text{s.t.} & \left\{ \begin{array}{l} Sx = T \\ x \geq \mathbf{0}_n \end{array} \right. \end{array}$$

We notice that a canonical problem can always be put into a standard form by introducing the slack variables $\xi$:

$$Sx \leq T \Leftrightarrow \{\xi \geq \mathbf{0}_{n_S} : Sx + I_{n_S}\xi = T\}$$

We obtain the following LP problem:

$$\begin{array}{rcl} y^\star & = & \arg\max d^\top y \\ & \text{s.t.} & \left\{ \begin{array}{l} My = N \\ y \geq \mathbf{0}_n \end{array} \right. \end{array}$$

where $d = (c, \mathbf{0}_{n_S})$, $y = (x, s)$, $M = \begin{pmatrix} S & I_{n_S} \end{pmatrix}$ and $N = T$. The technique of slack variables[5] can also be used when the contraint is $Sx \geq T$ and we have $Sx - \xi = T$. If we introduce lower and upper bounds ($x^- \leq x \leq x^+$), we can use the change of variable $y = x - x^-$. It follows that $y \geq \mathbf{0}_n$ and $I_n y \leq x^+ - x^-$. Since we have $x = x^- + y$, we obtain $c^\top x = c^\top x^- + c^\top y$ and $Sx \leq T \Leftrightarrow Sy \leq T - Sx^-$. Finally,we deduce that:

$$\left\{ \begin{array}{rcl} x^\star & = & \arg\max c^\top x \\ & \text{s.t.} & \left\{ \begin{array}{l} Sx \leq T \\ x \geq \mathbf{0}_n \end{array} \right. \end{array} \right. \iff \left\{ \begin{array}{rcl} y^\star & = & \arg\max c^\top y \\ & \text{s.t.} & \left\{ \begin{array}{l} \begin{pmatrix} S \\ I_n \end{pmatrix} y \leq \begin{pmatrix} T - Sx^- \\ x^+ - x^- \end{pmatrix} \\ y \geq \mathbf{0}_n \end{array} \right. \end{array} \right.$$

If some variables $x_i \in \mathbb{R}$, we can write $x_i = y_i - z_i$ where $y_i \geq 0$ and $z_i \geq 0$.

The previous analysis shows that we can always transform a general LP problem into a canonical or standard form. This is why most numerical packages consider the following general formulation:

$$\begin{array}{rcl} x^\star & = & \arg\min c^\top x \\ & \text{s.t.} & \left\{ \begin{array}{l} Ax = B \\ Cx \leq D \\ x^- \leq x \leq x^+ \end{array} \right. \end{array} \tag{A.2}$$

where $x$ is a $n \times 1$ vector, $c$ is a $n \times 1$ vector, $A$ is a $n_A \times n$ matrix, $B$ is a $n_A \times 1$ vector, $C$ is a $n_C \times n$ matrix, $D$ is a $n_C \times 1$ vector, and $x^-$ and $x^+$ are two $n \times 1$ vectors. If $n_A = 0$, there is no equality constraints. Similarly, there is no inequality constraints if $n_C = 0$. If there is no lower

[5] When we rewrite an inequality by substracting new variables, these last ones are also called surplus variables.

bounds or/and upper bounds, this implies that $x^- = -\infty \cdot \mathbf{1}_n$ and $x^+ = \infty \cdot \mathbf{1}_n$. A solution $x$ is said to be feasible if it satisfies all the constraints of the linear program (A.2). The set of feasible solutions is called the feasible space $\Omega$:

$$\Omega = \left\{x \in \mathbb{R}^n : Ax = B, Cx \leq D, x^- \leq x \leq x^+\right\}$$

Since $Ax = B$ and $Cx \leq D$ define two convex sets (a hyperplane and a closed half-space), $\Omega$ is a convex set. If $\Omega$ is not empty and $c^\top x$ is bounded below, then there is an optimal solution.

**Example 59** *We consider the following optimization problem:*

$$\begin{aligned}(x_1^\star, x_2^\star, x_3^\star) &= \arg\min x_1 + x_2 + x_3 \\ &s.t. \begin{cases} x_1 + x_2 + x_3 = 1 \\ 3x_1 + x_2 + 5x_3 \geq 2 \\ 2x_1 + x_2 + 3x_3 \leq s \\ 0 \leq x_i \leq 1 \end{cases}\end{aligned}$$

*If $s \geq 1.5$, the optimal solution is $(0, 0.75, 0.25)$. If $s < 1.5$, $\Omega = \emptyset$ and there is no solution.*

Let us consider the standard program: $x^\star = \arg\max f(x) = c^\top x$ subject to $Ax = b$. The Lagrange function is:

$$\mathcal{L}(x; \lambda) = c^\top x - \lambda^\top (Ax - b)$$

The first-order condition is:

$$\begin{cases} \partial_x \mathcal{L}(x; \lambda) = c - A^\top \lambda = \mathbf{0}_n \\ \partial_\lambda \mathcal{L}(x; \lambda) = Ax - b = \mathbf{0}_{n_A} \end{cases}$$

The optimal solution $(x^\star, \lambda^\star)$ satisfies the following system of equations: $Ax^\star = b$ and $A^\top \lambda^\star = c$. We also have $f(x^\star) = \mathcal{L}(x^\star, \lambda^\star) = c^\top x^\star - \lambda^{\star\top}(Ax^\star - b)$ and:

$$\mathcal{L}(x^\star, \lambda^\star) = \sum_{i=1}^n c_i x_i^\star - \sum_{j=1}^{n_A} \lambda_j^\star \sum_{i=1}^n A_{j,i} x_i^\star + \sum_{j=1}^{n_A} \lambda_j^\star b_j$$

Let us assume that we increase $b$ by a vector $\varepsilon \geq \mathbf{0}_{n_A}$. The Lagrange function becomes:

$$\begin{aligned}\mathcal{L}_\varepsilon(x^\star, \lambda^\star) &= \sum_{i=1}^n c_i x_i^\star - \sum_{j=1}^{n_A} \lambda_j^\star \sum_{i=1}^n A_{j,i} x_i^\star + \sum_{j=1}^{n_A} \lambda_j^\star (b_j + \varepsilon_j) \\ &= f(x^\star) + \sum_{j=1}^{n_A} \lambda_j^\star \varepsilon_j\end{aligned}$$

If we relax the $j^{\text{th}}$ constraint by a small value of $\varepsilon_j$, we change the objective function by $\lambda_j^\star \varepsilon_j$. If $\lambda_j^\star = 0$, then modifying locally the constraint has no impact. If $\lambda_j^\star < 0$, we have $f_\varepsilon(x^\star) < f(x^\star)$, implying that we have no incentive to change the value $b_j$ of the constraint, otherwise we will reduce the objective function. If $\lambda_j^\star > 0$, we have $f_\varepsilon(x^\star) > f(x^\star)$, meaning that we can improve the objective function. From an economic point of view, a linear program is usually a profit maximization, a production maximization or a cost minimization. In this case, we can ask ourselves what price $p_j$ we are willing to pay to increase the right-hand side value $b_j$ by one unit? By taking $\varepsilon_j = 1$, we obtain $p_j \leq \lambda_j^\star$ and $\lambda_j^\star$ is called the shadow or dual price. This explains why duality plays an important role in economics.

**Example 60** *We consider the following optimization problem:*

$$\begin{array}{rcl} x^\star & = & \arg\max 2x_2 + 3x_3 - x_1 \\ & s.t. & \left\{ \begin{array}{l} x_1 + x_2 + x_3 = 1 \\ 2x_1 + 5x_2 + 6x_3 = 0.2 \end{array} \right. \end{array}$$

The optimal solution is $x^\star = (1.45, 0, -0.45)$ and $\lambda^\star = (3, -1)$, and the objective function is equal to $f(x^\star) = 2.80$. The shadow prices are then equal to $+3$ for the first constraint and $-1$ for the second constraint. We do not want to increase the second constraint by $\varepsilon_2$ because it reduces the objective function by $\varepsilon_2$. Indeed, if $\varepsilon_2 = 0.04$, the new solution is $x^* = (1.44, 0, -0.44)$ and we have $f(x^*) = 2.76$. On the contrary, if we increase the first constraint by $\varepsilon_1$, we improve the objective function by $3\varepsilon_1$. For instance, if $\varepsilon_1 = 0.1$, the new solution is $x^* = (1.6, 0, -0.5)$ and we have $f(x^*) = 3.1$. Let us combine the two effects. If $(\varepsilon_1, \varepsilon_2) = (0.1, 0.04)$, we have $x^* = (1.59, 0, -0.49)$ and $f(x^*) = 3.06$. We verify that:

$$\begin{array}{rcl} f(x^\star) + \lambda_1^\star \varepsilon_1 + \lambda_2^\star \varepsilon_2 & = & 2.80 + 3 \times 0.1 - 1 \times 0.04 \\ & = & 3.06 \\ & = & f(x^*) \end{array}$$

If the primal problem is maximizing $c^\top x$ subject to $Ax \leq b$ and $x \geq \mathbf{0}_n$, then the dual problem is defined as:

$$\begin{array}{rcl} x^\star & = & \arg\min b^\top y \\ & \text{s.t.} & \left\{ \begin{array}{l} A^\top y \geq c \\ y \geq \mathbf{0}_m \end{array} \right. \end{array} \tag{A.3}$$

We notice that:

- The dual problem has a linear programming form;
- The maximization problem and the $\leq$ inequality type are changed into a minimization problem and a $\geq$ inequality type;
- Each dual variable $y_j$ may be assigned to a corresponding primal constraint $\sum_{i=1}^n A_{j,i} x_i \leq b_j$;
- The roles of the vectors $c$ and $b$ are switched: $c$ becomes the right-hand side of the constraints and $b$ the coefficients of the objective function;
- The matrix $A$ of the inequality constraints is transposed.

Let $\Omega_x = \{x : Ax \leq b, x \geq \mathbf{0}_n\}$ and $\Omega_y = \left\{y : A^\top y \geq c, y \geq \mathbf{0}_m\right\}$ be the primal and dual feasible spaces. The weak duality theorem states that[6]:

$$\forall x \in \Omega_x, y \in \Omega_y : c^\top x \leq b^\top y$$

This means that the objective value of the dual problem is an upper bound on the objective value of the primal problem, and vice versa. Using this property, we can also formulate the strong duality theorem: A primal feasible solution $x^\star$ is optimal if and only if there exists a dual feasible solution $y^\star$ such that $c^\top x^\star = b^\top y^\star$. We also deduce that $y^\star$ is the optimal solution of the dual LP problem.

[6] If $x \geq \mathbf{0}_n$ and $\alpha \geq \beta$, we have $\alpha^\top x \geq \beta^\top x$ because $\alpha_i x_i \geq \beta_i x_i$ and $\sum_{i=1}^n \alpha_i x_i \geq \sum_{i=1}^n \beta_i x_i$. Using the constraints $Ax \leq b$ and $A^\top y \geq c$, we deduce that $c^\top x = x^\top c \leq x^\top A^\top y = (Ax)^\top y \leq b^\top y$.

**Example 61** *We consider a classical ressource allocation problem. We would like to produce 3 goods, whose market prices are \$3, \$5 and \$7. The production of these goods requires some ressources, such as capital, labor, raw materials and land. The available ressources are respectively equal to 100, 50, 80 and 200. For the first good, the production of one unit needs 5 units of capital, 3 units of labor, 1 unit of raw materials and 1 unit of land. For the second good, the intermediary consumptions are 10, 2, 10 and 2, while they are equal to 4, 7, 8 and 4 for the third good.*

The problem is to maximize the revenue under allocation constraints. By definition, the revenue is the product of sold quantities and market prices:

$$\mathcal{R}evenue = 3x_2 + 5x_3 + 7x_1$$

If we consider the first ressource constraint, we have 100 units of capital that we can allocate between the three goods in the following way. We need 5 units of capital to produce one unit of the first good, 10 units of capital to produce one unit of the second good and 4 units of capital to produce one unit of the third good. The optimization problem is then defined as follows:

$$\begin{array}{rcl} x^\star & = & \arg\max 3x_2 + 5x_3 + 7x_1 \\ & & \text{s.t.} \left\{ \begin{array}{l} 5x_1 + 10x_2 + 4x_3 \leq 100 \\ 3x_1 + 2x_2 + 7x_3 \leq 50 \\ x_1 + 10x_2 + 8x_3 \leq 80 \\ x_1 + 2x_2 + 4x_3 \leq 200 \\ x_1 \geq 0, x_2 \geq 0, x_3 \geq 0 \end{array} \right. \end{array}$$

The optimal solution is $x_1^\star = 7.4390$, $x_2^\star = 5.3049$ and $x_3^\star = 2.4390$. The optimal value of the revenue is \$65.91. The computation of the Lagrange multipliers gives $\lambda_1^\star = 0.1555$, $\lambda_2^\star = 0.6707$, $\lambda_3^\star = 0.2104$ and $\lambda_4^\star = 0$. While the primal LP was a resource allocation problem, the dual LP is a resource valuation problem from an economic viewpoint. Indeed, $y_i$ is the implicit cost per unit associated with each resource $i$ and the objective is then to minimize the total cost of the resources:

$$\mathcal{C}ost = 100y_1 + 50y_2 + 80y_3 + 200y_4$$

Moreover, if we consider the first good, its market price $p_1$ is \$3, and its internal value to produce it is equal to $v_1 = 5y_1 + 3y_2 + y_3 + y_4$. Therefore, we have the following constraint $v_1 \geq p_1$. Finally, we deduce that the resource valuation problem is to minimize the total cost under the constraints $v_1 \geq p_1$, $v_2 \geq p_2$ and $v_3 \geq p_3$. Therefore, the dual problem is:

$$\begin{array}{rcl} y^\star & = & \arg\min 100y_1 + 50y_2 + 80y_3 + 200y_4 \\ & & \text{s.t.} \left\{ \begin{array}{l} 5y_1 + 3y_2 + y_3 + y_4 \geq 3 \\ 10y_1 + 2y_2 + 10y_3 + 2y_4 \geq 5 \\ 4y_1 + 7y_2 + 8y_3 + 4y_4 \geq 7 \\ y_1 \geq 0, y_2 \geq 0, y_3 \geq 0, y_3 \geq 0 \end{array} \right. \end{array}$$

The optimal solution is $y_1^\star = 0.1555$, $y_2^\star = 0.6707$, $y_3^\star = 0.2104$ and $y_4^\star = 0$. The optimal value of the dual objective function is \$65.91. The computation of the Lagrange multipliers gives $\vartheta_1^\star = 7.4390$, $\vartheta_2^\star = 5.3049$ and $\vartheta_3^\star = 2.4390$. We can make the following observations. First, the strong duality property is satisfied because $\mathcal{R}evenue\,(x^\star) = \mathcal{C}ost\,(y^\star) = \$65.91$. Second, we verify that $y^\star = \lambda^\star$ and $x^\star = \vartheta^\star$. The optimal solution of one problem is equal to the Lagrange coefficients of the second problem. Therefore, we interpret $y^\star$ as the shadow prices of the resources. Third, a shadow price $y_j^\star$ is equal to zero when the $j^{th}$ constraint is non-binding. Otherwise, it is strictly positive. If we

consider the previous example, the shadow price of the fourth resource is equal to zero because this resource is not scarce. In particular, we do not need to buy supplementary land to increase the revenue. Therefore, we are ready to pay zero for additional land. On the contrary, we can pay the supplementary unit up to \$0.1555 to buy more capital. If the price of capital is greater than \$0.1555, the increase of revenue will be lower than the increase of cost and we have no interest to increase the production capacity.

### Quadratic programming

A quadratic programming (QP) problem is an optimization problem with a quadratic objective function and linear inequality constraints:

$$\begin{aligned} x^\star &= \arg\min \frac{1}{2} x^\top Q x - x^\top R \\ &\text{s.t.} \quad Sx \leq T \end{aligned} \tag{A.4}$$

where $x$ is a $n \times 1$ vector, $Q$ is a $n \times n$ matrix and $R$ is a $n \times 1$ vector. We note that the system of constraints $Sx \leq T$ allows specifying linear equality constraints[7] $Ax = B$ or weight constraints $x^- \leq x \leq x^+$. Most numerical packages then consider the following formulation:

$$\begin{aligned} x^\star &= \arg\min \frac{1}{2} x^\top Q x - x^\top R \\ &\text{s.t.} \quad \begin{cases} Ax = B \\ Cx \leq D \\ x^- \leq x \leq x^+ \end{cases} \end{aligned} \tag{A.5}$$

because the problem (A.5) is equivalent to the canonical problem (A.4) with the following system of linear inequalities:

$$\begin{bmatrix} -A \\ A \\ C \\ -I_n \\ I_n \end{bmatrix} x \leq \begin{bmatrix} -B \\ B \\ D \\ -x^- \\ x^+ \end{bmatrix}$$

If the space $\Omega$ defined by $Sx \leq T$ is non-empty and if $Q$ is a symmetric positive definite matrix, the solution exists because the function $f(x) = \frac{1}{2} x^\top Q x - x^\top R$ is convex. In the general case where $Q$ is a square matrix, the solution may not exist.

The Lagrange function is also:

$$\mathcal{L}(x; \lambda) = \frac{1}{2} x^\top Q x - x^\top R + \lambda^\top (Sx - T)$$

We deduce that the dual problem is defined by:

$$\begin{aligned} \lambda^\star &= \arg\max \left\{ \inf_x \mathcal{L}(x; \lambda) \right\} \\ &\text{s.t.} \quad \lambda \geq 0 \end{aligned}$$

[7] This is equivalent to imposing that $Ax \geq B$ and $Ax \leq B$.

We note that $\partial_x \mathcal{L}(x;\lambda) = Qx - R + S^\top \lambda$. The solution to the problem $\partial_x \mathcal{L}(x;\lambda) = 0$ is then $x = Q^{-1}\left(R - S^\top \lambda\right)$. We obtain:

$$\begin{aligned}
\inf_x \mathcal{L}(x;\lambda) &= \frac{1}{2}\left(R^\top - \lambda^\top S\right) Q^{-1}\left(R - S^\top \lambda\right) - \left(R^\top - \lambda^\top S\right) Q^{-1} R + \\
&\quad \lambda^\top \left(S Q^{-1}\left(R - S^\top \lambda\right) - T\right) \\
&= \frac{1}{2} R^\top Q^{-1} R - \lambda^\top S Q^{-1} R + \frac{1}{2}\lambda^\top S Q^{-1} S^\top \lambda - R^\top Q^{-1} R + \\
&\quad 2\lambda^\top S Q^{-1} R - \lambda^\top S Q^{-1} S^\top \lambda - \lambda^\top T \\
&= -\frac{1}{2}\lambda^\top S Q^{-1} S^\top \lambda + \lambda^\top \left(S Q^{-1} R - T\right) - \frac{1}{2} R^\top Q^{-1} R
\end{aligned}$$

The dual program is another quadratic program:

$$\begin{aligned}
\lambda^\star &= \arg\min \frac{1}{2}\lambda^\top \bar{Q}\lambda - \lambda^\top \bar{R} \\
&\text{s.t.} \quad \lambda \geq 0
\end{aligned} \tag{A.6}$$

where $\bar{Q} = S Q^{-1} S^\top$ and $\bar{R} = S Q^{-1} R - T$.

**Alternating direction method of multipliers**

The alternating direction method of multipliers (ADMM) is an algorithm introduced by Gabay and Mercier (1976) to solve optimization problems that can be expressed as:

$$\begin{aligned}
\{x^\star, y^\star\} &= \arg\min_{(x,y)} f_x(x) + f_y(y) \\
&\text{s.t.} \quad Ax + By = c
\end{aligned} \tag{A.7}$$

where $A \in \mathbb{R}^{p\times n}$, $B \in \mathbb{R}^{p\times m}$, $c \in \mathbb{R}^p$, and the functions $f_x : \mathbb{R}^n \to \mathbb{R} \cup \{+\infty\}$ and $f_y : \mathbb{R}^m \to \mathbb{R} \cup \{+\infty\}$ are proper closed convex functions. Boyd *et al.* (2011) showed that the ADMM algorithm consists of the following three steps:

1. The $x$-update is:

$$x^{(k+1)} = \arg\min_x \left\{ f_x^{(k+1)}(x) := f_x(x) + \frac{\varphi}{2}\left\| Ax + By^{(k)} - c + u^{(k)} \right\|_2^2 \right\} \tag{A.8}$$

2. The $y$-update is:

$$y^{(k+1)} = \arg\min_y \left\{ f_y^{(k+1)}(y) := f_y(y) + \frac{\varphi}{2}\left\| Ax^{(k+1)} + By - c + u^{(k)} \right\|_2^2 \right\} \tag{A.9}$$

3. The $u$-update is:

$$u^{(k+1)} = u^{(k)} + \left( Ax^{(k+1)} + By^{(k+1)} - c \right) \tag{A.10}$$

In this approach, $u^{(k)}$ is the dual variable of the primal residual $r = Ax + By - c$ and $\varphi$ is the $\mathcal{L}_2$-norm penalty variable. The parameter $\varphi$ may be constant or it may change at each iteration. The ADMM algorithm benefits from the dual ascent principle and the multipliers method. The difference with the latter is that the $x$- and $y$-updates are performed alternately. This makes it more flexible, since the updates are equivalent to computing proximal operators for $f_x$ and $f_y$ independently. In practice, ADMM may be slow to converge at high accuracy, but is fast to converge at modest accuracy. Therefore, ADMM is a good candidate for solving large-scale machine learning problems where high accuracy does not necessarily lead to a better solution.

### A.1.3 Quadratic form

#### Definition

In mathematics, a quadratic form is a polynomial with terms all of degree two:

$$\mathcal{QF}(x_1,\dots,x_n)=\sum_{i=1}^{n}\sum_{j=1}^{n}a_{i,j}x_ix_j=x^\top Ax$$

where $A=(a_{i,j})$ is a $n\times n$ matrix. Since $x^\top Ax$ is a scalar, we have $\left(x^\top Ax\right)^\top=x^\top A^\top x$ and:

$$\begin{aligned}\mathcal{QF}(x_1,\dots,x_n) &= \frac{1}{2}\left(x^\top Ax+x^\top A^\top x\right)\\ &= \frac{1}{2}x^\top\left(A+A^\top\right)x\\ &= \frac{1}{2}x^\top Qx\end{aligned}$$

where $Q=A+A^\top$ is a symmetric matrix. We use the notation $\mathcal{QF}(x;Q)=\frac{1}{2}x^\top Qx$ to define a canonical quadratic form. A generalized quadratic form is a polynomial including terms with degrees one and zero[8]:

$$\mathcal{QF}(x;Q,R,c)=\frac{1}{2}x^\top Qx-x^\top R+c$$

#### Main properties

We list here some properties that are helpful when considering portfolio optimization:

- The multiplication of a quadratic form by a scalar $\varphi\geq 0$ remains a quadratic form:

$$\varphi\cdot\mathcal{QF}(w;Q,R,c)=\mathcal{QF}(w;\varphi Q,\varphi R,\varphi c)$$

- The sum of two quadratic forms is a quadratic form:

$$\mathcal{QF}(x;Q_1,R_1,c_1)+\mathcal{QF}(x;Q_2,R_2,c_2)=\mathcal{QF}(x;Q_1+Q_2,R_1+R_2,c_1+c_2)$$

- A quadratic form applied to the difference vector $x-y$ is a quadratic form in $x$:

$$\begin{aligned}\mathcal{QF}(x-y;Q,R,c) &= \frac{1}{2}(x-y)^\top Q(x-y)-(x-y)^\top R+c\\ &= \frac{1}{2}\left(x^\top Qx-2x^\top Qy+y^\top Qy\right)-x^\top R+y^\top R+c\\ &= \frac{1}{2}x^\top Qx-x^\top(R+Qy)+\frac{1}{2}y^\top Qy+y^\top R+c\\ &= \mathcal{QF}\left(x;Q,R+Qy,\frac{1}{2}y^\top Qy+y^\top R+c\right)\end{aligned}$$

  and a quadratic form in $y$:

$$\begin{aligned}\mathcal{QF}(x-y;Q,R,c) &= \frac{1}{2}y^\top Qy-y^\top(Qx-R)+\frac{1}{2}x^\top Qx-x^\top R+c\\ &= \mathcal{QF}\left(y;Q,Qx-R,\frac{1}{2}x^\top Qx-x^\top R+c\right)\end{aligned}$$

[8] We add the one-degree polynomial $-x^\top R$ instead of $+x^\top R$ in order to match the canonical form of a QP problem.

- When $Q$ is a diagonal matrix, the quadratic form reduces to:

$$\mathcal{QF}(x;Q,R,c)=\frac{1}{2}\sum_{i=1}^{n}q_{i,i}x_i^2-\sum_{i=1}^{n}r_ix_i+c$$

We deduce that:

$$\frac{1}{2}\sum_{i=1}^{n}q_ix_i^2=\mathcal{QF}(x;\mathcal{D}(q),\mathbf{0}_n,0)$$

where $q=(q_1,\ldots,q_n)$ is a $n\times 1$ vector and $\mathcal{D}(q)=\operatorname{diag}(q)$.

- Using the previous properties, we have:

$$\begin{aligned}\frac{1}{2}\sum_{i=1}^{n}q_i(x_i-y_i)^2 &= \mathcal{QF}(x-y;\mathcal{D}(q),\mathbf{0}_n,0)\\ &= \mathcal{QF}\left(x;\mathcal{D}(q),\mathcal{D}(q)\,y,\frac{1}{2}y^\top\mathcal{D}(q)\,y\right)\end{aligned}$$

- The square of the weighted sum is also a quadratic form:

$$\frac{1}{2}\left(\sum_{i=1}^{n}q_ix_i\right)^2=\frac{1}{2}\left(x^\top q\right)^2=\frac{1}{2}\left(x^\top q\right)\left(x^\top q\right)^\top=\frac{1}{2}x^\top qq^\top x^\top=\mathcal{QF}(x;\mathcal{T}(q),\mathbf{0}_n,0)$$

where $\mathcal{T}(q)=qq^\top$.

- We deduce that:

$$\begin{aligned}\frac{1}{2}\left(\sum_{i=1}^{n}q_i(x_i-y_i)\right)^2 &= \mathcal{QF}(x-y;\mathcal{T}(q),\mathbf{0}_n,0)\\ &= \mathcal{QF}\left(x;\mathcal{T}(q),\mathcal{T}(q)\,y,\frac{1}{2}y^\top\mathcal{T}(q)\,y\right)\end{aligned}$$

- The previous results can be extended when we consider partial sums:

$$\sum_{i\in\Omega}q_ix_i=\sum_{i=1}^{n}\mathbb{1}\{i\in\Omega\}\cdot q_ix_i=\sum_{i=1}^{n}(\omega_iq_i)\,x_i=\sum_{i=1}^{n}\tilde{q}_ix_i$$

where $\omega_i=\mathbb{1}\{i\in\Omega\}$ and $\tilde{q}_i=\omega_iq_i$. In a matrix form, we have:

$$\sum_{i\in\Omega}q_ix_i=(\omega\circ q)^\top x$$

where $\omega=(\omega_1,\ldots,\omega_n)$. We deduce that:

$$\begin{cases}\frac{1}{2}\sum_{i\in\Omega}q_ix_i^2=\mathcal{QF}(x;\mathcal{D}(\omega\circ q),\mathbf{0}_n,0)\\ \frac{1}{2}\sum_{i\in\Omega}q_i(x_i-y_i)^2=\mathcal{QF}\left(x;\mathcal{D}(\omega\circ q),\mathcal{D}(\omega\circ q)\,y,\frac{1}{2}y^\top\mathcal{D}(\omega\circ q)\,y\right)\\ \frac{1}{2}\left(\sum_{i\in\Omega}q_ix_i\right)^2=\mathcal{QF}(x;\mathcal{T}(\omega\circ q),\mathbf{0}_n,0)\\ \frac{1}{2}\left(\sum_{i\in\Omega}q_i(x_i-y_i)\right)^2=\mathcal{QF}\left(x;\mathcal{T}(\omega\circ q),\mathcal{T}(\omega\circ q)\,y,\frac{1}{2}y^\top\mathcal{T}(\omega\circ q)\,y\right)\end{cases}$$

We notice that $\mathcal{D}(\omega\circ q)=\operatorname{diag}(\omega\circ q)=\mathcal{D}(\omega)\,\mathcal{D}(q)$ and $\mathcal{T}(\omega\circ q)=(\omega\circ q)(\omega\circ q)^\top=\left(\omega\omega^\top\right)\circ qq^\top=\mathcal{T}(\omega)\circ\mathcal{T}(q)$.

### A.1.4 Nonnegative matrix

#### Definition

$A = (a_{i,j})$ is a nonnegative matrix if all the elements are greater than or equal to zero: $a_{i,j} \geq 0$. Here are some special cases:

- A positive matrix is one where all elements are strictly greater than zero.
- A stochastic matrix is a square nonnegative matrix whose rows or columns are probability vectors[9].
  - A right/row stochastic matrix is a stochastic matrix where each row sums to 1: $\sum_{j=1}^{n} a_{i,j} = 1$.
  - A left/column stochastic matrix is a stochastic matrix where each column sums to 1: $\sum_{i=1}^{n} a_{i,j} = 1$.
  - A doubly stochastic matrix is a right and left stochastic matrix.
- A substochastic matrix is a square nonnegative matrix whose rows or columns add up to at most 1.
  - $A$ is a right/row substochastic matrix if $\sum_{j=1}^{n} a_{i,j} \leq 1$.
  - $A$ is a left/column substochastic matrix if $\sum_{i=1}^{n} a_{i,j} \leq 1$.
  - $A$ is a doubly substochastic matrix if it is a right and left substochastic matrix.

#### Ordering properties

$A$ is greater than or equal to $B$ if and only if $A_{i,j} \geq B_{i,j}$ for all $i, j$. We use the notation $A \succeq B$. By definition, a square nonnegative matrix $A$ satisfies $A \succeq \mathbf{0}_{n,n}$. If $A$ is a stochastic matrix, we have $\mathbf{0}_{n,n} \preceq A \preceq \mathbf{1}_{n,n}$. Let $A$, $B$, $C$ and $D$ be square nonnegative matrices. We can show that:

(NN1) $A \succeq B \Rightarrow AC \succeq BC$;

(NN2) $A \succeq B \wedge C \succeq D \Rightarrow AC \succeq BD$;

(NN3) $A \succeq B \wedge C \succeq D \Rightarrow A + C \succeq B + D$;

(NN4) $A \succeq B \wedge k \geq 1 \Rightarrow A^k \succeq B^k$;

The proofs can be found in Desnos *et al.* (2023).

[9] This means that each entry is a real number between 0 and 1 and the sum of entries is equal to 1.

## A.2 Statistical and probability analysis

### A.2.1 Probability distributions

#### The Bernoulli distribution

The Bernoulli random variable $X$ takes the value 1 with success probability of $p$ and the value 0 with failure probability of $q = 1 - p$. We note $X \sim \mathcal{B}(p)$. The probability mass function may also be expressed as follows:

$$\Pr\{X = k\} = p^k (1-p)^{1-k} \qquad \text{with } k = 0, 1$$

We have $\mathbb{E}[X] = p$ and $\text{var}(X) = p(1-p)$.

#### The binomial distribution

The binomial random variable $X$ is the sum of $n$ independent Bernoulli random variables with the same probability of success $p$:

$$X = \sum_{i=1}^{n} \mathcal{B}_i(p)$$

We note $X \sim \mathcal{B}(n, p)$. The probability mass function is equal to:

$$\Pr\{X = k\} = \binom{n}{k} p^k (1-p)^{n-k} \qquad \text{with } k = 0, 1, \ldots, n$$

We have $\mathbb{E}[X] = np$ and $\text{var}(X) = np(1-p)$.

#### The geometric distribution

The geometric random variable $X$ is the number of Bernoulli trials needed to get one success. We note $X \sim \mathcal{G}(p)$. The probability mass function is equal to:

$$\Pr\{X = k\} = (1-p)^{k-1} p \qquad \text{with } k \in \mathbb{N}^\star$$

We have $\mathbb{E}[X] = 1/p$ and $\text{var}(X) = (1-p)/p^2$.

**Remark 133** *If we define $X$ as the number of failures before the first success, we have* $\Pr\{X = k\} = (1-p)^k p$ *with* $k \in \mathbb{N}$, $\mathbb{E}[X] = (1-p)/p$ *and* $\text{var}(X) = (1-p)/p^2$.

#### The Poisson distribution

The Poisson random variable $X$ is the number of times an event occurs in the unit interval of time. We note $X \sim \mathcal{P}(\lambda)$ where $\lambda$ is the parameter of the Poisson distribution. The probability mass function is equal to:

$$\Pr\{X = k\} = \frac{\lambda^k e^{-\lambda}}{k!} \qquad \text{with } k \in \mathbb{N}$$

We have $\mathbb{E}[X] = \text{var}(X) = \lambda$. The parameter $\lambda$ is then the expected number of events occurring in the unit interval of time.

### The 1- and $n$-diversity distributions

Let $\pi_n \in \mathbb{R}_+^n$ such that $\mathbf{1}^\top \pi_n = 1$. $\pi_n$ is then a probability distribution. The probability distribution $\pi_n^-$ is perfectly concentrated if there exists one observation $i_0$ such that $\pi_{n,i_0}^- = 1$ and $\pi_{n,i}^- = 0$ if $i \neq i_0$. When $n$ tends to $+\infty$, the limit distribution is noted $\pi_\infty^-$. On the opposite, the probability distribution $\pi_n^+$ such that $\pi_{n,i}^+ = 1/n$ for all $i = 1, \ldots, n$ has no concentration. $\pi_n^-$ and $\pi_n^+$ are respectively called 1- and $n$-diversity distributions.

### The negative binomial distribution

Probability distribution!Negative binomial distribution

The negative binomial distribution is a probability distribution used for modeling the frequency of an event. We denote it as $X \sim \mathcal{NB}(r, p)$, where $r > 0$ and $p \in [0, 1]$. The probability mass function is equal to:

$$\Pr\{X = k\} = \binom{r+k-1}{k} (1-p)^r p^k \qquad \text{with } k \in \mathbb{N}$$

We have $\mathbb{E}[X] = pr/(1-p)$ and $\text{var}(X) = pr/(1-p)^2$.

### The Poisson binomial distribution

The Poisson binomial distribution is the discrete probability distribution of a sum of independent Bernoulli trials that are not identically distributed [10]:

$$X = \sum_{i=1}^n \mathcal{B}(p_i) \sim \mathcal{PB}(p_1, \ldots, p_n)$$

The probability mass function is given by:

$$\Pr\{X = k\} = \sum_{\mathcal{E} \in \mathcal{F}_k} \prod_{i \in \mathcal{E}} p_i \prod_{j \in \mathcal{E}^c} (1 - p_j)$$

where $\mathcal{F}_k$ is the set of all subsets of $k$ integers that can be selected from $\{1, \ldots, n\}$ and $\mathcal{E}^c$ denotes the complement of the subset $\mathcal{E}$. The probability mass function can also be expressed as the convolution of the vectors $\{u_0, u_1, \ldots, u_n\}$ where $u_0 = 1$ and $u_i = (p_i, 1 - p_i)$. To calculate $\Pr\{X = k\}$, we deduce that the vector of discrete probabilities is the inverse Fourier transform of the vector $v_n$ where:

$$v_j = \left(1 + p_j + p_j \exp\left(-\frac{2\pi i}{n+1}\right)\right) v_{j-1}$$

and $v_0 = \mathbf{1}_{n+1}$. We have $\mathbb{E}[X] = \sum_{i=1}^n p_i$ and $\text{var}(X) = \sum_{i=1}^n p_i (1 - p_i)$.

### The uniform distribution

$X$ is a uniform random variable $\mathcal{U}_{[a,b]}$ if the density function is $f(x) = (b-a)^{-1}$ for $x \in [a, b]$. We deduce that the cumulative density function is equal to:

$$\mathbf{F}(x) = \begin{cases} 0 & \text{if } x \leq a \\ \dfrac{x-a}{b-a} & \text{if } x \in [a, b] \\ 1 & \text{if } x \geq b \end{cases}$$

[10] If $p_i = p_j$, we get the Binomial distribution.

We have:

$$\mathbb{E}[X] = \frac{a+b}{2}$$

and:

$$\text{var}(X) = \frac{(b-a)^2}{12}$$

The standard uniform distribution $\mathcal{U}_{[0,1]}$ is obtained with $a = 0$ and $b = 1$.

**Remark 134** *The uniform distribution is related to the probability integral transform. We assume that $X \sim \mathbf{F}$ is a continuous random variable. Let $U = \mathbf{F}(X)$ be the integral transform of $X$. Its cumulative distribution function $\mathbf{G}$ is equal to:*

$$\begin{aligned}
\mathbf{G}(u) &= \Pr\{U \leq u\} \\
&= \Pr\{\mathbf{F}(X) \leq u\} \\
&= \Pr\left\{X \leq \mathbf{F}^{-1}(u)\right\} \\
&= \mathbf{F}\left(\mathbf{F}^{-1}(u)\right) \\
&= u
\end{aligned}$$

*where $\mathbf{G}(0) = 0$ and $\mathbf{G}(1) = 1$. We deduce that $U$ is a standard uniform random variable.*

**The gamma distribution**

The gamma distribution is a two-parameter family of continuous probability distributions, whose support is $[0, \infty)$. We note $X \sim \mathcal{G}(\alpha, \beta)$ where $\alpha > 0$ and $\beta > 0$. $\alpha$ and $\beta$ are called the shape parameter and the rate parameter. The probability density function is equal to:

$$f(x) = \frac{\beta^\alpha x^{\alpha-1} e^{-\beta x}}{\Gamma(\alpha)}$$

where $\Gamma(\alpha)$ is the gamma function defined as:

$$\Gamma(\alpha) = \int_0^\infty t^{\alpha-1} e^{-t} \, \mathrm{d}t$$

The cumulative distribution function is the regularized gamma function:

$$\mathbf{F}(x) = \frac{\gamma(\alpha, \beta x)}{\Gamma(\alpha)}$$

where $\gamma(\alpha, x)$ is the lower incomplete gamma function defined as:

$$\gamma(\alpha, x) = \int_0^x t^{\alpha-1} e^{-t} \, \mathrm{d}t$$

We have $\mathbb{E}[X] = \alpha/\beta$ and $\text{var}(X) = \alpha/\beta^2$. We verify the following properties:

- $\mathcal{G}(1, \beta) \sim \mathcal{E}(\beta)$;
- if $X \sim \mathcal{G}(\alpha, \beta)$, then $cX \sim \mathcal{G}(\alpha, \beta/c)$ when $c > 0$;
- $\sum_{i=1}^n \mathcal{G}(\alpha_i, \beta) \sim \mathcal{G}(\sum_{i=1}^n \alpha_i, \beta)$.

**Remark 135** *The standard gamma distribution corresponds to $\mathcal{G}(\alpha, 1)$ and is denoted by $\mathcal{G}(\alpha)$.*

### The beta distribution

The beta distribution is a two-parameter family of continuous probability distributions defined on the interval $[0,1]$. We note $X \sim \mathcal{B}(\alpha,\beta)$ where $\alpha > 0$ and $\beta > 0$. The probability density function is equal to:

$$f(x) = \frac{x^{\alpha-1}(1-x)^{\beta-1}}{\mathfrak{B}(\alpha,\beta)}$$

where $\mathfrak{B}(\alpha,\beta)$ is the beta function defined as:

$$\mathfrak{B}(\alpha,\beta) = \int_0^1 t^{\alpha-1}(1-t)^{\beta-1}\,\mathrm{d}t = \frac{\Gamma(\alpha)\Gamma(\beta)}{\Gamma(\alpha+\beta)}$$

The cumulative distribution function is the regularized incomplete beta function:

$$\mathbf{F}(x) = \mathcal{IB}(x;\alpha,\beta) = \frac{\mathfrak{B}(x;\alpha,\beta)}{\mathfrak{B}(\alpha,\beta)}$$

where $\mathfrak{B}(x;\alpha,\beta)$ is the incomplete beta function defined as:

$$\mathfrak{B}(x;\alpha,\beta) = \int_0^x t^{\alpha-1}(1-t)^{\beta-1}\,\mathrm{d}t$$

We have $\mathbb{E}[X] = \alpha/(\alpha+\beta)$ and:

$$\mathrm{var}(X) = \frac{\alpha\beta}{(\alpha+\beta)^2(\alpha+\beta+1)}$$

### The exponential distribution

$X$ is an exponential random variable $\mathcal{E}(\lambda)$ if the density function is $f(x) = \lambda e^{-\lambda x}$ for $x \geq 0$. We deduce that $\mathbf{F}(x) = 1 - e^{-\lambda x}$. We have $\mathbb{E}[X] = 1/\lambda$ and $\mathrm{var}(X) = 1/\lambda^2$. More generally, we can show that $\mathbb{E}[X^n] = n!/\lambda^n$. This distribution verifies the lack of memory property:

$$\Pr\{X \geq s+t \mid X \geq s\} = \Pr\{X \geq t\}$$

for all $s \geq 0$ and $t \geq 0$.

### The normal distribution

Let $\mathbb{C}$ be a correlation matrix. We consider the standardized Gaussian random vector $X \sim \mathcal{N}(\mathbf{0},\mathbb{C})$ of dimension $n$. We note $\phi_n(x;\mathbb{C})$ the associated density function defined as:

$$\phi_n(x;\mathbb{C}) = (2\pi)^{-n/2}\left|\mathbb{C}\right|^{-1/2}\exp\left(-\frac{1}{2}x^\top\mathbb{C}^{-1}x\right)$$

We deduce that the expression of cumulative distribution function is:

$$\Phi_n(x;\mathbb{C}) = \int_{-\infty}^{x_1}\cdots\int_{-\infty}^{x_2}\phi_n(u;\mathbb{C})\,\mathrm{d}u$$

By construction, we have $\mathbb{E}[X] = \mathbf{0}$ and $\mathrm{cov}(x) = \mathbb{C}$. In the bivariate case, we use the notations $\phi_2(x_1,x_2;\rho) = \phi_2(x;\mathbb{C})$ and $\Phi_2(x_1,x_2;\rho) = \Phi_2(x;\mathbb{C})$ where $\rho = \mathbb{C}_{1,2}$ is the correlation between

the components $X_1$ and $X_2$. In the univariate case, we also consider the alternative notations $\phi(x) = \phi_1(x;1)$ and $\Phi(x) = \Phi_1(x;1)$. The density function reduces then to:

$$\phi(x) = \frac{1}{\sqrt{2\pi}} \exp\left(-\frac{1}{2}x^2\right)$$

Concerning the moments, we have $\mu(X) = 0$, $\sigma(X) = 1$, $\gamma_1(X) = 0$ and $\gamma_2(X) = 0$.

Adding a mean vector $\mu$ and a covariance matrix $\Sigma$ is equivalent to apply the linear transformation to $X$:

$$Y = \mu + \sigma X$$

where $\sigma = \text{diag}^{1/2}(\Sigma)$.

**The log-normal distribution**

Let $Z \sim \mathcal{N}(\mu, \sigma^2)$ be a normal-distributed random variable. $X = e^Z$ is a log-normal random variable and we note $X \sim \mathcal{LN}(\mu, \sigma^2)$. The probability distribution function is equal to:

$$f(x) = \frac{1}{x\sigma\sqrt{2\pi}} e^{-\frac{1}{2}\left(\frac{x-\mu}{\sigma}\right)^2}$$

whereas the cumulative distribution function has the following expression:

$$\mathbf{F}(x) = \Phi\left(\frac{\ln x - \mu}{\sigma}\right)$$

We have:

$$\mathbb{E}[X] = e^{\mu + \frac{1}{2}\sigma^2}$$

and:

$$\text{var}(X) = e^{2\mu+\sigma^2}\left(e^{\sigma^2} - 1\right)$$

**The inverse Gaussian distribution**

The inverse Gaussian distribution is a two-parameter family of continuous probability distribution, whose support is $[0, \infty)$. We note $X \sim \mathcal{IG}(\mu, \lambda)$ where $\mu > 0$ and $\lambda > 0$, $\mu$ and $\lambda$ are called the mean parameter and the shape parameter. The probability density function is equal to:

$$f(x) = \sqrt{\frac{\lambda}{2\pi x^3}} \exp\left(-\frac{\lambda}{2\mu^2 x}(x-\mu)^2\right)$$

while the cumulative density function has the following expression:

$$\mathbf{F}(x) = \Phi\left(\sqrt{\frac{\lambda}{x}}\left(\frac{x-\mu}{\mu}\right)\right) + \exp\left(2\frac{\lambda}{\mu}\right)\Phi\left(-\sqrt{\frac{\lambda}{x}}\left(\frac{x+\mu}{\mu}\right)\right)$$

We have $\mathbb{E}[X] = \mu$ and $\text{var}(X) = \mu^3/\lambda$. We verify the following properties:

- If $X \sim \mathcal{IG}(\mu, \lambda)$, then $cX \sim \mathcal{IG}(c\mu, c\lambda)$ when $c > 0$;
- If $X_i \sim \mathcal{IG}(\mu, \lambda)$, then $\sum_{i=1}^n X_i \sim \mathcal{IG}\left(n\mu, n^2\lambda\right)$;
- If $X \sim \mathcal{IG}(\mu, \lambda)$, then $\mathbb{E}\left[X^{-k}\right] = \mu^{-(2k+1)}\mathbb{E}\left(X^{k+1}\right)$ for $k \in \mathbb{N}^*$.

**The Pareto distribution**

The Pareto distribution is denoted by $\mathcal{P}(\alpha, x_-)$. We have:

$$f(x) = \frac{\alpha}{x}\left(\frac{x}{x_-}\right)^{-\alpha}$$

and:

$$\mathbf{F}(x) = 1 - \left(\frac{x}{x_-}\right)^{-\alpha}$$

where $x \geq x_-$, $\alpha > 0$ and $x_- > 0$. Concerning the first two moments, we obtain:

$$\mathbb{E}[X] = \frac{\alpha x_-}{\alpha - 1}$$

if $\alpha > 1$ and:

$$\text{var}(X) = \frac{\alpha x_-^2}{(\alpha-1)^2(\alpha-2)}$$

if $\alpha > 2$.

**Remark 136** *The Pareto distribution: can be parameterized as follows;*

$$\mathbf{F}(x) = 1 - \left(\frac{\theta + x}{\theta}\right)^{-\alpha}$$

*where $x \geq 0$, $\alpha > 0$ and $\theta > 0$. In this case, it is denoted by $\mathcal{P}(\alpha, \theta)$.*

**The generalized extreme value distribution**

The generalized extreme value distribution is denoted by $\mathcal{GEV}(\mu, \sigma, \xi)$. We have:

$$f(x) = \frac{1}{\sigma}\left(1 + \xi\left(\frac{x-\mu}{\sigma}\right)\right)^{-(1+1/\xi)} \exp\left(-\left(1 + \xi\left(\frac{x-\mu}{\sigma}\right)\right)^{-1/\xi}\right)$$

and:

$$\mathbf{F}(x) = \exp\left(-\left(1 + \xi\left(\frac{x-\mu}{\sigma}\right)\right)^{-1/\xi}\right)$$

where $x > \mu - \sigma/\xi$, $\sigma > 0$ and $\xi > 0$. Concerning the first two moments, we obtain:

$$\mathbb{E}[X] = \mu + \frac{\sigma}{\xi}(\Gamma(1-\xi) - 1)$$

if $\xi < 1$ and:

$$\text{var}(X) = \frac{\sigma^2}{\xi^2}\left(\Gamma(1-2\xi) - \Gamma^2(1-\xi)\right)$$

if $\xi < 1/2$.

**The generalized Pareto distribution**

The generalized Pareto distribution is denoted by $\mathcal{GPD}(\sigma, \xi)$. We have:

$$f(x) = \frac{1}{\sigma}\left(1 + \frac{\xi x}{\sigma}\right)^{-1/\xi - 1}$$

and:

$$\mathbf{F}(x) = 1 - \left(1 + \frac{\xi x}{\sigma}\right)^{-1/\xi}$$

where $x \geq 0$, $\sigma > 0$ and $\xi > 0$. Concerning the first two moments, we obtain:

$$\mathbb{E}[X] = \frac{\sigma}{1 - \xi}$$

if $\xi < 1$ and:

$$\text{var}(X) = \frac{\sigma^2}{(1 - \xi)^2 (1 - 2\xi)}$$

if $\xi < 1/2$.

**The Bates distribution**

Let $U_1, \ldots, U_n$ be a sequence of *iid* uniform random variables $\mathcal{U}_{[0,1]}$. The mean $\bar{U}_n$ follows the Bates distribution:

$$X := \bar{U}_n = \frac{1}{n}\sum_{k=1}^{n} U_k \sim \mathfrak{Bates}(n)$$

The support is $[0, 1]$. The probability density function is equal to[11]:

$$f(x) = \frac{n}{2(n-1)!}\sum_{k=0}^{n}(-1)^k \binom{n}{k}(nx - k)^{n-1}\,\text{sgn}(nx - k)$$

whereas the cumulative distribution function has the following expression:

$$\mathbf{F}(x) = \frac{1}{n!}\sum_{k=0}^{n}\mathbb{1}\{nx > k\}(-1)^k \binom{n}{k}(nx - k)^n$$

We have:

$$\mathbb{E}[X] = \frac{1}{2}$$

and

$$\text{var}(X) = \frac{1}{12n}$$

[11] If $k = nx$, $\text{sgn}(nx - k) = 0$.

**Conditional probability distribution in the Gaussian case**

Let us consider a Gaussian random vector defined as follows:

$$\begin{pmatrix} X \\ Y \end{pmatrix} \sim \mathcal{N}\left(\begin{pmatrix} \mu_x \\ \mu_y \end{pmatrix}, \begin{pmatrix} \Sigma_{x,x} & \Sigma_{x,y} \\ \Sigma_{y,x} & \Sigma_{y,y} \end{pmatrix}\right)$$

The conditional probability distribution of $Y$ given $X = x$ is a multivariate normal distribution. We have:

$$\mu_{y|x} = \mathbb{E}\left[Y \mid X = x\right] = \mu_y + \Sigma_{y,x}\Sigma_{x,x}^{-1}\left(x - \mu_x\right)$$

and:

$$\Sigma_{y,y|x} = \sigma^2\left[Y \mid X = x\right] = \Sigma_{y,y} - \Sigma_{y,x}\Sigma_{x,x}^{-1}\Sigma_{x,y}$$

We deduce that:

$$Y = \mu_y + \Sigma_{y,x}\Sigma_{x,x}^{-1}\left(x - \mu_x\right) + u$$

where $u$ is a centered Gaussian random variable with variance $\sigma^2 = \Sigma_{y,y|x}$. It follows that:

$$Y = \underbrace{\left(\mu_y - \Sigma_{y,x}\Sigma_{x,x}^{-1}\mu_x\right)}_{\beta_0} + \underbrace{\Sigma_{y,x}\Sigma_{x,x}^{-1}}_{\beta^\top}x + u$$

We recognize the linear regression of $Y$ on a constant and a set of exogenous variables $X$:

$$Y = \beta_0 + \beta^\top X + u$$

Moreover, we have:

$$\mathfrak{R}^2 = 1 - \frac{\sigma^2}{\Sigma_{y,y}} = \frac{\Sigma_{y,x}\Sigma_{x,x}^{-1}\Sigma_{x,y}}{\Sigma_{y,y}}$$

**Change of variables**

Let $X$ be a random variable whose probability density function is $f(x)$. We consider the change of the variable $Y = \varphi(X)$. If the function $\varphi$ is monotone, then the probability density function $g(y)$ of $Y$ is equal to:

$$g(y) = f(x)\left|\frac{\mathrm{d}x}{\mathrm{d}y}\right|$$

In the multivariate case, let $(X_1, \ldots, X_n)$ be the random vector with density function $f(x_1, \ldots, x_n)$. If the function $\varphi$ is bijective, we can show that the probability density function of $(Y_1, \ldots, Y_n) = \varphi(X_1, \ldots, X_n)$ is equal to:

$$g(y_1, \ldots, y_n) = f(x_1, \ldots, x_n)\left|\frac{1}{\det J_\varphi}\right|$$

where $J_\varphi$ is the Jacobian associated with the variable change.

**Ratio distribution**

Given two independent random variables $X$ and $Y$, the distribution of the random variable $Z = Y/X$ is a ratio distribution. We have:

$$\begin{aligned}
\mathbf{F}_z(z) &= \Pr\{Z \leq z\} \\
&= \Pr\left\{\frac{X}{Y} \leq z\right\} \\
&= \Pr\{X \geq zY, Y \leq 0\} + \Pr\{X \leq zY, Y > 0\} \\
&= \int_{-\infty}^{0}\int_{zy}^{\infty} f_{x,y}(x,y)\,\mathrm{d}x\,\mathrm{d}y + \int_{0}^{\infty}\int_{-\infty}^{zy} f_{x,y}(x,y)\,\mathrm{d}x\,\mathrm{d}y \\
&= \int_{-\infty}^{0}\int_{zy}^{\infty} f_x(x) f_y(y)\,\mathrm{d}x\,\mathrm{d}y + \int_{0}^{\infty}\int_{-\infty}^{zy} f_x(x) f_y(y)\,\mathrm{d}x\,\mathrm{d}y \\
&= \int_{-\infty}^{0}\left(\int_{zy}^{\infty} f_x(x)\,\mathrm{d}x\right) f_y(y)\,\mathrm{d}y + \int_{0}^{\infty}\left(\int_{-\infty}^{zy} f_x(x)\,\mathrm{d}x\right) f_y(y)\,\mathrm{d}y \\
&= \int_{-\infty}^{0}(1 - \mathbf{F}_x(zy)) f_y(y)\,\mathrm{d}y + \int_{0}^{\infty}\mathbf{F}_x(zy) f_y(y)\,\mathrm{d}y
\end{aligned}$$

and:

$$\begin{aligned}
f_z(z) &= \partial_z \Pr\{Z \leq z\} \\
&= -\int_{-\infty}^{0} y f_x(zy) f_y(y)\,\mathrm{d}y + \int_{0}^{\infty} y f_x(zy) f_y(y)\,\mathrm{d}y \\
&= \int_{-\infty}^{0} |y| f_x(zy) f_y(y)\,\mathrm{d}y + \int_{0}^{\infty} |y| f_x(zy) f_y(y)\,\mathrm{d}y \\
&= \int_{-\infty}^{\infty} |y| f_x(zy) f_y(y)\,\mathrm{d}y
\end{aligned}$$

In the case where $X \sim \mathcal{N}(\mu_x, \sigma_x^2)$ and $Y \sim \mathcal{N}(\mu_y, \sigma_y^2)$, we note $Z \sim \mathcal{NRD}(\mu_x, \sigma_x^2, \mu_y, \sigma_y^2)$, and Hinkley (1969) showed that:

$$\mathbf{F}_z(z) = \Phi_2\left(-\frac{\mu_y z - \mu_x}{\sigma_x\sigma_y a(z)}, -\frac{\mu_y}{\sigma_y}, \rho_z\right) + \Phi_2\left(\frac{\mu_y z - \mu_x}{\sigma_x\sigma_y a(z)}, \frac{\mu_y}{\sigma_y}, \rho_z\right)$$

and:

$$f_z(z) = \frac{b(z)}{\sigma_x\sigma_y\sqrt{2\pi}a^3(z)}\left(2\Phi\left(\frac{b(z)}{a(z)}\right) - 1\right)\exp\left(\frac{b^2(z) - ca^2(z)}{2a^2(z)}\right) + \frac{1}{\sigma_x\sigma_y a^2(z)\pi}\exp\left(-\frac{c}{2}\right)$$

where $a(z) = \sqrt{\frac{1}{\sigma_x^2}z^2 + \frac{1}{\sigma_y^2}}$, $b(z) = \frac{\mu_x}{\sigma_x^2}z + \frac{\mu_y}{\sigma_y^2}$, $c = \frac{\mu_x^2}{\sigma_x^2} + \frac{\mu_y^2}{\sigma_y^2}$ and $\rho_z = \frac{z}{\sigma_x a(z)}$. Depending on the parameter values, $Z$ has one or two modes. The moments of $Z$ do not exist. In the case where $\mu_x = \mu_y = 0$, $b(z) = 0$ and $c = 0$, which implies that $Z$ follows a Cauchy distribution:

$$f_z(z) = \frac{\sigma_x\sigma_y}{\pi\left(\sigma_y^2 z^2 + \sigma_x^2\right)}$$

The previous result can be easily extended to the correlated case, because $\mathbf{F}_z(z)$ has exactly the same expression with $a(z) = \sqrt{\frac{1}{\sigma_x^2}z^2 - 2\frac{\rho_{x,y}}{\sigma_x\sigma_y}z + \frac{1}{\sigma_y^2}}$ and $\rho_z = \frac{\sigma_y z - \rho_{x,y}\sigma_x}{\sigma_x\sigma_y a(z)}$.

### A.2.2 Copula functions

The concept of copula has been introduced by Sklar in 1959. During a long time, only a small number of people have used copula functions, more in the field of mathematics than this of statistics. The publication of Genest and MacKay (1986b) in the *American Statistician* marks a breakdown and opens areas of study in empirical modeling, statistics and econometrics. In what follows, we intensively use the materials developed in the books of Joe (1997), Nelsen (2006) and Roncalli (2020a).

#### Definition and main properties

Nelsen (2006) defines a bi-dimensional copula (or a 2-copula) as a function $\mathbf{C}$ which satisfies the following properties:

1. $\text{Dom}\,\mathbf{C} = [0,1] \times [0,1]$;
2. $\mathbf{C}(0,u) = \mathbf{C}(u,0) = 0$ and $\mathbf{C}(1,u) = \mathbf{C}(u,1) = u$ for all $u$ in $[0,1]$;
3. $\mathbf{C}$ is 2-increasing:

$$\mathbf{C}(v_1,v_2) - \mathbf{C}(v_1,u_2) - \mathbf{C}(u_1,v_2) + \mathbf{C}(u_1,u_2) \geq 0$$

for all $(u_1,u_2) \in [0,1]^2$, $(v_1,v_2) \in [0,1]^2$ such that $0 \leq u_1 \leq v_1 \leq 1$ and $0 \leq u_2 \leq v_2 \leq 1$.

This definition means that $\mathbf{C}$ is a cumulative distribution function with uniform margins:

$$\mathbf{C}(u_1,u_2) = \Pr\{U_1 \leq u_1, U_2 \leq u_2\}$$

where $U_1$ and $U_2$ are two uniform random variables.

Let us consider the function $\mathbf{C}^{\perp}(u_1,u_2) = u_1 u_2$. We have $\mathbf{C}^{\perp}(0,u) = \mathbf{C}^{\perp}(u,0) = 0$ and $\mathbf{C}^{\perp}(1,u) = \mathbf{C}^{\perp}(u,1) = u$. Since we have $v_2 - u_2 \geq 0$ and $v_1 \geq u_1$, it follows that $v_1(v_2-u_2) \geq u_1(v_2-u_2)$ and $v_1v_2 + u_1u_2 - u_1v_2 - v_1u_2 \geq 0$. We deduce that $\mathbf{C}^{\perp}$ is a copula function. It is called the product copula.

Let $\mathbf{F}_1$ and $\mathbf{F}_2$ be any two univariate distributions. It is obvious that $\mathbf{F}(x_1,x_2) = \mathbf{C}(\mathbf{F}_1(x_1),\mathbf{F}_2(x_2))$ is a probability distribution with margins $\mathbf{F}_1$ and $\mathbf{F}_2$. Indeed, $u_i = \mathbf{F}_i(x_i)$ defines a uniform transformation ($u_i \in [0,1]$). Moreover, we verify that $\mathbf{C}(\mathbf{F}_1(x_1),\mathbf{F}_2(\infty)) = \mathbf{C}(\mathbf{F}_1(x_1),1) = \mathbf{F}_1(x_1)$. Copulas are then a powerful tool to build a multivariate probability distribution when the margins are given. Conversely, Sklar (1959) proves that any bivariate distribution $\mathbf{F}$ admits such a representation:

$$\mathbf{F}(x_1,x_2) = \mathbf{C}(\mathbf{F}_1(x_1),\mathbf{F}_2(x_2)) \tag{A.11}$$

and that the copula $\mathbf{C}$ is unique provided the margins are continuous. This result is important, because we can associate to each bivariate distribution a copula function. We then obtain a canonical representation of a bivariate probability distribution: on one side, we have the margins or the univariate directions $\mathbf{F}_1$ and $\mathbf{F}_2$; on the other side, we have the copula $\mathbf{C}$ that links these margins and gives the dependence between the unidimensional directions.

If the joint distribution function $\mathbf{F}(x_1,x_2)$ is absolutely continuous, we obtain:

$$\begin{aligned} f(x_1,x_2) &= \partial_{1,2}\mathbf{F}(x_1,x_2) \\ &= \partial_{1,2}\mathbf{C}(\mathbf{F}_1(x_1),\mathbf{F}_2(x_2)) \\ &= c(\mathbf{F}_1(x_1),\mathbf{F}_2(x_2)) \cdot f_1(x_1) \cdot f_2(x_2) \end{aligned} \tag{A.12}$$

where $f(x_1, x_2)$ is the joint probability density function, $f_1$ and $f_2$ are the marginal densities and $c$ is the copula density:

$$c(u_1, u_2) = \partial_{1,2} \mathbf{C}(u_1, u_2)$$

We notice that the condition $\mathbf{C}(v_1, v_2) - \mathbf{C}(v_1, u_2) - \mathbf{C}(u_1, v_2) + \mathbf{C}(u_1, u_2) \geq 0$ is then equivalent to $\partial_{1,2} \mathbf{C}(u_1, u_2) \geq 0$ when the copula density exists. From Equation (A.12), we deduce that:

$$c(u_1, u_2) = \frac{f\left(\mathbf{F}_1^{-1}(u_1), \mathbf{F}_2^{-1}(u_2)\right)}{f_1\left(\mathbf{F}_1^{-1}(u_1)\right) \cdot f_2\left(\mathbf{F}_2^{-1}(u_2)\right)} \tag{A.13}$$

We obtain a second canonical representation based on density functions. For some copulas, there is no explicit analytical formula. This is the case of the Normal copula, which is equal to $\mathbf{C}(u_1, u_2; \rho) = \Phi\left(\Phi^{-1}(u_1), \Phi^{-1}(u_2); \rho\right)$. Using Equation (A.13), we can however characterize its density function:

$$\begin{aligned} c(u_1, u_2; \rho) &= \frac{2\pi\left(1-\rho^2\right)^{-1/2} \exp\left(-\frac{1}{2(1-\rho^2)}\left(x_1^2 + x_2^2 - 2\rho x_1 x_2\right)\right)}{(2\pi)^{-1/2} \exp\left(-\frac{1}{2}x_1^2\right) \cdot (2\pi)^{-1/2} \exp\left(-\frac{1}{2}x_2^2\right)} \\ &= \frac{1}{\sqrt{1-\rho^2}} \exp\left(-\frac{1}{2}\frac{\left(x_1^2 + x_2^2 - 2\rho x_1 x_2\right)}{(1-\rho^2)} + \frac{1}{2}\left(x_1^2 + x_2^2\right)\right) \end{aligned}$$

where $x_1 = \mathbf{F}_1^{-1}(u_1)$ and $x_2 = \mathbf{F}_2^{-1}(u_2)$. It is then easy to generate bivariate non-normal distributions.

**Example 62** *In Figure A.1, we have built a bivariate probability distribution by considering that the margins are a Student's distribution and a beta distribution. The copula function corresponds to the Normal copula such that its Kendall's tau is equal to* 60%.

### Fréchet classes and concordance ordering

The goal of Fréchet classes is to study the structure of the class of distributions with given margins. Let us first consider the bivariate case. The distribution function $\mathbf{F}$ belongs to the Fréchet class $(\mathbf{F}_1, \mathbf{F}_2)$ and we note $\mathbf{F} \in \mathcal{F}(\mathbf{F}_1, \mathbf{F}_2)$ if an only if the margins of $\mathbf{F}$ are $\mathbf{F}_1$ and $\mathbf{F}_2$, meaning that $\mathbf{F}(x_1, \infty) = \mathbf{F}_1(x_1)$ and $\mathbf{F}(\infty, x_2) = \mathbf{F}_2(x_2)$. Characterizing the Fréchet class $\mathcal{F}(\mathbf{F}_1, \mathbf{F}_2)$ is then equivalent to find the set $\mathcal{C}$ of copula functions:

$$\mathcal{F}(\mathbf{F}_1, \mathbf{F}_2) = \{\mathbf{F} : \mathbf{F}(x_1, x_2) = \mathbf{C}(\mathbf{F}_1(x_1), \mathbf{F}_2(x_2)), \mathbf{C} \in \mathcal{C}\}$$

Therefore this problem does not depend on the margins $\mathbf{F}_1$ and $\mathbf{F}_2$. We can show that the extremal distribution functions $\mathbf{F}^-$ and $\mathbf{F}^+$ of the Fréchet class $\mathcal{F}(\mathbf{F}_1, \mathbf{F}_2)$ are $\mathbf{F}^-(x_1, x_2) = \max(\mathbf{F}_1(x_1) + \mathbf{F}_2(x_2) - 1, 0)$ and $\mathbf{F}^+(x_1, x_2) = \min(\mathbf{F}_1(x_1), \mathbf{F}_2(x_2))$. $\mathbf{F}^-$ and $\mathbf{F}^+$ are called the Fréchet lower and upper bounds. We deduce that the corresponding copula functions are:

$$\mathbf{C}^-(u_1, u_2) = \max(u_1 + u_2 - 1, 0)$$

and:

$$\mathbf{C}^+(u_1, u_2) = \min(u_1, u_2)$$

Figure A.1: Example of a bivariate probability distribution with given margins

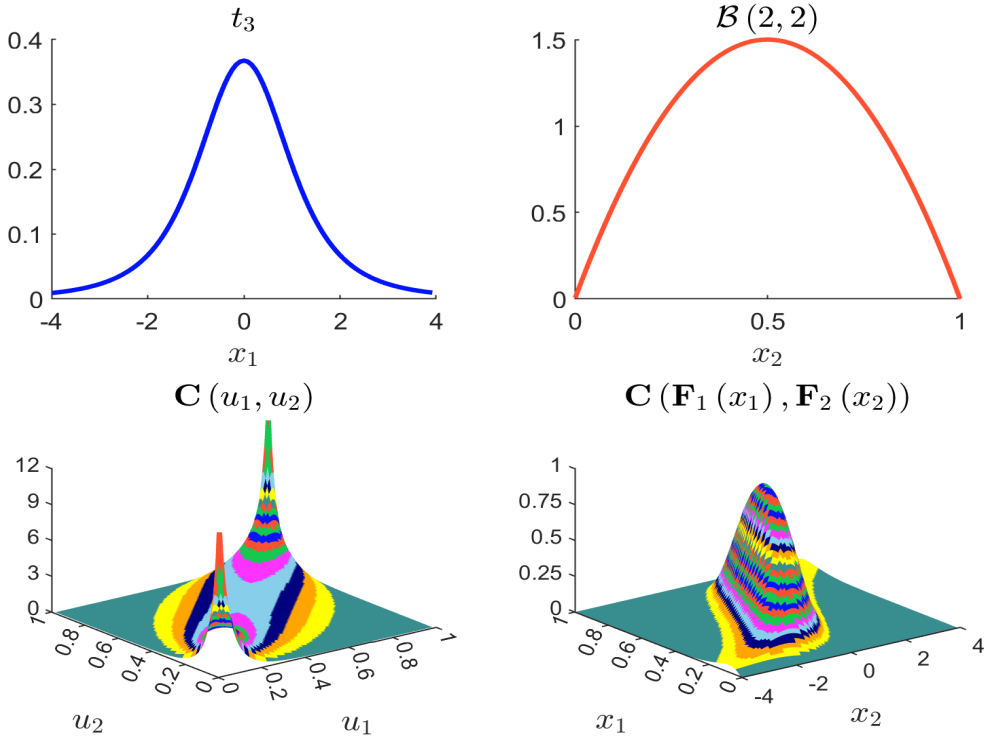


The extension of bivariate copulas to multivariate copulas is straightforward. Thus, the canonical decomposition of a multivariate distribution function is:

$$\mathbf{F}(x_1, \ldots, x_n) = \mathbf{C}(\mathbf{F}_1(x_1), \ldots, \mathbf{F}_n(x_n))$$

We note $\mathbf{C}_{\mathcal{E}}$ the sub-copula of $\mathbf{C}$ such that arguments that are not in the set $\mathcal{E}$ are equal to 1. For instance, with a dimension of 4, we have $\mathbf{C}_{12}(u, v) = \mathbf{C}(u, v, 1, 1)$ and $\mathbf{C}_{124}(u, v, w) = \mathbf{C}(u, v, 1, w)$. Let us consider the 2-copulas $\mathbf{C}_1$ and $\mathbf{C}_2$. It seems logical to build a copula of higher dimension with copulas of lower dimensions. In fact, the function $\mathbf{C}_1(u_1, \mathbf{C}_2(u_2, u_3))$ is not a copula in most cases. In the multivariate case, we define:

$$\mathbf{C}^-(u_1, \ldots, u_n) = \max\left(\sum_{i=1}^{n} u_i - n + 1, 0\right)$$

and:

$$\mathbf{C}^+(u_1, \ldots, u_n) = \min(u_1, \ldots, u_n)$$

We can show that $\mathbf{C}^+$ is a copula, but $\mathbf{C}^-$ does not belong to the set $\mathcal{C}$. Nevertheless, $\mathbf{C}^-$ is the best-possible bound, meaning that for all $(u_1, \ldots, u_n) \in [0,1]^n$, there is a copula that coincide with $\mathbf{C}^-$ (Nelsen, 2006). This implies that $\mathcal{F}(\mathbf{F}_1, \ldots, \mathbf{F}_n)$ has a minimal distribution function if and only if $\max\left(\sum_{i=1}^{n} \mathbf{F}_i(x_i) - n + 1, 0\right)$ is a probability distribution.

We now introduce a stochastic ordering on copulas. Let $\mathbf{C}_1$ and $\mathbf{C}_2$ be two copula functions. We say that the copula $\mathbf{C}_1$ is smaller than the copula $\mathbf{C}_2$ and we note $\mathbf{C}_1 \prec \mathbf{C}_2$ if we verify that $\mathbf{C}_1(u_1, u_2) \leq \mathbf{C}_2(u_1, u_2)$ for all $(u_1, u_2) \in [0,1]^2$. This stochastic ordering is called the concordance ordering and may be viewed as the first order of the stochastic dominance on probability

distributions. Using the previous results on Fréchet classes, we deduce that:

$$\mathbf{C}^- \prec \mathbf{C} \prec \mathbf{C}^+$$

for all $\mathbf{C} \in \mathcal{C}$. It follows that $\mathbf{C}^- \prec \mathbf{C}^\perp \prec \mathbf{C}^+$. A copula $\mathbf{C}$ has a positive quadrant dependence (PQD) if it satisfies the inequality $\mathbf{C}^\perp \prec \mathbf{C} \prec \mathbf{C}^+$. In a similar way, $\mathbf{C}$ has a negative quadrant dependence (NQD) if it satisfies the inequality $\mathbf{C}^- \prec \mathbf{C} \prec \mathbf{C}^\perp$. As it is a partial ordering, there exist copula functions $\mathbf{C}$ such that $\mathbf{C} \nsucc \mathbf{C}^\perp$ and $\mathbf{C} \nprec \mathbf{C}^\perp$. A copula function may then have a dependence structure that is neither positive or negative. In Figure A.2, we report the cumulative distribution function (above panel) and its contour lines (below panel) of the three copula functions $\mathbf{C}^-$, $\mathbf{C}^\perp$ and $\mathbf{C}^+$, which plays an important role to understand the dependance between unidimensional margins.

Figure A.2: The three copula functions $\mathbf{C}^-$, $\mathbf{C}^\perp$ and $\mathbf{C}^+$

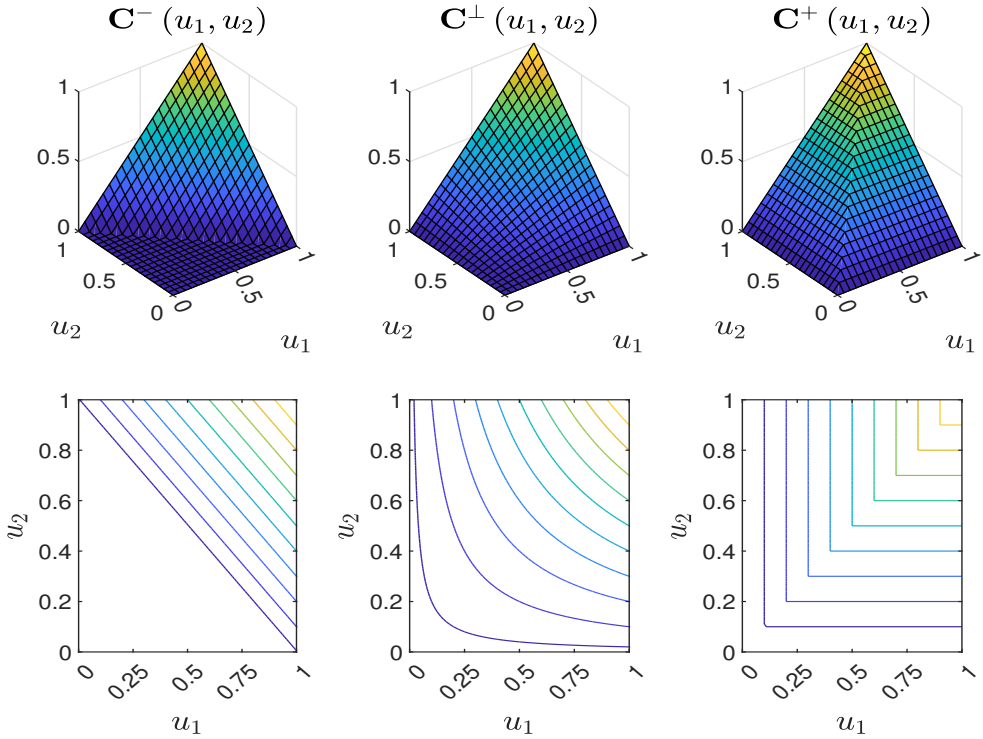


Let $\mathbf{C}_\theta(u_1,u_2) = \mathbf{C}(u_1,u_2;\theta)$ be a family of copula functions that depends on the parameter $\theta$. The copula family $\{\mathbf{C}_\theta\}$ is totally ordered if, for all $\theta_2 \geq \theta_1$, $\mathbf{C}_{\theta_2} \succ \mathbf{C}_{\theta_1}$ (positively ordered) or $\mathbf{C}_{\theta_2} \prec \mathbf{C}_{\theta_1}$ (negatively ordered). For instance, the Frank copula defined by:

$$\mathbf{C}(u_1,u_2;\theta) = -\frac{1}{\theta}\ln\left(1+\frac{\left(e^{-\theta u_1}-1\right)\left(e^{-\theta u_2}-1\right)}{e^{-\theta}-1}\right)$$

where $\theta \in \mathbb{R}$ is a positively ordered family. An illustration is showed in Figure A.3). For a given value $\alpha \in [0,1]$, we also verify that the level curves of $\mathbf{C}$ are in the triangle defined as follows:

$$\{(u_1,u_2) : \max(u_1+u_2-1,0) \leq \alpha, \min(u_1,u_2) \geq \alpha\}$$

Figure A.3: Concordance ordering of the Frank copula

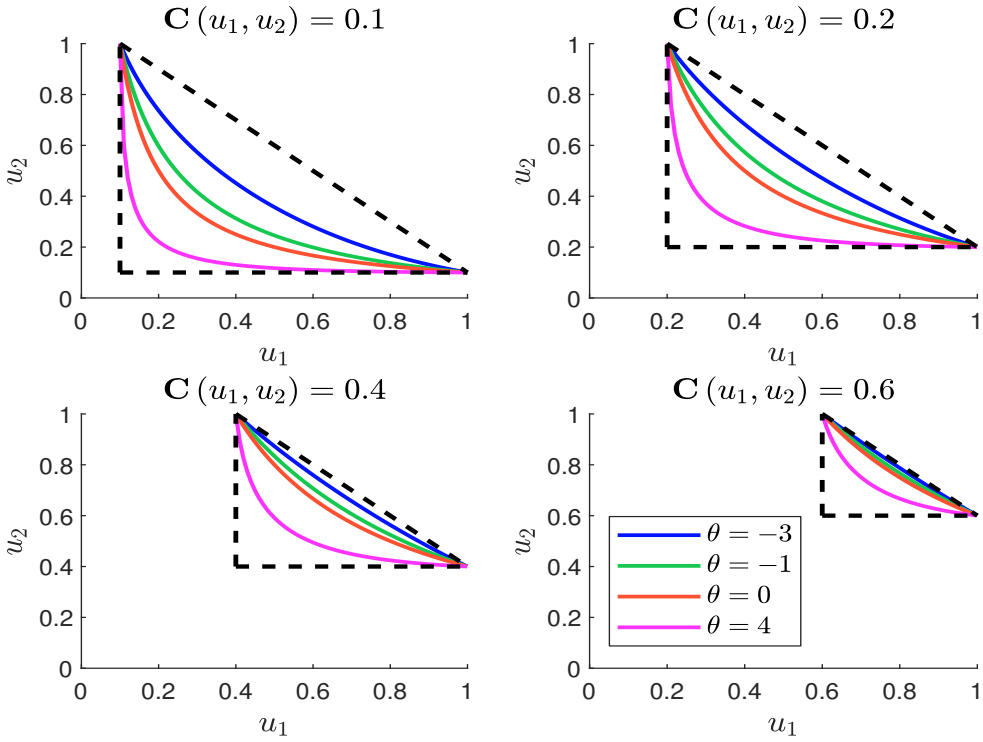


**Copula function and random vector**

Let $X = (X_1, X_2)$ be a random vector with distribution $\mathbf{F}$. We define the copula of $(X_1, X_2)$ by the copula of $\mathbf{F}$:

$$\mathbf{F}(x_1, x_2) = \mathbf{C}\langle X_1, X_2\rangle(\mathbf{F}_1(x_1), \mathbf{F}_2(x_2))$$

In what follows, we give the main results on the dependence of the random vector $X$ found in Nelsen (2006). We first consider the probabilistic interpretation of the three copula functions $\mathbf{C}^-$, $\mathbf{C}^\perp$ and $\mathbf{C}^+$:

- $X_1$ and $X_2$ are countermonotonic — or $\mathbf{C}\langle X_1, X_2\rangle = \mathbf{C}^-$ — if there exists a random variable $X$ such that $X_1 = f_1(X)$ and $X_2 = f_2(X)$ where $f_1$ and $f_2$ are respectively decreasing and increasing functions[12];
- $X_1$ and $X_2$ are independent if the dependence function is the product copula $\mathbf{C}^\perp$;
- $X_1$ are $X_2$ are comonotonic — or $\mathbf{C}\langle X_1, X_2\rangle = \mathbf{C}^+$ — if there exists a random variable $X$ such that $X_1 = f_1(X)$ and $X_2 = f_2(X)$ where $f_1$ and $f_2$ are both increasing functions[13].

Let us consider a uniform random vector $(U_1, U_2)$. We have $U_2 = 1 - U_1$ when $\mathbf{C}\langle X_1, X_2\rangle = \mathbf{C}^-$ and $U_2 = U_1$ when $\mathbf{C}\langle X_1, X_2\rangle = \mathbf{C}^+$. In the case of a standardized Gaussian random vector, we obtain $X_2 = -X_1$ when $\mathbf{C}\langle X_1, X_2\rangle = \mathbf{C}^-$ and $X_2 = X_1$ when $\mathbf{C}\langle X_1, X_2\rangle = \mathbf{C}^+$. If the marginals are log-normal, it follows that $X_2 = X_1^{-1}$ when $\mathbf{C}\langle X_1, X_2\rangle = \mathbf{C}^-$ and $X_2 = X_1$ when $\mathbf{C}\langle X_1, X_2\rangle = \mathbf{C}^+$. For these three examples, we verify that $X_2$ is a decreasing (resp. increasing) function of $X_1$ if

[12] We also have $X_2 = f(X_1)$ where $f = f_2 \circ f_1^{-1}$ is a decreasing function.
[13] In this case, $X_2 = f(X_1)$ where $f = f_2 \circ f_1^{-1}$ is an increasing function.

the copula function $\mathbf{C}\langle X_1, X_2\rangle$ is $\mathbf{C}^-$ (resp. $\mathbf{C}^+$). The concepts of counter- and comonotonicity concepts generalize the cases where the linear correlation of a Gaussian vector is equal to $-1$ or $+1$. Indeed, $\mathbf{C}^-$ and $\mathbf{C}^+$ define respectively perfect negative and positive dependence.

Let $(X_1, X_2)$ be a random vectors, whose copula is $\mathbf{C}\langle X_1, X_2\rangle$. If $h_1$ and $h_2$ are two increasing functions on $\operatorname{Im} X_1$ and $\operatorname{Im} X_2$, then we have:

$$\mathbf{C}\langle h_1(X_1), h_2(X_2)\rangle = \mathbf{C}\langle X_1, X_2\rangle$$

This means that copula functions are invariant under strictly increasing transformations of the random variables. To prove this theorem, we note $\mathbf{F}$ and $\mathbf{G}$ the probability distributions of the random vectors $(X_1, X_2)$ and $(Y_1, Y_2) = (h_1(X_1), h_2(X_2))$. The margins of $\mathbf{G}$ are:

$$\begin{aligned}
\mathbf{G}_1(y_1) &= \Pr\{Y_1 \leq y_1\} \\
&= \Pr\{h_1(X_1) \leq y_1\} \\
&= \Pr\left\{X_1 \leq h_1^{-1}(y_1)\right\} \quad \text{(because } h_1 \text{ is strictly increasing)} \\
&= \mathbf{F}_1\left(h_1^{-1}(y_1)\right)
\end{aligned}$$

and $\mathbf{G}_2(y_2) = \mathbf{F}_2\left(h_2^{-1}(y_2)\right)$. We deduce that $\mathbf{G}_1^{-1}(u_1) = h_1\left(\mathbf{F}_1^{-1}(u_1)\right)$ and $\mathbf{G}_2^{-1}(u_2) = h_2\left(\mathbf{F}_2^{-1}(u_2)\right)$. By definition, we have:

$$\mathbf{C}\langle Y_1, Y_2\rangle(u_1, u_2) = \mathbf{G}\left(\mathbf{G}_1^{-1}(u_1), \mathbf{G}_2^{-1}(u_2)\right)$$

Moreover, it follows that:

$$\begin{aligned}
\mathbf{G}\left(\mathbf{G}_1^{-1}(u_1), \mathbf{G}_2^{-1}(u_2)\right) &= \Pr\left\{Y_1 \leq \mathbf{G}_1^{-1}(u_1), Y_2 \leq \mathbf{G}_2^{-1}(u_2)\right\} \\
&= \Pr\left\{h_1(X_1) \leq \mathbf{G}_1^{-1}(u_1), h_2(X_2) \leq \mathbf{G}_2^{-1}(u_2)\right\} \\
&= \Pr\left\{X_1 \leq h_1^{-1}\left(\mathbf{G}_1^{-1}(u_1)\right), X_2 \leq h_2^{-1}\left(\mathbf{G}_2^{-1}(u_2)\right)\right\} \\
&= \Pr\left\{X_1 \leq \mathbf{F}_1^{-1}(u_1), X_2 \leq \mathbf{F}_2^{-1}(u_2)\right\} \\
&= \mathbf{F}\left(\mathbf{F}_1^{-1}(u_1), \mathbf{F}_2^{-1}(u_2)\right)
\end{aligned}$$

Because we have $\mathbf{C}\langle X_1, X_2\rangle(u_1, u_2) = \mathbf{F}\left(\mathbf{F}_1^{-1}(u_1), \mathbf{F}_2^{-1}(u_2)\right)$, we deduce that $\mathbf{C}\langle Y_1, Y_2\rangle = \mathbf{C}\langle X_1, X_2\rangle$.

We can interpret the copula function $\mathbf{C}\langle X_1, X_2\rangle$ as a standardization of the joint distribution after eliminating the effects of margins. Indeed, it is a comprehensive statistic of the dependence function between $X_1$ and $X_2$. Therefore, a non-comprehensive statistic will be a dependence measure if it can be expressed using $\mathbf{C}\langle X_1, X_2\rangle$. Following Nelsen (2006), a numeric measure $m$ of association between $X_1$ and $X_2$ is a measure of concordance if it satisfies the following properties:

1. $-1 = m\langle X, -X\rangle \leq m\langle \mathbf{C}\rangle \leq m\langle X, X\rangle = 1$;
2. $m\left\langle \mathbf{C}^{\perp}\right\rangle = 0$;
3. $m\langle -X_1, X_2\rangle = m\langle X_1, -X_2\rangle = -m\langle X_1, X_2\rangle$;
4. if $\mathbf{C}_1 \prec \mathbf{C}_2$, then $m\langle \mathbf{C}_1\rangle \leq m\langle \mathbf{C}_2\rangle$;

Using this last property, we have: $\mathbf{C} \prec \mathbf{C}^{\perp} \Rightarrow m\langle \mathbf{C}\rangle < 0$ and $\mathbf{C} \succ \mathbf{C}^{\perp} \Rightarrow m\langle \mathbf{C}\rangle > 0$. The concordance measure can then be viewed as a generalization of the linear correlation when the dependence function is not normal. Indeed, a positive quadrant dependence copula will have a positive concordance measure whereas a negative quadrant dependence copula will have a negative

concordance measure. Moreover, the bounds $-1$ and $+1$ are reached when the copula function is countermonotonic and comonotonic.

Among the several concordance measures, we find Kendall's tau and Spearman's rho, which play an important role in non-parametric statistics. Let us consider a sample of $n$ observations $\{(x_1, y_1), \ldots, (x_n, y_n)\}$ of the random vector $(X, Y)$. Kendall's tau is the probability of concordance — $(X_i - X_j) \cdot (Y_i - Y_j) > 0$ — minus the probability of discordance — $(X_i - X_j) \cdot (Y_i - Y_j) < 0$:

$$\tau = \Pr\{(X_i - X_j) \cdot (Y_i - Y_j) > 0\} - \Pr\{(X_i - X_j) \cdot (Y_i - Y_j) < 0\}$$

Spearman's rho is the linear correlation of the rank statistics $(X_{i:n}, Y_{i:n})$. We can also show that Spearman's rho has the following expression:

$$\varrho = \frac{\operatorname{cov}(\mathbf{F}_X(X), \mathbf{F}_Y(Y))}{\sigma(\mathbf{F}_X(X)) \cdot \sigma(\mathbf{F}_Y(Y))}$$

Schweizer and Wolff (1981) showed that Kendall's tau and Spearman's rho are concordance measures and have the following expressions:

$$\begin{aligned}
\tau &= 4 \iint_{[0,1]^2} \mathbf{C}(u_1, u_2) \, \mathrm{d}\mathbf{C}(u_1, u_2) - 1 \\
\varrho &= 12 \iint_{[0,1]^2} u_1 u_2 \, \mathrm{d}\mathbf{C}(u_1, u_2) - 3
\end{aligned}$$

From a numerical point of view, the following formulas should be preferred (Nelsen, 2006):

$$\begin{aligned}
\tau &= 1 - 4 \iint_{[0,1]^2} \partial_{u_1} \mathbf{C}(u_1, u_2) \, \partial_{u_2} \mathbf{C}(u_1, u_2) \, \mathrm{d}u_1 \, \mathrm{d}u_2 \\
\varrho &= 12 \iint_{[0,1]^2} \mathbf{C}(u_1, u_2) \, \mathrm{d}u_1 \, \mathrm{d}u_2 - 3
\end{aligned}$$

For some copulas, we have analytical formulas. For instance, we have:

| Copula | $\varrho$ | $\tau$ |
|---|---|---|
| Normal | $6\pi^{-1} \arcsin(\rho/2)$ | $2\pi^{-1} \arcsin(\rho)$ |
| Gumbel | ✓ | $(\theta - 1)/\theta$ |
| FGM | $\theta/3$ | $2\theta/9$ |
| Frank | $1 - 12\theta^{-1}(\mathbf{D}_1(\theta) - \mathbf{D}_2(\theta))$ | $1 - 4\theta^{-1}(1 - \mathbf{D}_1(\theta))$ |

where $\mathbf{D}_k(x)$ is the Debye function. The Gumbel (or Gumbel-Hougaard) copula is equal to:

$$\mathbf{C}(u_1, u_2; \theta) = \exp\left(-\left[(-\ln u_1)^\theta + (-\ln u_2)^\theta\right]^{1/\theta}\right)$$

for $\theta \geq 1$, whereas the expression of the Farlie-Gumbel-Morgenstern (or FGM) copula is:

$$\mathbf{C}(u_1, u_2; \theta) = u_1 u_2 (1 + \theta(1 - u_1)(1 - u_2))$$

for $-1 \leq \theta \leq 1$.

For illustration, we report in Figures A.4, A.5 and A.6 the level curves of several density functions built with Normal, Frank and Gumbel copulas. In order to compare them, the parameter of each copula is calibrated such that Kendall's tau is equal to 50%. This means that these 12 distributions functions have the same dependence with respect to Kendall's tau. However, the dependence is different from one figure to another, because their copula function is not the same. This is why Kendall's tau is not an exhaustive statistic of the dependence between two random variables.

Figure A.4: Contour lines of bivariate densities (Normal copula)

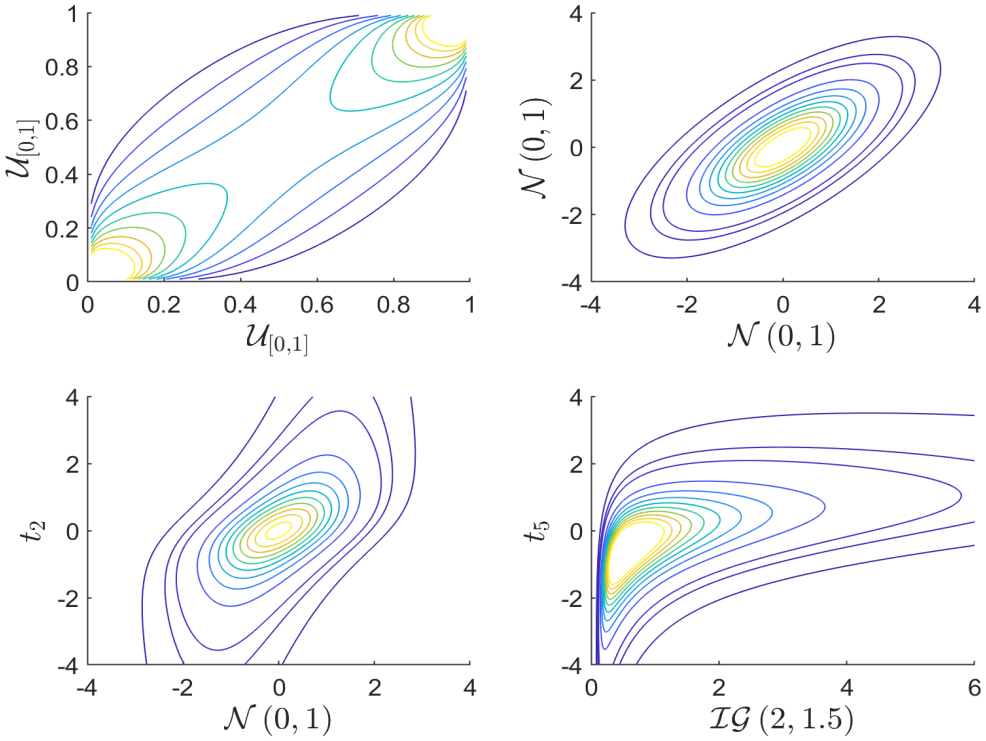


Figure A.5: Contour lines of bivariate densities (Frank copula)

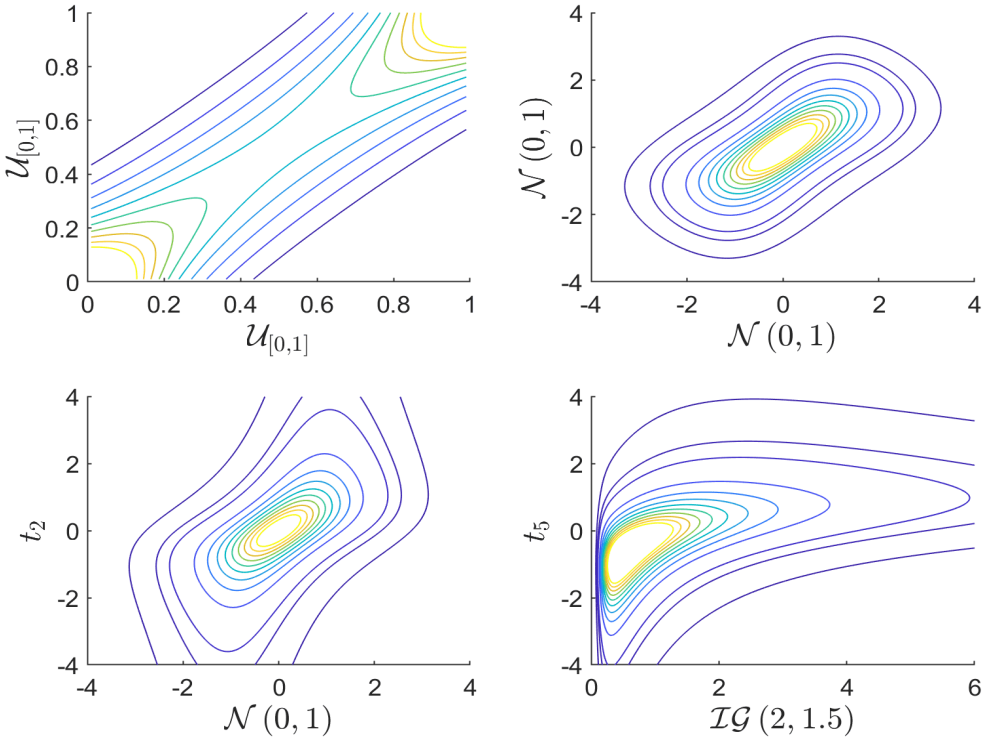

Figure A.6: Contour lines of bivariate densities (Gumbel copula)

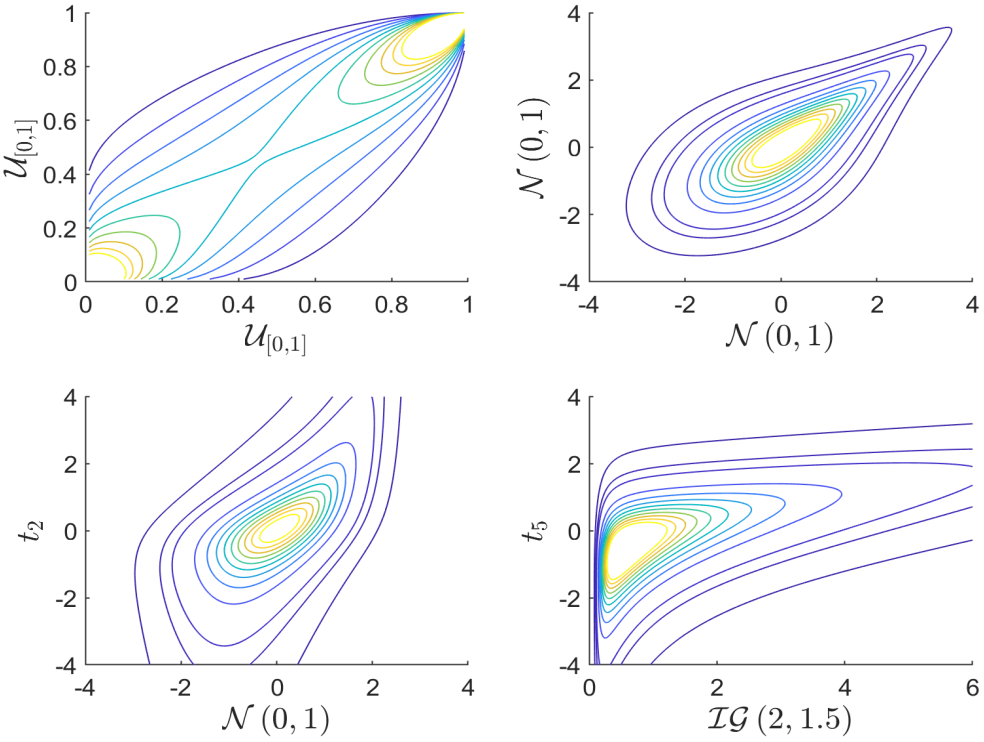


**Remark 137** *We can show that the linear correlation (or Pearson's correlation) is not a concordance measure (Roncalli, 2020a, pages 727-729). In particular, the lower and upper bounds $\rho\langle\mathbf{C}^-\rangle$ and $\rho\langle\mathbf{C}^+\rangle$ are not necessarily equal to $-1$ and $+1$. While the copula function is an invariant measure by increasing transformations, the Pearson's correlation is an invariant measure by increasing linear transformations. This is why the correlation is called a linear dependence measure.*

### Parametric copula functions

**Archimedean copulas** Genest and MacKay (1986b) define Archimedean copulas as follows:

$$\mathbf{C}(u_1,u_2)=\begin{cases}\varphi^{-1}(\varphi(u_1)+\varphi(u_2)) & \text{if } \varphi(u_1)+\varphi(u_2)\leq\varphi(0)\\ 0 & \text{otherwise}\end{cases}$$

where $\varphi$ a $C^2$ is a function which satisfies $\varphi(1)=0$, $\varphi'(u)<0$ and $\varphi''(u)>0$ for all $u\in[0,1]$. $\varphi(u)$ is called the generator of the copula function. If $\varphi(0)=\infty$, the generator is said to be strict. Genest and MacKay (1986a)MacKay, Jock link the construction of Archimedean copulas to the independence of random variables. Indeed, by considering the multiplicative generator $\lambda(u)=\exp(-\varphi(u))$, the authors show that:

$$\mathbf{C}(u_1,u_2)=\lambda^{-1}(\lambda(u_1)\lambda(u_2))$$

This means that:

$$\lambda(\Pr\{U_1\leq u_1,U_2\leq u_2\})=\lambda(\Pr\{U_1\leq u_1\})\times\lambda(\Pr\{U_2\leq u_2\})$$

In this case, the random variables $(U_1,U_2)$ become independent when the scale of probabilities has been transformed.

The product copula $\mathbf{C}^{\perp}$ is Archimedean and the associated generator is $\varphi(u) = -\ln u$. Concerning Fréchet copulas, only $\mathbf{C}^{-}$ is Archimedean with $\varphi(u) = 1 - u$. In Table A.1, we provide another examples of Archimedean copulas[14].

Table A.1: Archimedean copula functions

| Copula | $\varphi(u)$ | $\mathbf{C}(u_1, u_2)$ |
|---|---|---|
| Clayton | $u^{-\theta} - 1$ | $\left(u_1^{-\theta} + u_2^{-\theta} - 1\right)^{-1/\theta}$ |
| Frank | $-\ln \dfrac{e^{-\theta u} - 1}{e^{-\theta} - 1}$ | $-\dfrac{1}{\theta} \ln \left(1 + \dfrac{\left(e^{-\theta u_1} - 1\right)\left(e^{-\theta u_2} - 1\right)}{e^{-\theta} - 1}\right)$ |
| Gumbel | $(-\ln u)^{\theta}$ | $\exp\left(-\left(\tilde{u}_1^{\theta} + \tilde{u}_2^{\theta}\right)^{1/\theta}\right)$ |
| Joe | $-\ln\left(1 - (1-u)^{\theta}\right)$ | $1 - \left(\bar{u}_1^{\theta} + \bar{u}_2^{\theta} - \bar{u}_1^{\theta}\bar{u}_2^{\theta}\right)^{1/\theta}$ |

Nelsen (2006) showed that if $\varphi(t)$ is a strict generator, then we can build two-parameter Archimedean copulas by considering the following generator:

$$\varphi_{\alpha,\beta}(t) = \left(\varphi\left(t^{\alpha}\right)\right)^{\beta}$$

where $\alpha > 0$ and $\beta > 1$. For instance, if $\varphi(t) = t^{-1} - 1$, the two-parameter generator is $\varphi_{\alpha,\beta}(t) = \left(t^{-\alpha} - 1\right)^{\beta}$. Therefore, the corresponding copula function is defined by:

$$\mathbf{C}(u_1, u_2) = \left(\left[\left(u_1^{-\alpha} - 1\right)^{\beta} + \left(u_2^{-\alpha} - 1\right)^{\beta}\right]^{1/\beta} + 1\right)^{-1/\alpha}$$

This is a generalization of the Clayton copula, which is obtained when the parameter $\beta$ is equal to 1.

We can build multivariate Archimedean copulas in the following way:

$$\mathbf{C}(u_1, \ldots, u_n) = \varphi^{-1}\left(\varphi(u_1) + \ldots + \varphi(u_n)\right)$$

However, $\mathbf{C}$ is a copula function if and only if the function $\varphi^{-1}(u)$ is completely monotone (Nelsen, 2006):

$$(-1)^k \frac{\mathrm{d}^k}{\mathrm{d}u^k} \varphi^{-1}(u) \geq 0 \qquad \forall\, k \geq 1$$

For instance, the multivariate GumbelCopula function!Gumbel-Hougaard copula is defined by:

$$\mathbf{C}(u_1, \ldots, u_n) = \exp\left(-\left((-\ln u_1)^{\theta} + \ldots + (-\ln u_n)^{\theta}\right)^{1/\theta}\right)$$

**Normal copula** The Normal copula is the dependence function of the multivariate normal distribution with a correlation matrix $\rho$:

$$\mathbf{C}(u_1, \ldots, u_n; \rho) = \Phi_n\left(\Phi^{-1}(u_1), \ldots, \Phi^{-1}(u_n); \rho\right)$$

By using the canonical decomposition of the multivariate density function:

$$f(x_1, \ldots, x_n) = c(\mathbf{F}_1(x_1), \ldots, \mathbf{F}_n(x_n)) \prod_{i=1}^{n} f_i(x_i)$$

[14] We use the notations $\bar{u} = 1 - u$ and $\tilde{u} = -\ln u$.

we deduce that the probability density function of the Normal copula is:

$$c(u_1,\ldots,u_n,;\rho)=\frac{1}{|\rho|^{\frac{1}{2}}}\exp\left(-\frac{1}{2}x^\top\left(\rho^{-1}-I_n\right)x\right)$$

where $x_i=\Phi^{-1}(u_i)$. In the bivariate case, we obtain[15]:

$$c(u_1,u_2;\rho)=\frac{1}{\sqrt{1-\rho^2}}\exp\left(-\frac{x_1^2+x_2^2-2\rho x_1x_2}{2(1-\rho^2)}+\frac{x_1^2+x_2^2}{2}\right)$$

It follows that the expression of the bivariate Normal copula function is also equal to:

$$\mathbf{C}(u_1,u_2;\rho)=\int_{-\infty}^{\mathbf{\Phi}^{-1}(u_1)}\int_{-\infty}^{\mathbf{\Phi}^{-1}(u_2)}\phi_2(x_1,x_2;\rho)\,\mathrm{d}x_1\,\mathrm{d}x_2$$

where $\phi_2(x_1,x_2;\rho)$ is the bivariate normal density:

$$\phi_2(x_1,x_2;\rho)=\frac{1}{2\pi\sqrt{1-\rho^2}}\exp\left(-\frac{x_1^2+x_2^2-2\rho x_1x_2}{2(1-\rho^2)}\right)$$

Another expression of the bivariate Normal copula density is:

$$\mathbf{C}(u_1,u_2;\rho)=\int_0^{u_1}\Phi\left(\frac{\Phi^{-1}(u_2)-\rho\Phi^{-1}(u)}{\sqrt{1-\rho^2}}\right)\mathrm{d}u$$

**Student's $t$ copula** In a similar way, the Student's $t$ copula is the dependence function associated with the multivariate Student's $t$ probability distribution:

$$\mathbf{C}(u_1,\ldots,u_n;\rho,\nu)=\mathbf{T}_n\left(\mathbf{T}_\nu^{-1}(u_1),\ldots,\mathbf{T}_\nu^{-1}(u_n);\rho,\nu\right)$$

By using the definition of the cumulative distribution function:

$$\mathbf{T}_n(x_1,\ldots,x_n;\rho,\nu)=\int_{-\infty}^{x_1}\cdots\int_{-\infty}^{x_n}\frac{\Gamma\left(\frac{\nu+n}{2}\right)|\rho|^{-\frac{1}{2}}}{\Gamma\left(\frac{\nu}{2}\right)(\nu\pi)^{\frac{n}{2}}}\left(1+\frac{1}{\nu}x^\top\rho^{-1}x\right)^{-\frac{\nu+n}{2}}\mathrm{d}x$$

we can show that the copula density is then:

$$c(u_1,\ldots,u_n,;\rho,\nu)=|\rho|^{-\frac{1}{2}}\frac{\Gamma\left(\frac{\nu+n}{2}\right)\left[\Gamma\left(\frac{\nu}{2}\right)\right]^n}{\left[\Gamma\left(\frac{\nu+1}{2}\right)\right]^n\Gamma\left(\frac{\nu}{2}\right)}\frac{\left(1+\frac{1}{\nu}x^\top\rho^{-1}x\right)^{-\frac{\nu+n}{2}}}{\prod_{i=1}^n\left(1+\frac{x_i^2}{\nu}\right)^{-\frac{\nu+1}{2}}}$$

where $x_i=\mathbf{T}_\nu^{-1}(u_i)$. In the bivariate case, we deduce that the $t$ copula has the following expression:

$$\mathbf{C}(u_1,u_2;\rho,\nu)=\int_{-\infty}^{\mathbf{T}_\nu^{-1}(u_1)}\int_{-\infty}^{\mathbf{T}_\nu^{-1}(u_2)}\frac{1}{2\pi\sqrt{1-\rho^2}}\left(1+\frac{x_1^2+x_2^2-2\rho x_1x_2}{\nu(1-\rho^2)}\right)^{-\frac{\nu+2}{2}}\mathrm{d}x_1\,\mathrm{d}x_2$$

Like the Normal copula, we can obtain another expression, which is easier to manipulate. Let $(X_1,X_2)$ be a random vector whose probability distribution is $\mathbf{T}_2(x_1,x_2;\rho,\nu)$. Conditionally to $X_1=x_1$, we have:

$$\left(\frac{\nu+1}{\nu+x_1^2}\right)^{1/2}\frac{X_2-\rho x_1}{\sqrt{1-\rho^2}}\sim\mathbf{T}_{\nu+1}$$

[15]In the bivariate case, the parameter $\rho$ is the cross-correlation between $X_1$ and $X_2$, that is the element $(1,2)$ of the correlation matrix.

The conditional distribution $\mathbf{C}_{2|1}(u_1, u_2)$ is then equal to:

$$\mathbf{C}_{2|1}(u_1, u_2; \rho, \nu) = \mathbf{T}_{\nu+1}\left(\left(\frac{\nu+1}{\nu + \left[\mathbf{T}_\nu^{-1}(u_1)\right]^2}\right)^{1/2} \frac{\mathbf{T}_\nu^{-1}(u_2) - \rho\mathbf{T}_\nu^{-1}(u_1)}{\sqrt{1-\rho^2}}\right)$$

We deduce that:

$$\mathbf{C}(u_1, u_2; \rho, \nu) = \int_0^{u_1} \mathbf{C}_{2|1}(u, u_2; \rho, \nu)\, \mathrm{d}u$$

### A.2.3 Estimation methods

#### Linear regression

Let $Y$ and $X$ be two random vectors. We consider the conditional expectation problem:

$$y = \mathbb{E}[Y \mid X = x] = m(x)$$

The underlying idea is to find an estimate $\hat{m}(x)$ of the function $m(x)$. In the general case, this problem is extremely difficult to solve. However, if $(Y, X)$ is a Gaussian random vector, the function $m(x)$ can then be determined by considering the Gaussian linear model:

$$Y = \beta^\top X + u$$

where $u \sim \mathcal{N}(0, \sigma^2)$. Most of the time, the joint distribution of $(Y, X)$ is unknown. In this case, the linear model is estimated by applying least squares techniques[16] to a given sample $(\mathbf{Y}, \mathbf{X})$:

$$\mathbf{Y} = \mathbf{X}\beta + \mathbf{U}$$

**Derivation of the OLS estimator** We consider a training set of $n$ *iid* samples $(y_i, x_i)$. For the $i^{\text{th}}$ observation, we have:

$$y_i = \sum_{k=1}^{K} \beta_k x_{i,k} + u_i \tag{A.14}$$

The least squares estimate of the parameter vector $\beta$ is defined as follows:

$$\hat{\beta} = \arg\min \sum_{i=1}^{n} u_i^2$$

We introduce the following matrix notations: $\mathbf{Y}$ is the $n \times 1$ vector with elements $\mathbf{Y}_i = y_i$, $\mathbf{X}$ is the $n \times K$ matrix defined as follows:

$$\mathbf{X} = \begin{pmatrix} x_{1,1} & & x_{1,K} \\ & \ddots & \\ x_{n,1} & & x_{n,K} \end{pmatrix}$$

and $\mathbf{U}$ is the $n \times 1$ vector with elements $\mathbf{U}_i = u_i$. In this case, the system of equations (A.14) becomes:

$$\mathbf{Y} = \mathbf{X}\beta + \mathbf{U}$$

[16] In order to distinguish random variables and observations, we write matrices and vectors that are related to observations in bold style.

Let $\text{RSS}(\beta)$ be the residual sum of squares. We have:

$$\begin{aligned}\text{RSS}(\beta) &= \sum_{i=1}^{n} u_i^2 \\ &= \mathbf{U}^\top \mathbf{U} \\ &= \mathbf{Y}^\top \mathbf{Y} - 2\beta^\top \mathbf{X}^\top \mathbf{Y} + \beta^\top \mathbf{X}^\top \mathbf{X}\beta\end{aligned}$$

The least squares estimator verifies the set of normal equations $\partial_\beta \mathbf{U}^\top \mathbf{U} = \mathbf{0}$ and we deduce that $-2\mathbf{X}^\top \mathbf{Y} + 2\mathbf{X}^\top \mathbf{X}\hat{\beta} = \mathbf{0}$. The expression of the least squares estimator is then:

$$\hat{\beta} = \left(\mathbf{X}^\top \mathbf{X}\right)^{-1} \mathbf{X}^\top \mathbf{Y} \tag{A.15}$$

To obtain the expression of $\hat{\beta}$, we only need the assumption that the rank of the matrix $\mathbf{X}$ is $K$. In this case, $\hat{\beta}$ is the solution of the least squares problem. To go further, we assume that $(Y, X)$ is a Gaussian random vector. The solution of the conditional expectation problem $\mathbb{E}[Y \mid X = x] = m(x)$ is then:

$$\hat{m}(x) = x^\top \hat{\beta} = x^\top \left(\mathbf{X}^\top \mathbf{X}\right)^{-1} \mathbf{X}^\top \mathbf{Y}$$

It means that the prediction of $Y$ given that $X = x$ is equal to $\hat{y} = x^\top \hat{\beta}$. If we consider the training data $\mathbf{X}$, we obtain:

$$\hat{Y} = \hat{m}(\mathbf{X}) = \mathbf{X}\left(\mathbf{X}^\top \mathbf{X}\right)^{-1} \mathbf{X}^\top \mathbf{Y} = \mathbf{H}\mathbf{Y}$$

where $\mathbf{H} = \mathbf{X}\left(\mathbf{X}^\top \mathbf{X}\right)^{-1} \mathbf{X}^\top$ is called the '*hat*' matrix[17]. We notice that $\hat{m}(\mathbf{X})$ is a linear predictor of $\mathbf{Y}$.

**Statistical inference** Because $(Y, X)$ is a Gaussian random vector, it implies that $u = Y - \beta^\top X$ is a Gaussian random variable. We notice that:

$$\hat{\beta} = \left(\mathbf{X}^\top \mathbf{X}\right)^{-1} \mathbf{X}^\top \mathbf{Y} = \beta + \left(\mathbf{X}^\top \mathbf{X}\right)^{-1} \mathbf{X}^\top \mathbf{U}$$

By assuming the exogeneity of the variables $X$ — meaning that $\mathbb{E}[u \mid X = x] = 0$ — we deduce that $\hat{\beta}$ is an unbiased estimator:

$$\mathbb{E}\left[\hat{\beta}\right] = \beta + \left(\mathbf{X}^\top \mathbf{X}\right)^{-1} \mathbb{E}\left[\mathbf{X}^\top \mathbf{U}\right] = \beta$$

[17] We interpret $\mathbf{H}$ as the orthogonal projection matrix generated by $\mathbf{X}$ implying that $\mathbf{H}$ is idempotent, that is $\mathbf{H}\mathbf{H} = \mathbf{H}$. Indeed, we have:

$$\mathbf{H}\mathbf{H} = \mathbf{X}\left(\mathbf{X}^\top \mathbf{X}\right)^{-1} \mathbf{X}^\top \mathbf{X}\left(\mathbf{X}^\top \mathbf{X}\right)^{-1} \mathbf{X}^\top = \mathbf{X}\left(\mathbf{X}^\top \mathbf{X}\right)^{-1} \mathbf{X}^\top = \mathbf{H}$$

We recall that $\mathbf{U} \sim \mathcal{N}\left(0, \sigma^2 I_n\right)$. It follows that:

$$\begin{aligned}
\text{var}\left(\hat{\beta}\right) &= \mathbb{E}\left[\left(\hat{\beta}-\beta\right)\left(\hat{\beta}-\beta\right)^\top\right] \\
&= \mathbb{E}\left[\left(\mathbf{X}^\top\mathbf{X}\right)^{-1}\mathbf{X}^\top\mathbf{U}\mathbf{U}^\top\mathbf{X}\left(\mathbf{X}^\top\mathbf{X}\right)^{-1}\right] \\
&= \left(\mathbf{X}^\top\mathbf{X}\right)^{-1}\mathbf{X}^\top\mathbb{E}\left[\mathbf{U}\mathbf{U}^\top\right]\mathbf{X}\left(\mathbf{X}^\top\mathbf{X}\right)^{-1} \\
&= \left(\mathbf{X}^\top\mathbf{X}\right)^{-1}\mathbf{X}^\top\left(\sigma^2 I_n\right)\mathbf{X}\left(\mathbf{X}^\top\mathbf{X}\right)^{-1} \\
&= \sigma^2\left(\mathbf{X}^\top\mathbf{X}\right)^{-1}
\end{aligned}$$

We conclude that:

$$\hat{\beta} \sim \mathcal{N}\left(\beta, \sigma^2\left(\mathbf{X}^\top\mathbf{X}\right)^{-1}\right)$$

In most cases, $\sigma^2$ is unknown and we have to estimate it. The vector of residuals is:

$$\hat{\mathbf{U}} = \mathbf{Y} - \hat{\mathbf{Y}} = \mathbf{Y} - \mathbf{X}\hat{\beta}$$

We notice that $\mathbb{E}\left[\hat{\mathbf{U}}\right] = \mathbf{0}$ and $\text{var}\left(\hat{\mathbf{U}}\right) = \sigma^2\left(I_n - \mathbf{H}\right)$. Because $\text{RSS}\left(\hat{\beta}\right) = \hat{\mathbf{U}}^\top\left(I_n - \mathbf{H}\right)\hat{\mathbf{U}}$ is a quadratic form, we can show that:

$$\hat{\sigma}^2 = \frac{\text{RSS}\left(\hat{\beta}\right)}{n-K}$$

is an unbiased estimator of $\sigma^2$ and $\hat{\sigma}^2/\sigma^2 \sim \chi^2_{n-K}$. In order to measure the model quality, we consider the coefficient of determination or $R_c^2$. It is defined as follows:

$$R_c^2 = 1 - \frac{\text{RSS}\left(\hat{\beta}\right)}{\text{TSS}}$$

where $\text{TSS} = \sum_{i=1}^n (y_i - \bar{y})$ is the total sum of squares. We have $R_c^2 \leq 1$. A high (resp. low) level indicates a good (resp. bad) goodness-of-fit of the regression model.

**Lasso regression**

The lasso method consists in adding a $\mathcal{L}_1$-norm penalty function to the optimization function in order to obtain a sparse parameter vector $\theta$:

$$L_1(\theta) = \|\theta\|_1 = \sum_{k=1}^K |\theta_k|$$

For example, the lasso regression model is specified as follows (Tibshirani, 1996):

$$y_i = \sum_{k=1}^K \beta_k x_{i,k} + u_i \quad \text{s.t.} \quad \sum_{k=1}^K |\beta_k| \leq \tau$$

where $\tau$ is a scalar to control the sparsity. Using the notations introduced on page 1077, we have:

$$\begin{aligned}
\hat{\beta}(\tau) &= \arg\min\left(\mathbf{Y}-\mathbf{X}\beta\right)^\top\left(\mathbf{Y}-\mathbf{X}\beta\right) \\
&\text{s.t.} \quad \|\beta\|_1 \leq \tau
\end{aligned} \tag{A.16}$$

This problem is equivalent to the Lagrange optimization program $\hat{\beta}(\lambda) = \arg\min \mathcal{L}(\beta;\lambda)$ where[18]:

$$\begin{aligned}\mathcal{L}(\beta;\lambda) &= \frac{1}{2}(\mathbf{Y}-\mathbf{X}\beta)^\top(\mathbf{Y}-\mathbf{X}\beta)+\lambda\|\beta\|_1\\ &\propto \frac{1}{2}\beta^\top\left(\mathbf{X}^\top\mathbf{X}\right)\beta-\beta^\top\left(\mathbf{X}^\top\mathbf{Y}\right)+\lambda\|\beta\|_1\end{aligned}$$

The solution $\hat{\beta}(\lambda)$ can be found by solving the augmented QP program where $\beta=\beta^+-\beta^-$ under the constraints $\beta^+\geq\mathbf{0}$ and $\beta^-\geq\mathbf{0}$. We deduce that:

$$\begin{aligned}\|\beta\|_1 &= \sum_{k=1}^K\left|\beta_k^+-\beta_k^-\right|\\ &= \sum_{k=1}^K\left|\beta_k^+\right|+\sum_{k=1}^K\left|\beta_k^-\right|\\ &= \mathbf{1}^\top\beta^++\mathbf{1}^\top\beta^-\end{aligned}$$

Since we have:

$$\beta=\begin{pmatrix} I_K & -I_K\end{pmatrix}\begin{pmatrix}\beta^+\\ \beta^-\end{pmatrix}$$

the augmented QP program is specified as follows:

$$\begin{aligned}\hat{\theta} &= \arg\min\frac{1}{2}\theta^\top Q\theta-\theta^\top R\\ &\text{s.t. } \theta\geq\mathbf{0}\end{aligned}$$

where $\theta=(\beta^+,\beta^-)$, $\tilde{\mathbf{X}}=\begin{pmatrix}\mathbf{X} & -\mathbf{X}\end{pmatrix}$, $Q=\tilde{\mathbf{X}}^\top\tilde{\mathbf{X}}$ and $R=\tilde{\mathbf{X}}^\top\mathbf{Y}-\lambda\cdot\mathbf{1}$. If we denote $A=\begin{pmatrix} I_K & -I_K\end{pmatrix}$, we obtain $\hat{\beta}(\lambda)=A\hat{\theta}$.

**Remark 138** *If we consider Problem (A.16), we can also solve it using another augmented QP program:*

$$\begin{aligned}\hat{\theta} &= \arg\min\frac{1}{2}\theta^\top Q\theta-\theta^\top R\\ &s.t. \begin{cases} C\theta\geq D\\ \theta\geq\mathbf{0}\end{cases}\end{aligned}$$

*where* $Q=\tilde{\mathbf{X}}^\top\tilde{\mathbf{X}}$, $R=\tilde{\mathbf{X}}^\top\mathbf{Y}$, $C=-\mathbf{1}^\top$ *and* $D=-\tau$. *We again have* $\hat{\beta}(\tau)=A\hat{\theta}$.

We have:

$$\begin{aligned}\text{RSS}(\beta) &= (\mathbf{Y}-\mathbf{X}\beta)^\top(\mathbf{Y}-\mathbf{X}\beta)\\ &= \left(\mathbf{Y}-\mathbf{X}\left(\hat{\beta}^{\text{ols}}+\beta-\hat{\beta}^{\text{ols}}\right)\right)^\top\left(\mathbf{Y}-\mathbf{X}\left(\hat{\beta}^{\text{ols}}+\beta-\hat{\beta}^{\text{ols}}\right)\right)\\ &= \left(\mathbf{Y}-\mathbf{X}\hat{\beta}^{\text{ols}}\right)^\top\left(\mathbf{Y}-\mathbf{X}\hat{\beta}^{\text{ols}}\right)+2\left(\mathbf{Y}-\mathbf{X}\hat{\beta}^{\text{ols}}\right)^\top\mathbf{X}\left(\beta-\hat{\beta}^{\text{ols}}\right)+\\ &\quad\left(\beta-\hat{\beta}^{\text{ols}}\right)^\top\mathbf{X}^\top\mathbf{X}\left(\beta-\hat{\beta}^{\text{ols}}\right)\end{aligned}$$

[18] $\tau$ and $\lambda$ are related by the relationship $\tau=\left\|\hat{\beta}(\lambda)\right\|_1$.

We notice that:

$$\begin{aligned}
(*) &= \left(\mathbf{Y} - \mathbf{X}\hat{\beta}^{\text{ols}}\right)^{\top} \mathbf{X}\left(\beta - \hat{\beta}^{\text{ols}}\right) \\
&= \left(\mathbf{Y}^{\top} - \left(\hat{\beta}^{\text{ols}}\right)^{\top} \mathbf{X}^{\top}\right) \mathbf{X}\left(\beta - \hat{\beta}^{\text{ols}}\right) \\
&= \left(\mathbf{Y}^{\top} - \left(\left(\mathbf{X}^{\top}\mathbf{X}\right)^{-1} \mathbf{X}^{\top}\mathbf{Y}\right)^{\top} \mathbf{X}^{\top}\right) \mathbf{X}\left(\beta - \hat{\beta}^{\text{ols}}\right) \\
&= \left(\mathbf{Y}^{\top}\mathbf{X} - \left(\left(\mathbf{X}^{\top}\mathbf{X}\right)^{-1} \mathbf{X}^{\top}\mathbf{Y}\right)^{\top} \mathbf{X}^{\top}\mathbf{X}\right)\left(\beta - \hat{\beta}^{\text{ols}}\right) \\
&= \left(\mathbf{Y}^{\top}\mathbf{X} - \mathbf{Y}^{\top}\mathbf{X}\right)\left(\beta - \hat{\beta}^{\text{ols}}\right) \\
&= 0
\end{aligned}$$

Finally, we obtain:

$$\text{RSS}(\beta) = \text{RSS}\left(\hat{\beta}^{\text{ols}}\right) + \left(\beta - \hat{\beta}^{\text{ols}}\right)^{\top} \mathbf{X}^{\top}\mathbf{X}\left(\beta - \hat{\beta}^{\text{ols}}\right)$$

If we consider the equation $\text{RSS}(\beta) = c$, we distinguish three cases:

1. if $c < \text{RSS}\left(\hat{\beta}^{\text{ols}}\right)$, there is no solution;
2. if $c = \text{RSS}\left(\hat{\beta}^{\text{ols}}\right)$, there is one solution $\beta^{\star} = \hat{\beta}^{\text{ols}}$;
3. if $c > \text{RSS}\left(\hat{\beta}^{\text{ols}}\right)$, we have:

$$\left(\beta - \hat{\beta}^{\text{ols}}\right)^{\top} A\left(\beta - \hat{\beta}^{\text{ols}}\right) = 1$$

where:

$$A = \frac{\mathbf{X}^{\top}\mathbf{X}}{c - \text{RSS}\left(\hat{\beta}^{\text{ols}}\right)}$$

The solution $\beta^{\star}$ is an ellipsoid, whose center is $\hat{\beta}^{\text{ols}}$ and principal axes are the eigenvectors of the matrix $A$.

If we add the lasso constraint $\sum_{k=1}^{K} |\beta_k| \leq \tau$, the lasso estimator $\hat{\beta}(\tau)$ corresponds to the tangency between the diamond shaped region and the ellipsoid that corresponds to the possible maximum value of $c$. The diamond shape region due to the lasso constraint ensures that the lasso estimator is sparse:

$$\exists\, \eta > 0 : \forall\, \tau < \eta,\ \min\left(\hat{\beta}_1(\tau), \ldots, \hat{\beta}_K(\tau)\right) = 0$$

For example, the two-dimensional case is represented in Figure A.7. We notice that $\hat{\beta}_1(\tau)$ is equal to zero if $\tau < \eta$. This sparsity property is central for understanding the variable selection procedure.

**Example 63** *Using the data given in Table A.2, we consider the linear regression model:*

$$y_i = \beta_0' + \sum_{k=1}^{5} \beta_k' x_{i,k} + u_i \tag{A.17}$$

*The objective is to determine the importance of each variable.*

Figure A.7: Interpretation of the lasso regression

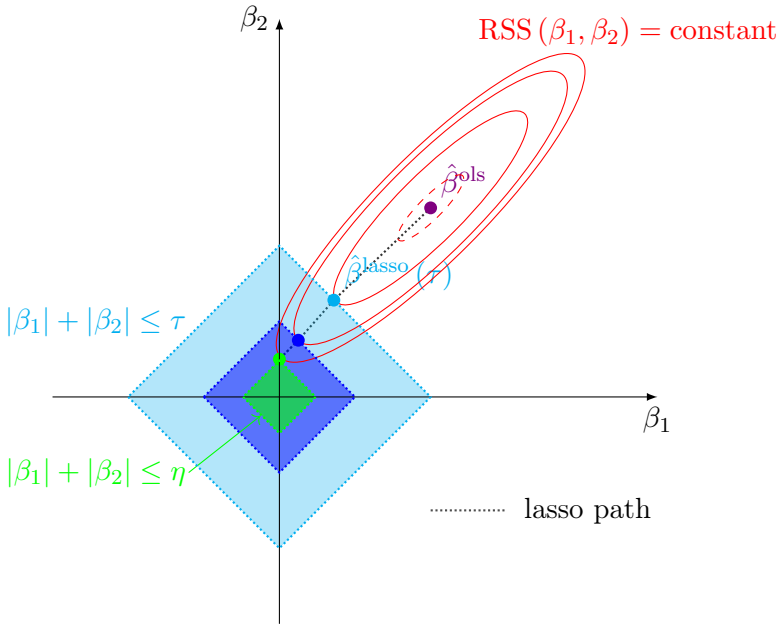


The lasso method can be used for ranking the variables. For that, we consider the following linear regression:

$$\tilde{y}_i = \sum_{k=1}^{5} \beta_k \tilde{x}_{i,k} + u_i$$

where $\tilde{y}_i$ and $\tilde{x}_{i,k}$ are the standardized data[19]:

$$\frac{y_i - \bar{y}}{s_y} = \sum_{k=1}^{5} \beta_k \left( \frac{x_{i,k} - \bar{x}_k}{s_{x_k}} \right) + u_i \tag{A.18}$$

Linear regressions (A.17) and (A.18) are related by the following equation:

$$y_i = \left( \bar{y} - \sum_{k=1}^{5} \frac{s_y \beta_k}{s_{x_k}} \bar{x}_k \right) + \sum_{k=1}^{5} \frac{s_y \beta_k}{s_{x_k}} x_{i,k} + s_y u_i$$

We deduce that $\beta_0' = \bar{y} - \sum_{k=1}^{5} (s_y / s_{x_k}) \beta_k \bar{x}_k$ and $\beta_k' = (s_y / s_{x_k}) \beta_k$. When performing lasso regression, we always standardize the data in order to obtain comparable beta's. Otherwise, the penalty function $\|\beta\|_1$ does not make a lot of sense. In Table A.3, we have estimated the lasso coefficients $\beta_k(\lambda)$ for different values of the shrinkage parameter $\lambda$. When $\lambda = 0$, we obtain the OLS estimate, and the lasso regression selects all the available variables. When $\lambda \to \infty$, the solution is $\hat{\beta}(\infty) = \mathbf{0}$, and the lasso regression selects no explanatory variables. In Table A.3, we verify that the number of selected variables is a decreasing function of $\lambda$. For instance, the lasso regression selects respectively four and three variables when $\lambda$ is equal to 0.9 and 2.5. It follows that the most important variable is the third one, followed by the first, second, fourth and fifth variables.

[19] The notations $\bar{x}_k$ and $s_{x_k}$ represent the mean and the standard deviation of the data $\{x_{i,k}, i = 1, \ldots, n\}$.

Table A.2: Data of the lasso regression problem

| $i$ | $y$ | $x_1$ | $x_2$ | $x_3$ | $x_4$ | $x_5$ |
|---|---|---|---|---|---|---|
| 1 | 3.1 | 2.8 | 4.3 | 0.3 | 2.2 | 3.5 |
| 2 | 24.9 | 5.9 | 3.6 | 3.2 | 0.7 | 6.4 |
| 3 | 27.3 | 6.0 | 9.6 | 7.6 | 9.5 | 0.9 |
| 4 | 25.4 | 8.4 | 5.4 | 1.8 | 1.0 | 7.1 |
| 5 | 46.1 | 5.2 | 7.6 | 8.3 | 0.6 | 4.5 |
| 6 | 45.7 | 6.0 | 7.0 | 9.6 | 0.6 | 0.6 |
| 7 | 47.4 | 6.1 | 1.0 | 8.5 | 9.6 | 8.6 |
| 8 | −1.8 | 1.2 | 9.6 | 2.7 | 4.8 | 5.8 |
| 9 | 20.8 | 3.2 | 5.0 | 4.2 | 2.7 | 3.6 |
| 10 | 6.8 | 0.5 | 9.2 | 6.9 | 9.3 | 0.7 |
| 11 | 12.9 | 7.9 | 9.1 | 1.0 | 5.9 | 5.4 |
| 12 | 37.0 | 1.8 | 1.3 | 9.2 | 6.1 | 8.3 |
| 13 | 14.7 | 7.4 | 5.6 | 0.9 | 5.6 | 3.9 |
| 14 | −3.2 | 2.3 | 6.6 | 0.0 | 3.6 | 6.4 |
| 15 | 44.3 | 7.7 | 2.2 | 6.5 | 1.3 | 0.7 |

Table A.3: Results of the lasso regression

| $\lambda$ | 0.0 | 0.9 | 2.5 | 5.5 | 7.5 |
|---|---|---|---|---|---|
| $\hat{\beta}_1(\lambda)$ | 0.4586 | 0.4022 | 0.3163 | 0.1130 | |
| $\hat{\beta}_2(\lambda)$ | −0.1849 | −0.2005 | −0.1411 | | |
| $\hat{\beta}_3(\lambda)$ | 0.8336 | 0.7265 | 0.5953 | 0.3951 | 0.2462 |
| $\hat{\beta}_4(\lambda)$ | −0.1893 | −0.1102 | | | |
| $\hat{\beta}_5(\lambda)$ | 0.0931 | | | | |
| $\left\|\hat{\beta}(\lambda)\right\|_1$ | 1.7595 | 1.4395 | 1.0527 | 0.5081 | 0.2462 |
| $\text{RSS}\left(\hat{\beta}(\lambda)\right)$ | 0.0118 | 0.0304 | 0.1180 | 0.4076 | 0.6306 |
| $R_c^2$ | 0.9874 | 0.9674 | 0.8735 | 0.5633 | 0.3244 |
| $\text{df}^{(\text{model})}$ | 5 | 4 | 3 | 2 | 1 |

In Figure A.8, we have reported the path of the lasso estimate $\hat{\beta}(\lambda)$ with respect to the scaling factor $\tau^\star \in [0,1]$, which is defined as follows:

$$\tau^\star = \frac{\tau}{\tau_{\max}} = \frac{\left\|\hat{\beta}(\lambda)\right\|_1}{\left\|\hat{\beta}(0)\right\|_1}$$

$\tau^\star$ is equal to zero when $\lambda \to \infty$ (no selected variable) and one when $\lambda = 0$, which corresponds to the OLS case. From this path, we verify the lasso ordering $x_3 \succ x_1 \succ x_2 \succ x_4 \succ x_5$.

### State space models

A state space model (SSM) includes a measurement equation and a transition equation. In the measurement equation, we define the relationship between an observable system and state variables, whereas the transition equation describes the dynamics of state variables. Generally, the state vector

Figure A.8: Variable selection with the lasso regression

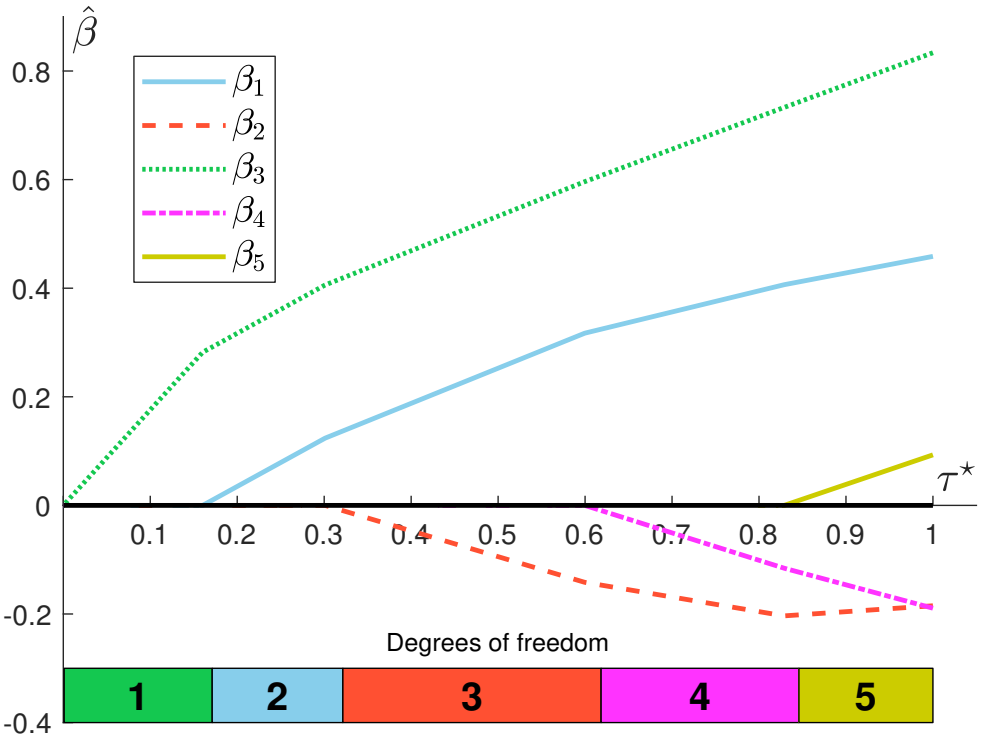


$\alpha_t$ is generated by a Markov linear process[20]:

$$\alpha_t = T_t\alpha_{t-1} + c_t + R_t\eta_t$$

where $\alpha_t$ is a $m \times 1$ vector, $T_t$ is a $m \times m$ matrix, $c_t$ is a $m \times 1$ vector and $R_t$ is a $m \times p$ matrix. In the case of a linear SSM, the measurement equation is given by:

$$y_t = Z_t\alpha_t + d_t + \epsilon_t$$

where $y_t$ is a $n$-dimensional time series, $Z_t$ is a $n \times m$ matrix, $d_t$ is a $n \times 1$ vector. We also assume that $\eta_t$ and $\epsilon_t$ are two independent white noise processes of dimension $p$ and $n$ with covariance matrices $Q_t$ and $H_t$.

**Kalman filtering** In the state space model, the variable $y_t$ is observable, but it is generally not the case of the state vector $\alpha_t$. The Kalman filter is a statistical tool to estimate the distribution function of $\alpha_t$. Let $\alpha_0 \sim \mathcal{N}(\hat{\alpha}_0, P_0)$ the initial position of the state vector. We note $\hat{\alpha}_{t|t}$ (or $\hat{\alpha}_t$) and $\hat{\alpha}_{t|t-1}$ the optimal estimators of $\alpha_t$ given the available information until time $t$ and $t-1$:

$$\begin{aligned}\hat{\alpha}_{t|t} &= \mathbb{E}[\alpha_t \mid \mathcal{F}_t] \\ \hat{\alpha}_{t|t-1} &= \mathbb{E}[\alpha_t \mid \mathcal{F}_{t-1}]\end{aligned}$$

$P_{t|t}$ (or $P_t$) and $P_{t|t-1}$ are the covariance matrices associated to $\hat{\alpha}_{t|t}$ and $\hat{\alpha}_{t|t-1}$:

$$\begin{aligned}P_{t|t} &= \mathbb{E}\left[(\hat{\alpha}_{t|t} - \alpha_t)(\hat{\alpha}_{t|t} - \alpha_t)^\top\right] \\ P_{t|t-1} &= \mathbb{E}\left[(\hat{\alpha}_{t|t-1} - \alpha_t)(\hat{\alpha}_{t|t-1} - \alpha_t)^\top\right]\end{aligned}$$

[20] The presentation is based on the book of Harvey (1990).

These different quantities are calculated thanks to the Kalman filter, which consists in a recursive algorithm[21] (Harvey, 1990):

$$\begin{cases} \hat{\alpha}_{t|t-1} = T_t \hat{\alpha}_{t-1|t-1} + c_t \\ P_{t|t-1} = T_t P_{t-1|t-1} T_t^\top + R_t Q_t R_t^\top \\ \hat{y}_{t|t-1} = Z_t \hat{\alpha}_{t|t-1} + d_t \\ v_t = y_t - \hat{y}_{t|t-1} \\ F_t = Z_t P_{t|t-1} Z_t^\top + H_t \\ \hat{\alpha}_{t|t} = \hat{\alpha}_{t|t-1} + P_{t|t-1} Z_t^\top F_t^{-1} v_t \\ P_{t|t} = \left(I_m - P_{t|t-1} Z_t^\top F_t^{-1} Z_t\right) P_{t|t-1} \end{cases}$$

where $\hat{y}_{t|t-1} = \mathbb{E}\left[y_t \mid \mathcal{F}_{t-1}\right]$ is the best estimator of $y_t$ given the available information until time $t-1$, $v_t$ is the innovation process and $F_t$ is the associated covariance matrix.

**Remark 139** *Harvey (1990) showed that we can directly calculate $\hat{\alpha}_{t+1|t}$ from $\hat{\alpha}_{t|t-1}$:*

$$\hat{\alpha}_{t+1|t} = \left(T_{t+1} - K_t Z_t\right) \hat{\alpha}_{t|t-1} + K_t y_t + c_{t+1} - K_t d_t$$

*where $K_t = T_{t+1} P_{t|t-1} Z_t^\top F_t^{-1}$ is the gain matrix. It follows that:*

$$\hat{\alpha}_{t+1|t} = T_{t+1} \hat{\alpha}_{t|t-1} + c_{t+1} + K_t \left(y_t - Z_t \hat{\alpha}_{t|t-1} - d_t\right)$$

*By recognizing the innovation process $v_t$, we obtain the following innovation representation:*

$$\begin{cases} y_t = Z_t \hat{\alpha}_{t|t-1} + d_t + v_t \\ \hat{\alpha}_{t+1|t} = T_{t+1} \hat{\alpha}_{t|t-1} + c_{t+1} + K_t v_t \end{cases}$$

**Estimation of unknown parameters** In many cases, the state space model depends on certain parameters that are unknown. Given a set $\theta$ of values for these unknown parameters, the Kalman filter may be applied to estimate the state vector $\alpha_t$. We have:

$$v_t \sim \mathcal{N}\left(\mathbf{0}, F_t\right)$$

where $v_t = y_t - \hat{y}_{t|t-1}$ is the innovation at time $t$ and $F_t = Z_t P_{t|t-1} Z_t^\top + H_t$ is the covariance matrix. If we change $\theta$ and we run the Kalman filter, we will obtain other values of $v_t$ and $F_t$, meaning that $v_t$ and $F_t$ depend on $\theta$. This is why we can write $v_t(\theta)$ and $F_t(\theta)$. We deduce that the likelihood function of the sample $\{y_1, \ldots, y_T\}$ is equal to:

$$\boldsymbol{\ell}(\theta) = -\frac{nT}{2} \ln(2\pi) - \frac{1}{2} \sum_{t=1}^{T} \left(\ln\left|F_t(\theta)\right| + v_t(\theta)^\top F_t(\theta)^{-1} v_t(\theta)\right)$$

We can then estimate the vector $\theta$ of unknown parameters by the method of maximum likelihood:

$$\hat{\theta} = \arg\max \boldsymbol{\ell}(\theta)$$

Once the ML estimate $\hat{\theta}$ is found, we can run again[22] the Kalman filter to estimate the other quantities $\hat{\alpha}_{t|t-1}$, $\hat{\alpha}_{t|t}$, $P_{t|t-1}$ and $P_{t|t}$.

[21] The algorithm is initialized with values $\hat{\alpha}_{0|0} = \hat{\alpha}_0$ and $P_{0|0} = P_0$.

[22] We say again, because computing the log-likelihood function requires one Kalman filter run, implying that many Kalman filter runs are used for maximizing the log-likelihood function.

**Time-invariant state space model** We consider the time-invariant model:

$$\begin{cases} y_t = Z\alpha_t + d + \epsilon_t \\ \alpha_t = T\alpha_{t-1} + c + R\eta_t \end{cases}$$

where $\epsilon_t \sim \mathcal{N}(\mathbf{0}, H)$ and $\eta_t \sim \mathcal{N}(\mathbf{0}, Q)$. If the state space model converges to a steady state, the estimators $(\hat{\alpha}_\infty, P_\infty)$ must satisfy the following equations:

$$\begin{cases} \hat{\alpha}_\infty = T\hat{\alpha}_\infty + c \\ P_\infty = TP_\infty T^\top + RQR^\top \end{cases}$$

It follows that the solution is:

$$\begin{cases} \hat{\alpha}_\infty = (I_m - T)^{-1} c \\ \text{vec}(P_\infty) = (I_{m^2} - T \otimes T)^{-1} \text{vec}\left(RQR^\top\right) \end{cases}$$

where $\hat{\alpha}_\infty$ and $P_\infty$ are the unconditional mean and covariance matrix of $\alpha_t$. Without any knowledge of the initial position $\alpha_0$, the best way to define $\hat{\alpha}_0$ and $P_0$ is then to use the steady state:

$$\begin{cases} \hat{\alpha}_0 = \hat{\alpha}_\infty \\ P_0 = P_\infty \end{cases}$$

In many state space models, the matrices $T$, $c$, $R$ and $Q$ depend on unknown parameters $\theta$, implying that $\hat{\alpha}_\infty$ and $P_\infty$ also depend on $\theta$. This means that when maximizing the log-likelihood function, the Kalman filter is initialized by values of $\hat{\alpha}_0$ and $P_0$ that depend on $\theta$. This is the main difference with time-varying state space model since the Kalman filter is initialized by fixed values of $\hat{\alpha}_0$ and $P_0$.

## A.3 Stochastic analysis

### A.3.1 Stochastic optimal control

### A.3.2 Jump-diffusion processes

## A.4 Spatial data

### A.4.1 Spherical coordinates

### A.4.2 Geographic coordinate systems

### A.4.3 Network common data form

# Appendix B

# Solutions to the Tutorial Exercises

## B.1 Exercises related to ESG risk

### B.1.1 Score normalization when the features are independent (Exercise 2.4.1)

### B.1.2 Probability distribution of ESG scores (Exercise 2.4.4)

1. (a) We have:

$$\boldsymbol{\mathcal{S}}_i^{(\mathrm{ESG})} = 0.4 \times \boldsymbol{\mathcal{S}}_i^{(\mathrm{E})} + 0.4 \times \boldsymbol{\mathcal{S}}_i^{(\mathrm{S})} + 0.2 \times \boldsymbol{\mathcal{S}}_i^{(\mathrm{G})}$$

We deduce the following results:

| Issuer | #1 | #2 | #3 | #4 | #5 | #6 | #7 | #8 |
|---|---|---|---|---|---|---|---|---|
| $\boldsymbol{\mathcal{S}}_i^{(\mathrm{E})}$ | −2.80 | −1.80 | −1.75 | 0.60 | 0.75 | 1.30 | 1.90 | 2.70 |
| $\boldsymbol{\mathcal{S}}_i^{(\mathrm{S})}$ | −1.70 | −1.90 | 0.75 | −1.60 | 1.85 | 1.05 | 0.90 | 0.70 |
| $\boldsymbol{\mathcal{S}}_i^{(\mathrm{G})}$ | 0.30 | −0.70 | −2.75 | 2.60 | 0.45 | 2.35 | 2.20 | 1.70 |
| $\boldsymbol{\mathcal{S}}_i^{(\mathrm{ESG})}$ | −1.74 | −1.62 | −0.95 | 0.12 | 1.13 | 1.41 | 1.56 | 1.70 |

(b) We obtain:

$$\boldsymbol{\mathcal{S}}^{(\mathrm{ESG})}(x_{\mathrm{ew}}) = \sum_{i=1}^{8} x_{\mathrm{ew},i} \times \boldsymbol{\mathcal{S}}_i^{(\mathrm{ESG})} = 0.2013$$

2. (a) We have:

$$\boldsymbol{\mathcal{S}}\left(x_{\mathrm{ew}}^{(n)}\right) = \sum_{i=1}^{n} x_{\mathrm{ew},i}^{(n)} \times \boldsymbol{\mathcal{S}}_i = \frac{1}{n}\sum_{i=1}^{n} \boldsymbol{\mathcal{S}}_i$$

We deduce that $\boldsymbol{\mathcal{S}}\left(x_{\mathrm{ew}}^{(n)}\right)$ follows a Gaussian distribution. Its mean is equal to:

$$\mathbb{E}\left[\boldsymbol{\mathcal{S}}\left(x_{\mathrm{ew}}^{(n)}\right)\right] = \frac{1}{n}\sum_{i=1}^{n} \mathbb{E}\left[\boldsymbol{\mathcal{S}}_i\right] = 0$$

whereas its standard deviation is equal to:

$$\sigma\left(\boldsymbol{\mathcal{S}}\left(x_{\mathrm{ew}}^{(n)}\right)\right) = \sqrt{\frac{1}{n^2}\sum_{i=1}^{n} \sigma^2\left(\boldsymbol{\mathcal{S}}_i\right)} = \frac{1}{\sqrt{n}}$$

Finally, we deduce that:

$$\boldsymbol{\mathcal{S}}\left(x_{\text{ew}}^{(n)}\right) \sim \mathcal{N}\left(0, \frac{1}{n}\right)$$

(b) The behavior of a well-diversified portfolio is close to an equally-weighted portfolio with $n$ sufficiently large. Therefore, the ESG score is close to zero because we have:

$$\lim_{n\to\infty} \boldsymbol{\mathcal{S}}\left(x_{\text{ew}}^{(n)}\right) = 0$$

(c) We have:

$$f_\alpha(t) = \alpha t^{\alpha-1}$$

The probability density function $f_\alpha(t)$ is reported in Figure B.1. We notice that the function $f_\alpha(t)$ tends to the dirac delta function when $\alpha$ tends to infinity:

$$\lim_{\alpha\to\infty} f_\alpha(t) = \delta_1(t) = \begin{cases} 0 & \text{if } t \neq 1 \\ +\infty & \text{if } t = 1 \end{cases}$$

Figure B.1: Probability density function $f_\alpha(t)$

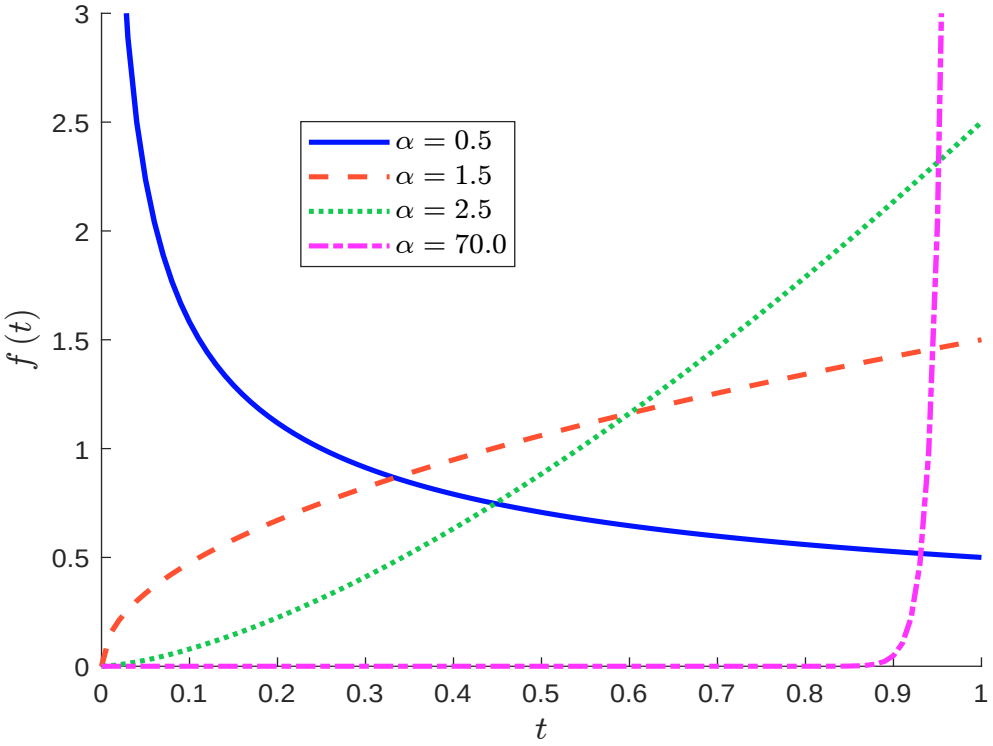


(d) To simulate $T_i$, we use the property of the probability integral transform: $U_i = \mathbf{F}_\alpha(T_i) \sim \mathcal{U}_{[0,1]}$. We deduce that:

$$T_i = \mathbf{F}_\alpha^{-1}(U_i) = U_i^{1/\alpha}$$

The algorithm for simulating the portfolio $x$ is then the following:

i. We simulate $n$ independent uniform random numbers $(u_1, \ldots, u_n)$;

ii. We compute the random variates $(t_1, \ldots, t_n)$ where:

$$t_i = u_i^{1/\alpha}$$

iii. We calculate the normalization constant:

$$c = \left( \sum_{i=1}^{n} t_i \right)^{-1} = \left( \sum_{i=1}^{n} u_i^{1/\alpha} \right)^{-1}$$

iv. We deduce the portfolio weights $x = (x_1, \ldots, x_n)$:

$$x_i = c \cdot t_i = c \cdot u_i^{1/\alpha} = \frac{u_i^{1/\alpha}}{\sum_{j=1}^{n} u_j^{1/\alpha}}$$

In Figure B.2, we have represented the composition of the portfolio $x$ for the 4 values of $\alpha$. The weights are ranked in descending order. We deduce that the portfolio $x$ is uniform when $\alpha \to \infty$. The parameter $\alpha$ controls the concentration of the portfolio. Indeed, when $\alpha$ is small, the portfolio is highly concentrated. It follows that the Herfindahl index $\mathcal{H}_\alpha(x)$ of the portfolio weights is a decreasing function of the parameter $\alpha$.

Figure B.2: Repartition of the portfolio weights in descending order

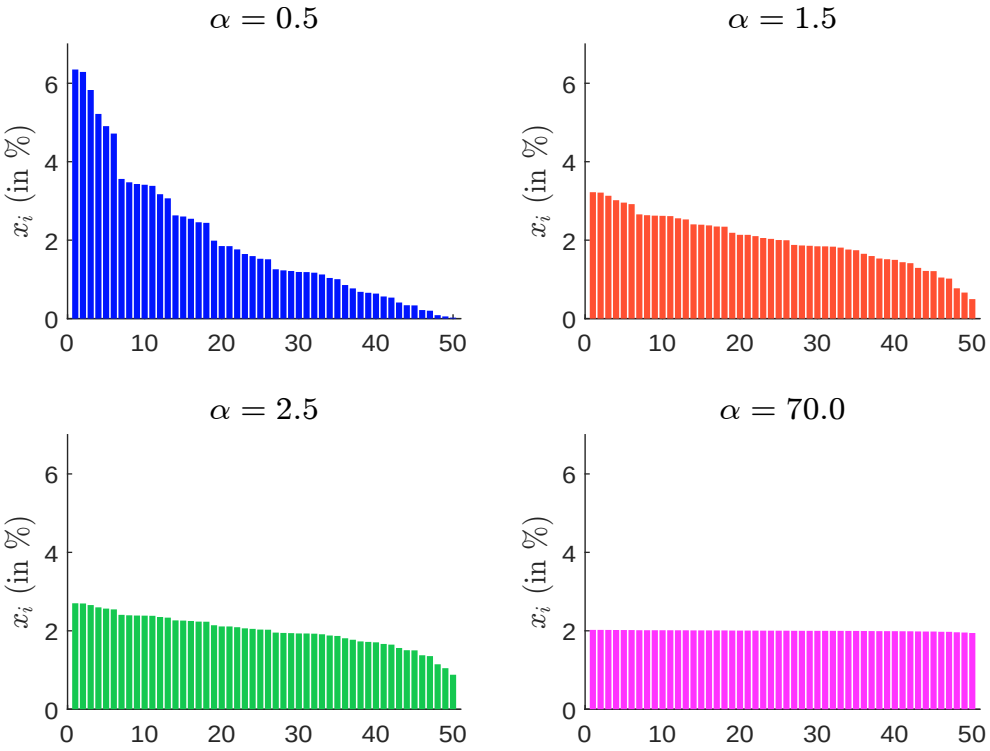


(e) We simulate $x = (x_1, \ldots, x_n)$ using the previous algorithm. The vector of ESG scores $\boldsymbol{\mathcal{S}} = (\boldsymbol{\mathcal{S}}_1, \ldots, \boldsymbol{\mathcal{S}}_n)$ is generated with normally-distributed random variables since we have $\boldsymbol{\mathcal{S}}_i \sim \mathcal{N}(0, 1)$. We deduce that the simulated value of the portfolio ESG score $\boldsymbol{\mathcal{S}}(x)$ is equal to:

$$\boldsymbol{\mathcal{S}}(x) = \sum_{i=1}^{n} x_i \cdot \boldsymbol{\mathcal{S}}_i$$

We replicate the simulation of $\boldsymbol{\mathcal{S}}(x)$ 50 000 times and draw the corresponding histogram in Figure B.3. We also report the fitted Gaussian distribution. We observe that the portfolio's ESG score $\boldsymbol{\mathcal{S}}(x)$ is equal to zero on average, and its variance is an increasing function of the portfolio concentration.

Figure B.3: Histogram of the portfolio ESG score $\boldsymbol{\mathcal{S}}(x)$

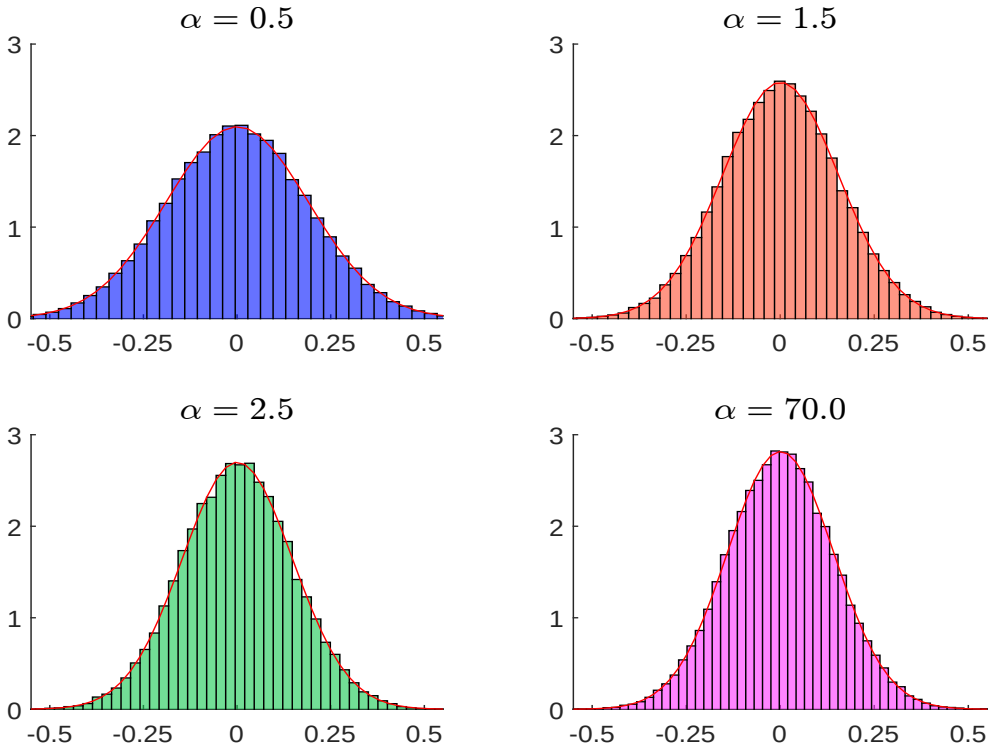


(f) Since $x_i \sim cT_i$, $x_i$ is an increasing function of $T_i$. We deduce that the copula function of $(T_i, \boldsymbol{\mathcal{S}}_i)$ is the same as the copula function of $(x_i, \boldsymbol{\mathcal{S}}_i)$. To simulate the Normal copula function $\mathbf{C}(u, v)$, we use the transformation algorithm based on the Cholesky decomposition:

$$\begin{cases} u_i = \Phi(g_i') \\ v_i = \Phi\left(\rho g_i' + \sqrt{1-\rho^2} g_i''\right) \end{cases}$$

where $g_i'$ and $g_i''$ are two independent random numbers from the probability distribution $\mathcal{N}(0, 1)$. Here is the algorithm to simulate the portfolios's ESG score $\boldsymbol{\mathcal{S}}(x)$:

i. We simulate $n$ independent normally-distributed random numbers $g_i'$and $g_i''$ and compute $(u_i, v_i)$:

$$\begin{cases} u_i = \Phi(g_i') \\ v_i = \Phi\left(\rho g_i' + \sqrt{1-\rho^2} g_i''\right) \end{cases}$$

ii. We compute the random variates $(t_1, \ldots, t_n)$ where $t_i = u_i^{1/\alpha}$;

iii. We deduce the vector of weights $x = (x_1, \ldots, x_n)$:

$$x_i = t_i \Big/ \sum_{j=1}^{n} t_j$$

iv. We simulate the vector of scores $\boldsymbol{\mathcal{S}} = (\boldsymbol{\mathcal{S}}_1, \ldots, \boldsymbol{\mathcal{S}}_n)$:

$$\boldsymbol{\mathcal{S}}_i = \Phi^{-1}(v_i) = \rho g_i' + \sqrt{1-\rho^2}\, g_i''$$

v. We calculate the portfolio score:

$$\boldsymbol{\mathcal{S}}(x) = \sum_{i=1}^{n} x_i \cdot \boldsymbol{\mathcal{S}}_i$$

Figure B.4: Histogram of the portfolio ESG score $\boldsymbol{\mathcal{S}}(x)$ ($\rho = 50\%$)

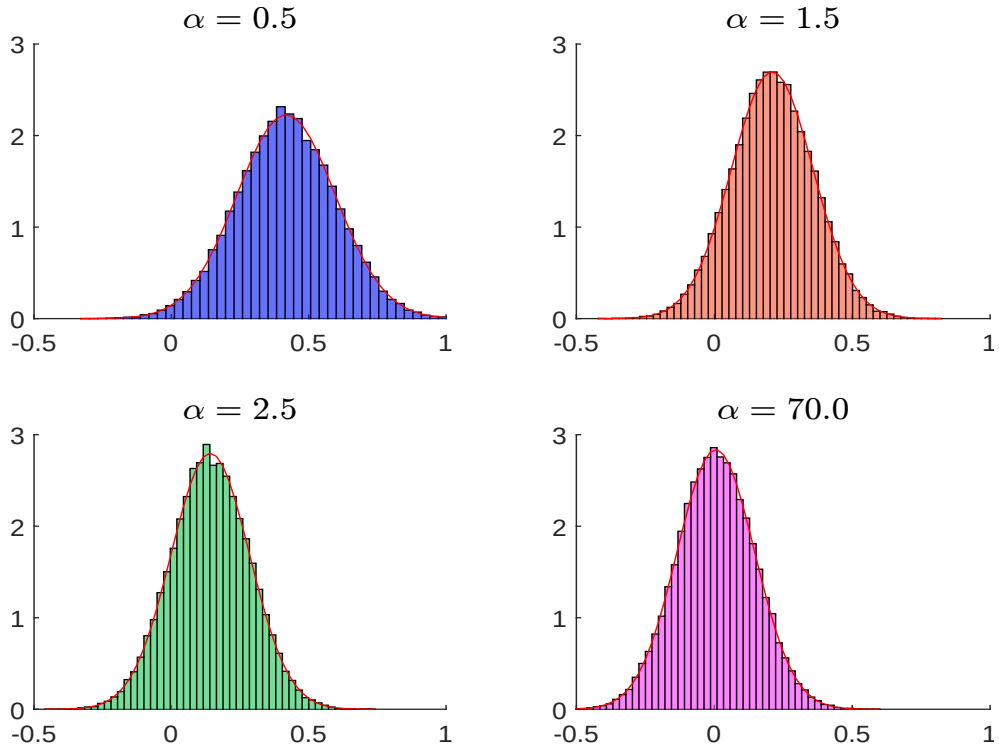


(g) In the independent case, we found that $\mathbb{E}[\boldsymbol{\mathcal{S}}(x)] = 0$. In Figure B.4, we notice that $\mathbb{E}[\boldsymbol{\mathcal{S}}(x)] \neq 0$ when $\rho$ is equal to 50%. Indeed, we obtain:

$$\mathbb{E}[\boldsymbol{\mathcal{S}}(x)] = \begin{cases} 0.418 & \text{if } \alpha = 0.5 \\ 0.210 & \text{if } \alpha = 1.5 \\ 0.142 & \text{if } \alpha = 2.5 \\ 0.006 & \text{if } \alpha = 70.0 \end{cases}$$

(h) In Figure B.5, we notice that there is a positive relationship between $\rho$ and $\mathbb{E}[\boldsymbol{\mathcal{S}}(x)]$ and the slope increases with the concentration of the portfolio.

(i) Big cap companies have more (financial and human) resources to develop an ESG policy than small cap companies. Therefore, we observe a positive correlation between the market capitalization and the ESG score of an issuer. It follows that ESG portfolios have generally a size bias. For instance, we generally observe that cap-weighted indexes have an ESG score which is greater than the average of ESG scores. In the previous questions, we verify that $\mathbb{E}[\boldsymbol{\mathcal{S}}(x)] \geq \mathbb{E}[\boldsymbol{\mathcal{S}}]$ when the Herfindahl index of the portfolio $x$ is high and the correlation between $x_i$ and $\boldsymbol{\mathcal{S}}_i$ is positive.

Figure B.5: Relationship between $\rho$ and $\mathbb{E}[\boldsymbol{\mathcal{S}}(x)]$

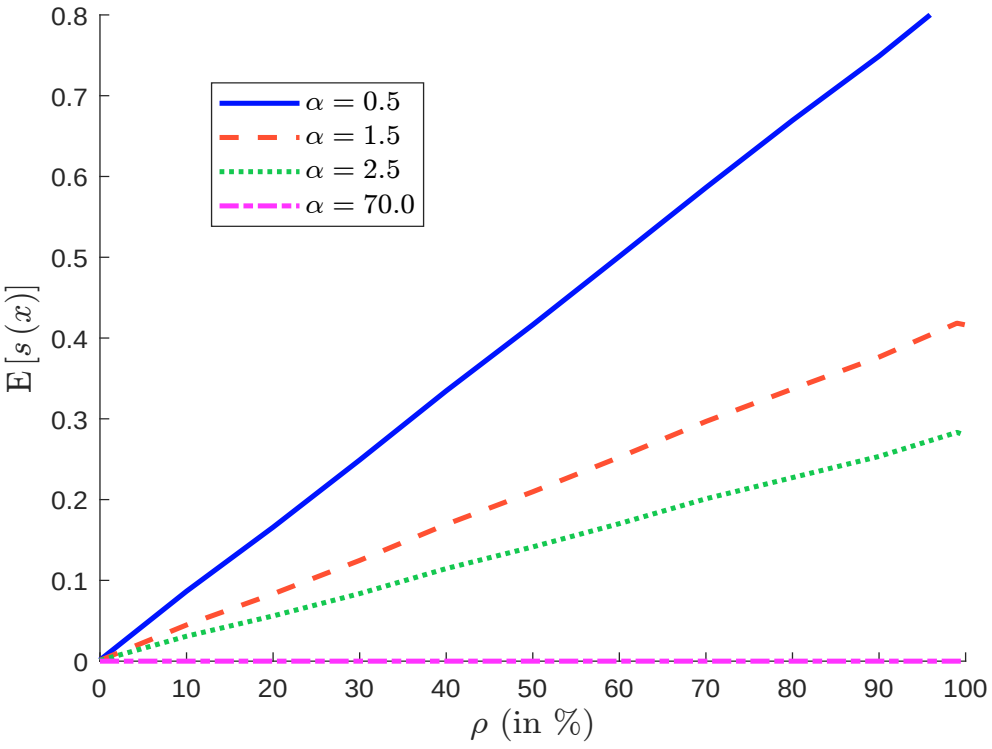


3. (a) We have:

$$\begin{aligned}\Pr\{\mathcal{R} = \mathbf{A}\} &= \Pr\{\boldsymbol{\mathcal{S}} \geq 1.5\} \\ &= 1 - \Phi(1.5) \\ &= 6.68\%\end{aligned}$$

and:

$$\begin{aligned}\Pr\{\mathcal{R} = \mathbf{B}\} &= \Pr\{0 \leq \boldsymbol{\mathcal{S}} < 1.5\} \\ &= \Phi(1.5) - \Phi(0) \\ &= 43.32\%\end{aligned}$$

Since the Gaussian distribution is symmetric around 0, we also have:

$$\Pr\{\mathcal{R} = \mathbf{C}\} = \Pr\{\mathcal{R} = \mathbf{B}\} = 43.32\%$$

and:

$$\Pr\{\mathcal{R} = \mathbf{D}\} = \Pr\{\mathcal{R} = \mathbf{A}\} = 6.68\%$$

The mapping function is then equal to:

$$\mathcal{M}_{\text{appring}}(\boldsymbol{\mathcal{S}}) = \begin{cases} \mathbf{A} & \text{if } \boldsymbol{\mathcal{S}} < -1.5 \\ \mathbf{B} & \text{if } -1.5 \leq \boldsymbol{\mathcal{S}} < 0 \\ \mathbf{C} & \text{if } 0 \leq \boldsymbol{\mathcal{S}} < 1.5 \\ \mathbf{D} & \text{if } \boldsymbol{\mathcal{S}} \geq 1.5 \end{cases}$$

(b) Since we have:

$$\Pr\{\mathcal{R}(t) = \mathbf{A}\} = \Pr\{\mathcal{R}(t) = \mathbf{B}\} = \Pr\{\mathcal{R}(t) = \mathbf{C}\} = \Pr\{\mathcal{R}(t) = \mathbf{D}\}$$

and:

$$\Pr\{\mathcal{R}(t) = \mathbf{A}\} + \Pr\{\mathcal{R}(t) = \mathbf{B}\} + \Pr\{\mathcal{R}(t) = \mathbf{C}\} + \Pr\{\mathcal{R}(t) = \mathbf{D}\} = 1$$

we deduce that:

$$\Pr\{\mathcal{R}(t) = \mathbf{A}\} = \frac{1}{4} = 25\%$$

and $\Pr\{\mathcal{R}(t) = \mathbf{B}\} = \Pr\{\mathcal{R}(t) = \mathbf{C}\} = \Pr\{\mathcal{R}(t) = \mathbf{D}\} = 25\%$. We want to find the breakpoints $(s_1, s_2, s_3)$ such that:

$$\begin{cases} \Pr\{\boldsymbol{\mathcal{S}} < s_1\} = 25\% \\ \Pr\{s_1 \leq \boldsymbol{\mathcal{S}} < s_2\} = 25\% \\ \Pr\{s_2 \leq \boldsymbol{\mathcal{S}} < s_3\} = 25\% \\ \Pr\{\boldsymbol{\mathcal{S}} \geq s_3\} = 25\% \end{cases}$$

We deduce that:

$$\begin{cases} s_1 = \Phi^{-1}(0.25) = -0.6745 \\ s_2 = \Phi^{-1}(0.50) = 0 \\ s_3 = \Phi^{-1}(0.75) = +0.6745 \end{cases}$$

The mapping function is then given by:

$$\mathcal{M}_{\text{appring}}(\boldsymbol{\mathcal{S}}) = \begin{cases} \mathbf{A} & \text{if } \boldsymbol{\mathcal{S}} < -0.6745 \\ \mathbf{B} & \text{if } -0.6745 \leq \boldsymbol{\mathcal{S}} < 0 \\ \mathbf{C} & \text{if } 0 \leq \boldsymbol{\mathcal{S}} < 0.6745 \\ \mathbf{D} & \text{if } \boldsymbol{\mathcal{S}} \geq 0.6745 \end{cases}$$

(c) We have:

$$\begin{cases} s_1 = \Phi^{-1}(0.10) = -1.2816 \\ s_2 = \Phi^{-1}(0.50) = 0 \\ s_3 = \Phi^{-1}(0.90) = +1.2816 \end{cases}$$

We deduce that the mapping function is equal to:

$$\mathcal{M}_{\text{appring}}(\boldsymbol{\mathcal{S}}) = \begin{cases} \mathbf{A} & \text{if } \boldsymbol{\mathcal{S}} < -1.2816 \\ \mathbf{B} & \text{if } -1.2816 \leq \boldsymbol{\mathcal{S}} < 0 \\ \mathbf{C} & \text{if } 0 \leq \boldsymbol{\mathcal{S}} < 1.2816 \\ \mathbf{D} & \text{if } \boldsymbol{\mathcal{S}} \geq 1.2816 \end{cases}$$

4. (a) The joint distribution of $(\boldsymbol{\mathcal{S}}(t-1), \Delta\boldsymbol{\mathcal{S}}(t))$ is:

$$\begin{pmatrix} \boldsymbol{\mathcal{S}}(t-1) \\ \Delta\boldsymbol{\mathcal{S}}(t) \end{pmatrix} \sim \mathcal{N}\left(\begin{pmatrix} 0 \\ 0 \end{pmatrix}, \begin{pmatrix} 1 & 0 \\ 0 & \sigma^2 \end{pmatrix}\right)$$

(b) Since we have:

$$\boldsymbol{\mathcal{S}}(t) = \boldsymbol{\mathcal{S}}(t-1) + \Delta\boldsymbol{\mathcal{S}}(t)$$

we deduce that:

$$\begin{pmatrix} \boldsymbol{\mathcal{S}}(t-1) \\ \boldsymbol{\mathcal{S}}(t) \end{pmatrix} = \begin{pmatrix} 1 & 0 \\ 1 & 1 \end{pmatrix} \begin{pmatrix} \boldsymbol{\mathcal{S}}(t-1) \\ \Delta\boldsymbol{\mathcal{S}}(t) \end{pmatrix}$$

We conclude that $(\boldsymbol{\mathcal{S}}(t-1), \boldsymbol{\mathcal{S}}(t))$ is a Gaussian random vector. We have:

$$\text{var}(\boldsymbol{\mathcal{S}}(t)) = 1 + \sigma^2$$

and:

$$\begin{aligned}\text{cov}(\boldsymbol{\mathcal{S}}(t-1), \boldsymbol{\mathcal{S}}(t)) &= \mathbb{E}[\boldsymbol{\mathcal{S}}(t-1) \cdot \boldsymbol{\mathcal{S}}(t)] \\ &= \mathbb{E}\left[\boldsymbol{\mathcal{S}}^2(t-1) + \boldsymbol{\mathcal{S}}(t-1) \cdot \Delta\boldsymbol{\mathcal{S}}(t)\right] \\ &= 1\end{aligned}$$

It follows that:

$$\begin{pmatrix} \boldsymbol{\mathcal{S}}(t-1) \\ \boldsymbol{\mathcal{S}}(t) \end{pmatrix} \sim \mathcal{N}(\mathbf{0}_2, \Sigma_\sigma)$$

where $\Sigma_\sigma$ is the covariance matrix:

$$\Sigma_\sigma = \begin{pmatrix} 1 & 1 \\ 1 & 1+\sigma^2 \end{pmatrix}$$

(c) We have:

$$\Pr\{\mathcal{R}(t-1) = \mathcal{R}_k\} = \Pr\{s_{k-1} \leq \boldsymbol{\mathcal{S}}(t-1) < s_k\} = \Phi(s_k) - \Phi(s_{k-1})$$

(d) We have:

$$\begin{aligned}(*) &= \Pr\{\mathcal{R}(t) = \mathcal{R}_k, \mathcal{R}(t-1) = \mathcal{R}_j\} \\ &= \Pr\{s_{k-1} \leq \boldsymbol{\mathcal{S}}(t) < s_k, s_{j-1} \leq \boldsymbol{\mathcal{S}}(t-1) < s_j\} \\ &= \Phi_2(s_j, s_k; \Sigma_\sigma) - \Phi_2(s_{j-1}, s_k; \Sigma_\sigma) - \Phi_2(s_j, s_{k-1}; \Sigma_\sigma) + \Phi_2(s_{j-1}, s_{k-1}; \Sigma_\sigma)\end{aligned}$$

where $\Phi_2(x, y; \Sigma_\sigma)$ is the bivariate Normal cdf with covariance matrix $\Sigma_\sigma$.

(e) We have:

$$\begin{aligned}p_{j,k} &= \Pr\{\mathcal{R}(t) = \mathcal{R}_k \mid \mathcal{R}(t-1) = \mathcal{R}_j\} \\ &= \frac{\Pr\{\mathcal{R}(t) = \mathcal{R}_k, \mathcal{R}(t-1) = \mathcal{R}_j\}}{\Pr\{\mathcal{R}(t-1) = \mathcal{R}_j\}} \\ &= \frac{\Phi_2(s_j, s_k; \Sigma_\sigma) + \Phi_2(s_{j-1}, s_{k-1}; \Sigma_\sigma)}{\Phi(s_j) - \Phi(s_{j-1})} - \frac{\Phi_2(s_{j-1}, s_k; \Sigma_\sigma) + \Phi_2(s_j, s_{k-1}; \Sigma_\sigma)}{\Phi(s_j) - \Phi(s_{j-1})}\end{aligned}$$

(f) We have:

$$\begin{aligned}\mathcal{T}(\mathcal{R}_k) &= \Pr\{\mathcal{R}(t) \neq \mathcal{R}_k \mid \mathcal{R}(t-1) = \mathcal{R}_k\} \\ &= 1 - \Pr\{\mathcal{R}(t) = \mathcal{R}_k \mid \mathcal{R}(t-1) = \mathcal{R}_k\} \\ &= 1 - p_{k,k}\end{aligned}$$

(g) We have:

$$\begin{aligned}\mathcal{T}(\mathcal{R}_1, \ldots, \mathcal{R}_K) &= \sum_{k=1}^{K} \Pr\{\mathcal{R}(t-1) = \mathcal{R}_k\} \cdot \mathcal{T}(\mathcal{R}_k) \\ &= \sum_{k=1}^{K} \Pr\{\mathcal{R}(t) \neq \mathcal{R}_k, \mathcal{R}(t-1) = \mathcal{R}_k\}\end{aligned}$$

Table B.1: ESG migration matrix (Question 3.a)

| Rating | $s_k$ | $p_k$ | Transition probability $p_{j,k}$ | | | | $\mathcal{T}(\mathcal{R}_k)$ |
|---|---|---|---|---|---|---|---|
| **D** | $-1.50$ | 6.68% | 92.96% | 7.04% | 0.00% | 0.00% | 7.04% |
| **C** | $0.00$ | 43.32% | 1.31% | 95.03% | 3.66% | 0.00% | 4.97% |
| **B** | $1.50$ | 43.32% | 0.00% | 3.66% | 95.03% | 1.31% | 4.97% |
| **A** | | 6.68% | 0.00% | 0.00% | 7.04% | 92.96% | 7.04% |
| $\mathcal{T}(\mathcal{R}_1,\ldots,\mathcal{R}_K)$ | | | | | | | 5.25% |

Table B.2: ESG migration matrix (Question 3.b)

| Rating | $s_k$ | $p_k$ | Transition probability $p_{j,k}$ | | | | $\mathcal{T}(\mathcal{R}_k)$ |
|---|---|---|---|---|---|---|---|
| **D** | $-0.67$ | 25.00% | 95.15% | 4.85% | 0.00% | 0.00% | 4.85% |
| **C** | $0.00$ | 25.00% | 5.27% | 88.38% | 6.35% | 0.00% | 11.62% |
| **B** | $0.67$ | 25.00% | 0.00% | 6.35% | 88.38% | 5.27% | 11.62% |
| **A** | | 25.00% | 0.00% | 0.00% | 4.85% | 95.15% | 4.85% |
| $\mathcal{T}(\mathcal{R}_1,\ldots,\mathcal{R}_K)$ | | | | | | | 8.23% |

Table B.3: ESG migration matrix (Question 3.c)

| Rating | $s_k$ | $p_k$ | Transition probability $p_{j,k}$ | | | | $\mathcal{T}(\mathcal{R}_k)$ |
|---|---|---|---|---|---|---|---|
| **D** | $-1.28$ | 10.00% | 93.54% | 6.46% | 0.00% | 0.00% | 6.46% |
| **C** | $0.00$ | 40.00% | 1.89% | 94.14% | 3.97% | 0.00% | 5.86% |
| **B** | $1.28$ | 40.00% | 0.00% | 3.97% | 94.14% | 1.89% | 5.86% |
| **A** | | 10.00% | 0.00% | 0.00% | 6.46% | 93.54% | 6.46% |
| $\mathcal{T}(\mathcal{R}_1,\ldots,\mathcal{R}_K)$ | | | | | | | 5.98% |

(h) The ESG migration matrices are given in Tables B.1, B.2 and B.3. We deduce that the ESG rating system defined in Question 3.a is the best rating system if we would like to reduce the monthly turnover of ESG ratings.

(i) The relationship between the parameter $\sigma$ and the turnover $\mathcal{T}(\mathcal{R}_1,\ldots,\mathcal{R}_K)$ is given in Figure B.6.

(j) The relationship between the number of notches $K$ and the turnover $\mathcal{T}(\mathcal{R}_1,\ldots,\mathcal{R}_K)$ is given in Figure B.7.

(k) An ESG rating system is mainly quantitative and highly depends on the mapping function. This is not the case of a credit rating system, which is mainly qualitative and discretionary. This explains that the turnover of an ESG rating system is higher than the turnover of a credit rating system. The stabilization of the ESG rating system implies to reduce the turnover $\mathcal{T}(\mathcal{R}_1,\ldots,\mathcal{R}_K)$, which depends on three factors: (1) the number of notches[1] $K$; (2) the volatility $\sigma$ of score changes; (3) the design of the ESG rating system $(s_1,\ldots,s_{K-1})$. The turnover $\mathcal{T}(\mathcal{R}_1,\ldots,\mathcal{R}_K)$ has a big impact on an ESG exclusion (or negative screening) policy, because it creates noisy short-term entry/exit positions that do not necessarily correspond to a decrease or increase of the long-term ESG risks.

[1]This is why ESG rating systems have less notches than credit rating systems.

Figure B.6: Relationship between $\sigma$ and $\mathcal{T}(\mathcal{R}_1, \ldots, \mathcal{R}_K)$

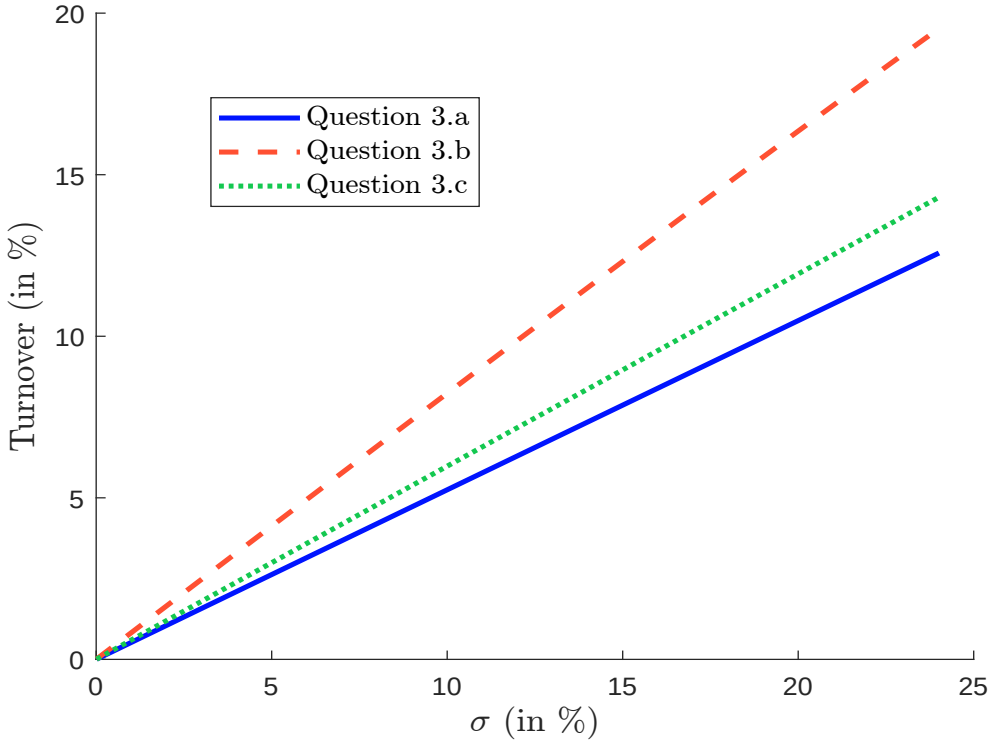


Figure B.7: Relationship between $K$ and $\mathcal{T}(\mathcal{R}_1, \ldots, \mathcal{R}_K)$

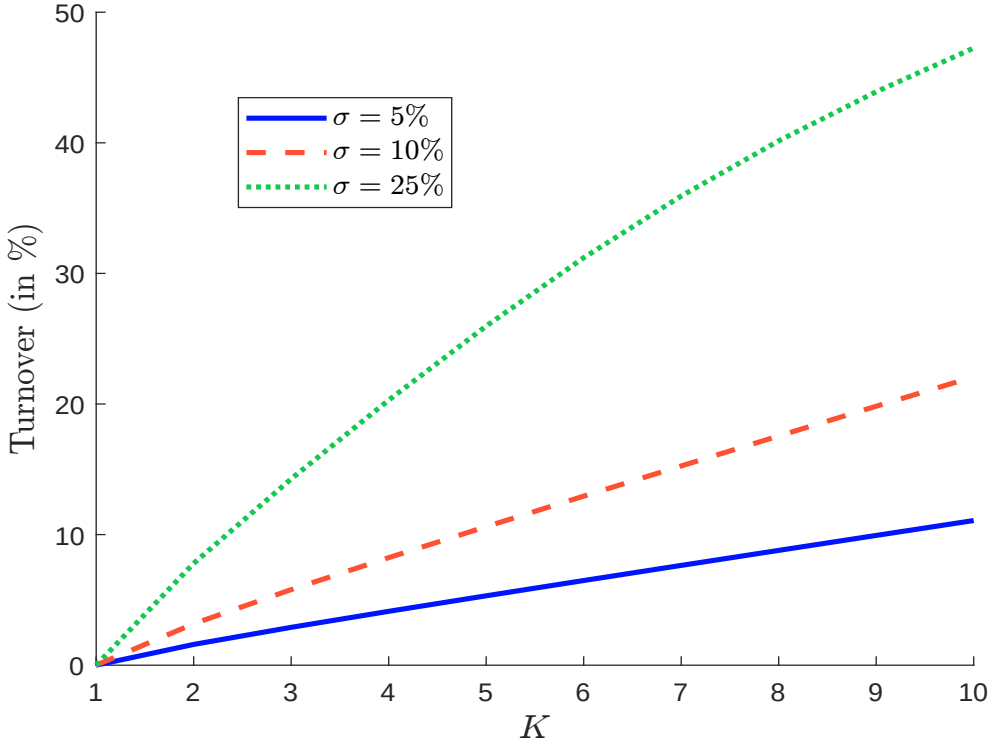

### B.1.3 Equity Portfolio optimization with ESG scores (Exercise 3.4.1)

1. We assume that the CAPM is valid.

   (a) Using the CAPM, we have:

   $$\mu_i = r + \beta_i (\mu_m - r)$$

   For instance, we have $\mu_1 = 1\% + 0.10 \times (6\% - 1\%) = 1.5\%$, $\mu_2 = 1\% + 0.30 \times 5\% = 2.5\%$. Finally, we obtain $\mu = (1.5\%, 2.5\%, 3.5\%, 5.5\%, 7.5\%, 11\%)$.

   (b) We have:

   $$\Sigma = \sigma_m^2 \beta\beta^\top + D$$

   where $D = \operatorname{diag}\left(\tilde{\sigma}_1^2, \ldots, \tilde{\sigma}_6^2\right)$. The numerical value of $\Sigma$ is:

   $$\Sigma = \begin{pmatrix} 293 & & & & & \\ 12 & 325 & & & & \\ 20 & 60 & 356 & & & \\ 36 & 108 & 180 & 424 & & \\ 52 & 156 & 260 & 468 & 797 & \\ 80 & 240 & 400 & 720 & 1\,040 & 1\,744 \end{pmatrix} \times 10^{-4}$$

   The computation of the asset volatility is equal to $\sigma_i = \sqrt{\Sigma_{i,i}}$. We deduce that $\sigma = (17.12\%, 18.03\%, 18.87\%, 20.59\%, 28.23\%, 41.76\%)$. The formula of the correlation is $\rho_{i,j} = (\sigma_i \sigma_j)^{-1} \Sigma_{i,j}$. We obtain the following correlation matrix expressed in %:

   $$\mathbb{C} = \begin{pmatrix} 100.00 & & & & & \\ 3.89 & 100.00 & & & & \\ 6.19 & 17.64 & 100.00 & & & \\ 10.21 & 29.09 & 46.33 & 100.00 & & \\ 10.76 & 30.65 & 48.81 & 80.51 & 100.00 & \\ 11.19 & 31.88 & 50.76 & 83.73 & 88.21 & 100.00 \end{pmatrix}$$

   (c) We have:

   $$w^* = \frac{\Sigma^{-1}(\mu - r\mathbf{1})}{\mathbf{1}^\top \Sigma^{-1}(\mu - r\mathbf{1})} = \begin{pmatrix} 0.94\% \\ 2.81\% \\ 5.28\% \\ 24.34\% \\ 29.06\% \\ 37.57\% \end{pmatrix}$$

   We deduce that $\mu(w^*) = w^{*\top}\mu = 7.9201\%$ and $\sigma(w^*) = \sqrt{w^{*\top}\Sigma w^*} = 28.3487\%$. The Sharpe ratio is then equal to:

   $$\mathrm{SR}(w^* \mid r) = \frac{7.9201\% - 1\%}{28.3487\%} = 0.2441$$

   Finally, the ESG score of the tangency portfolio is:

   $$\boldsymbol{\mathcal{S}}(w^*) = \sum_{i=1}^{6} w_i^* \boldsymbol{\mathcal{S}}_i = -2.0347$$

(d) We have:

$$\beta_i(w^*) = \frac{\mathbf{e}_i^\top \Sigma w^*}{\sigma^2(w^*)}$$

We obtain:

$$\beta(w^*) = \begin{pmatrix} 0.0723 \\ 0.2168 \\ 0.3613 \\ 0.6503 \\ 0.9393 \\ 1.4451 \end{pmatrix}$$

The computation of the implied expected return $\tilde{\mu}_i = r + \beta_i(w^*)(\mu(w^*) - r)$ gives:

$$\tilde{\mu} = \begin{pmatrix} 1.50\% \\ 2.50\% \\ 3.50\% \\ 5.50\% \\ 7.50\% \\ 11.00\% \end{pmatrix}$$

(e) We notice that $\beta_i(w^*) \neq \beta_i(w_m)$ but the risk premia deduced from the tangency portfolio are the same as those computed with the market portfolio. In fact, the market portfolio cannot coincide with the tangency portfolio because of the cash component. Let us assume that the allocation of $w_m$ is equal to $\alpha$ of the tangency portfolio $w^*$ and $1-\alpha$ of the risk-free asset. We deduce that:

$$\beta(w_m) = \frac{\Sigma w_m}{\sigma^2(w_m)} = \frac{\alpha \Sigma w^*}{\alpha^2 \sigma^2(w^*)} = \frac{1}{\alpha}\beta(w^*)$$

and:

$$\alpha = \frac{\beta_i(w^*)}{\beta_i(w_m)}$$

The computation gives $\alpha = 72.25\%$. The market portfolio $w_m$ is equal to 72.25% of the tangency portfolio $w^*$ and 27.75% of the risk-free asset. We have:

$$\begin{aligned} \mu(w_m) &= r + \alpha(\mu(w^*) - r) \\ &= 1\% + 72.25\% \times (7.9201\% - 1\%) \\ &= 6\% \end{aligned}$$

and:

$$\begin{aligned} \sigma(w_m) &= \alpha\,\sigma(w^*) \\ &= 72.25\% \times 28.3487\% \\ &= 20.48\% \end{aligned}$$

We deduce that:

$$\mathrm{SR}(w_m \mid r) = \frac{6\% - 1\%}{20.48\%} = 0.2441$$

Curiously, we do not obtain the true value of the Sharpe ratio:

$$\mathrm{SR}(w_m \mid r) = \frac{6\% - 1\%}{20\%} = 0.25$$

because the volatility $\sigma(w_m)$ is not equal to 20%. The reason is that the market portfolio computed with the tangency portfolio has an idiosyncratic risk. Indeed, we have:

$$\sqrt{w_m^\top (\sigma_m^2 \beta\beta^\top) w^\top} = 20\% < \sigma(w_m) = 20.48\%$$

Therefore, $w_m$ is not fully diversified because the number of assets is small ($n = 6$).

2. We consider long-only portfolios and we also impose a minimum threshold $\boldsymbol{\mathcal{S}}^\star$ for the portfolio ESG score:

$$\boldsymbol{\mathcal{S}}(w) = \sum_{i=1}^n w_i \boldsymbol{\mathcal{S}}_i \geq \boldsymbol{\mathcal{S}}^\star$$

(a) We have:

$$w^\star = \arg\min \frac{1}{2} w^\top \Sigma w - \gamma w^\top \mu$$
$$\text{s.t.} \begin{cases} \mathbf{1}_6^\top w = 1 \\ w^\top \boldsymbol{\mathcal{S}} \geq \boldsymbol{\mathcal{S}}^\star \\ \mathbf{0}_6 \leq w \leq \mathbf{1}_6 \end{cases}$$

Figure B.8: Impact of the minimum ESG score on the efficient frontier

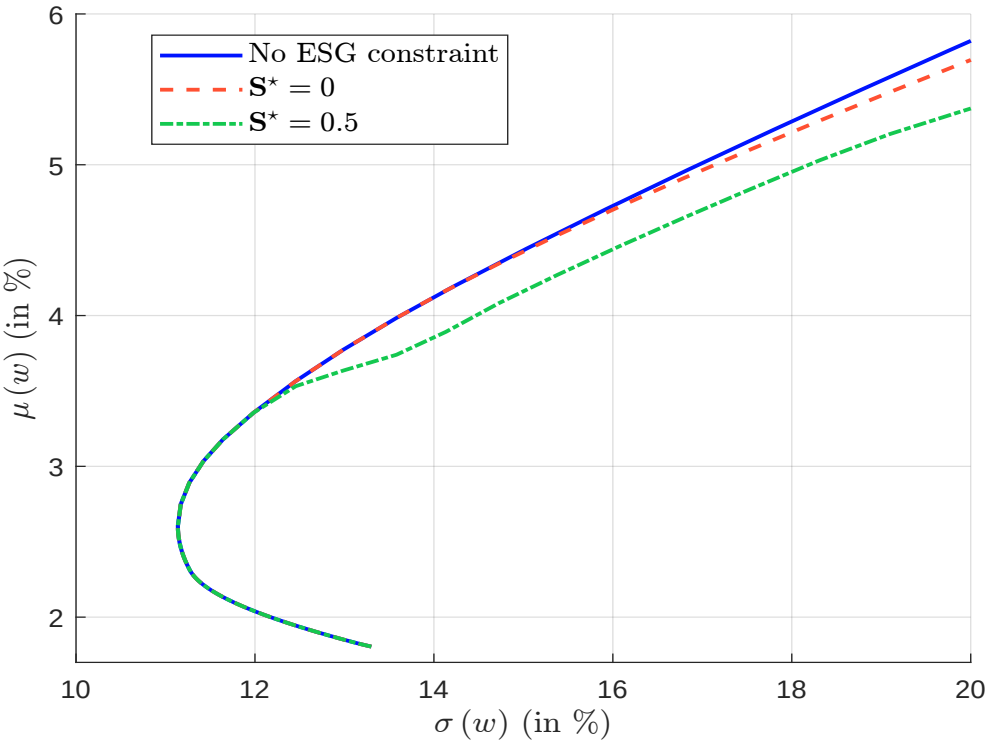


(b) We remind that the matrix form of the QP problem is:

$$w^\star = \arg\min \frac{1}{2} w^\top Q w - w^\top R$$
$$\text{s.t.} \begin{cases} Aw = B \\ Cw \leq D \\ w^- \leq w \leq w^+ \end{cases}$$

We deduce that $Q = \Sigma$, $R = \gamma\mu$, $A = \mathbf{1}_6^\top$, $B = 1$, $C = -\boldsymbol{\mathcal{S}}^\top$, $D = -\boldsymbol{\mathcal{S}}^\star$, $w^- = \mathbf{0}_6$ and $w^+ = \mathbf{1}_6$.

(c) To compute the efficient frontier, we consider several value of $\gamma \in [-1, 2]$. For each value of $\gamma$, we compute the optimal portfolio $w^\star$ and deduce its expected return $\mu(w^\star)$ and its volatility $\sigma(w^\star)$. In Figure B.8, we compare the results for the three cases: $\boldsymbol{\mathcal{S}}^\star = -\infty$, $\boldsymbol{\mathcal{S}}^\star = 0$ and $\boldsymbol{\mathcal{S}}^\star = 0.5$. We notice that imposing a positive ESG score has little impact, especially for low-volatility portfolios when $\sigma(w^\star) \leq 16\%$. This is not the case when $\boldsymbol{\mathcal{S}}^\star = 0.5$.

(d) Let $w^\star(\gamma)$ be the MVO portfolio when the risk tolerance is equal to $\gamma$. If we use a fine grid of $\gamma$ values, we can find the optimal value $\gamma^*$ by solving numerically the following optimization problem with the brute force algorithm:

$$\gamma^* = \arg\max \frac{\mu(w^\star(\gamma)) - r}{\sigma(w^\star(\gamma))} \qquad \text{for } \gamma \in [0, 2]$$

Then we deduce the tangency portfolio $w^* = w^\star(\gamma^*)$. We also compute the following statistics: $\mu(w^*) = w^{*\top}\mu$, $\sigma(w^*) = \sqrt{w^{*\top}\Sigma w^*}$, $\mathrm{SR}(w^* \mid r) = \sigma(w^*)^{-1}(\mu(w^*) - r)$ and $\boldsymbol{\mathcal{S}}(w^*) = w^{*\top}\boldsymbol{\mathcal{S}}$. Results are reported in Table B.4. In the case $\boldsymbol{\mathcal{S}}^\star = -\infty$, we retrieve the tangency portfolio, which has been found in Question 1.c. Moreover, we notice that the Sharpe ratio decreases when the minimum ESG score $\boldsymbol{\mathcal{S}}^\star$ increases.

Table B.4: Impact of the minimum ESG score on the efficient frontier

| $\boldsymbol{\mathcal{S}}^\star$ | $-\infty$ | 0 | 0.5 |
|---|---|---|---|
| $\gamma^*$ | 1.1613 | 0.8500 | 0.8500 |
| $w^*$ (in %) | 0.9360 | 9.7432 | 9.1481 |
| | 2.8079 | 16.3317 | 19.0206 |
| | 5.2830 | 31.0176 | 40.3500 |
| | 24.3441 | 5.1414 | 0.0000 |
| | 29.0609 | 11.6028 | 3.8248 |
| | 37.5681 | 26.1633 | 27.6565 |
| $\mu(w^*)$ (in %) | 7.9201 | 5.6710 | 5.3541 |
| $\sigma(w^*)$ $(in\%)$ | 28.3487 | 19.8979 | 19.2112 |
| $\mathrm{SR}(w^* \mid r)$ | 0.2441 | 0.2347 | 0.2266 |
| $\boldsymbol{\mathcal{S}}(w^*)$ | −2.0347 | 0.0000 | 0.5000 |

(e) We perform the same analysis as previously for several values $\boldsymbol{\mathcal{S}}^\star \in [-2.5, 2.5]$. Results are reported in Figure B.9. We verify that the Sharpe ratio is a decreasing function of $\boldsymbol{\mathcal{S}}^\star$.

(f) The market portfolio $w_m$ is then equal to:

$$w_m = \begin{pmatrix} 9.15\% \\ 19.02\% \\ 40.35\% \\ 0.00\% \\ 3.82\% \\ 27.66\% \end{pmatrix}$$

We deduce that $\mu(w_m) = 5.3541\%$, $\sigma(w_m) = 19.2112\%$, $\mathrm{SR}(w_m \mid r) = 0.2266$ and $\boldsymbol{\mathcal{S}}(w_m) = 0.5$.

Figure B.9: Relationship between the minimum ESG score $\boldsymbol{\mathcal{S}}^\star$ and the Sharpe ratio $\mathrm{SR}(w^* \mid r)$ of the tangency portfolio

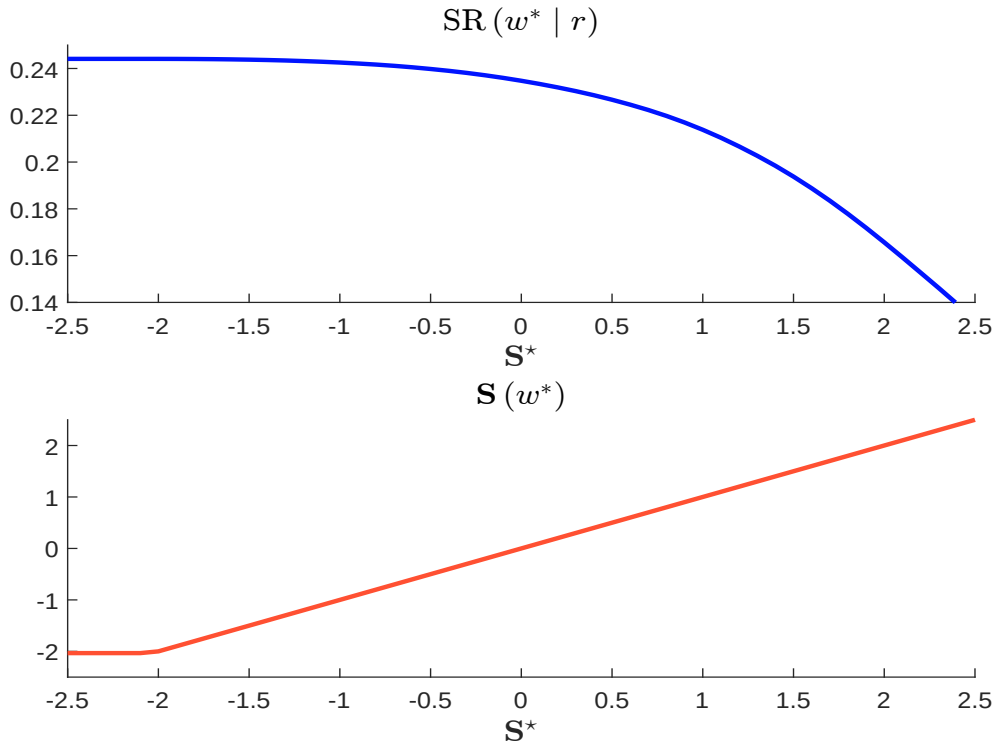


(f).i We have:

$$\beta_i(w_m) = \frac{\mathbf{e}_i^\top \Sigma w_m}{\sigma^2(w_m)}$$

and:

$$\tilde{\mu}_i(w_m) = r + \beta_i(w_m)(\mu(w_m) - r)$$

We deduce that the alpha return is equal to:

$$\begin{aligned} \alpha_i &= \mu_i - \tilde{\mu}_i(w_m) \\ &= (\mu_i - r) - \beta_i(w_m)(\mu(w_m) - r) \end{aligned}$$

Results are reported in Table B.5. We notice that $\alpha_i < 0$ for the first three assets and $\alpha_i > 0$ for the last three assets, implying that:

$$\begin{cases} \boldsymbol{\mathcal{S}}_i > 0 \Rightarrow \alpha_i < 0 \\ \boldsymbol{\mathcal{S}}_i < 0 \Rightarrow \alpha_i > 0 \end{cases}$$

(f).ii We have:

$$\beta(w_{\text{ew}} \mid w_m) = \frac{w_{\text{ew}}^\top \Sigma w_m}{\sigma^2(w_m)} = 0.9057$$

and:

$$\begin{aligned} \tilde{\mu}(w_{\text{ew}}) &= r + \beta(w_{\text{ew}} \mid w_m)(\mu(w_m) - r) \\ &= 1\% + 0.9057 \times (5.3541\% - 1\%) \\ &= 4.9435\% \end{aligned}$$

Table B.5: Computation of the alpha return due to the ESG constraint

| Asset | $\beta_i(w_m)$ | $\tilde{\mu}_i(w_m)$ (in %) | $\tilde{\mu}_i(w_m) - r$ (in %) | $\alpha_i$ (in bps) |
|---|---|---|---|---|
| 1 | 0.1660 | 1.7228 | 0.7228 | −22.28 |
| 2 | 0.4321 | 2.8813 | 1.8813 | −38.13 |
| 3 | 0.7518 | 4.2733 | 3.2733 | −77.33 |
| 4 | 0.8494 | 4.6984 | 3.6984 | 80.16 |
| 5 | 1.2395 | 6.3967 | 5.3967 | 110.33 |
| 6 | 1.9955 | 9.6885 | 8.6885 | 131.15 |

We deduce that:

$$\begin{aligned}\alpha(w_{\text{ew}}) &= \mu(w_{\text{ew}}) - \tilde{\mu}(w_{\text{ew}}) \\ &= 5.25\% - 4.9435\% \\ &= 30.65 \text{ bps}\end{aligned}$$

We verify that:

$$\alpha(w_{\text{ew}}) = \sum_{i=1}^{6} w_{\text{ew},i}\alpha_i = \frac{\sum_{i=1}^{6}\alpha_i}{6} = 30.65 \text{ bps}$$

The equally-weighted portfolio has a positive alpha. The main reason is that its ESG score is lower than the ESG score of the market portfolio:

$$\boldsymbol{\mathcal{S}}(w_{\text{ew}}) = -0.33 \ll \boldsymbol{\mathcal{S}}(w_m) = 0.50$$

3. The objective of the investor is twice. He would like to manage the tracking error risk of his portfolio with respect to the benchmark $b = (15\%, 20\%, 19\%, 14\%, 15\%, 17\%)$ and have a better ESG score than the benchmark. Nevertheless, this investor faces a long-only constraint because he cannot leverage his portfolio and he cannot also be short on the assets.

   (a) We have:

$$\boldsymbol{\mathcal{S}}(b) = \sum_{i=1}^{6} b_i \boldsymbol{\mathcal{S}}_i = -0.1620$$

   (b) We have:

$$\begin{cases} \boldsymbol{\mathcal{S}}(w \mid b) = (w-b)^\top \boldsymbol{\mathcal{S}} = 0.0470 \\ \mu(w \mid b) = (w-b)^\top \mu = -0.5 \text{ bps} \\ \sigma(w \mid b) = \sqrt{(w-b)^\top \Sigma (w-b)} = 2.8423\% \\ \text{IR}(w \mid b) = \dfrac{\mu(w \mid b)}{\sigma(w \mid b)} = -0.0018 \end{cases}$$

   The portfolio $w$ is not optimal since it improves the ESG score of the benchmark, but its information ratio is negative. Nevertheless, the expected excess return is close to zero (less than −1 bps).

   (c) We have $\boldsymbol{\mathcal{S}}(w \mid b) = 0.1305$, $\mu(w \mid b) = 29.5$ bps, $\sigma(w \mid b) = 2.4949\%$ and $\text{IR}(w \mid b) = 0.1182$. The portfolio $w$ has then a positive expected excess return of 29.5 bps and a tracking error volatility of 2.4949%. Moreover, it has a better ESG score than the benchmark since its excess ESG score is equal to 0.1305.

(d) The optimization problem is:

$$\begin{aligned} w^\star &= \arg\min \frac{1}{2}\sigma^2(w \mid b) - \gamma \boldsymbol{\mathcal{S}}(w \mid b) \\ &\text{s.t.} \begin{cases} \mathbf{1}_6^\top w = 1 \\ \mathbf{0}_6 \leq w \leq \mathbf{1}_6 \end{cases} \end{aligned}$$

(e) The objective function is equal to:

$$\begin{aligned} (*) &= \frac{1}{2}\sigma^2(w \mid b) - \gamma \boldsymbol{\mathcal{S}}(w \mid b) \\ &= \frac{1}{2}(w-b)^\top \Sigma (w-b) - \gamma (w-b)^\top \boldsymbol{\mathcal{S}} \\ &= \frac{1}{2} w^\top \Sigma w - w^\top (\Sigma b + \gamma \boldsymbol{\mathcal{S}}) + \underbrace{\left(\gamma b^\top \boldsymbol{\mathcal{S}} + \frac{1}{2} b^\top \Sigma b\right)}_{\text{does not depend on } w} \end{aligned}$$

We remind that the form of the QP problem is:

$$\begin{aligned} w^\star &= \arg\min \frac{1}{2} w^\top Q w - w^\top R \\ &\text{s.t.} \begin{cases} Aw = B \\ Cw \leq D \\ w^- \leq w \leq w^+ \end{cases} \end{aligned}$$

We deduce that $Q = \Sigma$, $R = \Sigma b + \gamma \boldsymbol{\mathcal{S}}$, $A = \mathbf{1}_6^\top$, $B = 1$, $w^- = \mathbf{0}_6$ and $w^+ = \mathbf{1}_6$.

(f) We solve the QP problem for several values of $\gamma \in [0, 5\%]$ and obtain Figure B.10.

(g) Using the QP numerical algorithm, we compte the optimal value $\sigma(w \mid b)$ for $\gamma = 0$ and $\gamma = 5\%$. Then, we apply the bisection algorithm to find the optimal value $\gamma^\star$ such that:

$$\sigma(w \mid b) = \sigma^\star$$

We obtain the results given in Table B.6.

Table B.6: Solution of the $\sigma$-problem

| Target $\sigma^\star$ | 0 | 1% | 2% | 3% | 4% |
|---|---|---|---|---|---|
| $\gamma^\star$ (in bps) | 0.000 | 4.338 | 8.677 | 13.015 | 18.524 |
| $w^\star$ (in %) | 15.000 | 15.175 | 15.350 | 15.525 | 14.921 |
| | 20.000 | 21.446 | 22.892 | 24.338 | 25.385 |
| | 19.000 | 23.084 | 27.167 | 31.251 | 35.589 |
| | 14.000 | 9.588 | 5.176 | 0.763 | 0.000 |
| | 15.000 | 12.656 | 10.311 | 7.967 | 3.555 |
| | 17.000 | 18.052 | 19.104 | 20.156 | 20.550 |
| $\boldsymbol{\mathcal{S}}(w^\star \mid b)$ | 0.000 | 0.230 | 0.461 | 0.691 | 0.915 |

(h) Using the QP numerical algorithm, we compte the optimal value $\boldsymbol{\mathcal{S}}(w \mid b)$ for $\gamma = 0$ and $\gamma = 5\%$. Then, we apply the bisection algorithm to find the optimal value $\gamma^\star$ such that:

$$\boldsymbol{\mathcal{S}}(w \mid b) = \boldsymbol{\mathcal{S}}^\star$$

Figure B.10: Efficient frontier of tracking a benchmark with an ESG score objective

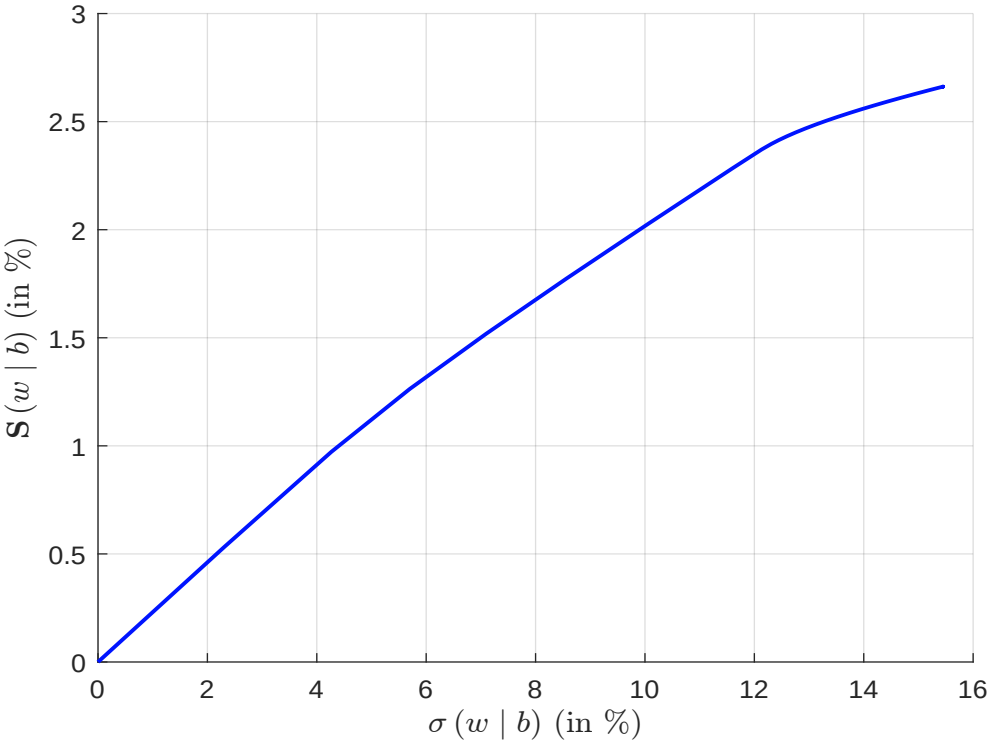


An alternative approach consists in solving the following optimization problem:

$$w^\star = \arg\min \frac{1}{2}\sigma^2(w \mid b)$$
$$\text{s.t.} \begin{cases} \mathbf{1}_6^\top w = 1 \\ \boldsymbol{\mathcal{S}}(w \mid b) = \boldsymbol{\mathcal{S}}^\star \\ \mathbf{0}_6 \leq w \leq \mathbf{1}_6 \end{cases}$$

It is easy to show that the QP problem is given by $Q = \Sigma$, $R = \Sigma b$, $A = \begin{pmatrix} \mathbf{1}_6^\top \\ \boldsymbol{\mathcal{S}}^\top \end{pmatrix}$, $B = \begin{pmatrix} 1 \\ \boldsymbol{\mathcal{S}}^\star + \boldsymbol{\mathcal{S}}^\top b \end{pmatrix}$, $w^- = \mathbf{0}_6$ and $w^+ = \mathbf{1}_6$. Finally, we obtain the results given in Table B.7.

Table B.7: Solution of the $\boldsymbol{\mathcal{S}}$-problem

| Target $\boldsymbol{\mathcal{S}}^\star$ | 0 | 0.1 | 0.2 | 0.3 | 0.4 |
|---|---|---|---|---|---|
| $\gamma^\star$ (in bps) | 0.000 | 1.882 | 3.764 | 5.646 | 7.528 |
| $w^\star$ (in %) | 15.000 | 15.076 | 15.152 | 15.228 | 15.304 |
| | 20.000 | 20.627 | 21.255 | 21.882 | 22.509 |
| | 19.000 | 20.772 | 22.544 | 24.315 | 26.087 |
| | 14.000 | 12.086 | 10.171 | 8.257 | 6.343 |
| | 15.000 | 13.983 | 12.966 | 11.949 | 10.932 |
| | 17.000 | 17.456 | 17.913 | 18.369 | 18.825 |
| $\sigma(w^\star \mid b)$ (in %) | 0.000 | 0.434 | 0.868 | 1.301 | 1.735 |

(i) For the best-in-class strategy, the optimization problem becomes:

$$w^\star = \arg\min \frac{1}{2}\sigma^2(w \mid b) - \gamma \boldsymbol{\mathcal{S}}(w \mid b) \quad \text{s.t.} \quad \begin{cases} \mathbf{1}_6^\top w = 1 \\ w_4 = w_5 = w_6 = 0 \\ \mathbf{0}_6 \leq w \leq \mathbf{1}_6 \end{cases}$$

The QP form is defined by $Q = \Sigma$, $R = \Sigma b + \gamma \boldsymbol{\mathcal{S}}$, $A = \mathbf{1}_6^\top$, $B = 1$, $w^- = \mathbf{0}_6$ and $w^+ = \begin{pmatrix} \mathbf{1}_3 \\ \mathbf{0}_3 \end{pmatrix}$. For the worst-in-class strategy, the optimization problem becomes:

$$w^\star = \arg\min \frac{1}{2}\sigma^2(w \mid b) - \gamma \boldsymbol{\mathcal{S}}(w \mid b) \quad \text{s.t.} \quad \begin{cases} \mathbf{1}_6^\top w = 1 \\ w_6 = 0 \\ \mathbf{0}_6 \leq w \leq \mathbf{1}_6 \end{cases}$$

The QP form is defined by $Q = \Sigma$, $R = \Sigma b + \gamma \boldsymbol{\mathcal{S}}$, $A = \mathbf{1}_6^\top$, $B = 1$, $w^- = \mathbf{0}_6$ and $w^+ = \begin{pmatrix} \mathbf{1}_5 \\ 0 \end{pmatrix}$. The efficient frontiers are reported in Figure B.11. The exclusion strategy has less impact than the selection strategy. This last one implies a high tracking error risk.

Figure B.11: Comparison of the efficient frontiers (ESG integration, best-in-class selection and worst-in-class exclusion)

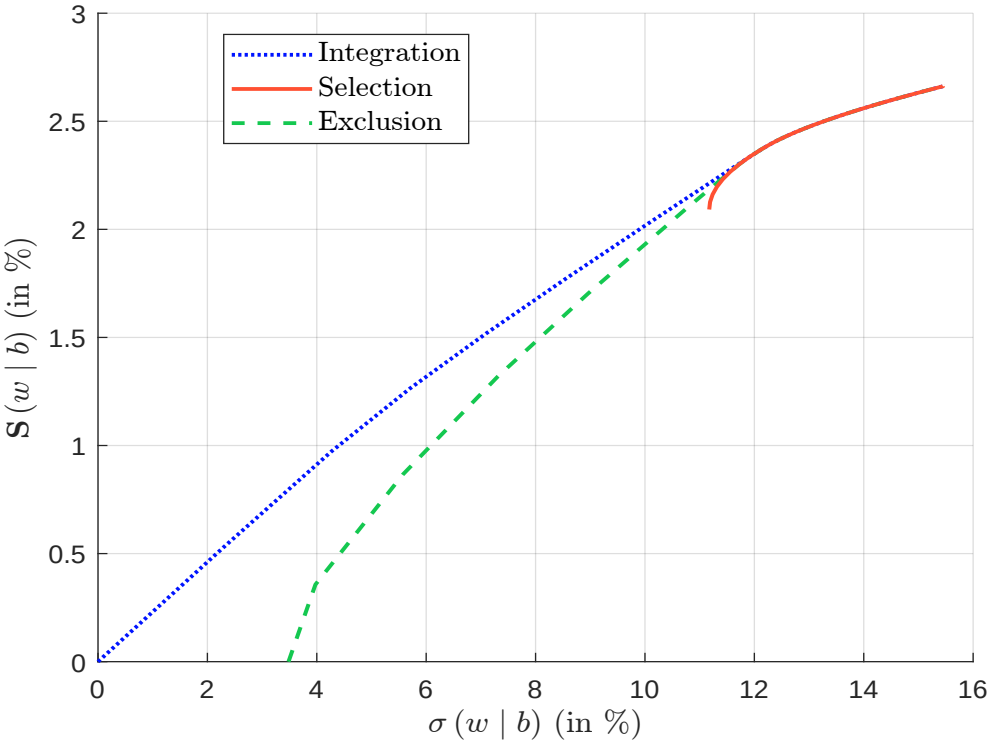

(j) We solve the first problem of Question 3.i with $\gamma = 0$ and obtain $\sigma(w \mid b) \geq 11.17\%$. When $\sigma(w^\star \mid b) = 11.17\%$, the corresponding optimal portfolio is:

$$w^\star = \begin{pmatrix} 16.31\% \\ 34.17\% \\ 49.52\% \\ 0\% \\ 0\% \\ 0\% \end{pmatrix}$$

**Remark 140** *The impact of ESG scores on optimized portfolios depends on their relationship with expected returns, volatilities, correlations, beta coefficients, etc. In the previous exercise, the results are explained because the best-in-class assets are those with the lowest expected returns and beta coefficients while the worst-in-class assets are those with the highest expected returns and beta coefficients. For instance, we obtain a high tracking error risk for the best-in-class selection strategy, because the best-in-class assets have low volatilities and correlations with respect to worst-in-class assets, implying that it is difficult to replicate these last assets with the other assets.*

### B.1.4 Calculating the prevalence of undernourishment (Exercise 5.5.1)

1. (a) We have:

$$\ln D = \ln X - \ln R \sim \mathcal{N}\left(\mu_d, \sigma_d^2\right)$$

where:

$$\mu_d = \mathbb{E}\left[\ln X - \ln R\right] = \mathbb{E}\left[\ln X\right] - \mathbb{E}\left[\ln R\right] = \mu_x - \mu_r$$

and:

$$\begin{aligned}
\sigma_d^2 &= \text{var}\left(\ln X - \ln R\right) \\
&= \text{var}\left(\ln X\right) + \text{var}\left(\ln R\right) - 2\,\text{cov}\left(\ln X, \ln R\right) \\
&= \sigma_x^2 + \sigma_r^2 - 2\rho\sigma_x\sigma_r
\end{aligned}$$

Thus, we deduce that $D = X/R$ is a log-normal random variable: $D \sim \mathcal{LN}\left(\mu_d, \sigma_d^2\right)$. It follows that:

$$\begin{aligned}
\text{PoU}^\star &= \Pr\{X < R\} \\
&= \Pr\{D < 1\} \\
&= \Pr\{\ln D < 0\} \\
&= \Phi\left(-\frac{\mu_d}{\sigma_d}\right) \\
&= \Phi\left(-\frac{\mu_x - \mu_r}{\sqrt{\sigma_x^2 + \sigma_r^2 - 2\rho\sigma_x\sigma_r}}\right)
\end{aligned}$$

(b) The probability density functions of $X$ and $R$ are given in Figure B.12.

(c) Figure B.13 illustrates the relationship between the correlation and the prevalence of undernourishment. We observe a decreasing function between $\rho$ and $\text{PoU}^\star$, because the standard deviation of $D$ is a decreasing function of the correlation between $X$ and $R$ and $\mu_x > \mu_r$. Conversely, if $\mu_x < \mu_r$, the relationship between $\rho$ and $\text{PoU}^\star$ becomes increasing.

(d) We have:

$$\text{PoU} = \Pr\{X < r_L\} = \Pr\{\ln X < \ln r_L\} = \Phi\left(\frac{\ln r_L - \mu_x}{\sigma_x}\right)$$

The relationship between $r_L$ and PoU is shown in Figure B.14.

(e) We deduce that:

$$\begin{aligned}
\text{PoU} = \text{PoU}^\star &\Leftrightarrow \Phi\left(\frac{\ln r_L^\star - \mu_x}{\sigma_x}\right) = \Phi\left(-\frac{\mu_x - \mu_r}{\sqrt{\sigma_x^2 + \sigma_r^2 - 2\rho_{x,r}\sigma_x\sigma_r}}\right) \\
&\Leftrightarrow \frac{\ln r_L^\star - \mu_x}{\sigma_x} = -\frac{\mu_x - \mu_r}{\sqrt{\sigma_x^2 + \sigma_r^2 - 2\rho_{x,r}\sigma_x\sigma_r}}
\end{aligned}$$

which implies:

$$r_L^\star = \exp\left(\mu_x - \frac{\left(\mu_x - \mu_r\right)\sigma_x}{\sqrt{\sigma_x^2 + \sigma_r^2 - 2\rho_{x,r}\sigma_x\sigma_r}}\right)$$

The calibration of $r_L^\star$ is shown in Figure B.15.

Figure B.12: Probability density functions of $X$ and $R$

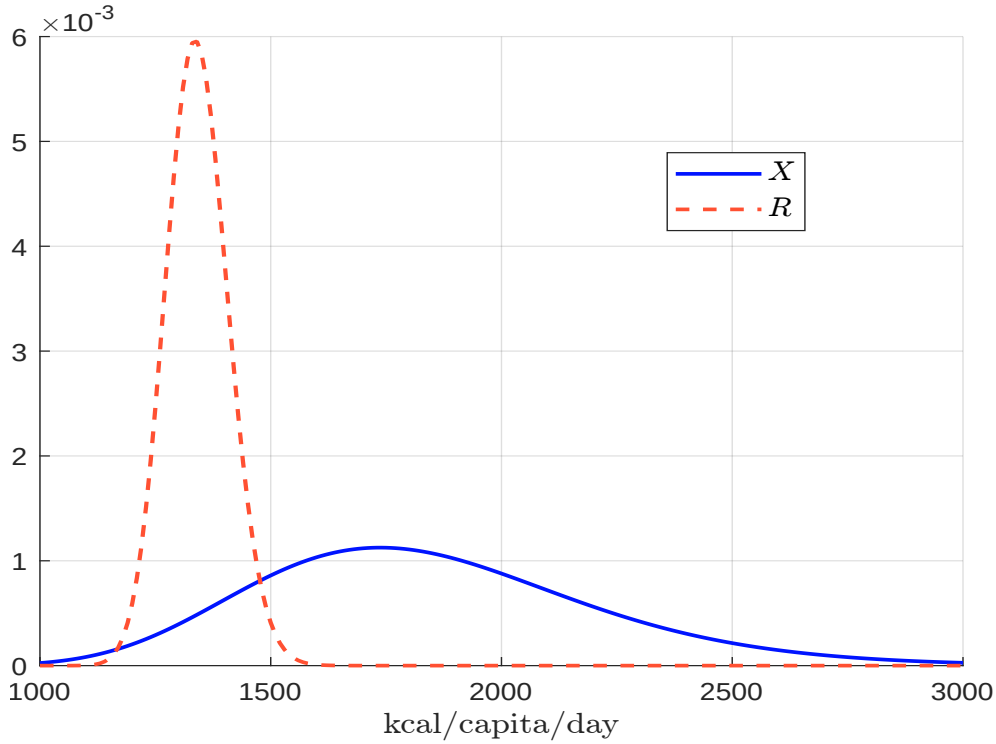


Figure B.13: Relationship between the correlation $\rho$ and the prevalence of undernourishment PoU$^\star$

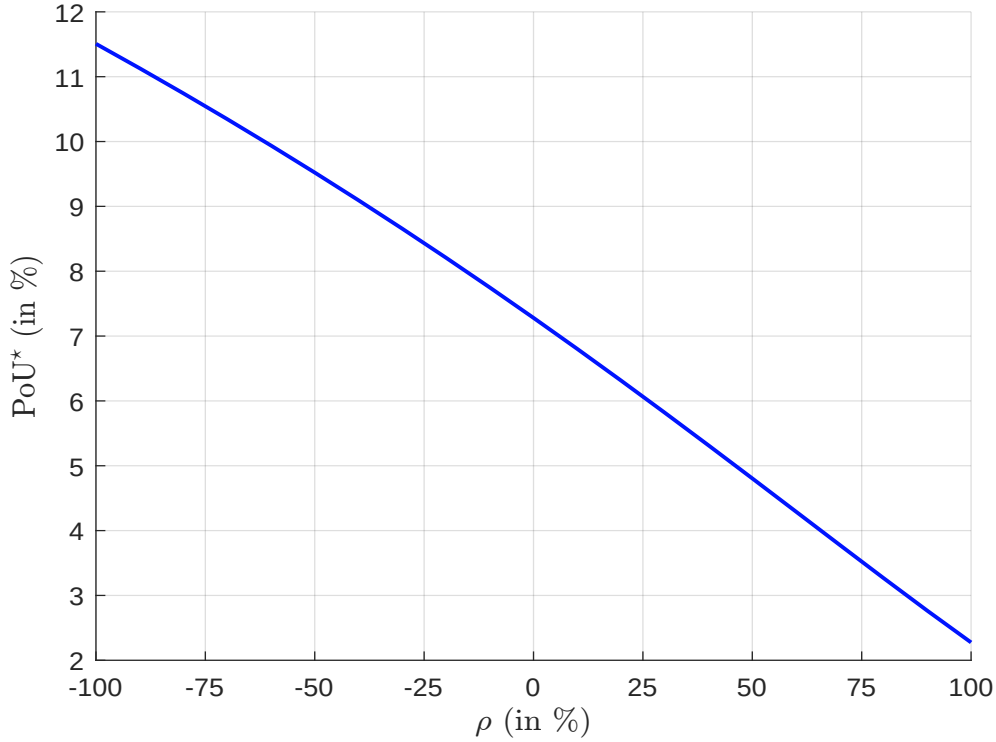

Figure B.14: Prevalence of undernourishment PoU

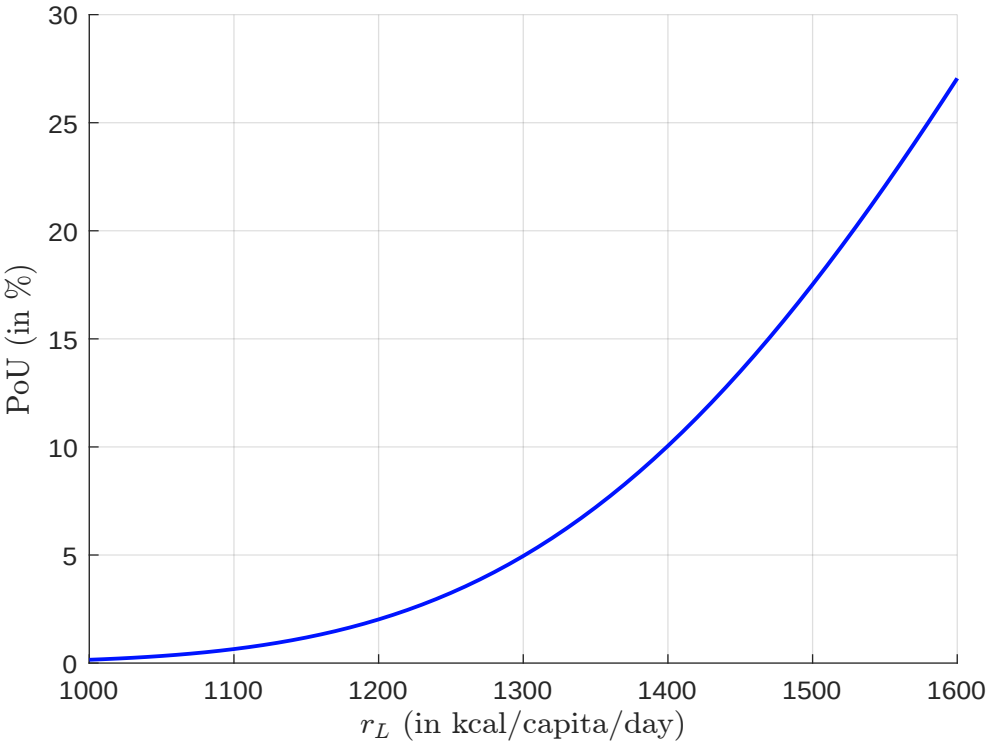


Figure B.15: Calibration of $r_L^\star$

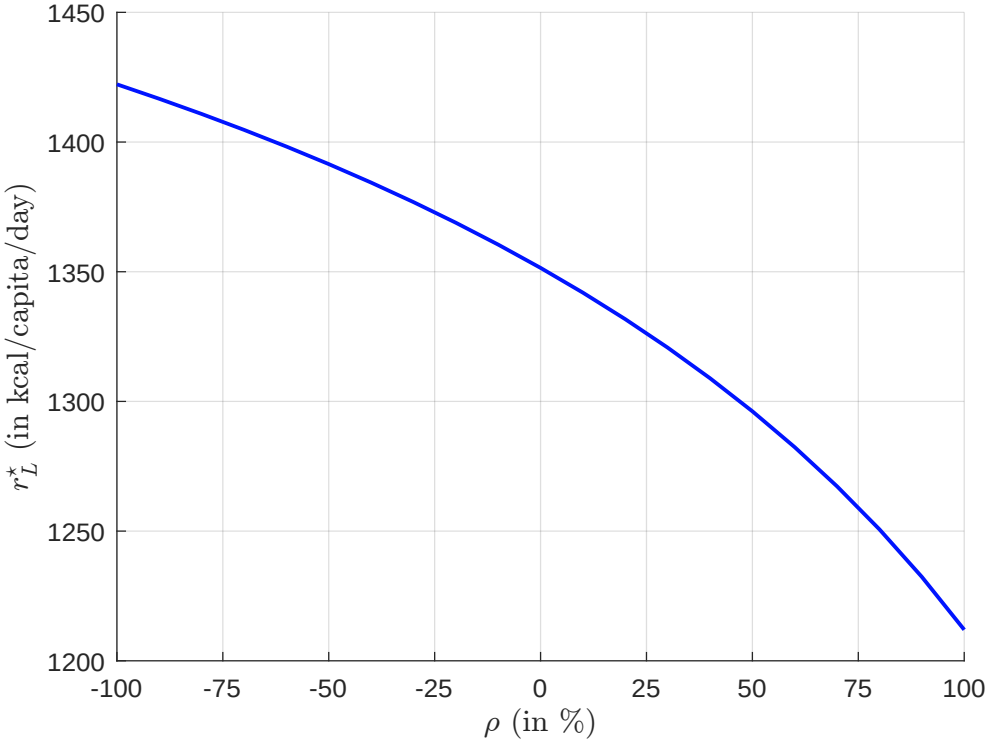

2. (a) We have:
$$\mu(X) = e^{\mu_x + \frac{1}{2}\sigma_x^2}$$
and:
$$\sigma^2(X) = e^{2\mu_x + \sigma_x^2}\left(e^{\sigma_x^2} - 1\right) = \mu^2(X)\left(e^{\sigma_x^2} - 1\right)$$

(b) We deduce that:
$$\text{CV}(X) = \frac{\sigma(X)}{\mu(X)} = \sqrt{e^{\sigma_x^2} - 1}$$

(c) We have:
$$\begin{aligned}\text{CV}(X) = \sqrt{e^{\sigma_x^2} - 1} &\Leftrightarrow e^{\sigma_x^2} = \text{CV}^2(X) + 1\\ &\Leftrightarrow \sigma_x = \sqrt{\ln\left(\text{CV}^2(X) + 1\right)}\end{aligned}$$
and:
$$\begin{aligned}\mu(X) = e^{\mu_x + \frac{1}{2}\sigma_x^2} &\Leftrightarrow \mu_x = \ln\mu(X) - \frac{1}{2}\sigma_x^2\\ &\Leftrightarrow \mu_x = \ln\mu(X) - \frac{1}{2}\ln\left(\text{CV}^2(X) + 1\right)\\ &\Leftrightarrow \mu_x = \ln\mu(X) - \ln\sqrt{\text{CV}^2(X) + 1}\\ &\Leftrightarrow \mu_x = \ln\frac{\mu(X)}{\sqrt{\text{CV}^2(X) + 1}}\end{aligned}$$

(d) The food available for human consumption is equal to:
$$\begin{aligned}Q_1 &= 349\,000 + 1\,025 - 40\,000 - (-1\,000) - 45\,000 - 9\,000 = 257\,025 \text{ tonnes}\\ Q_2 &= 50\,000 + 9\,010 - 1\,000 - 6\,000 - 500 - 500 = 51\,010 \text{ tonnes}\end{aligned}$$
We deduce that the ADEC value is:
$$\mu(X) = \frac{257\,025 \times 10^3 \times 3\,500 + 51\,010 \times 10^3 \times 500}{365 \times 10^6} = 2\,534.50 \text{ kcal/capita/day}$$

(e) Let $x_j^y$ be the average dietary energy consumption for the $j^{\text{th}}$ household expenditure decile. We have:
$$\sigma(X \mid Y) = \sqrt{\sum_{j=1}^{10} f_j\left(x_i^y - \bar{x}^y\right)^2} = 533.4906$$
where $f_j = 10\%$ is the frequency of each decile group and $\bar{x}^y = \sum_{j=1}^{10} f_j x_i^y$ is the mean. We verify that $\bar{x}^y = 2\,534.50 = \mu(X)$. It follows that:
$$\text{CV}(X \mid Y) = \frac{\sigma(X \mid Y)}{\mu(X \mid Y)} = \frac{533.4906}{2\,534.50} = 0.2105$$
We deduce that:
$$\text{CV}(X) = \sqrt{\text{CV}^2(X \mid Y) + \text{CV}^2(X \mid R)} = \sqrt{0.2105^2 + 0.20^2} = 0.2904$$

(f) We have:

$$\sigma_x = \sqrt{\ln\left(0.2904^2 + 1\right)} = 0.2845$$

and:

$$\mu_x = \ln \frac{2\,534.50}{\sqrt{0.2904^2 + 1}} = 7.7973$$

The prevalence of undernourishment is equal to:

$$\text{PoU} = \Phi\left(\frac{1\,850 - 7.7973}{0.2845}\right) = 16.75\%$$

Finally, the number of undernourished people is around 167 500:

$$\text{NoU} = N \cdot \text{PoU} = 10^6 \times 16.75\% = 167\,451$$

3. (a) We have:

$$\text{weight}^{\star}_{age,sex} = \text{BMI}_{age,sex}\,(p) \cdot \text{height}^2_{age,sex}$$

For example, we have:

$$\begin{aligned} \text{weight}^{\star}_{-3yr,female} &= \text{BMI}_{-3yr,female}\,(5\%) \cdot \text{height}^2_{-3yr,female} \\ &= 15.5 \times 0.80^2 \\ &= 9.92\,\text{kg} \end{aligned}$$

We obtain the following results:

| Age | −3 | 3–10 | 10–18 | 18–30 | 30–60 | 60+ |
|---|---|---|---|---|---|---|
| Female | 9.92 | 22.32 | 40.84 | 44.80 | 44.80 | 44.80 |
| Male | 12.00 | 23.83 | 42.44 | 54.73 | 54.73 | 54.73 |

This means that a 40-year-old woman is considered undernourished if she weighs less than 44.8 kg.

(b) The basal metabolic rate (BMR) is given by the Schofield equation:

$$\text{BMR}_{age,sex} = \alpha_{age,sex} + \beta_{age,sex} \cdot \text{weight}^{\star}_{age,sex}$$

For example, we have:

$$\begin{aligned} \text{BMR}_{-3yr,female} &= \alpha_{-3yr,female} + \beta_{-3yr,female} \cdot \text{weight}^{\star}_{-3yr,female} \\ &= -31.1 + 58.317 \times 9.92 \\ &= 547.40\,\text{kcal/capita/day} \end{aligned}$$

We obtain the following results:

| Age | −3 | 3–10 | 10–18 | 18–30 | 30–60 | 60+ |
|---|---|---|---|---|---|---|
| Female | 547 | 939 | 1 239 | 1 150 | 1 210 | 1 065 |
| Male | 684 | 1 045 | 1 409 | 1 516 | 1 501 | 1 229 |

(c) The minimum dietary energy requirement is equal to the physical activity level times the basal metabolic rate:

$$\text{MDER}_{age,sex} = \text{PAL}_{age,sex} \cdot \text{BMR}_{age,sex}$$

We obtain the following results:

| Age | −3 | 3–10 | 10–18 | 18–30 | 30–60 | 60+ |
|---|---|---|---|---|---|---|
| Female | 848 | 1 456 | 1 921 | 1 783 | 1 875 | 1 651 |
| Male | 1 060 | 1 620 | 2 184 | 2 350 | 2 326 | 1 904 |

This means that a 40-year-old woman is considered undernourished if her dietary energy consumption is less than 1 875 Calories per day.

(d) The minimum dietary energy requirement of the population is the weighted average of the different MDER values:

$$\text{MDER} = \sum_{sex} \sum_{age} f_{age,sex} \cdot \text{MDER}_{age,sex}$$

where $f_{age,sex}$ is the frequency of the group in the population. Finally, we obtain:

$$\text{MDER} = 1\,849.90\,\text{kcal/capita/day}$$

4. (a) FD indicates how many calories would be needed to ensure that undernourished would be eliminated if properly distributed.

(b) We have:

$$\begin{aligned}
\text{FD} &= \int_{x<r_L} (\bar{r} - x)\, f_x(x)\, \mathrm{d}x \\
&= \int_0^{r_L} \bar{r} f_x(x)\, \mathrm{d}x - \int_0^{r_L} x f_x(x)\, \mathrm{d}x \\
&= \bar{r} \int_0^{r_L} f_x(x)\, \mathrm{d}x - \frac{\int_0^{r_L} x f_x(x)\, \mathrm{d}x}{\int_0^{r_L} f_x(x)\, \mathrm{d}x} \int_0^{r_L} f_x(x)\, \mathrm{d}x \\
&= (\bar{r} - \mathbb{E}[X \mid X < r_L]) \cdot \Pr\{X < r_L\} \\
&= \text{PoU} \cdot (\bar{r} - \mathbb{E}[X \mid X < r_L])
\end{aligned}$$

The depth of the food deficit is the product of the prevalence of undernourishment and the difference between the average dietary energy requirement and the average dietary energy consumption, conditional on consumption being below the minimum requirement. Another expression is:

$$\text{FD} = \text{PoU} \cdot \mathbb{E}\left[(\bar{r} - X)_+ \mid X < r_L\right]$$

because $\bar{r} \geq r_L$. $\mathbb{E}\left[(\bar{r} - X)_+ \mid X < r_L\right]$ is the expected shortfall of food security.

(c) Following Roncalli (2020a, page 319), we introduce the notation $\Phi_c(x) = \Phi\left((x - \mu_x)/\sigma_x\right)$, and we calculate the conditional moment $\mu'_m(X) = \mathbb{E}[X^m \mid X < r_L]$ for $m \geq 1$ by using the change of variable $y = \ln x$:

$$\begin{aligned}
\mu'_m(X) &= \frac{1}{\Phi_c(\ln r_L)} \int_0^{r_L} \frac{x^m}{x\sigma_x\sqrt{2\pi}} \exp\left(-\frac{1}{2}\left(\frac{\ln x - \mu_x}{\sigma_x}\right)^2\right) \mathrm{d}x \\
&= \frac{1}{\Phi_c(\ln r_L)} \int_{-\infty}^{\ln r_L} \frac{1}{\sigma_x\sqrt{2\pi}} \exp\left(-\frac{1}{2}\left(\frac{y - \mu_x}{\sigma_x}\right)^2 + my\right) \mathrm{d}y
\end{aligned}$$

We have:

$$\begin{aligned} -\frac{1}{2}\left(\frac{y-\mu_x}{\sigma_x}\right)^2 + my &= -\frac{1}{2}\left(\frac{y^2 - 2y\left(\mu_x + m\sigma_x^2\right) + \mu_x^2}{\sigma_x^2}\right) \\ &= -\frac{1}{2}\left(\frac{y-\left(\mu_x + m\sigma_x^2\right)}{\sigma_x}\right)^2 + \left(m\mu_x + \frac{1}{2}m^2\sigma_x^2\right) \end{aligned}$$

We deduce that:

$$\mu'_m(X) = \frac{\exp\left(m\mu_x + m^2\sigma_x^2/2\right)}{\Phi_c(\ln r_L)} \int_{-\infty}^{\ln r_L} \frac{1}{\sigma_x\sqrt{2\pi}} \exp\left(-\frac{1}{2}\left(\frac{y-\left(\mu_x + m\sigma_x^2\right)}{\sigma_x}\right)^2\right) \mathrm{d}y$$

Using the change of variable $z = \dfrac{y-\left(\mu_x + m\sigma_x^2\right)}{\sigma_x}$, it follows that:

$$\mu'_m(X) = \frac{\exp\left(m\mu_x + m^2\sigma_x^2/2\right)}{\Phi_c(\ln r_L)} \int_{-\infty}^{z_L} \frac{1}{\sqrt{2\pi}} \exp\left(-\frac{1}{2}z^2\right) \mathrm{d}z$$

where:

$$z_L = \frac{\ln r_L - \left(\mu_x + m\sigma_x^2\right)}{\sigma_x}$$

Finally, we obtain:

$$\mu'_m(X) = \frac{\Phi_c\left(\ln r_L - m\sigma_x^2\right)}{\Phi_c(\ln r_L)} \exp\left(m\mu_x + \frac{1}{2}m^2\sigma_x^2\right)$$

and:

$$\mathbb{E}[X \mid X < r_L] = \mu'_1(X) = \frac{\Phi\left(\dfrac{\ln r_L - \mu_x - \sigma_x^2}{\sigma_x}\right)}{\Phi\left(\dfrac{\ln r_L - \mu_x}{\sigma_x}\right)} \exp\left(\mu_x + \frac{1}{2}\sigma_x^2\right)$$

The analytical expression of the depth of the food deficit is:

$$\mathrm{FD} = \bar{r}\Phi\left(\frac{\ln r_L - \mu_x}{\sigma_x}\right) - e^{\mu_x + \frac{1}{2}\sigma_x^2}\Phi\left(\frac{\ln r_L - \mu_x - \sigma_x^2}{\sigma_x}\right)$$

because:

$$\mathrm{PoU} = \Pr\{X < r_L\} = \Phi\left(\frac{\ln r_L - \mu_x}{\sigma_x}\right)$$

(d) The depth of the food deficit is equal to:

$$\begin{aligned} \mathrm{FD} &= 2\,500 \times \Phi\left(\frac{\ln 1\,850 - 7.7973}{0.2845}\right) - \\ &\quad \exp\left(7.7973 + \frac{1}{2}0.2845^2\right) \times \Phi\left(\frac{\ln 1\,850 - 7.7973 - 0.2845^2}{0.2845}\right) \\ &= 150.2968 \text{ kcal/capita/year} \end{aligned}$$

### B.1.5 Calculating the species-area relationship using the theory of island biogeography (Exercise 5.5.2)

1. (a) We have:

$$\begin{aligned} f'(x) &= ae^{b(x/c)^d} bd \left(\frac{x}{c}\right)^{d-1} \frac{1}{c} \\ &= \frac{abd}{c} \left(\frac{x}{c}\right)^{d-1} e^{b(x/c)^d} \end{aligned}$$

and:

$$\begin{aligned} f''(x) &= \frac{abd}{c}(d-1)\left(\frac{x}{c}\right)^{d-2} \frac{1}{c} e^{b(x/c)^d} + \frac{abd}{c}\left(\frac{x}{c}\right)^{d-1} e^{b(x/c)^d} bd \left(\frac{x}{c}\right)^{d-1} \frac{1}{c} \\ &= \frac{abd\,(d-1)}{c^2}\left(\frac{x}{c}\right)^{d-2} e^{b(x/c)^d} + \frac{ab^2d^2}{c^2}\left(\frac{x}{c}\right)^{2d-2} e^{b(x/c)^d} \\ &= \frac{abd}{c^2}\left(\frac{x}{c}\right)^{d-2}\left(d-1+bd\left(\frac{x}{c}\right)^d\right) e^{b(x/c)^d} \end{aligned}$$

Since $a$, $c$ and $d$ are positive, we deduce that $\frac{x}{c} \geq 0$, $e^{b(x/c)^d} \geq 0$ and:

$$f'(x) \geq 0 \Leftrightarrow b \geq 0$$

$f(x)$ is an increasing function of $x$ if the parameter $b$ is positive, otherwise $f(x)$ is a decreasing function of $x$. We have:

$$f''(x) \geq 0 \Leftrightarrow g(x;b) = \underbrace{b(d-1)}_{-/+} + \underbrace{b^2 d\left(\frac{x}{c}\right)^d}_{+} \geq 0$$

because we have:

$$0 \leq b^2 d\left(\frac{x}{c}\right)^d \leq b^2 d$$

We consider two cases:

i. $b = -1$
If $d \leq 1$, then $g(x;-1) = 1 - d + d\left(\frac{x}{c}\right)^d$, $f''(x) \geq 0$ and the function is convex. If $d > 1$, the function is neither convex nor concave.

ii. $b = 1$
If $d \geq 1$, then $g(x;1) = (d-1) + d\left(\frac{x}{c}\right)^d$, $f''(x) \geq 0$ and the function is convex. If $d \leq \frac{1}{2}$, then $g(0;1) = d - 1 < 0$, $g(c;1) = 2d - 1 \leq 0$, $f''(x) \leq 0$ and the function is concave. If $d \in \left(\frac{1}{2}, 1\right)$, the function is neither convex nor concave.

(b) We have[2]:

$$\frac{\partial \lambda(t)}{\partial S(t)} = -\frac{\beta_1 \lambda_0^2}{(1-e^{-1})S_s}\left(\frac{S(t)}{S_s}\right)^{\beta_1\lambda_0 - 1} e^{-\left(\frac{S(t)}{S_s}\right)^{\beta_1\lambda_0}} \leq 0$$

with:

$$\lambda(t_0) = \lambda_0 \frac{e^{-0} - e^{-1}}{1 - e^{-1}} = \lambda_0$$

[2] We set $a = \frac{\lambda_0}{1-e^{-1}}$, $b = -1$, $c = S_s$ and $d = \beta_1\lambda_0$.

and:

$$\lambda(t_s) = \lambda_0 \frac{e^{-1} - e^{-1}}{1 - e^{-1}} = 0$$

The second-order derivative is:

$$\frac{\partial^2 \lambda(t)}{\partial S(t)^2} = -\frac{\beta_1 \lambda_0^2}{(1 - e^{-1}) S_s^2} \left(\frac{S(t)}{S_s}\right)^{\beta_1 \lambda_0 - 2} \left(\beta_1 \lambda_0 - 1 - \beta_1 \lambda_0 \left(\frac{S(t)}{S_s}\right)^{\beta_1 \lambda_0}\right) e^{-\left(\frac{S(t)}{S_s}\right)^{\beta_1 \lambda_0}}$$

$\lambda(t)$ is convex if and only if $\beta_1 \lambda_0 \leq 1$. The function $\lambda(t)$ is plotted in Figure B.16. We verify that it is decreasing and convex for the first three sets of parameters because $\beta_1 \lambda_0 \leq 1$. For the last set of parameters, it is decreasing but not convex.

Figure B.16: Immigrate rate function $\lambda(t)$

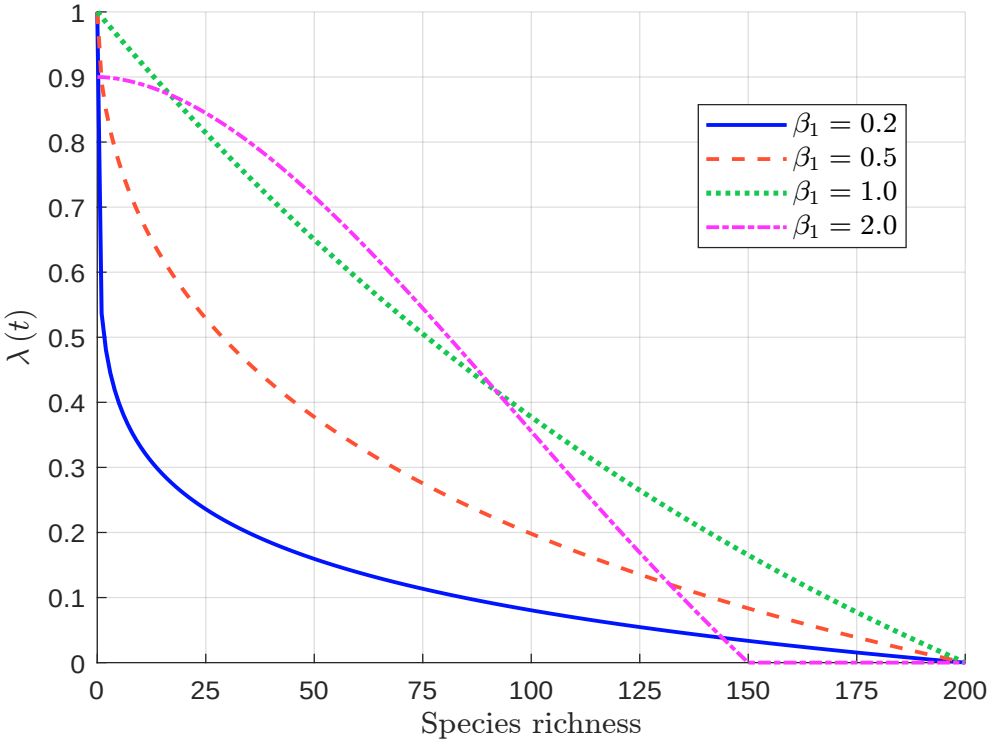


(c) We have[3]:

$$\frac{\partial \mu^{\text{long}}(t)}{\partial S(t)} = \frac{\beta_2 \mu_s^2}{(e^{-1} - 1) S_s} \left(\frac{S(t)}{S_s}\right)^{\beta_2 \mu_s - 1} e^{\left(\frac{S(t)}{S_s}\right)^{\beta_2 \mu_s}} \geq 0$$

with:

$$\mu^{\text{long}}(t_0) = \mu_s \frac{e^0 - 1}{e^1 - 1} = 0$$

and:

$$\mu^{\text{long}}(t_s) = \mu_s \frac{e^1 - 1}{e^1 - 1} = \mu_s$$

[3]We set $a = \frac{\mu_s}{e^{-1} - 1}$, $b = 1$, $c = S_s$ and $d = \beta_2 \mu_s$.

The second-order derivative is:

$$\frac{\partial^2 \mu^{\text{long}}(t)}{\partial S(t)^2} = \frac{\beta_2 \mu_s^2}{(e^{-1}-1) S_s^2} \left(\frac{S(t)}{S_s}\right)^{\beta_2 \mu_s - 2} \left(\beta_2 \mu_s - 1 + \beta_2 \mu_s \left(\frac{S(t)}{S_s}\right)^{\beta_2 \mu_s}\right) e^{\left(\frac{S(t)}{S_s}\right)^{\beta_2 \mu_s}}$$

$\mu^{\text{long}}(t)$ is convex if and only if $\beta_2 \mu_s \geq 1$ and concave if and only if $\beta_2 \mu_s \leq \frac{1}{2}$. The function $\mu^{\text{long}}(t)$ is plotted in Figure B.17. We verify that it is increasing and concave for the first two sets of parameters because $\beta_2 \mu_s \leq \frac{1}{2}$. For the last two sets of parameters, it is increasing and convex.

Figure B.17: Long-term extinction rate function $\mu^{\text{long}}(t)$

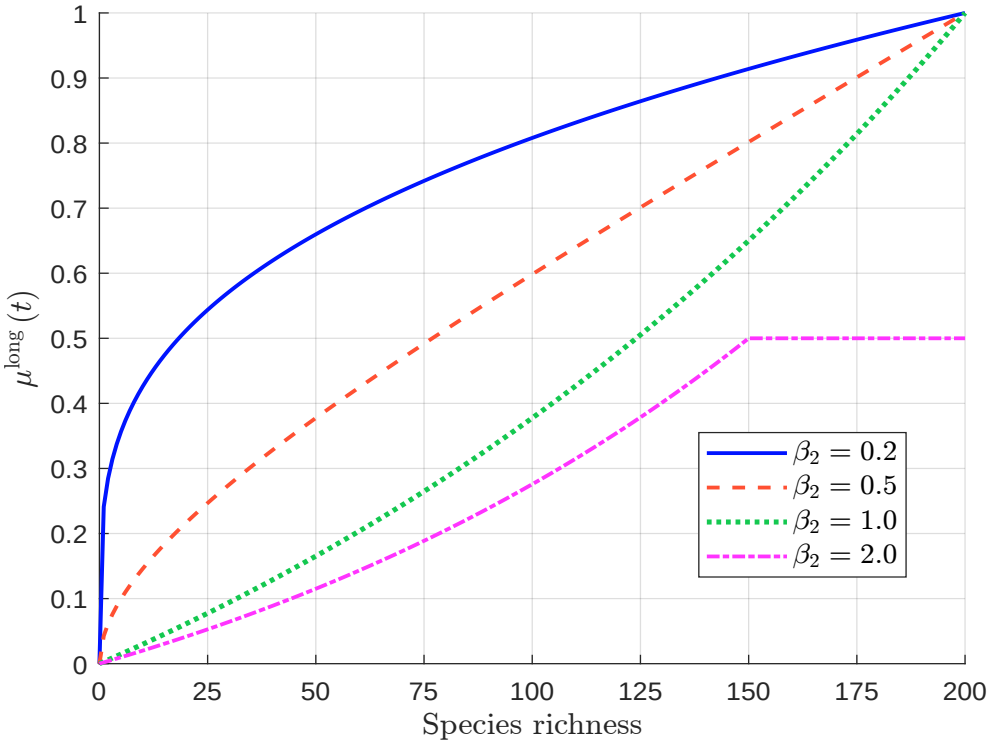


(d) $\mu^{\text{short}}(t)$ is the product of two positive and decreasing functions: $\lambda(t)$ and $\beta_3 \lambda(t) e^{-\beta_4 S(t)}$. We deduce that it is decreasing. We also have:

$$\mu^{\text{short}}(t_0) = \beta_3 \lambda_0 e^{-\beta_4 S_0} \leq \beta_3 \lambda_0$$

and:

$$\mu^{\text{short}}(t_s) = \beta_3 \lambda_s e^{-\beta_4 S_s} = 0$$

The function $\mu^{\text{short}}(t)$ is plotted in Figure B.18.

(e) We have:

$$\mu(t_0) = \mu^{\text{short}}(t_0) + \mu^{\text{long}}(t_0) = \mu^{\text{short}}(t_0) + 0 = \mu^{\text{short}}(t_0)$$

and:

$$\mu(t_s) = \mu^{\text{short}}(t_s) + \mu^{\text{long}}(t_s) = 0 + \mu_s = \mu_s$$

Figure B.18: Short-term extinction rate function $\mu^{\text{short}}(t)$

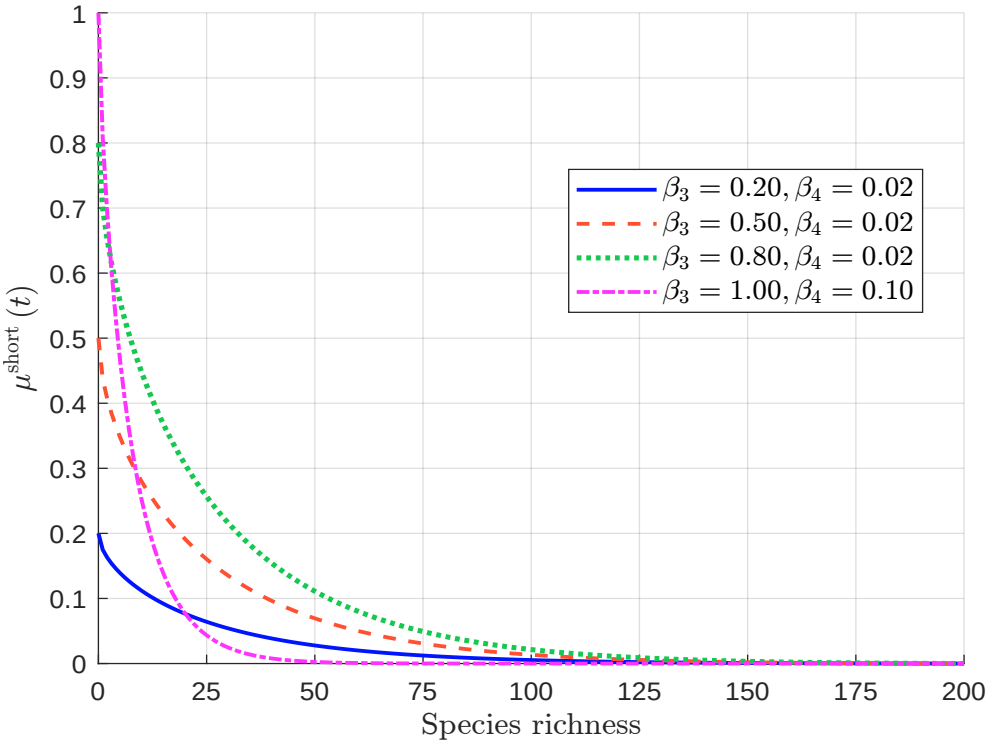


Figure B.19: Extinction rate function $\mu(t)$

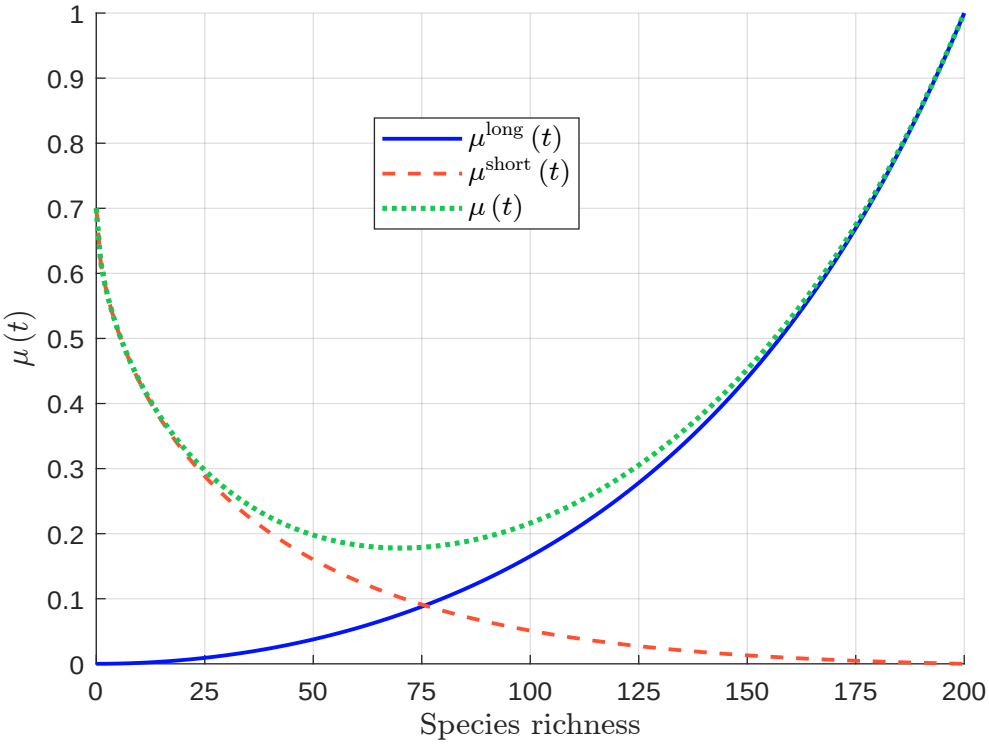

Figure B.19 illustrates the function $\mu(t)$. Since the extinction rate is the sum of two functions, $\mu^{\text{short}}(t)$ which is decreasing, and $\mu^{\text{long}}(t)$ which is increasing, $\mu(t)$ is not monotonic and can exhibit several shapes. However, for reasonable values of the parameters, we observe that $\mu(t)$ first decreases and then increases. This behavior arises because $\mu^{\text{short}}(t_0) > \mu^{\text{long}}(t_0)$ and $\mu^{\text{short}}(t_s) < \mu^{\text{long}}(t_s)$. Consequently, when $S(t)$ is low and close to zero, the short-term extinction rate dominates the long-term extinction rate, leading to a general decrease in $\mu(t)$. In contrast, when $S(t)$ is high and approaches the saturation state $S_s$, the long-term extinction rate becomes dominant, implying that $\mu(t)$ generally increases for high values of species richness. In summary, the extinction rate $\mu(t)$ has a U-shaped relationship with $S(t)$.

(f) An equilibrium occurs if and only if $\delta(t) = 0$ or $\lambda(t) = \mu(t)$. We deduce that such an equilibrium $S^\star$ is achieved if the following equation has at least one solution:

$$\lambda_0 \frac{e^{-\left(\frac{S^\star}{S_s}\right)^{\beta_1 \lambda_0}} - e^{-1}}{1 - e^{-1}} \left(1 - \beta_3 e^{-\beta_4 S^\star}\right) = \mu_s \frac{e^{\left(\frac{S^\star}{S_s}\right)^{\beta_2 \mu_s}} - 1}{e^1 - 1} \tag{B.1}$$

Figure B.20 shows the functions $\lambda(t)$ and $\mu(t)$. Solving Equation (B.1) gives $S^\star = 96.472$. This equilibrium is stable, because $\dfrac{\mathrm{d}S(t)}{\mathrm{d}t} < 0$ when $S(t) > S^\star$ and $\dfrac{\mathrm{d}S(t)}{\mathrm{d}t} > 0$ when $S(t) < S^\star$. This implies that any perturbation from $S^\star$ will return to the steady state $S^\star$.

(g) In Table B.8, we give the direction of variation of the functions $\lambda(t)$, $\mu^{\text{short}}(t)$, $\mu^{\text{long}}(t)$ and $\mu(t)$. We can then derive the table of variation of the net diversification rate $\delta(t) = \lambda(t) - \mu(t)$. When $\beta_3 = 0$, $\mu^{\text{short}}(t) = 0$ and $\delta(t)$ is a decreasing function with $\delta(t_0) = \delta_0 = \lambda_0 > 0$ and $\delta(t_s) = -\mu_s < 0$. We conclude that there is only one equilibrium. When $0 < \beta_3 \leq 1$, $\delta(t)$ increases up to a threshold $S^*$ and then decreases. We have $\delta_0 = \lambda_0(1 - \beta_3) > 0$ and $\delta(t_s) = -\mu_s < 0$. We obtain the table of variation of the net diversification rate given in Table B.9. When $\beta_3 > 1$, $\delta(t)$ has the same behavior as the previous case, but $\delta_0 = \lambda_0(1 - \beta_3) < 0$ and we obtain the table of variation of the net diversification rate given in Table B.10. We deduce that there are two equilibria $S_1^\star$ and $S_2^\star$, with $S_1^\star \leq S_2^\star$. The equilibrium $S_1^\star$ is unstable because $\dfrac{\mathrm{d}S(t)}{\mathrm{d}t} < 0$ when $S(t) < S_1^\star$ and $\dfrac{\mathrm{d}S(t)}{\mathrm{d}t} > 0$ when $S(t) > S_1^\star$. Only $S_2^\star$ is a stable steady state. Furthermore, the net diversification rate is negative when $S(t) < S_1^\star$, which means that $S(t + \mathrm{d}t) < S(t)$ and $S(t)$ tends to the equilibrium $S_0^\star = 0$.

(h) The simulations of the species richness process are presented in Figures B.22 and B.23. In the one-equilibrium case, the process $S(t)$ converges to the equilibrium $S^\star = 96.47$, regardless of the initial state $S_0$. In the three-equilibrium case, the process $S(t)$ converges to either $S_0^\star = 0$ or $S_2^\star = 97.35$, depending on the initial state $S_0$. The equilibrium $S_1^\star = 27.65$ is reached only if $S_0 = S_1^\star$. Otherwise, we get the equilibrium $S_0^\star = 0$ if $S_0 < S_1^\star$, and the equilibrium $S_2^\star = 97.35$ if $S_0 > S_1^\star$.

2. (a) We have:

$$\frac{\partial \mu(t)}{\partial \beta_2} = \frac{\mu_s^2}{e^1 - 1} e^{\left(\frac{S(t)}{S_s}\right)^{\beta_2 \mu_s}} \left(\frac{S(t)}{S_s}\right)^{\beta_2 \mu_s} \ln\left(\frac{S(t)}{S_s}\right) \leq 0$$

This means that the relationship $\mu(t)$ shifts downward as $\beta_2$ increases. Figure B.24 illustrates the equilibrium for the three values of $\beta_2$. From this, we deduce that if $\beta_2' \geq \beta_2$, then $S^\star(\beta_2') \geq S^\star(\beta_2)$.

Table B.8: Table of variation for the immigration and extinction rates

| $S$ | $0$ $\qquad\qquad$ $S^*$ $\qquad\qquad$ $S_s$ |
|---|---|
| $\lambda(t)$ | $\lambda_0 \searrow 0$ |
| $\mu^{\text{short}}(t)$ | $\beta_3\lambda_0 \searrow 0$ |
| $\mu^{\text{long}}(t)$ | $0 \nearrow \mu_s$ |
| $\mu(t)$ $(\beta_3 = 0)$ | $0 \nearrow \mu_s$ |
| $\mu(t)$ $(\beta_3 > 0)$ | $\beta_3\lambda_0 \searrow \mu^* \nearrow \mu_s$ |

Table B.9: Table of variation for the net diversification rate $\delta(t)$

| $S$ | $0$ $\qquad\qquad$ $S^*$ $\qquad\qquad$ $S^\star$ $\qquad\qquad$ $S_s$ |
|---|---|
| $\lambda(t) - \mu(t)$ $(0 < \beta_3 \leq 1)$ | $\delta_0 \nearrow \delta^* \searrow 0 \searrow -\mu_s$ |

Table B.10: Table of variation for the net diversification rate $\delta(t)$

| $S$ | $0$ $\qquad$ $S_1^\star$ $\qquad$ $S^*$ $\qquad$ $S_2^\star$ $\qquad$ $S_s$ |
|---|---|
| $\lambda(t) - \mu(t)$ $(\beta_3 > 1)$ | $\delta_0 \nearrow 0 \nearrow \delta^* \searrow 0 \searrow -\mu_s$ |

Figure B.20: Immigration rate $\lambda(t)$, extinction rate $\mu(t)$ and equilibrium $S^\star$

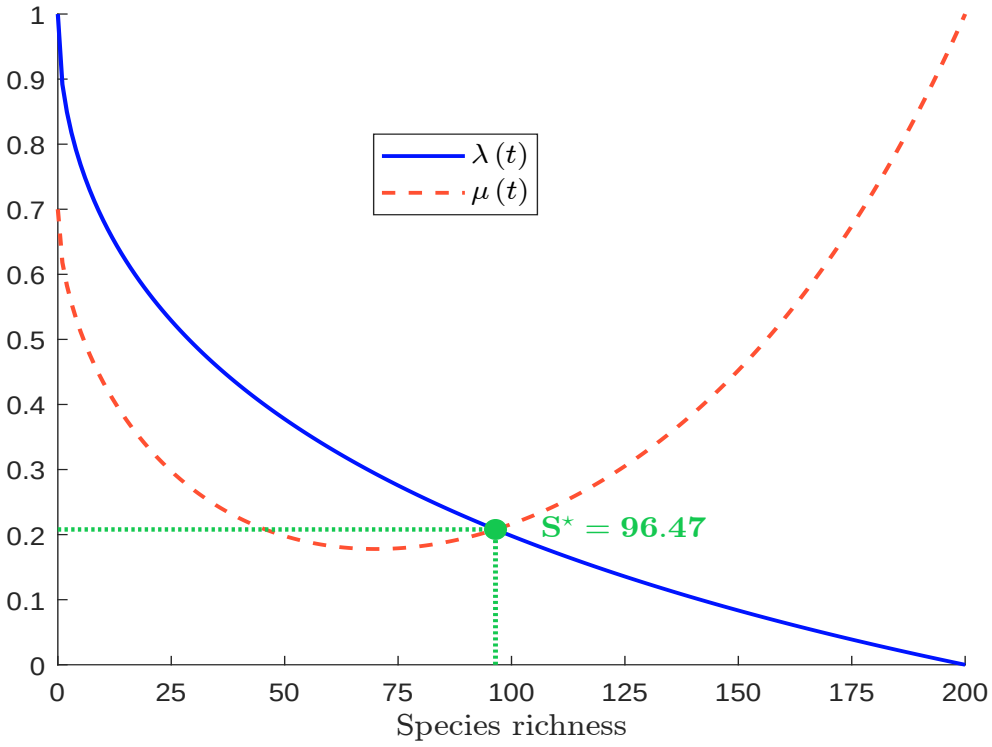


Figure B.21: The three-equilibrium case

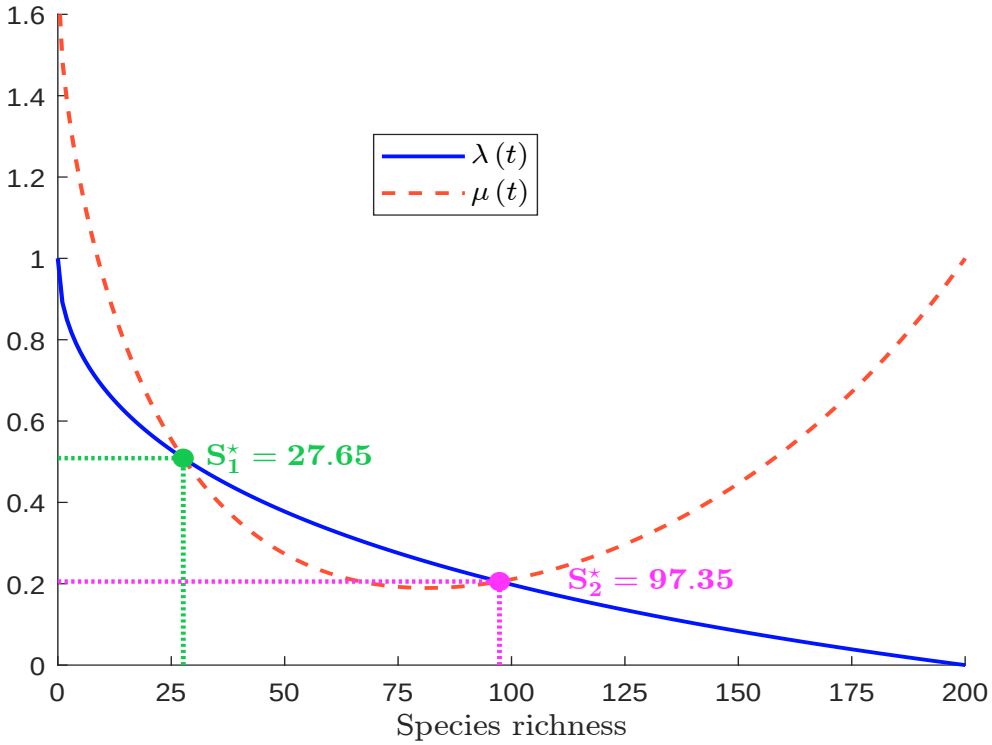

Figure B.22: Simulation of the species richness process under a one-equilibrium scenario

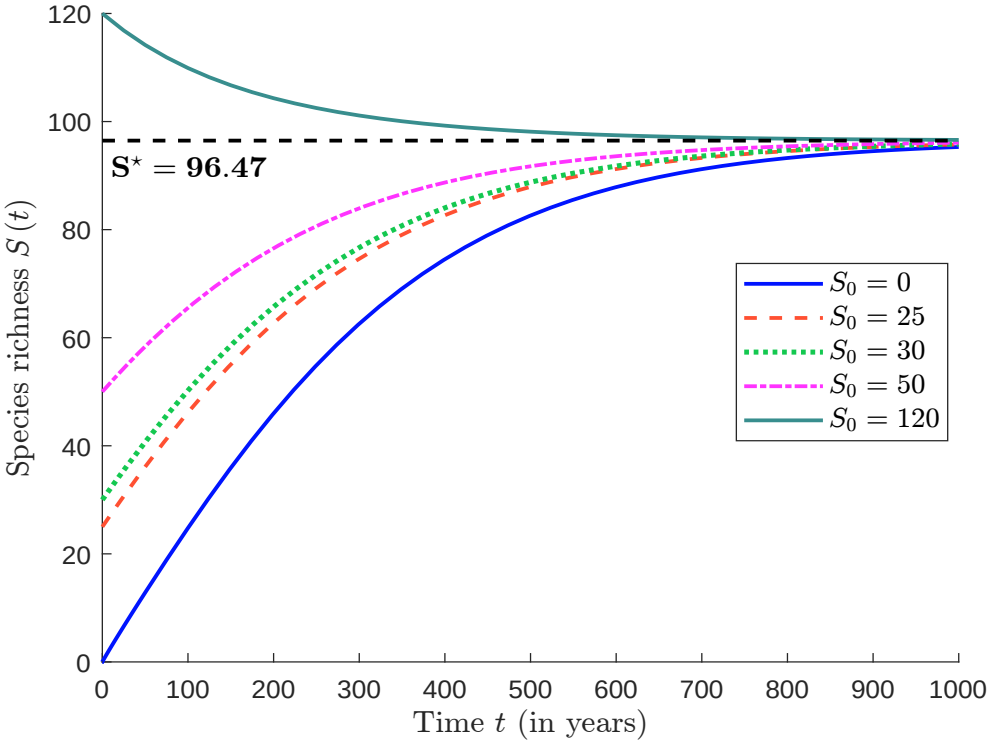


Figure B.23: Simulation of the species richness process under a three-equilibrium scenario

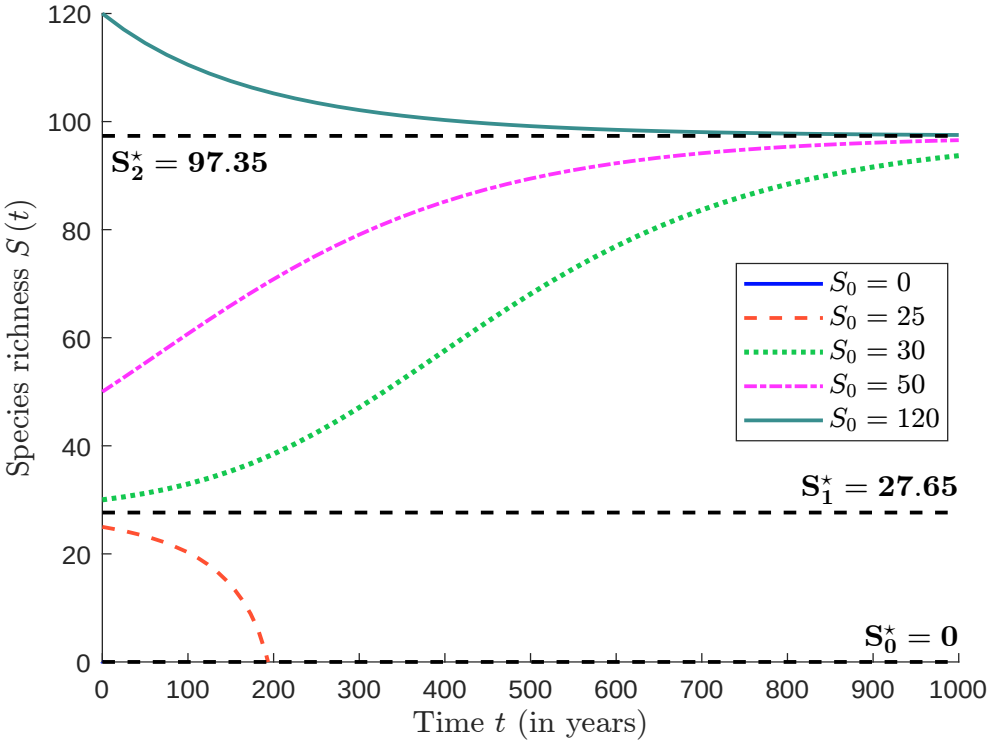

Figure B.24: How the equilibrium shifts with the parameter $\beta_2$

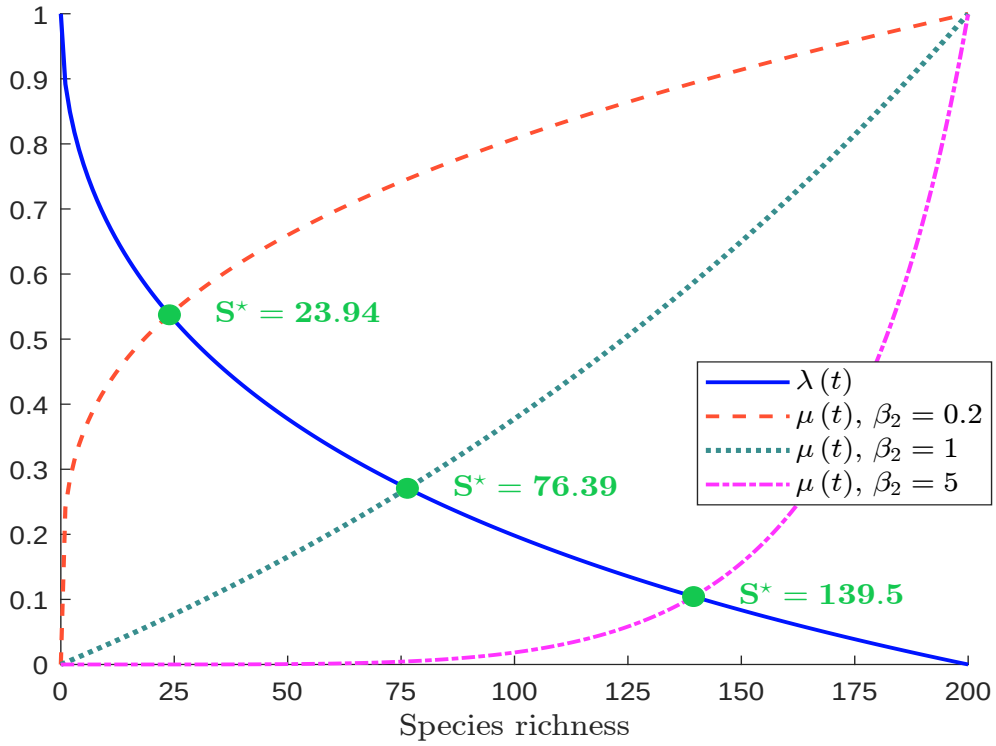


(b) The relationship between $\beta_2$ and $S^\star$ is shown in Figure B.25.

(c) We have:

$$\frac{\partial \mu(t)}{\partial \mu_s} = \frac{e^{\left(\frac{S(t)}{S_s}\right)^{\beta_2 \mu_s}} - 1}{e^1 - 1} + \frac{\beta_2 \mu_s}{e^1 - 1} e^{\left(\frac{S(t)}{S_s}\right)^{\beta_2 \mu_s}} \left(\frac{S(t)}{S_s}\right)^{\beta_2 \mu_s} \ln\left(\frac{S(t)}{S_s}\right)$$

Using the default parameter values and $S(t) = 100$, we find that $\partial_{\mu_s} \mu(t) = 0.045$ when $\mu_S = 1$ and $\partial_{\mu_s} \mu(t) = -0.047$ when $\mu_S = 5$. Since the derivative can be either positive or negative, we cannot determine the effect of $\mu_s$ on the equilibrium $S^\star$.

(d) The relationship between $\mu_s$ and $S^\star$ is shown in Figure B.26.

(e) We can assume that the relationship between $A$ and $\beta_2$ is increasing. In this case, we obtain the species-area relationship. We can also assume that the relationship between $A$ and $\mu_s$ is increasing. In this case, we retrieve the species-area relationship only if $\mu_s$ is greater than a threshold.

(f) We obtain the following estimated values for the parameters:

| Parameter | Power | Exponential | Kobayashi |
|---|---|---|---|
| $c$ | 74.513 | 82.098 | 73.539 |
| $z$ | 0.562 | 45.199 | 1.797 |

The fitted models are displayed in Figure B.27. We observe that the fitted curves closely align with the equilibrium curve predicted by the theory of island biogeography.

Figure B.25: Relationship between $\beta_2$ and $S^\star$

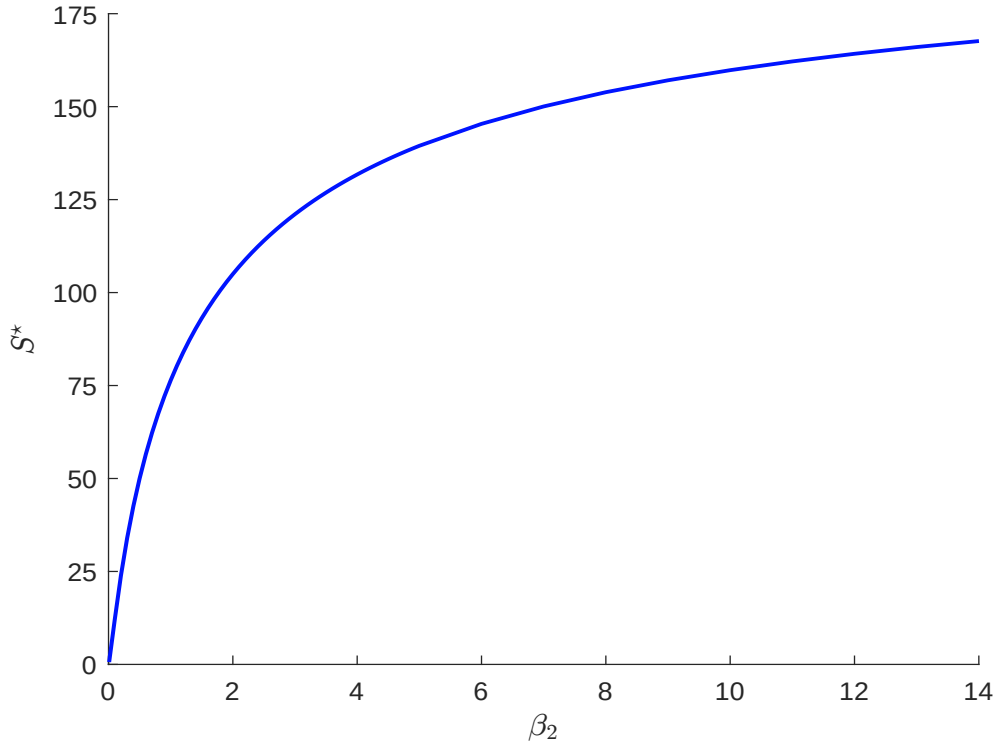


Figure B.26: Relationship between $\mu_s$ and $S^\star$

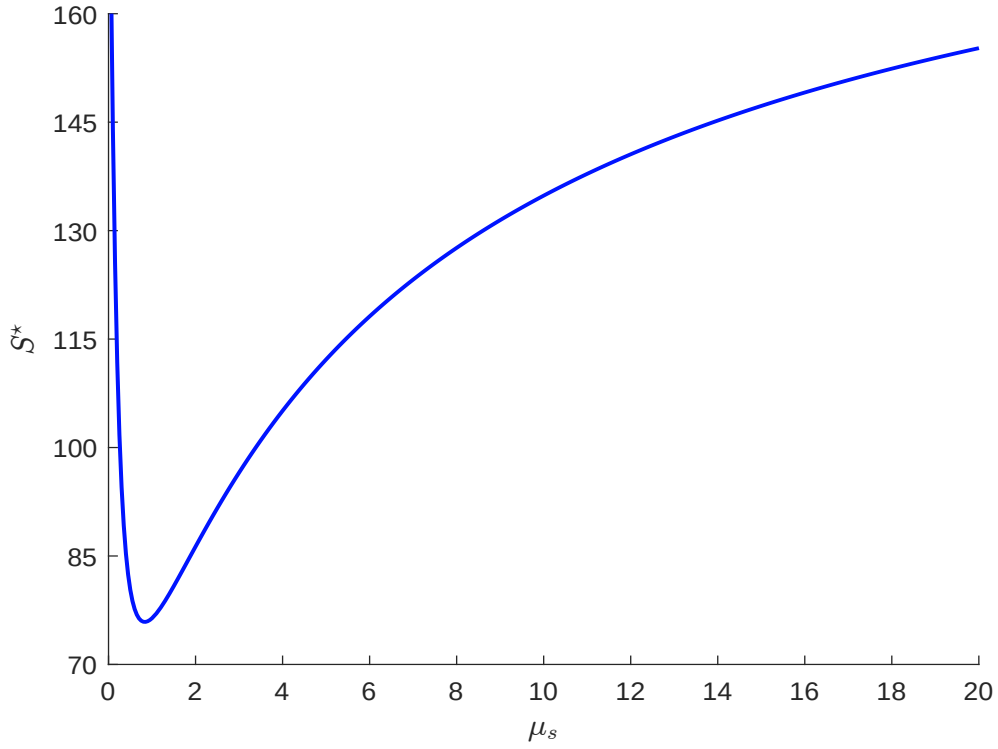

Figure B.27: Species-area relationship (TIB, power, exponential and Kobayashi models)

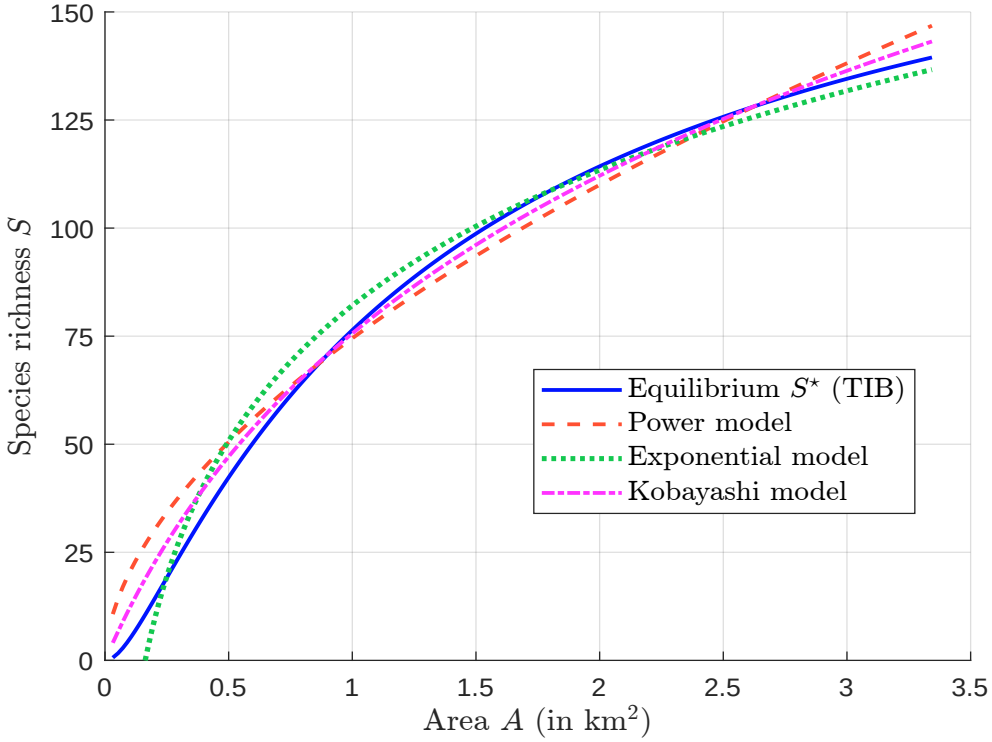


### B.1.6 Species abundance models (Exercise 5.5.3)

1. (a) We have:

$$\tilde{S}_a = \sum_{i=1}^{S} \tilde{S}_i$$

Assuming that the random variables $\tilde{S}_1, \ldots, \tilde{S}_S$ are independent, $\tilde{S}_a$ follows a Poisson binomial distribution:

$$\tilde{S}_a \sim \mathcal{PB}(p_1, \ldots, p_S)$$

The probability mass function is given by:

$$\Pr\left\{\tilde{S}_a = k\right\} = \sum_{\mathcal{E} \in \mathcal{F}_k} \prod_{i \in \mathcal{E}} p_i \prod_{j \in \mathcal{E}^c} (1 - p_j)$$

where $\mathcal{F}_k$ is the set of all subsets of $k$ integers that can be selected from $\{1, \ldots, n\}$ and $\mathcal{E}^c$ denotes the complement of the subset $\mathcal{E}$. From this, we deduce the expected value:

$$S_a = \mathbb{E}\left[\tilde{S}_a\right] = \mathbb{E}\left[\sum_{i=1}^{S} \tilde{S}_i\right] = \sum_{i=1}^{S} p_i$$

Given $p = (20\%, 30\%, 10\%, 65\%, 10\%)$, we obtain the following probability mass function for $\tilde{S}_a$:

| $k$ | 0 | 1 | 2 | 3 | 4 | 5 |
|---|---|---|---|---|---|---|
| $\Pr\left\{\tilde{S}_a = k\right\}$ | 15.88% | 43.79% | 30.85% | 8.48% | 0.97% | 0.04% |

The expected number of species is $S_a = 1.35$.

(b) Let $\pi$ be the probability that an individual occupies the subarea $a$. We have:

$$\pi = \frac{a}{A}$$

For example, if $A = 10\,\text{km}^2$, the occupancy probability is 20% when $a = 2\,\text{km}^2$. Let $\tilde{N}_i$ be the random variable indicating the number of individuals of species $i$ present in the subarea $a$. $\tilde{N}_i$ follows a binomial distribution with parameters $n_i$ (the total number of individuals of species $i$) and $\pi$. Thus, we have:

$$\Pr\left\{\tilde{N}_i = k\right\} = C_{n_i}^k \pi^k (1-\pi)^{n_i - k}$$

The probability $p_i$ of observing the species $i$ on the subarea is then:

$$\begin{aligned} p_i = \Pr\left\{\tilde{S}_i = 1\right\} &= \Pr\left\{\tilde{N}_i > 0\right\} \\ &= 1 - \Pr\left\{N_i = 0\right\} \\ &= 1 - (1-\pi)^{n_i} \\ &= 1 - \left(1 - \frac{a}{A}\right)^{n_i} \end{aligned}$$

Consequently, $\tilde{S}_a$ follows then a Poisson binomial distribution:

$$\tilde{S}_a \sim \mathcal{PB}\left(p_i = 1 - \left(1 - \frac{a}{A}\right)^{n_i}\right)$$

It follows that:

$$\begin{aligned} S_a &= \sum_{i=1}^{S} p_i \\ &= \sum_{i=1}^{S} \left(1 - \left(1 - \frac{a}{A}\right)^{n_i}\right) \\ &= S - \sum_{i=1}^{S} \left(1 - \frac{a}{A}\right)^{n_i} \end{aligned}$$

Given $(n_1, \ldots, n_5) = (10, 30, 25, 66, 8)$, $A = 10\,\text{km}^2$, and $a = 2\,\text{km}^2$, $\pi = 20\%$ and we obtain the following results:

| $k$ or $i$ | 0 | 1 | 2 | 3 | 4 | 5 |
|---|---|---|---|---|---|---|
| $p_i$ | | 89.26% | 59.04% | 99.62% | 73.79% | 83.22% |
| $\Pr\left\{\tilde{S}_a = k\right\}$ | 0.00% | 0.21% | 3.45% | 19.78% | 44.32% | 32.34% |

The expected number of species is $S_a = 4.05$.

(c) i. If the distribution is homogenous across species ($n_i = \frac{n}{S}$), we have:

$$p_i = 1 - \left(1 - \frac{a}{A}\right)^{\frac{n}{S}}$$

$\tilde{S}_a$ follows then a binomial distribution:

$$\tilde{S}_a \sim \mathcal{B}\left(S, p = 1 - \left(1 - \frac{a}{A}\right)^{\frac{n}{S}}\right)$$

The expected number of species is then equal to:

$$S_a = Sp = S\left(1 - \left(1 - \frac{a}{A}\right)^{\frac{n}{S}}\right)$$

ii. If the distribution is the most uneven ($n_i = 1$ for $i < S$ and $n_S = n - S + 1$), we have:

$$\begin{aligned} S_a &= S - \sum_{i=1}^{S-1}\left(1 - \frac{a}{A}\right)^1 - \left(1 - \frac{a}{A}\right)^{n-S+1} \\ &= S - (S-1)\left(1 - \frac{a}{A}\right) - \left(1 - \frac{a}{A}\right)^{n-S+1} \\ &= 1 + (S-1)\frac{a}{A} - \left(1 - \frac{a}{A}\right)^{n-S+1} \end{aligned}$$

iii. We have:

$$\begin{aligned} S_a &= S - \sum_{i=1}^{s}\left(1 - \frac{a}{A}\right)^1 - \sum_{i=s+1}^{S}\left(1 - \frac{a}{A}\right)^{n_{s+1}} \\ &= S - s\left(1 - \frac{a}{A}\right) - (S-s)\left(1 - \frac{a}{A}\right)^{n_{s+1}} \\ &= s\frac{a}{A} + (S-s)\left(1 - \left(1 - \frac{a}{A}\right)^{n_{s+1}}\right) \\ &= s\frac{a}{A} + (S-s)\left(1 - \left(1 - \frac{a}{A}\right)^{\frac{n-s}{S-s}}\right) \end{aligned}$$

If $s = 0$, we retrieve the most even model:

$$S_a = S\left(1 - \left(1 - \frac{a}{A}\right)^{\frac{n}{S}}\right)$$

If $s = S - 1$, we retrieve the most uneven model:

$$S_a = (S-1)\frac{a}{A} + \left(1 - \left(1 - \frac{a}{A}\right)^{\frac{n-S+1}{S-S+1}}\right) = 1 + (S-1)\frac{a}{A} - \left(1 - \frac{a}{A}\right)^{n-S+1}$$

iv. We have:

$$\begin{aligned} S_a &= \sum_{i=1}^{S}\left(1 - \left(1 - \frac{a}{A}\right)\left(1 + \frac{n_i a}{\kappa_i A}\right)^{-\kappa_i}\right) \\ &= S - \left(1 - \frac{a}{A}\right)\sum_{i=1}^{S}\left(1 + \frac{n_i a}{\kappa_i A}\right)^{-\kappa_i} \end{aligned}$$

v. We can approximate the harmonic sum by:

$$\sum_{k=i}^{S}\frac{1}{k} \approx \int_i^S \frac{1}{x}\,\mathrm{d}x = \ln\left(\frac{S}{i}\right)$$

We deduce that:

$$n_i = \frac{n}{S}\sum_{k=i}^{S}\frac{1}{k} \approx \frac{n}{S}\ln\left(\frac{S}{i}\right)$$

We have:

$$\left(1-\frac{a}{A}\right)^{n_i}=e^{\left(n_i\ln\left(1-\frac{a}{A}\right)\right)}=\exp\left(\frac{n}{S}\ln\left(\frac{S}{i}\right)\ln\left(1-\frac{a}{A}\right)\right)=\left(\frac{i}{S}\right)^{-\frac{n}{S}\ln\left(1-\frac{a}{A}\right)}$$

and:

$$\sum_{i=1}^{S}\left(1-\frac{a}{A}\right)^{n_i}=\sum_{i=1}^{S}\left(\frac{i}{S}\right)^{-\frac{n}{S}\ln\left(1-\frac{a}{A}\right)}\approx\int_0^S\left(\frac{x}{S}\right)^{-\frac{n}{S}\ln\left(1-\frac{a}{A}\right)}\,\mathrm{d}x$$

Using the change of variable $u=\dfrac{x}{S}$, we obtain:

$$\begin{aligned}\int_0^S\left(\frac{x}{S}\right)^{-\frac{n}{S}\ln\left(1-\frac{a}{A}\right)}\mathrm{d}x &= S\int_0^1 u^{-\frac{n}{S}\ln\left(1-\frac{a}{A}\right)}\,\mathrm{d}u\\ &= S\left[\frac{u^{-\frac{n}{S}\ln\left(1-\frac{a}{A}\right)+1}}{-\frac{n}{S}\ln\left(1-\frac{a}{A}\right)+1}\right]_0^1\\ &= \frac{S}{-\frac{n}{S}\ln\left(1-\frac{a}{A}\right)+1}\\ &= \frac{S^2}{S-n\ln\left(1-\frac{a}{A}\right)}\end{aligned}$$

Since we have:

$$S_a=S-\sum_{i=1}^{S}\left(1-\frac{a}{A}\right)^{n_i}\approx S-\frac{S^2}{S-n\ln\left(1-\frac{a}{A}\right)}=\frac{-Sn\ln\left(1-\frac{a}{A}\right)}{S-n\ln\left(1-\frac{a}{A}\right)}$$

we conclude that:

$$S_a=\frac{S\ln\left(1-\frac{a}{A}\right)}{\ln\left(1-\frac{a}{A}\right)-\frac{S}{n}}$$

(d) We have:

$$S_a=\sum_{i=1}^{S}p_i=\sum_j\sum_{i\in j}p_i=\sum_j s\left(j\right)p_j$$

where $p_j$ is the probability that a species with abundance $j$ is present in the subarea $a$. Since $p_j=1-\left(1-\dfrac{a}{A}\right)^j$, we get:

$$S_a=\sum_j s\left(j\right)\left(1-\left(1-\frac{a}{A}\right)^j\right)=S-\sum_j s\left(j\right)\left(1-\frac{a}{A}\right)^j$$

where $S=\sum_j s\left(j\right)$ is the total number of species. To calculate $S_a$ for the log-series distribution, we use a preliminary result: $\sum_{j=1}^{\infty}x^j/j$ is the series expansion for $-\ln\left(1-x\right)$ when $|x|<1$. We have:

$$S=\sum_{j=1}^{\infty}s\left(j\right)=\alpha\sum_{j=1}^{\infty}\frac{x^j}{j}=-\alpha\ln\left(1-x\right)$$

and:

$$\sum_{j=1}^{\infty} s(j)\left(1-\frac{a}{A}\right)^j = \alpha\sum_{j=1}^{\infty}\frac{x^j}{j}\left(1-\frac{a}{A}\right)^j = -\alpha\ln\left(1-x\left(1-\frac{a}{A}\right)\right)$$

We deduce that:

$$\begin{aligned} S_a &= -\alpha\ln(1-x)+\alpha\ln\left(1-x\left(1-\frac{a}{A}\right)\right) \\ &= \alpha\ln\left(\frac{1-x\left(1-\frac{a}{A}\right)}{1-x}\right) \\ &= \alpha\ln\left(1+\frac{x}{1-x}\frac{a}{A}\right) \end{aligned}$$

2. (a) Species $i$ is locally endemic to subarea $a \subseteq A$ if all the individuals of this species are found in $a$. Let $E_i \sim \mathcal{B}(\breve{p}_i)$ be the Bernoulli random variable that takes the value 1 if species $i$ is locally endemic to $a$. We have:

$$\breve{p}_i = \Pr\{E_i = 1\} = \prod_{k=1}^{n_i}\left(\frac{a}{A}\right) = \left(\frac{a}{A}\right)^{n_i}$$

(b) The expected number $E_a$ of locally endemic species is equal to:

$$E_a = \mathbb{E}[E_1+E_2+\ldots+E_S] = \sum_{i=1}^{S}\mathbb{E}[E_i] = \sum_{i=1}^{S}\breve{p}_i = \sum_{i=1}^{S}\left(\frac{a}{A}\right)^{n_i}$$

(c) Since we have $S_a = S - \sum_{i=1}^{S}\left(1-\frac{a}{A}\right)^{n_i}$ and $E_a = \sum_{i=1}^{S}\left(\frac{a}{A}\right)^{n_i}$, we deduce that:

$$S_{A-a} = S - \sum_{i=1}^{S}\left(1-\frac{A-a}{A}\right)^{n_i} = S - \sum_{i=1}^{S}\left(\frac{a}{A}\right)^{n_i}$$

and:

$$E_{A-a} = \sum_{i=1}^{S}\left(\frac{A-a}{A}\right)^{n_i} = \sum_{i=1}^{S}\left(1-\frac{a}{A}\right)^{n_i}$$

It follows that:

$$S_{A-a}+E_a = S - \sum_{i=1}^{S}\left(\frac{a}{A}\right)^{n_i} + \sum_{i=1}^{S}\left(\frac{a}{A}\right)^{n_i} = S$$

(d) We have:

$$T_a = S_a + E_a = S - \sum_{i=1}^{S}\left(1-\frac{a}{A}\right)^{n_i} + \sum_{i=1}^{S}\left(\frac{a}{A}\right)^{n_i}$$

It follows that:

$$\begin{aligned} \frac{\partial T_a}{\partial a} &= -\sum_{i=1}^{S} n_i\left(1-\frac{a}{A}\right)^{n_i-1}\left(-\frac{1}{A}\right) + \sum_{i=1}^{S} n_i\left(\frac{a}{A}\right)^{n_i-1}\left(\frac{1}{A}\right) \\ &= \frac{1}{A}\left(\sum_{i=1}^{S} n_i\left(1-\frac{a}{A}\right)^{n_i-1} + \sum_{i=1}^{S} n_i\left(\frac{a}{A}\right)^{n_i-1}\right) \\ &\geq 0 \end{aligned}$$

This implies that $T_a$ is an increasing function of $a$. Moreover, we have:

$$T_\emptyset = S_\emptyset + E_\emptyset = S - \sum_{i=1}^{S} \left(1 - \frac{0}{A}\right)^{n_i} + \sum_{i=1}^{S} \left(\frac{0}{A}\right)^{n_i} = S - S + 0 = 0$$

and:

$$T_A = S_A + E_A = S - \sum_{i=1}^{S} \left(1 - \frac{A}{A}\right)^{n_i} + \sum_{i=1}^{S} \left(\frac{A}{A}\right)^{n_i} = S - 0 + S = 2S$$

We deduce that:

$$0 \leq S_a + E_a \leq 2S$$

### B.1.7 Valuation of risks to life and health (Exercise 5.5.4)

1. Using Bayes theorem, we have:

$$\mathbf{S}(u \mid t) = \Pr\{\tau > u \mid \tau > t\} = \frac{\Pr\{\tau > u, \tau > t\}}{\Pr\{\tau > t\}} = \frac{\Pr\{\tau > u, t\}}{\Pr\{\tau > t\}} = \frac{\mathbf{S}(u)}{\mathbf{S}(t)}$$

2. Since $\mathrm{d}\mathbf{S}(t) = \partial \mathbf{S}(t)\ \mathrm{d}t = -f(t)\ \mathrm{d}t$, we can express the expected survival time as:

$$\mathbb{E}[\tau] = \int_0^\infty t f(t)\ \mathrm{d}t = -\int_0^\infty t\, \mathrm{d}\mathbf{S}(t)$$

Using integration by parts, we get:

$$\mathbb{E}[\tau] = -\left[t\mathbf{S}(t)\right]_0^\infty + \int_0^\infty \mathbf{S}(t)\ \mathrm{d}t = 0 + \int_0^\infty \mathbf{S}(t)\ \mathrm{d}t = \int_0^\infty \mathbf{S}(t)\ \mathrm{d}t$$

We deduce the conditional life expectancy for an individual alive at time $t$:

$$\mathrm{LE}(t) = \mathbb{E}[\tau \mid \tau > t] = \frac{\mathbb{E}[\mathbb{1}\{\tau > t\} \cdot \tau]}{\Pr\{\tau > t\}} = \frac{\int_t^\infty \mathbf{S}(u)\ \mathrm{d}u}{\mathbf{S}(t)} = \int_t^\infty \mathbf{S}(u \mid t)\ \mathrm{d}u$$

3. The expected present value of a payoff, taking into account the future lifetime, is given by:

$$\mathbb{E}[X; t, \varrho] = \int_t^\infty e^{-\varrho(u-t)} \mathbf{S}(u \mid t)\, X(u)\ \mathrm{d}u = \mathbb{E}[\delta(u)\, X(u)] \tag{B.2}$$

where $\delta(u) = B(t,u)\,\mathbf{S}(u \mid t)$ is the discount factor under uncertain lifetime and $B(t,u) = e^{-\varrho(u-t)}$ is the standard discount factor at time $u$. Therefore, we have:

$$\delta(u) = e^{-\varrho(u-t)} \Pr\{\tau > u \mid \tau > t\}$$

Equation (B.2) is the classical formula for the present value when the discount rate accounts for uncertainty about the individual's lifetime.

4. $\mathrm{DLE}(t; \varrho)$ is the mathematical expectation of the discounted survival time, given that the survival time exceeds $t$:

$$\mathrm{DLE}(t; \varrho) = \mathbb{E}\left[e^{-\varrho t}\tau \mid \tau > t\right]$$

Using integration by parts with $u = e^{-\varrho t}t$ and $v' = f(t)$, we can express the discounted life expectancy at $t = 0$ as:

$$\begin{aligned}
\text{DLE}(0;\varrho) &= \int_0^\infty e^{-\varrho t} t f(t)\,\mathrm{d}t \\
&= \left[-e^{-\varrho t}t\mathbf{S}(t)\right]_0^\infty + \int_0^\infty \left(-\varrho e^{-\varrho t}t + e^{-\varrho t}\right)\mathbf{S}(t)\,\mathrm{d}t \\
&= \int_0^\infty e^{-\varrho t}\mathbf{S}(t)\,\mathrm{d}t - \varrho\int_0^\infty e^{-\varrho t}t\mathbf{S}(t)\,\mathrm{d}t
\end{aligned}$$

because $u' = -\varrho e^{-\varrho t}t + e^{-\varrho t}$ and $v = -\mathbf{S}(t)$. We deduce that:

$$\text{DLE}(0;\varrho) = \text{LE}(0;\varrho) - \underbrace{\varrho\int_0^\infty e^{-\varrho t}t\mathbf{S}(t)\,\mathrm{d}t}_{\geq 0}$$

and:

$$\text{LE}(0;\varrho) \geq \text{DLE}(0;\varrho) = \int_0^\infty e^{-\varrho t} t f(t)\,\mathrm{d}t$$

The generalization to the case $t \neq 0$ is straightforward. Using the change of variable $x = u - t$, we obtain $\text{DLE}(t;\varrho) = \text{LE}(t;\varrho) - \varrho\int_0^\infty e^{-\varrho x}x\mathbf{S}(t+x)\,\mathrm{d}x$. Equality is achieved if and only if $\varrho = 0$.

5. Since $\mathbf{S}(t) = e^{-\lambda t}$, we have:

$$\begin{aligned}
\text{LE}(t;\varrho) &= \frac{1}{e^{-\lambda t}}\int_t^\infty e^{-\varrho(u-t)}e^{-\lambda u}\,\mathrm{d}u \\
&= \int_t^\infty e^{-(\varrho+\lambda)(u-t)}\,\mathrm{d}u \\
&= \left[\frac{e^{-(\varrho+\lambda)(u-t)}}{(\varrho+\lambda)}\right]_t^\infty \\
&= \frac{1}{\varrho+\lambda}
\end{aligned}$$

and:

$$\begin{aligned}
\text{DLE}(t;\varrho) &= \int_t^\infty e^{-\varrho(u-t)}(u-t)f(u\mid t)\,\mathrm{d}u \\
&= \int_t^\infty e^{-\varrho(u-t)}(u-t)\lambda e^{-\lambda(u-t)}\,\mathrm{d}u \\
&= \int_0^\infty \lambda e^{-(\varrho+\lambda)s}s\,\mathrm{d}s \\
&= \left[-\lambda s\frac{e^{-(\varrho+\lambda)s}}{(\varrho+\lambda)}\right]_0^\infty + \lambda\int_0^\infty \frac{e^{-(\varrho+\lambda)s}}{(\varrho+\lambda)}\,\mathrm{d}s \\
&= \lambda\left[-\frac{e^{-(\varrho+\lambda)s}}{(\varrho+\lambda)^2}\right]_0^\infty \\
&= \frac{\lambda}{(\varrho+\lambda)^2}
\end{aligned}$$

We verify that:

$$\mathrm{LE}(t;\varrho) = \left(1 + \frac{\varrho}{\lambda}\right) \mathrm{DLE}(t;\varrho) \geq \mathrm{DLE}(t;\varrho)$$

Moreover, we note that $\mathrm{LE}(t;\varrho)$ does not depend on time $t$ because exponential survival times satisfy the property of lack of memory.

6. (a) In the case of exponential survival time, we have:

$$\mathbb{E}[\tau] = \frac{1}{\lambda}$$

It follows that:

$$\lambda = \frac{1}{\mathbb{E}[\tau]} = \frac{1}{70} = 0.01429$$

For the Weibull distribution, we have:

$$\mathbb{E}[\tau] = a\Gamma\left(1 + \frac{1}{b}\right)$$

We deduce that:

$$a = \frac{\mathbb{E}[\tau]}{\Gamma\left(1 + \frac{1}{b}\right)} = \frac{70}{\Gamma\left(1 + \frac{1}{5}\right)} = 76.23871$$

The survival functions $\mathbf{S}(t)$ and $\mathbf{S}(u \mid t = 50)$ are shown in Figure B.28. It is evident that the exponential distribution is not suitable for modeling human lifetimes, as the probability of dying before reaching 50 years of age is approximately 50%. In contrast, the Weibull distribution provides a more realistic model for human lifetime.

(b) We have:

$$\mathrm{LE}(0;3\%) = \frac{1}{\varrho + \lambda} = \frac{1}{3\% + 1.43\%} = 22.58 \text{ years}$$

and:

$$\mathrm{DLE}(0;3\%) = \frac{\lambda}{(\varrho + \lambda)^2} = \frac{1.43\%}{(3\% + 1.43\%)^2} = 7.28 \text{ years}$$

The function $\mathrm{DLE}(t;\varrho)$ discounts lifetime too rapidly and is not a suitable approach for calculating present values while accounting for future lifetime.

(c) Figure B.29 shows the results. We observe that $\mathrm{LE}(t;\varrho)$ is a decreasing function with respect to both time $t$ and the discount rate $\varrho$. Using a standard discount rate of 3%, a life expectancy of 70 years corresponds to a discounted life expectancy of approximately 30 years at birth and 20 years at age 40.

7. (a) We have:

$$\begin{aligned}
\mathrm{QALE}(t;\varrho) &= \frac{1}{\mathbf{S}(t)} \int_t^\infty e^{-\varrho(u-t)} \mathbf{S}(u)\, Q(t)\, \mathrm{d}u \\
&= \left(\frac{1}{\mathbf{S}(t)} \int_t^\infty e^{-\varrho(u-t)} \mathbf{S}(u)\, \mathrm{d}u\right) \cdot Q(t) \\
&= \mathrm{LE}(t;\varrho) \cdot Q(t)
\end{aligned}$$

The quality-adjusted life expectancy is the product of the discounted life expectancy and the average quality of life weight.

Figure B.28: Survival function $\mathbf{S}(u \mid t)$

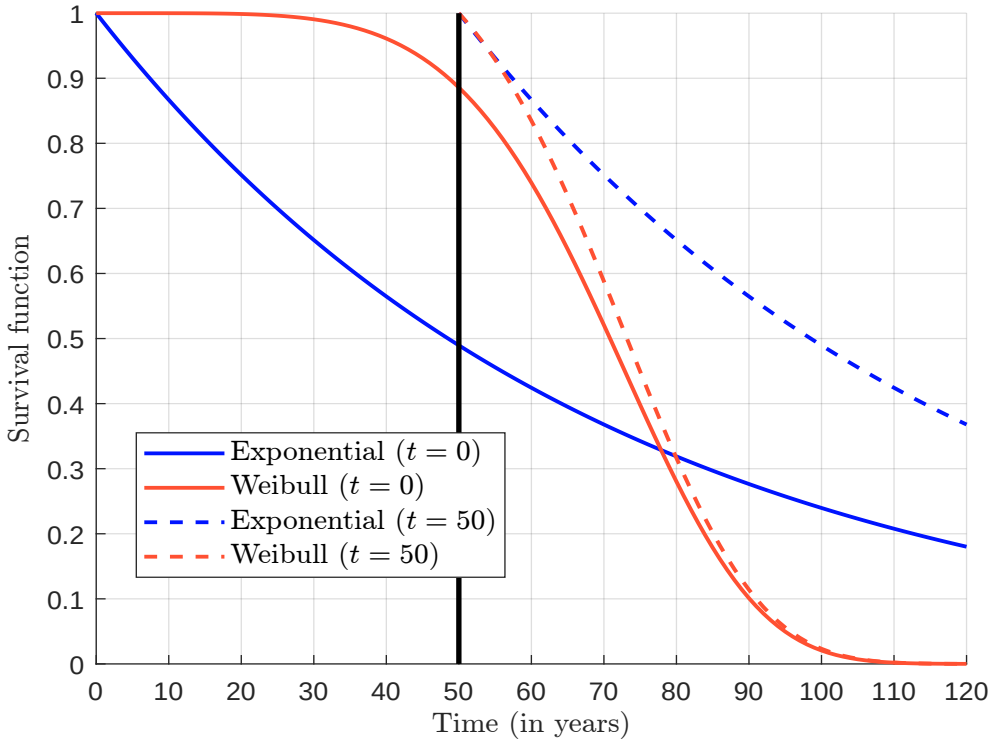


Figure B.29: Discounted lifetime expectancy $\mathrm{LE}(t; \varrho)$

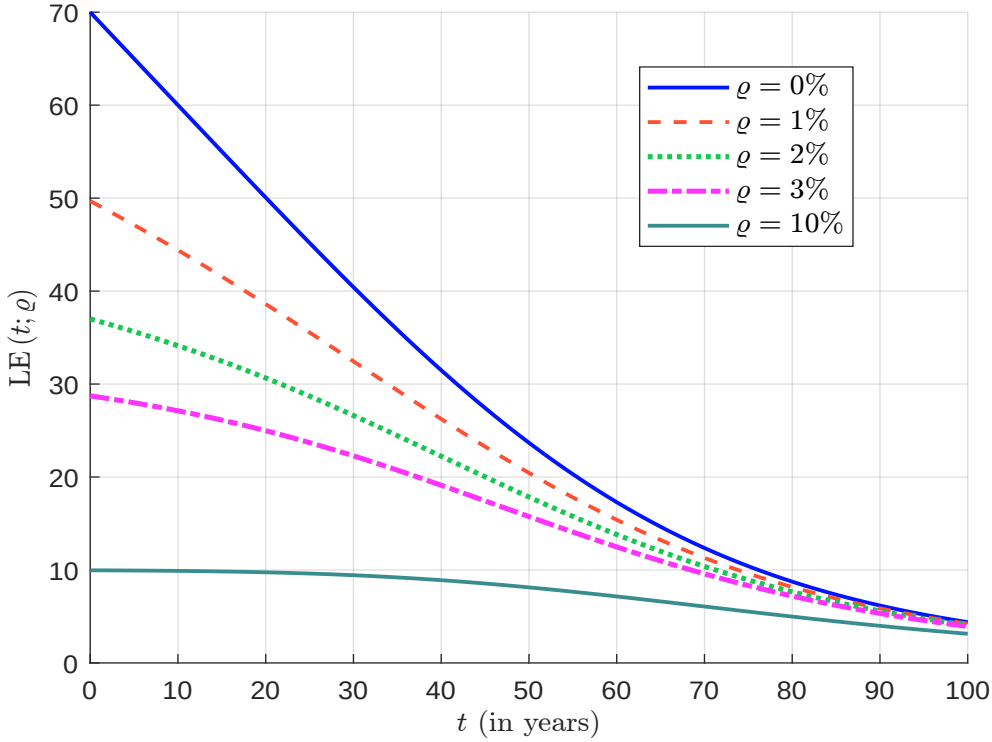

(b) Since $Q(t) \leq 1$, we deduce that:

$$0 \leq e^{-\varrho(u-t)} \frac{\mathbf{S}(u)}{\mathbf{S}(t)} Q(u) \leq e^{-\varrho(u-t)} \frac{\mathbf{S}(u)}{\mathbf{S}(t)}$$

and:

$$\int_t^\infty e^{-\varrho(u-t)} \frac{\mathbf{S}(u)}{\mathbf{S}(t)} Q(u)\, \mathrm{d}u \leq \int_t^\infty e^{-\varrho(u-t)} \frac{\mathbf{S}(u)}{\mathbf{S}(t)}\, \mathrm{d}u$$

We conclude that $\mathrm{QALE}(t;\varrho) \leq \mathrm{LE}(t;\varrho)$.

(c) $Q_1(t)$ is a piecewise linear function representing three phases of life. Before $t_1$, the quality of life is equal to 1. Between $t_1$ and $t_2$, the quality of life decreases linearly, reaching $1-\kappa_1$ at $t=t_2$. The rate of decrease per year in this phase is $\kappa_1/(t_2-t_1)$. In the third phase, between $t_2$ and $t_3$, the quality of life continues to decline linearly at a rate of $\kappa_2/(t_3-t_2)$. Figure B.30 shows the functions $\mathrm{LE}(t;\varrho)$, $\mathrm{QALE}_1(t;\varrho)$ calculated with $Q_1(t)$, and $\mathrm{QALE}_2(t;\varrho)$ calculated with $Q_2(t)$. The difference between $\mathrm{LE}(t;\varrho)$ and $\mathrm{QALE}_1(t;\varrho)$ is small, especially when $t \leq t_1$. It is more pronounced for large values of $t$ because quality of life is strongly affected when people are old. In contrast, $\mathrm{QALE}_2(t;\varrho)$ is much lower than $\mathrm{LE}(t;\varrho)$, because the quality of life decreases exponentially 2% per year.

Figure B.30: Discounted lifetime expectancy $\mathrm{LE}(t;\varrho)$

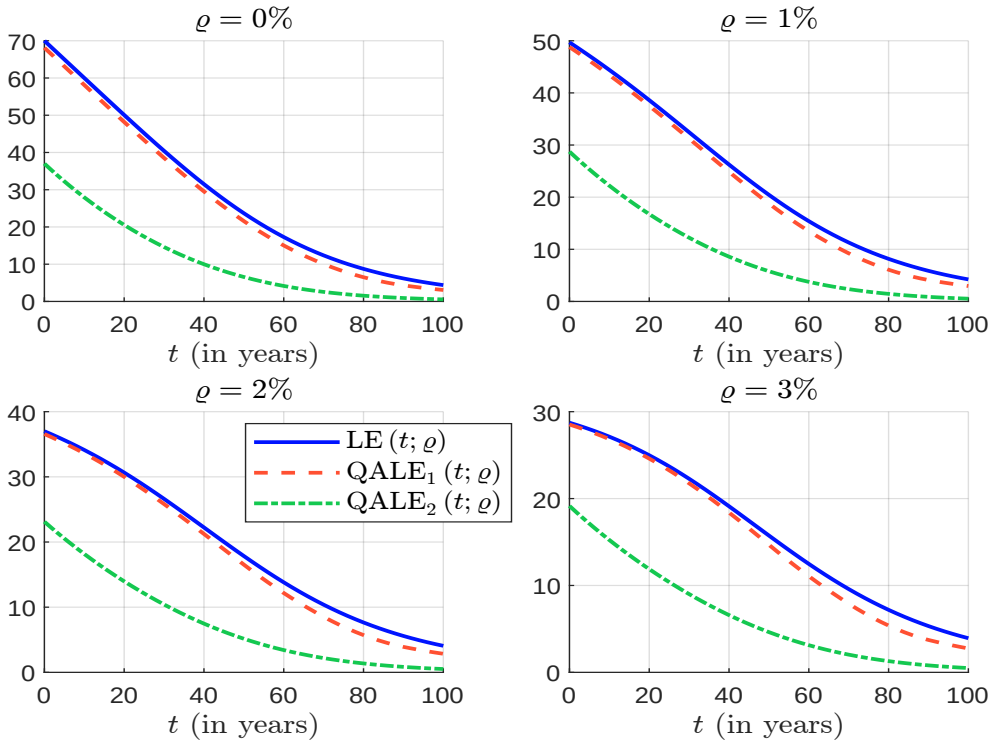


8. (a) We have:

$$\mathrm{VSL}(t) = \frac{v}{\Delta L(t)} = \frac{v}{\mathcal{R}(t) \cdot \Delta t}$$

We deduce that:

$$\mathrm{VSLY}(t) = \frac{\mathrm{VSL}(t) \cdot \Delta L}{\Delta \mathrm{LE}(t)} = \frac{\mathrm{VSL}(t)}{\mathrm{LE}(t;\varrho)}$$

and:

$$\text{VQALY}(t) = \frac{\text{VSL}(t) \cdot \Delta L}{\Delta\text{QALE}(t)} = \frac{\text{VSL}(t)}{\text{QALE}(t;\varrho)}$$

(b) Since $\Delta L(t) = \mathcal{R}(t) = \mathcal{I}(t)$ because $\Delta t = 1$ year, the associated payoff is:

$$X(t) = \text{VSL}(t) \cdot \mathcal{R}(t) = \text{VSL}(t) \cdot \Delta L(t)$$

It follows that:

$$X(t) = \text{VSLY}(t) \cdot \Delta\text{LE}(t) = \text{VQALY}(t) \cdot \Delta\text{QALE}(t)$$

(c) If $\text{VSL}(t)$ and $\mathcal{I}(t)$ are constant, we get:

$$\begin{aligned} \mathcal{G}(t;\varrho) &= \text{VSL} \cdot \left( \frac{1}{\mathbf{S}(t)} \int_t^\infty e^{-\varrho(u-t)} \mathbf{S}(u)\, \mathrm{d}u \right) \cdot \mathcal{I}(t) \\ &= \text{VSL} \cdot \text{LE}(t;\varrho) \cdot \Delta L \end{aligned} \tag{B.3}$$

The economic gain is the value of a statistical life multiplied by the discounted life expectancy and the expected number of lives saved.

(d) In the case of air pollution, $\mathcal{I}(t)$ is negative and the economic cost becomes:

$$\mathcal{C}(t;\varrho) = -\mathcal{G}(t;\varrho) = \text{VSL} \cdot \text{LE}(t;\varrho) \cdot \Delta L$$

where $\Delta L$ is the expected number of deaths due to air pollution. If we compare with the formula:

$$\mathcal{C} = \text{VSLY} \cdot \text{YLL}$$

we can deduce that the years of life lost (YLL) is equal to:

$$\text{YLL} = \Delta L \cdot \text{LE}(t;\varrho)$$

In this model, years of life lost is the product of the expected number of deaths and the discounted life expectancy. The traditional formula is:

$$\text{YLL} = \Delta L \cdot \Delta\tau$$

where $\Delta\tau$ is the difference between life expectancy without air pollution and life expectancy with air pollution. Therefore, we assume that:

$$\Delta\tau = \text{LE}(t;\varrho) = \frac{1}{\mathbf{S}(t)} \int_t^\infty e^{-\varrho(u-t)} \mathbf{S}(u)\, \mathrm{d}u$$

This means that we take the discount rate into account when calculating years of life lost.

(e) Results are reported in Table B.11. By construction, the life expectancy of an individual at age 0 is 70 years. Using a discount rate of 3%, the discounted life expectancy is 28.73 years. At age 40, the remaining life expectancy is 31.49 years, so the average lifetime of an individual alive at age 40 is 71.49 years. This corresponds to a discounted life expectancy of 19.11 years. At age 80, the remaining life expectancy is 8.74 years, so the average lifetime of an individual alive at age 80 is 88.74 years. The impact of the quality-of-life weight is shown in the second row. The estimated value of a statistical life is calculated as:

$$\text{VSL}(t) = \frac{\$1\,000}{1/10\,000} = \$10\,\text{mn}$$

Table B.11: Calculation of the economic gain $\mathcal{G}(t;\varrho)$

| Discount rate | $\varrho = 0\%$ | | | $\varrho = 3\%$ | | | Unit |
|---|---|---|---|---|---|---|---|
| Age | Birth | 40 years | 80 years | 0 | 40 years | 80 years | |
| LE $(t;\varrho)$ | 70.00 | 31.49 | 8.74 | 28.73 | 19.11 | 7.19 | years |
| QALE $(t;\varrho)$ | 68.13 | 29.54 | 6.50 | 28.52 | 18.39 | 5.38 | |
| VSL $(t)$ | | | 10 000 | | | | |
| VSLY $(t)$ | 143 | 318 | 1 144 | 348 | 523 | 1 390 | \$1 000 |
| VQALY $(t)$ | 147 | 339 | 1 538 | 351 | 544 | 1 858 | |
| VSL $(t)$ | 10 500 | 4 723 | 1 312 | 4 310 | 2 867 | 1 079 | |
| VSLY $(t)$ | | | 150 | | | | \$ 1000 |
| VQALY $(t)$ | 154 | 160 | 202 | 151 | 156 | 200 | |
| $\mathcal{G}(t;\varrho)$ | 36 750 | 7 437 | 573 | 6 191 | 2 740 | 388 | \$ |

We can then compute the value of a statistical life year. Assuming an age of 40 years and a discount rate of 3%, we obtain:

$$\text{VSLY}(40) = \frac{\text{VSL}(40)}{\text{LE}(40;3\%)} = \frac{\$10\,\text{mn}}{19.11} = \$523\,206$$

and:

$$\text{VQALY}(40) = \frac{\text{VSL}(40)}{\text{QALE}(40;3\%)} = \frac{\$10\,\text{mn}}{18.39} = \$543\,817$$

The assumption that VSL $(t)$ is constant is not realistic. For instance, the value per statistical life year for a newborn is \$142 857, while for an 80-year-old individual it is \$1 390 448. On the other hand, the assumption that VSLY $(t)$ is constant is more realistic, even if it does not fully match reality. In fact, we can expect VSLY $(40) \geq$ VSLY $(0)$ and VSLY $(40) \geq$ VSLY $(80)$. Finally, we calculate the economic gain using Equation (B.3). For example, assuming an age of 40 years and a discount rate of 3%, the economic gain is:

$$\mathcal{G}(40;3\%) = \$2\,866\,938 \times 19.11 \times \frac{5}{100\,000} = \$2\,740$$

We observe that the economic gain is greater for newborns than for older individuals.

## B.2 Exercises related to climate risk

### B.2.1 Equity and bond portfolio optimization with green preferences (Exercise 11.4.1)

1. (a) We have:

$$\mathcal{CI}_{i,j} = \frac{\mathcal{CE}_{i,j}}{Y_i}$$

For instance, if we consider the 8$^{\text{th}}$ issuer, we have[4]:

$$\begin{aligned}
\mathcal{CI}_{8,1} &= \frac{\mathcal{CE}_{8,1}}{Y_8} = \frac{5}{25} = 0.20 \text{ tCO}_2\text{e/\$ mn} \\
\mathcal{CI}_{8,2} &= \frac{\mathcal{CE}_{8,2}}{Y_8} = \frac{64}{25} = 2.56 \text{ tCO}_2\text{e/\$ mn} \\
\mathcal{CI}_{8,3} &= \frac{\mathcal{CE}_{8,3}}{Y_8} = \frac{199}{25} = 7.96 \text{ tCO}_2\text{e/\$ mn}
\end{aligned}$$

Since we have:

| Issuer | #1 | #2 | #3 | #4 | #5 | #6 | #7 | #8 |
|---|---|---|---|---|---|---|---|---|
| $\mathcal{CE}_{i,1}$ | 75 | 5 000 | 720 | 50 | 2 500 | 25 | 30 000 | 5 |
| $\mathcal{CE}_{i,2}$ | 75 | 5 000 | 1 030 | 350 | 4 500 | 5 | 2000 | 64 |
| $\mathcal{CE}_{i,3}$ | 24 000 | 15 000 | 1 210 | 550 | 500 | 187 | 30 000 | 199 |
| $Y_i$ | 300 | 328 | 125 | 100 | 200 | 102 | 107 | 25 |

we obtain:

| Issuer | #1 | #2 | #3 | #4 | #5 | #6 | #7 | #8 |
|---|---|---|---|---|---|---|---|---|
| $\mathcal{CI}_{i,1}$ | 0.25 | 15.24 | 5.76 | 0.50 | 12.50 | 0.25 | 280.37 | 0.20 |
| $\mathcal{CI}_{i,2}$ | 0.25 | 15.24 | 8.24 | 3.50 | 22.50 | 0.05 | 18.69 | 2.56 |
| $\mathcal{CI}_{i,3}$ | 80.00 | 45.73 | 9.68 | 5.50 | 2.50 | 1.83 | 280.37 | 7.96 |

(b) We have:

$$\mathcal{CI}_{i,1-2} = \frac{\mathcal{CE}_{i,1} + \mathcal{CE}_{i,2}}{Y_i} = \mathcal{CI}_{i,1} + \mathcal{CI}_{i,2}$$

and:

$$\mathcal{CI}_{i,1-3} = \mathcal{CI}_{i,1} + \mathcal{CI}_{i,2} + \mathcal{CI}_{i,3}$$

We deduce that:

| Issuer | #1 | #2 | #3 | #4 | #5 | #6 | #7 | #8 |
|---|---|---|---|---|---|---|---|---|
| $\mathcal{CI}_{i,1}$ | 0.25 | 15.24 | 5.76 | 0.50 | 12.50 | 0.25 | 280.37 | 0.20 |
| $\mathcal{CI}_{i,1-2}$ | 0.50 | 30.49 | 14.00 | 4.00 | 35.00 | 0.29 | 299.07 | 2.76 |
| $\mathcal{CI}_{i,1-3}$ | 80.50 | 76.22 | 23.68 | 9.50 | 37.50 | 2.12 | 579.44 | 10.72 |

(c) We have:

$$\begin{aligned}
\mathcal{CI}(b) &= \sum_{i=1}^{8} b_i \mathcal{CI}_i \\
&= 0.22 \times 80.50 + 0.19 \times 76.2195 + 0.17 \times 23.68 + 0.13 \times 9.50 + \\
&\quad 0.11 \times 37.50 + 0.08 \times 2.1275 + 0.06 \times 579.4393 + 0.04 \times 10.72 \\
&= 76.9427 \text{ tCO}_2\text{e/\$ mn}
\end{aligned}$$

[4] Because 1 ktCO$_2$e/\$ bn = 1 tCO$_2$e/\$ mn.

(d) i. We have:

$$b_i = \frac{MC_i}{\sum_{k=1}^{8} \text{MC}_k}$$

and $\sum_{k=1}^{8} \text{MC}_k = \$10$ tn. We deduce that:

$$\text{MC}_i = 10 \times b_i$$

We obtain the following values of market capitalization expressed in \$ bn:

| Issuer | #1 | #2 | #3 | #4 | #5 | #6 | #7 | #8 |
|---|---|---|---|---|---|---|---|---|
| $\text{MC}_i$ | 2 200 | 1 900 | 1 700 | 1 300 | 1 100 | 800 | 600 | 400 |

ii. Let $W$ be the wealth invested in the benchmark portfolio $b$. The wealth invested in asset $i$ is equal to $b_i W$. We deduce that the ownership ratio is equal to:

$$\varpi_i = \frac{b_i W}{\text{MC}_i} = \frac{b_i W}{b_i \sum_{k=1}^{n} \text{MC}_k} = \frac{W}{\sum_{k=1}^{n} \text{MC}_k}$$

When we invest in a capitalization-weighted portfolio, the ownership ratio is the same for all the assets. In our case, we have:

$$\varpi_i = \frac{1}{10 \times 1000} = 0.01\%$$

The ownership ratio is equal to 1 basis point.

iii. Using the financed emissions approach, the carbon emissions of our investment is equal to:

$$\begin{aligned} \boldsymbol{\mathcal{CE}}\,(\$1 \text{ bn}) &= 0.01\% \times (75 + 75 + 24\,000) + \\ &\quad 0.01\% \times (5\,000 + 5\,000 + 15\,000) + \\ &\quad \ldots + \\ &\quad 0.01\% \times (5 + 64 + 199) \\ &= 12.3045 \text{ ktCO}_2\text{e} \end{aligned}$$

iv. We compute the revenues of our investment:

$$Y\,(\$1 \text{ bn}) = 0.01\% \sum_{i=1}^{8} Y_i = \$0.1287 \text{ bn}$$

We deduce that the exact carbon intensity is equal to:

$$\boldsymbol{\mathcal{CI}}\,(\$1 \text{ bn}) = \frac{\boldsymbol{\mathcal{CE}}\,(\$1 \text{ bn})}{Y\,(\$1 \text{ bn})} = \frac{12.3045}{0.1287} = 95.6061 \text{ tCO}_2\text{e}/\$ \text{ mn}$$

We notice that the WACI of the benchmark underestimates the exact carbon intensity of our investment by 19.5%:

$$76.9427 < 95.6061$$

2. (a) The covariance matrix $\Sigma = (\Sigma_{i,j})$ is defined by:

$$\Sigma_{i,j} = \rho_{i,j}\sigma_i\sigma_j$$

We obtain the following numerical values (expressed in bps):

$$\Sigma = \begin{pmatrix} 484.0 & 352.0 & 385.0 & 237.6 & 616.0 & 253.0 & 200.2 & 382.8 \\ 352.0 & 400.0 & 375.0 & 234.0 & 400.0 & 276.0 & 130.0 & 377.0 \\ 385.0 & 375.0 & 625.0 & 360.0 & 700.0 & 402.5 & 227.5 & 507.5 \\ 237.6 & 234.0 & 360.0 & 324.0 & 612.0 & 331.2 & 175.5 & 391.5 \\ 616.0 & 400.0 & 700.0 & 612.0 & 1600.0 & 552.0 & 416.0 & 754.0 \\ 253.0 & 276.0 & 402.5 & 331.2 & 552.0 & 529.0 & 149.5 & 466.9 \\ 200.2 & 130.0 & 227.5 & 175.5 & 416.0 & 149.5 & 169.0 & 226.2 \\ 382.8 & 377.0 & 507.5 & 391.5 & 754.0 & 466.9 & 226.2 & 841.0 \end{pmatrix}$$

(b) The tracking error variance of portfolio $w$ with respect to benchmark $b$ is equal to:

$$\sigma^2(w \mid b) = (w-b)^\top \Sigma (w-b)$$

The carbon intensity constraint has the following expression:

$$\sum_{i=1}^{8} w_i \boldsymbol{\mathcal{CI}}_i \leq (1-\boldsymbol{\mathcal{R}})\,\boldsymbol{\mathcal{CI}}(b)$$

where $\boldsymbol{\mathcal{R}}$ is the reduction rate and $\boldsymbol{\mathcal{CI}}(b)$ is the carbon intensity of the benchmark. Let $\boldsymbol{\mathcal{CI}}^\star = (1-\boldsymbol{\mathcal{R}})\,\boldsymbol{\mathcal{CI}}(b)$ be the target value of the carbon footprint. The optimization problem is then:

$$\begin{aligned} w^\star &= \arg\min \frac{1}{2}\sigma^2(w \mid b) \\ &\text{s.t.} \quad \begin{cases} \sum_{i=1}^{8} w_i \boldsymbol{\mathcal{CI}}_i \leq \boldsymbol{\mathcal{CI}}^\star \\ \sum_{i=1}^{8} w_i = 1 \\ 0 \leq w_i \leq 1 \end{cases} \end{aligned}$$

We add the second and third constraints in order to obtain a long-only portfolio.

(c) The objective function is equal to:

$$f(w) = \frac{1}{2}\sigma^2(w \mid b) = \frac{1}{2}(w-b)^\top \Sigma (w-b) = \frac{1}{2}w^\top \Sigma w - w^\top \Sigma b + \frac{1}{2}b^\top \Sigma b$$

while the matrix form of the carbon intensity constraint is:

$$\boldsymbol{\mathcal{CI}}^\top w \leq \boldsymbol{\mathcal{CI}}^\star$$

where $\boldsymbol{\mathcal{CI}} = (\boldsymbol{\mathcal{CI}}_1, \ldots, \boldsymbol{\mathcal{CI}}_8)$ is the column vector of carbon intensities. Since $b^\top \Sigma b$ is a constant and does not depend on $w$, we can cast the previous optimization problem into a QP problem:

$$\begin{aligned} w^\star &= \arg\min \frac{1}{2}w^\top Q w - w^\top R \\ &\text{s.t.} \quad \begin{cases} Aw = B \\ Cw \leq D \\ w^- \leq w \leq w^+ \end{cases} \end{aligned}$$

We have $Q = \Sigma$, $R = \Sigma b$, $A = \mathbf{1}_8^\top$, $B = 1$, $C = \boldsymbol{\mathcal{CI}}^\top$, $D = \boldsymbol{\mathcal{CI}}^\star$, $w^- = \mathbf{0}_8$ and $w^+ = \mathbf{1}_8$.

(d) We have:

$$\begin{aligned}\boldsymbol{\mathcal{CI}}(b) &= 0.22 \times 0.50 + 0.19 \times 30.4878 + \ldots + 0.04 \times 2.76 \\ &= 30.7305 \text{ tCO}_2\text{e/\$ mn}\end{aligned}$$

We deduce that:

$$\boldsymbol{\mathcal{CI}}^\star = (1 - \boldsymbol{\mathcal{R}})\,\boldsymbol{\mathcal{CI}}(b) = 0.80 \times 30.7305 = 24.5844 \text{ tCO}_2\text{e/\$ mn}$$

Therefore, the inequality constraint of the QP problem is:

$$\begin{pmatrix} 0.50 & 30.49 & 14.00 & 4.00 & 35.00 & 0.29 & 299.07 & 2.76 \end{pmatrix} \begin{pmatrix} w_1 \\ w_2 \\ \vdots \\ w_7 \\ w_8 \end{pmatrix} \leq 24.5844$$

We obtain the following optimal solution:

$$w^\star = \begin{pmatrix} 23.4961\% \\ 17.8129\% \\ 17.1278\% \\ 15.4643\% \\ 10.4037\% \\ 7.5903\% \\ 4.0946\% \\ 4.0104\% \end{pmatrix}$$

The minimum tracking error volatility $\sigma(w^\star \mid b)$ is equal to 15.37 bps.

(e) In Table B.12, we report the optimal solution $w^\star$ (expressed in %) of the optimization problem for different values of $\boldsymbol{\mathcal{R}}$. We also indicate the carbon intensity of the portfolio (in $\text{tCO}_2\text{e/\$ mn}$) and the tracking error volatility (in bps). For instance, if $\boldsymbol{\mathcal{R}}$ is set to 50%, the weights of assets #1, #3, #4 and #8 increase whereas the weights of assets #2, #5, #6 and #7 decrease. The carbon intensity of this portfolio is equal to 15.3653 $\text{tCO}_2\text{e/\$ mn}$. The tracking error volatility is below 40 bps, which is relatively low.

(f) In this case, the inequality constraint $Cw \leq D$ is defined by:

$$C = \boldsymbol{\mathcal{CI}}_{1-3}^\top = \begin{pmatrix} 80.5000 \\ 76.2195 \\ 23.6800 \\ 9.5000 \\ 37.5000 \\ 2.1275 \\ 579.4393 \\ 10.7200 \end{pmatrix}^\top$$

and:

$$D = (1 - \boldsymbol{\mathcal{R}}) \times 76.9427$$

We obtain the results given in Table B.13.

Table B.12: Solution of the equity optimization problem (scope $\boldsymbol{\mathcal{SC}}_{1-2}$)

| $\boldsymbol{\mathcal{R}}$ | 0% | 20% | 30% | 50% | 70% |
|---|---|---|---|---|---|
| $w_1$ | 22.0000 | 23.4961 | 24.2441 | 25.7402 | 30.4117 |
| $w_2$ | 19.0000 | 17.8129 | 17.2194 | 16.0323 | 9.8310 |
| $w_3$ | 17.0000 | 17.1278 | 17.1917 | 17.3194 | 17.8348 |
| $w_4$ | 13.0000 | 15.4643 | 16.6964 | 19.1606 | 23.3934 |
| $w_5$ | 11.0000 | 10.4037 | 10.1055 | 9.5091 | 7.1088 |
| $w_6$ | 8.0000 | 7.5903 | 7.3854 | 6.9757 | 6.7329 |
| $w_7$ | 6.0000 | 4.0946 | 3.1418 | 1.2364 | 0.0000 |
| $w_8$ | 4.0000 | 4.0104 | 4.0157 | 4.0261 | 4.6874 |
| $\boldsymbol{\mathcal{CI}}(w)$ | 30.7305 | 24.5844 | 21.5114 | 15.3653 | 9.2192 |
| $\sigma(w \mid b)$ | 0.00 | 15.37 | 23.05 | 38.42 | 72.45 |

Table B.13: Solution of the equity optimization problem (scope $\boldsymbol{\mathcal{SC}}_{1-3}$)

| $\boldsymbol{\mathcal{R}}$ | 0% | 20% | 30% | 50% | 70% |
|---|---|---|---|---|---|
| $w_1$ | 22.0000 | 23.9666 | 24.9499 | 26.4870 | 13.6749 |
| $w_2$ | 19.0000 | 17.4410 | 16.6615 | 8.8001 | 0.0000 |
| $w_3$ | 17.0000 | 17.1988 | 17.2981 | 19.4253 | 24.1464 |
| $w_4$ | 13.0000 | 16.5034 | 18.2552 | 25.8926 | 41.0535 |
| $w_5$ | 11.0000 | 10.2049 | 9.8073 | 7.1330 | 3.5676 |
| $w_6$ | 8.0000 | 7.4169 | 7.1254 | 7.0659 | 8.8851 |
| $w_7$ | 6.0000 | 3.2641 | 1.8961 | 0.0000 | 0.0000 |
| $w_8$ | 4.0000 | 4.0043 | 4.0065 | 5.1961 | 8.6725 |
| $\boldsymbol{\mathcal{CI}}(w)$ | 76.9427 | 61.5541 | 53.8599 | 38.4713 | 23.0828 |
| $\sigma(w \mid b)$ | 0.00 | 21.99 | 32.99 | 104.81 | 414.48 |

(g) In Figure B.31, we report the relationship between the reduction rate $\boldsymbol{\mathcal{R}}$ and the tracking error volatility $\sigma(w \mid b)$. The choice of the scope has little impact when $\boldsymbol{\mathcal{R}} \leq 45\%$. Then, we notice a high increase when we consider the scope $1+2+3$. The portfolio's weights are given in Figure B.32. For assets #1 and #3, the behavior is divergent when we compare scopes $1+2$ and $1+2+3$.

3. (a) We have:

$$\begin{aligned} \text{MD}(b) &= \sum_{i=1}^{n} b_i \,\text{MD}_i \\ &= 0.22 \times 3.56 + 0.19 \times 7.48 + \ldots + 0.04 \times 7.96 \\ &= 5.96 \text{ years} \end{aligned}$$

and:

$$\begin{aligned} \text{DTS}(b) &= \sum_{i=1}^{n} b_i \,\text{DTS}_i \\ &= 0.22 \times 103 + 0.19 \times 155 + \ldots + 0.04 \times 155 \\ &= 210.73 \text{ bps} \end{aligned}$$

Figure B.31: Impact of the scope on the tracking error volatility

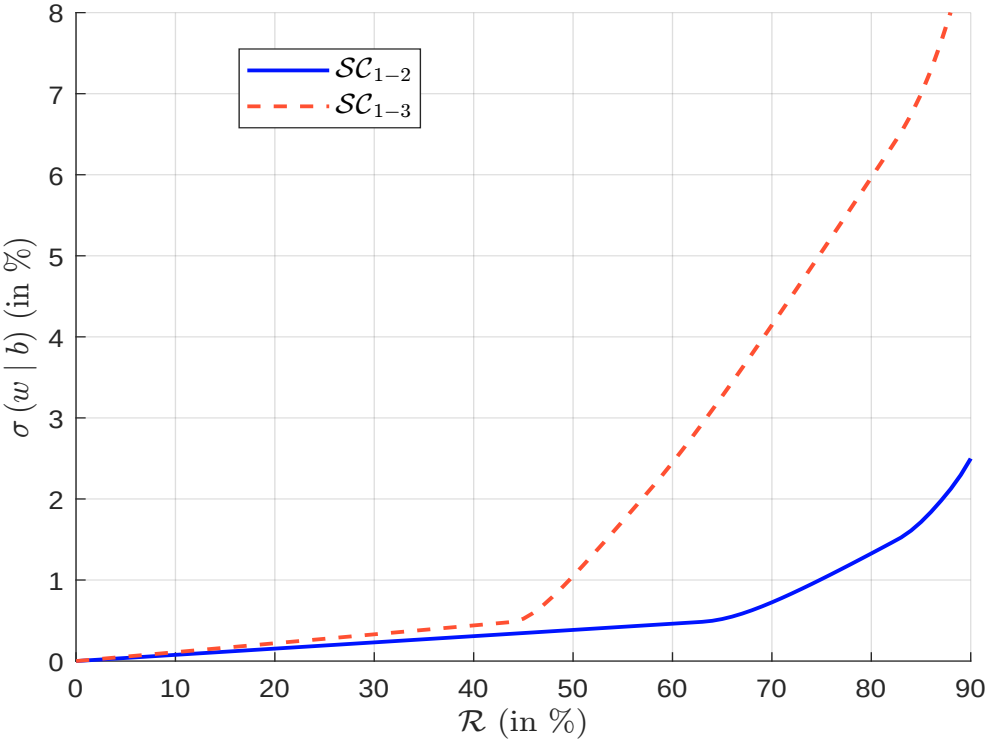


Figure B.32: Impact of the scope on the portfolio allocation (in %)

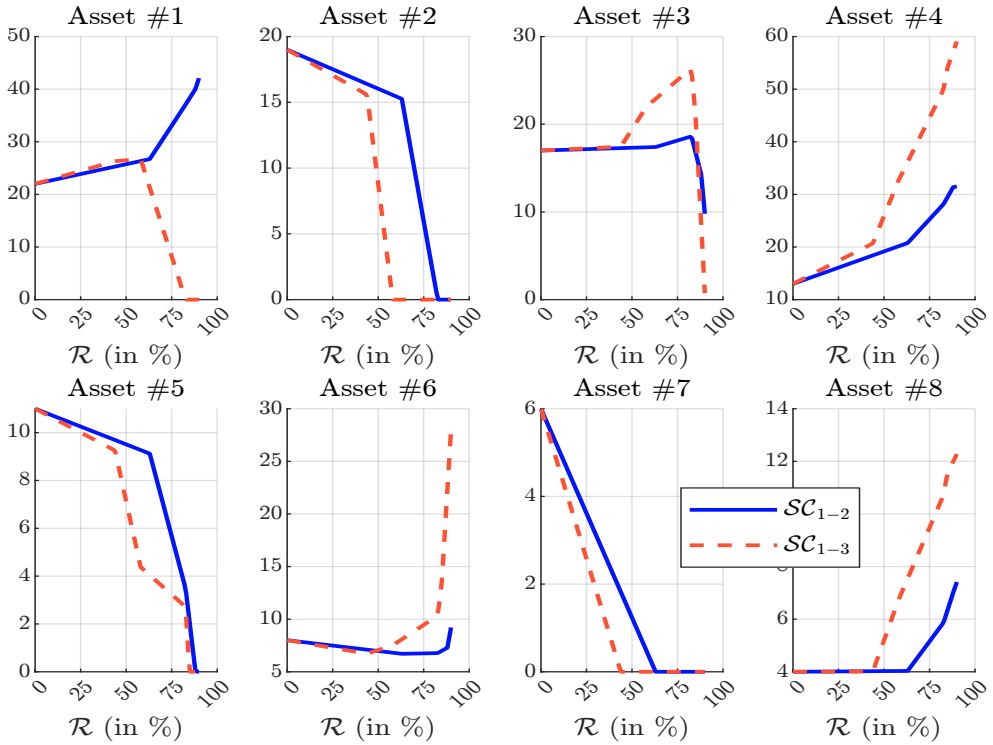

(b) We have:

$$\begin{cases} \text{MD}(w_{\text{ew}}) = 6.20 \text{ years} \\ \text{DTS}(w_{\text{ew}}) = 228.50 \text{ bps} \\ \sigma_{\text{AS}}(w_{\text{ew}} \mid b) = 17.03\% \\ \sigma_{\text{MD}}(w_{\text{ew}} \mid b) = 1.00 \text{ years} \\ \sigma_{\text{DTS}}(w_{\text{ew}} \mid b) = 36.19 \text{ bps} \end{cases}$$

(c) We have:

$$\begin{aligned} \mathcal{R}_{\text{AS}}(w \mid b) &= (w_1 - 0.22)^2 + (w_2 - 0.19)^2 + (w_3 - 0.17)^2 + (w_4 - 0.13)^2 + \\ &\quad (w_5 - 0.11)^2 + (w_6 - 0.08)^2 + (w_7 - 0.06)^2 + (w_8 - 0.04)^2 \end{aligned}$$

The objective function is then:

$$f(w) = \frac{1}{2}\mathcal{R}_{\text{AS}}(w \mid b)$$

The optimal solution is equal to:

$$w^\star = (17.30\%, 17.41\%, 20.95\%, 14.41\%, 10.02\%, 11.09\%, 0\%, 8.81\%)$$

The risk metrics are:

$$\begin{cases} \text{MD}(w^\star) = 5.96 \text{ years} \\ \text{DTS}(w^\star) = 210.73 \text{ bps} \\ \sigma_{\text{AS}}(w^\star \mid b) = 10.57\% \\ \sigma_{\text{MD}}(w^\star \mid b) = 0.43 \text{ years} \\ \sigma_{\text{DTS}}(w^\star \mid b) = 15.21 \text{ bps} \end{cases}$$

(d) We have[5]:

$$\begin{aligned} \mathcal{R}_{\text{MD}}(w \mid b) &= \left( \sum_{i=1,3,4,6} (w_i - b_i) \,\text{MD}_i \right)^2 + \left( \sum_{i=2,5,7,8} (w_i - b_i) \,\text{MD}_i \right)^2 \\ &= \left( \sum_{i=1,3,4,6} w_i \,\text{MD}_i - \text{MD}_1^\star \right)^2 + \left( \sum_{i=2,5,7,8} w_i \,\text{MD}_i - \text{MD}_2^\star \right)^2 \\ &= (3.56w_1 + 6.54w_3 + 10.23w_4 + 2.30w_6 - 3.4089)^2 + \\ &\quad (7.48w_2 + 2.40w_5 + 9.12w_7 + 7.96w_8 - 2.5508)^2 \end{aligned}$$

The objective function is then:

$$f(w) = \frac{\varphi_{\text{AS}}}{2}\mathcal{R}_{\text{AS}}(w \mid b) + \frac{\varphi_{\text{MD}}}{2}\mathcal{R}_{\text{MD}}(w \mid b)$$

The optimal solution is equal to:

$$w^\star = (16.31\%, 18.44\%, 17.70\%, 13.82\%, 11.67\%, 11.18\%, 0\%, 10.88\%)$$

The risk metrics are:

$$\begin{cases} \text{MD}(w^\star) = 5.93 \text{ years} \\ \text{DTS}(w^\star) = 210.73 \text{ bps} \\ \sigma_{\text{AS}}(w^\star \mid b) = 11.30\% \\ \sigma_{\text{MD}}(w^\star \mid b) = 0.03 \text{ years} \\ \sigma_{\text{DTS}}(w^\star \mid b) = 3.70 \text{ bps} \end{cases}$$

[5] We verify that $3.4089 + 2.5508 = 5.9597$ years.

(e) We have[6]:

$$\begin{aligned}\mathcal{R}_{\text{DTS}}(w \mid b) &= \left(\sum_{i=1,3,4,6}(w_i - b_i)\,\text{DTS}_i\right)^2 + \left(\sum_{i=2,5,7,8}(w_i - b_i)\,\text{DTS}_i\right)^2 \\ &= (103w_1 + 75w_3 + 796w_4 + 45w_6 - 142.49)^2 + \\ &\quad (155w_2 + 89w_5 + 320w_7 + 245w_8 - 68.24)^2\end{aligned}$$

The objective function is then:

$$f(w) = \frac{\varphi_{\text{AS}}}{2}\mathcal{R}_{\text{AS}}(w \mid b) + \frac{\varphi_{\text{MD}}}{2}\mathcal{R}_{\text{MD}}(w \mid b) + \frac{\varphi_{\text{DTS}}}{2}\mathcal{R}_{\text{DTS}}(w \mid b)$$

The optimal solution is equal to:

$$w^\star = (16.98\%, 17.21\%, 18.26\%, 13.45\%, 12.10\%, 9.46\%, 0\%, 12.55\%)$$

The risk metrics are:

$$\begin{cases}\text{MD}(w^\star) = 5.97 \text{ years} \\ \text{DTS}(w^\star) = 210.68 \text{ bps} \\ \sigma_{\text{AS}}(w^\star \mid b) = 11.94\% \\ \sigma_{\text{MD}}(w^\star \mid b) = 0.03 \text{ years} \\ \sigma_{\text{DTS}}(w^\star \mid b) = 0.06 \text{ bps}\end{cases}$$

(f) We summarize the results in Table B.14.

Table B.14: Solution of the bond optimization problem (scope $\boldsymbol{\mathcal{SC}}_{1-3}$)

| Problem | Benchmark | 3.(c) | 3.(d) | 3.(e) |
|---|---|---|---|---|
| $w_1$ | 22.0000 | 17.3049 | 16.3102 | 16.9797 |
| $w_2$ | 19.0000 | 17.4119 | 18.4420 | 17.2101 |
| $w_3$ | 17.0000 | 20.9523 | 17.6993 | 18.2582 |
| $w_4$ | 13.0000 | 14.4113 | 13.8195 | 13.4494 |
| $w_5$ | 11.0000 | 10.0239 | 11.6729 | 12.1008 |
| $w_6$ | 8.0000 | 11.0881 | 11.1792 | 9.4553 |
| $w_7$ | 6.0000 | 0.0000 | 0.0000 | 0.0000 |
| $w_8$ | 4.0000 | 8.8075 | 10.8769 | 12.5464 |
| $\text{MD}(w)$ | 5.9597 | 5.9597 | 5.9344 | 5.9683 |
| $\text{DTS}(w)$ | 210.7300 | 210.7300 | 210.7300 | 210.6791 |
| $\sigma_{\text{AS}}(w \mid b)$ | 0.0000 | 10.5726 | 11.3004 | 11.9400 |
| $\sigma_{\text{MD}}(w \mid b)$ | 0.0000 | 0.4338 | 0.0254 | 0.0308 |
| $\sigma_{\text{DTS}}(w \mid b)$ | 0.0000 | 15.2056 | 3.7018 | 0.0561 |
| $\boldsymbol{\mathcal{CI}}(w)$ | 76.9427 | 38.4713 | 38.4713 | 38.4713 |

(g) The goal is to write the objective function into a quadratic function:

$$\begin{aligned}f(w) &= \frac{\varphi_{\text{AS}}}{2}\mathcal{R}_{\text{AS}}(w \mid b) + \frac{\varphi_{\text{MD}}}{2}\mathcal{R}_{\text{MD}}(w \mid b) + \frac{\varphi_{\text{DTS}}}{2}\mathcal{R}_{\text{DTS}}(w \mid b) \\ &= \frac{1}{2}w^\top Q(b)\,w - w^\top R(b) + c(b)\end{aligned}$$

[6] We verify that $142.49 + 68.24 = 210.73$ bps.

where:

$$\begin{aligned}
\mathcal{R}_{\text{AS}}(w \mid b) &= (w_1 - 0.22)^2 + (w_2 - 0.19)^2 + (w_3 - 0.17)^2 + (w_4 - 0.13)^2 + \\
&\quad (w_5 - 0.11)^2 + (w_6 - 0.08)^2 + (w_7 - 0.06)^2 + (w_8 - 0.04)^2 \\
\mathcal{R}_{\text{MD}}(w \mid b) &= (3.56w_1 + 6.54w_3 + 10.23w_4 + 2.30w_6 - 3.4089)^2 + \\
&\quad (7.48w_2 + 2.40w_5 + 9.12w_7 + 7.96w_8 - 2.5508)^2 \\
\mathcal{R}_{\text{DTS}}(w \mid b) &= (103w_1 + 75w_3 + 796w_4 + 45w_6 - 142.49)^2 + \\
&\quad (155w_2 + 89w_5 + 320w_7 + 245w_8 - 68.24)^2
\end{aligned}$$

We use the analytical approach which is described in Section 11.1.3 on pages 961-966. Moreover, we rearrange the universe such that the first fourth assets belong to the first sector and the last fourth assets belong to the second sector. In this case, we have:

$$w = \left( \underbrace{w_1, w_3, w_4, w_6}_{\mathcal{S}ector_1}, \underbrace{w_2, w_5, w_7, w_8}_{\mathcal{S}ector_2} \right)$$

The matrix $Q(b)$ is block-diagonal:

$$Q(b) = \begin{pmatrix} Q_1 & \mathbf{0}_{4,4} \\ \mathbf{0}_{4,4} & Q_2 \end{pmatrix}$$

where the matrices $Q_1$ and $Q_2$ are equal to:

$$Q_1 = \begin{pmatrix} 11\,025.8400 & 8\,307.0600 & 82\,898.4700 & 4\,839.7000 \\ 8\,307.0600 & 6\,794.2900 & 61\,372.6050 & 3\,751.0500 \\ 82\,898.4700 & 61\,372.6050 & 636\,332.3225 & 36\,408.2250 \\ 4\,839.7000 & 3\,751.0500 & 36\,408.2250 & 2\,257.2500 \end{pmatrix}$$

and:

$$Q_2 = \begin{pmatrix} 25\,523.7600 & 14\,243.8000 & 51\,305.4400 & 39\,463.5200 \\ 14\,243.8000 & 8\,165.0000 & 29\,027.2000 & 22\,282.6000 \\ 51\,305.4400 & 29\,027.2000 & 104\,579.3600 & 80\,214.8800 \\ 39\,463.5200 & 22\,282.6000 & 80\,214.8800 & 61\,709.0400 \end{pmatrix}$$

The vector $R(b)$ is defined as follows:

$$R(b) = \begin{pmatrix} 15\,001.8621 \\ 11\,261.1051 \\ 114\,306.8662 \\ 6\,616.0617 \\ 11\,073.1996 \\ 6\,237.4080 \\ 22\,424.3824 \\ 17\,230.4092 \end{pmatrix}$$

Finally, the value of $c(b)$ is equal to:

$$c(b) = 12\,714.3386$$

Using a QP solver, we obtain the following numerical solution:

$$\begin{pmatrix} w_1 \\ w_3 \\ w_4 \\ w_6 \\ w_2 \\ w_5 \\ w_7 \\ w_8 \end{pmatrix} = \begin{pmatrix} 16.9796 \\ 18.2582 \\ 13.4494 \\ 9.4553 \\ 17.2102 \\ 12.1009 \\ 0.0000 \\ 12.5464 \end{pmatrix} \times 10^{-2}$$

We observe some small differences (after the fifth digit) because the QP solver is more efficient than a traditional nonlinear solver.

4. (a) The optimization problem is:

$$\begin{array}{rcl} w^\star & = & \arg\min \mathcal{D}\left(w \mid b\right) \\ & & \text{s.t.} \quad \begin{cases} \mathbf{1}_8^\top w = 1 \\ \boldsymbol{\mathcal{CI}}^\top w \leq \left(1 - \boldsymbol{\mathcal{R}}\right) \boldsymbol{\mathcal{CI}}\left(b\right) \\ \mathbf{0}_8 \leq w \leq \mathbf{1}_8 \end{cases} \end{array}$$

(b) We use the absolute value trick and obtain the following optimization problem:

$$\begin{array}{rcl} w^\star & = & \arg\min \dfrac{1}{2}\varphi_{\text{AS}} \displaystyle\sum_{i=1}^{8} \tau_{i,w} + \varphi_{\text{MD}} \sum_{j=1}^{2} \tau_{j,\text{MD}} + \varphi_{\text{DTS}} \sum_{j=1}^{2} \tau_{j,\text{DTS}} \\ & & \text{s.t.} \quad \begin{cases} \mathbf{1}_8^\top w = 1 \\ \mathbf{0}_8 \leq w \leq \mathbf{1}_8 \\ \boldsymbol{\mathcal{CI}}^\top w \leq \left(1 - \boldsymbol{\mathcal{R}}\right) \boldsymbol{\mathcal{CI}}\left(b\right) \\ \left|w_i - b_i\right| \leq \tau_{i,w} \\ \left|\sum_{i \in \boldsymbol{\mathcal{S}}ector_j} \left(w_i - b_i\right) \text{MD}_i\right| \leq \tau_{j,\text{MD}} \\ \left|\sum_{i \in \boldsymbol{\mathcal{S}}ector_j} \left(w_i - b_i\right) \text{DTS}_i\right| \leq \tau_{j,\text{DTS}} \\ \tau_{i,w} \geq 0, \tau_{j,\text{MD}} \geq 0, \tau_{j,\text{DTS}} \geq 0 \end{cases} \end{array}$$

We can now formulate this problem as a standard LP problem:

$$\begin{array}{rcl} x^\star & = & \arg\min c^\top x \\ & & \text{s.t.} \quad \begin{cases} Ax = B \\ Cx \leq D \\ x^- \leq x \leq x^+ \end{cases} \end{array}$$

where $x$ is the $20 \times 1$ vector defined as follows:

$$x = \begin{pmatrix} w \\ \tau_w \\ \tau_{\text{MD}} \\ \tau_{\text{DTS}} \end{pmatrix}$$

The $20 \times 1$ vector $c$ is equal to:

$$c = \begin{pmatrix} \mathbf{0}_8 \\ \dfrac{1}{2}\varphi_{\text{AS}}\mathbf{1}_8 \\ \varphi_{\text{MD}}\mathbf{1}_2 \\ \varphi_{\text{DTS}}\mathbf{1}_2 \end{pmatrix}$$

The equality constraint is defined by $A = \begin{pmatrix} \mathbf{1}_8^\top & \mathbf{0}_8^\top & \mathbf{0}_2^\top & \mathbf{0}_2^\top \end{pmatrix}$ and $B = 1$. The bounds are $x^- = \mathbf{0}_{20}$ and $x^+ = \infty \cdot \mathbf{1}_{20}$. For the inequality constraint, we have[7]:

$$Cx \leq D \Leftrightarrow \begin{pmatrix} I_8 & -I_8 & \mathbf{0}_{8,2} & \mathbf{0}_{8,2} \\ -I_8 & -I_8 & \mathbf{0}_{8,2} & \mathbf{0}_{8,2} \\ C_{\text{MD}} & \mathbf{0}_{2,8} & -I_2 & \mathbf{0}_{2,2} \\ -C_{\text{MD}} & \mathbf{0}_{2,8} & -I_2 & \mathbf{0}_{2,2} \\ C_{\text{DTS}} & \mathbf{0}_{2,8} & \mathbf{0}_{2,2} & -I_2 \\ -C_{\text{DTS}} & \mathbf{0}_{2,8} & \mathbf{0}_{2,2} & -I_2 \\ \boldsymbol{\mathcal{CI}}^\top & \mathbf{0}_{1,8} & 0 & 0 \end{pmatrix} x \leq \begin{pmatrix} b \\ -b \\ \text{MD}^\star \\ -\text{MD}^\star \\ \text{DTS}^\star \\ -\text{DTS}^\star \\ (1 - \boldsymbol{\mathcal{R}})\,\boldsymbol{\mathcal{CI}}\,(b) \end{pmatrix}$$

where:

$$C_{\text{MD}} = \begin{pmatrix} 3.56 & 0.00 & 6.54 & 10.23 & 0.00 & 2.30 & 0.00 & 0.00 \\ 0.00 & 7.48 & 0.00 & 0.00 & 2.40 & 0.00 & 9.12 & 7.96 \end{pmatrix}$$

and:

$$C_{\text{DTS}} = \begin{pmatrix} 103 & 0 & 75 & 796 & 0 & 45 & 0 & 0 \\ 0 & 155 & 0 & 0 & 89 & 0 & 320 & 245 \end{pmatrix}$$

The $2 \times 1$ vectors $\text{MD}^\star$ and $\text{DTS}^\star$ are respectively equal to $(3.4089, 2.5508)$ and $(142.49, 68.24)$.

(c) We obtain the following solution:

$$\begin{aligned} w^\star &= (18.7360, 15.8657, 17.8575, 13.2589, 11, 9.4622, 0, 13.8196) \times 10^{-2} \\ \tau_w^\star &= (3.2640, 3.1343, 0.8575, 0.2589, 0, 1.4622, 6, 9.8196) \times 10^{-2} \\ \tau_{\text{MD}} &= (0, 0) \\ \tau_{\text{DTS}} &= (0, 0) \end{aligned}$$

In Table B.15, we compare the two solutions[8]. They are very close. In fact, we notice that the LP solution matches perfectly the MD and DTS constraints, but has a higher AS risk $\sigma_{\text{AS}}(w \mid b)$. If we note the two solutions $w^\star(\mathcal{L}_1)$ and $w^\star(\mathcal{L}_2)$, we have:

$$\begin{cases} \mathcal{R}(w^\star(\mathcal{L}_2) \mid b) = 1.4524 < \mathcal{R}(w^\star(\mathcal{L}_1) \mid b) = 1.5584 \\ \mathcal{D}(w^\star(\mathcal{L}_2) \mid b) = 13.9366 > \mathcal{D}(w^\star(\mathcal{L}_1) \mid b) = 12.3982 \end{cases}$$

There is a trade-off between the $\mathcal{L}_1$- and $\mathcal{L}_2$-norm risk measures. This is why we cannot say that one solution dominates the other.

[7] $C$ is a $25 \times 8$ matrix and $D$ is a $25 \times 1$ vector.

[8] The units are the following: % for the weights $w_i$, and the active share metrics $\sigma_{\text{AS}}(w \mid b)$ and $\mathcal{D}_{\text{AS}}(w \mid b)$; years for the modified duration metrics $\text{MD}(w)$, $\sigma_{\text{MD}}(w \mid b)$ and $\mathcal{D}_{\text{MD}}(w \mid b)$; bps for the duration-times-spread metrics $\text{DTS}(w)$, $\sigma_{\text{DTS}}(w \mid b)$ and $\mathcal{D}_{\text{DTS}}(w \mid b)$; $\text{tCO}_2\text{e}/\$$ mn for the carbon intensity $\text{DTS}(w)$.

Table B.15: Solution of the bond optimization problem (scope $\boldsymbol{\mathcal{SC}}_{1-3}$)

| Problem | Benchmark | 3.(e) | 4.(c) |
|---|---|---|---|
| $w_1$ | 22.0000 | 16.9796 | 18.7360 |
| $w_2$ | 19.0000 | 17.2102 | 15.8657 |
| $w_3$ | 17.0000 | 18.2582 | 17.8575 |
| $w_4$ | 13.0000 | 13.4494 | 13.2589 |
| $w_5$ | 11.0000 | 12.1009 | 11.0000 |
| $w_6$ | 8.0000 | 9.4553 | 9.4622 |
| $w_7$ | 6.0000 | 0.0000 | 0.0000 |
| $w_8$ | 4.0000 | 12.5464 | 13.8196 |
| $\mathrm{MD}\,(w)$ | 5.9597 | 5.9683 | 5.9597 |
| $\mathrm{DTS}\,(w)$ | 210.7300 | 210.6791 | 210.7300 |
| $\sigma_{\mathrm{AS}}\,(w \mid b)$ | 0.0000 | 11.9400 | 12.4837 |
| $\sigma_{\mathrm{MD}}\,(w \mid b)$ | 0.0000 | 0.0308 | 0.0000 |
| $\sigma_{\mathrm{DTS}}\,(w \mid b)$ | 0.0000 | 0.0561 | 0.0000 |
| $\mathcal{D}_{\mathrm{AS}}\,(w \mid b)$ | 0.0000 | 25.6203 | 24.7964 |
| $\mathcal{D}_{\mathrm{MD}}\,(w \mid b)$ | 0.0000 | 0.0426 | 0.0000 |
| $\mathcal{D}_{\mathrm{DTS}}\,(w \mid b)$ | 0.0000 | 0.0608 | 0.0000 |
| $\boldsymbol{\mathcal{CI}}\,(w)$ | 76.9427 | 38.4713 | 38.4713 |

# Bibliography


Aboumahboub T, Auer C, Bauer N, ..., and Ueckerdt F (2020). *REMIND — REgional Model of INvestments and Development*. Technical Documentation, Version 2.1.0.

Abrams, P. A. (2009). When Does Greater Mortality Increase Population Size? The Long History and Diverse Mechanisms underlying the Hydra Effect. *Ecology Letters*, 12(5), pp. 462-474.

Admati, A. R., and Pfleiderer, P. (2009). The "Wall Street Walk" and Shareholder Activism: Exit as a Form of Voice. *Review of Financial Studies*, 22(7), pp. 2645-2685.

Agrawal, A., and Hockerts, K. (2021). Impact Investing: Review and Research Agenda. *Journal of Small Business & Entrepreneurship*, 33(2), pp. 153-181.

Aizen, M. A., Aguiar, S., Biesmeijer, J. C., ..., and Seymour, C. L. (2019). Global Agricultural Productivity is Threatened by Increasing Pollinator Dependence without a Parallel Increase in Crop Diversification. *Global change biology*, 25(10), pp. 3516-3527.

Aizen, M. A., Garibaldi, L. A., Cunningham, S. A., and Klein, A. M. (2009). How Much Does Agriculture Depend on Pollinators? Lessons from Long-term Trends in Crop Production. *Annals of Botany*, 103(9), pp. 1579-1588.

Åkerman, M. (2003). What Does 'Natural Capital' Do? The Role of Metaphor in Economic Understanding of the Environment. *Environmental Values*, 12(4), pp. 431-448.

Albuquerque, R., Koskinen, Y., and Zhang, C. (2019). Corporate Social Responsibility and Firm Risk: Theory and Empirical Evidence. *Management Science*, 65(10), pp. 4451-4469.

Alesina, A., Özler, S., Roubini, N., and Swagel, P. (1996). Political Instability and Economic Growth. *Journal of Economic Growth*, 1, pp. 189-211.

Alessi, L., and Battiston, S. (2022). Two Sides of the Same Coin: Green Taxonomy Alignment versus Transition Risk in Financial Portfolios. *International Review of Financial Analysis*, 102319.

Algeo, T. J., and Shen, J. (2024). Theory and Classification of Mass Extinction Causation. *National Science Review*, 11, nwad237, 21 pages.

Alkemade, R., Van Oorschot, M., Miles, L., Nellemann, C., Bakkenes, M., and Ten Brink, B. (2009). GLOBIO3: A Framework to Investigate Options for Reducing Global Terrestrial Biodiversity Loss. *Ecosystems*, 12, pp. 374-390.

Allen, M., Axelsson, K., Caldecott, B., Hale, T., Hepburn, C., Hickey, C., Mitchell-Larson, E., Malhi, Y., Otto, F., Seddon, N., and Smith, S. (2020). The Oxford Principles for Net Zero Aligned Carbon Offsetting. *Report*, September, 13 pages.

Alley, R. B., Anandakrishnan, S., Christianson, K., Horgan, H. J., Muto, A., Parizek, B. R., Pollard, D., and Walker, R. T. (2015). Oceanic Forcing of Ice-Sheet Retreat: West Antarctica and More. *Annual Review of Earth and Planetary Sciences*, 43, pp. 207-231.

Almond, R. E. A., Grooten, M., Juffe Bignoli, D., and Petersen, T. (Eds) (2022). Living Planet Report 2022 — Building a Nature-positive Society. *Report*, WWF.

Altman, E. I. (1968). Financial Ratios, Discriminant Analysis and the Prediction of Corporate Bankruptcy. *Journal of Finance*, 23(4), pp. 589-609.

Anderson, S. J., Kubiszewski, I., and Sutton, P. C. (2024). The Ecological Economics of Light Pollution: Impacts on Ecosystem Service Value. *Remote Sensing*, 16(14), 2591, 11 pages.

Andersson, M., Bolton, P., and Samama, F. (2016). Hedging Climate Risk. *Financial Analysts Journal*, 72(3), pp. 13-32.

Anthoff, D., and Tol, R. S. J. (2014). *The Climate Framework for Uncertainty, Negotiation and Distribution (Fund)*. Technical Description, Version 3.9.

Antràs, P., Chor, D., Fally, T., and Hillberry, R. (2012). Measuring the Upstreamness of Production and Trade Flows. *American Economic Review*, 102(3), pp. 412-416.

Apergis, N., Poufinas, T., and Antonopoulos, A. (2022). ESG Scores and Cost of Debt. *Energy Economics*, 112, 106186.

Appel, I. R., Gormley, T. A., and Keim, D. B. (2016). Passive Investors, Not Passive Owners. *Journal of Financial Economics*, 121(1), pp. 111-141.

Archer, D., and Pierrehumbert, R. (Eds) (2011). *The Warming Papers: The Scientific Foundation for the Climate Change Forecast*. John Wiley & Sons.

Arditi, R., and Ginzburg, L. R. (1989). Coupling in Predator-prey Dynamics: Ratio-dependence. *Journal of Theoretical Biology*, 139(3), pp. 311-326.

Arlidge, W. N. S., Bull, J. W., Addison, P. F. E., ..., and Milner-Gulland, E. J. (2018). A Global Mitigation Hierarchy for Nature Conservation. *BioScience*, 68(5), pp. 336-347.

Armstrong, R. A., and McGehee, R. (1980). Competitive Exclusion. *American Naturalist*, 115(2), pp. 151-170.

Armstrong McKay, D. I., Staal, A., Abrams, J. F., ..., and Lenton, T. M. (2022). Exceeding 1.5°C Global Warming Could Trigger Multiple Climate Tipping Points. *Science*, 377(6611), eabn7950, 11 pages.

Arrhenius, S. (1896). On the Influence of Carbonic Acid in the Air upon the Temperature of the Ground. *The London, Edinburgh, and Dublin Philosophical Magazine and Journal of Science*, 41(251), pp. 237-276.

Arrhenius, S. (1908). *Worlds in the Making: The Evolution of the Universe*. Harper.

Arrhenius, O. (1921). Species and Area. *Journal of Ecology*, 9(1), pp. 95-99.

Attig, N., El Ghoul, S., Guedhami, O., and Suh, J. (2013). Corporate Social Responsibility and Credit Ratings. *Journal of Business Ethics*, 117, pp. 679-694.

Attridge, S., and Engen, L. (2019). Blended Finance in the Poorest Countries: The Need for a Better Approach. *ODI Report*, Overseas Development Institute, April, 76 pages.

Atz, U., Van Holt, T., Liu, Z. Z., and Bruno, C. C. (2022). Does Sustainability Generate Better Financial Performance? Review, Meta-analysis, and Propositions. *Journal of Sustainable Finance & Investment*, 13(1), pp. 802-825.

Autorité de Contrôle Prudentiel et de Résolution (2021). A First Assessment of Financial Risks Stemming from Climate Change: The Main Results of the 2020 Climate Pilot Exercise. *Analyses et synthèses*, 122-2021, 4 May 2021.

Avramov, D., Cheng, S., Lioui, A., and Tarelli, A. (2022). Sustainable Investing with ESG Rating Uncertainty. *Journal of Financial Economics*, 145(2), pp. 642-664.

Azar, J., Duro, M., Kadach, I., and Ormazabal, G. (2021). The Big Three and Corporate Carbon Emissions around the World. *Journal of Financial Economics*, 142(2), pp. 674-696.

Bailon, M., Bor, A. M., and Redín, J. G. (2024). *Biodiversity Measurement Approaches — A Practitioner's Guide for Financial Institutions*. November, 86 pages.

Baker, M., Bergstresser, D., Serafeim, G., and Wurgler, J. (2022). The Pricing and Ownership of US Green Bonds, *Annual Review of Financial Economics*, 14, pp. 415-437.

Balitzky, S., and Mosson, N. (2024). Impact Investing — Do SDG Funds Fulfil their Promises?. *ESMA TRV Risk Analysis*, February, 17 pages.

Bambach, R. K. (2006). Phanerozoic Biodiversity Mass Extinctions. *Annual Review of Earth Planetary Sciences*, 34(1), pp. 127-155.

Bandeira, B., Jamet, J.-L., Jamet, D., and Ginoux, J.-M. (2013). Mathematical Convergences of Biodiversity Indices. *Ecological Indicators*, 29, pp. 522-528.

Bank of England (2022). Results of the 2021 Climate Biennial Exploratory Scenario (CBES). *Report*, 24 May 2022.

Barahhou, I., Ben Slimane, M., Oulid Azouz, N., and Roncalli, T. (2022). Net Zero Investment Portfolios — Part 1. The Comprehensive Integrated Approach. *SSRN*, 4283998.

Barahhou, I., Ferreira, P., and Maalej, Y. (2023). A Framework to Align Sovereign Bond Portfolios with Net Zero Trajectories. *SSRN*, 4515462.

Barber, B. M., Morse, A., and Yasuda, A. (2021). Impact Investing. *Journal of Financial Economics*, 139(1), pp. 162-185.

Barko, T., Cremers, M., and Renneboog, L. (2022). Shareholder Engagement on Environmental, Social, and Governance Performance. *Journal of Business Ethics*, 180(2), pp. 777-812.

Barlow, J., Lennox, G. D., Ferreira, J., ..., and Gardner, T. A. (2016). Anthropogenic Disturbance in Tropical Forests Can Double Biodiversity Loss from Deforestation. *Nature*, 535(7610), pp. 144-147.

Barnett, M. L., and Salomon, R. M. (2006). Beyond Dichotomy: The Curvilinear Relationship between Social Responsibility and Financial Performance. *Strategic Management Journal*, 27(11), pp. 1101-1122.

Barnosky, A. D., Matzke, N., Tomiya, S., ..., and Ferrer, E. A. (2011). Has the Earth's Sixth Mass Extinction Already Arrived?. *Nature*, 471, pp. 51-57.

Basel Committee on Banking Supervision (2022). Principles for the Effective Management and Supervision of Climate-related Financial Risks. *Guidelines*, 15 June 2022, 15 pages.

Basel Committee on Banking Supervision (2023). Disclosure of Climate-related Financial Risks. *Consultative Document*, 29 November 2023, 38 pages.

Bathiany, S., Notz, D., Mauritsen, T., Raedel, G., and Brovkin, V. (2016). On the Potential for Abrupt Arctic Winter Sea Ice Loss. *Journal of Climate*, 29(7), pp. 2703-2719.

Batista, M., and Karawia, A. (2009). The Use of the Sherman-Morrison-Woodbury Formula to Solve Cyclic Block Tri-diagonal and Cyclic Block Penta-diagonal Linear Systems of Equations. *Applied Mathematics and Computation*, 210(2), pp. 558-563.

Bauer, R., and Hann, D. (2010). Corporate Environmental Management and Credit Risk. *SSRN*, 1660470.

Bauer, R., Koedijk, K., and Otten, R. (2005). International Evidence on Ethical Mutual Fund Performance and Investment Style. *Journal of Banking & Finance*, 29(7), pp. 1751-1767.

Beabout, G. R., and Schmiesing, K. E. (2003). Socially Responsible Investing: An Application of Catholic Social Thought. *Logos: A Journal of Catholic Thought and Culture*, 6(1), pp. 63-99.

Beaugrand, G., Kléparski, L., Luczak, C., Goberville, E., and Kirby, R. R. (2024). A Niche-based Theory of Island Biogeography. *Ecology and Evolution*, 14(6), e11540, 14 pages.

Bebchuk, L. A., and Hirst, S. (2019). The Specter of the Giant Three. *NBER*, 25914.

Becker, M. G., Martin, F., and Walter, A. (2022). The Power of ESG Transparency: The Effect of the New SFDR Sustainability Labels on Mutual Funds and Individual Investors. *Finance Research Letters*, 47 (Part B), 102708.

Begon, M., & Townsend, C. R. (2021). *Ecology: From Individuals to Ecosystems*. Fifth edition, John Wiley & Sons, 864 pages.

Bekjarovski, F., and Brière, M. (2018). Shareholder Activism: Why Should Investors Care?. *Amundi Discussion Paper*, 30.

Ben Dor, A., Guan, J., Kelleher, A., Lauretig, A., Preclaw, R., and Zeng, X. (2022). ESG and Alternative Data: Capturing Corporates' Sustainability-Related Activities with Job Postings. *Journal of Financial Data Science*, 4(1), pp. 130-144.

Ben Slimane, M. (2021). Bond Index Tracking with Genetic Algorithms. *ResearchGate*, 350756323.

Ben Slimane, M., Brard, E., Le Guenedal, T., Roncalli, T., and Sekine, T. (2019a). ESG Investing in Fixed Income: It's Time to Cross the Rubicon. *SSRN*, 3683477.

Ben Slimane, M., Da Fonseca, D., and Mahtani, V. (2020). Facts and Fantasies about the Green Bond Premium. *ResearchGate*, 348650560.

Ben Slimane, M., and De Jong, M. (2017). Bond Liquidity Scores. *Journal of Fixed Income*, 27(1), pp. 77-82.

Ben Slimane, M., Le Guenedal, T., Roncalli, T., and Sekine, T. (2019b). ESG Investing in Corporate Bonds: Mind the Gap. *SSRN*, 3683472.

Ben Slimane, M., Lucius, D., Roncalli, T., and Xu, J. (2023b). Net Zero Investment Portfolios — Part 2. The Core-Satellite Approach. *SSRN*, 4611418.

Ben Slimane, M., Roncalli, T., and Semet, R. (2023a). Green vs. Social Bond Premium. *SSRN*, 4448651.

Ben Slimane, M., and Menchaoui, G. (2023). Bond Portfolio Optimisation and Mixed Integer Programming. *ResearchGate*, 376687891.

Bengis, R. G., Leighton, F. A., Fischer, J. R., Artois, M., Mörner, T., and Tate, C. M. (2004). The Role of Wildlife in Emerging and Re-emerging Zoonoses. *Revue Scientifique et Technique (International Office of Epizootics)*, 23(2), pp. 497-512.

Bennani, L., Le Guenedal, T., Lepetit, F., Ly, L., Mortier, V., Roncalli, T., and Sekine, T. (2018). How ESG Investing Has Impacted the Asset Pricing in the Equity Market. *SSRN*, 3316862.

Benton, M. J. (1995). Diversification and extinction in the history of life. *Science*, 268(5207), pp. 52-58.

Benton, M. J. (2015). *When Life Nearly Died: The Greatest Mass Extinction of All Time*. Thames & Hudson, 336 pages.

Berg, F., Kölbel, J. F., and Rigobon, R. (2022). Aggregate Confusion: The Divergence of ESG Ratings. *Review of Finance*, 26(6), pp. 1315-1344.

Berger, L., Speare, R., Daszak, P., ..., and Parkes, H. (1998). Chytridiomycosis Causes Amphibian Mortality Associated with Population Declines in the Rain Forests of Australia and Central America. *Proceedings of the National Academy of Sciences*, 95(15), pp. 9031-9036.

Berk, J., and Van Binsbergen, J. H. (2024). The Impact of Impact Investing. *Journal of Financial Economics*, forthcoming.

Bernard, J., Boiral, O., Guillaumie, L., and Brotherton, M. C. (2023). Does Proxy Voting Really Promote Corporate Sustainability?. *Corporate Governance: An International Review*, 31(3), pp. 445-463.

Bernstein, A. S., Ando, A. W., Loch-Temzelides, T., ..., and Dobson, A. P. (2022). The Costs and Benefits of Primary Prevention of Zoonotic Pandemics. *Science Advances*, 8(5), eabl4183, 13 pages.

Berrada, T., Engelhardt, L., Gibson, R., and Krueger, P. (2022). The Economics of Sustainability Linked Bonds. *Swiss Finance Institute Research Paper*, 22-26.

Betts, M. G., Wolf, C., Ripple, W. J., ..., and Levi, T. (2017). Global Forest Loss Disproportionately Erodes Biodiversity in Intact Landscapes. *Nature*, 547(7664), pp. 441-444.

Bicknell, J. E., Struebig, M. J., and Davies, Z. G. (2015). Reconciling Timber Extraction with Biodiversity Conservation in Tropical Forests using Reduced-impact Logging. *Journal of Applied Ecology*, 52(2), pp. 379-388.

Billio, M., Costola, M., Hristova, I., Latino, C., and Pelizzon, L. (2021). Inside the ESG Ratings: (Dis)agreement and Performance. *Corporate Social Responsibility and Environmental Management*, 28(5), pp. 1426-1445.

Bingler, J. A., Kraus, M., Leippold, M., and Webersinke, N. (2022). Cheap Talk and Cherry-Picking: What ClimateBert has to Say on Corporate Climate Risk Disclosures. *Finance Research Letters*, 47(B), 102776, June.

Black, F. (1972). Capital Market Equilibrium with Restricted Borrowing. *Journal of Business*, 45(3), pp. 444-455.

Black, F. and Litterman, R. B. (1991). Asset Allocation: Combining Investor Views with Market Equilibrium. *Journal of Fixed Income*, 1(2), pp. 7-18.

Black, F. and Litterman, R. B. (1992). Global Portfolio Optimization. *Financial Analysts Journal*, 48(5), pp. 28-43.

Blehert, D. S., Hicks, A. C., Behr, M., ..., and Stone, W. B. (2009). Bat White-Nose Syndrome: An Emerging Fungal Pathogen?. *Science*, 323(5911), pp. 227.

Board of Governors of the Federal Reserve System (2011). Supervisory Guidance of Model Risk Management. Joint Publication with the Office of the Comptroller of the Currency. *Supervision and Regulation Letters*, SR 11-7, April.

Board of Governors of the Federal Reserve System (2021). Interagency Statement on Model Risk Management for Bank Systems Supporting Bank Secrecy Act/Anti-Money Laundering Compliance. Joint Publication with the Federal Deposit Insurance Corporation andthe Office of the Comptroller of the Currency. *Interagency Statement*, April.

Bobbink, R., Hicks, K., Galloway, J., ..., and De Vries, W. (2010). Global Assessment of Nitrogen Deposition Effects on Terrestrial Plant Diversity: A Synthesis. *Ecological Applications*, 20(1), pp. 30-59.

Boffo, R., and Patalano, R. (2020). ESG Investing: Practices, Progress and Challenges. *Report*, OECD Paris.

Böhringer, C. (2003). The Kyoto Protocol: A Review and Perspectives. *Oxford Review of Economic Policy*, 19(3), pp. 451-466.

Bolin, B., and Eriksson, E. (1958). Changes in the Carbon Dioxide Content of the Atmosphere and Sea due to Fossil Fuel Combustion. In Bolin, B. (Ed.), *The Atmosphere and the Sea in Motion: Scientific Contributions to the Rossby Memorial Volume*, Rockefeller Institute Press, pp. 130-142.

Bolton, P., and Kacperczyk, M. (2021). Do Investors Care about Carbon Risk?. *Journal of Financial Economics*, 142(2), pp. 517-549.

Bolton, P., Kacperczyk, M., and Samama, F. (2022). Net-zero Carbon Portfolio Alignment. *Financial Analysts Journal*, 78(2), pp. 19-33.

Bolton, P., Musca, X., and Samama, F. (2020). Global Public-Private Investment Partnerships: A Financing Innovation with Positive Social Impact. *Journal of Applied Corporate Finance*, 32(2), pp. 31-41.

Bosetti, V., Carraro, C., Galeotti, M., Massetti, E., and Tavoni, M. (2006). A World Induced Technical Change Hybrid Model. *Energy Journal*, 27, Special Issue #2, pp. 13-37.

Bosmans, P., and de Mariz, F. (2023). The Blue Bond Market: A Catalyst for Ocean and Water Financing. *Journal of Risk and Financial Management*, 16(3), 184, 48 pages.

Boston Consulting Group (2023a). The Voluntary Carbon Market: 2022 Insights and Trends. *Report*, January, 21 pages.

Boston Consulting Group (2023b). Sustainability in Private Equity, 2023. *Report*, October, 32 pages.

Bouyé, E., and Menville, D. (2021). The Convergence of Sovereign Environmental, Social and Governance Ratings. *Policy Research Working Paper*, World Bank, 9583.

Bowen, H. R. (1953). *Social Responsibilities of the Businessman.* Harper & Row.

Bowker, G. C. (2000). Biodiversity Datadiversity. *Social Studies of Science*, 30(5), pp. 643-683.

Boyd, S., Parikh, N., Chu, E., Peleato, B., and Eckstein, J. (2010). Distributed Optimization and Statistical Learning via the Alternating Direction Method of Multipliers. *Foundations and Trends® in Machine learning*, 3(1), pp. 1-122.

Brander, M., Ascui, F., Scott, V., and Tett, S. (2021). Carbon Accounting for Negative Emissions Technologies. *Climate Policy*, 21(5), pp. 699-717.

Breidert, C. (2006). *Estimation of Willingness-to-pay: Theory, Measurement, Application.* Springer.

Brière, M., Keip, M., and Le Berthe, T. (2022). Artificial Intelligence for Sustainable Finance: Why it may Help. *Amundi Institute Research Paper*, October 2022.

Brière, M., Pouget, S., and Ureche-Rangau, L. (2020). BlackRock vs Norway Fund at Shareholder Meetings: Institutional Investors' Votes on Corporate Externalities. In Bank for International Settlements (Ed.), *Evolving Practices in Public Investment Management*, Proceedings of the Seventh Public Investors Conference, pp. 81-108.

Brière, M., and Ramelli, S. (2021). Green Sentiment, Stock Returns, and Corporate Behavior. *SSRN*, 3850923.

Brito-Ramos, S., Cortez, M. C., and Silva, F. (2024a). Do Sustainability Signals Diverge? An Analysis of Labeling Schemes for Socially Responsible Investments. *Business & Society*, forthcoming.

Brito-Ramos, S., Cortez, M. C., Covachev, S., and Silva, F. (2024b). In Labels we Trust? The Influence of Sustainability Labels in Mutual Fund Flows. *SSRN*, 4748816.

Broccardo, E., Hart, O. D., and Zingales, L. (2022). Exit versus Voice. *Journal of Political Economy*, 130(12), pp. 3101-3145.

Broecker, W. S. (1975). Climatic Change: Are we on the Brink of a Pronounced Global Warming?. *Science*, 189(4201), pp. 460-463.

Brown, J. H. (1999). The Legacy of Robert MacArthur: From Geographical Ecology to Macroecology. *Journal of Mammalogy*, 80(2), pp. 333-344.

Brummitt, C. D., Barnett, G., and D'Souza, R. M. (2015). Coupled Catastrophes: Sudden Shifts Cascade and Hop among Interdependent Systems. *Journal of The Royal Society Interface*, 12(112), 20150712, 12 pages.

Budyko, M. I. (1969). The Effect of Solar Radiation Variations on the Climate of the Earth. *Tellus*, 21(5), pp. 611-619.

Bugg-Levine, A., and Emerson, J. (2011). *Impact Investing: Transforming How We Make Money While Making a Difference*. John Wiley & Sons, 310 pages.

Burivalova, Z., Purnomo, Orndorff, S., Truskinger, A., Roe, P., and Game, E. T. (2021). The Sound of Logging: Tropical Forest Soundscape Before, During, and After Selective Timber Extraction. *Biological Conservation*, 254, 108812, 6 pages.

Burke, M., Driscoll, A., Lobell, D. B., and Ermon, S. (2021). Using Satellite Imagery to Understand and Promote Sustainable Development. *Science*, 371(6535), March.

Busch, T., Bruce-Clark, P., Derwall, J., Eccles, R., Hebb, T., Hoepner, A., Klein, C., Krueger, P., Paetzold, F., Scholtens, B. and Weber, O. (2021). Impact Investments: A Call for (Re)Orientation. *SN Business & Economics*, 1, pp. 1-13.

Busch, T., Pruessner, E., Oulton, W., Palinska, A., and Garrault, P. (2024). Methodology for Eurosif Market Studies on Sustainability-related Investments. *Eurosif Report*, February, 30 pages.

Butchart, S. H. M., Resit Akçakaya, H., Chanson, J., ..., and Hilton-Taylor, C. (2007). Improvements to the Red List Index. *PloS One*, 2(1), e140.

Calabrese, E. J., and Mattson, M. P. (2017). How Does Hormesis Impact Biology, Toxicology, and Medicine?. *npj Aging and Mechanisms of Disease*, 3(13), 8 pages.

Calel, R., and Stainforth, D. A. (2017a). On the Physics of Three Integrated Assessment Models. *Bulletin of the American Meteorological Society*, 98(6), pp. 1199-1216.

Calel, R., and Stainforth, D. A. (2017b). On the Physics of Three Integrated Assessment Models: Supplement. *Internet Supplementary Materials*, https://doi.org/10.1175/BAMS-D-16-0034.1.

Callendar, G. S. (1938). The Artificial Production of Carbon Dioxide and its Influence on Temperature. *Quarterly Journal of the Royal Meteorological Society*, 64(275), pp. 223-240.

Calvin, K., Patel, P., Clarke, L., ..., and Wise, M. (2019). GCAM v5.1: Representing the Linkages between Energy, Water, Land, Climate, and Economic Systems. *Geoscientific Model Development*, 12, 677-698.

Capelle-Blancard, G., Crifo, P., Diaye, M. A., Scholtens, B., and Oueghlissi, R. (2019). Sovereign Bond Yield Spreads and Sustainability: An Empirical Analysis of OECD Countries. *Journal of Banking & Finance*, 98, pp. 156-169.

Capelle-Blancard, G., and Monjon, S. (2014). The Performance of Socially Responsible Funds: Does the Screening Process Matter?. *European Financial Management*, 20(3), pp. 494-520.

Carbone, L., Nergadze, S. G., Magnani, E., ..., and Giulotto, E. (2006). Evolutionary Movement of Centromeres in Horse, Donkey, and Zebra. *Genomics*, 87(6), pp. 777-782.

Cardinale, B. J., Duffy, J. E., Gonzalez, A., ..., and Naeem, S. (2012). Biodiversity Loss and its Impact on Humanity. *Nature*, 486(7401), pp. 59-67.

Carey, M. (2010). *In the Shadow of Melting Glaciers: Climate Change and Andean Society*. Oxford University Press.

Carney, M. (2015). Breaking the Tragedy of the Horizon — Climate Change and Financial Stability. *Speech given at Lloyd's of London*, 29 September 2015.

Carney, M. (2019). Fifty Shades of Green. *Finance and Development*, 56(4), pp. 12-15.

Carroll, A. B. (1999). Corporate Social Responsibility: Evolution of a Definitional Construct. *Business & Society*, 38(3), pp. 268-295.

Carroll, A. B., and Shabana, K. M. (2010). The Business Case for Corporate Social Responsibility: A Review of Concepts, Research and Practice. *International Journal of Management Reviews*, 12(1), pp. 85-105.

Carson, R. (1962). *Silent Spring*. Houghton Mifflin Harcourt Publishing Company.

Case, T. J., and Gilpin, M. E. (1974). Interference Competition and Niche Theory. *Proceedings of the National Academy of Sciences*, 71(8), pp. 3073-3077.

Catling, D. C., and Zahnle, K. J. (2020). The Archean Atmosphere. *Science Advances*, 6(9), eaax1420, pp. 1-16.

Cawthorn, D. M., and Hoffman, L. C. (2015). The Bushmeat and Food Security Nexus: A Global Account of the Contributions, Conundrums and Ethical Collisions. *Food Research International*, 76, pp. 906-925.

Cazzolla Gatti, R., Reich, P. B., Gamarra, J. G. P., ..., and Liang, J. (2022). The Number of Tree Species on Earth. *Proceedings of the National Academy of Sciences*, 119(6), e2115329119, 11 pages.

CDP (2022). Accounting of Scope 2 Emissions — CDP Climate Change Questionnaire. *Technical Note*, Version 9.0, March.

Ceballos, G., Ehrlich, P. R., Barnosky, A. D., García, A., Pringle, R. M., and Palmer, T. M. (2015). Accelerated Modern Human-induced Species Losses: Entering the Sixth Mass Extinction. *Science Advances*, 1(5), e1400253, 5 pages.

Ceballos, G., Ehrlich, P. R., and Dirzo, R. (2017). Biological Annihilation via the Ongoing Sixth Mass Extinction Signaled by Vertebrate Population Losses and Declines. *Proceedings of the National Academy of Sciences*, 114(30), pp. E6089-E6096.

Cedergreen, N., Ritz, C., and Streibig, J. C. (2005). Improved Empirical Models Describing Hormesis. *Environmental Toxicology and Chemistry: An International Journal*, 24(12), pp. 3166-3172.

Chaber, A. L., Moloney, G. K., Renault, V., ..., and Gaubert, P. (2023). Examining the International Bushmeat Traffic in Belgium: A Threat to Conservation and Public Health. *One Health*, 17, 100605, 8 pages.

Chafik, L., Holliday, N. P., Bacon, S., and Rossby, T. (2022). Irminger Sea is the Center of Action for Subpolar AMOC Variability. *Geophysical Research Letters*, 49(17), e2022GL099133, 11 pages.

Chambers, D., Dimson, E., and Quigley, E. (2020). To Divest or to Engage? A Case Study of Investor Responses to Climate Activism. *Journal of Investing*, 29(2), pp. 10-20.

Chao, A. (1984). Nonparametric Estimation of the Number of Classes in a Population. *Scandinavian Journal of Statistics*, 11(4), pp. 265-270.

Chao, A. (1987). Estimating the Population Size for Capture-Recapture Data with Unequal Catchability. *Biometrics*, 43(4), pp. 783-791.

Charnay, B., Wolf, E. T., Marty, B., and Forget, F. (2020). Is the Faint Young Sun Problem for Earth Solved?. *Space Science Reviews*, 216(90), pp. 1-29.

Charney, J. G., Arakawa, A., Baker, D. J., Bolin, B., Dickinson, R. E., Goody, R. M., Leith, C. E., Stommel, H. M., and Wunsch, C. I. (1979). *Carbon Dioxide and Climate: A Scientific Assessment*. US National Academy of Sciences, 22 pages.

Charney, J. G., Fjörtoft, R., and von Neumann, J. (1950). Numerical Integration of the Barotropic Vorticity Equation. *Tellus*, 2(4), pp. 237-254.

Chatterji, A. K., Durand, R., Levine, D. I., and Touboul, S. (2016). Do Ratings of Firms Converge? Implications for Managers, Investors and Strategy Researchers. *Strategic Management Journal*, 37(8), pp. 1597-1614.

Chazdon, R. L., Brancalion, P. H. S., Laestadius, L., ..., and Wilson, S. J. (2016). When is a Forest a Forest? Forest Concepts and Definitions in the Era of Forest and Landscape Restoration. *Ambio*, 45(5), pp. 538-550.

Chen, T., Dong, H., and Lin, C. (2020). Institutional Shareholders and Corporate Social Responsibility. *Journal of Financial Economics*, 135(2), pp. 483-504.

Chen, Z., Van Khoa, L. D., Teoh, E. N., Nazir, A., Karuppiah, E. K., and Lam, K. S. (2018). Machine Learning Techniques for Anti-money Laundering (AML) Solutions in Suspicious Transaction Detection: A Review. *Knowledge and Information Systems*, 57(2), pp. 245-285.

Cherief, A., Sekine, T., and Stagnol, L. (2025). A Novel Nature-based Risk Index: Application to Acute Risks and their Financial Materiality on Corporate Bonds. *Ecological Economics*, 228, 108427, 10 pages.

Chertow, M. R. (2000). The IPAT Equation and its Variants. *Journal of Industrial Ecology*, 4(4), pp. 13-29.

Chesson, P. (1990). MacArthur's Consumer-Resource Model. *Theoretical Population Biology*, 37(1), pp. 26-38.

Chesson, P. (2000). Mechanisms of Maintenance of Species Diversity. *Annual Review of Ecology and Systematics*, 31(1), pp. 343-366.

Chiappini, H., Marinelli, N., Jalal, R. N., and Birindelli, G. (2023). Past, Present and Future of Impact Investing and Closely Related Financial Vehicles: A Literature Review. *Sustainability Accounting, Management and Policy Journal*, 14(7), pp. 232-257.

Chin, L., Cojoianu, T., Hoepner, A., Moreno, D., Patil, R., and Vu, A. (2023). NZAOA Evidence on the Paris Alignment of Members' Disclosure, Proxy Voting, and Fossil Fuel Bond Investing. *Climate Votes Report*, January, 114 pages.

Chiquier, S., Patrizio, P., Bui, M., Sunny, N., and Mac Dowell, N. (2022). A Comparative Analysis of the Efficiency, Timing, and Permanence of $CO_2$ Removal Pathways. *Energy & Environmental Science*, 15(10), pp. 4389-4403.

Chowdhry, B., Davies, S. W., and Waters, B. (2019). Investing For Impact. *Review of Financial Studies*, 32(3), pp. 864-904.

Clark, C. M., and Tilman, D. (2008). Loss of Plant Species After Chronic Low-level Nitrogen Deposition to Prairie Grasslands. *Nature*, 451(7179), pp. 712-715.

Claus, J., and Thomas, J. (2001). Equity Premia as Low as Three Percent? Evidence from Analysts' Earnings Forecasts for Domestic and International Stock Markets. *Journal of Finance*, 56(5), pp. 1629-1666.

Climate Bonds Initiative (2019). Climate Bonds Standard Version 3.0. *Guidelines*, December, 34 pages.

Climate Bonds Initiative (2022). Sustainable Debt — Global State of the Market 2021. *Report*, April, 38 pages.

Climate Bonds Initiative (2023). Sustainable Debt — Global State of the Market 2022. *Report*, April, 32 pages.

Climate Bonds Initiative (2024b). Climate Bonds Standard Version 4.1. *Guidelines*, February, 71 pages.

Climate Bonds Initiative (2024b). Sustainability-Linked Bonds: Building a High-Quality Market. *Report*, March, 36 pages.

Climate Bonds Initiative (2024c). Sustainable Debt — Global State of the Market 2023. *Report*, May, 30 pages.

Climate Disclosure Standards Board (2021a). Application Guidance for Water-related Disclosures. *CDSB Framework*, August 2021.

Climate Disclosure Standards Board (2021b). Application Guidance for Biodiversity-related Disclosures. *CDSB Framework*, November 2021.

Climate Disclosure Standards Board (2021c). TCFD Good Practice Handbook. *Report*, November 2021.

Cline, W. R. (1992). *The Economics of Global Warming*. Institute for International Economics.

Cohen, A. J., Brauer, M., Burnett, R., ..., and Forouzanfar, M. H. (2017). Estimates and 25-year Trends of the Global Burden of Disease Attributable to Ambient Air Pollution: An Analysis of Data from the Global Burden of Diseases Study 2015. *The Lancet*, 389(10082), pp. 1907-1918.

Cointe, B., and Guillemot, H. (2023). A History of the 1.5°C Target. *WIREs Climate Change*, 14(3), e824, 11 pages.

Cojoianu, T., Hoepner, A., Lin, Y., Van der Merve, K., and Vu, A. (2021). NZAOA Climate Voting Transparency and Benchmarking Report. *Climate Votes Report*, December, 75 pages.

Coleman, B. D. (1981). On Random Placement and Species-Area Relations. *Mathematical Biosciences*, 54(3-4), pp. 191-215.

Colman, R., and Soden, B. J. (2021). Water Vapor and Lapse Rate Feedbacks in the Climate System. *Reviews of Modern Physics*, 93(4), 045002, 90 pages.

Colwell, R. K., and Coddington, J. A. (1994). Estimating Terrestrial Biodiversity Through Extrapolation. *Philosophical Transactions of the Royal Society of London Series B: Biological Sciences*, 345(1311), pp. 101-118.

Colwell, R. K., Mao, C. X., and Chang, J. (2004). Interpolating, Extrapolating, and Comparing Incidence-based Species Accumulation Curves. *Ecology*, 85(10), pp. 2717-2727.

Commissariat Général au Développement Durable (2020). L'empreinte carbone des Français reste stable. *Report*, 4 pages, January.

Condit, R., Pitman, N., Leigh Jr, E. G., ..., and Hubbell, S. P. (2002). Beta-Diversity in Tropical Forest Trees. *Science*, 295(5555), pp. 666-669.

Connor, E. F., and McCoy, E. D. (1979). The Statistics and Biology of the Species-Area Relationship. *The American Naturalist*, 113(6), pp. 791-833.

Convention on Biological Diversity (2022). *15/4 Kunming-Montreal Global Biodiversity Framework*. Conference of the Parties, 16 pages.

Convergence (2024). State of Blended Finance 2024. *Report*, April, 93 pages.

Cooper, E. W., and Uzun, H. (2015). Corporate Social Responsibility and the Cost of Debt. *Journal of Accounting & Finance*, 15(8), pp. 11-29.

Coppola, D., Lauritano, C., Palma Esposito, F., Riccio, G., Rizzo, C., and de Pascale, D. (2021). Fish Waste: From Problem to Valuable Resource. *Marine Drugs*, 19(2), 116, 39 pages.

Coqueret, G. (2022). *Perspectives in Sustainable Equity Investing*. CRC Press.

Cortez, M. C., Silva, F., and Areal, N. (2009). The Performance of European Socially Responsible Funds. *Journal of Business Ethics*, 87(4), pp. 573-588.

Costanza, R., D'Arge, R., De Groot, R., ..., and Van den Belt, M. (1997). The Value of the World's Ecosystem Services and Natural Capital. *Nature*, 387(6630), pp. 253-260.

Costanza, R., and Daly, H. E. (1992). Natural Capital and Sustainable Development. *Conservation Biology*, 6(1), pp. 37-46.

Costanza, R., De Groot, R., Sutton, P., ..., and Turner, R. K. (2014). Changes in the Global Value of Ecosystem Services. *Global Environmental Change*, 26, pp. 152-158.

Cowie, R. H., Bouchet, P., and Fontaine, B. (2022). The Sixth Mass Extinction: Fact, Fiction or Speculation?. *Biological Reviews*, 97(2), pp. 640-663.

Cox, G. M., Halverson, G. P., Stevenson, R. K., ..., and Macdonald, F. A. (2016). Continental Flood Basalt Weathering as a Trigger for Neoproterozoic Snowball Earth. *Earth and Planetary Science Letters*, 446, pp. 89-99.

Craig, H. (1961). Isotopic Variations in Meteoric Waters. *Science*, 133(3465), pp. 1702-1703.

Crifo, P., Diaye, M. A., and Oueghlissi, R. (2015). Measuring the Effect of Government ESG Performance on Sovereign Borrowing Cost. *Quarterly Review of Economics & Finance*, 66, pp. 13-20.

Crippa, M., Guizzardi, D., Pagani, F., ..., and Vignati, E. (2023). GHG Emissions of All World Countries. *Publications Office of the European Union*, JRC134504, 268 pages.

Crowther, D., and Aras, G. (2008). *Corporate Social Responsibility*. Bookboon.

Crutzen, P. J. and Stoermer, E. F. (2000). The Anthropocene. *IGBP Global Change News*, 41, pp. 17-18.

Cui, W., Marsland III, R., and Mehta, P. (2024). Les Houches Lectures on Community Ecology: From Niche Theory to Statistical Mechanics. *arXiv*, 2403.05497.

Curtis, P. G., Slay, C. M., Harris, N. L., Tyukavina, A., and Hansen, M. C. (2018). Classifying Drivers of Global Forest Loss. *Science*, 361(6407), pp. 1108-1111.

Daily, G. C. (1997). Introduction: What Are Ecosystem Services. In Daily, G. C. (Ed.), *Nature's Services: Societal Dependence On Natural Ecosystems*, Island Press, Chapter 1, pp. 1-10.

Daly, H. E. (1968). On Economics as a Life Science. *Journal of Political Economy*, 76(3), pp. 392-406.

Daniel, K. D., Litterman, R. B., and Wagner, G. (2016). Applying Asset Pricing Theory to Calibrate the Price of Climate Risk. *NBER*, 22795.

Daniel, K. D., Litterman, R. B., and Wagner, G. (2019). Declining $CO_2$ Price Paths. *Proceedings of the National Academy of Sciences*, 116(42), pp. 20886-20891.

Dansgaard, W. (1964). Stable Isotopes in Precipitation. *Tellus*, 16(4), pp. 436-468.

Dasgupta, P. (2021). *The Economics of Biodiversity: The Dasgupta Review*. London: HM Treasury, February, 610 pages.

Daubanes, J. X., Mitali, S. F., and Rochet, J-C. (2021). Why Do Firms Issue Green Bonds?. *Swiss Finance Institute Research Paper*, 21-97.

Davies, S. W., and Van Wesep, E. D. (2018). The Unintended Consequences of Divestment. *Journal of Financial Economics*, 128(3), pp. 558-575.

Davis, S. J., and Caldeira, K. (2010). Consumption-based Accounting of $CO_2$ Emissions. *Proceedings of the National Academy of Sciences*, 107(12), pp. 5687-5692.

Davis, A. P., Chadburn, H., Moat, J., O'Sullivan, R., Hargreaves, S., and Lughadha, E. N. (2019). High Extinction Risk for Wild Coffee Species and Implications for Coffee Sector Sustainability. *Science Advances*, 5(1), eaav3473, 9 pages.

Davis, G. F., and Kim, E. H. (2007). Business Ties and Proxy Voting by Mutual Funds. *Journal of Financial Economics*, 85(2), pp. 552-570.

De Groot, R., Brander, L., Van Der Ploeg, S., ..., and Van Beukering, P. (2012). Global Estimates of the Value of Ecosystems and Their Services in Monetary Units. *Ecosystem Services*, 1(1), pp. 50-61.

De Palma, A., Hoskins, A., Gonzalez, R. E., ..., and Purvis, A. (2021). Annual Changes in the Biodiversity Intactness Index in Tropical and Subtropical Forest Biomes, 2001–2012. *Scientific Reports*, 11(1), 20249, 13 pages.

De Queiroz, K. (2007). Species Concepts and Species Delimitation. *Systematic biology*, 56(6), pp. 879-886.

De Ryck, J., Driesen, K., Verhelst, J., and Lammerant, J. (2024). *Assessment of Biodiversity Measurement Approaches for Businesses and Financial Institutions*. Update Report 5 on behalf of the EU Business & Biodiversity Platform, October, 272 pages.

De Vos, J. M., Joppa, L. N., Gittleman, J. L., Stephens, P. R., and Pimm, S. L. (2015). Estimating the Normal Background Rate of Species Extinction. *Conservation Biology*, 29(2), pp. 452-462.

Dechezleprêtre, A., Rivers, N., and Stadler, B. (2019). The Economic Cost of Air Pollution: Evidence from Europe. *OECD Economics Department Working Papers*, 1584, 62 pages.

Del Monte-Luna, P., Nakamura, M., Vicente, A., ..., and Lluch-Cota, S. E. (2023). A Review of Recent and Future Marine Extinctions. *Cambridge Prisms: Extinction*, 1, e13, 9 pages.

Delmas, R. J., Ascencio, J. M., and Legrand, M. (1980). Polar Ice Evidence that Atmospheric $CO_2$ 20,000 yr BP was 50% of Present. *Nature*, 284(5752), pp. 155-157.

Delmas, M. A., and Burbano, V. C. (2011). The Drivers of Greenwashing. *California Management Review*, 54(1), pp. 64-87.

Demartini, A. (2020). Provision of Non-financial Data: Mapping of Stakeholders, Products and Services. *AMF Risks and Trend Mapping*, December.

Dengler, J. (2009). Which Function Describes the Species-Area Relationship Best? A Review and Empirical Evaluation. *Journal of Biogeography*, 36(4), pp. 728-744.

Dennig, F., Budolfson, M. B., Fleurbaey, M., Siebert, A., and Socolow, R. H. (2015). Inequality, Climate Impacts on the Future Poor, and Carbon Prices. *Proceedings of the National Academy of Sciences*, 112(52), pp. 15827-15832.

Derwall, J., and Koedijk, K. (2009). Socially Responsible Fixed-income Funds. *Journal of Business Finance & Accounting*, 36(1-2), pp. 210-229.

Derwall, J., and Verwijmeren, P. (2007). Corporate Governance and the Cost of Equity Capital: Evidence from GMI's Governance Rating. *European Centre for Corporate Engagement Research Note*, 6(1), 11 pages.

Descombes, P., Wisz, M. S., Leprieur, F., ..., and Pellissier, L. (2015). Forecasted Coral Reef Decline in Marine Biodiversity Hotspots under Climate Change. *Global Change Biology*, 21(7), pp. 2479-2487.

Desnos, B., Le Guenedal, T., Morais, P., and Roncalli, T. (2023). From Climate Stress Testing to Climate Value-at-Risk: A Stochastic Approach. *SSRN*, 4497124, 182 pages.

Deutz, A., Heal, G. M., Niu, R., ..., and Tobin-de la Puente, J. (2020). *Financing Nature: Closing the Global Biodiversity Financing Gap*. The Paulson Institute, The Nature Conservancy, and the Cornell Atkinson Center for Sustainability, 262 pages.

Di Franco, E., Pierson, P., Di Iorio, L., ..., and Guidetti, P. (2020). Effects of Marine Noise Pollution on Mediterranean Fishes and Invertebrates: A Review. *Marine Pollution Bulletin*, 159, 111450, 10 pages.

Diagne, C., Leroy, B., Vaissière, A. C., ..., and Courchamp, F. (2021). High and Rising Economic Costs of Biological Invasions Worldwide. *Nature*, 592(7855), pp. 571-576.

Diaz, D. B., and Moore, F. C. (2017a). Quantifying the Economic Risks of Climate Change. *Nature Climate Change*, 7(11), pp. 774-782.

Diaz, D. B., and Moore, F. C. (2017b). Quantifying the Economic Risks of Climate Change: Supplementary Information. Available at www.nature.com/articles/nclimate3411.

Dicks, L. V., Breeze, T. D., Ngo, H. T., ..., and Potts, S. G. (2021). A Global-scale Expert Assessment of Drivers and Risks Associated With Pollinator Decline. *Nature Ecology & Evolution*, 5(10), pp. 1453-1461.

Dietrich, J. P., Bodirsky, B. L., Humpenöder, F., ..., and Popp, A. (2019). MAgPIE 4 — A Modular Open-source Framework for Modeling Global Land Systems. *Geoscientific Model Development*, 12(4), pp. 1299-1317.

Dietzenbacher, E., Los, B., Stehrer, R., Timmer, M. P., and De Vries, G. (2013). The Construction of World Input-Output Tables in the WIOD Project. *Economic Systems Research*, 25(1), pp. 71-98.

Dimson, E., Karakaş, O., and Li, X. (2015). Active Ownership. *Review of Financial Studies*, 28(12), pp. 3225-3268.

Dimson, E., Karakaş, O., and Li, X. (2021). Coordinated Engagements. *SSRN*, 3209072.

Dimson, E., Kreutzer, I., Lake, R., Sjo, H., and Starks, L. T. (2013). Responsible Investment and the Norwegian Government Pension Fund Global. *Strategy Council 2013*, Report, 34 pages, 11 November 2013.

Dinerstein, E., Olson, D. M., Joshi, A., ..., and Saleem, M. (2017). An Ecoregion-based Approach to Protecting Half the Terrestrial Realm. *BioScience*, 67(6), pp. 534-545.

Dirzo, R., Young, H. S., Galetti, M., Ceballos, G., Isaac, N. J. B., and Collen, B. (2014). Defaunation in the Anthropocene. *Science*, 345(6195), pp. 401-406.

Disley, E., Giacomantonio, C., Kruithof, K., and Sim, M. (2016). The Payment by Results Social Impact Bond Pilot at HMP Peterborough: Final Process Evaluation Report. *RAND Europe Research Series*, February, 73 pages.

Disley, E., Rubin, J., Scraggs, E., Burrowes, N., and Culley, D. (2011). Lessons Learned from the Planning and Early Implementation of the Social Impact Bond at HMP Peterborough. *RAND Europe Research series*, May, 86 pages.

Diz-Pita, E., and Otero-Espinar, M. V. (2021). Predator-prey Models: A Review of Some Recent Advances. *Mathematics*, 9(15), 1783, 34 pages.

Dommenget, D. (2022). An Introduction to Climate Dynamics. *Lectures Notes for the Undergraduate Course in Climate Dynamics*, 408 pages.

Drei, A., Le Guenedal, T., Lepetit, F., Mortier, V., Roncalli, T. and Sekine, T. (2019). ESG Investing in Recent Years: New Insights from Old Challenges. *SSRN*, 3683469.

Drucker, P. F. (1954). *The Practice of Management*. Harper & Row.

Drucker, P. F. (1984). The New Meaning of Corporate Social Responsibility. *California Management Review*, 26(2), pp. 53-63.

Duarte, C. M., Agusti, S., Barbier, E., ..., and Worm, B. (2020). Rebuilding Marine Life. *Nature*, 580(7801), pp. 39-51.

Ducoulombier, F. (2021). Understanding the Importance of Scope 3 Emissions and the Implications of Data Limitations. *Journal of Impact and ESG Investing*, 1(4), pp. 63-71.

Dudás, F., and Naffa, H. (2020). The Predictive Role of Country-Level ESG Indicators. *Economy and Finance*, 7(4), pp. 441-453.

Easton, P. D. (2004). PE Ratios, PEG Ratios, and Estimating the Implied Expected Rate of Return on Equity Capital. *Accounting Review*, 79(1), pp. 73-95.

Eccles, R. G., Lee, L. E., and Stroehle, J. C. (2020). The Social Origins of ESG: An Analysis of Innovest and KLD. *Organization & Environment*, 33(4), pp. 575-596.

Eccles, R. G., Shandal, V., Young, D., and Montgomery, B. (2023). Private Equity Should Take the Lead in Sustainability. In Young, D., and Reeves, M. (Eds), *Sustainable Business Model Innovation*, De Gruyter, Chapter 21, pp. 203-214.

Eccles, R. G., and Stroehle, J. C. (2018). Exploring Social Origins in the Construction of Environmental, Social and Governance Measures. *SSRN*, 3212685.

Ecosystem Marketplace (2023a). All in on Climate: The Role of Carbon Credits in Corporate Climate Strategies. *Report*, October, 36 pages.

Ecosystem Marketplace (2023b). State of the Voluntary Carbon Markets 2023. *Insights Report*, November, 28 pages.

Edmans, A. (2009). Blockholder Trading, Market Efficiency, and Managerial Myopia. *Journal of Finance*, 64(6), pp. 2481-2513.

Edmans, A. (2011). Does the Stock Market fully Value Intangibles? Employee Satisfaction and Equity Prices. *Journal of Financial Economics*, 101(3), pp. 621-640.

Edmans, A. (2014). Blockholders and Corporate Governance. *Annual Review of Financial Economics*, 6, pp. 23-50.

Edmans, A., Levit, D., and Schneemeier, J. (2022). Socially Responsible Divestment. European Corporate Governance Institute, *Finance Working Paper*, 823, April.

Ehlers, T., and Packer, F. (2017). Green Bond Finance and Certification. *BIS Quarterly Review*, September, pp. 89-104.

Eilers, E. J., Kremen, C., Smith Greenleaf, S., Garber, A. K., and Klein, A. M. (2011). Contribution of Pollinator-mediated Crops to Nutrients in the Human Food Supply. *PLoS One*, 6(6), e21363, 6 pages.

El Ghoul, S., Guedhami, O., Kwok, C. C., and Mishra, D. R. (2011). Does Corporate Social Responsibility Affect the Cost of Capital?. *Journal of Banking & Finance*, 35(9), pp. 2388-2406.

Eliwa, Y., Aboud, A., and Saleh, A. (2021). ESG Practices and the Cost of Debt: Evidence from EU Countries. *Critical Perspectives on Accounting*, 79, 102097, 21 pages.

Emerson, J. (2003). The Blended Value Proposition: Integrating Social and Financial Returns. *California Management Review*, 45(4), pp. 35-51.

ENCORE (2024). *ENCORE: Exploring Natural Capital Opportunities, Risks and Exposure*. www.encorenature.org.

EPICA community members (2004). Eight Glacial Cycles from an Antarctic Ice Core. *Nature*, 429(6992), pp. 623-628.

Ehrlich, P. R. (1995). The Scale of the Human Enterprise and Biodiversity Loss. In Lawton, J.H., and May, R. M. (Eds), *Extinction Rates*, Oxford University Press, Chapter 14, pp. 214-226.

Escher, B. I., Stapleton, H. M., and Schymanski, E. L. (2020). Tracking Complex Mixtures of Chemicals in our Changing Environment. *Science*, 367(6476), pp. 388-392.

European Banking Authority (2014). Regulatory Technical Standards on the Conditions for Assessing the Materiality of Extensions and Changes of Internal Approaches for Credit, Market and Operational Risk. *Technical Standards, Guidelines & Recommendations*, July.

European Banking Authority (2023). EBA Progress Report on Greenwashing Monitoring and Supervision. *Report*, 2023/16, 74 pages.

European Central Bank (2022). 2022 Climate Risk Stress Test. *Report*, July 2022.

European Commission (2022a). Targeted Consultation on the Functioning of the ESG Ratings Market in the European Union and on the Consideration of ESG Factors in Credit Ratings. *Consultation Document*, April 2022.

European Commission (2022b). Targeted Consultation on the Functioning of the ESG Ratings Market in the European Union and on the Consideration of ESG Factors in Credit Ratings. *Summary Report*, August 2022.

European Environment Agency (2024a). *The Costs to Health and the Environment from Industrial Air Pollution in Europe — 2024 Update*. Briefing 24/2023, January, 18 pages.

European Environment Agency (2024b). *Estimating the External Costs of Industrial Air Pollution — Trends 2012–2021*. Technical Note, January, 177 pages.

European Financial Reporting Advisory Group (2022). Draft European Sustainability Reporting Standards (Appendix II — CSRD Requirements for the Development of sustainability Reporting Standards and their Coverage by the draft ESRS). *Draft*, November, 20 pages.

European Fund and Asset Management Association (2023a). Fact Book 2023. *Trends in European Investment Funds*, 21st Edition, June, 326 pages.

European Fund and Asset Management Association (2023b). The SFDR Fund Market — State of Play. *Market Insights*, 12, June, 8 pages.

European Investment Bank (2021). Measuring the EIB Group's Impact — Methods and Studies. *Report*, October, 46 pages.

European Securities and Markets Authority (2022). ESMA's Technical Advice to the European Commission on Integrating Sustainability Risks and Factors in MiFID II. *Final Report*, September 2022.

European Securities and Markets Authority (2023). Final Report on Draft RTS on the Review of PAI and Financial Product Disclosures in the SFDR Delegated Regulation. *Report*, JC-2023-55, 4 December 2023, 221 pages.

European Securities and Markets Authority (2024). EU Alternative Investment Funds 2023. *Market Report*, ESMA50-524821-3095, 30 January 2024, 53 pages.

European Sustainable Investment Forum (2018). *2018 European SRI Study*. November.

European Sustainable Investment Forum (2021). *2021 Eurosif Report: Fostering Investor Impact — Placing it at the Heart of Sustainable Finance*. October, 45 pages.

Eze, M. O., George, S. C., and Hose, G. C. (2021). Dose-Response Analysis of Diesel Fuel Phytotoxicity on Selected Plant Species. *Chemosphere*, 263, 128382, 10 pages.

Fa, J. E., Peres, C. A., and Meeuwig, J. (2002). Bushmeat Exploitation in Tropical Forests: An Intercontinental Comparison. *Conservation Biology*, 16(1), pp. 232-237.

Fabozzi, F. J., Ma, K. C., and Oliphant, B. J. (2008). Sin Stock Returns. *Journal of Portfolio Management*, 35(1), pp. 82-94.

Fahrig, L. (2003). Effects of Habitat Fragmentation on Biodiversity. *Annual Review of Ecology, Evolution, and Systematics*, 34(1), pp. 487-515.

Fahrig, L. (2017). Ecological Responses to Habitat Fragmentation per se. *Annual Review of Ecology, Evolution, and Systematics*, 48(1), pp. 1-23.

Fahrig, L., Arroyo-Rodríguez, V., Bennett, J. R., ..., and Watling, J. I. (2019). Is Habitat Fragmentation Bad for Biodiversity?. *Biological Conservation*, 230, pp. 179-186.

Fama E. F., and French, K. R. (1993). Common Risk Factors in the Returns on Stocks and Bonds. *Journal of Financial Economics*, 33(1), pp. 3-56.

Fatica, S., Panzica, R., and Rancan, M. (2021). The Pricing of Green Bonds: Are Financial Institutions Special?. *Journal of Financial Stability*, 54, 100873.

Fattorini, S., Borges, P. A., Dapporto, L., and Strona, G. (2017). What Can the Parameters of the Species-Area Relationship (SAR) Tell Us? Insights from Mediterranean Islands. *Journal of Biogeography*, 44(5), pp. 1018-1028.

Faulwasser, T. , Kellett, C. M., and Weller, S. R. (2018). *MPC-DICE: Model Predictive Control — Dynamic Integrated model of Climate and Economy*. Code source available at https://github.com/cmkellett/MPC-DICE.

Fawcett, T. (2006). An Introduction to ROC Analysis. *Pattern Recognition Letters*, 27(8), pp. 861-874.

Feenstra, R. C., Inklaar, R., and Timmer, M. P. (2015). The Next Generation of the Penn World Table. *American Economic Review*, 105(10), pp. 3150-3182.

Fender, I., McMorrow, M., Sahakyan, V., and Zulaica, O. (2019). Green Bonds: The Reserve Management Perspective. *BIS Quarterly Review*, September, pp. 49-53.

Feulner, G. (2012). The Faint Young Sun Problem. *Reviews of Geophysics*, 50(2), RG2006, 29 pages.

Fichtner, J., Heemskerk, E. M., and Garcia-Bernardo, J. (2017). Hidden Power of the Big Three? Passive Index Funds, Re-concentration of Corporate Ownership, and New Financial Risk. *Business and Politics*, 19(2), pp. 298-326.

Figueiredo, L., Krauss, J., Steffan-Dewenter, I., and Sarmento Cabral, J. (2019). Understanding Extinction Debts: Spatio-temporal Scales, Mechanisms and A Roadmap for Future Research. *Ecography*, 42(12), pp. 1973-1990.

Financial Stability Board (2015). Financial Reforms — Progress on the Work Plan for the Antalya Summit. *Chair's Letter to G20 Finance Ministers and Central Bank Governors*.

Finster, M., Wood, M., and Raja, S. N. (2005). The Apgar Score has Survived the Test of Time. *Journal of the American Society of Anesthesiologists*, 102(4), pp. 855-857.

Fisher, R. A., Corbet, A. S., and Williams, C. B. (1943). The Relation between the Number of Species and the Number of Individuals in a Random Sample of an Animal Population. *Journal of Animal Ecology*, 12(1), pp. 42-58.

Flammer, C. (2021). Corporate Green Bonds. *Journal of Financial Economics*, 142(2), pp. 499-516.

Flammer, C., Giroux, T., and Heal, G. M. (2024). Blended Finance. *NBER*, 32287.

Flammer, C., Giroux, T., and Heal, G. M. (2025). Biodiversity Finance. *Journal of Financial Economics*, 164, 103987, 15 pages.

Fletcher Jr, R. J., Didham, R. K., Banks-Leite, C., ..., and Haddad, N. M. (2018). Is Habitat Fragmentation Good for Biodiversity?. *Biological Conservation*, 226, pp. 9-15.

Flörke, M., Kynast, E., Bärlund, I., Eisner, S., Wimmer, F., and Alcamo, J. (2013). Domestic and Industrial Water Uses of the Past 60 Years as a Mirror of Socio-economic Development: A Global Simulation Study. *Global Environmental Change*, 23(1), pp. 144-156.

Food and Agriculture Organization of the United Nations (2019). *The State of the World's Biodiversity for Food and Agriculture*. FAO Commission on Genetic Resources for Food and Agriculture, prepared by Bélanger J., and Pilling D. (Eds), February, 572 pages.

Food and Agriculture Organization of the United Nations (2020). *Global Forest Resources Assessment 2020 — Key Findings*. 16 pages.

Food and Agriculture Organization of the United Nations (2022). *Blue Transformation — Roadmap 2022–2030: A Vision for FAO's Work on Aquatic Food Systems*. 40 pages.

Food and Agriculture Organization of the United Nations (2023a). FRA 2025: Terms and Definitions. *Forest Resources Assessment Working Paper*, 194, 29 pages.

Food and Agriculture Organization of the United Nations (2023b). *World Food and Agriculture — Statistical Yearbook 2023*. November, 384 pages.

Food and Agriculture Organization of the United Nations (2024a). *The State of Food Security and Nutrition in the World 2024 – Financing to End Hunger, Food Insecurity and Malnutrition in all its Forms*. September, 316 pages.

Food and Agriculture Organization of the United Nations (2024b). *The State of World Fisheries and Aquaculture 2024 — Blue Transformation in action*. October, 264 pages.

Foster, G. L., Royer, D. L., and Lunt, D. J. (2017). Future Climate Forcing Potentially without Precedent in the last 420 Million Years. *Nature Communications*, 8, 14845, 8 pages.

Fourier, J. (1824). Remarques générales sur les températures du globe terrestre et des espaces planétaires. *Annales de Chimie et de Physique*, 27, pp. 136-167.

France Invest & Forum pour l'investissement responsable (2021). Impact Investing: A Demanding Definition For Listed and Non-listed Products. *Guidelines*, March, 19 pages.

Frankignoul, C., and Hasselmann, K. (1977). Stochastic Climate Models, Part II Application to Sea-surface Temperature Anomalies and Thermocline Variability. *Tellus*, 29(4), pp. 289-305.

Frazzini, A., and Pedersen, L. H. (2014). Betting Against Beta. *Journal of Financial Economics*, 111(1), pp. 1-25.

Freeman, R. E. (2004). *Strategic Management: A Stakeholder Approach*. Pitman.

Freshfields Bruckhaus Deringer (2005). A Legal Framework for the Integration of Environmental, Social and Governance Issues into Institutional Investment. *UNEP Report*, October.

Fretwell, S. D. (1975). The Impact of Robert MacArthur on Ecology. *Annual Review of Ecology and Systematics*, 6, pp. 1-13.

Friede, G., Busch, T., and Bassen, A. (2015). ESG and Financial Performance: Aggregated Evidence from more than 2000 Empirical Studies. *Journal of Sustainable Finance & Investment*, 5(4), pp. 210-233.

Friederich, D., Kaack, L. H., Luccioni, A., and Steffen, B. (2021). Automated Identification of Climate Risk Disclosures in Annual Corporate Reports. *arXiv*, 2108.01415.

Friedlingstein, P., O'Sullivan, M., Jones, M. W., ..., and Zheng, B. (2022). Global Carbon Budget 2022. *Earth System Science Data*, 14(11), pp. 4811-4900.

Friedman, M. (1962). *Capitalism and Freedom*. University of Chicago Press.

Friedman, M. (1970). The Social Responsibility of Business Is to Increase Its Profits. *New York Times Magazine*, September 13, Section SM, pp. 17 (reproduced in Zimmerli, W. Ch., Holzinger, M., and Richter, K. (Eds). (2007), *Corporate Ethics and Corporate Governance*, Springer, pp. 173-178).

Friedrich, O., Norris, R. D., and Erbacher, J. (2012). Evolution of Middle to Late Cretaceous Oceans — A 55 my Record of Earth's Temperature and Carbon Cycle. *Geology*, 40(2), pp. 107-110.

Fujimori, S., Hasegawa, T., and Masui, T. (2017). AIM/CGE V2.0: Basic Feature of the Model. In Fujimori, S., Kainuma, M., and Masui, T. (Eds), *Post-2020 Climate Action: Global and Asian Perspectives*, Springer, pp. 305-328.

Fuller, R., Landrigan, P. J., Balakrishnan, K., ..., and Yan, C. (2022). Pollution and Health: A Progress Update. *The Lancet Planetary Health*, 6(6), e535-e547.

Fuss, S., Lamb, W. F., Callaghan, ..., and Minx, J. C. (2018). Negative Emissions — Part 2: Costs, Potentials and Side Effects. *Environmental Research Letters*, 13(6), 063002, 47 pages.

Gabay, D., and Mercier, B. (1976). A Dual Algorithm for the Solution of Nonlinear Variational Problems via Finite Element Approximation. *Computers & Mathematics with Applications*, 2(1), pp. 17-40.

Gambhir, A., Butnar, I., Li, P. H., Smith, P., and Strachan, N. (2019). A Review of Criticisms of Integrated Assessment Models and Proposed Approaches to Address These, Through the Lens of BECCS. *Energies*, 12(9), 1747.

Gantchev, N. (2013). The Costs of Shareholder Activism: Evidence from a Sequential Decision Model. *Journal of Financial Economics*, 107(3), pp. 610-631.

Gantchev, N., Gredil, O. R., and Jotikasthira, C. (2019). Governance under the Gun: Spillover Effects of Hedge Fund Activism. *Review of Finance*, 23(6), pp. 1031-1068.

Garibaldi, L. A., Steffan-Dewenter, I., Winfree, R., ..., and Klein, A. M. (2013). Wild Pollinators Enhance Fruit Set of Crops Regardless of Honey Bee Abundance. *Science*, 339(6127), pp. 1608-1611.

Gaston, K. J. (2010). Biodiversity. In Sodhi, N. S., and Ehrlich, P. R. (Eds), *Conservation Biology for All*, Oxford University Press, Chapter 2, pp. 27-44.

Gaston, K. J., and Spicer, J. I. (2004). *Biodiversity: An Introduction*. Second Edition, Wiley-Blackwell, 208 pages.

Gatti, L. V., Basso, L. S., Miller, J. B., ..., and Neves, R. A. (2021). Amazonia as a Carbon Source Linked to Deforestation and Climate Change. *Nature*, 595(7867), pp. 388-393.

Gebhardt, W. R., Lee, C. M., and Swaminathan, B. (2001). Toward an Implied Cost of Capital. *Journal of Accounting Research*, 39(1), pp. 135-176.

Geczy, C., Jeffers, J. S., Musto, D. K., and Tucker, A. M. (2021). Contracts with (Social) Benefits: The Implementation of Impact Investing. *Journal of Financial Economics*, 142(2), pp. 697-718.

Gemechu, E. D., Butnar, I., Llop, M., and Castells, F. (2014). Economic and Environmental effects of $CO_2$ Taxation: An Input-output Analysis for Spain. *Journal of Environmental Planning and Management*, 57(5), pp. 751-768.

Genest, C., and MacKay, J. (1986a). Copules Archimédiennes et Familles de Lois Bidimensionnelles dont les Marges sont données. *Canadian Journal of Statistics*, 14(2), pp. 145-159.

Genest, C., and MacKay, J. (1986b), The Joy of Copulas: Bivariate Distributions with Uniform Marginals, *American Statistician*, 40(4), pp. 280-283.

Gentleman, W., Leising, A., Frost, B., Strom, S., and Murray, J. (2003). Functional Responses for Zooplankton Feeding on Multiple Resources: A Review of Assumptions and Biological Dynamics. *Deep Sea Research Part II: Topical Studies in Oceanography*, 50(22-26), pp. 2847-2875.

Gerard, B. (2019). ESG and Socially Responsible Investment: A Critical Review. *Beta*, 33(1), pp. 61-83.

GHG Protocol (2004). The Greenhouse Gas Protocol: A Corporate Accounting and Reporting Standard. *Standards*.

GHG Protocol (2011). The Value Chain (Scope 3) Standard. *Standards*.

GHG Protocol (2013). Technical Guidance for Calculating Scope 3 Emissions: Supplement to the Corporate Value Chain (Scope 3) Accounting & Reporting Standard. *Standards*.

GHG Protocol (2015). GHG Protocol Scope 2 Guidance: An Amendment to the GHG Protocol Corporate Standard. *Standards*.

Ghosh, B., and Kar, T. K. (2013). Maximum Sustainable Yield and Species Extinction in a Prey-predator System: Some New Results. *Journal of Biological Physics*, 39, pp. 453-467.

Gianfrate, G., and Peri, M. (2019). The Green Advantage: Exploring the Convenience of Issuing Green Bonds. *Journal of Cleaner Production*, 219, pp. 127-135.

Gianoncelli, A., Gaggiotti, G., Boiardi, P., and Picón Martínez, A. (2019). 15 Years of Impact — Taking Stock and Looking Ahead. *EVPA Report*, 112 pages.

Gibbard, P., Walker, M., Bauer, A., ..., and Ruddiman, W. (2022). The Anthropocene as an Event, not an Epoch. *Journal of Quaternary Science*, 37(3), pp. 395-399.

Giglio, S., Maggiori, M., Stroebel, J., Tan, Z., Utkus, S., and Xu, X. (2023a). Four Facts about ESG Beliefs and Investor Portfolios. *NBER*, 31114

Giglio, S., Kuchler, T., Stroebel, J., and Zeng, X. (2023b). Biodiversity Risk. *NBER*, 31137.

Gillan, S. L., and Starks, L. T. (2000). Corporate Governance Proposals and Shareholder Activism: The Role of Institutional Investors. *Journal of Financial Economics*, 57(2), pp. 275-305.

Gillingham, K., and Stock, J. H. (2018). The Cost of Reducing Greenhouse Gas Emissions. *Journal of Economic Perspectives*, 32(4), pp. 53-72.

Gilpin, M. E., Case, T. J., and Ayala, F. J. (1976). $\theta$-selection. *Mathematical Biosciences*, 32(1-2), pp. 131-139.

Gini, C. (1921). Measurement of Inequality of Incomes. *Economic Journal*, 31(121), pp. 124-126.

Girona, M. M., Morin, H., Gauthier, S., and Bergeron, Y. (Eds) (2023). *Boreal Forests in the Face of Climate Change: Sustainable Management*. Springer Nature, Advances in Global Change Research, 14, 837 pages.

Gleason, H. A. (1922). On the Relation Between Species and Area. *Ecology*, 3(2), pp. 158-162.

Global Development Network (2021). Measuring Impacts — The Experience of the EIB-GDN Programme. *Report*, 114 pages.

Global Impact Investing Network (2021). *Impact Investing: A Guide to this Dynamic Market*. January, 20 pages.

Global Sustainable Investment Alliance (2013). *2012 Global Sustainable Investment Review*. January, 46 pages.

Global Sustainable Investment Alliance (2015). *2014 Global Sustainable Investment Review*. February, 36 pages.

Global Sustainable Investment Alliance (2017). *2016 Global Sustainable Investment Review*. March, 31 pages.

Global Sustainable Investment Alliance (2019). *2018 Global Sustainable Investment Review*. April, 29 pages.

Global Sustainable Investment Alliance (2021). *2020 Global Sustainable Investment Review*. July, 32 pages.

Global Sustainable Investment Alliance (2023). *2022 Global Sustainable Investment Review*. November, 47 pages.

Gluszek, S., Viollaz, J., Mwinyihali, R., Wieland, M., and Gore, M. L. (2021). Using Conservation Criminology to Understand the Role of Restaurants in the Urban Wild Meat Trade. *Conservation Science and Practice*, 3(5), e368, 13 pages.

Gode, D., and Mohanram, P. (2003). Inferring the Cost of Capital using the Ohlson-Juettner Model. *Review of Accounting Studies*, 8, pp. 399-431.

Goedkoop, M., Heijungs, R., Huijbregts, M., De Schryver, A., Struijs, J., and Van Zelm, R. (2009). *ReCiPe 2008*. First edition, 132 pages.

Goldreyer, E. F., Ahmed, P., and Diltz, J. D. (1999). The Performance of Socially Responsible Mutual Funds: Incorporating Sociopolitical Information in Portfolio Selection. *Managerial Finance*, 25(1), pp. 23-36.

Gollier, C. (2010). Ecological Discounting. *Journal of Economic Theory*, 145(2), pp. 812-829.

Gollier, C. (2013). *Pricing the Planet's Future: The Economics of Discounting in an Uncertain World*. Princeton University Press.

Gollier, C., and Pouget, S. (2022). Investment Strategies and Corporate Behaviour with Socially Responsible Investors: A Theory of Active Ownership. *Economica*, 89(356), pp. 997-1023.

Golub, G. H., and Van Loan, C. F. (2013). *Matrix Computations*. Fourth edition, Johns Hopkins University Press.

Gombeer, S., Nebesse, C., Musaba, P., ..., and Verheyen, E. (2021). Exploring the Bushmeat Market in Brussels, Belgium: A Clandestine Luxury Business. *Biodiversity and Conservation*, 30, pp. 55-66.

Gompers, P., Ishii, J., and Metrick, A. (2003). Corporate Governance and Equity Prices. *Quarterly Journal of Economics*, 118(1), pp. 107-156.

Gonçalves, T. C., Dias, J., and Barros, V. (2022). Sustainability Performance and the Cost of Capital. *International Journal of Financial Studies*, 10(3), 63, 32 pages.

González-Martín, J., Kraakman, N. J. R., Pérez, C., Lebrero, R., and Muõoz, R. (2021). A State-of-the-art Review on Indoor Air Pollution and Strategies for Indoor Air Pollution Control. *Chemosphere*, 262, 128376, 16 pages.

Goosse, H., Kay, J. E., Armour, K. C., ..., and Vancoppenolle, M. (2018). Quantifying Climate Feedbacks in Polar Regions. *Nature Communications*, 9(1), 1919, 13 pages.

Gordon, H. S. (1954). The Economic Theory of a Common-Property Resource: The Fishery. *Journal of Political Economy*, 62(2), pp. 124-142.

Gotelli, N. J., and Colwell, R. K. (2001). Quantifying Biodiversity: Procedures and Pitfalls in the Measurement and Comparison of Species Richness. *Ecology Letters*, 4(4), pp. 379-391.

Gouriéroux, C. (1992). Courbes de Performance, de Sélection et de Discrimination. *Annales d'Économie et de Statistique*, 28(4), pp. 107-123.

Gouriéroux, C., and Jasiak, J. (2007). *The Econometrics of Individual Risk: Credit, Insurance, and Marketing*. Princeton University Press.

Goutelle, S., Maurin, M., Rougier, F., ..., and Maire, P. (2008). The Hill Equation: A Review of Its Capabilities in Pharmacological Modelling. *Fundamental & Clinical Pharmacology*, 22(6), pp. 633-648.

Graff Zivin, J., and Neidell, M. (2013). Environment, Health, and Human Capital. *Journal of Economic Literature*, 51(3), pp. 689-730.

Gratcheva, E. M., Emery, T., and Wang, D. (2020). Demystifying Sovereign ESG. *Report*, World Bank, Equitable Growth, Finance and Institutions Insight, December.

Gray, A. (2019). The Ecology of Plant Extinction: Rates, Traits and Island Comparisons. *Oryx*, 53(3), pp. 424-428.

Gregory, A., Tharyan, R., and Whittaker, J. (2014). Corporate Social Responsibility and Firm Value: Disaggregating the Effects on Cash Flow, Risk and Growth. *Journal of Business Ethics*, 124(4), pp. 633-657.

Green, J. L., and Ostling, A. (2003). Endemics-Area Relationships: The Influence of Species Dominance and Spatial Aggregation. *Ecology*, 84(11), pp. 3090-3097.

Grewal, J., Serafeim, G., and Yoon, A. (2016). Shareholder Activism on Sustainability Issues. *SSRN*, 2805512.

Grossman, B. R., and Sharpe, W. F. (1986). Financial Implications of South African Divestment. *Financial Analysts Journal*, 42(4), pp. 15-29.

Grubb, M., Wieners, C., and Yang, P. (2021). Modeling Myths: On DICE and Dynamic Realism in Integrated Assessment Models of Climate Change Mitigation. *WIREs Climate Change*, 12(3), e698.

Gupta, J., and Vegelin, C. (2016). Sustainable Development Goals and Inclusive Development. *International Environmental Agreements: Politics, Law and Economics*, 16, pp. 433-448.

Gupta, K. (2018). Environmental Sustainability and Implied Cost of Equity: International Evidence. *Journal of Business Ethics*, 147(2), pp. 343-365.

Gutierrez, M. S. (2008). *Economic Activity and Atmospheric Pollution in Spain: An Input-output Approach*. PhD Thesis, Universitat de Barcelona.

Haddad, N. M., Brudvig, L. A., Clobert, J., ..., and Townshend, J. R. (2015). Habitat Fragmentation and its Lasting Impact on Earth's Ecosystems. *Science Advances*, 1(2), e1500052, 9 pages.

Halley, J. M., Monokrousos, N., Mazaris, A. D., Newmark, W. D., and Vokou, D. (2016a). Dynamics of Extinction Debt Across Five Taxonomic Groups. *Nature Communications*, 7(1), 12283, 6 pages.

Halley, J. M., Monokrousos, N., Mazaris, A. D., Newmark, W. D., and Vokou, D. (2016b). Supplementary Information. *Nature Communications*, 7(1), 12283, 34 pages.

Hallmann, C. A., Sorg, M., Jongejans, E., ..., and De Kroon, H. (2017). More than 75 Percent Decline over 27 Years in Total Flying Insect Biomass in Protected Areas. *PloS One*, 12(10), e0185809, 21 pages.

Hammitt, J. K. (2023). Consistent Valuation of a Reduction in Mortality Risk using Values per Life, Life Year, and Quality-Adjusted Life Year. *Health Economics*, 32(9), pp. 1964-1981.

Hammitt, J. K., and Robinson, L. A. (2011). The Income Elasticity of the Value per Statistical Life: Transferring Estimates Between High and Low Income Populations. *Journal of Benefit-Cost Analysis*, 2(1), 28 pages.

Hand, D., Sunderji, S., Nova, N. and De, I. (2021). Impact Investing Decision-making: Insights on Financial Performance. *GIIN Report*, January, 55 pages.

Hand, D., Ringel, B., and Danel, A. (2022). Sizing the Impact Investing Market: 2022. *GIIN Report*, October, 17 pages.

Hanemann, W. M. (2008). What is the Economic Cost of Climate Change?. *Working Paper*, University of California, Berkeley, 1071.

Hänsel, M. C., Drupp, M. A., Johansson, D. J., ..., and Sterner, T. (2020). Climate Economics Support for the UN Climate Targets. *Nature Climate Change*, 10(8), pp. 781-789.

Hansen, J. E., Lacis, A., Rind, D., Russell, G., Stone, P., Fung, I., Ruedy, R., and Lerner, J. (1984). Climate Sensitivity: Analysis of Feedback Mechanisms. In Hansen, J. E., and Takahashi, T. (Eds), *Climate Processes and Climate Sensitivity*, 29, pp. 130-163.

Hansen, J. E., Sato, M., Russell, G., and Kharecha, P. (2013a). Climate Sensitivity, Sea Level and Atmospheric Carbon Dioxide. *Philosophical Transactions of the Royal Society A: Mathematical, Physical and Engineering Sciences*, 371(2001), 20120294, 31 pages.

Hansen, M. C., Potapov, P. V., Moore, R., ..., and Townshend, J. R. (2013b). High-Resolution Global Maps of 21st-century Forest Cover Change. *Science*, 342(6160), pp. 850-853.

Hanski, I., and Ovaskainen, O. (2002). Extinction Debt at Extinction Threshold. *Conservation Biology*, 16(3), pp. 666-673.

Hanski, I., and Ovaskainen, O. (2003). Metapopulation Theory for Fragmented Landscapes. *Theoretical Population Biology*, 64(1), pp. 119-127.

Hanski, I., Zurita, G. A., Bellocq, M. I., and Rybicki, J. (2013). Species-fragmented Area Relationship. *Proceedings of the National Academy of Sciences*, 110(31), pp. 12715-12720.

Hardin, G. (1968). The Tragedy of the Commons. *Science*, 162(3859), pp. 1243-1248.

Hasselmann, K. (1976). Stochastic Climate Models, Part I. Theory. *Tellus*, 28(6), pp. 473-485.

Hartigan Jr, J. (2017). *Care of the Species: Races of Corn and the Science of Plant Biodiversity*. University of Minnesota Press, 376 pages.

Hartmann, D. L. (2016). *Global Physical Climatology*. Second edition, Elsevier Science.

Harvey, A. C. (1990). *Forecasting, Structural Time Series Models and the Kalman Filter*. Cambridge University Press.

Hastie, T., Tibshirani, R., and Friedman, J.H. (2009). *The Elements of Statistical Learning*. Second edition, Springer.

Havlìk, P., Valin, H., Mosnier, A., ..., and Hasegawa, T. (2018). *GLOBIOM Documentation*. International Institute for Applied Systems Analysis.

Hays, J. D., Imbrie, J., and Shackleton, N. J. (1976). Variations in the Earth's Orbit: Pacemaker of the Ice Ages. *Science*, 194(4270), pp. 1121-1132.

He, F., and Hubbell, S. P. (2011). Species-Area Relationships Always Overestimate Extinction Rates from Habitat Loss. *Nature*, 473(7347), pp. 368-371.

He, F., and Legendre, P. (2002). Species Diversity Patterns Derived from Species-Area Models. *Ecology*, 83(5), pp. 1185-1198.

Heeb, F., Kölbel, J. F., Paetzold, F., and Zeisberger, S. (2023). Do Investors Care About Impact?. *Review of Financial Studies*, 36(5), pp. 1737-1787.

Hein, L., Bagstad, K. J., Obst, C., ..., and Caparrós, A. (2020). Progress in Natural Capital Accounting for Ecosystems. *Science*, 367(6477), pp. 514-515.

Held, I. M., and Soden, B. J. (2006). Robust Responses of the Hydrological Cycle to Global Warming. *Journal of Climate*, 19(21), pp. 5686-5699.

Henry, P. B., and Miller, C. (2009). Institutions Versus Policies: A Tale of Two Islands. *American Economic Review*, 99(2), pp. 261-267.

Heras-Saizarbitoria, I., Urbieta, L., and Boiral, O. (2022). Organizations' Engagement with Sustainable Development Goals: From Cherry-picking to SDG-washing?. *Corporate Social Responsibility and Environmental Management*, 29(2), pp. 316-328.

Hersbach, H., Bell, B., Berrisford, P., ..., and Thépaut, J. N. (2020). The ERA5 Global Reanalysis. *Quarterly Journal of the Royal Meteorological Society*, 146(730), pp. 1999-2049.

Heywood, V. H. (1995). *The Global Biodiversity Assessment*. UNEP & Cambridge University Press, 1140 pages.

High-Level Expert Group on Sustainable Finance (2018). Financing a Sustainable European Economy. *Final Report*, January.

Hilderink, M. H., and De Winter, I. I. (2021). No Need to Beat Around the Bushmeat — The Role of Wildlife Trade and Conservation Initiatives in the Emergence of Zoonotic Diseases. *Heliyon*, 7, e07692, 10 pages.

Hinkley, D. V. (1969). On the Ratio of Two Correlated Normal Random Variables. *Biometrika*, 56(3), pp. 635-639.

Hirschman, A. O. (1970). *Exit, Voice, and Loyalty: Responses to Decline in Firms, Organizations, and States*. Harvard University Press.

Hjort, J., Streletskiy, D., Doré, G., Wu, Q., Bjella, K., and Luoto, M. (2022). Impacts of Permafrost Degradation on Infrastructure. *Nature Reviews Earth & Environment*, 3(1), pp. 24-38.

Hoegh-Guldberg, O. I., Beal, D., Chaudhry, T., ..., and Smits, M. (2015). Reviving the Ocean Economy: The Case for Action. *WWF Report*, April, 60 pages.

Hoffman, P. F., Kaufman, A. J., Halverson, G. P., and Schrag, D. P. (1998). A Neoproterozoic Snowball Earth. *Science*, 281(5381), pp. 1342-1346.

Hoffman, P. F., and Schrag, D. P. (2002). The Snowball Earth Hypothesis: Testing the Limits of Global Change. *Terra Nova*, 14(3), pp. 129-155.

Hölker, F., Wolter, C., Perkin, E. K., and Tockner, K. (2010). Light Pollution as a Biodiversity Threat. *Trends in Ecology & Evolution*, 25(12), pp. 681-682.

Holling, C. S. (1959a). The Components of Predation as Revealed by a Study of Small-mammal Predation of the European Pine Sawfly. *Canadian Entomologist*, 91(5), pp. 293-320.

Holling, C. S. (1959b). Some Characteristics of Simple Types of Predation and Parasitism. *Canadian Entomologist*, 91(7), pp. 385-398.

Hong, H., and Kacperczyk, M. (2009). The Price of Sin: The Effects of Social Norms on Markets. *Journal of Financial Economics*, 93(1), pp. 15-36.

Hope, C. (2011). The PAGE09 Integrated Assessment Model: A Technical Description. *Cambridge Judge Business School Working Paper*, 4.

Höchstädter, A. K., and Scheck, B. (2015). What's in a Name: An Analysis of Impact Investing Understandings by Academics and Practitioners. *Journal of Business Ethics*, 132, pp. 449-475.

Howard, P. H., and Sterner, T. (2017). Few and not so Far Between: A Meta-analysis of Climate Damage Estimates. *Environmental and Resource Economics*, 68(1), pp. 197-225.

Hübel, B. (2022). Do Markets Value ESG Risks in Sovereign Credit Curves?. *Quarterly Review of Economics and Finance*, 85, pp. 134-148.

Humphrey, J. E., Lee, D. D., and Shen, Y. (2012). Does it Cost to be Sustainable?. *Journal of Corporate Finance*, 18(3), pp. 626-639.

Huppmann, D., Gidden, M., Fricko, ..., and Krey, V. (2019). The MESSAGEix Integrated Assessment Model and the ix Modeling Platform (ixmp): An Open Framework for Integrated and Cross-cutting Analysis of Energy, Climate, the Environment, and Sustainable Development. *Environmental Modelling & Software*, pp. 112, 143-156.

Hurlbert, S. H. (1971). The Nonconcept of Species Diversity: A Critique and Alternative Parameters. *Ecology*, 52(4), pp. 577-586.

Hutchinson, G. E. (1961). The Paradox of the Plankton. *American Naturalist*, 95(882), pp. 137-145.

Hutchinson, M. C., and Lucey, B. (2024). A Bibliometric and Systemic Literature Review of Biodiversity Finance. *Finance Research Letters*, 105377, 7 pages.

Institute for Global Environmental Strategies (IGES) (2022). *Nationally Determined Contributions (NDC) Database Version 7.7*. Source: https://pub.iges.or.jp/pub/iges-ndc-database.

Interagency Working Group on Social Cost of Greenhouse Gases (2021). *Technical Support Document: Social Cost of Carbon, Methane, and Nitrous Oxide, Interim Estimates under Executive Order 13990*. United States Government, 2021.

Intergovernmental Panel on Climate Change (1999). Procedures for the Preparation, Review, Acceptance, Adoption, Approval and Publication of IPCC Reports. *Appendix A to the Principles Governing IPCC Work*, 29 pages.

Intergovernmental Panel on Climate Change (2006). 2006 IPCC Guidelines for National Greenhouse Gas Inventories. Prepared by the National Greenhouse Gas Inventories Programme, Eggleston H. S., Buendia L., Miwa K., Ngara T. and Tanabe K. (Eds).

Intergovernmental Panel on Climate Change (2007). Climate Change 2007: The Physical Science Basis — Contribution of Working Group I to the Fourth Assessment Report of the IPCC. *Report*.

Intergovernmental Panel on Climate Change (2013). Climate Change 2013: The Physical Science Basis — Contribution of Working Group I to the Fifth Assessment Report of the IPCC. *Report*.

Intergovernmental Panel on Climate Change (2014a). Climate Change 2014: Mitigation of Climate Change — Contribution of Working Group III to the Fifth Assessment Report of the IPCC. *Report*.

Intergovernmental Panel on Climate Change (2014b). Climate Change 2014: Synthesis Report — Contribution of Working Groups I, II and III to the Fifth Assessment Report of the IPCC. *Report*, 151 pages.

Intergovernmental Panel on Climate Change (2018). Global Warming of 1.5°C. *Special Report*, 616 pages.

Intergovernmental Panel on Climate Change (2019). *2019 Refinement to the 2006 IPCC Guidelines for National Greenhouse Gas Inventories*. Prepared by Calvo Buendia, E., Tanabe, K., Kranjc, A., Baasansuren, J., Fukuda, M., Ngarize, S., Osako, A., Pyrozhenko, Y., Shermanau, P. and Federici, S. (Eds).

Intergovernmental Panel on Climate Change (2021). Climate Change 2021: The Physical Science Basis — Contribution of Working Group I to the Sixth Assessment Report of the IPCC. *Report*.

Intergovernmental Panel on Climate Change (2022). Climate Change 2022: Mitigation of Climate Change — Contribution of Working Group III to the Sixth Assessment Report of the IPCC. *Report*.

Intergovernmental Science-Policy Platform on Biodiversity and Ecosystem Services (2016). *The Assessment Report of the Intergovernmental Science-Policy Platform on Biodiversity and Ecosystem Services on Pollinators, Pollination and Food Production*. IPBES secretariat, prepared by Potts, S.G., Imperatriz-Fonseca, V. L., and Ngo H. T. (Eds), 552 pages.

Intergovernmental Science-Policy Platform on Biodiversity and Ecosystem Services (2019). *Global Assessment Report on Biodiversity and Ecosystem Services of the Intergovernmental Science-Policy Platform on Biodiversity and Ecosystem Services*. IPBES secretariat, prepared by Brondízio, E. S., Settele, J., Díaz, S., and Ngo, H. T. (Eds), 1144 pages.

Intergovernmental Science-Policy Platform on Biodiversity and Ecosystem Services (2019). *Thematic Assessment Report on Invasive Alien Species and their Control*. IPBES secretariat, prepared by Roy, H. E., Pauchard, A., Stoett, P., and Renard Truong, T. (Eds.), 952 pages.

International Association of Insurance Supervisors (2021). Supervision of Climate-related Risks in the Insurance Sector. *Application Paper*, May, 37 pages.

International Association of Insurance Supervisors (2023). Public Consultation on Climate Risk Supervisory Guidance — Part One. *Consultation Document*, March, 12 pages.

International Capital Market Association (2021a). Green Bond Principles — Voluntary Process Guidelines for Issuing Green Bonds. *Guidelines*, June.

International Capital Market Association (2021b). Social Bond Principles — Voluntary Process Guidelines for Issuing Social Bonds. *Guidelines*, June.

International Capital Market Association (2022). Green, Social and Sustainability Bonds: A High-Level Mapping to the Sustainable Development Goals. *Report*, June.

International Capital Market Association (2023). Bonds to Finance the Sustainable Blue Economy. *Report*, September, 33 pages.

International Energy Agency (2017). Energy Technology Perspectives 2017: Catalysing Energy Technology Transformations. *Flagship Report*, June.

International Energy Agency (2021). Net Zero by 2050: A Roadmap for the Global Energy Sector. *Report*, July.

International Energy Agency (2022). Direct Air Capture: A Key Technology for Net Zero. *Report*, April, 76 pages.

International Finance Corporation (2020). Green Bond Handbook: A Step-by-step Guide to Issuing a Green Bond. *Guidelines*.

International Finance Corporation (2022). Blue Finance — Guidance for Financing the Blue Economy, Building on the Green Bond Principles and the Green Loan Principles. *Guidelines*, January.

International Organization of Securities Commissions (2021). Environmental, Social and Governance (ESG) Ratings and Data Products Providers. *Report*, 23 November 2021, 56 pages.

International Organization of Securities Commissions (2023). Supervisory Practices to Address Greenwashing. *Report*, 4 December 2023, 94 pages.

International Sustainability Standards Board (2022a). IFRS S1 General Requirements for Disclosure of Sustainability-related Financial Information. *Exposure Draft*, March.

International Sustainability Standards Board (2022b). IFRS S2 Climate-related Disclosures. *Exposure Draft*, March.

Israel, R. B., Rosenthal, J. S., and Wei, J. Z. (2001). Finding Generators for Markov Chains via Empirical Transition Matrices, with Applications to Credit Ratings. *Mathematical Finance*, 11(2), pp. 245-265.

ISS Governance (2022). Climate & Voting: 2021 Review and Global Trends. *Insights Report*, May.

IUCN (2012). *IUCN Red List Categories and Criteria*. Version 3.1, second edition, 32 pages.

IUCN (2022). *The IUCN Red List of Threatened Species*. Version 2022-1, www.iucnredlist.org.

IUCN (2024a). *The IUCN Red List of Threatened Species*. Version 2024-1, www.iucnredlist.org.

IUCN (2024b). *Summary Statistics*. Version 2024-1, www.iucnredlist.org.

Izzo, M. F., and Magnanelli, B. S. (2012). Does it Pay or Does Firm Pay? The relation Between CSR Performance and the Cost of Debt. *SSRN*, 1986131.

Jackson, E. T. (2013). Interrogating the Theory of Change: Evaluating Impact Investing where It Matters Most. *Journal of Sustainable Finance & Investment*, 3(2), pp. 95-110.

Jackson, J. B., Kirby, M. X., Berger, W. H., ..., and Warner, R. R. (2001). Historical Overfishing and the Recent Collapse of Coastal Ecosystems. *Science*, 293(5530), pp. 629-637.

Jahnke, P. (2019). Ownership Concentration and Institutional Investors' Governance through Voice and Exit. *Business and Politics*, 21(3), pp. 327-350.

Jarrow, R.A., Lando, D., and Turnbull, S.M. (1997). A Markov Model for the Term Structure of Credit Risk Spreads. *Review of Financial Studies*, 10(2), pp. 481-523.

Jaulin, T., Le Berthe, T., Deixonne, F., and De Vecchi, V. (2022). EU Sustainable Finance Action Plan: State of Play. *Amundi ESG Thema*, 11, 13 pages.

Jeevanjee, N. (2023). Climate Sensitivity from Radiative-Convective Equilibrium: A Chalkboard Approach. *American Journal of Physics*, 91(9), pp. 731-745.

Jensen, M. C. (1968). The Performance of Mutual Funds in the Period 1945–1964. *Journal of Finance*, 23(2), pp. 389-416.

Jensen, M. C. (1993). The Modern Industrial Revolution, Exit, and the Failure of Internal Control Systems. *Journal of Finance*, 48(3), pp. 831-880.

Jensen, M. C., and Meckling, W. H. (1976). Theory of the Firm: Managerial Behavior, Agency Costs and Ownership Structure. *Journal of Financial Economics*, 3(4), pp. 305-360.

Jewell, J., and Cherp, A. (2020). On the Political Feasibility of Climate Change Mitigation Pathways: Is it Too Late to Keep Warming Below 1.5°C?. *WIREs Climate Change*, 11(1), e621, 12 pages.

Jha, A., and Cox, J. (2015). Corporate Social Responsibility and Social Capital. *Journal of Banking & Finance*, 60, pp. 252-270.

Joe, H. (1997). *Multivariate Models and Dependence Concepts*. Monographs on Statistics and Applied Probability, 73, Chapman & Hall.

Johansen, D. F., and Vestvik, R. A. (2020). The Cost of Saving our Ocean — Estimating the Funding Gap of Sustainable Development Goal 14. *Marine Policy*, 112, 103783, 12 pages.

Johnson, S. A., Moorman, T. C., and Sorescu, S. (2009). A Reexamination of Corporate Governance and Equity Prices. *Review of Financial Studies*, 22(11), pp. 4753-4786.

Jolles, A. E. (2007). Population Biology of African Buffalo (*Syncerus caffer*) at Hluhluwe-iMfolozi Park, South Africa. *African Journal of Ecology*, 45(3), pp. 398-406.

Jondeau, E., Mojon, B., and Pereira da Silva, L. A. (2021). Building Benchmark Portfolios with Decreasing Carbon Footprints. *Swiss Finance Institute Research Paper*, 21-91.

Jones, K. C., and De Voogt, P. (1999). Persistent Organic Pollutants (POPs): State of the Science. *Environmental Pollution*, 100(1-3), pp. 209-221.

Jones, M. W., Peters, G. P., Gasser, T., ..., and Le Quéré, C. (2023). National Contributions to Climate Change due to Historical Emissions of Carbon Dioxide, Methane, and Nitrous Oxide since 1850. *Scientific Data*, 10(1), 23 pages.

Jones, T. M. (1980). Corporate Social Responsibility Revisited, Redefined. *California Management Review*, 22(3), pp. 59-67.

Joos, F., Roth, R., Fuglestvedt, J. S., ..., and Weaver, A. J. (2013). Carbon Dioxide and Climate Impulse Response Functions for the Computation of Greenhouse Gas Metrics: A Multi-model Analysis. *Atmospheric Chemistry and Physics*, 13(5), pp. 2793-2825.

Joppa, L. N., Luers, A., Willmott, E., Friedmann, S. J., Hamburg, S. P., and Broze, R. (2021). Microsoft's Million-Tonne $CO_2$-Removal Purchase — Lessons for Net Zero. *Nature*, 597(7878), pp. 629-632.

Jorion, P. (2003). Portfolio Optimization with Tracking-Error Constraints. *Financial Analysts Journal*, 59(5), pp. 70-82.

Jouzel, J. (2013). A Brief History of Ice Core Science over the last 50 yr. *Climate of the Past*, 9(6), pp. 2525-2547.

Jouzel, J., Masson-Delmotte, V., Cattani, O., ..., and Wolff, E. W. (2007). Orbital and Millennial Antarctic Climate Variability over the Past 800,000 Years. *Science*, 317(5839), pp. 793-796.

Kaplan, R. S., Ramanna, K., and Roston, M. (2023). Accounting for Carbon Offsets — Establishing the Foundation for Carbon-trading Markets. *Harvard Business School Working Paper*, 23-050, 16 pages.

Kapraun, J., Latino, C., Scheins, C., and Schlag, C. (2021). (In)-credibly Green: Which Bonds Trade at a Green Bond Premium?. *SSRN*, 3347337.

Kar, T. K., and Ghosh, B. (2013). Impacts of Maximum Sustainable Yield Policy to Prey-predator Systems. *Ecological Modelling*, 250, pp. 134-142.

Kaufmann, D., Kraay, A., and Mastruzzi, M. (2010). The Worldwide Governance Indicators: Methodology and Analytical Issues. *World Bank Policy Research Working Paper*, 5430 (SSRN, 1682130).

Kavvathas, D. (2001). Estimating Credit Rating Transition Probabilities for Corporate Bonds. *SSRN*, 248421.

Kaya, Y., and Yokobori, K. (Eds) (1997). *Environment, Energy, and Economy: Strategies for Sustainability*. United Nations University Press, 393 pages.

Keeling, C. D. (1960). The Concentration and Isotopic Abundances of Carbon Dioxide in the Atmosphere. *Tellus*, 12(2), pp. 200-203.

Keeling, C. D., Bacastow, R. B., Bainbridge, A. E., Ekdahl Jr, C. A., Guenther, P. R., Waterman, L. S., and Chin, J. F. S. (1976). Atmospheric Carbon Dioxide Variations at Mauna Loa Observatory, Hawaii. *Tellus*, 28(6), pp. 538-551.

Keeling, C. D. (1978). The Influence of Mauna Loa Observatory on the Development of Atmospheric $CO_2$ Research. In Miller, J (Ed.), *Mauna Loa Observatory: A 20th Anniversary Report*, National Oceanic and Atmospheric Administration Special Report, pp. 36-54.

Keeling, C. D., Piper, S. C., Bacastow, R. B., Wahlen, M., Whorf, T. P., Heimann, M., and Meijer, H. A. (2001). Exchanges of Atmospheric $CO_2$ and $^{13}CO_2$ with the Terrestrial Biosphere and Oceans from 1978 to 2000. I. Global aspects. *Scripps Institution of Oceanography, San Diego, SIO Reference Series*, 01-06, 28 pages.

Kellett, C. M., Faulwasser, T., and Weller, S. R. (2016). *DICE-2013R-mc — A Matlab/CasADi Implementation of Vanilla DICE-2013R*. Code source available at https://github.com/cmkellett/DICE2013R-mc.

Kellett, C. M., Weller, S. R., Faulwasser, T., Grüne, L., and Semmler, W. (2019). Feedback, Dynamics, and Optimal Control in Climate Economics. *Annual Reviews in Control*, 47, pp. 7-20.

Kelly, D. L., and Kolstad, C. D. (1999). Integrated Assessment Models for Climate Change Control. In Folmer, H., and Tietenberg, T. (Eds), *International Yearbook of Environmental and Resource Economics 1999/2000*, Edward Elgar, pp. 171-197.

Kemp, L., Xu, C., Depledge, J., ..., and Lenton, T. M. (2022). Climate Endgame: Exploring Catastrophic Climate Change Scenarios. *Proceedings of the National Academy of Sciences*, 119(34), e2108146119, 9 pages.

Khaled, R., Ali, H., and Mohamed, E. K. (2021). The Sustainable Development Goals and Corporate Sustainability Performance: Mapping, Extent and Determinants. *Journal of Cleaner Production*, 311, 127599.

Khanchel, I., and Lassoued, N. (2022). ESG Disclosure and the Cost of Capital: Is there a Ratcheting Effect over Time?. *Sustainability*, 14(15), 9237, 19 pages.

Kiehl, J. T., and Trenberth, K. E. (1997). Earth's Annual Global Mean Energy Budget. *Bulletin of the American Meteorological Society*, 78(2), pp. 197-208.

Kitchen, A. M., Gese, E. M., and Schauster, E. R. (1999). Resource Partitioning Between Coyotes and Swift Foxes: Space, Time, and Diet. *Canadian Journal of Zoology*, 77(10), pp. 1645-1656.

Kitzes, J. (2013). An Introduction to Environmentally-extended Input-output Analysis. *Resources*, 2(4), pp. 489-503.

Klein, A. M., Vaissière, B. E., Cane, J. H., ..., and Tscharntke, T. (2007). Importance of Pollinators in Changing Landscapes for World Crops. *Proceedings of the Royal Society B: Biological Sciences*, 274(1608), pp. 303-313.

Kleinberg, R. L. (2020). The Global Warming Potential Misrepresents the Physics of Global Warming Thereby Misleading Policy Makers. *EarthArXiv*, November.

Klose, A. K., Karle, V., Winkelmann, R., and Donges, J. F. (2020). Emergence of Cascading Dynamics in Interacting Tipping Elements of Ecology and Climate. *Royal Society Open Science*, 7(6), 200599, 18 pages.

Kofoworola, O., Dodd, N., Boyano, A., Konstantas, A., Wolf, O., Alessi, L., and Ossola, E. (2019). Development of EU Ecolabel Criteria for Retail Financial Products — Technical Report 2.0. *Joint Research Centre Technical Report*, December, 119 pages.

Kölbel, J. F., Leippold, M., Rillaerts, J., and Wang, Q. (2022). Ask BERT: How Regulatory Disclosure of Transition and Physical Climate Risks Affects the CDS Term Structure. *Swiss Finance Institute Research Paper*, 21-19.

Kolbert, E. (2014). *The Sixth Extinction: An Unnatural History*. Henry Holt and Company, 319 pages.

Köppl, A., and Schratzenstaller, M. (2023). Carbon Taxation: A Review of the Empirical Literature. *Journal of Economic Surveys*, 37(4), pp. 1353-1388.

Kostant, P. C. (1999). Exit, Voice and Loyalty in the Course of Corporate Governance and Counsel's Changing Role. *Journal of Socio-Economics*, 28(3), pp. 203-246.

Konstantas, A., Faraca, G. Dodd, N., Kofoworola, O., Boyano, A., Wolf, O., Alessi, L., and Ossola, E. (2019). Development of EU Ecolabel Criteria for Retail Financial Products — Technical Report 4.0. *Joint Research Centre Technical Report*, March, 141 pages.

Kremen, C. (2005). Managing Ecosystem Services: What Do We Need to Know about Their Ecology?. *Ecology letters*, 8(5), pp. 468-479.

Krueger, P., Sautner, Z., and Starks, L. T. (2020). The Importance of Climate Risks for Institutional Investors. *Review of Financial Studies*, 33(3), pp. 1067-1111.

Kruse, H., Kirkemo, A. M., and Handeland, K. (2004). Wildlife as Source of Zoonotic Infections. *Emerging Infectious Diseases*, 10(12), pp. 2067-2072.

Kuipers, K. J. J., May, R., and Verones, F. (2021). Considering Habitat Conversion and Fragmentation in Characterisation Factors for Land-use Impacts on Vertebrate Species Richness. *Science of the Total Environment*, 801, 149737, 10 pages.

Kurtz, L. (1999). Investment in Minority-Owned Media: A Social Investor's Perspective. *Federal Communications Law Journal*, 51(3), pp. 681-691.

Kuussaari, M., Bommarco, R., Heikkinen, R. K., ..., and Steffan-Dewenter, I. (2009). Extinction Debt: A Challenge for Biodiversity Conservation. *Trends in Ecology & Evolution*, 24(10), pp. 564-571.

Kvenvolden, K. A. (1988). Methane Hydrates and Global Climate. *Global Biogeochemical Cycles*, 2(3), pp. 221-229.

Lafortune, G., Fuller, G., Moreno, J., Schmidt-Traub,G., and Kroll, C. (2018). SDG Index and Dashboards: Detailed Methodological Paper. *Supplementary Materials*, September, 56 pages.

Lamb, W. F., Wiedmann, T., Pongratz, J., ..., and Minx, J. (2021). A Review of Trends and Drivers of Greenhouse Gas Emissions by Sector from 1990 to 2018. *Environmental Research Letters*, 16(7), 073005.

Landrigan, P. J., Fuller, R., Acosta, N. J. R., ..., and Zhong, M. (2018). The *Lancet* Commission on Pollution and Health. *The Lancet*, 391(10119), pp. 462-512.

Langway, C. C. (2008). The History of Early Polar Ice Cores. *Cold Regions Science and Technology*, 52(2), pp. 101-117.

Lapola, D. M., Pinho, P., Barlow, J., ..., and Walker, W. S. (2023). The Drivers and Impacts of Amazon Forest Degradation. *Science*, 379(6630), eabp8622, 11 pages.

Larcker, D. F., Tayan, B., and Copland, J. R. (2018). The Big Thumb on the Scale: An Overview of the Proxy Advisory Industry. *Harvard Law School Forum on Corporate Governance*, 9 pages, 14 June 2018.

Larcker, D. F., and Watts, E. M. (2020). Where's the Greenium?. *Journal of Accounting and Economics*, 69(2-3), 101312.

Larsen, B. B., Miller, E. C., Rhodes, M. K., and Wiens, J. J. (2017). Inordinate Fondness Multiplied and Redistributed: The Number of Species on Earth and the New Pie of Life. *Quarterly Review of Biology*, 92(3), pp. 229-265.

Le Guenedal, T. (2019). Economic Modeling of Climate Risks. *SSRN*, 3693661.

Le Guenedal, T., Drobinski, P., and Tankov, P. (2021). Measuring and Pricing Cyclone-Related Physical Risk Under Changing Climate. *SSRN*, 3850673.

Le Guenedal, T., Drobinski, P., and Tankov, P. (2022). Cyclone Generation Algorithm Including a Thermodynamic Module for Integrated National Damage Assessment (CATHERINA 1.0) Compatible with Coupled Model Intercomparison Project (CMIP) Climate Data. *Geoscientific Model Development*, 15(21), pp. 8001-8039.

Le Guenedal, T., Lombard, F, Roncalli, T., and Sekine, T. (2022). Net Zero Carbon Metrics. *SSRN*, 4033686.

Le Guenedal, T., and Roncalli, T. (2022). Portfolio Construction with Climate Risk Measures. In Jurczenko, E. (Ed.), *Climate Investing: New Strategies and Implementation Challenges*, Wiley, December 2022, pp. 49-86.

Leakey, R. E., and Lewin, R. (1995). *The Sixth Extinction: Patterns of Life and the Future of Humankind*. Doubleday, 271 pages.

Lebreton, L., Slat, B., Ferrari, F., ..., and Reisser, J. (2018). Evidence that the Great Pacific Garbage Patch is Rapidly Accumulating Plastic. *Scientific Reports*, 8(1), pp. 1-15.

Legesse, F., Degefa, S., and Soromessa, T. (2022). Valuation Methods in Ecosystem Services: A Meta-analysis. *World Journal of Forest Research*, 1(1), pp. 1-12.

Leite, P., and Cortez, M. C. (2016). The Performance of European Socially Responsible Fixed-Income Funds. *SSRN*, 2726094.

Lelieveld, J., Evans, J. S., Fnais, M., Giannadaki, D., and Pozzer, A. (2015). The Contribution of Outdoor Air Pollution Sources to Premature Mortality on a Global Scale. *Nature*, 525(7569), pp. 367-371.

Lemoine, D. (2020). *DICE-2016R-Matlab*. Code source available at https://github.com/dlemoine1/DICE-2016R-Matlab.

Lenssen, N. J., Schmidt, G. A., Hansen, J. E., Menne, M. J., Persin, A., Ruedy, R., and Zyss, D. (2019). Improvements in the GISTEMP Uncertainty Model. *Journal of Geophysical Research: Atmospheres*, 124(12), pp. 6307-6326.

Lenton, T. M. (2011). Early Warning of Climate Tipping Points. *Nature Climate Change*, 1(4), pp. 201-209.

Lenton, T. M., Held, H., Kriegler, E., Hall, J. W., Lucht, W., Rahmstorf, S., and Schellnhuber, H. J. (2008). Tipping Elements in the Earth's Climate System. *Proceedings of the National Academy of Sciences*, 105(6), pp. 1786-1793.

Lenton, T. M., Rockström, J., Gaffney, O., Rahmstorf, S., Richardson, K., Steffen, W., and Schellnhuber, H. J. (2019). Climate Tipping Points — Too Risky to Bet Against. *Nature*, 575(7784), pp. 592-595.

Leontief, W. W. (1936). Quantitative Input and Output Relations in the Economic Systems of the United States. *Review of Economics and Statistics*, 18(3), pp. 105-125.

Leontief, W. W. (1941). *Structure of American Economy, 1919–1929: An Empirical Application of Equilibrium Analysis*. Harvard University Press.

Leontief, W. (1970). Environmental Repercussions and the Economic Structure: An Input-output Approach. *Review of Economics and Statistics*, 52(3), pp. 262-271.

Lesiv, M., Schepaschenko, D., Buchhorn, M., ..., and Fritz, S. (2022). Global Forest Management Data for 2015 at a 100 m Resolution. *Scientific Data*, 9(1), 199, 14 pages.

Letts, C. W., Ryan, W., and Grossman, A. (1997). Virtuous Capital: What Foundations Can Learn from Venture Capitalists. *Harvard Business Review*, 75, pp. 36-50.

Levit, D. (2019). Soft Shareholder Activism. *Review of Financial Studies*, 32(7), pp. 2775-2808.

Levit, D., Malenko, N., and Maug, E. (2024). Trading and Shareholder Democracy. *Journal of Finance*, 79(1), pp. 257-304.

Lewis, S. L., and Maslin, M. A. (2015). Defining the Anthropocene. *Nature*, 519(7542), pp. 171-180.

Lezmi, E., Roncalli, T, and Xu, J. (2022). Multi-Period Portfolio Optimization. *SSRN*, 4078043.

Lhotellier J., Less, E. Bossanne, E., and Pesnel, S. (2017). Modélisation et évaluation du poids carbone de produits de consommation et biens d'équipements. *ADEME Report*, September.

Liang, S., Wang, D., He, T., and Yu, Y. (2019). Remote Sensing of Earth's Energy Budget: Synthesis and Review. *International Journal of Digital Earth*, 12(7), pp. 737-780.

Lin, K., Kabel, A., Parker, S., and Joye, C. (2019). Are ESG Alpha and Beta Benefits in Corporate Bonds a Mirage?. *SSRN*, 3352950.

Lisiecki, L. E., and Raymo, M. E. (2005). A Pliocene-Pleistocene Stack of 57 Globally Distributed benthic $\delta^{18}$O Records, *Paleoceanography*, 20(1), 17 pages.

Liu, W., Xie, S. P., Liu, Z., and Zhu, J. (2017). Overlooked Possibility of a Collapsed Atlantic Meridional Overturning Circulation in Warming Climate. *Science Advances*, 3(1), e1601666, 7 pages.

Liu, P. R., and Raftery, A. E. (2021). Country-based Rate of Emissions Reductions Should Increase by 80% Beyond Nationally Determined Contributions to Meet the 2°C Target. *Communications Earth & Environment*, 2(1):29, 10 pages.

Livingston, J. E., and Rummukainen, M. (2020). Taking Science by Surprise: The Knowledge Politics of the IPCC Special Report on 1.5 Degrees. *Environmental Science & Policy*, 112, pp. 10-16.

Loehle, C., and Eschenbach, W. (2012). Historical Bird and Terrestrial Mammal Extinction Rates and Causes. *Diversity and Distributions*, 18(1), pp. 84-91.

Löffler, K. U., Petreski, A., and Stephan, A. (2021). Drivers of Green Bond Issuance and New Evidence on the "Greenium". *Eurasian Economic Review*, 11(1), pp. 1-24.

Lomolino, M. V. (2001). The Species-Area Relationship: New Challenges for an Old Pattern. *Progress in Physical Geography*, 25(1), pp. 1-21.

Longcore, T., and Rich, C. (2004). Ecological Light Pollution. *Frontiers in Ecology and the Environment*, 2(4), pp. 191-198.

Lotka, A. J. (1925). *Elements of Physical Biology*. First edition, Williams and Wilkins Company, 495 pages.

Lorenz, M. O. (1905). Methods of Measuring the Concentration of Wealth. *Journal of the American Statistical Association*, 9(70), pp. 209-219.

Lucas, R. E. (1993). Making A Miracle. *Econometrica*, 61(2), pp. 251-272.

Ludwig, D., Hilborn, R., and Walters, C. (1993). Uncertainty, Resource Exploitation, and Conservation: Lessons from History. *Science*, 260(5104), pp. 17-36.

Lueck, D. (2002). The Extermination and Conservation of the American Bison. *Journal of Legal Studies*, 31(S2), pp. 609-652.

MacArthur, R. H. (1957). On the Relative Abundance of Bird Species. *Proceedings of the National Academy of Sciences*, 43(3), pp. 293-295.

MacArthur, R. H. (1958). Population Ecology of Some Warblers of Northeastern Coniferous Forests. *Ecology*, 39(4), pp. 599-619.

MacArthur, R. (1970). Species Packing and Competitive Equilibrium for Many Species. *Theoretical Population Biology*, 1(1), pp. 1-11.

MacArthur, R. H., and Levins, R. (1964). Competition, Habitat Selection, and Character Displacement in a Patchy Environment. *Proceedings of the National Academy of Sciences*, 51(6), pp. 1207-1210.

MacArthur, R. H., and Wilson, E. O. (1967). *The Theory of Island Biogeography*. Princeton University Press, 203 pages.

Mace, G. M. (1998). Getting the Measure of Extinction. *People Planet*, 7(4):9, PMID: 12348876.

Mace, G. M., and Baillie, J. E. M. (2007). The 2010 Biodiversity Indicators: Challenges for Science and Policy. *Conservation Biology*, 21(6), pp. 1406-1413.

Mack, R. N., Simberloff, D., Lonsdale, W. M., Evans, H., Clout, M., and Bazzaz, F. A. (2000). Biotic Invasions: Causes, Epidemiology, Global Consequences, and Control. *Ecological Applications*, 10(3), pp. 689-710.

MacLeod, M., Arp, H. P. H., Tekman, M. B., and Jahnke, A. (2021). The Global Threat from Plastic Pollution. *Science*, 373(6550), pp. 61-65.

Mair, L., Bennun, L. A., Brooks, T. M., ..., and McGowan, P. J. (2021). A Metric for Spatially Explicit Contributions to Science-based Species Targets. *Nature Ecology & Evolution*, 5(6), pp. 836-844.

Malenko, A., Malenko, N., and Spatt, C. S. (2021). Creating Controversy in Proxy Voting Advice. *NBER*, 29036.

Maltais, A., and Nykvist, B. (2020). Understanding the Role of Green Bonds in Advancing Sustainability. *Journal of Sustainable Finance & Investment*, pp. 1-20.

Malthus, T. R. (1798). *An Essay on the Principle of Population*. First edition, J. Johnson.

Manabe, S., and Wetherald, R. T. (1967). Thermal Equilibrium of the Atmosphere with a Given Distribution of Relative Humidity. *Journal of the Atmospheric Sciences*, 24(3), pp. 241-259.

March, A., Failler, P., and Bennett, M. (2023). Challenges when Designing Blue Bond Financing for Small Island Developing States. *ICES Journal of Marine Science*, 80(8), pp. 2244-2251.

Mardones, C., and Mena, C. (2020). Economic, Environmental and Distributive Analysis of the Taxes to Global and Local Air Pollutants in Chile. *Journal of Cleaner Production*, 259, 120893.

Margolis, J. D., Elfenbein, H. A., and Walsh, J. P. (2009). Does it Pay to be Good... and does it Matter? A Meta-analysis of the Relationship between Corporate Social and Financial Performance. *SSRN*, 1866371.

Markowitz H. M. (1952), Portfolio Selection. *Journal of Finance*, 7(1), pp. 77-91.

Markowitz H. M. (1956). The Optimization of a Quadratic Function Subject to Linear Constraints. *Naval Research Logistics Quarterly*, 3(1-2), pp. 111-133.

Martellini, L., and Vallée, L. S. (2021). Measuring and Managing ESG Risks in Sovereign Bond Portfolios and Implications for Sovereign Debt Investing. *Journal of Portfolio Management*, 47(9), pp. 198-223.

Martin, M. (2013). Making Impact Investible. *SSRN*, 2272553.

Matos, P. (2020). *ESG and Responsible Institutional Investing around the World: A Critical Review*. CFA Institute Research Foundation.

Matsusaka, J. G., Ozbas, O., and Yi, I. (2021). Can Shareholder Proposals Hurt Shareholders? Evidence from Securities and Exchange Commission No-action-letter Decisions. *Journal of Law and Economics*, 64(1), pp. 107-152.

Matsusaka, J. G., and Shu, C. (2024). Robo-Voting: Does Delegated Proxy Voting Pose a Challenge for Shareholder Democracy?. *SSRN*, 4564648.

Matthews, T. J., and Whittaker, R. J. (2015). On the Species Abundance Distribution in Applied Ecology and Biodiversity Management. *Journal of Applied Ecology*, 52(2), pp. 443-454.

May, R. M. (1975). Patterns of Species Abundance and Distribution. In Cody, M., and Diamond, J. (Eds), *Ecology and Evolution of Communities*, Harvard University Press, pp. 81-120.

May, R. M. (1988). How Many Species are there on Earth?. *Science*, 241(4872), pp. 1441-1449.

May, R. M. (2010). Tropical Arthropod Species, More or Less?. *Science*, 329(5987), pp. 41-42.

McCahery, J. A., Sautner, Z., and Starks, L. T. (2016). Behind the Scenes: The Corporate Governance Preferences of Institutional Investors. *Journal of Finance*, 71(6), pp. 2905-2932.

McCarthy, D. P., Donald, P. F., Scharlemann, J. P. W., ..., and Butchart, S. H. (2012). Financial Costs of Meeting Global Biodiversity Conservation Targets: Current Spending and Unmet Needs. *Science*, 338(6109), pp. 946-949.

McGill, B. J., Etienne, R. S., Gray, J. S., ..., and White, E. P. (2007). Species Abundance Distributions: Moving Beyond Single Prediction Theories to Integration within an Ecological Framework. *Ecology Letters*, 10(10), pp. 995-1015.

McKibbin, W. J., and Wilcoxen, P. J. (2002). The Role of Economics in Climate Change Policy. *Journal of Economic Perspectives*, 16(2), pp. 107-129.

McKinsey (2022). *The Net-zero Transition — What it Would Cost, What it Could Bring*. January 2022, 224 pages.

McKinsey (2024). Private Markets: A Slower Era. *Report*, March, 66 pages.

Medina, A., De La Cruz, A., and Tang, Y. (2022). Corporate Ownership and Concentration. *OECD Corporate Governance Working Papers*, 27, 50 pages.

Megaeva, K., Engelen, P. J., and Van Liedekerke, L. (2021). A Comparative Study of European Sustainable Finance Labels. *SSRN*, 3790435.

Megaeva, K., Engelen, P. J., and Van Liedekerke, L. (2023). New Trends in European Sustainable Finance Labels. *SSRN*, 4688587.

Meijer, L. J. J., Van Emmerik, T., Van Der Ent, R., Schmidt, C., and Lebreton, L. (2021). More than 1000 Rivers Account for 80% of Global Riverine Plastic Emissions into the Ocean. *Science Advances*, 7(18), eaaz5803, 13 pages.

Meinshausen, M., Lewis, J., McGlade, C., ..., Hackmann, B. (2022). Realization of Paris Agreement Pledges may limit Warming just below 2°C. *Nature*, 604(7905), pp. 304-309.

Meinshausen, M., Raper, S. C. B., and Wigley, T. M. L. (2011). Emulating Coupled Atmosphere-Ocean and Carbon Cycle Models with a Simpler Model, MAGICC6 — Part 1: Model Description and Calibration. *Atmospheric Chemistry and Physics*, 11(4), pp. 1417-1456.

Mejino-López, J., and Oliu-Barton, M. (2024). How Much Does Europe Pay for Clean Air?. *Bruegel Working Paper*, 15/2024, June, 49 pages.

Menif, M., Redon, N., and Husson-Traore, A. C. (2023). Fonds durables labellisés en Europe au 31 juillet 2023. *Novethic Publication*, 4 pages.

Menz, K. M. (2010). Corporate Social Responsibility: Is it Rewarded by the Corporate Bond Market? A Critical Note. *Journal of Business Ethics*, 96(1), pp. 117-134.

Merlivat, L., and Jouzel, J. (1979). Global Climatic Interpretation of the Deuterium-Oxygen 18 Relationship for Precipitation. *Journal of Geophysical Research: Oceans*, 84(C8), pp. 5029-5033.

Millennium Ecosystem Assessment (2005). Ecosystems and Human Well-being: Synthesis. *Report*, 155 pages, www.millenniumassessment.org.

Miller, R. E., and Blair, P. D. (2009). *Input-output Analysis: Foundations and Extensions*. Second edition, Cambridge University Press.

Mintzberg, H. (1983). The Case for Corporate Social Responsibility. *Journal of Business Strategy*, 4(2), pp. 3-13.

Minx, J. C., Lamb, W. F., Callaghan, M. W., ..., and del Mar Zamora Dominguez, M. (2018). Negative Emissions — Part 1: Research Landscape and Synthesis. *Environmental Research Letters*, 13(6), 063001, 29 pages.

Minx, J. C., Wiedmann, T., Wood, R., ..., and Ackerman, F. (2009). Input-output Analysis and Carbon Footprinting: An Overview of Applications. *Economic Systems Research*, 21(3), pp. 187-216.

Mio, C., Panfilo, S., and Blundo, B. (2020). Sustainable Development Goals and the Strategic Role of Business: A Systematic Literature Review. *Business Strategy and the Environment*, 29(8), pp. 3220-3245.

Mishra, B. (2018). Social Impact Measurement and Investment: Methods, Limitations and Challenges. *Transcience*, 9(1), pp. 20-51.

Missemer, A. (2018). Natural Capital as an Economic Concept, History and Contemporary Issues. *Ecological Economics*, 143, pp. 90-96.

Mitchell, R. K., Agle, B. R., and Wood, D. J. (1997). Toward a Theory of Stakeholder Identification and Salience: Defining the Principle of Who and What Really Counts. *Academy of Management Review*, 22(4), pp. 853-886.

Mittermeier, R. A., Turner, W. R., Larsen, F. W., Brooks, T. M., and Gascon, C. (2011). Global Biodiversity Conservation: The Critical Role of Hotspots. In Zachos, F. E., and Habel, J. C. (Eds), *Biodiversity Hotspots: Distribution and Protection of Conservation Priority Areas*, Springer, Chapter 1, pp. 3-22.

Moler, C., and Van Loan, C.F. (2003). Nineteen Dubious Ways to Compute the Exponential of a Matrix, Twenty-Five Years Later. *SIAM Review*, 45(1), pp. 3-49.

Moody's (2022). Sovereign Default and Recovery Rates, 1983–2021. *Report*, April.

Mooney, H. A., and Ehrlich, P. R. (1997). Ecosystem Services: A Fragmentary History. In Daily, G. C. (Ed.), *Nature's Services: Societal Dependence On Natural Ecosystems*, Island Press, Chapter 2, pp. 11-19.

Moore, F. C., Rising, J., Lollo, N., ..., and Anthoff, D. (2018). Mimi-PAGE, An Open-source Implementation of the PAGE09 Integrated Assessment Model. *Scientific Data*, 5, 180187.

Moore, G. W. K., Våge, K., Renfrew, I. A., and Pickart, R. S. (2022). Sea-ice Retreat Suggests Re-organization of Water Mass Transformation in the Nordic and Barents Seas. *Nature Communications*, 13(67), 8 pages.

Mora, C., Tittensor, D. P., Adl, S., Simpson, A. G., and Worm, B. (2011). How Many Species are there on Earth and in the Ocean?. *PLoS biology*, 9(8), e1001127, 8 pages.

Morice, C. P., Kennedy, J. J., Rayner, N. A., ..., and Simpson, I. R. (2021). An Updated Assessment of Near-surface Temperature Change from 1850: The HadCRUT5 Data Set. *Journal of Geophysical Research: Atmospheres*, 126(3), e2019JD032361, 28 pages.

Morningstar (2023). Investing in Times of Climate Change 2023?. *Morningstar Manager Research Report*, 54 pages, September 2023.

Morningstar (2024a). Global Sustainable Fund Flows: Q4 2023 in Review. *Morningstar Manager Research Report*, 45 pages, January 2024.

Morningstar (2024b). SFDR Article 8 and Article 9 Funds: Q4 2023 in Review. *Morningstar Manager Research Report*, 44 pages, January 2024.

Moskowitz, M. (1972). Choosing Socially Responsible Stocks. *Business and Society Review*, 1(1), pp. 71-75.

MSCI (2020). MSCI ESG Ratings Methodology. *Methodology Document*, April.

MSCI (2022). MSCI ESG Ratings Methodology. *Executive Summary*, June.

MSCI ESG Research (2024). MSCI SDG Alignment Methodology. *Methodology Document*, January, 51 pages.

Müller-Wenk, R. (1998). Land Use — The Main Threat to Species: How to Include Land Use in LCA. Institut für Wirtschaft und Ökologie, Universität St. Gallen, *IWÖ Discussion Paper*, 64, 46 pages.

Murphy, K. J. (1985). Corporate Performance and Managerial Remuneration: An Empirical Analysis. *Journal of Accounting and Economics*, 7(1-3), pp. 11-42.

Myers, N. (1988). Threatened Biotas: "Hot Spots" in Tropical Forests. *Environmentalist*, 8, pp. 187-208.

Myers, N. (1990). The Biodiversity Challenge: Expanded Hot-spots Analysis. *Environmentalist*, 10(4), pp. 243-256.

Myers, N., Mittermeier, R., Mittermeier, C. G., Da Fonseca, G. A. B., and Kent, J. (2000). Biodiversity Hotspots for Conservation Priorities. *Nature*, 403, pp. 853-858.

Myers, R. A., Hutchings, J. A., and Barrowman, N. J. (1997). Why Do Fish Stocks Collapse? The Example of Cod in Atlantic Canada. *Ecological Applications*, 7(1), pp. 91-106.

Myers, R. A., and Worm, B. (2003). Rapid Worldwide Depletion of Predatory Fish Communities. *Nature*, 423(6937), pp. 280-283.

Myllyvirta, L. (2020). Quantifying the Economic Costs of Air Pollution from Fossil Fuels. *Centre for Research on Energy and Clean Air (CREA)*, *Working Paper*, February, 14 pages.

Naidu, R., Biswas, B., Willett, I. R., ..., and Aitken, R. J. (2021). Chemical Pollution: A Growing Peril and Potential Catastrophic Risk to Humanity. *Environment International*, 156, 106616, 12 pages.

Naiken, L. (2002). Keynote Paper: FAO Methodology for Estimating the Prevalence of Undernourishment. In *Measurement and Assessment of Food Deprivation and Undernutrition*, Proceedings of the International Scientific Symposium convened by the Agriculture and Economic Development Analysis Division, FAO, Rome, 26-28 June 2002.

Nasi, R., Brown, D., Wilkie, D., Bennett, E., Tutin, C., Van Tol, G., and Christophersen, T. (2008). *Conservation and Use of Wildlife-based Resources: The Bushmeat Crisis*. Secretariat of the Convention on Biological Diversity and Center for International Forestry Research, CBD Technical Series, 33, 50 pages.

Nasi, R., Taber, A., and Van Vliet, N. (2011). Empty Forests, Empty Stomachs? Bushmeat and Livelihoods in the Congo and Amazon Basins. *International Forestry Review*, 13(3), pp. 355-368.

National Academies of Sciences, Engineering, and Medicine (2019). *Negative Emissions Technologies and Reliable Sequestration: A Research Agenda*. The National Academy Press, 510 pages.

NBIM (2020). Shareholder Voting Process — Asset Management Perspective. *Report*, March.

Nelsen, R. B. (2006). *An Introduction to Copulas*. Second edition, Springer.

Nemet, G. F., Callaghan, M. W., Creutzig, F., ..., and Smith, P. (2018). Negative Emissions — Part 3: Innovation and Upscaling. *Environmental Research Letters*, 13(6), 063003, 31 pages.

Newbold, S. C., and Marten, A. L. (2014). The Value of Information for Integrated Assessment Models of Climate Change. *Journal of Environmental Economics and Management*, 68(1), pp. 111-123.

Newman, M. C. (2019). *Fundamentals of Ecotoxicology — The Science of Pollution*. Fifth edition, CRC Press, 708 pages.

Ng, A. C., and Rezaee, Z. (2015). Business Sustainability Performance and Cost of Equity Capital. *Journal of Corporate Finance*, 34, pp. 128-149.

NGFS (2022). NGFS Scenarios for Central Banks and Supervisors. *Report*, September.

NGFS (2024). Nature-related Financial Risks: A Conceptual Framework to Guide Action by Central Banks and Supervisors. *Report*, July, 50 pages.

Noss, R. F., Platt, W. J., Sorrie, B. A., ..., and Peet, R. K. (2015). How Global Biodiversity Hotspots May Go Unrecognized: Lessons from the North American Coastal Plain. *Diversity and Distributions*, 21(2), pp. 236-244.

Nordhaus, W. D. (1977). Economic Growth and Climate: the Carbon Dioxide Problem. *American Economic Review*, 67(1), pp. 341-346.

Nordhaus, W. D. (1992). An Optimal Transition Path for Controlling Greenhouse Gases. *Science*, 258(5086), pp. 1315-1319.

Nordhaus, W. D. (2007). A Review of the Stern Review on the Economics of Climate Change. *Journal of Economic Literature*, 45(3), pp. 686-702.

Nordhaus, W. D. (2008). *A Question of Balance: Weighing the Options on Global Warming Policies*. Yale University Press.

Nordhaus, W. D. (2017a). Revisiting the Social Cost of Carbon. *Proceedings of the National Academy of Sciences*, 114(7), pp. 1518-1523.

Nordhaus, W. D. (2017b). Integrated Assessment Models of Climate Change. *NBER Reporter*, 3, September, pp. 16-20.

Nordhaus, W. D. (2018a). Evolution of Modeling of the Economics of Global Warming: Changes in the DICE Model, 1992–2017. *Climatic Change*, 148(4), pp. 623-640.

Nordhaus, W. D. (2018b). Projections and Uncertainties about Climate Change in An Era of Minimal Climate Policies. *American Economic Journal: Economic Policy*, 10(3), pp. 333-360.

Nordhaus, W. D. (2019). *Climate Change: The Ultimate Challenge for Economics*. *American Economic Review*, 109(6), pp. 1991-2014.

Nordhaus, W. D., and Boyer, J. G. (1999). Requiem for Kyoto: An Economic Analysis of the Kyoto Protocol. *Energy Journal*, 20(1), pp. 93-130.

Nordhaus, W. D., and Boyer, J. G. (2000). *Warming the World: Economic Models of Global Warming*. MIT Press.

Nordhaus, W. D., and Sztorc, P. (2013). *DICE 2013R: Introduction and User's Manual*. Yale University, Second Edition, October.

Nordhaus, W. D., and Yang, Z. (1996). A Regional Dynamic General-equilibrium Model of Alternative Climate-change Strategies. *American Economic Review*, 86(4), pp. 741-765.

Norris, J. R. (1997). *Markov Chains*. Cambridge Series in Statistical and Probabilistic Mathematics, Cambridge University Press.

North Greenland Ice Core Project members (2004). High-resolution Record of Northern Hemisphere Climate Extending into the Last Interglacial Period. *Nature*, 431(7005), pp. 147-151.

Nurk, S., Koren, S., Rhie, A., ..., and Phillippy, A. M. (2022). The Complete Sequence of a Human Genome. *Science*, 376(6588), pp. 44-53.

O'Donohoe, N., Leijonhufvud, C., Saltuk, Y., Bugg-Levine, A., and Brandenburg, M. (2010). Impact Investments: An Emerging Asset Class. J.P. Morgan Global Research & Rockefeller Foundation, *Report*, 96 pages.

O'Neill, B. C., Kriegler, E., Ebi, K. L., ..., and Solecki, W. (2017). The Roads Ahead: Narratives for Shared Socioeconomic Pathways Describing World Futures in the 21st Century. *Global Environmental Change*, 42, pp. 169-180.

O'Neill, B. C., Kriegler, E., Riahi, K., Ebi, K. L., Hallegatte, S., Carter, T. R., Mathur, R., and Van Vuuren, D. P. (2014). A New Scenario Framework for Climate Change Research: The Concept of Shared Socioeconomic Pathways. *Climatic Change*, 122, pp. 387-400.

Oberthür, S., and Ott, H. E. (1995). The First Conference of the Parties. *Environmental Policy and Law*, 25(4-5), pp. 144-156.

Oberthür, S., and Ott, H. E. (1999). *The Kyoto Protocol: International Climate Policy for the 21st Century*. Springer, 358 pages.

Observatoire de la Responsabilité Sociétale des Entreprises (2001). Guide des Organismes d'Analyse Sociétale et Environnementale. *Report*, October.

Observatoire de la Responsabilité Sociétale des Entreprises (2007). Guide to Sustainability Analysis Organisations — Profiles. *Report*, December.

OECD (2021). Biodiversity, Natural Capital and the Economy: A Policy Guide for Finance, Economic and Environment Ministers. *OECD Environment Policy Papers*, 26, May, 83 pages.

OECD (2022). *Global Plastics Outlook: Policy Scenarios to 2060*. OECD Publishing, Paris.

Ohlson, J. A., and Juettner-Nauroth, B. E. (2005). Expected EPS and EPS Growth as Determinants of Value. *Review of Accounting Studies*, 10, pp. 349-365.

Ohlmann, M., Miele, V., Dray, S., Chalmandrier, L., O'connor, L., and Thuiller, W. (2019). Diversity Indices for Ecological Networks: A Unifying Framework using Hill Numbers. *Ecology letters*, 22(4), pp. 737-747.

Oikonomou, I., Brooks, C., and Pavelin, S. (2014). The Effects of Corporate Social Performance on the Cost of Corporate Debt and Credit Ratings. *Financial Review*, 49(1), pp. 49-75.

Olhnuud, A., Liu, Y., Makowski, D., ..., and Van der Werf, W. (2022). Pollination Deficits and Contributions of Pollinators in Apple Production: A Global Meta-analysis. *Journal of Applied Ecology*, 59(12), pp. 2911-2921.

Ollerton, J., Winfree, R., and Tarrant, S. (2011). How Many Flowering Plants are Pollinated by Animals?. *Oikos*, 120(3), pp. 321-326.

Olson, D. M., Dinerstein, E., Wikramanayake, E. D., ..., and Kassem, K. R. (2001). Terrestrial Ecoregions of the World: A New Map of Life on Earth. *BioScience*, 51(11), pp. 933-938.

Olson, D. M., and Dinerstein, E. (2002). The Global 200: Priority Ecoregions for Global Conservation. *Annals of the Missouri Botanical Garden*, 89(2), pp. 199-224.

Orlitzky, M., Schmidt, F. L., and Rynes, S. L. (2003). Corporate Social and Financial Performance: A Meta-analysis. *Organization Studies*, 24(3), pp. 403-441.

Ortiz, J. D., and Jackson, R. (2022). Understanding Eunice Foote's 1856 Experiments: Heat Absorption by Atmospheric Gases. *Notes and Records*, 76(1), pp. 67-84.

Ott, W. R. (1978). *Environmental Indices: Theory and Practice*. Ann Arbor Science, 371 pages.

Ott, W. R., and Thorn, G. C. (1976). Air Pollution Index Systems in the United States and Canada. *Journal of the Air Pollution Control Association*, 26(5), pp. 460-470.

Park, T. (1962). Beetles, Competition, and Populations. *Science*, 138(3548), pp. 1369-1375.

Parrenin, F., Barnola, J. M., Beer, J., ..., and Wolff, E. (2007). The EDC3 Chronology for the EPICA Dome C Ice Core. *Climate of the Past*, 3(3), pp. 485-497.

Pástor, L., Stambaugh, R. F., and Taylor, L. A. (2021). Sustainable Investing in Equilibrium. *Journal of Financial Economics*, 142(2), pp. 550-571.

Pástor, L., Stambaugh, R. F., and Taylor, L. A. (2022). Dissecting Green Returns. *Journal of Financial Economics*, 146(2), pp. 403-424.

Pauli, G. A. (2010). *The Blue Economy: 10 Years, 100 Innovations, 100 Million Jobs*. Paradigm Publications.

Pauly, D., Christensen, V., Guénette, S., ..., and Zeller, D. (2002). Towards Sustainability in World Fisheries. *Nature*, 418(6898), pp. 689-695.

Pauly, D., Watson, R., and Alder, J. (2005). Global Trends in World Fisheries: Impacts on Marine Ecosystems and Food Security. *Philosophical Transactions of the Royal Society B: Biological Sciences*, 360(1453), pp. 5-12.

Pausata, F. S. R., Gaetani, M., Messori, G., Berg, A., de Souza, D. M., Sage, R. F., and DeMenocal, P. B. (2020). The Greening of the Sahara: Past Changes and Future Implications. *One Earth*, 2(3), pp. 235-250.

Pearce, D. (1988). Economics, Equity and Sustainable Development. *Futures*, 20(6), pp. 598-605.

Pearce, D. (1998). Auditing the Earth: The Value of the World's Ecosystem Services and Natural Capital. *Environment: Science and Policy for Sustainable Development*, 40(2), pp. 23-28.

Pearce, D., Putz, F. E., and Vanclay, J. K. (2003). Sustainable Forestry in the Tropics: Panacea or Folly?. *Forest Ecology and Management*, 172(2-3), pp. 229-247.

Pedersen, L. H., Fitzgibbons, S., and Pomorski, L. (2021). Responsible Investing: The ESG-Efficient Frontier. *Journal of Financial Economics*, 142(2), pp. 572-597.

Pereira, H. M., Ferrier, S., Walters, M., ..., and Wegmann, M. (2013). Essential Biodiversity Variables. *Science*, 339(6117), pp. 277-278.

Pereira, P., Cortez, M. C., and Silva, F. (2019). Socially Responsible Investing and the Performance of Eurozone Corporate Bond Portfolios. *Corporate Social Responsibility and Environmental Management*, 26(6), pp. 1407-1422.

Peres, C. A. (2010). Overexploitation. In Sodhi, N. S., and Ehrlich, P. R. (Eds), *Conservation Biology for All*, Oxford University Press, Chapter 6, pp. 107-130.

Peres, C. A., and Palacios, E. (2007). Basin-wide Effects of Game Harvest on Vertebrate Population Densities in Amazonian Forests: Implications for Animal-mediated Seed Dispersal. *Biotropica*, 39(3), pp. 304-315.

Pérez Roda, M. A., Gilman, E., Huntington, T., Kennelly, S. J., Suuronen, P., Chaloupka, M. and Medley, P. A. H. (2019). A Third Assessment of Global Marine Fisheries Discards. *FAO Fisheries and Aquaculture Technical Paper*, 633, 78 pages.

Perrin, S., and Roncalli, T. (2020). Machine Learning Optimization Algorithms & Portfolio Allocation. In Jurczenko, E. (Ed.), *Machine Learning for Asset Management: New Developments and Financial Applications*, Wiley, Chapter 8, pp. 261-328.

Peters, G. P., Andrew, R. M., Canadell, J. G., ..., and Nakicenovic, N. (2017). Key Indicators to Track Current Progress and Future Ambition of the Paris Agreement. *Nature Climate Change*, 7(2), pp. 118-122.

Peters, G. P., and Hertwich, E. G. (2008). $CO_2$ Embodied in International Trade with Implications for Global Climate Policy. *Environmental Science & Technology*, 42(5), pp. 1401-1407.

Peters, G. P., Minx, J. C., Weber, C. L., and Edenhofer, O. (2011). Growth in Emission Transfers via International Trade from 1990 to 2008. *Proceedings of the National Academy of Sciences*, 108(21), pp. 8903-8908.

Petit, J. R., Jouzel, J., Raynaud, D., ..., and Stievenard, M. (1999). Climate and Atmospheric History of the Past 420,000 Years from the Vostok Ice Core, Antarctica. *Nature*, 399(6735), pp. 429-436.

Phenix Capital (2023). Private Debt Funds at a Glance. *Phenix Report*, June, 23 pages.

Phenix Capital (2024a). Impact Fund Universe Report. *Phenix Report*, January, 32 pages.

Phenix Capital (2024b). Biodiversity Funds at a Glance. *Phenix Report*, April, 30 pages.

Phenix Capital (2024c). Blue Economy Funds at a Glance. *Phenix Report*, May, 40 pages.

Phenix Capital (2024d). Private Debt Funds at a Glance. *Phenix Report*, June, 23 pages.

Phillips, N. A. (1956). The General Circulation of the Atmosphere: A Numerical Experiment. *Quarterly Journal of the Royal Meteorological Society*, 82(352), pp. 123-164.

Pimm, S. L., and Brooks, T. M. (2000). The Sixth Extinction: How Large, Where, and When. In Raven, P. H. (Ed.), *Nature and Human Society: The Quest for a Sustainable World — Proceedings of the 1997 Forum on Biodiversity*, National Academic Press, Chapter 4, pp. 46-62.

Pimm, S. L., Russell, G. J., Gittleman, J. L., and Brooks, T. M. (1995). The Future of Biodiversity. *Science*, 269(5222), pp. 347-350.

Pindyck, R. S. (2012). Uncertain Outcomes and Climate Change Policy. *Journal of Environmental Economics and Management*, 63(3), pp. 289-303.

Pindyck, R. S. (2013). Climate Change Policy: What Do the Models Tell Us?. *Journal of Economic Literature*, 51(3), pp. 860-872.

Pindyck, R. S. (2017). The Use and Misuse of Models for Climate Policy. *Review of Environmental Economics and Policy*, 11(1), pp. 100-114.

PitchBook (2023). 2023 Impact Investing Update. *Report*, December, 19 pages.

PitchBook (2024). The State of Private Market ESG and Impact Investing in 2024. *Report*, March, 14 pages.

Plass, G. N. (1956). The Carbon Dioxide Theory of Climatic Change. *Tellus*, 8(2), pp. 140-154.

Polbennikov, S., Desclée, A., Dynkin, L., and Maitra, A. (2016). ESG Ratings and Performance of Corporate Bonds. *Journal of Fixed Income*, 26(1), pp. 21-41.

Pointer, M. D., Gage, M. J. G., and Spurgin, L. G. (2021). Tribolium Beetles as a Model System in Evolution and Ecology. *Heredity*, 126(6), pp. 869-883.

Polis, G. A., Myers, C. A., and Holt, R. D. (1989). The Ecology and Evolution of Intraguild Predation: Potential Competitors that Eat Each Other. *Annual Review of Ecology and Systematics*, 20, pp. 297-330.

Pollan, M. (2007). *The Omnivore's Dilemma: A Natural History of Four Meals*. Penguin, 480 pages.

Pope III, C. A., and Dockery, D. W. (2006). Health Effects of Fine Particulate Air Pollution: Lines That Connect. *Journal of the Air & Waste Management Association*, 56(6), pp. 709-742.

Popp, D. (2004). ENTICE: Endogenous Technological Change in the DICE Model of Global Warming. *Journal of Environmental Economics and Management*, 48(1), pp. 742-768.

Potapov, P. V., Hansen, M. C., Pickens, A., ..., and Kommareddy, A. (2022). The Global 2000-2020 Land Cover and Land Use Change Dataset derived from the Landsat Archive: First Results. *Frontiers in Remote Sensing*, 3, 856903, 22 pages.

Pottier, A., Espagne, E., Perrissin Fabert, B., and Dumas, P. (2015). The Comparative Impact of Integrated Assessment Models' Structures on Optimal Mitigation Policies. *Environmental Modeling & Assessment*, 20, pp. 453-473.

Potts, S. G., Biesmeijer, J. C., Kremen, C., Neumann, P., Schweiger, O., and Kunin, W. E. (2010). Global Pollinator Declines: Trends, Impacts and Drivers. *Trends in Ecology & Evolution*, 25(6), pp. 345-353.

Potts, S. G., Imperatriz-Fonseca, V., Ngo, H. T., ..., and Vanbergen, A. J. (2016). Safeguarding Pollinators and Their Values to Human Well-being. *Nature*, 540(7632), pp. 220-229.

Pouillet, C. (1838). *Mémoire sur la chaleur solaire, sur les pouvoirs rayonnants et absorbants de l'air atmosphérique et sur la température de l'espace*. Bachelier, Paris.

Powers, D. M. (2011). Evaluation: From Precision, Recall and F-measure to ROC, Informedness, Markedness and Correlation. *Journal of Machine Learning Technologies*, 2(1), pp 37-63.

Pratt, S. P., and Grabowski, R. J. (2008). *Cost of Capital*. John Wiley & Sons, 778 pages.

Prequin (2023). ESG in Alternatives 2023. *Insights+*, June, 31 pages.

Preston, F. W. (1948). The Commonness and Rarity of Species. *Ecology*, 29(3), pp. 254-283.

Preston, F. W. (1960). Time and Space and the Variation of Species. *Ecology*, 41(4),pp. 612-627.

Primack, R. B. (2014). *Essentials of Conservation Biology*. Sixth edition, Sinauer Associates & Oxford University Press, 603 pages.

Principles for Responsible Investment (2018a). How ESG Engagement Creates Value for Investors and Companies. *Report*, April, 32 pages.

Principles for Responsible Investment (2018b). Impact Investing Market Map. *Report*, August, 112 pages.

Principles for Responsible Investment (2019a). A Practical Guide to ESG integration in Sovereign Debt. *Report*, August, 63 pages.

Principles for Responsible Investment (2019). Private Equity. *An Introduction to Responsible Investment*, October, 7 pages.

Principles for Responsible Investment (2019c). Active Owenership 2.0: The Evolution Stewardship Urgently Needs. *Report*, November, 12 pages.

Principles for Responsible Investment (2020). Screening. *An Introduction to Responsible Investment*, May, 8 pages.

Principles for Responsible Investment (2021a). Stewardship. *An Introduction to Responsible Investment*, February, 10 pages.

Principles for Responsible Investment (2021b). Making Voting Count. *Report*, March, 17 pages.

Principles for Responsible Investment (2022a). Discussing Divestment: Developing an Approach when Pursuing Sustainability Outcomes in Listed Equities. *Report*, April, 19 pages.

Principles for Responsible Investment (2022b). PRI's Regulation Database. *Database*, Q1 2022.

Principles for Responsible Investment (2022c). Real Estate. *An Introduction to Responsible Investment*, July, 10 pages.

Principles for Responsible Investment (2023). ESG Incorporation in Direct Lending — A Guide For Private Debt Investors. *Report*, September, 27 pages.

Principles for Responsible Investment (2024). Infrastructure. *An Introduction to Responsible Investment*, February, 10 pages.

Quinn, T. J., and Deriso, R. B. (1999). *Quantitative Fish Dynamics*. Oxford University Press, 560 pages.

Rader, R., Bartomeus, I., Garibaldi, L. A., ..., and Woyciechowski, M. (2016). Non-bee Insects are Important Contributors to Global Crop Pollination. *Proceedings of the National Academy of Sciences*, 113(1), pp. 146-151.

Rahman, M. T., Sobur, M. A., Islam, M. S., ..., and Ashour, H. M. (2020). Zoonotic Diseases: Etiology, Impact, and Control. *Microorganisms*, 8(9), 1405, 34 pages.

Raimo, N., Caragnano, A., Zito, M., Vitolla, F., and Mariani, M. (2021). Extending the Benefits of ESG Disclosure: The Effect on the Cost of Debt Financing. *Corporate Social Responsibility and Environmental Management*, 28(4), pp. 1412-1421.

Ramanathan, V. (1975). Greenhouse Effect Due to Chlorofluorocarbons: Climatic Implications. *Science*, 190(4209), pp. 50-52.

Ramanathan, V., Cicerone, R. J., Singh, H. B., and Kiehl, J. T. (1985). Trace Gas Trends and Their Potential Role in Climate Change. *Journal of Geophysical Research: Atmospheres*, 90(D3), pp. 5547-5566.

Ramirez, A. G., Monsalve, J., González-Ruiz, J. D., Almonacid, P., and Peña, A. (2022). Relationship between the Cost of Capital and Environmental, Social, and Governance Scores: Evidence from Latin America. *Sustainability*, 14, 5012, 15 pages.

Ramírez-Delgado, J. P., Di Marco, M., Watson, J. E. M., ..., and Venter, O. (2022). Matrix Condition Mediates the Effects of Habitat Fragmentation on Species Extinction Risk. *Nature Communications*, 13(1), 595, 10 pages.

Rao, N. D., Sauer, P., Gidden, M., and Riahi, K. (2019). Income Inequality Projections for the Shared Socioeconomic Pathways (SSPs). *Futures*, 105, pp. 27-39.

Ratto, F., Simmons, B. I., Spake, R., ..., and Dicks, L. V. (2018). Global Importance of Vertebrate Pollinators for Plant Reproductive Success: A Meta-analysis. *Frontiers in Ecology and the Environment*, 16(2), pp. 82-90.

Raup, D. M., and Sepkoski, J. J. (1982). Mass Extinctions in the Marine Fossil Record. *Science*, 215(4539), pp. 1501-1503.

Raupach, M. R., Marland, G., Ciais, P., Le Quéré, C., Canadell, J. G., Klepper, G., and Field, C. B. (2007). Global and Regional Drivers of Accelerating $CO_2$ Emissions. *Proceedings of the National Academy of Sciences*, 104(24), pp. 10288-10293.

RBB Economics (2014). Cost Pass-through: Theory, Measurement, and Potential Policy Implications. *A Report prepared for the Office of Fair Trading*, February, 210 pages.

Reeder, N., and Colantonio, A. (2013). Measuring Impact and Non-financial Returns in Impact Investing: A Critical Overview of Concepts and Practice. *Working Paper*, London School of Economics, 39 pages.

Refinitiv (2022). Environmental, Social and Governance Scores from Refinitiv. *Report*, May.

Renneboog, L., Ter Horst, J., and Zhang, C. (2008). Socially Responsible Investments: Institutional Aspects, Performance, and Investor Behavior. *Journal of Banking & Finance*, 32(9), pp. 1723-1742.

RepRisk (2022). RepRisk Methodology Overview. *Report*, July.

RepRisk (2023). On the Rise: Navigating the Wave of Greenwashing and Social Washing. *Report*, October.

Revelle, R., and Suess, H. E. (1957). Carbon Dioxide Exchange between Atmosphere and Ocean and the Question of an Increase of Atmospheric $CO_2$ during the Past Decades. *Tellus*, 9(1), pp. 18-27.

Reynolds, J. D. and Peres, C. A. (2006). Overexploitation. In Groom, M. J., Meffe, G. K., and Carroll, C. R. (Eds), *Principles of Conservation Biology*, Third edition, Sinauer Associates, Chapter 8, pp 253-277.

Riahi, K., Van Vuuren, D. P., Kriegler, E., ..., and Tavoni, M. (2017). The Shared Socioeconomic Pathways and Their Energy, Land Use, and Greenhouse Gas Emissions Implications: An Overview. *Global Environmental Change*, 42, pp. 153-168.

Rice, R. E., Gullison, R. E., and Reid, J. W. (1997). Can Sustainable Management Save Tropical Forests?. *Scientific American*, 276(4), pp. 44-49.

Richardson, K., Steffen, W., Lucht, W., ..., and Rockström, J. (2023). Earth Beyond Six of Nine Planetary Boundaries. *Science Advances*, 9(37), eadh2458, 16 pages.

Richardson, L. F. (1922). *Weather Prediction by Numerical Process*. Cambridge University Press.

Richters, O., Bertram, C., Kriegler, E., ..., and Zwerling, M. (2022). NGFS Climate Scenario Database. *Technical Documentation*, V3.1, November.

Rickards, R. B. (1977). Patterns of Evolution in the Graptolites. In Halam, A. (Ed.), *Developments in Palaeontology and Stratigraphy — Patterns of Evolution as Illustrated by the Fossil Record*, 5, Elsevier, Chapter 10, pp. 333-358.

Ripple, W. J., Abernethy, K., Betts, M. G., ..., and Young, H. (2016). Bushmeat Hunting and Extinction Risk to the World's Mammals. *Royal Society Open Science*, 3(10), 160498, 16 pages.

Ripple, W. J., Wolf, C., Newsome, T. M., ..., and Worm, B. (2019). Are We Eating the World's Megafauna to Extinction?. *Conservation Letters*, 12(3), e12627.

Ritchie, P. D., Clarke, J. J., Cox, P. M., and Huntingford, C. (2021). Overshooting Tipping Point Thresholds in A Changing Climate. *Nature*, 592(7855), pp. 517-523.

Ritz, C. (2010). Toward a Unified Approach to Dose-Response Modeling in Ecotoxicology. *Environmental Toxicology and Chemistry*, 29(1), pp. 220-229.

Ritz, C., Baty, F., Streibig, J. C., and Gerhard, D. (2015). Dose-Response Analysis using R. *PloS One*, 10(12), e0146021, 13 pages.

Rockström, J., Steffen, W., Noone, K., ..., and Foley, J. (2009). A Safe Operating Space for Humanity. *Nature*, 461(7263), pp. 472-475.

Rohde, R. A., and Hausfather, Z. (2020). The Berkeley Earth Land/Ocean Temperature Record. *Earth System Science Data*, 12(4), pp. 3469-3479.

Rohde, R. A., and Muller, R. A. (2005). Cycles in Fossil Diversity. *Nature*, 434(7030), pp. 208-210.

Roll, R. (1992). A Mean/Variance Analysis of Tracking Error. *Journal of Portfolio Management*, 18(4), pp. 13-22.

Roncalli, T. (2013). *Introduction to Risk Parity and Budgeting*. Chapman and Hall/CRC Financial Mathematics Series.

Roncalli, T. (2017). Alternative Risk Premia: What Do We Know?. in Jurczenko, E. (Ed.), *Factor Investing: From Traditional to Alternative Risk Premia*, Elsevier.

Roncalli, T. (2020a). *Handbook of Financial Risk Management*. Chapman and Hall/CRC Financial Mathematics Series.

Roncalli, T. (2020b). ESG & Factor Investing: A New Stage has been Reached. *Amundi Viewpoint*, May.

Roncalli, T., Le Guenedal, T., Lepetit, F., Roncalli, T., and Sekine, T. (2020). Measuring and Managing Carbon Risk in Investment Portfolios. *arXiv*, 2008.13198.

Roncalli, T., Le Guenedal, T., Lepetit, F., Roncalli, T., and Sekine, T. (2021). The Market Measure of Carbon Risk and its Impact on the Minimum Variance Portfolio. *Journal of Portfolio Management*, 47(9), pp. 54-68.

Roncalli, T., and Semet, R. (2024). The Economic Cost of the Carbon Tax. *SSRN*, 4755259.

Roques, L., Hosono, Y., Bonnefon, O., and Boivin, T. (2015). The Effect of Competition on the Neutral Intraspecific Diversity of Invasive Species. *Journal of Mathematical Biology*, 71, pp. 465-489.

Rosati, B., Moote, K., Kumar, R., and Maiolo, M. (2022). A Look Back at the 2022 Proxy Season. *Report*, Georgeson LLC.

Rose, S. K., Diaz, D. B., and Blanford, G. J. (2017a). Understanding the Social Cost of Carbon: A Model Diagnostic and Inter-comparison Study. *Climate Change Economics*, 8(02), 1750009.

Rose, S. K., Diaz, D. B., and Blanford, G. J. (2017b). Understanding the Social Cost of Carbon: A Model Diagnostic and Inter-comparison Study: Supplementary Material. Available at https://doi.org/10.1142/S2010007817500099.

Rosenzweig, M. L. (1995). *Species Diversity in Space and Time*. Cambridge University Press, 436 pages.

Ross, S. (1976). The Arbitrage Theory of Capital Asset Pricing. *Journal of Economic Theory*, 13(3), pp. 341-360.

Rossberg, A. G. (2022). Quantifying Biodiversity Impact. *Technical Report*, Queen Mary University of London, 16 pages.

Rossberg, Axel G., O'Sullivan, J. D., Malysheva, S., and Shnerb, N. M. (2023). A Metric for Tradable Biodiversity Credits Linked to the Living Planet Index and Global Species Conservation. *arXiv*, 2111.03867.

Rössler, O. E. (1976). An Equation for Continuous Chaos. *Physics Letters A*, 57(5), pp. 397-398.

Royer, D. L., Berner, R. A., MontaÃśez, I. P., Tabor, N. J., and Beerling, D. J. (2004). $CO_2$ as a Primary Driver of Phanerozoic Climate. *GSA Today*, 14(3), pp. 4-10.

Rudd, A. (1979). Divestment of South African Equities: How Risky?. *Journal of Portfolio Management*, 5(3), pp. 5-10.

Russell, S. (2023). Estimating and Reporting the Comparative Emissions Impacts of Products. World Resources Institute, *Working Paper*, 26 pages.

Sachs, J. D., Lafortune, G., and Fuller, G. (2024). The SDGs and the UN Summit of the Future. *Sustainable Development Report 2024*, Dublin University Press, DOI:10.25546/108572.

Sachs, J. D., Schmidt-Traub, G., Mazzucato, M., Messner, D., Nakicenovic, N., and Rockström, J. (2019). Six Transformations to Achieve the Sustainable Development Goals. *Nature Sustainability*, 2(9), pp. 805-814.

Sætra, H. S. (2021). A Framework for Evaluating and Disclosing the ESG Related Impacts of AI with the SDGs. *Sustainability*, 13(15), 8503.

Sagan, C. (1986). *Dragons of Eden: Speculations on the Evolution of Human Intelligence*. Ballantine Books.

Sala, O. E., Stuart Chapin III, F. , Armesto, J. J., ..., and Wall, D. H. (2000). Global Biodiversity Scenarios for the Year 2100. *Science*, 287(5459), pp. 1770-1774.

Sánchez-Bayo, F., and Wyckhuys, K. A. G. (2019). Worldwide Decline of the Entomofauna: A Review of its Drivers. *Biological Conservation*, 232, pp. 8-27.

Sassi, O., Crassous, R., Hourcade, J-C., Gitz, V., Waisman, H-D., and Guivarch, C. (2010). IMACLIM-R: A Modelling Framework to Simulate Sustainable Development Pathways. *International Journal of Global Environmental Issues*, 10 (1-2), pp. 5-24.

Sautel, O., Mini, C., Bailly, H., and Dieye, R. (2022). *La tarification du carbone et ses répercussions. Exposition sectorielle au surcoût carbone.* Les Notes de La Fabrique, Presses des Mines.

Sayre, R., Karagulle, D., Frye, C., ..., and Possingham, H. (2020). An Assessment of the Representation of Ecosystems in Global Protected Areas using New Maps of World Climate Regions and World Ecosystems. *Global Ecology and Conservation*, 21, e00860, 21 pages.

Schaefer, M. B. (1954). Some Aspects of the Dynamics of Populations Important to the Management of Commercial Marine Fisheries. *Bulletin of the Inter-American Tropical Tuna Commission*, 1(2), pp. 27-56.

Scheringer, M., Strempel, S., Hukari, S., Ng, C. A., Blepp, M., and Hungerbuhler, K. (2012). How Many Persistent Organic Pollutants Should We Expect?. *Atmospheric Pollution Research*, 3(4), pp. 383-391.

Schijns, R., Froese, R., Hutchings, J. A., and Pauly, D. (2021). Five Centuries of Cod Catches in Eastern Canada. *ICES Journal of Marine Science*, 78(8), pp. 2675-2683.

Schipper, A. M., Hilbers, J. P., Meijer, J. R., ..., and Huijbregts, M. A. (2020). Projecting Terrestrial Biodiversity Intactness with GLOBIO 4. *Global Change Biology*, 26(2), pp. 760-771.

Schleussner, C. F., Rogelj, J., Schaeffer, M., ..., and Hare, W. (2016). Science and Policy Characteristics of the Paris Agreement Temperature Goal. *Nature Climate Change*, 6(9), pp. 827-835.

Schmeller, D. S., Weatherdon, L. V., Loyau, A., ..., and Regan, E. C. (2018). A Suite of Essential Biodiversity Variables for Detecting Critical Biodiversity Change. *Biological Reviews*, 93(1), pp. 55-71.

Schneider, V. A., Graves-Lindsay, T., Howe, K., ..., and Church, D. M. (2017). Evaluation of GRCh38 and de novo Haploid Genome Assemblies Demonstrates the Enduring Quality of the Reference Assembly. *Genome Research*, 27(5), pp. 849-864.

Scholes, R. J., and Biggs, R. (2005). A Biodiversity Intactness Index. *Nature*, 434(7029), pp. 45-49.

Schramade, W. (2017). Investing in the UN Sustainable Development Goals: Opportunities for Companies and Investors. *Journal of Applied Corporate Finance*, 29(2), pp. 87-99.

Schulp, C. J. E., Thuiller, W., and Verburg, P. H. (2014). Wild Food in Europe: A Synthesis of Knowledge and Data of Terrestrial Wild Food as an Ecosystem Service. *Ecological Economics*, 105, pp. 292-305.

Schulte, P., Alegret, L., Arenillas, I., ..., and Willumsen, P. S. (2010). The Chicxulub Asteroid Impact and Mass Extinction at the Cretaceous-Paleogene Boundary. *Science*, 327(5970), pp. 1214-1218.

Schuur, E. A. G., McGuire, A. D., Schädel, C., ..., and Vonk, J. E. (2015). Climate Change and the Permafrost Carbon Feedback. *Nature*, 520(7546), pp. 171-179.

Schweizer, B., and Wolff, E. F. (1981). On Nonparametric Measures of Dependence for Random Variables. *Annals of Statistics*, 9(4), pp. 879-885.

Sellers, W. D. (1969). A Global Climatic Model based on the Energy Balance of the Earth-atmosphere System. *Journal of Applied Meteorology and Climatology*, 8(3), pp. 392-400.

Semet, R. (2020). The Social Issue of ESG Analysis. *SSRN*, 3838372.

Semet, R., Roncalli, T., and Stagnol, L. (2021). ESG and Sovereign Risk: What is Priced in by the Bond Market and Credit Rating Agencies?. *SSRN*, 3940945.

Senkowski, C. K., and McKenney, M. G. (1999). Trauma Scoring Systems: A Review. *Journal of the American College of Surgeons*, 189(5), pp. 491-503.

Sepkoski, J. J. (2002). A Compendium of Fossil Marine Animal Genera. In Jablonski, D., and Foote, M. (Eds), *Bulletins of American paleontology*, 363, 560 pages.

ShareAction (2019). Voting Matters — Are Asset Managers using their Proxy Votes for Climate Action?. *Rankings & Surveys*, November.

ShareAction (2020). Voting Matters 2020 — Are Asset Managers using their Proxy Votes for Action on Climate and Social Issues?. *Rankings & Surveys*, December.

ShareAction (2021). Voting Matters 2021 — Are Asset Managers using their Proxy Votes for Action on Climate and Social Issues?. *Rankings & Surveys*, December.

ShareAction (2023). Voting Matters 2022. *Rankings & Surveys*, January.

ShareAction (2024). Voting Matters 2023 — Are Asset Managers using their Proxy Votes for Action on Climate and Social Issues?. *Rankings & Surveys*, January.

Sharfman, M. P., and Fernando, C. S. (2008). Environmental Risk Management and the Cost of Capital. *Strategic Management Journal*, 29(6), pp. 569-592.

Sharpe, W. F. (1964). Capital Asset Prices: A Theory of Market Equilibrium under Conditions of Risk. *Journal of Finance*, 19(3), pp. 425-442.

Shepherd, A., Ivins, E., Rignot, E., and the IMBIE team (2020). Mass Balance of the Greenland Ice Sheet from 1992 to 2018. *Nature*, 579(7798), pp. 233-239.

Sherwood, S. C., Webb, M. J., Annan, J. D., ..., and Zelinka, M. D. (2020). An Assessment of Earth's Climate Sensitivity using Multiple Lines of Evidence. *Reviews of Geophysics*, 58(4), e2019RG000678, 92 pages.

Shields, G., and Veizer, J. (2002). Precambrian Marine Carbonate Isotope Database: Version 1.1. *$G^3$: Geochemistry, Geophysics, Geosystems*, 3(6), pp. 1-12.

Shine, K. P., Fuglestvedt, J. S., Hailemariam, K., and Stuber, N. (2005). Alternatives to the Global Warming Potential for Comparing Climate Impacts of Emissions of Greenhouse Gases. *Climatic Change*, 68(3), pp. 281-302.

Shu, C. (2024). The Proxy Advisory Industry: Influencing and Being Influenced. *Journal of Financial Economics*, 154, 103810.

Simberloff, D. (2010). Invasive Species. In Sodhi, N. S., and Ehrlich, P. R. (Eds), *Conservation Biology for All*, Oxford University Press, Chapter 7, pp. 131-152.

Simberloff, D., Martin, J. L., Genovesi, P., ..., and Vilà, M. (2013). Impacts of Biological Invasions: What's What and The Way Forward. *Trends in Ecology & Evolution*, 28(1), pp. 58-66.

Simpson, G. G. (1952). How Many Species. *Evolution*, 6(3), pp. 342

Skaife, H. A., Collins, D. W., and LaFond, R. (2004). Corporate Governance and the Cost of Equity Capital. *SSRN*, 639681.

Sekercioglu, C. H. (2010). Ecosystem Function and Services. In Sodhi, N. S., and Ehrlich, P. R. (Eds), *Conservation Biology for All*, Oxford University Press, Chapter 3, pp. 45-72.

Skidmore, A. K., Coops, N. C., Neinavaz, E., ..., and Wingate, V. (2021). Priority List of Biodiversity Metrics to Observe From Space. *Nature Ecology & Evolution*, 5(7), pp. 896-906.

Sklar, A. (1959). Fonctions de Répartition à $n$ Dimensions et leurs Marges. *Publications de l'Institut de Statistique de l'Université de Paris*, 8(1), pp. 229-231.

Smith, K. T., Lopez, B., Vignieri, S., and Wible, B. (2023). Losing the Darkness. *Science*, 380(6650), pp. 1116-1117.

So, I., and Staskevicius, A. (2015). Measuring the 'Impact' in Impact Investing. *Report*, Harvard Business School, 58 pages.

Social Finance (2009). Social Impact Bonds: Rethinking Finance for Social Outcomes. *Report*, August, 8 pages.

Sodhi, N. S. and Ehrlich, P. R. (2010). *Conservation Biology for All*. Oxford University Press, 351 pages.

Solé, M., Kaifu, K., Mooney, T. A., ..., and André, M. (2023). Marine Invertebrates and Noise. *Frontiers in Marine Science*, 10, 1129057, 34 pages.

Solomon, M. E. (1949). The Natural Control of Animal Populations. *Journal of Animal Ecology*, 18, pp. 1-35.

S&P Dow Jones Indices (2022). S&P DJI ESG Score. *Methodology*, May.

Spalding, C., and Hull, P. M. (2021). Towards Quantifying the Mass Extinction Debt of the Anthropocene. *Proceedings of the Royal Society B (Biological Sciences)*, 288(1949), 20202332, 9 pages.

Stanton, E. A. (2011). Negishi Welfare Weights in Integrated Assessment Models: The Mathematics of Global Inequality. *Climatic Change*, 107(3-4), pp. 417-432.

Starks, L. T. (2023). Presidential Address: Sustainable Finance and ESG Issues — *Value* versus *Values*. *Journal of Finance*, 78(4), pp. 1837-1872.

Steffen, W., Broadgate, W., Deutsch, L., Gaffney, O., and Ludwig, C. (2015). The Trajectory of the Anthropocene: The Great Acceleration. *Anthropocene Review*, 2(1), pp. 81-98.

Steffen, W., Richardson, K., Rockström, J., ..., and Sörlin, S. (2015). Planetary Boundaries: Guiding Human Development on a Changing Planet. *Science*, 347(6223), pp. 736 & 1259855 (10 pages).

Steffen, W., Rockström, J., Richardson, K., ..., and Schellnhuber, H. J. (2018). Trajectories of the Earth System in the Anthropocene. *Proceedings of the National Academy of Sciences*, 115(33), pp. 8252-8259.

Stehfest, E., van Vuuren, D. P., Kram, T., and Bouwman, L. (2014), *Integrated Assessment of Global Environmental Change with IMAGE 3.0: Model Description and Policy Applications*. Netherlands Environmental Assessment Agency.

Stephens, G. L., O'Brien, D., Webster, P. J., Pilewski, P., Kato, S., & Li, J.-L. (2015). The Albedo of Earth. *Reviews of Geophysics*, 53(1), pp. 141-163.

Stephenson, P. J., and Stengel, C. (2020). An Inventory of Biodiversity Data Sources for Conservation Monitoring. *PloS One*, 15(12), e0242923.

Stern, N. (2007). *The Economics of Climate Change: The Stern Review*. Cambridge University Press.

Stern, N., and Taylor, C. (2007). Climate Change: Risk, Ethics, and the Stern Review. *Science*, 317(5835), pp. 203-204.

Stevens, C. J., Dise, N. B., Mountford, J. O., and Gowing, D. J. (2004). Impact of Nitrogen Deposition on the Species Richness of Grasslands. *Science*, 303(5665), pp. 1876-1879.

Stokes, C. R., Abram, N. J., Bentley, M. J., ..., and Whitehouse, P. L. (2022). Response of the East Antarctic Ice Sheet to Past and Future Climate Change. *Nature*, 608(7922), pp. 275-286.

Strevens, C. M. J., and Bonsall, M. B. (2011). The Impact of Alternative Harvesting Strategies in a Resource-Consumer Metapopulation. *Journal of Applied Ecology*, 48(1), pp. 102-111.

Strogatz, S. H. (2015). *Nonlinear Dynamics and Chaos: With Applications to Physics, Biology. Chemistry, and Engineering*. Westview Press, Second Edition, 528 pages.

Sukhatme, P. V. (1961). The World's Hunger and Future Needs in Food Supplies. *Journal of the Royal Statistical Society: Series A*, 124(4), pp. 463-508.

Svartzman, R., Espagne, E., Gauthey, J., ..., and Vallier, A. (2021). A "Silent Spring" for the Financial System? Exploring Biodiversity-Related Financial Risks in France. *Banque de France Working Paper*, 826, August, 95 pages.

Svenning, J. C., Lemoine, R. T., Bergman, J., ..., and Pedersen, R. Ø. (2024). The Late-Quaternary Megafauna Extinctions: Patterns, Causes, Ecological Consequences and Implications for Ecosystem Management in the Anthropocene. *Cambridge Prisms: Extinction*, 2, e5, 27 pages.

Syeed, M. M. M., Hossain, M. S., Karim, M. R., Uddin, M. F., Hasan, M., and Khan, R. H. (2023). Surface Water Quality Profiling Using the Water Quality Index, Pollution Index and Statistical Methods: A Critical Review. *Environmental and Sustainability Indicators*, 18, 100247, 23 pages.

Taft, R. J., and Mattick, J. S. (2003). Increasing Biological Complexity is Positively Correlated with the Relative Genome-wide Expansion of Non-protein-coding DNA Sequences. *Genome Biology*, 5(1), pp. 1-24.

Tang, D. Y., and Zhang, Y. (2020). Do Shareholders Benefit from Green Bonds?. *Journal of Corporate Finance*, 61, 101427.

Tanner, J. T. (1975). The Stability and the Intrinsic Growth Rates of Prey and Predator Populations. *Ecology*, 56(4), pp. 855-867.

Tanzer, S. E., and Ramírez, A. (2019). When Are Negative Emissions Negative Emissions?. *Energy & Environmental Science*, 12(4), pp. 1210-1218.

Taskforce on Nature-related Financial Disclosures (2023). Recommendations of the Taskforce on Nature-related Financial Disclosures. *Final Report*, September, 154 pages.

Task Force on Climate-related Financial Disclosures (2017). Recommendations of the Task Force on Climate-related Financial Disclosures. *Final Report*, June.

Task Force on Climate-related Financial Disclosures (2021a). Implementing the Recommendations of the Task Force on Climate-related Financial Disclosures. *Implementation Guidance*, October.

Task Force on Climate-related Financial Disclosures (2021b). Guidance on Metrics, Targets, and Transition Plans. *Implementation Guidance*, October.

Task Force on Climate-related Financial Disclosures (2022). 2022 Status Report. *Status Report*, October, 145 pages.

Task Force on Climate-related Financial Disclosures (2023). 2023 Status Report. *Status Report*, October, 161 pages.

Taylor, L. H., Latham, S. M., and Woolhouse, M. E. J. (2001). Risk Factors for Human Disease Emergence. *Philosophical Transactions of the Royal Society B: Biological Sciences*, 356(1411), pp. 983-989.

Technical Expert Group on Sustainable Finance (2019a). TEG Final Report on Climate Benchmarks and Benchmarks' ESG Disclosures. *Report*, September.

Technical Expert Group on Sustainable Finance (2019b). Handbook of Climate Transition Benchmarks, Paris-Aligned Benchmarks and Benchmarks' ESG Disclosures. *Report*, December.

Technical Expert Group on Sustainable Finance (2020). TEG Final Report on the EU Taxonomy. *Report*, March.

Terlouw, T., Bauer, C., Rosa, L., and Mazzotti, M. (2021). Life Cycle Assessment of Carbon Dioxide Removal Technologies: A Critical Review. *Energy & Environmental Science*, 14(4), pp. 1701-1721.

Testa, F., Iraldo, F., Vaccari, A., and Ferrari, E. (2015). Why Eco-labels can be Effective Marketing Tools: Evidence from a Study on Italian Consumers. *Business Strategy and the Environment*, 24(4), pp. 252-265.

Thangavel, P., Park, D., and Lee, Y. C. (2022). Recent Insights into Particulate Matter ($PM_{2.5}$)-mediated Toxicity in Humans: An Overview. *International Journal of Environmental Research and Public Health*, 19(12), 7511, 22 pages.

Thinking Ahead Institute (2023). The Asset Owner 100. *Report*, November, 67 pages.

Thogmartin, W. E., Wiederholt, R., Oberhauser, K., ..., and Lopez-Hoffman, L. (2017). Monarch Butterfly Population Decline in North America: Identifying the Threatening Processes. *Royal Society Open Science*, 4(9), 170760, 16 pages.

Thompson, B. S. (2022). Blue Bonds for Marine Conservation and a Sustainable Ocean Economy: Status, Trends, and Insights from Green Bonds. *Marine Policy*, 144, 105219, 10 pages.

Thompson, I. D., Guariguata, M. R., Okabe, K., Bahamondez, C., Nasi, R., Heymell, V., and Sabogal, C. (2013). An Operational Framework for Defining and Monitoring Forest Degradation. *Ecology and Society*, 18(2), Art. 20, 23 pages.

Thornhill, G. D., Collins, W. J., Kramer, R. J., ..., and Zhang, J. (2021). Effective Radiative Forcing from Emissions of Reactive Gases and Aerosols — A Multi-model Comparison. *Atmospheric Chemistry and Physics*, 21(2), pp. 853-874.

Thurstan, R. H., Brockington, S., and Roberts, C. M. (2010). The Effects of 118 Years of Industrial Fishing on UK Bottom Trawl Fisheries. *Nature Communications*, 1(15), 6 pages.

Tibshirani, R. (1996). Regression Shrinkage and Selection via the Lasso. *Journal of the Royal Statistical Society B*, 58(1), pp. 267-288.

Tilman, D (1982). *Resource Competition and Community Structure*. Monographs in Population Biology, 17, Princeton University Press.

Tilman, D., May, R. M., Lehman, C. L., and Nowak, M. A. (1994). Habitat Destruction and the Extinction Debt. *Nature*, 371(6492), pp. 65-66.

Timmer, M. P., Dietzenbacher, E., Los, B., Stehrer, R., and De Vries, G. J. (2015). An Illustrated User Guide to the World Input-Output Database: The Case of Global Automotive Production. *Review of International Economics*, 23(3), pp. 575-605.

Tjørve, E. (2003). Shapes and Functions of Species-Area Curves: A Review of Possible Models. *Journal of Biogeography*, 30(6), pp. 827-835.

Tobin J. (1958). Liquidity Preference as Behavior Towards Risk. *Review of Economic Studies*, 25(2), pp. 65-86.

Tol, R. S. J. (1997). On the Optimal Control of Carbon Dioxide Emissions: An Application of FUND. *Environmental Modeling & Assessment*, 2, pp. 151-163.

Tol, R. S. J. (1999). Kyoto, Efficiency, and Cost-effectiveness: Applications of FUND. *Energy Journal*, 20(1), pp. 131-156.

Tol, R. S. J. (2022). A Meta-analysis of the Total Economic Impact of Climate Change. *arXiv*, 2207.12199.

Tonello, M. (2022). Shareholder Voting Trends (2018–2022). *Report*, The Conference Board.

Townsend, B. (2020). From SRI to ESG: The Origins of Socially Responsible and Sustainable Investing. *Journal of Impact and ESG Investing*, 1(1), pp. 10-25.

Trenberth, K. E., Fasullo, J. T., and Kiehl, J. T. (2009). Earth's Global Energy Budget. *Bulletin of the American Meteorological Society*, 90(3), pp. 311-324.

Triantis, K. A., Guilhaumon, F., and Whittaker, R. J. (2012). The Island Species-Area Relationship: Biology and Statistics. *Journal of Biogeography*, 39(2), pp. 215-231.

Trinks, A., Ibikunle, G., Mulder, M., and Scholtens, B. (2022). Carbon Intensity and the Cost of Equity Capital. *Energy Journal*, 43(2), pp. 181-214.

Turner, K., Lenzen, M., Wiedmann, T., and Barrett, J. (2007). Examining the Global Environmental Impact of Regional Consumption Activities — Part 1: A Technical Note on Combining Input-output and Ecological Footprint Analysis. *Ecological Economics*, 62(1), pp. 37-44.

Tyndall, J. (1861). On the Absorption and Radiation of Heat by Gases and Vapours, and on the Physical Connexion of Radiation, Absorption, and Conduction — The Bakerian Lecture. *The London, Edinburgh, and Dublin Philosophical Magazine and Journal of Science*, 22(146), pp. 169-194.

United Nations (1992a). Report of the United Nations Conference on Environment and Development. *Report*, A/CONF.151/26(I), 12 August 1992, 5 pages.

United Nations (1992b). Non-legally Binding Authoritative Statement of Principles for a Global Consensus on the Management, Conservation and Sustainable Development of All Types of Forests. *Report*, A/CONF.151/26(III), 12 August 1992.

United Nations (1992c). Agenda 21. *Report*, 351 pages.

United Nations (1992d). United Nations Framework Convention on Climate Change. *International Treaty*, 33 pages.

United Nations (2023). The Sustainable Development Goals Report 2023: Special Edition. *Report*, July, 80 pages.

United Nations Economic Commission for Europe (2022). Carbon Neutrality in the UNECE Region: Integrated Life-cycle Assessment of Electricity Sources. *Report*, April.

United Nations Environment Programme (2022). Advancing Delivery on Decarbonisation Targets. *Second Progress Report*, September.

United Nations Framework Convention on Climate Change (1997). *Kyoto Protocol*. Conference of the Parties, 24 pages.

United Nations Framework Convention on Climate Change (2004). *The First Ten Years*. Bonn, Germany, Climate Change Secretariat, 99 pages.

United Nations Framework Convention on Climate Change (2012). *Doha Amendment to the Kyoto Protocol*. Conference of the Parties, 6 pages.

United Nations Framework Convention on Climate Change (2015). *Paris Agreement*. Conference of the Parties, 16 pages.

United Nations Framework Convention on Climate Change (2023a). Long-term Low-emission Development Strategies. *Synthesis Report by the Secretariat*, 41 pages, 14 November 2023.

United Nations Framework Convention on Climate Change (2023b). Nationally Determined Contributions under the Paris Agreement. *Synthesis Report by the Secretariat*, 45 pages, 14 November 2023.

United Nations Office on Drugs and Crimes (2024). *World Wildlife Crime Report 2024: Trafficking in Protected Species*. May, 242 pages.

US Environmental Protection Agency (2024). *Technical Assistance Document for the Reporting of Daily Air Quality — the Air Quality Index (AQI)*. EPA-454/B-24-002, May, 32 pages.

Valentine, J. W. (1970). How Many Marine Invertebrate Fossil Species? A New Approximation. *Journal of Paleontology*, 44(3), pp. 410-415.

Van Bruggen, A. H., He, M. M., Shin, K., ..., and Morris Jr, J. G. (2018). Environmental and Health Effects of the Herbicide Glyphosate. *Science of the Total Environment*, 616, pp. 255-268.

Van der Ploeg, S., and de Groot, R. (2010). *The TEEB Valuation Database — A Searchable Database of 1310 Estimates of Monetary Values of Ecosystem Services*. Foundation for Sustainable Development, www.teebweb.org.

Van Loan, C. F. (1978). Computing Integrals Involving the Matrix Exponential. *IEEE Transactions on Automatic Control*, 23(3), pp. 395-404.

Van Valen, L. (1973). A New Evolutionary Law. *Evolutionary Theory*, 1, pp. 1-30.

Vance, S. C. (1975). Are Socially Responsible Corporations Good Investment Risks. *Management Review*, 64(8), pp. 19-24.

Vano, J. A., Wildenberg, J. C., Anderson, M. B., Noel, J. K., and Sprott, J. C. (2006). Chaos in Low-dimensional Lotka-Volterra Models of Competition. *Nonlinearity*, 19(10), pp. 2391âĂŞ2404.

Veizer, J., Ala, D., Azmy, K., ..., and Strauss, H. (1999). $^{87}Sr/^{86}Sr$, $\delta^{13}C$ and $\delta^{18}O$ Evolution of Phanerozoic Seawater. *Chemical Geology*, 161(1-3), pp. 59-88.

Veizer, J., Godderis, Y., and François, L. M. (2000). Evidence for Decoupling of Atmospheric $CO_2$ and Global Climate during the Phanerozoic Eon. *Nature*, 408(6813), pp. 698-701.

Venålåinen, A., Lehtonen, I., Laapas, M., Ruosteenoja, K., Tikkanen, O. P., Viiri, H., Ikonen, V. P., and Peltola, H. (2020). Climate Change Induces Multiple Risks to Boreal Forests and Forestry in Finland: A Literature Review. *Global Change Biology*, 26(8), pp. 4178-4196.

Venter, J. C., Adams, M. D., Myers, E. W., ..., and Kalush, F. (2001). The Sequence of the Human Genome. *Science*, 291(5507), pp. 1304-1351.

Verhulst, P. F. (1838). Notice sur la loi que la population poursuit dans son accroissement. *Correspondance Mathématique et Physique*. 10, pp. 113-121.

Viscusi, W. K., and Masterman, C. J. (2017). Income Elasticities and Global Values of a Statistical Life. *Journal of Benefit-Cost Analysis*, 8(2), pp. 226-250.

Vitousek, P. M., Mooney, H. A., Lubchenco, J., and Melillo, J. M. (1997). Human Domination of Earth's Ecosystems. *Science*, 277(5325), pp. 494-499.

Volterra, V. (1928). Variations and Fluctuations of the Number of Individuals in Animal Species Living Together. *ICES Journal of Marine Science*, 3(1), pp. 3-51.

Vose, R. S., Huang, B., Yin, X., ..., and Zhang, H. M. (2021). Implementing Full Spatial Coverage in NOAA's Global Temperature Analysis. *Geophysical Research Letters*, 48(4), 2020GL090873.

Wackernagel, M., and Rees, W. (1996). *Our Ecological Footprint: Reducing Human Impact on the Earth*. New Society Publishers.

Wagner, G., and Weitzman, M. L. (2015). *Climate Shock: The Economic Consequences of a Hotter Planet*. Princeton University Press.

Wake, D. B., and Vredenburg, V. T. (2008). Are We in the Midst of the Sixth Mass Extinction? A View from the World of Amphibians. *Proceedings of the National Academy of Sciences*, 105, pp. 11466-11473.

Waldron, A., Mooers, A. O., Miller, D. C., ..., and Gittleman, J. L. (2013). Targeting Global Conservation Funding to Limit Immediate Biodiversity Declines. *Proceedings of the National Academy of Sciences*, 110(29), pp. 12144-12148.

Walker, W. H., Bumgarner, J. R., Walton, J. C., ..., and DeVries, A. C. (2020). Light Pollution and Cancer. *International Journal of Molecular Sciences*, 21(24), 9360, 18 pages.

Wang, F., Xiang, L., Leung, K. S. Y., .., and Tiedje, J. M. (2024). Emerging Contaminants: A One Health Perspective. *The Innovation*, 5(4), 100612, 32 pages.

Wang, Z., Walker, G. W., Muir, D. C. G., and Nagatani-Yoshida, K. (2020). Toward A Global Understanding of Chemical Pollution: A First Comprehensive Analysis of National and Regional Chemical Inventories. *Environmental Science & Technology*, 54(5), pp. 2575-2584.

Wang, H. L., Weng, Y. Y., and Pan, X. Z. (2023). Comparison and Analysis of Mitigation Ambitions of Parties' Updated Nationally Determined Contributions. *Advances in Climate Change Research*, 14(1), pp. 4-12.

Warner, M. E. (2013). Private Finance for Public Goods: Social Impact Bonds. *Journal of Economic Policy Reform*, 16(4), pp. 303-319.

Warren, M. S., Maes, D., van Swaay, C. A. M., ..., and Ellis, S. (2021). The Decline of Butterflies in Europe: Problems, Significance, and Possible Solutions. *Proceedings of the National Academy of Sciences*, 118(2), e2002551117, 10 pages.

Watanabe, K. (2015). Potato Genetics, Genomics, and Applications. *Breeding Science*, 65(1), pp. 53-68.

Waters, C. N., Zalasiewicz, J., Summerhayes, ..., and Wolfe, A. P. (2016). The Anthropocene is Functionally and Stratigraphically Distinct from the Holocene. *Science*, 351(6269), page 137.

Watson, J. E. M., Evans, T., Venter, O., ..., and Lindenmayer, D. (2018). The Exceptional Value of Intact Forest Ecosystems. *Nature Ecology & Evolution*, 2(4), pp. 599-610.

Weart, S. (2023). *The Discovery of Global Warming*. American Institute of Physics, https://history.aip.org/climate/index.htm.

Weitzman, M. L. (2007). A Review of the Stern Review on the Economics of Climate Change. *Journal of Economic Literature*, 45(3), pp. 703-724.

Weitzman, M. L. (2009). On Modeling and Interpreting the Economics of Catastrophic Climate Change. *Review of Economics and Statistics*, 91(1), pp. 1-19.

Weitzman, M. L. (2010). What is the "Damages Function" for Global Warming — And What Difference Might it Make?. *Climate Change Economics*, 1(1), pp. 57-69.

Weitzman, M. L. (2012). GHG Targets as Insurance against Catastrophic Climate Damages. *Journal of Public Economic Theory*, 14(2), pp. 221-244.

Weldon, C., Du Preez, L. H., Hyatt, A. D., Muller, R., and Speare, R. (2004). Origin of the Amphibian Chytrid Fungus. *Emerging Infectious Diseases*, 10(12), pp. 2100-2105.

Wepprich, T., Adrion, J. R., Ries, L., Wiedmann, J., and Haddad, N. M. (2019). Butterfly Abundance Declines over 20 Years of Systematic Monitoring in Ohio, USA. *PLoS One*, 14(7), e0216270, 21 pages.

Westveer, J., Freeman, R., McRae, L., Marconi, V., Almond, R. E. A., and Grooten, M. (2022). A Deep Dive into the Living Planet Index. *Technical Report*, WWF.

Weyant, J. P., and Hill, J. N. (1999). Introduction and Overview. *Energy Journal*, 20(1), pp. vii-xliv.

Whittaker, R. H. (1960). Vegetation of the Siskiyou Mountains, Oregon and California. *Ecological Monographs*, 30(3), pp. 279-338.

Whittaker, R. H. (1965). Dominance and Diversity in Land Plant Communities: Numerical Relations of Species Express the Importance of Competition in Community Function and Evolution. *Science*, 147(3655), pp. 250-260.

Whittaker, R. H., Harrison, S., and Damschen, E. (2022). Plant Community Data Collected by Robert H. Whittaker in the Siskiyou Mountains, Oregon and California, USA. *Ecology*, 103(9), e3764, https://doi.org/10.1002/ecy.3764.

Who Cares Wins (2004). Connecting Financial Markets to a Changing World. *Conference Report*, December.

Who Cares Wins (2005). Investing for Long-Term Value — Integrating Environmental, Social and Governance Value Drivers in Asset Management and Financial Research. *Conference Report*, October.

Wiedmann, T. (2009). A Review of Recent Multi-region Input-output Models used for Consumption-based Emission and Resource Accounting. *Ecological Economics*, 69(2), pp. 211-222.

Wiedmann, T., Lenzen, M., Turner, K., and Barrett, J. (2007). Examining the Global Environmental Impact of Regional Consumption Activities — Part 2: Review of Input-output Models for the Assessment of Environmental Impacts Embodied in Trade. *Ecological Economics*, 61(1), pp. 15-26.

Wiedmann, T., and Minx, J. (2008). A Definition of 'Carbon Footprint'. In Pertsova, C. C. (Ed.), *Ecological Economics Research Trends*, Nova Science Publishers, Chapter 1, pp. 1-11.

Wiens, J. J. (2023). How Many Species are there on Earth? Progress and Problems. *PLoS biology*, 21(11), e3002388, 4 pages.

Wilkie, D. S., Bennett, E. L., Peres, C. A., and Cunningham, A. A. (2011). The Empty Forest Revisited. *Annals of the New York Academy of Sciences*, 1223(1), pp. 120-128.

Williamson, O. E. (1970). *Corporate Control and Business Behavior*. Prentice-Hall.

Willig, M. R., Kaufman, D. M., and Stevens, R. D. (2003). Latitudinal Gradients of Biodiversity: Pattern, Process, Scale, and Synthesis. *Annual Review of Ecology, Evolution, and Systematics*, 34(1), pp. 273-309.

Wilson, E. O. (1989). Threats to Biodiversity. *Scientific American*, 261(3), pp. 108-117.

Wood, D. J. (1991). Corporate Social Performance Revisited. *Academy of Management Review*, 16(4), pp. 691-718.

Wood, D., Thornley, B., and Grace, K. (2013). Institutional Impact Investing: Practice and Policy. *Journal of Sustainable Finance & Investment*, 3(2), pp. 75-94.

World Bank (2022). The Global Health Cost of $PM_{2.5}$ Air Pollution: A Case for Action Beyond 2021. *International Development in Focus*, January, 89 pages.

World Economic Forum (2020a). *Nature Risk Rising: Why the Crisis Engulfing Nature Matters for Business and the Economy*. January, 36 pages.

World Economic Forum (2020b). *New Nature Economy Report II: The Future of Nature and Business*. July, 111 pages.

World Health Organization (2009). *Principles for Modelling Dose-Response for the Risk Assessment of Chemicals*. Environmental Health Criteria, 239, 163 pages.

World Health Organization (2006). *Air Quality Guidelines — Global Update 2005*. August, 496 pages.

World Health Organization (2021). *WHO Global Air Quality Guidelines — Particulate Matter ($PM_{2.5}$ and $PM_{10}$), Ozone, Nitrogen Dioxide, Sulfur Dioxide and Carbon Monoxide*. Geneva, 300 pages.

World Meteorological Organization (1982). Meeting of Experts on Potential Climatic Effects of Ozone and Other Minor Trace Gases (13-17 September 1982). *Report (GORMP)*, 14, 35 pages.

World Ocean Review (2015). *Sustainable Use of Our Oceans — Making Ideas Work*. Volume 4, 78 pages, worldoceanreview.com.

Worm, B., Barbier, E. B., Beaumont, N., ..., and Watson, R. (2006). Impacts of Biodiversity Loss on Ocean Ecosystem Services. *Science*, 314(5800), pp. 787-790.

Worm, B., Hilborn, R., Baum, J. K., ..., and Zeller, D. (2009). Rebuilding Global Fisheries. *Science*, 325(5940), pp. 578-585.

Wratten, S. D., Gillespie, M., Decourtye, A., Mader, E., and Desneux, N. (2012). Pollinator Habitat Enhancement: Benefits to Other Ecosystem Services. *Agriculture, Ecosystems & Environment*, 159, pp. 112-122.

Wright, D. A., and Welbourn, P. (2002). *Environmental Toxicology*. Environmental Chemistry Series Book 11, Cambridge University Press, 656 pages.

Wunderling, N., Donges, J. F., Kurths, J., and Winkelmann, R. (2021). Interacting Tipping Elements Increase Risk of Climate Domino Effects under Global Warming. *Earth System Dynamics*, 12(2), pp. 601-619.

Yaari, M. E. (1965). Uncertain Lifetime, Life Insurance, and The Theory of The Consumer. *Review of Economic Studies*, 32(2), pp. 137-150.

Yamano, N., and Guilhoto, J. J. M. (2020). $CO_2$ Emissions Embodied in International Trade and Domestic Final Demand: Methodology and Results using the OECD Inter-Country Input-Output Database. *OECD Working Paper*, 2020/11, 55 pages.

Yuan, Y., Lu, L. Y., Tian, G., and Yu, Y. (2020). Business Strategy and Corporate Social Responsibility. *Journal of Business Ethics*, 162(2), pp. 359-377.

Zachos, J. C., Dickens, G. R., and Zeebe, R. E. (2008). An Early Cenozoic Perspective on Greenhouse Warming and Carbon-cycle Dynamics. *Nature*, 451(7176), pp. 279-283.

Zachos, J., Pagani, M., Sloan, L., Thomas, E., and Billups, K. (2001). Trends, Rhythms, and Aberrations in Global Climate 65 Ma to Present. *Science*, 292(5517), pp. 686-693.

Zalles, V., Harris, N., Stolle, F., and Hansen, M. C. (2024). Forest Definitions Require a Re-think. *Communications Earth & Environment*, 5(1), 620, 4 pages.

Zeller, D., Cashion, T., Palomares, M., and Pauly, D. (2018). Global Marine Fisheries Discards: A Synthesis of Reconstructed Data. *Fish and Fisheries*, 19(1), pp. 30-39.

Zerbib, O. D. (2019). The Effect of Pro-environmental Preferences on Bond Prices: Evidence from Green Bonds. *Journal of Banking & Finance*, 98, pp. 39-60.

Zerbib, O. D. (2022). A Sustainable Capital Asset Pricing Model (S-CAPM): Evidence from Environmental Integration and Sin Stock Exclusion. *Review of Finance*, 26(6), pp. 1345-1388.

Zhan, J. X., and Santos-Paulino, A. U. (2021). Investing in the Sustainable Development Goals: Mobilization, Channeling, and Impact. *Journal of International Business Policy*, 4(1), pp. 166-183.

Zhang, S., Qiao, S., Yu, J., ..., and Wang, X. (2021). Bat and Pangolin Coronavirus Spike Glycoprotein Structures Provide Insights into SARS-CoV-2 Evolution. *Nature Communications*, 12(1), 1607, 12 pages.

Zhang, X., Zhong, T., Liu, L., and Ouyang, X. (2015). Impact of Soil Heavy Metal Pollution on Food Safety in China. *Plos One*, 10(8), e0135182, 14 pages.

Zohary, D., and Hopf, M. (1988). *Domestication of Plants in the Old World. The Origin and Spread of Cultivated Plants in West Asia, Europe, and the Nile Valley.* Clarendon Press, 249 pages. Fourth edition in 2012 with Weiss, E., Oxford University Press, 264 pages.

# Subject Index


## A

Abatement cost, 756, 759, 944
Abundance, 366, 439–452, 540, 541
Accounting, 609, 905
Active management, 137, 146, 179, 180, 202, 230, 991
Active ownership, *see* Shareholder activism
Active share, 957, 960, 990, 998, 1012
Additionality, 300, 305
Aerosol, 656, 658, 674
Afforestation, *see* Forest management
Age dating model, 632, 637
Agenda 21, 724
Aichi biodiversity targets, 549–551, 553
Air pollution, 468, 481–500
Air quality guidelines (AQG), 481, 495
Air quality index (AQI), 483
Airbone fraction, 649
Albedo, 623, 627, 662, 674, 676, 677, 689
Alpha return, 146, 155, 156, 230
Alternating direction method of multipliers (ADMM), 966, 1053
Alternative data, 71
Alternative fuels infrastructure regulation (AFIR), 744
Amazon rainforest, 699, 701, 708
Ambient air pollution, *see* Outdoor air pollution
Announced pledges scenario (APS), 785, 1014
Annual general meeting (AGM), 11, 575, 577, 580, 604
Antarctica, 621, 632, 633, 635, 640
Anthropocene, 384, 624–626
Anthropogenic features, 624, 642, 656–658
Arctic winter sea ice, 699, 702
Artificial intelligence (AI), 27
Assessment Report (IPCC)
  · AR1, 5, 710
  · AR2, 727
  · AR4, 730
  · AR5, 730, 782
  · AR6, 5, 676, 711–712, 782, 788, 1000
  · SR15, 711, 731, 782, 786, 993
Asset manager, 1, 6, 312, 597–604, 947
Asset owner, 1, 6, 605–607, 947
Asset selection, 1, 948–1017, 1024
Asset tracking, 73, 557, 1035
Atlantic meridional overturning circulation (AMOC), 698–702, 708
Atlantic thermohaline circulation, *see* Atlantic meridional overturning circulation (AMOC)
Atmosphere, 614–624, 647, 649, 658, 660–673, 760–764
Avoided emissions, 301, 901

## B

Background extinction rate, 379, 381
Backlash in ESG, 6
Backtesting, 108
Barents sea, 702
Basel Committee on Banking Supervision, 15
Benchmarks Regulation (BMR), 36
Benefit corporation (B-Corp), 295, 304
Best-in-class, 44, 153, 177, 180, 181, 186, 187, 193, 201
Beta coefficient, **145**, 146, 155, 161, 163, 165, 168, 177
Bifurcation theory, 692–698
Biocapacity, 422
Biodiversity, 5, 33, **62–65**, 73, 221, 255, 295, 326, 351, **365–564**, 564–571, 626, 656, 658, 724, 750, 940, 1024, 1107–1135
Biodiversity finance, 559–564
Biodiversity intactness index (BII), 544

Biodiversity investing, *see* Biodiversity finance
Bioenergy with carbon capture and storage (BECCS), 900, 905, 906, 919
Biological pollution, 468
Birth-death model, 375, 434
Bisection algorithm, 141, 1047
Black body, 659–667, 671, 672, 675
Blended finance, 309, 312, 354–362
Blue bond, 351–353, 560
Blue finance, 351–353
Body mass index (BMI), 424, 541, 565
Bond picking, *see* Asset selection
Bond yield, 213, 218, 274, 352, 359
Bonus point system, *see* Grading system
Boreal forest, 373, 699, 702
Broken-stick model (biodiversity), 445, 446, 451, 569, 1126–1127
Buildings, 945
Bushmeat crisis, 503, 535
Business-as-usual, 1, 137, 710, 732, 734, 991

## C

Cap-and-trade system, 902
Capital asset pricing model, *see* CAPM
Capital market line, 143, 144
CAPM, **144–146**, 148, 151, 155, 158, 163, 165, 166, 193, 194, 210, 227
Carbon border adjustment mechanism (CBAM), 740, 743, 749
Carbon budget, **914–919**, 993–996
Carbon capture, use, and storage (CCUS), 890, 901, 905, 906
Carbon credits, 902, 904
Carbon cycle, 1034
Carbon dioxide ($CO_2$), 21, 497, 615–618, 621, 627, 632, 641, 647–655, 785, 869–874
Carbon dioxide removal (CDR), 899, 905
Carbon Disclosure Project, *see* CDP
Carbon emissions, 734, 760, 823, 826, **870–906**, 991
Carbon footprint, 22, 823, 869, **870**, 895, 907, 952
· *See also* Carbon emissions, Carbon intensity
Carbon intensity, 651, 761, 823–832, 895, **907–913**, 991, 1016
Carbon isotope, 382, 627–629
Carbon momentum, 927, 1001–1005
Carbon monoxide (CO), 468, 470, 478, 482, 483
Carbon offsetting, 899–906
Carbon sink, 12, 701, 730, 761, 1034
Carbon target, 929–932, 1015
Carbon tax, 273, 759, 767, 776, 846–865, 944, 1014
Carbon trend, 920–928, 1004, 1015
Carbon velocity, 926
Carry, 199, 955
Carrying capacity, 508, 509, 512, 519
CDP, 22, 66
Cement, 647, 649
Ceres, 5
Chaos theory, 514, 520, 695, 696
Chapman-Kolmogorov equation, 118, 125, 130
Chemical pollution, 468
Circular economy, 33, 54, 474, 945
Clausius-Clapeyron equation, 678
Climate Action 100+, 10, 583, 587, 604
Climate Bonds Initiative (CBI), 251
Climate investing, 265, 559, 947
Climate scenario, 782
Climate sensitivity, 617, 621, 623, 640, **670–698**
Climate transition benchmark, *see* CTB
Coal, 617, 649
Coalition for environmentally responsible economies, *see* Ceres
Collaborative engagement, 11, 583, 586
Community investing, 42, 69, 307, 349
Competition model, 520–524
Competitive exclusion principle, 524
Compliance carbon market, *see* Cap-and-trade system
Concentration-response function (CRF), *see* Dose-response relationship
Concessional loan, 299, 308, 309, 352, 355
Conditional expectation, 1064
Conditional probability distribution, 1064, 1077
Conference of Parties, *see* COP
Confusion matrix, 105
Conservation biology, 366, 394, 503, 554
Constant mix strategy, 1026–1028
Consumer price index, 811

Consumer-resource model, 522
Consumption-based inventory, 819–821, 836–846, 1014
Contaminant, 467, 471, 475, 477, 487, 497
Controversy risk, 6, 27, 71, 210, 341
Convention on Biological Diversity (CBD), 5, 62, 540, 549–554, 559, 724
Conventional bond, 268, 1022
COP, 13, 272, 549, 559, 727, 947
Copula function, 82, 134, 1066–1077
· Archimedean, 1074
· Clayton, 1075
· Farlie-Gumbel-Morgenstern, 1072
· Frank, 1069, 1075
· Fréchet, 1067, 1075
· Gumbel-Hougaard, 1072, 1075
· Joe, 1075
· Multivariate copula, 1068
· Negative quadrant dependence, 1069, 1071
· Normal, 361, 1067, 1075
· Positive quadrant dependence, 1069, 1071
· Product, 1066, 1070, 1075
· Scale invariance property, 1071
· Student's $t$, 1076
Coral reefs, 398, 549, 560, 702, 703
Core portfolio, 1018–1019
Core-satellite portfolio, 200, 991, 1017–1029
Corporate carbon footprint (CCF), 907
Corporate social responsibility (CSR), 3, 25, 67, 539, 573, 574
Corporate Sustainability Reporting Directive, *see* CSRD
Correlation, 59, 75, 84, 165, 199, 361, 954, 1028
Cost of capital, 209–226
Cost of debt, 213–226
Cost of equity, 209–213
Cost-push price model, 809
Covariance matrix, 84, 138, 160, 161, 164, 166, 167, 188, 948, 1028
Covered bond, 268
Cradle-to-gate, 906, 907
Cradle-to-grave, 906, 907
Credit enhancement, 355
Credit rating, 199, 214, 223, 268, 352, 355
Credit rating agency, 25, 28, 131, 226
Credit risk, 202, 206, 223, 357, 359, 1022
Credit scoring, 75, 77
Credit spread, 213, 274
CSRD, 16, 35, 39, 739
CTB, 35, 36, 265, 916, 991–993, 1008

## D

Damage function, 756, 759
Data quality, 65, 486, 491, 540
Death, *see* Mortality
Decarbonization, *see* Portfolio decarbonization
Decarbonization pathway, 919, 929–932, 991–996
Default time, 358, 569, 570, 1129, 1131
Deforestation, 61, 239, 432, 459–463
Demand-pull quantity model, 807
Depth of the food deficit, 566, 1112
Deuterium, 634, 637, 640
Development finance institution (DFI), 308, 312, 354, 364
Development impact bond (DIB), 348
DICE model, **750–773**, 775
Dietary energy consumption (DEC), 424–427, 564, 1110
Direct air carbon capture with carbon storage (DACCS), 900, 905, 919
Disability-adjusted life years (DALY), 489
Discount rate, 211, 500, 570, 767, 771–773, 776, 1129, 1134, 1135
Discounted cash flow model (DCF), 211
Discriminant curve, 98–100
Diversification risk, 1008
Diversity index, 63
Divestment, 4, 44, 313, 584, 967
Dividend discount model (DDM), 211
DNSH, 33, 230, 254, 332, 421, 939, 940
Do no significant harm, *see* DNSH
Dose-response relationship, 477–481
Double materiality, 19, 40, 319, 417, 539, 562
Downstream, 547, 827
Downstreamness, 832
Dry powder, 288, 342
Dual inverse matrix, *see* Leontief inverse matrix
Dual problem, 1050, 1052
Due diligence questionnaire (DDQ), 66, 70
Duration risk, 201, 203, 1022

Duration-times-spread factor (DTS), 206, 954, 955, 958, 978, 990, 998, 1012

## E

Earth Summit, 5, 549, 723–725
East Antarctic ice sheet, 702
East Antarctic subglacial basins, 701
Ecological diversity, 366, 373–374, 541
Ecological footprint, 422, 869
Ecoregion, 373
Ecosystem, 351, 366, 394–427, 477
Ecosystem diversity, *see* Ecological diversity
Ecosystem service, 394–402, 540, 547
Ecotoxicology, 477
Effective temperature, 662–664, 672
Efficient frontier, **138–142**, 144, 149, 154, 169, 172–176, 188, 189, 970, 971
Effort sharing regulation (ESR), 742
Eigendecomposition, 120, 812, 817, 1045
El Niño Southern Oscillation (ENSO), 699
Elasticity (economics), 494, 501, 751, 767, 773, 851–853, 860
Electricity, 945, 993, 1018
Emission factor, 881–882
Emissions trading system (ETS), 31, 740–742, 749
Emissivity, 659, 662, 667–669, 673, 674, 676, 678
Endemic species, 393, 450, 466, 569, 1128
Endemics-area curve, 450–454, 569, 1128
Energy balance model (EBM), 659–698
Energy efficiency directive (EED), 744
Energy performance of buildings directive (EPBD), 745
Engage behind the scenes, 575
Engagement, 11, 12, 44, 303, **573**
Enhanced weathering, 900, 905
Environmental toxicology, 477
Environmentally-extended input-output model, **807**, 894, 1016
Eora, 821
Equilibrium climate sensitivity (ECS), 682, 686–688
Equity tranche, *see* Junior tranche
ESG
- · Data, **54–73**
- · Definition, 1
- · Integration, 44, 297, 792
- · Investment strategy, 42–45, 153, 947
- · Market growth, 42–48
- · Metrics, 66
- · Rating agency, 2, 5, 15, **25–28**
- · Rating model, 112–132
- · Scoring, **53–136**
- · Uncertainty, 74

ESG investing, 1, 42–48, 559
ESMA, 16, 28, 268, 335
ESRS, 365, 739
European Commission, 1, 16
European ESG Template (EET), 37
European Financial Reporting Advisory Group (EFRAG), 16, 40
European Green Deal, 16, 30, 31, 557, 740
European Investment Bank (EIB), 253, 268, 306, 308, 322, 362
European Project for Ice Coring in Antarctica (EPICA), 640
European Securities and Markets Authority, *see* ESMA
European Sustainability Reporting Standards, *see* ESRS
European Sustainable Finance Action Plan, 30
European Sustainable Investment Forum, *see* Eurosif
Eurosif, 7, 317
Evenness, 366, 439, 441, 568, 1125
Exclusion, 35, 252, 253, 998, 1000, 1002, 1011, 1017, 1018
Exiobase, 821, 832–835
Exit, *see* Divestment
Expected return, 138, 948, 955
Exported emissions, 836–846
Extinct in the wild, 383, 385
Extinction, 64, 375, 380, 428, 502
Extinction debt, 387–391, 394
Extinction event, *see* Mass extinction
Extinction rate, 375, 377, 389, 434
Extirpation, 375
Extra-financial rating agency, *see* ESG/Rating agency

## F

Faint young Sun paradox, 627
Feedback, 674–682, 690, 692, 695
Fiduciary duty, 5

Financed emissions, 894
Financial inclusion, *see* Microfinance
Financial materiality, *see* Single materiality
Financial Stability Board (FSB), 14, 23
First law of thermodynamics, 659
First-loss capital, *see* Junior tranche
Fit for 55 package, 30, 31, 733, 740–748
Fixed quota, 513
Flaring, 649, 746
Food security, 44, 55, 63, 281, 328, 363, 412–427, 534, 750
Food web, 524
Foreign direct investment (FDI), 334
Forest loss, 455–463
Forest management, 22, 300, 455–463, 533–539, 701, 723, 899, 904, 905
Founder crops, 419
Fragmentation, 432–463
Fréchet class, 1067
Frequency, 660
Freshwater, 373, 395, 505–507, 656, 658
FuelEU maritime regulation, 745
Functional response, 517, 518
FUND model, 750, 774, 775
Fundraising, 288, 289, 292

## G

Gas, 649
Gause's law, *see* Competitive exclusion principle
GCAM model, 774, 777, 778, 793, 798, 801
Gender equality, 56, 326, 328, 341, 363
General circulation model (GCM), 622, 623, 760, 761, **1034**
Genetic diversity, 366–370, 540, 541, 550
Genus/genera, 370, 372, 374, 375, 381
Geologic time scale (GTS), 624, 625
Geometric model (biodiversity), 444, 446, 451
GHG emissions, *see* Carbon emissions
GHG Protocol, 18, 19, **21**, 22, 830, 874, 878
GICS, 834, **973–977**, 979, 1021–1023
Gini coefficient, 57, 59, 102, 104, 793, 796
Glasgow Financial Alliance for Net Zero (GFANZ), 12, 947, 991
Global Biodiversity Framework (GBF), 549, 551–555
Global Compact initiative, *see* UN Global Compact
Global Impact Investing Network (GIIN), 299, 307, 312
Global Industry Classification Standard, *see* GICS
Global Reporting Initiative (GRI), 5, 18
Global stratotype section and point (GSSPS), 625
Global Sustainable Investment Alliance, *see* GSIA
Global Sustainable Investment Review, *see* GSIR
Global warming, 618–624, 994
Global warming potential (GWP), 655, 785, 869, **870–874**
GLOBIO, 541
GLOBIOM model, 774, 778, 793, 798, 801, 802
Glyphosate, 490
Grading system, 252, 253
Graph theory, 79
Gray body, 667, 673
Green bond, 35, 44, 200, 229, **267–280**, 357, 560, 1022
Green Bond Principles (GBP), 21, 251, 267
Green capex, 942, 1002
Green footprint, 1002
Green intensity, 33, 938, 1002, 1018
Green loan, 266
Green revenue share, 36, 939–941, 1002
Green-to-brown ratio, 36, 942
Greenhouse effect, 614–617, 664–668
Greenhouse gas, 16, 21, 497, 617, 647–655, 760, 761, 782–784, 870, 876, 878, 883
Greenhushing, 251, 289
Greenium, 273–280
Greenland, 632, 633, 639, 645
Greenland Ice Core Project (GRIP), 632
Greenland ice sheet, 699, 701, 708
Greenland Ice Sheet Project (GISP), 632
Greenness, 33, 255, **938–942**, 1000
Greenwashing, 13, 16, 71, 244, 248–251, 268, 286, 317, 604, 930, 933
GSIA, 7
GSIR, 7
Gulf Stream, *see* Atlantic meridional overturning circulation (AMOC)

## H

Habitat loss, 387, 432–463
Harvest, 508–517, 533
Health concerns, 470, 486–491
Heat capacity, 670, 675, 691, 698
Heavy metal, 467, 469, 471, 475, 490, 495, 497, 499
Hedging, 1039
Herbicide, 487, 490
Herfindahl index, 63, 86, 134
High climate impact sector, 36, 979
High-Level Expert Group on sustainable finance, *see* HLEG
Hill number, 63
HLEG, 16, 30
Holocene, 384, 624
Hormesis, 478
Hotspot (biodiversity), 393
Household air pollution, *see* Indoor air pollution
Hunting, 533–537
Hydrogen, 744, 746, 945
Hydrogen isotope, 634
Hysteresis, 694, 706

## I

Ice age, 617, 624
Ice cap, 615
Ice core, 632
Ice-albedo feedback, 623, 627, 676–677, 689, 695
Impact bond, *see* Social impact bond (SIB)
Impact investing, 44, 65, **297–364**
Impact materiality, 40
Implied temperature rating (ITR), 932, 945, 1001–1003
Imported emissions, 332, 836–846
Income inequality, 59, 217, 793
Index fund, 229
Index sponsor, 27
Indoor air pollution, 468, 489, 491, 493
Industrial Revolution, 625, 642
Industry, 945
Inequalities, 326, 363, 492, 777, 793
Inflation risk, 847, 849, 856
Information ratio, 149
Infrastructure, 287, 289, 294, 1024
Input-output analysis, 807, 1016
Input-output model, *see* Environmentally-extended Input-output model
Inside-out materiality, *see* Impact materiality
Insurance Distribution Directive (IDD), 39
Integrated assessment model, **750–802**
Intentionality, 300, 305
Intergovernmental Panel on Climate Change, *see* IPCC
Intergovernmental Science-Policy Platform on Biodiversity and Ecosystem Services, *see* IPBES
International Association of Insurance Supervisors (IAIS), 16
International Energy Agency (IEA), 785, 918, 919, 929, 991
International Finance Corporation (IFC), 4, 304, 306, 308, 351, 362
International Organization of Securities Commissions (IOSCO), 15
International Sustainability Standards Board (ISSB), 18, 245, 556, 739
Invasive species, 463–466, 468, 517, 550, 552, 553, 555
Inventory boundary, 878
Investment manager, *see* Asset manager
Investor-pays principle, 27
IPAT equation, 651
IPBES, 384, 395, 410, 555–556
IPCC, 5, 12, 624, 710–712, 723, 782, 786, 788
Irminger sea, 701, 702
Isotope, 627, 628, **634**
Isotope ratio, 627–629, 632, 640
Issuer-pays principle, 28
IUCN Red List, 383, 385–387, 409, 535, 545, 551

## J

Japan Sustainable Investment Forum (JSIF), 7
Junior tranche, 309, 356–361

## K

Kalman filter, 926, 1084
Kaya identity, 651, 735–738
Keeling curve, 621, 622
Kendall's tau, 1067, 1072
Kofi Annan (UN Secretary-General), 3, 8

Kolmogorov equation, *see* Chapman-Kolmogorov equation
Kolmogorov-Smirnov test, **102**
Kunming-Montreal Global Biodiversity Framework, *see* Global Biodiversity Framework (GBF)
Kyoto Protocol, 5, 21, 617, 727–730, 874

## L

Label, 246–257
Labrador sea, 701, 702
Lack of memory property, 127, 1060, 1131
Lagrange function, 141, 170, 1049, 1052, 1080
Land Use, Land-Use Change, and Forestry, *see* LULUCF
Land-use change, 647, 656, 658, 904
Lapse rate, 678
Lasso regression, 93, 194, **1079–1084**
Lead pollution, 467, 482, 487, 491
Leontief inverse matrix, 808–813, 824, 829
Liability risk, 14
Life cycle assessment (LCA), 543, 893, 901, 907
Life expectancy, 489, 569, 1129–1131, 1134
Light pollution, 471
Linear programming (LP), 963–965, 999, 1006, 1019, **1048–1052**
Linear regression, 145, 920, 921, 1064, **1077–1079**, 1081
Linear trend model, 920, 1004
Liquidity risk, 1008, 1011
Living Planet Index (LPI), 62, 541
Local linear trend (LLT), 926
Log-linear trend model, 921, 1004
Log-logistic model, 478
Log-normal model (biodiversity), 444–446
Log-series model (biodiversity), 445, 446, 450, 451, 569, 1127
Logistic growth model, 508, 510, 511, 518–520, 528
Longwave radiation, 660, 661, 668
Lorenz curve, 57, 102–104
Lotka-Volterra equations, 508–524
LULUCF, 55, 730, 742

## M

MAGGIC model, 775, 781
MagPIE model, 775, 777, 780, 798, 801
Maize (*Zea mays*), 420–421
Marginal abatement cost (MAC), 759, 944
Marine ice sheet instability (MISI), 701
Mark Carney, 13, 504
Market portfolio, 138, 146, 154
Markov chain
· Continuous-time, 125–129
· Discrete-time, 97, 117–125
· Stationary distribution, 97, 120
Markov generator, 125
Markov property, 118
Mass extinction, 380, 428
Materials, 945
Matrix exponential, 126, 1046
Matrix function, 1045
Matrix logarithm, 127, 1046
Matrix power, 811–813, 817
Maximum likelihood estimation, 446, 525, 1085
Maximum sustainable yield (MSY), 509–511, 526
Mean species abundance (MSA), 64, 541–542, 563
Mean-variance portfolio, *see* Efficient frontier or Portfolio optimization
Measurability, 300, 305, 320, 324
Megafauna, 502, 503
MESSAGE model, 775, 777, 779, 782, 793, 798, 801, 802
Methane ($CH_4$), 21, 497, 617, 632, 655, 746, 869–874
Mezzanine tranche, 356–358
Michael Jantzi, 26
Microfinance, 42, 44, 281, 299, 301, 345, 362–364
MiFID, 37, 38
Milankovitch cycle, 627, 640
Minimum dietary energy requirement (MDER), 424–427, 565, 1112
Minimum variance portfolio, 139
Mitigation risk, 33
Modified duration, 206, 954, 955, 958, 978, 998
Momentum strategy (ESG), 44, 177
Monsoon, 699, 702
Moral hazard, 273
Morbidity, 489–494, 497
Mortality, 328, 477, 481, 487–494, 497, 501,

569
Mountain glacier, 702
Multi-regional input-output (MRIO), 814–817
Multilateral development bank (MDB), 312, 354
Multivariate probability distribution
· Normal distribution, 83, 151, 158, 1060, 1064, 1075
· Student's $t$ distribution, 1076
· *See also* Copula function
Mutual fund, 229
Mutual fund separation theorem, 138, 142

## N

NACE, 33, 940, 977, 979, 1022
Nationally determined contribution (NDC), 730, 732–738, 1015
Nationally Recognized Statistical Rating Organization, 28
Natural capital, 396–402
Natural language processing (NLP), 27, 71
Negative emissions, 899
Negative emissions technology (NET), 900, 905
Negative externality, 40, 273, 574, 751
Negative screening, 42, 584
Negishi welfare weights, 776
Net diversification rate, 377, 434
Net Zero Asset Managers initiative (NZAM), 13, 588, 991
Net Zero Asset Owner Alliance (NZAOA), 12, 607, 991, 993, 1019
Net-zero
· Alliance, 12, 991
· Definition, 12, 902
· Financing, 273
· Investment portfolio, 35, 914, 927, **991–1028**
· Scenario, 723, 786, 798, 919, 929, 930, **991**
Network for Greening the Financial System , *see* NGFS
Neumann series, 811, 812, 823
NFRD, 13, 16, 35, 39
NGFS, 14, 797–802
NICE model, 777
Nitrogen dioxide ($NO_2$), 468, 470, 482, 483, 497
Nitrous oxide ($N_2O$), 497, 655
Noise pollution, 473
Non-Financial Reporting Directive, *see* NFRD
Nonnegative matrix, 1056
Norm-based screening, 44, 584
North Greenland Ice Core Project (NGRIP), 632, 639

## O

Ocean, 761, 1034
Ocean acidification, 656, 658
Ocean fertilization, 900
Office of Credit Ratings, 28
Oil, 649
One Planet Sovereign Wealth Funds (OPSWF), 13, 607
Operational boundary, 878
Organismal diversity, 366, 370–371, 394, 550
Organizational boundary, 876, 878
Origination rate, 375, 377, 384, 389, 434
Outdoor air pollution, 468, 489, 491, 493
Outside-in materiality, *see* Single materiality
Overexploitation, 502–539
Overfishing, 502, 524–532
Oxygen isotope, 634
Ozone ($O_3$), 468, 482, 483, 487, 617, 618, 656, 658, 699

## P

PAB, 35, 36, 265, 916, 991–993, 1008
$\mathcal{PAC}$ framework, 929–935, 1001, 1015
PAGE model, 750, 774, 775
PAI indicator, 37, 39, 63, 233–242, 335, 365
Paris aligned benchmark, *see* PAB
Paris Climate Agreement, 5, 10, 28, 185, 587, 727, 730–738
Part per billion (ppb/ppbv), 468, 637, 640
Part per million (ppm/ppmv), 468, 621, 637, 729
Particulate matter (PM), 468, 470, 481–484, 487, 489–493, 499
Pass-or-fail system, 252, 253
Pass-through, 851–865
Passive management, 137, 187, 188, 229, 991
Pay-for-failure bond, *see* Sustainability-linked bond (SLB)
Pay-for-success bond, *see* Social impact bond (SIB)

Pee Dee Belemnite (PDB), 628
Performance curve, 98–100
Permafrost, 699, 701, 702
Perron-Frobenius theorem, 812
Persistent organic pollutant (POP), 469, 471, 472
Pesticide, 325, 410, 411, 415, 469, 471, 477, 552, 559
Phanerozoic era, 374–382, 624, 630–641
Philanthropic investing, 299, 307, 310, 315, 362, 364
Philanthropy, 584
Photosphere, 662
Phylum/phyla, 370, 372, 385
Physical risk, 14, 23, 73, 295, 642, 751, 756, 797–799, 801, **1033–1036**
Pitchfork bifurcation, 694
Planck feedback, 675
Planck's law, 659–660
Planetary boundaries, 656–658
Plastic pollution, 473, 486, 552, 558
Ploidy, 368
$PM_{2.5}/PM_{10}$, *see* Particulate matter
Pollination, 402–411, 473, 555
Pollutant, *see* Contaminant
Pollution, 33, 467–500
Population growth, 504, 508, 735, 751–754
Portfolio alignment, 997–999, 1008
Portfolio decarbonization, **967–989**, 997–999
Portfolio optimization, **138–150**, 152, 170–176, **948–1017**
Portfolio rebalancing, 1000
Positive screening, 44
Potentially disappeared fraction (PDF), 543
Power, *see* Electricity
Predator-prey model, 508–520
Preference ordering, 92, 114, 117
Prevalence of undernourishment, 423–427, 564–566, 1107–1113
PRI, 8–10, 583, 587
Primary market, 272, 1017
Principal adverse impacts, *see* PAI indicator
Principles for Responsible Investment, *see* PRI
Private debt, 287, 294, 301, 310, 345, 353, 364
Private equity, 287, 289, 292, 299, 301, 310, 313, 323, 342, 345, 347, 353
Probability distribution
· Bates distribution, 84, 1063
· Bernoulli distribution, 1057
· Beta distribution, 88, 89, 1060, 1067
· Binomial distribution, 1057, 1125
· Diversity distribution, 63, 1058
· Exponential distribution, 361, 570, 672, 872, 1060, 1122, 1131
· Gamma distribution, 1059
· Generalized extreme value distribution, 1062
· Generalized Pareto distribution, 1063
· Geometric distribution, 1057
· Inverse Gaussian distribution, 1061
· Log-logistic distribution, 478
· Log-normal distribution, 152, 444, 478, 1061, 1070
· Normal distribution, 83, 88, 179, 679, 1060
· Pareto distribution, 1062
· Poisson binomial distribution, 1058, 1124, 1125
· Poisson distribution, 1057
· Ratio distribution, 688, 1065
· Reciprocal normal distribution, 686
· Uniform distribution, 95, **1058**, 1063, 1066
· Weibull distribution, 478, 570, 1131
Probability integral transform, 88, 361, 1059
Producer price index, 811
Product carbon footprint (PCF), 819, 907
Production-based inventory, 819–821, 1014
Productivity, 363, 486, 494, 495, 501
Project bond, 268
Proxy voting, 26, 27, 44, 593
Pulse event, 381, 392

## Q

Quadratic form, 948, 955–1055
Quadratic programming (QP), 139, 149, 948, 950, 955, 1004, 1005, 1019, **1052–1053**, 1080
Quality-adjusted life year (QALY), 500, 571, 1134, 1135

## R

Radiative forcing, 615, 640, 658, 674, 686–688, 762, 783, 871
Radiative relaxation timescale, 671

Ramsey rule, 771–773
Randomized controlled trial (RCT), 322
Rank-abundance distribution, 440–444, 568
Rating migration matrix, **117–132**
Rating model, **112–132**
Real asset, 229, 287, 294–296, 564
Real estate, 296, 1025
Reanalysis, 644
Red List Index (RLI), 64, 541, 553
Reduction rate, 916
Reforestation, *see* Forest management
ReFuelEU aviation regulation, 745
Regulation policy, **28–42**, 230–245, 739–749
Relaxation timescale, 389, 683, 694, 696, 697
REMIND model, 775, 777, 780, 793, 798, 801
Renewable energy, 31, 744, 904
Renewable energy directive (RED), 744
Reporting
· Biodiversity, 14, 22, 41, 556
· Climate, 21
· Sustainability, 18, 301
REPowerEU, 30, 31
Representative concentration pathway (RPC), 716, 782
Reputational risk, 6, 71
Resource extraction, 502–539
Revenue bond, 268
Rhinoceros, 502, 537, 538, 560
RIA Canada, 7
RIAA, 7
RICE model, 776
Risk factor model, 163–169
Risk premium, **145**, 147, 151–169, 176
Risk-aversion coefficient, 139
Risk-free asset, 142
Risk-tolerance coefficient, 139, 144, 152, 153, 155, 948, 955
Robo-voting, 594
ROC curve, 104–108
Rössler model, 696

## S

Saddle-node bifurcation, 694, 696
Satellite portfolio, 1019–1025
Say on climate, 581, 604
Say on pay, 581
Schur decomposition, 122, 1045
Scope 1 emissions, 880–882, 894, 1008
Scope 2 emissions, 885–891, 1008
Scope 3 emissions, 891–1016
Scope 4 emissions, 901
Scoring model, **75–109**, 540
Screening, 42, 1024
SDGs, **19**, 317, **325–341**, 346, 353, 363, 563, 724
Second party opinion, 268
Secondary market, 272, 1017
Sector neutrality, 179, 200, 201, 951, 953, 983, 1008, 1017
Sectoral decarbonization, 993, 1018
Securitization, 268, 355, 357
Security and Exchange Commission (SEC), 16, 28
Selection curve, 98–100
Self-decarbonization, 36, 927, 1000–1001, 1005, 1006, 1018
Senior tranche, 309, 356–361
Sepkoski curve, 374
SFDR, 16, 35, **36–37**, 39, 45, 230–242, 365
Shadow price, 1049, 1051
Shannon entropy, 63, 95–97
ShareAction, 580, 581, 597
Shared socioeconomic pathway (SSP), 716, 791
Shared socioeconomic pathways (SSP), 793
Shareholder activism, 44, 574
Shareholder resolution, 11, 579
Sharpe ratio, 143, 145, 147, 172
Sherman-Morrison-Woodbury formula, 167, 1046
Shortwave radiation, 660, 661, 668
Signaling theory, 45
Silent Spring, 469
Simpson index, *see* Herfindahl index
Sin stock, 3, 178
Single materiality, 19, 40, 76
Slack variable, 1048
Snowball Earth hypothesis, 627, 628
Social bond, 44, 229, **281–283**, 1022
Social Bond Principles (SBP), 21, 281
Social climate fund, 742
Social cost of carbon (SCC), *see* Carbon tax
Social impact bond (SIB), 313, 348
Social outcomes contract (SOC), *see* Social impact bond (SIB)
Socially responsible investing, *see* SRI

Soil pollution, 475, 490
Solar radiation, 616, 627, 662–666
Sovereign bond, 1012–1016
Sovereign risk, 27, 1012–1016
Spearman's rho, 1072
Speciation, 375, 384
Speciation rate, *see* Origination rate
Species, 366, 370–371
Species abundance distribution (SAD), 440–446, 568–569, 1124–1129
Species accumulation curve (SAC), 446–450
Species diversity, *see* Organismal diversity
Species rarefaction curve, 447
Species richness, 366, 389–391, 428, 434, 441, 448, 540, 1121–1122
Species threat abatement and restoration (STAR), 545–546
Species-area relationship (SAR), 434–439, 450–454, 568, 1122, 1124
Spectral density function, 660, 661
SPO, *see* Second party opinion
SRI, 1, 298, 315
Standard Mean Ocean Water (SMOW), 634
State space model, 1083–1086
Stated policies scenario (STEPS), 785, 1014
Stefan-Boltzmann law, 659
Stewardship, 573
Stock picking, *see* Asset selection
Stranded asset, 584, 944
Strategic asset allocation (SAA), 1026
Stratosphere, 667
Strong duality theorem, 1050
Substochastic matrix, 812, 830, 854, 1056
Suitability Test (MiFID II), 38
Sulfur dioxide ($SO_2$), 468, 470, 482, 483, 497
Sullivan Principles, 4
Supervised learning, 75
Supply chain, 67, 295, 579, 580, 807, 821, 830, 860, 862, 905
Survival function, 377, 435, 500, 569–571, 872, 1129–1135
Survival time, *see* Default time
Sustainability bond, **266–287**, 1022
Sustainability Disclosure Requirements (SDRs), 244
Sustainability preferences, 39
Sustainability-linked bond (SLB), 266, 285, 1022
Sustainable Blue Economy (SBE), 62, 351
Sustainable Development Goals, *see* SDGs
Sustainable finance, **1**, 246, 297
Sustainable Finance Disclosure Regulation, *see* SFDR
Sustainable investment forum, 7
Symbiosis, 521

## T

TAB, 35
Taiga, *see* Boreal forest
Tangency portfolio, 138, **142–144**, 144, 145, 151, 155, 176
Target population, 281, 348, 350
Target setting
· Engagement, 12, 44, 1015
· Net-zero, 12, 929–932
Task force on Climate-related Financial Disclosures, *see* TCFD
Taskforce on Nature-related Financial Disclosures, *see* TNFD
Taxonomic tree (biology), 370–372
Taxonomy
· Brown taxonomy, 35
· ESG taxonomy, 58, 59, 70
· EU Taxonomy Regulation, 16, **33–35**, 37, 39, 255, 365, 938
· Green taxonomy, 33, 938–939, 1024
· Social taxonomy, 35
Taxonomy-aligning benchmark, *see* TAB
TCFD, 9, 14, 18, **23**
Technical assistance facility (TAF), 355
Technical Expert Group on sustainable finance (TEG), 16, 31, 33, 36
Temperature, 614–646, 663, 665, 668, 669, 674, 756–764
Temperature anomaly, 642–646, 699, 708
Temperature scale, 630
Temperature score, *see* Implied temperature rating (ITR)
Thematic investing, 44, 303, 317, 1024
Theory of island biogeography (TIB), 433–434, 566–568, 1114–1122
Tipping element, 699
Tipping point, 12, 656–658, 689–709, 781
TNFD, 395, 556–557
Total factor productivity, 754
Total solar irradiance, 615, 659

Toxicity, 472, 477–481
Tracking error risk, 148, 187, 192, 203, 948, 950, 957, 1027–1028
Tragedy of the commons, 504
Tragedy of the horizon, 14, 504
Tranching, 355–361
Transcritical bifurcation, 694
Transition bond, 266, 287
Transition probability matrix, *see* Rating migration matrix
Transition risk, 14, 23, 33, 295, 751, 756, 768, 797–799, 801, **943–945**, 999, 1012, 1017
Transparency challenge, 28
Transportation, 945, 993
Tree model, 77–93
Troposphere, 667, 671
Trucost, 832–835
Tundra, 373, 699, 702
Twin bond, 274, 276
Two-fund separation theorem, *see* Mutual fund separation theorem, 144

## U

Ultraviolet, 661
UN Framework Convention on Climate Change, *see* UNFCCC
UN Global Compact, 3, 4, 44, 335, 351
UN PRI, *see* PRI
UNFCCC, 5, 12, 272, 710, 724–727, 730
United Nations, 3
United Nations Environment Programme (UNEP), 5, 351, 624, 710, 723
Unsupervised learning, 75, 95, 108
Upstream, 547, 823–835
Upstreamness, 831
US SIF, 7
Utility function, 139, 152, 160, 169, 299, 337, 767, 777

## V

Valdez Principles, 5
Value of a statistical life (VSL), 492, 497–501, 569–571, 1129–1135
Value of life year (VOLY), *see* Value per statistical life year (VSLY)
Value per statistical life year (VSLY), 497–499, 501, 571, 1133–1135
Values, 3, 13, 39, 297
VBDO, 7
Venture capital, 287, 289, 299, 307, 342, 345
Voice, 582
Volatile organic compound (VOC), 469, 497, 499
Voluntary carbon market (VCM), 902, 904
Voting policy, 11, 44, 580, **593–607**
Voting principles, 595

## W

Warren Buffet, 71
Waste management, 394, 945
Water pollution, 432, 475, 476, 486–488, 491, 499, 561
Water security, 22, 33, 656, 701, 945
Water vapor, 615, 616, 678
Wavelength, 660
Weighted average carbon intensity (WACI), 832, 910, 913, 980, 1004
Weighted average cost of capital (WACC), 209
West African monsoon, 699, 702
West Antarctic ice sheet, 699, 701, 708
West Antarctic Ice Sheet project (WAIS), 632
White body, 662
Willingness-to-pay (WTP), 313, 314, 398, 500, 501
WIOD, 814–817, 832–835
WITCH model, 775, 793
World Health Organization (WHO), 58
World input-output database, *see* WIOD
World Meteorological Organization (WMO), 5, 624, 710
Worst-in-class, 42

## X

Xenodiversity, *see* Invasive species

## Y

Years lived with disability (YLD), 489, 490, 492
Years of life lost (YLL), 489, 571, 1134
Yield, *see* Bond yield
Yield to maturity, 213, 274, 275

## Z

Zero-order model, 662–668
Zoonotic disease, 538
$z$-score, 77, 87

# Author Index


**A**

Abernethy, Katharine, 535
Aboud, Ahmed, 213
Aboumahboub, Tino, 774
Abram, Nerilie J., 701, 702
Abrams, Jesse F., 699, 700, 703, 708
Abrams, Peter A., 524
Acosta, Nereus J. R., 487
Adams, Mark D., 369
Addison, Prue F. E., 561
Adger, William Neil, 717
Adl, Sina, 371
Admati, Anat R., 585
Adrion, Jeffrey R., 410
Agle, Bradley R., 574
Agrawal, Anirudh, 313
Aguiar, Sebastián, 403, 404
Agusti, Susana, 532
Ahmed, Parvez, 199
Aizen, Marcelo A., 403, 404, 406
Åkerman, Maria, 396
Ala, Davin, 639
Albuquerque, Rui, 213
Alcamo, Joseph, 505
Alder, Jackie, 525
Alegret, Peter, 382
Alesina, Alberto, 217
Alessi, Lucia, 257, 941
Algeo, Thomas J., 381, 382, 428, 429
Ali, Heba, 333
Alkemade, Rob, 542
Allen, Myles, 902, 903, 905
Alley, Richard B., 701
Almonacid, Paula, 213
Almond, Rosamunde E. A., 62
Altman, Edward I., 75, 77
Anandakrishnan, Sridhar, 701
Anderson, M. B., 521, 522
Anderson, Sharolyn J., 473
Andersson, Mats, 947, 967
Ando, Amy W., 538
Andrew, Robbie M., 738
Annan, James D., 679, 681, 688
Anthoff, David, 774
Antonopoulos, Alexandros, 213
Antràs, Pol, 831
Apergis, Nicholas, 213
Appel, Ian R., 588, 589
Arakawa, Akio, 623
Aras, Güler, 574
Archer, David, 618–620
Arditi, Roger, 519
Areal, Nelson, 199
Arenillas, Ignacio, 382
Arlidge, William N. S., 561
Armesto, Juan J., 428
Armour, Kyle C., 676
Armstrong McKay, David I., 699, 700, 703, 708
Armstrong, Robert A., 524
Arp, Hand Peter H., 473
Arrhenius, Olof, 434
Arrhenius, Svante, 616–618
Arroyo-Rodríguez, Víctor, 433
Artois, Marc, 538
Ascencio, Jean-Marc, 617
Ascui, Francisco, 905
Attig, Najah, 213
Attridge, Samantha, 334
Atz, Ulrich, 137
Auer, Cornelia, 774
Autorité de Contrôle Prudentiel et de Résolution (ACPR), 16
Avramov, Doron, 159–162
Axelsson, Kaya, 902, 903, 905
Ayala, Ted J., 513

Azar, José, 591
Azmy, Karem, 639

## B

Bacastow, Robert B., 622, 718
Bacon, Sheldon, 701
Bagstad, Kenneth J., 401
Bahamondez, Carlos, 463
Baillie, Jonathan E. M., 539
Bailly, Hugo, 853, 860
Bailon, Martha, 547, 548
Bainbridge, Arnold E., 718
Baker, D. James, 623
Baker, Malcolm, 269, 273
Bakkenes, Michel, 542
Balakrishnan, Kalpana, 487–489
Balitzky, Sara, 335, 336
Bandeira, Benjamin, 64
Bank of England (BoE), 16
Banks-Leited, Cristina, 433
Barahhou, Inès, 896–900, 911–913, 928, 941, 942, 979–984, 989, 990, 998–1002, 1006–1016
Barber, Brad M., 313, 314
Barbier, Edward, 532
Barbier, Edward B., 525
Barko, Tamas, 577
Barlow, Jos, 461, 463
Bärlund, Ilona, 505
Barnett, George, 703, 704, 706, 708
Barnett, Michael L., 178
Barnola, Jean-Marc, 637
Barnosky, Anthony D., 380, 381, 384, 387
Barrett, John, 836
Barros, Victor, 213
Barrowman, Nicholas J., 526
Bartomeus, Ignasi, 405, 410
Basel Committee on Banking Supervision (BCBS), 15
Bassen, Alexander, 137, 178
Basso, Luana S., 701
Bathiany, Sebastian, 702
Batista, Milan, 1047
Battiston, Stefano, 941
Baty, Florent, 478
Bauer, Andrew, 626
Bauer, Christian, 905
Bauer, Nico, 774
Bauer, Rob, 199, 213
Baum, Julia K., 532
Bazzaz, Fakhri A., 464
Beabout, Gregory R., 2
Beal, Douglas, 352
Beaugrand, Gregory, 566
Beaumont, Nicola, 525
Bebchuk, Lucian A., 591
Becker, Martin G., 260
Beer, Juerg, 637
Beerling, David J., 639
Begon, Michael, 513
Behr, Melissa, 464
Bekjarovski, Filip, 575, 576
Bell, Bill, 645
Bellocq, M. Isabel, 439
Ben Dor, Arik, 73
Ben Slimane, Mohamed, 157, 200–205, 213–215, 217, 277, 279, 280, 283, 896–900, 911–913, 928, 941, 942, 955, 966, 979–984, 989–991, 998–1002, 1006–1013, 1018–1023, 1027, 1028
Bengis, Roy G., 538
Bennani, Leila, 179–183, 185, 187–192, 197
Bennett, Elisabeth, 535
Bennett, Elizabeth L., 533
Bennett, Joseph R., 433
Bennett, Michael, 353
Bennun, Leon A., 545, 546
Bentley, Michael J., 701, 702
Benton, Michael J., 381
Berg, Alexis, 702
Berg, Florian, 27, 70, 74, 159
Berger, Lee, 464
Berger, Wolfgang H., 524
Bergeron, Yves, 702
Bergman, Juraj, 502
Bergstresser, Daniel, 269, 273
Berk, Jonathan B., 313
Bernard, Julie, 594
Berner, Robert A., 639
Bernstein, Aaron S., 538
Berrada, Tony, 286
Berrisford, Paul, 645
Bertram, Christoph, 797, 798
Betts, Matthew G., 463, 535
Betts, Richard Arthur, 717
Bicknell, Jake E., 534

Biesmeijer, Jacobus C., 403, 404, 408
Biggs, Reinette, 544
Billio, Monica, 75
Billups, Katharina, 640
Bingler, Julia Anna, 72
Birindelli, Giuliana, 313
Biswas, Bhabananda, 468
Bjella, Kevin, 702
Black, Fisher, 147, 148
Blair, Peter D., 807, 810, 819, 821
Blanford, Geoffrey J., 775, 776
Blehert, David S., 464
Blepp, Markus, 472
Blundo, Benedetta, 334
Board of Governors of the Federal Reserve System (FRB), 53
Bobbink, Roland, 475
Bodirsky, Benjamin Leon, 774
Boffo, Riccardo, 28
Böhringer, Christoph, 729
Boiardi, Priscilla, 315, 316
Boiral, Olivier, 341, 594
Boivin, Thomas, 517
Bolin, Bert, 621, 623, 710
Bolton, Patrick, 157, 357, 947, 967, 993, 998
Bommarco, Riccardo, 387, 389
Bonnefon, Oli, 517
Bonsall, Michael B., 524
Bor, Anne-Marie, 547, 548
Borges, Paulo A. V., 436–438
Bosetti, Valentina, 774
Bosmans, Pieter, 352
Boston Consulting Group (BCG), 294, 904
Bouchet, Philippe, 384, 387
Bouwman, Lex, 774
Bouyé, Eric, 58, 59
Bowen, Howard R., 3, 574
Bowker, Geoffrey C., 64
Boyano, Alicia, 257
Boyd, Stephen, 1053
Boyer, Joseph G., 729, 758
Brancalion, Pedro H. S., 455
Brandenburg, Margot, 307
Brander, Luke, 398
Brander, Matthew, 905
Brard, Eric, 200, 201, 203, 214, 215
Brauer, Michael, 58
Breeze, Tom D., 408, 410, 411
Breidert, Christoph, 314
Brière, Marie, 71, 273, 575, 576, 580, 938
Brito-Ramos, Sofia, 258
Broadgate, Wendy, 504, 505
Broccardo, Eleonora, 585
Brockington, Simon, 526, 527
Broecker, Wallace S., 623
Brooks, Chris, 199, 213
Brooks, Thomas M., 378–380, 384, 393, 435, 545, 546
Brotherton, Marie-Christine, 594
Brovkin, Victor, 702
Brown, David, 535
Brown, James H., 523
Broze, Rafael, 905
Bruce-Clark, Peter, 317, 318
Brudvig, Lars A., 433
Brummitt, Charles D., 703, 704, 706, 708
Bruno, Christopher C., 137
Buchhorn, Marcel, 461
Budolfson, Mark B., 777
Budyko, Mikhail I., 623, 677
Bugg-Levine, Antony, 307
Bui, Mai, 905
Bull, Joseph W., 561
Bumgarner, Jacob R., 473
Burbano, Vanessa Cuerel, 248, 249
Burivalova, Zuzana, 534
Burke, Marshall, 73
Burnett, Richard, 58
Burrowes, Nina, 349
Busch, Timo, 137, 178, 317–319
Butchart, Stuart H.M., 64
Butnar, Isabela, 781, 782, 850

## C

Calabrese, Edward J., 478
Caldecott, Ben, 902, 903, 905
Caldeira, Ken, 651, 717, 836
Calel, Raphael, 760, 762, 763
Callaghan, Max W., 900
Callendar, Guy Stewart, 618
Calvin, Katherine, 774, 778
Canadell, Josep G., 651, 717, 738
Cane, James H., 402–404
Capelle-Blancard, Gunther, 178, 217
Carbone, Lucia, 377
Cardinale, Bradley J., 62

Carey, Mark, 702
Carney, Mark, 14, 504, 575
Carraro, Carlo, 774
Carroll, Archie B., 3, 574
Carson, Rachel, 469
Carter, Timothy R., 791, 793
Case, Ted J., 513, 520
Cashion, Tim, 532
Castells, Francesc, 850
Catling, David C., 626
Cattani, Olivier, 640
Cawthorn, Donna-Mareè, 535
Cazzolla Gatti, Roberto, 450
CDP, 885
Ceballos, Gerardo, 380, 384, 387
Cedergreen, Nina, 478
Chaber, Anne-Lise, 535
Chadburn, Helen, 418, 419
Chafik, Léon, 701
Chalmandrier, Loïc, 64
Chaloupka, Milani, 531, 532
Chambers, David, 585
Chang, Jing, 450
Chanson, Janice, 64
Chao, Anne, 448
Charnay, Benjamin, 627
Charney, Jule G., 622, 623
Chatterji, Aaron K., 27
Chaudhry, Taz, 352
Chazdon, Robin L., 455
Chen, Tao, 588
Chen, Zhiyuan, 75
Cheng, Si, 159–162
Cherief, Amina, 559
Cherp, Aleh, 731
Chertow, Marian R., 651
Chesson, Peter, 522, 524
Cheung, William Wai Lung, 717
Chiappini, Helen, 313
Chin, John F. S., 718
Chin, Lauren, 607
Chiquier, Solene, 905
Chor, Davin, 831
Chowdhry, Bhagwan, 350
Christensen, Villy, 525
Christianson, Knut, 701
Christophersen, Tim, 535
Chu, Eric, 1053
Ciais, Philippe, 651, 715, 717
Cicerone, Ralph J., 617
Clark, Christopher M., 475
Clarke, Joseph J., 698
Clarke, Leon, 774, 778
Claus, James, 212
Climate Bonds Initiative (CBI), 266, 267, 269, 283, 285, 286
Climate Disclosure Standards Board (CDSB), 23
Clobert, Jean, 433
Clout, Michael, 464
Coddington, Jonathan A., 450
Cohen, Aaron J., 58
Cointe, Béatrice, 731
Cojoianu, Theodor, 607
Colantonio, Andrea, 321
Coleman, Bernard D., 568
Collen, Ben, 384
Collins, Daniel W., 213
Collins, William J., 688
Colman, Robert, 678
Colwell, Robert K., 450
Commissariat Général au Développement Durable, 846
Condit, Richard, 443
Connor, Edward F., 435
Convention on Biological Diversity (CBD), 551–553
Convergence, 355, 362
Cooper, Elizabeth W., 213
Coops, Nicholas C., 540
Copland, James R., 593, 594
Coppola, Daniela, 532
Coqueret, Guillaume, 137, 178, 213
Corbet, A. Steven, 444
Cortez, Maria Céu, 199, 258
Costanza, Robert, 63, 397–400
Costola, Michele, 75
Covachev, Svetoslav, 258
Cowie, Robert H., 384, 387
Cox, Grant M., 629
Cox, James, 574
Cox, Peter M., 698
Craig, Harmon, 634
Crassous, Renaud, 774
Cremers, Martijn, 577
Creutzig, Felix, 900

Crifo, Patricia, 217
Crippa, Monica, 734
Crowther, David, 574
Crutzen, Paul J., 624
Cui, Wenping, 523
Culley, Deirdre, 349
Cunningham, Andrew A., 533
Cunningham, Saul A., 406
Curtis, Philip G., 461, 462

## D

D'Arge, Ralph, 63, 397–399
D'Souza, Raissa M., 703, 704, 706, 708
Da Fonseca, Dany, 157, 277, 279
Da Fonseca, Gustavo A. B., 393
Daily, Gretchen C., 394
Daly, Herman E., 397, 819
Damschen, Ellen, 441
Danel, Alexander, 342, 347
Daniel, Kent D., 758, 759
Dansgaard, Willi, 632, 634
Dapporto, Leonardo, 436–438
Dasgupta, Partha, 402
Daszak, Peter, 464
Daubanes, Julien Xavier, 272, 273
Davies, Shaun William, 350, 586
Davies, Zoe G., 534
Davis, Aaron P., 418, 419
Davis, Gerald F., 594
Davis, Steven J., 651, 836
De Groot, Rudolf, 63, 397–400
De Jong, Marielle, 955
De La Cruz, Adriana, 589–591
De Mariz, Frederic, 352
De Palma, Adriana, 544, 545
De Pascale, Donatella, 532
De Queiroz, Kevin, 370
De Ryck, Jo, 547, 548
De Schryver, An, 543
De Souza, Danielle Maia, 702
De Vecchi, Viola, 32
De Vos, Jurriaan M., 380
De Vries, Gaaitzen, 815
De Winter, Iris I., 538
De, Indrani, 313
Dechezleprêtre, Antoine, 494, 495
Decourtye, Axel, 408
Degefa, Sileshi, 401
Deixonne, Florent, 32
Del Monte-Luna, Pablo, 384
Delmas, Magali A., 248, 249
Delmas, Robert J., 617
Demartini, Anne, 26, 27
DeMenocal, Peter B., 702
Dengler, Jürgen, 436
Dennig, Francis, 777
Depledged, Joanna, 691
Deriso, Richard B., 513
Derwall, Jeroen, 199, 213, 317, 318
Desclée, Albert, 199
Descombes, Patrice, 702
Desnos, Baptiste, 807, 830, 832–836, 851, 856–860, 1056
Deutsch, Lisa, 504, 505
Deutz, Andrew, 551, 554, 555
Di Franco, Eugenio, 473
Di Iorio, Lucia, 473
Di Marco, Moreno, 433
Diagne, Christophe, 466
Dias, João, 213
Diaye, Marc-Arthur, 217
Diaz, Delavane B., 775, 776
Dickens, Gerald R., 640
Dickinson, Robert E., 623
Dicks, Lynn V., 408, 410, 411
Didham, Raphael K., 433
Dietrich, Jan Philipp, 774
Dietzenbacher, Erik, 815
Dieye, Rokhaya, 853, 860
Diltz, J. David, 199
Dimson, Elroy, 185, 585, 588, 592
Dinerstein, Eric, 373
Dirzo, Rodolfo, 384
Dise, Nancy B., 475
Disley, Emma, 349
Diz-Pita, Erika, 520
Dockery, Douglas W., 490
Dodd, Nicholas, 257
Dommenget, Dietmar, 665
Donald, Paul F., 551
Dong, Hui, 588
Donges, Jonathan F., 703–705, 707–709
Doré, Guy, 702
Dray, Stéphane, 64
Drei, Angelo, 179, 183–187, 192
Driesen, Kim, 547, 548

Driscoll, Anne, 73
Drobinski, Philippe, 73
Drucker, Peter F., 574
Drupp, Moritz A., 771, 773
Du Preez, Louis H., 464
Duarte, Carlos Manuel, 532, 717
Ducoulombier, Frédéric, 894
Dudás, Fanni, 217
Duffy, J. Emmett, 62
Dumas, Patrice, 776
Durand, Rodolphe, 27
Duro, Miguel, 591
Dynkin, Lev, 199

## E

Easton, Peter D., 212
Ebi, Kristie L., 791–793
Eccles, Robert G., 25, 26, 292, 293, 317, 318
Eckstein, Jonathan, 1053
Ecosystem Marketplace, 904
Edenhofer, Ottmar, 713, 836
Edmans, Alex, 178, 583, 585, 586
Ehlers, Torsten, 268, 273
Ehrlich, Paul R., 365, 380, 384, 387, 394, 428, 504
Eilers, Elisabeth J., 406, 407
Eisner, Stephanie, 505
Ekdahl Jr, Carl A., 718
El Ghoul, Sadok, 178, 210, 213
Elfenbein, Hillary Anger, 137
Eliwa, Yasser, 213
Emerson, Jed, 307
Emery, Teal, 58, 75
ENCORE, 395
Engelen, Peter-Jan, 246, 252
Engelhardt, Leonie, 286
Engen, Lars, 334
EPICA community members, 640
Erbacher, Jochen, 640
Eriksson, Erik, 621
Ermon, Stefano, 73
Eschenbach, Willis, 380
Escher, Beate I., 471
Espagne, Etienne, 402, 776
Etienne, Rampal S., 440, 441
European Banking Authority (EBA), 53, 250, 251
European Central Bank (ECB), 16
European Commission (EC), 1, 28
European Environment Agency (EEA), 497–499, 501
European Financial Reporting Advisory Group (EFRAG), 39
European Fund and Asset Management Association (EFAMA), 258–260
European Investment Bank (EIB), 321–323
European Securities and Markets Authority (ESMA), 231, 233, 235, 259
European Sustainable Investment Forum (Eurosif), 42, 186, 357
Evans, Harry, 464
Evans, John S., 490
Evans, Tom, 463
Eze, Michael O., 478

## F

Fa, Julia E., 535
Fabozzi, Frank J., 178
Fahrig, Lenore, 433
Failler, Pierre, 353
Fally, Thibault, 831
Fama, Eugene F., 179
Faraca Giorgia, 257
Fasullo, John T., 668
Fatica, Serena, 277
Fattorini, Simone, 436–438
Faulwasser, Timm, 759, 763, 768
Fawcett, Tom, 106
Feenstra, Robert C., 754
Fender, Ingo, 279
Fergus, Glen, 630, 631
Fernando, Chitru S., 209, 210, 213
Ferrari, E., 246
Ferrari, Francesco, 474
Ferreira, Joice, 463
Ferreira, Philippe, 1012, 1014–1016
Ferrier, Simon, 540
Feulner, Georg, 627
Fichtner, Jan, 591
Field, Christopher B., 651, 717
Figueiredo, Ludmilla, 387
Financial Stability Board, 14
Finster, Mieczyslaw, 75
Fischer, John R., 538
Fisher, Ronald Aylmer, 444

Fitzgibbons, Shaun, 137, 169–171, 173, 176, 177
Fjörtoft, Ragnar, 622
Flammer, Caroline, 272, 273, 277, 309, 559
Fletcher Jr, Robert J., 433
Fleurbaey, Marc, 777
Flörke, Martina, 505
Fnais, Mohammed, 490
Fontaine, Benoît, 384, 387
Food and Agriculture Organization (FAO), 415, 417, 424, 456, 457, 459, 460, 528, 531
Forget, François, 627
Forum pour l'investissement responsable (FIR), 300, 303
Foster, Gavin L., 641, 642
Fourier, Joseph, 614
France Invest, 300, 303
Francois, Louis M., 639
Frankignoul, Claude, 622
Frazzini, Andrea, 148
Freeman, R. Edward., 3, 574
Freeman, Robin, 62
French, Kenneth R., 179
Freshfields Bruckhaus Deringer, 5
Fretwell, Stephen D., 523
Fricko, Oliver, 774
Friede, Gunnar, 137, 178
Friederich, David, 72
Friedlingstein, Pierre, 647–650, 652–654, 715–717, 836, 842
Friedman, Jerome H., 75
Friedman, Milton, 3, 574
Friedmann, S. Julio, 905
Friedrich, Oliver, 640
Froese, Rainer, 526, 527
Frost, Bruce, 518
Frye, Charlie, 374
Fuglestvedt, Jan S., 871, 874
Fujimori, Shinichiro, 715, 717, 774
Fuller, Grayson, 21, 328, 337
Fuller, Richard, 487–489
Fung, Inez, 676
Fuss, Sabine, 900

## G

Gabay, Denis, 1053
Gaetani, Marco, 702
Gaffney, Owen, 504, 505, 699
Gage, Matthew J. G., 524
Gaggiotti, Gianluca, 315, 316
Galeotti, Marzio, 774
Galetti, Mauro, 384
Galloway, Jim, 475
Gamarra, Javier G. P., 450
Gambhir, Ajay, 781, 782
Game, Edward T., 534
Gantchev, Nickolay, 584
Garber, Andrea K., 406, 407
García, Andrés, 380, 384, 387
Garcia-Bernardo, Javier, 591
Garibaldi, Lucas A., 405, 406, 410
Garrault, Pierre, 317, 319
Gascon, Claude, 393
Gasser, Thomas, 655
Gaston, Kevin J., 365–367, 374, 375, 394, 504
Gatti, Luciana V., 701
Gauthey, Julien, 402
Gauthier, Sylvie, 702
Gebhardt, William R., 212
Geczy, Christopher, 313
Gemechu, Eskinder Demisse, 850
Genest, Christian, 1066, 1074
Genovesi, Piero, 464
Gentleman, Wendy, 518
George, Simon C., 478
Gerard, Bruno, 199
Gerhard, Daniel, 478
Gese, Eric M., 521
GHG Protocol, 21, 22, 885
Ghosh, Bapan, 520
Giacomantonio, Chris, 349
Gianfrate, Gianfranco, 277
Giannadaki, Despina, 490
Gianoncelli, Alessia, 315, 316
Gibbard, Philip, 626
Gibson, Rajna, 286
Gidden, Matthew, 774, 793
Giglio, Stefano, 48, 559
Gillan, Stuart, 574, 586, 588, 589
Gillespie, Mark, 408
Gillingham, Kenneth, 759
Gilman, Eric, 531, 532
Gilpin, Michael E., 513, 520
Gini, Corrado, 65
Ginoux, Jean-Marc, 64

Ginzburg, Lev R., 519
Giorgi, Filippo, 717
Girona, Miguel Montoro, 702
Giroux, Thomas, 309, 559
Gittleman, John L., 378–380, 435
Gitz, Vincent, 774
Gleason, Henry Allan, 435
Global Development Network, 321
Global Impact Investing Network (GIIN), 299
Global Sustainable Investment Alliance (GSIA), 7, 42, 45–48, 186, 229
Gluszek, Sarah, 535
Goberville, Eric, 566
Godderis, Yves, 639
Gode, Dan, 212
Goedkoop, Mark, 543
Goldreyer, Elizabeth F., 199
Gollier, Christian, 592, 773
Golub, Gene H., 1046, 1047
Gombeer, Sophie, 535
Gompers, Paul, 178
Gonçalves, Tiago Cruz, 213
González-Ruiz, Juan David, 213
Gonzalez, Andrew, 62
Gonzalez, Ricardo E., 544, 545
González-Martín, Javier, 468
Goody, Richard M., 623
Goosse, Hugues, 676
Gordon, H. Scott, 509
Gore, Meredith L., 535
Gormley, Todd A., 588, 589
Gotelli, Nicholas J., 450
Gouriéroux, Christian, 97, 99, 100
Goutelle, Sylvain, 480
Gowing, David J., 475
Grabowski, Roger J., 211
Grace, Katie, 311
Graff Zivin, Joshua, 495
Gratcheva, Ekaterina M., 58, 75
Graves-Lindsay, Tina, 369
Gray, Alan, 380
Gray, John S., 440, 441
Gredil, Oleg R., 584
Green, Jessica L., 451–453
Gregory, Alan, 213
Grewal, Jody, 592
Grooten, Monique, 62
Grossman, Allen, 307
Grossman, Blake R., 4
Grubb, Michael, 774
Grüne, Lars, 759, 763, 768
Guan, Jingling, 73
Guariguata, Manuel R., 463
Guedhami, Omrane, 178, 210, 213
Guénette, Sylvie, 525
Guenther, Peter R., 718
Guilhaumon, François, 436
Guilhoto, Joaquim J. M., 836, 842–845
Guillaumie, Laurence, 594
Guillemot, Hélène, 731
Guivarch, Céline, 774
Guizzardi, Diego, 734
Gullison, Raymond E., 533, 534
Gupta, Joyeeta, 327
Gupta, Kartick, 213
Gutierrez, Monica Serrano, 809

## H

Haddad, Nick M., 410, 433
Hailemariam, Kinfe, 874
Haines, Andy P., 717
Hale, Thomas, 902, 903, 905
Hall, Jim W., 691, 699
Hallegatte, Stéphane, 717, 791, 793
Halley, John M., 389, 390
Hallmann, Caspar A., 409
Halverson, Galen P., 627, 629
Hamburg, Steven P., 905
Hammitt, James K., 500, 501, 569, 571
Hand, Dean, 313, 342, 347
Handeland, Kjell, 538
Hanemann, W. Michael, 758
Hann, Daniel, 213
Hänsel, Martin C., 771, 773
Hansen, James E., 623, 624, 640, 645, 676, 716
Hansen, Matthew C., 455, 461, 462
Hanski, Ilkka, 391, 439
Hardin, Garrett, 504
Hargreaves, Serene, 418, 419
Harris, Nancy, 455
Harris, Nancy L., 461, 462
Harrison, Susan, 441
Hart, Oliver D., 585
Hartigan Jr, John, 420
Hartmann, Dennis L., 659, 664, 665, 674, 675

Harvey, Andrew C., 1084, 1085
Hasan, Mahady, 476
Hasegawa, Tomoko, 774
Hasselmann, Klaus, 622, 716, 717
Hastie, Trevor, 75
Hausfather, Zeke, 645
Havlìk, Petr, 715, 717, 774
Hays, James D., 617
He, Fangliang, 451–454, 568
He, Miaomiao, 490
He, Tao, 668
Heal, Geoffrey M., 309, 551, 554, 555, 559
Hebb, Tessa, 317, 318
Heeb, Florian, 313
Heemskerk, Eelke M., 591
Heijungs, Reinout, 543
Heikkinen, Risto K., 387, 389
Heimann, Martin, 622
Hein, Lars, 401
Held, Hermann, 691, 699
Held, Isaac M., 718
Henry, Peter Blair, 217
Hepburn, Cameron, 902, 903, 905
Heras-Saizarbitoria, Iñaki, 341
Herrero, Mario, 717
Hersbach, Hans, 645
Hertwich, Edgar G., 836
Heymell, Victoria, 463
Heywood, Vernon Hilton, 367
Hickey, Conor, 902, 903, 905
Hicks, Alan C., 464
Hicks, Kevin, 475
High-Level Expert Group on Sustainable Finance (HLEG), 30
Hilbers, Jelle P., 542, 543
Hilborn, Ray, 502, 532
Hilderink, M. H., 538
Hill, Jennifer N., 729
Hillberry, Russell, 831
Hinkley, David V., 1065
Hirschman, Albert O., 582, 583
Hirst, Scott, 591
Hjort, Jan, 702
Höchstädter, Anna Katharina, 307, 313
Hockerts, Kai, 313
Hoegh-Guldberg, Ove I., 352, 717
Hoepner, Andreas, 317, 318, 607
Hoffman, Louwrens C., 535
Hoffman, Paul F., 627
Hölker, Franz, 471
Holliday, N. Penny, 701
Holling, Crawford S., 517
Holt, Robert D., 520, 521
Hong, Harrison, 178, 210
Hope, Chris, 774, 775
Hopf, Maria, 419
Horgan, Huw J., 701
Hose, Grant C., 478
Hoskins, Andrew, 544, 545
Hosono, Yuzo, 517
Hossain, Md Shakhawat, 476
Hourcade, Jean-Charles, 774
Howard, Peter H., 758
Howe, Kerstin, 369
Hristova, Iva, 75
Huang, Boyin, 645, 646
Hubbell, Stephen P., 452, 454
Hübel, Benjamin, 217
Huijbregts, Mark, 543
Hukari, Sirja, 472
Hull, Pincelli M., 378, 391, 392
Humpenöder, Florian, 774
Humphrey, Jacquelyn E., 213
Hungerbuhler, Konrad, 472
Huntingford, Chris, 698
Huntington, Tim, 531, 532
Huppmann, Daniel, 774
Hurlbert, Stuart H., 447
Husson-Traore, Anne-Catherine, 258
Hutchings, Jeffrey A., 526, 527
Hutchinson, G. Evelyn, 524
Hutchinson, Mark C., 559
Hyatt, Alex D., 464

## I

Ibikunle, Gbenga, 213
Ikonen, Veli-Pekka, 702
Imbrie, John, 617
Imperatriz-Fonseca, Vera, 410
Inklaar, Robert, 754
Institute for Global Environmental Strategies, 732, 734
Interagency Working Group on Social Cost of Greenhouse Gases, 750
Intergovernmental Panel on Climate Change (IPCC), 12, 676, 678, 686–688, 691,

731, 782, 786, 788, 882, 890, 916, 993, 1000
Intergovernmental Science-Policy Platform on Biodiversity and Ecosystem Services (IPBES), 384, 395, 405, 408, 464, 466, 504, 539
International Association of Insurance Supervisors (IAIS), 16
International Capital Market Association (ICMA), 21, 267, 281, 351
International Energy Agency (IEA), 12, 782, 901, 918, 919, 930, 932, 935–937, 992, 1014
International Finance Corporation (IFC), 2, 267, 268
International Organization of Securities Commissions (IOSCO), 15, 16
International Sustainability Standards Board (ISSB), 19
Iraldo, Fabio, 246
Isaac, Nick J., 384
Ishii, Joy, 178
Islam, Md Saiful, 538
Israel, Robert B., 127
ISS Governance, 581
IUCN, 64, 383, 385–388
Ivins, Erik, 701
Izzo, Maria Federica, 213

## J

Jackson, Jeremy B., 524
Jackson, Roland, 616
Jahnke, Annika, 473
Jahnke, Patrick, 585
Jalal, Raya Nabeel-Ud-Din, 313
Jamet, Dominique, 64
Jamet, Jean-Louis, 64
Jarrow, Robert A., 125
Jasiak, Joann, 97
Jaulin, Timothée, 32
Jeevanjee, Nadir, 682
Jeffers, Jessica S., 313
Jensen, Michael C., 146, 574
Jewell, Jessica, 731
Jha, Anand, 574
Joe, Harry, 1066
Johansen, Despina F., 353
Johansson, Daniel J. A., 771, 773
Johnson, Shane A., 178
Jolles, Anna E., 512
Jondeau, Eric, 998
Jones, Matthew W., 647–650, 652–655, 836, 842
Jones, Phil D., 717
Jones, Thomas M., 574
Jongejans, Eelke, 409
Joos, Fortunat, 871
Joppa, Lucas N., 380, 905
Joshi, Anup, 373
Jotikasthira, Chotibhak, 584
Jouzel, Jean, 632, 634, 635, 637, 638, 640, 715
Joye, Christopher, 199
Juettner-Nauroth, Beate E., 212
Juffe Bignoli, Diego, 62

## K

Kaack, Lynn H., 72
Kabel, Ashley, 199
Kacperczyk, Marcin, 157, 178, 210, 993, 998
Kadach, Igor, 591
Kaifu, Kenzo, 473
Kaplan, Robert S., 905
Kapraun, Julia, 277
Kar, T. K., 520
Karagulle, Deniz, 374
Karakaş, Oğuzhan, 588, 592
Karawia, Abdelrahman, 1047
Karim, Md Rajaul, 476
Karle, Volker, 703–705, 707, 708
Karuppiah, Ettikan Kandasamy, 75
Kato, Seiji, 662, 676
Kaufman, Alan J., 627
Kaufman, Dawn M., 394
Kaufmann, Daniel, 58
Kavvathas, Dimitrios, 131
Kay, Jennifer E., 676
Kaya, Yoichi, 651
Keeling, Charles D., 621, 622, 718
Keim, Donald B., 588, 589
Keip, Matthieu, 71
Kelleher, Adam, 73
Kellett, Christopher M., 759, 763, 768
Kelly, David L., 750
Kemp, Luke, 691
Kennedy, John J., 643–645
Kennelly, Steven J., 531, 532

Kent, Jennifer, 393
Khaled, Raneem, 333
Khan, Razib Hayat, 476
Khanchel, Imen, 213
Kharecha, Pushker, 640
Kiehl, Jeffrey T., 617, 668
Kim, E. Han, 594
Kirby, Michael X., 524
Kirby, Richard R., 566
Kirkemo, Anne-Mette, 538
Kitchen, Ann M., 521
Kitzes, Justin, 821
Klein, Alexandra-Maria, 402–404, 406, 407
Klein, Christian, 317, 318
Kleinberg, Robert L., 872–875
Kléparski, Loick, 566
Klepper, Gernot, 651
Klose, Ann Kristin, 703–705, 707, 708
Koedijk, Kees, 199
Kofoworola, Oyeshola, 257
Kölbel, Julian F., 27, 70, 73, 74, 159, 313
Kolbert, Elizabeth, 384
Kolstad, Charles D., 750
Konstantas, Antonios, 257
Köppl, Angela, 856
Koren, Sergey, 369
Koskinen, Yrjö, 213
Kostant, Peter C., 583
Kraakman, Norbertus, 468
Kraay, Aart, 58
Kram, Tom, 774
Kramer, Ryan J., 688
Kraus, Mathias, 72
Krauss, Jochen, 387
Kremen, Claire, 394, 406–408
Kreutzer, Idar, 185
Kriegler, Elmar, 691, 699, 713, 717, 791–793, 797, 798
Krueger, Philipp, 286, 317, 318, 589
Kruithof, Kristy, 349
Kruse, Hilde, 538
Kubiszewski, Ida, 473
Kuchler, Theresa, 559
Kuipers, Koen J. J., 543
Kumar, Rajeev, 580–582
Kunin, William E., 408
Kurths, Jürgen, 708, 709
Kurtz, Lloyd, 307, 313
Kuussaari, Mikko, 387, 389
Kvenvolden, Keith A., 617
Kwok, Chuck C., 178, 210
Kynast, Ellen, 505

## L

Laapas, Mikko, 702
Lacis, Andrew, 676
Laestadius, Lars, 455
LaFond, Ryan, 213
Lafortune, Guillaume, 21, 328, 337
Lake, Rob, 185
Lam, Kim Sim, 75
Lamb, William F., 836, 900
Lammerant, Johan, 547, 548
Lando, David, 125
Landrigan, Philip J., 487–489
Langway, Chester C., 632, 633
Lapola, David M., 461
Larcker, David F., 277, 593, 594
Larsen, Brendan B., 371
Larsen, Frank W., 393
Lassoued, Naima, 213
Latham, Sophia M., 538
Latino, Carmelo, 75, 277
Lauretig, Adam, 73
Lauritano, Chiara, 532
Le Berthe, Tegwen, 32, 71
Le Guenedal, Théo, 73, 166, 167, 179–192, 197, 200–205, 213–215, 217, 750, 768–770, 807, 830, 832–836, 851, 856–860, 895, 920, 926, 927, 930, 932–937, 977, 1001, 1047, 1056
Le Quéré, Corinne, 651
Leakey, Richard E., 384
Lebrero, Raquel, 468
Lebreton, Laurent, 474, 475
Lee, Charles M., 212
Lee, Darren D., 213
Lee, Linda-Eling, 26
Lee, Young-Chul, 490
Legendre, Pierre, 451–453, 568
Legesse, Fekadu, 401
Legrand, Michel, 617
Lehman, Clarence L., 387, 391
Lehtonen, Ilari, 702
Leigh Jr, Egbert G., 443
Leighton, Frederick A., 538

Leijonhufvud, Christina, 307
Leippold, Markus, 72, 73
Leiserowitz, Anthony A., 716, 717
Leising, Andrew, 518
Leite, Paulo, 199
Leith, Cecil E., 623
Lelieveld, Jos, 490
Lemoine, Derek, 768
Lemoine, Rhys T., 502
Lennox, Gareth D., 463
Lenssen, Nathan J., 645
Lenton, Timothy M., 691, 692, 699
Lenzen, Manfred, 836
Leontief, Wassily W., 807, 819
Lepetit, Frédéric, 166, 167, 179–192, 197, 1047
Leprieur, Fabien, 702
Lerner, Jean, 676
Leroy, Boris, 466
Lesiv, Myroslava, 461
Letts, Christine W., 307
Leung, Kelvin Sze-Yin, 471
Levine, David I., 27
Levins, Richard, 522
Levit, Doron, 583, 585, 592
Lewin, Roger, 384
Lewis, Jared, 735
Lewis, Simon L., 624, 625
Lezmi, Edmond, 966
Li, Jui-lin, 662, 676
Li, Pei-Hao, 781, 782
Li, Xi, 588, 592
Liang, Shunlin, 668
Lin, Chen, 588
Lin, Kai, 199
Lin, Yanan, 607
Lioui, Abraham, 159–162
Lisiecki, Lorraine E., 639
Litterman, Robert B., 147, 758, 759
Liu, Lei, 475
Liu, Peiran R., 733, 735
Liu, Wei, 702
Liu, Yunhui, 402
Liu, Zhengyu, 702
Liu, Zongyuan Zoe, 137
Livingston, Jasmine E., 731
Llop, Maria, 850
Lobell, David B., 73, 717
Loch-Temzelides, Ted, 538
Loehle, Craig, 380
Löffler, Kristin Ulrike, 277
Lollo, Niklas, 774, 775
Lombard, François, 920, 926, 927, 930, 932–937, 977, 1001
Lomolino, Mark V., 434, 435
Longcore, Travis, 471
Lonsdale, W. Mark, 464
Lopez, Bianca, 473
Lorenz, Max O., 65
Los, Bart, 815
Lotka, Alfred J., 508
Loyau, Adeline, 540
Lu, Louise Yi, 574
Lubchenco, Jane, 428
Lucas Jr, Robert E., 217
Luccioni, Alexandra, 72
Lucey, Brian, 559
Lucht, Wolfgang, 656–658, 691, 699
Lucius, Dorianne, 991, 998, 999, 1006, 1018–1021, 1023, 1027, 1028
Luczak, Christophe, 566
Ludwig, Cornelia, 504, 505
Ludwig, Donald, 502
Lueck, Dean, 503, 512
Luers, Amy, 905
Lunt, Daniel J., 641, 642
Luoto, Miska, 702
Ly, Lai, 179–183, 185, 187–192, 197

## M

Ma, K. C., 178
Maalej, Yassine, 1012, 1014–1016
Mac Dowell, Niall, 905
MacArthur, Robert H., 387, 433, 434, 445, 522, 524
Mace, Georgina M., 375, 539
Mack, Richard N., 464
MacKay, Jock, 1066, 1074
MacLeod, Matthew, 473
Mader, Eric, 408
Maes, Dirk, 409, 410
Maggiori, Matteo, 48
Magnanelli, Barbara Sveva, 213
Magnani, Elisa, 377
Mahtani, Vivek, 157, 277, 279
Maibach, Edward Wile, 717

Maiolo, Michael, 580–582
Mair, Louise, 545, 546
Maitra, Anando, 199
Makowski, David, 402
Malenko, Andrey, 594
Malenko, Nadya, 592, 594
Malhi, Yadvinder Singh, 717, 902, 903, 905
Maltais, Aaron, 272
Malthus, Thomas Robert, 508
Malysheva, Svetlana, 547
Manabe, Syukuro, 622, 624, 716–718
Mao, Chang Xuan, 450
March, Antaya, 353
Marconi, Valentina, 62
Mardones, Cristian, 850
Margolis, Joshua D., 137
Marinelli, Nicoletta, 313
Markowitz, Harry M., 138, 139
Marland, Gregg, 651
Marsland III, Robert, 523
Martellini, Lionel, 217
Marten, Alex L., 758
Martin, Fabio, 260
Martin, Jean-Louis, 464
Martin, Maximilian, 315
Marty, Bernard, 627
Maslin, Mark A., 624, 625
Massetti, Emanuele, 774
Masson-Delmotte, Valérie, 640, 715
Masterman, Clayton J., 501
Mastruzzi, Massimo, 58
Masui, Toshihiko, 774
Mathur, Ritu, 791, 793
Matos, Pedro, 178
Matsusaka, John G., 579, 594
Matthews, Thomas J., 443
Mattick, John S., 368
Mattson, Mark P., 478
Matzke, Nicholas, 380, 381, 384, 387
Maug, Ernst, 592
Maurin, Michel, 480
Mauritsen, Thorsten, 702
May, Robert M., 371, 387, 391, 445
May, Roel, 543
Mazaris, Antonios D., 389, 390
Mazzotti, Marco, 905
Mazzucato, Mariana, 334
McCahery, Joseph A., 577, 583
McCarthy, Donal P., 551
McCoy, Earl D., 435
McGehee, Richard, 524
McGill, Brian J., 440, 441
McGlade, Christophe, 735
McGuire, Anthony David, 701
McKenney, Mark G., 75
McKibbin, Warwick J., 944
McKinsey, 273, 287, 289, 293
McMorrow, Mike, 279
McRae, Louise, 62
Meckling, William H., 574
Medina, Alejandra, 589–591
Medley, Paul A. H., 531, 532
Meeuwig, Jessica, 535
Megaeva, Karina, 246, 252
Mehta, Pankaj, 523
Meijer, Harro A., 622
Meijer, Johan R., 542, 543
Meijer, Lourens J. J., 474, 475
Meinshausen, Malte, 735, 774
Mejino-López, Juan, 495–497
Melillo, Jerry M., 428
Mena, Camilo, 850
Menchaoui, Ghassen, 966
Menif, Myriam, 258
Menne, Matthew J., 645
Menville, Diane, 58, 59
Menz, Klaus-Michael, 199, 213
Mercier, Bertrand, 1053
Merlivat, Liliane, 634
Messner, Dirk, 334
Messori, Gabriele, 702
Metrick, Andrew, 178
Miele, Vincent, 64
Miles, Lera, 542
Millennium Ecosystem Assessment, 395
Miller, Conrad, 217
Miller, Daniel C., 551
Miller, Elizabeth C., 371
Miller, John B., 701
Miller, Ronald E., 807, 810, 819, 821
Mini, Caroline, 853, 860
Mintzberg, Henry, 574
Minx, Jan Christoph, 821, 836, 869, 900
Mio, Chiara, 334
Mishra, Bibhu, 321
Mishra, Dev R., 178, 210

Missemer, Antoine, 396
Mitali, Shema Frédéric, 272, 273
Mitchell, Ronald K., 574
Mitchell-Larson, Eli, 902, 903, 905
Mittermeier, Cristina G., 393
Mittermeier, Russell A., 393
Moat, Justin, 418, 419
Mohamed, Ehab K. A., 333
Mohanram, Partha, 212
Mojon, Benoît, 998
Moler, Cleve, 1046
Moloney, Georgia Kate, 535
Monjon, Stéphanie, 178
Monokrousos, Nikolaos, 389, 390
Monsalve, Julián, 213
Montañez, Isabel P., 639
Montgomery, Benedicte, 292, 293
Moody's, 131
Mooers, Arne O., 551
Moomaw, William, 624
Mooney, Harold A., 394, 428
Mooney, T. Aran, 473
Moore, Frances C., 774–776
Moore, G. W. Kent, 702
Moore, Rebecca, 461
Moorman, Theodore C., 178
Moote, Kilian, 580–582
Mora, Camilo, 371
Morais, Philippe, 807, 830, 832–836, 851, 856–860, 1056
Moreno, Diana, 607
Moreno, Jorge, 328
Morice, Colin P., 643–645
Morin, Hubert, 702
Mörner, Torsten, 538
Morningstar, 231–233, 235, 242, 258–265
Morse, Adair, 313, 314
Mortier, Vincent, 179–192, 197
Moskowitz, Milton, 3
Mosnier, Aline, 774
Mosson, Natacha, 335, 336
Motomura, Isao, 444
Mountford, J. Owen, 475
MSCI, 68, 70, 338–341
Muñoz, Raúl, 468
Muir, Derek C. G., 468
Mulder, Machiel, 213
Muller, Reinhold, 464
Muller, Richard A., 374–377
Murphy, Kevin J., 574
Murray, James, 518
Musaba, Prescott, 535
Musca, Xavier, 357
Musto, David K., 313
Muto, Atsu, 701
Mwinyihali, Robert, 535
Myers, Christopher A., 520, 521
Myers, Eugene W., 369
Myers, Norman, 393
Myers, Ransom A., 525, 526
Myllyvirta, Lauri, 491, 492

## N

Naffa, Helena, 217
Nagatani-Yoshida, Kakuko, 468
Naidu, Ravi, 468
Naiken, Loganaden, 424
Nakamura, Miguel, 384
Nakicenovic, Nebojsa, 334
Nasi, Robert, 463, 535
National Academies of Sciences, Engineering, and Medicine (NASEM), 901
Nazir, Amril, 75
Nebesse, Casimir, 535
Neidell, Matthew, 495
Neinavaz, Elnaz, 540
Nellemann, Christian, 542
Nelsen, Roger B., 1066, 1068, 1070–1072, 1075
Nemet, Gregory F., 900
Nergadze, Solomon G., 377
Network for Greening the Financial System (NGFS), 395, 797, 799
Neumann, Peter, 408
Newbold, Stephen C., 758
Newman, Michael C., 477
Newmark, William D., 389, 390
Newsome, Thomas M., 502, 503
Ng, Anthony C., 213
Ng, Carla A., 472
Ngo, Hien T., 408, 410, 411
Noel, Jeffrey K., 521, 522
Noone, Kevin, 656
Nordhaus, William D., 715, 717, 718, 729, 750, 751, 754, 756, 758–760, 762, 768, 773, 774, 776

Norges Bank Investment Management (NBIM), 593
Norris, James R., 117, 122
Norris, Richard D., 640
North Greenland Ice Core Project members, 639
Noss, Reed F., 393
Notz, Dirk, 702
Nova, Noshin, 313
Nowak, Martin A., 387, 391
Nurk, Sergey, 369
Nykvist, Björn, 272

## O

O'Brien, Denis, 662, 676
O'Connor, Louise, 64
O'Donohoe, Nick, 307
O'Neill, Brian C., 791–793
O'Sullivan, Jacob D., 547
O'Sullivan, Michael, 647–650, 652–654, 836, 842
O'Sullivan, Robert, 418, 419
Oberhauser, Karen, 410
Obersteiner, Michael, 717
Oberthür, Sebastian, 727
Observatoire de la Responsabilité Sociétale des Entreprises (ORSE), 25
Obst, Carl, 401
Ohlmann, Marc, 64
Ohlson, James A., 212
Oikonomou, Ioannis, 199, 213
Okabe, Kimiko, 463
Olhnuud, Aruhan, 402
Oliphant, Becky J., 178
Oliu-Barton, Miquel, 495–497
Ollerton, Jeff, 408
Olson, David M., 373
Oppenheimer, Michael G., 624, 717
Organisation for Economic Co-operation and Development (OECD), 402
Orlitzky, Marc, 137
Ormazabal, Gaizka, 591
Orndorff, Samantha, 534
Ortiz, Joseph D., 616
Ossola, Elisa, 257
Ostling, Annette, 451–453
Otero-Espinar, M. Victoria, 520
Ott, Hermann E., 727
Otten, Roger, 199
Otto, Friederike, 902, 903, 905
Oueghlissi, Rim, 217
Oulid Azouz, Noureddine, 896–900, 911–913, 928, 941, 942, 979–984, 989, 990, 998–1002, 1006–1013
Oulton, Will, 317, 319
Our World in Data, 60, 61, 458, 461, 488, 538
Ouyang, Xiaoying, 475
Ovaskainen, Otso, 391
Ozbas, Oguzhan, 579
Özler, Sule, 217

## P

Pérez, Cristina, 468
Packer, Frank, 268, 273
Paetzold, Falko, 313, 317, 318
Pagani, Federico, 734
Pagani, Mark, 640
Palacios, Erwin, 534
Palinska, Aleksandra, 317, 319
Palma Esposito, Fortunato, 532
Palmer, Todd. M., 384, 387
Palomares, Maria, 532
Pan, Xun-Zhang, 735
Panfilo, Silvia, 334
Panzica, Roberto, 277
Parikh, Neal, 1053
Parizek, Byron R., 701
Park, Duckshin, 490
Park, Thomas, 524
Parker, Stephen, 199
Parrenin, Frédéric, 637
Pástor, Luboš, 137, 151–155, 157, 160, 164, 276
Patalano, Robert, 28
Patel, Pralit, 774, 778
Patil, Richa, 607
Patrizio, Piera, 905
Pauli, Gunter A., 352
Pauly, Daniel, 525–527, 532
Pausata, Francesco S. R., 702
Pavelin, Stephen, 199, 213
Pearce, David, 396, 397, 533
Pedersen, Lasse Heje, 137, 148, 169–171, 173, 176, 177
Peleato, Borja, 1053
Pelizzon, Loriana, 75

Peltola, Heli, 702
Peña, Alejandro, 213
Pereira da Silva, Luiz A., 998
Pereira, Henrique Miguel, 540
Pereira, Patrícia, 199
Peres, Carlos A., 502, 503, 533–535, 539
Pérez Roda, Maria Amparo, 531, 532
Peri, Mattia, 277
Perkin, Elizabeth K., 471
Perrin, Sarah, 948, 966
Perrissin Fabert, Baptiste, 776
Persin, Avraham, 645
Peters, Glen P., 655, 717, 738, 836
Petersen, Tanya, 62
Petit, Jean-Robert, 632, 635, 637, 638
Petreski, Aleksandar, 277
Pfleiderer, Paul, 585
Phenix Capital, 345, 346, 353, 354, 364, 563
Phillips, Norman A., 622
Pickart, Robert S., 702
Pickens, Amy, 461
Picón Martínez, Arnau, 315, 316
Pierrehumbert, Raymond, 618–620, 716
Pierson, Patricia, 473
Pilewski, Peter, 662, 676
Pimm, Stuart L., 378–380, 384, 435
Pindyck, Robert S., 758, 781
Pinho, Patricia, 461
Piper, Stephen C., 622
PitchBook, 289–291, 342–344
Pitman, Nigel, 443
Plass, Gilbert Norman, 621
Platt, William J., 393
Pointer, Michael D., 524
Polbennikov, Simon, 199
Polis, Gary A., 520, 521
Pollan, Michael, 420
Pollard, David, 701
Pomorski, Lukasz, 137, 169–171, 173, 176, 177
Pongratz, Julia, 836
Pope III, C. Arden, 490
Popp, David, 776
Potapov, Peter V., 461
Pottier, Antonin, 776
Potts, Simon G., 408, 410
Poufinas, Thomas, 213
Pouget, Sébastien, 580, 592
Pouillet, Claude, 615
Powers, David Martin, 104
Pozzer, Andrea, 490
Pratt, Shannon P., 211
Preclaw, Ryan, 73
Prequin, 289
Preston, Frank W., 443, 444
Primack, Richard B., 365, 428, 465
Principles for Responsible Investment (PRI), 28, 42, 59, 294–296, 304, 573, 586, 588, 593
Pringle, Robert M., 380, 384, 387
Pruessner, Eric, 317, 319
Purnomo, 534
Putz, Francis E., 533

## Q

Qiao, Shuyuan, 538
Quigley, Ellen, 585
Quinn, Terrance J., 513

## R

Rader, Romina, 405, 410
Raedel, Gaby, 702
Raftery, Adrian E., 733, 735
Rahman, Md Tanvir, 538
Rahmstorf, Stefan, 691, 699, 713
Raja, Srinivasa N., 75
Ramanathan, Veerabhadran, 617
Ramanna, Karthik, 905
Ramelli, Stefano, 938
Ramirez, Ana Gabriela, 213
Ramírez, Andrea, 900, 905, 906
Ramírez-Delgado, Juan Pablo, 433
Rancan, Michela, 277
Rao, Narasimha D., 793
Raper, Sarah C. B., 774
Ratto, Fabrizia, 405
Raup, David M., 380, 381
Raupach, Michael R., 651
Raymo, Maureen E., 639
Raynaud, Dominique, 632, 635, 637, 638
Rayner, Nick A., 643–645
RBB Economics, 851, 852
Redín, Julen González, 547
Redín, Julen González, 548
Redon, Nicolas, 258
Reeder, Neil, 321
Rees, William, 422, 869

Refinitiv, 69, 70
Reich, Peter B., 450
Reid, John W., 533, 534
Renault, Véronique, 535
Renfrew, Ian A., 702
Renneboog, Luc, 313, 577
RepRisk, 72, 249–251
Resit Akçakaya, H., 64
Revelle, Roger, 621
Reynolds, John D., 533
Rezaee, Zabihollah, 213
Rhie, Arang, 369
Rhodes, Matthew K., 371
Riahi, Keywan, 715–717, 791, 793
Riccio, Gennaro, 532
Rice, Richard E., 533, 534
Rich, Catherine, 471
Richardson, Katherine, 656–658, 699
Richardson, Lewis F., 622
Richters, Oliver, 797, 798
Rickards, Barrie, 380
Ries, Leslie, 410
Rignot, Eric, 701
Rigobon, Roberto, 27, 70, 74, 159
Rillaerts, Jordy, 73
Rind, David, 676
Ringel, Ben, 342, 347
Ripple, William J., 463, 502, 503, 535
Rising, James, 774, 775
Ritchie, Hannah, *see* Our World in Data
Ritchie, Paul D., 698
Ritz, Christian, 478
Rivers, Nicholas, 494, 495
Rizzo, Carmen, 532
Roberts, Callum M., 526, 527
Robinson, Lisa A., 501
Rochet, Jean-Charles, 272, 273
Rockström, Johan, 326, 334, 656, 699, 713
Roe, Paul, 534
Rogelj, Joeri, 730
Rohde, Robert A., 374–377, 645
Roll, Richard, 149
Roncalli, Théo, 166, 167, 1047
Roncalli, Thierry, 13, 53, 58, 75, 95, 138, 144, 148, 166, 167, 179–195, 197, 200–205, 211, 213–215, 217–226, 279, 280, 283, 309, 356, 807, 830, 832–836, 851, 856–860, 862–866, 895–900, 911–913, 920, 926–928, 930, 932–937, 941, 942, 948, 954, 966, 977, 979–984, 989–991, 998–1002, 1006–1013, 1018–1023, 1027, 1028, 1047, 1056, 1066
Roques, Lionel, 517
Rosa, Lorenzo, 905
Rosati, Brigid, 580–582
Rose Niu, 551, 554, 555
Rose, Steven K., 775, 776
Rosenthal, Jeffrey S., 127
Rosenzweig, Michael L., 436
Ross, Stephen A., 148
Rossberg, A. G., 547
Rossby, Thomas, 701
Rössler, Otto E., 696
Roston, Marc, 905
Roth, Raphael, 871
Roubini, Nouriel, 217
Rougier, Florent, 480
Royer, Dana L., 639, 641, 642
Rubin, Jennifer, 349
Rudd, Andrew, 4
Ruedy, Reto, 645, 676
Rummukainen, Markku, 731
Ruosteenoja, Kimmo, 702
Russell, Gareth J., 378–380, 435
Russell, Gary, 640, 676
Russell, Stephen, 901
Ryan, William, 307
Rybicki, Joel, 439
Rynes, Sara L., 137

## S

Sabogal, Cesar, 463
Sachs, Jeffrey D., 21, 328, 334, 337
Sætra, Henrik Skaug, 21
Sagan, Carl, 630
Sage, Rowan F., 702
Sahakyan, Vahe, 279
Sala, Osvaldo E., 428
Saleh, Ahmed, 213
Salomon, Robert M., 178
Saltuk, Yasemin, 307
Samama, Frédéric, 357, 947, 967, 993, 998
Sánchez-Bayo, Francisco, 409
Santos-Paulino, Amelia U., 334
Sarmento Cabral, Juliano, 387
Sassi, Olivier, 774

Sato, Makiko, 640
Sauer, Petra, 793
Sautel, Olivier, 853, 860
Sautner, Zacharias, 577, 583, 589
Sayre, Roger, 374
Schädel, Christina, 701
Schaefer, Milner B., 509
Schaeffer, Michiel, 730
Scharlemann, Jörn. P. W., 551
Schauster, Edward R., 521
Scheck, Barbara, 307, 313
Scheins, Christopher, 277
Schellnhuber, Hans Joachim, 691, 699, 713, 715
Schepaschenko, Dmitry, 461
Scheringer, Martin, 472
Schijns, Rebecca, 526, 527
Schipper, Aafke M., 542, 543
Schlag, Christian, 277
Schleussner, Carl-Friedrich, 730
Schmeller, Dirk S., 540
Schmidt, Christian, 474, 475
Schmidt, Frank L., 137
Schmidt, Gavin A., 645
Schmidt-Traub, Guido, 328, 334
Schmiesin, Kevin E., 2
Schneemeier, Jan, 585
Schneider, Valerie A., 369
Scholes, Robert J., 544
Scholtens, Bert, 213, 217, 317, 318
Schrag, Daniel P., 627
Schramade, Willem, 334
Schratzenstaller, Margit, 856
Schulp, Catharina J. E., 412
Schulte, Peter, 382
Schuur, Edward, A., 701
Schweiger, Oliver, 408
Schweizer, Berthold, 1072
Schymanski, Emma L., 471
Scott, Vivian, 905
Scraggs, Emily, 349
Seddon, Nathalie, 902, 903, 905
Sekercioglu, Cagan H., 394
Sekine, Takaya, 166, 167, 179–192, 197, 200–205, 213–215, 217, 559, 920, 926, 927, 930, 932–937, 977, 1001, 1047
Sellers, William D., 623, 677
Semet, Raphaël, 58, 59, 217–226, 279, 280, 283, 862–866, 1022
Semmler, Willi, 759, 763, 768
Seneviratne, Sonia Isabelle, 717
Senkowski, Christopher K., 75
Sepkoski, Joseph John, 375, 380, 381
Serafeim, George, 269, 273, 592
Shabana, Kareem M., 574
Shackleton, Nicholas J., 617
Shandal, Vinay, 292, 293
Sharfman, Mark P., 209, 210, 213
Sharpe, William F., 4, 138, 144, 145
Shen, Jun, 381, 382, 428, 429
Shen, Yaokan, 213
Shepherd, Andrew, 701
Sherwood, Steven C., 679, 681, 688
Shields, Graham, 628
Shin, Keumchul, 490
Shine, Keith P., 874
Shnerb, Nadav M., 547
Shu, Chong, 594
Siebert, Asher, 777
Silva, Florinda, 199, 258
Sim, Megan, 349
Simberloff, Daniel, 464, 465
Simmons, Benno I., 405
Simpson, Alastair G. B., 371
Simpson, George Gaylord, 379, 380
Singh, Hanwant B., 617
Sitch, Stephen A., 717
Sjo, Hege, 185
Skaife, Hollis Ashbaugh, 213
Skidmore, Andrew K., 540
Sklar, Abe, 1066
Slat, Boyan, 474
Slay, Christy M., 461, 462
Sloan, Lisa, 640
Smith Greenleaf, Sarah, 406, 407
Smith, Keight T., 473
Smith, Pete, 717, 781, 782
Smith, Steve, 902, 903, 905
So, Ivy, 321
Sobur, Md Abdus, 538
Social Finance, 348
Socolow, Robert H., 777
Soden, Brian J., 678, 718
Sodhi, Navjot S., 365, 428
Solé, Marta, 473

Solomon, Maurice E., 517
Sorescu, Sorin, 178
Sorg, Martin, 409
Soromessa, Teshome, 401
Sorrie, Bruce A., 393
Spake, Rebecca, 405
Spalding, Christopher, 378, 391, 392
Spatt, Chester S., 594
Speare, Rick, 464
Spicer, John I., 365, 366, 374, 375, 394, 504
Sprott, Julien Clinton, 521, 522
Spurgin, Lewis G., 524
Staal, Arie, 699, 700, 703, 708
Stadler, Balazs, 494, 495
Stagnol, Lauren, 58, 217–226, 559
Stainforth, David A., 760, 762, 763
Stambaugh, Robert F., 137, 151–155, 157, 160, 164, 276
Stanton, Elizabeth A., 777
Stapleton, Heather M., 471
Starks, Laura T., 185, 297, 298, 574, 577, 583, 586, 588, 589
Staskevicius, Alina, 321
Steffan-Dewenter, Ingolf, 387, 405
Steffen, Bjarne, 72
Steffen, Will, 504, 505, 656–658, 699
Stehfest, Elke, 774
Stehrer, Robert, 815
Stengel, Carrie, 64
Stephan, Andreas, 277
Stephens, Graeme L., 662, 676
Stephens, Patrick R., 380
Stephenson, P. J., 64
Stern, Nicholas, 771, 773
Sterner, Thomas, 758
Stevens, Carly J., 475
Stevens, Richard D., 394
Stevenson, Ross K., 629
Stock, James H., 759
Stoermer, Eugene F., 624
Stokes, Chris R., 701, 702
Stolle, Fred, 455
Stommel, Henry M., 623
Stone, Peter, 676
Strachan, Neil, 781, 782
Streibig, Jens Carl, 478
Streletskiy, Dmitry, 702
Strempel, Sebastian, 472
Strevens, Chloë M. J., 524
Stroebel, Johannes, 48, 559
Stroehle, Judith C., 25, 26
Strogatz, Steven H., 692, 694
Strom, Suzanne, 518
Strona, Giovanni, 436–438
Struebig, Matthew J., 534
Struijs, Jaap, 543
Stuart Chapin III, F., 428
Stuber, Nicola, 874
Suess, Hans E., 621
Suh, Jungwon, 213
Sukhatme, Pandurang Vasudeo, 423, 424
Summerhayes, Colin, 625
Sunderji, Sophia, 313
Sunny, Nixon, 905
Sutton, Paul, 398, 400
Sutton, Paul C., 473
Suuronen, Petri, 531, 532
Svartzman, Romain, 402
Svenning, Jens-Christian, 502
Swagel, Phillip, 217
Swaminathan, Bhaskaran, 212
Syeed, M. M. Mahbubul, 476
Sztorc, Paul, 750, 751, 754, 756, 758, 762, 774

## T

Taber, A., 535
Tabor, Neil J., 639
Taft, Ryan J., 368
Tan, Zhenhao, 48
Tang, Dragon Yongjun, 277
Tang, Yun, 589–591
Tankov, Peter, 73
Tanner, James T., 518
Tanzer, Samantha Eleanor, 900, 905, 906
Tarelli, Andrea, 159–162
Tarrant, Sam, 408
Task Force on Climate-related Financial Disclosures (TCFD), 23, 25
Taskforce on Nature-Related Financial Disclosures (TNFD), 395
Taskforce on Nature-related Financial Disclosures (TNFD), 557, 558
Tate, Cynthia M., 538
Tavoni, Massimo, 774
Tayan, Brian, 593, 594
Taylor, Chris, 773

Taylor, Louise H., 538
Taylor, Lucian A., 137, 151–155, 157, 160, 164, 276
Technical Expert Group on Sustainable Finance (TEG), 33, 36, 894, 979, 991
Tekman, Mine B., 473
Ten Brink, Ben, 542
Teoh, Ee Na, 75
Ter Horst, Jenke, 313
Terlouw, Tom, 905
Testa, Francesco, 246
Tett, Simon, 905
Thangavel, Prakash, 490
Tharyan, Rajesh, 213
Thogmartin, Wayne E., 410
Thomas, Chris D., 717
Thomas, Ellen, 640
Thomas, Jacob, 212
Thompson, Benjamin S., 353
Thompson, Ian D., 463
Thornhill, Gillian D., 688
Thornley, Ben, 311
Thuiller, Wilfried, 64, 412
Thurstan, Ruth H., 526, 527
Tian, Gaoliang, 574
Tibshirani, Robert, 75, 1079
Tikkanen, Olli-Pekka, 702
Tilman, David, 387, 391, 475, 523
Timmer, Marcel P., 754, 815
Tittensor, Derek P., 371
Tjørve, Even, 436
Tobin, James, 138, 142
Tockner, Klement, 471
Tol, Richard S. J., 717, 718, 729, 758, 774, 775
Tomiya, Susumu, 380, 381, 384, 387
Tonello, Matteo, 580, 583
Touboul, Samuel, 27
Townsend, Blaine, 3, 5
Townsend, Colin R., 513
Trenberth, Kevin E., 668, 713, 717
Triantis, Kostas A., 436
Trinks, Arjan, 213
Truskinger, Anthony, 534
Tucker, Anne M., 313
Turnbull, Stuart M., 125
Turner, Karen, 836
Turner, Will R., 393
Tutin, Caroline, 535
Tyndall, John, 616
Tyukavina, Alexandra, 461, 462

## U

Uddin, Mohammad Faisal, 476
UN Framework Convention on Climate Change (UNFCCC), 728, 735
United Nations (UN), 327, 329, 723–726
United Nations Economic Commission for Europe (UNECE), 890
United Nations Environment Programme (UNEP), 12
United Nations Office on Drugs and Crimes (UNDOC), 537
Urbieta, Laida, 341
Ureche-Rangau, Loredana, 580
US Environmental Protection Agency (EPA), 484, 485
Utkus, Stephen, 48
Uzun, Hatice, 213

## V

Vaccari, Alessandra, 246
Våge, Kjetil, 702
Vaissière, Anne-Charlotte, 466
Vaissière, Bernard E., 402–404
Valentine, James W., 379, 380
Valin, Hugo, 774
Vallée, Lou-Salomé, 217
Van Binsbergen, Jules H., 313
Van Bruggen, Ariena H., 490
Van Der Ent, Ruud, 474, 475
Van der Merve, Kate, 607
Van der Ploeg, Sander, 398
Van Emmerik, Tim, 474, 475
Van Holt, Tracy , 137
Van Khoa, Le Dinh, 75
Van Liedekerke, Luc, 246, 252
Van Loan, Charles F., 129, 1046, 1047
Van Oorschot, Mark, 542
Van Swaay, Chris A. M., 409, 410
Van Tol, Gijs, 535
Van Valen, Leigh, 379, 380
Van Vliet, Nathalie, 535
Van Vuuren, Detlef P., 716, 717, 774, 791, 793
Van Wesep, Edward Dickersin, 586
Van Zelm, Rosalie, 543

Vance, Stanley C., 3
Vanclay Jerome K., 533
Vano, J. A., 521, 522
Vegelin, Courtney, 327
Veizer, Ján, 628, 639
Venålåinen, Ari, 702
Venter, J. Craig, 369
Venter, Oscar, 463
Verburg, Peter H., 412
Verhelst, Jolien, 547, 548
Verhulst, Pierre-François, 508, 509
Verones, Francesca, 543
Verwijmeren, Patrick, 213
Vestvik, Rolf A., 353
Vicente, Alba, 384
Vignieri, Sacha, 473
Viiri, Heli, 702
Viollaz, Julie, 535
Viscusi, W. Kip, 501
Vitousek, Peter M., 428
Vokou, Despoina, 389, 390
Volterra, Vito, 508
Von Neumann, John, 622
Vose, Russell S., 645, 646
Vredenburg, Vance T., 384
Vu, Anh, 607

## W

Wackernagel, Mathis, 422, 869
Wagner, Gernot, 758, 759
Wahlen, Martin, 622
Waisman, Henri, 774
Wake, David B., 384
Waldron, Anthony, 551
Walker, Glen W., 468
Walker, Michael, 626
Walker, Ryan T., 701
Walker, William H., 473
Walsh, James P., 137
Walter, Andreas, 260
Walters, Carl, 502
Walters, Michele, 540
Walton, James C., 473
Wang, Dieter, 58, 75
Wang, Dongdong, 668
Wang, Fang, 471
Wang, Hai-Lin, 735
Wang, Qian, 73
Wang, Zhanyun, 468
Warner, Mildred E., 313
Warren, Martin S., 409, 410
Watanabe, Kazuo, 368
Waterman, Lee S., 718
Waters, Brian, 350
Waters, Colin N., 625
Watson, James E. M., 433, 463
Watson, Reg, 525
Watts, Edward M., 277
Weart, Spencer, 624
Weatherdon, Lauren V., 540
Webb, Mark J., 679, 681, 688
Weber, Christopher L., 836
Weber, Olaf, 317, 318
Webersinke, Nicolas, 72
Webster, Peter J., 662, 676
Wei, Jason Z., 127
Weiss, Ehud, 419
Weitzman, Martin L., 758, 771
Welbourn, Pamela, 477
Weldon, Ché, 464
Weller, Steven R., 759, 763, 768
Weng, Yu-Yan, 735
Wepprich, Tyson, 410
Westveer, Judith, 62
Wetherald, Richard T., 622, 718
Weyant, John P., 729
Whittaker, Julie, 213
Whittaker, Robert H., 441, 443
Whittaker, Robert J., 436, 443
Who Cares Wins, 4, 5
Whorf, Timothy P., 622
Wible, Brad, 473
Wiederholt, Ruscena, 410
Wiedmann, Jerome, 410
Wiedmann, Thomas, 821, 836, 869
Wieland, Michelle, 535
Wieners, Claudia, 774
Wiens, John J., 371
Wigley, Tom M. L., 713, 774
Wikramanayake, Eric D., 373
Wilcoxen, Peter J., 944
Wildenberg, Joe C., 521, 522
Wilkie, David, 535
Wilkie, David S., 533
Willett, Ian R., 468
Williams, Carrington Bonsor, 444

Williamson, Oliver E., 574
Willig, Michael R., 394
Willmott, Elizabeth, 905
Wilson, Edward O., 365, 387, 428, 433, 434
Wimmer, Florian, 505
Winfree, Rachael, 405, 408
Winkelmann, Ricarda, 703–705, 707–709
Wisz, Mary S., 702
Wolf, Christopher, 463, 502, 503
Wolf, Eric T., 627
Wolf, Oliver, 257
Wolff, Edward F., 1072
Wolter, Christian, 471
Wood, David, 311
Wood, Donna J., 574
Wood, Margaret, 75
Wood, Richard, 821
Woolhouse, Mark E. J., 538
World Bank, 489, 490, 493
World Economic Forum (WEF), 401, 429, 431
World Health Organization (WHO), 480, 481
World Meteorological Organization (WMO), 617
World Ocean Review, 400
Worm, Boris, 371, 525, 526, 532
Wratten, Stephen D., 408
Wright, David A., 477
Wu, Qingbai, 702
Wunderling, Nico, 708, 709
Wunsch, Carl I., 623
Wurgler, Jeffrey, 269, 273
Wyckhuys, Kris A. G., 409

## X

Xiang, Leilei, 471
Xie, Shang-Ping, 702
Xu, Chi, 691
Xu, Jiali, 966, 991, 998, 999, 1006, 1018–1021, 1023, 1027, 1028
Xu, Xiao, 48

## Y

Yamano, Norihiko, 836, 842–845
Yang, Pu, 774
Yang, Zili, 776
Yasuda, Ayako, 313, 314
Yi, Irene, 579
Yin, Xungang, 645, 646
Yokobori, Keiichi, 651
Yoon, Aaron, 592
Young, David, 292, 293
Young, Hillary S., 384
Yu, Jinfang, 538
Yu, Yangxin, 574
Yu, Yunyue, 668
Yuan, Yuan, 574

## Z

Zachos, James C., 640
Zahnle, Kevin J., 626
Zalasiewicz, Jan, 625
Zalles, Viviana, 455
Zeebe, Richard E., 640
Zeisberger, Stefan, 313
Zeller, Dirk, 532
Zeng, Xiaming, 73
Zeng, Xuran, 559
Zerbib, Olivier David, 157, 276, 277
Zhan, James X., 334
Zhang, Chendi, 213, 313
Zhang, Shuyuan, 538
Zhang, Xiuying, 475
Zhang, Yupu, 277
Zhong, Taiyang, 475
Zhu, Jiang, 702
Zingales, Luigi, 585
Zohary, Daniel, 419
Zulaica, Omar, 279
Zurita, Gustavo A., 439
Zyss, Daniel, 645